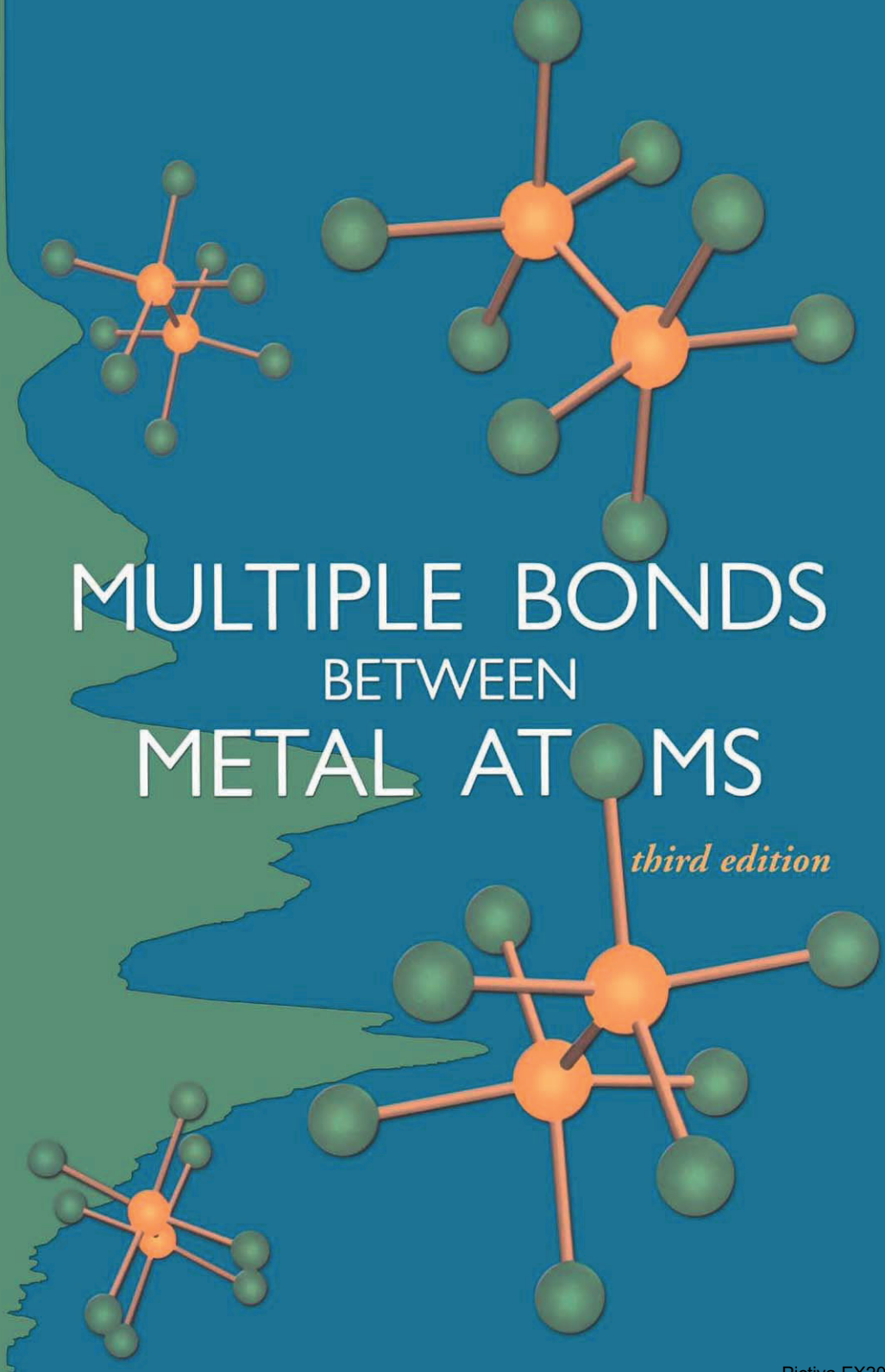


MULTIPLE BONDS BETWEEN METAL ATOMS

third edition

Pictiva EX2004
Samsung v Pictiva
IPR2024-01094

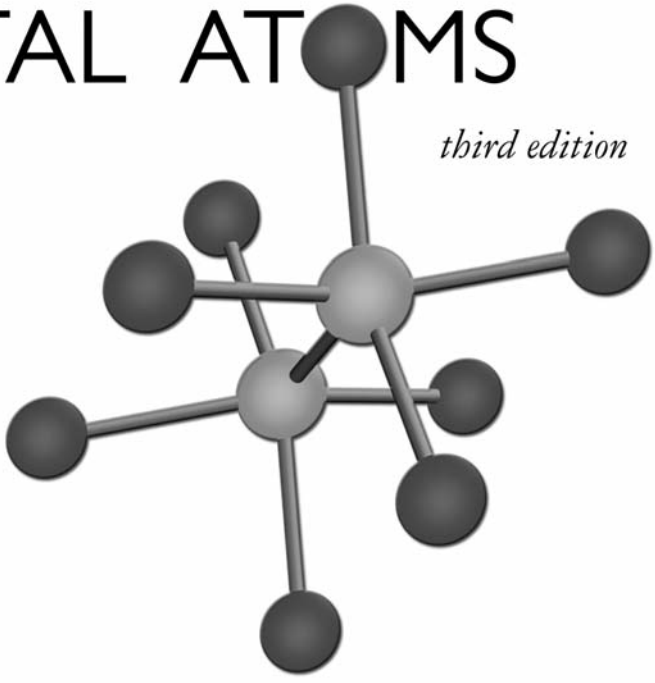
Edited by
F. Albert Cotton, Carlos A. Murillo, and Richard A. Walton

Multiple Bonds Between Metal Atoms

Pictiva EX2004
Samsung v Pictiva
IPR2024-01094

MULTIPLE BONDS BETWEEN METAL ATOMS

third edition



Edited by

F. Albert Cotton, Carlos A. Murillo and Richard A. Walton

Springer Science and Business Media, Inc. • 2005

Pictiva EX2004
Samsung v Pictiva
IPR2024-01094

Springer Science and Business Media, Inc.
New York, Boston, Dordrecht, London, Moscow

Published in the United States by
Springer Science and Business Media, Inc., New York

© Carlos A. Murillo, 2005
The second edition of this work was published by Oxford University Press, New York, 1993
The first edition of this work was published by John Wiley & Sons, New York, 1982

All rights reserved. This work may not be translated or copied in whole or in part without the written permission of the publisher (Springer Science and Business Media, Inc., 233 Spring Street, New York, NY 10013, USA), except for brief excerpts in connection with reviews or scholarly analysis. Use in connection with any form of information storage and retrieval, electronic adaptation, computer software, or by similar or dissimilar methodology now known or hereafter developed is forbidden.

The use in this publication of trade names, trademarks, service marks and similar terms, even if they are not identified as such, is not to be taken as an expression of opinion as to whether or not they are subject to proprietary rights.

Cover and Interior design by Debbie Murillo.
Printed in the United States of America. (BS/DH)

Library of Congress Cataloging in Publication Data
ISBN 0-387-22605-2 (Hardbound)
ISBN 0-387-22 (eBook)
Printed on acid-free paper.

9 8 7 6 5 4 3 2 1

SPIN 10860606

springeronline.com

Pictiva EX2004
Samsung v Pictiva
IPR2024-01094

To all of our past and present coworkers

Pictiva EX2004
Samsung v Pictiva
IPR2024-01094

Preface to the Third Edition

Since the second edition of this book there has been so much published in the field that two points seemed clear. One was a sense that a new, up-to-date monograph was needed. The other was the reluctance of two or even three people to undertake the daunting task of covering all the ground. Our response was to call on others to help and, thus, to produce the present, multiauthored volume. Each of the contributing authors was in a position to write authoritatively, from hands-on research experience. We are confident that this has led to a better book than the three of us would have produced. As always in a book where different chapters are written by different authors, there is some variation in style and we chose not to try to smooth it all out.

In every chapter the objective has been to be comprehensive, if not encyclopedic. Putting it a little differently, we, and the other authors, have aimed to mention all pertinent literature references, although the amount of emphasis accorded each paper necessarily varies.

Since the volume of literature to cover is now so large, a few topics that might have been included (or were in the second edition) have been omitted or are covered only in limited detail. Notable ones are the treatment of metal-metal bonding in edge-sharing and face-sharing bioctahedra, and metal cluster compounds of rhenium. Also, the vast field of catalysis by dirhodium compounds has been restricted to only the area of chiral catalysts.

The physical properties and bonding of many compounds are, in general, described in two places, to varying degrees. There are some specific reports regarding properties of compounds of certain metals in the first fifteen chapters. Comprehensive discussions (i. e., not element specific) are provided in Chapter 16.

To assist the user of this book a few comments about how it is organized and indexed are pertinent. Because of the element by element (or group of elements) organization, and the division of each chapter into numerous sections and subsections, as well as the extensive tables of compounds, the table of contents plays the part of an index to a major extent. The index itself is thus limited to general topics and concepts that turn up often throughout the book. Individual compounds are, in most instances, not listed there.

Pictiva EX2004
Samsung v Pictiva
IPR2024-01094

Many other people contributed to the production of this volume in addition to those who wrote chapters that were not written by the editors themselves. We are very grateful to these authors, but we are also much indebted to others. The word indispensable must be reserved for Mrs. Debbie Murillo. She created the book from the scattered and mangled fragments available after the tragic and utterly unexpected illness of Ms. Beverly Moore, who contributed much to preparing early drafts. For Debbie's mastery of computerized book publishing as well as her selfless devotion to the task, we owe her a debt that cannot be fully repaid. We have also had major assistance from Dr. Xiaoping Wang and Mr. Dino Villagrán in preparing many of the illustrations, and we thank Mrs. Julie Zercher for efforts in searching computer files.

F. Albert Cotton
Texas A&M University

Carlos A. Murillo
Texas A&M University

Richard A. Walton
Purdue Universtiy

Pictiva EX2004
Samsung v Pictiva
IPR2024-01094

Forward to the Second Edition

Jack Lewis
Cambridge University

The recognition of the multiple bond in $[Re_2Cl_8]^{2-}$ by F. A. Cotton was a clear landmark in the development of inorganic transition metal chemistry. Prior to 1960 the mere existence of metal–metal bonding had been under considerable debate. The determination of the structures of $Mn_2(CO)_{10}$ and $Re_2(CO)_{10}$ by Dahl, Ishishi, and Rundle in 1957 established beyond any doubt that molecules occurred containing bonding between metal centres rather than metal interactions, possibly occurring via the agency of bridging groups as is $Fe_2(CO)_9$. The presence of multiple bonding between metals was recognized, again by Cotton, in the trimeric ion $[Re_3Cl_{12}]^{3-}$. However, as with the iron carbonyl $Fe_2(CO)_9$ the presence of bridging between the metals, in this instance by chloride atoms, left the alternative interpretation of the cause of diamagnetism in this molecule as arising via the bridging groups. The determination of the structure of the $[Re_2Cl_8]^{2-}$ ion established both the presence of an unsupported metal–metal bond and a high multiple (quadruple) bond between the metal centres. The trauma in the chemical community of exceeding a bond order of three, the limit of the bonding modes observed in the *p* block, and the unequivocal establishing of a multiple bond between transition metals, was great. It was however considered by many to be an 'anomaly', a rare bonding mode. The subsequent work of Cotton and co-workers has established that this molecule is in fact the progenitor of a vast new area of chemistry. This book documents how progress was made in this field. The synthetic methods were developed in a logical manner and the whole force of both structural methods and theoretical interpretation of the bonding was applied to the problems in a masterly way. It provides a prime example of the present day application of chemical methods in mapping this field of chemistry that has now been uncovered, and in particular the importance of X-ray crystallography as a structural tool.

The appearance of the first edition of this book in 1981 was heralded as the authoritative exposition of this area of chemistry and illustrated the vast amount of work and interest that had been generated during the initial twenty years of study. The second edition, a decade later shows how the interest in this field has been maintained and in certain aspects increased to incorporate the majority of the *d*-block elements. The utility of multiple metal bonded

Pictiva EX2004
Samsung v Pictiva
IPR2024-01094

molecules in general synthetic chemistry is well illustrated and what had certainly appeared as an interesting but possibly unique molecule proved to be the genesis of a wide and fundamental area of chemistry. Metal–metal bonding is now accepted as a major pattern in the transition metal complexes, particularly in low oxidation states. The vast range of molecules containing multiple bonding between the metal centres is a reflection of the significant contribution to chemistry made by Cotton and his co-workers.

The authors are to be complimented on maintaining the standard they set in that first edition, their insight into the fascinating study, and their lucid presentation.

Pictiva EX2004
Samsung v Pictiva
IPR2024-01094

Preface to the Second Edition

By mid-1981, with the manuscript for the first edition in the hands of the publishers, we had little inkling that the field of multiple metal–metal bond chemistry would continue to grow at the same explosive rate as it had through much of the 1970s. However, in the intervening 10 years, far more work has been published in the area than in all the period prior to 1981. This spectacular growth of new advances in the field, which continues to this day, along with the favorable response that the first edition received, prompted us to embark on the preparation of a second edition of *Multiple Bonds between Metal Atoms*. The present text is the result.

We have endeavored to include not only those topics that appeared in the first edition, but all significant advances that have been published since. The coverage of the literature in the field is complete up to December 1990, with most of the literature that appeared throughout 1991, during the final stages of manuscript preparation, also being cited. Any omissions of work prior to the end of 1990 are inadvertent. To bring the coverage, at least of the most important topics, as nearly up to date as possible, we have added a short additional chapter (Chapter 11) which includes literature from late 1991 and early 1992.

The dramatic increase in the literature in this field has necessitated some compromise in the depth of coverage of certain topics in order to keep the text size within reasonable bounds. Also, certain topics have grown much more rapidly than others and are therefore afforded more detailed coverage than in the first edition. While there has been some significant reshuffling in the organization, the text is generally along similar lines to those employed previously. Chapters 1-4 cover the same topics as those in the first edition, although Chapter 2 now includes all types of multiply bonded dirhenium and ditechnetium compounds, instead of just those that contain quadruple bonds. Triply-bonded dimolybdenum(III) and ditungsten(III) compounds of the type L_3MML_3 constitute such an important and extensive area of chemistry that they are now afforded coverage in a separate chapter (Chapter 5). There has also been such a dramatic growth in the chemistry of multiply bonded dimetal compounds of the platinum metals, and many of their closely allied singly-bonded analogs, that separate chapters are now devoted to the chemistry of diruthenium and diosmium compounds (Chapter 6), singly-bonded dirhodium (II)

Pictiva EX2004
Samsung v Pictiva
IPR2024-01094

compounds (Chapter 7), and compounds of the other platinum metals, especially those of diplatinum(III) (Chapter 8). There are many other classes of multiply bonded compounds that bear an important and, in some cases, close relationship to those of the types L_3MML_3, L_4MML_4, and L_5MML_5 which are the principal focus of this text. These comprise the following: higher nuclearity clusters (trinuclear, tetranuclear, hexanuclear, and octanuclear); various organometallics, such as the mixed cyclopentadienylcarbonyl compounds $(\eta^5\text{-}C_5R_5)_2M_2(CO)_n$ (e.g., $(\eta^5\text{-}C_5Me_5)_2Mo_2(CO)_4$); edge-sharing and face-sharing bioctahedra; simple diatomic molecules. All are discussed together in Chapter 9. Finally, Chapter 10, which contains the most important physical, spectroscopic, and theoretical results that have been obtained on compounds discussed in earlier chapters, follows closely the format of Chapter 8 in the first edition, except for the omission of diatomic molecules now covered in Chapter 9.

As before, we appreciate the invaluable assistance of our many friends and colleagues who have continued to ply us with preprints and other interesting tidbits of information on unpublished results. These insights have helped us greatly throughout the preparation of this manuscript. In this regard, a particular word of thanks is due to our good friend Professor Malcolm H. Chisholm. One of us (R. A. W.) is most grateful to Keng-Yu (Ivan) Shih for his critical reading of several chapters. Once again, we are particularly grateful for the wonderful secretarial assistance of Mrs Rita Biederstedt and Mrs Irene Casimiro who have patiently helped us overcome many obstacles in the preparation of both editions of this text. This edition is dedicated to both of them, with our profound thanks for their help in this and many other of our scientific endeavours.

F. Albert Cotton,
College Station, Texas

Richard A. Walton
West Lafayette, Indiana

March 1992

Pictiva EX2004
Samsung v Pictiva
IPR2024-01094

Forward to the First Edition

Roald Hoffmann
Cornell University

Our central science progresses, but often by uncoordinated steps. Experiments are done here, perceived as important there, fruitfully extended elsewhere. There are satisfactions, to be sure, in the interactive, perforce international nature of modern chemistry. Yet most advances at the frontiers of our lively discipline seem small in scope, chaotic.

Occasionally does one encounter a large chunk of chemistry that is the coherent outcome of the work of one group. Initial observations evolve into an idea. This idea leads to the synthesis of novel molecules or new measurements and to the recognition of an entirely new structural type or a different mechanism. The new field expands, seemingly without limit. All this takes time, for the minds and hands of men and women must be engaged in the effort. The careful observer of the chemical scene seeks out such rare achievements. For when the tangled web of our experience is so transformed, by one person, into symmetries of pristine order and the chemical equivalent of the rich diversity of pattern of an oriental carpet—it is then that one encounters a moment of intellectual pleasure that really makes one feel good about being a chemist.

Such a story is that of metal–metal multiple bonding. A recognition of the structural and theoretical significance of the Re–Re quadruple bond by F. A. Cotton in 1964 was followed by a systemic and rational exploration of metal–metal bonding across the transition series. Cotton and his able co-workers have made most such complexes. The consistent and proficient use of X-ray crystallography results in their studies, not only for structure determination but as an inspiration to further synthetic chemistry, has served as a model for modern inorganic research. Much of the chemistry of metal–metal multiple-bonded species—and interesting chemistry it is indeed—is due to F. A. Cotton and his students. Throughout this intellectual journey into fresh chemistry they have been guided by a lucid theoretical framework. Their bounteous achievement is detailed in this book. I want to record here my personal thanks to them for providing us with the psychological satisfaction of viewing a scientific masterpiece.

Pictiva EX2004
Samsung v Pictiva
IPR2024-01094

Preface to the First Edition

The renaissance of inorganic chemistry that began in the 1950s has been propelled by the discovery of new and important classes of inorganic molecules, many of which do not conform to classical bonding theories. Among these landmark discoveries has been the isolation and structural characterization of transition metal compounds that possess multiple metal-metal bonds. From the seminal discoveries in this area in the early 1960s has developed a complex and fascinating chemistry. This chemistry is simultaneously different from but very relevant to the classical chemistry of the majority of the transition elements. Since the synthetic methodologies, reaction chemistries, and bonding theories are now remarkably well understood, we felt the topic had reached a level of maturity sufficient to justify a comprehensive treatise.

The content of this book encompasses all the classes of compounds currently known to possess, or suspected of possessing, metal-metal bonds of order two or greater, as well as some compounds with single bonds that have a close formal relationship to the multiple bonds. Synthetic procedures, reaction chemistries, spectroscopic properties, and bonding theories are discussed in detail for these molecules, and, in addition, we have attempted to place in historical perspective the most important discoveries in this field. Since both of us have worked in this field for many years, much of our discussion inevitably takes on a rather personal flavor, particularly in our treatment of the circumstances surrounding many of the major advances. We have endeavored to cover all the pertinent literature that was in our hands by the end of December 1980. When possible, we have also referred to those key developments that may have emerged during the early part of 1981, while the manuscript was in press.

Throughout the preparation of the manuscript we were fortunate to have the assistance of many friends and colleagues who not only provided us with valuable information on unpublished results, but on occasion critically read various sections of the text and otherwise helped us surmount minor hurdles. We especially appreciate the assistance of Professors M. H. Chisholm, D. A. Davenport, F. G. A. Stone, O. Glemser, and B. E. Bursten. We also thank the various authors and editors who kindly gave us permission to reproduce diagrams from their papers; the appropriate numbered reference is given in the captions to those figures that were reproduced

Pictiva EX2004
Samsung v Pictiva
IPR2024-01094

directly from the literature or were modified so slightly as to retain an essential similarity to those in the original publications. Finally, we appreciate the expert patient secretarial assistance of Mrs Rita Biederstedt and Mrs Irene Casimiro in the preparation of the manuscript.

F. Albert Cotton
College Station, Texas

Richard A. Walton
West Lafayette, Indiana

June 1981

Pictiva EX2004
Samsung v Pictiva
IPR2024-01094

Contributors

Panagiotis Angaridis
Department of Chemistry
Texas A&M University
P.O. Box 30012
College Station, TX 77842-3012
angaridi@umich.edu

John F. Berry
Department of Chemistry
Texas A&M University
P.O. Box 30012
College Station, TX 77842-3012
berry@mpi-muelheim.mpg.de

Helen T. Chifotides
Department of Chemistry
Texas A&M University
P.O. Box 30012
College Station, TX 77842-3012
chifotides@mail.chem.tamu.edu

Malcolm H. Chisholm
Department of Chemistry
The Ohio State University
Columbus, OH 43210-1185
chisholm@chemistry.ohio-state.edu

Pictiva EX2004
Samsung v Pictiva
IPR2024-01094

F. Albert Cotton
Department of Chemistry
Texas A&M University
P.O. Box 30012
College Station, TX 77842-3012
cotton@tamu.edu

Michael P. Doyle
Department of Chemistry and Biochemistry
University of Maryland
College Park, MD 20742
mdoyle3@umd.edu

Kim R. Dunbar
Department of Chemistry
Texas A&M University
P.O. Box 30012
College Station, TX 77842-3012
dunbar@mail.chem.tamu.edu

Judith L. Eglin
Los Alamos National Laboratory
P.O. Box 1663
Los Alamos, NM 87545
eglin@lanl.gov

Carl B. Hollandsworth
Department of Chemistry
The Ohio State University
Columbus, OH 43210-1185
cholland@chemistry.ohio-state.edu

Carlos A. Murillo
Department of Chemistry
Texas A&M University
P.O. Box 30012
College Station, TX 77842-3012
murillo@tamu.edu

Pictiva EX2004
Samsung v Pictiva
IPR2024-01094

Tong Ren
Department of Chemistry
University of Miami
Coral Gables, FL 33124-0431
tren@miami.edu

Alfred P. Sattelberger
ADSR Office, MS A127
Los Alamos National Laboratory
P.O. Box 1663
Los Alamos, NM 87545
sattelberger@lanl.gov

Daren J. Timmons
Department of Chemistry
Virginia Military Institute
Lexington, VA 24450
TimmonsDJ@vmi.edu

Richard A. Walton
Department of Chemistry
Purdue University
West Lafayette, IN 47907-2084
rawalton@purdue.edu

Pictiva EX2004
Samsung v Pictiva
IPR2024-01094

Contents

Introduction and Survey

1.1 Prolog 1
- 1.1.1 From Werner to the new transition metal chemistry 1
- 1.1.2 Prior to about 1963 2

1.2 How It All Began 3
- 1.2.1 Rhenium chemistry from 1963 to 1965 3
- 1.2.2 The recognition of the quadruple bond 7
- 1.2.3 Initial work on other elements 8

1.3 An Overview of the Multiple Bonds 12
- 1.3.1 A qualitative picture of the quadruple bond 13
- 1.3.2 Bond orders less than four 15
- 1.3.3 Oxidation states 15

1.4. Growth of the Field 16

1.5 Going Beyond Two 19

Complexes of the Group 5 Elements

2.1 General Remarks 23

2.2 Divanadium Compounds 23
- 2.2.1 Triply-bonded divanadium compounds 24
- 2.2.2 Metal–metal vs metal–ligand bonding 27
- 2.2.3 Divanadium compounds with the highly reduced V_2^{3+} core 27

2.3 Diniobium Compounds 29
- 2.3.1 Diniobium paddlewheel complexes 29
- 2.3.2 Diniobium compounds with calix[4]arene ligands and related species 31

2.4 Tantalum 32

Pictiva EX2004
Samsung v Pictiva
IPR2024-01094

Chromium Compounds

3.1 Dichromium Tetracarboxylates 35
3.1.1 History and preparation 35
3.1.2 Properties of carboxylate compounds 38
3.1.3 Unsolvated $Cr_2(O_2CR)_4$ compounds 40

3.2 Other Paddlewheel Compounds 43
3.2.1 The first 'supershort' bonds 43
3.2.2 2-Oxopyridinate and related compounds 47
3.2.3 Carboxamidate compounds 50
3.2.4 Amidinate compounds 52
3.2.5 Guanidinate compounds 56

3.3 Miscellaneous Dichromium Compounds 57
3.3.1 Compounds with intramolecular axial interactions 57
3.3.2 Compounds with Cr–C bonds 60
3.3.3 Other pertinent results 61

3.4 Concluding Remarks 65

Molybdenum Compounds

4.1 Dimolybdenum Bridged by Carboxylates or Other O,O Ligands 69
4.1.1 General remarks 69
4.1.2 $Mo_2(O_2CR)_4$ compounds 70
4.1.3 Other compounds with bridging carboxyl groups 79
4.1.4 Paddlewheels with other O,O anion bridges 92

4.2 Paddlewheel Compounds with O,N, N,N and Other Bridging Ligands 95
4.2.1 Compounds with anionic O,N bridging ligands 95
4.2.2 Compounds with anionic N,N bridging ligands 98
4.2.3 Compounds with miscellaneous other anionic bridging ligands 103

4.3 Non-Paddlewheel Mo_2^{4+} Compounds 105
4.3.1 $Mo_2X_8^{4-}$ and $Mo_2X_6(H_2O)_2^{2-}$ compounds 105
4.3.2 $[Mo_2X_8H]^{3-}$ compounds 108
4.3.3 Other aspects of dimolybdenum halogen compounds 109
4.3.4 $M_2X_4L_4$ and $Mo_2X_4(LL)_2$ compounds 111
4.3.5 Cationic complexes of Mo_2^{4+} 130
4.3.6 Complexes of Mo_2^{4+} with macrocyclic, polydentate and chelate ligands 132
4.3.7 Alkoxide compounds of the types $Mo_2(OR)_4L_4$ and $Mo_2(OR)_4(LL)_2$ 134

Pictiva EX2004
Samsung v Pictiva
IPR2024-01094

4.4 Other Aspects of Mo_2^{4+} Chemistry 136
4.4.1 Cleavage of Mo_2^{4+} compounds 136
4.4.2 Redox behavior of Mo_2^{4+} compounds 137
4.4.3 Hydrides and organometallics 142
4.4.4 Heteronuclear Mo–M compounds 145
4.4.5 An overview of Mo–Mo bond lengths in Mo_2^{4+} compounds 148

4.5 Higher-order Arrays of Dimolybdenum Units 148
4.5.1 General concepts 148
4.5.2 Two linked pairs with carboxylate spectator ligands 154
4.5.3 Two linked pairs with nonlabile spectator ligands 155
4.5.4 Squares: four linked pairs 160
4.5.5 Loops: two pairs doubly linked 162
4.5.6 Rectangular cyclic quartets 164
4.5.7 Other structural types 166

Tungsten Compounds

5.1 Multiple Bonds in Ditungsten Compounds 183

5.2 The W_2^{4+} Tetracarboxylates 183

5.3 W_2^{4+} Complexes Containing Anionic Bridging Ligands Other Than Carboxylate 189

5.4 W_2^{4+} Complexes without Bridging Ligands 191
5.4.1 Compounds coordinated by only anionic ligands 191
5.4.2 Compounds coordinated by four anionic ligands and four neutral ligands 192

5.5 Multiple Bonds in Heteronuclear Dimetal Compounds of Molybdenum and Tungsten 196

5.6 Paddlewheel Compounds with W_2^{5+} or W_2^{6+} Cores 197

$X_3M{\equiv}MX_3$ Compounds of Molybdenum and Tungsten

6.1 Introduction 203

6.2 Homoleptic $X_3M{\equiv}MX_3$ Compounds 204
6.2.1 Synthesis and characterization of homoleptic M_2X_6 compounds 204
6.2.2 Bonding in M_2X_6 compounds 208
6.2.3 $X_3M{\equiv}MX_3$ Compounds as Molecular Precursors to Extended Solids 210

6.3 $M_2X_2(NMe_2)_4$ and $M_2X_4(NMe_2)_2$ Compounds 210

Pictiva EX2004
Samsung v Pictiva
IPR2024-01094

6.4 Other $M_2X_2Y_4$, $M_2X_{6-n}Y_n$ and Related Compounds 212
6.4.1 $Mo_2X_2(CH_2SiMe_3)_4$ compounds 215
6.4.2 1,2-$M_2R_2(NMe_2)_4$ compounds and their derivatives 217

6.5 M_4 Complexes: Clusters or Dimers? 218
6.5.1 Molybdenum and tungsten twelve-electron clusters $M_4(OR)_{12}$ 218
6.5.2 $M_4X_4(OPr^i)_8$ (X = Cl, Br) and $Mo_4Br_3(OPr^i)_9$ 220
6.5.3 $W_4(p\text{-tolyl})_2(OPr^i)_{10}$ 221
6.5.4 $W_4O(X)(OPr^i)_9$, (X = Cl or OPr^i) 221
6.5.5 $K(18\text{-crown-}6)_2Mo_4(\mu_4\text{-}H)(OCH_2Bu^t)_{12}$ 221
6.5.6 Linked M_4 units containing localized MM triple bonds 222

6.6 M_2X_6L, $M_2X_6L_2$ and Related Compounds 223
6.6.1 $Mo_2(CH_2Ph)_2(OPr^i)_4(PMe_3)$ and $[Mo_2(OR)_7]^-$ 223
6.6.2 $M_2(OR)_6L_2$ compounds and their congeners 224
6.6.3 Amido-containing compounds 226
6.6.4 $Mo_2Br_2(CHSiMe_3)_2(PMe_3)_4$ 228
6.6.5 Calix[4]arene complexes 228

6.7 Triple Bonds Uniting Five- and Six-Coordinate Metal Atoms 229

6.8 Redox Reactions at the M_2^{6+} Unit 230

6.9 Organometallic Chemistry of $M_2(OR)_6$ and Related Compounds 232
6.9.1 Carbonyl adducts and their products 232
6.9.2 Isocyanide complexes 234
6.9.3 Reactions with alkynes 234
6.9.4 Reactions with C≡N bonds 236
6.9.5 Reactions with C=C bonds 237
6.9.6 Reactions with H_2 240
6.9.7 Reactions with organometallic compounds 241
6.9.8 $(\eta^5\text{-}C_5H_4R)_2W_2X_4$ compounds where R = Me, Pr^i and X = Cl, Br 241

6.10 Conclusion 242

Technetium Compounds

7.1 Synthesis and Properties of Technetium 251

7.2 Preparation of Dinuclear and Polynuclear Technetium Compounds 252

7.3 Bonds of Order 4 and 3.5 252

7.4 Tc_2^{6+} and Tc_2^{5+} Carboxylates and Related Species with Bridging Ligands 257

Pictiva EX2004
Samsung v Pictiva
IPR2024-01094

7.5 Bonds of Order 3 261

7.6 Hexanuclear and Octanuclear Technetium Clusters 265

Rhenium Compounds

8.1 The Last Naturally Occurring Element to Be Discovered 271

8.2 Synthesis and Structure of the Octachlorodirhenate(III) Anion 273

8.3 Synthesis and Structure of the Other Octahalodirhenate(III) Anions 278

8.4 Substitution Reactions of the Octahalodirhenate(III) Anions that Proceed with Retention of the Re_2^{6+} Core 280
- 8.4.1 Monodentate anionic ligands 280
- 8.4.2 The dirhenium(III) carboxylates 282
- 8.4.3 Other anionic ligands 292
- 8.4.4 Neutral ligands 298

8.5 Dirhenium Compounds with Bonds of Order 3.5 and 3 302
- 8.5.1 The first metal–metal triple bond: $Re_2Cl_5(CH_3SCH_2CH_2SCH_3)_2$ and related species 302
- 8.5.2 Simple electron-transfer chemistry involving the octahalodirhenate(III) anions and related species that contain quadruple bonds 303
- 8.5.3 Oxidation of $[Re_2X_8]^{2-}$ to the nonahalodirhenate anions $[Re_2X_9]^{n-}$ (n = 1 or 2) 307
- 8.5.4 Re_2^{5+} and Re_2^{4+} halide complexes that contain phosphine ligands 309
- 8.5.5 Other Re_2^{5+} and Re_2^{4+} complexes 359
- 8.5.6 Other dirhenium compounds with triple bonds 360

8.6 Dirhenium Compounds with Bonds of Order Less than 3 361

8.7 Cleavage of Re–Re Multiple Bonds by σ-donor and π-acceptor Ligands 361
- 8.7.1 σ-Donor ligands 362
- 8.7.2 π-Acceptor ligands 363

8.8 Other Types of Multiply Bonded Dirhenium Compounds 363

8.9 Postscript on Recent Developments 364

Pictiva EX2004
Samsung v Pictiva
IPR2024-01094

Ruthenium Compounds

9.1 Introduction 377

9.2 Ru_2^{5+} Compounds 378
- 9.2.1 Ru_2^{5+} compounds with O,O'-donor bridging ligands 382
- 9.2.2 Ru_2^{5+} compounds with N,O-donor bridging ligands 391
- 9.2.3 Ru_2^{5+} compounds with N,N'-donor bridging ligands 396

9.3 Ru_2^{4+} Compounds 404
- 9.3.1 Ru_2^{4+} compounds with O,O'-donor bridging ligands 405
- 9.3.2 Ru_2^{4+} compounds with N,O-donor bridging ligands 409
- 9.3.3 Ru_2^{4+} compounds with N,N'-donor bridging ligands 411

9.4 Ru_2^{6+} Compounds 414
- 9.4.1 Ru_2^{6+} compounds with O,O'-donor bridging ligands 415
- 9.4.2 Ru_2^{6+} compounds with N,N'-donor bridging ligands 416

9.5 Compounds with Macrocyclic Ligands 422

9.6 Applications 422
- 9.6.1 Catalytic activity 422
- 9.6.2 Biological importance 423

Osmium Compounds

10.1 Syntheses, Structures and Reactivity of Os_2^{6+} Compounds 431

10.2 Syntheses and Structures of Os_2^{5+} Compounds 437

10.3 Syntheses and Structures of Other Os_2 Compounds 438

10.4 Magnetism, Electronic Structures, and Spectroscopy 439

10.5 Concluding Remarks 444

Iron, Cobalt and Iridium Compounds

11.1 General Remarks 447

11.2 Di-iron Compounds 447

11.3 Dicobalt Compounds 451
- 11.3.1 Tetragonal paddlewheel compounds 451
- 11.3.2 Trigonal paddlewheel compounds 453
- 11.3.3 Dicobalt compounds with unsupported bonds 454
- 11.3.4 Compounds with chains of cobalt atoms 455

Pictiva EX2004
Samsung v Pictiva
IPR2024-01094

11.4 Di-iridium Compounds 455
11.4.1 Paddlewheel compounds and related species 455
11.4.2 Unsupported Ir–Ir bonds 458
11.4.3 Other species with Ir–Ir bonds 459
11.4.4 Iridium blues 461

Rhodium Compounds

12.1 Introduction 465

12.2 Dirhodium Tetracarboxylato Compounds 466
12.2.1 Preparative methods and classification 466
12.2.2 Structural studies 469

12.3 Other Dirhodium Compounds Containing Bridging Ligands 493
12.3.1 Complexes with fewer than four carboxylate bridging groups 493
12.3.2 Complexes supported by hydroxypyridinato, carboxamidato and other (N, O) donor monoanionic bridging groups 505
12.3.3 Complexes supported by amidinato and other (N, N) donor bridging groups 512
12.3.4 Complexes supported by sulfur donor bridging ligands 521
12.3.5 Complexes supported by phosphine and (P, N) donor bridging ligands 524
12.3.6 Complexes supported by carbonate, sulfate and phosphate bridging groups 527

12.4 Dirhodium Compounds with Unsupported Rh–Rh Bonds 528
12.4.1 The dirhodium(II) aquo ion 528
12.4.2 The $[Rh_2(NCR)_{10}]^{4+}$ cations 529
12.4.3 Complexes with chelating and macrocyclic nitrogen ligands 530

12.5 Other Dirhodium Compounds 533
12.5.1 Complexes with isocyanide ligands 533
12.5.2 Rhodium blues 536

12.6. Reactions of Rh_2^{4+} Compounds 540
12.6.1 Oxidation to Rh_2^{5+} and Rh_2^{6+} species 540
12.6.2 Cleavage of the Rh–Rh bond 547

12.7 Applications of Dirhodium Compounds 547
12.7.1 Catalysis 547
12.7.2 Supramolecular arrays based on dirhodium building blocks 548
12.7.3 Biological applications of dirhodium compounds 555
12.7.4 Photocatalytic reactions 566
12.7.5 Other applications 567

Pictiva EX2004
Samsung v Pictiva
IPR2024-01094

Chiral Dirhodium(II) Catalysts and Their Applications

13.1 Introduction 591

13.2 Synthetic and Structural Aspects of Chiral Dirhodium(II) Carboxamidates 591

13.3 Synthetic and Structural Aspects of Dirhodium(II) Complexes Bearing Orthometalated Phosphines 599

13.4 Dirhodium(II) Compounds as Catalysts 605

13.5 Catalysis of Diazo Decomposition 607

13.6 Chiral Dirhodium(II) Carboxylates 609

13.7 Chiral Dirhodium(II) Carboxamidates 611

13.8 Catalytic Asymmetric Cyclopropanation and Cyclopropenation 613
- 13.8.1 Intramolecular reactions 613
- 13.8.2 Intermolecular reactions 616
- 13.8.3 Cyclopropenation 617
- 13.8.4 Macrocyclization 617

13.9 Metal Carbene Carbon-Hydrogen Insertion 619
- 13.9.1 Intramolecular reactions 619
- 13.9.2 Intermolecular reactions 624

13.10 Catalytic Ylide Formation and Reactions 624

13.11 Additional Transformations of Diazo Compounds Catalyzed by Dirhodium(II) 626

13.12 Silicon-Hydrogen Insertion 626

Nickel, Palladium and Platinum Compounds

14.1 General Remarks 633

14.2 Dinickel Compounds 633

14.3 Dipalladium Compounds 634
- 14.3.1 A singly bonded Pd_2^{6+} species 634
- 14.3.2 Chemistry of Pd_2^{5+} and similar species 635
- 14.3.3 Other compounds with Pd–Pd interactions 636

14.4 Diplatinum Compounds 636
- 14.4.1 Complexes with sulfate and phosphate bridges 642
- 14.4.2 Complexes with pyrophosphite and related ligands 644
- 14.4.3 Complexes with carboxylate, formamidinate and related ligands 646

Pictiva EX2004
Samsung v Pictiva
IPR2024-01094

14.4.4 Complexes containing monoanionic bridging ligands with N,O and N,S donor sets 648
14.4.5 Unsupported Pt–Pt bonds 656
14.4.6 Dinuclear Pt_2^{5+} species 657
14.4.7 The platinum blues 658
14.4.6 Other compounds 661

Extended Metal Atom Chains

15.1 Overview 669

15.2 EMACs of Chromium 671

15.3 EMACs of Cobalt 686

15.4 EMACs of Nickel and Copper 694

15.5 EMACs of Ruthenium and Rhodium 701

15.6 Other Metal Atom Chains 702

Physical, Spectroscopic and Theoretical Results

16.1 Structural Correlations 707
16.1.1 Bond orders and bond lengths 707
16.1.2 Internal rotation 710
16.1.3 Axial ligands 712
16.1.4 Comparison of second and third transition series homologs 713
16.1.5 Disorder in crystals 715
16.1.6 Rearrangements of M_2X_8 type molecules 718
16.1.7 Diamagnetic anisotropy of M–M multiple bonds 720

16.2 Thermodynamics 721
16.2.1 Thermochemical data 721
16.2.2 Bond energies 722

16.3 Electronic Structure Calculations 724
16.3.1 Background 724
16.3.2 $[M_2X_8]^{n-}$ and $M_2X_4(PR_3)_4$ species 725
16.3.3 The $M_2(O_2CR)_4$ (M = Cr, Mo, W) molecules 728
16.3.4 $M_2(O_2CR)_4R'_2$ (M = Mo, W) compounds 729
16.3.5 Dirhodium species 731
16.3.6 Diruthenium compounds 732
16.3.7 M_2X_6 molecules (M = Mo, W) 733
16.3.8 Other calculations 738

Pictiva EX2004
Samsung v Pictiva
IPR2024-01094

16.4 Electronic Spectra 738
16.4.1 Details of the δ manifold of states 739
16.4.2 Observed δ→δ* transitions 744
16.4.3 Other electronic absorption bands of Mo_2, W_2, Tc_2 and Re_2 species 751
16.4.4 Spectra of Rh_2, Pt_2, Ru_2 and Os_2 compounds 756
16.4.5 CD and ORD spectra 758
16.4.6 Excited state distortions inferred from vibronic structure 760
16.4.7 Emission spectra and photochemistry 762

16.5 Photoelectron Spectra 766
16.5.1 Paddlewheel molecules 766
16.5.2 Other tetragonal molecules 772
16.5.3 M_2X_6 molecules 773
16.5.4 Miscellaneous other PES results 774

16.6 Vibrational Spectra 775
16.6.1 M–M stretching vibrations 775
16.6.2 M–L stretching vibrations 781

16.7 Other types of Spectra 783
16.7.1 Electron Paramagnetic Resonance 783
16.7.2 X-Ray spectra, EXAFS, and XPS 785

Abbreviations 797

Index 811

Pictiva EX2004
Samsung v Pictiva
IPR2024-01094



Introduction and Survey

F. Albert Cotton and Carlos A. Murillo, *Texas A&M University*
Richard A. Walton, *Purdue University*

1.1 Prolog

1.1.1 From Werner to the new transition metal chemistry

From the time of Alfred Werner (*c.* 1900) until the early 1960s, the chemistry of the transition metals was based entirely on the conceptual framework established by Alfred Werner.[1] This Wernerian scheme has as its essential feature the concept of a single metal ion surrounded by a set of ligands. It focuses attention on the characteristics of the individual metal ion, the interaction of the metal ion with the ligand set, and the geometrical and chemical characteristics of this ligand set. It is true that following Werner there was an enormous development and refinement of his central concept. Progress occurred notably in the following areas: metal carbonyls and other compounds where the metal 'ion' is formally not an ion; sophisticated analysis of the electronic structures of complexes; understanding of the thermodynamics and kinetics pertaining to the stabilities and transformations of complexes; structural studies that vastly increase the range of geometries now deemed important (i.e. coordination numbers of five and those greater than six); an appreciation of the role of metal ions in biological systems; recognition that ligands, especially organic ones, are not passive but that their behavior is often greatly modified by being attached to a metal atom, in some cases allowing metal atoms to act catalytically.

However, all of these advances constitute *continuous* (evolutionary) progress. They expand upon, augment, 'orchestrate' so to speak, Werner's theme, and that theme is, in essence, *one-center coordination chemistry.*

But the transition metals have another chemistry: *multicenter chemistry,* or the chemistry of compounds with direct metal-to-metal bonds. The recognition and rapid development of this second kind of transition metal chemistry, *non-Wernerian transition metal chemistry,* began in the period 1963-65, and constitutes a *discontinuous* (revolutionary) step in the progress of chemistry. We see in it the creation and elaboration of a new conceptual scheme, one which is becoming as important an intellectual innovation in chemistry as was the Wernerian idea in its time, or the ideas of Kekulé, and of van't Hoff and Le Bel in their time. The recognition of the existence of a wholly new and previously entirely unrecognized chemistry of the transition metals, which constitute more than half of the periodic table, is certainly an important fundamental step in the progress of chemistry.

Pictiva EX2004
Samsung v Pictiva
IPR2024-01094

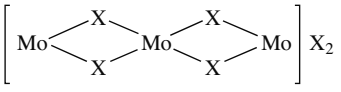
One of the aspects of this overall development of multicenter transition metal chemistry obviously constitutes an innovation with respect to the entire science of chemistry, namely, the recognition that there exist chemical bonds of an order higher than triple. The existence of quadruple bonds was first recognized in 1964, and since then more than a thousand compounds containing them have been prepared and characterized with unprecedented thoroughness by virtually every known physical and theoretical method, as well as by a wide-ranging investigation of their chemistry.

It is especially to be noted that compounds containing quadruple bonds are in most cases not at all exotic, unstable, or difficult to obtain. On the contrary, many of them can be (and are) easily prepared by undergraduate chemistry students and they 'live out in the air with us'. Perhaps the most astonishing thing about this chemistry is that it was discovered so late.

1.1.2 Prior to about 1963

It is well to begin with the following observation. Werner, of course, recognized the existence of polynuclear complexes and, indeed, he wrote quite a number of papers on that subject.[2] However, the compounds he dealt with were regarded (and correctly so) as simply the result of conjoining two or more mononuclear complexes through shared ligand atoms. The properties of these complexes were accounted for entirely in terms of the various *individual* metal atoms and the local sets of metal-ligand bonds. No direct M–M interactions of any type were considered and the concept of a metal-metal bond remained wholly outside the scope of Wernerian chemistry, even in polynuclear complexes.

Before Werner's time, however, there were a few compounds in the literature that could not be accommodated correctly by the coordination theory. The earliest was chromous acetate, to which we shall return later (p. 10). In the period 1857-61, the Swedish chemist Christian Wilhelm Blomstrand[3] and co-workers investigated the dichloride and dibromide of molybdenum and found them to have some surprising properties. For example, only one third of the halide ions could be precipitated with Ag^+, thus indicating that the smallest possible molecular formula is Mo_3X_6. Werner himself in the several editions of his *Neuere Anschauungen auf dem Gebiete der Anorganischen Chemie* proposed the following formulation:



Towards the middle and end of Werner's life, further discoveries inconsistent with his theory were made. From 1905 to 1910 Blondel and others[4] reported dinuclear Pt^{III} compounds, which we now know to contain Pt–Pt bonded $[Pt_2(SO_4)_4]^{2-}$ ions. In 1907, '$TaCl_2{\cdot}2H_2O$' (which, as shown below, was later correctly formulated as $Ta_6Cl_{14}{\cdot}7H_2O$) was reported.[5] During the 1920s Lindner[6] and others attempted to account for the composition of these and other compounds by imaginative (but chimerical) polynuclear structures in which *metal-metal bonds were not included.*

It was only with the advent of X-ray crystallography and its evolution into a tool capable of handling reasonably large structures that the existence of non-Wernerian transition metal chemistry could be recognized with certainty and the character of the compounds exemplifying it disclosed in detail. The first such experimental results were provided by C. Brosset,[7] who showed that the lower chlorides of molybdenum contain octahedral groups of metal atoms with Mo–Mo distances even shorter (~2.6 Å) than those in metallic molybdenum (2.725 Å). Brosset's publications did not, apparently, stimulate any further research activity.

It was also Brosset[8] who showed that $K_3W_2Cl_9$ contained a binuclear anion, $[W_2Cl_9]^{3-}$, with the tungsten atoms so close together that "[t]hey are, apparently, within these pairs, in

Pictiva EX2004
Samsung v Pictiva
IPR2024-01094

some way bound together." This promising insight was not pursued.

In 1950, an X-ray diffraction experiment, albeit of an unconventional type carried out on aqueous solutions, showed that $Ta_6Cl_{14}\cdot 7H_2O$ and its bromide analog, as well as the corresponding niobium compounds, also contain octahedral groups of metal atoms[9] with rather short M–M distances (~ 2.8 Å). As before, these remarkable observations did not lead to any further exploration of such chemistry.

It was not until 1963, in fact, that attention was effectively focused on non-Wernerian coordination compounds. It was observed at about the same time in two different laboratories[10,11] that '$ReCl_4^-$' actually contains triangular Re_3 groups in which the Re–Re distances (2.47 Å) are very much shorter than those (2.75 Å) in metallic rhenium. In one report[10] not only was the molecular structure described very precisely, the electronic structure was discussed in detail, leading to the explicit conclusion[10] that the rhenium atoms are united by a set of three Re–Re double bonds. This work was important because it was the basis for:

1. the first explicit recognition that direct metal–metal bonds can be very strong and can play a crucial role in transition metal chemistry, and
2. the first formal recognition that there is an entire class of such compounds to which the name *metal atom cluster compounds* was then applied.[12,13]

In $[Re_3Cl_{12}]^{3-}$ it was first shown that metal–metal bonds may be multiple, since the MO analysis[10(a),12] of this cluster clearly shows that there are six doubly occupied bonding MOs covering the three Re–Re edges of the triangle, thus giving the MO equivalent of double bonds.

It should be noted that during the period of time just considered there were developments in the field of metal carbonyl chemistry that also led to the consideration of direct metal–metal bonds as stereoelectronic elements of molecular structure. In 1938 the first evidence for the structure of a polynuclear metal carbonyl compound, $Fe_2(CO)_9$, was obtained by X-ray crystallography. To account for the diamagnetism of the compound, it was considered necessary to postulate a pairing of two electron spins, each of which formally originated from a different metal atom. For many years it was taken as obvious that there exists an Fe–Fe bond. The structural integrity does not require such an assumption because there are three bridging carbonyl groups. Today there are convincing (though not entirely conclusive) theoretical arguments in favor of spin coupling via the carbonyl bridges without direct Fe–Fe bonding. It was not until 1957, with the determination of the $Mn_2(CO)_{10}$ structure,[14] that unequivocal evidence for metal–metal bond formation in metal carbonyls was obtained.

1.2 How It All Began

1.2.1 Rhenium chemistry from 1963 to 1965

By mid-1963, further studies of the chemistry of the trinuclear cluster anion $[Re_3Cl_{12}]^{3-}$ had led to the recognition that the trinuclear Re_3 cluster with Re–Re double bonds was the essential stereoelectronic feature of much of the chemistry of rhenium(III), particularly that which used the so-called trihalides as the starting materials. Both the chloride and bromide of Re^{III} had been shown to contain these Re_3 clusters.[15]

However, it was precisely the use of these Re^{III} halides as starting materials that posed a practical problem, since their preparation is tedious and time consuming. The idea of obtaining the trinuclear complexes by reduction in aqueous solution of the readily available $[ReO_4]^-$ ion to give, for example, $[Re_3Cl_{12}]^{3-}$ was very attractive. The devising of such an aqueous route into trinuclear Re^{III} chemistry was regarded at MIT as perhaps the one remaining task to be carried out before leaving the field of Re^{III} chemistry. During the autumn of 1963, Dr. Neil Curtis (later Professor of Chemistry at Victoria University in Wellington, New

Pictiva EX2004
Samsung v Pictiva
IPR2024-01094

Zealand) was a visiting research associate at MIT, and he set about trying this, with the added objective of obtaining mixed clusters, such as $[Re_2OsCl_{12}]^{2-}$, by using a mixture of $[ReO_4]^-$ and an osmium compound.

Neither of the original goals has ever been attained because, after a few exploratory experiments, a far more interesting result was obtained by Curtis. He found that by using concentrated aqueous hydrochloric acid as the reaction medium and hypophosphorous acid as the reducing agent (with or without the presence of any osmium compound), the product was an intense blue solution from which materials such as a beautiful royal-blue solid of composition $CsReCl_4$ could be isolated. Since this substance had the same empirical formula as the red $Cs_3Re_3Cl_{12}$ we were keenly interested in learning its true nature.

By a coincidence, of a sort that seems to occur rather often in research, there was another visiting research associate in the group at the same time, namely, Dr Brian Johnson (today Professor of Chemistry, Cambridge University), who had been checking a rather puzzling report from the USSR[16] to the effect that reduction of $[ReO_4]^-$ in hydrochloric acid by hydrogen gas under pressure gave $[ReCl_6]^{3-}$. This was obviously relevant to Curtis's work, since it suggested that aqueous reduction of $[ReO_4]^-$ might give (previously unknown) mononuclear Re^{III} chloro complexes. An even more remarkable feature of this curious report was that the precipitated '$M^I_3ReCl_6$' compounds displayed a variety of colors, depending on the counterion, M^I. Johnson showed quickly that the claim of $[ReCl_6]^{3-}$ salts was erroneous[17] and that the compounds were in fact the rather uninteresting, very familiar, $M^I_2ReCl_6$ salts. The variety of colors displayed is not easy to explain with certainty, but probably arose from incorporation of impurities. The reaction conditions cause serious corrosion of the steel bomb in which the reaction is conducted.

However, it had also been claimed[16] that there was a dark-blue/green product, to which the formula K_2ReCl_4, was assigned. Johnson found that there was indeed such a product and, in view of its apparent similarity to Curtis's new blue '$CsReCl_4$,' we immediately wondered if the Soviet chemists had simply got their formula wrong and that they really had '$KReCl_4$.' It did not take long to show that this was precisely the case and that the substance had the empirical formula $KReCl_4{\cdot}H_2O$. Since it formed better-looking crystals than did the cesium compound (which, incidentally, is actually $CsReCl_4{\cdot}{}^1/_2H_2O$[18] before drying), and these had a small triclinic unit cell, we considered $KReCl_4{\cdot}H_2O$ to be the preferred subject for an X-ray crystallographic study. Mr C. B. Harris (now Professor of Chemistry, University of California, Berkeley), who was just beginning his doctoral research and had never previously done a crystal structure, began a study of these crystals.

The Soviet chemical literature was also examined more carefully to see if there were any further reports of interest on the chemistry of lower-valent rhenium. It was found that between 1952 and 1958 V. G. Tronev and co-workers had published three papers[16,19,20] that described an assortment of low-oxidation state rhenium halide complexes in which the metal oxidation state was proposed to be +2. Much of the impetus for their investigations was a search for analogies between the chemistry of rhenium and platinum, an approach which no doubt prejudiced them in favor of the Re^{II} oxidation state. The existence of most of the compounds described in their 1952[19] and 1954[16] reports has never been substantiated, for example, products such as '$Re(C_5H_5N)_4Cl_2$,' '$Re(C_5H_5N)_2Cl_2$,' and 'Re(thiourea)$_4Cl_2$.' Two compounds—namely, the 'K_2ReCl_4' already mentioned and blue-green '$(NH_4)_2ReCl_4$,' which was also obtained by the action of hydrogen under pressure upon solutions of NH_4ReO_4 in concentrated hydrochloric acid at 300 °C—were further discussed in 1958 when Kotel'nikova and Tronev[20] published a more substantial contribution, entitled 'Study of the Complex Compounds of Divalent Rhenium.' Additional details were reported for the various materials emanating from a work-up of the blue solutions produced by these hydrogen reductions of perrhenate ($KReO_4$) in concen-

Pictiva EX2004
Samsung v Pictiva
IPR2024-01094

trated hydrochloric acid. In addition to the rhenium(IV) salts such as K_2ReCl_6, a remarkable variety of low-oxidation state products of spurious and largely unsubstantiated formulas (e.g., H_2ReCl_4, $KHReCl_4$, $ReCl_2{\cdot}4H_2O$, $ReCl_2{\cdot}2H_2O$, $H_2ReCl_4{\cdot}2H_2O$, $KHReCl_4{\cdot}2H_2O$, and $NH_4HReCl_4{\cdot}2H_2O$) were mentioned. Other than rhenium and chlorine microanalyses and an occasional oxidation state determination by the old method of I. and W. Noddack[21] (see below), no further characterizations were described that supported these formulations.

With respect to the oxidation state determinations, which Kotel'nikova and Tronev reported as supporting the oxidation state *+2* for rhenium, two points are pertinent. First, this method (which involves treatment with basic chromate, with intent to oxidize all rhenium to Re^{VII}, while reducing an equivalent amount of chromium to Cr_2O_3, which is filtered off and weighed) has often been found unreliable. Second, however, when this procedure was repeated at MIT on one of our own compounds,[22] it gave an oxidation number of $+2.9\pm0.2$. Presumably, the Soviet chemists, for whatever reason, obtained results that they thought required an oxidation number of +2 and, accordingly, adjusted the number of cations, usually by postulating the otherwise unsupported H^+, to make this consistent with the analytical data they had.

Before we leave our discussion of these rather confused and largely erroneous early results, consideration of two additional points is appropriate. First, Kotel'nikova and Tronev[20] observed the formation of a gray-green material, formulated as $(C_5H_5NH)HReCl_4$, upon the addition of pyridine to an acetone solution of '$H_2ReCl_4{\cdot}2H_2O$' that had been acidified with concentrated hydrochloric acid. Second, a variety of products, obtained when '$H_2ReCl_4{\cdot}2H_2O$' was dissolved in glacial acetic acid, were described[20] once again as derivatives of rhenium(II), namely $ReCl_2{\cdot}4CH_3COOH$, $ReCl_2{\cdot}2CH_3COOH{\cdot}H_2O$, $ReCl_2{\cdot}CH_3COOH{\cdot}H_2O$, $ReCl_2{\cdot}CH_3COOH$, and $ReCl_2{\cdot}CH_3COOH{\cdot}C_5H_5N$. The isolation of both $(C_5H_5NH)HReCl_4$ and $ReCl_2{\cdot}CH_3COOH$ is of significance since, while both were incorrectly formulated,[20] they are now known to have been genuine products that contain quadruple rhenium–rhenium bonds.

Except for one more brief report in 1962, describing[23] the formation of crystalline $(C_5H_5NH)HReCl_4$, by hydrogen reduction of a hydrochloric acid solution of the rhenium(IV) complex $ReCl_4(C_5H_5N)_2$ in an autoclave, the work of Tronev *et al.* was not further examined, by the authors themselves or anyone else, until 1963. We return now to that story.

While Harris was carrying out his crystallographic study of '$KReCl_4{\cdot}H_2O$,' proceeding rather slowly and deliberately (since he was learning X-ray crystallography as he went), a new issue of the *Zhurnal Strukturnoi Khimii* was received at MIT, and we noted that it contained an article[24] dealing with, '(pyH)$HReCl_4$.' Since we did not read Russian, it was not immediately clear what was being reported, though tables and figures within the article implied that it was reporting a structure determination. Fortunately, S. J. Lippard, a graduate student in the group (now Professor of Chemistry at MIT), had completed a crash course in Russian the previous summer at Harvard University and he was able to enlighten us. The paper reported that (in Lippard's translation, which is substantively identical to but in exact wording slightly different from the commercial translation that appeared nearly a year later):

> Eight chlorine atoms constitute a square prism with two rhenium atoms lying within the prism, whereby each rhenium atom is surrounded by four neighboring chlorine atoms situated at the apices of a strongly flattened tetragonal pyramid. The apices of two such pyramids approach each other generating the prism. In such a structure, each rhenium atom has for its neighbors one rhenium atom, at a distance of 2.22 Å and four chlorine atoms at a distance of 2.43 Å. As a result, the dimeric ion $[Re_2Cl_8]^{4-}$ is generated.

Pictiva EX2004
Samsung v Pictiva
IPR2024-01094

With regard to the structural situation of the H atoms present in the formula, the following statements were made:

> The isolated $[Re_2Cl_8]^{4-}$ grouping is bonded ionically to the pyridinium ion $[C_5H_5NH]^+$ carrying a positive charge, and its free hydrogen ions. . . . The detached free hydrogen ion is identified as situated on a fourfold position, which is electrostatically stable. It may be surmised that four hydrogen atoms are situated between Cl_{II} atoms on centers of symmetry . . . and serve to bond the $[Re_2Cl_4]^{4-}$ groups even further to each other.

In addition to the completely unprecedented Re-to-Re distance of only 2.22 Å and a puzzling discussion of the structural role of the 'hydrogen ions' (also sometimes called 'hydrogen atoms'), there had been, according to the experimental section of the paper, severe difficulty with crystal twinning. For all these reasons, we felt that this work was probably in error, possibly because the twinning problem had not, in fact, been successfully handled. Harris therefore hurried to complete his work on '$KReCl_4 \cdot H_2O$.'

To our considerable surprise, he found an anion essentially identical in structure to that described by the Soviet workers. There were some slight quantitative discrepancies, which we later resolved by carrying out a better refinement of the Soviet structure. The structure of the $[Re_2Cl_8]^{2-}$ ion, exactly as found and reported by C. B. Harris[25] in $K_2Re_2Cl_8 \cdot 2H_2O$, is shown in Fig. 1.1.

While Harris was completing his structural work, several others in the laboratory had also prepared a number of new compounds containing the $[Re_2Cl_8]^{2-}$ ion, using both our method (H_3PO_2 reduction) and the Tronev method (high-pressure H_2 reduction), and shown that:

1. the same products were obtained by both methods, although the former was far more practical, and
2. that the charge on the Re_2Cl_8 unit was indeed 2- and not 4-, as believed by the Soviet workers.

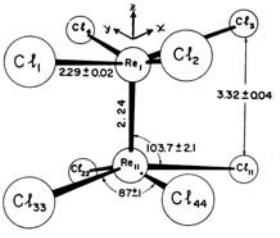


Fig. 1.1. The structure of the $[Re_2Cl_8]^{2-}$ ion as originally reported in ref. 25. A cartesian coordinate system has been added.

To round out this section, it is pertinent to note several other publications during the period in question, even though they had no bearing on the recognition of the existence of the Re–Re quadruple bond. There were two other very short Soviet papers (neither of which became known to us until much later, anyway) in which a few additional, misformulated, compounds were reported. One[26(a)] described compounds said to have the compositions $ReCl_2 \cdot CH_3CO_2H \cdot L$, with L = H_2O, C_5H_5N, or $(NH_2)_2CS$, while the other[26(b)] reported substances said to have the formulas $(ReCl_2 \cdot CH_3CO_2H \cdot H_2O)_2$, $Re_2Cl_3 \cdot 3CH_3CO_2H \cdot H_2O$, $(ReCl \cdot 2CH_3CO_2H)_2$, $ReCl_2 \cdot CH_3CO_2H \cdot H_2O$, $ReCl_2 \cdot CH_3CO_2H \cdot 2$thiourea, and $ReCl_2 \cdot CH_3CO_2H \cdot$pyridine. As to possible structures, little was said, none of which was correct.

Pictiva EX2004
Samsung v Pictiva
IPR2024-01094

Finally, in late 1963 there was a paper[27] reporting that reactions of rhenium(III) chloride with neat carboxylic acids give diamagnetic, orange products with molecular formulas $[ReCl(O_2CR)_2]_2$. It was proposed, by analogy with the known structure of Cu^{II} acetate, that the compounds were molecular, with bridging carboxylato groups and terminal chloride ligands.

1.2.2 The recognition of the quadruple bond

In only one of the Soviet papers discussed in the preceding section was anything said about the bonding in the putative Re^{II} compounds, namely in the structural paper,[24] where the following statement was made:

> It should be noted that the Re–Re distance ~2.22 Å is less than the Re–Re distance in the metal . . . . The decrease in the Re–Re distance in this structure, compared with the Re–Re distance in the metal, indicates that the valence electrons of rhenium also take part in the formation of the Re–Re bond. This may explain the diamagnetism of this compound.

Although it appears that at least by 1977,[28] the Russian school fully endorsed the concept of the quadruple bond, they appeared to have remained quite ambivalent for some time about the related problems of composition (i.e. the oxidation state of the rhenium and the question of whether hydrogen is present) and bonding, and the discussions in their papers are sometimes confusing, even as late as 1970. Thus, there is a paper[29] entitled 'Crystal Structure of Re_2Cl_4-$[CH_3COO(H)]_2{\cdot}(H_2O)$, with a Dimeric Complex Ion,' in which it was stated that, "In the two (α and β) modifications of $(pyH)HRe^{II}Br_4$ the authors found triple ($1\sigma + 2\pi$) Re–Re bonds." The correct formulas and oxidation numbers for at least some of their compounds still appeared to elude them. In the formula used in the title, the appearance of '(H)' is certainly an arresting feature, but what it is meant to imply was left entirely to the reader's imagination, unless it was an attempt to evade 'the question of whether acetic acid is found as a neutral molecule or as an acetate ion.' The authors described that question as one which "remains unclear."

Taha and Wilkinson[27] did come to grips with the question of bonding in their $[ReCl(OCOR)_2]_2$ compounds (for which they did have the correct formulas). They drew a structure with *no Re–Re bond* and explicitly stated that "it is not necessary to invoke metal–metal bonding to account for the diamagnetism."

The explanation for the remarkable structure of the $[Re_2Cl_8]^{2-}$ ion was put forward by one of the editors of this book in 1964.[30] Prior to this the chemistry of the $[Re_2Cl_8]^{2-}$ ion had been extensively clarified.[22] We had shown that the ion could be prepared much more conveniently from $[ReO_4]^-$ using an open beaker with H_3PO_2 as the reducing agent, that the analogous bromide could be made, that it reacted with carboxylic acids to give the Taha and Wilkinson[27] compounds, and that this reaction is reversible.[22]

$$[Re_2Cl_8]^{2-} \underset{\text{excess HCl}}{\overset{\text{excess } RCO_2H}{\rightleftharpoons}} Re_2(O_2CR)_4Cl_2$$

The existence of a bond between the rhenium atoms was proposed and explained in September 1964, as follows:[30]

> The fact that $[Re_2Cl_8]^{2-}$ has an eclipsed, rather than a staggered, structure (that is, not the structure to be expected on considering only the effects of repulsions between chlorine atoms) is satisfactorily explained when the Re–Re multiple bonding is examined in detail. To a first approximation, each rhenium atom uses a set of s, p_x, p_y, $d_{x^2-y^2}$ hybrid orbitals to form its four Re–Cl bonds. The remain-

Pictiva EX2004
Samsung v Pictiva
IPR2024-01094

> ing valence shell orbitals of each rhenium may then be used for metal-to-metal bonding as follows. (i) On each rhenium d_{z^2}–p_z hybrids overlap to form a very strong σ bond. (ii) The d_{xz}, d_{yz}, pair on each rhenium can be used to form two fairly strong π-bonds. Neither the σ nor the π bonds impose any restriction on rotation about the Re–Re axis. These three bonding orbitals will be filled by six of the eight Re *d* electrons. (iii) There remains now, on each rhenium atom, a d_{xy} orbital containing one electron. In the eclipsed configuration these overlap to a fair extent (about one third as much as one of the π overlaps) to give a δ bond, with the two electrons becoming paired. This bonding scheme is in accord with the measured diamagnetism of the $[Re_2Cl_8]^{2-}$ ion. If, however, the molecule were to have a staggered configuration, the δ bonding would be entirely lost (d_{xy}-d_{xy}, overlap would be zero). . . . Since the Cl–Cl repulsion energy tending to favor the staggered configuration can be estimated to be only a few kilocalories per mole, the δ-bond energy is decisive and stabilizes the eclipsed configuration. This would appear to be the first quadruple bond to be discovered.

In a full paper[31] that followed shortly, this proposal was elaborated in detail and supported with numerical estimates of *d*-orbital overlap. It was proposed that Re–Re quadruple bonds also occur in the $Re_2(O_2CR)_4X_2$ molecules. Finally, the correlation of metal–metal distances with bond orders ranging from <1 to 4 was explicitly discussed, and the concept of an entire gamut of M–M bond orders in an entire field of non-Wernerian compounds was introduced. This broad, synthetic view (and preview) of the field, which is in the nature of a Kuhnian paradigm shift, was presented in more detail very soon after in a review article.[32]

The quadruple-bond chemistry of rhenium was opened up quickly in several papers,[33,34] and before the end of 1966 the first metal–metal triple bond had also been reported[35] in the dirhenium compound $Re_2Cl_5(CH_3SCH_2CH_2SCH_3)_2$, which is obtained from the $[Re_2Cl_8]^{2-}$ ion.

Today the concept of quadruple bonds is no longer novel, with about 1500 compounds known to contain them, and the physical and theoretical characterization of them is very comprehensive, as this book will show. However, prior to 1964 quadruple bonds were totally unknown, and the idea even seemed to alarm some organic chemists, who took some time to accept the fact that *d*-orbitals can do things that *s*- and *p*-orbitals cannot. The newness of the concept of a quadruple bond is well illustrated by Linus Pauling's comment[36] (1960) that no one had ever presented evidence "justifying the assignment to any molecule of a structure involving a quadruple bond between a pair of atoms." Actually, the notion of quadruple bonds had been broached earlier, when Langmuir had proposed[37] to G. N. Lewis that the structure for nitrogen and carbon monoxide might involve "a quadruple bond such that two atomic kernels lie together inside a single octet," but this possibility (not surprisingly) was quickly eliminated as a realistic description of the bonding in any homonuclear or heteronuclear diatomic molecule formed by nonmetals.

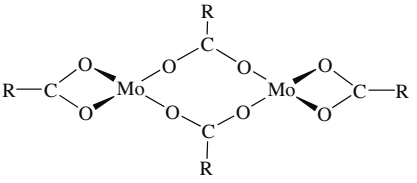
1.2.3 Initial work on other elements

Molybdenum and technetium

The reaction of molybdenum carbonyl with carboxylic acids was apparently examined for the first time in 1959, when the reaction with benzoic acid was reported[38] to yield a compound of empirical formula $Mo(C_6H_5CO_2)_2$. It was suggested that this substance might be either mononuclear or an infinite polymer, but, in either case "a novel type of oxygen *chelate* complex . . . where, in addition, the arene nucleus is bound to the metal atom by a sandwich-type bond, as in the arene metal carbonyls."

Pictiva EX2004
Samsung v Pictiva
IPR2024-01094

When, in 1960, it was shown[39] that several aliphatic acids also react with $Mo(CO)_6$ to form "$(RCOO)_2Mo$" compounds, the arene–metal structure for the benzoate was pronounced "unlikely." For all of these compounds an infinite polymer structure with tetrahedrally coordinated metal atoms and no metal–metal bonding was suggested. When this same work was reported more fully in 1964, it was suggested[40] that dinuclear molecules (which were pictured as shown below) are present and that, since they "are diamagnetic, this is consistent with tetrahedral coordination by oxygen, . . . with both bridging and chelating carboxylate groups." Again, no metal–metal bonding was even mentioned as a possibility. Clearly, at this time the true nature of these substances was entirely unrecognized.



It was not until late 1964 that such recognition occurred. By then the existence of quadruple bonds in $[Re_2X_8]^{2-}$ and $Re_2(O_2CR)_4X_2$ compounds had been proposed, as outlined above in Sections 1.2.1 and 1.2.2, and an X-ray investigation of a recently reported[41] technetium compound, $(NH_4)_3Tc_2Cl_8{\cdot}2H_2O$, had been completed. The formula of this compound prompted those who reported it to observe that "the stoichiometry of the $[Tc_2Cl_8]^{3-}$ ion is unusual and it seems to have no analogs." One of us was immediately struck by its similarity to $[Re_2Cl_8]^{2-}$ and, within a few months, had shown[42a] that the $[Tc_2Cl_8]^{3-}$ ion had a structure very similar to that of the $[Re_2Cl_8]^{2-}$ ion, especially in that the conformation was eclipsed. The Tc–Tc distance was even shorter (2.13(1) Å) than the Re–Re quadruple bond distance (2.24 Å), which seemed consistent with the fact that Tc atoms are inherently a little smaller than Re atoms. The correct explanation for the presence of an additional electron in the $[Tc_2Cl_8]^{3-}$ ion was not at that time evident and the issue was not addressed.

Just as the findings on the $[Tc_2Cl_8]^{3-}$ ion were being prepared for publication, it was learned by letter from Prof. Ronald Mason (then of Sheffield University) that he had determined the crystal structure of '$(CH_3COO)_2Mo$' and found the molecular unit to be as shown in Fig. 1.2. The Mo–Mo distance is nearly the same as the Tc–Tc distance and, since Mo^{II} is isoelectronic with Re^{III}, it seemed clear that $Mo_2(O_2CCH_3)_4$ contains a quadruple bond and that it is a group 6 analog to the $Re_2(O_2CR)_4X_2$ type of group 7 compound. We invited Mason to publish his molybdenum acetate structure back-to-back with our $[Tc_2Cl_8]^{3-}$ structure, and he agreed. The two manuscripts were submitted together on 30 November 1964, and appeared together in early 1965.[42] In our communication on $[Tc_2Cl_8]^{3-}$ we observed that on the basis of these new results on two compounds formed by metals in the second transition series:

> It appears that the formation of extremely short, presumably quadruple, bonds between d^4-ions of the second- and third-row transition elements may be quite general.

Subsequent events have shown that this statement erred only in being too cautious.

The chemistry of quadruply bonded Mo_2^{4+} derivatives did not undergo further development until late 1967, when a young Yugoslavian chemist, Jurij V. Brenčič (Professor of Inorganic Chemistry, University of Ljubljana), joined the MIT group and took up the problem of finding the right conditions for the reaction

$$Mo_2(O_2CCH_3)_4 + 8HCl \rightarrow [Mo_2Cl_8]^{4-} + 4H^+ + 4CH_3CO_2H$$

Pictiva EX2004
Samsung v Pictiva
IPR2024-01094

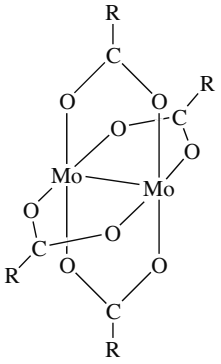


Fig. 1.2. The structure of the dinuclear molybdenum(II) acetate molecule, as first reported by Lawton and Mason in 1965.

which is analogous to our earlier reaction for the smooth interconversion of $[Re_2Cl_8]^{2-}$ and $Re_2(O_2CCH_3)_4Cl_2$. It turned out that unless conditions were carefully controlled, a variety of products were obtained, many of which were insoluble and, for that and other reasons, difficult to characterize.[43] Brenčič sorted out this confusion, and by July of 1968 we were able to submit a report of the preparation and X-ray verification of the first of several compounds containing the $[Mo_2Cl_8]^{4-}$ ion.[44]

It was with this discovery that a decade of virtually exponential growth of the field of M–M multiple bonds commenced. The compounds containing the $[Mo_2Cl_8]^{4-}$ ion are entirely stable thermally and toward the atmosphere (like those of $[Re_2Cl_8]^{2-}$); they have provided the starting points for a host of chemical, physical, and theoretical investigations.

In 1979 it was recognized[45] that several compounds containing Mo–Mo quadruple bonds had been made as early as 1962[46] and 1964[47] but were not at all understood at that time. It was found that Mo^{III} chloride and bromide reacted with liquid ammonia, methylamine, and dimethylamine to produce what were believed to be solvolysis products with suggested stoichiometries such as $MoX_2(NH_2)\cdot 3NH_3$, $MoBr(NHMe)_2\cdot{}^2/_3NH_2Me$, and $MoBr_2(NMe_2)\cdot NHMe_2$. It is now[45] clear that these are $Mo_2X_4L_4$ type molecules; for example, '$MoBr_2(NMe_2)\cdot NHMe_2$' is actually $Mo_2Br_4(NHMe_2)_4$ and may be smoothly converted to $Mo_2Br_4(PPr^n{}_3)_4$, which is also obtained by action of $PPr^n{}_3$ on $[Mo_2Br_8]^{4-}$.

Thus the prehistory of Mo–Mo quadruple bonds resembles that of rhenium in that several key compounds had been made prior to 1964, but no one had the remotest idea what they really were until after the true nature of the $[Re_2Cl_8]^{2-}$ ion was made clear.[30,31]

Chromium

The prehistory of the Cr–Cr quadruple bonds is fairly extensive. Astonishing as it may seem, the story begins with work published as early as 1844. In that year Eugène Peligot (Fig. 1.3) reported for the first time[48,49] that from bright blue aqueous solutions of chromium(II) ions, he could isolate, upon addition of sodium or potassium acetate, "little red transparent crystals. . . . which decompose upon exposure for a few moments to air." The method of preparation, the properties, and the analytical data leave no doubt at all that the compound Peligot prepared is $Cr_2(O_2CCH_3)_4(H_2O)_2$. Because of uncertainties prevalent at the time as to the molecular versus atomic weight of hydrogen, the empirical formula given was $CrC_4H_4O_5$; upon multiplying the number of H atoms by two, this formula becomes precisely correct. Moreover, Peligot showed that thermal decomposition gave an oxide weighing 41.8% of the original weight of the salt:

Pictiva EX2004
Samsung v Pictiva
IPR2024-01094

this is in good agreement with the ratio of the molecular weight of Cr_2O_3 to the molecular weight of $Cr_2(O_2CCH_3)_4(H_2O)_2$.

Over many decades following Peligot's report of the acetate of Cr^{II}, virtually nothing new was learned about this or other Cr^{II} carboxylates. It was not until 1916 that an advance occurred. It was shown[50] that from blue aqueous solutions of Cr^{II}, conveniently made by electrolytic reduction of acidic Cr^{III} solutions and protected from air by a layer of ligroin, the following red compounds could be isolated by addition of the sodium or other requisite carboxylate salt:

$$Cr(HCO_2)_2 \cdot 2H_2O$$
$$NH_4Cr(HCO_2)_3$$
$$Cr(CH_2OHCO_2)_2 \cdot H_2O$$
$$Cr[CH_2(CO_2)_2] \cdot 2H_2O$$

Aside from elemental analysis and the observation that dilute aqueous solutions of these red solids were blue, their properties were not elucidated. In 1925 the formate and malonate were again described, but not further studied.[51]

The first articulated realization that chromium(II) acetate might be of unusual interest is to be found (more than a century after the discovery of the acetate) in a paper by King and Garner[52] in 1950, who noted that "the orange-tan and red colors [of the anhydrous and hydrated acetate, respectively] and their moderately low solubility in water suggest a different type of bonding of the chromium from that in the typical blue and very soluble salts of dipositive chromium. . . ." They were prompted by this consideration to make the first magnetic susceptibility measurements on any chromous carboxylate, and they discovered that neither anhydrous nor hydrated chromium(II) acetate possesses any unpaired electrons. This is in sharp contrast to all of the blue chromium(II) compounds and the aquo ion, which have four unpaired electrons. To explain this result, they postulated a tetrahedral structure which, according to the valence bond ideas prevalent at the time, would utilize a set of d^3s hybrid orbitals on the chromium atom, thus relegating the four *d*-electrons to the remaining two *d*-orbitals with their spins paired. This explanation is, of course, wrong, but the important observation that there are no unpaired electrons is one of the two points of departure for our present day understanding of the chromium(II) carboxylates.



Fig. 1.3. Eugène-Melchoir Peligot (1811-90), the discoverer of chromium(II) carboxylates, worked on problems ranging from the physiology of silkworms to inorganic chemical analyses. He was the first to isolate metallic uranium, thus distinguishing it from UO_2, previously believed to be the element itself. Photo supplied by the Dains Collection, Spencer Research Library, The University of Kansas.

The other key development was the observation, in 1953, that hydrated chromium(II) acetate is isomorphous with hydrated copper(II) acetate and therefore binuclear, with bridging carboxyl groups.[53] Unfortunately, the structure was not quantitatively determined, and the Cr–Cr distance was estimated to be the same as the Cu–Cu distance, namely 2.64 Å. The suggestion was also made that the diamagnetism could be attributed to "a direct bond . . . between the two chromium atoms." The fact that at this distance two Cu atoms could not form a strong enough bond to pair even two electrons, whereas a pairing of eight electrons was required in the chromium case, was not, apparently, considered inconsistent with this proposal.

Pictiva EX2004
Samsung v Pictiva
IPR2024-01094

In 1956 Figgis and Martin,[54] as part of a very lengthy and detailed analysis of the electronic structure of the binuclear acetate of copper(II), devoted a few lines to the chromium(II) compound. They suggested that a set of weak *d–d* interactions, one σ, two π, and one δ, could occur and that "the resulting exchange is apparently sufficient effectively to pair the spins of the eight electrons occupying 3*d* levels in each chromous acetate molecule and to account for the observed diamagnetism." This hesitant but perceptive analysis of the chromous acetate molecule might well, under more auspicious circumstances, have led directly to a purposeful examination of the broader potentialities for the existence of M–M multiple bonds. Instead, however, chromium(II) acetate seems to have been thought of as a singular oddity and prompted no further work.

The dichromium carboxylates did not become integrated into the main stream of research on M–M multiple bonds until much later (1970), when an accurate measurement of the crystal structure of $Cr_2(O_2CCH_3)_4(H_2O)_2$ was carried out.[55] This showed that the Cr–Cr distance is actually 2.362(1) Å, which made it reasonable to speak of "the quadruple M–M interaction as a strong one." In the meantime beginning in 1964, S. Herzog and W. Kalies published a series of papers[56] showing that many essentially diamagnetic, red to brown compounds, $Cr_2(O_2CR)_4L_2$, could be made, where R might be virtually any C_nH_{2n+1} group and the ligand L (which might or might not be present) could be virtually any simple donor, such as H_2O, ROH, or an amine. Although these essentially preparative studies did nothing to clarify the nature of the compounds, they did show the important point that a large class of compounds was at hand.

It is also interesting that in 1964 F. Hein and D. Tille[57] reported a yellow, pyrophoric microcrystalline compound to which they assigned the formula $Cr(o\text{-}MeOC_6H_4)_2$, as well as orange-yellow '$Cr(o\text{-}MeOC_6H_4)_2{\cdot}LiBr{\cdot}3Et_2O$.' Both were observed to have very low magnetic moments (*c*. 0.5 BM), and for the former a bridged binuclear structure was proposed by which "erklärt sich die Herabsetzung des Paramagnetismus aus einer Wechselwirkung benachbarter 3*d*-Orbitale der beiden Chromatome, deren Abstande nahezu dem entsprich, der in metallischen Zustand vorliegt." Here, again, we have work that could have led on to the discovery of M–M multiple bonds, but was in fact aborted and abandoned at that time, and only many years later[58] was its true significance shown. Indeed, the second of the two compounds mentioned above not only contains a Cr–Cr quadruple bond, it contains the shortest known metal–metal bond, 1.830(4) Å!

Once more, as with rhenium and molybdenum, there existed prior to 1964 a number of significant experimental observations, all capable of revealing the existence of M–M quadruple bonds if properly interpreted. However, *none of them were properly interpreted* until after the formal proposal of a genuine, strong quadruple bond in $[Re_2Cl_8]^{2-}$, whereupon a coherent understanding of all the earlier scattered observations became possible, and was soon developed.

1.3 An Overview of the Multiple Bonds

As noted in the Preface, the extent of the literature on M–M multiple bonds is so great that this book can deal only with those compounds that fall within three structural categories. In the first, and by far the largest, are those compounds that have each of two metal atoms forming a square or square pyramidal MX_4 arrangement. For molybdenum and tungsten only, there are $L_3M{\equiv}ML_3$ molecules, which will be discussed in Chapter 6. Thirdly, there is now emerging class of EMAC (extended metal atom chain) compounds which have three or more metal atoms in a linear arrangement and surrounded by ligands. These compounds are reviewed in Chapter 15. Our plan is to discuss synthetic methods, structures and properties of these compounds first, and only at the end (Chapter 16) to discuss in more detail the electronic structures and some physical and theoretical techniques used to elucidate them. However, the descriptive

Pictiva EX2004
Samsung v Pictiva
IPR2024-01094

material can be effectively organized only within the framework of a qualitative picture of the M–M bonding, the relationship between the different bond orders, and the electronic properties of the metal atoms that facilitate M–M multiple bond formation. Therefore, we now give a broad qualitative overview of the electronic structures of M–M multiple bonds.

1.3.1 A qualitative picture of the quadruple bond

The components of the M–M quadruple bonds include the key elements in most other multiple bonds between pairs of metal atoms. Therefore, a discussion of quadruple bonds provides a good introduction to all of the others.

A quadruple bond can occur only with transition metals, because orbitals of angular momentum quantum number 2 (*d*-orbitals) or higher (*f, g*, etc., orbitals) are required. In fact, the quadruple bond can be formulated using only *d*-orbitals, and by considering only *d*-orbital overlaps a picture that is qualitatively and even semiquantitatively reliable can be obtained. When two metal atoms approach each other, only five nonzero overlaps between pairs of *d*-orbitals on the two atoms are possible because of the symmetry properties. These five nonzero overlaps are those between corresponding pairs, that is, d_{z^2} with d_{z^2}, d_{xz} with d_{xz} etc. The coordinate axes shown in Fig. 1.1 may be used to define the orbitals.

The positive overlap of the two d_{z^2}-orbitals, $d_{z^2}^{(1)} + d_{z^2}^{(2)}$, gives rise to a σ-bonding orbital. There is, of course, a corresponding antibonding σ-orbital formed by negative overlap, $d_{z^2}^{(1)} - d_{z^2}^{(2)}$. The $d_{xz}^{(1)} + d_{xz}^{(2)}$ and $d_{yz}^{(1)} + d_{yz}^{(2)}$ overlaps can each give rise to a π-bond; these two are equivalent, but orthogonal, and hence constitute a degenerate pair. Again, there are the corresponding π^*-orbitals resulting from the negative overlaps. Lastly, there are the bonding and antibonding (δ and δ*) combinations of the d_{xy}-orbitals. The remaining pair of *d*-orbitals, $d_{x^2-y^2}$ on each metal atom, can also overlap to form bonding and antibonding combinations, but both qualitative reasoning and calculations show that each of them interacts primarily with the set of four ligands on its own metal atom. In this way they make a strong contribution to metal–ligand bonding but have very little to do with M–M bonding.

Using the basic Hückel concept, namely, that MO energies are proportional to overlap integrals, at least for similar types of orbitals, and noting that these overlaps must increase in the order $\delta << \pi < \sigma$, we expect the orbitals to be ordered in energy as follows, beginning with the most stable:

$$\sigma < \pi << \delta < \delta^* << \pi^* < \sigma^*$$

These considerations are summarized in Fig. 1.4.

For the $[Re_2Cl_8]^{2-}$ ion we have eight electrons to be placed in these orbitals, since the rhenium atoms are in the formal oxidation state III, leaving 7 - 3 = 4 electrons for each one. These eight electrons just fill the bonding orbitals giving a configuration we can represent as $\sigma^2\pi^4\delta^2$. There are four pairs of bonding electrons and no antibonding electrons. According to the conventional MO theory definition of bond order,

$$\text{bond order} = \frac{n_b - n_a}{2}$$

where n_b and n_a designate the number of electrons occupying bonding and antibonding orbitals, respectively, the bond is of order 4. It is a quadruple bond. It is worthwhile emphasizing that bond order here is being used in an *ordinal* and not a *metrical* sense; it is simply a statement of the *net number of electron pairs*—or halves thereof—that are serving to bind the two atoms together. It does not explicitly or implicitly provide a measure of bond strength, except in the broadest qualitative sense. Indeed, the four components, σ, two π, δ, vary considerably in their contributions to total bond strength, that of the δ component being very small (<10 per cent).

Pictiva EX2004
Samsung v Pictiva
IPR2024-01094

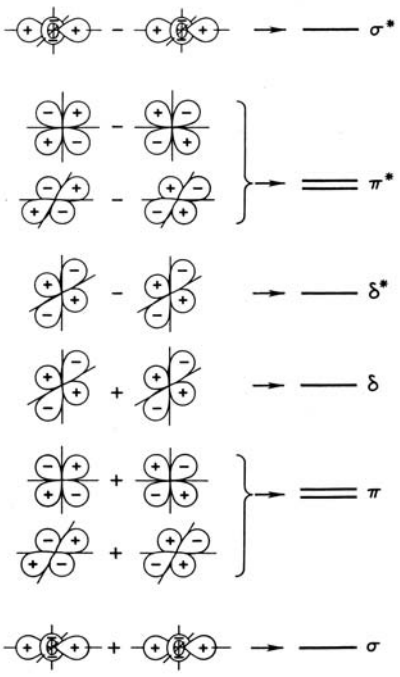


Fig. 1.4. Diagram of the overlaps of *d*-orbitals and the resulting energy levels as they are involved in the formation of M–M multiple bonds in a $X_4M–MX_4$ structure. In practice, the ordering of orbitals, especially those having antibonding nature, might differ.

It is worthwhile to note, parenthetically, that a simple valence bond or hybridized orbital description of the quadruple bond is possible.[59]

The $\sigma^2\pi^4\delta^2$ description of a quadruple bond unequivocally accounts for its two most conspicuous features: its extreme shortness and its tendency to impose an eclipsed configuration. Obviously the high multiplicity (i.e. the presence of four pairs of bonding electrons) will account for the shortness. The conformational preference is also unambiguously explained. The σ-bond is, of course, cylindrically symmetrical. A *pair* of π-bonds is also cylindrically symmetrical. For one of these the amplitude of the wave function as a function of an angle χ, measured from the *x*-axis around the bond in the *xy*-plane, is proportional to $\sin^2\chi$. For the other π-bond, perpendicular to the first one, the angular dependence is given by $\cos^2\chi$. Thus, the combined π wave function has an angular dependence of $\cos^2\chi + \sin^2\chi$, which is, by a well-known trigonometric identity, a constant, viz. unity. Hence the $\sigma^2\pi^4$ part of the bond is insensitive to the angle of internal rotation.

The δ component of the bond, however, is markedly angle sensitive. As shown in Fig. 1.5, the $d_{xy}^{(1)} + d_{xy}^{(2)}$ overlap has its maximum value when the two $ReCl_4$ moieties are precisely eclipsed and it has a value of zero when the rotational conformation is precisely staggered. Thus, any rotation away from the eclipsed conformation causes a loss of δ-bond energy and, when carried to the limit of precise staggering, causes complete disappearance of the δ-bond. It is this dependence of the δ-bond on rotation angle that opposes the tendency of nonbonded repulsions to favor a staggered conformation.

This argument does *not* predict that the *fully* eclipsed conformation is preferred, but only that a conformation approaching the eclipsed one should be preferred. In many crystal structures the crystallographic symmetry (e.g., a center of inversion between the metal atoms) dic-

Pictiva EX2004
Samsung v Pictiva
IPR2024-01094

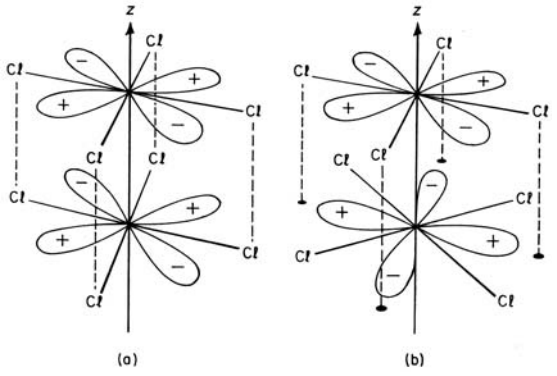


Fig 1.5. The relationship of one d_{xy}-orbital to the other for (a) an eclipsed structure and (b) a fully staggered one.

tates that the average of the torsional angles is, in fact, exactly zero. However, in other cases net torsional rotation does occur, to the extent of a few degrees. It should be noted that the dependence of the δ overlap[60] on the angle of internal rotation χ is given by cos2χ. Therefore, considerable deviation from perfect eclipsing can occur without serious loss of δ-bonding. Indeed a rotation of 30°, that is, two thirds of the way towards the fully staggered conformation, causes a loss of only half of the δ overlap. The interplay of the inherent preference of the δ bond for an eclipsed configuration and all of the other intramolecular forces (bonded and nonbonded) in determining molecular structures is very complex. Only a few efforts have been made to tackle these problems by molecular modeling (or molecular mechanics).[61]

1.3.2 Bond orders less than four

The energy level diagram shown in Fig. 1.4 shows that within the tetragonal structural framework of two metal atoms surrounded by eight ligand atoms with an eclipsed relationship of the two MX_4 halves, many ground state electron configurations are possible.[62] Bond orders may vary, in steps of $^1/_2$, from $^1/_2$ to 4, as shown in Fig. 1.6. It will be noted that all bond orders except 4 can result in two ways. Those to the left of 4 may be called "electron-poor" and those to the right "electron-rich." Not shown in Fig. 1.6 are electron-poor bonds of orders $^1/_2$ to $2^1/_2$ because, to date, no real examples within the tetragonal geometry specified are known.

It must also be noted that there is another much more limited but important structural motif for multiple metal–metal bonding. Molybdenum and tungsten form a large number of triply-bonded compounds[63,64] of the trigonal type $L_3M{\equiv}ML_3$, with D_{3d} symmetry, shown by the representative example, $Mo_2(NMe_2)_6$, in Fig. 1.7. These compounds, which are fully reviewed in Chapter 6, have an acetylene-like triple bond ($\sigma^2\pi^4$) and an ethane-like structure.

1.3.3 Oxidation states

The most common oxidation states for the M_2^{n+} units in paddlewheel complexes correspond to values of n of 4, 5, and 6. A few electrochemical studies have shown values outside that range but it was not until very recently that compounds with V_2^{3+}, Os_2^{7+}, and Re_2^{7+} cores have been characterized structurally and by other techniques (Chapters 2, 10 and 8, respectively). The difficulties in finding compounds with values below the common range (such as n = 3) lie in that oxidation numbers of less than 2+ are not common in transition metal chemistry, except with pi-acid ligands which generally do not occur in paddlewheel complexes. For values of n greater than 6, it has generally been thought that the decrease in the size of the ion with in-

Pictiva EX2004
Samsung v Pictiva
IPR2024-01094

creasing oxidation number would weaken overlap in the metal–metal bond too severely. An increase in atomic charge would also create repulsion between metal centers, further diminishing the strength of the metal-metal bonding. However, the examples of n = 3 and 7 recently found open up possibilities of finding appropriate ligands that could stabilize still more compounds with oxidation numbers outside the common range.

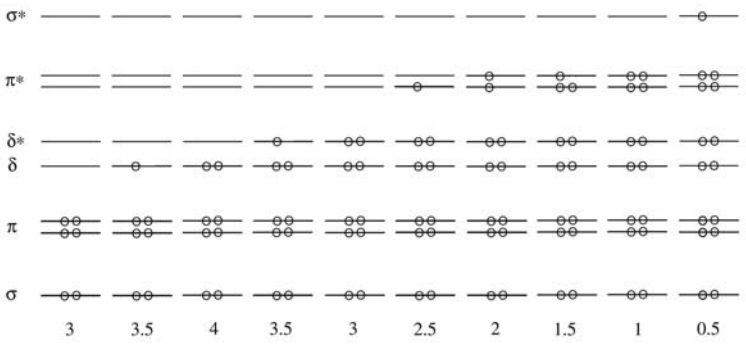


Fig. 1.6. A diagramatic representation of how M–M bond orders can change by removal of δ-electrons or addition of antibonding electrons. Ordering can change for antibonding orbitals.

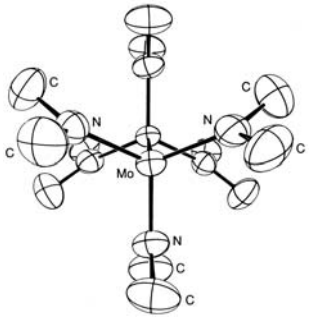


Fig. 1.7. The $Mo_2(NMe_2)_6$ molecule which has a $\sigma^2\pi^4$ triple bond.

1.4. Growth of the Field

Two ways in which the field has grown since 1965 are:

1. In the range of metallic elements it embraces.
2. In the number and variety of compounds.

With regard to the range of metallic elements, the expansion of the field can be seen in Fig. 1.8. There are now more than 4000 compounds, and elements in all of the groups 5 to 10 are represented. The only two elements among these eighteen for which no compound pertinent to this monograph has been reported are manganese and tantalum.

The vast majority of the tetragonal compounds have homonuclear M_2^{n+} cores, but a few heteronuclear ones[65] have been known since 1975 when $MoW(O_2CCMe_3)_4$ was reported and 1976 when $CrMo(O_2CCMe)_4$ was reported. Since then several dozen compounds with MoW cores have been described, as well as two with RuOs cores. Only in 1999 were the first compounds

Pictiva EX2004
Samsung v Pictiva
IPR2024-01094

V	Cr	Mn	Fe	Co	Ni
Nb	***Mo*** 1-9	***Tc*** 1-9	Ru	Rh	Pd
Ta	W	***Re*** 1-9	Os	Ir	Pt

1965

V	***Cr*** 10-99	Mn	Fe	Co	Ni
Nb	***Mo*** 100-499	***Tc*** 1-9	***Ru*** 10-99	***Rh*** 10-99	Pd
Ta	***W*** 1-9	***Re*** 100-499	***Os*** 1-9	Ir	***Pt*** 1-9

1980

V	***Cr*** 100-499	Mn	Fe	***Co*** 3	***Ni*** 1-9
Nb	***Mo*** 500-999	***Tc*** 1-9	***Ru*** 100-499	***Rh*** 100-499	Pd
Ta	***W*** 10-99	***Re*** 100-499	***Os*** 10-49	***Ir*** 3	***Pt*** <99

1990

V 11	***Cr*** >500	Mn	***Fe*** 3	***Co*** 8	***Ni*** 1-9
Nb 7	***Mo*** >1100	***Tc*** >50	***Ru*** >500	***Rh*** >1500	***Pd*** 3
Ta	***W*** >110	***Re*** >550	***Os*** ~70	***Ir*** 9	***Pt*** >100

2003

Fig. 1.8. An element by element inventory of the number of compounds containing M_2^{n+} cores from 1965 to 2003.

of the (Porph)MM'(Porph') type reported; compounds with metal atoms from different groups, namely, MoRu, WRu and MoRe cores are now known.[65]

In the preceding pages, two structural motifs for tetragonal compounds have been mentioned, namely, the square parallelepiped $[M_2X_8]^{n-}$ type and the $M_2(O_2CR)_4L_n$ (n = 0, 1, 2) type. It is appropriate at this point to give an overview of the structural types that occur most frequently and some of the designators used to distinguish isomers when they occur.

Structural types for $M_2X_{8-n}L_n$ molecules

While there are relatively few $[M_2X_8]^{n-}$ species, there are a large number of substitution products, $[M_2X_{8-n}L_n]$, where L is a neutral ligand and n may run from 1 to 4. All of the species with n = 2, 3 and 4 have isomers, and there is a notation for designating them. The eight ligand positions are numbered as shown in Fig. 1.9 where the M_2 unit is taken to be vertical, and these numbers are used to specify the relative placement of the ligands L, always using the smallest possible numbers. Particularly important examples of isomeric compounds employing this scheme are also shown.

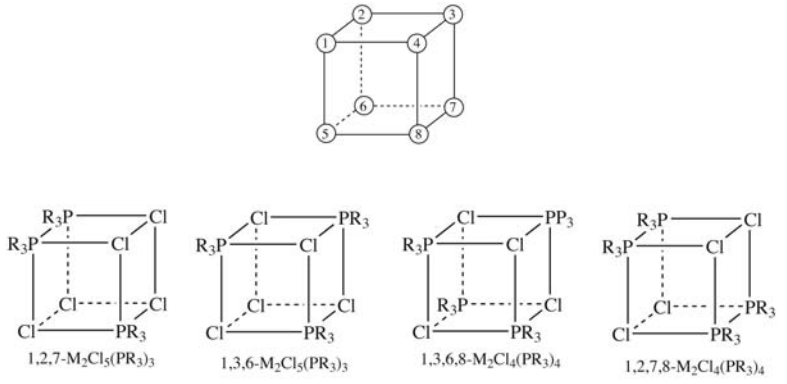


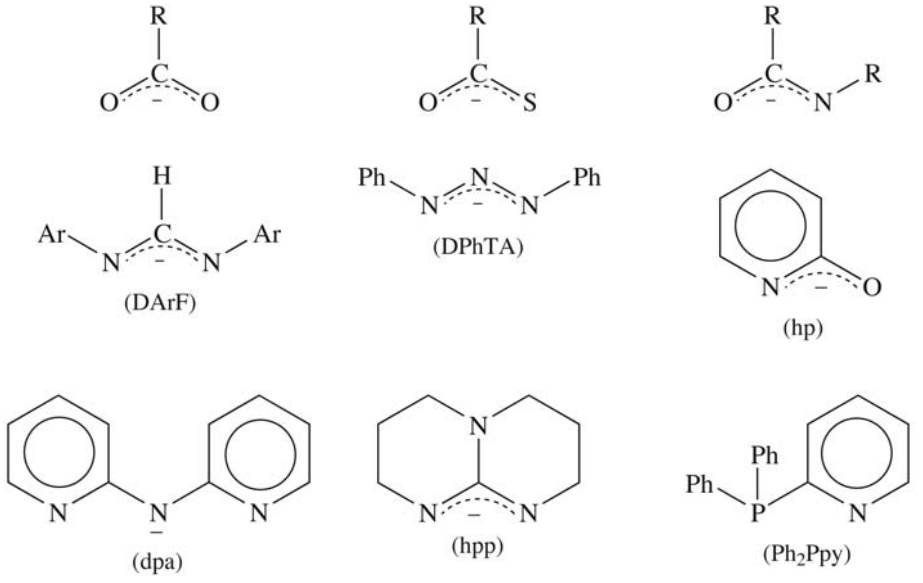
Fig. 1.9. Notation for isomers of $M_2Cl_5(PR_3)_3$ and $M_2Cl_4(PR_3)_4$ molecules.

Pictiva EX2004
Samsung v Pictiva
IPR2024-01094

Paddlewheel structures

Compounds having four bidentate, three-atom ligands that bridge the metal atoms, as in the case of the tetracarboxylate shown in Fig. 1.2, are called *paddlewheel* compounds. There are a great many ligands that occur in such structures. Table 1.1 displays a few of the most common ones and their abbreviations. A longer list of abbreviations is given in the Appendix. A paddlewheel molecule may have 0, 1 or 2 axial ligands.

Table 1.1. Representative ligands found in paddlewheel complexes



Several of the important ligands (or classes of ligand) that occur in paddlewheel complexes are unsymmetrical. This opens the possibility of *regioisomers*, as depicted in Fig. 1.10, where the notation is also shown. Compounds in which there is a mixture of paddlewheel type ligands (especially RCO_2^-) and monodentate ligands (anionic or neutral) are numerous.

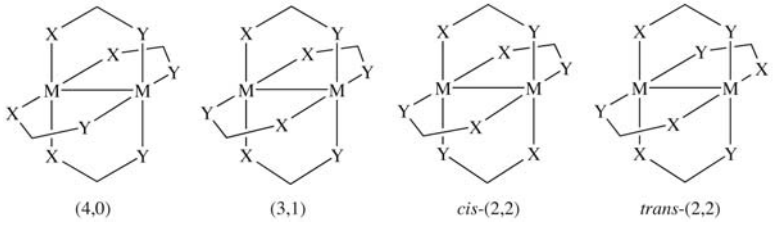


Fig. 1.10. Designators for regioisomers of paddlewheel molecules with unsymmetrical ligands

Pictiva EX2004
Samsung v Pictiva
IPR2024-01094

1.5 Going Beyond Two

In approximately the past decade, compounds containing more than one pair of metal atoms or chains of more than two metal atoms have made their appearance. Such compounds are obtained in three different ways:

1. By linking dimetal units through axial linkers, Fig. 1.11(a).
2. By linking dimetal units through equatorial linkers, Fig. 1.11(b) and 1.11(c).
3. By making *extended metal atom chains*, EMACs, Fig. 1.11(d).

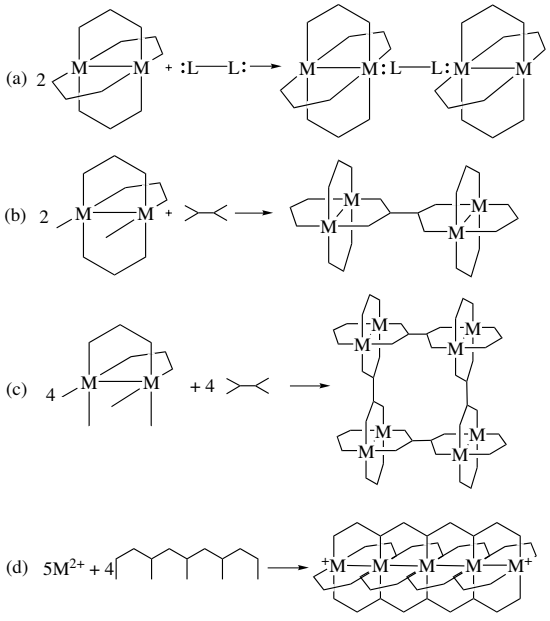


Fig. 1.11. (a) Axially linking two dimetal moieties. (b) Equatorially linking two dimetal moieties. (c) Equatorially linking four dimetal moieties. (d) Formation of EMACs.

Actually, there are some rather old examples of linking dimetal units by difunctional axial linkers although attention to this kind of synthesis has markedly increased lately. Many compounds of this kind are formed by those dimetal units that tend to bind axial ligands most strongly, particularly Cr_2^{4+}, $Ru_2^{5+,6+}$ and Rh_2^{4+}, and details will be found in Chapters 3, 9 and 12, respectively. Linking dimetal units by equatorially-bridging bifunctional ligands began only in the 1990s, with the first linkers being dicarboxylic acids.[66] Of the many reported products, the most numerous are dimers (with Mo_2, W_2 and Ru_2 end units), triangles (with Mo_2 and Rh_2 corners) and squares (with Mo_2, Rh_2 and Ru_2 corners). It has also been shown that diamides may serve as linkers. The main key to success in this chemistry is the use of spectator ligands (i.e., those not involved in bridging) that are not labile. Amidinates are well suited, but carboxylates present difficulties. Specific compounds will be discussed in Chapters 4, 5, 9 and 12 for Mo_2-, W_2-, Ru_2- and Rh_2- based oligomers, respectively.

Molecules with linear chains of three to eleven metal atoms, EMACs, wrapped with four polydentate ligands, are now known for the metallic elements Cr, Co, Ni, Cu, Ru and Rh. They are reviewed in Chapter 15. In some cases the metal atoms are evenly spaced, with fractional bonds between each neighboring pair of metal atoms, but in others the metal atoms pair off and form stronger bonds like those found in dinuclear molecules. For example Cr_5 species can be described as Cr≡Cr···Cr≡Cr···Cr.

Pictiva EX2004
Samsung v Pictiva
IPR2024-01094

References

1 (a) A. Werner, *Neuere Anschauungen auf dem Gebiete der anorganischen Chemie,* Braunschweig, 1905; (b) see P. Pfeiffer in *Great Chemists,* ed. E. Farber, Interscience, New York, 1961, p. 1233; (c) excellent general reviews of Werner's publications are to be found in G. B. Kauffman, *Coord. Chem. Rev.* **1973**, *11,* 161; **1974**, *12,* 105; **1975**, *I5,* 1 ; see also ref. 2.
2. G. B. Kauffman, *Coord. Chem. Rev.* **1973**, *9,* 339, provides a comprehensive review of Werner's publications.
3. C. W. Bloomstrand, *J. Prakt. Chem.* **1857**, *71,* 449; **1859**, *77,* 88; **1861**, *82,* 433.
4. M. Blondel, *Ann. Chim. Phys.,* **1905**, *8,* 110; L. Wöhler and W. Frey, *Z. Electrochem.* **1909**, *15,* 132; M. Delepine, *Compt. Rend.* **1910**, *150,* 104.
5. M. C. Chabrié, *C. R. Acad. Sci.,* **1907**, *144,* 804; W. H. Chapin, *J. Am. Chem. Soc.* **1910**, *32,* 327; H. S. Harned, *J. Am. Chem. Soc.* **1913**, *35,* 1078.
6. K. Lindner, *Z. anorg. allg. Chem.* **1927**, *162,* 203, and numerous earlier papers cited therein.
7. C. Brosset. *Arkiv Kemi, Miner. Geol.* **1946**, *A20* (7); *A22* (11).
8. C. Brosset, *Arkiv Kemi, Miner. Geol.* **1935**, *128,* No. 7; *Nature* **1935**, *135,* 874.
9. P. A. Vaughan, J . H. Sturtivant, and L. Pauling, *J. Am. Chem. Soc.* **1950**, *72,* 5477.
10. (a) J. A. Bertrand, F. A. Cotton, and W. A. Dollase, *J. Am. Chem. Soc.* **1963**, *85,* 1349; (b) *idem., Inorg. Chem.* **1963**, *2,* 1166.
11. W. I. Robinson, J. E. Fergusson, and B. R. Penfold, *Proc. Chem. Soc.* **1963**, 116.
12. F. A. Cotton and T. E. Haas, *Inorg. Chem.* **1964**, *3,* 10.
13. F. A. Cotton, *Inorg. Chem.* **1964**, *3,* 1217.
14. L. F. Dahl, E. Ishishi and R. E. Rundle, *J. Chem. Phys.* **1957**, *26,* 1750.
15. (a) F. A. Cotton and J. T. Mague, *Proc. Chem. Soc.* **1964**, 233; (b) *idem., Inorg. Chem.* **1964**, *3,* 1402; (c) F. A. Cotton and S. J. Lippard, *J. Am. Chem. Soc.* **1964**, *86,* 4497; (d) F. A. Cotton, S. J. Lippard and J. T. Mague, *Inorg. Chem.* **1965**, *4,* 508; (c) J. Gelinek and W. Rudorff, *Naturwiss.* **1964**, *51,* 85.
16. V. G. Tronev and S. M. Bondin, *Khim. Redk. Elem. Akad. Nauk SSSR* **1954**, *1,* 40.
17. F.A. Cotton and B. F. G. Johnson, *Inorg. Chem.* **1964**, *3,* 780.
18. F. A. Cotton and W. T. Hall, *Inorg. Chem.* **1977**, *16.* 1867.
19. V. G. Tronev and S. M. Bondin, *Dokl. Akad. Nauk SSSR,* **1952**, *86,* 87.
20. A. S. Kotel'nikova and V. G. Tronev, *Russ. J. Inorg. Chem.* **1958**, *3,* 268.
21. I. Noddack and W. Noddack, *Z. anorg. a1lg. Chem.* **1933**, *215,* 182.
22. F. A. Cotton, N. F. Curtis, B. F. G. Johnson and W. R. Robinson, *Inorg. Chem.* **1965**, *4,* 326.
23. G. K. Babeshkina and V. G. Tronev, *Zh. Neorg. Khim.* **1962**, *7,* 215.
24. V. G. Kuznetzov and P. A. Koz'min, *J. Struct. Chem.* **1963**, *4,* 49.
25. F. A. Cotton and C. B. Harris, *Inorg. Chem.* **1965**, *4,* 330.
26. (a) A. S. Kotel'nikova and G. A. Vinogradova, *Dokl. Akad. Nauk SSSR* **1963**, *152,* 621; (b) *idem., Zh. Neorg. Khim.* **1964**, *9,* 307.
27. F. Taha and G. Wilkinson, *J. Chem. Soc.* **1963**, 5406.
28. M. A. Porai-Koshits and Yu. N. Mikhailov, *Zh. Strukt. Khim.* **1977**, *18*, 983.
29. P. A. Koz'min, M. D. Surazhskaya and V. G. Kuznetsov, *J. Struct. Chem.* **1970**, *11*, 291.
30. F. A. Cotton, N. F. Curtis, C. B. Harris, B. F. G. Johnson, S. J. Lippard, J. T. Mague, W. R. Robinson and J. S. Wood, *Science* **1964**, *145*, 1305.
31. F. A. Cotton, *Inorg. Chem.* **1965**, *4,* 334.
32. F. A. Cotton, *Quart. Rev,* **1966**, *20*, 389.
33. F. A. Cotton, N. F. Curtis and W. R. Robinson, *Inorg. Chem.,* **1965**, *4,* 1696.
34. F. A. Cotton, C. Oldham and W. R. Robinson, *Inorg. Chem.* **1966**, *5*, 1798.
35. M. J. Bennett, F. A. Cotton and R. A. Walton, *J. Am. Chem. Soc.* **1966**, *88,* 3866.
36. L. Pauling. *The Nature of the Chemical Bond,* 3rd ed. Cornell University Press, Ithaca, NY, 1960, p. 64.
37. G. N. Lewis, *Valence and the Structure of Atoms and Molecules,* The Chemical Catalog Company, Inc., New York, 1923, p. 127.

Pictiva EX2004
Samsung v Pictiva
IPR2024-01094

38. E. W. Abel, A. Singh and G. Wilkinson, *J. Chem. Soc.* **1959**, 3097.
39. E. Bannister and G. Wilkinson, *Chem. Ind. (London)* **1960**, 319.
40. T. A. Stephenson. E. Bannister and G. Wilkinson, *J. Chem. Soc.* **1964**, 2538.
41. J. D. Eakins, D. G. Humphries and C. E. Mellish, *J. Chem. Soc.* **1063**, 6012.
42. (a) F. A. Cotton and K. W. Bratton, *J. Am. Chem. Soc.* **1965**, *87*, 921. (b) D. Lawton and R. Mason, *J. Am. Chem. Soc.* **1965**, *87*, 921.
43. One paper had already appeared and, while Brenčič was working, another came out in which a great variety of compounds (many of which we could never reproduce) were reported and assigned fascinating but unsupported structures, none of which has ever been confirmed. See the following: I. R. Anderson and J. C. Sheldon, *Aust. J. Chem.* **1965**, *18*, 271; G. B. Allison, I. R. Anderson and J. C. Sheldon, *Aust. J. Chem.* **1967**, *20*, 869.
44. J. V. Brenčič and F. A. Cotton, *Inorg. Chem.* **1969**, *8*, 7.
45. J. E. Armstrong, D. A. Edwards, J. J. Maguire and R. A. Walton, *Inorg. Chem*. **1979**, *18*, 1172.
46. D. A. Edwards and G. W. A. Fowles, *J. Less-Common Met.* **1962**, *4*, 512.
47. D. A. Edwards *J. Less-Common Met.* **1964**, 7, 159.
48. E. Peligot, *C. R. Acad. Sci.* **1844**, *19*, 609.
49. E. Peligot, *Ann. Chim. Phys.* **1844**, *12*, 528.
50. W. Traube and A. Goodson, *Chem. Ber.* **1916**, *49,* 1679.
51. W. Traube, E. Burmeister and R. Stahn, *Z. anorg. allg. Chem.* **1925**, *147*, 50.
52. W. R. King, Jr and C. S. Garner, *J. Chem. Phys.* **1950**, *18*, 689.
53. J. N. van Niekerk, F. R. L. Schoening and J. F. de Wet, *Acta Crystallogr.* **1953**, *6*, 501.
54. B. N. Figgis and R. L. Martin, *J. Chem. Soc.* **1956**, 3837.
55. F. A. Cotton, B. G. DeBoer, M. D. LaPrade, J. R. Pipal and D. A. Ucko, *J. Am. Chem. Soc.* **1970**, *92*, 2926; *idem., Acta Crystallogr.* **1971**, *B27*, 1664.
56. S. Herzog and W. Kalies, *Z. Chem.* **1964**, *4,* 183; *Z. anorg. allg. Chem.* **1964**, 329, 83; *Z. Chem.,* 1965, 5, 273; *Z. Chem.* **1966**, *6,* 344; Z. *anorg. allg. Chem.* 1967, 351, 237; *Z. Chem.* **1968**, *8,* 81.
57. F. Hein and D. Tille, *Z. anorg. allg. Chem.* **1964**, *329*, 72.
58. F. A. Cotton and S. Koch, *Inorg. Chem.* **1978**, *17*, 2021.
59. L. Pauling, *Proc. Natl. Acad. Sci. USA* **1975**, *72*, 3799; 4200.
60. F. A. Cotton, P. E. Fanwick, J. W. Fitch, H. D. Glicksman and R. A. Walton, *J. Am. Chem. Soc.* **1979**, *101*, 1752.
61. (a) J. C. A. Boeyens and F. M. M. O'Neill, *Inorg. Chem.* **1995**, *34*, 1988. (b) J. Bacsa and J. C. A. Boeyens, *J. Organomet. Chem*. **2000**, *596*, 159.
62. F. A. Cotton, *Chem. Soc. Rev.* **1983**, *12*, 35.
63. M. H. Chisholm and F. A. Cotton, *Acc. Chem. Res.* **1978**, *11*, 356.
64. M. H. Chisholm and I. P. Rothwell, *J. Am. Chem. Soc.* **1980**, *102*, 5950.
65. J. P. Collman and R. Boulatov, *Angew. Chem. Int. Ed.* **2002**, *41*, 3948.
66. (a) R. H. Cayton, M. H. Chisholm, J. C. Huffman, E. B. Lobkovsky, *J. Am. Chem. Soc*. **1991**, *113*, 8709. (b) F. A. Cotton, C. Lin and C. A. Murillo, *Acc. Chem. Res*. **2001**, *34*, 759.

Pictiva EX2004
Samsung v Pictiva
IPR2024-01094

2

Complexes of the Group 5 Elements

Carlos A. Murillo,
Texas A&M University

2.1 General Remarks

Paddlewheel compounds having two dimetal units, each with a square planar configuration, and each group parallel to the other are relatively new in group 5. With other transition metal atoms, this type of atom arrangement is commonly found for M_2^{n+} units where n = 4, 5 or 6. This means that the oxidation state for each metal atom is between 2 and 3. It has been generally thought that when the formal oxidation numbers are higher the atoms shrink so much that good orbital overlap necessary for metal–metal bond formation is not attained. Oxidation numbers of less than two are not common in inorganic compounds of the first transition series, with the exception of Cu or when compounds are stabilized by π-donors such as carbonyl groups which are not generally covered in this monograph. Therefore only a few examples of compounds with values of n outside the range 4-6 are known. For the group 5 elements, compounds in which the metal atom has an oxidation number of three are commonly found forming edge-sharing bioctahedra, not paddlewheel compounds. Lower oxidation numbers such as two give rise to only a few coordination complexes for vanadium; an even lesser number is known for niobium and tantalum. Therefore part of the challenge in synthesizing metal–metal bonded paddlewheel compounds of the group 5 elements is the development of appropriate synthetic procedures that produce precursors in low oxidation states. Most of the compounds of the paddlewheel type for vanadium and niobium have the metal atom in the divalent state in a d^3 electronic configuration. The overlap of these d^3–d^3 atoms give triply bonded dimetal units with an expected electronic configuration of $\sigma^2\pi^4$ or a variation thereof.

2.2 Divanadium Compounds

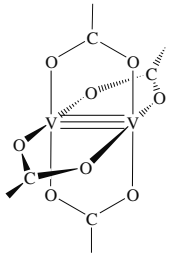
Theoretical calculations at the Fenske-Hall and Hartree-Fock level for the model system $V_2(O_2CH)_4$, which had been carried out in the mid-eighties, indicate that multiple bonds between vanadium atoms should be stable.[1] The calculations clearly show the possible existence of paddlewheel molecules of the type **2.1** and predict a vanadium-to-vanadium triple bond length between 2.0 and 2.1 Å with a $\sigma^2\pi^4$ electronic configuration for the V_2^{4+} unit. However, all efforts to synthesize V_2(carboxylato)$_4$ compounds from the reaction of carboxylates and a few known V^{2+} starting materials available[2] (e.g., $V(H_2O)_6(CF_3SO_3)_2$, $[V_2Cl_3(THF)_6]_2[Zn_2Cl_6]$ or $VCl_2(py)_4$) fail to produce dinuclear complexes.[3] These reactions give oxo-centered trinuclear

Pictiva EX2004
Samsung v Pictiva
IPR2024-01094

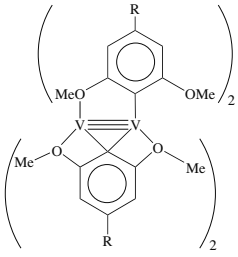
species of the type $[V_3(\mu_3\text{-}O)(\text{carboxylato})_6L_3]^{n+}$, where n = 0, 1 and L = a neutral donor molecule such as H_2O, THF or py.

Likewise, early attempts at reacting formamidinates with divalent starting materials such as $VCl_2(py)_4$ gave only mononuclear compounds. An example is *trans*-$V(py)_2(DTolF)_2$ which is made by reacting *trans*-$VCl_2(py)_4$ with LiDTolF, DTolF = *N*,*N*'-di-*p*-tolylformamidinate.[4]

A triple bond between vanadium atoms has been claimed for two compounds of the type **2.2** for R = H[5] and OCH_3[6] which have V–V distances of 2.200(2) and 2.223(2) Å, respectively. However, these compounds are better described as edge-sharing bioctahedra (ESBO), not paddlewheel compounds. A reaction of *trans*-$(tmeda)_2VCl_2$ (tmeda = tetramethylethylendiamine) and the amidate salt, $Na(PhNC(CH_3)O)$ gives another ESBO compound but without metal–metal bonding. This is $\{[PhNC(CH_3)O]_4V\}_2(tmeda)$.[7]



2.1



2.2

2.2.1 Triply-bonded divanadium compounds

The first paddlewheel compound containing the triply-bonded V_2^{4+} core was prepared after a systematic study of the chemistry of V^{2+}. The key step in the synthesis is the use of a THF solution of $VCl_3(THF)_3$ which is reduced with one equivalent of $NaEt_3BH$. The reddish-purple solution of $VCl_2(THF)_n$ reacts with LiDTolF to produce the air-sensitive, diamagnetic compound $V_2(DTolF)_4$ in yields as high as 90%:[8]

$$2VCl_2(THF)_n + 4LiDTolF \xrightarrow{THF} V_2(DTolF)_4 + 4LiCl$$

Crystals from toluene solutions layered with hexanes at -70 °C produce $V_2(DTolF)_4$·toluene which belong to a tetragonal system. The compound has a short V–V distance of 1.978(2) Å and the structure shown in Fig. 2.1.[8] This structure is of the same type as other dinuclear formamidinato complexes having four bridging ligands and it is homologous to that of the dimolybdenum and ditungsten complexes mentioned in Chapters 4 and 5, respectively. When crystallization is carried out at -70 °C from solutions of the compound in neat toluene, an orthorhombic form with a V–V distance of 1.974(4) Å is obtained.[9]

The $V_2(DTolF)_4$ molecule is very stable in THF, toluene, and benzene solutions as long as they are protected from oxygen. In the presence of dry oxygen, they react to produce reddish orange $V_2O_2(DTolF)_4$ and the corresponding greenish monomer $VO(DTolF)_2$.[9] In pyridine solution, the dinuclear $V_2(DTolF)_4$ species is stable for short periods of time. An analysis of the ^1H NMR spectra of the solid that remains after pyridine solutions are dried shows that the dinuclear unit remains intact after 1 h at room temperature. However, if the solutions are refluxed in neat pyridine, the color rapidly changes from red to purple due to the formation of *trans*-$V(py)_2(DTolF)_2$.

Pictiva EX2004
Samsung v Pictiva
IPR2024-01094

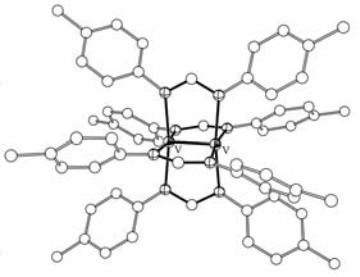
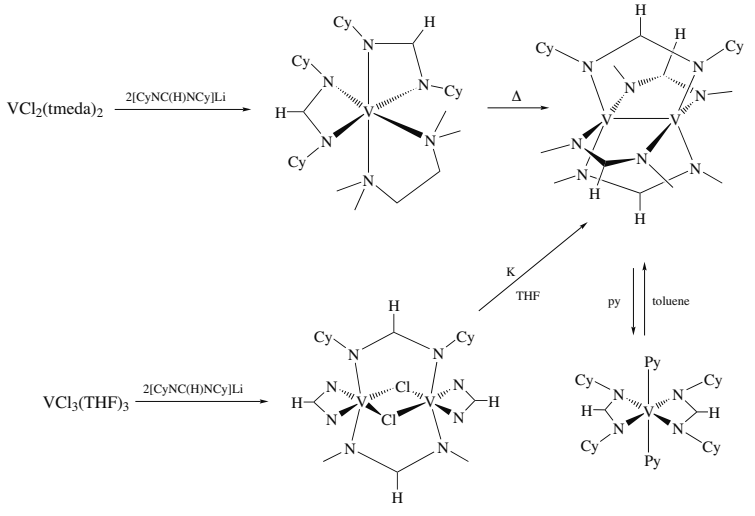


Fig. 2.1. The paddlewheel molecule in the tetragonal form of $V_2(DTolF)_4$·toluene.

The method of preparation of $V_2(DTolF)_4$ has been shown to be very useful for the synthesis of other triply-bonded divanadium compounds with a variety of formamidinate, aminopyridinate and guanidinate ligands.[10,11] However, special precautions must be taken when reacting ligands with electron-withdrawing substituents that disfavor the formation of vanadium–vanadium bonds. Thus, for *N*,*N*'-di-*p*-chlorophenylformamidinate ($D^{Cl}PhF$), reaction time must be limited to 15 min to avoid formation of oily substances.[10] Less basic formamidinates such as *N*,*N*'-di-2,5-chlorophenylformamidinate do not produce dinuclear compounds and only the corresponding tris-chelated mononuclear complex $Li(THF)_4[V(form\text{-}amidinate)_3]$ can be isolated. Attempts to carry out the reaction at higher temperatures led to cleavage of the formamidinate groups.[10] An alternative method of synthesis of V–V bonded compounds begins with the reaction of *trans*-$VCl_2(tmeda)_2$[12,13] and LiDCyF (DCyF = *N*,*N*'-dicyclohexylformamidinate) in toluene at room temperature. This produces the mononuclear compound $V(tmeda)(DCyF)_2$ which upon heating gives dinuclear $V_2(DCyF)_4$ with a V–V distance of 1.968(2) Å. This compound, like $V_2(DTolF)_4$, reacts with pyridine to give the mononuclear complex *trans*-$V(py)_2(DCyF)_2$ which in turn reverts to the dinuclear species in refluxing toluene.[13] An alternative route to $V_2(DCyF)_4$ is reaction of $VCl_3(THF)_3$ with LiDCyF to produce $(\eta^2\text{-}DCyF)V(\mu\text{-}Cl)_2(\mu\text{-}DCyF)_2V(\eta^2\text{-}DCyF)$ which can be reduced in THF by potassium metal.[13] These reactions are summarized in the chart:



All compounds that have been structurally characterized are listed in Table 2.1. Compounds with a V_2^{4+} core are diamagnetic and have the typical paddlewheel structure, Fig. 2.1, with

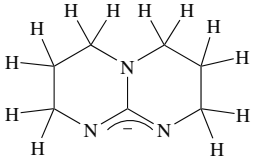
Pictiva EX2004
Samsung v Pictiva
IPR2024-01094

V–V bond distances ranging from 1.932(1) Å for $V_2(hpp)_4$ to 1.988(1) Å for $V_2(DAniF)_4$, where hpp is the anion of 1,3,4,6,7,8-hexahydro-2*H*-pyrimido[1,2-*a*]pyrimidinate, **2.3**, and DAniF is *N*,*N*'-di-*p*-anisylformamidinato. The longer distances correspond to the formamidinates, while the shorter ones belong to compounds with more basic aminopyridinate (ap) and guanidinate ligands, e.g., hpp and 1,2,3-triphenylguanidinate (TPG). The later is shown in Fig. 2.2. It should be noted that the V–V bonds are the only metal–metal bonds, other than the so-called supershort Cr–Cr quadruple bonds, that are shorter than 2.0 Å. The formal shortness ratio, FSR (see Section 3.2.1), which is a measure of the bond shortness normalized to atomic size, range from 0.790 for $V_2(hpp)_4$ to 0.812 for $V_2(DAniF)_4$. These FSRs are similar to those for the supershort Cr_2 bonds, the smallest of which is 0.770 for $Cr_2(2\text{-MeO-5-Me}C_6H_4)$.

Table 2.1. Structural data for divanadium paddlewheel compounds

Compound	r(V–V)[a] (Å)	core	ref.
$V_2(hpp)_4$	1.932(1)	V_2^{4+}	11
$V_2(ap)_4 \cdot 2C_6H_6$	1.942(1)	V_2^{4+}	10
$V_2(TPG)_4 \cdot 4C_6H_6$	1.952(1)	V_2^{4+}	10
$V_2(DCyF)_4$	1.968(2)	V_2^{4+}	12,13
$V_2(DTolF)_4 \cdot C_7H_8$[b]	1.978(2)	V_2^{4+}	8,9
$V_2(DTolF)_4 \cdot C_7H_8$[c]	1.974(4)	V_2^{4+}	9
$V_2(D^{Cl}PhF)_4$[d]	1.974(1) 1.982(1)	V_2^{4+}	10
$V_2(DPhF)_4$[d]	1.978(1) 1.979(1)	V_2^{4+}	10
$V_2(DAniF)_4$	1.988(1)	V_2^{4+}	10
$K_3(THF)_3[V_2(DPhF)_4]$	1.929(1)	V_2^{3+}	10,15
$[K(18\text{-crown-6})(THF)_2][V_2(DPhF)_4]$	1.924(2)	V_2^{3+}	10

[a] Distances are given with up to 3 decimal digits.
[b] Tetragonal form.
[c] Orthorhombic form.
[d] Two independent molecules.



2.3

The electrochemistry of some of V_2^{4+} species has been studied. While no reversible oxidation occurs, the cyclic voltammograms in THF solutions containing 0.1 M $Bu^n_4NPF_6$ and using Ag/AgCl reference electrodes show a reversible wave at negative potentials. The reduction wave appears at an $E_{1/2}$ of -1.23, -1.46, -1.77, -1.82 and -1.99 V for $V_2(D^{Cl}PhF)_4$, $V_2(DPhF)_4$, $V_2(DAniF)_4$, $V_2(ap)_4$ and $V_2(TPG)_4$, respectively.[10] This shows that as the ligands become more basic the reduction is more difficult.

Pictiva EX2004
Samsung v Pictiva
IPR2024-01094

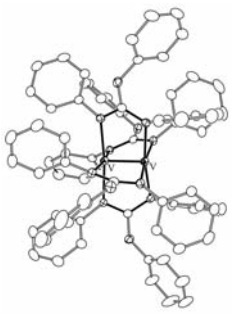
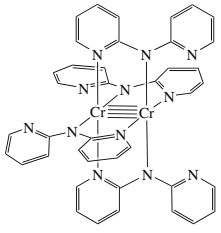


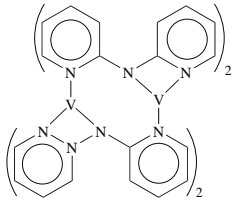
Fig. 2.2. The triply-bonded V_2^{4+} unit bridged by 1,2,3-triphenylguanidinate ligands in $V_2(TPG)_4 \cdot 4C_6H_6$.

2.2.2 Metal–metal vs metal–ligand bonding

As mentioned above, the use of electron-withdrawing substituents in formamidinate ligands such in *N*,*N*'-di-3,5-chlorophenylformamidinate or *N*,*N*'-di-*p*-trifluoromethylformamidinate prevents the formation of V–V bonds and a tris-chelating species is favored.[10] Reaction of $V_2(DTolF)_4$ and pyridine also gives six-coordinate mononuclear species.[9] Interestingly, reaction of $VCl_2 \cdot n$THF with the anion of 2,2'-dipyridylamine (dpa) which is well known to form compounds such as **2.4** having metal-metal bonds, fails to produce V–V bonds in **2.5** which have two six-coordinate vanadium species.[14] The difference between these two types of compounds is that in **2.5** the four groups that were dangling in **2.4** form two bonds to each metal atom and the M–M bond disappears. This indicates that there is a fine line between the formation of the metal–metal bond and the metal–ligand bonds.



2.4



2.5

2.2.3 Divanadium compounds with the highly reduced V_2^{3+} core

Chemical reduction of $V_2(DPhF)_4$ with potassium graphite in THF allows the isolation of the first four-bladed paddlewheel complex with a V_2^{3+} core in $K(THF)_3[V_2(DPhF)_4]$.[15] During the reaction, which proceeds according to

$$V_2(DPhF)_4 + KC_8 \xrightarrow{THF} K(THF)_3[V_2(DPhF)_4] + 8C$$

the red-brown, diamagnetic V_2^{4+} complex is transformed to a dark-green, paramagnetic complex with a V_2^{3+} core. The compound is extremely air-sensitive and must be crystallized quickly at temperatures below -10 °C. Otherwise it reverts to the triply-bonded diamagnetic species. An X-ray study reveals that the paddlewheel structure is conserved but the V–V bond contracts significantly to a distance of 1.929(1) Å, a difference of 0.05 Å when compared to the neutral species.[15,10] The shortening of this bond is due the increase of bond order from 3 to 3.5 upon

Pictiva EX2004
Samsung v Pictiva
IPR2024-01094

addition of an electron. The magnitude of the change, which is similar to that obtained upon oxidation of Mo_2(carboxylato)$_4$ compounds discussed in Chapter 4, suggests that the additional electron resides in the δ-orbital and that the dimetal core has a $\sigma^2\pi^4\delta$ configuration. The average V–N distance increases from 2.101[3] to 2.142[3] Å upon reduction.

As shown in Fig. 2.3, the K^+ cation is found in one of the pockets between two of the formamidinate ligands but the distances to the N atoms of over 3.0 Å are too long to be considered of chemical importance. This type of association of an alkali metal cation with some ligands of an M_2 paddlewheel molecule has been observed also in $Nb_2(hpp)_4$ (Section 2.3.1) and $W_2(hpp)_4$ (Chapter 5) and creates a few minor distortions to the angles between paddles.

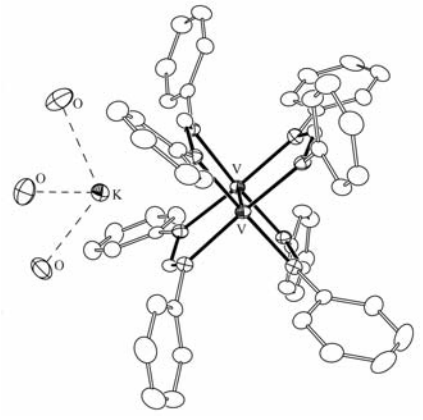


Fig. 2.3. The structure of $K(THF)_3[V_2(DPhF)_4]$ that has a highly reduced V_2^{3+} core showing the position of the potassium ions between the paddles of the anion.

The potassium cation can be easily removed from the pocket by addition of a crown ether.[10] This gives the more stable complex $[K(18\text{-crown-}6)(THF)_2][V_2(DPhF)_4]$ which does not revert to the V_2^{4+} species as long as it is protected from oxygen. The V–V distance of 1.924(2) Å is the same within 3σ to that in $K(THF)_3[V_2(DPhF)_4]$ (1.929(1) Å). This supports the notion that the presence or absence of the alkali metals in the pockets between paddles does not alter the metal–metal interaction.

Although the reduced species can be formally considered to provide an example of a rare monovalent oxidation state for the vanadium atom, this is not the best view as the additional electron is introduced into the δ bonding orbital, where it is delocalized on the V_2^{3+} core. This is supported by EPR results. A frozen THF solution of $K(THF)_3[V_2(DPhF)_4]$ at 6 K gave a 15-line spectrum which indicates that the electron is coupled to each ^{51}V ($I = {}^7/_2$) atom equally. A simulation of the main feature gives a *g* value of 1.9999. Although this value is close to the free-electron value, the complicated hyperfine splitting pattern indicates that the unpaired electron is localized on the metal core.[10,15]

These are the first structurally characterized compounds with an M_2^{3+} core in a tetragonal paddlewheel environment. There are only four other compounds known to contain such core but they are in a trigonal paddlewheel environment (with only three bridging ligands, not four bridging groups). In the latter, M = Fe and Co and they are discussed in Sections 11.2 and 11.3.2, respectively. A compound that has been isolated in the solid state and presumed to have a Co_2^{3+} core bridged by four benzamidinate ligands is mentioned in Section 11.3.1.

Pictiva EX2004
Samsung v Pictiva
IPR2024-01094

2.3 Diniobium Compounds

Divalent compounds of niobium can be classified as mononuclear, polynuclear and organometallic.[16] Paramagnetic, octahedral NbX_2L_4 , X = Cl and L = PMe_3, $^1/_2$dmpe[17] or X = OAr and L = $^1/_2$dmpe[18] are prepared by reduction of higher oxidation state niobium chlorides or aryloxides with sodium amalgam. Potassium graphite, KC_8, works best for the reduction of $NbCl_4(THF)_2$ in pyridine in the preparation of *trans*-$NbCl_2(py)_4$.[19] A few anionic species of the type $[Nb_2Cl_6(THT)_3]^{2-}$ and $[Nb_2Cl_5(THT)(py)_3]^-$ are also known.[20] In these face-sharing bioctahedral (FSBO) complexes there are formal triple bonds between the metal atoms, but the Nb–Nb distances of *c.* 2.6 Å are rather long. These FSBO compounds are not covered in this monograph which is devoted to paddlewheel and some related complexes. The M–M distances in paddlewheel compounds are given in Table 2.2.

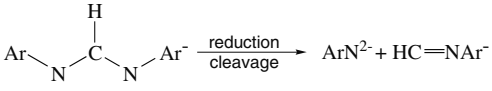
Table 2.2. Structural data for diniobium compounds

Compound	r(Nb–Nb)[a] (Å)	core	ref.
$Nb_2(hpp)_4$	2.204(1)	Nb_2^{4+}	22,23
$Nb_2(hpp)_4{\cdot}Na(C_2H_5)_3BH$	2.219(1)	Nb_2^{4+}	23
$Nb_2(hpp)_4{\cdot}2Na(C_2H_5)_3BH$	2.206(1)	Nb_2^{4+}	23
$Nb_2(azin)_4{\cdot}2LiCl{\cdot}4THF$	2.278(2)	Nb_2^{4+}	23
$Nb_2(azin)_4{\cdot}4THF$	2.263(1)	Nb_2^{4+}	25
$Nb_2(azin)_4{\cdot}2LiCl{\cdot}6THF$	2.268(1)	Nb_2^{4+}	26
$Na_4Nb_2(calix)_2{\cdot}10C_4H_8O_2$	2.385(2)	Nb_2^{4+}	28

[a] Distances are given with up to 3 decimal digits.

2.3.1 Diniobium paddlewheel complexes

Early attempts at preparing paddlewheel complexes having diniobium or ditantalum units analogous to V_2(formamidinato)$_4$ were stymied not only by the lack of divalent species that could be used as starting materials but mainly by another severe difficulty: under the reaction conditions necessary to reduce the precursor to the divalent state, ligands such as formamidinates, **2.6**, readily cleave.[21]



2.6

To avoid the cleavage of the ligands, the more robust guanidinate hpp ligand **2.3** was the first to be used to prepare compounds of the paddlewheel type.[22] The hpp ligand is more resistant toward cleavage because of the support provided by other bonds within it. The compound $Nb_2(hpp)_4$ was made in 17% yield by reacting $NbCl_3$(DME) with a mixture of Lihpp and KC_8 in THF. The yield was improved to *c.* 47% when lithium naphthalenide was used as reducing agent instead of the less soluble KC_8:[23]

$$2NbCl_3(DME) + 2Na(naphthalenide) + 4Li(hpp) \longrightarrow Nb_2(hpp)_4 + 4LiCl + 2NaCl + naphthalene + 2DME$$

The green, air-sensitive compound is diamagnetic and has a centrosymmetric structure with the four hpp ligands forming bridges between two niobium atoms at a distance of 2.204(1) Å.[22]

Pictiva EX2004
Samsung v Pictiva
IPR2024-01094

This Nb–Nb distance is shorter by *c.* 0.4 Å than the corresponding distances in FSBO compounds mentioned earlier but it is 0.27 Å longer than that found in the isostructural vanadium complex cited in Section 2.2.1. Also, it is significantly shorter than that in niobium itself (2.85 Å) which is one of the most refractory metals (mp 2468 °C). The diamagnetic nature of the compound and the short Nb–Nb distance are consistent with an electronic structure of the type $\sigma^2\pi^4$ with no unpaired electrons. The structure was predicted (genuinely, before the compound was made) by density functional theory.[24] The calculated Nb–Nb distance is 2.225 Å for the model compound $Nb_2(HNCHNH)_4$ and the calculated Nb–N distance is 2.20 Å which is the same in $Nb_2(hpp)_4$.

When $Nb_2(hpp)_4$ is placed in contact with $NaEt_3BH$, the solubility properties change dramatically. While $Nb_2(hpp)_4$ is relatively insoluble in THF but soluble in toluene, a new species is formed which is soluble in THF but insoluble in toluene. Crystallization of mixtures of these reagents provide crystals of $Nb_2(hpp)_4{\cdot}NaEt_3BH$ and $Nb_2(hpp)_4{\cdot}2NaEt_3BH$. In these compounds, the sodium atoms are between paddles of the paddlewheel structure as shown in Fig. 2.4 for $Nb_2(hpp)_4{\cdot}2NaEt_3BH$.[23] Even though there are small deviations in the N–Nb–N angles relative to those of $Nb_2(hpp)_4$, the Nb–Nb distances are essentially unchanged (see Table 2.2). These are 2.206(1) and 2.219(1) Å for $Nb_2(hpp)_4{\cdot}2NaEt_3BH$ and $Nb_2(hpp)_4{\cdot}NaEt_3BH$, respectively.

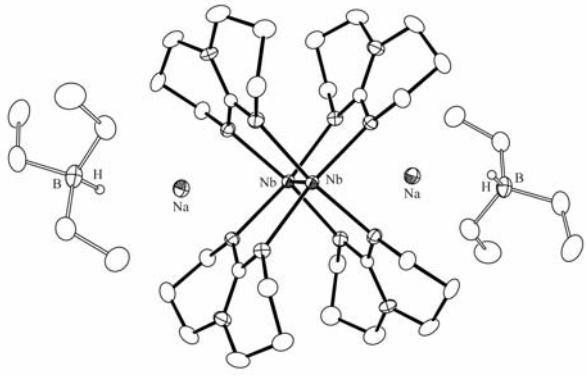
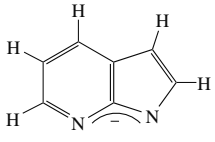


Fig. 2.4. The structure of $Nb_2(hpp)_4{\cdot}2NaEt_3BH$ showing the puckering of the guanidinate ligand hpp and the position of the sodium cations between the clefts of the neutral, triply-bonded paddlewheel unit.

The generality of the synthetic method of preparation of paddlewheel compounds with ligands protected from possible cleavage is shown by using the lithium salt of 7-azaindole, Li(azin) (**2.7**) in place of Lihpp:



2.7

From THF solutions, crystals of composition $Nb_2(azin)_4{\cdot}2LiCl{\cdot}4THF$ are obtained.[23] The structure consists of two niobium atoms spanned by four azin ligands giving a Nb–Nb distance of 2.278(2) Å. There are also some very weak interactions with axial chloride ions. The Nb···Cl separation is 2.849(3) Å. Thus it is unlikely that the lengthening of *c.* 0.07 Å of the

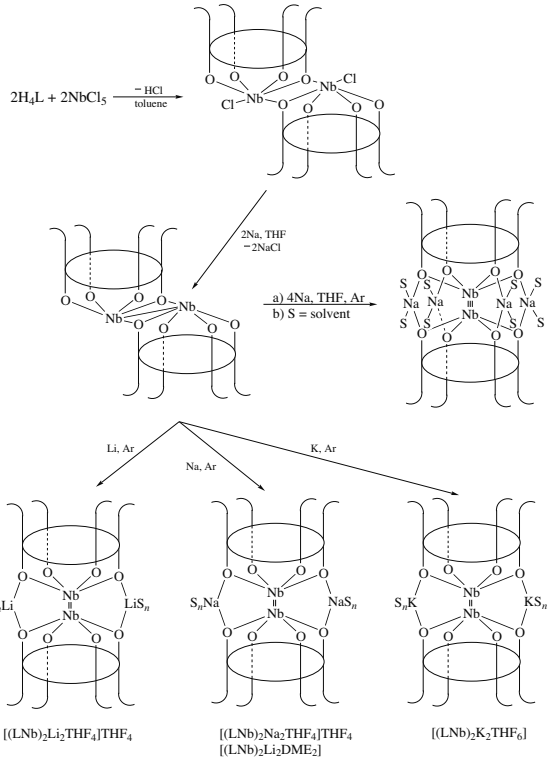
Pictiva EX2004
Samsung v Pictiva
IPR2024-01094

Nb–Nb distance relative to that in $Nb_2(hpp)_4$ is due to such interactions. This is more likely due to the geometrical character of the azin ligand which imposes a wider bite. The compound has been shown to be diamagnetic by the NMR spectrum.

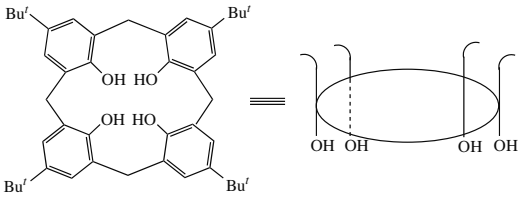
There are two additional compounds having a Nb_2^{4+} core and four bridging azin groups. One was obtained by reaction of $Li(TMEDA)Nb_2Cl_5$ with 4 equiv of potassium 7-azaindolyl which affords $Nb_2(azin)_4 \cdot 2THF$. This is described as red-orange and diamagnetic with a Nb–Nb distance of 2.263(1) Å.[25] This compound does not have any chemically significant axial interactions. The other compound was made similarly by using the lithium salt of 7-azaindole. The compound, described as blue, has the formula $Nb_2(azin)_4 \cdot 2LiCl \cdot 6THF$. The structure is similar to those described above and the Nb–Nb distance of 2.268(1) Å is essentially unchanged but this compound like $Nb_2(azin)_4 \cdot 2LiCl \cdot 4THF$ has very weak Nb···Cl interactions with the corresponding distance being 2.733(2) Å.[26] The odd thing about this compound is that it is described as being paramagnetic with a μ_{eff} at room temperature that corresponds to *one* unpaired electron. This value drops to *c.* 0.6 μ_B at very low temperatures (nearly 0 K). This is in sharp contrast with the other two azin compounds which are diamagnetic and give very good ^1H NMR data.

2.3.2 Diniobium compounds with calix[4]arene ligands and related species

There is a series of compounds which have Nb_2^{n+} units, n = 4, 6, and 8, which correspond to formal bond orders of 3, 2 and 1, respectively.[27-30] Some reactions that lead to these compounds have been summarized[31] and are presented in the following scheme where the bond orders are shown by the number of lines between Nb atoms. The calix[4]arene, H_4L, that is typically employed is the *p-tert*-butyl derivative shown as **2.8** and the solvent S can be dioxane, diglyme or THF.



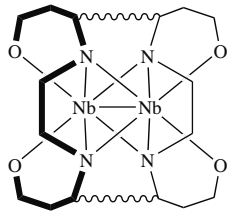
Pictiva EX2004
Samsung v Pictiva
IPR2024-01094



2.8

Many of these diamagnetic compounds have been characterized by X-ray crystallography. The Nb–Nb distances vary accordingly to the bond order. For example, the Nb–Nb singly-bonded compounds have distances of about 2.75 Å,[28] the doubly bonded Nb–Nb compounds have distances of *c.* 2.65 Å,[30] while those with Nb–Nb triple bonds have distances of *c* 2.38 Å.[28] The latter is slightly longer than those in Nb_2 triply-bonded, paddlewheel complexes (see Table 2.2).

Another series of compounds with formal Nb–Nb bonds are those obtained by reductive coupling of Nb(Bu^t-salophen)Cl_3, where Bu^t-salophen is *N*,*N*'-*o*-phenylenebis(salicylidenamine), which forms dinuclear compounds with C–C bonds across two imino groups of the ligand to give the Nb–Nb singly bonded compound Nb_2(Bu^t-*salophen$_2$*), **2.9**, where Bu^t-*salophen$_2$* represents a coupled salophen ligand.[32] This has a Nb–Nb bond distance of 2.653(1) Å. This can be reduced further by potassium to a transient compound that contains a Nb–Nb double bond.



2.9

2.4 Tantalum

As for niobium, there are only a few compounds with divalent tantalum atoms. Examples are the mononuclear $TaCl_2L_4$, L = PMe_3, $^1/_2$dmpe,[16] and the dinuclear FSBO complexes of the type $[Ta_2X_6(THT)_3]^{2-}$,[20] the latter have long Ta–Ta distances of *c.* 2.6 Å. The FSBO compounds are not covered here. There are also Ta–Ta bonds in some low-valent halides and oxides, an example being $Na_{0.74}Ta_3O_6$[33] which is isomorphous with $NaNb_3O_5F$.[34] The metal–metal bond distance in $Na_{0.74}Ta_3O_6$ is 2.673 Å.

A report of a compound containing unsupported Ta^{III}–Ta^{III} bonds has appeared.[35] However, this has been shown to be in error.[36] The correct formula is $[(Cy_2N)_2ClTa(\mu\text{-}H)]_2$ (Cy = cyclohexyl) which has a $Ta^{IV}(\mu\text{-}H)_2Ta^{IV}$ core. To date, there are no known paddlewheel compounds.

References

1. F. A. Cotton, M. P. Diebold and I. Shim, *Inorg. Chem.* 1985, *24*, 1510.
2. G. J. Leigh and J. S. de Souza, *Coord. Chem. Rev.* 1996, *154*, 71.
3. F. A. Cotton, M. W. Extine, L. R. Falvello, D. B. Lewis, G. E. Lewis, C. A. Murillo, W. Schwotzer, M. Tomás and J. M. Troup, *Inorg. Chem.* 1986, *25*, 3505.

Pictiva EX2004
Samsung v Pictiva
IPR2024-01094

4. F. A. Cotton and R. Poli, *Inorg. Chim. Acta* **1988**, *141*, 91.
5. F. A. Cotton and M. Millar, *J. Am. Chem. Soc*. **1977**, *99*, 7886.
6. F. A. Cotton, G. E. Lewis and G. N. Mott, *Inorg. Chem*. **1983**, *22*, 560.
7. J. J. H. Edema, A. Meetsma, F. van Bolhuis and S. Gambarotta, *Inorg. Chem*. **1991**, *30*, 2056.
8. F. A. Cotton, L. M. Daniels and C. A. Murillo, *Angew. Chem. Int. Ed. Engl.* **1992**, *31*, 737.
9. F. A. Cotton, L. M. Daniels and C. A. Murillo, *Inorg. Chem*. **1993**, *32*, 2881.
10. F. A. Cotton, E. A. Hillard, C. A. Murillo and X. Wang, *Inorg. Chem.* **2003**, *42*, 6063.
11. F. A. Cotton and D. J. Timmons, *Polyhedron* **1998**, *17*, 179.
12. P. Berno, S. Hao, R. Minhas and S. Gambarotta, *J. Am. Chem. Soc.* **1994**, *116*, 7417.
13. S. Hao, P. Berno, R. K. Minhas and S. Gambarotta, *Inorg. Chim. Acta* **1996**, *244*, 37.
14. F. A. Cotton, L. M. Daniels, C. A. Murillo and H.-C. Zhou, *Inorg. Chim. Acta* **2000**, *305*, 69.
15. F. A. Cotton, E. A. Hillard and C. A. Murillo, *J. Am. Chem. Soc.* **2003**, *125*, 2026.
16. See for example: F. Calderazzo, G. Pampaloni, L. Rocchi, J. Strähle and K. Wurst, *Angew. Chem., Int. Ed. Engl*. **1991**, *30*, 102; F. Calderazzo, U. Englert, G. Pampaloni and L. Rocchi, *Angew. Chem., Int. Ed. Engl.* **1992**, *31*, 1235.
17. M. L. Luetkens, W. L. Elcesser, J. C. Huffman and A. P. Sattelberger, *Inorg. Chem*. **1984**, *23*, 1235.
18. T. W. Coffindaffer, B. D. Steffy, I. P. Rothwell, K. Folting, J. C. Huffman and W. E. Streib, *J. Am. Chem. Soc*. **1989**, *111*, 4742.
19. M. A. Araya, F. A. Cotton, J. H. Matonic and C. A. Murillo, *Inorg. Chem*. **1995**, *34*, 5424.
20. See for example: F. A. Cotton and M. Shang, *Inorg. Chim. Acta* **1994**, *227*, 191 and references therein.
21. F. A. Cotton, L. M. Daniels, C. A. Murillo and X. Wang, *Inorg. Chem*. **1997**, *36*, 896.
22. F. A. Cotton, J. H. Matonic and C. A. Murillo, *J. Am. Chem. Soc*. **1997**, *119*, 7889.
23. F. A. Cotton, J. H. Matonic and C. A. Murillo, *J. Am. Chem. Soc*. **1998**, *120*, 6047.
24. F. A. Cotton and X. Feng, *J. Am. Chem. Soc*. **1997**, *119*, 7514.
25. M. Tayebani, K. Feghali, S. Gambarotta and G. P. A. Yap, *Inorg. Chem*. **2001**, *40*, 1399.
26. M. Tayebani, K. Feghali, S. Gambarotta, G. P. A. Yap and L. K. Thompson, *Angew. Chem. Int. Ed.* **1999**, *38*, 3659.
27. A. Caselli, E. Solari, R. Scopelliti and C. Floriani, *J. Am. Chem. Soc.* **2000**, *122*, 538.
28. A. Zanotti-Gerosa, E. Solari, L. Giannini, C. Floriani, A. Chiesi-Villa and C. Rizzoli, *J. Am. Chem. Soc.* **1998**, *120*, 437.
29. A. Caselli, E. Solari, R. Scopelliti and C. Floriani, *J. Am. Chem. Soc.* **1999**, *121*, 8296.
30. A. Caselli, E. Solari, R. Scopelliti, C. Floriani, N. Re, C. Rizzoli and A. Chiesi-Villa, *J. Am. Chem. Soc.* **2000**, *122*, 3652.
31. F. A. Cotton, L. M. Daniels, C. Lin and C. A. Murillo, *Inorg. Chim. Acta* **2003**, *347*, 1.
32. C. Floriani, E. Solari, F. Franceschi, R. Scopelliti, P. Belanzoni and M. Rosi, *Chem. Eur. J.* **2001**, *7*, 3052.
33. B. Harbrecht and A. Ritter, *Z. anorg. allg. Chem.* **1999**, *625*, 178.
34. J. Köhler and A. Simon, *Angew. Chem. Int., Ed. Engl*. **1986**, *25*, 996.
35. L. Scoles, K. B. P. Ruppa and S. Gambarotta, *J. Am. Chem. Soc.* **1996**, *118*, 2529.
36. F. A. Cotton, L. M. Daniels, C. A. Murillo and X. Wang, *J. Am. Chem. Soc*. **1996**, *118*, 12449.

Pictiva EX2004
Samsung v Pictiva
IPR2024-01094

3

Chromium Compounds

F. Albert Cotton,
Texas A&M University

3.1 Dichromium Tetracarboxylates

Chromium is unique among the elements of the first transition series in its ability to form many compounds with multiple bonds in Cr_2^{4+} complexes. While many if not all of these can be formally called quadruple bonds, in the sense that they entail one σ, two π and one δ interaction, the strengths of these bonds, as evidenced by the Cr–Cr distances, vary widely. The Cr–Cr distances range from about 1.83 Å to about 2.60 Å, all within a generally similar geometrical arrangement (paddlewheel) of ligands. Needless to say, this extraordinary variation has been the subject of a great deal of theoretical activity, and will be given attention later in this chapter.

3.1.1 History and preparation

We begin with the $Cr_2(O_2CR)_4$ compounds since they are, by far, the longest known. In Section 1.2.3 the early (1844) discovery of hydrated chromium (II) acetate, $Cr_2(O_2CCH_3)_4(H_2O)_2$, by Peligot and the extension of this work to the preparation and (nonstructural) characterization of a large number of similar compounds with other carboxylic acids, especially by Herzog and Kalies, were mentioned. In more recent years additional compounds have been made, but the most significant advances have been the structural characterization of over 40 of these compounds since 1970, and the recent (2000) crystallographic characterization of a $Cr_2(O_2CR)_4$ molecule with no axial ligation and a supershort bond (1.966 Å).

It will be convenient to have in mind from the outset that the vast majority of tetracarboxylate compounds have the types of structure shown in Fig. 3.1. The axial positions are filled either by separate ligands L or by the oxygen atoms of other $Cr_2(O_2CR)_4$ molecules. In the latter case infinite chains are built up. A list of structurally characterized tetracarboxylate compounds is presented in Table 3.1.

Dichromium tetracarboxylato compounds are generally air-sensitive, especially in solution, and they must be prepared and handled in an inert atmosphere. Today, nitrogen or argon would be used. Peligot, working at a time when the laboratory staples of today were not available (and for argon, not even known), used CO_2.[1]

Pictiva EX2004
Samsung v Pictiva
IPR2024-01094

Peligot made the acetate by the addition of NaO_2CCH_3 in approximately the stoichiometric quantity, to a fairly dilute aqueous solution of $CrCl_2$, obtaining an immediate precipitate of the slightly soluble hydrated acetate:

$$2Cr^{2+}(aq) + 4CH_3CO_2^- + 2H_2O = Cr_2(O_2CCH_3)_4(H_2O)_2(s)$$

By heating this deep-red hydrate for about two hours at 100-110 °C, the brown, noncrystalline, anhydrous material can be obtained. Peligot's method is presented in full contemporary detail in *Inorganic Syntheses*[2] and *Brauer's Handbuch*.[3]

Table 3.1. Structures of dichromium tetracarboxylates

R	L	Cr–Cr (Å)	Cr–L (Å)	ref.
	A. $Cr_2(O_2CR)_4L_2$			
H	H_2O[a]	2.373(2)	2.268(4)	4
		2.360(2)	2.210(6)	4
H	py	2.408(1)	2.308(3)	14a
H	HCO_2^-	2.451(1)	2.224(2)	14a
H	4-NMe_2-py	2.443(1)	2.270(4)	44
H	4-CN-py	2.385(3)	2.34[1]	44
CH_3	CH_3CO_2H	2.300(1)	2.306(3)	13
CH_3	H_2O	2.362(1)	2.272(3)	5
CH_3	piperidine	2.342(2)	2.338(7)	13
CH_3	pyridine	2.369(2)	2.335(5)	6
CH_3	$(pyrazine)_{2/2}$[b]	2.295(5)	2.314(10)	6
CH_3	4-CN-py	2.315[2]	2.327[4]	44
CH_3	4-NMe_2-py	2.411(1)	2.279(4)	44
CH_3	CH_3CN	2.389(2)	2.326(3)	39
2,4,6-$(Me_2CH)_3C_6H_2$	CH_3CN	2.395(1)	2.326(6)	39
CF_3	Et_2O	2.541(1)	2.244(3)	14a
Ph	$PhCO_2H$	2.352(3)	2.295(7)	14a
2-phenyl-Ph	THF	2.316(3)	2.275(6)	35
9-anthracenyl	$(CH_3OCH_2CH_2OCH_3)_{2/2}$	2.283(2)	2.283(5)	14a
O[c]	H_2O	2.214(1)	2.300(3)	13
$OCMe_3$	THF	2.367(3)	2.268(7)	7
CMe_3	pyridine	2.359(3)	2.325(8)	44
CMe_3	4-NH_2-py	2.379(1)	2.282(2)	44
CMe_3	4-CN-py	2.335(1)	2.334(2)	44
CMe_3	2-CN-py	2.327(1)	2.388(4)	44
NEt_2	Et_2HN	2.384(2)	2.452(8)	8
$CH_2NH_3^+$	Cl	2.524(1)	2.581(1)	9
$CH_2NH_3^+$	Br	2.513(1)	2.736(1)	9
C_2H_5	NCS	2.467(3)	2.249(3)	21
CPh_3	Et_2O	2.303(4)	2.30(1)	36
CPh_3	½pyridine	2.383(4)	2.31(4)	36
CPh_3	$(C_6H_6)_{2/2}$	2.256(4)	3.299(2)[d]	36
CPh_3	$(1,4\text{-}F_2C_6H_4)_{2/2}$	2.176(3)	3.388(2)[d]	36
CPh_3	$(1,4\text{-}Me_2C_6H_4)_{2/2}$	2.291(3)	3.310(2)[d]	36
$CClH_2/CH_3$	pyridine	2.367(2)	2.336(6)	44
$CClH_2$	4-CN-py	2.408(4)	2.23(2)	44

Pictiva EX2004
Samsung v Pictiva
IPR2024-01094

R	L	Cr–Cr (Å)	Cr–L (Å)	ref.
CF_2H	4-NMe_2-py	2.500(1)	2.246(9)	44
CF_2H	4-$C(CH_3)_3$-py	2.514(1)	2.299(9)	44
$CpFe(CO)_2CH_2$	$CpFe(CO)_2CH_2CO_2H$	2.307(1)	2.246(2)	10
B. Chains of $Cr_2(O_2CR)_4$ molecules[e]				
CH_3	–	2.288(2)	2.327(4)	34
$C(CH_3)_3$	–	2.388(4)	2.44(1)	14
2-PhC_6H_4	–	2.348(2)	2.309(5)	35
C. Bare $Cr_2(O_2CR)_4$ molecules				
CH_3	–	1.966(14)	–	37
2,4,6-$(Me_2CH)_3C_6H_2$	–	1.9662(5)	–	39

[a] There are two crystallographically independent $Cr_2(O_2CH)_4(H_2O)_2$ molecules in the cell.
[b] Notation indicates one axial ligand connects $Cr_2(O_2CR)_4$ molecules.
[c] The bridging ligands are carbonate ions.
[d] Cr to ring center. See text.
[e] See Fig. 3.1.

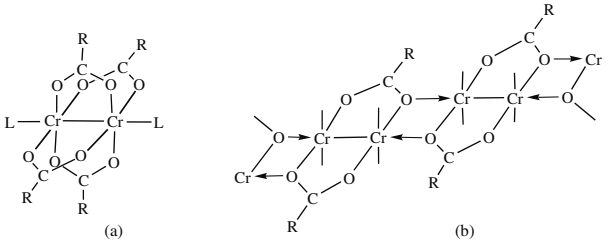


Fig. 3.1. (a) The general structure of a $Cr_2(O_2CR)_4L_2$ molecule. (b) The formation of infinite chains of $Cr_2(O_2CR)_4$ molecules by oxygen bridge bonding. Above and below each Cr_2 unit are two more RCO_2 groups not fully shown.

Quite similar methods have been used for the preparation of other $Cr_2(O_2CR)_4$ compounds,[2,3,11,12] often with the use of ethanol rather than water as a solvent for the longer-chain fatty acids and their sodium salts. As with the acetate, the initial products are hydrates or ethanolates that can be easily desolvated by heating in vacuum. By recrystallization in the presence of donor ligands L or using such ligands as the solvent, a great variety of $Cr_2(O_2CR)_4L_2$ products may easily be prepared,[11] for example, the piperidine diadduct[13] of the acetate, whose structure is shown in Fig. 3.2.

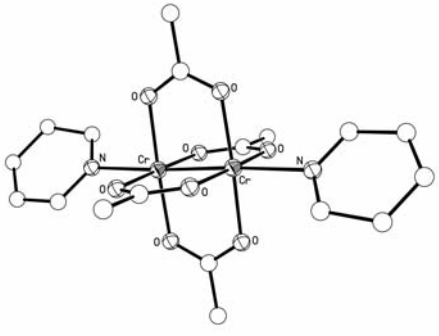


Fig. 3.2. The structure of the dipiperidine adduct of dichromium tetraacetate.

Pictiva EX2004
Samsung v Pictiva
IPR2024-01094

Other methods of preparation[14] have been introduced, based on the idea of displacing the anion of a weak acid from a di- or mononuclear Cr^{II} complex. One method uses the dichromium tetracarbonato anion (to be discussed in more detail below) and the other employs the π-complex $(\eta^5\text{-}C_5H_5)_2Cr$.

$$[Cr_2(CO_3)_4]^{4-} + 4CF_3CO_2H + 4H^+ = Cr_2(O_2CCF_3)_4 + 4H_2O + 4CO_2$$

$$2(\eta^5\text{-}C_5H_5)_2Cr + 6PhCO_2H = Cr_2(O_2CPh)_4(PhCO_2H)_2 + 4C_5H_6$$

Reactions of acids with $(\eta^5\text{-}C_5H_5)_2Cr$ do not always lead to the $Cr_2(O_2CR)_4$ product. In the case of CF_3CO_2H, a complex, mixed-valence compound, $(\eta^5\text{-}C_5H_5)Cr^{III}(\mu\text{-}O_2CCF_3)_3Cr^{II}(\mu\text{-}O_2CCF_3)_3Cr^{III}(\eta^5\text{-}C_5H_5)$, was obtained.[15] A method[16] which has not been widely used but may have merit in selected cases, involves treatment of $CrCl_3$ in THF with $NaBH_4$, extraction of the blue product into benzene, and addition of a benzene solution of the carboxylic acid. The products are the THF adducts, $Cr_2(O_2CR)_4(THF)_2$. Chromium(II) acetate, either as the hydrate or in anhydrous form, is widely used as a convenient starting material for the preparation of many other Cr^{II} compounds.

It is convenient to mention here the $[Cr_2(CO_3)_4]^{4-}$ ion, which has been isolated in yellow hydrated salts of Li^+, Na^+, K^+, Rb^+, Cs^+, NH_4^+, and Mg^{2+}. The earliest work was done around the turn of the century by Baugé,[17] but the modern work of Ouahes and coworkers[18-20] should be consulted for details concerning the preparation[18] and for characterization.[19,20] X-ray studies of the magnesium[19] and ammonium[13] salts have shown the presence of dinuclear $[Cr_2(O_2CO)_4(H_2O)_2]^{4-}$ ions (see Fig. 3.3) very similar in structure to the $Cr_2(O_2CR)_4(H_2O)_2$ molecules in hydrated carboxylates, but with a significantly shorter Cr–Cr bond.

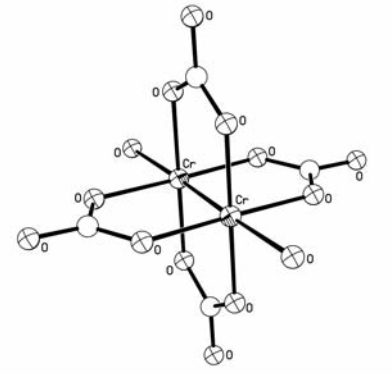


Fig. 3.3. The structure of the $[Cr_2(O_2CO)_4(H_2O)_2]^{4-}$ ion found in the ammonium salt.

3.1.2 Properties of carboxylate compounds

From the earliest days it was reported that $Cr_2(O_2CR)_4(L_{ax})_2$ compounds display weak paramagnetism (typically corresponding to 0.3-0.5 BM). In some cases at least part of this may be due to impurities, probably Cr^{III}. In several cases where the Cr–Cr distances are long there is also evidence that the Cr_2^{4+} unit displays genuine paramagnetism of its own, attributable to thermal population of a paramagnetic excited state.[21,22] There are several possible specifications of the nature of this excited state.

In 1992 this question was fully investigated.[23] It was recognized that if the singlet-triplet gap is sufficiently small relative to kT at room temperature, it will cause anomalous tempera-

Pictiva EX2004
Samsung v Pictiva
IPR2024-01094

ture dependence of the ^1H NMR spectrum, according to the equation below, in which E_{ST} is the energy difference between a triplet state and the ground singlet state, Δ is the shift in the magnetic field at which resonance is actually observed (at a fixed frequency), C is a collection of fundamental constants, A is the hyperfine coupling constant, T is the temperature (K).

$$\Delta = \frac{CA}{kT}\left(3 + e^{E_{ST}/kT}\right)^{-1}$$

By fitting data to this equation at various temperatures, E_{ST} values were obtained for several $Cr_2(O_2CR)_4L_2$ compounds. When these are plotted against the Cr–Cr distance, a good linear relationship is found, as shown in Fig. 3.4.

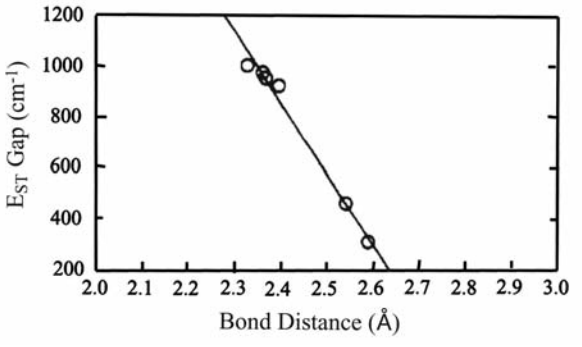


Fig. 3.4. Plot of the singlet-triplet gap (E_{ST}) for some $Cr_2(O_2CR)_4L_2$ compounds.

Because the acetate has been widely employed as an aqueous reductant, its kinetic and equilibrium properties in aqueous states have been extensively studied. $Cr_2(O_2CCH_3)_4(H_2O)_2$ is not very soluble in water, but solutions up to at least 10 mM are obtainable, and the binuclear structure found in the solid persists in solution; the visible spectra of solutions in water (and other solvents) closely resemble the spectrum of the solid.[24-26] It has been shown that the important equilibria in aqueous solution (25 °C, ionic strength 1.0 mol/liter of $NaClO_4$) are the following:

$$Cr_2(O_2CCH_3)_4 = 2Cr(O_2CCH_3)_2 \qquad pK = 4.35$$

$$Cr(O_2CCH_3)_2 = Cr(O_2CCH_3)^+ + CH_3CO_2^- \qquad pK = -0.8$$

$$Cr(O_2CCH_3)^+ = Cr^{2+} + CH_3CO_2^- \qquad pK = -0.9$$

It is also known that $Cr_2(O_2CCH_3)_4$ is soluble in acetic acid where it is also predominantly in the dinuclear form and, not surprisingly, this continues to be true in mixed H_2O/CH_3CO_2H solvents, for some of which the dissociation constant has been evaluated.[27]

In aqueous solution to which other ligands are added, $Cr_2(O_2CCH_3)_4(H_2O)_2$ can react simply by having these ligands, e.g., SCN^-,[21] N_2H_4,[28] replace the axial water molecules, or it may react more extensively, as with polydentate ligands,[29,30] to give mononuclear products. The rate-determining step for these cleavage reactions is the dissociation of the dinuclear Cr_2^{4+} to a mononuclear species, for which the rate constant at 25 °C in 1.0 M $NaClO_4$ is 505 ± 10 s^{-1}.

There has also been a study of the chromium(II) ion in aqueous formate solution,[31] from which it was concluded that the following equilibrium occurs:

$$2Cr(O_2CH)^+ + HCO_2^- = Cr_2(O_2CH)_3^+ \qquad K = (2.9 \pm 0.2)\ M^{-2}$$

Pictiva EX2004
Samsung v Pictiva
IPR2024-01094

As in the previously mentioned reaction of $Cr_2(O_2CCH_3)_4$ with EDTA and other polydentate reagents, the rate laws[29,32] are indicative of a mechanism in which dissociation plays a key role. In a few reactions (e.g., with $[Co(NH_3)_5Cl]^{2+}$ and $[Co(C_2O_4)_3]^{3-}$), dissociation alone is rate-controlling, but with slower oxidations more complex behavior was found.

Some thermodynamic characteristics of chromium(II) acetate have been reported.[33] The enthalpy of dehydration of $Cr_2(O_2CCH_3)_4(H_2O)_2$ to give solid $Cr_2(O_2CCH_3)_4 + 2H_2O$ is 94 ± 9 or 96 ± 8 kJ mol^{-1} according to the method of measurement. The ΔH of sublimation of $Cr_2(O_2CCH_3)_4$ is reported to be 300 ± 10 kJ mol^{-1} as compared to 171 ± 7 kJ mol^{-1} for the molybdenum analog. This large difference has been ascribed to the strong intermolecular association in $Cr_2(O_2CCH_3)_4$ (see Fig. 3.1) as compared to the much weaker association in the Mo compound.

3.1.3 Unsolvated $Cr_2(O_2CR)_4$ compounds

The $Cr_2(O_2CR)_4$ molecules have such a strong tendency to coordinate electron pair donors in the axial positions that such molecules are very difficult to obtain without axial coordination. Although a number of unsolvated compounds have been reported, only two have been studied structurally, those with R = CH_3[34] and CMe_3.[14] These and other unsolvated compounds are insufficiently soluble in noncoordinating solvents to permit the growth of good crystals from solution, and, of course, the use of a coordinating solvent gives only crystals of $Cr_2(O_2CR)_4(solvent)_2$, where there is a solvent molecule in each axial site. Crystals were obtained, in these two cases, by vacuum sublimation. The volatilities are not very great and the crystals obtained were not of the highest quality. In each case, the X-ray studies revealed an infinite chain structure of the type shown in Fig. 3.1(b). Thus, axial coordination occurs even in these unsolvated compounds by association of the molecules to form infinite chains.

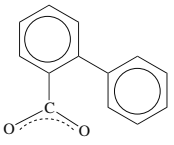
The question of how long the Cr–Cr bond would be in an isolated $Cr_2(O_2CR)_4$ molecule, that is, when axial coordination of any kind is entirely absent, has provoked several efforts to isolate such a species. Logically there are only two approaches, given the fact, as just mentioned, that even when no independent ligands are present, $Cr_2(O_2CR)_4$ molecules tend to associate with themselves. One potentially general approach is to employ an R group of such size and shape as to deny access to any form of axial ligand. However, this is much more easily said than done, since the position of the R group is not close to the axial sites and rotation about the bond from the carboxyl group to the α-carbon atom of the R group allows even the large 9-anthracenyl group to avoid interfering with axial coordination.[14] Even with a sterically appropriate R group, there is the question of sufficient solubility and other factors necessary for obtaining X-ray quality crystals. This approach has not yet been successful, but has produced some interesting results, nonetheless.

Another approach is to recognize that to prevent association of $Cr_2(O_2CR)_4$ molecules it is not necessary to block absolutely all access to the axial positions, but only to screen the carboxyl oxygen atoms so that they cannot use their lone pairs to reach the metal atom of an adjacent molecule. The $Cr_2(O_2CR)_4$ molecule with such an R group would still be able to have small axial ligands (i.e. to form some $Cr_2(O_2CR)_4L_2$ derivatives), but if it had suitable solubility to be crystallized from a noncoordinating solvent, a structure built of nonassociated, nonsolvated $Cr_2(O_2CR)_4$ molecules might be obtained. The first R group chosen was 2-phenylphenyl,[35] giving the carboxyl group **3.1**, and it was hoped that in the $Cr_2[O_2CC_6H_4(C_6H_5)]_4$ molecule two pendant phenyl groups would be directed toward each end of the $Cr_2(O_2Cbiph)_4$ molecule, thus preventing chain growth at either end.

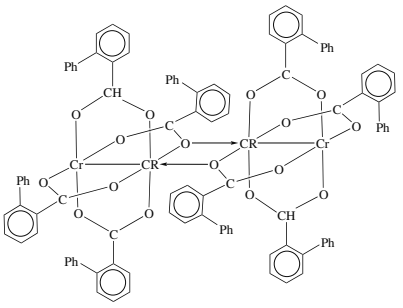
When this compound was prepared in THF the result, $Cr_2(O_2Cbiph)_4(THF)_2$, was exactly as anticipated, with two pendant phenyl groups directed each way and not interfering with the axial coordination of the two THF molecules. The compound was next prepared in toluene

Pictiva EX2004
Samsung v Pictiva
IPR2024-01094

with the object of obtaining unassociated, uncoordinated molecules. However, an unanticipated result was obtained, as shown schematically in **3.2**. In each of two $Cr_2(O_2Cbiph)_4$ molecules, all pendant phenyl groups have oriented themselves to one end, thus preventing the use of oxygen atoms on that end for association. The unencumbered ends of the two $Cr_2(O_2Cbiph)_4$ molecules, however, have united, to produce a dimer.

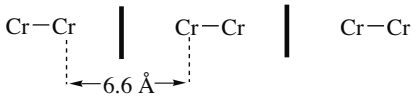


3.1



3.2

In another early effort[36] to obtain a crystalline sample of a $Cr_2(O_2CR)_4$ compound having no axial ligation the group R was chosen to be triphenylmethyl, Ph_3C, and the compound was crystallized from benzene. Once again, the desired goal was not achieved because of the enormous avidity of $Cr_2(O_2CR)_4$ compounds for some kind of axial ligation. In $Cr_2(O_2CCPh_3)_4{\cdot}C_6H_6$, the steric requirements of the large CPh_3 groups lead to a tetragonal packing of the molecules in which there are parallel infinite chains of the type shown schematically in **3.3**, with a benzene molecule centered between every neighboring Cr pair, perpendicular to the chain direction. The Cr–Cr distance within each Cr_2 unit, 2.256(4) Å , the shortest one yet found in any crystalline $Cr_2(O_2CR)_4L_{0,1,2}$ type compound, is still relatively long. MO calculations[36] show that the reason for this lengthening is that the benzene molecules donate electron density from their filled π-orbitals (e_1) to the π*-orbitals of the Cr_2 units. This was the first recognized case of donation to the π* rather the σ* orbitals.



3.3

Two similar compounds with *p*-$C_6H_4F_2$ and *p*-$C_6H_4(CH_3)_2$ were also examined.[36] They are essentially isostructural with $Cr_2(O_2CCPh_3)_4{\cdot}C_6H_6$. The results of substituting axial π donors that are less and more electron-donating than benzene, are qualitatively exactly what would be expected. In the *p*-$C_6H_4F_2$ compound the Cr–Cr bond is shorter, 2.176(3) Å, and in the *p*-$C_6H_4(CH_3)_2$ compound it is longer, 2.291(3) Å.

While the crystallographic approach to determining the length of a Cr–Cr bond in a $Cr_2(O_2CR)_4$ molecule *entirely* lacking axial ligation remained at this time a failure, another general approach, that of examining a molecule in the gas phase, was pursued successfully.[37] It had long been known that some $Cr_2(O_2CR)_4$ compounds are moderately volatile[38] (mass spectra display parent ion peaks). The gas-phase structure would have to be determined by electron diffraction, thus requiring that the subject molecule be small; only the formate and the acetate are small enough to meet this criterion, and the formate is thermally unstable. It is also neces-

Pictiva EX2004
Samsung v Pictiva
IPR2024-01094

sary that there be a sufficient vapor pressure at a temperature where no decomposition products whatsoever are formed because these would contribute to (and vitiate) the measured diffraction pattern. It was finally found that the acetate can be used, provided it is handled in a system that excludes all contact of the vapor with metal surfaces. At metal surfaces decomposition occurs.

Even with the relatively simple acetate molecule, deconvolution of the radial distribution function to reveal the Cr–Cr distance in the presence of many others of similar magnitude was a process requiring the expert application of the most sophisticated methods. The end result[37] was the determination of the Cr–Cr distance as 1.966(14) Å. Despite the technical difficulty of the work, this is a reliable result, although unfounded doubts had been expressed.

Finally, in 2000, the quest for an X-ray characterized $Cr_2(O_2CR)_4$ compound in which there is no axial ligation of any kind was rewarded.[39] The compound is shown in Fig. 3.5. The R group is 2,4,6-triisopropylphenyl. The Cr–Cr bond length is 1.9662(5) Å. This, it may be noted, perfectly confirms the report based on electron diffraction in the vapor phase of 1.966(14) Å for the acetate. It was also shown that the addition of axial ligands greatly lengthens the Cr–Cr bond, to 2.3892(2) Å for the $Cr_2(O_2CR)_4(NCCH_3)_2$ compound. (This is almost identical to the Cr–Cr distance in $Cr_2(O_2CCH_3)_4(NCCH_3)_2$.

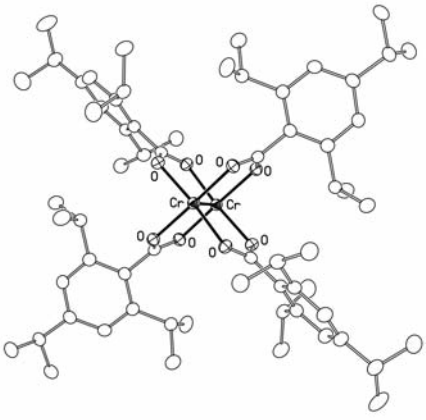


Fig. 3.5. The molecular structure of the molecule $Cr_2(O_2CR)_4$, R = 2,4,6-tri-iso-propylphenyl.

Prior to the experimental study of $Cr_2[O_2C(2,4,6\text{-}Pr^i)_3C_6H_2]_4$ there had been considerable theoretical discussion as to whether the axial or the equatorial ligands had the greater influence on the Cr–Cr bond length.[40-43] There was decidedly much to be said in favor of the former, but theorists espoused the latter, basing themselves on the results of Hartree-Fock calculations. There is no longer any point in recounting this controversy because one good experiment[39] has definitively resolved it. For those interested, however, Chapter 4 of the 2nd edition of this book may be consulted.

There are two striking facts about the data in Table 3.1. One is that the range of Cr–Cr distances is large and the other is that even the shortest ones where axial ligands are present are much longer than the longest Mo–Mo quadruple bond length. In 1984 a systematic effort was made to see if the Cr–Cr distances could be correlated with axial ligand basicity when the bridging RCO_2^- ion was kept constant, or with the strength of the acid. Qualitative correlations of both these types were found,[44] as well as an inverse relationship between Cr–Cr distance and axial Cr–N distance for various substituted pyridines.

Pictiva EX2004
Samsung v Pictiva
IPR2024-01094

The heteronuclear compound $CrMo(O_2CCH_3)_4$ was made[45] by reaction of $Mo(CO)_6$ with acetic acid in the presence of excess $Cr_2(O_2CCH_3)_4$ (Cr/Mo ratio of *c.* 5). It was the first authenticated compound containing a heteronuclear quadruple bond, although others have since been made. The most interesting thing about this compound is the length of the Cr–Mo bond, 2.050(1) Å, in comparison with the Cr–Cr and Mo–Mo bond lengths in the homonuclear acetates, which are 1.966(12) and 2.093(1) Å, respectively. This indicates that when the chromium atom is bonded to a molybdenum atom, rather than to another chromium atom, and no axial ligands are present, it manifests the bonding capabilities that might have been expected of it, since the Cr–Mo bond is shorter than the Mo–Mo bond, but longer than the Cr–Cr bond, by about the expected difference of the Cr and Mo atomic radii. The reason for this behavior has been explored by ab initio molecular orbital calculations.[46] It is found that the Cr–Mo interaction leads to orbital populations essentially similar to those in the Mo–Mo case, but very different from those in the Cr–Cr case.

3.2 Other Paddlewheel Compounds

3.2.1 The first 'supershort' bonds

As noted in Section 1.4, a major role in the growth of the field of quadruply bonded M–M compounds has been played by bridging ligands that are stereoelectronically similar to the carboxylate ions. Nowhere has this been more important than for the dichromium compounds. Prior to the preparation of the first compound containing such a ligand, the only large class of quadruply bonded Cr_2 compounds was the carboxylates, mostly $Cr_2(O_2CR_4)L_2$ compounds with rather long and remarkably sensitive Cr–Cr bonds, that vary through the range of 2.2-2.6 Å. There are also a few organodichromium compounds, to be discussed in Section 3.3, in which Cr–Cr distances are in the range of 1.95-2.00 Å. It was not clear, however, whether these latter highly air-sensitive and poorly characterized compounds had any broad significance or were only isolated curiosities.

It was the preparation and characterization of $Cr_2(DMP)_4$, (DMP = 2,6-dimethoxyphenyl) whose structure is shown in Fig. 3.6 that initiated the development of a broad, systematic chemistry of dichromium compounds with very short, unmistakably quadruple bonds. At the time it was discovered,[47,48] the Cr–Cr bond distance of 1.847(1) Å in $Cr_2(DMP)_4$ was considered so surprisingly short as to raise the question of whether there might, somehow, be an error in the structure determination. This was recognized to be exceedingly unlikely, since every phase of the crystallographic structure determination on $Cr_2(DMP)_4$ had proceeded routinely.

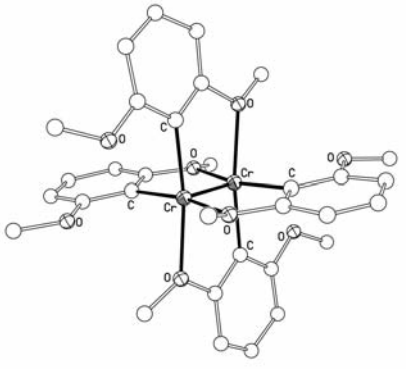
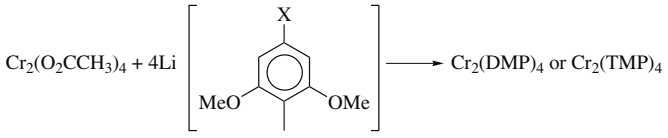


Fig. 3.6. The molecular structure of $Cr_2(2,6\text{-dimethoxyphenyl})_4$, $Cr_2(DMP)_4$.

Pictiva EX2004
Samsung v Pictiva
IPR2024-01094

There had been no indication of twinning, disorder, or the like, the other bond lengths and angles were all normal, and, in general, a crystal structure determination is so overdetermined mathematically (data-to-parameter ratio typically 5/1 or higher) that major error is almost inconceivable. Nonetheless, to be fully certain that no subtle, unrecognized error had crept in, the structure of the chemically almost identical compound, $Cr_2(TMP)_4$, where TMP is the 2,4,6-trimethoxyphenyl anion, was determined.[48,49] This molecule affords a crystal structure that is totally independent of the $Cr_2(DMP)_4$ structure, and thus provides a totally separate and independent measurement of the Cr–Cr distance. The result was 1.849(2) Å, which is statistically indistinguishable from that for $Cr_2(DMP)_4$.

$Cr_2(DMP)_4$ and $Cr_2(TMP)_4$ were rather easily prepared by the reactions:



DMP, X = H
TMP, X = OMe

Both compounds are beautifully crystalline orange-red solids that can be handled in air for several minutes without decomposition, although solutions are immediately attacked by air. Surprisingly, the solid $Mo_2(DMP)_4$ analog is extremely sensitive to oxygen.

The Cr–Cr bonds in $Cr_2(DMP)_4$ and $Cr_2(TMP)_4$ are extraordinarily short compared to any other known metal-metal bonds, but to go beyond a mere qualitative comment of this kind and make a quantitative comparison, not only with other M–M bonds but with all other bonds, a scheme that takes account of the inherent sizes of the atoms in a bond is needed. For example, it is not surprising that a C–C bond is shorter than an Si–Si bond because carbon atoms are smaller than silicon atoms. On the other hand, the fact that the P–P distance in the P_2 molecules (1.89 Å) is far shorter than the usual Si–Si distance (2.34 Å) is highly significant, since the P and Si atoms are not expected to differ much in intrinsic size. The significance, of course, is that we are comparing a triple bond, P≡P, with a single bond.

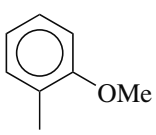
A convenient, broadly applicable set of 'atomic sizes' is provided by the set of R_1 radii worked out many years ago by Pauling.[50] The meaning of the absolute values of these radii is irrelevant so long as they afford a correct measure of the relative sizes of the atoms, which they do. We then define a 'formal shortness ratio', FSR, for a bond A–B as follows:

$$\mathrm{FSR_{AB}} = \frac{D_{\mathrm{A\text{-}B}}}{R_1{}^{\mathrm{A}} + R_1{}^{\mathrm{B}}}$$

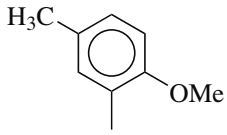
The FSR for the Cr–Cr bond in $Cr_2(DMP)_4$ is found to be $1.847/(2\times1.186) = 0.779$, while those for the Cr–Cr and Mo–Mo bonds in the unsolvated acetates are 0.965 and 0.807, and that for the Re–Re bond in $[Re_2Cl_8]^{2-}$ is 0.869. Thus we see that when due allowance is made for the inherently smaller size of the chromium atom, the Cr–Cr bond in $Cr_2(DMP)_4$ is exceptionally short even when compared to other quadruple bonds. We shall return to this point later, but first we describe several other dichromium compounds with even shorter bonds.

Examination of the structure of $Cr_2(DMP)_4$ shows that while one methoxy oxygen atom on each DMP ligand is essential because it is coordinated to a chromium atom, the other one appears to be superfluous. The question thus arises whether a comparable compound could be obtained with the 2-methoxyphenyl ion, **3.4**, derived from anisole. In fact, $Cr_2(2\text{-}MeOC_6H_4)_4$ had already been reported, twice,[51,52] but never well characterized.

Pictiva EX2004
Samsung v Pictiva
IPR2024-01094

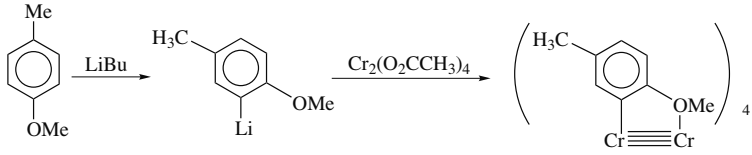


3.4



3.5

It is an air- and moisture-sensitive yellow solid with very low solubility in common solvents, and recrystallization appeared impractical. Because of the very low solubility, a polymeric structure had been proposed by one group,[52] although the other workers[51] suggested a dinuclear, bridged structure of the correct type. With the idea of getting a compound that might have higher solubility without differing significantly in the stereochemistry close to the chromium atoms, the anion derived from *p*-methylanisole, **3.5**, was used, and the corresponding $Cr_2(2\text{-}MeO\text{-}5\text{-}MeC_6H_3)_4$ compound was prepared[53] by the reaction:



This pyrophoric substance resembles the anisole compound very closely, including low solubility, but fortunately crystals, albeit small ones, were obtained and the structure was determined. It is shown in Fig. 3.7. This compound has an even shorter Cr–Cr distance than $Cr_2(DMP)_4$, namely, 1.828(2) Å, and this remains the shortest known metal–metal bond in an isolable compound.

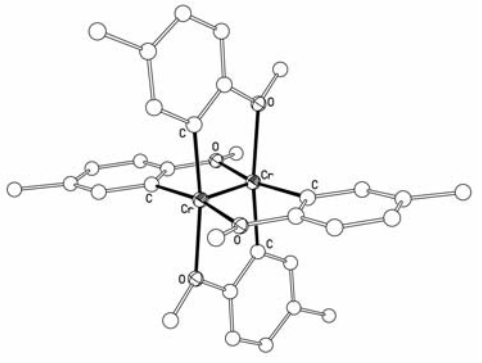


Fig. 3.7. The molecular structure of $Cr_2(2\text{-}MeO\text{-}5\text{-}MeC_6H_3)_4$.

In addition to $Cr_2(2\text{-}MeOC_6H_4)_4$, Hein and Tille[54] had also reported a compound containing the phenoxide dianion **3.6** with a proposed formula of $Li_2Cr(C_6H_4O)_2{\cdot}LiBr{\cdot}3Et_2O$. It has been found that this compound can indeed be prepared[55] and that the presence of LiBr in the reaction mixture, as well as in the product, greatly enhances the tractability of the substance from the point of view of obtaining good crystals. The crystal structure[55] shows that the unit of interest is that in Fig. 3.8. In this centrosymmetric unit the Cr–Cr distance is 1.830(4) Å, which is, statistically, indistinguishable from that in $Cr_2(2\text{-}MeO\text{-}5\text{-}MeC_6H_3)_4$. The Br^- ions are well coordinated to the Li^+ ions, and the Cr···Br distances are too long (3.226(2) Å) to signify bonding.

Pictiva EX2004
Samsung v Pictiva
IPR2024-01094

Finally, in this same period of time, and still using oxophenyl-type ligands, one more important compound was studied.[56] The fact that the Cr–Cr bonds are enormously shorter (*c.* 1.83 Å) when four oxophenyl-type ligands are present than when there are four carboxyl groups (*c.* 1.97 Å) posed the interesting question as to what the Cr–Cr distance would be if the ligand set consisted of two of each type. By using the ligand **3.7**, where the t-butyl groups are so large as to inhibit the simultaneous attachment of four such ligands, it proved possible to obtain a product in which only two of the four acetate groups of $Cr_2(O_2CCH_3)_4$ are replaced. The crystal structure of the resulting compound, shown in Fig. 3.9, has the intended ligand arrangement, and the Cr–Cr distance is 1.862(1) Å.

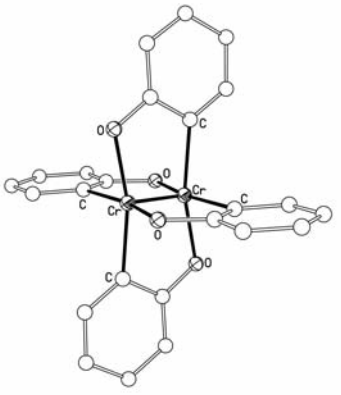
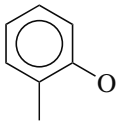
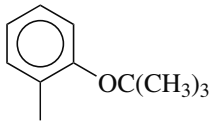


Fig. 3.8. The molecular structure of the Cr_2(2-oxophenyl)$_4$ portion of $Li_6Cr_2(OC_6H_4)_4Br_2(Et_2O)_6$.



3.6



3.7

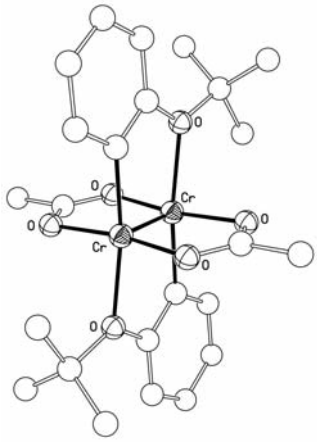


Fig. 3.9. The molecular structure of $Cr_2(O_2CCH_3)_2$(2-$Me_3COC_6H_4)_2$.

Pictiva EX2004
Samsung v Pictiva
IPR2024-01094

We conclude this section by returning to the subject of the formal shortness ratios (FSRs) for the supershort Cr–Cr bonds. We have now introduced the shortest ones of all, and a comparison with other very short bonds of all kinds can be made. In Table 3.2 are listed, in order of increasing FSR, a number of M–M bonds, as well as other chemical bonds with very small FSRs. It can be seen that among homonuclear bonds, only the N≡N and C≡C bonds are as short as the M–M quadruple bonds typically are, and even these are not as short as the shortest Cr–Cr bonds.

Table 3.2. Formal shortness ratios for some chemical bonds

Compound	Bond	FSR
$Cr_2(2\text{-}MeO\text{-}5\text{-}MeC_6H_3)_4$	Cr≡Cr	0.767
$Li_6Cr_2(C_6H_4O)_4Br_2{\cdot}6Et_2O$	Cr≡Cr	0.771
$Cr_2[2,6\text{-}(MeO)_2C_6H_3]_4$	Cr≡Cr	0.779
$Cr_2(O_2CCH_3)_2(C_6H_4OBu^t)_2$	Cr≡Cr	0.785
HCCH	C≡C	0.783[a]
N_2	N≡N	0.786[a]
$Mo_2(hpp)_4$[b]	Mo≡Mo	0.797
$CrMo(O_2CCH_3)_4$	Cr≡Mo	0.826
$[Cr_2(CH_3)_8]^{4-}$	Cr≡Cr	0.835
$Re_2(hpp)_4Cl_2$[c]	Re≡Re	0.854
P_2	P≡P	0.860
$[Re_2Cl_8]^{2-}$	Re≡Re	0.869

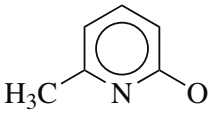
[a] Pauling does not list R_1 for N or C; their single bond radii, 0.70 and 0.77, have been used here.
[b] Shortest Mo–Mo. See F. A. Cotton and D. J. Timmons, *Polyhedron* **1998**, *17*, 179.
[c] F. A. Cotton, J. Gu, C. A. Murillo and D. J. Timmons, *J. Chem. Soc., Dalton Trans.* **1999**, 3741.

The first examples of extremely short Cr–Cr quadruple bonds in $Cr_2(DMP)_4$, $Cr_2(TMP)_4$ and a few other compounds containing related 2-oxophenyl ligands prompted a systematic search for more ligands that would support very short Cr–Cr bonds. This effort has been very fruitful and the following sections will discuss such compounds in detail. When the $Cr_2(DMP)_4$ and $Cr_2(TMP)_4$ compounds were first reported, the Cr–Cr bonds were described as "super-short" because lengths <1.9 Å were so far below those in any previously known metal-metal bonded compounds. Since this time (*c.* 1978) Cr–Cr bonds throughout the range 1.83-2.2 Å have been found, and the basis for any particular line of demarcation, such as 1.9 Å or 2.0 has become debatable.

3.2.2 2-Oxopyridinate and related compounds

In the search that ensued following the discovery of the compounds just discussed in Section 3.2.1 for more Cr_2^{4+} compounds with very short Cr–Cr bonds, the next important class of ligands were the anions of substituted 2-hydroxypyridines, chosen because of their structural similarity to the **3.4 - 3.7** ligands. The first of these was the 6-methyl compound, **3.8**, abbreviated mhp. The preparation of $Cr_2(mhp)_4$ was carried out by adding NaOMe to a solution of $Cr_2(O_2CCH_3)_4$, followed by Hmhp. Upon recrystallization from CH_2Cl_2, the yellow crystalline product $Cr_2(mhp)_4{\cdot}CH_2Cl_2$ was obtained.[57] The molecular structure is shown in Fig 3.10. The hydrated acetate can also be used as a starting material, in which case $Cr_2(mhp)_4{\cdot}H_2O$ is obtained, from which the water can be expelled by heating to 100 °C in vacuum. $Cr_2(mhp)_4$ or its solvates are remarkably stable; they are unaffected by water vapor, and atmospheric oxygen attacks them so slowly that only after several weeks in air is surface discoloration (to green) noticeable. $Cr_2(mhp)_4$ is one of the most air-stable chromium(II) compounds known.

Pictiva EX2004
Samsung v Pictiva
IPR2024-01094



3.8

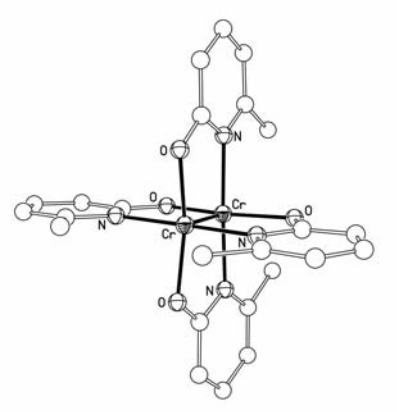
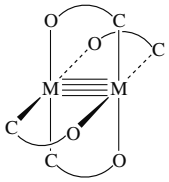


Fig. 3.10. The molecular structure of $Cr_2(mhp)_4$.

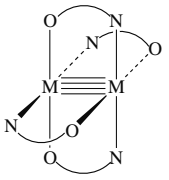
It was found that $Mo_2(mhp)_4$ can be prepared in a similar way. Since there was no $W_2(O_2CCH_3)_4$ available as a starting material, direct reaction of $W(CO)_6$ with Hmhp in refluxing diglyme was tried and found to give an excellent yield of $W_2(mhp)_4$. For the molybdenum compound a similar reaction with $Mo(CO)_6$ is also a practical preparative method of comparable efficiency to the reaction of the mhp anion with the acetate, but the reaction of $Cr(CO)_6$ with Hmhp in diglyme takes place so slowly as to make this a distinctly inferior preparative reaction. The isolation of the three $M_2(mhp)_4$ (M = Cr, Mo, W) compounds marked the first time homologous multiply-bonded dimetal compounds from the same group in the periodic table had been reported.

The structure of $Cr_2(mhp)_4$ (Fig. 3.10) displays a very short Cr–Cr distance (1.889(1) Å). The molybdenum and tungsten compounds are isostructural and form isotypic crystals. It will be noted, upon comparing Figs. 3.6 and 3.10, that there is a qualitative difference between the ligand arrangements (regioisomerism) in the $Cr_2(DMP)_4$ and $Cr_2(mhp)_4$ molecules. In the former the ligands are arranged with unlike ligand atoms *trans* (**3.9**), while in the latter like atoms are *trans* (**3.10**). Thus, in the former case a center of symmetry is possible and the idealized symmetry is C_{2h}. In the latter case there can be no inversion center and the idealized symmetry is D_{2d}. Both of these structure types are found in many other M_2L_4 compounds, and there is no general way of predicting which one will be preferred. They are evidently of very similar stability as far as the metal–metal and metal–ligand bonding are concerned, and the choice in any given case may depend on the interplay of many small non-bonded attractions and repulsions, and perhaps also on crystal packing.

Pictiva EX2004
Samsung v Pictiva
IPR2024-01094

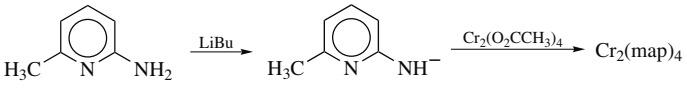


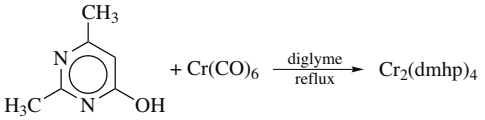
3.9



3.10

Two other closely similar Cr_2L_4 compounds were soon made by the following reactions.[58,59]





These two molecules closely resemble the $Cr_2(mhp)_4$ molecule in having a D_{2d} arrangement of ligands and in having very short bonds, with Cr–Cr distances of 1.870(3) Å in $Cr_2(map)_4$ and 1.907(3) Å in $Cr_2(dmhp)_4$. It became very clear that a vast array of bridging ligands that are stereo-electronic analogs of carboxylate anions can also serve to support M–M multiple bonds.

A later example of a molecule of this type provided a surprise. With the 6-chloro-2-oxopyridine anion (chp) the $Cr_2(chp)_4$ molecule was prepared from $Cr_2(O_2CCH_3)_4$ and found to have the D_{2d} structure, like all the closely related ones.[60] However, the Cr–Cr distance here is longer than in the other cases, viz. 1.955(2) Å. The reason for this has still not been determined, but two hypotheses were considered. One is that lone pairs on the chlorine atoms may interact weakly with the metal atom orbitals, perhaps placing some electron density into the π*-orbital, thus weakening the Cr–Cr bond. The other is that the electron withdrawing effect of the Cl atoms weakens the donor strength of the ring nitrogen atoms and that this, in a manner not completely clear, weakens the Cr–Cr bond.

As a seemingly straightforward way of choosing between these two hypotheses, the preparation of the analogous compound with fluorine atoms in place of the chlorine atoms, $Cr_2(fhp)_4$, was undertaken.[61] It was reasoned that the fluorine atoms of the fhp^- ligands would have less of a donor interaction with the π*-orbitals of the chromium atoms but more of an electron withdrawing effect. Thus, in $Cr_2(fhp)_4$ the Cr–Cr distance should be longer than in $Cr_2(chp)_4$ if the inductive effect dominates but shorter if the donation to metal π-orbitals is the principal factor.

It turned out that this well-designed experiment was foiled by another example of regioisomerism in paddlewheel complexes (see Section 1.4). The fhp complex was indeed obtained but it was a regioisomer of the $Cr_2(chp)_4$ compound, as shown in Fig. 3.11. The four fhp ligands all point in the same direction, thus leaving one axial position unencumbered and coordinated by a THF molecule. Apparently this can happen because, unlike CH_3 or Cl, the F atom is small enough that four of them will fit on one end and the formation of the additional axial bond to THF stabilizes this structure. The presence of a tightly bound axial THF (Cr–O = 2.266 Å would cause the Cr–Cr bond to be very long, 2.150(2) Å.

Pictiva EX2004
Samsung v Pictiva
IPR2024-01094

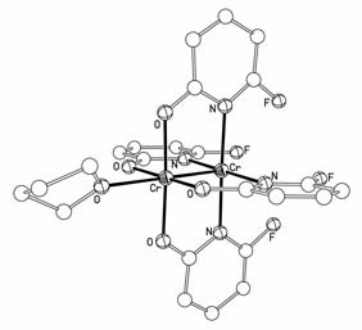


Fig. 3.11. The structure of the $Cr_2(fhp)_4(THF)$ molecule.

Table 3.3 lists the structures of the earliest compounds just discussed in sections 3.2.1 and 3.2.2, having extremely short Cr–Cr bonds.

Table 3.3. Some compounds with very short Cr–Cr bonds

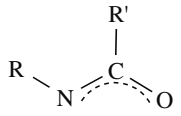
Ligands	d_{Cr-Cr} (Å)	ref.
$(DMP)_4$	1.847 (1)	47,48
$(TMP)_4$	1.849 (2)	48,49
$[(2\text{-}Bu^tO)C_6H_4]_2(O_2CMe)_2$	1.862 (1)	56
$[(2\text{-}MeO)(5\text{-}Me)C_6H_3]_4$	1.828 (2)	53
$(2\text{-oxophenyl})_4$	1.830 (4)	55
$(mhp)_4$	1.889 (1)	57
$(map)_4$	1.870 (3)	58
$(dmhp)_4$	1.907 (3)	59
$(chp)_4$	1.955 (2)	60
$(fhp)_4(THF)$	2.150 (2)	61

3.2.3 Carboxamidate compounds

From the stability of the $Cr_2(oxopyridinate)_4$ compounds, it was inferred that $Cr_2(carboxamidate)_4$ compounds, where the carboxamidate ligand is **3.11**, would also be stable. The first one reported,[62,63] contains the $PhNC(CH_3)O$ ligand and has the structure shown in Fig. 3.12. The Cr–Cr bond length is 1.873(4) Å. A number of other carboxamidate compounds have since been made, and all with known structures are listed in Table 3.4. Those with no axial ligands or very weak ones (CH_2Cl_2, CH_2Br_2) have short Cr–Cr bonds (< 2.00 Å). Unligated $Cr_2(carboxamidate)_4$ molecules are easy to obtain, even if solvated ones are initially isolated, by driving off the coordinated solvent molecules, and $Cr_2(carboxamidate)_4$ molecules do not associate as most $Cr_2(O_2CR)_4$ molecules do. The increase in the Cr–Cr distance by about 0.07 Å upon replacing Ph by 2-xylyl has no obvious explanation.

It is, however, easy to introduce axial ligands to bare $Cr_2(carboxamidate)_4$ molecules. This has been exploited to demonstrate the dominant influence of axial ligation, first with a series of axially ligated molecules derived from the unligated molecule[64] shown in Fig. 3.13. With very weak axial ligands, the Cr–Cr distance increases only a little (see Table 3.4). With the addition of first one and then two axial THF molecules, the distance increases to 2.023(1) and then 2.221(3) Å. With the addition of two axial pyridine ligands, the increase is huge, to 2.354(5) Å. The structure of this compound is shown in Fig. 3.14. Completely consistent with this trend are the observations on three other $Cr_2(carboxamidate)_4$ molecules, as seen in Table 3.4.

Pictiva EX2004
Samsung v Pictiva
IPR2024-01094



3.11

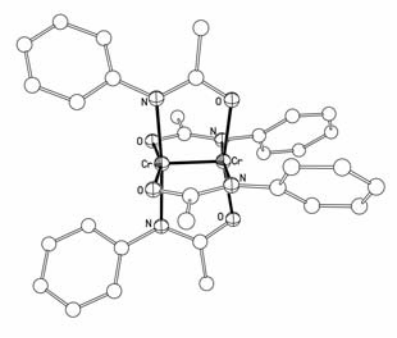


Fig. 3.12. The structure of $Cr_2(PhNC(CH_3)O)_4$.

Table 3.4. Structures of Cr_2 carboxamidate compounds

R	R'	Axial ligand(s)	Cr–Cr, Å	ref.
Ph	Me	—	1.873 (4)	62,63
Me_3C	Me	—	1.866 (2)	64
2,6-Me_2Ph	Me	—	1.937 (2)	65
2,6-Me_2Ph	Me	CH_2Cl_2	1.949 (2)	66
2,6-Me_2Ph	Me	CH_2Br_2	1.961 (4)	67
2,6-Me_2Ph	Me	THF	2.023 (1)	66
2,6-Me_2Ph	Me	2THF	2.221 (3)	66
2,6-Me_2Ph	Me	2py	2.354 (5)	66
Ph	PhNH	—	1.873 (4)	68
Ph	PhNH	2THF	2.246 (2)	66,68
$Me_2NC_6H_4$	CH_3	THF	2.006 (2)	66

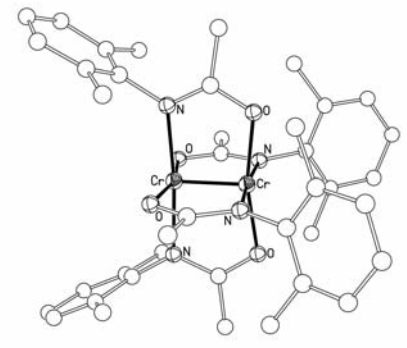


Fig. 3.13. The structure of $Cr_2[(2\text{-xylyl})NC(CH_3)O]_4$.

Pictiva EX2004
Samsung v Pictiva
IPR2024-01094

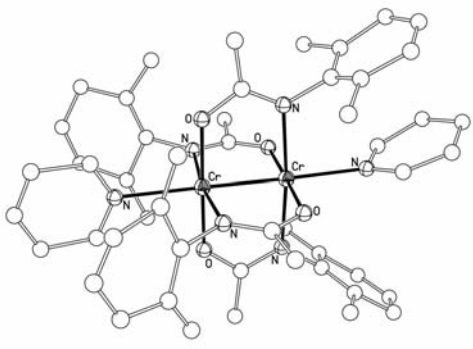
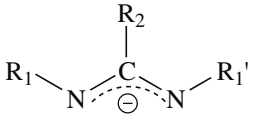


Fig. 3.14. The structure of $Cr_2[(2\text{-xylyl})NC(CH_3)O]_4(py)_2$.

The behavior of $Cr_2(carboxamidate)_4$ compounds in response to axial ligation was reported in 1979 and 1980, and yet for years theoreticians continued to insist[69-77] that it was not axial ligation but some property of *carboxylate* ligands that made Cr–Cr bonds long in axially ligated tetracarboxylates. The message to be drawn from the behavior of the $Cr_2(carboxamidate)_4$ compounds, namely, that we must consider very seriously the possibility that the dichotomy of supershort and long (quadruple) Cr–Cr bonds is due primarily to the absence or presence of axial ligands went unnoticed. The lesson to be learned from these events is that clear inference from experimental facts is more likely to be right than the results of calculations of uncertain reliability. There is a well known German adage that makes this point: "Die Theorie leitet; das Experiment entscheidet."

3.2.4 Amidinate compounds

Amidinate-bridged paddlewheel compounds of M_2^{4+} units have emerged as one of the more important classes. A general formula for amidinate ligands is **3.12**. While it is in principle possible for R_1 and R_1' to be different, such unsymmetrical ligands are difficult to make and have played no role, except in cases where R_1 is 2-pyridyl and R_1' is not.



3.12

The first amidinate compound[78] of Cr_2^{4+} reported was prepared in a manner that is representative of the most common one from all $M_2(amidinate)_4$ compounds:

$$CH_3N(H)C(Ph){=}NCH_3 \xrightarrow{LiBu} \xrightarrow{Cr_2(O_2CCH_3)_4} Cr_2[CH_3NC(Ph)NCH_3]_4$$

In this paddlewheel structure, shown in Fig. 3.15, the Cr–Cr distance, 1.843(2) Å, is extremely short.

At about the same time as the first amidinate compound was obtained, the first triazinate[79] was also obtained by the following reaction:

$$Li_4[Cr_2(CH_3)_8] + 4PhN(H)NNPh \rightarrow Cr_2(PhN_3Ph)_4 + 4CH_4 + 4LiCH_3$$

Pictiva EX2004
Samsung v Pictiva
IPR2024-01094

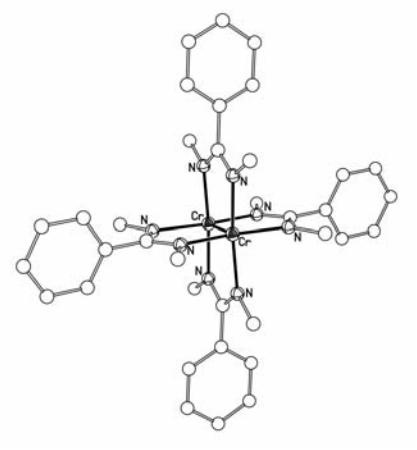


Fig. 3.15. The structure of $Cr_2[MeNC(Ph)NMe]_4$.

This is a rare instance of the $[Cr_2(CH_3)_8]^{4-}$ ion being used as a starting material. $Cr_2(PhN_3Ph)_4$, in which there is a very short Cr–Cr bond, 1.858 (1) Å, is still the only triazinate compound of Cr_2^{4+} known. Its structure is shown in Fig. 3.16.

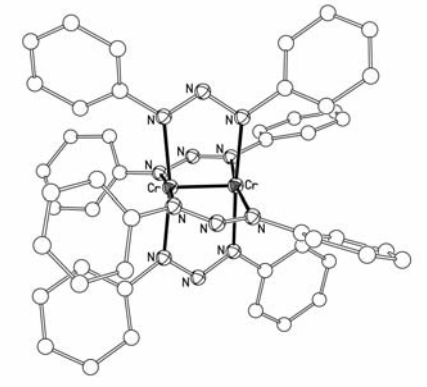


Fig. 3.16. The structure of $Cr_2(PhN_3Ph)_4$.

Beginning with the first reported amidinate compound in 1979, a great many other Cr_2 (amidinate)$_4$ compounds have been made and characterized. While all of those with no special features appear to be quite stable, with very short Cr–Cr distances, a number of bond-weakening features may be introduced. Most of these involve the building in of axial interactions and will be discussed in Section 3.3.1.

The vast majority of the known amidinate compounds of Cr_2^{4+} have formamidinate ligands, that is, those in which R_2 in **3.12** is hydrogen, and most of these have $R_1 = R_1' =$ aryl. Those with known structures are listed in Table 3.5. Curiously, what might be called the parent of this series of diaryl formamidinates, the diphenyl compound, has not been reported but no doubt it resembles the *p*-tolyl compound[80] closely. Others listed in Table 3.5 serve to determine the effect of substituents on the Cr–Cr distances. Generally the effects are small and show no meaningful pattern. In the case of the pentafluorophenyl compound,[81] it is probably the electronegativity of the C_6F_5 groups that causes a significant effect, in the expected direction.

Pictiva EX2004
Samsung v Pictiva
IPR2024-01094

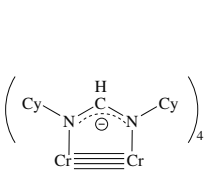
Table 3.5. Structures of formamidinate compounds of Cr_2^{4+}

R in RNC(H)NR	Cr–Cr, Å	ref.
p-tolyl	1.930(2)	80
o-fluorophenyl	1.968(2)	81
m-fluorophenyl	1.916(1)	81
p-fluorophenyl	1.917(6)	81
pentafluorophenyl	2.012(1)	81
3,5-difluorophenyl	1.906(1)	81
o-tolyl	1.925(1)	82
cyclohexyl	1.913(3)	83
(*o*-Clphenyl)$_3$(μ-Cl)	1.940(1)	84
(*o*-Brphenyl)$_3$(μ-Cl)	1.940(2)	82
cis-(o-MeOphenyl)$_2$(O_2CCH_3)$_2$	2.037(1)	85
p-Clphenyl	1.907(1)	86
3,5-dichlorophenyl†	1.916(1)	86
m-CF_3phenyl†	1.902(1)	86
m-(CH_3O)phenyl†	1.918(1)	86
o-(CH_3O)phenyl	2.140(2)	82
o-Clphenyl	2.208(2)	82
o-Brphenyl	2.272(2)	82
p-C_6H_5Ph	1.928(2)	81
[(Me_2HC)NC(H)N(Me_2HC)]$_3$(μ-BH_4)	1.844(2)	87
trans-[(Xyl)NC(H)N(Xyl)]$_2$(O_2CCH_3)$_2$(THF)$_2$	2.342(1)	85
[(Xyl)NC(H)N(Xyl)]$_2$(μ-Cl)$_2$(THF)$_2$	2.612(1)	85

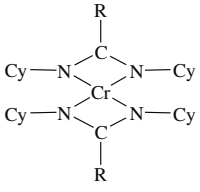
† Also mentioned[86] without structures: 3,4-Cl_2, *p*-CF_3, *p*-OCH_3

It is evident that ortho substituents can have relatively large effects,[82] with the Cr–Cr distances increasing in the order CH_3, Cl, CH_3O, Br. This will be discussed in Section 3.3.1.

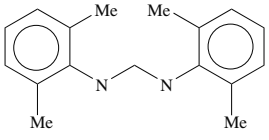
What appears to be a purely steric factor in controlling the formation of Cr_2(amidinate)$_4$ compounds was explored[83] in the compounds **3.13** and **3.14**. In **3.14**, the R groups are either methyl or 2-(Me_2NCH_2)C_6H_4. While the dinuclear compound **3.13** is a typical paddlewheel with a Cr–Cr bond length of 1.913(3) Å, when the ligands with substituents, even as small as CH_3, on the middle carbon atom were employed, only the mononuclear products, **3.14**, were isolated. This was attributed to the forcing down of the cyclohexyl groups with consequent reduction of the bite angle of the amidinates, to the extent that they prefer to chelate rather than span even the short Cr–Cr quadruple bond.



3.13



3.14



3.15

Two compounds[87] having a mixture of amidinate ligands and others have the formula Cr_2[RNC(H)CNR]$_3$(μ-BH_4), with R = $(CH_3)_2CH$ and *c*-C_6H_{11}. The structure of the former has been reported and it has Cr–Cr =1.844(2) Å. Other mixed ligand complexes were obtained

Pictiva EX2004
Samsung v Pictiva
IPR2024-01094

deliberately[85] by using the formamidinate ligand **3.15**. Here the steric hindrance caused by the methyl groups prevents the xylyl rings from occupying all bridging positions, so as to form a paddlewheel compound. Instead, only two can be accomodated in a transoid fashion. Thus, when $Cr_2(O_2CCH_3)_4$ is used as a starting material the transoid molecule shown in Fig. 3.17 is obtained.[85] Axial THF molecules are not excluded, and as a result, the Cr–Cr bond becomes quite long, viz., 2.342(1) Å. When $CrCl_2$ is the starting material the molecule shown in Fig 3.18 is obtained, in which the Cr–Cr distance is so long (2.612(1) Å) that little or no Cr–Cr bonding exists.[85] By using the formamidine with *o*-$MeOC_6H_4$ groups on the nitrogen atoms a cisoid molecule, Fig. 3.19, is obtained. Note that there are intramolecular axial interactions (a subject discussed generally in Section 3.3.1) which cause a lengthening of the Cr–Cr bond to 2.037(1) Å.

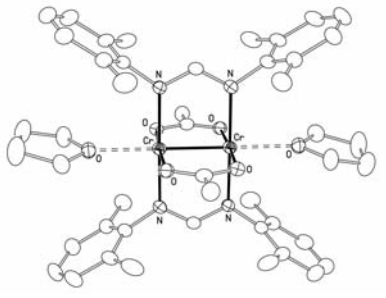


Fig. 3.17. The structure of $Cr_2(DXylF)_2(O_2CCH_3)_2(THF)_2$.

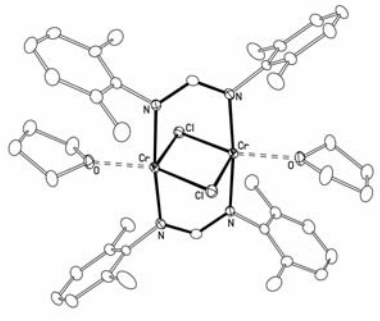


Fig. 3.18. The structure of $Cr_2(DXylF)_2(\mu\text{-}Cl)_2(THF)_2$.

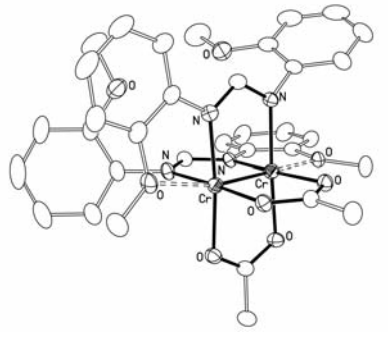
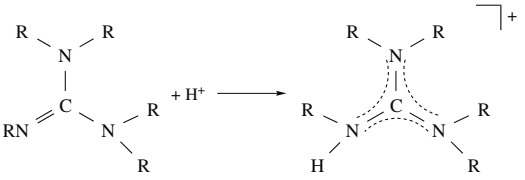


Fig. 3.19. The structure of $Cr_2(DAni^oF)_2(O_2CCH_3)_2$.

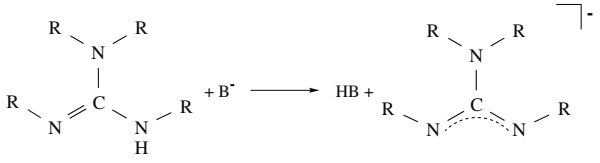
Pictiva EX2004
Samsung v Pictiva
IPR2024-01094

3.2.5 Guanidinate compounds

While guanidines are best known as very strong organic bases (**3.16**), they can also be deprotonated (**3.17**) to give N–C–N bridging ligands. These ligands have the ability to stabilize higher oxidation states of M_2^{n+} cores in general, but some special results are obtained in the case of dichromium species.

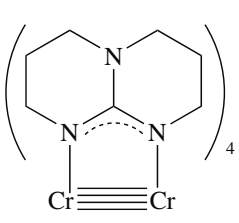


3.16

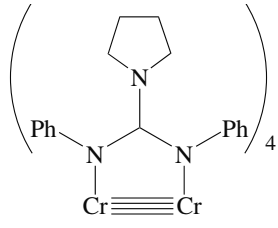


3.17

The first guanidinate compound of Cr_2^{4+}, **3.18**, was made with a bicyclic guanidinate anion, abbreviated hpp.[88] It is not in itself an especially remarkable compound, although it does have one of the shortest known Cr–Cr bonds, 1.852(1) Å. It led, however, to efforts to prepare other Cr_2^{4+} compounds[89,90] with guanidinate bridges. One of these, **3.19**, provided an unexpected breakthrough. The cyclic voltammogram of this compound displays a reversible oxidation at 0.02 V vs Ag/AgCl. Never before had any dichromium compound been oxidized electrochemically without decomposition. This cation was then isolated by oxidation with $AgPF_6$ and has the structure shown in Fig. 3.20. The only significant structural change, although small, caused by oxidation was an increase of 0.022 Å in the Cr–Cr bond length, from 1.903(4) to 1.925(1) Å. A solid state measurement of the magnetic susceptibility as well as an EPR measurement at X-band frequency (9.5 GHz) confirmed the presence of one unpaired electron, with a *g*-value of 2.00 ± 0.02. However, the question of where this electron is located was not correctly settled until a later EPR study[90] was done at W-band frequency (95 GHz). This showed that the odd electron is located in the Cr_2^{5+} core rather than delocalized over the ligand π orbitals.



3.18



3.19

A measurement of the PES of **3.18** in the gas phase[91] gave a δ ionization energy of 4.76 eV, which is a surprising low value.

Pictiva EX2004
Samsung v Pictiva
IPR2024-01094

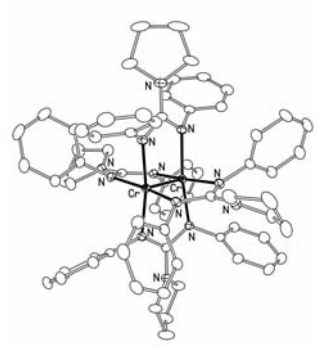


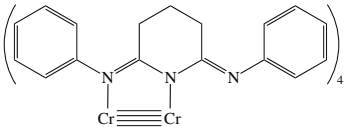
Fig. 3.20. The structure of the cation of the tetrakis (guanidinate) dichromium compound, **3.19**.

3.3 Miscellaneous Dichromium Compounds

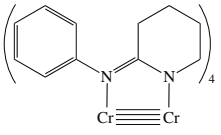
3.3.1 Compounds with intramolecular axial interactions

Cr–L_{ax} interactions are those whose effect is to place electron density in σ* or π* orbitals. In either case there is weakening and lengthening of the Cr–Cr bonds, as has already been discussed for the cases where the ligands, $L_{ax,}$ are exogenous, that is, independent molecules. This includes the self-association of $Cr_2(O_2CR)_4$ molecules, discussed in Section 3.1.3. The subject of this section are special cases where the axial ligands are covalently attached to the bridging ligands. It is not always clear whether the axial interaction is with the σ* or the π* orbitals, or perhaps both. A possible but unproven early example that was discovered serendipitously, $Cr_2(chp)_4$,[60] has already been mentioned (Section 3.2.2).

A designed, unambiguous case of axial π interactions[92] occurs in red $Cr_2(DPhIP)_4$, **3.20**, where the Cr–Cr bond length is 2.265(1) Å. The lengthening effect of the axial ligation is evident by comparison with $Cr_2(PhIP)_4$, **3.21**, in which the Cr–Cr bond length is 1.858(1) Å. The structure of $Cr_2(DPhIP)_4$ is shown in Fig. 3.21, where it can be seen that at each end there are two pendant pyridyl groups that are placed so as to donate their lone pair electron density into the chromium π* orbitals as shown in Fig. 3.22. A similar but less extreme case is presented by comparing the Cr–Cr bond length (1.940[5] Å) in $Cr_2(dpa)_4$[92] with that (1.870(3) Å) in $Cr_2(map)_4$.[58] The ligands in these two compounds are shown in **3.22** and **3.23**, respectively.



3.20



3.21

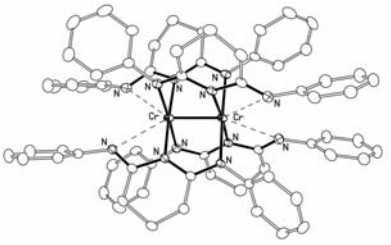


Fig. 3.21. The structure of the $Cr_2(DPhIP)_4$ molecule.

Pictiva EX2004
Samsung v Pictiva
IPR2024-01094

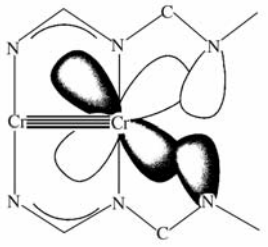
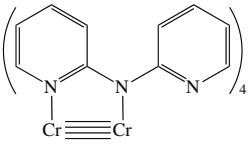
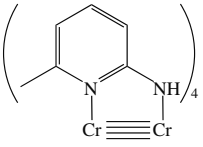


Fig. 3.22. The manner in which the appended nitrogen atoms of the ligand **3.20** are able to donate lone-pair electron density to a Cr_2 π^* orbital.



3.22



3.23

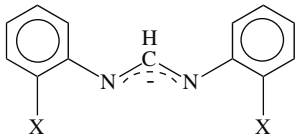
It is part of the design of **3.20** that the axially interacting lone pairs on the dangling nitrogen atoms are at distances where they can reach only the π^* but not the σ^* orbitals of the Cr_2^{4+} unit. The result for $Cr_2(DPhIP)_4$ provides support for the previous proposal (Section 3.1.3) that the Cr–Cr distance of 2.256(4) Å in $Cr_2(O_2CCPh_3)_4 \cdot C_6H_6$ is a result of the donation of C_6H_6 π electron density into the Cr–Cr π^* orbitals.

However, the story is not yet complete on $Cr_2(DPhIP)_4$. It occurs in another crystal form where the color is orange, not red, and the Cr–Cr distance is only 2.155(1) Å. Of course, this is still an elongation of about 0.30 Å. To explain this, it is necessary to look more closely at the structures. As indicated by Fig. 3.22, maximum donation to the π^* orbitals occurs when the dangling pyridyl ligand and hence, the centroid of the nitrogen lone pair, lies in the same plane as the rest of the ligand. However, rotation about the C–N bond can move the lone pair out of this optimal orientation. This is what happens in the orange crystals (Cr–Cr = 2.155(1) Å) compared to the red ones (Cr–Cr = 2.265(1) Å).

As for $Cr_2(dpa)_4$, there is a much smaller lengthing due to axial π^* interaction because of an even greater "misdirection" of the nitrogen lone pairs. The increase from $Cr_2(map)_4$, **3.23**, to $Cr_2(dpa)_4$, **3.22**, is only 0.07 Å.

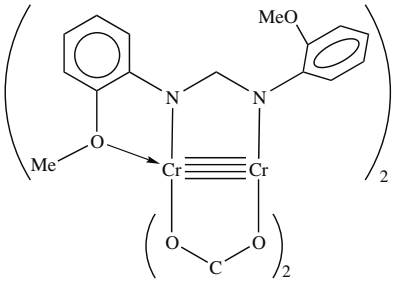
Three other examples of the effect of intramolecular donation into Cr_2 σ^* orbitals have been reported.[82] They have already been mentioned in Section 3.2.4 and listed in Table 3.5. These were made using ligands of type **3.24**. For X = Me, the Cr–C distance is 1.925(1) Å, and there is no significant donation into any axial orbital. When X is a potential donor, it probably reaches down into the region of the Cr–Cr σ^* orbital, although this is not certain. In the series X = MeO, Cl, Br, the Cr–Cr bond lengths greatly increase, to 2.140(2), 2.208(2), and 2.272(2) Å, respectively. Clearly, as the ortho substituents get bigger and "softer" they donate more electron density into the axial orbitals. In these three cases, only one such interaction occurs on each end, rather than two at each end, because only one donor atom at a time can occupy the axial region.

Pictiva EX2004
Samsung v Pictiva
IPR2024-01094



3.24

A molecule with only two o-methoxyphenylformamidinate ligands, **3.25**, has also been made.[85] Here again, one methoxy oxygen atom at each end can be an axial donor mainly to the σ* orbital. In this case, the Cr–Cr bond length is 2.037(2) Å.



3.25

Yet another phenomenon that arises with ligands that have dangling donor atoms is that they can chelate additional metal atoms and hold one or two in axial positions. We mention first the novel case[93] of $Cr_2(DPhIP)_4$, where, as discussed earlier in this section, the dangling imino nitrogen atoms give rise to axial π* interactions that take the Cr–Cr bond from 1.858(1) Å in $Cr_2(PhIP)_4$ to 2.265(1) Å in $Cr_2(DPhIP)_4$. This molecule reacts with CuCl to form a product in which a Cu^+ is held at each axial position, at distances of 2.628(2) Å and 2.689(2) Å, and the Cr–Cr bond contracts to 1.906(2) Å. It appears that the Cu^+ ions have virtually no effect on the Cr–Cr bond.

An interesting example of how the introduction of axial metal atoms can strengthen intramolecular axial interactions, and thus weaken the Cr–Cr bond, is provided by the last two compounds[94] in Table 3.6. In $Cr_2(pyphos)_4$ there is enough axial interaction by two phosphorus atoms at each end to lengthen the Cr–Cr bond from 1.90 Å (about that in $Cr_2(mhp)_4$) to 2.015(5) Å. When the two platinum atoms are anchored in place (at Cr–Pt distances of 2.810 ± 0.01 Å) the Cr–Cr distance goes to 2.389(9) Å. Those who reported these results referred to the platinum atoms acting as "axial donors to the quadruple Cr–Cr bond." However, this may be a multiple interaction since the platinum atom has all of its *d* orbitals except $d_{x^2-y^2}$ filled.

Table 3.6. Structures with intramolecular axial interactions

Compound	Cr–Cr, Å	ref.
$Cr_2(PhIP)_4$	1.858 (1)	92
$Cr_2(DPhIP)_4$	2.265 (1)	92
$[Cr_2(DPhIP)_4Cu_2][CuCl_2]_2$	1.906 (2)	93
$Cr_2(dpa)_4$	1.943 (2)	92
$Cr_2(dpa)_4 \cdot 2CH_2Cl_2$	1.940 (1)	92
$Cr_2(pyphos)_4$	2.015 (5)	94
$Cr_2(pyphos)_4(Me_2Pt)_2$	2.389 (9)	94

Pictiva EX2004
Samsung v Pictiva
IPR2024-01094

3.3.2 Compounds with Cr–C bonds

Some of these have already been mentioned in Section 3.2.1, namely $Cr_2(DMP)_4$ and several similar or related ones. Others will now be described.

A phosphine ylid ligand occurs in $Cr_2[(CH_2)P(CH_3)_2]_4$.[95,96] The structure in which the Cr–Cr bond length is 1.895(3) Å, is shown in Fig. 3.23.

The two compounds, $Li_4(THF)_4[Cr_2Me_8]$ and $Li_4(THF)_4[Cr_2(C_4H_8)_4]$, have been reported and their structures described.[97-99] Both contain eclipsed Cr–C_4 sets of bonds, and the Cr–Cr distances are 1.980(5) and 1.975(5) Å. These structures clearly imply the presence of Cr–Cr quadruple bonds. However, whether they can be regarded as true $[Cr_2X_8]^{4-}$ compounds is a moot point. A $(THF)Li^+$ ion is located between each opposing pair of RCCr–CrCR components, with distances such that the Li^+ ions might be regarded as forming part of five-membered Li−C−Cr−Cr−C rings. It may be noted that only lithium compounds of this type have been reported, and there is no indication in the literature that the preparation of a $Cr_2R_8^{4+}$ compound with any other cation has been attempted.

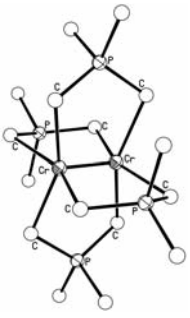
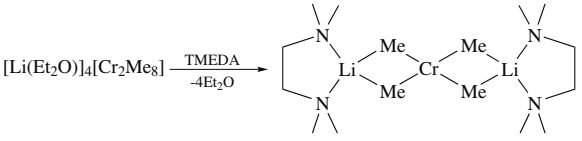


Fig. 3.23. The structure of $Cr_2[(CH_2)_2P(CH_3)_2]_4$.

It has more recently been reported[100] that the octamethyl compound with diethyl ether in place of THF can be made and that it undergoes the following reaction with excess *N*,*N*,*N*',*N*'-tetramethylethylenediamine (TMEDA):



It is also reported that on addition of excess THF the dinuclear $(LiTHF)_4Cr_2Me_8$ is formed. The compound $[Li(TMEDA)]_2[CrMe_4]$ has a square coordinated Cr^{II} with four unpaired electrons.

Another molecule having Cr–C bonds is the allyl molecule, $Cr_2(C_3H_5)_4$, which is one of the earliest Cr_2^{4+} compounds to be structurally characterized.[101,102] The planes of the allyl groups all lie parallel to the Cr–Cr bond. This pyrophoric compound, which has a molybdenum analog, is easily made by reaction of $CrCl_3$ with an excess of allyl Grignard, or by reduction of $Cr(C_3H_5)_3$ with C_2H_5Li.[103] It is a brownish-black solid with a metallic luster. Both structure determinations are imprecise, but give a Cr–Cr distance of about 1.97-1.98 Å.

An unusual organometallic compound is $Cr_2(C_8H_8)_3$, with one bridging C_8H_8 and two that are each attached to only one metal atom. It has isostructural molybdenum and tungsten analogs. The Cr–Cr distance is 2.214(1) Å.[104] There are two methods of preparation, one from $CrCl_3$ and $Na_2C_8H_8$[105] and the other by passing chromium atom vapor into C_8H_8.[106]

Pictiva EX2004
Samsung v Pictiva
IPR2024-01094

The only compound with four-membered ligands, 1,2-$(NMe_2)(CH_2)C_6H_4$, bridging the two chromium atoms is also an organometallic compound. It contains two of the above ligands and two CH_3CO_2 and has the structure[107] shown in Fig. 3.24, with a Cr–Cr distance of 1.870(1) Å.

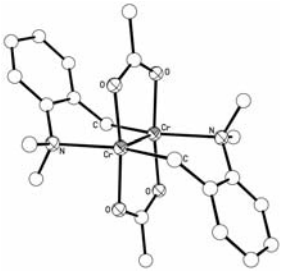


Fig. 3.24. The structure of trans-$Cr_2(O_2CCH_3)_2[1,2\text{-}(NMe_2)(CH_2)C_6H_4]_2$.

A curious, and unique organometallic compound[108] is $Cr_2(CH_2SiMe_3)_2(\mu\text{-}CH_2SiMe_3)_2(PMe_3)_2$, with the structure shown schematically in Fig. 3.25.

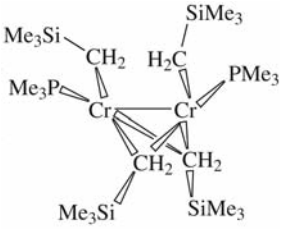


Fig. 3.25. A schematic depiction of the molecule $Cr_2(CH_2SiMe_3)_2(\mu\text{-}CH_2SiMe_3)_2(PMe_3)_2$.

3.3.3 Other pertinent results

Preparation of the $Cr_2(tmtaa)_2$ molecule,[109,110] Fig. 3.26, is rather easy, there being five distinct methods, and it is very stable. The Cr–Cr bond (length 2.10(1) Å) appears to be only a triple bond on the basis of MO calculations.[109] The reported partial paramagnetism[110] may imply a singlet-triplet equilibrium, but a study of the temperature dependence is needed. The eclipsed conformation of the two N_4Cr groups is probably a consequence of the nesting of the two macrocyclic rings. $Cr_2(tmtaa)_2$ is the only Cr–Cr bonded molecule that is indubitably without bridging ligands (i.e., it is not a paddlewheel).

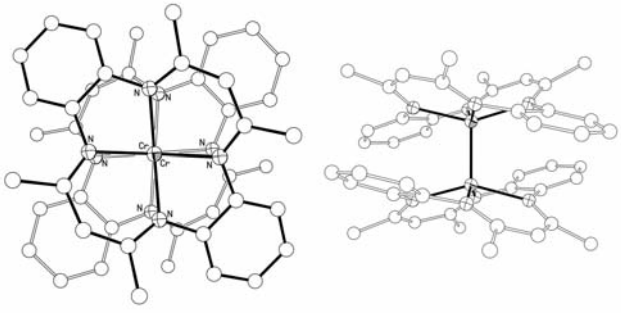


Fig. 3.26. The structure of the $Cr_2(tmtaa)_2$ molecule.

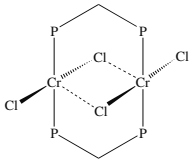
Pictiva EX2004
Samsung v Pictiva
IPR2024-01094

In the presence of excess pyridine, the molecule splits and when THF is added in large excess the dinuclear species forms again, as shown in the following equation:

$$Cr_2(tmtaa)_2 \underset{-4py}{\overset{+4py}{\rightleftharpoons}} 2\ \textit{trans}\text{-}Cr(tmtaa)py_2$$

Based on these observations the energy of the Cr–Cr bond may be expressed as a multiple of the Cr–py bond energy. If ΔG is about zero, the Cr–Cr bond enthalpy would be more than *four* times the Cr–py bond enthalpy, allowing for the fact that $T\Delta S$ must be positive (by perhaps 5-10 kcal mol^{-1}) and from each broken Cr–Cr bond *four* Cr–py bonds are formed.

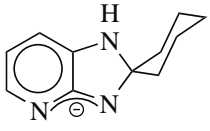
An attempt has been made to make a molecule with a Cr–Cr bond but only two bridges. A molecule with the desired stoichiometry, $Cr_2Cl_4(dmpm)_2$, was made,[111] but it is highly paramagnetic and has the structure shown in **3.26** with a Cr–Cr distance of 3.24 Å. No $[Cr_2X_8]^{4-}$ or $Cr_2X_4L_4$ molecules, analogous to those formed by molybdenum, tungsten, technetium or rhenium appear to exist. All reported compounds of the stoichiometry CrX_2L_2, $MCrX_3$ and M_2CrX_4 are paramagnetic, with four unpaired electrons per Cr atom.



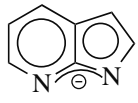
3.26

Divergent-bite ligands.[112]

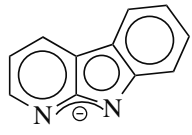
Most paddlewheel complexes with four N–C–N type bridging ligands tend to have short Cr–Cr bonds and no axial ligands. However, the short Cr–Cr bonds are possible only when the bridging ligands can have a sufficiently small "bite", as in the amidinates, where the nitrogen lone pairs naturally point approximately along parallel lines, and can even toe in somewhat without much strain. However, there are some N–C–N type ligands for which the ligand structure dictates that the preferred bonding directions for the nitrogen atoms naturally diverge and toeing in is resisted. This is always true when a 6-membered ring and a 5-membered ring are fused with one nitrogen atom in each, as in **3.27**, **3.28**, and **3.29**. There is enough flexibility in ligand **3.27** (CHIP) so that $Cr_2(CHIP)_4$ shows only moderate lengthening of the Cr–Cr bond. In two different crystalline compounds the bond lengths are 2.016 Å and 2.125(2) Å. The molecule containing the shorter of these Cr–Cr bonds is shown in Fig. 3.27.



3.27



3.28



3.29

With the 7-azaindolate ligand, azin, **3.28**, the tendency of the ligand to lengthen the Cr–Cr bond has a dominant effect. As indicated in Fig. 3.28, for a typical Cr–N bond length, the placement of Cr atoms exactly in the directions expected for the nitrogen donor orbitals would lead to a very long distance indeed. In the first Cr_2^{4+} compound reported with four azin ligands,[113] there are also two axial interactions with DMF ligands and the Cr–Cr distance is very long, 2.604(2) Å.

Pictiva EX2004
Samsung v Pictiva
IPR2024-01094

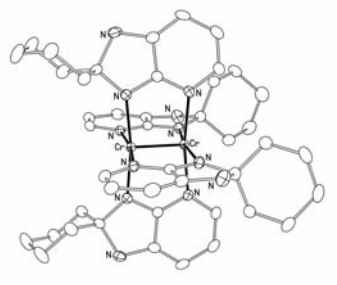


Fig. 3.27. The structure of $Cr_2(CHIP)_4$.

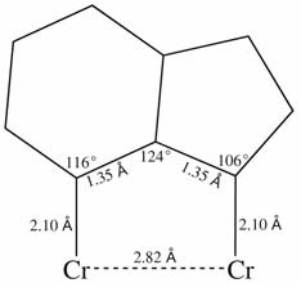


Fig. 3.28. Calculated geometric parameters for an azin ligand with a typical Cr–N bond of 2.10 Å.

A compound[114] containing the $[Cr_2(azin)_4Cl_2]^{2-}$ ion (Cr···Cl = 2.606 Å) has also been examined, and here, too, there is probably no Cr–Cr bond, since the Cr···Cr distance is 2.688(2) Å. This structure is shown in Fig. 3.29. One feature of interest, however, is that the azin ligands all show end-for-end disorder, with superposed 5- and 6-membered rings showing up in each ring position. Azin shows this tendency in other $M_2(azin)_4$ compounds, and to avoid it was one of the reasons why the carb ligand was employed in the compound mentioned earlier.

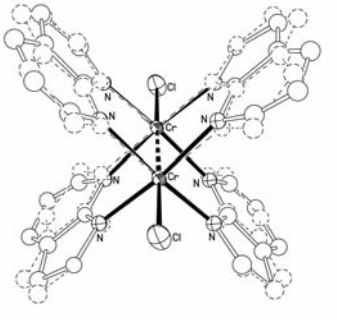


Fig. 3.29. The structure of the $Cr_2(azin)_4Cl_2^{2-}$ anion.

The carboline (carb) ligand, **3.29** is very rigid and gives two compounds with much longer Cr–Cr distances and with an axial Cl^- ligand at one end. One of these, $[Cr_2(carb)_4Cl]^+$, shown in Fig. 3.30, has a Cr–Cr distance of 2.5301(1) Å and the other, $Cr_2(carb)_4Cl\cdots Li(acetone)$ has a distance of 2.517(1) Å.

Pictiva EX2004
Samsung v Pictiva
IPR2024-01094

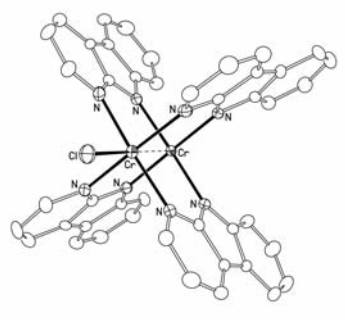
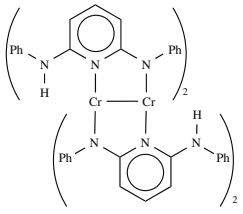


Fig. 3.30. The structure of $Cr_2(carb)_4$.

Two other complexes with divergent-bite ligands contain the ligands oxindolate,[115] (Cr–Cr = 2.495(4) Å) and saccharinate,[116] (Cr–Cr = 2.550(4) Å and 2.591(1) Å in two different compounds.

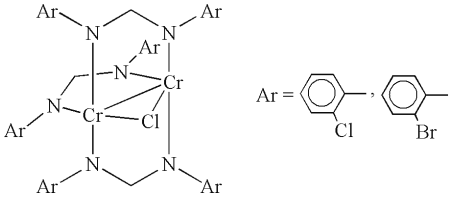
The compound **3.30** has been isolated in two crystal modifications[117] but the molecule has essentially the same structure in both with a Cr–Cr distance of 1.874[2] Å. The structure is not at all surprising, but the ^{1}H NMR spectrum of the compound displays a very interesting feature not seen anywhere else. The exceptionally high diamagnetic anisotropy of quadruple bonds has been established in many compounds on the basis of the large downfield shift of protons (such as the methine proton in a formamidinate) that are located over the center of the M–M bond. In **3.30**, the protons on the amino nitrogen atoms are located in a region of space where a large upfield shift would be expected and that is what is observed. The signal is shifted 3.0 to 4.5 ppm from where it would normally have been expected.



3.30

A-frames.

Two Cr_2^{4+} compounds with A-frame structures are known,[82,84] namely, those shown in **3.31**. In spite of the perturbation of the regular paddlewheel structure, both retain very short Cr–Cr distances, 1.940 (1) Å and 1.940(2) Å for the *o*-Cl and *o*-Br compounds, respectively. In order to allow this the Cr–Cl–Cr angles are extremely small, namely, about 46.7°. These are the most acute angles ever observed in an M–Cl–M unit.



3.31

Pictiva EX2004
Samsung v Pictiva
IPR2024-01094

3.4 Concluding Remarks

The number of isolated dichromium compounds is large, probably several hundred. Counting only those for which there are crystal structures, there are at least 110. Many of the earliest carboxylates, of course, have never been structurally characterized and have not been discussed here individually. Another entity not discussed here is the gaseous Cr_2 molecule, in which the Cr–Cr distance is about 1.68 Å. The entire range of Cr–Cr distances in isolable compounds, from *c.* 1.83 Å to *c.* 2.7 Å, occurs within a common paddlewheel arrangement of ligands. The problem posed by this is how best to formulate the interactions between the chromium atoms and explain why they vary so much. It has been established, empirically, that axial ligation is the most important factor influencing Cr–Cr bond lengths.

While all Cr^{II}–Cr^{II} interactions can, presumably, be regarded as having σ, π and δ components, these are not distinctly separated as in analogous Mo^{II}–Mo^{II} compounds. The strengths of these interactions, like all others, must vary inversely with Cr–Cr distance. At distances <2.00 Å it seems reasonable to assign $\sigma^2\pi^4\delta^2$ quadruple bonds. At much longer distances it is clear that the δ bonding becomes so weak that population of a state based on a triplet δδ* configuration is easily detected and quantified, as discussed in Section 3.1.2. Over the entire range of Cr–Cr distances all of the orbital overlaps, σσ, ππ and δδ will vary continuously. It is possible that at the longest distances, the covalence in the Cr–Cr interactions might be negligible and the interaction regarded as mere antiferromagnetic coupling. However, there are no criteria, either experimental or theoretical, for drawing any line of demarcation, and probably none exists.

The failure of Hartree-Foch calculations to provide a useful description of the bonding in Cr_2^{4+} compounds was referred to in Section 3.1.3. The source of the difficulty lies in the severe problem of electron correlation, a matter that was addressed in an instructive way by M. B. Hall.[69] Clearly, calculations without any allowance for configuration interaction[70,71] give hopelessly erroneous results. The idea of distinct LCAO-MOs, each occupied by an electron pair, is too simple an approximation, although it serves well for Mo_2^{4+} compounds. Even efforts to salvage it by adding heavy corrections for configuration interaction[72-77] are of doubtful value. Neither generalized valence bond calculations nor DFT have given anything like satisfactory results either. The only calculations that have given any theoretical inkling that a bare $Cr_2(O_2CR)_4$ molecule could have a Cr–Cr distance below 2.00 Å were done by a complete-active-space, self-consistent-field (CASSCF) method applied to $Cr_2(O_2CH)_4$.[118] A measurement of the photoelectron spectrum[119] of $Cr_2[(p\text{-tol})NC(H)N(p\text{-tol})]_4$ showed that the nominal σ, π and δ orbitals, together with some ligand-based orbitals, are all bunched together in a range of 0.81 eV.

References

1. E. Peligot, *C. R. Acad. Sci.*, **1844**, *19*, 609; *Ann. Chim. Phys.* **1844**, *12*, 528.
2. L. R. Ocone and B. P. Block, *Inorg. Synth.* **1966**, *8*, 125.
3. G. Brauer, *Handbuch der präparativen anorganischen Chemie*, Bd. 2, Enke, Stuttgart, 1962.
4. F. A. Cotton and G. W. Rice, *Inorg. Chem.* **1978**, *17*, 688.
5. F. A. Cotton, B. G. DeBoer, M. D. LaPrade, J. R. Pipal and D. A. Ucko, *Acta Crystallogr.* **1971**, *B27*, 1664.
6. F. A. Cotton and T. R. Felthouse, *Inorg. Chem.* **1980**, *19*, 328.
7. M. H. Chisholm, F. A. Cotton, M. W. Extine and D. C. Rideout, *Inorg. Chem.* **1979**, *18,* 120.
8. M. H. Chisholm, F. A. Cotton, M. W. Extine and D. C. Rideout, *Inorg. Chem.* **1978**, *17,* 3536.
9. M. Ardon, A. Bino, S. Cohen and T. R. Felthouse, *Inorg. Chem.* **1984**, *23*, 3450.
10. F. A. Cotton and G. Schmid, *Inorg. Chim. Acta* **1997**, *254*, 233.

Pictiva EX2004
Samsung v Pictiva
IPR2024-01094

11. S. Herzog and W. Kalies, *Z. anorg. allg. Chem.* **1964**, *329*, 83; *Z. anorg. allg. Chem*. **1967**, *351*, 237; *Z. Chem*. **1964**, *5*, 183.
12. P. Sharrock, T. Theophanides and F. Brisse, *Can. J. Chem*. **1973**, *51*, 2963.
13. F. A. Cotton and G. W. Rice, *Inorg. Chem*. **1978**, *17*, 2004.
14. (a) F. A. Cotton, M. W. Extine, and G. W. Rice, *Inorg. Chem*. **1978**, *17*, 176; (b) L. Bennes, J. Kalousova, and J. Votinsky, *J. Organomet. Chem*. **1985**, *290*, 147.
15. F. A. Cotton and G. W. Rice, *Inorg. Chim. Acta* **1978**, *27*, 75.
16. A. A. Pasynskii, I. L. Eremenko, T. C. Idrisov and V. T. Kalinnikov, *Koord. Khim.* **1977**, *3*, 1205.
17. See, for example, F. Baugé, *Ann. Chim. Phys*. **1900**, *19*, 158 and earlier references therein.
18. R. Ouahes, J. Amiel and H. Suquei, *Rev. Chim. Min*. **1970**, 7, 789.
19. R. Ouahes, H. Pezerat and J. Gayoso, *Rev. Chim. Min*. **1970**, 7, 849.
20. R. Ouahes, B. Devallez and J. Amiel, *Rev. Chim. Min*. **1970**, 7, 855.
21. P. D. Ford, L. F. Larkworthy, D. C. Povey and A. J. Roberts, *Polyhedron* **1983**, *2*, 1317.
22. C. J. Bilgrien, R. S. Drago, C. J. O'Connor and N. Wong, *Inorg. Chem*. **1988**, *27*, 1410.
23. F. A. Cotton, H. Chen, L. M. Daniels and X. Feng, *J. Am. Chem. Soc*. **1992**, *114*, 8980.
24. C. Furlani, *Gazz. Chim. Ital*. **1957**, *87*, 885.
25. L. Dubicki and R. L. Martin, *Inorg. Chem*. **1966**, *5* , 2203.
26. R. D. Cannon, *J. Chem. Soc. (A)* **1968**, 1098; R. D. Cannon and M. J. Gholami, *J. Chem, Soc., Dalton Trans*. **1976**, 1574.
27. L. M. Wilson and R. D. Cannon, *Inorg. Chem*. **1988**, *27*, 2382.
28. J. M. Bellerby, D. A. Edwards and D. Thompsett, *Inorg. Chim. Acta* **1986**, *117*, L31.
29. R. D. Cannon and J. S. Stillman, *Inorg. Chem*. **1975**, *14*, 2202; 2207.
30. R. D. Cannon and M. J. Gholami, *Bull. Chem. Soc. Jpn*. **1982**, *55*, 594.
31. E. H. Abbott and J. M. Mayer, *J. Coord. Chem*. **1977**, **6**, 135.
32. L. M. Wilson and R. D. Cannon, *Inorg. Chem*. **1985**, *24*, 4366.
33. A. S. Carson, *J. Chem. Thermodynamics* **1984**, *16*, 427.
34. F. A. Cotton, C. E. Rice and G. W. Rice, *J. Am. Chem. Soc*. **1977**, *99*, 4704.
35. F. A. Cotton and J. L. Thompson, *Inorg. Chem*. **1981**, *20*, 1292.
36. F. A. Cotton, X. Feng, P. A. Kibala and M. Matusz, *J. Am. Chem. Soc*. **1988**, *110*, 2807.
37. S. N. Ketkar and M. Fink, *J. Am. Chem. Soc*. **1985**, *107*, 338.
38. N. V. Gerbeleu, G. A. Popovich, K. M. Indrichan and G. A. Timko, *Russ. J. Inorg. Chem*. **1983**, *28*, 1720.
39. F. A. Cotton, E. A. Hillard, C. A. Murillo and H.-C. Zhou, *J. Am. Chem. Soc*. **2000**, *122*, 416.
40. R. A. Kok and M. B. Hall, *J. Am. Chem. Soc*. **1983**, *105*, 676.
41. R. Wiest and M. Bénard, *Chem. Phys. Lett*. **1983**, *98*, 102.
42. R. A. Kok and M. B. Hall, *Inorg. Chem*. **1985**, *24*, 1542.
43. R. B. Davy and M. B. Hall, *J. Am. Chem. Soc*. **1989**, *111*, 1268.
44. F. A. Cotton and W. Wang, *Nouv. J. Chim*. **1984**, *8*, 331.
45. C. D. Garner, R. G. Senior and T. J. King, *J. Am. Chem. Soc*. **1976**, *98*, 3526.
46. R. Wiest and M. Bénard, *Theor. Chim. Acta* **1984**, *66*, 65.
47. F. A. Cotton, S. Koch and M. Millar, *J. Am. Chem. Soc*. **1977**, *99*, 7372.
48. F. A. Cotton, S. A. Koch and M. Millar, *Inorg. Chem*. **1978**, *17*, 2087.
49. F. A. Cotton and M. Millar, *Inorg. Chim. Acta* **1977**, *25*, L105.
50. L. Pauling, *The Nature of the Chemical Bond*, 3rd ed, Cornell University Press, 1960, p. 403.
51. F. Hein and D. Tille, *Z. anorg. allg. Chem*. **1964**, *329*, 72.
52. R. P. A. Sneeden and H. H. Zeiss, *J. Organomet. Chem*. **1973**, *47*, 125.
53. F. A. Cotton, S. A. Koch and M. Millar, *Inorg. Chem*. **1978**, *17*, 2084.
54. F. Hein and D. Tille, *Monatsber. Dtsch. Akad. Wiss. Berlin*, **1962**, *4*, 414.
55. F. A. Cotton and S. Koch, *Inorg. Chem*. **1978**, *17*, 2021.
56. F. A. Cotton and M. Millar, *Inorg. Chem*. **1978**, *17*, 2014.
57. F. A. Cotton, P. E. Fanwick, R. H. Niswander and J. C. Sekutowski, *J. Am. Chem. Soc*. **1978**, *100*, 4725.

Pictiva EX2004
Samsung v Pictiva
IPR2024-01094

58. F. A. Cotton, R.H. Niswander and J. C. Sekutowski, *Inorg. Chem*. **1978**, *17*, 3541.
59. F. A. Cotton, R. H. Niswander and J. C. Sekutowski, *Inorg. Chem*. **1979**, *18*, 1152.
60. F. A. Cotton, W. H. Ilsley and W. Kaim, *Inorg. Chem*. **1980**, *19*, 1453.
61. F. A. Cotton, L. R. Falvello, S. Han and W. Wang, *Inorg. Chem*. **1983**, *22*, 4106.
62. A. Bino, F. A. Cotton and W. Kaim, *J. Am. Chem. Soc*. **1979**, *101*, 2506.
63. A. Bino, F. A. Cotton and W. Kaim, *Inorg. Chem*. **1979**, *18*, 3030.
64. F. A. Cotton and W. Wang, unpublished work.
65. S. Baral, F. A. Cotton and W. H. Ilsley, *Inorg. Chem*. **1981**, *20*, 2696.
66. F. A. Cotton, W. H. Ilsley and W. Kaim, *J. Am. Chem. Soc*. **1980**, *102*, 3475.
67. F. A. Cotton, W. H. Ilsley and W. Kaim, *J. Am. Chem. Soc*. **1980**, *102*, 3464.
68. F. A. Cotton, W. H. Ilsley and W. Kaim, *Angew. Chem., Int. Ed. Engl*. **1979**, *18*, 874.
69. M. B. Hall, *Polyhedron* **1987**, *6*, 697.
70. C. D. Garner, I. H. Hillier, M. F. Guest, J. C. Green and A. W. Coleman, *Chem. Phys. Lett*. **1976**, *41*, 91.
71. P. Correa de Mello, W. D. Edwards and M. C. Zerner, *J. Am. Chem. Soc*. **1982**, *104*, 1440; *Int. J. Quantum Chem*. **1983**, *23*, 425.
72. M. Bénard, *J. Chem. Phys*. **1979**, *71*, 2546.
73. M. F. Guest, I. H. Hillier and C. D. Garner, *Chem. Phys. Lett*. **1977**, *48*, 587.
74. M. Bénard and A. Veillard, *Nouv. J. Chim*. **1977**, *1*, 97.
75. M. Bénard, *J. Am. Chem. Soc*. **1978**, *100*, 2354.
76. P. M. Atha, I. H. Hillier and M. F. Guest, *Mol. Phys*. **1982**, *46,* 437.
77. P. M. Atha, I. H. Hillier, A. A. MacDowell and M. F. Guest, *J. Chem. Phys*. **1982**, 77, 195.
78. A. Bino, F. A. Cotton and W. Kaim, *Inorg. Chem*. **1979**, *18*, 3566.
79. F. A. Cotton, G. W. Rice and J. C. Sekutowski, *Inorg. Chem*. **1979**, *18*, 1143.
80. F. A. Cotton and T. Ren, *J. Am. Chem. Soc*. **1992**, *114*, 2237.
81. F. A. Cotton, C. A. Murillo and I. Pascual, *Inorg. Chem*. **1999**, *38*, 2182.
82. F. A. Cotton, L. M. Daniels, C. A. Murillo and P. Schooler, *J. Chem. Soc., Dalton Trans*. **2000**, 2007.
83. S. Hao, S. Gambarotta, C. Bensimon and J. J. H. Edema, *Inorg. Chim. Acta 1993*, *213*, 65.
84. F. A. Cotton, C. A. Murillo and I. Pascual, *Inorg. Chem. Commun*. **1999**, *2*, 101.
85. F. A. Cotton, L. M. Daniels, C. A. Murillo and P. Schooler, *J. Chem. Soc., Dalton Trans*. **2000**, 2001.
86. K. M. Carlton-Day, J. L. Eglin, C. Lin, L. T. Smith, R. J. Staples and D. O. Wipf, *Polyhedron* **1999**, *18*, 817.
87. M. Dionne, S. Hao and S. Gambarotta, *Can. J. Chem*. **1995**, *73*, 1126.
88. F. A. Cotton and D. J. Timmons, *Polyhedron* **1998**, *17*, 179.
89. F. A. Cotton, L. M. Daniels, P. Huang and C. A. Murillo, *Inorg. Chem*. **2002**, *41*, 317.
90. F. A. Cotton, N. S. Dalal, E. A. Hillard, P. Huang, C. A. Murillo and C. M. Ramsey, *Inorg. Chem*. **2003**, *42*, 1388.
91. F. A. Cotton, N. E. Gruhn, J. Gu, P. Huang, D. L. Lichtenberger, C. A. Murillo, L. O. Van Dorn and C. C. Wilkinson, *Science* **2002**, *298*, 1971.
92. F. A. Cotton, L. M. Daniels, C. A. Murillo, I. Pascual and H.-C. Zhou, *J. Am. Chem. Soc*. **1999**, *121*, 6856.
93. F. A. Cotton, C. A. Murillo, L. E. Roy and H.-C. Zhou, *Inorg. Chem*. **2000**, *39*, 1743.
94. K. Mashima, M. Tanaka, K. Tani, A. Nakamura, S. Takeda, W. Mori and K. Yamaguchi, *J. Am. Chem. Soc*. **1997**, *119*, 4307.
95. F. A. Cotton, B. E. Hanson, W. H. Ilsley and G. W. Rice, *Inorg. Chem*. **1979**, *18*, 2713.
96. E. Kurras, U. Rosenthal, M. Mennenga, G. Oehme and G. Engelhardt, *Z. Chem*. **1974**, *14*, 160.
97. E. Kurras and J. Otto, *J. Organomet. Chem*. **1965**, *4*, 114.
98. J. Krausse, G. Marx and G. Schödl, *J. Organomet. Chem*. **1970**, *21*, 159.
99. J. Krausse and G. Schödl, *J. Organomet. Chem*. **1971**, *27*, 59.
100. S. Hao, S. Gambarotta and C. Bensimon, *J. Am. Chem. Soc*. **1992**, *114*, 3556.

Pictiva EX2004
Samsung v Pictiva
IPR2024-01094

101. T. Aoki, A. Furusaki, Y. Tomiie, K. Ono and K. Tanaka, *Bull. Chem. Soc. Jpn*. **1969**, *42*, 545.
102. G. Albrecht and D. Stock, *Z. Chem*. *1967*, 7, 321.
103. S. I. Beilin, S. B. Golstein, B. A. Dolgoplosk, L. Sh. Guzman and E. I. Tinyakova, *J. Organomet. Chem*. **1977**, *142*, 145.
104. D. J. Brauer and C. Krüger, *Inorg. Chem*. **1976**, *15*, 2511.
105. H. Breil and G. Wilke, *Angew. Chem*. **1966**, *78*, 942.
106. P. L. Timms and T. W. Turney, *J. Chem. Soc., Dalton Trans*. **1976**, 2021.
107. F. A. Cotton and G. N. Mott, *Organometallics* **1982**, *1*, 302.
108. R. A. Andersen, R. A. Jones, G. Wilkinson, M. B. Hursthouse and K. M. Abdul, *J. Chem. Soc., Chem. Commun*. **1977**, 283.
109. F. A. Cotton, J. Czuchajowska and X. Feng, *Inorg. Chem*. **1990**, *29*, 4329.
110. J. J. H. Edema, S. Gambarotta, P. van der Sluis, W. J. J. Smeets and A. L. Spek, *Inorg. Chem*. **1989**, *28*, 3782.
111. F. A. Cotton, R. L. Luck and K.-A. Son, *Inorg. Chim. Acta* **1990**, *168*, 3.
112. F. A. Cotton, L. M. Daniels, C. A. Murillo and H.-C. Zhou, *Inorg. Chim. Acta* **2000**, *300-302*, 319.
113. J. J. H. Edema, S. Gambarotta, A. Meetsma, F. van Bolhuis, A. L. Spek and W. J. J. Smeets, *Inorg. Chem*. **1990**, *29*, 2147.
114. F. A. Cotton, C. A. Murillo and H.-C. Zhou, *Inorg. Chem*. **2000**, *39*, 3728.
115. F. A. Cotton and W. Wang, *Polyhedron* **1985**, *4*, 1735
116. (a) F. A. Cotton, G. E. Lewis, C. A. Murillo, W. Schwotzer and G. Valle, *Inorg. Chem*. **1984**, *23*, 4038; (b) N. M. Alfaro, F. A. Cotton, L. M. Daniels and C. A. Murillo, *Inorg. Chem*. **1992**, *31*, 2718.
117. F. A. Cotton, L. M. Daniels, P. Lei, C. A. Murillo and X. Wang, *Inorg. Chem*. **2001**, *40*, 2778.
118. K. Andersson, C. W. Bauschlicher, Jr., B. J. Persson and B. O. Roos, *Chem. Phys. Lett*. **1996**, *257*, 238.
119. D. L. Lichtenberger, M. A. Lynn and M. H. Chisholm, *J. Am. Chem. Soc*. **1999**, *121*, 12167.

Pictiva EX2004
Samsung v Pictiva
IPR2024-01094

4

Molybdenum Compounds

F. Albert Cotton,
Texas A&M University

4.1 Dimolybdenum Bridged by Carboxylates or Other O,O Ligands

4.1.1 General remarks

There are more M_2^{n+} compounds with multiply-bonded M_2^{n+} units having M = Mo than any other metal (although Rh_2^{4+} compounds (Chapter 12), in which there is a *single* bond, are more numerous). The total number of Mo_2^{n+} compounds, is over 1100, of which about 550 have been crystallographically characterized.

The somewhat muddled early preparative work on $Mo_2(O_2CR)_4$ compounds has been reviewed in Chapter 1. Productive development of the field followed closely on the structural characterization of $Mo_2(O_2CCH_3)_4$.[1] This structure as later redetermined more precisely,[2] is shown in Fig. 4.1; the Mo–Mo distance is 2.093(1) Å, a typical value for Mo–Mo quadruple bonds.

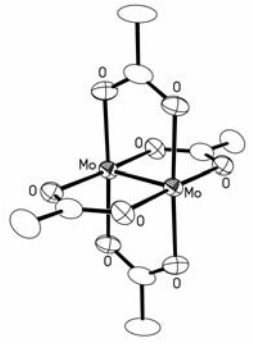


Fig. 4.1. The structure of $Mo_2(O_2CCH_3)_4$ as first accurately reported.

The conversion of $Mo_2(O_2CCH_3)_4$ to $Mo_2Cl_8^{4-}$, and the definitive structural characterization of this anion, Fig. 4.2, were reported in 1969.[3] The observation that the $Mo_2Cl_8^{4-}$ anion is stereoelectronically analogous to $Re_2Cl_8^{2-}$ was a critical breakthrough in the evolution of Mo_2^{4+} chemistry.

Pictiva EX2004
Samsung v Pictiva
IPR2024-01094

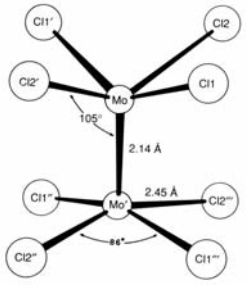


Fig. 4.2. The structure of the $Mo_2Cl_8^{4-}$ ion in $K_4Mo_2Cl_8{\cdot}H_2O$, exactly as first reported in 1969.

4.1.2 $Mo_2(O_2CR)_4$ compounds

Preparation of $Mo_2(O_2CR)_4$ compounds.

Synthesis of the carboxylates from a mononuclear starting material, molybdenum hexacarbonyl, was first described by Wilkinson and co-workers. The procedure used by Wilkinson,[4-6] namely, heating $Mo(CO)_6$ with the carboxylic acid (and the anhydride if available) either alone or in diglyme, still remains a good general method for preparing these complexes[7-10] although modifications of this procedure have sometimes been used. Such modifications include the use of solvents other than diglyme (for example, decalin, 1,2-dichlorobenzene, and toluene),[8,11] a different carbonyl precursor (for example, $Mo(CO)_4[(CH_3)_2NCH_2CH_2N(CH_3)_2]$),[11] and carboxylate exchange reactions utilizing the acetate $Mo_2(O_2CCH_3)_4$ as the starting material.[8,12-19] While other methods have been reported for the synthesis of the carboxylates, these usually involve starting materials that are themselves first prepared from $Mo_2(O_2CCH_3)_4$ (e.g. salts of the $[Mo_2Cl_8]^{4-}$ anion). However, one unusual exception is the preparation of the formate $Mo_2(O_2CH)_4$ from $[Mo(\eta^6\text{-}C_6H_5Me)(\eta^3\text{-}C_3H_5)Cl]_2$.[20] Other examples are the reaction of $MoCl_3(THF)_3$ with Zn and acetic acid to give $Mo_2(O_2CCH_3)_4$,[21] and the reduction of $MoCl_3$ by Na/Hg in the presence of NaO_2CCF_3 to produce very pure $Mo_2(O_2CCF_3)_4$.[22] As far as the range of carboxylate ligands that have been used to form neutral complexes of the type $Mo_2(O_2CR)_4$ is concerned, these have included formic acid,[13] several alkyl,[3,19a] halo-alkyl,[3,8,12] and aryl monocarboxylic acids,[3,9] as well as dicarboxylic acids[14] and mixed mono- and di-carboxylates.[19b,c] Another interesting and important group of complexes are those in which chiral ligands are used, e.g., mandelic acid.[23] Deuterated derivatives can also be prepared, for example $Mo_2(O_2CCD_3)_4$, a compound whose vibrational spectral properties have been of interest.[24]

While the formation of $Mo_2(O_2CCH_3)_4$ from $Mo(CO)_6$ is the single most important synthesis of a dimolybdenum(II) carboxylate, this reaction proceeds in low yield (15-20%) when pure acetic acid or a mixture of the acid and its anhydride is used.[10] Superior yields (80%) are obtained only when a solvent such as diglyme or 1,2-dichlorobenzene (mixed with a small amount of hexane) is used. The fate of the remaining molybdenum has been established in a variety of subsequent studies.[25] It is converted to one or more higher oxidation state trinuclear species of the type $[Mo_3X_2(O_2CCH_3)_6(H_2O)_3]^{n+}$ where the Mo_3X_2 unit is a trigonal bipyramid in which the axial or capping units, X, are either O or CCH_3, or one of each. There are Mo–Mo single bonds in these clusters.

In addition to $Mo_2(O_2CCH_3)_4$, the structure of which is shown in Fig. 4.1, a number of other structures of $Mo_2(O_2CR)_4$ compounds have been reported. All of these are listed in Table 4.1. The structure of the acetate is prototypical for most of them; in this type of structure there

Pictiva EX2004
Samsung v Pictiva
IPR2024-01094

are no exogenous axial ligands and the $Mo_2(O_2CR)_4$ molecules are strung together in infinite chains, very similar to the chains found in $Cr_2(O_2CCH_3)_4$, shown in Fig. 3.1b. In all these cases, the Mo–Mo quadruple bond lengths are about the same, *c.* 2.10 Å. The intermolecular Mo···O links are quite long (2.60-2.90 Å) compared to the intramolecular Mo–O bonds (*c.* 2.10 Å).

Table 4.1. Structures of $Mo_2(O_2CR)_4$ compounds

Compound	Crystal Sym.	Virtual Sym.	Mo–Mo	Twist[a]	ref.
$Mo_2(O_2CH)_4$	1	D_{4h}	2.091(2)	1.0	13
$Mo_2(O_2CH)_4$	1	D_{4h}	2.093(1)	0	35
	1	D_{4h}	2.092(1)	≈0	35
$Mo_2(O_2CH)_4$	1	D_{4h}	2.091(1)	0	35
$Mo_2(O_2CH)_4$	1	D_{4h}	2.091(1)	0	28
$Mo_2(O_2CH)_4(H_2O)_2$	1	D_{4h}	2.100(1)	0	28
$Mo_2(O_2CH)_4$·KCl	1	D_{4h}	2.109(2)	0	35
	1	D_{4h}	2.102(2)	0	35
$Mo_2(O_2CCH_3)_4$	1	D_{4h}	2.093(1)	0	2
$Mo_2(O_2CCH_3)_4$·NaO_2CCH_3·HO_2CCH_3	1	D_{4h}	2.093(1)	0	33
$Mo_2(O_2CCH_3)_4$(μ-dmpe)	1	D_{4h}	2.105(3)	0	49
$Mo_2(O_2CCH_3)_4$(μ-tmed)	1	D_{4h}	2.103(1)	0	49
$[Mo_2(O_2CCH_3)_4$(N,N'-dmed)$]_\infty$ dmed = $Me(H)NCH_2CH_2N(H)Me$	$\bar{1}$	C_{2v}	2.124(2)	NR	50
$[Mo_2(O_2CCH_3)_4$(N,N'-pda)$]_\infty$ pda = $H_2NCH_2CH_2CH_2NH_2$	1	C_{2v}	2.130(2)	NR	50
$Mo_2(O_2CCH_3)_4$(μ-4,4'-bipyridine)·THF	1	C_{2h}	2.103(1)	0	51
		C_{2h}	2.104(1)	0	51
$Mo_2(O_2CCH_3)_4(4,4'$-bipyr$)]_n$·*n*THF	$\bar{1}$	D_{4h}	2.104(1)	zero	52
$(pyH)_2[Mo_2(O_2CCH_3)_4)Br_2]$	4/*m*	D_{4h}	2.101(1)	0	53
$(pyH)_2[Mo_2(O_2CCH_3)_4)I_2]$	1	D_{4h}	2.103(1)	0	53
	1	D_{4h}	2.103(1)	0	53
$(pyH)_2[Mo_2(O_2CCH_3)_4)I_2]$	4/*mmm*	D_{4h}	2.102(1)	0	53
$(PipH)_2[Mo_2(O_2CCH_3)_4I_2]$	$\bar{1}$	D_{4h}	2.100(3)	zero	54
$Mo_2(O_2CCF_3)_4$	1	D_{4h}	2.090(4)	0	12
$Mo_2(O_2CCF_3)_4(py)_2$	1	D_{4h}	2.129(2)	0	29
$Mo_2(\eta^1$-$O_2CCF_3)_4(bpy)_2$	1	C_{2h}	2.129(1)[b]	0	55
$Mo_2(O_2CCF_3)_4(PBu^n_3)_2$	1	C_{2h}	2.105(1)	0	22
$Mo_2(O_2CCF_3)_4(PEt_2Ph)_2$	1	C_{2h}	2.100(1)	0	56
$Mo_2(O_2CCF_3)_4(PMePh_2)_2$	1	D_{4h}	2.128(1)	≈0	57
$Mo_2(O_2CCF_3)_4(PMePh_2)_2$	1	C_{2h}	2.107(2)	0	56
$(Bu_4N)_2[Mo_2(O_2CCF_3)_4Br_2]$	1	D_{4h}	2.134(2)	0	58
$(Bu_4N)_2[Mo_2(O_2CCF_3)_4I_2]$	1	D_{4h}	2.140(2)	0	
	1	D_{4h}	2.136(2)	0	
$[Mo_2(O_2CCF_3)_4$(DM-DCNQI)·$C_6H_6]_n$	$\bar{1}$	D_{4h}	2.127(2)	zero	59
$[Mo_2(O_2CCF_3)_4(TCNQ)_{0.5}$·*m*-xylene$]_2$·$[Mo_2(O_2CCF_3)_4$·*m*-xylene$]$	$\bar{1}$ (chain)	D_{4h}	2.113(1)	NR	60
	$\bar{1}$ (molec.)	D_{4h}	2.113(1)	zero	
$Mo_2(O_2CCF_3)_4$·9,10-anthraquinone$]_n$	$\bar{1}$	D_{4h}	2.107(1)	NR	61
$[Mo_2(O_2CCF_3)_4$·bpy$]_n[Mo_2(O_2CCF_3)_4]$·$(bpy)_2$	Dimer: $\bar{1}$	D_{4h}	2.124(1)	zero	62
	Chain: 1	D_{4h}	2.128(1)	NR	

Pictiva EX2004
Samsung v Pictiva
IPR2024-01094

Compound	Crystal Sym.	Virtual Sym.	Mo–Mo	Twist[a]	ref.
$Mo_2(O_2CCF_3)_4(FPA)_2$ FPA = (ferrocenyl)(4-pyridyl)ethyne	$\bar{1}$	D_{4h}	2.142(1)	zero	63
$Mo_2(O_2CCF_3)_4(\eta^1\text{-}HO_2CCF_3)_3\cdot 2Hdpa$	$\bar{1}$	D_{4h}	2.131(1)	zero	64
$[Mo_2(O_2CCF_3)_4(1,4\text{-nq})]_n\cdot nC_6H_6$ nq = naphthoquinone	$\bar{1}$	D_{4h}	2.117(1)	zero	65
$Mo_2(O_2CCF_3)_4$-bis(2,6-di-*t*-butyl-*p*-benzoquinone)	$\bar{1}$	D_{4h}	2.114(1)	zero	66
$\alpha\text{-}Mo_2(O_2CCMe_3)_4$	1	D_{4h}	2.088(1)	≈0	37
$\beta\text{-}Mo_2(O_2CCMe_3)_4$	1	D_{4h}	2.087(1)	0	38
$\gamma\text{-}Mo_2(O_2CCMe_3)_4$	1	D_{4h}	2.087(1)	0	38
$[Mo_2(O_2CCMe_3)_4\cdot bpy]_n$	$\bar{1}$	D_{4h}	2.092(1) 2.099(1)	zero	67
$Mo_2(O_2CC_6H_5)_4$	1	D_{4h}	2.096(1)	0	37
$Mo_2(O_2C\text{adamantyl})_4\cdot 2THF$	$\bar{1}$	D_{4h}	2.087(1)	zero	68
	$\bar{1}$	D_{4h}	2.087(1)	zero	
$Mo_2(O_2CC_6H_5)_4(diglyme)_2$	1	D_{4h}	2.100(1)	0	69
$Mo_2(O_2CC_6H_4\text{-}2\text{-}Ph)_4$	1	D_{4h}	2.082(1)	0	15
$(Ph_4P)_2[Mo_2(O_2CC_6H_5)_4Cl_2]\cdot 2CH_2Cl_2$	1	D_{4h}	2.128(1)	0	70
$(Ph_4P)_2[Mo_2(O_2CC_6H_5)_4Br_2]\cdot 2CH_2Br_2$	1	D_{4h}	2.123(1)	0	71
$Mo_2(\mu\text{-}O_2CC_6H_3(NH_3)_2)_4Cl_8\cdot 16H_2O$	$\bar{1}$	D_{4h}	2.107(1)	zero	72
$Mo_2(O_2CC_6H_4\text{-}3\text{-}NO_2)_4(py)_2\cdot 2py$	$\bar{1}$	D_{4h}	2.125(1) 2.123(1)	zero	50
$Mo_2(O_2CC_6H_4Ph)_4$	1	D_{4h}	2.096(1)	NR	73
$Mo_2(O_2CC_6H_4Ph)_4py_2$	$\bar{1}$	D_{4h}	2.111(1)	zero	73
$Mo_2(\mu\text{-}O_2CC_6H_4\text{-}2\text{-}PPh_2)_4(MeOH)_2$	$\bar{1}$	D_{4h}	2.112(1)	zero	74
$[Mo_2(\mu\text{-}O_2CC_6H_4\text{-}4\text{-}P(O)Ph_2)_4\cdot 4EtOH]_n$	$\bar{1}$	D_{4h}	2.125(2)	zero	74
$Mo_2(O_2C\text{-}o\text{-}C_6H_4Cl)_4\cdot 4THF$	$\bar{1}$	D_{4h}	2.103(1)	zero	75
$Mo_2(O_2C\text{-}o\text{-}C_6H_4Br)_4\cdot 2THF$	$\bar{1}$	D_{4h}	2.101(1)	zero	75
$Mo_2(O_2C\text{-}o\text{-}C_6H_4I)_4\cdot 2THF$	$\bar{1}$	D_{4h}	2.106(1)	zero	75
$Mo_2(O_2C\text{-}o\text{-}C_6H_4NO_2)_4$	$\bar{1}$	D_{4h}	2.094(1) 2.096(1)	zero	75
$Mo_2(TiPB)_4$ TiPB = 2,4,6-triisopropylbenzoate	$\bar{1}$	D_{4h}	2.076(1)	zero	27
$Mo_2(salicylate)_4\cdot 1,2\text{-}C_6H_4Cl_6$	1	C_{2h}	2.092(1)	0	76
	1	C_{2h}	2.094(1)	≈0	76
$Mo_2(salicylate)_4(diglyme)_2$	1	C_{2h}	2.101(1)	0	76
$Mo_2(D\text{-mandelate})_4\cdot 2THF$	1	C_4	2.104(1)	≈0	23
	1	C_4	2.101(1)	≈0	
$Mo_2(O_2CC_4H_3S)_4(THF)_2$	1	C_{2h}	2.102(1)	0	77
$Mo_2(FCA)_4(NCCH_3)(DMSO)\cdot 2DMSO$	1	D_{4h}	2.105(1)	0	16
$Mo_2(O_2CCH_3)_2(FCA)_2(py)_2$	1	C_{2h}	2.107(2)	0	16
$Mo_2(O_2CPBu^t_2)_4\cdot 2C_6H_6$	1	D_{4h}	2.092(3)	0	78,79
$[Mo_2(O_2CCH_2NH_3)_4](SO_4)_2\cdot 4H_2O$	4	D_{4h}	2.115(1)	0	80
$[Mo_2(O_2CCH_2NH_3)_4]Cl_4\cdot 3H_2O$	1	D_{4h}	2.112(1)	0	81
$[Mo_2(O_2CCH_2NH_3)_4]Cl_4\cdot 2^2/_3H_2O$	1	D_{4h}	2.103(1)	0	81
	1	D_{4h}	2.107(1)	0	
	1	D_{4h}	2.110(1)	0	

Pictiva EX2004
Samsung v Pictiva
IPR2024-01094

Compound	Crystal Sym.	Virtual Sym.	Mo–Mo	Twist[a]	ref.
$[Mo_2(glygly)_4]Cl_4{\cdot}6H_2O$	1	D_{2h}	2.106(1)	0	82
$[Mo_2(L\text{-leu})_4]Cl_2(PTS)_2{\cdot}2H_2O$	1	C_{4h}	2.108(1)	≈0	83
	1	C_{4h}	2.111(1)	≈0	
$[Mo_2(D\text{-phe})_2(L\text{-phe})_2I_2]I_2{\cdot}6H_2O$	1	D_{4h}	2.114(1)	0	84
$[Mo_2(D\text{-tyr})_2(L\text{-tyr})_2I_2]I_2{\cdot}6H_2O$	1	D_{4h}	2.116(1)	0	84
$[Mo_2(D\text{-phgly})_2(L\text{-phgly})_2](PTS)_4{\cdot}4H_2O$	1	D_{4h}	2.113(1)	0	84
$[Mo_2(D\text{-val})_2(L\text{-val})_2](ZnCl_4)_2{\cdot}4H_2O$	1	D_{4h}	2.104(1)	0	85
$[Mo_2(D\text{-leu})_2(L\text{-leu})_2]\text{-}Cl_2(PTS)_2{\cdot}2H_2O$	1	D_{4h}	2.114(1)	0	85
$[Mo_2(O_2CC_5H_4NH)_4Cl_2]Cl_2{\cdot}6H_2O$	1	D_{4h}	2.122(1)	0	77
$Mo_2(O_2CNEt_2)_4$	$\bar{1}$	D_{4h}	2.067(2)	zero	86
$Mo_2(glycolate)_4{\cdot}2H_2O$	$\bar{1}$	D_{4h}	2.103(1)	zero	87
$Mo_2(O_2CCPh_3)_4{\cdot}3CH_2Cl_2$	$\bar{4}$	D_{4h}	2.076(1)	zero	26
$Mo_2(R\text{-ibp})_2(S\text{-ibp})_2$ ibp = ibuprofen	$\bar{1}$	D_{4h}	2.085(2)	zero	88
$Mo_2(OSCPh)_4(OPPh_3)_2$	$\bar{1}$	C_{2h}	2.153(1)	zero	89
$Mo_2[O_2CC_6H_3(OH)_2]_4{\cdot}KCl$	2	D_{4h}	2.106(4)	≈0	90

[a] Zero means rigorously 0; 0 means reported to be ≈0; ≈0 means not reported but apparently ≈0; NR means not reported and uncertain.

[b] The distance given in ref. 55 is in error.

There are two small groups of dimolybdenum tetracarboxylates that differ structurally from the $Mo_2(O_2CCH_3)_4$ model. In one group large R groups interfere with the intermolecular interactions required to form chains. This group includes $Mo_2(O_2CCPh_3)_4$,[26] $Mo_2(O_2CC_6H_4\text{-}2\text{-}Ph)_4$,[15] and $Mo_2[O_2C(2,4,6\text{-}Pr^iC_6H_2)]_4$.[27] The other cases where chain formation does not occur are those in which exogenous axial ligands are present, such as $Mo_2(O_2CH)_4(H_2O)_2$[28] and $Mo_2(O_2CCF_3)_4(py)_2$[29] and others listed in Table 4.1. In many cases, the exogenous ligands are bidentate and link the $Mo_2(O_2CR)_4$ groups into infinite chains, some linear and others zigzag. In all cases, the axial Mo···L distances are very long and it must be concluded that axial bonding to the $Mo_2(O_2CR)_4$ molecules is always weak. This is in contrast to the strong axial bonding to $Cr_2(O_2CR)_4$ compounds.

The crystals of $Mo_2(OCCPh_3)_4{\cdot}3CH_2Cl_2$[26] have the $Mo_2(O_2CCPh_3)_4$ molecules perfectly aligned parallel to one crystallographic axis and this compound allowed the use of the polarized single-crystal visible spectrum to show definitively the location of the $\delta \rightarrow \delta^*$ absorption band.[30]

The minimal influence of axial coordination on the Mo–Mo bond length is best shown by comparison of the gas phase structures of $Mo_2(O_2CCH_3)_4$[31] and $Mo_2(O_2CCF_3)_4$,[32] determined by electron diffraction, with the structures of the crystalline solids. For the acetate the distance in the isolated, gas-phase molecule, 2.079(3) Å, is *c.* 0.01 Å shorter than that in the crystal, 2.093(1) Å. For the trifluoroacetate, the gas and solid values are 2.105(9) Å and 2.090(4) Å. In neither case is the difference significant. The series of complexes $Mo_2[O_2C(CH_2)_nCH_3]_4$, where n = 3-9, exhibit a liquid crystalline phase between their crystalline and isotropic liquid phases.[19a] This liquid crystalline behavior, the first for materials incorporating M–M multiple bonds, reflects the breakdown of intermolecular Mo···O bonding.

For the structurally characterized $Mo_2(O_2CR)_4$ compounds listed in Table 4.1, a few other observations may be made. The structural characterization of the double salt $\{Mo_2(O_2CCH_3)_4{\cdot}NaO_2CCH_3{\cdot}HO_2CCH_3\}$ shows the presence of the usual binuclear

Pictiva EX2004
Samsung v Pictiva
IPR2024-01094

$Mo_2(O_2CCH_3)_4$ unit together with pairs of hydrogen-bonded acetate/acetic acid units.[33] In another structural study of $Mo_2(O_2CCH_3)_4$, the electron-density distribution in crystals of the acetate was determined by single-crystal X-ray diffractometry at 293K.[34] The form of the deformation-density map was accounted for in terms of the usual representation of a quadruple Mo–Mo bond. In the case of $Mo_2(O_2CH)_4$, structure determinations have been carried out on three different anhydrous forms, one orthorhombic (subsequently designated α)[13,35] and two monoclinic (β and γ),[35] as well as on the complex $Mo_2(O_2CH)_4 \cdot KCl$ in which the usual $Mo_2(O_2CH)_4$ molecules are linked in zig-zag chains by weak chloride bridges (Mo···Cl *c.* 2.86 Å) in such a way that two independent $Mo_2(O_2CH)_4$ units are present.[35] The $Mo_2(O_2CH)_4$ molecule is also present in the 'monohydrate' $Mo_2(O_2CH)_4 \cdot H_2O$, which actually contains $Mo_2(O_2CH)_4$ and $Mo_2(O_2CH)_4(H_2O)_2$ units with Mo–Mo distances of 2.091(1) and 2.100(1) Å, respectively. In a subsequent study of the Raman and infrared spectra of $Mo_2(O_2CH)_4$ and '$Mo_2(O_2CH)_4 \cdot H_2O$', the investigators neglected to treat the hydrate as a mixture of the anhydrous and dihydrated forms.[36] The pivalate complex $Mo_2(O_2CCMe_3)_4$ has also been structurally characterized in three different polymorphic forms.[37,38]

In $Mo_2(O_2CR)_4$ compounds generally, the carboxyl groups are kinetically labile. Apart from occasional random observations, and the well-known fact, to be discussed in detail later, that many $Mo_2(O_2CR)_4$ compounds can be prepared from the tetra-acetate by the reaction,

$$Mo_2(O_2CMe)_4 + \text{excess } RCO_2H \rightarrow Mo_2(O_2CR)_4$$

there have been three detailed studies of the exchange process. One[39] dealt with the system with $Mo_2(O_2CH)_4/Mo_2(O_2CCF_3)_4$ and all four intermediates in acetone solution. At equilibrium the six species are statistically distributed, within experimental error, as shown in Fig. 4.3. It is notable that the cisoid and transoid isomers of $Mo_2(O_2CH)_2(O_2CCF_3)_2$ are present in the statistical ratio of 2:1, indicating no detectable trans influence, nor any preference for the polar cisoid isomer in the somewhat polar solvent. The rates of attainment of equilibrium at several temperatures were also measured, but not quantitatively interpreted. Equilibrium was reached in *c.* 30 min, beginning with a mixture of the two end members $Mo_2(O_2CH)_4$ and $Mo_2(O_2CCF_3)_4$.

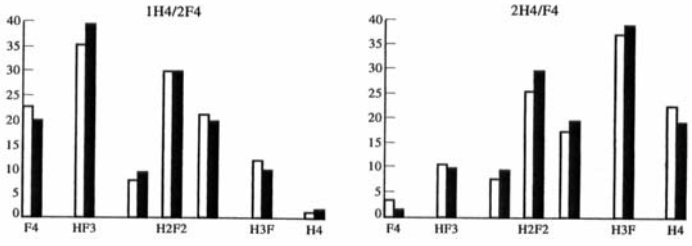


Fig. 4.3. The observed (open bars) and statistical (filled bars) percentages of the five kinds of $(CF_3CO_2)_v(HCO_2)_{4-v}$ molecules in 2:1 and 1:2 mixed solutions. The "observed" values for $v = 4$ (F4) are not literally observed but calculated from the other observed values. In each case the bars for the total H_2F_2 are flanked by those for the *cis* and *trans* isomers.

The lability of the $Mo_2(O_2CBu^t)_4/Mo_2(O_2CCF_3)_4$ system has also been demonstrated,[40] and again the exchange processes occur rapidly (*c.* 1 h) at ambient temperature. In this report some suggestions were made as to the mechanism of the exchange reactions.

A kinetic study was made of the reaction between $Mo_2(O_2CCF_3)_4$ and NaO_2CCF_3 in acetonitrile.[41] This reaction was monitored by ^{19}F NMR spectroscopy and, not surprisingly, the

Pictiva EX2004
Samsung v Pictiva
IPR2024-01094

data point to the existence of the adduct $[Mo_2(O_2CCF_3)_4O_2CCF_3]^-$ in solution. The following mechanism was proposed:[41]

$$[Mo_2(O_2CCF_3)_4O_2CCF_3]^- + \overset{*}{C}F_3CO_2^- \xrightarrow{\text{fast}} [Mo_2(O_2CCF_3)_4O_2C\overset{*}{C}F_3]^- + CF_3CO_2^-$$

$$[Mo_2(O_2CCF_3)_4O_2C\overset{*}{C}F_3]^- \xrightarrow{k_s} [Mo_2(O_2CCF_3)_3(O_2C\overset{*}{C}F_3)O_2CCF_3]^-$$

The only well-defined example of a $Mo_2(O_2CR)_4$ compound with chiral carboxylates is Mo_2(D(-)mandelate)$_4$ (mandelic acid = PhCH(OH)CO_2H), which was prepared by the reaction of an aqueous solution of Mo_2^{4+} (generated by admixing $K_4Mo_2(SO_4)_4$, $Ba(CF_3SO_3)_2$ and CF_3SO_3H in water) with D-mandelic acid.[23] Other starting materials, specifically $K_4Mo_2Cl_8$ and $(NH_4)_5Mo_2Cl_9{\cdot}H_2O$, have been used to prepare this isomer as well as the analogous derivatives with racemic and L-mandelic acid,[42,43] and comparative studies have been made of the infrared[42,43] and electronic absorption and CD spectra of these isomers.[43,44] This work is of particular relevance to the discovery that various chiral ligands (e.g., carboxylic acids, glycols, amino alcohols, substituted thiophosphinic acids, and esters of thiophosphonic acid) coordinate to $Mo_2(O_2CCH_3)_4$ and that the signs of the observed CD and ORD effects of the complexes can be used to determine the absolute configurations of the ligands.[45-48] While the structures of the species have not been determined, partial displacement of the acetate probably occurs in many cases.

Even when crystallographic data are not available for some molybdenum(II) carboxylates, such as the chloroacetate derivatives[8] and certain insoluble bis(dicarboxylato) complexes,[14] the similarity of the electronic absorption spectra and/or Raman-active ν(Mo–Mo) modes (at *c.* 400 cm^{-1}) of these complexes to those of authentic quadruply-bonded complexes such as $Mo_2(O_2CCH_3)_4$,[23,30,91,92] supports the belief that they all contain the $Mo_2(O_2CR)_4$ moiety. Since a detailed consideration of the spectroscopic properties (especially electronic absorption, Raman and PES) and electronic structures of the dimolybdenum carboxylates is provided in Chapter 16, only a few of their other properties will be mentioned here. The volatility of $Mo_2(O_2CCH_3)_4$ and $Mo_2(O_2CCF_3)_4$ and the proof, via electron diffraction studies, that the dinuclear structure is retained in the vapor-phase accords with the observation that an abundant molecular ion peak $[Mo_2(O_2CR)_4]^+$ is seen in the mass spectra of the formate, acetate, difluoroacetate, trifluoroacetate and propionate.[9,12,13,93] This property has also proved to be useful in identifying individual components in mixtures of complexes of the type $Mo_2(O_2CC_6H_5)_n(O_2CCH_2OCH_3)_{4-n}$.[17] The volatility of such compounds has permitted the measurement of the X-ray photoelectron spectra (XPS) and/or valence-shell photoelectron spectra (PES) of the formate, acetate, pivalate and trifluoroacetate,[13,20,94,95] studies that are extremely important to an understanding of their electronic structures. The ^{95}Mo NMR spectra of a series of $Mo_2(O_2CR)_4$ compounds (R = CH_3, $CHCl_2$, CF_3, Pr^n, Pr^i, Bu^n and Bu^t) have been recorded.[96] These resonances were detected in the range 3656-4148 ppm, making them one of the most deshielded classes of molybdenum compounds so far discovered.

Two unusual $Mo_2(O_2CR)_4$ species are the compounds $Mo_2(O_2CNMe_2)_4$[97] and $Mo_2(O_2CPBu^t_2)_4$.[78,79] The former complex is prepared through the insertion of CO_2 into the Mo–NMe_2 bonds of triply bonded complexes of the type 1,2-$Mo_2(NMe_2)_4R_2$, followed by the reductive elimination of alkene and alkane:[97]

$$Mo_2(NMe_2)_4R_2 + CO_2 \text{ (excess)} \rightarrow Mo_2(O_2CNMe_2)_4 + \text{alkane} + \text{alkene} \quad (R = Et, Pr^i, Bu)$$

In a related study of the reaction of CO_2 with 1,2-$Mo_2(NMe_2)_4(PBu^t_2)_2$ the dimolybdenum(III) complex $Mo_2(O_2CNMe_2)_2(O_2CPBu^t_2)_2(NMe_2)_2$ was isolated; this converts in solution to

Pictiva EX2004
Samsung v Pictiva
IPR2024-01094

the quadruply-bonded complex $Mo_2(O_2CPBu^t_2)_4$, which has been characterized by X-ray crystallography.[78,79]

Another interesting group comprises several cationic dimolybdenum(II) species that contain amino acid ligands. The yellow glycine complex $[Mo_2(O_2CCH_2NH_3)_4]Cl_4 \cdot nH_2O$ was the first to be prepared[80] in powder form from the reaction of glycine with $K_4Mo_2Cl_8$ in hydrochloric acid. The crystalline sulfate analog $[Mo_2(O_2CCH_2NH_3)_4](SO_4)_2 \cdot 4H_2O$ is readily produced by anion exchange and a structure determination[80] revealed the usual tetracarboxylato-bridged dimolybdenum unit. Because of the particular orientation of the $-CH_2NH_3$ groups, this cation is of S_4 symmetry (Fig. 4.4). There are very long and weak axial interactions between each molybdenum atom and two oxygen atoms from a sulfate group.



Fig. 4.4. The core structure of the $[Mo_2(O_2CCH_2NH_3)_4]^{4+}$ units in $[Mo_2(O_2CCH_2NH_3)_4](SO_4)_2 \cdot 4H_2O$.

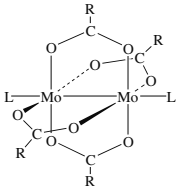
Later work[81] succeeded in obtaining the chloride salt in crystalline form by two methods. In the first of these, the original procedure[80] was utilized but modified by using more dilute reaction solutions and employing slow mixing of an aqueous solution containing $K_4Mo_2Cl_8$ and glycine with a 2 M solution of hydrochloric acid. This gave the trihydrate $[Mo_2(O_2CCH_2NH_3)_4]Cl_4 \cdot 3H_2O$ which had the expected structure with a Mo–Mo distance of 2.112(1) Å and very weak axial coordination (r(Mo···Cl) = 2.882(1) Å).[81] An alternative and less direct method was found to give a different hydrate $[Mo_2(O_2CCH_2NH_3)_4]Cl_4 \cdot 2^2/_3H_2O$.[81] When $Cs_3Mo_2Cl_8H$ is reacted with a 1 M aqueous solution of glycine a violet species is generated which may be absorbed on a cation-exchange column.[98] If the violet species is eluted with 1 M hydrochloric acid and the eluant is then stored at 0 °C under nitrogen, reduction to yellow crystalline $[Mo_2(O_2CCH_2NH_3)_4]Cl_4 \cdot 2^2/_3H_2O$ takes place. The structure of this hydrate has three crystallographically independent molecules, each residing on a crystallographic center of inversion (Table 4.1).

Since the initial work on these glycinate complexes, a variety of related systems have been prepared and structurally characterized. The first of these were the salts $[Mo_2(glygly)_4]Cl_4 \cdot 6H_2O$ (glygly = glycylglycine)[82] and $[Mo_2(L\text{-leu})_4]Cl_2(PTS)_2 \cdot 2H_2O$ (leu = leucine; PTS = *p*-toluenesulfonate),[83] which were prepared by reaction of $K_4Mo_2Cl_8$ with the appropriate amino acid in dilute hydrochloric acid. In both crystals, very long and weak axial Mo···Cl interactions are present. The use of this same synthetic procedure but with the *racemic* amino acid in place of the chiral *D* or *L* form has enabled Bino[84,85] to prepare several complexes of the $[Mo_2(D\text{-amino acid})_2(L\text{-amino acid})_2]^{4+}$ type (amino acid = phenylalanine,[84] tyrosine,[84] *C*-phenylglycine,[84] leucine,[85] and valine[85]). These are listed in Table 4.1. In all instances, the four bridging amino acids ligands are coordinated to the Mo_2^{4+} unit in the cyclic order DDLL. In three of these structures, viz. $[Mo_2(D\text{-leu})_2(L\text{-leu})_2]Cl_2(PTS)_2 \cdot 2H_2O$,[85] $[Mo_2(D\text{-phe})_2(L\text{-phe})_2]I_4$[84] and

Pictiva EX2004
Samsung v Pictiva
IPR2024-01094

$[Mo_2(D\text{-tyr})_2(L\text{-tyr})_2]I_4{\cdot}6H_2O$,[84] there are long weak Mo···halide axial interactions. While anhydrous complexes of stoichiometry $Mo_2(\beta\text{-alanine})_4$ and $Mo_2(glycine)_4$ are said to be formed from the reactions of these acids with $Mo_2Cl_4(PEt_3)_4$,[99] the structures of these materials have not been determined. Nicotinic acid (pyridine-3-carboxylic acid) reacts with $(pyH)_3Mo_2Cl_8H$ in oxygen-free hydrochloric acid to form the complex $[Mo_2(\mu\text{-}O_2CC_5H_4NH)_4]Cl_2{\cdot}6H_2O$.[77]

$Mo_2(O_2CR)_4$ compounds are capable of forming diadducts as first noted by Wilkinson,[6] although he did not know the structures of either the adducts or their parent compounds. In general these adducts have structures of type **4.1**. The ones Wilkinson made were the dipyridine adducts of the acetate and the benzoate. These two compounds readily lose the bound pyridine, and it was not until several years later that the first adduct was structurally characterized. Following the synthesis and structure determination of the trifluoroacetate $Mo_2(O_2CCF_3)_4$,[12] its pyridine adduct was obtained upon dissolution in pyridine. The complex appears to be stable indefinitely when stored under nitrogen or argon at −20 °C. While the Mo–N distances (2.548(8) Å) are quite long, this interaction is sufficient to lead to a lengthening of the Mo–Mo bond by 0.039(6) Å relative to that in the parent $Mo_2(O_2CCF_3)_4$.[12] In comparison to other dimolybdenum(II) complexes, the effect of axial coordination upon the metal–metal distance in $Mo_2(O_2CCF_3)_4(py)_2$ appears to be atypically large.



4.1

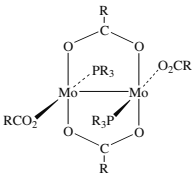
Other adducts that have been prepared from the parent carboxylates include $Mo_2(O_2CCHCl_2)_4L_2$ (L = pyridine or DMSO),[100] $Mo_2(O_2CH)_4L_2$ (L = DMSO, $HCONH_2$, $HCONMe_2$, $HCONEt_2$, CH_3CONMe_2, CH_3CONEt_2, sulfolane, or tetramethylthiourea),[36] $Mo_2(O_2CCF_3)_4L_2$ (L = Me_3PO or quinuclidine),[101] $Mo_2(O_2CCF_3)_4(AsR_3)_2$ (R = Et or Ph),[102] and the thermally unstable methanolate $Mo_2(O_2CCF_3)_4(CH_3OH)_2$.[101] The trifluoroacetate $Mo_2(O_2CCF_3)_4$ has been reacted with the radical ligand Tempo (2,2,6,6,-tetramethylpiperindinyl-1-oxy) to form the bis(nitroxyl) radical adduct $Mo_2(O_2CCF_3)_4(Tempo)_2$. Interestingly, magnetic susceptibility measurements show no signs of an exchange interaction down to 4.2 K.[103] This is in contrast to the magnetic behavior of the dirhodium(II) $Rh_2(O_2CCF_3)_4(Tempo)_2$, with which the molybdenum complex is isomorphous.[103]

Thermodynamic data have been obtained from calorimetric measurements on toluene solutions of several 1:1 and 2:1 adducts of $Mo_2(O_2CC_3F_7)_4$ with CH_2CN, py, DMSO, DMA, etc.[104] A comparison of these data with those for the analogous dirhodium(II) complexes indicates that the $Mo_2(O_2CCF_3)_4$ is the weaker Lewis acid.

Of the neutral 1:2 adducts that are known, those involving phosphine ligands are the most interesting. Although the adduct $Mo_2(O_2CCF_3)_4(PPh_3)_2$ has been known since the early 1970s,[22,101] it was not until 1980 that the first detailed study of the reactions of a dimolybdenum(II) carboxylate with a wide range of phosphine ligands was reported.[105] Based upon a combined ^1H, ^{19}F and ^{31}P NMR and infrared spectral study on the adducts $Mo_2(O_2CCF_3)_4(PR_3)_2$, it was concluded that they fall into two structural classes.[105] Some possess a structure of the type shown in **4.1** (L = PPh_3, $P(C_6H_{11})_3$, PBu^t_3 and $P(SiMe_3)_3$). $^{31}P\{^1H\}$ NMR spectroscopy showed that these adducts are extensively dissociated in $CDCl_3$ solution.[105] Other complexes, which are

Pictiva EX2004
Samsung v Pictiva
IPR2024-01094

formed with PMe_3, PMe_2Ph, PEt_3, PEt_2Ph and PBu^n_3,[22,56,105] have structures in which there are both bidentate bridging and monodentate trifluoroacetate groups as represented in **4.2**. The complex $Mo_2(O_2CCF_3)_4(PMePh_2)_2$ is unusual in existing in both structural forms; this has been confirmed by crystal structure determinations on the orange-yellow (**4.1**)[57] and red-orange (**4.2**)[56] isomeric forms (Table 4.1). X-ray crystal structures have also been reported for the **4.2** type complexes $Mo_2(O_2CCF_3)_4(PEt_2Ph)_2$[56] and $Mo_2(O_2CCF_3)_4(PBu^n_3)_2$.[22] The structure of the type **4.1** complex $Mo_2(O_2CCF_3)_4(PPh_3)_2$ has also been determined,[56] but not fully refined. The spectroscopic properties of the arsine complexes $Mo_2(O_2CCF_3)_4(AsR_3)_2$ (R = Et or Ph) are consistent with structure type **4.1**.[102]



4.2

A criterion for predicting which phosphine adduct will have which structure has been developed. This is based on a cone angle versus basicity relationship: type **4.2** complexes are formed only by the smallest and most basic phosphines.[105] In a related context, it has been reported[106] that the predominant species in pyridine-containing solutions of $Mo_2(O_2CCF_3)_4$ is the 1:4 adduct $Mo_2(O_2CCF_3)_4(py)_4$ and not $Mo_2(O_2CCF_3)_4(py)_2$, the latter being isolated upon crystallization. The former complex is believed to have a structure in which two of the trifluoroacetate groups are monodentate. This result indicates that the type **4.1**/**4.2** structural behavior may not be restricted to phosphine ligands.

Although the aforementioned 1:2 adducts are most easily prepared by the direct reaction of the phosphine with the dimolybdenum(II) carboxylate, other procedures are possible. Thus, the benzoate complex $Mo_2(O_2CC_6H_5)_4(PBu^n_3)_2$ has been obtained by the treatment of $Mo_2Br_4(PBu^n_3)_4$ with benzoic acid (1:4 mole proportions) in refluxing benzene.[107] Also, mixed phosphine complexes can be formed, as in the case of $Mo_2(O_2CCF_3)_4(PEt_3)(PBu^n_3)$ which is produced when equimolar quantities of $Mo_2(O_2CCF_3)_4(PEt_3)_2$ and $Mo_2(O_2CCF_3)_4(PBu^n_3)_2$ are mixed in toluene at −80 °C.[22]

While some bidentate phosphines ($Me_2PCH_2PMe_2$, $Ph_2PCH_2PPh_2$ and $Me_2PCH_2CH_2PMe_2$) react with $Mo_2(O_2CCF_3)_4$, the products remain less well characterized than adducts with monodentate phosphines, although in some of them monodentate trifluoroacetate groups and chelating phosphine ligands may be present.[105] In contrast, the polymeric acetate complex $[Mo_2(O_2CCH_3)_4(\mu\text{-dmpe})]_\infty$ and its amine analog $[Mo_2(O_2CCH_3)_4(\mu\text{-tmed})]_\infty$ are well characterized.[49] In each, there are infinite zig-zag chains of $Mo_2(O_2CCH_3)_4$ linked by the bridging $Me_2ACH_2CH_2AMe_2$ ligands (A = N or P). Both have structures of type **4.1**. With the complex $[Mo_2(O_2CCH_3)_4(\mu\text{-dmed})]_\infty$ (dmed = $MeNHCH_2CH_2NHMe$, the chain structure is kinked due to hydrogen bonding effects.[108] Polymeric chain compounds $[Mo_2(O_2CCH_3)_4(\mu\text{-L})]_\infty$ have also been prepared and characterized in the case of L being pyrazine, 4,4'-bipyridine, and 1,4-diazabicyclo[2.2.2]octane.[51]

The use of the phosphine adducts $Mo_2(O_2CR)_4(PR_3)_2$ as precursors to other dimolybdenum compounds has scarcely been examined. The one exception is a report that $Mo_2(O_2CCF_3)_4(PR_3)_2$ (R = Et or Ph) act as templates for the self condensation of 2-aminobenzaldehyde to give dimolybdenum species that contain a tetradentate macrocyclic ligand.[109] The structures of these complexes remain to be definitively established.

Pictiva EX2004
Samsung v Pictiva
IPR2024-01094

The 1:2 adduct $Mo_2(O_2CCF_3)_4(bpy)_2$ is an unusual complex since it has a centrosymmetric structure consisting of unbridged neutral Mo_2 units with four η^1-O_2CCF_3 groups and chelating bpy ligands.[55] It is prepared by reacting acetone solutions of $Mo_2(O_2CCF_3)_4$ and bpy in a 1:2 ratio and from the thermal and photochemical conversion of $[Mo_2(\mu\text{-}O_2CCF_3)_2(bpy)_2](O_2CCF_3)_2$. The correct Mo–Mo distance, however, is 2.129(1) Å, not 2.077(1) Å.

Another important group of adducts are those involving monoanionic ligands, for example $Mo_2(O_2CH)_4{\cdot}KCl$.[35] It is formed from solutions of $K_4Mo_2Cl_8{\cdot}2H_2O$ in 90% formic acid and has been shown to contain intact $Mo_2(O_2CH)_4$ units which are linked by weak chloride bridges to give an infinite zig-zag chain structure. However, a more extensive series of halide-containing complexes have been obtained by the use of organic cations. One of the earliest studies was that described by Garner and Senior,[110] who isolated 1:1 adducts of the type $Et_4N[Mo_2(O_2CCF_3)_4X]$, where X = Cl, Br, I, CF_3CO_2 and $SnCl_3^-$, together with certain 1:2 adducts $(Et_4N)_2[Mo_2(O_2CCF_3)_4X_2]$, where X = Br and I, by mixing dichloromethane solutions of $Mo_2(O_2CCF_3)_4$ and the appropriate Et_4NX salt. These adducts appear to be more stable than those formed by neutral donors, an observation that was attributed to the lattice energy of the salts. A series of structural studies on the complexes $(Bu_4N)_2[Mo_2(O_2CCF_3)_4X_2]$ (X = Cl or Br)[70,71] have confirmed that they all have structures with short Mo–Mo distances and long axial Mo–X bonds. For example, in the case of $(Ph_4P)_2[Mo_2(O_2CC_6H_5)_4Cl_2]$[70] the Mo–Cl distance of 2.88 Å is similar to that in $Mo_2(O_2CH)_4{\cdot}KCl$ (*c.* 2.86 Å).[35] The aforementioned complexes are prepared directly from the parent $Mo_2(O_2CR)_4$ compounds. The azido complex $(Ph_4P)_2[Mo_2(O_2CC_6H_5)_4(N_3)_2]$ has also been prepared, but upon its dissolution in dichloromethane N_2 is evolved and the dichloride adduct is formed.[70]

A useful spectroscopic probe of the existence of significant Mo–L_{ax} interactions is provided by the reduction in the Raman active ν(Mo–Mo) mode upon complex formation. For example, ν(Mo–Mo) of solid $Mo_2(O_2CCH_3)_4$ and $Mo_2(O_2CCF_3)_4$ occur at 406 and 397 cm^{-1}, respectively,[12,92] and both frequencies shift approximately -30 cm^{-1} upon formation of the bis-pyridine adducts.[29] This Raman frequency shift, together with variations in the electronic absorption spectra, has been used to probe the nature of the interaction of neutral or anionic base ligands with a variety of dimolybdenum(II) carboxylates.[29,36,49,100,101,107,110]

4.1.3 Other compounds with bridging carboxyl groups

There are many compounds in which one, two, or three, but not four carboxyl groups span the Mo_2^{4+} core. Those with known structures are listed in Table 4.2. Compounds of this class are generally obtained by partial replacement of RCO_2 ligands in $Mo_2(O_2CR)_4$ compounds. The overwhelming majority contain acetate ion, but compounds containing $PhCO_2^-$, $CF_3CO_2^-$, $Me_3CCO_2^-$ and others are also known.

There are very few examples of dimolybdenum(II) complexes in which three carboxylate groups are present. Attempts to prepare $(Et_3N)_2[Mo_2(O_2CCF_3)_4Cl_2]$ led to the unplanned discovery[110] of $(Et_3N)_2[Mo_2(O_2CCF_3)_3Cl_3]$. Other complexes with three carboxylate ligands are the various salts of composition $M^I{}_2[Mo_2(O_2CH)_3Cl_3]{\cdot}HCl{\cdot}2H_2O$ (M^I = NH_4, K, Rb or Cs) and $Cs[Mo_2(O_2CH)_3(SO_4)]{\cdot}2H_2O$, which have been isolated by reacting mixtures of NH_4O_2CH and M^ICl with $K_4Mo_2Cl_8$, $(NH_4)_3Mo_2Cl_9{\cdot}H_2O$ or $(NH_4)_4[Mo_2(SO_4)_4]{\cdot}2H_2O$.[111,112] Characterization of these complexes is based primarily on their vibrational spectra[111,112] but in the case of $M^I{}_2[Mo_2(O_2CH)_3Cl_2]{\cdot}Cl{\cdot}2H_2O$ (M = NH_4 or Rb) full crystal structure data are available.[112,113] The eclipsed $[Mo_2(O_2CH)_3Cl_2]^-$ anions have Mo–Mo distances of 2.099(3) Å and 2.106(3) Å, respectively, but the nature of the axial ligands (Cl^- and/or H_2O) could not be discerned because of a disorder problem.

Pictiva EX2004
Samsung v Pictiva
IPR2024-01094

Table 4.2. Other Compounds with Carboxylate Ligands

Compound [a]	Crystal sym.	Virtual sym. [b]	*r*(Mo–Mo) (Å)	Twist Angle (°) [c]	ref
$[Mo_2(O_2CCH_3)_3(S_2CPEt_3)(OPEt_3)]BF_4$	1	C_s	2.138(1)	0	114
$Mo_2(O_2CCH_3)_3(BAII)\cdot C_6H_6$	1	C_s	2.106(1)	0	115
$(Ph_4As)_2[Mo_2(O_2CCH_3)_2Cl_4]\cdot 2CH_3OH$	1	D_{2h}	2.086(2)	≈0	116,117
cis-$Mo_2(O_2CCH_3)_2(NCCH_3)_4(SO_3CF_3)_2\cdot 2CF_3SO_3H\cdot THF$	m	C_{2v}	2.132(4)	0	118
cis-$[Mo_2(O_2CCH_3)_2(NCCH_3)_6](BF_4)_2$	m	C_{2v}	2.134(2)	0	118
trans-$[Mo_2(O_2CCH_3)_2(\mu\text{-dmpe})_2](BF_4)_2\cdot CH_3CN$	$\bar{1}$	D_{2h}	2.099(1)	0	119
	$\bar{1}$	D_{2h}	2.096(1)	0	
trans-$Mo_2(O_2CCH_3)_2(CH_2SiMe_3)_2(PMe_3)_2$	$\bar{1}$	C_{2h}	2.098(1)	0	120
trans-$Mo_2(O_2CCH_3)_2(CH_2Ph\text{-}p\text{-}Me)_2(PMe_3)_2$	$\bar{1}$	C_{2h}	2.108(2)	0	121
	$\bar{1}$	C_{2h}	2.107(1)	0	
trans-$Mo_2(O_2CCH_3)_2(OSiMe_3)_2(PMe_3)_2$	$\bar{1}$	C_{2h}	2.114(1)	0	122
trans-$Mo_2(O_2CCH_3)_2Cl_2(PBu^n{}_3)_2$	$\bar{1}$	C_{2h}	2.099(1)	0	123
trans-$Mo_2(O_2CCH_3)_2Cl_2(PPh_3)_2$	$\bar{1}$	C_{2h}	2.091(1)	0	124
trans-$Mo_2(O_2CCMe_3)_2Cl_2(PEt_3)_2$	$\bar{1}$	C_{2h}	2.098(1)	0	125
cis-$Mo_2(O_2CCMe_3)_2Cl_2(PEt_3)_2$	1	C_2	2.113(1)	0	125
trans-$Mo_2(O_2CCH_3)_2Cl_2(Ph_2Ppy)_2\cdot 2CH_2Cl_2$	$\bar{1}$	C_{2h}	2.190(1)	0	126
$Mo_2(O_2CCH_3)Cl_3(PMe_3)_3\cdot 0.5C_7H_8$	m	C_s	2.121(2)	0	127
cis-$Mo_2(O_2CCH_3)_2(acac)_2$	1	C_{2v}	2.129(1)	0	116
cis-$Mo_2(O_2CCH_3)_2[PhNC(CH_3)CHC\text{-}(CH_3)O]_2$	1	C_2	2.131(1)	0	128
cis-$Mo_2(O_2CCH_3)_2[(pz)_2BEt_2]_2$	1	C_s	2.129(1)	2.6	129
cis-$Mo_2(O_2CCH_3)_2[(pz)_3BH]_2$	1	C_s	2.147(3)	3.4	129
cis-$Mo_2(O_2CCH_3)_2(pdc)_2(OPPh_3)\cdot 1.5C_6H_6$	1	C_s	2.134(1)	0	114
trans-$Mo_2(O_2CCH_3)_2\{[(2,6\text{-xylyl})N]_2CCH_3\}_2(THF)_2\cdot 2THF$	$\bar{1}$	D_{2h}	2.107(1)	0	130
trans-$Mo_2(O_2CCH_3)_2[o\text{-}(Me_2N)C_6H_4CH_2]_2$	$\bar{1}$	C_i	2.065(1)	0	131
trans-$Mo_2(O_2CCH_3)_2(7\text{-azaindolyl})_2\cdot 2DMF$	$\bar{1}$	C_{2h},C_{2v}	2.112(1)	0	132
trans-$Mo_2(O_2CCH_3)_2[Al(OPr^i)_4]_2$	$\bar{1}$	C_{2h}	2.079(1)	0	133

Pictiva EX2004
Samsung v Pictiva
IPR2024-01094

Compound [a]	Crystal sym.	Virtual sym. [b]	r(Mo–Mo) (Å)	Twist Angle (°)[c]	ref
cis-$[Mo_2(O_2CCH_3)_2(en)_2][ax\text{-}en)(O_2CCH_3)_2]\cdot en$	m	C_{2v}	2.125(1)	0	134(a)
$Mo_2(O_2CCH_3)(ambt)_3\cdot 2THF$	1	C_s	2.093(3)	1.9	135
$Mo_2(O_2CCH_3)[(PhN)_2CCH_3]_3$	1	C_{2v}	2.082(1)	0	130
$(C_5N_2H_5)\{Mo_2(O_2CCH_3)[CH_3Ga(C_5N_2H_5)O]_4\}\cdot 2THF$	mm	C_{2v}	2.127(1)	0	136
trans-$[Mo_2(\mu\text{-}O_2CCH_3)_2(\mu\text{-}dppma)_2(CH_3CN)_2](BF_4)_2\cdot 4CH_3CN$	$\bar{1}$	D_{2h}	2.113(1)	Zero	137
			2.130(1)		
trans-$[Mo_2(\mu\text{-}O_2CCH_3)_2(\mu\text{-}dppma)_2(BF_4)_2]\cdot 2CH_2Cl_2$	$\bar{1}$	D_{2h}	2.115(1)	Zero	137
			2.111(1)		
trans-$[Mo_2(\mu\text{-}O_2CCH_3)_2(\mu\text{-}dppma)_2(NCC(CH_3)_3)_2](BF_4)_2\cdot 0.5(C_4H_{10}O,C_6H_{14})$	1	D_{2h}	2.115(1)	0.8	137
			2.116(1)	7.8	
trans-$[Mo_2(\mu\text{-}O_2CCH_3)_2(\mu\text{-}dppma)_2(NCC_6H_3)_2](BF_4)_2$	$\bar{1}$	D_{2h}	2.131(1)	Zero	138
trans-$[Mo_2(\mu\text{-}O_2CCH_3)_2(\mu\text{-}dppma)_2(NCC_6H_4C{\equiv}CH)_2](BF_4)_2$	$\bar{1}$	D_{2h}	2.131(1)	Zero	137
$Mo_2(O_2CCH_3)(triphos)Br_3\cdot 2CH_2Br_2$	1	C_1	2.132(3)	13.6	139
trans-$[Mo_2(O_2CCH_3)_2((Ph_2PCH_2)_2PPh)_2](BF_4)_2\cdot 2CH_2Cl_2$	$\bar{1}$	C_{2h}	2.119(3)	Zero	140
trans-$[Mo_2(O_2CCH_3)_2(dpmp\text{-}O)_2](BF_4)_2\cdot 2CH_2Cl_2$ dpmp-O = $Ph_2PCH_2PPhCH_2P(O)Ph_2$	$\bar{1}$	C_{2h}	2.141(2)	Zero	140
cis-$[Mo_2(O_2CCH_3)_2(dpnapy\text{-}N,P)_2](BF_4)_2\cdot C_7H_8\cdot 2CH_2Cl_2$	1	C_2	2.119(1)	NR	141
trans-$[Mo_2(O_2CCH_3)_2(dpnapy\text{-}N,P)_2](BF_4)_2\cdot 5C_6H_6$	$\bar{1}$	C_{2h}	2.099(2)	Zero	141
trans-$[Mo_2(O_2CCH_3)_2(dppma)_2(NC_5H_4CMe_3)_2](BF_4)_2\cdot CH_2Cl_2$	$\bar{1}$	D_{2h}	2.150(1)	Zero	142
$Mo_2Cl_2(O_2CCH_3)_2(py)_2\cdot CH_2Cl_2$	1	C_2	2.131(1)	NR	143
trans-$Mo_2(O_2CCH_3)_2[PhC(NSiMe_3)_2]_2$	2	D_{2h}	2.069(1)	NR	144
cis-$Mo_2(O_2CCH_3)_2[PhC(NSiMe_3)_2]_2$	2	C_{2v}	2.124(1)	NR	144
trans-$Mo_2Cl_2(OCCH_3)_2(dppa)_2\cdot 2CH_3OH$	$\bar{1}$	D_{2h}	2.152(2)	Zero	145
trans-$[Mo_2(O_2CCH_3)_2(dppa)_2(CH_3CN)_2](BF_4)_2\cdot CH_3CN$	$\bar{1}$	D_{2h}	2.133(1) 2.136(1)	Zero	146
trans-$[Mo_2(O_2CCH_3)_2Cl_2(dppma)_2]\cdot 2CH_3CN$	2	D_{2h}	2.172(1)	10	147
trans-$[Mo_2(O_2CCH_3)_2(\mu\text{-}dppa)_2](BF_4)_2$	$\bar{1}$	D_{2h}	2.112(1)	Zero	148
$[Mo_2(O_2CCH_3)_2(pynp)_2](BF_4)_2\cdot 3CH_3CN$	1	C_2	2.124(1)	NR	149

Pictiva EX2004
Samsung v Pictiva
IPR2024-01094

Compound [a]	Crystal sym.	Virtual sym. [b]	r(Mo–Mo) (Å)	Twist Angle (°) [c]	ref
cis-[Mo_2(mphamnp)$_2$(O_2CCH_3)$_2$]·C_5H_{12} Hmphamnp = 2-acetamido-5-methyl-7-phenyl-1,8-naphthyridine	2	C_2	2.097(2)	NR	150
[Mo_2PtBr_2(pyphos)$_2$(O_2CCH_3)$_2$]$_2$·4CH_2Cl_2	1	C_s	2.096(1)	4.8[4]	151
Mo_2(O_2CCH_3)$_2$($SSiMe_3$)$_2$(PEt$_3$)$_2$	$\bar{1}$	C_{2h}	2.110(1)	Zero	152
Mo_2(O_2CCH_3)$_2$(H$_2$-calix[4]arene)]·THF·C_6H_6	1	C_s	2.126(1)	~0	153
Mo_2(O_2CCH_3)$_3$($D^{o\text{-}OMe}$PhF)	1	C_{2v}	2.093(1)	NR	154
trans-Mo_2(O_2CCH_3)$_2$($D^{o\text{-}OMe}$PhF)$_2$·2CH_2Cl_2	1	D_{2h}	2.108(1)	NR	154
Mo_2(O_2CCH_3)($D^{o\text{-}OMe}$PhF)Cl$_2$(PMe_3)$_2$	1	C_1	2.124(1)	NR	154
[Bu^n_4N]$_3$[Mo_2(O_2CCH_3)$_3$(CN)$_6$]	1	C_{2v}	2.114(2)	3.5	155
[Mo_2PdCl_2(pyphos)$_2$(O_2CCH_3)$_2$]$_2$·2CH_2Cl_2·Et_2O	1	C_s	2.083(6)	NR	156
			2.099(6)		
trans-[Mo_2(μ-O_2CCH_3)$_2$(μ-2-(diphenylphosphino)-6-(pyrazol-1-yl)pyridine)$_2$][BF_4]$_2$	$\bar{1}$	C_{2h}	2.153(1)	Zero	157
[Mo_2(O_2CCH_3)$_2$(dppm)$_2$][BF_4]$_2$·3CH_3CN	1	D_{2h}	2.132(1)	NR	158
[Mo_2(O_2CCH_3)$_2$(dppe)$_2$][BF_4]$_2$	$\bar{1}$	C_{2h}	2.093(1)	Zero	158
Mo_2(O_2CCH_3)$_2$(dppee)$_2$][BF_4]$_2$·2CH_3CN	$\bar{1}$	C_{2h}	2.144(1)	Zero	158
Mo_2Cl_3(O_2CCH_3)(η^3-tetraphos-2)·THF	1	C_1	2.126(3)	13.2	159
Mo_2(O_2CCH_3)Cl_3(η^3-triphos)·2CH_2Cl_2	1	C_1	2.121(3)	11.4	159
			2.134(3)	11.7	
Mo_2(O_2CCF_3)$_3$Cl(NCC_2H_5)	1	C_s	2.127(2)	0	160
Mo_2(O_2CCF_3)$_2$Cl$_2$(NCC_2H_5)$_2$	1	C_2	2.134(2)	0	160
(Bu_4N)$_2$[Mo_2(O_2CCF_3)$_2$Br$_4$]	1	D_{2h}	2.098(1)	0	58
cis-[Mo_2(O_2CCF_3)$_2$(bpy)$_2$][O_2CCF_3)$_2$	1	C_{2v}	2.181(2)	0	55
{[*trans*-Mo_2(O_2CCF_3)$_2$(μ-dppa)]$_3$(μ_6-CO_3)(μ_2-Cl)$_3$}F·4CH_2Cl_2·2Et_2O	2	D_{3h}	2.153(1)	NR	161
			2.155(1)		
{[*trans*-Mo_2(O_2CCF_3)$_2$(μ-dppa)]$_3$(μ_6-CO_3)(μ_2-Br)$_3$}F·4CH_2Cl_2·2Et_2O	2	D_{3h}	2.152(1)	NR	161
			2.148(1)		
{[*trans*-Mo_2(O_2CCF_3)$_2$(μ-dppa)]$_3$(μ_6-CO_3)(μ_2-I)$_3$}F·4CH_2Cl_2·2Et_2O	2	D_{3h}	2.150(1)	NR	161
			2.154(1)		

Pictiva EX2004
Samsung v Pictiva
IPR2024-01094

Compound [a]	Crystal sym.	Virtual sym. [b]	r(Mo–Mo) (Å)	Twist Angle (°) [c]	ref
trans-$Mo_2(O_2CCF_3)_2(D^{p\text{-}OMe}PhF)_2$	$\bar{1}$	D_{2h}	2.133(2)	Zero	154
trans-$Mo_2(O_2CCF_3)_2(PPhpy_2)_2$(ax-$O_2CCF_3)_2$	$\bar{1}$	C_{2v}	2.190(1)	Zero	162
trans-$Mo_2(O_2CCF_3)_2(Ppy_3)_2$(ax-$O_2CCF_3)_2$	$\bar{1}$	C_{2v}	2.188(1)	Zero	162
cis-$Mo_2(O_2CCF_3)_2Br_2(\eta^2$-Hdpa)·$2CH_2Cl_2$	1	C_s	2.152(4)	NR	64
			2.158(4)		
$[Mo_2(O_2CCF_3)_3(MeNHCH_2CH_2NHMe)_2]O_2CCF_3$	1	C_{2v}	2.132(2)	~0	163
$[Mo_2(O_2CCF_3)_2(S,S$-dach$)_2(CH_3CN)_2](BF_4)_2$	2	C_{2v}	2.155(1)	~0	164
			2.154(1)		
$Mo_2(O_2CCF_3)_2(R,R$-dach$)_2(CH_3CN)_2]BF_4$	2	C_{2v}	2.153(1)	~0	164
			2.153(1)		
$(NH_4)_2[Mo_2(O_2CH)_3Cl_2]Cl\cdot nH_2O$			2.099(3)	0	113
$Rb_2[Mo_2(O_2CH)_3Cl_2]Cl\cdot nH_2O$			2.106(3)	0	113
trans-$Mo_2(O_2CC_6H_5)_2Br_2(PBu^n_3)_2$	$\bar{1}$	C_{2h}	2.091(3)	0	165
trans-$[Mo_2(O_2CPh)_2(dpmp)_2](BF_4)_2\cdot 4CH_2Cl_2$	$\bar{1}$	C_{2h}	2.131(4)	Zero	140
trans-$[Mo_2(O_2CPh)_2(dpmp\text{-}O)_2](BF_4)_2\cdot 4CH_2Cl_2$	$\bar{1}$	C_{2h}	2.141(2)	Zero	140
$(Et_4N)_2(Mo_2(O_2CC_6H_5)_2(WS_4)_2$	$\bar{1}$	C_{2h}	2.144(1)	Zero	166
$Mo_2(O_2CC_6H_5)_2((NMe_3Si)_2CC_6H_5)_2$	2	C_{2v}	2.083(1)	NR	167
$Mo_2(O_2CC_6H_5)_2(dppa)_2Cl_2\cdot 2CH_3CH_2OH$	$\bar{1}$	D_{2h}	2.158(1)	Zero	168
$Mo_2(O_2CC_6H_5)_2(dppa)_2Br_2\cdot 2C_7H_8$	$\bar{1}$	D_{2h}	2.176(1)	Zero	168
$Mo_2(O_2CC_6H_5)_2(dppa)_2I_2\cdot CH_3CH_2OH\cdot NCCH_3$	1	D_{2h}	2.164(1)	NR	168
trans-$[Mo_2(O_2CCMe_3)_2(dpmp)_2](BF_4)_2$	$\bar{1}$	C_{2h}	2.115(1)	Zero	140
$[Mo_2PtCl_2(pyphos)_2(O_2CCMe_3)_2]_2\cdot CH_2Cl_2$	1	C_s	2.094(1)	2.5[5]	151
$[Mo_2PtBr_2(pyphos)_2(O_2CCMe_3)_2]_2\cdot CH_2Cl_2$	1	C_s	2.096(1)	3.7[2]	151
$[Mo_2PtI_2(pyphos)_2(O_2CCMe_3)_2]_2\cdot CH_2Cl_2$	1	C_s	2.102(1)	3.4[2]	151
$Mo_2(O_2CCMe_3)_3(2\text{-}CH_2\text{-}6\text{-}Mepy)\cdot 0.5C_6H_6$	1	C_s	2.083(1)	NR	169
$[Mo_2(O_2CCMe_3)_2(\alpha,\alpha'$-bipyrimidine$)_2](BF_4)_2\cdot 2CH_3CN$	1	C_{2v}	2.151(1)	NR	169
$[Bu^n_4N](Mo_2(O_2CCMe_3)_5)$	1	C_{4v}	2.104(1)	NR	170

Pictiva EX2004
Samsung v Pictiva
IPR2024-01094

Compound [a]	Crystal sym.	Virtual sym. [b]	r(Mo–Mo) (Å)	Twist Angle (°) [c]	ref
$Mo_2(O_2CCH_2NH_3)_2(NCS)_4 \cdot H_2O$	1	C_{2v}	2.132(2)	0	171
	1	C_{2v}	2.134(2)	0	
Mo_2(*L*-isoleucine)$_2(NCS)_4 \cdot 4.5H_2O$	1	C_{2v}	2.154(5)	0	171
	1	C_{2v}	2.145(5)	0	
Mo_2(*D*-valine)(*L*-valine)$(NCS)_4 \cdot 1.5H_2O$	1	C_{2v}	2.139(1)	0	85
$Mo_2\{\mu\text{-}[(CO)_9Co_3(\mu_3\text{-}CCO_2)]\}_4[(CO)_9Co_3(\mu_3\text{-}CCO_2H)]_2$	$\bar{1}$	D_{4h}	2.113(1)	Zero	172
$Mo_2\{\mu\text{-}[(CO)_9Co_3(\mu_3\text{-}CCO_2)]\}_3(O_2CCH_3) \cdot C_7H_8$	m or 2	D_{4h}	NR	NR	172
$Mo_2(O_2CCH_2\text{-}p\text{-}C_6H_4OH)_4 \cdot 2THF$	$\bar{1}$	D_{4h}	2.097(1)	Zero	173
$Mo_2(O_2CC(OH)(C_6H_5)_2)_4 \cdot 4THF$	$\bar{1}$	D_{4h}	2.104(1)	Zero	
$[Mo_2(O_2CCHF_2)_2(bpy)_2(CH_3CN)(BF_4)]BF_4$	m	C_s	2.143(1)	0.3	174
$Mo_6(O_2CCHF_2)_{12}(bpy)_4 \cdot 4CH_3CN$	$\bar{1}$	C_{2h}	2.123(2)	Zero	
			2.174(1)		
cis-$[Mo_2(O_2CCH_2Cl)_2(CH_3CN)_6](BF_4)_2$	2	C_{2v}	2.140(2)	NR	146
trans-$[Mo_2Cl_2(O_2C(CH_2)_2CH_3)_2(\mu\text{-dppa})_2] \cdot 4CH_2Cl_2$	$\bar{1}$	D_{2h}	2.172(1)	Zero	148
trans-$[Mo_2Br_2(O_2C(CH_2)_2CH_3)_2(\mu\text{-dppa})_2] \cdot 4CH_2Cl_2$	$\bar{1}$	D_{2h}	2.167(2)	Zero	148
trans-$Mo_2(O_2CCH_2CH_2CH_3)_2(D^{p\text{-}OMe}PhF)_2$	$\bar{1}$	D_{2h}	2.109(1)	Zero	154
$Mo_2(O_2CCHF_2)_2(9\text{-EtAH})_2(CH_3CN)_2](BF_4)_2 \cdot 2CH_3CN$ 9-EtAH = N,N'-9-ethyladenine	2	C_2	2.144(2)	~0	175

[a] Where more than one set of data is given for any complex this signifies that more than one crystallographically independent molecule is present in the crystal.

[b] This is a (partly subjective) estimate of the symmetry that would be possessed by the central unit consisting of the two metal atoms and those portions of the ligands (usually the 8-10 donor atoms) that have an important influence on the electronic structure of the Mo_2 unit if it were not subject to any distortion by its neighbors in the crystal. Schoenflies symbols are used.

[c] NR means not reported

Pictiva EX2004
Samsung v Pictiva
IPR2024-01094

The complex $[Mo_2(O_2CCH_3)_3(S_2CPEt_3)(OPEt_3)]BF_4$ is formed upon reacting $Mo_2(O_2CCH_3)_4$ with the zwitterionic ligand S_2CPEt_3 in THF in the presence of HBF_4.[114] The structure of the purple/black crystals showed that an axially coordinated Et_3PO ligand was present; it is evidently formed by reaction of the S_2CPEt_3 ligand with water.[114] Several complexes of stoichiometry $Mo_2(O_2CCH_3)_3$(BAII), where BAII represents a planar tridentate bis(arylimino)isoindoline ligand, have been prepared from $Mo_2(O_2CCH_3)_4$.[115,176]

Electronic absorption and ^1H NMR spectral measurements have been made on derivatives where the aryl group is pyridyl, 4-methylpyridyl, 4-ethylpyridyl and 4,6-dimethylpyridyl,[115,176,177] and the crystal structure of the dark-green pyridyl derivative has been determined (Fig. 4.5). The tridentate nitrogen ligand binds so that one of its pyridyl nitrogen atoms is coordinated at one of the axial sites. Another example is encountered when toluene solutions of $Mo_2(O_2CCF_3)_4$ are treated with Me_3SiCl and C_2H_5CN below 0 °C.[160] The orange-red crystals that form have the unusual composition $\{Mo_2(O_2CCF_3)_3Cl(NCC_2H_5)\cdot Mo_2(O_2CCF_3)_2Cl_2(NCC_2H_5)_2\}$; the two molecules jointly comprise the crystallographic asymmetric unit.[160] Their structures are represented in 4.3 and 4.4 and the Mo–Mo distances listed in Table 4.2. They pack to form infinite chains of alternating molecules through weak intermolecular Mo···Cl and Mo···O bridges.

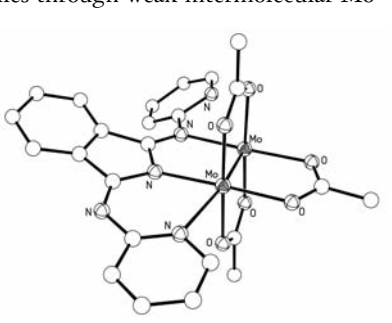
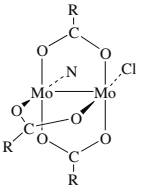
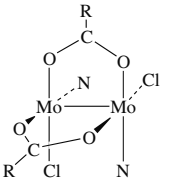


Fig. 4.5. The structure of $Mo_2(O_2CCH_3)_3$[bis(pyridylimino)isoindoline].



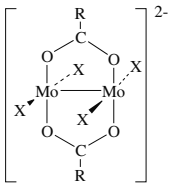
4.3



4.4

Further substitution of carboxylate groups by halide ions can occur to give anions of stoichiometry $[Mo_2(O_2CR)_2X_4]^{2-}$, as in the cases of $(Ph_4As)_2[Mo_2(O_2CCH_3)_2Cl_4]\cdot 2H_2O$[116,117] and $(Bu_4N)_2[Mo_2(O_2CCF_3)_2Br_4]$,[58] which are prepared directly from the parent carboxylates upon their reaction with Ph_4AsCl and Bu_4NBr, respectively. The crystal structures of these complexes have been determined (Table 4.2) and each found to possess a *trans* arrangement of carboxylate ligands and an eclipsed rotational geometry as shown in 4.5. While the spectroscopic properties of $(Ph_4As)_2[Mo_2(O_2CCH_3)_2Cl_4]$, specifically its Raman-active ν(Mo–Mo) mode at 380 cm^{-1} and $\delta \rightarrow \delta^*$ electronic absorption transition at 20,200 cm^{-1}, lie between the corresponding features in the spectra of $Mo_2(O_2CCH_3)_4$ and $K_4Mo_2Cl_8$, the Mo–Mo distance is the shortest of the three complexes.

Pictiva EX2004
Samsung v Pictiva
IPR2024-01094



4.5

In addition to the nitrile-containing molecules $Mo_2(O_2CCF_3)_3Cl(NCC_2H_5)$ and $Mo_2(O_2CCF_3)_2Cl_2(NCC_2H_5)_2$ there are several cationic dimolybdenum(II) species that contain carboxylate and nitrile ligands in the coordination sphere. All those that have been fully characterized contain the $[Mo_2(O_2CCH_3)_2]^{2+}$ moiety, although the number of coordinated nitrile ligands varies; these species can be considered as an intermediate stage in the conversion of $Mo_2(O_2CCH_3)_4$ to $[Mo_2(NCCH_3)_8]^{4+}$ (see Section 4.3.5).[178,179] Treatment of acetonitrile suspensions of $Mo_2(O_2CCH_3)_4$ with stoichiometric amounts of the noncomplexing acids CF_3SO_3H and $HBF_4{\cdot}Et_2O$ has been described[180] as forming materials of composition $[Mo_2(O_2CCH_3)_2(NCCH_3)_4](SO_3CF_3)_2$ and $[Mo_2(O_2CCH_3)_2(NCCH_3)_5](BF_3OH)_2$, respectively, that were characterized by spectroscopic means. A recipe similar to that used to prepare the first of these complexes was later found to give the crystalline complex $Mo_2(O_2CCH_3)_2(NCCH_3)_4(O_3SCF_3)_2$.[118] A crystal structure determination revealed[118] a *cis*-arrangement of acetate groups, and weakly axially bound triflate anions. The use of $(Et_3O)BF_4$ in place of $HBF_4{\cdot}Et_2O$ gave the hexakis(acetonitrile) complex *cis*-$[Mo_2(O_2CCH_3)_2(NCCH_3)_6](BF_4)_2$, whose structure resembles that of the triflate derivative except that additional acetonitrile ligands have replaced the $[CF_3CO_2]^-$ anions in the axial sites,[118] as shown in Fig. 4.6. There is a large discrepancy between the Mo–N distances of the equatorially and axially bound nitrile ligands (*c.* 2.15 Å versus 2.70 Å).[118] The same complex is also formed when $(Et_3O)BF_4$ is replaced by $(Me_3O)BF_4$,[181,182] a procedure that can be adapted to give the formato complex $[Mo_2(O_2CH)_2(NCCH_3)_4](BF_4)_2$.[182] The isolation of only a tetrakis complex in the latter case (albeit impure) indicates that the axially bound nitriles are very labile, and in accord with this expectation the NMR spectra of the acetonitrile complex show that the equatorial and axial CH_3CN ligands interchange rapidly.[182] This has also been shown to be the case with $[Mo_2(O_2CBu^t)_2(NCCH_3)_6]^{2+}$, a species which also undergoes a rapid reaction with $Mo_2(O_2CBu^t)_4$ according to the following equilibrium:[183]

$$Mo_2(O_2CBu^t)_4 + [Mo_2(O_2CBu^t)_2]^{2+} \underset{}{\overset{CH_3CN}{\rightleftharpoons}} 2[Mo_2(O_2CBu^t)_3]^+$$

The lability of the acetonitrile ligands of *cis*-$[Mo_2(O_2CCH_3)_2(NCCH_3)_6](BF_4)_2$ has been shown by the reactions of this complex with the $Me_2PCH_2CH_2PMe_2$ (dmpe) and with the chiral ligand (2*S*,3*S*)-bis(diphenylphosphino)butane(*S*,*S*-dppb) to give *trans*-$[Mo_2(O_2CCH_3)_2(\mu\text{-dmpe})_2](BF_4)_2$ and $[Mo_2(O_2CCH_3)_2(S,S\text{-dppb})(NCCH_3)_2](BF_4)_2$, respectively.[119] The X-ray crystal structure of the former complex shows that the dmpe ligands bridge the Mo atoms so as to maintain a rigorously eclipsed rotational geometry. The rings adopt a half chair conformation, like that of cyclohexane, but they possess opposite chirality so as to give the complex an overall D_{2h} symmetry. This geometry is retained in solution.[119] Reaction of $[Mo_2(O_2CCH_3)_2(CH_3CN)_6]^{2+}$ with 1,4,7-trithiacyclononane (TTCN) affords the compounds $[(TTCN)Mo(\mu\text{-}O_2CCH_3)_2Mo(NCCH_3)_3](BF_4)_2$ and $[(TTCN)Mo(\mu\text{-}O_2CCH_3)_2Mo(TTCN)](BF_4)_2$ which are formed in stepwise fashion. The first of these reacts with KX in aqueous solution to form blue species of stoichiometry $(TTCN)Mo(\mu\text{-}O_2CCH_3)_2MoX_2$ (X = Cl, Br, SCN or OCN).[184]

Pictiva EX2004
Samsung v Pictiva
IPR2024-01094

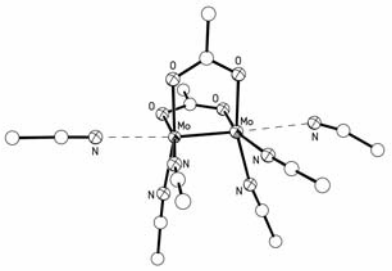
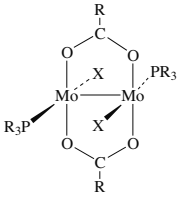


Fig. 4.6. The cation in *cis*-$[Mo_2(O_2CCH_3)_2(CH_3CN)_4(ax\text{-}CH_3CN)_2](BF_4)_2$.

An extensive series of dimolybdenum(II) carboxylate complexes are those of stoichiometry $Mo_2(O_2CR)_2X_2(PR_3)_2$, where X represents an alkyl, amido, siloxy or halide ligand. The first alkyl derivatives to be isolated were obtained by the reaction of $Mg(CH_2SiMe_3)_2$ and $Mg(CH_2CMe_3)_2$ with mixtures of $Mo_2(O_2CCH_3)_4$ and PMe_3 with a MgR_2: $Mo_2(O_2CCH_3)_4$ reaction stoichiometry of 2:1.[185,186] The benzyl and *p*-methyl benzyl complexes of this type were prepared by a similar procedure,[121] as were the pivalate complexes $Mo_2(O_2CCMe_3)_2R_2(PMe_2Et)_2$ (R = CH_2SiMe_3 or CH_2CMe_3).[122] X-ray crystal structure determinations on $Mo_2(O_2CCH_3)_2(CH_2SiMe_3)_2(PMe_3)_2$[120] and $Mo_2(O_2CCH_3)_2(CH_2Ph\text{-}p\text{-}Me)_2(PMe_3)_2$[121] have shown that these complexes possess the centrosymmetric *trans* structure represented in **4.6**. The P–Mo–C angles of *c.* 142° are probably a consequence of the steric demands of the alkyl and phosphine ligands. The phenyl and 4-fluorophenyl complexes of stoichiometry $Mo_2(O_2CCH_3)R_3(PMe_3)_3$, where R = Ph or 4-F-Ph, are the products of the reaction between $Mo_2(O_2CCH_3)_4$ and the magnesium diaryl in diethyl ether containing an excess of trimethylphosphine.[187] In the absence of phosphine, decomposition has been found to occur. An unsymmetrical structure is clearly in order, and this is supported by NMR spectroscopy.[187]



4.6

The acetate $Mo_2(O_2CCH_3)_4$ reacts in diethyl ether with $LiN(SiMe_3)_2$, $LiN(SiMe_2H)_2$ or $LiN(SiMe_3)(Me)$ in the presence of tertiary phosphines (PMe_3, PEt_3 or PMe_2Ph) to give red pentane-soluble complexes of the type $Mo_2(O_2CCH_3)_2(NR_2)_2(PR_3)_2$. Infrared and NMR ($^1H$, ^{13}C and ^{31}P) spectroscopy have been used[188] to demonstrate that the particular isomer formed is dependent upon the nature of the NR_2 ligand. With $[N(SiMe_2H)_2]^-$ the structure is similar to **4.6**, but the other two silylamido ligands apparently give the isomer in which the pairs of PR_3 and silylamido groups are *trans* to each other on different molybdenum atoms. The analogous pivalate complex $Mo_2(O_2CCMe_3)_4$ has been reported[188] to react in a similar fashion, with the exception that the bis(trimethylsilyl)amido complexes are of stoichiometry $Mo_2(O_2CCMe_3)_3[N(SiMe_3)_2]_2](PR_3)$ (PR_3 = PMe_3, PEt_3 or PMe_2Ph). The compounds $Mo_2(O_2CCF_3)_2[N(SiMe_3)_2]_2(PMe_3)_2$[188] and $Mo_2(O_2CCMe_3)_2[N(SiMe_2H)_2]_2(PMe_2Et)_2$[122] have also been described.

The preparation of the siloxy complexes, $Mo_2(O_2CCMe_3)_2(OSiMe_3)_2(PR_3)_2$ (PR_3 = PMe_3 or PMe_2Et) from the reaction of $Mo_2(O_2CCMe_3)_4$, $LiOSiMe_3$, and PR_3 in diethyl ether, has been re-

Pictiva EX2004
Samsung v Pictiva
IPR2024-01094

ported.[122] The crystal structure of the acetate complex $Mo_2(O_2CCH_3)_2(OSiMe_3)_2(PMe_3)_2$ shows[122] the geometry to be as in **4.6**; the Mo–Mo distance of 2.114(1) Å is similar to the distances reported for the structurally characterized alkyl derivatives (Table 4.2) and the P–Mo–O(siloxyl) angle (149°) is slightly larger than the P–Mo–C angles of these same two alkyl complexes.

Several procedures that have been utilized to prepare halide complexes of the type $Mo_2(O_2CR)_2X_2(PR'_3)_2$ R = alkyl or aryl; X = Cl or Br; PR'_3 = monodentate phosphine) are as follows:

$$Mo_2(O_2CCH_3)_4 + AlCl_3 + PPh_3 \rightarrow Mo_2(O_2CCH_3)_2Cl_2(PPh_3)_2^{189}$$

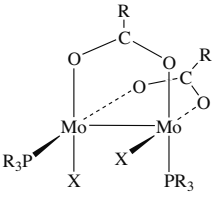
$$Mo_2(O_2CR)_4 + Me_3SiX + PR'_3 \rightarrow Mo_2(O_2CR)_2X_2(PR'_3)_2^{123\text{-}125,190}$$

(R = CH_3 or CMe_3; X = Cl or Br; R' = Me, Et, Bu^n or Ph)

$$Mo_2X_4(PR'_3)_4 + RCO_2H \rightarrow Mo_2(O_2CR)_2X_2(PR'_3)_2^{107,125}$$

(X = Cl or Br; R' = Et or Bu^n; R = CMe_3, Ph or 2,4,6-Me_3Ph)

While molecules of this type were first synthesized by San Filippo and coworkers[107,165] with the use of the third of these methods, the second method has subsequently become the most popular one. It is adaptable to a range of Me_3SiX reagents and can also be used to prepare compounds of the type $Mo_2Cl_4L_4$ (see Section 4.3.4) by the complete expulsion of all the carboxylate ligands.[123] The THF complex $Mo_2(O_2CCH_3)_2Cl_2(THF)_2$ has also been prepared by this same type of procedure. X-ray structure determinations have been carried out on several of these derivatives (Table 4.2) and, with one exception, they have been found[125] to possess the centrosymmetric *trans* structure **4.6**, like that of their alkyl[120,121] and siloxy[122] analogs. The exception is $Mo_2(O_2CCMe_3)_2Cl_2(PEt_3)_2$ which has been isolated and structurally characterized in both its *trans* (**4.6**) and *cis* (**4.7**) isomeric forms.[125] The isomers designated as α- and β-$Mo_2(O_2CCH_3)_2X_2(PEt_3)_2$ by Green *et al.*[123] probably correspond to structures **4.7** and **4.6**, respectively.



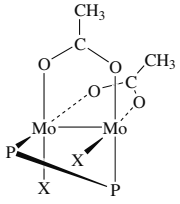
4.7

The lability of the PPh_3 ligand of *trans*-$Mo_2(O_2CCH_3)_2Cl_2(PPh_3)_2$ has been demonstrated by the conversion of this complex to the related PEt_3 and PBu^n_3 derivatives.[123] These reactions proceed by a stepwise dissociative mechanism as shown[122] by studies of the reactions of $Mo_2(O_2CCMe_3)_2X_2(PMe_2Et)_2$ X = CH_2SiMe_3, CH_2CMe_3, CH_3, Cl, Br, I, $N(SiMe_2H)_2$ or $OSiMe_3$) with PMe_3 at low temperatures to give $Mo_2(O_2CCMe_3)_2X_2(PMe_2Et)(PMe_3)$. From the magnitude of the $^3J_{PP}$ coupling constants, the structural *trans* effect was deduced to be alkyl > halide > amide > siloxy, an order that mirrors the kinetic *trans* effect.[122]

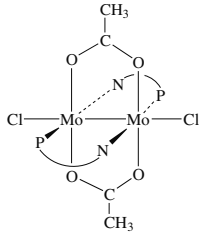
The aforementioned phosphine lability is further shown by the reaction of $Mo_2(O_2CCH_3)_2Cl_2(PPh_3)_2$ with the bidentate phosphine $Ph_2PCH_2PPh_2$ (dppm) in THF to give red-violet $Mo_2(O_2CCH_3)_2Cl_2(\mu\text{-dppm})$ when short reaction times are used.[190] As an al-

Pictiva EX2004
Samsung v Pictiva
IPR2024-01094

ternative synthetic route to the latter compound, the THF complex $Mo_2(O_2CCH_3)_2Cl_2(THF)_2$ has been reacted with dppm.[123] The complex $Mo_2(O_2CCH_3)_2Cl_2(\mu\text{-dppm})_2$ is unstable and decomposes to $Mo_2Cl_4(\mu\text{-dppm})_2$ in both solution and the solid state.[123,190] Compounds of the type $Mo_2(O_2CCH_3)_2X_2(\mu\text{-LL})$ (X = Cl or Br) that are much more stable than the dppm complex have been isolated in the case of LL = $Ph_2PCH_2CH_2PPh_2$, *cis*-$Ph_2PCH{=}CHPPh_2$ and 1,2-$C_6H_4(PPh_2)_2$,[190] and, on the basis of their spectroscopic and electrochemical properties, they have all been assigned the type of structure shown in **4.8**. While none of these bidentate phosphines react to form the 1:2 complexes of the type $Mo_2(O_2CCH_3)_2X_2(\mu\text{-LL})_2$, the 2-(diphenylphosphino)pyridine ligand forms such a compound.[126] Red crystalline *trans*-$Mo_2(O_2CCH_3)_2Cl_2(\mu\text{-}Ph_2Ppy)_2$ is produced, along with $Mo_2(CCH_3)_4$, upon heating $Mo_2Cl_4(Ph_2Ppy)_2$ with acetic acid. However, it is not isolated when $Mo_2(O_2CCH_3)_4$ is treated with Me_3SiCl and Ph_2Ppy since this reaction gives insoluble green $Mo_2Cl_4(Ph_2Ppy)_2$. The crystal structure of *trans*-$Mo_2(O_2CCH_3)_2Cl_2(\mu\text{-}Ph_2Ppy)_2$ shows[126] that this compound is centrosymmetric (**4.9**), although the Mo–Mo–Cl units are bent (*c.* 163°).



4.8



4.9

With the ligand $Ph_2PN(H)PPh_2$ (dppa) stable compounds such as that shown in Fig. 4.7 can be obtained[168] by the stoichiometric reactions:

$$Mo_2(O_2CCH_3)_4 + 2Me_3SiX + 2dppa \rightarrow \textit{trans}\text{-}Mo_2(O_2CCH_3)_2(dppa)_2(\textit{ax}\text{-}X)_2$$

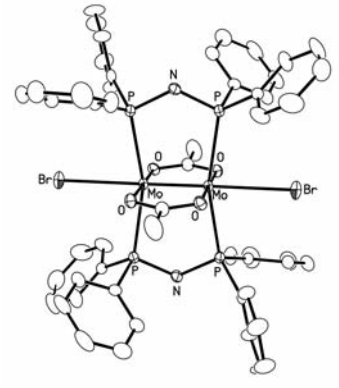


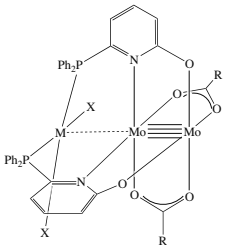
Fig. 4.7. The structure of $Mo_2(O_2CCH_3)_2(dppa)_2Br_2$.

The pyphos ligand, (2-Ph_2P)(6-O)py, has been exploited to allow additional metal ions (Pd^{2+}, Pt^{2+}) to be held in the axial positions of Mo_2^{4+} units. For example the type of molecule (which dimerizes) shown in **4.10** has been made[151] with R = CH_3 or CMe_3 and X = Cl, Br or I.

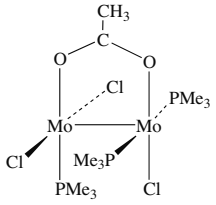
When $Mo_2(O_2CCH_3)_4$ is reacted with a mixture of LiCl (3 equiv) and PMe_3 in THF the mono(acetate) complex $Mo_2(O_2CCH_3)Cl_3(PMe_3)_3$ can be isolated in almost quantitative yield.[127]

Pictiva EX2004
Samsung v Pictiva
IPR2024-01094

Its X-ray crystal structure has been determined and shows a geometry (**4.11**) that minimizes repulsions between the PMe_3 ligands. This complex slowly converts to $Mo_2Cl_4(PMe_3)_4$ and $Mo_2(O_2CCH_3)_4$ when dissolved in THF.[127]



4.10



4.11

Of the remaining examples of reactions in which two of the carboxylate groups of $Mo_2(O_2CR)_4$ are displaced, most involve the binding of monoanionic *bridging* ligands. Exceptions to this include the reactions of $Mo_2(O_2CCH_3)_4$ with sodium acetylacetonate and lithium (4-phenylimino)-2-pentanonide in THF which lead to the formation of $Mo_2(O_2CCH_3)_2(acac)_2$[116] and $Mo_2(O_2CCH_3)_2[PhNC(CH_3)CHC(CH_3)O]_2$.[128] These compounds have a *cis* disposition of acetates and chelating $acac^-$ and $[PhNC(CH_3)CHC(CH_3)O]^-$ ligands. A more complicated system involves the reactions between $Mo_2(O_2CCH_3)_4$ and pyrazolylborate ligands.[129] With sodium diethyldipyrazolylborate, the reaction stoichiometry was adjusted to afford either red $Mo_2(O_2CCH_3)_2[(pz)_2BEt_2]_2$ or blue $Mo_2[(pz)_2BEt_2]_4$ (whose structure could not be determined) using 1,2-dimethoxyethane and toluene, respectively, as the reaction solvents. The structure of the mixed ligand complex (recrystallized from carbon disulfide) is similar to those of *cis*-$Mo_2(O_2CCH_3)_2(acac)_2$ and *cis*-$Mo_2(O_2CCH_3)_2[PhNC(CH_3)CHC(CH_3)O]_2$. A related complex, $Mo_2(O_2CCH_3)_2[(pz)_3BH]_2$, has been obtained using $KHB(pz)_3$ in place of $NaEt_2B(pz)_2$ and it too possesses a *cis* arrangement of acetate groups (Fig. 4.8).[129] This complex was prepared in order to ascertain whether the availability of three nitrogen donor atoms in each ligand (compared to two in $Et_2B(pz)_2^-$) would force the formation of two axial Mo–N bonds. In fact only one such axial bond is formed (at 2.45 Å) but it is far longer than the normal equatorial Mo–N bond lengths.[129] It appears that while the steric and conformational demands of one $HB(pz)_3$ ligand permit the approach of a pyrazolyl nitrogen atom at one of the axial sites, a similar conformation for two of these ligands within the dinuclear complex is not possible.

A complex with pairs of *cis* acetates and bridging monoanionic ligands is $Mo_2(O_2CCH_3)_2(\mu\text{-pdc})_2(OPPh_3)$, which is prepared by reacting $Mo_2(O_2CCH_3)_4$ with the potassium salt of the dithiocarbamate of pyrrole (Kpdc) and Ph_3PO.[114] *Trans* isomers of this general type are encountered in the case of the THF adduct of the bis(xylyl)acetamidinato complex *trans*-$Mo_2(O_2CCH_3)_2\{[(2,6\text{-xylyl})N]_2CCH_3\}_2$,[130] the *o*-(dimethylamino)benzyl ligand complex *trans*-$Mo_2(O_2CCH_3)_2[o\text{-}(Me_2N)C_6H_4CH_2]_2$,[131] the DMF adduct of *trans*-$Mo_2(O_2CCH_3)_2(7\text{-azaindolyl})_2$[132] and *trans*-$Mo_2(O_2CC_6H_5)_2[(Me_3SiN)_2CPh]_2$.[132] These compounds have all been prepared directly from $Mo_2(O_2CCH_3)_4$. Structural information is contained in Table 4.2. Interest in molybdenum-based catalysts has led to an investigation of the reaction between $Mo_2(O_2CCH_3)_4$ and aluminum isopropoxide. In decalin this reaction was found to yield the orange complex $Mo_2Al_2(O_2CCH_3)_2(OPr^i_7)_8$ which may be purified by sublimation.[191] Its structure consists of an eclipsed Mo_2O_8 skeleton, with a Mo–Mo distance of 2.079(1) Å, containing two acetate bridges in a *trans* disposition and two $[Al(OPr^i)_4]$ bridges.[133,191] The interest in this molecule lies in its reaction with oxygen and the potential this offers of oxidizing ligand groups.

Pictiva EX2004
Samsung v Pictiva
IPR2024-01094

The bis-carboxylate complexes $Mo_2(O_2CCH_3)_2(mhp)_2$ (mph is the anion of 2-methyl-6-hydroxypyridine)[192] and $Cs_2[Mo_2(O_2CH)_2(SO_4)_2]\cdot 2H_2O$[111,112] have been described; full details of their structures have not been established although the standard enthalpy of formation of $Mo_2(O_2CCH_3)_2(mhp)_2$ has been determined.[192]

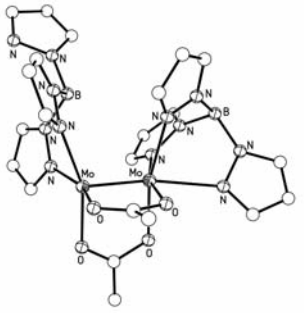


Fig. 4.8. The structure of $Mo_2(O_2CCH_3)_2[HB(pz)_3]_2$.

When solutions of the amino acid complexes $[Mo_2(O_2CCH_2NH_3)_4]^{4+}$, $[Mo_2(L\text{-isoleu})_4]^{4+}$, and $[Mo_2(D\text{-val})_2(L\text{-val})_2]^{4+}$, which are generated by dissolving $K_4Mo_2Cl_8$ in acidified aqueous solutions of the appropriate amino acid, are mixed with KNCS, the red crystalline species $Mo_2(\text{amino acid})_2(NCS)_4\cdot nH_2O$ are formed.[85,171] Each of these complexes has been structurally characterized (Table 4.2), and each possesses a cisoid arrangement of the amino acid ligands and four N-bonded NCS^- groups.

While $Mo_2(O_2CCF_3)_4$ reacts with pyridine to form the fairly stable 1:2 adduct,[29] reactions of this carboxylate with 2,2'-bipyridyl (bpy) are quite complicated. With 1:2 mole proportions of reagents ($Mo_2(O_2CCF_3)_4$:bpy) four different 'adducts' (two 1:1 and two 1:2) have been isolated[55,193] depending upon the choice of solvent. It was suggested (mainly on the basis of infrared spectral data) that these complexes possess structures in which the bpy ligands are chelating and the carboxylate ligands are present in one or more of the following modes – bidentate bridging, bidentate chelating, monodentate, and outer-sphere.[193] The crystal structure of a 1:2 adduct has shown it to be the ion-pair $[Mo_2(\mu\text{-}O_2CCF_3)_2(bpy)_2](O_2CCF_3)_2$.[55] This compound undergoes thermal and photochemical conversion to $Mo_2(\eta^1\text{-}O_2CCF_3)_4(bpy)_2$.[55] When $Mo_2(O_2CCF_3)_4$ is reacted with bpy in dichloromethane in the presence of $(Et_3O)BF_4$ the complex $[Mo_2(O_2CCF_3)_2(bpy)_2](BF_4)_2\cdot Et_2O$ is produced.[193] In the absence of $(Et_3O)BF_4$, the 1:1 adduct $[Mo_2(O_2CCF_3)_3(bpy)]^+[O_2CCF_3]^-$ is the principal product.[193] The reaction of $Mo_2(O_2CCH_3)_4$ with neat ethylenediamine (en)[134(a)] gives $[Mo_2(O_2CCH_3)_2(en)_4](O_2CCH_3)_2\cdot en$, which contains two *cis* bridging acetate ligands, two en bridges, and two monodentate terminally bound en ligands, which are disordered. This complex converts back to $Mo_2(O_2CCH_3)_4$ when heated at 120 °C in the solid state.[134(a)] When $Mo_2(O_2CCH_3)_4$ in en is reacted with K_2Te_4, the $[Mo_4Te_{16}(en)_4]^{2-}$ ion is formed.[134(b)] This tetranuclear molybdenum cluster actually contains pairs of confacial bioctahedral Mo_2^{6+} units with an Mo–Mo bond distance of 2.469(3) Å.[134(b)]

A few examples are known of dimolybdenum(II) complexes in which there is a single carboxylate bridge present. The compound $Cs_3[Mo_2(O_2CH)(SO_4)_3]\cdot 2H_2O$ has been described[111,112] but not yet fully characterized. Two complexes that contain one acetate and three other ligand bridges are $Mo_2(O_2CCH_3)(ambt)_3\cdot 2THF$ (THF is present as lattice solvent and ambt is the anion of 2-amino-4-methylbenzothiazole)[135] and $Mo_2(O_2CCH_3)[(PhN)_2CCH_3]_3$.[129] In both cases the anionic ligand is generated by treatment of the protonated form with Bu^nLi in THF/hexane, and then reacted with $Mo_2(O_2CCH_3)_4$. A more complicated molecule is the

Pictiva EX2004
Samsung v Pictiva
IPR2024-01094

ion-pair complex $(C_3N_2H_5)^+\{Mo_2(O_2CCH_3)[CH_3Ga(C_3N_2H_3)O]_4\}^-$, which was obtained as its bis-THF solvate upon reacting $Mo_2(O_2CCH_3)_4$ with $Na[CH_3Ga(C_3N_2H_3)_3]$ (i.e. the tridentate anionic ligand methyl(tris-pyrazolyl)gallate) in THF.[136] During the course of this reaction the $[CH_3Ga(C_3N_2H_3)_3]^-$ anion hydrolyzed to give the hexadentate ligand that was identified by a crystal structure determination.[136] The ion-pair is present in the gas phase as shown by the mass spectrum of this complex.[136] The first example of an alkyne addition to a metal–metal quadruple bond has been encountered in the reaction between $Mo_2(O_2CCH_3)_4$ and 4-$MeC_6H_4C{\equiv}CH$ in ethylenediamine.[194] Two alkyne containing isomers are formed in an approximate 1:1 ratio, and the X-ray crystal structure of one isomer revealed the structure to be that of the salt $[Mo_2(\mu\text{-}4\text{-}MeC_6H_4CCH)(\mu\text{-}O_2CCH_3)(en)_4](O_2CCH_3)_3{\cdot}2en$, in which the trication contains a perpendicular alkyne bridge and a Mo–Mo distance of 2.489(3) Å. The latter is consistent with a double bond.[194]

4.1.4 Paddlewheels with other O,O anion bridges

Relatively few are known, mainly those with $\mu\text{-}SO_4^{2-}$, $\mu\text{-}HPO_4^{2-}$ and $\mu\text{-}HAsO_4^{2-}$. The known structures as well as structures of some thio analogs are presented in Table 4.3.

Table 4.3. Dimolybdenum compounds with polyoxoanion bridges

Compound	Crystal sym.	Virtual sym.	*r*(Mo–Mo) Å	Twist angle	ref.
$K_4[Mo_2(SO_4)_4]{\cdot}2H_2O$	$\bar{1}$	C_{4h}	2.110(3)	0	195
$K_3[Mo_2(SO_4)_4]{\cdot}3.5H_2O$	1	C_{4h}	2.164(3)	~0	196
$Cs_2[Mo_2(HPO_4)_4(H_2O)_2]$	1	C_{4h}	2.223(2)	~0	197
$(pyH)_3[Mo_2(HPO_4)_4Cl_{2/2}]$	$\bar{1}$	C_{4h}	2.232(1)	0	197
$(pyH)_2[Mo_2(HAsO_4)_4(H_2O)_2]$	$\bar{1}$	C_{4h}	2.265(1)	0	198
$Mo_2[O_2P(OPh)_2]_4{\cdot}2H_2O$	$\bar{1}$	C_{4h}	2.141(2)	0	199
$Mo_2(OSPEt_2)_4(THF)$	$\bar{4}$	D_{4h}	2.128(2)	0	200
$Mo_2(S_2PEt_2)_4(THF)$	$\bar{1}$	C_{4h}	2.123(1)	0	200
$Mo_2(\mu\text{-}S_2PEt_2)_2(\kappa\text{-}S_2PEt_2)_2$	1	C_{2v}	2.137(1)	–	200

The compound $K_4[Mo_2(SO_4)_4]$ was first reported[201] in 1971 and the crystalline dihydrate was characterized crystallographically[202] soon after. Its structure is shown in Fig. 4.9. There are several good synthetic routes.[195,201-204] The $[Mo_2(SO_4)_4]^{4-}$ ion is red, diamagnetic, and has an absorption band at *c.* 520 nm which is presumed to correspond to the $\delta \rightarrow \delta^*$ transition. It is easily oxidized to the $[Mo_2(SO_4)_4]^{3-}$ ion,[196,205,206] which forms the crystalline compound $K_3[Mo_2(SO_4)_4]{\cdot}3.5H_2O$.

The structure of $K_3Mo_2(SO_4)_4{\cdot}3.5H_2O$ resembles that of $K_4Mo_2(SO_4)_4{\cdot}2H_2O$ except for the presence of axially bound water molecules (Mo–O distance of 2.550(4) Å) in place of sulfate oxygen.[195,196] The Mo–Mo distance is longer in the 3– ion (2.167(1) versus 2.111(1) Å) in accord with the loss of half of the δ-bond upon oxidation from $\sigma^2\pi^4\delta^2$ to $\sigma^2\pi^4\delta^1$. The magnetic and EPR spectrum[195,207] of this complex are in accord with the ground state configuration being $\sigma^2\pi^4\delta^1$.

The $[Mo_2(SO_4)_4]^{3-}$ anion has also been obtained in compounds with the formula $K_4[Mo_2(SO_4)_4]X{\cdot}4H_2O$ (X = Cl or Br) by the hydrogen peroxide oxidation of a solution of $K_4Mo_2Cl_8$ in 2 M H_2SO_4 and 0.3 M HCl, or 0.5 M HBr, to which is added KX.[208,209] These molecules are structurally similar to $K_3[Mo_2(SO_4)_4]{\cdot}3.5H_2O$ (the Mo–Mo distances are the same) but possess Mo···X axial interactions in place of Mo···OH_2. The presence of these continu-

Pictiva EX2004
Samsung v Pictiva
IPR2024-01094

ous, linear ···Mo–Mo···X···Mo–Mo···X··· chains confers properties that are advantageous in the study of the electronic structure and spectroscopic properties of the $[Mo_2(SO_4)_4]^{3-}$ anion.[209]

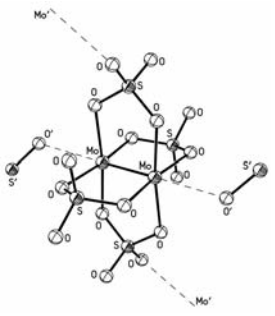


Fig. 4.9. The structure of the $[Mo_2(SO_4)_4]^{4-}$ ion in $K_4[Mo_2(SO_4)_4]\cdot 2H_2O$. The linking of these ions to one another is also shown. The water molecules are not coordinated to molybdenum atoms.

Solutions of $K_3[Mo_2(SO_4)_4]\cdot 3.5H_2O$ in 2 M H_2SO_4 are blue and have spectroscopic properties (e.g., λ_{max} at 412 nm) that are in accord[207] with the preservation of the $[Mo_2(SO_4)_4]^{3-}$ ion or a structurally related, partly aquated sulfate complex. Solutions in other strong acids (hydrochloric or *p*-toluenesulfonic acid) turn a deep red color as disproportionation to Mo_2^{4+} and Mo_2^{6+} species occurs.[207,210] This disproportionation reaction can be reversed upon the addition of K_2SO_4, the blue complex $K_3[Mo_2(SO_4)_4]\cdot 3.5H_2O$ being regenerated.[207] The Mo_2^{6+} species cannot be isolated.

An interesting derivative of $[Mo_2(SO_4)_4]^{4-}$ has been prepared in virtually quantitative yield by the reaction of $Mo_2(O_2CCH_3)_4$ with concentrated H_2SO_4 in pyridine.[211] This molecule is of composition $Mo_2(SO_4)_2(py)_8$, and has been shown by X-ray crystallography to be centrosymmetric with a *trans* arrangement of bridging sulfate groups and three kinds of pyridine molecule. Four pyridines are bound in equatorial sites, two in axial sites, and two more are present in interstitial positions.[211] The Mo–Mo bond length is 2.134(2) Å.

Displacement of the acetate ligands of $Mo_2(O_2CCH_3)_4$, by methylsulfonate and trifluoromethylsulfonate can be accomplished[212,213] to produce the analogous ligand-bridged dimolybdenum(II) complexes $Mo_2(O_3SCH_3)_4$ and $Mo_2(O_3SCF_3)_4$. Temperatures of close to 100 °C were required for the reaction between these sulfonic acids and $Mo_2(O_2CCH_3)_4$, the reaction with CH_3SO_3H having been carried out in diglyme. While purification of $Mo_2(O_3SCF_3)_4$ can be accomplished by sublimation to afford air-sensitive crystals, it has in fact proven difficult to remove the last traces of acetate impurity.[213] In an attempt to circumvent this problem an alternative synthetic procedure was investigated, namely, the reaction of $Mo_2(O_2CH)_4$ with CF_3SO_3H and $(CF_3SO_2)_2O$.[178] However, this gives the hydrate $[Mo_2(O_3SCF_3)_2(H_2O)_4](CF_3SO_3)_2$ which cannot be dehydrated, although its reaction with acetonitrile affords $[Mo_2(NCCH_3)_8](CF_3SO_3)_4$ (see Section 4.3.5). An ethanol solution of $Mo_2(O_3SCF_3)_4$ when treated with formic acid yields the formate complex $Mo_2(O_2CH)_4$.[213] The methylsulfonate complex $Mo_2(O_3SCH_3)_4$ has been converted to the 1:2 adducts $Mo_2(O_3SCH_3)_4L_2$ (L = γ-butyrolactone or dimethylformamide), to the mixed methylsulfonate-halide complexes $(Me_4N)_2[Mo_2(O_3SCH_3)_2Cl_4]$ and $(Bu_4N)_2[Mo_2(O_3SCH_3)_2X_4]$ (X = Br or I) upon reaction with the appropriate substituted ammonium halide, and to the octakis(isothiocyanato)dimolybdate(II) anion upon stirring with a dimethoxyethane solution of NH_4NCS.[212] The reaction of '$Mo_2(O_3SCF_3)_4$' (or more probably $[Mo_2(O_3SCF_3)_2(H_2O)_4](CF_3SO_3)_2$) with 1,5,9,13-tetrathiacyclohexadecane yields several products,[214] in none of which is there a Mo–Mo multiple bond.

Pictiva EX2004
Samsung v Pictiva
IPR2024-01094

Phosphate-, arsenate-, diarylphosphate-, phosphinate-, and phosphonate-bridged complexes of Mo_2^{4+}, Mo_2^{5+} and Mo_2^{6+}.

While further oxidation of $[Mo(SO_4)_4]^{3-}$ to give an isolable species with a triple bond has not been observed, the formation of the triply-bonded dimolybdenum(III) species $[Mo_2(HPO_4)_4]^{2-}$ takes place very easily. Simply by dissolving $K_4Mo_2Cl_8{\cdot}2H_2O$ in aqueous 2 M H_3PO_4 and allowing the solution to stand in an open beaker for 24 h, with larger cations such as Cs^+ or pyridinium also present, purple crystalline materials containing this triply-bonded species are formed.[197] The structures of both $Cs_2[Mo_2(HPO_4)_4(H_2O)_2]$, which has axial water molecules, and $(pyH)_3[Mo_2(HPO_4)_4]Cl$, in which there are infinite chains with shared Cl^- ions occupying axial positions, have been determined. While the hydrogen atoms of the HPO_4^{2-} ligands were not observed, it is easy to tell where they are from the outer P–O distances. One on each ligand is about 1.48 Å (P=O) and the other is about 1.54 Å (P–OH). The O=P–OH moieties are so arranged that the overall symmetry of the $[Mo_2(HPO_4)_4]^{2-}$ ion is C_{4h}; however, the inner Mo_2O_8 portion of the ion has effective D_{4h} symmetry and the bonding can be simply understood as a $\sigma^2\pi^4$ configuration. The bromide salt $(pyH)_3[Mo_2(HPO_4)_4]Br$ has been prepared starting from $Mo_2(O_2CCH_3)_4$, and is isostructural with its chloride analog.[198] Both the chloride and bromide complexes show Raman-active ν(Mo–Mo) modes at *c.* 360 cm^{-1} and have very similar electronic absorption spectra.[198,215]

While the above complexes[197] were the first dimolybdenum phosphates to be isolated, Bino showed[210] soon thereafter that light-purple colored solutions of $[Mo_2(HPO_4)_4]^{2-}$ in 2 M H_3PO_4 could be reduced by zinc amalgam under nitrogen first to pale-blue/gray Mo_2^{5+} and then to deep-red Mo_2^{4+} phosphate species. Later, solutions of the dimolybdenum(II) complex $[Mo_2(HPO_4)_4]^{4-}$ were generated by the reactions of $K_4Mo_2Cl_8$, $K_4Mo_2(SO_4)_4$ or $[Mo_2(aq)]^{4+}$ with H_3PO_4 under anaerobic conditions.[216] The one-electron oxidation of this species was carried out to afford the paramagnetic salt $K_3Mo_2(HPO_4)_4$. While neither of the species $[Mo_2(HPO_4)_4]^{4-}$ or $[Mo_2(HPO_4)_4]^{3-}$ has been structurally characterized by X-ray crystallography, the close structural relationship between them is shown by the reversibility of their electrochemical properties. Cyclic voltammetric measurements on 2 M H_3PO_4 solutions of $[Mo_2(HPO_4)_4]^{4-}$ (with use of a glassy carbon electrode) show redox processes at –0.67 and –0.25 V versus SCE that have been attributed to the (3–/4–) and (2–/3–) couples, respectively.[216] Whereas $[Mo_2(HPO_4)_4]^{4-}$ reacts thermally in 2M H_3PO_4 to produce $[Mo_2(HPO_4)_4]^{3-}$ and H_2 over a period of several days, UV irradiation ($\lambda \geq 335$ nm) leads to the facile production of $[Mo_2(HPO_4)_4]^{2-}$ and H_2, by one-electron steps via the high energy $\pi \rightarrow \pi^*$ excited state.[216,217] The thermal reaction is believed to involve the slow conversion of $[Mo_2(HPO_4)_4]^{4-}$ to $[Mo_2(HPO_4)_4]^{2-}$ which then reacts in an ensuing comproportionation reaction with $[Mo_2(HPO_4)_4]^{4-}$ to give $[Mo_2(HPO_4)_4]^{3-}$.

In addition to the extensive photochemical studies that have been carried out on these phosphate complexes,[216,217] detailed measurements have been made on the electronic absorption spectra of the 4–, 3–, and 2– anions,[215,216] and the magnetic properties and EPR spectrum of $K_3[Mo_2(HPO_4)_4]$ which possesses the $\sigma^2\pi^4\delta^1$ configuration, have been examined down to 5 K.[216]

Several dimolybdenum(III) arsenate analogs of these phosphato complexes have been prepared, namely, $Cs_2[Mo_2(HAsO_4)_4]{\cdot}3H_2O$, $(pyH)_2[Mo_2(HAsO_4)_4]{\cdot}2H_2O$, and $(pyH)_3[Mo_2(HAsO_4)_4]X$ (X = Cl or Br). In the case of $(pyH)_2[Mo_2(HAsO_4)_4]{\cdot}2H_2O$ its identity was confirmed by X-ray crystallography.[198] The structure of the $[Mo_2(HAsO_4)_4]^{2-}$ anion is closely akin to that of its phosphate analog, with a Mo–Mo triple bond distance of 2.265(1) Å. The Mo–Mo stretching frequencies of these arsenate complexes (*c.* 330 cm^{-1}) are a little lower than those in the Raman spectra of their phosphate analogs (*c.* 360 cm^{-1}).[198,215]

Pictiva EX2004
Samsung v Pictiva
IPR2024-01094

The dimolybdenum(II) diphenylphosphato complex $Mo_2[O_2P(OPh)_2]_4$ is formed upon addition of excess $(PhO)_2PO_2H$ to $Mo_2(O_3SCF_3)_4$ in methanol.[199] While complete displacement of the triflate ligands occurs in this reaction, the use of $Mo_2(O_2CCH_3)_4$ in place of $Mo_2(O_2SCF_3)_4$ gives a product in which only partial replacement of acetate ligands has occurred. The tetrakisdiphenylphosphate complex has also been prepared from $(NH_4)_5Mo_2Cl_9 \cdot H_2O$.[218] The crystal structure of the THF adduct $Mo_2[O_2P(OPh)_2]_4 \cdot 2THF$ has been determined; the two THF molecules are bound weakly in axial positions (Mo–O = 2.656(9) Å).[199] This complex readily undergoes a one-electron oxidation as shown by cyclic voltammetry and chemical oxidation with $[(\eta^5\text{-}C_5H_5)_2Fe]PF_6$. The resulting product, $\{Mo_2[O_2P(OPh)_2]_4\}PF_6$, is paramagnetic with magnetic susceptibility and EPR spectral properties in accord with the presence of one unpaired electron.[199]

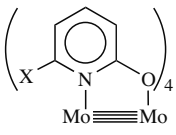
Measurements of the electronic absorption spectra of $Mo_2[O_2P(OPh)_2]_4$ and its one-electron oxidized congener show that the $\delta \rightarrow \delta^*$ transition shifts from *c.* 20,000 cm^{-1} to *c.* 6,500 cm^{-1}.[199] In the case of the Mo_2^{4+} complex, the chemistry of the $^1(\delta\delta^*)$ excited state has been examined.[217,218] In the solid state and solution, this complex exhibits weak luminescence upon excitation into the $\delta^2 \rightarrow \delta\delta^*$ absorption band. Solutions of $Mo_2[O_2P(OPh)_2]_4$ in 1,2-dichloroethane undergo the following photoreaction when excited with visible light ($\lambda \geq 530$ nm):[218]

$$2Mo_2[O_2P(OPh)_2]_4 + ClCH_2CH_2Cl \xrightarrow{h\nu\ (\geq 530\ nm)} 2Mo_2[O_2P(OPh)_2]_4Cl + CH_2CH_2$$

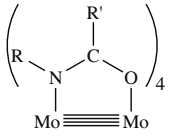
4.2 Paddlewheel Compounds with O,N, N,N and Other Bridging Ligands

4.2.1 Compounds with anionic O,N bridging ligands

These compounds fall into two main classes: (1) those with 2-oxopyridine type ligands (**4.12**), and those with noncyclic amidate ligands (**4.13**). We include here also several thio analogs. Structural data are collected in Table 4.4.



4.12



4.13

There are two main methods of preparation for the 2-oxopyridine compounds, namely, the reaction of the free ligand or its monoanion with $Mo_2(O_2CCH_3)_4$ or $Mo(CO)_6$.[220,222-236,238-240]. In general, these compounds do not have axial ligands; the structure of $Mo_2(mhp)_4$ is shown in Fig. 4.10 where the ligand arrangement gives D_{2d} symmetry to the central $Mo_2N_4O_4$ core. The structures of the chp and dmhp molecules are similar. In contrast, the fhp ligand gives a structurally different product, $Mo_2(fhp)_4THF$, in which all fhp ligands point in the same direction.[223] This completely blocks one axial position but leaves the other one free to accommodate the axial THF molecule. With mhp and chp it is impossible to have all four substituents (Me or Cl) at the same end. Since four F atoms can fit at one end, they do so and this allows one more bond, to axial THF at the other end, to be formed.

Pictiva EX2004
Samsung v Pictiva
IPR2024-01094

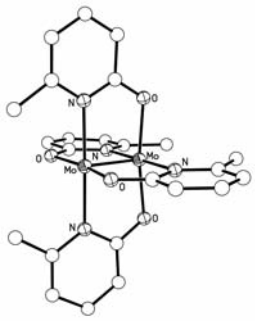


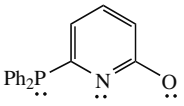
Fig. 4.10. The $Mo_2(mhp)_4$ molecule as found in $Mo_2(mhp)_4{\cdot}CH_2Cl_2$. Note the D_{2d} symmetry of the $Mo_2N_4O_4$ core.

Table 4.4. Structures of Mo_2^{4+} compounds with anionic O,N bridging ligands

Compound	Crystal sym.	Virtual sym.	*r*(Mo–Mo) (Å)	Twist Angle (°)	ref.
$Mo_2(mhp)_4$	1	D_{2d}	2.067(1)	≈0	219
$Mo_2(mhp)_4{\cdot}CH_2Cl_2$	1	D_{2d}	2.065(1)	1.3	220
$Mo_2(mhp)_4{\cdot}CH_3OH$	1	D_{2d}	2.068(1)	≈0	219
cis-$Mo_2(mhp)_2Cl_2(PEt_3)_2$	1	C_2	2.103(1)	≈0	221
$Mo_2(chp)_4$	1	D_{2d}	2.085(1)	3.1	222
$Mo_2(fhp)_4{\cdot}THF$	1	C_{4v}	2.092(1)	≈0	223
$Mo_2(dmhp)_4{\cdot}diglyme$	1	D_{2d}	2.072(1)	0.3	224
$[Mo_2(mhp)_3(CH_3CN)_2](BF_4){\cdot}2CH_3CN$	1	C_s	2.103(1)	NR	169
$Mo_2(pyphos)_4{\cdot}CH_2Cl_2$	1	D_{2d}	2.098(2)	≈0	225
$Mo_2(pyphos)_4{\cdot}2CH_2Cl_2$	$\bar{1}$	C_{2h}	2.103(1)	zero	226
$Mo_2(pyphos)_4Pd_2(TCNE)_2$	2	D_{2d}	2.097(2)	NR	227
$Mo_2(pyphos)_4Pd_2Cl_2(CH_2Cl_2)$	2	D_{2d}	2.106(2)	NR	227
$Mo_2(pyphos)_4Pd_2Cl_4$	2	D_{2d}	2.096(3)	NR	225
$Mo_2(pyphos)_4Pd_2Br_4$	2	D_{2d}	2.095(4)	NR	225
$Mo_2(pyphos)_4Pt_2Cl_4$	2	D_{2d}	2.101(2)	NR	225
Mo_2(2-O-7-Me-naphthyridine)$_4$	$\bar{1}$	D_{2d}	2.090(4)	1	228
Mo_2(2-S-7-Me-naphthyridine)$_4$	2	D_{2d}	2.131(2)	8	228
$Mo_2[Bu^tNC(CH_3)O]_4$	$\bar{1}$	C_{2h}	2.063(1)	0	229
$Mo_2[PhNC(CH_3)O]_4{\cdot}2THF$	$\bar{1}$	C_{2h}	2.086(2)	0	230
$Mo_2[PhNC(CMe_3)O]_4$	$\bar{1}$	C_{2h}	2.070(1)	0	231
$Mo_2[(2,6\text{-xylyl})NC(CH_3)O]_4{\cdot}2CH_2Cl_2$	1	C_{2v}	2.083(2)	≈0	232
$Mo_2[(2,6\text{-xylyl})NC(CH_3)O]_4{\cdot}2CH_2Br_2$	1	C_{2v}	2.086(2)	≈0	233
$Mo_2[(2,6\text{-xylyl})NC(H)O]_4{\cdot}2THF$	2	D_{2d}	2.113(1)	≈0	231
$Mo_2[(2,6\text{-xylyl})NC(CH_3)O)]_4{\cdot}2THF$	1	C_{2v}	2.097(3)	≈0	234
	2	C_{2v}	2.093(2)	≈0	234
$Mo_2[(2,6\text{-xylyl})NC(CH_3)O]_4{\cdot}py{\cdot}C_6H_6$	1	C_{2v}	2.101(1)	≈0	234
$Mo_2[(2,6\text{-xylyl})NC(CH_3)O]_4{\cdot}4\text{-pic}$	2	C_{2v}	2.102(1)	≈0	234
Mo_2(2-mq)$_4$	1	D_{2d}	2.089(1)	≈0	235
$Mo_2(dmmp)_4{\cdot}CH_2Cl_2$	1	D_{2d}	2.083(1)	≈0	236
$Mo_2[MeNC(PPh_2)S]_4$	1	D_{2d}	2.083(1)	≈0	237
$Mo_2[MeNC(PPh_2)S]_2[MeNC(S)PPh_2]_2$	$\bar{1}$	C_i	2.104(2)	0	237

Pictiva EX2004
Samsung v Pictiva
IPR2024-01094

The pyphos ligand, 4.14, is a special case because the substituent at the 6-position, Ph_2P, is also a potential electron donor. The structure of $Mo_2(pyphos)_4$ is shown in Fig. 4.11, where the presence of two Ph_2P "claws" at each end can be seen. In a series of papers[225-227,241] K. Mashima and A. Nakamura have shown how these "claws" can be used to capture Pd^{2+}, Pd^{1+} and Pd^0 atoms and also Pt^{2+} ion, and they have explored the chemistry of the various tetranuclear species. The presence of the captured metal atoms has very little effect on the Mo–Mo bond lengths although small changes occur in the ν(Mo–Mo) frequencies in the Raman spectra.



4.14

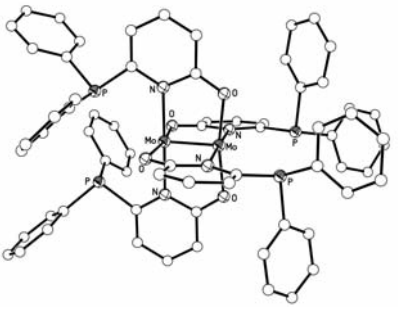


Fig. 4.11. The structure of the $Mo_2(pyphos)_4$ molecule showing how two Ph_2P "claws" are in place at each end for capturing other metal atoms such as Pd and Pt.

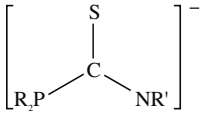
The compounds with noncyclic amidate bridging ligands are generally prepared by reaction of $Mo_2(O_2CCH_3)_4$ with the ligand in anionic form.[229-233] Both C_{2h} and D_{2h} arrangements of the $Mo_2N_4O_4$ core are found.[230,232-234] The particular amidato ligand $CH_3C(O)NH$ arises in several compounds[242,243] as the hydrolysis product of the CH_3CN ligand. It is believed that this normally very slow hydrolysis is catalyzed by the metal atoms.

For $Mo_2(mhp)_4$, the standard enthalpy of formation has been determined.[192] Mass spectral measurements on $Mo_2(mhp)_4$, $MoW(mhp)_4$ and $Mo_2[pyNC(O)CH_3]_4$ have confirmed[220,238,244,245] that the dinuclear structure is retained in the vapor phase and an extensive PES study has been carried out on $Mo_2(mhp)_4$,[244] as well as a gas phase XPS study of $Mo_2(mhp)_4$.[94] The Raman spectra of the molybdenum-containing mhp complexes gave M–M stretching frequencies of 504, 425 and 384 cm^{-1} for the Cr–Mo, Mo–Mo and Mo–W bonds.[220,246] In the case of the polar molecule $Mo_2(fhp)_4 \cdot THF$, the ν(Mo–Mo) mode has been assigned to a band at *c.* 430 cm^{-1}.[223]

The reaction of $Mo_2(mhp)_4$ with a cesium halide and the appropriate hydrogen halide in refluxing methanol produces $Cs_4Mo_2X_8$ (X = Cl or Br).[247] When a $Bu_4NI/HI(g)/THF$ mixture is used, $Mo_2(mhp)_4$ is converted to $(Bu_4N)_2Mo_4I_{11}$.[247] The synthetic utility of $Mo_2(mhp)_4$ is further shown by its reactions with $Mo_2X_4(PR_3)_4$ to form complexes of the type $Mo_2X_2(mhp)_2(PR)_2$.[248] An alternative synthetic strategy involves reacting $Mo_2(mhp)_4$ with Me_3SiCl in the presence of PR_3.[221]

Several dimolybdenum complexes containing the ligand type 4.15, with R' = Ph or Me, have been examined.[237] Both N,P and N,S modes of bridging are found. A molecule with the latter is shown in Fig. 4.12.

Pictiva EX2004
Samsung v Pictiva
IPR2024-01094



4.15

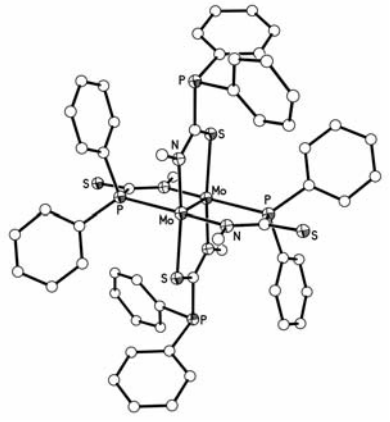
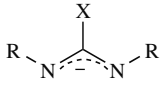


Fig. 4.12. The structure of the green isomer of $Mo_2[Ph_2PC(S)NMe]_4$ showing the occurence of both N,S, and N,P coordination modes.

4.2.2 Compounds with anionic N,N bridging ligands

Anionic bridging ligands with the type of anionic structure shown as **4.16** have emerged as especially important. Table 4.5 lists structurally characterized molecules that contain only one Mo_2^{4+} unit bridged by at least one such ligand. Compounds containing two or more Mo_2^{4+} units connected by linkers are treated in Section 4.5 and compounds in which the dimolybdenum unit has been oxidized to Mo_2^{5+} or Mo_2^{6+} are discussed in Section 4.4.2.



4.16

Pictiva EX2004
Samsung v Pictiva
IPR2024-01094

Table 4.5. Compounds with anionic N,N bridging ligands

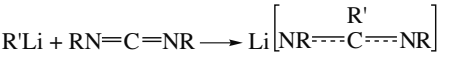
Compound	Crystal sym.	Virtual sym.	*r*(Mo–Mo) (Å)	Twist Angle (°)	ref.
$Mo_2[EtC(O)Npy]_4$	1	D_{2d}	2.083(1)	≈0	249
	1	D_{2d}	2.087(1)	≈0	
	1	D_{2d}	2.081(1)	≈0	
$Mo_2(map)_4 \cdot 2THF$	1	D_{2d}	2.070(1)	1.6	239
$Mo_2(PhNpy)_4$	$\bar{1}$	C_{2h}	2.073(2)	0	240
	$\bar{1}$	C_{2h}	2.068(2)	0	
$Mo_2[(PhN)_2CPh]_4$	2	D_{4h}	2.090(1)	≈0	250
$Mo_2\{[(p\text{-tol})N]_2CH\}_4$	4	D_{4h}	2.085(4)	3.2	251
$Mo_2(N_3Ph_2)_4 \cdot {}^1/_2C_7H_8$	1	D_{4h}	2.083(2)	10.5	252
$Mo_2(DPhF)_4$	$\bar{1}$	D_{4h}	2.094(1)	zero	253
$Mo_2(D^{3,5\text{-}Cl_2}PhF)_4$	$\bar{1}$	D_{4h}	2.096(1)	zero	253
$Mo_2(D^{m\text{-}Cl}PhF)_4$	$\bar{1}$	D_{4h}	2.097(1)	zero	254
$Mo_2(DAniF)_4$	$\bar{1}$	D_{4h}	2.096(1)	zero	254
$Mo_2(D^{p\text{-}Cl}PhF)_4$	$\bar{1}$	D_{4h}	2.090(1)	zero	255
$Mo_2(D^{p\text{-}Br}PhF)_4$	$\bar{1}$	D_{4h}	2.087(2)	zero	256
$Mo_2(azin)_4(Me_2CO)_2$	$\bar{1}$	C_{2h}	2.135(1)	zero	257
$Mo_2(azin)_4(THF)_2$	$\bar{1}$	C_{2h}	2.124(1)	zero	257
$Mo_2(ambt)_4 \cdot THF$	$\bar{1}$	C_{2h}	2.103(1)	0	135
$Mo_2(acbt)_4 \cdot THF$	$\bar{1}$	C_{2h}	2.117(1)	0	135
$[(C_7H_7)NH_3][Mo_2(\mu\text{-}(HNC(CH_3)NC_7H_7))(CH_3CN)_6](BF_4)_4 \cdot 3CH_3CN$	1	C_s	2.157(1)	NR	242
trans-$Mo_2(O_2CCH_3)_2[PhC(NSi(CH_3)_3)_2]_2$	2	D_{2h}	2.069(1)	NR	144
cis-$Mo_2(O_2CCH_3)_2[PhC(NSi(CH_3)_3)_2]_2$	2	C_{2v}	2.124(1)	NR	144
$Mo_2(DPhIP)_4$	1	D_{2h}	2.114(1)	NR	258
$Mo_2(DPhIP)_4(CH_3CN)(CuCl_2)_2 \cdot 2CH_3CN$	1	D_{2h}	2.078(1)	NR	258
$Mo_2(DPhIP)_2(O_2CCH_3)_2$	$\bar{1}$	C_{2h}	2.089(1)	NR	258
$Mo_2(DpyF)_4$	$\bar{1}$	D_{4h}	2.110(1)	0	259
$[Mo_2(DpyF)_4Co][CoCl_4]$	2	C_{2v}	2.115(5)	NR	259

Pictiva EX2004
Samsung v Pictiva
IPR2024-01094

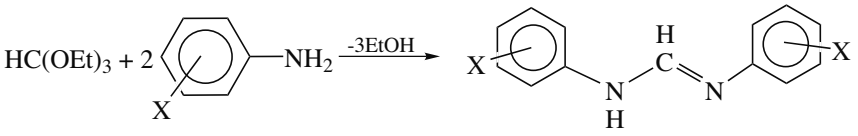
Compound	Crystal sym.	Virtual sym.	*r*(Mo–Mo) (Å)	Twist Angle (°)	ref.
$[Mo_2(DpyF)_4Cu_4Cl_2](CuCl_2)_2$	2	D_{2d}	2.127(1)	NR	259
$Mo_2(HBPAP)_4$	1	D_{2d}	2.081(1)	NR	260
$[Mo_2(O_2CCH_3)_2(pynp)_2](BF_4)_2$	1	C_2	2.124(1)	≈0	149
cis-$[Mo_2(mphamnp)_2(O_2CCH_3)_2]\cdot C_5H_{12}$	2	C_2	2.097(2)	NR	150
Hmphamnp = 2-acetamido-5-methyl-7-phenyl-1,8-naphthyridine					
trans-$[Mo_2(mbznnp)_4]$	1	D_{2d}	2.091(3)	*c.* 1	150
mbznnp = 2-benzylamino-7-methyl-1,8-naphthyridine					
cis-$[Mo_2(mphonp)_4]\cdot Et_2O$	$\bar{1}$	C_{2h}	2.079(2)	zero	150
Hmphonp = 5-methyl-7-phenyl-1,8-naphthyridin-2-one					
trans-$[Mo_2(mphonp)_4]\cdot Et_2O$	1	D_{2d}	2.084(1)	*c.* 3	150
$Mo_2(\mu\text{-dpa})_4$	2	D_{2d}	2.097(1)	3.4	64
Hdpa = bis(2-pyridyl)amine					
$Mo_2(TPG)_4$	2	D_{4h}	2.084(1)	4.5	261
$Mo_2(hpp)_4$	$\bar{1}$	D_{4h}	2.067(1)	zero	262
cis-$Mo_2(DAniF)_2(calix)$	1	C_{2v}	2.118(3)	≈0	263
			2.122(3)	≈0	
			2.125(3)	≈0	
			2.127(3)	≈0	
trans-$\{Mo_2[(C_6H_5N)_2CH]_2py_4\}(BF_4)_2$	$\bar{1}$	D_{2h}	2.107(2)	≈0	264
$\{Mo_2[(C_6H_5N)_2CH](CH_3CN)_6\}(BF_4)_3$	1	C_{2v}	2.149(1)	≈0	264
	1	C_{2v}	2.151(1)	≈0	
cis-$\{Mo_2(C_6H_5N)_2CH]_2(CH_3CN)_4\}(BF_4)_2$	1	C_{2v}	2.146(1)	≈0	264
cis-$\{Mo_2[(p\text{-}MeOC_6H_4N)_2CH]_2(CH_3CN)_4\}(BF_4)_2$	1	C_{2v}	2.144(1)	≈0	264
$\{Mo_2[(p\text{-}MeOC_6H_4N)_2CH](CH_3CN)_6\}(BF_4)_3$	1	C_{2v}	2.152(1)	≈0	265

Pictiva EX2004
Samsung v Pictiva
IPR2024-01094

The ligands of type **4.16** come in a variety of shapes and sizes, but the largest class is the amidinates, in which X is C–H or C–R. The former are called formamidinates and there are more of these than any other kind. All amidinate complexes of Mo_2^{4+} are fairly easily made by reaction of $Mo_2(O_2CCH_3)_4$ with the amidinate anion although other preparative reactions are known. The amidines themselves (or their anions) are also easy to make from carbodiimides according to the reaction:



For the special case of diaryl formamidinates, **4.17**, the use of triethylorthoformate and a primary amine allows for a very wide choice of substituents on the nitrogen atoms, as shown in the following reaction:

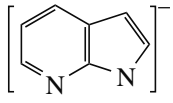


4.17

While practically all the amidinates that have been used are symmetrical, unsymmetrical ones, PhNC(H)N(2-py) being an important example, can be made in other ways.[266]

Other ligands mentioned in Table 4.5 are triazinates, RN_3R^-, 2-aminopyridines, especially anilinopyridine (pyNPh), 7-azaindole, **4.18** (azin), and map, the amino analog of mhp. These compounds have no special features, although the azin ligand gives relatively long Mo–Mo bonds. In addition to $Mo_2(Ph_2N_3)_4$ which is of known structure, the $Mo_2(tol_2N_3)_4$ compound is also known.[97] It was made in an unusual way, as shown in the following reaction:

$$Mo_2R_2(NMe_2)_4 + 4(p\text{-tol})N(H)NN(p\text{-tol}) \rightarrow Mo_2[N_3(p\text{-tol})_2]_4 + 4HNMe_2 + \text{alkane} + \text{alkene}$$



4.18

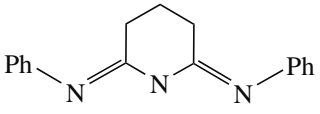
The first reported $Mo_2(amidinate)_4$ compound contained the N,N'-diphenylbenzamidinate ligand, $(PhN)_2CPh^-$. This and its di-*p*-tolyl analog were obtained by reacting the amidine with $Mo(CO)_6$ in a refluxing hydrocarbon.[250] Both products displayed strong resonance-enhanced Raman lines at 412 cm^{-1}, indicative of the quadruple bonds present. Subsequent work[251,267] showed that this synthetic method was generally valid, especially for formamidines. However, an alternative method in which a formamidinate anion reacts with $Mo_2(O_2CCH_3)_4$ is now generally preferred.

The most thoroughly investigated $Mo_2(amidinate)_4$ compounds are those in which the amidinate is a diarylformamidinate,[268] of the type **4.17**. As the six entries in Table 4.5 show, the Mo–Mo distance is essentially insensitive to the substituents on the aryl groups, even though the Hammett σ parameters cover an enormous range, from −0.27 to +0.74. It is also true that the HOMO–LUMO (δ–δ*) gap is essentially insensitive to the changes in aryl groups. How-

Pictiva EX2004
Samsung v Pictiva
IPR2024-01094

ever, the absolute energy of the HOMO is very sensitive and this shows up dramatically in the oxidation potentials measured electrochemically, as will be discussed fully in Section 4.4.2.

The anionic ligand DPhIP, **4.19**, forms a paddlewheel complex,[258] $Mo_2(DPhIP)_4$, in which the Mo–Mo distance is long compared to those in other Mo_2^{4+} paddlewheel complexes with N,N bridging ligands. As shown in Fig. 4.13(a), the longer-than-expected Mo–Mo distance (i.e., 2.114(1) Å instead of about 2.07 Å) may be attributed to donation of lone-pair electron density of the four non-bonded nitrogen atoms into the π* orbitals. When two Cu^I atoms are introduced, as shown in Fig. 4.13(b), they become the receptors for this electron density and the Mo–Mo distance decreases to 2.078 Å.



4.19

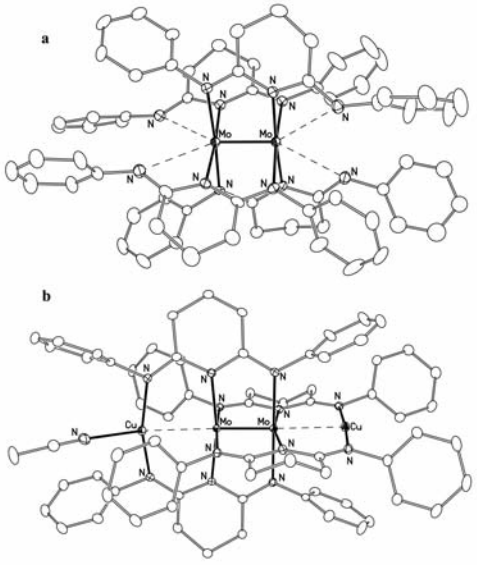
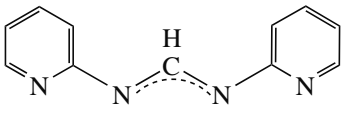


Fig. 4.13. (a) The $Mo_2(DPhIP)_4$ molecule. (b) The $[Mo_2(DphIP)_4Cu_2(CH_3CN)]^{2+}$ cation. The four N → Mo dative interactions in (a) are replaced by N → Cu bonds in (b) thereby decreasing the Mo–Mo distance from 2.114(1) Å to 2.078(1) Å.

With the bridging ligand DpyF, **4.20**, which has the potential to form several regioisomers of $Mo_2(DpyF)_4$, only one, in which all four ligands employ the two central nitrogen atoms, was isolated.[259] The eight dangling py groups do not interact with the axial positions of the Mo_2^{4+} units. This molecule can, however, interact with additional cations (Co^{2+}, Cu^+) through its pyridyl nitrogen atoms to give the two compounds listed below it in Table 4.5. These acquired metal ions show little or no interaction with the central Mo_2^{4+} unit.

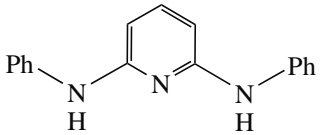
The $Mo_2(HBPAP)_4$ compound[260] (see **4.21** for H_2BPAP) as well as its chromium analog have paddlewheel structures in which four N–H hydrogen atoms are located close to the axial positions of the dimetal units. As a result of the large diamagnetic anisotropy of the M_2 unit, their chemical shifts are *c.* 3 ppm upfield from where they would normally be expected.

Pictiva EX2004
Samsung v Pictiva
IPR2024-01094



DpyF

4.20



H_2BPAP

4.21

Several Mo_2L_4 paddlewheels have been made in which L is a substituted naphthyridine.[150] In only one case,[149] $[Mo_2(O_2CCH_3)_2(pynp)_2]^{2+}$, where pynp represents 2-(2-pyridyl)-1,8-naphthyridine, does the napthyridine moiety itself bridge the metal atoms. Instead, in other cases one such nitrogen atom and an adjacent NR^- or O^- form an NCN or NCO bridging group.

Finally, there are two paddlewheel compounds in which the bridging groups are guanidinate anions, $Mo_2(TPG)_4$ and $Mo_2(hpp)_4$. The chief interest of both of these, particularly the latter, is the degree to which guanidinates stabilize the higher oxidation states, Mo_2^{5+} and Mo_2^{6+}. This topic will be discussed at length in Section 4.4.2

4.2.3 Compounds with miscellaneous other anionic bridging ligands

Mono- and dithiocarboxylates.

Many $Mo_2(OSCR)_4$ and $Mo_2(S_2CR)_4$ compounds are known; among the former are those with R = CH_3, Ph, $C_5H_4FeC_5H_5$[269-271] and among the dithiocarboxylates are those with R = CH_3, Ph and *p*-tolyl.[269,272,273] In addition there are dithiocarbonates (xanthates) $ROCS_2^-$ (R = Me, Et, Pr^i, Pr^n, Bu^n or CH_2Ph),[269,273-275] thioxanthates $RSCS_2^-$ (R = Et, Pr^i, Bu^t or CH_2Ph),[273] and dithiocarbamates $R_2NCS_2^-$ (R = Et, Pr^i or Ph.)[269,273] In most instances, these complexes are prepared[269,273-275] by the direct reaction of $Mo_2(O_2CCH_3)_4$ with an alkali metal or ammonium salt for the appropriate ligand in methanol, ethanol or THF. Some syntheses, particularly for the $Mo_2(OSCR)_4$ and $Mo_2(S_2CR)_4$ compounds, have been achieved[269,270,273] through use of the free acids RCOSH and RCS_2H. However, in the case of the odoriferous phenyl- and methyldithiocarboxylic acids it is preferable to react $Mo_2(O_2CCH_3)_4$ directly with the reagents CH_3CS_2MgBr and $PhCS_2MgBr$ without first converting the latter to the free acids or some suitable salt.[272] The complexes $Mo_2(S_2CPh)_4$ and $Mo_2(S_2CC_5H_4FeC_5H_5)_4$ have been reported to form upon the slow thermal decarbonylation of the mononuclear species $Mo(CO)_3(S_2CR)_2$.[271]

Crystal structure determinations on the tetrahydrofuran solvates $Mo_2(S_2CR)_4{\cdot}2THF$ (R = CH_3 or Ph) have confirmed[272] that these are indeed quadruply bonded dimolybdenum(II) complexes with Mo–Mo distances of 2.133 Å and 2.139 Å, respectively. A lengthening of *c.* 0.04 Å compared to $Mo_2(O_2CR)_4$ compounds may be attributed partly to the presence of two weakly bound axial THF molecules but must also reflect the steric and electronic properties of the RCS_2^- ligands. The similarity of the electronic absorption spectra[270] of $Mo_2(S_2CPh)_4$ and $Mo_2(OSCPh)_4$, together with mass spectral evidence for a dinuclear structure in the case of the monothiocarboxylates[269,270] implies that a close structural relationship exists between $Mo_2(S_2CR)_4$ and $Mo_2(OSCR)_4$. The structure of $Mo_2(OSCPh)_4(OPPh_3)_2$ shows the effect of axial coordination, with an Mo–Mo bond length of 2.152 Å.[89]

The xanthates, $Mo_2(S_2COR)_4$, which, like the monothio- and dithiocarboxylate derivatives are red in color, also exhibit the expected paddlewheel structure. A crystal structure determination on $Mo_2(S_2COEt)_4{\cdot}2THF$, has shown[134] the presence of an eclipsed Mo_2S_8 skeleton and Mo–Mo distance (2.125(1) Å) which is only a little shorter than the Mo–Mo distance in $Mo_2(S_2CR)_4$. While a definitive structure determination is not yet in hand for a thioxanthate

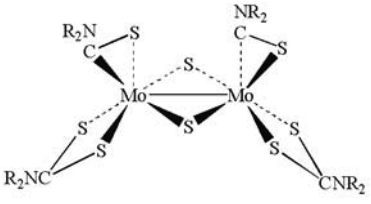
Pictiva EX2004
Samsung v Pictiva
IPR2024-01094

derivative, the available spectroscopic characterizations[273] on $Mo_2(S_2CSR)_4$ are in accord with the expected ligand-bridged structure.

The xanthantes exhibit an interesting reaction chemistry which in some ways resembles that of $Mo_2(O_2CCF_3)_4$. The ethyl and isopropyl derivatives form 1:2 adducts with ligands such as pyridine, several of which are quite stable in the solid state,[269,275] and $Mo_2(S_2COEt)_4$ reacts with halide ions to form salts such as $[Ph_3PCH_2Ph]_2[Mo_2(S_2COEt)_4X_2]$ (X = Br or I) and $\{[Ph_3PCH_2Ph][Mo_2(S_2COEt)_4Cl]\}_n$.[276]

In the original synthesis of $Mo_2(S_2COEt)_4$ by reacting $Mo_2(O_2CCH_3)_4$ with an excess of potassium xanthate, a green product of unknown stoichiometry was also isolated.[274] Some time later this was shown[276] to be a salt of the $[Mo_2(S_2COEt)_5]^-$ anion. This species can also be prepared by reacting $Mo_2(S_2COEt)_4$ with a stoichiometric amount of KS_2COEt and precipitated as its $[Ph_4As]^+$ or $[Ph_3PCH_2Ph]^+$ salt;[276] the related isopropyl derivative $[Mo_2(S_2COPr^i)_5]^-$ has also been prepared by this means.[275] The mixed xanthates $[Mo_2(S_2COR)_4(S_2COR')]^-$ (R = Me, R' = Et; R = Et, R' = Me) together with $[Mo_2(S_2COR)_4(S_2CR)]^-$ and $[Mo_2(S_2COR)_4(OSCR)]^-$ have also been obtained. Both dinuclear and tetranuclear[276] structures have been proposed for the $[Mo_2(S_2COR)_5]^-$ anions on the basis of their spectrosopic[275,276] and conductance[276] properties, but the structural questions have not yet been resolved by a crystal structure determination.

The reactions between $Mo_2(O_2CCH_3)_4$ and dialkyldithiocarbamates are more complicated than those involving the other sulfur ligands.[269,273,277] While genuine quadruply-bonded $Mo_2(S_2CNR_2)_4$ compounds may indeed exist,[269,273] and there is spectroscopic evidence[273] in support of this contention, the most stable complexes isolated from this system are the green dimolybdenum(IV) complexes $Mo_2S_2(S_2CNR_2)_2(SCNR_2)_2$, where R is Et or Pr. These novel complexes contain a bridging Mo_2S_2 sulfide unit, two conventional chelating dithiocarbamate ligands, and two thiocarboxamide ligands ($SCNR_2$), the latter arising from cleavage of a C–S bond of each of two dithiocarbamates (see **4.22**).[277] The short Mo–C distance (2.069 Å) indicates[277] carbenoid character in the Mo–C bond involving each of the thiocarboxamido functions, and a Mo–Mo distance of 2.705 Å implies a Mo–Mo interaction.



4.22

The complexes $Mo_2S_2(S_2CNR_2)_2(SCNR_2)_2$ may be viewed as being derived from $Mo_2(S_2CNR_2)_4$ via an internal irreversible redox reaction whereby the metal is oxidized (Mo^{II} to Mo^{IV}) and two of the ligands are reduced. This reaction points to the existence of a rich and interesting redox chemistry for many species containing the $[Mo_2S_8]$ core. Bromine and iodine react with stoichiometric amounts of $Mo_2(S_2COR)_4$ (R = Et or Pr^i) in chlorocarbon solvents or THF to produce crystalline solids of composition $Mo_2(S_2COR)_4X_2$.[278] These turn out not to be products of a 'simple' oxidative addition of X_2 to a Mo–Mo quadruple bond, whereby a triple bond would result, but instead involve a major change in the bonding mode of all four xanthate ligands.[278] From the structure determination of the dimolybdenum(III) complex $Mo_2(S_2COEt)_4I_2$ (see Fig. 4.14), two xanthate ligands were found to be chelating while the remaining two coordinate in an extraordinary bridging manner.[278] Each of the latter may be considered to be acting as a bidentate, three-electron donor to one metal atom while at the same time contributing

Pictiva EX2004
Samsung v Pictiva
IPR2024-01094

four electrons, as a tridentate donor, to the other metal atom. The observed Mo–Mo distance of 2.720(3) Å probably corresponds to a bond order of one. Other examples of the oxidation of such complexes include the conversion of $Mo_2(S_2CNR_2)_4$ to compounds that contain the $Mo_2O_3^{4+}$ core,[269,279,280] but in these instances the products do not contain a Mo–Mo bond.

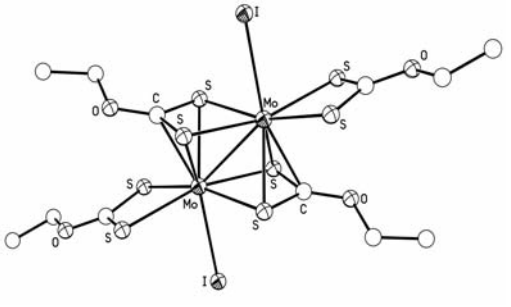


Fig. 4.14. The structure of $Mo_2(S_2COEt)_4I_2$.

The only monothiocarbamate paddlewheel molecule is $Mo_2(OSCNPr^i_2)_4$, prepared from $Mo_2(O_2CCH_3)_4$ and $Li(OSCNPr^i_2)$ in ethanol[281] It has an Mo–Mo distance of 2.112(1) Å.

Dichloromethane solutions of xanthate, thioxanthate and dithiocarboxylate complexes exhibit similar electrochemistry,[273] including a common quasi-reversible one-electron reduction in the potential range −1.4 to −2.2 V (versus SCE). A second reduction at more cathodic potentials is irreversible, the electron transfer being followed by dissociation of a ligand which is itself electrochemically active. The xanthates and thioxanthates are irreversibly oxidized at approximately +0.8 and +0.9 V, respectively.[273]

The dithiocarbamates exhibit a reduction in the vicinity of −2.1 V and an oxidation in the range +0.1 to +0.4 V. Controlled potential electrolysis of a dichloromethane solution of $Mo_2(S_2CNPr^i_2)_4$ at potentials anodic of the oxidation wave leads to the formation of $Mo_2(S_2CNPr^i_2)_2(SCNPr^i_2)_2$, as identified by its characteristic cyclic voltammogram.[273]

Other compounds that may contain Mo–Mo quadruple bonds, although structural data are lacking, are $(Ph_4As)_4Mo_4(C_4S_4)_4$,[282] and a substance formed upon reaction of $K_4Mo_2Cl_8$ with $(NH_4)_2MoS_4$ in 1 M aqueous KCl which has been formulated as $K_4[Mo_2(MoS_4)_4]$.

A few thiophosphorus compounds are known.[200,269] These include $Mo_2(S_2PPh_2)_4$ and $Mo_2(S_2PEt_2)_4$. The latter exists in isomeric forms. Unsolvated $Mo_2(S_2PEt_2)_4$ has two bridging and two chelating ligands whereas $Mo_2(S_2PEt_2)_4$·THF has a paddlewheel structure with an axial THF. The Mo–Mo distances are 2.137(1) Å and 2.123(1) Å, respectively. Apparently $Mo_2(S_2PMe_2)_4$ behaves similarly,[283] but no bond distances have been reported. It is surprising that there should be so little difference between the Mo–Mo distances in the two structures.

There are compounds containing $F_2PS_2^-$ ligands,[269] viz., $Mo_2(S_2PF_2)_4$, $Mo_2(S_2PF_2)_2(O_2CCF_3)_2$ and $Mo_2(S_2PF_2)_2(O_2CCH_3)_2$. NMR spectroscopy indicates paddlewheel structures for all three with *trans* configurations in the two mixed ligand compounds. $Mo_2(OSPEt_2)_4$·THF is isostructural with $Mo_2(S_2PEt_2)_4$·THF with an Mo–Mo distance of 2.128(2) Å.[200]

4.3 Non-Paddlewheel Mo_2^{4+} Compounds

4.3.1 $Mo_2X_8^{4-}$ and $Mo_2X_6(H_2O)_2^{2-}$ compounds

As early as 1965[284] it was shown that the following reversible interconversions occur:

$$Re_2Cl_8^{2-} + 4RCO_2H = ClRe(O_2CR)_4ReCl + 4HCl + 2Cl^-$$

Pictiva EX2004
Samsung v Pictiva
IPR2024-01094

Thus, when the $Mo_2(O_2CCH_3)_4$ structure was reported,[1] the idea of proceeding in an analogous way to make the new anion $Mo_2Cl_8^{4-}$, which would be a stereoelectronic analog of $Re_2Cl_8^{2-}$, was soon shown to be valid. The first reported compound[3] of the $Mo_2Cl_8^{4-}$ ion was $K_4Mo_2Cl_8{\cdot}2H_2O$. The Mo–Mo distance of 2.139 Å and the rigorously eclipsed rotational conformation attested to the existence of a quadruple bond between the molybdenum atoms. The structure, exactly as originally reported, is shown in Fig. 4.2. It is interesting to note that it was in this structure that the tendency of $M_2X_8^{n-}$ and related species to display a type of disorder in which some of the quasicubic M_2X_8 units are oriented at 90° to the principal orientation (in this case about 7%) was first observed. For an extended discussion of this type of disorder, see Section 16.1.5. Table 4.6 lists all $Mo_2X_8^{4-}$ and $Mo_2X_6(H_2O)_2^{2-}$ compounds for which crystal structures are known.

Table 4.6. Structures of $[Mo_2X_8]^{4-}$ and $[Mo_2X_6(H_2O)_2]^{2-}$ compounds

Compound	Crystal sym.	Virtual sym.	*r*(Mo–Mo) (Å)		Twist Angle (°)	ref.
$K_4Mo_2Cl_8{\cdot}2H_2O$	2/*m*	D_{4h}	2.139(4)		0	3
$(enH_2)_2Mo_2Cl_8{\cdot}2H_2O$	$\bar{1}$	D_{4h}	2.134(1)		0	285
$(NH_4)_5Mo_2Cl_9{\cdot}H_2O$	m	D_{4h}	2.150(5)		0	286
$(pipH_2)_2Mo_2Cl_8{\cdot}4H_2O$	$\bar{1}$	D_{4h}	2.129(3)		0	287
$[H_3N(CH_2)_3NH_3]_2[Mo_2Cl_8]{\cdot}4H_2O$	$\bar{1}$	D_{4h}	2.125(2)	53%	0	288
			2.123(2)	47%	0	
$[H_3N(CH_2)_4NH_3]_2[Mo_2Cl_8]$	$\bar{1}$	D_{4h}	2.132(2)		0	288
$(NH_4)_4Mo_2Br_8$	4/*mmm*	D_{4h}	2.135(2)		0	290
$(NH_4)_4Mo_2(NCS)_8{\cdot}4H_2O$	$\bar{1}$	D_{4h}	2.162(1)		0	291
$(NH_4)_4Mo_2(NCS)_8{\cdot}6H_2O$	$\bar{1}$	D_{4h}	2.174(1)		0	291
	$\bar{1}$	D_{4h}	2.177(1)		0	
$Li_4Mo_2(CH_3)_8{\cdot}4THF$	$\bar{1}$	D_{4h}	2.148(2)		0	292
$[Bu^n_4N]_4[Mo_2(CN)_8]{\cdot}8CHCl_3$	$\bar{1}$	D_{4h}	2.122(2)		0	155
$(morphH)_2[Mo_2Cl_6(H_2O)_2]$	$\bar{1}$	C_{2h}	2.118(1)		0	293
$(morphH)_2[Mo_2Br_6(H_2O)_2]$	$\bar{1}$	C_{2h}	2.114(2)		0	293
$(pyH)_3[Mo_2Br_6(H_2O)_2]Br$	2	C_2	2.130(4)		≈0	294
$(picH)_2[Mo_2Br_6(H_2O)_2]$	$\bar{1}$	C_{2h}	2.122(2)		0	295
$(pyH)_2[Mo_2I_6(H_2O)_2]$	$\bar{1}$	C_{2h}	2.115(1)		0	296
$(picH)_2[Mo_2I_6(H_2O)_2]$	$\bar{1}$	C_{2h}	2.116(1)		0	297

The preparation of $K_4Mo_2Cl_8{\cdot}2H_2O$ triggered extensive investigations of reactions between $Mo_2(O_2CCH_3)_4$ and hydrohalic acids under a wide variety of experimental conditions, as will now be described. First, it should be mentioned that the conversions of $Mo_2(O_2CR)_4$ to $[Mo_2X_8]^{4-}$ by halide ions proceed through the intermediacy of mixed halide-carboxylate species such as $[Mo_2(O_2CR)_4X_2]^{2-}$, $[Mo_2(O_2CR)_3X_3]^{2-}$, and $[Mo_2(O_2CR)_2X_4]^{2-}$, which have been considered previously in Section 4.1.3.

The reactions of $Mo_2(O_2CCH_3)_4$ with hydrohalic acids (HCl, HBr) to produce $Mo_2X_8^{4-}$ ions must be conducted under carefully controlled conditions or oxidative cleavage will occur, leading to $[MoOX_4]^-$ (X = Cl, Br) anions,[298,299] or $[MoCl_5(H_2O)]^{2-}$.[300]

The conditions used to convert $Mo_2(O_2CCH_3)_4$ to $K_4Mo_2Cl_8{\cdot}H_2O$,[3] namely reaction at *c.* 0 °C in constant-boiling hydrochloric acid, were soon adapted to the synthesis of other such salts. These included $(enH_2)_2Mo_2Cl_8{\cdot}2H_2O$,[285] where $enH_2 = H_3NCH_2CH_2NH_3$, and $(NH_4)_5Mo_2Cl_9{\cdot}H_2O$,[286] which were structurally characterized and shown to contain the

Pictiva EX2004
Samsung v Pictiva
IPR2024-01094

eclipsed $[Mo_2Cl_8]^{4-}$ anion (Fig. 4.2). The anhydrous salt $K_4Mo_2Cl_8$ is formed, instead of the dihydrate, when the concentrated hydrochloric acid is saturated with HCl gas.[301] Similar procedures were used subsequently by others to prepare $Rb_5Mo_2Cl_9{\cdot}H_2O$,[290] $Rb_4Mo_2Cl_8$,[302] and $Cs_4Mo_2Cl_8$,[302] while the salt $(pipH_2)_2Mo_2Cl_8{\cdot}4H_2O$ (pip = piperazine) was isolated[287] by reacting $(morphH)_2Mo_2Cl_6(H_2O)_2$ (see below) with $(pipH_2)Cl_2$ in hydrochloric acid. This complex has a structure like that of other salts of the $[Mo_2Cl_8]^{4-}$.[287] Adaption of this general synthetic method to the related bromide systems by Brenčič and co-workers[290,303] and others[101] has permitted the isolation of $(NH_4)_4Mo_2Br_8$, $Cs_4Mo_2Br_8$, and $(NH_4)_5Mo_2Br_9{\cdot}H_2O$. In the case of $(NH_4)_4Mo_2Br_8$, the synthesis is actually best approached[290] via the sulfate complex $(NH_4)_4Mo_2(SO_4)_4{\cdot}2H_2O$, the latter being prepared by the reaction of $(NH_4)_5Mo_2Cl_9{\cdot}H_2O$ with $(NH_4)_2SO_4$ in cold 1 M sulfuric acid.

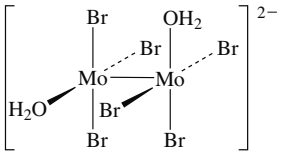
$(NH_4)_5Mo_2Br_9{\cdot}H_2O$ and $Rb_5Mo_2Cl_9{\cdot}H_2O$ have been shown[290] to be isostructural with $(NH_4)_5Mo_2Cl_9{\cdot}H_2O$ and therefore they contain the $[Mo_2X_8]^{4-}$ anions. A crystal structure determination of $(NH_4)_4Mo_2Br_8$ has revealed[290] the expected eclipsed $[Mo_2Br_8]^{4-}$ anion of D_{4h} symmetry and a Mo–Mo distance of 2.135(2) Å. An attempt to synthesize $K_4CrMoCl_8$ by the reaction of $CrMo(O_2CCH_3)_4$ with a solution of KCl dissolved in concentrated hydrochloric acid saturated with HCl gas afforded only $K_4Mo_2Cl_8{\cdot}2H_2O$.[304]

The spectroscopic properties of salts of the $[Mo_2X_8]^{4-}$ anions, (X = Cl or Br) have been of considerable interest and importance and are discussed in some detail in Chapter 16. Of additional note are the ^{95}Mo NMR spectra that have been reported for $K_4Mo_2Cl_8$ and $Cs_4Mo_2Br_8{\cdot}2H_2O$.[96]

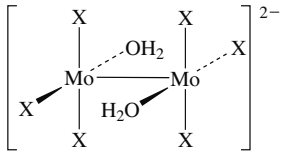
In addition to salts containing the $[Mo_2Cl_8]^{4-}$ and $[Mo_2Br_8]^{4-}$ anions, various halide 'deficient' species have been isolated and structurally characterized. The first one to be isolated, $K_3Mo_2Cl_7{\cdot}2H_2O$, was obtained by adding alcohol to solutions that would otherwise have produced $K_4Mo_2Cl_8{\cdot}2H_2O$ if allowed to crystallize slowly.[301] On the other hand, $Rb_3Mo_2Cl_7{\cdot}2H_2O$ separates from constant boiling hydrochloric acid solutions that contain $Mo_2(O_2CCH_3)_4$ and RbCl without the addition of alcohol.[301] A bromide analog, $Cs_3Mo_2Br_7{\cdot}2H_2O$, was later prepared by Brenčič *et al*.[303] and found to crystallize in the same space group and to have similar cell dimensions as $Rb_3Mo_2Cl_7{\cdot}2H_2O$. A full crystal structure has yet to be carried out on any of these alkali metal salts. However, the pyridinium salt $(pyH)_3Mo_2Br_7{\cdot}2H_2O$, which was prepared by reacting $(NH_4)_5Mo_2Cl_9{\cdot}H_2O$ in hydrobromic acid with pyridinium bromide, has been shown[294] to be the double salt $(pyH)_3[Mo_2Br_6(H_2O)_2]Br$. The $[Mo_2Br_6(H_2O)_2]^{2-}$ anion in this salt possesses a Mo–Mo distance of 2.130(4) Å and a structure as represented in **4.23**. Whether the alkali metal salts have such a structure is unknown. Actually, the $[Mo_2X_6(H_2O)_2]^{2-}$ anions (X = Cl, Br or I) are particularly well characterized species, structure determinations having been carried out on several pyridinium and 4-methylpyridinium salts of the type $(pyH)_2[Mo_2X_6(H_2O)_2]$ and $(picH)_2[Mo_2X_6(H_2O)_2]$, as well as the morpholinium derivatives $(morphH)_2[Mo_2X_6(H_2O)_2]$ (Table 4.6).[293,295-297] However, in all these instances the anions are centrosymmetric (**4.24**) and therefore differ from the structure of $(pyH)_3[Mo_2Br_6(H_2O)_2]Br$, although in each the rotational geometry is eclipsed. Compared to the corresponding $[Mo_2X_8]^{4-}$ anions, the Mo–Mo distances in the $[Mo_2X_6(H_2O)_2]^{2-}$ species are shorter by up to ≈0.02 Å, no doubt reflecting the decreased anion charge in the latter species. Their preparation is quite straightforward,[293,295,297,305] and involves halide exchange reactions in hydrohalic acid media in the presence of the appropriate amine hydrohalide in the case of the pyridinium and 4-methylpyridinium salts. Thus, $(picH)_2[Mo_2Br_6(H_2O)_2]$ is obtained from $(NH_4)_5Mo_2Cl_9{\cdot}H_2O$[295] while $(pyH)_2[Mo_2I_6(H_2O)_2]$ and $(picH)_2[Mo_2I_6(H_2O)_2]$ are prepared via $(pyH)_3Mo_2Br_7{\cdot}2H_2O$ and $(picH)_2[Mo_2Br_6(H_2O)_2]_2$, respectively.[296,297] The morpholinium salts are obtained from $(morphH)_4Mo_2Cl_8$ and $(NH_4)_4Mo_2Br_8$.[293] The electronic absorption, infrared, and Raman spectra of the series of complexes $(morphH)_2[Mo_2X_6(H_2O)_2]$ (X = Cl or Br) and $(pyH)_2[Mo_2I_6(H_2O)_2]$

Pictiva EX2004
Samsung v Pictiva
IPR2024-01094

have been studied in considerable detail;[306] these properties accord with the presence of Mo–Mo quadruple bonds.



4.23



4.24

Although kinetic studies on the reaction of $Mo_2(O_2CCH_3)_4$ with halide ion have not been reported, the reverse reaction, namely, the reaction of acetic acid with equilibrated solutions of $K_4Mo_2Cl_8$ in hydrochloric acid, *p*-toluenesulfonic acid, and mixtures of these two acids has been studied.[41,307] Several mechanisms have been advocated for these reactions.

It is a little surprising that no compounds containing $Mo_2F_8^{4-}$ or $Mo_2I_8^{4-}$ ions have been reported. On the other hand the $Mo_2(NCS)_8^{4-}$ ion[291] and $Mo_2(CN)_8^{4-}$ ion[308-310] are well characterized. The $Mo_2Cl_8^{4-}$ ion (as well as $Mo_2Cl_8H^{3-}$) are reducing agents and deoxygenating agents, known to convert sulfoxides to sulfides.[311]

4.3.2 $[Mo_2X_8H]^{3-}$ compounds

The red or violet colored salts of the $[Mo_2X_8]^{4-}$ and $[Mo_2X_6(H_2O)_2]^{2-}$ anions that are formed from $Mo_2(O_2CCH_3)_4$ are the obvious non-redox halide substitution products of the carboxylate. However, unlike the corresponding substitution chemistry of $Re_2(O_2CR)_4Cl_2$, that of $Mo_2(O_2CR)_4$ can also be more complicated. At around the time of the synthesis and structure elucidation of $K_4Mo_2Cl_8{\cdot}2H_2O$,[3] it was reported[312] that the reaction between $Mo_2(O_2CCH_3)_4$ and RbCl or CsCl in deoxygenated 12 N hydrochloric acid at temperatures higher than those used to produce $[Mo_2Cl_8]^{4-}$, namely 60 °C or thereabouts, afforded high yields of green-yellow $Rb_3Mo_2Cl_8$ or $Cs_3Mo_2Cl_8$. These would appear to be Mo(+2.5) derivatives and a crystal structure determination on $Rb_3Mo_2Cl_8$, with which the cesium salt was found to be isostructural, led to the proposal[312] that the binuclear anions were best described as confacial bioctahedra (M_2X_9) with one-third of the bridging halogen atoms absent. A similar structural situation was believed to exist with the bromide salt $Cs_3Mo_2Br_8$ which was later prepared[313] by an analogous procedure. Sheldon and coworkers had also described[314] a series of salts containing the $[Mo_2X_8]^{3-}$ anions (X = Cl or Br). Their attempts to identify the molybdenum oxidation state by using the ferric-permanganate titration method was puzzling since solutions of these complexes in 4 –12 M hydrochloric acid gave oxidation numbers of +3 rather than +2.5.

Some years later, $Rb_3Mo_2Cl_8$ and $Cs_3Mo_2Br_8$ were found to be diamagnetic, a result inconsistent with the non-integral oxidation number of +2.5. These complexes were reinvestigated[315] and reformulated as the dimolybdenum(III) species $[Mo_2X_8H]^{3-}$ on the basis of deuterium and tritium labeling experiments and infrared spectroscopy (ν(Mo–H–Mo) at $\approx 1260\ cm^{-1}$).[315] Accordingly, the overall reaction of $Mo_2(O_2CCH_3)_4$ with the hydrohalic acids may be represented as follows:

$$Mo_2(O_2CCH_3)_4 + 8HX \rightarrow [Mo_2X_8H]^{3-} + 3H^+ + 4CH_3CO_2H$$

This reaction appears to be quantitative when carried out at temperatures of 60 °C and above, and with the exclusion of oxygen. It constituted the first example of an oxidative-addition reaction involving a well-defined metal–metal bond.

Pictiva EX2004
Samsung v Pictiva
IPR2024-01094

There is a disorder of the μ-H and μ-X atoms in the alkali metal salts that prevented the identification of the hydrogen atom in $Rb_3Mo_2X_8H$ and $Cs_3Mo_2X_8H$ by crystallographic means. However, the pyridinium salt $(pyH)_3Mo_2Cl_8H$, which can be prepared by the usual method, exhibits no disorder problem thereby permitting its structure solution,[316,317] including the location of the bridging hydrogen atom. With a Mo–Mo distance of 2.371(1) Å, a value which is similar to those in $Rb_3Mo_2Cl_8H$ (2.38(1) Å)[312] and $Cs_3Mo_2Br_8H$ (2.439(7) Å),[313] the presence of a fairly strong Mo–Mo bond is evident. The terminal Mo–Cl bonds *trans* to μ-H are significantly longer (by 0.10 Å) than those *trans* to μ-Cl. Refinement of the μ-H atom gave a Mo–H distance of *c.* 1.7 Å. These complexes bear a close structural relationship to the nonahalodimolybdate(III) anions except for the substantially shorter Mo–Mo distance in $[Mo_2Cl_8H]^{3-}$ compared to $[Mo_2Cl_9]^{3-}$ (by *c.* 0.28 Å). Subsequently, similar structures were determined for the $[Mo_2Cl_8H]^{3-}$ anion in the salts $(Et_4N)_2(H_5O_2)[Mo_2Cl_8H]$,[317] $(Et_4N)_3(H_5O_2)$-$[Mo_2Cl_8H][MoOCl_4(H_2O)]$,[298] and $(Me_4N)_3Mo_2Cl_8H$,[318]all of which have been prepared by the addition of R_4NCl to solutions of $Mo_2(O_2CCH_3)_4$ in hot 12 M HCl. The structure determination of $(Me_4N)_3Mo_2Cl_8H$ was carried out with the use of both X-ray and neutron diffraction methods.[318] The Mo–Mo and Mo–H bond lengths were determined by neutron diffraction to be 2.357(3) Å and 1.823[7] Å, respectively. The bromo and iodo complexes $(Me_4N)_2(H_7O_3)$-$[Mo_2Br_8H]^{3-}$[319] and $(Et_4N)_2(H_7O_3)[Mo_2I_8H]^{3-}$[320] have been obtained by analogous procedures to these, and both salts structurally characterized. The Mo-Mo distances are 2.384(4) Å and 2.408(2) Å, respectively, and although neither anion is disordered the μ-H ligands were not located.

Various other compounds that contain the $[Mo_2Cl_8H]^{3-}$ anion have been prepared by oxidation of $Mo_2(O_2CCH_3)_4$, including $(Bu_4N)^+$, $(4\text{-MepyH})^+$, piperdinium, 8-hydroxyquinolinium and phenanthrolinium salts.[321,322] The magnetic and spectroscopic properties and thermal characteristics of these compounds have been measured.[321,322] The phosphonium salts $(R_3PH)_3Mo_2Cl_8H$ (R = Et or Pr^n), have been prepared[323] by the treatment of $Mo_2(mhp)_4$ with gaseous HCl and R_3P in ethanol. These species show a resonance at δ −3.7 (R = Et) and δ −3.6 (R = Pr^n) in their ^1H NMR spectra (recorded in CD_3CN) that is assignable to the μ-H ligand.[323] While the mixed metal carboxylate $MoW(O_2CCMe_3)_4$ is not converted into $[MoWCl_8]^{4-}$ upon treatment with hydrochloric acid, Katovic and McCarley[324,325] have prepared Cs_3MoWCl_8H, a complex that is isostructural with $Rb_3Mo_2Cl_8H$ but whose Mo–W distance of 2.445(3) Å is longer than the Mo–Mo distance in $Rb_3Mo_2Cl_8H$. This metal–metal bond lengthening which occurs upon formation of the heteronuclear dimer is in contrast to the bond shortening in the carboxylate dimer $MoW(O_2CCMe_3)_4$ compared to $Mo_2(O_2CCMe_3)_4$. A detailed comparison has been made of the vibrational spectra of $[Mo_2Cl_8H]^{3-}$ and $[MoWCl_8H]^{3-}$ and symmetric and asymmetric ν(M–H–M) modes assigned.[325]

4.3.3 Other aspects of dimolybdenum halogen compounds

A variety of studies that have focused upon the interrelationships between $[Mo_2X_8]^{4-}$, $[Mo_2X_8H]^{3-}$ and the closely related $[Mo_2X_9]^{3-}$ species. A cyclic voltammetric study of the electrochemical oxidation of $K_4Mo_2Cl_8$ in 6 M HCl has shown[326] that a single oxidation wave is present at +0.5 V (versus SCE) with a shape very close to that expected for a reversible process. However, except at high sweep rates (500 mVs^{-1}) the corresponding reduction peak was absent. For solutions of $[Mo_2Cl_8]^{4-}$ in the nonaqueous, basic $AlCl_3$-ImCl melt system (ImCl = 1-methyl-3-ethylimidazolium chloride), two one-electron oxidations have been measured. With a glassy carbon electrode, these are at $E_{1/2} \approx -0.31$ V and $E_{p,a}$ *c.* +0.3 V.[327] The first (reversible) oxidation generates $[Mo_2Cl_8]^{3-}$; the second (irreversible) oxidation gives $[Mo_2Cl_9]^{3-}$. When protonic impurities are present in these melts the $[Mo_2Cl_8H]^{3-}$ anion is generated. This

Pictiva EX2004
Samsung v Pictiva
IPR2024-01094

problem can be circumvented by the addition of $EtAlCl_2$, to the melt.[328] This gives cleaner electrochemistry, with $E_{1/2}$ = −0.16 V and $E_{p,a}$ in the range 0.3 to 0.4 V (the value depending upon sweep rate) with the use of a Pt working electrode. A comparison of these data with the electrochemical properties of $Mo_2Cl_4(PR_3)_4$ compounds (Section 4.3.4) shows that the oxidation of $[Mo_2Cl_8]^{4-}$ to $[Mo_2Cl_8]^{3-}$ is much more cathodic than that of $Mo_2Cl_4(PR_3)_4$ to $[Mo_2Cl_4(PR_3)_4]^{+}$. It has also been suggested[327] that the oxidation observed at +0.5 V in the cyclic voltammogram of $K_4Mo_2Cl_8$ in 6 M HCl[326] is actually the irreversible second oxidation (i.e. $[Mo_2Cl_8]^{3-} \rightarrow [Mo_2Cl_9]^{3-}$), since the first oxidation should be overlapped by the H^+/H_2 redox couple in this medium, and therefore obscured.

A detailed study has been made of the redox chemistry interrelating $[Mo_2Cl_8]^{4-}$, $[Mo_2Cl_8H]^{3-}$ and $[Mo_2Cl_9]^{3-}$ in the basic ambient temperature molten salt $AlCl_3$–ImCl by employing electrochemistry and visible absorption spectroscopy.[327,328] The electrochemical behavior of $[Mo_2Cl_8H]^{3-}$ in $AlCl_3$–ImCl[327] is quite different from that reported for solutions of $[Mo_2Cl_8H]^{3-}$ in CH_2Cl_2 and CH_3CN.[323]

The kinetics of the oxidative addition of 6-12 M HCl to $[Mo_2Cl_8]^{4-}$ has been shown[329] to be first order in $[Mo_2Cl_8]^{4-}$ and to obey a linear dependence with respect to the acidity function. The $[Mo_2Cl_8H]^{3-}$ anion decomposes in hydrochloric acid solutions (<3 M) to yield H_2 and a hydroxy-bridged dimolybdenum(III) dimer. The 254 nm irradiation of $[Mo_2Cl_8]^{4-}$ in 3 M HCl has been found[206] to produce $[Mo_2Cl_8H]^{3-}$, probably through the reaction of H_2O with a ligand-to-metal charge transfer excited state of $[Mo_2Cl_8]^{4-}$. In a subsequent step, this anion decomposes thermally to yield 1 mole of hydrogen gas and the dimolybdenum(III) dimer $[Mo_2(\mu\text{-}OH)_2(aq)]^{4+}$. A similar reaction of $[Mo_2Br_8]^{4-}$ occurs in 3 M hydrobromic acid.[206] No photoactivity was associated with irradiation of the $\delta \rightarrow \delta^*$ absorption band (located at ≈ 500 nm) of $[Mo_2X_8]^{4-}$, an observation that was attributed[206] to the persistence of strong metal–metal bonding in low lying $\delta\delta^*$ and $\delta\pi^*$ excited states.

While the oxidation of $[Mo_2Cl_8]^{4-}$ to $[Mo_2Cl_8H]^{3-}$ is clearly a quite facile process, the reversal of this reaction has been accomplished both in the basic $AlCl_3$–ImCl melt system[327,328] and in aqueous hydrohalic acid solutions. In the latter media, Bino and Gibson[204] have shown that $[Mo_2X_8H]^{3-}$ and $[Mo_2X_9]^{3-}$ are reduced in a Jones reductor (amalgamated zinc) to afford a deep red solution containing Mo_2^{4+}, from which $K_4Mo_2Cl_8{\cdot}2H_2O$, $Mo_2(O_2CCH_3)_4$ and $K_4Mo_2(SO_4)_4{\cdot}2H_2O$ can be crystallized upon addition of the appropriate anion. A similar conversion of $[Mo_2Cl_9]^{3-}$ and $[Mo_2Cl_8H]^{3-}$ to $[Mo_2Cl_8I]^{4-}$ can be accomplished with the use of chromium(II) chloride in 6 M HCl.[330]

In addition to the reactions of $Mo_2(O_2CCH_3)_4$ with aqueous hydrohalic acids that afford halo-anions of dimolybdenum, two other reaction systems yield halide phases under different reaction conditions. These are:

1. reactions of solid $Mo_2(O_2CCH_3)_4$ with the gaseous hydrogen halides at elevated temperatures;
2. reactions with the gaseous hydrogen halides in non-aqueous media.

The first of these leads to phases of composition MoX_2 as first demonstrated in the case of X = Cl. The brown powder that is formed upon reacting $Mo_2(O_2CCH_3)_4$ with dry gaseous HCl at 300 °C and which analyzes as molybdenum(II) chloride, has been designated as β-$MoCl_2$.[6,331,332] Much more recently, this halide has been prepared by the reaction between $Mo_2(O_2CCH_3)_4$ and $AlCl_3$ in refluxing chlorobenzene.[333] Its chemical reactions[331-334] and spectroscopic properties[333,335] show that this phase is not structurally related to α-$MoCl_2$, in which a hexanuclear cluster of molybdenum atoms is present. However, there is evidence[334,336] that heating the β-isomer at 350 °C leads to its conversion to α-$MoCl_2$. The corresponding treatment of $Mo_2(O_2CCH_3)_4$ with hydrogen bromide and iodide at 300°C has been found to afford

Pictiva EX2004
Samsung v Pictiva
IPR2024-01094

β-$MoBr_2$ and β-MoI_2.[331,337] Another study of molybdenum bromide phases has also led to the isolation of a material purported to be β-$MoBr_2$ (a dark green solid).[338] However, the properties of this phase are not the same as those of β-$MoBr_2$ that is prepared from $Mo_2(O_2CCH_3)_4$.[331]

In view of the ease of converting the β-MoX_2 phases to complexes of the type $Mo_2X_4L_4$ (L = pyridine or tertiary phosphine), it was originally suggested[331,337] that they be formulated as $[Mo_2X_4]_n$, i.e the parent halides of the $[Mo_2X_8]^{4-}$ anions. However, there is now evidence[333] that these phases contain *tetranuclear* units, which would also react to form $Mo_2X_4L_4$ molecules.

An interesting observation[339] is that the thermal decomposition of $Mo_2Cl_4(NHEt_2)_4$ proceeds in four stages, whereby the $NHEt_2$ is totally removed between 305 and 380 °C to give $MoCl_2$. This may well be another route to β-$MoCl_2$, but further study is necessary.

The reactions of $Mo_2(O_2CCH_3)_4$ with HX(g) in methanol lead, in all instances, to oxidation of the molybdenum and, in the presence of the appropriate $Bu^n_4N^+$ salts, to the crystallization of the salts $(Bu_4N)MoOCl_4$, $(Bu_4N)Mo_2Br_6$ and $(Bu_4N)_2Mo_4I_{11}$.[340] Thus, the extent of oxidation decreases in the order Cl > Br > I. $(Bu_4N)MoOCl_4$ is a well characterized Mo^V complex but $(Bu_4N)Mo_2Br_6$ is of unknown structure, and therefore of uncertain nuclearity, although its chemical reactions have been interpreted[340] in terms of the retention of a strongly bonded Mo–Mo unit. The paramagnetic iodide cluster (μ_{eff} = 1.95 BM and g_{av} = 2.03 at room temperature)[340] has been obtained by an alternative procedure that was devised by McCarley and co-workers.[341] The tetranuclear structure of $(Bu_4N)_2Mo_4I_{11}$ has been confirmed by X-ray crystallography.[341]

A material of composition $(Bu_4N)_2Mo_2Br_6$ has been prepared[342] from the reaction of $Mo(CO)_6$ with Bu_4NBr and dibromoethane in chlorobenzene. It is believed to be the one-electron reduced congener of $(Bu_4N)Mo_2Br_6$. A study has been conducted on its reactions with monodentate and bidentate phosphine ligands,[343] and both mononuclear and dinuclear complexes have been isolated (see Section 4.3.4).

4.3.4 $M_2X_4L_4$ and $Mo_2X_4(LL)_2$ compounds

In the majority of these compounds, X is a halogen (most often Cl), but others (e.g., NCS, NCO, R, OR, C≡CR) also occur. The most common neutral ligands, L and LL, are mono- and diphosphines, but more recently $Mo_2X_4L_4$ molecules with L = amine have been prepared.

Starting materials that are most commonly used (but with many exceptions) are as follows:

1. A dimolybdenum halide that can itself easily be prepared from $Mo_2(O_2CCH_3)_4$, i.e. $K_4Mo_2Cl_8$, $(NH_4)_4Mo_2Br_8$, $(NH_4)_5Mo_2Cl_9{\cdot}H_2O$, $Cs_3Mo_2X_8H$ (X = Cl or Br) or $(picH)_2[Mo_2X_6(H_2O)_2]$ (X = Br or I).
2. A mixture of $Mo_2(O_2CCH_3)_4$ or $Mo_2(O_2CCF_3)_4$ and Me_3SiX (X = Cl, Br or I).
3. The dimolybdenum(II) carbonyl halides $Mo_2X_4(CO)_8$; this is particularly important in the case of X = I.
4. A preformed complex of the type $Mo_2X_4L_4$ (L is a monodentate ligand such as py or PR_3) that is prepared by one of the three above methods and undergoes ligand exchanges (i.e., $Mo_2X_4L_4 + 4L' \rightarrow Mo_2X_4L'_4 + 4L$).

Table 4.7 lists a large number of (though not all) compounds and the starting materials from which they have been made. Table 4.8 lists the $Mo_2X_4L_4$ compounds for which structural data are known, and Table 4.9 lists the $Mo_2X_4(LL)_2$ compounds.

Pictiva EX2004
Samsung v Pictiva
IPR2024-01094

Table 4.7. $Mo_2X_4L_4$ and $Mo_2X_4(LL)_2$ compounds and the starting materials used in their synthesis

Compound[a]	Synthetic starting materials
$Mo_2X_4(NH_3)_4$; (X = Cl, Br or I)	$Mo_2X_4(py)_4$ (X = Cl, Br or I),[303,305] $Mo_2I_4(4\text{-pic})_4$[305]
$Mo_2X_4(HNMe_2)_4$; (X = Cl or Br)	MoX_3 (X = Cl or Br)[344,345]
$Mo_2Cl_4(NMe_3)_4$	$MoCl_3$[346]
$Mo_2X_4(py)_4$; (X = Cl, Br or I)	$Cs_3Mo_2X_8H$,[347] $(NH_4)_5Mo_2Cl_9\cdot H_2O$,[348] $Mo_2Cl_4(dtdd)_2$,[347] β-MoX_2 (X = Cl, Br or I),[331,337] $Cs_3Mo_2Br_7\cdot 2H_2O$,[303] $(picH)_2[Mo_2Br_6(H_2O)_2]$,[295] $(Bu_4N)Mo_2Br_6$[340]
$Mo_2X_4(4\text{-pic})_4$; (X = Cl, Br or I)	$(NH_4)_5Mo_2Cl_9\cdot H_2O$,[349] $(picH)_2[Mo_2X_6(H_2O)_2]$ (X = Br or I)[305,349]
$Mo_2X_4(3\text{-pic})_4$; (X = Cl or Br)	$Cs_3Mo_2X_8H$[350]
$Mo_2X_4(3,4\text{-lut})_4$; (X = Cl or Br)	$Cs_3Mo_2X_8H$[350]
$Mo_2X_4(3,5\text{-lut})_4$; (X = Cl or Br)	$Cs_3Mo_2X_8H$[350]
$Mo_2X_4(4\text{-Bu}^t\text{py})_4$; (X = Cl or Br)	$Cs_3Mo_2X_8H$[350]
$Mo_2Cl_4(4\text{-Bu}^t\text{py})_4$	$Mo_2Cl_6(THF)$[351]
$Mo_2Cl_4(RNH_2)_4$; (R = Et, Pr^n, Bu^t or Cy)	$Mo_2Cl_6(THF)_3$[352]
$[Mo_2Cl_4(pyz)_2]_n$	$(NH_4)_5Mo_2Cl_9\cdot H_2O$[350]
$Mo_2Cl_4(2,6\text{-Me}_2\text{pyz})_4$	$(NH_4)_5Mo_2Cl_9\cdot H_2O$[350]
$Mo_2X_4(bpy)_2$ (X = Cl, Br or I)	$(NH_4)_5Mo_2Cl_9\cdot H_2O$[350] $Mo_2Cl_4(dtd)_2$,[347] $Mo_2X_4(py)_4$ (X = Br or I),[305,347] $Mo_2I_4(4\text{-pic})_4$,[305] $(Bu_4N)_2Mo_4I_{11}$[340]
$Mo_2Cl_4(phen)_2$	$Mo_2Cl_4(py)_4$[348]
$Mo_2X_4(NCR)_4$; (X = Cl, Br or I; R = Me, Et or Ph)	$Mo_2Cl_4(SMe_2)_4$,[347] $[MoI_2(THF)_n]_x$ (via $Mo_2I_4(CO)_8$)[353]
$Mo_2Cl_4(dpa)_2$	$(NH_4)_5Mo_2Cl_9\cdot H_2O$[354]
$Mo_2Cl_4(amp)_2$	$(NH_4)_5Mo_2Cl_9\cdot H_2O$[354]
$Mo_2Cl_4(8\text{-aq})_2$	$(NH_4)_5Mo_2Cl_9\cdot H_2O$[354]
$Mo_2Cl_4(Ph_2Ppy)_2$	$K_4Mo_2Cl_8$,[355] $(NH_4)_5Mo_2Cl_9\cdot H_2O$,[355] $Mo_2Cl_4(py)_4$,[355] $Mo_2Cl_4(PBu^n_3)_4$,[355] $Mo_2(O_2CCH_3)_4/Me_3SiCl$[126]
$Mo_2X_4(PR_3)_4$ (X = Cl, Br or I; PR_3 = PMe_3, PEt_3, PPr^n_3, PBu^n_3, PH_2Ph, PMe_2Ph, PEt_2Ph, $PHPh_2$, $PMePh_2$ or $PEtPh_2$)	$K_4Mo_2Cl_8$,[331,356] $(NH_4)_5Mo_2Cl_9\cdot H_2O$,[347,357,358] $Cs_3Mo_2Br_8H$,[347] β-MoX_2 (X = Cl, Br or I),[331,337] $Mo_2Br_4(py)_4$,[347] $(Bu_4N)Mo_2Br_6$,[340] $MoH_4(PMePh_2)_4$,[359] $Mo_2I_4(NCR)_4$ (via $Mo_2I_4(CO)_8$),[353] $Mo_2X_4(CO)_8$ (X = Cl, Br or I),[360-362] $MoCl_3(THF)_3/Zn$,[21] $Mo_2(O_2CCH_3)_4/Me_3SiCl$[123,363]
$Mo_2Cl_4(PR_3)_4$; (PR_3 = PMe_3, PMe_2Ph or $PHEt_2$)	$Mo_2Cl_4(NHEt_2)_4$[364]
$Mo_2Cl_4(PPh_3)_2(CH_3OH)_2$	$(NH_4)_5Mo_2Cl_9\cdot H_2O$[365]
$Mo_2Cl_4[P(OMe)_3]_4$	$(NH_4)_5Mo_2Cl_9\cdot H_2O$[357]

Pictiva EX2004
Samsung v Pictiva
IPR2024-01094

Compound[a]	Synthetic starting materials
$Mo_2Cl_4[P(OMe)Ph_2]_4$	$(NH_4)_5Mo_2Cl_9{\cdot}H_2O$[358]
$Mo_2Cl_4(AsR_3)_4$; (R = Me or Et)	$K_4Mo_2Cl_8$,[366] $Cs_4Mo_2Cl_8$[102]
$Mo_2Br_4(AsEt_3)_4$	$Cs_3Mo_2Br_8H$[102]
$Mo_2Cl_4(dmpm)_2$	$K_4Mo_2Cl_8$,[367] $Mo_2(O_2CCH_3)_4/Me_3SiCl$[367]
$Mo_2X_4(dppm)_2$	$K_4Mo_2Cl_8$,[368] $Mo_2X_4(PEt_3)_4$ (X = Cl or Br),[368] $Mo_2(O_3SMe)_4$,[369] $MoCl_3(THF)_3/Zn$,[21] $Mo_2(O_2CCH_3)_4/Me_3SiX$
(X = Cl, Br or I)	(X = Cl, Br or I),[123,370,371] $Mo_2I_4(CO)_8$[371]
α-$Mo_2Cl_4(dmpe)_2$	$(NH_4)_5Mo_2Cl_9{\cdot}H_2O$[347]
β-$Mo_2X_4(dmpe)_2$; (X = Cl or Br)	$Mo_2X_4(PEt_3)_4$ (X = Cl or Br)[372,373]
β-$Mo_2Cl_4(depe)_2$	$K_2Mo_2Cl_8$[374]
α-$Mo_2Cl_4(dedp)_2$	$K_2Mo_2Cl_8$[375]
α-$Mo_2X_4(dppe)_2$; (X = Cl or Br)	$K_2Mo_2Cl_8$[368,376] $(NH_4)_4Mo_2Br_8$,[377] $Mo_2Cl_4(py)_4$,[376] $Mo_2(O_2CCF_3)_4/Me_3SiCl$[378]
β-$Mo_2X_4(dppe)_2$	$K_4Mo_2Cl_8$,[376] $Mo_2X_4(PEt_3)_4$ (X = Cl or Br),[368] $Mo_2Cl_4(PBu^n_3)_4$,[368] $Mo_2Cl_4(py)_4$,[376] $(Bu_4N)Mo_2Br_6$,[340]
(X = Cl, Br or I)	$Mo_2(O_2CCH_3)_4/Me_3SiX$ (X = Cl or I),[123,379] $Mo_2(O_2CCF_3)_4/Me_3SiX$ (X = Cl or Br)[377,378]
α-$Mo_2X_4(dppee)_2$; (X = Cl or Br)	$K_4Mo_2Cl_8$,[380] $(NH_4)_4Mo_2Br_8$,[380] $Mo_2(O_2CCH_3)_4/Me_3SiX$[380]
β-$Mo_2X_4(dppee)_2$; (X = Cl or Br)	$K_4Mo_2Cl_8$,[380] $(NH_4)_4Mo_2Br_8$,[380] $Mo_2(O_2CCH_3)_4/Me_3SiX$[380]
$Mo_2I_4(dppee)_2$	$Mo_2(O_2CCH_3)_4/Me_3SiI$[380]
α-$Mo_2Cl_4(dpdt)_2$	$K_4Mo_2Cl_8$[375]
β-$Mo_2Cl_4(dpdt)_2$	$Mo_2(O_2CCF_3)_4/Me_3SiCl$[375]
α-$Mo_2Cl_4(dpdbp)_2$	$K_4Mo_2Cl_8$[381]
β-$Mo_2Cl_4(dpdbp)_2$	$Mo_2(O_2CCF_3)_4/Me_3SiCl$[381]
α-$Mo_2Cl_4(dptpe)_2$	$K_4Mo_2Cl_8$[382,383]
α-$Mo_2Cl_4(R\text{-dppp})_2$	$K_4Mo_2Cl_8$[383]
β-$Mo_2X_4(S,S\text{-dppp})_2$; (X = Cl or Br)	$K_4Mo_2Cl_8$,[384] $Mo_2(O_2CCF_3)_4/Me_3SiX$[384]
α-$Mo_2X_4(dppbe)_2$; (X = Cl or Br)	$K_4Mo_2Cl_8$,[385] $(NH_4)_5Mo_2Cl_9{\cdot}H_2O$,[385] $(NH_4)_4Mo_2Br_8$[385]
β-$Mo_2Cl_4[(R,R)\text{-diop}]_2$	$K_4Mo_2Cl_8$[386]
β-$Mo_2Cl_4[(S,S)\text{-diop}]_2$	$K_4Mo_2Cl_8$[386]
α-$Mo_2Cl_4(dppp)_2$	$K_4Mo_2Cl_8$,[376] $Mo_2Cl_4(py)_4$[376]
β-$Mo_2X_4(dppp)_2$; (X = Cl or Br)	$K_4Mo_2Cl_8$,[376] $(NH_4)_5Mo_2Cl_9{\cdot}H_2O$,[387] $Mo_2Cl_4(py)_4$,[376] $(NH_4)_4Mo_2Br_8$[387]
$Mo_2Cl_4(PPr^n_3)_2(dppp)$	$Mo_2Cl_4(PPr^n_3)_4$[376]

Pictiva EX2004
Samsung v Pictiva
IPR2024-01094

Compound[a]	Synthetic starting materials
β-$Mo_2X_4(dppp)_2$; (X = Cl or Br)	$K_4Mo_2Cl_8$,[388] $Mo_2(O_2CCF_3)_4/Me_3SiBr$[388]
β-$Mo_2Cl_4(tdpm)_2$	$(NH_4)_5Mo_2Cl_9{\cdot}H_2O$[370]
β-Mo_2Cl_4(*S*,*S*-bppm)$_2$	$K_4Mo_2Cl_8$[389]
β-$Mo_2X_4(arphos)_2$[b]; (X = Cl or Br)	$K_4Mo_2Cl_8$,[368] $(Bu_4N)Mo_2Br_6$[340]
$Mo_2Cl_4(dpae)_2$	$K_4Mo_2Cl_8$[368]
$Mo_2Cl_4(diars)_2$	$K_4Mo_2Cl_8$[368]
$Mo_2X_4(DMF)_4$; (X = Cl or Br)	$Mo_2Cl_4(dtdd)_2$,[347] $Mo_2Br_4(SMe_2)_4$[347]
$Mo_2X_4(SR_2)_4$; (X = Cl or Br; R = Me or Et)	$(NH_4)_5Mo_2Cl_9{\cdot}H_2O$,[347] $Mo_2Br_4(py)_4$[347]
$Mo_2Cl_4(dth)_2$	$(NH_4)_5Mo_2Cl_9{\cdot}H_2O$[347]
$Mo_2Cl_4(dto)_2$	$(NH_4)_5Mo_2Cl_9{\cdot}H_2O$[390]
$Mo_2X_4(dtd)_2$ (X = Cl or Br)	$(NH_4)_5Mo_2Cl_9{\cdot}H_2O$[347] $Mo_2Br_4(DMF)_4$[347]
$Mo_2Cl_4(dtdd)_2$	$(NH_4)_5Mo_2Cl_9{\cdot}H_2O$[347]

[a] The prefixes α and β signify different isomeric forms. These structural differences are discussed in the text.

[b] For X = Cl a mixture of α- and β-isomers is formed when $(NH_4)_5Mo_2Cl_9{\cdot}H_2O$ is used as the synthetic starting material (see ref. 376).

Pictiva EX2004
Samsung v Pictiva
IPR2024-01094

Table 4.8. Structures of $Mo_2X_4L_4$ compounds[a,b]

Compound	Crystal Sym.	Virtual Sym.	Mo–Mo, Å	Twist Angle (°)	ref.
A. L = Phosphine					
$Mo_2F_4(PMe_3)_4$	$\bar{4}3m$	D_{2d}	2.110(5)	≈0	391
$Mo_2Cl_4(PMe_3)_4$	2	D_{2d}	2.130(1)	0	356
	1	D_{2d}	2.131(1)	~0	392
$[Mo_2I_2(PBu^n_3)_2]_2(\mu\text{-}I)_4$	222	D_{2h}	2.129[3]	≈0	393
$Mo_2(C{\equiv}CH)_4(PMe_3)_4$	2	D_{2d}	2.134(1)	NR	394
$Mo_2(C{\equiv}CCH_3)_4(PMe_3)_4$	1	D_{2d}	2.141(1)	1.5	395
			2.140(1)		
$Mo_2(C{\equiv}CCMe_3)_4(PMe_3)_4$	1	D_{2d}	2.132(3)	~0	395
$Mo_2(C{\equiv}CPr^i)_4(PMe_3)_4$	1	D_{2d}	2.10(1)	?	396
$Mo_2(C{\equiv}CSiMe_3)_4(PMe_3)_4$	*m*	D_{2d}	2.136(1)	1	395
$Mo_2Cl_4(PHEt_2)_4$	2	D_{2d}	2.137(1)	2	364
$Mo_2Cl_4(\eta^1\text{-dmpm})_4$	222	D_{2d}	2.137(1)	~0	364
$Mo_2Cl_4[(Ph_2P)_2py]_2$	$\bar{1}$	C_{2h}	2.149(1)	0	397
$Mo_2Cl_4[(NCCH_2CH_2)_3P]_2(MeCN)_2{\cdot}2MeCN$	2	C_{2v}	2.143(1)	~0	398
$Mo_2Cl_4[(NCCH_2CH_2)_3P]_2(EtCN)_2$	*m2m*	C_{2v}	2.139(2)	0	398
$Mo_2Cl_4[(NCCH_2CH_2)_3P]_2(Pr^iCN)_2{\cdot}Pr^iCN$	1	C_{2v}	2.146(1)	3	398
$Mo_2Br_4(PMe_3)_4$	2	D_{2d}	2.125(1)	≈0	366
$Mo_2I_4(PMe_3)_4$	1	D_{2d}	2.127(1)	≈0	366
$Mo_2I_4(PMe_3)_4{\cdot}2THF$	2	D_{2d}	2.129(1)	≈0	360,362
$Mo_2Cl_4(PEt_3)_4$	$\bar{4}3m$	D_{2d}	2.141(9)	0	358
$Mo_2Cl_4(PMe_2Ph)_4$	2	D_{2d}	2.129(1)	≈0	358
$Mo_2Cl_4(PMePh_2)_4{\cdot}C_6H_6$	1	D_{2d}	2.135(1)	≈0	363
$Mo_2Cl_4(PHPh_2)_4$	1	D_{2d}	2.147(1)	≈0	358
$Mo_2Cl_4(PPh_3)_2(CH_3OH)_2$	$\bar{1}$	C_{2h}	2.143(1)	0	365
$Mo_2(NCO)_4(PMe_3)_4$	2	D_{2d}	2.134(1)	≈0	399
$Mo_2(NCS)_4(PMe_3)_4$	2	D_{2d}	2.134(1)	1.5	399
$Mo_2(CH_3)_4(PMe_3)_4$	2	D_{2d}	2.153(1)	≈0	400
$Mo_2Cl_4(PNP)(PHCy_2)$	1	C_s	2.147(1)	≈0	401
B. L = Nitrogen atom donors					
1,3,6,8-$Mo_2Cl_4(NHEt_2)_4$	2	D_{2d}	2.133(1)	8.7(1)	339
$Mo_2Cl_4(NH_2Pr^n)_4$	222	D_{2d}	2.118(2)	7.7	352
$Mo_2Cl_4(NH_2Bu^i)_4$	1	D_{2d}	2.131(1)	3.9	352
			2.134(1)	NR	
$Mo_2Cl_4(NH_2Cy)_4$	222	D_{2d}	2.117(1)	2.8	352
$Mo_2Cl_4[S\text{-}NH_2(1\text{-cyclohexylethyl})]_4$	222	D_{2d}	2.127(4)	~6	402
$Mo_2Cl_4[R\text{-}NH_2(1\text{-cyclohexylethyl})]_4$	222	D_{2d}	2.121(4)	~6	402
$Mo_2Cl_4(4\text{-pic})_4{\cdot}CHCl_3$	$\bar{1}$	D_{2h}	2.143(6)	0	351[a]
$Mo_2Br_4(4\text{-pic})_4$	$\bar{1}$	D_{2h}	2.150(2)	0	349
1,3,6,8-$Mo_2Cl_4(4\text{-pic})_4$	1	D_{2d}	2.150(1)	9	351
1,3,5,7-$Mo_2Cl_4(3,5\text{-lut})_4$	1	D_{2h}	2.142(1)	2	351
1,3,6,8-$Mo_2Cl_4(3,5\text{-lut})_4$	2	D_{2d}	2.139(1)	9	351

Pictiva EX2004
Samsung v Pictiva
IPR2024-01094

Compound	Crystal Sym.	Virtual Sym.	Mo–Mo, Å	Twist Angle (°)	ref.
$Mo_2Cl_4(4\text{-}Bu^tpy)_4\cdot C_6H_5$	$\bar{1}$	D_{2h}	2.142(1)	0	351
$Mo_2Cl_4(4\text{-}Bu^tpy)_4\cdot{}^2/_3THF$	$\bar{1}$	D_{2h}	2.140(1)	0	351
	1	D_{2d}	2.138(1)	5	351
$Mo_2Cl_4(4\text{-}Bu^tpy)_4\cdot{}^3/_4C_6H_{14}$	1	D_2	2.141(1)	8	351
$Mo_2Cl_4(4\text{-}Bu^tpy)_4\cdot{}^4/_3CH_2Cl_2$	1	D_2	2.136(2)	14	351
	1	D_2	2.150(2)	19	
$Mo_2Cl_4(4\text{-}Bu^tpy)_4\cdot C_6H_6$	2	D_2	2.157(1)	22	351
$Mo_2Cl_4(4\text{-}Bu^tpy)_4\cdot$acetone	1	D_2	2.147(1)	22	403
$Mo_2Br_4(4\text{-}Bu^tpy)_4\cdot 2C_6H_6$	$\bar{1}$	D_{2h}	2.148(2)	0	404
$Mo_2Cl_4(NH_2Pr^n)_2(PMe_3)_2$	2	C_{2v}	2.125(1)	NR	405
$Mo_2Cl_4(NH_2Cy)_2(PMe_3)_2$	1	C_{2v}	2.129(1)	NR	405
$Mo_2Cl_4(NH_2Cy)_2(PMe_2Ph)_2$	1	C_{2v}	2.128(1)	NR	405
C. X = alkoxide					
$Mo_2(OPr^i)_4py_4$	1	D_{2d}	2.195(1)	NR	406
$Mo_2(OCH_2CMe_3)_4(NHMe_2)_4$	*m*	D_{2d}	2.133(3)	NR	406
$Mo_2(OPr^i)_4(HOPr^i)_4$	4	D_{2d}	2.110(3)	~0	407,406
$Mo_2(O\text{-}c\text{-}Pen)_4(HO\text{-}c\text{-}Pen)_4$	1	D_{2d}	2.113(3)	NR	406
$Mo_2(OCH_2CMe_3)_4(PMe_3)_4$	1	D_{2d}	2.218(2)	~0	407,406
$Mo_2(OCH_2CMe_3)_4(HNMe_2)_4$	1	D_{2d}	2.133(2)	~0	407
$Mo_2(OC_6F_5)_4(PMe_3)_4$	$\bar{1}$	C_{2h}	2.146(2)	0	408
$Mo_2(OC_6F_5)_4(HNMe_2)_4$	2	D_{2d}	2.140(2)	~0	409
D. Miscellaneous structures					
$Mo_2Cl_4(SEt_2)_4$	1	D_{2d}	2.144(1)	~0	410
$Mo_2Cl_2(HBpz)_2$	1	C_2	2.155(1)	27	411
$Mo_2Br_2(HBpz)_2$	1	C_2	2.156(1)	28	411
$Mo_2I_4(NCPh)_4$	2	D_{2d}	2.144(5)	4	353
$Mo_2(\eta^1\text{-}O_2CCF_3)_4(bpy)_2$	$\bar{1}$	C_{2h}	2.129(1)[c]	0	55
$Mo_2(\mu\text{-}CH_2SiMe_2CH_2)(CH_2SiMe_3)_2(PMe_3)_3$	1	S_s	2.164(1)	d	412

[a] When more than one crystallographically independent molecule is present, all independent Mo–Mo distances and χ angles are listed.
[b] The idealized symmetry of the central Mo_2L_8 core.
[c] The distance given in the reference (2.077 Å) is in error, although the structure is otherwise correct.
[d] This has Mo^I and Mo^{III} atoms with 4 and 3 Mo–L bonds, respectively.

Table 4.9. Structures of $Mo_2X_4(LL)_2$ compounds with LL = diphosphine or polyphosphine

Compound[a]	Crystal Sym.	Virtual Sym.[b]	Mo–Mo, Å	Twist Angle (°)	ref.
$Mo_2Cl_4(dmpm)_2$	$\bar{1}$	C_{2h}	2.125(1)	0	367
$Mo_2Cl_4(dmpm)_2\cdot{}^1/_2H_2O\cdot 1{}^1/_3CH_3OH$	4/*mmm*	C_{2h}	2.134(4)	0	367
$Mo_2Cl_4(dmpm)$	2	D_{2h}	2.127(1)	≈0	
$Mo_2Br_4(dmpm)_2$	$\bar{1}$	D_{2h}	2.127(1)	zero	413
$Mo_2Cl_4(dmdppm)_2$	1	C_2	2.152(1)	18	414
$Mo_2I_4(dmpm)_2$	1	D_2	2.132(2)	11	413

Pictiva EX2004
Samsung v Pictiva
IPR2024-01094

Compound[a]	Crystal Sym.	Virtual Sym.[b]	Mo–Mo, Å	Twist Angle (°)	ref.
$Mo_2Cl_4(dippm)_2$	1	D_2	2.170(1)	30	415
$Mo_2Cl_4(dppm)_2 \cdot 2(CH_3)_2CO$	$\bar{1}$	C_{2h}	2.138(1)	0	369
$Mo_2Cl_4(dppm) \cdot 2CH_2Cl_2$	1	D_{2h}	2.150(1)	NR	364
$Mo_2(NCS)_4(dppm)_2 \cdot 2(CH_3)_3CO$	1	C_2	2.167(3)	13.3	369
$Mo_2Br_4(dppm)_2 \cdot 2THF$	$\bar{1}$	C_{2h}	2.138(1)	0	370
$Mo_2Cl_4(tdpm)_2 \cdot 2CH_2Cl_2$	1	C_2	2.148(1)	20	370
$Mo_2I_4(dppm)_2 \cdot 2C_7H_8$	1	C_{2h}	2.139(1)	≈0	371
$Mo_2I_4(dppm)_2$	$\bar{1}$	C_{2h}	2.178(3)	0	416
	1	C_2	2.152(2)	17	
β-$Mo_2Cl_4(dmpe)_2$	2	D_2	2.183(3)	40.0	372
β'-$Mo_2Cl_4(dmpe)_2$[c]	D_2	D_2	2.168(1)	33.8	373
β-$Mo_2Br_4(dmpe)_2$	1	D_2	2.169(2)	36.5	373
β-$Mo_2Cl_4(depe)_2$	D_2	D_2	2.173(2)	43.7	374
α-$Mo_2Cl_4(dppe)_2 \cdot THF$	$\bar{1}$	C_{2h}	2.140(2)	0	417
β-$Mo_2Cl_4(dppe)_2$	1	D_2	2.183(3)	30.5	378
β-$Mo_2Br_4(dppe)_2$	1	D_2	2.177(8)	31.1	418
β-$Mo_2I_4(dppe)_2 \cdot {}^2/_3CH_2Cl_2$	$\bar{1}$	C_{2h}	2.129(5)	0	379
	1	D_2	2.180(4)	27.9	
β-$Mo_2I_4(dppe)_2 \cdot C_7H_8$	1	D_2	2.179(3)	25.7	379
β-$Mo_2Cl_4(dppee)_2$	1	D_2	2.163(2)	25.5	380
anti-α-$Mo_2Cl_4(dpdt)_2 \cdot 2CH_3OH$	$\bar{1}$	C_{2h}	2.147(1)	0	375
anti-α-$Mo_2Cl_4(dpdbp)_2$	$\bar{1}$	C_{2h}	2.149(1)	0	381
β-$Mo_2Cl_4(S,S\text{-dppb})_2 \cdot THF$	1	D_2	2.147(3)	24	384
β-$Mo_2Cl_4(S,S\text{-dppb})_2 \cdot 4CH_3CN$	1	D_2	2.144(2)	22	384
β-$Mo_2Br_4(S,S\text{-dppb})_2$	1	D_2	2.147(6)	21.7[d]	384
	1	D_2	2.152(6)		
β-$Mo_2Cl_4(dpcp)_2 \cdot 0.5THF$	2	D_2	2.159(2)	≈22	419
β-$Mo_2Br_4(dpcp)_2 \cdot 0.5THF$	2	D_2	2.155(4)	≈22	419
β-$Mo_2I_4(dpcp)_2 \cdot THF$	2	D_2	2.151(3)	≈22	419
β-$Mo_2Br_4(arphos)_2$	1	C_2	2.167(4)	30	420
β-$Mo_2Cl_4(dppp)_2$	1	D_2	2.156(3)	70.3	387
	1	D_2	2.144(4)	68.5	
β-$Mo_2Cl_4[(R,R)\text{-diop}]_2 \cdot {}^3/_4CH_2Cl_2$	1	D_2	2.149(1)	78	386
β-$Mo_2Cl_4(S,S\text{-bppm})_2$	1	C_{2h}	2.128(2)	≈0	389
$Mo_2(OPr^i)_4(dmpe)_2$	2	C_2	2.236(1)	NR	421
$Mo_2(NCS)_4(Ph_2Ppy)_2 \cdot 2THF \cdot 2C_7H_8$	2	C_2	2.191(1)	11.0	422
$Mo_2Cl_4(dppa)_2$	1	D_2	2.134(1)	14	423
$Mo_2Br_4(dppa)_2 \cdot 2THF$	1	D_2	2.137(1)	15	423
$Mo_2Cl_4(dppa)_2 \cdot 2H_2O$	2	D_{2h}	2.13(1)	23	145
$Mo_2Cl_4(triphos)PEt_3$	1	C_1	2.159(2)	12	424
$Mo_2Cl_4(triphos)_2$	$\bar{1}$	C_i	2.149(6)	0	424
meso-Mo_2Cl_4(tetraphos-1)	1	C_1	2.186(1)	31	425

Pictiva EX2004
Samsung v Pictiva
IPR2024-01094

Compound[a]	Crystal Sym.	Virtual Sym.[b]	Mo–Mo, Å	Twist Angle (°)	ref.
meso-Mo_2Br_4(tetraphos-1)·CH_2Cl_2	1	C_1	2.195(3)	31	425
			2.183(3)	31	425
meso-Mo_2Br_4(tetraphos-1)·1.5THF	1	C_1	2.195(1)	29	425
rac-Mo_2Cl_4(tetraphos-1)·CH_2Cl_2	2	C_2	2.155(1)	18	426,425
rac-Mo_2Br_4(tetraphos-1)·0.5CH_2Cl_2	2	C_2	2.152(1)	19	425
rac-$Mo_2Cl_4(PEt_3)(\eta^3$-tetraphos-2)·C_6H_6	1	C_1	2.132(3)	12	427
α-Mo_2Cl_4[1,2-bis(2,5-dimethylphospholene)-benzene]$_2$·CH_2Cl_2	1	C_{2h}	2.147(1)	5	428
$Mo_2(NCS)_4(dppb)_2$·CH_3NO_2	2	D_2	2.172(3)	26	429
			2.154(3)	22	
$Mo_2Cl_4(bdppp)_2$·2CH_2Cl_2	$\bar{1}$	C_{2h}	2.149(1)	0	397
trans-$Mo_2Cl_4(2\text{-}Ph_2P\text{-}6\text{-}Cl\text{-}py)_2$	$\bar{1}$	C_{2h}	2.136(3)	zero	157
trans-$Mo_2Cl_4(Ph_2PCH_2CO_2Me)_2$	$\bar{1}$	C_{2h}	2.145(1)	zero	430

[a] When more than one crystallographically independent molecule is present, all independent Mo–Mo distances and X angles are listed.
[b] The idealized symmetry of the Mo_2^{4+} and its eight equatorial ligand atoms.
[c] The prime signifies a different crystal form.
[d] Average P–Mo–Mo–P torsion angle for two independent molecules.

The first report of halide complexes of the type $Mo_2X_4L_4$ was that of San Filippo,[357] who isolated the phosphine complexes $Mo_2Cl_4(PR_3)_4$, where PR_3 = PEt_3, PPr^n_3, PBu^n_3 or PMe_2Ph, and the phosphite analog $Mo_2Cl_4[P(OMe)_3]_4$, upon reacting $(NH_4)_5Mo_2Cl_9$·H_2O with the appropriate ligand in methanol under oxygen-free conditions. An interesting feature which was discovered in the ^{1}H NMR spectra of $Mo_2Cl_4(PR_3)_4$ (and incidentally, in the related spectra of $Re_2Cl_6(PR_3)_2$)[357] is the substantial deshielding of the ligand α-methylene protons as a consequence of the diamagnetic anisotropy associated with the M–M multiple bonds. Similar effects have subsequently been seen (Section 16.1.7) in the NMR spectra of other complexes that contain multiple bonds. In a later paper, San Filippo *et al*.[347] reported a more extensive series of complexes of the type $Mo_2X_4L_4$ (X = Cl or Br) which were prepared both from reactions of monodentate or bidentate ligands with $(NH_4)_5Mo_2Cl_9$·H_2O or $Cs_3Mo_2X_8H$, and via ligand exchange reactions from other preformed $Mo_2X_4L_4$ complexes. Use of the latter method included the preparation of the acetonitrile and benzonitrile complexes $Mo_2Cl_4(NCR)_4$ from $Mo_2Cl_4(SMe_2)_4$, and the conversion of the pyridine complex $Mo_2Br_4(py)_4$ to $Mo_2Br_4(SMe_2)_4$, $Mo_2Br_4(bpy)_2$, and $Mo_2Br_4(PBu^n_3)_4$. $Mo_2Cl_4(SMe_2)_4$ and $Mo_2Br_4(py)_4$ were in turn prepared from $(NH_4)_5Mo_2Cl_9$·H_2O and $Cs_3Mo_2Br_8H$, respetively.[347] With the use of these procedures, San Filippo *et al*.[347] were able to establish the existence of such complexes with a variety of nitrogen, sulfur, and phosphorus donors plus the dimethylformamide complex $Mo_2Cl_4(DMF)_4$.

Following this early work,[347,357] a large number of complexes that contain monodentate (L) or bidentate (LL) ligands have been prepared. In a few instances, complexes of these types have been generated in solution only, e.g., $Mo_2Cl_4(PR_3)_4$, where PR_3 = $P(OCH_2CH_2Cl)_3$, $P(OCH_2)_3CEt$, $PClPh_2$ and $P(CH{=}CH_2)_3$.[357] While the best strategies for preparing these complexes usually involve the use of well-defined dimolybdenum(III) or dimolybdenum(II) starting materials, other procedures exist that are of interest and significance in their own right even though they may not be the synthetic method of choice. Examples include the conversion of the methylsulfonate complex $Mo_2(O_3SCH_3)_4$ (prepared from $Mo_2(O_2CCH_3)_4$)[212] to $Mo_2Cl_4(dppm)_2$

Pictiva EX2004
Samsung v Pictiva
IPR2024-01094

upon its reaction with a methanol solution of Me_4NCl followed by the addition of a solution of dppm in dimethoxyethane.[369] The treatment of the methyl derivative $Mo_2(CH_3)_4(PMe_3)_4$ itself prepared from $Mo_2(O_2CCH_3)_4$, with conc. HCl in methanol produces the blue chloride $Mo_2Cl_4(PMe_3)_4$.[226]

The only compounds containing X = F are $Mo_2F_4(PMe_3)_4$ and $Mo_2F_4(PMe_2Ph)_4$. The anion $Mo_2F_8^{4-}$ is unknown, and the preparation of these compounds[391] was accomplished by the reaction:

$$Mo_2(CH_3)_4(PR_3)_4 \xrightarrow{OR} Mo_2F_4(PR_3)_4 + 4CH_4$$

where "Olah's reagent" (OR) is a 70% solution of HF in pyridine. The compounds are relatively unstable, especially toward visible light, but are well characterized by ^{19}F and ^{31}P NMR, and the structure of $Mo_2F_4(PMe_3)_4$ was confirmed by X-ray crystallography (Mo–Mo = 2.110(5) Å).

The reactions of acetone solutions of $(Bu_4N)Mo_2Br_6$ with pyridine, PEt_3, PPr^n_3, dppe or arphos result in reduction of this bromo-anion and the formation of $Mo_2Br_4L_4$ and $Mo_2Br_4(LL)_2$ compounds.[340] This starting material is of uncertain nuclearity but it could well be tetranuclear. Indeed, other reactions are known in which tetranuclear molybdenum clusters degrade to dinuclear species. Thus, the 2,2'-bipyridyl complex $Mo_2I_4(bpy)_2$ is formed upon prolonged reflux of an acetonitrile solution of $(Bu_4N)_2Mo_4I_{11}$, with bpy.[340] Also, the β-MoX_2 phases (X = Cl, Br or I),[331,337] which are believed to contain tetranuclear clusters of molybdenum atoms[333] react with an excess of monodentate PR_3 to afford $Mo_2X_4(PR_3)_4$. The reactions of the salt $(Bu_4N)_2Mo_2Br_6$ (formally the one-electron reduced congener of $(Bu_4N)Mo_2Br_6$)[340,342] with PEt_3, PEt_2Ph, dppe and $(Ph_2PCH_2CH_2)_2PPh$ (bdpp) are said[343] to give complexes of the type $(Bu_4N)[Mo_2Br_5L_2]$, $(Bu_4N)[Mo_2Br_3L_4]$ or $Mo_2Br_4L_4$, depending upon the choice of reaction conditions. However, the complexes that are formulated as $Mo_2Br_4(PEt_3)_4$, $Mo_2Br_4(PEt_2Ph)_4$ and $Mo_2Br_4(dppe)_2$ are described[343] as being orange in color, quite different from the colors that are normally associated with authentic samples of these complexes (blue-purple for the PEt_3 and PEt_2Ph complexes, green for α-$Mo_2Br_4(dppe)_2$ and red-brown for β-$Mo_2Br_4(dppe)_2$).[331,368,377] Accordingly, some question exists as to the true identity of these particular products.[343]

A curious route to complexes of the type $Mo_2X_4(PR_3)_4$ is the reaction of molybdenum atoms with oxalyl chloride to give a material that upon extraction into THF and treatment with PEt_3 affords $Mo_2Cl_4(PEt_3)_4$.[431] A route to $Mo_2Br_4(PMe_3)_4$ involves the decomposition of the triply bonded dimolybdenum(III) complex $Mo_2Br_2(=CHSiMe_3)_2(PMe_3)_4$ in hydrocarbon solvents:[432]

$$3Mo_2Br_2(=CHSiMe_3)_2(PMe_3)_4 \rightarrow Mo_2Br_4(PMe_3)_4 + 2MoBr(\equiv CSiMe_3)(PMe_3)_4 + 2Me_4Si + Me_3SiCH=CHSiMe_3 + \text{other product(s)}$$

There are also the very slow reactions between the trihalides MoX_3 and tertiary phosphines in refluxing ethanol or toluene to give $Mo_2X_4(PR_3)_4$ (X = Cl, Br or I; R = Me, Et or Pr^n).[345,433] Since the solid-state structures of $MoCl_3$[434] and $MoBr_3$[435] are based on face-sharing MoX_6 octahedra with adjacent metal atoms drawn together in pairs (Mo–Mo = 2.76 Å in $MoCl_3$ and 2.92 Å in $MoBr_3$), the formation of $Mo_2X_4(PR_3)_4$ may involve the cleavage of the halide bridges and retention and enhancement of the Mo–Mo interactions of the trihalides. The dimethylamine and trimethylamine complexes $Mo_2X_4(HNMe_2)_4$ (X = Cl or Br) and $Mo_2Cl_4(NMe_3)_4$ have been prepared from the trihalides.[344-346] In the case of the bromide/dimethylamine system, these results corrected an earlier formulation of the product as the solvolyzed molybdenum(III) complex $MoBr_2(NMe_2)\cdot NHMe_2$.[436] Both of the dimethylamine complexes are readily convertible to $Mo_2X_4(PPr^n_3)_4$, thereby supporting[345] this structural formulation.

In contrast to the relatively sluggish reactivity of the trihalides themselves, the THF complexes $MoCl_3(THF)_3$[21] or $Mo_2Cl_6(THF)_3$[352,351] provide much more convenient routes. Also, the

Pictiva EX2004
Samsung v Pictiva
IPR2024-01094

comproportionation reaction between $MoI_3(PMe_3)_3$ and $Mo(CO)_6$ in refluxing toluene gives $Mo_2I_4(PMe_3)_4$.[362] Other examples are known where a higher oxidation state mononuclear molybdenum complex is reduced in a 'one-pot' reaction to give $Mo_2X_4(PR_3)_4$ compounds. When an excess of hydrochloric acid is added to the hydride $MoH_4(PMePh_2)_4$, monomeric $MoCl_3(PMePh_2)_3$ is formed, but when THF is used as the reaction solvent and the HCl:$MoH_4(PMePh_2)_4$ stoichiometric ratio is adjusted to 2:1, then the green complex $Mo_2Cl_4(PMePh_2)_4$ can be isolated.[359] This reaction represents formally the reductive elimination of hydrogen and the coupling of pairs of low oxidation state coordinatively unsaturated molybdenum monomers. Attempts to purify this green compound were thwarted[359] by its conversion to a more stable blue isomer. A similar result was obtained by Luck and Morris[440,439] who prepared this same complex in its green and blue forms by a comproportionation reaction involving the reaction of $Mo(\eta^6\text{-PhPMePh})(PMePh_2)_3$ with $MoCl_4(THF)_2$. The complex $Mo_2Cl_4(PMe_2Ph)_4$ was prepared by a similar procedure, as was $Mo_2Cl_4(PEt_2Ph)_4$ although in an impure form.[439] Another example of a mononuclear to dinuclear transformation is that reported by Sharp and Schrock,[437] who found that the sodium amalgam reduction of a THF solution of $MoCl_4$ and PBu^n_3 gave $Mo_2Cl_4(PBu^n_3)_4$ via the intermediacy of $MoCl_4(PBu^n_3)_2$.

In addition to the methods outlined in Table 4.7, an additional but little-used strategy is halide exchange, which has been used[438] to convert $Mo_2Cl_4(dppm)$, to its bromo and iodo analogs by reaction with NaX in acetone. However, a problem with this method is ensuring that complete halide replacement occurs.[416] Phosphine exchange can also be used, as in the conversion of $Mo_2Cl_4(PMePh_2)_4$ to $Mo_2Cl_4(PMe_3)_4$.[439] In a few instances the synthesis of compounds of the type $\beta\text{-}Mo_2X_4(LL)_2$ is best approached by allowing the preformed α-isomer to isomerize to the more thermodynamically stable β-form in solution, e.g. $\beta\text{-}Mo_2Cl_4(dptpe)_2$ and $\beta\text{-}Mo_2Cl_4(R\text{-}dppp)_2$ whose preparations have not been reported by any other means.[383] In a related context, other solution reactions of note include the slow conversions (ligand redistribution reactions) of $Mo_2(O_2CCH_3)Cl_3(PMe_3)_3$ in THF to a mixture of $Mo_2Cl_4(PMe_3)_4$ and $Mo_2(O_2CCH_3)_4$,[127] and of $Mo_2(O_2CCH_3)_2Cl_2(dppm)_2$ to $Mo_2Cl_4(dppm)_2$ in several solvents.[123,190]

Most molecules of the $Mo_2X_4L_4$ type are the 1,3,6,8 isomers,[356,358,362,363,366] presumably because the usually larger L ligands best avoid one another that way. However molecules of the type $Mo_2Cl_4(Rpy)_4$, where Rpy may be 4-Mepy, 4-Bu^{t}py or 3,5-Me_2py, are remarkable in their capacity to present themselves with a variety of rotation angles about the Mo–Mo bond in different crystals.[351] Some are close to having D_{2h} symmetry (1,3,5,7), some close to D_{2d} (1,3,6,8) and a few are well in between with only D_2 symmetry. In the D_{2d} and D_{2h} structures there is essentially full δ overlap and it must be small differences in intramolecular nonbonded forces that decide the outcome. For the D_2 structures, where much of the δ overlap has to be lost, various nonbonded interactions evidently dominate. A subsequent study[403] of these molecules by spectroscopy in solution and DFT calculations (B3LYP with large basis sets) led to two principal conclusions: (1) The D_{2h} (1,3,5,7) conformation, though frequently found in crystals, is the least stable in solution or the vapor phase. (2) The relative stabilities of the D_{2d} (1,3,6,8) and D_2 conformations are both solvent-dependent and temperature-dependent.

The vast majority of $Mo_2X_4L_4$ and $Mo_2L_4(LL)_4$ compounds have mono- or diphosphines as neutral ligands, but before proceeding to these the $Mo_2X_4(amine)_4$ compounds will be discussed. In fact, the first $Mo_2X_4L_4$ compound ever reported[436] (1962) was then thought to be $MoBr_2(NMe_2)\cdot NHMe_2$, rather than, as now recognized, $Mo_2Br_4(NHMe_2)_4$. Later investigations established the existence of $Mo_2Cl_4(NHMe_2)_4$ and $Mo_2Cl_4(NMe_3)_4$ as well.[344-346]

The three $Mo_2X_4(amine)_4$ compounds just mentioned were prepared from Mo^{III} starting materials. Yields were low and the way in which reduction of some of the molybdenum occurs remains obscure. More recently, the preparation and chemical reactions of $Mo_2X_4(amine)_4$ com-

Pictiva EX2004
Samsung v Pictiva
IPR2024-01094

pounds were further studied.[339] While spontaneous reduction of $Mo_2Cl_6(THF)_3$ in the presence of $NHEt_2$ does occur to give low yields of $Mo_2Cl_4(NHEt_2)_4$, the use of Na/Hg as a reductant allows efficient preparation:

$$Mo_2Cl_6(THF)_3 + 2Na/Hg + 4NHEt_2 \rightarrow Mo_2Cl_4(NHEt_2)_4$$

By similar reactions, $Mo_2Cl_4(amine)_4$ compounds with the primary amines NH_2Et, NH_2Pr^n, NH_2Bu^t and NH_2Cy have been prepared in almost quantitative yield and characterized.[352]

It is a general characteristic of the $Mo_2X_4(amine)_4$ compounds that the amines may be displaced by phosphines. This point was studied in detail[364] for $Mo_2Cl_4(NHEt_2)_4$, where displacement is facile, and it was shown that the $Mo_2X_4(PR_3)_4$ compounds with PR_3 = PMe_3, PMe_2Ph, $PHEt_2$, η^1-$Me_2PCH_2PMe_2$ and η^1-$Me_2PCH_2CH_2PMe_2$ are obtained smoothly. The latter two are quite novel in that the normally bidentate dmpm and dmpe ligands are attached to metal atoms by only one phosphorus atom, with the other one dangling, as shown in Fig. 4.15 for $Mo_2Cl_4(\eta^1\text{-dmpm})_4$. On heating, this compound expels two dmpm molecules to form the previously known ß-$Mo_2Cl_4(dmpm)_2$:

$$Mo_2Cl_4(\eta^1\text{-dmpm})_4 \rightarrow Mo_2Cl_4(\eta^2,\mu\text{-dmpm})_2 + 2dmpm$$

The $Mo_2Cl_4(\eta^1\text{-dmpe})_4$ compound also decomposed on heating, but in a complex way that led to an unidentified solid. When $Mo_2Cl_4(NHEt_2)_4$ reacted with dppa and dppm the products were the conventional $Mo_2Cl_4(LL)_2$ molecules.

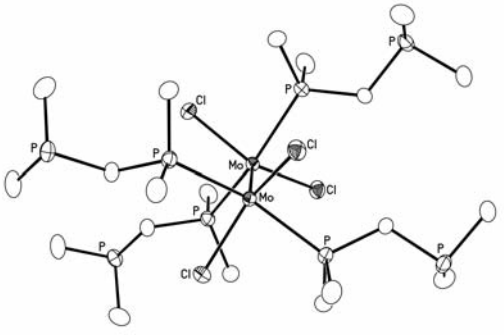


Fig. 4.15. The structure of 1,3,6,8-$Mo_2Cl_4(\eta^1\text{-dmpm})_4$.

For the $Mo_2Cl_4(NH_2R)_4$ compounds, replacement of the NH_2R by phosphines is less facile than for $NHEt_2$; replacement proceeds only halfway at ambient temperature and heating is necessary to go all the way to an $Mo_2Cl_4(PR_3)_4$ product. Also, back reaction occurs. It was possible to show in detail the stepwise nature of these reactions.[405] The general results are summarized in Fig. 4.16, although the details vary with the particular amine and phosphine used, depending particularly on the basicity of the latter. The overall pattern displays a "stereochemical hysteresis," in that the forward and reverse paths are not identical. The reason for this is the large difference in the *trans* influence of phosphines and amines; the former is far greater. Thus, the action of PR_3 on $Mo_2Cl_4(PR_3)(NH_2R)_3$ leads to isomer (*3*) of the $Mo_2Cl_4(PR_3)_2(NH_2R)_2$ intermediate, whereas the action of NH_2R on $Mo_2Cl_4(PR_3)_3(NH_2R)$ leads to isomer (*4*) because the preference is always to replace a ligand opposite to a PR_3 group rather than one opposite to a NH_2R group.

The blue mixed-ligand complex $Mo_2Cl_4(PPh_3)_2(CH_3OH)_2$ was isolated[365] during attempts to prepare $Mo_2Cl_4(PPh_3)_4$ through reaction of $(NH_4)_5[Mo_2Cl_9]\cdot H_2O$ with PPh_3 in methanol. It

Pictiva EX2004
Samsung v Pictiva
IPR2024-01094

is the centrosymmetric isomer with a 1,3,5,7 distribution of neutral ligands. Upon dissolution in benzene it is converted to a brown complex of stoichiometry $[MoCl_2(PPh_3)]_n$. Reaction of the latter material with the trialkyl phosphines PEt_3 or PBu^n_3 in benzene at 25 °C converts it to diamagnetic brownish-yellow complexes that proved to be tetranuclear $Mo_4Cl_8(PR_3)_4$.[365] The chemistry of these and other tetranuclear molybdenum complexes is dealt with in Section 4.5.6.

An interesting subtlety addressed in the X-ray structure determination of $Mo_2Cl_4(PMePh_2)_4$,[363] concerns the relationship between the green and blue forms of this complex. These two forms had been encountered in prior synthetic studies[359,439,440] and their electronic absorption and ^{31}P NMR spectra were found[359] to be essentially the same. However, there are some differences in their low frequency infrared spectra[359] and their electrochemical properties are quite different (see below).[439] Based on the crystal structure of the blue form, which is the 1,3,6,8-isomer, it has been suggested[363] that the difference lies in the orientation of the $PMePh_2$ ligands about the Mo–P bonds. The blue form is the form with the least degree of repulsive contact (S_4 symmetry).[363]

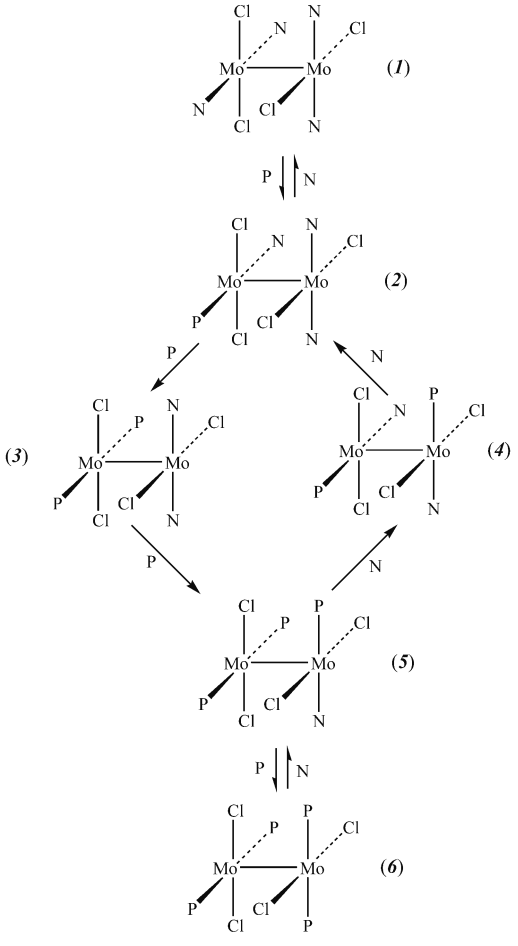


Fig. 4.16. The interconversion of $Mo_2Cl_4(PR_3)_4$ and $Mo_2Cl_4(NRH_2)_4$ compounds, showing the dual pathway. For simpicity the neutral ligands are represented by P and N.

Pictiva EX2004
Samsung v Pictiva
IPR2024-01094

Studies of electronic absorption spectra (particularly the $\delta \rightarrow \delta^*$ transition),[102,331,347,350,353,358,361,366,404,439] low frequency infrared spectroscopy (ν(Mo–X)).[102,331,346,347,350,354] Raman spectroscopy (ν(Mo–Mo)),[102,347,350,366,404,441] and ^{31}P NMR spectroscopy[248,362,363,439] have been used to identify compounds as containing $Mo_2X_4L_4$ molecules. The presence of a $\delta \rightarrow \delta^*$ transition close to 600 nm, two infrared-active ν(Mo–X) modes, a Raman-active ν(Mo–Mo) mode at *c.* 350 cm^{-1}, and a singlet in the $^{31}P\{^1H\}$ spectrum are particularly characteristic. Excited state spectra have been studied in considerable detail for $Mo_2X_4(PMe_3)_4$,[442-444] $Mo_2Cl_4(PBu^n_3)_4$,[445] and $Mo_2Cl_4(NCCH_3)_4$,[445] and the gas-phase PE spectrum of $Mo_2Cl_4(PMe_3)_4$ has been recorded and interpreted in terms of the $\sigma^2\pi^4\delta^2$ configuration.[446] The latter spectroscopic studies[442-446] are discussed in more detail in Chapter 16.

We turn now to the $Mo_2X_4(LL)_2$ class of compounds, in which the bidentate ligands, LL, are almost always diphosphines. The structures that have been established by X-ray crystallography are listed in Table 4.9.

The structure of the complexes that contain a single atom between the two donor atoms of the LL ligands are relatively simple as shown in Fig. 4.17 in the case of the monoclinic form of β-$Mo_2Cl_4(dmpm)_2$.[367] This molecule, which possesses a rigorously eclipsed rotation geometry and bridging dmpm ligands has the phosphorus atoms in the 1,3,5,7 arrangement. Most of the molecules that contain diphosphinomethane ligands do not have precisely eclipsed structures. As Table 4.9 shows, twist angles of 30° or more are observed. The dppm complexes $Mo_2X_4(dppm)_2$ (X = Cl, Br or I) show a similar structure[371] although $Mo_2I_4(dppm)_2$, when grown from CH_2Cl_2/CH_3OH, crystallizes with two independent molecules in the unit cell, one of which is centrosymmetric with an average torsional angle (χ) of zero, while the other possesses no crystallographically imposed symmetry and has an average χ of 17°.[416] This result demonstrates clearly that crystal packing forces can play an important role in determining the exact rotational geometry. The complex $Mo_2Cl_4(tdpm)_2$ (tdpm = $(Ph_2P)_3CH$) can be considered as containing a modified dppm ligand.[370] It resembles the aforementioned structures but with an uncomplexed Ph_2P unit replacing one of the hydrogen atoms of the bridgehead CH_2 group. Also, the molecule assumes a partially staggered conformation (χ = 20[3]°), presumably because of the steric bulkiness of the extra PPh_2 group.[370]

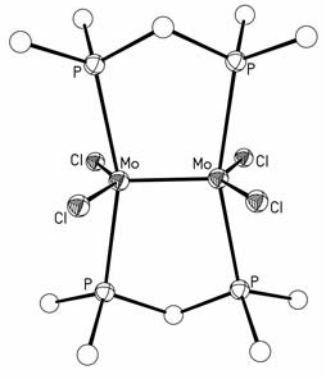
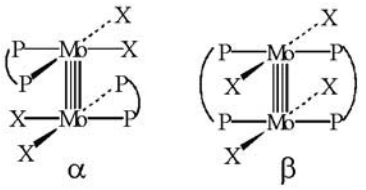


Fig. 4.17. The structure of the monoclinic form of β-$Mo_2Cl_4(dmpm)_2$.

When the LL ligands have the two donor atoms separated by two (or even three) carbon atoms they may be attached to the Mo_2X_4 unit in either of two ways, as shown in 4.25 for biphosphines.

Pictiva EX2004
Samsung v Pictiva
IPR2024-01094



4.25

In the β isomers it should be noted that the fusion of two 6-membered rings along the Mo–Mo bond results, in every case but one (see below), in a non-zero torsion angle about this bond. Apart from any influence that packing forces may have, the angle of rotation reflects a balance between conformational preferences of the rings and the retention of δ-bonding. It has been estimated[420] that with a torsion angle of 30° about half of the δ-bond strength is retained.

The actual occurrence of α and β isomers was first recognized for molybdenum compounds (although analogous ones were already known for $Re_2X_4(LL)_2$ molecules) when $Mo_2Cl_4(LL)_2$ compounds containing dppe, arphos and dpae ligands were made and structurally characterized.[340,368]

Following this early work a profusion of both α and β isomers of $Mo_2X_4(LL)_2$ compounds have been made and characterized structurally, spectroscopically and in other ways. The vast majority of the structures that have been determined crystallographically are those of β isomers because these are generally more stable than their α analogs. Some α isomers have been observed to isomerize to their β analogs, and in many cases the α isomer has not been observed. The twist angles in β isomers range from ~0° to ~70°, but the majority are in the range of 20° to 40°. The only case in which both α and β isomers of the same stoichiometry have been characterized crystallographically is $Mo_2Cl_4(dppe)_2$.[378,417] There is also one case, β-$Mo_2I_4(dppe)_2$·0.67CH_2Cl_2, in which two independent molecules are present, one with X = 27.9° and the other 0°. The latter is shown in Fig. 4.18.

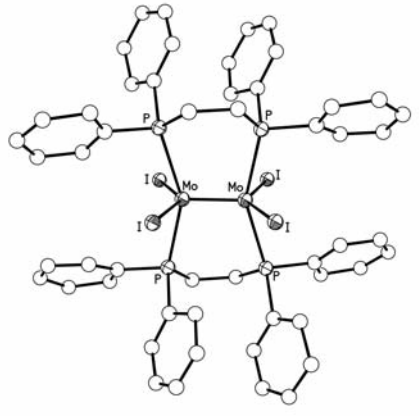


Fig. 4.18. The structure of the eclipsed rotomer (χ = 0) of β-$Mo_2I_4(dppe)_2$.

For several of these structures, different kinds of structural disorder have been encountered. In the cases of β'-$Mo_2Cl_4(dmpe)_2$[373] and β-$Mo_2Cl_4(depe)_2$[374] there is a disorder of the Cl and phosphine ligands that imparts a higher crystal symmetry than that of the individual molecules. Specifically, there is a twofold axis coincident with the Mo–Mo axis, and two other

Pictiva EX2004
Samsung v Pictiva
IPR2024-01094

twofold axes perpendicular to the Mo–Mo axis. For β-$Mo_2Cl_4(dmpe)_2$ there is also another form of disorder that is found with some other β-$Mo_2X_4(LL)_2$ molecules listed in Table 4.9. This is an orientation disorder involving primary (or major) and secondary (or minor) orientations of the Mo_2 unit that are essentially orthogonal. This disorder is quite commonly encountered with β-$Mo_2X_4(LL)_2$ compounds and is of the same kind as that commonly found in dirhenium halide chemistry (Chapter 8). The primary and secondary molecules at a given crystallographic site are conformational enantiomers; although the populations of the two conformers at a given site are not equal, the crystals as a whole are racemic. However, with the use of a chiral phosphine ligand such as *S*,*S*-dppb [i.e., *S*,*S*-2,3-bis (diphenylphosphino)butane] chiral molecules can be obtained. The complexes β-Mo_2X_4(*S*,*S*-dppb)$_2$ have been characterized by X-ray crystallography although several other well authenticated chiral molecules, such as β-Mo_2Cl_4(*R*-dppp)$_2$ (*R*-dppp = *R*-1,2-bis(diphenylphosphino)propane), have not. A general discussion of the chiral character of these and other closely related dimolybdenum(II) complexes[383,384,419,447-449] is given in Section 16.4.5.

Another interesting structural feature is seen in the case of α- and β-isomers of $Mo_2Cl_4(dpdt)_2$ (dpdt = $Ph_2PCH_2CH_2P(p\text{-tol})_2$), where because of the unsymmetric nature of the ligand these two isomers can exist in *syn* and *anti* forms. The *anti*-α-isomer has been crystallographically characterized (Table 4.9) and ^1H NMR spectroscopy has been used to study the α- and β-forms.[375,381] In the case of the α-isomers, a combination of the structural data and ^1H NMR spectroscopy has been used[382] to obtain the diamagnetic anisotropies of Mo–Mo quadruple bonds.

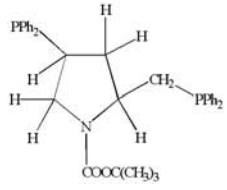
The large body of structural data now available on the α- and β-$Mo_2X_4(LL)_2$ compounds clearly shows[370,372,374,379] that there is an inverse linear relationship between the Mo–Mo bond distances and cos(2χ), where χ is the average torsional (twist) angle. This correlation is a direct consequence of the strength of the δ component of the quadruple bond being a function of cos(2χ).[420] As χ increases so the δ component weakens. From this it follows that since the $\delta \rightarrow \delta^*$ transition energies are a function of δ-bond strength, there should also be a relationship between the $\delta \rightarrow \delta^*$ electronic transition and cos(2χ). This has been shown[373,379] to be the case, and its further interpretation is discussed in Section 16.4.1.

The relative stabilities and interconversion of α and β isomers in solution have been studied. A unimolecular mechanism involving internal rotation of the Mo_2 unit within the ligand cage is supported.[377,417] Although the equilibrium constant may strongly favor the β-isomer in the $\alpha \rightleftharpoons \beta$ equilibrium, the α-isomer can be obtained from the β-isomer by the use of a solvent system that permits selective precipitation of the α-form. This has been demonstrated through the conversion of β-$Mo_2Cl_4(dpdt)_2$ to α-$Mo_2Cl_4(dpdt)_2$.[375] The case of α-$Mo_2X_4(dppbe)_2$ (X = Cl or Br) is unusual in that the β-isomers have not been detected.[385] The apparent failure to form β-$Mo_2X_4(dppbe)_2$ is most likely a consequence of the rigidity of the dppbe ligand and its inability to bridge the two molybdenum atoms.

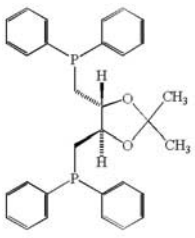
In addition to the complexes that contain bridging phosphine (and/or arsine) ligands and five- or six-membered rings, a few examples are known of β-$Mo_2X_4(LL)_2$ type compounds where the ring size is larger. The complex β-$Mo_2Cl_4(dppp)_2$ (dppp or 1,3-dppp = $Ph_2P(CH_2)_3PPh_2$)[376] contains two fused seven-membered rings, and has a disorder of the type where there are two perpendicular orientations of the Mo_2 unit.[387] The average twist angles for the primary and secondary orientations of the two independent molecules in the unit cell are close to 70°, reflecting this increase in ring size. There are two examples of structurally characterized dimolybdenum(II) complexes in which eight-membered rings are present. These are β-Mo_2Cl_4[(*R*,*R*)-diop]$_2$ (the related isomer β-Mo_2Cl_4[(*S*,*S*)-diop]$_2$ has also been prepared although its crystal structure has not been determined),[386] and β-Mo_2Cl_4(*S*,*S*-bppm)$_2$,[389] both of which contain chiral phosphine ligands. Schematic representations of the diop ligand (as its *R*,*R* and *S*,*S* enantiomorphs) and

Pictiva EX2004
Samsung v Pictiva
IPR2024-01094

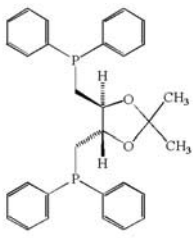
S,*S*-bppm are given in **4.26** and **4.27**. The conformational preference of each of these chiral ligands essentially effects an asymmetric synthesis and thereby produces only one of the possible configurational isomers. In these two instances, quite different twists are encountered, β-Mo_2Cl_4[(*R*,*R*)-diop]$_2$ having a very large torsional angle (78°), while β-Mo_2Cl_4(*S*,*S*-bppm)$_2$ is essentially eclipsed with each of the *S*,*S*-bppm ligands being bound through a phosphorus atom and its keto oxygen atom. The polydentate phosphine $Ph_2PCH_2CH_2P(Ph)CH_2CH_2P(Ph)CH_2CH_2PPh_2$(tetraphos-1) reacts with $K_4Mo_2Cl_4$ in methanol to give Mo_2Cl_4(tetraphos-1) in which the ligand has both bridging and chelating functionalities.[426] The crystal contains the racemic *R*,*R* and *S*,*S* enantiomers.



4.26



R,*R*



S,*S*

4.27

The $^{31}P\{^1H\}$ NMR spectra of several of these complexes have been measured and generally consist of a singlet at room temperature, viz. $Mo_2Cl_4(dmpm)_2$,[367] $Mo_2X_4(dppm)_2$ (X = Cl, Br or I),[371,438] and α- and β-$Mo_2Cl_4(dppee)_2$.[380] In the case of α- and β-$Mo_2Cl_4(dppee)_2$, the resonances are at δ +35.9 and δ +16.8 (spectra recorded in CD_2Cl_2),[380] the upfield shift of the latter compound being typical of the greater shielding associated with six-membered rings compared to that of their five-membered analogs. The spectrum of β-$Mo_2I_4(dppe)_2$ shows no signal at room temperature, but a broad resonance appears as the temperature is lowered and by −80 °C it is a sharp singlet.[379] This temperature dependence is indicative of a low-energy fluxional process. For β-Mo_2Cl_4(*S*,*S*-bppm)$_2$, singlets at δ +32.5 and δ −7.8 are assignable to the coordinated and free phosphine donor sites on the bppm ligand.[389]

The reaction chemistry of the $Mo_2X_4L_4$ and $Mo_2X_4(LL)_2$, compounds falls into two main categories, namely, non-redox ligand substitution reactions and redox chemistry in which the molybdenum unit is preserved. Ligand substitution reactions of the type $Mo_2X_4L_4 + 4L' \rightarrow Mo_2X_4L'_4 + 4L$ have already been mentioned in the context of the synthetic strategies used to prepare tetrahalodimolybdenum(II) complexes. Halide substitution reactions have also been reported; the reaction of $Mo_2Cl_4(dppm)_2$ with NaX (X = Br or I) in acetone has been used to prepare $Mo_2X_4(dppm)_2$.[438] In the reactions between $Mo_2X_4(PBu^n_3)_4$, where X = Cl or Br, and carboxylic acids, it was found[107] that when $Mo_2X_4(PBu^n_3)_4$ and benzoic acid were reacted in refluxing benzene one of three complexes, viz. $Mo_2(O_2CPh)_2X_2(PBu^n_3)_2$, $Mo_2(O_2CPh)_4(PBu^n_3)_2$ or $Mo_2(O_2CPh)_4$, could be isolated depending upon the reaction conditions. Under similar conditions, alkyl carboxylic acids form only $Mo_2(O_2CR)_4$.[107] The crystal structure of $Mo_2(O_2CPh)_2Br_2(PBu^n_3)_2$ shows[165] it to be centrosymmetric with a transoid arrangement of bridging benzoate ligands. The formation of $Mo_2(O_2CPh)_2Br_2(PBu^n_3)_2$ is similar to the reaction course that is encountered upon refluxing a mixture of 7-azaindole and $Mo_2Cl_4(PEt_3)_4$ in benzene.[450] The emerald green complex $Mo_2(C_7H_5N_2)_2Cl_2(PEt_3)_2$ contains two monanionic 7-azaindolyl ligands and has a structure analogous to that of $Mo_2(O_2CPh)_2Br_2(PBu^n_3)_2$ although the Mo–Mo bond is distinctly longer (by *c.* 0.03 Å).

Pictiva EX2004
Samsung v Pictiva
IPR2024-01094

In a similar manner, the reactions between $Mo_2X_4(PR_3)_4$ (X = Cl or Br; PR_3 = PEt_3, PMe_2Ph or $PMePh_2$) and 2-hydroxy-6-methylpyridine (Hmhp) or 2,4-dimethyl-6-hydroxypyrimidine (Hdmhp) in toluene give $Mo_2(mhp)_2X_2(PR_3)_2$ or $Mo_2(dmhp)_2X_2(PEt_3)_2$.[248] In the case of the mhp complexes, an alternative synthetic procedure is to react $Mo_2X_4(PR_3)_4$ with $Mo_2(mhp)_4$, and similar strategies can be used to prepare the complexes $Mo_2Cl_3(mhp)(PR_3)_3$ and $Mo_2Cl(mhp)_3(PR_3)$.[248] An X-ray crystal structure determination has been carried out on *cis*-$Mo_2(mhp)_2Cl_2(PEt_3)_2$.[221]

There are several reactions in which the Mo–Mo bond of $Mo_2X_4L_4$ and $Mo_2X_4(LL)_2$ is cleaved by π-acceptor ligands. While the reactions of $Mo_2X_4(dppm)_2$ (X = Cl, Br or I) with an equivalent of RNC (R = Pr^i or Bu^t) in the presence of $TlPF_6$ (in THF) or KPF_6 (in acetone) give $[Mo_2X_3(dppm)_2(CNR)]PF_6$,[438] an excess of RNC leads to seven-coordinate mononuclear complexes. The properties of $[Mo_2X_3(dppm)_2(CNR)]PF_6$ are in accord[438] with a structure similar to that of the parent tetrahalo species.

A variety of electrochemical studies have demonstrated the relative ease with which phosphine containing complexes of the types $Mo_2X_4L_4$ and $Mo_2X_4(LL)_2$ undergo one-electron oxidations, which in some instances are reversible. Cyclic voltammetric measurements have been carried out on many of these complexes and the important results are summarized in Table 4.10. The first such study was carried out on solutions of $Mo_2Cl_4(PR_3)_4$ (R = Et or Pr^n), α-$Mo_2Cl_4(dppe)_2$, and β-$Mo_2Br_4(dppe)_2$ in 0.2 M $(Bu_4N)PF_6$–CH_2Cl_2 and revealed the presence of a quasi-reversible one-electron oxidation in the range +0.35 to +0.54 V versus SCE.[451] Subsequently, a much more extensive range of complexes has been studied,[248,367,379,380,385,438,439,452-456] with CH_2Cl_2 and THF used as solvents. No redox activity was observed for solutions of $Mo_2Cl_4[P(OMe_3)_3]_4$ and $Mo_2Cl_4[P(OMe)Ph_2]_4$ in CH_2Cl_2.[454] Since the $E_{1/2}$(ox) values for solutions of $Mo_2X_4(PR_3)_4$ in THF are generally shifted by *c.* +0.3 V relative to those observed in CH_2Cl_2, this has permitted the observation of a one electron reduction ($E_{1/2}$(red)) for several of these complexes when the former solvent is used. Occasionally, this process has been observed even in CH_2Cl_2 (Table 4.10) and, in the case of the complexes with bidentate phosphines, a one-electron reduction is readily accessible in both solvents. In some instances, measurements on the same complex have been carried out in independent studies in different laboratories. Generally, very similar results have been obtained. The data reported in Table 4.10 for $Mo_2Cl_4(PMe_2Ph)_4$ refer to the stable blue form (see above). A THF solution of the green form is said[439] to have $E_{1/2}$(ox) = +0.28 V and $E_{1/2}$(red) = −0.95 V versus SCE under similar experimental conditions. The difference in potentials for these two forms seems too great in view of the close similarities of their other properties.

For the set of complexes $Mo_2X_4(PMe_3)_4$ (X = Cl, Br or I), the ease of oxidation and difficulty of reduction are both in the order Cl > Br > I. This 'inverse' halide order is opposite to that expected on electronegativity grounds, but it does reflect the tendency for low-valent iodides to be more stable than bromides, and these in turn more stable than chlorides.[457] This order, which has been attributed to the effects of metal(*d*)-to-halide(*d*) back bonding,[452] is also seen in the first oxidation ($E_{1/2}$(ox) (1)) of the dirhenium(II) complexes $Re_2X_4(PR_3)_4$. The order Cl > Br for $E_{1/2}$(ox) is followed for the other pairs of chloride/bromide complexes with monodentate phosphines, but this order is not so clear-cut in the case of the complexes that contain bidentate phosphines (see Table 4.10). For the pairs of α- and β-isomers of the type $Mo_2X_4(LL)_2$, differences in the $E_{1/2}$(ox) (or $E_{p,a}$) and $E_{1/2}$(red) values[380] do not provide a ready means of distinguishing between such isomers. For a series of chloride complexes, $Mo_2Cl_4(PR_3)_4$, a fairly good correlation was found[454] to exist between the $E_{1/2}$(ox) (or $E_{p,a}$) values and the δ → δ* transition energies. These compounds become more difficult to oxidize as the electron withdrawing nature of the PR_3 substituents increases and the δ → δ* energy decreases.

Pictiva EX2004
Samsung v Pictiva
IPR2024-01094

Table 4.10. Cyclic voltammetric data for dimolybdenum(II) complexes of the types $Mo_2X_4L_4$ and $Mo_2X_4(LL)_2$, X = Cl, Br, I, NCO or NCS)

Compound	$E_{1/2}$(ox)	$E_{1/2}$(red)	Other processes	Solvent	Reference electrode	ref.
$Mo_2Cl_4(PMe_3)_4$	+0.74	−1.70		THF	SCE	452[d]
	+0.77	−1.62		THF	Ag/AgCl	399
	+0.47			CH_2Cl_2	SCE	452[e]
	+0.50	−1.72		CH_2Cl_2	Ag/AgCl	399
$Mo_2Br_4(PMe_3)_4$	+0.87	−1.48		THF	SCE	452
	+0.59			CH_2Cl_2	SCE	452
$Mo_2I_4(PMe_3)_4$	+0.88	−1.28		THF	SCE	452
	+0.96	−1.17		THF	Ag/AgCl	399
	+0.73	−1.35		CH_2Cl_2	Ag/AgCl	399
$Mo_2Cl_4(PEt_3)_4$	+0.67	−1.81		THF	SCE	452
	+0.35			CH_2Cl_2	SCE	451,452[e]
	+0.40		$E_{p,a}$ = +1.43	CH_2Cl_2	Ag/AgCl	248
$Mo_2Br_4(PEt_3)_4$	+0.76	−1.59		THF	SCE	452
	+0.54		$E_{p,a}$ = +1.44	CH_2Cl_2	Ag/AgCl	248
$Mo_2Cl_4(PPr^n_3)_4$	+0.65	−1.89		THF	SCE	452
	+0.38			CH_2Cl_2	SCE	451,452[e]
$Mo_2Cl_4(PBu^n_3)_4$	+0.64	−1.92		THF	SCE	433
	+0.38			CH_2Cl_2	SCE	433[c,f]
$Mo_2Cl_4(PH_2Ph)_4$	≈+1.2[a,b]			CH_2Cl_2	Ag/AgCl	454
$Mo_2Cl_4(PMe_2Ph)_4$	+0.80	−1.63		THF	SCE	439
	+0.56		$E_{p,a}$ = +1.50	CH_2Cl_2	Ag/AgCl	248[e]
$Mo_2Br_4(PMe_2Ph)_4$	+0.74		$E_{p,a}$ = +1.47	CH_2Cl_2	Ag/AgCl	248
$Mo_2Cl_4(PEt_2Ph)_4$	+0.60			CH_2Cl_2	Ag/AgCl	454
$Mo_2Cl_4(PHPh_2)_4$	+0.92[b]			CH_2Cl_2	Ag/AgCl	454
$Mo_2Cl_4(PMePh_2)_4$	+0.88[b]	−1.54		THF	SCE	439
	+0.62		$E_{p,a}$ = +1.69	CH_2Cl_2	Ag/AgCl	248[e]
$Mo_2Br_4(PMePh_2)_4$	+0.66		$E_{p,a}$ = +1.5	CH_2Cl_2	Ag/AgCl	248
$Mo_2Cl_4(PEtPh_2)_4$	+0.63[b]			CH_2Cl_2	Ag/AgCl	454
$Mo_2Cl_4(dmpm)_2$	+0.49	−1.75[c]	$E_{p,a}$ = +1.25	CH_2Cl_2	Ag/AgCl	367
$Mo_2Cl_4(dppm)_2$	+0.66	−1.5[c]		CH_2Cl_2	Ag/AgCl	438
$Mo_2Br_4(dppm)_2$	+0.71	−1.28[c]		CH_2Cl_2	Ag/AgCl	438
$Mo_2I_4(dppm)_2$	+0.77[b]	−1.03[c]	$E_{p,a}$ = +1.21	CH_2Cl_2	Ag/AgCl	438
α-$Mo_2Cl_4(dppe)_2$	+0.61[b]	−1.26		CH_2Cl_2	Ag/AgCl	380[g]
β-$Mo_2Cl_4(dppe)_2$	+0.59	−1.37		CH_2Cl_2	Ag/AgCl	380
α-$Mo_2Br_4(dppe)_2$	+0.65[b]	−1.15		CH_2Cl_2	Ag/AgCl	380
β-$Mo_2Br_4(dppe)_2$	+0.59	−1.07		CH_2Cl_2	Ag/AgCl	380[g]
β-$Mo_2I_4(dppe)_2$	+0.62	−1.04[c]		CH_2Cl_2	Ag/AgCl	379
α-$Mo_2Cl_4(dppee)_2$	+0.58[b]	−1.18		CH_2Cl_2	Ag/AgCl	380
β-$Mo_2Cl_4(dppee)_2$	+0.75[b]	−1.29		CH_2Cl_2	Ag/AgCl	380
α-$Mo_2Br_4(dppee)_2$	+0.64[b]	−1.04		CH_2Cl_2	Ag/AgCl	380
β-$Mo_2Br_4(dppee)_2$	+0.77[b]	−1.07		CH_2Cl_2	Ag/AgCl	380

Pictiva EX2004
Samsung v Pictiva
IPR2024-01094

Compound	$E_{1/2}$(ox)	$E_{1/2}$(red)	Other processes	Solvent	Reference electrode	ref.
α-$Mo_2Cl_4(dppbe)_2$	+0.45[b]	−1.23[c]		CH_2Cl_2	Ag/AgCl	385
$Mo_2(NCO)_4(PMe_3)_4$	+0.83[b]	−1.42		THF	Ag/AgCl	399
	+0.60	−1.57		CH_2Cl_2	Ag/AgCl	399
$Mo_2(NCS)_4(PMe_3)_4$	+1.0[b]	−0.93	$E_{1/2}$(red) = −1.95	THF	Ag/AgCl	399
	+1.0[b]	−1.01		CH_2Cl_2	Ag/AgCl	399
$Mo_2(NCS)_4(PEt_3)_4$	+0.80	−1.17		CH_2Cl_2	SCE	451
$Mo_2(NCS)_4(dppm)_2$	+0.84[b]	−0.80	$E_{p,c}$ = −1.60	CH_2Cl_2	SCE	451
$Mo_2(NCS)_4(dppe)_2$	+0.74[b]	−0.85	$E_{1/2}$(red) = −1.58	CH_2Cl_2	SCE	451

[a] This process is described as being at a potential near the solvent limit.
[b] $E_{p,a}$ value.
[c] $E_{p,c}$ value.
[d] Similar data reported in ref. 439. Values of $E_{1/2}$(ox) = +0.65 V and $E_{1/2}$(red) = −1.82 V have been reported with the use of a silver quasi-reference electrode (see ref. 455).
[e] Values of $E_{1/2}$(ox) are given in ref. 454 for CH_2Cl_2 solutions of several $Mo_2Cl_4(PR_3)_4$ complexes. The values quoted (versus Ag/AgCl) are anywhere between 0.04 V and 0.14 V more positive than those cited in this table depending upon the identity of PR_3.
[f] Similar data reported in ref. 452.
[g] Similar data reported in ref. 451.

The one-electron oxidation and one-electron reduction of the phosphine complexes generate species that possess the electronic configurations $\sigma^2\pi^4\delta^1$ and and $\sigma^2\pi^4\delta^2\delta^{*1}$, respectively, and therefore contain Mo–Mo bond orders of 3.5. While several attempts have been made to isolate salts of the monocations, these efforts have met with limited success. Solutions of the paramagnetic EPR-active $[Mo_2Cl_4(PPr^n_3)_4]^+$ cation in CH_2Cl_2 have been generated electrochemically at *c.* 0 °C,[451] while $[Mo_2Cl_4(PBu^n_3)_4]PF_6$ has been formed at −78 °C with the use of $[Ag(NCMe)_4]PF_6$ as oxidant.[453] These species decompose rapidly at room temperature. An interesting case of electrogenerated chemiluminescence has been encountered in the case of $Mo_2Cl_4(PMe_3)_4$ dissolved in $(Bu_4N)BF_4$-THF by pulsing the potential of the Pt electrode between −1.95 and +0.7 V (versus a Ag quasi-reference electrode).[458] Emission results from the electron-transfer reaction between the $[Mo_2Cl_4(PMe_3)_4]^-$ and $[Mo_2Cl_4(PMe_3)_4]^+$ species that are generated.

$$[Mo_2Cl_4(PMe_3)_4]^- + [Mo_2Cl_4(PMe_3)_4]^+ \rightarrow \{Mo_2Cl_4(PMe_3)_4\}^* + Mo_2Cl_4(PMe_3)_4$$

$$\{Mo_2Cl_4(PMe_3)_4\}^* \rightarrow Mo_2Cl_4(PMe_3)_4 + h\nu$$

Electrogenerated chemiluminescence has also been observed upon electrochemical reduction of $Mo_2Cl_4(PMe_3)_4$ in the presence of $[S_2O_8]^{2-}$ when the potential is pulsed between −0.5 and −2.0 V. The mechanism involves the reaction of $[Mo_2Cl_4(PMe_3)_4]^-$ with $SO_4^{\cdot-}$.[458]

A different technique has been used to study the arsine complexes $Mo_2X_4(AsEt_3)_4$ (X = Cl or Br), namely, rotating electrode polarography.[102] Solutions of these complexes in CH_3CN show oxidations at $E_{1/2}$ = +0.56 V (X = Cl) and $E_{1/2}$ = +0.6 V (X = Br) versus SCE. Controlled potential electrolysis at 0 °C has been used to generate solutions of the paramagnetic EPR-active monocations, which can be re-reduced to their neutral parents.[102] The $[Mo_2X_4(AsEt_3)_2]^+$ cations have also been characterized by electronic absorption spectroscopy.

In addition to the simple one-electron transfer reactions that these complexes undergo, there are numerous reactions in which the Mo_2^{4+} core is oxidized to Mo_2^{6+}, the resulting complexes containing confacial bioctahedral or edge-sharing bioctahedral structures. The com-

Pictiva EX2004
Samsung v Pictiva
IPR2024-01094

plexes $Mo_2Cl_4(PR_3)_4$ (R = Et or Pr^n) are oxidized in refluxing CH_2Cl_2–CCl_4, mixtures to give red $(R_3PCl)_3Mo_2Cl_9$,[331] and this same anion is also generated from $Mo_2Cl_4(dppm)_2$ and α-$Mo_2Cl_4(dppe)_2$ under similar conditions;[368] it can be precipitated as its Et_4N^+ salt from the latter reaction solutions. The oxidations of $Mo_2Cl_4(PR_3)_4$, where PR_3 = PEt_3, PBu^n_3or $PEtPh_2$, also proceed photochemically. A maroon colored compound purported to be $Mo_2Cl_6(PEtPh_2)_3$ was prepared[459] by broad band UV photolysis of a dichloromethane solution of $Mo_2Cl_4(PEtPh_2)_4$. The reaction of $Mo_2I_4(PMe_3)_4$ with I_2 in toluene affords $(Me_3PH)[Mo_2(\mu\text{-}I)_3I_4(PMe_3)_2]$,[460] while the oxidation of $Mo_2Cl_4(PMe_3)_4$ with $PhICl_2$ gives $(Me_3PH)[Mo_2Cl_7(PMe_3)_2]$, which can be isolated in both *syn* and *gauche* isomeric forms.[461]

Oxidative addition reactions to β-$Mo_2X_4(LL)_2$ molecules are numerous.[390,462-468] They yield edge-sharing bioctahedra in which the LL ligands continue to bridge the metal atoms with the phosphorus atoms trans at each molybdenum atom. The complex $Mo_2(\mu\text{-}SPh)(\mu\text{-}Cl)Cl_4(\mu\text{-}dppm)_2$ is isolated in low yield (8%) through the reaction of $Mo_2Cl_4(dppm)_2$ with PhSSPh in CH_2Cl_2.[466] In some cases there is a change in the bonding mode of the dmpe and dppe ligands from bridging to chelating, and dichloromethane may serve as a chlorinating agent. The reactions of RSSR with $Mo_2Cl_4(dto)_2$ afford $Mo_2(SR)_2Cl_4(dto)_2$ compounds which can also be obtained by reacting $K_4Mo_2Cl_8$ or $(NH_4)_3Mo_2Cl_9{\cdot}H_2O$ with dto and EtSSEt or PhSSPh in refluxing methanol. These later reactions certainly proceed through the intermediacy of $Mo_2Cl_4(dto)_2$.[467,468]

4.3.5 Cationic complexes of Mo_2^{4+}

There are only a few compounds that contain the Mo_2^{4+} core entirely surrounded by neutral ligands so that a $[Mo_2L_8]^{4+}$ or $[Mo_2L_{10}]^{4+}$ complex results. The first such cation, Mo_2^{4+}(aq), was prepared in solution[201] in 1971, but no solid compound of it has ever been reported and it is not known whether the coordination sphere has 8 or 10 water molecules. The solution was prepared by adding $Ba(SO_3CF_3)_2$ to $K_4Mo_2(SO_4)_4$ dissolved in 0.01 M CF_3SO_3H.[202,201] The solution of the cation, which has electronic absorption bands at 370 and 504 nm, is stable if not exposed to light or oxygen. Green $[Mo_2(\mu\text{-}OH)_2(aq)]^{4+}$ is formed with evolution of H_2 when a solution of Mo_2^{4+}(aq) in 1 M CF_3SO_2H is irradiated at 254 nm.[206] The kinetics and mechanism of reaction with NCS^- and $HC_2O_4^-$ have been investigated.[469] From X-ray absorption edge and EXAFS spectra the Mo–Mo distance in the Mo_2^{4+}(aq) ion has been estimated to be 2.12 Å.[470]

The $[Mo_2(CH_3CN)_n]^{4+}$ (n = 8, 9, 10) ions are well established and some of their chemistry has been studied. Structural results are collected in Table 4.11. $[Mo_2(CH_3CN)_8](CF_3SO_3)_4$ was obtained as a blue crystalline solid.[178] It readily loses CH_3CN and reacts with acetic acid to form $Mo_2(O_2CCH_3)_4$. $[Mo_2(CH_3CN)_{10}](BF_4)_4$ may be prepared[158,179] by reaction of $Mo_2(O_2CCH_3)_4$ and HBF_4 in Et_2O. This compound is also rather unstable, but gives large dark-blue crystals from acetonitrile. X-ray crystallography reveals a centrosymmetric $[Mo_2(CH_3CN)_8(ax\text{-}CH_3CN)_2]^{4+}$ ion (Fig. 4.19) with a Mo–Mo distance of 2.187(1) Å. More recently $[Mo_2(CH_3CN)_9](BF_4)_4$ has been structurally defined with C_{4v} symmetry and an Mo–Mo distance of 2.180(1) Å.[243] These are the only cationic Mo_2^{4+} complexes that have been crystallographically defined.

Pictiva EX2004
Samsung v Pictiva
IPR2024-01094

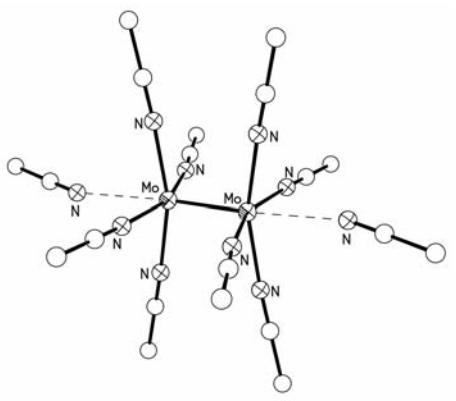


Fig. 4.19. The $[Mo_2(NCCH_3)_{10}]^{4+}$ cation as found in $[Mo_2(NCCH_3)_{10}](BF_4)_4{\cdot}2CH_3CN$.

Some reactions of the $[Mo_2(CH_3CN)_{8\text{-}10}]^{4+}$ ions have been studied.[242] The compound $[Mo_2(\mu\text{-}CH_3CONH)(CH_3CN)_6](BF_4)_3$ is obtained by reaction of $[Mo_2(CH_3CN)_8](BF_4)_4$ with CH_3CONH_2 in *c.* 60% yield or by reaction of $[Mo_2(CH_3CN)_8](BF_4)_4$ with H_2O in *c.* 70% yield. Hydrolysis of CH_3CN occurs in the latter reaction. The compound $[Mo_2(\mu\text{-}CH_3CONH)(CH_3CN)_6](BF_4)_3$ reacts with dppm to give $[Mo_2(\mu\text{-}CH_3CONH)(\mu\text{-dppm})_2(CH_3CN)_2](BF_4)_3$. Reaction of toluidine with $[Mo_2(CH_3CN)_8]^{4+}$ produces $[Mo_2(\mu\text{-}(HNCMeNtol)(CH_3CN)_6]^{4+}$. $[Mo_2(CH_3CN)_9](BF_4)_4$ reacts[243] with dppe to produce an adduct with a very complex structure in which an Mo–Mo bond (2.180(1) Å) is multiply bridged, and this in turn reacts with traces of water at low temperature to generate another complex product in which the dppe is lost and one CH_3CN is hydrolyzed to an acetamido anion, which bridges through its nitrogen atom only. However, by reaction of the dppe intermediate with excess water the cation $[Mo_2(NHC(CH_3)O)_2(CH_3CN)_4]^{2+}$ is formed, in which the Mo–Mo distance is 2.144(2) Å.

Table 4.11. Structures of $[Mo_2(CH_3CN)_{8\text{-}10}]^{4+}$ compounds and their reaction products

Compound	Crystal sym.	Virtual sym.	*r*(Mo–Mo)	Twist angle	ref.
$[Mo_2(CH_3CN)_8(ax\text{-}CH_3CN)_2](BF_4)_4{\cdot}2CH_3CN$	$\bar{1}$	D_{4h}	2.187(1)	zero	179
$[Mo_2(CH_3CN)_8(ax\text{-}CH_3CN)](BF_4)_4$	4	C_{4v}	2.180(1)	≈0	243
$[Mo_2(CH_3C(O)NH)(CH_3CN)_6](BF_4)_3$	1	C_s	2.183(1)	NR	242
$[Mo_2(CH_3C(O)NH)_2(CH_3CN)_4](BF_4)_2$	1	C_2	2.144(2)	NR	243
$[Mo_2(CH_3C(O)NH)py_5(OH)](BF_4)_2$	1	C_s	2.149(1)	NR	242
$[Mo_2(CH_3C(O)NH)(dppm)_2(CH_3CN)_2](BF_4)_3$	1	C_s	2.146(2)	NR	242
$(CH_3C_6H_4NH_3)[Mo_2(HNC(CH_3)Ntol)\text{-}(CH_3CN)_6](BF_4)_4$	1	C_s	2.157(1)	NR	242

The compound $[Mo(en)_4]Cl_4$ forms upon heating neat ethylenediamine with $K_4Mo_2Cl_8$ and was isolated[202] as orange crystals upon adding hydrochloric acid to an aqueous solution of the crude product. Such a recrystallization in the presence of *p*-toluenesulfonic acid produces the *p*-toluenesulfonate salt.[202] $[Mo_2(en)_4]^{4+}$ has its $\delta \rightarrow \delta^*$ electronic transition at 20,900 cm^{-1} and, like $[Mo_2(aq)]^{4+}$, is irreversibly oxidized under a variety of conditions; cyclic voltammetry measurements have shown that this complex exhibits an irreversible oxidation at +0.78 V versus SCE.[202] The analogous complex $[Mo_2(R\text{-pn})_4]Cl_4$, where *R*-pn = (*R*)-1,2-diaminopropane, has also been prepared[471] by a similar procedure. The CD spectrum of this complex in 0.1 M HCl

Pictiva EX2004
Samsung v Pictiva
IPR2024-01094

has been interpreted in terms of a structure with bridging *R*-pn ligands and a staggered rotational geometry (χ between 45 and 90°).

A complex formulated as $[Mo_2(EtCO_2CH_3)_4](CF_3SO_3)_4$ and proposed to contain ethyl acetate bridges, may be a further example of cationic species.[213]

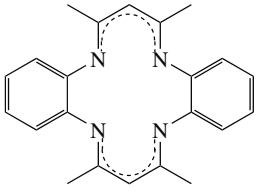
4.3.6 Complexes of Mo_2^{4+} with macrocyclic, polydentate and chelate ligands

Compounds that have been crystallographically characterized are listed in Table 4.12.

Table 4.12. Structures of Mo_2^{4+} compounds with macrocyclic or chelating ligands

Compound	Crystal sym.	Virtual sym.	*r*(Mo–Mo)	Twist angle	ref.
$Mo_2(Bu^tC(O)CHC(O)Bu^t)_4$	$\bar{1}$	D_{2h}	2.147(1)	zero	472
$Mo_2(acacen)_2$	$\bar{1}$	C_{2h}	2.168(1)	0	473
$Mo_2(Bu^t\text{-salophen})_2$	1	C_1	2.203(1)	88	474
$Mo_2(tmtaa)_2$	1	D_{2d}	2.175(1)	90	475
$Mo_2(TPP)_2$	1	D_{2d}	2.239(1)	18	476
$Mo_2(o\text{-}Me_2NCH_2C_6H_4)_4$	1	C_2	2.145(1)	11	477
$Mo_2(Et_2Bpz_2)_2[Et_2B(OH)pz]_2$	1	D_{2d}	2.156(1)	15	478

The macrocyclic ligand $tmtaa^{2-}$, shown as **4.28**, as Li_2tmtaa reacts with $Mo_2(O_2CCH_3)_4$ to give a brown-black product $Mo_2(tmtaa)_2$.[475,479] The tmtaa ligands are rotated 90° relative to one another which still gives two sets of Mo–N bonds that are essentially eclipsed, but allows the two saddle-shaped ligands to fit snugly together. Cyclic voltammetry of solutions of this complex in $(Bu_4N)PF_6$–CH_3CN shows four redox processes, two of which correspond to oxidations and two to reductions.[479] Oxidation at room temperature with $[(\eta^5\text{-}C_5H_5)_2Fe]PF_6$ affords dark-purple paramagnetic $[Mo_2(tmtaa)_2]PF_6$,[479] whose structure is very similar to that of $Mo_2(tmtaa)_2$. The Mo–Mo distance (2.221(1) Å) is 0.046 Å longer than that in $Mo_2(tmtaa)_2$, as a result of removing one δ electron.



4.28

The treatment of $Mo_2(tmtaa)_2$ with the mild oxidant tetracyanoethylene (TCNE) in toluene or acetonitrile gives the biradical compound $[Mo_2(tmtaa)_2]^+(TCNE)^-$, which has been characterized by EPR spectroscopy.[480] This complex decomposes to $[MoO(tmtaa)]^+[C_3(CN)_5]^-$ in the presence of a trace amount of water, and this compound can in turn be converted to the dimolybdenum radical anion $[Mo_2(tmtaa)_2]^-$ upon reaction with Na/Hg in THF.[480] The later species is formed more directly by the reduction of $Mo_2(tmtaa)_2$ with Na/Hg.[479] When $Mo_2(O_2CCH_3)_4$ reacts with H_2tmtaa, only two cisoid molecules of acetic acid are displaced and the tmtaa forms two bonds to each molybdenum atom, thereby bridging them.

Several dimolybdenum(II) porphyrin complexes, $Mo_2(Por)_2$, have been prepared in which there is an unsupported Mo–Mo quadruple bond. These have usually been prepared by the vacuum pyrolysis of mononuclear Mo(Por)(PhC≡CPh),[481] where Por represents the dianionic

Pictiva EX2004
Samsung v Pictiva
IPR2024-01094

porphyrin ligand, and/or from the reaction of $MoCl_2(CO)_4$ with the free porphyrin (H_2Por) in oxygen-free toluene in the presence of lutidine.[482] These methods have been used to prepare derivatives where Por = octaethylporphyrinato (OEP), mono-*meso*-substituted OEP-X (where X = formyl, nitro, amine or isocyanate), and *meso*-tetra-*p*-tolylporphyrinato (TTP). By utilizing a mixture of H_2(OEP) and H_2(OEP–CHO) in the second of these procedures, a separable mixture of $Mo_2(OEP)_2$, $Mo_2(OEP)(OEP–CHO)$ and $Mo_2(OEP–CHO)_2$ was obtained.[482] Variable temperature ^{1}H NMR studies of the *meso*-substituted derivatives have provided solution evidence for the presence of Mo–Mo bonds and an activation energy of 10.0 ± 0.5 kcal mol^{-1} for the barrier to rotation about the Mo–Mo bonds. The resonance Raman spectrum of $Mo_2(OEP)_2$ has yielded a Mo–Mo stretching frequency of 341 cm^{-1}, from which an Mo–Mo distance of 2.23 Å has been estimated.[483]

In one instance a complex has been prepared in which the two porphyrin rings are constrained to be eclipsed by employing a rigid biphenylene bridge to link them. This complex, Mo_2DPB, contains the tetraanion 1,8-bis[5-2,8,13,17-tetraethyl-3,7,12,18-tetramethyl)porphyrin]biphenylene and is prepared by reacting H_4DPB with $MoCl_2(CO)_4$ followed by chromatography.[484] Only in the case of $Mo_2(TPP)_2$, which is the initial product from the reaction of $Mo(CO)_6$ with tetraphenylporphyrin (H_2TPP), has the structure been determined by X-ray crystallography (Table 4.6).[476]

There are several molecules in which Mo^{II}, which are either bis-chelated or coordinated by a tetradentate ligand, are linked by an unbridged quadruple bond. For example, the reaction of $Mo_2(O_2CCH_3)_4$ with $Na[Et_2Bpz_2]$ (pz = 2-pyrazolyl) yields several products,[478] one of which is $Mo_2(Et_2Bpz_2)_2(Et_2B(OH)pz)_2$. One ligand of each type is chelated to each Mo atom and the $N_3OMoMoN_3O$ core is nearly eclipsed. An organometallic example is $Mo_2(o\text{-}Me_2NCH_2C_6H_4)_4$, in which two $C_6H_4CH_2NMe_2$ ligands are chelated to each Mo atom in a cis relationship.[477]

The structural characterization of the eclipsed β-diketonate complex $Mo_2(Bu^tCOCHCOBu^t)_4$ has also been carried out[472] following the synthesis of several complexes of the type $Mo_2(RCOCHCOR)_4$. The reduction of the mononuclear molybdenum(IV) complex Mo(acacen)Cl_2, where acacen^{2-} = *N*,*N*'-ethylenebis(acetylacetoneiminato), with sodium in THF in the presence of diphenylacetylene, affords the dimolybdenum(II) complex Mo_2(acacen)$_2$, whose structure is shown in Fig. 4.20.[473] The role of the PhC≡CPh in the synthesis of this complex may be similar to that in the preparation of various porphyrin complexes of dimolybdenum(II). A comparable complex of a salophen ligand has also been made.[474]

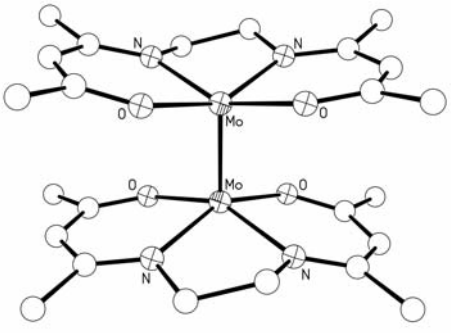
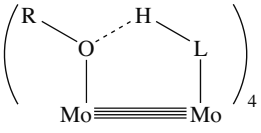


Fig. 4.20. The structure of the Mo_2(acacen)$_2$ molecule.

Pictiva EX2004
Samsung v Pictiva
IPR2024-01094

4.3.7 Alkoxide compounds of the types $Mo_2(OR)_4L_4$ and $Mo_2(OR)_4(LL)_2$

Several such complexes have been prepared and characterized. Entry to this chemistry has involved dimethylamido dimolybdenum(III) starting materials. The first such study, reported in 1984[407] showed that the reaction of 1,2-$Mo_2(Bu^i)_2(NMe_2)_4$ with isopropyl or neopentyl alcohol in hexane results in β-hydrogen atom transfer to form isobutylene, isobutane and $Mo_2(OR)_4(HNMe_2)_4$ (R = Pr^i or CH_2CMe_3). Ligand exchange reactions have been used to prepare $Mo_2(OPr^i)_4L_4$, where L = py, $MeNH_2$, Pr^iOH or PMe_3, and $Mo_2(OCH_2CMe_3)_4(PMe_3)_4$.[406,407] X-ray structure determinations on $Mo_2(OPr^i)_4L_4$ (L = py or Pr^iOH) and $Mo_2(OCH_2CMe_3)_4L_4$ (L = Me_2NH or PMe_3) have confirmed[406,407] that each of these complexes is the 1,3,6,8 isomer. The Mo–Mo distances (Table 4.8) are typical of Mo–Mo quadruple bonds, although the mixing of filled oxygen *p*-orbitals with empty Mo–Mo δ* and π* MOs probably tends to make the Mo–Mo bonds slightly longer and weaker than those in similar halide complexes. However, in the cases of $Mo_2(OPr^i)_4(HOPr^i)_4$ and $Mo_2(OCH_2CMe_3)_4(HNMe_3)_4$, the Mo–Mo bonds are actually shorter than expected because of the formation of strong hydrogen bonds of the type represented in **4.29**.



4.29

Similar chemistry with aryloxide ligands has been shown to occur by treating $Mo_2(NMe_2)_6$ with C_6F_5OH and 3,5-$Me_2C_6H_3OH$. The former reaction, when carried out in toluene or a pyridine–benzene mixture and with the use of a large excess of C_6F_5OH (10-12 equivalents), affords the complex $Mo_2(OC_6F_5)_4(HNMe_2)_4$.[409] Its structure, of the 1,3,6,8 type, is shown in Fig. 4.21. The reaction of $Mo_2(NMe_2)_6$ with four equiv of 3,5-$Me_2C_6H_3OH$ in hexane gives deep blue $Mo_2(OC_6H_3\text{-}3,5\text{-}Me_2)_4(HNMe_2)_4$ in 15-30% yield; this yield is increased to 65% if Me_2NH is added to the initial reaction mixture.[455] A crystal of the novel Mo_2^{7+} complex $Mo_2(\mu\text{-}NMe_2)(\mu\text{-}OC_6H_3\text{-}3,5\text{-}Me_2)_2(OC_6H_3\text{-}3,5\text{-}Me_2)_4(HNMe_2)_2$ has been isolated from this reaction and structurally characterized (the Mo–Mo distance is 2.414(1) Å).[455] The reaction of $Mo_2(OC_6H_3\text{-}3,5\text{-}Me_2)_4(HNMe_2)_4$ with PMe_3 produces $Mo_2(OC_6H_3\text{-}3,5\text{-}Me_2)_4(PMe_3)_4$; both complexes have electronic absorption spectra characteristic of Mo_2^{4+} complexes with the δ → δ* transition at 584 and 673 nm, respectively. Interestingly, the redox properties of these two complexes are markedly different from those of the halide complexes of the type $Mo_2X_4L_4$. Cyclic voltammograms on solutions in $(Bu_4N)PF_6$–THF show two one-electron oxidations at $E_{1/2}$ = −0.15 V and $E_{p,a}$ = +0.31 V versus Ag/AgCl for the Me_2NH complex and at $E_{1/2}$ = −0.40 V and $E_{1/2}$ = +0.24 V versus Ag/AgCl for the PMe_3 derivative. While the oxidation of $Mo_2(OC_6H_3\text{-}3,5\text{-}Me_2)_4(HNMe_2)_4$ is chemically irreversible, the PMe_3 complex can be oxidized electrochemically to its yellow-brown, EPR-active monocation. While this process is reversible, the second oxidation is not.[455]

The green compound, $Mo_2(OC_6F_5)_4(PMe_3)_4$, obtained from the reaction of C_6F_5OH with $Mo_2(CH_3)_4(PMe_3)_4$[408] is the 1,2,7,8 isomer, although the Mo–Mo distance is about the same as that in 1,3,6,8-$Mo_2(OC_6F_5)_4(HNMe_2)_4$. Reactions of $Mo_2(CH_3)_4(PR_3)_4$ (PR_3 = PMe_3 or PMe_2Ph) with the fluoroalcohols C_6F_5OH, CF_3CH_2OH and $(CF_3)_2CHOH$ all seem to proceed in a similar fashion but the structures of the products (other than $Mo_2(OC_6F_5)_4(PMe_3)_4$) have not yet been determined.[408]

Pictiva EX2004
Samsung v Pictiva
IPR2024-01094

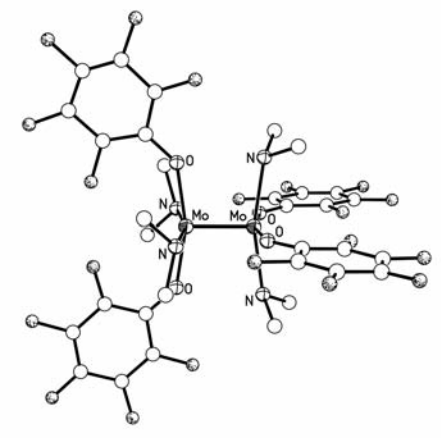
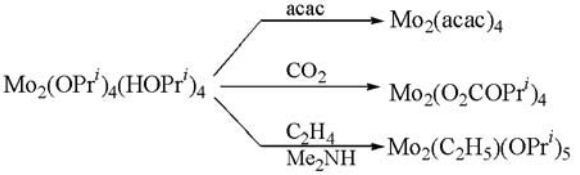
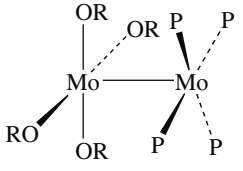


Fig. 4. 21. The structure of the $Mo_2(OC_6F_5)_4(NHMe_2)_4$ molecule.

The $Mo_2(OR)_4L_4$ compounds show some interesting chemistry. There are preliminary reports[407] of the following reactions:



The reaction of $Mo_2(OPr^i)_4(HOPr^i)_4$ with dmpe in hexane gives[421] $Mo_2(OPr^i)_4(dmpe)_2$, which can also be obtained from reaction of $Mo_2(Bu^i)_2(NMe_2)_4$ with $Pr^i(OH)$ (> 4 equivalents) and dmpe (2 equivalents) in a hydrocarbon solvent. The structure of this compound is of the 1,2,3,4–$Mo_2X_4(LL)_2$ type as shown in **4.30**, but the conformation is also staggered. The Mo–Mo bond distance and staggered geometry are in accord with a triple bond.[421] The electronic structures of the model species $X_4Mo–Mo(PH_3)_4$ (X = OH or Cl) have been investigated by the SCF-Xα-SW method.[485] It has been concluded the π-donor ligands such as alkoxides inhibit the formation of a polar δ-bond between the two metal centers by interacting strongly with the Mo^{IV}-based d_{xy} orbital. This would result in a Mo–Mo bond order of three in *any* ligand conformation; the staggered geometry is preferred for steric reasons. The preferences for the structure $(Pr^iO)_4MoMo(dmpe)_2$ over β-$Mo_2(OPr^i)_4(dmpe)_2$ apparently reflects the greater steric demands of the isopropoxide ligands as compared to the halide ligands.[485]



4.30

Pictiva EX2004
Samsung v Pictiva
IPR2024-01094

4.4 Other Aspects of Mo_2^{4+} Chemistry

4.4.1 Cleavage of Mo_2^{4+} compounds

The red phosphido compound, $Mo_2(\mu\text{-}PBu^t_2)_2(PBu^t_2)_2$, can be prepared by the interaction of $LiPBu^t_2$ with $Mo_2(O_2CCH_3)_4$ in diethyl ether at −78 °C.[486] This compound has a 'butterfly' structure and a short Mo–Mo distance (2.209(1) Å) that accords with a multiple bond. The $^{31}P\{^1H\}$ NMR spectrum of this complex shows two sharp singlets, which is evidence that this structure is retained in solution.[486]

The interaction between $Mo_2(O_2CCH_3)_4$, Me_3SiI, and I_2 in THF results in oxygen abstraction from the solvent and the formation of the salt $[Mo_2(\mu\text{-}O)(\mu\text{-}I)(\mu\text{-}O_2CCH_3)I_2(THF)_4]^+$-$[MoOI_4(THF)]^-$ and $I(CH_2)_4I$.[487] The cation contains a metal–metal bonded Mo_2^{7+} core.

A further reaction of note is that between $Mo_2(O_2CCH_3)_4$ and the sodium salt of 2-mercaptopyridine in ethanol. This affords a green solid which upon exposure to oxygen is converted into red $Mo_2O_3(C_5H_4NS)_4$,[390] a complex that contains two terminal Mo=O units and a linear Mo–O–Mo bridge. This reaction is analogous to the reaction between $Re_2(O_2CCH_3)_4Cl_2$ and sodium diethyldithiocarbamate which produces $Re_2O_3(S_2CNEt_2)_4$. A similar reaction course to this has been found[488] to lead to the formation of $Mo_2O_3(SC_4H_3N_2)_2(py)_2$ when $Mo_2(O_2CCH_3)_4$ is reacted with 2-mercaptopyrimidine in methanol and the reaction precipitate is dissolved in pyridine. The dithiocarbamate complex $Mo_2(S_2CNEt_2)_4$ is readily oxidized by air to give $Mo_2O_3(S_2CNEt_2)_4$,[279] while its oxidation with I_2 in THF affords $Mo_2O_3(S_2CNEt_2)_2I_2(THF)_2$.[280]

The pyridine complexes $Mo_2X_4(py)_4$ (X = Cl or Br) are oxidized to *mer*-$MoX_3(py)_3$ in the presence of an excess of pyridine under forcing reaction conditions.[489] This is an especially noteworthy reaction since the $Mo_2X_4(py)_4$ compounds are themselves best prepared[347] from the dimolybdenum(III) species $Cs_3Mo_2X_8H$. Another group of cleavage reactions that involve σ-donor ligands include the formation of *trans*-$MoBr_2(dppe)_2$, as one of the products of the reaction between $(NH_4)_4Mo_2Br_8$ and $Ph_2PCH_2CH_2PPh_2$,[377] and *trans*-$MoX_2(dppee)_2$ (X = Cl or Br; dppee = *cis*-$Ph_2PCH{=}CHPh_2$), which are formed in small quantities when $K_4Mo_2Cl_8$ and $(NH_4)_4Mo_2Br_8$ are reacted with dppee in refluxing *n*-propanol for several days.[380] The compounds *trans*-$MoX_2(dppbe)_2$ (X = Cl or Br; dppbe = 1,2-bis(diphenylphosphino)benzene) can be obtained in quite good yield by a similar procedure, together with some $[MoOX(dppbe)_2]X{\cdot}nH_2O$.[385]

Like other multiply bonded dimetal complexes, those of quadruply bonded Mo_2^{4+} are in many instances cleaved by π-acceptor ligands such as CO, NO, and isocyanides.[490] Note that there are also examples where π-acceptor ligands give products in which a dimolybdenum unit is retained, such as the conversion of $Mo_2(O_2CCH_3)_4$ to the alkyne complex $[Mo_2(\mu\text{-}4\text{-}MeC_6H_4CCH)(\mu\text{-}O_2CCH_3)(en)_4](O_2CCH_3)_3{\cdot}2en$.[194] The reactions of $Mo_2Cl_4(PR_3)_4$ (PR_3 = PEt_3 or PBu^t_3) with CO in toluene give mononuclear $Mo(CO)_3(PR_3)_2Cl_2$ and *trans*-$Mo(CO)_4(PR_3)_4$ as the only identifiable products. In a similar fashion, a variety of phosphine complexes of the type $Mo_2X_4(PR_3)_4$, where X = Cl or Br and PR_3 = PEt_3, PBu^n_3 or $PEtPh_2$, and $Mo_2X_4(LL)_2$, where X = Cl or NCS and LL = dppe or dppm, react with NO in dichloromethane to yield the mononuclear complexes $Mo(NO)_2X_2L_2$ and $Mo(NO)_2X_2(LL)$.[491] These reactions constitute a useful general synthetic method for obtaining dinitrosyls of molybdenum. On the other hand, the cleavage of $Mo_2(CH_3)_4(PMe_3)_4$ by NO gives a yellow complex of stoichiometry $Mo_2O(NO)_2(ONCH_3)_2(Me_3PO)_2$.[492] In a related study, it was found that the only identifiable products from the reactions of nitrosyl chloride with $K_4Mo_2Cl_8$ and $Mo_2(O_2CCH_3)_4$ were those in which fission of the Mo–Mo bond had occurred. After work-up of the reaction mixtures, $K_2Mo(NO)Cl_5$ and $Mo(NO)Cl_3(Ph_3PO)_2$ (upon the addition of triphenylphosphine oxide) were isolated.[493]

Pictiva EX2004
Samsung v Pictiva
IPR2024-01094

A suspension of $Mo_2(O_2CCH_3)_4$ in methanol reacts quickly with phenyl isocyanide[494a] and other aryl isocyanides[494b] to yield $Mo(CNAr)_6$. This reduction to Mo^0 is in contrast to the related reactions of $Mo_2(O_2CR)_4$ (R = CH_3 or CF_3) and $K_4Mo_2Cl_8$ with alkyl isocyanides,[495,496] where the Mo–Mo bond is cleaved but the products that result, the $[Mo(CNR)_7]^{2+}$ ions, where R = Me, CMe_3 or C_6H_{11}, are derivatives of Mo^{II}. This difference in reaction course is in accord with previously documented differences between the stabilities of homoleptic aryl and alkyl isocyanide complexes of molybdenum, viz. $Mo(CNAr)_6$ versus $[Mo(CNR)_7]^{2+}$. When the phosphine-containing complexes $Mo_2Cl_4(dppm)_2$, $Mo_2Cl_4(dppe)_2$, and $Mo_2Cl_4(PR_3)_4$ (PR_3 = PEt_3, PPr^n_3 or $PEtPh_2$) are used in place of $Mo_2(O_2CCH_3)_4$, seven-coordinate mixed phosphine-alkyl isocyanide complexes are formed. The $[MoCNR)_5(dppm)]^{2+}$, $[Mo(CNR)_5(dppe)]^{2+}$, $[Mo(CNR)_5(PR_3)_2]^{2+}$ and $[Mo(CNR)_6(PR_3)]^{2+}$ cations have been isolated as their PF_6^- salts.[497] A detailed study of the reactions of $Mo_2X_4(dppm)_2$ (X = Cl, Br or I) with RNC (R = Pr^i or Bu^t) has shown[438] that with one equivalent of RNC in the presence of $TlPF_6$ (in THF) or KPF_6 (in acetone), the dimolybdenum(II) complexes $[Mo_2X_3(dppm)_2(CNR)]PF_6$ are formed. When an excess of RNC is used, cleavage of the Mo–Mo bond occurs to give $[MoX(CNR)_4(dppm)]^+$, which is in turn converted into $[Mo(CNR)_5(dppm)]^{2+}$ and finally $[Mo(CNR)_7]^{2+}$.[438]

4.4.2 Redox behavior of Mo_2^{4+} compounds

The Mo_2^{4+} core has a $\sigma^2\pi^4\delta^2$ electron configuration. The δ electrons are not strongly bound, and the LUMO, δ^*, is relatively low in energy. The possibilities of one- and two-electron oxidations and reductions under normally accessible chemical conditions therefore suggest themselves. Obviously, the nature of the ligands surrounding the Mo_2^{4+} core will strongly affect these possibilities. The electrochemical behavior of $Mo_2X_4L_4$ and $Mo_2X_4(LL)_2$ compounds has already been discussed in Section 4.3.4.

There are two main ways to study the redox behavior. One is by electrochemistry (usually the cyclic voltammetry (CV) or differential pulse voltammetry (DPV) methods are used), and the other is by employing chemical oxidants or reductants to produce isolable amounts of the desired products. Commonly, the electrochemistry provides a basis for choosing the most suitable redox reagent, with $FcPF_6$, $AgPF_6$ being the most often used oxidants. Some observed electrochemical oxidation data are present in Table 4.13.

No simple $[Mo_2X_8]^{3-}$ ion has been isolated. A solution of $K_4Mo_2Cl_8$ in 6 M HCl shows an oxidation at about 500 mV vs SCE, but the oxidation product, presumably $[Mo_2Cl_8]^{3-}$, appears to be very short lived.[326]

There is only one instance in which chemical reduction has led to an isolable product containing an Mo_2^{3+} core.[506] This is shown in the following reaction:

$$1,3,6,8\text{-}Mo_2(C{\equiv}CSiMe_3)_4(PMe_3)_4 \xrightarrow[\text{crypt-222}]{K(C_{10}H_8)} [K(\text{crypt-222})][Mo_2(C{\equiv}CSiMe_3)_4(PMe_3)_4]$$

The necessity of a very strong reductant is in accord with the observation by CV in THF that the reduction potential lies 2.13 V negative from the Fc/Fc^+ potential. This and other studies of $Mo_2(C{\equiv}CR)_4(PMe_3)_4$ compounds[394,395,507,508] (and their W analogs) have shown that there is major interaction of the π and/or π^* orbitals of the acetylide ligands with the δ and/or δ^* orbitals of the dimetal units.

It has also been reported that pulse radiolysis of a methanol solution of $Mo_2(O_2CCF_3)_4$ gave rise to a new electronic absorption band at 780 nm.[509] This band, which decayed rapidly, was assigned to the $[Mo_2(O_2CCF_3)_4]^-$ ion.

Pictiva EX2004
Samsung v Pictiva
IPR2024-01094

Table 4.13. Some electrode potentials for Mo_2^{4+}/Mo_2^{5+} processes in paddlewheel compoundsa

Compound		$E_{1/2}$ (mV)	ref.
$Mo_2(O_2CC_3H_7)_4$		450	326
$Mo_2(O_2CC_3H_7)_4$	in EtOH	300	
$Mo_2(O_2CC_3H_7)_4$	in CH_3CN	390	
$[Mo_2(O_2C(2,4,6\text{-}Pr^i{}_3C_6H_2)]_4$		621	498
$[Mo_2(O_2C(2,4,6\text{-}Pr^i{}_3C_6H_2)]_4$	in EtOH	488	
$[Mo_2(O_2C(2,4,6\text{-}Pr^i{}_3C_6H_2)]_4$	in CH_3CN	462	
$Mo_2[(O_2C(3,5\text{-}C_6H_3(OH)_2]_4$	in C_6H_5CN	530	90
$[Mo_2(SO_4)_4]^{4-}/[Mo_2(SO_4)_4]^{3-}$	in 9 M H_2SO_4	220 (vs SCE)	195
$Mo_2(DArF)_4$	Ar = *p*-$MeOC_6H_4$	142	499,500,501
	Ar = *p*-MeC_6H_4	231	
	Ar = C_6H_5	316	
	Ar = *m*-MeO	356	
	Ar = *p*-ClC_6H_4	499	
	Ar = *m*-ClC_6H_4	581	
	Ar = *m*-CF_3	660	
	Ar = *p*-$MeC(O)C_6H_4$	676	
	Ar = *p*-$CF_3C_6H_4$	693	
$Mo_2(DAniF)_3$(uracilate)		172	502
$Mo_2(DAniF)_3(O_2CC{\equiv}CH)$		351	503
$Mo_2(DAniF)_3(O_2CCH{=}CH_2)$		217	503
$Mo_2(DAniF)_3(O_2CCH{=}CH{-}CH{=}CH_2)$		225	503
$Mo_2(hpp)_4$	in $Bu_4NBF_4{\cdot}3$toluene	−1271	504
$Mo_2[(PhN)_2CN(H)Ph]_4$		−50	505

[a] In CH_2Cl_2 solutions vs Ag/AgCl with Bu_4NBF_4 supporting electrolyte, where Fc/Fc^+ has a value of 440 mV, unless otherwise stated.

The indirect synthesis of a compound[510] that could reasonably be assigned a Mo_2^{2+} core occurred when the $[Mo_2Cl_8]^{4-}$ ion was reacted with $F_2PN(CH_3)PF_2$ to produce $Mo_2[(F_2PN(CH_3)PF_2]_4Cl_2$, which has the structure shown in Fig. 4.22. The rotational conformation is twisted 21° and the Mo–Mo distance is 2.457(1) Å. Oxidation of Mo_2^{4+} compounds to isolable Mo_2^{5+} and Mo_2^{6+} species has often been observed. All of these isolated oxidation products have been obtained with paddlewheel ligands present. The first observations[326] were made electrochemically on $Mo_2(O_2CPr^n)_4$. This was shown to undergo "quasireversible" oxidation in CH_3CN, CH_2Cl_2 and EtOH to $[Mo_2(O_2CPr^i)_4]^+$ which had a half-life of *c.* 10^{-2} s at ambient temperature. EPR spectroscopy at 77 K (g_{av} = 1.941) showed the presence of one unpaired electron delocalized over two molybdenum atoms.

The cyclic voltammogram of $Mo_2(O_2CCH_3)_4$ in methanol is similar to that of the butyrate, with $E_{1/2}$ = +0.24 V versus Ag/AgCl,[18] while measurements on solutions of $Mo_2(O_2CCMe_3)_4$ in acetonitrile (0.1 M in Bu_4NBF_4) and THF (0.2 M in Bu_4NPF_6) have given $E_{1/2}$ values of +0.38 V versus SCE[511] and +0.86 V versus Ag wire,[19] respectively (note the difference in referencing procedures). In the case of DMF solutions of the ferrocenyl species $Mo_2(O_2CCH_3)_2(FCA)_2(py)_2$ and $Mo_2(FCA)_4(CH_3CN)(DMSO)$, where FCAH = ferrocenemonocarboxylic acid, a reversible oxidation occurred near the potential of the ferrocene–ferrocenium couple but further oxidation led to the destruction of the complexes.[16] Cyclic voltammetric measurements on DMF solutions of the 2-acetoxybenzoate complex showed that oxidation of the monocation was followed by a rapid and irreversible decomposition of the complex.[18]

Pictiva EX2004
Samsung v Pictiva
IPR2024-01094

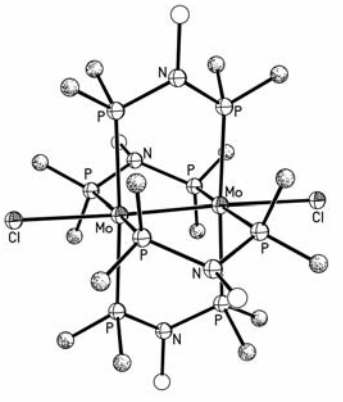


Fig. 4.22. The structure of $Mo_2[F_2PN(CH_3)PF_2]_4Cl_2$. This chiral molecule has idealized D_4 symmetry.

Oxidation of $Mo_2(O_2CR)_4$ (R = C_2H_5, CMe_3 or Ph) in 1,2-dichloroethane by iodine was reported[11] to afford $[Mo_2(O_2CR)_4]I_3$ products which have relatively narrow EPR signals (g = 1.93 ± 0.01). In another early report of a chemical oxidation, CCl_4 in CH_2Cl_2 oxidized $(Ph_4P)_2[Mo_2(O_2CPh)_4Cl_2]$ to give $(Ph_4P)_2[Mo_2(O_2CPh)_4Cl_4]$, but here the paddlewheel structure was changed to that of an edge-sharing bioctahedron.[512]

It was not until relatively recently that compounds containing $[Mo_2(O_2CR)_4]^+$ ions were actually prepared and the ions studied in more detail.[513] The three compounds prepared were $[Mo_2(2,4,6\text{-}Pr^i_3C_6H_2)_4]X$ (X = BF_4, PF_6) and $[Mo_2(O_2CCMe_3)_4]PF_6$. All have Mo–Mo distances in the range 2.136(1)-2.151(1) Å, which may be compared with the Mo–Mo distances of the neutral $Mo_2(O_2CR)_4$ compounds of *c.* 2.09 Å. There has never been any indication that $[Mo_2(O_2CR)_4]^{2+}$ ions can be obtained.

The earliest isolated and well-characterized example of an Mo_2^{5+} compound was the $[Mo_2(SO_2)_4]^{3-}$ ion, which was discovered[196] by chance in 1973. Attempts to recrystallize $K_4[Mo_2(SO)_4)_4]\cdot 2H_2O$ gave small amounts of the oxidized species. It was then found that it can be obtained in good yield by using an air stream to oxidize a solution of $K_4[Mo_2(SO_4)_4]\cdot 2H_2O$ in 2 M H_2SO_4 until the color changes from red to pale blue. It is also possible to form $[Mo_2(SO_4)_4]^{3-}$ from $[Mo_2(SO_4)_4]^{4-}$ by irradiating the former in 5 M H_2SO_4 with ultraviolet light (254 nm).[206,205] The Mo–Mo distance in $[Mo_2(SO_4)_4]^{3-}$ is 2.167(1) Å as compared to 2.111(1) Å in $[Mo_2(SO_4)_4]^{4-}$.

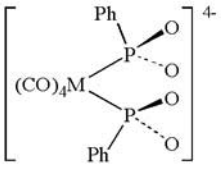
Further oxidation of the $[Mo_2(SO_4)_4]^{3-}$ ion to an isolable compound of the triply-bonded $(\sigma^2\pi^4)$ $[Mo_2(SO_4)_4]^{2-}$ ion has not been accomplished, but the similar $[Mo_2(HPO_4)_4]^{2-}$ ion can be made simply by dissolving $K_4Mo_2Cl_8\cdot 2H_2O$ in aqueous 2 M H_3PO_4 and exposing the solution to air for 24 h. When large cations such as Cs^+ and pyH^+ are present, purple crystalline products are obtained.[197] An electrochemical study[216] of the $[Mo_2(HPO_4)_4]^{2-}$ ion showed that reductions to the 3^- ans 4^- ions require potentials of −0.25 and −0.67 V versus SCE in 2 M H_3PO_4 solution.

The ability of bridging ligands such as SO_4^{2-} and HPO_4^{2-} to stabilize Mo_2^{5+} and Mo_2^{6+} cores better than uninegative bridging ligands such as the carboxylate ions, is essentially electrostatic in nature: the large amount of negative charge surrounding the Mo_2^{n+} core makes higher values of n more attainable and stable.

An interesting sequel to the story of the sulfato and phosphato complexes of Mo_2^{5+} and Mo_2^{6+} began with a report[514] in 1989 of compounds alleged to contain the Mo_2^{4+} core com-

Pictiva EX2004
Samsung v Pictiva
IPR2024-01094

plexed by two ligands, L, of the type **4.31**. The complex anions, $[Mo_2L_2]^{4-}$, were accompanied by only two +1 cations, but the presence, at an unstated location, of two H^+ ions was postulated in the one case where a structure was reported.[514] Moreover, the Mo–Mo distance was found to be 2.186(2) Å. In 2002 the suspicious character of these compounds was cleared up.[515] An abundance of evidence shows that they are complexes of the Mo_2^{6+} core. The highly oxidized core is stabilized by the total of eight negative charges, the Mo–Mo distance is consistent with a bond order of three, and the postulated protons are not present. A drawing of the $[Mo_2L_2]^{2-}$ anion in one of the four compounds studied is presented in Fig. 4.23. This structure (and the absence of any other cations, protons or otherwise) was exhaustively characterized by crystallography employing four polymorphs of $[NBu^n_4]_2Mo_2L_4$ where L is the anion **4.31** with M = Mo. All of the pertinent data are listed in Table 4.14.



4.31

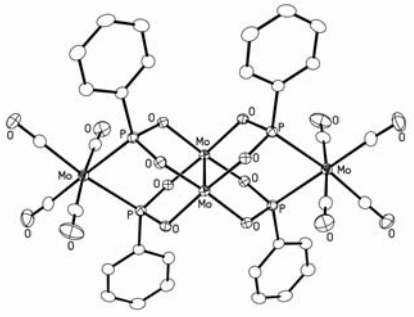


Fig. 4.23. The dianion in $(NBu^n_4)_2\{Mo_2[Mo_2(CO)_4(PhPO_2)_2]_2\}$.

Table 4.14. Structural data for $(NBu^n_4)_2Mo_2[Mo(CO)_4(PPhO_2)_2]_2$

Space group	Mo–Mo distance	Remarks
$P2_1/n$	2.178(8)	no solvent, neutron diffraction
$P2_1/n$	2.190(1)	no solvent, X-ray diffraction
$P2_1/n$	2.223(1)	axial THF molecules
$P\bar{1}$	2.193(1)	CH_2Cl_2 present
*P*bca	2.187(1)	no solvent

The fact that the ligand **4.31** has the ability to stabilize the Mo_2^{6+} core, however, does not entirely account for the formation of the $[Mo_2L_2]^{2-}$ ions, since the preparations all begin with $Mo_2(O_2CCH_3)_4$ or another Mo_2^{4+} compound and no recognized oxidizing agent is used. The explanation is that the solvent, CH_2Cl_2 or C_2H_5OH, in which the reaction is carried out oxidizes

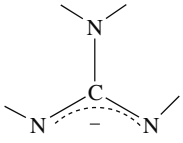
Pictiva EX2004
Samsung v Pictiva
IPR2024-01094

the initially formed $[Mo_2L_2]^{4-}$ complex. In the non-oxidizing solvent THF a reversible wave corresponding to the process

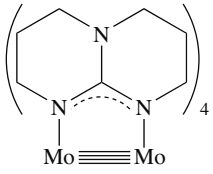
$$[Mo_2L_2]^{2-} \underset{-e}{\overset{+e}{\rightleftharpoons}} [Mo_2L_2]^{3-}$$

was observed at −1.54 V vs Ag/AgCl, showing that even the mildest oxidizing agents can take Mo_2^{4+} to Mo_2^{6+} when it is coordinated by two **4.31** ions. The use of the **4.31** type ligands represents the extreme known limit of employing highly charged ionic ligands to stabilize highly charged M_2^{n+} cores. These ligands have not yet been used with any cores other than Mo_2^{6+}.

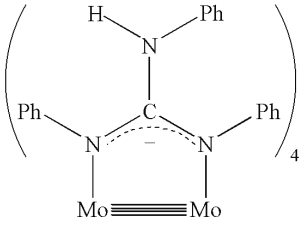
In addition to this "ionic ligand" approach, there is also a "covalent ligand" or "noninnocent ligand" approach to the stabilization of highly oxidized M_2^{n+} cores. This approach, which also originated with Mo_2^{n+} chemistry (but has been extended to W_2^{n+}, Re_2^{n+} and several other metals) is based on guanidinate type ligands, **4.32**. The first two examples of neutral paddlewheel complexes[504,505,516] with guanidinate bridges are those with L = hpp (**4.33**) and 1,2,3-triphenylguanidinate (**4.34**) as ligands. In both cases it was immediately noted that oxidation occurs readily and the oxidation products can be easily isolated and characterized. From **4.33** $Mo_2(hpp)_4(BF_4)_2$ was obtained[517] and shown to have a Mo–Mo distance of 2.142(2) Å, which is 0.075 Å longer than that in $Mo_2(hpp)_4$, as a result of the combined effects of two δ electrons being lost and the charges on the Mo_2 unit increasing from +4 to +6. Similarly, for the oxidation of Mo_2(1,2,3-triphenylguanidinate)$_4$ to the corresponding Mo_2^{5+} compound, the Mo–Mo distance increases from 2.084(1) to 2.119(1) Å.



4.32



4.33



4.34

The $Mo_2(hpp)_4$ molecule is so easily oxidized that it cannot dissolve in dichloromethane without undergoing the following reactions:[518]

$$Mo_2(hpp)_4 \xrightarrow{CH_2Cl_2} Mo_2(hpp)_4Cl \xrightarrow{O_2/CH_2Cl_2} Mo_2(hpp)_4Cl_2$$

In $Mo_2(hpp)_4Cl$ the Mo–Mo distance is 2.128(1) Å and in $Mo_2(hpp)_4Cl_2$ it is 2.174(1) Å.

The electrochemistry of the two Mo_2(guanidinate)$_4$ molecules is truly remarkable when compared to that of all other Mo_2 paddlewheel compounds. Whereas the most easily oxidized $Mo_2(DArF)_4$ molecule (Ar = *p*-anisyl) has an Mo_2^{4+}/Mo_2^{5+} potential of +142 mV, for the $Mo_2(hpp)_4$ molecule the corresponding oxidation occurs at −1271 mV, and the $[Mo_2(hpp)_4]^+/[Mo_2(hpp)_4]^{2+}$ potential is −444 mV. For $Mo_2[(PhN)_2CNHPh]_4$, the corresponding potentials are −50 mV and +850 mV. The basis for the extraordinary ability of guanidinate ligands to stabilize the higher oxidation states of M_2^{n+} cores in general is still under study.

An important study of the influence of the ligands on the Mo_2^{4+}/Mo_2^{5+} potential was reported in 1995 by Ren *et al.*[499,500] They found that for a series of $Mo_2(DArF)_4$ compounds with various Ar groups the voltage varied systematically with the Hammett σ constant for the sub-

Pictiva EX2004
Samsung v Pictiva
IPR2024-01094

stituents in the XC_6H_4 aryl groups. This is shown in Fig. 4.24 where the potentials have been corrected for errors in the original data that resulted from contamination by H_2O.[501]

The most extensive electrochemical studies have been carried out on compounds with pairs of Mo_2^{4+} cores linked by dicarboxylic anions, diamidato anions, SO_4^{2-} ions, etc. These results are all presented in Sections 4.5.1 to 4.5.7.

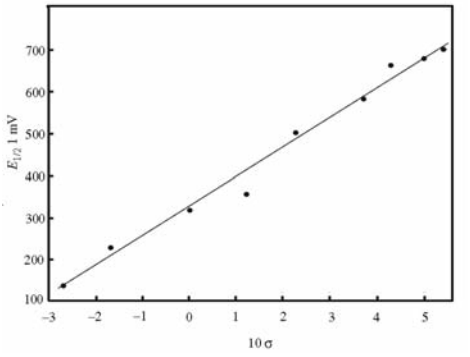


Fig. 4.24. The linear relationship of the oxidation potentials of $Mo_2(DArF)_4$ compounds to the Hammett σ-parameters of the aryl groups.

4.4.3 Hydrides and organometallics

There is a curious phosphine hydride molecule, $(Me_3P)_3HMo(\mu\text{-}H)_2MoH(PMe_3)_3$, which was prepared by reaction of $Mo_2(O_2CCH_3)_4$ with Na/Hg in THF in the presence of excess PMe_3 under 3 atm pressure of hydrogen.[519,520] It is a centrosymmetric edge-sharing bioctahedron, but is of interest here because the Mo–Mo distance within the $Mo_2(\mu\text{-}H)_2$ unit is very short, viz., 2.194(3) Å. The ^1H NMR spectrum is consistent with retention of this structure in solution. It is pyrophoric and reacts rapidly with alkyl halides, olefins, acetylenes, CO and H_2S, but no defined products were isolated.[520]

Like the isoelectronic species $[Re_2(CH_3)_8]^{2-}$ and $[Cr_2(CH_3)_8]^{4-}$, the octamethyldimolybdate anion $[Mo_2(CH_3)_8]^{4-}$ has been prepared and successfully characterized.[292] The pyrophoric lithium salts $Li_4Mo_2(CH_3)_8{\cdot}4L$, L = diethyl ether, tetrahydrofuran or 1,4-dioxane, were prepared[292] by reacting $Mo_2(O_2CCH_3)_5$ with diethyl ether solutions of MeLi followed by recrystallization from the appropriate ether solvent. The structure of the anion, as determined in the THF solvate, is that of the familiar centrosymmetric, eclipsed Mo_2L_8 unit of D_{4h} symmetry, with a short Mo–Mo distance, 2.148(2) Å. The ether molecules do not bind axially to the $[Mo_2(CH_3)_8]^{4-}$ ions, probably reflecting the low electrophilicity of this anion. An alternative route to $Li_4Mo_2(CH_3)_8{\cdot}4THF$ involves the reaction of methyllithium with the *mononuclear* starting material $MoCl_3(THF)_3$ in diethyl ether at −30 °C,[521] although at the time this reaction was first reported it was not recognized as leading to a quadruply-bonded dimolybdenum complex.

$Li_4Mo_2(CH_3)_8{\cdot}4$ether complexes are thermally stable at room temperature in the absence of oxygen and moisture. They react rapidly with acetic acid-acetic anhydride at −78 °C to regenerate $Mo_2(O_2CCH_3)_4$. The ether solvent molecules are replaceable by, for example, ammonia, pyridine, acetonitrile, acetamide, and hexamethylphosphoramide, but the products of many other reactions have not been identified owing to their instability and/or insolubility.

In the presence of trimethylphosphine, $Mo_2(O_2CCH_3)_4$ reacts with $Mg(CH_3)_2$ at 25 °C to afford the blue, air-stable, and volatile complex $Mo_2(CH_3)_4(PMe_3)_4$. While dimethyl-

Pictiva EX2004
Samsung v Pictiva
IPR2024-01094

phenylphosphine forms the analogous dimer $Mo_2(CH_3)_4(PMe_2Ph)_4$, complexes with methyldiphenylphosphine, triphenylphosphine, and trimethylphosphite could not be obtained.[186] The complex $Mo_2(CH_3)_4(PEt_3)_4$ has been prepared[522] from $Mo_2(O_2CCMe_3)_4$, MeMgCl and PEt_3 in diethyl ether, followed by crystallization at −10 °C. This complex undergoes rapid exchange with excess PMe_2Ph or PMe_3 in toluene solution to give $Mo_2(CH_3)_4(PMe_2Ph)_4$ or $Mo_2(CH_3)_4(PMe_3)_4$.[522] It has been shown[400] subsequently that the preparation of $Mo_2(CH_3)_4(PR_3)_4$ from the reaction between $Mg(CH_3)_2$, $Mo_2(O_2CCH_3)_4$ and PR_3 requires rigorously chloride-free conditions if contamination by $Mo_2Cl_4(PMe_3)_4$ is to be avoided. This can be accomplished by the use of $Mg(CH_3)_2$ prepared from $Hg(CH_3)_2$. The preparative method that uses the Grignard reagent CH_3MgCl[522] also introduces chloride contaminants.[400] Indeed, the reaction between $Mo_2(O_2CCH_3)_4$, $PhCH_2MgCl$ and PMe_3 in THF at −78 °C affords the mixed chloride-alkyl $Mo_2Cl_3(CH_2Ph)(PMe_3)_4$.[400]

The NMR spectra of the complexes $Mo_2(CH_3)_4(PR_3)_4$ are similar,[186,522] and are in accord with a structure like that found for their halide analogs. These structural conclusions have been confirmed[400] by X-ray crystal structure determinations on $Mo_2(CH_3)_4(PMe_3)_4$ and $Mo_2(CH_3)_4(PMe_2Ph)_4$, as well as on $Mo_2Cl_3(CH_2Ph)(PMe_3)_4$. An earlier report[522] on the structure of $Mo_2(CH_3)_4(PMe_3)_4$ has been shown[400] to be vitiated by serious contamination from chloride-containing impurities.

The phosphine-exchange reactions of $Mo_2(CH_3)_4(PEt_3)_4$ with PMe_2Ph and PMe_3 in toluene have been shown by NMR spectroscopy to occur in a stepwise fashion through a *dissociative* mechanism.[400] The driving force for these reactions is believed to be the relief of steric congestion as PEt_3 is replaced by the smaller PMe_2Ph or PMe_3 ligands. In further studies of their reactivity, it has been shown that the $Mo_2(CH_3)_4(PR_3)_4$ compounds (PR_3 = PMe_3, PEt_3 or PMe_2Ph) react with CO (18 atm) at room temperature in benzene to give acetone and compounds of the type $Mo(CO)_{6-x}(PR_3)_x$ (x = 0-3). The reaction rates are in the order PEt_3 >> PMe_2Ph > PMe_3, suggesting that the rate determining step involves PR_3 dissociation.

The reaction of an excess of $Mg(CH_2SiMe_3)_2$ with a mixture of $Mo_2(O_2CCH_3)_4$ and PMe_3 leads to an air-sensitive compound of formula $Mo_2(CH_2SiMe_3)_2[(CH_2)_2SiMe_2](PMe_3)_3$ whose structure is represented in Fig. 4.25.[186] A related complex containing trimethylphosphite has also been isolated.[186] This unusual molecule has a metal–metal bond distance (*c.* 2.16 Å) that seems at first sight to be in accord with a quadruple bond. It contains two electronically different metal atoms that may be represented formally as Mo^{I} and Mo^{III}, a situation that would be compatible with a Mo–Mo quadruple bond that included a dative component, or a triple bond. This may be another example like $Mo_2(OPr^i)_4(dmpe)_2$, of an intramolecular disproportionation reaction. In this complex the two metal atoms are bridged by a $(CH_2)_2SiMe_2$ group that could form by the elimination of a γ-hydrogen from a terminal $MoCH_2SiMe_2$ unit.

Mixed alkyl phosphine complexes of Mo_2^{4+} may also be obtained through the reactions of trimethylphosphine with the triply-bonded dimolybdenum(III) complexes $Mo_2Br_2(CH_2CMe_3)_4$ and $Mo_2Br_2(CH_2SiMe_3)_4$.[523] The neopentyl derivative affords $Mo_2(CH_2CMe_3)_4(PMe_3)_4$ while $Mo_2Br_2(CH_2SiMe_3)_4$ yields $Mo_2Br_2(CH_2SiMe_3)_2(PMe_3)_4$,[524] but both are the consequence of reductive eliminations.

Several alkynyl-substituted, quadruply bonded complexes of the type $Mo_2(\eta^1\text{-CCR})_4(PMe_3)_4$ (R = $CHMe_2$, CMe_3, $SiMe_3$ or Ph) have been prepared by the reaction of LiCCR with $Mo_2Cl_4(PMe_3)_4$ in diethyl ether-dimethoxyethane mixtures.[507] Their electronic absorption and resonance Raman spectra show characteristics that are manifestations of the conjugation between the $[\delta,\delta^*]$ orbitals of the Mo_2^{4+} core and the $[\pi, \pi^*]$ orbitals of the CCR ligands.

Pictiva EX2004
Samsung v Pictiva
IPR2024-01094

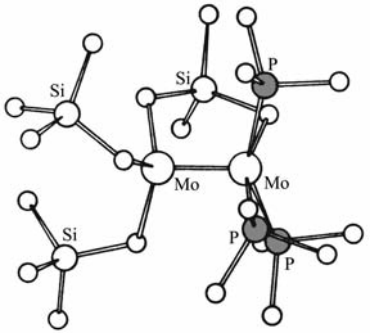


Fig. 4.25. The structure of $Mo_2(CH_2SiMe_3)_2[(CH_3)_2SiMe_2](PMe_3)_3$.

Two other important organometallic derivatives are the allyl and cyclooctatetraene (COT) compounds $Mo_2(C_3H_5)_4$ and $Mo_2(COT)_3$. The former has been prepared either by reaction of $MoCl_5$ with allylmagnesium chloride in diethyl ether,[525,526] or by treating $Mo_2(O_2CCH_3)_4$ with four equivalents of allyllithium or allylmagnesium bromide.[292] The cyclooctatetraene derivative has been obtained by a procedure that involves reduction of a mixture of $MoCl_5$ in THF by $K_2C_8H_8$ to give the black crystalline complex $Mo_2(COT)_3$.[527] Both molecules may be construed as possessing Mo–Mo quadruple bonds but the rather low symmetry of these molecules and the complex ligand array has not encouraged a detailed treatment of the bonding in either case.

The use of $Mo_2(\eta^3\text{-}C_3H_5)_4$ as a precursor complex for the preparation of active catalysts containing Mo_2 species on alumina or silica is well documented.[528-533] The catalysts show high activities for ethylene or 1,3-butadiene hydrogenation, propene metathesis, and other important organic reactions. The thermodynamic and kinetic stability of the isomers of $Mo_2(\eta^3\text{-}C_3H_5)_4$ and its methylallyl analog have been studied[534] as well as their Lewis base catalyzed isomerization. The reactions of β-diketones with $Mo_2(\eta^3\text{-}C_3H_5)_4$ afford $Mo_2(\mu_2\text{-}\eta^3\text{-}C_3H_5)_2(\eta^2\text{-L})_2$, where L = acac, tfac and hfac,[535] while reaction of $Mo_2(\eta^3\text{-}C_3H_5)_4$ with carbon monoxide induces the reductive elimination of two pairs of allylic ligands and the formation of mononuclear $Mo(\eta^4\text{-}1,5\text{-hexadiene})(CO)_4$.[536]

The orange, diamagnetic phosphine ylid compound, $Mo_2[(CH_2)_2PMe_2]_4$, can be obtained by both of the following reactions:[537]

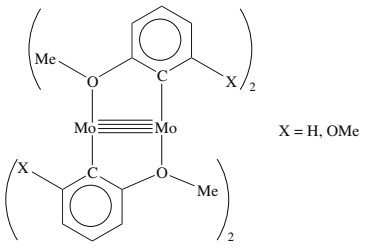
$$MoCl_3(THF)_3 + Li[(CH_2)_2PMe_2] \rightarrow Mo_2[(CH_2)_2PMe_2]_4$$

$$Li_4[Mo_2Me_8] + 4Me_4PCl \rightarrow Mo_2[(CH_2)_2PMe_2]_4 + 8CH_4 + 4LiCl$$

In the first one the oxidation product from the $Li[(CH_2)_2PMe_2]$ was not identified. The second reaction illustrates the utility of $Li_4[Mo_2Me_8]$ as a synthon, although it has not been widely exploited as such. The Mo–Mo distance in the tetrakis ylid molecule is 2.082(2) Å; the molecule has an inversion center and virtual C_{4h} symmetry.[538]

There are two compounds[187,539,540] in which the Mo_2^{4+} unit is bridged by four 2-methoxyphenyl or 2,6-dimethoxyphenyl groups (**4.35**). There is an exceptionally short quadruple bond in the $Mo_2(2,6\text{-dimethoxyphenyl})_4$ molecule,[540] namely, 2.064(1) Å, the structure of which is shown in Fig. 4.26.

Pictiva EX2004
Samsung v Pictiva
IPR2024-01094



4.35

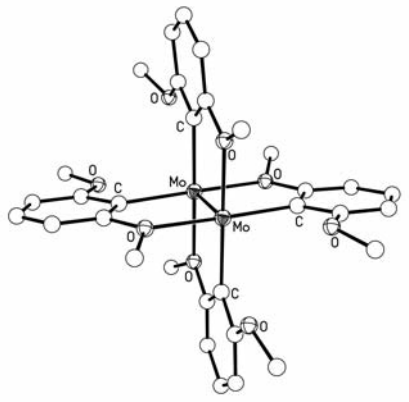


Fig. 4.26. The structure of the Mo_2(2,6-dimethoxyphenyl)$_4$ molecule.

4.4.4 Heteronuclear Mo–M compounds

Apart from a few compounds containing MoRe, MoRu and MoOs bonds (*vide infra*) this class of compounds is limited to those with MoCr and MoW bonds. All the known structures are listed in Table 4.15. Incidentally, no CrW compound has been reported.

Table 4.15. Structures of Mo–M compounds

Formula	Mo–M	ref.
$MoCr(O_2CCH_3)_4$	2.050(1)	304
$MoW(O_2CCMe_3)_4$	2.080(1)	324
$MoW(O_2CCMe_3)_4I$	2.194(2)	541
$MoW(mhp)_4$	2.091(1)	246
$MoWCl_4(PMe_3)_4$	2.209(2)	439
$(PMe_3)_2Cl_2MoWCl_2(PMePh_2)_2$	2.207(1)	439
$MoWCl_4(PMePh_2)_4$	2.210(4)	439
	2.207(4)	439
$MoWCl_4(PMe_2Ph)_4$	2.208(1)	542
$MoWBr_4(PMe_2Ph)_4$	2.209(1)	543
$(PMe_2Ph)_2Cl_2MoWCl_2(PMe_2Ph)(PPh_3)$ $(PMe_2Ph)(PPh_3)Cl_2MoWCl_2(PMe_2Ph)_2$	2.216(1)	542
β-$MoWCl_4(dppm)_2$	2.211(1)	544
β-$MoWCl_4(dppe)_2$	2.243(1)	544

Pictiva EX2004
Samsung v Pictiva
IPR2024-01094

Formula	Mo–M	ref.
β-$MoWCl_4(dmpm)_2$	2.193(2)	545
[(OEP)MoRu(TPP)]PF_6	2.181(2)	546
[(TPP)MoRu(OEP)]PF_6	2.211(2)	547
[(OEP)MoOs(TPP)]PF_6	2.238(3)	548
[(TPP)MoRe(OEP)]PF_6	2.235(1)	547

The two tetraacetato molecules, $CrMo(O_2CCH_3)_4$ and $MoW(O_2CCH_3)_4$ are well characterized. The former was made in 30% yield by addition of $Mo(CO)_6$, dissolved in a mixture of acetic acid, acetic anhydride and CH_2Cl_2, to a refluxing solution of $Cr_2(O_2CCH_3)_4(H_2O)_2$ in acetic acid/acetic anhydride.[304] It can also be obtained by reaction of $Mo_2Br_4(CO)_8$ with an excess of $CrCl_2$ in acetic acid.[549] Yellow, volatile $CrMo(O_2CCH_3)_4$ is isomorphous with $Mo_2(O_2CCH_3)_4$ and the Cr–Mo distance, 2.050(1) Å, is between those in $Mo_2(O_2CCH_3)_4$ and gaseous $Cr_2(O_2CCH_3)_4$. It displays a parent ion peak in the mass spectrum and has a Raman-active Cr–Mo stretching mode at 394 cm^{-1}. Impure $CrMo(O_2CCF_3)_4$ has been obtained by treatment of $CrMo(O_2CCH_3)_4$ with CF_3COOH.[304]

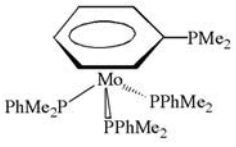
The yellow, crystalline $MoW(O_2CCMe_3)_4$ was made by refluxing a 1:3 mixture of $Mo(CO)_6$ and $W(CO)_6$ with pivalic acid in *o*–dichlorobenzene.[11,541] The initial product consists of about 70% $MoW(O_2CCMe_3)_4$ and 30% $Mo_2(O_2CCMe_3)_4$. The separation and purification of the pure MoW compound was accomplished by oxidizing it to $MoW(O_2CCMe_3)_4I$, separating this, then reducing it back to $MoW(O_2CCMe_3)_4$ by Zn in acetonitrile. The compound shows a parent ion peak in the mass spectrum and it has an Mo–W distance[324] of 2.080(1) Å, which is but slightly shorter than that in $Mo_2(O_2CCMe_3)_4$, 2.088(2) Å.[35] In the compound $MoW(O_2CCMe_3)_4I$,[541] the iodine atom is bonded to the tungsten atom and the structure is ordered, with a Mo–W distance of 2.194(2) Å.

Similarly, $MoW(mhp)_4$ is formed[246] by refluxing a 3:2 mixture of $Mo(CO)_6$ and $W(CO)_6$ with Hmhp in a mixture of diglyme/heptane. Like its pivalate analog, $MoW(mhp)_4$ can be purified, and thereby freed of any $Mo_2(mhp)_4$ contaminant, by oxidation with iodine to $[MoW(mhp)_4]^+$ followed by reduction with zinc amalgam.[246] The dichloromethane solvate $MoW(mhp)_4{\cdot}CH_2Cl_2$ is isomorphous with the other members of the mhp series, and the Mo–W distance of 2.091 Å falls between the corresponding Mo–Mo and W–W distances, but is shorter by 0.022(2) Å than the average of the latter two. A very small amount of impure $CrMo(mhp)_4$ has also been obtained, both by a procedure analogous to that used to prepare $MoW(mhp)_4$[247] and also upon treating $CrMo(O_2CCH_3)_4$ with Na(mhp) in ethanol.

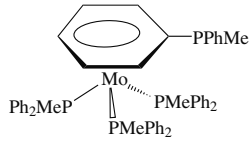
An elegant, efficient and general route to certain complexes of the MoW^{4+} core was first reported in 1984[440] and in more detail in 1987.[439] It takes advantage of the reactivity of the phosphine arene complexes **4.36** and **4.37**, with WCl_4, as illustrated in the following equation:

$$(\eta^6\text{-PhPMe}_2)\text{Mo(PPhMe}_2)_3 + \text{WCl}_4(\text{PPh}_3)_2 \rightarrow (\text{PPhMe}_2)_2\text{Cl}_2\text{MoWCl}_2(\text{PPhMe}_2)_2 + 2\text{PPh}_3$$

With this approach the two compounds $MoWCl_4(PMe_2Ph)_4$ and $MoWCl_4(PMePh_2)_4$ were obtained. Small amounts of the $Mo_2Cl_4(PR_3)_4$ compounds were also formed.



4.36



4.37

Pictiva EX2004
Samsung v Pictiva
IPR2024-01094

By taking advantage of the ability of the smaller, more basic PMe_3 to replace the larger, less basic $PMePh_2$, the following reactions were accomplished:

$$MoWCl_4(PMePh_2)_4 + nPMe_3 \xrightarrow{n=2} MoWCl_4(PMe_3)_2(PMePh_2)_2$$

$$MoWCl_4(PMePh_2)_4 + nPMe_3 \xrightarrow{n=4} MoWCl_4(PMe_3)_4$$

or

In general these MoW compounds crystallize so the two kinds of metal atoms are disordered over the two metal atom sites. This leads to a situation where the reported uncertainties in the bond lengths and angles undoubtedly underestimate the actual ones. The structure of the mixed phosphine complex is an exception to this because the PMe_3 ligands are both on the molybdenum atom and the $PMePh_2$ ligands are both on the tungsten atom, and the molecules are ordered. This structure is shown in Fig. 4.27.

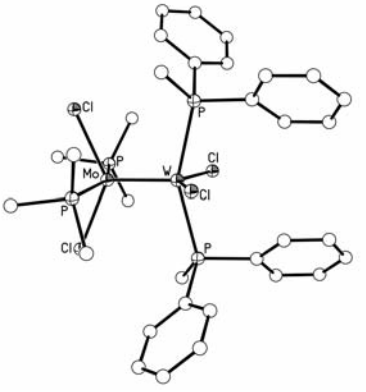


Fig. 4.27. The structure of $(PMe_3)_2Cl_2MoWCl_2(PMePh_2)_2$.

In a modification[542] of the above procedure, PPh_3 was included in the reaction of $(\eta^6\text{-PhPMe}_2)Mo(PMe_2Ph)_3$ with $WCl_4(PPh_3)_2$. This led to the formation of a mixture of $(PMe_2Ph)_2Cl_2MoWCl_2(PMe_2Ph)(PPh_3)$ and $(PMe_2Ph)(PPh_3)Cl_2MoW(PMe_2Ph)_2$, which co-crystallize with the Mo and W atoms disordered. The compound $MoWBr_4(PMe_2Ph)_4$ has been made by reaction of $(\eta^6\text{-PhPMe}_2)Mo(PMe_2Ph)_3$ with WBr_5.[543]

It should be noted that the type of reaction used to make the $MoWCl_4(PMe_nPh_{3-n})_4$ molecules is also effective for making the $Mo_2X_4(PMe_nPh_{3-n})_4$ molecules if $MoCl_4(THF)_2$ is used in place of $WCl_4(PPh_3)_2$. However, as already noted in Section 4.3.4 the homonuclear molecules can be obtained in more conventional ways.

Extensive studies have been made of $MoWCl_4(diphos)_2$ compounds,[544,545] which were obtained by the action of the diphosphines on $MoWCl_4(PMePh_2)_4$. The diphosphines employed were dppm, dppe, dmpm and dmpe. As with the homonuclear $Mo_2X_4(diphos)_2$ compounds, two isomeric types, α and β, occur. No X-ray structures of α-$MoWCl_4(diphos)_2$ molecules have been reported but there is NMR evidence for their existence.

In general the MoW compounds resemble their homonuclear analogs. The polarity of the MoW bond is probably small and has no significant effect on the properties of the compounds. An electronic absorption band in the region of 630-650 nm has been reported for several of them and is presumed to be due to a $\delta \rightarrow \delta^*$ transition. Several of the $MoWCl_4(PR_3)_4$ compounds appear to undergo oxidation at *c.* +0.45 V versus Ag/AgCl, but there is no report of any such oxidation having been carried out chemically. The photoelectron spectrum[550] of

Pictiva EX2004
Samsung v Pictiva
IPR2024-01094

$MoWCl_4(PMe_3)_4$ shows three resolved peaks that have been assigned to δ, π and σ electrons, in increasing order of energy.

There are only a few reported compounds containing MM' multiple bonds between metal atoms from different groups of the periodic table; all of them have the metal atoms embraced by porphyrin rings and all have been made by J. P. Collman et al.[546-548,551] Those that contain molybdenum are (OEP)MoRu(TPP), [(OEP)MoRu(TPP)]PF_6, (OEP)MoOs(OEP), [(OEP)MoOs(TPP)]PF_6, [(TPP)MoOs(OEP)]PF_6 and [(TPP)MoRe(OEP)]PF_6. Their electronic structures are probably all as expected; the physical properties do not suggest otherwise.

4.4.5 An overview of Mo–Mo bond lengths in Mo_2^{4+} compounds

At the end of 2001, a search of the Cambridge Crystallographic Database was made to determine the range and distribution of Mo–Mo distances in compounds with Mo_2^{4+} cores.[552] This resulted in 465 compounds for which both the reported distances and the assignment of an Mo_2^{4+} core are believed to be correct. A histogram of these data is shown in Fig. 4.28. All of the distances have been rounded off to the second decimal place. In the range of 2.18-2.19 Å are nine compounds in which the torsion angles about the Mo–Mo bond are 26-40°, and thus a major part (40-70%) of the δ bonding has been abolished. Were it not for this, these distances would probably have been 0.03-0.05 Å shorter. For nearly all of the remaining "long" bonds, there is some plausible reason for elongation.

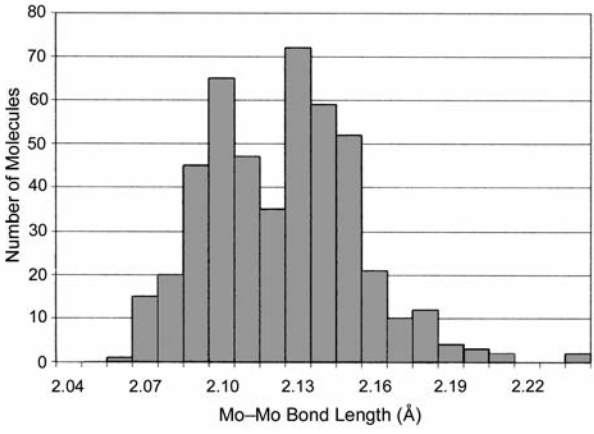


Fig. 4.28. A histogram of Mo-Mo quadruple bond lengths.

The conclusion of this survey is that the "normal" range for Mo_2^{4+} bond lengths is 2.06 to 2.17 Å. Within this range the histogram shows a bimodal distribution, which can be ascribed to the fact that paddlewheel compounds tend to have shorter bonds (2.06-2.12 Å). These conclusions, while not to be taken as inviolable rules, provide a reliable guide to the distances that may reasonably be expected in compounds to be reported in the future.

4.5 Higher-order Arrays of Dimolybdenum Units

4.5.1 General concepts

The terms supramolecular or higher-order array are used to designate any conglomeration of two or more M_2^{n+} (usually with $n = 4$) units. We are concerned here with arrays of Mo_2^{n+} units, but such arrays have also been made with other species of M_2^{n+} units (W_2^{n+}, Re_2^{n+}, Rh_2^{4+}, Ru_2^{5+}) and are discussed in their appropriate chapters.

Pictiva EX2004
Samsung v Pictiva
IPR2024-01094

In the supramolecular arrays there are two types of ligands:

1. *linkers*, that connect dimetal units with one or more others, and
2. *spectator ligands*, which fill all the positions around the dimetal unit that are not occupied by linkers.

The dimolybdenum units that have been used are of the two types shown as (a) and (b) in Fig. 4.29 along with a generic representation of a linker, (c). The four main types of supramolecular structures are shown in Fig. 4.30 although there are a few others that will be mentioned later.

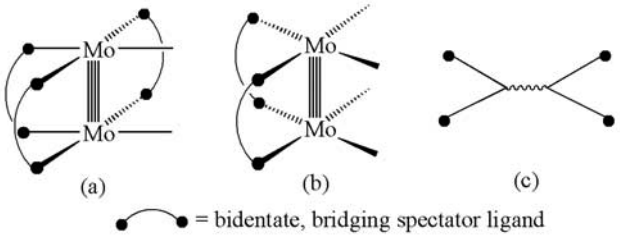


Fig. 4.29. The two types of dimolybdenum fragments, (a) and (b), that can be connected by linkers, (c), to form supramolecular arrays.

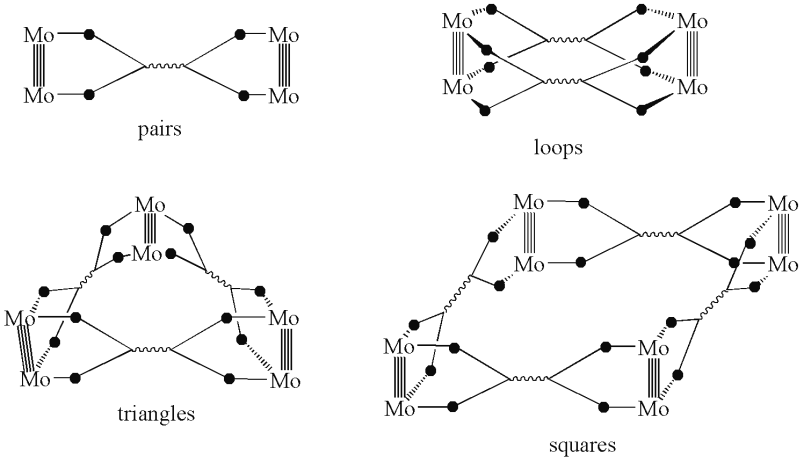


Fig. 4.30. The four most common types of supramolecular arrays, with the spectator ligands omitted for clarity.

It is clear that the unit (a) in Fig. 4.29 is suited to form only the pairs shown in Fig. 4.30 when the linkers are of the type shown in (c). For the type of dimolybdenum fragment shown as (b) in Fig. 4.29, it might seem that only squares could be expected, because of the 90° angle subtended at the Mo_2 unit by the carboxyl planes of the two adjacent linkers. However, this is too simplistic a view. It is obvious that if the linkers are inherently bent, loops will naturally be favored.

Less obvious is the possibility of forming triangles, since the 60° corner angles of a triangle are far from the 90° angles favored by the type (b) units shown in Fig. 4.29. And yet triangles are sometimes formed, for thermodynamic reasons.

Pictiva EX2004
Samsung v Pictiva
IPR2024-01094

In order to have a $\Delta G°$ of zero for the reaction in which triangles become squares,

$$4\{[Mo_2]_3L_3\} = 3\{[Mo_2]_4L_4\} \qquad \Delta G° = \Delta H° - T\Delta S°$$

(where we abbreviate the dimolybdenum core plus its spectator ligands as $[Mo_2]$) $\Delta H°$ must equal $T\Delta S°$. Now there is considerable strain entailed in forming triangles relative to forming squares which could arise from any or all of three principal distortions:

1. making the angles subtended at metal atoms by the linkers less than 90°;
2. curving and twisting linkers;
3. twisting the angle of internal rotation about the Mo–Mo quadruple bond away from the preferred eclipsed conformation.

The accumulation of strain energies in the triangle must make a negative contribution to $\Delta H°$ in the above equation; that is, squares are enthalpically preferred to triangles.

However, the entropy change as four moles of triangles are converted to three moles of squares is negative so the $-T\Delta S°$ will be positive and tend to offset the negative $\Delta H°$ term. Rough estimates[553] of both $\Delta H°$ and $-T\Delta S°$ (at *c.* 300 K) suggest that each of these terms might have an absolute value of 10-15 kcal mol^{-1}. Since the entropy contribution should be practically independent of the exact identity of the linker, the most promising strategy for obtaining triangles instead of squares is to employ linkers that are flexible – avoiding, however, those that actually prefer (or demand) to be bent since, as already noted, they will give rise to loops for enthalpic reasons alone.

So far, only one successful preparation of a triangle containing $[Mo_2]$ components has been reported.[554] The two carboxyl groups in the linker are at the 1 and 4 positions of a cyclohexane ring, and this ring is flexible enough to provide, at a low enthalpic cost, the curvature in the sides necessary for the triangle, as shown in Fig. 4.31. This may be contrasted with the result of using the *p*-xylenediyldicarboxylate which can equally well have the linear conformation **4.38**(a), that would make possible the formation of a square, or the bent one **4.38**(b) which favors a loop. The formation of a loop is even more entropically favored than a triangle, so that this linker, in conformation **4.38**(b), could have been predicted to give rise to a loop in preference to a square or even a triangle and, as shown in Section 4.5.6, this is what it does.

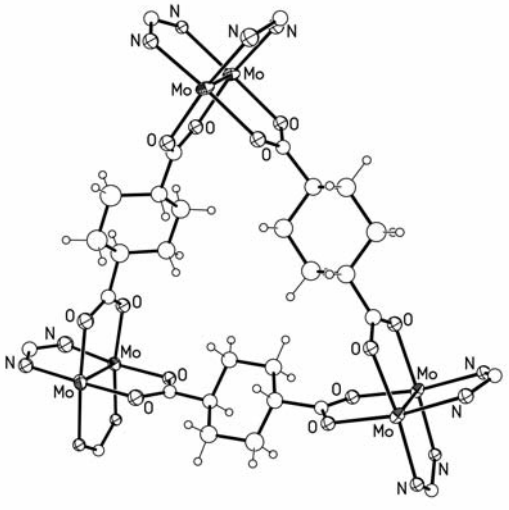
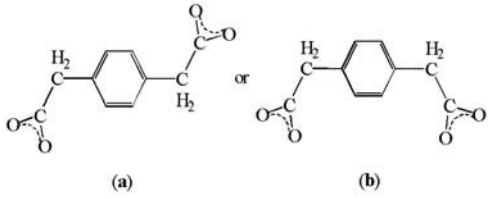


Fig. 4.31. The core of the structure of the molecular triangle $[(DAniF)_2Mo_2(O_2CC_6H_{10}CO_2)]_3$.

Pictiva EX2004
Samsung v Pictiva
IPR2024-01094

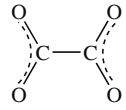


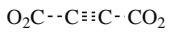
4.38

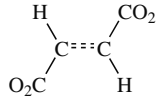
In the following subsections, the entire range of supramolecular assemblies afforded by $[Mo_2]$ units (pairs, squares, loops and others) will be discussed. The one and only triangle so far reported was mentioned above. A list of all of the dianions that have been used to link Mo_2^{4+} cores into supramolecular arrays is presented in Table 4.16. The numbers assigned there will be used to identify these linkers in all subsequent lists and tables.

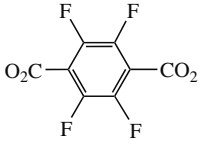
Table 4.16. Linkers that have been used to make supramolecular structures of Mo_2^{4+} components.

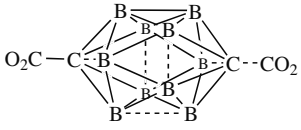
A. Dicarboxylates

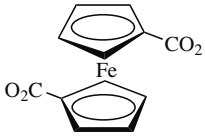

A1

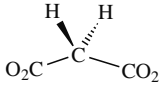

A2

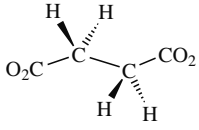

A3

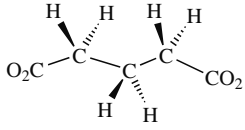

A4

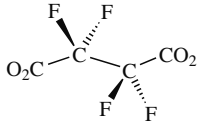

A5

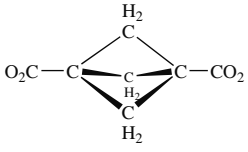

A6

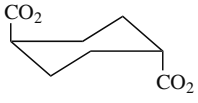

A7

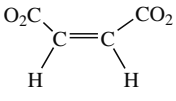

A8

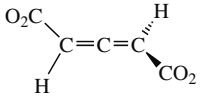

A9

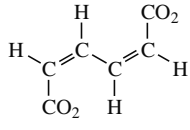

A10


A11

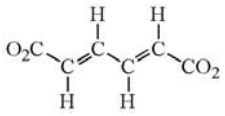

A12


A13

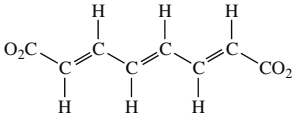

A14


A15

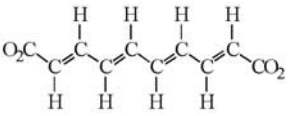
Pictiva EX2004
Samsung v Pictiva
IPR2024-01094



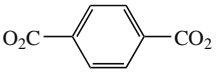
A16



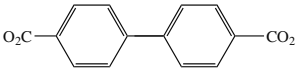
A17



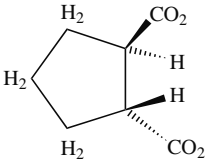
A18



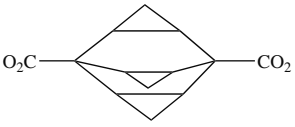
A19



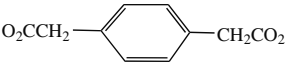
A20



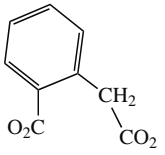
A21



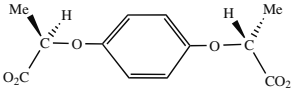
A22



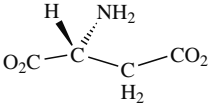
A23



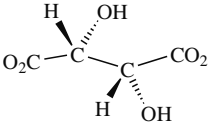
A24



A25

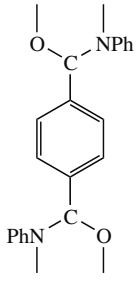


A26

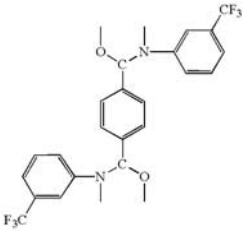


A27

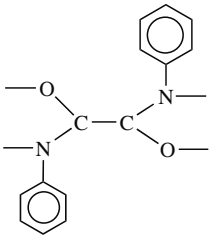
B. Diamidates



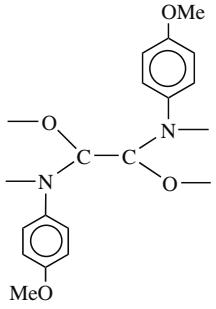
B1



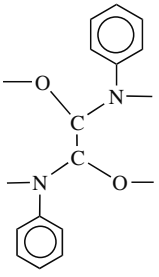
B2



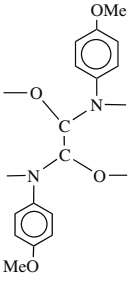
B3



B4

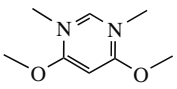


B5

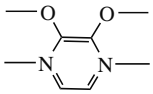


B6

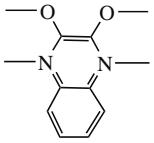
Pictiva EX2004
Samsung v Pictiva
IPR2024-01094



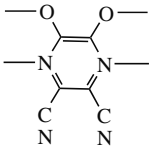
B7



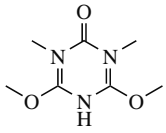
B8



B9



B10



B11

C. Tetrahedral XY_4^{2-} linkers

SO_4^{2-}	MoO_4^{2-}	WO_4^{2-}
C1	**C2**	**C3**
$Zn(OMe)_4^{2-}$	$Co(OMe)_4^{2-}$	
C4	**C5**	

Communication through linkers.

One of the most interesting questions raised by the supramolecular compounds described in this section is the extent to which an electronic change (oxidation or excitation) in one Mo_2^{4+} unit will be communicated to the other, or others, in the same higher-order assembly. One convenient way to explore this subject is by electrochemistry, and this has been done on the majority of the supramolecular compounds. The accessible oxidation potentials may be determined by cyclic voltammetry (CV) or by differential pulse voltammetry (DPV), and the difference between the first and second ones, $\Delta E_{1/2}$, (and any succeeding ones) provides a measure of communication.

In the case of a "dimer of dimers" type molecule (Sections 4.5.2 and 4.5.3) $\Delta E_{1/2}$ is related to the stabilities of the neutral, +1, and +2 species by the following equations, in which we continue to use $[Mo_2]$ as a shorthand for the dimolybdenum unit together with its spectator ligands and L for the linker. We first define the comproportionation constant, K_c, and then a form of the Nernst equation in which 25.69 is the numerical value of the requisite combination of fundamental constants when $\Delta E_{1/2}$ is in millivolts. For cases where $\Delta E_{1/2}$ is small, it is best evaluated from the pulse voltammogram by employing a method due to Richardson and Taube.[555]

$$K_c = \frac{[\{[Mo_2]L[Mo_2]\}^+]^2}{[\{[Mo_2]L[Mo_2]\}][\{[Mo_2]L[Mo_2]\}^{2+}]}$$

$$K_c = \exp(\Delta E_{1/2}/25.69)$$

The smallest value of the comproportionation constant, K_c, is 4 for purely statistical reasons. If the linkers simply insulate one $[Mo_2]$ group from the other in the $[Mo_2]L[Mo_2]^+$ ion the second oxidation will be as easy as the first (except for the statistical factor) and we will have

$$\Delta E_{1/2} = 25.69 \ln 4 = 35.6 \text{ mV}$$

On the other hand if the +1 ion is fully delocalized, removal of the second electron will be significantly more difficult than the first and $\Delta E_{1/2}$ values typically exceed 400 mV. Actually, a $\Delta E_{1/2}$ value as low as 36 would occur only when the linker is very long so that the electrostatic

Pictiva EX2004
Samsung v Pictiva
IPR2024-01094

repulsive effect would be reduced effectively to zero. For the majority of linkers that have been used $\Delta E_{1/2}$ values in the range 100-400 mV have been measured. Such compounds are variously called "moderately coupled," "partly delocalized" or "class II," the latter term derived from the Robin-Day classification of charge transfer systems.[556]

The theoretical problems raised by these intermediately coupled systems are formidable and are much discussed elsewhere.[557] The work on supramolecular systems of $[Mo_2]$ units, but especially on $[Mo_2]L[Mo_2]$ molecules and their +1 and +2 ions provides an abundance of new results concerning electronic communication through linkers. Not only are the results new, but they present certain advantages not generally afforded by other classes of compounds, such as those in which mononuclear complexes (e.g., of Ru^{2+}/Ru^{3+}) or organometallic moieties (e.g., ferrocene/ferrocenium) are linked. In the $[Mo_2]L[Mo_2]$ compounds the nature of the orbitals (δ_{Mo-Mo}) from which electrons are removed is unambiguous and their interactions with linker orbitals are well-defined. Moreover, the structural changes in going from Mo_2^{4+} to Mo_2^{5+}, especially in the Mo–Mo distances, are independently well-established and in each compound they can be determined crystallographically to sufficient accuracy (≤0.001 Å) that the distinction between Mo_2^{4+}, two $Mo_2^{4.5+}$ in a delocalized system, and Mo_2^{5+}, is always clear. The change at each step is about 0.025(1) Å. Moreover, as in other systems, magnetic susceptibilities, EPR and electronic spectra also provide valuable information.

The very schematic representation of a linker in Fig. 4.29(c) indicates only one essential feature, namely that there be two end portions, each consisting of a bent triatomic group with the two outer atoms being donor atoms capable of spanning the two Mo atoms in an Mo_2^{n+} unit. In fact, a very large number of species, mostly dianions, can meet this simple prescription. Table 4.16 is a list of all of those that have actually been used in structurally characterized compounds.

4.5.2 Two linked pairs with carboxylate spectator ligands

The first efforts to link Mo_2^{4+} units into larger arrays[558] were made by employing the following class of reactions:

$$x\text{Mo}_2(\text{O}_2\text{CCMe}_3)_4 + y\text{HO}_2\text{CXCO}_2\text{H} \rightleftharpoons \frac{x}{2}[\text{Mo}_2(\text{O}_2\text{CCMe}_3)_3]_2(\text{O}_2\text{CXCO}_2) + x\text{Me}_3\text{CO}_2\text{H} \quad \text{(when x = 2y)}$$

$$\text{and/or} \quad x[\text{Mo}_2(\text{O}_2\text{CCMe}_3)_2](\text{O}_2\text{CXCO}_2) + 2x\text{Me}_3\text{CO}_2\text{H} \quad \text{(when } x = y\text{)}$$

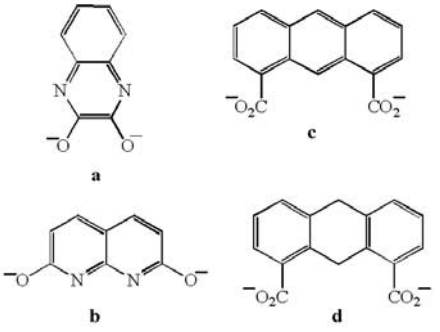
At equilibrium the relative amounts of the two stoichiometric products will depend on the ratio x/y. The major products were the 2:1 type. It was implied that the 1:1 type might also be formed, but none have ever been isolated and it is not known if they might be linear chains, triangles, squares, etc.

Several products of the 2:1 type were obtained (as well as some tungsten analogs) each of which had two $Mo_2(O_2CCMe_3)_3$ units linked by a dicarboxylate ion (oxalate, $^-O_2C(1,4\text{-}C_6F_4)CO_2^-$, $^-O_2C(1,1'\text{Fc})CO_2^-$) or by the linkers **4.39**(a) through **4.39**(d). Of all these compounds only the one with the linker **4.39**(b) was subjected to structure determination by X-ray crystallography, because of the well-known lability of carboxyl groups.[39-41]

Despite the fact that it has never been possible to carry out a conventional single-crystal X-ray structural characterization of any $(RCO_2)_3M_2O_2CXCO_2M_2(O_2CR)_3$ compound, such compounds have been extensively studied. From powder diffraction data the crystal packing of the $(Bu^tCO_2)_3Mo_2(O_2CCO_2)\text{-}Mo_2(O_2CBu^t)_3$ and $(Bu^tCO_2)_3Mo_2(O_2CC_6H_4CO_2)Mo(O_2CBu^t)_3$ molecules was assessed in a semiquantitative way.[559-561]

Pictiva EX2004
Samsung v Pictiva
IPR2024-01094

On the basis of these results Chisholm and coworkers have carried out many interesting physical and theoretical studies[562-566] of the $(Bu^tCO_2)_3Mo_2(O_2CXCO_2)Mo_2(O_2CBu^t)_3$ compounds and their tungsten analogs. For example, EPR spectra and related physical evidence have led to the conclusion that for oxalato-bridged molecules with both Mo_2 and W_2, the monocations are delocalized, while for $O_2CC_6F_4CO_2$-bridged species, only the W_2 compound is delocalized. These conclusions are, in part, surprising. For the W_2 oxalato-bridged compound the comproportionation constant was reported[558] to be *c.* 10^{12}, so that delocalization is expected, and for the $O_2CC_6F_4CO_2$-bridged compound of molybdenum $K_c = 13$, so that localization is expected. However, for both of the other compounds said to be delocalized, K_c values (10^4-10^5) are below the value of *c.* 10^6 often cited as the approximate lower limit for delocalization. This, of course, rises the question (which will not be discussed here) of what "delocalization" really means, especially with respect to time scales of various spectroscopies.



4.39

It is particularly worth mentioning that spectroscopic and DFT molecular orbital studies of the oxalato-bridged and $O_2CC_6F_4CO_2$-bridged compounds of both Mo_2^{4+} and W_2^{4+} have been reported.[560,561] For all four compounds the interactions between the M_2^{4+} δ and δ* orbitals and the π orbitals of the bridging ligands are extensive when the molecules are planar. Planarity is electronically favored, although rotational barriers about the C–C bonds are less than 10 kcal mol^{-1} according to the DFT calculations. The visible spectra are dominated by MLCT transitions. The Mo–Mo stretching modes (by Raman spectroscopy) are at 395-400 cm^{-1} for the Mo_2^{4+} compounds and about 311 cm^{-1} for those of W_2^{4+}. In preliminary communications of this work, calculations of more extended compounds (none of which have been made) were also reported briefly[564,565] and several overviews of this area have been presented.[562,563]

It has more recently been shown that 2,5-thiophenedicarboxylate can also serve as a bridge between $Mo_2(O_2CCMe_3)_3$ groups.[567]

4.5.3 Two linked pairs with nonlabile spectator ligands

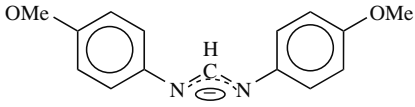
The pernicious consequences of the lability of carboxylate ligands with regard to efforts to isolate and study molecules containing two or more dimetal units are overcome by using ligands that are stereoelectronic to carboxylates but less labile.[568,569] Amidinate ligands serve this purpose well and experience has shown that one particular ligand, $DAniF^-$, **4.40**, is extremely suitable. Thus, by employing $(DAniF)_3Mo_2^+$ rather than $(RCO_2)_3Mo_2^+$, stable crystalline "dimers of dimers" in which a virtually unlimited range of O_2CXCO_2 and other types of linkers may be incorporated are readily accessible. Table 4.17 lists all neutral compounds of the type $(DAniF)_3Mo_2(linker)Mo_2(DAniF)_3$ that have been isolated and studied.

Pictiva EX2004
Samsung v Pictiva
IPR2024-01094

The first two compounds,[570a] reported in 1998, were obtained by the reactions:

$$2Mo_2(DAniF)_3Cl_2 + 2NaHBEt_3 + (NBu^n_4)_2O_2C–X–CO_2 \rightarrow$$
$$Mo_2(DAniF)_3O_2C–X–CO_2Mo_2(DAniF)_3 + 2NaCl + 2NBu^n_4Cl + 2BEt_3 + H_2$$

in which X represents either nothing (i.e., the linker is oxalate) or 1,4-C_6F_4. The complete structure of the oxalato-bridged molecule is shown in Fig. 4.32. In 2001 a total of twelve compounds of this type were reported,[570b] in which the linkers were A1 to A12 in Table 4.16. In addition to extending the range of linkers, this report introduced a better method of preparation in which the $(DAniF)_3Mo_2Cl_2$ compound (previously used together with $NaHBEt_3$) is first dissolved in CH_3CN and treated with Zn to produce, in situ, a solution of $[(DAniF)_3Mo_2(CH_3CN)_2]^+$, from which the excess Zn is removed by filtration. This avoids the formation of unwanted products that sometimes result from reaction of $NaHBEt_3$ with the linker. All twelve compounds were crystallographically characterized.



4.40

Table 4.17. Compounds with two linked $Mo_2(DAniF)_3^+$ units

	Distances, Å				
Linker[a]	Mo–Mo bond distances[b]		$Mo_2\cdots Mo_2$ distance	$\Delta E_{1/2}$, mV	ref.
A1	2.090		6.94	212	570
A2	2.095	2.095	9.54	150	570
A3	2.086	2.087	9.19	145	570
A4	2.090		11.30	87	570
A5	2.088		11.61	69	570
A6	2.087		10.95	75	570
A7	2.088	2.089	7.65	108	570
A8	2.090	2.092	9.21	100	570
A9	2.084	2.088	9.01	112	570
A10	2.086	2.087	9.06	121	570
A11	2.082	2.088	10.30	95	570
A12	2.087	2.088	9.78	69	570
A13	2.090	2.093	7.69	172	571
A14	2.092		9.40	130	571
A15	2.087	2.087	10.35	125	571
A16	2.087		11.58	105	571
A17	2.086		13.92	75	571
A18	2.090		16.16	65	571
A19	2.090		11.24	100	572
A20	2.082		15.45	na	573
A22	2.092	2.092	11.10	66	574
A26	2.101	2.086	9.03	na	575
A27	2.088	2.088	9.02	na	575
B1	2.089		11.38	112	576
B2	2.089		11.38	105	576

Pictiva EX2004
Samsung v Pictiva
IPR2024-01094

	Distances, Å				
Linker[a]	Mo–Mo bond distances[b]		$Mo_2\cdots Mo_2$ distance	$\Delta E_{1/2}$, mV	ref.
B3	2.07		7.10	191	577
B4	2.094		7.08	190	577
B5	2.093		6.32	540	577
B6	2.095		6.33	523	577
B7	2.084	2.089	7.26	187	502
B8	2.092		7.08	258	502
B9	2.090		7.09	308	502
B10	2.095		7.13	263	502
B11	2.096	2.097	7.32	152	502
C1	2.090	2.094	6.01	228	578
C2	2.108	2.119	6.01	311	578
C3	2.110	2.117	6.08	285	578
C4	2.117	2.111	6.55	212	579,580
C5	2.116	2.114	6.56	207	579,580

[a] Identification numbers are given in Table 4.16.
[b] When the Mo_2 units are crystallographically independent, both are given. Esd in each case is 0.001 Å or less.

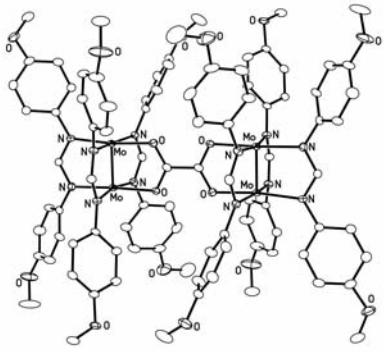


Fig. 4.32. The structure of the $[(DAniF)_3Mo_2]_2(O_2CCO_2)$ molecule.

In 2003 six more $[Mo_2]L[Mo_2]$ compounds having dicarboxylate linkers were reported.[571] This work was focused on dicarboxylates with conjugated, unsaturated chains of carbon atoms, namely A3, A13, A14, A15, A16, A17 and A18 in Table 4.16. In this and a closely following paper,[581] the interactions between the δ orbitals of the Mo_2^{4+} cores and the π orbitals of the linkers were examined by both spectroscopy and DFT calculations. It was concluded that with saturated linkers (e.g., succinate) or others in which no continuous orbital overlap connects one Mo_2^{4+} core to the other, the lowest energy absorption band is localized in each of the independent, non-interacting Mo_2^{4+} chromophores. However, with linkers such as A1, A2, A3, A13, A15, A16, A17 and A18, the lowest transitions are best described as Mo_2^{4+} δ to linker π* MLCT transitions.

The $(DAniF)_3Mo_2(O_2C–X–CO_2)Mo_2(DAniF)_3$ compounds cover a range of $\Delta E_{1/2}$ values of 213 mV to 65 mV and the distances between the centers of the two Mo_2^{4+} unit go from 6.95 Å to 16.15 Å. The magnitude of $\Delta E_{1/2}$ is proportional to the ΔG on introducing a positive charge on the second Mo_2^{4+} unit after one is already present on the first one. In the absence of any form of interaction between the two charges other than one that follows Coulomb's Law, and with

Pictiva EX2004
Samsung v Pictiva
IPR2024-01094

the further assumption that the effective dielectric constant for the medium that separates the two charges is the same in all compounds, a plot of $\Delta E_{1/2}$ vs the Mo_2^{4+} to Mo_2^{4+} distance, d, should be linear. Of course, the effective dielectric constant probably does vary, the Mo_2^{5+} to Mo_2^{5+} distance in the product may not always differ by the same amount from the Mo_2^{4+} to Mo_2^{4+} distance in the neutral molecules, and the end-to-end distances in conformationally non-rigid molecules may be different in solution from what they are in the crystals. Thus, even if the only energy of interaction were Coulombic, perfect adherence to a linear relationship could not be expected. However, major and non-random deviation would vitiate the idea of a purely Coulombic interaction.

In Fig. 4.33 the $\Delta E_{1/2}$ values have been plotted vs d for 19 compounds. Filled circles are for linkers that are either saturated or for other reasons (such as the orthogonality of the π bonds in A14 or the non-planarity of A19) are expected to be poor electronic connectors. These data provide no support for the concept of a linear relationship based on a predominantly Coulombic interaction. Presumably the animadversions already noted, and probably other special features of individual linkers, are too important to ignore.

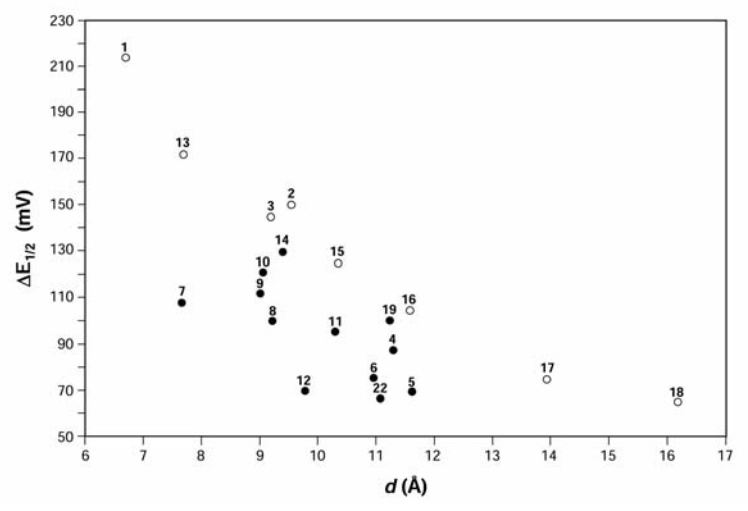


Fig. 4.33. A plot of $\Delta E_{1/2}$ vs the distance between Mo_2^{4+} centers in some compounds with linked $(DAniF)_3Mo_2^{+}$ units. The numbers refer to the linkers in Table 4.16.

It is interesting to see that the seven compounds (open circles) with unsaturated moieties connecting the carboxyl groups plus the oxalate bridge (which is planar) form a much better behaved set. The relationship is not linear, but curvature is expected if an electronic connection through the π systems which falls off with $1/d^n$ ($n > 1$) is superimposed on the Coulombic behavior. Both the Coulombic and the non-Coulombic interactions should go to zero as $d \rightarrow \infty$, and therefore the points should approach a limiting value of $\Delta E_{1/2} = 35.6$ mV, as explained in Section 4.5.1. This does not seem inconsistent with the limited data available.

Diamidate linkers.

Dicarboxylates are not the only linkers that have produced interesting compounds with linked pairs of $Mo_2(DAniF)_3^{+}$ units. A closely related class are diamidate dianions, several of which are shown in Table 4.16. They are of two types, open chain[577] and cyclic.[502] The compounds made so far with diamidate linkers are listed in Table 4.17. With linkers B1 and B2

Pictiva EX2004
Samsung v Pictiva
IPR2024-01094

compounds analogous to the one linked by the terephthalic acid dianion were obtained.[576] In these molecules the dimolybdenum units are far apart and there is considerable non-planarity in the linkers. Thus, it is not surprising that the $\Delta E_{1/2}$ values (*c.* 100 mV) are relatively small.

The linkers B3-B6 provide more interesting results. In Table 4.16 the bond-like lines projecting from the N and O atoms indicate the directions in which bonds may be formed to the Mo_2^{4+} units. B3 and B4 correspond to the same orientation (designated α) of the central C–C bond as in the oxalate linker, whereby a separate 5-membered ring is formed about each Mo_2 group. B5 and B6 lead to the formation of a 6-membered ring about each Mo_2 group, with the two rings fused along a common C–C bond. This arrangement is designated β. It has not been seen with the oxalate linker.

The structures of the α and β isomers formed by the B4 and B6 linkers are shown in Fig. 4.34. In the α isomer it may be noted that the two Mo_2 units are perpendicular, whereas in the oxalate-bridged molecule they are coplanar.

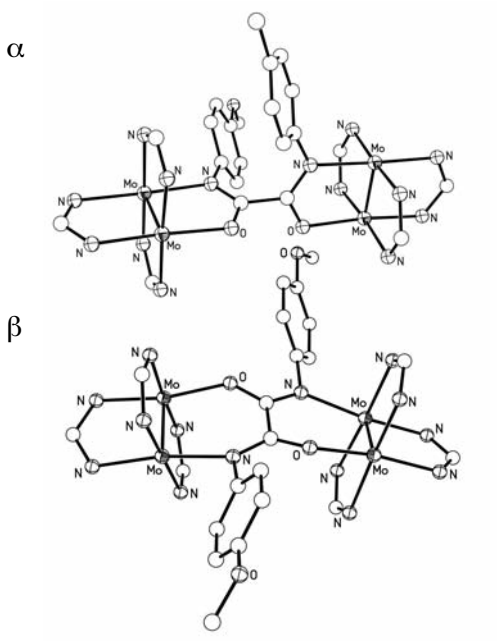


Fig. 4.34. The structures of α and β isomers formed by the diamidate linkers B4 and B6.

As the data in Table 4.17 show, there is a major difference in the abilities of the α and β diamidate linkers to couple the Mo_2 redox centers, far beyond what could be attributed to the small difference in the Mo_2 to Mo_2 distances in these isomers. The $\Delta E_{1/2}$ values for the α isomers (*c.* 190 mV) are about the same as $\Delta E_{1/2}$ for the oxalate linked compound (212 mV)[503], as expected. The C–C single bond connecting the two halves of the molecule is a barrier to communication. In the β structure communication is greatly enhanced by the existence of a naphthalene-like π system.

There are five compounds in which cyclic diamidate dianions, B7-B11, are the linkers.[502] These provide a range of $\Delta E_{1/2}$ values indicative of relatively weak coupling (B7, B11) to moderate (B8, B10) to fairly strong (B9). No detailed explanation for these variations has been given.

Pictiva EX2004
Samsung v Pictiva
IPR2024-01094

Tetrahedral linkers.

Five tetrahedral linkers, shown in Table 4.16 as C1-C5 have been investigated. The first three compounds[578] which have sulfate, molybdate and tungstate ions as linkers have shorter Mo_2 to Mo_2 distances than any found in compounds with dicarboxylate or diamidate linkers. It should be noted that in all cases, a tetrahedral linker requires the two Mo_2^{4+} units to be orthogonal to each other. For the compounds with C1, C2 and C3 linkers, no oxidized products have yet been isolated.

The linkers C4 and C5 are remarkable in that there is no evidence for their independent existence. Instead, they are both formed and trapped between the dimolybdenum units when $Mo_2(DAniF)_3^+$, $ZnCl_2$ (or $CoCl_2$) and $NaOCH_3$ are all present in acetonitrile solution and the products crystallize out.[579] In each of the five cases, the $\Delta E_{1/2}$ values (Table 4.17) indicate that the coupling of the $[Mo_2]$ units, although better than for any dicarboxylate linker, is only moderate. In accord with this, structural studies[580] show that the monocations of the compounds with both the C4 and C5 linkers are localized. The monocation with C4 is shown in Fig. 4.35. Thus, in the C4 case there are Mo–Mo distances of 2.116 Å and 2.151 Å, and in the C5 case they are 2.113 Å and 2.151 Å. Localization is confirmed by EPR measurements.

In the doubly-oxidized zinc-bridged compound, the two Mo_2^{5+} distances are 2.147(1) and 2.151 Å. EPR and magnetic susceptibility data fully support the idea that there is only negligible communication between the Mo_2^{n+} units through these $(MeO)_2M(OMe)_2^{2-}$ linkers. The +2 cation behaves as a simple diradical with neither ferromagnetic nor antiferromagnetic coupling.

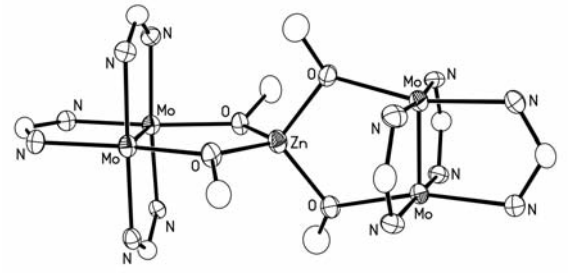


Fig. 4.35. The structure of the $[(DAniF)_3Mo_2]_2[Zn(OMe)_4]$ monocation.

4.5.4 Squares: four linked pairs

By a simple adaptation of the synthetic methods just described for making molecules with two linked Mo_2^{4+} units, a general method for making molecules with four linked Mo_2^{4+} units was devised.[582] The first reported compounds were the oxalato-bridged molecule, along with those having the dianions of tetrafluoroterephthalic acid and ferrocenedicarboxylic acid (A1, A4 and A6 in Table 4.16). The procedure is summarized in the following equation:

$$4[Mo(DAniF)_2(CH_3CN)_4](BF_4)_2 + 4(Bu^n{}_4N)_2O_2CXCO_2 \rightarrow$$
$$[Mo(DAniF)_2(O_2CXCO_2)]_4 + 8(Bu^n{}_4N)(BF_4)$$

Shortly thereafter,[583] squares with linkers A2, A3, A5 and A20 (Table 4.16) were also reported. Those that have been structurally characterized are listed in Table 4.18. The structures of four representative squares are shown in Fig. 4.36.

Pictiva EX2004
Samsung v Pictiva
IPR2024-01094

Table 4.18. Structural data for molecular squares with $Mo_2(DAniF)_3^+$ corners

Linkers	Mo–Mo distance (Å)		ref.
A1[a]	2.087(1)	2.094(1)	582,583
A3[a]	2.087(1)	2.089(1)	583
A6[a]	2.084(1)	2.075(1)	582,583
A20[a]	2.075(4)	2.082(3)	583
	2.082(4)	2.089(4)	
CO_3^{2-}	2.092(4)	2.098(2)	584

[a] As listed in Table 4.16.

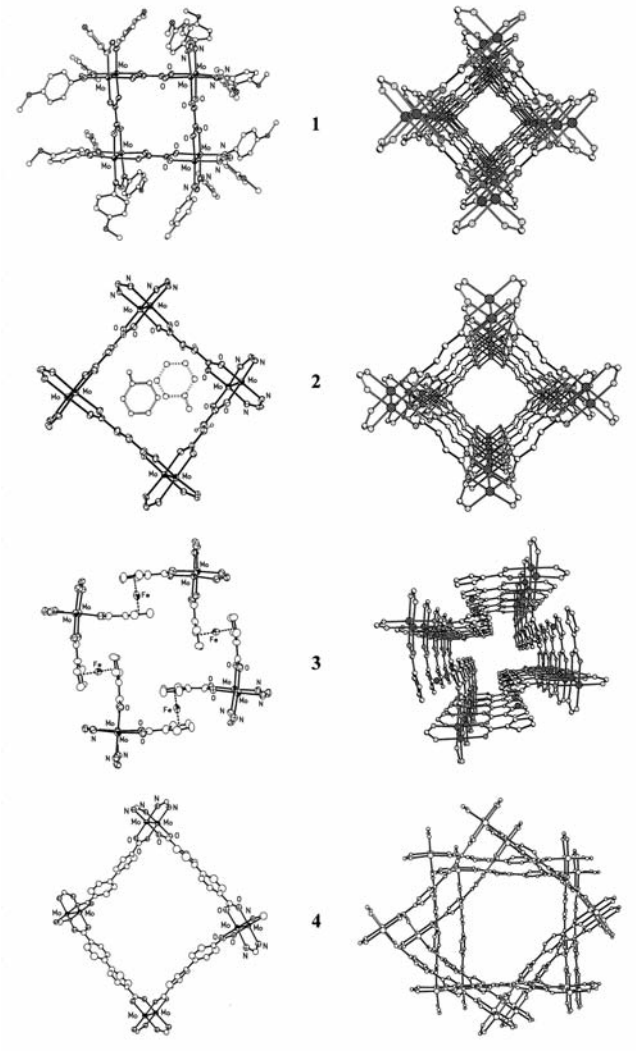


Fig. 4.36. Four molecular square molecules and their crystal stacking patterns.

Pictiva EX2004
Samsung v Pictiva
IPR2024-01094

The electrochemistry of each of the seven reported squares has been examined, but a satisfactory understanding of the results is lacking. For example, for the oxalato square, three one-electron oxidations are clearly resolved. The separation, $\Delta E_{1/2}$, between the first (407 mV) and second (567 mV) is only 160 mV as compared to a $\Delta E_{1/2}$ for $Mo_2(DAniF)_3(O_2CCO_2)Mo_2(DAniF)_3$ of 212 mV. As shown in Fig. 4.37, there are two possible sequences for the successive oxidation steps. In comparing these sequences with each other as well as with the results for the oxalate square the following points arise:

a. The main difference is in step (2) and it could be argued that the lower $\Delta E_{1/2}$ just mentioned for the square favors the assumption of sequence A.
b. However, the $\Delta E_{1/2}$ pertinent to step (3) for the oxalate equals only 94 mV, and this is not to be expected for either sequence.
c. There is no indication that step (4) occurs.

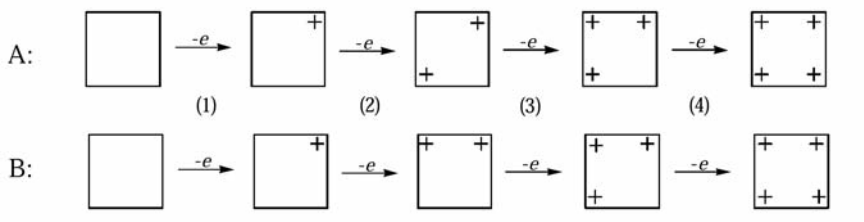


Fig. 4.37. Two possible sequences for the successive oxidations of a square.

In fact, step (4) has not been observed for any of the seven squares, and with linkers that are expected to give weaker coupling steps (2) and (3) are practically undifferentiated. For the $O_2CC{\equiv}CCO_2$ bridged square, for example, there is a one-electron oxidation at 518 mV and then two overlapping oxidations at 621 mV. In cases of even weaker coupling, as illustrated by the $O_2CC_6F_4CO_2$ square, steps (1), (2) and (3) are all undifferentiated. Communication occurring in the squares clearly needs further study.

Another characteristic of all the squares is the stacking of the molecules in their crystals. This is illustrated for four of them in Fig. 4.36. In three of these the squares are stacked "in register," and this is the usual pattern. However, for the $O_2CC_6H_4C_6H_4CO$ square there is an alternation from one level to the next. In many of the stacks small solvent molecules (e.g., CH_2Cl_2, toluene) are present in the interior, sometimes ordered and sometimes not.

An atypical square[585] is shown in Fig. 4.38. The linkers are carbonate ions and one ligand position on each Mo_2^{4+} unit is occupied by a molecule of H_2O. This is the only molecular square for which all four successive oxidations have been observed. The first two presumably arise from oxidations at opposite corners and the last two at the remaining corners.

4.5.5 Loops: two pairs doubly linked

The use of inherently bent linkers to form loops has been demonstrated in six instances.[586-588] The six linkers used are shown in Table 4.16 (A7, A14, A21, A23-A25) and the compounds are listed in Table 4.19. Linkers A14, A21 and A25 are chiral; the loops made with A14 and A21 are racemic (one *R* and one *S* linker), but in the loop made with A25 both linkers in the same molecule have the same (*RR* or *SS*) chirality. In all cases, the loops are stacked in the crystals. Fig. 4.39 shows the molecular structure of the chiral loop made with the ligand A25. The stereochemistry of this loop is rather unusual.[587] The molecule is a second-order Möbius strip, that is, a Möbius type ring with two twists rather than just one. It may be noted that linker A13 should be able to form a loop, but this has not been attempted.

Pictiva EX2004
Samsung v Pictiva
IPR2024-01094

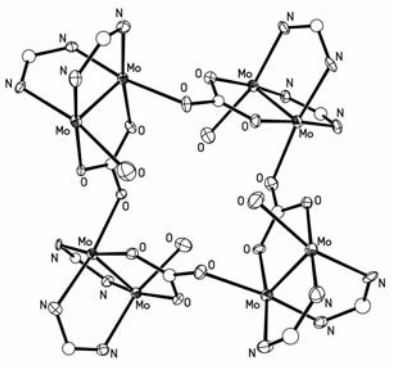


Fig. 4. 38. The core of the square formed by four $[(DAniF)_2(H_2O)Mo_2]^{2+}$ units and four carbonate ions.

Table 4.19. Properties of loops

Linker[a]	Distances, Å			$\Delta E_{1/2}$, mV	ref.
	Mo–Mo bond distances[b]		$Mo_2\cdots Mo_2$ separation		
A7	2.088		6.51	109	586
A14	2.098		8.19	80	588
A21	2.088		na	irrev	586
A23	2.086	2.094	9.62	91	586
A24	2.088	2.092	6.27	179	586
A25	2.081		na	<70	587

[a] See Table 4.16.

[b] If the Mo_2 units are crystallographically independent both are given.

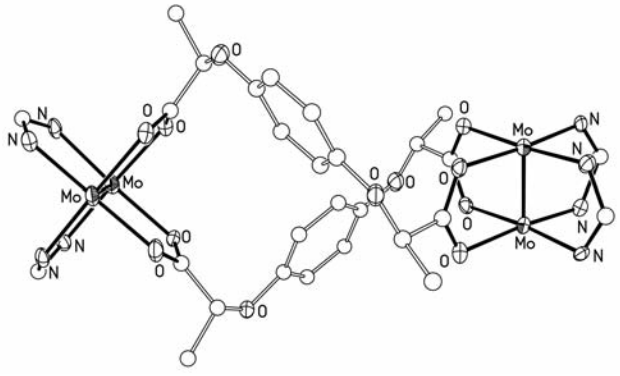


Fig. 4. 39. The chiral structure of the molecular loop molecule formed by $[(DAniF)_2Mo_2]^{2+}$ units with two *SS* linkers of type A25 (Table 4.16).

There are two cases where the same linker has been employed to make a pair with two $Mo_2(DAniF)_3$ units and also a loop with two $Mo_2(DAniF)_2$ units. As shown by the following comparisons, this seems to make very little difference in the communication between the two

Pictiva EX2004
Samsung v Pictiva
IPR2024-01094

Mo_2^{4+} units. Even though in the loops the number of linkers is doubled and the distances are *c.* 1.2 Å shorter, the communication ($\Delta E_{1/2}$) is either no better or poorer.

Table 4.19. Comparison of Loops and Pairs

Linker		$Mo_2 \cdots Mo_2$ distance	$\Delta E_{1/2}$, mV
malonate	pair	7.65	108
	loop	6.51	109
allenedicarboxylate	pair	9.40	130
	loop	8.19	80

4.5.6 Rectangular cyclic quartets

The title of this section refers to molecules in which two Mo_2^{4+} units are linked into a rectangle. There are four types as shown schematically in Fig. 4.40. Note that in (a) and (c) the quadruple bonds persist, in (b) there is partial oxidation and in (d) there has been a cyclic 2+2 addition to give a metalla- cyclobutadiyne ring. Known compounds of types (a) and (c) and key structural data are listed in Table 4.20.

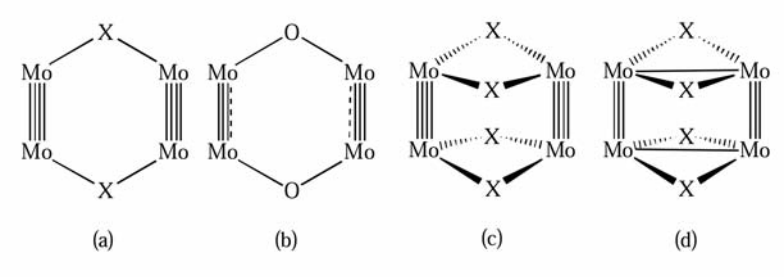


Fig. 4.40. Four structural types of rectangular cyclic arrays in which Mo_2^{n+} units are linked by small bridging anions.

Table 4.20. Rectangular cyclic compounds of types (a) and (c)

Compound	Mo–Mo, Å	$Mo_2 \cdots Mo_2$, Å
	Type (a) structures	
$[Mo_2(DTolF)_3]_2(\mu\text{-}H)_2$	2.093(1)	3.532(1)
$[Mo_2(DAni)_3]_2(\mu\text{-}H)_2$	2.086(4)	3.48(1)
$[Mo_2(DTolF)_3]_2(\mu\text{-}OH)_2$	2.107(1)	4.073(1)
	Type (c) structures	
$[Mo_2(DTolF)_2]_2(\mu\text{-}Cl)_4$	2.118(1)	3.592(1)
$[Mo_2(DPh^fF)_2]_2(\mu\text{-}Cl)_4$	2.123(1)	3.563(1)
$[Mo_2(DAniF)_2]_2(\mu\text{-}Cl)_4$	2.119(1)	3.601(1)
$[Mo_2(DAniF)_2]_2(\mu\text{-}Br)_4$	structure not reported	
$[Mo_2(DAniF)_2]_2(\mu\text{-}I)_4$	2.117(1)	3.915(1)
$[Mo_2I_2(PBu^n{}_3)_2]_2(\mu\text{-}I)_4$	2.129(3)	3.998(3)

In type (a) X may be H (with either DAniF or DTolF as spectator ligands) or OH (with DTolF).[393,589,590] The structure of $[Mo_2(DAniF)_3]_2(\mu\text{-}H)_2$ is shown in Fig. 4.41. The hydrido compounds resist hydrolysis by water but are decomposed by acid. The presence of the

Pictiva EX2004
Samsung v Pictiva
IPR2024-01094

hydrogen atom bridges has been confirmed by neutron diffraction (Mo–H = 1.84(2) Å). The compounds are obtained in 60-70% yield by the reaction:

$$2Mo_2(DArF)_3Cl_2 + 4NaHBEt_3 \rightarrow Mo_2(DArF)_3(\mu\text{-}H)_2Mo_2(DArF)_3$$

The OH-bridged product was obtained when $Mo_2(DTolF)_3Cl_2$ was reduced by metallic potassium in the presence of KOH. It is converted by atmospheric oxygen to the di-oxo compound,[393] in which the dimolybdenum units are $[Mo_2(DTolF)_3]^{2+}$. Since the oxo-bridged compound displays a normal ^1H NMR spectrum the electron spins in these two units are coupled across the μ-O bridges. In the OH-bridged compound[393,590] the Mo–Mo quadruple bond lengths are 2.107(1) Å, whereas in the O-bridged molecule, the Mo–Mo distances of 2.140(2) Å are consistent with the bond order of 3.5.

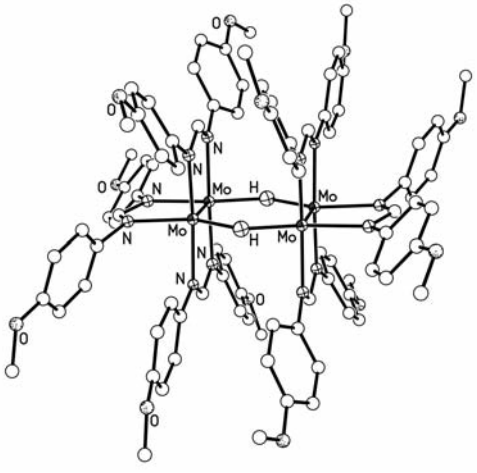
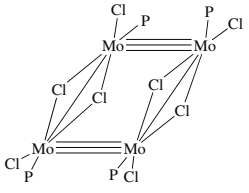


Fig. 4.41. The structure of the $[(DAniF)_3Mo_2]_2(\mu\text{-}H)_2$ molecule as determined by neutron diffraction.

The first compounds with a central structure of type (d) were reported by McCarley and coworkers,[365] who obtained both $Mo_4Cl_8(PBu^n_3)_4$ and $Mo_2Cl_8(PEt_3)_4$ by an indirect route commencing with $Mo_2Cl_4(PPh_3)_2(CH_3OH)_2$. The second of these compounds consists of $Mo_4Cl_4(PEt_3)_4(\mu\text{-}Cl)_4$ molecules, in which the arrangement of Cl and PPh_3 ligands is as shown in 4.42. Later on it was recognized[591] that these centrosymmetric molecules are actually packed in a disordered fashion, as shown in Fig. 4.42. The report of $Mo_4Cl_4(PEt_3)_4(\mu\text{-}Cl)_4$ was followed several years later[592] by the development of other synthetic methods and the report of six more compounds of the same type, although none was structurally confirmed. Soon after that $Mo_2Cl_4[P(OMe)_3]_4(\mu\text{-}Cl)_4$ was obtained[593] and shown by crystallography to have the 4.41 type structure.



4.41

Pictiva EX2004
Samsung v Pictiva
IPR2024-01094

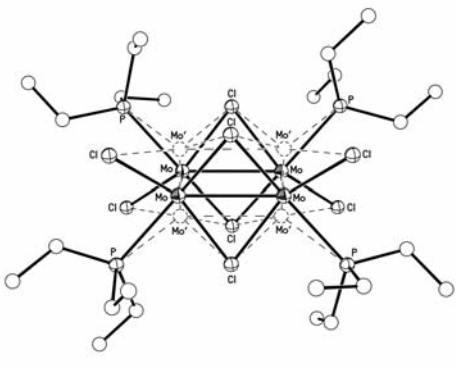


Fig. 4.42. The disordered packing of $[Mo_2(PEt_3)_2Cl_2]_2(\mu\text{-}Cl)_4$ molecules. The minor orientation is shown by broken lines.

In all of the molecules with structures of type (d) two quadruple Mo–Mo bonds originally present in the starting materials have combined in a 2+2 cyclo addition to generate a rectangle of molybdenum atoms in which Mo–Mo single bonds bridged by μ-Cl or other μ-X atoms have been formed. In place of the initial $\sigma^2\pi^4\delta^2$ bonds there now remain $\sigma^2\pi^4$ triple bonds. The newly formed single bonds have Mo–Mo distances of about 2.90 Å (i.e., much shorter than the non-bonded distances of *c.* 3.60 Å in type (c) structures) and the remaining Mo–Mo triple bond lengths are *c.* 2.21 Å.

Although the $Mo_4I_4(PBu^n_3)_4(\mu\text{-}I)_4$ molecule was prepared in the expectation that it too would have a structure of type (d), its properties led to the suggestion[592] that it might actually be of type (c). A later X-ray study confirmed this.[393] The reason it does not conform is presumably that the large μ-I atoms make it impossible for the Mo–Mo single bonds to be formed, as in (d), and thus the Mo–Mo quadruple bonds remain intact, as in (c).

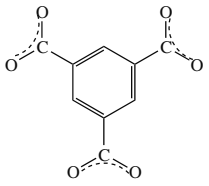
Two unique molecules resulted from attempts to employ dmpm or dppm instead of monodentate neutral ligands in forming cyclobutadiyne type molecules.[594] The preparations were carried out in methanol and $\mu\text{-}OCH_3$ groups are present in the products. In the simpler case $Mo_2Cl_4(\mu\text{-dppm})_2(\mu\text{-}Cl)_2(\mu\text{-}OCH_3)_2$ was formed, in which the Mo–Mo triple bond distances are 2.224(1) Å and the Mo–Mo single bonds, each bridged by μ-Cl and $\mu\text{-}OCH_3$, have lengths of 2.814(1) Å. In the other case, $Mo_4Cl_4(\mu\text{-dmpm})_2(\mu\text{-}Cl)_3(\mu\text{-}OCH_3)_3(\mu_4\text{-}O)$ there is a quadruply bridging oxygen atom; two of the Mo–Mo distances are about 2.45 Å and the others are *c.* 2.65 Å and 2.71 Å. The electronic structure was not discussed.

One final point should be noted. All of the rectangular compounds discussed here are made from quadruply-bonded Mo_2^{4+} starting materials. There are also some rectangular Mo_4 compounds that are made from Mo_2^{6+} triply-bonded starting materials, in which the Mo≡Mo bonds are retained and there are no Mo–Mo single bonds but only pairs of μ-X atoms linking the Mo≡Mo moieties. Such compounds are discussed in Chapter 6.

4.5.7 Other structural types

The most interesting trifunctional linker is the anion of trimesic acid, **4.42**. It readily combines with three $Mo_2(DAniF)_3^+$ units to form the structure[595] shown in Fig. 4.43. For this molecular propeller, three strongly overlapping electrochemical oxidations have been observed with a separation of only 112 mv from the first to the third, indicating relatively poor communication through the trimesate ion.

Pictiva EX2004
Samsung v Pictiva
IPR2024-01094



4.42

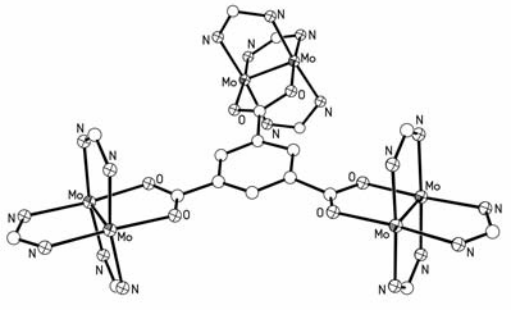


Fig. 4. 43. The "molecular propeller", in which three $(DAniF)_3Mo_2^{+}$ units are attached to a central trimesate anion, $1,3,5\text{-}C_6H_3(CO_2^{-})_3$.

A more impressive result was obtained[596,597] when 4.42 is combined with $Mo_2(DAniF)_2^{2+}$ in the ratio of 4 to 6 to give the structure shown in Fig. 4.44. This remarkable structure, which has a rhodium analog, is a concentric superposition of an octahedron (vertices at the centers of Mo_2^{4+} units) and a tetrahedron (vertices at the centers of the trimesate rings). A number of oxidations were seen in the CV/DPV scans, but so bunched together in a range of about 250 mV that an interpretation was not possible.

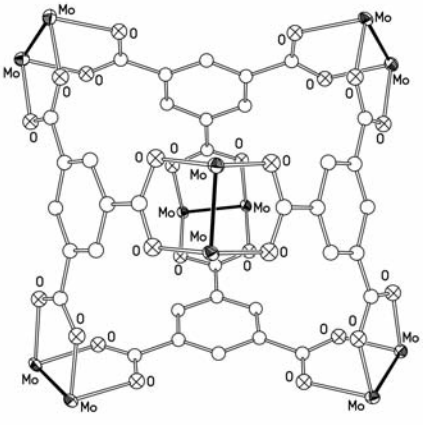
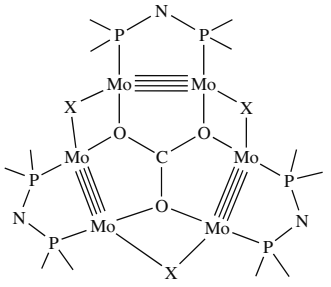


Fig. 4.44. The core structure of the tetrahedral/octahedral molecule that assembles four trimesate anions and six $(DAniF)_2Mo_2^{2+}$ ions.

The participation of the carbonate ion in the formation of a square has already been mentioned (Section 4.5.4). In that case its inherent three-fold symmetry does not influence the sym-

Pictiva EX2004
Samsung v Pictiva
IPR2024-01094

metry of the product. On the other hand, the carbonate ion has been used to make molecules[161] of the type shown schematically as 4.44. Strong coupling among the three dimolybdenum components might be expected but, unfortunately, the electrochemistry of these molecules was not investigated.



X = Cl, Br, I
CF_3CO_2 groups above and below are omitted

4.43

References:

1. D. Lawton and R. Mason, *J. Am. Chem. Soc*. 1965, *87*, 921.
2. F. A. Cotton, Z. C. Mester and T. R. Webb, *Acta Crystallogr*. 1974, *B30*, 2768.
3. J. V. Brenčič and F. A. Cotton, *Inorg. Chem.* 1969, *8*, 7.
4. E. W. Abel, A. Singh and G. Wilkinson, *J. Chem. Soc*. 1959, 3097.
5. E. Bannister and G. Wilkinson, *Chem. Ind. (London)* 1960, 319.
6. T. A. Stephenson, E. Bannister and G. Wilkinson, *J. Chem. Soc*., 1964, 2538.
7. G. Holste and H. Schafer, *Z. anorg. allg. Chem*. 1972, *391*, 263.
8. G. Holste, *Z. anorg. allg. Chem*. 1975, *414*, 81.
9. E. Hochberg, P. Walks and E. H. Abbott, *Inorg. Chem.* 1974, *13*, 1824.
10. A. B. Brignole and F. A. Cotton, *Inorg. Synth*. 1972, *13*, 81.
11. R. E. McCarley, J. L. Templeton, T. J. Colburn, V. Katovic and R. J. Hoxmeier, *Adv. Chem. Ser*. 1976, *No. 150*, 318.
12. F. A. Cotton and J. G. Norman, Jr, *J. Coord. Chem*. 1971, *1*, 161.
13. F. A. Cotton, J. G. Norman, Jr, B. R. Stults and T. R. Webb, *J. Coord. Chem*. 1976, 5, 217.
14. R. J. Mureinik, *J. Inorg. Nucl. Chem*. 1976, *38*, 1275.
15. F. A. Cotton and J. L. Thompson, *Inorg. Chem.* 1981, *20*, 3887.
16. F. A. Cotton, L. R. Falvello, A. H. Reid, Jr and J. H. Tocher, *J. Organomet. Chem*. 1987, *319*, 87.
17. G. M. McCann and H. Ryan, *Inorg. Chim. Acta* 1987, *133*, 11.
18. A. Carvill, P. Higgins, G. M. McCann, H. Ryan and A. Shiels, *J. Chem. Soc., Dalton Trans*. 1989, 2435.
19. (a) R. H. Cayton, M. H. Chisholm and F. D. Darrington, *Angew. Chem., Int. Ed. Engl*. 1990, *29*, 1481. (b) R. H. Cayton and M. H. Chisholm, *J. Am. Chem. Soc*. 1989, *111*, 8921. (c) R. H. Cayton, M. H. Chisholm, J. C. Huffman and E. B. Lobkovsky, *Angew. Chem., Int. Ed. Engl*. 1991, *30*, 862.
20. A. W. Coleman, J. C. Green, A. J. Hayes, E. A. Seddon, D. R. Lloyd and Y. Niwa, *J. Chem. Soc., Dalton Trans*. 1979, 1057.
21. E. Carmona, A. Galindo, L. Sánchez, A. J. Nielson and G. Wilkinson, *Polyhedron*, 1984, *3*, 347.
22. D. J. Santure and A. P. Sattelberger, *Inorg. Chem.* 1985, *24*, 3477.
23. F. A. Cotton, L. R. Falvello and C. A. Murillo, *Inorg. Chem.* 1983, *22*, 382.
24. R. J. H. Clark, A. J. Hempleman and M. Kurmoo, *J. Chem. Soc*. 1988, 973.
25. See for example: F. A. Cotton, *Polyhedron*, 1986, *5*, 3 and references cited therein.
26. F. A. Cotton, L. M. Daniels, P. A. Kibala, M. Matusz, W. J. Roth, W. Schwotzer, W. Wang and B. Zhong, *Inorg. Chim. Acta* 1994, *215, 9*.

Pictiva EX2004
Samsung v Pictiva
IPR2024-01094

27. F. A. Cotton, L. M. Daniels, E. A. Hillard and C. A. Murillo, *Inorg. Chem.* **2002**, *41*, 1639.
28. P. A. Koz'min, M. D. Surazhskaya and T. B. Larina, *Russ. J. Inorg. Chem.* **1980**, *25*, 702.
29. F. A. Cotton and J. G. Norman, Jr., *J. Am. Chem. Soc*., **1972**, *94*, 5967.
30. F. A. Cotton and B. Zhong, *J. Am. Chem. Soc*. **1990**, *112*, 2256.
31. M. H. Kelley and M. Fink, *J. Chem. Phys*. **1982**, *76*, 1407.
32. C. D. Garner, I. H. Hillier, I. B. Walton and B. Beagley. *J. Chem. Soc., Dalton Trans*. **1979**, 1279.
33. D. L. Kepert, B. W. Skelton and A. H. White, *Aust. J. Chem*. **1980**, *33*, 1847.
34. K. Hino, Y. Saito and M. Benard, *Acta Crystallogr*. **1981**, *B37*, 2164.
35. G. A. Robbins and D. S. Martin, *Inorg. Chem.* **1984**, *23*, 2086.
36. E. L. Akhmedov, A. S. Kotel'nikova, O. N. Evstaf'eva, Yu. Ya. Kharitonov, A. N. Smirnov, A. Yu. Tsivadze, I. Z. Babievskaya and A. M. Abbasov, *Sov. J. Coord. Chem*. **1987**, *13*, 273.
37. F. A. Cotton, M. Extine and L. D. Gage, *Inorg. Chem.* **1978**, *17*, 172.
38. D. S. Martin and H.-W. Huang, *Inorg. Chem.* **1990**, *29*, 3674.
39. H. Chen and F. A. Cotton, *Polyhedron* **1995**, *14*, 2221.
40. M. H. Chisholm and A. M. Macintosh, *J. Chem. Soc., Dalton Trans.* **1999**, 1205.
41. K. Teramoto, Y. Sasaki, K. Migita, M. Iwaizumi and K. Saito, *Bull. Chem. Soc. Jpn.* **1979**, *52*, 466.
42. E. L. Akhmedov, A. S. Kotel'nikova and O. N. Evstaf'eva, *Russ. J. Inorg. Chem*. **1980**, *25*, 1810.
43. I. F. Golovaneva, E. L. Akhmedov and A. S. Kotel'nikova, *Sov. J. Coord. Chem*. **1986**, *12*, 531.
44. I. F. Golovaneva, E. L. Akhmedov, A. S. Kotel'nikova and R. N. Shchelokov, *Dokl. Chem*. **1985**, *284*, 315.
45. G. Snatzke, U. Wagner and H. P. Wolff, *Tetrahedron* **1981**, *37*, 349.
46. J. Engel, R. Geiger, G. Snatzke and U. Wagner, *U., Chem.-Ztg*. **1981**, *105*, 85.
47. J. Omelanczuk and G. Snatzke, *Angew. Chem., Int. Ed. Engl*. **1981**, *20*, 786.
48. A. Svensson, *Chemica Scripta* **1983**, *22*, 157.
49. M. C. Kerby, B. W. Eichhorn, J. A. Creighton and K. P. C. Vollhardt, *Inorg. Chem.* **1990**, *29*, 1319.
50. M. H. Chisholm, J. C. Huffman, S. S. Iyer and M. A. Lynn, *Inorg. Chim. Acta* **1996**, *243*, 283.
51. M. Handa, K. Kasamatsu, K. Kasuga, M. Mikuriya and T. Fujii, *Chem. Lett*. **1990**, 1753.
52. (a) M. Handa, M. Mikuriya, T. Kotera, K. Yamada, T. Nakao, H. Matsumoto and K. Kasuga, *Bull. Chem. Soc. Jpn.* **1995**, *68*, 2567. (b) F. H. Herbstein, S. Hu and M. Kapon, *Acta Crystallogr.* **2002**, *B58*, 884.
53. L. Golic, I. Leban and P. Segedin, *Croat. Chem. Acta*, **1984**, *57*, 565.
54. P. Segedin, *Acta Chim. Slov.* **1995**, *42*, 349.
55. J. M. Matonic, S.-J. Chen, S. P. Perlepes, K. R. Dunbar and G. Christou, *J. Am. Chem. Soc.* **1991**, *113*, 8169.
56. F. A. Cotton and D. G. Lay, *Inorg. Chem.* **1981**, *20*, 935.
57. G. S. Girolami and R. A. Andersen, *Inorg. Chem.* **1982**, *21*, 1318.
58. F. A. Cotton and P. E. Fanwick, *Inorg. Chem.* **1983**, *22*, 1327.
59. X. Ouyang, C. Campana and K. R. Dunbar, *Inorg. Chem.* **1996**, *35*, 7188.
60. C. Campana, K. R. Dunbar and X. Ouyang, *Chem. Commun*. **1996**, 2427.
61. M. Handa, H. Sono, K. Kasamatsu, K. Kasuga, M. Mikuriya and S. Ikenoue, *Chem. Lett*. **1992**, 453.
62. M. Handa, K. Yamada, T. Nakao, K. Kasuga, M. Mikuriya and T. Kotera, *Chem. Lett.* **1993**, 1969.
63. W.-M. Xue, F. E. Kuhn, E. Herdtweck and Q. Li, *Eur. J. Inorg. Chem*. **2001**, 213.
64. M. -C. Suen, Y.-Y. Wu, J.-D. Chen, T.-C. Keng and J.-C. Wang, *Inorg. Chim. Acta* **1999**, *288*, 82.
65. M. Handa, H. Matsumoto, D. Yoshioka, R. Nukada, M. Mikuriya, I. Hiromitsu and K. Kasuga, *Bull. Chem. Soc. Jpn*. **1998**, *71*, 1811.
66. M. Handa, H. Matsumoto, T. Namura, T. Nagaoka, K. Kasuga, M. Mikuriya, T. Kotera and R. Nukada, *Chem. Lett*. **1995**, 903.
67. M. Handa, M. Mikuriya, R. Nukada, H. Matsumoto and K. Kasuga, *Bull. Chem. Soc. Jpn*. **1994**, 67, 3125.
68. F. A. Cotton, L. Labella and M. Shang, *Inorg. Chim. Acta* **1992**, *197*, 149.

Pictiva EX2004
Samsung v Pictiva
IPR2024-01094

69. D. M. Collins, F. A. Cotton and C. A. Murillo, *Inorg. Chem.* **1976**, *15*, 2950.
70. K. Jansen, K. Dehnicke and D. Fenske, *Z. Naturforsch*. **1985**, *40b*, 13.
71. H. Goesmann, D. Fenske, H.-W. Swidersky and K. Dehnicke, *Z. anorg. allg. Chem*. **1988**, *566*, 83.
72. B. Udovic, I. Leban and P. Segedin, *Croat. Chem. Acta* **1999**, *72*, 477.
73. F. A. Cotton and D. de O. Silva, *Polyhedron* **1996**, *15*, 4079.
74. S.-M. Kuang, P. E. Fanwick and R. A. Walton, *Inorg. Chem. Commun*. **2002**, *5*, 134.
75. T. Liwporncharoenvong and R. L. Luck, *Inorg. Chim. Acta*, **2002**, *340*, 147.
76. F. A. Cotton and G. N. Mott, *Inorg. Chim. Acta* **1983**, *70*, 159.
77. F. A. Cotton, L. R. Falvello, A. H. Reid, Jr. and W. J. Roth, *Acta Crystallogr*. **1990**, *C46*, 1815.
78. W. E. Buhro, M. H. Chisholm, K. Folting and J. C. Huffman, *Inorg. Chem.* **1987**, *26*, 3087.
79. W. E. Buhro, M. H. Chisholm, J. D. Martin, J. C. Huffman, K. Folting and W. E. Streib, *J. Am. Chem. Soc*. **1989**, *111*, 8149.
80. F. A. Cotton and T. R. Webb, *Inorg. Chem.* **1976**, *15*, 68.
81. A. Bino, F. A. Cotton and P. E. Fanwick, *Inorg. Chem.* **1979**, *18*, 1719.
82. A. Bino and F. A. Cotton, *J. Am. Chem. Soc*. **1980**, *102*, 3014.
83. A. Bino, F. A. Cotton and P. E. Fanwick, *Inorg. Chem.* **1980**, *19*, 1215.
84. F. Apfelbaum-Tibika and A. Bino, *Inorg. Chem.* **1984**, *23*, 2902.
85. F. Apfelbaum and A. Bino. *Inorg. Chim. Acta* **1989**, *155*, 191.
86. A. Belforte, D. B. Dell'Amico, F. Calderazzo, M. Devillers and U. Englert, *Inorg. Chem.* **1993**, *32*, 2282.
87. T. S. Barnard, F. A. Cotton, L. M. Daniels and C. A. Murillo, *Inorg. Chem. Commun*. **2002**, *5*, 527.
88. F. A. Cotton and D. de O. Silva, *Inorg. Chim. Acta* **1996**, *249*, 57.
89. M. Cindric, V. Vrdoljak, D. Matkovic-Calogovic and B. Kamenar, *Acta Crystallogr.* **1996**, *C52*, 3016.
90. T. Liwporncharoenvong and R. L. Luck, *J. Am. Chem. Soc*. **2001**, *123*, 3615.
91. D. S. Martin, R. A. Newman and P. E. Fanwick, *Inorg. Chem.* **1982**, *21*, 3400.
92. W. K. Bratton, F. A. Cotton, M. Debeau and R. A. Walton, *J. Coord. Chem*. **1971**, *1*, 121.
93. T. R. Webb, J. D. Pollard, G. W. Goodloe and M. L. McKee, *Inorg. Chim. Acta* **1995**, *229*, 127.
94. P. A. Atha, J. C. Campbell, C. D. Garner, I. H. Hillier and A. A. MacDowell, *J. Chem. Soc., Dalton Trans*. **1983**, 1085.
95. (a) D. L. Lichtenberger and C. H. Blevins, II, *J. Am. Chem. Soc*. **1984**, *106*, 1636. (b) D. L. Lichtenberger and J. G. Kristofzski, *J. Am. Chem. Soc*. **1987**, *109*, 3458.
96. B. P. Shehan, M. Kony, R. T. C. Brownlee, M. J. O'Connor and A. G. Wedd, *J. Magn. Reson*. **1985**, *63*, 343.
97. (a) M. H. Chisholm, D. A. Haitko and C. A. Murillo, *J. Am. Chem. Soc.* **1978**, *100*, 6262. (b) M. J. Chetcuti, M. H. Chisholm, K. Folting, D. A. Haitko and J. C. Huffman, *J. Am. Chem. Soc*. **1982**, *104*, 2138.
98. A. Bino and M. Ardon, *J. Am. Chem. Soc*. **1977**, *99*, 6446.
99. P. Salagre and J. E. Sueiras, *Transition Met. Chem*. **1985**, *10*, 191.
100. G. Holste, *Z. anorg. allg. Chem*. **1978**, *438*, 125.
101. A. P. Ketteringham and C. Oldham, *J. Chem. Soc., Dalton Trans*. **1973**, 1067.
102. J. Ribas, G. Jugie and R. Poilblanc, *Transition Met. Chem*. **1983**, *8*, 93.
103. (a) T.-Y. Dong, D. N. Hendrickson, T. R. Felthouse and H.-S. Shieh, *J. Am. Chem. Soc*. **1984**, *106*, 5373. (b) T. R. Felthouse, T.-Y. Dong, D.N. Hendrickson, H.-S. Shieh and M. R. Thompson, *J. Am. Chem. Soc*. **1986**, *108*, 8201.
104. R. S. Drago, J. R. Long and R. Cosmano, *Inorg. Chem.* **1982**, *21*, 2196.
105. G. S. Girolami, V. V. Mainz and R. A. Andersen, *Inorg. Chem.* **1980**, *19*, 805.
106. T. R. Webb and T.-Y. Dong, *Inorg. Chem.* **1982**, *21*, 114.
107. J. San Filippo, Jr and H. J. Sniadoch, *Inorg. Chem.* **1976**, *15*, 2209.
108. B. W. Eichhorn, M. C. Kerby, K. J. Ahmed and J. C. Huffman, *Polyhedron* **1991**, *10*, 2573.
109. A. Sahajpal and P. Thornton, *Polyhedron* **1988**, *7*, 2715.
110. C. D. Garner and R. G. Senior, *J. Chem. Soc., Dalton Trans*. **1975**, 1171.

Pictiva EX2004
Samsung v Pictiva
IPR2024-01094

111. E. L. Akhmedov, A. S. Kotel'nikova and A. N. Smirnov, *Bull. Acad. Sci. USSR* **1981**, 346.
112. E. L. Akhmedov, A. S. Kotel'nikova and O. N. Evstaf'eva, *Sov. J. Coord. Chem*. **1981**, 7, 595.
113. (a) P. A. Koz'min, T. B. Larina and M. D. Surazhskaya, *Koord. Khim*. **1981**, 7, 634. (b) P. A. Koz'min, *Sov. J. Coord. Chem*. **1986**, *12*, 374.
114. D. M. Baird, P. E. Fanwick and T. Barwick, *Inorg. Chem.* **1985**, *24*, 3753.
115. D. M. Baird, K. Y. Shih, J. H. Welch and R. D. Bereman, *Polyhedron* **1989**, *8*, 2359.
116. C. D. Garner, S. Parkes, I. B. Walton and W. Clegg, *Inorg. Chim. Acta* **1978**, *31*, L451.
117. W. Clegg, C. D. Garner, S. Parkes and I. B. Walton, *Inorg. Chem.* **1979**, *18*, 2250.
118. F. A. Cotton, A. H. Reid, Jr and W. Schwotzer, *Inorg. Chem.* **1985**, *24*, 3965.
119. L. J. Farrugia, A. McVitie and R. D. Peacock, *Inorg. Chem*. **1988**, *27*, 1257.
120. M. B. Hursthouse and K. M. A. Malik, *Acta Crystallogr.* **1979**, *835*, 2709.
121. S. M. Beshouri, P. E. Fanwick, I. P. Rothwell, *Inorg. Chim. Acta* **1987**, *129*, 87.
122. G. S. Girolami, V. V. Mainz and R. A. Andersen, *J. Am. Chem. Soc.* **1982**, *104*, 2041.
123. M. L. H. Green, G. Parkin, J. Bashkin, J. Fail and K. Prout, *J. Chem. Soc., Dalton Trans*. **1982**, 2519.
124. F. A. Cotton and G. L. Powell, *Polyhedron* **1985**, *4*, 1669.
125. J. D. Arenivar, V. V. Mainz, H. Ruben. R. A. Andersen and A. Zalkin, *Inorg. Chem*. **1982**, *21*, 2649.
126. F. A. Cotton and M. Matusz, *Polyhedron* **1988**, 7, 2201.
127. P. A. Bates, A. J. Nielson and J. M. Waters, *Polyhedron* **1987**, *6*, 2111.
128. F. A. Cotton, W. H. Ilsley and W. Kaim, *Inorg. Chim. Acta* **1979**, *37*, 267.
129. D. M. Collins. F. A. Cotton and C. A. Murillo, *Inorg. Chem*. **1976**, *15*, 1861.
130. F. A. Cotton, W. H. Ilsley and W. Kaim, *Inorg. Chem*. **1981**, *20*, 930.
131. F. A. Cotton and G. N. Mott, *Organometallics* **1982**, *1*, 302.
132. F. Allaire and A. L. Beauchamp, *Inorg. Chim. Acta* **1989**, *156*, 241.
133. J. Lamotte, O. Dideberg, L. Dupont and P. Durbut, *Cryst. Struct. Commun*. **1981**, *10*, 59.
134. (a) B. W. Eichhorn, M. C. Kerby, R. C. Haushalter and K. P. C. Vollhardt, *Inorg. Chem*. **1990**, *29*, 723. (b) B. W. Eichhorn, R. C. Haushalter, F. A. Cotton and B. Wilson, *Inorg. Chem*. **1988**, *27*, 4084.
135. F. A. Cotton and W. H. Ilsley. *Inorg. Chem*. **1981**, *20*, 572.
136. K. R. Breakell, S. J. Rettig, A. Storr and J. Trotter, *Can. J. Chem*. **1983**, *61*, 1659.
137. W.-M. Xue, F. E Kühn, G. Zhang, E. Herdtweck and G. Raudaschl-Sieber, *J. Chem. Soc., Dalton Trans.* **1999**, 4103.
138. W.-M. Xue, F. E Kühn, G. Zhang, E. Herdtweck and G. Raudaschl-Sieber, *J. Chem. Soc., Dalton Trans.* **1999**,4103.
139. M.-C. Suen, S.-F. Chiang, J.-D. Chen, S.-S. Chern and C.-D. Hsiao, *J. Chin. Chem. Soc. (Taipei)* **1998**, *45*, 263.
140. T. Tanase, T. Igoshi and Y. Yamamoto, *Inorg, Chim. Acta* **1997**, *256*, 61.
141. T. Tanase, T. Igoshi, K. Kobayashi and Y. Yamamoto, *J. Chem. Res.* **1998**, *538*, 2140.
142. W.-M. Xue, F.E. Kuhn, G. Zhang and E. Herdtweck, *J. Organomet. Chem.* **2000**, *596*, 177.
143. J.-D. Chen, F. A. Cotton, and S.-J. Kang, *Inorg. Chim. Acta* **1991**, *190*, 103.
144. G. Zou and T. Ren, *Inorg. Chim. Acta* **2000**, *304*, 305.
145. Y.-Y. Wu, J.-D. Chen, L.-S. Liou and J.-C. Wang, *Inorg. Chim Acta* **1997**, *258*, 193.
146. F. A. Cotton and F. E. Kühn, *Inorg. Chim. Acta* **1996**, *252*, 257.
147. F. A. Cotton, F. E. Kühn and A. Yokochi, *Inorg. Chim. Acta* **1996**, *252*, 251.
148. G.-W. Tseng, M.-C. Suen, J.-D. Chen, J.-J. Huang, Y. W. Chen-Yang, T.-C. Keng and J.-C. Wang, *J. Chin. Chem. Soc. (Taipei)* **1999**, *46*, 545.
149. (a) C. S. Campos-Fernández, X. Ouyang and K. R. Dunbar, *Inorg. Chem.* **2000**, *39*, 2432. (b) C. S. Campos-Fernández, L. M. Thomson, J. R. Galán-Mascarós, X. Ouyang and K. R. Dunbar, *Inorg. Chem.* **2002**, *41*, 1523.
150. M. Mintert and W. S. Sheldrick, *Chem. Ber.* **1996**, *129*, 683.
151. H. Nakano, A. Nakamura and K. Mashima, *Inorg. Chem. 1996, 35*, 4007.

Pictiva EX2004
Samsung v Pictiva
IPR2024-01094

152. (a) F. A. Cotton, L. M. Daniels, C. Lin and C. A. Murillo, *Chem. Commun.* **1999**, 841. (b) F. A. Cotton, C. Lin and C. A. Murillo, *Inorg. Chem.* **2001**, *40*, 6413.
153. (a) J. A. Acho and S. J. Lippard, *Inorg. Chim. Acta* **1995**, *229*, 5. (b) J. A. Acho, T. Ren, J. W. Yun and S. J. Lippard, *Inorg. Chem.* **1995**, *34*, 5226.
154. Y.-Y. Wu, J.-D. Chen, L.-S. Liou and J.-C. Wang, *Inorg. Chim. Acta* **2002**, *336*, 71.
155. S. L. Bartley, S. N. Bernstein and K. R. Dunbar, *Inorg. Chim. Acta* **1993**, *213*, 213.
156. K. Mashima, H. Nakano and A. Nakamura, *J. Am. Chem. Soc.* **1993**, *115*, 11632.
157. S.-M.Kuang, P. E. Fanwick and R. A. Walton, *Inorg. Chim. Acta* **2000**, *305*, 102.
158. F. A. Cotton, J. L. Eglin, and K.J. Wiesinger, *Inorg. Chim. Acta* **1992**, *195*, 11.
159. C.-T. Lee, S.-F. Chiang, C.-T. Chen, J.-D. Chen and C. D. Hsiao, *Inorg. Chem.* **1996**, *35*, 2930.
160. P. Agaskar and F. A. Cotton, *Inorg. Chim. Acta* **1984**, *83*, 33.
161. M.-C. Suen, G.-W. Tseng, J.-D. Chen, T.-C. Keng and J.-C. Wang, *Chem. Commun.* **1999**, 1185.
162. G. Zhang, J. Zhao, G. Raudascho-Sieber, E. Herdtweck and F. E. Kühn, *Polyhedron* **2002**, *21*, 1737.
163. K. J. Snowden, T. R. Webb and B. Snoddy, *Inorg. Chem.* **1993**, *32*, 3541.
164. C.-Y. Pan, M.-C.Suen, Y.-Y. Wu, J.-D. Chen, T.-C. Keng and J.-C. Wang, *Inorg. Chim. Acta* **2001**, *312*, 111.
165. J. A. Potenza, R. J. Johnson and J. San Filippo, Jr, *Inorg. Chem*. **1976**, *15*, 2215.
166. M. A. Greaney and E. I. Stiefel, *Chem. Commun.* **1992**, 1679.
167. A. Zinn, F. Weller and K. Dehnicke, *Z. anorg. allg. Chem.* **1991**, *594*, 106.
168. D. I. Arnold, F. A. Cotton and F. E. Kühn, *Inorg. Chem.* **1996**, *35*, 4733.
169. R. H. Cayton, M. H. Chisholm, E. F. Putilina, K. Folting, J. C. Huffman and K. G. Moodley, *Inorg. Chem.* **1992**, *31*, 2928.
170. R. H. Cayton, S. T. Chacon, M. H. Chisholm and K. Folting, *Polyhedron,* **1993**, *12*, 415.
171. A. Bino and F. A. Cotton, *Inorg. Chem*. **1979**, *18*, 1381.
172. W. Cen, P. Linderfeld and T. P. Fehlner, *J. Am. Chem. Soc.* **1992**, *114*, 5451.
173. T. Liwporncharoenvong, T. Lu and R. L. Luck, *Inorg. Chim. Acta* **2002**, *329*, 51.
174. E. F. Day, J. C. Huffman, K. Folting and G. Christou, *J. Chem. Soc., Dalton Trans.* **1997**, 2837.
175. E. F. Day, C. A. Crawford, K. Folting, K. R. Dunbar and G. Christou, *J. Am. Chem. Soc.* **1994**, *116*, 9339.
176. D. M. Baird, R. Hassen and W. K. Kim, *Inorg. Chim. Acta* **1987**, *130*, 39.
177. D. M. Baird and K.-Y. Shih, *Polyhedron* **1991**, *10*, 229.
178. J. M. Mayer and E. H. Abbott, *Inorg. Chem.* **1983**, *22*, 2774.
179. F. A. Cotton and K. J. Wiesinger, *Inorg. Chem.* **1991**, *30*, 871.
180. J. Telser and R. S. Drago, *Inorg. Chem.* **1984**, *23*, 1798.
181. W. Clegg, G. Pimblett and C. D. Garner, *Polyhedron*, **1986**, *5*, 31.
182. G. Pimblett, C. D. Garner and W. Clegg, *J. Chem. Soc., Dalton Trans*. **1986**, 1257.
183. J. M. Calas, R. H. Cayton and M. H. Chisholm, *Inorg. Chem.* **1991**, *30*, 358.
184. H.-J. Kuppers and K. Wieghardt, *Polyhedron* **1989**, *8*, 1770.
185. R. A. Andersen, R. A. Jones, G. Wilkinson, M. B. Hursthouse and K. M. Abdul Malik, *J. Chem. Soc., Chem. Commun*. **1977**, 283.
186. R. A. Anderson, R. A. Jones and G. Wilkinson, *J. Chem. Soc., Dalton Trans*. **1978**, 446.
187. R. A. Jones and G. Wilkinson, *J. Chem. Soc., Dalton Trans*. **1979**, 472.
188. V. V. Mainz and R. A. Andersen, *Inorg. Chem*. **1980**, *19*, 2165.
189. T. R. Ryan and R. E. McCarley, *Inorg. Chem*. **1982**, *21*, 2072.
190. M. Bakir and R. A. Walton, *Polyhedron* **1988**, *7*, 1279.
191. L. Hocks, P. Durbut and Ph. Teyssie, *J. Mol. Catal*. **1980**, *7*, 75.
192. K. J. Cavell. C. D. Garner, J. A. Martinho-Simoss. G. Pilcher, H. Al-Samman, H. A. Skinner, G. Al-Tekhin. I. B. Walton and M. T. Zafarani-Moattar, *J. Chem. Soc., Faraday Trans. 1* **1981**, *77*, 2927.
193. C. D. Garner and R. G. Senior, *J. Chem. Soc., Dalton Trans*. **1976**, 1041.
194. M. C. Kerby, B. W. Eichhorn, L. Dovikew and K. P. C. Vollhardt, *Inorg. Chem*. **1991**, *30*, 156.

Pictiva EX2004
Samsung v Pictiva
IPR2024-01094

195. F. A. Cotton, B. A. Frenz, E. Pedersen and T. R. Webb, *Inorg. Chem*. **1991**, *30*, 156.
196. F. A. Cotton, B. A. Frenz and T. R. Webb, *J. Am. Chem. Soc.* **1973**, *95*, 4431.
197. (a) A. Bino and F. A. Cotton, *Angew. Chem., Int. Ed. Engl.* **1979**, *18*, 462. (b) A. Bino and F. A. Cotton, *Inorg. Chem.* **1979**, *18*, 3562.
198. J. Ribas, R. Poilblanc, C. Sourisseau, X. Solans, J. L. Brianso and C. Miravitlles, *Transition Met. Chem.* **1983**, *8*, 244.
199. (a) J. R. Morrow and W. C. Trogler, *Inorg. Chem.* **1989**, *28*, 615. (b) T.-L. Hsu, I.-J. Chang, D. L. Ward and D. G. Noccera, *Inorg. Chem.* **1994**, *33*, 2932.
200. J. H. Burk, G. E. Whitwell, II, J. T. Lemley and J. M. Burlitch, *Inorg. Chem.* **1983**, *22*, 1306.
201. A. R. Bowen and H. Taube, *J. Am. Chem. Soc*. **1971**, *93*, 3287.
202. A. R. Bowen and H. Taube, *Inorg. Chem.* **1974**, *13*, 2245.
203. C. L. Angell, F. A. Cotton, B. A. Frenz and T. R. Webb, *J. Chem. Soc., Chem. Commun.* **1973**, 399.
204. A. Bino and D. Gibson, *J. Am. Chem. Soc.* **1980**, *102*, 4277.
205. D. K. Erwin, G. L. Geoffroy, H. B. Gray, G. S. Hammond, E. I. Solomon, W. C. Trogler and A. A. Zagars, *J. Am. Chem. Soc.* **1977**, *99*, 3620.
206. W. C. Trogler, D. K. Erwin, G. L. Geoffroy and H. B. Gray, *J. Am. Chem. Soc.* **1978**, *100*, 1160.
207. A. Pernick and M. Ardon, *J. Am. Chem. Soc.* **1975**, *97*, 1255.
208. A. Bino and F. A. Cotton, *Inorg. Chem.* **1979**, *18*, 1159.
209. A. Bino, F. A. Cotton, D. O. Marler, S. Farquharson, B. Hutchinson, B. Spencer and J. Kincaid, *Inorg. Chim. Acta* **1987**, *133*, 295.
210. A. Bino, *Inorg. Chem.* **1981**, *20*, 623.
211. F. A. Cotton and A. H. Reid, Jr, *Nouv. J. Chim.* **1984**, *8*, 203.
212. E. Hochberg and E. H. Abbott, *Inorg. Chem.* **1978**, *17*, 506.
213. E. H. Abbott, F. Schoenewolf, Jr. and T. Backstrom, *J. Coord. Chem.* **1974**, *3*, 255.
214. J. Cragel, Jr, V. B. Pett, M. D. Glick and R. E. DeSimone, *Inorg. Chem.* **1978**, *17*, 2885.
215. M. D. Hopkins, V. M. Miskowski and H. B. Gray, *J. Am. Chem. Soc.* **1986**, *108*, 959.
216. I.-J. Chang and D. G. Nocera, *J. Am. Chem. Soc.* **1987**, *109*, 4901.
217. C. M. Partigianoni, I.-J. Chang and D. G. Nocera, *Coord. Chem. Rev.* **1990**, *97*, 105.
218. I.-J. Chang and D. G. Nocera, *Inorg. Chem.* **1989**, *28*, 4311.
219. W. Clegg, C. D. Garner, L. Akhter and M. H. Al-Samman, *Inorg. Chem.* **1983**, *22*, 2466.
220. F. A. Cotton, P. E. Fanwick, R. H. Niswander and J. C. Sekutowski, *J. Am. Chem. Soc.* **1978**, *100*, 4725.
221. P. E. Fanwick, *Inorg. Chem.* **1985**, *24*, 258.
222. F. A. Cotton, W. H. Ilsley and W. Kaim, *Inorg. Chem.* **1980**, *19*, 1453.
223. F. A. Cotton, L. R. Falvello, S. Han and W. Wang, *Inorg. Chem.* **1983**, *22*, 4106.
224. F. A. Cotton, R. H. Niswander and J. C. Sekutowski, *Inorg. Chem.* **1979**, *18*, 1152.
225. K. Mashima, N. Nakano and A. Nakamura, *J. Am. Chem. Soc.* **1996**, *118*, 9083.
226. K. Mashima, N. Nakano, T. Mori, H. Takaya and A. Nakamura, *Chem. Lett*. **1992**, 185.
227. K. Mashima, A. Fukumoto, N. Nakano, Y. Kaneda, K. Tami and A. Nakamura, *J. Am. Chem. Soc.* **1998**, *120*, 12151.
228. W. S. Sheldrick and M. Mintert, *Inorg. Chim. Acta* **1994**, *219*, 23.
229. D. L. Lichtenberger, J. G. Kristofzski and M. A. Bruck, *Acta Crystallogr.* **1988**, *C44*, 1523.
230. A. Bino, F. A. Cotton and W. Kaim, *Inorg. Chem.* **1979**, *18*, 3030.
231. F. A. Cotton, W. H. Ilsley, and W. Kaim, *Inorg. Chem.* **1980**, *19*, 3586.
232. F. A. Cotton, W. H. Ilsley and W. Kaim, *J. Am. Chem. Soc.* **1980**, *102*, 3475.
233. S. Baral, F. A. Cotton and W. H. Ilsley, *Inorg. Chem.* **1981**, *20*, 2696.
234. S. Baral, F. A. Cotton, W. H. Ilsley and W. Kaim, *Inorg. Chem.* **1982**, *21*, 1644.
235. P. E. Fanwick, J. S. Qi, Y.-P. Wu and R. A. Walton, *Inorg. Chim. Acta* **1990**, *168*, 159.
236. F. A. Cotton, R. H. Niswander and J. C. Sekutowski, *Inorg. Chem.* **1979**, *18*, 1149.
237. H. P. M. M. Ambrosius, F. A. Cotton, L. R. Falvello, H. T. J. M. Hintzen, T. J. Melton, W. Schwotzer, M. Tomas and J. G. M. Van Der Linden, *Inorg. Chem.* **1984**, *23*, 1611.
238. F. A. Cotton, W. H. Ilsley and W. Kaim, *Inorg. Chem.* **1979**, *18*, 2717.

Pictiva EX2004
Samsung v Pictiva
IPR2024-01094

239. F. A. Cotton, R. H. Niswander and J. C. Sekutowski, *Inorg. Chem.* **1978**, *17*, 3541.
240. A. R. Chakravarty, F. A. Cotton and E. S. Shamshoum, *Inorg. Chem.* **1984**, *23*, 4216.
241. K. Mashima, H. Nakano and A. Nakamura, *J. Am. Chem. Soc.* **1993**, *115*, 11632.
242. F. A. Cotton, L. M. Daniels, S. C. Haefner and F. E. Kühn, *Inorg. Chim. Acta* **1999**, *287*, 159.
243. F. A. Cotton, L M. Daniels, C. A. Murillo and X. Wang, *Polyhedron* **1998**, *17*, 2781.
244. B. E. Bursten, F. A. Cotton, A. H. Cowley, B. E. Hanson, M. Lattman and G. G. Stanley, *J. Am. Chem. Soc.* **1979**, *101*, 6244.
245. P. E. Fanwick, B. E. Bursten and G. B. Kaufmann, *Inorg. Chem.* **1985**, *24*, 1165.
246. F. A. Cotton and B. E. Hanson, *Inorg. Chem.* **1978**, *17*, 3237.
247. D. DeMarco, T. Nimry and R. A. Walton, *Inorg. Chem.* **1980**, *19*, 575.
248. W. S. Harwood, S. M. Kennedy, F. E. Lytle. J.-S. Qi and R. A. Walton, *Inorg. Chem.* **1987**, *26*, 1784.
249. F. A. Cotton, L. M. Daniels, E. A. Hillard and C. A. Murillo, *Inorg. Chem.* **2002**, *41*, 2466.
250. F. A. Cotton, T. Inglis, M. Kilner and T. R. Webb, *Inorg. Chem.* **1975**, *14*, 2023.
251. F. A. Cotton, X. Feng, and M. Matusz, *Inorg. Chem.* **1989**, *28*, 594.
252. F. A. Cotton, G. W. Rice and J. C. Sekutowski, *Inorg. Chem.* **1979**, *18*, 1143.
253. C. Lin, J. D. Protasiewicz, E. T. Smith and T. Ren, *Inorg. Chem.* **1996**, *35*, 6422.
254. C. Lin, J. D. Protasiewicz, E. T. Smith and T. Ren, *Chem. Commun.* **1995**, 2257.
255. M. A. Lynn, H. D. Selby, M. D. Carducci, M. A. Bruck, C. Grittini and D. L. Lichtenberger, *Acta Crystallogr.* **2001**, *57E*, m57.
256. M. A. Lynn, H. D. Selby, M. D. Carducci, M. A. Bruck, C. Grittini and D. L. Lichtenberger, *Acta Crystallogr.* **2001**, *57E*, m70.
257. F.A. Cotton, L. M. Daniels, C. A. Murillo and H.-C. Zhou, *Inorg. Chim. Acta* **2000**, *300-302*, 319.
258. F. A. Cotton, C. A. Murillo, L. E. Roy and H.-C. Zhou, *Inorg. Chem.* **2000**, *39*, 1743.
259. R. Clérac, F. A. Cotton, K. R. Dunbar, C. A. Murillo and X. Wang, *Inorg, Chem.* **2001**, *40*, 420.
260. L. M. Daniels, P. Lei, C. A. Murillo and X. Wang, *Inorg. Chem.* **2001**, *40*,2778.
261. P. J. Bailey, S. F. Bone, L. A. Mitchell, S. Parsons, K. J. Taylor and L. J. Yellowlees, *Inorg. Chem.* **1997**, *36*, 867.
262. F. A. Cotton and D. J. Timmons, *Polyhedron* **1998**, *17*, 179.
263. F. A. Cotton, L. M. Daniels, C. Lin and C. A. Murillo, *Inorg. Chim. Acta* **2003**, *347*, 1.
264. M. H. Chisholm, F. A. Cotton, L. M. Daniels, K. Folting, J. C. Huffman, S. S. Iyer, C. Lin, A. M. Macintosh and C. A. Murillo, *Dalton Trans.* **1999**, *1387*.
265. M. H. Chisholm, F. A. Cotton, L. M. Daniels, K. Folting, J. C. Huffman, S. S. Iyer, C. Lin, A. M. Macintosh and C. A. Murillo, *Dalton Trans.* **1999**, *1387*.
266. F. A. Cotton, P. Lei, C. A. Murillo and L.-S. Wang, *Inorg. Chim. Acta* **2003**, *349*, 165.
267. W. H. DeRoode, K. Vrieze, E. A. Koerner von Gustorf and A. Ritter, *J. Organomet. Chem.* **1977**, *135*, 183.
268. T. Ren, *Coord. Chem. Rev.* **1998**, *175*, 43.
269. D. F. Steele and T. A. Stephenson, *Inorg. Nucl. Chem. Lett.* **1973**, *9*, 777.
270. G. Holste, *Z. anorg. allg. Chem.* **1976**, *425*, 57.
271. M. Nakamoto, K. Tanaka and T. Tanaka, *Inorg. Chim. Acta* **1987**, *132*, 193.
272. F. A. Cotton, P. E. Fanwick, R. H. Niswander and J. C. Sekutowski, *Acta Chem. Scand.* **1978**, *A32*, 663.
273. P. Vella and J. Zubieta, *J. Inorg. Nucl. Chem.* **1978**, *40*, 477.
274. L. Ricard, P. Karagiannidis and R. Weiss, *Inorg. Chem.* **1973**, *12*, 2179.
275. T. R. Webb, C.-C. Cheng, E. Heavlin and R. A. Little, *Inorg. Chim. Acta* **1981**, *49*, 107.
276. J. A. Goodfellow and T. A. Stephenson, *Inorg. Chim. Acta* **1980**, *44*, L45.
277. L. Ricard, J. Estienne and R. Weiss, *Inorg. Chem.* **1973**, *12*, 2182.
278. F. A. Cotton, M. W. Extine and R.H. Niswander, *Inorg. Chem.* **1978**, *17*, 692.
279. D. M. Baird and S. D. Croll, *Polyhedron* **1986**, *5*, 1931.
280. D. M. Baird, A. L. Rheingold, S. D. Croll and A. T. DiCenso, *Inorg. Chem.* **1986**, *25*, 3458.
281. A. D. Calcaterra, S. B. Kimble, T. L. Groy and T. M. Brown, *Inorg. Chem. Acta* **1998**, *267*, 101.

Pictiva EX2004
Samsung v Pictiva
IPR2024-01094

282. R. Grenz, F. Gotzfried, U. Nagel and W. Beck, *Chem. Ber.* **1986**, *119*, 1217.
283. M. Q. Islam, W. E. Hill and T. R. Webb, *J. Fluorine Chem.* **1990**, *48*, 429.
284. F. A. Cotton, N. F. Curtis, B. F. G. Johnson and W. R. Robinson, *Inorg. Chem.* **1965**, *4*, 326.
285. J. V. Brenčič and F. A. Cotton, *Inorg. Chem.* **1969**, *8*, 2698.
286. J. V. Brenčič and F. A. Cotton, *Inorg. Chem.* **1970**, *9*, 346.
287. I. Leban and P. Segedin, *Inorg. Chim. Acta* **1984**, *85*, 181.
288. F. A. Cotton, J. H. Matonic and D. de O. Silva, *Inorg. Chim. Acta* **1995**, *234*, 115.
289. Reference deleted.
290. J. V. Brenčič, I. Leban and P. Segedin, *Z. anorg. allg. Chem.* **1976**, *427*, 85.
291. A. Bino, F. A. Cotton and P. E. Fanwick, *Inorg. Chem.* **1979**, *18*, 3558.
292. F. A. Cotton, J. M. Troup, T. R. Webb, D. H. Williamson and G. Wilkinson, *J. Am. Chem. Soc.* **1974**, *96*, 3824.
293. J. V. Brenčič, L. Golic and P. Segedin, *Inorg. Chim. Acta* **1982**, *57*, 247.
294. J. V. Brenčič, I. Leban and P. Segedin, *Z. anorg. allg. Chem*. **1978**, *444*, 211.
295. J. V. Brenčič and P. Segedin, *Z. anorg. allg. Chem.* **1976**, *423*, 266.
296. J. V. Brenčič and P. Segedin, *Inorg. Chim. Acta* **1978**, *29*, L281.
297. J. V. Brenčič and L. Golic, *J. Cryst. Mol. Struct.* **1977**, *7*, 183.
298. A. Bino and F. A. Cotton, *J. Am. Chem. Soc.* **1979**, *101*, 4150.
299. A. Bino and F. A. Cotton, *Inorg. Chem.* **1979**, *18*, 2710.
300. J. V. Brenčič and F. A. Cotton, *Inorg. Synth.* **1972**, *13*, 170.
301. J. V. Brenčič and F. A. Cotton, *Inorg. Chem.* **1970**, *9*, 351.
302. R. J. H. Clark and M. L. Franks, *J. Am. Chem. Soc.* **1975**, *97*, 2691.
303. J. V. Brenčič, D. Dobcnik and P. Segedin, *Monatsh. Chem.* **1974**, *105*, 944.
304. (a) C. D. Garner and R. G. Senior, *J. Chem. Soc., Chem. Commun.* **1974**, 580. (b) C. D. Garner, R. G. Senior and T. J. King, *J. Am. Chem. Soc.* **1976**, *98*, 647.
305. J. V. Brenčič, D. Dobcnik and P. Segedin, *Monatsh. Chem.* **1976**, *107*, 395.
306. V. K. Ceylan, C. Sourisseau and J. V. Brenčič, *J. Raman Spectrosc.* **1985**, *16*, 128.
307. R. J. Mureinik, *Inorg. Chim. Acta* **1977**, *23*, 103.
308. S. L. Bartley, S. N. Bernstein and K. R. Dunbar, *Inorg. Chim. Acta* **1993**, *213*, 213.
309. I. M. Bell, R. J. H. Clark and D. G. Humphrey, *J. Chem. Soc., Dalton Trans*. **1997**, 1225.
310. R. J. H. Clark, S. Firth, A. Sella, V. M. Miskowski and M. D. Hopkins, *J. Chem. Soc., Dalton Trans*. **2000**, 2928.
311. R. G. Nuzzo, H. J. Simon and J. San Filippo, Jr., *J. Org. Chem.* **1977**, *42*, 568.
312. M. J. Bennett, J. V. Brenčič and F. A. Cotton, *Inorg. Chem.* **1969**, *8*, 1060.
313. F. A. Cotton, B. A. Frenz and Z. C. Mester, *Acta Crystallogr.* **1973**, *B15*, 15.
314. G. B. Allison, I. R. Anderson, W. van Bronswyk and J. C. Sheldon, *Aust. J. Chem.* **1969**, *22*, 1097.
315. F. A. Cotton and B. J. Kalbacher, *Inorg. Chem.* **1976**, *15*, 522.
316. A. Bino and F. A. Cotton, *Angew. Chem., Int. Ed. Engl.* **1979**, *18*, 332.
317. A. Bino, B. E. Bursten, F. A. Cotton and A. Fang, *Inorg. Chem.* **1982**, *21*,3755.
318. F. A. Cotton, P. C. W. Leung, W. J. Roth, A. J. Schultz and J. M. Williams, *J. Am. Chem. Soc.* **1984**, *106*, 117.
319. A. Bino, *Inorg. Chim. Acta* **1985**, *101*, L7.
320. A. Bino and S. Luski, *Inorg. Chim. Acta* **1986**, *86*, L35.
321. A. M. Mityukov, V. V. Zelentsov, P. E. Kazin, N. A. Subbotina, A. I. Zhirov, and M. G. Felin, *Russ. J. Inorg. Chem.* **1987**, *32*, 1706.
322. A. M. Mityukov, V. V. Zelentsov, N. A. Subbotina, P. E. Kazin, A. I. Zhirov and M. G. Felin, *Russ. J. Inorg. Chem.* **1998**, *33*, 351.
323. J. L. Pierce, D. DeMarco and R. A. Walton, *Inorg. Chem.* **1983**, *22*, 9.
324. V. Katovic and R. E. McCarley, *J. Am. Chem. Soc.* **1978**, *100*, 5586.
325. V. Katovic and R. E. McCarley, *Inorg. Chem.* **1978**, *17*, 1268.
326. F. A. Cotton and E. Pedersen, *Inorg. Chem.* **1975**, *14*, 399.

Pictiva EX2004
Samsung v Pictiva
IPR2024-01094

327. R. T. Carlin and R. A. Osteryoung, *Inorg. Chem.* **1988**, *27*, 1482.
328. R. T. Carlin and R. A. Osteryoung, *Inorg. Chem.* **1988**, *27*, 3675.
329. S. S. Miller and A. Haim. *J. Am. Chem. Soc.* **1983**, *105*, 5624.
330. C. Mertis, M. Kravaritous, A. Shehadeh and D. Katakis, *Polyhedron* **1987**, *6*, 1975.
331. H. D. Glicksman, A. D. Hamer, T. J. Smith and R. A. Walton, *Inorg. Chem.* **1976**, *15*, 2205.
332. G. B. Allison, I. R. Anderson and J. C. Sheldon, *Aust. J. Chem.* **1969**, *22*, 1091.
333. W. W. Beers and R. E. McCarley, *Inorg. Chem.* **1985**, *24*, 472.
334. G. Holste and H. Schafer, *J. Less-Common Met.* **1970**, *20*, 164.
335. A. D. Hamer and R. A. Walton, *Inorg. Chem*. **1974**, *13*, 1446.
336. A. P. Mazhara, A. A. Opalovskii, V. E. Fedorov and S. D. Kirik, *Russ. J. Inorg. Chem.* **1977**, *22*, 991.
337. H. D. Glicksman and R. A. Walton, *Inorg. Chem.* **1978**, *17*, 200.
338. S. A. Ryabov, A. S. Alikhanyan, V. D. Butskii and V. S. Pervov, *Russ. J. Inorg. Chem.* **1989**, *34*, 570.
339. F. A. Cotton, E. V. Dikarev and S. Herrero, *Inorg. Chem.* **1998**, *37*, 5862.
340. H. D. Glicksman and R. A. Walton, *Inorg. Chem.* **1978**, *17*, 3197.
341. S. Stensvad, B. J. Helland, M. W. Babich, R. A. Jacobson and R. E. McCarley, *J. Am. Chem. Soc.* **1978**, *100*, 6257.
342. J. Latorre, J. Soto, P. Salagre and J. E. Sueiras, *Transition Met. Chem.* **1984**, *9*, 447.
343. P. Salagre, J. E. Sueiras, X. Solans and G. Germain, *J. Chem. Soc., Dalton Trans.* **1985**, 2263.
344. D. A. Edwards and J.J. Maguire, *Inorg. Chim. Acta* **1977**, *25*, L47.
345. J. E. Armstrong, D. A. Edwards, J. J. Maguire and R. A. Walton, *Inorg. Chem.* **1979**, *18*, 1172.
346. K. R. Millington, S. R. Wade. G. R. Willey and M. G. B. Drew, *Inorg. Chim. Acta* **1984**, *89*, 185.
347. J. San Filippo, Jr, H. J. Sniadoch and R. L. Grayson, *Inorg. Chem.* **1974**, *13*, 2121.
348. J. V. Brenčič, D. Dobcnik and P. Segedin, *Monatsh. Chem.* **1974**, *105*, 142.
349. J. V. Brenčič, L. Golic, I. Leban and P. Segedin, *Monatsh. Chem.* **1979**, *110*, 1221.
350. K. W. Ewing and S. I. Shupack, *Polyhedron* **1985**, *4*, 2069.
351. F. A. Cotton, E. V. Dikarev, S. Herrero and B. Modec, *Inorg. Chem*. **1999**, *38*, 4882.
352. F. A. Cotton, E. V. Dikarev and S. Herrero, *Inorg. Chem*. **1999**, *38*, 2649.
353. F. A. Cotton and R. Poli, *J. Am. Chem. Soc.* **1988**, *110*, 830.
354. D. A. Edwards, G. Uden, W. S. Mialki and R. A. Walton, *Inorg. Chim. Acta* **1980**, *40*, 25.
355. T. J. Barder, F. A. Cotton, G. L. Powell, S. M. Tetrick and R. A. Walton, *J. Am. Chem. Soc.* **1984**, *106*, 1323.
356. F. A. Cotton, M. W. Extine, T. R. Felthouse, B. W. Kolthammer and D. G. Lay, *J. Am. Chem. Soc.* **1981**, *103*, 4040.
357. J. San Filippo, Jr, *Inorg. Chem.* **1972**, *11*, 3140.
358. F. A. Cotton, L. M. Daniels, G. L. Powell, A. J. Kahaian, T. J. Smith and E. F. Vogel, *Inorg. Chim. Acta* **1988**, *144*, 109.
359. E. Carmona-Guzman and G. Wilkinson, *J. Chem. Soc., Dalton Trans.* **1977**, 1716.
360. F. A. Cotton and R. Poli, *J. Am. Chem. Soc.* **1986**, *108*, 5628.
361. F. A. Cotton and R. Poli, *Inorg. Chem.* **1986**, *25*, 3624.
362. F. A. Cotton and R. Poli, *Inorg. Chem.* **1987**, *26*, 3228.
363. F. A. Cotton, J. Czuchajowska and R. L. Luck, *J. Chem Soc., DaltonTrans.* **1991**, 579.
364. F. A. Cotton, E. V. Dikarev and S. Herrero, *Inorg. Chem*. **1998**, *37*, 490.
365. R. N. McGinnis, T. R. Ryan and R. E. McCarley, *J. Am. Chem. Soc.* **1978**, *100*, 7900.
366. M. D. Hopkins, W. P. Schaefer, M. J. Bronikowski, W. H. Woodruff, V. M. Miskowski, R. F. Dallinger and H. B. Gray, *J. Am. Chem. Soc.* **1987**, *109*, 408.
367. F. A. Cotton, L. R. Falvello, W. S. Harwood, G. L. Powell and R. A. Walton, *Inorg. Chem.* **1986**, *25*, 3949.
368. S. A. Best, T. J. Smith and R. A. Walton, *Inorg. Chem.* **1978**, *17*, 99.
369. E. H. Abbott, K. S. Bose, F. A. Cotton, W. T. Hall and J. C. Sekutowski, *Inorg. Chem.* **1978**, *17*, 3240.

Pictiva EX2004
Samsung v Pictiva
IPR2024-01094

370. F. L. Campbell, III, F. A. Cotton and G. L. Powell, *Inorg. Chem.* **1984**, *23*, 4222.
371. F. A. Cotton, K. R. Dunbar and R. Poli, *Inorg. Chem.* **1986**, *25*, 3700.
372. F. A. Cotton and G. L. Powell, *Inorg. Chem.* **1983**, *22*, 1507.
373. F. L. Campbell, III, F. A. Cotton and G. L. Powell, *Inorg. Chem.* **1985**, *24*, 177.
374. F. L. Campbell, III, F. A. Cotton and G. L. Powell, *Inorg. Chem.* **1985**, *24*, 4384.
375. F. A. Cotton and S. Kitagawa, *Inorg. Chem.* **1987**, *26*, 3463.
376. N. F. Cole, D. R. Derringer, E. A. Fiore, D. J. Knoechel, R. K. Schmitt and T. J. Smith, *Inorg. Chem.* **1985**, *24*, 1978.
377. P. A Agaskar, F. A. Cotton, D. R. Derringer, G. L. Powell, D. R. Root and T. J. Smith, *Inorg. Chem.* **1985**, *24*, 2786.
378. P. A. Agaskar and F. A. Cotton, *Inorg. Chem.* **1984**, *23*, 3383.
379. F. A. Cotton, K. R. Dunbar and M. Matusz, *Inorg. Chem.* **1986**, *25*, 3641.
380. M. Bakir, F. A. Cotton, L. R. Falvello, C. Q. Simpson and R. A. Walton, *Inorg. Chem.* **1988**, *27*, 4197.
381. F. A. Cotton and S. Kitagawa, *Polyhedron* **1988**, 7, 463.
382. F. A. Cotton and S. Kitagawa, *Polyhedron* **1988**, 7, 1673.
383. I. F. Frazer, A. McVitie and R. D. Peacock, *J. Chem. Res. (S)* **1984**, 420.
384. P. A. Agaskar, F. A. Cotton, I. F. Fraser, L. Manojlovic-Muir, K. W. Muir and R. D. Peacock, *Inorg. Chem.* **1986**, *25*, 2511.
385. M. Bakir, F. A. Cotton, M. M. Cudahy, C. Q. Simpson, T. J. Smith, E. F. Vogel and R. A. Walton, *Inorg. Chem.* **1988**, *27*, 2608.
386. J.-D. Chen, F. A. Cotton and L. R. Falvello, *J. Am. Chem. Soc.* **1990**, *112*, 1076.
387. F. A. Cotton, L. R. Falvello, D. R. Root, T. J. Smith and K. Vidyasager, *Inorg. Chem.* **1990**, *29*, 1328.
388. Unpublished results cited in ref. 384. See ref. 419 for full details.
389. J.-D. Chen and F. A. Cotton, *Inorg. Chem.* **1990**, *29*, 1797.
390. F. A. Cotton, P. E. Fanwick and J. W. Fitch, III, *Inorg. Chem.* **1978**, *17*, 3254.
391. F. A. Cotton and K. J. Wiesinger, *Inorg. Chem.* **1992**, *31*, 920.
392. G.-S. Jung, B.-G. Park and S.-W. Lee, *Bull. Korean Chem. Soc.* **1997**, *18*, 213.
393. F. A. Cotton, L. M. Daniels, I. Guimet, R. W. Henning, G. T. Jordan IV, C. A. Murillo and A. J. Schultz, *J. Am. Chem. Soc.* **1998**, *120*, 12531.
394. T. C. Stoner, S. J. Geib and M. D. Hopkins, *Angew. Chem., Int. Ed. Engl.* **1993**, *32*, 409.
395. K. D. John, V. M. Miskowski, M. A. Vance, R. F. Dallinger, L. C. Wang, S. J. Geib and M. D. Hopkins, *Inorg. Chem.* **1998**, *37*, 6858.
396. T. C. Stoner, W. P. Schaefer, R. E. Marsh and M. D. Hopkins, *J. Cluster Sci.* **1994**, *5*, 107.
397. F. A. Cotton, E.V. Dikarev, G. T. Jordan, IV, C. A. Murillo and M. A. Petrukhina, *Inorg. Chem.* **1998**, *37*, 4611.
398. F. A. Cotton, L. M. Daniels, S. C. Haefner and E. N. Walke, *Inorg. Chim. Acta* **1996**, *247*, 105.
399. F. A. Cotton and M. Matusz, *Inorg. Chem.* **1988**, *27*, 2127.
400. F. A. Cotton and K. J. Wiesinger, *Inorg. Chem.* **1990**, *29*, 2594.
401. H.-F. Lang, P. E. Fanwick and R. A. Walton, *Inorg. Chim. Acta* **2002**, *329*, 1.
402. H.-L. Chen, C.-T. Lee, C.-T. Chen, J.-D. Chen, L.-S. Liou and J.-C.Wang, *J. Chem. Soc., Dalton Trans.* **1998**, 31.
403. F. A. Cotton, E. V. Dikarev, J. Gu, S. Herrero and B. Modec, *J. Am. Chem. Soc*. **1999**, *121*, 11758.
404. K. J. Ewing, S. I. Shupack and A. L. Rheingold, *Polyhedron* **1990**, *9*, 1209.
405. F. A. Cotton, E. V. Dikarev and S. Herrero, *Inorg. Chem*. **2000**, *39*, 609.
406. M. H. Chisholm, K. Folting, J. C. Huffman, E. F. Putilina, W. E. Streib and R. J. Tatz, *Inorg. Chem.* **1993**, *32*, 3771.
407. M. H. Chisholm, K. Folting, J. C. Huffman and R. J. Tatz, *J. Am. Chem. Soc.* **1984**, *106*, 1153.
408. F. A. Cotton and K. J. Wiesinger, *Inorg. Chem.* **1991**, *30*, 750.
409. R. G. Abbott, F. A. Cotton and L. R. Falvello, *Inorg. Chem.* **1990**, *29*, 514.
410. F. A. Cotton and P. E. Fanwick, *Acta Crystallogr.* **1980**, *B36*, 457.

Pictiva EX2004
Samsung v Pictiva
IPR2024-01094

411. C.-T. Lee, J.-D. Chen, L.-S. Liou and J.-C. Wang, *Inorg. Chim. Acta* **1996**, *249*, 115.
412. M. B. Hursthouse and K. M. A. Malik, *Transition Met. Chem.* **1995**, *20*, 574.
413. F. A. Cotton, K. R. Dunbar, B. Hong, C. A. James, J. M. Matonic and J. L. C. Thomas,*Inorg. Chem.* **1993**, *32*, 5183.
414. F. A. Cotton, J. L. Eglin and C. A. James, *Inorg. Chim. Acta* **1993**, *204*, 175.
415. H.-F. Lang, P. E. Fanwick and R. A. Walton, *Inorg. Chim. Acta* **2001**, *322*, 17.
416. P. E. Fanwick, W. S. Harwood and R. A. Walton, *Inorg. Chim. Acta* **1986**, *122*, 7.
417. P. A. Agaskar and F. A. Cotton, *Inorg. Chem.* **1986**, *25*, 15.
418. P. A. Agaskar and F. A. Cotton, *Rev. Chim. Minerale* **1985**, *22*, 302.
419. J.-D. Chen, F. A. Cotton and E. C. DeCanio, *Inorg. Chim. Acta* **1990**, *176*, 215.
420. F. A. Cotton, P. E. Fanwick, J. W. Fitch, H. D. Glicksman and R. A. Walton, *J. Am. Chem. Soc.* **1979**, *101*, 1752.
421. M. H. Chisholm, J. C. Huffman and W. G. Van Der Sluys, *J. Am. Chem. Soc.* **1987**, *109*, 2514.
422. F. A. Cotton and M. Matusz, *Inorg. Chim. Acta* **1989**, *157*, 223.
423. D. I. Arnold, F. A. Cotton and F. E. Kühn, *Inorg. Chem.* **1996**, *35*, 5764.
424. C.-T. Lee, W.-K. Yang, J.-D. Chen, L.-S. Liou and J.-C. Wang, *Inorg. Chim. Acta* **1998**, *274*, 7.
425. J.-D. Chen, F. A. Cotton and B. Hong, *Inorg. Chem.* **1993**, *32*, 2343.
426. J.-D. Chen and F. A. Cotton, *Inorg. Chem.* **1991**, *30*, 6.
427. F. A. Cotton and B. Hong, *Inorg. Chem.* **1993**, *32*, 2354.
428. C.-T. Lee, J.-D. Chen, Y. W. Chen-Yang, L.-S. Liou and J.-C. Wang, *Polyhedron* **1997**, *16*, 473.
429. A. A. Aitchison, L. J. Farrugia and R. D. Peacock, *Acta Crystallogr.* **1991**, *47C*, 2556.
430. S.-M. Kuang, D. A. Edwards, P. E. Fanwick and R. A. Walton, *Inorg. Chim. Acta* **2003**, *342*, 267.
431. P. R. Brown, F. G. N. Cloke and M. L. H. Green, *Polyhedron* **1985**, *4*, 869.
432. K. J. Ahmed, M. H. Chisholm and J. C. Huffman, *Organometallics* **1985**, *4*, 1168.
433. F. A. Cotton and R. Poli, *Inorg. Chem.* **1987**, *26*, 1514.
434. H. Schafer, H. G. von Schnering, J. Tillack, F. Kuhnen, H. Wohrle and H. Bauman, *Z. anorg. allg. Chem.* **1967**, *353*, 281.
435. D. Babel, *J. Solid State Chem.* **1972**, *4*, 410.
436. D. A. Edwards and G. W. A. Fowles, *J. Less-Common Met.* **1962**, *4*, 512.
437. P. R. Sharp and R. R. Schrock, *J. Am. Chem. Soc.* **1980**, *102*, 1430.
438. W. S. Harwood, J.-S. Qi and R. A. Walton, *Polyhedron* **1986**, *5*, 15.
439. R. L. Luck, R. H. Morris and J. F. Sawyer, *Inorg. Chem.* **1987**, *26*, 2422.
440. R. L. Luck and R. H. Morris, *J. Am. Chem. Soc.* **1984**, *106*, 7978.
441. J. San Filippo, Jr, and H. J. Sniadoch, *Inorg. Chem.* **1973**, *12*, 2326.
442. M. D. Hopkins and H. B. Gray, *J. Am. Chem. Soc.* **1984**, *106*, 2468.
443. M. D. Hopkins, T. C. Zietlow, V. M. Miskowski and H. B. Gray, *J. Am. Chem. Soc.* **1985**, *107*, 510.
444. M. D. Hopkins, V. M. Miskowski and H. B. Gray, *J. Am. Chem. Soc.* **1988**, *110*, 1787.
445. J. R. Winkler, D. G. Nocera and T. L. Netzel, *J. Am. Chem. Soc.* **1986**, *108*, 4451.
446. F. A. Cotton, J. L. Hubbard, D. L. Lichtenberger and I. Shim, *J. Am. Chem. Soc.* **1982**, *104*, 679.
447. P. A. Agaskar, F. A. Cotton, I. F. Fraser and R. D. Peacock, *J. Am. Chem. Soc.* **1984**, *106*, 1851.
448. S. Christie, I. F. Fraser, A. McVitie and R. D. Peacock, *Polyhedron* **1986**, *5*, 35.
449. I. F. Fraser, A. McVitie and R. D. Peacock, *Polyhedron* **1986**, *5*, 39.
450. F. A. Cotton, D. G. Lay and M. Millar, *Inorg. Chem.* **1978**, *17*, 186.
451. T. Zietlow, D. D. Klendworth, T. Nimry, D. J. Salmon and R. A. Walton, *Inorg. Chem.* **1981**, *20*, 947.
452. T. C. Zietlow, M. D. Hopkins and H. B. Gray, *J. Am. Chem. Soc.* **1986**, *108*, 8266.
453. R. R. Schrock, L. G. Sturgeoff and P. R. Sharp, *Inorg. Chem.* **1983**, *22*, 2801.
454. D. S. Hanselman and T.J. Smith, *Polyhedron* **1988**, *7*, 2679.
455. T. W. Coffindaffer, G. P. Niccolai, D. Powell, I. P. Rothwell and J. C. Huffman, *J. Am. Chem. Soc.* **1985**, *107*, 3572.

Pictiva EX2004
Samsung v Pictiva
IPR2024-01094

456. R. Bhattacharyya, G. P. Bhattacharjee, A. K. Mitra and A. B. Chatterjee, *J. Chem. Soc., Dalton Trans.* **1984**, 487.
457. R. A. Walton, *Prog. Inorg. Chem.* **1972**, *16*, 1.
458. J. Ouyang, T. C. Zietlow, M. D. Hopkins, F.-R. F. Fan, H. B. Gray and A. J. Bard, *J. Phys. Chem.* **1986**, *90*, 3841.
459. W. C. Trogler and H. B. Gray, *Nouv. J. Chim.* **1977**, *1*, 475.
460. F. A. Cotton and R. Poli, *Inorg. Chem,* **1987**, *26*, 3310.
461. F. A. Cotton and R. L. Luck, *Inorg. Chem.* **1989**, *28*, 182.
462. J. M. Canich, F. A. Cotton, L. M. Daniels and D. B. Lewis, *Inorg. Chem.* **1987**, *26*, 4046.
463. F. A. Cotton, L. M. Daniels, K. R. Dunbar, L. R. Falvello, C. J. O'Connor and A. C. Price, *Inorg. Chem.* **1991**, *30*, 2509.
464. P. A. Agaskar, F. A. Cotton, K. R. Dunbar, L. R. Falvello and J. C. O'Connor, *Inorg. Chem.* **1987**, *26*, 4051.
465. J. K. Bera, P. S. Szalay and K. R. Dunbar, *Inorg. Chem*. **2002**, *41*, 3429.
466. J. M. Canich, F. A. Cotton, K. R. Dunbar and L. R. Falvello, *Inorg. Chem.* **1988**, *27*, 804.
467. F. A. Cotton and G. L. Powell, *J. Am. Chem. Soc.* **1984**, *106*, 3371.
468. F. A. Cotton, M. P. Diebold, C. J. O'Connor and G. L. Powell, *J. Am. Chem. Soc.* **1985**, *107*, 7438.
469. J. E. Finholt, P. Leupin and A. G. Sykes, *Inorg. Chem.* **1983**, *22*, 2315.
470. S. P. Cramer, P. K. Eidem, M. T. Paffett, J. R. Winkler, Z. Dori and H. B. Gray, *J. Am. Chem. Soc.* **1983**, *105*, 799.
471. R. D. Peacock and I. F. Fraser, *Inorg. Chem.* **1985**, *24*, 989.
472. M. H. Chisholm, K. Folting and E. F. Putilina, *Inorg. Chem.* **1992**, *31*, 1510.
473. G. Pennesi, C. Floriani, A. Chiesi-Villa and C. Guastini, *J. Chem. Soc., Chem. Commun.* **1988**, 350.
474. C. Floriani, E. Solari, F. Franceschi, R. Scopelliti, P. Belanzoni and M. Rosi, *Chem. Eur. J.* **2001**, 7, 3052.
475. F. A. Cotton, J. Czuchajowska and X. Feng, *Inorg. Chem.* **1990**, *29*, 4329.
476. C.-H. Yang, S. J. Dzugan and V. L. Goedken, *J. Chem. Soc., Chem. Commun.* **1986**, 1313.
477. F. A. Cotton and G. N. Mott, *Inorg. Chem.* **1981**, *20*, 3896.
478. F. A. Cotton, B. W. S. Kolthammer and G. N. Mott, *Inorg. Chem.* **1981**, *20*, 3890.
479. (a) D. Mandon, J.-M. Giraudon, L. Toupet, J. Sala-Pala and J. E. Guerchais, *J. Am. Chem. Soc.* **1987**, *109*, 3490. (b) J. M. Kerbaol, E. Furet, J. E. Guerchais, Y. Le Mest, J. Y. Saillard, J. Sala-Pala and L. Toupet, *Inorg. Chem.* **1993**, *32*, 713.
480. (a) J.-M. Giraudon. J. E. Guerchais, J. Sala-Pala and L. Toupet, *J. Chem. Soc., Chem. Commun.* **1988**, 921. (b) J.-M. Giraudon, J. Sala-Pala, J. E. Guerchais, Y. Le Mest and L. Toupet, *Inorg. Chem.* **1991**, *30*, 891.
481. J. P. Collman, C. E. Barnes and L. K. Woo, *Proc. Natl. Acad. Sci. USA* **1983**, *80*, 7684.
482. J. P. Collman and L. K. Woo, *Proc. Natl. Acad. Sci. USA* **1984**, *81*, 2592.
483. C. D. Tait, J. M. Garner, J. P. Collman, A. P. Sattelberger and W. H. Woodruff, *J. Am. Chem. Soc.* **1989**, *111*, 9072.
484. J. P. Collman, K. Kim and J. M. Garner, *J. Chem. Soc., Chem. Commun.* **1986**, *1711*.
485. B. E. Bursten and W. F. Schneider, *Inorg. Chem.* **1989**, *28*, 3292.
486. R. A. Jones, J. G. Lasch, N. C. Norman, B. R. Whittlesey and T. C. Wright, *J. Am. Chem. Soc.* **1983**, *105*, 6184.
487. F. A. Cotton and R. Poli, *Polyhedron* **1987**, *6*, 2181.
488. F. A. Cotton and W. H. Ilsley, *Inorg. Chim. Acta* **1982**, *59*, 213.
489. J. San Filippo, Jr. and M. A. Schaefer King, *Inorg. Chem.* **1976**, *15*, 1228.
490. R. A. Walton, *ACS Symp. Ser.* **1981**, *No. 155*, 207.
491. T. Nimry, M. A. Urbancic and R. A. Walton, *Inorg. Chem.* **1979**, *18*, 691.
492. A. R. Middleton and G. Wilkinson, *J. Chem. Soc., Dalton Trans.* **1981**, 1898.
493. K. E. Voss, J. D. Hudman and J. Kleinberg, *Inorg. Chim. Acta* **1976**, *20*, 79.

Pictiva EX2004
Samsung v Pictiva
IPR2024-01094

494. (a) K. R. Mann, M. Cimolino, G. L. Geoffroy, G. S. Hammond, A. A. Orio, G. Albertin and H. B. Gray, *Inorg. Chim. Acta* **1976**, *16*, 97. (b) D. A. Bohling, K. R. Mann, S. Enger, T. Gennett, M. J. Weaver and R. A. Walton, *Inorg. Chim. Acta* **1985**, *97*, L51.
495. P. Bryant, F. A. Cotton, J. C. Sekutowski, T. E. Wood and R. A. Walton, *J. Am. Chem. Soc.* **1979**, *101*, 6588.
496. G. S. Girolami and R. A. Andersen, *J. Organomet. Chem.* **1979**, *182*, C43.
497. T. E. Wood, J. C. Deaton, J. Corning, R. E. Wild and R. A. Walton, *Inorg. Chem.* **1980**, *19*, 2614.
498. F. A. Cotton, L. M. Daniels, E. A. Hillard and C. M. Murillo, *Inorg. Chem.* **2002**, *41*, 1639.
499. C. Lin, J. D. Protasiewicz, E. T. Smith and T. Ren, *J. Chem. Soc., Chem. Commun.* **1995**, 2257.
500. C. Lin, J. D. Protasiewicz, E. T. Smith and T. Ren, *Inorg. Chem.* **1996**, *35*, 6422.
501. These corrections are based on personal communications with Dr. T. Ren. The data given in Table 4.13 are corrected data.
502. F. A. Cotton, J. P. Donahue, C. A. Murillo, L. M. Pérez and R. Yu, *J. Am. Chem. Soc.* **2003**, *125*, 8900.
503. F. A. Cotton, J. P. Donahue and C. A. Murillo, *J. Am. Chem. Soc.* **2003**, *125*, 5436.
504. F. A. Cotton, L. M. Daniels, C. A. Murillo, D. J. Timmons and C. C. Wilkinson, *J. Am. Chem. Soc.* **2002**, *124*, 9249.
505. (a) P. J. Bailey, S. F. Bone, L. A. Mitchell, S. Parsons, K. J. Taylor and L. J. Yellowlees, *Inorg. Chem.* **1997**, *36*, 867. (b) P. J. Bailey, S. F. Bone, L. A. Mitchell, S. Parsons, K. J. Taylor and L. J. Yellowlees, *Inorg. Chem.* **1997**, *36*, 1337.
506. K. D. John, T. C. Stoner and M. D. Hopkins, *Organometallics* **1997**, *16*, 4948.
507. T. C. Stoner, R. F. Dallinger and M. D. Hopkins, *J. Am. Chem. Soc.* **1990**, *112*, 5651.
508. T. C. Stoner, S. J. Geib and M. D. Hopkins, *J. Am. Chem. Soc.* **1992**, *114*, 4201.
509. J. H. Baxendale, C. D. Garner, R. G. Senior and P. Sharpe, *J. Am. Chem Soc.* **1976**, *98*, 637.
510. F. A. Cotton, W. H. Ilsley and W. Kaim, *J. Am. Chem. Soc.* **1980**, *102*, 1918.
511. D. J. Santure, J. C. Huffman and A. P. Sattelberger, *Inorg. Chem.* **1985**, *24*, 371.
512. K. Jansen, K. Dehnicke and D. Fenske, *Z. Naturforsch.* **1987**, *42b*, 1097.
513. F. A. Cotton, L. M. Daniels, E. A. Hillard and C. A. Murillo, *Inorg. Chem.* **2002**, *41*, 1639.
514. L. H. Wong, C. Valdez, E. J. Gabe and F. L. Lee, *Polyhedron* **1989**, *8*, 2339.
515. F. A. Cotton, L. M. Daniels, C. Y. Liu, C. A. Murillo, A. J. Schultz and X. Wang, *Inorg. Chem.* **2002**, *41*, 4232.
516. F. A. Cotton and D. J. Timmons, *Polyhedron* **1998**, *17*, 179.
517. F. A. Cotton, L. M. Daniels, C. A. Murillo and D. J. Timmons, *Chem. Commun.* **1997**, 1449.
518. F. A. Cotton, C. A. Murillo, X. Wang and C. C. Wilkinson, *Inorg. Chim. Acta,* **2003**, *351*,183.
519. R. A. Jones, K. W. Chiu, G. Wilkinson, A. M. R. Galas and H. B. Hursthouse, *J. Chem. Soc., Chem. Commun.* **1980**, 408.
520. K. W. Chiu, R. A. Jones, G. Wilkinson, A. M. R. Galas and Hursthouse, J. *Chem. Soc., Dalton Trans,* **1981**, 1892.
521. B. Heyn and C. Haroske, *Z. Chem.* **1972**, *12*, 338.
522. G. S. Girolami, V. V. Mainz, R. A. Anderson, S. H. Vollmer and V. W. Day, *J. Am. Chem. Soc.* **1981**, *103*, 3955.
523. M. H. Chisholm and I. P. Rothwell, *J. Am. Chem. Soc.* **1980**, *102*, 5950.
524. M. H. Chisholm, personal communication.
525. G. Wilke, B. Bogdanovic, P. Hardt, P. Heimbach, W. Kerm, M. Kroner, W. Oberkirch, K. Tanaka, E. Steinrucke, W. Walters and H. Zimmerman, *Angew. Chem., Int. Ed. Engl.* **1966**, *5*, 151.
526. F. A. Cotton and J. R. Pipal, *J. Am. Chem. Soc.* **1971**, *93*, 5441.
527. F. A. Cotton, S. A. Koch, A. J. Schultz and J. M. Williams, *Inorg. Chem.* **1978**, *17*, 2093.
528. J. P. Candlin and H. Thomas, *Adv. Chem. Ser.* **1974**, *132*, 212.
529. Y. Iwasawa, M. Yamagishi and S. Ogasawara, *J. Chem. Soc., Chem. Commun.* **1980**, 871.
530. Y. Iwasawa, S. Ogasawara, Y. Sato and H. Kuroda, *Proceedings of the Climax Fourth International Conference on the Chemistry and Uses of Molybenum* **1982**, 283.
531. Y. Iwasawa, Y. Sato and H. Kuroda, *J. Catal.* **1983**, *82*, 289.

Pictiva EX2004
Samsung v Pictiva
IPR2024-01094

532. Y. Iwasawa and M. Yamagishi, *J. Catal.* **1983**, *82*, 373.
533. W. P. McKenna and E. M. Eyring, *J. Mol. Catal.* **1985**, *29*, 363.
534. R. J. Blau, M. S. Goetz, R. R. Howe, C. J. Smith, R.-J. Tsay and U. Siriwardane, *Organometallics* **1991**, *10*, 3259.
535. R. J. Blau, M. S. Goetz and R.-J. Tsay, *Polyhedron* **1991**, *10*, 605.
536. R. J. Blau and U. Siriwardane, *Organometallics* **1991**, *10*, 1627.
537. E. Kurras, H. Mennenga, G. Oehme, U. Rosenthal and G. Engelhardt, *J. Organomet. Chem.* **1975**, *84*, C13.
538. F. A. Cotton, B. E. Hanson, W. H. Ilsley and G. W. Rice, *Inorg. Chem.* **1979**, *18*, 2713.
539. F. A. Cotton, S. Kosk and M. Millar, *J. Am. Chem. Soc.* **1977**, *99*, 7372.
540. F. A. Cotton, S. A. Kosk and M. Millar, *Inorg. Chem.* **1978**, *17*, 2087.
541. V. Katovic, J. L. Templeton, R. J. Hoxmeier and R. E. McCarley, *J. Am. Chem. Soc.* **1975**, *97*, 5300.
542. F. A. Cotton, L. R. Falvello, C. A. James and R. L. Luck, *Inorg. Chem.* **1990**, *29*, 4759.
543. F. A. Cotton, J. L. Eglin and C. A. James, *Inorg. Chem.* **1993**, *32*, 681.
544. F. A. Cotton and C. A. James, *Inorg. Chem.* **1992**, *31*, 5298.
545. F. A. Cotton, K. R. Dunbar, B. Hong, C. A. James, J. H. Matonic and J. L. C. Thomas, *Inorg. Chem.* **1993**, *32*, 5183.
546. J. P. Collman, S. T. Harford, S. Franzen, A. P. Shreve and W. H. Woodruff, *Inorg. Chem.* **1999**, *38*, 2093.
547. J. P. Collman and R. Boulatov, *Angew. Chem. Int. Ed.* **2002**, *41*, 3948.
548. J. P. Collman, S. T. Harford, S. Franzen, J.-C. Marchon, P. Maldivi, A. P. Shreve and W. H. Woodruff, *Inorg. Chem.* **1999**, *38*, 2085.
549. J. C. Menezes and C. C. Romao, *Polyhedron*, **1990**, *9*, 1237.
550. G. M. Bancroft, J. Bice, R. H. Morris and R. L. Luck, *J. Chem. Soc., Chem. Commun.* **1986**, 898.
551. J. P. Collman, R. Boulatov and J. P. Jameson, *Angew. Chem. Int. Ed.* **2001**, *40*, 1271.
552. F. A. Cotton, L. M. Daniels, E. A. Hillard and C. A. Murillo, *Inorg. Chem.* **2002**, *41*, 2466.
553. F. A. Cotton and R. A. Marcus, unpublished work.
554. (a) F. A. Cotton, C. Lin and C. A. Murillo, *J. Chem. Soc., Dalton Trans.* **1998**, 3151. (b) F. A. Cotton, J. P. Donahue, C. Lin and C. A. Murillo, *Inorg. Chem.* **2001**, *40*, 1234.
555. D. E. Richardson and H. Taube, *Inorg. Chem.* **1981**, *20*, 1278.
556. M. B. Robin and P. Day, *Adv. Inorg. Chem. Radiochem.* **1967**, *10*, 247.
557. K. D. Demadis, C. M. Hartshorn and T. J. Meyer, *Chem. Rev.* **2001**, *101*, 2655.
558. R. H. Cayton, M. H. Chisholm, J. C. Huffman and E. B. Lobkovsky, *J. Am. Chem. Soc.* **1991**, *113* 8709.
559. M. H. Chisholm, P. J. Wilson and P. M. Woodward, *Chem. Commun.* **2002**, 566.
560. B. E. Bursten, M. H. Chisholm, R. J. H. Clark, S. Firth, C. M. Hadad, A. M. Macintosh, P. J. Wilson, P. M. Woodward and J. M. Zeleski, *J. Am. Chem. Soc.* **2002**, *124*, 3050.
561. B. E. Bursten, M. H. Chisholm, R. J. H. Clark, S. Firth, C. M. Hadad, A. M. Macintosh, P. J. Wilson, P. M. Woodward and J. M. Zeleski, *J. Am. Chem. Soc.* **2002**, *124*, 12244.
562. M. H. Chisholm, *J. Organomet. Chem.* **2002**, *641*, 15.
563. M. H. Chisholm, *Dalton Trans.* **2003**, 3821.
564. B. E. Bursten, M. H. Chisholm, C. M. Hadad, J. Li and P. J. Wilson, *Chem. Commun.* **2001**, 2382.
565. B. E. Bursten, M. H. Chisholm, C. M. Hadad, J. Li and P. J. Wilson, *Isr. J. Chem.* **2001**, *41*, 187.
566. M. H. Chisholm, B. D. Pate, P. J. Wilson and J. M. Zeleski, *Chem. Comm.* **2002**, 1084.
567. M. J. Byrnes and M. H. Chisholm, *Chem. Commun.* **2002**, 2040.
568. F. A. Cotton, C. Lin and C. A. Murillo, *Acc. Chem. Res.* **2001**, *34*, 759.
569. F. A. Cotton, C. Lin and C. A. Murillo, *Proc. Nat. Acad. Sci.* **2002**, *99*, 4810.
570. (a) F. A. Cotton, C. Lin and C. A. Murillo, *J. Chem. Soc., Dalton Trans.* **1998**, 3151. (b) F. A. Cotton, J. P. Donahue, C. Lin and C. A. Murillo, *Inorg. Chem.* **2001**, *40*, 1234.
571. F. A. Cotton, J. P. Donahue and C. A. Murillo, *J. Am. Chem. Soc.* **2003**, *125*, 5436.
572. F. A. Cotton, J. P. Donahue and C. A. Murillo, *J. Am. Chem. Soc.* **2003**, *125*, 5436.

Pictiva EX2004
Samsung v Pictiva
IPR2024-01094

573. F. A. Cotton, C. Lin and C. A. Murillo, unpublished work.
574. F. A. Cotton, C. A. Murillo and R. Yu, unpublished work.
575. F. A. Cotton, J. P. Donahue and C. A. Murillo, *Inorg. Chem. Commun.* **2002**, *5*, 59.
576. F. A. Cotton, L. M. Daniels, J. P. Donahue, C. Y. Liu and C. A. Murillo, *Inorg. Chem.* **2002**, *41*, 1354.
577. F. A. Cotton, C. Y. Liu, C. A. Murillo, D. Villagrán and X. Wang, *J. Am. Chem. Soc.* **2003**, *125*, 13564.
578. F. A. Cotton, J. P. Donahue and C. A. Murillo, *Inorg. Chem.* **2001**, *40*, 2229.
579. F. A. Cotton, C. Y. Liu, C. A. Murillo and X.Wang, *Inorg. Chem.* **2003**, *42*, 4619.
580. F. A. Cotton, N. S. Dalal, C. Y. Liu, C. A. Murillo, J. M. North and X. Wang, *J. Am. Chem. Soc.* **2003**, *125*, 12945.
581. F. A. Cotton, J. P. Donahue, C. A. Murillo and L. M. Pérez, *J. Am. Chem. Soc*. **2003**, *125*, 5486.
582. F. A. Cotton, L. M. Daniels, C. Lin and C. A. Murillo, *J. Am. Chem. Soc.* **1999**, *121*, 4538.
583. F. A. Cotton, C. Lin and C. A. Murillo, *Inorg. Chem.* **2001**, *40*, 478.
584. F. A. Cotton, C. Lin and C. A. Murillo, *J. Am. Chem. Soc*, **2001**, *123*, 2670.
585. F. A. Cotton, C. Lin and C. A. Murillo, *J. Am. Chem. Soc*. **2001**, *123*, 2670.
586. F. A. Cotton, C. Lin and C. A. Murillo, *Inorg. Chem.* **2001**, *40*, 472.
587. J. F. Berry, F. A. Cotton, S. A. Ibragimov, C. A. Murillo and X. Wang, *J. Chem. Soc., Dalton Trans.* **2003**, 4297.
588. F. A. Cotton, J. P. Donahue, C. A. Murillo and R. Yu, unpublished work.
589. F. A. Cotton, L. M. Daniels, G. T. Jordan IV, C. Lin and C. A. Murillo, *J. Am. Chem. Soc.* **1998**, *120*, 3398.
590. F. A. Cotton, L. M. Daniels, G. T. Jordan IV, C. Lin and C. A. Murillo, *Inorg. Chem. Commun.* **1998**, *1*, 109.
591. F. A. Cotton and M. Shang, *J. Cluster Sci.* **1991**, *2*, 121.
592. T. R. Ryan and R. E. McCarley, *Inorg. Chem.* **1982**, *21*, 2072.
593. F. A. Cotton and G. L. Powell, *Inorg. Chem.* **1983**, *22*, 871.
594. F. A. Cotton, B. Hong and M. Shang, *Inorg. Chem.* **1993**, *32*, 4876.
595. F. A. Cotton, C. Lin and C. A. Murillo, *Inorg. Chem. Commun.* **2001**, *4*, 130.
596. F. A. Cotton, L. M. Daniels, C. Lin and C. A. Murillo, *Chem. Commun*. **1999**, 841.
597. F. A. Cotton, C. Lin and C. A. Murillo, *Inorg. Chem*. **2001**, *40*, 6413.

Pictiva EX2004
Samsung v Pictiva
IPR2024-01094

5

Tungsten Compounds

Judith L. Eglin,
Los Alamos National Laboratory

5.1 Multiple Bonds in Ditungsten Compounds

In contrast to the ease of preparation of the other group 6 elements Cr and Mo, the syntheses of critical ditungsten starting materials have been notably difficult. Specifically, W_2^{4+} tetracarboxylates $W_2(O_2CR)_4$ and salts of the $[W_2Cl_8]^{4-}$ anion have not shown the synthetic utility of the Mo_2^{4+} analogs. Therefore, progress in the synthesis, structural characterization, and reactivity studies of W_2^{4+} compounds has relied on new developments in synthetic methodologies and new ligand types.

The more than fifty structurally characterized quadruply bonded W_2^{4+} compounds fall into three primary categories: classic paddlewheel complexes with four bridging anionic ligands both with and without axially coordinated neutral ligands,[1-22] compounds coordinated by only anionic ligands,[23-26] and compounds coordinated by four anionic ligands and neutral ligands.[1,27-42] In Section 5.2, the first attempts to synthesize the tetracarboxylates of the type $W_2(O_2CR)_4$, culminating in their successful isolation and characterization in the early 1980's, are described. Subsequent sections focus on the comparatively small but growing number of other W_2^{4+} and MoW^{4+} quadruply bonded complexes and paddlewheel compounds with either W_2^{5+} or W_2^{6+} cores. The W–W distances of the structurally characterized ditungsten complexes are provided in Table 5.1. A list of other synthesized but not structurally characterized W_2^{4+} complexes is provided in Table 5.2.

5.2 The W_2^{4+} Tetracarboxylates

Following the successful preparation of $Mo_2(O_2CCH_3)_4$ from $Mo(CO)_6$ by Wilkinson and co-workers,[43] three reports[44-46] appeared between 1969 and 1973 that described the analogous reaction between acetic acid and $W(CO)_6$. In two of these studies,[44,45] the thermal reaction between $W(CO)_6$ and acetic acid-acetic anhydride was investigated. The third report[46] described attempts to prepare $W_2(O_2CCH_3)_4$ by photolysis of a 1:2 stoichiometric mixture of $W(CO)_6$ and acetic acid in benzene. None of these early investigations yielded the yellow-brown solids of the acetate derivative.[17,18,21] The use of other carboxylic acids, either alone or mixed with the corresponding anhydrides, in place of acetic acid produces brown complexes of approximate formula $[W(O_2CR)_2]_x$, where R = Ph, *p*-$CH_3C_6H_4$, C_6F_5, C_3H_7 or C_3F_7.[45] Oxidation state titrations on several of the products gave oxidation numbers for tungsten close to +2.0.

Pictiva EX2004
Samsung v Pictiva
IPR2024-01094

Table 5.1. Structurally characterized compounds with a quadruply bonded W_2^{4+} core listed by increasing W–W bond length

Compound	W–W (Å)	ref.
$W_2(dmhp)_4 \cdot 0.5(diglyme)$	2.155(2)	2
$W_2(hpp)_4 \cdot 2NaHBEt_3$	2.1608(5)	3
$W_2(mhp)_4 \cdot CH_2Cl_2$	2.161(1)	4
$W_2(hpp)_4$	2.1617(4)	68
$W_2(dmhp)_4 \cdot (diglyme)$	2.163(1)	2
$W_2(map)_4 \cdot 2THF$	2.164(1)	5
$W_2(ap)_4 \cdot {}^2/_3THF$	2.168(2)	6
	2.164(2)	
$W_2(dmhp)_2[(PhN)_2N]_2 \cdot 2THF$	2.169(1)	7
$W_2(dmhp)_2[\mu\text{-}(PhN)_2CCH_3]_2 \cdot 2THF$	2.174(1)	8
$W_2[O_2CC_6H_2\text{-}2,4,6\text{-}(CH_3)_3]_4 \cdot 2CH_3C_6H_5$	2.176(1)	9
$W_2(chp)_4$	2.177(1)	10
$W_2(fhp)_4 \cdot THF$	2.185(2)	11
$W_2(DTolF)_4 \cdot C_7H_8$	2.187(1)	12
$W_2(O_2CEt)_4$	2.189(1)	13
$W_2(D^{Cl_2}PhF)_4$	2.1920(3)	14
$W_2(D^{p\text{-}Cl}PhF)_4$	2.1924(2)	22
$W_2(O_2C(CH_2)_2CH_3)_4$	2.194(3)	15
$W_2(D^{m\text{-}Me}PhF)_4$	2.1957(6)	22
$W_2(O_2CC_6H_5)_4 \cdot 2THF$	2.196(1)	9,16
$W_2[O_2CC_6H_4(4\text{-}OCH_3)]_4 \cdot 2THF$	2.203(1)	9
$W_2(O_2CCF_3)_4 \cdot {}^2/_3(diglyme)$	2.211(2)	17
	2.207(2)	
$W_2(O_2CBu^t)_4 \cdot 2PPh_3$	2.218(1)	18
$W_2(\mu\text{-}O_2CCF_3)_2(\eta^1\text{-}O_2CCF_3)_2(PBu^n_3)_2$	2.224(1)	19
$W_2(azin)_4 \cdot 2THF$	2.227(2)	20
$W_2(\mu\text{-}O_2CBu^t)_3(\eta^1\text{-}O_2CBu^t)(PMePh_2)_2$	2.2345(9)	1
$W_2(O_2CCF_3)_4 \cdot 2PPh_3$	2.240(1)	21
	2.243(1)	
$W_2Cl_4(NH_2Cy)_4$	2.2455(5)	27
$W_2(\mu\text{-}O_2CCF_3)(O_2CCF_3)_3(PMe_3)_3$	2.246(1)	19
$Na_4(TMEDA)_4[W_2Cl_8]$	2.259(1)	26
	2.254(1)	
$W_2Cl_4(4\text{-}Bu^t\text{-}py)_4 \cdot 4\text{-}Bu^t\text{-}py$	2.259(1)	28
$W_2Cl_4(4\text{-}Bu^t\text{-}py)_4 \cdot C_7H_8$	2.2602(8)	28
$W_2Cl_4(4\text{-}Bu^t\text{-}py)_4 \cdot (CH_3)_2CO$	2.2605(6)	28
$W_2Cl_4(PMe_3)_4$	2.262(1)	29,30
$Li_4W_2(CH_3)_xCl_{8-x} \cdot 4THF$	2.263(2)	25
$W_2Cl_4(4\text{-}Bu^t\text{-}py)_4$	2.2631(6)	28
$\beta\text{-}W_2Br_4(dppm)_2$	2.2632(1)	31
$Li_4W_2(CH_3)_8 \cdot 4Et_2O$	2.264(1)	25
$W_2Cl_4(PBu^n_3)_4 \cdot C_7H_8$	2.267(1)	32
$W_2(CCMe)_2Cl_2(PMe_3)_4$	2.268(1)	33
$\beta\text{-}W_2Cl_4(dppm)_2$	2.269(1)	34
$W_2Cl_4(PMePh_2)_4 \cdot C_6H_6$	2.2728(7)	35

Pictiva EX2004
Samsung v Pictiva
IPR2024-01094

Compound	W–W (Å)	ref.
α-$W_2Cl_4(dppp)_2$	2.274(2)	36
$W_2(CCMe)_4(PMe_3)_4$	2.2742(9)	37
α-$W_2Cl_4(dppe)_2$·0.5H_2O	2.281(1)	30,38
α-$W_2Cl_4(dmpe)_2$·(toluene)	2.287(1)	29,30
[W_2{*p*-Bu^t-calix[4](O)$_4$}$_2$(μ-Na)$_4$]	2.292(1)	24
$W_2(μ\text{-}O_2CC_6H_5)_2I_2(μ\text{-}dppm)_2$	2.2925(6)	39
α-$W_2Cl_4(depe)_2$	2.2950(7)	40
β-$W_2Cl_4(Pr^i_2PCH_2CH_2CH_2PPr^i_2)_2$	2.297(1)	41
$W_2(μ\text{-}O_2CC_6H_5)_2Br_2(μ\text{-}dppa)_2$·2THF	2.299(1)	42
β-$W_2Cl_4(dppe)_2$	2.314(1)	30,38
$W_2(TPP)_2$	2.352(1)	90
$W_2(C_8H_8)_3$	2.375(1)	23

Table 5.2. Other compounds with a W_2^{4+} core

Compound	ref.	Compound	ref.
[W(OEP)]$_2$	91	[W_2(O$_2$CBu^t)$_3$]$_2$(2,5-TH(CO$_2$)$_2$)	66
[W(TOEP)]$_2$	92,122	$W_2(O_2CBu^t)_2Cl_2(PMe_3)_2$	1
$W_2(μ\text{-}mhp)_2(μ\text{-}TFA)_2$	17	$W_2(O_2CC_6H_5)_2Cl_2(μ\text{-}dppa)_2$·2THF	42
$W_2(TFA)_4$	21	$W_2(O_2CC_6H_5)_2I_2(μ\text{-}dppa)_2$·2THF	42
$W_2(TFA)_4$·2PMe_3	19	$W_2(O_2CC_6H_5)_2Cl_2(μ\text{-}dppm)_2$	39
$W_2(TFA)_4$·2PEt_3	19	$W_2(O_2CC_6H_5)_2Br_2(μ\text{-}dppm)_2$	39
$W_2(O_2CC_6H_5)_4$	45	$W_2Cl_4(3\text{-}Bu^n\text{-}py)_4$	28
$W_2(O_2CC_6H_4CH_3)_4$	45	$W_2Cl_4(NH_2Pr^n)_4$	27
$W_2(O_2CC_6F_5)_4$	45	$W_2Cl_4(NH_2Bu^t)_4$	27
$W_2(O_2CC_3F_7)_4$	45	$Na_4(THF)_x[W_2Cl_8]$	87
$W_2(O_2CCH_3)_4$	13,18	$Na_4(DME)_4[W_2Cl_8]$	87
$W_2(O_2CBu^t)_4$	1,13,	$W_2Cl_4(PMePh_2)_4$	86
	18,87	$W_2Cl_4(PMe_2Ph)_4$	31
$W_2(O_2CBu^t)_4$·2PMe_2Ph	1	$W_2Cl_4(PBu^n_3)_4$	86
$W_2(O_2C(CH_2)_6CH_3)_4$	15	$W_2Cl_4(PEt_3)_4$	97
$W_2(O_2C(CF_2)_6CF_3)_4$	15	$W_2Cl_4(PPr^n_3)_4$	150
$W_2[O_2CC_6H_4(4\text{-}CN)]_4$·2THF	9	$W_2Cl_4(PEt_3)_3(PMe_3)$	97
$W_2(μ\text{-}O_2CCCo_3(CO)_3)_3(μ\text{-}O_2CCF_3)$·2THF	148	$W_2Cl_4(PEt_3)_2(PMe_3)_2$	97
$W_2(μ\text{-}O_2CCCo_3(CO)_3)_4$	149	$W_2Cl_4(PEt_3)_3(PMe_2Ph)$	97
$W_2(O_2CBu^t)_4]_2$·2Bu^{t}CONMe$_2$	13	$W_2Cl_4(PEt_3)_2(PMe_2Ph)_2$	97
$W_2(O_2CMe)_4$·2MeCONMe$_2$	13	$W_2Cl_4(PEt_3)_3(PMePh_2)$	97
$W_2(O_2CEt)_4$·2EtCONMe$_2$	13	$W_2Cl_4(PBu^n_3)_3(PMe_3)$	97
$W_2(2\text{-}THCO_2)_4$	66	$W_2Cl_4(PBu^n_3)_3(PMe_2Ph)$	97
$W_2(3\text{-}THCO_2)_4$	66	$W_2Cl_4(PBu^n_3)_2(PMe_2Ph)_2$	97
$W_2(μ\text{-}O_2CBu^t)(O_2CBu^t)_3(PMe_3)_2$	1	$W_2Cl_4(PBu^n_3)_3(PMePh_2)$	97
$W_2(μ\text{-}O_2CBu^t)(O_2CBu^t)_3(PMe_2Ph)_2$	1	$W_2Br_4(PMe_2Ph)_4$	31
$W_2(μ\text{-}O_2CBu^t)_2(O_2CBu^t)_2(PMe_3)_2$	1	$W_2Br_4(PMePh_2)_4$	31
[W_2(O$_2$CBu^t)$_3$]$_2$(O$_2$CCO$_2$)	65	$W_2(CCBu^t)_4(PMe_3)_4$	99
[W_2(O$_2$CBu^t)$_3$]$_2$(O$_2$C-1,4-C$_6$F$_4$-CO$_2$)	65	β-$W_2Cl_4(dppa)_2$·2THF	42
[W_2(O$_2$CBu^t)$_3$]$_2$(O$_2$C-1,8-C$_{14}$H$_8$-CO$_2$)	65	α-$W_2Cl_4(dmpe)_2$	86
[W_2(O$_2$CBu^t)$_3$]$_2$(O$_2$C-1,4-C$_{14}$H$_{10}$-CO$_2$)	65	α-$W_2Cl_4(dppe)_2$	86
[W_2(O$_2$CBu^t)$_3$]$_2$(O$_2$C(C$_5$H$_4$)Fe(C$_5$H$_4$)CO$_2$)	65		

Pictiva EX2004
Samsung v Pictiva
IPR2024-01094

Unfortunately, none of these products afforded single crystals suitable for a crystal structure determination, and spectroscopic characterizations failed to confirm their identity as $W_2(O_2CR)_4$, so their relationship to now characterized acetate products remains unclear. In many of these reactions, a large proportion of the tungsten species remained in solution. Work-up of the reaction filtrates showed that the main products were trinuclear clusters having a $[W_3O_2(O_2CR)_6]^{n+}$ core.[47,48]

Following these early unsuccessful attempts to prepare an authentic tetracarboxylate with a W_2^{4+} core, the first structural characterization was reported for $W_2(O_2CCF_3)_4 \cdot {}^2/_3$(diglyme).[17] This compound was synthesized by Sattelberger et. al. by reduction at -20 °C of $W_2Cl_6(THF)_4$ (later reformulated as $NaW_2Cl_7(THF)_5$)[49] with 2 equiv of sodium amalgam followed by subsequent addition of $Na(O_2CCF_3)$.[17] While this method failed to provide a direct route to $W_2(O_2CCH_3)_4$,[18] this compound can be prepared by the metathesis of $W_2(O_2CCF_3)_4$ with $(Bu_4N)O_2CCH_3$ in toluene.[18] With the synthesis of $W_2(O_2CCF_3)_4$, a route to ditungsten tetracarboxylates was established and provided the experimental foundation for the synthesis of a variety of $W_2(O_2CCR_3)_4$ compounds.[17,18,21,50]

An alternative synthetic procedure involves reduction of a mixture of WCl_4 and sodium trifluoroacetate with Na/Hg in THF at 0 °C.[21] The pivalate analog is prepared by this method,[18] and the reaction also provides a convenient route to the corresponding tetraarylcarboxylate derivatives $W_2(O_2CAr)_4$ (Ar = Ph, C_6H_4-*p*-OMe, and C_6H_2-2,4,6-Me_3).[9,16] Based on the synthesis of other W_2^{4+} materials such as $W_2Cl_4(PMePh_2)_4$,[31] $NaBEt_3H$ has also been used as reducing agent as in the synthesis of $W_2(O_2CPh)_4$ from WCl_4 and NaO_2CPh.[39] Another useful method for the synthesis of alkyl carboxylate analogs involves room temperature reaction of hydrocarbon solutions of 1,2-$W_2Et_2(NMe_2)_4$ with acid anhydrides $(RCO)_2O$, where R = CH_3, C_2H_5, or CMe_3 with product yields in the range of 40 to 65%, after recrystallization. The general reaction is shown in the following equation:[13]

$$1,2\text{-}W_2Et_2(NMe_2)_4 + 4(RCO_2)_2O \rightarrow W_2(O_2CR)_4 + 4RCONMe_2 + C_2H_4 + C_2H_6$$

The crystal structures of several tetraalkyl and tetraaryl carboxylate derivatives have been determined, both with and without axially coordinated ether molecules such as THF or diglyme. In $W_2(O_2CC_2H_5)_4$, weak intermolecular W–O axial interactions (2.665(4) Å) link the dinuclear units into infinite chains.[13] The bis-toluene solvate of $W_2(O_2CC_6H_2$-2,4,6-$Me_3)_4$ is the only W_2^{4+} tetracarboxylate known to lack axial interactions.[9] A summary of the W–W bond lengths for the structurally characterized derivatives is provided in Table 5.1 and the structure of $W_2(O_2CC_6H_5)_4 \cdot 2THF$ is shown in Fig. 5.1.[9] Note that the shorter W–W bond length in $W_2(O_2CC_6H_2$-2,4,6-$Me_3)_4$ can possibly be ascribed to the absence of axial ligands, a structural effect that is seen in other tetracarboxylate M_2^{4+} complexes of the group 6 elements.

The air-sensitive alkyl tetracarboxylate complexes can be sublimed,[18,21] and give an intense parent ion multiplet in the mass spectra which provides conclusive evidence that these dinuclear complexes can survive intact in the vapor phase. This has allowed measurement of the UV photoelectron spectra of $W_2(O_2CCF_3)_4$[51] and $W_2(O_2CCH_3)_4$[52] in the gas phase. The spectrum for gaseous $W_2(O_2CCH_3)_4$ is very similar to that in a thin film.[52] The δ ionizations of $Mo_2(O_2CCF_3)_4$ and $W_2(O_2CCF_3)_4$ appear at 8.76 and 7.39 eV, respectively,[51] a difference that correlates with the much greater susceptibility of W_2^{4+} complexes to oxidation and oxidative-addition reactions. This trend is also reflected in the electrochemical properties of $W_2(O_2CR)_4$ (R = CH_3 or CMe_3).[18] The $E_{1/2}$(ox) values measured for acetonitrile solutions of these complexes (-0.37 V and -0.40 V, respectively, versus SCE) are *c.* 0.8 V more negative than for the Mo_2^{4+} analogs.[18] The pivalate complex is easily oxidized to the paramagnetic EPR-active salt $[W_2(O_2CCMe_3)_4]I$ upon treatment with I_2 in benzene,[18] a reaction that is similar to the oxidations of $Mo_2(O_2CCMe_3)_4$

Pictiva EX2004
Samsung v Pictiva
IPR2024-01094

and $MoW(O_2CCMe_3)_4$ (Section 5.5). Other important spectroscopic characterizations carried out on these W_2^{4+} tetracarboxylates include the ^{183}W NMR spectra of the trifluoroacetate[21] and pivalate,[18] and the assignment of the $\delta \rightarrow \delta^*$ transition for several of the alkyl[18] and aryl[9] tetracarboxylate derivatives.

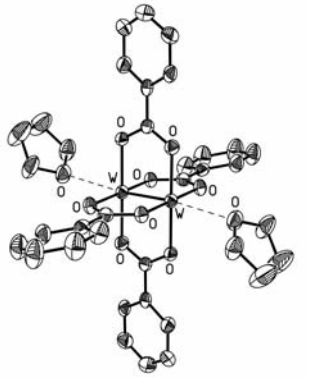


Fig. 5.1. The structure of $W_2(O_2CC_6H_5)_4 \cdot 2THF$. The W–O(THF) separations are *c*. 2.6 Å.

The ability of $W_2(O_2CR)_4$ compounds to form axial adducts has already been discussed with reference to the ether ligands THF and diglyme (Table 5.1). In addition, triphenylphosphine reacts with $W_2(O_2CR)_4$ (R = CF_3 or CMe_3)[18,21] to form $W_2(O_2CR)_4(PPh_3)_2$. Both complexes have been structurally characterized and have axially bound triphenylphosphine molecules.[18,21] The weakening of the W–W bond of $W_2(O_2CR)_4$ by axial W–L interactions is reflected by changes in the Raman active ν(W–W) modes. This is illustrated by the shift in ν(W–W) from 310 cm^{-1} in $W_2(O_2CCF_3)_4$ to 280 cm^{-1} in $W_2(O_2CCF_3)_4(PPh_3)_2$,[21] and from 313 cm^{-1} in $W_2(O_2CCMe_3)_4$ to 287 cm^{-1} in $W_2(O_2CCMe_3)_4(PPh_3)_2$.[18]

In contrast to reactions of PPh_3 with $W_2(O_2CCF_3)_4$ and $W_2(O_2CCMe_3)_4$ leading to 1:2 adducts that contain axially bound phosphine ligands,[18,21] the behavior of $W_2(O_2CCF_3)_4$ with other phosphine ligands (PMe_3, PEt_3, and PBu^n_3) is more complex.[19] Toluene solutions of $W_2(O_2CCF_3)_4$ react with these three trialkylphosphine ligands to yield red to red-orange, air-sensitive 1:2 adducts. The ^{19}F and $^{31}P\{^1H\}$ NMR spectra (+25 to -50 °C) support the presence of a single isomer with the phosphine ligands bound equatorially and two bridging bidentate and two monodenate trifluoroacetate ligands.[19] A single crystal X-ray structure determination for $W_2(\mu\text{-}O_2CCF_3)_2(\eta^1\text{-}O_2CCF_3)_2(PBu^n_3)_2$ confirms[19] the presence of a single isomer in the solid state. Similar to the dimolybdenum analog,[53-55] $W_2(O_2CCF_3)_4$ can react with phosphine ligands to give axial (D_{4h} symmetry) or equatorial (C_{2h} symmetry) adducts. An unusual isomer is $W_2(O_2CBu^t)_3(\eta^1\text{-}O_2CBu^t)(PMePh_2)_2$ with one axially and one equatorially coordinated phosphine ligand and an equatorially coordinated carboxylate ligand.[1]

Reactions of $W_2(O_2CCF_3)_4$ or $W_2(\mu\text{-}O_2CCF_3)_2(\eta^1\text{-}O_2CCF_3)_2(PMe_3)_2$ with an excess of PMe_3 yields the corresponding dark-green 1:3 adduct.[19] $W_2(\mu\text{-}O_2CCF_3)(\eta^1\text{-}O_2CCF_3)_3(PMe_3)_3$ is stable in solution at room temperature but loses a molecule of PMe_3 to form $W_2(\mu\text{-}O_2CCF_3)_2(\eta^1\text{-}O_2CCF_3)_2(PMe_3)_2$ when heated in benzene.[19] The ^{19}F and $^{31}P\{^1H\}$ NMR spectra indicate that $W_2(\mu\text{-}O_2CCF_3)_2(\eta^1\text{-}O_2CCF_3)_2(PMe_3)_2$ has the same structure in solution (with equatorially bound phosphine ligands) as that found in the solid state by X-ray crystallography. A comparison of the spectroscopic properties of $W_2(\mu\text{-}O_2CCF_3)(\eta^1\text{-}O_2CCF_3)_3(PMe_3)_3$ and the previously reported molybdenum analog $Mo_2(\mu\text{-}O_2CCF_3)(\eta^1\text{-}O_2CCF_3)_3(PMe_3)_3$[56] suggests that these complexes are isostructural. However, the differences that exist in solution between

Pictiva EX2004
Samsung v Pictiva
IPR2024-01094

$Mo_2(O_2CCF_3)_4(PR_3)_2$ and $W_2(O_2CCF_3)_4(PR_3)_2$, and between $Mo_2(\mu\text{-}O_2CCF_3)(\eta^1\text{-}O_2CCF_3)_3(PMe_3)_3$ and $W_2(\mu\text{-}O_2CCF_3)(\eta^1\text{-}O_2CCF_3)_3(PMe_3)_3$, have been linked to differences in the M–P bond strengths (W–P > Mo–P).[19]

Unlike the Mo_2^{4+} tetracarboxylates that have served as key starting materials in the development of multiply bonded dimolybdenum chemistry, the related W_2^{4+} compounds have more limited use as synthetic precursors. The ease of oxidation of $W_2(O_2CR)_4$ is a hindrance in designing synthetic procedures for preparation and subsequent reactivity studies of the tetracarboxylates.[57] However, $W_2(O_2CPh)_4$ is a synthetic precursor that is easily prepared by reduction of WCl_4 with $NaBEt_3H$ followed by addition of NaO_2CPh.[39] Unlike the reaction of $Mo_2(O_2CCF_3)_4$ with Me_3SiX where X is Cl, Br, or I and bidentate phosphine ligands such as dppm to produce $Mo_2X_4(\mu\text{-dppm})_2$ compounds, only a maximum of three of the benzoate ligands can be replaced upon oxidative addition of HBr to the W_2^{4+} core.[58-61] For the reaction of $W_2(O_2CPh)_4$ with dppm and Me_3SiBr, the presence of acid from the halide source in the reaction mixture promotes the loss of a third carboxylate ligand and the formation of the W_2^{6+} complex with a bridging hydride $W_2(\mu\text{-H})(\mu\text{-}O_2CPh)Br_4(\mu\text{-dppm})_2\cdot 2THF$.[39] By using halide sources such as Me_3SiI or the zinc salts $ZnCl_2$, $ZnBr_2$ or ZnI_2 to eliminate acid, the compounds $W_2(\mu\text{-}O_2CPh)_2X_2(\mu\text{-dppm})_2$ were made (X is Cl, Br, or I) and these still retained two of the benzoate ligands.[39] The structure of $W_2(\mu\text{-}O_2CPh)_2X_2(\mu\text{-dppm})_2$ is shown in Fig. 5.2.

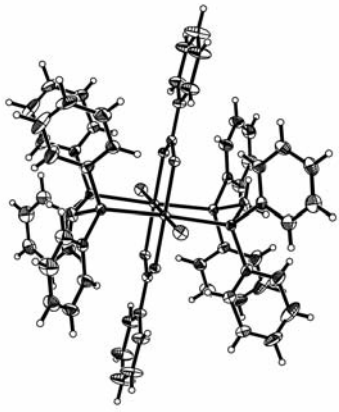


Fig. 5.2. The structure of $W_2(O_2CPh)_2(dppm)_2I_2$.

The presence of an acid may be required to protonate the third and fourth carboxylate groups from the ditungsten core as in the dimolybdenum analogs where acids drive the reactions to completion.[29,62,63] The formation of oxidative addition products does not occur in Mo_4^{2+} chemistry as demonstrated by the preparation of $K_4Mo_2Cl_8$ in a highly acidic reaction medium.[64]

Dinuclear compounds are of interest in the synthesis of oligomers, and the tetracarboxylate $W_2(O_2CBu^t)_4$ has been used as a precursor in the synthesis of two W_2^{4+} cores linked by dicarboxylates with either a perpendicular or parallel alignment of the W–W bonds.[65] Using a simple substitution reaction, five new precursors to oligomeric materials have been synthesized, namely $[W_2(O_2CBu^t)_3]_2(O_2CCO_2)$, $[W_2(O_2CBu^t)_3]_2(O_2C\text{-}1,4\text{-}C_6F_4\text{-}CO_2)$, $[W_2(O_2CBu^t)_3]_2(O_2C\text{-}1,8\text{-}C_{14}H_8\text{-}CO_2)$, $[W_2(O_2CBu^t)_3]_2(O_2C\text{-}1,4\text{-}C_{14}H_{10}\text{-}CO_2)$, and $[W_2(O_2CBu^t)_3]_2(O_2C(C_5H_4)Fe(C_5H_4)CO_2)$.[65] The work has been expanded to include the thienylcarboxylates in order to further understand the electronic properties of the parent paddlewheel compounds $W_2(2\text{-}THCO_2)_4$[66] and $W_2(3\text{-}THCO_2)_4$[66] in addition to the tetranuclear species $[W_2(O_2CBu^t)_3]_2(2,5\text{-}TH(CO_2)_2)$[66].

Pictiva EX2004
Samsung v Pictiva
IPR2024-01094

5.3 W_2^{4+} Complexes Containing Anionic Bridging Ligands Other Than Carboxylate

An organometallic compound with a W–W quadruple bond is the cyclo-octatetraene derivative $W_2(COT)_3$ prepared by reaction of WCl_4 and $K_2C_8H_8$ in tetrahydrofuran.[67] One of the COT ligands is a bridging dianion while the others are monoanions, with one COT^- bound to each of the W atoms. $W_2(COT)_3$ is isostructural with the molybdenum analog.[23,67]

The nitrogen-containing monoanionic ligands hpp,[3,68] mhp,[4] chp,[10] fhp,[11] dmhp,[2] map,[5] DTolF,[12] $D^{Cl_2}PhF$,[14] $D^{p\text{-}Cl}PhF$,[22] $D^{m\text{-}Me}PhF$,[22] azin,[20] and ap[6] form W_2^{4+} paddlewheel compounds with W–W bond lengths similar to those of the tetracarboxylates (Table 5.1). The dark-red purple $W_2(mhp)_4$ complex was the first one of this series to be reported. It forms upon refluxing $W(CO)_6$ (not WCl_4) with 2-hydroxy-6-methylpyridine (Hmhp) in diglyme.[4] $W_2(mhp)_4$ is isostructural with the Cr and Mo analogs.[4] Both $W_2(mhp)_4$ and $MoW(mhp)_4$ display readily accessible one-electron oxidations.[69] The $E_{1/2}$ values (from cyclic voltammetry) for these complexes in acetonitrile solutions are -0.35 V and -0.16 V, respectively, versus SCE.[69]

Some of these anionic ligands allow the syntheses of homologous series of Cr, Mo, and W compounds as in the case of the anions of 2,4-dimethyl-6-hydroxypyrimidine (Hdmhp),[2] 2-hydroxy-6-chloropyridine (Hchp),[10] 1,3,4,6,7,8-hexahydro-2*H*-pyrimido[1,2-*a*]pyrimidine (Hhpp),[3,68,70] 2-amino-6-methylpyridine (Hmap),[5] and 2-hydroxy-6-fluoropyridine (Hfhp).[11] The reactions of the first two of these ligands with $W(CO)_6$ produce $W_2(dmhp)_4$ and $W_2(chp)_4$.[2,10] Interestingly, this synthetic strategy does not always work in the synthesis of W_2^{4+} complexes as shown by the reaction of $W(CO)_6$ with *N*,*N*'-di-3,5-xylylformamidine. This reaction yields $W_2(\mu\text{-}CO)_2[\mu\text{-}HC(NR)_2]_2[HC(NR)_2[(RN)CH(NR)CH_2]$, where R = 3,5-xylyl, a complex that probably contains a W–W double bond (the W–W length is 2.464(3) Å).[71,72] In contrast, $Cr(CO)_6$ and $Mo(CO)_6$ react with this formamidine to yield the expected M_2^{4+} quadruply-bonded complexes.[71] The tungsten complex coordinated by dmhp can be obtained as two diglyme solvates, $W_2(dmhp)_4 \cdot 1/2$diglyme or $W_2(dmhp)_4 \cdot$diglyme.[2] As shown in Table 5.1, the W–W bond lengths of these two forms differ very little.[2]

The complex derived from 2-hydroxy-6-fluoropyridine is prepared as the 1:1 adduct with THF by Na/Hg reduction of a THF solution containing Na(fhp) and WCl_4.[11] As the Cr and Mo analogs, $W_2(fhp)_4$ has a polar structure with four bridging fhp ligands orientated in the same direction; a THF molecule is axially coordinated to the metal atom bonded to four oxygen atoms.[11] A synthetic procedure similar to that used to prepare $W_2(fhp)_4$ has been adapted for the synthesis of $W_2(ap)_4$ (ap is 2-anilinopyridine), a complex that contains an eclipsed $[W_2N_8]$ core.[6] Cyclic voltammetric measurements on solutions of $W_2(ap)_4$ in THF indicate the presence of a very accessible oxidation at $E_{1/2}$ = -0.067 V versus Ag/AgCl and a one-electron reduction at -0.84 V.[6]

For hpp,[3,68] DTolF,[12] $D^{Cl_2}PhF$,[14] $D^{p\text{-}Cl}PhF$),[22] and $D^{m\text{-}Me}PhF$,[22] the W_2^{4+} paddlewheel compounds are synthesized by low temperature reduction of WCl_4 with either Na/Hg or $NaBEt_3H$ followed by addition of the appropriate deprotonated ligand. The core structure of $W_2(D^{m\text{-}Me}PhF)_4$ is shown in Fig. 5.3.[22] For $W_2(hpp)_4$,[3,68] the use of the reducing agent $NaBEt_3H$ results in interstitial $NaBEt_3H$, and the structure of $W_2(hpp)_4 \cdot 2NaBEt_3H$ (2.1608(5) Å)[3] was determined. Reaction of $W_2(hpp)_4Cl_2$ in refluxing THF with potassium metal provides a synthetic pathway to $W_2(hpp)_4$ (2.1617(4) Å).[68] The room temperature reaction of four equivalents of Hhpp with the triply bonded compounds 1,2-$W_2Bu^i_2(NMe_2)_4$ or 1,2-$W_2(p\text{-tolyl})_2(NMe_2)_4$ in benzene results in the generation of isobutene and isobutylene, respectively and formation of $W_2(hpp)_4$.[73] This is a very strong reducing agent.[68] Remarkably in the gas-phase, the onset of the ionization of $W_2(hpp)_4$ (3.51 eV) is nearly 0.4 eV lower in energy than Cs.[74]

The compounds $W_2(azin)_4$[20] and $W_2(map)_4$[5] are made by substitution reactions. The former, $W_2(azin)_4$,[20] results in 75% yield from the reaction of $W_2(O_2CPh)_4$ with four equivalents

Pictiva EX2004
Samsung v Pictiva
IPR2024-01094

of Li(azin) in hexanes. The reaction of $W_2(mhp)_4$ with the lithium salt of 2-amino-6-methylpyridine (Hmap) leads to displacement of the mhp ligands and formation of $W_2(map)_4$.[5] The solvates $M_2(map)_4 \cdot 2THF$ (M = Cr, Mo, or W) are isomorphous,[5] and the W–W bond length is very similar to that in $W_2(mhp)_4$ and other complexes of this type. Other examples of ligand displacement reactions are encountered for $W_2(dmhp)_4$. Two of the dmhp ligands can be replaced by reacting $W_2(dmhp)_4$ with the lithium salts of *N,N'*-diphenylacetamidine and 1,3-diphenyltriazine, $Li[(PhN)_2CCH_3]$ and $Li[(PhN)_2N]$ respectively, in THF.[7,8] The thermally stable but air-sensitive complexes $W_2(dmhp)_2[(PhN)_2CCH_3]_2 \cdot 2THF$ and $W_2(\mu\text{-}dmhp)_2[(PhN)_2N]_2 \cdot 2THF$ contain a transoid arrangement of bridging ligands.

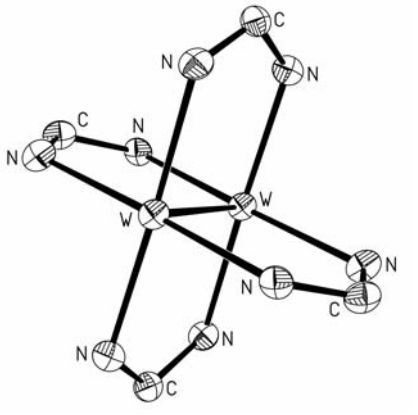


Fig. 5.3. The core of $W_2(D^{m\text{-}Me}PhF)_4$.

Similar to the tetracarboxylates, W_2^{4+} complexes with nitrogen-containing, anionic bridging ligands are easily oxidized. Reactions of $W_2(mhp)_4$ with gaseous HCl or HBr in methanol yield $[W_2X_9]^{3-}$, rather than $[W_2X_8]^{4-}$.[2,75] A similar reaction of HCl(g) with $W_2(mhp)_4$ or $W_2(dmhp)_4$ in methanol or ethanol in the presence of PEt_3 or PPr^n_3 affords a route to the doubly bonded W_2^{6+} complexes $W_2(\mu\text{-}OR)_2Cl_4(OR)_2(ROH)_2$ (R = CH_3 or C_2H_5).[75,76] These compounds contain a $\sigma^2\pi^2$ ground state electronic configuration and have been the subject of detailed structural, spectroscopic, and theoretical studies[76,77] as well as studies of their chemical reactivity.[78-80] The W_2^{6+} complexes $W_2(\mu\text{-}H)(\mu\text{-}Cl)Cl_4(\mu\text{-}dppm)_2$ and $W_2(\mu\text{-}H)(\mu\text{-}Cl)Cl_4(py)_4$ have been prepared[57,81] by reactions of $W_2(mhp)_4$ with Me_3SiCl and dppm or pyridine in methanol. The dppm complex has been structurally characterized,[57] as has the 4-ethylpyridine adduct synthesized from $W_2(\mu\text{-}H)(\mu\text{-}Cl)Cl_4(py)_4$ by ligand exchange at 100 °C.[81] The conversion of $W_2(mhp)_4$ to the W_2^{5+} complex $W_2(mhp)_3^{Cl_2}$ and subsequent structural characterization of the dichloromethane solvate has shown that a very short W–W bond is retained (2.214(2) Å).[82] Other oxidative addition reactions include the addition of chloroalkanes to $W_2(hpp)_4$ to yield $W_2(hpp)_4Cl_2$.[74]

When the tetraformamidinate complex $W_2(D^{Cl_2}PhF)_4$ is dissolved in a toluene/hexanes solution and exposed to moisture and oxygen, oxidative addition occurs to result in $W_2(\mu\text{-}OH)_2(\mu\text{-}D^{Cl_2}PhF)_2(\eta^2\text{-}D^{Cl_2}PhF)_2$.[14] This edge sharing bioctahedral W_2^{6+} compound is shown in Fig. 5.4. It has a rather short W–W bond length of 2.3508(3) Å, indicating a strong $\sigma^2\pi^2\delta^2$ interaction.

Pictiva EX2004
Samsung v Pictiva
IPR2024-01094

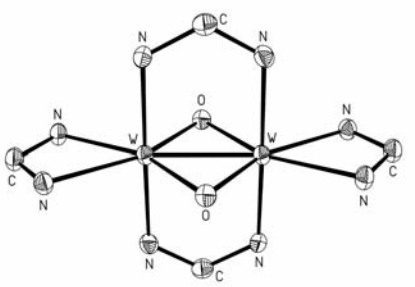


Fig. 5.4. The core of $W_2(\mu\text{-}OH)_2(\mu\text{-}D^{Cl_2}PhF)_2(\eta^2\text{-}D^{Cl_2}PhF)_2$.

5.4 W_2^{4+} Complexes without Bridging Ligands

5.4.1 Compounds coordinated by only anionic ligands

The first species prepared and unambiguously shown to possess W–W quadruple bonds were salts of the anion $[W_2(CH_3)_8]^{4-}$ and the partially chlorinated ana1ogs.[25,83,84] Reaction of either WCl_4 or WCl_5 with methyllithium at temperatures below 0 °C leads to the red anion $[W_2(CH_3)_8]^{4-}$ when a 1-2 molar excess of $LiCH_3$ is used.[84] $Li_4W_2(CH_3)_8$ can be crystallized as either the diethyl ether or tetrahydrofuran solvate $Li_4W_2(CH_3)_8{\cdot}4L$. With only about a 0.5 molar excess of $LiCH_3$, reduction to W^{II} is accomplished but there is insufficient $LiCH_3$ remaining in solution to displace all of the Cl ligands by CH_3 and accordingly the mixed methyl-chloro species $Li_4W_2(CH_3)_{8-x}Cl_x{\cdot}4L$ (L = Et_2O or THF) are formed.[83,84] For the latter, different reaction conditions yield different CH_3:Cl ratios (2.7-4.6) but with no obvious preference for any particular stoichiometry. These methyl compounds are extremely sensitive to air and moisture and are thermally unstable except at low temperatures.[84] Crystal structure determinations on $Li_4W_2(CH_3)_8{\cdot}4Et_2O$ and $Li_4W_2(CH_3)_{8-x}Cl_x{\cdot}4THF$ confirmed the existence of an eclipsed W_2L_8 geometry of idealized D_{4h} symmetry. and short W–W bond lengths.[25,83]

These $[W_2(CH_3)_8]^{4-}$ species are historically very important not only because these complete the first triad of homologous compounds containing metal-metal multiple bonds but more importantly because the existence of $[W_2(CH_3)_8]^{4-}$ suggested that compounds containing the $[W_2Cl_8]^{4-}$ anion should be isolable. This conclusion was supported by SCF-Xα-SW calculations on $[W_2Cl_8]^{4-}$ which predicted an electronic structure similar to that for $[Mo_2Cl_8]^{4-}$.[85]

While several phosphine-containing derivatives of $[W_2Cl_8]^{4-}$ were prepared first,[86] the development of a successful synthetic route to salts of $[W_2Cl_8]^{4-}$ was reported in 1982.[26] The Na/Hg reduction of WCl_4 in THF proceeds first to a green W_2^{6+} complex,[49,86,87] and then to an intensely blue colored species. Work-up of this solution at 0 °C has afforded $Na_4(THF)_xW_2Cl_8$ as a reactive blue powder.[26,87] Attempts to increase the yield of $[W_2Cl_8]^{4-}$ by performing a reduction of WCl_4 with Na/Hg in the presence of additional chloride ions were unsuccessful.[87] In one such instance, $[(Ph_3P)_2N]Cl$ was used as the chloride source but this resulted in dark violet crystals of $[(Ph_3P)_2N]_2W_2Cl_9$.[88,89]

The THF molecules in $Na_4(THF)_xW_2Cl_8$(x = 1-2) can be replaced by bidentate ethers and amines such as dimethoxyethane (DME) and tetramethylethylenediamine (TMEDA).[26,87] The salts, $Na_4(DME)_4W_2Cl_8$ and $Na_4(TMEDA)_4W_2Cl_8$, display a band at ~600 nm in their electronic absorption spectra that can be assigned to the δ→δ* transition of the $[W_2Cl_8]^{4-}$anion.[26,87] A crystal structure of $Na_4(TMEDA)_4W_2Cl_8$ has confirmed the existence of the $[W_2Cl_8]^{4-}$ anion in this salt.[26] The W–W bond lengths of 2.259(1) and 2.254(1) Å for the two independent

Pictiva EX2004
Samsung v Pictiva
IPR2024-01094

$[W_2Cl_8]^{4-}$ ions in the unit cell are about 0.11-0.13 Å longer than the Mo–Mo lengths in salts of $[Mo_2Cl_8]^{4-}$. This M–M bond lengthening is typical of that found between analogous quadruply bonded W–W and Mo–Mo species.

Samples of $Na_4(THF)_xW_2Cl_8$ react with phosphine ligands (PMe_3 and PBu^n_3) to form $W_2Cl_4(PR_3)_4$ in essentially quantitative yield.[87] The $[W_2Cl_8]^{4-}$ ion also reacts[87] with 6-methyl-2-hydroxypyridine (Hmhp) in the presence of Et_3N to yield the known quadruply bonded W_2^{4+} complex $W_2(mhp)_4$ (Section 5.3). A similar reaction with a THF solution containing pivalic acid and Et_3N at -30 °C has been used to obtain $W_2(O_2CCMe_3)_4$ as a yellow powder.[87]

Another nitrogen based ligand, tetraphenylporphyrin ($TPPH_2$) reacts with $W(CO)_6$ in refluxing decalin for 24 h to yield the black product $W_2(TPP)_2$ in 90% yield.[90] This compound has a long W–W bond length of 2.352(1) Å,[90] and a barrier to rotation of the porphyrin ligand of 11.3 kcal mol^{-1}, as estimated from NMR line shape analysis. The rotational barrier has been taken as a measure of the δ bond strength, but it should be noted that steric interactions between the porphyrin ligands and non-bonding electronic interactions are reflected in the rotational barrier. Other porphyrin complexes include derivatives of 2,3,7,8,12,13,17,18-octaethylporphyrin (OEP)[91] and *meso*-(4'-tolyl)octaethylporphyrin) (TOEP),[92] e. g., $W_2(OEP)_2$ and $W_2(TOEP)_2$, respectively. With a rotational barrier of 12.9 kcal mol^{-1} for $W_2(TOEP)_2$, the strength of the ditungsten δ bond strength appears greater than the dimolybdenum δ bond strength in isostructural metalloporphyrin compounds.[92]

In addition to these known compounds, a recent article predicts the presence of a tungsten-tungsten quadruple bond in complexes of the hypothetical phase $Ca_2W_6O_8$.[93] Based on Hückel analysis of the bonding, metallic behavior is expected.

5.4.2 Compounds coordinated by four anionic ligands and four neutral ligands

While $W_2Cl_4(PR_3)_4$ complexes have been prepared by the reaction of PR_3 with $Na_4(THF)_xW_2Cl_8$, the most convenient preparative route involves reduction of a mixture of WCl_4 and the monodentate phosphine ligand in THF with Na/Hg or $NaBEt_3H$ as shown below.[35,36,42,86,87]

$$2WCl_4 + 4Na/Hg + 4PR_3 \xrightarrow{THF} W_2Cl_4(PR_3)_4 + 4NaCl$$

$$2WCl_4 + 4NaBEt_3H + 4PR_3 \xrightarrow{THF} W_2Cl_4(PR_3)_4 + 4NaCl + 2H_2 + 4BEt_3$$
$$(PR_3 = PMe_3, PMe_2Ph, PMePh_2 \text{ or } PBu^n_3)$$

If only one equivalent of Na/Hg or $NaBEt_3H$ is used in the preceding reaction, red crystalline, edge-sharing bioctahedral complexes, $W_2Cl_6(PR_3)_4$, are obtained.[86,94] Upon treatment with a further equivalent of Na/Hg, $W_2Cl_6(PR_3)_4$ is converted to $W_2Cl_4(PR_3)_4$ for PR_3 = PMe_3 and PMe_2Ph.[86,94] When the quantity of the phosphine is limited to 1.5 equiv, then the face-sharing bioctahedral complexes such as $W_2Cl_6(PMe_2Ph)_3$ and $W_2Cl_6(PBu^n_3)_3$ are formed.[94] The first complexes of the type $W_2Br_6(PMe_2Ph)_3$ and $W_2Br_6(PMe_3)_3$ were synthesized by replacing WCl_4 with WBr_5 and adjusting the amounts of the reducing agents Na/Hg or $NaBEt_3H$ to compensate for the change in oxidation state.[94] Reduction of WBr_5 with 3 equiv of $NaBEt_3H$ and subsequent addition of PMe_2Ph or $PMePh_2$ resulted in the first synthesis of compounds with a W_2Br_4 core and formation of $W_2Br_4(PMe_2Ph)_4$ and $W_2Br_4(PMePh_2)_4$.[31]

Based upon $^{31}P\{^1H\}$ NMR data,[87] the Raman spectrum of $W_2Cl_4(PBu^n_3)_4$ (ν(W–W) at 260±10 cm^{-1}),[86] detailed electronic absorption[29,95] and photoelectron[96] studies, and crystal structure determinations of $W_2Cl_4(PMe_3)_4$[29,30] and $W_2Cl_4(PBu^n_3)_4$,[32] these ditungsten complexes are isostructural with their Mo_2^{4+} analogs. Using $^{31}P\{^1H\}$ NMR spectroscopy to monitor the

Pictiva EX2004
Samsung v Pictiva
IPR2024-01094

exchange reactions, $W_2Cl_4(PEt_3)_4$ and $W_2Cl_4(PBu^n_3)_4$ react with PMe_3, PMe_2Ph, and $PMePh_2$ to form a series of W_2Cl_4 mixed-phosphine complexes, $W_2Cl_4(PEt_3)_3(PMe_3)$, $W_2Cl_4(PEt_3)_2(PMe_3)_2$, $W_2Cl_4(PEt_3)_3(PMe_2Ph)$, $W_2Cl_4(PEt_3)_2(PMe_2Ph)_2$, $W_2Cl_4(PEt_3)_3(PMePh_2)$, $W_2Cl_4(PBu^n_3)_3(PMe_3)$, $W_2Cl_4(PBu^n_3)_3(PMe_2Ph)$, $W_2Cl_4(PBu^n_3)_2(PMe_2Ph)_2$, and $W_2Cl_4(PBu^n_3)_3(PMePh_2)$.[97] The results of the phosphine ligand exchange studies suggest that the exchange reactions proceed by an interchange dissociative mechanism, with the entering group within the W_2^{4+} coordination sphere at the axial coordination site before the rate-determining phosphine displacement step.[97]

Another synthetic method[86] involves the thermal decomposition of *trans*-$WCl_2(PMe_3)_4$ and *mer*-$WCl_3(PMe_3)_3$. The decomposition in refluxing dibutyl ether proceeds as follows:

$$\textit{trans}\text{-}WCl_2(PMe_3)_4 \xrightarrow[\text{reflux}]{Bu_2O} 0.5W_2Cl_4(PMe_3)_4 + 2PMe_3$$

$$\textit{mer}\text{-}WCl_3(PMe_3)_3 \xrightarrow[\text{reflux}]{Bu_2O} 0.25W_2Cl_4(PMe_3)_4 + 0.5WCl_4(PMe_3)_3 + 0.5PMe_3$$

Interestingly, $W_2I_4(CO)_8$ has not been useful for the preparation of complexes of the type $W_2I_4(PR_3)_4$,[98] even though the related molybdenum analog has been used to prepare $Mo_2X_4(PR_3)_4$ compounds. The asymmetrical compound 1,1-$W_2(C{\equiv}CMe)_2Cl_2(PMe_3)_4$ has been prepared[33] from the reaction between $W_2Cl_4(PMe_3)_4$ and LiC≡CMe in dimethoxyethane. Both the W–W bond length (2.268(l) Å) and the W–C bond length (2.13 Å) are consistent with the presence of significant W–C π interaction.[33] $W_2(C{\equiv}CMe)_4(PMe_3)_4$ and $W_2(C{\equiv}CBu^t)_4(PMe_3)_4$ are prepared similarly using four equivalents of LiCCMe or LiCCBu^t and $W_2Cl_4(PMe_3)_4$ in dimethoxyethane solution.[99] Only a slight lengthening of the W–W bond length for $W_2(C{\equiv}CMe)_4(PMe_3)_4$ (2.276(1) Å) is observed upon the addition of the two alkynyl ligands.[37]

The first synthesis of W_2^{4+} complexes containing monodentate nitrogen based ligands was recently achieved. Unlike the W_2^{6+} complex $W_2(\mu\text{-}H)(\mu\text{-}Cl)Cl_4(py)_4$[57,81] prepared from $W_2(mhp)_4$, the synthesis of $W_2Cl_4(4\text{-}Bu^t\text{-}py)_4$ is performed by reduction of WCl_4 by either KC_8 or $NaBEt_3H$ at low temperature in THF, followed by the addition of the amine. A similar reaction occurs with either pyridine derivatives, 4-*tert*-butylpyridine and 3-*n*-butylpyridine,[28] or primary amines resulting in $W_2Cl_4(NH_2R)_4$ complexes where R is Pr^n, Bu^t, or Cy.[27] Unlike the monodentate phosphine derivatives,[35,36,42,86,87] the crystal structure of $W_2Cl_4(4\text{-}Bu^t\text{-}py)_4$ has an eclipsed centrosymmetric structure where the pyridine groups face each other across the dimetal unit.[28] In contrast, complexes with primary amines retain a D_{2d} geometry with a *trans* arrangement of the amine ligands analogous to that of mondentate phosphine ligands.[27]

The reactions of toluene solutions of $W_2Cl_4(PBu^n_3)_4$ with the bidentate phosphine ligands 1,2-bis(dimethylphosphino)ethane (dmpe),[29,30] 1,2-bis(diphenylphosphino)ethane (dppe),[30,38] 1,3-bis(diphenylphosphino)propane (dppp),[36] 1,2-bis(diphenylphosphino)amine (dppa),[42] and 1,2-bis(diethylphosphino)ethane (depe),[40] produce green α-$W_2Cl_4(\eta^2\text{-}PP)_2$ isomers. With the exception of α-$W_2Cl_4(\eta^2\text{-}dppa)_2$, the compounds have been structurally characterized. As an example the core of α-$W_2Cl_4(\eta^2\text{-}dppp)_2$ is shown in Fig. 5.5.

Unique to this series of compounds is $W_2Cl_4(dppe)_2$ where both the green (α) and brown (β) isomers of $W_2Cl_4(dppe)_2$ have been isolated and structurally characterized.[30,38] Notable is the lengthening of the W–W bond in going from the α to the β-form of $W_2Cl_4(dppe)_2$ (2.281(1) Å versus 2.314(1) Å). This is a consequence of the staggered rotational conformation in the β-isomer (twisted 31.3° from the eclipsed conformation) which leads to a weakening of the angle-sensitive δ-bond. Only the β-isomer has been isolated and characterized for the phosphine ligands $Pr^i_2P(CH_2)_3PPr^i_2$ (dippp),[41] $Ph_2PNHPPh_2$ (dppa),[42] and $Ph_2PCH_2PPh_2$ (dppm).[34] The purple complex β-$W_2Cl_2(\mu\text{-dippp})_2$ has been prepared[41] by reduction of a mixture of WCl_4 and $Pr^i_2P(CH_2)_2PPr^i_2$ with Na/Hg. The W–W bond length is between those of the α- and β-

Pictiva EX2004
Samsung v Pictiva
IPR2024-01094

isomers of $W_2Cl_4(dppe)_2$ and, in accord with this result, the P–W–W–P torsional angle of this chiral molecule is 75.9°.[41] The complex $W_2Cl_4(\mu\text{-dppm})_2$ has been prepared by the reaction of $W_2Cl_4(PBu^n{}_3)_4$ with bis(diphenylphosphino)methane in a mixture of hexane and toluene.[34] This air-sensitive compound exhibits a $\delta \rightarrow \delta^*$ electronic transition at 730 nm. It is structurally similar to $Mo_2Cl_4(\mu\text{-dppm})_2$, but has a longer M–M bond length (2.269(1) Å versus 2.138(1) Å) and unlike its molybdenum analog possesses a slightly twisted geometry (average χ = 17°).[34] The only structurally characterized quadruply bonded W_2Br_4 complex, $W_2Br_4(\mu\text{-dppm})_2$,[31] has an eclipsed geometry that more closely resembles those of the $Mo_2X_4(\mu\text{-dppm})_2$ compounds where X is Cl, Br, or I[59,63,100-102] rather than that of $W_2Cl_4(\mu\text{-dppm})_2$, with a torsional angle of 17.25°.[34] The slightly shorter W–W bond length in $W_2Br_4(\mu\text{-dppm})_2$ (2.263(1)Å) in comparison to $W_2Cl_4(\mu\text{-dppm})_2$ (2.269(1)Å) is attributed to the torsion angle in $W_2Cl_4(\mu\text{-dppm})_2$ that results in a weaker δ bond.[31,34,103]

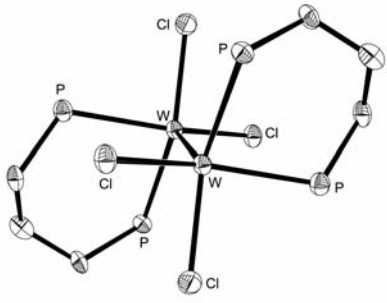


Fig. 5.5. The core of α-$W_2Cl_4(\eta^2\text{-dppp})_2$.

Using variable temperature $^{31}P\{^1H\}$ NMR spectroscopy as a probe, the position of the low lying triplet state in $W_2Cl_4(\mu\text{-dppm})_2$ and $W_2Cl_4(\mu\text{-dppe})_2$ was investigated.[104] Based on a weakening of the δ bond strength with increased torsion angles, the temperature dependence of the upfield chemical shifts to the singlet-triplet spin equilibrium allows the singlet-triplet state energy separation to be determined. For $W_2Cl_4(\mu\text{-dppm})_2$ and $W_2Cl_4(\mu\text{-dppe})_2$ with torsion angles of 17.3 and 58.7°, respectively, the energy separations between the $^1\delta^2$ and $^3\delta\delta^*$ states are -2650(20) and -1400(60) cm^{-1}.[104]

The much greater ease of oxidation of W_2^{4+} complexes compared to the Mo_2^{4+} analogs is reflected in the marked differences between the electrochemical properties of $W_2Cl_4(PBu^n{}_3)_4$ and $Mo_2Cl_4(PBu^n{}_3)_4$. For example, while solutions of $W_2Cl_4(PBu^n{}_3)_4$ in THF and CH_2Cl_2 exhibit $E_{1/2}$(ox) values of +0.04 V and -0.24 V versus SCE, respectively,[87] the corresponding values for $Mo_2Cl_4(PBu^n{}_3)_4$ are +0.64 V and +0.38 V. The tungsten complex has been oxidized chemically to the paramagnetic and EPR-active salt $[W_2Cl_4(PBu^n{}_3)_4]PF_6$ using $[Ag(NCMe)_4]PF_6$ as the oxidant.[87] When $W_2Cl_4(PBu^n{}_3)_4$ is heated with acetic acid in glyme, oxidation occurs to yield the red trinuclear W^{4+} cluster $W_3O_3Cl_5(O_2CCH_3)(PBu^n{}_3)_3$.[30,87,105] The reaction between benzoic acid (2 equiv) and $W_2Cl_4(PBu^n{}_3)_4$ (1 equiv) in benzene produces $W_2(\mu\text{-H})(\mu\text{-Cl})(\mu\text{-}O_2CPh)_2Cl_2(PBu^n{}_3)_2$,[106] the product of the oxidative addition of HCl to $W_2(O_2CPh)_2Cl_2(PBu^n{}_3)_2$. This behavior contrasts with the relative ease of producing $Mo_2(\mu\text{-}O_2CR)_2X_2(PBu^n{}_3)_2$ and $Mo_2(O_2CR)_4$ by reactions of $Mo_2X_4(PBu^n{}_3)_4$ with carboxylic acids.

There are other well documented examples of oxidative addition reactions involving W–W quadruple bonds.[107] The reaction of Cl_2 with $W_2Cl_4(dppe)_2$ affords $W_2(\mu\text{-Cl})_2Cl_4(dppe)_2$,[61] while Cl_2 (or CH_2Cl_2) oxidizes $W_2Cl_4(\mu\text{-dppm})_2$ and $W_2Cl_4(\mu\text{-dmpm})_2$ (prepared *in situ* from

Pictiva EX2004
Samsung v Pictiva
IPR2024-01094

$W_2Cl_4(PBu^n_3)_4$ and $Me_2PCH_2PMe_2$) to $W_2(\mu\text{-}Cl)_2Cl_4(\mu\text{-}dppm)_2$ and $W_2(\mu\text{-}Cl)_2Cl_4(\mu\text{-}dmpm)_2$.[108] Similar reactions between $W_2Cl_4(\mu\text{-}dppm)_2$ and Ph_2E_2 (E = S or Se) yield complexes of the types $W_2(\mu\text{-}Cl)(\mu\text{-}EPh)Cl_4(\mu\text{-}dppm)_2$ and $W_2(\mu\text{-}EPh)_2Cl_4(\mu\text{-}dppm)_2$.[109] The quantitative oxidative addition of CH_3I to $W_2Cl_4(\mu\text{-}dppm)_2$ has been achieved using visible irradiation ($\lambda > 435$ nm), whereas the thermal reactions of this complex with alkyl iodides yield $W_2Cl_5I(\mu\text{-}dppm)_2$ and $W_2Cl_4I_2(\mu\text{-}dppm)_2$.[110] The susceptibility of $W_2Cl_4(\mu\text{-}dppm)_2$ to oxidative addition is probably the explanation for why $W_2(\mu\text{-}H)(\mu\text{-}Cl)Cl_4(\mu\text{-}dppm)_2$ was obtained during unsuccessful attempts to prepare $W_2Cl_4(\mu\text{-}dppm)_2$ from the reaction between $W_2Cl_4(PBu^n_3)_4$ with dppm in toluene for 12 h.[57] The target complex $W_2Cl_4(\mu\text{-}dppm)_2$ was later prepared by a similar procedure using toluene:hexane solvent mixtures and a reduction in reaction time to 4 h.[34] Attempts to prepare $W_2Cl_4(\mu\text{-}dmpm)_2$ by the reaction of $W_2Cl_4(PBu^n_3)_4$ with $Me_2PCH_2PMe_3$ in toluene/hexane solvent mixtures led[111] instead to the W_2^{7+} complex $[Cl_2W(\mu\text{-}Cl)(\mu\text{-}dmpm)_2(\mu\text{-}PMe_2)WCl(\eta^2\text{-}CH_2PMe_2)]Cl$.

An unusual reaction occurs upon treating $W_2Cl_4(PMe_3)_4$ with H_2 (3 atm) and Na/Hg in THF at 75 °C. The product appears to be $W_2(\mu\text{-}H)(\mu\text{-}PMe_2)H_4(PMe_3)_5$; the W–W bond length is 2.588(1) Å, but the number of hydride ligands in this diamagnetic complex is not known for certain.[112] Hydrogen present due to the use of the reducing agent $NaBEt_3H$ results in the formation of $W_2(\mu\text{-}H)_2(\mu\text{-}O_2CC_6H_5)_2Cl_2(PPh_3)_2$ (2.3500(12) Å).[113] A high yield (72%) bulk preparation of $W_2(\mu\text{-}H)_2Cl_4(\mu\text{-}dppm)_2$ results by reducing WCl_4 with $NaBEt_3H$ in THF at low temperature and the subsequent addition of dppm. Without the isolation of an intermediate monodentate phosphine ligand complex such as $W_2Cl_4(PBu^n_3)_4$, the H_2 formed as a by-product of the reduction oxidatively adds to the W_2^{4+} core.[114] The W–W bond length of 2.3918(7) Å for $W_2(\mu\text{-}H)_2Cl_4(\mu\text{-}dppm)_2$ is only 0.12 Å longer than $W_2Cl_4(\mu\text{-}dppm)_2$ (2.269(1) Å).[34,114] Only a 42.8% yield of the purple complex $W_2(\mu\text{-}H)_2Cl_4(\mu\text{-}dppa)_2$ is obtained when the same synthetic methodology is used with the bidentate phosphine ligand dppa is used instead of dppm.[42] With a relatively short W–W bond length of 2.407(2) Å for $W_2(\mu\text{-}H)_2Cl_4(\mu\text{-}dppa)_2$, the $^{31}P\{^1H\}$ NMR spectra of $W_2(\mu\text{-}H)_2Cl_4(\mu\text{-}dppm)_2$ and $W_2(\mu\text{-}H)_2Cl_4(\mu\text{-}dppa)_2$ confirm the presence of a large HOMO-LUMO gap and the diamagnetism of complexes of this type.[42]

Oxidative addition to the W–W quadruple bond occurs when acetonitrile is used as solvent in attempts to prepare $W_2Cl_4(\mu\text{-}dppm)_2$ and $W_2Cl_4(\mu\text{-}dppm)_2(\eta^2\text{-}\mu\text{-}CH_3CN)$ is synthesized instead.[115] As shown in Fig. 5.6, the N–C of the acetonitrile molecule is perpendicular to the W–W bond (2.4981(10) Å) and the C–C–N bond angle is no longer linear (116.3(7)°). The $^{31}P\{^1H\}$ NMR spectrum of the molecule has an AA'BB' pattern with multiplets centered at 4 and 15 ppm, indicating the acetonitrile is not fluxional on the NMR time scale.

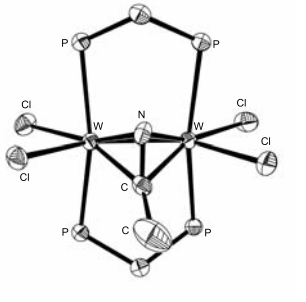


Fig. 5.6. The core of $W_2Cl_4(\mu\text{-}dppm)_2(\eta^2\text{-}\mu\text{-}CH_3CN)$.

Pictiva EX2004
Samsung v Pictiva
IPR2024-01094

5.5 Multiple Bonds in Heteronuclear Dimetal Compounds of Molybdenum and Tungsten

Quadruply bonded MoW heteronuclear dimetal complexes are relatively rare because of the difficulties in synthesizing the materials. This class of complexes has been the subject of reviews by Morris and Collman.[116,117] The heteronuclear MoW tetracarboxylates have been synthesized by refluxing a 3:1 mixture of $W(CO)_6$/$Mo(CO)_6$ in *o*-dichlorobenzene with pivalic acid to form a 70:30 mixture of $MoW(O_2CC(CH_3)_3)_4$/$Mo_2(O_2CC(CH_3)_3)_4$.[118] The mixture can be separated by selective iodination to result in the precipitation of gray $[MoW(O_2CC(CH_3)_3)_4]I$ (2.194(2) Å). Yellow $MoW(O_2CC(CH_3)_3)_4$ (2.080(1) Å)[119] is sublimed after the MoW^{4+} product is obtained from the reduction of the MoW^{5+} precursor with zinc powder.[118] Upon reaction with a saturated hydrochloric acid and addition of either CsCl or RbCl, oxidative addition at the dinuclear core occurs and the MoW^{6+} salts Cs_3MoWCl_8H or Rb_3MoWCl_8H (2.445(3) Å) are formed.[119,120]

Other bridging ligands such as the anion of 2-hydroxy-6-methylpyridine, 2,3,7,8,12,13,17,18-octaethylporphyrin, and *meso*-(4'-tolyl)octaethylporphyrin allow the preparation of $MoW(mhp)_4$, $MoW(OEP)_4$ and $MoW(TOEP)_4$, respectively.[121,122] Similar to the tetracarboxylate analog,[118] the mhp derivative can be made by refluxing a mixture of $Mo(CO)_6$, $W(CO)_6$, and Hmhp in a ratio of 1:1.5:5, in diglyme/heptane, to produce a mixture of $Mo_2(mhp)_4$ and $MoW(mhp)_4$.[121] Oxidation with iodine, separation of the brown precipitate formed, and subsequent reduction with zinc amalgam results in $MoW(mhp)_4$ in a 20% yield. The Mo–W bond length is 2.091 (1) Å.[121] Substitution of $Cr(CO)_6$ for $Mo(CO)_6$ does not yield $CrW(mhp)_4$. The compounds $MoW(OEP)_4$ and $MoW(TOEP)_4$ are prepared by refluxing a 1.25:6:1 ratio of the porphyrin, $W(CO)_6$, and $Mo(CO)_6$ in decalin.[122] Unlike the preparation of $MoW(O_2CC(CH_3)_3)_4$ and $MoW(mhp)_4$, a mixture of $Mo_2(OEP)_4$ or $Mo_2(TOEP)_4$, $MoW(OEP)_4$ or $MoW(TOEP)_4$, and $W_2(OEP)_4$ or $W_2(TOEP)_4$ were prepared and isolated by titration with ferrocenium hexafluorphosphate to allow the isolation of the cations $[MoW(OEP)_4]PF_6$ or $[MoW(TOEP)_4]PF_6$. Upon reduction with cobaltocene, the corresponding MoW^{4+} complexes were isolated. Based on ^1H variable temperature NMR spectra, the rotation barrier for $MoW(TOEP)_4$ is 10.6 kcal mol^{-1},[122] slightly smaller than the value determined for $W_2(TOEP)_2$.[92]

The most extensive series of heteronuclear MoW complexes are those of composition $MoWCl_4(PR_3)_4$ in which the quadruple bond is not supported by bridging ligands. For PR_3 = $PMePh_2$ or PMe_2Ph derivatives, the best method of preparation is to react the mononuclear compounds $Mo(\eta^6\text{-}PhPMePh)(PMePh_2)_3$ or $Mo(\eta^6\text{-}PhPMe_2)(PMe_2Ph)_3$ with $WCl_4(PPh_3)_2$ in benzene.[123,124] Substitution of $WBr_4(PPh_3)_2$ for $WCl_4(PPh_3)_2$ provides a synthetic route to $MoWBr_4(PMe_2Ph)_4$ and $MoWBr_4(PMePh_2)_4$.[31]

The lability of the phosphine ligands is illustrated by the following substitution reaction:[124]

$$MoWCl_4(PMePh_2)_4 \xrightarrow{1\text{ h, }40\ ^oC,\ PMe_3} (Me_3P)_2Cl_2MoWCl_2(PMePh_2)_2 \xrightarrow{3\text{ h, }60\ ^oC,\ PMe_3}$$

$$\square\ (Me_3P)_2Cl_2\ MoWCl_2(PMe_3)_2$$

These reactions reflect the expected trend in metal-phosphorus bond strengths, Mo–P < W–P. The PMe_3 containing complexes $MoWCl_2(PMe_3)_2(PMePh_2)_2$ and $MoWCl_2(PMe_3)_4$ have similar electronic absorption spectra (recorded in benzene) to those of $MoWCl_4(PMePh_2)_4$ and $MoWCl_4(PMe_2Ph)_4$ with the $\delta \rightarrow \delta^*$ transition in the region 650 to 635 nm.[124] Also, the cyclic voltammograms of THF solutions of all four complexes resemble one another very closely with $E_{1/2}$(ox) at +0.45 V and $E_{1/2}$(red) at -1.8 V versus SCE. Other examples of $(MoW)^{4+}$ mixed-

Pictiva EX2004
Samsung v Pictiva
IPR2024-01094

phosphine ligand complexes are obtained when the reaction of $Mo(\eta^6\text{-}PhPMe_2)(PMe_2Ph)_3$ with $WCl_4(PPh_3)_2$ is carried out in the presence of excess PPh_3. In this case, the mixed-phosphine ligand complex $(PhMe_2P)_2Cl_2MoWCl_2(PMe_2Ph)(PPh_3)$ is formed first and then undergoes partial isomerization to $(PhMe_2P)(Ph_3P)Cl_2MoWCl_2(PMe_2Ph)_2$.[125] The reactions of these isomers with THF lead to displacement of the PPh_3 ligand.[125]

The $^{31}P\{^1H\}$ NMR spectra[31,124,125] are consistent with structures of the corresponding Mo_2^{4+} and W_2^{4+} analogs with one Mo replaced by W, and X = Cl, Br and L = PR_3. X-ray crystal structures have been reported for several of the complexes. A structure determination for $MoWCl_4(PMe_3)_2(PMePh_2)_2$ revealed a Mo–W bond length of 2.207(1) Å.[124] However, for $MoWCl_4(PR_3)_4$, where PR_3 = PMe_3 (2.2092(7) Å),[124] PMe_2Ph (2.207(3) Å),[125] or $PMePh_2$ (2.210(4) and 2.207(4) Å),[124] and $MoWBr_4(PMe_2Ph)_4$ (2.209(1) Å),[31] there is a disorder of the Mo and W atoms. For both $MoWCl_4(PMe_2Ph)_4$ and $MoWBr_4(PMe_2Ph)_4$, there is evidence of a 14 and 5% contamination of the crystals by $Mo_2Cl_4(PMe_2Ph)_4$ and $Mo_2Br_4(PMe_2Ph)_4$, respectively.[31,125] The structural characterization of the isomers of composition $MoWCl_4(PMe_2Ph)_3(PPh_3)$ has been carried out on a mixed crystal of these complexes.[125]

For the bidentate phosphine ligands dppe, dmpe, and dppm, the starting material $MoWCl_4(PMePh_2)_4$ is reacted with the appropriate bidentate phosphine in either 1-propanol [dmpe and dppm] or methanol [dppe].[126] α-$MoWCl_4(dppe)_2$, α-$MoWCl_4(dmpe)_2$ (2.234(4) Å), and $MoWCl_4(\mu\text{-}dppm)_2$ (2.2110(7) Å) are formed by heating the corresponding reaction mixture, while $MoWCl_4(\mu\text{-}dppe)_2$ (2.243(1) Å) is formed from α-$MoWCl_4(dppe)_2$ upon reflux in 1-propanol for 36 h. In contrast, $MoWCl_4(\mu\text{-}dmpm)_2$ (2.193(2) Å)[127] is prepared by stirring a solution of $MoWCl_4(PMePh_2)_4$ and dmpm in a hexane/benzene solvent mixture for 1 h.[126] As in the case of the monodentate phosphine derivatives, a disorder of the metal sites, Mo and W, is observed in the crystal structures.[126, 127]

5.6 Paddlewheel Compounds with W_2^{5+} or W_2^{6+} Cores

A variety of compounds have been synthesized with either a W_2^{5+} or W_2^{6+} core and include triply bonded molecules such as $W_2(OC_6F_5)_6(NHMe_2)_2$, related molecules without bridging ligands, and edge-sharing or face-sharing bioctahedral geometries.[14,42,61,87,94,113-115,128-141] When limited to ditungsten compounds with chelating anionic ligands, the paucity of W_2^{5+} or W_2^{6+} compounds is apparent. One of the two examples with a bridging carboxylate was synthesized in 1985 by the reaction of I_2 in benzene with $W_2(O_2CCMe_3)_4$. The paramagnetic W_2^{5+} salt, $[W_2(O_2CCMe_3)_4]I$, retains the paddlewheel framework.[18] Supported by three bridging pivalate ligands, the cation $[W_2(O_2CBu^t)_3(O_2CBu^t)_2]^+$ is synthesized by reaction of $W_2(O_2CBu^t)_6$ with either Et_3OBF_4 or $Me_3SiO_3SCF_3$ in CH_2Cl_2 at room temperature.[142] The W_2^{6+} core has a distorted pentagonal pyramid geometry supported by three bridging and two chelating pivalate ligands. Loss of the anion of 2-hydroxy-6-methylpyridine results in formation of the paramagnetic orange-brown W_2^{5+} molecule $W_2(mhp)_3Cl_2$ upon refluxing $W_2(mhp)_4$ in diglyme with $AlCl_3$. Subsequent structural characterization of the dichloromethane solvate of $W_2(mhp)_3Cl_2$ has shown that a very short W–W bond (Table 5.3) is retained (2.214(2) Å).[82]

A series of W_2^{5+} and W_2^{6+} compounds has been synthesized with the anion of 1,3,4,6,7,8-hexahydro-2*H*-pyrimido[1,2-*a*]pyrimidine (hpp). The $W_2(hpp)_4Cl$ molecule has been structurally characterized as $W_2(hpp)_4Cl$ and $W_2(hpp)_4Cl_{0.5}Cl_{0.5}$ with W–W bond lengths of 2.2131(8) Å and 2.209(1) Å, respectively.[3] Surprisingly the W–Cl bond lengths vary rather significantly from 2.938(4) Å to 2.842(9) Å for $W_2(hpp)_4Cl$ and $W_2(hpp)_4Cl_{0.5}Cl_{0.5}$. While $W_2(hpp)_4Cl$ is prepared by layering a purple THF solution of $W_2Cl_4(NH_2Pr^n)_4$ over a THF solution of Lihpp, $W_2(hpp)_4Cl_{0.5}Cl_{0.5}$ is synthesized by reacting a THF solution of Lihpp with $W_2Cl_4(NH_2Pr^n)_4$ in toluene and layering the filtered solution with diethyl ether.

Pictiva EX2004
Samsung v Pictiva
IPR2024-01094

Table 5.3. Structurally characterized paddlewheel type compounds with W_2^{5+} or W_2^{6+} cores

Compound	W–W (Å)	ref.
W_2^{5+}		
$W_2(hpp)_4Cl_{0.5}Cl_{0.5}$	2.209(1)	3
$W_2(hpp)_4Cl$	2.2131(8)	3
$W_2(mhp)_3Cl_2$	2.214(2)	82
$[W_2(O_2CBu^t)_4]BF_4$	2.2762(14)	142
	2.2824(13)	
W_2^{6+}		
$W_2(hpp)_4Cl_2{\cdot}6CDCl_3$	2.2328(2)	73
$W_2(hpp)_4Cl_2{\cdot}4CH_2Cl_2$	2.2497(8)	68
$W_2(hpp)_4Cl_2$	2.250(2)	3
$[NH_2Me_2]_2W_2[(p\text{-}tert\text{-}butylcalix[4]arene)_2]$	2.2926(1)	145
$[W_2(p\text{-}tert\text{-}butylcalix[8]arene)Na_2(MeCN)_5]{\cdot}5MeCN$	2.2976(6)	143
$(NH_2Me_2)W_2[(p\text{-}tert\text{-}butylcalix[4]arene)][(p\text{-}tert\text{-}buylcalix[4]arene)H]$	2.3039(8	144,146
$[W_2(p\text{-}tert\text{-}butylcalix[4]arene)_2\{\mu\text{-}Na(pyridine)_2\}\{\mu\text{-}Na(pyridine)_3\}]{\cdot}2THF$	2.313(1)	24,147

The W_2^{6+} molecule, $W_2(hpp)_4Cl_2$, is synthesized by the reaction of WCl_4 in THF with one equivalent of $NaEt_3BH$ in the presence of Lihpp. The green-brown compound has been reported with W–W bond lengths of 2.250(2) Å and 2.2497(8) Å for the complexes $W_2(hpp)_4Cl_2$, shown in Fig. 5.7,[3] and $W_2(hpp)_4Cl_2{\cdot}4CH_2Cl_2$,[68] respectively. An alternate synthesis involves the reaction of eight equivalents of the free ligand Hhpp with the triply bonded compound $W_2Cl_2(NMe_2)_4$ in a melt for 12-15 h with evolution of $HNMe_2$.[73] A crystal structure of the $CDCl_3$ adduct $W_2(hpp)_4Cl_2{\cdot}6CDCl_3$ contains a W–W bond length of 2.2328(2) Å.[73]

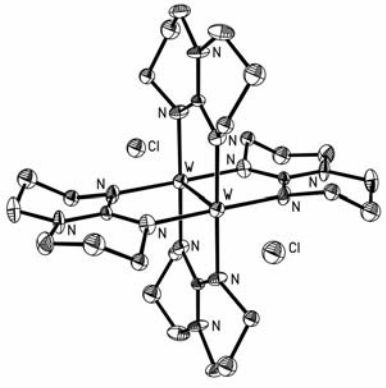


Fig. 5.7. The structure of $W_2(hpp)_4Cl_2$. The W···Cl separation of over 3.0 Å is too long to be a significant bonding interaction.

The majority of W_2^{6+} compounds result from the reaction of tungsten species with calixarene ligands.[24,143-147] The reaction of WCl_6 with the ligand *p-tert*-butylcalix[8]areneH_8 and subsequent reduction with sodium amalgam in toluene yields the orange-brown complex $[W_2(p\text{-}tert\text{-}butylcalix[8]arene)Na_2(MeCN)_5]{\cdot}5MeCN$ with a tungsten-tungsten triple bond length of 2.2976(6) Å and a torsion angle of 39.4°,[143] similar to the compound $[W_2(p\text{-}tert\text{-}butylcalix[4]arenetetrol)_2(\mu\text{-}Na(pyridine)_2\{\mu\text{-}Na(pyridine)_3\}]$ with a tungsten-tungsten bond distance of 2.313(1) Å.[24,147]

Pictiva EX2004
Samsung v Pictiva
IPR2024-01094

The triply bonded compound $W_2(NMe_2)_6$ reacts with *p-tert*-buylcalix[4]arene in toluene and retains the tungsten-tungsten triple bond to form $[NH_2Me_2]_2W_2$[(*p-tert*-buylcalix[4]arene)$_2$] (2.2926(1) Å).[145] Reaction of $[NH_2Me_2]_2W_2$[(*p-tert*-buylcalix[4]arene)$_2$] and W_2[{(*p-tert*-buylcalix[4]arene)H}$_2$] (formed by the reaction of (*p-tert*-buylcalix[4]arene)H_4 and $W_2(OBu^t)_6$ in benzene) result in the triply bonded compound $(NH_2Me_2)W_2$[(*p-tert*-buylcalix[4]arene)[(*p-tert*-buylcalix[4]arene)H] (2.3039(8) Å).[144,146]

References

1. P. Mountford and J. A. G. Williams, *J. Chem. Soc., Dalton Trans.* **1993**, 877.
2. F. A. Cotton, R. H. Niswander and J. C. Sekutowski, *Inorg. Chem.* **1979**, *18*, 1152.
3. F. A. Cotton, P. Huang, C. A. Murillo and D. J. Timmons, *Inorg. Chem. Commun.* **2002**, *5*, 501.
4. F. A. Cotton, P. E. Fanwick, R. H. Niswander and J. Sekutowski, *J. Am. Chem. Soc.* **1978**, *100*, 4725.
5. F. A. Cotton, R. H. Niswander and J. C. Sekutowski, *Inorg. Chem.* **1978**, *17*, 3541.
6. A. R. Chakravarty, F. A. Cotton and E. S. Shamshoum, *Inorg. Chem.* **1984**, *23*, 4216.
7. F. A. Cotton, W. H. Ilsley and W. Kaim, *Inorg. Chem.* **1980**, *19*, 1450.
8. F. A. Cotton, W. H. Ilsley and W. Kaim, *Inorg. Chem.* **1979**, *18*, 3569.
9. F. A. Cotton and W. Wang, *Inorg. Chem.* **1984**, *23*, 1604.
10. F. A. Cotton, W. H. Ilsley and W. Kaim, *Inorg. Chem.* **1980**, *19*, 1453.
11. F. A. Cotton, L. R. Falvello, S. Han and W. Wang, *Inorg. Chem.* **1983**, *22*, 4106.
12. F. A. Cotton and T. Ren, *J. Am. Chem. Soc.* **1992**, *114*, 2237.
13. M. H. Chisholm, H. T. Chiu and J. C. Huffman, *Polyhedron* **1984**, *3*, 759.
14. K. M. Carlson-Day, J. L. Eglin, L. T. Smith and R. J. Staples, *Inorg. Chem.* **1999**, *38*, 2216.
15. D. Baxter, R. Cayton, M. H. Chisholm, J. C. Huffman, E. Putilina, S. Tagg, J. Wesemann, J. Zwanziger and F. Darrington, *J. Am. Chem. Soc.* **1994**, *116*, 4551.
16. F. A. Cotton and W. Wang, *Inorg. Chem.* **1982**, *21*, 3859.
17. A. P. Sattelberger, K. W. McLaughlin and J. C. Huffman, *J. Am. Chem. Soc.* **1981**, *103*, 2880.
18. D. J. Santure, J. C. Huffman and A. P. Sattelberger, *Inorg. Chem.* **1985**, *24*, 371.
19. D. J. Santure, J. C. Huffman and A. P. Sattelberger, *Inorg. Chem.* **1984**, *23*, 938.
20. F. A. Cotton, L. R. Falvello and W. Wang, *Inorg. Chim. Acta* **1997**, *261*, 77.
21. D. J. Santure, K. W. McLaughlin, J. C. Huffman and A. P. Sattelberger, *Inorg. Chem.* **1983**, *22*, 1877.
22. J. L. Eglin, L. T. Smith and R. J. Staples, *Inorg. Chim. Acta* **2003**, *351*, 217.
23. F. A. Cotton and S. A. Koch, *J. Am. Chem. Soc.* **1977**, *99*, 7371.
24. L. Giannini, E. Solari, C. Floriani, N. Re, A. Chiesi-Villa and C. Rizzoli, *Inorg. Chem.* **1999**, *38*, 1438.
25. D. M. Collins, F. A. Cotton, S. A. Koch, M. Millar and C. A. Murillo, *Inorg. Chem.* **1978**, *17*, 2017.
26. F. A. Cotton, G. N. Mott, R. R. Schrock and L. G. Sturgeoff, *J. Am. Chem. Soc.* **1982**, *104*, 6781.
27. F. A. Cotton, E. V. Dikarev and S. Herrero, *Inorg. Chem. Commun.* **1999**, *2*, 98.
28. F. A. Cotton, E. V. Dikarev, J. D. Gu, S. Herrero and B. Modec, *Inorg. Chem.* **2000**, *39*, 5407.
29. F. A. Cotton, M. W. Extine, T. R. Felthouse, B. W. S. Kolthammer and D. G. Lay, *J. Am. Chem. Soc.* **1981**, *103*, 4040.
30. F. A. Cotton, T. R. Felthouse and D. G. Lay, *J. Am. Chem. Soc.* **1980**, *102*, 1431.
31. F. A. Cotton, J. L. Eglin and C. A. James, *Inorg. Chem.* **1993**, *32*, 681.
32. F. A. Cotton, J. G. Jennings, A. C. Price and K. Vidyasagar, *Inorg. Chem.* **1990**, *29*, 4138.
33. T. C. Stoner, S. J. Geib and M. D. Hopkins, *J. Am. Chem. Soc.* **1992**, *114*, 4201.
34. J. M. Canich and F. A. Cotton, *Inorg. Chim. Acta* **1988**, *142*, 69.
35. F. A. Cotton, J. L. Eglin and C. A. James, *Acta Crystallogr.* **1993**, *C49*, 893.
36. J. L. Eglin, E. J. Valente, K. R. Winfield and J. D. Zubkowski, *Inorg. Chim. Acta* **1996**, *245*, 81.

Pictiva EX2004
Samsung v Pictiva
IPR2024-01094

37. K. D. John, V. M. Miskowski, M. A. Vance, R. F. Dallinger, L. C. Wang, S. J. Geib and M. D. Hopkins, *Inorg. Chem.* **1998**, *37*, 6858.
38. F. A. Cotton and T. Felthouse, *Inorg. Chem.* **1981**, *20*, 3880.
39. K. M. Carlson-Day, J. L. Eglin, C. Lin, T. Ren, E. J. Valente and J. D. Zubkowski, *Inorg. Chem.* **1996**, *35*, 4727.
40. K. M. Carlson-Day, J. L. Eglin, K. M. Huntington and R. J. Staples, *Inorg. Chim. Acta* **1998**, *271*, 49.
41. M. D. Fryzuk, C. G. Kreiter and W. S. Sheldrick, *Chem. Ber.* **1989**, *122*, 851.
42. J. L. Eglin, L. T. Smith, R. J. Staples, E. J. Valente and J. D. Zubkowski, *J. Organomet. Chem.* **2000**, *596*, 136.
43. T. A. Stephenson, E. Bannister and G. Wilkinson, *J. Chem. Soc.* **1964**, 2538.
44. T. A. Stephenson and D. Whittaker, *Inorg. Nucl. Chem. Lett.* **1969**, *5*, 569.
45. F. A. Cotton and M. Jeremic, *Synth. Inorg. Metal-Org. Chem.* **1971**, *1*, 265.
46. G. Holste, *Z. anorg. allg. Chem.* **1973**, *398*, 249.
47. A. Bino, F. A. Cotton, Z. Dori, S. Koch, H. Kueppers, M. Millar and J. C. Sekutowski, *Inorg. Chem.* **1978**, *17*, 3245
48. A. Bino, K. F. Hesse and H. Kueppers, *Acta Crystallogr.* **1980**, *B36*, 723.
49. D. J. Bergs, M. H. Chisholm, K. Folting, J. C. Huffman and K. A. Stahl, *Inorg. Chem.* 1988, 27, 2950.
50. D. J. Santure and A. P. Sattelberger, *Inorg. Synth.* **1989**, *26*, 219.
51. G. M. Bancroft, E. Pellach, A. P. Sattelberger and K. W. McLaughlin, *J. Chem. Soc., Chem. Commun.* **1982**, 752.
52. D. L. Lichtenberger and J. G. Kristofzski, *J. Am. Chem. Soc.* **1987**, *109*, 3458.
53. G. S. Girolami and R. A. Andersen, *Inorg. Chem.* **1982**, *21*, 1318
54. F. A. Cotton and D. G. Lay, *Inorg. Chem.* **1981**, *20*, 935.
55. D. J. Santure and A. P. Sattelberger, *Inorg. Chem.* **1985**, *24*, 3477
56. G. S. Girolami, V. V. Mainz and R. A. Andersen, *Inorg. Chem.* **1980**, *19*, 805.
57. P. E. Fanwick, W. S. Harwood and R. A. Walton, *Inorg. Chem.* **1987**, *26*, 242.
58. F. A. Cotton, L. R. Falvello, W. S. Harwood, G. L. Powell and R. A. Walton, *Inorg. Chem.* **1986**, *25*, 3949.
59. F. A. Cotton, K. R. Dunbar and R. Poli, *Inorg. Chem.* **1986**, *25*, 3700.
60. J. D. Chen, F. A. Cotton and L. R. Falvello, *J. Am. Chem. Soc.* **1990**, *112*, 1076.
61. P. A. Agaskar, F. A. Cotton, K. R. Dunbar, L. R. Falvello and C. J. O'Connor, *Inorg. Chem.* **1987**, *26*, 4051.
62. F. A. Cotton, L. M. Daniels, G. L. Powell, A. J. Kahaian, T. J. Smith and E. F. Vogel, *Inorg. Chim. Acta* **1988**, *144*, 109.
63. M. D. Hopkins, W. P. Schaefer, M. J. Bronikowski, W. H. Woodruff, V. M. Miskowski, R. F. Dallinger and H. B. Gray, *J. Am. Chem. Soc.* **1987**, *109*, 408.
64. J. V. Brenčič and F. A. Cotton, *Inorg. Chem.* **1970**, *9*, 351.
65. R. H. Cayton, M. H. Chisholm, J. C. Huffman and E. B. Lobkovsky, *J. Am. Chem. Soc.* **1991**, *113*, 8709.
66. M. J. Byrnes and M. H. Chisholm, *Chem. Commun.* **2002**, 2040.
67. F. A. Cotton, S. A. Koch, A. J. Schultz and J. M. Williams, *Inorg. Chem.* **1978**, *17*, 2093
68. F. A. Cotton, P. Huang, C. A. Murillo and X. Wang, *Inorg. Chem. Commun.* **2003**, *6*, 121.
69. B. E. Bursten, F. A. Cotton, A. H. Cowley, B. E. Hanson, M. Lattman and G. G. Stanley, *J. Am. Chem. Soc.* **1979**, *101*, 6244.
70. F. A. Cotton and D. J. Timmons, *Polyhedron* **1998**, *17*, 179.
71. W. H. deRoode, K. Vrieze, E. A. Koerner von Gustorf and A. Ritter, *J. Organomet. Chem.* **1977**, *135*, 183.
72. J. D. Schagen and H. Schenk, *Crystallogr. Struct. Commun.* **1978**, *7*, 223.
73. M. H. Chisholm, J. Gallucci, C. M. Hadad, J. C. Huffman and P. J. Wilson, *J. Am. Chem. Soc.* **2003**, *125*, 16040.

Pictiva EX2004
Samsung v Pictiva
IPR2024-01094

74. F. A. Cotton, N. E. Gruhn, J. Gu, P. Huang, D. L. Lichtenberger, C. A. Murillo, L. O. VanDorn and C. C. Wilkinson, *Science* **2002**, *298*, 1971.
75. D. DeMarco, T. Nimry and R. A. Walton, *Inorg. Chem.* **1980**, *19*, 575.
76. L. B. Anderson, F. A. Cotton, D. DeMarco, A. Fang, W. H. Ilsley, B. W. S. Kolthammer and R. A. Walton, *J. Am. Chem. Soc.* **1981**, *103*, 5078.
77. F. A. Cotton, L. R. Falvello, M. F. Fredrich, D. DeMarco and R. A. Walton, *J. Am. Chem. Soc.* **1983**, *105*, 3088.
78. F. A. Cotton, D. DeMarco, B. W. S. Kolthammer and R. A. Walton, *Inorg. Chem.* **1981**, *20*, 3048.
79. W. S. Harwood, D. DeMarco and R. A. Walton, *Inorg. Chem.* **1984**, 23, 3077.
80. J. Savard and H. Alper, *Can. J. Chem.* **1988**, *66*, 2483.
81. R. T. Carlin and R. E. McCarley, *Inorg. Chem.* **1989**, *28*, 2604.
82. T. R. Ryan and R. E. McCarley, *Croatica Chem. Acta* **1995**, *68*, 769.
83. D. M. Collins, F. A. Cotton, S. Koch, M. Millar and C. A. Murillo, *J. Am. Chem. Soc.* **1977**, *99*, 1259.
84. F. A. Cotton, S. Koch, K. Mertis, M. Millar and G. Wilkinson, *J. Am. Chem. Soc.* **1977**, *99*, 4989.
85. F. A. Cotton and B. J. Kalbacher, *Inorg. Chem.* **1977**, *16*, 2386.
86. P. R. Sharp and R. R. Schrock, *J. Am. Chem. Soc.* **1980**, *102*, 1430.
87. R. R. Schrock, L. G. Sturgeoff and P. R. Sharp, *Inorg. Chem.* **1983**, *22*, 2801.
88. F. A. Cotton, L. R. Falvello, G. N. Mott, R. R. Schrock and L. G. Sturgeoff, *Inorg. Chem.* **1983**, *22*, 2621.
89. C. Mertis and N. Psaroudakis, *Polyhedron* **1989**, *8*, 469.
90. J. C. Kim, V. L. Goedken and B. M. Lee, *Polyhedron* **1996**, *15*, 57.
91. J. P. Collman, J. M. Garner and L. K. Woo, *J. Am. Chem. Soc.* **1989**, *111*, 8141.
92. J. P. Collman, J. M. Garner, R. T. Hembre and Y. Ha, *J. Am. Chem. Soc.* **1992**, *114*, 1292.
93. M. M. Balakrishnarajan, P. Kroll, M. J. Bucknum and R. Hoffmann, *New J. Chem.* **2004**, *28*, 185.
94. F. A. Cotton and S. K. Mandal, *Inorg. Chem.* **1992**, *31*, 1267.
95. M. D. Hopkins, V. M. Miskowski and H. B. Gray, *J. Am. Chem. Soc.* **1988**, *110*, 1787.
96. F. A. Cotton, J. L. Hubbard, D. L. Lichtenberger and I. Shim, *J. Am. Chem. Soc.* **1982**, *104*, 679.
97. M. H. Chisholm and J. M. McInnes, *J. Chem. Soc., Dalton Trans.* **1997**, 2735.
98. F. A. Cotton, L. R. Falvello and R. Poli, *Polyhedron* **1987**, *6*, 1135.
99. T. Stoner, W. P. Schaefer, R. E. Marsh and M. D. Hopkins, *J. Cluster Science* **1994**, *5*, 107.
100. S. A. Best, T. J. Smith and R. A. Walton, *Inorg. Chem.* **1978**, *17*, 99.
101. E. H. Abbott, K. S. Bose, F. A. Cotton, W. T. Hall and J. C. Sekutowski, *Inorg. Chem.* **1978**, *17*, 3240.
102. F. L. Campbell, F. A. Cotton and G. L. Powell, *Inorg. Chem.* **1985**, *24*, 177.
103. M. C. Milletti, *Polyhedron* **1993**, *12*, 401.
104. F. A. Cotton, J. L. Eglin, B. Hong and C. A. James, *Inorg. Chem.* **1993**, *32*, 2104.
105. F. A. Cotton, T. R. Felthouse and D. G. Lay, *Inorg. Chem.* **1981**, *20*, 2219.
106. F. A. Cotton and G. N. Mott, *J. Am. Chem. Soc.* **1982**, *104*, 5978.
107. T.-L. C. Hsu, S. A. Helvoigt, C. M. Partigianoni, C. Turro and D. G. Nocera, *Inorg. Chem.* **1995**, *34*, 6186.
108. J. A. M. Canich, F. A. Cotton, L. M. Daniels and D. B. Lewis, *Inorg. Chem.* **1987**, *26*, 4046.
109. J. A. M. Canich, F. A. Cotton, K. R. Dunbar and L. R. Falvello, *Inorg. Chem.* **1988**, *27*, 804.
110. C. M. Partigianoni and D. G. Nocera, *Inorg. Chem.* **1990**, *29*, 2033.
111. F. A. Cotton, J. A. M. Canich, R. L. Luck and K. Vidyasagar, *Organometallics* **1991**, *10*, 352.
112. K. W. Chiu, R. A. Jones, G. Wilkinson, A. M. R. Galas and M. B. Hursthouse, *J. Chem. Soc., Dalton Trans.* **1981**, 487.
113. K. M. Carlson-Day, T. E. Concolino, J. L. Eglin, C. Lin, T. Ren, E. J. Valente and J. D. Zubkowski, *Polyhedron* **1996**, *15*, 4469.
114. T. E. Concolino, J. L. Eglin, E. J. Valente and J. D. Zubkowski, *Polyhedron* **1997**, *16*, 4137.
115. J. L. Eglin, E. M. Hines, E. J. Valente and J. D. Zubkowski, *Inorg. Chim. Acta* **1995**, *229*, 113.
116. R. H. Morris, *Polyhedron* **1987**, *6*, 793.

Pictiva EX2004
Samsung v Pictiva
IPR2024-01094

117. J. P. Collman and R. Boulatov, *Angew. Chem. Int. Ed.* **2002**, *41*, 3948.
118. V. Katovic, J. L. Templeton, R. J. Hoxmeier and R. E. McCarley, *J. Am. Chem. Soc.* **1975**, *97*, 5300.
119. V. Katovic and R. E. McCarley, *J. Am. Chem. Soc.* **1978**, *100*, 5586.
120. V. Katovic and R. E. McCarley, *Inorg. Chem.* **1978**, *17*, 1268.
121. F. A. Cotton and B. E. Hanson, *Inorg. Chem.* **1978**, *17*, 3237
122. J. P. Collman, S. T. Harford, S. Franzen, T. A. Eberspacher, R. K. Shoemaker and W. H. Woodruff, *J. Am. Chem. Soc.* **1998**, *120*, 1456.
123. R. L. Luck and R. H. Morris, *J. Am. Chem. Soc.* **1984**, *106*, 7978.
124. R. L. Luck, R. H. Morris and J. F. Sawyer, *Inorg. Chem.* **1987**, *26*, 2422.
125. F. A. Cotton, L. R. Falvello, C. A. James and R. L. Luck, *Inorg. Chem.* **1990**, *29*, 4759.
126. F. A. Cotton and C. A. James, *Inorg. Chem.* **1992**, *31*, 5298.
127. F. A. Cotton, K. R. Dunbar, B. Hong, C. A. James, J. H. Matonic and J. L. C. Thomas, *Inorg. Chem.* **1993**, *32*, 5183.
128. R. G. Abbott, F. A. Cotton and L. R. Falvello, *Inorg. Chem.* **1990**, *29*, 514.
129. M. H. Chisholm, I. P. Parkin, W. E. Streib and K. S. Folting, *Polyhedron* **1991**, *10*, 2309.
130. M. H. Chisholm, K. S. Kramer, J. D. Martin, J. C. Huffman, E. B. Lobkovsky and W. E. Strieb, *Inorg. Chem.* **1992**, *31*, 4469.
131. F. A. Cotton, E. V. Dikarev and W.-Y. Wong, *Inorg. Chem.* **1997**, *36*, 80.
132. F. A. Cotton, E. V. Dikarev, N. Nawar and W.-Y. Wong, *Inorg. Chem.* **1997**, *36*, 559.
133. F. A. Cotton, E. V. Dikarev and W.-Y. Wong, *Inorg. Chem.* **1997**, *36*, 902.
134. F. A. Cotton, E. V. Dikarev, N. Nawar and W.-Y. Wong, *Inorg. Chim. Acta* **1997**, *262*, 21.
135. F. A. Cotton, E. V. Dikarev and W.-Y. Wong, *Polyhedron* **1997**, *16*, 3893.
136. M. H. Chisholm, K. Folting and D.-D. Wu, *Acta Crystallogr.* **1998**, *C54*, 225.
137. J. T. Barry, S. T. Chacon, M. H. Chisholm, V. F. DiStasi, J. C. Huffman, W. E. Streib and W. G. Van Der Sluys, *Inorg. Chem.* **1993**, *32*, 2322.
138. S. T. Chacon, M. H. Chisholm, W. E. Streib and W. G. Van Der Sluys, *Inorg. Chem.* **1989**, *28*, 5.
139. F. A. Cotton, J. L. Eglin and C. J. James, *Inorg. Chem.* **1993**, *32*, 687.
140. K. M. Carlson-Day, J. L. Eglin, E. J. Valente and J. D. Zubkowski, *Inorg. Chim. Acta* **1996**, *244*, 151.
141. K. M. Carlson-Day, J. L. Eglin, E. J. Valente and J. D. Zubkowski, *Inorg. Chim. Acta* **1999**, *284*, 300.
142. T. A. Budzichowski, M. H. Chisholm, J. C. Huffman, K. S. Kramer and M. G. Fromhold, *Inorg. Chim. Acta* **1993**, *213*, 141.
143. V. C. Gibson, C. Redshaw and M. R. J. Elsegood, *Chem. Commun.* **2002**, 1200.
144. M. H. Chisholm, K. Folting, W. E. Streib and D.-D. Wu, *Inorg. Chem.* **1999**, *38*, 5219.
145. U. Radius and J. Attner, *Eur. J. Inorg. Chem.* **1998**, 299.
146. M. H. Chisholm, K. Folting, W. E. Streib and D.-D. Wu, *Chem. Commun.* **1998**, 379.
147. L. Giannini, E. Solari, A. Zanotti-Gerosa, C. Floriani, A. Chiesi-Villa and C. Rizzoli, *Angew. Chem. Int. Ed. Engl*. **1997**, *36*, 753.
148. V. Calvo-Pérez, T. P. Fehlner and A. L. Rheingold, *Inorg. Chem.* **1996**, *35*, 7289.
149. T. P. Fehlner, V. Calvo-Pérez and W. Cen, *J. Electr. Spectrosc. Related Phenom.* **1993**, *66*, 29.
150. P. E. Fanwick, W. S. Harwood and R. A. Walton, *Inorg. Chem.* **1987**, *26*, 242.

Pictiva EX2004
Samsung v Pictiva
IPR2024-01094

6

$X_3M{\equiv}MX_3$ Compounds of Molybdenum and Tungsten

Malcolm H. Chisholm and Carl B. Hollandsworth,
The Ohio State University

6.1 Introduction

After the dimetal unit within the cubic X_4MMX_4 structural motif, the $X_3M{\equiv}MX_3$ compounds of Mo and W provide the most pertinent examples of coordination complexes having metal–metal multiple bonds. For the most part $X_3M{\equiv}MX_3$ compounds have staggered conformations with MMX bond angles within the range 100-105° which has led to the common description as "ethane-like" dimers. This terminology, though descriptively useful, is not totally accurate. There is, to date, no evidence for the existence of their monomeric counterparts, although Cummins and coworkers have made monomeric Mo complexes with extremely bulky amide ligands.[1-3]

Moreover, unlike substituted ethane derivatives, a number of eclipsed $X_3M{\equiv}MX_3$ ground state geometries are known which calls into question the optimum enthalpic geometry of the $X_3M{\equiv}MX_3$ species. It is, however, a very striking testimony to the strength of MM multiple bonding that $X_3M{\equiv}MX_3$ species exist in preference to the bridged-ligand structures (e.g., $X_2M_2(\mu\text{-}X)_2M_2X_2$) which have been known for many M(III) compounds with attendant uninegative ligands such as amides, alkoxides, halides, and thiolates.[4]

As a result of the three M–X σ-bonds formed at each metal and the formation of the MM triple bond, each metal attains a share of 12 electrons. With ligands X that are capable of π-donation (e.g., amide, alkoxide, or thiolate), the metal atoms may increase their effective electron count and thereby formally satisfy the EAN rule. However, such π-buffering leaves the metal atoms susceptible to nucleophilic attack by σ-donating ligands and the $X_3M{\equiv}MX_3$ compounds commonly increase their coordination numbers through association of neutral Lewis bases. This increase in coordination number can also be achieved by transforming the X^- ligands into bidentate ligands such as in the replacement of alkoxides with carboxylates. The inherent coordinative unsaturation of $X_3M{\equiv}MX_3$ compounds allows uptake of a wide variety of substrates by the dinuclear center.

If this substrate is redox active, very interesting and often unusual reactions can be observed. Research in the Chisholm group over the last three decades has elucidated much of the coordination chemistries of $X_3M{\equiv}MX_3$ compounds. This work has also focused on connecting the chemistries of M≡M bonds with those of MM single, double and quadruple bonds for M = Mo and W. Singly- and doubly-bonded compounds can be accessed by oxidative-addition reactions

Pictiva EX2004
Samsung v Pictiva
IPR2024-01094

at the M≡M bond and, conversely, reductive elimination leads to quadruply bonded species. Much of this closely related chemistry involving the reactivities of $X_3M{\equiv}MX_3$ compounds is summarized within this chapter.

6.2 Homoleptic $X_3M{\equiv}MX_3$ Compounds

6.2.1 Synthesis and characterization of homoleptic M_2X_6 compounds

The first member in the $X_3M{\equiv}MX_3$ series was $Mo_2(CH_2SiMe_3)_6$ (Fig. 6.1) formed in a metathetic reaction involving Me_3SiCH_2MgBr and a molybdenum trihalide.[5] Also claimed, though without full structural characterization were $Mo_2(CH_2Ph)_6$[5], $W_2(CH_2CMe_3)_6$[6], and $W_2(CH_2SiMe_3)_6$.[5] These compounds were formed in metathetic reactions involving $MoCl_5$ or WCl_6. The yellow $Mo_2(CH_2SiMe_3)_6$ (m.p. 99 °C) and orange-brown $W_2(CH_2SiMe_3)_6$ (m.p. 110 °C) were volatile and sublimed *in vacuo* at 10^{-4} torr at 100–120 °C. These alkyl compounds are hydrocarbon soluble, diamagnetic, and stable to dry air in the solid-state for short periods of time but are oxidized by air in solution. Their NMR spectra indicated only one type of alkyl ligand.

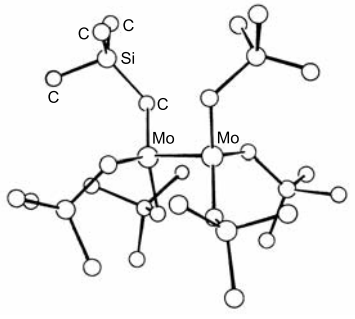


Fig. 6.1. The structure of $Mo_2(CH_2SiMe_3)_6$.

As is now well known, metathetic reactions involving Mo and W halides are extremely complex and lead to the formation of several different compounds via redox reactions and C–H bond activation processes. Subsequently, compounds such as the paramagnetic d^1-Mo(V) alkylidene, $(Me_3SiCH_2)_3Mo{=}CHSiMe_3$ and the diamagnetic alkylidyne bridged complex $[(Me_3SiCH_2)_2W]_2(\mu\text{-}CSiMe_3)_2$ were also discovered as products in these reactions.[7] Alkyl for alkoxide group exchange involving $M_2(OR)_6$ compounds proved a cleaner route to the homoleptic M_2R_6 compounds. This was first noted by Rothwell[8] and further explored by Gilbert.[9] Bonding parameters for the structurally characterized homoleptic alkyls are given in Table 6.1. Notably absent are homoleptic compounds with β-hydrogen-containing alkyl ligands.

Table 6.1. Structural parameters for homoleptic M_2X_6 compounds

M	X	M–M[a]	M–X[b]	M–M–X[c]	sym[d]	ref.
Mo	CH_2SiMe_3	2.167	2.13	100	s	5
Mo	CH_2SiMe_2Ph	2.170	2.11	100	s	10
Mo	CH_2Ph	2.175	2.16	98	s	8
Mo	CH_2CMe_2Ph	2.176	2.13	98	s	10
Mo	⅓ $(OCHMe_2)_3N$	2.177	1.95	99	s	11
Mo	½ $NPr^i(CH_2)_2Pr^iN$	2.188	1.97	101	e	12
Mo	½ $NMe(CH_2)_2MeN$	2.190	1.97	102	e	15

Pictiva EX2004
Samsung v Pictiva
IPR2024-01094

M	X	M–M[a]	M–X[b]	M–M–X[c]	sym[d]	ref.
Mo	½ $OCMe_2CMe_2O$	2.194	1.89	99	e	13
Mo	NMe_2	2.214	1.98	103	s	14,15
Mo	⅓ $Si_7O_{12}Cy_7$	2.215	1.90	102	s	16
Mo	½ (S)-(-)-$OCPh_2CH_2CH_2O$	2.217	1.90	100	e	17
Mo	glucofuranoside[g]	2.218	1.90	102	s	18
Mo	$SeC_6H_2Me_3$	2.218	2.44	97	s	19
Mo	OCH_2Bu^t	2.222	1.87	103	s	20
Mo	SMes	2.228	2.33	97	s	21,22
Mo	$OCMe(CF_3)_2$	2.230	1.88	98	s	23
Mo	$OCMe_2Ph$	2.238	1.89	101	s	9
Mo	$O_2Si(OBu^t)_2$	2.240	1.91[e]	96	e	24
W	CH_2Ph	2.249	2.16	98	s	10
W	CH_2SiMe_3	2.255	2.14	102	s	25
Mo	O-1,4-dipentyl-[2,2,2]-bicyclooctyl	2.258	1.89	104	s	26
W	CH_2SiMe_2Ph	2.259	2.11	102	s	10
W	½ $NMe(CH_2)_2MeN$	2.265	1.97	102	e	13
W	½ $OCMe_2CMe_2O$	2.274	1.90	100	e	27
W	O_2CBu^t	2.292	2.10[e]	96	e	28
W	NMe_2	2.292	1.97	103	s	29,30
W	SeMes	2.300	2.43	97	s	19
Mo	½ COT	2.302	na[f]	na[f]	e	31
W	$OCMe(CF_3)_2$	2.309	1.88	101	s	9
W	SMes	2.312	2.32	97	s	22
W	OPr^i	2.315	1.87	106	s	32
W	$OSiMe_2Bu^t$	2.324	1.93	100	s	33
W	OBu^t	2.333	1.89	109	s	h
W	glucofuranoside[g]	2.334	1.87	109	s	18
W	(+)-mentholate	2.338	1.88	104	s	34
W	OCy	2.340	1.87	107	s	27
W	O-1,4-dipentyl-[2,2,2]-bicyclooctyl	2.341	1.88	105	s	26
W	½ $OCMe_2CH_2CMe_2O$	2.360	1.87	110	e	35-37
W	½ 1,4-TMS_2-COT	2.363	na[f]	na[f]	e	h
W	½ COT	2.375	na[f]	na[f]	e	31

[a] Å, ± 0.001 Å
[b] Å, ± 0.01 Å
[c] °, ± 0.1 °
[d] s = staggered, e = eclipsed
[e] disregarding axial coordination
[f] for COT compounds there are a variety of M–C bond lengths ranging from 2.22(1) to 2.56(1) Å
[g] anion of 1,2:5,6-di-O-isopropylidene-α-D-glucofuranose
[h] M. H. Chisholm, J. C. Gallucci, and C. B. Hollandsworth, unpublished results

The amides $M_2(NMe_2)_6$ were subsequently discovered[14, 15, 38-41] and based on the well-known alcoholysis of metal amides, the alkoxides $M_2(OR)_6$ were synthesized.[20, 42-44] The original preparation of the dimetal amides involved reactions of metal chlorides $MoCl_3$, $MoCl_5$, WCl_4, or WCl_6 with $LiNMe_2$ in mixed hydrocarbon/ether solutions.[15,30] Again, the reactions were complex, giving many products such as mononuclear $W(NMe_2)_6$[45] and $Mo(NMe_2)_4$.[46,47] The compounds $Mo(NMe_2)_4$ and $Mo_2(NMe_2)_6$ were separable by their different volatilities. $Mo(NMe_2)_4$

Pictiva EX2004
Samsung v Pictiva
IPR2024-01094

sublimes at *c.* 40–60 °C at 10^{-2} torr whereas $Mo_2(NMe_2)_6$ sublimes at *c.* 80–100 °C. $W_2(NMe_2)_6$ has similar volatility to $W(NMe_2)_6$ and both sublime at *c.* 80–100 °C at 10^{-2} torr. The pure mononuclear amide is rather sparingly soluble in hydrocarbon solvents, giving ruby-like cubic crystals[45] but mixtures of the mononuclear and dinuclear amides co-crystallize giving crystals of $W_2(NMe_2)_6 \cdot W(NMe_2)_6$.[30] Crystals of pure $W_2(NMe_2)_6$ have also been obtained.[30] Because these compounds crystallize in different space groups, a rapid unit cell determination can differentiate between the three species once they are separated. Also, $W_2(NMe_2)_6$ is pale yellow whereas $W(NMe_2)_6$ is red and the 1:1 crystals appear orange.

Improved syntheses of the dinuclear amides followed by using different halide starting materials, $MoCl_3(dme)$[23] and $NaW_2Cl_7(thf)_5$.[6] The pure $M_2(NMe_2)_6$ compounds when sublimed are fluffy and pale yellow powders. They are soluble and stable in dry, deoxygenated hydrocarbon solvents but extremely reactive to air in both the solid-state and in solution. Attempts to prepare other dinuclear, homoleptic amides usually failed except in the case of $Mo_2(NMeEt)_6$ and $Mo_2(NEt_2)_6$ which are well-characterized.[15] With the more bulky NEt_2 ligand the mixed chloro/amido compound $W_2Cl_2(NEt_2)_4$ was also well-characterized.[48] Subsequently, others working with bulky primary amides have obtained similar dinuclear amido-chlorides having MM triple bonds.[49-51]

The molecular structure of $Mo_2(NMe_2)_6$ is shown in Fig. 1.7 (see page 16). The molecule has virtual D_{3d} symmetry and the NMe_2 ligands are arranged so that six Me–N bonds lie over the M≡M bond, and six lie away. These proximal and distal methyl groups exhibit markedly different chemical shifts in their ^1H and ^{13}C NMR spectra because of the large magnetic anisotropy induced by the M≡M unit. Those lying over the triple bond are deshielded (δ 4 ppm in ^1H NMR) and those lying away are shielded (δ 2 ppm) relative to the typical chemical shift (3 ppm) for a metal amide.[52] However, rapid rotation about the M–N bond occurs on the NMR time scale at high temperatures (*c.* 70 to 80 °C), giving a single resonance as an average of the proximal and distal chemical shifts. From dynamic NMR line broadening and coalescence behavior the activation energy for rotation about the M–N bond has been estimated to be 12 kcal mol^{-1} for $Mo_2(NMe_2)_6$. The ^1H NMR spectrum of $Mo_2(NMeEt)_6$ shows similar but slightly more complex variable temperature behavior as a result of the interconversion of several rotamers having different ratios of proximal and distal methyl and ethyl groups.[15]

Reactions employing $WCl_4(Et_2O)_2$ or $MoCl_3(dme)$ and the lithium salt of *N*,*N*′-dimethylethylenediamine led to the isolation of the pale yellow, crystalline $M_2(MeNCH_2CH_2NMe)_3$ compounds in which the bidentate diamide spans the M≡M bond and leads to a near eclipsed M_2N_6 skeleton.[13] The eclipsed geometry arises from the strain formed within the resulting six-membered ring incorporating the M≡M bond. A related *N*,*N*′-diisopropyldiamide, $Mo_2(Pr^iNCH_2CH_2NPr^i)_3$, was recently reported as the product from the reaction between $MoCl_3(dme)$ and the dilithioamide salt. It too had an eclipsed structure.[53] The initial preparation of these near-eclipsed M_2N_6-containing dimers was prompted by the prediction of Albright and Hoffmann that M_2X_6 compounds should be eclipsed in order to maximize the MM bonding.[54] As seen in Table 6.1 the MM bond distances are slightly shorter for these compounds.

Homoleptic, dinuclear alkoxides, $M_2(OR)_6$, can be obtained by the addition of at least six equivalents of alcohol to the $M_2(NR_2)_6$ amides:[20]

$$M_2(NMe_2)_6 + 6ROH \rightarrow M_2(OR)_6 + 6HNMe_2$$

In several instances, competing reactions occur and only tetranuclear alkoxide clusters are obtained by this method. These clusters will be discussed in Section 6.5. However, the use of bulky, usually tertiary alkoxides guarantees the formation of dinuclear species. In the case of molybdenum, a fairly extensive series of $Mo_2(OR)_6$ compounds was isolated via this route,

Pictiva EX2004
Samsung v Pictiva
IPR2024-01094

namely for R = CH_2Bu^t, Pr^i, Bu^t, CHMePh, $SiMe_3$, and $SiEt_3$.[20] Subsequently, Gilbert noted that several fluorinated alkoxides could be prepared by the direct reaction between $MoCl_3$(dme) and the lithium or sodium alkoxide, thus avoiding the metal amide intermediate altogether.[23] Less sterically demanding alcohols such as methanol, ethanol, or *n*-propanol react with $M_2(NMe_2)_6$ to generate $Mo_4(OR)_{16}$ compounds in which the M≡M bond is no longer present.

The alcoholysis reactions of $W_2(NMe_2)_6$ are more complex for several reasons:

1. The W≡W bond is more labile toward oxidation than the Mo≡Mo bond.
2. The W≡W bond is more labile toward dimerization to form W_4 clusters.
3. $W_2(OR)_6$ complexes are more Lewis acidic than their molybdenum counterparts, and thus they more easily form adducts with Lewis bases.
4. The W alkoxides are thermally unstable above *c.* 60 °C.

This having been stated, a number of $W_2(OR)_6$ compounds are now known, the most useful being $W_2(OBu^t)_6$ which despite forming dark red, needle-like crystals have only recently been properly characterized on crystals grown from a thf/Bu^tOH mixture.[56] The asymmetric unit of this polymorph of $W_2(OBu^t)_6$ contains 1.5 molecules. The dimer that is contained within the unit cell has one main W–W orientation that comprises 80% of the W_2 electron density and four other orientations of approximately 5% each. The half-dimer has one, almost 100%, W–W orientation and this dimer provides the most reliable bonding parameters for $W_2(OBu^t)_6$.

Closely related compounds, such as $W_2(O\text{-}c\text{-}C_6H_{11})_6$ and $W_2(OSiMe_2Bu^t)_6$ have been structurally characterized and those along with other structurally characterized $W_2(OR)_6$ compounds are listed in Table 6.1. Notable among the later synthesized alkoxides of $(W{\equiv}W)^{6+}$ are those with chiral groups, such as (+)-*D*-menthol, that may allow the ditungsten template to act as a chiral Lewis acid, as was also noted by Heppert, et al. in their synthesis of mixed alkoxide/binolates.[57] Whereas most $Mo_2(OR)_6$ alkoxides are volatile and sublime at *c.* 60–100 °C and 10^{-2} torr, the $W_2(OR)_6$ alkoxides tend to decompose under such conditions, so the preferred purification method for the alkoxides of tungsten is crystallization from hydrocarbon solvents.

The complexities of these alcoholyses are exemplified by the reaction between $W_2(NMe_2)_6$ and Pr^iOH. This reaction has been shown to give $W_2(OPr^i)_6(HNMe_2)_2$,[58] the carbide $W_4(C)(NMe)(OPr^i)_{12}$,[59] and the bis-hydride $W_4(H)_2(OPr^i)_{12}$[55,60] along with homoleptic alkoxides $W_2(OPr^i)_6$ and $W_4(OPr^i)_{12}$.[32] A better route to $(W{\equiv}W)^{6+}$ compounds having secondary and primary alkoxides involves the alcoholysis of $W_2(OBu^t)_6$ whereby Bu^tOH is liberated and most easily removed from the product mixture under reduced pressure as a hydrocarbon azeotrope. This method was used in the low temperature preparation of $W_2(OPr^i)_6$ where $W_4(OPr^i)_{12}$ cluster formation is kinetically retarded.[61] At higher temperatures, however, this reaction gives the tetranuclear clusters or their alcohol adducts, $W_4(OR)_{12}(HOR)$.[62]

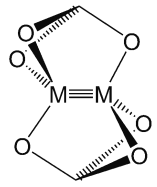
Reactions involving pinacol, $Me_2C(OH)C(OH)Me_2$ gave the yellow pinacolate complexes $M_2(OCMe_2CMe_2O)_3$, which like the ethylenediamides, have structures in which the central M_2O_6 skeleton is nearly eclipsed.[27] The majority of other structurally characterized $M_2(OR)_6$ compounds have staggered M_2O_6 skeleta except when factors associated with the packing of extremely bulky ligands give a nearly eclipsed skeleton as noted in Table 6.1.

Also included in Table 6.1 are data for the complexes formed in reactions with triols[11] and trisilylanols.[16] These reactions result in M_2L_2 complexes where the tridentate ligand L chelates to one metal and spans the MM bond to occupy one coordination site of the other metal as depicted in 6.1. The carbohydrate derivatives prepared by Floriani are closely related to these triolate structures.[18]

The homoleptic compounds $W_2(O_2CBu^t)_6$ and M_2COT_3 (where M = Mo, W) are also listed in Table 6.1. The carboxylates act as bidentate ligands and in these compounds, each metal

Pictiva EX2004
Samsung v Pictiva
IPR2024-01094

atom forms five M–O bonds in the plane perpendicular to the MM axis together with an additional, weak, axial W–O bond. There are two O_2CR ligands spanning the MM bond.



6.1

In the M_2COT_3 complexes, one COT ligand straddles the MM bond such that five carbon atoms are within bonding distance of each metal. The other two COT ligands are terminally-bound in an η^4-fashion resembling a butadiene ligand, as seen for the recently synthesized 1,4-*bis*-trimethylsilyl-substituted compound shown in Fig. 6.2.[63] The MM bond order in M_2COT_3 has been variously described as quadruple or double based on the diamagnetism of the compound and qualitative electronic structure arguments. However, recent DFT calculations suggest that this may be viewed as a M≡M triple bond and, as can be seen from Table 6.1, the MM distances are closer to those of the M_2X_6 species than those of MM quadruple or double bonds.[64]

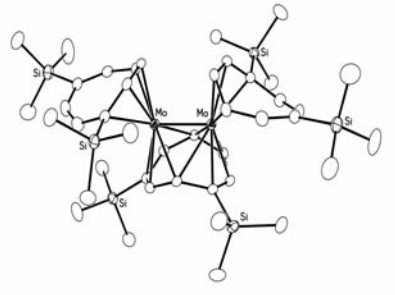


Fig. 6.2. The structure of $Mo_2(COT\text{-}TMS_2)_3$.

The homoleptic mesityl thiolates and selenates, $M_2(EC_6H_2Me_3)_6$ have been prepared via similar metathesis reactions using the mesityl-thiol[21,22] or selenol.[19,65] The thiolates (red) and selenates (red-brown) are crystalline and have staggered M_2E_6 skeletons. Attempts to obtain suitable crystal structures of other thiolates such as $M_2(SBu^t)_6$ have been unsuccessful, possibly due to the same issues of W–W disorder that appear in the structure of $W_2(OBu^t)_6$.

6.2.2 Bonding in M_2X_6 compounds

As can be seen from an inspection of Table 6.1 the MM bond distances in the homoleptic M_2X_6 compounds span a small range of about 2.15 to 2.35 Å. For a related pair of compounds, the MM distance is longer by *c.* 0.08 Å for the W compound despite the fact that the M–X bond distances (where X = C, N, O, S, or Se) are either comparable or slightly shorter. The MM distances are roughly 0.1 Å longer than those seen in MM quadruply bonded compounds.[4] The origin of the longer W≡W distance compared to Mo≡Mo, is almost certainly due to increased core-core repulsions. There have been both experimental[66] and theoretical[67] attempts to estimate the bond strength of MM triple bonds. Although there are uncertainties that arise with

Pictiva EX2004
Samsung v Pictiva
IPR2024-01094

each approach, a reasonable numerical value of 60 and 90 kcal mol^{-1} is accepted for the M≡M bond strength, where M = Mo and W, respectively.

The bonding in these M_2X_6 compounds can be considered qualitatively as follows. Taking the M–M axis as the *z*-axis, each metal forms three MX σ-bonds using s, p_x, and p_y hybrids and forms the MM triple bond using metal d_{z^2} and d_{xz}, d_{yz} orbitals. This leads to the formation of a cylindrical triple bond of MM configuration $\sigma^2\pi^4$ for these d^3-d^3 complexes. In addition, each metal may use its d_{xy} and $d_{x^2-y^2}$ orbitals to form π-bonds to the X ligands (if they are available and of suitable energy). For NR_2 ligands, these are oriented in such a way as to maximize amide to metal π-bonding, though only two π-bonds delocalized over three M–N σ-bonds can be formed from ligand to metal π-donation. A consideration of the M–N bond distances (1.96 Å on average) in relation to related $M–C_{sp^3}$ bond distances (2.14 Å on average) certainly supports the importance of this π-donation. In the case of alkoxides the MOC angles are normally in the range 130–150° and the alkyl groups are disposed in either a proximal or distal manner with respect to the M–M bond. In this case, oxygen pπ donation can occur and the relatively short M–O distances (1.88 Å on average) support this view. A similar argument can be made for the thiolates and selenates, but based on M–E distances (E = S, Se) this π-donation is believed to be less important than for the alkoxides. The M_2X_6 compounds are therefore electronically of the 18-electron count, though the amide and alkoxide ligands provide a π-buffering effect.

Electronic structure calculations have been undertaken on these M_2X_6 compounds and generally support the preceding qualitative bonding description.[68] In C_3-symmetry there can be extensive mixing of MX σ and the MM bonding and antibonding orbitals. This is particularly prominent when the metal and ligand orbitals are of similar energy as is the case for the homoleptic alkyls. In the case of alkoxides, the more electronegative oxygen gives a greater energy separation and the photoelectron spectra of $M_2(OR)_6$ compounds reveals that the first ionizations can be assigned to ionizations from the MM π- and σ-based orbitals. Ionization from the π-orbitals requires roughly 1 eV more energy than from the δ-bond of a MM quadruple bond. In the case of the $M_2(NR_2)_6$ compounds the ionization from the nonbonding NR_2 lone pair π combinations is close in energy to the ionization from the MM π-bonding orbital. Calculations on model thiolates $M_2(SH)_6$ also indicate that the HOMO is a sulfur-based lone pair combination. The influence of Xpπ to Mdπ donation is to raise the energy of the HOMO, which is the MM π-bonding MO, and it has been suggested that this labilizes the M≡M bond in $M_2(OR)_6$ compounds.[69] The LUMO in these compounds is a metal-based π*δ combination which too has some ligand pπ contribution. The color of these compounds, yellow to red, arises from the HOMO→LUMO transition which may be viewed as a MM π to π* transition.[27]

Raman spectra have been recorded for some of these M_2X_6 compounds with the intent of identifying and quantifying the MM stretching frequency. The earliest attempt examined the compounds $M_2(NMe_2)_6$ and $M_2(NMe_2\text{-}d_6)_6$ and concluded that it was not possible to identify a Raman band uniquely associated with ν(MM).[15,30] The bands in the region expected for ν(MM) and ν(MN) all showed significant shifts upon deuteration. Subsequent work by Dallinger, Gilbert, and coworkers who examined both $M_2(CH_2EMe_3)_6$ (where E = C or Si) and $M_2(OR)_6$ (where R = Bu^t, $Bu^t\text{-}d_8$, CMe_2CF_3 and 1-adamantyl) were able to assign ν(MoMo) in the range 360–380 cm^{-1} and ν(WW) from 274–304 cm^{-1}.[26] Based on the known values of ν(MM) in quadruply-bonded complexes their numerical values appear very reasonable and for related pairs of compounds the ratio ν(MoMo)/ν(WW) is found to be 1.30, close to that predicted assuming an equivalent force constant for each triple bond, namely 1.38. This work has subsequently been extended to include computation of the Raman bands and a re-evaluation of the spectra of the $M_2(NMe_2)_6$ compounds.[26]

Pictiva EX2004
Samsung v Pictiva
IPR2024-01094

6.2.3 $X_3M{\equiv}MX_3$ Compounds as Molecular Precursors to Extended Solids

Some of the M_2X_6 compounds have been examined as molecular precursors to ceramic materials. Upon heating $W_2(OBu^t)_6$ to 200 °C under a stream of dry N_2, the alkoxide decomposes to give WO_2 with the elimination of isobutylene, Bu^tOH, and trace amounts of water.[70] The $Mo_2(OBu^t)_6$ species is more thermally robust, but in the presence of trace amounts of water decomposes to MoO_2 at *c.* 250 °C. $Mo_2(OPr^i)_6$ sublimed at 120 °C under 1 atm of N_2, but $W_2(OPr^i)_6$ decomposed to give a mixture of tungsten metal and W_2C.[71] A similar product mixture was obtained in the decomposition of $W_2(O\text{-}c\text{-}C_6H_{11})_6$ whereas the Mo analog gave exclusively Mo_2C. The introduction of benzyl ligands in the compounds $M_2(CH_2Ph)_2(OR)_4$ triggered decompositions at lower temperatures, around 120 °C, and significantly changed the product distribution.[71]

In a somewhat related study, Tilley and Su showed that the siloxide $Mo_2[O_2Si(OBu^t)_2]_3$ decomposed upon heating to give MoO_2 as the only crystalline phase, whereas the W analog gave W(s) and WO_2.[24] However, in both decompositions an amorphous ceramic phase was formed containing metallic Mo or W along with Si and O. McCarley and coworkers have also investigated the use of $Mo_2(OR)_6$ compounds and $Mo_2(NMe_2)_6$ in a sol-gel approach to forming Mo_2O_3.[72] They were unsuccessful in this attempt, but did discover MoO(OH), a new species that could be converted to Mo_3O_5 and $LiMoO_2$ (along with other molecular species such as $Mo_3(OH)_9(NMe_2)\cdot\frac{1}{2}HNMe_2$) by reacting with Li_2CO_3.

6.3 $M_2X_2(NMe_2)_4$ and $M_2X_4(NMe_2)_2$ Compounds

A large class of compounds of the general formula 1,2-$M_2X_2(NMe_2)_4$ is now known and the majority has been prepared from metathetic reactions involving 1,2-$M_2Cl_2(NMe_2)_4$. These important starting materials are prepared from the reaction between two equivalents of Me_3SiCl and $M_2(NMe_2)_6$ compounds in a hydrocarbon solvent, typically hexane, benzene or toluene. If a concentrated or near saturated solution of the $M_2(NMe_2)_6$ compound is employed, the 1,2-$M_2Cl_2(NMe_2)_4$ compounds are formed as orange microcrystalline powders.[73] Evidence has been presented that these reactions are catalyzed by adventitious HCl or $HNMe_2$ which allow for the replacement of the NMe_2 ligands as seen in the equations below. However, oxidative addition of Me_3SiCl followed by reductive elimination of $Me_3Si{-}NMe_2$ is also possible though unlikely.[74]

$$Me_3SiCl + NHMe_2 \rightleftharpoons Me_3SiNMe_2 + HCl$$

$$M_2(NMe_2)_6 + HCl \rightleftharpoons M_2Cl(NMe_2)_5 + HNMe_2$$

If an excess of Me_3SiCl is employed, further chloride for amide exchange occurs leading to insoluble products. The $M_2Cl_2(NMe_2)_4$ compounds can be further purified by sublimation. In solution and in the solid-state, the dichlorides adopt the *anti* rotamer and the barrier to M–N bond rotation is notably higher than that in the $M_2(NMe_2)_6$ compounds.[73] The 1,2-$M_2Cl_2(NMe_2)_4$ compounds have been employed as starting materials in a large number of metathetic reactions employing organolithium or Grignard reagents, leading to the isolation of a wide range of compounds of the type 1,2-$M_2R_2(NMe_2)_4$. Examples include R = Me,[41] Et,[75] Bu,[76] Pr^i,[76] Bu^i,[76] Ph,[77] *o*- and *p*-tolyl,[77] CH_2Ph,[77] CPh_3,[78] CH_2SiMe_3,[76] CH_2CMe_3,[76] $CH(SiMe_3)_2$,[79] $SiPh_3$,[78] $GePh_3$,[78,80] $Si(SiMe_3)_3$,[81] $SnPh_3$,[78] $Sn(SnMe_3)_3$,[77,81] PBu^t_2,[82] $AsBu^t_2$,[83] $OCPh_3$,[84] $OSiPh_3$,[84] $OB(mesityl)_2$,[85] SBu^t,[86] Cp,[87,88] C_5H_4Me,[89] indenyl,[87,89] allyl,[90] and 3-methylallyl.[90] A number of bridging groups have also been employed, e.g., X_2 = 1,1′-$(C_5H_4)_2Fe$,[91] $(\text{-}CH_2\text{-})_4$[92], and COT.[93] Notably absent in this series are alkenyl and alkynyl complexes and attempts to prepare such compounds have always resulted in the formation of insoluble byproducts.[94] Reactions employing LiCPhCPhCPhCPhLi and 1,2-$W_2Cl_2(NMe_2)_4$ gave $W_2(NMe_2)_4(\mu\text{-CPh})(\mu\text{-}C_3Ph_3)$ via C–C

Pictiva EX2004
Samsung v Pictiva
IPR2024-01094

reductive cleavage and it is likely that some similar reaction occurs in reactions employing alkynyl and alkenyllithium reagents.[94]

The majority of the 1,2-$M_2R_2(NMe_2)_4$ compounds where R represents a σ-carbon bonded ligand exist as a mixture of *anti* and *gauche* rotamers in solution that interconvert slowly on the NMR timescale with $\Delta G^{\neq}$ of 20-24 kcal mol^{-1}. One rotameric form of 1,2-$M_2R_2(NMe_2)_4$ tends to be the most stable due to steric factors. In fact, *gauche* 1,2-$Mo_2[CH(SiMe_3)_2]_2(NMe_2)_4$ is air-stable in the crystalline state for days at room temperature, which is a result of the presence of the bulky $CH(SiMe_3)_2$ groups.[95] The 1,2-*ortho*- and 1,2-*para*-tolyl compounds revealed that there is an extremely low barrier to rotation about the M–C σ bond in contrast to the M–N bonds consistent with the view that the latter arises from electronic considerations, Npπ to Mdπ donation, and not from steric factors. In fact, the solid-state structure of the *ortho*-tolyl complex showed that the C_6 plane was offset 90° with respect to alignment with the MM axis. Another notable feature of the β-hydrogen-containing alkyl groups is their thermal stability. Many can be sublimed at temperatures near 100 °C at 10^{-2} torr and they are relatively inert to decomposition by β-H elimination processes despite the fact that the metal-atoms are formally unsaturated. This has been attributed to the important role of the π-donor ligands in bonding to metal d-orbitals that otherwise would be available for (CH)–M interactions.

For allyl, Cp, and indenyl ligands, the focus of attention was on the relative π-donor properties of the ligands. In all cases, η^3-coordination was observed which suggests that Cp and indenyl ligands compete effectively with dimethylamides as π-donors. In the case of allyl ligands, a bridged structure was observed with a relatively long WW distance for a $(M{\equiv}M)^{6+}$ compound (2.48 Å). Electronic structure calculations imply that there is a significant interaction between all three allyl π-MOs at the $(M{\equiv}M)^{6+}$ center and, in particular, π_3 of the allyl can receive electron density from the MM π-orbitals. A similar kind of bonding description can be formulated for $W_2COT(NMe_2)_4$ where the COT ligand spans the WW triple bond. In solution, the COT ligand is evidently fluxional on the NMR time-scale and rotation occurs by a 1,2-site exchange in a similar manner to that seen recently in the corresponding alkoxides, $W_2COT(OR)_4$.[96]

From reactions between $W_2Cl_2(NMe_2)_4$ and two equivalents of $LiPR_2$, the compounds 1,2-$W_2(PR_2)_2(NMe_2)_4$ have been isolated and fully characterized.[97,98] For R = Bu^t, the relatively long W–P bond distances and the pyramidal coordination at phosphorus clearly indicate that Ppπ to Wdπ-bonding is less significant than Npπ to Wdπ bonding. In the case of R = Ph, bridged compounds are formed and for R = cyclohexyl, both unbridged and bridged isomers were obtained and shown to interconvert:

$$1,2\text{-}W_2(PCy_2)_2(NMe_2)_4 \rightleftharpoons W_2(\mu\text{-}PCy_2)_2(NMe_2)_4$$

Similar bridged structures were seen for $W_2(PPh_2)_2(NMe_2)_4$ and $W_2(PPh_2)_2(OBu^t)_4$. The structures of bridged and unbridged molecules are compared in Fig. 6.3. Most notable in the bridged isomer is the non-planar W_2P_2 unit. The origin of this puckering was traced to electronic factors where d^3-d^3 MM bonding is maximized.

The compounds $M_2(NMe_2)_6$ are also labile to reactions with REH where E is a chalcogen and R is an extremely bulky and/or strongly electron withdrawing group. The replacement of NMe_2 ligands leads to compounds of the form $M_2(NMe_2)_2(ER)_4$. The series where M = W, E = O and R = CMe_2CF_3, $CMe(CF_3)_2$ and $C(CF_3)_3$ was studied in detail to ascertain the influence of the fluorinated alkyl substituents.[99] These studies included single crystal X-ray, VT NMR and UV-visible spectroscopy. The introduction of the CF_3 groups has a pronounced effect in stabilizing the MM π and σ and Npπ-based ionizations and this effect increases with the successive replacement of each methyl by trifluoromethyl. Also in these compounds, the lowest energy ionization bands clearly reveal the removal of the degeneracy of the MM π MO's.

Pictiva EX2004
Samsung v Pictiva
IPR2024-01094

As a result of the poor π-donation from the fluorinated alkoxides, the remaining NMe_2 ligands π-donate more strongly as evidenced by higher M–N rotational barriers and shorter M–N bond distances. The average M–N bond length is 1.91 Å in $W_2(NMe_2)_2(OCMe(CF_3)_2)_4$ compared to a W–N bond length of 1.96 Å in $W_2(NMe_2)_6$.

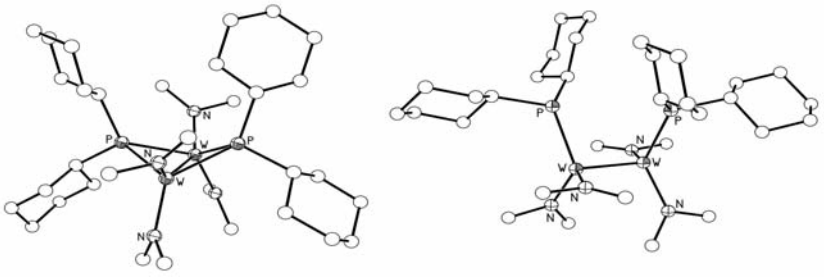
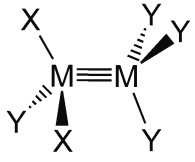


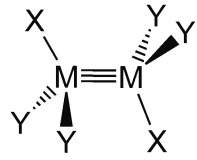
Fig. 6.3. Structural comparison of bridged and unbridged isomers of $W_2(PCy_2)_2(NMe_2)_4$.

6.4 Other $M_2X_2Y_4$, $M_2X_{6-n}Y_n$ and Related Compounds

Compounds in which the central $(M{\equiv}M)^{6+}$ unit is supported by a set of mixed uninegative ligands of the form $M_2X_{6-n}Y_n$ constitute the largest group of compounds having M≡M bonds. The ligands X and Y may be monodentate, e.g., as in alkyl, amide and alkoxide, or bidentate as in a carboxylate or β-diketonate and may bind to the binuclear center by spanning the metal–metal bond or by chelating to one metal center. In the latter case, the metal center expands its coordination number first in the equatorial plane and then axially as was seen earlier for $W_2(O_2CNMe_2)_6$[108] and $W_2(O_2CBu^t)_6$[28]. Most compounds of this type have the formula $M_2X_2Y_4$ and nearly all are symmetrically substituted about the M_2 unit. There are, however, notable exceptions even though the isomerization of 1,1- and 1,2-$M_2X_2Y_4$ (**6.2** and **6.3** respectively) isomers has been shown to have a significant kinetic barrier.[101]



6.2



6.3

Perhaps the most notable feature of this class of compounds is the virtual absence of members in which one or more of the groups directly bridge the two metal atoms as is so common for the amide, alkoxide, halide and thiolate ligands. Only for some phosphide groups is μ-PR_2 bonding thermodynamically preferred. This again testifies to the energetic importance of preserving the MM $\sigma^2\pi^4$ electronic configuration in these d^3-d^3 dinuclear complexes. In some cases, the bonding mode of the ligand X is η^n or μ-η^n,η^n, as for certain hydrocarbon ligands such as Cp, indenyl, allyl or COT. In all of these compounds, the MM bond distances span a very small range from 2.2 to 2.4 Å and for otherwise equivalent complexes, the MoMo distances are shorter than their WW counterparts by roughly 0.08 Å. Table 6.2 summarizes pertinent structural parameters for $M_2X_2Y_4$ compounds while others such as $M_2X_aY_bZ_c$ (where $a + b + c = 6$) are presented in Table 6.3. Table 6.4 summarizes data regarding the M–NR_2 rotational barriers in some compounds of the form $M_2X_2(NR_2)_4$ where X is a variety of ligands; R = Me/Et.

Pictiva EX2004
Samsung v Pictiva
IPR2024-01094

Table 6.2. Structural parameters for selected $M_2X_2Y_4$ compounds

M	X	Y	M–M[a]	M–X[a]	M–Y[a]	geom.[b]	ref.
Mo	*p*-tolyl	NMe_2	2.20	2.16	1.95	a	77
Mo	Et	NMe_2	2.20	2.16	1.95	g	76
Mo	Me	NMe_2	2.20	2.17	1.96	a	102
Mo	½ $(CH_2)_4$	NMe_2	2.20	2.17	1.96	g	92
Mo	CH_2Ph	NMe_2	2.20	2.18	1.95	g	77
Mo	Cl	NMe_2	2.20	2.35	1.93	a	100
Mo	$Sn(SnMe_3)_3$	NMe_2	2.20	2.78	1.95	a	81
Mo	OBu^t	CH_2SiMe_3	2.21	1.87	2.13	a	5,103
Mo	$OSi(OBu^t)_3$	NMe_2	2.21	1.96	1.93	a	104
Mo	PBu^t_2	NMe_2	2.21	2.48	1.98	a	82
Mo	I	NMe_2	2.21	2.70	1.95	a	91
Mo	OPr^i	SeMes	2.22	1.87	2.43	a	65
Mo	SBu^t	NMe_2	2.22	2.36	1.95	a	86
Mo	$AsBu^t_2$	NMe_2	2.22	2.62	1.97	a	83
Mo	$Si(SiMe_3)_3$	NMe_2	2.22	2.67	1.95	a	81
Mo	OPr^i	SMes	2.23	1.88	2.31	a	105
Mo	$OCPh_3$	NMe_2	2.23	1.92	1.96	a	84
Mo	*o*-tolyl	NMe_2	2.23	2.17	1.94	g	77
Mo	NMe_2	½ OArO[d,e]	2.25	1.92	1.92	g	106
Mo	$OSi(OBu^t)_3$	OBu^t	2.25	1.93	1.87	a	104
Mo	NMe_2	½ OArO[d,e]	2.26	1.92	1.93	g	106
Mo	CH_2SiMe_3	$Bu^tNCCH_2SiMe_3$	2.26	2.26	2.12	g	107
W	Me	O_2CNEt_2	2.27	2.20	2.11	na	108
W	Me	NEt_2	2.28	2.17	1.97	a	41
W	O_3SCF_3	NMe_2	2.29	2.07	1.92	a	109
W	½ 1,1'-Cp_2Fe	NMe_2	2.29	2.16	1.96	g	91
W	2-Me-allyl	NMe_2	2.29	2.18	1.96	a	110
W	Cl	NMe_2	2.29	2.33	1.94	a	100
W	PCy_2	NMe_2	2.29	2.40	1.98	g	97
W	$OSiPh_3$	NMe_2	2.30	1.93	1.94	a	84
W	Cl	NEt_2	2.30	2.33	1.94	a	48
W	SBu^t	NMe_2	2.30	2.35	1.95	a	f
W	Br	NEt_2	2.30	2.48	1.90	a	73
W	$AsBu^t_2$	NMe_2	2.30	2.59	1.96	a	83
W	$GePh_3$	NMe_2	2.30	2.63	1.95	a	80
W	I	NMe_2	2.30	2.68	1.94	a	73
W	OPr^i	SeMes	2.31	1.86	2.44	a	65
W	$OCPh_3$	NMe_2	2.31	1.96	1.94	g	84
W	½ Me_4BINO	OBu^t	2.32	1.93	1.87	g	111
W	CH_2SiMe_3	NMe_2	2.32	2.19	1.95	g	79
W	PBu^t_2	NMe_2	2.32	2.40	1.97	g	82
W	OBu^t	SBu^t	2.33	1.81	2.30	a	69
W	indenyl	NMe_2	2.34	2.36 - 2.54	1.97	g	87
W	Cl	$HNBu^t$	2.34	2.31	1.98	g	112
W	Cp	NMe_2	2.35	2.27[c]	1.96	g	g, 87

Pictiva EX2004
Samsung v Pictiva
IPR2024-01094

M	X	Y	M–M[a]	M–X[a]	M–Y[a]	geom.[b]	ref.
W	½ COT	OBu^t	2.39	2.24 - 2.45	1.92	e	96
W	½ COT	NMe_2	2.43	2.23 - 2.47	1.99	e	93
W	allyl	NMe_2	2.48	2.22 - 2.44	1.95	e	90

[a] Å, ± 0.01 Å.
[b] a = *anti*, g = *gauche*, e = eclipsed, na = not applicable.
[c] W-to-ring centroid.
[d] OArO = 2,2'-ethylidenebis(4,6-di-*tert*-butylphenoxide).
[e] Two diastereomeric isomers were characterized.
[f] M. H. Chisholm, J. C. Gallucci, C. B. Hollandsworth, unpublished crystal structure of $W_2(SBu^t)_2(NMe_2)_4$.
[g] M. H. Chisholm, J. C. Gallucci, C. B. Hollandsworth, unpublished crystal structure of $W_2Cp_2(NMe_2)_4$.

Table 6.3. $M_2X_aY_bZ_c$ Compounds (where $a + b + c = 6$ or 7)

M	X	a	Y	b	Z	c	color	ref.
Mo	Et	1	OBu^t	5			red	113
Mo	Pr	1	OBu^t	5			red	113
Mo	Bu	1	OBu^t	5			red	113
Mo	Et	1	OPr^i	5			yellow	113
Mo	Pr	1	OPr^i	5			yellow	113
Mo[a]	CH_2Ph	2	PMe_3	1	OPr^i	4	yellow	113
Mo	CH_2Ph	2	Py	1	OPr^i	4	yellow	113
W[b]	I	1	NMe_2	5			orange-brown	91
Mo[c]	I	1	NMe_2	5			orange-brown	91
W[d]	PPh_2	1	NMe_2	5			orange-brown	91
W	Me	1	NMe_2	5			orange-brown	91
W	CH_2Ph	1	NMe_2	5			dark brown	91
W	CH_2-*o*-tolyl	1	NMe_2	5			yellow-orange oil	91
Mo	CH_2Ph	1	NMe_2	5			yellow-orange oil	91
W	CH_2SiMe_3	1	I	1	NMe_2	4	orange oil	91
Mo	CH_2Ph	1	CH_2SiMe_3	1	NMe_2	4	yellow-orange oil	91

[a] For $Mo_2(CH_2Ph)_2(OPr^i)_4(PMe_3)$, Mo–Mo = 2.235(1) Å, Mo–C (av.) = 2.22(1) Å, Mo–P = 2.581(1) Å, and Mo–O (av.) = 1.88(1) Å.
[b] For $W_2I(NMe_2)_5$, W–W = 2.298 (1) Å, W–I = 2.688(1) Å, W–N (av.) = 1.94(1) Å.
[c] For $Mo_2I(NMe_2)_5$ Mo–Mo = 2.211(1) Å, Mo–I = 2.80(1) Å, Mo–N (av.) = 1.93(1) Å.
[d] For $W_2(PPh_2)(NMe_2)_5$, W–W = 2.304(1) Å, W–P = 2.432(4) Å, W–N (av.) = 1.95(1).

Table 6.4. M–N Bond rotation parameters for 1,2-$M_2X_2(NR_2)_4$ compounds[108]

M	X	R	Config[a]	$\Delta G^{\neq}_{MN}$[b]	T_c (°C)	M–N[c]	ref.
Mo	PBu^t_2	Me	a	7.1(2)	-108	1.98	82
W	PBu^t_2	Me	a	7.3(2)	-103	1.96	82,97
W[d]	PBu^t_2	Me	g	7.5(1)	-103	1.97	82,97
Mo[d]	PBu^t_2	Me	g	8.2(1)	-88	1.98	82
W	PCy_2	Me	g	9.0(1)	-69	1.97	97
W	P(*p*-FPh)$_2$	Me	a/g	9.4(5)	-65	n.r.[e]	97
W	PEt_2	Me	a/g	9.8(2)	-49	n.r.[e]	97
W	P(*p*-tolyl)$_2$	Me	a/g	10.6(3)	-33	n.r.[e]	97

Pictiva EX2004
Samsung v Pictiva
IPR2024-01094

M	X	R	Config[a]	$\Delta G^{\neq}_{MN}$[b]	T_c (°C)	M–N[c]	ref.
W	CpMe	Me	g	11(2)	-60	1.97	89
W	indenyl	Me	g	11(2)	-60	1.96	89
W	NMe_2	Me	a/g	11.2(2)	-35(2)	1.97	30
W[d]	PBu^t_2	Me	g	11.3(1)	-17	1.97	82,97
Mo[d]	PBu^t_2	Me	g	11.5(1)	-13	1.98	82
W	$P(SiMe_3)_2$	Me	a	11.5(1)	-10	1.96	97
Mo	NMe_2	Me	a/g	11.5(2)	-30(2)	1.98	15
W	PPh_2	Me	a/g	12.0(1)	0	n.r.[e]	97
W	NEt_2	Et	g	13.3(4)	10(5)	n.r.[e]	30
Mo	NEt_2	Et	g	13.6(2)	16(5)	n.r.[e]	15
W	Cl	Me	a	13.9	n.r.[e]	1.94	100
Mo	CH_2Ph	Me	a/g	14	-45	1.95	77
Mo	*p*-tolyl	Me	a/g	14	-45	1.95	77
Mo	*o*-tolyl	Me	a/g	14	-45	1.94	77
Mo	Cl	Me	a	14.1	n.r.[e]	1.93	100
W	Br	Et	a	15.3(4)	-25	1.91	73
W	I	Et	a	15.3(4)	-25	1.94	73
W	Cp	Me	g	16.1	25	1.96	f, 87
Mo	$Sn(SnMe_3)_3$	Me	a	16.4(5)	90(5)	1.95	81
W	$Sn(SnMe_3)_3$	Me	a	16.8(5)	90(5)	n.r.[e]	81
W	½COT	Me	g	n.r.[e]	-40	1.98	93

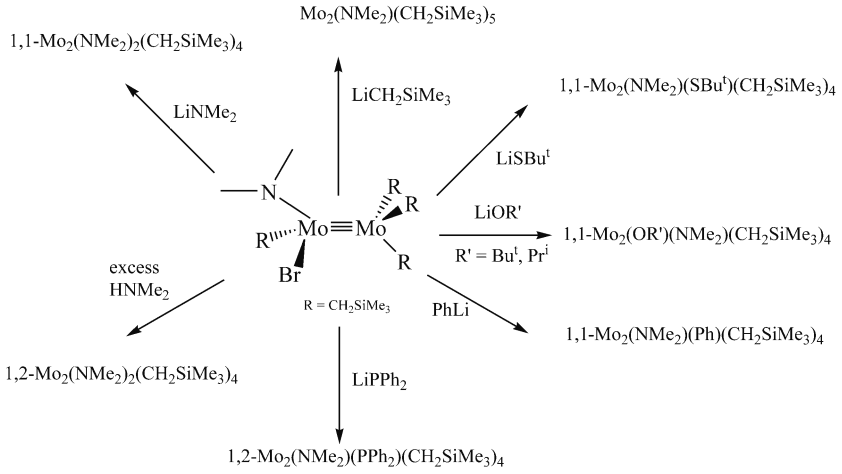
[a] a = *anti*, g = *gauche*, a/g = mixture of *anti* and *gauche* isomers.
[b] kcal mol^{-1}.
[c] Å ± 0.01 Å.
[d] Two different M–N bonds rotational barriers are seen in *gauche* $M_2(Bu^t_2P)_2(NMe_2)_4$ compounds where M = Mo, W.
[e] n.r. = not reported.
[f] M. H. Chisholm, J. C. Gallucci, and C. B. Hollandsworth, unpublished crystal structure of $W_2Cp_2(NMe_2)_4$.

6.4.1 $Mo_2X_2(CH_2SiMe_3)_4$ compounds

Hydrocarbon solutions of $Mo_2(CH_2SiMe_3)_6$ react with 2 equiv of anhydrous HBr to give the orange, hydrocarbon soluble, crystalline compound 1,2-$Mo_2Br_2(CH_2SiMe_3)_4$. Based upon spectroscopic data, this dibromide adopts the *anti* rotamer in solution and in the solid-state.[103,115] The bromide ligands in $Mo_2Br_2(CH_2SiMe_3)_4$ are substitutionally labile and a wide variety of $Mo_2(X)(Y)(CH_2SiMe_3)_4$ compounds have been prepared by metathetic reactions e.g., X = Y = alkyl, amide, alkoxide, thiolate, phosphide, and X ≠ Y where Y = CH_2SiMe_3, O_2CNMe_2, OBu^t.[101,116] Many of these compounds were obtained as oils or waxy solids. Two compounds were crystallographically characterized, 1,2-$Mo_2(OBu^t)_2(CH_2SiMe_3)_4$[116] and 1,2-$Mo_2(NMe_2)(PPh_2)(CH_2SiMe_3)_4$[101] and both were found to have the *anti*-staggered rotamer in the solid-state. Studies of this class of compounds revealed unequivocal information concerning the solution dynamic behavior of $M_2X_nY_{6-n}$ compounds and the complexities of the seemingly simple metathetic exchange reactions at the $(M{\equiv}M)^{6+}$ center. For example, 1,2-$Mo_2Br_2(CH_2SiMe_3)_4$ was found to undergo metathesis reactions in hydrocarbon solvents with excess $HNMe_2$ or two equivalents of $LiNMe_2$ to give 1,2-$Mo_2(NMe_2)_2(CH_2SiMe_3)_4$ and 1,1-$Mo_2(NMe_2)_2(CH_2SiMe_3)_4$, respectively. Initially, it was thought that 1,1-$Mo_2(NMe_2)_2(CH_2SiMe_3)_4$ was a kinetic product which in the presence of an excess of $HNMe_2$ isomerized to the 1,2-isomer. However, the 1,1-$Mo_2(NMe_2)_2(CH_2SiMe_3)_4$ isomer was subsequently shown to undergo aminolysis with $NH(CD_3)_2$ *without* 1,1- to 1,2-isomerization.[101] Moreover, it was shown that the reactions

Pictiva EX2004
Samsung v Pictiva
IPR2024-01094

involving 1,2-$Mo_2Br_2(CH_2SiMe_3)_4$ and each of $LiNMe_2$ and $HNMe_2$, proceeded via the common intermediate 1,1-$Mo_2Br(NMe_2)(CH_2SiMe_3)_4$.[101] Finally, it was shown that the isomerization of 1,1- to 1,2-$Mo_2(NMe_2)_2(CH_2SiMe_3)_4$ could be catalyzed by the presence of Me_2NH_2Br and this allowed for speculation concerning the mechanism of metathetic exchange at the $(Mo{\equiv}Mo)^{6+}$ center. However, as shown in Scheme 6.1, the ability to isolate kinetically persistent 1,1- and 1,2-isomers (that do not interconvert even at 100 °C) indicates that a relatively high barrier to ligand exchange between the two metal atoms exists.



Scheme 6.1. Reactions of 1,1-$Mo_2Br(NMe_2)R_4$ where R = CH_2SiMe_3.

The dynamic behavior of this class of compounds led to the first direct observation of rotation about a triple bond by variable temperature NMR studies. These studies complemented studies of 1,2-$M_2X_2(NMe_2)_4$ compounds, vide infra, and the rotational barriers about M–NR_2 bonds are listed in Table 6.4. The restricted rotation about the M–NMe_2 bond arises from the preferred alignment of the CNC unit along the Mo≡Mo axis to allow Npπ to Mod_{xy} π-bonding. This gives rise to the proximal and distal methyl groups with respect to the M≡M bond and does not disrupt the MM π-bonding orbitals, which utilize the Md_{xz}, and Md_{yz} atomic orbitals. For the series of compounds 1,1-$Mo_2(NMe_2)(X)(CH_2SiMe_3)_4$, the rate of proximal to distal exchange follows the order X = NMe_2 > OBu^t > SBu^t > CH_2SiMe_3 ≅ Ph > Br which correlates well with the relative σ/π-donating ability of the X ligands.[101] The electronegative bromide ligand leads to the highest rotational barrier. Steric factors can also greatly influence M–NMe_2 rotational barriers as was argued for the $M_2R_2(NMe_2)_4$ compounds where R = $Si(SiMe_3)_3$ and $CH(SiMe_3)_2$.[79,117]

For some compounds, such as 1,2-$Mo_2X_2(CH_2SiMe_3)_4$ where X = Br or OBu^t, it is not possible to determine whether they exist in solution exclusively in the *anti* rotameric form or if *anti* to *gauche* isomerization is too fast to be frozen out. The cases of 1,1-$Mo_2(NMe_2)_2(CH_2SiMe_3)_4$ and 1,2-$Mo_2(NMe_2)(PPh_2)(CH_2SiMe_3)_4$ have been examined in detail.[101] In general, the low barriers to rotation about the M≡M bond are consistent with the view that a cylindrical triple bond of $\sigma^2\pi^4$ configuration should have no inherent electronic barrier. For a molecule of the type 1,2-$M_2X_2R_4$, steric factors may influence this barrier, and for a *gauche* rotamer with C_2 symmetry, the degeneracy of the MM π_x and π_y MO's is removed. Herein some electronic barrier may be introduced when the *gauche* rotamer is thermodynamically preferred, but in all cases that have been studied, these barriers, when measurable, are small.

Pictiva EX2004
Samsung v Pictiva
IPR2024-01094

6.4.2 1,2-$M_2R_2(NMe_2)_4$ compounds and their derivatives

Particular attention was given to the chemistry of 1,2-$Mo_2R_2(NMe_2)_4$ compounds with respect to developing the organometallic chemistry of dinuclear molybdenum and tungsten compounds. Early attempts at investigating reductive elimination from the dinuclear center focused on 1,2-$Mo_2R_2(NMe_2)_4$ compounds where R contained a β-hydrogen atom, such as in the ethyl and isopropyl ligand. It was found that insertion of CO_2 into the MN bond was accompanied by β-CH activation leading to reductive elimination of ethane and ethene. Furthermore, in labeling studies, it was shown that this involved transfer of the β-H atom of one alkyl ligand to the α-carbon of the other ligand:

$$1,2\text{-}Mo_2(CH_2CD_3)_2(NMe_2)_4 + 4CO_2 \rightarrow Mo_2(O_2CNMe_2)_4 + CH_2{=}CD_2 + CH_2D{-}CD_3$$

A similar reductive elimination was observed in the reactions of β-H alkyl containing molybdenum compounds with 1,3-diaryltriazines which gave $Mo_2(ArNNNAr)_4$, alkane, and alkene.[118]

Related 1,2-$W_2R_2(NMe_2)_4$ compounds are less prone to reductive elimination though reactions of these compounds with symmetrical anhydrides R'CO_2COR' (where R' = Me, Bu^i, Ph) provide a useful and general synthetic route to WW quadruply bonded carboxylate compounds:

$$W_2R_2(NMe_2)_4 + 4R'CO_2COR' \rightarrow W_2(O_2CR')_4 + 4R'CONMe_2 + \text{alkane} + \text{alkene}$$

For alkyl compounds lacking β-hydrogen atoms, the reaction with acid anhydrides gave compounds of formula $W_2R_2(O_2CR')_4$ which have the unusual structure in which the axial sites of the paddlewheel $W_2(O_2CR')_4$ are ligated by alkyl ligands.[117] Particularly noteworthy in the structures of $W_2R_2(O_2CR')_4$ compounds are the short WW distances, comparable to those found in species with ditungsten quadruple bonds. One exception, however is seen in the reaction of $W_2Cp_2(NMe_2)_4$ with propionic anhydride which gave incomplete substitution forming $W_2Cp_2(O_2CEt)_3(NMe_2)$. Electronic structure calculations indicated that $W_2R_2(O_2CR')_4$ compounds most likely have the unusual bonding configuration of $\pi^4\delta^2$, lacking a formal σ-bond component to the ditungsten multiple bond. This situation is similar to that found for the molecule C_2, which also contains an unusually short C–C distance for a diatomic molecule formally lacking a σ-bond. In both cases, however, there is slight, residual σ-bonding as a result of the fact that occupied σ-orbitals are slightly more bonding in character than the populated σ* MO's are antibonding.[119,120]

The structure involving axial alkyl ligation, is in marked contrast to the structure seen in $W_2Me_2(O_2CNMe_2)_4$ wherein each tungsten center forms five bonds in a pentagonal plane perpendicular to the W≡W bond axis.[108] However, there would appear to be little difference in energy between these two structural forms as seen from the study of the compound $W_2(CH_2CMe_3)_2(O_2CMe)_2(S_2CNEt_2)_2$.[121] The axially ligated $W_2R_2(O_2CR')_4$ compounds were thermally labile to reductive elimination via a WC homolysis reaction with the stability order R = Me_3CCH_2 > Me > Ph > $PhCH_2$ which correlates with the accepted stability of organic radicals. The molybdenum analogs were more prone to reductive elimination and only the neopentyl complex $Mo_2(CH_2CMe_3)_2(O_2CMe)_4$ has been found stable enough for characterization.[122]

Reactions of 1,2-$M_2R_2(NMe_2)_4$ compounds with alcohols showed a similar trend in that reductive elimination was more favorable for M = Mo. The reactions proceed under kinetic control in which the amides are replaced by alkoxides:[113,123]

$$1,2\text{-}M_2R_2(NMe_2)_4 + R'OH\ (\text{excess}) \rightarrow 1,2\text{-}M_2R_2(OR')_4 + 4HNMe_2$$

When the alkyl ligand R contains β-hydrogen atoms, e.g., R = Et, Pr, Pr^i, CH_2CHMe_2, and for M = Mo, reductive elimination occurs during the course of the reactions to give an alkane and an alkene. When R = Bu^i and R' = Pr, the compound $Mo_2(OPr^i)_4(HOPr^i)_4$ is obtained in

Pictiva EX2004
Samsung v Pictiva
IPR2024-01094

contrast to $W_2(Bu^i)_2(OPr^i)_4$. In the presence of a chelating diphosphine ligand, the compound $Mo_2(OPr^i)_4(dmpe)_2$ was obtained wherein d^6-Mo^0 and d^2-Mo^{4+} centers were united by a formal Mo_2^{4+} quadruple bond.[124]

In contrast, $W_2COT(NMe_2)_4$ reacts with sterically demanding alcohols, ROH (where R = CH_2Bu^t, Pr^i, Bu^t), to give clean alkoxide for amide exchange products $W_2COT(OR)_4$.[96] Reactions with less sterically demanding alcohols, R'OH (where R = Me, Et, Pr) give the dimerized products $[W_2COT(OR')_4]_2$ where two $W_2COT(\mu\text{-}OR')(OR')_2$ units are connected via two symmetrical μ-OR' bridges.[125] The ditungsten COT alkoxides do not eliminate COT-H_2 even when dissolved in neat alcohol. Dissolving $W_2COT(OBu^t)_4$ in excess Pr^iOH gives $W_2COT(OPr^i)_4$ quantitatively. However, preliminary studies indicate that $W_2COT(NMe_2)_4$ reacts with Bu^tSH (excess) to make exclusively the COT-eliminated product $W_2(SBu^t)_2(NMe_2)_4$. This seems to suggest that under conditions of alcoholysis or thiolysis, there is a point at which either amine ($HNMe_2$) or alkyl (COT-H_2) can preferentially eliminate.

Preliminary studies also suggest that $W_2Cp_2(NMe_2)_4$ is unreactive towards bulky alcohols such as Bu^tOH.[126] This result indicates that the amide might be sterically inaccessible to alcohols. However, reactions with excess CF_3CH_2OH give a variety of products. Observations on the $W_2COT(NMe_2)_4$ and $W_2Cp_2(NMe_2)_4$ alcoholysis reactions tend to suggest that alkyl elimination is preferred only in some cases over amine elimination, despite the fact that thermodynamically alkyl exchange should be preferred as M–C bonds are weaker than M–N bonds. It is likely that the formation of an intermediate, having the incoming alcohol hydrogen-bonded to the dinuclear complex plays an important role in deciding the preference for alkyl vs. amine elimination. Efforts are underway to better understand the mechanisms of alcoholysis (and thiolysis) of both $W_2COT(NMe_2)_4$ and 1,2-$Cp_2W_2(NMe_2)_4$.

6.5 M_4 Complexes: Clusters or Dimers?

The coupling or oligomerization of MM triple bonds has been a topic of longstanding interest to the Chisholm group. In 1978, they speculated about the reversibility of the reaction below, wherein a metathesis of $(M{\equiv}M)^{6+}$ bonds could occur.[127] However, studies of the species present in solution upon both thermal and photochemical excitation provided no evidence for the metathesis product $Cp_2MoW(CO)_4$.

$$Cp_2Mo_2(CO)_4 + Cp_2W_2(CO)_4 \rightarrow 2Cp_2MoW(CO)_4$$

The mixed metal compound is formed in a thermal or photochemical reaction employing the two $Cp_2M_2(CO)_6$ compounds (M = Mo and W). The compound $Cp_2MoW(CO)_4$ can be detected readily by mass spectrometry and is probably formed by the following reaction sequence:

$$\text{(i)}\quad Cp_2M_2(CO)_6 + h\nu \rightarrow 2CpM(CO)_3\ (M = Mo, W)$$
$$\text{(ii)}\quad CpM(CO)_3 \rightarrow CpM(CO)_2 + CO$$
$$\text{(iii)}\quad CpMo(CO)_2 + CpW(CO)_2 \rightarrow Cp_2MoW(CO)_4$$

Subsequently, several M_4 clusters were made via coupling of two $(M{\equiv}M)^{6+}$ units supported by alkoxide ligands. This work is described in the following sections.

6.5.1 Molybdenum and tungsten twelve-electron clusters $M_4(OR)_{12}$

The reversible coupling of two $W_2(OPr^i)_6$ molecules was discovered in 1986.[128] The addition of secondary and bulky primary alcohols (Pr^i, CH_2Bu^t, CH_2-cyclopentyl, CH_2-cyclobutyl, and CH_2Pr^i) to $W_2(OBu^t)_6$ leads to black crystalline clusters $W_4(OR)_{12}$ and/or $W_4(OR)_{12}(HOR)$.[129,130] The molybdenum analogs $Mo_4(OR)_{12}$ and $Mo_4(OR)_{12}(HOR)$ are formed for the less sterically-

Pictiva EX2004
Samsung v Pictiva
IPR2024-01094

demanding alkoxide ligands but not for R = Pr^i and CH_2Bu^t which remain as dinuclear species.[129,130]

The compound $W_4(OPr^i)_{12}$ was crystallographically characterized along with $W_2(OPr^i)_6$; the unit cell contained one dinuclear and one tetranuclear species.[32] The tetranuclear structure is shown in Fig. 6.4. The central W_4 unit is diamond-shaped having alternating short, 2.5 Å and long, WW distances, 2.8 Å, with a significant backbone WW interaction of 2.7 Å. The low temperature ^1H NMR spectrum is consistent with expectations based on the C_{2h} symmetry found in the solid state. Upon raising the temperature, two dynamic processes are observed,[61] one of which is intramolecular and the other involves the reversible dissociation of the tetranuclear compound to $W_2(OPr^i)_6$:

$$W_4(OPr^i)_{12} \rightleftharpoons 2W_2(OPr^i)_6$$

The intramolecular process involves the site exchange of the bridging alkoxides without exchange with the terminal OPr^i ligands. Also one set of terminal ligands exchanges sites but these do not exchange with the other set of terminal ligands. The wing-tip alkoxides may be classified in a pair-wise manner as proximal and distal with respect to the orientation of the methine vector. The terminal alkoxide ligands of the wingtip metals thus interconvert as do the bridging groups, but these transformations do not involve the backbone alkoxides.

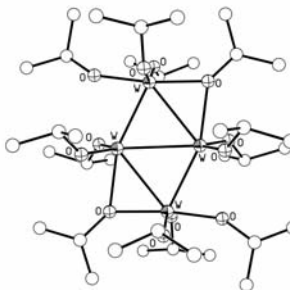
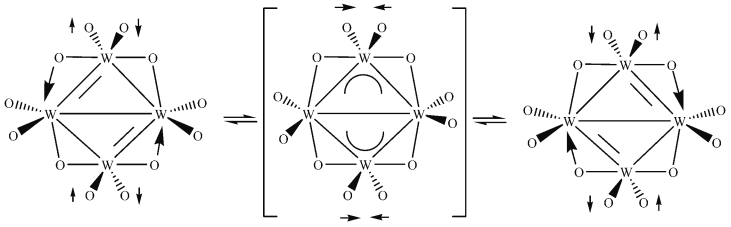


Fig. 6.4. Structure of the butterfly $W_4(OPr^i)_{12}$ cluster.

The explanation proposed for this dynamic process was that the C_{2h}-W_4 cluster oscillates about the more symmetric diamond W_4 structure wherein the WW distances are equivalent. This leads to the bridging groups becoming equivalent without exchange with the terminal groups. Concomitant with this dynamic process is a correlated motion of the wing-tip alkoxides. The process is shown schematically in Scheme 6.2 and was called the *Bloomington Shuffle*. The energy of activation of this intramolecular process was estimated to be 13 kcal mol^{-1}. This was determined from the line broadening seen at low temperatures in ^1H NMR spectra. At room temperature the dissociative equilibrium is clearly evident by NMR spectroscopy although it is never rapid on the NMR time scale.

The thermodynamic parameters of this equilibrium were found to be ΔH^o = -16 kcal mol^{-1} and ΔS^o = +60 eu, together with the activation parameters $\Delta H^{\neq}$ = 5 kcal mol^{-1} and $\Delta S^{\neq}$ = +38 eu for the forward (dissociative), and $\Delta H^{\neq}$ = 10 kcal mol^{-1} and $\Delta S^{\neq}$ = -40 eu for the back (associative reaction).[61] The tetranuclear cluster is favored on enthalpic grounds but disfavored by entropy. The low enthalpic barrier to the association of two M–M bonds is noteworthy and contrasts with organic pπ–pπ systems for which the process would be symmetry forbidden according to the Woodward-Hoffman rules.[131-133]

Pictiva EX2004
Samsung v Pictiva
IPR2024-01094



Scheme 6.2. The Bloomington shuffle.

This 12-electron W_4 cluster was also compared to cyclobutadiene in a theoretical analysis of the bonding in the cluster. The descent from D_{4h} to C_{2h} symmetry was reasonably traced to a second order Jahn-Teller distortion.[32] The preference for the diamond W_4 geometry relative to the rectangular C_4H_4-like ground state structure could also be traced to the importance of W_d-W_d orbital interactions, which favor the diamond structure, due to increased W(1)–W(1)' metal–metal bonding.

The $W_4(OPr^i)_{12}$ cluster appears to be unique amongst the $M_4(OR)_{12}$ clusters as it is the only one found to exhibit a dissociative equilibrium. Also the NMR spectra of other compounds of formula $M_4(OR)_{12}$ (M = Mo, W) cannot be rationalized by the diamond structure but rather by the adoption of a M_4 cluster structure which has a marked asymmetric distribution of alkoxide ligands. This implies that the oxidation states of the metal atoms are not all the same. Such asymmetry is also reflected in the MM distances.[130]

6.5.2 $M_4X_4(OPr^i)_8$ (X = Cl, Br) and $Mo_4Br_3(OPr^i)_9$

The reaction between $Mo_2(OPr^i)_6$ and acetylchloride or Me_3SiCl in hexane leads to a black insoluble compound that was characterized by single crystal X-ray crystallography as $Mo_4Cl_4(OPr^i)_8$.[134] The molecule lies on a crystallographic C_4 axis. There are four terminal MoCl bonds and eight bridging alkoxide ligands, four lying above and four below a molybdenum square [Mo–Mo (av.) = 2.41(1) Å]. Quite remarkably, the related $Mo_4Br_4(OPr^i)_8$ has a butterfly-Mo_4 unit with terminal MoBr bonds and edge- and face-bridging alkoxides.[135] The chloride and bromide structures are shown in Fig. 6.5. The solution structures of $Mo_4X_3(OPr^i)_9$ molecules, X = Cl, Br and I, can be reliably correlated with the butterfly structure by NMR spectroscopy, and this conclusion was firmly established by crystallography for X = Br, wherein one of the wingtip terminal MoBr bonds is replaced by a terminal alkoxide ligand.[135]

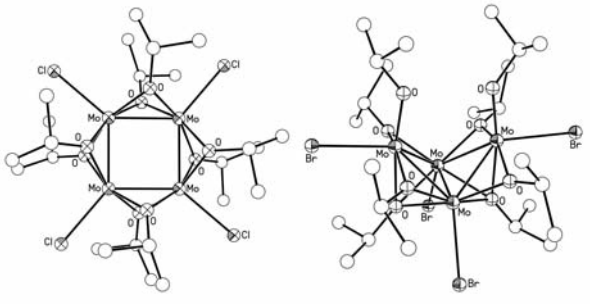


Fig. 6.5. Structures of the square cluster $Mo_4Cl_4(OPr^i)_8$ (left) and the butterfly $Mo_4Br_4(OPr^i)_8$ cluster (right).

Pictiva EX2004
Samsung v Pictiva
IPR2024-01094

The bonding in these tetranuclear halide clusters was examined by Fenske-Hall Molecular Orbital (FHMO) calculations on the model compounds $M_4X_4(OH)_8$.[136] The square and butterfly structures are fragments of the well-known cube-octahedral clusters $M_6(\mu_3\text{-}X)_8L_6$. The preference for MoX bonds to occupy terminal sites can be understood in terms of a radial cluster influence. In order to maximize MM bonding within the cluster, the ligands with weaker *trans* influence, in this case halides, occupy radial positions.[136]

6.5.3 $W_4(p\text{-tolyl})_2(OPr^i)_{10}$

The unusual cluster $W_4(p\text{-tolyl})_2(OPr^i)_{10}$ was prepared by adding Pr^iOH to hexane solutions of $W_2(p\text{-tolyl})_2(NMe_2)_4$.[137] The cluster has a planar central W_4 moiety with an "open edge" in the sense that two tungsten atoms are held together through the agency of an alkoxide bridge rather than by a direct MM bond (M(1)–M(4) = 3.01 Å). The structure may be viewed as a perturbation of the $W_4(OPr^i)_{12}$ structure described previously.

6.5.4 $W_4O(X)(OPr^i)_9$, (X = Cl or OPr^i)

Two other 12-electron W_4 clusters were obtained from the degradation of the alkoxides in $W_4(OPr^i)_{12}$ upon heating in solution: $W_4O(Cl)(OPr^i)_9$ and $W_4O(OPr^i)_{10}$.[138,139] NMR data reveal these products to be structurally related although only the cluster $W_4O(Cl)(OPr^i)_9$ was characterized in the solid state. The structure has a "$WCl(OPr^i)$" unit capping a triangular "$W_3(\mu\text{-}O)(\mu\text{-}OPr)_2(OPr^i)_6$" fragment. The WW distances in the latter are all long (2.85 – 2.96 Å) while the three W–W distances to the capping tungsten atom are short (2.49 Å). This short distance is indicative of some multiple bond order and the bonding in these clusters was examined by Extended Huckel Molecular Orbital (EHMO) calculations and an interesting analogy was drawn between these clusters and PtL_2 capped metal carbonyl clusters.[138,139]

6.5.5 $K(18\text{-crown-}6)_2Mo_4(\mu_4\text{-}H)(OCH_2Bu^t)_{12}$

The addition of hydride anion from either KH or $NaHBEt_3$ to solutions of $Mo_2(OR)_6$, where R = Pr^i and CH_2Bu^t, leads to the formation of the anionic cluster $[Mo_4(\mu_4\text{-}H)(OR)_{12}]^-$ whose structure is shown in Fig. 6.6.[140] Evidently, addition of H^- to $Mo_2(OR)_6$ yields a nucleophilic $[Mo_2(H)(OR)_7]^-$ moiety which attacks another $Mo_2(OR)_6$ molecule. The structure is related to that seen for $Mo_4Br_4(OPr^i)_8$, and evidence for the μ_4-H ligand came from both crystallographic data and EHMO calculations.[140,141]

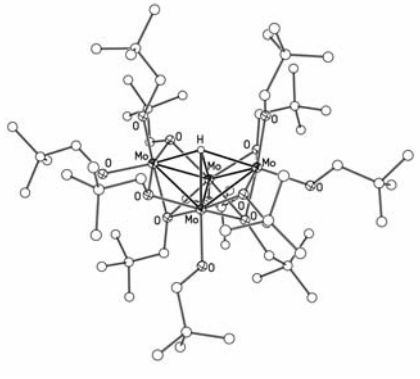


Fig. 6.6. Structure of the μ_4-hydrido-bridged anion in $K[Mo_4(\mu_4\text{-}H)(OCH_2Bu^t)_{12}]$.

Pictiva EX2004
Samsung v Pictiva
IPR2024-01094

As noted earlier, there are interesting analogies in the bonding of early transition metal alkoxide clusters and later transition metal carbonyl clusters. However, perhaps the most amazing characteristic of these 12-electron clusters of Mo and W is the variety of geometries seen for the M_4 unit. Clearly, the MM bonding is very sensitive or responsive to the steric and electronic constraints of the attendant ligands. This is even further underscored by a consideration of the linked M≡M bonded dimers to be described next.

6.5.6 Linked M_4 units containing localized MM triple bonds

It was previously noted that $Mo_2(OPr^i)_6$ does not show any tendency to form $Mo_4(OPr^i)_{12}$ akin to its tungsten analog. However, with less sterically-demanding alkoxide ligands, clusters are formed. In an attempt to study the nature of the "dimerization" process, $Mo_2(OPr^i)_6$ and methanol were allowed to react in hydrocarbon solvents. An initial "dimer of dimers" was characterized as $[Mo_2(OPr^i)_4(\mu\text{-OMe})(\mu\text{-}OPr^i)]_2$.[142] Its structure, Fig. 6.7, has a rectangular Mo_4 unit containing two localized Mo≡Mo bonds of 2.22 Å brought together by alkoxide bridges for non-bonding MoMo distances of 3.5 Å.

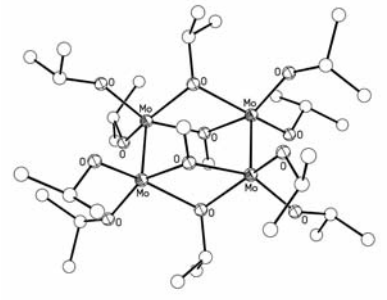


Fig. 6.7. Structure of the mixed alkoxide cluster $[Mo_2(OPr^i)_4(\mu\text{-OMe})(\mu\text{-}OPr^i)]_2$.

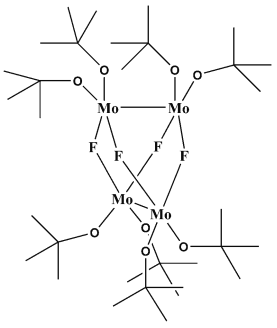
Another rectangular Mo_4-containing molecule, $[Mo_2(OPr^i)_4(\mu\text{-}OPr^i)(\mu\text{-F})]_2$, was obtained from the reaction between $Mo_2(OPr^i)_6$ and two equivalents of PF_3. Here the "dimer of dimers" was readily cleaved by the addition of PMe_3 which gave $Mo_2(OPr^i)_6$ and $Mo_2F_2(OPr^i)_4(PMe_3)_2$.[143] Treatment of a hydrocarbon solution of $Mo_2(OBu^t)_6$ with two equivalents of PF_3 gave $Mo_4(\mu\text{-F})_4(OBu^t)_8$ as depicted in 6.4.[143,144] Once again, the differing MoMo distances of 2.25 Å and 3.7 Å leave no doubt that the localized triple bonds have been retained. This is further supported by the fact that treatment of $Mo_4(\mu\text{-F})_4(OBu^t)_8$ with 4 equiv of PMe_3 yields $Mo_2(F)_2(OBu^t)_4(PMe_3)_2$. The reactions are:

$$2[Mo_2(OBu^t)_6] + 4PF_3 \rightarrow Mo_4F_4(OBu^t)_8 + 4PF_2OBu^t$$

$$Mo_4F_4(OBu^t)_8 + 4PMe_3 \rightarrow 2[Mo_2(F)_2(OBu^t)_4(PMe_3)_2]$$

From the reaction between 1,2-$Mo_2Br_2(CH_2SiMe_3)_4$ and water in the presence of pyridine, the unusual compound $Mo_4O_2(CH_2SiMe_3)_8$ was obtained.[145] The notable feature of this structure shown in Fig. 6.8 is that each molybdenum atom is three-coordinate and the local ethane-like $W_2O_2C_4$ core is *gauche*, whereas in the previously described linked $(Mo{\equiv}Mo)^{6+}$ species each Mo atom is four coordinate such that each "$L_4Mo{\equiv}MoL_4$" fragment is square pyramidal.

Pictiva EX2004
Samsung v Pictiva
IPR2024-01094



6.4

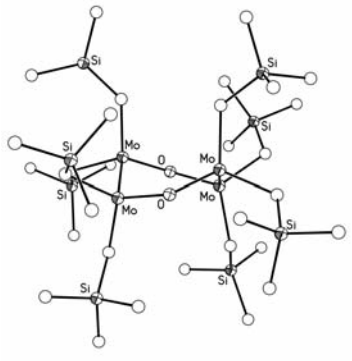


Fig. 6.8. Structure of $Mo_4(O)_2(CH_2SiMe_3)_8$.

6.6 M_2X_6L, $M_2X_6L_2$ and Related Compounds

This class of compounds arises from the ability of the homoleptic $X_3M{\equiv}MX_3$ compounds to expand their coordination sphere either by direct association with a Lewis base or by virtue of the fact that one X ligand can be replaced by a uninegative bidentate group. A notable feature of this class of compounds is the drive to form symmetrically-substituted compounds. Each metal atom tends to be surrounded by an identical set of ligands and when this does not occur, each metal atom at least enjoys the same coordination number. Because of this observation, particular attention has been given to the following exceptions.

6.6.1 $Mo_2(CH_2Ph)_2(OPr^i)_4(PMe_3)$ and $[Mo_2(OR)_7]^-$

The addition of PMe_3 to 1,2-$Mo_2(CH_2Ph)_2(OPr^i)_4$ in hydrocarbon solvents was studied in great detail by ^{31}P and ^1H VT NMR spectroscopy and revealed the facile nature of benzyl for alkoxide exchange between metal centers.[146] The symmetrically substituted compound $Mo_2(CH_2Ph)_2(OPr^i)_4(PMe_3)_2$ is formed in this reaction and is thermodynamically favored like its structurally characterized analog 1,2-$Mo_2(CH_2Ph)_2(OPr^i)_4$(dmpm). However, the unsymmetrically substituted compound $(PMe_3)(PhCH_2)_2(Pr^iO)Mo{\equiv}Mo(OPr^i)_3$ is present at room temperature and was structurally characterized, and it is shown in Fig. 6.9. In solution, this compound is labile to PMe_3 dissociation to reform the symmetrically substituted ethane-like compound 1,2-$Mo_2(CH_2Ph)_2(OPr^i)_4$. Given the kinetic persistence of 1,1- and 1,2-$M_2X_2Y_4$ isomers, the significance of this Lewis base facilitated migration of groups between the metal centers becomes apparent.

Pictiva EX2004
Samsung v Pictiva
IPR2024-01094

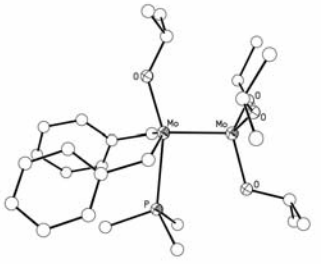


Fig. 6.9. Structure of $(PMe_3)(PhCH_2)_2(Pr^iO)Mo{\equiv}Mo(OPr^i)_3$.

The addition of KOR to $M_2(OR)_6$ compounds was studied for M = Mo and W and R = Bu^t, Pr^i and CH_2Bu^t.[147] In the presence of 18-crown-6, the K^+ (crown) salts of the anions $M_2(OR)_7^-$ and $M_2(OR)_8^{2-}$ were isolated. Most significantly, the $M_2(OR)_7^-$ anions contained a single bridging alkoxide group for M = Mo and R = Pr^i. The Mo≡Mo distance of 2.22 Å was only slightly longer than that found in $Mo_2(OPr^i)_6$. In solution, the anionic alkoxide is fluxional on the NMR time scale. Even at -80 °C only one set of alkoxide resonances is visible. Again this attests to the facility of ligand transfer between the metal atoms in a M_2X_6L type of complex.

6.6.2 $M_2(OR)_6L_2$ compounds and their congeners

In the reactions between $M_2(NMe_2)_6$ compounds and alcohols, the dimethylamine that is liberated can coordinate to the dinuclear center to give dimethylamine adducts of the type $M_2(OR)_6(HNMe_2)_2$.[58,148] The $HNMe_2$ ligands are kinetically labile and may be readily replaced by other Lewis bases. Thus, in the reaction between $W_2(NMe_2)_6$ and isopropanol in the presence of pyridine, the black crystalline compound $W_2(OPr^i)_6(py)_2$ is formed[149] whereas in a related reaction involving ethanol in the presence of en'' ligands, $W_2(OEt)_6(Me(H)NCH_2CH_2N(H)Me)$ is formed.[58] Even sterically bulky alkoxide ligands such as those present in $W_2(OBu^t)_6$ and $W_2(OCMe_2CF_3)_6$ will undergo reversible Lewis base association reactions[150] in solution with pyridine, 4-methylpyridine and isocyanides:

$$M_2(OR)_6 + 2L \rightleftharpoons M_2(OR)_6L_2$$

The geometries of these $M_2(OR)_6L_2$ complexes are largely determined by steric factors. The two square planar $M(OR)_3L$ units are united by a M≡M bond that is typically only 0.05 Å longer than in the unligated complex. Staggered geometries about the M≡M bond are common but amine to alkoxide hydrogen bonding can favor an eclipsed geometry. Structural data for such compounds are given in Table 6.5.

Table 6.5. Compounds of the form $X_4M{\equiv}MX_4$ containing intramolecular hydrogen-bonding

Compound	Donor	Acceptor	M–M[a]	ref.
cis,*cis*-$Mo_2(OC_6F_5)_4(NMe_2)_2(HNMe_2)_2$	NHR_2	OR	2.22	151
$Mo_2[OCH(CF_3)_2]_5(NMe_2)(HNMe_2)_2$	NHR_2	OR	2.24	152
$Mo_2(OBu^t)_4(NHPh)_2(NH_2Ph)_2$	NHR/ NHR_2	OR	2.25	153
trans-$W_2Cl_4(NHCy)_2(NH_2Cy)_2$	NHR	Cl	2.29	154
trans-$W_2Cl_4(NHBu^t)_2(NH_2Bu^t)_2$	NHR	Cl	2.29	50,155
$W_2Cl_3(NHBu^t)_2(NH_2Bu^t)(PPh_2NPOPh_2)$	NHR	Cl	2.30	154
trans-$W_2Cl_4(NHBu^t)_2(PMe_3)_2$	NHR	Cl	2.31	156
trans-$W_2Cl_4(NHBu^t)_2(PMe_3)_2$	NHR	Cl	2.31	156
trans-$W_2Cl_4(NHBu^t)_2(PMe_2Ph)_2$	NHR	Cl	2.31	156

Pictiva EX2004
Samsung v Pictiva
IPR2024-01094

trans-$W_2Cl_4(NHEt)_2(NH_2Et)_2$	NHR	Cl	2.31	155,157
trans-$W_2Cl_4(NHBu^t)_2(PPr_3)_2$	NHR	Cl	2.32	156
cis,*cis*-$W_2Cl_4(NHBu^t)_2$(dmpm)	NHR	Cl	2.32	158
cis-$W_2Cl_4(NHCy)_2(PMe_3)_2$	NHR	Cl	2.32	154
cis-$W_2Cl_4(NHBu^t)_2(PMe_3)_2$	NHR	Cl	2.32	154
1,1,2-$W_2Cl_3(OBu^t)_3(NHMe_2)_2$	NHR	OR	2.32	159
$W_2(OBu^t)_4(NHPh)_2(NH_2Ph)_2$	NHR/ NHR_2	OR	2.32	153
cis-$W_2Cl_4(NHBu^t)_2(PMe_3)_2$	NHR	Cl	2.33	156
cis,*cis*-$W_2Cl_4(NHBu^t)_2$(dmpe)	NHR	Cl	2.33	158
cis,*cis*-$W_2Cl_4(NHBu^t)_2$(dppm)	NHR	Cl	2.33	158
cis,*cis*-$W_2(OC_6F_5)_4(NMe_2)_2(HNMe_2)_2$	NHR_2	OR	2.34	b
$W_2(OPr^i)_6(HNMe_2)_2$	NHR_2	OR	2.34	58
cis,*cis*-$W_2Cl_4(NHBu^t)_2$(dppe)	NHR	Cl	2.35	158

[a] Å, ± 0.01 Å

[b] M. H. Chisholm, J. C. Gallucci, C. B. Hollandsworth, unpublished crystal structure of $W_2(OC_6F_5)_4(NMe_2)_2$-$(HNMe_2)_2$.

The dynamic equilibrium is slow enough to be monitored by variable temperature NMR studies which reveal the cooperative nature of the binding and releasing of the ligands, L. At higher temperatures, entropy favors the unligated $M_2(OR)_6$ compounds whereas, at low temperatures, the enthalpy of ligation dominates. The position of equilibrium is very sensitive to steric factors associated with the alkoxide and the Lewis base. Also the relative electron-donating properties of the alkoxide play a significant role following the donicity order $Me_3CO > Me_2CF_3CO > Me(CF_3)_2CO$. Ease of adduct formation follows the inverse order of alkoxide donicity. The tertiary phosphine adducts $W_2(OCH_2CMe_3)_6(PMe_3)_2$ and $W_2(OCH_2CMe_3)_6$-$(Me_2PCH_2CH_2PMe_2)$ show interesting ^{31}P NMR spectra as a result of the dynamic equilbria just described and also because of the presence of ^{183}W, I = ½, *c.* 14% natural abundance, which gives rise to a satellite spectrum reflecting the magnetically different ^{31}P nuclei in the mixed $^{183}W{\equiv}W$ isotopomer. Addition of alkoxide anions to $M_2(OR)_6$ compounds has also been noted to give $M_2(OR)_8^{2-}$ anions supported by lithium, potassium, or $H_2NMe_2^+$ cations.[147,160] For the latter, the presence of excess, acidic alcohol, causes formation of $(H_2NMe_2)(OR)$ from the reaction of liberated $HNMe_2$ and ROH. The salt can then add to $W_2(OR)_6$ to give $(H_2NMe_2)_2[W_2(OR)_8]$ species in which the $H_2NMe_2^+$ cations form strong hydrogen bonding interactions to the alkoxide ligands.

A pair of four-coordinate, triply-bonded dimetal centers also arises when two alkoxide ligands are replaced by a *bidentate* chelating ligand such as a carboxylate or acac ligand. In the case of $M_2(OR)_4(acac)_2$ compounds, the acac acts as chelating group to each metal center resulting in unbridged four-coordinated metal atoms.[161] A similar unbridged MM bond was seen in the $W_2R_2(OPr^i)_2(Bu^t\text{-acac})_2$ compounds, where R = Et, Ph, CH_2Ph or Bu, and Bu^t-acac = 2,5-di-*tert*-butylpentanedienylate.[162]

Insertion of CO_2 into the M-OR bond occurs reversibly for $M_2(OR)_6$ compounds to give the alkylcarbonate $M_2(OR)_4(O_2COR)_2$ compounds[163] which like their carboxylate analogs[164] have four coordinate metal centers and two mutually *cis*, bridging carboxylates.

A related double insertion also occurs in the reactions of $M_2(OR)_6$ and organic isocyanates and the compounds $Mo_2(OPr^i)_4(N(Ph)C(O)OPr^i)_2$ and $W_2(OBu^t)_4(N(Ph)C(O)OBu^t)_2$ were structurally characterized.[165] The structure of the tungsten compound is shown in Fig. 6.10. Here there is a *trans* O–W–N arrangement such that each metal is in an equivalent environment. In the case of the Mo_2-containing compound, the bridging groups are *cis* but symmetrically disposed so that each metal center forms three M–O bonds and one M–N bond.[165] In a subsequent

Pictiva EX2004
Samsung v Pictiva
IPR2024-01094

study,[166] it was found that an initial adduct was formed in which the phenylisocyanate molecule bridged to two metal centers and the product resulting from subsequent insertion into a metal-alkoxide bond was isolated as the PMe_3 adduct. These structures are depicted in **6.5** and **6.6**.

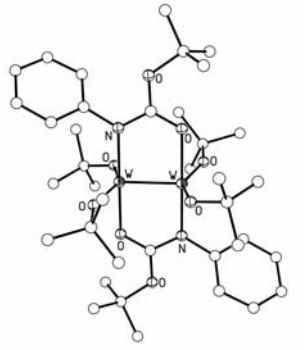
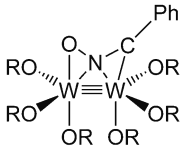
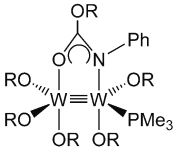


Fig. 6.10. Structure of $W_2(OBu^t)_4(N(Ph)C(O)OBu^t)_2$.



6.5



6.6

6.6.3 Amido-containing compounds

The homoleptic $M_2(NMe_2)_6$ compounds do not form Lewis base adducts, although once replacement of the NMe_2 groups occurs by less electron donating groups, Lewis base adduct formation is common. For example, $M_2Cl_2(NMe_2)_4$ compounds react with tertiary phosphine ligands and a variety of mixed chloroamido phosphine complexes have been characterized including $W_2Cl_2(NMe_2)_4(dmpm)$, $W_2Cl_3(NMe_2)_3(PMe_2Ph)_2$, and $W_2Cl_4(NMe_2)_2(PMe_2Ph)_2$ by single crystal X-ray diffraction studies.[167] Notable within this series are the W–N bond distances which decrease as more Cl groups are introduced to the tungsten center. Also the rotational barrier about the W–N bonds reflects these changes and increases with increasing NMe_2 $p\pi$ to $Wd\pi$ donation. Similarly in the reactions of fluoroalkoxides, mixed amido/ alkoxide/amine complexes have often been isolated and a particularly interesting series of compounds was isolated in a study of the reactions between $Mo_2(NMe_2)_6$ and pentafluorophenol, C_6F_5OH.[151] These include $Mo_2(OC_6F_5)_4(NMe_2)_2(HNMe_2)_2$, $Mo_2(OC_6F_5)_5(NMe_2)(HNMe_2)_2$, and the MoMo quadruply bonded complex $Mo_2(OC_6F_5)_4(HNMe_2)_4$ as well as $(Me_2NH_2)[Mo_2(OC_6F_5)_6(HNMe_2)_2]$, which has a formal bond order of 3.5. Aside from the occurrence of redox reaction products in what is seemingly a simple alcoholysis reaction, the product $Mo_2(OC_6F_5)_5(NMe_2)(HNMe_2)_2$ warrants special note. The structure of this compound is shown in Fig. 6.11.

The two four-coordinate metal centers are staggered but, surprisingly, four phenolate groups are bonded to one Mo atom while the other has one phenolate and one NMe_2 group, along with two dimethylamines. The $(Mo{\equiv}Mo)^{6+}$ center is thus polar having one Mo^{4+} and one Mo^{2+} center. The Mo≡Mo distance of 2.214(1) Å is unexceptional and consistent with a MoMo triple bond. It can be thought of as having one dative component from the Mo^{2+} center to the Mo^{4+} akin to that in carbon monoxide where oxygen provides four of the six electrons employed to form the triple bond.

Pictiva EX2004
Samsung v Pictiva
IPR2024-01094

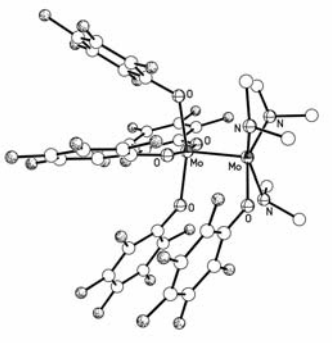


Fig. 6.11. Structure of $Mo_2(OC_6F_5)_5(NMe_2)(HNMe_2)_2$.

Reactions with reduced tungsten halides (as in THF solutions of NaW_2Cl_7),[6] with bulky primary amines have also been shown to give mixed chloroamido amine complexes such as $W_2Cl_4(N(H)Bu^t)_2(H_2NBu^t)_2$.[50] Also in a rare example of the replacement of an alkoxide by an amide, it was found that $M_2(OBu^t)_6$ compounds react with aniline to form the mixed amide/alkoxide/amine complexes $M_2(OBu^t)_4(N(H)Ph)_2(N(H)_2Ph)_2$ with the liberation of Bu^tOH.[48] In these compounds, significant N–H···Cl or N–H···O hydrogen bonds exist across the M≡M bond and thus favor the eclipsed geometry, as noted in Table 6.5.

Reactions involving 1,2-$M_2Cl_2(NMe_2)_4$ wherein the chloride ligands are replaced by bidentate uninegative ligands gave compounds containing 2-oxy-6-methylpyridine,[168] 1,3-di-*p*-tolyltriazenido,[169] and 6-methyl-2-pyridylmethyl.[170] Ditolyltriazene reacts with both $Mo_2(NMe_2)_6$[169] and 1,2-$Mo_2Me_2(NMe_2)_4$ to replace one NMe_2 group from each Mo atom but the structures of the products are quite different. In $Mo_2(NMe_2)_4(ArNNNAr)_2$, the triazenido ligands are chelating whereas in $Mo_2Me_2(NMe_2)_2(ArNNNAr)_2$, they bridge the $(Mo{\equiv}Mo)^{6+}$ bond. These two structures are shown in Fig. 6.12.

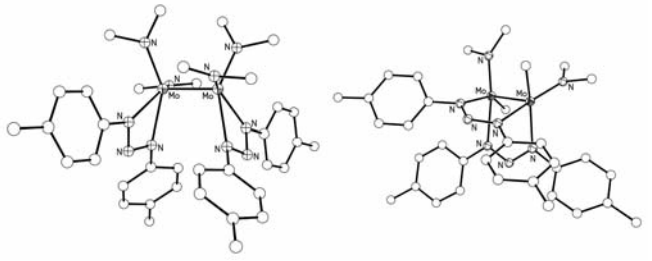


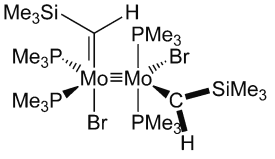
Fig. 6.12. Structures of $Mo_2(NMe_2)_4(\eta^2\text{-}ArNNNAr)_2$ and $Mo_2Me_2(NMe_2)_2(\mu\text{-}ArNNNAr)_2$.

$W_2(NMe_2)_6$ and 1,3-diphenyltriazene react similarly to give $W_2(NMe_2)_4(PhNNNPh)_2$ which is structurally similar to its molybdenum analog. However, $Mo_2R_2(NMe_2)_4$ and $W_2R_2(NMe_2)_4$ compounds where R = ethyl and benzyl react quite differently with 1,3-diaryl triazenes.[77, 118] The molybdenum compounds undergo reductive elimination to yield the MoMo quadruply bonded compound $Mo_2(ArNNNAr)_4$, whereas the tungsten compounds give $W_2R_2(NMe_2)_2(ArNNNAr)_2$, which are analogs of $Mo_2Me_2(NMe_2)_2(ArNNNAr)_2$ shown in Fig. 6.12. Similar reactions occur with $M_2R_2(NMe_2)_4$ compounds and carbon dioxide. The molybdenum compounds are more susceptible to reductive elimination via alkyl group disproportionation as noted earlier. The benzyl complexes undergo reductive elimination by a radical process.[76]

Pictiva EX2004
Samsung v Pictiva
IPR2024-01094

6.6.4 $Mo_2Br_2(CHSiMe_3)_2(PMe_3)_4$

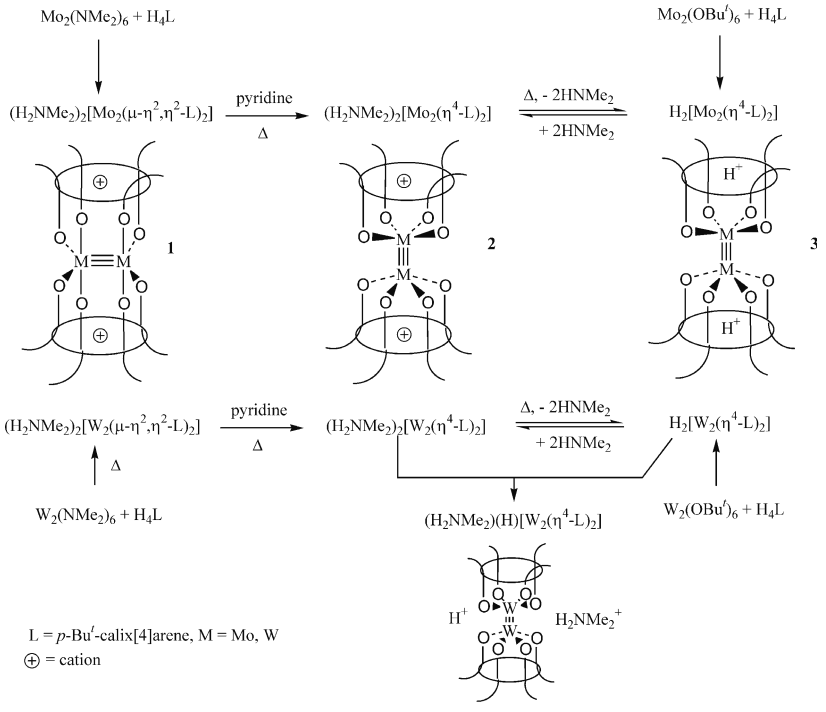
The compounds $M_2(CH_2R)_6$ where R = CMe_3, $SiMe_3$ and Ph do not react with Lewis bases but the compound 1,2-$Mo_2Br_2(CH_2SiMe_3)_4$ does. The addition of PMe_3 induces alkane elimination via α-hydrogen activation and leads to an unusual dinuclear *bis*-alkylidene complex, $Mo_2Br_2(CHSiMe_3)_2(PMe_3)_4$.[171,172] In the solid-state, this complex possesses C_2 symmetry. The PMe_3 ligands are mutually *trans* and the central $Mo_2Br_2C_2P_4$ skeleton is eclipsed as depicted in **6.7**. The HCSi planes are aligned with the $(Mo{\equiv}Mo)^{6+}$ axis such that the carbene-Mo π-bond does not compete with the MoMo π-bond. The $(Mo{\equiv}Mo)^{6+}$ distance 2.276(1) Å is well within the normal range for Mo≡Mo bonds.



6.7

6.6.5 Calix[4]arene complexes

Reactions between *p-tert*-butylcalix[4]arenes and $M_2(NMe_2)_6$ or $M_2(OR)_6$ compounds leads to the formation of products where each metal is bonded to four oxygen atoms. Interestingly, in these reactions kinetic products of substitution were shown to have the calix[4]arene spanning the Mo≡Mo bond. However, these compounds isomerized to the thermodynamic products upon heating in the presence of donor ligands such as pyridine as shown in Scheme 6.3 where ⊕ represents $H_2NMe_2^+$ hydrogen-bonded to the respective calixarene.[173, 174]



Scheme 6.3. Some reactions of M_2(calixarene)$_2$ compounds.

Pictiva EX2004
Samsung v Pictiva
IPR2024-01094

6.7 Triple Bonds Uniting Five- and Six-Coordinate Metal Atoms

This is a small but interesting group of compounds. As noted earlier, there are compounds of the type $W_2R_2(O_2CMe_3)_4$ where R = CH_3, CH_2Ph and CH_2CMe_3[117,119-120] and $Mo_2(CH_2CMe_3)_2(O_2CMe)_4$[122] that have very short MM distances comparable to MM quadruple bond distances. They have the ubiquitous paddlewheel geometry with additional axial alkyl ligation as seen for $W_2(CH_2Ph)_2(O_2CEt)_4$ in Fig. 6.13.

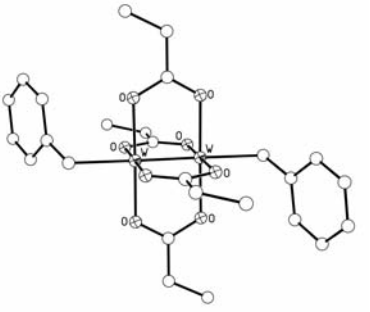
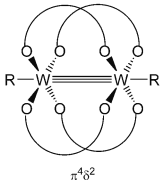
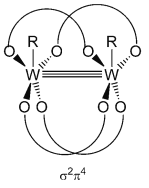


Fig. 6.13. Structure of $W_2(CH_2Ph)_2(O_2CEt)_4$.

A similar geometry is seen in the compounds $M_2(hpp)_4Cl_2$ which are formed either by oxidation of the highly reducing $M_2(hpp)_4$ complexes or from the melt reaction involving $M_2Cl_2(NMe_2)_4$ and > 4 equivalents of Hhpp.[175,176] These are noteworthy for having abnormally long M–Cl axial bonds of ≥ 3 Å. The former compounds, $M_2R_2(O_2CR')_4$, share a valence MO configuration MM $\pi^4\delta^2$ and the latter MM $\pi^4\sigma^2$, where the HOMO is MM σ- bonding and M–Cl σ* in character. This contrasts with the structure seen for $W_2Me_2(O_2CNEt_2)_4$ where each metal atom forms five bonds in a pentagonal plane.[108] Here the MM bonding configuration is $\sigma^2\pi^4$. However, subtle factors can induce a transformation from one structure to another as seen in the replacement of two acetate ligands by dithiocarbamate ligands in the compound $W_2(CH_2CMe_3)_2(O_2CMe)_2(S_2CNEt_2)_2$.[121] The latter has a WW bond of configuration $\sigma^2\pi^4$. An analysis of the frontier molecular orbitals indicated there should be no significant electronic barrier to the interconversion of these two structures, **6.8** and **6.9**, and furthermore, that the nitrogen lone pairs in $R_2NCO_2^{1-}$ and $R_2NCS_2^{1-}$ ligands had a destabilizing influence on the $\pi^4\delta^2$ triple bond as in **6.8** thus favoring the $\sigma^2\pi^4$ configuration seen in **6.9**.[121]



6.8



6.9

Finally, for metal atoms forming six bonds to ligands as in $W_2(O_2CBu^t)_6$[28] and $W_2(O_2CNMe_2)_6$,[108] there is only one possibility, namely that five bonds are formed in the xy plane and one additional bond along the $(W{\equiv}W)^{6+}$ axis. In these compounds, the EAN rule is satisfied and the triple bond is of configuration $\sigma^2\pi^4$. NMR spectroscopy indicates that these molecules are fluxional on the NMR time scale. To these structural motifs we can add the more common geometries for dinuclear metal complexes, namely edge-shared and face-shared

Pictiva EX2004
Samsung v Pictiva
IPR2024-01094

bioctahedral which too can exist in equilibrium.[177] This is further testimony to the remarkable coordination modes available to the M_2^{6+} unit.[178]

6.8 Redox Reactions at the M_2^{6+} Unit

In 1979, Chisholm speculated about redox reactions of $(M{\equiv}M)^{6+}$ complexes and anticipated that these compounds should enter into redox reactions wherein the M≡M bond order was systematically changed. Moreover, it was suggested that the dinuclear center could act as a template for catalytic reactions.[179] As has been noted already, 1,2-dialkyl and -diaryl compounds were found to enter into reductive elimination reactions leading to the formation of MM quadruple bonds. The first examples of the oxidative conversion of a MM triple bond to a double or single bond are shown[180] in the following reactions:

$$Mo_2(OPr^i)_6 + Pr^iOOPr^i \rightarrow Mo_2(OPr^i)_8$$

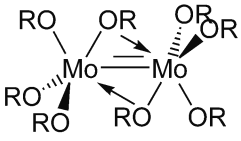
$$Mo_2(OPr^i)_6 + 2X_2 \rightarrow Mo_2(OPr^i)_6X_4, \text{ where X = Cl, Br and I}$$

Subsequently, it was shown that the octaalkoxide anions $[M_2(OR)_8]^{2-}$ could be cleanly converted to $M_2(OR)_8$ compounds:

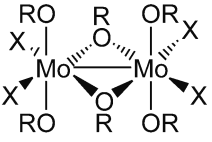
$$K_2M_2(OR)_8 + PPh_3Br_2 \rightarrow M_2(OR)_8 + 2KBr + PPh_3$$

The latter reaction afforded access to $W_2(OCH_2Bu^t)_8$, with a formal W=W double bond, which has now been shown to have an extensive organometallic chemistry.[181-184]

Oxidative addition reactions invariably led to bridge formation and the structure of the $Mo_2(OPr^i)_8$[47] and $Mo_2(OPr^i)_6X_4$ compounds[180] are shown schematically in **6.10** and **6.11**. The related $W_2(OCH_2Bu^t)_8$ compound is polymeric and is believed to have an extended chain structure of face sharing $(W{=}W)^{8+}$ units linked by alkoxide bridges.



6.10



6.11

In an equatorial-axial bridged bipyramid, the M=M bond of about 2.5 Å can be formulated as having a σ- and a δ- component but lacking a π component. In a pair of d^1-d^1 edge-sharing octahedra, the M–M single bond of length *c.* 2.7 Å is of σ^2 origin, being formed from one of the t_{2g}-t_{2g} interactions.

Alcohols have also been found to oxidatively add to $W_2(OR)_6$ compounds to give hydrido-bridged structures such as that seen in $[W_2(\mu\text{-}H)OPr^i)_7]_2$.[55,60] In the solid state, this compound contains a chain of four tungsten atoms, and the WW distances alternate between short, long, and short (2.45, 3.30 and 2.45 Å, respectively). This is consistent with the view that two confacial $(W{=}W)^{8+}$ units are linked together by a pair of alkoxide bridges. It is intriguing that this molecule is fluxional on the NMR time-scale giving rise to only one type of alkoxide signal even at -80 °C. The hydride signal appears downfield at about 20 ppm and is flanked by satellites due to coupling to two equivalent ^{183}W nuclei. The tetranuclear structure of $[W_2(H)(OPr^i)_7]_2$ is readily broken by the addition of Lewis bases or NaOR in diglyme. Consequently, $Na[W_2(H)(OPr^i)_8]$ has been structurally characterized as the diglyme adduct.[185] Although the reaction pathway leading to the oxidative addition of alcohol was a matter of considerable discussion, it was eventually argued that it is a base promoted addition.[185]

Pictiva EX2004
Samsung v Pictiva
IPR2024-01094

α-Diketones R'C(O)C(O)R' were also found to react with $W_2(OR)_6$ compounds to give W–W singly bonded complexes $W_2(OR)_6(OC(R')C(R')O)_2$ with W–W distances of *c.* 2.75 Å when R = Bu^t or Pr^i and R' = Me, Ph and *p*-tolyl.[186] The α-diketone ligands are essentially reduced to diolates and chelate to the metal center.

In a similar manner $Mo_2(OR)_6$ compounds (R = Pr^i and CH_2Bu^t) and $W_2(OPr^i)_6(py)_2$ were found to react with 9,10-phenanthrenequinone and tetrachloro-1,2-benzoquinone to give $(M–M)^{10+}$ units.[95] Also, it was found that 1,4-diisopropyl-1,4-diazobutadiene adds to give the $(M{=}M)^{8+}$ complex $Mo_2(OPr^i)_6(Pr^iNCHCHNPr^i)_2$ along with $Mo_2(OPr^i)_5(Pr^iNCHCHNPr^i)_2$.[187]

$Mo_2(OR)_6$ compounds and arylazides react to give imido compounds such as $[Mo(OBu^t)_2(NAr)(\mu\text{-}NAr)]_2$ with complete loss of the MM bond and loss of one alkoxide ligand per metal atom.[188] Diaryldiazoalkanes, Ph_2CN_2 react with $M_2(OR)_6$ to give $Mo_2(OPr^i)_6(N_2CPh_2)_2(py)$ and $W_2(OBu^t)_6(N_2CPh_2)_2$. In each compound, the diazoalkane is reduced to a hydrazone ligand, $N_2CPh_2^{2-}$. In the tungsten compound, there is a fused trigonal bipyramidal geometry with a pair of bridging N_2CPh_2 ligands and a WW bond length of 2.67 Å. However, in the Mo structure, there are terminal $N–N{=}CAr_2$ nitrene type ligands and three bridging alkoxides spanning a MoMo bond of distance 2.66 Å.

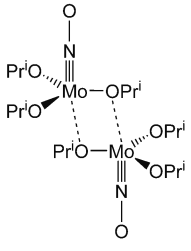
The compounds $M_2(OR)_6$ undergo facile reactions with dry O_2 and for M = Mo, the reaction is complex and dependent on the nature of R. For tungsten, the only observed product is $W_2O_3(OBu^t)_6$ of unknown structure.[189] For $Mo_2(OBu^t)_6$, the product was a thermally sensitive, yellow, volatile liquid $MoO_2(OBu^t)_2$.[190] For $Mo_2(OR)_6$ compounds where R = Pr^i and CH_2Bu^t, a more complex reaction sequence was observed and a variety of products were isolated from careful studies of O_2 uptake.[191] These included $MoO_2(OR)_2(bpy)$, $MoO(OR)_4$, $Mo_3(O)(OR)_{10}$, $Mo_4O_4(OR)_4(py)_4$ and $Mo_6O_{10}(OR)_{12}$. The green, oxo- capped triangular Mo^{4+}-containing clusters, $Mo_3(\mu_3\text{-}O)(\mu_3\text{-}OR)(\mu_2\text{-}OR)_3(OR)_6$, where R = Pr^i or CH_2Bu^t, were shown[192] to be formed by the following reaction:

$$M_2(OR)_6 + MO(OR)_4 \rightarrow M_3(O)(OR)_{10}$$

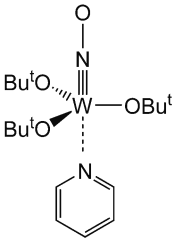
This reaction proved quite general for both Mo and W when R = Pr^i and CH_2Bu^t and the analogous, mixed metal MoW_2 and Mo_2W containing clusters were also prepared in this way.[193,194] In a subsequent study, an imido capped triangular cluster $W_3(\mu_3\text{-}NH)(OPr^i)_{10}$ was isolated and was almost certainly formed in a manner similar to that shown above.

Reactions involving P_4 and $W_2(OR)_6$ compounds yielded products derived from cleavage of the W≡W bond: $W(\eta^3\text{-}P_3)(OCH_2Bu^t)_3(HNMe_2)$[195] and $W_3(\mu_3\text{-}P)(OCH_2Bu^t)_9$[196] along with evidence of the phosphide $(Bu^tO)_3W{\equiv}P$. This evidence was provided by a unique trapping experiment employing $Cr(CO)_5(THF)$.[197]

The compounds $Mo_2(OR)_6$ react with nitric oxide to give products where the M≡M bond is cleaved and the compounds $[Mo(OPr^i)_3NO]_2$[198] and $W(OBu^t)_3(NO)(py)$[199] were structurally characterized and shown to have the molecular forms depicted in **6.12** and **6.13** below.



6.12



6.13

Pictiva EX2004
Samsung v Pictiva
IPR2024-01094

In both nitrosyl-adduct structures, the metal adopts a trigonal bipyramidal coordination environment with the linear nitrosyl ligand in an axial site. The M–N bond is depicted as a triple bond to emphasize that in this reaction with NO, the M≡M bond is formally replaced by two M≡N bonds. The compounds show extremely low values of ν(NO) as a result of extensive metal dπ to NOπ* back-bonding with ν(NO) = 1640 cm^{-1} (M = Mo) and 1555 cm^{-1} (M = W). Moreover, the M–N distances, *c.* 1.74 Å are comparable to those seen in the compounds $(Bu^tO)_3W{\equiv}N$[200] and $(Bu^tO)_3Mo{\equiv}N$.[200,201]

In contrast to these reactions that give nitrosyl derivatives, the compound $W_2(OSiMe_2Bu^t)_6$ reacts with NO to produce oxotungsten compounds: $WO(SiMe_2Bu^t)_4$ and $WO_2(OSiMe_2Bu^t)_2$.[202] The same products are formed in reactions involving N_2O. Evidently, in the reactions involving NO and $W_2(OSiMe_2Bu^t)_6$, N–N bond formation occurs leading to O atom transfer and N_2 liberation.

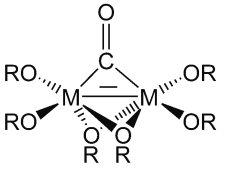
There are also various reactions that lead to complete loss of the MM bond as a result of redox reactions. For example, $W_2(OBu^t)_6$ reacts with nitrosobenzene and nitrobenzene to give the oxoimido tungsten complex $(Bu^tO)_2(PhN)W(\mu\text{-}O)(\mu\text{-}OBu^t)_2W(OBu^t)_2(NPh)$.[203] With bpy, $M_2(OR)_6$ compounds give products of redox disproportionation. The $Mo(OPr^i)_2(bpy)_2$ compound was shown to be an interesting molecule containing the d^2-*cis*-MoO_2N_4 core. With an excess of aryl or *t*-butylisocyanide ligands or carbon monoxide, $M(CNR)_6$ or $M(CO)_6$ compounds are formed along with M^{6+} metal alkoxides.[204] This provides a very efficient preparation of labeled $M(CO)_6$ compounds in reactions employing ^{13}CO or $C^{18}O$. The latter are only sparingly soluble in alkane solvents and so are readily separated from the other more soluble transition metal alkoxide products.

6.9 Organometallic Chemistry of $M_2(OR)_6$ and Related Compounds

Many of the reactions described in this section can be viewed as a redox reactions between π-acceptor, reducible organic molecules and the electron donating $(M{\equiv}M)^{6+}$ center. The presence of alkoxides or related π-donor ligands is ideal as the donor and steric properties can be modified in subtle ways. The flexible M–O–C angle allows for π-buffering and the ability of the alkoxide ligands to go between terminal and bridging positions make the $(M{\equiv}M)^{6+}$ center a remarkably responsive template for substrate binding and activation.[205]

6.9.1 Carbonyl adducts and their products

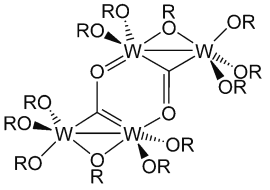
Carbon monoxide adds reversibly to $Mo_2(OBu^t)_6$ to form a 1:1 adduct[206] while tungsten forms $W_2(OBu^t)_6(CO)$ as a more kinetically persistent adduct.[207] Both compounds adopt a common structure having a carbonyl ligand bridging two metal atoms that are in a square pyramidal environment with the M–C bond in the axial position shown in **6.14**. The most notable feature of these monocarbonyls is the low value of ν(CO): 1575 cm^{-1} (M = W) and 1625 cm^{-1} (M = Mo). Hence in **6.14**, the C–O and MM bonds are shown as double bonds [M=M = 2.50(1) Å (for M = Mo), 2.53(1) Å (for M = W), and C=O = 1.25 Å], and these compounds can be viewed as inorganic analogs of cyclopropenone.[208,209]



6.14

Pictiva EX2004
Samsung v Pictiva
IPR2024-01094

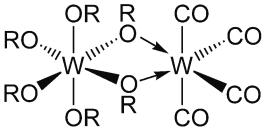
With less sterically demanding alkoxide ligands, closely related compounds $M_2(OR)_6(\mu\text{-}CO)(py)_2$ have been isolated.[207,210] Here the pyridine ligands bind in a *trans* position to the M–C bond. However, the py ligands are labile, and in solution the tungsten complex $W_2(OPr^i)_6(\mu\text{-}CO)(py)_2$ reacts by py dissociation to give the tetranuclear complex $W_4(\mu\text{-}CO)_2(OPr^i)_{12}(py)_2$.[211] The addition of Pr^iOH to $W_2(OBu^t)_6(\mu\text{-}CO)$ leads to $W_4(\mu\text{-}CO)_2(OPr^i)_{12}$, **6.15**.[207,210]



6.15

The reaction that takes a $W_2(\mu\text{-}CO)$ compound to a $W_4(\mu\text{-}CO)_2$ containing compound comes about with an increase in W–W distance, from 2.50 to 2.67 Å and an increase in CO distance from 1.25 to 1.35 Å. The W–C distance decreases from 2.00 to 1.95 Å. These changes are consistent with a further reduction of the CO ligand and an oxidation of the ditungsten center. A good case can be made that in **6.15** the C–O bond and W–W bond distances represent single bonds and the chemical shift of the bridging carbonyl carbon at 310 ppm is in the range often seen for μ-alkylidyne carbon atoms. The W–O distances associated with the $W_4(\mu\text{-}CO)_2$ moiety are 1.97 Å which is comparable to an alkoxide O to W distance. This is indicative of Opπ to Wdπ donation. The reduction of the CO ligand in this sequence of reactions arises from the combination of W_2 dπ to CO π* back-bonding and Opπ to Wdπ donation. The former reduces the CO π bond by adding electron density to the CO π* molecular orbital and the latter by removing electron density from the filled CO π bonds by Opπ to Wdπ donation. Recognition of this fact led to investigations of the reactivity between $W_4(OR)_{12}$ compounds and CO and the alcoholysis reaction between $W_2(OBu^t)_6(\mu\text{-}CO)$ and Pr^iOH in the presence of $W_2(OBu^t)_6$. In both cases, reductive cleavage of CO was observed with the formation of tetranuclear $W_4(\mu\text{-}C)$ containing clusters.[212]

In the presence of more than one equiv of CO, higher carbonylated complexes have been obtained such as $Mo(OBu^t)_2(py)_2(CO)_2$, $Mo_2(OPr^i)_8(CO)_2$,[213] and $W_2(OPr^i)_6(CO)_4$ (**6.16**).[214] In **6.16** a $W^{VI}(OR)_6$ acts as a bidentate ligand to $W^0(CO)_4$.[214] These compounds reveal how redox disproportionation occurs leading to $M(CO)_6$ and higher oxidation state metal alkoxides $M(OBu^t)_4$ or $W(OPr^i)_6$.

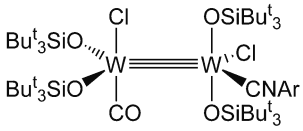


6.16

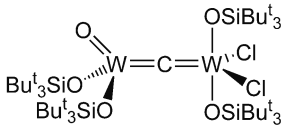
Changing from alkoxides to siloxides or fluoroalkoxides changes the nature of CO uptake at the $(M{\equiv}M)^{6+}$ center. $W_2(OCMe_2CF_3)_6(CO)_2$ is a compound of the type $M_2(OR)_6L_2$ with two terminal η^1-CO ligands that are disposed so as to maximize MM and M to CO π-bonding.[215] The same formation of $W_2(OR)_6(CO)_2$ is seen for R = Me_2Bu^tSi and 2,6-$Me_2C_6H_3$.

The ethane-like dimer $W_2Cl_2(silox)_4$ also reacts with CO to give a carbonyl adduct of type shown in **6.17** when ArNC is replaced by CO. Upon heating to 120 °C over 4 h this compound looses CO and reacts to give the oxo-carbide shown in **6.18**.[216]

Pictiva EX2004
Samsung v Pictiva
IPR2024-01094



6.17



6.18

Carbon monoxide has also been found to react with the compounds $W_2Cl_2(NMe_2)_4$ and $W_2(NMe_2)_2(OCMe_2CF_3)_4$ to give terminal carbonyl adducts and products of CO insertion into the amide bonds.[215,217]

6.9.2 Isocyanide complexes

As noted earlier, $M_2(OR)_6$ reacts in the presence of excess arylisocyanide to give $M(CNAr)_6$ by disproportionation. However, monoisocyanide adducts of ditungsten hexaalkoxides have been isolated and fully characterized.[218] The compounds $W_2(OBu^t)_6(CNAr)$ and $W_2(OPr^i)_6(CNAr)(py)$, where Ar = 2,6-$C_6H_3Me_2$, were similar to their carbonyl adducts in having WW distances of *c.* 2.52 Å, which are comparable to M≡M bonds. These compounds also have bridging isocyanide ligands. However, the bridging isocyanides were asymmetrically bonded and had C–N–C angles of *c.* 130 °. The μ-CNC plane was aligned along the WW axis and a theoretical investigation into the bonding revealed that this was favored by W_2 to CNC backbonding. In solution, these compounds are fluxional and it was not possible to freeze out the inversion at nitrogen of the bridging isonitrile ligand on the NMR time scale.

The compound $W_2Cl_2(silox)_4$ was noted to form a *bis*-isocyanide complex and a carbonyl-isocyanide complex $W_2Cl_2(silox)_4(CO)(CNAr)$ which, based on NMR studies, was assigned the structure shown in **6.17**.[216]

6.9.3 Reactions with alkynes

Alkynes and $Mo_2(OR)_6$ compounds were first noted to react via adduct formation and CC coupling reactions.[219,220] This led to characterization of the compounds $Mo_2(OPr^i)_6(\mu\text{-}C_2H_2)(py)_2$ and $Mo_2(OCH_2Bu^t)_6(\mu\text{-}C_4H_4)(py)$. $W_2(OBu^t)_6$ and the alkynes RC≡CR where R = Me, Et and Pr were shortly thereafter reported to enter into the metathesis reaction, the Schrock "Chop Chop" reaction:[221]

$$W_2(OBu^t)_6 + RC{\equiv}CR \rightarrow 2[W(OBu^t)_3(CR)]$$

Schrock, et al. extended this to a general route to $(Bu^tO)_3W{\equiv}CR$ compounds by employing terminal alkynes.[221] They also reported $(Bu^tO)_3Mo{\equiv}CPh$ could be prepared similarly.[222] The reactions between $W_2(OR)_6$ compounds and alkynes were subsequently shown to be very sensitive to the nature of the steric and electronic properties of the R groups.

Compounds such as $W_2(OPr^i)_6(\mu\text{-}C_2H_2)(py)_2$, $W_2(OCH_2Bu^t)_6(\mu\text{-}C_2Me_2)(py)_2$, and $W_2(OPr^i)_6(\mu\text{-}C_4R_4)(\eta^2\text{-}C_2R_2)$, where R = Me and H were also structurally characterized.[223] The alkyne adducts were shown to enter into C–C coupling reactions with alkynes and nitriles.[58,224-225] The ethyne adduct $W_2(OBu^t)_6(\mu\text{-}C_2H_2)(py)$ was shown to exist in equilibrium with the methylidyne complexes $(Bu^tO)_3W{\equiv}CH$ on the basis of the following double labeling experiment:[226]

$$W_2(OBu^t)_6(\mu\text{-}C_2D_2)(py) + W_2(OBu^t)_6(\mu\text{-}^{13}C_2H_2)(py) \rightleftharpoons 2W_2(OBu^t)_6(\mu\text{-}H^{13}CCD)(py)$$

Further evidence for the generality of the equilibrium between alkyne adducts and $(Bu^tO)_3W{\equiv}CR$ compounds was presented based on trapping experiments. The addition of CO to $(Bu^tO)_3W{\equiv}CMe$ in hydrocarbon solutions gave the butyne adduct $W_2(OBu^t)_6(\mu\text{-}C_2Me_2)(CO)$.[227]

Pictiva EX2004
Samsung v Pictiva
IPR2024-01094

Addition of CO to $(Bu^tO)_3W{\equiv}C{-}(CH_2)_n{-}C{\equiv}W(OBu^t)_3$ gave $W_2(OBu^t)_6(\mu\text{-}C_2(CH_2)_n)(CO)$ where $n = 4$ and 5.[228]

The compounds $(Bu^tO)_3W{\equiv}CR$ are alkyne metathesis catalysts[229,230] and react via the reversible formation of metallacyclobutadienes. In reactions between alkynes and $W_2[OCH(CF_3)_2]_6$, $W_2(OC_6H_3\text{-}2,6\text{-}Me_2)_6$ or $W_2[OCMe_2(CF_3)]_6$ tungstacyclobutadiene complexes $(RO)_3WC_3Et_3$ were isolated and characterized.[231,232]

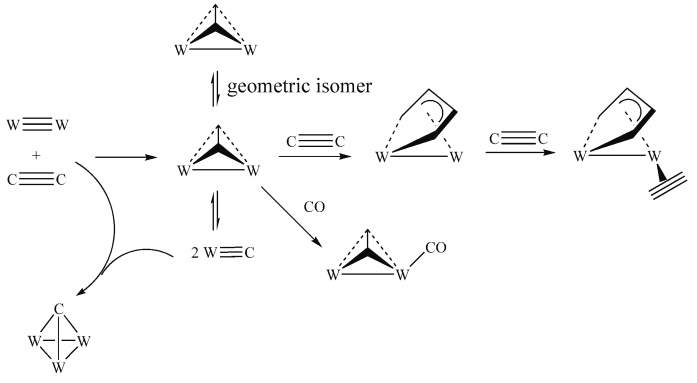
In reactions between certain $W_2(OR)_6$ compounds and alkynes where the alkyne to $W_2(OR)_6$ ratio is 1:3, alkylidyne capped tritungsten clusters such as $W_3(\mu\text{-}CMe)(OPr^i)_9$ are formed.[128, 233] These products form as a result of the alkyne metathesis reaction being followed by a comproportionation between the reactive $(RO)_3W{\equiv}CR'$ species and the $W_2(OR)_6$ starting material. In the reaction between $W_2(OPr^i)_6$ and 3-hexyne, the M≡M/C≡C metathesis reaction, alkyne-alkyne coupling and formation of the alkylidyne clusters are all competitive reactions.[234]

The general scheme of reactions for alkynes and $M_2(OR)_6$ is shown in Scheme 6.4. The alkyne adducts have μ-perpendicular alkyne ligands that span MM bonds of distance *c*. 2.65 Å. A notable feature of these compounds is the presence of long CC (alkyne) distances that fall in the range 1.38 to 1.44 Å. These are longer than those typically seen in alkyne adducts such as $Co_2(CO)_6(\mu\text{-}C_2H_2)$ that have distances in the range 1.30-1.35 Å. Also, it was noted from the spectroscopic studies of $\mu\text{-}^{13}C_2H_2$ compounds that the carbon-carbon coupling constants were very small, in the range of 12-24 Hz. These are notably smaller than the 56 Hz coupling in $Co_2(CO)_6(\mu\text{-}C_2H_2)$ which in turn can be compared to 256 Hz in free acetylene. This, together with the observed long CC distances testifies to the rehybridization of the alkyne upon binding to the $(M{\equiv}M)^{6+}$ center. The compounds can be viewed as dimetallatetrahedranes and the following reversible reaction as an internal redox reaction.[235]

$$(RO)_6M_2(\mu\text{-}C_2R_2') \rightleftharpoons 2[(RO)_3M{\equiv}CR']$$

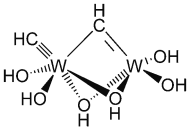
Notable in this context is the observation that addition of donor ligands such as quinuclidine drive the equilibrium to the right while acceptors such as CO capture the alkyne adduct. Also, whereas this equilbrium is often seen for W, it has not been observed for Mo which is easier to reduce and harder to oxidize.

A theoretical investigation into the reaction pathway leading to the cleavage of the CC bond as shown in the equation above, implicated the asymmetrical transition state shown in **6.19**.[236] The WW distance is 2.63 Å and the CC bond is clearly broken as one CH group becomes a terminal alkylidyne and the other is bridging.



Scheme. 6.4. Reactions of alkynes with $(W{\equiv}W)^{6+}$.

Pictiva EX2004
Samsung v Pictiva
IPR2024-01094



6.19

As noted earlier, the nature of the alkoxide group also influences the reaction pathway. Whereas $W_2(OBu^t)_6$ and ethyne establish the equilibrium shown in the equation above, $W_2(OSiMe_2Bu^t)_6$ reacts to form a kinetically labile μ-ethyne adduct that yields $W_2(OSiMe_2Bu^t)_5(\mu\text{-}\eta^1,\eta^2\text{-}C_2H)$ with elimination of Bu^tMe_2SiOH. The eliminated silanol then enters into reaction with the ethyne adduct leading to μ-vinyl (μ-$CHCH_2$) and the μ-ethylidyne complex $W_2(OSiMe_2Bu^t)_7(\mu\text{-}CCH_3)$.[33]

Whereas the dichloride $W_2Cl_2(silox)_4$ failed to react with alkynes, the bis-hydrido complex $W_2H_2(silox)_4$ reacts at low temperatures with RC≡CR' to give kinetically labile alkyne adducts $W_2(\mu\text{-}H)_2(silox)_4(\mu\text{-}RCCR')$ where R = R' = H,Me; R = H, R' = Ph. Based on spectroscopic data, these compounds were proposed to have C_2 molecular symmetry with a μ-perpendicular alkyne and asymmetric hydride bridges.[237] Upon warming, these compounds eliminate H_2 and give alkylidyne bridged compounds $W_2(silox)_4(\mu\text{-}CR)_2$, with a planar central W_2C_2 ring. For R = Me, W≡W = 2.72 Å and W≡C = 1.95 Å.

The introduction of alkyl or benzyl groups in compounds of the type 1,2-$W_2R_2(OPr^i)_4$ leads to some fascinating reactions with alkynes. Alkyne adducts such as $W_2(CH_2Ph)_2(OPr^i)_4(\mu\text{-}C_2Me_2)$, are formed along with products derived from α-hydrogen activation, such as $W_2(H)(OPr^i)_4(\mu\text{-}CPh)(\mu\text{-}C_4Me_4)_2$. Other compounds such as $W_2(Pr)_2(OPr^i)_4(\mu\text{-}C_2Me_2)_2$, $W_2(\mu\text{-}C_2Me_2)_2(OPr^i)_4$, and $W_4(\mu\text{-}CEt)_2(\mu\text{-}C_2Me_2)_2(\eta^2\text{-}C_2Me_2)_2(OPr^i)_6$, are formed from alkyne metathesis and from C–C couplings and α- or β-hydrogen activation.[238-241]

Addition of alkynes to mixed chloride-dimethylamide compounds also led to μ-alkyne adducts and in a study of the reaction between ethyne and $W_2Cl_3(NMe_2)_3$ in the presence of PR_3, the formation of the μ-vinyl ligand in $(PR_3)Cl_2W(\mu\text{-}NMe_2)(\mu\text{-}\eta^1,\eta^2\text{-}CHCH_2)(\mu\text{-}\eta^2\text{-}CH_2NMe)WCl(NMe_2)(PR_3)$ was observed by hydrogen atom transfer from a dimethylamide ligand.[242] This formation of a $\mu\text{-}\eta^2\text{-}CH_2NMe$ ligand provides a clue to the likely first step in the reaction between $W_2(NMe_2)_6$ and Pr^iOH that leads to the carbido-imido cluster compound $W_4(\mu_4\text{-}C)(\mu\text{-}NMe)(OPr^i)_{12}$.[59]

The replacement of alkoxide by thiolate groups shuts down reactions with alkynes as evidenced by the lack of reactivity of $M_2(OBu^t)_2(SBu^t)_4$.[69] Calculations on model compounds indicate that the alkoxide ligands are much stronger π-donor ligands than thiolates and thus labilize the MM π-bonding MO's.[69] Furthermore, replacement of *t*-butoxide by *o*-tolyl thiolate[243] converts an alkylidyne to a μ-alkyne complex:

$$2[(Bu^tO)_3W{\equiv}CPh] + 6C_7H_8SH \rightarrow W_2(SC_7H_8)_6(\mu\text{-}C_2Ph_2) + 6Bu^tOH$$

6.9.4 Reactions with C≡N bonds

$W_2(OBu^t)_6$ and organic nitriles enter into the Schrock "Chop Chop Reaction" to give an equivalent of the alkylidyne complex $(Bu^tO)_3W{\equiv}CR$ and the nitride $(Bu^tO)_3W{\equiv}N$. However, this reaction is unique to tungsten as $Mo_2(OBu^t)_6$ and related molybdenum alkoxides are inert to reaction with acetonitrile at ambient temperature. The reaction is also very sensitive to the nature of the alkoxide and replacement of *t*-butoxide by fluorinated alkoxides or siloxides greatly reduces the propensity of the reductive cleavage reaction. Schrock noted that acetonitrile binds reversibly to $W_2[OCMe_2CF_3]_6$ to give an adduct of the form $W_2(OR_F)_6L_2$.[231] Sub-

Pictiva EX2004
Samsung v Pictiva
IPR2024-01094

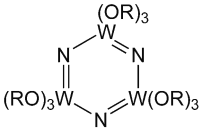
sequently, the binding of acetonitrile to $M_2(OCMe_2CF_3)_6$ was studied in some detail. Adduct formation was enthalpically favored for tungsten (where ΔH^o = 26(1) kcal mol^{-1}) relative to molybdenum (where ΔH^o = 22(1) kcal mol^{-1}).[244] Arylnitriles bind less strongly and undergo the following metathesis reactions.

$$W_2(OCMe_2CF_3)_6 + 2ArC{\equiv}N \rightarrow 2[(CF_3Me_2CO)_3WN] + ArC{\equiv}CAr$$

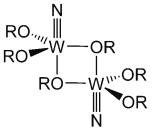
$$W_2(OSiMe_2Bu^t)_6 + 2ArC{\equiv}N \rightarrow [(Bu^tMe_2SiO)_3W{\equiv}N]_2 + ArC{\equiv}CAr$$

A similar reaction was observed for $W_2(OSiMe_2Bu^t)_6$ and the nitridotungsten compounds were shown to adopt the trimeric and dimeric structures shown below in **6.20** and **6.21** for $OCMe_2CF_3$ and $OSiMe_2Bu^t$, respectively.[244,245]

Studies of the kinetics of this reductive cleavage reaction indicated that the reaction was suppressed by excess benzonitrile and the active species leading to cleavage was proposed to be a mononitrile adduct $W_2(OR)_6(NCPh)$.[244,246]



6.20



6.21

Although $Mo_2(OR)_6$ compounds do not react with alkyl or aryl nitriles, beyond showing reversible adduct formation, Me_2NCN was found to form a 1:1 adduct with a structure wherein the C≡N bond bridges the two metal atoms.[247] Based on the C–N and MoMo distances, this complex was formulated as having double bonds and as such provides a model for a reactive intermediate on the pathway to reductive cleavage of the CN bonds. The analogous reaction with $W_2(OBu^t)_6$ led to C≡N cleavage,[247] although in a reaction involving the less bulky neopentoxide, a compound $W_2(OCH_2Bu^t)_6(NCNMe_2)_3$ was obtained and structurally characterized.[248] This compound contained three $NCNMe_2^{2-}$ ligands, each bound to the ditungsten center in a different manner. This reaction proceeds with complete cleavage and loss of the WW bond.

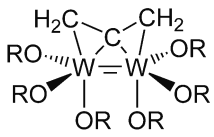
6.9.5 Reactions with C=C bonds

Allene adds to $W_2(OBu^t)_6$ to give a 1:1 adduct and a 2:1 adduct. The 1:1 adduct contains a V-shaped bridging allene as depicted by **6.22** and an essentially eclipsed W_2O_6 skeleton.[249,250] The WW distance in the green 1:1 allene adduct is 2.58 Å which indicates extensive backbonding to the μ-allene ligand. By NMR spectroscopy, the two methylene carbons and their protons are equivalent. However, the methylene protons appear to be coupled to both tungsten nuclei in an equivalent manner, which led to the suggestion that the μ-allene ligand was fluxional on the NMR time scale. Due to backbonding, the allene in this compound can be construed as an $(allene)^{2-}$ ligand.

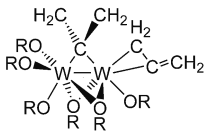
Addition of allene to this 1:1 allene adduct yields the 2:1 allene adduct which, in the solid state, has the structure depicted by **6.23**.[249,250] The bridging allene can now be considered as a metallated η^3-allyl group while the terminal η^2-allene is typical of allenes bonded to mononuclear metal centers.

Addition of CO also leads to the formation of a dimetallaallyl, $W_2(OBu^t)_6[(\mu\text{-}\eta^1,\eta^3\text{-}C(CH_2)_2](CO)_2$ having the structure depicted in **6.24**.[250] An allene adduct of $W_2(OCMe_2CF_3)_6$ of structural type seen in **6.22**, was also characterized.[150] Carbodiimides ArN=C–NAr, which are isoelectronic with allenes were also found to give structurally related 1:1 adducts.[150,251]

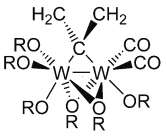
Pictiva EX2004
Samsung v Pictiva
IPR2024-01094



6.22



6.23



6.24

Ethylene adds to $W_2(OCH_2Bu^t)_6$ to give a 2:1 adduct.[252,253] The structure, shown in Fig. 6.14, bonding and dynamic behavior of this molecule proved particularly interesting.[253] The reversible uptake of ethylene occurs in a cooperative manner and in the 2:1 ethene adduct, the C–C axes are perpendicular to the WW axis and the two C_2 units may be viewed as metallacyclopropanes where C–C = 1.45 Å and W–C = 2.14 Å. There are four bridging alkoxide ligands that span the WW bond of distance 2.53 Å in an asymmetric manner forming four short W–O distances, 2.00 Å and four long W–O distances, 2.31 Å. The two C_2 units are orthogonal to each other so as to maximize Wdπ to ethylene π^* back-bonding. Tungsten-olefin bond rotation is restricted on the NMR time scale and the olefinic protons appear as an ABCD spin system. The two carbon atoms are chemically inequivalent and in the ^{13}C labeled compound derived from reaction with $^{13}C_2H_4$, $^1J_{CC}$ is 67 Hz.

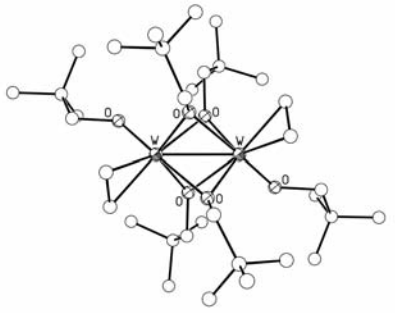


Fig. 6.14. Structure of $W_2(OCH_2Bu^t)_6(C_2H_4)_2$.

This compound reacts further with ethylene to give an alkylidyne bridged metallacyclic compound $W_2(\mu\text{-}CCH_2CH_2CH_2)(OR)_6$ with the elimination of ethane. This reaction[254] proved to be general for $W_2(OR)_6$ compounds where R = Pr^i, *c*-C_5H_9 and *c*-C_6H_{11}.

$$W_2(OR)_6 + 3C_2H_4 \rightarrow W_2(\mu\text{-}CCH_2CH_2CH_2)(OR)_6 + C_2H_6$$

In the case of R = Pr^i, the reaction pathway was found[254] to proceed by the reversible formation of a metallacyclopentane ethylene complex:

$$W_2(OPr^i)_6 + 3C_2H_4 \rightleftharpoons W_2(OPr^i)_6(CH_2)_4(\eta^2\text{-}C_2H_4) \rightarrow W_2(\mu\text{-}CCH_2CH_2CH_2)(OPr^i)_6 + C_2H_6$$

In $W_2(OPr^i)_6(CH_2)_4(\eta^2\text{-}C_2H_4)$ the η^2-ethene ligand can again be viewed as a metallacyclopropane and the WW distance of 2.65 Å is consistent with a $(M–M)^{10+}$ center.

$W_2(OCH_2Bu^t)_6(py)_2$ reacts with 1,3-butadiene and isoprene to form 1:1 adducts in which all four carbon atoms of the conjugated diene are coordinated to the dinuclear center in a $\mu\text{-}\eta^1,\eta^4$-manner[255, 256] as in Fig. 6.15. This addition was reversible and in the presence of H_2, the 1,3-dienes were selectively hydrogenated to the 3-enes.[257] α-Olefins were also found to be hydrogenated by $W_2(OCH_2Bu^t)_6(py)_2$ in the presence of H_2.[257]

Pictiva EX2004
Samsung v Pictiva
IPR2024-01094

Ene-yne couplings have been observed in reactions involving $W_2(OSiMe_2Bu^t)_6(\mu\text{-}C_2H_2)(py)$ and ethene and allene. The hydrido alkylidyne bridged compound $W_2(H)(\mu\text{-}CCH{=}CHMe)(OSiMe_2Bu^t)_6$ and the analogous bridged compound $W_2(H)(\mu\text{-}CC(=CH_2)(CH=CH_2)(OSiMe_2Bu^t)_6$ were formed, respectively.[258,259]

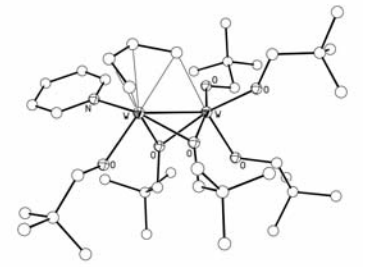
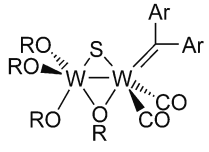


Fig. 6.15. Structure of $W_2(OCH_2Bu^t)_6(\mu\text{-}\eta^1,\eta^4\text{-}C_4H_6)(py)$.

α,β-Unsaturated aldehydes and ketones were found to add to $W_2(OR)_6$ compounds to form 1,2- and 1,4-adducts.[260] Aldehydes and ketones undergo reductive cleavage of the C=O bond to give oxo-alkylidene complexes which are themselves capable of undergoing CC coupling with CO bond cleavage in further reactions with aldehydes and ketones.[261-264] This forms the basis of a selective two step olefination reaction. The first step, the reduction of the first aldehyde or ketone is quite general but the second step is less efficient and does not proceed in high yield for aryl or bulky alkyl substituted ketones. Rather interestingly, the product in the first step is a $(W{-}W)^{10+}$ containing compound having a terminal oxo group and a bridging alkylidene. The reaction involving *c*-C_3H_5CHO gave a cyclopropylidene complex and this was taken as evidence that the C=O bond cleavage did not proceed via a radical process or one in which significant positive charge was localized on the ketonic carbon atom.[263] However, the reaction involving cyclohexanone gave a product of vinyligous coupling. An overall scheme for the olefination reaction and its competing side reactions is shown in Scheme 6.5.

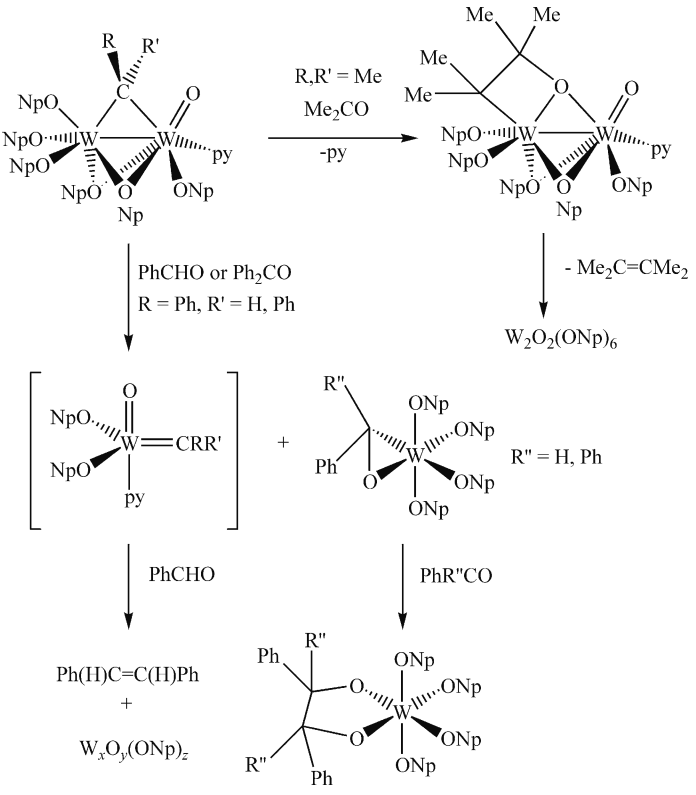
Diarylthiones, $Ar_2C{=}S$, also undergo reductive cleavage of the C=S bond yielding sulfido bridged complexes of the structural type depicted in **6.25**. The PMe_3 adduct, $W_2(OCH_2Bu^t)_6(S)(CPh_2)(PMe_3)$ was structurally characterized.[265] In this study, the kinetics of the reductive cleavage of $(p\text{-}XC_6H_4)_2C{=}S$ compounds was studied by NMR spectroscopy as a function of X, where X = NMe_2, OMe, Me, H, F, Cl and CF_3. Both electron donating and electron withdrawing groups accelerated the rates of reaction. From Eyring plots, the activation parameters $\Delta H^{\neq}$ = 10.2(2) kcal mol^{-1}, $\Delta S^{\neq}$ = -29(1) eu were obtained for $Ph_2C{=}S$ cleavage.



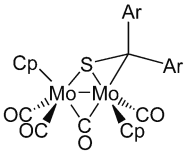
6.25

A general reaction scheme was proposed involving the initial reversible formation of a 1:1 adduct followed by an irreversible cleavage.[265] The kinetic parameters were compared with those for the reversible uptake of $Et_2NC{\equiv}N$ by $Mo_2(OCH_2Bu^t)_6$ to give the $\mu\text{-}\eta^1,\eta^2$-CN adduct. A further analogy was made with the $\mu\text{-}\eta^1,\eta^2\text{-}SCPh_2$ adduct of $Cp_2Mo_2(CO)_4$ which has the structure depicted in **6.26**.[266]

Pictiva EX2004
Samsung v Pictiva
IPR2024-01094



Scheme 6.5. Some reactions of ditungsten oxo/alkylidene compounds with ketones.



6.26

6.9.6 Reactions with H_2

Although H_2 is not usually observed to add directly to the M≡M bond (see Section 6.9.8), it has been noted to react with attendant metal-carbon bonds as in the hydrogenation of 1,3-dienes and α-olefins.[257] Also, in reaction with $W_2(Bu^i)_2(OPr^i)_4$, a complex reaction ensues leading to the unusual octahedral cluster $W_6H_5(CPr^i)(OPr^i)_{12}$.[267] This cluster has the central skeleton shown in Fig. 6.16 and has the unusual property of being sufficiently kinetically slow toward bridge to terminal exchange that the reactivity of bridging and terminal hydrides can be distinguished within the same molecule.

The terminal W–H group participates in the hydrogenation of ethene while the other hydrides do not. The stepwise coupling of W_2 units containing hydride ligands formed by hydrogenation of the butyl ligands, together with α-CH activation, presumably leads to formation of this W_6 cluster. In the presence of chelating diphosphines, dinuclear $W_2H_2(OPr^i)_4(dmpe)_2$ and tetranuclear $W_4(H)_4(OPr^i)_8(dmpm)_3$ complexes were isolated.

Pictiva EX2004
Samsung v Pictiva
IPR2024-01094

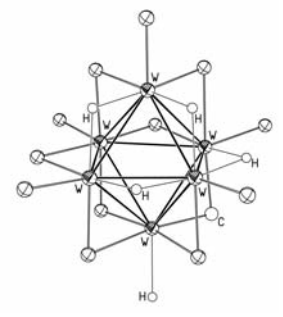


Fig. 6.16. The core in $W_6H_5(CPr^i)(OPr^i)_{12}$.

6.9.7 Reactions with organometallic compounds

This is a relatively unexplored field of chemistry although the following indicates the potential for this area of research.

The compound $Fe_2(CO)_6(\mu\text{-}S_2)$ was shown to react with $W_2(OPr^i)_6(py)_2$ to give a planar "$Fe_2W_2(\mu\text{-}S)_2$" containing cluster, $Fe_2W_2(OPr^i)_6(CO)_5(\mu\text{-}S)_2(py)$ having both WW and FeW bonds.[268] The reaction could be viewed as an oxidative addition to the WW triple bond.

Alkynylplatinum(II) compounds enter into a complex series of reactions with $W_2(OBu^t)_6$ and from the reactions involving *trans*-$Pt(C{\equiv}CH)_2(PMe_2Ph)_2$, the dicarbido compounds $(Bu^tO)_3W{\equiv}C{-}C{\equiv}W(OBu^t)_3$ and *trans*-$(PMe_2Ph)_2Pt[C_2W_2(OBu^t)_5]_2$ were isolated and fully characterized.

From the reaction between $CpCo(C_2H_4)_2$ and $W_2(OCH_2Bu^t)_6$, the compound $CpCoW_2(OCH_2Bu^t)_6$ was isolated and fully characterized.[271] As shown in Fig. 6.17, this molecule contains unsupported Co–W bonds of distance 2.28 and 2.34 Å. The WW distance of 2.50 Å is typical of a double bond distance and an interesting analogy can be made with this addition of a CpCo fragment across a W≡W bond with that of the addition of CO across W≡W.[271]

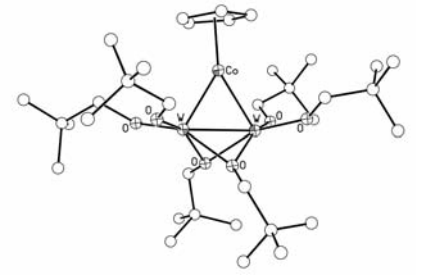


Fig. 6.17. Structure of $CpCoW_2(OCH_2Bu^t)_6$.

6.9.8 $(\eta^5\text{-}C_5H_4R)_2W_2X_4$ compounds where R = Me, Pr^i and X = Cl, Br

$Cp_2W_2X_4$ compounds exhibit η^5-bound Cp rings, in contrast to aforementioned, slipped η^3-Cp-dimethylamides: $W_2Cp_2(NMe_2)_4$, $W_2(MeCp)_2(NMe_2)_4$, and $W_2(indenyl)_2(NMe_2)_4$. Green and Mountford discovered these halo-compounds formed in the reactions of piano-stool $(RCp)WX_4$ compounds (where R = Me, Pr^i and X = Cl, Br) with Na(Hg). The solid state structure of $(Pr^iCp)_2W_2Cl_4$ revealed an unbridged $(W{\equiv}W)^{6+}$ bond of distance 2.368(1) Å and

Pictiva EX2004
Samsung v Pictiva
IPR2024-01094

an *anti*-conformation for the central 1,2-$W_2Cp_2Cl_4$ skeleton.[272, 273] The presence of the unbridged W≡W bond is in contrast to the related compounds $[CpMX_2]_2$ which have either four halide bridges (for M = Cr) or two halide bridges (for M = Mo).[274]

This lack of halide bridging testifies to the increasing importance of MM bonding in descending from Cr to W within the group 6 transition metals. However, as can be seen in Table 6.2, the ditungsten distance in $(Pr^iCp)_2W_2Cl_4$ is slightly longer than those seen for most compounds of formula 1,2-$M_2X_2Y_4$.

The addition of chelating Lewis bases such as $Me_2P(CH_2)_2PMe_2$ or the addition of halide ions to these compounds leads to the formation of bridged species with disruption of the M≡M bond.[275] CO reacts with them to form $[Cp'WCl(CO)]_2(\mu\text{-}Cl)_2$ which contains a rather long WW bond of 2.965(1) Å. Nitriles add to these compounds to form 1:1 adducts in which the nitrile bridges the ditungsten center in a $\mu\text{-}\eta^1,\eta^2$ fashion. A similar structure was proposed for a 1:1 isocyanide adduct.

Alkynes react with these $Cp'_2W_2X_4$ species to give both alkyne adducts and products from alkyne coupling.[276] The product from simple alkyne addition exhibits a relatively long W—W bond of 2.795(3) Å while the alkyne moiety within exhibits a long μ-(CC) distance of 1.41(4) Å which is indicative of the formation of a dimetallatetrahedrane. The skewed alkyne bridge (25° dihedral between WW and CC) was the subject of an EHMO computational study by Mountford who concluded that steric and not electronic factors were responsible for the unique alkyne coordination geometry.[277]

The perpendicular nature of the $\mu\text{-}C_4Me_4$ bridging ligand in the alkyne-coupled product, $(\eta^5\text{-}MeCp)_2W_2Cl_4(\mu_2\text{-}C_4Me_4)$ contrasts with that for analogous $M_2(OR)_6(\mu\text{-}C_4R'_4)$ compounds. Again, a rather long WW distance of 2.930(1) Å is observed for the alkyne-coupled product, possibly as a result of steric crowding around each tungsten atom.

The compounds $Cp'_2W_2X_4$ are unique among ditungsten compounds in showing reversible reactivity with H_2 at room temperature to give the hydrido-bridged species: $Cp'_2W_2X_4(\mu\text{-}H)_2$.[278] The bridging hydride was formulated based upon NMR spectroscopic data including the appearance of hydride resonances at δ 1.2 with $J^{183}{}_{W\text{-}}{}^1{}_H$ = 112-116 Hz and T_1 ~ 1-2 s at –90 °C. Several other oxidative addition reactions were noted for reactions involving HCl, HSR and HPR_2 compounds. Notable among these was the complex $(\eta^5\text{-}Pr^iCp)_2W_2Cl_3(\mu\text{-}H)(\mu\text{-}Cl)(\mu\text{-}PPh_2)(PMe_3)$ which was structurally characterized.

6.10 Conclusion

The coordination chemistry of the $X_3M{\equiv}MX_3$ "ethane-like dimers" of molybdenum and tungsten is rich and varied. Though the chemistry of the $(Mo{\equiv}Mo)^{6+}$ and $(W{\equiv}W)^{6+}$ units are very similar, there are significant differences. The ditungsten center is notably more readily oxidized and this leads to a much more extensive organometallic chemistry of small, unsaturated organic molecules. Many of these reactions lead to the reduction and cleavage of C—X multiple bonds. In contrast, reductive eliminations occur more readily from the Mo_2^{6+} center to give Mo_2^{4+} compounds having MM quadruple bonds. Furthermore, the ditungsten compounds are much more labile towards forming clusters. The organometallic chemistry of the $M_2(OR)_6$ compounds bears a superficial resemblance to that of the $Cp_2M_2(CO)_4$ compounds, though it is evident that despite the difference in formal oxidation states, the $M_2(OR)_6$ compounds are more reactive as electron reservoirs.

Pictiva EX2004
Samsung v Pictiva
IPR2024-01094

References

1. C. C. Cummins, *Chem. Commun.* **1998**, 1777.
2. C. C. Cummins, *Prog. Inorg. Chem.* **1998**, *47*, 685.
3. P. T. Wolczanski, *Polyhedron* **1995**, *14*, 3335.
4. F. A. Cotton, G. Wilkinson, C. A. Murillo and M. Bochmann, *Advanced Inorganic Chemistry,* 6th ed. John Wiley & Sons: New York, 1999.
5. F. Huq, W. Mowat, A. Shortland, A. C. Skapski and G. Wilkinson, *Chem. Commun.* **1971**, 1079.
6. M. H. Chisholm, B. W. Eichhorn, K. Folting, J. C. Huffman, C. D. Ontiveros, W. E. Streib and W. G. Van der Sluys, *Inorg. Chem.* **1987**, *26*, 3182.
7. R. A. Andersen, M. H. Chisholm, J. F. Gibson, W. W. Reichert, I. P. Rothwell and G. Wilkinson, *Inorg. Chem.* **1981**, *20*, 3934.
8. S. M. Beshouri, I. P. Rothwell, K. Folting, J. C. Huffman and W. E. Streib, *Polyhedron* **1986**, *5*, 1191.
9. T. M. Gilbert, C. B. Bauer, A. H. Bond and R. D. Rogers, *Polyhedron* **1999**, *18*, 1293.
10. T. M. Gilbert, C. B. Bauer and R. D. Rogers, *Polyhedron* **1999**, *18*, 1303.
11. M. H. Chisholm, A. M. Macintosh, J. C. Huffman, D. Wu, E. R. Davidson, R. J. H. Clark and S. Firth, *Inorg. Chem.* **2000**, *39*, 3544.
12. W. H. Armstrong and P. J. Bonitatebus, Jr. *Z. Kristallogr.* **1999**, *214*, 241.
13. T. P. Blatchford, M. H. Chisholm and J. C. Huffman, *Inorg. Chem.* **1987**, *26*, 1920.
14. M. H. Chisholm and W.W. Reichert, *J. Am. Chem. Soc.* **1974**, *96*, 1249.
15. M. H. Chisholm, F. A. Cotton, B. A. Frenz, W. W. Reichert, L. W. Shive and B. R. Stults, *J. Am. Chem. Soc.* **1976**, *98*, 4469.
16. T. A. Budzichowski, S. T. Chacon, M. H. Chisholm, F. J. Feher and W. Streib, *J. Am. Chem. Soc.* **1991**, *113*, 689.
17. M. H. Chisholm, K. Folting, J. C. Huffman, H. Li, A. M. Macintosh and D.-D.Wu, *Polyhedron* **2000**, *19*, 375.
18. U. Piarulli, D. N. Williams, C. Floriani, G. Gervasio and D. Viterbo, *J. Organomet. Chem.* **1995**, *503*, 185.
19. M. H. Chisholm, J. C. Huffman, I. P. Parkin and W. E. Streib, *Polyhedron* **1990**, *9*, 2941.
20. M. H. Chisholm; F. A. Cotton; C. A. Murillo; W. W. Reichert, *Inorg. Chem.* **1977**, *16*, 1801.
21. M. H. Chisholm, J. F. Corning and J. C. Huffman, *J. Am. Chem. Soc.* **1983**, *105*, 5924.
22. M. H. Chisholm, J. F. Corning, K. Folting and J. C. Huffman, *Polyhedron* **1985**, *4*, 383.
23. T. M. Gilbert, A. M. Landes and R. D. Rogers, *Inorg. Chem.* **1992**, *31*, 3438.
24. K. Su and T. D. Tilley, *Chem. Mater.* **1997**, *9*, 588.
25. M. H. Chisholm, F. A. Cotton, M. Extine and B. R. Stults, *Inorg. Chem.* **1976**, *15*, 2252.
26. T. M. Gilbert, J. C. Littrell, C. E. Talley, M. A. Vance, R. F. Dallinger and R. D.Rogers, *Inorg. Chem.* **2004**, *43*, 1762.
27. M. H. Chisholm, K. Folting, M. Hampden-Smith and C. A. Smith, *Polyhedron* **1987**, *6*, 1747.
28. M. H. Chisholm, J. A. Heppert, D. M. Hoffman and J. C. Huffman, *Inorg. Chem.* **1985**, *24*, 3214.
29. F. A. Cotton, B. R. Stults, J. M. Troup, M. H. Chisholm and M. Extine, *J. Am. Chem. Soc.* **1975**, *97*, 1242.
30. M. H. Chisholm, F. A. Cotton, M. Extine and B. R. Stults, *J. Am. Chem. Soc.* **1976**, *98*, 4477.
31. F. A. Cotton, S. A. Koch, A. J. Schultz and J. M. Williams, *Inorg. Chem.* **1978**, *17*, 2093.
32. M. H. Chisholm, D. L. Clark, K. Folting, J. C. Huffman and M. Hampden-Smith, *J. Am. Chem. Soc.* **1987**, *109*, 7750.
33. M. H. Chisholm, C. M. Cook, J. C. Huffman and W. E. Streib, *J. Chem. Soc., Dalton Trans.* **1991**, 929.
34. I. P. Parkin and K. Folting, *J. Chem. Soc., Dalton Trans.* **1992**, 2343.
35. M. H. Chisholm, I. P. Parkin, K. Folting, E. B. Lubkovsky and W. E. Streib, *Chem. Commun.* **1991**, 1673.
36. M. H. Chisholm, J.-H. Huang, J. C. Huffman and I. P. Parkin, *Inorg. Chem.* **1997**, *36*, 1642.
37. M. H. Chisholm, I. P. Parkin, K. Folting and E. Lobkovsky, *Inorg. Chem.* **1997**, *36*, 1636.

Pictiva EX2004
Samsung v Pictiva
IPR2024-01094

38. M. H. Chisholm, F. A. Cotton, B. A. Frenz and L. W. Shive, *Chem. Commun.* **1974**, 480.
39. M. H. Chisholm and M. Extine, *J. Am. Chem. Soc.* **1975**, *97*, 5625.
40. M. H. Chisholm, M. Extine and W. W. Reichert, *Adv. Chem. Ser.* **1976**, *150*, 273.
41. M. H. Chisholm, F. A. Cotton, M. Extine, M. Millar and B. R. Stults, *Inorg. Chem.* **1976**, *15*, 2244.
42. M. H. Chisholm, W. W. Reichert, F. A. Cotton and C. A. Murillo, *J. Am. Chem. Soc.* **1977**, *99*, 1652.
43. M. H. Chisholm and F. A. Cotton, *Acc. Chem. Res.* **1978**, *11*, 356.
44. M. Akiyama, M. H. Chisholm, F. A. Cotton, M. W. Extine and D. A. Haitko, *Inorg. Chem.* **1979**, *18*, 2266.
45. D. C. Bradley, M. H. Chisholm, C. E. Heath and M. B. Hursthouse, *Chem. Commun.* **1969**, 1261.
46. D. C. Bradley and M. H. Chisholm, *J. Chem. Soc., Perkin Trans.* **1971**, 2741.
47. M. H. Chisholm, F. A. Cotton and M. W. Extine, *Inorg. Chem.* **1978**, *17*, 1329.
48. M. H. Chisholm, F. A. Cotton, M. Extine, M. Millar and B. R. Stults, *J. Am. Chem. Soc.* **1976**, *98*, 4486.
49. D. C. Bradley, M. B. Hursthouse and H. R. Powell, *J. Chem. Soc., Dalton Trans.* **1989**, 1537.
50. D. C.Bradley, R. J. Errington, M. B. Hursthouse and R. L. Short, *J. Chem. Soc., Dalton Trans.* **1986**, 1305.
51. S. M. Holmes, D. F. Schafer, P. T. Wolczanski and E. B. Lobkovsky, *J. Am. Chem. Soc.* **2001**, *123*, 10571.
52. D. C.Bradley and M. H. Chisholm, *Acc. Chem. Res.* **1976**, *9*, 273.
53. W. H. Armstrong and P. J. Bonitatebus, Jr., *Z. Kristallogr.* **1999**, *214*, 243.
54. T. A. Albright and R. Hoffmann, *J. Am. Chem. Soc.* **1978**, *100*, 7736.
55. M. Akiyama, D. Little, M. H. Chisholm, D. A. Haitko, F. A. Cotton and M. W. Extine, *J. Am. Chem. Soc.* **1979**, *101*, 2504.
56. M.H. Chisholm, J.A. Gallucci, and C. B. Hollandsworth, unpublished results.
57. S. D. Dietz, N. W. Eilerts and J. A. Heppert, *Angew. Chem.* **1992**, *104*, 67. (See also *Angew. Chem., Int. Ed. Engl.*, **1992**, *31*, 66).
58. M. J. Chetcuti, M. H. Chisholm, J. C. Huffman and J. Leonelli, *J. Am. Chem. Soc.* **1983**, *105*, 292.
59. M. H. Chisholm, K. Folting, J. C. Huffman, J. Leonelli, N. S. Marchant, C. A. Smith and L. C. E. Taylor, *J. Am. Chem. Soc.* **1985**, *107*, 3722.
60. M. Akiyama, M. H. Chisholm, F. A. Cotton, M. W. Extine, D. A. Haitko, J. Leonelli and D. Little, *J. Am. Chem. Soc.* **1981**, *103*, 779.
61. M. H. Chisholm, D. L. Clark and M. J. Hampden-Smith, *J. Am. Chem. Soc.* **1989**, *111*, 574.
62. M. H. Chisholm, K. Folting, J. C. Huffman, J. A. Klang and W. E. Streib, *Organometallics* **1989**, *8*, 89.
63. M. H. Chisholm, J. A. Gallucci and C. B. Hollandsworth, unpublished results.
64. B. E. Bursten, M. H. Chisholm, M. L. Drummond and C. B. Hollandsworth, unpublished results.
65. M. H. Chisholm, I. P. Parkin, J. C. Huffman and W. B. Streib, *Chem. Commun.* **1990**, 920.
66. J. A. Connor, G. Pilcher, H. A. Skinner, M. H. Chisholm and F. A. Cotton, *J. Am. Chem. Soc.* **1978**, *100*, 7738.
67. B. E. Bursten, F. A. Cotton, J. C. Green, E. A. Seddon and G. G. Stanley, *J. Am. Chem. Soc.* **1980**, *102*, 4579.
68. B. E. Bursten, F. A. Cotton, M. B. Hall and R. C. Najjar, *Inorg. Chem.* **1982**, *21*, 302.
69. M. H. Chisholm, E. R. Davidson, J. C. Huffman and K. B. Quinlan, *J. Am. Chem. Soc.* **2001**, *123*, 9652.
70. D. V. Baxter, M. H. Chisholm, V. F. DiStasi and J. A. Klang, *Chem. Mater.* **1991**, *3*, 221.
71. D. V. Baxter, M. H. Chisholm, V. F. DiStasi and S. T. Haubrich, *Chem. Mater.* **1995**, *7*, 84.
72. J. A. Hollingshead, M. T. Tyszkiewicz and R. E. McCarley, *Chem. Mater.* **1993**, *5*, 1600.
73. M. H. Chisholm, F. A. Cotton, M. W. Extine, M. Millar and B. R. Stults, *Inorg. Chem.* **1977**, *16*, 320.
74. G. Trinquier and R. Hoffmann, *Organometallics* **1984**, *3*, 370.

Pictiva EX2004
Samsung v Pictiva
IPR2024-01094

75. M. H. Chisholm, D. A. Haitko and C. A. Murillo, *J. Am. Chem. Soc.* **1978**, *100*, 6262.
76. M. H. Chisholm, D. A. Haitko, K. Folting and J. C. Huffman, *J. Am. Chem. Soc.* **1981**, *103*, 4046.
77. M. J. Chetcuti, M. H. Chisholm, K. Folting, D. A. Haitko, J. C. Huffman and J. Janos, *J. Am. Chem. Soc.* **1983**, *105*, 1163.
78. M. H. Chisholm, G. J. Gama and I. P. Parkin, *Polyhedron* **1993**, *12*, 961.
79. M. H. Chisholm, B. W. Eichhorn, K. Folting and J. C. Huffman, *Inorg. Chim. Acta* **1988**, *144*, 193.
80. M. H. Chisholm, I. P. Parkin and J. C. Huffman, *Polyhedron* **1991**, *10*, 1215.
81. M. H. Chisholm, H. T. Chiu, K. Folting and J. C. Huffman, *Inorg. Chem.* **1984**, *23*, 4097.
82. W. E. Buhro, M. H. Chisholm, K. Folting and J. C. Huffman, *J. Am. Chem. Soc.* **1987**, *109*, 905.
83. M. H. Chisholm, J. C. Huffman and J. W. Pasterczyk, *Inorg. Chem.* **1987**, *26*, 3781.
84. M. H. Chisholm, I. P. Parkin, J. C. Huffman, E. M. Lobkovsky and K. Folting, *Polyhedron* **1991**, *10*, 2839.
85. M. H. Chisholm, K. Folting, S. T. Haubrich and J. D. Martin, *Inorg. Chim. Acta* **1993**, *213*, 17.
86. M. H. Chisholm, J. F. Corning and J. C. Huffman, *Inorg. Chem.* **1983**, *22*, 38.
87. M. H. Chisholm, M. J. Hampden-Smith, J. C. Huffman, J. D. Martin, K. A. Stahl and K. G. Moodley, *Polyhedron* **1988**, 7, 1991.
88. M. H. Chisholm, J. A. Gallucci and C. B. Hollandsworth. Unpublished crystal structure of $W_2Cp_2(NMe_2)_4$.
89. R. H. Cayton, M. H. Chisholm, K. Folting, J. L. Wesemann and K. G. Moodley, *J. Chem. Soc., Dalton Trans.* **1997**, *16*, 3161.
90. R. H. Cayton, M. H. Chisholm, M. J. Hampden-Smith, J. C. Huffman and K. G. Moodley, *Polyhedron* **1992**, *11*, 3197.
91. H. Schulz, K. Folting, J. C. Huffman, W. E. Streib and M. H. Chisholm, *Inorg. Chem.* **1993**, *32*, 6056.
92. M. J. Chetcuti, M. H. Chisholm, H. T. Chiu and J. C. Huffman, *Polyhedron* **1985**, *4*, 1213.
93. R. H. Cayton, S. T. Chacon, M. H. Chisholm, K. Folting and K. G. Moodley, *Organometallics* **1996**, *15*, 992.
94. M. H. Chisholm, unpublished results.
95. T. P. Blatchford, M. H. Chisholm and J. C. Huffman, *Inorg. Chem.* **1988**, *27*, 2059.
96. B. E. Bursten, M. H. Chisholm, M. L. Drummond, J. C. Gallucci and C. B. Hollandsworth, *J. Chem. Soc., Dalton Trans.* **2002**, 4077.
97. W. E. Buhro, M. H. Chisholm, K. Folting, J. C. Huffman, J. D. Martin and W. E. Streib, *J. Am. Chem. Soc.* **1988**, *110*, 6563.
98. W. E. Buhro, M. H. Chisholm, J. D. Martin, J. C. Huffman, K. Folting and W. E. Streib, *J. Am. Chem. Soc.* **1989**, *111*, 8149.
99. T. A. Budzichowski, M. H. Chisholm, D. B. Tiedtke, N. E. Gruhn and D. L. Lichtenberger, *Polyhedron* **1998**, *17*, 705.
100. M. Akiyama, M. H. Chisholm, F. A. Cotton, M. W. Extine and C. A. Murillo, *Inorg. Chem.* **1977**, *16*, 2407.
101. M. H. Chisholm, D. R. Click, J. C. Huffman, *Organometallics* **2000**, *19*, 3916.
102. M. H. Chisholm, F. A. Cotton, M. W. Extine and C. A. Murillo, *Inorg. Chem.* **1978**, *17*, 2338.
103. M. H. Chisholm, K. Folting, J. C. Huffman and I. P. Rothwell, *Organometallics* **1982**, *1*, 251.
104. K. L. Fujdala and T. D. Tilley, *Chem. Mater.* **2004**, *16*, 1035.
105. M. H. Chisholm, J. F. Corning and J. C. Huffman, *Inorg. Chem.* **1984**, *23*, 754.
106. M. H. Chisholm, K. Folting, W. E. Streib and D.-D.Wu, *Inorg. Chem.* **1998**, *37*, 50.
107. J. E. Hill, P. E. Fanwick and I. P. Rothwell, *Polyhedron* **1992**, *11*, 2825.
108. M. H. Chisholm, F. A. Cotton, M. W. Extine and B. R. Stults, *Inorg. Chem.* **1977**, *16*, 603.
109. M. H. Chisholm, K. S. Kramer, J. D. Martin, J. C. Huffman, E. B. Lobkovsky and W. E. Streib, *Inorg. Chem.* **1992**, *31*, 4469.

Pictiva EX2004
Samsung v Pictiva
IPR2024-01094

110. M. H. Chisholm, M. J. Hampden-Smith, J. C. Huffman and K. G. Moodley, *J. Am. Chem. Soc.* **1988**, *110*, 4070.
111. S. D. Dietz, N. W. Eilerts, J. A. Heppert and M. D. Morton, *Inorg. Chem.* **1993**, *32*, 1698.
112. S. M. Holmes, D. F. Schafer, II, P. T. Wolczanski and E. B. Lobkovsky, *J. Am. Chem. Soc.* **2001**, *123*, 10571.
113. M. H. Chisholm and R. J. Tatz, *Organometallics* **1986**, *5*, 1590.
114. J. W. Pasterczyk, Ph. D. Dissertation, Indiana University, Bloomington, IN, 1988.
115. M. H. Chisholm and I. P. Rothwell, *Chem. Commun.* **1980**, 985.
116. M. H. Chisholm, *ACS Symposium Series* **1981**, *155*, 17.
117. M. H. Chisholm, D. M. Hoffman, J. C. Huffman, W. G. Van der Sluys and S. Russo, *J. Am. Chem. Soc.* **1984**, *106*, 5386.
118. M. J. Chetcuti, M. H. Chisholm, K. Folting, D. A. Haitko and J. C. Huffman, *J. Am. Chem. Soc.* **1982**, *104*, 2138.
119. M. H. Chisholm, D. L. Clark, J. C. Huffman, W. G. Van der Sluys, E. M. Kober, D. L. Lichtenberger and B. E. Bursten, *J. Am. Chem. Soc.* **1987**, *109*, 6796.
120. M. D. Braydich, B. E. Bursten, M. H. Chisholm, and D. L. Clark, *J. Am. Chem. Soc.* **1985**, *107*, 4459.
121. M. H. Chisholm, D. L. Clark, J. C. Huffman and W. G. Van der Sluys, *J. Am. Chem. Soc.* **1987**, *109*, 6817.
122. M. H. Chisholm, J. C. Huffman and W. Van der Sluys, *Inorg. Chim. Acta* **1986**, *116*, L13.
123. M. H. Chisholm, B. W. Eichhorn, K. Folting, J. C. Huffman and R. J. Tatz, *Organometallics* **1986**, *5*, 1599.
124. M. H. Chisholm, J. C. Huffman and W. G. Van Der Sluys, *J. Am. Chem. Soc.* **1987**, *109*, 2514.
125. M. H. Chisholm, J. C. Gallucci and C. B. Hollandsworth, *J. Organomet. Chem.* **2003**, *684*, 269.
126. M. H. Chisholm and C. B. Hollandsworth, unpublished results.
127. M. H. Chisholm M. W. Extine, R. L. Kelly, W. C. Mills, C. A. Murillo, L. A. Rankel and W. W. Reichert, *Inorg. Chem.* **1978**, *17*, 1673.
128. M. H. Chisholm, D. L. Clark, K. Folting and J. C. Huffman, *Angew. Chem.* **1986**, *98*, 1021.
129. M. H. Chisholm, K. Folting, C. E. Hammond and M J. Hampden-Smith, *J. Am. Chem. Soc.* **1988**, *110*, 3314.
130. M. H. Chisholm, K. Folting, C. E. Hammond, M. J. Hampden-Smith and K. G. Moodley, *J. Am. Chem. Soc.* **1989**, *111*, 5300.
131. R. B. Woodward and R.Hoffmann, *The Conservation of Orbital Symmetry*, Academic Press: New York, 1970.
132. R. B. Woodward and R. Hoffmann, *Angew. Chem., Int. Ed. Eng.* **1969**, *8*, 781.
133. R. Hoffmann and R. B. Woodward, *Acc. Chem. Res.* **1968**, *1*, 17.
134. M. H. Chisholm, R. J. Errington, K. Folting and J. C. Huffman, *J. Am. Chem. Soc.* **1982**, *104*, 2025.
135. M. H. Chisholm, D. L. Clark, R. J. Errington, K. Folting and J. C. Huffman, *Inorg. Chem.* **1988**, *27*, 2071.
136. B. E. Bursten, M. H. Chisholm and D. L. Clark, *Inorg. Chem.* **1988**, *27*, 2084.
137. M. H. Chisholm, K. Folting, B. W. Eichhorn and J. C. Huffman, *J. Am. Chem. Soc.* **1987**, *109*, 3146.
138. M. H. Chisholm, C. E. Hammond, J. C. Huffman and J. D. Martin, *Polyhedron* **1990**, *9*, 1829.
139. M. H. Chisholm, K. Folting, C. E. Hammond, J. C. Huffman and J. D. Martin, *Angew. Chem.* **1989**, *101*, 1399.
140. T. A. Budzichowski, M. H. Chisholm, J. C. Huffman and O. Eisenstein, *Angew. Chem.* **1994**, *106*, 203
141. T. A. Budzichowski, M. H. Chisholm, J. C. Huffman, K. S. Kramer and O. Eisenstein, *J. Chem. Soc., Dalton Trans.* **1998**, 2563.
142. M. H. Chisholm, C. E. Hammond, M. Hampden-Smith, J. C.Huffman and W. G. Van der Sluys, *Angew. Chem.* **1987**, *99*, 937.

Pictiva EX2004
Samsung v Pictiva
IPR2024-01094

143. M. H. Chisholm, D. L. Clark and J. C. Huffman, *Polyhedron* **1985**, *4*, 1203.
144. M. H. Chisholm, J. C. Huffman and R. L. Kelly, *J. Am. Chem. Soc.* **1979**, *101*, 7100.
145. M. H. Chisholm, D. R. Click and J. C. Huffman, *J. Organomet. Chem.* **2000**, *614-615*, 238.
146. M. H. Chisholm, K. Folting, J. C. Huffman, K. S. Kramer and R. J. Tatz, *Organometallics* **1992**, *11*, 4029.
147. T. A. Budzichowski, M. H. Chisholm, K. Folting, J. C. Huffman and W. E. Streib, *J. Am. Chem. Soc.* **1995**, *117*, 7428.
148. M. H. Chisholm, F. A. Cotton, M. W. Extine and W. W. Reichert, *J. Am. Chem. Soc.* **1978**, *100*, 153.
149. M. Akiyama, M. H. Chisholm, F. A. Cotton, M. W. Extine, D. A. Haitko, D. Little and P. E. Fanwick, *Inorg. Chem.* **1979**, *18*, 2266.
150. T. A. Budzichowski, M. H. Chisholm, K. Folting, J. C. Huffman, W. E. Streib and D. B. Tiedtke, *Polyhedron* **1998**, *17*, 857.
151. R. G. Abbott, F. A. Cotton and L. R. Falvello, *Inorg. Chem.* **1990**, *29*, 514.
152. R. G. Abbott, Ph.D. Dissertation, Texas A&M University, College Station, TX, 1988.
153. M. H. Chisholm, I. P. Parkin, W. E. Streib and K. S. Folting, *Polyhedron* **1991**, *10*, 2309.
154. F. A. Cotton, E. V. Dikarev, N. Nawar and W.-Y. Wong, *Inorg. Chim. Acta* **1997**, *262*, 21.
155. F. A. Cotton, E. V. Dikarev, N. Nawar and W.-Y.Wong, *Inorg. Chem.* **1997**, *36*, 559.
156. F. A. Cotton and Z. Yao, *J. Cluster Sci.* **1994**, *5*, 11.
157. F. A. Cotton, E. V. Dikarev, W.-Y. Wong, *Inorg. Chem.* **1997**, *36*, 3268.
158. F. A. Cotton, E. V. Dikarev and W.-Y. Wong, *Inorg. Chem.* **1997**, *36*, 80.
159. M. H. Chisholm, K. Folting and D.-D. Wu, *Acta Crystallogr.,* **1998**, *C54*, 225.
160. M. H. Chisholm and C. B. Hollandsworth. Unpublished crystal structure of $(H_2NMe_2)_2[W_2OCH_2CF_3)_8]$.
161. M. H. Chisholm, K. Folting, J. C. Huffman and A. L. Ratermann, *Inorg. Chem.* **1984**, *23*, 613.
162. M. H. Chisholm, E. F. Putilina, K. Folting and W. E. Streib, *J. Cluster Sci.* **1994**, *5*, 67.
163. M. H. Chisholm, F. A. Cotton, M. W. Extine and W. W. Reichert, *J. Am. Chem. Soc.* **1978**, *100*, 1727.
164. M. H. Chisholm, J. C. Huffman and C. C. Kirkpatrick, *Inorg. Chem.* **1983**, *22*, 1704.
165. M. H. Chisholm, F. A. Cotton, K. Folting, J. C. Huffman, A. L. Ratermann and E. S. Shamshoum, *Inorg. Chem.* **1984**, *23*, 4423.
166. F. A. Cotton and E. S. Shamshoum, *J. Am. Chem. Soc.* **1985**, *107*, 4662.
167. K. J. Ahmed, M. H. Chisholm, K. Folting, J. C. Huffman, *Inorg. Chem.* **1985**, *24*, 4039.
168. M. H. Chisholm, K. Folting, J. C. Huffman and I. P. Rothwell, *Inorg. Chem.* **1981**, *20*, 1854.
169. M. H. Chisholm, D. A. Haitko, J. C. Huffman and K. Folting, *Inorg. Chem.* **1981**, *20*, 171.
170. M. H. Chisholm, K. Folting, J. C. Huffman and I. P. Rothwell, *Inorg. Chem.* **1981**, *20*, 1496.
171. K. J. Ahmed, M. H. Chisholm, I. P. Rothwell and J. C. Huffman, *J. Am. Chem. Soc.* **1982**, *104*, 6453.
172. K. J. Ahmed, M. H. Chisholm and J. C. Huffman, *Organometallics* **1985**, *4*, 1168.
173. M. H. Chisholm, K. Folting, W. E. Streib and D.-D. Wu, *Chem. Commun.* **1998**, 379.
174. M. H. Chisholm, K. Folting, W. E. Streib and D.-D. Wu, *Inorg. Chem.* **1999**, *38*, 5219.
175. M. H. Chisholm, J. C. Gallucci, C. M. Hadad, J. C. Huffman and P. J. Wilson, *J. Am. Chem. Soc.* **2003**, *125*, 16040.
176. F. A. Cotton, N. E. Gruhn, J. Gu, P. Huang, D. L. Lichtenberger, C. A. Murillo, L. O. Van Dorn and C. C. Wilkinson, *Science* **2002**, *298*, 1971.
177. S. T. Chacon, M. H. Chisholm, W. E. Streib and W. Van der Sluys, *Inorg. Chem.* **1989**, *28*, 5.
178. M. H. Chisholm, *Acc. Chem. Res.* **1990**, *23*, 419.
179. M. H. Chisholm, *Advances in Chemistry Series* **1979**, *173*, 396.
180. M. H. Chisholm, C. C. Kirkpatrick and J. C. Huffman, *Inorg. Chem.* **1981**, *20*, 871.
181. M. H. Chisholm, K. Folting, M. A. Lynn, W. E. Streib and D. B. Tiedtke, *Angew. Chem., Int. Ed. Eng.* **1997**, *36*, 52.
182. M. H. Chisholm, W. E. Streib, D. B. Tiedtke and D.-D. Wu, *Chem. Eur. J.* **1998**, *4*, 1470.

Pictiva EX2004
Samsung v Pictiva
IPR2024-01094

183. M. H. Chisholm, D. R. Click, J. C. Gallucci, C. M. Hadad and P. J. Wilson, *Organometallics* **2003**, *22*, 4725.
184. M. H. Chisholm, D. R. Click, J. C. Gallucci and C. M. Hadad, *J. Chem. Soc., Dalton Trans.* **2003**, 3205.
185. M. H. Chisholm, J. C. Huffman and C. A. Smith, *J. Am. Chem. Soc.* **1986**, *108*, 222.
186. M. H. Chisholm, J. C. Huffman and A. L. Ratermann, *Inorg. Chem.* **1983**, *22*, 4100.
187. M. H. Chisholm, K. Folting, J. C. Huffman and J. J. Koh, *Polyhedron* **1989**, *8*, 123.
188. M. H. Chisholm, K. Folting, J. C. Huffman and A. L. Ratermann, *Inorg. Chem.* **1982**, *21*, 978.
189. C. C. Kirkpatrick, Ph.D Dissertation, Indiana University, Bloomington, IN, 1982.
190. M. H. Chisholm, K. Folting, J. C. Huffman, C. C. Kirkpatrick and and A. L. Ratermann, *J. Am. Chem. Soc.* **1981**, *103*, 1305.
191. M. H. Chisholm, K. Folting, J. C. Huffman and C. C. Kirkpatrick, *Inorg. Chem.* **1984**, *23*, 1021.
192. M. H. Chisholm, K. Folting, J. C. Huffman and C. C. Kirkpatrick, *J. Am. Chem. Soc.* **1981**, *103*, 5967.
193. M. H. Chisholm, F. A. Cotton, A. Fang and E. M. Kober, *Inorg. Chem.* **1984**, *23*, 749.
194. M. H. Chisholm, K. Folting, J. C. Huffman and E. M. Kober, *Inorg. Chem.* **1985**, *24*, 241.
195. M. H. Chisholm, J. C. Huffman and J. W. Pasterczyk, *Inorg. Chim. Acta* **1987**, *133*, 17.
196. M. H. Chisholm, K. Folting and J. W. Pasterczyk, *Inorg. Chem.* **1988**, *27*, 3057.
197. M. Scheer, K. Schuster, T. A. Budzichowski, M. H. Chisholm, and W. E. Streib, *Chem. Commun.* **1995**, 1671.
198. M. H. Chisholm, F. A. Cotton, M. W. Extine and R. L. Kelly, *J. Am. Chem. Soc.* **1978**, *100*, 3354.
199. M. H. Chisholm, F. A. Cotton, M. W. Extine and R. L. Kelly, *Inorg. Chem.* **1979**, *18*, 116.
200. M. H. Chisholm, D. M. Hoffman and J. C. Huffman, *Inorg. Chem.* **1983**, *22*, 2903.
201. D. M. T. Chan, M. H. Chisholm, K. Folting, J. C. Huffman and N. S. Marchant, *Inorg. Chem.* **1986**, *25*, 4170.
202. M. H. Chisholm, C. M. Cook, K. Folting and W. E. Streib, *Inorg. Chim. Acta* **1992**, *198-200*, 63.
203. F. A. Cotton and E. S. Shamshoum, *J. Am. Chem. Soc.* **1984**, *106*, 3222.
204. M. H. Chisholm, J. F. Corning, K. Folting, J. C. Huffman, A. L. Ratermann, I. P. Rothwell and W. E. Streib, *Inorg. Chem.* **1984**, *23*, 1037.
205. M. H. Chisholm, *Chemtracts: Inorg. Chem.* **1992**, *4*, 273.
206. M. H. Chisholm, F. A. Cotton, M. W. Extine and R. L. Kelly, *J. Am. Chem. Soc.* **1979**, *101*, 7645.
207. M. H. Chisholm, D. M. Hoffman and J. C. Huffman, *Organometallics* **1985**, *4*, 986.
208. K. T. Potts and J. S. Baum, *Chem. Rev.* **1974**, *74*, 189.
209. K. Komatsu and T. Kitagawa, *Chem. Rev.* **2003**, *103*, 1371.
210. M. H. Chisholm, J. C. Huffman, J. Leonelli and I. P. Rothwell, *J. Am. Chem. Soc.* **1982**, *104*, 7030.
211. F. A. Cotton and W. Schwotzer, *J. Am. Chem. Soc.* **1983**, *105*, 4955.
212. M. H. Chisholm, C. E. Hammond, V. J. Johnston, W. E. Streib and J. C. Huffmann, *J. Am. Chem. Soc.* **1992**, *114*, 7056.
213. M. H. Chisholm, J. C. Huffman and R. L. Kelly, *J. Am. Chem. Soc.* **1979**, *101*, 7615.
214. F. A. Cotton and W. Schwotzer, *J. Am. Chem. Soc.* **1983**, *105*, 5639.
215. T. A. Budzichowski, M. H. Chisholm, D. B. Tiedtke, J. C. Huffman and W. E. Streib, *Organometallics* **1995**, *14*, 2318.
216. R. L. Miller, P. T. Wolczanski and A. L. Rheingold, *J. Am. Chem. Soc.* **1993**, *115*, 10422.
217. K. J. Ahmed and M. H. Chisholm, *Organometallics* **1986**, *5*, 185.
218. M. H. Chisholm, D. L. Clark, D. Ho and J. C. Huffman, *Organometallics* **1987**, *6*, 1532.
219. M. H. Chisholm, J. C. Huffman and I. P. Rothwell, *J. Am. Chem. Soc.* **1981**, *103*, 4245.
220. M. H. Chisholm, K. Folting, J. C. Huffman and I. P. Rothwell, *J. Am. Chem. Soc.* **1982**, *104*, 4389.
221. a) R. R. Schrock, M. L. Listemann and L. G. Sturgeoff, *J. Am. Chem. Soc.* **1982**, *104*, 4291. b) M L. Listemann and R. R. Schrock, *Organometallics* **1985**, *4*, 74.
222. H. Strutz and R. R. Schrock, *Organometallics* **1984**, *3*, 1600.

Pictiva EX2004
Samsung v Pictiva
IPR2024-01094

223. M. H. Chisholm, K. Folting, D. M. Hoffman, J. C. Huffman and J. Leonelli, *Chem. Commun.* **1983**, 589.
224. M. H. Chisholm, D. M. Hoffman and J. C. Huffman, *J. Am. Chem. Soc.* **1984**, *106*, 6806.
225. M. H. Chisholm, D. M. Hoffman and J. C. Huffman, *J. Am. Chem. Soc.* **1984**, *106*, 6815.
226. M. H. Chisholm, K. Folting, D. M. Hoffman and J. C. Huffman, *J. Am. Chem. Soc.* **1984**, *106*, 6794.
227. M. H. Chisholm, B. K. Conroy, J. C. Huffman and N. S. Marchant, *Angew. Chem., Int. Edit. Engl.* **1986**, *25*, 446.
228. M. H. Chisholm, K. Folting, J. C. Huffman and E. A. Lucas, *Organometallics* **1991**, *10*, 535.
229. R. R. Schrock, *Science* **1983**, *219*, 13.
230. R. R. Schrock, J. H. Freudenberger, M. L. Listemann and L. G. McCullough, *J. Mol. Cat.* **1985**, *28*, 1.
231. J. H. Freudenberger, S. F. Pedersen and R. R. Schrock, *Bull. Chem. Soc. Fr.* **1985**, 349.
232. J. H. Freudenberger, R. R. Schrock, M. R. Churchill, A. L. Rheingold and J. W. Ziller, *Organometallics* **1984**, *3*, 1563.
233. M. H. Chisholm, D. M. Hoffman and J. C. Huffman, *Inorg. Chem.* **1984**, *23*, 3683.
234. M. H. Chisholm, B. K. Conroy and J. C. Huffman, *Organometallics* **1986**, *5*, 2384.
235. M. H. Chisholm, B. K. Conroy, B. W. Eichhorn, K. Folting, D. M. Hoffman, J. C. Huffman and N. S. Marchant, *Polyhedron* **1987**, *6*, 783.
236. M. H. Chisholm, K. B. Quinlan and E. R. Davidson, *J. Am. Chem. Soc.* **2002**, *124*, 15351.
237. R. L. M. Chamberlin, D. C. Rosenfeld, P. T. Wolczanski and E. B. Lobkovsky, *Organometallics* **2002**, *21*, 2724.
238. M. H. Chisholm, B. W. Eichhorn, K. Folting and J. C. Huffman, *Organometallics* **1989**, *8*, 49.
239. M. H. Chisholm, B. W. Eichhorn and J. C. Huffman, *Chem. Commun.* **1985**, 861.
240. M. H. Chisholm, B. W. Eichhorn and J. C. Huffman, *Organometallics* **1987**, *6*, 2264.
241. M. H. Chisholm, B. W. Eichhorn and J. C. Huffman, *Organometallics* **1989**, *8*, 69; 80.
242. K. J. Ahmed, M. H. Chisholm, K. Folting and J. C. Huffman, *J. Am. Chem. Soc.* **1986**, *108*, 989.
243. M. H. Chisholm, E. R. Davidson, M. Pink and K. B. Quinlan, *Inorg. Chem.* **2002**, *41*, 3437.
244. M. H. Chisholm, K. Folting, M. L. Lynn, D. B. Tiedtke, F. Lemoigno and O. Eisenstein, *Chem. Eur. J.* **1999**, *5*, 2318.
245. M. H. Chisholm, K. Folting-Streib, D. B. Tiedtke, F. Lemoigno and O. Eisenstein, *Angew. Chem., Int. Ed. Engl.* **1995**, *34*, 110.
246. M. H. Chisholm, *Chem. Record* **2001**, *1*, 12.
247. M. H. Chisholm, J. C. Huffman and N. L. Marchant, *J. Am. Chem. Soc.* **1983**, *105*, 6162.
248. M. H. Chisholm, K. Folting, J. C. Huffman and N. S. Marchant, *Polyhedron* **1984**, *3*, 1033.
249. R. H. Cayton, S. T. Chacon, M. H. Chisholm, M. J. Hampden-Smith, J. C. Huffman, K. Folting, P. D. Ellis and B. A. Huggins, *Angew. Chem.* **1989**, *101*, 1547.
250. S. T. Chacon, M. H. Chisholm, K. Folting, J. C. Huffman and M. J. Hampden-Smith, *Organometallics* **1991**, *10*, 3722.
251. F. A. Cotton, W. Schwotzer and E. S. Shamshoum, *Organometallics* **1985**, *4*, 461.
252. R. H. Cayton, S. T. Chacon, M. H. Chisholm and J. C. Huffman, *Angew. Chem.* **1990**, *29*, 1026.
253. S. T. Chacon, M. H. Chisholm, O. Eisenstein and J. C. Huffmann, *J. Am. Chem. Soc.* **1992**, *114*, 8497.
254. M. H. Chisholm, J. C. Huffman and M. J. Hampden-Smith, *J. Am. Chem. Soc.* **1989**, *111*, 5284.
255. J. T. Barry, J. C. Bollinger, M. H. Chisholm, K. C. Glasgow, J. C. Huffman, E. A. Lucas, E. B. Lubkovsky and W. E. Streib, *Organometallics* **1999**, *18*, 2300.
256. M. H. Chisholm, J. C. Huffman, E. A. Lucas and E. B. Lubkovsky, *Organometallics* **1991**, *10*, 3424.
257. J. T. Barry and M. H. Chisholm, *Chem. Commun.* **1995**, 1599.
258. S. T. Chacon, M. H. Chisholm, C. M. Cook, M. H. Hampden-Smith and W. E. Streib, *Angew. Chem., Int. Edit. Engl.* **1992**, *31*, 462.
259. M. H. Chisholm, C. M. Cook, J. C. Huffman and W. E. Streib, *Organometallics*, **1993**, *12*, 2677.

Pictiva EX2004
Samsung v Pictiva
IPR2024-01094

260. M. H. Chisholm, E. A. Lucas, A. C. Sousa, J. C. Huffman, K. Folting, E. B. Lobkovsky and W. E. Streib, *Chem. Commun.* **1991**, 847.
261. M. H. Chisholm, K. Folting and J. A. Klang, *Organometallics* **1990**, *9*, 602.
262. M. H. Chisholm, K. Folting and J. A. Klang, *Organometallics* **1990**, *9*, 607.
263. M. H. Chisholm, J. C. Huffman, E. A. Lucas, A. Sousa and W. E. Streib, *J. Am. Chem. Soc.* **1992**, *114*, 2710.
264. M. H. Chisholm, K. Folting, K. C. Glasgow, E. Lucas and W. E. Streib, *Organometallics* **2000**, *19*, 884.
265. T. A. Budzichowski, M. H. Chisholm and K. Folting, *Chem. Eur. J.* **1996**, *2*, 110.
266. H. Alper, N. D. Silavwe, G. I. Birnbaum and F. R. Ahmed, *J. Am. Chem. Soc.* **1979**, *101*, 6582.
267. M. H. Chisholm, K. Folting, K. S. Kramer and W. E. Streib, *J. Am. Chem. Soc.* **1997**, *119*, 5528.
268. M. H. Chisholm, J. C. Huffman and J. J. Koh, *Polyhedron* **1989**, *8*, 127.
269. R. J. Blau, M. H. Chisholm, K. Folting and R. J. Wang, *Chem. Commun.* **1985**, 1582.
270. R. J. Blau, M. H. Chisholm, K. Folting and R. J. Wang, *J. Am. Chem. Soc.* **1987**, *109*, 4552.
271. M. H. Chisholm, V. J. Johnston, O. Eisenstein and W. E. Streib, *Angew. Chem.* **1992**, *104*, 889. See also *Angew. Chem., Int. Ed. Engl*., **1992**, 19311997), 1896).
272. M. L. H. Green and P. Mountford, *J. Chem. Soc., Chem. Commun.* **1989**, 732.
273. M. L. H. Green, J. D. Hubert and P. Mountford, *J. Chem. Soc., Dalton Trans.* **1990**, 3793.
274. J. C. Green, M. L. H. Green, P. Mountford and M. J. Parkington, *J. Chem. Soc., Dalton Trans.* **1990**, 3407.
275. Q. Feng, M. Ferrer, M. L. H. Green, P. Mountford and V. S. B. Mtetura, *J. Chem. Soc., Dalton Trans.* **1992**, 1205.
276. Q. Feng, M. L. H. Green and P. Mountford, *J. Chem. Soc., Dalton Trans.* **1992**, 2171.
277. P. Mountford, *J. Chem. Soc., Dalton Trans.* **1994**, 1843.
278. Q. Feng, M. Ferrer, M. L. H. Green, P. Mountford and V. S. B. Mtetura, *J. Chem. Soc., Dalton Trans.* **1991**, 1397.

Pictiva EX2004
Samsung v Pictiva
IPR2024-01094

7

Technetium Compounds

Alfred P. Sattelberger,
Los Alamos National Laboratory

7.1 Synthesis and Properties of Technetium

Technetium was the first man-made element and isotopes ^{95}Tc and ^{97}Tc were obtained by Perrier and Segré in 1937 by bombarding molybdenum with deuterons.[1,2] Today, 21 isotopes of element 43 are known with mass numbers from 90-111 and all are radioactive. The longest-lived isotope is ^{98}Tc ($t_{1/2} = 4.2\times10^6$ years), but the most readily available isotope is ^{99}Tc ($t_{1/2} = 2.1\times10^5$ years). The latter is isolated in large quantities from spent nuclear fuel and constitutes approximately 6% of the fission product yield.[3] Ammonium pertechnetate is readily available in gram quantities with a radiopurity of >99% from Oak Ridge National Laboratory.[4] All other starting materials, including technetium metal, trace their origins to ammonium pertechnetate.

The ^{99}Tc isotope is a weak β-emitter ($E_{max} = 0.292$ MeV). The decay properties of ^{99}Tc allow handling of the isotope during normal chemical operations in quantities up to *c.* 1 g. With this mass limitation, special shielding precautions are not necessary since the low energy β radiation is completely absorbed by ordinary glassware. It is prudent to remember that ^{99}Tc, like all radionuclides, is a potential health hazard and protective gloves, lab coats, and safety glasses are essential at all times when working with ^{99}Tc compounds. Additional care must be exercised with volatile compounds such as Tc_2O_7, $Me_3SiOTcO_3$, and $Tc_2(CO)_{10}$ to avoid inhalation and the unwanted spread of radioactivity. The author's collaborators have safely carried out numerous synthetic reactions and spectroscopic characterizations in laboratories designed for low-level radioactivity using efficient fume hoods and Schlenk and glove box techniques and following, in our case, Department of Energy approved handling and monitoring procedures.

Because technetium bears a close electronic relationship to rhenium, the occurrence of analogous compounds, including those containing metal–metal multiple bonds, is to be expected, but the radioactive nature of technetium has served to limit the development of Tc chemistry relative to its heavier congener Re. As one striking comparison, thirteen binary halides have been reported for rhenium, but only three binary halides of technetium (TcF_6, TcF_5, and $TcCl_4$) are reasonably well characterized.[5] Logic predicts a plethora of exciting Tc chemistry yet to be discovered. Several recent review articles have been published that contain accounts of the chemistry, properties, and structures[6-9] of dinuclear and polynuclear technetium compounds. These sources should be consulted for additional details.

Pictiva EX2004
Samsung v Pictiva
IPR2024-01094

7.2 Preparation of Dinuclear and Polynuclear Technetium Compounds

A few words on the methods of synthesis employed in the preparation of dinuclear and polynuclear technetium compounds seem appropriate. Synthetic methodologies fall into one of three categories: (1) moderate temperature (100-250 °C) reduction of higher-valent mononuclear Tc precursors in concentrated aqueous hydrohalic acid solution using molecular hydrogen (30-50 atm) as the reductant; (2) reduction of higher-valent mononuclear precursors using chemical reductants other than H_2, either in aqueous acid or non-aqueous solvents; (3) substitution and/or redox reactions involving pre-formed dinuclear complexes. Russian chemists have been advocates for the first method while American and European chemists have traditionally opted for the latter two strategies. Each has its attendant advantages and disadvantages. The hydrogen reductions do require the use of high-pressure stainless steel autoclaves. The use of glass test tubes inside the autoclave minimizes corrosion of the stainless steel. Russian chemists have isolated a wide variety of dinuclear and polynuclear Tc compounds by systematically varying the experimental parameters (such as time, Tc and acid concentration, temperature, pressure, cool-down rate). Structurally characterized technetium compounds containing Tc–Tc multiple bonds are presented in Table 7.1.

7.3 Bonds of Order 4 and 3.5

The original entry into the chemistry of Tc–Tc multiple bonds was afforded by the work of Eakins, Humphreys, and Mellish[10] who discovered that the reaction of $(NH_4)_2TcCl_6$ or $MgTcCl_6$ with zinc in concentrated hydrochloric acid at roughly 100 °C gave a mixture which could be used to prepare the deeply colored salts $(NH_4)_3Tc_2Cl_8{\cdot}2H_2O$, $YTc_2Cl_8{\cdot}9H_2O$ and $K_3Tc_2Cl_8{\cdot}2H_2O$:

$$4(NH_4)_2TcCl_6 + 3Zn \xrightarrow{12\ M\ HCl} 2(NH_4)_3Tc_2Cl_8{\cdot}2H_2O + 2NH_4Cl + 3ZnCl_2$$

The average Tc oxidation state of *c.* +2.5 was established via oxidative titrations using ceric sulfate or basic peroxide. In dilute hydrochloric acid or water, the compounds decompose rapidly by oxidation and hydrolysis. The British work[10] was published shortly before the structural characterization of $K_2Re_2Cl_8{\cdot}2H_2O$ and, accordingly, the authors' conclusions were limited to the observation that "the stoichiometry of the $[Tc_2Cl_8]^{3-}$ ion is unusual, and it seems to have no analogs." Cotton and Pedersen[11] published an improvement in the original synthetic procedures some years ago.

Following the completion of the original structural work on $K_2Re_2Cl_8{\cdot}2H_2O$, the full structural characterization of a salt containing the $[Tc_2Cl_8]^{3-}$ anion became an important objective. Black crystalline $(NH_4)_3Tc_2Cl_8{\cdot}2H_2O$ was chosen for this study and a structure solution revealed the presence of the $[Tc_2Cl_8]^{3-}$ anion having the same non-bridged, eclipsed M_2Cl_8 structure as $[Re_2Cl_8]^{2-}$.[12,13] The very short Tc–Tc distance of 2.13(1) Å was indicative of a strong metal–metal bond. The paramagnetism of the ammonium and yttrium salts (μ_{eff} = 1.78±0.03 B.M.)[11,12,14,15] is consistent with the anion possessing a $\sigma^2\pi^4\delta^2\delta^{*1}$ electronic configuration, a conclusion supported by SCF-Xα-SW calculations (see Chapter 16).[16,17] Frozen solution EPR spectral measurements on $YTc_2C1_8{\cdot}9H_2O$ at X- and Q-band frequencies revealed the expected coupling of one unpaired electron to two equivalent Tc nuclei each with a nuclear spin of $^9/_2$.[11] The spectrum was analyzed to afford $g_{\parallel}$ = 1.912 and $g_{\perp}$ = 2.096. The values are consistent with the odd electron occupying the b_{1u} δ^* orbital.[18] Every indication is that $[Tc_2Cl_8]^{3-}$ contains a Tc–Tc bond of order 3.5 in contrast with the recognition of the first Re–Re multiple bond as being one of order four.

Unlike $[Re_2Cl_8]^{3-}$, the stability of the $[Tc_2Cl_8]^{3-}$ anion has been demonstrated on a number of occasions since the original synthesis and structural characterization. However, some later work is confusing and contradictory. Glinkina *et al.*[19] described the reduction of solutions of ammonium or potassium pertechnetate in concentrated hydrochloric acid by hydrogen under

Pictiva EX2004
Samsung v Pictiva
IPR2024-01094

Table 7.1. Structurally characterized technetium compounds with Tc–Tc multiple bonds.

Compound	Tc–Tc (Å)	ref.
Bonds of order 4.0		
$(Bu_4N)_2Tc_2Cl_8$	2.147(4)	30
$Tc_2(O_2CCMe_3)_4Cl_2$	2.192(1)	39
$[Tc_2(O_2CMe)_4](TcO_4)_2$	2.149(1)	51,52
$[Tc_2(O_2CCH_3)_2Cl_4(dma)_2]$	2.1835(7)	42
$K_2[Tc_2(SO_4)_4]\cdot 2H_2O$	2.155(1)	7
Bonds of order 3.5		
$K_3Tc_2Cl_8\cdot nH_2O$	2.117(2)	20,21
$(NH_4)_3Tc_2Cl_8\cdot 2H_2O$	2.13(1)	12,13
$Y[Tc_2Cl_8]\cdot 9H_2O$	2.105(2)	22
$(C_5H_5NH)_3Tc_2Cl_8$	2.1185(5)	23
$Tc_2(hp)_4Cl$	2.095(1)	53
$Tc_2(O_2CCH_3)_4Cl$	2.117(1)	46
$K[Tc_2(O_2CCH_3)_4Cl_2]$	2.1260(5)	45
$Tc_2(O_2CCH_3)_4Br$	2.112(1)	49
$[Tc_2Cl_4(PMe_2Ph)_4]PF_6$ (orthorhombic)	2.109(1)	57
$[Tc_2Cl_4(PMe_2Ph)_4]PF_6$ (monoclinic)	2.106(1)	57
$[Tc_2Cl_4(PMe_2Ph)_4]PF_6\cdot 0.5THF$	2.107(1)	57
$Tc_2Cl_5(PMe_2Ph)_3$	2.109(1)	57
$Tc_2(DPhF)_4Cl\cdot C_7H_8$	2.119(2)	54
$Tc_2(DTolF)_3Cl_2$	2.094(1)	54
Bonds of order 3.0		
$K_2[Tc_2Cl_6]$	2.044(1), 2.047(1), 2.042(1)	59,60
$Tc_2Cl_4(PEt_3)_4$	2.133(3)	61
$Tc_2Cl_4(PMe_2Ph)_4$	2.127(1)	61
$Tc_2Cl_4(PMePh_2)_4\cdot C_6H_6$	2.138(1)	61
α-$Tc_2Cl_4(dppe)_2$	2.15(1)	58
β-$Tc_2Cl_4(dppe)_2$	2.117(1)	58
β-$Tc_2Cl_4(dppm)_2$	2.1126(7)	65
$[Tc_2(NCCH_3)_8(CF_3SO_3)_2](BF_4)_4\cdot CH_3CN$	2.122(1)	66
Hexanuclear cluster compounds		
$[(CH_3)_4N]_3\{[Tc_6(\mu\text{-}Cl)_6Cl_6]Cl_2\}$	2.16(1), 2.69(1)	72
$[(CH_3)_4N]_2[Tc_6(\mu\text{-}Cl)_6Cl_6]$	2.22(1), 2.57(1)	73
$[(C_2H_5)_4N]_2\{[Tc_6(\mu\text{-}Br)_6Br_6]Br_2\}$	2.188(5), 2.66(2)	74
$[(CH_3)_4N]_3\{[\ Tc_6(\mu\text{-}Br)_6Br_6]Br_2\}$	2.154(5), 2.702(2)	74
Octanuclear cluster compounds		
$\{[Tc_8(\mu\text{-}Br)_8Br_4]Br\}\cdot 2H_2O$	2.146(2), 2.521(2), 2.687(23)	77
$[H(H_2O)_2]\{[Tc_8(\square\text{-}Br)_8Br_4]Br\}$	2.155(3), 2.531(2), 2.70(2)	79
$[H(H_2O)_2]_2\{[Tc_8(\square\text{-}Br)_8Br_4]Br_2\}$	2.152(9), 2.520(9), 2.69(1)	78
$[(C_4H_9)_4N]_2\{[Tc_6(\square\text{-}Br)4(\square\text{-}I)_4Br_2I_2]I_2\}$	2.162(9), 2.507(2), 2.704(10)	81
$[Fe(C_5H_5)_2]_3\{Tc_6(\square\text{-}I)_6I_6]I_2\}$	2.17(1), 2.67(1)	52

Pictiva EX2004
Samsung v Pictiva
IPR2024-01094

pressure at 170 °C to produce dark blue solutions from which salts with the compositions $K_8(Tc_2Cl_8)_3 \cdot 4H_2O$, $(NH_4)_8(Tc_2Cl_8)_3 \cdot 2H_2O$, or $Cs_8(Tc_2Cl_8)_3 \cdot 2H_2O$ could be isolated. In spite of these complexes having spectral and magnetic properties clearly in accord with the presence of the $[Tc_2Cl_8]^{3-}$ anion, these workers describe the oxidation number of technetium as being 2.67 on the basis of oxidation state titrations. Furthermore, they cited the results of an X-ray crystallographic study[20] that purportedly showed "that technetium exists as the binuclear anionic octachloroditechnetate complex $\{[Tc_2Cl_8]_3\}^{8-}$, in which technetium has an average valency of 2.67". Actually, the cited report[20] describes no such result. Rather, the publication discusses the structures of $K_3Tc_2Cl_8 \cdot 2H_2O$ and $Cs_3Tc_2Cl_8 \cdot 2H_2O$ using crystals provided by Glinkina and Kuzina.[19] The potassium and cesium salts were described[20] as being isostructural with $(NH_4)_3Tc_2Cl_8 \cdot 2H_2O$, and for $K_3Tc_2Cl_8 \cdot 2H_2O$ a Tc–Tc distance of 2.10 Å was obtained. Since this structure determination was of relatively poor quality, a further structural study was carried out on a sample of $K_3Tc_2Cl_8 \cdot nH_2O$ prepared by cation exchange from $YTc_2Cl_8 \cdot 9H_2O$.[21] As before, the $[Tc_2Cl_8]^{3-}$ anion was found to have virtual D_{4h} symmetry and to be very similar in structure to the $[Re_2Cl_8]^{2-}$ anion (Fig. 7.1). The Tc–Tc distance of 2.117(2) Å was determined with greater precision than before. The structure of the yttrium salt $Y[Tc_2Cl_8] \cdot 9H_2O$ was determined several years later.[22] The Tc–Tc distance is 2.105(1) Å, and the counter cation proved to be $[Y(H_2O)_8]^{3+}$.

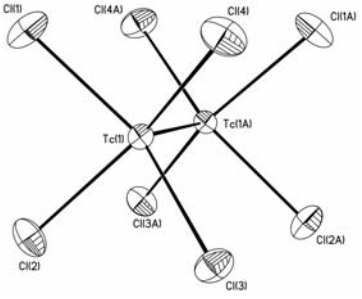


Fig. 7.1. Structure of the $[Tc_2Cl_8]^{3-}$ anion in $K_3Tc_2Cl_8 \cdot nH_2O$.

The ease of conversion of technetium(IV) to $[Tc_2Cl_8]^{3-}$ has also been demonstrated by the high pressure hydrogen reduction (30 atm H_2, 160 °C, 5 h) of the pyridinium and quinolinium salts of $[TcCl_6]^{2-}$ in 11 M HCl to $(pyH)_3Tc_2Cl_8 \cdot 2H_2O$ described as forming dark-brown crystals,[23] and $(quinH)_3Tc_2Cl_8 \cdot 2H_2O$ which is olive colored.[24] Similar reductions of Tc(VII) or Tc(IV) species in hydrobromic acid have been used to obtain brown $M_3[Tc_2Br_8] \cdot 2H_2O$ (M = NH_4 or K).[25]

The ease of producing $[Tc_2Cl_8]^{3-}$, rather than $[Tc_2Cl_8]^{2-}$, was long considered a rather curious result. Shown experimentally[11] in 1975, $[Tc_2Cl_8]^{3-}$ (as its yttrium salt) is reversibly oxidized to $[Tc_2Cl_8]^{2-}$ at +0.14 V versus SCE in mixtures of hydrochloric acid and ethanol (1:9 v/v). The resulting product gave no EPR signal and is likely diamagnetic. With a lifetime in solution of at least 5 min, it seemed reasonable to conclude[11] that a "suitably designed effort to isolate (it) might be successful." Accordingly, in 1977, a communication by Schwochau et al.[26] describing their isolation and characterization of $(Bu_4N)_2Tc_2Cl_8$ was received with considerable interest. An olive-green complex of this stoichiometry was described as being prepared by the hypophosphorous acid (H_3PO_2) reduction of $[TcO_4]^-$ in hydrochloric acid followed by the addition of Bu_4NCl. The synthetic details presented were minimal, i.e., quantities of reactants, HCl concentration, temperature, and the duration of the reaction were not provided in the report.

Pictiva EX2004
Samsung v Pictiva
IPR2024-01094

The diamagnetic product was said to be isomorphous with $(Bu_4N)_2Re_2Cl_8$ and to possess an electronic absorption spectrum similar to that of the latter complex with its $\delta \rightarrow \delta^*$ transition located at about 700 nm. Thus the authors concluded 'that there seems to be no more doubt about the existence of a stable dinegative octachloroditechnetate(III) which closely resembles the analogous rhenium complex in magnetic, structural and spectroscopic properties.'

In order to establish definitely the structure of $(Bu_4N)_2Tc_2Cl_8$ by X-ray crystallography this system was reinvestigated in 1979.[27] However, an attempt to reproduce the hypophosphorous acid reduction procedure of Schwochau *et al*.[26] afforded dark-green $(Bu_4N)TcOCl_4$ that was easily converted to the bis(triphenylphosphine)iminium salt, $[(Ph_3P)_2N]TcOCl_4$.[27] The infrared spectra of both salts revealed the characteristic $\nu(Tc{=}O)$ mode at *c*. 1020 cm^{-1} and an X-ray crystallographic analysis of $[(Ph_3P)_2N]TcOCl_4$ confirmed the presence of the distorted square pyramidal $[TcOCl_4]^-$ anion.[27] A second report on the synthesis of $(Bu_4N)_2Tc_2Cl_8$ via H_3PO_2 reduction of pertechnetate was published by Schwochau in 1981.[28] In this report, the synthetic details were provided, as well as the fact that the desired compound was isolated in only 10% yield starting from NH_4TcO_4.[28] A note in a 1995 review article by Kryutchkov[7] claims that the Schwochau[28] procedure can be optimized to obtain much higher yields of $(Bu_4N)_2Tc_2Cl_8$.

In between the two Schwochau publications,[26,28] Preetz and Peters[29] reported a successful preparation of $(Bu_4N)_2Tc_2Cl_8$, together with grey-blue $(Bu_4N)_3Tc_2Cl_8$, by a procedure that involved the mossy zinc reduction of $(NH_4)_2TcCl_6$ in aqueous HCl followed by cation exchange using Bu_4NCl. The green complex $(Bu_4N)_2Tc_2Cl_8$ can be converted to the carmine-red bromide derivative $(Bu_4N)_2Tc_2Br_8$ by dissolving it in aqueous acetone/HBr.[29] Raman and electronic absorption spectral data supported the proposed formulations, but the successful completion of an X-ray crystal structure determination on $(Bu_4N)_2Tc_2Cl_8$ provided the incontrovertible proof as to the structure of the $[Tc_2Cl_8]^{2-}$ anion.[30] $(Bu_4N)_2Tc_2Cl_8$ is isostructural with $(Bu_4N)_2Re_2Cl_8$ and, like the latter, possesses a quadruply bonded dimetal unit with an eclipsed rotational geometry. While there is disorder associated with the orientation of the $[Tc_2Cl_8]^{2-}$ ions, the structure is of high precision; the Tc–Tc distance is 2.147(4) Å; the weighted average of Tc–Tc distances of 2.151(1) Å and 2.133(3) Å for the major and minor orientations.[30] Actually, the Tc–Tc distance of 2.147(4) Å poses an interesting dilemma since it is *longer* than the Tc–Tc distances in the NH_4^+, K^+, and Y^{3+} salts of $[Tc_2Cl_8]^{3-}$ (see above). This trend is, of course, the opposite expected based upon a simple bond length/bond order correlation argument, but the explanation is probably similar to that advanced to explain metal–metal bond length changes in the series $[Re_2Cl_4(PMe_2Ph)_4]^{n+}$ (n = 0, 1 or 2),[31] namely, as the formal bond order increases (and the metal core charge increases) there is some decrease in the strength of the σ- and/or π-bonding contributions to the Tc–Tc bond because of orbital contraction.

One result not readily explained concerns the electrochemical redox characteristics of the $[Tc_2Cl_8]^{2-}/[Tc_2Cl_8]^{3-}$ couple. In a mixed hydrochloric acid-ethanol solvent (1:9 by volume) the $[Tc_2Cl_8]^{3-}$ ion is reversibly oxidized to $[Tc_2Cl_8]^{2-}$ at +0.14 V versus SCE.[11] Solutions of $(Bu_4N)_2Tc_2Cl_8$ in 0.1 M Bu_4NClO_4/CH_2Cl_2 are characterized by $E_{1/2}$ = -0.13 V versus SCE at a rotating platinum electrode,[30] demonstrating the solvent dependence of the electrochemical potential for this process. However, partial solvolysis of the $[Tc_2Cl_8]^{3-}$ ion is likely to occur in HCl-EtOH solutions. In this context, it should be noted that spectrophotometric methods have been used to investigate the stability of solutions of the $[Tc_2X_8]^{3-}$ anions (X = Cl or Br) in hydrohalic acids as a function of metal and acid concentration both in the presence and absence of air.[32-34] At HCl concentrations below ~3 M in the absence of air, $[Tc_2Cl_8]^{3-}$ hydrolyzes to mixed aquo-chloro species of the type $[Tc_2Cl_{8-n}(H_2O)_n]^{(3-n)-}$.[32]

In 1994, Preetz and coworkers published a definitive synthetic/spectroscopic paper that provided new information on the solution behavior of the octachloro- and octabromoditechnetate

Pictiva EX2004
Samsung v Pictiva
IPR2024-01094

anions and described high yield syntheses for all four $[Tc_2X_8]^{n-}$dimers (X = Cl, Br; n = 2, 3).[35] Their improved preparative route for $(Bu_4N)_2Tc_2Cl_8$ starts with the tetrabutylammonium salt of $[TcO_4]^-$ which is first reduced to $(Bu_4N)TcOCl_4$ via treatment with concentrated aqueous HCl. The compound $(Bu_4N)TcOCl_4$ is then dissolved in THF and treated dropwise with a THF solution containing 2 equiv of $(Bu_4N)BH_4$. The latter step provides a brown intermediate (not characterized) that is isolated and dried, dissolved in methylene chloride, and then treated with gaseous HCl and air. The green $(Bu_4N)_2Tc_2Cl_8$ is crystallized by adding ether and cooling to *c*. -30 °C:

$$(Bu^n{}_4N)TcO_4 \xrightarrow{12\ M\ HCl} (Bu^n{}_4N)TcOCl_4 \xrightarrow[+\ 2(Bu^n{}_4N)BH_4\ -\ H_2,\ -B_2H_6]{THF} \text{brown intermediate}$$

$$\text{brown intermediate} \xrightarrow[HCl(g),\ air]{CH_2Cl_2} (Bu^n{}_4N)_2Tc_2Cl_8$$

The overall yield of $(Bu_4N)_2Tc_2Cl_8$, starting from $(NH_4)TcO_4$, is nearly 80%. A similar procedure, via $(Bu_4N)TcOBr_4$ and bromine-free HBr(g), provides $(Bu_4N)_2Tc_2Br_8$ in comparable yield. The $[Tc_2X_8]^{2-}$ anions can be interconverted by dissolution in methylene chloride and treatment with the appropriate gaseous hydrogen halide:

$$[Tc_2Cl_8]^{2-} \underset{CH_2Cl_2/HCl(g)}{\overset{CH_2Cl_2/HBr(g)}{\rightleftharpoons}} [Tc_2Br_8]^{2-}$$

Green $(Bu_4N)_2Tc_2Cl_8$ and carmine-red $(Bu_4N)_2Tc_2Br_8$ are both diamagnetic crystalline solids that contain Tc–Tc quadruple bonds. A structure determination of $(Bu_4N)_2Tc_2Br_8$ has yet to be performed. The compounds are stable in dry air and can be stored under argon in the dark for several years without signs of decomposition. Solutions of either complex are stable in dry methylene chloride or acetone for several days; extended exposure to air results in oxidation to the corresponding hexahalogenotechnetate(IV) ions, $[TcX_6]^{2-}$. The $(Bu_4N)_2Tc_2X_8$ salts are only sparingly soluble in concentrated aqueous HX and on warming disproportionate:

$$3[Tc_2X_8]^{2-} + 4X^- \xrightarrow{\text{conc. HX}} 2[Tc_2X_8]^{3-} + 2[TcX_6]^{2-}$$

The ready availability of $(Bu_4N)_2Tc_2X_8$ should pave the way for further elaborations of Tc–Tc quadruple bond chemistry.

Grey-blue $(Bu_4N)_3Tc_2Cl_8$ and golden $(Bu_4N)_3Tc_2Br_8$ can be prepared, in good yield, from the corresponding $(Bu_4N)_2Tc_2X_8$ salts by dissolution of the latter in acetone and treatment with one equivalent of $(Bu_4N)BH_4$:[35]

$$(Bu^n{}_4N)_2Tc_2Cl_8 + (Bu^n{}_4N)BH_4 \xrightarrow{(CH_3)_2CO} (Bu^n{}_4N)_3Tc_2Cl_8 + 0.5H_2 + 0.5B_2H_6$$

Both salts are paramagnetic with Tc–Tc bond orders of 3.5.

Neither of the $(Bu_4N)_3Tc_2X_8$ salts has been characterized by X-ray crystallography. The solids are very sensitive to air and water but can be stored for several weeks in a dry argon atmo-

Pictiva EX2004
Samsung v Pictiva
IPR2024-01094

sphere in the absence of light. Both salts are readily soluble in methylene chloride but the solutions are photo-labile and decompose rather rapidly. On the other hand, both salts are readily soluble *and* stable in the respective air- and halogen-free, constant-boiling aqueous hydrohalic acid. Addition of KCl, RbCl or CsCl to these solutions results in the precipitation of the alkali metal salt, $M_3Tc_2X_8$. The synthesis and the low energy optical spectrum ($\delta \rightarrow \delta^*$ transition) of $Cs_3Tc_2Br_8$ have been described in considerable detail.[36]

As can be gleaned from the foregoing paragraphs, the solution stability of the $[Tc_2X_8]^{2-}$ and $[Tc_2X_8]^{3-}$ anions is very much solvent dependent. With rigorous exclusion of air and water, the $[Tc_2X_8]^{2-}$ anions are stable in organic solvents and unstable in concentrated aqueous hydrohalic acid. In contrast, the $[Tc_2X_8]^{3-}$ anions are stable in concentrated aqueous HX and unstable in organic solvents. These properties have undoubtedly contributed to some of the difficulties encountered in earlier chemical and physical studies of these systems.

In addition to the aforementioned structural studies and measurements of the EPR spectra and magnetic properties of salts of the $[Tc_2Cl_8]^{3-}$ anions, other physicochemical investigations have included the X-ray photoelectron spectrum of $K_3Tc_2Cl_8 \cdot 2H_2O$; as part of a larger investigation devoted to the measurement of the Tc 3*d* binding energies.[37] Normal coordinate analyses have been performed on the $[Tc_2X_8]^{2-/3-}$ (X = Cl, Br) ions. The calculated force constants for the Tc–Tc multiple bonds range from 2.67 mdyne/Å for $[Tc_2Br_8]^{2-}$ to 4.86 mdyne/Å for $[Tc_2Cl_8]^{3-}$.[35] The thermal decomposition of $(NH_4)_3Tc_2Cl_8 \cdot 2H_2O$ has been found to yield technetium metal via the intermediacy of $(NH_4)_2TcCl_6$, TcNCl, and TcN.[38]

7.4 Tc_2^{6+} and Tc_2^{5+} Carboxylates and Related Species with Bridging Ligands

While quadruply bonded, carboxylate-bridged Re_2^{6+} complexes of the type $Re_2(O_2CR)_4X_2$ are well known and easily prepared, comparable Tc_2^{6+} carboxylate compounds are still quite rare and were, until the development of reliable routes to $(Bu_4N)_2Tc_2X_8$, difficult to isolate. The first such example, for which there was definitive structural proof, was the pivalate $Tc_2(O_2CCMe_3)_4Cl_2$.[39] The compound was prepared in very low yield, as red crystals, by the reaction of $(NH_4)_3Tc_2Cl_8$ with molten pivalic acid in a nitrogen atmosphere. The structure of $Tc_2(O_2CCMe_3)_4Cl_2$ resembles closely that of its rhenium analog (Fig. 7.2); the Tc–Tc bond length of 2.192(1) Å is longer than in $(Bu_4N)_2Tc_2Cl_8$ (2.147(4) Å),[30] a complex that does not contain axial Tc–ligand bonds that weaken the Tc–Tc bond. Subsequently, the diamagnetic acetate complex $Tc_2(O_2CCH_3)_4Cl_2$ was prepared as cherry-red crystals from the reaction between $KTcO_4$, hydrochloric acid, and acetic acid in a hydrogen atmosphere.[40] The reaction of $(Bu_4N)_2[Tc_2X_8]$ with acetic acid/acetic anhydride provides $Tc_2(O_2CCH_3)_4Cl_2$ and orange-red $Tc_2(O_2CCH_3)_4Br_2$ in excellent yield.[41] By analogy with known rhenium chemistry, other carboxylic acid/acid anhydride reactions could be a source of as yet unknown $Tc_2(O_2CR)_4X_2$ derivatives. A thorough analysis of the low temperature (80 K) IR and Raman spectra of the $Tc_2(O_2CCH_3)_4X_2$ complexes allowed assignments of the metal–metal, metal–ligand and intraligand vibrations. The Tc–Tc stretching vibration is found at 319 cm^{-1} for the chloro compound, and at 310 cm^{-1} for the bromo derivative. A normal coordinate analysis provided a Tc–Tc force constant of 4.08 mdyne/Å for the chloride and 3.99 mdyne/Å for the bromide.[41]

The deep green complex $[Tc_2(O_2CCH_3)_2Cl_4(H_2O)_2]$ has been prepared by reaction of acetic anhydride and HBF_4 with $[Tc_2Cl_8]^{2-}$.[42] Subsequent treatment with Lewis bases such as dmf, dma, dmso, $Ph_3P{=}O$, or pyridine results in substitution of the water ligands providing complexes of general composition $[Tc_2(O_2CCH_3)_2Cl_4L_2]$.[42] The X-ray crystal structure of $Tc_2(O_2CCH_3)_2Cl_4(dma)_2$ reveals a *cis* arrangement of the bridging acetate ligands and the terminal chlorides. The dma ligands are axial and coordinate via the amido oxygen atoms (Fig. 7.3). The Tc–Tc distance is 2.1835(7) Å, significantly longer than in $[Tc_2Cl_8]^{2-}$. The elongation of the Tc–Tc bond is due to the presence

Pictiva EX2004
Samsung v Pictiva
IPR2024-01094

of strongly bound axial ligands that weaken the Tc–Tc bond. Electronic spectra show only minor dependence on the Lewis base. The $\delta \rightarrow \delta^*$ transitions are found in the range of 648-652 nm for all adducts.[43] The correlation between the donor strength of the axial bases and the Tc–Tc vibrational mode was studied,[43] and a linear relationship between the donor number and $\nu_{Tc\text{-}Tc}$ was discovered. For the strongest donor pyridine, the Tc–Tc stretching vibration is at 282 cm^{-1}; for the weakest donor, H_2O, it is at 311 cm^{-1}.

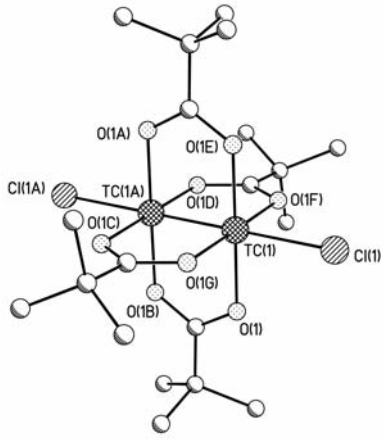


Fig. 7.2. Structure of $Tc_2(O_2CCMe_3)_4Cl_2$.

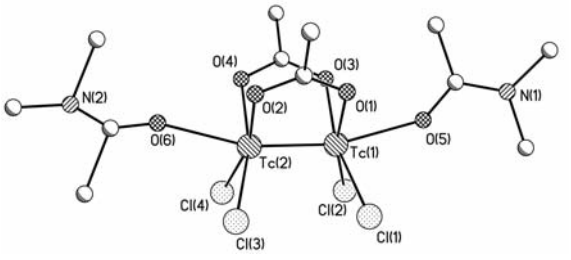


Fig. 7.3. Structure of *cis*-$Tc_2(O_2CCH_3)_2Cl_4(dma)_2$.

Reaction of $K_3Tc_2Cl_8 \cdot 2H_2O$ and glacial acetic acid in an atmosphere of argon or hydrogen at 120 °C and 30 atm in an autoclave has been used to prepare the crystalline Tc_2^{5+} derivatives $Tc_2(O_2CCH_3)_4Cl$ (green) and $K[Tc_2(O_2CCH_3)_4C1_2]$ (pale brown), admixed with K_2TcCl_6 (argon atmosphere) or a material speculated to be a Tc^{2+} complex (hydrogen atmosphere).[44] The complexes $Tc_2(O_2CCH_3)_4Cl$ and $K[Tc_2(O_2CCH_3)_4Cl_2]$ are clearly authentic derivatives of the Tc_2^{5+} core. Both compounds are paramagnetic and EPR-active, and possess magnetic moments in accord with the presence of a $\sigma^2\pi^4\delta^2\delta^{*1}$ ground state electronic configuration.[44] A comparison of their X-ray photoelectron spectra has been made; the Tc $3d_{5/2}$ binding energy is 255.8 eV for both compounds.[37] X-ray crystal structure determinations on $K[Tc_2(O_2CCH_3)_4Cl_2]$ and $Tc_2(O_2CCH_3)_4Cl$ have been completed.[45,46] The former salt contains the dinuclear $[Tc_2(O_2CCH_3)_4Cl_2]^-$ anion with Tc–Tc and Tc–Cl distances of 2.126(1) Å and 2.589(1) Å, respectively.[45] The complex $Tc_2(O_2CCH_3)_4Cl$ has a structure with chains of $[Tc_2(O_2CCH_3)_4]^+$ units linked by bridging chloride ligands.[46] Note that there is a longer Tc–Tc distance in $Tc_2(O_2CCMe_3)_4Cl_2$[39] compared to $[Tc_2(O_2CCMe_3)_4Cl_2]^-$.[45,47] A related green bromide compound, $Tc_2(O_2CCH_3)_4Br$, has been prepared[48] from the reaction of

Pictiva EX2004
Samsung v Pictiva
IPR2024-01094

$M_2Tc_2Br_6 \cdot 2H_2O$ (M = NH_4 or K; see below), and acetic acid at 230-250 °C under argon. The structure of $Tc_2(O_2CCH_3)_4Br$ is quite similar to that of $Tc_2(O_2CCH_3)_4Cl$. The Tc–Tc separation is 2.112(1) Å.[49] The magnetic susceptibilities and frozen solution (MeOH) EPR of $Tc_2(O_2CCH_3)_4Cl$, $K[Tc_2(O_2CCH_3)_4Cl_2]$ and $Tc_2(O_2CCH_3)_4Br$ have been measured.[50] The values of μ_{eff} are 1.78±0.05 B.M. for the first two compounds and ~2.0 B.M. for the bromide, the higher value apparently due to the presence of K_2TcBr_6 as an impurity. The EPR spectral parameters coincide within experimental error, viz., $g_{\parallel}$ = 1.85±0.03 and $g_{\perp}$ = 2.13±0.03 for all three compounds.

Aerial oxidation of solutions of $[Tc_2(O_2CCH_3)_4Cl_2]^-$ provided a low yield of red crystals which proved to be the Tc_2^{6+} complex, $[Tc_2(O_2CCH_3)_4](TcO_4)_2$.[51,52] The structure is similar to $Tc_2(O_2CCMe_3)_4Cl_2$ with a paddlewheel $[Tc_2(O_2CCH_3)_4]^{2+}$ core axially ligated by a single oxygen of each pertechnetate anion. The Tc–Tc distance of 2.149(1) Å is 0.04 Å shorter than that in $Tc_2(O_2CCMe_3)_4Cl_2$ and the Tc–O_{ax} distances average 2.153(5) Å.[51,52]

A compound that bears a close structural relationship to $Tc_2(O_2CCH_3)_4Cl$ is the dark green complex $Tc_2(hp)_4Cl$, which is prepared by reacting $(NH_4)_3Tc_2Cl_8$ with molten 2-hydroxypyridine.[53] It is paramagnetic (g = 2.046 from the EPR spectrum) and exhibits a Raman active ν(Tc–Tc) mode at 383 cm^{-1}. The parent ion has been detected in the mass spectrum, while in the solid-state the structure resembles $Tc_2(O_2CCH_3)_4Cl$ and consists of infinite chains of $[Tc_2(hp)_4]^+$ units (the Tc–Tc distance is 2.095(1) Å) symmetrically linked by bridging chloride ligands.[53] Perhaps the most interesting feature of the compound is the visible absorption spectrum measured on single crystals at 5 K (see Chapter 16). The lowest energy transition at 12,194 cm^{-1} is z polarized and consistent with the assignment as a δ→δ* transition.

As discussed in Chapter 1, the use of aryl amidinate ligands, $[ArNC(R)NAr]^-$, relatives of more common carboxylate ligands, has become increasingly prominent in the field of metal–metal multiple bond research. The success of these ligands derives, at least in part, from their enhanced π-basicity relative to carboxylate ligands. Seeking examples of this class of compound in technetium chemistry, Cotton and coworkers examined reactions of Tc_2^{4+} compounds of the type $Tc_2Cl_4(PR_3)_4$ (see below), and reasoned that treatment of $Tc_2Cl_4(PR_3)_4$ with molten aryl formamidines, ArN(H)C(H)NAr, might liberate volatile PR_3 and HCl(g), produced by the transfer of H^+ from the formamidine to the Cl^- ligands, and drive the reaction to equilibrium and concomitant formation of $Tc_2(ArNC(H)NAr)_4$. Instead, the reactions produced two types of higher-valent formamidinate complexes in low to moderate yield:[54]

$$Tc_2Cl_4(PR_3)_4 + HDPhF \xrightarrow{140\text{-}160\ ^\circ C,\ vacuum} Tc_2(DPhF)_3Cl_2 + Tc_2(DPhF)_4Cl$$

$$HCl + PR_3$$

Both reddish-purple $Tc_2(DTolF)_3Cl_2$ and red-orange $Tc_2(DPhF)_4Cl$ were structurally characterized.[54] The structure of $Tc_2(DTolF)_3Cl_2$ can be described as a variant of the familiar paddlewheel variety in which one of the bridging formamidinate ligands has been replaced by two chloride anions. At 2.0937(6) Å, the metal–metal bond length in $Tc_2(DTolF)_3Cl_2$ is among the shortest known Tc–Tc bonds. The structure of a related complex, $Tc_2(DPhF)_4Cl$, consists of four bridging formamidinate ligands in the traditional lantern motif (Fig. 7.4). The Tc–Tc bond length of 2.119(2) Å is more typical of structurally characterized complexes with a Tc_2^{5+} core. The chloride ligand occupies an axial position along the four-fold axis at a rather short distance of 2.450(4) Å from one of the Tc atoms. Unlike the situation in $Tc_2(hp)_4Cl$, there are no bridging chloride interactions in solid $Tc_2(DPhF)_4Cl$. The electrochemistry of the Tc_2^{5+}

Pictiva EX2004
Samsung v Pictiva
IPR2024-01094

formamidinate complexes, measured in methylene chloride/0.1 M $(Bu_4N)PF_6$, is rich with a reversible one-electron oxidation and a one-electron reduction for each complex. The potentials for $Tc_2(DTolF)_3Cl_2$ occur at -0.2 V and -1.5 V; those for $Tc_2(DPhF)_4Cl$ are -0.46 and -1.73 V (vs. Fc^+/Fc). Based on the electrochemistry, it is reasonable to postulate that compounds of the type $Tc_2[ArNC(H)NAr]_4Cl_2$ and $Tc_2[ArNC(H)NAr]_4$ might be isolable.[54]

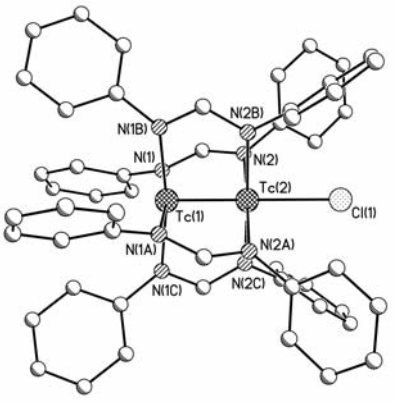


Fig. 7.4. Structure of $Tc_2(DPhF)_4Cl$.

Spin-restricted SCF-Xα-SW calculations were performed on the model complexes $Tc_2(HNCHNH)_4Cl$ and $Tc_2(HNCHNH)_3Cl_2$. For both systems the HOMO is the δ* orbital, and the (primarily) metal-based orbital ordering was calculated to be $\sigma<\pi<\delta<\delta^*<\pi^*<\sigma^*$.[54]

A green μ-sulfato complex of composition $K_2Tc_2(SO_4)_4{\cdot}2H_2O$ has been obtained[55] by treating $K_3Tc_2Cl_8{\cdot}2H_2O$ with 8 M sulfuric acid at ~100 °C for 1 h followed by slow cooling to room temperature. The structure of $K_2Tc_2(SO_4)_4{\cdot}2H_2O$ has been determined by P. A. Koz'min and coworkers,[7] and is similar to that of $[Re_2(SO_4)_4(H_2O)_2]^{2-}$.[56] The Tc–Tc distance is 2.155(1) Å.[7]

A penultimate set of Tc_2^{5+} species to discuss in this section are the $[Tc_2Cl_4(PR_3)_4]^+$ cations and the related neutral $Tc_2Cl_5(PR_3)_4$ complexes.[57] Mild chemical oxidation of purple $Tc_2Cl_4(PMe_2Ph)_4$ (see Section 7.5) with $[Fc]PF_6$ in acetonitrile provides green $[Tc_2Cl_4(PMe_2Ph)_4]PF_6$ in 82% yield. If the same reaction is carried out in the presence of additional chloride ion, one of the phosphines is substituted to give neutral, orange $Tc_2Cl_5(PMe_2Ph)_3$. Both complexes are paramagnetic, consistent with a ground state $\sigma^2\pi^4\delta^2\delta^{*1}$ electronic configuration. The X-ray crystal structure shows that the cation $[Tc_2Cl_4(PMe_2Ph)_4]^+$ adopts an eclipsed structure with an arrangement of ligands similar to that observed for the neutral counterpart (Fig. 7.5). The Tc–Tc bond length is 2.1074(9) Å compared to a Tc–Tc separation of 2.127(1) Å in the neutral Tc_2^{4+} counterpart $Tc_2Cl_4(PMe_2Ph)_4$. In this case, the bond length change is consistent with an increase in bond order (3 to 3.5) due to the removal of an electron from the δ* orbital.[57] The complex $Tc_2Cl_5(PMe_2Ph)_3$ is structurally similar to $[Tc_2Cl_4(PMe_2Ph)_4]PF_6$, and consists also of two eclipsed ML_4 fragments with a relatively short Tc–Tc separation of 2.1092(4) Å. Both $[Tc_2Cl_4(PMe_2Ph)_4]PF_6$ and $Tc_2Cl_5(PMe_2Ph)_3$ exhibit well resolved EPR spectra in frozen solution as expected for molecules with $\sigma^2\pi^4\delta^2\delta^{*1}$ ground states.[57]

Another cationic Tc_2^{5+} complex has recently been mentioned in the literature. Treatment of a pink methylene chloride solution containing β-$Tc_2Cl_4(dppe)_2$ with 1 equiv of the one-electron oxidant $NOPF_6$ provides a green solution from which green crystals of (presumably) $[Tc_2Cl_4(dppe)_2]PF_6$ are isolated.[58] No additional details are available at this time.

Pictiva EX2004
Samsung v Pictiva
IPR2024-01094

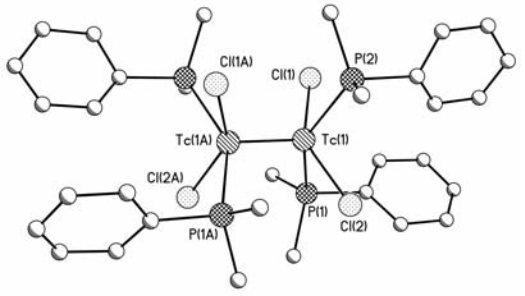


Fig. 7.5. Structure of the cation in $[Tc_2Cl_4(PMe_2Ph)_4]PF_6$.

7.5 Bonds of Order 3

The possibility that Tc_2^{4+} compounds can be prepared was first investigated by Spitsyn and co-workers,[25,33,48] and culminated in the successful structural characterization of such species.[59] It was first reported that reductions of mixtures that contained $MTcO_4$, M_2TcX_6, $M_3Tc_2X_8{\cdot}2H_2O$, or M_2TcOX_5 (M = NH_4 or K; X = Cl, Br) and concentrated HX in an H_2 atmosphere, and in an autoclave, affords brown or black crystalline Tc_2^{4+} compounds $M_2Tc_2X_6{\cdot}2H_2O$ (X = Cl or Br). While the details of the structures of $M_2Tc_2X_6{\cdot}2H_2O$ were not established for some time, clearly the properties of these compounds were consistent with the presence of a ditechnetium structural unit. The complexes dissolve readily in hot hydrohalic acid forming brown solutions that are rapidly oxidized in air, initially to $[Tc_2X_8]^{3-}$ and then to $[TcX_6]^{2-}$. The X-ray photoelectron spectra of $K_2Tc_2X_6{\cdot}2H_2O$ showed Tc 3d binding energies lower than those of Tc_2^{5+} compounds.[37]

The successful solution of the single crystal X-ray structure of $K_2Tc_2Cl_6$ was described a few years later.[59] Crystals of $K_2Tc_2Cl_6{\cdot}2H_2O$ from the mother liquor were unsuitable for X-ray analysis. However, a crystal of anhydrous $K_2Tc_2Cl_6$ was found above the meniscus of the mother liquor and structurally characterized. The structure is composed of potassium cations and polymeric $\{[Tc_2Cl_6]^{2-}\}_n$ anions (Fig. 7.6); the latter consist of "$[Tc_2Cl_8]$" fragments, possessing a staggered rotational geometry and a very short Tc–Tc distance of 2.044(1) Å, that are linked through chloride bridges. The assertion that the Tc–Tc bond has a multiplicity greater than four "since the M–M distance is about 0.1 Å shorter than the analogous distance in $[Tc_2Cl_8]^{2-}$ with a quaternary Tc–Tc bond",[59] is questionable. It is much more likely that $\{[Tc_2Cl_6]^{2-}\}_n$ are species that contain Tc–Tc triple bonds. Subsequently, this structural result has been verified and the observed Tc–Tc distance reinterpreted in terms of a triple bond.[60] It is reasonable to suppose[25,59] that the diamagnetic $[Tc_2X_6]^{2-}$ anions are intermediates in the formation of higher nuclearity clusters like $[Tc_6X_{12}]^{-}$ and $[Tc_6X_{12}]^{2-}$, which are discussed in Section 7.6.

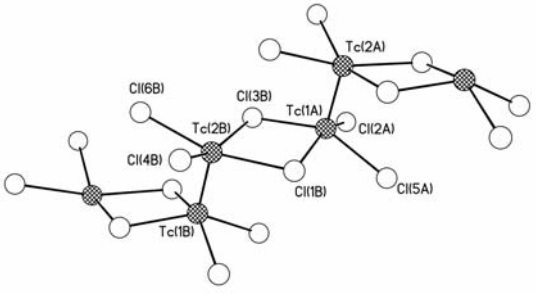
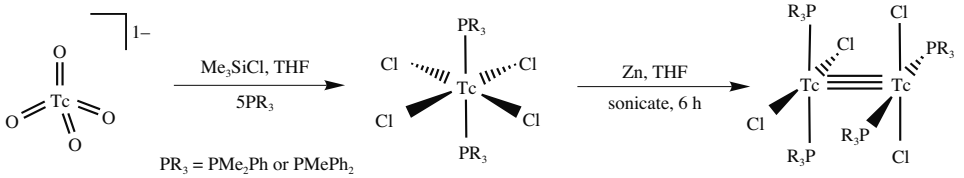


Fig. 7.6. Structure of polymeric $K_2Tc_2Cl_6$ showing the zig-zag chains of $[Tc_2Cl_8]$ units.

Pictiva EX2004
Samsung v Pictiva
IPR2024-01094

A series of triply metal–metal-bonded Tc_2^{4+} tertiary phosphine complexes of the general formula $Tc_2Cl_4(PR_3)_4$ have been prepared and characterized.[61] These compounds are intermediates for a number of other ditechnetium complexes in the same, higher (see Section 7.4), or lower oxidation states. The $Tc_2Cl_4(PR_3)_4$ complexes are prepared from mononuclear Tc^{4+} precursors of the type *trans*-$TcCl_4(PR_3)_2$. The starting materials with the alkyl phosphines PEt_3 and PPr^n_3 are prepared as blue solids via exchange with the known bis-triphenylphosphine compound *trans*-$TcCl_4(PPh_3)_2$.[62] Precursors with less basic phosphines, viz., *trans*-$TcCl_4(PMe_2Ph)_2$ and *trans*-$TcCl_4(PMePh_2)_2$, are prepared as green crystalline solids by treating a suspension of NH_4TcO_4 in THF with chlorotrimethylsilane and excess PR_3 followed by column chromatography on silica gel.[61] The mononuclear phosphine complexes are then combined with 1 equiv of zinc powder in dry, O_2-free benzene or THF in a Schlenk flask. Sonication (in a commercially available ultrasonic water cleaning bath) of the suspensions for 6 h results in almost quantitative yield of the air-sensitive purple $Tc_2Cl_4(PR_3)_4$ compounds that can be recrystallized from benzene/$(Me_3Si)_2O$:

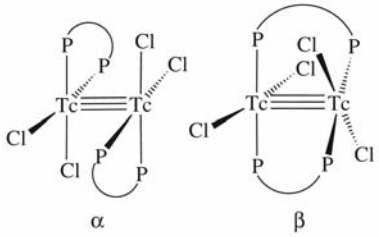


The complexes are readily soluble in aromatic solvents, THF, and methylene chloride. They are diamagnetic, exhibit sharp ^1H and $^{31}P\{^1H\}$ NMR spectra, and show a series of weak absorptions in the VIS/NIR region between 488 and 770 nm. The spectroscopic features, as might be expected, are quite similar to those of the related Re_2^{4+} compounds, $Re_2Cl_4(PR_3)_4$. Therefore, the lowest energy bands near 770 nm may be assigned as forbidden $\delta^* \rightarrow \pi^*$ transitions by analogy with that of the lowest energy transition in $Re_2Cl_4(PPr^n_3)_4$.[63] The structures of three of the complexes were elucidated. All consist of two *trans*-$TcCl_2(PR_3)_2$ fragments that are rotated 90° with respect to each other, to give an eclipsed geometry with approximate D_{2d} symmetry. The Tc–Tc distances are 2.133(3) Å, 2.127(1) Å, and 2.1384(5) Å for the PEt_3, PMe_2Ph and $PMePh_2$ complexes, respectively. Two reversible oxidation couples were measured electrochemically. Depending on the phosphine ligand, the first oxidation wave is found between -0.48 (PEt_3) and -0.26 V ($PMePh_2$) and the second at +0.88 and +0.92 V vs. Fc^+/Fc, respectively. The reversibility implies that syntheses of the mono- and dicationic species $[Tc_2Cl_4(PR_3)_4]^{2+/+}$ are possible. Indeed, mild chemical oxidation of $Tc_2Cl_4(PMe_2Ph)_4$ with $FcPF_6$ in acetonitrile produced green $[Tc_2Cl_4(PMe_2Ph)_4]^+$ in high yield (see Section 7.4). An attempt to oxidize $Tc_2Cl_4(PMe_2Ph)_4$ to $[Tc_2Cl_4(PMe_2Ph)_4]^{2+}$ with 2 equiv of $[p\text{-}BrC_6H_4)_3N]SbCl_6$ in acetonitrile was unsuccessful and resulted in the isolation and structural characterization of the monomeric Tc(IV) adduct $TcCl_4(PMe_2Ph)_2 \cdot 2SbCl_3$.[64]

Treatment of $Tc_2Cl_4(PR_3)_4$ (PR_3 = PEt_3 or PMe_2Ph) with 2 equiv of bis(diphenylphosphino)ethane (dppe) in refluxing toluene results in displacement of the monodentate phosphine ligands and formation of the pale pink β-isomer of $Tc_2Cl_4(dppe)_2$ (60% yield) whose structure was determined by X-ray crystallography,[58] and is depicted in 7.1. The β-$Tc_2Cl_4(dppe)_2$ isomer has a twist or torsion angle of 35(2) Å and a Tc–Tc separation of 2.117(1) Å. When $Tc_2Cl_4(PMe_2Ph)_4$ is refluxed with a ten-fold excess of dppe for 1 h, the mauve α-isomer of $Tc_2Cl_4(dppe)_2$ is formed in 80% isolated yield. The α-isomer has an eclipsed conformation and an average Tc–Tc bond length of 2.15[1] Å. Davison and coworkers have examined the reaction of $Tc_2Cl_4(PEt_3)_4$ with 2 equiv of bis(dimethylphosphino)methane (dppm) in refluxing benzene

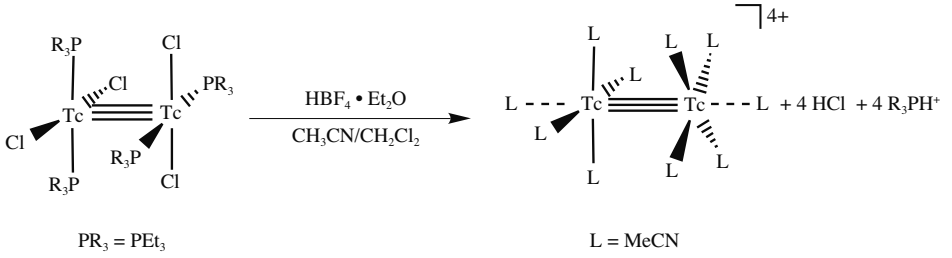
Pictiva EX2004
Samsung v Pictiva
IPR2024-01094

and obtained a 60% yield of the fuchsia colored $Tc_2Cl_4(\mu\text{-dppm})_2$. Crystallographic studies of the complex confirm the β-isomer with a twist angle of *c.* 51° and a Tc–Tc bond length of 2.1126(7) Å.[65]



7.1

Acidification of acetonitrile/methylene chloride solution (1:5) of $Tc_2Cl_4(PEt_3)_4$ with $HBF_4(Et_2O)$ (>8 equiv) followed by heating to *c.* 50 °C provides the bright blue solvated Tc_2^{4+} complex $[Tc_2(NCCH_3)_{10}](BF_4)_4$ in 80% isolated yield:[66]



Blue crystals are obtained by recrystallization from acetonitrile/ether. The procedure was adopted from a similar one that Dunbar and coworkers used to prepare $[Re_2(NCCH_3)_{10}](BF_4)_4$.[67,68] The dinuclear tetracation can also be prepared, albeit in lower yields, from higher valent starting materials such as $(Bu_4N)_2TcCl_6$ and $(Bu_4N)_2Tc_2Cl_8$.[66] Attempts to obtain a satisfactory structure from X-ray data collected on $[Tc_2(NCCH_3)_{10}](BF_4)_4$ were unsuccessful. Treatment of $[Tc_2(NCCH_3)_{10}](BF_4)_4$ with 8 equiv of thallium triflate, $Tl(O_3SCF_3)$, gave the triflate substituted complex $[Tc_2(NCCH_3)_8(O_3SCF_3)_2](BF_4)_2$ as a blue solid. It consists of two $Tc(NCCH_3)_4$ fragments which are linked by a short Tc–Tc triple bond of 2.122(1) Å. The pseudo-planar $[Tc(NCCH_3)_4]$ units are staggered with respect to each other, resulting in a torsion angle of 43.5° (Fig. 7.7).

If the axial triflate ligands are ignored, the remainder of the cation has approximate D_{4d} symmetry. A ground-state configuration of $\sigma^2\pi^4\delta^2\delta^{*2}$ is expected. The absence of δ-bonding between the technetium atoms implies a low energy rotation barrier between the two fragments, and the molecule adopts the sterically favored staggered geometry. The ^{1}H NMR spectrum of $[Tc_2(NCCH_3)_{10}](BF_4)_4$ in CD_3NO_2 contained two separate signals for coordinated acetonitrile at δ 3.0 and δ 2.0 ppm in a ratio of 4:1. These are assigned as the equatorial and axial nitrile ligands, respectively. The ^{1}H NMR spectrum of the same complex in CD_3CN initially shows resonances for the equatorial nitriles at δ 2.95 and free CH_3CN at δ 1.95 ppm, i.e., the axial nitriles rapidly exchange with the deuterated solvent. The electrochemistry of $[Tc_2(NCCH_3)_{10}](BF_4)_4$ in acetonitrile/0.1 M $(Bu_4N)PF_6$ shows a reversible one electron reduction at -0.82 V vs Fc^+/Fc which prompted a search for the $[Tc_2(NCCH_3)_{10}]^{3+}$ cation.

Pictiva EX2004
Samsung v Pictiva
IPR2024-01094

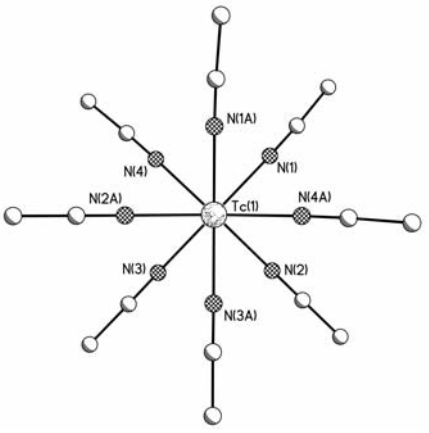
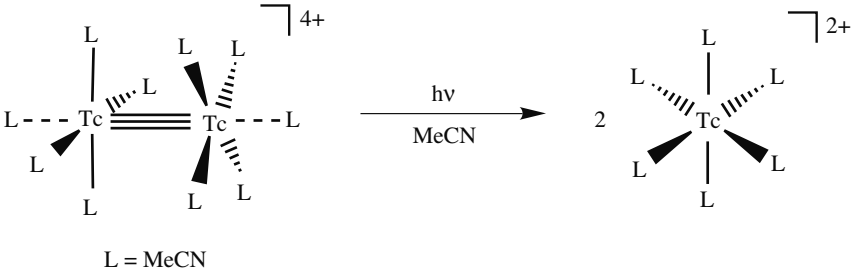


Fig. 7.7. View of the $[Tc_2(NCCH_3)_8]$ unit of $[Tc_2(NCCH_3)_8(O_3SCF_3)_2](BF_4)_2$ looking down the Tc–Tc bond.

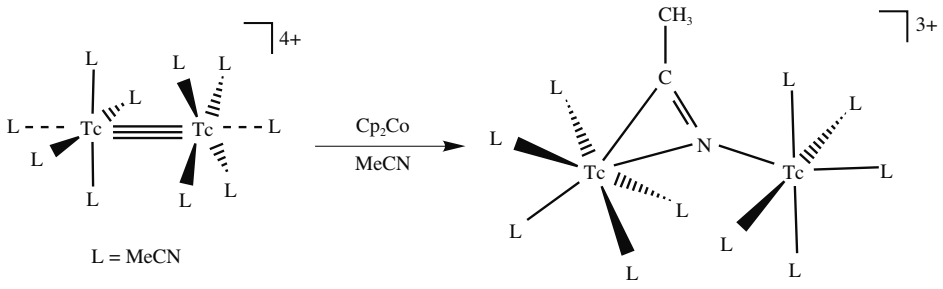
Bright blue acetonitrile solutions of $[Tc_2(NCCH_3)_{10}](BF_4)_4$ gradually lose their color when exposed to fluorescent light. While initially this color change was believed to be a consequence of deterioration of the glove box atmosphere where the samples were stored, this is not the case. Rather, a rare example of the photochemical scission of a metal–metal multiple bond was discovered.[69]



In this case $[Tc_2(NCCH_3)_{10}]^{4+}$ is converted to the solvated mononuclear Tc^{2+} complex $[Tc(NCCH_3)_6]^{2+}$. Under preparative conditions, using a 1000 W Hg vapor lamp, concentrated solutions of $[Tc_2(NCCH_3)_{10}](BF_4)_4$ are photolyzed for *c.* 90 min and pale yellow $[Tc(NCCH_3)_6](BF_4)_2$ (95% yield) is precipitated by careful addition of diethyl ether. The structure of $[Tc(NCCH_3)_6](BF_4)_2$ was determined and revealed a Tc center coordinated to six acetonitrile ligands, with almost ideal octahedral symmetry. The magnetic moment of the low spin d^5 complex is 2.1 B.M. as determined by the Evans method. Monitoring of the photochemical reaction indicated the process is not a simple one-step conversion. At least two intermediates are involved in the formation of the final product. A possible mechanism could be photoexcitation to a mixed-valent, charge-separated Tc^{1+}–Tc^{3+} species that undergoes bond cleavage and subsequent comproportionation to the observed Tc^{2+} species. Of note, $[Tc_2(NCCH_3)_{10}]^{4+}$ is stable in refluxing acetonitrile and the Re–Re triple bond of $[Re_2(NCCH_3)_{10}]^{4+}$ cannot be broken under similar photolytic conditions.[69]

Reduction of $[Tc_2(NCCH_3)_{10}](BF_4)_4$ in acetonitrile with 1 equiv of cobaltocene leads to a red-brown mixed-valence Tc^{1+}–Tc^{2+} complex $[Tc_2(NCCH_3)_{11}](BF_4)_3$ as shown in the following equation.[70]

Pictiva EX2004
Samsung v Pictiva
IPR2024-01094



The reaction is performed at ambient temperature, and the product is isolated in 70% yield. The X-ray crystal structure reveals an unusual μ,η^1,η^2 coordination mode of one of the acetonitrile ligands which is bridging via its nitrogen atom between Tc centers and through the nitrile carbon to one of the Tc centers. The Tc–Tc separation is 4.04(2) Å indicating the total loss of metal–metal bonding. The electrochemical reduction of $[Tc_2(NCCH_3)_{10}]^{4+}$ at -0.82 V in acetonitrile is reversible using scan rates ranging from 20 mV/s to 250 mV/s. On the chemical time scale, the cation $[Tc_2(NCCH_3)_{10}]^{4+}$ is reduced and then undergoes reaction and rearrangement to the final (isolated) product. Electrochemical studies indicate the mixed-valence complex can be further reduced at -1.12 V, probably to a bridged Tc^{1+}–Tc^{1+} complex. The observed oxidation at +0.25 V would correspond to a bridged Tc^{2+}–Tc^{2+} complex. Although these compounds have not been isolated, the observed redox chemistry is unparalleled among homoleptic acetonitrile complexes.

7.6 Hexanuclear and Octanuclear Technetium Clusters

For a particular metal oxidation state, an increase in cluster size should be paralleled by a decrease in the average M–M bond order. An example of this trend is provided by the pair of Mo^{2+} cluster anions $[Mo_2Cl_8]^{4-}$ and $[Mo_6Cl_{14}]^{2-}$ where the Mo–Mo bond order decreases from four to one as the number of pairwise Mo–Mo interactions for each Mo atom increases from one to four. For octahedral Tc^{3+} and Re^{3+}clusters based upon the 24-electron M_6^{18+} cores, the average M–M bond order should be one, like that for the isoelectronic Mo_6^{12+} core. This expectation has not been realized for Tc and Re as halo species of the types $[M_6X_{12}]^{6+}$ or M_6X_{18} have not yet been prepared. A related question is how the properties and structures of Tc (or Re) hexanuclear clusters might change as the electron count *increases*, i.e., as the average metal oxidation state decreases. This question, to some degree at least, has been answered with the synthesis of molecules containing Tc_6^{12+}, Tc_6^{11+}, and Tc_6^{10+} cores.

The reduction of $(Me_4N)_2TcCl_6$ or $(Me_4N)TcO_4$ in concentrated hydrochloric acid by molecular hydrogen (30-50 atm) in an autoclave at 140-180 °C yields a mixture of dark brown almost black crystals of different geometric shapes.[25,71] These crystals are a mixture of two hexanuclear species, brown $(Me_4N)_3\{[Tc_6Cl_6(\mu\text{-}Cl)_6]Cl_2\}$ and black $(Me_4N)_2[Tc_6Cl_6(\mu\text{-}Cl)_6]$. The former is formed in high yield at 140-150 °C under an initial H_2 pressure of 30-50 atm. Optimal conditions for the synthesis of $(Me_4N)_2[Tc_6Cl_6(\mu\text{-}Cl)_6]$ are more forcing and require temperatures of 160-180 °C. The $\{[Tc_6Cl_6(\mu\text{-}Cl)_6]Cl_2\}^{3-}$ and $[Tc_6Cl_6(\mu\text{-}Cl)_6]^{2-}$ clusters are derivatives of Tc_6^{11+} and Tc_6^{10+} cores with 31- and 32-electron counts, respectively. Both compounds have been described as being paramagnetic. While a magnetic moment of ~1.7 B.M. for $(Me_4N)_3\{[Tc_6(\mu\text{-}Cl)_6Cl_6]Cl_2\}$ is consistent with the presence of one unpaired electron, a value of ~1.1 B.M. reported for $(Me_4N)_2[(Tc_6Cl_6)Cl_6]$, as well as an EPR signal, may be due to the presence of a paramagnetic impurity. The trigonal prismatic structure of the chloro anions is as represented in Fig. 7.8.[72,73] The unsupported rectangular edge Tc–Tc bonds are very short, 2.16(1) Å for the $[Tc_6Cl_{12}]^{-}$ anion and 2.22(1) Å for $[Tc_6Cl_{12}]^{2-}$, whereas

Pictiva EX2004
Samsung v Pictiva
IPR2024-01094

the triangular edge distances are indicative of much weaker Tc–Tc bonding. The average Tc–Tc distances for the latter bonds are 2.69(1) Å and 2.57(1) Å, respectively, in the two structures. The related 31e$^-$ trigonal prismatic bromide cluster $(Me_4N)_3\{[Tc_6(\mu\text{-}Br)_6Br_6]Br_2\}$has been synthesized by the reaction of the analogous chloride complex with concentrated hydrobromic acid at 180 °C under a pressure of H_2 in an autoclave.[74] The structure is similar to $(Me_4N)_3\{[Tc_6(\mu\text{-}Cl)_6Cl_6]Cl_2\}$ with Tc–Tc distances of 2.154(5) Å and 2.702(2) Å.[74] When $(Et_4N)_2TcCl_6$ is reduced by H_2 in concentrated hydrobromic acid under similar conditions, a different cluster is obtained. The resulting dark brown salt is $(Et_4N)_2\{[Tc_6(\mu\text{-}Br)_6Br_6]Br_2\}$, a derivative of the diamagnetic Tc_6^{12+} core with a 30-electron count.[74] The structure of this anion is similar to those of the 31- and 32-electron species with Tc–Tc distances in $(Et_4N)_2\{[Tc_6(\mu\text{-}Br)_6Br_6]Br_2\}$ of 2.188(5) Å and 2.66(2) Å.[74]

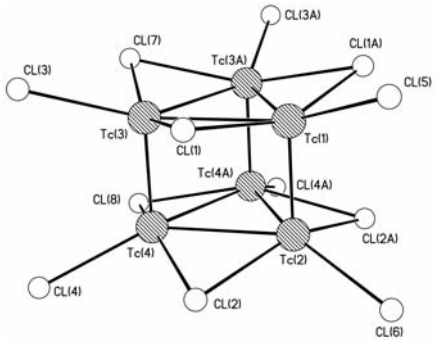


Fig. 7.8. Structure of the trigonal prismatic cluster anion, $[Tc_6Cl_6(\mu\text{-}Cl)_6]^-$ in $(Me_4N)_3\{[Tc_6(\mu\text{-}Cl)_6Cl_6]Cl_2$. Capping chloride ions have been omitted. The structure of $[Tc_6Cl_6(\mu\text{-}Cl)_6]^{2-}$ is similar.

A detailed treatment of the bonding in 30- to 32-electron chloro clusters by Wheeler and Hoffmann has shown that 30 electrons are involved in the metal–metal bonding and the additional one or two electrons occupy a weakly antibonding Tc–Tc orbital that is π* with respect to the dinuclear species and weakly bonding in the triangles.[75,76] The 30 electrons are partitioned between three electron-rich Tc≡Tc bonds and six Tc–Tc single bonds. The model developed for the hexanuclear chloro compounds does not fit the 30- and 31-electron bromide clusters. Here the Tc–Tc bond length *decreases* on going from Tc_6^{12+} to Tc_6^{11+} which is inconsistent with population of an a_2'' orbital that is π-antibonding within the dimers. It would seem that additional theoretical work will be needed to fully understand the bonding in these remarkable compounds.

Additional technetium cluster compounds of even higher nuclearity are synthesized from concentrated HBr and HI solutions. The series of octanuclear Tc bromide cluster compounds $[Tc_8(\mu\text{-}Br)_8Br_4]Br{\cdot}2H_2O$,[77,78] $(H_5O_2)[Tc_8(\mu\text{-}Br)_8Br_4]Br$,[78,79] and $(H_5O_2)_2[Tc_8(\mu\text{-}Br)_8Br_4]Br_2$[78] has been described and all are based upon the cluster unit shown in Fig. 7.9. The $[Tc_8(\mu\text{-}Br)_8Br_4]^+$ cluster has properties consistent with the presence of one unpaired electron.[80] The four types of Tc–Tc bonds in these clusters have quite different distances, as illustrated in the case of the $[Tc_8(\mu\text{-}Br)_8Br_4]^+$ cluster by values for the distances Tc(1)–Tc(2), Tc(1)–Tc(4), Tc(3)–Tc(4), and Tc(3)–Tc(4A) of 2.145(2) Å, 2.689(2) Å, 2.521(2) Å and 2.147(2) Å, respectively. The clusters clearly possess four Tc–Tc bonds of high multiplicity. A consideration of the bonding in this cluster type has led to the conclusion[75] that these four Tc–Tc bonds are electron-rich triple bonds and similar to the triple bonds present in trigonal prismatic $[Tc_6Cl_{12}]^{n-}$ clusters (see above). These four Tc_2 units are then bound together by overlap of five δ and δ* type orbitals, four of which are associated mainly with bonds around the rhomboidal top and bottom faces,

Pictiva EX2004
Samsung v Pictiva
IPR2024-01094

while the remaining pair of δ- and δ*-orbitals are concentrated on atoms located in the prisms' shared face.[75] The mixed bromide-iodide cluster $(Bu_4N)_2[Tc_8(\mu\text{-}Br)_4(\mu\text{-}I)_4Br_2I_2]I_2$ has been reported as the product of the reaction of $(H_5O_2)_2[Tc_8(\mu\text{-}Br)_8Br_4]Br_2$ with concentrated hydriodic acid and NBu^n_4OH in acetone. The identity of the cluster was confirmed by a single crystal X-ray structure determination.[81] In addition, an unusual ferrocinium salt of the Tc iodide cluster anion $\{[Tc_6(\mu\text{-}I)_6I_6]I_2\}^{3-}$ has been isolated and structurally characterized.[52]

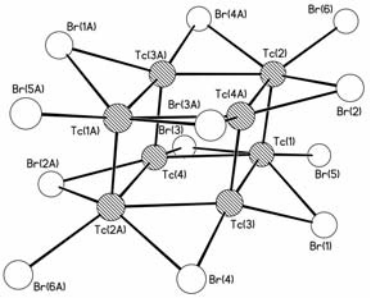


Fig. 7.9. Structure of $[Tc_8(\mu\text{-}Br)_8Br_4]^+$ cation in $[Tc_8(\mu\text{-}Br)_8Br_4]Br{\cdot}2H_2O$.

References

1. C. Perrier and E. Segré, *J. Chem. Phys.* **1937**, *5*, 712.
2. C. Perrier and E. Segré, *Nature (London)* **1937**, *140*, 193.
3. K. V. Kotegov, O. N. Pavlov and V. P. Shvedov, *Adv. Inorg. Chem. Radiochem.* **1968**, *2*, 1.
4. The Oak Ridge isotope catalog is available online at http://www.ornl.gov/isotopes/catalog.html
5. F. A. Cotton, G. Wilkinson, C. A. Murillo and M. Bochmann, *Advanced Inorganic Chemistry*, 6 th ed., John Wiley and Sons: New York, 1999, Chapter 18-D.
6. R. Alberto, in *Comprehensive Coordination Chemistry II, Vol. 5* (Eds.: J. A. McCleverty and T. J. Meyer), Elsevier Science, Inc.: London, 2004, p. 127.
7. S. V. Kryutchkov, *Topics in Current Chemistry* **1996**, *176*, 189.
8. S. V. Kryutchkov, *Russ. Chem. Rev.* **1998**, *67*, 883.
9. G. Bandoli, A. Dolmella, M. Porchia, F. Refosco and F. Tisato, *Coord. Chem. Rev.* **2001**, *214*, 43.
10. J. D. Eakins, D. G. Humphreys and C. E. Mellish, *J. Chem. Soc.* **1963**, 6012.
11. F. A. Cotton and E. Pedersen, *Inorg. Chem.* **1975**, *14*, 383.
12. F. A. Cotton and W. K. Bratton, *J. Am. Chem. Soc.* **1965**, *87*, 921.
13. W. K. Bratton and F. A. Cotton, *Inorg. Chem.* **1970**, *9*, 789.
14. Y. V. Rakitin, S. V. Kryuchkov, A. I. Aleksandrov, A. F. Kuzina, N. V. Nemtsev, B. G. Ershov and V. I. Spitsyn, *Dokl. Phys. Chem.* **1983**, *269*, 253.
15. Y. V. Rakitin and V. I. Nefedov, *Russ. J. Inorg. Chem.* **1984**, *29*, 294.
16. F. A. Cotton and B. J. Kalbacher, *Inorg. Chem.* **1977**, *16*, 2386.
17. F. A. Cotton, P. E. Fanwick, L. D. Gage, B. Kalbacher and D. S. Martin, *J. Am. Chem. Soc.* **1977**, *99*, 15642.
18. F. A. Cotton and E. Pedersen, *J. Am. Chem. Soc.* **1975**, *97*, 303.
19. M. I. Glinkina, A. F. Kuzina and V. I. Spitsyn, *Russ. J. Inorg. Chem.* **1973**, *18*, 210.
20. P. A. Koz'min and G. N. Novitskaya, *Russ. J. Inorg. Chem.* **1972**, *17*, 1652.
21. F. A. Cotton and L. W. Shive, *Inorg. Chem.* **1975**, *14*, 2032.
22. F. A. Cotton, A. Davison, V. W. Day, M. F. Fredrich, C. Orvig and R. Swanson, *Inorg. Chem.* **1982**, *21*, 1211.
23. V. I. Spitsyn, A. F. Kuzina, A. A. Oblova and L. I. Belyaeva, *Dokl. Akad. Nauk. SSSR* **1977**, *237*, 1126.

Pictiva EX2004
Samsung v Pictiva
IPR2024-01094

24. V. I. Spitsyn, A. F. Kuzina, A. A. Oblova, S. V. Kryuchkov and L. I. Belyaeva, *Dokl. Acad. Nauk. SSSR* **1977**, *237*, 1412.
25. V. I. Spitsyn, A. F. Kuzina, A. A. Oblova and S. V. Kryuchkov, *Russ. Chem. Rev.* **1985**, *54*, 373.
26. K. Schwochau, K. Hedwig, H. J. Schenk and O. Greis, *Inorg. Nucl. Chem. Lett.* **1977**, *13*, 77.
27. F. A. Cotton, A. Davison, V. W. Day, L. D. Gage and H. S. Trop, *Inorg. Chem.* **1979**, *18*, 3024.
28. K. Schwochau, in *In Handbuch der Präparativen Anorganischen Chemie, Vol. 26* (Ed.: G. Brauer), Enke: Stuttgart: Germany, **1981**, 1597.
29. W. Preetz and G. Peters, *Z. Naturforsch.* **1980**, *35b*, 797.
30. F. A. Cotton, L. Daniels, A. Davison and C. Orvig, *Inorg. Chem.* **1981**, *20*, 3051.
31. F. A. Cotton, K. R. Dunbar, L. R. Falvello, M. Tomás and R. A. Walton, *J. Am. Chem. Soc.* **1983**, *105*, 4950.
32. V. I. Spitsyn, A. F. Kuzina and S. V. Kryuchkov, *Russ. J. Inorg. Chem.* **1980**, *25*, 406.
33. S. V. Kryuchkov, A. F. Kuzina and V. I. Spitsyn, *Russ. J. Inorg. Chem.* **1983**, *28*, 1124.
34. S. V. Kryuchkov and A. E. Simonov, *Bull. Acad. Sci. USSR* **1987**, *36*, 1991.
35. W. Preetz, G. Peters and D. Bublitz, *J. Cluster Sci.* **1994**, *5*, 83.
36. G. Peters, J. Scowronek and W. Preetz, *Z. Naturforsch.* **1992**, *47A*, 591.
37. V. N. Gerasimov, S. V. Kryuchkov, A. F. Kuzina, V. M. Kulakov, S. V. Pirozhkov and V. I. Spitsyn, *Dokl. Phys. Chem.* **1982**, *266*, 688.
38. V. I. Spitsyn, A. F. Kuzina, S. V. Kryuchkov and A. E. Simonov, *Russ. J. Inorg. Chem.* **1987**, *32*, 1278.
39. F. A. Cotton and L. D. Gage, *Nouv. J. Chim.* **1977**, *1*, 441.
40. L. I. Zaitseva, A. S. Kotel'nikova and A. A. Rezvov, *Russ. J. Inorg. Chem.* **1980**, *25*, 1449.
41. J. Skowronek and W. Preetz, *Z. Naturforsch.* **1992**, *47B*, 482.
42. J. Skowronek, W. Preetz and S. M. Jessen, *Z. Naturforsch.* **1991**, *46B*, 1305.
43. J. Skowronek and W. Preetz, *Z. anorg. allg. Chem.* **1992**, *615*, 73.
44. V. I. Spitsyn, B. Baierl, S. V. Kryuchkov, A. F. Kuzina and M. Varen, *Dokl. Akad. Nauk.* **1981**, *256*, 608.
45. P. A. Koz'min, T. B. Larina and M. D. Surazhskaya, *Sov. J. Coord. Chem.* **1982**, *8*, 451.
46. P. A. Koz'min, T. B. Larina and M. D. Surazhskaya, *Koord. Khim.* **1981**, *7*, 1719.
47. V. I. Nefedov and P. A. Koz'min, *Inorg. Chim. Acta* **1982**, *64*, L177.
48. S. V. Kryuchkov, A. F. Kuzina and V. I. Spitsyn, *Dokl. Chem.* **1982**, *266*, 304.
49. P. A. Koz'min, T. B. Larina and M. D. Surazhskaya, *Koord. Khim.* **1983**, *9*, 1114.
50. Y. V. Radikin, S. V. Kryuchkov, A. I. Aleksandrov, A. F. Kuzina, N. V. Nemtsev, B. G. Ershov and V. I. Spotzin, *Dokl. Akad. Nauk. SSSR* **1983**, *269*, 253.
51. N. A. Baturin, K. E. German, M. S. Grigoriev and S. V. Kryuchkov, *Sov. J. Coord. Chem.* **1991**, *17*, 732.
52. M. S. Grigoriev and S. V. Kryutchkov, *Radiochim. Acta* **1993**, *63*, 187.
53. F. A. Cotton, P. F. Fanwick and L. D. Gage, *J. Am. Chem. Soc.* **1980**, *102*, 1570.
54. F. A. Cotton, S. C. Haefner and A. P. Sattelberger, *Inorg. Chem.* **1996**, *35*, 7350.
55. S. V. Kryuchkov and A. E. Simonov, *Sov. J. Coord. Chem.* **1990**, *16*, 191.
56. F. A. Cotton, B. A. Frenz and L. W. Shive, *Inorg. Chem.* **1975**, *14*, 649.
57. F. A. Cotton, S. C. Haefner and A. P. Sattelberger, *Inorg. Chem.* **1996**, *35*, 1831.
58. F. A. Cotton, L. M. Daniels, S. C. Haefner and A. P. Sattelberger, *Inorg. Chim. Acta* **1999**, *288*, 69.
59. S. V. Kryuchkov, M. S. Grigorev, A. F. Kuzina, B. F. Gulev and V. I. Spitsyn, *Dokl. Chem.* **1986**, *288*, 147.
60. F. A. Cotton, L. M. Daniels, L. R. Falvello, M. S. Grigoriev and S. V. Kryuchkov, *Inorg. Chim. Acta* **1991**, *189*, 53.
61. C. J. Burns, A. K. Burrell, F. A. Cotton, S. C. Haefner and A. P. Sattelberger, *Inorg. Chem.* **1994**, *33*, 2257.
62. J. E. Fergusson and P. F. Heveldt, *J. Inorg. Nucl. Chem.* **1976**, *38*, 2231.
63. B. E. Bursten, F. A. Cotton, P. E. Fanwick, G. G. Stanley and R. A. Walton, *J. Am. Chem. Soc.* **1982**, *105*, 2606.

Pictiva EX2004
Samsung v Pictiva
IPR2024-01094

64. F. A. Cotton, S. C. Haefner and A. P. Sattelberger, *Inorg. Chim. Acta* **1998**, *271*, 187.
65. E. Freiberg, A. Davison, A. G. Jones and W. M. Davis, *Inorg. Chem. Commun.* **1999**, *2*, 516.
66. J. C. Bryan, F. A. Cotton, L. M. Daniels, S. C. Haefner and A. P. Sattelberger, *Inorg. Chem.* **1995**, *34*, 1875.
67. S. N. Bernstein and K. R. Dunbar, *Angew. Chem., Int. Ed. Engl.* **1992**, *31*, 1360.
68. S. L. Bartley, S. N. Bernstein and K. R. Dunbar, *Inorg. Chim. Acta* **1993**, *213*, 213.
69. F. A. Cotton, S. C. Haefner and A. P. Sattelberger, *J. Am. Chem. Soc.* **1996**, *118*, 5486.
70. F. A. Cotton, S. C. Haefner and A. P. Sattelberger, *Inorg. Chim. Acta* **1997**, *266*, 55.
71. K. E. German, S. V. Kryuchkov, A. F. Kuzina and V. I. Spitsyn, *Dokl. Chem.* **1986**, *288*, 139.
72. P. A. Koz'min, T. B. Larina and M. D. Surazhskaya, *Dokl. Phys. Chem.* **1983**, *271*, 577.
73. P. A. Koz'min, M. D. Surazhskaya and T. B. Larina, *Sov. J. Coord. Chem.* **1985**, *11*, 888.
74. S. V. Kryuchkov, M. S. Grigoriev, A. I. Yanovskii, Y. T. Struchkov and V. I. Spitsyn, *Dokl. Chem.* **1988**, *297*, 520.
75. R. A. Wheeler and R. Hoffmann, *J. Am. Chem. Soc.* **1986**, *108*, 6605.
76. R. A. Wheeler and R. Hoffmann, *Angew. Chem.* **1986**, *98*, 828.
77. S. V. Kryuchkov, M. S. Grigoriev, A. F. Kuzina, B. F. Gulev and V. I. Spitsyn, *Dokl. Chem.* **1986**, *288*, 172.
78. V. I. Spitzin, S. V. Kryuchkov, M. S. Grigoriev and A. F. Kuzina, *Z. anorg. allg. Chem.* **1988**, *563*, 136.
79. P. A. Koz'min, M. D. Surazhskaya and T. B. Larina, *Dokl. Phys. Chem.* **1982**, *265*, 656.
80. S. V. Kryuchkov, A. F. Kuzina and V. I. Spitzin, *Z. anorg. allg. Chem.* **1988**, *563*, 153.
81. S. V. Kryuchkov, M. S. Grigoriev, A. I. Yanovskii, Y. T. Struchkov and V. I. Spitsyn, *Dokl. Chem.* **1988**, *301*, 219.

Pictiva EX2004
Samsung v Pictiva
IPR2024-01094

8

Rhenium Compounds

Richard A. Walton,
Purdue University

8.1 The Last Naturally Occurring Element to Be Discovered

One reason so much of the chemistry of rhenium was not developed until the last few decades is that the element itself was not discovered until 1925. In its relationship to its group 7 congeners, rhenium is rather special. In all other groups of transition elements, the 4*d* element is about as common as the 5*d* element and in several cases it served as a guide to the properties that might be helpful in isolating the heaviest member of the group. This was the case with hafnium, for example, which was identified only two years earlier than rhenium. The 4*d* element in group 7 is, of course, technetium and it is not found in Nature. Indeed in its initial isolation from the products of deuteron bombardment of molybdenum a number of years later (1939) the standard scenario was reversed. Prior knowledge of the chemistry of rhenium helped in designing procedures to separate technetium. Of course, the 3*d* element can provide some guidance as to the chemistry of its heavier congeners, but it always differs far more from the heavier two than they do from each other.

Beginning in about 1922 Dr. Walter Noddack and Dr. Ida Tacke (who in 1926 became Mrs. Noddack), see Fig. 8.1, who were employed in the Physico-Technical Testing Office in Berlin began to search for both element 43 (technetium) and element 75 (rhenium) in a number of ores that were known to contain the elements with similar atomic numbers. It was already recognized in those days that elements of odd atomic number (Z) were systematically less abundant than those of even Z and Noddack and Tacke were able to make an approximate forecast of the extent to which they might have to concentrate various ores before either of the missing elements would become detectable. They counted on similarities to manganese chemistry in designing their concentration procedures and expected to use X-ray spectra to detect the new elements.

After several years of work, an approximately 100,000-fold concentration of the group 7 elements in a sample of the mineral gadolinite was accomplished. With Dr. Otto Berg of the Siemens Company, an X-ray spectroscopic analysis revealed that element 75 was present. Using the mineral columbite a ponderable quantity of the element was isolated as the oxide, Re_2O_7, and it was named rhenium after the river Rhine. The X-ray spectra were also thought to have lines for element 43, but later work leaves no doubt that this was an error. By 1928-1929 gram quantities of rhenium had been isolated and detailed study of the chemistry was begun.[1]

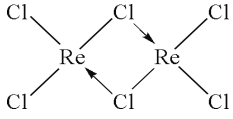
Pictiva EX2004
Samsung v Pictiva
IPR2024-01094



Fig. 8.1. Walter and Ida (Tacke) Noddack, the discoverers of the element rhenium. These photographs were kindly provided by Professor Otto Glemser.

It is remarkable that rhenium chemistry has proved to be the vehicle for the discovery of the first examples of *all* the multiple bonds, double, triple, and quadruple, between transition metal atoms. Rhenium trichloride and bromide were discovered[2,3] in 1933 and a short time later the complexes of empirical formula $RbReCl_4$ and $CsReCl_4$ were reported.[4] However, these compounds were not correctly formulated as Re_3 clusters with Re–Re double bonds until 1963. As late as 1962 in an authoritative review[5] of "Recent Developments in the Chemistry of Rhenium and Technetium" it was stated that:

> The well-known diamagnetic four-coordinate complexes of Re^{III} include the $[ReCl_4]^-$ ion. The simple Re^{III} chloride and bromide are presumably dimeric with halogen bridges, viz.



The correct formulation[6] of these compounds, with their double bonds, was soon followed by the recognition[7] of the quadruple bond in $[Re_2Cl_8]^{2-}$ and the first triple bond[8] in $Re_2Cl_5(CH_3SCH_2CH_2SCH_3)_2$. The events leading to about this point are reviewed in Chapter 1. Our purpose now is to present systematically the chemistry of dirhenium compounds with Re–Re multiple bonds. The literature up to the end of 1991 was covered comprehensively in the two previous editions of *Multiple Bonds Between Metal Atoms*[9,10] and in a review published in 1985.[11] Since the publication of the second edition,[10] a more limited review of recent aspects of the chemistry of Tc and Re compounds that contain M–M bonds has become available.[12] The present chapter will cover the literature up to the end of 2003 in a fully comprehensive fashion, but some topics will not be afforded the same detailed coverage they received in the previous edition, so the earlier text[10] may still serve as a useful reference.

Although the chemistry of triangular $[Re_3]^{9+}$ clusters that contain Re=Re bonds was covered in previous editions of this text,[9,10] these compounds will not be reviewed in this new addition. Instead, all higher nuclearity halide clusters of rhenium in which Re–Re multiple bonds are present will be the subject of a separate review that will be published elsewhere.[438]

Pictiva EX2004
Samsung v Pictiva
IPR2024-01094

8.2 Synthesis and Structure of the Octachlorodirhenate(III) Anion

While the high pressure reduction of $KReO_4$ and NH_4ReO_4 by molecular hydrogen in concentrated hydrochloric acid is interesting for historical reasons as an early route to salts of the $[Re_2Cl_8]^{2-}$ anion,[13,14] this method has subsequently been used little. Among the reasons for this are corrosion of the pressure bomb and other practical difficulties such as the competing formation of $[ReCl_6]^{2-}$.[15-17] In addition, the salt $(Bu_4N)_2Re_2Cl_8$, whose favorable solubility properties in a wide range of organic solvents make it the obvious choice for exploring the chemical reactivity of $[Re_2Cl_8]^{2-}$, is available in good yield by more desirable routes. Nonetheless, the hydrogen reduction method does have certain features of note. It has in the past been the only source of the potassium and ammonium salts of $[Re_2Cl_8]^{2-}$. These salts were in turn used as intermediates for the synthesis of other alkali metal salts of $[Re_2Cl_8]^{2-}$, such as the cesium compound $Cs_2Re_2Cl_8{\cdot}H_2O$.[18] More recently, the autoclave reduction of $(Et_4N)ReO_4$ by dihydrogen in hydrochloric acid has been used to prepare $(Et_4N)_2Re_2Cl_8$.[19] As might be expected, the ammonium and rubidium compounds, which are isolated as dihydrates, are isostructural with $K_2Re_2Cl_8{\cdot}2H_2O$,[20] whereas $Cs_2Re_2Cl_8{\cdot}H_2O$ has a different structure,[18,20,21] although all of them contain the $[Re_2Cl_8]^{2-}$ anion.

The synthesis of the tetra-*n*-butylammonium salt $(Bu_4N)_2Re_2Cl_8$ in 1965 by the hypophosphorous acid reaction of $[ReO_4]^-$ in aqueous hydrochloric acid provided ready access to a salt of $[Re_2Cl_8]^{2-}$ that had good solubility in a variety of polar organic solvents;[14,22] this was important in enabling studies of the reaction chemistry of $[Re_2Cl_8]^{2-}$ to be carried out in non-aqueous media. The major disadvantage of this synthetic method is the relatively low yield (<40%) in which this salt is isolated, so that over the years alternative synthetic routes have been sought. These have included the reaction of Re_3Cl_9 with an excess of molten diethylammonium chloride which leads to the disruption of the Re_3 cluster and the formation of $(Et_2NH_2)_2Re_2Cl_8$.[23,24] This method in turn suffers from one important disadvantage, namely, it requires a ready source of Re_3Cl_9. Another route involves the reaction of the rhenium(III) benzoate complex $Re_2(O_2CPh)_4Cl_2$, itself a compound that contains a Re–Re quadruple bond (see Section 8.4.2), with gaseous hydrogen chloride in methanol in the presence of cations such as tetra-*n*-butylammonium and tetraphenylarsonium.[25] This non-aqueous procedure has been adapted to produce the $[Re_2Br_8]^{2-}$ and $[Re_2I_8]^{2-}$ anions (see Section 8.3). A slight variation of this method, employing alkyl carboxylates of the type $Re_2(O_2CR)_4Cl_2$ in concentrated hydrochloric acid, has been used to prepare $(Ph_4As)_2Re_2Cl_8$ and $Cs_2Re_2Cl_8{\cdot}H_2O$.[14,21] There are other reactions in which $[Re_2Cl_8]^{2-}$ can be generated,[26-28] including some that involve mononuclear starting materials,[26,27] but these are not useful synthetic routes.

All of the preceding synthetic routes to $(Bu_4N)_2Re_2Cl_8$ and other salts with solubilizing organic cations have now been replaced by a much more convenient method. This straightforward one-pot synthesis involves the reaction of $(Bu_4N)ReO_4$ with refluxing benzoyl chloride at *c.* 210 °C, followed by the addition of an HCl(g) saturated solution of $[Bu_4N]^+$ in ethanol.[29] By this means, $(Bu_4N)_2Re_2Cl_8$ can be prepared easily, quickly and in very high yield (*c.* 90%).

$$2(Bu_4N)ReO_4 + 8PhCOCl \rightarrow (Bu_4N)_2Re_2Cl_8 + \text{organic products}$$

It is believed[29(a)] that this reaction proceeds via the intermediacy of $Re_2(O_2CPh)_2Cl_4$, with the role of PhCOCl being to reduce and chlorinate the rhenium centers and couple them via the agency of benzoate bridges. The complex $ReOCl_3(PPh_3)_2$ can be used as an alternative starting material,[29(a)] but since it is itself prepared from $[ReO_4]^-$ this offers no real advantage.

The compound $(Bu_4N)_2Re_2Cl_8$ undergoes cation exchange reactions with various organic mono- and dications to afford other salts of the $[Re_2Cl_8]^{2-}$ anion.[30,31] In the case of $(R_3PCH_2CH_2PR_3)Re_2Cl_8$ (R = Cy or Ph), the reactions of the phosphine R_3P with either

Pictiva EX2004
Samsung v Pictiva
IPR2024-01094

$(Bu_4N)_2Re_2Cl_8$ or *cis*-$Re_2(\mu\text{-}O_2CCH_3)_2Cl_4(py)_2$ in refluxing 1,2-dichloroethane can be used to give these salts.[31] Alternatively, salts with organic cations can be obtained[32] directly from solutions of $[Re_2Cl_8]^{2-}$ that are generated by the reaction of $(Bu_4N)ReO_4$ with PhCOCl,[29] without first isolating $(Bu_4N)_2Re_2Cl_8$.

Crystal structure determinations on the salts $Cs_2Re_2Cl_8{\cdot}H_2O$ and $(Bu_4N)_2Re_2Cl_8$ have, in recent years, confirmed the essential structural features first established for the $[Re_2Cl_8]^{2-}$ anion in its potassium[7(c)] and pyridinium salts and discussed at some length in Chapter 1. The unit cell of the cesium salt $Cs_2Re_2Cl_8{\cdot}H_2O$ contains four $[Re_2Cl_8]^{2-}$ anions, two of which are anhydrous and the other two hydrated, with both axial positions occupied by water molecules (r(Re–O) = 2.66(3) Å).[21] The Re–Re distance in the hydrated anion is, as expected, slightly longer (2.252(2) Å) than in the anhydrous species (2.237(2) Å). This result corrected an earlier structure determination[18,20] that had led to the erroneous conclusion that $[Re_2Cl_8(H_2O)_2]^{2-}$ had an appreciably *shorter* Re–Re distance than $[Re_2Cl_8]^{2-}$ (2.210 Å versus 2.226 Å).

The structure of the tetra-*n*-butylammonium salt $(Bu_4N)_2Re_2Cl_8$ is of importance for two reasons. First it established the structure of the salt from which most of the reaction chemistry of the $[Re_2Cl_8]^{2-}$ anion has been developed (vide infra). Second, the study of the polarized crystal spectrum[33] of this complex, so important to unraveling the details of the electronic structure of this molecule, required prior knowledge of the crystal structure. The usual eclipsed rotational conformation with a Re–Re distance of 2.222(2) Å was found[33] in the structure determination. However, a complication in the structure solution was the observation that $(Bu_4N)_2Re_2Cl_8$ possesses a subtle form of disorder (Fig. 8.2), which is of a kind found subsequently with many other species of the type M_2X_8, including other salts of the $[Re_2X_8]^{2-}$ anions. When this type of orientational disorder is encountered it is usually a 2-fold disorder like that in $(Bu_4N)_2Re_2Cl_8$, although examples of 3-fold disorder also are known.[19,31,32,34] The effect of high pressure on the structure of $(Bu_4N)_2Re_2Cl_8$ in dichloromethane has subsequently been investigated[35] and the gas-phase electronic structure of the intact $[Re_2Cl_8]^{2-}$ anion has also been probed.[36]

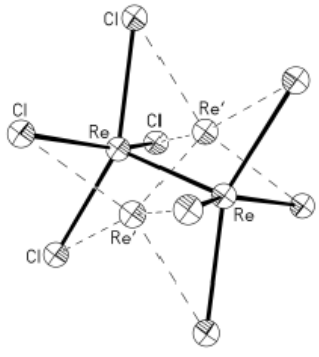


Fig. 8.2. The structure of the $[Re_2Cl_8]^{2-}$ anion in $(Bu_4N)_2Re_2Cl_8$. The Re atoms are in positions with an occupation number of 73.89% while the Re' atoms are those with an occupation number of 26.11%. The common midpoint of the two Re-Re lines is a crystallographic center of inversion.

Since the report of the full structural characterization of $(Bu_4N)_2Re_2Cl_8$ in 1976,[33] crystal structure determinations have been carried out on a large number of salts that contain the $[Re_2Cl_8]^{2-}$ anion.[19,28,30-32,37-42] In most instances the anions are required by crystallographic symmetry to possess rigorously eclipsed rotational geometries (as reflected by a twist angle

Pictiva EX2004
Samsung v Pictiva
IPR2024-01094

χ of zero), but in a few cases a small twisting is encountered. The Re–Re distances that have been determined for all the $[Re_2Cl_8]^{2-}$ salts are presented in Table 8.1, together with all other available structural data for compounds, to be discussed in due course, that contain Re–Re quadruple bonds, including salts of other octahalodirhenate(III) anions (Section 8.3). Some of these data are also included in a fairly extensive review published by Koz'min and Surazhskaya in 1980.[43] The individual references should be consulted for information on the salts that show orientational disorder of the $[Re_2X_8]^{2-}$ anions (vide supra), although much of the work published pre-1995 has been reviewed.[32,34] See also section 16.1.5.

Table 8.1. Structural Data for Dirhenium(III) Compounds Containing Re–Re Quadruple Bonds

Compound	r(Re–Re)(Å)[a]	Twist Angle (°)[b]	ref.
A. Compounds with No Bridging Ligands			
$(Bu_4N)_2Re_2F_8{\cdot}2Et_2O$	2.188(3)	c	48
$K_2Re_2Cl_8{\cdot}2H_2O$	2.241(7)	0	7(c)
$Cs_2Re_2Cl_8{\cdot}H_2O$: $[Re_2Cl_8]^{2-}$	2.237(2)	0	21
$[Re_2Cl_8(H_2O)_2]^{2-}$	2.252(2)	0	21
$(NH_4)_2Re_2Cl_8{\cdot}2H_2O$	2.234(1)	0	37
$(C_5H_5NH)_2Re_2Cl_8$	2.244(15)	0	44
$[2,4,6\text{-}(CH_3)_3C_5H_2NH]_2Re_2Cl_8$	2.246(8)	0	d
$(Et_4N)_2Re_2Cl_8$	2.2146(7)	0	19
$(Bu_4N)_2Re_2Cl_8$	2.222(2)	0	33
$[(DMF)_2H]_2Re_2Cl_8$	2.221(1)	0	38
$[(CH_3)_2NH_2]_2Re_2Cl_8$	2.235(2)	c	38
	2.234(2)	c	38
$(Pr^n{}_3PH)_2Re_2Cl_8$	2.216(2)	0	39
$(Ph_3MeP)_2Re_2Cl_8$	2.218(1)	0	39
$[ReCl_2(depe)_2]_2Re_2Cl_8$	2.213(1)	0	40
$[Rh_2(O_2CCH_3)_2(NCMe)_6]Re_2Cl_8$	2.226(4)	c	41
	2.216(3)	c	41
	2.211(3)	c	41
$(Ph_4P)_2Re_2Cl_8{\cdot}2CH_2Cl_2$	2.222(1)	0	42
$(Ph_4P)_2Re_2Cl_8{\cdot}2CH_3CN$	2.229(2)	0	28
$(morphH)_2Re_2Cl_8$	2.222(1)	0	30
$[1,6\text{-}C_6H_{12}(NH_3)_2]Re_2Cl_8$	2.2326(7)	0	32
$(Ph_3PCH_2CH_2PPh_3)Re_2Cl_8$	2.2221(6)	0	31
$[(p\text{-}MeOC_6H_4)_3MeP]_2Re_2Cl_8$	2.2231(6)	0	142(b)
	2.2157(7)	0	142(b)
$Cs_2Re_2Br_8$	2.228(4)	0	49
$(Bu_4N)_2Re_2Br_8$	2.226(4)	0	51
$(Ph_3MeP)_2Re_2Br_8$	2.226(1)	0	39
$(Bu_4N)_2Re_2I_8$	2.245(3)	0	60
$(Ph_4As)_2Re_2(NCS)_8[(CH_3)_2CO]_2$	2.270(1)	0	67
$(Ph_4As)_2Re_2(NCS)_8(C_5H_5N)_2$	2.296(1)	0	67
$(Bu_4N)_2Re_2(NCS)_8(dto)$	2.2854(3)	0	68
$Li_2Re_2(CH_3)_8{\cdot}2(C_2H_5)_2O$	2.178(1)	0	72
$Re_2Cl_4(acac)_2(DMSO)_2$	2.2650(5)	0	145
$Re_2Cl_4(acac)_2(acacH)_2$	2.236(1)	0	146

Pictiva EX2004
Samsung v Pictiva
IPR2024-01094

Compound	r(Re–Re)(Å)[a]	Twist Angle (°)[b]	ref.
$(Ph_4As)Re_2Cl_7(PBu^n_3)$	2.219(3)	c	194
$(Ph_4As)Re_2Cl_7(PBu^n_2Ph)$	2.209(1)	8.7	195
	2.218(1)	1.7	195
$(Ph_4As)Re_2Cl_7(PBu^nPh_2)$	2.220(1)	4.7	194
$(Ph_4As)Re_2Cl_7(PPhBzMe)$	2.2196(8)	11.6	193
$(Bu_4N)_4[Re_2Cl_7(PMe_3)]_2[Re_2Cl_8]\cdot 2CH_2Cl_2$	2.210(1)[e]	4.9	185
$Re_2Cl_6(PMe_3)_2$ (cubic form)	2.208(1)	0	179
(monoclinic form)	2.209(1)[f]	0	185
$Re_2Cl_6(PEt_3)_2$	2.222(3)	0	187(a)
$Re_2Cl_6(PEt_3)_2\cdot C_7H_8$	2.219(1)	0	187(b)
$Re_2Cl_6(PMe_2Ph)_2$	2.215(1)	0	180
	2.212(1)	0	180
$Re_2Cl_6(PMePh_2)_2$	2.227(1)	0	188
$Re_2Cl_4(OEt)_2(PPh_3)_2$	2.231(1)	1.4	98
$Re_2Cl_4(OMe)_2[P(p\text{-}MeOPh)_3]_2$	2.2476(4)	≈0	143
$Re_2Cl_3(OEt)_3(PPh_3)_2$	2.2399(12)	1.2	143
1,3-Re_2Cl_6(dppf)	2.2444(3)	4.8	190
1,3-Re_2Cl_6(dppf)$\cdot 4C_6H_4Cl_2$	2.2390(6)	≈0	190
$[1,3,6,8\text{-}Re_2Cl_4(PMe_2Ph)_4](PF_6)_2\cdot CH_3CN$	2.215(2)	≈0	243
$(Bu_4N)Re_2Cl_7$(dth)	2.257(1)	2.4	211
$(Bu_4N)Re_2Cl_7$(dto)	2.248(1)	2.3	211
B. Compounds with Carboxylato Bridges			
$Re_2(O_2CC_6H_5)_4Cl_2\cdot 2CHCl_3$	2.235(2)	0	89
$Re_2[O_2CC(CH_3)_3]_4Cl_2$	2.236(1)	0	90
$Re_2[O_2CC(CH_3)_3]_4Br_2$	2.234(1)	0	90
$Re_2(O_2CC_3H_7)_4(ReO_4)_2$	2.251(2)	0	78
$Re_2(O_2CCH_3)_4Cl_2$	2.2240(5)	0	91
$Re_2[O_2C(2\text{-biphenyl})]_4Cl_2\cdot 2CH_2Cl_2$	2.2363(7)	0	83
$Re_2(O_2CAd)_4Cl_2\cdot 4CHCl_3$	2.2300(5)	0	81
$Re_2[O_2CCHCo_2(CO)_6]_4Cl_2$	2.240(1)	0	88
$Re_2[O_2CC(CH_3)_3]_3Cl_3$	2.229(2)	≈0	114
$Re_2(O_2CH)_3Cl_3$	2.223(1)	c	107
$Re_2[O_2CCH(CH_3)_2]_3Cl_2(ReO_4)$	2.259(3)	2.6	77
$Re_2(O_2CCH_3)_2Cl_4$	2.208(1)	0	110,111
$Re_2(O_2CCH_3)_2Br_4$	2.216(3)	0	112
$Re_2(O_2CC_6H_5)_2I_4$	2.198(1)	0	58
$Re_2[O_2CC(CH_3)_3]_2Cl_4$	2.209(2)	≈0	114
$Re_2(O_2CCH_3)_2Cl_4(H_2O)_2$	2.224(5)	5.8	120
$Re_2(O_2CCH_3)_2Cl_4(DMSO)_2$	2.237(1)	0	121
$Re_2(O_2CCH_3)_2Cl_4(DMF)_2$	2.239(2)	c	122
$[Re_2(O_2CCH_3)_2Cl_4(pyz)]_2(\mu\text{-pyz})$	2.240(2)	≈0	102
$[Re_2(O_2CCH_3)_2Cl_4(\mu\text{-pyz})]_n$	2.2358(8)	≈0	102
$[Re_2(O_2CCH_3)_2Cl_4(\mu\text{-}4,4'\text{-bpy})]_n$	2.2512(4)	≈0	102
$[Re_2(O_2CCH_3)_2Cl_4(\mu\text{-dppmO}_2)]_n$	2.2438(4)	≈0	102
$[Re_2(O_2CCH_3)_2Cl_4(INA)_2]_n$	2.2493(4)	0	124
$(Bu_4N)Re_2(O_2CCH_3)_2Cl_5\cdot(CH_3)_2CO$	2.236(1)	≈0	101

Pictiva EX2004
Samsung v Pictiva
IPR2024-01094

Compound	r(Re–Re)(Å)[a]	Twist Angle (°)[b]	ref.
$Re_2(O_2CH)_2Cl_4(DPF)_2$	2.238(2)	c	104
$[(C_2H_5)_3NH]Re_2(O_2CH)_3Cl_4{\cdot}HCO_2H$[g]	2.244(3)	0	106
$(NH_4)_2Re_2(O_2CH)_2Cl_6$	2.260(5)	0	123
$Re_2(O_2CPh)_2Cl_4(THF)_2{\cdot}THF$	2.225(1)	0	101
$[ReCl_2(dpcp)_2]Re_2(O_2CPh)_2Cl_6{\cdot}CHCl_3$	2.237(2)	0	101
$(Bu_4N)Re_2(O_2CCF_3)Cl_6$	2.2361(5)	c	88
$Re_2(O_2CCH_3)_2(CH_3)_2(\eta^1\text{-}O_2CCH_3)_2$	2.177(1)	0	132
$Re_2(O_2CCH_3)_2Cl_2(CH_3)_2(DMSO)$	2.184(1)	c	132
$Re_2(O_2CC_2H_5)_2(9\text{-EtA})_2Cl_2{\cdot}EtOH{\cdot}C_6H_{14}$	2.2455(10)	0	134
$Re_2(O_2CC_2H_5)(mhp)_2Cl_3$	2.204(1)	1.8	136
$Re_2(O_2CCH_3)Cl_3(OMe)_2(PCyPh_2)_2$	2.2872(15)	≈0	143
	2.2851(6)	≈0	143
C. Other Compounds			
$Na_2[Re_2(SO_4)_4(H_2O)_2]{\cdot}6H_2O$	2.214(1)	0	150
$Cs_2[Re_2(HPO_4)_4(H_3PO_4)_2]$	2.224(1)	0	153
$Re_2(hp)_4Cl_2$	2.206(2)	0	154
$Re_2(mhp)_2Cl_4(Hmhp){\cdot}(CH_3)_2CO$	2.210(1)	3.6	136
$Re_2(chp)_3Cl_3$	2.2015(7)	1.4	156
$Re_2(mp)_4Cl_2{\cdot}2C_6H_6$	2.2453(4)	4.0	157
$Re_2(C_7H_4NS_2)_4Cl_2{\cdot}CH_2Cl_2$	2.2716(3)	18.0	158
$Re_2[(PhN)_2CPh]_2Cl_4$	2.177(2)	0	159
$Re_2[(PhN)_2CPh]_2Cl_4{\cdot}THF$	2.209(1)	6.0	159
$Re_2[(PhN)_2CCH_3]_2Cl_4$	2.178(1)	3.8	160
$Re_2[(CH_3N)_2CPh]_4Cl_2{\cdot}CCl_4$	2.208(2)	0	160
$Re_2[(p\text{-}CH_3C_6H_4N)_2CH]_4Cl_2{\cdot}3C_6H_6$	2.2759(3)	0	161
$Re_2[(p\text{-}CH_3C_6H_4N)_2CH]_4Cl_2{\cdot}2CH_2Cl_2$	2.2705(5)	1.6	161
$Re_2[(p\text{-}CH_3C_6H_4N)_2CH]_4(OMe)_2{\cdot}3C_6H_6$	2.3047(2)	≈0	161
$Re_2[(p\text{-}MeOC_6H_4N)_2CH]_4Cl_2$	2.2777(3)	≈0	162
$\{Re_2[(p\text{-}MeOC_6H_4N)_2CH]_4Cl\}BF_4$	2.2239(9)	≈0	163
$Re_2[(m\text{-}MeOC_6H_4N)_2CH]_4Cl_2{\cdot}2CH_2Cl_2$	2.2765(6)	≈0	162
$Re_2[(3,4\text{-}Cl_2C_6H_3N)_2CH]_4Cl_2{\cdot}2CH_2Cl_2$	2.2783(4)	≈0	162
$Re_2[(3,5\text{-}Cl_2C_6H_3N)_2CH]_4Cl_2{\cdot}4CH_2Cl_2$	2.2734(3)	≈0	162
$Re_2[(3,5\text{-}Cl_2C_6H_3N)_2CH]_4Cl_2{\cdot}THF$	2.2840(5)	≈0	162
$Re_2[(PhN)_2CH]_3Cl_3$	2.2318(8)	c	164
$Re_2[(PhN)_2CH]_3Cl_3{\cdot}2CH_3CN$	2.2288(9)	c	164
$Re_2[(PhN)_2CH]_2Cl_4$	2.177(1)[g]	≈0	164
$Re_2[(PhN)_2CH]_2Cl_4(H_2O){\cdot}2THF$	2.2198(3)	≈0	165
$Re_2(hpp)_4Cl_2$	2.1913(12)	0	166
$Re_2(hpp)_3Cl_3{\cdot}(CH_3)_2CO$	2.189(2)	≈0	166
cis-$Re_2(PhNCHO)_4Cl_2$	2.2491(5)	0	165
cis-$Re_2[PhNC(CH_3)O]_4Cl_2{\cdot}2CH_3CN$	2.2304(6)	≈0	168
cis-$Re_2[HNC(Ph)O]_4Cl_2$	2.2218(8)	1.3	168
	2.2181(6)	≈0	168
cis-$Re_2[PhNC(Ph)O]_4Cl_2{\cdot}2CH_2Cl_2$	2.2350(4)	1.8	168
trans-$Re_2[\mu\text{-}XylNC(CH_3)O]_4Cl_2{\cdot}2Et_2O$	2.2364(5)	1.7	168
trans-$Re_2[\mu\text{-}XylNC(CH_3)O]_4(N_3)_2{\cdot}CH_2Cl_2$	2.2477(3)	c	169

Pictiva EX2004
Samsung v Pictiva
IPR2024-01094

Compound	r(Re–Re)(Å)[a]	Twist Angle (°)[b]	ref.
trans-$Re_2[\mu\text{-}XylNC(CH_3)O]_4(NCS)_2\cdot 0.83CHCl_3$	2.2324(5)	c	169
$(Bu_4N)\{Re_2[\mu\text{-}HNC(CH_3)O_2]_2Cl_5\}\cdot 3CH_2Cl_2$	2.2395(5)	c	171
$(Bu_4N)_2\{Re_2[\mu\text{-}HNC(CH_3O]Cl_6\}_2$	2.229(1)	0	172
$(Bu_4N)\{Re_2[\mu\text{-}HNC(Ph)O]Cl_6\}\cdot 0.5CH_2Cl_2$	2.2209(5)	c	173
$(Bu_4N)\{[Re_2Cl_6(DMF)_2]_2[\mu\text{-}HNC(O)C_6H_4C(O)NH]\}$	2.2317(7)	c	174
$(Bu_4N)Re_2Cl_7(bdppp)\cdot CH_2Cl_2$	2.275(1)	h	196
	2.280(1)	h	196
$Re_2Cl_6(S,S\text{-}isodiop)\cdot CH_2Cl_2$	2.224(2)	≈0	201

[a] Where more than one set of data is given for any complex this signifies that more than one crystallographically independent molecule is present in the crystal. In cases where orientational disorder occurs, the Re–Re distance given is that for the dirhenium unit with the highest occupancy or is a weighted average of the distances.

[b] This is the average torsion angle χ_{av}. An angle of ≈0 means 1.0° or less.

[c] Not reported but evidently close to zero.

[d] W. R. Robinson, Ph.D. Thesis, Massachusetts Institute of Technology, 1966.

[e] This is the Re–Re distance for the $[Re_2Cl_7(PMe_3)]^-$ anion.

[f] This distance is the average for two crystallographically independent molecules in the asymmetric unit.

[g] In ref. 106 the space group is reported as $P2_1/c$ with $Z = 2$. This would require $\bar{1}$ crystal symmetry, which is inconsistent with the reported structure. Accordingly, Z must equal 4 not 2.

[h] All the L–Re–Re–L torsion angles are reported as being less than 12° for the two independent molecules.

8.3 Synthesis and Structure of the Other Octahalodirhenate(III) Anions

The other three octahalodirhenate(III) anions are all known though none is as extensively characterized nor so important in the discovery and development of the chemistry of compounds containing M–M multiple bonds as the classic $[Re_2Cl_8]^{2-}$ anion. Of the remaining anions, the most recent one to be discovered is the $[Re_2F_8]^{2-}$ anion, which has been prepared by reacting an excess of $Bu_4NF\cdot 3H_2O$ with $(Bu_4N)_2Re_2Cl_8$ in freshly distilled dichloromethane.[45] While the structure of the resulting salt, $(Bu_4N)_2Re_2F_8\cdot 4H_2O$, was not confirmed for some time, its spectroscopic properties[45,46] provided good support for this formulation. Later, this was substantiated by an EXAFS structure determination which yielded a Re–Re bond distance of 2.22 Å.[47] Subsequently, the dark blue etherate $(Bu_4N)_2Re_2F_8\cdot 2Et_2O$ was prepared[48] by the reaction of $(Bu_4N)_2Re_2Cl_8$ with Bu_4NF in anhydrous CH_2Cl_2 followed by recrystallization from acetone/diethylether. Its crystal structure shows[48] the Re–Re distance to be 2.188(3) Å and that a Et_2O molecule is coordinated to one of the Re atoms thereby lowering the symmetry of the anion. The shortness of the Re–F distances in both structure determinations[47,48] suggests the presence of significant Re–F π interactions. Surprisingly, studies on salts of the $[Re_2F_8]^{2-}$ anion have been very limited.

The first accurate structure determination of the $[Re_2Br_8]^{2-}$ anion was carried out on the cesium salt $Cs_2Re_2Br_8$, which was prepared by the hypophosphorous acid reduction of $KReO_4$ in 48% aqueous hydrobromic acid with CsBr present.[49] The Re–Re bond length of 2.228(4) Å is very similar to that found for salts of the $[Re_2Cl_8]^{2-}$ anion (Table 8.1), and it has the same eclipsed rotational geometry. This structure determination on $Cs_2Re_2Br_8$ was published several years after an early structure determination on the pyridinium salt "$(C_5H_5NH)HReBr_4$" by Koz'min et al.[50] It was concluded that this substance exists in two crystalline modifications with both structures being "constructed from the dimeric anions $[Br_4Re{\equiv}ReBr_4]^{4-}$ (or $[HBr_4Re{\equiv}ReBr_4H]^{2-}$) and the pyridinium cations $[C_5H_5NH]^+$." The Re–Re bond lengths for these two forms were said[50] to range from 2.207(3) to 2.27 Å. In view of the structural data for

Pictiva EX2004
Samsung v Pictiva
IPR2024-01094

$[Re_2Cl_8]^{2-}$ which are listed in Table 8.1, the first of these distances seems too short while the second one is too long.

In addition to the preparative method described above for $Cs_2Re_2Br_8$,[49] a much simpler method for the synthesis of many salts of the octabromodirhenate(III) anion involves the halide exchange reactions of $[Re_2Cl_8]^{2-}$. This necessitates the evaporation of a methanol solution of the appropriate $[Re_2Cl_8]^{2-}$ salt that contains 48% aqueous hydrobromic acid until crystallization of the olive-green salt is complete.[14,22,24] This exchange reaction proceeds in almost quantitative yield and is ideal for the preparation of $(Bu_4N)_2Re_2Br_8$. The crystal structure of this salt shows[51] a structure similar to that of its chloro analog including the same type of crystallographic disorder (see Section 8.2). The only other structural determinations on salts of the $[Re_2Br_8]^{2-}$ anion has been carried out on $[(DMA)_2H]_2Re_2Br_8$ (DMA = dimethylacetamide)[52,53] and $(Ph_3MeP)_2Re_2Br_8$.[39] In contrast to the structures of $(Bu_4N)_2Re_2Br_8$ and $(Ph_3MeP)_2Re_2Br_8$, where there are two orientations of the Re_2 units,[39,51] in the case of $[(DMA)_2H]_2Re_2Br_8$ the disorder involves three orientations of the mutually perpendicular Re_2 units within the ordered arrangement of bromide ligands.[53]

An alternative method for preparing $(Bu_4N)_2Re_2Br_8$ involves the treatment of solutions of the dirhenium(III) benzoate complex $Re_2(O_2CPh)_4Cl_2$ (see Section 8.4.2) in methanol or ethanol with hydrogen bromide in the presence of tetra-*n*-butylammonium bromide.[25] This strategy works equally well for the preparation of $(Bu_4N)_2Re_2Cl_8$ and $(Bu_4N)_2Re_2I_8$:

$$Re_2(O_2CPh)_4Cl_2 + 8HX + 2Bu_4N^+ \xrightarrow[\text{reflux}]{\text{ROH}} (Bu_4N)_2Re_2X_8 + 4PhCO_2H + 4H^+ + 2Cl^-$$

Not only did this reaction constitute the first general synthetic route to all three of these halo-anions, but it was the first time that a route to the $[Re_2I_8]^{2-}$ anion had been discovered.[25] One year later (1979), a procedure related to the one described above for the synthesis of $(Bu_4N)_2Re_2I_8$ was reported.[54] This reaction, which is the more convenient one of the two synthetic procedures, is as follows:

$$(Bu_4N)_2Re_2X_8 + 8HI \xrightarrow[20\ ^\circ C]{CH_2Cl_2} (Bu_4N)_2Re_2I_8 + 8HX$$
$$X = Cl \text{ or } Br$$

The conversion of the edge-sharing bioctahedral dirhenium(IV) complex $(Bu_4N)_2Re_2Br_{10}$ to $(Bu_4N)_2Re_2Br_8$ has been reported to occur when the former compound is reacted with Hg at 100 °C in a vacuum.[55] While other salts of the $[Re_2Br_8]^{2-}$ anion have been reported, specifically $(morphH)_2Re_2Br_8$[30] and $[(\eta^5\text{-}C_5H_5)_2Fe]_2Re_2Br_8$,[56] neither has been fully characterized by X-ray crystallography although the spectroscopic and magnetic properties of the ferrocenium salt have been reported.[56]

As it turns out, the use of a non-aqueous solvent is essential for the preparation of pure $[Re_2I_8]^{2-}$ (vide supra) since it had been demonstrated in earlier studies,[57,58] that the treatment of dirhenium(III) carboxylates with 55% aqueous HI produces $Re_2(O_2CR)_4I_2$ and/or $Re_2(O_2CR)_2I_4$ but not $[Re_2I_8]^{2-}$. At that time, it was not at all clear that $[Re_2I_8]^{2-}$ would exist, although it had been noted[58] that if the most likely bonded and non-bonded Re–Re, Re–I and I–I contacts for $[Re_2I_8]^{2-}$ were considered, then there was no obvious *steric* reason why this anion would not exist. Prior to the full structure determination of $(Bu_4N)_2Re_2I_8$ its Raman spectrum had been studied[46,59] and interpreted in terms of the expected eclipsed structure for the $[Re_2I_8]^{2-}$ anion. The crystal structure of this complex, which was determined in 1988,[60] confirms its close structural relationship to the chloro and bromo analogs. However, unlike $(Bu_4N)_2Re_2X_8$ (X = Cl or Br) there is a three-fold disorder of the Re_2 units within the essentially cubic ar-

Pictiva EX2004
Samsung v Pictiva
IPR2024-01094

ray of eight iodide ligands.[60] The Re–Re distance of 2.245(3) Å is close to Re–Re distances in other $[Re_2X_8]^{2-}$species (X = Cl or Br) (see Table 8.1). While on the subject of the structural identity of the $[Re_2I_8]^{2-}$ anion, the isolation of the compound $Re_4I_8(CO)_6$ is of relevance.[61] It is prepared by the I_2 oxidation of $Re_2I_2(CO)_6(THF)_2$ in heptane, and has a structure that can be viewed formally as involving interactions between two $[Re(CO)_3]^+$ fragments and $[Re_2I_8]^{2-}$; this association occurs via bent Re–I–Re bridges that involve six of the iodine atoms of $[Re_2I_8]^{2-}$. As a consequence of this interaction, which gives rise to $[(CO)_3ReI_3]$ units, the rotational conformation within the Re_2I_8 unit is staggered rather than eclipsed and, as a result, the Re–Re bond length is longer (2.279(1) Å)[61] than that found in the eclipsed $[Re_2I_8]^{2-}$ species (Table 8.1). In accord with the usual bonding scheme for Re_2L_8 species, as the conformation changes from eclipsed to staggered, the d_{xy}–d_{xy} overlap diminishes and the metal-metal bond order decreases from four to three as the δ contribution is lost.

8.4 Substitution Reactions of the Octahalodirhenate(III) Anions that Proceed with Retention of the Re_2^{6+} Core

The synthesis and structural elucidation of the octahalodirhenate(III) anions has been paralleled by studies of their chemical reactivity particularly in the cases of $[Re_2Cl_8]^{2-}$ and $[Re_2Br_8]^{2-}$. The reactions of these anions fall into three main categories: (1) substitution reactions in which a metal-metal bonded Re_2^{6+} core is retained, (2) redox reactions that give rise to products wherein the Re–Re bond order is less than four and in which ligand substitution reactions may also have occurred, and (3) reactions in which the metal-metal bond is disrupted. Since the latter reaction course is also encountered with compounds that contain Re–Re bond orders other than four (especially Re–Re triple bonds), such reactions are most conveniently treated all together in a separate section (see Section 8.7).

In this section, we consider the non-redox substitution reactions of the octahalodirhenate(III) anions and the chemistry of the compounds that result. We will also consider those compounds that while they may not have been prepared directly from the $[Re_2X_8]^{2-}$ anions, are derived formally from them by ligand for halide substitutions. Since the chemistry of the dirhenium(III) carboxylates is so extensive, these compounds will be considered on their own in Section 8.4.2.

8.4.1 Monodentate anionic ligands

Halide exchange reactions occur very readily, as has already been noted in Section 8.2. Thus, the reactions of $(Bu_4N)_2Re_2Cl_8$ with 48% aqueous hydrobromic acid have been used to prepare $(Bu_4N)_2Re_2Br_8$[14,22] and, in addition, the mixed haloanions $[Re_2Cl_2Br_6]^{2-}$, $[Re_2Cl_3Br_5]^{2-}$ and $[Re_2Cl_6Br_2]^{2-}$.[62] Since few experimental details were reported for the mixed haloanions[62] it is not clear how easy it is to control the stoichiometry of these reactions. However, a few other methods exist for the preparation of mixed haloanions that involve less obvious but more controllable procedures, such as the preparations of $(Et_3PCl)_2Re_2Cl_4Br_4$ from $Re_2Br_4(PEt_3)_4$ (see Section 8.5.4) and $(Bu_4N)_2Re_2Cl_6Br_2$ from $Re_2Cl_6(AsBu^n{}_2Ph)_2$ (see Section 8.4.4).

Since the Re_2^{6+} core is preserved in exchange reactions between $(Bu_4N)_2Re_2Cl_8$ and HBr(aq), it can be expected that other coordinating anions will react in a similar fashion towards $[Re_2X_8]^{2-}$. Among the first systems to be investigated were those involving the reactions between $(Bu_4N)_2Re_2Cl_8$ and an excess of thiocyanate and selenocyanate.[63-65] Both NaSCN and KSeCN react with $(Bu_4N)_2Re_2Cl_8$ in non-aqueous media to produce dark red $(Bu_4N)_2Re_2(NCS)_8$ and purple $(Bu_4N)_2Re_2(NCSe)_8$, respectively.[63-65] In the case of $[Re_2(NCS)_8]^{2-}$, cation replacement reactions have been used[63] to produce other salts, all of which display the same spectral properties as $(Bu_4N)_2Re_2(NCS)_8$. Initial infrared spectral characterizations on salts of both

Pictiva EX2004
Samsung v Pictiva
IPR2024-01094

these dianions were interpreted in terms of *N*-bound thiocyanate and selenocyanate,[63-65] and electronic absorption spectral measurements[66] led to the conclusion that the δ bond is weaker in $[Re_2(NCS)_8]^{2-}$ than $[Re_2Cl_8]^{2-}$ and $[Re_2Br_8]^{2-}$. Much more recently, these interpretations have been substantiated by crystal structure determinations of the salts $(Ph_4As)_2Re_2(NCS)_8(L)_2$ (L = $(CH_3)_2CO$ or C_5H_5N).[67] Both structures contain 'solvent' molecules (acetone or pyridine) that are weakly bound axially, the Re–O and Re–N distances being 2.56(1) Å and 2.54(1) Å respectively.[67] This might be expected to result in a slight lengthening of the Re–Re bonds and, indeed, the measured distances of 2.270(1) Å and 2.296(1) Å, are longer than the corresponding distances in other $[Re_2X_8]^{2-}$ species (X = Cl, Br or I) (see Table 8.1). This bond lengthening is also encountered in the complex $(Bu_4N)_2Re_2(NCS)_8(\mu\text{-dto})$[68] in which the weakly bridging 3,6-dithiaoctane ligand links $[Re_2(NCS)_8]^{2-}$ anions into infinite centrosymmetric chains (Fig. 8.3); the Re–S distance is 3.0072(8) Å.

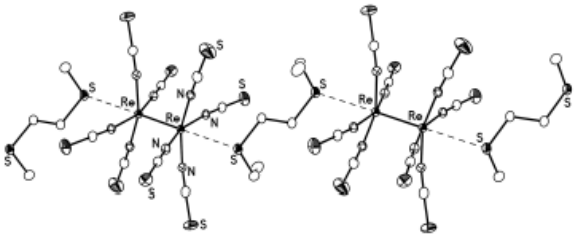
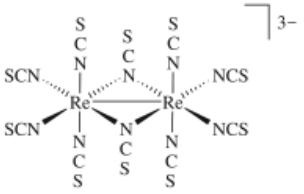


Fig. 8.3. The structure of the infinite centrosymmetric chains present in $(Bu_4N)_2Re_2(NCS)_8$·dto.

Whereas reflux in acidified methanol produces the octa(isothiocyanato)dirhenate(III) anion in the aforementioned reactions, the use of acetone as the reaction solvent produces solutions from which the red-brown rhenium(IV) complex $(Bu_4N)_2Re(NCS)_6$ and a dark green material, originally formulated[63] as $(Bu_4N)_3Re_2(NCS)_{10}(CO)_2$, can be isolated. Several years later the true identity of this complex was established by X-ray crystallography.[69] The structure of the anion is as shown in **8.1** and reveals at once the reason for the earlier misinterpretation of the infrared spectral data, namely, the presence of two *N*-bridging NCS ligands, a structural form of this ligand not previously documented. The Re–Re distance of 2.613(1) Å in this edge-shared bioctahedral complex implies the existence of a metal-metal bond, although its order is unknown and cannot be inferred from the magnitude of the Re–Re distance alone. The D_{2h} symmetry of the Re_2N_{10} core is consistent with the unpaired electron being delocalized equally over both metal atoms i.e. it is a (+3.5, +3.5) mixed-valence complex rather than being localized (+4, +3). However, it can safely be concluded that some degree of Re–Re multiple bonding exists in this species.[70] Electrochemical studies have shown that $[Re_2(NCS)_8]^{2-}$ converts to $[Re_2(NCS)_{10}]^{4-}$ in the presence of free $[NCS]^-$ and that the latter species is readily oxidized to $[Re_2(NCS)_{10}]^{3-}$ (**8.1**) in the presence of oxygen,[70] thereby explaining why the edge-shared bioctahedral $[Re_2(NCS)_{10}]^{3-}$ is so easily formed in the reaction between $[Re_2Cl_8]^{2-}$ and excess $[NCS]^-$.[63] It has also been established that at room temperature the one-electron oxidation of $[Re_2(NCS)_8]^{2-}$ to $[Re_2(NCS)_8]^-$ is followed by conversion of the latter to $[Re_2(NCS)_{10}]^{2-}$ via a $[NCS]^-$ scavenging mechanism involving the sacrifice of some unoxidized $[Re_2(NCS)_8]^{2-}$ (see also Section 8.5.2). More recently, the synthesis and crystal structures of a pair of salts that contain the $[Re_2(NCS)_{10}]^{n-}$ anions (n = 2 or 3) have been reported.[71] Crystals of the bis(ethylenedithio)tetrathiafulvalene salts of compositions $(BEDT\text{-}TTF)_3Re_2(NCS)_{10}\cdot 2CH_2Cl_2$ and $(BEDT\text{-}TTF)_2Re_2(NCS)_{10}\cdot C_6H_5CN$ were prepared by electrooxidation techniques, and both complexes shown to have structures like

Pictiva EX2004
Samsung v Pictiva
IPR2024-01094

8.1, with Re–Re distances of 2.602(1) Å for the $[Re_2(NCS)_{10}]^{3-}$ anion and 2.615(1) Å for the analogous $[Re_2(NCS)_{10}]^{2-}$ species.[71]



8.1

Although salts of the homoleptic methyl species $[Re_2(CH_3)_8]^{2-}$ have been obtained, and one such compound structurally characterized (Table 8.1),[72] they have not been prepared directly from the octahalodianions but rather from the dirhenium(III) carboxylates. Consequently, their chemistry is described in Section 8.4.2.

8.4.2 The dirhenium(III) carboxylates

The dirhenium(III) carboxylates $Re_2(O_2CR)_4X_2$, $Re_2(O_2CR)_3X_3$ and $Re_2(O_2CR)_2X_4$ (X = Cl, Br or I) not only have a very extensive chemistry in their own right but they have also occupied a crucial place in the development of the chemistry of the quadruple bond. A review of some of this chemistry, as seen from the perspective of Russian workers in the field, was published[73] just prior to the publication of the second edition of *Multiple Bonds Between Metal Atoms*.[10]

Discovery, synthesis and structure

The recognition that rhenium(III) carboxylates of the type $Re_2(O_2CR)_{4-x}Cl_{2+x}$ (x = 0, 1 or 2) contain Re–Re quadruple bonds followed closely upon the heels of the structural characterization of the $[Re_2Cl_8]^{2-}$ anion and the original treatment of its bonding.[7] Prior to that time, those literature reports that described low oxidation state rhenium carboxylates often failed to take into account the possibility of metal-metal bonding and in some cases explicitly precluded it. Accordingly, this early literature (pre-1965) is replete with erroneous conclusions concerning the nature of the materials that were purported to be formed.

The first report on low oxidation state rhenium carboxylates appears to be that published in 1958 by Kotel'nikova and Tronev[13] who obtained a variety of products from the reactions between solutions containing "$H_2ReCl_4{\cdot}2H_2O$" and glacial acetic acid. The formulation of the products as derivatives of rhenium(II) (i.e. $ReCl_2{\cdot}4CH_3COOH$, $ReCl_2{\cdot}2CH_3COOH{\cdot}H_2O$, $ReCl_2{\cdot}CH_3COOH{\cdot}H_2O$, $ReCl_2{\cdot}CH_3COOH$ and $ReCl_2{\cdot}CH_3COOH{\cdot}C_5H_5N$)[13] is clearly incorrect, stemming in part from a failure to recognize that the solutions of "$H_2ReCl_4{\cdot}2H_2O$" contained, in reality, $[Re_2Cl_8]^{2-}$. While further work in this period[74,75] failed to establish the correct structural identity of these complexes, they were eventually assigned dimeric formulations.

Quite independently of the earlier Russian work, Taha and Wilkinson[76] had, in their investigations into the reactions of rhenium(III) chloride (at the time of unknown structure) with mixtures of the lower monocarboxylic acids and the appropriate anhydride (when available), isolated crystalline orange products of stoichiometry $[Re(O_2CR)_2Cl]_n$. The absence of air was essential for the reactions to proceed in this fashion (vide infra). Molecular weight measurements indicated that these complexes were dimeric and Taha and Wilkinson[76] concluded that they most likely possessed the copper(II) acetate type of structure with terminally bound chlorines in the axial coordination sites. However, they further concluded[76] that in spite of the diamagnetism of the complexes it was not necessary "to invoke metal-metal bonding to account for the

Pictiva EX2004
Samsung v Pictiva
IPR2024-01094

diamagnetism" and indeed explicitly reasoned against its existence. The lability of the chloride ligands was demonstrated[76] by the reactions of $[Re_2(O_2CC_3H_7)_2Cl]_2$ with AgSCN and Ag_2SO_4. It is clear that the orange complexes formulated correctly by Taha and Wilkinson[76] as the dirhenium(III) complex $[Re(O_2CCH_3)_2Cl]_2$ and incorrectly by Kotel'nikova and Vinogradova[75] as $(ReCl{\cdot}2CH_3COOH)_2$ are one and the same thing.

When the reactions between rhenium(III) chloride and the carboxylic acids were carried out in the presence of dry air or oxygen a mixture of purple $[ReOCl(O_2CR)_2]_2$ and orange $[ReO_2(O_2CR)_2]_2$ was said[76] to be produced. Both complexes were believed at the time to contain carboxylate and oxo-bridges and therefore to possess rhenium in an oxidation state higher than +3. However, later work by Lock and co-workers[77,78] clarified the structural nature of these species.

While the reduction of $KReO_4$ by hydrogen in hydrohalic acid (HCl or HBr)/carboxylic acid mixtures has continued to be used by Kotel'nikova and co-workers[79,80] as a means of preparing the dirhenium(III) carboxylates, $Re_2(O_2CR)_4X_2$, the readily availability of high yield synthetic routes to $(Bu_4N)_2Re_2X_8$ (X = Cl, Br or I)[22,29,54] provides a much more convenient synthetic procedure. The reaction of $(Bu_4N)_2Re_2Cl_8$ with an alkyl carboxylic acid, usually admixed with the appropriate anhydride and using oxygen and moisture free reaction conditions, is an excellent method for preparing $Re_2(O_2CR)_4Cl_2$.[14,24,57,81]

$$(Bu_4N)_2Re_2Cl_8 + 4RCO_2H \rightarrow Re_2(O_2CR)_4Cl_2 + 4HCl + 2Bu_4NCl$$

This strategy is readily applicable to the related bromide[24,57,81] and iodide[25] derivatives. Interestingly, in the reactions between $[Re_2X_8]^{2-}$ (X = Cl or Br) and monochloroacetic and monobromoacetic acids to prepare $Re_2(O_2CCH_2Cl)_4Cl_2$ and $Re_2(O_2CCH_2Br)_4Br_2$, halide ligand exchange also occurs (e.g., $[Re_2Cl_8]_2 + CH_2BrCO_2H \rightarrow Re_2(O_2CCH_2Br)_4Br_2$).[82]

In the case of the aryl carboxylic acids, the complexes are best prepared through carboxyl exchange utilizing the acetates.[57,83]

$$Re_2(O_2CCH_3)_4X_2 + 2ArCO_2H \rightarrow Re_2(O_2CAr)_4X_2 + 4CH_3CO_2H$$

As an alternative to starting with the $[Re_2Br_8]^{2-}$ and $[Re_2I_8]^{2-}$ anions, the following reaction[84] of the pre-formed chloro-complexes $Re_2(O_2CR)_4Cl_2$ with liquid HBr or HI can be used:

$$Re_2(O_2CR)_4Cl_2 + 2HX \rightarrow Re_2(O_2CR)_4X_2 + 2HCl$$

Note that in the presence of an excess of HX and the appropriate Bu_4NX salt, the latter reaction proceeds further to regenerate $(Bu_4N)_2Re_2X_8$ (see Section 8.3).[25] The synthesis of the orange formate complex $Re_2(O_2CH)_4Cl_2$ has been accomplished through the reaction of $(NH_4)_2Re_2(O_2CH)_2Cl_6$ or $Re_2(O_2CH)_3Cl_3$ with formic acid at 70-80 °C in the presence of metallic zinc;[85,86] the role of the zinc in these reactions is unclear. The infrared spectral properties of this complex have been compared with those of the analogous bromide although details for the preparation of $Re_2(O_2CH)_4Br_2$ were not described.[85]

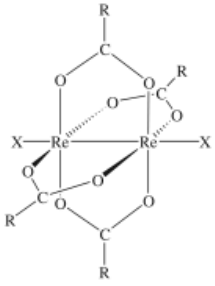
The homoleptic acetate complex $Re_2(O_2CCH_3)_6$, which probably possesses the structure $Re_2(\mu\text{-}O_2CCH_3)_4(\eta^1\text{-}O_2CCH_3)_2$, has been isolated as the major product when the dirhenium octahydride complex $Re_2H_8(PPh_3)_4$ reacts with acetic acid/acetic anhydride mixtures in 1,2-dichlorobenzene.[87] This brown compound is very insoluble in most solvents but can be converted into $Re_2(O_2CCH_3)_4Cl_2$ when reacted with gaseous hydrogen chloride in ethanol.

Recently, the first trifluoroacetate complex of dirhenium(III) was obtained by the solvothermal reaction of $(Bu_4N)_2Re_2Cl_8$ with $CF_3COOH/(CF_3CO)_2O$ mixtures.[88] This affords the complex $(Bu_4N)Re_2(O_2CCF_3)Cl_6$ (yield not reported), along with a reduced dirhenium by-product $Re_2(\mu\text{-}Cl)_2(CO)_6$. The reaction of $(Bu_4N)_2Re_2(O_2CCF_3)Cl_6$ with the organometallic carboxylic

Pictiva EX2004
Samsung v Pictiva
IPR2024-01094

acid $(CO)_6Co_2CHCCO_2H$ gives the mixed-metal complex $Re_2[O_2CCCHCo_2(CO)_6]_4Cl_2$,[88] which is similar structurally to other $Re_2(O_2CR)_4Cl_2$ carboxylates.

Several dirhenium(III) carboxylates of the type $Re_2(O_2CR)_4X_2$ have been fully characterized structurally[78,81,83,88-91] and all are found to have the basic 'paddlewheel' structure represented in **8.2**. These compounds, along with their Re–Re bond lengths, are listed in Table 8.1. From a historical perspective the most important structural determination was that carried out on the chloroform solvate of the dirhenium(III) benzoate, $Re_2(O_2CPh)_4Cl_2{\cdot}2CHCl_3$.[89] This structure determination established that the Re–Re quadruple bond had indeed been retained upon substitution of the chloride ligands of the parent $[Re_2Cl_8]^{2-}$ anion by four bridging benzoate ligands. A further significant feature in the structure of the benzoate complex is the weakness of the axial Re–Cl bonds (r(Re–Cl) = 2.49 Å). In fact, the latter feature is common in the structures of all the dirhenium(III) carboxylate complexes of this type.



8.2

The weakness of the axial Re–Cl bonds in $Re_2(O_2CR)_4Cl_2$ is reflected in their substitutional lability; this fact has already mentioned in the case of the reactions of $Re_2(O_2CR)_4Cl_2$ with liquid HBr and HI to give $Re_2(O_2CR)_4X_2$ (X = Br or I).[84] A further illustration is found in the recent report of the reactions of the pivalate complex $Re_2(O_2CCMe_3)_4Cl_2$ with $Na[M(CO)_5CN]$ to form the linear μ-cyano bridged complexes $Re_2(O_2CCMe_3)_4[\mu\text{-}NCM(CO)_5]_2$ (M = Cr, Mo or W).[92] These complexes have been characterized primarily on the basis of their spectroscopic properties. Although detailed mechanistic studies of the halide substitution in complexes that contain the Re_2^{6+} core are quite rare, one such investigation by Webb and Espenson[93] established that the reaction $Re_2(O_2CC_2H_5)_4Cl_2 + Br^- \rightarrow Re_2(O_2CC_2H_5)_4ClBr + Cl^-$ in acetonitrile proceeds by a two-step mechanism involving loss of Cl^- prior to coordination of Br^-. This reaction is subject to catalysis by trace amounts of such neutral donors as pyridine, DMF, urea, water, etc., an effect that has been ascribed[93] to the nucleophilic character of the catalysts and their ability to stabilize the coordinatively unsaturated $[Re_2(O_2CC_2H_5)_4Cl]^+$ species.

The preceding discussion has focused on the carboxylate complexes of the type $Re_2(O_2CR)_4X_2$, which represent the maximum extent to which substitution of the halide ligands of the parent $[Re_2X_8]^{2-}$ anions may occur. Bearing in mind the description by Kotel'nikova et al[13,74,75] of materials that were said to be $(ReCl_2{\cdot}CH_3COOH{\cdot}H_2O)_2$ and $Re_2Cl_3{\cdot}(CH_3COOH)_3{\cdot}H_2O$, the existence of $Re_2(O_2CR)_2X_4$ and $Re_2(O_2CR)_3X_3$, representing intermediate degrees of substitution of $[Re_2X_8]^{2-}$, seemed likely. Indeed, Kotel'nikova and co-workers later published several reports[79,80,94,95] that provided details of the experimental conditions necessary for the conversion of $KReO_4$ and K_2ReX_6 to $Re_2(O_2CR)_2X_4(H_2O)_2$ (R = CH_3, C_2H_5, $(CH_3)_2CH$, $(CH_3)_3C$ or C_6H_5; X = Cl or Br) through the high pressure hydrogen reduction of these reagents in mixtures of HX and RCO_2H. Several mixed halide derivatives of the type $Re_2(O_2CCH_3)_2Cl_{4-x}Br_xL_2$ (L = DMF, DMSO, or DMA) were obtained serendipitously as by-products during the autoclave synthesis

Pictiva EX2004
Samsung v Pictiva
IPR2024-01094

of $Re_2(O_2CCH_3)_2Br_4L_2$.[96] It appears that the presence of chloride in these products arose from impurities that had been adsorbed on the wall of the autoclave from previous experiments that had involved an HCl-containing reaction mixture.

An alternative and very convenient synthesis of $Re_2(O_2CCH_3)_2X_4(H_2O)_2$ (X = Cl or Br) and $Re_2(O_2CC_2H_5)_2Cl_4(H_2O)_2$ that has been developed involves the reaction of $(Bu_4N)_2Re_2X_8$ with acetic or propionic anhydride and 48% aqueous HBF_4.[97,98] The blue trichloroacetate complex $Re_2(O_2CCCl_3)_2Cl_4$ is produced[97] when $(Bu_4N)_2Re_2Cl_8$ is added to molten trichloroacetic acid.

When the aforementioned hydrated acetato complexes $Re_2(O_2CR)_2X_4(H_2O)_2$ (X = Cl or Br) are reacted with neutral donor ligands (L) such as pyridine, 4-methylpyridine, dimethylacetamide, DMF, DMSO and Ph_3PO, the coordinated water molecules are displaced to give $Re_2(O_2CR)_2X_4L_2$.[79,98,99] The relationship between the Raman active Re–Re stretching frequency and the donor properties of the monodentate neutral ligands in complexes of the type $Re_2(O_2CCH_3)_2Cl_4L_2$ has been examined.[100] The pyridine complex $Re_2(O_2CCH_3)_2Cl_4(py)_2$, which is formed upon treatment of an aqueous solution of $Re_2(O_2CCH_3)_2Cl_4(H_2O)_2$ with pyridine, must be identical with the material described by Kotel'nikova and Vinogradova[74] as "$(ReCl_2{\cdot}CH_3COOH{\cdot}C_5H_5N)_2$". Also, a close similarity in the spectroscopic properties of this group of complexes (including the hydrates) implies[79] that they are closely related structurally. Crystal structure determinations on representative members of this series (vide infra) have shown that in all instances except one, namely the benzoate containing $[Re_2(O_2CPh)_2Cl_6]^{2-}$ anion, as present in the salt $[ReCl_2(dpcp)_2]Re_2(O_2CPh)_2Cl_6$,[101] there is a cis-arrangement of bridging carboxylate groups and the ligands L are axially bound; accordingly, they are usually represented as *cis*-$Re_2(O_2CR)_2X_4L_2$. This is also true in the case of the chloride complex $(Bu_4N)Re_2(O_2CCH_3)_2Cl_5$, which consists of individual *cis*-$Re_2(O_2CCH_3)_2Cl_4$ units linked into infinite chains by bridging axial chloride ligands.[101] While $Re_2(O_2CPh)_2Cl_4(THF)_2{\cdot}THF$ has the usual cis structure, the bis-chloride adduct $[Re_2(O_2CPh)_2Cl_6]^{2-}$, possesses a transoid arrangement of carboxylate ligands.[101]

More recently, it has been reported that $Re_2(O_2CR)_2X_4(H_2O)_2$ reacts with the symmetrical linker ligands pyrazine, 4,4'-bipyridine and methylenebis(diphenylphosphine oxide) to form insoluble polymeric complexes of the type $[Re_2(O_2CCH_3)_2Cl_4(LL)]_n$ in which the cis structure of the $Re_2(O_2CCH_3)_2Cl_4$ unit is preserved.[102] In addition, the non-polymeric pyrazine complex $[Re_2(O_2CCH_3)_2Cl_4(pyz)]_2(\mu\text{-pyz})$ has been isolated in which both terminally bound and bridging pyrazine ligands are present.[102]

Several formato complexes that are derived from $Re_2(O_2CH)_2Cl_4$ are known. The entry to this chemistry is through $(NH_4)_2Re_2(O_2CH)_2Cl_6$, a complex that is formed by the reaction of $(NH_4)_2Re_2Cl_8$ with formic acid.[85,103] The corresponding Cs^+ salt has also been prepared and shows very similar infrared spectral properties to $(NH_4)_2Re_2(O_2CH)_2Cl_6$.[85] Treatment of this complex with DMF or diphenylformamide in formic acid gives *cis*-$Re_2(O_2CH)_2Cl_4(DMF)_2$ and *cis*-$Re_2(O_2CH)_2Cl_4(DPF)_2$.[85,104,105] On the other hand, with triethylamine as the base, the blue-green crystalline salt $[(C_2H_5)_3NH]Re_2(O_2CH)_3Cl_4{\cdot}HCO_2H$ is formed.[106] The crystal structure of this salt suggests that it is best considered as a derivative of $Re_2(O_2CH)_2Cl_4$. The pyridine adduct $Re_2(O_2CH)_2Cl_4(py)_2$ is formed from $(NH_4)_2Re_2Cl_8{\cdot}2H_2O$ in the presence of formic acid and pyridine.[105] The pyrolysis of $Re_2(O_2CH)_2Cl_4L_2$ (L = DPF, DMF or py) has been reported to form $ReCl(CO)_5$ and ReO_2 as the main decomposition products.[105] While the formate complex $Re_2(O_2CH)_2Br_4(DMF)_2$ has been described as precipitating when a solution of $K_2Re_2Br_8{\cdot}2H_2O$ is treated with formic acid and DMF,[85] it remains poorly characterized.

Since the tetrakis(formate) derivative $Re_2(O_2CH)_4Cl_2$ (vide supra) can be prepared from $(NH_4)_2Re_2(O_2CH)_2Cl_6$, it is logical that, with the careful manipulation of the reaction conditions, $Re_2(O_2CH)_3Cl_3$ can also be prepared from this same starting material upon its reac-

Pictiva EX2004
Samsung v Pictiva
IPR2024-01094

tion with formic acid.[85,86,107] A few other examples of carboxylates of the type $Re_2(O_2CR)_3X_3$ are known. Thus, while $Re_2(O_2CCH_3)_2X_4L_2$ complexes are converted into $Re_2(O_2CCH_3)_4X_2$ upon prolonged reflux with glacial acetic acid,[79,97] much milder and more controlled reactions have been used to convert $Re_2(O_2CCH_3)_2X_4(H_2O)_2$[97] and $Re_2(O_2CCH_3)_2X_4$[79] (X = Cl or Br) into $Re_2(O_2CCH_3)_3X_3$. However, as discussed below, an additional method for preparing $Re_2(O_2CR)_3X_3$ compounds is through the thermal decomposition of $Re_2(O_2CR)_4X_2$.

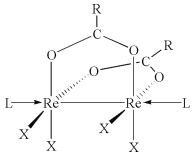
Thermal studies have shown[95,108,109] that the axial ligands L of $Re_2(O_2CCH_3)_2X_4L_2$ can be lost on heating, although it is apparent that this can be a complex process. The most thoroughly studied systems are the hydrates; the volatile anhydrous acetates $Re_2(O_2CCH_3)_2X_4$ are formed following loss of H_2O.[95] X-ray structure determinations on anhydrous $Re_2(O_2CCH_3)_2X_4$ have shown[110-112] that a trans arrangement of acetate ligands is present, thereby establishing that the loss of the axially bound ligand molecules is accompanied by a *cis* → *trans* isomerization. This isomerization process is reversed upon the re-addition of the axial ligand.[113] The thermal decomposition of several carboxylates of the type $Re_2(O_2CR)_4X_2$ (X = Cl or Br; R = CH_3, C_2H_5, $(CH_3)_2CH$, $(CH_3)_3C$ and C_6H_5) has also been found to yield $Re_2(O_2CR)_2X_4$ compounds under a flow of inert gas (Ar or N_2),[112] but the stoichiometry of the reactions are quite complex and, in the case of $Re_2(O_2CC_2H_5)_4Cl_2$, appreciable quantities of $Re_2(O_2CC_2H_5)_3Cl_3$ are also said to be produced.[112] The latter observation is in accord with earlier results from the thermal decomposition of the pivalate complex $Re_2(O_2CCMe_3)_4Cl_2$ in vacuo. At a temperature of 240 °C the major product is pink $Re_2(O_2CCMe_3)_3Cl_3$, whereas at 260 °C green $Re_2(O_2CCMe_3)_2(HO_2CCMe_3)Cl_4$ is produced.[114] Resublimation of the latter complex at 160 °C in a sealed tube leads to loss of the molecule of pivalic acid and the formation of green crystals of $Re_2(O_2CCMe_3)_2Cl_4$.[114]

There are other reactions that afford some of these same carboxylates, by less obvious pathways than the ones that start from $[Re_2X_8]^{2-}$, i.e., the starting materials do not already contain a Re–Re quadruple bond. Thus, at the beginning of this section (8.4.2) we described the reactions of trinuclear rhenium(III) chloride with alkyl carboxylic acids. The complexes $[Re(O_2CR)_2Cl]_2$ which had been isolated in this fashion by Taha and Wilkinson[76] are the same orange colored species $Re_2(O_2CR)_4Cl_2$ that were later prepared in a more logical fashion[14] directly from $[Re_2Cl_8]^{2-}$. Another example is rhenium(IV) chloride, $[\beta\text{-}ReCl_4]_\infty$, which can be converted into $Re_2(O_2CCH_3)_4Cl_2$ upon reflux with acetic acid, and also to dark blue $Re_2(O_2CCH_3)_2Cl_4(H_2O)_2$.[115] However, perhaps the most interesting system, is *trans*-$ReOX_3(PPh_3)_2$ (X = Cl or Br). The reactions of these mononuclear complexes are rather complicated and the products that are formed depend critically upon the reaction conditions.[116] Mixtures of red *trans*-$ReCl_4(PPh_3)_2$, purple $Re_2OCl_3(O_2CR)_2(PPh_3)_2$ (the latter originally mis-formulated as lacking the oxygen) and/or dark green $Re_2OCl_5(O_2CR)(PPh_3)_2$ are obtained upon heating *trans*-$ReOCl_3(PPh_3)_2$ with carboxylic acids in boiling toluene. Structural studies[117,118] on $Re_2OCl_5(O_2CC_2H_5)(PPh_3)_2$ and $Re_2OCl_3(O_2CC_2H_5)_2(PPh_3)_2$ revealed the correct formula for the latter and showed that these complexes are carboxylate bridged edge-sharing bioctahedral dirhenium compounds that contain Re–Re bonds. Although the Re–Re bond distances are quite short (2.51-2.52 Å) it is not clear what these values imply in terms of the metal-metal bond orders. Upon prolonged hearing of $Re_2OCl_3(O_2CR)_2(PPh_3)_2$ with more carboxylic acid the quadruply-bonded complexes $Re_2(O_2CR)_4Cl_2$ are produced.[116] Alternatively, the latter may be prepared in fairly high yield by the direct reaction of *trans*-$ReOCl_3(PPh_3)_2$ with the refluxing acid anhydride. Accordingly, $Re_2OCl_5(O_2CR)(PPh_3)_2$ and $Re_2OCl_3(O_2CR)_2(PPh_3)_2$ represent intermediate stages of reduction in the conversion of $ReOCl_3(PPh_3)_2$ to $Re_2(O_2CR)_4Cl_2$. From the reactions between *trans*-$ReOBr_3(PPh_3)_2$ and the carboxylic acids or their anhydrides, the related bromide complexes $Re_2(O_2CR)_4Br_2$ can be prepared.[116]

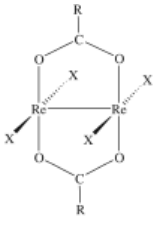
Pictiva EX2004
Samsung v Pictiva
IPR2024-01094

Around the time of the structure report on $Re_2(O_2CPh)_4Cl_2$,[89] which was the first for a quadruply-bonded compound of the type $Re_2(O_2CR)_4Cl_2$, Koz'min et al[119] described preliminary details of a structure determination on the carboxylate complex they represented as $ReCl_2{\cdot}CH_3COO(H){\cdot}2H_2O$. Three years later the full structure report appeared,[120] the complex continuing to be represented incorrectly as containing rhenium(II) and acetic acid i.e. $Re_2Cl_4[CH_3COO(H)]^2{\cdot}2H_2O$. The Re–Re bond length (2.224(5) Å) is consistent with a quadruple bond, and there are axially bound water molecules (r(Re–O) = 2.50 Å) and a *cis*-arrangement of bridging acetate groups. This same type of structure (**8.3**) has been found for all complexes of the type $Re_2(O_2CR)_2X_4L_2$ that have been structurally characterized (R = H when L = DPF; R = CH_3 when L = H_2O, DMSO or DMF),[104,120-122] including $(NH_4)_2Re_2(O_2CH)_2Cl_6$ in which L = Cl^-. The axial Re–Cl distances in the latter complex are very long (2.71 Å) relative to the equatorial Re–Cl bond lengths (2.31 Å).[123] The polymeric ligand-bridged complexes $[Re_2(O_2CCH_3)_2Cl_4(\mu\text{-LL})]_n$, where LL = pyz, 4,4'-bpy or $dppmO_2$, as well as $[Re_2(O_2CCH_3)_2Cl_4(pyz)]_2(\mu\text{-pyz})$, also contain the **8.3** unit; all these compounds have been crystallographically characterized (Table 8.1).[102] Polymeric complexes have also been isolated with isonicotinamide (INA) and nicotinamide as the axial ligands.[124] In these cases, polymerization arises from strong intermolecular hydrogen-bond interactions. A further variation of **8.3** is seen in the structure of the formate complex $[(C_2H_5)_3NH]Re_2(O_2CH)_3Cl_4{\cdot}HCO_2H$, in which *cis*-$Re_2(O_2CH)_2Cl_4$ units are linked by axially bridging formate ligands to form polymeric chains.[106] The structures that are based on **8.3** are listed in Table 8.1.

As was mentioned earlier in this section, ligand loss from *cis*-$Re_2(O_2CR)_2X_4L_2$ produces $Re_2(O_2CR)_2X_4$, which have been shown to possess the symmetric trans structure **8.4**. In the structures of the acetate complexes $Re_2(O_2CCH_3)_2X_4$, the Re–Re bond distances are 2.2084(3) Å for X = Cl and 2.216(3) Å for X = Br; the neighboring dinuclear units are linked via weak Re–X···Re bridges (2.887(1) Å for X = Cl and *c.* 3.09 Å for X = Br).[110-112] These structures are very similar to those reported earlier for $Re_2(O_2CPh)_2I_4$[58] and $Re_2(O_2CCMe_3)_2Cl_4$,[114] which in turn resemble the centrosymmetric structures of the amidinate complexes $Re_2[(PhN)_2CPh]_2Cl_4$ and $Re_2[(PhN)_2CCH_3]_2Cl_4$ that are discussed in Section 8.4.3. The blue chloro complex $Re_2(O_2CCH_3)_2Cl_4$ preserves its identity in the gas phase as shown by mass spectral measurements.[111]



8.3



8.4

Turning now to the 3:3 complexes $Re_2(O_2CR)_3X_3$, the pivalate complex $Re_2(O_2CCMe_3)_3Cl_3$ can be considered to have the prototype structure (Fig. 8.4). It represents a situation that is intermediate between $Re_2(O_2CR)_4Cl_2$ and $Re_2(O_2CR)_2Cl_4$. Parallel chains of $[Re_2(O_2CCMe_3)_3Cl_2]^+$ units are linked by bridging Cl^- ligands that are shared between the axial positions of successive $[Re_2(O_2CCMe_3)_3Cl_2]^+$ ions in the chains.[114] A similar structure was reported around the same time for the formate complex $Re_2(O_2CH)_3Cl_3$.[107]

With the basic structural information available for the three main groups of dirhenium(III) carboxylates, it is now appropriate to return to the question of the structures of complexes for-

Pictiva EX2004
Samsung v Pictiva
IPR2024-01094

mulated by Taha and Wilkinson[76] as $[ReOCl(O_2CR)]_2$ and $[ReO_2(O_2CR)]_2$ that they obtained upon refluxing Re_3Cl_9 with carboxylic acids in the presence of oxygen. Lock and co-workers[77,78] have shown by structural studies on the two butyrate derivatives that these complexes are in reality $[Re_2(O_2CR)_3Cl_2]ReO_4$ and $[Re_2(O_2CR)_4](ReO_4)_2$, respectively, so they correspond to known structural types, i.e. $Re_2(O_2CCMe_3)_3Cl_3$ and $Re_2(O_2CCMe_3)_4Cl_2$, with perrhenate substituted for *axial* halide.

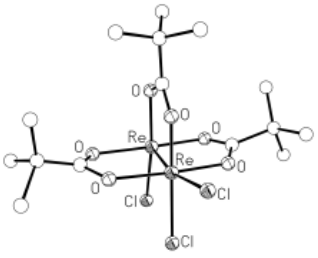


Fig. 8.4. The structure of $Re_2(O_2CCMe_3)_3Cl_3$ showing the formula unit.

In addition to studies of the thermal decomposition of various formato complexes of dirhenium(III)[86,105] and ^{1}H NMR spectral studies of the isomerization between *trans*-$Re_2(O_2CR)_2X_4$ and *cis*-$Re_2(O_2CR)_2X_4L_2$,[113] an assortment of carboxylates, namely, $Re_2(O_2CCH_3)_4Br_2$, *trans*-$Re_2(O_2CCH_3)_2X_4$ (X = Cl or Br), *cis*-$Re_2(O_2CCH_3)_2X_4L_2$ (L = py, DMSO, etc.), $Re_2(O_2CH)_2Cl_4L_2$ (L = DMF or DMSO), and $(NH_4)_2Re_2(O_2CH)_2Cl_6$ have been studied by ^{35}Cl or ^{81}Br NQR spectroscopy and the results compared with data for salts containing the $[Re_2Cl_8]^{2-}$ and $[Re_2Br_8]^{2-}$ anions.[125]

Reactions in which the Re_2^{6+} core is preserved

In this section, we consider those non-redox reactions of the dirhenium(III) carboxylates in which the dirhenium unit remains intact. Most redox reactions of these carboxylates, and reactions in which the Re–Re quadruple bond is cleaved, are discussed in Sections 8.5 and 8.7, respectively.

On the basis of the previous discussions of the synthetic procedures that have been used to obtain the dirhenium(III) carboxylates, the interconversions shown below are well documented and need not be considered in any further detail. Suffice it to say that the reversibility of these reactions serves to illustrate dramatically the stability of the Re–Re quadruple bond. Note that these same reactions are also encountered in the case of the various dirhenium(III) formate complexes.[85] Thus, $(NH_4)_2Re_2(O_2CH)_2Cl_6$, $Re_2(O_2CH)_3Cl_3$ and $Re_2(O_2CH)_4X_2$ (X = Cl or Br) all react with NH_4Cl in conc HCl to give $(NH_4)_2Re_2Cl_8{\cdot}2H_2O$.[85]

$$[Re_2X_8]^{2-} \rightleftharpoons \textit{cis}\text{-}Re_2(O_2CR)_2X_4L_2 \rightleftharpoons Re_2(O_2CR)_3X_3 \rightleftharpoons Re_2(O_2CR)_4X_2$$

$$\textit{cis}\text{-}Re_2(O_2CR)_2X_4L_2 \underset{-2L}{\overset{+2L}{\rightleftharpoons}} \textit{trans}\text{-}Re_2(O_2CR)_2X_4$$

Behavior related to that mentioned above is encountered in the reactions of $Re_2(O_2CCH_3)_4Cl_2$ with the gaseous hydrogen halides (HX).[126-128] In all instances, these reactions, when carried out at 300-350 °C, lead to complete displacement of the acetate groups and the formation of the trinuclear rhenium(III) halides Re_3X_9. In the case of the reaction with HCl(g), the bright blue solid that is formed as an intermediate[126] has been shown to be *trans*-$Re_2(O_2CCH_3)_2Cl_4$.[111]

Pictiva EX2004
Samsung v Pictiva
IPR2024-01094

The synthetic utility of the dirhenium(III) carboxylates is further shown by their usefulness in providing a convenient entry to various alkyl derivatives that contain the Re_2^{6+} core. The interaction of the benzoate $Re_2(O_2CPh)_4Cl_2$ with methyllithium in diethyl ether produces[72] $Li_2Re_2(CH_3)_8{\cdot}2Et_2O$, a diamagnetic red crystalline complex. It is air- and water-sensitive but thermally stable. Addition of tetramethylethylenediamine or 1,10-phenanthroline to ether solutions of $Li_2Re_2(CH_3)_8{\cdot}2Et_2O$ yields pyrophoric $Li_2Re_2(CH_3)_8{\cdot}$tmed and $Li_2Re_2(CH_3)_8{\cdot}$phen. The etherate, $Li_2Re_2(CH_3)_8{\cdot}2Et_2O$, can also be produced by the reaction of rhenium(V) chloride with methyllithium. This is an especially significant reaction since it constitutes a relatively rare example of the formation of a Re–Re quadruple bond from a *mononuclear* starting material without the use of *bridging* ligands. The crystal structure of $Li_2Re_2(CH_3)_8{\cdot}2Et_2O$ has been determined[72] and reveals the short Re–Re bond (Table 8.1) and eclipsed configuration that are so characteristic of the presence of a Re–Re quadruple bond.

The reactions of $Li_2Re_2(CH_3)_8{\cdot}2Et_2O$ with various monodentate tertiary phosphines gives $Re_2(CH_3)_6(PR_3)_2$ in good yield,[129] a reaction course analogous to that in which the $[Re_2X_8]^{2-}$ anions are converted to $Re_2X_6(PR_3)_2$ (Section 8.4.4). Mixed alkyl-carboxylato complexes can be obtained starting from either $Re_2(O_2CCH_3)_4Cl_2$ or $[Re_2(CH_3)_8]^{2-}$. The treatment of $Re_2(O_2CCH_3)_4Cl_2$ with R_2Mg reagents in diethyl ether produces red crystalline $Re_2(O_2CCH_3)_2R_4$, where R = $CH_2Si(CH_3)_3$, $CH_2C(CH_3)_3$, $CH_2C(CH_3)_2Ph$ or CH_2Ph.[130] The trimethylsilylmethyl and neopentyl derivatives are quite air stable. When $Re_2(O_2CCH_3)_4Cl_2$ reacts with three equivalents of bis-2-methoxyphenylmagnesium, the diamagnetic dark green dirhenium(III) complex $Re_2(2\text{-}CH_3OC_6H_4)_6$ is produced.[131] This complex is of unknown structure although it probably retains a Re–Re quadruple bond; its ^1H and ^{13}C NMR spectra are consistent[131] with aryl groups in two different environments.

The addition of glacial acetic acid and acetic anhydride to $Li_2Re_2(CH_3)_8{\cdot}2Et_2O$ gives the bright red air-stable complex $Re_2(O_2CCH_3)_4(CH_3)_2$. Its crystal structure has been determined (Fig. 8.5), revealing[132] that it does not have the $Re_2(O_2CR)_4Cl_2$ type structure. Two acetate groups bridge the quadruply-bonded pair of rhenium atoms while a chelate acetate and terminal methyl group are bound to each metal atom.[132] The oxygen atoms of the chelating acetate ligands that occupy the axial coordination sites of the dinuclear complex (along the Re–Re axis) are, as expected, weakly bound (2.46 Å versus 2.02-2.12 Å for the equatorial Re–O bonds).[132] It has been suggested,[133] that the treatment of $Re_2(O_2CH)_4Br_2$ with Et_3Al leads to $Re_2(O_2CH)_4Et_2$ and perhaps $Re_2(O_2CH)_4H_2$, prior to cleavage of the Re–Re bond to give mononuclear products. However, neither complex has been isolated and definitively characterized.[133]

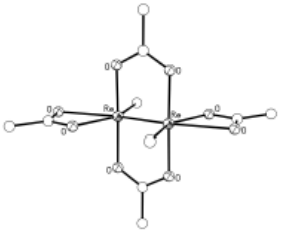


Fig. 8.5. The structure of $Re_2(O_2CCH_3)_4(CH_3)_2$.

Treatment of $Re_2(O_2CCH_3)_4(CH_3)_2$ with chlorine in dichloromethane and with methanol gives[130] purple-mauve powders of stoichiometry $[Re(O_2CCH_3)Cl(CH_3)]_n$ and $[Re(O_2CCH_3)(OCH_3)(CH_3)]_n$, respectively. These two materials probably bear a close structural relationship to one another. The chloro-derivative is soluble in dimethylsulfoxide from which air stable crystals of $Re_2(O_2CCH_3)_2Cl_2(CH_3)_2{\cdot}$DMSO have been grown. The basic structure of this complex[132]

Pictiva EX2004
Samsung v Pictiva
IPR2024-01094

shows a close resemblance to that of *trans*-$Re_2(O_2CCH_3)_2Cl_4$, with a DMSO ligand occupying only *one* of its two available axial coordination sites. A rather surprising feature in the structures of the methyl derivatives $Re_2(O_2CCH_3)_2Cl_2(CH_3)_2$·DMSO and $Re_2(O_2CCH_3)_4(CH_3)_2$ is the shortness of the Re–Re bonds (Table 8.1) even though both complexes contain axial ligands.[132] These appear to be examples of molecules for which the presence of axial ligands does not lead to an obvious weakening of the Re–Re bond.

The substitution of all four carboxylate groups in $Re_2(O_2CR)_4X_2$ (especially when R = CH_3 and X = Cl) by other monoanionic *bridging* ligands has often been used to prepare compounds of the type $Re_2(\mu\text{-bridge})_4X_2$. This procedure often constitutes a convenient alternative to the use of $[Re_2X_8]^{2-}$. These reactions are more appropriately discussed in Section 8.4.3, along with those of the $[Re_2X_8]^{2-}$ anions with monoanionic bidentate ligands. However, note the possibility of obtaining complexes in which there are mixed sets of carboxylate and other monoanionic bridging ligands. Such an example is the complex $Re_2(O_2CEt)_2(9\text{-EtA})_2Cl_2$ in which there are *cis*-pairs of bridging propionate and the bridging anion of the DNA nucleobase adenine, the latter being bound through its N1 and N6 positions.[134]

The substitution chemistry of $Re_2(O_2CCH_3)_2X_4L_2$ (X = Cl or Br; L = H_2O or 4-methylpyridine) has also proved synthetically useful,[135] although many of the reactions of these compounds lead to Re_2^{5+} and Re_2^{4+} species (see Section 8.5.4). Examples of non-redox substitution chemistry include reactions with 2-hydroxypyridine and with 2-methyl-6-hydroxypyridine in THF or acetone which afford $Re_2(hp)_2Cl_4$·Hhp·THF and $Re_2(mhp)_2X_4$·Hmhp·S (S = THF or $(CH_3)_2CO$), respectively (for further details see Section 8.4.3).[136] While $Re_2(O_2CCH_3)_2Cl_4(H_2O)_2$ reacts with an excess of Hhp in acetonitrile or ethanol to give $Re_2(hp)_4Cl_2$, the Hmhp ligand reacts with $Re_2(O_2CCH_3)_2X_4(H_2O)_2$ (X = Cl or Br) in a different fashion when nitrile solvents R'CN (R' = CH_3 or C_2H_5) are used. The latter reactions afford products of the type $Re_2(O_2CR')(mhp)_2X_3$, in which the bridging carboxylate ligands is formed by hydrolysis of the R'CN solvent.[136]

A variety of interesting and synthetically useful reactions that involve dirhenium(III) carboxylates and tertiary phosphine ligands have been examined. Several of these lead to Re_2^{5+} and Re_2^{4+} products and so are discussed in Section 8.5.4, while others will be considered here. Most of these involve products in which all of the carboxylato ligands have been replaced but in a couple of cases a carboxylate ligand is retained. In the case of the reaction between $Re_2(O_2CPh)_4Cl_2$ and PMe_3 in ethanol in the presence of traces of air (or a small amount of H_2O_2) an unusual centrosymmetric 'dimer of dimers' complex $[(PMe_3)_3ClRe(\mu\text{-}O_2CPh)Re(O)]_2(\mu\text{-}O)_2$ is obtained, the structure of which is shown in Fig. 8.6.[137] The rhenium centers in each dirhenium unit have distinctly different coordination environments i.e. $P_3ClORe–ReO_4$, and it has been suggested that this unit can be considered formally as Re(IV)–Re(II) or Re(V)–Re(I). The Re–Re bond distance of 2.3396(8) Å is consistent with a Re–Re multiple bond. Other examples that give rise to this general type of intramolecular disproportionation had been encountered previously. Thus the reaction of $Re_2(O_2CCH_3)_4Cl_2$ with $Cy_2PCH_2PCy_2$ produces both $ReOCl(\eta^2\text{-dcpm})_2$ and *trans*-$Re_2(\mu\text{-}O_2CCH_3)_2Cl_2(\mu\text{-dcpm})_2$ (see Section 8.5.4), the mononuclear Re(III) product subsequently converting to $O_3ReReCl(\eta^2\text{-dcpm})_2$ (**8.5**) upon exposure to O_2.[138] The Re–Re distance in **8.5** is 2.5398(6) Å and therefore signifies a bond order less than four. A formal description of this compound as a Re(VI)–Re(I) system seems reasonable.[138] In an even earlier report it was shown that the reactions of the bis-acetato complex *cis*-$Re_2(O_2CCH_3)_2Cl_4(H_2O)_2$ with $Me_2PCH_2PMe_2$ gives a compound that is related structurally to **8.5**, namely, $O_3ReReCl_2(dmpm)_2$.[139] This reaction, like the aforementioned one that gives **8.5**, might proceed through a mononuclear intermediate. In the dmpm compound, the two metal centers have coordination numbers of four and seven as shown in **8.6**, rather than four and six as

Pictiva EX2004
Samsung v Pictiva
IPR2024-01094

in **8.5**. The Re–Re bond length of 2.4705(5) Å is shorter by *c*. 0.07 Å than that in **8.5**. *Ab initio* SCF and CI studies on the model species $O_3ReReCl_2(H_2PCH_2PH_2)_2$ have been interpreted[140] in terms of a charge distribution Re(V)–Re(III) (i.e. d^2–d^4), with the short, strong Re–Re bond represented in terms of a σ-donation from $[ReO_3]^-$ to $[ReCl_2(H_2PCH_2PH_2)_2]^+$



8.5 **8.6**

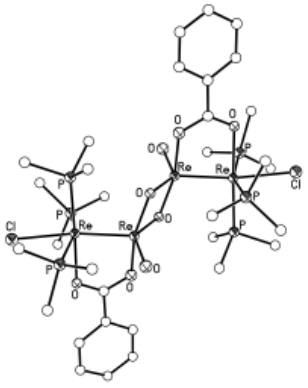


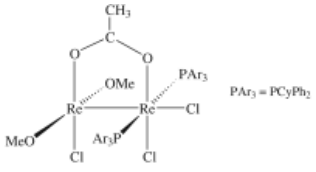
Fig. 8.6. The structure of the "dimer of dimers" molecule $[(PMe_3)_3ClRe(\mu\text{-}O_2CPh)Re(O)]_2(\mu\text{-}O)_2$.

While $Re_2(O_2CCH_3)_2Cl_4L_2$ (L = H_2O or py) react with PMe_3, PMe_2Ph and $PMePh_2$ in alcohol solvents (ROH) to give the Re_2^{4+} complexes $Re_2Cl_4(PR_3)_4$ (Section 8.5.4), a quite different reaction course ensues with the phosphine ligand PPh_3 and other triarylphosphines.[98,141-143] Upon reacting *cis*-$Re_2(O_2CCH_3)_2Cl_4(H_2O)_2$ in methanol with PAr_3 ligands that have relatively low basicities (pK_a values of 1.0-4.6) and moderately large cone angles (145-165°) the unsymmetrical Re_2^{6+} methoxides $(MeO)_2Cl_2ReReCl_2(PAr_3)_2$ (PAr_3 = PPh_3, P(*p*-tolyl)$_3$, P(*m*-tolyl)$_3$, P(*p*-ClPh)$_3$ and P(*p*-MeOPh)$_3$) are formed.[98,141-143] In the case of PPh_3 this same type of product has been obtained for the bromide and with other alkoxide ligands, i.e. $Re_2X_4(OR)_2(PPh_3)_2$ (X = Cl or Br; R = CH_3, C_2H_5, *n*-C_3H_7 or *i*-C_3H_7).[98,141] The reaction of *cis*-$Re_2(O_2CCH_3)_2Cl_4(H_2O)_2$ with P(*p*-MeOPh)$_3$ in methanol have also been found[142] to produce the tetranuclear complex $Re_2(\mu\text{-}O)_4Cl_4[P(p\text{-}MeOPh)_3]_4$. The mixed halide-alkoxide products are different structurally from the Re(III)–Re(III) derivatives $Re_2X_6(PR_3)_2$ (see Sec. 8.4.4) since they possess the unsymmetrical mixed-valence Re(IV)–Re(II) structure shown in Fig. 8.7. Both $Re_2Cl_4(OEt)_2(PPh_3)_2$ and $Re_2Cl_4(OMe)_2[P(p\text{-}MeOPh)_3]_2$ have been crystallographically characterized; the Re–Re distances are 2.231(1) Å and 2.2476(4) Å, respectively.[98,141,143] The very short Re–Re distance and eclipsed rotational geometry are in accord with the retention of a Re–Re quadruple bond, with one component of this bond being dative in character in the sense Re(1) → Re(2), i.e. Re≣Re. These are interesting and relatively rare examples of intramolecular disproportionation reactions that occur at a metal-metal multiple bond without change in the formal metal-metal bond order. Indeed, they were the first examples of their kind to be reported.[98,141] In the case of

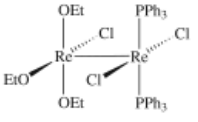
Pictiva EX2004
Samsung v Pictiva
IPR2024-01094

the more basic phosphines $PCyPh_2$ and PBz_3, which have cone angles of 153° and 165°, respectively, their reactions with *cis*-$Re_2(O_2CCH_3)_2Cl_4(H_2O)_2$ in methanol afford $Re_2(\mu\text{-}O_2CCH_3)Cl_3(OMe)_2(PCyPh_2)_2$ (see **8.7**), which has a slightly longer Re–Re quadruple bond distance because of the presence of an axial Re–Cl bond (see Table 8.1), and the paramagnetic Re_2^{5+} complex $Re_2(\mu\text{-}O_2CCH_3)Cl_4(PBz_3)_2$ (see Section 8.5.4), respectively. The tris-ethoxide complex $Re_2Cl_3(OEt)_3(PPh_3)_2$, which has a structure similar to that of $Re_2Cl_4(OEt)_2(PPh_3)_2$ but with one Re–Cl bond replaced by Re–OEt (see **8.8**) is formed by the reactions of $Re_2Cl_4(OEt)_2(PPh_3)_2$ or $Re_2Cl_6(PPh_3)_2$ (Section 8.4.4) with NaOEt in ethanol.[143]

Finally, note should be made of some screening studies that have been carried out involving the use of $[Re_2(O_2CC_2H_5)_4]SO_4$ and several derivatives of the type *cis*-$Re_2(O_2CR)_2X_4(H_2O)_2$ as anti-tumor agents.[144]



8.7



8.8

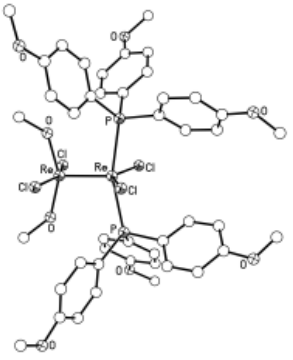


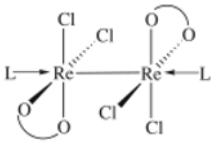
Fig. 8.7. The structure of $Re_2Cl_4(OMe)_2[P(p\text{-}MeOPh)_3]_2$, an example of an intramolecular disproportionation product.

8.4.3 Other anionic ligands

In addition to substitution reactions that involve monodentate anionic ligands (Section 8.4.1) and bridging carboxylate ligands (Section 8.4.2) there is also an extensive body of literature that deals with the reactions of the $[Re_2X_8]^{2-}$ anions, and in some cases carboxylate complexes of the types $Re_2(O_2CR)_4Cl_2$ and $Re_2(O_2CR)_2Cl_4L_2$, with bidentate monoanionic and dianionic ligands. In most instances such ligands bridge the dirhenium unit, but in a few cases chelation is found to occur. Examples of the latter are encountered in the formation of $Re_2X_4(acac)_2$ and $Re_2X_4(acac)_2L_2$ (X = Cl or Br; L = DMSO, DMF or acacH) by the reactions of $(NH_4)_2Re_2X_8{\cdot}2H_2O$ with acetylacetone.[145-147] The structures of the DMSO and acetylacetone adducts $Re_2Cl_4(acac)_2L_2$ have been determined[145,146] (see **8.9**) and the presence of a quadruple bond confirmed (Table 8.1). The axial Re–O distance involving the neutral acacH ligand is very long (2.63 Å); this compares to distances of 2.01-2.02 Å for the chelating equatorial acac

Pictiva EX2004
Samsung v Pictiva
IPR2024-01094

anions.[146] Another case, albeit an unusual one, is found in the mixed-metal quadruply bonded porphyrin complex [(TPP)MoRe(OEP)]PF_6.[148] In the dimetal cation the Mo–Re distance is 2.236 Å and the porphyrin ligands are perfectly eclipsed. This is one of several of several heterodinuclear complexes with multiple metal-metal bonds.[149]



8.9

The reactions of $(Bu_4N)_2Re_2Cl_8$ with sulfate/sulfuric acid mixtures and with phosphoric acid have been shown to produce complexes whose structures are of the 'acetate type',[150-152] in which the anionic ligands bridge the two metal atoms. These results further support the idea that substitution of some or all of the halide ligands of $[Re_2X_8]^{2-}$ usually leads to products in which the Re–Re quadruple bond (Table 8.1) is retained. The tetrakis(sulfato) derivative $(NH_4)_2Re_2(SO_4)_4(H_2O)_2$ has also been prepared by the reaction of conc H_2SO_4 with various dirhenium(III) formate complexes.[85] The structure of the $[Re_2(SO_4)_4(H_2O)_2]^{2-}$ anion is shown in Fig. 8.8 and reveals the presence of two weakly bound water molecules (r(Re–O) = 2.28 Å). Like the carboxylate complexes $Re_2(O_2CR)_4Cl_2$, the sulfate $Na_2Re_2(SO_4)_4{\cdot}8H_2O$ may be reconverted to $(Bu_4N)_2Re_2Cl_8$ upon reaction with refluxing hydrochloric acid in the presence of Bu_4NCl.[150] A compound that is closely related to this sulfate complex is formed upon reacting $(Bu_4N)_2Re_2Cl_8$ with phosphoric acid in methanol. Addition of CsCl to the resulting reaction mixture affords pale-blue crystalline $Cs_2[Re_2(HPO_4)_4(H_2O)_2]$, whereas the use of pyridine in place of CsCl gives the anhydrous pyridinium salt $(pyH)_2Re_2(HPO_4)_4$.[152] The crystal structure of the closely related derivative $Cs_2[Re_2(HPO_4)_4(H_3PO_4)_2]$ has been determined by Koz'min and co-workers.[153] Its preparation, which was different from that used to obtain $Cs_2[Re_2(HPO_4)_4(H_2O)_2]$, involves the high pressure reduction of $KReO_4$ in a 2:1 mixture of H_3PO_4 and HCl at 330 °C, followed by the addition of $(NH_4)H_2PO_4$ and CsCl to accelerate the crystallization of the complex. As expected, the two H_3PO_4 molecules are axially bound and the Re–Re bond length (2.224(1) Å) is similar to that of the sulfate complex (2.214(1) Å).

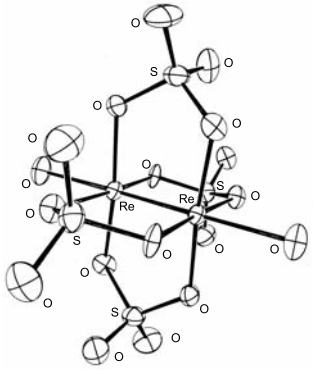


Fig. 8.8. The structure of the $[Re_2(SO_4)_4(H_2O)_2]^{2-}$ anion present in $Na_2Re_2(SO_4)_4{\cdot}8H_2O$.

Pictiva EX2004
Samsung v Pictiva
IPR2024-01094

The complex with 2-hydroxypyridine, $Re_2(hp)_4Cl_2$,[154] whose structure is represented in **8.10**, is of importance since this type of ligand system has proved to be especially effective in stabilizing dimetal units. The Re–Re bond distance of 2.206(2) Å is about 0.03 Å shorter than that in the carboxylates of the type $Re_2(O_2CR)_4X_2$ (Table 8.1). This compound was first obtained by reacting $(Bu_4N)_2Re_2Cl_8$ with molten 2-hydroxypyridine. It has also been prepared by a method that can easily be adaptable to its bromo and iodo analogs, viz., the reaction of $(Bu_4N)_2Re_2X_8$ (X = Cl, Br or I) with Hhp in refluxing *n*-pentanol.[155] The complexes $Re_2(hp)_2Cl_4(Hhp)$, and $Re_2(mhp)_2X_4(Hmhp)\cdot S$ (X = Cl or Br; S (solvent of crystallization) = THF or $(CH_3)_2CO$) have also been prepared, but not from $(Bu_4N)_2Re_2X_8$; instead, the bis(acetate) complexes $Re_2(O_2CCH_3)_2X_4L_2$ (X = Cl or Br; L = H_2O or 4-Mepy—see Section 8.4.2) were used as the starting materials with THF or acetone as the reaction solvent.[136] The coordinated Hmhp molecule in $Re_2(mhp)_2X_4(Hmhp)\cdot(CH_3)_2CO$ can be substituted by 4-methylpyridine to give $Re_2(mhp)_2X_4(4\text{-Mepy})$.[136] The reaction of $Re_2(hp)_2Cl_4(Hhp)$ with excess Hhp in hot ethanol affords the tetrakis derivative $Re_2(hp)_4Cl_2$.[136] The structure of $Re_2(mhp)_2Cl_4(Hmhp)$ is shown in Fig. 8.9 and reveals the presence of a trans arrangement of mhp ligands and an axially bound Hmhp ligand; the Re–Re distance of 2.210(1) Å is similar to that in *trans*-$Re_2(O_2CCH_3)_2Cl_4$ (Section 8.4.2). The mhp ligands are bound in a polar fashion, i.e., they are orientated in the same direction so as to give a dimetal unit that has $[ReCl_2O_2]$ and $[ReCl_2N_2]$ units. Formally at least, the Re centers can be considered to differ in oxidation state, viz., Re(IV) and Re(II), respectively. However, the ability of the mhp ligands to delocalize charge makes these systems behave more like symmetrical quadruply bonded Re(III)–Re(III) species than mixed-valent Re(IV)–Re(II) derivatives. The mixed carboxylate-mhp species $Re_2(O_2CR)(mhp)_2X_3$ (R = CH_3 or C_2H_5; X = Cl or Br) are also known;[136] their chemistry is considered elsewhere (see Section 8.4.2). Another complex that contains a 2-hydroxypyridine ligand is $Re_2(\mu\text{-chp})_2(\eta^2\text{-chp})Cl_3$, which is formed from the reaction of $Re_2(O_2CCH_3)_4Cl_2$ and molten 2-hydroxy-6-chloropyridine.[156] It has a structure in which there are two trans head-to-head bridging chp ligands (i.e. similar to $Re_2(mhp)_2Cl_4(Hmhp)$) and one chelating chp ligand with its nitrogen atom bound in an axial position. The Re–Re distance is normal (see Table 8.1).

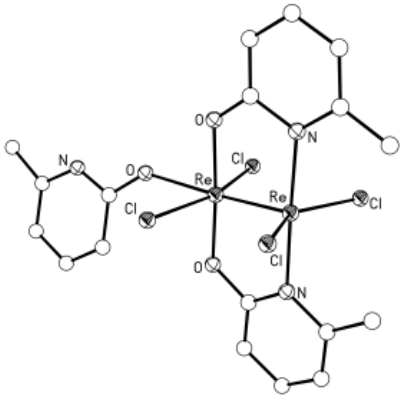
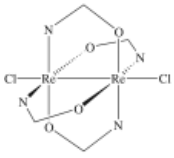


Fig. 8.9. The structure of $Re_2(mhp)_2Cl_4(Hmhp)$.

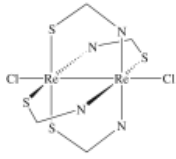
The sulfur-containing analogs of $Re_2(\mu\text{-hp})_4X_2$ are formed when 2-mercaptopyridine is reacted with $(Bu_4N)_2Re_2X_8$ (X = Cl or Br).[157] The formation of $Re_2(\mu\text{-mp})_4X_2$ probably occurs via the intermediacy of $Re_2(mp)_2X_4$. The bis-acetate complexes *cis*-$Re_2(O_2CCH_3)_2X_4L_2$ (X = Cl

Pictiva EX2004
Samsung v Pictiva
IPR2024-01094

or Br; L = H_2O or py) can be used as alternative starting materials to $(Bu_4N)_2Re_2X_8$.[157] The structural characterization of $Re_2(\mu\text{-mp})_4Cl_2$ shows that there is a small twisting about the Re–Re bond (torsion angles range from 0.8° to 11.8°) but the Re–Re quadruple bond distance is close to that in $Re_2(hp)_4Cl_2$ (Table 8.1). However, what is surprising is that the stereoisomer that is formed is the one with a 3:1 orientation of the μ-mp ligands (**8.11**), while the *cis* 2:2 isomeric form is obtained in the case of $Re_2(hp)_4Cl_2$ (**8.10**). There is no obvious reason for this difference, which may simply be the consequence of solubility differences between the different stereoisomers in the reaction solvents. Indeed, the structural characterization of the compound $Re_2(\mu\text{-}C_7H_4NS_2)_4Cl_2$, which contains bridging *N*,*S*-benzothiazole-2-thiolate ligands, has shown that there is cis 2:2 orientation, like that in $Re_2(hp)_4Cl_2$.[158] In this molecule, there is a significant deviation from an eclipsed conformation such that the average torsion angle χ_{av} is 18.0°. As a consequence, the Re–Re distance is a little longer (by *c*. 0.026 Å) than that in $Re_2(\mu\text{-mp})_4Cl_2$. The synthetic procedure for obtaining $Re_2(\mu\text{-}C_7H_4NS_2)_4Cl_2$ used $Re_2Cl_6(PPh_3)_2$ (see Section 8.4.4) rather than $(Bu_4N)_2Re_2Cl_8$.[158]



8.10



8.11

There is now a fairly extensive body of synthetic and structural data for dirhenium(III) complexes that contain bridging amidate, amidinate and related monoanionic ligands. The first of these to be reported was the bis-*N*,*N*'-diphenylbenzamidinato complex $Re_2[(PhN)_2CPh]_2Cl_4$ along with its mono-THF solvate, both of which have the expected ligand-bridged structure with a trans disposition of amidinate ligands.[159] In the case of the solvated derivative, the THF molecule occupies one of the empty coordination sites colinear with the Re–Re bond. As a result, the Re–Re distance of 2.209(1) Å is longer than that in the complex lacking THF (2.177(1) Å). Other examples of structurally characterized amidinato-bridged complexes that were reported in earlier studies are $Re_2[(PhN)_2CCH_3]_2Cl_4$ and $Re_2[(CH_3N)_2CPh]_4Cl_2$ (Table 8.1).[160] The structure of the first of these is very similar to that of $Re_2[(PhN)_2CPh]_2Cl_4$, while the tetrakis-*N*,*N*'-dimethylbenzamidinato complex is noteworthy because the methyl groups keep the chloride ligands at a greater distance than that encountered in $Re_2(O_2CR)_4Cl_2$ compounds. As a result, the Re–Re distance in this amidinato complex is shorter (by 0.027 Å).[160]

The most thoroughly studied of the amidinate ligand systems are the diarylformamidinates $[ArNC(H)NAr]^-$ (abbreviated DArF). The first report on dirhenium(III) complexes that contain these bridges appeared in 1992 and involved the synthesis of the compound $Re_2(DTolF)_4Cl_2$ by the reaction of molten di-*p*-tolylformamidine with $Re_2(O_2CCH_3)_4Cl_2$.[161] This complex can be reduced by Na/Hg to produce $Re_2(DTolF)_4Cl$ and $Re_2(DTolF)_4$ (see Section 8.5.5) and substitution of the axial Re–Cl bonds by methoxide gives $Re_2(DTolF)_4(OMe)_2$. Structural characterization of $Re_2(DTolF)_4Cl_2$ and $Re_2(DTolF)_4(OMe)_2$ shows that the Re–Re bond length in the methoxide is longer by *c*. 0.03 Å (Table 8.1). Subsequently, a variety of other complexes of the type $Re_2(DArF)_4Cl_2$ have been prepared by a procedure similar to that used for $Re_2(DTolF)_4Cl_2$, and the structures of several of them determined crystallographically (see Table 8.1).[162] Extensive electrochemical characterizations have been carried on the series of compounds for which the aryl rings XC_6H_4 or $X_2C_6H_3$ contains the following substituent(s) X: H, *p*-Me, *p*-MeO, *m*-MeO, *p*-Cl, *m*-Cl, *p*-CF_3, *m*-CF_3, 3,4-Cl_2 and 3,5-Cl_2.[161,162] One of the axial

Pictiva EX2004
Samsung v Pictiva
IPR2024-01094

Re–Cl bonds in $Re_2[(p\text{-}MeOC_6H_4N)_2CH]_4Cl_2$ can be replaced by BF_4^- to form the compound $\{Re_2[(p\text{-}MeOC_6H_4N)_2CH]_4Cl\}BF_4$ in which the Re–Re bond distance is shortened by *c.* 0.05 Å compared to its parent; a F atom of the BF_4^- anion is at a distance of 4.502 Å to the coordinatively unsaturated Re atom.[163]

Only one diarylformamidinate ligand has to date been found to form the pair of complexes $Re_2(DArF)_2Cl_4$ and $Re_2(DArF)_3Cl_3$, namely when Ar = phenyl.[164,165] They resemble structurally the carboxylate-bridged complexes of these same types (vide supra). The compound $Re_2(DPhF)_3Cl_3$ was prepared by the reactions of $Re_2Cl_5(PMePh_2)_3$ and $Re_2Cl_4(PEt_3)_4$ (see Section 8.5.4) with *N*,*N*'-diphenylformamidine, and converted into *trans*-$Re_2(DPhF)_2Cl_4$ upon treatment with $HBF_4{\cdot}Et_2O$ in CH_3CN/CH_2Cl_2.[164] The mechanisms of these redox reactions are unknown. Later it was found that the compound *trans*-$Re_2(DPhF)_2Cl_4$ could be prepared in good yield by a non-redox procedure involving the reaction of $(Bu_4N)_2Re_2Cl_8$ with the formamidine in molten state or in refluxing 1,2-dichlorobenzene.[165] The compounds have been structurally characterized and the Re–Re distances follow the expected trends. This distance in $Re_2(DPhF)_2Cl_4(H_2O){\cdot}2THF$, which contains an axially bound H_2O molecule, that is in turn H-bonded to two THF molecules (see Fig. 8.10), is longer (by *c.* 0.04 Å) than that in *trans*-$Re_2(DPhF)_2Cl_4$.

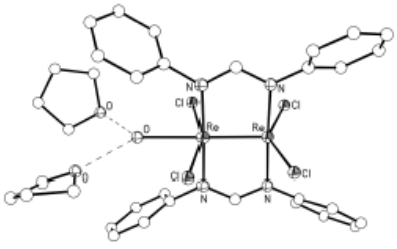


Fig. 8.10. The structure of *trans*-$Re_2(DPhF)_2Cl_4(H_2O){\cdot}2THF$.

Other monoanionic bridging ligands that contain *N*,*N* donor atom sets include the anion of 1,3,4,6,7,8-hexahydro-2*H*-pyrimido[1,2-*a*]pyrimidine, which reacts as its Li^+ salt with $(Bu_4N)_2Re_2Cl_8$ to give $Re_2(\mu\text{-hpp})_4Cl_2$ and $Re_2(\mu\text{-hpp})_3Cl_3$, both of which have been structurally characterized (Table 8.1).[166] The tetrakis-hpp complex was also prepared by the use of molten Hhpp. DFT calculations have been utilized to compare the electronic structures of $Re_2(HNCHNH)_4Cl_2$ and $Re_2(hpp)_4Cl_2$.[166] The anions of *N*6,*N*6-dimethyladenine and 7-azaindole have been used to prepare $Re_2(\mu\text{-dmad})_4X_2$ (X = Cl or Br) (from $Re_2(O_2CCH_3)_4X_2$) and $Re_2(\mu\text{-aza})_4Cl_2$ (from $(Bu_4N)_2Re_2Cl_8$), which have been characterized by NMR spectroscopy.[167] Different relative orientations of these unsymmetrical ligands about the Re–Re bond lead to mixtures of stereoisomers.

When $Re_2(O_2CCH_3)_4Cl_2$ is reacted with molten amides, μ-amidato complexes of the type $Re_2[(\mu\text{-}RNC(R')O]_4Cl_2$ are formed.[165,168] Attempts to isolate $Re_2[\mu\text{-}RNC(R')O]_2Cl_4$ compounds have not yet been successful.[165] Most of the $Re_2[\mu\text{-}RNC(R')O]_4Cl_2$ complexes, all of which contain N,O ligand bridges, have been characterized by X-ray crystallography. Each Re atom contains *cis* or *trans*- ReN_2O_2 planar units and an axial Re–Cl bond; this *cis* or *trans* designation is used in Table 8.1 to differentiate these geometries. For the synthesis of $Re_2(\mu\text{-}CyNCHO)_4Cl_2$, the compound $(Bu_4N)_2Re_2Cl_8$ was used in place of $Re_2(O_2CCH_3)_4Cl_2$.[165] The lability of the terminal Re–Cl bonds in *trans*-$Re_2[\mu\text{-}XylNC(CH_3)O]_4Cl_2$ towards substitution by N_3^-, NCS^-, NCO^-, H_2O, py and 4,4'-bpy has been examined and the crystal structures of the azide and thio-

Pictiva EX2004
Samsung v Pictiva
IPR2024-01094

cyanate substituted products determined.[169] Studies of the electronic absorption spectra of some of the compounds have shown[168] that the $\delta \rightarrow \delta^*$ transitions are at higher energies than those of $Re_2(O_2CR)_4Cl_2$ molecules. Amidato-bridged compounds that contain the *cis*-ReN_2O_2 geometry are prone to react with oxygen in aqueous media; in the case of $Re_2[\mu\text{-}PhNC(CH_3)O]_4Cl_2$ the unsymmetrical tetranuclear complex $\{Re_4[\mu\text{-}PhNC(CH_3)O]_6Cl(\mu\text{-}O)(\mu\text{-}OH)(MeOH)_3\}(ReO_4)_2$ has been isolated when methanol is present.[170] This complex contains two quadruply bonded $\{Re_2[\mu\text{-}PhNC(CH_3)O]_3\}^{3+}$ core units (see Fig. 8.11). The Re–Re bond distances in this compound are 2.213(2) Å and 2.200(2) Å; data for this compound are not listed in Table 8.1. Mass spectrometry studies have shown[170] that the basic structural integrity of this tetranuclear Re compound is retained in the gas phase.

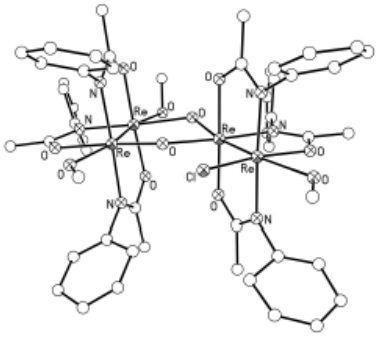


Fig. 8.11. The structure of the $\{Re_4[\mu\text{-}PhNC(CH_3)O]_6Cl(\mu\text{-}O)(\mu\text{-}OH)(MeOH)_3\}^{2+}$ cation. The two quadruply bonded $Re_2[\mu\text{-}PhNC(CH_3)O]_3$ units are bridged by an oxo and hydroxo ligand; one Cl and three methanol ligands occupy the four remaining coordination sites about the two dirhenium cores.

Dirhenium(III) amidate complexes have also been prepared from $(Bu_4N)_2Re_2Cl_8$ by the hydrolysis of acetonitrile and benzonitrile. The salts $(Bu_4N)\{Re_2[\mu\text{-}HNC(CH_3)O]_2Cl_5\}$,[171] $(Bu_4N)_2[\{Re_2[\mu\text{-}HNC(CH_3)O]Cl_6\}_2]$[172] and $(Bu_4N)\{Re_2[\mu\text{-}HNC(Ph)O]Cl_6\}$[173] have been structurally characterized (see Table 8.1). In the bis-acetamidate complex the amidate ligands are cis to one another in a head-to-head fashion (i.e. *cis*-ReN_2 and *cis*-ReO_2), although NMR spectroscopy has been interpreted in terms of the structure being best represented as $(Bu_4N)\{Re_2[\mu\text{-}HNC(CH_3)O][\mu\text{-}NC(CH_3)OH]Cl_5\}$ (at least in solution).[171] The monoacetamidate complex is linked into a dimer-of-dimers by bridging chlorides.[172] The complexes $(Bu_4N)\{Re_2[\mu\text{-}HNC(CH_3)O]_2Cl_5\}$ and $(Bu_4N)\{Re_2[\mu\text{-}HNC(Ph)O]Cl_6\}$ react with $Ph_2PCH_2PPh_2$ to form the paramagnetic Re_2^{5+} compounds $Re_2[\mu\text{-}HNC(R)O]Cl_4(\mu\text{-}dppm)_2$, where R = CH_3 or Ph.[171,173] Another instance where hydrolysis leads to an μ-amidate complex has been encountered in the reaction of $(Bu_4N)_2Re_2Cl_8$ with 1,4-dicyanobenzene in aqueous ethanol.[174] Extraction of the product into DMF enabled crystals of the centrosymmetric diamidate-bridged complex $(Bu_4N)_2\{[Re_2Cl_6(DMF)]_2[\mu\text{-}HNC(O)C_6H_4C(O)NH]\}$ to be isolated and structurally characterized.

A substitution reaction of a different type involving the dirhenium(III) carboxylates is encountered in the case of the reaction between $Re_2(O_2CCH_3)_4Cl_2$ and $(Bu_4N)MoS_4$ in acetonitrile.[175] This is said to afford $(Bu_4N)_2Re_2Mo_4S_{16}$, in which the Re–Re quadruple bond is believed to be preserved and $[MoS_4]^{2-}$ ligands either bridge the dirhenium unit or chelate the individual rhenium atoms.

Pictiva EX2004
Samsung v Pictiva
IPR2024-01094

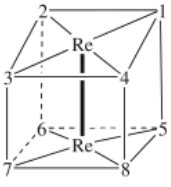
8.4.4 Neutral ligands

Although reactions with neutral donors sometimes involve metal-metal bond cleavage as a dominant reaction course, there are many examples where such reactions give products that bear a close structural relationship to $[Re_2X_8]^{2-}$. The best known are the phosphine complexes of the type $Re_2X_6(PR_3)_2$, many of which are formed upon reacting methanol solutions of $[Re_2Cl_8]^{2-}$ and $[Re_2Br_8]^{2-}$ with monodentate tertiary phosphines (*e.g.*, the series PPh_3, $PEtPh_2$, PEt_2Ph and PEt_3) under mild reaction conditions.[22,176-178] The PMe_3 complex $Re_2Cl_6(PMe_3)_2$ cannot be obtained by this method, but only by resorting to the one-electron oxidation of the crystalline complex 1,2,7-$Re_2Cl_5(PMe_3)_3{\cdot}Bu_4NCl$,[179] which is in turn prepared from $(Bu_4N)_2Re_2Cl_8$ (see Section 8.5.4).

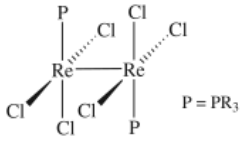
$$Re_2Cl_5(PMe_3)_3{\cdot}(Bu_4NCl) + NOBF_4 \xrightarrow{CH_2Cl_2} Re_2Cl_6(PMe_3)_2 + PMe_3 + NO + (Bu_4N)BF_4$$

A similar procedure has also been used to prepare $Re_2Cl_6(PMe_2Ph)_2$; in this case the $NOBF_4$ oxidation of 1,2,7-$Re_2Cl_5(PMe_2Ph)_3$ is carried out in the presence of one equivalent of added Bu_4NCl.[180] As we shall see in Sect 8.5.4, it is very easy to obtain reduced Re_2^{5+} and Re_2^{4+} species by the reaction of $(Bu_4N)_2Re_2X_8$ with monodentate tertiary phosphines, so much so that reduced complexes are often the predominant products. In the case of the reaction between $(Bu_4N)_2Re_2Cl_8$ and PMe_3, the only rhenium(III) compound that has been isolated is the edge-shared bioctahedral complex $Re_2(\mu\text{-}Cl)_2Cl_4(PMe_3)_4$, in which there is no metal-metal bond (the Re–Re distance is 3.8476(4) Å).[179] Bioctahedral dirhenium(III) complexes have also been isolated with other phosphines, and in some instances they may be intermediates in reactions where lower oxidation state complexes are formed by a disproportionation process; examples of these bioctahedral species include $(Bu_4N)_2[Re_2(\mu\text{-}PPh_2)_2Cl_6(PPh_2H)_2]$,[181] $(Bu_4N)[Re_2(\mu\text{-}Cl)_2Cl_5(PEt_3)_3]$,[182] $Re_2(\mu\text{-}PEt_2)_2Cl_4(PEt_2H)_4$[183] and $Re_2(\mu\text{-}I)_2I_4(PMe_3)_4$.[184] As yet, there is no instance where an iodide complex of the type $Re_2I_6(PR_3)_2$ has been isolated.

Several crystal structure determinations have been carried out on chloro complexes of the type $Re_2Cl_6(PR_3)_2$. On the basis of the ligand atom numbering scheme shown in **8.12**, the structures are all of the type 1,7-$Re_2Cl_6(PR_3)_2$ (**8.13**) and the Re–Re distances span the narrow range 2.208-2.227(1) Å.[179,180,185-188]



8.12



8.13

An interesting structural variation is encountered in the case of the mixed halide-alkoxide complexes $Re_2X_4(OR)_2(PPh_3)_2$ and $Re_2Cl_3(OEt)_3(PPh_3)_2$.[98,141-143] As mentioned already in Section 8.4.2 these compounds are, in reality, the mixed-valent dirhenium(IV,II) species $(RO)_2X_2ReReX_2(PAr_3)_2$ in which a Re–Re quadruple bond is still preserved (see Table 8.1 for structural information). Formally, they are derivatives of the 1,3-$Re_2Cl_6(PR_3)_2$ isomers that have not yet been isolated with *monodentate* phosphines. Indeed it has been pointed out that the syntheses of 1,2- and 1,3- isomers of $Re_2Cl_6(PR_3)_2$ are improbable except by resorting to chelating diphosphines.[189] This has been accomplished in the case of the reaction of $(Bu_4N)_2Re_2Cl_6$ with the chelating phosphine 1,1'-bis(diphenylphosphino)ferrocene.[190] The

Pictiva EX2004
Samsung v Pictiva
IPR2024-01094

structure of $Re_2Cl_6(dppf)$ is shown in Fig. 8.12 and is clearly an example of a 1,3-$Re_2Cl_6(PR_3)_2$ molecule. What is almost certainly a very close structural analog of $Re_2Cl_6(dppf)$ is isolated by the reaction of $(Bu_4N)_2Re_2Cl_8$ with bis[2-(diphenylphosphino)phenyl]ether.[191] Its spectroscopic and electrochemical properties are very similar to those of $Re_2Cl_6(dppf)$; it only differs from $Re_2Cl_6(dppf)$ in having a weak axially bound ether O atom in place of the unbound Fe atom of $Re_2Cl_6(dppf)$.[191] The salt $(Bu_4N)Re_2Cl_7(P\frown O\frown P)$ is formed when 4,6-bis(diphenylphosphino) dibenzofuran is reacted with $(Bu_4N)_2Re_2Cl_8$; in this case, the potentially tridentate phosphino-ether ligand is probably η^1-phosphine bound, so the compound is structurally similar to species of the type $[Re_2Cl_7(PR_3)]^-$ (vide infra).[191(b)]

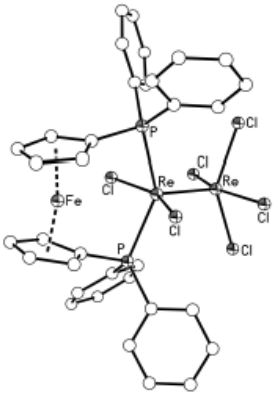


Fig. 8.12. The structure of $Re_2Cl_6(dppf)$.

The kinetics of the stepwise replacement of two chlorides of $[Re_2Cl_8]^{2-}$ by tertiary phosphine and arsine ligands has been examined.[192] Measurements were carried out in dichloromethane solution and involved the ligands PEt_2Ph, $AsEt_2Ph$, $PBu^n_{3-x}Ph_x$ and $AsBu^n_{3-x}Ph_x$ (x = 1-3); the reactions proceed as shown in the scheme below, with $k_2 > k_1$ and $k_{-2} >> k_{-1}$. All the reactions studied followed second-order kinetics, in accord with associative mechanisms. When these Group 5 ligands are used in large excess, then reduction of the Re_2^{6+} core occurs (Section 8.5.4). Through the reactions of $Re_2Cl_6(PR_3)_2$ (PR_3 = PBu^n_3, PBu^n_2Ph, PBu^nPh_2 or PPhBzMe) with Ph_4AsCl in CH_2Cl_2, samples of $(Ph_4As)Re_2Cl_7(PR_3)$ have been isolated.[192,193] The identities of all these salts have been confirmed by X-ray crystallography (Table 8.1).[193-195] Similarly, it was found that the reaction of $Re_2Cl_6(AsBu^n_2Ph)_2$ with Bu_4NBr in CH_2Cl_2 affords $(Bu_4N)_2Re_2Cl_6Br_2$.[192] The interesting mixed-salt $(Bu_4N)_4[Re_2Cl_7(PMe_3)]_2[Re_2Cl_8]$, that contains both $[Re_2Cl_7(PMe_3)]^-$ and $[Re_2Cl_8]^{2-}$ anions, has been prepared and structurally characterized.[185] It is formed when the Re_2^{5+} complex 1,2,7-$Re_2Cl_5(PMe_3)_3{\cdot}Bu_4NCl$ is oxidized with $NOBF_4$ in the presence of an additional equivalent of Bu_4NCl.[185] Examples of the dicationic tetrakis(phosphine) species $[Re_2Cl_4(PR_3)_4]^{2+}$ are also known; these are formed by the two-electron oxidation of $Re_2Cl_4(PR_3)_4$ and are discussed in Section 8.5.4.

$$[Re_2Cl_8]^{2-} + PR_3 \underset{k_{-1}}{\overset{k_1}{\rightleftharpoons}} [Re_2Cl_7(PR_3)]^- + Cl^- \qquad \text{Step 1}$$

$$[Re_2Cl_7(PR_3)]^- + PR_3 \underset{k_{-2}}{\overset{k_2}{\rightleftharpoons}} Re_2Cl_6(PR_3)_2 + Cl^- \qquad \text{Step 2}$$

In a study of the chemistry of trirhenium(III) cluster alkyls, Wilkinson and co-workers[196] discovered that they undergo cleavage reactions to yield dirhenium(III) or dirhenium(II) com-

Pictiva EX2004
Samsung v Pictiva
IPR2024-01094

plexes. When the methyl derivatives $Re_3(CH_3)_9$ or $Re_3(CH_3)_9(PR_3)_3$ are treated with a large excess of tertiary phosphine, the centrosymmetric quadruply-bonded dirhenium(III) complexes $Re_2(CH_3)_6(PR_3)_2$ (PR_3 = PMe_3, PMe_2Ph or PEt_2Ph) are produced.[196]

Anionic dirhenium(III) species have also been obtained with diphosphines. The best characterized example is $(Bu_4N)Re_2Cl_7$(bdppp) which has an unsymmetrical structure $[PCl_4ReReCl_3N]$, wherein which an uncoordinate phosphorus atom of the 2,6-bis(diphenylphosphino)pyridine ligand blocks, but does not bind to, the axial position of the coordinatively unsaturated metal center.[197] The bidentate ligands $Ph_2PC{\equiv}CPPh_2$ and *trans*-$Ph_2PCH{=}CHPPh_2$ (abbreviated LL), which are capable of forming intermolecular bridges, react with $(Bu_4N)_2Re_2Cl_8$ in methanol-conc HCl mixtures to give $(Bu_4N)_2[(Re_2Cl_7)_2(\mu\text{-LL})]$, in which pairs of monoanionic $[Re_2Cl_7L]^-$ units are linked through LL bridges.[198] Interestingly, when the chelating form of $Ph_2PCH{=}CHPPh_2$ (*cis*-dppee) is used in place of *trans*-$Ph_2PCH{=}CHPPh_2$, cleavage of the Re–Re quadruple bond predominates to give *trans*-$[ReCl_2(dppee)_2]Cl$.[199] The latter reaction course is commonly encountered when bidentate phosphine and arsine ligands are used that have two bridgehead carbons between the group 5 donor atoms. The best known example is the reaction of $(Bu_4N)_2Re_2Cl_8$ with $Ph_2PCH_2CH_2PPh_2$ in acetonitrile which gives the paramagnetic complex $(dppe)Cl_2Re(\mu\text{-}Cl)_2ReCl_2(dppe)$.[200]

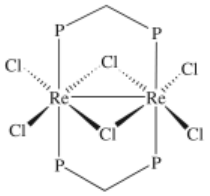
A neutral complex that contains only a single bridging ligand is β-Re_2Cl_6(S,S-isodiop), where isodiop is the zwitterionic ligand $Ph_2PCH_2CH(O)\overline{CHOC(Me)_2P(Ph)_2CH_2}$.[201] It is formed by the reaction of $Re_2(O_2CCH_3)_2Cl_4$ with S,S-diop and Me_3SiCl in THF, and involves the rearrangement of S,S-diop (S,S-diop is (+)-2,3-*O*-isopropylidene-2,3-dihydroxy-1,4-bis(diphenylp hosphino)butane) to S,S-isodiop, a ligand that coordinates through a P and O atom.[201] This was the first example of a structurally characterized chiral dirhenium(III) complex.

Another set of reactions that should be mentioned are those between $(Bu_4N)_2Re_2X_8$ and diphosphines in which only a single bridgehead atom separates the phosphorus atoms. This is exemplified by the case of the dark purple, diamagnetic complex $Re_2Cl_6(\mu\text{-dppm})_2$, which is the product of the reaction between $(Bu_4N)_2Re_2Cl_8$ and $Ph_2PCH_2PPh_2$ in acetonitrile, acetone or dichloromethane.[202,203] When an alcohol is used as the reaction solvent, the mixed chloroalkoxides $Re_2Cl_5(OR)(\mu\text{-dppm})_2$ (R = CH_3, C_2H_5, *n*-C_3H_7 or *n*-C_4H_9) are produced.[203] In a theoretical analysis of d^4–d^4 M_2L_{10} complexes by Hoffmann and his coworkers[204] the extreme cases of diamagnetic, unbridged, $[Re_2Cl_8L_2]^{2-}$ type 'Cotton structures' with short Re–Re distances, and the paramagnetic di-μ-chloro bridged 'Walton complexes', *e.g.* $Re_2Cl_6(dppe)_2$ (see Section 8.7), with long Re–Re separations were considered. It was suggested that $Re_2Cl_6(dppm)_2$, which had first been reported in 1976, might represent the case of an intermediate di-μ-chloro bridged, metal-metal double-bonded structure ($\sigma^2\pi^2\delta^{*2}\delta^2$ configuration). A few years later,[203] this was confirmed to be the case when the crystal structure of this compound showed it to be $Re_2(\mu\text{-}Cl)_2Cl_4(\mu\text{-dppm})_2$ (**8.14**). The Re–Re distance of 2.616(1) Å is fully in accord with a Re–Re double bond.[203] A crystal structure determination on the ethoxide derivative $Re_2Cl_5(OEt)(\mu\text{-dppm})_2$ showed it to be similar to that of $Re_2Cl_6(\mu\text{-dppm})_2$, with an ethoxide group in place of one of the terminal chloride ligands.[203] Subsequently, the isostructural complex $Re_2Cl_6(\mu\text{-dmpm})_2$ was prepared by reacting a CH_2Cl_2 solution of $(Bu_4N)_2Re_2Cl_8$ with one of $Me_2PCH_2PMe_2$ in acetone at room temperature; the Re–Re distance is 2.5807(4) Å.[205]

An interesting property of $Re_2Cl_6(\mu\text{-dppm})_2$ is its rich redox chemistry. The cyclic voltammograms of its solutions in Bu_4NPF_6-CH_2Cl_2 show four metal-based couples in the potential range +1.8 to -1.8 V (vs. Ag/AgCl).[203,206] Two of these correspond to one-electron oxidations, and two are one-electron reductions. An oxidation at +0.81 V and reduction at -0.54 V can be accessed with the use of NOX (X = BF_4^- or PF_6^-) as oxidant and $(\eta^5\text{-}C_5H_5)_2Co$ as reductant to give $[Re_2Cl_6(\mu\text{-dppm})_2]X$ and $[(\eta^5\text{-}C_5H_5)_2Co][Re_2Cl_6(\mu\text{-dppm})_2]$, respectively.[206] The crys-

Pictiva EX2004
Samsung v Pictiva
IPR2024-01094

tal structure determination of a salt of the paramagnetic $[Re_2Cl_6(\mu\text{-dppm})_2]^+$ cation, showed that the structure of the parent $Re_2Cl_6(\mu\text{-dppm})_2$ is retained, although the Re–Re bond distance increases to 2.6823(6) Å. The monocation and monoanion are believed to each possess Re–Re bond orders of 1.5 with ground state configurations of $\sigma^2\pi^2\delta^{*2}\delta^1$ and $\sigma^2\pi^2\delta^{*2}\delta^2\pi^{*1}$, respectively.[206]

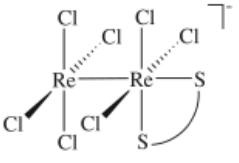


8.14

Several other metal-metal bonded edge-sharing bioctahedral compounds have been prepared from $(Bu_4N)_2Re_2Cl_8$ including $Re_2Cl_6(\mu\text{-dppa})_2$,[203] $Re_2Cl_6(\mu\text{-}Ph_2Ppy)_2$[207] and $Re_2(\mu\text{-SEt})_2Cl_4(dto)_2$;[208] they all very likely contain Re=Re bonds.

In the case of neutral sulfur donors, a few complexes in which a Re–Re quadruple bond is present have been obtained. The reactions of tetramethylthiourea and 2,5-dithiahexane with $(Bu_4N)_2Re_2X_8$ (X = Cl or Br) form complexes of the type $Re_2X_6L_2$ under mild reaction conditions.[97] The formation of quadruply bonded $Re_2X_6(tmtu)_2$ (X = Cl or Br) contrasts with the corresponding reactions of $[Re_2X_8]^{2-}$ with thiourea in acetone or acidified methanol (HCl or HBr) whereupon cleavage of the Re–Re bond occurs to give $ReX_3(tu)_3$ (Section 8.7).[97]

While the 2,5-dithiahexane compounds $Re_2X_6(dth)_2$ (X = Cl or Br), which can be prepared from $(Bu_4N)_2Re_2X_8$,[97] have yet to be structurally characterized by X-ray crystallography, there is no doubt that they are authentic derivatives of the quadruple Re–Re bond. Studies on their reactivity have established[209] that they can be converted in very high yield to other dirhenium(III) complexes is which quadruple bonds are present, namely, $Re_2X_6(PPh_3)_2$ and $Re_2(O_2CCH_3)_4X_2$, thereby implying that such a bond is also present in $Re_2X_6(dth)_2$. Although spectroscopic studies[62,210] failed to resolve the structural question, the subsequent structure characterizations of closely related systems suggests that the structure of $Re_2X_6(dth)_2$ is that of a symmetrical Re_2^{6+} complex, with chelating dth ligands and sulfur atoms coordinated in both axial and equatorial positions. With use of relatively mild reaction conditions Powell and coworkers[211] have been able to isolate the salts $(Bu_4N)Re_2Cl_7(dth)$ and $(Bu_4N)_2Re_2Cl_7(dto)$. Both have the structure represented in **8.15**, and this group of compounds therefore bears a close relationship to those of the types $Re_2X_6(PR_3)_2$ and $[Re_2Cl_7(PR_3)_2]^-$ (vide supra), although the sulfur ligands are bidentate. The axial Re–S bond distances in $(Bu_4N)Re_2Cl_7(dth)$ and $(Bu_4N)Re_2Cl_7(dto)$ are longer by *c.* 0.4 Å than the corresponding equatorial Re–S bonds. The compounds $(Bu_4N)Re_2Cl_7(SS)$ (SS = dth or dto) are probably intermediates in the reduction of $(Bu_4N)_2Re_2Cl_8$ to the triply-bonded, paramagnetic complexes $Re_2Cl_5(SS)_2$ (see Section 8.5.1).



8.15

Pictiva EX2004
Samsung v Pictiva
IPR2024-01094

8.5 Dirhenium Compounds with Bonds of Order 3.5 and 3

Much of this chemistry has been developed through a careful and deliberate mapping-out of the redox chemistry of compounds that contain a Re–Re quadruple bond.[212] The explicit recognition that quadruple metal-metal bonds exist and that they may be represented by the ground state electronic configuration $\sigma^2\pi^4\delta^2$, provides a framework upon which to consider bonds of lower orders. We shall see that there are two classes of molecules possessing metal-metal triple bonds, namely, those that contain two electrons less (i.e. $\sigma^2\pi^4$, 'electron-poor' triple bonds), or two more (i.e. $\sigma^2\pi^4\delta^2\delta^{*2}$, 'electron-rich' triple bonds) than is necessary for a full quadruple bond. In the case of dirhenium chemistry, the electron-rich triple bond is much more commonly encountered, as is the related odd-electron configuration $\sigma^2\pi^4\delta^2\delta^{*1}$, in which the metal-metal bond order is 3.5. Since the publication of the second edition of this text,[10] it is this area of dirhenium chemistry that has experienced the most dramatic growth.

8.5.1 The first metal–metal triple bond: $Re_2Cl_5(CH_3SCH_2CH_2SCH_3)_2$ and related species

The first redox reaction involving the $[Re_2X_8]^{2-}$ anions, which also generated the first metal-metal triple bond, was encountered[97] in the reaction between $(Bu_4N)_2Re_2Cl_8$ and 2,5-dithiahexane. While reaction in methanol was found to afford $Re_2Cl_6(dth)_2$, upon refluxing these reagents in acetonitrile beautiful red-black dichroic crystals were obtained that exhibited spectroscopic properties quite different from those of this dirhenium(III) complex. The crystal structure revealed[213] that this was in fact a truly remarkable substance which, as shown in Fig. 8.13, has two unique features. First, in spite of the retention of a very short Re–Re bond (2.293(2) Å)[213] the molecule is surprisingly unsymmetrical, being composed of $[ReCl_4]$ and $[Re(dth)_2Cl]$ units. This result, when taken in conjunction with the paramagnetism of the complex (1.72 BM per dimetal unit), led originally to the suggestion[213] that it be considered as the 'zwitterion' $Cl_4Re(III)–Re(II)(dth)_2Cl$, i.e., $Cl_4\bar{R}e–\overset{+}{R}e(dth)_2Cl$. Second, the molecule possesses a *staggered* rotational configuration, the first such instance to be encountered for a dimetal complex then recognized as possessing a metal-metal multiple bond. Another point of interest is the way in which *weak* intermolecular Re–Cl···Re bridges link the dimetal units together to form a 'molecular wire'. The absence of a δ bond in this structure led to the conclusion[213] that $Re_2Cl_5(dth)_2$ was an example (the first one known) of a molecule containing a metal-metal triple bond. Incidentally, the original suggestion of a 'zwitterionic' formulation[213] arose out of the anticipation that the alternative Re(IV)–Re(I) formulation (i.e. non-zwitterionic) would be less likely because of the great disparity in oxidation numbers. However, as was pointed out subsequently,[212] the Re(IV)–Re(I) case is certainly not untenable since this would simply entail making one of the components to the triple bond a Re(IV)–Re(I) dative contribution (i.e. Re≒Re). This possibility seems reasonable in light of the electronic and molecular structure of the mixed-valent Re(IV)–Re(II) complexes $(RO)_2X_2ReReX_2(PPh_3)_2$ (Section 8.4.2).[98,141,143] In any event, the electronic structure can best be represented as $\sigma^2\pi^4$, i.e. a bond of order 3, with an additional unpaired electron occupying a singly degenerate orbital localized on that rhenium atom which is bound to four chloride ligands. While many other complexes that contain the Re_2^{5+} core have subsequently been prepared, with few exceptions these possess a $\sigma^2\pi^4\delta^2\delta^{*1}$ electronic configuration, with the unpaired electron in a singly degenerate orbital delocalized over both metal nuclei, and thus having a metal-metal bond order of 3.5. Consequently, $Re_2Cl_5(dth)_2$ is accorded special attention in our present discussion because of its historical significance and since it remains to this day something of a curiosity. It is only relatively recently that other compounds of this type have been prepared and characterized. The pair of paramagnetic complexes $Re_2X_5(dto)_2$ (X = Cl or Br) have been prepared from $(Bu_4N)_2Re_2X_8$ and structurally characterized.[68] The Re–Re distances are 2.2772(8) Å (X = Cl)

Pictiva EX2004
Samsung v Pictiva
IPR2024-01094

and 2.2826(6) Å (X = Br), comparing closely with that reported for $Re_2Cl_5(dth)_2$. The only significant structural difference from $Re_2Cl_5(dth)_2$ is the absence of weak axial intermolecular Re–X···Re interactions in the case of $Re_2X_5(dto)_2$. Cyclic voltammetric measurements on solutions of $Re_2X_5(dto)_2$ in 0.1 M Bu_4NPF_6-CH_2Cl_2 show the presence of reversible one-electron reductions at $E_{1/2}$ = -0.61 V (X = Cl) and $E_{1/2}$ = -0.42 V (X = Br) vs. Ag/AgCl.[68] There is good evidence that compounds of these type $Re_2X_5(SS)_2$ (SS = dth or dto) are formed via the intermediacy of the Re_2^{6+} complexes $(Bu_4N)Re_2X_7(SS)$ (see Section 8.4.4).[211(b)]

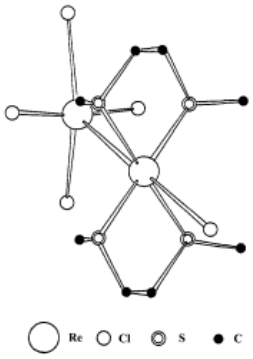


Fig. 8.13. The structure of $Re_2Cl_5(dth)_2$.

8.5.2 Simple electron-transfer chemistry involving the octahalodirhenate(III) anions and related species that contain quadruple bonds

Studies of the electron transfer chemistry on quadruply bonded dirhenium complexes have been carried out, utilizing both electrochemical techniques and chemical redox reagents. The earliest attempt to study the electrochemistry of the $[Re_2X_8]^{2-}$ anions involved the polarographic reduction of acetonitrile solutions of $(Bu_4N)_2Re_2X_8$ (X = Cl, Br or NCS).[214] This study was important because it demonstrated the feasibility of using electrochemical techniques to study these species and, furthermore, it revealed that the reduction $[Re_2Cl_8]^{2-} + e \rightarrow [Re_2Cl_8]^{3-}$, occurring at an $E_{1/2}$ of -0.82 V (vs. SCE), gave a rhenium species that was analogous to that of the already structurally characterized $[Tc_2Cl_8]^{3-}$ anion. Six years after the publication of this paper,[214] the results of more detailed electrochemical studies of $[Re_2Cl_8]^{2-}$ and $[Re_2Br_8]^{2-}$ were reported;[215] dc polarograms for acetonitrile solutions of these two species were in accord with the earlier results. Cyclic voltammograms (CV) were also recorded and, with HMD (hanging mercury drop) and Pt electrodes, reduction waves were found for $[Re_2Cl_8]^{2-}$ at -0.85 V and approximately -1.45 V. Controlled potential electrolysis experiments[215] gave a value of n close to 1 for the first reduction. Although it was claimed[215] that this reduction represents a reversible process, the $i_{p,a}/i_{p,c}$ current ratio does not appear to be unity for any of the sweep rates used (between 50 and 500 mV s^{-1}). The reduction which is at the more negative potential is clearly electrochemically irreversible. Two reduction processes were also detected by cyclic voltammetry for acetonitrile solutions of $(Bu_4N)_2Re_2Br_8$.[215]

An independent polarographic and cyclic voltammetric study of $(Bu_4N)_2Re_2Cl_8$ confirmed[216] the presence of the quasi-reversible reduction close to -0.85 V, but evidence for a second reduction was not obtained thereby throwing doubt upon the existence of $[Re_2Cl_8]^{4-}$. In the CVs of $(Bu_4N)_2Re_2Cl_8$ shown in Fig. 8.14, the $i_{p,a}/i_{p,c}$ ratios for the process at -0.85 V was found to approach a value of unity for a sweep rate of 500 mV s^{-1} but decreased rapidly with decreasing sweep rate. The variation of $i_{p,a}/i_{p,c}$ is due to the rapid and irreversible decomposition of the

Pictiva EX2004
Samsung v Pictiva
IPR2024-01094

reduced product $[Re_2Cl_8]^{3-}$. The resulting (unidentified) chemical product is characterized by $E_{p,a} \simeq$ -0.3 V (Fig. 8.14). A suggestion by Hendriksma and van Leeuwen[215] that the electrochemically reduced solutions of $[Re_2Cl_8]^{2-}$ exhibit electronic absorption spectra with features due to $[Re_2Cl_8]^{3-}$ was later refuted.[217]

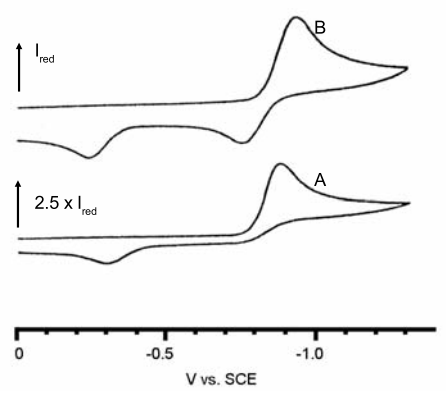


Fig. 8.14. The cyclic voltammogram of $(Bu_4N)_2Re_2Cl_8$ in acetonitrile (10^4 M) using a Pt electrode and 0.1 M Bu_4NClO_4 as supporting electrolyte. Sweep rates are (A) 20 mV s^{-1} and (B) 200 mV s^{-1}

Measurements of the CV's of acetonitrile and dichloromethane solutions of $(Bu_4N)_2Re_2Cl_8$, with Bu_4NPF_6 as the supporting electrolyte, have also revealed a reversible looking process that can be attributed to the $[Re_2Cl_8]^{1-/2-}$ couple.[218-221] This is best shown for the measurements in dichloromethane, where $E_{1/2}$ values for the $[Re_2Cl_8]^{1-/2-}$ and $[Re_2Cl_8]^{2-/3-}$ couples of +1.20 V and -0.87 V (vs. Ag/AgCl),[220] and +1.25 V and -0.85 V (vs. SCE),[221] were obtained in two independent studies. By resorting to low temperature spectroelectrochemical measurements, Heath and Raptis[222] were able to show conclusively that in 1:1CH_2Cl_2/CH_3CN solution at 220 K successive reversible oxidations of $[Re_2Cl_8]^{2-}$ to $[Re_2Cl_8]^{-}$ and $[Re_2Cl_8]^{0}$ occur. Both the paramagnetic species $[Re_2Cl_8]^{-}$ and $[Re_2Cl_8]^{3-}$ have been characterized by electronic absorption spectroscopy at low temperatures and their $\delta \rightarrow \delta^*$ transitions (at 4650 cm^{-1} and 6950 cm^{-1}, respectively) identified.[222,223] There is a close relationship between the various $[Re_2Cl_8]^{n-}$ and $[Re_2Cl_9]^{(n-1)}$ species that will be dealt with in Section 8.5.3.

The $[Re_2Cl_8]^{3-}$ anion has also been generated and characterized in a molten salt medium. Electrochemical measurements on solutions of $[Re_2Cl_8]^{2-}$ in the aluminum chloride-1-methyl-3-ethylimidazolium chloride molten salt have shown[224] that it can be reduced to $[Re_2Cl_8]^{3-}$ at a glassy-carbon electrode in a reversible electrode process ($E_{1/2}$ *c.* -0.58 V vs. the Al^{3+}/Al couple). Bulk electrolysis with the use of a Pt-gauze electrode gives solutions of $[Re_2Cl_8]^{3-}$ that are stable in the absence of oxygen and which have been characterized by electronic absorption and EPR spectroscopy.[225] These properties confirm the $\sigma^2\pi^4\delta^2\delta^{*1}$ electronic configuration.

Another important example of simple electron-transfer reactions involving quadruply bonded dirhenium(III) complexes is provided by the $[Re_2(NCS)_8]^{2-}$ anion. The polarographic reductions of acetonitrile solutions of $(Bu_4N)_2Re_2(NCS)_8$, which were seen[214] at -0.04 V and -0.71 V vs. SCE (with 0.5 M Bu_4NClO_4 as supporting electrolyte), are apparently genuine since CV measurements on dichloromethane solutions of $(Bu_4N)_2Re_2(NCS)_8$ at room temperature (with Bu_4NPF_6 as supporting electrolyte) revealed[226] electrochemical reductions with $E_{1/2}$ = -0.10 V and $E_{1/2}$ = -0.82 V versus SSCE, as well as an oxidation at $E_{1/2}$ = +1.03 V. Low temperature spectroelectrochemical characterizations of $[Re_2(NCS)_8]^{-}$ and $[Re_2(NCS)_8]^{3-}$ by IR and electron-

Pictiva EX2004
Samsung v Pictiva
IPR2024-01094

ic absorption spectroscopic techniques were carried out subsequently.[70,223] These studies, which were carried out on THF[70] or *n*-PrCN[223] solutions of $(Bu_4N)_2Re_2(NCS)_8$, also addressed the formation of the second one-electron reduced species, $[Re_2(NCS)_8]^{4-}$, which was characterized by IR spectroscopy.[70] The temperature dependence of the chemically reversible $[Re_2(NCS)_8]^{3-/4-}$ couple at temperatures of 290 K and below was interpreted[223] in terms of the 3- (9e) anion being eclipsed and the 4- (10e) anion having a staggered rotational geometry. Companion electrochemical studies[70,227] on the electrochemical properties of $[Re_2(\mu\text{-}NCS)_2(NCS)_8]^{n-}$ species (n = 1-4) has helped provide an explanation for the ease with which $[Re_2(NCS)_8]^{2-}$ is chemically oxidized to $[Re_2(NCS)_{10}]^{3-}$ (see Section 8.4.1).[63]

The electrochemical results we have discussed so far pertain to anions that contain ligands with no particular ability to stabilize low oxidation states, at least to the extent that these species can be isolated in the solid state. In contrast, the cyclic voltammograms of dichloromethane solutions of the phosphine derivatives $Re_2X_6(PR_3)_2$ (X = Cl or Br and PR_3 = PEt_3, PPr^n_3, PEt_2Ph, $PMePh_2$ and $PEtPh_2$)[228] exhibit an electrochemically reversible reduction with an $E_{1/2}$ value between +0.06 and -0.13 V versus SCE. These data, along with results for other $Re_2X_6(PR_3)_2$ complexes, and for a few closely allied $[Re_2Cl_7(PR_3)]^-$ anions that have been reported since these early studies,[228] are listed in Table 8.2. All data given for the $Re_2X_6(PR_3)_2$ complexes are presumably for the 1,7-isomers, except in the case of $Re_2Cl_6(dppf)$, which is a 1,3-isomer type.[190] Clearly, the reductions of $Re_2X_6(PR_3)_2$ to $[Re_2X_6(PR_3)_2]^-$ occur at much more positive potentials than does the reduction of $[Re_2Cl_8]^{2-}$ to $[Re_2Cl_8]^{3-}$, in accord with the greater ability of phosphines (compared to halide) to stabilize low oxidation states. Furthermore, the electrochemically generated anions $[Re_2X_6(PR_3)_2]^-$ were found to have reasonable stability as evidenced by EPR spectral meaurements.[228] Subsequently, it was found possible to prepare salts of some of the $[Re_2Cl_6(PR_3)_2]^-$ anions through the use of cobaltocene as a one-electron reducing agent.[178,190] These reactions, when carried out in acetone or dichloromethane, proceed as follows:

$$Re_2Cl_6(PR_3)_2 + (\eta^5\text{-}C_5H_5)_2Co \rightarrow [(\eta^5\text{-}C_5H_5Co][Re_2Cl_6(PR_3)_2]$$

$$PR_3 = PEt_3,\ PPr^n_3,\ PMePh_2,\ PEtPh_2 \text{ or dppf}$$

Interestingly, in a few instances several compounds of the type $(Bu_4N)Re_2Cl_6(PR_3)_2$, where PR_3 = PPr^n_3, PEt_2Ph or ½($Ph_2P(CH_2)_3PPh_2$), have been prepared directly by the reaction of the phosphine with $(Bu_4N)_2Re_2Cl_8$; these kinetic products must proceed via dirhenium(III) phosphine intermediates.[182,189] They are discussed further in Section 8.5.4.

Several of the $Re_2X_6(PR_3)_2$ complexes exhibit a second reduction at more negative potentials ($E_{1/2} \simeq$ -0.9 V),[178,228] but the resultant species $[Re_2X_6(PR_3)_2]^{2-}$ are not very stable chemically. Further mention is made of the redox chemistry of $Re_2X_6(PR_3)_2$ when the related properties of compounds such as those of the types $Re_2X_5(PR_3)_3$ and $Re_2X_4(PR_3)_4$ are discussed in Section 8.5.4.

In contrast to the behavior presented in Table 8.2 for the $Re_2X_6(PR_3)_2$ and $[Re_2Cl_7(PR_3)]^-$ species, the alkoxide-containing complexes of the type $Re_2X_4(OR)_2(PAr_3)_2$ display markedly different electrochemical properties, with a one-electron oxidation between +0.76 and +1.01 V and a one-electron reduction between -0.63 and -0.38 V versus Ag/AgCl, the $E_{1/2}$ values depending on the nature of the X, R and Ar groups.[98,143] This difference clearly reflects pronounced differences in the electronic structures of these two sets of complexes. In the case of the 'mixed-valent' Re(IV)–Re(II) alkoxide complexes, i.e. $(RO)_2X_2ReReX_2(PAr_3)_2$, the oxidation may be associated formally with a metal-based orbital that has more 'Re(II)' character and the reduction with the 'Re(IV)' center.

Pictiva EX2004
Samsung v Pictiva
IPR2024-01094

Table 8.2. Voltammetric $E_{1/2}$ values for the dirhenium(III) complexes $Re_2X_6(PR_3)_2$ and related species in dichloromethane

Compound	$E_{1/2}$(red)(1)[a]	$E_{1/2}$(red)(2)[a]	ref.
$Re_2Cl_6(PMe_3)_2$	+0.01[b]	-1.03[b]	179
$Re_2Cl_6(PEt_3)_2$	-0.10	-1.17[c]	228(b)
$Re_2Cl_6(PPr^n_3)_2$	-0.11		228(b)
$Re_2Cl_6(PBu^n_3)_2$	-0.13		228(b)
$Re_2Cl_6(PMe_2Ph)_2$	-0.05[d]	-0.92[d]	243
$Re_2Cl_6(PEt_2Ph)_2$	0.00	-0.95	228(b)
$Re_2Cl_6(PMePh_2)_2$	+0.02	-0.95	228(b)
$Re_2Cl_6(PEtPh_2)_2$	-0.02	-0.99	228(b)
$Re_2Cl_6(PBu^nPh_2)_2$	-0.37[d]		194
Re_2Cl_6(dppf)	-0.03[b]		190
$Re_2Br_6(PEt_3)_2$	+0.02		228(b)
$Re_2Br_6(PMePh_2)_2$	+0.06	-0.85	228(b)
$Re_2Br_6(PEtPh_2)_2$	+0.03		228(b)
$(Bu_4N)_4[Re_2Cl_7(PMe_3)]_2Re_2Cl_8$	-0.39[b,e]		185
$(Ph_4As)Re_2Cl_7(PBu^nPh_2)$	-0.34[d]		194
$(Bu_4N)Re_2Cl_7$(μ-bdppp)	+0.03[b]	-0.75[b]	196

[a] In volts vs. the saturated sodium chloride calomel electrode (SSCE) with a Pt–bead working electrode; 0.1 M Bu_4NPF_6 (TBAH) or similar salt as supporting electrolyte.

[b] vs. Ag/AgCl.

[c] This is an $E_{p,c}$ value which can be inferred from data reported for the $[Re_2Cl_6(PEt_3)_2]^-$ anion (ref. 182); vs. Ag/AgCl.

[d] vs. SCE.

[e] The $[Re_2Cl_8]^{2-}$ anion in this complex has processes at $E_{1/2}$(ox) = 1.21 V and $E_{1/2}$(red) = -0.87 V.

Just as the phosphine-containing complexes $Re_2X_6(PR_3)_2$ exhibit a very accessible and reversible reduction (Table 8.2), so also do the quadruply bonded carboxylates of the type $Re_2(O_2CR)_4X_2$ (R = an alkyl or aryl group; X = Cl, Br or I),[84,229] as well as the analogous 2-hydroxypyridinato and 2-mercaptopyridine complexes $Re_2(hp)_4X_2$ (X = Cl, Br or I)[155] and $Re_2(mp)_4X_2$ (X = Cl or Br)[157] (see Table 8.3). For the carboxylate complexes, the reduction potentials show a linear dependence upon the nature of the halogen (becoming more negative in the order I < Br < Cl) and upon the Taft σ* parameter for R.[84] The reduced anions $[Re_2(O_2CR)_4X_2]^-$ and $[Re_2(hp)_4X_2]^-$ are quite stable and EPR spectral measurements show that they all possess the $\sigma^2\pi^4\delta^2\delta^{*1}$ ground state electronic configuration.[84,155] Cobaltocene can be used to prepare the salts $[(\eta^5\text{-}C_5H_5)_2Co][Re_2(O_2CR)_4Cl_2]$ (R = Pr^n, CMe_3 or Ph)[178] and $[(\eta^5\text{-}C_5H_5)_2Co][Re_2(hp)_4X_2]$ (X = Cl or Br),[155] thereby demonstrating the considerable stability of these paramagnetic species and the ready accessibility of Re–Re bonds of order 3.5. Note that in the case of $Re_2(mp)_4X_2$, a one-electron oxidation is observed near the limit of the CV scans; for X = Cl, $E_{1/2}$(ox) = +1.21 V but for X = Br the process is irreversible with $E_{p,a} \simeq +1.30$ V.[157] Recent measurement of the CV of the heterometallic complex $Re_2[O_2CCHCo_2(CO)_6]_4Cl_2$ (i.e. R = $CCHCo_2(CO)_6$) has shown that the one-electron reduction (measured using a vitreous carbon electrode) have an $E_{1/2}$ value of -0.33 V versus SCE.[88]

Electrochemical studies of the $[Re_2]^{6+}/[Re_2]^{5+}$ couple have been reported for other groups of dirhenium(III) complexes, but in none of these cases has the simple one-electron reduced species been isolated. Cyclic voltammetric data for *cis*-$Re_2(O_2CR)_2X_4L_2$ complexes (recorded in CH_2Cl_2 or CH_3CN) show[98] that the $E_{1/2}$ values occur over the range -0.47 V to -0.27 V vs. Ag/AgCl, the value being dependent primarily on the nature of X (Cl or Br), with only a small

Pictiva EX2004
Samsung v Pictiva
IPR2024-01094

dependence on L. For the diaryl formamidinate complexes $Re_2(\mu\text{-DArF})_4Cl_2$, two sequential electrochemical reductions in dichloromethane have often been observed, the second presumably corresponding to the $[Re_2]^{5+}/[Re_2]^{4+}$ process.[161,162] The dependence of this electrochemistry on the nature of the aryl substituents has been examined in some detail,[162] and in the case of $Re_2(DTolF)_4Cl_2$ the chemical reductions to $Re_2(DTolF)_4Cl$ and $Re_2(DTolF)_4$ have been accomplished; these reductions involve the stepwise loss of a terminal Cl^- ligand (see Section 8.5.5).[161] Cyclic voltammetric data have also been reported for $Re_2(DPhF)_3Cl_3$,[164] $Re_2(DPhF)_2Cl_4$[165] and the μ-amidato complexes $Re_2(RNCHO)_4Cl_2$ (R = Ph or Cy);[165] a one-electron reduction is observed in dichloromethane in each case.

Table 8.3. Voltammetric $E_{1/2}$ values for the dirhenium(III) carboxylates, $Re_2(O_2CR)_4X_2$, and related complexes $Re_2(hp)_4X_2$ and $Re_2(mp)_4X_2$ in dichloromethane[a]

R[b]	Cl	Br	I
Me_3C	-0.42	-0.35	-0.31
C_2H_5	-0.34	-0.27	-0.20
C_3H_7	-0.34	-0.28	-0.21
$PhCH_2$	-0.24	-0.18	-0.13
p-$CH_3OC_6H_4$	-0.42	-0.35	-0.31
p-$CH_3C_6H_4$	-0.35	-0.29	-0.26
Ph	-0.27	-0.22	-0.18
hp[c]	-0.73	-0.67	-0.55
mp[d]	-0.54	-0.51	–

[a] Data taken from ref. 84 unless otherwise stated; in volts vs. SCE with a Pt–bead working electrode and 0.1 M Bu_4NPF_6 (TBAH) as supporting electrolyte.
[b] R is the alkyl or aryl substituent except in the case of the hp and mp complexes.
[c] Data for $Re_2(hp)_4X_2$ taken from ref. 155; vs. Ag/AgCl.
[d] Data for $Re_2(mp)_4X_2$ taken from ref. 157; vs. Ag/AgCl.

Quite different redox behavior is encountered in the case of $Re_2(\mu\text{-hpp})_4Cl_2$. Rather than an accessible reduction to Re_2^{5+} being observed, the cyclic voltammogram of this complex in dichloromethane shows two one-electron oxidations at $E_{1/2}$ = +0.058 V and +0.733 V vs Ag/AgCl.[230] Oxidation with $[(\eta^5\text{-}C_5H_5)_2Fe]PF_6$ produces $[Re_2(\mu\text{-hpp})_4Cl_2]PF_6$, which is the first paddlewheel complex with an Re_2^{7+} core and a bond order of 3.5.[230] The Re–Re bond distance of 2.2241(4) Å is a little longer than that for the quadruple bond in $Re_2(\mu\text{-hpp})_4Cl_2$.[166]

8.5.3 Oxidation of $[Re_2X_8]^{2-}$ to the nonahalodirhenate anions $[Re_2X_9]^{n-}$ (n = 1 or 2)

The first study undertaken to explore the consequence of *oxidizing* the $[Re_2Cl_8]^{2-}$ and $[Re_2Br_8]^{2-}$ anions was that carried out by Bonati and Cotton who, in 1966, investigated the products obtained by the action of halogens (Cl_2 and Br_2). Treatment of $[Re_2Cl_8]^{2-}$ and $[Re_2Br_8]^{2-}$ with chlorine and bromine, respectively, in dichloromethane or acetonitrile leads to the dirhenium(IV) complex anions $[Re_2X_9]^-$ which are dark green (X = Cl) or dark red (X = Br) in color.[231] The salts $(Bu_4N)Re_2X_9$ are quite stable in the solid-state but their solutions are easily reduced (under a variety of conditions) to produce either $(Bu_4N)_2Re_2X_9$, containing rhenium (+3.5), or the $(Bu_4N)_2Re_2X_8$ starting materials.[231] The 'intermediate' oxidation state anion $[Re_2Cl_9]^{2-}$ is readily reoxidizable to $[Re_2Cl_9]^-$. The various methods that were discovered in this early study[231] were subsequently refined in some cases.[221,232]

The close relationship that exists between various $[Re_2Cl_8]^{n-}$ and $[Re_2Cl_9]^{(n-1)-}$ species has been well documented by the elegent low temperature spectroelectrochemical studies of Heath and Raptis.[222] Not only have the coupled chemical-electrochemical relationships been mapped

Pictiva EX2004
Samsung v Pictiva
IPR2024-01094

out as shown in Fig. 8.15, but dichloromethane solutions of many of the unstable species have been characterized by electronic absorption spectroscopy.[222,223,233] The electrochemical and spectroscopic properties of solutions of the $[Re_2Cl_9]^-$ and $[Re_2Cl_9]^-$ anions in basic aluminum chloride-1-methyl-3-ethylimidazolium chloride room temperature molten salts have also been measured.[224,234]

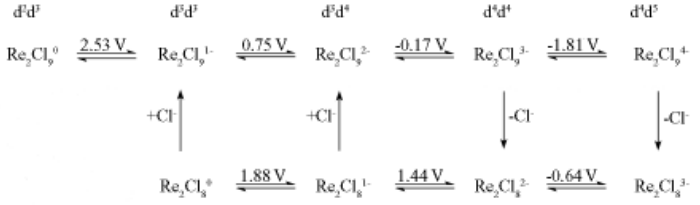


Fig. 8.15. Summary of the relationship between $[Re_2Cl_8]^{n-}$ and $[Re_2Cl_9]^{(n-1)-}$ species as demonstrated by low temperature spectroelectrochemical techniques. The potentials are versus a Ag/AgCl reference electrode.

Another close relationship between $[Re_2Cl_8]^{2-}$ and the $[Re_2Cl_9]^{n-}$ anions (n = 1 or 2) was encountered during studies of the photochemistry of $[Re_2Cl_8]^{2-}$ which involves the electron-transfer chemistry of the luminescent excited state $[Re_2Cl_8]^{2-*}$. This state is an $\delta\delta^*$ singlet and behaves as a strong oxidant and moderately good reductant.[218,219] Various electron acceptors (e.g. TCNE and chloroanil) quench the $[Re_2Cl_8]^{2-*}$ luminescence in non-aqueous solvents to produce $[Re_2Cl_8]^-$ and the reduced acceptor; the products back-react rapidly to give starting materials. The luminescence is also quenched by electron donor secondary and tertiary aromatic amines (e.g. *N*,*N*,*N*',*N*'-tetramethyl-*p*-phenylenediamine) in acetonitrile solution.[218] Thus the $\delta\delta^*$ singlet provides a facile route to the powerful oxidant $[Re_2Cl_8]^-$, a species that has its own interesting chemistry. For example, it reacts with Cl^- to generate $[Re_2Cl_9]^{2-}$; this demonstrates that the Cl^- trapping reaction efficiently competes with the very fast back-reaction between $[Re_2Cl_8]^-$ and $[TCNE]^-$ or $[chloranil]^-$.[221] In these experiments, the reaction stops at the $[Re_2Cl_9]^{2-}$ stage, because these particular quenchers cannot oxidize $[Re_2Cl_9]^{2-}$ to $[Re_2Cl_9]^-$. However, with quenchers such as 2,3-dichloro-5,6-dicyano-1,4-benzoquinone the oxidized species $[Re_2Cl_9]^-$ is produced.[221]

Several structural studies on $(Bu_4N)Re_2Cl_9$ have been carried out.[233,235,236] The $[Re_2Cl_9]^-$ anion has long been viewed as a derivative of β-$ReCl_4$, the latter containing Re_2Cl_9 units which are strung together by sharing terminal chlorine atoms (the structure can be represented as $Re_2Cl_7Cl_{2/2}$).[186] The expectation of a close structural relationship between β-$ReCl_4$ and $[Re_2Cl_9]^-$ has been confirmed by a crystal structure determination on $(Bu_4N)Re_2Cl_9$.[233,235,236] This revealed that the anion possesses a confacial bioctahedral metal-metal bonded structure; the Re–Re distance is 2.704(1) Å. The structure of the dianion has been determined in the salt $(Et_4N)_2Re_2Cl_9$.[233] Interestingly, the Re–Re distance in the lower oxidation state species, which formally has the *lower* bond order, is shorter by *c*. 0.23 Å (2.473(4) Å). An explanation for this shortening may lie in the occurrence of enhanced *d*-orbital overlap and diminished electrostatic repulsion in the more reduced species.[233] The synthesis and structural characterization of $(PCl_4)Re_2Cl_9$,[237] $(SCl_3)Re_2Cl_9$,[238] and $(Ph_4P)Re_2Cl_9$[239] have been reported more recently; the Re–Re bond distances are 2.724(2) Å, 2.722(2) Å and 2.780 Å, respectively.

The close relationship between the reactivities of the nonachlorodirhenate anions $[Re_2Cl_9]^{n-}$, $[Re_2Cl_8]^{2-}$ and β-$ReCl_4$ has been well documented.[115,240] Many of the reactions of β-$ReCl_4$ are typical of those of $[Re_2Cl_8]^{2-}$ itself; most noteworthy is the relative ease of converting β-$ReCl_4$ into $[Re_2Cl_8]^{2-}$ and $[Re_2Cl_9]^{2-}$.[115,240]

Pictiva EX2004
Samsung v Pictiva
IPR2024-01094

8.5.4 Re_2^{5+} and Re_2^{4+} halide complexes that contain phosphine ligands

The single most important class of complexes that contain the electron-rich metal-metal triple bond ($\sigma^2\pi^4\delta^2\delta^{*2}$ electronic configuration) are Re_2^{4+} complexes of stoichiometry $Re_2X_4(PR_3)_4$ (X = Cl, Br or I; PR_3 is a monodentate tertiary phosphine) and the analogous compounds $Re_2X_4(LL)_2$, where LL represents a bidentate phosphine and/or arsine ligand. These compounds, and closely related ones such as $Re_2X_5(PR_3)_3$, constitute the topic of the first part of the present section. Note that the $Re_2X_5(PR_3)_3$ and $Re_2X_4(PR_3)_4$ compounds are formally derivatives of the $[Re_2X_8]^{3-}$ and $[Re_2X_8]^{4-}$ anions, neither of which has yet been stabilized in the solid state.

Monodentate phosphines

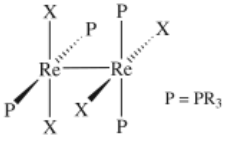
We have previously considered two important cases of the redox activity of the $[Re_2X_8]^{2-}$ anions where the structural integrity of the dirhenium unit is retained in the products, one a reduction (involving the dth ligand), the other involving halogen oxidation to $[Re_2X_9]^{-}$. However, by far the most extensive series of redox reactions investigated to date are those that involve the reduction of $[Re_2X_8]^{2-}$ in the presence of tertiary phosphines. This work was originally an outgrowth of studies of the reactions of phosphines with the trinuclear rhenium(III) cluster Re_3Cl_9. In the reaction between triethylphosphine and this chloride, using forcing reaction conditions, the major product[177] was glittering black crystals of stoichiometry $[ReCl_2(PEt_3)_2]_n$, that proved to be the dinuclear complex $Re_2Cl_4(PEt_3)_4$. Similar products were isolated in reactions between Re_3Cl_9 and PPr^n_3 and PEt_2Ph, whereas with $PMePh_2$ and $PEtPh_2$ the intermediate oxidation state complexes $Re_2Cl_5(PRPh_2)_3$ (R = Me or Et) were formed.[177] Such trinuclear to dinuclear transformations were subsequently found to occur upon reacting Re_3Br_9 (or $Re_3Br_9(THF)_3$) with PMe_3, PPr^n_3 and $PEtPh_2$,[241,242] and Re_3I_9 with PPr^n_3,[127] to afford the corresponding dirhenium(II) complexes $Re_2X_4(PR_3)_4$. When trimethylphosphine is added to solutions of the mixed chloride-alkyl cluster $Re_3Cl_3(CH_2SiMe_3)_6$ in light petroleum or diethylether reductive cleavage occurs to give $Re_2Cl_2(CH_2SiMe_3)_2(PMe_3)_4$,[196] a reaction clearly analogous to the reductive cleavage of Re_3Cl_9 by tertiary phosphines that leads to $Re_2Cl_4(PR_3)_4$.[177]

Since it seemed at the time[177] that the synthesis of dinuclear complexes of the types $Re_2Cl_4(PR_3)_4$ and $Re_2Cl_5(PR_3)_3$ could be more logically approached via the quadruply bonded $[Re_2Cl_8]^{2-}$ anion, such a possibility was explored. It was noted in Section 8.4.4 that *monodentate* phosphines react with the $[Re_2Cl_8]^{2-}$ and $[Re_2Br_8]^{2-}$ ions to yield the simple substitution products $Re_2X_6(PR_3)_2$, when *mild reaction conditions* are used. However, in refluxing acetone or alcohol reduction was indeed found to occur,[177] to an extent that appeared to depend upon the basicity of the phosphine, to give either $Re_2Cl_4(PR_3)_4$ or $Re_2Cl_5(PR_3)_3$ as products. In the period between the original discovery[177] and the early 1990's, this chemistry was developed to include the isolation and characterization of a range of compounds of the type $Re_2X_4(PR_3)_4$, with X = Cl, Br or I and PR_3 = PMe_3, PEt_3, PPr^n_3, PMe_2Ph, PEt_2Ph, $PMePh_2$ or $PEtPh_2$.[25,177,178,243-246] To access the $PMePh_2$ and $PEtPh_2$ complexes of this type, rather than $Re_2Cl_5(PRPh_2)_3$ (R = Me or Et),[177] $NaBH_4$ was added to the reaction mixtures to serve as a reducing agent.[245,246] Even with the more basic phosphines, this reagent enhances the rate of formation of the $Re_2Cl_4(PR_3)_4$ products. In the reaction that led to $Re_2Cl_4(PEtPh_2)_4$, the red brown polyhydride complex $Re_2(\mu\text{-}H)_4H_4(PEtPh_2)_4$ was also formed.[246]

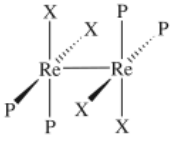
The first structure determination on a Re_2^{4+} complex of the type $Re_2X_4(PR_3)_4$ was carried out on $Re_2Cl_4(PEt_3)_4$, which was shown to have the eclipsed non-centrosymmetric structure represented in **8.16**.[247] With the use of the nomenclature first suggested by Cotton (see **8.12**)[248] this structure is that of a 1,3,6,8-$Re_2X_4(PR_3)_4$ isomer. This structure was later redetermined[249] with the use of a different space group. The Re–Re distance of 2.250(4) Å is consistent with a triple bond. In this structure,[247,249] there is a three-fold orientational disorder of the Re–Re unit. This

Pictiva EX2004
Samsung v Pictiva
IPR2024-01094

may or may not be the case in other compounds of this type or closely similar molecules; for other structures that are mentioned in this section and are based upon the L_4ReReL_4 geometry, the original references can be consulted to see whether this type of disorder is present or not. The structure determination of $Re_2Cl_4(PEt_3)_4$ was followed by those of $Re_2Cl_4(PMe_2Ph)_4$,[243] $Re_2Cl_4(PMePh_2)_4$,[245] $Re_2Cl_4(PMe_3)_4$[250] and $Re_2X_4(PPr^n_3)_4$ (X = Cl or Br).[250] In all cases, these have the 1,3,6,8 structure (**8.16**) and similar Re–Re bond distances (see Table 8.4). As we shall discuss shortly, isomers of the 1,2,7,8-type, as represented in structure **8.17**, have been obtained in more recent studies. A compilation of all the mixed halide-phosphine complexes with multiply bonded Re_2^{4+} and Re_2^{5+} cores that have been structurally characterized is available in Table 8.4, together with a listing of the Re–Re distances.



8.16



8.17

Table 8.4. Structural data for mixed halide-phosphine complexes of Re_2^{4+} and Re_2^{5+} that contain Re–Re bonds of order 3 or 3.5

Compound	r(Re–Re)(Å)[a]	Rotational Geometry[b]	ref.
A. Re_2^{4+} Compounds			
1,3,6,8-$Re_2Cl_4(PMe_3)_4$	2.247(1)	eclipsed	250
1,2,7,8-$Re_2Cl_4(PMe_3)_4$	2.414(8)	eclipsed	179
1,2,7,8-$Re_2Cl_4(PMe_3)_3(PEt_2H)$	2.253(2)	eclipsed	262
1,3,6,8-$Re_2Cl_4(PEt_3)_4$	2.250(4)	eclipsed	249
1,3,6,8-$Re_2Cl_4(PPr^n_3)_4$	2.252(2)	eclipsed	250
1,2,7,8-$Re_2Cl_4(PEt_2H)_4$	2.2533(8)	eclipsed	183
1,3,6,8-$Re_2Cl_4(PMe_2Ph)_4$	2.241(1)	eclipsed	243
1,2,7,8-$Re_2Cl_4(PMe_2Ph)_4$	2.261(1)	eclipsed	180
	2.258(1)	eclipsed	180
1,2,7,8-$Re_2Cl_4(PMe_2Ph)_3(PEt_2H)\cdot CH_2Cl_2$	2.247(1)	staggered	262
1,3,6,8-$Re_2Cl_4(PMePh_2)_4\cdot C_6H_6$	2.260(1)	eclipsed	245
1,3,6,8-$Re_2Cl_4(PMePh_2)_4\cdot (CH_3)_2CO$	2.255(0)	eclipsed	245
1,3,6,8-$Re_2Br_4(PPr^n_3)_4$	2.253(4)	eclipsed	250
1,3,6,8-$Re_2I_4(PMe_3)_4\cdot CH_2Cl_2$	2.2541(8)	eclipsed	184
1,3,6,8-$Re_2I_4(PMe_2Ph)_4$	2.258(1)	staggered	184
1,3,6,8-$Re_2I_4(PEt_2Ph)_4$	2.2698(7)	eclipsed	184
$(Bu_4N)[1,2,7\text{-}Re_2Cl_5(PMe_3)_3]$	2.2354(7)	staggered	261
$(Bu_4N)[1,2,7\text{-}Re_2Cl_5(PMe_2Ph)_3]$	2.2388(7)	staggered	262
α-$Re_2Cl_4(dppe)_2\cdot 4C_6H_6$	2.2650(6)	eclipsed	277
α-$Re_2Cl_4(dppe)_2\cdot$dppe	2.2544(8)	eclipsed	277
β-$Re_2Cl_4(dppe)_2$	2.244(1)	staggered	266
α-$Re_2Cl_4(dppee)_2\cdot$PrOH	2.250(1)	eclipsed	276
	2.265(1)	eclipsed	276

Pictiva EX2004
Samsung v Pictiva
IPR2024-01094

Compound		r(Re–Re)(Å)[a]	Rotational Geometry[b]	ref.
β-$Re_2Cl_4(dppee)_2$		2.242(3)	staggered	276
α-$Re_2Cl_4(depe)_2$		2.2608(6)	eclipsed	279
β-$Re_2Cl_4(depe)_2$		2.211(1)	staggered	278
α-$Re_2Cl_4(dmpe)_2{\cdot}CH_3OH$		2.266(1)	eclipsed	274
α-$Re_2Cl_4(dppp)_2$		2.264(1)	eclipsed	273
α-$Re_2Cl_4(dppp)_2{\cdot}4CH_2Cl_2$		2.2559(8)	eclipsed	189
β-$Re_2Cl_4(dpae)_2$		2.231(2)	staggered	272
$Re_2Cl_4(\mu\text{-}dppm)_2$		2.234(3)[e]	staggered	274
		2.2497(4)[e]	staggered	294
		2.2368(5)	staggered	294
$Re_2(CH_3)_4(\mu\text{-}dppm)_2$		2.284(7)	staggered	289
$Re_2(NCBH_3)_4(\mu\text{-}dppm)_2(H_2O)_2{\cdot}2THF$		2.2874(5)	staggered	290
$Re_2[N(CN)_2]_4(\mu\text{-}dppm)_2(DMF)_2{\cdot}3DMF$		2.2960(5)	staggered	291
$Re_2Cl_4(\mu\text{-}dppa)_2{\cdot}(CH_3)_2CO$		2.2417(5)	staggered	288
$Re_2Cl_4(\mu\text{-}dppE)_2{\cdot}CH_2Cl_2$		2.2448(5)	staggered	287
$Re_2Cl_4(\mu\text{-}dcpm)_2$		2.2256(4)	staggered	294
		2.2267(4)	staggered	294
$Re_2Cl_4(\mu\text{-}dmpm)_3$	(orthorhombic form)	2.309(2)	staggered	295
	(monoclinic form)	2.3157(4)	staggered	295
$[Re_2Cl_3(dpmp)_2]Cl$		2.307(1)	staggered	297
$[Re_2Cl_3(dpmp)_2]PF_6$		2.300(1)	staggered	297
$Re_2Cl_4(\mu\text{-}dppm)(PMe_3)_2{\cdot}0.75C_7H_8$		2.238(1)	staggered	285
		2.242(1)	staggered	285
β-$Re_2Cl_4(dppm)(dppe)$		2.237(1)	staggered	298
$Re_2Cl_3(Ph_2Ppy)_2[(C_6H_5)(C_6H_4Ppy]$		2.336(2)	staggered	207,301
$Re_2Cl_4(Ph_2Ppy)_2(PEt_3)$		2.270(1)	staggered	207
$[Re_2Cl_2(Ph_2Ppy)_4](PF_6)_2{\cdot}2(CH_3)_2CO$		2.300(1)	staggered	207
$Re_2Cl_4(bdppp)_2$		2.2342(6)	eclipsed	197
$Re_2Cl_2(pyphos)_2(pyphosH){\cdot}CH_3CN$		2.2693(3)	eclipsed	302
cis-$Re_2(\mu\text{-}O_2CCH_3)_2Cl_2(\mu\text{-}dppm)_2$		2.315(1)	staggered	271
cis-$Re_2(\mu\text{-}O_2CCH_3)_2(NCBH_3)_2(\mu\text{-}dppm)_2{\cdot}CH_2Cl_2$		2.2938(7)	staggered	325
cis-$Re_2(\mu\text{-}O_2CC_5H_4N)_2Cl_2(\mu\text{-}dppm)_2{\cdot}2C_2H_5OH$		2.3271(4)	staggered	320
$[cis\text{-}Re_2(\mu\text{-}O_2CC_5H_4N)_2(O_3SCF_3)_2(\mu\text{-}dppm)_2Pt(dbbpy)]_2\text{-}(O_3SCF_3)_4{\cdot}2.37CH_2Cl_2{\cdot}1.18H_2O$		2.2839(15)	staggered	320
cis-$Re_2(\mu\text{-}O_2CC_6H_{10}CO_2Et)_2Cl_2(\mu\text{-}dppm)_2{\cdot}2C_2H_5OH$		2.3120(5)	staggered	323
$[cis\text{-}Re_2(\mu\text{-}O_2CC_6H_{10}CO_2H)_2Cl_2(\mu\text{-}dppm)_2]_2\text{-}(\mu\text{-}O_2CC_6H_{10}CO_2){\cdot}7C_2H_4Cl_2$		2.3172(9)	staggered	322
$\{[cis\text{-}Re_2Cl_2(\mu\text{-}dppm)_2](\mu\text{-}O_2CC_6H_4CO_2)\}_3{\cdot}2C_6H_6{\cdot}H_2O$		2.3192(12)[f]	staggered	322
		2.3186(13)[f]		
		2.3185(12)[f]		
cis-$Re_2Cl_2(\mu\text{-}dppm)_2[(\mu\text{-}O_2CC_5H_4)_2Fe]{\cdot}1.43C_2H_5OH$		2.3218(3)	eclipsed	323
cis-$Re_2(\mu\text{-}O_2CCH_3)_2Cl_2(\mu\text{-}dppa)_2$		2.3067(5)	staggered	284
cis-$Re_2(\mu\text{-}O_2CC_6H_4\text{-}4\text{-}PPh_2)_2Cl_2(\mu\text{-}dppm)_2{\cdot}2C_2H_5OH$		2.3040(2)	staggered	321

Pictiva EX2004
Samsung v Pictiva
IPR2024-01094

Compound	r(Re–Re)(Å)[a]	Rotational Geometry[b]	ref.
cis-Re(μ-$O_2CC_6H_4$-4-PPh_2)$_2$$Cl_2$(μ-dppm)$_2$($Pd_2Cl_4$)	2.3295(6)	staggered	321
trans-Re_2(μ-O_2CCH_3)$_2$$Cl_2$(μ-dppm)$_2$·$C_7H_8$·2$H_2O$	2.2763(7)	eclipsed	314
trans-Re_2(μ-O_2C-3-C_5H_4N)$_2$$Cl_2$(μ-dppm)$_2$	2.2931(3)	eclipsed	315
trans-Re_2(μ-O_2CCH_3)$_2$$Cl_2$(μ-dppE)$_2$·$CH_3OH$	2.2861(6)	staggered	287
trans-Re_2(μ-O_2C-4-quin)$_2$$Cl_2$(μ-dppE)$_2$	2.2808(4)	staggered	321(b)
trans-Re_2(μ-O_2CCH_3)$_2$$Cl_2$(μ-cdpp)$_2$·$CH_3OH$	2.2871(5)	eclipsed	286
	2.2858(5)	eclipsed	286
[Re_2(μ-O_2CCH_3)Cl_2(μ-dmpm)$_3$]Cl·2H_2O·CH_2Cl_2	2.304(1)	staggered	317
Re_2(pic)Cl_3(μ-dppm)$_2$	2.2816(4)	staggered	315
Re_2(pic)Cl_3(μ-dppm)$_2$·CH_2Cl_2	2.2937(4)	staggered	315
2Re_2(pic)Cl_3(μ-dppm)$_2$·Re_2Cl_6(μ-dppm)$_2$·2.172CH_2Cl_2	2.2841(5)	staggered	315
Re_2[(O_2C-2-(EtO_2C-3-)py]Cl_3(μ-dppm)$_2$·CH_2Cl_2	2.2752(2)	staggered	315
Re_2[(O_2C-2-(HO_2C-4-)py]Cl_3(μ-dppm)$_2$·CH_2Cl_2·C_6H_6	2.2713(5)	staggered	315
Re_2(dipic)Cl_2(μ-dppm)$_2$·3C_6H_6 (Isomer **A**)	2.2750(10)	staggered	315
Re_2(dipic)Cl_2(μ-dppm)$_2$·0.5CH_2Cl_2 (Isomer **B**)	2.2512(3)	staggered	315
Re_2(dipic)Cl_2(μ-dppm)$_2$·2CH_2Cl_2 (Isomer **C**)	2.2583(3)	staggered	316
Re_2(HnicO)$_2$$Cl_2$(μ-dppm)$_2$	2.3035(6)	staggered	316
Re_2(picO)$_2$(μ-dppm)$_2$·H_2O	2.3139(3)	staggered	316
Re_2(μ-SH)$_2$$Cl_2$(μ-dppm)$_2$·0.5$CH_2Cl_2$	2.2577(5)	eclipsed	326
Re_2(μ-S_2CMe_2)Cl_2(μ-dppm)$_2$·CH_2Cl_2	2.2544(6)	eclipsed	326
Re_2(acac)Cl_3(μ-dppm)$_2$	2.2542(5)	staggered	329
Re_2(acac)$_2$$Cl_2$(μ-dppm)$_2$·($C_2H_5$)$_2$O	2.2968(3)	staggered	329
Re_2Cl_3(μ-dmpm)$_2$(NO)	2.379(1)	staggered	311
B. Re_2^{5+} Compounds			
[1,3,6,8-Re_2Cl_4(PMe_3)$_4$]ReO_4	2.205(1)	eclipsed	250
[1,3,6,8-Re_2Cl_4(PMe_3)$_4$]Cl·CH_2Cl_2	2.2152(9)	eclipsed	260
[1,3,6,8-Re_2Cl_4(PMe_3)$_4$]I·CH_2Cl_2	2.2122(7)	eclipsed	184
[1,3,6,8-Re_2Cl_4(PMe_2Ph)$_4$]PF_6·0.5THF	2.218(1)	eclipsed	243
1,3,6-Re_2Cl_5(PMe_3)$_3$	2.2182(7)	eclipsed	248
1,3,6-Re_2Cl_5(PMe_3)$_3$·0.5CH_2Cl_2	2.211(1)	eclipsed	259
1,2,7-Re_2Cl_5(PMe_3)$_3$·Bu^n_4NCl	2.2274(8)	staggered	259
1,3,6-/1,2,7-Re_2Cl_5(PMe_3)$_3$	2.2183(8)[c]	eclipsed	259
	2.2261(5)[d]	staggered	259
1,2,7-Re_2Cl_5(PMe_3)$_3$	2.226(1)	staggered	248
1,3,6-Re_2Cl_5(PMe_2Ph)$_3$	2.219(1)	eclipsed	180
1,2,7-Re_2Cl_5(PMe_2Ph)$_3$	2.2313(4)	staggered	180
1,3,6-Re_2Cl_5(PEt_3)$_2$	2.221(2)	eclipsed	248
1,3,6-Re_2Cl_5(PPr^n_3)$_3$ (trigonal form)	2.2284(9)	eclipsed	189
(orthorhombic form)	2.220(1)	eclipsed	182
1,3,6-Re_2Cl_5(PPr^n_3)$_3$·0.25C_6H_{14}	2.2224(7)	eclipsed	182
1,3,6-Re_2Cl_5(PCy_2H)$_3$·CH_2Cl_2·0.5C_6H_{14}	2.223(1)	staggered	181
1,3,6-Re_2Cl_5(PEt_2Ph)$_3$	2.2262(3)	eclipsed	253
1,3,6-Re_2Cl_5($Ph_2PCH_2CO_2Me$)$_3$	2.2318(3)	eclipsed	263

Pictiva EX2004
Samsung v Pictiva
IPR2024-01094

Compound	r(Re–Re)(Å)[a]	Rotational Geometry[b]	ref.
1,3,6-$Re_2I_5(PMe_3)_3$	2.235(1)	eclipsed	184
$(Bu_4N)[1,6\text{-}Re_2Cl_6(PPr^n_3)_2]$	2.2211(6)	staggered	189
$(Bu_4N)[1,7\text{-}Re_2Cl_6(PPr^n_3)_2$	2.2141(4)	staggered	189
$(Bu_4N)[1,7\text{-}Re_2Cl_6(PEt_2Ph)_2]$	2.2273(4)	eclipsed	189
	2.2278(5)	eclipsed	189
$(Bu_4N)[1,7\text{-}Re_2I_6(PEt_3)_2]\cdot 0.33C_6H_6$	2.233(1)	staggered	184
	2.240(1)	eclipsed	184
$(Bu_4N)[1,2\text{-}Re_2Cl_6(dppp)]$	2.2458(5)	staggered	189
$[ReCl_2(o\text{-}P2)_2][1,2\text{-}Re_2Cl_6(o\text{-}P2)]\cdot 4CH_2Cl_2$	2.2402(9)	eclipsed	281
$Re_2Cl_5(\mu\text{-}dppm)_2\cdot 2C_7H_8$	2.263(1)	eclipsed	303
cis-$[Re_2(\mu\text{-}O_2CCH_3)_2Cl_2(\mu\text{-}dppa)_2]PF_6$	2.2757(5)	staggered	284
cis-$[Re_2(\mu\text{-}O_2CCH_3)_2Cl_2(\mu\text{-}Ph_2Ppy)_2]PF_6$	2.261(1)	eclipsed	319
trans-$[Re_2(\mu\text{-}O_2CCH_3)_2Cl_2(\mu\text{-}dippm)_2]\text{-}Cl_{0.74}(ReO_4)_{0.26}\cdot CHCl_3$	2.2705(3)	eclipsed	293
trans-$[Re_2(\mu\text{-}O_2CCH_3)_2Cl_2(\mu\text{-}dcpm)_2]Cl_{0.8}(ReO_4)_{0.2}$	2.271(2)	eclipsed	138
$Re_2(\mu\text{-}O_2CCH_3)Cl_4(\mu\text{-}dppm)_2\cdot 2(CH_3)_2CO$	2.300(1)	eclipsed	271
$Re_2(\mu\text{-}O_2CC_5H_4N)Cl_4(\mu\text{-}dppm)_2$	2.3055(3)	staggered	323
$[Re_2Cl_4(\mu\text{-}dppm)_2]_2(\mu\text{-}O_2CC_6H_4CO_2)\cdot 1.5C_2H_4Cl_2$	2.2939(6)	eclipsed	322
$Re_2[(\mu\text{-}HNC(CH_3)O]Cl_4(\mu\text{-}dppm)_2\cdot 4CH_2Cl_2\cdot 0.833\text{-}C_2H_5OH$	2.3011(3)	eclipsed	171
$Re_2[\mu\text{-}HNC(Ph)O]Cl_4(\mu\text{-}dppm)_2$	2.3129(7)	eclipsed	173
$Re_2(\mu\text{-}O_2CCH_3)Cl_4(PPh_3)_2\cdot H_2O$	2.2165(7)	eclipsed	318
$Re_2(\mu\text{-}O_2CCH_3)Cl_4(\eta^3\text{-}\mathbf{L}_1)$[g]	2.2454(3)	eclipsed	191(b)
$Re_2(\mu\text{-}O_2CCH_3)Cl_4(\eta^3\text{-}\mathbf{L}_2)$[g]	2.2403(4)	eclipsed	191(b)
$Re_2(\mu\text{-}O_2CCH_3)Cl_4(\eta^3\text{-}\mathbf{L}_3)\cdot C_6H_6$[g]	2.2804(4)	eclipsed	191(b)
$Re_2(\mu\text{-}O_2CCH_3)Cl_4(\eta^3\text{-}\mathbf{L}_4)$[g]	2.2596(3)	eclipsed	191(b)
$Re_2(\mu\text{-}O_2CC_6H_4\text{-}2\text{-}PPh_2)Cl_4(\eta^3\text{-}\mathbf{L}_1)$[g]	2.2390(3)	eclipsed	191(b)
$Re_2(\mu\text{-}O_2C\text{-}4\text{-}quin)Cl_4(\eta^3\text{-}\mathbf{L}_1)$[g]	2.2536(4)	eclipsed	191(b)
$Re_2(\mu\text{-}O_2CC_6H_4\text{-}2\text{-}PPh_2Cl_4(\eta^3\text{-}\mathbf{L}_3)\cdot C_2H_5OH$[g]	2.2651(4)	eclipsed	191(b)
$Re_2(\mu\text{-}O_2C\text{-}4\text{-}quin)Cl_4(\eta^3\text{-}\mathbf{L}_3)\cdot C_2H_5OH$[g]	2.2694(3)	eclipsed	191(b)
$[Re_2Cl_4(\eta^3\text{-}\mathbf{L}_1)]_2(\mu\text{-}O_2CC_6H_4CO_2)\cdot 2C_2H_5OH$[g]	2.2424(4)	eclipsed	191(b)
$[Re_2Cl_3(\mu\text{-}dppm)_2(mq)]PF_6$	2.2540(5)	eclipsed	328

[a] Unless otherwise indicated, where more than one set of data is given for any complex this signifies that more than one crystallographically independent molecule is present in the crystal. In cases where orientational disorder occurs, the Re–Re distance given is that for the dirhenium unit with the highest occupancy or is a weighted average of the distances.

[b] A compound is designated as having a "staggered" geometry if χ_{av} exceeds an arbitrarily chosen value of 10°.

[c] Distance for the 1,3,6-isomer.

[d] Distance for the 1,2,7-isomer.

[e] These are different monoclinic forms of $Re_2Cl_4(\mu\text{-}dppm)_2$.

[f] These are the distances for each of the three dirhenium units in the molecule.

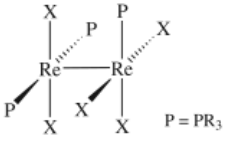
[g] This compound contains a tridentate donor designated as $\mathbf{L}_n$, the identity of which is given in the text (see also ref. 191(b)).

There is no doubt that the 1,3,6,8-$Re_2X_4(PR_3)_4$ compounds possess a $\sigma^2\pi^4\delta^2\delta^{*2}$ ground state electronic configuration, a conclusion that was supported by relativistic Xα-SW calculations

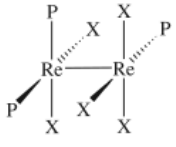
Pictiva EX2004
Samsung v Pictiva
IPR2024-01094

on the hypothetical molecule $Re_2Cl_4(PH_3)_4$[251] and gas-phase photoelectron spectral studies on volatile $Re_2Cl_4(PMe_3)_4$.[244] With this configuration there is no net δ bond, and thus no inherent electronic barrier to rotation about the Re–Re bond. An eclipsed rather than a staggered rotational geometry is clearly a consequence of steric factors in the case of this particular isomeric form (**8.16**). The striking similarity between the spectroscopic and electrochemical properties (vide infra) of the compounds of the type $Re_2X_4(PR_3)_4$ (X = Cl, Br or I) that have been considered up to this point leaves little doubt that they all possess the 1,3,6,8-$Re_2X_4(PR_3)_4$ structure.

Let us now return to the paramagnetic $Re_2X_5(PR_3)_3$ compounds (X = Cl or Br) that were also isolated and characterized in the first report[177] of Re_2^{4+} and Re_2^{5+} compounds. As mentioned already, these compounds are obtained when the tertiary phosphine is $PRPh_2$ (R = Me or Et). In all cases they contain a Re–Re bond order of 3.5 and a $\sigma^2\pi^4\delta^2\delta^{*1}$ ground state electronic configuration. It had already been reported long ago[22] that with PPh_3 only the insoluble, unreduced compounds $Re_2X_6(PPh_3)_2$ are formed (presumably as the 1,7-isomers) consistent with the extent of reduction being dependent on the basicity (and steric bulk) of the phosphine. Subsequently, several other compounds of the type $Re_2Cl_5(PR_3)_3$ were obtained by other less direct means. In the period leading up to the publication of the second edition of this text,[10] these procedures involved both the reduction of $Re_2Cl_6(PR_3)_2$ and the oxidation of the analogous $Re_2Cl_4(PR_3)_4$ compounds. An early example was encountered in the reaction between $(Bu_4N)_2Re_2Cl_8$ and PEt_3 in methanol-conc HCl which gave a separable mixture of $Re_2Cl_4(PEt_3)_4$ and $Re_2Cl_5(PEt_3)_3$.[178] The latter compound was also obtained in high yield upon the treatment of the Re_2^{5+} compound $[(\eta^5\text{-}C_5H_5)_2Co]Re_2Cl_6(PEt_3)_2$ (see Section 8.5.2) with PEt_3 at room temperature,[178] and it is also the product (as are other compounds of this type) from the reaction between $[Re_2Cl_4(PEt_3)_4]^+$ and Cl^-, as first carried out in an electrochemical cell.[228] The latter behavior will be discussed a little later when we deal with the electrochemical properties of these complexes. The compound $Re_2Cl_5(PPr^n_3)_3$ has been prepared by the reaction of $Re_2Cl_4(PPr^n_3)_4$ with ethanol which results in disproportionation to give a mixture of $ReCl(CO)_3(PPr^n_3)_2$ and $Re_2Cl_5(PPr^n_3)_3$.[252] Finally, we mention here the chlorine oxidation of $Re_2Cl_4(PMe_3)_4$ in dichloromethane which, depending on the reaction conditions, gives either the 1,3,6-isomer represented in structure **8.18** or the 1,2,7-isomer shown in **8.19**.[248] The latter product (**8.19**) requires the presence of an equivalent of PMe_3 in the reaction medium. These isomers do not interconvert. This contribution[248] is important because it first established the existence of isomers for compounds of this type; X-ray crystal structures were reported[248] for both isomers of $Re_2Cl_5(PMe_3)_3$ as well as 1,3,6-$Re_2Cl_5(PEt_3)_3$ (Table 8.4). More recently, the crystal structure of 1,3,6-$Re_2Cl_5(PEt_2Ph)_3$ was reported.[253] It should be noted that isomers of the types 1,3,5- and 1,2,5-$Re_2X_5(PR_3)_3$ could easily isomerize to **8.18** and **8.19**, respectively, by a simple 90° rotation about the Re–Re bond, and so may not be isolable.



8.18



8.19

It is noteworthy that the same products $Re_2Cl_6(PR_3)_2$, $Re_2Cl_5(PR_3)_3$ and $Re_2Cl_4(PR_3)_4$ are formed when the dirhenium(IV) complex $(Bu_4N)Re_2Cl_9$ is used in place of $(Bu_4N)_2Re_2Cl_8$ in reactions with certain phosphines. Thus, with PPh_3, $PEtPh_2$ and PEt_3 the products are $Re_2Cl_6(PPh_3)_2$, $Re_2Cl_5(PEtPh_2)_3$ and $Re_2Cl_4(PEt_3)_4$, respectively.[254] The reduction of $[Re_2Cl_9]^-$ to

Pictiva EX2004
Samsung v Pictiva
IPR2024-01094

$Re_2Cl_4(PEt_3)_4$ represents formally a four-electron reduction of a metal-metal bonded dinuclear species in which a metal-metal bond is retained and also constitutes a unique example of a redox reaction in which the starting material and product both possess a different type of metal-metal triple bond ($\sigma^2\pi^4$ and $\sigma^2\pi^4\delta^2\delta^{*2}$, respectively).

The redox chemistry of $Re_2X_4(PR_3)_4$ that has been cited previously, together with that of compounds of the types $Re_2X_5(PR_3)_3$ and $Re_2X_6(PR_3)_2$, accords very nicely with the notion that these Re_2^{n+} species are representatives of the $\sigma^2\pi^4\delta^2$ (n = 6), $\sigma^2\pi^4\delta^2\delta^{*1}$ (n = 5), and $\sigma^2\pi^4\delta^2\delta^{*2}$ (n = 4) configurations. In the case of $Re_2X_4(PR_3)_4$, such redox chemistry is quite extensive and examples of chemical and electrochemical oxidations are very well documented. Among examples of chemical oxidations are those in which CCl_4 oxidizes $Re_2Cl_4(PEt_3)_4$ and $Re_2Br_4(PEt_3)_4$ to produce the Et_3PCl^+ salts $(Et_3PCl)_2Re_2Cl_8$ and $(Et_3PCl)_2Re_2Cl_4Br_4$.[177] In the latter reaction, a quantity of $Re_2Cl_4Br_2(PEt_3)_2$ is also formed through the reaction of $(Et_3PCl)_2Re_2Cl_4Br_4$ with some of the free phosphine that is released during the oxidation.[177] Additional examples of chlorocarbon oxidations that produce the $[Re_2Cl_8]^{2-}$ anion are those of $Re_2Cl_4(PEt_3)_4$ and $Re_2Cl_5(PEtPh_2)_3$.[177] Other oxidations include the conversion of $Re_2Cl_4(PEt_3)_4$ to $Re_2Cl_6(PEt_3)_2$ by methanolic-HCl,[177] and the aerial oxidation of $Re_2X_4(PR_3)_4$ which produces the cations $[Re_2X_4(PR_3)_4]^+$ and/or their neutral analogs $Re_2X_5(PR_3)_3$.[25,177,217] The latter oxidations can be accomplished cleanly via electrochemical methods as we shall now discuss.

The oxidation of the dinuclear rhenium(II) compounds $Re_2X_4(PR_3)_4$ has been studied by electrochemistry, the cyclic voltammetric technique having proved especially convenient. The original studies on $Re_2X_4(PR_3)_4$, coupled with related ones on $Re_2X_5(PR_3)_3$ and $Re_2X_6(PR_3)_2$ (see Table 8.2),[228] showed that the electrochemical oxidations of $Re_2X_4(PR_3)_4$ to $[Re_2X_4(PR_3)_4]^+$ and $[Re_2X_4(PR_3)_4]^{2+}$ (Table 8.5) are followed by the conversion of these cations to $Re_2X_5(PR_3)_3$ and then $Re_2X_6(PR_3)_2$ via coupled chemical steps.[228] Electrochemical data for various $Re_2X_5(PR_3)_3$ complexes are also given in Table 8.5; note that the 1,3,6- and 1,2,7-isomers of $Re_2Cl_5(PMe_3)_3$ have quite different sets of values for $E_{1/2}$(ox) and $E_{1/2}$(red).[248] A noteworthy feature of these systems is that the conversion of $Re_2X_4(PR_3)_4$ to $Re_2X_6(PR_3)_2$ proceeds by both EECC and ECEC coupled electrochemical(E) - chemical(C) reaction series (see Schemes 8.1 and 8.2); the difference between them is the selection of the potential used for the oxidation of $Re_2X_4(PR_3)_4$. This is demonstrated in Fig. 8.16, where curve B shows the appearance of the processes at $E_{1/2}$(ox) = +0.31 V and $E_{1/2}$(red) = -0.88 V that signal the formation of $Re_2Cl_5(PPr^n_3)_3$ following the bulk oxidation of $Re_2Cl_4(PPr^n_3)_4$ to the monocation. Curve C shows that both $Re_2Cl_5(PPr^n_3)_3$ and $Re_2Cl_6(PPr^n_3)_2$ (the latter characterized by $E_{1/2}$(red) = -0.11 V) are formed upon oxidation at +1.0 V (i.e. to $[Re_2Cl_4(PPr^n_3)_4]^{2+}$). The mechanism of the chemical reactions that follow the electrochemical oxidations of $Re_2X_4(PR_3)_4$ involves the reaction between halide ion and $[Re_2X_4(PR_3)_4]^+$ or $[Re_2X_4(PR_3)_4]^{2+}$ to produce $Re_2X_5(PR_3)_3$ and $[Re_2X_5(PR_3)_3]^+$, respectively. $[Re_2X_5(PR_3)_3]^+$ then reacts further with X^- to form the final product, $Re_2X_6(PR_3)_2$.[228(b)] The halide ion that is available for these reactions, as originally carried out,[228] is generated by the disruption of a very small proportion of the dirhenium complex (almost certainly through reaction with adventitious oxygen). These mechanisms were confirmed later in separate experiments[243] that involved the addition of halide ion to pure samples of $[Re_2X_4(PR_3)_4]^+$ and $[Re_2X_4(PR_3)_4]^{2+}$ (vide infra).

$$[Re_2X_4(PR_3)_4]^0 \xrightarrow{-e} [Re_2X_4(PR_3)_4]^+$$
$$[Re_2X_4(PR_3)_4]^+ \xrightarrow{-e} [Re_2X_4(PR_3)_4]^{2+}$$
$$[Re_2X_4(PR_3)_4]^{2+} \xrightarrow{+X^-} [Re_2X_5(PR_3)_3]^+$$
$$[Re_2X_5(PR_3)_3]^+ \xrightarrow{+X^-} [Re_2X_6(PR_3)_2]^0$$

Scheme 8.1. EECC process.

$$[Re_2X_4(PR_3)_4]^0 \xrightarrow{-e} [Re_2X_4(PR_3)_4]^+$$
$$[Re_2X_4(PR_3)_4]^+ \xrightarrow{+X^-} [Re_2X_5(PR_3)_3]^0$$
$$[Re_2X_5(PR_3)_3]^0 \xrightarrow{-e} [Re_2X_5(PR_3)_3]^+$$
$$[Re_2X_5(PR_3)_3]^+ \xrightarrow{+X^-} [Re_2X_6(PR_3)_2]^0$$

Scheme 8.2. ECEC process.

Pictiva EX2004
Samsung v Pictiva
IPR2024-01094

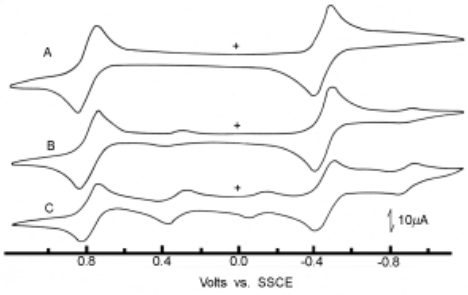


Fig. 8.16. Cyclic voltammograms in 0.2 M Bu_4NPF_6-dichloromethane. (A) $Re_2Cl_4(PPr^n_3)_4$; (B) solution A following oxidation at +0.1 V; (C) solution A following oxidation at +1.0 V.

Table 8.5. Voltammetric $E_{1/2}$ Values for Mixed Halide-Phosphine Complexes of Re_2^{4+} and Re_2^{5+} in Dichloromethane[a]

A. Re_2^{4+} Compounds

Compound	$E_{1/2}$(ox)(2)	$E_{1/2}$(ox)(1)	ref.
1,3,6,8-$Re_2Cl_4(PMe_3)_4$	+0.96[b]	-0.23[b]	244
1,2,7,8-$Re_2Cl_4(PMe_3)_4$	+1.12[b]	-0.16[b]	179
1,3,6,8-$Re_2Cl_4(PEt_3)_4$	+0.80	-0.42	228(b)
1,3,6,8-$Re_2Cl_4(PP^n_3)_4$	+0.79	-0.44	228(b)
1,3,6,8-$Re_2Cl_4(PBu^n_3)_4$	+0.82	-0.44	228(b)
1,2,7,8-$Re_2Cl_4(PEtH)_4$	+1.14[b]	+0.03[b]	183
1,3,6,8-$Re_2Cl_4(PMe_2Ph)_4$	+0.83	-0.30	228(b)
1,2,7,8-$Re_2Cl_4(PMe_2Ph)_4$	+0.98[b]	-0.17[b]	180
1,2,7,8-$Re_2Cl_4(PMe_2Ph)_3(PEt_2H)$	+1.22[b]	+0.37[b]	262
1,3,6,8-$Re_2Cl_4(PEt_2Ph)_4$	+0.85	-0.25	228(b)
1,3,6,8-$Re_2Cl_4(PEtPh_2)_4$	+0.84	-0.29	246
1,3,6,8-$Re_2Br_4(PMe_3)_4$	+1.01[b]	-0.11[b]	244
1,3,6,8-$Re_2Br_4(PEt_3)_4$	+0.83	-0.31	228(b)
1,3,6,8-$Re_2Br_4(PPr^n_3)_4$	+0.84	-0.38	228(b)
1,3,6,8-$Re_2Br_4(PBu^n_3)_4$	+0.82	-0.40	228(b)
1,3,6,8-$Re_2I_4(PMe_3)_4$	+0.98[b]	-0.02[b]	184
1,3,6,8-$Re_2I_4(PEt_3)_4$	+0.77	-0.27	228(b)
1,3,6,8-$Re_2I_4(PPr^n_3)_4$	+0.85	-0.22	228(b)
1,3,6,8-$Re_2I_4(PBu^n_3)_4$	+0.83	-0.25	228(b)
1,3,6,8-$Re_2I_4(PMe_2Ph)_4$	+0.94[b]	-0.01[b]	184
α-Re_2Cl_4(dmpe)$_2$	+1.10[b,c]	+0.21[b]	275
α-Re_2Br_4(depe)$_2$	+1.07[b,c]	+0.02[b]	275
α-Re_2Cl_4(dppe)$_2$	+1.05[b]	+0.27[b]	276
α-Re_2Br_4(dppe)$_2$	+1.03[b]	+0.29[b]	276
α-Re_2Cl_4(dppee)$_2$	+1.05[b]	+0.30[b]	275
α-Re_2Br_4(dppee)$_2$	≈1.0[b]	+0.33[b]	275
α-Re_2Cl_4(dppbe)$_2$	+1.14[b,c]	+0.29[b]	280
β-Re_2Cl_4(depe)$_2$	+0.88[b]	+0.08[b]	275
β-Re_2Br_4(depe)$_2$	+0.89[b]	+0.13[b]	275

Pictiva EX2004
Samsung v Pictiva
IPR2024-01094

A. Re_2^{4+} Compounds

Compound	$E_{1/2}$(ox)(2)	$E_{1/2}$(ox)(1)	ref.
β-$Re_2Cl_4(dppe)_2$	+1.04	+0.23	282
β-$Re_2Br_4(dppe)_2$	+0.97	+0.22	282
β-$Re_2I_4(dppe)_2$	+0.92	+0.29	282
β-$Re_2Cl_4(dppee)_2$	+1.13[b]	+0.24[b]	275
β-$Re_2Br_4(dppee)_2$	+1.15[b]	+0.34[b]	275
β-$Re_2Cl_4(arphos)_2$	+1.07	+0.23	282
β-$Re_2Br_4(arphos)_2$	+1.01	+0.24	282
β-$Re_2I_4(arphos)_2$	+0.91	+0.28	282
$Re_2Cl_4(\mu\text{-}dppm)_2$	+0.87[b,f]	+0.29[b,f]	288
$Re_2Br_4(\mu\text{-}dppm)_2$	+0.94[b]	+0.34[b]	288
$Re_2I_4(\mu\text{-}dppm)_2$	+0.95[b]	+0.34[b]	288
$Re_2(NCBH_3)_4(\mu\text{-}dppm)_2$[g]		+0.98[b]	290
$Re_2(CH_3)_4(\mu\text{-}dppm)_2$	+0.59[b]	-0.14[b]	289
$Re_2Cl_4(\mu\text{-}dppa)_2$	+0.94[b,f]	+0.40[b,f]	288
$Re_2Br_4(\mu\text{-}dppa)_2$	+1.05[b]	+0.41[b]	284
$Re_2Cl_4(\mu\text{-}dppE)_2$	+0.92[b]	+0.37[b]	287
$Re_2Cl_4(\mu\text{-}dcpm)_2$	+0.93[b]	-0.05[b]	285
$Re_2Cl_4(\mu\text{-}dpam)_2$	+0.84[b]	+0.32[b]	288
$Re_2Br_4(\mu\text{-}dpam)_2$	+0.92[b]	+0.37[b]	288
$Re_2Cl_4(\mu\text{-}dmpm)_3$	+1.30[b,c]	+0.53[b]	295
$Re_2Br_4(\mu\text{-}dmpm)_3$	+1.33[b,c]	+0.58[b]	296
$Re_2Cl_4(\mu\text{-}dppm)(PMe_3)_2$	+1.28[b,c]	+0.58[b]	244,299
$Re_2Cl_4(\mu\text{-}dppa)(PMe_3)_2$	+1.26[b,c]	+0.65[b]	244
$Re_2Cl_4(\mu\text{-}dppm)(PEt_3)_2$	+1.15[b,c]	+0.55[b]	244
$Re_2Cl_4(\mu\text{-}dppa)(PMe_2Ph)_2$	+1.37[c,d]	+0.64[d]	203
$Re_2Cl_4(\mu\text{-}dcpm)(PMe_3)_2$	+1.40[b,c]	+0.49[b]	285
β-$Re_2Cl_4(dppm)(dppe)$	+0.96[b]	+0.32[b]	298
β-$Re_2Cl_4(dppm)(arphos)$	+0.88[b]	+0.31[b]	298
β-$Re_2Cl_4(dppa)(dppe)$	+1.00[b]	+0.35[b]	298
$Re_2Cl_4(\mu\text{-}dppm)_2(PMe_3)$	+1.29[b,c]	+0.30[b]	300
$Re_2Br_4(\mu\text{-}dppm)_2(PMe_3)$	+1.31[b,c]	+0.38[b]	300
$Re_2Cl_4(\mu\text{-}dppm)_2[P(OMe)_3]$	+1.39[b,c]	+0.31[b]	300
$Re_2Cl_4(\mu\text{-}dppm)_2[P(OEt)_3]$	+1.41[b,c]	+0.29[b]	300
$Re_2Cl_4(\mu\text{-}dppm)_2[P(OPh)_3]$	+1.66[b,c]	+0.43[b]	300
$Re_2Cl_4(Ph_2Ppy)_3$	+1.20[d]	+0.41[d]	207
$Re_2Cl_3(Ph_2Ppy)_2[(C_6H_5)(C_6H_4)Ppy]$	+1.06[d]	+0.24[d]	207
$Re_2Cl_4(Ph_2Ppy)_2(PEt_3)$	+1.15[c,d]	+0.27[d]	207
$Re_2Cl_4(Ph_2Ppy)_2(PBu^n_3)$	+1.19[c,d]	+0.27[d]	207
$[Re_2Cl_2(Ph_2Ppy)_2](PF_6)_2$		+1.38[d,h]	207
$Re_2Cl_4(bdppp)_2$	+0.85[b]	-0.07[b]	197
$Re_2Cl_2(pyphos)_2(pyphosH)$	+1.00[b]	+0.22[b]	302

B. Re_2^{5+} Compounds

Compound	$E_{1/2}$(ox)	$E_{1/2}$(red)	ref.
1,3,6-$Re_2Cl_5(PMe_3)_3$	+0.46[b]	-0.75[b]	248
1,2,7-$Re_2Cl_5(PMe_3)_3$[e]	+0.68[b]	-0.48[b]	248
1,3,6-$Re_2Cl_5(PEt_3)_3$	+0.34	-0.88	228(b)

Pictiva EX2004
Samsung v Pictiva
IPR2024-01094

B. Re_2^{5+} Compounds

Compound	$E_{1/2}$(ox)	$E_{1/2}$(red)	ref.
1,3,6-$Re_2Cl_5(PPr^n_3)_3$	+0.31	-0.88	228(b)
1,3,6-$Re_2Cl_5(PCy_2H)_3$	+0.52[b]	-0.66[b]	181
1,3,6-$Re_2Cl_5(PMe_2Ph)_3$	+0.46[d]	-0.65[d]	243
1,2,7-$Re_2Cl_5(PMe_2Ph)_3$	+0.75[b]	-0.40[b]	180
1,3,6-$Re_2Cl_5(PEtPh_2)_3$	+0.44	-0.66	228(b)
1,3,6-$Re_2Cl_5(Ph_2PCH_2CO_2Me)_3$	+0.66[b]	-0.46[b]	263
1,3,6-$Re_2Cl_5(Ph_2PCH_2CO_2Et)_3$	+0.61[b]	-0.44[b]	263
1,3,6-$Re_2Br_5(PMePh_2)_3$	+0.48	-0.55	228(b)
1,3,6-$Re_2Br_5(PEtPh_2)_3$	+0.45	-0.59	228(b)
(Bu_4N)[1,2-Re_2Cl_6(dppp)]	+0.39[b]		189
$Re_2Cl_5(\mu$-dppm$)_2$	+0.51[d]	-0.36[d,i]	203

[a] Unless otherwise stated, data are in volts vs. the saturated sodium chloride calomel electrode (SSCE) with a Pt-bead working electrode and 0.1 M Bu_4NPF_6(TBAH) as supporting electrolyte.
[b] Versus Ag/AgCl.
[c] $E_{p,a}$ value
[d] Versus SCE.
[e] The reduced complex (Bu_4N)[1,2,7-$Re_2Cl_5(PMe_3)_3$] is reported to have $E_{1/2}$(ox) values of +0.73 V and -0.46 V vs. Ag/AgCl. (ref 261)
[f] Values are similar to those reported vs. SCE (see ref 203).
[g] This complex has an irreversible reduction with $E_{p,c}$ = -1.14V vs. Ag/AgCl. (ref 290).
[h] Reductions observed at $E_{1/2}$ = -0.82 V and -1.6 V vs. SCE. (ref 207)
[i] $E_{p,c}$ value

Standard electrochemical rate constants k have been measured by ac voltammetry for the two sequential one-electron transfers of $Re_2X_4(PMe_2Ph)_4$ (X = Cl or Br) and other triply bonded Re_2^{4+} complexes including $Re_2X_4(PMe_3)_4$, as well as for $Re_2Cl_5(PMe_2Ph)_3$ and $Re_2Cl_6(PMe_3)_2$.[255] Measurements were carried out in dichloromethane, acetonitrile and *N*,*N*-dimethylformamide at platinum electrodes and established the electrochemical reversibility that is in accord with fast electron transfer. In dichloromethane and acetonitrile, k for the first oxidation step of the dirhenium(II) complexes was invariably larger than for the second oxidation; for example, the k values for the +/0 and 2+/+ couples of $Re_2Cl_4(PMe_2Ph)_4$ in CH_2Cl_2 are 0.65 and 0.28 cm s^{-1}, respectively.[255] More recently, the kinetics of the electron self-exchange reaction of the redox couples $[Re_2X_4(PMe_2Ph)_4]^{0/+}$ (X = Cl or Br) have been measured in CH_2Cl_2 as a function of temperature and concentration by ^{1}H NMR line-broadening experiments.[256] The values of the self-exchange rate constants (at 298 K) are 2.3×10^{-8} M^{-1} s^{-1} for X = Cl and 4.2×10^{8} M^{-1} s^{-1} for X = Br. In addition, the kinetics of outer-sphere oxidation of $Re_2Br_4(PMe_2Ph)_4$ by cobalt(III) has been studied.[257]

From the very low value of the potential for the first oxidation of $Re_2X_4(PR_3)_4$ (Table 8.5) it is apparent that mild oxidants should be capable of generating $[Re_2X_4(PR_3)_4]^+$. The salt $NOPF_6$ proved to be an excellent oxidant in this regard, and earlier work led to the isolation of $[Re_2X_4(PEt_3)_4]PF_6$ (X = Cl or Br) by such a procedure.[228(b)] Spectroscopic characterizations, using EPR and electronic absorption spectroscopy,[228(b)] showed that these monocations possess the expected $\sigma^2\pi^4\delta^2\delta^{*1}$ ground-state electronic configuration. In a later study, a comparison was made of the low temperature (5 K) electronic absorption spectrum of $Re_2Cl_4(PPr^n_3)_4$ and its one-electron oxidized congener $[Re_2Cl_4(PPr^n_3)_4]PF_6$.[251] The trimethylphosphine complexes $[Re_2X_4(PMe_3)_4]PF_6$ (X = Cl or Br) have also been prepared by this method,[244] while $[Re_2Cl_4(PMe_3)_4]ReO_4$ has been obtained by the aerial oxidation of $Re_2Cl_4(PMe_3)_4$.[250]

Pictiva EX2004
Samsung v Pictiva
IPR2024-01094

It has also been found that $NOPF_6$ can access the second oxidation of $Re_2X_4(PMe_3)_4$; by this means $Re_2Cl_4(PMe_2Ph)_4$ was oxidized cleanly in two one-electron steps to give $[Re_2Cl_4(PMe_2Ph)_4]PF_6$ and $[Re_2Cl_4(PMe_2Ph)_4](PF_6)_2$.[243] In a similar fashion, the reversible one-electron oxidation of the $Re_2X_5(PR_3)_3$ complexes can be accomplished through the use of $NOPF_6$; for example, $Re_2Cl_5(PMePh_2)_3$ has been oxidized to $[Re_2Cl_5(PMe_2Ph)_3]PF_6$.[178] Of particular note is the observation that the treatment of $[Re_2Cl_4(PMe_2Ph)_4]PF_6$ and $[Re_2Cl_4(PMe_2Ph)_4](PF_6)_2$ with Cl^- forms $Re_2Cl_5(PMe_2Ph)_3$ and $Re_2Cl_6(PMe_2Ph)_2$, respectively,[243] thereby confirming the EECC and ECEC mechanisms that were proposed in Schemes 8.1 and 8.2 (vide supra).

The isolation and structural characterization of the complexes $Re_2Cl_4(PMe_2Ph)_4$, $[Re_2Cl_4(PMe_2Ph)_4]PF_6$, and, $[Re_2Cl_4(PMe_2Ph)_4](PF_6)_2$ provided the first opportunity to probe the structural changes that take place in a series of complexes that possess M–M bond orders of 3, 3.5, and 4 and *identical* sets of monodentate ligands.[243] The same basic eclipsed rotational geometry is preserved in all three complexes (D_{2d} virtual symmetry), the structures being as depicted in **8.16**. It is also clear that the electrochemical properties of these complexes accord with only minimal structural changes accompanying the electron transfer processes.[255] Of most interest is the trend in Re–Re bond lengths which are 2.241(1) Å, 2.218(1) Å and 2.215(2) Å, respectively (see Tables 8.1 and 8.4). Apparently, the Re–Re distances do not respond in a simple and predictable way to δ bond order changes because, with the increase in metal core charge (as the dimetal unit is oxidized), there is some decrease in the strength of the σ and/or π bonding contributions to the Re–Re bond resulting from orbital contraction. The X-ray photoelectron spectra (XPS) of representative complexes of the types $Re_2X_6(PR_3)_3$, $Re_2X_5(PR_3)_3$, $[Re_2X_4(PR_3)_4]PF_6$ and $Re_2X_4(PR_3)_4$ have been recorded,[228(b),258] and although the binding energies of the core Re(4f) electrons are in the expected order ($Re_2^{6+} > Re_2^{5+} > Re_2^{4+}$), interpretations of these chemical shifts are complicated by relaxation effects that occur during the core ionization.

The use of cobaltocene to reduce the complexes of the type $Re_2Cl_6(PR_3)_2$ by one electron to give $[(\eta^5\text{-}C_5H_5)_2Co][Re_2Cl_6(PR_3)_2]$ has already been discussed in Section 8.5.2. Likewise, this reagent was shown to reduce $Re_2Cl_5(PMePh_2)_3$ to the Re_2^{4+} complex $[(\eta^5\text{-}C_5H_5)_2Co][Re_2Cl_5(PMePh_2)_3]$ upon admixing acetone solutions of the reactants.[178] This reaction could be expected based on the cyclic voltammetric data reported in Table 8.5 for this complex. Both types of anions react further with an equivalent of the appropriate phosphine ligand with substitution of a halide ligand and the formation of the appropriate neutral mixed halide-phosphine complex,[178] as the following reactions show:

$$[(C_5H_5)_2Co][Re_2Cl_6(PEt_3)_2] + PEt_3 \xrightarrow{CH_2Cl_2} Re_2Cl_5(PEt_3)_3 + [(C_5H_5)_2Co]^+ + Cl^-$$

$$[(C_5H_5)_2Co][Re_2Cl_5(PMePh_2)_3] + PMePh_2 \xrightarrow{CH_2Cl_2} Re_2Cl_4(PMePh_2)_4 + [(C_5H_5)_2Co]^+ + Cl^-$$

The key reactions we have discussed that lead to the interconversion of the various mixed halide-monodentate tertiary phosphine complexes of Re_2^{6+}, Re_2^{5+} and Re_2^{4+} are summarized in the redox scheme shown in Fig. 8.17. We now focus our attention on the more recent developments in the field that started in the mid-1990's, many of which have taken advantage of the transformations that are given in Fig. 8.17. Most important among these contributions are those of Cotton and co-workers who re-visited this chemistry with a further investigation[259] of the isomeric 1,3,6- and 1,2,7-$Re_2Cl_5(PMe_3)_3$ compounds (see structures **8.18** and **8.19**, respectively) that had first been reported in 1990.[248] By minor modifications of the original reaction conditions[248] a form of $Re_2Cl_5(PMe_3)_3$ was isolated that contained both 1,3,6- and 1,2,7-isomers in the same unit cell, as well as a new crystalline modification of composition 1,3,6-$Re_2Cl_5(PMe_3)_3 \cdot 0.5CH_2Cl_2$. The compound 1,2,7-$Re_2Cl_5(PMe_3)_3 \cdot Bu^n_4NCl$ was formed by the

Pictiva EX2004
Samsung v Pictiva
IPR2024-01094

reaction of $(Bu_4N)_2Re_2Cl_8$ with PMe_3 in 1-propanol at room temperature.[259] All three compounds were structurally characterized (see Table 8.4). Several of the $Re_2Cl_5(PMe_3)_3$ compounds have proven to be useful starting materials. Thus, 1,2,7-$Re_2Cl_5(PMe_3)_3$ can be reduced to its monoanion by cobaltocene, and this in turn reacts with PMe_3 to give 1,2,7,8-$Re_2Cl_4(PMe_3)_4$, which was the first example of this type of isomer to be isolated (see structure **8.17** and Table 8.4).[179] This isomer has different cyclic voltammetric properties from those of 1,3,6,8-$Re_2Cl_4(PMe_3)_4$ (Table 8.5). When $NOBF_4$ is used to oxidize the compound 1,2,7-$Re_2Cl_5(PMe_3)_3$·Bu_4NCl by one-electron , the Re_2^{6+} complex 1,7-$Re_2Cl_6(PMe_3)_2$ is formed.[179] Both the aforementioned reactions involving 1,2,7-$Re_2Cl_5(PMe_3)_3$ are of types that have been discussed previously and are represented in Fig. 8.17. The reaction between 1,2,7-$Re_2Cl_5(PMe_3)_3$·Bu_4NCl and $NOBF_4$ is different in the presence of an additional equivalent of Bu_4NCl; in this case, both $Re_2Cl_6(PMe_3)_2$ and the mixed-salt $(Bu_4N)_4[Re_2Cl_7(PMe_3)]_2[Re_2Cl_8]$ are formed (see Section 8.4.4).[185] The reduction of 1,2,7-$Re_2Cl_5(PMe_3)_3$ to form 1,3,6,8-$Re_2Cl_4(PMe_3)_4$, which occurs when the former compound is reacted with PMe_3 in 1-propanol, proceeds via the intermediacy of the Re_2^{5+} complex $[1,3,6,8\text{-}Re_2Cl_4(PMe_3)_4]Cl$ which has been isolated and structurally characterized (Table 8.4).[260] The isomerization and substitution that occurs when 1,2,7-$Re_2Cl_5(PMe_3)_3$ converts to $[1,3,6,8\text{-}Re_2Cl_4(PMe_3)_4]Cl$ may in turn proceed[260] via the intermediacy of the confacial bioctahedral Re_2^{5+} complex $(Me_3P)_2ClRe(\mu\text{-}Cl)_3ReCl(PMe_3)_4$, a compound that has been isolated separately (vide infra).[261]

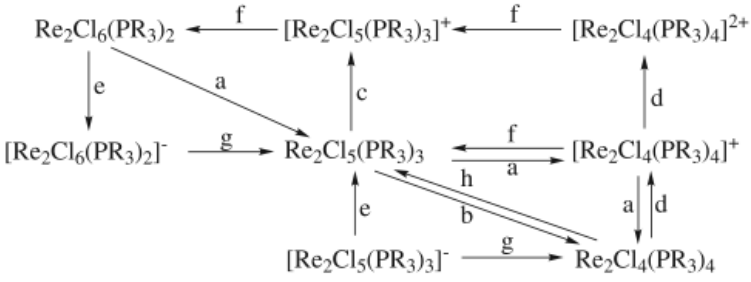


Fig. 8.17. Reaction scheme for mixed halide-monodentate tertiary phosphine complexes containing the Re_2^{n+} cores (n = 6, 5 or 4). The chemical reactions are as follows: (a) reaction with PR_3 at room temperature; (b) reaction with PR_3 under reflux; (c) reaction with $NO^+PF_6^-$ in CH_2Cl_2 at room temperature; (d) reaction with $NO^+PF_6^-$ in CH_3CN at room temperature; (e) reaction with Cp_2Co in acetone at room temperature; (f) reaction with one-equivalent of Cl^- (g) reaction with one equivalent of PR_3; (h) Cl_2 oxidation. Note: (1) the reduction of $Re_2Cl_6(PR_3)_2$ to $[Re_2Cl_6(PR_3)_2]^-$ may occur in some instances directly from the reaction of $[Re_2Cl_8]^{2-}$ with PR_3; (2) the oxidation of $Re_2Cl_4(PR_3)_4$ to $[Re_2Cl_4(PR_3)_4]^+$ is possible with other oxidants, including O_2.

Another entry into PMe_3 complexes that contain the Re_2^{5+} and Re_2^{4+} cores is through the paramagnetic, non metal-metal bonded, edge-shared bioctahedral complex 1,3,5,7-$Re_2(\mu\text{-}Cl)_2Cl_4(PMe_3)_4$, which is the main product from the reaction of $(Bu_4N)_2Re_2Cl_8$ with PMe_3 in benzene at room temperature.[179,261] Reduction of this compound with one or two equivalents of KC_8 in toluene (or toluene/CH_2Cl_2) affords the confacial bioctahedron $Re_2(\mu\text{-}Cl)_3Cl_2(PMe_3)_4$ (mentioned above) and 1,2,7,8-$Re_2Cl_4(PMe_3)_4$, respectively. The Re–Re distance in $Re_2(\mu\text{-}Cl)_3Cl_2(PMe_3)_4$ is 2.686(1) Å.[261] When the reduction with 2 equiv of KC_8 is carried out in benzene in the presence of Bu_4NCl the Re_2^{4+} complex $(Bu_4N)[1,2,7\text{-}Re_2Cl_5(PMe_3)_3]$ is formed.[261] The latter compound is also obtained when 1,2,7-$Re_2Cl_5(PMe_3)_3$·Bu_4NCl is reduced with KC_8; like its neutral congener 1,2,7-$Re_2Cl_5(PMe_3)_3$[248,259] it has a partially staggered rotational

Pictiva EX2004
Samsung v Pictiva
IPR2024-01094

geometry (χ_{av} = 24.4° versus 16.0° in 1,2,7-$Re_2Cl_5(PMe_3)_3$). Under other conditions $Re_2(\mu\text{-}Cl)_2Cl_4(PMe_3)_4$ can react to give mononuclear Re(III) or Re(IV) species.[261]

Chemistry similar to that described above for the PMe_3 complexes of Re_2^{5+} and Re_2^{4+} has been developed with several other phosphines, including PMe_2Ph. The relatively low cone angle phosphines PMe_3 and PMe_2Ph give very similar products. Depending on the choice of solvent, $(Bu_4N)_2Re_2Cl_8$ reacts with PMe_2Ph at room temperature to form 1,3,6- and/or 1,2,7-$Re_2Cl_5(PMe_2Ph)_3$.[180] The 1,2,7-isomer reacts with cobaltocene (in the presence of PMe_2Ph) and with $NOBF_4$ (in the presence of Bu_4NCl) to afford 1,2,7,8-$Re_2Cl_4(PMe_2Ph)_4$ and 1,7-$Re_2Cl_6(PMe_2Ph)_2$, respectively,[180] closely mirroring the behavior of 1,2,7-$Re_2Cl_5(PMe_3)_3$. The structures and electrochemical properties of the pairs of analogous PMe_3 and PMe_2Ph compounds are very similar (Tables 8.1, 8.2, 8.4 and 8.5). The reduction of 1,2,7-$Re_2Cl_5(PMe_2Ph)_3$ with KC_8 in toluene/CH_2Cl_2, followed by the addition of an equivalent of Bu_4NCl, gives $(Bu_4N)[1,2,7\text{-}Re_2Cl_5(PMe_2Ph)_3]$;[262] this compound is similar structurally to its PMe_3 analog (see Table 8.4). When the reduction of 1,2,7-$Re_2Cl_5(PMe_2Ph)_3$ by KC_8 is carried out in the presence of PEt_2H, the mixed phosphine complex 1,2,7,8-$Re_2Cl_4(PMe_2Ph)_3(PEt_2H)$ is formed.[262] A similar compound, 1,2,7,8-$Re_2Cl_4(PMe_3)_3(PEt_2H)$, has been obtained, albeit in low yield and admixed with other products, when 1,2,7-$Re_2Cl_5(PMe_3)_3$ is reduced with cobaltocene and the reduced anion reacted with PEt_2H.[262] Both of these mixed-phosphine complexes have been structurally characterized (Table 8.4), and they differ only in their rotational geometries in the solid state, with a χ_{av} value of 30.1° for the PMe_2Ph complex and 3.0° for its PMe_3 analog.[262] The 1,2,7,8 ligand arrangement has (to date) been encountered only when the phosphine ligands have relatively small cone angles, i.e., PMe_3, PMe_2Ph and PEt_2H.

As already mentioned in Section 8.5.2, salts of the $[1,7\text{-}Re_2Cl_6(PR_3)_2]^-$ anions can be generated by electrochemical means from their neutral Re_2^{6+} precursors,[228] and also by their reaction with the one-electron reductant cobaltocene.[178,190] In addition, the salts $(Bu_4N)Re_2Cl_6(PR_3)_2$, where PR_3 is PEt_3, PPr^n_3 or PEt_2Ph, have been isolated[182,189] as the kinetic products in the reactions of these phosphines with $(Bu_4N)_2Re_2Cl_8$ in 1-propanol at room temperature; the PEt_2Ph derivative was also obtained (although much more slowly) in benzene.[189] The X-ray crystal structures of $(Bu_4N)Re_2Cl_6(PPr^n_3)_2$ and $(Bu_4N)Re_2Cl_6(PEt_2Ph)_2$ have been determined (Table 8.4). In the case of the PPr^n_3 complex, both 1,7 and 1,6 isomeric forms exist in the solid state although in solution only one form (presumably the 1,7 isomer) is present.[189] Both the 1,6- and 1,7-isomers of $[Re_2Cl_6(PPr^n_3)_2]^-$ have partially staggered rotational geometries, while the PEt_2Ph complex is eclipsed.[189] The 1,3,6-$Re_2Cl_5(PPr^n_3)_3$ complex was also isolated in different polymorphic forms during the course of these studies,[182,189] each of which was characterized crystallographically (Table 8.4).

In the reaction between $(Bu_4N)_2Re_2Cl_8$ and PEt_3 or PPr^n_3 in the non-polar solvent benzene,[182] it is apparent that disproportionation occurs to give the dirhenium Re_2^{5+} products $(Bu_4N)Re_2Cl_6(PR_3)_2$ or $Re_2Cl_5(PR_3)_3$ along with mononuclear *trans*-$ReCl_4(PR_3)_2$. These disproportionations proceed by way of dirhenium(III) intermediates, which in the case of the PEt_3 reaction has been identified as the unsymmetrical edge-shared bioctahedral complex $(Bu_4N)[(Et_3P)_2Cl_2Re(\mu\text{-}Cl)_2ReCl_3(PEt_3)]$.[182] In the case of these specific phosphines, the disproportionation can be represented as:

$$3Re_2^{6+} \rightarrow 2Re_2^{5+} + 2Re^{4+}$$

Similar disproportionation behavior occurs with PEt_2H[183] and PCy_2H[181] when non-polar solvents are used, although the stoichiometries of the disproportionation processes are different in each case, and in turn differ from that given above for the PEt_3 and PPr^n_3 reactions. In the reactions with these secondary phosphines, Re_2^{5+} and Re_2^{4+} complexes have been isolated and

Pictiva EX2004
Samsung v Pictiva
IPR2024-01094

structurally characterized, namely, 1,2,7,8-$Re_2Cl_4(PEt_2H)_4$ and 1,3,6-$Re_2Cl_5(PCy_2H)_3$. Their structural and electrochemical properties are given in Tables 8.4 and 8.5.

Other examples of 1,3,6-$Re_2Cl_5(PR_3)_3$ are encountered with the phosphine-ester complexes $Re_2Cl_5(Ph_2PCH_2CO_2R)_3$, where R = Me or Et, which are prepared when $(Bu_4N)_2Re_2Cl_8$ and $Ph_2PCH_2CO_2H$ are reacted together in refluxing methanol or ethanol.[263]

It has become abundantly clear from several of these studies,[181-183] that the reduction reactions that occur between $(Bu_4N)_2Re_2Cl_8$ and monodentate tertiary phosphines are greatly influenced by the reaction temperature, in some cases by the proportions of reactants, and (most importantly) by the choice of solvent. The solvent affects the reaction rate, the product solubility, and the reaction mechanism; alcohol solvents are implicated as being intimately involved in the reaction mechanism, while in non-polar solvents such as benzene, toluene, hexanes and dichloromethane a disproportionation mechanism seems to predominate (as demonstrated for PEt_3, PPr^n_3, PEt_2H and PCy_2H).[181-183]

A re-investigation of the reactions between $(Bu_4N)_2Re_2I_8$ with PR_3 ligands, which were originally carried out with ethanol or acetone as the reaction solvent and were shown to afford 1,3,6,8-$Re_2I_4(PR_3)_4$ complexes,[25] has provided further insights into these systems.[184] The use of either ethanol or benzene as the solvent at room temperature or below affords the isomers 1,3,6,8-$Re_2I_4(PR_3)_4$ (PR_3 = PMe_3, PEt_3, PMe_2Ph or PEt_2Ph); the structures of several of these compounds were established by X-ray crystallography (Table 8.4). In the reaction of $(Bu_4N)_2Re_2I_8$ with PMe_3 in benzene, the paramagnetic complex $Re_2(\mu\text{-}I)_2I_4(PMe_3)_4$ was isolated in high yield as a kinetic product.[184] At room temperature it disproportionates to give some 1,3,6,8-$Re_2I_4(PMe_3)_4$, and when reduced with a two-fold excess of KC_8 in toluene/dichloromethane it gives this same Re_2^{4+} complex along with a small amount of 1,3,6-$Re_2I_5(PMe_3)_3$ (Table 8.4). The analogous reaction of PEt_3 with $(Bu_4N)_2Re_2I_8$ in benzene affords $(Bu_4N)[1,7\text{-}Re_2I_6(PEt_3)_2]$ as a kinetic product; its formation along with a Re(IV) species presumably occurs by a disproportionation mechanism.[184]

While the reductions of $[Re_2Cl_8]^{2-}$ and $[Re_2I_8]^{2-}$ by PR_3 ligands are similar, there are several important differences.[184] One of these is the much faster rate of reduction of $[Re_2I_8]^{2-}$ in ethanol, the solvent itself probably being involved in the reduction. While the same kinetic products are formed in benzene (i.e. $Re_2(\mu\text{-}X)_2X_4(PMe_3)_4$ and $[Re_2X_6(PEt_3)_2]^-$) they are less stable for X = I. Also, the disproportionation products in this solvent are different, e.g., 1,3,6,8-$Re_2I_4(PR_3)_4$ versus 1,2,7-$Re_2Cl_5(PR_3)_3$. The different results of PR_3 substitution on $[Re_2I_8]^{2-}$ versus $[Re_2Cl_8]^{2-}$ has been explained[184] by the trans effect order $Cl^- > PR_3 > I^-$.

In subsequent sections we will encounter additional aspects of the chemical reactivity of $Re_2X_4(PR_3)_4$ complexes. These will include the susceptibility of these Re≡Re bonds to cleavage by π-acceptor ligands to afford mononuclear complexes (see Section 8.7). The use of $Re_2Cl_4(PR_3)_4$ as synthons for the preparation of the dirhenium octahydrides $Re_2H_8(PR_3)_4$ is also of note (see Section 8.8),[264] as is the reaction of $Re_2Cl_4(PEt_3)_4$ with H_2 in dichloromethane at 60 °C and 120 atm to give $(Et_4N)[Re_2(\mu\text{-}H)(\mu\text{-}Cl)_2Cl_4(PEt_3)_2]$; the dirhenium(III) anion contains a short Re–Re distance (2.349(1) Å).[265] An especially important reaction is the conversion of $Re_2X_4(PR_3)_4$ to complexes of the types $Re_2X_4(LL)(PR_3)_2$ and $Re_2X_4(LL)_2$, where LL represents a bidentate (chelating or bridging) phosphine and/or arsine ligand.[202] The latter reactions are discussed in the following sections.

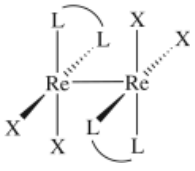
Bidentate phosphines and arsines containing two or three bridgehead groups

For convenience, we will first deal with complexes that contain $R_2X(CH_2)_nYR_2$ ligands (R = alkyl or aryl; X = Y = P or As, and X = P when Y = As), or close analogs thereof, in which n = 2 or 3, and then with those cases in which there is only a single bridgehead group

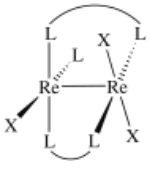
Pictiva EX2004
Samsung v Pictiva
IPR2024-01094

present between the two donor atoms (i.e. n = 1). The first studies that were carried out involved the reactions of $(Bu_4N)_2Re_2X_8$ (X = Cl or Br) with the bidentate ligands 1,2-bis(diphenylphosphino)ethane (dppe) and 1-diphenylphosphino-2-diphenylarsinoethane (arphos) in refluxing acetonitrile, from which the triply bonded dirhenium(II) compounds $Re_2Cl_4(dppe)_2$, $Re_2Cl_4(arphos)_2$ and $Re_2Br_4(arphos)_2$ were isolated in low yield (< 12%).[202] The reactions of $(Bu_4N)_2Re_2I_8$ with dppe and arphos in refluxing acetone for short periods lead to the iodide complexes $Re_2I_4(dppe)_2$ and $Re_2I_4(arphos)_2$ in much higher yields (60% and 30%, respectively) than those of their chloride and bromide analogs.[25] The difference arises because in the chloride and bromide cases quite stable di-μ-halo bridged complexes, $Re_2(\mu\text{-}X)_2X_4(LL)_2$, are also formed.[200,202,209] A higher yield synthetic procedure utilized the reactions between $Re_2Cl_4(PEt_3)_4$ and dppe or arphos to afford $Re_2Cl_4(dppe)_2$ and $Re_2Cl_4(arphos)_2$.[202] The arphos complex can also be prepared by reacting $Re_2Cl_5(PEtPh_2)_3$ with arphos in refluxing benzene. The mechanism for these reactions may well involve a disproportionation step similar to those that can occur in the reduction reactions of $[Re_2X_8]^{2-}$ with monodentate phosphines (vide supra).

The reversal of these substitution reactions has been accomplished in the case of the reaction between $Re_2Cl_4(arphos)_2$ and PEt_3 which gives 1,3,6,8-$Re_2Cl_4(PEt_3)_4$, thereby implying that a close structural similarity exists between the $Re_2X_4(PR_3)_4$ and $Re_2X_4(LL)_2$ compounds. However, differences between the spectroscopic properties of $Re_2Cl_4(LL)_2$ and 1,3,6,8-$Re_2Cl_4(PR_3)_4$ led to the proposal[202] that although a *trans*-$ReCl_2P_2$ (or *trans*-$ReCl_2PAs$) geometry is preserved in the $Re_2Cl_4(LL)_2$ compounds, they have significantly different structures from $Re_2Cl_4(PR_3)_4$. Specifically, rather than the complexes containing an eclipsed rotational geometry and chelating LL ligands (i.e. as in structure **8.20**), it was suggested[202] that the bidentate ligands (LL) bridge the two metal atoms within the dimer thereby conferring a staggered rotational geometry (**8.21**). This was confirmed by a structure determination on $Re_2Cl_4(dppe)_2$ (Fig. 8.18).[266] The Re–Re distance of 2.244(1) Å is very similar to those in the Re_2^{4+} complexes $Re_2X_4(PR_3)_4$ (Table 8.4), which is to be expected since these complexes possess the same ligand sets, the same *trans*-$Re_2Cl_2P_2$ geometry and the same Re–Re bond order. The electronic configuration $\sigma^2\pi^4\delta^2\delta^{*2}$ which is germane to $Re_2Cl_4(PR_3)_4$ imposes no rotational barrier, so with the displacement of PR_3 by dppe (or arphos) the conformational preference of the chair-like $Re_2C_2P_2$ rings that result (Fig. 8.18) apparently dominates, thereby ensuring the staggered conformation. In this structure the Cl–Re–Re–Cl and P–Re–Re–P torsional angles are 51° and 39°. Their deviations from 45° are doubtless attributable to the conformational demands of the six-membered rings.[266] Subsequently, structures of the types represented by **8.20** and **8.21** were given the notation α-$M_2X_4(LL)_2$ and β-$M_2X_4(LL)_2$, respectively,[267] a terminology that is still in common use, so that the aforementioned isomer is represented as β-$Re_2Cl_4(dppe)_2$.



8.20



8.21

The structure determination of β-$Re_2Cl_4(dppe)_2$ was an important milestone for several reasons, not the least of which is that it constituted the first example of its kind; many such complexes are now known, including several of dimolybdenum(II) and ditungsten(II). Also, this structure shows several characteristics that are often shared by other complexes with a structure

Pictiva EX2004
Samsung v Pictiva
IPR2024-01094

like **8.21**. Each crystal site is occupied by one or the other of two β-$M_2X_4(LL)_2$ molecules, one orientation being far more prominent than the other.[34] This sort of orientational disorder is related to that seen with the $[Re_2X_8]^{2-}$ anions (see Section 8.3), and is such that the M_2 units of the principal and secondary molecules have the same midpoint and are approximately perpendicular. A consequence of the fused six-membered ring systems and the twisted geometry is that at each site, the principal and secondary isomers have opposite chiralities. Indeed, the chirality of such complexes has been of considerable interest, and this has led subsequently to the isolation of the first configurationally chiral dirhenium complex Re_2Cl_4(*S*,*S*-dppb)$_2$, where *S*,*S*-dppb = *S*,*S*-2,3-bis(diphenylphosphino)butane, and its oxidized dication $[Re_2Cl_4$(*S*,*S*-dppb)$_2]^{2+}$ (vide infra).[268,269] The CD spectrum of the quadruply bonded dication implies that it has the Λ absolute configuration with a twist of less than 45°.[268] The sort of twisting first encountered in the β-$Re_2X_4(LL)_2$ complexes (structure **8.21**), was later found in the related molybdenum and tungsten complexes of this stoichiometry (Chaps. 4 and 5).[34] For example, the structure of the β-isomer of Mo_2Br_4(arphos)$_2$[270] has been determined, the mean torsional angle being *c.* 30°. Since quadruply bonded Mo_2^{4+} (and W_2^{4+}) compounds have a $\sigma^2\pi^4\delta^2$ configuration, the bond order will in these instances be reduced by rotation away from a full eclipsed structure unlike the situation with triply-bonded Re_2^{4+}. The mean torsional angle of 30° is in accord with a bond order of *c.* 3.5 for β-Mo_2Br_4(arphos)$_2$.[270]



Fig. 8.18. The structure of the $Re_2Cl_4P_4$ skeleton in β-Re_2Cl_4(dppe)$_2$ showing the staggered rotational geometry and the *cis*-decalin-like fusion of the two $Re_2C_2P_2$ chair-like rings.

As an alternative to using $(Bu_4N)_2Re_2X_8$ (X = Cl, Br or I) and $Re_2X_4(PEt_3)_4$ (X = Cl or Br) as the starting materials for the synthesis of β-$Re_2X_4(LL)_2$,[25,202] the reactions of *cis*-$Re_2(O_2CCH_3)_2X_4(H_2O)_2$ (X = Cl, Br or I) with dppe have been successfully employed to prepare β-Re_2X_4(dppe)$_2$.[271] In view of the general usefulness and availability of these carboxylate starting materials, this strategy has considerable merit. The compound β-Re_2Cl_4(dpae)$_2$ (dpae = $Ph_2AsCH_2CH_2AsPh_2$) has been isolated as one of the products in the reaction between $(Bu_4N)_2Re_2Cl_8$ and dpae in refluxing *n*-butanol;[272] an earlier report[202] had described this reaction as yielding Re_2Cl_6(dpae)$_2$. An X-ray structural analysis of β-Re_2Cl_4(dpae)$_2$ crystals showed signs of Re_2Cl_6(dpae) as a minor component.[272]

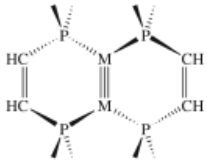
Five years after the isolation of the first examples of β-isomers of $Re_2X_4(LL)_2$, the complex Re_2Cl_4(dppp)$_2$ (dppp = $Ph_2P(CH_2)_3PPh_2$) was obtained from the reaction of $(Bu_4N)_2Re_2Cl_8$ and dppp in refluxing acetonitrile.[273] An X-ray crystal structure determination showed it to be the α-isomer and to have a structure as represented in **8.20**, in which the two dppp ligands each chelate to a single metal atom and the conformation is eclipsed.[273] More recently, this same compound was found to be the major product when toluene was used as the reaction solvent and the mixture refluxed for 4 days; the structure of a crystal of composition

Pictiva EX2004
Samsung v Pictiva
IPR2024-01094

α-$Re_2Cl_4(dppp)_2 \cdot 4CH_2Cl_2$ was reported (Table 8.4).[189] A couple of years after the initial characterization of α-$Re_2Cl_4(dppp)_2$,[273] a second such compound, viz. α-$Re_2Cl_4(dmpe)_2$ (dmpe = $Me_2P(CH_2)_2PMe_2$), was prepared from the reaction of $(Bu_4N)_2Re_2Cl_8$ with dmpe in methanol-conc HCl at room temperature. Its structure is similar to that of α-$Re_2Cl_4(dppp)_2$, with a Re–Re distance of 2.266(1) Å (Table 8.4).[274]

It is now known that for most $R_2ECH_2CH_2ER_2$ ligands both α and β forms can be isolated and many have been structurally characterized. The first such pairs to be isolated and characterized were the α- and β-isomers of $Re_2X_4(dppee)_2$ (X = Cl or Br; dppee = cis-$Ph_2PCH{=}CHPPh_2$)[275] and the X-ray crystal structures of the chloro complexes determined (Table 8.4).[276] The green α forms are produced in low yields when $(Bu_4N)_2Re_2X_8$, or $Re_2Cl_6(PBu^n_3)_2$ in the case of the chloride system, are reacted with cis-dppee in refluxing methanol (acidified with conc HX) or ethanol; these conversions are accompanied by some cleavage of the dirhenium starting materials to give mononuclear complexes (see Section 8.7).[275] The brown β isomers are quite easily prepared through the use of $Re_2X_4(PR_3)_4$ (X = Cl or Br; R = Et or Pr^n) and their reaction with cis-dppee in refluxing benzene.[275] This success in preparing both α and β isomers of a particular $Re_2X_4(LL)_2$ complex eventually led to the successful preparation of α-$Re_2X_4(dppe)_2$ (X = Cl or Br), using a procedure similar to that described for the analogous complexes containing cis-dppee.[276] The crystal structures of two compounds that contain α-$Re_2Cl_4(dppe)_2$ have been reported, namely, α-$Re_2Cl_4(dppe)_2 \cdot 4C_6H_6$ and α-$Re_2Cl_4(dppe)_2 \cdot$dppe.[277]

The complexes β-$Re_2X_4(dppee)_2$ are of special significance in that they constitute the first examples of compounds that contain the unsaturated ring system represented in **8.22**.[275,276] The resulting six-membered ring conformations are of a type well known for cyclohexene, namely, a flattened chair or half-chair.



8.22

The synthons $(Bu_4N)_2Re_2Cl_8$ and $Re_2X_4(PR_3)_4$ (X = Cl when PR_3 = PEt_3 and X = Br when PPr^n_3) have been used to prepare the isomeric pairs α- and β-$Re_2X_4(depe)_2$, where depe is $Et_2PCH_2CH_2PEt_2$.[275,278,279] The structures of the two isomers of the chloro complex show the usual features, with the α-form being eclipsed and having a slightly longer Re–Re bond than the staggered β-form.[278,279]

The compound α-$Re_2Cl_4(dppbe)_2$ (dppbe = 1,2-bis(diphenylphosphino)benzene) has been prepared by the reaction between $Re_2Cl_4(PPr^n_3)_4$ and dppbe in benzene or toluene.[280] The electrochemical properties of α-$Re_2Cl_4(dppbe)_2$ (see Table 8.5), as well as its low frequency infrared spectral properties, which closely resemble those of other α-$Re_2Cl_4(LL)_2$ complexes,[273,275,276] support the structural assignment. The β-isomer has not been isolated, which is to be expected in view of the more rigid nature of this ligand.

In addition to the extensive series of Re_2^{4+} complexes that contain $R_2E(CH_2)_nER_2$ ligands (n = 2 or 3) and which have been the subject of this section, a few compounds are known in which the paramagnetic Re_2^{5+} core is present. One of these is the salt $[(\eta^5\text{-}C_5H_5)_2Co][1,3\text{-}Re_2Cl_6(dppf)]$, that is formed by the cobaltocene reduction of $Re_2Cl_6(dppf)$ and in which the anion has a structure of the type 1,3-$Re_2Cl_6(PR_3)_2$ (see **8.12**).[190] Another one is the salt $(Bu_4N)Re_2Cl_6(dppp)$,

Pictiva EX2004
Samsung v Pictiva
IPR2024-01094

which is formed in the reaction of $(Bu_4N)_2Re_2Cl_8$ with 1,3-bis(diphenylphosphino)propane and is apparently an intermediate in the formation of α-$Re_2Cl_4(dppp)_2$.[189] It is a kinetic product of the reaction in toluene (at reflux) and acetonitrile (at room temperature), and an X-ray crystal structure determination shows it to have the expected 1,2-$Re_2Cl_6(PR_3)_2$ structure for the anion (Table 8.4).[189] A third example, which like the dppp complex has a 1,2-structure for the anion, is formed when the tetrathiafulvalene ligand *o*-$\{Ph_2P\}_2(CH_3)_2TTF$ (abbreviated *o*-P2) is reacted with $(Bu_4N)_2Re_2Cl_8$ in refluxing ethanol.[281] The mixed-nuclearity salt [*trans*-$ReCl_2$(*o*-P2)$_2$][1,2-Re_2Cl_6(*o*-P2)] is obtained in high yield, the mononuclear cation being formed by non-reductive cleavage of some of the $[Re_2Cl_8]^{2-}$ anion. Reaction of this compound with cobaltocene reduces the cation to *trans*-$ReCl_2$(*o*-P2) and forms (η^5-C_5H_5)[1,2-Re_2Cl_6(*o*-P2)].[281]

Like their analogs with monodentate phosphines, the dirhenium(II) compounds of the types α- and β-$Re_2X_4(LL)_2$ exhibit two accessible one-electron oxidations. Electrochemical measurements on dichloromethane solutions of many of these complexes (see Table 8.5) have shown that the first process is reversible and that the potentials can be accessed by several one-electron oxidants.[255,275,276,282] The kinetics of outer-sphere oxidation of β-$Re_2X_4(dppee)_2$ (X = Cl or Br) by Co(III) has been studied.[257] Several β-$Re_2X_4(LL)_2$ complexes have been oxidized chemically to paramagnetic β-$[Re_2X_4(LL)_2]PF_6$ by $NOPF_6$ in acetonitrile (X = Cl when LL = depe, dppe, dppe or arphos; X = Br when LL = dppee),[275,282] and in a few instances the second oxidation has been achieved to give diamagnetic quadruply bonded β-$[Re_2Cl_4(LL)_2](PF_6)_2$ (LL = depe, dppe or S,S-dppb).[268,275] Note that β-$[Re_2Cl_4(LL)_2]^+$ cations do not appear to react with Cl^-,[282] in contrast to the reactivity of $[Re_2Cl_4(PR_3)_4]^+$ to afford $Re_2Cl_5(PR_3)_3$ (vide supra). The monocationic species are EPR-active,[275,282] and both monocations and dications retain the staggered rotational conformation of their parents as a result of the dominant conformational demands of the bridging phosphine ligands. Thus, the β-$[Re_2Cl_4(LL)_2]^+$ cations most probably possess a metal-metal bond order closer to 3, rather than that of 3.5, which would be expected in a system, like $[Re_2X_4(PR_3)_4]^+$, where the rotational conformation is fully eclipsed. In a couple of instances, the related α isomers have been oxidized successfully; both α-$[Re_2Cl_4(dppee)_2]PF_6$ and α-$[Re_2Cl_4(dppp)_2]PF_6$ have been obtained through the use of ferrocenium hexafluorophosphate as the oxidant.[276]

As a consequence of the shift of $E_{1/2}$(ox) to more positive potentials for $Re_2X_4(LL)_2$ relative to $Re_2X_4(PR_3)_4$ (Table 8.5), the reduction of $Re_2X_4(LL)_2$ to the monoanions $[Re_2X_4(LL)_2]^-$ becomes feasible. By the use of acetonitrile as solvent, in which $[Re_2Cl_4(dppe)_2]PF_6$ is soluble, and a hanging mercury drop electrode, an irreversible reduction in the potential range -1.6 to -1.7 V has been observed.[282] This monoanion may possess a Re–Re bond order of 2.5. Also, in the cyclic voltammograms of α-$Re_2Cl_4(dppe)_2$, α-$Re_2Br_4(dppe)_2$ and α-$Re_2Cl_4(dppbe)_2$ (recorded in 0.1 M Bu_4NPF_6-CH_2Cl_2),[276,280] irreversible reductions have been measured between -1.4 and -1.6 V vs. Ag/AgCl.

While the complexes α-$Re_2X_4(LL)_2$ and β-$Re_2X_4(LL)_2$ have some limited chemical reactivity, such as the conversion of β-$Re_2Cl_4(dppe)_2$ to $Re_2H_8(dppe)_2$,[264] and the reactions of β-$Re_2Cl_4(dppe)_2$ and β-$Re_2Cl_4(arphos)_2$ with CCl_4 to regenerate the $[Re_2Cl_8]^{2-}$ anion,[202] their oxidized congeners are much more reactive. This has been shown in studies detailing some of the reactions of β-$[Re_2X_4(LL)_2]PF_6$ (X = Cl when LL = depe, dppe or arphos; X = Br when LL = dppe or arphos).[275,283] While their neutral precursors do not react with nitriles RCN (R = Me or Et), the salts β-$[Re_2X_4(LL)_2]PF_6$ react with these donors in the presence of $TlPF_6$ to give paramagnetic β-$[Re_2X_3(LL)_2(NCR)](PF_6)_2$. The latter complexes can be reduced to diamagnetic β-$[Re_2X_3(LL)_2(NCR)]PF_6$ with the use of $LiBEt_3H$ or cobaltocene as reductants.[275,283] In all instances, spectroscopic and electrochemical data support the retention of the staggered rotational geometry of the parent species β-$[Re_2X_4(LL)_2]^{n+}$ (n = 0 or 1). The same is true of the

Pictiva EX2004
Samsung v Pictiva
IPR2024-01094

products formed from the reactions between β-$[Re_2X_4(LL)_2]PF_6$ (LL = dppe or arphos) and the isocyanide ligands RNC (R = Pr^i or Bu^t) in CH_2Cl_2.[283] However, in these instances reduction to β-$[Re_2X_3(LL)_2(CNR)]PF_6$ occurs, although these Re_2^{4+} complexes can be oxidized to paramagnetic β-$[Re_2X_3(LL)_2(CNR)](PF_6)_2$ with the use of $NOPF_6$ as the oxidant.[283]

Bidentate and tridentate phosphines and arsines containing a single bridgehead group

The most famous of these is the ligand $Ph_2PCH_2PPh_2$ (dppm). Although it can chelate, dppm shows a propensity for bridging two metal atoms. This is the situation in the case of $Re_2X_4(\mu\text{-dppm})_2$ (X = Cl or Br), which were first prepared[202] from the reactions between $Re_2X_4(PPr^n_3)_4$ and dppm in benzene. Note that in this early report $Re_2Br_4(\mu\text{-dppm})_2$ is referred to as β-$[ReBr_2(dppm)_2]_n$. When $Re_2Cl_4(PEt_3)_4$ is used in place of $Re_2Cl_4(PPr^n_3)_4$, the mixed phosphine complex $Re_2Cl_4(\mu\text{-dppm})(PEt_3)_2$ can be isolated (vide infra). Improved methods for obtaining $Re_2Cl_4(\mu\text{-dppm})_2$ include the reaction of $Re_2Cl_6(PPr^n_3)_2$ with dppm in methanol,[203,274] although in diethyl ether the product is $Re_2Cl_5(\mu\text{-dppm})_2$ (vide infra).[203] However, perhaps the best method for preparing all three halide complexes of the type $Re_2X_4(\mu\text{-dppm})_2$ (X = Cl, Br or I) involves the reactions between *cis*-$Re_2(O_2CCH_3)_2X_4L_2$ (L = H_2O, 4-Mepy, DMF or DMSO) and dppm in refluxing ethanol.[271] These reactions, which proceed via the intermediacy of $Re_2(O_2CCH_3)X_4(\mu\text{-dppm})_2$ (at least in the case of X = Cl or Br), are part of an extensive chemistry involving mixed carboxylate-dppm complexes of dirhenium that will be discussed more fully a little later. The synthesis of $Re_2Cl_4(\mu\text{-dppm})_2$ by this route can be simplified by use of a one-pot reaction between $(Bu_4N)_2Re_2Cl_8$, CH_3CO_2Na and dppm in ethanol.[271]

Several compounds analogous to $Re_2X_4(\mu\text{-dppm})_2$ have been prepared by the use of procedures similar to those described above. By such means the compounds $Re_2X_4(\mu\text{-dppa})_2$ (X = Cl or Br; dppa = $Ph_2PNHPPh_2$),[203,284] $Re_2Cl_4(\mu\text{-dcpm})_2$ (dcpm = $Cy_2PCH_2PCy_2$),[285] $Re_2Cl_4(\mu\text{-cdpp})_2$ (cdpp = $Ph_2PC(CH_2)_2PPh_2$),[286] $Re_2Cl_4(\mu\text{-dppE})_2$ (dppE = 1,1-bis(diphenylphosphino)ethene)[287] and $Re_2X_4(\mu\text{-dpam})_2$ (dpam = $Ph_2AsCH_2AsPh_2$)[288] have been obtained. Another compound of the type $Re_2X_4(\mu\text{-dppm})_2$ is the tetramethyl derivative $Re_2(CH_3)_4(\mu\text{-dppm})_2$ which is obtained by methylating the chloride complex with CH_3Li.[289] The compound $Re_2(NCBH_3)_4(\mu\text{-dppm})_2(H_2O)_2\cdot 2THF$ has been prepared from the reaction between $Re_2Cl_4(\mu\text{-dppm})_2$ and $NaBH_3CN$ in methanol,[290] and similar reactions with $Na[N(CN)_2]$ and $K[C(CN)_3]$ give $Re_2[N(CN)_2]_4(\mu\text{-dppm})_2$ and $Re_2[C(CN)_3]_4(\mu\text{-dppm})_2$, respectively.[291] The structure of the dicyanamide complex has been confirmed on a crystal of composition $Re_2[N(CN)_2]_4(\mu\text{-dppm})_2(DMF)_2\cdot 3DMF$.[291] The structure of this compound[291] closely resembles that of $Re_2(NCBH_3)_4(\mu\text{-dppm})_2(H_2O)_2\cdot 2THF$[290] and both compounds contain axially bound ligand molecules (Table 8.4). A different kind of behavior is encountered when $Re_2Cl_4(\mu\text{-dppm})_2$ is reacted with $(Bu^n_4N)CN$ in dichloromethane; cyanide for chloride substitution occurs plus coordination of additional cyanide to give the salt $(Bu_4N)_2Re_2(CN)_6(\mu\text{-dppm})_2$, in which a long Re–Re single bond is present and two of the CN^- ligands adopt an unusual η^2-(σ,π) bridging arrangement.[292]

Although the compound $Re_2Cl_4(\mu\text{-dippm})_2$ (dippm = bis(di-iso-propylphosphino)methane) may well be formed in solution from the reaction between $(Bu_4N)_2Re_2Cl_8$ (or $Re_2Cl_4(PMe_3)_4$) and dippm, all attempts to isolate it have so far failed.[293] It is in any event quite reactive and easily decomposes; in the presence of O_2 the complex $Re_2O_3Cl_4(\mu\text{-dippm})_2$ is formed.[293] In contrast to the ease of making $Re_2Cl_4(\mu\text{-cdpp})_2$, the closely related complex $Re_2Cl_4[\mu\text{-(2,2-dppp)}]_2$ (2,2-dppp = $Ph_2PCMe_2PPh_2$) cannot be obtained because the strong chelating tendency of this phosphine results in Re–Re bond cleavage to give *trans*-$ReCl_2(2,2\text{-dppp})_2$.[286]

The first of the aforementioned $Re_2X_4(\mu\text{-LL})_2$ compounds to be structurally characterized was $Re_2Cl_4(\mu\text{-dppm})_2$.[274] Subsequently, several of these compounds were characterized by X-ray

Pictiva EX2004
Samsung v Pictiva
IPR2024-01094

crystallography, the results of which are summarized in Table 8.4. All show the same structural features, as typified in Fig. 8.19 by the structure of $Re_2Cl_4(\mu\text{-dcpm})_2$, which clearly reveals the staggered rotational geometry.[294] The extent of twisting can be defined in terms of the averages of the Cl–Re–Re–Cl and P–Re–Re–P torsion angles which are 43.6° and 39.0°, respectively, for the molecule shown in Fig. 8.19.

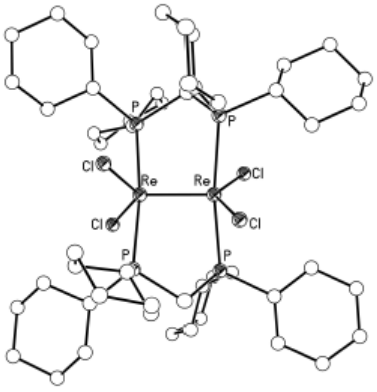


Fig. 8.19. The structure of $Re_2Cl_4(\mu\text{-dcpm})_2$.

The group of complexes of the type $Re_2X_4(\mu\text{-LL})_2$, have very similar spectroscopic and electrochemical properties. The spectroscopic characterizations have included electronic absorption spectroscopy and ^1H and $^{31}P\{^1H\}$ NMR spectroscopy.[285-290,294] Also, the low frequency infrared spectrum of $Re_2Cl_4(dppm)_2$ shows two ν(Re–Cl) modes (335 s and 309 s cm^{-1}) that mirror those found in the related spectrum of $\beta\text{-}Re_2Cl_4(dppe)_2$ at 333 and 303 cm^{-1}.[202] The cyclic voltammetric properties of these complexes (Table 8.5), which resemble the behavior of the other dirhenium(II) complexes with bidentate phosphines and arsines, are discussed later in Section 8.5.4 when the redox chemistry of these complexes is considered.

An interesting and surprising result was obtained when attempts were made to prepare the bis(dimethylphosphino)methane complex $Re_2Cl_4(\mu\text{-dmpm})_2$. The reactions of dmpm with $(Bu_4N)_2Re_2Cl_8$ in methanol and with $Re_2Cl_4(PPr^n_3)_4$ in ethanol-toluene gave red crystalline $Re_2Cl_4(\mu\text{-dmpm})_3$,[295] and the bis-dmpm complex has so far defied all attempts to isolate it. The crystal structure of this complex was determined on different crystalline forms both of which are essentially the same (Table 8.4 and Fig. 8.20). The rotational conformation is staggered, and there is a two-fold axis passing through the methylene carbon atom of one dmpm ligand and the mid-point of the Re–Re bond. This defines the unique dmpm ligand (Fig. 8.20), which has a helical sense opposite to that of the other two, thereby making interconversions of the enantiomers by simple internal rotation about the Re–Re bond impossible. Not surprisingly, this results in a complex ^1H NMR spectrum.[295] The cyclic voltammetric properties of this complex show the presence of two accessible one-electron oxidations (Table 8.4).[295] The related bromide derivative $Re_2Br_4(\mu\text{-dmpm})_3$ has also been prepared and characterized (Table 8.4).[296]

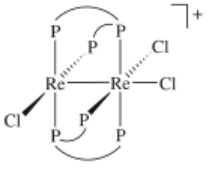
With use of the tridentate phosphine bis[(diphenylphosphino)methyl]phenylphosphine, the 1:1 salts $[Re_2Cl_3(dpmp)_2]X$ (X = Cl or PF_6) have been isolated upon reacting this ligand with $(Bu_4N)_2Re_2Cl_8$ in methanol.[297] The structure of the cation in both salts is the same (**8.23**), with a staggered rotational geometry and the dpmp ligand doubly bridging the dirhenium unit.[297]

Pictiva EX2004
Samsung v Pictiva
IPR2024-01094

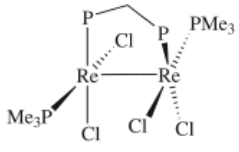


Fig. 8.20. The structure of the monoclinic form of $Re_2Cl_4(\mu\text{-dmpm})_3$.

A variety of mixed-phosphine complexes that contain the dppm, dppa and dcpm ligands are also known. The first of these to be prepared was $Re_2Cl_4(\mu\text{-dppm})(PEt_3)_2$, which is obtained as a purple solid upon heating a mixture of $Re_2Cl_4(PEt_3)_4$ and dppm in benzene.[202] Later, the PMe_3 complexes $Re_2Cl_4(\mu\text{-LL})(PMe_3)_2$, where LL = dppm, dppa or dcpm, were obtained by a closely related procedure.[244,285] The compound $Re_2Cl_4(\mu\text{-dppm})(PMe_3)_2$ has also been prepared by reacting $Re_2Cl_4(\mu\text{-dppm})_2$ with an excess of PMe_3, by heating a 1:1 mixture of $Re_2Cl_4(PMe_3)_2$ and $Re_2Cl_4(\mu\text{-dppm})_2$ in 1-butanol and, quite unexpectedly, upon reacting the tripodal ligand $HC(PPh_2)_3$ with $Re_2Cl_4(PMe_3)_4$ in hot ethanol.[298,299] In the direct reaction of $Re_2Cl_4(\mu\text{-dppm})_2$ with PMe_3, the 1:1 adduct $Re_2Cl_4(\mu\text{-dppm})_2(PMe_3)$ is formed as an isolable intermediate.[300] This complex, as well as its bromide analog and the corresponding phosphite derivatives $Re_2Cl_4(dppm)_2[P(OR)_3]$ (R = Me, Et or Ph), have been characterized on the basis of their spectroscopic and electrochemical properties (Table 8.5).[300] ^1H and $^{31}P\{^1H\}$NMR spectroscopy has been used to show that $Re_2Cl_4(\mu\text{-LL})(PMe_3)_2$ possess structure **8.24**, a conclusion that was confirmed by an X-ray crystal structure determination on $Re_2Cl_4(\mu\text{-dppm})_2(PMe_3)_2$.[285] These complexes, as well as the compound $Re_2Cl_4(\mu\text{-dppa})(PMe_2Ph)_2$,[203] have redox properties that are typical of triply bonded Re_2^{4+} species (Table 8.5).[244]



8.23

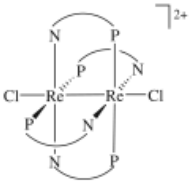


8.24

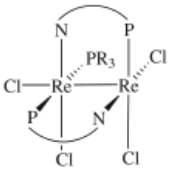
The compounds $Re_2Cl_4(\mu\text{-dppm})(PMe_3)_2$ and $Re_2Cl_4(\mu\text{-dppa})(PMe_3)_2$ are converted to the β isomers of $Re_2Cl_4(dppm)(dppe)$, $Re_2Cl_4(dppm)(arphos)$ and $Re_2Cl_4(dppa)(dppe)$ upon their reaction with dppe or arphos in 1-butanol.[298] Alternative synthetic strategies for $Re_2Cl_4(dppm)(dppe)$ include the reaction of $Re_2Cl_4(PMe_3)_4$ with 2 equiv of dppm and 1 equiv of dppe, and the reaction of $Re_2Cl_4(\mu\text{-dppm})_2$ with dppe.[298] The spectroscopic and electrochemical properties (Table 8.5) of these mixed phosphine ligand complexes are in accord with their possessing a structure of the type shown in **8.21**, with both bidentate ligands in a bridging transoid disposition to one another. This has been confirmed by a crystal structure determination of $Re_2Cl_4(\mu\text{-dppm})(\mu\text{-dppe})$.[298]

Pictiva EX2004
Samsung v Pictiva
IPR2024-01094

Several Re_2^{4+} compounds have been isolated that contain bridging ligands with N and P donor atoms rather than a pair of P atoms. A complex that is related to $Re_2X_4(\mu\text{-dmpm})_3$ is $Re_2Cl_4(\mu\text{-}Ph_2Ppy)_3$, which is formed from the reactions between $(Bu_4N)_2Re_2Cl_8$ or $Re_2Cl_6(PBu^n{}_3)_2$ and 2-(diphenylphosphino)pyridine in methanol.[207,301] The Ph_2Ppy ligand, like dppm, can bridge two metal atoms but in this instance the bridging atoms are N and P. While the complex $Re_2Cl_4(\mu\text{-}Ph_2Ppy)_3$ has not been structurally characterized, it may have a structure related to that of $Re_2X_4(\mu\text{-dmpm})_3$. However, this compound quite easily eliminates HCl to give the ortho-metalated complex $Re_2Cl_3(\mu\text{-}Ph_2Ppy)_2[(C_6H_5)(C_6H_4)Ppy]$,[207,301] the first example of an ortho-metalation reaction occurring at a multiple bond in a molecule of the M_2L_8 type. The structure of $Re_2Cl_3(\mu\text{-}Ph_2Ppy)_2[(C_6H_5)(C_6H_4)Ppy]$ is shown in Fig. 8.21.[207,301] Another product from this same reaction is the dirhenium(II) salt $[Re_2Cl_2(\mu\text{-}Ph_2Ppy)_4]Cl_2$. It can be metathesized with KPF_6 to give $[Re_2Cl_2(Ph_2Ppy)_4](PF_6)_2$, a compound whose structure (represented in **8.25**) has been determined by X-ray crystallography.[207] This complex constitutes a rare example of a multiply bonded dimetal unit bridged by four *neutral* bridging ligands. In addition, the bis-Ph_2Ppy complexes $Re_2Cl_4(\mu\text{-}Ph_2Ppy)_2(PR_3)$ (R = Et or Bu^n) are the major products when $Re_2Cl_6(PR_3)_2$ are reacted with Ph_2Ppy in acetone.[207] They have the structure shown in **8.26**, based upon an X-ray crystal structure determination of the PEt_3 derivative. Note that the structures represented in **8.25** and **8.26** are both staggered with χ_{av} torsion angles of 16.5° and 18.5°, respectively.[207]



8.25



8.26

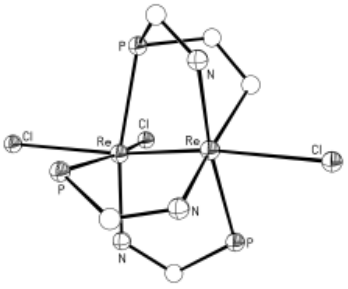


Fig. 8.21. The structure of $Re_2Cl_3(Ph_2Ppy)_2[(C_6H_5)(C_6H_4)Ppy]$ showing the central portion of the molecule with the phenyl and pyridyl rings omitted in order to emphasize the tridentate bonding mode of the orthometalated ligand.

While the electrochemical behavior of $Re_2Cl_4(\mu\text{-}Ph_2Ppy)_3$, $Re_2Cl_3(\mu\text{-}Ph_2Ppy)_2[(C_6H_5)(C_6H_4)Ppy]$ and $Re_2Cl_4(\mu\text{-}Ph_2Ppy)_2(PR_3)$ shows a close resemblance to that of other triply bonded Re_2^{4+} complexes, the properties of $[Re_2Cl_2(\mu\text{-}Ph_2Ppy)_4](PF_6)_2$ are different (Table 8.5).[207] Apparently, there is increase in the effective positive charge at the dirhenium core in this dication relative to the other Ph_2Ppy complexes, so that both the δ^* (the HOMO) and π^* (the LUMO) orbitals fall in energy, thereby making oxidation (from δ^*) more difficult and reduction (through addition of electrons to π^*) much easier.

Pictiva EX2004
Samsung v Pictiva
IPR2024-01094

The reaction of $(Bu_4N)_2Re_2Cl_8$ with the potentially tridentate *P*,*N*,*P* ligand 2,6-bis(diphenylphosphino)pyridine in refluxing methanol affords the complex $Re_2Cl_4(\mu\text{-bdppp})_2$, in which the pair of bdppp ligands bridge in a trans head-to-tail fashion through N and P atoms.[197] The other Ph_2P group on each bdppp ligand is uncoordinated, and these are positioned so as to block access to the axial sites; the non-bonding Re···P distances are 2.98 Å and 3.11 Å. The conversion of $(Bu_4N)_2Re_2Cl_8$ to $Re_2Cl_4(\mu\text{-bdppp})_2$ proceeds via $(Bu_4N)Re_2Cl_7(bdppp)$ (see Section 8.4.4).[197]

Another ligand that possesses a bridging *N*,*P* donor set is 6-diphenylphosphino-2-pyridone (pyphosH). However, it differs from Ph_2Ppy and bdppp in being able to bond in both neutral and anionic forms. It reacts with $(Bu_4N)_2Re_2Cl_8$, $Re_2(\mu\text{-}O_2CCH_3)_4Cl_2$ and *cis*-$Re_2(\mu\text{-}O_2CCH_3)_2Cl_4(H_2O)_2$ in refluxing acetonitrile to give the diamagnetic Re_2^{4+} complex $Re_2Cl_2(\mu\text{-pyphos})_2(\mu\text{-pyphosH})$, in which the three bridging pyphos/pyphosH ligands are *N*,*P* bound. The two cis head-to-tail anionic pyphos ligands have their O atoms located in the vicinity of the axial sites of the dirhenium core (Re···O distances of 2.42 and 2.56 Å).[302] The uncoordinated OH group of the pyphosH ligand forms a strong intermolecular hydrogen bond with the uncoordinated O atom of an adjacent symmetry related molecule such that the dirhenium units are linked into dimers-of-dimers (see Fig. 8.22).[302]

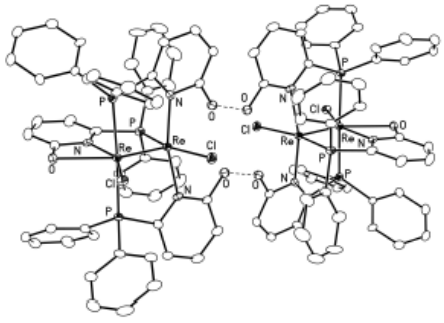


Fig. 8.22. The structure of $Re_2Cl_2(\mu\text{-pyphos})_2(\mu\text{-pyphosH})$ showing how pairs of these molecules are linked into dimers-of-dimers by intermolecular H-bonds.

Redox chemistry of $Re_2X_4(\mu\text{-LL})_2$ compounds when LL = R_2PXPR_2

Of all the mixed halide-phosphine complexes of Re_2^{4+}, those that contain a bridging bidentate phosphine with a *single* bridgehead group between the two donor atoms possess the richest reaction chemistry. Like most triply bonded dirhenium(II) complexes, those of the type $Re_2X_4(\mu\text{-LL})_2$, where X = Cl, Br or I and LL = dppm, dppa, dppE, dcpm or dpam, exhibit well-defined electrochemical behavior with two reversible one-electron oxidations in the cyclic voltammograms of solutions in 0.1 M Bu_4NPF_6-CH_2Cl_2 (Table 8.5). In the case of $Re_2Cl_4(\mu\text{-dppm})_2$, this redox chemistry has been coupled with the reaction chemistry of the cations that are generated. Thus, the reaction of Cl^- with the one-electron oxidation product $[Re_2Cl_4(\mu\text{-dppm})_2]^+$ ($E_{1/2}$ = +0.27 V vs. SCE) produces $Re_2Cl_5(\mu\text{-dppm})_2$.[203] If the latter complex is in turn oxidized to $[Re_2Cl_5(\mu\text{-dppm})_2]^+$, which can be accomplished at a potential of *c.* +0.6 V vs. SCE (Table 8.5), and this oxidation product reacted with Cl^-, then the dirhenium(III) complex $Re_2Cl_6(\mu\text{-dppm})_2$ is formed.[203] The latter compound, which can also be synthesized by other means (see Sec. 8.4.4), possesses a μ-dichloro-bridged structure (**8.14**) with a Re–Re double bond.[203] The Re_2^{5+} complex $Re_2Cl_5(\mu\text{-dppm})_2$ has also been prepared from the reactions of $(Bu_4N)_2Re_2Cl_8$ with dppm in reagent grade acetone[303] and of $Re_2Cl_6(PPr^n_3)_2$ with dppm in

Pictiva EX2004
Samsung v Pictiva
IPR2024-01094

diethyl ether.[203] It is paramagnetic, and shows a broad and complex X-band EPR spectrum that is in accord with the unpaired electron being coupled to two Re nuclei, each with a spin 5/2.[303] A crystal structure determination confirms that the dppm ligands are bridging, and that the structure most closely resembles that of $Re_2Cl_4(\mu\text{-dppm})_2$ with the additional (fifth) chloride ligand being co-linear with the Re–Re bond. The Re–Re distance of 2.263(1) Å, which is about 0.03 Å longer than that in $Re_2Cl_4(\mu\text{-dppm})_2$,[274] reflects the presence of an axial Re–Cl bond.

The conversion of $Re_2Cl_4(\mu\text{-dppm})_2$ to $Re_2Cl_5(\mu\text{-dppm})_2$ and $Re_2Cl_6(\mu\text{-dppm})_2$ can be summarized as follows:

$$\underset{\sigma^2\pi^4\delta^2\delta^{*2}}{Re_2Cl_4(dppm)_2} \xrightarrow[+Cl^-]{-e} \underset{\sigma^2\pi^4\delta^2\delta^{*1}}{Re_2Cl_5(dppm)_2} \xrightarrow[+Cl^-]{-e} \underset{\sigma^2\pi^2\delta^{*2}\delta^2}{Re_2Cl_6(dppm)_2}$$

Bond order = 3 3.5 2

The second step, namely, the conversion of $Re_2Cl_5(\mu\text{-dppm})_2$ to $Re_2Cl_6(\mu\text{-dppm})_2$, represents an interesting case of a reaction in which the oxidation of the Re_2^{5+} core to Re_2^{6+} results in a reduction in the Re–Re bond order, rather than an increase in bond order to 4.

The net two-electron oxidation of $Re_2Cl_4(\mu\text{-dppm})_2$ to $Re_2Cl_6(\mu\text{-dppm})_2$ has also been accomplished by the direct chlorination of the former complex in THF.[304] This type of 2-electron oxidative addition to the Re≡Re bond of $Re_2X_4(\mu\text{-LL})_2$ compounds has been encountered in several other instances. Thus, a related oxidation to give an edge-shared bioctahedral complex occurs when $Re_2Cl_4(\mu\text{-dppm})_2$ is reacted with Ph_2Se_2 in toluene to form $Re_2Cl_4(\mu\text{-SePh})_2(\mu\text{-dppm})_2$.[305] The Ph_2PH ligand also oxidatively adds to the Re≡Re bond of $Re_2X_4(\mu\text{-dppm})_2$ (X = Cl or Br) and $Re_2Cl_4(\mu\text{-dpam})_2$ to give $Re_2(\mu\text{-X})(\mu\text{-PPh}_2)HX_3(\mu\text{-LL})_2$ which contains a terminal Re–H bond.[306] Monophenylphosphine likewise reacts with $Re_2X_4(\mu\text{-dppm})_2$ to give $Re_2(\mu\text{-X})(\mu\text{-PHPh})HX_3(\mu\text{-dppm})_2$,[306(b)] but when H_2S is used the edge-shared bioctahedral compounds that are formed have the structure $Re_2(\mu\text{-H})(\mu\text{-SH})X_4(\mu\text{-dppm})_2$, in which the hydride ligand bridges the two metal centers.[307] More complicated redox chemistry is involved in the oxidation of $Re_2X_4(\mu\text{-dppm})_2$ by dioxygen.[308] The initial products are the weakly paramagnetic, edge-shared bioctahedral complexes $Re_2(\mu\text{-O})(\mu\text{-X})(O)X_3(\mu\text{-dppm})_2$ in which a Re–Re bond is absent. The formation of these compounds precedes further oxidation to dinuclear and mononuclear oxo-Re(V) compounds.[308-310]

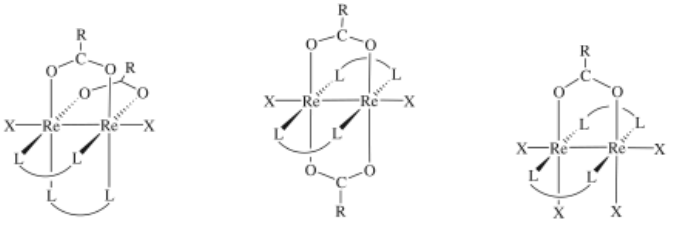
While $NOPF_6$ can be used to oxidize $Re_2X_4(dmpm)_3$ (X = Cl or Br) to $[Re_2X_4(dmpm)_3]PF_6$, the resultant chloride complex reacts with an additional equivalent of $NOPF_6$ to produce the diamagnetic nitrosyl complex $Re_2Cl_5(\mu\text{-dmpm})_2(NO)$ in which the Re–Re distance is 2.379(1) Å and one of the dmpm ligands from the precursor complex has been lost.[311] This compound can be treated formally as a Re_2^{4+} derivative if we consider the nitrosyl ligand as NO^+.

A different type of redox behavioir is encountered when $Re_2Cl_4(\mu\text{-dppm})_2$ is reacted with 7,7'8,8'-tetracyano-*p*-quinodimethane and 2,5-dimethyl-*N*,*N*'-dicyanoquinonediimine to afford the complexes $[Re_2Cl_4(\mu\text{-dppm})_2]_2(\mu\text{-TCNQ})$ and $[Re_2Cl_4(\mu\text{-dppm})_2]_2(\mu\text{-DM-DCNQI})$.[312,313] Both complexes have been characterized by X-ray crystallography and were shown to contain organocyanide bridges linking two $Re_2Cl_4(dppm)_2$ molecules through equatorial positions. Based upon the spectroscopic, magnetic and electrochemical properties of these two complexes it is reasonable to conclude[312,313] that significant change transfer occurs between the dirhenium units and both of these polycyano acceptor molecules. The Re–Re distances in the crystals of composition $[Re_2Cl_4(\mu\text{-dppm})_2]_2(\mu\text{-L})\cdot 10THF$ are 2.2895(4) Å (L = TCNQ) and 2.2986(5) Å (L = DM-DCNQI),[313] both of which are longer than the distance in $Re_2Cl_4(\mu\text{-dppm})_2$ by *c.* 0.05 Å.

Pictiva EX2004
Samsung v Pictiva
IPR2024-01094

Complexes that contain carboxylate and other anionic ligands in conjunction with halides and phosphines

A quite extensive chemistry has been developed in the last few years for Re_2^{4+} and Re_2^{5+} complexes that contain mixed carboxylate/halide/phosphine ligand sets. The most thoroughly studied compounds are of the types $Re_2(\mu\text{-}O_2CR)_2X_2(\mu\text{-}LL)_2$ and $Re_2(\mu\text{-}O_2CR)X_4(\mu\text{-}LL)$, where LL represents a ligand such as dppm. These complexes were first encountered during studies that involved the reactions of tetrakis(carboxylato)dirhenium(III) complexes $Re_2(\mu\text{-}O_2CR)_4X_2$ (R = CH_3, C_2H_5 or C_6H_5; X = Cl or Br) with dppm in methanol or ethanol.[271] The reaction products consisted of mixtures of *cis* and *trans*-$Re_2(\mu\text{-}O_2CR)_2X_2(\mu\text{-dppm})_2$ (structures **8.27** and **8.28**). Because of the quite different redox properties of these isomers (Table 8.6) they could be separated and purified by making use of different oxidants to selectively oxidize them to their paramagnetic monocations. This is shown by the scheme in Fig. 8.23.[271] When the bis-carboxylate complexes $Re_2(\mu\text{-}O_2CR)_2X_4L_2$ are used as starting materials instead of $Re_2(\mu\text{-}O_2CR)_4X_2$, the chemistry becomes more complex and involves the formation of the Re_2^{5+} complexes $Re_2(\mu\text{-}O_2CR)X_4(\mu\text{-dppm})_2$ as intermediates; these species can undergo reductive decarboxylation to give $Re_2X_4(\mu\text{-dppm})_2$ or react with more carboxylate ion in hot methanol to afford *cis*-$Re_2(\mu\text{-}O_2CR)_2X_2(dppm)_2$.[271] The structure of $Re_2(\mu\text{-}O_2CCH_3)Cl_4(\mu\text{-dppm})_2$, which has been determined by X-ray crystallography, is that shown in **8.29**. The paramagnetic, EPR-active complexes $Re_2(\mu\text{-}O_2CR)X_4(dppm)_2$ have a well-defined redox chemistry with a reversible one-electron oxidation and an irreversible reduction (see Table 8.6).[271] The reactions of $(Bu_4N)_2Re_2X_8$ (X = Cl or Br) with various combinations of dppm and the appropriate carboxylic acid/anhydride or carboxylate salt in alcohol solvents have also been used as a means by which $Re_2(\mu\text{-}O_2CR)X_4(\mu\text{-dppm})_2$, *cis*-$Re(\mu\text{-}O_2CR)_2X_2(\mu\text{-dppm})_2$ and $Re_2X_4(\mu\text{-dppm})_2$ can be formed.[271] Compounds analogous to $Re_2(\mu\text{-}O_2CR)Cl_4(\mu\text{-dppm})_2$ have been obtained in the case of the amidate complexes $Re_2[\mu\text{-HNC(R)O}]Cl_4(\mu\text{-dppm})_2$ when R = CH_3 or Ph (see Section 8.4.3).[171,173] Both are paramagnetic Re_2^{5+} species and they have been characterized by X-ray crystallography (see Table 8.4).



8.27 **8.28** **8.29**

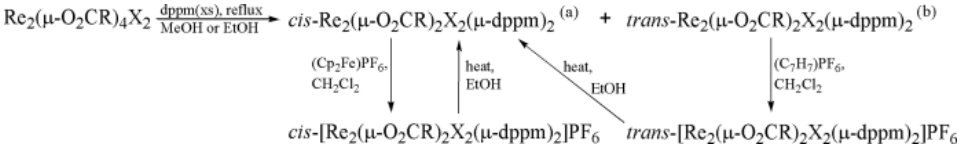


Fig. 8.23. Reaction scheme showing the products of the reactions of $Re_2(\mu\text{-}O_2CR)_4X_2$ (R = CH_3, C_2H_5, C_6H_5; X = Cl or Br) with dppm.
Footnotes: (a) The formation of the cis isomer is favored by long reaction times (several days) and $Re_2(\mu\text{-}O_2CR)_4X_2$:dppm stoichiometric ratios of *c.* 1:6. (b) The formation of the trans isomer is favored by shorter reaction times (one day or less) and stoichiometric ratios of 1:<4.

Pictiva EX2004
Samsung v Pictiva
IPR2024-01094

Table 8.6. Voltammetric $E_{1/2}$ values for mixed carboxylate-halide-phosphine complexes of Re_2^{4+} and Re_2^{5+} in dichloromethane[a]

Compound	$E_{1/2}$(ox) (2)	$E_{1/2}$(ox) (1)	$E_{p,c}$	ref.
A. Re_2^{4+} Compounds				
cis-$Re_2(\mu\text{-}O_2CCH_3)_2Cl_2(\mu\text{-}dppm)_2$	+1.34	+0.28	-	271
cis-$Re_2(\mu\text{-}O_2CC_2H_5)_2Cl_2(\mu\text{-}dppm)_2$	+1.38	+0.30	-	271
cis-$Re_2(\mu\text{-}O_2CCCl_3)_2Cl_2(\mu\text{-}dppm)_2$	b	+0.60	-	271
cis-$Re_2(\mu\text{-}O_2CC_6H_5)_2Cl_2(\mu\text{-}dppm)_2$	+1.38	+0.30	-	271
cis-$Re_2(\mu\text{-}O_2C\text{-}4\text{-}C_5H_4N)_2Cl_2(\mu\text{-}dppm)_2$	b	+0.45	-	320
cis-$Re_2(\mu\text{-}O_2CC_6H_4\text{-}4\text{-}PPh_2)_2Cl_2(\mu\text{-}dppm)_2$	+1.40	+0.33	-	321(b)
cis-$Re_2(\mu\text{-}O_2C\text{-}4\text{-}quin)_2Cl_2(\mu\text{-}dppm)_2$	b	+0.49	-	321(b)
cis-$Re_2(\mu\text{-}O_2CC_6H_4\text{-}4\text{-}PPh_2)_2Cl_2(\mu\text{-}dppm)_2(AuCl)_2$	+1.44[c]	+0.40	-	321(b)
cis-$Re_2Cl_2(\mu\text{-}dppm)_2[\mu\text{-}O_2CC_6H_4\text{-}4\text{-}N\text{-}(CH_2PPh_2)_2(PdCl_2)]_2$	+1.25	+0.31	-	321(b)
cis-$Re_2(\mu\text{-}O_2CC_6H_{10}CO_2Et)_2Cl_2(\mu\text{-}dppm)_2$	+1.39	+0.32	-	323
cis-$Re_2Cl_2(\mu\text{-}dppm)_2[(\mu\text{-}O_2CC_5H_4)_2Fe]$	+1.29	+0.31	-	323
cis-$Re_2(\mu\text{-}O_2CCH_3)]_2Br_2(\mu\text{-}dppm)_2$	+1.41	+0.35	-	271
cis-$Re_2(\mu\text{-}O_2CC_2H_5)_2Br_2(\mu\text{-}dppm)_2$	+1.41	+0.35	-	271
cis-$Re_2(\mu\text{-}O_2CCCl_3)_2Br_2(\mu\text{-}dppm)_2$	b	+0.67	-	271
cis-$Re_2(\mu\text{-}O_2CC_6H_5)_2Br_2(\mu\text{-}dppm)_2$	+1.37	+0.36	-	271
cis-$Re_2(\mu\text{-}O_2CCH_3)_2(NCBH_3)_2(\mu\text{-}dppm)_2$	b	+0.60	-1.29, -1.48	325
cis-$Re_2(\mu\text{-}O_2CCH_3)Cl_2(\mu\text{-}dppa)_2$	+1.39	+0.35	-1.58	284
cis-$Re_2(\mu\text{-}O_2CCH_3)_2Br_2(\mu\text{-}dppa)_2$	+1.40	+0.39	-1.52	284
cis-$Re_2(\mu\text{-}O_2CCH_3)_2Br_2(\mu\text{-}dpam)_2$	+1.38	+0.28	-	314
cis-$Re_2(\mu\text{-}O_2CC_6H_5)_2Br_2(\mu\text{-}dpam)_2$	+1.31	+0.20	-	314
cis-$Re_2(\mu\text{-}O_2CCH_3)_2Cl_2(\mu\text{-}Ph_2Ppy)_2$	+1.20	+0.11	-	319
cis-$Re_2(\mu\text{-}O_2CC_2H_5)_2Cl_2(\mu\text{-}Ph_2Ppy)_2$	+1.18	+0.10	-	319
cis-$Re_2(\mu\text{-}O_2CC_2H_5)_2Br_2(\mu\text{-}Ph_2Ppy)_2$	+1.22	+0.14	-	319
trans-$Re_2(\mu\text{-}O_2CCH_3)_2Cl_2(\mu\text{-}dppm)_2$	+0.93	-0.27	-	271
trans-$Re_2(\mu\text{-}O_2CC_2H_5)_2Cl_2(\mu\text{-}dppm)_2$	+0.93	-0.29	-	271
trans-$Re_2(\mu\text{-}O_2CC_6H_5)_2Cl_2(\mu\text{-}dppm)_2$	+1.00	-0.25	-	271
trans-$Re_2(\mu\text{-}O_2C\text{-}4\text{-}C_5H_4N)_2Cl_2(\mu\text{-}dppm)_2$	+1.17	-0.08	-	314
trans-$Re_2(\mu\text{-}O_2C\text{-}3\text{-}C_5H_4N)_2Cl_2(\mu\text{-}dppm)_2$	+1.11	-0.12	-	315
trans-$Re_2(\mu\text{-}O_2CCH_3)_2Br_2(\mu\text{-}dppm)_2$	+0.97	-0.21	-	271
trans-$Re_2(\mu\text{-}O_2CC_6H_5)_2Br_2(\mu\text{-}dppm)_2$	+1.00	-0.22	-	271
trans-$Re_2(\mu\text{-}O_2CCH_3)_2Cl_2(\mu\text{-}dppa)_2$	+0.97[d]	-0.22[d]	-	284
trans-$Re_2(\mu\text{-}O_2CCH_3)_2Br_2(\mu\text{-}dppa)_2$	+0.99[d]	-0.19[d]	-	284
trans-$Re_2(\mu\text{-}O_2CCH_3)_2Cl_2(\mu\text{-}dmpm)_2$	+0.76[d]	-0.42[d]	-	317
trans-$Re_2(\mu\text{-}O_2CCH_3)_2Cl_2(\mu\text{-}dippm)_2$	+0.79[d]	-0.50[d]	-	293
trans-$Re_2(\mu\text{-}O_2CCH_3)_2Cl_2(\mu\text{-}dcpm)_2$	+0.78	-0.51	-	138
trans-$Re_2(\mu\text{-}O_2CCH_3)_2Cl_2(\mu\text{-}dppE)_2$	+0.97	-0.27	-	287
trans-$Re_2(\mu\text{-}O_2CC_6H_4\text{-}4\text{-}PPh_2)_2Cl_2(\mu\text{-}dppE)_2$	+1.05	-0.23	-	321(b)
trans-$Re_2(\mu\text{-}O_2CC_6H_4\text{-}4\text{-}PPh_2)_2Cl_2(\mu\text{-}dppE)_2(AuCl)_2$	+1.06	-0.15	-	321(b)
trans-$Re_2(\mu\text{-}O_2C\text{-}4\text{-}quin)_2Cl_2(\mu\text{-}dppE)_2$	+1.13	-0.12	-	321(b)
trans-$Re_2(\mu\text{-}O_2CCH_3)_2Cl_2(\mu\text{-}cdpp)_2$	+0.96	-0.33	-	286
trans-$Re_2(\mu\text{-}O_2CCH_3)_2Br_2(\mu\text{-}dpam)_2$	+1.01	-0.24	-	314

Pictiva EX2004
Samsung v Pictiva
IPR2024-01094

Compound	$E_{1/2}$(ox) (2)	$E_{1/2}$(ox) (1)	$E_{p,c}$	ref.
trans-$Re_2(\mu\text{-}O_2CC_6H_5)_2Br_2(\mu\text{-dpam})_2$	+1.03	-0.25	-	314
$[Re_2(\mu\text{-}O_2CCH_3)Cl_2(\mu\text{-dmpm})_3]Cl$	-	+0.75	-1.48	317
$[Re_2(\mu\text{-}O_2CC_2H_5)Cl_2(\mu\text{-dmpm})_3]Cl$	-	+0.69	-1.55	317
$[Re_2(\mu\text{-}O_2CCH_3)Br_2(\mu\text{-dmpm})_3]Br$	-	+0.74	-1.52	317
$[Re_2(\mu\text{-}O_2CC_2H_5)Br_2(\mu\text{-dmpm})_3]Br$	-	+0.73	-1.48	317
B. Re_2^{5+} Compounds				
$Re_2(\mu\text{-}O_2CCH_3)Cl_4(\mu\text{-dppm})_2$	-	+0.52	-0.60	271
$Re_2(\mu\text{-}O_2CC_2H_5)Cl_4(\mu\text{-dppm})_2$	-	+0.49	-0.58	271
$Re_2(\mu\text{-}O_2CC_5H_4N)Cl_2(\mu\text{-dppm})_2$	-	+0.57	-0.53	323
$Re_2(\mu\text{-}O_2CCH_3)Br_4(\mu\text{-dppm})_2$	-	+0.55	-0.52	271
$Re_2(\mu\text{-}O_2CCH_3)Cl_4(\mu\text{-dmpm})_2$	-	+0.39	-0.69	139(b)
$Re_2(\mu\text{-}O_2CC_2H_5)Cl_4(\mu\text{-dmpm})_2$	-	+0.40	-0.70	139(b)
$Re_2(\mu\text{-}O_2CCH_3)Br_4(\mu\text{-dmpm})_2$	-	+0.42	-0.64	139(b)
$Re_2(\mu\text{-}O_2CCH_3)Cl_4(\mu\text{-dppa})_2$	-	+0.49	-0.53	284
$Re_2(\mu\text{-}O_2CCH_3)Br_4(\mu\text{-dppa})_2$	-	+0.57	-0.39	284
$Re_2(\mu\text{-}O_2CCH_3)Cl_4(PPh_3)_2$	-	+0.56[c]	-0.62[e]	318
$Re_2(\mu\text{-}O_2CCH_3)Br_4(PPh_3)_2$	-	+0.58[c]	-0.58[e]	318
$Re_2(\mu\text{-}O_2CCH_3)Cl_4[P(CH_2Ph)_3]_2$	-	+0.54	-0.67[e]	143
$Re_2(\mu\text{-}O_2CCH_3)Cl_4(PMePh_2)_2$	-	+0.48	-0.65[e]	142(b)
$Re_2(\mu\text{-}O_2CCH_3)Cl_4[P(C_6H_4\text{-}4\text{-}OMe)_3]_2$	-	+0.47	-0.67[e]	142(b)
$Re_2(\mu\text{-}O_2CCH_3)Cl_4(Ph_2Ppy)_2$	-	+0.47	-0.56[e]	318
$Re_2(\mu\text{-}O_2CC_2H_5)Cl_4(Ph_2Ppy)_2$	-	+0.49	-0.49[e]	318
$Re_2(\mu\text{-}O_2CCH_3)Br_4(Ph_2Ppy)_2$	-	+0.58	-0.40[e]	318
$Re_2(\mu\text{-}O_2CCH_3)Cl_4(\eta^3\text{-}\mathbf{L}_1)$[f]	-	+0.42	-1.03[e]	191(b)
$Re_2(\mu\text{-}O_2CCH_3)Cl_4(\eta^3\text{-}\mathbf{L}_2)$[f]	-	+0.42	-1.00[e]	191(b)
$Re_2(\mu\text{-}O_2CCH_3)Cl_4(\eta^3\text{-}\mathbf{L}_3)$[f]	-	+0.36	-1.09[e]	191(b)
$Re_2(\mu\text{-}O_2CCH_3)Cl_4(\eta^3\text{-}\mathbf{L}_4)$[f]	-	+0.30	-1.10[e]	191(b)
$Re_2(\mu\text{-}O_2CCH_3)Cl_4(\eta^3\text{-}\mathbf{L}_5)$[f]	-	+0.33	-1.11[e]	191(b)
$Re_2(\mu\text{-}O_2CC_6H_4\text{-}4\text{-}PPh_2)Cl_4(\eta^3\text{-}\mathbf{L}_1)$[f]	-	+0.39	-1.02	191(b)
$Re_2(\mu\text{-}O_2CC_6H_4\text{-}2\text{-}PPh_2)Cl_4(\eta^3\text{-}\mathbf{L}_1)$[f]	-	+0.37	-1.06	191(b)
$Re_2(\mu\text{-}O_2C\text{-}4\text{-quin})Cl_4(\eta^3\text{-}\mathbf{L}_1)$[f]	-	+0.44	-0.97	191(b)
$Re_2(\mu\text{-}O_2CC_6H_4\text{-}4\text{-}PPh_2)Cl_4(\eta^3\text{-}\mathbf{L}_3)$[f]	-	+0.37	-1.06	191(b)
$Re_2(\mu\text{-}O_2CC_6H_4\text{-}2\text{-}PPh_2)Cl_4(\eta^3\text{-}\mathbf{L}_3)$[f]	-	+0.34	-1.10	191(b)
$Re_2(\mu\text{-}O_2C\text{-quin})Cl_4(\eta^3\text{-}\mathbf{L}_3)$[f]	-	+0.40	-1.01	191(b)
$[Re_2Cl_4(\eta^3\text{-}\mathbf{L}_1)]_2(\mu\text{-}O_2CC_6H_4CO_2)$[f]	-	+0.43[g]	-1.00[g]	191(b)
$[Re_2Cl_4(\eta^3\text{-}\mathbf{L}_3)]_2(\mu\text{-}O_2CC_6H_4CO_2)$[f]	-	+0.39[g]	-1.05[g]	191(b)

[a] Unless otherwise stated, data are in volts vs the Ag/AgCl electrode with a Pt-bead working electrode and 0.1 M Bu_4NPF_6(TBAH) as supporting electrolyte.

[b] $E_{1/2}$(ox)(2) beyond the limits of the measurement.

[c] $E_{p,a}$ value

[d] Potentials are based upon CV measurements on a salt of the monocation of the neutral Re_2^{4+} complex. In this instance the neutral *trans*-$Re_2(\mu\text{-}O_2CCH_3)_2Cl_2(\mu\text{-LL})_2$ complex has not been isolated.

[e] $E_{1/2}$(red) value.

[f] This compound contains a tridentate donor designated as $\mathbf{L}_n$, the identity of which is given in the text (see also ref. 191(b)).

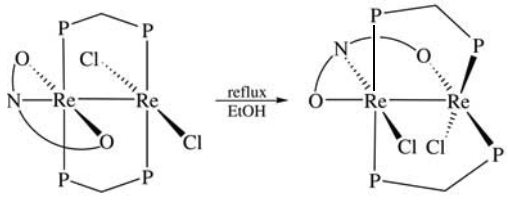
[g] These processes are broadened due to weak electronic coupling between the pairs of dirhenium units.

Pictiva EX2004
Samsung v Pictiva
IPR2024-01094

A related chemistry has been developed in the case of the dppa complexes.[284] The main differences from the dppm system are as follows. First, in the dppa system, complexes of the type *trans*-$[Re_2(\mu\text{-}O_2CCH_3)_2X_2(\mu\text{-}LL)_2]X$ are important intermediates in the formation of *cis*-$Re_2(\mu\text{-}O_2CCH_3)_2X_2(\mu\text{-}dppa)_2$ but the same does not appear to be the case with the analogous dppm complexes. Second, the reductive decarboxylation of $Re_2(\mu\text{-}O_2CR)X_4(\mu\text{-}dppm)_2$ to give $Re_2X_4(\mu\text{-}dppm)_2$ occurs more rapidly than does their reaction with carboxylate ion to give *trans*-$[Re_2(\mu\text{-}O_2CR)_2X_2(\mu\text{-}dppm)_2]X$.[271] This is in contradistinction to the behavior of $Re_2(\mu\text{-}O_2CCH_3)X_4(\mu\text{-}dppa)_2$, which readily converts to *trans*-$[Re_2(\mu\text{-}O_2CCH_3)_2X_2(\mu\text{-}dppa)_2]X$ in the presence of an excess of dppa.[284]

The most direct and easiest means of obtaining the cis and trans isomers of $Re_2(\mu\text{-}O_2CR)_2X_2(\mu\text{-}LL)_2$ is the most obvious one, namely, the reaction of $Re_2X_4(\mu\text{-}LL)_2$ with a source of the appropriate carboxylate anion. This has been demonstrated in the case of the reactions of $Re_2Cl_4(\mu\text{-}dppm)_2$ and $Re_2Br_4(\mu\text{-}dpam)_2$ with $[PPN]O_2CR$ (PPN = $(Ph_3P)_2N^+$; R = CH_3, C_2H_5, C_6H_5 or 4-C_5H_5N) in CH_2Cl_2 at room temperature give *trans*-$Re_2(\mu\text{-}O_2CR)_2X_2(\mu\text{-}LL)_2$.[314] If the reactions are carried out in refluxing ethanol, the cis isomers are obtained in the case of R = CH_3 or C_2H_5, a mixture of cis and trans for R = C_6H_5, and only the trans form when R = 4-C_5H_5N. Upon heating *trans*-$Re_2(\mu\text{-}O_2CR)_2Cl_2(\mu\text{-}dppm)_2$ (R = CH_3 or C_2H_5) in ethanol, isomerization to *cis*-$Re_2(\mu\text{-}O_2CR)_2Cl_2(\mu\text{-}dppm)_2$ occurs, signifying that this is indeed the thermodynamically favored form when LL = dppm.[314] Recently, the trans isomer that contains nicotinate (pyridine-3-carboxylate) has been prepared by this same method.[315]

When $Re_2Cl_4(\mu\text{-}dppm)_2$ is reacted with pyridine-2-carboxylic acids, or their $[PPN]^+$ salts, more complicated structures are obtained because the pyridine N is involved in forming *N,O* chelate rings.[315] With py-2-CO_2H, py-2,3-$(CO_2H)_2$ and py-2,4-$(CO_2H)_2$, complexes of the type $Re_2(\eta^2\text{-}N,O)Cl_3(\mu\text{-}dppm)_2$ are formed in which the μ-dppm ligands are bound in a *trans*, *cis* fashion, with the chelating pyridine carboxylate ligand being coordinated to the Re atom that has the trans disposition of P atoms.[315] With the $[PPN]^+$ salt of pyridine-2,6-dicarboxylic acid ($dipicH_2$), both kinetic and thermodynamic products of composition $Re_2(dipic)Cl_2(\mu\text{-}dppm)_2$ are formed; the former species (**8.30**) is favored at room temperature and converts quantitatively to the thermodynamically stable form (**8.31**) when refluxed in ethanol. This conversion occurs by a partial "merry-go-round" process that results in a switch from a *trans*,*trans* to *trans*,*cis* coordination of the dppm ligands. Both isomers have been structurally characterized; they are labeled as isomer **A** and **B**, respectively, in Table 8.4. Note that a third isomer (**C**) has been isolated by the reaction of *cis*-$Re_2(\mu\text{-}O_2CCH_3)_2Cl_2(\mu\text{-}dppm)_2$ with $dipicH_2$ and contains a *cis*,*cis* coordination of the μ-dppm ligands.[316]



8.30 **8.31**

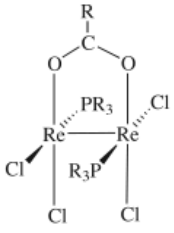
While the synthesis of $Re_2(\mu\text{-}O_2CR)_2X_2(\mu\text{-}LL)_2$ compounds directly from $Re_2X_4(\mu\text{-}LL)_2$ is the most logical synthetic route, compounds such as $Re_2Cl_4(\mu\text{-}dppm)_2$ are often themselves best prepared from $(Bu_4N)_2Re_2Cl_8$ via the intermediacy of the carboxylate complexes $Re_2(\mu\text{-}O_2CCH_3)Cl_4(\mu\text{-}dppm)_2$ (see earlier discussion in Section 8.5.4).[271] Accordingly, the reactions

Pictiva EX2004
Samsung v Pictiva
IPR2024-01094

of $Re_2(\mu\text{-}O_2CCH_3)_4Cl_2$ and *cis*-$Re_2(\mu\text{-}O_2CCH_3)_2X_4L_2$ (X = Cl or Br; L = H_2O, py or 4-Mepy) have continued to be used to prepare Re_2^{4+} and Re_2^{5+} carboxylate complexes. The phosphines dcpm,[138] dippm,[293] dppE,[287] and cdpp[286] have been reacted with $Re_2(\mu\text{-}O_2CCH_3)_4Cl_2$ in refluxing methanol to produce either neutral *trans*-$Re_2(\mu\text{-}O_2CCH_3)_2Cl_2(\mu\text{-LL})_2$ (LL = dppE or cdpp)[286,287] or the cationic species *trans*-$[Re_2(\mu\text{-}O_2CCH_3)_2Cl_2(\mu\text{-LL})]^+$ (LL = dcpm or dippm).[138,293] These compounds have been structurally characterized and their structures resemble closely those of the neutral and cationic cis and trans isomers in the case of LL = dppm or dppa (Table 8.4). The cyclic voltammetric data for these complexes are compared in Table 8.6.

Various mixed carboxylate-dmpm complexes have been prepared through the use of $Re_2(\mu\text{-}O_2CR)_4X_2$ (X = Cl or Br) and $Re_2Cl_4(\mu\text{-dmpm})_3$ as starting materials. Salts of the *trans*-$[Re_2(\mu\text{-}O_2CR)_2X_2(\mu\text{-dmpm})_2]^+$ and $[Re_2(\mu\text{-}O_2CR)X_2(\mu\text{-dmpm})_3]^+$ cations have been obtained,[317] and the acetate complexes $[Re_2(\mu\text{-}O_2CCH_3)X_2(\mu\text{-dmpm})_3]PF_6$ have been oxidized by $NOPF_6$ to the paramagnetic 1:2 salts $[Re_2(\mu\text{-}O_2CCH_3)X_2(\mu\text{-dmpm})_3](PF_6)_2$. When dmpm is reacted with *cis*-$Re_2(\mu\text{-}O_2CR)_2X_4L_2$ (X = Cl or Br; R = CH_3 or C_2H_5; L = H_2O or py) the compounds $Re_2(\mu\text{-}O_2CCH_3)X_4(\mu\text{-dmpm})_2$ and $Re_2(\mu\text{-}O_2CC_2H_5)Cl_4(\mu\text{-dmpm})_2$ can be isolated.[139] Note that $Re_2(\mu\text{-}O_2CCH_3)Cl_4(\mu\text{-dmpm})_2$ reacts further with dmpm to afford $Re_2Cl_4(\mu\text{-dmpm})_3$,[139(b)] and it has been reacted with Ph_2PH as a route to $Re_2(\mu\text{-Cl})(\mu\text{-}PPh_2)HCl_3(\mu\text{-dmpm})_2$.[306(b)]

A comparison has also been made of the reactions between *cis*-$Re_2(\mu\text{-}O_2CCH_3)_2X_4L_2$ (X = Cl or Br; L = H_2O, py or 4-Mepy) and Ph_2Ppy or PPh_3 in refluxing ethanol or acetone.[318,319] Both ligands form similar dark red paramagnetic complexes $Re_2(\mu\text{-}O_2CCH_3)X_4(Ph_2Ppy)_2$ and $Re_2(\mu\text{-}O_2CCH_3)X_4(PPh_3)_2$, which are in turn related to $Re_2(\mu\text{-}O_2CR)X_4(\mu\text{-LL})_2$ (LL = dppm or dppa). A single crystal X-ray structure determination on $Re_2(\mu\text{-}O_2CCH_3)Cl_4(PPh_3)_2$ shows it to contain an eclipsed rotational geometry as in **8.32**, and a short Re–Re distance (Table 8.4).[318] This structure is related to that in **8.29**, except that with only two monodentate phosphines present the two axial Re–Cl bonds (in **8.29**) now switch to become equatorial bonds. In the case of the Ph_2Ppy ligand, longer reaction times favor the formation of *cis*-$Re_2(\mu\text{-}O_2CR)_2X_2(\mu\text{-}Ph_2Ppy)_2$ (X = Cl when R = CH_3 or C_2H_5 and X = Br when R = C_2H_5).[319] These same compounds are formed when the dirhenium(II) complexes $Re_2X_4(\mu\text{-}Ph_2Ppy)_2(PEt_3)$ (X = Cl or Br) are reacted with NaO_2CR in refluxing methanol for 1 day.[319] Oxidation of *cis*-$Re_2(\mu\text{-}O_2CCH_3)_2Cl_2(\mu\text{-}Ph_2Ppy)_2$ with $[(\eta^5\text{-}C_5H_5)_2Fe]PF_6$ gives the paramagnetic monocationic species which has been characterized by X-ray crystallography (Table 8.4).[319]

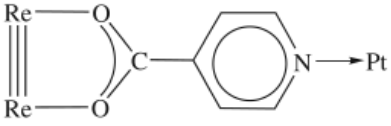


8.32

The triphenylphosphine ligands in $Re_2(\mu\text{-}O_2CCH_3)Cl_4(PPh_3)_2$ are easily replaced by certain monodentate phosphines (i.e. $P(CH_2Ph)_3$, $P(C_6H_4\text{-}4\text{-}OMe)_3$ and $PMePh_2$) to form other $Re_2(\mu\text{-}O_2CCH_3)Cl_4(PR_3)_2$ complexes, and also by bidentate dppm, dppa and dppE to give $Re_2(\mu\text{-}O_2CCH_3)Cl_4(\mu\text{-LL})_2$, all in high yield.[142(b)] The aforementioned tribenzylphosphine complex $Re_2(\mu\text{-}O_2CCH_3)Cl_4[P(CH_2Ph)_3]_2$ has also been prepared by the reaction between *cis*-$Re_2(\mu\text{-}O_2CCH_3)_2Cl_4(H_2O)_2$ and this phosphine in refluxing methanol.[143]

Pictiva EX2004
Samsung v Pictiva
IPR2024-01094

Of all the Re_2^{4+} and Re_2^{5+} mixed carboxylate/halide/phosphine complexes that have been isolated, the two that have generated the greatest interest are *cis*-$Re_2(\mu\text{-}O_2CCH_3)_2Cl_2(\mu\text{-}dppm)_2$ and $Re_2(\mu\text{-}O_2CCH_3)Cl_4(\mu\text{-}dppm)_2$, primarily as a result of the lability of their acetate ligands and, consequently, their use as synthons. The displacement of the μ-acetato ligands in *cis*-$Re_2(\mu\text{-}O_2CCH_3)_2X_2(\mu\text{-}dppm)_2$ upon reaction with trichloroacetic acid provides a route to *cis*-$Re_2(\mu\text{-}O_2CCCl_3)_2X_2(\mu\text{-}dppm)_2$,[271] while the reaction of the chloro complex with isonicotinic acid gives *cis*-$Re_2(\mu\text{-}O_2C\text{-}4\text{-}C_5H_4N)_2Cl_2(\mu\text{-}dppm)_2$, which has in turn been used to prepare the hybrid mixed-metal molecular squares $[cis\text{-}Re_2(\mu\text{-}O_2CC_5H_4N)_2X_2(\mu\text{-}dppm)_2PtL_2]_2(O_3SCF_3)_4$, where X = Cl for L = PEt_3 and X = O_3SCF_3 for L = dbbpy.[320] The latter compounds, which contain triply bonded Re_2^{4+} and planar Pt(II) units at the corners, contain bridging isonicotinate as the linker ligands; the connectivity (**8.33**) has been established by an X-ray crystal structure determination of the supramolecular assembly with L = PEt_3.[320] A variety of behavior has been found upon the reaction of *cis*-$Re_2(\mu\text{-}O_2CCH_3)_2Cl_2(\mu\text{-}dppm)_2$ with the picolinic (picH), dipicolinic ($dipicH_2$), 2-hydroxynicotinic (HnicOH) and 6-hydroxypicolinic (HpicOH) acids. Picolinic acid gives $Re_2(pic)Cl_3(\mu\text{-}dppm)_2$, which is identical to the product formed upon the reaction of [PPN]pic with $Re_2Cl_4(\mu\text{-}dppm)_2$,[315] while the other acids form $Re_2(dipic)Cl_2(\mu\text{-}dppm)_2$, *cis*-$Re_2(HnicO)_2Cl_2(\mu\text{-}dppm)_2$ and *cis*-$Re_2(picO)_2(\mu\text{-}dppm)_2$, respectively.[316] The dipicolinate complex is the third isomeric form of this compound (isomer **C**), and the compound formed from 6-hydroxypicolinic acid involves the coordination of two cis tridentate $picO^{2-}$ ligands that displace both the acetate groups and the two terminal chloride ligands. All these compounds have been characterized by X-ray crystallography (Table 8.4).[316]



8.33

The reactions of *cis*-$Re_2(\mu\text{-}O_2CCH_3)_2Cl_2(\mu\text{-}dppm)_2$ and *trans*-$Re_2(\mu\text{-}O_2CCH_3)_2Cl_2(\mu\text{-}dppE)_2$ with substituted benzoic acids of the type 4-$XC_6H_4CO_2H$ (X = Ph_2P, $Ph_2P(O)$, $Ph_2P(S)$ or $Ph_2P(O)CH_2$) and with quinoline-4-carboxylic acid lead to displacement of the acetato ligands and retention of the *cis* and *trans* stereochemistries.[321] The electrochemical properties of these products are similar to those of the parent molecules (representative data only are given in Table 8.6), and the X-ray crystal structures of the complexes *cis*-$Re_2(\mu\text{-}O_2CC_6H_4\text{-}4\text{-}PPh_2)_2Cl_2(\mu\text{-}dppm)_2$ and *trans*-$Re_2(\mu\text{-}O_2C\text{-}4\text{-}quin)_2Cl_2(\mu\text{-}dppm)_2$ have been determined (Table 8.4).[321] The use of the pendant donor atoms in these complexes to coordinate other metal centers has been demonstrated in the case of the two structurally characterized compounds cited above through the synthesis of mixed-metal complexes that contain Au(I) and Pd(II). The isolated products include the interesting mixed Re_2Pd_2 complex *cis*-$Re_2(\mu\text{-}O_2C_6H_4\text{-}4\text{-}PPh_2)_2Cl_2(\mu\text{-}dppm)_2(Pd_2Cl_4)$, that has a structure (Fig. 8.24) which can be considered to be that of a molecular "tweezer".[321] A different type of Re_2Pd_2 assembly has been obtained by the reaction of *cis*-$Re_2(\mu\text{-}O_2CCH_3)_2Cl_2(\mu\text{-}dppm)_2$ with $PdCl_2[(Ph_2PCH_2)_2N\text{-}4\text{-}C_6H_4CO_2H]$, the latter reagent containing a free carboxylic acid group.[321(b)]

Studies have been made of the reactions between dicarboxylic acids and *cis*-$Re_2(\mu\text{-}O_2CCH_3)_2Cl_2(\mu\text{-}dppm)_2$ and $Re_2(\mu\text{-}O_2CCH_3)Cl_4(\mu\text{-}dppm)_2$.[322-324] The bis-acetate reacts with terephthalic acid to give the triangular assembly $\{[Re_2Cl_2(\mu\text{-}dppm)_2](\mu\text{-}O_2CC_6H_4CO_2)\}_3$ (Fig. 8.25), in which the three $[Re{\equiv}Re]^{4+}$ units have very similar Re–Re bond distances (Table 8.4).[322] Electrochemical measurements show[322,323] that the Re_2 units are only very weakly coupled. While a

Pictiva EX2004
Samsung v Pictiva
IPR2024-01094

similar triangular structure is probably formed with *trans*-1,4-cyclohexanedicarboxylate when 1:1 proportions of reagents are used,[323] the use of a higher proportion of this diacid gives the complex $[cis\text{-}Re_2(\mu\text{-}O_2CC_6H_{10}CO_2H)_2Cl_2(\mu\text{-}dppm)_2]_2(\mu\text{-}O_2CC_6H_{10}CO_2)$. In the solid-state its structure consists of this "dimer-of-dimers" unit which is linked into an infinite zig-zag chain-like polymer through intermolecular hydrogen-bonds involving the "free" carboxylic acid groups of the cis $\mu\text{-}O_2CC_6H_{10}CO_2H$ ligands.[322,323] The diacid 1,1'-ferrocenedicarboxylic acid reacts with $cis\text{-}Re_2(\mu\text{-}O_2CCH_3)_2Cl_2(\mu\text{-}dppm)_2$ to give exclusively the trimetallic compound $cis\text{-}Re_2Cl_2(\mu\text{-}dppm)_2[(\mu\text{-}O_2CC_5H_4)_2Fe]$,[323] rather than a compound in which the acid serves to bridge the dirhenium units, as occurs with dimolybdenum(II) to form a "dimer-of-dimers" or supramolecular square. The structure of this complex has been determined (see Table 8.4) as well as its electrochemical properties (Table 8.6).

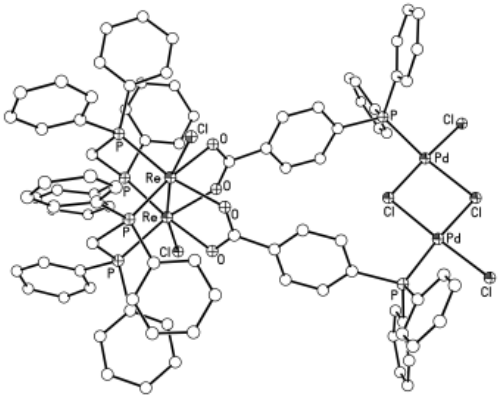


Fig. 8.24. The structure of the Re_2Pd_2 moleculer "tweezer" complex $cis\text{-}Re_2(\mu\text{-}O_2CC_6H_4\text{-}4\text{-}PPh_2)_2Cl_2(\mu\text{-}dppm)_2(Pd_2Cl_4)$.

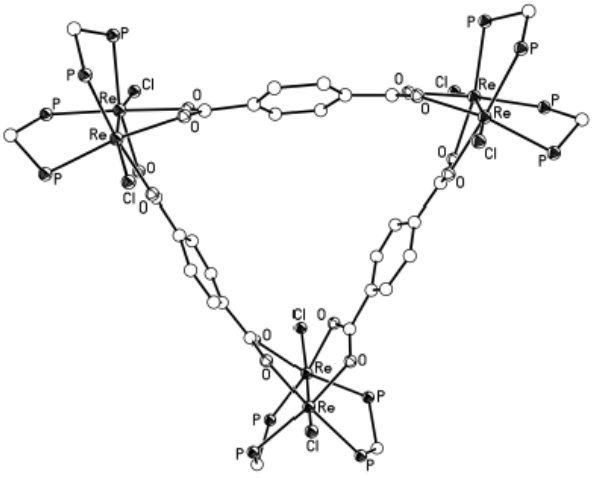
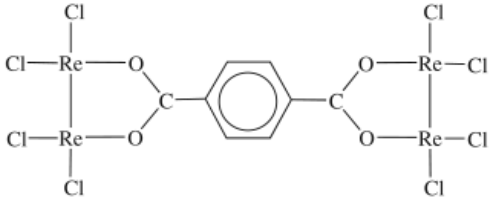


Fig. 8.25. The structure of the molecule $\{[Re_2Cl_2(\mu\text{-}dppm)_2](\mu\text{-}O_2CC_6H_4CO_2)\}_3$ with the phenyl groups omitted.

Pictiva EX2004
Samsung v Pictiva
IPR2024-01094

The paramagnetic mono-acetate complex $Re_2(\mu\text{-}O_2CCH_3)Cl_4(\mu\text{-}dppm)_2$ also reacts with carboxylic acids in a fashion similar to that of *cis*-$Re_2(\mu\text{-}O_2CCH_3)_2Cl_2(\mu\text{-}dppm)_2$. Isonicotinic acid gives the expected product $Re_2(\mu\text{-}O_2CC_5H_4N)Cl_4(\mu\text{-}dppm)_2$ (see Tables 8.4 and 8.6),[323] while with terephthalic acid the "dimer-of-dimers" complex $[Re_2Cl_4(\mu\text{-}dppm)_2]_2(\mu\text{-}O_2CC_6H_4CO_2)$ is formed.[322] Its structure is represented in **8.34** (with the trans sets of dppm ligands omitted).[322] Similar dicarboxylate-bridged complexes are formed with the use of adipic acid, 4,4'-biphenyldicarboxylic acid and fumaric acid.[323] When *trans*-1,4-cyclohexanedicarboxylic acid is reacted with $Re_2(\mu\text{-}O_2CCH_3)Cl_4(\mu\text{-}dppm)_2$ in refluxing ethanol, the only product isolated was the reduced Re_2^{4+} complex *cis*-$Re_2(\mu\text{-}O_2CC_6H_{10}CO_2Et)_2Cl_2(\mu\text{-}dppm)_2$ (see Tables 8.4 and 8.6).[323] The interactions between the paramagnetic centers in $[Re_2Cl_4(\mu\text{-}dppm)_2]_2(\mu\text{-L})$, where L = terephthalate, adipate, 4,4'-biphenyldicarboxylate or fumarate, have been probed by magnetic susceptibility and/or cyclic voltammetric and differential pulsed voltammetric measurements.[323] Only in the case of the terephthate and fumarate bridged complexes is there evidence for weak coupling.



8.34

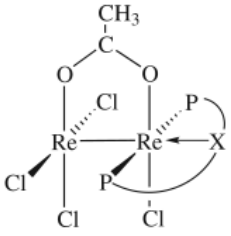
When the alkyne carboxylic acids $HO_2CC{\equiv}CCO_2H$ and $CH_3C{\equiv}CCO_2H$ are refluxed with $Re_2(\mu\text{-}O_2CCH_3)Cl_4(\mu\text{-}dppm)_2$, decarboxylation occurs to give the paramagnetic μ-alkyne and diamagnetic μ-carbyne complexes $Re_2(\mu\text{-Cl})(\mu\text{-}\eta^2\text{-HCCH})Cl_4(\mu\text{-}dppm)_2$ and $Re_2(\mu\text{-Cl})(\mu\text{-}CCH_2CH_3)Cl_4(\mu\text{-}dppm)_2$.[324] Both reactions are believed to proceed via the formation of the Re_2^{5+} alkynoates. The crystal structures of the edge-sharing bioctahedral products show that the Re–Re bond distances are 2.6567(5) Å and 2.5277(6) Å, respectively; these values are consistent with Re–Re bond orders of 1.5 and 2.

Other examples of substitution reactions involving *cis*-$Re_2(\mu\text{-}O_2CR)_2Cl_2(\mu\text{-}dppm)_2$ include that of the acetate complex with $NaBH_3CN$ in THF which gives *cis*-$Re_2(\mu\text{-}O_2CCH_3)_2(NCBH_3)_2(\mu\text{-}dppm)_2$, while the reactions of *cis*-$Re_2(\mu\text{-}O_2CC_2H_5)_2Cl_2(\mu\text{-}dppm)_2$ with nitriles RCN in the presence of $HBF_4{\cdot}Et_2O$ or HPF_6(aq) provide a route to salts of the *cis*-$[Re_2Cl_2(\mu\text{-}dppm)_2(NCR)_4]^{2+}$ cations.[325] The exposure of *cis*-$Re_2(\mu\text{-}O_2CR)_2Cl_2(\mu\text{-}dppm)_2$ (R = Me or Et) to gaseous H_2S in the presence of $HBF_4{\cdot}Et_2O$ gives either *cis*-$Re_2(\mu\text{-}SH)_2Cl_2(\mu\text{-}dppm)_2$, when THF or $CHCl_3$ is used as the solvent, or the *gem*-dithiolato complexes *cis*-$Re_2(\mu\text{-}S_2CR^1R^2)Cl_2(\mu\text{-}dppm)_2$ and *cis*-$Re_2(\mu\text{-}S_2CHR^2)Cl_2(\mu\text{-}dppm)_2$ in the presence of ketones (R^1R^2CO) and aldehydes (R^2CHO).[326] Single crystal X-ray structural characterizations of *cis*-$Re_2(\mu\text{-}SH)_2Cl_2(\mu\text{-}dppm)_2$ and *cis*-$Re_2(\mu\text{-}S_2CMe_2)Cl_2(\mu\text{-}dppm)_2$ show that both complexes possess similar cradle-like geometries and short Re–Re distances that accord with retention of the electron-rich Re–Re triple bond (Table 8.4). The electrochemical properties of this series of compounds are very similar, with two oxidations ($E_{p,a} \simeq 1.4$ V and $E_{1/2}(ox) \simeq 0.65$ V versus Ag/AgCl) and a one-electron reduction with $E_{1/2}(red) \simeq -1.6$ V versus Ag/AgCl being observed in all cases.[326]

A different structural type of mixed carboxylate/halide/phosphine complex is obtained when the synthon *cis*-$Re_2(\mu\text{-}O_2CCH_3)_2Cl_4(H_2O)_2$ is reacted with tridentate ligands that contain P_2O and P_2N donor sets.[191] The complexes that are formed are derivatives of the Re_2^{5+} core and all have the same unsymmetrical structure shown in **8.35**, in which an O or N atom is weakly bound in

Pictiva EX2004
Samsung v Pictiva
IPR2024-01094

an axial position. The ligands that have been used are bis[2-(diphenylphosphino)phenyl]ether, 4,6-bis(diphenylphosphino)dibenzofuran, 2,6-bis(diphenylphosphinomethyl)pyridine, bis[2-(diphenylphosphino)ethyl]amine and N,N-bis[2-(diphenylphosphino)ethyl]trimethylacetamide and these are designated as $\mathbf{L}_1$, $\mathbf{L}_2$, $\mathbf{L}_3$, $\mathbf{L}_4$ and $\mathbf{L}_5$, respectively, in Tables 8.4 and 8.6 where details of the X-ray crystal structures and electrochemical data for the complexes are given.[191] The lability of the acetate group in these complexes has been demonstrated by reactions of certain of these complexes (those that contain ligands $\mathbf{L}_1$ and $\mathbf{L}_3$) with 4-$Ph_2PC_6H_4CO_2H$, 2-$Ph_2PC_6H_4CO_2H$ and quin-4-CO_2H, to give products that have structures and properties very similar to those of the μ-acetato derivatives (Tables 8.4 and 8.6).[191(b)] These same two acetate complexes also react with terephthalic acid to give $[Re_2Cl_4(\eta^3\text{-}\mathbf{L}_1)]_2(\mu\text{-}O_2CC_6H_4CO_2)$ and $[Re_2Cl_4(\eta^3\text{-}\mathbf{L}_3)_2](\mu\text{-}O_2CC_6H_4CO_2)$, the structure of the first of these having been established by X-ray crystallography.[191] Magnetic susceptibility and cyclic voltammetric measurements show that any electronic coupling between the paramagnetic individual Re_2^{5+} units is at most very weak.[191(b)]

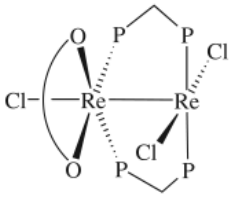


8.35

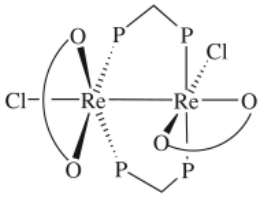
A few examples exist of Re_2^{4+} and Re_2^{5+} complexes that contain bidentate monoanionic ligands, other than carboxylates, in combination with halide and phosphine donor sets. These ligands may bridge the two metal centers or chelate to only one of them. Bis(μ-hydrosulfido) and μ-*gem*-dithiolato complexes prepared from *cis*-$Re_2(\mu\text{-}O_2CR)_2Cl_2(\mu\text{-dppm})_2$ have already been mentioned.[326] The reaction of $Re_2X_4(\mu\text{-dppm})_2$ (X = Cl or Br) with 2-mercaptoquinoline (2-mqH) affords the 1:1 adducts $Re_2X_4(\mu\text{-dppm})_2(2\text{-mqH})$ that can undergo a reversible one-electron oxidation with $[(\eta^5\text{-}C_5H_5)_2Fe]PF_6$ to give $[Re_2X_4(\mu\text{-dppm})_2(2\text{-mqH})]PF_6$. This oxidation is followed by the slow elimination of HX to give paramagnetic $[Re_2X_3(\mu\text{-dppm})_2(2\text{-mq})]PF_6$ in which, in addition to two bridging dppm ligands, there is also a bridging 2-mq ligand bound through its N and S (thiol) atoms.[327,328] A crystal structure determination on the chloride derivative shows the Re–Re distance to be 2.2540(5) Å.[328] The neutral compounds $Re_2X_3(\mu\text{-dppm})_2(2\text{-mq})$ are formed by the electrochemical reduction of the paramagnetic cations and from $Re_2X_4(\mu\text{-dppm})_2(2\text{-mqH})$ by treatment with the strong base DBU.[328]

The reaction of $Re_2Cl_4(\mu\text{-dppm})_2$ with Tl(acac) affords $Re_2(acac)_2Cl_2(\mu\text{-dppm})_2$ (**8.37**) via the intermediacy of $Re_2(acac)Cl_3(\mu\text{-dppm})_2$ (**8.36**).[329] These are the first examples of β-diketonate complexes of Re_2^{4+} and both have been characterized by X-ray crystallography (Table 8.4), and found to have *cis*, *trans* sets of ReP_2 units as shown in **8.36** and **8.37**.[329]

Pictiva EX2004
Samsung v Pictiva
IPR2024-01094



8.36



8.37

Reactions of $Re_2X_4(\mu\text{-}LL)_2$ compounds with carbon monoxide, isocyanides, nitriles and related ligands

By far the most extensive reaction chemistry for the $Re_2X_4(\mu\text{-}LL)_2$ compounds has been developed from their reactions with organic ligands such as CO, isocyanides, nitriles and alkynes, some of which involve multi-electron redox changes at the dirhenium unit. Selected aspects of this chemistry are covered in several earlier short overviews of the subject,[212,330,331] and these can be consulted for additional insights. One simplifying feature in surveying this chemistry is that, to date, it has involved predominantly the reactions of $Re_2X_4(\mu\text{-dppm})_2$ (X = Cl or Br), although there can be little doubt that related compounds will generally behave similarly and this has been shown to be the situation with the few other systems that have been studied.

We will discuss first the compounds that are formed exclusively with CO, alkyl and aryl isocyanides, nitriles or alkynes, and then turn our attention to compounds that contain two or three of these ligands in combination. Finally we will mention briefly other small molecules such as CS_2 and SO_2. Structural data for some of the key complexes that have been characterized by X-ray crystallography and which retain Re–Re multiple bonds are summarized in Table 8.7.

A thorough investigation has been made of the reactions between $Re_2X_4(\mu\text{-dppm})_2$ (X = Cl or Br) and carbon monoxide.[332-335] The chloride compounds that have been prepared are shown in Fig. 8.26, along with the structures of the 1:1, 1:2 and 1:3 complexes (**8.38 - 8.40**) as based upon single crystal X-ray structure determinations (see Table 8.7).[332-334] The analogous bromide complexes have been prepared in all cases, and the structure of the monocarbonyl has also been established by X-ray crystallography and shown to be like **8.38**.[335] Two (CO) modes are observed in the infrared spectra of the monocarbonyls and these vary in their relative intensities depending on the solvent used. This information, along with NMR spectral data which clearly indicates that a fluxional process is occurring in solution, suggests that isomers are present, as is also the case for the mono-isocyanide species $Re_2X_4(\mu\text{-dppm})_2(CNR)$ (vide infra). A partial X-ray structure determination on a single crystal of the second isomer of $Re_2Cl_4(\mu\text{-dppm})_2(CO)$ showed that it has an open structure with no bridging ligands other than dppm.[335] Its structure is probably closely akin to one of the structure types encountered with mono-isocyanide adducts of $Re_2Cl_4(\mu\text{-LL})_2$ compounds (vide infra). Although the dicarbonyl complex $Re_2Cl_4(\mu\text{-dppm})_2(CO)_2$ has been characterized by X-ray crystallography,[332] a disorder problem made it impossible to say if the two CO ligands are cis or trans to each other with respect to the Re–Re axis. However, in light of the derivatization of this dicarbonyl with isocyanides and nitriles, and the structural characterization of these complexes as well as that of the related complex $Re_2Cl_4(\mu\text{-dppE})_2(CO)_2$,[287] it is clear that the CO ligands are cis as shown in **8.39**. The Re–Re bond distance of 2.584(1) Å is far longer than bonds observed in triply bonded complexes with a Re_2^{4+} core, and this complex can be viewed[332] as possessing a Re–Re double bond.

Pictiva EX2004
Samsung v Pictiva
IPR2024-01094

Table 8.7. Structural data for selected dirhenium complexes that contain Re–Re multiple bonds and are formed from the reactions of $Re_2X_4(\mu\text{-LL})_2$ (X = Cl or Br) with carbon monoxide, isocyanides, and nitriles[a]

Compound	r(Re–Re)Å	Structure Description[b]	ref.
$Re_2Cl_4(\mu\text{-dppm})_2(CO)$	2.338(1)	A-frame-like (μ-Cl) (**8.38** in Fig. 8.26)	333
$Re_2Cl_4(\mu\text{-dppm})_2(CO)_2$	2.584(1)	edge-shared bioctahedron(μ-Cl,CO)[c] (**8.39** in Fig. 8.26)	332
$Re_2HCl_3(\mu\text{-dppm})_2(CO)_2$	2.605(1)	edge-shared bioctahedron (μ-H,Cl)[c]	337
$[Re_2Cl_3(\mu\text{-dppm})_2(CO)_3]PF_6$	2.582(1)	edge-shared bioctahedron (μ-Cl,CO)[c] (**8.40** in Fig. 8.26)	334
$[Re_2Cl_3(\mu\text{-dmpm})_3(CO)]PF_6$	2.3565(7)	open bioctahedron	338
$Re_2Cl_4(\mu\text{-dppm})_2(CNBu^t)$	2.30(1)	A-frame-like (μ-Cl) (similar to **8.38**)	341
$Re_2Cl_4(\mu\text{-dppm})_2(CNXyl)$	2.3195(9)	A-frame-like (μ-Cl) (similar to **8.38**)	342
$Re_2Cl_4(\mu\text{-dcpm})_2(CNXyl)\cdot(CH_3)_2CO$	2.2887(3)	open structure (**8.42**)	342
$Re_2Cl_4(\mu\text{-dcpm})_2(CNBu^t)_2\cdot CH_2Cl_2$	2.3797(3)	open bioctahedron (**8.43**)	342
$Re_2Cl_4(\mu\text{-dppE})_2(CNBu^t)_2\cdot 3C_2H_4Cl_2$	2.3497(4)	open bioctahedron (**8.43**)	342
$[Re_2Cl_3(\mu\text{-dppE})_3(CNBu^t)_3]Cl$	2.3451(10)	open bioctahedron (**8.44**)	342
$[Re_2Cl_3(\mu\text{-dppm})_2(NCMe)_2]Cl$	2.272(5)	structure **8.41** with L = MeCN	349
$[Re_2Cl_3(\mu\text{-dppm})_2(NCEt)_2]PF_6$	2.2661(9)	structure **8.41** with L = EtCN	300
$[Re_2Cl_3(\mu\text{-dppm})_2(NCPh)_2]PF_6$	2.270(1)	structure **8.41** with L = PhCN	345
$[Re_2Cl_3(\mu\text{-dppm})_2(NCPh)_2]Cl\cdot 2CH_2Cl_2$	2.2835(5)	structure **8.41** with L = PhCN	349
$[Re_2Cl_3(\mu\text{-dppm})_2(1,2\text{-}NCC_6H_4CN)_2]PF_6$	2.265(1)	structure **8.41** with L = 1,2-NCC_6H_4CN	325
$[Re_2Cl_3(\mu\text{-dppm})_2(1,4\text{-}NCC_6H_4CN)_2]PF_6$	2.2637(12)	structure **8.41** with L = 1,4-NCC_6H_4CN	348
$Re_2Br_4(\mu\text{-dppm})_2(CO)(CNBu^t)\cdot CH_2Cl_2\cdot 2.5C_6H_6$	2.3805(14)	open bioctahedron (**8.49**)	335
$Re_2Cl_4(\mu\text{-dppm})_2(CO)(CNXyl)\cdot CH_3OH$	2.581(2)	edge-shared bioctahedron (μ-Cl,CO)[c] (**8.48**)	333
$[Re_2Br_3(\mu\text{-dppm})_2(CO)(CNXyl)]O_3SCF_3$	2.298(1)	structure **8.41** with L = CO, XylNC	335
$[Re_2Cl_3(\mu\text{-dppm})_2(CO)(NCMe)]O_3SCF_3$	2.2881(7)	structure **8.41** with L = CO, MeCN	355
$[Re_2Cl_3(\mu\text{-dppm})_2(CO)_2(NCEt)]PF_6\cdot CH_2Cl_2\cdot 1/2Et_2O$	2.586(1)	edge-shared bioctahedron (μ-Cl,CO)[c] (similar to **8.50** in Fig. 8.28)	356
$Re_2Cl_3(\mu\text{-dppm})_2(CO)_2(CNPr^i)$	2.718(1)	edge-shared bioctahedron (μ-Cl,CO)[c]	358
$[Re_2Cl_3(\mu\text{-dppm})_2(CO)_2(CNBu^t)]PF_6\cdot 2CH_2Cl_2$	2.605(1)	edge-shared bioctahedron (μ-Cl,CO)[d] (**8.51** in Fig. 8.28)	358
$[Re_2Br_3(\mu\text{-dppm})_2(CO)_2(CNXyl)]O_3SCF_3\cdot Me_2CHC(O)Me$	2.5853(13)	edge-shared bioctahedron (μ-Br,CO)[c] (similar to **8.50** in Fig. 8.28)	359
$[Re_2Cl_3(\mu\text{-dppE})_2(CO)_2(CNXyl)]O_3SCF_3\cdot 1.53CH_2Cl_2$	2.5767(5)	edge-shared bioctahedron (μ-Cl,CO)[c] (similar to **8.50** in Fig. 8.28)	287
$[Re_2Cl_3(\mu\text{-dppm})_2(CO)(CNBu^t)_2](PF_6)_{0.5}(OMe)_{0.5}$	2.379(1)	open bioctahedron (similar to **III** and **IV** in Fig. 8.29)	357,363

Pictiva EX2004
Samsung v Pictiva
IPR2024-01094

Compound	r(Re–Re)Å	Structure Description[b]	ref.
$[Re_2Cl_3(\mu\text{-dppm})_2(CO)(CNXyl)_2](ReO_4)_{0.82}Cl_{0.18}$	2.576(1)	edge-shared bioctahedron (μ-Cl,CO)[c] (isomer **VI** in Fig. 8.30)	364
$Re_2Cl_3(\mu\text{-dppm})_2(CO)(CNXyl)_2$	2.7155(9)	edge-shared bioctahedron (μ-Cl,CNXyl)[c] (isomer **V** in Fig. 8.30)	362
$[Re_2Cl_3(\mu\text{-dppm})_2(CO)(CNXyl)_2]O_3SCF_3\cdot CH_2Cl_2$	2.3833(8)	open bioctahedron (isomer **VII** in Fig 8.30)	353
$[Re_2Br_3(\mu\text{-dppm})_2(CO)(CNXyl)_2]O_3SCF_3\cdot MeCN$	2.3792(7)	open bioctahedron (isomer **VII** in Fig 8.30)	359
$[Re_2Cl_3(\mu\text{-dppm})_2(CO)(CNXyl)(NCMe)]O_3SCF_3\cdot MeCN$	2.378(3)	open bioctahedron (similar to **III** in Fig. 8.29 with MeCN in place of Bu^{t}NC)	354
$[Re_2Cl_3(\mu\text{-dppm})_2(CO)(NCMe)_2]ReO_4\cdot MeCN$	2.5669(4)	edge-shared bioctahedron (μ-Cl,CO)[c]	355
$[Re_2Cl_3(\mu\text{-dppm})_2(CO)(PMe_3)_2]Cl\cdot 0.5CH_2Cl_2$	2.6021(6)	edge-shared bioctahedron (μ-Cl,CO)[c]	377
$[Re_2Cl_3(\mu\text{-dppm})_2(CO)_2(PMe_3)]PF_6$	2.593(1)	edge-shared bioctahedron (μ-Cl,CO)[c]	378
$\{Re_2Cl_3(\mu\text{-dppm})_2(CO)_2[P(OEt)_3]\}PF_6$	2.595(1)[e]	edge-shared bioctahedron (μ-Cl,CO)[c]	378
$Re_2Cl_3[C(CN)_3](\mu\text{-dppm})_2(CNXyl)\cdot H_2O$	2.2766(10)	open structure (**8.52**)	291
$Re_2Cl_2[C(CN)_3]_2(\mu\text{-dppm})_2(CNXyl)\cdot 2CHCl_3$	2.2856(5)	open structure (**8.53**)	291
$Re_2Cl_3[C(CN)_3](\mu\text{-dppE})_2(CO)_2\cdot C_2H_4Cl_2$	2.5823(6)	edge-shared bioctahedron (μ-Cl,CO)[c]	291
$Re_2Cl_3[C(CN)_3](\mu\text{-dppm})_2(CO)(CNXyl)\cdot 0.436C_2H_4Cl_2$	2.5672(3)	edge-shared bioctahedron (μ-Cl,CO)[c]	291
$Re_2Cl_3[C(CN)_3](\mu\text{-dppm})_2(CO)(CNXyl)\cdot C_2H_4Cl_2$	2.23776(3)	open bioctahedron (similar to **III** in Fig. 8.29 with $[C(CN)_3]^-$ in place of Bu^{t}NC)	291
$\{[Re_2Cl_3(\mu\text{-dppm})_2(CO)_2]_2[\mu\text{-}N(CN)_2]\}Cl\cdot 5C_2H_4Cl_2$	2.5839(7)	two edge-shared bioctahedra (μ-Cl,CO)[c] linked by μ-$[N(CN)_2]$	370
$[Re_2Cl_3(\mu\text{-dppE})_2(CO)_2]_2[\mu\text{-}Ni(CN)_4]\cdot 6CH_2Cl_2$	2.5768(5)	two-edge-shared bioctahedra (μ-Cl,CO)[c] linked by μ-$[Ni(CN)_4]$ (see Fig. 8.31)	370
$Re_2Cl_3(\mu\text{-dppm})_2(CO)_2[(\mu\text{-NC})W(CO)_5]$	2.5898(4)	edge-shared bioctahedron (μ-Cl,CO)[c]	291
$[Re_2Cl_3(\mu\text{-dppE})_2(CO)_2(\mu\text{-NCS})]_2[Pd_2Cl_2(SCN)_2]\cdot 10C_6H_6$	2.5775(4)	two-edge shared bioctahedra (μ-Cl,CO)[c] linked by μ-$[Pd_2(\mu\text{-SCN})(\mu\text{-NCS})Cl_2(SCN)_2]$	291,371

[a] Only compounds that contain no more than three of these ligands, either alone or in combination with one another, are listed.
[b] All structures contain a pair of trans bridging dppm, dcpm or dppE ligands. Other bridging ligands, when present, are given in parentheses, as are any references to the structures if cited elsewhere in the text.
[c] Edge-shared bioctahedron with a symmetrical all-cis arrangement of halide ligands.
[d] Edge-shared bioctahedron with an unsymmetrical arrangement of halide ligands.
[e] Two crystallographically independent and essentially identical molecules are present in the unit cell.

Pictiva EX2004
Samsung v Pictiva
IPR2024-01094

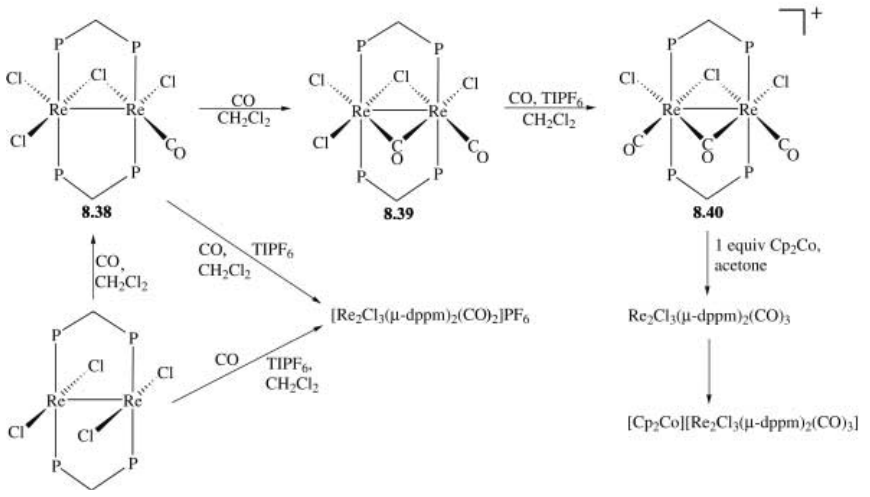
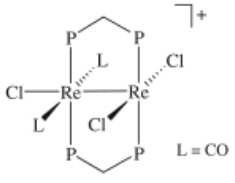


Fig. 8.26. Reaction scheme showing the products of the reactions of $Re_2Cl_4(\mu\text{-dppm})_2$ with carbon monoxide.

In the presence of $TlPF_6$, a Re–X bond is labilized and the products are $[Re_2X_3(\mu\text{-dppm})_2(CO)_2]PF_6$ or $[Re_2X_3(\mu\text{-dppm})_2(CO)_3]PF_6$, depending upon whether $Re_2X_4(\mu\text{-dppm})_2(CO)$ or $Re_2X_4(\mu\text{-dppm})_2(CO)_2$, respectively, is used as the reactant (see Fig. 8.26).[334] The similarity between the electrochemical and NMR spectral properties of $[Re_2X_3(\mu\text{-dppm})_2(CO)_2]PF_6$[334] and those of the structurally characterized nitrile complexes $[Re_2X_3(\mu\text{-dppm})_2(NCR)_2]PF_6$ (vide infra) argues for a structure like **8.41** for the bis-carbonyl cations. Support for this comes from their infrared spectra which show the presence of only terminal carbonyl ligands.[334]



8.41

The aforementioned carbonyl complexes exhibit well-defined electrochemical behavior,[332-334] with several redox states quite readily accessible. This is clearly demonstrated in the case of $[Re_2X_3(\mu\text{-dppm})_2(CO)_3]PF_6$ (X = Cl or Br), which can be reduced by cobaltocene in a stepwise fashion to give the lower valent complexes $Re_2X_3(\mu\text{-dppm})_2(CO)_3$ and $[(\eta^5\text{-}C_5H_5)_2Co][Re_2X_3(\mu\text{-dppm})_2(CO)_3]$ (see Fig. 8.26).[334] Another aspect of the redox chemistry of the carbonyl complexes is encountered in the case of the halogen oxidation of $Re_2X_4(\mu\text{-dppm})_2(CO)$ (X = Cl or Br) to give the cationic species $[Re_2X_5(\mu\text{-dppm})_2(CO)]^+$. A crystal structure determination of $[Re_2Cl_5(\mu\text{-dppm})_2(CO)]PF_6$ showed that the cation has the edge-shared bioctahedral structure $[Re_2(\mu\text{-Cl})_2(\mu\text{-dppm})_2Cl_3(CO)]^+$ with a formal Re=Re bond (the distance is 2.6607(4) Å).[336]

An interesting mixed hydride-carbonyl complex is formed upon reacting $Re_2Cl_4(\mu\text{-dppm})_2$ with various carbonyl clusters in the presence of H_2 and, also, from its reaction with H_2/CO gas mixtures in refluxing toluene.[337] The structure of $Re_2(\mu\text{-H})(\mu\text{-Cl})Cl_2(\mu\text{-dppm})_2(CO)_2$ is that of a symmetrical edge-shared bioctahedron with an all-cis arrangment of chloride ligands and a bridging hydride ligand.[337]

Pictiva EX2004
Samsung v Pictiva
IPR2024-01094

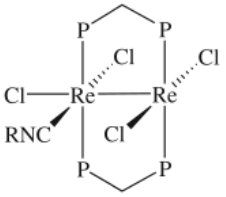
The carbonyl complexes $Re_2Cl_4(\mu\text{-dppE})_2(CO)_2$ and $[Re_2Cl_3(\mu\text{-dppE})_2(CO)_3]O_3SCF_3$ have been prepared from $Re_2Cl_4(\mu\text{-dppE})_2$[287] but, surprisingly, $Re_2Cl_4(\mu\text{-dcpm})_2$ does not react with CO[285] although it does convert to 1:1 and 1:2 complexes with isocyanides (vide infra). Even though the compound $Re_2Cl_4(\mu\text{-dmpm})_2$ does not exist, the tris-dmpm complex $Re_2Cl_4(\mu\text{-dmpm})_3$ is very stable[295] and has been found to react at room temperature with CO in the presence of $TlPF_6$ to form $[Re_2Cl_3(CO)(\mu\text{-dmpm})_3]PF_6$,[338] which has an open bioctahedral structure with a terminal CO ligand in an equatorial position and a short Re–Re distance (see Table 8.7). The dicarbonyl complexes $[Re_2X_2(CO)_2(dmpm)_3](H_2PO_4)_2$ (X = Cl or Br) are produced upon reacting $[Re_2(\mu\text{-}O_2CCH_3)X_2(\mu\text{-dmpm})_3]PF_6$ with CO in deoxygenated acetone/HPF_6(aq) mixtures.[338,339] These compounds have a structure that can be represented as $[Re_2(\mu\text{-}X)_2(\mu\text{-dmpm})(CO)_2(dmpm)_2]^{2+}$, in which a Re–Re single bond is present (2.918(2) Å) and two of the original bridging dmpm ligands have switched to a chelating mode.[338,339]

In contrast to the simple carbonylation reactions that $Re_2X_4(\mu\text{-dppm})_2$ undergo (Fig. 8.26), the tetramethyl complex $Re_2(CH_3)_4(\mu\text{-dppm})_2$ reacts with CO to give the di-μ-methylene complex $Re_2(\mu\text{-}CH_2)_2(CO)_4(\mu\text{-dppm})_2$ in which a long Re–Re single bond is present.[289] Structure determinations on two different crystals of this complex that contain solvent THF or CH_2Cl_2 molecules show that the $[Re_2(\mu\text{-dppm})_2]$ units possess chair and boat conformations, respectively.

The reactions of $Re_2X_4(\mu\text{-dppm})_2$ with one equivalent of an isocyanide, RNC (R = Me, Bu^t or Xyl), give the monoisocyanide adducts $Re_2X_4(\mu\text{-dppm})_2(CNR)$ in high yield.[340-342] A partial crystal structure determination of $Re_2Cl_4(\mu\text{-dppm})_2(CNBu^t)$ showed that like the analogous monocarbonyl complex it has an A-frame-like structure (**8.38**) with a Re–Re distance of *c.* 2.30 Å.[341] Based upon a qualitative treatment of the bonding, this distance can be considered to represent a slightly weakened triple bond. Because of a disorder involving the terminal Bu^tNC and Cl ligands trans to the Cl-bridge, the full structure could not be solved. However, more recently, a similar disorder in $Re_2Cl_4(\mu\text{-dppm})_2(CNXyl)$ was satisfactorily modeled and the structure solved (see Table 8.7).[342]

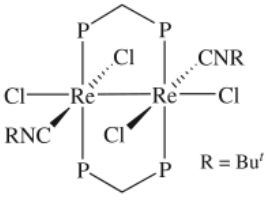
The cyclic voltammetric properties of these 1:1 complexes show that like other triply bonded dirhenium(II) species they possess two accessible one-electron oxidations.[341] Another interesting property is the presence of two ν(C≡N) modes in the infrared spectra at frequencies characteristic of a terminally coordinated RNC ligands.[341] These findings indicate that the complexes exist as a mixture of isomers, as is the case for $Re_2X_4(\mu\text{-dppm})_2(CO)$ (vide supra), but only one of which forms suitable crystals for a crystallographic determination. These isomers interconvert rapidly on the NMR time scale. However, oxidation of these complexes with $NOPF_6$ forms $[Re_2X_4(\mu\text{-dppm})_2(CNR)]PF_6$ (X = Cl or Br)[341] which show one ν(C≡N) mode in their infrared spectra, indicating that only a single isomer is now present. The structure of this other isomer is most likely that shown in **8.42**, based upon studies of the 1:1 complexes $Re_2Cl_4(\mu\text{-dppE})_2(CNXyl)$ and $Re_2Cl_4(\mu\text{-dcpm})_2(CNXyl)$.[342] Although both these compounds have solution properties that resemble closely those of $Re_2Cl_4(\mu\text{-dppm})_2(CNXyl)$, an X-ray crystal structure determination of $Re_2Cl_4(\mu\text{-dcpm})_2(CNXyl)$ revealed that the structure is as shown in **8.42** with a Re–Re triple bond (see Table 8.7).[342] The halogen oxidation of $Re_2X_4(\mu\text{-dppm})_2(CNR)$ (X = Cl or Br; R = Bu^t or Xyl) affords salts of the edge-shared bioctahedral cations $[Re_2(\mu\text{-}X)_2(\mu\text{-dppm})_2X_3(CNR)]^+$; the chloride complexes have been reduced by cobaltocene to the neutral paramagnetic Re_2^{5+} complexes $Re_2(\mu\text{-}X)_2(\mu\text{-dppm})_2X_3(CNR)$.[336]

Pictiva EX2004
Samsung v Pictiva
IPR2024-01094



8.42

A variety of complexes with two or three RNC ligands present have also been isolated and some of these structurally characterized.[340,342] Which compound is isolated depends upon the reaction conditions and the identity of the phosphine ligand in the $Re_2X_4(\mu\text{-LL})_2$ precursor compound. The first such study, which involved the treatment of $Re_2Cl_4(\mu\text{-dppm})_2$ with two equivalents of Bu^{t}NC in acetone in the presence of PF_6^-, gave yellow and green isomers of stoichiometry $[Re_2Cl_3(\mu\text{-dppm})_2(CNBu^t)_2]PF_6$.[340,343] A comparison of their infrared, ^{1}H NMR and $^{31}P\{^1H\}$ NMR spectra show that these isomers are structurally very different, with the green isomer very likely having a structure that is similar to **8.41** (with L = Bu^{t}NC). Subsequently, the salts $[Re_2Cl_3(\mu\text{-dppE})_2(CNBu^t)_2]X$ were prepared with X = O_3SCF_3 or PF_6, and shown to have properties very similar to those of the green isomeric form of the dppm complex.[342] A novel complex that contains a μ-iminyl ligand, $[Re_2Cl_3(\mu\text{-C=NHBu}^t)(\mu\text{-dppm})_2(CNBu^t)_2]PF_6$, has been isolated as a by-product in the synthesis of the green isomer and has been structurally characterized.[343,344] It has an edge-shared bioctahedral structure with an all-cis arrangement of chloride ligands, a symmetrically bridging μ-C=NHBu^t ligand and a Re–Re distance of 2.704(1) Å. This blue, paramagnetic compound exhibits a well-defined X-band EPR spectrum. In the absence of salts such as TlO_3SCF_3 or $TlPF_6$, $Re_2Cl_4(\mu\text{-dppm})_2$ reacts with 2 equiv of Bu^{t}NC to give $Re_2Cl_4(\mu\text{-dppm})_2(CNBu^t)_2$ via the intermediacy of the 1:1 complex, but this product could not be separated from some $[Re_2Cl_3(\mu\text{-dppm})_2(CNBu^t{}_3]^+$ (vide infra) which is formed.[342] However, the bis-isocyanide complexes $Re_2Cl_4(\mu\text{-dppE})_2(CNBu^t)_2$ and $Re_2Cl_4(\mu\text{-dcpm})_2(CNBu^t)_2$ can be isolated and both have the same symmetrical structure shown in **8.43** with axial Re–Cl bonds, and quite short Re–Re distances (see Table 8.7).[342] The dppE complex possesses a staggered rotational geometry in the solid state while the dcpm complex is rigorously eclipsed.[342] The 1:2 complexes with XylNC have not yet been isolated.

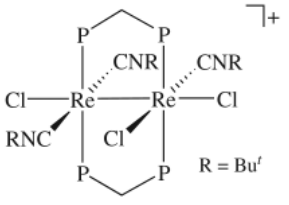


8.43

Complexes that contain three isocyanide ligands i.e. $[Re_2Cl_3(\mu\text{-dppm})_2(CNR)_3]^+$ (R = Bu^t or Xyl), have been isolated as their PF_6^- salts from the reactions of $Re_2Cl_4(\mu\text{-dppm})_2$ or the mixed isocyanide-nitrile complex $[Re_2Cl_3(\mu\text{-dppm})_2(CNBu^t)(NCEt)]PF_6$ (vide infra) with *c.* 4 equiv of Bu^{t}NC and of $[Re_2Cl_3(\mu\text{-dppm})_2(CNXyl)(NCPh)]PF_6$ (vide infra) with 2.5 equiv of XylNC.[343] While the stoichiometries of these two complexes are identical, their electrochemical redox properties are very different. This suggests that they have different structures. Reduction of the monocation $[Re_2Cl_3(\mu\text{-dppm})_2(CNXyl)_3]PF_6$ with cobaltocene yields the neutral paramagnetic

Pictiva EX2004
Samsung v Pictiva
IPR2024-01094

complex $Re_2Cl_3(dppm)_2(\mu\text{-}CNXyl)_3$ containing (formally at least) the Re_2^{3+} core, while oxidation with $NOPF_6$ gives the paramagnetic dication $[Re_2Cl_3(\mu\text{-}dppm)_2](CNXyl)_3](PF_6)_2$. The related green Bu^tNC derivative $[Re_2Cl_3(\mu\text{-}dppm)_2(CNBu^t)_3]PF_6$ does not possess any reversible redox chemistry.[343] In a more recent study, the Bu^tNC complex $[Re_2Cl_3(\mu\text{-}dppm)_2(CNBu^t)_3]^+$ was isolated as its Cl^- salt from the direct reaction of Bu^tNC with $Re_2Cl_4(\mu\text{-}dppm)_2$, and the pair of salts $[Re_2Cl_3(\mu\text{-}dppE)_2(CNBu^t)_3]X$ (X = Cl or PF_6) were likewise prepared from $Re_2Cl_4(\mu\text{-}dppE)_2$.[342] An X-ray crystal structure determination carried out on $[Re_2Cl_3(\mu\text{-}dppE)_2(CNBu^t)_3]Cl$ has established that it has the open bioctahedral structure shown in **8.44**, with a staggered rotational geometry and a short Re–Re distance (see Table 8.7).[342] It seems certain that the related $[Re_2Cl_3(\mu\text{-}dppm)_2(CNBu^t)_3]^+$ species has this same structure. Although all attempts to date have failed to solve the crystal structure of a salt of the $[Re_2Cl_3(\mu\text{-}dppm)_2(CNXyl)_3]^+$ cation, a partially refined structure of its neutral reduced congener $Re_2Cl_3(\mu\text{-}dppm)_2(CNXyl)_3$ has confirmed that it is the edge-shared bioctahedron $(XylNC)ClRe(\mu\text{-}Cl)(\mu\text{-}CNXyl)(\mu\text{-}dppm)_2ReCl(CNXyl)$ with an all-cis arrangement of XylNC ligands and a Re–Re distance of 2.73 Å.[342]



8.44

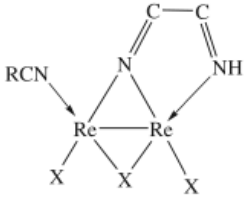
A variety of nitriles react with $Re_2X_4(\mu\text{-}dppm)_2$, including the polycyano acceptor molecules TCNQ and DM-DCNQI that form neutral complexes of the type $[Re_2Cl_4(\mu\text{-}dppm)_2]_2(\mu\text{-}L)$, in which the organocyanide bridges link two $Re_2Cl_4(\mu\text{-}dppm)_2$ through equatorial positions.[312,313] These compounds are discussed in the section dealing with the redox chemistry of $Re_2X_4(\mu\text{-}LL)_2$ compounds. Simple organic nitriles RCN react very readily with $Re_2Cl_4(dppm)_2$ in the presence of KPF_6 to yield the stable, bis-nitrile complexes $[Re_2Cl_3(\mu\text{-}dppm)_2(NCR)_2]PF_6$.[345] In the original study of this system, the nitriles where R = Me, Et, Ph, or 4-PhC_6H_4 were used,[345] although a wider range of them has subsequently been studied, including a few di- and trinitrile ligands (such as 1,2- and 1,4-dicyanobenzene and tris(2-cyanoethyl)phosphine) which bind through only one of their nitrile groups.[325,346-348] Several related bromide complexes have been isolated;[346] it should be noted that the insoluble complex that is formed upon reacting $(Bu_4N)_2Re_2Br_8$ with dppm in refluxing acetonitrile, and which had originally been formulated as "α-$[ReBr_2(dppm)]_n$",[202] is in fact $[Re_2Br_3(\mu\text{-}dppm)_2(NCMe)_2]Br$.[346] The use of $^{31}P\{^1H\}$ NMR spectroscopy to monitor the formation of $[Re_2Cl_3(\mu\text{-}dppm)_2(NCEt)_2]Cl$ in the reaction between $Re_2Cl_4(\mu\text{-}dppm)_2$ and propionitrile shows that these reactions occur in a two step fashion, in which a RCN ligand first coordinates to one of the Re atoms of $Re_2Cl_4(\mu\text{-}dppm)_2$ to generate a 1:1 adduct, possibly having a molecular A-frame-like structure (see **8.38**), followed by the addition of a second nitrile ligand to the same Re atom with concomitant loss of Cl^- to generate $[Re_2Cl_3(\mu\text{-}dppm)_2(NCEt)_2]^+$.[345] These conclusions have been supported by a detailed electrochemical study of the formation of these complexes.[347] The acetonitrile, propionitrile, benzonitrile, 1,2-dicyanobenzene and 1,4-dicyanobenzene complexes have all been structurally characterized and found to have a structure like that shown in **8.41** (L = RCN) (see also Table 8.7).[300,325,345,348,349] The Re–Re bond lengths are very similar to one another, although longer than in the parent $Re_2Cl_4(\mu\text{-}dppm)_2$, and the molecules have staggered rotational geometries.

Pictiva EX2004
Samsung v Pictiva
IPR2024-01094

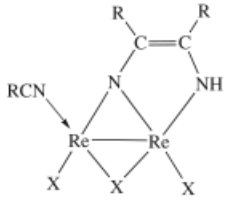
The bis-nitrile salts react cleanly with $NOPF_6$ to generate the paramagnetic EPR-active dications $[Re_2Cl_3(dppm)_2(NCR)_2](PF_6)_2$,[206] which possess the Re_2^{5+} core and a $\sigma^2\pi^4\delta^2\delta^{*1}$ ground-state electronic configuration.

A few bis-nitrile complexes have been isolated with phosphine ligands other than dppm, namely, $[Re_2Cl_3(\mu\text{-cdpp})_2(NCR)_2]PF_6$ (R = Me or Et)[286] and $[Re_2Cl_3(\mu\text{-dppa})_2(NCR)_2]PF_6$ (R = Et or Ph).[348] They resemble closely their μ-dppm analogs.

Several of the bis-nitrile complexes react with further nitrile under reflux conditions to afford the green paramagnetic complexes $[Re_2X_3(\mu\text{-}HN_2C_2R_2)(\mu\text{-dppm})_2(NCR)]PF_6$ (X = Cl or Br; R = Me, Et, Pr^i or Ph),[346,350] in which the dimetal unit has served as a template for the reductive coupling of two nitrile ligands. The lability of the nitrile ligand (RCN) in these complexes has been demonstrated by carrying out nitrile exchange reactions, and their structural identity has been confirmed by an X-ray structure analysis of a salt of the edge-shared bioctahedral $[Re_2Br_3(\mu\text{-}HN_2C_2Me_2)(\mu\text{-dppm})_2(NCMe)]^+$ cation, which has shown that the coupled nitrile ligands exhibit a novel μ_2-η^2 bonding mode.[346,350] The Re–Re distance in this complex is 2.666(1) Å. Distances within the five-membered metallacycle ring, formed from the coupled nitrile ligands, can best be rationalized in terms of contributions from a singly deprotonated diimine ligand (**8.45**), and a triply deprotonated ene-diamine ligand (**8.46**). The treatment of these complexes with either $[(\eta^5\text{-}C_5H_5)_2Fe]PF_6$ in acetone or $NOPF_6$ in CH_2Cl_2 leads to oxidation, and the formation of the red, diamagnetic salts $[Re_2X_3(\mu\text{-}HN_2C_2R_2)(\mu\text{-dppm})_2(NCR)](PF_6)_2$.[346,350] This chemistry has recently been extended to the analogous reactions between $Re_2Cl_4(\mu\text{-dppa})_2$ and propionitrile, which has led to the isolation of $[Re_2Cl_3(\mu\text{-}HN_2C_2Et_2)(\mu\text{-dppa})_2(NCEt)]Cl$ and the oxidized salt $[Re_2Cl_3(\mu\text{-}HN_2C_2Et_2)(\mu\text{-dppa})_2(NCEt)](PF_6)_2$.[348]



8.45



8.46

The reaction of $Re_2Cl_4(\mu\text{-dppm})_2$ with acetylene at room temperature in dichloromethane or acetone affords both 1:2 and 1:3 complexes as shown in the reaction scheme in Fig. 8.27.[351] These complexes have structures that resemble those of the corresponding carbonyl complexes (structures **8.39** and **8.40** in Fig. 8.26) with the important difference that the acetylene complexes contain Re–Re single bonds; the Re–Re bond distances are 2.8094(3) Å and 2.8613(5) Å, respectively. The bis-acetylene complex has also been isolated in the case of $Re_2Br_4(\mu\text{-dppm})_2$. The compound $Re_2Cl_4(\mu\text{-dppm})_2(\mu\text{:}\eta^2,\eta^2\text{-HCCH})(\eta^2\text{-HCCH})$ can be derivatized by isocyanides, while the two terminally bound η^2-acetylene ligands in the tris-acetylene complex are readily displaced by CO and XylNC (see Fig. 8.27). In all cases the products retain the Re–Re single bonds of the parent molecules.[351] A quite different and novel reaction course ensues when $Re_2Cl_4(\mu\text{-dppm})_2$ is treated with 1,7-octadiyne.[352] In this case, the starting material serves as a reagent for the 2-electron reductive cyclization of the diyne and as a template to stabilize the resulting $[C_8H_7Re_2]$ bridging unit shown in structure **8.47**, in which a quadruply bonded Re_2^{6+} core is present (the Re–Re distance is 2.2647(3) Å). The $\mu\text{-}C_8H_7$ ligand is formally trianionic.

Very extensive series of mixed carbonyl-isocyanide, carbonyl-nitrile and carbonyl-isocyanide-nitrile complexes have been prepared starting from the preformed adducts Re_2Cl_4-

Pictiva EX2004
Samsung v Pictiva
IPR2024-01094

(μ-dppm)$_2$(CO), Re_2Cl_4(μ-dppm)$_2$(CO)$_2$ and Re_2Cl_4(μ-dppm)$_2$(CNR). The products of these reactions typically have edge-sharing bioctahedral or open-bioctahedral structures which lead to a dependence of bond order upon structure type. Up to five CO, RNC and RCN ligands in combination with one another have been incorporated into the coordination sphere of the $[Re_2(\mu\text{-}LL)_2]$ unit. Once again, the cases where LL is the dppm ligand dominate this chemistry. A complicating factor in some of this chemistry is the existence of structural isomerism, the important features of which are discussed below. Because this chemistry is now so extensive and quite complicated, only a few key aspects of each type of compound will be discussed but the literature citations are complete and can be consulted for further details. The coverage of these specific compounds will be followed by a consideration of complexes that result from combining alkynes with compounds that contain RNC and CO ligands and, finally, other related compounds of interest.

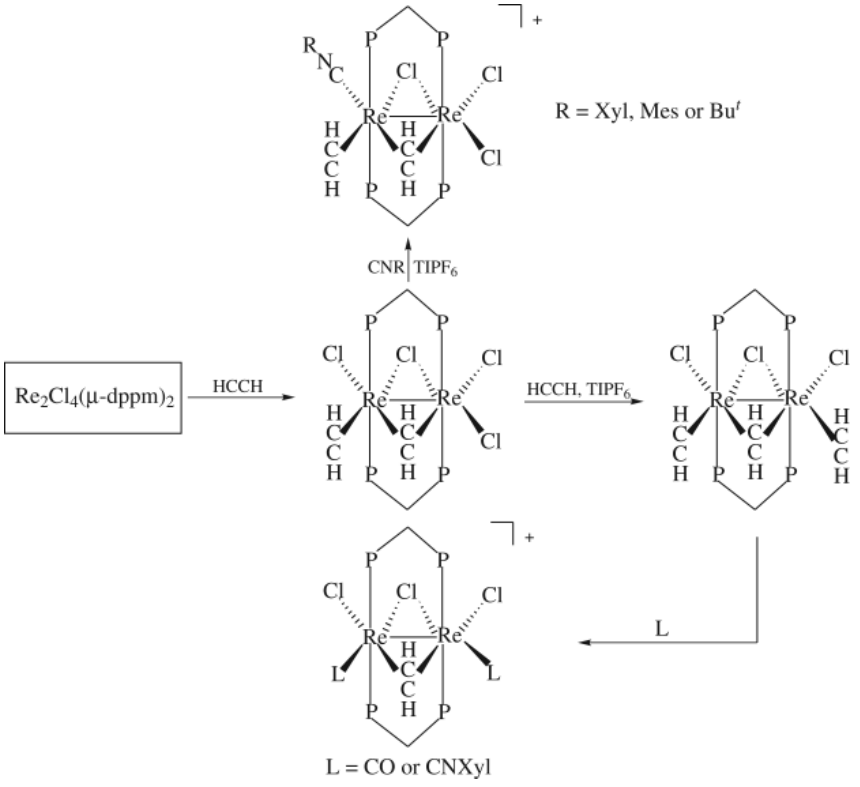
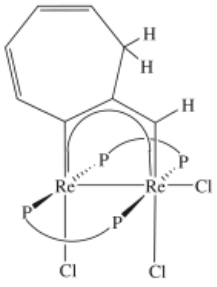


Fig. 8.27. Reaction scheme showing the products of the reactions Re_2Cl_4(μ-dppm)$_2$ with acetylene.

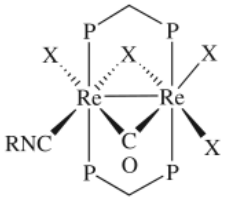
The first study involved the reactions of the monocarbonyl Re_2Cl_4(μ-dppm)$_2$(CO) in acetone with one equivalent of an isocyanide to form the neutral complexes of stoichiometry Re_2Cl_4(μ-dppm)$_2$(CO)(CNR) (R = Pr^i, Bu^t, xylyl or mesityl).[333] A comparison of their infrared spectral properties shows that the alkyl isocyanide derivatives have both their π-acceptor ligands terminally bound, but in the aryl isocyanide derivatives the CO ligand bridges the Re–Re bond. Their electrochemical properties and hence their electronic configurations are

Pictiva EX2004
Samsung v Pictiva
IPR2024-01094

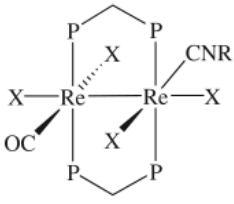


8.47

very different. An X-ray crystal structure of $Re_2Cl_4(\mu\text{-dppm})_2(CO)(CNXyl)$ has shown that the CO and XylNC ligands are cis to one another and the Re–Re distance accords with a double bond (Table 8.7); this structure is in all important respects the same as that of $Re_2Cl_4(\mu\text{-dppm})_2(CO)_2$ (see **8.39** in Fig. 8.26) and is shown in **8.48** (X = Cl). The structures of the Bu^tNC and Pr^iCN derivatives are almost certainly like that shown in **8.49** (X = Cl), based upon the spectroscopic properties of these complexes and their similarity to the bromide analog $Re_2Br_4(\mu\text{-dppm})_2(CO)(CNBu^t)$, which has been prepared by a similar procedure and characterized by X-ray crystallography (Table 8.7).[335] This structure contains a Re–Re triple bond rather than the double bond that is present in compounds with structure **8.48**. This is shown by the difference between the Re–Re bond distances in $Re_2Cl_4(\mu\text{-dppm})_2(CO)(CNXyl)$ (**8.48**) and $Re_2Br_4(\mu\text{-dppm})_2(CO)(CNBu^t)$ (**8.49**) which are 2.581(1) Å and 2.3805(14) Å, respectively. The compound $Re_2Br_4(\mu\text{-dppm})_2(CO)(CNXyl)$ has also been prepared when acetone is used as the reaction solvent and has this same open bioctahedral structure.[335] When the precursor compound $Re_2Cl_4(\mu\text{-dppm})_2(CO)$ is reacted with an equivalent of XylNC in acetonitrile (instead of acetone) it forms $Re_2Cl_4(\mu\text{-dppm})_2(CO)(CNXyl)$ which has structure **8.49** rather than **8.48**.[353] This was the first case of structural isomerism with compounds of the type $Re_2X_4(\mu\text{-LL})_2(CO)(CNR)$.



8.48



8.49

Those isomers of $Re_2X_4(\mu\text{-dppm})_2(CO)(CNR)$ that have the open bioctahedral structure **8.49** (X = Cl or Br; R = Bu^t or Xyl) react with TlO_3SCF_3 in the absence of another donor molecule to give the cationic species $[Re_2X_3(\mu\text{-dppm})_2(CO)(CNR)]^+$ with a structure like that of their bis-carbonyl or bis-nitrile analogs (see **8.41**).[335,354] This transformation occurs through labilization of the Re–X bond that is trans to the XylNC ligand and CO transfer from the adjacent Re atom. The structure of $[Re_2Br_3(\mu\text{-dppm})_2(CO)(CNXyl)]^+$ has been determined crystallographically.[335]

When the monocarbonyls $Re_2X_4(\mu\text{-dppm})_2(CO)$ (X = Cl or Br) are reacted with stoichiometric quantities of nitrile ligands RCN (R = Me or Ph) in the presence of TlY (Y = PF_6 or O_3SCF_3) the compounds $[Re_2X_3(\mu\text{-dppm})_2(CO)(NCR)]Y$ and $[Re_2X_3(\mu\text{-dppm})_2(CO)(NCR)_2]Y$

Pictiva EX2004
Samsung v Pictiva
IPR2024-01094

are formed in high yield.[333,355] Crystal structure determinations on salts of $[Re_2Cl_3(\mu\text{-dppm})_2(CO)(NCMe)]^+$ and $[Re_2Cl_3(\mu\text{-dppm})_2(CO)(NCMe)_2]^+$ (see Table 8.7) have shown[355] that the structures resemble closely **8.41** and **8.40**, respectively; in the case of the bis-nitrile complex, the CO ligand is bridging with the acetonitrile molecules cis to it. These mixed CO/acetonitrile complexes readily interconvert upon the addition or loss of CH_3CN.[355] When salts of the $[Re_2X_3(\mu\text{-dppm})_2(CO)(NCMe)_2]^+$ cations are oxidized with X_2, the products are the same as those formed by $Re_2X_4(\mu\text{-dppm})_2(CO)$, viz, $[Re_2(\mu\text{-}X_2)(\mu\text{-dppm})_2X_3(CO)]^+$.[336]

The lability of one of the Re–Cl bonds of $Re_2Cl_4(\mu\text{-dppm})_2(CNR)$ (R = But or Xyl) has been demonstrated by the conversion of these 1:1 adducts to $[Re_2Cl_3(\mu\text{-dppm})_2(CNR)(NCR')]PF_6$ upon their reaction with R'CN (R' = Me, Et or Ph) and KPF_6.[343] The resulting complexes have very similar electrochemistry and electronic absorption and NMR spectral properties to those of the structurally characterized bis-nitrile salts (vide supra). The available evidence supports a structure closely akin to **8.41**, with the isocyanide and nitrile ligands being coordinated to the same rhenium atom. They can be oxidized chemically with $NOPF_6$ to yield the paramagnetic dications $[Re_2Cl_3(\mu\text{-dppm})_2(CNR)(NCR')](PF_6)_2$, which show[343] complex EPR spectra comparable to those of the oxidized bis-nitrile analogs.

The incorporation of mixed-sets of three CO,RNC and/or RCN ligands can easily be accomplished by the reactions of $Re_2X_4(\mu\text{-dppm})_2(CO)_2$ (**8.39** in Fig. 8.26) and the isomers of $Re_2X_4(\mu\text{-dppm})_2(CO)(CNR)$ (**8.48** and **8.49**) with additional equivalents of RNC or RCN ligands in the presence of Tl^+ salts that can labilize a Re–X bond, as in the conversion of $Re_2Cl_4(\mu\text{-dppm})_2(CO)_2$ to $[Re_2Cl_3(\mu\text{-dppm})_2(CO)_3]^+$ (Fig. 8.26). Thus, salts of stoichiometry $[Re_2Cl_3(\mu\text{-dppm})_2(CO)_2(NCR)]PF_6$ (R = Me, Et or Ph)[356] have been prepared by reacting the dicarbonyl $Re_2Cl_4(\mu\text{-dppm})_2(CO)_2$ with an excess of nitrile in the presence of $TlPF_6$. In the case of the acetonitrile derivative, it has also been obtained by reacting the all-cis complex $[Re_2Cl_3(\mu\text{-dppm})_2(CO)(NCMe)_2]PF_6$ with CO in dichloromethane.[357] An X-ray crystal structure of $[Re_2Cl_3(dppm)_2(CO)_2(NCEt)]PF_6$ shows an all-cis arrangement of chloride ligands. The structure is just like that of $[Re_2Cl_3(\mu\text{-dppm})_2(CO)_3]^+$ (**8.40**) except a terminal carbonyl ligand cis to the μ-CO ligand has been replaced by a propionitrile molecule.[356] The salts $[Re_2Cl_3(\mu\text{-dppm})_2(CO)_2(NCR)]PF_6$ can be reduced to the paramagnetic, EPR-active neutral species $Re_2Cl_3(\mu\text{-dppm})_2(CO)_2(NCR)$ upon their reaction with cobaltocene in acetone.[356] The analogous mixed carbonyl-isocyanide complexes $[Re_2Cl_3(\mu\text{-dppm})_2(CO)_2(CNR)]PF_6$ (R = Pr^i, Bu^t or Xyl) have been prepared by reacting $Re_2Cl_4(\mu\text{-dppm})_2(CO)_2$ with RNC in the presence of $TlPF_6$,[356,358] or the displacement of the nitrile ligand of $[Re_2Cl_3(\mu\text{-dppm})_2(CO)_2(NCR)]PF_6$ by RNC.[356,357] The isocyanide complexes possess a well defined electrochemistry just like that of their nitrile analogs, including a very accessible reversible reduction. The reduction of these mixed carbonyl-isocyanide salts to the neutral, paramagnetic species $Re_2Cl_3(dppm)_2(CO)_2(CNR)$, has been achieved chemically using cobaltocene, and also electrochemically. The complexes of stoichiometry $[Re_2Cl_3(\mu\text{-dppm})_2(CO)_2(CNR)]PF_6$ that have been prepared by the aforementioned methods, possess the all-cis structure **8.50** that is shown in Fig. 8.28. This is the same basic structure as determined for the propionitrile derivative,[356] as well as for the reduced complex $Re_2Cl_3(\mu\text{-dppm})_2(CO)_2(CNPr^i)$.[358] The dicarbonyl complex $Re_2Cl_4(\mu\text{-dppE})_2(CO)_2$ reacts with XylNC and 2,5-dimethylbenzonitrile in the presence of TlO_3SCF_3 to give this same type of complex with structures like **8.50**.[287]

Other routes to complexes of stoichiometry $[Re_2Cl_3(\mu\text{-dppm})_2(CO)_2(CNR)]PF_6$ involve exposing the monoisocyanide $Re_2Cl_4(\mu\text{-dppm})_2(CNR)$ or the mixed carbonyl-isocyanide $Re_2Cl_4(\mu\text{-dppm})_2(CO)(CNR)$ to an atmosphere of CO in the presence of $TlPF_6$.[358] However, these methods can give rise to geometric isomers as shown in Fig. 8.28. The isomer derived from $Re_2Cl_4(\mu\text{-dppm})_2(CNR)$ (R = Bu^t or Xyl) and $Re_2Cl_4(\mu\text{-dppm})_2(CO)(CNBu^t)$ possesses

Pictiva EX2004
Samsung v Pictiva
IPR2024-01094

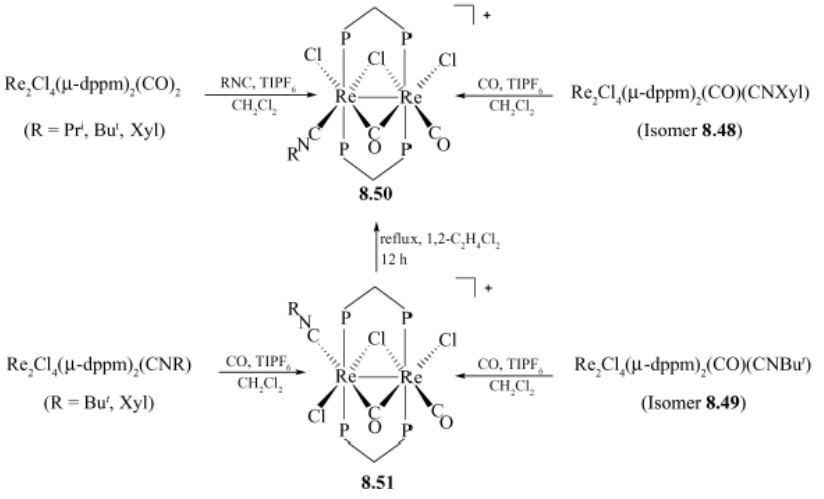


Fig. 8.28. Reaction scheme showing the syntheses, structures and isomerization of mixed carbonyl-isocyanide complexes $[Re_2Cl_3(\mu\text{-dppm})_2(CO)_2(CNR)]PF_6$.

an unsymmetric arrangement of ligands in the equatorial plane (**8.51**) as shown by an X-ray crystal structure of $[Re_2Cl_3(\mu\text{-dppm})_2(CO)_2(CNBu^t)]PF_6$.[358] The Re–Re distance is similar to those of all the other edge-shared bioctahedral complexes listed in Table 8.7. This isomer is also formed by the carbonylation of the complex $[Re_2Cl_3(\mu\text{-dppm})_2(CO)(CNXyl)(NCMe)]O_3SCF_3$, which has an open bioctahedral structure and a labile acetonitrile ligand.[354] Isomerization to the more thermodynamically stable all-cis form occurs upon heating 1,2-dichloroethane solutions of these species over a period of several hours (Fig. 8.28). A bromo analog $[Re_2Br_3(\mu\text{-dppm})_2(CO)_2(CNXyl)]O_3SCF_3$ has also been structurally characterized and shown to have structure **8.50**, with Br in place of Cl.[359] It is prepared by the reaction of CO with $[Re_2Br_3(\mu\text{-dppm})_2(CO)(CNXyl)]O_3SCF_3$ (structure similar to **8.41**).[359] Different isomers of $[Re_2Cl_3(\mu\text{-dcpm})_2(CO)_2(CNXyl)]O_3SCF_3$ have been obtained starting from $Re_2Cl_4(\mu\text{-dcpm})_2(CNXyl)$, but their structures have not yet been determined crystallographically although one of the isomers probably has a structure resembling **8.51**.[360]

Structural isomerism has also been encountered in the case of salts of $[Re_2Cl_3(\mu\text{-dppm})_2(CO)(CNR)_2]^+$, where R = Bu^t or Xyl and the two RNC ligands can be the same or different. Examples were first encountered by reacting the structurally dissimilar isomers of $Re_2Cl_4(\mu\text{-dppm})_2(CO)(CNR)$ (R = Bu^t or Xyl), which can have structures **8.48** or **8.49**, with nitriles (R'CN) and isocyanides (R'NC) in the presence of $TlPF_6$, whereby complexes of the types $[Re_2Cl_3(\mu\text{-dppm})_2(CO)(CNR)(NCR')]PF_6$ and $[Re_2Cl_3(\mu\text{-dppm})_2(CO)(CNR)(CNR')]PF_6$ (R≠R') are formed.[357] The crystal structure of the acetonitrile complex $[Re_2Cl_3(\mu\text{-dppm})_2(CO)(CNXyl)(NCCH_3)]O_3SCF_3$ has confirmed that it has an open bioctahedral structure; this isomer is formed from the isomer of $Re_2Cl_4(\mu\text{-dppm})_2(CO)(CNXyl)$ with structure **8.49**.[354] The nitrile ligands R'CN are labile and are readily displaced by CO and R'NC.[354,357,361] This chemistry is quite extensive, and leads to complexes that can exist in several isomeric forms, e.g. $[Re_2Cl_3(\mu\text{-dppm})_2(CO)(CNBu^t)(CNXyl)]PF_6$ has been isolated and characterized in four forms, two of which are edge-shared bioctahedra (with μ-CO or μ-CNXyl ligands)[357,362] and two are open bioctahedra.[354,357,361] These structures are represented in Fig. 8.29 along with the Re–Re bond order that is present in each. The XylNC-bridged isomer **I** converts to the more thermodynamically stable **II** upon refluxing solutions in 1,2-dichloroethane.[357] As we shall see,

Pictiva EX2004
Samsung v Pictiva
IPR2024-01094

similar isomers are encountered when both isocyanides are the same (namely XylNC) but in this case the chemistry is even more complex.

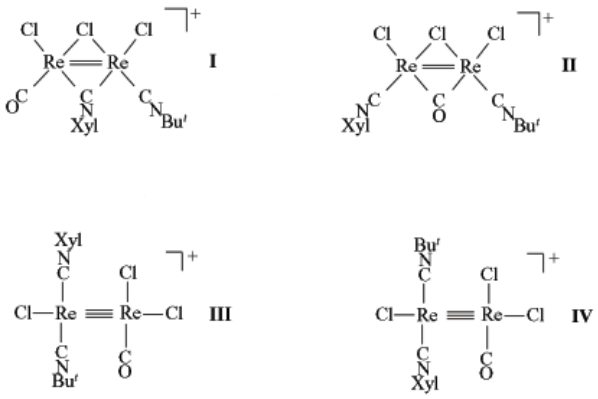


Fig. 8.29. Structural isomers of the dirhenium cation $[Re_2Cl_3(\mu\text{-dppm})_2(CO)(CNBu^t)(CNXyl)]^+$ with the bridging dppm ligand omitted for clarity.

The complex $[Re_2Cl_3(\mu\text{-dppm})_2(CO)(CNBu^t)_2]^+$ has so far been identified in only one isomeric form and this has an open bioctahedral structure like those for isomers **III** and **IV** in Fig. 8.29. The Re–Re bond distance is typical of a triple bond (see Table 8.7).[357,363] It is prepared by the reaction of $[Re_2Cl_3(\mu\text{-dppm})_2(CO)(CNBu^t)(NCMe)]PF_6$ with Bu^tNC and of $Re_2Cl_4(\mu\text{-dppm})_2(CO)(CNBu^t)$ (**8.49**) with Bu^tNC (1 equiv) and $TlPF_6$.[357,358] Because $Re_2Cl_4(\mu\text{-dppm})_2(CO)(CNXyl)$ exists as two stable isomers (structures **8.48** and **8.49**),[333,353] this leads to a quite extensive isomer chemistry in the case of the bis-XylNC cation $[Re_2Cl_3(\mu\text{-dppm})_2(CO)(CNXyl)_2]^+$ which is formed by reacting these isomers with XylNC in the presence of K^+ or Tl^+ salts although, as we shall see, other precursors and procedures can also be used. Three of the isomers have a very close structural relationship to those of $[Re_2Cl_3(\mu\text{-dppm})_2(CO)(CNBu^t)(CNXyl)]^+$ that are shown in Fig. 8.29. The isomers of $[Re_2Cl_3(\mu\text{-dppm})_2(CO)(CNXyl)_2]^+$, along with those of the bromo analog that have been identified, are shown in Fig. 8.30.[353,354,359,361,362,364-367] The formal Re–Re bond orders are also indicated for each of the structures, and it can be seen that these are 3, 2, 1 or 0. Isomers **V** (yellow) and **VI** (green) are formed as separable mixtures by reacting $Re_2Cl_4(\mu\text{-dppm})_2(CO)$ or $Re_2Cl_4(\mu\text{-dppm})_2(CO)(CNXyl)$ (**8.48**) with XylNC.[358,364] These reactions give the chloride salts which can be exchanged with $[PF_6]^-$, $[O_3SCF_3]^-$ or $[ReO_4]^-$.[358,364] Both isomers have a rich redox chemistry that consists of a one-electron oxidation and two one-electron reductions, the first reduction being very accessible ($E_{1/2}$ ca -0.1 V and *c.* -0.25 V vs. Ag/AgCl for **V** and **VI**, respectively).[358,364] In the case of **V**, reduction with cobaltocene has been used to prepare the neutral complex $Re_2Cl_3(\mu\text{-dppm})_2(CO)(CNXyl)_2$ which can be reoxidized by $[(\eta^5\text{-}C_5H_5)_2Fe]PF_6$ (with preservation of structure).[362] Crystal structure determinations on this one-electron reduction product of **V**,[362] and of a salt of **VI**,[364] have established the structures shown in Fig. 8.30 for these two isomers (see also Table 8.7). The neutral reduced complex $Re_2Cl_3(\mu\text{-dppm})_2(CO)(CNXyl)_2$ (isomer **V**) has a formal Re–Re bond order of 1.5. Isomer **V** converts irreversibly to **VI** when solutions in 1,2-dichloroethane are refluxed.[358,364]

The third isomer of $[Re_2Cl_3(\mu\text{-dppm})_2(CO)(CNXyl)_2]^+$ (labeled **VII** in Fig. 8.30) is prepared by the reaction of $Re_2Cl_4(\mu\text{-dppm})_2(CO)(CNXyl)$ (**8.49**) with XylNC in the presence of TlO_3SCF_3.[353] It is also formed when the acetonitrile complex $[Re_2Cl_3(\mu\text{-dppm})_2(CO)(CNXyl)(NCMe)]O_3SCF_3$, which has an open bioctahedral structure, is reacted with XylNC.[354] The

Pictiva EX2004
Samsung v Pictiva
IPR2024-01094

bromo analog is formed in low yield along with isomeric forms **IX** and **X**, by reacting $[Re_2Br_3(\mu\text{-dppm})_2(CO)(CNXyl)]Y$ ($Y = PF_6$ or O_3SCF_3) with XylNC (1 equiv).[359] A higher yield route involves the reaction of $[Re_2Br_3(\mu\text{-dppm})_2(CO)(CNXyl)(NCMe)]O_3SCF_3$ with XylNC.[361] Its crystal structure has been determined (Table 8.7). The thermal isomerization of **VII** to **VIII** occurs in essentially quantitative yield when solutions of **VII** (X = Cl or Br) in 1,2-dichloroethane (and other solvents) are heated at reflux.[361,365] The paramagnetic mixed-valence isomers **VIII** contain no Re–Re bond; for X = Cl, the Re–Re distance is 3.321(1) Å. The most likely mechanism for this isomerization is a "merry-go-round" process.[361,365]

Isomer **IX** (Fig 8.30), which is obtained only in the case of X = Br, is formed as the major product in the reactions of $[Re_2X_3(\mu\text{-dppm})_2(CO)(CNXyl)]Y$ ($Y = PF_6$ or O_3SCF_3) with XylNC and of $Re_2Br_4(\mu\text{-dppm})_2(CO)(CNBu^t)$ with XylNC and TlY.[359] This product is actually a mixture of isomers, both of which have the basic structure shown for **IX** in Fig. 8.30, but they differ in having either boat or chair conformations for the $Re_2(\mu\text{-dppm})_2$ unit.[366] These conformational isomers have been separated,[366] and both have been shown to have long Re–Re single bonds (3.03 - 3.05 Å).[359,366]

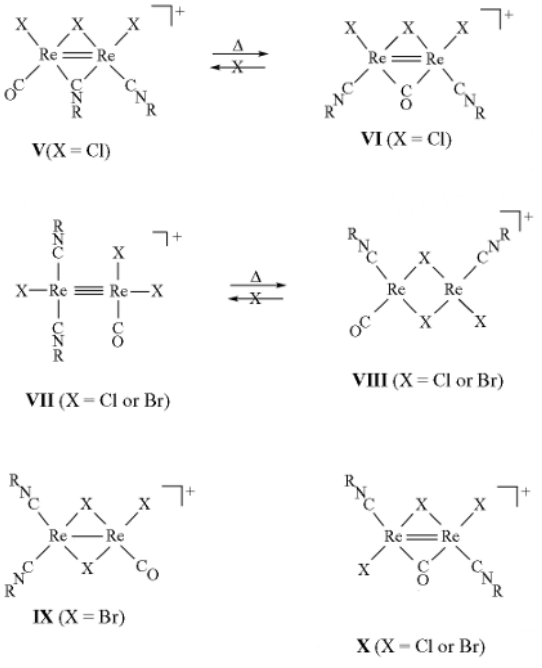


Fig. 8. 30. Structural isomers (**V**-**X**) of the dirhenium cations $[Re_2Cl_3(\mu\text{-dppm})_2(CO)(CNXyl)_2]^+$ that have been identified. All have been characterized by X-ray crystallography except **X** whose proposed structure is based upon its spectroscopic properties and chemical reactivity. The bridging dppm ligands are omitted for clarity.

The final isomer of $[Re_2X_3(\mu\text{-dppm})_2(CO)(CNXyl)_2]^+$ is **X**, which has been identified for both X = Cl and Br. It has been obtained in only very small amounts in the case of X = Br,[359] but is obtained in very high yield when $[Re_2Cl_3(\mu\text{-dppm})_2(CO)(CNXyl)]O_3SCF_3$ is reacted with 1 equiv of XylNC in dichloromethane. It has not yet been characterized by X-ray crystallography, so the structure given in Fig. 8.30 is tentative.[367] Interestingly, it reacts with a further equivalent of XylNC in the presence of TlO_3SCF_3 to form[367] one of several known isomers of $[Re_2Cl_2(\mu\text{-dppm})_2(CO)(CNXyl)_3]^+$, as we shall shortly discuss.

Pictiva EX2004
Samsung v Pictiva
IPR2024-01094

The only other system that gives complexes of composition $[Re_2X_3(\mu\text{-LL})_2(CO)(CNR)_2]Y$ is $[Re_2Cl_3(\mu\text{-dcpm})_2(CO)(CNBu^t)_2]Y$ (Y = Cl or O_3SCF_3), which can be isolated in two isomeric forms by the carbonylation of $Re_2Cl_4(\mu\text{-dcpm})_2(CNBu^t)_2$.[360] Both isomers have been characterized on the basis of electrochemical and spectroscopic measurements but in neither case is the structure known for certain.

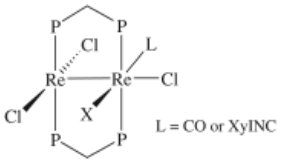
The reactions of $Re_2Cl_4(\mu\text{-dppm})_2(CO)$ (**8.38**), $Re_2Cl_4(\mu\text{-dppm})_2(CO)(CNXyl)$ (**8.49**) and $[Re_2Cl_3(\mu\text{-dppm})_2(CO)(CNXyl)_2]O_3SCF_3$ (isomer **VII** in Fig. 8.30) in dichloromethane with the requisite number of equivalents of TlO_3SCF_3 and XylNC that are necessary to give a compound of stoichiometry $[Re_2Cl_2(\mu\text{-dppm})_2(CO)(CNXyl)_3](O_3SCF_3)_2$, successfully produce such a product but in each case a different isomer is formed.[368] These isomers do not interconvert and each undergoes two reversible one-electron reductions when reacted with cobaltocene; for one of these isomers, the reduced products are similar structurally to the parent, while for the other two the first one-electron reduction is followed by isomerization to a different structure.[368(b)] These redox processes can be reversed chemically with the use of the oxidants $[(\eta^5\text{-}C_5H_5)_2Fe]PF_6$ or $NOPF_6$. In some cases the reduced products undergo further slow isomerization in solution to give additional isomers which, in turn, have their own reversible redox chemistry.[368(b)] In total, the $[Re_2Cl_2(\mu\text{-dppm})_2(CO)(CNXyl)_3]^{n+}$ species (n = 2, 1, or 0) have been found to exist in seven distinct forms which possess Re–Re bond orders of 3, 2, 1.5, 1 or 0.[368(b)] These bond orders depend on the specific bioctahedral structure that each species has and on its charge. In all cases, the crystallographic characterizations have shown that there is a large variation in the degree of Cl, CO and XylNC ligand bridging in the different complexes. The structural data for these complexes are not listed in Table 8.7; the original literature reference [368(b)] should be consulted for full details.

It has been possible to increase the number of π-acceptor ligands bound to the dirhenium core by reacting several of the fully reduced neutral compounds of the type $Re_2Cl_2(\mu\text{-dppm})_2(CNXyl)_3$ with 1 equiv each of XylNC and TlO_3SCF_3.[369] These reactions give the same symmetrical edge-shared bioctahedral complex $[Re_2(\mu\text{-Cl})(\mu\text{-CO})(\mu\text{-dppm})_2(CNXyl)_4]O_3SCF_3$ which has a Re–Re single bond. When acetonitrile is used in place of XylNC these reactions give rise to three different isomeric forms of $[Re_2Cl(\mu\text{-dppm})_2(CO)(CNXyl)_3(NCMe)]O_3SCF_3$.[369]

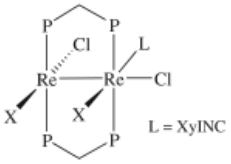
Another group of compounds are those that contain CO and/or RNC ligands in combination with anionic or neutral cyanide-containing ligands that have the potential to act as linkers to form polymetallic assemblies.[291,370,371] The reactions of $Re_2Cl_4(\mu\text{-dppm})_2(L)$ (L = CO or XylNC) (**8.38**), the edge-shared bioctahedral complexes $Re_2Cl_4(\mu\text{-dppm})_2(CO)(L)$ (L = CO or XylNC) and $Re_2Cl_4(\mu\text{-dppE})_2(CO)_2$ (**8.39** and **8.48**), and the open bioctahedral complex $Re_2Cl_4(\mu\text{-dppm})_2(CO)(CNXyl)$ (**8.49**) with $Na[N(CN)_2]$ and $K[C(CN)_3]$ in methanol result in the substitution of one Re–Cl bond except in the case of $Re_2Cl_4(\mu\text{-dppm})_2(CNXyl)$ for which a second bond can be substituted to form $Re_2Cl_2[N(CN)_2]_2(\mu\text{-dppm})_2(CNXyl)$ and $Re_2Cl_2[C(CN)_3]_2(\mu\text{-dppm})_2(CNXyl)$.[291,370] In all instances the $[N(CN)_2]^-$ and $[C(CN)_3]^-$ ligands coordinate through a single cyano group as shown by single crystal structure determination on representative complexes from each group (see Table 8.7).[291]

The structures of the complexes derived from $Re_2Cl_4(\mu\text{-dppm})_2(L)$ are shown in **8.52** and **8.53** (where X = $N(CN)_2$ or $C(CN)_3$) and are similar to that of $Re_2Cl_4(\mu\text{-dcpm})_2(CNXyl)$ (**8.42**). The compounds that are formed from $Re_2Cl_4(\mu\text{-dppm})_2(CO)(L)$ (L = CO or XylNC) and $Re_2Cl_4(\mu\text{-dppE})_2(CO)_2$ have structures that resemble those of the parent edge-shared bioctahedra (**8.39** in Fig. 8.26 and **8.48**) with substitution of the Re–Cl bond cis to the μ-CO ligand, while for the open bioctahedron $Re_2Cl_4(\mu\text{-dppm})_2(CO)(CNXyl)$(**8.49**) the Re–Cl bond that is trans to XylNC is replaced by $[N(CN)_2]^-$ or $[C(CN)_3]^-$.[291,370] These reactions resemble those in which these same precursors are reacted with RNC or RCN ligands in the presence of Tl^+ (vide supra).

Pictiva EX2004
Samsung v Pictiva
IPR2024-01094



8.52



8.53

The potential of using complexes that contain terminally bound $[N(CN)_2]$ and $[C(CN)_3]$ ligands to generate polymetallic assemblies has been demonstrated by the reactions of $Re_2Cl_3[N(CN)_2](\mu\text{-dppm})_2(CO)_2$ and $Re_2Cl_3[C(CN)_3](\mu\text{-dppm})_2(CO)_2$ with $Re_2Cl_4(\mu\text{-dppm})_2(CO)_2$; the resulting "dimer-of-dimers" complexes contain the $\{[Re_2Cl_3(\mu\text{-dppm})_2(CO)_2]_2(\mu\text{-L})\}^+$ cations, one of which (with L = $N(CN)_2$) has been characterized crystallographically (see Table 8.7).[370] Neutral species that contain coupled dirhenium units linked by $[Ni(CN)_4]$ have been prepared[370] by the reaction of the nitrile-containing, edge-shared bioctahedral complexes $[Re_2Cl_3(\mu\text{-LL})_2(CO)(L)(NCMe)]PF_6$ (LL = dppE when L = CO, and LL = dppm when L = CO or Xyl) with $(Bu^n_4N)_2Ni(CN)_4$:

$$2[Re_2Cl_3(\mu\text{-LL})_2(CO)(L)(NCMe)]PF_6 + (Bu^n_4N)_2Ni(CN)_4 \rightarrow [Re_2Cl_3(\mu\text{-LL})_2(CO)(L)(NCMe)]_2[\mu\text{-Ni}(CN)_4] + 2Bu^n_4NPF_6$$

The structure of one of these molecules, as present in a crystal of composition $[Re_2Cl_3(\mu\text{-dppE})_2(CO)_2]_2[\mu\text{-Ni}(CN)_4]\cdot 6CH_2Cl_2$, is given in Fig. 8.31. Electrochemical studies have established that electronic communication occurs between the dirhenium units and that this interaction is greatest in the case of the $[N(CN)_2]$ and $[C(CN)_3]$ bridged complexes.[370] Other mixed-metal cyano-bridged complexes have been obtained by the reactions of the edge-shared bioctahedron $Re_2Cl_4(\mu\text{-dppE})_2(CO)_2$ with $(Et_4N)[W(CO)_5CN]$, *trans*-$Pt(CN)_2(CNBu^t)_2$ and *trans*-$Rh[N(CN)_2](CO)(PPh_3)_2$ in the presence of $TlPF_6$ or TlO_3SCF_3.[291] The reaction of $Re_2Cl_4(\mu\text{-dppm})_2(CO)_2$ with $(Et_4N)[W(CO)_5CN]$ has also been reported.[291] The structures of the products are similar to one another; that of $Re_2Cl_3(\mu\text{-dppm})_2(CO)_2[(\mu\text{-NC})W(CO)_5]$ has been determined by X-ray crystallography (see Table 8.7).[291] An interesting case of so-called "spontaneous self-assembly" is encountered in the reaction of $Re_2Cl_4(\mu\text{-dppE})_2(CO)_2$ (**8.39**) with NaSCN and Pd(1,5-COD)Cl_2. The reaction proceeds via the intermediacy of $Re_2Cl_3(NCS)(\mu\text{-dppE})_2(CO)_2$ to give the complex $[Re_2Cl_3(\mu\text{-dppE})_2(CO)_2(\mu\text{-NCS})]_2Pd_2(\mu\text{-SCN})(\mu\text{-NCS})Cl_2$, in which the neutral Re_4Pd_2 unit can be considered to arise from the combination of two $[Re_2Cl_3(\mu\text{-dppE})_2(CO)_2]^+$ cations and a centrosymmetric $[Pd_2(\mu\text{-SCN})(\mu\text{-NCS})Cl_2(SCN)_2]^{2-}$ anion.[291,371] The X-ray crystal structure of this compound was determined (see Table 8.7).[291,371]

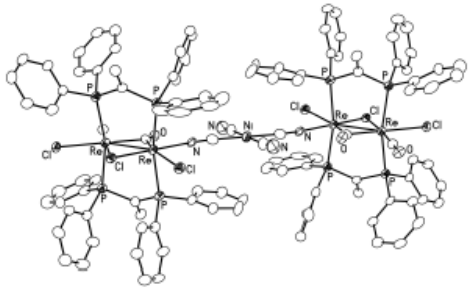
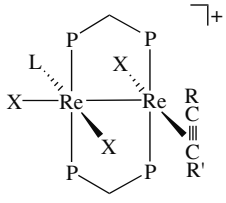


Fig. 8.31. The structure of the Re_4Ni complex $\{[Re_2Cl_3(\mu\text{-dppE})_2(CO)_2]_2(\mu\text{-Ni}(CN)_4\}$.

Pictiva EX2004
Samsung v Pictiva
IPR2024-01094

The reactions of acetylene with $Re_2X_4(\mu\text{-dppm})_2$ (X = Cl or Br) give dirhenium complexes that contain η^2 and/or $\mu{:}\eta^2,\eta^2$ bound ethyne molecules (see Fig. 8.27). When the compounds $Re_2X_4(\mu\text{-dppm})_2(L)$ (L = CO or CNR) and $Re_2Cl_4(\mu\text{-dppm})_2(CO)(L)$ (L = CO (**8.39**) or CNXyl (**8.48**)) are reacted with alkynes the chemistry becomes more complicated. The Re–Re triple bond is retained in the adducts of the type $[Re_2X_3(\mu\text{-dppm})_2(L)(\eta^2\text{-RCCR}')]Y$ that are formed in the reactions of RCCR' with $Re_2X_4(\mu\text{-dppm})_2(CO)$ and $Re_2X_4(\mu\text{-dppm})_2(CNR)$ (R = Bu^t or Xyl) in the presence of $TlPF_6$ or TlO_3SCF_3.[372,373] With the monocarbonyl complex, both internal and terminal alkynes were used[372] while the mono-isocyanide complexes were reacted with terminal alkynes only.[373] The ethyne complexes $[Re_2X_3(\mu\text{-dppm})_2(CO)(\eta^2\text{-HCCH})]PF_6$ have also been prepared by the treatment of the mixed CO/nitrile compound $[Re_2X_3(\mu\text{-dppm})_2(CO)(NCR)_2]PF_6$ with acetylene.[355] The structural similarities of these 1:1 alkyne adducts was shown by infrared and NMR spectroscopy, by cyclic voltammetric measurements, and by representative X-ray structures on crystals of composition $[Re_2Cl_3(\mu\text{-dppm})_2(CO)(\eta^2\text{-MeCCEt})]PF_6$[372] and $[Re_2Cl_3(\mu\text{-dppm})_2(CNBu^t)(\eta^2\text{-HCCH})]O_3SCF_3{\cdot}CH_3C(O)OC_2H_5$.[373] The Re–Re distances are 2.3407(4) Å and 2.3171(5) Å, respectively, and the structures of the cations involve different coordination numbers for the two Re centers (i.e. $[(L)X_2Re(\mu\text{-dppm})_2ReX(\eta^2\text{-RCCR}')]^+$) and an anti arrangement of the L and η^2-RCCR' ligands (see **8.54**). NMR spectroscopy has shown that these complexes are sterochemically rigid at room temperature.[372,373]

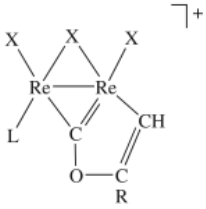


8.54

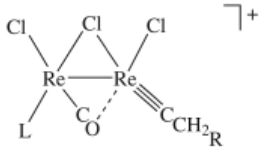
When the η^2-alkyne adducts $[Re_2Cl_3(\mu\text{-dppm})_2(CO)(\eta^2\text{-RCCH})]Y$ (R = H, Pr^n, Bu^n or Ph; Y = PF_6 or O_3SCF_3) are reacted with tertiary phosphines PR_3 (R_3 = Me_3, Et_3, Me_2Ph or $MePh_2$) resonance stabilized ylides are formed that are of composition $[Re_2Cl_3(\mu\text{-dppm})_2(CO)\{C(R)CH(PR_3)\}]Y$.[374] A Re–Re triple bond is retained as shown by an X-ray structure determination of a crystal of composition $[Re_2Cl_3(\mu\text{-dppm})_2(CO)\{C(Pr^n)CH(PMe_2Ph)\}]O_3SCF_3{\cdot}0.87C_7H_8$ (Re–Re distance 2.311(1) Å).[374] The structure resembles that of **8.54** except that the η^2-RCCH ligand is converted to the η^1-bound ylide $C(R)CH(PR_3)$.

When the edge-shared bioctahedral complexes $Re_2X_4(\mu\text{-dppm})(CO)(L)$ (X = Cl or Br; L = CO or XylNC) (**8.39** and **8.48**) react with terminal alkynes RCCH (R = H, Pr^n, Bu^n, Ph or p-tol) at room temperature in the presence of $TlPF_6$ they convert to the diamagnetic complexes $[Re_2(\mu\text{-X})(\mu\text{-COC(R)CH})X_2(L)(\mu\text{-dppm})_2]PF_6$ (structure **8.55**; μ-dppm ligands omitted for clarity), in which the reductive coupling of the μ-CO ligand and the alkyne leads to a 3-metallafuran ring.[375] These reactions, which are regiospecific, proceed through reaction intermediates of the type $[Re_2X_3(\mu\text{-dppm})_2(CO)(L)(\eta^2\text{-RCCH})]^+$.[375] Structure determinations have shown that the Re–Re distances are in the range 2.55-2.57 Å, but the assignment of bond order is not clear-cut.[375] Under certain conditions the 3-metallafuran ring can undergo ring opening to afford paramagnetic mixed-valence dirhenium alkylidyne complexes of the type represented by **8.56**.[376] These reactions have been carried out only in the case of X = Cl, and the resulting complexes (one unpaired electron) can be reduced by cobaltocene to their neutral diamagnetic congeners, which probably do not contain a Re–Re bond.[376(b)]

Pictiva EX2004
Samsung v Pictiva
IPR2024-01094



8.55



8.56

A few examples of mixed CO/PR_3 (or $P(OR)_3$) and $CO/RNC/PR_3$ (or $P(OR)_3$) complexes are also known. These are prepared from $Re_2Cl_4(\mu\text{-dppm})_2(CO)$,[377] $Re_2Cl_4(\mu\text{-dppm})(CO)_2$[378] and $Re_2Cl_4(\mu\text{-dppm})_2(CO)(CNR)$ (R = Bu^t or Xyl),[378] and structures that have been determined by X-ray crystallography are listed in Table 8.7. The structures of $[Re_2X_3(\mu\text{-dppm})_2(CO)(PMe_3)_2]Y$ (X = Cl or Br; Y = Cl, PF_6 or BPh_4) and $[Re_2Cl_3(\mu\text{-dppm})_2(CO)\{P(OR)_3\}_2]PF_6$ (R = Me or Et) have been established by a single crystal X-ray structure analysis of a salt of $[Re_2Cl_3(\mu\text{-dppm})_2(CO)(PMe_3)_2]^+$ (Table 8.7).[377] The yellow-green diamagnetic complexes $[Re_2X_3(\mu\text{-dppm})_2(CO)_2(PMe_3)]PF_6$ and $[Re_2X_3(\mu\text{-dppm})_2(CO)_2\{P(OR)_3\}]PF_6$ (R = Me or Et), and the dark blue, paramagnetic, one-electron reduced neutral complex $Re_2Cl_3(\mu\text{-dppm})_2(CO)_2(PMe_3)$ have been prepared.[378] Single crystal X-ray structure analyses (Table 8.7) have shown that $[Re_2Cl_3(\mu\text{-dppm})_2(CO)_2(PMe_3)]PF_6$ and $[Re_2Cl_3(\mu\text{-dppm})_2(CO)_2\{P(OEt)_3\}]PF_6$ have an all-cis structure like **8.50** with unsymmetrical carbonyl bridges.[378] The reactions of $Re_2Cl_4(\mu\text{-dppm})_2(CO)(CNR)$ (R = Bu^t or Xyl) with PMe_3 and $TlPF_6$ yield $[Re_2Cl_3(\mu\text{-dppm})_2(CO)(CNR)(PMe_3)]PF_6$ in which the structure of the neutral precursor is retained, i.e., when R = Bu^t the structure is similar to isomer **IV** in Fig. 8.29, with PMe_3 in place of XylNC, while for R = Xyl the structure resembles **8.50** (Fig. 8.28), with PMe_3 in place of the terminal CO.[378]

A few complexes that are derived from $Re_2X_4(\mu\text{-dppm})_2$ (X = Cl or Br) and contain CS ligands have been prepared by their reaction with carbon disulfide.[379] A similar reaction occurs with $Re_2Br_4(\mu\text{-dpam})_2$.[379] These oxidative addition reactions afford the edge-shared bioctahedral dirhenium(III) complexes $Re_2(\mu\text{-S})(\mu\text{-X})X_3(\mu\text{-dppm})(CS)$, which can be derivatized by reaction with organic nitriles, isocyanides, and CO in the presence of $TlPF_6$ to give $[Re_2(\mu\text{-S})(\mu\text{-X})X_2(\mu\text{-dppm})_2(CS)(L)]PF_6$.[379,380] The crystal structure of the complex with X = Br and L = EtCN shows a long Re–Re distance (2.949(1) Å) that implies the presence of a surprisingly weak metal-metal bond.[379] The complexes of the types $Re_2(\mu\text{-S})(\mu\text{-X})X_3(\mu\text{-LL})_2(CS)$ and $[Re_2(\mu\text{-S})(\mu\text{-X})X_2(\mu\text{-dppm})(CS)(L)]PF_6$ are converted to the analogous $\mu\text{-}SO_2$ complexes when reacted with $NOPF_6$ in the presence of O_2.[380,381] These oxygenation reactions are catalytic in $NOPF_6$. The $\mu\text{-}SO_2$ complexes possess two reversible one-electron reductions both of which can be accessed in some cases with the use of cobaltocene as the reductant.[380,381] When $Re_2Cl_4(\mu\text{-dppm})_2$ is treated with SO_2 in tetrahydrofuran, a major product is the paramagnetic complex $Re_2(\mu\text{-Cl})(\mu\text{-}SO_2)Cl_4(\mu\text{-dppm})_2$, which has a Re–Re bond distance of 2.6289(3) Å.[382] The mechanism of the reaction that leads to this product is clearly quite complicated since it involves oxidation of the Re_2^{4+} core and the incorporation of an additional Cl^- ligand, presumably through the sacrifice of some of the $Re_2Cl_4(\mu\text{-dppm})_2$ starting material.

8.5.5 Other Re_2^{5+} and Re_2^{4+} complexes

A few additional examples of authentic triply bonded Re_2^{4+} complexes are known of which the homoleptic allyl complex $Re_2(C_3H_5)_4$ is one of the most thoroughly characterized. Rhenium(V) chloride is reacted with allylmagnesium chloride in diethyl ether to give a yellow-brown solution from which orange crystals of $Re_2(C_3H_5)_4$ may be isolated.[383] The crystal

Pictiva EX2004
Samsung v Pictiva
IPR2024-01094

structure of this complex showed[384] that an important difference exists from that of the isostructural pair $Cr_2(C_3H_5)_4$ and $Mo_2(C_3H_5)_4$. Unlike the latter complexes, which possess terminal and symmetrically bridging allyl groups, $Re_2(C_3H_5)_4$ has four chemically equivalent terminal $Re(\eta^3\text{-}C_3H_5)$ bonds (D_{2d} symmetry). The Re–Re distance of 2.225(7) Å is consistent with those of other Re_2^{4+} derivatives (Table 8.4). The He I photoelectron spectrum of $Re_2(C_3H_5)_4$ has been recorded; the data confirm the prediction from relativistic SCF-X_α-SW calculations that this complex has a $\sigma^2\pi^4\delta^2\delta^{*2}$ configuration, but with a substantial amount of Re-to-allyl π back donation occurring primarily via interaction of the filled Re δ and δ^* orbitals with the allyl π^* levels.[385]

The novel $[Re_2(NCCH_3)_{10}]^{4+}$ cation has been isolated as its BF_4^- salt, following protonation of $[Re_2Cl_8]^{2-}$ or $Re_2Cl_4(PPr^n_3)_4$ with $HBF_4{\cdot}Et_2O$ in CH_3CN/CH_2Cl_2, and its $[Mo_6O_{19}]^{2-}$ salt has been structurally characterized.[292,386] The Re–Re bond length in this dirhenium(II) complex is 2.259(4) Å and the two halves of the cation are almost perfectly staggered with respect to one another (χ_{av} = 44.5°). The kinetics of exchange of the eight equatorial acetonitrile ligands has been determined in CD_3CN by ^1H NMR spectroscopy.[387]

The vacuum pyrolyses of the rhenium(II) porphyrin complexes $Re(Por)(PEt_3)_2$, where Por is the dianion of octaethylporphyrin (OEP) or tetra(*p*-tolyl)porphyrin, produce the triply bonded complexes $Re_2(Por)_2$.[388,389] Like their halide-phosphine analogs of the type $Re_2X_4(PR_3)_4$, they can be oxidized in two one-electron steps to give the corresponding Re_2^{5+} and Re_2^{6+} derivatives. Thus, the treatment of $Re_2(OEP)_2$ with $[(\eta^5\text{-}C_5H_5)_2Fe]BF_4$ in acetonitrile and $AgBF_4$ in toluene affords $[Re_2(OEP)_2]BF_4$ and $[Re_2(OEP)_2](BF_4)_2$, respectively.[388] Both of these oxidations are believed to be metal-centered, the first giving rise to the expected paramagnetic ground state.[388] The resonance Raman and infrared spectra of the $[Re_2(OEP)_2]^{n+}$ species (n = 0–2) have been measured. In the case of $[Re_2(OEP)_2]^+$, exitation at 514.5 nm gives a weak Raman peak at 290 cm^{-1} that has been assigned to ν(Re–Re); a Re–Re bond distance of 2.20 Å has been estimated from this stretching frequency.[390] The synthesis of the porphyrin complex $Re_2(AHEDMP)_2$, where $H_2AHEDMP$ is 5-(4-methoxyphenyl)-2,3,7,8,13,17-hexaethyl-12,18-dimethylporphyrin,[391] as well as the phthalocyaninato complex $Re_2(pc)_2$,[392] are similar to those reported for $Re_2(Por)_2$. The compound $Re_2(pc)_2$ has an eclipsed rotational geometry, a Re–Re distance of 2.285(2) Å, and a Raman-active ν(Re–Re) mode at 240 cm^{-1}.[392]

The reduction of quadruply bonded complex $Re_2(DTolF)_4Cl_2$ (Section 8.4.3) by Na/Hg gives the complexes $Re_2(DTolF)_4Cl$ and $Re_2(DTolF)_4$.[161] Dark purple crystals of composition $Re_2(DTolF)_4{\cdot}C_6H_6$ have been characterized by X-ray crystallography; the Re–Re distance is 2.344(2) Å.[161] This complex may have the novel triple bond configuration $\sigma^2\pi^4\delta^2\pi^{*2}$ based upon the results of SCF-Xα calculations.[161]

8.5.6 Other dirhenium compounds with triple bonds

In addition to the chloride phase β-$ReCl_4$ and the nonahalo species $[Re_2(\mu\text{-}X)_3X_6]^-$ (see Section 8.5.3), all of which contain bridging halide ligands, a few compounds of Re_2^{8+} are known in which bridging ligands are not present and the Re–Re bonding can be considered in terms of the electron-poor $\sigma^2\pi^4$ ground state configuration.

Rhenium tetrafluoride is believed to exist as Re_2F_8 molecules in the vapor phase with an eclipsed D_{4h} conformation and a Re≡Re bond.[393] There are several structurally characterized ternary oxides containing a lanthanide metal together with rhenium, with the latter in an oxidation state of +4 to +5. In two cases,[394,395] there are Re(IV) ions present in Re_2O_8 units having D_{4h} symmetry and Re–Re distances consistent with the presence of triple bonds between the rhenium atoms. In $La_4Re_2O_{10}$,[394] the overall structure can be thought of as distorted fluorite structure, with each La^{3+} and each Re_2^{8+} ion occupying a distorted cube of eight oxide ions.

Pictiva EX2004
Samsung v Pictiva
IPR2024-01094

The Re_2^{8+} unit elongates its "cube" into a square parallelepiped, with four long edges (3.10 Å) parallel to the Re–Re bond and eight others that are much shorter (2.64 Å). The Re–Re distance is 2.259(1) Å, the Re–O distances are 1.915(3) Å and the Re–Re–O angles are 102.7(1)°. In $La_6Re_4O_{18}$[395] the rhenium atoms are two kinds. Half of them are Re(V) and are present in Re_2O_{10} units consisting of octahedra sharing an edge with a Re–Re double bond (2.456(5) Å), while the others are present as Re(IV) in Re_2O_8 units with virtual D_{4h} symmetry and the Re–Re distance is 2.235(6) Å. The mean Re–O distance is 1.914(16) Å. Other examples of phases with edge-shared bioctahedral Re_2O_{10} units are known, including some that are formally Re_2^{9+}.[396]

The compound $[(Bu^t{}_3SiO)_2ReO]_2$, which possesses a $[O_3ReReO_3]$ core, is prepared by treating *cis*-$ReOCl_3(PEt_3)_2$ with $TlOSiBu^t{}_3$. It has a structure with terminal Re=O bonds and a Re–Re bond distance of 2.3593(6) Å.[397] The Re–Re bond is comprised of the usual σ- and π-bonding orbitals.

8.6 Dirhenium Compounds with Bonds of Order Less than 3

Multiply bonded dirhenium complexes that contain Re–Re bond orders between three and one are comparatively rare. In the preceding sections, we have considered several compounds that contain double bonds, as in the case of the edge-shared bioctahedral compounds $Re_2(\mu\text{-}Cl)_2Cl_4(\mu\text{-}LL)_2$ where, for example, LL = dppm, dmpm or dppa (see Sections 8.4.4 and 8.5.4).[203,205] These compounds are relevant to the theme of this text since they are derived from other multiply bonded dirhenium complexes. A variety of dirhenium(IV,III), dirhenium (IV,IV) and dirhenium(V,V) complexes are known that contain $[Re_2(\mu\text{-}O)_2]$ bridging units and short Re–Re distances, but since these complexes are not prepared from discrete multiply bonded dirhenium compounds, they will not be considered in any detail. Examples include the dirhenium(IV,IV) complex $K_4[Re_2(\mu\text{-}O)_2(C_2O_4)_4]\cdot 3H_2O$,[398,399] and bis(μ-oxo) complexes of dirhenium(IV,IV) and dirhenium(IV,III) that contain 1,4,7-triazacyclononane,[400] and tris(2-pyridylmethyl)amine and its (6-methyl-2-pyridyl)methyl derivatives.[401,402] The Re–Re distances in this selection of complexes span the narrow range 2.36-2.43 Å. Also of note is the homoleptic alkoxide complex $Re_2(\mu\text{-}OMe)_2(OMe)_8$, in which the Re–Re distance of 2.5319(7) Å can be viewed[403] as a double bond. It is prepared by the unusual procedure of reacting ReF_6 with $Si(OMe)_4$ at low temperature.[403] There are also some ternary rhenium oxide phases where a case can be made for Re–Re double bonds.[394,404]

A good candidate for a species containing a bond of order 2.5 has been encountered in the case of β-$[Re_2Cl_4(dppe)_2]^-$ (dppe = $Ph_2PCH_2CH_2PPh_2$); this anion is very unstable and has only been generated electrochemically.[282] The one-electron oxidation and one-electron reduction of $Re_2Cl_6(\mu\text{-}dppm)_2$, which can be accomplished using $NOPF_6$ and cobaltocene, give paramagnetic ions that possess metal-metal bond orders of 1.5 characterized by the ground state configurations $\sigma^2\pi^2\delta^{*2}\delta^1$ and $\sigma^2\pi^2\delta^{*2}\delta^2\pi^{*1}$, respectively (Section 8.4.4).[206]

There are also several organometallic dirhenium complexes in which the presence of a Re–Re double bond has been proposed on structural grounds and/or adherence to an 18-electron count (see Section 8.8 for further details).

8.7 Cleavage of Re–Re Multiple Bonds by σ-donor and π-acceptor Ligands

There are a variety of reactions in which dinuclear complexes with Re–Re quadruple or triple bonds are cleaved by σ-donor or π-acceptor ligands to give mononuclear species or ligand-bridged dirhenium complexes in which there is no Re–Re bond. These can be the major reaction products or reaction intermediates, or minor products that accompany the formation of products in which a metal-metal bonded dimetal unit is retained. Since many of these reactions have been mentioned in previous sections they will not be dealt with in great detail

Pictiva EX2004
Samsung v Pictiva
IPR2024-01094

here. A few representative cases will be cited. In some instances, especially with π-acceptor ligands, these reactions have proved to be excellent methods for preparing certain classes of mononuclear complexes.[405]

8.7.1 σ-Donor ligands

Although the most extensive series of reactions are those involving phosphines (vide infra), others of note include the reactions of $(Bu_4N)_2Re_2X_8$ (X = Cl or Br) with thiourea in acetone or acidified methanol to give $ReX_3(tu)_3$.[97] These reactions are unusual because the related tetramethylthiourea ligand affords the quadruply bonded compounds $Re_2X_6(tmtu)_2$. An interesting product is formed from the reaction of $(Bu_4N)_2Re_2Cl_8$ with Li_2S_3 in THF. The mononuclear complex is of stoichiometry $(Bu_4N)ReS_9$, the tetragonal pyramidal $[ReS_9]^-$ anion containing two chelating S_4^{2-} chains and a Re=S unit.[406] An example of a reaction that leads to cleavage of the Re–Re bond of $Re_2(\mu\text{-}O_2CCH_3)_4Cl_2$ occurs when this compound is warmed with an acetone solution of sodium diethyldithiocarbamate. The resulting orange-brown crystals were identified as $Re_2(\mu\text{-}O)(O)_2(S_2CNEt_2)_4$.[407] Another interesting and related case of Re–Re bond cleavage, in this instance involving the Re≡Re bond, occurs in the reaction between $Re_2X_4(\mu\text{-dppm})_2$ (X = Cl or Br) and dioxygen.[308] The initial product is the edge-shared bioctahedral complex $Re_2(\mu\text{-}O)(\mu\text{-}X)(O)X_3(\mu\text{-dppm})_2$ in which a Re–Re bond is absent and the bridging dppm ligands help stabilize a "dirhenium(IV)" complex. Further reaction with O_2 then forms $Re_2(\mu\text{-}O)(O)_2Cl_4(\mu\text{-dppm})_2$ in which a linear O=Re–O–Re=O unit is present and the dppm ligands still bridge the two Re(V) centers.[308]

While the reaction between $(Bu_4N)_2Re_2Cl_8$ and NaSCN in methanol produces quadruply bonded $(Bu_4N)_2Re_2(NCS)_8$, the use of acetone as the reaction solvent produces solutions from which $(Bu_4N)_2[Re(NCS)_6]$ and $(Bu_4N)_3[Re_2(\mu\text{-}NCS)_2(NCS)_8]$ can be isolated (see Section 8.4.1). Clearly the solvent plays an important role in the course of this reaction. Another case of solvent participation involving cleavage of the Re–Re quadruple bond is that induced by ultraviolet irradiation of acetonitrile solutions of $(Bu_4N)_2Re_2Cl_8$.[408] Two monomeric rhenium(III) products, tan-colored $(Bu_4N)[ReCl_4(NCMe)_2]$ and orange $ReCl_3(NCMe)_3$, have been isolated from a preparative scale photolysis.[408] Cleavage occurs upon irradiation at 366 nm (or higher energies) but not at energies comparable to the $\delta\rightarrow\delta^*$ transition energy of $[Re_2Cl_8]^{2-}$. This implies that reaction occurs via one of the excited states higher than that derived from the $\delta\rightarrow\delta^*$ transition.

Cleavage by phosphine donors constitutes the most thoroughly investigated systems of this kind. One of the best characterized of these systems is that involving the reaction of $(Bu_4N)_2Re_2Cl_8$ with $Ph_2PCH_2CH_2PPh_2$ in acetonitrile which gives the paramagnetic, centrosymmetric dimer $Re_2(\mu\text{-}Cl)_2Cl_4(dppe)_2$.[22,200,209] This type of complex has more recently been isolated in reactions of $(Bu_4N)_2Re_2X_8$ with monodentate phosphines, examples being $Re_2(\mu\text{-}X)_2X_4(PMe_3)_4$, where X = Cl or I.[179,184,261] This type of compound can in turn react further to give mononuclear Re(III) or Re(IV) complexes and/or multiply bonded $Re_2X_5(PR_3)_3$ or $Re_2X_4(PR_3)_4$ complexes, often by diproportionation mechanisms (see Sections 8.4.4 and 8.5.4 for further details). A fairly common product from the reaction between $(Bu_4N)_2Re_2Cl_8$ and a *bidentate* phosphine is a mononuclear complex of the type *trans*-$[ReX_2(PP)_2]X$, although reaction conditions (solvent, temperature, proportions of reagents) are usually important in dictating the reaction course. Examples of this non-redox cleavage have been encountered when PP = dppe,[22,276] *cis*-$Ph_2PCH{=}CHPPh_2$,[199,275] $Et_2PCH_2CH_2PEt_2$,[40] $(p\text{-}MeC_6H_4)_2PCH_2CH_2P(C_6H_4Me\text{-}p)_2$,[40] and 1,2-bis(diphenylphosphino)benzene.[280] In one such study, the compound $[trans\text{-}ReCl_2(depe)_2]_2Re_2Cl_8$ was isolated and structurally characterized.[40] In a few instances, mononuclear rhenium(II) compounds have been isolated and structurally characterized; examples are *trans*-$ReCl_2(dppe)_2$,[276] *trans*-$ReCl_2(dppee)_2$,[199] *trans*-$ReCl_2(dppbe)_2$,[280] *trans*-$ReCl_2[\eta^2\text{-}HC(PPh_2)_3]$[299] and *trans*-$ReCl_2(2,2\text{-dppp})_2$.[286] Other in-

Pictiva EX2004
Samsung v Pictiva
IPR2024-01094

teresting examples of dirhenium products in which a Re–Re bond is absent are the confacial, bioctahedral dirhenium(II) complexes $[Re_2(\mu\text{-}X)_3(triphos)_2]Y$, where Y = Cl, Br, O_3SCF_3 or BPh_4. These are formed by reacting *cis*-$Re_2(\mu\text{-}O_2CCH_3)_2X_4L_2$ (X = Cl or Br; L = py or H_2O) with $CH_3C(CH_2PPh_2)_3$ in refluxing ethanol.[409]

8.7.2 π-Acceptor ligands

Without the constraints imposed on the dimetal unit by intramolecular bridging ligands such as $Ph_2PCH_2PPh_2$ (see Section 8.5.4), quadruply and triply bonded dirhenium complexes are readily cleaved by π-acceptors such as carbon monoxide and alkyl and aryl isocyanides. Thus, the reactions between carbon monoxide and $Re_2X_4(PR_3)_4$, where X = Cl or Br and R = Et or Pr^n, in refluxing ethanol, toluene or acetonitrile afford 17-electron *trans*-$ReX_2(CO)_2(PR_3)_2$ as major products.[252,410,411] These reactions are quite complicated since complexes of the types $Re_2Cl_5(PR_3)_3$, $Re_2Cl_6(PR_3)_2$, $ReX(CO)_3(PR_3)_2$, $ReX(CO)_4(PR_3)$ and *trans*-$ReCl_4(PR_3)_2$ are also formed; disproportionation mechanisms may be involved. A comparative study has been made of the carbonylation of the series of complexes $Re_2Cl_4(PMe_2Ph)_4$, $[Re_2Cl_4(PMe_2Ph)_4]PF_6$ and $[Re_2Cl_4(PMe_2Ph)_4](PF_6)_2$; the major reaction products are $ReCl(CO)_3(PMe_2Ph)_2$, $ReCl(CO)_2(PMe_2Ph)_3$ and/or $ReCl_3(CO)(PMePh)_3$.[412] The reaction of $(Bu_4N)_2Re_2Cl_8$ in acetonitrile with CO at 100 atm. and ≈90 °C gives $ReCl(CO)_5$ as the major product and the ionic compound $[cis\text{-}Re(CO)_2(NCMe)_4]_2ReCl_6$ as a minor one.[413]

In the case of the alkyl isocyanide ligands RNC, salts of the stable homoleptic cations $[Re(CNR)_6]^+$ (R = Bu^t or cyclohexyl) can be obtained in good yield from $Re_2(\mu\text{-}O_2CR)_4Cl_2$ (R = CH_3 or C_6H_5).[414] When the triply bonded complexes $Re_2Cl_4(PR_3)_4$ (R = Et or Pr^n) are treated with these same isocyanides, a similar reaction course ensues to give the cationic species $[Re(CNR)_4(PR_3)_2]^+$ which can be isolated as their PF_6^- salts.[414] In contrast to these results, the comparatively halide-rich phases $(Bu_4N)_2Re_2X_8$ (X = Cl or Br) and $Re_2Cl_6(PEtPh_2)_2$ give the mononuclear rhenium(III) complexes $[Re(CNR)_5X_2]PF_6$ (X = Cl or Br) and $[Re(CNR)_4(PEtPh_2)Cl_2]PF_6$, respectively.[414] A similar complex with Me_3SiCH_2NC has been obtained from $Re_2(\mu\text{-}O_2CCH_3)_4Cl_2$.[415] Related behavior has been encountered in the reactions of aryl isocyanides ArNC (Ar = phenyl, *p*-tolyl, 2,6-dimethylphenyl, 2,4,6-trimethylphenyl and 2,4,6-tri-*tert*-butylphenyl) with the complexes $Re_2(\mu\text{-}O_2CCH_3)_4Cl_2$ and $(Bu_4N)_2Re_2Cl_8$.[220,416] In refluxing methanol, these reactions usually provide an excellent high yield synthetic route to $[Re(CNAr)_6]PF_6$.[220] When the reactions between ArNC and $(Bu_4N)_2Re_2Cl_8$ are conducted at room temperature, then Re(III)-containing intermediates of the types $[Re(CNAr)_6]_2Re_2Cl_8$, $[Re(CNAr)_6][ReCl_4(CNAr)_2]$, and $ReCl_3(CNAr)_3$ can be isolated.[220] In the case of the 2,4,6-tri-*tert*-butylphenylisocyanide ligand, the pentakis(isocyanide) derivatives $Re(CNR)_5X$ (X = Cl or Br) have been obtained.[416] While the aforementioned reactions lead eventually to stable mononuclear rhenium(I) complexes, one exception is the green rhenium(IV) complex $Bu_4N[ReCl_5(CNMe)]$; this has been obtained as a major reaction product from the treatment of $(Bu_4N)_2Re_2Cl_8$ with MeNC.[417]

While these cleavage reactions have been of considerable synthetic value, little in the way of mechanistic information is available.

8.8 Other Types of Multiply Bonded Dirhenium Compounds

There are several kinds of organometallic and hydrido dirhenium complexes in which a case can be made for the presence of multiple Re–Re bonds, but which do not possess electronic structures that bear a simple and straightforward relationship to the $\sigma^2\pi^4\delta^2\delta^{*n}$ (n = 0, 1 or 2) configurations that are present in the complexes that are the principal focus of this chapter. In accord with the theme of this text most of these compounds will not be discussed, since they

Pictiva EX2004
Samsung v Pictiva
IPR2024-01094

do not have multiply bonded $L_4M–ML_4$ or $L_5M–ML_5$ structures and they cannot be prepared from or be converted to such species. These compounds often contain CO or cyclopentadienyl ligands and most, but not all, contain ligand bridges. Multiple bonding in these instances can often be inferred by assuming an 18-electron count for the metal centers. Examples include compounds such as $(\eta^5\text{-}C_5Me_5)_2Re_2(\mu\text{-}CO)_3$,[418] $(\eta^5\text{-}C_5Me_5)_2Re_2(\mu\text{-}Cl)_2Cl_2$[419] and $Re_2(\mu\text{-}CSiMe_3)_2(CH_2SiMe_3)_4$.[420] However, there are two exceptions that will be mentioned briefly. One of these is $(\eta^5\text{-}C_5Me_5)_2Re_2(CO)_4$,[421] a compound with a very extensive reaction chemistry,[422] which has a structure with two semi-bridging CO ligands and a Re–Re distance of 2.723(1) Å. The other exception is $Re_2(\equiv CCMe_3)_2(OR)_4$ in which the Re–Re bond lengths of 2.3836(8) Å (R = $OCMe(CF_3)_2$) and 2.396(1) Å (R = Bu^t) accord with the presence of unsupported Re=Re bonds.[423] The reason these compounds are highlighted is that Fenske-Hall MO calculations on the model species $[CpRe(CO)_2]_2$ and $[HCRe(OH)_2]_2$ are consistent with both having Re–Re double bonds, corresponding to $\sigma^2\pi^4\delta^2\ \delta^{*2}\pi^{*2}$ and $\sigma^2\pi^2$ metal-based bonding configurations, respectively.[424]

One other group of complexes that merits brief mention are dirhenium complexes that contain mixed hydride-phosphine ligand sets since their chemistry is closely connected to that of compounds of Re_2^{6+} and Re_2^{4+}. When the triply bonded mixed chloride-phosphine complexes $Re_2Cl_4(PR_3)_4$ (PR_3 = PMe_3, PEt_3, PPr^n_3, PMe_2Ph, PEt_2Ph, $PMePh_2$, $^1/_2$dppm or $^1/_2$dppe) are reacted with $LiAlH_4$ in glyme (or THF), the corresponding dirhenium octahydrides $Re_2H_8(PR_3)_4$ can be isolated following hydrolysis and work-up of the reaction mixtures.[264] In related reactions, the complexes $Re_2H_8(PPh_3)_4$ and $Re_2H_8(AsPh_3)_4$ have been prepared by treating the quadruply bonded compound $Re_2Cl_6(PPh_3)_2$ with $NaBH_4$ in the presence of added PPh_3,[425,426] and mixtures of $(Bu_4N)_2Re_2Cl_8$ and excess PPh_3 and $AsPh_3$ with $NaBH_4$.[246,427] The triphenylstibine derivative $Re_2H_8(SbPh_3)_4$ can be prepared from $(Bu_4N)_2Re_2Cl_8$, but this method leads to samples contaminated with $Re_2H_6(SbPh_3)_6$.[428] A similar strategy has been used to prepare mixed phosphine-phosphine, phosphine-arsine and phosphine-stibine complexes of the types $Re_2H_8(PR_2Ph)_2(EPh_3)_2$ and $Re_2H_8(PRPh_2)_3(EPh_3)$ (R = Me or Et; E = P, As or Sb) through the reaction of $Re_2Cl_6(PR_2Ph)_2$ and $Re_2Cl_5(PRPh_2)_3$, respectively, with the appropriate stoichiometric amount of EPh_3 and an excess of $NaBH_4$ in ethanol at -10 °C.[427] The close relationship that exists between the $Re_2H_8(PR_3)_4$ compounds and the triply and quadruply bonded dirhenium synthetic starting materials is further demonstrated by the reactions of $Re_2H_8(PPh_3)_4$ with carbon tetrachloride and the allyl halides C_3H_5X (X = Cl or Br) that produce $(Ph_3PCl)_2Re_2Cl_8$ and $(Ph_3PC_3H_5)_2Re_2X_8$, respectively.[425] In a similar manner, the salt $(Ph_3PH)_2Re_2Cl_8$ is formed when $Re_2H_8(PPh_3)_4$ is treated with methanol saturated with gaseous hydrogen chloride.[425] Also, $Re_2H_8(PPh_3)_4$ is converted into the quadruply bonded complex $Re_2(\mu\text{-}O_2CCH_3)_4(O_2CCH_3)_2$ when it is reacted with acetic acid/acetic anhydride mixtures in 1,2-dichlorobenzene.[87]

8.9 Postscript on Recent Developments

The material presented in Sections 8.1-8.8 covers the literature on multiple bond dirhenium chemistry through mid-2003. The few contributions that were published in the latter half of 2003, just prior to the submission of the final version of the manuscript, are briefly summarized in this postscript section. The literature references are cited along with the sections where the chemistry of these compounds are discussed in more detail.

Re_2^{6+} Complexes

The glycinium and β-alaninium salts of the octachlorodirhenate(III) anion (see Section 8.2 and Table 8.1) have been synthesized and structurally characterized. The compounds $(\beta\text{-}AlaH)_2Re_2Cl_8$ and $(GlyH)_4[Re_2Cl_8]Cl_2$ have Re–Re distances of 2.2374(8) Å and

Pictiva EX2004
Samsung v Pictiva
IPR2024-01094

2.2407(3) Å, respectively, with the latter compound having an unusually large value of 16.2° for the Cl–Re–Re–Cl torsion angle. In the salt $(GlyH)_2Re_2Cl_8{\cdot}H_2O$ there are structurally distinct $(GlyH)_2Re_2Cl_8(H_2O)_2$ and $(GlyH)_2Re_2Cl_8$ molecules present and these have Re–Re distances of 2.2418(5) Å and 2.2306(5) Å, respectively; in the former molecule the H_2O molecules are H-bonded to Cl ligands and $(GlyH)^+$ cations.[429]

Further studies have been carried out on the hydrolysis of nitrile ligands in the presence of $(Bu_4N)_2Re_2Cl_8$ that give Re_2^{6+} complexes with μ-amidate ligands (see Section 8.4.3 and Table 8.1). In the earlier studies,[171-174] acetonitrile, benzonitrile and 1,4-dicyanobenzene were hydrolyzed, while the most recent work focused on 2-,3-, and 4-cyanophenol. Crystals with the compositions $(Bu_4N)\{Re_2[\mu\text{-}HNC(C_6H_4\text{-}2\text{-}OH)O]Cl_6\}{\cdot}CH_2Cl_2$, $(Bu_4N)\{Re_2[\mu\text{-}HNC(C_6H_4\text{-}3\text{-}OH)O]Cl_6\}$ and $(Bu_4N)\{Re_2[\mu\text{-}HNC(C_6H_4\text{-}4\text{-}OH)O]Cl_6\}{\cdot}S$ (where S = 1.81 CH_2Cl_2 or C_6H_6) were structurally characterized and the variations in the Re-Re distances found to be minimal (range 2.2171(5) to 2.2284(19) Å).[430] A recent spectroscopic study[431] has led to the first direct observation of luminescence from the low-lying $^3\delta\delta^*$ excited state of a formamidinate complex of the type $Re_2(DArF)_4Cl_2$ (Ar = *p*-MeO).

The reaction of *cis*-$Re_2(\mu\text{-}O_2CCH_3)_2Cl_4(H_2O)_2$ (Section 8.4.2) with picolinic acid in methanol/ethanol gives the edge-sharing bioctahedral dirhenium(III) complex $Re_2(\mu\text{-}OMe)(\mu{:}\eta^2\text{-}pic)(\eta^2\text{-}pic)_3Cl$ (Re–Re bond distance 2.4588(4) Å), whereas in an acetone/ethanol solvent mixture mononuclear $ReO(\eta^2\text{-}pic)_2Cl$ is formed.[432] Further examples of the cleavage of the Re–Re quadruple bonds of $Re_2(O_2CR)_4Cl_2$ (R = CH_3 or Ph) by RNC ligands to give salts of $[Re(CNR)_6]^+$(see Section 8.7) have been reported in the case of isocyano-carborane ligands.[433]

Re_2^{4+} and Re_2^{5+} Complexes

The reactions of $Re_2Cl_4(\mu\text{-}dppm)_2$ with 2-hydroxypyridine, 2-hydroxynicotinic acid (HnicOH) and 6-hydroxypicolinic acid (HpicOH) give the 2-pyridonate complexes $Re_2(\eta^2\text{-}hp)Cl_3(\mu\text{-}dppm)_2$, $Re_2(\eta^2\text{-}HnicO)Cl_3(\mu\text{-}dppm)_2$ and $Re_2(\mu\text{-}picO)_2(\mu\text{-}dppm)_2$,[434] the latter complex being identical to the product from the reaction of *cis*-$Re_2(\mu\text{-}O_2CCH_3)_2Cl_2(\mu\text{-}dppm)_2$ with HpicOH.[316] Another example of an edge-sharing bioctahedral complex of the type $[Re_2Cl_3(\mu\text{-}dppm)_2(CO)_2(NCR)]X$ (R = 4-C_5H_4N and X = O_3SCF_3) (see Section 8.5.4) has been structurally characterized.[435]

Reactions in which the Re-Re bond is cleaved or the bond order reduced have been reported. Salts of the mononuclear Re(II) cation $[Re(triphos)(NCCH_3)_3]^{2+}$ have been prepared from $[Re_2(NCCH_3)_{10}](BF_4)_4$ (Section 8.5.5),[436] while the confacial bioctahedral Re_2^{7+} complexes $Re_2(\mu\text{-}SR')_3X_4(PR_3)_2$ are formed by the reactions of both $Re_2X_4(PEt_2Ph)_4$(X = Cl or Br) and $Re_2Cl_5(PMePh_2)_3$ with various disulphide ligands R'SSR' (R = Me, Et or Ph).[437] The Re–Re bond distances (range 2.458(2) to 2.4870(8) Å) are indicative of the presence of multiple Re–Re bonding.

References

1. (a) G. F. Druce, *Rhenium*, Cambridge University Press: Cambridge, 1948, gives an account that is complete through the date of publication, including a complete bibliography; (b) F. Habashi, *CIM Bulletin* **1985**, *78*, pp 90-91; (c) See also M. E. Weeks and H. M. Leicester, *The Discovery of the Elements* 7th Edn., Journal of Chemical Education, 1968, pp. 823-829 for early references; (d) R. Colton, *The Chemistry of Rhenium and Technetium,* John Wiley and Sons, N.Y., 1965.
2. W. Geilmann, F. W. Wrigge and W. Blitz, *Z. anorg. allg. Chem.* **1933**, *214*, 248.
3. H. Hagen and A. Sieverts, *Z. anorg. allg. Chem.* **1935**, *215*, 111.
4. W. Geilmann and F. W. Wrigge, *Z. anorg. allg. Chem.* **1935**, *233*, 144.
5. J. E. Fergusson, W. Kirkham and R. S. Nyholm, in *Rhenium* B. W. Gonser, Ed., Elsevier, N.Y., **1962**, pp. 36.

Pictiva EX2004
Samsung v Pictiva
IPR2024-01094

6. See, for example, (a) J. A. Bertrand, F. A. Cotton and W. A. Dollase, *Inorg. Chem.* **1963**, *2*, 1166. (b) W. T. Robinson, J. E. Fergusson and B. R. Penfold, *Proc. Chem. Soc.* **1963**, 116; (c) F. A. Cotton and J. T. Mague, *Inorg. Chem.* **1964**, *3*, 1402; (d) F. A. Cotton and T. E. Haas, *Inorg. Chem.* **1964**, *3*, 10.
7. (a) F. A. Cotton, N. F. Curtis, C. B. Harris, B. F. G. Johnson, S. J. Lippard, J. T. Mague, W. R. Robinson and J. S. Wood, *Science* **1964**, *145*, 1305. (b) F. A. Cotton, *Inorg. Chem.* **1965**, *4*, 334. (c) F. A. Cotton and C. B. Harris, *Inorg. Chem.* **1965**, *4*, 330.
8. M. J. Bennett, F. A. Cotton and R. A. Walton, *J. Am. Chem. Soc.* **1966**, *88*, 3866.
9. F. A. Cotton and R. A. Walton, *Multiple Bonds Between Metal Atoms* 1st edn, J. Wiley & Sons, New York, 1982.
10. F. A. Cotton and R. A. Walton, *Multiple Bonds Between Metal Atoms* 2nd edn, Oxford University Press, Oxford, 1993.
11. F. A. Cotton and R. A. Walton, *Structure and Bonding (Berlin)* **1985**, *62*, pp 2-12.
12. T. E. Concolino and J. L. Eglin, *J. Cluster Sci.* **1997**, *8*, pp 482.
13. A. S. Kotel'nikova and V. G. Tronev, *Russ. J. Inorg. Chem.* **1958**, *3*, 268.
14. F. A. Cotton, N. F. Curtis, B. F. G. Johnson and W. R. Robinson, *Inorg. Chem.* **1965**, *4*, 326.
15. A. S. Kotel'nikova, M. I. Glinkina, T. V. Misailova and V. G. Lebedev, *Russ. J. Inorg. Chem.* **1976**, *21*, 547.
16. A. S. Kotel'nikova, T. V. Misailova, I. Z. Babievskaya and V. G. Lebedov, *Russ. J. Inorg. Chem.* **1978**, *23*, 1326.
17. I. F. Golovaneva, T. V. Misailova, A. S. Kotel'nikova and A. V. Shtemenko, *Russ. J. Inorg. Chem.* **1986**, *31*, 517.
18. P. A. Koz'min, G. N. Novitskaya, V. G. Kuznetsov and A. S. Kotel'nikova, *J. Struct. Chem.* **1971**, *11*, 861.
19. K. E. German, M. S. Grigor'ev, F. A. Cotton, S. V. Kryuchkov and L. Falvello, *Sov. J. Coord. Chem.* **1991**, *17*, 663.
20. P. A. Koz'min, G. N. Novitskaya and V. G. Kuznetsov., *J. Struct. Chem.* **1973**, *11*, 629.
21. F. A. Cotton and W. T. Hall, *Inorg. Chem.* **1977**, *16*, 1867.
22. F. A. Cotton, N. F. Curtis and W. R. Robinson, *Inorg. Chem.* **1965**, *4*, 1696.
23. R. A. Bailey and J. A. McIntyre, *Inorg. Chem.* **1966**, *5*, 1940.
24. A. B. Brignole and F. A. Cotton, *Inorg. Synth.* **1972**, *13*, 81.
25. H. D. Glicksman and R. A. Walton, *Inorg. Chem.* **1978**, *17*, 3197.
26. A. P. Ginsberg, *Chem. Commun.* **1968**, 857.
27. H. Gehrke, Jr. and G. Eastland, *Inorg. Chem.* **1970**, *9*, 2722.
28. A. Noll and U. Muller, *Z. anorg. allg.Chem.* **2001**, *627*, 803.
29. (a) T. J. Barder and R. A. Walton, *Inorg. Chem.* **1982**, *21*, 2510. (b) T. J. Barder and R. A. Walton, *Inorg. Synth.* **1985**, *23*, 116.
30. N. A. Baturin, K. E. German, M. S. Grigor'ev, S. V. Kryuchkov, V. A. Kucherenko, V. V. Obruchikov and V. A. Pustovalov, *Sov. J. Coord. Chem.* **1992**, *18*, 945.
31. S. S. Lau, W. Wu, P. E. Fanwick and R. A. Walton, *Polyhedron* **1997**, *16*, 3649.
32. F. A. Cotton, J. H. Matonic and D. de O. Silva, *Inorg. Chim. Acta* **1995**, *234*, 115.
33. F. A. Cotton, B. A. Frenz, B. R. Stultz and T. R. Webb, *J. Am. Chem. Soc.* **1976**, *98*, 2768.
34. F. A. Cotton and J. L. Eglin, *Inorg. Chim. Acta* **1992**, *198-200*, 13.
35. D. E. Morris, C. D. Tait, R. B. Dyer, J. R. Schoonover, M. D. Hopkins, A. P. Sattelberger and W. H. Woodruff, *Inorg. Chem.* **1990**, *29*, 3447 and references cited therein.
36. X.-B. Wang and L.-S. Wang, *J. Am. Chem. Soc.* **2000**, *122*, 2096.
37. P. A. Koz'min, M. D. Surazhskaya and T. B. Larina, *Sov. J. Coord. Chem.* **1979**, *5*, 593.
38. P. A. Koz'min, A. S. Kotel'nikova, M. D. Surazhskaya, T. B. Larina, Sh. A. Bagirov, and T. V. Misailova, *Sov. J. Coord. Chem.* **1978**, *4*, 1183.
39. F. A. Cotton, A. C. Price, R. C. Torralba and K. Vidyasagar, *Inorg. Chim. Acta* **1990**, *175*, 281.
40. F. A. Cotton and L. M. Daniels, *Inorg. Chim. Acta* **1988**, *142*, 255.
41. K. R. Dunbar, L. E. Pence and J. L. C. Thomas, *Inorg. Chim. Acta* **1994**, *217*, 79.

Pictiva EX2004
Samsung v Pictiva
IPR2024-01094

42. F. Weller, K. Jansen and K. Dehnicke, *Acta Crystallogr.* **1987**, *C43*, 2437.
43. P. A. Koz'min and M. D. Surazhskaya, *Sov. J. Coord. Chem.* **1980**, *6*, 309.
44. See footnote 19 in W. K. Bratton and F. A. Cotton, *Inorg. Chem.* **1969**, *8*, 1299.
45. G. Peters and W. Preetz, *Z. Naturforsch* **1979**, *34b*, 1767.
46. R. J. H. Clark and M. J. Stead, *Inorg. Chem.* **1983**, *22*, 1214.
47. S. D. Conradson, A. P. Sattelberger and W. H. Woodruff, *J. Am. Chem. Soc.* **1988**, *110*, 1309.
48. G. Henkel, G. Peters, W. Preetz and J. Skowronek, *Z. Naturforsch.* **1990**, *45b*, 469.
49. F. A. Cotton, B. G. DeBoer and M. Jeremic, *Inorg. Chem.* **1970**, *9*, 2143.
50. P. A. Koz'min, V. G. Kuznetsov and Z. V. Popova, *J. Struct. Chem.* **1965**, *6*, 624.
51. H. W. Huang and D. S. Martin, *Inorg. Chem.* **1985**, *24*, 96.
52. P. A. Koz'min, M. D. Surazhskaya and T. B. Larina, *Chem. Abs.* **1982**, *97*, 136870u.
53. P. A. Koz'min, *Sov. J. Coord. Chem.* **1986**, *12*, 374.
54. W. Preetz and L. Rudzik, *Angew. Chem., Int. Ed. Engl.* **1979**, *18*, 150.
55. P. Hollmann and W. Preetz, *Z. Naturforsch.* **1992**, *47b*, 1491.
56. (a) B. G. Antipov, S. V. Kryuchkov, V. N. Gerasimov, M. S. Grigor'ev, P. E. Kazin, V. V. Kharitonov, V. G. Maksimov, S. V. Moisa, V. V. Sergeev and T. K. Yurik, *Russ. J. Coord. Chem.* **1995**, *9*, 685. (b) *Idem*, *Radiochim. Acta* **1994**, *64*, 191.
57. F. A. Cotton, C. Oldham and W. R. Robinson, *Inorg. Chem.* **1966**, *5*, 1798.
58. W. K. Bratton and F. A. Cotton, *Inorg. Chem.* **1969**, *8*, 1299.
59. W. Preetz, G. Peters and L. Rudzik, *Z. Naturforsch.* **1979**, *34b*, 1240.
60. F. A. Cotton, L. M. Daniels and K. Vidyasagar, *Polyhedron* **1988**, *7*, 1667.
61. F. Calderazzo, F. Marchetti, R. Poli, D. Vitali and P. F. Zanazzi, *J. Chem. Soc., Dalton Trans.* **1982**, 1665.
62. C. Oldham and A. P. Ketteringham, *J. Chem. Soc., Dalton Trans*. **1973**, 2304.
63. F. A. Cotton, W. R. Robinson, R. A. Walton and R. Whyman, *Inorg. Chem.* **1967**, *6*, 929.
64. R. R. Hendriksma, *Inorg. Nucl. Chem. Lett.* **1972**, *8*, 1035.
65. R. R. Hendriksma, *J. Inorg. Nucl. Chem.* **1972**, *34*, 1581.
66. T. Nimry and R. A. Walton, *Inorg. Chem.* **1977**, *16*, 2829.
67. F. A. Cotton and M. Matusz, *Inorg. Chem.* **1987**, *26*, 3468.
68. B. J. Heyen, J. G. Jennings, G. L. Powell, W. B. Roach, D. W. Thurman and L. M. Daniels, *Polyhedron* **2001**, *20*, 783.
69. F. A. Cotton, A. Davison, W. H. Ilsley and H. S. Trop, *Inorg. Chem.* **1979**, *18*, 2719.
70. R. J. H. Clark and D. G. Humphrey, *Inorg. Chem.* **1996**, *35*, 2053.
71. C. J. Kepert, M. Kurmoo and P. Day, *Inorg. Chem.* **1997**, *36*, 1128.
72. F. A. Cotton, L. D. Gage, K. Mertis, L. W. Shive and G. Wilkinson, *J. Am. Chem. Soc.* **1976**, *98*, 6922.
73. A. S. Kotel'nikova, *Sov. J. Coord. Chem.* **1991**, *17*, 459.
74. A. S. Kotel'nikova and G. A. Vinogradova, *Dokl. Akad. Nauk. SSSR* **1963**, *152*, 621.
75. A. S. Kotel'nikova and G. A. Vinogradova, *Russ. J. Inorg. Chem.* **1964**, *9*, 168.
76. F. Taha and G. Wilkinson, *J. Chem. Soc.* **1963**, 5406.
77. C. Calvo, N. C. Jayadevan and C. J. L. Lock, *Can. J. Chem.* **1969**, *47*, 4213.
78. C. Calvo, N. C. Jayadevan, C. J. L. Lock and R. Restivo, *Can. J. Chem.* **1970**, *48*, 219.
79. A. V. Shtemenko, A. S. Kotel'nikova, B. A. Bovykin and I. F. Golovaneva, *Russ. J. Inorg. Chem.* **1986**, *31*, 225.
80. I. F. Golovaneva, B. A. Bovykin, A. V. Shtemenko, A. S. Kotel'nikova, T. V. Misailova and V. P. Shram, *Russ. J. Inorg. Chem.* **1987**, *32*, 213.
81. A. V. Shtemenko, A. A. Golichenko and K. V. Domasevitch, *Z. Naturforsch*. **2001**, *56b*, 381.
82. C. Oldham and A. P. Ketteringham, *Inorg. Nucl. Chem. Lett.* **1974**, *10*, 361.
83. F. A. Cotton, L. M. Daniels, J. Lu and T. Ren, *Acta Crystallogr.* **1997**, *C53*, 714.
84. V. Srinivasan and R. A. Walton, *Inorg. Chem.* **1980**, *19*, 1635.
85. N. S. Osmanov, T. V. Misailova, A. S. Kotel'nikova, O. N. Evstaf'eva, I. Z. Babievskaya, I. K. Kireeva and I. A. Dzhavadova, *Russ. J. Inorg. Chem.* **1988**, *33*, 353.

Pictiva EX2004
Samsung v Pictiva
IPR2024-01094

86. N. S. Osmanov, T. A. Abbasova and A. S. Kotel'nikova, *Russ. J. Inorg. Chem.* **1995**, *40*, 85.
87. C. J. Cameron, P. E. Fanwick, M. Leeaphon and R. A. Walton, *Inorg. Chem.* **1989**, *28*, 1101.
88. A. Vega, V. Calvo, J. Manzur, E. Spodine and J.-Y. Saillard, *Inorg. Chem.* **2002**, *41*, 5382.
89. M. J. Bennett, W. K. Bratton, F. A. Cotton and W. R. Robinson, *Inorg. Chem.* **1968**, 7, 1570.
90. D. M. Collins, F. A. Cotton and L. D. Gage, *Inorg. Chem.* **1979**, *18*, 1712.
91. P. A. Koz'min, M. D. Surazhskaya, T. B. Larina, A. S. Kotel'nikova and T. V. Misailova, *Chem. Abs.* **1980**, *93*, 213705r.
92. F. E. Kühn, I. S. Goncalves, A. D. Lopes, J. P. Lopes, C. C. Romao, W. Wachter, J. Mink, L. Hajba, A. J. Parola, F. Pina and J. Sotomayor, *Eur. J. Inorg. Chem.* **1999**, 295.
93. T. R. Webb and J. H. Espenson, *J. Am. Chem. Soc.* **1974**, *96*, 6289.
94. A. V. Shtemenko, I. F. Golovaneva, A. S. Kotel'nikova and T. V. Misailova, *Russ. J. Inorg. Chem.* **1980**, *25*, 704.
95. A. V. Shtemenko, Sh. A. Bagirov, A. S. Kotel'nikova, V. G. Lebedev, O. I. Kazymov and A. I. Alieva, *Russ. J. Inorg. Chem.* **1981**, *26*, 58.
96. P. A. Koz'min, M. D. Surazhskaya, T. B. Larina, A. V. Shtemenko, A. S. Kotel'nikova and I. F. Golovaneva, *Sov. J. Coord. Chem.* **1981**, 7, 386.
97. F. A. Cotton, C. Oldham and R. A. Walton, *Inorg. Chem.* **1967**, *6*, 214.
98. A. R. Chakravarty, F. A. Cotton, A. R. Cutler and R. A. Walton, *Inorg. Chem.* **1986**, *25*, 3619.
99. T. V. Misailova, A. S. Kotel'nikova, I. F. Golovaneva, O. N. Evstaf'eva and V. G. Lebedev, *Russ. J. Inorg. Chem.* **1981**, *26*, 343.
100. J. Skowronek and W. Preetz, *Z. anorg. allg. Chem*. **1992**, *615*, 73.
101. F. A. Cotton, E. C. DeCanio, P. A. Kibala and K. Vidyasagar, *Inorg. Chim. Acta* **1991**, *184*, 221.
102. Y. Ding, S. S. Lau, P. E. Fanwick and R. A. Walton, *Inorg. Chim. Acta* **2000**, *300-302*, 505.
103. A. S. Kotel'nikova, P. A. Koz'min and M. D. Surazhskaya, *Zh. Strukt. Khim.* **1969**, *10*, 1128.
104. P. A. Koz'min, M. D. Surazhskaya, T. B. Larina, A. S. Kotel'nikova and N. S. Osmanov, *Sov. J. Coord. Chem.* **1979**, *5*, 1484.
105. N. S. Osmanov, T. A. Abbasova and A. S. Kotel'nikova, *Russ. J. Inorg. Chem.* **1997**, *42*, 61.
106. N. S. Osmanov, A. S. Kotel'nikova, P. A. Koz'min, T. A. Abbasova, M. D. Surazhskaya and T. B. Larina, *Russ. J. Inorg. Chem.* **1988**, *33*, 457.
107. P. A. .Koz'min, M. D. Surazhskaya, T. B. Larina, Sh. A. Bagirov, N. S. Osmanov, A. S. Kotel'nikova and T. B. Misailova, *Sov. J. Coord. Chem.* **1979**, *5*, 1229.
108. A. S. Kotel'nikova, A. S. Moskovkin, T. V. Misailova, I. V. Miroshnichenko and Sh. A. Bagirov, *Russ. J. Inorg. Chem.* **1980**, *25*, 1656.
109. A. V. Shtemenko, A. A. Bovykin, V. P. Shram, A. S. Kotel'nikova, I. F. Golovaneva and A. V. Steblevskii, *Russ. J. Inorg. Chem.* **1985**, *30*, 1753.
110. P. A. Koz'min, M. D. Surazhskaya and T. B. Larina, *Sov. J. Coord. Chem*. **1979**, *5*, 1201.
111. S. M. V. Esjornson, P. E. Fanwick and R. A. Walton, *Inorg. Chim. Acta* **1989**, *162*, 165.
112. P. A. Koz'min, M. D. Surazhskaya and T. B. Larina, *Russ. J. Inorg. Chem.* **1981**, *26*, 57.
113. V. A. Mikhalev, *Russ. J. Gen. Chem.* **2001**, *71*, 1.
114. F. A. Cotton, L. D. Gage and C. E. Rice, *Inorg. Chem.* **1979**, *18*, 1138.
115. F. A. Cotton, W. R. Robinson and R. A. Walton, *Inorg. Chem.* **1967**, *6*, 223.
116. G. Rouschias and G. Wilkinson, *J. Chem. Soc., A* **1966**, 465.
117. F. A. Cotton and B. M. Foxman, *Inorg. Chem.* **1968**, 7, 1784.
118. F. A. Cotton, R. Eiss and B. M. Foxman, *Inorg. Chem.* **1969**, *8*, 950.
119. P. A. Koz'min, M. D. Surazhskaya and V. G. Kuznetsov, *J. Struct. Chem.* **1967**, *8*, 983.
120. P. A. Koz'min, M. D. Surazhskaya and V. G. Kuznetsov, *J. Struct. Chem.* **1970**, *11*, 291.
121. P. A. Koz'min, M. D. Surazhskaya and T. B. Larina, *Sov. J. Coord. Chem.* **1979**, *5*, 471.
122. M. D. Surazhskaya, T. B. Larina, P. A. Koz'min, A. S. Kotel'nikova and T. V. Misailova, *Sov. J. Coord. Chem.* **1978**, *4*, 1091.
123. P. A. Koz'min, M. D. Surazhskaya and T. B. Larina, *J. Struct. Chem*. **1974**, *15*, 56.
124. J. K. Bera, T.-T. Vo, R. A. Walton and K. R. Dunbar, *Polyhedron* **2003**, *22*, 3009.
125. A. I. Kuz'min, A. V. Shtemenko and A. S. Kotel'nikova, *Russ. J. Inorg. Chem.* **1980**, *25*, 1662.

Pictiva EX2004
Samsung v Pictiva
IPR2024-01094

126. H. D. Glicksman, A. D. Hamer, T. J. Smith and R. A. Walton, *Inorg. Chem.* **1976**, *15*, 2205.
127. H. D. Glicksman and R. A. Walton, *Inorg. Chem.* **1978**, *17*, 200.
128. H. D. Glicksman and R. A. Walton, *Inorg. Synth.* **1980**, *20*, 46.
129. P. Edwards, K. Mertis, G. Wilkinson, M. B. Hursthouse and K. M. Abdul Malik, *J. Chem. Soc., Dalton Trans.* **1980**, 334.
130. R. A. Jones and G. Wilkinson, *J. Chem. Soc., Dalton Trans*. **1978**, 1063.
131. R. A. Jones and G. Wilkinson, *J. Chem. Soc., Dalton Trans*. **1979**, 472.
132. M. B. Hursthouse and K. M. Abdul Malik, *J. Chem. Soc., Dalton Trans*. **1979**, 409.
133. E. G. Ismailov, A. A. Medzhidov, Ya. A. Abbasov, N. S. Osmanov and A. S. Kotel'nikova, *Dokl. Phys. Chem.* **1987**, *295*, 710.
134. M. E. Prater, D. J. Mindiola, X. Ouyang and K. R. Dunbar, *Inorg. Chem. Commun.* **1998**, *1*, 475.
135. R. A. Walton, *J. Cluster Sci.* **1994**, *5*, 173.
136. A. R. Cutler, S. M. V. Esjornson, P. E. Fanwick and R. A. Walton, *Inorg. Chem.* **1988**, *27*, 287.
137. F. A. Cotton, E. V. Dikarev and M. A. Petrukhina, *Inorg. Chim. Acta* **2002**, *334*, 67.
138. J. K. Bera, P. E. Fanwick and R. A. Walton, *Inorg. Chem.* **2001**, *40*, 2914.
139. (a) I. Ara, P. E. Fanwick and R. A. Walton, *J. Am. Chem. Soc.* **1991**, *113*, 1429. (b) I. Ara, P. E. Fanwick and R. A. Walton, *Inorg. Chem.* **1992**, *31*, 3211.
140. M. Costas, T. Leininger, G.-H. Jeung and M. Bénard, *Inorg. Chem.* **1992**, *31*, 3317.
141. A. R. Chakravarty, F. A. Cotton, A. R. Cutler, S. M. Tetrick and R. A. Walton, *J. Am. Chem. Soc.* **1985**, *107*, 4795.
142. (a) S. S. Lau, P. E. Fanwick and R. A. Walton, *J. Chem. Soc., Dalton Trans.* **1999**, 2273. (b) J. K. Bera, S. S. Lau, P. E. Fanwick and R. A. Walton, *J. Chem. Soc., Dalton Trans.* **2000**, 4277.
143. S. S. Lau, P. E. Fanwick and R. A. Walton, *Inorg. Chim. Acta* **2000**, *308*, 8.
144. G. W. Eastland, G. Yang and T. Thompson, *Meth. Find. Exptl. Clin. Pharmacol.* **1983**, *5*, 435.
145. N. S. Osmanov, M. D. Surazhskaya, T. A. Abbasova, T. B. Larina, A. S. Kotel'nikova and P. A. Koz'min, *Dokl. Phys. Chem.* **1989**, *304*, 21.
146. N. S. Osmanov, M. D. Surazhskaya, T. A. Abbasova, T. B. Larina, A. S. Kotel'nikova and P. A. Koz'min, *Russ. J. Inorg. Chem.* **1993**, *38*, 941.
147. N. S. Osmanov and T. A. Abbasova, *Russ. J. Inorg. Chem.* **1998**, *38*, 92.
148. J. P. Collman, R. Boulatov and G. B. Jameson, *Angew. Chem., Int. Ed.* **2001**, *40*, 1271.
149. J. P. Collman and R. Boulatov, *Angew. Chem., Int. Ed.* **2002**, *41*, 3948.
150. F. A. Cotton, B. A. Frenz and L. W. Shive, *Inorg. Chem.* **1975**, *14*, 649.
151. O. N. Evstaf'eva, A. S. Kotel'nikova, T. V. Misailova, N. S. Osmanov and R. N. Shchelokov, *Russ. J. Coord. Chem.* **1996**, *22*, 691.
152. (a) C. J. Cameron and R. A. Walton, unpublished work (1983). (b) C. J. Cameron, Ph.D. Thesis, Purdue University, 1983.
153. P. A. Koz'min, M. D. Surazhskaya, T. B. Larina, A. S. Kotel'nikova, and T. V. Misailova, *Dokl. Phys. Chem.* **1985**, *280*, 114.
154. F. A. Cotton and L. D. Gage, *Inorg. Chem.* **1979**, *18*, 1716.
155. A. R. Cutler and R. A. Walton, *Inorg. Chim. Acta* **1985**, *105*, 219.
156. F. A. Cotton and T. Ren, *Polyhedron* **1992**, *11*, 811.
157. R. M. Tylicki, W. Wu, P. E. Fanwick and R. A. Walton, *Inorg. Chem.* **1995**, *34*, 988.
158. K. T. Horne, G. L. Powell and L. M. Daniels, *Acta Crystallogr.* **2002**, *C58*, m292.
159. F. A. Cotton and L. W. Shive, *Inorg. Chem.* **1975**, *14*, 2027.
160. F. A. Cotton, W. H. Ilsley and W. Kaim, *Inorg. Chem.* **1980**, *19*, 2360.
161. F. A. Cotton and T. Ren, *J. Am. Chem. Soc.* **1992**, *114*, 2495.
162. J. L. Eglin, C. Lin, T. Ren, L. Smith, R. J. Staples and D. O. Wipf, *Eur. J. Inorg. Chem.* **1999**, 2095.
163. T. Barclay, J. L. Eglin and L. T. Smith, *Polyhedron* **2001**, *20*, 767.
164. F. A. Cotton, L. M. Daniels and S. C. Haefner, *Inorg. Chim. Acta* **1999**, *285*, 149.
165. N. D. Reddy, P. E. Fanwick and R. A. Walton, *Inorg. Chim. Acta* **2001**, *319*, 224.
166. F. A. Cotton, J. Gu, C. A. Murillo and D. J. Timmons, *J. Chem. Soc., Dalton Trans*. **1999**, 3741.

Pictiva EX2004
Samsung v Pictiva
IPR2024-01094

167. A.-M. Lebuis and A. L. Beauchamp, *Inorg. Chim. Acta* **1994**, *216*, 131.
168. F. A. Cotton, J. Liu and T. Ren, *Polyhedron* **1994**, *13*, 807.
169. D. P. Lydon, T. R. Spalding and J. F. Gallagher, *Polyhedron* **2003**, *22*, 1281.
170. F. A. Cotton, J. Lu and Y. Huang, *Inorg. Chem.* **1996**, *35*, 1839.
171. T. E. Concolino, J. L. Eglin and R. J. Staples, *Polyhedron* **1999**, *18*, 915.
172. R. W. McGraff, N. C. Dopke, R. K. Hayashi, D. R. Powell and P. M. Treichel, *Polyhedron* **2000**, *19*, 1245.
173. C. B. Bauer, T. E. Concolino, J. L. Eglin, R. D. Rogers and R. J. Staples, *J. Chem. Soc., Dalton Trans.* **1998**, 2813.
174. K. J. Nelson, R. W. McGaff and D. R. Powell, *Inorg. Chim. Acta* **2000**, *304*, 130.
175. V. P. Fedin, Yu. V. Mironov, M. N. Sokolov and V. E. Fedorov, *Bull. Acad. Sci. USSR* **1987**, *36*, 171.
176. J. San Filippo, Jr., *Inorg. Chem.* **1972**, *11*, 3140.
177. J. R. Ebner and R. A. Walton, *Inorg. Chem.* **1975**, *14*, 1987.
178. K. R. Dunbar and R. A. Walton, *Inorg. Chem.* **1985**, *24*, 5.
179. F. A. Cotton, E. V. Dikarev and M. A. Petrukhina, *J. Am. Chem. Soc.* **1997**, *119*, 12541.
180. F. A. Cotton, E. V. Dikarev and M. A. Petrukhina, *Inorg. Chem.* **1998**, *37*, 1949.
181. P. A. Angaridis, F. A. Cotton, E. V. Dikarev and M. A. Petrukhina, *Inorg. Chim. Acta* **2002**, *332*, 47.
182. F. A. Cotton, E. V. Dikarev and M. A. Petrukhina, *Inorg. Chem.* **1999**, *38*, 3384.
183. F. A. Cotton, E. V. Dikarev and M. A. Petrukhina, *Inorg. Chem.* **1998**, *37*, 6035.
184. P. Angaridis, F. A. Cotton, E. V. Dikarev and M. A. Petrukhina, *Polyhedron* **2001**, *20*, 755.
185. F. A. Cotton, E. V. Dikarev and M. A. Petrukhina, *Inorg. Chem.* **2001**, *40*, 5716.
186. M. J. Bennett, F. A. Cotton, B. M. Foxman and P. F. Stokely, *J. Am. Chem. Soc.* **1967**, *89*, 2759.
187. (a) F. A. Cotton and B. M. Foxman, *Inorg. Chem.* **1968**, 7, 2135. (b) F. A. Cotton and K. Vidyasagar, *Inorg. Chim. Acta* **1989**, *166*, 105.
188. F. A. Cotton, M. P. Diebold and W. J. Roth, *Inorg. Chim. Acta* **1988**, *144*, 17.
189. F. A. Cotton, E. V. Dikarev and M. A. Petrukhina, *Inorg. Chem.* **1999**, *38*, 3889.
190. N. D. Reddy, P. E. Fanwick and R. A. Walton, *Inorg. Chem.* **2001**, *40*, 1732.
191. (a) S.-M. Kuang, P. E. Fanwick and R. A. Walton, *Inorg. Chem. Commun*. **2001**, *4*, 745 and **2002**, *5*, 175. (b) S.-M. Kuang, P. E. Fanwick and R. A. Walton, *Inorg. Chem.* **2002**, *41*, 405.
192. J. Ferry, P. McArdle and M. J. Hynes, *J. Chem. Soc., Dalton Trans.* **1989**, 767.
193. P. McArdle, M. Rabbitte and D. Cunningham, *Inorg. Chim. Acta* **1995**, *229*, 95.
194. J. Ferry, J. Gallagher, D. Cunningham and P. McArdle, *Inorg. Chim. Acta* **1989**, *164*, 185.
195. J. Ferry, J. Gallagher, D. Cunningham and P. McArdle, *Inorg. Chim. Acta* **1990**, *172*, 79.
196. P. Edwards, K. Mertis, G. Wilkinson, M. B. Hursthouse and K. M. Abdul Malik, *J. Chem. Soc., Dalton Trans*. **1980**, 334.
197. F. A. Cotton, E. V. Dikarev, G. T. Jordan IV, C. A. Murillo and M. A. Petrukhina, *Inorg. Chem.* **1998**, *37*, 4611.
198. M. Bakir and R. A. Walton, *Polyhedron* **1987**, *6*, 1925.
199. M. Bakir, P. E. Fanwick and R. A. Walton, *Polyhedron* **1987**, *6*, 907.
200. J. A. Jaecker, W. R. Robinson and R. A. Walton, *J. Chem. Soc., Dalton Trans*. **1975**, 698.
201. J.-D. Chen and F. A. Cotton, *J. Am. Chem. Soc.* **1991**, *113*, 2509.
202. J. R. Ebner, D. R. Tyler and R. A. Walton, *Inorg. Chem.* **1976**, *15*, 833.
203. T. J. Barder, F. A. Cotton, D. Lewis, W. Schwotzer, S. M. Tetrick and R. A. Walton, *J. Am. Chem. Soc.* **1984**, *106*, 2882.
204. (a) S. Shaik and R. Hoffmann, *J. Am. Chem. Soc.* **1980**, *102*, 1194. (b) S. Shaik, R. Hoffmann, R. C. Fisel and R. H. Summerville, *J. Am. Chem. Soc.* **1980**, *102*, 4555.
205. J. M. Canich, F. A. Cotton, L. M. Daniels and D. B. Lewis, *Inorg. Chem.* **1987**, *26*, 4046.
206. K. R. Dunbar, D. Powell and R. A. Walton, *Inorg. Chem.* **1985**, *24*, 2842.
207. T. J. Barder, F. A. Cotton, G. L. Powell, S. M. Tetrick and R. A. Walton, *J. Am. Chem. Soc.* **1984**, *106*, 1323.

Pictiva EX2004
Samsung v Pictiva
IPR2024-01094

208. B. J. Heyen and G. L. Powell, *Inorg. Chem.* **1990**, *29*, 4574.
209. J. A. Jaecker, D. P. Murtha and R. A. Walton, *Inorg. Chim. Acta* **1975**, *13*, 21.
210. D. G. Tisley and R. A. Walton, *J. Mol. Struct*. **1973**, *17*, 401.
211. (a) B. J. Heyen and G. L. Powell, *Polyhedron* **1988**, 7, 1207. (b) B. J. Heyen, J. G. Jennings and G. L. Powell, *Inorg. Chim. Acta* **1995**, *229*, 241.
212. R. A. Walton, in *Metal-Metal Bonds and Clusters in Chemistry and Catalysis* Ed. J. P. Fackler, Jr., Plenum Press, New York, **1990**, pp. 7-17.
213. (a) M. J. Bennett, F. A. Cotton and R. A. Walton, *J. Am. Chem. Soc.* **1966**, *88*, 3866. (b) M. J. Bennett, F. A. Cotton and R. A. Walton, *Proc. Roy. Soc.* **1968**, *A303*, 175.
214. F. A. Cotton, W. R. Robinson and R. A. Walton, *Inorg. Chem.* **1967**, *6*, 1257.
215. R. R. Hendriksma and H. P. van Leeuwen, *Electrochim. Acta* **1973**, *18*, 39.
216. F. A. Cotton and E. Pedersen, *Inorg. Chem.* **1975**, *14*, 383.
217. J. R. Ebner and R. A. Walton, *Inorg. Chim. Acta* **1975**, *14*, L45.
218. D. G. Nocera and H. B. Gray, *J. Am. Chem. Soc.* **1981**, *103*, 7349.
219. D. G. Nocera, A. W. Maverick, J. R. Winkler, C. Che and H. B. Gray, *ACS Symp. Ser.* **1983**, *No. 211*, 21.
220. C. J. Cameron, S. M. Tetrick and R. A. Walton, *Organometallics* **1984**, *3*, 240.
221. D. G. Nocera and H. B. Gray, *Inorg. Chem.* **1984**, *23*, 3686.
222. G. A. Heath and R. G. Raptis, *Inorg. Chem.* **1991**, *30*, 4108.
223. G. A. Heath and R. G. Raptis, *J. Am. Chem. Soc.* **1993**, *115*, 3768.
224. S. K. D. Strubinger, I.-W. Sun, W. E. Cleland, Jr. and C. L. Hussey, *Inorg. Chem.* **1990**, *29*, 993.
225. S. K. D. Strubinger, C. L. Hussey and W. E. Cleland, Jr., *Inorg. Chem.* **1991**, *30*, 4276.
226. J. E. Hahn, T. Nimry, W. R. Robinson, D. J. Salmon and R. A. Walton, *J. Chem. Soc., Dalton Trans.* **1978**, 1232.
227. S. P. Best, R. J. H. Clark and D. G. Humphrey, *Inorg. Chem.* **1995**, *34*, 1013.
228. (a) D. J. Salmon and R. A. Walton, *J. Am. Chem. Soc.* **1978**, *100*, 991. (b) P. Brant, D. J. Salmon and R. A. Walton, *J. Am. Chem. Soc.* **1978**, *100*, 4424.
229. F. A. Cotton and E. Pedersen, *J. Am. Chem. Soc.* **1975**, *97*, 303.
230. J. F. Berry, F. A. Cotton, P. Huang and C. A. Murillo, *Dalton Trans.* **2003**, 1218.
231. F. Bonati and F. A. Cotton, *Inorg. Chem.* **1967**, *6*, 1353.
232. C. Mertis and N. Psaroudakis, *Polyhedron* **1989**, *8*, 469.
233. G. A. Heath, J. E. McGrady, R. G. Raptis and A. C. Willis, *Inorg. Chem.* **1996**, *35*, 6838.
234. S. K. D. Strubinger, I.-W. Sun, W. E. Cleland, Jr. and C. L. Hussey, *Inorg. Chem.* **1990**, *29*, 4246.
235. P. F. Stokely, Ph.D. Thesis, Massachusetts Institute of Technology, 1969.
236. F. A. Cotton and D. A. Ucko, *Inorg. Chim. Acta* **1972**, *6*, 161.
237. A. J. Baranov, G. V. Khvorykh and S. I. Troyanov, *Z. anorg. allg.Chem.* **1999**, *625*, 1240.
238. S. Rabe and U. Müller, *Z. anorg. allg.Chem.* **2000**, *626*, 830.
239. W. Preetz and S. Strueb, *Z. anorg. allg.Chem.* **1998**, *624*, 578.
240. R. A. Walton, *Inorg. Chem.* **1971**, *10*, 2534.
241. H. D. Glicksman and R. A. Walton, *Inorg. Chim. Acta* **1976**, *19*, 91.
242. P. R. Brown, F. G. N. Cloke, M. L. H. Green and R. C. Tovey, *J. Chem. Soc., Chem. Commun.* **1982**, 519.
243. F. A. Cotton, K. R. Dunbar, L. R. Falvello, M. Tomas and R. A. Walton, *J. Am. Chem. Soc.* **1983**, *105*, 4950.
244. D. R. Root, C. H. Blevins, D. L. Lichtenberger, A. P. Sattelberger and R. A. Walton, *J. Am. Chem. Soc.* **1986**, *108*, 953.
245. F. A. Cotton, J. Czuchajowska and R. L. Luck, *J. Am. Chem. Soc., Dalton Trans.* **1991**, 579.
246. P. Brant and R. A. Walton, *Inorg. Chem.* **1978**, *17*, 2674.
247. (a) F. A. Cotton, B. A. Frenz, J. R. Ebner and R. A. Walton, *J. Chem. Soc., Chem. Commun.* **1974**, 4. (b) F. A. Cotton, B. A. Frenz, J. R. Ebner and R. A. Walton, *Inorg. Chem.* **1976**, *15*, 1630.
248. F. A. Cotton, A. C. Price and K. Vidyasagar, *Inorg. Chem.* **1990**, *29*, 5143.
249. F. A. Cotton, L. M. Daniels, M. Shang and Z. Yao, *Inorg. Chim. Acta* **1994**, *215*, 103.

Pictiva EX2004
Samsung v Pictiva
IPR2024-01094

250. F. A. Cotton, J. G. Jennings, A. C. Price and K. Vidyasagar, *Inorg. Chem.* **1990**, *29*, 4138.
251. B. E. Bursten, F. A. Cotton, P. E. Fanwick, G. G. Stanley and R. A. Walton, *J. Am. Chem. Soc.* **1983**, *105*, 2606.
252. C. A. Hertzer, R. E. Myers, P. Brant and R. A. Walton, *Inorg. Chem.* **1978**, *17*, 2383.
253. K. T. Hovne, G. L. Powell and L. M. Daniels, *Acta Crystallogr.* **2002**, *C58*, m302.
254. C. A. Hertzer and R. A. Walton, *Inorg. Chim. Acta* **1977**, *22*, L10.
255. K. A. Conner, T. Gennett, M. J. Weaver and R. A. Walton, *J. Electroanal. Chem.* **1985**, *196*, 69.
256. J. Coddington and S. Wherland, *Inorg. Chem.* **1997**, *36*, 6235.
257. J. Coddington and S. Wherland, *Inorg. Chem.* **1996**, *35*, 4023.
258. J. R. Ebner and R. A. Walton, *Inorg. Chem.* **1975**, *14*, 2289.
259. F. A. Cotton and E. V. Dikarev, *Inorg. Chem.* **1996**, *35*, 4738.
260. F. A. Cotton, E. V. Dikarev and M. A. Petrukhina, *Inorg. Chem. Commun.* **1999**, *2*, 28.
261. F. A. Cotton, E. V. Dikarev and M. A. Petrukhina, *Inorg. Chem.* **2001**, *40*, 6825.
262. P. A. Angaridis, F. A. Cotton, E. V. Dikarev and M. A. Petrukhina, *Inorg. Chim. Acta* **2002**, *330*, 173.
263. S.-M. Kuang, D. A. Edwards, P. E. Fanwick and R. A. Walton, *Inorg. Chim. Acta* **2003**, *342*, 267.
264. (a) P. E. Fanwick, D. R. Root and R. A. Walton, *Inorg. Chem.* **1989**, *28*, 395. (b) P. E. Fanwick, D. R. Root and R. A. Walton, *Inorg. Chem.* **1989**, *28*, 3203.
265. S. Bucknor, F. A. Cotton, L. R. Falvello, A. H. Reid, Jr. and C. D. Schmulbach, *Inorg. Chem.* **1987**, *26*, 2954.
266. F. A. Cotton, G. G. Stanley and R. A. Walton, *Inorg. Chem.* **1978**, *17*, 2099.
267. S. A. Best, T. J. Smith and R. A. Walton, *Inorg. Chem.* **1978**, *17*, 99.
268. I. F. Fraser and R. D. Peacock, *J. Chem. Soc., Chem. Commun.* **1985**, 1727.
269. R. D. Peacock, *Polyhedron* **1987**, *6*, 715.
270. F. A. Cotton, P. E. Fanwick, J. W. Fitch, H. D. Glicksman and R. A. Walton, *J. Am. Chem. Soc.* **1979**, *101*, 1752.
271. A. R. Cutler, D. R. Derringer, P. E. Fanwick and R. A. Walton, *J. Am. Chem. Soc.* **1988**, *110*, 5024.
272. J. Ferry, J. Gallagher, D. Cunningham and P. McArdle, *Polyhedron* **1989**, *8*, 1733.
273. N. F. Cole, F. A. Cotton, G. L. Powell and T. J. Smith, *Inorg. Chem.* **1983**, *22*, 2618.
274. T. J. Barder, F. A. Cotton, K. R. Dunbar, G. L. Powell, W. Schwotzer and R. A. Walton, *Inorg. Chem.* **1985**, *24*, 2550.
275. L. B. Anderson, M. Bakir and R. A. Walton, *Polyhedron* **1987**, *6*, 1483.
276. M. Bakir, F. A. Cotton, L. R. Falvello, K. Vidyasagar and R. A. Walton, *Inorg. Chem.* **1988**, *27*, 2460.
277. J. L. Eglin, L. T. Smith, E. J. Valente and J. D. Zubkowski, *Inorg. Chim. Acta* **1998**, *268*, 151.
278. F. L. Campbell, III, F. A. Cotton and G. L. Powell, *Inorg. Chem.* **1985**, *24*, 4384.
279. K. M. Carlson-Day, J. L. Eglin, K. M. Huntington and R. J. Staples, *Inorg. Chim. Acta* **1998**, *271*, 49.
280. D. Esjornson, M. Bakir, P. E. Fanwick, K. S. Jones and R. A. Walton, *Inorg. Chem.* **1990**, *29*, 2055.
281. C. E. Uzelmeier, S. L. Bartley, M. Fourmigué, R. Rogers, G. Grandinetti and K. R. Dunbar, *Inorg. Chem.* **1998**, *37*, 6706.
282. P. Brant, H. D. Glicksman, D. J. Salmon and R. A. Walton, *Inorg. Chem.* **1978**, *17*, 3203.
283. L. B. Anderson, S. M. Tetrick and R. A. Walton, *J. Chem. Soc., Dalton Trans.* **1986**, 55.
284. D. R. Derringer, P. E. Fanwick, J. Moran and R. A. Walton, *Inorg. Chem.* **1989**, *28*, 1384.
285. F. A. Cotton, A. Yokochi, M. J. Siwajek and R. A. Walton, *Inorg. Chem.* **1998**, *37*, 372.
286. N. D. Reddy, P. E. Fanwick and R. A. Walton, *Inorg. Chim. Acta* **2001**, *314*, 189.
287. S.-M. Kuang, P. E. Fanwick and R. A. Walton, *Inorg. Chim. Acta* **2000**, *300-302*, 434.
288. M. T. Costello, D. R. Derringer, P. E. Fanwick, A. C. Price, M. I. Rivera, E. Scheiber, E. W. Siurek III, and R. A. Walton, *Polyhedron* **1990**, *9*, 573.
289. M. Ganesan, P. E. Fanwick and R. A. Walton, *J. Organomet. Chem*. **2003**, *671*, 166.

Pictiva EX2004
Samsung v Pictiva
IPR2024-01094

290. K.-Y. Shih, P. E. Fanwick and R. A. Walton, *Inorg. Chem.* **1991**, *30*, 3971.
291. S.-M. Kuang, P. E. Fanwick and R. A. Walton, *Inorg. Chem.* **2001**, *40*, 5682.
292. S. L. Bartley, S. N. Bernstein and K. R. Dunbar, *Inorg. Chim Acta* **1993**, *213*, 213.
293. H.-F. Lang, P. E. Fanwick and R. A. Walton, *Inorg. Chim. Acta* **2001**, *322*, 17.
294. J. K. Bera, P. E. Fanwick and R. A. Walton, *Inorg. Chim. Acta* **2000**, *311*, 138.
295. L. B. Anderson, F. A. Cotton, L. R. Falvello, W. S. Harwood, D. Lewis and R. A. Walton, *Inorg. Chem.* **1986**, *25*, 3637.
296. I. Ara and R. A. Walton, *Inorg. Chim. Acta* **1992**, *198-200*, 787.
297. F. A. Cotton and M. Matusz, *Inorg. Chem.* **1987**, *26*, 984.
298. P. E. Fanwick, D. R. Root and R. A. Walton, *Inorg. Chem.* **1986**, *25*, 4832.
299. M. J. Siwajek, W. Wu and R. A. Walton, *Inorg. Chim. Acta* **1995**, *235*, 421.
300. P. E. Fanwick, J.-S. Qi, K.-Y. Shih and R. A. Walton, *Inorg. Chim. Acta* **1990**, *172*, 65.
301. T. J. Barder, S. M. Tetrick, R. A. Walton, F. A. Cotton and G. L. Powell, *J. Am. Chem. Soc.* **1983**, *105*, 4090.
302. S.-M. Kuang, P. E. Fanwick and R. A. Walton, *J. Chem. Soc., Dalton Trans.* **2002**, 2501.
303. F. A. Cotton, L. W. Shive and B. R. Stults, *Inorg. Chem.* **1976**, *15*, 2239.
304. S. M. V. Esjornson, Ph.D. Thesis, Purdue University, 1989.
305. F. A. Cotton and K. R. Dunbar, *Inorg. Chem.* **1987**, *26*, 1305.
306. (a) I. Ara, P. E. Fanwick and R. A. Walton, *Polyhedron* **1989**, *8*, 1689. (b) I. Ara, P. E. Fanwick and R. A. Walton, *J. Cluster Sci.* **1992**, *3*, 83.
307. K.-Y. Shih, P. E. Fanwick and R. A. Walton, *J. Cluster Sci.* **1991**, *2*, 259.
308. S. L. Bartley, K. R. Dunbar, K.-Y. Shih, P. E. Fanwick and R. A. Walton, *Inorg. Chem.* **1993**, *32*, 1341.
309. K.-Y. Shih, P. E. Fanwick and R. A. Walton, *Inorg. Chim. Acta* **1993**, *212*, 23.
310. K.-Y. Shih, P. E. Fanwick and R. A. Walton, *Inorg. Chim. Acta* **1993**, *213*, 247.
311. I. Ara, P. E. Fanwick and R. A. Walton, *Inorg. Chem.* **1991**, *30*, 1973.
312. K. R. Dunbar and S. L. Bartley, *Angew. Chem., Int. Ed. Engl.* **1991**, *301*, 448.
313. S. L. Bartley, M. J. Bazile, Jr., R. Clérac, H. Zhao, X. Ouyang and K. R. Dunbar, *Dalton Trans.* **2003**. 2937.
314. D. R. Derringer, E. A. Buck, S. M. V. Esjornson, P. E. Fanwick and R. A. Walton, *Polyhedron* **1990**, *9*, 743.
315. S. K. Chattopadhyay, P. E. Fanwick and R. A. Walton, *Inorg. Chem.* **2003**, *42*, 4954.
316. S. K. Chattopadhyay, P. E. Fanwick and R. A. Walton, *Dalton Trans.* **2003**, 3617.
317. I. Ara, P. E. Fanwick and R. A. Walton, *Inorg. Chem.* **1991**, *30*, 1227.
318. A. R. Cutler, P. E. Fanwick and R. A. Walton, *Inorg. Chem.* **1987**, *26*, 3811.
319. P. W. Schrier, D. R. Derringer, P. E. Fanwick and R. A. Walton, *Inorg. Chem.* **1990**, *29*, 1290.
320. J. K. Bera, B. W. Smucker, R. A. Walton and K. R. Dunbar, *Chem. Commun.* **2001**, 2562.
321. (a) S.-M. Kuang, P. E. Fanwick and R. A. Walton, *Inorg. Chem.* **2002**, *41*, 1036. (b) S.-M. Kuang, P. E. Fanwick and R. A. Walton, *Inorg. Chim. Acta* **2002**, *338*, 219.
322. J. K. Bera, P. Angaridis, F. A. Cotton, M. A. Petrukhina, P. E. Fanwick and R. A. Walton, *J. Am. Chem. Soc.* **2001**, *123*, 1515.
323. J. K. Bera, R. Clérac, P. E. Fanwick and R. A. Walton, *J. Chem. Soc., Dalton Trans.* **2002**, 2168.
324. J. K. Bera, P. E. Fanwick and R. A. Walton, *J. Chem. Soc., Dalton Trans.* **2001**, 109.
325. D. R. Derringer, K.-Y. Shih, P. E. Fanwick and R. A. Walton, *Polyhedron* **1991**, *10*, 79.
326. (a) K.-Y. Shih, P. E. Fanwick and R. A. Walton, *J. Chem. Soc., Chem. Commun.* **1992**, 375. (b) K.-Y. Shih, P. E. Fanwick and R. A. Walton, *Inorg. Chem.* **1992**, *31*, 3663.
327. P. E. Fanwick, J.-S. Qi, Y.-P. Wu and R. A. Walton, *Inorg. Chim. Acta* **1990**, *168*, 159.
328. P. E. Fanwick, J.-S. Qi and R. A. Walton, *Inorg. Chem.* **1990**, *29*, 3787.
329. M. Ganesan, P. N. Kapoor, P. E. Fanwick and R. A. Walton, *Inorg. Chem. Commun.* **2002**, *5*, 1073.
330. A. C. Price and R. A. Walton, *Polyhedron* **1987**, *6*, 729.
331. R. A. Walton, *Polyhedron* **1989**, *8*, 1689.

Pictiva EX2004
Samsung v Pictiva
IPR2024-01094

332. F. A. Cotton, L. M. Daniels, K. R. Dunbar, L. R. Falvello, S. M. Tetrick and R. A. Walton, *J. Am. Chem. Soc.* **1985**, *107*, 3524.
333. F. A. Cotton, K. R. Dunbar, A. C. Price, W. Schwotzer and R. A. Walton, *J. Am. Chem. Soc.* **1986**, *108*, 4843.
334. P. E. Fanwick, A. C. Price and R. A. Walton, *Inorg. Chem.* **1987**, *26*, 3920.
335. W. Wu, P. E. Fanwick and R. A. Walton, *Inorg. Chem.* **1995**, *34*, 5810.
336. J. Chantler, D.A. Kort, P. E. Fanwick and R. A. Walton, *J. Organomet. Chem.* **2000**, *596*, 27.
337. S. J. Chen and K. R. Dunbar, *Inorg. Chem.* **1990**, *29*, 529.
338. I. Ara, P. E. Fanwick and R. A. Walton, *Inorg. Chem.* **1993**, *32*, 2958.
339. I. Ara, P. E. Fanwick and R. A. Walton, *Polyhedron* **1992**, *11*, 2431.
340. L. B. Anderson, T. J. Barder and R. A. Walton, *Inorg. Chem.* **1985**, *24*, 1421.
341. L. B. Anderson, T. J. Barder, D. Esjornson, R. A. Walton and B. E. Bursten, *J. Chem. Soc., Dalton Trans.* **1986**, 2607.
342. Y. Ding, S.-M. Kuang, M. J. Siwajek, P. E. Fanwick and R. A. Walton, *Inorg. Chem.* **2000**, *39*, 2676.
343. L. B. Anderson, T. J. Barder, F. A. Cotton, K. R. Dunbar, L. R. Falvello and R. A. Walton, *Inorg. Chem.* **1986**, *25*, 3629.
344. T. J. Barder, D. Powell and R. A. Walton, *J. Chem. Soc., Chem. Commun.* **1985**, 550.
345. T. J. Barder, F. A. Cotton, L. R. Falvello and R. A. Walton, *Inorg. Chem.* **1985**, *24*, 1258.
346. D. Esjornson, D. R. Derringer, P. E. Fanwick and R. A. Walton, *Inorg. Chem.*, **1989**, *28*, 2821.
347. G. N. Holder, T. A. Leach, C. T. Eagle and L. A. Bottomley, *Trans. Met. Chem.* **1995**, *20*, 409.
348. J. Chantler, P. E. Fanwick and R. A. Walton, *Inorg. Chim. Acta* **2000**, *305*, 215.
349. T. E. Concolino, J. L. Eglin, C. E. Hadden, R. P. Hicks, R. J. Staples, E. J. Valente and J. D. Zubkowski, *J. Cluster Sci.* **2000**, *11*, 109.
350. D. Esjornson, P. E. Fanwick and R. A. Walton, *Inorg. Chem.* **1988**, *27*, 3067.
351. M. Ganesan, K.-Y. Shih, P. E. Fanwick and R. A. Walton, *Inorg. Chem.* **2003**, *42*, 1241.
352. M. Ganesan, P. E. Fanwick and R. A. Walton, *Organometallics* **2003**, *22*, 870.
353. W. Wu, P. E. Fanwick and R. A. Walton, *J. Cluster Sci.***1996**, 7, 155.
354. W. Wu, J. A. Subramony, P. E. Fanwick and R. A. Walton, *Inorg. Chem.* **1996**, *35*, 6785.
355. J. Chantler, P. E. Fanwick and R. A. Walton, *J. Organomet. Chem.* **2000**, *604*, 219.
356. F. A. Cotton, K. R. Dunbar, L. R. Falvello and R. A. Walton, *Inorg. Chem.* **1985**, *24*, 4180.
357. P. E. Fanwick, A. C. Price and R. A. Walton, *Inorg. Chem.* **1988**, *27*, 2601.
358. L. B. Anderson, F. A. Cotton, K. R. Dunbar, L. R. Falvello, A. C. Price, A. H. Reid and R. A. Walton, *Inorg. Chem.* **1987**, *26*, 2717.
359. W. Wu, P. E. Fanwick and R. A. Walton, *Inorg. Chem.* **1996**, *35*, 5484.
360. M. J. Siwajek and R. A. Walton, *J. Cluster Sci.* **2000**, *11*, 511.
361. Y. Ding, D. A. Kort, W. Wu, P. E. Fanwick and R. A. Walton, *J. Organomet. Chem.* **1999**, *573*, 87.
362. W. Wu, P. E. Fanwick and R. A. Walton, *Organometallics* **1997**, *16*, 1538.
363. P. E. Fanwick, A. C. Price and R. A. Walton, *Inorg. Chem.* **1987**, *26*, 3087.
364. W. Wu, P. E. Fanwick and R. A. Walton, *Inorg. Chim. Acta* **1996**, *242*, 81.
365. W. Wu, P. E. Fanwick and R. A. Walton, *J. Am. Chem. Soc.* **1996**, *118*, 13091.
366. (a) W. Wu, P. E. Fanwick and R. A. Walton, *Chem. Commun.* **1997**, 755. (b) W. Wu, P. E. Fanwick and R. A. Walton, *Inorg. Chem.* **1998**, *37*, 3122.
367. W. Wu, P. E. Fanwick and R. A. Walton, *J. Cluster Sci.* **1997**, *8*, 547.
368. (a) W. Wu, P. E. Fanwick and R. A. Walton, *Inorg. Chem.* **1997**, *36*, 3810. (b) Y. Ding, W. Wu, P. E. Fanwick and R. A. Walton, *Inorg. Chem.* **1999**, *38*, 1918.
369. Y. Ding, P. E. Fanwick and R. A. Walton, *Inorg. Chem.* **1999**, *38*, 5165.
370. S.-M. Kuang, P. E. Fanwick and R. A. Walton, *Inorg. Chem.* **2002**, *41*, 147.
371. S.-M. Kuang, P. E. Fanwick and R. A. Walton, *Inorg. Chem.* **2000**, *39*, 2968.
372. K.-Y. Shih, P. E. Fanwick and R. A. Walton, *Organometallics* **1993**, *12*, 347.
373. D. A. Kort, W. Wu, P. E. Fanwick and R. A. Walton, *Trans. Met. Chem.* **1995**, *20*, 625.

Pictiva EX2004
Samsung v Pictiva
IPR2024-01094

374. K.-Y. Shih, R. M. Tylicki, W. Wu, P. E. Fanwick and R. A. Walton, *Inorg. Chim. Acta* **1995**, *229*, 105.
375. (a) K.-Y. Shih, P. E. Fanwick and R. A. Walton, *J. Am. Chem. Soc.* **1993**, *115*, 9319. (b) K.-Y. Shih, P. E. Fanwick and R. A. Walton, *Organometallics* **1994**, *13*, 1235.
376. (a) K.-Y. Shih, P. E. Fanwick and R. A. Walton, *J. Chem. Soc., Chem. Commun.* **1994**, 861. (b) K.-Y. Shih, P. E. Fanwick and R. A. Walton, *Organometallics* **1995**, *14*, 448.
377. J.-S. Qi, P. E. Fanwick and R. A. Walton, *Polyhedron* **1990**, *9*, 565.
378. J.-S. Qi, P. E. Fanwick and R. A. Walton, *Inorg. Chem.* **1990**, *29*, 457.
379. J.-S. Qi, P. W. Schrier, P. E. Fanwick and R. A. Walton, *Inorg. Chem.* **1992**, *31*, 258.
380. K. J. Kolodsick, P. W. Schrier and R. A. Walton, *Polyhedron* **1994**, *13*, 457.
381. (a) J.-S. Qi, P. W. Schrier, P. E. Fanwick and R. A. Walton, *J. Chem. Soc., Chem. Commun.* **1991**, 1737. (b) P. W. Schrier, P. E. Fanwick and R. A. Walton, *Inorg. Chem.* **1992**, *31*, 3929.
382. M. Ganesan, P. E. Fanwick and R. A. Walton, *Inorg. Chim. Acta* **2003**, *343*, 391.
383. A. F. Masters, K. Mertis, J. F. Gibson and G. Wilkinson, *Nouv. J. Chim.* **1977**, *1*, 389.
384 F. A. Cotton and M. W. Extine, *J. Am. Chem. Soc.* **1978**, *100*, 3788.
385. F. A. Cotton, G. G. Stanley, A. H. Cowley and M. Lattman, *Organometallics* **1988**, 7, 835.
386. S. N. Bernstein and K. R. Dunbar, *Angew. Chem., Int. Ed. Engl.* **1992**, *31*, 1360.
387. A. Døssing and A. van Lelieveld, *Inorg. Chim. Acta* **2001**, *322*, 130.
388. J. P. Collman, J. M. Garner and L. K. Woo, *J. Am. Chem. Soc.* **1989**, *111*, 8141.
389. J. P. Collman and H. J. Arnold, *Acc. Chem. Res.* **1993**, *26*, 586.
390. C. D. Tait, J. M. Garner, J. P. Collman, A. P. Sattelberger and W. H. Woodruff, *J. Am. Chem. Soc.* **1989**, *111*, 9072.
391. J. P. Collman, J. M. Garner, R. T. Hembre and Y. Ha, *J. Am. Chem. Soc.* **1992**, *114*, 1292.
392. M. Göldner, H. Hücksträdt, K. S. Murray, B. Moubaraki and H. Homborg, *Z. anorg. allg. Chem.* **1998**, *624*, 288.
393. N. I. Girichеva, G. V. Girichev, S. B. Lapshina, S. A. Shl'ykov, Yu. A. Politov, V. D. Butskii and V. S. Pervov, *J. Struct. Chem.* **1993**, *34*, 214. (See also, *Dokl Akad. Nauk.* **1992**, *325*, 761.)
394. K. Waltersson, *Acta Crystallogr.* **1976**, *B32*, 1485.
395. J.-P. Besse, G. Baud, R. Chevalier and M. Gasperin, *Acta Crystallogr.* **1978**, *B34*, 3532.
396. See, for example, (a) L. Chi, J. F. Britten and J. E. Greedan, *J. Solid State Chem.* **2003**, *172*, 451. (b) W. Jeitschko, D. H. Heumannskämper, U. C. Rodewald and M. S. Schriewar-Pöttgen, *Z. anorg. allg. Chem.* **2000**, *626*, 80.
397. R. E. Douthwaite, P. T. Wolczanski and E. Merschrod, *Chem. Commun.* **1998**, 2591.
398. T. Lis, *Acta Crystallogr.* **1975**, *B31*, 1594.
399. J. W. Atkinson, M.-C. Hong, D. A. House, P. Kyritsis, Y.-J. Li, M. Nasreldin and A. G. Sykes, *J. Chem. Soc., Dalton Trans.* **1995**, 3317.
400. G. Böhm, K. Wieghardt, B. Nuber and J. Weiss, *Inorg. Chem.* **1991**, *30*, 3464.
401. T. Takahira, K. Umakoshi and Y. Sasaki, *Acta Crystallogr.* **1994**, *C50*, 1870.
402. H. Sugimoto, M. Kamei, K. Umakoshi, Y. Sasaki and M. Suzuki, *Inorg. Chem.* **1996**, *35*, 7082.
403. J. C. Bryan, D. R. Wheeler, D. L. Clark, J. C. Huffman and A. P. Sattelberger, *J. Am. Chem. Soc.* **1991**, *113*, 3184.
404. See, for example, I. Wentzell, H. Fuess, J. W. Bats and A. K. Cheetham, *Z. anorg. allg. Chem.* **1985**, *528*, 48, and references cited therein.
405. R. A. Walton, *ACS Symposium Ser.* **1981**, *155*, 207.
406. F. A. Cotton, P. A. Kibala and M. Matusz, *Polyhedron* **1988**, 7, 83.
407. D. G. Tisley, R. A. Walton and D. L. Wills, *Inorg. Nucl. Chem. Lett.* **1971**, 7, 523.
408. G. L. Geoffroy, H. B. Gray and G. S. Hammond, *J. Am. Chem. Soc.* **1974**, *96*, 5565.
409. (a) M. T. Costello, P. W. Schrier, P. E. Fanwick and R. A. Walton, *Inorg. Chim. Acta* **1993**, *212*, 157. (b) M. J. Siwajek, Y. Ding, P. E. Fanwick and R. A. Walton, *J. Cluster Sci.* **2000**, *11*, 243.
410. C. A. Hertzer and R. A. Walton, *J. Organomet. Chem.* **1977**, *124*, C15.
411. S. Bucknor, F. A. Cotton, L. R. Falvello, A. H. Reid, Jr. and C. D. Schmulbach, *Inorg. Chem.* **1986**, *25*, 1021.

Pictiva EX2004
Samsung v Pictiva
IPR2024-01094

412. K. R. Dunbar and R. A. Walton, *Inorg. Chim. Acta* **1984**, *87*, 185.
413. F. A. Cotton, L. M. Daniels and C. D. Schmulbach, *Inorg. Chim. Acta* **1983**, *75*, 163.
414. J. D. Allison, T. E. Wood, R. E. Wild and R. A. Walton, *Inorg. Chem.* **1982**, *21*, 3540.
415. S. Bouguillon and M. Dartiguenave, *J. Coord. Chem.* **1994**, *31*, 257.
416. C. J. Cameron, D. R. Derringer and R. A. Walton, *Inorg. Chim. Acta* **1989**, *165*, 141.
417. F. A. Cotton, P. E. Fanwick and P. A. McArdle, *Inorg. Chim. Acta* **1979**, *35*, 289.
418. J. K. Hoyano and W. A. G. Graham, *J. Chem. Soc., Chem. Commun.* **1982**, 27.
419. W. A. Herrmann, R. A. Fischer and E. Herdtweck, *J. Organomet. Chem.* **1987**, *329*, C1.
420. M. Bochmann, G. Wilkinson, A. M. R. Galas, M. B. Hursthouse and K. M. Abdul Malik, *J. Chem. Soc., Dalton Trans.* **1980**, 1797.
421. C. P. Casey, H. Sakaba, P. N. Hazin and D. R. Powell, *J. Am. Chem. Soc.* **1991**, *113*, 8165.
422. See, for example: (a) C. P. Casey, R. S. Carino, R. K. Hayashi and K. D. Schladetzky, *J. Am. Chem. Soc.* **1996**, *118*, 1617. (b) C. P. Casey, R. S. Carino, H. Sakaba and R. K. Hayashi, *Organometallics* **1996**, *15*, 2640; (c) C. P. Casey, R. S. Carino and H. Sakaba, *Organometallics* **1997**, *16*, 41.
423. R. Toreki, R. R. Schrock and M. G. Vale, *J. Am. Chem. Soc.* **1991**, *113*, 3610.
424. T. A. Barckholtz, B. E. Bursten, G. P. Niccolai and C. P. Casey, *J. Organomet. Chem.* **1994**, *478*, 153.
425. J. D. Allison, C. J. Cameron and R. A. Walton, *Inorg. Chem.* **1983**, *22*, 1599.
426. C. J. Cameron, G. A. Moehring and R. A. Walton, *Inorg. Synth.* **1990**, *27*, 14.
427. M. T. Costello, G. A. Moehring and R. A. Walton, *Inorg. Chem.* **1990**, *29*, 1578.
428. M. T. Costello, P. E. Fanwick, K. E. Meyer and R. A. Walton, *Inorg. Chem.* **1990**, *29*, 4437.
429. A. V. Shtemenko, O. V. Kozhura, A. A. Pasenko and K. V. Domasevitch, *Polyhedron* **2003**, *22*, 1547.
430. M. Dequeant, J. L. Eglin, M. K. Graves-Brook and L. T. Smith, *Inorg. Chim. Acta* **2003**, *351*, 141.
431. P. M. Bradley, L. T. Smith, J. L. Eglin and C. Turro, *Inorg. Chem.* **2003**, *42*, 7360.
432. S. Chattopadhyay, P. E. Fanwick and R. A. Walton, *Inorg. Chem. Commun*. **2003**, *6*, 1358.
433. P. Schaffer, J. F. Britten, A. Davison, A. G. Jones and J. F. Valliant, *J. Organomet. Chem*. **2003**, *680*, 323.
434. S. Chattopadhyay, P. E. Fanwick and R. A. Walton, *Inorg. Chim. Acta*, **2004**, *357*, 764.
435. D. A. Kort, N. D. Reddy, P. E. Fanwick and R. A. Walton, *Ind. J. Chem*. **2003**, *42A*, 2277.
436 E. J. Schelter, J. K. Bera, J. Bacsa, J. R. Galán-Mascarós and K. R. Dunbar, *Inorg. Chem*. **2003**, *42*, 4256.
437. C. P. Chaney, L. E. T. Hibbard, K. T. Horne, T. L. C. Howe, G. L. Powell and D. W. Thurman, *Polyhedron* **2003**, *22*, 2625.
438. R. A. Walton, *J.Cluster Sci.* **2004**, *15*, 559.

Pictiva EX2004
Samsung v Pictiva
IPR2024-01094

9

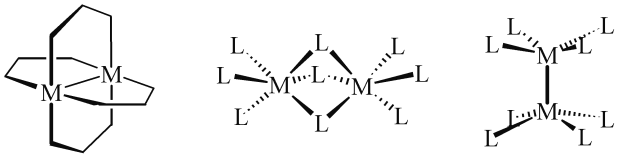
Ruthenium Compounds

Panagiotis Angaridis,
Texas A&M University

9.1 Introduction

In the previous edition of this book the chapter on Ru_2 compounds was rather short, covering in only a few pages the small number of compounds known at that time. However, since then a variety of new Ru_2 compounds have been synthesized, structurally characterized, and studied using theoretical and spectroscopic methods providing a better understanding of the Ru–Ru bond and its reactivity.

The Ru_2 complexes have been found to adopt either the paddlewheel (**9.1**a), or the face-sharing bioctahedral structures (**9.1**b). The lack of the tetragonal prismatic structure (**9.1**c) is surprising, since it is a common structural motif for dimetal compounds of Mo, W, Tc, Re, and Os. The majority of Ru_2 complexes adopt the paddlewheel structure, in which four monoanionic, three-atom donor ligands are bridging two multiply-bonded Ru atoms. Typical examples of bridging ligands with O,O'-, N,O- and N,N'-donor atoms are shown in Fig. 9.1.



a **b** **c**

9.1

Complexes of the paddlewheel framework have been isolated in three different formal oxidation states: Ru_2^{4+}, Ru_2^{5+}, and Ru_2^{6+}. Those with the Ru_2^{5+} core are the most common, while those having the Ru_2^{4+} and Ru_2^{6+} cores represent the most recent additions to the Ru_2 family. Recent electrochemical experiments have given support for the existence of Ru_2^{7+} complexes; however, attempts to synthesize such complexes have been unsuccessful. This chapter describes the syntheses, properties and electronic structures of paddlewheel Ru_2 compounds classified according to the oxidation state of the dimetal unit and the ligand type.

Pictiva EX2004
Samsung v Pictiva
IPR2024-01094

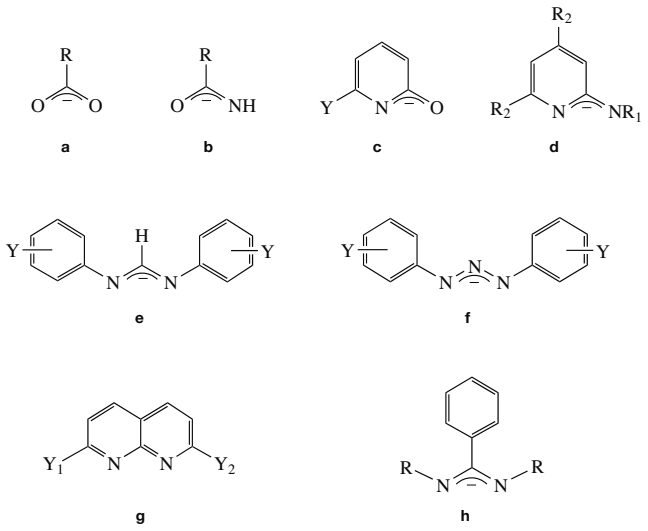


Fig. 9.1. Generic examples of bridging ligands with O,O'-, N,O- and N,N'-donor atoms used in Ru_2 complexes of the paddlewheel framework: (a) carboxylate, (b) amidate, (c) oxopyridinate, (d) aminopyridinate, (e) formamidinate, (f) triazenate, (g) naphthyridine and (h) benzamidinate.

9.2 Ru_2^{5+} Compounds

Complexes of the Ru_2^{5+} core are the most common and stable Ru_2 complexes. They have been often designated as mixed-valent $Ru^{2+}Ru^{3+}$ or Ru_2(II,III); however, since the two Ru atoms are equivalent, they should be referred to as having Ru_2^{5+} cores. The stability of this oxidation state can be attributed to the half-filled highest occupied molecular orbitals, the nearly degenerate π^* and δ^* molecular orbitals, which give rise to an electronic configuration with three unpaired electrons, $(\pi^*\delta^*)^3$, as discussed later. Structurally characterized compounds of this type together with their corresponding Ru–Ru bond lengths are given in Table 9.1.

Table 9.1. Structurally characterized paddlewheel Ru_2^{5+} compounds

Compound	*r*(Ru–Ru) (Å)	ref.
O,O'-donor bridging ligands		
carboxylate ligands		
$Ru_2(O_2CPr^n)_4Cl$	2.281(4)	6
$[Ru_2(O_2CMe)_4(H_2O)_2]BF_4$	2.248(1)	7
$Cs[Ru_2(O_2CMe)_4Cl_2]$	2.286(2)	7
$Ru_2(O_2CMe)_4Cl{\cdot}2H_2O$	2.267(1)	7
$K[Ru_2(O_2CH)_4Cl_2]$	2.290(1)	7
$Ru_2(O_2CEt)_4Cl$	2.292(7)	7
$Ru_2(O_2CC(Me)=CHEt)_4Cl$	2.281(1)	8
$Ru_2(O_2CMe)_4Cl$	2.281(3)	9
$Ru_2(O_2CC_6H_4$-*p*-$OMe)_4Cl{\cdot}0.25H_2O$	2.286[2]	10
$Ru_2(O_2CPh)_4Cl$	2.290(1)	11
$Ru_2(O_2C(Me)C=CH_2)_4Cl$	2.289[2]	12
$Ru_2(O_2CH)_4Br$	2.290[2]	13

Pictiva EX2004
Samsung v Pictiva
IPR2024-01094

Compound	r(Ru–Ru) (Å)	ref.
$Ru_2(O_2CCF_3)_4(O_2CCF_3)$	2.278(1)	14
$Ru_2(O_2CEt)_4(O_2CEt)$	2.273(1)	14
$[Ru_2(O_2CMe)_4(O_2CMe)_2]H{\cdot}0.7H_2O$	2.265(1)	14
$[Ru_2(O_2CPh)_4(O_2CPh)]{\cdot}PhCO_2H$	2.278[2]	15
$[Ru_2(O_2CMe)_4(PhPO_3H)_2]H{\cdot}H_2O$	2.267(2)	16
$[Ru_2(O_2CMe)_4(HPhPO_2)_2]H$	2.272(1)	16
$[Ru_2(O_2CEt)_4(phz)]BF_4$	2.276(1)	17
$[Ru_2(O_2CBu^t)_4(nitph)]BF_4{\cdot}2$benzene	2.266(1)	18
$Ru_2(O_2CC_4H_4N)_4Cl(THF){\cdot}THF{\cdot}H_2O$	2.268(1)	19
$Ru_2(O_2CBu^t)_4Cl(H_2O)$	2.274(2)	20
$Ru_2(O_2CPr^i)_4Cl(THF)$	2.272(2)	20
$Ru_2(O_2CPr^i)_4Cl(OPPh_3)$	2.279(1)	21
$[Ru_2(O_2CCH_2CH_2OPh)_4I_2][Ru_2(O_2CCH_2CH_2OPh)_4(H_2O)_2]{\cdot}H_2O$	2.310(2) 2.265(2)	22
$Ru_2(O_2CCH_2CH_2OPh)_4Cl(H_2O){\cdot}2MeOH$	2.279(3)	22
$Ru_2(O_2CCMePh_2)_4Cl(H_2O)$	2.284(1)	22
$[Ru_2(O_2CMe)_4(H_2O)_2]PF_6{\cdot}3H_2O$	2.265(1)	23
$[Ru_2(O_2CMe)_4(DMF)_2]PF_6$	2.262(3)	23
$[Ru_2(O_2CMe)_4(DMF)_2]PF_6{\cdot}DMF$	2.265(2)	23
$[Ru_2(O_2CMe)_4(DMSO)_2]PF_6$	2.271(2)	23
$[Ru_2(O_2CMe)_4Cl(OPPh_3)_2]PF_6{\cdot}CH_2ClCH_2Cl$	2.267(1)	24
$[Ru_2(O_2CCH_2OEt)_4Cl][Ru_2(O_2CCH_2OEt)_4Cl_2]$- $[Ru_2(O_2CCH_2OEt)_4(H_2O)_2]{\cdot}3H_2O$	2.277(1) 2.294(2) 2.261(1)	25
$[Ru_2(O_2CMe)_4(PCy_3)_2]PF_6{\cdot}CH_2Cl_2$	2.427(1)	26
$[RuCl(MeCN)_4(PPh_3)]_2[Ru_2(O_2CC_6H_4\text{-}p\text{-}OMe)_4Cl_2]{\cdot}0.5Et_2O{\cdot}0.75H_2O$	2.299(1)	30
$[Ru_2(O_2CC_6H_4\text{-}p\text{-}Bu^t)_4(THF)_2]OH$	2.260(1)	35
$[Ru_2(O_2CC_4H_3S)_4(OPPh_3)_2]BF_4{\cdot}2H_2O$	2.275(1)	36
$[Ru_2(O_2CMe)_4(urea)_2][Ru_2(O_2CMe)_4(Pr^nOH)_2](PF_6)_2$	2.264(1) 2.259(1)	38
$[Ru_2(O_2CMe)_4(tmu)_2]PF_6$	2.275(1)	38
$[Ru_2(O_2CMe)_4(tmtu)_2]PF_6{\cdot}2CH_2ClCH_2Cl$	2.301(2)	38
$[Ru_2(O_2CMe)_4(tht)_2]PF_6$	2.285(4)	39
$[Ru_2(O_2CMe)_4(quinoline)_2]PF_6{\cdot}$quinoline	2.282(2)	40
$[Ru_2(O_2CMe)_4(quin)_2]PF_6$	2.292(1)	41
$[Ru_2(O_2CMe)_4(4\text{-}Mepy)_2]PF_6$	2.279[2]	41
$[Ru_2(O_2CMe)_4(py)_2]PF_6{\cdot}0.5H_2O$	2.281[10]	41
$[Ru_2(O_2CMe)_4(4\text{-}CNpy)_2]PF_6{\cdot}CH_2ClCH_2Cl$	2.274(1)	41
$[Ru_2(O_2CMe)_4(4\text{-}Phpy)_2]PF_6{\cdot}H_2O$	2.279[7]	41
$[Ru_2(O_2CMe)_4](N(CN)_2){\cdot}MeCN$	2.279(1)	42
$[Ru_2(O_2CMe)_4](C(CN)_3)$	2.276(1)	42
$[Ru_2(O_2CBu^t)_4]_3(H_2O)[Fe(CN)_6]{\cdot}4H_2O$	2.273(5) 2.292(3)	45
$\{[Ru_2(O_2CBu^t)_4(H_2O)](\mu\text{-}TCNQ)[Ru_2(O_2CBu^t)_4(H_2O)]\}(BF_4)_2$	2.263(1)	46

Pictiva EX2004
Samsung v Pictiva
IPR2024-01094

Compound	*r*(Ru–Ru) (Å)	ref.
$[Ru_2(O_2CPh)_4(EtOH)_2][Ru_2(O_2CPh)_4(HSO_4)_2]$	2.265(2)	49
	2.272(2)	
$[Ru_2(O_2CFc)_4(Pr^nOH)_2]PF_6{\cdot}Pr^nOH$	2.260(4)	50
$[Ru_2(Fcpe)_4(Pr^nOH)_2]PF_6{\cdot}3Pr^nOH$	2.262(2)	51
$[Ru_2(O_2CRc)_4(Pr^nOH)_2]PF_6{\cdot}Pr^nOH$	2.260(10)	51
$Ru_2(O_2CMe)_4Cl$	2.287(2)	62
$Ru_2(O_2CCMePh_2)_4Cl$	2.289(1)	67
$Ru_2(O_2CBu^n)_4Cl$	2.290(1)	68
$Ru_2(O_2CCH{=}CHCH{=}CHMe)_4Cl$	2.286(1)	72
$Ru_2(O_2CCH_2OMe)_4Cl$	2.290(1)	72
$[Ru_2(O_2CBu^t)_4(tempo)_2][Ru_2(O_2CBu^t)_4(H_2O)_2](BF_4)_2$	2.273(1)	73
	2.260(1)	
$[Ru_2(O_2CBu^t)_4(nitme)_2]BF_4{\cdot}2CH_2Cl_2$	2.272(1)	74
$[Ru_2(O_2CBu^t)_4(nitme)_2][Ru_2(O_2CBu^t)_4(H_2O)_2](BF_4)_2{\cdot}2CH_2Cl_2$	2.275(1)	74
	2.262(1)	
$[Ru_2(O_2CBu^t)_4(nitet)_2][Ru_2(O_2CBu^t)_4(H_2O)_2](BF_4)_2{\cdot}2CH_2Cl_2$	2.273(2)	74
	2.256(1)	
$[Ru_2(O_2CBu^t)_4(nitme)_2][Ru_2(O_2CBu^t)_4(H_2O)_2](BF_4)_2{\cdot}2CH_2Cl_2$	2.275(1)	75
	2.262(1)	
$[Ru_2(O_2CBu^t)_4(nitph)]BF_4{\cdot}$benzene	2.266(1)	76
$[Ru_2(O_2CBu^t)_4(nitph)(H_2O)]BF_4{\cdot}2CH_2Cl_2$	2.265(1)	77
$[Ru_2(O_2CBu^t)_4(p\text{-nitpy})]BF_4{\cdot}1.5CH_2Cl_2$	2.272(1)	78
$[Ru_2(O_2CBu^t)_4(m\text{-nitpy})_2]BF_4$	2.276(1)	79
$[Ru_2(O_2CBu^t)_4(p\text{-nitpy})_2]BPh_4{\cdot}0.5CH_2Cl_2$	2.282(1)	79
$\{Ru_2(O_2CMe)_4[NCRu(PPh_3)_2(\eta^5\text{-}C_5H_5)]SbF_6{\cdot}CHCl_3$	2.296(1)	119
$Ru_2(O_2CC_{10}H_{15})_3(O_2CO)(MeOH)_2{\cdot}2MeOH$	2.254(1)	147
$[Ru_2(O_2CC_6H_4\text{-}p\text{-}Me)_4(THF)_2]BF_4$	2.262(2)	152
O,O'-donor bridging ligands other than carboxylates		
$Na_3[Ru_2(O_2CO)_4]{\cdot}6H_2O$	2.254[7]	80
$Na_3[Ru_2(O_2CO)_4]{\cdot}6H_2O$	2.251[2]	81
$K_3[Ru_2(O_2CO)_4]{\cdot}4H_2O$	2.251(1)	81
$K_4[Ru_2(HPO_4)_3(PO_4)(H_2O)_2]$	2.305(1)	82
$K_2H[Ru_2(SO_4)_4(H_2O)_2]{\cdot}4H_2O$	2.303(1)	83
$(NH_4)_3[Ru_2(hedp)_2]{\cdot}2H_2O$	2.347(1)	85
N,O-donor bridging ligands		
amidate ligands		
trans-(2,2)-$Ru_2(ONHCPh)_4Cl{\cdot}$MeOH	2.293(2)	87
trans-(2,2)-$Ru_2(ONHCC_6H_4\text{-}p\text{-}Cl)_4Cl{\cdot}$MeOH	2.296[1]	88
[*trans*-(2,2)-$Ru_2(ONHCC_6H_4\text{-}p\text{-}Bu^t)_4(OPPh_3)_2]BF_4$	2.281[3]	89
[*trans*-(2,2)-$Ru_2(ONHCC_4H_3S)_4(THF)_2]SbF_6{\cdot}0.5$cyclohexane	2.286(2)	90
oxopyridinate ligands		
(4,0)-$Ru_2(hp)_4Cl(Hhp)$	2.286(1)	96
$Ru_2(O_2CMe)(chp)_3Cl{\cdot}CH_2Cl_2$	2.282(4)	97
$[(4,0)\text{-}Ru_2(chp)_4]_2(BF_4)_2{\cdot}4CH_2Cl_2$	2.254(1)	98
(4,0)-$Ru_2(fhp)_4Cl$	2.284(1)	99

Pictiva EX2004
Samsung v Pictiva
IPR2024-01094

Compound	*r*(Ru–Ru) (Å)	ref.
(4,0)-$Ru_2(chp)_4Cl{\cdot}CH_2Cl_2$	2.281(1)	100
(4,0)-$Ru_2(chp)_4(OMe)$	2.256(1)	101
trans-$Ru_2(O_2CMe)_2(mhp)_2Cl{\cdot}0.5CH_2Cl_2$	2.278(2)	102
$[(4,0)\text{-}Ru_2(chp)_4(THF)]BF_4{\cdot}2THF$	2.266(1)	103
$[(4,0)\text{-}Ru_2(chp)_4(py)]BF_4{\cdot}$hexane·py	2.270(1)	104
$\{[(4,0)\text{-}Ru_2(chp)_4](\mu\text{-pyz})[(4,0)\text{-}Ru_2(chp)_4]\}(BF_4)_2{\cdot}4CH_2Cl_2$	2.267(1)	104
N,N'-donor bridging ligands		
aminopyridinate ligands		
(4,0)-$Ru_2(ap)_4Cl$	2.275(3)	96
trans-$Ru_2(O_2CMe)_2(ap)_2Cl(Hap){\cdot}CH_2Cl_2$	2.308(1)	97
$Ru_2(O_2CMe)_3(admp)Cl{\cdot}3CH_2Cl_2$	2.277[2]	108
trans-$Ru_2(O_2CMe)_2(admp)_2Cl{\cdot}2.5CH_2Cl_2$	2.274(1)	108
$Ru_2(O_2CMe)(admp)_3Cl{\cdot}$Hadmp·benzene	2.283(1)	108
(4,0)-$Ru_2(2,4,6\text{-}F_3ap)_4Cl$	2.296*	109
(3,1)-$Ru_2(2,4,6\text{-}F_3ap)_4Cl$	2.284*	109
(4,0)-$Ru_2(2,5\text{-}F_2ap)_4Cl$	2.284*	109
(3,1)-$Ru_2(2,6\text{-}F_2ap)_4Cl$	2.286*	109
(4,0)-$Ru_2(2\text{-Meap})_4Cl$	2.279*	109
$[(4,0)\text{-}Ru_2(ap)_4(H_2O)]SbF_6{\cdot}Et_2O$	2.288(1)	111
(4,0)-$Ru_2(ap)_4(C{\equiv}CPh){\cdot}2CH_2Cl_2$	2.319(2)	112
(4,0)-$Ru_2(ap)_4(C{\equiv}CSiMe_3)$	2.316(1)	113
(4,0)-$Ru_2(ap)_4(C{\equiv}CCH_2OMe)$·hexane	2.323(1)	113
(4,0)-$Ru_2(ap)_4(C{\equiv}CC{\equiv}CSiMe_3){\cdot}$MeC(O)OEt	2.330(1)	114
$[(4,0)\text{-}Ru_2(ap)_4](\mu\text{-}C{\equiv}CC{\equiv}C)[(4,0)\text{-}Ru_2(ap)_4]{\cdot}8H_2O$	2.332[3]	116
$[(4,0)\text{-}Ru_2(ap)_4](\mu\text{-}C{\equiv}CC{\equiv}CC{\equiv}CC{\equiv}C)[(4,0)\text{-}Ru_2(ap)_4]{\cdot}$THF·MeOH	2.329(1)	117
(4,0)-$Ru_2(ap)_4(CN){\cdot}2$THF $\cdot H_2O$	2.336(2)	118
(4,0)-$Ru_2(2\text{-Meap})_4(CN){\cdot}2CH_2Cl_2$	2.304(5)	118
$\{(4,0)\text{-}Ru_2(ap)_4[NCFe(dppe)(\eta^5\text{-}C_5H_5)]\}SbF_6{\cdot}CH_2Cl_2$	2.280(2)	119
$\{(4,0)\text{-}Ru_2(ap)_4[NCRu(PPh_3)_2(\eta^5\text{-}C_5H_5)]\}SbF_6{\cdot}CH_2ClCH_2Cl$	2.287(2)	119
$\{(3,1)\text{-}Ru_2(2\text{-Fap})_4[NCFe(dppe)(\eta^5\text{-}C_5H_5)]\}SbF_6{\cdot}2CH_2ClCH_2Cl$	2.284(2)	119
(3,1)-$Ru_2(2\text{-Fap})_4Cl{\cdot}CH_2Cl_2$	2.286(1)	120
(3,1)-$Ru_2(2\text{-Fap})_4Cl(NO)$	2.420(1)	120
$Ru_2(O_2CMe)(HNC_5H_3NMe)_3Cl$	2.287(2)	123
formamidinate ligands		
$Ru_2(DTolF)_4Cl{\cdot}$hexane	2.370(2)	125
trans-$Ru_2(O_2CMe)_2(DAni^{o}F)(Ani^{o}Ph^{o\text{-}O}F)$	2.311(1)	127
$Ru_2(O_2CMe)(DAni^{o}F)_2(Ani^{o}Ph^{o\text{-}O}F)$	2.312(1)	127
cis-$Ru_2(DAniF)_2(O_2CMe)_2Cl{\cdot}H_2O$	2.319(1)	128
$\{[cis\text{-}Ru_2(DAniF)_2Cl(H_2O)](\mu\text{-}O_2CCO_2)\}_4{\cdot}$MeCN·2hexane·$12H_2O$	2.332[2]	128
$\{[cis\text{-}Ru_2(DAniF)_2Cl(4\text{-}Bu^tpy)](\mu\text{-}O_2CC_6H_4CO_2)\}_4{\cdot}17CH_2ClCH_2Cl{\cdot}$hexane	2.332[2]	128
$\{[Ru_2(DAniF)_3Cl]_2(\mu\text{-}O_2CC_6H_4CO_2){\cdot}$4.5benzene	2.329[2]	129
$Ru_2(O_2CMe)(DPhF)_3Cl{\cdot}$HDPhF	2.320(1)	130
$Ru_2(O_2CMe)(DPhF)_3Cl{\cdot}2$THF	2.325(2)	130
$Ru_2(O_2CC_6H_4\text{-}p\text{-}OC_{10}H_{21})(DPhF)_3Cl$	2.325(1)	130
$Ru_2(O_2CMe)_3(DXyl^{2,6}F)Cl(THF){\cdot}0.5$THF	2.305(1)	131

Pictiva EX2004
Samsung v Pictiva
IPR2024-01094

Compound	r(Ru–Ru) (Å)	ref.
$Ru_2(O_2CMe)_3(DXyl^{2,6}F)Cl(HDXyl^{2,6}F)$·toluene	2.333(1)	131
trans-$Ru_2(O_2CMe)_2(DXyl^{2,6}F)_2Cl(THF)$	2.326(1)	131
trans-$Ru_2(O_2CMe)_2(DXyl^{2,6}F)_2Cl$·2toluene	2.316(1)	131
$Ru_2(DAniF)_4Cl$·$0.5CH_2Cl_2$	2.396(1)	131
$Ru_2(DPhF)_4Cl$·pentane	2.339(1)	132
$Ru_2(DPhF)_4(C{\equiv}CPh)$	2.400[2]	132
$Ru_2(DPh^{m\text{-}Cl}F)_4(C{\equiv}CPh)$·hexane	2.387(1)	133
$Ru_2(DPh^{3,5\text{-}diCl}F)_4(C{\equiv}CPh)$·$4CH_2Cl_2$	2.429(1)	133
$Ru_2(DAni^{m}F)_4(C{\equiv}CC{\equiv}CSiMe_3)$	2.506(1)	135
naphthyridine ligands		
$Ru_2(O_2CMe)_3(bcnp)$·$2H_2O$	2.265[5]	136
trans-$Ru_2(O_2CMe)_2(mephonp)_2Cl$·$3CHCl_3$	2.285(1)	137
other N,N'-donor bridging ligands		
$Ru_2(O_2CMe)_3(admpym)Cl(MeOH)$	2.290(1)	138
$[Na(THF)_2][Ru_2(O_2CMe)_2(5\text{-}Clsalpy)_2]$·THF	2.295(1)	139
[K(18-crown-6)][$Ru_2(O_2CMe)_2(salpy)_2$]·toluene	2.300(1)	140
[Na(18-crown-6)(OC_4H_8)(H_2O)][$Ru_2(O_2CMe)_2(5\text{-}Mesalpy)_2$]·0.5THF	2.297[2]	140
[Na(18-crown-6)(THF)(H_2O)][$Ru_2(O_2CMe)_2(5\text{-}Clsalpy)_2$]·0.5THF	2.288[2]	140
[Na(18-crown-6)(THF)(H_2O)][$Ru_2(O_2CMe)_2(5\text{-}Brsalpy)_2$]·0.5THF	2.291[2]	140
[K(18-crown-6)][$Ru_2(O_2CMe)_2(5\text{-}NO_2salpy)_2$]·2toluene	2.283(1)	140
[$Li_2(THF)_4Cl$][$Ru_2(5\text{-}Clsalpy)_3$]·THF	2.313(1)	141
$Ru_2(dmat)_4Cl$·CH_2Cl_2	2.432(1)	142
[$Ru_2(DTolTA)_4(MeCN)$]BF_4	2.373(1)	169

* no esds reported.

9.2.1 Ru_2^{5+} compounds with O,O'-donor bridging ligands

Carboxylate ligands

Paddlewheel Ru_2^{5+} compounds with carboxylate bridges were the first to be discovered and represent the majority of the Ru_2^{5+} complexes. The first syntheses were reported by Wilkinson and Stephenson in 1966.[1] By refluxing $RuCl_3$·xH_2O in a mixture of a carboxylic acid and its anhydride, compounds of the general type $Ru_2(O_2CR)_4Cl$ (R = Me, Et, Pr^n) were synthesized. The synthesis of Ru_2^{5+} tetraformate was achieved the following year using a similar method.[2] Two other synthetic procedures appeared later: one involved reaction of 'ruthenium[(III),(IV)] chloride' with acetic acid in a sealed stainless steel container to form the product in low yield,[3] while the other was a modification of the original synthesis in which LiCl and O_2 were added to the reaction mixture improving the yield to >80%.[4] Other Ru_2^{5+} tetracarboxylates have been obtained via metathesis reactions by refluxing a solution of a $Ru_2(O_2CR)_4Cl$ complex in the presence of another carboxylic acid R'CO_2H or its salt.[5]

The first insight into the structures of Ru_2^{5+} tetracarboxylates was gained in 1969, when the crystal structure of $Ru_2(O_2CPr^n)_4Cl$ (Fig. 9.2) was published by Cotton and coworkers.[6] This provided the first evidence of the existence of a strong Ru–Ru bond, with a bond order of 2.5 and a short distance of 2.281(4) Å. The compound exhibits a polymeric structure in which Ru_2^{5+} units bridged by four butyrate ligands, $[Ru_2(O_2CPr^n)_4]^+$, are linked by Cl^- ions into an infinite zig-zag chain.

Pictiva EX2004
Samsung v Pictiva
IPR2024-01094

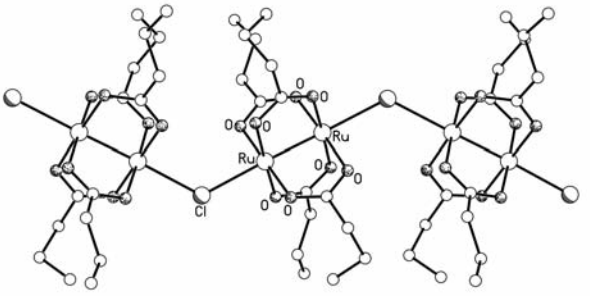


Fig. 9.2. Part of the polymeric zig-zag chain structure of $Ru_2(O_2CPr^n)_4Cl$.

Subsequent structural characterization of other $Ru_2(O_2CR)_4X$ compounds (X = halide) showed that in the solid state they form similar polymeric chain structures which can be either linear (Fig. 9.3a) as in $Ru_2(O_2CEt)_4Cl$[7] and $Ru_2(O_2CC(Me)=CHEt)_4Cl$,[8] or bent (Fig. 9.3b) as in $Ru_2(O_2CMe)_4Cl$,[9] $Ru_2(O_2CC_6H_4$-*p*-$OMe)_4Cl$,[10] $Ru_2(O_2CPh)_4Cl$,[11] $Ru_2(O_2C(Me)C=CH_2)_4Cl$[12] and $Ru_2(O_2CH)_4Br$.[13] The last of the above series of polymers exhibits an extremely bent structure with ∠Ru–Br–Ru ~110°. The type of polymeric structure (linear or bent) a particular Ru_2^{5+} tetracarboxylate adopts does not depend on the nature of the substituents R of the carboxylate bridges. Similar polymeric structures are also observed in $Ru_2(O_2CR)_4X$ compounds when X is not a halide, but a bifunctional linker. Examples of this type of polymers are $Ru_2(O_2CEt)_4(O_2CEt)$,[14] $[Ru_2(O_2CPh)_4(O_2CPh)]\cdot(HO_2CPh)$,[15] and $[Ru_2(O_2CMe)_4(HPhPO_2)_2]H$.[16] In the first two compounds the chains result from the direct bonding between the Ru_2^{5+} units and the linkers $EtCO_2^-$, and $PhCO_2^-$, respectively, while in the latter the chain is supported by H-bonding. Neutral bifunctional molecules can also be linkers between Ru_2^{5+} tetracarboxylate units, like phz in $[Ru_2(O_2CEt)_4(phz)]BF_4$,[17] and nitph in $[Ru_2(O_2CBu^t)_4(nitph)]BF_4$.[18]

Some Ru_2^{5+} tetracarboxylates exhibit non-polymeric structures in the solid state. These are of the general formula $Ru_2(O_2CR)_4XL$, in which the ligands X and L (X = halide, L = neutral ligand, or solvent molecule) are axially coordinated to the Ru_2^{5+} unit (Fig. 9.3c). Examples of this type of compound include $Ru_2(O_2CC_4H_4N)_4Cl(THF)$,[19] $Ru_2(O_2CCHMe_2)_4Cl(THF)$,[20] and $Ru_2(O_2CCHMe_2)_4Cl(OPPh_3)$.[21] The factors which determine whether a particular compound will adopt the polymeric or non-polymeric structure remain unclear. However, it has been proposed that they are related to the presence of branched chains in the substituents of the carboxylate bridges and to the type of axial ligand.[20-22]

Another type of non-polymeric structure includes the diadducts of the formula $[Ru_2(O_2CR)_4L_2]Y$ (Fig. 9.3d). In these complexes the axial ligands L can either be anions while Y is a positively charged ion, as in $K[Ru_2(O_2CH)_4Cl_2]$,[7] or neutral donor molecules with Y being a negatively charged ion, as in $[Ru_2(O_2CMe)_4(DMF)_2]PF_6$[23] and $[Ru_2(O_2CMe)_4(OPPh_3)_2]PF_6$.[24]

There are also reports of Ru_2^{5+} tetracarboxylates that exist as pairs of discrete anionic and cationic units of the type $[Ru_2(O_2CR)_4X_2][Ru_2(O_2CR)_4L_2]$ (Fig. 9.3e), where X is an anion and L is a neutral ligand, as in $[Ru_2(O_2CH_2CH_2OPh)_4I_2][Ru_2(O_2CH_2CH_2OPh)_4(H_2O)_2]$.[22] Of interest is the compound $Ru_2(O_2CCH_2OEt)_4Cl$ in which both the discrete anionic-cationic dinuclear units and the polymeric chain coexist.[25]

Pictiva EX2004
Samsung v Pictiva
IPR2024-01094

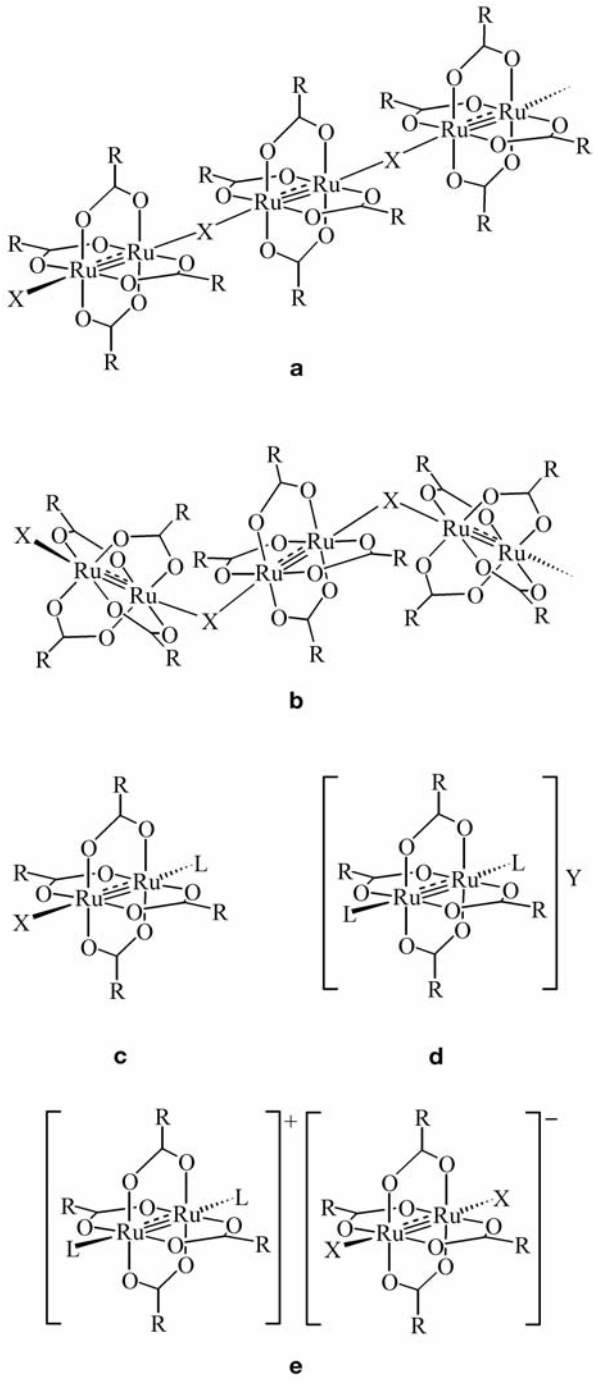


Fig. 9.3. Structural types of Ru_2^{5+} tetracarboxylates: (a) polymeric linear chain (X = anionic ligand), (b) polymeric zig-zag chain (X = anionic ligand), (c) non-polymeric monoadduct (X = anionic ligand, L = neutral ligand), (d) nonpolymeric diadduct (L = neutral ligand and Y = counter-anion, or L = anionic ligand and Y = counter-cation). (e) anion-cation pair (X = anionic ligand, L = neutral ligand).

Pictiva EX2004
Samsung v Pictiva
IPR2024-01094

As listed in Table 9.1, the Ru–Ru bond lengths of Ru_2^{5+} tetracarboxylates lie in the narrow range of 2.248-2.310 Å (an exception is discussed in the following paragraph). They show a very small dependence on the nature of the carboxylate bridge and the axially coordinated ligands. However, the diadducts exhibit slightly shorter Ru–Ru bond lengths than the corresponding polymeric compounds, as shown in $[Ru_2(O_2CMe)_4(H_2O)_2]BF_4$ and $Ru_2(O_2CMe)_4Cl$ in which the Ru–Ru bond lengths are 2.248(1) and 2.267(1) Å, respectively.[7]

The only compound exhibiting a Ru–Ru bond distance outside the aforementioned range is $[Ru_2(O_2CMe)_4(PCy_3)_2]PF_6$.[26] The remarkably long distance of 2.427(1) Å is attributed to the strong electron donating nature of the axial PCy_3 ligands, which increases the anti-bonding σ* electron density between the two metals that weakens the Ru–Ru bond. Typically, reactions of $Ru_2(O_2CR)_4Cl$ compounds with phosphines do not result in the formation of diadducts. This is because the phosphines prefer to coordinate to the equatorial instead of the axial positions of the dimetal core to maximize their π-back bonding. As a result they displace the equatorial ligands causing the disintegration of the paddlewheel structure and giving a number of decomposition products, such as oxo-centered trimers, oxo-bridged dimers and other mononuclear compounds, depending on the reaction conditions.[27-30] However, for $[Ru_2(O_2CMe)_4(PCy_3)_2]^+$ steric factors (cone angle of PCy_3 ~170°) force the PCy_3 ligands to coordinate axially to the Ru_2^{5+} unit minimizing in this way their π-accepting ability.

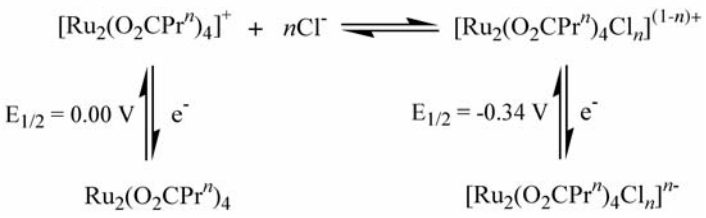
Similarly to the reactions with phosphines, Ru_2^{5+} tetracarboxylate compounds react with diphosphines (P–P), Grignard reagents (or other Lewis bases which are also π-acceptors) resulting in the disintegration of the dimetal core and the formation of mononuclear complexes such as $Ru(O_2CR)_2(P–P)_2$, $RuCl_2(P–P)_2$,[31,32] and $Ru(c\text{-}C_6H_{11})_4$,[33] respectively. In contrast, reactions with Lewis bases which are not π-acceptors result in axial mono- or diadducts. The enthalpies of formation of such adducts of $Ru_2(O_2CPr^n)_4Cl$ with various Lewis bases, such as py, DMSO, acetone and MeCN, were determined in a calorimetric study conducted by Drago *et al.* from which it was concluded that $Ru_2(O_2CR)_4Cl$ compounds are stronger Lewis acids than $Rh_2(O_2CR)_4$ and $Mo_2(O_2CR)_4$ compounds.[34]

The axial halide X in polymeric and non-polymeric $Ru_2(O_2CR)_4X$ compounds can be easily removed as AgX upon reaction with $AgBF_4$, or $AgPF_6$. This leaves both of the axial positions of the dimetal unit available for coordination by solvent molecules, L, resulting in diadducts of the general type $[Ru_2(O_2CR)_4L_2]^+$.[35,36] The axially coordinating solvent molecules can be exchanged with neutral O-, N- or S-donor ligands forming new diadducts. Examples of such ligands include DMSO,[23] Ph_3PO,[37] urea,[38] THT,[39] quinoline,[40] and py.[41] With bifunctional ligands, such as phz, nitph, $N(CN)_2^-$, $C(CN)_3^-$ and 9,10-anthraquinone, the same exchange reactions take place to form cationic, or neutral one-dimensional polymeric chains,[17,18,42,43] while with polyfunctional ligands, like $[Fe(CN)_6]^{3-}$, $[Cr(CN)_6]^{3-}$, and $[Co(CN)_6]^{3-}$, three-dimensional coordination polymers are obtained.[44,45] Unexpectedly, the reaction of $[Ru_2(O_2CBu^t)_4(H_2O)_2]BF_4$ with the polyfunctional ligand TCNQ results in the complex $\{[Ru_2(O_2CBu^t)_4(H_2O)](\mu\text{-TCNQ})[Ru_2(O_2CBu^t)_4(H_2O)]\}(BF_4)_2$ instead of a two- or three-dimensional polymer.[46]

Substitution reactions of the bridging carboxylate ligands are of special interest, since they offer a synthetic route to Ru_2^{5+} paddlewheel complexes with different types of bridging ligands. As mentioned, reactions of $Ru_2(O_2CR)_4X$ compounds with an excess of other carboxylic acids, $R'CO_2H$, or their salts (e.g., NaO_2CR') result in new $Ru_2(O_2CR')_4X$ compounds. Analogous reactions with other three-atom bridging ligands (e.g., amidates, oxopyridinates, aminopyridinates, formamidinates, triazinates) can take place and under appropriate conditions some or all of the RCO_2^- groups can be substituted resulting in new types of complexes. Such reactions will be considered in more detail in the following sections, where the syntheses of Ru_2^{5+} compounds with bridging ligands other than carboxylates will be discussed.

Pictiva EX2004
Samsung v Pictiva
IPR2024-01094

The first electrochemical study on Ru_2^{5+} tetracarboxylates was reported in 1972 for $Ru_2(O_2CMe)_4Cl$ and showed a single redox wave at a potential of +0.06 V vs SCE which was assigned to the reduction $Ru_2^{5+} + e^- \rightarrow Ru_2^{4+}$.[3] This process was later described as quasi-reversible.[47] A more extensive electrochemical study of $Ru_2(O_2CPr^n)_4Cl$ showed that the potential of this one-electron reduction process varies between 0.0 and -0.4 V, depending on the electrolyte and the solvent.[48] For example, while in CH_2Cl_2 with $Bu^n_4NClO_4$ as electrolyte the compound exhibits a two-step reduction, in a coordinating solvent or using Bu^n_4NCl as electrolyte a one-step reduction is observed for which the potential is shifted cathodically. This behavior (shown in **9.2**) is attributed to the association equilibria between $[Ru_2(O_2CPr^n)_4]^+$, Cl^- ions and solvent molecules. Compounds of the type $Ru_2(O_2CR)_4L$, where L = an anionic ligand other than halide, and diadducts of the type $[Ru_2(O_2CR)_4L_2]^+$, where L = a neutral ligand, exhibit similar electrochemical behavior to the $Ru_2(O_2CR)_4X$ compounds, where X = halide. Cyclic voltammetry measurements showed a quasi-reversible (or sometimes reversible) reduction wave at potentials between 0.0 and -0.8 V vs SCE.[38-40,49-52] Ru_2^{5+} compounds with a mixed set of bridging carboxylates have also been studied.[53]



9.2

The chemical reduction of Ru_2^{5+} tetracarboxylates has been the subject of a series of kinetic studies. The one-electron reduction of $[Ru_2(O_2CMe)_4]^+$ with Ti^{3+} in 1.0 M $LiCF_3SO_3/CF_3SO_3H$ shows that the reaction follows a two-term, pH-dependent rate law, suggesting that both Ti^{3+} and $Ti(OH)^{2+}$species are effective reducing agents; however, the reduction is faster for $Ti(OH)^{2+}$.[54] Analogous results are obtained from the study of the reduction of $[Ru_2(O_2CMe)_4]^+$ with oxalato complexes of Ti^{3+}.[55] There is a similar study in which the Ti^{3+} ion is complexed with N-(2-hydroxyethyl)-ethylenediaminetriacetic acid.[56]

Kinetic studies have also been employed to monitor the substitution of the axial ligands and the equatorial carboxylate ligands. For the former type of reactions it has been shown that in $[Ru_2(O_2CMe)_4(H_2O)_2]^+$, the H_2O molecules are rapidly displaced by Cl^- ions to give the complexes $Ru_2(O_2CMe)_4Cl(H_2O)$ and $[Ru_2(O_2CMe)_4Cl_2]^-$, with equilibrium constants for the first and second substitutions being 15 and 3.7 M^{-1}, respectively.[57] For the latter, the substitution reaction of $[Ru_2(O_2CEt)_4]^+$ with oxalate anions was studied which gives complexes with mixed $EtCO_2^-$/oxalate ligand sets. In this case the replacement of the $EtCO_2^-$ groups by the oxalate anions takes place in a stepwise fashion, followed by a slow decomposition process.[58]

The determination of the electronic structure of this type of compounds has been rather challenging. Magnetic susceptibility measurements for the $Ru_2(O_2CR)_4Cl$ compounds (R = Me, Et, Pr^n), which showed magnetic moments of 3.6 to 4.4 BM per Ru_2^{5+} unit,[1] and the EPR spectrum of $Ru_2(O_2CPr^n)_4Cl$,[48] which suggested a quartet ground state, were consistent with the presence of three unpaired electrons delocalized over the Ru_2^{5+} unit. However, early attempts to correlate these data with the electronic spectra of Ru_2^{5+} tetracarboxylate compounds by constructing a qualitative molecular orbital diagram based on the $Re_2Cl_8^{2-}$ model were unsuccessful.[3,6]

Pictiva EX2004
Samsung v Pictiva
IPR2024-01094

A detailed theoretical analysis of the electronic structure of Ru_2 tetracarboxylates reported by Norman and coworkers in the late 1970s provided an interpretation of the above experimental data.[59,60] SCF-Xα-SW calculations performed for $Ru_2(O_2CH)_4$, $[Ru_2(O_2CH)_4]^+$, and $[Ru_2(O_2CH)_4Cl_2]^-$, (HCO_2^- was used as a model of a carboxylate bridge) showed that Ru_2^{5+} tetracarboxylates do not exhibit the electronic configuration $\sigma^2\pi^4\delta^2\delta^{*2}\pi^*$ which is common for other dimetal complexes. Instead, the π* and δ* molecular orbital levels are very close in energy (almost degenerate), regardless of the identity of the axial ligands and the use of a spin-restricted or spin-unrestricted model, giving rise to the electronic configuration $\sigma^2\pi^4\delta^2(\pi^*\delta^*)^3$ (Fig. 9.4). The fact that these almost degenerate π* and δ* molecular orbitals are half-filled may be the reason for the higher stability of the Ru_2^{5+} tetracarboxylates compared to their Ru_2^{4+} analogs.

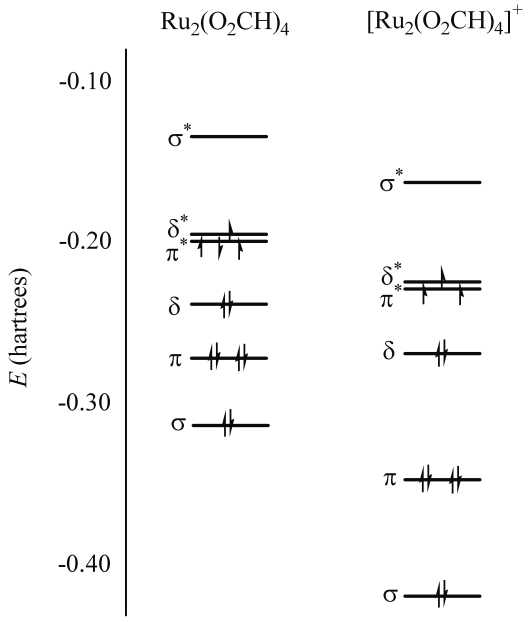


Fig. 9.4. The theoretically calculated molecular orbital energies of $Ru_2(O_2CH)_4$ and $[Ru_2(O_2CH)_4]^+$ using the SCF-Xα-SW method.

Based on this electronic structure, assignments of the bands in the electronic[1,47] and resonance Raman spectra[61] were suggested by Norman.[60] In solution all Ru_2^{5+} tetracarboxylates exhibit a strong band at 21,000-22,000 cm^{-1} which does not show any dependence on the alkyl substituent, R, of the carboxylate bridge, and a weak band at ~9,000 cm^{-1}. The former band, which was originally proposed to be a δ→δ* transition, has been reassigned to a charge transfer π(Ru–O, Ru_2) → π*(Ru_2) transition, with the π level having ~75% Ru–O π character, while the weak near-IR band has been assigned to the δ(Ru_2) → δ*(Ru_2) transition. Experiments using single crystal polarized optical spectroscopy and other studies supported Norman's assignments.[62] By using resonance Raman spectroscopy, Clark and Ferris showed that the band at 21,000-22,000 cm^{-1} is a dipole-allowed *z*-polarized π→π* transition,[63] while, Gray and Miskowski by using single crystal polarized optical spectroscopy provided evidence that the band at ~9,000 cm^{-1} is a *z*-polarized δ→δ* transition.[64] The rest of the electronic absorption

Pictiva EX2004
Samsung v Pictiva
IPR2024-01094

spectra of the Ru_2^{5+} tetracarboxylate compounds has been examined in great detail by Gray and Miskowski.[65]

Early variable temperature magnetic susceptibility measurements for $Ru_2(O_2CPr^n)_4Cl$ showed that this compound exhibits Curie-Weiss behavior in the temperature range 35-300 K, but at temperatures below 35 K there is a deviation (Fig. 9.5).[48,66] Due to the polymeric chain structure of this compound, its magnetic behavior at lower temperatures was originally attributed to a combination of a contribution from antiferromagnetic exchange between the Ru_2^{5+} units and a large zero-field splitting. However, attempts to model the results of these magnetic measurements led to the conclusion that the system can be better modeled as if there is no intermolecular antiferromagnetic exchange but only a large zero-field splitting (a value ~70 cm^{-1} was calculated for the zero-field splitting parameter, D). Therefore, each of the $[Ru_2(O_2CPr^n)_4]^+$ units of the polymeric chain behaves as an independent unit with $S = {}^3/_2$. This can be explained in terms of the bent polymeric chain structure of the compound, ∠Ru–Cl–Ru ~125°, which does not allow optimum orbital overlap between the paramagnetic Ru_2^{5+} units and the Cl^- linkers necessary for sufficient intermolecular antiferromagnetic interaction.

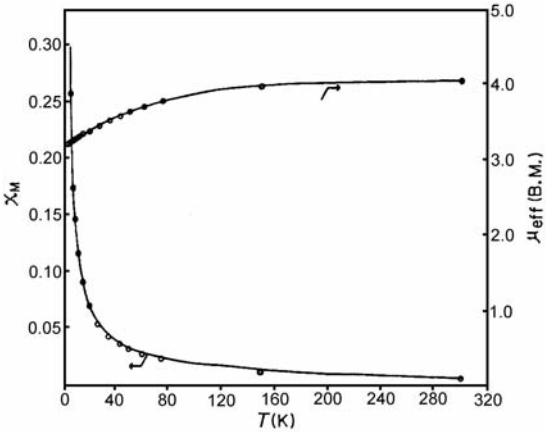


Fig. 9.5. Plots of the temperature dependence of molar magnetic susceptibility and effective magnetic moment for $Ru_2(O_2CPr^n)_4Cl$.

In contrast to $Ru_2(O_2CPr^n)_4Cl$, variable temperature magnetic susceptibility measurements for $Ru_2(O_2CCMePh_2)_4Cl$, which exhibits a linear polymeric chain structure with ∠Ru–Cl–Ru = 180°, show that at temperatures below 70 K together with a large zero-field splitting, an interdimer antiferromagnetic coupling also exists with a coupling constant J = -10 cm^{-1}, revealing that the geometry of the polymeric structure of $Ru_2(O_2CR)_4Cl$ compounds affects their magnetic behavior.[67] A correlation between the ∠Ru–Cl–Ru and the magnitude of the interdimer antiferromagnetic coupling has been proposed, according to which the latter increases as the ∠Ru–Cl–Ru approaches 180° and becomes smaller for more acute angles.[68] Indeed, for the compounds $Ru_2(O_2CEt)_4Cl$, $Ru_2(O_2CC(Me)=CHEt)_4Cl$ and $Ru_2(O_2CCMePh)_4Cl$, in which ∠Ru–Cl–Ru ~180°, together with a large zero-field splitting (D ~70 cm^{-1}) there is an antiferromagnetic exchange interaction between the Ru_2^{5+} units with coupling constants ranging from -8 to -13 cm^{-1},[69] while in the compounds $Ru_2(O_2CBu^n)_4Cl$ and $Ru_2(O_2C\text{-}n\text{-}C_7H_{15})_4Cl$ in which 125° < ∠Ru–Cl–Ru < 180°, the coupling is weaker with coupling constants -1 and -5 cm^{-1}, respectively.[68]

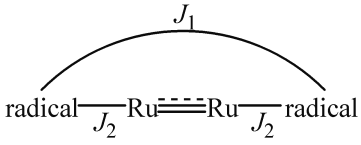
Pictiva EX2004
Samsung v Pictiva
IPR2024-01094

In the case of polymeric Ru_2^{5+} tetracarboxylate compounds with linear or slightly bent chain structures linked by ligands other than halides, like $[Ru_2(O_2CMe)_4(pyz)]BPh_4$,[70] $[Ru_2(O_2CMe)_4(4,4'\text{-dipy})]PF_6$,[71] $[Ru_2(O_2CMe)_4(dabco)]PF_6$,[71] and $[Ru_2(\mu\text{-}O_2CMe)_4](N(CN)_2)$,[42] a small, but not negligible, degree of interdimer antiferromagnetic coupling is also suggested to exist (the coupling constants range from -1 to -3 cm^{-1}) together with a large zero-field splitting. In compounds of this type the axial ligand linking the Ru_2^{5+} units is of great importance, since the antiferromagnetic coupling effect becomes less important when longer linkers are used, as there is a lengthening of the distance between the interacting Ru_2^{5+} units.

A strong dependence of the magnetic behavior on the axial ligands is also observed in the three-dimensional coordination polymers $[Ru_2(O_2CMe)_4]_3[M(CN)_6]$ (M = Cr, Fe, and Co) with a Prussian blue type of structure.[44] The data for the compound with the diamagnetic $[Co(CN)_6]^{3-}$ linker show that there are no interactions between the paramagnetic Ru_2^{5+} units (a value of 0 K was calculated for the Weiss constant, θ). For the $[Cr(CN)_6]^{3-}$ analog, there are antiferromagnetic interactions between the adjacent spin sites (θ ~ -40 K). However, for the paramagnetic linker $[Fe(CN)_6]^{3-}$ the data suggest that there are ferromagnetic interactions between the adjacent Ru_2^{5+} units with θ ~0.7 K, while at 8 K a transition from short range ferromagnetic interactions to long range magnetic ordering takes place.

For the Ru_2^{5+} tetracarboxylates with non-polymeric structures the situation is simpler, because the Ru_2^{5+} units are not connected together and no coupling between them is expected. Indeed, measurements on the diadduct $[Ru_2(O_2CCHMePh)_4(H_2O)_2]BPh_4$ over the temperature range 6-300 K fit a model involving only a large zero-field splitting (D ~70 cm^{-1}) and no intermolecular antiferromagnetic coupling.[70] However, a recent study of the magnetic properties of the non-polymeric $Ru_2(O_2CBu^t)_4Cl$ and $Ru_2(O_2CC_4H_4N)_4Cl$ indicates that these complexes exhibit a weak intermolecular antiferromagnetic coupling, which is not associated with spin-exchange between adjacent Ru_2^{5+} units as in the polymeric compounds (since these are not bridged by a linker), but allowed by a through-space pathway.[72]

The magnetic properties of Ru_2^{5+} carboxylate compounds with axially coordinated nitroxide radicals, such as tempo,[73] nitme,[74,75] nitet,[74] nitph,[18,76,77] *p*-pynit[78,79] and *m*-pynit[79] are of special interest, since these compounds exhibit two types of magnetic interactions: between the two axially coordinated radicals through the dimetal core (with coupling constant J_1) and between the dimetal core and the radicals (with coupling constant J_2) as shown in **9.3**. For the discrete dimer $[Ru_2(O_2CBu^t)_4(nitme)_2]BF_4$ both ferromagnetic interactions between the Ru_2 core and the nitme ligands (J_2 = 5 cm^{-1}) and antiferromagnetic interactions between the nitme ligands (J_1 = -40 cm^{-1}) are observed.[74] In contrast, in $[Ru_2(O_2CBu^t)_4(tempo)_2][Ru_2(O_2CBu^t)_4(H_2O)_2](BF_4)_2$ the cation $[Ru_2(O_2CBu^t)_4(tempo)_2]^+$ exhibits only a large antiferromagnetic interaction between the Ru_2 core and the nitroxide radical with J_2 = -130 cm^{-1}, and no coupling between the two axial nitroxide ligands (J_1 = 0).[73] In the cases of the polymeric chain compounds $[Ru_2(O_2CBu^t)_4(nitph)]BF_4$[18] and $[Ru_2(O_2CBu^t)_4(p\text{-pynit})]BF_4$[78] only magnetic interactions between the Ru_2 units and the nitme ligands are observed, with J_2 coupling constants -100 and 20 cm^{-1}, respectively. In the last two polymeric compounds only localized coupling is observed.



9.3

Pictiva EX2004
Samsung v Pictiva
IPR2024-01094

O,O'-donor bridging ligands other than carboxylates

Other non-carboxylate-type O,O'-donor bridging ligands that have also been used for the synthesis of Ru_2^{5+} paddlewheel compounds include CO_3^{2-}, SO_4^{2-}, $H_nPO_4^{-3+n}$, and hedp.

The polymeric compound $K_3[Ru_2(O_2CO)_4]\cdot 6H_2O$ was first reported to be synthesized from $Ru_2(O_2CMe)_4$ and an excess of K_2CO_3 in H_2O according to the disproportionation reaction:

$$5Ru_2(O_2CMe)_4 + 16K_2CO_3 \rightarrow 2Ru + 4K_3[Ru_2(O_2CO)_4]\cdot 6H_2O + 20K(O_2CMe).^{80}$$

$Na_3[Ru_2(O_2CO)_4]\cdot 6H_2O$ was made from $K_3[Ru_2(O_2CO)_4]\cdot 6H_2O$ by ion exchange. However, although the room temperature magnetic moments of these two compounds (~ 4.1 BM) suggest that they are Ru_2^{5+} species, the precise oxidation state of the Ru_2 unit could not be inferred from the crystallographic data (for the Na^+ salt, the formula appears to be $Na_{3.5}[Ru_2(O_2CO)_4]\cdot 6H_2O$).

Alternatively, $M_3[Ru_2(O_2CO)_4]\cdot xH_2O$ compounds (M = Na and x = 6, M = K and x = 4), respectively) have been synthesized from the ligand substitution reaction of $Ru_2(O_2CMe)_4Cl$ with excess of M_2CO_3 in H_2O:

$$Ru_2(O_2CMe)_4Cl + 4M_2CO_3 \rightarrow M_3[Ru_2(O_2CO)_4]\cdot xH_2O + 4M(O_2CMe) + MCl.^{81}$$

The crystal structures of the compounds obtained by this method were accurately determined as $K_3[Ru_2(O_2CO)_4]\cdot 4H_2O$ and $Na_3[Ru_2(O_2CO)_4]\cdot 6H_2O$, establishing in this way unequivocally the oxidation states of the metal and the stoichiometries. They show that each one of the $Ru_2(O_2CO)_4$ units participates with two O atoms in the formation of axial bonds with two neighboring $Ru_2(O_2CO)_4$ units resulting in two-dimensional layers (Fig. 9.6). The average Ru–Ru bond length of 2.251 Å (Table 9.1) falls in the range of Ru_2^{5+} tetracarboxylates and is consistent with the $\sigma^2\pi^4\delta^2(\pi^*\delta^*)^3$ electronic configuration.

These Ru_2^{5+} tetracarbonates have been used as starting materials for the preparation of $K_3[Ru_2(SO_4)_4(H_2O)_2]\cdot 2H_2O$ and $K_4[Ru_2(HPO_4)_3(PO_4)(H_2O)_2]$.[82] Although the former was originally synthesized by a different synthetic method which involved the reaction of $[Ru_2(O_2CMe)_4]^+$ with H_2SO_4,[83] the utilization of $[Ru_2(O_2CO)_4]^{3-}$ offers a fast, convenient and high-yield synthesis due to the ease of expelling CO_2 in acidic media. The crystal structure of $[Ru_2(SO_4)_4(H_2O)_2]^{3-}$, determined as $K_2H[Ru_2(SO_4)_4(H_2O)_2]\cdot 4H_2O$, shows the expected paddlewheel structure similar to those of Mo, Rh, and Pt compounds,[83] while that of $K_4[Ru_2(HPO_4)_3(PO_4)(H_2O)_2]$ reveals the existence of a three-dimensional network in which the dimetal units are held together by H-bonds between the axially coordinating H_2O molecules and O atoms of the bridging ligands.[82] The Ru–Ru bond lengths of 2.303(1) and 2.305(1) Å for $K_2H[Ru_2(SO_4)_4(H_2O)_2]\cdot 4H_2O$ and $K_4[Ru_2(HPO_4)_3(PO_4)(H_2O)_2]$, respectively (Table 9.1), are slightly longer than the corresponding Ru–Ru distances in Ru_2^{5+} tetracarboxylates and tetracarbonates, but they are still in the typical range for Ru_2^{5+} compounds with three unpaired electrons and the $\sigma^2\pi^4\delta^2(\pi^*\delta^*)^3$ electronic configuration, as it is indicated by the room temperature magnetic moment of $K_3[Ru_2(SO_4)_4(H_2O)_2]\cdot 2H_2O$.[82,84]

The related Ru_2^{5+} compound with bridging phosphonate ligands $(NH_4)_3[Ru_2(hedp)_2]\cdot 2H_2O$ has been synthesized by the hydrothermal reaction between $RuCl_3\cdot xH_2O$ and $H_4hedp\cdot H_2O$.[85] It exhibits a two-dimensional layer structure similar to those of $K_3[Ru_2(O_2CO)_4]\cdot 4H_2O$ and $Na_3[Ru_2(O_2CO)_4]\cdot 6H_2O$, with a Ru–Ru bond length of 2.347(1) Å (Table 9.1). This distance is much longer than the distances for most Ru_2^{5+} compounds, due to the larger "bite" of the phosphonate ligands. Magnetic susceptibility measurements show that its room temperature magnetic moment is ~4.2 BM per dimer, which implies the presence of Ru_2^{5+} units with three unpaired electrons, while at low temperatures weak ferromagnetic interactions between the Ru_2^{5+} units within each layer are observed.

Pictiva EX2004
Samsung v Pictiva
IPR2024-01094

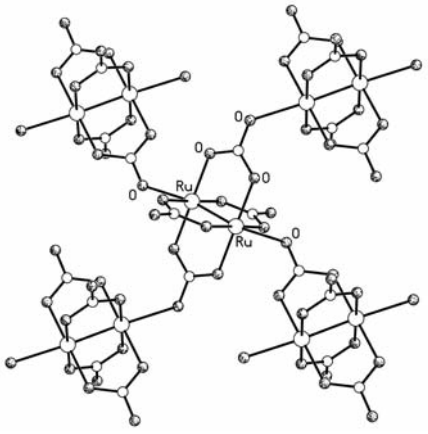


Fig. 9.6. The structure of the polymeric anion in $Na_3[Ru_2(O_2CO)_4]$.

9.2.2 Ru_2^{5+} compounds with N,O-donor bridging ligands

Amidate ligands

The Ru_2^{5+} tetraamidates are synthesized from the substitution reactions of $Ru_2(O_2CMe)_4Cl$ with excess of molten amides ($RCONH_2$) at elevated temperatures.[86] Attempts to synthesize such compounds from reactions in $MeOH/H_2O$ mixtures have been unsuccessful.

Structural data, although they are limited since only four compounds have been crystallographically characterized, show that in the solid state Ru_2^{5+} tetraamidates exhibit two structural types. Compounds of the type $Ru_2(ONHCR)_4Cl$ show polymeric structures similar to the Ru_2^{5+} tetracarboxylate analogs, in which the $[Ru_2(ONHCR)_4]^+$ units form infinite zig-zag chains through axial Cl^- ions, as in $Ru_2(ONHCPh)_4Cl$[87] (Fig. 9.7) and $Ru_2(ONHCC_6H_4\text{-}p\text{-}Cl)_4Cl$.[88] There are also discrete diadducts of the type $[Ru_2(ONHCR)_4L_2]Y$, as in the compounds $[Ru_2(ONHCC_6H_4\text{-}p\text{-}Bu^t)_4(OPPh_3)_2]BF_4$[89] and $[Ru_2(ONHCC_4H_3S)_4(THF)_2]SbF_6$.[90] The Ru–Ru distances are between 2.281 and 2.296 Å (Table 9.1). Similarly to the carboxylate analogs, the diadducts exhibit shorter distances than the polymeric compounds.

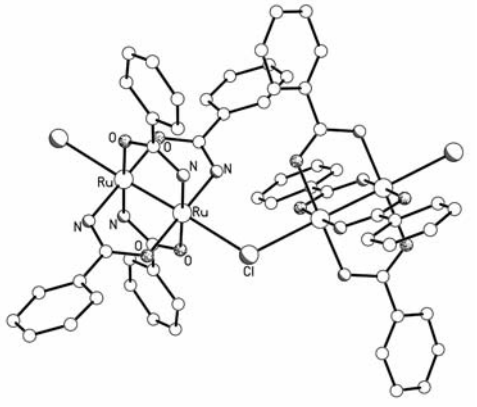


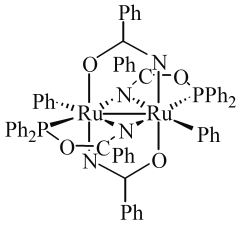
Fig. 9.7. Part of the polymeric zig-zag chain structure of $Ru_2(ONHCPh)_4Cl$.

Pictiva EX2004
Samsung v Pictiva
IPR2024-01094

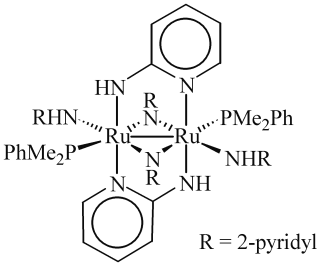
Since amidates have two different donor atoms, N and O, the arrangement of four such ligands around the Ru_2^{5+} unit can give rise to four possible regioisomers as shown in Fig. 1.10. So far, only non-polar *trans*-(2,2) regioisomers have been isolated.

The $Ru_2(ONHCR)_4Cl$ compounds react with Ag^+ reagents in the presence of coordinating solvents or other suitable ligands to give diadducts, such as $[Ru_2(ONHCC_4H_3S)_4(THF)_2]SbF_6$.[90] The axial Ru–Cl bonds can also be cleaved by strong polar solvents, such as DMSO.

A few unusual reactions of Ru_2^{5+} tetraamidates with phosphines have been reported. When the substituent R group of the bridging amidate ligand is a phenyl or aryl group, the phosphine undergoes metal-assisted P–C bond cleavage, resulting in the transfer of a phenyl (or aryl) group from the phosphine to the Ru atoms to give edge-sharing bioctahedral Ru(III)Ru(III) compounds. For example, the reaction of $Ru_2(ONHCPh)_4Cl$ with Ph_3P gives $Ru_2(ONHCPh)_2(Ph)_2[Ph_2POC(Ph)N]_2$ (**9.4**a), in which the metal atoms are in a slightly distorted octahedral environment at a distance of 2.566(1) Å from each other, indicative of a Ru–Ru single bond.[91] Similar reactions occur between $Ru_2(ONHCPh)_4Cl$ and $(p\text{-Me-}C_6H_4)_3P$, and $Ru_2(ONHCC_6H_3\text{-}3,5\text{-}(MeO)_2)_4Cl$ and Ph_3P, in which the Ru–Ru distances of the resulting compounds are 2.570(2) Å and 2.567[1] Å, respectively.[92] In another case, reaction of $Ru_2(ONHCPh)_4Cl$ and Li(ap) followed by addition of PMe_2Ph results in the edge-sharing bioctahedral complex **9.4**b which has a Ru–Ru single bond of 2.573(2) Å.[93]



a



b

9.4

Electrochemical experiments for $Ru_2(ONHCCF_3)_4Cl$ in different solvents, and using various concentrations of Cl^- ions show a medium-dependent reduction process, similarly to $Ru_2(O_2CPr^n)_4Cl$.[86] While in strongly coordinating solvents, or in the presence of excess of Cl^- ions, a single one-electron reduction process is observed at mild potentials (0.0 to -0.35 V), in non-coordinating solvents two- or three-step reduction processes occur. These are attributed to the association equilibria between $[Ru_2(ONHCCF_3)_4]^+$, Cl^- ions and solvent molecules.

Of interest is the electrochemical behavior of $Ru_2(ONHCMe)_4Cl$.[94] The cyclic and the differential pulse voltammograms in DMSO using LiCl as electrolyte (Fig. 9.8) show three one-electron processes, one oxidation (+0.47 V) and two reductions (-0.96 and -1.22 V vs SCE). These have been assigned to the processes $[Ru_2(ONHCMe)_4]^+ \rightarrow [Ru_2(ONHCMe)_4]^{2+} + e^-$, $[Ru_2(ONHCMe)_4]^+ + e^- \rightarrow Ru_2(ONHCMe)_4$, and $Ru_2(ONHCMe)_4 + e^- \rightarrow [Ru_2(ONHCMe)_4]^-$, respectively. The first reduction process described by the second equation, typically occurs at less negative potentials than for $Ru_2(O_2CR)_4Cl$ and other $Ru_2(ONHCR)_4Cl$ compounds. This substantial cathodic shift is attributed to the high basicity of the MeCONH ligand compared to the others, and this is probably responsible for the observation of the oxidation process described by the first equation. An explanation of the exact nature of the doubly reduced species in the second reduction process has not been given. An oxidation process is also observed in

Pictiva EX2004
Samsung v Pictiva
IPR2024-01094

$Ru_2(ONHCCMe_3)_4Cl$, which also shows a complex redox behavior with a dependence on solvent and concentration of Cl^- ions.[95]

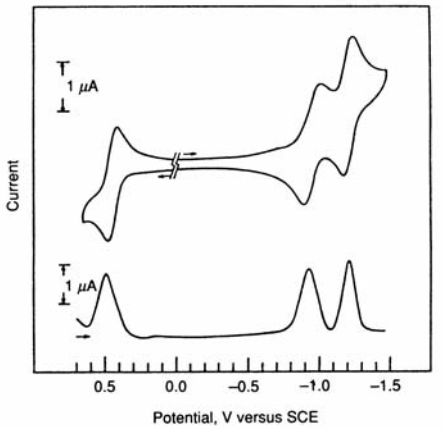


Fig. 9.8. Cyclic voltammogram (top) and differential pulse voltammogram (bottom) of $Ru_2(ONHCMe)_4Cl$ in DMSO.

Room temperature magnetic susceptibility measurements of Ru_2^{5+} tetraamidates show magnetic moments of ~4.0 BM per Ru_2^{5+} unit, which are indicative of a quartet ground state and suggest the $\sigma^2\pi^4\delta^2(\pi^*\delta^*)^3$ electronic configuration. Structural data give support to this electronic configuration. The Ru–Ru bond distances in Ru_2^{5+} tetraamidates are similar to those for the Ru_2^{5+} teracarboxylates, for which it is known that they exhibit a quartet state and the $\sigma^2\pi^4\delta^2(\pi^*\delta^*)^3$ electronic configuration. Any change from the quartet state would entail a change in the number of π^* electrons. Since the number of π^* electrons has a large effect on the Ru–Ru bond length, any compound that does not have a quartet ground state ought to display a Ru–Ru bond distance outside of the range observed for Ru_2^{5+} tetracarboxylates. Conversely, all Ru_2^{5+} compounds with Ru–Ru bond lengths in that range may be presumed to have the $\sigma^2\pi^4\delta^2(\pi^*\delta^*)^3$ electronic configuration.

Variable temperature magnetic susceptibility measurements for polymeric compounds $Ru_2(ONHCR)_4Cl$ and discrete diadducts $[Ru_2(ONHCR)_4L_2]Y$ show Curie-Weiss behavior over the temperature range of 70-290 K, which is consistent with three unpaired electrons.[89,90] However, below 70 K a deviation from the Curie-Weiss behavior is observed, which is attributed to a large zero-field splitting (D ~ 45-70 cm^{-1}) together with a weak, but not negligible, antiferromagnetic coupling with coupling constants ranging form -0.1 to -2.9 cm^{-1}. It has been proposed that in the polymeric compounds the coupling takes place through the bridging Cl^- ions, while in the diadducts a through-space antiferromagnetic interaction is present, similar to some of the non-polymeric Ru_2^{5+} tetracarboxylates.[72]

Oxopyridinate ligands

The first structurally characterized Ru_2^{5+} tetraoxopyridinate complex, $Ru_2(hp)_4Cl(Hhp)$ (Fig. 9.9), was synthesized by reacting $Ru_2(O_2CMe)_4Cl$ with an excess of molten Hhp.[96] A few other compounds of this type have been prepared in a similar way. By careful temperature control of these reactions, partial substitution of the acetate groups by Xhp ligands can be accomplished and complexes of the general type $Ru_2(O_2CMe)_{4-x}(Xhp)_xCl$ (x = 1, 2, 3) can be synthesized. An example is the synthesis of $Ru_2(O_2CMe)(chp)_3Cl$, which is obtained from the reaction of $Ru_2(O_2CMe)_4Cl$ with Hchp in boiling MeOH.[97]

Pictiva EX2004
Samsung v Pictiva
IPR2024-01094

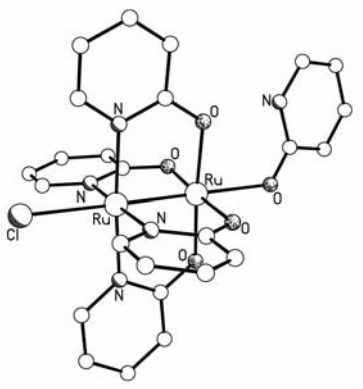


Fig. 9.9. The structure of $Ru_2(hp)_4Cl(Hhp)$.

In the solid state, the majority of Ru_2^{5+} tetraoxopyridinates exist as discrete paddlewheel complexes. However, there are a few cases in which association occurs, as in $[Ru_2(chp)_4]_2(BF_4)_2$ which crystallizes as a dimer with bonds between the O atom of one $Ru_2(chp)_4$ unit and the axial position of the other and vice versa (Fig. 9.10).[98]

The Ru–Ru bond lengths (Table 9.1) lie in the narrow range of 2.254-2.286 Å, similar to the Ru_2^{5+} tetracarboxylates, and they do not show any dependence on the substituents of the bridging Xhp ligands. However, they are affected by the axial ligands, since complexes without axial ligands exhibit shorter Ru–Ru bond lengths than those with axial ligands, as shown in $[Ru_2(chp)_4]_2(BF_4)_2$ and $Ru_2(chp)_4Cl$, in which the Ru–Ru distances are 2.254(1) and 2.281(1) Å, respectively.

Although all possible regioisomers are known for tetraoxopyridinate complexes of other metals, for $Ru_2(Xhp)_4Cl$ complexes only the polar (4,0) arrangement has been observed, possibly due to the strong preference of the Ru_2 complexes for axial coordination. In the polar arrangement (4,0) the preference for axial coordination is accommodated, since all the X groups of the bridging Xhp ligands are placed at one axial site leaving the other one unencumbered for the formation of an axial Ru–Cl bond. A second factor which plays an important role in determining the structures of the Ru_2^{5+} tetraoxopyridinates is the bulk of the X groups. For X groups with small steric demand, e.g., X = H or F, the polar arrangement is adopted with the bridging Xhp ligands in an eclipsed conformation.[96,99] When X is larger, e.g., X = Cl, in order to relieve the repulsions between the Cl atoms which are in close proximity a twist of the Xhp ligands is induced (torsion angle ~19°).[100,101] For the bulkier Me groups, the polar arrangement would result in so great a twist of the bridging ligands that all attempts to prepare a polar complex $Ru_2(mhp)_4Cl$ have been unsuccessful. Only the complex *trans*-$Ru_2(O_2CMe)_2(mhp)_2Cl$ has been isolated, which has two mhp ligands oriented in the same direction (Fig. 9.11).[102]

Reactions of $Ru_2(Xhp)_4Cl$ complexes with Ag^+ reagents result in the removal of the axial halide leaving an open position available for coordination by suitable ligands, L (e.g., THF, pyridine, $CF_3SO_3^-$), and forming monoadducts of the general type $[Ru_2(Xhp)_4L]^+$. Diadducts do not form because the polar arrangement of the bridging Xhp ligands makes the second axial site inaccessible.[103,104] Upon reactions with π-acceptor reagents, such as PMe_3 or CNC_6H_{11}, mononuclear decomposition products are obtained.[105] However, in the case of reactions with $Me_3SnC{\equiv}CPh$, the paddlewheel structure is retained (even with excess of $Me_3SnC{\equiv}CPh$), and mono-alkynyl Ru_2^{5+} complexes are isolated.[106]

Pictiva EX2004
Samsung v Pictiva
IPR2024-01094

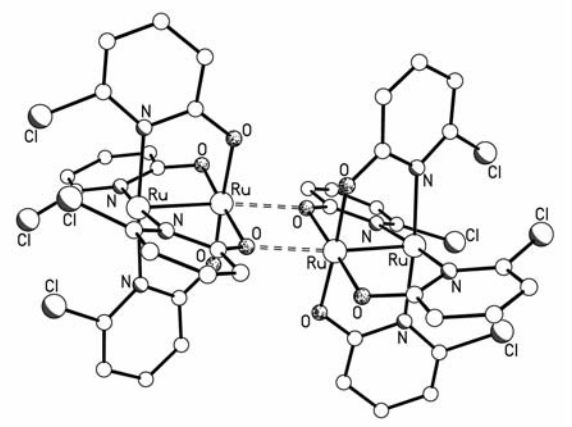


Fig. 9.10. The structure of the cation in $[Ru_2(chp)_4]_2(BF_4)_2$.

Cyclic voltammetry measurements of $Ru_2(Xhp)_4Cl$ compounds show two metal-centered redox processes: a one-electron oxidation which corresponds to $Ru_2^{5+} \rightarrow Ru_2^{6+} + e^-$ and a one-electron reduction which corresponds to $Ru_2^{5+} + e^- \rightarrow Ru_2^{4+}$.[99,102,107] The electrochemical behavior of the Ru_2^{5+} oxopyridinates is similar to that of Ru_2^{5+} carboxylate and amidate analogs, which indicates that the polar arrangement of the Xhp ligands does not result in any significant electronic differences.

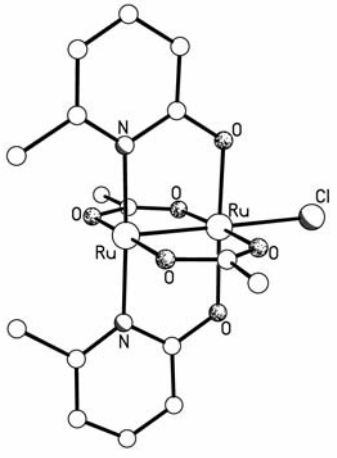


Fig. 9.11. The structure of *trans*-$Ru_2(O_2CMe)_2(mhp)_2Cl$.

Magnetic data for Ru_2^{5+} tetraoxopyridinates are very limited. An early magnetic measurement conducted for $Ru_2(hp)_4Cl(Hhp)$ showed a room temperature magnetic moment of ~4.6 BM, which is indicative of three unpaired electrons, and the $\sigma^2\pi^4\delta^2(\pi^*\delta^*)^3$ electronic configuration was proposed.[96] Structural data support this electronic configuration, as the Ru–Ru bond lengths of Ru_2^{5+} tetraoxopyridinates fall in the same range with those reported for Ru_2^{5+} tetracarboxylates.

The only available variable temperature magnetic susceptibility study is for $[Ru_2(chp)_4(py)]BF_4$ and $\{[(chp)_4Ru_2](\mu\text{-pyz})[Ru_2(chp)_4]\}(BF_4)_2$, in which two $[Ru_2(chp)_4]^+$ units are linked by a pyz

Pictiva EX2004
Samsung v Pictiva
IPR2024-01094

molecule (Fig. 9.12).[104] Both complexes exhibit similar magnetic behavior: Curie-Weiss behavior in the temperature range 70-300 K with room temperature magnetic moments ~4.0 BM, and a decrease in their magnetic moments below 70 K, attributed primarily to the zero-field splitting effect. Due to this similarity, it was proposed that in $[(chp)_4Ru_2](\mu\text{-pyz})[Ru_2(chp)_4]\}(BF_4)_2$ there are no significant magnetic exchange interactions between the Ru_2^{5+} units.

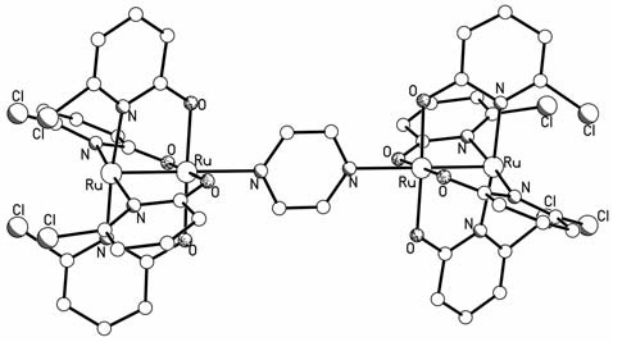


Fig. 9.12. The structure of the cation in $\{[(chp)_4Ru_2](\mu\text{-pyz})[Ru_2(chp)_4]\}(BF_4)_2$.

9.2.3 Ru_2^{5+} compounds with N,N'-donor bridging ligands

Aminopyridinate ligands

The Ru_2^{5+} tetraaminopyridinates are synthesized by reacting $Ru_2(O_2CMe)_4Cl$ with excess of molten aminopyridines (HXap) at elevated temperatures. By careful control of the experimental conditions of these reactions complexes with a mixed set of aminopyridinate/acetate ligands can be selectively synthesized.[97,108] For example, by reacting $Ru_2(O_2CMe)_4Cl$ with excess of Hadmp in MeOH at room temperature the mono-substituted complex is obtained, while a second admp ligand is introduced when the reaction takes place in boiling THF; further substitution is carried out at higher temperatures using molten Hadmp.

In the solid state, Ru_2^{5+} aminopyridinates exist as discrete molecules, as it is shown by the crystal structure of $Ru_2(ap)_4Cl$ in Fig. 9.13.[96] $Ru_2(O_2CMe)_3(admp)Cl$ is an exception, as it dimerizes due to the interaction of an O atom of a bridging acetate ligand with the axial position of the Ru_2^{5+} unit of a neighboring molecule and vice versa.[108]

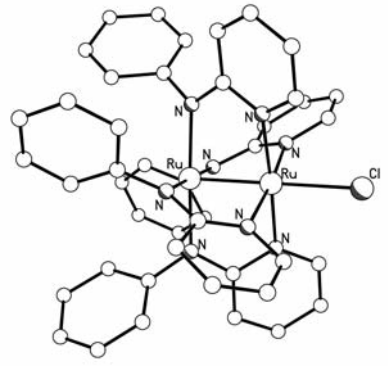


Fig. 9.13. The structure of $Ru_2(ap)_4Cl$.

Pictiva EX2004
Samsung v Pictiva
IPR2024-01094

In most $Ru_2(Xap)_4Cl$ compounds the polar arrangements (4,0) and (3,1) are preferred even though sometimes they result in distortions of the eclipsed geometry of the paddlewheel structures due to the steric requirements of the aryl substituents of the bridging aminopyridinate ligands, as shown in the structures of the (3,1) and (4,0) regioisomers of $Ru_2(2,4,6\text{-}F_3ap)_4Cl$ which display torsion angles of ~17 and ~24º, respectively.[109] It has been suggested that this is due to the strong preference of the Ru_2 complexes for axial coordination: in the (4,0) regioisomer all the aryl substituents surround one axial site, leaving the other axial site unencumbered allowing the coordination of the Cl^- ion. However, there are cases in which other than the (4,0) and (3,1) arrangements are preferred, depending on the basicity of the aminopyridinate ligands. For example, while $Ru_2(2\text{-}Meap)_4Cl$ is obtained only as the (4,0) regioisomer, $Ru_2(F_5ap)_4Cl$ is obtained as a mixture of all possible regioisomers.[109,110]

The axial Cl^- ion of Ru_2^{5+} aminopyridinates can be replaced by other ligands upon reactions with suitable reagents. For example, $Ru_2(ap)_4Cl$ reacts with $AgSbF_6$ in wet MeOH to give $[Ru_2(ap)_4(H_2O)](SbF_6)$.[111] In addition, $Ru_2(ap)_4Cl$ reacts with LiC≡CPh in 1:5 ratio resulting in the formation of the mono-alkynyl Ru_2^{5+} complex $Ru_2(ap)_4(C{\equiv}CPh)$ (Fig. 9.14).[112] A number of similar complexes of the type $Ru_2(ap)_4[(C{\equiv}C)_mY]$ (m = 1, 2 and Y = H, $SiMe_3$, CH_2COMe) have been obtained by this method.[113-115] An attractive extension of such reactions is the synthesis of complexes composed of two Ru_2^{5+} tetraaminopyridinate units linked through the axial positions with linear alkynyl-type of ligands, such as $[(ap)_4Ru_2](\mu\text{-}C{\equiv}C)[Ru_2(ap)_4]$ and $[(ap)_4Ru_2](\mu\text{-}C{\equiv}CC{\equiv}C)[Ru_2(ap)_4]$ (Fig. 9.15).[116,117] These are synthesized by treating $Ru_2(ap)_4Cl$ with an excess of the corresponding dilithiated alkynyl reagent.

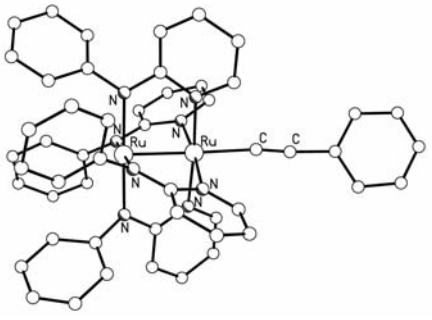


Fig. 9.14. The structure of $Ru_2(ap)_4(C{\equiv}CPh)$.

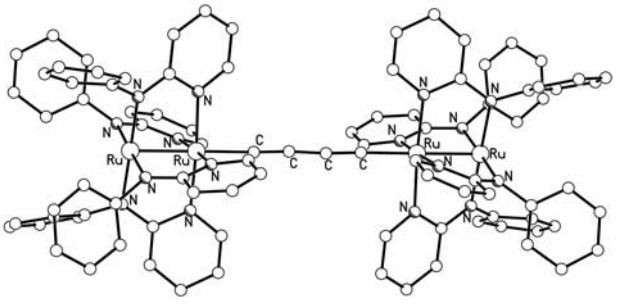


Fig. 9.15. The structure of $[(ap)_4Ru_2](\mu\text{-}C{\equiv}CC{\equiv}C)[Ru_2(ap)_4]$.

Pictiva EX2004
Samsung v Pictiva
IPR2024-01094

The axial Cl^- ions can also be replaced by CN^- in stoichiometric reactions giving monocyano adducts,[118] or other cyanide-containing mononuclear organometallic complexes resulting in the formation of compounds such as $\{Ru_2(ap)_4[NCFe(dppe)(\eta^5\text{-}C_5H_5)]\}^+$ and $\{Ru_2(ap)_4[NCRu(PPh_3)_2(\eta^5\text{-}C_5H_5)]\}^+$.[119]

The Ru_2^{5+} tetraaminopyridinates react with strong π-acceptors, like NO, without decomposition. More specifically, $Ru_2(2\text{-}Fap)_4Cl$ reacts with NO to form the axial NO-adduct $Ru_2(2\text{-}Fap)_4Cl(NO)$ in which the bridging ap ligands adopt the (3,1) arrangement in order to minimize the steric repulsions with the phenyl substituents.[120] Finally, the complex $Ru_2(O_2CMe)_2(ap)_2Cl(Hap)$ reacts with dmpm in the presence of Me_3SiCl and $NaBPh_4$ to form the Ru_2^{4+} compound $[Ru_2(ap)_2(dmpm)_2Cl]BPh_4$, which is the only crystallographically characterized Ru_2^{4+} compound with bridging aminopyridinate ligands.[121]

Cyclic voltammetry measurements of Ru_2^{5+} tetraaminopyridinates show that their electrochemical behavior is strongly influenced by the solvent. Electrochemical measurements for a series of complexes conducted in THF, DMF and DMSO show a single one-electron, metal-centered oxidation and two one-electron, metal-centered reduction processes.[122] However, in CH_2Cl_2 one reduction and two oxidation processes are observed which are assigned to $Ru_2^{5+} + e^- \rightarrow Ru_2^{4+}$, $Ru_2^{5+} \rightarrow Ru_2^{6+} + e^-$ and $Ru_2^{6+} \rightarrow Ru_2^{7+} + e^-$, respectively. These processes are sensitive to the isomer type.[109] For example, the potential of the first oxidation for the (3,1) regioisomer of $Ru_2(F_5ap)_4Cl$ in CH_2Cl_2 is shifted cathodically by ~170 mV compared to that of the (4,0) regioisomer, while the analogous process for the *trans*-(2,2) regioisomer is shifted cathodically by ~320 mV.[110] The potentials of the first oxidation and the reduction processes are also influenced by the substituents on the aryl groups of the aminopyridinate ligands and linear free-energy relationships have been established between the electrode potentials for these processes and the Hammett parameters of the substituents.[109]

The axial ligands also influence the redox behavior of Ru_2^{5+} tetraaminopyridinates significantly. The cyclic voltammogram of $Ru_2(2\text{-}Fap)_4Cl(NO)$ in CH_2Cl_2 shows two reversible, one-electron reductions and a reversible, one-electron oxidation at potentials which are shifted to more positive values compared to those in $Ru_2(2\text{-}Fap)_4Cl$.[120] The stabilization of the low-valent redox level of the Ru_2 core is explained by the strong π-accepting ability of the NO ligand. Complexes with alkynyl ligands of the type $Ru_2(ap)_4[(C{\equiv}C)_mY]$ (m = 1, 2, and Y = H, $SiMe_3$, CH_2COMe) undergo two one-electron redox processes, a reduction and an oxidation.[113] In this case a cathodic shift of the potentials, relative to the analogous processes in the parent complex $Ru_2(ap)_4Cl$ is observed. This is attributed to the strong nucleophilic character of the C≡CR ligands. For complexes of the type $[(ap)_4Ru_2][\mu\text{-}(C{\equiv}C)_n][Ru_2(ap)_4]$ (n = 1, 2, 3, 4, and 6), cyclic voltammetry measurements show that the linear alkynyl chains mediate significant electronic communication between the Ru_2^{5+} units. While the mono-alkynyl complex $Ru_2(ap)_4(C{\equiv}CPh)$ shows two quasi-reversible redox processes (an oxidation and a reduction), the compound $[(ap)_4Ru_2](\mu\text{-}C{\equiv}C)[Ru_2(ap)_4]$ exhibits four quasi-reversible, and one irreversible, one-electron redox processes. The strength of the electronic communication decreases as the length of the carbon chain increases.[116,117]

Complexes with a mixed set of bridging ligands of the type $Ru_2(O_2CMe)_{4-x}(admp)_xCl$ (x = 1, 2, 3) exhibit two redox processes, a one-electron oxidation which becomes easier as the number of aminopyridinate ligands increases, and an one-electron reduction of increasing difficulty with the number of aminopyridinate ligands.[108] However, the analogous mixed-ligand Ru_2^{5+} complex $Ru_2(O_2CMe)(HNC_5H_3NMe)_3Cl$ shows three metal-based redox processes, which have been assigned to the oxidation of the Ru_2^{5+} core to Ru_2^{6+} and the reductions to Ru_2^{4+} and further to a rare Ru_2^{3+} species.[123]

Pictiva EX2004
Samsung v Pictiva
IPR2024-01094

As shown in Table 9.1, the Ru–Ru bond lengths in Ru_2^{5+} aminopyridinates fall in the range of 2.274 to 2.336 Å (Ru_2(2-Fap)$_4$Cl(NO) is an exception; see below). Although these distances do not show any dependence on the arrangement and the substitution of the bridging aminopyridinate ligands, they are significantly affected by the axial coordination: the complexes with axial alkynyl ligands exhibit longer Ru–Ru bond lengths. For example, the Ru–Ru bond distances in $Ru_2(ap)_4(C{\equiv}CPh)$[112] and $Ru_2(ap)_4(C{\equiv}CC{\equiv}CSiMe_3)$[114] are 2.319(3) and 2.330(1) Å, respectively, and they are longer than that of 2.275(3) Å in the parent complex $Ru_2(ap)_4Cl$. These rather elongated Ru–Ru bonds are attributed to the electron donating character of the alkynyl ligands, which result in an increase of the anti-bonding σ* electron density between the two metal atoms and weakening of the Ru–Ru bond.

The compound Ru_2(2-Fap)$_4$Cl(NO) exhibits a Ru–Ru bond length of 2.420(1) Å, which is significantly longer than that in all other Ru_2^{5+} tetraaminopyridinate complexes.[120] Given the nature of NO, this could reflect a reduction of the Ru_2^{5+} core to Ru_2^{4+}. Indeed, the formulation $Ru_2^{4+}(NO)^+$ is supported by an almost linear Ru–N–O angle. The lowering of the oxidation state from Ru_2^{5+} to Ru_2^{4+} implies addition of an electron to the anti-bonding orbitals of the dimetal unit which results in the observed lengthening of the Ru–Ru bond.

Room temperature magnetic measurements for the Ru_2^{5+} tetraaminopyridinates show magnetic moments in the range 3.8-4.0 BM, indicating the presence of three unpaired electrons.[110,112,124] Considering that the Ru–Ru bond lengths of Ru_2^{5+} tetraaminopyridinates fall almost in the same range as those reported for Ru_2^{5+} tetracarboxylates, the two types of compounds should exhibit the same electronic configuration, i.e., $\sigma^2\pi^4\delta^2(\pi^*\delta^*)^3$. Room temperature magnetic measurements conducted for the series of complexes with a mixed set of bridging admp/acetate ligands of the type $Ru_2(O_2CMe)_{4-x}(admp)_xCl$ (x = 1, 2, 3) also indicate the presence of three unpaired electrons. However, the magnetic moment of $Ru_2(admp)_4Cl$ implies the presence of only one unpaired electron.[108] The explanation that was given is that the four admp ligands cause a destabilization of the δ* orbital resulting in the $\sigma^2\pi^4\delta^2\pi^{*3}$ electronic configuration.

Formamidinate ligands

Ru_2^{5+} tetraformamidinates are synthesized from the reactions of $Ru_2(O_2CMe)_4Cl$ with excess of molten formamidines (HDArF), a method that was used for the synthesis of the first complex of this type to be reported, $Ru_2(DTolF)_4Cl$.[125] Alternatively, they can be synthesized from stoichiometric ligand metathesis reactions by refluxing $Ru_2(O_2CMe)_4Cl$ with the appropriate formamidine in the presence of Et_3N in THF.[126] By careful control of the reaction conditions or by using formamidines with appropriate substituents on the aryl rings complexes with a mixed set of formamidinate/acetate ligands of the type $Ru_2(O_2CMe)_{4-x}(DArF)_xCl$ (x = 1, 2, 3) can be synthesized in a controlled manner.[127-130] For example, the reaction of $Ru_2(O_2CMe)_4Cl$ with HDAniF in 1:2 ratio in refluxing THF (~70ºC) results in the synthesis of *cis*-$Ru_2(O_2CMe)_2(DAniF)_2Cl$.[128] In contrast, the reaction of $Ru_2(O_2CMe)_4Cl$ with HDXyl^{2,6}F gives the bis-substituted complex $Ru_2(O_2CMe)_2(DXyl^{2,6}F)_2Cl$ only at ~150 ºC, while the DXyl^{2,6}F ligands are forced in a *transoid* arrangement due to the steric requirements imposed by the methyl substituents of the aryl rings.[131] In addition, the reaction of $Ru_2(O_2CMe)_4Cl$ with excess of HDAniF in refluxing toluene gives the fully substituted complex $Ru_2(DAniF)_4Cl$, while the analogous reaction in boiling MeOH is not a substitution reaction but a disproportionation, which results in the Ru_2^{4+} complex $Ru_2(DAniF)_4$ and the edge-sharing bioctahedral Ru(III)Ru(III) compound $[Ru_2(OMe)_2(O_2CMe)_2(HDAniF)_4]Cl_2$.[131]

In the solid state, Ru_2^{5+} tetraformamidinates exist as discrete paddlewheel structures, which do not associate (either via the axial Cl^- ions as in Ru_2^{5+} carboxylate compounds, or directly as

Pictiva EX2004
Samsung v Pictiva
IPR2024-01094

in Ru_2^{5+} oxopyridinates and aminopyridinates) due to the steric requirements of the aryl groups of the bridging formamidinate ligands. An example of a Ru_2^{5+} tetraformamidinate complex is shown in Fig. 9.16.[131] Ligands known to coordinate axially are Cl^- ions, alkynyl groups, and solvent molecules, such as THF.

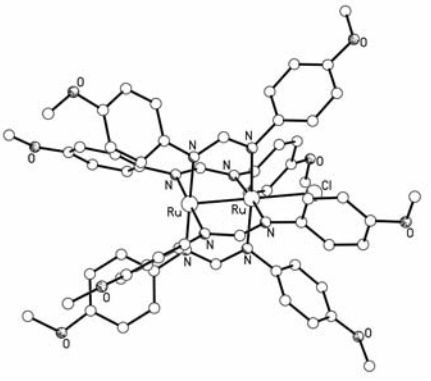


Fig. 9.16. The structure of $Ru_2(DAniF)_4Cl$.

The axial Cl^- ion of $Ru_2(DArF)_4Cl$ complexes can be replaced either by strongly coordinating solvent molecules (e.g., MeOH), or by anionic ligands, such as alkynyls. For example, reaction of $Ru_2(DPhF)_4Cl$ with LiC≡CPh in 1:5 ratio gives $Ru_2(DPhF)_4(C{\equiv}CPh)$.[132] A few other similar compounds of the type $Ru_2(DArF)_4[(C{\equiv}C)_mY]$ (Ar = Ph, $Ph^{m\text{-}Cl}$, $Ph^{3,5\text{-}diCl}$, Ani^m, Y = Ph, $SiMe_3$, m = 1, 2) have been synthesized by this method.[115,133]

In complexes with a mixed set of formamidinate and acetate bridging ligands substitution of the labile acetate ligands can take place. The reaction of $Ru_2(O_2CMe)(DPhF)_3Cl$ with *p*-(*n*-decyloxy)benzoic acid results in $Ru_2(O_2CC_6H_4\text{-}p\text{-}OC_{10}H_{21})(DPhF)_3Cl$,[130] whereas the reaction of $Ru_2(O_2CMe)(DAniF)_3Cl$ with the dicarboxylic acid 1,4-$HO_2CC_6H_4CO_2H$ gives the molecular pair $[Ru_2(DAniF)_3Cl](\mu\text{-}O_2CC_6H_4CO_2)[Ru_2(DAniF)_3Cl]$.[129] In an analogous way, *cis*-$Ru_2(O_2CMe)_2(DAniF)_2Cl$ reacts with the dicarboxylic acids HO_2CCO_2H and $HO_2CC_6H_4CO_2H$ to form the molecular squares $\{[cis\text{-}Ru_2(DAniF)_2Cl](\mu\text{-}O_2CCO_2)\}_4$ (Fig. 9.17) and $\{[cis\text{-}Ru_2(DAniF)_2Cl](\mu\text{-}O_2CC_6H_4CO_2)\}_4$, respectively.[128]

Cyclic voltammetry measurements of $Ru_2(DArF)_4Cl$ complexes show a reversible, one electron, metal-based oxidation process and an irreversible reduction process, which correspond to $Ru_2^{5+} \rightarrow Ru_2^{6+} + e^-$ and $Ru_2^{5+} + e^- \rightarrow Ru_2^{4+}$, respectively.[125,126,134] In some cases an additional irreversible redox wave has also been observed, which was assigned to the axial chloride-free redox couple Ru_2^{5+}/Ru_2^{4+}. The potentials of these processes are dependent on the substitution on the aryl groups of the ligand and linear correlations between the electrode potentials of the redox processes and the substituent's Hammett constants have been established.[126] The monoalkynyl Ru_2^{5+} tetraformamidinate complexes exhibit analogous redox processes, an irreversible oxidation and a reversible reduction, but the electrode potentials of the redox waves are cathodically shifted compared to those of the corresponding $Ru_2(DArF)_4Cl$ compounds.[133]

The Ru–Ru bond distances for Ru_2^{5+} formamidinates lie in a wide range of 2.305 to 2.506 Å (Table 9.1). These distances, which are longer than those observed in the Ru_2^{5+} tetracarboxylates, do not depend on the substituents of the aryl groups, but they are strongly influenced by the nature of the axial ligand. Shorter Ru–Ru bond lengths are observed in complexes in which the axial ligand is a Cl^- ion, while longer ones are observed when the axial ligand is an alkynyl anion, e.g., the Ru–Ru distance in $Ru_2(DAni^mF)_4(C{\equiv}CC{\equiv}CSiMe_3)$ is 2.506(1) Å.[135] The alkynyl

Pictiva EX2004
Samsung v Pictiva
IPR2024-01094

bonding interaction with the Ru_2^{5+} core has been studied in a series of $Ru_2(DArF)_4(C{\equiv}CPh)$ complexes using IR spectroscopy.[133] Based on the dependence of $\nu(C{\equiv}C)$ on the substituents of the formamidinates, it was concluded that there is a strong Ru–C_α σ-bonding interaction (d_π–π back bonding interaction is also present in a small degree). This strong σ-bonding interaction increases the antibonding σ* electron density between the two metals resulting in the lengthening of the Ru–Ru bond.

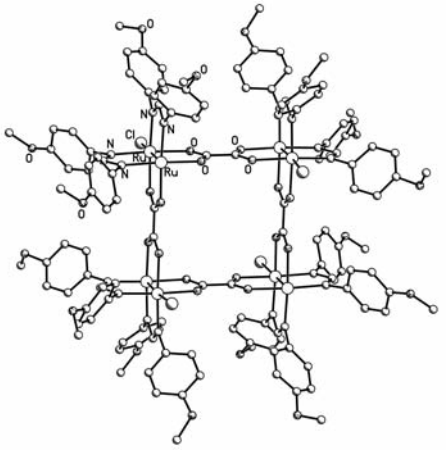


Fig. 9.17. The structure of the molecular square $\{[cis\text{-}Ru_2(DAniF)_2Cl](\mu\text{-}O_2CCO_2)\}_4$.

The Ru_2^{5+} tetraformamidinates exhibit room temperature magnetic moments in the range 3.64-3.97 BM, which is indicative of the presence of three unpaired electrons and corresponds to the $\sigma^2\pi^4\delta^2(\pi^*\delta^*)^3$ electronic configuration.[126] In addition, the temperature dependence of the magnetic moment of $Ru_2(DTolF)_4Cl$ at 300 K shows that its magnetic moment has a value of 3.66 BM, but at temperatures below ~100 K there is a deviation from the Curie-Weiss behavior, as the magnetic moment decreases. This deviation was ascribed to zero-field splitting (D ~50 cm^{-1}), since any type of interdimer antiferromagnetic interaction was excluded.[125]

Room temperature magnetic susceptibility measurements for complexes with a mixed set of bridging formamidinate/acetate ligands have also corresponded to the $\sigma^2\pi^4\delta^2(\pi^*\delta^*)^3$ electronic configuration.[127-129] In the case of the molecular squares $\{[cis\text{-}Ru_2(DAniF)_2Cl](\mu\text{-}O_2CCO_2)\}_4$ and $\{[cis\text{-}Ru_2(DAniF)_2Cl](\mu\text{-}O_2CC_6H_4CO_2)\}_4$ variable temperature magnetic susceptibility studies show that in the square with the shorter oxalate bridges there is a weak antiferromagnetic coupling between the Ru_2^{5+} units (θ ~ -5 K), while in the terephthalate analog the coupling is negligible.[128] Analogously, no coupling was observed between the two Ru_2^{5+} units in the compound $[Ru_2(DAniF)_3Cl](\mu\text{-}O_2CC_6H_4CO_2)[Ru_2(DAniF)_3Cl]$.[129]

Naphthyridine ligands

There are only two known Ru_2^{5+} naphthyridine complexes, $Ru_2(O_2CMe)_3(bcnp)$[136] (Fig. 9.18) and $trans\text{-}Ru_2(O_2CMe)_2(mephonp)_2Cl$[137] (Fig. 9.19). These were synthesized from the reactions of $Ru_2(O_2CMe)_4Cl$ with the corresponding naphthyridine in MeOH under mild conditions. Complexes with four bridging naphthyridine ligands have not been reported. This is probably due to the fact that the high temperatures and long reaction times that appear to be necessary for the syntheses of the fully substituted complexes are associated with reduction of the Ru_2^{5+} core to Ru_2^{4+} (see section 9.3.3).

Pictiva EX2004
Samsung v Pictiva
IPR2024-01094

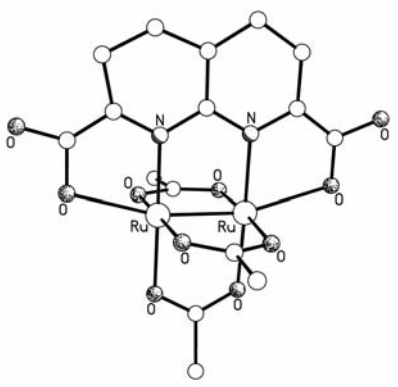


Fig. 9.18. The structure of $Ru_2(O_2CMe)_3(bcnp)$.

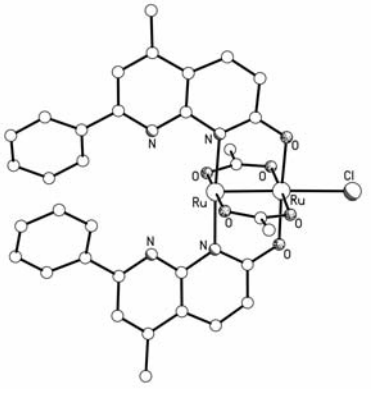


Fig. 9.19. The structure of *trans*-$Ru_2(O_2CMe)_2(mephonp)_2Cl$.

The crystal structure of *trans*-$Ru_2(O_2CMe)_2(mephonp)_2Cl$ (Fig. 9.19) shows a polar arrangement of the mephonp ligands.[137] As for the similar Ru_2^{5+} complex *trans*-$Ru_2(O_2CMe)_2(mhp)_2Cl$,[102] the strong preference of the Ru_2^{5+} unit for axial coordination favors the polar and *transoid* arrangement of the bridging mephonp ligands, regardless of the steric crowding that this preference may cause (there is a twist angle of ~6°). Interestingly, the mephonp ligands, which can adopt either the N,O or the N,N' coordination mode, prefer the N,O coordination, since this leaves one axial site unencumbered for coordination of the Cl^- ion that stabilizes the molecule. The Ru–Ru bond lengths in $Ru_2(O_2CMe)_3(bcnp)$ and *trans*-$Ru_2(O_2CMe)_2(mephonp)_2Cl$ are 2.285(1) and 2.265[5] Å, respectively (Table 9.1). These are within the range of the Ru–Ru distances observed in Ru_2^{5+} tetracarboxylates. Although there are no magnetic measurements that would give some information about the electronic structure of these complexes, the observed Ru–Ru bond lengths give an indication for the $\sigma^2\pi^4\delta^2(\pi^*\delta^*)^3$ electronic configuration.

Other N,N'-donor bridging ligands

Other N,N'-donor bridging ligands that have been used in complexes with the Ru_2^{5+} core include: admpym, a series of 5-Rsalpy ligands, dmat and DTolTA.

Reaction of $Ru_2(O_2CMe)_4Cl$ with Hadmpym in MeOH results in the synthesis of $Ru_2(O_2CMe)_3(admpym)Cl(MeOH)$ which exhibits a Ru–Ru bond length of 2.290(1) Å

Pictiva EX2004
Samsung v Pictiva
IPR2024-01094

(Table 9.1).[138] This complex undergoes three one-electron redox processes, one oxidation and two reductions, which correspond to the processes $Ru_2^{5+} \rightarrow Ru_2^{6+} + e^-$, $Ru_2^{5+} + e^- \rightarrow Ru_2^{4+}$, and $Ru_2^{4+} + e^- \rightarrow Ru_2^{3+}$, respectively. Variable temperature magnetic susceptibility measurements show a ground state with $S = {}^3/_2$, arising from the $\sigma^2\pi^4\delta^2(\pi^*\delta^*)^3$ electronic configuration.

Complexes of the type $[Ru_2(O_2CMe)_2(5\text{-Rsalpy})_2]^-$ have been synthesized from the reactions of $Ru_2(O_2CMe)_4Cl$ with the dianionic, tridentate ligands 5-Rsalpy (R = H, Me, Cl, Br, NO_2) in 1:2 ratio.[139,140] In the solid state, these complexes are isolated by using K^+ or Na^+(18-crown-6) as counter-cations, and they display either discrete paddlewheel structures (Fig. 9.20), or one-dimensional polymeric chain structures formed by the interactions of the alkali metals with the phenolate O atoms of the $[Ru_2(O_2CMe)_2(5\text{-Rsalpy})_2Cl]^-$ units (Fig. 9.21). The 5-Rsalpy ligands are at *transoid* positions exhibiting a bridging/axial chelating coordination mode. The Ru–Ru bond lengths are in the range 2.283-2.300 Å. Electrochemical studies of these complexes reveal four redox processes: a metal-centered reduction of the Ru_2^{5+} core to Ru_2^{4+}, two metal-centered oxidations to Ru_2^{6+} and an unusual Ru_2^{7+} core, while a fourth redox process is assigned to a ligand-based oxidation. The temperature dependence of the magnetic susceptibility supports the $\sigma^2\pi^4\delta^2(\pi^*\delta^*)^3$ electronic configuration.

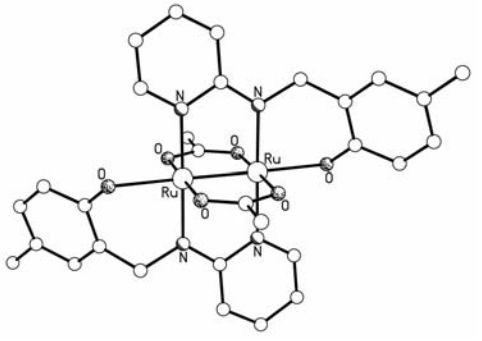


Fig. 9.20. The structure of $[Ru_2(O_2CMe)_2(5\text{-Mesalpy})_2]^-$.

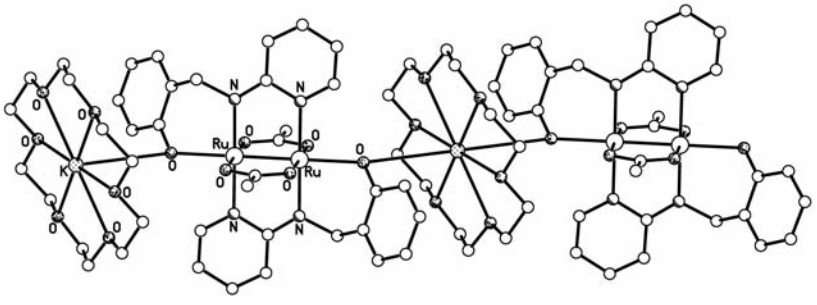


Fig. 9.21. The polymeric structure of $[K(18\text{-crown-6})][Ru_2(O_2CMe)_2(salpy)_2]$.

A similar reaction of $Ru_2(O_2CMe)_4Cl$ with 5-Clsalpy in 1:3 ratio results in the complete substitution of the acetate ligands and the formation of $Li_2(THF)_4Cl[Ru_2(5\text{-Clsalpy})_3]$ with a Ru–Ru bond length of 2.313(1) Å.[141] In this complex one of the 5-Clsalpy ligands embraces the dimetal unit in a bridging/axial chelating coordination mode, while the other two ligands adopt a bridging/equatorial chelating coordination mode.

Pictiva EX2004
Samsung v Pictiva
IPR2024-01094

The complexes $Ru_2(dmat)_4Cl$, synthesized from the reaction of $Ru_2(O_2CMe)_4Cl$ with excess of molten Hdmat, and $[Ru_2(DTolTA)_4(MeCN)]BF_4$, obtained from the reaction of $Ru_2(DTolTA)_4$ with $AgBF_4$ in MeCN, exhibit an electronic structure that is not common for Ru_2^{5+} complexes.[142,169] Their room temperature magnetic moments of 1.70 and 1.88 BM, respectively, are consistent with the presence of one unpaired electron, suggesting either the $\sigma^2\pi^4\delta^2\delta^{*2}\pi^{*1}$ or the $\sigma^2\pi^4\delta^2\pi^{*3}$ electronic configuration. The unusually long Ru–Ru distances of 2.432(1) Å of the former and 2.373(1) Å of the latter (compared to other Ru_2^{5+} complexes) support the latter electronic configuration, since the presence of three electrons in the π^* molecular orbitals is expected to result in a substantial lengthening of the Ru–Ru bond, whereas the lengthening of the Ru–Ru bond caused by the presence of electrons in the δ^* molecular orbital would have been small. The destabilization of the δ^* molecular orbital is attributed to an interaction with suitable molecular orbitals of the highly basic dmat and DTolTA ligands.

9.3 Ru_2^{4+} Compounds

Complexes of the paddlewheel framework with a Ru_2^{4+} core, together with those with a Ru_2^{6+} core discussed in the following section, represent the other two main families of Ru_2 compounds. The Ru_2^{4+} compounds that have been structurally characterized along with their corresponding Ru–Ru bond lengths are listed in Table 9.2.

Table 9.2. Structurally characterized Ru_2^{4+} paddlewheel compounds

Compound	r(Ru–Ru) (Å)	ref.
O,O′-donor bridging ligands		
carboxylate ligands		
$Ru_2(O_2CPh)_4(PhCO_2H)_2$	2.263(1)	15
$[RuCl(MeCN)_3(PPh_3)_2]_2[Ru_2(O_2CC_6H_4\text{-}p\text{-}Me)_4Cl_2]\cdot 4H_2O$	2.291(2)	30
$Ru_2(O_2CCF_3)_4(THF)_2$	2.276(3)	80
$Ru_2(O_2CEt)_4(NO)_2$	2.515(4)	80
$Ru_2(O_2CCF_3)_4(NO)_2$	2.532(4)	80
$Ru_2(O_2CMe)_4(THF)_2$	2.260(2)	143
$Ru_2(O_2CMe)_4(THF)_2$	2.261(3)	144
$Ru_2(O_2CMe)_4(H_2O)_2$	2.262(3)	144
$Ru_2(O_2CEt)_4(acetone)_2$	2.260(3)	144
$Ru_2(O_2CC_{10}H_{15})_4(MeOH)_2\cdot 2MeOH$	2.281(1)	147
$Ru_2(O_2CCH(OH)Ph)_4(H_2O)_2$	2.266[2]	148
$Ru_2(O_2CCPh_3)_4(H_2O)(EtOH)\cdot 2EtOH$	2.252(2)	149
$Ru_2(O_2CC(O)Ph)_4(THF)_2$	2.274(1)	151
$Ru_2(O_2CC_6H_4\text{-}p\text{-}Me)_4(THF)_2\cdot 2THF$	2.269(1)	152
$Ru_2(O_2CC_6H_4\text{-}p\text{-}Me)_4(MeCN)_2\cdot 3MeCN$	2.276(1)	152
$Ru_2(O_2CCF_3)_4(phz)$	2.311(1)	157
$[Ru_2(O_2CCF_3)_4]_2(\mu_4\text{-}TCNQ)\cdot 3toluene$	2.287(1)	159
$Ru_2(O_2CCF_3)_4(tempo)_2$	2.293(1)	163
N,O-donor bridging ligands		
oxopyridinate ligands		
$(4,0)\text{-}Ru_2(chp)_4(THF)\cdot THF$	2.261(1)	98
trans-$(2,2)\text{-}Ru_2(chp)_4$	2.248(1)	98
trans-$(2,2)\text{-}Ru_2(mhp)_4\cdot CH_2Cl_2$	2.238(1)	164
trans-$(2,2)\text{-}Ru_2(mhp)_4$	2.235(1)	165
trans-$(2,2)\text{-}Ru_2(bhp)_4\cdot 1.5benzene$	2.259(1)	165

Pictiva EX2004
Samsung v Pictiva
IPR2024-01094

Compound	r(Ru–Ru) (Å)	ref.
$[(3,1)\text{-}Ru_2(chp)_4]_2\cdot CH_2Cl_2$	2.247[1]	165
$(4,0)\text{-}Ru_2(fhp)_4(THF)$	2.274(1)	166
other N,O-donor bridging ligands		
$[Ru_2(O_2CMe)_{2-x}(O_2CCF_3)_x(9\text{-}EtGH)_2(MeOH)_2](O_2CCF_3)_2\cdot 2MeOH\cdot 0.5Et_2O$ (x = 0.18)	2.322(13)	214
N,N'-donor bridging ligands		
formamidinate ligands		
$[Ru_2(DAniF)_3Cl_{0.12}]_2(\mu\text{-}O_2CC_6H_4CO_2)\cdot 6THF$	2.416(1)	129
$Ru_2(DAniF)_4$	2.454(1)	131
$Ru_2(DTolF)_4\cdot 2benzene$	2.474(1)	167
$Ru_2(DPhF)_4(CO)\cdot 4CH_2Cl_2$	2.554(1)	168
triazenate ligands		
$Ru_2(DPhTA)_4$	2.399(1)	169
$Ru_2(DTolTA)_4(MeCN)$	2.407(1)	169
$Ru_2(DTolTA)_4\cdot 3toluene$	2.417(2)	170
naphthyridine ligands		
$trans\text{-}Ru_2(O_2CMe)_2(mephonp)_2\cdot 2CHCl_3$	2.268(2)	137
$Ru_2(mephonp)_4(H_2O)\cdot 0.5MeOH\cdot 1.5C_6H_4Cl_2$	2.238(2)	137
$cis\text{-}[Ru_2(O_2CMe)_2(pynp)_2](PF_6)_2\cdot 2MeOH$	2.298(1)	172
$[Ru_2(O_2CMe)_3(bpnp)]PF_6$	2.28(2)	173
$Ru_2(meonp)_4\cdot 2benzene$	2.258(2)	174

9.3.1 Ru_2^{4+} compounds with O,O'-donor bridging ligands

Carboxylate ligands

Despite the fact that the mild reduction potentials for the Ru_2^{5+} tetracarboxylates indicated that the one-electron reduced Ru_2^{4+} analogs were chemically accessible,[3,48] it was not until 1984 that Wilkinson and coworkers reported the synthesis of the first Ru_2^{4+} tetracarboxylate. $Ru_2(O_2CMe)_4(THF)_2$ (Fig. 9.22) was made by reacting $Ru_2(O_2CMe)_4Cl$ with the Grignard reagent Me_3SiCH_2MgCl (the latter acting as one-electron reducing agent).[143] A more efficient synthetic method for Ru_2^{4+} tetracarboxylates was reported the following year which involved reactions of Na^+ or Li^+ salts of the appropriate carboxylic acids with a "blue solution of $RuCl_3$" (a MeOH solution of $RuCl_3\cdot xH_2O$ that has been reduced with H_2). A number of $Ru_2(O_2CR)_4L_2$ complexes (R = H, Me, CH_2Cl, Et, Ph, and L = H_2O, THF, MeOH, acetone, MeCN) were made following this synthetic method.[144] Exchange reactions of $Ru_2(O_2CH)_4$ (the compound obtained in the best yield from the above mentioned synthetic method) with suitable salts of different carboxylates also result in new Ru_2^{4+} tetracarboxylates. However, this procedure fails to give $Ru_2(O_2CCF_3)_4$, whereas the reaction of $Ru_2(O_2CMe)_4$ with AgO_2CCF_3 results in $Ru_2(O_2CMe)_4(O_2CCF_3)$. $Ru_2(O_2CCF_3)_4$ can be made by refluxing $Ru_2(O_2CMe)_4$ in a $CF_3CO_2H/(CF_3CO)_2O$ mixture in the presence of NaO_2CCF_3,[80] or by reaction of $RuCl_3\cdot xH_2O$ with AgO_2CCF_3.[145]

Reduction of Ru_2^{5+} tetracarboxylates can also be used for the synthesis of compounds of this type. For example, the complex $Ru_2(asp)_4Cl$ is converted to $Ru_2(asp)_4(NO)$ by heating its MeOH solution in the presence of $AgNO_3$.[146] In another case $K_3[Ru_2(O_2CO)_4]$ reacts with 1-adamantylcarboxylic acid in $MeOH/H_2O$ solution to yield the Ru_2^{4+} tetraadamantylcarboxylate complex.[147] Furthermore, reaction of $Ru_2(O_2CMe)_4Cl$ with mandelic acid gives $Ru_2(mandelate)_4$,[148] which serves as a starting material in carboxylate exchange reactions to

Pictiva EX2004
Samsung v Pictiva
IPR2024-01094

give other Ru_2^{4+} tetracarboxylate compounds.[149] Although the mechanism of these reductions is not clear, it has been proposed that they proceed via a disproportionation pathway, which in the case of $Ru_2(mandelate)_4$ can be described with the equation:

$$6Ru_2(mandelate)_4Cl + 8H_2O \rightarrow 3Ru_2(mandelate)_4 + 2[Ru_3(\mu_3\text{-}O)(mandelate)_6(H_2O)_3]Cl + 4HCl$$

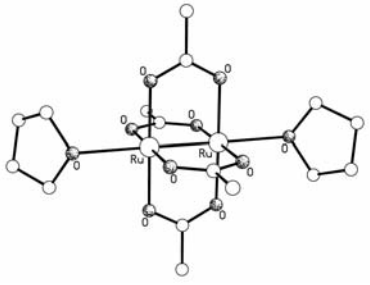


Fig. 9.22. The structure of $Ru_2(O_2CMe)_4(THF)_2$.

Alternatively, chemical reduction of Ru_2^{5+} tetracarboxylates using either $CrCl_2$,[150] or Zn/Hg[151] can also be used to prepare their Ru_2^{4+} analogs.

The Ru_2^{4+} tetracarboxylates have a high affinity for axial coordination. In coordinating solvents they exist as discrete diadducts of the general type $Ru_2(O_2CR)_4L_2$, where L is a solvent molecule. The same type of structure is maintained in the solid state. However, in non-coordinating solvents oligomerization takes place by intermolecular interactions between the O atoms of the bridging carboxylate ligand of one molecule with the axial position of another molecule.[152]

The Ru–Ru bond lengths of the $Ru_2(O_2CR)_4L_2$ compounds fall in the range of 2.252-2.311 Å, (there are two exceptions that are discussed in the following paragraph). They do not show any significant dependence on the substituent R of the carboxylate bridge or the type of the axial donor ligand L. However, they are slightly longer than those in the Ru_2^{5+} teracarboxylate analogs (e.g., Ru–Ru = 2.262(3) Å in $Ru_2(O_2CMe)_4(H_2O)_2$[144] and Ru–Ru = 2.248(1) Å in $[Ru_2(O_2CMe)_4(H_2O)_2]BF_4$).[7]

The compounds with metal-metal bond lengths outside of the aforementioned range are $Ru_2(O_2CEt)_4(NO)_2$ and $Ru_2(O_2CCF_3)_4(NO)_2$, with Ru–Ru distances of 2.515(4) and 2.532(4) Å, respectively.[80] Early attempts to explain these exceptions suggested that the complexes could be considered as Ru^{I}–Ru^{I} complexes, with both NO ligands donating their odd π^* electrons to the Ru_2 unit, resulting in the electronic configuration $\sigma^2\pi^4\delta^2\pi^{*4}\delta^{*2}$ and a diamagnetic ground state. However, this is not consistent with the short Ru–N bond lengths, the bent coordination mode of the NO groups ($\angle$Ru–N–O = 153°) and the low NO stretching frequencies (1745-1805 cm^{-1}). Thus, the long Ru–Ru distances are probably due to strong σ interactions, while the rest of the data suggest a strong delocalization of the π^* electron density over the ONRu-RuNO chain. Theoretical calculations for the $Ru_2(O_2CR)_4(NO)_2$ (R = H, CF_3) compounds have been conducted and their PES spectra have been reported.[153-155] However, the results of these studies do not lead to a good understanding of the electronic structures of these compounds.

The Ru_2^{4+} tetracarboxylates react with Lewis bases (e.g., THF, acetone, H_2O) which occupy the axial positions forming $Ru_2(O_2CR)_4L_2$ diadducts.[80] These axial ligands can be removed by heating under vacuum to give unsolvated compounds. As for the Ru_2^{5+} analogs, their reactions with Lewis bases that are also π-acceptors result in the cleavage of the metal-metal bond.

Pictiva EX2004
Samsung v Pictiva
IPR2024-01094

Mononuclear cleavage products of the type $Ru(O_2CR)_2(PPh_3)_2$ and $Ru(O_2CR)_2(CNBu^t)_4$ are obtained from reactions with Ph_3P and Bu^tNC, respectively. A variety of mononuclear Ru carbonyl compounds are also isolated from reactions with CO. Surprisingly, excess pyridine also reacts with the $Ru_2(O_2CR)_4$ (R = Me, CF_3) compounds to give the cleavage products $Ru(O_2CR)_2(py)_4$. With $Ru_2(O_2CCF_3)_4$, but not the other $Ru_2(O_2CR)_4$ compounds, MeCN also causes cleavage to give $[Ru(O_2CCF_3)_2(MeCN)_5]O_2CCF_3$.

Reactions of $Ru_2(O_2CR)_4$ compounds with bifunctional N-donor ligands, such as pyz, phz, and DMDCNQI, result in the formation of one-dimensional polymeric chain structures.[156-158] More extended architectures are obtained when polyfunctional ligands are used, as shown in the reaction of $Ru_2(O_2CCF_3)_4$ with TCNQ which gives a two-dimensional network $[Ru_2(O_2CCF_3)_4]_2(\mu_4\text{-TCNQ})$.[159] However, upon reaction of $Ru_2(O_2C(CH_2)_6CH_3)_4$ with the polyfunctional ligand TCNE a redox reaction occurs instead.[156]

Electrochemical measurements show that Ru_2^{4+} tetracarboxylates are easily oxidized to their Ru_2^{5+} analogs: a reversible or a quasi-reversible one electron oxidation is observed close to a potential where reduction of the Ru_2^{5+} species takes place. A study of a series of $Ru_2(O_2CR)_4$ (R = H, Me, CH_2Cl, Et, Ph, CF_3) compounds reveals that the oxidation potentials are highly dependent on the solvent and the substituent R of the carboxylate bridges.[80,144] For solvents that can axially coordinate to the Ru_2^{4+} unit, the stronger the coordination of the donor solvent, the easier the oxidation becomes. Furthermore, substituents R with strong electron withdrawing ability result in more difficult oxidations. For example, the oxidation of $Ru_2(O_2CCH_2Cl)_4$ in THF is more difficult than the oxidation of $Ru_2(O_2CEt)_4$ with potentials of +0.29 V and -0.03 V, respectively, whereas $Ru_2(O_2CCF_3)_4$ shows a much more positive oxidation potential in acetone at +1.03 V.

The electronic structure of compounds of this type has been quite controversial. Room temperature magnetic susceptibility measurements on $Ru_2(O_2CR)_4$ and $Ru_2(O_2CR)_4L_2$ complexes showed magnetic moments in the range of 1.9-2.2 BM, which indicates the presence of two unpaired electrons.[144] This means that the electronic configuration can either be $\sigma^2\pi^4\delta^2\pi^{*3}\delta^{*1}$ or $\sigma^2\pi^4\delta^2\delta^{*2}\pi^{*2}$. Early theoretical calculations at the SCF-Xα-SW level performed for $Ru_2(O_2CH)_4$ predicted the former,[60] while *ab initio* Hartree-Fock calculations conducted later led to the conclusion that the ground state can be better described by the latter.[154] In each case the difference in the calculated energies of the two electronic configurations is too small to allow a definite assignment of the ground state. In addition, regardless of their paramagnetic nature, no EPR spectra have been observed for this type of compounds (probably due to large zero-field splitting),[80,144] while PES studies on $Ru_2(O_2CH)_4$ and $Ru_2(O_2CCF_3)_4$ have been inconclusive.[153-155]

Structural data support the $\sigma^2\pi^4\delta^2\delta^{*2}\pi^{*2}$ electronic configuration. Considering that the Ru–Ru distances of Ru_2^{4+} tetracarboxylates are similar to those of the corresponding Ru_2^{5+} compounds, for which the electronic configuration is $\sigma^2\pi^4\delta^2(\pi^*\delta^*)^3$, it is expected the additional electron in the Ru_2^{4+} tetracaboxylates should enter a δ^* molecular orbital. The lengthening of the Ru–Ru bond caused by an additional electron in a δ^* molecular orbital is very small and can be counterbalanced by the decrease of the electrostatic repulsion between the Ru centers (lower mean oxidation state). It should be noted that addition of an electron to a π^* molecular orbital should result in a substantial lengthening of the Ru–Ru bond. Recent DFT calculations predict a ground state electronic configuration in agreement with that suggested by the structural data.[160]

Variable temperature magnetic susceptibility studies have also been helpful in the assignment of the ground state electronic configuration. A study on Ru_2^{4+} long-chain alkyl tetracarboxylates over the temperature range of 6-400 K concluded that the ground state has a singlet component and that there is a thermally accessible triplet excited state, but it was

Pictiva EX2004
Samsung v Pictiva
IPR2024-01094

not possible to distinguish between the two possible ground state electronic configurations mentioned above.[150] However, another study provided adequate and very persuasive evidence for the $\sigma^2\pi^4\delta^2\pi^{*2}\delta^{*2}$ electronic configuration.[148] The temperature dependence of the magnetic susceptibility of the complexes $Ru_2(O_2CMe)_4$ and $Ru_2(O_2CPh)_4$ over the temperature range of 6-298 K showed that the room temperature magnetic moment of ~2.8 BM per Ru_2 unit tends towards zero as the temperature is lowered (Fig. 9.23). This implies a non-magnetic ground state at low temperatures, despite the fact that there are unpaired electrons at room temperature. This behavior is consistent with a $\pi^{*2}\delta^{*2}$ electronic configuration that results in a $^3A_{2g}$ ground state, which in turn splits under spin-orbit coupling into an ^3E_g state with $m_S = \pm 1$ and a much lower in energy A_{1g} state ($m_S = 0$) (**9.5**). The two states are separated by a large zero-field splitting (a value of ~250 cm^{-1} was calculated for the zero-field splitting parameter, D). As shown in Fig. 9.23, there is an excellent agreement of this model and the experimental data.

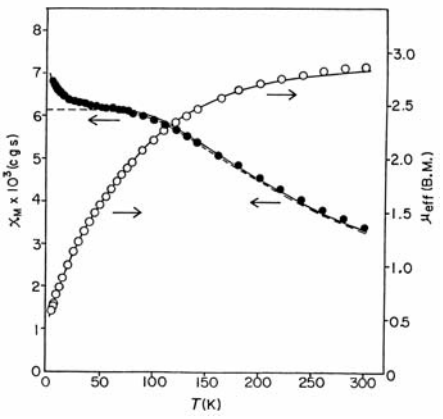
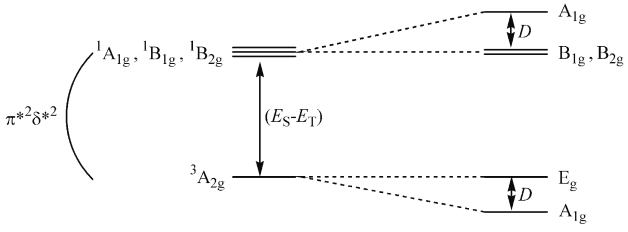


Fig. 9.23. Plots of the molar magnetic susceptibility and effective magnetic moment versus temperature for $Ru_2(O_2CMe)_4$.

Magnetic measurements conducted for the polymeric compounds $Ru_2(O_2C(CH_2)_{10}CH_3)_4(pz)$[161] and $Ru_2(O_2CCF_3)_4(phz)$[157] show that in both compounds there is an appreciable contribution of a large zero-field splitting arising from the $S = 1$ ground state to the resulting magnetic moments (D = 250-300 cm^{-1}). However, for the former the data were inconclusive as to whether any interdimer antiferromagnetic coupling exists, while the data for the latter suggest that the Ru_2^{4+} units are weakly antiferromagnetically coupled with a coupling constant of -3 cm^{-1}. Other Ru_2^{4+} tetracarboxylates linked by pyz, 4,4'-bipy, and dabco have also been studied, and show no interdimer interactions.[162]



9.5

Pictiva EX2004
Samsung v Pictiva
IPR2024-01094

The polymeric compound with a two-dimensional network structure $[Ru_2(O_2CCF_3)_4]_2(\mu_4$-TCNQ) exhibits a low magnetic moment at room temperature ($\chi_M T$ = 0.678 cm^3Kmol^{-1}) which decreases as the temperature approaches 0 K.[159] Although the contribution of the zero-field splitting to the decrease of the magnetic moment at lower temperatures is significant, the data are in accordance with the existence of a strong antiferromagnetic interaction between the Ru_2^{4+} units.

The complexes with axially coordinating nitroxide radicals $Ru_2(O_2CCF_3)_4(tempo)_2$ and $Ru_2(O_2CC_6F_5)_4(tempo)_2$, which have a large zero-field splitting within the dimetal unit (D ~240 cm^{-1}), display strong antiferromagnetic interactions between the Ru_2 core and the nitroxide radical with J_2 = -263 and -234 cm^{-1}, respectively,[163] which are much larger than those in the Ru_2^{5+} analog $[Ru_2(O_2CCMe_3)_4(tempo)_2]^+$.[73] No coupling was observed between the two axially coordinating tempo ligands (J_1 = 0).

9.3.2 Ru_2^{4+} compounds with N,O-donor bridging ligands

Oxopyridinate ligands

Prior to the isolation of any other Ru_2^{4+} compound, $Ru_2(mhp)_4$ (Fig. 9.24) was prepared in low yield (8%) from the reaction of $Ru_2(O_2CMe)_4Cl$ with Na(mhp) in 1981.[164] It was later shown that by employing a Ru_2^{4+} tetracarboxylate instead of a Ru_2^{5+} tetracarboxylate as starting material in such a reaction, higher yields of $Ru_2(mhp)_4$ can be obtained.[165] Other Ru_2^{4+} tetraoxopyridinates, like $Ru_2(chp)_4$, $Ru_2(fhp)_4$, and $Ru_2(bhp)_4$, have been synthesized following a similar synthetic strategy, i.e., from the reactions of $Ru_2(O_2CMe)_4$ with either an excess of the molten hydroxypyridines, or stoichiometric amounts of their Na^+ salts (methods which are comparable to those employed for the synthesis of analogous Cr_2^{4+} and Mo_2^{4+} compounds).

The majority of Ru_2^{4+} tetraoxopyridinates exist as discrete paddlewheel complexes, which do not associate through the axial positions to form polymers, except for some cases in which dimerization occurs (see below). Axial ligands are usually coordinating solvent molecules. The Ru–Ru bond lengths span from 2.235 to 2.274 Å (Table 9.2), and they do not show any dependence on the bridging oxopyridinate ligand and the steric effect of the coordination mode. However, axial ligation results in longer Ru–Ru bonds.

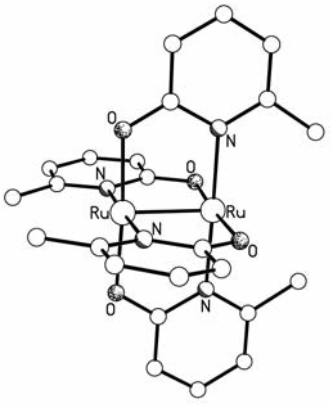


Fig. 9.24. The structure of $Ru_2(mhp)_4$.

The major factor determining the preferred regioisomer for the Ru_4^{4+} tetraoxopyridinates is not the axial ligation as in $Ru_2(Xhp)_4Cl$ compounds, but the size of the X group in the Xhp ligand. For large X groups, like Br and Me, the *trans*-(2,2) regioisomers form, since only two

Pictiva EX2004
Samsung v Pictiva
IPR2024-01094

large substituents X can be accommodated at each end. In contrast, for smaller substituents, like F and Cl, the polar arrangements (4,0) and (3,1) are preferred. In this latter case any steric hindrance that might be imposed due to the X substituents at one axial site can be overcome by the stabilization gained from the coordination of a ligand to the unencumbered axial site. For example, in the (4,0) regioisomer of $Ru_2(fhp)_4$ a THF molecule coordinates to the open axial position.[166] Stabilization can also be gained through dimerization. For example, $Ru_2(chp)_4$, when isolated as the (3,1) regioisomer, dimerizes in the absence of coordinating solvents as shown in Fig. 9.25.[165] The last compound has also been isolated as the *trans*-(2,2) regioisomer.[98]

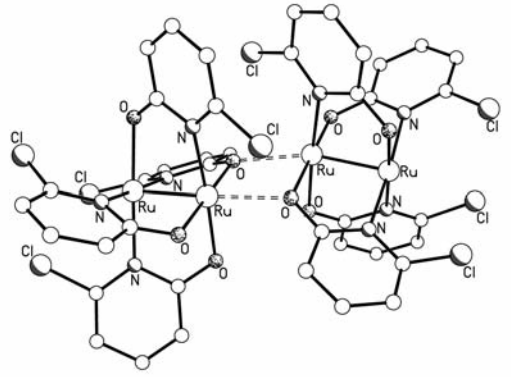


Fig. 9.25. The structure of the (3,1) regioisomer of $Ru_2(chp)_4$.

The $Ru_2(Xhp)_4$ complexes exhibit room temperature magnetic moments of ~2.5 BM, indicative of two unpaired electrons.[165] As for the Ru_2^{4+} tetracarboxylates, there are two possible electronic configurations, $\sigma^2\pi^4\delta^2\pi^{*3}\delta^{*1}$ or $\sigma^2\pi^4\delta^2\delta^{*2}\pi^{*2}$. The PES of $Ru_2(mhp)_4$ shows three peaks of approximately equal intensities at ionization energies of 5.8, 6.3, and 6.8 eV.[164] These energies were assigned to π^*, δ^*, and δ, respectively. It was asserted that this spectrum "suggests" a $\delta^*\pi^{*3}$ electronic configuration. However, it is equally compatible, if not more so with a $\delta^{*2}\pi^{*2}$ electronic configuration (because the δ and δ^* peaks are of about equal intensity rather than in a 2:1 ratio).

Structural data clearly favor the $\sigma^2\pi^4\delta^2\delta^{*2}\pi^{*2}$ electronic configuration since the Ru–Ru distances in Ru_4^{4+} oxopyridinates (2.235 to 2.274 Å) fall in the range of the $Ru_2(O_2CR)_4Cl$ compounds, which are known to have two π^* electrons. Additional support for the electronic configuration is provided by variable temperature magnetic measurements. The complexes $Ru_2(mhp)_4$, $Ru_2(chp)_4$, $Ru_2(bhp)_4$, and $Ru_2(fhp)_4$ exhibit similar magnetic behavior[165,166] with room temperature magnetic moments of ~2.5 BM that drop to an extrapolated value of 0 BM as the temperature approaches 0 K, as in the $Ru_2(O_2CR)_4$ compounds. This behavior is not consistent with a $\pi^{*3}\delta^{*1}$ configuration or a singlet-triplet Boltzmann distribution based on $\pi^{*3}\delta^{*1}$ and π^{*4} electronic configurations, since these would lead to qualitatively different types of behavior as a function of temperature. However, the magnetic data are consistent with a ground state derived from $\sigma^2\pi^4\delta^2\delta^{*2}\pi^{*2}$ configuration, which results in a ${}^3A_{2g}$ state that is split by spin-orbit coupling (D ~ 200-250 cm^{-1}) to give a lower state with $M_s = 0$.

Quantitative support for the above mentioned electronic configuration comes from SCF-Xα theoretical calculations for the $Ru_2(Xhp)_4$ compounds, in which the Xhp ligand was modeled by the ONHCH fragment.[166]

Pictiva EX2004
Samsung v Pictiva
IPR2024-01094

9.3.3 Ru_2^{4+} compounds with N,N'-donor bridging ligands

Formamidinate ligands

The Ru_2^{4+} tetraformamidinates are usually synthesized by ligand metathesis reactions of $Ru_2(O_2CMe)_4$ with stoichiometric amounts of Li^+ salts of formamidinates.[167] Alternatively, they can be synthesized from their Ru_2^{5+} analogs either by bulk electrolysis,[168] or by reduction with Zn.[129] They are isolated as air-sensitive solids which give normal ^{1}H NMR spectra.

Upon reactions with Lewis bases which are also strong π-acceptors, like CO, $Ru_2(DArF)_4$ compounds give axial adducts without disruption of the Ru–Ru bond, in contrast to their carboxylate analogs which react with CO to decompose to mononuclear species. For example, $Ru_2(DPhF)_4$ reacts with CO to give $Ru_2(DPhF)_4(CO)$.[168] Attempts made to isolate the bis-CO adduct have been unsuccessful.

The cyclic voltammogram of $Ru_2(DTolF)_4$ shows two redox processes: a reversible oxidation at +1.163 V and a reversible reduction at -0.118 V. However, the electrochemical behavior of this compound is not very well understood, since the oxidation potential suggests that it should be stable towards oxygen, which is not true.[167]

In the solid state $Ru_2(DArF)_4$ compounds exist as discrete molecules which do not associate, as shown by the structure of $Ru_2(DTolF)_4$ (Fig. 9.26).[167] There are only three crystallographically characterized complexes of this type (Table 9.2). Two of them, $Ru_2(DAniF)_4$ and $Ru_2(DTolF)_4$, exhibit similar Ru–Ru bond lengths at 2.454(1) and 2.474(1) Å, respectively. However, the third one, $Ru_2(DPhF)_4(CO)$, displays a much longer Ru–Ru bond length of 2.554(1) Å, which is comparable with the distances observed in $Ru_2(O_2CEt)_4(NO)_2$ and $Ru_2(O_2CCF_3)_4(NO)_2$.[80]

The Ru–Ru distances of Ru_2^{4+} tetraformamidinates are the longest observed among the Ru_2^{4+} paddlewheel complexes. Even though it has been proposed that this might be due to the larger "bite" angle of the bridging formamidinates, the real reason is electronic in nature. Generally, for Ru_2^{4+} compounds there are three possible electronic configurations: $\sigma^2\pi^4\delta^2\pi^{*4}$, $\sigma^2\pi^4\delta^2\pi^{*3}\delta^{*1}$, $\sigma^2\pi^4\delta^2\pi^{*2}\delta^{*2}$, depending on the ordering of the π* and δ* molecular orbitals levels and their energy separation. The diamagnetism of $Ru_2(DArF)_4$ compounds (as indicated by their normal ^{1}H NMR spectra) together with the long Ru–Ru distances suggest that the frontier electrons are paired in the strongly antibonding π*, rather than in the weakly antibonding δ* molecular orbital, as the lengthening of the Ru–Ru bond caused by the pairing of electrons in the δ* molecular orbital would have been very small. As a result, the $\sigma^2\pi^4\delta^2\pi^{*4}$ electronic configuration was proposed.

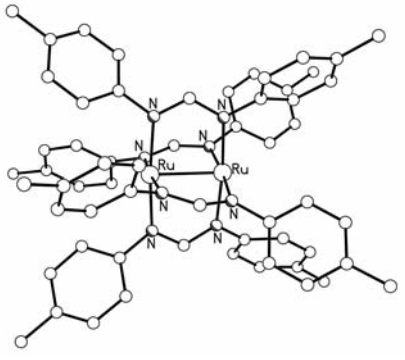


Fig. 9.26. The structure of $Ru_2(DTolF)_4$.

Pictiva EX2004
Samsung v Pictiva
IPR2024-01094

SCF-Xα theoretical calculations on the $Ru_2(HNCHNH)_4$ model compound support the above mentioned electronic configuration.[167] The formamidinate ligands interact with the Ru_2^{4+} core raising the energy of the δ* molecular orbital above that of the π* orbital. As a result, the HOMO is a fully occupied π* molecular orbital and the LUMO is a δ* molecular orbital. The π*–δ* separation, calculated at ~1.18 eV, is large enough to prevent any appreciable population of higher magnetic states at room temperature.

Triazenate ligands

The Ru_2^{4+} tetratriazenates can be synthesized from the stoichiometric ligand metathesis reactions of $Ru_2(O_2CMe)_4$ with Li^+ salts of triazenates (DArTA).[80] They are isolated as air-stable solids which give normal ^1H NMR spectra.

The $Ru_2(DArTA)_4$ complexes generally do not react with weak Lewis bases (e.g., THF, acetone, MeCN) to give axial adducts; however, $Ru_2(DTolTA)_4$ gives a mono-MeCN adduct.[169] Similarly to their formamidinate analogs, they react with Lewis bases which are also strong π-acceptors to form adducts. For example, $Ru_2(DPhTA)_4$ reacts with NO and CO to form strong bis-adducts and with the bulkier Bu^{t}NC to form a mono adduct. However, it does not react with py nor PPh_3. This lack of reactivity is almost certainly due to steric constraints imposed by the bulky phenyl groups of the DPhTA ligands.[80]

Cyclic voltammetry measurements of $Ru_2(DPhTA)_4$ show three redox processes. The NO, CO, and Bu^{t}NC axial adducts of $Ru_2(DPhTA)_4$ show similar redox behavior.[80] For the latter complexes the potentials of the reduction and the first oxidation processes vary considerably, which gives an indication that these are metal-based processes corresponding to $Ru_2^{4+} + e^- \rightarrow Ru_2^{3+}$ and $Ru_2^{4+} \rightarrow Ru_2^{5+} + e^-$, respectively. However, the second oxidation wave appears almost invariantly at the same potential (~ +1.30 V), which suggests that this redox process may be associated with the ligand and not with the dimetal core.

In the solid state, Ru_2^{4+} tetratriazenates exist as discrete molecules which do not associate, as shown by the structure of $Ru_2(DTolTA)_4$ in Fig. 9.27.[170] The Ru–Ru bond lengths lie in the range of 2.399 to 2.417 Å (Table 9.2). Although shorter than those in the Ru_2^{4+} tetraformamidinates, these distances are significantly longer than those of most of the Ru_2^{4+} paddlewheel compounds. Interestingly, the Ru–Ru bond length of 2.407(1) Å in $Ru_2(DTolTA)_4(MeCN)$[169] is slightly shorter than the corresponding distance of 2.417(2) Å in $Ru_2(DTolTA)_4$.[170] For most Ru_2 compounds, axial ligation causes an elongation of the M–M bond distance, since the σ donation of the ligand increases the anti-bonding σ* electron density between the two metals. In this case it appears that along with the σ donation of the axially coordinated MeCN, there is a moderate π-back donation from the π* metal orbitals to the empty π* orbitals of MeCN, which partially cancels the lengthening of the Ru–Ru bond distance caused by σ donation.

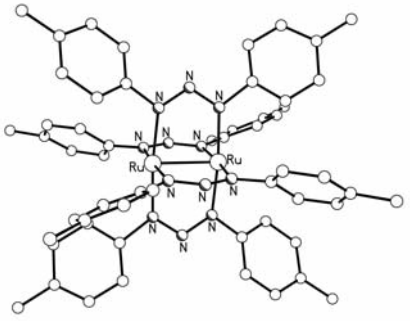


Fig. 9.27. The structure of $Ru_2(DTolTA)_4$.

Pictiva EX2004
Samsung v Pictiva
IPR2024-01094

The long Ru–Ru bond lengths of Ru_2^{4+} tetratriazenates together with their diamagnetism (as indicated by their normal ^{1}H NMR spectra) suggest the $\sigma^2\pi^4\delta^2\pi^{*4}$ electronic configuration. This is supported by SCF-Xα theoretical calculations carried out on the simplified computational model $Ru_2(HNNNH)_4$, which show a strong interaction between the δ^* orbital of the Ru_2^{4+} core and the $p\pi$ lone pair of the ligands.[171] The δ^* molecular orbital is higher in energy than the π^* molecular orbital by ~1 eV. The large π^*–δ^* separation indicates that the δ^* is thermally inaccessible at room temperature, resulting in a singlet ground state.

Naphthyridine ligands

The Ru_2^{4+} naphthyridine compounds are synthesized by reacting $Ru_2(O_2CMe)_4Cl$ and excess of naphthyridines (or their Na^+ salts) either in molten naphthyridines, or by prolonged reflux in MeOH, a process that causes the reduction to a Ru_2^{4+} core. For the neutral naphthyridines to replace negatively charged acetate groups, suitable counter ions (e.g., PF_6^-) are required.[172] When naphthyridines with substituents that can coordinate axially to the dimetal unit are used, only partial substitution of the acetate groups of $Ru_2(O_2CMe)_4Cl$ takes place. For example, in the complexes *cis*-$[Ru_2(O_2CMe)_2(pynp)_2](PF_6)_2$[172] (Fig. 9.28) and $[Ru_2(O_2CMe)_3(bpnp)]PF_6$ [173] the substituents at the 2 and 7 positions of the bridging naphthyridine ligands block the axial positions preventing further substitution.

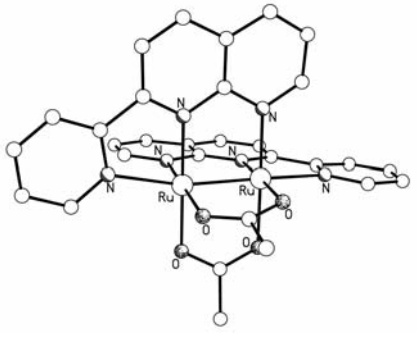


Fig. 9.28. The structure of the cation in $[Ru_2(O_2CMe)_2(pynp)_2](PF_6)_2$.

In the case of the naphthyridinone ligand mephonp, which can adopt either the N,O or the N,N' coordination mode, while in the Ru_2^{5+} complex *trans*-$Ru_2(O_2CMe)_2(mephonp)_2Cl$ the mephonp ligands prefer the N,O coordination mode, in the Ru_2^{4+} analog *trans*-$Ru_2(O_2CMe)_2(mephonp)_2$ the N,N' coordination mode is adopted.[137] The same preference for the N,N' coordination is observed in $Ru_2(meonp)_4$, although there is a twist of ~18° from the eclipsed configuration due to the steric requirement of the methyl substituents of the meonp ligands (Fig. 9.29).[174] However, in the analogous complex $Ru_2(mephonp)_4$ the crowding of the adjacent phenyl substituents of the mephonp ligands allows only three of the bridging naphthyridinone ligands to adopt the N,N' coordination mode, while the fourth one is N,O-coordinated.[137]

Electrochemical data for Ru_2^{4+} naphthyridines show multiple redox processes due to both the Ru_2^{4+} core and the naphthyridine ligands. For example, the cyclic voltammogram of *cis*-$[Ru_2(O_2CMe)_2(pynp)_2](PF_6)_2$ shows four reversible, one-electron, ligand-based reductions and an irreversible, one-electron, metal-based oxidation at ~ +0.85 V.[175] Free pynp exhibits a single two-electron reduction. However, in *cis*-$[Ru_2(O_2CMe)_2(pynp)_2](PF_6)_2$ the two-electron process for each one of the two ligands is separated into two one-electron processes, which suggests that the mixed-valence intermediates are stabilized by delocalized bonding. The high potential of

Pictiva EX2004
Samsung v Pictiva
IPR2024-01094

the one-electron metal-based oxidation at ~ +0.85 V gives an indication of the greater stability of the Ru_2^{4+} core relative to that of the Ru_2^{5+} core in this environment.

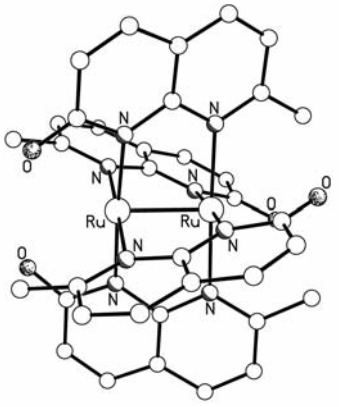


Fig. 9.29. The structure of $Ru_2(meonp)_4$.

The Ru–Ru bond lengths of Ru_2^{4+} naphthyridines fall in the range 2.238-2.298 Å (Table 9.2), which is similar to those of the Ru_2^{4+} tetracarboxylates and tetraoxopyridinates. In addition, magnetic measurements conducted for the complexes $[Ru_2(O_2CMe)_3(bpnp)]PF_6$ and $Ru_2(meonp)_4$ show room temperature magnetic moments of 2.79 and 2.51 BM, respectively, which are consistent with the presence of two unpaired electrons.[173,174] These structural and magnetic data give support to the $\sigma^2\pi^4\delta^2\delta^{*2}\pi^{*2}$ electronic configuration.

9.4 Ru_2^{6+} Compounds

Paddlewheel complexes having a Ru_2^{6+} core are relatively new additions to the family of Ru_2 compounds. Other types of Ru_2^{6+} complexes that have been previously reported include compounds without bridging ligands, such as Ru_2(dibenzotetraaza[14]annulene)$(BF_4)_2$,[176] $Ru_2(CH_2SiMe_3)_6$,[177] trihalo-bridged face-sharing bioctahedral compounds of the general type $[Ru_2X_9]^{3-}$,[178,179] and a variety of edge-sharing bioctahedral compounds with single-atom and three-atom bridging ligands.[92,93] There are claims of paddlewheel Ru_2^{6+} carboxylate compounds,[53,180] but such compounds do not exist.[14] From the absence of an oxidation process in the cyclic voltammograms there would be no reason to expect these or any other $[Ru_2(O_2CR)_4]^{2+}$ species to be stable. However, with the use of either highly charged O,O'-donor, or electron rich bridging ligands in combination with suitable axial ligands, the higher oxidation state (Ru_2^{6+}) becomes more favorable. The structurally characterized compounds of the Ru_2^{6+} core along with their corresponding Ru–Ru distances are given in Table 9.3.

Table 9.3. Structurally characterized Ru_2^{6+} paddlewheel compounds

Compound	*r*(Ru–Ru) (Å)	ref.
O,O'-donor bridging ligands		
$Cs_2[Ru_2(SO_4)_4(H_2O)_2]$	2.343(1)	83
N,N'-donor bridging ligands		
aminopyridinate ligands		
(4,0)-$Ru_2(F_5ap)_4(C{\equiv}CPh)_2$	2.441(1)	110,183
(3,1)-$Ru_2(F_5ap)_4(C{\equiv}CPh)_2$	2.475(1)	110
trans-(2,2)-$Ru_2(F_5ap)_4(C{\equiv}CPh)_2$	2.473(1)	110

Pictiva EX2004
Samsung v Pictiva
IPR2024-01094

Compound	*r*(Ru–Ru) (Å)	ref.
(4,0)-$Ru_2(ap)_4(C{\equiv}CC{\equiv}CSiMe_3)_2$	2.472(1)	114
(4,0)-$Ru_2(ap)_4(CN)_2{\cdot}CH_2Cl_2{\cdot}MeOH$	2.449[4]	118
(3,1)-$Ru_2(2\text{-}Fap)_4(CN)_2{\cdot}CH_2Cl_2$	2.456(5)	118
$[(4,0)\text{-}Ru_2(ap)_4Cl][FeCl_4]{\cdot}2.5CH_2Cl_2$	2.301(1)	181
$Ru_2(F_5ap)_3(F_4Oap)Cl{\cdot}CH_2Cl_2{\cdot}0.5$benzene	2.336(1)	182
(4,0)-$Ru_2(ap)_4(C{\equiv}CPh)_2$	2.471(1)	184
(4,0)-$Ru_2(ap)_4(C{\equiv}CPh)(C{\equiv}CSiMe_3)$	2.434(1)	184
(4,0)-$Ru_2(ap)_4(C{\equiv}CSiPr^i_3)(C{\equiv}CC{\equiv}CSiMe_3)$	2.458(1)	185
(4,0)-$Ru_2(ap)_4(C{\equiv}CC{\equiv}CH)(C{\equiv}CSiMe_3)$	2.466(1)	185
formamidinate ligands		
$Ru_2(DPhF)_4(C{\equiv}CPh)_2$	2.556[2]	132
$Ru_2(DPhF)_4(CN)_2{\cdot}2.5CH_2Cl_2{\cdot}0.5$hexane	2.539(1)	132
$Ru_2(DAni^mF)_4(C{\equiv}CC{\equiv}CSiMe_3)_2$	2.599(1)	135
$Ru_2(DPhF)_4(C{\equiv}CPh)_2$	2.556(1)	187
$Ru_2(DPh^{p\text{-}Cl}F)_4(C{\equiv}CPh)_2{\cdot}2$benzene	2.555(1)	188
$(Me_3SiC{\equiv}CC{\equiv}C)[Ru_2(DPhF)_4](\mu\text{-}C{\equiv}CC{\equiv}CC{\equiv}CC{\equiv}C)[Ru_2(DPhF)_4]\text{-}(C{\equiv}CC{\equiv}CSiMe_3){\cdot}4$toluene$\cdot 2$hexane	2.559[2]	189
$[(Bu^t_2bipy)(CO)_3Re](py\text{-}4\text{-}C{\equiv}C)[Ru_2(DTolF)_4](4\text{-}C{\equiv}C\text{-}py)\text{-}[Re(CO)_3(Bu^t_2bipy)]$	2.567(1)	190
benzamidinate ligands		
$Ru_2(DMeBz)_4Cl_2{\cdot}4$THF	2.323(1)	191
$Ru_2(DMeBz)_4(C{\equiv}CSiMe_3)_2$	2.450(1)	191
$Ru_2(DMeBz)_4(C{\equiv}CC{\equiv}CH)_2$	2.456(1)	191
$Ru_2(DMeODMeBz)_4Cl_2{\cdot}2CH_2Cl_2$	2.316(1)	192
$Ru_2(DEtBz)_4Cl_2$	2.340(1)	192
$Ru_2(DEtBz)_4(C{\equiv}CPh)_2$	2.459(1)	192
$Ru_2(DEtBz)_4(C{\equiv}CSiMe_3)_2$	2.461(1)	192
$Ru_2(DMeODMeBz)_4(C{\equiv}CSiPr^i_3)_2$	2.476(1)	192
$Ru_2(m\text{-}MeODMeBz)_4(C{\equiv}CPh)_2$	2.448(1)	193
$Ru_2(DMeBz)_4(C{\equiv}CC_6H_4\text{-}p\text{-}NO_2)_2{\cdot}2CH_2Cl_2$	2.459(1)	193
$[Ru_2(DMeBz)_4](BF_4)_2$	2.265(1)	194
$[Ru_2(DMeBz)_4](NO_3)_2$	2.287(1)	194
other N,N'-donor bridging ligands		
$[Ru_2(dmat)_4Cl]PF_6$	2.333(1)	142
$Ru_2(hpp)_4Cl_2$	2.321(1)	195

9.4.1 Ru_2^{6+} compounds with O,O'-donor bridging ligands

The ability of "hard", highly charged O,O'-donor bridging ligands, such as SO_4^{2-} and $H_nPO_4^{-3+n}$, to stabilize the dimetal units in their higher oxidation states is well established. Examples are the Mo_2^{5+} and Mo_2^{6+} complexes $[Mo_2(SO_4)_4]^{3-}$ and $[Mo_2(HPO_4)_4(H_2O)]^{2-}$ (see Chapter 4). In 1989 the syntheses of the first Ru_2^{6+} compounds $K_2[Ru_2(SO_4)_4(H_2O)_2]$ and $Cs_2[Ru_2(SO_4)_4(H_2O)_2]$ and the crystal structure of the latter, which revealed a Ru–Ru bond length of 2.343(1) Å (Table 9.3), were reported.[83,84] The room temperature magnetic moments of both the K^+ and Cs^+ salts were ~4.5 BM which is in accordance with the presence of four unpaired electrons and the $\sigma^2\pi^4\delta\pi^{*2}\delta^*$ electronic configuration.

A more convenient synthetic route for the above complexes utilizes $K_3[Ru_2(O_2CO)_4]{\cdot}4H_2O$ as starting material to prepare the Ru_2^{5+} sulfate and phosphate compounds which are sub-

Pictiva EX2004
Samsung v Pictiva
IPR2024-01094

sequently electrochemically oxidized to yield the corresponding Ru_2^{6+} compounds.[82] Variable temperature magnetic susceptibility measurements for $K_2[Ru_2(SO_4)_4(H_2O)_2]$ confirm the $\sigma^2\pi^4\delta\pi^{*2}\delta^*$ electronic configuration. This is consistent with the Ru–Ru bond length of 2.343(1) Å in $Cs_2[Ru_2(SO_4)_4(H_2O)_2]$, a distance that is slightly longer than that of 2.303(1) Å in the Ru_2^{5+} complex $[Ru_2(SO_4)_4(H_2O)_2]^{3-}$ which is known to possess the $\sigma^2\pi^4\delta^2(\pi^*\delta^*)^3$ electronic configuration.[83] The lengthening of the metal to metal distance on going from the Ru_2^{5+} to the Ru_2^{6+} complex is a combined effect of the loss of a δ electron and the higher mean oxidation state which tends to weaken the Ru–Ru bonding interactions.

9.4.2 Ru_2^{6+} compounds with N,N'-donor bridging ligands

The possible existence of Ru_2^{6+} compounds with N,N'-donor bridging ligands had been originally suggested by electrochemical experiments on some Ru_2^{5+} compounds. A variety of Ru_2^{6+} compounds have been synthesized with the use of electron-rich N,N'-donor ligands, like aminopyridinates, formamidinates, benzamidinates and hpp, with or without the assistance of axial ligands.

Aminopyridinate ligands

Based on their structural characteristics Ru_2^{6+} tetraaminopyridinates can be divided into two groups: those without and those with axial ligands with σ donor and π acceptor ability. Examples of the former are $[Ru_2(ap)_4Cl][FeCl_4]$, $[Ru_2(ap)_4F]PF_6$ and $[Ru_2(ap)_4(H_2O)_2]CF_3SO_3$. These are synthesized via simple oxidation reactions of $Ru_2(ap)_4Cl$ with various oxidizing agents, such as Ag^+ and $[(\eta^5\text{-}C_5H_5)_2Fe]^+$.[181] Another compound, $Ru_2(F_5ap)_3(F_4Oap)Cl$, shown in Fig. 9.30, was synthesized serendipitously from the reaction of the (3,1) regioisomer of $Ru_2(F_5ap)_4Cl$ and a trace peroxide in THF.[182] Only two complexes of this type have been characterized crystallographically, $[Ru_2(ap)_4Cl][FeCl_4]$ and $Ru_2(F_5ap)_3(F_4Oap)Cl$ with Ru–Ru bond lengths of 2.301(1) and 2.336(1) Å, respectively (Table 9.3).

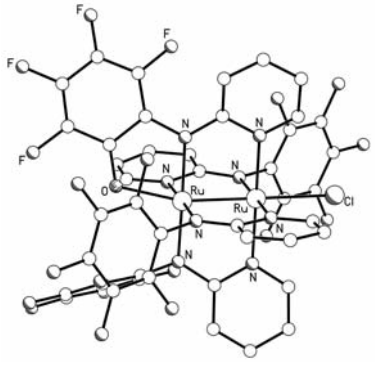


Fig. 9.30. The structure of $Ru_2(F_5ap)_3(F_4Oap)Cl$.

The room temperature magnetic moments of the above compounds are ~2.9 BM, which indicate the presence of two unpaired electrons.[181] Thus, the ground state electronic configuration of these compounds can either be $\sigma^2\pi^4\delta^2\pi^{*2}$ or $\sigma^2\pi^4\delta^2\pi^{*1}\delta^{*1}$. Structural data favor the former considering that the Ru–Ru bond length in $[Ru_2(ap)_4Cl][FeCl_4]$ is only 0.026 Å longer than the corresponding distance in $Ru_2(ap)_4Cl$, which has three unpaired electrons and the electronic configuration $\sigma^2\pi^4\delta^2(\pi^*\delta^*)^3$.[96] Since the bond lengthening is so small, it is likely that the electron is removed from a δ* molecular orbital upon oxidation, because removal of such an electron is expected to bring only a small shortening of the bond which is offset by

Pictiva EX2004
Samsung v Pictiva
IPR2024-01094

an electrostatic repulsion between the Ru centers (higher mean oxidation state). On the other hand, removal of an electron from a π* molecular orbital would result in a substantial shortening of the Ru–Ru bond.

The second group of Ru_2^{6+} tetraaminopyridinates involves complexes with strongly bound σ donor and π acceptor ligands in axial positions, such as alkynyls and CN^-. In a reinvestigation of the reactions between Ru_2^{5+} tetraaminopyridinates with excess of Li^+ salts of alkynyls from which mono-alkynyl Ru_2^{5+} complexes are synthesized,[112] both the mono-alkynyl and the bis-alkynyl Ru_2^{6+} tetraaminopyridinate complex $Ru_2(F_5ap)_4(C{\equiv}CPh)_2$ were obtained in the reaction mixture and chromatographically separated.[183] Other complexes of the type $Ru_2(Xap)_4[(C{\equiv}C)_mY]_2$ (Y = H, Ph, $SiMe_3$, $SiPr^i_3$ and *m* = 1, 2) have been synthesized from similar reactions.[114,184] An interesting extension is the synthesis of Ru_2^{6+} complexes with two different types of axially bound alkynyl ligands, such as $Ru_2(ap)_4(C{\equiv}CC{\equiv}CH)(C{\equiv}CSiMe_3)$.[185] Both the work-up conditions and the choice of the starting materials are crucial for the distribution of the products of these reactions. In the reaction of $Ru_2(ap)_4Cl$ with $Li(C{\equiv}CC{\equiv}CSiMe_3)$ exposure of the reaction mixture to air is necessary in order to increase the yield of the bis-alkynyl complex $Ru_2(ap)_4(C{\equiv}CC{\equiv}CSiMe_3)_2$ (Fig. 9.31).[114] The analogous reaction of $Ru_2(F_5ap)_4Cl$ with excess of $Li(C{\equiv}CPh)$ is more complicated, since $Ru_2(F_5ap)_4Cl$ exists as a mixture of the (4,0), (3,1) and *trans*-(2,2) regioisomers, and the product distribution depends on the type of isomer used as starting material, with the *trans*-(2,2) regioisomer giving the bis-acetylide compound as the only product.[110]

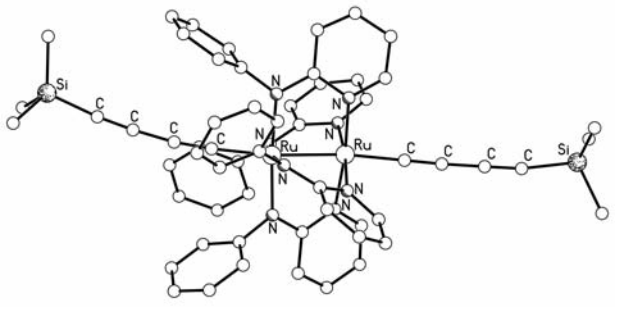
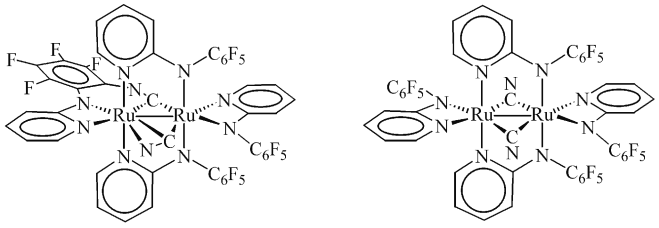


Fig. 9.31. The structure of $Ru_2(ap)_4(C{\equiv}CC{\equiv}CSiMe_3)_2$.

All the bis-alkynyl Ru_2^{6+} tetraaminopyridinates are isolated as air- and moisture-stable solids which exhibit well resolved ^1H NMR spectra. At least one very intense C≡C stretching band is observed at ~2100 cm^{-1} in the IR spectra, while the analogous mono-alkynyl complexes and organic alkynyl compounds exhibit only weak C≡C stretching bands. This could possibly be attributed to strong coupling between the two axial alkynyl ligands due to conjugation.[115]

The Ru_2^{6+} complexes with two axially coordinated CN^- ligands, like $Ru_2(ap)_4(CN)_2$ and $Ru_2(2\text{-}Meap)_4(CN)_2$, are synthesized from the reactions of Ru_2^{5+} tetraaminopyridinates with excess of CN^- and exposure of the reaction mixture to air.[118] When Ru_2^{5+} tetraaminopyridinates with less basic ligands are used as starting materials, such as $Ru_2(2\text{-}Fap)_4Cl$, $Ru_2(2,4,6\text{-}F_3ap)_4Cl$, $Ru_2(F_5ap)_4Cl$, edge-sharing bioctahedral complexes of the type $Ru_2(\mu\text{-}F_xap)_2(\eta^2\text{-}F_xap)[\mu\text{-}(o\text{-}NC)F_{x-1}ap](\mu\text{-}CN)$ can also be isolated depending on the reaction conditions. For example, $Ru_2(2\text{-}Fap)_4Cl$ reacts with excess of CN^- at room temperature to give the dicyanide adduct and at 70 ºC to give $Ru_2(\mu\text{-}2\text{-}Fap)_2(\eta^2\text{-}2\text{-}Fap)[\mu\text{-}(o\text{-}NC)ap]\text{-}(\mu\text{-}CN)$,[118] while $Ru_2(F_5ap)_4Cl$ gives only $Ru_2(\mu\text{-}F_5ap)_2(\eta^2\text{-}F_5ap)[\mu\text{-}(o\text{-}NC)F_4ap](\mu\text{-}CN)$ (**9.6a**) and $Ru_2(\mu\text{-}F_5ap)_2(\eta^2\text{-}F_5ap)_2(\mu\text{-}CN)_2$ (**9.6b**).[186]

Pictiva EX2004
Samsung v Pictiva
IPR2024-01094



a b

9.6

Electrochemical studies of the bis-alkynyl and bis-cyano Ru_2^{6+} tetraaminopyridinates reveal three reversible, metal-centered, one-electron processes, one oxidation and two reductions which correspond to Ru_2^{7+}, Ru_2^{5+} and Ru_2^{4+} complexes, respectively.[110,118] These processes are irreversible for complexes with terminal C≡CH groups.[185] For the different regioisomers of $Ru_2(F_5ap)_4(C{\equiv}CPh)_2$, an anodic shift for the oxidation and cathodic shifts for the reduction waves are observed proceeding from the (4,0) regioisomer to the (3,1) and to the *trans*-(2,2) regioisomer.[110]

The Ru–Ru bond lengths of the bis-alkynyl and bis-cyano Ru_2^{6+} tetraaminopyridinates fall in the range of 2.434 to 2.475 Å (Table 9.3). These are longer than the corresponding distances in the Ru_2^{6+} complex $[Ru_2(ap)_4Cl][FeCl_4]$ and the mono-alkynyl or the mono-cyano Ru_2^{5+} complexes. This difference can be attributed to the presence of the second axial alkynyl or cyano ligand, which further increases the antibonding σ* electron density between the two Ru atoms resulting in the lengthening of the Ru–Ru bond.

Considering that complexes of this type are diamagnetic (as it is shown by their normal ^{1}H NMR spectra)[110,118] and that the electronic configuration of the corresponding mono-alkynyl and mono-cyano Ru_2^{5+} tetraaminopyridinates is $\sigma^2\pi^4\delta^2(\pi^*\delta^*)^3$, the electronic configuration of $\sigma^2\pi^4\delta^2\delta^{*2}$ could be suggested for these Ru_2^{6+} compounds. However, this is not consistent with the observed long Ru–Ru bond lengths (2.434 to 2.475 Å), since the removal of an antibonding π* electron could not possibly lengthen the Ru–Ru bond from 2.33 to 2.47 Å. Because the Ru orbitals used to form axial bonds with σ donor ligands are also used to form the Ru–Ru σ bond, and because the alkynyl ligands are strong σ donors, these orbitals are deeply involved in the formation of the two axial Ru–C σ bonds with the alkynyl ligands. As a result, the Ru–Ru σ bond is essentially cancelled and the electron configuration of the metal-metal bonding orbitals becomes $\pi^4\delta^2\pi^{*4}$. This leaves the Ru_2^{6+} core with a single net δ bond, which explains satisfactorily the observed long Ru–Ru bond lengths.

Formamidinate ligands

The only type of Ru_2^{6+} tetraformamidinates known are those with two axially bound σ donor and π acceptor ligands. The first compound of this type, $Ru_2(DPhF)_4(C{\equiv}CPh)_2$, was synthesized from the reaction of $Ru_2(DPhF)_4Cl$ with excess of $Li(C{\equiv}CPh)$.[187] Others have been made similarly from reactions of $Ru_2(DArF)_4Cl$ and excess of Li^+ salts of CN^-,[132] or alkynyl ligands of the general type $Y(C{\equiv}C)_m$ (m = 1, 2, and Y = Ph, $SiMe_3$),[135,188] followed by exposure of the reaction mixture to air and chromatographic purification which elutes only the bis-alkynyl Ru_2^{6+} complexes. Only one case has been reported in which both the mono- and bis-alkynyl complexes can be separated by chromatography: these are the complexes $Ru_2(DPhF)_4(C{\equiv}CC{\equiv}CSiMe_3)$ and $Ru_2(DPhF)_4(C{\equiv}CC{\equiv}CSiMe_3)_2$.[135] The formation of these types of complexes is influenced by the donor properties of the bridging formamidinate ligands; compounds with strong electron-

Pictiva EX2004
Samsung v Pictiva
IPR2024-01094

withdrawing substituents form faster and they are isolated in higher yields than those with electron-donating substituents.[188]

Cyclic voltammetry studies show three reversible, one-electron, metal-centered processes, one oxidation and two reductions, corresponding to $Ru_2^{6+} \rightarrow Ru_2^{7+} + e^-$, $Ru_2^{6+} + e^- \rightarrow Ru_2^{5+}$ and $Ru_2^{5+} + e^- \rightarrow Ru_2^{4+}$, respectively.[188] The potential for each one of these processes depends on the substitution on the aryl groups of the formamidinate ligands. Linear correlations between these potentials and the substituent's Hammett constants for a series of compounds of the type $Ru_2(DArF)_4(C{\equiv}CPh)_2$ have been established.

Complexes of this type are isolated as air- and moisture-stable solids which are not thermally stable (most of them decompose above 50 ºC under vacuum) and they show normal ^1H NMR spectra. Their IR spectra show one very intense band at ~2100 cm^{-1} corresponding to C≡C stretching frequency, indicative of a strong coupling between the two axial alkynyl ligands due to the conjugation through the Ru_2^{6+} unit.[115]

Due to the rich electronic nature of Ru_2^{6+} units and the π-conjugation mediated by the alkynyl ligands, a variety of polymetallic Ru_2^{6+} alkynyl complexes have been synthesized and investigated as potential 'molecular wires'. For example, $(Me_3SiC{\equiv}CC{\equiv}C)[Ru_2(DPhF)_4]$-$(\mu$-$C{\equiv}CC{\equiv}CC{\equiv}CC{\equiv}C)[Ru_2(DPhF)_4](C{\equiv}CC{\equiv}CSiMe_3)$ has a total length of ~3.5 nm and exhibits rich electrochemistry compared to that of the related complex $Ru_2(DPhF)_4(C{\equiv}CC{\equiv}CSiMe_3)_2$ complex.[189] However, even though electronic delocalization occurs, the redox processes are not reversible. In contrast, the hetero-metallic complex $[(Bu^t_2bipy)(CO)_3Re](py$-4-$C{\equiv}C)$-$[Ru_2(DTolF)_4](4$-$C{\equiv}C$-$py)[Re(CO)_3(Bu^t_2bipy)]$ displays electronic delocalization with reversible redox couples.[190]

The crystal structures of bis-alkynyl Ru_2^{6+} tetraformamidinates show deviations from the eclipsed configuration and distorted axial alkynyl ligands (∠Ru–Ru–C ~160º), as shown in the structure of $Ru_2(DPhF)_4(C{\equiv}CPh)_2$ in Fig. 9.32. Based on theoretical calculations, it has been proposed that the origin of these distortions is electronic in nature and they have been attributed to a second-order Jahn-Teller effect.[188]

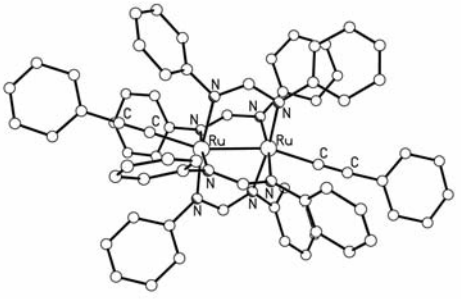


Fig. 9.32. The structure of $Ru_2(DPhF)_4(C{\equiv}CPh)_2$.

The Ru–Ru bond lengths fall in the range of 2.539 to 2.599 Å (Table 9.3). These distances are longer than those in the mono-alkynyl Ru_2^{5+} tetraformamidinates. The reason for this difference is the nature of the Ru_2-alkynyl bonding interaction in the two types of compounds. In the mono-alkynyl Ru_2^{5+} tetraformamidinates the Ru_2^{5+}-alkynyl bonding interaction is mainly a σ bonding interaction, but in the bis-alkynyl Ru_2^{6+} tetraformamidinates, it is a combination of σ bonding and d_π-π* back-bonding interaction.[188] As a result, not only the anti-bonding σ* electron density is increased, but also the π electron density is removed from the Ru_2^{6+} core

Pictiva EX2004
Samsung v Pictiva
IPR2024-01094

resulting in the lengthening of the Ru–Ru bond. This gives a satisfactory explanation of the extremely elongated Ru–Ru bond of 2.599(1) Å observed in $Ru_2(DAni^mF)_4(C{\equiv}CC{\equiv}CSiMe_3)_2$.[135]

The long Ru–Ru bond lengths of these compounds together with their diamagnetism (as indicated by their well resolved ^1H NMR spectra) suggest that the electronic configuration is $\pi^4\delta^2\pi^{*4}$. As in the case of the analogous Ru_2^{6+} aminopyridinates, the Ru–Ru σ bond is cancelled due to the formation of the Ru–C σ bonds with the strong σ donor alkynyl ligands. Theoretical calculations support this assignment and show that the Ru d_{z^2} orbitals needed for the Ru–Ru σ bond are engaged in Ru–C σ bonding and σ* antibonding molecular orbitals, leaving the Ru_2^{6+} core with a net single δ bond.[188]

Benzamidinate ligands

The first reported Ru_2^{6+} complex with bridging benzamidinate ligands, $Ru_2(DMeBz)_4Cl_2$ (Fig. 9.33), was synthesized from the reaction of $Ru_2(O_2CMe)_4Cl$ with HDMeBz in the presence of Et_3N and LiCl in THF.[191] Two other complexes of this type, $Ru_2(DMeODMeBz)_4Cl_2$ and $Ru_2(DEtBz)_4Cl_2$, have been synthesized in a similar way.[192] As discussed in section 9.2.3, the analogous reactions of $Ru_2(O_2CMe)_4Cl$ with formamidines give the corresponding tetraformamidinate compounds maintaining the Ru_2^{5+} core unoxidized. This difference can be attributed to the high basicity of the benzamidinate ligands which stabilizes higher oxidation states.

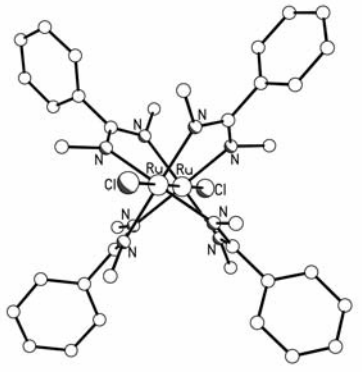


Fig. 9.33. The structure of $Ru_2(DMeBz)_4Cl_2$.

The axial Cl^- ions in the above complexes can be removed in reactions with excess of Li^+ salts of alkynyl reagents to give bis-alkynyl Ru_2^{6+} tetrabenzamidinates.[191-193] In addition, $Ru_2(DMeBz)_4Cl_2$ reacts with $AgBF_4$ and $AgNO_3$ to yield complexes with weakly coordinating axial ligands, $[Ru_2(DMeBz)_4](BF_4)_2$ and $[Ru_2(DMeBz)_4](NO_3)_2$, respectively.[194] These two axial chloride-free complexes offer an alternative route for the synthesis of bis-alkynyl Ru_2^{6+} tetrabenzamidinates under very mild reaction conditions.[193]

Cyclic voltammetry measurements of bis-chloro Ru_2^{6+} tetrabenzamidinates show three one-electron, metal-based redox processes: a quasi-reversible oxidation, a reversible reduction and an irreversible reduction, which correspond to the formation of Ru_2^{7+}, Ru_2^{5+} and Ru_2^{4+} complexes, respectively.[191,192] Three redox processes are also observed in the electrochemistry of the complexes $[Ru_2(DMeBz)_4](BF_4)_2$ and $[Ru_2(DMeBz)_4](NO_3)_2$, which however are less reversible with anodically shifted potentials.[194] The corresponding bis-alkynyl complexes exhibit similar redox behavior, but the redox waves are cathodically shifted due to the strong donating ability of the alkynyl ligands.[191-193]

Pictiva EX2004
Samsung v Pictiva
IPR2024-01094

Based on their Ru–Ru distances, which fall in the wide range of 2.265-2.476 Å as shown in Table 9.3, Ru_2^{6+} tetrabenzamidinates can be grouped in two categories. One category is formed by compounds with axial alkynyl ligands which exhibit long Ru–Ru distances that vary from 2.448 to 2.476 Å, while the other category contains complexes with axial Cl^- ions or weakly coordinating BF_4^- and NO_3^- ions with much shorter Ru–Ru distances from 2.265 to 2.340 Å. The differences in the distances of the two types of compounds reflect their different electronic structures. In the complexes without axial alkynyl ligands the Ru–Ru bond lengths are similar to those observed in $[Ru_2(ap)_4Cl][FeCl_4]$[181] and $Ru_2(F_5ap)_3(F_4Oap)Cl$.[182] Magnetic measurements show that they are paramagnetic with room temperature magnetic moments of ~3.0 BM which indicate the presence of two unpaired electrons.[191,194] This is consistent either with the $\sigma^2\pi^4\delta^2\pi^{*2}$ or $\sigma^2\pi^4\delta^2\pi^{*1}\delta^{*1}$ electronic configurations. By analogy to the Ru_2^{6+} aminopyridinates without axial alkynyl ligands, the observed Ru–Ru bond lengths favor the $\sigma^2\pi^4\delta^2\pi^{*2}$ electronic configuration. The bis-alkynyl Ru_2^{6+} tetrabenzamidinates display Ru–Ru bond lengths that are comparable to those of bis-alkynyl Ru_2^{6+} tetraaminopyridinates. In addition, they are diamagnetic, as indicated by their normal ^{1}H NMR spectra.[191] These data suggest that their electronic configuration is $\pi^4\delta^2\pi^{*4}$. Similarly to the analogous Ru_2^{6+} tetraaminopyridinates, the formation of the Ru–C σ bonds with the strong σ donor alkynyl ligands cancels the formation of the Ru–Ru σ bond.

Other N,N'-donor bridging ligands

Two other N,N'-donor, electron rich ligands that are known to stabilize the dimetal units in high oxidation states are the guanidinate derivative hpp and dmat.

The complex $Ru_2(hpp)_4Cl_2$ (Fig. 9.34) is synthesized by reacting $Ru_2(O_2CMe)_4Cl$ with an excess of molten Hhpp.[195] The Ru–Ru bond length of 2.321(1) Å is very close to those of the bis-chloro Ru_2^{6+} tetrabenzamidinates, but much shorter than those of the corresponding diamagnetic Ru_2^{6+} complexes with axial alkynyl ligands (Table 9.3).

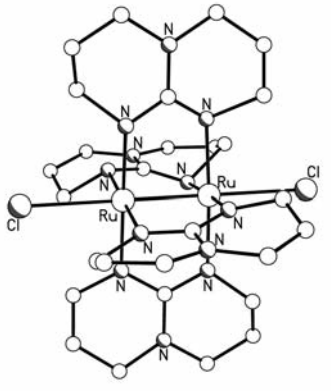


Fig. 9.34. The structure of $Ru_2(hpp)_4Cl_2$.

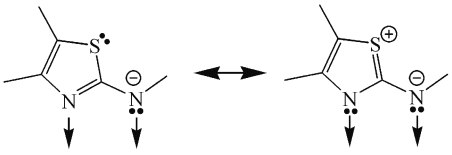
Electrochemical studies show two one-electron, metal-centered redox processes: an oxidation at +0.55 V and a reduction at -0.60 V vs SCE, which correspond to $Ru_2^{6+} \rightarrow Ru_2^{7+} + e^-$ and $Ru_2^{6+} + e^- \rightarrow Ru_2^{5+}$, respectively. These are cathodically shifted with respect to the potentials of the bis-chloro Ru_2^{6+} tetrabenzamidinates[191,192] and they suggest that hpp is more electron rich than benzamidinates. The mild oxidation potential of $Ru_2(hpp)_4Cl_2$ implies that the one-electron oxidized $[Ru_2(hpp)_4Cl_2]^+$ ion might be accessible; however, all attempts to generate it

Pictiva EX2004
Samsung v Pictiva
IPR2024-01094

chemically or electrochemically have been unsuccessful and only decomposition products have been obtained.

The room temperature magnetic moment of $Ru_2(hpp)_4Cl_2$ is 2.78 BM, which implies the presence of two unpaired electrons. Thus, the electronic configuration can either be $\sigma^2\pi^4\delta^2\pi^{*2}$ or $\sigma^2\pi^4\delta^2\pi^{*1}\delta^{*1}$. No information can be obtained from EPR, since the complex is EPR silent. However, since $Ru_2(hpp)_4Cl_2$ is isoelectronic with the $Ru_2(DMeBz)_4Cl_2$ and the two complexes have similar Ru–Ru bond lengths, it is assumed that the electronic configuration is $\sigma^2\pi^4\delta^2\pi^{*2}$.

The complex $[Ru_2(dmat)_4Cl]PF_6$ is synthesized by bulk electrolysis of $Ru_2(dmat)_4Cl$ in the presence of $TBAPF_6$.[142] The stabilization of the Ru_2^{6+} oxidation state is due to the high basicity of dmat, as indicated by its resonance structures in **9.7**. Its room temperature magnetic moment is 2.89 BM, which suggests the presence of two unpaired electrons. Considering that the Ru–Ru bond length of 2.333(1) Å of this complex is similar to those observed in the Ru_2^{6+} tetraaminopyridinates without axial alkynyl ligands[181,182] and the bis-chloro Ru_2^{6+} tetrabenzamidinates,[191] the electronic configuration $\sigma^2\pi^4\delta^2\pi^{*2}$ has been proposed.



9.7

9.5 Compounds with Macrocyclic Ligands

The only Ru_2^{n+} compounds that have Ru–Ru bonds unsupported by bridging ligands are those of the type LRu–^{n}RuL, where –^{n} is a bond order of 2 to 3 and L represents a four-nitrogen macrocyclic ring. The earliest examples[196] were the $Ru_2(tmtaa)_2^n$ (n = 0, +1, +2). From structural data[197] and magnetic measurements, it was established that the electron configurations are $\sigma^2\pi^4\delta^2\delta^{*2}\pi^{*2}$, $\sigma^2\pi^4\delta^2\delta^{*2}\pi^*$ and $\sigma^2\pi^4\delta^2\delta^{*2}$, respectively.

A series of compounds in which L is a porphyrin ligand (TPP^{2-}, OEP^{2-} or TPP^{2-}) has also been prepared and studied.[198-201] In terms of bonding, magnetism and structure these compounds differ little from the $Ru_2(tmtaa)_2^n$ species, but there are more of them and more extensive data. They react with neutral donors to give Ru(porph)L products.[202,203]

Mixed $RuOs(porph)_2$ compounds have also been obtained,[204,205] as have some (porph)RuMo(porph') and (porph)RuW(porph') compounds.[205,206]

With alkyl (Me, Et) substituted corroles (cor), the Ru_2^{6+} core is stabilized in (cor)Ru–Ru(cor) molecules,[207] but reduction to Ru_2^{5+} and Ru_2^{4+}, as well as oxidations to Ru_2^{7+} and Ru_2^{8+} compounds can be carried out electrochemically,[208] although none of these oxidized or reduced species have been isolated.

9.6 Applications

9.6.1 Catalytic activity

The study of catalytic activity of Ru_2 compounds is limited to Ru_2 tetracarboxylate complexes. Early studies using $Ru_2(O_2CMe)_4$ and $Ru_2(O_2CMe)_4Cl$ showed that hydrogenation of alkenes and alkynes occurs in methanolic solution of fluoroboric acid in the presence of PPh_3.[209]

Pictiva EX2004
Samsung v Pictiva
IPR2024-01094

Since the active catalysts in these processes have not been isolated and characterized, the formation of a mononuclear Ru^{2+} complex that does the catalysis cannot be ruled out.

Room temperature hydrogenation of alk-1-ene by $Ru_2(O_2CR)_4$ (R = CH_3 or CF_3) in the presence of 1 atm of H_2 has also been reported.[210] The suggested mechanism for this process is described by the following equations:

$$Ru_2(O_2CMe)_4 + H_2 \rightarrow HRu_2(O_2CMe)_3 + H^+ + CH_3COO^-$$

$$HRu_2(O_2CMe)_3 + \text{alkene} \rightarrow Ru_2(O_2CMe)_3(\text{alkyl})$$

$$Ru_2(O_2CMe)_3(\text{alkyl}) + H^+ + CH_3COO^- \rightarrow Ru_2(O_2CMe)_4 + \text{alkane}$$

No isomerization of the mono-alkenes is observed, suggesting irreversible alkyl formation. The slower rates of hydrogenation observed when the trifluoroacetate analog was used as catalyst are expected because of the slower H_2 uptake by the electron poor dimetal core of $Ru_2(O_2CCF_3)_4$.

In addition, $Ru_2(O_2CMe)_4$ has been found to catalyze the competitive cyclopropanation and cross-metathesis of alkenes.[211] Small amounts of $Ru_2(O_2CMe)_4$ added to a mixture containing styrene and norbornene together with ethyldiazoacetate (N_2CHCO_2Et) form cyclopropanated styrene and norbornene in 35-40% and 2% yields, respectively. The reaction is believed to be initiated by addition of N_2CHCO_2Et to $Ru_2(O_2CMe)_4$ which results in the formation of a carbene species, $Ru{=}CHCO_2Et$, that subsequently reacts with an olefin to form metallocyclobutane. This can facilitate metathesis or release of cyclopropane to give back the metal catalyst ready to react with another molecule of N_2CHCO_2Et.

Recently, $Ru_2(O_2CMe)_4$ has been used as catalyst for the reaction of diazacoumarin with ROH at 90 °C in alcohol or hexafluorobenzene as solvent to form 3-alkoxy-4-hydroxycoumarin, in yields of 35-95%, as a result of insertion into the O–H bond of the alcohols.[212]

9.6.2 Biological importance

The Ru_2^{5+} tetracarboxylate complexes have been used in antitumor activity studies. $Ru_2(O_2CMe)_4Cl$ and $Ru_2(O_2CEt)_4Cl$ show a small activity against P388 leukemia cells, but unfortunately the poor to moderate aqueous solubilities of these compounds did not allow tests with increased concentrations.[213]

In attempts to gain insight into the mechanism of antitumor activity, the binding of guanine bases to Ru_2^{5+} tetracarboxylate complexes has been studied. The compound $[Ru_2(O_2CMe)_{2-x}(O_2CCF_3)_x(9\text{-EtGH})_2(MeOH)_2](O_2CCF_3)_2 \cdot 2MeOH \cdot 0.5Et_2O$ (x = 0.18) (Fig. 9.35)[214] is obtained by reacting $Ru_2(O_2CMe)_4Cl$ with AgO_2CCF_3 in refluxing CF_3COOH and addition of two equivalents of 9-EtGH. It contains a Ru_2^{4+} core with the two metals separated by 2.322(13) Å and the two 9-EtGH groups in a *cis* head to tail (HT) fashion. The reactivity of $Ru_2(O_2CMe)_4Cl$ towards adenine and adenosine has also been studied.[215] Although no crystal structures were reported, the products of the reactions were characterized by several physicochemical methods and were found to be a 1:1 adduct for adenine, which forms a polymeric chain with the adenine bridging the Ru_2^{5+} units through the axial positions, and a typical diadduct $[Ru_2(O_2CMe)_4(adenosine)_2]Cl$ for adenosine. The importance of these complexes, besides the binding of biologically relevant ligands, lies on their lesser toxicity compared to other diruthenium complexes, a property that allows the use of increased concentrations in antitumor activity tests.

Pictiva EX2004
Samsung v Pictiva
IPR2024-01094

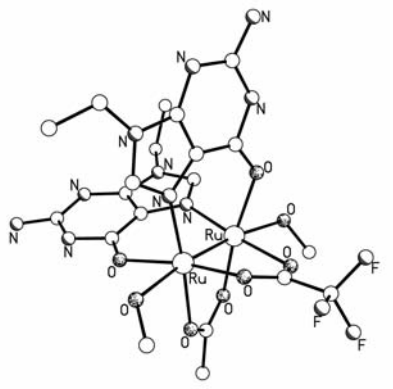


Fig. 9.35. The structure of the cation in $[Ru_2(O_2CMe)_{2-x}(O_2CCF_3)_x(9\text{-EtGH})_2(MeOH)_2](O_2CCF_3)_2$ ($x = 0.18$).

A series of Ru_2^{5+} complexes of the type $[Ru_2(O_2CR)_4L_2]^+$ (R = Me, CH=CH-Fc, *m*-$C_6H_4SO_3^-$, *p*-$C_6H_4SO_3^-$, L = Im, 1-MeIm, EtOH, H_2O) having different water solubility and reduction potentials (Ru_2^{5+}/Ru_2^{4+}) was tested for anti-neoplastic activity against P388 leukemia cells.[216] The compounds that showed significant activity were the water soluble *m*-$C_6H_4SO_3^-$, *p*-$C_6H_4SO_3^-$ substituted complexes, and $[Ru_2(O_2CMe)_4(H_2O)_2]PF_6$. The others did not show any activity in the range of concentration used in the study due to their lack of water solubility.

References

1. T. A. Stephenson and G. Wilkinson, *J. Inorg. Nucl. Chem.* **1966**, *28*, 2285.
2. M. Mukaida, T. Nomura and T. Ishimori, *Bull. Chem. Soc. Jpn*. **1967**, *40*, 2462.
3. M. Mukaida, T. Nomura and T. Ishimori, *Bull. Chem. Soc. Jpn.* **1972**, *45*, 2143.
4. R. W. Mitchell, A. Spencer and G. Wilkinson, *J. Chem. Soc., Dalton Trans.* **1973**, 846.
5. M. C. Barral, R. Jiménez-Aparicio, C. Rial, E. C. Royer, M. J. Saucedo and F. A. Urbanos, *Polyhedron* **1990**, *9*, 1723.
6. M. J. Bennet, K. G. Caulton and F. A. Cotton, *Inorg. Chem.* **1969**, *8*, 1.
7. A. Bino, F. A. Cotton and T. R. Felthouse, *Inorg. Chem*. **1979**, *18*, 2599.
8. M. C. Barral, R. Jiménez-Aparicio, D. Pérez-Quintanilla, E. Pinilla, J. L. Priego, E. C. Royer and F. A. Urbanos, *Polyhedron* **1999**, *18*, 371.
9. T. Togano, M. Mukaida and T. Nomura, *Bull. Chem. Soc. Jpn*. **1980**, *53*, 2085.
10. B. K. Das and A. R. Chakravarty, *Polyhedron* **1991**, *10*, 491.
11. M. Abe, Y. Sasaki, T. Yamaguchi and T. Ito, *Bull. Chem. Soc. Jpn*. **1992**, *65*, 1585.
12. M. McCann, A. Carvill, P. Guinan, P. Higgins, J. Campbell, H, Ryan, M. Walsh, G. Ferguson and J. Gallagher, *Polyhedron* **1991**, *10*, 2273.
13. T. Kimura, T. Sakurai, M. Shima, T. Togano, M. Mukaida and T. Nomura, *Bull. Chem. Soc. Jpn*. **1982**, *55*, 3927.
14. F. A. Cotton, M. Matusz and B. Zhong, *Inorg. Chem*. **1988**, *27*, 4368.
15. M. Spohn, J. Strähle and W. Hiller, *Z. Naturforsch.* **1986**, *41b*, 541.
16. M. McCann, E. Murphy, C. Cardin and M. Convery, *Polyhedron* **1993**, *12*, 1725.
17. F. A. Cotton, Y. Kim and T. Ren, *Inorg. Chem.* **1992**, *31*, 2723.
18. M. Handa, Y. Sayama, M. Mikuriya, R. Nukada, I. Hiromitsu and K. Kasuga, *Chem. Lett.* **1996**, 201.
19. M. C. Barral, R. Jiménez-Aparicio, E. C. Royer, C. Ruíz-Valero, M. J. Saucedo and F. A. Urbanos, *Inorg. Chem*. **1994**, *33*, 2692.

Pictiva EX2004
Samsung v Pictiva
IPR2024-01094

20. M. C. Barral, R. Jiménez-Aparicio, J. L. Priego, E. C. Royer, M. J. Saucedo, F. A. Urbanos and U. Amador, *J. Chem. Soc., Dalton Trans*. **1995**, 2183.
21. M. C. Barral, R. Jiménez-Aparicio, J. L. Priego, E. C. Royer, F. A. Urbanos and U. Amador, *J. Chem. Soc., Dalton Trans*. **1997**, 863.
22. M. C. Barral, R González-Prieto, R. Jiménez-Aparicio, J. L. Priego, M. R. Torres and F. A. Urbanos, *Eur. J. Inorg. Chem*. **2003**, 2339.
23. K. D. Drysdale, E. J. Beck, T. S. Cameron, K. N. Robertson and M. A. S. Aquino, *Inorg. Chim. Acta* **1997**, *256*, 243.
24. M. C. Barral, R. Jiménez-Aparicio, E. C. Royer, C. Ruiz-Valero, F. A. Urbanos, E. Gutiérrez-Puebla and A. Monge, *Polyhedron* **1989**, *8*, 2571.
25. M. C. Barral, R. Jiménez-Aparicio, J. L. Priego, E. C. Royer, F. A. Urbanos and U. Amador, *Inorg. Chem*. **1998**, *37*, 1413.
26. G. G. Briand, M. W. Cooke, T. S. Cameron, H. M. Farrell, T. J. Burchell and M. A. S. Aquino, *Inorg. Chem.* **2001**, *40*, 3267.
27. S. K. Mandal and A. R. Chakravarty, *Inorg. Chim. Acta* **1987**, *132*, 157.
28. B. K. Das and A. R. Chakravarty, *Inorg. Chem.* **1990**, *29*, 1783.
29. B. K. Das and A. R. Chakravarty, *Inorg. Chem.* **1990**, *29*, 2078.
30. B. K. Das and A. R. Chakravarty, *Inorg. Chem.* **1992**, *31*, 1395.
31. E. B. Boyar, P. A. Harding, S. D. Robinson and C. P. Brock, *J. Chem. Soc., Dalton Trans.* **1986**, 1771.
32. F. A. Cotton, M. P. Diebold and M. Matusz, *Polyhedron* **1987**, *6*, 1131.
33. P. Stavropoulos, P. D. Savage, R. P. Tooze, G. Wilkinson, G.; B. Hussain, M. Motevalli and M. B. Hursthouse, *J. Chem. Soc., Dalton Trans.* **1987**, 557.
34. R. S. Drago, R. Cosmano and J. Telser, *Inorg. Chem.* **1984**, *23*, 4514.
35. M. C. Barral, R. Jiménez-Aparicio, J. L. Priego, E. C. Royer, E. Gutiérrez-Puebla and C. Ruíz-Valero, *Polyhedron* **1992**, *11*, 2209.
36. M. C. Barral, R. Jiménez-Aparicio, J. L. Priego, E. C. Royer, M. J. Saucedo, F. A. Urbanos and U. Amador, *Polyhedron* **1995**, *14*, 2419.
37. F. A. Urbanos, M. C. Barral and R. Jiménez-Aparicio, *Polyhedron* **1988**, *7*, 2597.
38. M. W. Cooke, C. A. Murphy, T. S. Cameron, E. J. Beck, G. Vamvounis and M. A. S. Aquino, *Polyhedron* **2002**, *21*, 1235.
39. H. J. Gilfoy, K. N. Robertson, T. S. Cameron and M. A. S. Aquino, *Inorg. Chim. Acta* **2002**, *331*, 330.
40. H. J. Gilfoy, K. N. Robertson, T. S. Cameron and M. A. S. Aquino, *Acta Crystallogr.* **2001**, *E57*, m496.
41. G. Vamvounis, J. F. Caplan, T. S. Cameron, K. N. Robertson and M. A. S. Aquino, *Inorg. Chim. Acta* **2000**, *304*, 87.
42. H. Miyasaka, R. Clérac, C. S. Campos-Fernández and K. R. Dunbar, *Inorg. Chem*. **2001**, *40*, 1663.
43. D. Yoshioka, M. Handa, H. Azuma, M. Mikuriya, I. Hiromitsu and K. Kasuga, *Mol. Cryst. Liq. Cryst*. **2000**, *342*, 133.
44. Y. Liao, W. W. Shum and J. S. Miller, *J. Am. Chem. Soc*. **2002**, *124*, 9336.
45. D. Yoshioka, M. Mikuriya and M. Handa, *Chem. Lett*. **2002**, 1044.
46. M. Handa, D. Yoshika, Y. Sayama, K. Shiomi, M. Mikuriya, I. Hiromitsu and K. Kasuga, *Chem. Lett.* **1999**, 1033.
47. C. R. Wilson and H. Taube, *Inorg. Chem.* **1975**, *14*, 2276.
48. F. A. Cotton and E. Pedersen, *Inorg. Chem*. **1975**, *14*, 388.
49. M. McCann, A. Carvill, C. Cardin and M. Convery, *Polyhedron* **1993**, *12*, 1163.
50. M. W. Cooke, C. A. Murphy, T. S. Cameron, J. C. Swarts and M. A. S. Aquino, *Inorg. Chem. Commun*. **2000**, *3*, 721.
51. M. W. Cooke, T. S. Cameron, K. N. Robertson, J. C. Swarts and M. A. S. Aquino, *Organometallics* **2002**, *21*, 5962.
52. M. McCann and E. Murphy, *Polyhedron* **1992**, *11*, 2327.

Pictiva EX2004
Samsung v Pictiva
IPR2024-01094

53. P. Higgins and G. M. McCann, *J. Chem. Soc., Dalton Trans.* **1988**, 661.
54. J. E. Earley, R. N. Bose and B. H. Berrie, *Inorg. Chem.* **1983**, *22*, 1836.
55. A. O. Oyetunji, O. O. Olubuyide, J. F. Ojo and J. E. Earley, *Polyhedron* **1991**, *10*, 829.
56. M. Zhu, A. O. Oyetunji, K. Lu and J. E. Earley, *Polyhedron* **1989**, *8*, 577.
57. A. C. Dema and R. N. Bose, *Inorg. Chem.* **1989**, *28*, 2711.
58. M. Everhart and J. E. Earley, *Polyhedron* **1988**, *7*, 1393.
59. J. G. Norman Jr. and H. J. Kolari, *J. Am. Chem. Soc.* **1978**, *100*, 791.
60. J. G. Norman Jr., G. E. Renzoni and D. A. Case, *J. Am. Chem. Soc.* **1979**, *101*, 5256.
61. R. J. H. Clark and M. R. Franks, *J. Chem. Soc., Dalton Trans*. **1976**, 1825.
62. D. S. Martin, R. A. Newman and L. M. Vlasnik, *Inorg. Chem.* **1980**, *19*, 3404.
63. R. J. H. Clark and L. H. Ferris, *Inorg. Chem.* **1981**, *20*, 2759.
64. V. M. Miskowski, T. M. Loehr and H. B. Gray, *Inorg. Chem.* **1987**, *26*, 1098.
65. V. M. Miskowski and H. B. Gray, *Inorg. Chem*. **1988**, *27*, 2501.
66. J. Telser and R. S. Drago, *Inorg. Chem.* **1984**, *23*, 3114.
67. F. A. Cotton, Y. Kim and T. Ren, *Polyhedron* **1993**, *12*, 607.
68. F. D. Cukiernik, D. Luneau, J.-C. Marchon and P. Maldivi, *Inorg. Chem.* **1998**, *37*, 3698.
69. R. Jiménez-Aparicio, F. A. Urbanos and J. M. Arrieta, *Inorg. Chem.* **2001**, *40*, 613.
70. F. D. Gukiernik, A.-M. Giroud-Godquin, P. Maldivi and J.-C. Marchon, *Inorg. Chim. Acta* **1994**, *215*, 203.
71. E. J. Beck, K. D. Drysdale, L. K. Thompson, L. Li, C. A. Murphy and M. A. S. Aquino, *Inorg. Chim. Acta* **1998**, *279*, 121.
72. M. C. Barral, R. Jiménez-Aparicio, D. Pérez-Quintanilla, J. L. Priego, E. C. Royer, M. R. Torres and F. A. Urbanos, *Inorg. Chem.* **2000**, *39*, 65.
73. M. Handa, Y. Sayama, M. Mikuriya, R. Nukada, I. Hiromitsu and K. Kasuga, *Bull. Chem. Soc. Jpn*. **1995**, *68*, 1647.
74. Y. Sayama, M. Handa, M. Mikuriya, I. Hiromitsu and K. Kasuga, *Bull. Chem. Soc. Jpn*. **2003**, *76*, 769.
75. Y. Sayama, M. Handa, M. Mikuriya, I. Hiromitsu and K. Kasuga, *Chem. Lett.* **1999**, 453.
76. M. Handa, Y. Sayama, M. Mikuriya, R. Nukada, I. Hiromitsu and K. Kasuga, *Bull. Chem. Soc. Jpn.* **1998**, *71*, 119.
77. Y. Sayama, M. Handa, M. Mikuriya, I. Hiromitsu and K. Kasuga, *Bull. Chem. Soc. Jpn.* **2001**, *74*, 2129.
78. Y. Sayama, M. Handa, M. Mikuriya, I. Hiromitsu and K. Kasuga, *Chem. Lett*. **1998**, 777.
79. Y. Sayama, M. Handa, M. Mikuriya, I. Hiromitsu and K. Kasuga, *Bull. Chem. Soc. Jpn*. **2000**, *73*, 2499.
80. A. J. Lindsay, G. Wilkinson, M. Motevalli and M. B. Hursthouse, *J. Chem. Soc., Dalton Trans.* **1987**, 2723.
81. F. A. Cotton, L. Labella and M. Shang, *Inorg. Chem.* **1992**, *31*, 2385.
82. F. A. Cotton, T. Datta, L. Labella and M. Shang, *Inorg. Chim. Acta* **1993**, *203*, 55.
83. I. V. Kuz'menko, A. N. Zhilyaev, T. A. Fomina, M. A. Porai-Koshits and J. B. Baranovskii, *Russ. J. Inorg. Chem*. **1989**, *34*, 1457.
84. A. N. Zhilyaev, T. A. Fomina, I. V. Kuz'menko, A. V. Rotov and J. B. Baranovskii, *Russ. J. Inorg. Chem*. **1989**, *34*, 532.
85. X.-Y. Yi, L.-M. Zheng, W. Xu and S. Feng, *Inorg. Chem.* **2003**, *42*, 2827.
86. T. Malinsky, D. Chang, F. N. Feldmann, J. L. Bear and K. M. Kadish, *Inorg. Chem.* **1983**, *22*, 3225.
87. A. R. Chakravarty and F. A. Cotton, *Polyhedron* **1985**, *4*, 1957.
88. A. R. Chakravarty, F. A. Cotton and D. A. Tocher, *Polyhedron* **1985**, *4*, 1097.
89. M. C. Barral, R. Jiménez-Aparicio, J. L. Priego, E. C. Royer, F. A. Urbanos, A. Monge and C. Ruíz-Valero, *Inorg. Chim. Acta* **1993**, *12*, 2947.
90. M. C. Barral, I. de la Fuente, R. Jiménez-Aparicio, J. L. Priego, M. R. Torres and F. A. Urbanos, *Polyhedron* **2001**, *20*, 2537.

Pictiva EX2004
Samsung v Pictiva
IPR2024-01094

91. A. R. Chakravarty, F. A. Cotton and D. A. Tocher, *J. Am. Chem. Soc.* **1984**, *106*, 6409.
92. A. R. Chakravarty and F. A. Cotton, *Inorg. Chem.* **1985**, *24*, 3584.
93. A. R. Chakravarty, F. A. Cotton and D. A. Tocher, *Inorg. Chem.* **1984**, *23*, 4030.
94. M. Y. Chavan, F. N. Feldmann, X. Q. Lin, J. L. Bear and K. M. Kadish, *Inorg. Chem*. **1984**, *23*, 2373.
95. K. Ryde and D. A. Tocher, *Inorg. Chim. Acta* **1986**, *118*, L49.
96. A. R. Chakravarty, F. A. Cotton and D. A. Tocher, *Inorg. Chem.* **1985**, *24*, 172.
97. A. R. Chakravarty and F. A. Cotton, *Inorg. Chim. Acta* **1985**, *105*, 19.
98. F. A. Cotton, Y. Kim and A. Yokochi, *Inorg. Chim. Acta* **1995**, *236*, 55.
99. A. Chakravarty, F. A. Cotton and W. Schwotzer, *Polyhedron* **1986**, *5*, 1821.
100. A. Chakravarty, F. A. Cotton and D. A. Tocher, *Inorg. Chem.* **1985**, *24*, 1263.
101. K.-T. Youm, Y. Kim and M.-J. Jun, *Acta Crystollogr*. **1999**, *C55*, 1483.
102. A. Chakravarty, F. A. Cotton and D. A. Tocher, *Inorg. Chem.* **1985**, *24*, 2857.
103. F. A. Cotton and A. Yokochi, *Polyhedron* **1998**, *17*, 959.
104. F. A. Cotton, Y. Kim and T. Ren, *Inorg. Chem.* **1992**, *31*, 2608.
105. F. A. Cotton and A. Yokochi, *Inorg. Chim. Acta* **1998**, *275*, 557.
106. F. A. Cotton, S.-E. Stiriba and A. Yokochi, *J. Organomet. Chem.* **2000**, *595*, 300.
107. A. R. Chakravarty, F. A. Cotton, D. A. Tocher and J. H. Tocher, *Polyhedron* **1985**, *4*, 1475.
108. F. A. Cotton and A. Yokochi, *Inorg. Chem*. **1998**, *37*, 2723.
109. K. M. Kadish, L.-L.Wang, A. Thuriere, E. Van Caemelbecke and J. L. Bear, *Inorg. Chem*. **2003**, *42*, 834.
110. J. L. Bear, Y. Li, B. Han, E. Van Caemelbecke and K. M. Kadish, *Inorg. Chem*. **1997**, *36*, 5449.
111. L. Gao, L. Zhang and Z. Chen, *Acta Crystollogr.* **2003**, *E59*, m419.
112. A. R. Chakravarty and F. A. Cotton, *Inorg. Chim. Acta* **1986**, *113*, 19.
113. G. Zou, J. C. Alvarez and T. Ren, *J. Organomet. Chem*. **2000**, *596*, 152.
114. G.-L. Xu and T. Ren, *Organometallics* **2001**, *20*, 2400.
115. S. K. Hurst and T. Ren, *J. Organomet. Chem*. **2003**, *670*, 188.
116. T. Ren, G. Zou and J. C. Alvarez, *Chem. Commun*. **2000**, 1197.
117. G.-L. Xu, G. Zou, Y.-H. Ni, M. C. DeRosa, R. J. Crutchley and T. Ren, *J. Am. Chem. Soc.* **2003**, *125*, 10057.
118. J. L. Bear, W. Z. Chen, B. Han, S. Huang, L.-L. Wang, A. Thuriere, E. Van Caemelbecke, K. M. Kadish and T. Ren, *Inorg. Chem*. **2003**, *42*, 6230.
119. L.-Y. Zhang, J.-L. Chen, L.-X. Shi and Z.-N. Chen, *Organometallics* **2002**, *21*, 5919.
120. J. L. Bear, J. Wellhoff, G. Royal, E. Van Caemelbecke, S. Eapen and K. M. Kadish, *Inorg. Chem*. **2001**, *40*, 2282.
121. A. R. Chakravarty, F. A. Cotton and L. R. Falvello, *Inorg. Chem*. **1986**, *25*, 214.
122. K. M. Kadish, L.-L. Wang, A. Thuriere, L. Giribabu, R. Garcia, E. Van Caemelbecke and J. L. Bear, *Inorg. Chem*. **2003**, *42*, 8309.
123. H. J. McCarthy and D. A. Tocher, *Polyhedron* **1992**, *11*, 13.
124. D. A. Tocher, *Inorg. Chim. Acta* **1986**, *115*, 51.
125. F. A. Cotton and T. Ren, *Inorg. Chem.* **1995**, *34*, 3190.
126. C. Lin, T. Ren, E. J. Valente, J. D. Zubkowski and E. T. Smith, *Chem. Lett.* **1997**, 753.
127. T. Ren, V. DeSilva, G. Zou, C. Lin, L. M. Daniels, C. F. Campana and J. C. Alvarez, *Inorg. Chem. Commun.* **1999**, *2*, 301.
128. P. Angaridis, J. F. Berry, F. A. Cotton, C. A. Murillo and X. Wang, *J. Am. Chem. Soc*. **2003**, *125,* 10327.
129. P. Angaridis, J. F. Berry, F. A. Cotton, P. Lei, C. Lin, C. A. Murillo and D. Villagrán, *Inorg. Chem. Commun.* **2004**, *7*, 9.
130. M. C. Barral, S. Herrero, R. Jiménez-Aparicio, M. R. Torres and F. A. Urbanos, *Inorg. Chem. Commun.* **2004**, *7*, 42.
131. P. Angaridis, F. A. Cotton, C. A. Murillo, D Villagrán and X. Wang, *Inorg. Chem*. **2004**, *43*, 8290.

Pictiva EX2004
Samsung v Pictiva
IPR2024-01094

132. J. L. Bear, B. Han, S. Huang and K. M. Kadish, *Inorg. Chem*. **1996**, *35*, 3012.
133. C. Lin, T. Ren, E. J. Valente and J. D. Zubkowski, *J. Organomet. Chem.* **1999**, *579*, 114.
134. T. Ren, *Coord. Chem. Rev.* **1998**, *175*, 43.
135. G. Xu and T. Ren, *Inorg. Chem.* **2001**, *40*, 2925.
136. J.-P. Collin, A. Jouaiti, J.-P. Sauvage, W. C. Kaska, M. A. McLoughlin, N. L. Keder, W. T. A. Harrison and G. D. Stucky, *Inorg. Chem.* **1990**, *29*, 2238.
137. M. Mintert and W. S. Sheldrick, *Inorg. Chim. Acta* **1995**, *236*, 13.
138. C. Kachi-Terajima, H. Miyasaka, T. Ishii, K. Sugiura and M. Yamashita, *Inorg. Chim. Acta* **2002**, *332*, 210.
139. H. Miyasaka, C. Kachi-Terajima, T. Ishii and M. Yamashita, *J. Chem. Soc., Dalton Trans*. **2001**, 1929.
140. H. Miyasaka, T. Izawa, K. Sugiura and M. Yamashita, *Inorg. Chem.* **2003**, *42*, 7683.
141. H. Miyasaka, K. Sugiura and M. Yamashita, *Inorg. Chem. Commun.* **2003**, *6*, 1078.
142. M. Ebihara, N. Nagaya, N. Kawashima and T. Kawamura, *Inorg. Chim. Acta* **2003**, *351*, 305.
143. A. J. Lindsay, R. P. Tooze, M. Motevalli, M. B. Hursthouse and G. Wilkinson, *J. Chem. Soc., Chem. Commun.* **1984**, 1383.
144. A. J. Lindsay, G. Wilkinson, M. Motevalli and M. B. Hursthouse, *J.Chem. Soc., Dalton. Trans*. **1985**, 2321.
145. P. Sarkhel, S. C. Sarker, A. K. Gupta and R. K. Poddar, *Transition Met. Chem*. **1996**, *21*, 250.
146. A. Carvill, P. Higgins, G. M. McCann, H. Ryan and A. Shiels, *J. Chem. Soc., Dalton Trans*. **1989**, 2435.
147. F. A. Cotton, L. Labella and M. Shang, *Inorg. Chim. Acta* **1992**, *197*, 149.
148. F. A. Cotton, V. M. Miskowski and B. Zhong, *J. Am. Chem. Soc*. **1989**, *111*, 6177.
149. F. A. Cotton, L. M. Daniels, P. A. Kibala, M. Matusz, W. J. Roth, W. Schwotzer, W. Wang and B. Zhong, *Inorg. Chim. Acta* **1994**, *215*, 9.
150. P. Maldivi, A. M. Giroud-Godquin, J.-C. Marchon, D. Guillon and A. Skoulios, *Chem. Phys. Lett*. **1989**, *157*, 552.
151. M. C. Barral, R. Jiménez-Aparicio, J. L. Priego, E. C. Royer, F. A. Urbanos and U. Amador, *Inorg. Chim. Acta* **1998**, *279*, 30.
152. M. H. Chisholm, G. Christou, K. Folting, J. Huffmann, C. A. James, J. A. Samuels, J. L. Wesemann and W. H. Woodruff, *Inorg. Chem*. **1996**, *35*, 3643.
153. G. E. Quelch, I. H. Hillier and M. F. Guest, *J. Chem. Soc., Dalton Trans*. **1990**, 3075.
154. D. L. Clark, J. C. Green, C. M. Redfern, G. E. Quelch, I. H. Hillier and M. F. Guest, *Chem. Phys. Lett*. **1989**, *154*, 326.
155. D. L. Clark, J. C. Green and C. M. Redfern, *J. Chem. Soc., Dalton Trans*. **1989**, 1037.
156. J. L. Wesemann and M. H. Chisholm, *Inorg. Chem*. **1997**, *36*, 3258.
157. H. Miyasaka, R. Clérac, C. S. Campos-Fernández and K. R. Dunbar, *J. Chem. Soc., Dalton Trans*. **2001**, 858.
158. S. C. Huckett, C. A. Arrington, C. J. Burns, D. L. Clark and B. I. Swanson, *Synthetic Metals* **1991**, *41-43*, 2769.
159. H. Miyasaka, C. S. Campos-Fernández, R. Clérac and K. R. Dunbar, *Angew. Chem. Int. Ed.* **2000**, *39*, 3831.
160. G. Estiú, F. D. Cukiernik, P. Maldivi and O. Poizat, *Inorg. Chem*. **1999**, *38*, 3030.
161. L. Bonnet, F. D. Gukiernik, P. Maldivi, A.-M. Giroud-Godquin, J.-C. Marchon, M. Ibn-Elhaj, D. Guillon and A. Skoulios, *Chem. Mater*. **1994**, *6*, 31.
162. M. Handa, D. Yoshioka, M. Mikuriya, I. Hiromitsu and K. Kasuga, *Mol. Cryst. Liq. Cryst.* **2002**, *376*, 257.
163. A. Cogne, E. Belorizky, J. Laugier and P. Rey, *Inorg. Chem*. **1994**, *33*, 3364.
164. M. Berry, C. D. Garner, I. H. Hillier, A. A. MacDowell and W. Clegg, *Inorg. Chim. Acta* **1981**, *53*, L61.
165. F. A. Cotton, T. Ren and J. L. Eglin, *J. Am. Chem. Soc.* **1990**, *112*, 3439.
166. F. A. Cotton, T. Ren and J. L. Eglin, *Inorg. Chem.* **1991**, *30*, 2552.

Pictiva EX2004
Samsung v Pictiva
IPR2024-01094

167. F. A. Cotton and T. Ren, *Inorg. Chem.* **1991**, *19*, 3675.
168. K. M. Kadish, B. Han, J. Shao, Z. Ou and J. L. Bear, *Inorg. Chem*. **2001**, *40*, 6848.
169. F. A. Cotton, L. R. Falvello, T. Ren and K. Vidyasagar, *Inorg. Chim. Acta* **1992**, *194*, 163.
170. F. A. Cotton and M. Matusz, *J. Am. Chem. Soc.* **1988**, *110*, 5761.
171. F. A. Cotton and X. Feng, *Inorg. Chem.* **1989**, *28*, 1180.
172. C. S. Campos-Fernández, X. Ouyang and K. R. Dunbar, *Inorg. Chem.* **2000**, *39*, 2432.
173. E. Binamira-Soriaga, N. L. Keder and W. C. Kaska, *Inorg. Chem.* **1990**, *29*, 3167.
174. W. S. Sheldrick and M. Mintert, *Inorg. Chim. Acta* **1994**, *219*, 23.
175. C. S. Campos-Fernández, L. M. Thomson, J. R. Galán-Mascarós, X. Ouyang and K. R. Dunbar, *Inorg. Chem.* **2002**, *41*, 1523.
176. L. F. Warren and V. L. Goedken, *J. Chem. Soc., Chem. Commun.* **1978**, 909.
177. R. P. Tooze, G. Wilkinson, M. Motevalli and M. B. Hursthouse, *J. Chem. Soc., Dalton Trans.* **1986**, 2711.
178. B. J. Kennedy, G. A. Heath and T. J. Khoo, *Inorg. Chim. Acta* **1991**, *190*, 265.
179. M. B. Hursthouse, R. A. Jones, K. M. Abdul Malik and G. Wilkinson, *J. Am. Chem. Soc.* **1979**, *101*, 4128.
180. M. G. B. Drew, P. Higgins and G. M. McCann, *J. Chem. Soc., Chem. Commun.* **1987**, 1385.
181. F. A. Cotton and A. Yokochi, *Inorg. Chem.* **1997**, *36*, 567.
182. J. L. Bear, Y. Li, B. Han, E. Van Caemelbecke and K. M. Kadish, *Inorg. Chem.* **1996**, *35*, 3035.
183. Y. Li, B. Han, K. M. Kadish and J. L. Bear, *Inorg. Chem*. **1993**, *32*, 4175.
184. G. Xu and T. Ren, *J. Organomet. Chem*. **2002**, *655*, 239.
185. T. Ren, *Organometallics* **2002**, *21*, 732.
186. J. L. Bear, Y. Li, J. Cui, B. Han, E. Van Caemelbecke, T. Phan and K. M. Kadish, *Inorg. Chem*. **2000**, *39*, 857.
187. J. L. Bear, B. Han and S. Huang, *J. Am. Chem. Soc*. **1993**, *115*, 1175.
188. C. Lin, T. Ren, E. J. Valente and J. D. Zubkowski, *J. Chem. Soc., Dalton Trans*. **1998**, 571.
189. K.-T. Wong, J.-M. Lehn, S.-M. Peng and G.-H. Lee, *Chem. Commun*. **2000**, 2259.
190. J.-L. Zuo, E. Herdtweck and F. E. Kühn, *J. Chem. Soc., Dalton Trans*. **2002**, 1244.
191. G. Xu, C. Campana and T. Ren, *Inorg. Chem.* **2002**, *41*, 3521.
192. G.-L. Xu, C. G. Jablonski and T. Ren, *J. Organomet. Chem.* **2003**, *683*, 388.
193. S. K. Hurst, G.-L. Xu and T. Ren, *Organometallics* **2003**, *22*, 4118.
194. G.-L. Xu, C. G. Jablonski and T. Ren, *Inorg. Chim. Acta* **2003**, *343*, 387.
195. J. L. Bear, Y. Li, B. Han and K. M. Kadish, *Inorg. Chem.* **1996**, *35*, 1395.
196. L. F. Warren and V. L. Goedken, *J. Chem. Soc., Chem. Commun*. **1978**, 909.
197. V. L. Goedken, private communication.
198. (a) J. P. Collman and S. T. Harford, *Inorg. Chem*. **1998**, *37*, 4152. (b) J. P. Collman, C. E. Barnes, T. J. Collins, P. J. Brothers, J. Galluci and J. A. Ibers, *J. Am. Chem. Soc*. **1981**, *103*, 7030. (c) J. P. Collman, C. E. Barnes, P. N. Swepston and J. A. Ibers, *J. Am. Chem. Soc*. **1984**, *106*, 3500.
199. J. P. Collman, J. W. Prodolliet and C. R. Leidner, *J. Am. Chem. Soc*. **1986**, *108*, 2916.
200. H. Asahina, M. B. Zisk, B. Hedman, J. T. McDevitt, J. P. Collman and K. O. Hodgson, *J. Chem. Soc., Chem. Commun*. **1989**, 1360.
201. C. D. Tait, J. M. Garner, J. P. Collman, A. P. Sattelberger and W. H. Woodruff, *J. Am. Chem. Soc*. **1989**, *111*, 7806.
202. B. R. James, A. Pacheco, S. J. Rettig and J. A. Ibers, *Inorg. Chem*. **1988**, *27*, 2414.
203. (a) J. P. Collman, P. J. Brothers, L. McElwee-White, E. Rose and L. J. Wright, *J. Am. Chem. Soc*. **1985**, *107*, 4570. (b) J. P. Collman, J. T. McDevitt, G. T. Yee, C. R. Leidner, L. G. McCullough, W. A. Little and J. B. Torrance, *Proc. Natl. Acad. Sci. USA*, **1986**, *83*, 4581. (c) J. P. Collman, J. T. Mc Devitt, C. R. Leidner, G. T. Yee, J. B. Torrance and W. A. Little, *J. Am. Chem. Soc*. **1987**, *109*, 4606.
204. J. P. Collman, H. J. Arnold, J. P. Fitzgerald and K. J. Weissman, *J. Am. Chem. Soc*. **1993**, *115*, 9309.

Pictiva EX2004
Samsung v Pictiva
IPR2024-01094

205. J. P. Collman, S. T. Hartford, S. Franzen, J.-C. Marchon, P. Maldivi, A. P. Shreve and W. H. Woodruff, *Inorg. Chem*. **1999**, *38*, 2085.
206. J. P. Collman, S. T. Hartford, S. Franzen, A. P. Shreve and W. H. Woodruff, *Inorg. Chem*. **1999**, *38*, 2093.
207. F. Jérôme, B. Billier, J.-M. Barbe, E. Espinosa, S. Dahaoui, C. Lecomte and R. Guillard, *Angew. Chem. Int. Ed*. **2000**, *39*, 4051.
208. K. M. Kadish, F. Burdet, F. Jérôme, J.-M. Barbe, Z. Ou, J. Shao and R. Guillard, *J. Organometal. Chem*. **2002**, *652*, 69.
209. P. Legzdins, R. W. Mitchell, G. L. Rempel, J. D. Ruddick and G. Wilkinson, *J. Chem. Soc. (A)* **1970**, 3322.
210. A. J. Lindsay, G. McDermott and G. Wilkinson, *Polyhedron* **1988**, 7, 1239.
211. A. F. Noels, A. Demonceau, E. Carlier, A. J. Hubert, R.-L. Márquez-Silva and R. A. Sánchez-Delgado, *J. Chem. Soc., Chem. Commun.* **1988**, 783.
212. S. Cenini, G. Cravotto, G. B. Giovenzana, G. Palmisano, A. Penoni and S. Tollari, *Tetrahedron Lett.* **2002**, *43*, 3637.
213. B. K. Keppler, M. Henn, U. M. Juhl, M. R. Berger, R. Niebl and F. E. Wagner, *Prog. Clin. Biochem. Med.* **1989**, *10*, 41.
214. C. A. Crawford, E. F. Day, V. P. Saharan, K. Folting, J. C. Huffman, K. R. Dunbar and G. Christou, *Chem. Commun*. **1996**, 1113.
215. S. Gangopadbyay and P. K. Gangopadbyay, *J. Inorg. Biochem.* **1997**, 175.
216. C. E. J. Van Rensburg, E. Kreft, J. C. Swarts, S. R. Dalrymple, D. M. MacDonald, M. W. Cooke and M. A. S. Aquino, *Anticancer Res*. **2002**, *22*, 889.

Pictiva EX2004
Samsung v Pictiva
IPR2024-01094

10

Osmium Compounds

Tong Ren,
University of Miami

The chemistry of diosmium compounds containing metal–metal bonds bears much similarity to the chemistry of diruthenium compounds, and its progress closely tracked that of diruthenium in the 1980's. While diruthenium chemistry has flourished during the last fifteen years (see preceding chapter), diosmium chemistry has lagged, which is likely attributable to the prohibitive cost of Os raw materials. Nevertheless, some interesting aspects have emerged since the publication of the second edition of this book, and a description of diosmium chemistry in its entirety is attempted in this chapter.

10.1 Syntheses, Structures and Reactivity of Os_2^{6+} Compounds

The first Os_2 compound containing an Os–Os multiple bond was $Os_2(hp)_4Cl_2$, which was obtained by refluxing $OsCl_3$ with 2-hydroxypyridine in ethanol under a nitrogen atmosphere.[1] This compound was crystallized as both the diethylether and acetonitrile solvates, and crystal structures were determined for both forms. The diosmium molecule, shown in Fig. 10.1, adopts a paddlewheel motif having four hp ligands coordinated to the Os_2 to give the 2,2 regioisomer. The Os–Os distances are 2.344 and 2.357 Å in the diethylether and acetonitrile solvates, respectively, which firmly establish the existence of an Os–Os triple bond.

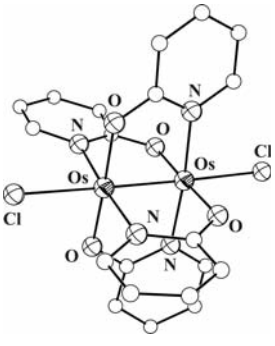


Fig. 10.1. The structure of $Os_2(hp)_4Cl_2$.

Pictiva EX2004
Samsung v Pictiva
IPR2024-01094

Discovery of $Os_2(hp)_4Cl_2$ was immediately followed by the isolation of $Os_2(O_2CMe)_4Cl_2$ from the reaction between a hydrochloric acid solution of $OsCl_6^{2-}$, prepared by the reduction of OsO_4 with $FeCl_2$, and acetic acid/anhydride.[2,3] Other $Os_2(O_2CR)_4Cl_2$ compounds (R = CH_2Cl, Et, Pr^n, and 2-PhC_6H_4) have been synthesized from $Os_2(O_2CMe)_4Cl_2$ using carboxylate exchange reactions.[3-5] Crystal structures of $Os_2(O_2CR)_4Cl_2$ with R = CH_3, C_2H_5, *n*-C_3H_7 (Fig. 10.2) and 2-PhC_6H_4 have been determined,[4-6] and the Os–Os bond lengths are within a narrow range of 2.301 – 2.318 Å. The axial chloro ligands in tetracarboxylates can be readily displaced with bromo ligands by treating $Os_2(O_2CR)_4Cl_2$ with anhydrous HBr at -78 °C.[7]

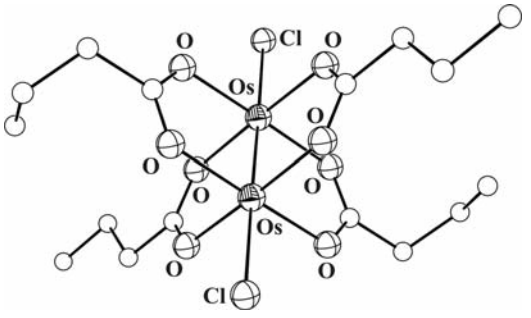


Fig. 10.2. The structure of $Os_2(O_2CC_3H_7)_4Cl_2$.

In addition to being the precursor of other tetracarboxylates, $Os_2(O_2CMe)_4Cl_2$ also serves as a convenient starting material for many diosmium compounds supported by other bridging bidentate ligands enumerated below. $Os_2(hp)_4Cl_2$ was obtained from refluxing $Os_2(O_2CMe)_4Cl_2$ with excess 2-hydroxypyridine in methanol.[3] Molten reaction between $Os_2(O_2CMe)_4Cl_2$ and benzamide resulted in $Os_2(PhCONH)_4Cl_2$,[8] which was converted to $Os_2(PhCONH)_4Br_2$ when recrystallized in the presence of Me_4NBr.[9] X-ray diffraction studies revealed that the benzamidato ligands adopt the cis-(2,2) arrangement around the Os_2 core in both cases and the Os–Os bond lengths are 2.369 and 2.383 Å for axial Cl and Br adducts, respectively, which are slightly elongated from that of $Os_2(hp)_4Cl_2$. A molten reaction between $Os_2(O_2CMe)_4Cl_2$ and 6-chloro-2-hydroxypyridine in a sealed Pyrex tube resulted in $Os_2(chp)_2Cl_4(H_2O)$ in addition to $Os_2(chp)_4Cl$ (see below).[10] $Os_2(chp)_2Cl_4(H_2O)$ was converted to $Os_2(chp)_2Cl_4(py)$ and X-ray analysis revealed that two bridging chp ligands are trans to each other, four chloro ligands occupy the remaining equatorial sites, and H_2O/py occupies the axial position.[11] A molten reaction between $Os_2(O_2CMe)_4Cl_2$ and *N*,*N*'-di(*p*-tolyl)formamidine (HDTolF) furnished $Os_2(DTolF)_4Cl_2$, which has the longest Os–Os bond length (2.467 Å) among all known Os_2^{6+} paddlewheel species, and an almost eclipsed arrangement of DTolF ligands (0.1° N–Os–Os'–N' torsion angle).[12] Brief refluxing of $Os_2(O_2CMe)_4Cl_2$ with Me_3SiCl and 2-anilinopyridine in toluene led to an unsymmetrical compound $Os_2(ap)_3Cl_3$ (Fig. 10.3), where the Os–Os distance was determined to be 2.392 Å.[13] Fully substituted $Os_2(ap)_4Cl_2$ was obtained recently from the prolonged reflux of $Os_2(O_2CMe)_4Cl_2$ and 2-anilinopyridine with the aid of an acetic acid scrubbing apparatus. For single crystals obtained from CH_3OH/CH_2Cl_2 solution, X-ray analysis revealed a *cis*-(2,2) arrangement of ap ligands (Fig. 10.4), an Os–Os distance of 2.396(1) Å, and an averaged N-Os–Os'-N' torsional angle of 5°.[14] Surprisingly, crystals obtained from hexanes/CH_2Cl_2 solution contain the (3,1)-isomer instead, which exhibits similar dimensions.[15] $Os_2(ap)_4Cl_2$ undergoes facile reaction with LiC_2Ph to yield $Os_2(ap)_4(C_2Ph)_2$, the first Os_2-alkynyl complex, which was crystallized as either the (3,1)-isomer from hexanes/THF solution or the cis-(2,2)-isomer from CH_3OH/CH_2Cl_2 (Fig. 10.5).[15] Upon alkynylation, the Os–Os bond elon-

Pictiva EX2004
Samsung v Pictiva
IPR2024-01094

gates about 0.06 Å in the cis-(2,2) isomer and 0.08 Å in (3,1) isomer. Similar to the original preparation of $Os_2(hp)_4Cl_2$, $Os_2(hpp)_4Cl_2$ was synthesized in 30% yield from refluxing $OsCl_3$ with four equivalents of Hhpp in ethanol.[16] X-ray structural analysis revealed an Os–Os bond length of 2.379 Å, the shortest among Os_2^{6+} compounds containing *N*,*N*'-bidentate ligands, and an eclipsed configuration of hpp ligands (0° N–Os–Os'–N' torsion angle as imposed by $\bar{4}$/mmm crystallographic symmetry).[16,17]

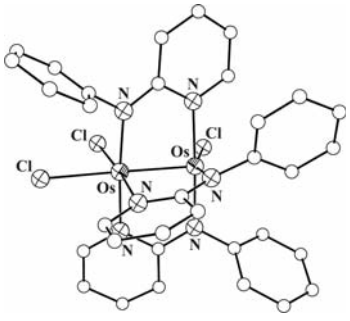


Fig. 10.3. The structure of $Os_2(PhNPy)_3Cl_3$.

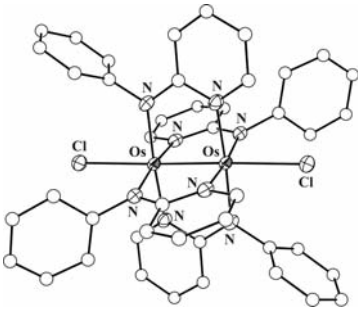


Fig. 10.4. The structure of *cis*-(2,2)-$Os_2(PhNPy)_4Cl_2$.

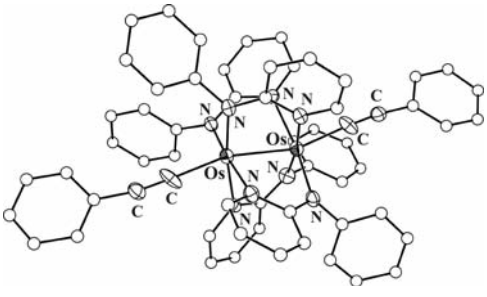


Fig. 10.5. The structure of *cis*-(2,2)-$Os_2(PhNPy)_4(C_2Ph)_2$.

In an attempt to prepare axial phosphine adducts having an $Os_2(O_2CMe)_4$ core, gentle refluxing of $Os_2(O_2CMe)_4Cl_2$ and Ph_3P in acetic acid resulted in *cis*-$Os_2(O_2CCH_3)_2(Ph_2PC_6H_4)_2Cl_2$, where the ortho-metallated $Ph_2P(C_6H_4)$ group functions as a P,C-bidentate bridging ligand.[18,19] *cis*-$Os_2(O_2CC_2H_5)_2(Ph_2PC_6H_4)_2Cl_2$ was prepared similarly. Crystal structures of both ortho-metal-

Pictiva EX2004
Samsung v Pictiva
IPR2024-01094

lated products were determined, and very short Os–Os bond lengths (2.271 and 2.272 Å) were revealed.[19] *cis*-$Os_2(O_2CCH_3)_2(Ph_2PC_6H_4)_2Cl_2$ reacts with Me_3SiCl to afford $Os_2Cl_4(Ph_2PC_6H_4)_2$ (Fig. 10.6) where the Os–Os bond (2.231 Å) was shortened further. This compound exhibits an unusually distorted geometry around the Os_2 core that is best described as two trigonal bipyramidal (TBP) Os centers fused at the equatorial position (Fig. 10.6).

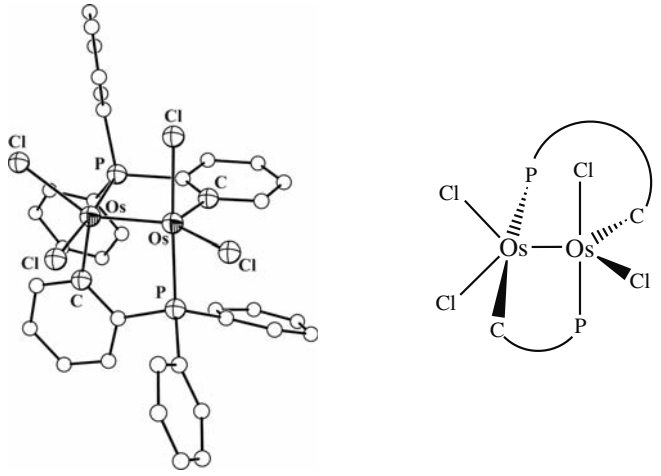


Fig. 10.6. The structure of $Os_2Cl_4(Ph_2PC_6H_4)_2$.

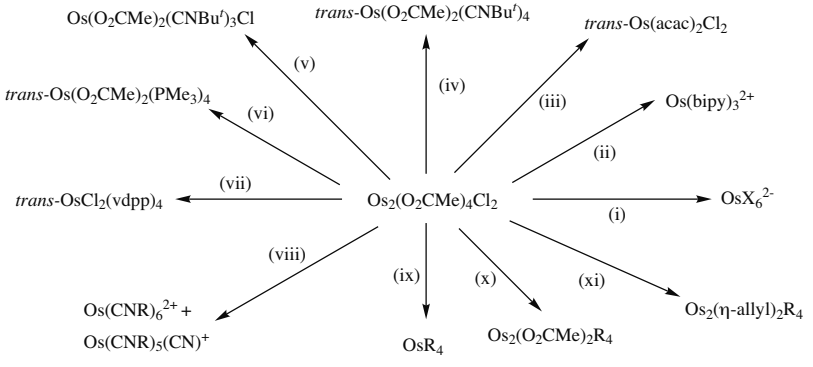
While the Os–Os bond is retained in the aforementioned bridging ligand exchange reactions, $Os_2(O_2CR)_4Cl_2$ also undergoes facile Os–Os bond cleavage with many nucleophiles to yield a number of mononuclear Os complexes as summarized in Scheme 10.1.[3,20-23] Reactions between $Os_2(O_2CMe)_4Cl_2$ and Grignard reagent MgRCl are most peculiar and yielded drastically different products depending on the nature of R. Cleavage products, OsR_4, were isolated with R as cyclohexyl and 2-methylcyclohexyl.[21,22] On the other hand, the partially alkylated dinuclear compounds $Os_2(O_2CMe)_2R_4$ were produced with R as CH_2SiMe_3 and CH_2CMe_3.[24,25] Although these compounds were described as crystalline, structures were not determined. While $Os_2(O_2CMe)_2R_4$ could not be further alkylated with MgRCl in large excess, it reacts with $Mg(C_3H_5)Br$ to yield $Os_2(\eta^3\text{-}C_3H_5)_2R_4$. An X-ray diffraction study of $Os_2(\eta^3\text{-}C_3H_5)_2(CH_2CMe_3)_4$ (Fig. 10.7) revealed the shortest Os–Os bond length known: 2.194 Å. Both $Os_2(O_2CMe)_2R_4$ and $Os_2(\eta^3\text{-}C_3H_5)_2(CH_2CMe_3)_4$ are diamagnetic.

Table 10.1 The diosmium paddlewheel species and related compounds

Compound	Os–Os, Å	Os–X_{ax}, Å	Color	μ/B.M. (T/K)	ref.
		Os_2^{6+}			
$Os_2(hp)_4Cl_2{\cdot}2Et_2O$	2.344(2)	2.47/2.50	Purple	1.70(280)	1,5
$Os_2(hp)_4Cl_2{\cdot}2MeCN$	2.357(1)	2.505(5)	Red	--	1
$Os_2(O_2CCH_3)_4Cl_2$	2.314(1)	2.448(2)	Brown	1.65(288)	6
$Os_2(O_2CC_2H_5)_4Cl_2$	2.316(2)	2.430(5)	Brown	1.60 (300)	6
$Os_2(O_2CC_3H_7)_4Cl_2$	2.301(1)	2.417(3)	Dark green	1.63 (300)	4
$Os_2(O_2CCMe_3)_4Cl_2$	NA	NA	Green-brown	2.15 (300)	26
$Os_2(O_2CCH_3)_2(Ph_2PC_6H_4)_2Cl_2$	2.271(1)	2.372(2)	Black	0.41 (295)	19
$Os_2(O_2CC_2H_5)_2(Ph_2PC_6H_4)_2Cl_2$	2.272(1)	2.396(2)	Black	0.10 (295)	19
$Os_2(DTolF)_4Cl_2$	2.467(1)	2.48	Purple	1.40 (300)	12

Pictiva EX2004
Samsung v Pictiva
IPR2024-01094

Compound	Os–Os, Å	Os–X_{ax}, Å	Color	μ/B.M. (T/K)	ref.
$Os_2(PhCONH)_4Cl_2$	2.367(3)	2.47-2.51	Dark green	1.76 (298)	8,9
$Os_2(PhCONH)_4Br_2$	2.383(2)	2.59-2.63	Dark green	NA	9
$Os_2(ap)_3Cl_3$	2.392(1)	2.449(5)	Dark blue	2.06 (308)	13
$Os_2(CH_2CMe_3)_4(\eta^3\text{-}C_3H_5)_2$	2.194(3)	---	Orange	Diamag.	25
$Os_2Cl_4(chp)_2(py)$	2.322(1)	2.238(14)	Red	NA	10,11
$Os_2Cl_4(chp)_2(H_2O)$	2.293(1)	2.246(9)	Dark purple	1.65 (298)	10,11
$Os_2(Ph_2PC_6H_4)_2Cl_4$	2.231(1)	---	Brown	NA	27
$Os_2(O_2CC_6H_4\text{-}2\text{-}Ph)_4Cl_2$	2.318(1)	2.38	Brown	1.90 (300)	5
$Os_2(hpp)_4Cl_2$	2.379(2)	2.67	Dark red	See text	16,17
cis-(2,2)-$Os_2(ap)_4Cl_2$	2.396[1]	2.53	Dark blue	2.76 (293)	14
(3,1)-$Os_2(ap)_4Cl_2$	2.391(1)	2.512(4) 2.590(4)	Dark blue	---	15
cis-(2,2)-$Os_2(ap)_4(C_2Ph)_2$	2.456(1)	2.029(9) 2.040(9)	Dark red	Diamag.	15
(3,1)-$Os_2(ap)_4Cl_2(C_2Ph)_2$	2.471(1)	2.126(16) 1.973(13)	Dark red	Diamag.	15
		Os_2^{5+}			
$Os_2(chp)_4Cl$	2.348(1)	2.433(2)	Brown	2.90 (298)	10
$Os_2(fhp)_4Cl$	2.341(1)	2.487(7)	Brown	3.70 (298)	28
$Os_2Cl_4(Ph_2Ppy)_2(O_2CMe)\cdot 2CH_2Cl_2$	2.395(1)	2.428(6)	Brown	NA	29,30
$Os_2Cl_4(Ph_2Ppy)_2(O_2CMe)\cdot 2Me_2CO$	2.388(1)	2.436(2)	Brown	NA	30
$[Os_2(chp)_4(py)](BF_4)$	2.3361(9)	2.22(2)	Dark brown	3.0 (300)	31
$\{[Os_2(chp)_4]_2(\mu\text{-}N,N'\text{-}pyrazine)\}(BF_4)_2$	2.334(1)	2.26(2)	Dark brown	3.6/Os_2(300)	31
		Os_2^{7+}			
$[Os_2(hpp)_4Cl_2](PF_6)\cdot 2$acetone	2.3309(4)	2.520(1)	Deep purple	1.3 B.M.	32
$[Os_2(hpp)_4Cl_2](PF_6)\cdot$hexane	2.3290(6)	2.543(2)	Deep purple	--	32



Scheme 10.1. Os–Os bond cleavage reactions. (i) aqueous HCl or HBr; (ii) bipy; (iii) acetylacetone; (iv) Na + $CNBu^t$; (v) $CNBu^t$; (vi) PMe_3; (vii) vdpp, LiCl, reflux in toluene; (viii) (a) $Pb(NO_3)_2$, KPF_6; (b) CNR; (ix) MgRCl, R = cyclohexyl; (x) MgRCl, R= CH_2SiMe_3 and CH_2CMe_3; (xi) (a) $Mg(CH_2CMe_3)Cl$; (b) $Mg(C_3H_5)Br$

Pictiva EX2004
Samsung v Pictiva
IPR2024-01094

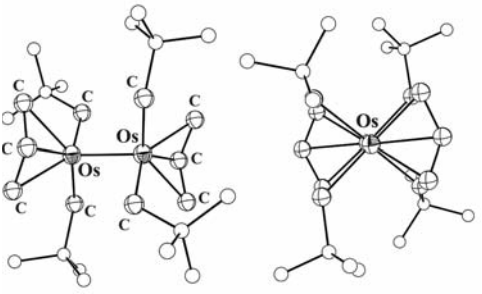


Fig. 10.7. The structure of $Os_2(\eta^3\text{-allyl})_2(CH_2Bu^t)_4$; (a) labeled plot and (b) viewed along Os1–Os2 vector

The compound $Os_2(O_2CMe)_4Cl_2$ reacts with hydrohalic acids (HCl, HBr) to yield either $[OsX_6]^{2-}$ in aqueous solution[3] or $[Os_2X_8]^{2-}$ in anhydrous ethanol.[33,34] $[Os_2I_8]^{2-}$ was obtained by treating $(Bu_4N)_2[Os_2Cl_8]$ with gaseous HI in CH_2Cl_2, and crystallized via slow diffusion of toluene into a CH_2Cl_2 solution.[35] More recently, $[Os_2Br_8]^{2-}$ was isolated from the reaction between H_2OsBr_6 and C_5Me_5H in the mixture of 48% HBr and ethanol (or methanol), representing the only example of $[Os_2X_8]^{2-}$ synthesis directly from a mononuclear source.[36]

$$4H_2OsBr_6 + 4C_5Me_5H + 3C_2H_5OH \rightarrow [(C_5Me_5)_2OsH]_2[Os_2Br_8] + 16HBr + 3CH_3CHO$$

While they resemble the quadruply bonded $[Mo_2X_8]^{4-}$ and $[Re_2X_8]^{2-}$ anions in formulation, $[Os_2X_8]^{2-}$ anions are unique in that the majority adopt a staggered configuration,[33-38] indicating the absence of a net δ–bond. The Os–Os bond lengths in $[Os_2X_8]^{2-}$ (Fig. 10.8a) are generally short and within a narrow range of 2.182– 2.231 Å despite the large variation in the size of X. As with some other $[M_2X_8]^{2-}$ species, the Os_2 core is sometimes disordered within the cage defined by eight halide ligands in several cases (see Table 2). A rare tetraosmium cluster $[Os_4I_{14}]^{2-}$ (Fig. 10.8b),[38] where two $[Os_2I_8]^{2-}$ units were fused through edge-sharing, was obtained by recrystallizing $[Os_2I_8]^{2-}$ from ethanol/CH_2Cl_2.

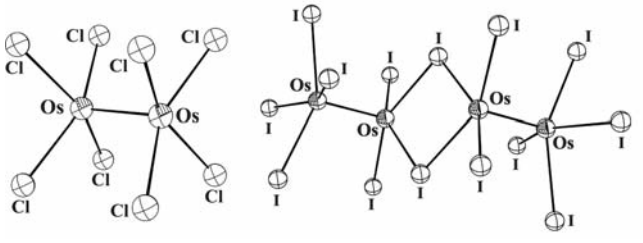
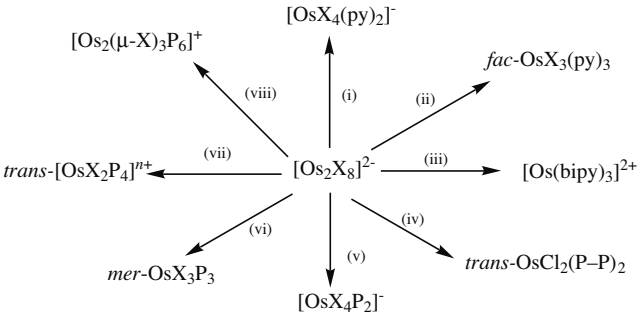


Fig. 10.8. (a) The structure of $[Os_2Cl_8]^{2-}$; (b) The structure of $[Os_4I_{14}]^{2-}$.

The anion $[Os_2X_8]^{2-}$ readily reacts with various nitrogen and phosphorus donor ligands to yield either the mononuclear Os(III)/Os(II) complexes or face-sharing bioctohedral $[Os_2(\mu\text{-}X)_3(PR)_6]^+$ complexes, as summarized in the scheme below.[39] No simple substitution reaction to give, for example, an $Os_2X_6L_2$ molecule has been observed. The crystal structure of $[Os_2(\mu\text{-}Cl)_3(PEt_3)_6]PF_6$ was determined, and the long Os···Os distance (3.47 Å) therein clearly indicates the absence of an Os–Os bond. $[Os_2Cl_8]^{2-}$ reacts with cyclic triaza ligands L to yield $LOsCl_3$ (L = TACN and Me_3TACN, where TACN is 1,4,7-triazacyclononane), which can be converted to $[LOs(\mu\text{-}Cl)_3OsL]^{3+}$ upon refluxing in triflic acid.[40] Os–Os bonding was deduced based on an Os–Os distance of 2.67 Å from a partially refined structure of $[(TACN)Os(\mu\text{-}Cl)_3Os(TACN)](PF_6)_3$.

Pictiva EX2004
Samsung v Pictiva
IPR2024-01094



Scheme 10.2. (i) heat in DMF containing 5 equiv. py, X = Cl; (ii) reflux in neat py, X = Cl; (iii) 10 equiv. bipy in methanol; (iv) bidentate phosphine (P–P) in ethanol; (v) 2.5 equiv. phosphine (P) in *n*-PrOH, 0 °C - room temp.; (vi) 5.5 equiv. P in methanol, reflux; (vii) *n* = 1, 3 equiv. P in methanol, room temp.; *n* = 0, 9 equiv. P in methanol reflux; (viii) 7.5 equiv. P in ethanol, reflux

Table 10.2. Compounds of the $Os_2X_8^{2-}$ type

Compound	Os–Os, Å	Mean Torsional Angle (deg)	Color	Comment	ref.
$(PPN)_2Os_2Cl_8$	2.195(2)	14	Green	3-fold disorder	33
	2.206(1)	12	Green	2-fold disorder	34
	2.212(1)	0	Brown	2-fold disorder	34
$(Bu_4N)_2Os_2Cl_8$	2.182(1)	49	Green	No disorder	37
$(PMePh_3)_2Os_2Cl_8$	2.209(1)	0	Pink	2-fold disorder	35
$(Ph_3PCH_2CH_2PPh_3)(Os_2Cl_8)$	2.190(1)	49	Green	No disorder	41
$(Bu_4N)_2Os_2Br_8$	2.196(1)	47	Green	No disorder	37
$(Bu_4N)_2Os_2I_8$	2.217(1)	47	Brown	No disorder	35
$(PMePh_3)_2[Os_4I_{14}]$	2.231(1)	46	Black	No disorder	38
$[Cp^*_2OsH]_2Os_2Br_8$	2.219(2), 2.222(2)	0	Brown	3-fold disorder	36

Edge sharing bioctahedral (ESBO) $[Os_2(\mu\text{-}X)_2X_8]^{2-}$ species with X as Cl^- or Br^- have been synthesized from OsX_6^{2-}.[42,43] While all ESBO W_2 and Re_2 compounds are metal–metal bonded, the Os–Os distance in $Os_2(\mu\text{-}Br)_2Br_8^{2-}$ is 3.788(3) Å, consistent with the absence of an Os–Os bond.[42] Reductive halide extrusion of $Os_2(\mu\text{-}X)_2X_8^{2-}$ at -35 °C resulted in the face-sharing $[Os_2^{III}(\mu\text{-}X)_3X_6]^{3-}$ species, and the X-ray structural analysis of a bromo complex revealed an Os–Os bond length of 2.779 Å,[44] based on which the presence of a σ(Os–Os) bond is suggested.

10.2 Syntheses and Structures of Os_2^{5+} Compounds

Soon after their discoveries, both $Os_2(hp)_4Cl_2$ and $Os_2(O_2CR)_4Cl_2$ were chemically reduced with cobaltocene to the corresponding monoanions $[Os_2(hp)_4Cl_2]^-$ and $[Os_2(O_2CR)_4Cl_2]^-$,[45] but the structures of these Os_2^{5+} complexes were not determined. The Os_2^{6+} core was reduced also to an Os_2^{5+} core during the metathesis reactions between $Os_2(O_2CCH_3)_4Cl_2$ and 6-X-2-hydroxypyridine (X = F or Cl) to result in $Os_2(Xhp)_4Cl$.[10,28] Crystallographic analysis revealed that both compounds adopt the (4,0) arrangement: the Xhp ligands are so arranged that all X-atoms are placed around the axial position opposite to the one occupied by the chloro ligand. Clearly, the accommodation of four pyridine substituents X necessitates the loss of an axial Cl from the Os_2 core, and consequently its reduction. The Os–Os distances are 2.341(1) and 2.348(1) Å for

Pictiva EX2004
Samsung v Pictiva
IPR2024-01094

X = F and Cl, respectively, which are almost identical to that of $Os_2(hp)_4Cl_2$. A plausible explanation is that the bond elongation due to the gain of an antibonding electron is cancelled out by the bond shortening caused by the reduction of electrostatic repulsion between two Os atoms in the Os_2^{5+} core. It is also interesting to note that the Os–Os distances in $Os_2(Xhp)_4Cl$ are about 0.06 Å longer than the Ru-Ru distances for the isostructural $Ru_2(Xhp)_4Cl$ compounds.[46,47]

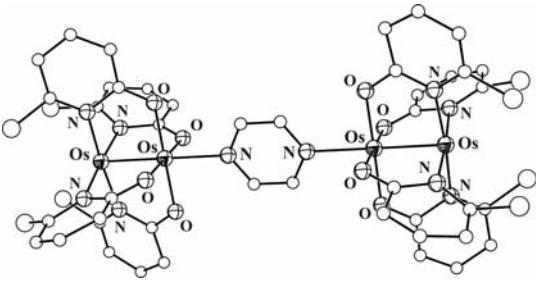


Fig. 10.9. The structure of $\{[Os_2(chp)_4]_2(\mu\text{-N,N'-pyrazine})\}^{2+}$.

The complex $Os_2Cl_4(Ph_2Ppy)_2(O_2CMe)$ was the unexpected product (30% yield) from the reaction between $Os_2(O_2CMe)_4Cl_2$ and Ph_2Ppy in the presence of Me_3SiCl,[29] and its yield was significantly improved by reacting $Os_2(O_2CMe)_4Cl_2$ and Ph_2Ppy in the presence of an excess of LiCl.[30] The species $Os_2Cl_4(Ph_2Ppy)_2(O_2CMe)$ crystallized as both CH_2Cl_2 and acetone solvates, and Os–Os distances are 2.395 and 2.388 Å, respectively.[30] Reaction between $Os_2(chp)_4Cl$ and $[Ag(NCMe)_4](BF_4)$ resulted in $[Os_2(chp)_4(NCMe)](BF_4)$. The axial acetonitrile in the latter complex ion was displaced by either pyridine to yield $[Os_2(chp)_4(py)](BF_4)$, or pyrazine to yield $\{[Os_2(chp)_4]_2(\mu\text{-N,N'-pyrazine})\}(BF_4)_2$ (Fig. 10.9),[31] and nearly identical Os–Os distances were found for $[Os_2(chp)_4(py)]^+$ (2.336 Å) and $\{[Os_2(chp)_4]_2(\mu\text{-N,N'-pyrazine})\}^{2+}$ (2.334 Å).

10.3 Syntheses and Structures of Other Os_2 Compounds

The compounds $[Os(Porp)]_2$ were synthesized from the pyrolysis of $Os(Porp)(py)_2$ (Porp = TPP, TTP, OEP, and OETAP),[48,49] while heterometallic dimer [(Porp)OsMo(OEP)] was isolated from the mixture produced from the pyrolysis of $Os(Porp)py_2$ and $Mo(OEP)(\eta^2\text{-PhCCPh})$.[50,51] Using a cofacial bis(porphyrin) linked with biphenylene (DPB), an heterometallic dimer OsRu(DPB) was isolated as a dark brown solid from the pyrolysis of $Os(py)_2(DPB)Ru(py)_2$.[52] Later, [(OEP)OsRu(OETAP)] was isolated from the mixture produced via the co-pyrolysis of $Ru(OETAP)(py)_2$ and $Os(OEP)(py)_2$,[49,53] and [(OEP)OsW(OEP)] from the co-pyrolysis of $Os(OEP)(py)_2$ and $W(OEP)(PEt_3)_2$. Structural details of these compounds would be very interesting since the Os–Os and Os–M' bonds are not sustained by bridging ligands. The only reported structure, however, is that of $[(TPP)OsMo(OEP)]^+(PF_6)^-$ (Fig. 10.10), where the Os–Mo bond length is 2.238(3) Å.[51] While the Os–Mo bond order should be 3.5 based on the valence electron count, the single δ-type electron is probably nonbonding, judging from the nearly staggered configuration adopted by the Os–N_4 and Mo–N'_4 cores (N–Os–Mo–N' = 42.1°).

The Os–Os bonds in $[Os(Porp)]_2$ can be readily cleaved by a nucleophilic ligand. $Os_2(OEP)_2$ reacts with a simple nucleophilic ligand L (L = CO, py, and THF) to yield mononuclear *trans*-$Os(OEP)L_2$ and the reaction rate is proportional to the ligand field strength of L: the reaction with CO is complete in seconds, py in minutes, and THF in days.[54] The compound $Os_2(OEP)_2$ reacts with several linear bidentate linkers L-L (L-L = pyrazine, 4,4'-bipyridine and 1,4-diazabicyclo[2.2.2]octane) to yield insoluble polymers $\{Os(OEP)(\mu\text{-L-L})\}_\infty$, which can be oxidatively

Pictiva EX2004
Samsung v Pictiva
IPR2024-01094

doped with either I_2 or $NOPF_6$ resulting in conductive polymers.[54,55] The cation $[Os_2(TTP)_2]^{2+}$ was also used as precursor to mononuclear $Os^{IV}(TTP)$ complexes.[56]

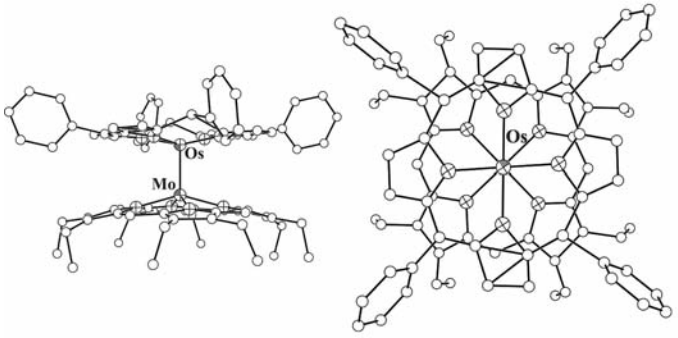
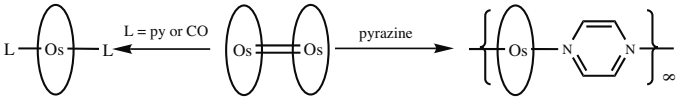


Fig. 10.10. The structure of [(TPP)OsMo(OEP)]$^+$ viewed from the side (left) and along the Os–Mo bond (right, Os–N_4 plane at the front and labeled).



Scheme 10.3. Reactions between $[Os(Porp)]_2$ and nucleophiles

In a related example, the reaction of $OsCl_3$ with molten o-cyanobenzamide in excess yielded $(Pc)OsL_x$, which produced a peak corresponding to $[(Pc)Os]_2$ (m/e = 1407) in a FD mass spectrometer.[57] Subsequently, the structure of "Os(Pc)" prepared from the pyrolysis of $Os(Pc)(py)_2$ was analyzed with a wide angle X-ray scattering technique and a dimeric structure was deduced with an estimated Os–Os bond length of 2.38 Å.[58]

Although the ease of undergoing one-electron oxidation has been established for many Os_2^{6+} species through voltammetric studies, it is not until recently that the first Os_2^{7+} complex, $[Os_2(hpp)_4Cl_2](PF_6)$, was isolated from the chemical oxidation of $Os_2(hpp)_4Cl_2$ by ferrocenium.[32] The Os–Os bond lengths determined for the acetone and hexane solvates are 2.331(1) and 2.329(1) Å, respectively, and the shortening from that of the neutral parent $Os_2(hpp)_4Cl_2$ (2.379(2) Å) is consistent with the loss of a δ* electron.

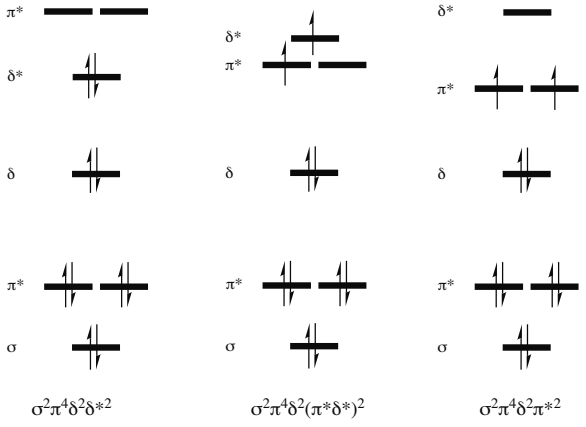
10.4 Magnetism, Electronic Structures, and Spectroscopy

While the most common dinuclear species of other 5d metals, namely those having W_2^{4+} and Re_2^{6+} cores, are typically diamagnetic, paramagnetism has been the hallmark for the majority of the Os_2^{6+} species, especially those having paddlewheel motifs. Paramagnetism of Os_2^{n+} species was first uncovered in $Os_2(O_2CR)_4Cl_2$, where μ_{eff} measured using the Evans technique decreases from 1.15 B.M. per Os (1.6 per Os_2) at 300 K to 1.0 B.M. per Os at *c.* 200 K.[3] While the diamagnetic ground state $\sigma^2\pi^4\delta^2\delta^{*2}$ (Scheme 10.4) was clearly ruled out, data obtained were insufficient to distinguish between two possible $S = 1$ configurations: $\sigma^2\pi^4\delta^2\pi^{*2}$ and $\sigma^2\pi^4\delta^2(\delta^*\pi^*)^2$.[3] A later study of the magnetic susceptibility of $Os_2(O_2CC_6H_4\text{-}2\text{-}C_6H_5)_4Cl_2$ over a temperature range of 5 – 300 K ruled out the possibility of $\sigma^2\pi^4\delta^2\pi^{*2}$, but modeling based on the $\sigma^2\pi^4\delta^2(\delta^*\pi^*)^2$ configuration was not performed.[5] Subsequently, a detailed analysis of the magnetic properties for $Os_2(O_2CCMe_3)_4Cl_2$ was accomplished based on the $\sigma^2\pi^4\delta^2(\delta^*\pi^*)^2$ configuration, for which the temperature dependence of the effective magnetic moment μ_{eff} was derived:[26]

Pictiva EX2004
Samsung v Pictiva
IPR2024-01094

$$\mu^2_{eff} = \left(\frac{g_{eff}}{4}\right)^2\left[1 + \frac{8}{x}\right]$$

where x = D/k_BT, and D is the zero-field splitting parameter for the ^3E_u state derived from the $\sigma^2\pi^4\delta^2(\delta^*\pi^*)^2$ configuration. This deceptively simple equation yielded a satisfactory fit of data between 30 – 350 K for $Os_2(O_2CCMe_3)_4Cl_2$. This study, together with the short Os–Os bond lengths observed, firmly establishes the existence of Os–Os triple bonds in $Os_2(O_2CR)_4Cl_2$ compounds.



Scheme 10.4. Possible ground state configurations for Os_2^{6+} paddlewheel species.

All three paddlewheel Os_2^{6+} compounds supported by the *N*,*N*'-bidentate ligands (DTolF, hpp and ap) exhibit elongated Os–Os bonds in comparison with those of $Os_2(O_2CR)_4Cl_2$ compounds, and are paramagnetic. Temperature-dependence of the measured μ_{eff} for $Os_2(DTolF)_4Cl_2$ resembles that reported for diruthenium(II) compounds supported by both carboxylates and hydroxypyridinates,[59,60] and a satisfactory fit according to the following relationship was achieved (Fig. 10.11):[5]

$$\mu^2_{eff} = 2g_{eff}^2\left[\frac{e^{-x} + (2/x)(1-e^{-x})}{1 + 2e^{-x}}\right]$$

where x = D/k_BT, and D is the zero-field splitting parameter for the $^3A_{1g}$ state derived from the $\sigma^2\pi^4\delta^2\pi^{*2}$ configuration. A very long Os–Os bond is also consistent with the $\sigma^2\pi^4\delta^2\pi^{*2}$ assignment. SCF-Xα calculations, both non- and relativistic, performed on the model compound $Os_2[HNC(H)NH]_4Cl_2$ revealed a HOMO(π^*)-LUMO(δ^*) gap of 1.13 eV, which is attributed to the substantial destabilization of δ^*(Os–Os) by the π_{nb}(N-C-N) orbitals.[12] $Os_2(hpp)_4Cl_2$, on the other hand, exhibits a very small, temperature-independent paramagnetism (TIP, 4.1 x 10^{-5} emu/mol; 0.3 B.M. per Os_2) over the temperature range of 10 – 300 K, which is best explained by a singlet ground state $\sigma^2\pi^4\delta^2\delta^{*2}$ with a low-lying triplet excited state.[16] Consistent with the weak antibonding nature of δ^* orbital, the Os–Os bond length in $Os_2(hpp)_4Cl_2$ is 0.08 Å shorter than that of $Os_2(DTolF)_4Cl_2$. The one-electron oxidation product of $Os_2(hpp)_4Cl_2$ has an effective magnetic moment of 1.3 B.M., and a very small *g* value (0.79) determined from the X-band EPR spectrum.[32] The recently reported $Os_2(ap)_4Cl_2$ has an Os–Os bond length ca. 0.02 Å longer than that of $Os_2(hpp)_4Cl_2$, and an effective magnetic moment of 2.76 B.M. per Os_2 unit. Effective magnetic moments of diosmium compounds tend to be much lower

Pictiva EX2004
Samsung v Pictiva
IPR2024-01094

than the spin-only values ($\mu = [n(n+2)]^{1/2}$; n is the number of unpaired electrons) because of the large spin-orbit coupling intrinsic to Os. Hence, the high effective moment of $Os_2(ap)_4Cl_2$ is peculiar.

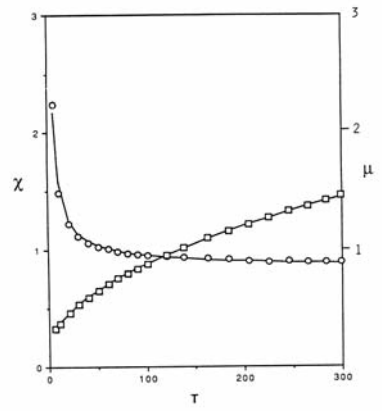


Fig. 10.11. Temperature dependence of magnetic susceptibility (χ, x 10^{-3} cgs) and effective magnetic moment (μ, B.M.) of $Os_2(DTolF)_4Cl_2$ (taken from ref. 61).

The ground state configuration of $Os_2(hp)_4Cl_2$ was initially assigned as diamagnetic $\sigma^2\pi^4\delta^2\delta^{*2}$ on the basis of a relatively short Os–Os bond (2.344(2) Å).[1] Measurement of its magnetic susceptibility between 5 – 300 K revealed a room temperature magnetic moment of 1.7 B.M. and overall dependence described by the equation on the previous page, implying a ground state configuration of $\sigma^2\pi^4\delta^2\pi^{*2}$.[5] Although the χ–T dependence is unavailable, both the Os–Os bond length and room temperature effective moment (1.76 B.M.) of $Os_2(PhCONH)_4Cl_2$ are consistent with a $\sigma^2\pi^4\delta^2\pi^{*2}$ ground state.[9] Small room-temperature μ_{eff} values were reported for $Os_2(O_2CCH_3)_2$-$(Ph_2PC_6H_4)_2Cl_2$ (0.29 B.M./Os) and $Os_2(O_2CC_2H_5)_2(Ph_2PC_6H_4)_2Cl_2$ (0.07 B.M./Os),[18] while the magnetism of the compound $Os_2Cl_4(Ph_2PC_6H_4)_2$ remains unknown.[27] These orthometallated species have the shortest Os–Os bond lengths (2.23 – 2.27 Å) among all paddlewheel diosmium species, which supports $\sigma^2\pi^4\delta^2\delta^{*2}$ as the most probable ground state configuration. The weak paramagnetism in these compounds is certainly worthy of further investigation, although the presence of a paramagnetic impurity cannot be excluded.

The $[Os_2X_8]^{2-}$ anions are all diamagnetic with very short Os–Os bond lengths (2.20 – 2.22 Å), which is consistent with a closed-shell ground state and an Os–Os triple bond. A $\sigma^2\pi^4\delta^2\delta^{*2}$ ground state was derived from the SCF Xα calculation of $Os_2Cl_8^{2-}$ in the eclipsed configuration, where the π^* orbital (LUMO) was found to be 1.5 eV above the δ^* orbital (HOMO).[37] On the basis of both the Xα results of the eclipsed $Os_2Cl_8^{2-}$ and symmetry considerations, it was concluded that four valence electrons from the δ-type orbitals on both Os centers are accommodated in a nonbonding e_2^4 shell in the staggered $Os_2Cl_8^{2-}$.[37] Hence, the staggered $Os_2X_8^{2-}$ has a $\sigma^2\pi^4$ ground state configuration and an Os–Os triple bond.

The earliest studies of $[Os_2(O_2CR)_4Cl_2]^{1-}$ and $[Os_2(hp)_4Cl_2]^{1-}$ found their room temperature magnetic moments (ca. 2.70 B.M.) much higher than those of the corresponding Os_2^{6+} parent compounds,[45] indicating the S = 3/2 nature for Os_2(II,III) molecules. An EPR study of the latter anion also revealed a pattern consistent with a M_S = 1/2 ground state in thermal equilibrium with a M_S = 3/2 state, both the consequence of zero-field splitting of an S = 3/2 configuration. Subsequently, magnetic properties of $Os_2(chp)_4Cl$ and its derivatives were care-

Pictiva EX2004
Samsung v Pictiva
IPR2024-01094

fully examined,[10] which yielded both an effective moment of 2.90 B.M. and an EPR spectrum similar to that of $[Os_2(hp)_4Cl_2]^{1-}$. The ground state configuration for all Os_2^{5+} species appears to be $\sigma^2\pi^4\delta^2\pi^{*2}\delta^{*1}$. This description fits the structural data as well: the Os–Os bond length in $Os_2(chp)_4Cl$ (2.348(1) Å) is identical to that of $Os_2(hp)_4Cl_2$ (2.344(2) and 2.357(1) Å) within the experimental errors, since the added δ* electron in $Os_2(chp)_4Cl$ is only weakly antibonding. Magnetic susceptibilities over a temperature range of 2 – 300 K were measured for both $[Os_2(chp)_4(py)]BF_4$ and $\{[Os_2(chp)_4]_2(\mu\text{-pyrazine})\}(BF_4)_2$.[31] The temperature dependence of the former was modeled with a zero-field splitting of the $S = 3/2$ state, which corroborated the ground state configuration derived from previous EPR studies. Compared with $[Os_2(chp)_4(py)]BF_4$, $\{[Os_2(chp)_4]_2(\mu\text{-pyrazine})\}(BF_4)_2$ exhibited a much faster decay in the effective moment as temperature decreases, which is indicative of a significant antiferromagnetic coupling in the bridged compound.

Details about the Os–Os bonding in $[Os(Porp)]_2$ remain elusive due to the absence of single crystal X-ray structures. Temperature-dependent magnetic properties are consistent with a ground state configuration of $\sigma^2\pi^4\delta^2\delta^{*2}\pi^{*2}$ for $[Os(Porp)]_2$ in analogy to that of Ru_2^{4+} compounds,[53] and an Os–Os double bond.

The majority of Os_2 compounds are deeply colored, reflecting the strong charge transfer nature of electronic absorption spectra as the result of Os-ligand orbital mixings. However, quantitative analysis of these spectroscopic signatures remains rare. A careful examination of both the solution and solid state (CsI pellet and single crystal) absorption spectra of $Os_2(O_2CR)_4X_2$, (R = Me, Pr^n and Bu^t, X = Cl and Br) provided detailed assignments of the observed transitions.[26] Solution studies of $Os_2(O_2CCMe_3)_4X_2$ with X = Cl, Br, and BF_4^- (Fig. 10.12) revealed that the intense peaks at 394 nm for Cl and 455 nm for Br are the ligand to metal charge transfer (LMCT) transitions from axial ligand X to the Os_2 center. Analysis of single crystal polarized absorption spectra of $Os_2(O_2CCMe_3)_4Cl_2$ (Fig. 10.13) yielded assignments of δ→δ* band at 850 nm and π*→δ* band at 1200 nm, and vibronic progression of *c.* 220 cm^{-1} in both bands assigned as ν(Os–Os) in the excited states.

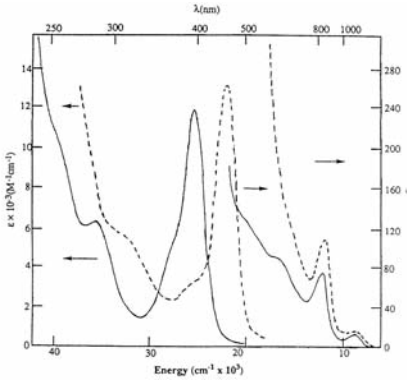


Fig. 10.12. Solution spectra of $Os_2(O_2CCMe_3)_4Cl_2$ (solid line) and $Os_2(O_2CCMe_3)_4Br_2$ (dashed line) at room temperature (taken from ref. 26).

It was noted that $[Os_2Cl_8]^{2-}$ undergoes two reversible one-electron oxidations at 235 K, which were assigned as

$$[Os_2Cl_8]^{2-} \overset{-e^-}{\rightleftharpoons} [Os_2Cl_8]^{-} \overset{-e^-}{\rightleftharpoons} [Os_2Cl_8]^{0}$$

Pictiva EX2004
Samsung v Pictiva
IPR2024-01094

Spectroelectrochemical characterization of $[Os_2Cl_8]^-$ was carried out at 233 K (Fig. 10.14), from which the $\delta \rightarrow \delta^*$ transition was unambiguously identified at a ν_{max} of 4600 cm^{-1}.[62] The observed $\nu(\delta \rightarrow \delta^*)$ is substantially lower than those observed in $[Re_2Cl_8]^{3-}$ (6950 cm^{-1})[63] and $[Tc_2Cl_8]^{3-}$ (6800 cm^{-1}),[64] reflecting a significant deviation from the eclipsed configuration in $[Os_2Cl_8]^{1-}$.[65]

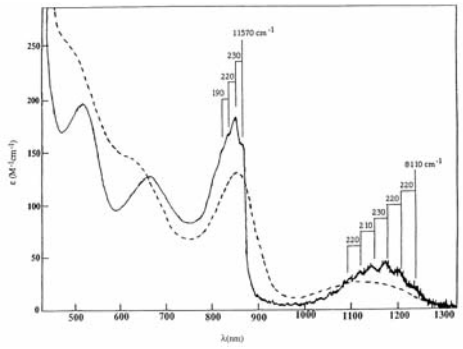


Fig. 10.13. Electronic spectra of the (110) face of a single crystal of $Os_2(O_2CCMe_3)_4Cl_2$ (parallel c polarization) at 20 (solid line) and 295 K(dashed line) (taken from ref. 26).

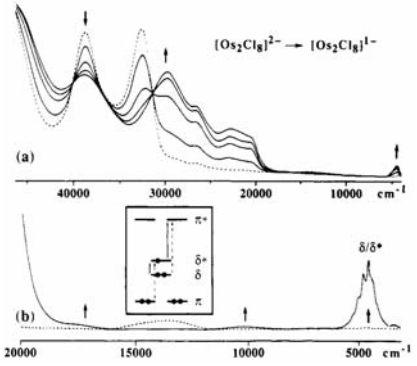
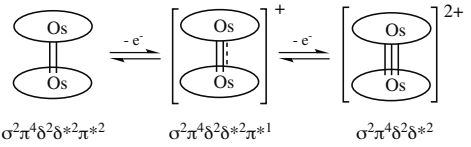


Fig. 10.14. Spectroelectrochemical data for $[Os_2Cl_8]^{2-}$. (a) Spectral changes as oxidation progresses; (b) Spectrum of $[Os_2Cl_8]^{1-}$ showing three visible and near infrared transitions and their assignments (inset) (taken from ref. 62).

While the majority of infrared and Raman spectroscopic data were reported as part of rudimentary characterizations of Os_2 compounds, resonance enhanced Raman data allow inferences as to Os–Os bond strengths. A resonance Raman study of $Os_2(O_2CCH_3)_4Cl_2$ and $Os_2(O_2CCD_3)_4Cl_2$ revealed an Os–Os stretching frequency at 229 cm^{-1},[66] and a similar study of $Os_2(O_2CCH_2Cl)_4Cl_2$, $Os_2(O_2CC_2H_5)_4Cl_2$, and $Os_2(O_2CC_3H_7)_4Cl_2$ yielded ν(Os–Os) ranging from 228 to 236 cm^{-1}.[67] These values are consistent with the triple bond nature of these Os_2 species, considering that the ν(M-M) determined for other 5*d* paddlewheel species are 304 cm^{-1} for $W_2(O_2CCH_3)_4$ (quadruple bond),[68] 288 cm^{-1} for $Re_2(O_2CCH_3)_4Cl_2$ (quadruple bond),[69] and 158 cm^{-1} for $[Pt_2(P_2O_5H_2)_4Cl_2]^{4-}$ (single bond).[70] A resonance Raman study of both $[Os(Porp)]_2$ and its oxidized derivatives revealed that the Os–Os stretching frequency progressively increases with the increasing oxidation state: 233 cm^{-1} for $[Os_2]$, 254 cm^{-1} for $[Os_2]^{1+}$ and 266 cm^{-1} for

Pictiva EX2004
Samsung v Pictiva
IPR2024-01094

$[Os_2]^{2+}$,[71] which are consistent with the stepwise removal of π* electrons and consequently the increase of Os–Os bond order from 2 to 3 (Scheme 10.5).



Scheme 10.5. Change of the ground state configuration of $[Os(porp)]_2$ upon oxidations.

10.5 Concluding Remarks

The chemistry of diosmium compounds is clearly dominated by compounds with an Os_2^{6+} core. Recent isolation of an Os_2^{7+} compound[32] supported by hpp revealed diosmium compounds of higher oxidation state as a promising new focus area. Paddlewheel species having an Os_2^{6+} core display the propensity of axial halide ligation (Table 1) that is reminiscent of Ru_2^{5+} species, which should enable axial coordination of non-trivial ligands through metathesis. Theoretical understanding of diosmium species is limited to a few SCF-Xα calculations performed between late 80s and early 90s. Calculations capable of treating the relativistic effect accurately are much needed in providing better understanding of structures, magnetism and spectroscopy.

References

1. F. A. Cotton and J. L. Thompson, *J. Am. Chem. Soc.* **1980**, *102*, 6437.
2. D. S. Moore, A. S. Alves and G. Wilkinson, *J. Chem. Soc., Chem. Comm.* **1981**, 1164.
3. T. Behling, G. Wilkinson, T. A. Stephenson, D. A. Tocher and M. D. Walkinshaw, *J. Chem. Soc., Dalton Trans.* **1983**, 2109.
4. T. A. Stephenson, D. A. Tocher and M. D. Walkinshaw, *J. Organomet. Chem.* **1982**, *232*, c51.
5. F. A. Cotton, T. Ren and M. J. Wagner, *Inorg. Chem.* **1993**, *32*, 965.
6. F. A. Cotton, A. R. Chakravarty, D. A. Tocher and T. A. Stephenson, *Inorg. Chim. Acta* **1984**, *87*, 115.
7. T. W. Johnson, S. M. Tetrick and R. A. Walton, *Inorg. Chim. Acta* **1990**, *167*, 133.
8. A. R. Chakravarty, F. A. Cotton and D. A. Tocher, *Inorg. Chim. Acta* **1984**, *89*, L15.
9. A. R. Chakravarty, F. A. Cotton and D. A. Tocher, *Inorg. Chem.* **1985**, *24*, 1334.
10. F. A. Cotton, K. R. Dunbar and M. Matusz, *Inorg. Chem.* **1986**, *25*, 1585.
11. F. A. Cotton, K. R. Dunbar and M. Matusz, *Inorg. Chem.* **1986**, *25*, 1589.
12. F. A. Cotton, T. Ren and J. L. Eglin, *Inorg. Chem.* **1991**, *30*, 2559.
13. A. R. Chakravarty, F. A. Cotton and D. A. Tocher, *Inorg. Chem.* **1984**, *23*, 4693.
14. T. Ren, D. A. Parrish, J. R. Deschamps, J. L. Eglin, G.-L. Xu, W.-Z. Chen, M. H. Moore, T. L. Schull, S. K. Pollack, R. Shashidhar and A. P. Sattelberger, *Inorg. Chim. Acta* **2004**, *357*, 1313.
15. Y.-H. Shi, W.-Z. Chen, G.-L. Xu, J. L. Eglin, A. P. Sattelberger, C. Hare and T. Ren, manuscript in preparation.
16. R. Clérac, F. A. Cotton, L. M. Daniels, J. P. Donahue, C. A. Murillo and D. J. Timmons, *Inorg. Chem.* **2000**, *39*, 2581.
17. F. A. Cotton, C. A. Murillo, X. Wang and C. C. Wilkinson, *Inorg. Chim. Acta* **2003**, *351*, 191.
18. A. R. Chakravarty, F. A. Cotton and D. A. Tocher, *J. Chem. Soc., Chem. Commun.* **1984**, 501.
19. A. R. Chakravarty, F. A. Cotton and D. A. Tocher, *Inorg. Chem.* **1984**, *23*, 4697.
20. S. M. Tetrick and R. A. Walton, *Inorg. Chem.* **1985**, *24*, 3363.
21. R. P. Tooze, P. Stavropoulos, M. Motevalli, M. B. Hursthouse and G. Wilkinson, *J. Chem. Soc., Chem. Commun.* **1985**, 1139.

Pictiva EX2004
Samsung v Pictiva
IPR2024-01094

22. P. Stavropoulos, P. D. Savage, R. P. Tooze, G. Wilkinson, B. Hussain, M. Motevalli and M. B. Hursthouse, *J. Chem. Soc., Dalton Trans.* **1987**, 557.
23. F. A. Cotton, M. P. Diebold and M. Matusz, *Polyhedron* **1987**, *6*, 1131.
24. R. P. Tooze, M. Motevalli, M. B. Hursthouse and G. Wilkinson, *J. Chem. Soc., Chem. Commun*. **1984**, 799.
25. R. P. Tooze, G. Wilkinson, M. Motevalli and M. B. Hursthouse, *J. Chem. Soc., Dalton Trans.* **1986**, 2711.
26. V. M. Miskowski and H. B. Gray, *Topics Cur. Chem.* **1997**, *191*, 41.
27. F. A. Cotton and K. R. Dunbar, *J. Am. Chem. Soc.* **1987**, *109*, 2199.
28. F. A. Cotton and M. Matusz, *Polyhedron* **1987**, *6*, 1439.
29. F. A. Cotton, K. R. Dunbar and M. Matusz, *Polyhedron* **1986**, *5*, 903.
30. F. A. Cotton and M. Matusz, *Inorg. Chim. Acta* **1988**, *143*, 45.
31. F. A. Cotton, Y. M. Kim and D. L. Shulz, *Inorg. Chim. Acta* **1995**, *236*, 43.
32. F. A. Cotton, N. S. Dalal, P. Huang, C. A. Murillo, A. C. Stowe and X. Wang, *Inorg. Chem.* **2003**, *42*, 670.
33. P. E. Fanwick, M. K. King, S. M. Tetrick and R. A. Walton, *J. Am. Chem. Soc.* **1985**, *107*, 5009.
34. P. E. Fanwick, S. M. Tetrick and R. A. Walton, *Inorg. Chem.* **1986**, *25*, 4546.
35. F. A. Cotton and K. Vidyasagar, *Inorg. Chem.* **1990**, *29*, 3197.
36. C. L. Gross, S. R. Wilson and G. S. Girolami, *Inorg. Chem.* **1995**, *34*, 2582.
37. P. A. Agaskar, F. A. Cotton, K. R. Dunbar, L. R. Falvello, S. M. Tetrick and R. A. Walton, *J. Am. Chem. Soc.* **1986**, *108*, 4850 .
38. F. A. Cotton and K. Vidyasagar, *Inorg. Chim. Acta* **1989**, *166*, 109.
39. P. E. Fanwick, I. F. Fraser, S. M. Tetrick and R. A. Walton, *Inorg. Chem.* **1987**, *26*, 3786.
40. D. C. Ware, M. M. Olmstead, R. Wang and H. Taube, *Inorg. Chem.* **1996**, *35*, 2576.
41. S. S. Lau, W. G. Wu, P. E. Fanwick and R. A. Walton, *Polyhedron* **1997**, *16*, 3649.
42. F. A. Cotton, S. A. Duraj, C. C. Hinckley, M. Matusz and W. J. Roth, *Inorg. Chem.* **1984**, *23*, 3080.
43. G. A. Heath, D. G. Humphrey and K. S. Murray, *J. Chem. Soc., Dalton Trans.* **1998**, 2417.
44. S. F. Gheller, G. A. Heath, D. C. R. Hockless, D. G. Humphrey and J. E. McGrady, *Inorg. Chem.* **1994**, *33*, 3986.
45. S. M. Tetrick, V. T. Coombe, G. A. Heath, T. A. Stephenson and R. A. Walton, *Inorg. Chem.* **1984**, *23*, 4567.
46. A. R. Chakravarty, F. A. Cotton and D. A. Tocher, *Inorg. Chem.* **1985**, *24*, 172.
47. A. R. Chakravarty, F. A. Cotton and W. Schwotzer, *Polyhedron* **1986**, *5*, 1821.
48. J. P. Collman, C. E. Barnes and L. K. Woo, *Proc. Natl. Acad. Sci., USA* **1983**, *80*, 7684.
49. J. P. Collman and H. J. Arnold, *Acc. Chem. Res.* **1993**, *26*, 586.
50. J. P. Collman, H. J. Arnold, K. J. Weissman and J. M. Burton, *J. Am. Chem. Soc.* **1994**, *116*, 9761.
51. J. P. Collman, S. T. Harford, S. Franzen, A. P. Shreve and W. H. Woodruff, *Inorg. Chem.* **1999**, *38*, 2093.
52. J. P. Collman and J. M. Garner, *J. Am. Chem. Soc.* **1990**, *112*, 166.
53. H. A. Godwin, J. P. Collman, J.-C. Marchon, P. Maldivi, G. T. Yee and B. J. Conklin, *Inorg. Chem.* **1997**, *36*, 3499.
54. J. P. Collman, J. T. McDevitt, C. R. Leidner, G. T. Yee, J. B. Torrance and W. A. Little, *J. Am. Chem. Soc.* **1987**, *109*, 4606.
55. J. P. Collman, J. T. McDevitt, G. T. Yee, C. R. Leidner, L. G. McCullough, W. A. Little and J. B. Torrance, *Proc. Natl. Acad. Sci., USA* **1986**, *83*, 4581.
56. J. P. Collman, D. S. Bohle and A. K. Powell, *Inorg. Chem.* **1993**, *32*, 4004.
57. M. Hanack and P. Vermehren, *Inorg. Chem.* **1990**, *29*, 134.
58. R. Caminiti, M. P. Donzello, C. Ercolani and C. Sadun, *Inorg. Chem.* **1998**, *37*, 4210.
59. F. A. Cotton, V. M. Miskowski and B. Zhong, *J. Am. Chem. Soc.* **1989**, *111*, 6177.
60. F. A. Cotton, T. Ren and J. L. Eglin, *J. Am. Chem. Soc.* **1990**, *112*, 3439.

Pictiva EX2004
Samsung v Pictiva
IPR2024-01094

61. T. Ren Ph.D. Dissertation, Texas A&M University, 1990.
62. S. F. Gheller, G. A. Heath and R. G. Raptis, *J. Am. Chem. Soc.* **1992**, *114*, 7924.
63. G. A. Heath and R. G. Raptis, *Inorg. Chem.* **1991**, *30*, 4106.
64. F. A. Cotton, P. E. Fanwick, L. D. Gage, B. Kalbacher and D. S. Martin, *J. Am. Chem. Soc.* **1977**, *99*, 5642.
65. F. A. Cotton and D. G. Nocera, *Acc. Chem. Res.* **2000**, *33*, 483.
66. R. J. H. Clark, A. J. Hempleman and D. A. Tocher, *J. Am. Chem. Soc.* **1988**, *110*, 5968.
67. R. J. H. Clark and A. J. Hempleman, *J. Chem. Soc., Dalton Trans.* **1988**, 2601.
68. D. J. Santure, J. C. Huffman and A. P. Sattelberger, *Inorg. Chem.* **1985**, *24*, 371.
69. C. Oldham, J. E. D. Davies and A. P. Ketteringham, *J. Chem. Soc., Chem. Comm.* **1971**, 572.
70. M. Kurmoo and R. J. H. Clark, *Inorg. Chem.* **1985**, *24*, 4420.
71. C. D. Tait, J. M. Garner, J. P. Collman, A. P. Sattelberger and W. H. Woodruff, *J. Am. Chem. Soc.* **1989**, *111*, 7806.

Pictiva EX2004
Samsung v Pictiva
IPR2024-01094

11

Iron, Cobalt and Iridium Compounds

Carlos A. Murillo,
Texas A&M University

11.1 General Remarks

There is a rich and extensive chemistry of the group 8 element ruthenium (see Chapter 9) which has a large number of Ru_2^{n+} paddlewheel compounds, n = 4, 5, and 6. For the heaviest of the elements in this group (Os) there is also a substantial number of compounds having Os–Os bond orders of 2, 2.5 and 3 (see Chapter 10). However, no parallel in the chemistry of iron has been found yet.

Likewise, the extensive chemistry that has been discovered for metal–metal bonded Rh_2^{4+} and Rh_2^{5+} species that contain L_4MML_4 and L_5MML_5 structures based upon planar ML_4 or square pyramidal ML_5 geometries has led to the expectation that related, isoelectronic compounds of the group 9 elements Co and Ir should exist. However, the number of d^7–d^7 compounds of these elements is very limited. In this chapter we will focus our attention primarily on dimetal complexes for which each metal unit possesses a square planar configuration and the two square planes (with or without additional axial ligands) are parallel to each other and analogous metal–metal bonded compounds with two parallel triangular planes.

11.2 Di-iron Compounds

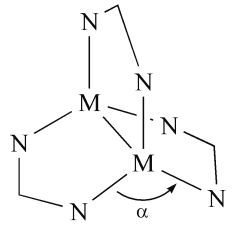
Compounds with Fe–Fe bonds without π-donor ligands, such as carbonyl, are scarce. To date, there is one family of paddlewheel compounds in which the presence of Fe–Fe bonds is unmistakable. The first such compound was initially prepared in low yield by reacting the diphenylformamidine-containing Fe^{II} compound $FeCl_2(HDPhF)_2$ and butyllithium which produces an unusual trigonal paddlewheel (also referred as a trigonal lantern) complex $Fe_2(DPhF)_3$ having an Fe_2^{3+} core and a very short Fe–Fe bond distance of 2.2318(8) Å.[1] This distance is 0.25 Å shorter than that of 2.48 Å found in metallic iron. The reduction of the iron atom presumably proceeds through the attachment of a butyl group to the coordinatively unsaturated metal center followed by β-elimination. The hydride ion which remains could react with a coordinated HDPhF molecule to produce the corresponding bridging anion. An improved synthesis has been devised by adding the hydride reducing agent, $NaEt_3BH$, before the deprotonating agent methyllithium.[2] The net reaction is:

$$2FeCl_2(HDPhF)_2 + NaEt_3BH + 4LiMe \rightarrow Fe_2(DPhF)_3 + LiDPhF + 3LiCl + NaCl + \tfrac{1}{2}H_2 + BEt_3 + 4CH_4$$

Pictiva EX2004
Samsung v Pictiva
IPR2024-01094

In this manner the analogous benzamidinate compound $Fe_2(DPhBz)_3$ has been made. This has an even shorter Fe–Fe bond of 2.198(2) Å. Indeed this is the shortest Fe–Fe distance in any iron containing compound. These compounds are the first paddlewheel complexes having an M_2^{3+} core in which each metal atom has a formal oxidation number of +1.5.

The core of these compounds, which also has Co analogs (see Section 11.3.2), is represented in **11.1**. The molecular structures of the two compounds show that there are three amidinate bridges spanning the Fe_2^{3+} unit. In $Fe_2(DPhF)_3$, the formamidinato groups are not evenly distributed around the iron–iron line segment. One of the ring–ring dihedral angles, α, is opened (132.6°) while the other two are compressed (116.2 and 111.2°) relative to the ideal 120°. Thus the core of this molecule can be described as having C_{2v} symmetry. For the benzamidinate complex $Fe_2(DPhBz)_3$ there is no distortion and the core has virtual D_{3h} symmmetry. The reason for the distortion in $Fe_2(DPhF)_3$ has been attributed to the packing of the molecules in the crystal. This is shown in Fig. 11.1. The molecules are aligned along a crystallographic two-fold axis in such a way that two of the hydrogen atoms of two phenyl rings of adjacent molecules point toward the faces of phenyl rings of adjacent molecules, leading to a restrained packing arrangement that is accommodated by the open intramolecular dihedral angle. Theoretical calculations are consistent with this explanation as they indicate that the total energy of the ground state for the model compound $Fe_2(HNCHNH)_3$ does not change significantly as a function of the dihedral angle.[3] A very detailed study of electron density maps ruled out the existence of any other species, such as a hydride ion, contributing to the distortion.



11.1

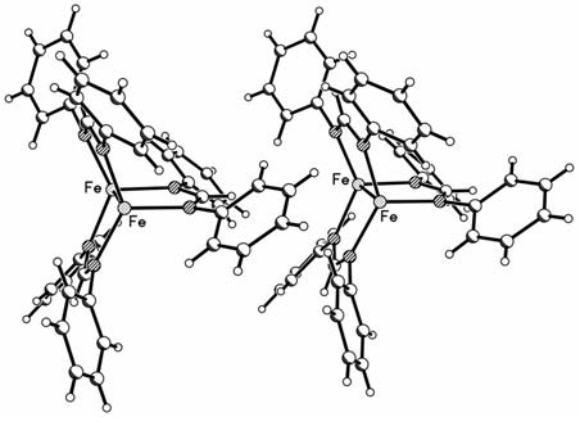


Fig. 11.1. Packing of $Fe_2(DPhF)_3$ molecules along the *b* axis which coincides with a crystallographic two-fold axis. In a given molecule, two DPhF ligands, related to each other by the two-fold axis, are pushed apart by Van der Waals contacts breaking the ideal D_{3h} symmetry.

Pictiva EX2004
Samsung v Pictiva
IPR2024-01094

Another remarkable characteristic of these compounds is their magnetism. At room temperature, the μ_{eff} values for the formamidinate and benzamidinate compounds are 7.81 and 7.53 BM, respectively, indicating the presence of seven unpaired electrons for each molecule. An EPR spectrum of $Fe_2(DPhF)_3$ in a frozen toluene glass gives two signals corresponding to *g* values of 1.99 and 7.94. If axial symmetry is assumed, the spectrum is consistent with an *S* value of $^7/_2$. This unusual value for a small dinuclear molecule containing a metal of the first transition series not only is consistent with the bulk magnetic measurements but also with Xα-SW and *ab initio* with configuration interaction (CI) calculations. These have been carried out for both the regular D_{3h} and the distorted C_{2v} symmetries for the model compound $Fe_2(HNCHNH)_3$. For these, the standard orbital ordering common for tetragonal paddlewheel compounds and based on D_{4h} symmetry is no longer valid and that based on D_{3h} is shown in Fig. 11.2. According to the Xα-SW calculations the energies of the metal–metal based orbitals σ* and π* (5e'' and $4a_2''$) resulting from the linear combinations of the d_{z^2} and d_{xz} and d_{yz}, and those of the delta-type bonding and antibonding orbitals (7e' and 6e'') resulting from the linear combination of d_{xy} and $d_{x^2-y^2}$, are all within a close energy range of 1 eV. By assuming single occupation of all these closely spaced orbitals, the electronic configuration $(a_1')^2(e')^2(e')^2(e'')^1(e'')^1(a_2')^1(e')^1(e')^1(e'')^1(e'')^1$ or $\sigma^2\pi^2\pi^2\pi^{*1}\pi^{*1}\sigma^{*1}\delta^1\delta^1\delta^{*1}\delta^{*1}$ with seven unpaired electrons is obtained. The latter can be abbreviated as $\sigma^2\pi^4\pi^{*2}\sigma^{*1}\delta^2\delta^{*2}$. The calculated equilibrium Fe–Fe distance in the ground state is 2.27 Å as compared to 2.2318 and 2.198 Å in $Fe_2(DPhF)_3$ and $Fe_2(DPhBz)_3$, respectively. The Fe–Fe bond order is 1.5.

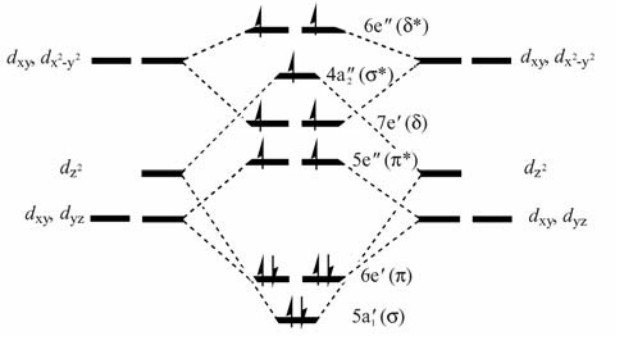


Fig. 11.2. A schematic electron distribution for trigonal paddlewheel molecules with Fe_2^{3+} cores showing the seven unpaired electrons in the closely spaced orbitals. Data are from ref. 3.

By eliminating the use of the reducing agent $NaEt_3BH$ for the preparation of $Fe_2(DPhF)_3$, a compound having an Fe_2^{4+} core is formed with four formamidinate bridges.[4] However, the molecular structure is significantly different from those found in other paddlewheel $M_2(RNXNR)_4$ compounds. A two-fold axis bisects the Fe–Fe vector and lies between the planes formed by the Fe–Fe–N–C–N rings. In contrast to the other compounds known with this stoichiometry but different metal centers (see for example those of cobalt described in Section 11.3.1), there are significant distortions as shown in Fig. 11.3. Two *trans* bridges are pulled towards one end of the molecule while the other opposite pair are pulled in the opposite direction. The core symmetry is thus reduced from the frequently encountered D_{4h} to D_{2d} symmetry. There is also significant asymmetry in the Fe–N distances; two are short (*c.* 2.00 Å) and two are long (*c.* 2.17 Å). The inter-iron separation of 2.462(2) Å [5] is *c.* 0.26 Å longer than those in $Fe_2(amidinate)_3$, discussed above, and only slightly shorter than that in the non-metal–metal

Pictiva EX2004
Samsung v Pictiva
IPR2024-01094

bonded, formamidinate compound $Ni_2(DTolF)_4$ which is discussed in Section 14.2. This distance is similar to those in metal–metal bonded complexes having the heavier congener Ru as shown in Chapter 9. Since this molecule is so distorted and the iron–iron separation is long, it is difficult to decide if a metal–metal bond exists. No theoretical calculations have been done on this molecule. Interestingly, a similar reaction with the benzamidinate analog gave a dinuclear molecule with similar stoichiometry but with two bridging and two chelating benzamidinate ligands. The iron–iron separation of more than 3 Å rules out the possibility of any metal–metal bonding interactions.

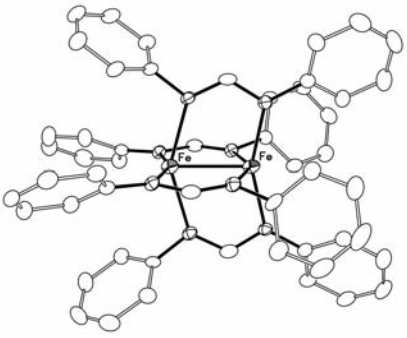
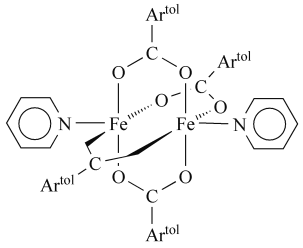


Fig. 11.3. The distorted tetragonal paddlewheel molecule in $Fe_2(DPhF)_4$.

Several compounds having two iron(II) atoms and carboxylate groups have been made.[6,7] Most of them have long Fe···Fe separations which are consistent with the absence of metal–metal bonding. There is a series of tetragonal paddlewheel compounds that have been made with four bulky, bridging carboxylate anions of the type O_2CAr^{tol}, where O_2CAr^{tol} is 2,6-di(*p*-tolyl)benzoate with pyridine-type ligands in axial positions. One compound, $Fe_2(O_2CAr^{tol})_4(4\text{-}Bu^t\text{-}py)_2$, has an Fe···Fe separation of 2.823(1) Å.[8] The compound **11.2** undergoes a reversible one-electron oxidation ($E_{1/2}$ = -0.216 V vs $FeCp_2^+/FeCp_2$ in CH_2Cl_2).[9] Chemical oxidation with Cp_2FePF_6 or $AgCF_3SO_3$ generates dark green solutions containing the $[Fe_2(O_2CAr^{tol})_4\text{-}(4\text{-}Bu^t\text{-}py)_2]^+$ cation. The pyridine and THF analogs are also known. The derivative $[Fe_2(O_2CAr^{tol})_4(4\text{-}Bu^t\text{-}py)_2](CF_3SO_3)$ has been structurally characterized. The Fe···Fe separation shortens relative to that of the precursor from 2.823(3) Å to 2.713(3) Å. Even though the iron–iron separation shrinks with the increase of charge, it is unlikely that metal–metal bonding is significant in these highly paramagnetic compounds.

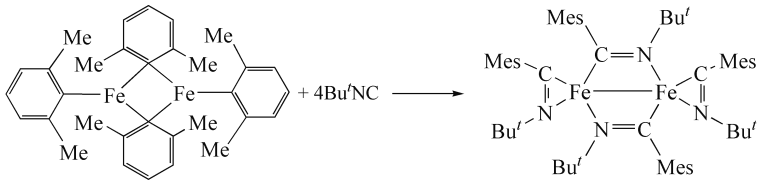


11.2

Finally there is a short Fe–Fe distance of 2.371(4) Å in the organometallic compound $\{\eta^2\text{-}C(Mes)=NBu^t\}_2Fe_2\{\mu\text{-}C(Mes)=NBu^t\}_2$, where Mes = 2,4,6-$Me_3C_6H_2$.[10] This is made ac-

Pictiva EX2004
Samsung v Pictiva
IPR2024-01094

cording to the equation below by insertion of the isonitrile Bu^{t}NC into a C–Fe bond in Fe_2Mes_4 which also has a relatively short iron–iron separation of 2.617(1) Å.[11] This type of compound falls outside the scope of this book and no further discussion will be provided.



11.3 Dicobalt Compounds

There are only a few dinuclear compounds with Co–Co bonds. These are of the classical paddlewheel type with four bridging ligands, and a few which have a trigonal paddlewheel structure. There are also some with unsupported metal–metal bonds.

11.3.1 Tetragonal paddlewheel compounds

The first authentic Co_2^{4+} paddlewheel complex that contains a Co–Co single bond is $Co_2[(p\text{-tol})_2N_3]_4$, in which the strong stabilizing effect of a triazenido ligand towards an M_2^{4+} unit is used to advantage.[12] This compound is prepared by the interaction of anhydrous $CoCl_2$ with $[(p\text{-tol})_2N_3]^-$ in THF at -78 ºC. This moisture-sensitive, diamagnetic complex has been structurally characterized as its bis-toluene solvate and shown to possess a very short Co–Co separation of 2.265(2) Å. A more efficient synthetic procedure for the preparation of the corresponding amidinate complexes appears to be the reaction of $CoCl_2(amidine)_2$ and methyllithium that gives highly pure paddlewheel complexes in good yield according to:

$$CoCl_2(amidine)_2 + 4LiMe \rightarrow Co_2(amidinate)_4 + 4LiCl + 4CH_4$$

This has been used to make the corresponding diphenylformamidinato and benzamidinato compounds $Co_2(DPhF)_4$ and $Co_2(DPhBz)_4$.[13] These two compounds cannot be made from anhydrous $CoCl_2$ as in the synthesis of $Co_2(DTolTA)_4$.

In solution, the red-brown tetra-bridged species are sensitive to the laboratory atmosphere giving solutions with deep blue color containing μ_4-oxotetracobalt species but crystals of the tetra-bridged compounds can be handled for a few days in air without noticeable decomposition. The Co–Co single bond distance in the formamidinate compound shown in Fig. 11.4 is 2.3735(7) Å and that of the benzamidinate analog is 2.302(1) Å.[14] The torsion angles in these diamagnetic compounds are in the range of 15.5 and 17°. The full pairing of the electrons in these d^7–d^7 complexes contrasts with the antiferromagnetic bis-quinoline adduct of $Co_2(O_2CPh)_4$ in which the non-bonded Co···Co separation is more than 2.8 Å.[15,16]

As shown in Table 11.1, there is a significant increase of the Co–Co distances with a Co_2^{4+} core in going from the DTolTA to the DPhBz to the DPhF compound, a pattern similar to that in the corresponding dirhodium compounds (see Chapter 12). Theoretical calculations indicate that these changes are probably due to geometric constraints imposed by the ligands, but other factors, such as the basicity of the ligand set, cannot be ruled out. An early Xα-SW calculation[17] on the model species $Co_2(HNNNH)_4$ failed to predict the expected $\sigma^2\pi^4\delta^2\delta^{*2}\pi^{*4}$ configuration that would be consistent with the diamagnetism of the molecules and a single σ bond between the cobalt atoms. However, later calculations using configuration interaction (CI) methods correctly predict different Co–Co distances for the three known $Co_2(amidinato)_4$ compounds. The results of the calculations show that the single bond configuration $\sigma^2\sigma^{*0}$ is

Pictiva EX2004
Samsung v Pictiva
IPR2024-01094

always the leading term in the CI wavefunction of the ground state for each compound. Therefore, it is justified to assign a single σ bond between the metal atoms in all these compounds and an overall electronic configuration of $\sigma^2\pi^4\delta^2\delta^{*2}\pi^{*4}$.

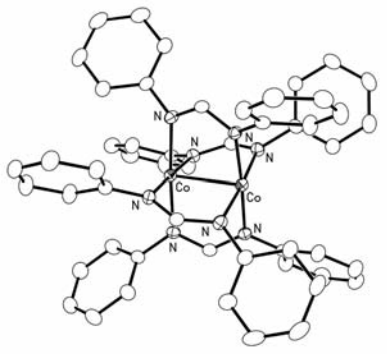


Fig. 11.4. The structure of $Co_2(DPhF)_4$. The molecule resides on a crystallographic two-fold axis that passes through the midpoint of the Co–Co single bond.

Table 11.1. Structural data for dicobalt compounds

Compound	r(Co–Co)[a] (Å)	core	ref.
$Co_2(DTolTA)_4 \cdot 2C_6H_5Me$	2.265(2)	Co_2^{4+}	12
$Co_2(DPhBz)_4$	2.302(1)	Co_2^{4+}	14
$Co_2(DPhF)_4$	2.374(1)	Co_2^{4+}	13
$[Co_2(DPhBz)_4]PF_6 \cdot 2.4CH_2Cl_2$[b]	2.322(2) 2.332(2)	Co_2^{5+}	13
$Co_2(DPhF)_3$	2.385(1)	Co_2^{3+}	18,19
$Co_2(DPhBz)_3$	2.320(1)	Co_2^{3+}	19
$Ba_3[Co_2(CN)_{10}] \cdot 13H_2O$[c]	2.798(2) 2.794(2)	Co_2^{4+}	20,21
$[Co_2(CNCH_3)_{10}](ClO_4)_4$	2.74(1)	Co_2^{4+}	22

[a] Distances are given with up to 3 decimal digits.
[b] Two independent molecules.
[c] Two independent determinations.

Electrochemical studies of $Co_2(DPhBz)_4$ in CH_2Cl_2 solution reveal the existence of two reversible one-electron oxidation waves ($E_{1/2}$ of 0.29 and 1.45 V vs SCE) and one quasi-reversible reduction which has been assigned to a Co_2^{3+} species. Bulk controlled-potential electrolysis of $Co_2(DPhBz)_4$ at 0.50 V in CH_2Cl_2 using Bu_4NPF_6 as electrolyte revealed that one electron per molecule is involved in the first oxidation. The EPR spectrum of an electrochemically generated (but not fully characterized) reduced species formulated as containing the anion $[Co_2(DPhBz)_4]^-$ gives an axial signal with $g_\perp$ of 2.26 and $g_\parallel$ of 2.01. The $g_\parallel$ is split into 15 equally spaced lines.

An EPR spectrum of the oxidized $[Co_2(DPhBz)_4]^+$ cationic species shows a signal at $g = 1.98$ (g_3) split into 15 equally spaced lines by the two ^{59}Co ions ($I = {}^7/_2$, 100% abundance). The $g_\perp$, or possibly the g_1 and g_2 signals, is complex and overlaps with a portion of the g_3 signal. The splitting of the g_3 is consistent with the odd-electron spin density being localized on both cobalt atoms. The oxidized form has been crystallographically characterized in

Pictiva EX2004
Samsung v Pictiva
IPR2024-01094

$[Co_2(DPhBz)_4]PF_6{\cdot}2.4CH_2Cl_2$. Two independent molecules in the crystal give metal–metal separations of 2.322(2) and 2.332(2) Å which are slightly longer than those in the neutral molecule (2.302(1) Å). This is of course counter-intuitive if one thinks that the elimination of an electron in an antibonding orbital should increase the bond order from 1 to 1.5. Theoretical calculations showed that upon oxidation the ground state is $^2B_{1u}$ and the $\sigma^2\delta^{*1}$configuration is the dominant configuration in the CI wavefunction. Because the electron is being removed from a δ^* orbital, it has a negligible effect on the length of the metal–metal bond and the intermetallic repulsion due to the increase on the charge in the metal atoms appears to dominate.

11.3.2 Trigonal paddlewheel compounds

Compounds with Co_2^{3+} cores have been crystallographically characterized also but the structures do not correspond to the proposed tetra-bridged $[Co_2(DPhBz)_4]^-$ anion mentioned above. Instead these are similar to those of iron discussed in Section 11.2. There are only three bridging amidinato ligands spanning the dicobalt core which gives a trigonal paddlewheel or trigonal lantern structure. The first such compound $Co_2(DPhF)_3$, shown in Fig. 11.5, is prepared in low yield by reaction of $CoCl_2(HDPhF)_2$ and Bu^nLi.[18] The yield is improved to 63% by addition of the reducing agent $NaEt_3BH$ before adding butyllithium:[19]

$$2CoCl_2(HDPhF)_2 + NaEt_3BH \xrightarrow{4LiBu} Co_2(DPhF)_3 + 3LiCl + NaCl + LiDPhF + \tfrac{1}{2}H_2 + BEt_3 + 3BuH$$

In this manner a benzamidinate analog has also been prepared.

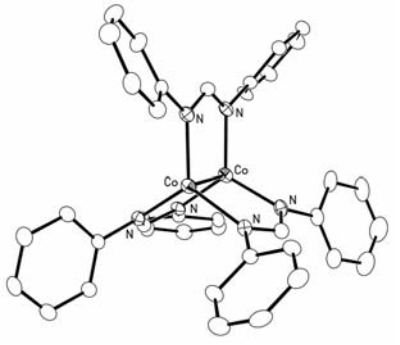


Fig. 11.5. The structure of $Co_2(DPhF)_3$ showing the idealized D_{3h} symmetry.

The Co–Co distances are 2.385(1) Å for $Co_2(DPhF)_3$ and 2.3201(9) Å for $Co_2(DPhBz)_3$. The core of the molecules comes very close to having D_{3h} symmmetry. The three N–Co–Co–N torsion angles have an average of only *c.* 4° and the dihedral angles between ligand planes lie in the range of 115 to 127°. It should be noted that in $Fe_2(DPhF)_3$ there is a clear deviation from three-fold symmetry but this was attributed to packing forces (see Section 11.2). The corresponding cobalt analog is not isostructural and the molecules pack in such a way that no marked distortion is engendered. The room temperature magnetic susceptibilities of the compounds with the Co_2^{3+} cores are consistent with an electronic ground state having $S = {}^3/_2$ with a very low-lying $S = {}^5/_2$ state.

The large difference in the M–M bond lengths in the $M_2(amidinato)_3$ compounds with Fe–Fe distances of 2.232(1) and 2.198(2) Å and Co–Co distances of 2.385(1) and 2.320(1) Å for the formamidinato and benzamidinato derivatives is quite remarkable. A study of the electronic structure of the iron compounds (see Section 11.2) leads to the expectation that the two additional electrons in the cobalt analog should occupy π^* orbitals which then become fully

Pictiva EX2004
Samsung v Pictiva
IPR2024-01094

occupied (Fig. 11.2), leading to an electronic configuration $\sigma^2\pi^2\pi^2\pi^{*2}\pi^{*2}\sigma^{*1}\delta^1\delta^1\delta^{*1}\delta^{*1}$. As shown schematically in Fig. 11.6, the σ* (4a'') orbitals, the doubly degenerate δ orbitals, (7e'), and the corresponding δ* antibonding orbitals are all singly occupied. Thus, there are five unpaired electrons in these $Co_2(amidinate)_3$ compounds, and a bond order of 0.5

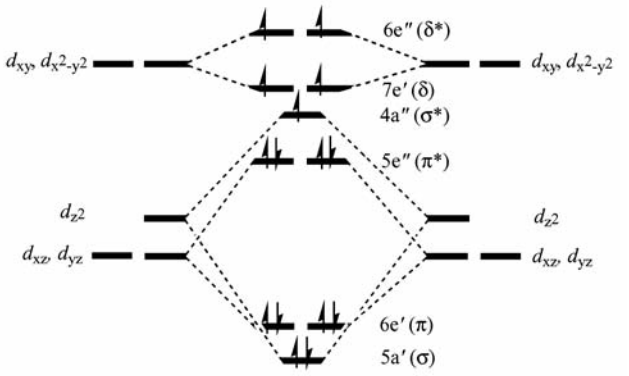


Fig. 11.6. A schematic electron distribution for trigonal paddlewheel molecules with Co_2^{3+} cores. Data are from ref. 3.

11.3.3 Dicobalt compounds with unsupported bonds

An air-stable ruby-red compound of the dinuclear anion $[Co_2(CN)_{10}]^{6-}$ has been prepared and characterized as the barium salt $Ba_3[Co_2(CN)_{10}]\cdot 13H_2O$. The crystal structure, done by two independent research groups, is shown in Fig. 11.7. The Co_2^{4+} unit lies on a crystallographic two-fold axis which bisects the Co–Co bond of 2.798(2) Å according to one group[20] or 2.794(2) Å in the other determination.[21] The four equatorial groups are tilted slightly towards the Co–Co unit. The $[Co(CN)_5]^{3-}$ groups are rotated 4.5° relative to one another about the Co–Co bond from an ideal D_{4d} geometry. The five independent Co–N bond lengths are equal within experimental error and average 2.151(4) Å. The barium cations, $[Co_2(CN)_{10}]^{6-}$ anions, and several water molecules are linked by several types of coordination bridges to give a very tight and cross-linked three-dimensional array which presumably explains the unusual stability towards oxidation.

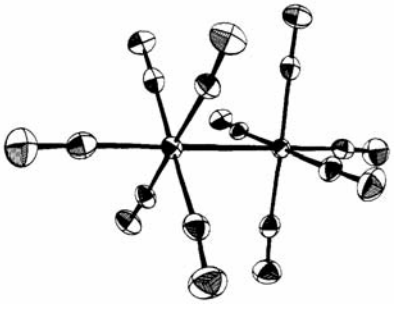


Fig. 11.7. The $[Co_2(CN)_{10}]^{6-}$ anion with an unsupported Co–Co bond.

Pictiva EX2004
Samsung v Pictiva
IPR2024-01094

A similar compound, $[Co_2(CNCH_3)_{10}](ClO_4)_4$, contains stronger π-acceptor ligands and $[Co_2(CNCH_3)_{10}]^{4+}$ cations.[22] In the solid state this is red and diamagnetic. The monomer $[Co(CNCH_3)_5](ClO_4)_2$ has also been isolated; this is green and paramagnetic. The two forms are present in solution. The Co–Co distance in the dimer is 2.74(1) Å. Perhaps the best known compound with an unsupported Co–Co bond is $Co_2(CO)_8$. Because these compounds contain π-donor ligands, they fall out of the scope of this book and no further discussion will be provided.

11.3.4 Compounds with chains of cobalt atoms

Many compounds are known to contain extended metal atom chains of three and five Co atoms in which metal–metal bonding exists. These are presented in Chapter 15.

11.4 Di-iridium Compounds

Dinuclear paddlewheel-type complexes with elements of the third transition series from tungsten to platinum are relatively well-known, an exception being iridium. These complexes typically have two metal atoms linked by four bridging ligands; some have axial ligands also. Depending on the electronic configuration of the metal atoms and the type of ligands, metal–metal bond orders can vary from 0.5 to 4. For the lighter congener rhodium (Chapter 12), there are many compounds containing a Rh_2^{4+} core with four monoanionic bridging ligands and a single metal–metal bond consistent with a $\sigma^2\pi^4\delta^2\delta^{*2}\pi^{*4}$ electronic configuration.

For iridium the number of such compounds is far smaller. Earlier work provided the first examples of metal–metal bonded compounds of other than the paddlewheel types. The di-iridium(I) compound $(Ph_3P)(CO)Ir(\mu\text{-}PPh_2)_2Ir(CO)(PPh_3)$[23,24] was the first one to be formulated as containing an Ir–Ir double bond on the basis of the short Ir–Ir bond distance (*c.* 2.55 Å) and adherence to the EAN rule. However, this bond-order, bond-length correlation remains suspect in view of the propensity of $\mu\text{-}PR_2$ ligands to favor short metal–metal contacts. Subsequently, other di-iridium compounds that are believed to contain Ir–Ir multiple bonds have been prepared and characterized, but few possess structures of the L_4MML_4 or L_5MML_5 types. In this chapter we consider only the latter type and some closely related species. Others, mainly organometallic compounds, are not considered in detail as they remain outside of the main thrust of this monograph.

11.4.1 Paddlewheel compounds and related species

The one example of a di-iridium complex with an Ir_2^{4+} core and four identical monoanionic bridging ligands is the green formamidinate derivative $Ir_2(DTolF)_4$, which is prepared[25] in small yields by the reaction between $(COD)Ir(\mu\text{-}DTolF)_2Ir(O_2CCF_3)_2(H_2O)$, where DTolF = $[(p\text{-tolN})_2CH]^-$ and COD = 1,5-cyclo-octadiene, and 2 equiv of HDTolF in toluene. It is isostructural with its dirhodium analog (see Section 12.3.3) and has an Ir–Ir distance of 2.524(3) Å as shown in Table 11.2.

Table 11.2. Structural data for di-iridium compounds

Compound[a]	r(Ir–Ir)[a] (Å)	r(Ir–L)[b] (Å)	core	ref.
$Ir_2(DTolF)_4$	2.524(3)		Ir_2^{4+}	25
$[Ir_2(\mu\text{-}NC_5H_4)_2(\mu\text{-}DTolF)_2(py)_2(CH_3CN)_2]BPh_4{\cdot}2CH_3CN$	2.518(1)	2.13[1]	Ir_2^{4+}	27
$[Ir_2(\mu\text{-}DTolF)_2(CH_3CN)_6](BF_4)_2$	2.601(1)	2.18[2]	Ir_2^{4+}	28
$[Ir_2(\mu\text{-}DAniF)_2(CH_3CN)_6](BF_4)_2{\cdot}2CH_3CN$	2.602(1)	2.209(5)	Ir_2^{4+}	29
$Ir_2(\mu\text{-}DAniF)_4(\eta^1\text{-}O_2CCF_3){\cdot}2CH_2Cl_2$	2.507(1)	2.139(8)	Ir_2^{5+}	29

Pictiva EX2004
Samsung v Pictiva
IPR2024-01094

Compound[a]	r(Ir–Ir)[a] (Å)	r(Ir–L)[b] (Å)	core	ref.
$Ir_2(\mu\text{-}D^{Cl}PhF)_4(\eta^1\text{-}O_2CCF_3)\cdot 2CH_2Cl_2$	2.513(1)	2.16(2)	Ir_2^{5+}	29
$Ir_2(hpp)_4Cl_2$	2.495(1)	2.643[6]	Ir_2^{6+}	30
$Ir_2(pc^{2-})_2(py)_2$	2.707(1)	2.32[2]	Ir_2^{4+}	32
$Ir_2(tfepma)_2Cl_2(CH_3CN)_2$	2.753(1)	2.433[1]	Ir_2^{4+}	31

[a] Distances are given with up to 3 decimal digits.

[b] In some cases the average Ir–L bond lengths are quoted. In these instances the estimated derivation, which is given in square brackets, is calculated as $[\ ] = [\sum_n \Delta_i^2/n/(n-1)]^{1/2}$, in which Δ_i is the derivation of the ith of n values from the arithmetic mean of the set.

This chemistry was developed following the discovery[26] that the reaction between the di-iridium(I) compound $Ir_2(\mu\text{-DTolF})_2(COD)_2$ and 2 equiv of AgO_2CCF_3 produces the unusual complex $(COD)Ir(\mu\text{-DTolF})_2Ir(O_2CCF_3)_2(H_2O)$ in which there is an $Ir^I \rightarrow Ir^{III}$ dative bond. The Ir^{III} center contains two monodentate trifluoroacetate ligands, and an axial water molecule that can be displaced easily by other donor ligands (e.g., DMSO, py, and CH_3CN). The Ir–Ir distance in the dark-red pyridine adduct is quite short (2.774(1) Å). The reaction that produces $(COD)Ir(\mu\text{-DTolF})_2Ir(O_2CCF_3)_2(py)$ can also give the complex $[Ir_2(\mu\text{-}NC_5H_4)_2(\mu\text{-DTolF})(py)_4]O_2CCF_3\cdot py$, which results from orthometalation of two pyridine ligands.[27] A metathesis reaction of this complex with $NaBPh_4$ in acetonitrile has been used to prepare $[Ir_2(\mu\text{-}NC_5H_4)_2(\mu\text{-DTolF})(py)_2(NCCH_3)_2]BPh_4\cdot 2CH_3CN$ in which two acetonitrile ligands occupy the axial sites. The Ir–Ir distance in the latter compound is 2.518(1) Å. The X-ray crystal structure determination of this di-iridium species (Fig. 11.8) was not able to distinguish between a head-to-head and head-to-tail arrangement of the two orthometalated pyridine ligands.

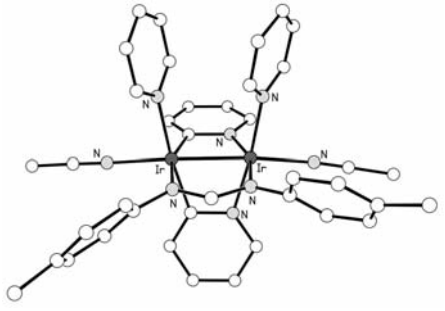


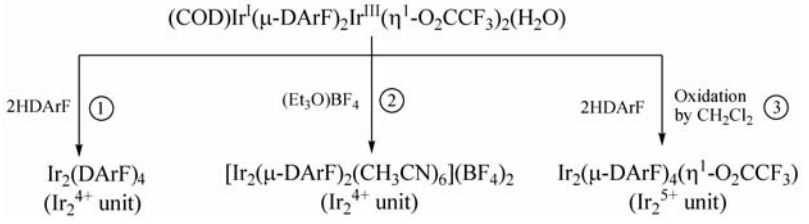
Fig. 11.8. The $[Ir_2(\mu\text{-}NC_5H_4)_2(\mu\text{-DTolF})(py)_2(NCCH_3)_2]^+$ cation.

When the mixed-valent compound with the $Ir^I \rightarrow Ir^{III}$ dative bond is allowed to react with $(Et_3O)BF_4$ in acetonitrile, the compound $[cis\text{-}Ir_2(DTolF)_2(MeCN)_6](BF_4)_2$ forms.[28] Since the number of bridging ligands is only two, the Ir–Ir distance of 2.601(1) Å is longer than the distance in compounds with four bridging ligands. The cyclic voltammogram reveals an irreversible reduction and a reversible oxidation wave with the $E_{1/2}$ of the latter at +0.77 V vs Ag/AgCl. Analogs containing *N,N'*-di-*p*-anisylformamidinato (DAniF) and *N,N'*-di-*p*-chlorophenylformamidinato ($D^{Cl}PhF$) ligands have been made.[29] The former has been characterized by X-ray crystallography and has an Ir–Ir distance of 2.6019(4) Å (see Table 11.2).

In the presence of trifluoroacetate anions, these Ir_2^{4+} species react with chlorinated solvents such as CH_2Cl_2 to give compounds of the type $Ir_2(\mu\text{-DArF})_4(\eta^1\text{-}O_2CCF_3)$. The metal–metal distances of these Ir_2^{5+} compounds are 2.507(1) and 2.513(1) Å for the DAniF and $D^{Cl}PhF$

Pictiva EX2004
Samsung v Pictiva
IPR2024-01094

derivatives, respectively. The structure of the *p*-anisyl derivative given in Fig. 11.9 shows that only one of the two axial sites is occupied by an oxygen atom of the triflate anion. The EPR spectrum of $Ir_2(\mu\text{-DAniF})_4(\eta^1\text{-}O_2CCF_3)$ in frozen CH_2Cl_2 solution at -100 °C is consistent with the presence of an unpaired electron; it shows a ground state of $S = {}^1/_2$ with a g_{iso} of 2.14. The preparations of these compounds from the $Ir^I \rightarrow Ir^{III}$ precursor are summarized in the following chart:



There is also a compound with an Ir_2^{6+} core which does not have precedent in the chemistry of rhodium. This is the guanidinate compound $Ir_2(hpp)_2Cl_2$ where hpp is the anion of 1,3,4,6,7,8-hexahydro-2*H*-pyrimido[1,2-*a*]pyrimidate. The compound has a paddlewheel structure with four bridging hpp ligands and two axial chlorine atoms and a short Ir–Ir distance of 2.495(1) Å.[30] It is paramagnetic with two unpaired electrons.

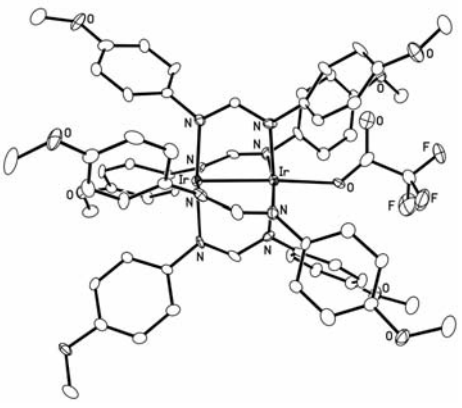


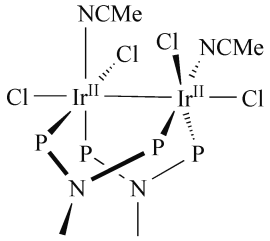
Fig. 11.9. The structure of $Ir_2(\mu\text{-DAniF})_4(\eta^1\text{-}O_2CCF_3)$.

As listed in Table 11.2, the Ir–Ir distances of the paddlewheel compounds with all-nitrogen donor ligands decrease slightly as the charge in the Ir_2 core increases. This variation is consistent with the change from a single bond in the Ir_2^{4+} unit to a formal bond order of 1.5 in Ir_2^{5+} to a double bond in Ir_2^{6+}. Unfortunately it is hard to make stronger correlations because there are not enough structurally characterized compounds to make comparisons and one cannot rule out that this correlation might be fortuitous. Therefore it is hard to tell the precise electronic configuration of these Ir_2^{n+} cores solely on the basis of their structures without comprehensive theoretical calculations that are still lacking. However, the limited magnetic data are consistent with the electronic configurations $\sigma^2\pi^4\delta^2\delta^{*2}\pi^{*4}$, $\sigma^2\pi^4\delta^2\delta^{*2}\pi^{*3}$ and $\sigma^2\pi^4\delta^2\delta^{*2}\pi^{*2}$ for $n = 4$, 5 and 6, respectively.

A large number of di-iridium compounds have mixed-valence cores stabilized by diphosphazane ligands of the type tfepma (tfepma is the neutral molecule bis(bis(trifluoro-

Pictiva EX2004
Samsung v Pictiva
IPR2024-01094

ethoxy)phosphino)methylamine, $MeN[P(OCH_2CF_3)_2]_2$).[31] The precursor $Ir_2(tfepma)_3Cl_2$ has a core with Ir^0 and Ir^{II} centers. These react with $PhICl_2$ in CH_2Cl_2 to give Ir^I/Ir^{III} compounds which upon heating with an excess of $PhICl_2$ in CH_3CN give complexes such as **11.3** which has two bridging tfepma groups and two Ir^{II} atoms with a long Ir–Ir distance of 2.752(1) Å.



11.3

11.4.2 Unsupported Ir–Ir bonds

Controlled thermal decomposition of di(acido)phthalocyaninatoiridates in an inert, high-boiling solvent such as 1-chloronaphthalene or under reduced pressure at a temperature of less than 350 °C produces a blue, diamagnetic di(iridiumphthalocyaninate(2-)), $(Irpc^{2-})_2$.[32] This is soluble in pyridine yielding a blue-violet, diamagnetic compound of composition $Ir_2(pc^{2-})_2(py)_2$. This is a dimeric compound with an Ir–Ir distance of 2.707(1) Å. Each Ir atom is surrounded by a phthalocyaninato dianion and a pyridine molecule occupying the axial position. A differential pulse voltammogram shows four quasi-reversible one electron transfer processes at -1.34, -0.82, 0.55 and 0.82 V. The process at 0.55 V is assigned to the redox couple $\{Ir_2(pc^{2-})_2(py)_2/[Ir_2(pc^{2-})(pc^{-})(py)_2]^+$ by comparison to the electronic spectrum of the product of oxidation by iodine. The Ir–Ir stretching vibration at 135 cm^{-1} is selectively enhanced in the FT-Raman spectrum.

A compound that bears a close relationship is the di-iridium(II)octaethylporphyrin dimer $[Ir(OEP)]_2$. While this has not been structurally characterized, it almost certainly possesses an unsupported Ir–Ir single bond. It is prepared by the photolysis of $Ir(OEP)CH_3$ in C_6D_6[33] but an improved and convenient synthesis uses the reaction of M(OEP)H, M = Ir and Rh, with 2,2,6,6-tetramethyl-1-piperdinoxy (TEMPO):[34]

$$2M(OEP)H + 2TEMPO \rightarrow M_2(OEP)_2 + 2TEMPOH$$

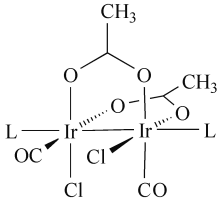
The iridium compound reacts[35] in a similar fashion to its dirhodium(II) analog (Section 12.4.3) including alkene insertion and the oxidative addition of alkyl C–H bonds. These reactions probably proceed through the intermediacy of the metalloradical $[Ir(OEP)]^{\bullet}$ which is formed by homolytic dissociation of the Ir–Ir bond.

An early example that might have an unsupported Ir–Ir bond is the Ir_2^{4+} complex $Ir_2(Tcbiim)_2(CO)_4(NCCH_3)_2$ (Tcbiim is the dianion of tetracyanobisimidazole) whose isolation was reported[36] in 1985. It is prepared by the electrolysis of salts of the mononuclear iridium(I) species $[Ir(CO)_2(Tcbiim)]^-$ in acetonitrile at a Pt anode. While the structure of this compound has not been determined, it can be derivatized by reaction with $P(OEt)_3$ to give $Ir_2(Tcbiim)_2(CO)_2(NCCH_3)_2[P(OEt)_3]_2$, a compound with an unsupported Ir–Ir bond and a linear P–Ir–Ir–P unit. The Ir–Ir distance is 2.826(2) Å. The equatorial plane about each iridium atom contains *cis* sets of CO and CH_3CN ligands; there is staggered rotation geometry with a C–Ir–Ir–C torsional angle of 44.4°.

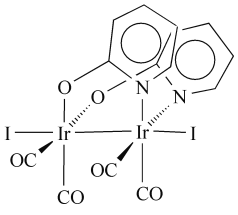
Pictiva EX2004
Samsung v Pictiva
IPR2024-01094

11.4.3 Other species with Ir–Ir bonds

In addition to the structurally characterized complex $Ir_2(Tcbiim)_2(CO)_2(NCCH_3)_2[P(OEt_3)_2]_2$ mentioned at the end of the previous section, there are several other di-iridium(II) compounds that contain carbonyl ligands. Recent examples are those of the type **11.4** which has two *cis* bridging acetate groups, one chloride ion and a carbonyl group at the equatorial position of each iridium atom. Solvent molecules such as CH_3CN, DMSO, pyridine and 4-isopropylpyridine (4-Pr^{i}py) can occupy axial positions.[37] The first three compounds have moderately short Ir–Ir distances of 2.569(1), 2.5980(5) and 2.5918(5) Å, respectively. These have the formula $[Ir_2(\mu\text{-}O_2CCH_3)_2Cl_2(CO)_2L_2]$ and they are prepared by a one-step reaction of H_2IrCl_6 with lithium acetate in the presence of O_2 and a mixture of acetic acid and acetic anhydride. Compounds where L = PPh_3, PCy_3, $P(OPh)_3$, $AsPh_3$ and $SbPh_3$ have slightly longer Ir–Ir distances in the range 2.620(1)-2.694(1) Å.[38] Cyclic voltammograms show a one-electron quasi-reversible oxidation wave. Electrolytic or radiolytic one-electron oxidations of the py and 4-Pr^{i}py compounds give cationic radicals, which show pseudo-axially symmetric EPR spectra suggesting that the odd electron is in the δ_{IrIr}* orbital. A somewhat related compound is the α-pyridonate-bridged (hp) **11.5** which has the formula $HH\text{-}Ir_2(hp)_2(CO)_4I_2$. In this compound the pyridonate (2-hydroxypyridinate) ligands are *cis* and in a head-to-head arrangement.[39] The Ir–Ir distances in two crystallographically independent molecules are 2.643(1) and 2.635(1) Å.



11.4



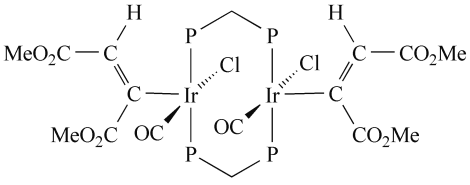
11.5

The reaction of $Ir_2Cl_2(CO)_2(\mu\text{-dppm})_2$ with H_2 affords the dihydrido complex $Ir_2H_2Cl_2(CO)_2(\mu\text{-dppm})_2$ in which the hydrido ligands are believed to be mutually *cis* on adjacent metal atoms.[40] This complex reacts with 1 equiv of $MeO_2CC{\equiv}CCO_2Me$ to give $Ir_2HCl_2(\eta^1\text{-}MeO_2CC{=}CHCO_2Me)(CO)_2(\mu\text{-dppm})_2$ in which alkyne insertion into one of the Ir–H bonds has occurred. A double alkyne insertion occurs upon reacting $MeO_2CC{\equiv}CCO_2Me$ with $[Ir_2H_2C1(CO)_2(\mu\text{-dppm})_2]BF_4$ in dichloromethane; a major product is the di-iridium(II) complex $Ir_2Cl_2(MeO_2CC{=}CHCO_2Me)_2(CO)_2(\mu\text{-dppm})_2$. This compound has the structure depicted in **11.6** with a very long Ir–Ir separation (3.013(1) Å and 3.022(1) Å for the two crystallographically independent molecules within the asymmetric unit). These long separations have been attributed to steric crowding about the Ir atoms in a molecule in which there is an eclipsed rotational geometry.

Another carbonyl-containing di-iridium complex that has been structurally characterized is the tetracarbonyl derivative $Ir_2(\mu\text{-pyS})_2(CH_2I)I(CO)_4$, where pyS is the monanion of 2-mercaptopyridine.[41] It is prepared by the oxidative-addition reaction of CH_2I_2 with $Ir_2(\mu\text{-pyS})_2(CO)_4$ at room temperature upon exposure to direct sunlight or irradiation with a 150 W incandescent lamp. Similar reactions occur with I_2 and with CH_3I to give $Ir_2(\mu\text{-pyS})_2I_2(CO)_4$ and $Ir_2(\mu\text{-pyS})_2(CH_3)I(CO)_4$, respectively. The lability of the iodide ligand in $Ir_2(\mu\text{-pyS})_2(CH_2I)I(CO)_4$ has been demonstrated by the preparation of $Ir_2(\mu\text{-pyS})_2(CH_2I)X(CO)_4$ (X = C1 or Br). The structure of $Ir_2(\mu\text{-pyS})_2(CH_2I)I(CO)_4$, which has been determined by X-ray crystallography, is

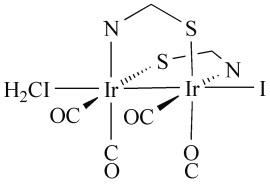
Pictiva EX2004
Samsung v Pictiva
IPR2024-01094

depicted in **11.7**; there is a cisoid head-to-tail arrangement of pyS ligands and a relatively short Ir–Ir distance (2.695(2) Å).



11.6

Just as iodine oxidatively adds to $Ir_2(\mu\text{-}pyS)_2(CO)_4$ upon exposure to sunlight to give $Ir_2(\mu\text{-}pyS)_2I_2(CO)_4$, a similar reaction of a dichloromethane solution of $Ir_2(\mu\text{-}C_7H_4NS_2)_2(CO)_4$, where $C_7H_4NS_2$ is the benzothiazole-2-thiolate anion, affords $Ir_2(\mu\text{-}C_7H_4NS_2)_2I_2(CO)_4$.[42] Its structure is similar to **11.7** with an Ir–Ir single bond length of 2.676(2) Å. If the reaction with I_2 is carried out in toluene the intermediate tetranuclear cluster $Ir_4(\mu\text{-}C_7H_4NS_2)_4I_2(CO)_8$ can be isolated (see Section 11.4.4). The tetranuclear complex reacts rapidly with another equivalent of I_2 in dichloromethane by a light-assisted step to give the dinuclear species $Ir_2(\mu\text{-}C_7H_4NS_2)_2I_2(CO)_4$; this conversion also involves a switch in the coordination mode of the pairs of benzothiazole-2-thiolate ligands from a head-to-head to a head-to-tail arrangement. A relevant review on controlling the molecular architecture of low nuclearity rhodium and iridium complexes using bridging N–C–X (X = N, O, S) ligands has appeared.[43]



11.7

A few di-iridium(II) complexes that contain the 2,5-di-isocyano-2,5-dimethylhexane ligand (abbreviated TMB) have been prepared and characterized. The compounds $[Ir_2(TMB)_4X_2](BPh_4)_2$ (X = Cl, Br or I) are prepared by titrating acetonitrile solutions of the di-iridium(I) compounds $[Ir_2(TMB)_4](BPh_4)_2$ with X_2.[44,45] The X-ray structure of crystals of composition $[Ir_2(TMB)_4I_2](BPh_4)_2{\cdot}1.5(CH_3)_2CO$ shows this compound to be isostructural with its rhodium analog $[Rh_2(TMB)_4Cl_2](PF_6)_2$; the Ir–Ir distance is 2.803(4) Å and the C–Ir–Ir–C torsion angle is 31°, values that are close to those of 2.770(3) Å and 33°, respectively, which have been determined for the dirhodium analog. Evidence for the interconversion of Δ- and Λ-type enantiomers has been obtained from ^{1}H NMR spectroscopy, while detailed studies have been made of the vibrational and electronic absorption spectral properties of the $[Ir_2(TMB)_4X_2]^{2+}$ cations. When solutions that contain the di-iridium(I) cation $[Ir_2(TMB)_4]^{2+}$ are irradiated in the presence of hydrogen atom donors such as 1,4-cyclohexadiene, the dihydrido species $[Ir_2(TMB)_4H_2]^{2+}$ is generated; this can be isolated as its crystalline BPh_4^- salt.[46] A structure determination on a crystal of $[Ir_2(TMB)_4H_2](BPh_4)_2{\cdot}C_7H_8$ showed a close structural relationship to that of the di-iodo derivative but with a Ir–Ir distance (2.920(2) Å) that was longer by *c.* 0.1 Å than that of $[Ir_2(TMB)_4I_2]^{2+}$ although the rotational geometries are very similar. The linear H–Ir–Ir–H unit is characterized by ν(Ir–H) and ν(Ir–Ir) vibrational frequencies of 1940 and 136 cm^{-1},

Pictiva EX2004
Samsung v Pictiva
IPR2024-01094

respectively; the Raman-active ν(Ir–Ir) mode in the spectra of the chloride, bromide, and iodide complexes decreases from 140 to 128 to 116 cm^{-1}.

While an assortment of other compounds that contain Ir–Ir single bonds are well documented, these do not possess the structural features that accord with the theme of this chapter. Examples include such structurally characterized complexes as (COD)IIr(μ-I)$_2$IrI(COD)[47] and (COD)ClIr(μ-SPh)$_2$IrCl(COD),[48] where COD = 1,5-cyclo-octadiene, which possess Ir–Ir distances of 2.914(1) and 2.800(1) Å, respectively, but with each Ir center exhibiting an approximately square-pyramidal metal–ligand coordination sphere. In other instances no Ir–Ir bond whatsoever may exist in di-iridium(II) complexes. Such an example is encountered in the case of $Ir_2\{\mu\text{-}1,8\text{-}(NH)_2C_{10}H_6\}(\mu\text{-}CH_2)I_2(CO)_2)PPh_3)_2$ in which the Ir···Ir separation is 3.0306(4) Å.[49] The absence of an Ir–Ir bond accords with the EAN rule.

11.4.4 Iridium blues

These compounds are named after the family of deeply colored platinum compounds known as platinum blues (Section 14.4.7). The term *blue* has been used to describe a class of compounds, independent of their color, that are mainly tetrametallic (or a multiple thereof) chains with at least one unsupported metal–metal bond, in which the metal atoms possess nonintegral oxidation numbers. For iridium (and also rhodium), most of the work has been done by the groups of Ciriano and Oro in Zaragoza and has been reviewed.[50]

In dichloromethane solution, iodine oxidatively adds to $Ir_2(\mu\text{-}C_7H_4NS_2)_2(CO)_4$, where $C_7H_4NS_2$ is the benzothiazole-2-thiolate anion, to afford $Ir_2(\mu\text{-}C_7H_4NS_2)_2I_2(CO)_4$. If the reaction with I_2 is carried out in toluene the intermediate tetranuclear cluster $Ir_4(\mu\text{-}C_7H_4NS_2)_4I_2(CO)_8$ can be isolated. Its structure is shown in Fig. 11.10 and reveals that the outer Ir–Ir bonds are shorter than the inner, unsupported Ir–Ir bond (2.73l(2) Å versus 2.828(2) Å). The bridging benzothiazole-2-thiolate ligands are bound in a head-to-head fashion. Structurally this diamagnetic complex resembles the linear tetranuclear species $[Rh_4(1,3\text{-di-isocyanopropane})_8Cl]^{5+}$ (see Section 12.4.3) and certain platinum blues. It can be considered to arise from the coupling of two radical species $[Ir_2(\mu\text{-}C_7H_4NS_2)_2I(CO)_4]^{\bullet}$. This tetranuclear dichroic (black, golden-green) compound shows all the characteristics of the platinum blues (four metal atoms with an average fractional oxidation number of 1.5 and bound by an unsupported metal–metal bond).

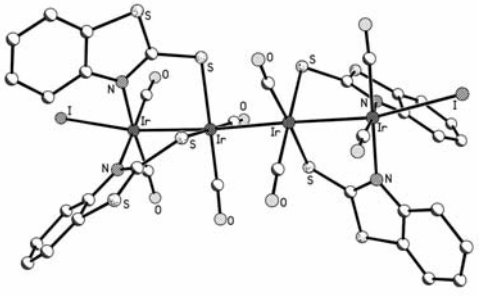


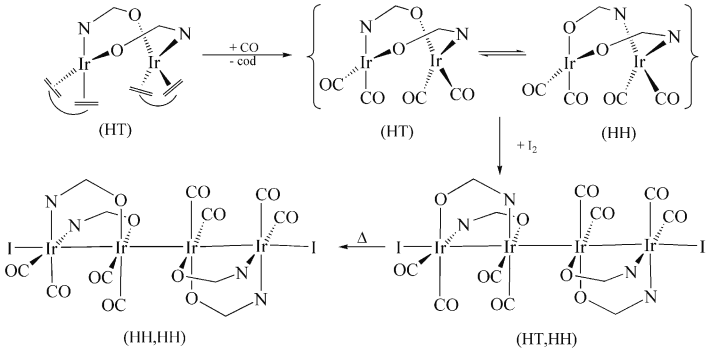
Fig. 11.10. The structure of the linear molecule in *iridium blue* $Ir_4(\mu\text{-}C_7H_4NS_2)_4I_2(CO)_8$.

Bright purple, EPR silent solutions are obtained by mixing the pyrazolyl (pz) compounds $Ir_2(pz)_2(CNBu^t)_4$ and $[Ir_2(pz)_2(CNBu^t)_4(CH_3CN)_2]PF_6$ of which there are also rhodium analogs. Oxidation of $Ir_2(pz)_2(CNBu^t)_4$ with iodine (in a 1:1 molar ratio) in acetonitrile yields a neutral red complex $[Ir_2(pz)_2(I)_2(CNBu^t)_4]_2$.[51] This tetranuclear complex has iodine atoms at each of the

Pictiva EX2004
Samsung v Pictiva
IPR2024-01094

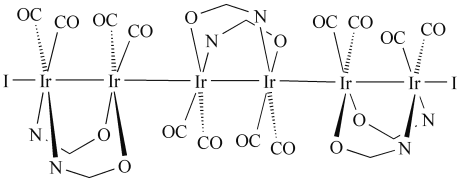
axial positions. The outer Ir–Ir distances of 2.727(1) Å are crystallographically equivalent and the inner Ir–Ir distance of 2.804(1) Å is significantly longer than the outer distances.

Other iridium blues have been made using α-pyridonate (hp) bridging ligands according to the sequence:[52]



The precursor is the head-to-tail $Ir_2(hp)_2(COD)_2$ complex which upon carbonylation gives a mixture of head-to-head and head-to-tail $Ir_2(hp)_2(CO)_4$. Upon oxidation with iodine below 0 °C the unusual HT,HH-$[Ir_2(hp)_2(I)(CO)_4]_2$ iridium blue forms in 75% yield; it has an average oxidation number of 1.5+ per iridium atom. The outer Ir–Ir distances are 2.692 and 2.711(1) Å and the inner and unsupported Ir–Ir distance is 2.779(1) Å. If the oxidation is carried out at 50 °C, *cis*-$[Ir_2(hp)_2(I)(CO)_4]_2$ is obtained. This has the more common HH, HH arrangement and outer Ir–Ir distances of 2.702(2) Å and an inner and unsupported distance of 2.750(2) Å. In the two complexes, the two dinuclear moities are arranged in an almost *transoid* conformation.

Finally there is a hexanuclear iridium chain compound having the formula HH,HT,HH-$[Ir_6(hp)_6(I)_2(CO)_{12}]$ in which the formal oxidation number of each iridium atom is +1.33. This is made by oxidation of $Ir_2(hp)_2(CO)_4$ with iodine in a 3:1 molar ratio at 0 °C which gives an EPR silent, dark-blue solution from which a crystalline solid having a copper-like aspect is isolated in 75% yield. The crystal structure shows a hexanuclear chain formed by an almost linear array in which two HH-$[Ir_2(hp)_2(I)(CO)_4]$ units sandwich an HT-$[Ir_2(hp)_2(CO)_4]$ complex as shown in **11.8**. The six iridium atoms are linked by metal–metal bonds, two of which are unsupported by bridging ligands. The unsupported Ir–Ir distances in the range of 2.776(2) to 2.793(1) Å are longer than those with pyridonate bridges (range of 2.685(1) to 2.710(1) Å in two independent molecules). The relative conformation of the dinuclear units around the unsupported metal–metal bonds is staggered and almost *transoid*. These structural features are similar to those found in the tetranuclear complex HT,HH-$[Ir_2(hp)_2(I)(CO)_4]_2$.



11.8

Pictiva EX2004
Samsung v Pictiva
IPR2024-01094

References

1. F. A. Cotton, L. M. Daniels, L. R. Falvello and C. A. Murillo, *Inorg. Chim. Acta* **1994**, *219*, 7.
2. F. A. Cotton, L. M. Daniels, L. R. Falvello, J. H. Matonic and C. A. Murillo, *Inorg. Chim. Acta* **1997**, *256*, 269.
3. F. A. Cotton, X. Feng and C. A. Murillo, *Inorg. Chim. Acta* **1997**, *256*, 303.
4. F. A. Cotton, L. M. Daniels and C. A. Murillo, *Inorg. Chim. Acta* **1994**, *224*, 5.
5. F. A. Cotton, L. M. Daniels, J. H. Matonic and C. A. Murillo, *Inorg. Chim. Acta* **1997**, *256*, 277.
6. D. Lee and S. J. Lippard, *J. Am. Chem. Soc. 1998,* 120, 12153.
7. C. R. Randall, L. Shu, Y.-M. Chiou, K. S. Hagen, M. Ito, N. Kitajima, R. J. Lachicotte, Y. Zang and L. Que, Jr., *Inorg. Chem.* **1995**, *34*, 1036.
8. D. Lee, J. Du Bois, D. Petasis, M. P. Hendrich, C. Krebs, B. H. Huynh and S. J. Lippard, *J. Am. Chem. Soc.* **1999**, *121*, 9893.
9. D. Lee, C. Krebs, B. H. Huynh, M. P. Hendrich and S. J. Lippard, *J. Am. Chem. Soc.* **2000**, *122*, 5000.
10. A. Klose, E. Solari, C. Floriani, A. Chiesi-Villa, C. Rizzoli and N. Re, *J. Am. Chem. Soc.* **1994**, *116*, 9123.
11. H. Müller, W. Seidel and H. Görls, *J. Organomet. Chem.* **1993**, *445*, 133.
12. F. A. Cotton and R. Poli, *Inorg. Chem.* **1987**, *26*, 3652.
13. F. A. Cotton, L. M. Daniels, X. Feng, D. J. Maloney, J. H. Matonic and C. A. Murillo, *Inorg. Chim. Acta 1997, 256*, 291.
14. L.-P. He, C.-L. Yao, M. Naris, J. C. Lee, J. D. Korp and J. L. Bear, *Inorg. Chem.* **1992**, *31*, 620.
15. J. Catterick, M. B. Hursthouse, P. Thornton and A. J. Welch, *J. Chem. Soc., Dalton Trans*. **1977**, 223.
16. Y. Cui, F. Zheng and J. Huang, *Acta Cryst.* **1999**, *C55*, 1067.
17. F. A. Cotton and X. Feng, *Inorg. Chem.* **1989**, *28*, 1180.
18. F. A. Cotton, L. M. Daniels, D. J. Maloney and C. A. Murillo, *Inorg. Chim. Acta* **1996**, *249*, 9.
19. F. A. Cotton, L. M. Daniels, D. J. Maloney, J. H. Matonic and C. A. Murillo, *Inorg. Chim. Acta* **1997**, *256*, 283.
20. G. L. Simon, A. W. Adamson and L. F. Dahl, *J. Am. Chem. Soc.* **1972**, 94, 7654.
21. L. D. Brown, K. N. Raymond and S. Z. Goldberg, *J. Am. Chem. Soc.* **1972**, *94*, 7664.
22. F. A. Cotton, T. G. Dunne and J. S. Wood, *Inorg. Chem.* **1964**, *3*, 1495.
23. P. L. Bello, C. Benedicenti, G. Caglio and W. Manassero, *J. Chem. Soc., Chem. Commun*. **1973**, 946.
24. R. Mason, I. Soetofte, S. D. Robinson and M. F. Uttley, *J. Organomet. Chem*. **1972**, *46*, C61.
25. F. A. Cotton and R. Poli, *Polyhedron* **1987**, *6*, 1625.
26. F. A. Cotton and R. Poli, *Inorg. Chem.* **1987**, *26*, 590.
27. F. A. Cotton and R. Poli, *Organometallics* **1987**, *6*, 1743.
28. K. R. Dunbar, S. O. Majors and J.-S. Sun, *Inorg. Chim. Acta* **1995**, *229*, 373.
29. F. A. Cotton, C. Lin and C. A. Murillo, *Inorg. Chem.* **2000**, *39*, 4574.
30. F. A. Cotton, C. A. Murillo and D. J. Timmons, *Chem. Commun.* **1999**, 1427.
31. A. F. Heyduk and D. G. Nocera, *J. Am. Chem. Soc.* **2000**, *122*, 9415.
32. H. Hückstädt and H. Homborg, *Z. anorg. allg. Chem.* **1997**, *623*, 369.
33. K. J. Del Rossi and B. B. Wayland, *J. Chem. Soc., Chem. Commun*. **1986**, 1653.
34. K. S. Chan and Y.-B. Leung, *Inorg. Chem.* **1994**, *33*, 3187.
35. K. J. D. Rossi, X.-X. Zhang, B. B. Wayland, *J. Organomet. Chem.* **1995**, *504*, 47.
36. P. G . Rasmussen, J. E. Anderson, O. H. Bailey, M. Tamres and J. C. Bayón, *J. Am. Chem. Soc*. **1985**, *107*, 279.
37. N. Kanematsu, M. Ebihara and T. Kawamura, *J. Chem. Soc., Dalton Trans.* **1999**, 4413.
38. N. Kanematsu, M. Ebihara and T. Kawamura, *Inorg. Chim. Acta* **2001**, *323*, 96.
39. C. Tejel, M. A. Ciriano, B. E. Villarroya, J. A. López, F. J. Lahoz and L. A. Oro, *Angew. Chem. Int. Ed.* **2003**, *42*, 530.
40. B. R. Sutherland and M. Cowie, *Organometallics* **1985**, *4*, 1801.

Pictiva EX2004
Samsung v Pictiva
IPR2024-01094

41. M. A. Ciriano, F. Viguri, L. A. Oro, A. Tiripicchio and M. Tiripicchio-Camellini, *Angew. Chem., Int. Ed. Engl*. **1987**, *26*, 444.
42. M. A. Ciriano, S. Sebastián, L. A. Oro, A. Tiripicchio, M. Tiripicchio-Camellini and F. J. Lahoz, *Angew. Chem., Int. Ed. Engl*. **1988**, *27*, 402.
43. L. A. Oro, M. A. Ciriano, J. J. Pérez-Torrente and B. E. Villarroya, *Coord. Chem. Rev.* **1999**, *193-195*, 941.
44. V. M. Miskowski, T. P. Smith, T. M. Loehr and H. B. Gray, *J. Am. Chem. Soc*. **1985**, *107*, 7925.
45. A. W. Maverick, T. P. Smith, E. F. Maverick and H. B. Gray, *Inorg. Chem.* **1987**, *26*, 4336.
46. D. C. Smith, R. E. Marsh, W. P. Schaefer, T. M. Loehr and H. B. Gray, *Inorg. Chem.* **1990**, *29*, 534.
47. F. A. Cotton, P. Lahuerta, M. Sanaú and W. Schwotzer, *J. Am. Chem. Soc*. **1985**, *107*, 8284.
48. F. A. Cotton, P. Lahuerta, J. Latorre, M. Sanau, I. Solana and W. Schwotzer, *Inorg. Chem.* **1988**, *27*, 2131.
49. M. J. Fernández, J. Modrego, F. J. Lahoz, J. A. López and L. A. Oro, *J. Chem. Soc., Dalton Trans*. **1990**, 2587.
50. C. Tejel, M. A. Ciriano and L. A. Oro, *Chem. Eur. J.* **1999**, *5*, 1131.
51. C. Tejel, M. A. Ciriano, J. A. López, F. J. Lahoz and L. A. Oro, *Angew. Chem. Int. Ed.* **1998**, *37*, 1542.
52. C. Tejel, M. A. Ciriano, B. E. Villarroya, R. Gelpi, J. A. López, F. J. Lahoz and L. A. Oro, *Angew. Chem. Int. Ed.* **2001**, *40*, 4084.

Pictiva EX2004
Samsung v Pictiva
IPR2024-01094

12

Rhodium Compounds

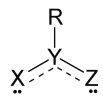
Helen T. Chifotides and Kim R. Dunbar,
Texas A&M University

12.1 Introduction

Dirhodium compounds have a prominent role in the field of metal-metal bond chemistry. Their fascinating properties span diverse fields such as catalysis,[1-5] antitumor metallopharmaceuticals,[6] phototherapeutic agents,[7-9] photochemistry,[10-12] and design of supramolecular arrays.[13-15] A key factor in stabilizing Rh_2^{4+} units is the formation of Rh–Rh single bonds, the lengths of which are generally in the range 2.35-2.45 Å. In terms of a simplified molecular orbital picture, eight of the 14 electrons are distributed in the σ-, π-, δ-orbitals and the remaining six electrons occupy the π*- and δ*-orbitals, resulting in a net Rh–Rh bond order of one and no unpaired electrons.

Paddlewheel dirhodium compounds with Rh_2^{4+} and Rh_2^{5+} cores are the focus of the present chapter. These generally possess one or two axial (*ax*) ligands but the Rh–Rh bond length is essentially insensitive to the presence of σ-donor *ax* ligands. This has recently been supported by the synthesis of a dirhodium tetracarboxylate compound entirely lacking *ax* ligation.[16] Mononuclear Rh(II) compounds are comparatively rare[17] and are not currently discussed. An excellent review of Rh_2^{4+} chemistry that covers the literature up to mid-1981, published by T. R. Felthouse,[18] is complemented by another comprehensive review published in 1983.[19] A number of additional but shorter reviews that cover specific aspects of Rh_2^{4+} chemistry have been published since the early 1980s.[20-25] The last two decades have witnessed an exponential growth of the number of structurally characterized dirhodium compounds and an effort has been made to compile them in the present chapter. The compounds have been classified according to the ligands that are coordinated to the dirhodium core in equatorial (*eq*) positions. The bridging ligands generally are uninegative, bent, trinuclear anions of the general type 12.1 with X–Z distances similar to the Rh–Rh distances. The general classification includes compounds supported by: (1) carboxylato (12.2) and thiocarboxylato (12.3) groups, (2) (N, O) (12.4-12.6), (3) (N, N) (12.7-12.10), (4) (S, N), (S, O) and (S, S) donor and (5) phosphine bridging groups, (6) dianionic bridging ligands, and (7) ligands that do not span the Rh–Rh bond. The last section addresses the applications of dirhodium compounds with the exception of catalysis which is covered in Chapter 13. We apologize to those scientists whose work may have been inadvertently omitted.

Pictiva EX2004
Samsung v Pictiva
IPR2024-01094

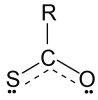


12.1



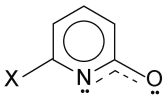
carboxylates

12.2



thiocarboxylates

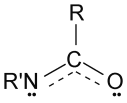
12.3



6-X-oxopyridinates

X = H; hp
X = CH_3; mhp
X = Cl; chp
X = F; fhp

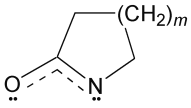
12.4



carboxamidates

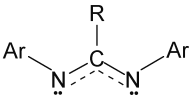
R = CH_3, R' = H; acetamidates
R = CF_3, R' = H; trifluoroacetamidates
R = CH_3, R' = Ph; *N*-phenylacetamidates
R = Ph, R' = H; benzamidates

12.5



m = 1; 2-pyrrolidinate (pyro)
m = 2; 2-valerolactamate (vall)

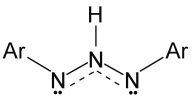
12.6



amidinates

R = H, Ar = Ph; DPhF
R = H, Ar = *p*-Tol; DTolF
R = H, Ar = *p*-OCH_3; DAniF
R = CH_3, Ar = Ph; DPhAc
R = Ph, Ar = Ph; DPhBz

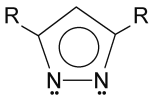
12.7



triazenides

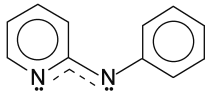
Ar = Ph; DPhTA
Ar = *p*-Tol; DTolTA

12.8



pyrazolates (pz)

12.9



anilinopyridinates (ap)

12.10

12.2 Dirhodium Tetracarboxylato Compounds

12.2.1 Preparative methods and classification

Dirhodium carboxylate complexes are most commonly obtained by reduction of Rh(III) compounds in alcohols which presumably act as the reducing agent, but mechanistic details are unknown. Compounds of the general type $Rh_2(O_2CR)_4L_n$ (n = 1 or 2) were first obtained by refluxing salts of $[RhCl_6]^{3-}$ in aqueous formic acid, a reaction that affords the dark-green product $Rh_2(O_2CH)_4(H_2O)$.[26,27] This compound is believed to exhibit a structure consisting of $Rh_2(O_2CH)_4(H_2O)_2$ units and $Rh_2(O_2CH)_4$ chains.[28] Other early preparative methods employed $Rh(OH)_3{\cdot}H_2O$ in a refluxing carboxylic acid[29] or an alcohol and carboxylic acid mixture,[30] but these methods result in low yields due to formation of considerable quantities of rhodium metal. The most efficient general synthetic method for dirhodium tetraacetate involves refluxing $RhCl_3{\cdot}3H_2O$ under N_2 in a mixture of sodium acetate, acetic acid and ethanol,[31-34] as illustrated in the following equation:

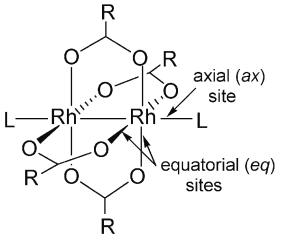
Pictiva EX2004
Samsung v Pictiva
IPR2024-01094

$$RhCl_3 \cdot H_2O \xrightarrow[EtOH/reflux,\ N_2]{CH_3CO_2H\ +\ CH_3CO_2Na} Rh_2(O_2CCH_3)_4 \cdot x EtOH$$

The red solution of Rh(III) becomes dark green after *c.* 1 h of reflux, and the green solid product precipitates from solution. Although prolonged refluxing causes deposition of rhodium metal, the overall yields for most $Rh_2(O_2CC_nH_{2n+1})_4$ compounds are quite good (80-85%).[31] The halocarboxylate compounds (e.g., R = CF_3, CCl_3, $CHCl_2$) are prepared in a similar fashion but yields are lower.[35] Ligand exchange reactions of the acetate with excess carboxylic acid proceed in nearly quantitative yields[29,30,36,37] and constitute one of the best methods for preparing various carboxylate derivatives, including those supported by mixed carboxylate ligand sets.[38,39] The carbonate complex $[Rh_2(CO_3)_4]^{4-}$ [40] (Section 12.3.6) can also be employed as a starting material for dirhodium carboxylate compounds with yields that range from 50 to 90%.[41] Reduction of $RhCl_3$ by dimethylformamide, in the presence of dimethylammonium acetate, has been suggested as a method to synthesize dirhodium tetraacetate in yields that are comparable to those previously described.[42]

The thermal stabilities of carboxylate complexes vary,[43-46] and most decompose at temperatures > 200 ºC with concomitant formation of Rh metal. A notable exception is $Rh_2(O_2CCF_3)_4$, which sublimes at *c.* 350 ºC prior to decomposition; this property, coupled with its high Lewis acidity, has ushered the way to crystallization of dirhodium adducts with very weak donor molecules that cannot be obtained by conventional methods. These compounds are prepared by a technique referred to as '*solventless synthesis*',[47-60] which is based on a sublimation-deposition procedure in the absence of solvent molecules that very often compete with weak donor ligands for *ax* coordination. In this manner, the isolation of crystalline dirhodium adducts of ostensibly '*innocent*' molecules, such as naphthalene and other polycyclic aromatic hydrocarbons, has been achieved.[53,57] Liquid secondary ion mass spectrometry has been employed in studying the fragmentation patterns of various dirhodium carboxylate compounds.[61]

Dirhodium tetracarboxylate complexes generally are air-stable solids that readily form adducts with a variety of donor ligands which occupy *ax* positions. A conspicuous feature of $Rh_2(O_2CR)_4L_2$ compounds is the sensitivity of their colors to the identity of the *ax* ligands, due to the influence of *ax* bonding on the energy of the LUMO (σ*) orbital.[16,29,62] Blue or green products are usually obtained with oxygen donors, red or violet with nitrogen donors, and burgundy or orange with sulfur or phosphorus donors.[19] The $Rh_2(O_2CR)_4L_2$ adducts with the discrete paddlewheel structure **12.11** comprise the largest class of Rh_2^{4+} compounds, due to the extensive range of R groups and the plethora of ligands L (Lewis bases) that coordinate to the *ax* positions.



12.11

Pictiva EX2004
Samsung v Pictiva
IPR2024-01094

In addition to the familiar R groups CH_3, CF_3, C_2H_5, *n*-C_3H_7, *n*-C_3F_7, CMe_3, C_6H_5, and C_6F_5 encountered in $Rh_2(O_2CR)_4L_2$ carboxylate compounds, other substituents include linear chain *n*-alkanoates ($C_nH_{2n+1}CO_2^-$; *n* = 5, 7 or 11),[63,64] CH_3OCH_2,[65] $(CH_2)_nPh$ (*n* = 2 or 3),[66,67] CPh_3,[38,68] C_6H_4-2-Ph,[38] C_6H_2-2,4,6-(*p*-tol)$_3$,[39] C_6H_2-3,4,5-(OEt)$_3$,[69] C_6H_4-4-OC_nH_{2n+1} (*n* = 8-14),[70] C_6H_4-2-OH (salicylate),[71-73] sulfosalicylate,[74] 1,3,5-triisopropylphenyl,[16,75] l-adamantyl,[38] (1*S*)-3-oxo-4,7,7-trimethyl-2-oxabicyclo[2.2.1]heptyl,[76] methoxytrifluoromethylphenylmethyl,[77-90] 2-hydroxy-1,3-propanedicarboxylic acid,[91] and Br_2calix[4]arene.[92] Complexes based on carboxylates derived from the amino acids $CH_3CH(NH_2)CO_2H$ (α-alanine),[93] $NH_2(CH_2)_2CO_2H$ (β-alanine),[94-96] pyrrolidine-2-carboxylic acid (*S*-proline) and derivatives,[97-99] tethered proline rings,[100,101] *S*-leucine[98] as well as those of other optically active carboxylate ligands have been studied.[33,102-108] Compounds with chiral bridging ligands are presented in detail in Chapter 13 (catalysis). Moreover, compounds supported by glutaric ($HO_2C(CH_2)_3CO_2H$)[93] and other chelating dicarboxylic acids[109-116] have been reported. Complexes with bridging thiocarboxylate ions such as CH_3COS^-,[117-121] $C_6H_5COS^-$,[122-124] Bu^t-COS^-,[125] and those of thiosalicylic acids[126-128] are known as well.

Dirhodium tetracarboxylate complexes that exhibit the paddlewheel structure **12.11** are among the most well-studied $M_2(O_2CR)_4L_n$ (*n* = 1 or 2) compounds and surpass all others in the plethora of *ax* ligands. The seemingly infinite variety of *ax* ligands L that form complexes with $Rh_2(O_2CR)_4$ includes molecules with almost all common donor atoms such as nitrogen, oxygen, sulfur, carbon, phosphorus, arsenic, antimony, selenium, halogens and others.

Nitrogen-donor adducts of the dirhodium carboxylate family constitute the largest class of compounds. Adducts have been reported with molecular nitrogen,[129] ammonia,[26,27,29,72,130-133] aliphatic and cyclic amines,[29,30,66,130,134,135] pyridines[27,29,30,39,66,93,110,112,124,130-133,136-153] and other aromatic nitrogen containing ligands,[65,135,154-160] 4-ferrocenylpyridine and ferrocenyl-4-pyridylacetylene,[161,162] pyrimidines,[146,163-165] aromatic,[112,155,158,166] and polyfunctional amines such as ethylenediamine,[72] guanidine and its derivatives,[133,167] durene diamine,[155] phenazine,[155] sulfadiazine,[168] and triazenes.[146,169] In addition, *ax* adducts with *N,N*'-di-*p*-tolylformamidine (HDTolF),[170] 2,2'-dipyridylamine (Hdpa),[171] cyclam and other tri- and tetradentate nitrogen containing macrocycles,[172] imidazole and substituted imidazole ligands,[66,67,141,173-177] isonicotinate groups,[178] nicotinamide and isonicotinamide,[179,180] various nucleobases and their derivatives,[181-191] $tRNA^{phe}$,[192] the ester of vitamin B1,[193] cytochrome *c*[174,194] as well as with amino acids and peptides are known.[141,174] Other *ax* ligands with nitrogen donors include nitriles,[29,38,75,136,137,142,195-199] cyanide based electron acceptors,[200-203] cyanoscorpionate ligands,[204] tpy,[205,206] pyrazines and substituted pyrazines,[207-209] 1,8-pyrazine-capped 5,12-dioxocyclams,[210] thiazepines,[211] substituted thiazoles,[212-214] diphenylcarbazides,[215] nitric oxide,[29,134,216-218] nitrite,[26,27] *N*-bound nitroxide free radicals,[219] and $[NCX]^-$ (X = O, S, Se) anions.[220,221]

Axial complexes with H_2O[222] and DMSO[29] are among the first oxygen-donor carboxylate adducts to be studied and subsequently were further investigated.[28, 51,131,142,196,223-229] Adducts with other oxygen-donor molecules include those with methanol[38,76,186,230,231] ethanol,[68,71,106,232] acetone,[75,233] THF,[49,106,142,196] DMF,[142,231,234,235] urea,[236] dimethylsulfone,[237] dimethylselenoxide,[238] *ax* acetate groups,[144,239,240] sterically hindered lanostanols,[241] quinones,[242] and *O*-bound organic nitroxide radicals[219,243-246] or their 4-hydroxyl substituted counterparts.[247]

Sulfur-donor adducts with *S*-bound DMSO have been reported for the tetraacetate, propionate, butyrate, benzoate and tetrakis(trifluoroacetate) dirhodium dimers.[51,226,227,248,249] Other sulfur-donor adducts include those with diethylsulfide[43] and dibenzylsulfide,[250,251] benzylthiol,[252] sulfur containing aminoacids,[253] tetrahydrothiophene,[226] tetrathiafulvalene,[254] *N,N*'-dimethylthioformamide (DMTF),[255] thiourea and thioacetamide,[72,166,256,257] *N,N*'-dimethyl-*O*-ethylthiocarbamate (DMTC),[255] other thiocarbonyl donors,[258] thiosemicarbazidedi-

Pictiva EX2004
Samsung v Pictiva
IPR2024-01094

acetate,[166,259] 1,4,7-trithiacyclononane,[172] and cyclooctasulfur (S_8);[56] the S_8 adduct was obtained by the '*solventless*' synthesis method. The gas-phase reaction of $Rh_2(O_2CCF_3)_4$ with Me_2SeO affords the unusual compound $[Rh_2(O_2CCF_3)_4(Me_2Se)]_\infty$ wherein the Se atom is coordinated to the dirhodium core.[238]

Ligands that form *ax* Rh–C bonds with dirhodium carboxylato compounds include CN^-,[260] CO [136,261-263] ($Rh_2(\mu\text{-}O_2CCH_3)_4(CO)_2$ is prepared at -20° C in CH_2Cl_2),[261] various isocyanides,[264-266] and olefins.[267-273] The first reported dirhodium tetrakis(trifluoroacetate) olefin 1:2 complex is that with (–)-*trans*-caryophyllene,[274] which was followed by two other compounds with arene coordination to *ax* sites of the dirhodium core.[75,92] It was not until the introduction of the '*solventless synthesis*' strategy that adducts of the extremely strong Lewis acid dirhodium tetrakis-(trifluoroacetate) with weak π-donor molecules such as ethene,[55] substituted alkynes,[52,59] benzene and hexamethylbenzene,[48,53] as well as with a series of polycyclic aromatic hydrocarbons,[57] the geodesic polyarene corannulene[58] and hemibuckminsterfullerene[59] were isolated and structurally characterized. Direct attachment of C=C double bonds to *ax* positions of the dirhodium unit is observed in the 1:1 polymeric chain complex of 1,4-benzoquinone.[275,276] In the same vein, *ax* interactions are established between the carbene CH_2: group and the Rh_2^{4+} core in the carbenoid 1,3,4,5-tetramethylimidazol-2-ylidene (temyl) adduct $Rh_2(O_2CCMe_3)_4(\eta^1\text{-temyl})$.[277]

Investigations of *ax* phosphorus-donor adducts initiated with PPh_3,[30,35] followed by preparative and structural studies of $Rh_2(O_2CCH_3)_4$ with PF_3,[217,261] PPh_3,[278,279] $P(OPh)_3$,[261,278] $P(OMe)_3$,[217,261] $Ph_2P(MeOC_6H_4)$,[280] bicyclic phosphites[281,282] and 2-pyridylphosphine ligands.[283] In addition, products were isolated from the reaction of $Rh_2(O_2CCF_3)_4$ with PPh_3 and $P(OPh)_3$,[284] $Rh_2(O_2CC_2H_5)_4$ with PPr^i_3 and PCy_3,[285] and $Rh_2(OSCR)_4$ (R = CH_3, Bu^t or Ph) with PPh_3.[125] Detailed multinuclear NMR and UV-visible spectral studies have been reported for the 1:1 and 1:2 adducts of $Rh_2(O_2CR)_4$ (R = CH_3, C_2H_5, C_3H_7 or Ph) with phosphines and phosphites which exist in equilibrium in solution,[286-289] whereas ^{19}F and ^{31}P NMR spectra of $Rh_2(O_2CCF_3)_4$ adducts with PX_3 (X = Ph, OPh, Cy) have been employed to distinguish *ax* from mixed *ax/eq* coordination of the PX_3 ligands.[142,290] Carboxylate adducts with As or Sb as donor atoms, i.e., $Rh_2(O_2CR)_4(YPh_3)_2$,[250,291] Y = As, Sb and $Rh_2(O_2CR)_4L_2$, L = $Ph_2AsCH_2PPh_2$ or $Ph_2As(CH_2)_nAsPh_2$,[292] *n* = 2, 4, have been reported.

The assortment of *ax* ligands for dirhodium carboxylate $[Rh_2(O_2CCH_3)_4X_2]^{2-}$ (X = Cl, Br, I) complexes includes halide anions; several of the salts have been structurally characterized.[42,293-296] The betaine complex $[Rh_2(O_2CCH_2NMe_3)_4Cl_2]Cl_2\cdot 4H_2O$, which contains axially coordinated chloride ligands,[297] and the unprecedented diiodine bridged adduct $\{[Rh_2(O_2CCF_3)_4I_2]\cdot I_2\}_\infty$[54] have been the subject of single crystal X-ray studies.

12.2.2 Structural studies

The first accurate structural determination of a $Rh_2(O_2CR)_4L_2$ compound was reported in 1970 for $Rh_2(O_2CCH_3)_4(H_2O)_2$ (Fig. 12.1);[223,224] this structure serves as the prototype for all $Rh_2(O_2CR)_4L_2$ structures. In Table 12.1 a compendium of the structural data for Rh_2^{4+} tetracarboxylate complexes, including monothiocarboxylate (**12.2**) and chelating dicarboxylic acid compounds, is provided. The entries in Table 12.1 are grouped according to the type of carboxylate ligand and within the subgroup by the donor atom of the *ax* ligand. With a few exceptions noted below, the majority of tetracarboxylato Rh–Rh distances are in the range 2.35-2.45 Å. The Rh–Rh bond length is rather insensitive to the presence of σ-donor *ax* ligands. The latter is corroborated by comparing structural data for $Rh_2(TiPB)_4$ (TiPB: anion of 2,4,6-triisopropyl benzoic acid), which lacks *entirely ax* interactions, and $Rh_2(TiPB)_4(Me_2CO)_2$.[16,75] The Rh–Rh distance in the former (2.350(1) Å) is only slightly shorter, by 0.02 Å, than that in the latter (2.370[1] Å), which has *ax* ligands. In contrast, the Cr–Cr bond in $Cr_2(TiPB)_4$ is dramatically

Pictiva EX2004
Samsung v Pictiva
IPR2024-01094

shortened by *c.* 0.4 Å when deprived of *ax* ligands.[16,75] The shortest Rh–Rh distances for tetracarboxylate compounds are encountered in $Rh_2(TiPB)_4$ with no *ax* ligands (2.350(1) Å) and the monoadduct $Rh_2(TiPB)_4(NCCH_3)$ (2.354(1) Å).[16,75] Other tetracarboxylate complexes with short Rh–Rh distances are $[Rh_2(TiPB)_3(\mu\text{-}O_2CCH_3)(TiPBH)]_2$ (2.358[1] Å)[75] and $\{Rh_2(O_2CC_3H_7)_4\}_\infty$ (2.366(1) Å),[298] which have one or both *ax* sites associated with a neighboring dirhodium unit, as well as $Rh_2(O_2CCPh_3)_4(EtOH)_2$ (2.365(1) Å) with two exogenous *ax* ligands.[68] The longest Rh–Rh distances are encountered among the tetracarboxylate compounds with phosphine and nitric oxide *ax* ligands, e.g., $Rh_2(O_2CCF_3)_4(PPh_3)_2$ (2.486(1) Å),[284] $Rh_2(O_2CC_2H_5)_4(NO)_2$ (2.512(2) Å),[218] $Rh_2(O_2CCH_3)_4(NO)_2$ (2.513(1) Å),[218] and $Rh_2(O_2CC_3H_7)_4(NO)_2$ (2.519(1) Å).[218] The monothiocarboxylate compounds $Rh_2(OSCBu^t)_4(PPh_3)_2$[125] and $Rh_2(\mu\text{-}OSCCH_3)_4(CH_3CSOH)_2$[117,118] exhibit Rh–Rh distances of 2.584(1) Å and 2.550(3) Å, respectively, which are longer than those in $Rh_2(O_2CR)_4L_2$.[121] These long distances apparently are a consequence of the large '*bite*' angle of $RCSO^-$ type ligands.[299] Efforts have been made to correlate Rh–Rh distances with the Lewis basicity of the *ax* ligands L,[261] but it does not appear that any simple relationship exists; this is presumably due to the fact that electronic and steric factors[299-301] as well as packing forces influence the Rh–Rh bond distance (e.g., comparison of the Rh–Rh and Rh–N distances for $Rh_2(O_2CCH_3)_4L_2$, L = py and Et_2NH, indicates that both are longer for the Et_2NH adduct; see Table 12.1).[134,138] The difference of 0.01 Å between the Rh–Rh bond distances of $Rh_2(O_2CCF_3)_4(DMSO)_2$[227] and the deuterated analog $Rh_2(O_2CCF_3)_4(DMSO\text{-}d_6)_2$,[228] which are two chemically identical compounds that differ only in the crystal packing arrangements, lends further credibility to this argument.

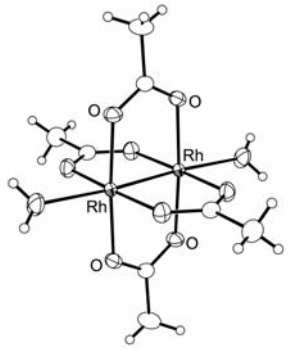


Fig. 12.1. Molecular structure of $Rh_2(O_2CCH_3)_4(H_2O)_2$.

Pictiva EX2004
Samsung v Pictiva
IPR2024-01094

Table 12.1. Structural data for paddlewheel Rh_2^{4+} tetracarboxylato compounds

Compound	r (Rh–Rh)[a] (Å)	r (Rh–L_{ax})[b] (Å)	Donor atom(s)	ref.
$Rh_2(O_2CH)_4(H_2O)$	2.38[c]	2.45[c]	O	28,302
$Na[Rh_2(\mu\text{-}O_2CH)_4(\mu_3\text{-}\eta^1{:}\eta^1{:}\eta^1\text{-}O_2CH)(H_2O)]\cdot H_2O$	2.390(1)	2.257(2)[d] 2.309(2)[d]	O	235
$Rh_2(O_2CH)_4(DMF)_2$	2.397(1)	2.261(1)	O	235
$[Rh_2(O_2CCH_3)_4]_\infty$[e]	2.415(3)	2.506(2)[f]	O[g]	312
$Rh_2(O_2CCH_3)_4(H_2O)_2$	2.386(1)	2.310(3)	O	223,224
$Na[Rh_2(\mu\text{-}O_2CCH_3)_4(\eta^1\text{-}O_2CCH_3)(\eta^1\text{-}HO_2CCH_3)]$[h]	2.383(1)	2.279(2)	O[h]	240
$Na_2[Rh_2(O_2CCH_3)_4Cl_2]\cdot 4H_2O$	2.387(1)	2.564(1)	Cl	296
$Li_2[Rh_2(O_2CCH_3)_4Cl_2]\cdot 8H_2O$	2.397(1)	2.601(1)	Cl	294
$[Rh_2(O_2CCH_3)_4Cl_2](Me_2NH_2)_2$	2.399(1)	2.563(1) 2.592(1)	Cl	42
$(GudH)_2[Rh_2(O_2CCH_3)_4Cl_2]$	2.397(2)	2.571(6) 2.610(5)	Cl	293
$[C(NH_2)_3]_2[Rh_2(O_2CCH_3)_4Cl_2]$	2.396(1)	2.585(1)	Cl	295
$Rh_2(O_2CCH_3)_4(MeOH)_2$	2.378(1)	2.288(3)	O	230
$Rh_2(O_2CCH_3)_4(DMF)_2$	2.383(3)	2.308(4)	O	234
$[Rh_2(O_2CCH_3)_4(Me_2SeO)_2]\cdot 2CH_2Cl_2$	2.394(1)	2.290(5)	O	238
$Rh_2(O_2CCH_3)_4(CO)_2$	2.420(1)	2.092(4)	C	217,261
$Rh_2(O_2CCH_3)_4(NHEt_2)_2$	2.402(1)	2.301(5)	N	134
$Rh_2(O_2CCH_3)_4(NO)(NO_2)$	2.454(1)	1.933(4)[i] 2.010(4)[i]	N	134,217
$Rh_2(O_2CCH_3)_4(NO)_2$	2.513(1)	1.947(3)	N	218
$Rh_2(O_2CCH_3)_4(Ds\text{-}im)_2$	2.390(1)	2.237(3)	N	218
$Rh_2(O_2CCH_3)_4(Ds\text{-}pip)_2$	2.398(1)	2.272(6)	N	218
$Rh_2(O_2CCH_3)_4(1\text{-}MeAdo)_2\cdot H_2O$	2.401(1)	2.295(5)	N	184
$Rh_2(O_2CCH_3)_4(tRNA^{phe})_2$	2.4[j]	2.4[j]	N	192
$Rh_2(O_2CCH_3)_4(theophylline)_2$	2.412(6)	2.23(3)	N	185

Pictiva EX2004
Samsung v Pictiva
IPR2024-01094

Compound	r (Rh–Rh)[a] (Å)	r (Rh–L_{ax})[b] (Å)	Donor atom(s)	ref.
$Rh_2(O_2CCH_3)_4$(caffeine)$_2$	2.395(1)	2.315(9)	N	185
$Rh_2(O_2CCH_3)_4$(metro)$_2$	2.388(1)	2.240(5)	N	67
$Rh_2(O_2CCH_3)_4$(tmph)$_2$·1.5H_2O	2.405(1)	2.284(8)	N	193
$Rh_2(O_2CCH_3)_4$(AZ)$_2$·4DMAA	2.373(3)	2.23(1)	N	188
$Rh_2(O_2CCH_3)_4$(Roll-3696)$_2$	2.399(1)	2.248(4)	N	173
$Rh_2(O_2CCH_3)_4$(HDTolF)$_2$·$CHCl_3$	2.412(1)	2.309(4)	N	170
$Rh_2(O_2CCH_3)_4$(py)$_2$	2.396(1)	2.223(2) 2.231(3)	N	138
$Rh_2(O_2CCH_3)_4$(py)$_2$[k]	2.400(1)	2.258(4)	N	144
$[Rh_2(O_2CCH_3)_4(\mu_2\text{-dapy})]_\infty$	2.420(1) 2.398(1)	2.365(5)[l] 2.325(5)[m]	N	145
$Rh_2(O_2CCH_3)_4(\eta^1\text{-ampy})_2$[n]	2.417(3) 2.400(2)	2.36(1)[l] 2.30(1)[m]	N	145
$[Rh_2(O_2CCH_3)_4(\mu_2\text{-ammpy})\cdot 0.5CH_3CN]_\infty$	2.410(1)	2.25(1)[l] 2.31(1)[m]	N	147
$Rh_2(O_2CCH_3)_4(\eta^1\text{-dmp})_2$	2.414(1)	2.403(4)	N	146
$Rh_2(O_2CCH_3)_4(\eta^1\text{-damt})_2$	2.401(1)	2.315(9)	N	146
$Rh_2(O_2CCH_3)_4(\eta^1\text{-dmapd})_2$	2.412(1)	2.370(6)	N	146
$Rh_2(O_2CCH_3)_4(\eta^1\text{-aampy})_2$	2.411(1)	2.439(4)	N	145
$Rh_2(O_2CCH_3)_4(\eta^1\text{-daapy})_2$	2.404(1)	2.388(6)	N	145,148
$Rh_2(O_2CCH_3)_4(\eta^1\text{-Hdpa})_2$	2.404(1)	2.294(4)	N	171
$Rh_2(O_2CCH_3)_4$(4-CN-py)$_2$·CH_3CN	2.393(1)	2.244(4)	N[o]	143
$[Rh_2(O_2CCH_3)_4(\mu_2\text{-}\eta^1\text{:}\eta^1\text{-btp})]_\infty$	2.387(1)	2.237(6)	N	149
$[Rh_2(O_2CCH_3)_4(\mu_2\text{-}\eta^1\text{:}\eta^1\text{-dmpyethybz})\cdot CH_2Cl_2]_\infty$	2.401[c]	2.247[c]	N	150
$[Rh_2(O_2CCH_3)_4(\mu_2\text{-}\eta^1\text{:}\eta^1\text{-tpyethebz})\cdot 2CH_2Cl_2]_\infty$	2.408(1) 2.407(1)	2.300(3) 2.306(3)	N	305
$Rh_2(O_2CCH_3)_4(\eta^1\text{-tpy})_2$[p]	2.401(1)	2.337(7)	N	205
$Rh_2(O_2CCH_3)_4(\eta^1\text{-tpy})_2$[q]	2.408(1)	2.323(2)	N	206
$Rh_2(O_2CCH_3)_4(\eta^1\text{-Cl-tpy})_2$	2.405(1)	2.359(6)	N	206

Pictiva EX2004
Samsung v Pictiva
IPR2024-01094

Compound	r (Rh–Rh)[a] (Å)	r (Rh–L_{ax})[b] (Å)	Donor atom(s)	ref.
$Rh_2(O_2CCH_3)_4(plpyz)_2$	2.387(1)	2.224(3)	N	209
$\{Rh_2(O_2CCH_3)_4[Cu_2(1,8\text{-pyrazine-capped 5,12-dioxocyclam})_2]_2\}\cdot CH_3CO_2C_2H_5$	2.389(1)	2.249(4)	N	210
$Rh_2(O_2CCH_3)_4(HDPhTA)_2$	2.407(2)	2.301(8)	N	169
$Rh_2(O_2CCH_3)_4(adbtz)_2$	2.402(2)	2.287(8)	N	211
$Rh_2(O_2CCH_3)_4(admpym)_2$	2.414(1)	2.368(3)	N	163
$Rh_2(O_2CCH_3)_4(admpym)_2\cdot H_2O$	2.415(1)	2.376(5)	N	163
$Rh_2(O_2CCH_3)_4(trimethoprim)_2\cdot 2C_6H_6\cdot CH_3OH$	2.409(1)	2.289(2)	N	164
$Rh_2(O_2CCH_3)_4(pyrimethamine)_2$	2.409(1)	2.365(3)	N	164
$[Rh_2(O_2CCH_3)_4(AAMP)\cdot 3.5H_2O]_\infty$	2.405(1) 2.404(1)	2.293(7)[r] 2.291(9)[s]	N	165
$Rh_2(O_2CCH_3)_4(NCCH_3)_2$	2.384(1)	2.258(6)	N	195
$Rh_2(O_2CCH_3)_4(1,1\text{-TCNE})\cdot C_6H_6$	2.389(3) 2.367(3)	2.24(3) 2.19(3)	N	202
$Rh_2(O_2CCH_3)_4(trans\text{-}1,2\text{-TCNE})_2\cdot C_6H_6\cdot C_8H_{10}$	2.372(1) 2.373(1)	2.185(6) 2.181(7)	N	202
$Rh_2(O_2CCH_3)_4(NCPhCN)\cdot CH_3COCH_3$	2.391(1)	2.239(5)	N	198
$Rh_2(O_2CCH_3)_4(NCPhCN)\cdot 2CH_3OH$	2.391(1)	2.236(4)	N	198
$Rh_2(O_2CCH_3)_4(NCPhCN)\cdot EtOH$	[t]	[t]	N	198
$Rh_2(O_2CCH_3)_4(NCPhCN)\cdot THF$	2.383(1)	2.226(3)	N	198
$Rh_2(O_2CCH_3)_4(NCPhCN)\cdot C_6H_6$	2.389(1)	2.237(2)	N	198
$[Rh_2(O_2CCH_3)_4(stf\text{-}CN)_2]\cdot 6CHCl_3$	2.384(1)	2.202(7)	N	199
$[Rh_2(O_2CCH_3)_4(CNPh)]_2$	2.398(1)	2.109(4) 2.373[c,f]	C O[g]	279
$Rh_2(O_2CCH_3)_4(CNPh)_2$	2.427(1)	2.133(3)	C	266
$Rh_2(O_2CCH_3)_4(CNPhCF_3)_2$	2.418(1)	2.122(3)	C	266
$Rh_2(O_2CCH_3)_4(CNPhNMe_2)_2$	2.424(1)	2.148(4)	C	266
$[Rh_2(O_2CCH_3)_4(PPh_3)]_2$	2.407(1)	2.423(1) 2.405[c,f]	P O[g]	279
$Rh_2(O_2CCH_3)_4(PPh_3)_2$	2.451(1)	2.477(1)	P	278

Pictiva EX2004
Samsung v Pictiva
IPR2024-01094

Compound	r (Rh–Rh)[a] (Å)	r (Rh–L_{ax})[b] (Å)	Donor atom(s)	ref.
$Rh_2(O_2CCH_3)_4(PF_3)_2$	2.430(3)	2.42(1)	P	261
$Rh_2(O_2CCH_3)_4[P(OPh)_3]_2{\cdot}C_6H_5Me$	2.443(1)	2.412(1)	P	217,261,278
$Rh_2(O_2CCH_3)_4[P(OMe)_3]_2$	2.456(1)	2.437(5)	P	261
$\{Rh_2(O_2CCH_3)_4[Ph_2P(o\text{-}MeOC_6H_4)]\}_2$	2.414(1)	2.455(1)[a] 2.043(3)[f] 2.437(3)[f]	P O[g]	280
$Rh_2(O_2CCH_3)_4\{\eta^1\text{-}(S,R)\text{-CPFA-}P\}_2$	2.453(1)	2.561(2)	P	311
$Rh_2(O_2CCH_3)_4(AsPh_3)_2$	2.427(1)	2.576(1)	As	250
$Rh_2(O_2CCH_3)_4(SbPh_3)_2$	2.421(4)	2.732(4)	Sb	250
$Rh_2(O_2CCH_3)_4(DMSO)_2$	2.406(1)	2.451(1)	S	226
$Rh_2(O_2CCH_3)_4(DMTF)_2$	2.418(1)	2.546(1)	S	255
$Rh_2(O_2CCH_3)_4(THT)_2$	2.413(1)	2.517(1)	S	226
$Rh_2(O_2CCH_3)_4(ttf)_2$	2.408(2)	2.519(4)	S	254
$Rh_2(O_2CCH_3)_4(SHCH_2Ph)_2$	2.402(1)	2.551(2)	S	252
$Rh_2(O_2CCH_3)_4[S(CH_2Ph)_2]_2$	2.406(3)	2.561(5)	S	250
$Rh_2(O_2CCH_3)_4(DMTC)_2$	2.409(1)	2.614(3)	S	255
$Rh_2(O_2CCH_3)_4(dmptsczda)_2$	2.413(1)	2.519(2)	S	259
$\{Rh_2(O_2CCH_3)_4(\mu_2\text{-}Se_2C_5H_8)\}_\infty$[e]	2.415(3)	2.625(6)[v]	Se	312
$Rh_2(O_2CCH_3)_4[5\text{-nitro-2-(chromone-2-carboxyl-amino)-1,3-thiazole}]_2{\cdot}2CHCl_3$	2.388[c]	2.259[c]	N	213
$Rh_2(O_2CCH_3)_4[5\text{-nitro-2-(2-thienoylamino)-1,3-thiazole}]_2{\cdot}CH_2Cl_2$	2.383(1)	2.241(4)	N	212
$\{[Rh_2(O_2CCH_3)_2][\textit{cis}\text{-}ReCl_2(dppm)_2(O_2CC_5H_4N\text{-}4)_2]{\cdot}1.5C_3H_6O{\cdot}2CH_2Cl_2{\cdot}H_2O\}_\infty$	2.417(6)	2.22(2)	N	178
$\{Rh_2(O_2CCH_3)_4(nicotinamide)_2{\cdot}2Me_2CO\}_\infty$	2.397(1)	2.224(5)	N	179
$\{Rh_2(O_2CCH_3)_4(isonicotinamide)_2{\cdot}2Me_2CO\}_\infty$	2.403(1)	2.205(7)	N	179
$\{[Rh_2(O_2CCH_3)_4][Ni(bpbg)_2]\}_\infty$	2.411(2)	2.319(9)	N	148
$Rh_2(O_2CCH_3)_4(diphenylcarbazide)_2$	2.39(2)	2.31(4)	N	215
$Rh_2(O_2CCH_3)_4(Acr\text{-}4\text{-}carboxamide)_2$	2.403(1) 2.407(1)	2.339(6) 2.349(5)[w]	N	154
$Rh_2(O_2CCH_3)_4(AcrNMe_2)_2$	2.409(1)	2.344(3)	N	65

Pictiva EX2004
Samsung v Pictiva
IPR2024-01094

Compound	r (Rh–Rh)[a] (Å)	r (Rh–L_{ax})[b] (Å)	Donor atom(s)	ref.
$\{[Rh_2(\mu\text{-}O_2CCH_3)_4(\mu_2\text{-}\eta^1\text{:}\eta^1\text{-}O_2CCH_3)_2][Rh(tmtaa)(PhC{\equiv}CPh)]_2\}\cdot 2C_6H_6$[h]	2.384(1)	2.227(4)	O[h]	144
$[Rh_2(O_2CCF_3)_4]_\infty$	2.381(1)	2.337(4)	O[g]	47
$Rh_2(O_2CCF_3)_4(H_2O)_2$	2.396(2)	2.25(1)	O	196
$Rh_2(O_2CCF_3)_4(H_2O)_2\cdot 2DTBN$	2.409(1)	2.243(2)	O	247
$Rh_2(O_2CCF_3)_4(EtOH)_2$	2.396(2) 2.409(2)	2.28(1) 2.26(1)	O	232
$Rh_2(O_2CCF_3)_4(NCCH_3)_2$	2.418(1)	2.201(5)	N	196
$Rh_2(O_2CCF_3)_4(Me_2CO)_2$	2.406(1)	2.252(4)	O	315
$Rh_2(O_2CCF_3)_4(Me_2CO)_2\cdot C_6H_6$	2.407(3)	2.239(5)	O	233
$[Rh_2(O_2CCF_3)_4(Me_2CO)]_2$[x]	2.396(1)	2.410(7)[f] 2.208(7)[y]	O	315
$[Rh_2(O_2CCF_3)_4(Me_2CO)]_2$	2.398(1)	2.374(4)[f] 2.525(4)[f] 2.196(4)[y]	O	315
$Rh_2(O_2CCF_3)_4(DMSO)_2$	2.419(1)	2.236(3)	O	227
$[Rh_2(O_2CCF_3)_4]_7(DMSO)_8$	2.398(3) 2.417(2) 2.425(2) 2.398(2)	2.451(4)[z] 2.410(4)[z] 2.522(5)[z] 2.23(1)[aa] 2.27(1)[aa] 2.24(1)[aa]	O[bb] S	51
$[Rh_2(O_2CCF_3)_4(\mu\text{-DMSO-}\mathit{O})]_\infty$	2.407(1) 2.416(1)	2.299(5) 2.375(5)	O	51
$\{[Rh_2(O_2CCF_3)_4]_3(\mu\text{-DMSO-}\mathit{S,O})_2\}_\infty$	2.391(1) 2.426(2)	2.449(3)[z] 2.386(6)[f] 2.219(7)[cc]	S O	51
$Rh_2(O_2CCF_3)_4(DMSO\text{-}d_6)_2$	2.409(1) 2.407(1)	2.263(3) 2.234(3)	O	228
$\{Rh_2(O_2CCF_3)_4(Me_2SeO)\cdot 0.5C_6H_6\}_\infty$	2.418(1)	2.295(5)	O	238

Pictiva EX2004
Samsung v Pictiva
IPR2024-01094

Compound	r (Rh–Rh)[a] (Å)	r (Rh–L_{ax})[b] (Å)	Donor atom(s)	ref.
$Rh_2(O_2CCF_3)_4(Me_2SeO)_2$	2.422(1)	2.244(6)	O	238
$Rh_2(O_2CCF_3)_4(Me_2SO_2)_2$	2.401(1)	2.291(3)	O	237
	2.399(1)	2.284(3)		
$[Rh_2(O_2CCF_3)_4(THF)]_2$	2.391(1)	2.214(7)	O	49
		2.406(6)[f]	O[g]	
$[Rh_2(O_2CCF_3)_4(THF)]_\infty$	2.407(2)	2.385(6)	O	49
$Rh_2(O_2CCF_3)_4(THF)_2$	2.397(1)	2.210(8)	O	196
$\{Rh_2(O_2CCF_3)_4(Me_2Se)\}_\infty$	2.428(3)	2.590(3)	Se	238
$Rh_2(O_2CCF_3)_4(PPh_3)_2$	2.486(1)	2.494(2)	P	284
$Rh_2(O_2CCF_3)_4[P(OPh)_3]_2$	2.470(1)	2.422(2)	P	284
$[Rh_2(O_2CCF_3)_4(S_8)]_\infty$	2.420(1)	2.516(1)	S	56
		2.578(1)		
$[Rh_2(O_2CCF_3)_4]_3(S_8)_2$	2.419(3)	2.484(6)	S	56
	2.412(4)	2.507(6)		
		2.567(6)		
$\{[Rh_2(O_2CCF_3)_4I_2]\cdot I_2\}_\infty$	2.417(1)	2.836(1)	I	54
	2.415(1)	2.824(1)		
$\{Rh_2(O_2CCF_3)_4[Rh_2(\mu\text{-}O_2CCF_3)_2(CO)_4]_2\}_\infty$[dd]	2.412(1)	2.790(1)[ee]		50,310
		2.960(1)[ff]		
		3.062(1)[gg]		
$[Rh_2(O_2CCF_3)_4]_2(\mu_2\text{-}Me_2CO)[Cu_2(O_2CCF_3)_4]$	2.399(1)	2.392(1)[f]	O	315
		2.217(1)[y]		
$[Rh_2(\mu\text{-}O_2CCF_3)_4(\mu_2\text{-}\eta^1\text{:}\eta^1\text{-btp})][Rh_2(\mu\text{-}O_2CCF_3)_2(\eta^1\text{-}O_2CCF_3)_2(\eta^1\text{-btp})_2]$	2.420(1)	2.212(7)	N	149
	2.565(1)[hh]	2.230(7)		
$Rh_2(O_2CCF_3)_4(Tempo)_2$	2.417(1)	2.220(2)	O	243,244
$Rh_2(O_2CCF_3)_4(Tempol)_2$	2.405(1)	2.240(3)	O[ii]	247
$Rh_2(O_2CCF_3)_4(NITPh)_2$	2.412(1)	2.239(3)	O	219,245
$[Rh_2(O_2CCF_3)_4(IMMe)]_\infty$	2.419(1)	2.188(5)	N	219
		2.320(5)	O	

Pictiva EX2004
Samsung v Pictiva
IPR2024-01094

Compound	r (Rh–Rh)[a] (Å)	r (Rh–L_{ax})[b] (Å)	Donor atom(s)	ref.
$Rh_2(O_2CCF_3)_4(IMMe)_2$	2.432(1)	2.237(4)	N	219,245
$[Rh_2(O_2CCF_3)_4(NITMe)]_\infty$	2.407(1)	2.268(5)	O	219
$Rh_2(O_2CCF_3)_4[\eta^2$-(–)-*trans*-caryophyllene$]_2$	2.461(1)	2.46(1) 2.62(1)	C	274
$\{Rh_2(O_2CCF_3)_4(\mu_2\text{-}\eta^2\text{:}\eta^2\text{-}C_2H_4)\}_\infty$	2.424[c]	2.484(3)	C	55
$Rh_2(O_2CCF_3)_4(\eta^2\text{-}Ph_2C_2)_2$	2.432(1)	2.550(4)[ij] 2.510(4)[ij]	C	52
$[Rh_2(O_2CCF_3)_4(\mu_2\text{-}\eta^2\text{:}\eta^2\text{-}Ph_2C_2)]_\infty$	2.426(1)	2.499(5)[ij] 2.489(5)[ij] 2.696(5)[kk] 2.750(6)[kk]	C	52
$[Rh_2(O_2CCF_3)_4(Me_2CO)]_2(\mu_2\text{-}\eta^2\text{:}\eta^2\text{-}C_4I_2)$	2.413(1)	2.60(1)[ij] 2.63(1)[ij] 2.214(8)[ll]	C O	59
$[Rh_2(O_2CCF_3)_4(\mu_2\text{-}\eta^2\text{:}\eta^2\text{-}C_6H_6)]_\infty$	2.412(1)	2.646(6) 2.678(6)	C	53
$\{Rh_2(O_2CCF_3)_4[\mu_2\text{-}\eta^2\text{:}\eta^2\text{-}p\text{-}(CH_3)_2C_6H_4]\}_\infty$	2.417(1)	2.598(7) 2.770(7)	C	53
$[Rh_2(O_2CCF_3)_4(\mu_2\text{-}\eta^2\text{:}\eta^2\text{-}C_{10}H_8)]_\infty$	2.422(2)	2.609(9) 2.567(9)	C	53
$[Rh_2(O_2CCF_3)_4(\mu_2\text{-}\eta^2\text{:}\eta^2\text{-}C_6Me_6)]_\infty$	2.422(1)	2.770(6) 2.787(6)	C	48
$[Rh_2(O_2CCF_3)_4(\mu_2\text{-}\eta^2\text{:}\eta^2\text{-}C_{12}H_8)]_\infty$[mm]	2.430(2)	2.65(1) 2.66(1) 2.47(1) 2.53(1)	C	57
$[Rh_2(O_2CCF_3)_4(\mu_2\text{-}\eta^2\text{:}\eta^2\text{-}C_{12}H_{10})]_\infty$[nn]	2.429(1)	2.599(6) 2.647(6)[oo]	C	57

Pictiva EX2004
Samsung v Pictiva
IPR2024-01094

Compound	r (Rh–Rh)[a] (Å)	r (Rh–L_{ax})[b] (Å)	Donor atom(s)	ref.
$[Rh_2(O_2CCF_3)_4(\mu_2\text{-}\eta^2\text{:}\eta^2\text{-}C_{14}H_{10})]_\infty$[pp]	2.429(1)	2.574(6) 2.603(5)[oo]	C	57
$[Rh_2(O_2CCF_3)_4(\mu_2\text{-}\eta^2\text{:}\eta^2\text{-}C_{14}H_{10})]_\infty$[qq]	2.425(1)	2.615(6) 2.627(6) 2.556(5) 2.563(6)	C	57
$[Rh_2(O_2CCF_3)_4(\mu_2\text{-}\eta^2\text{:}\eta^2\text{-}C_{16}H_{10})]_\infty$[rr]	2.430(1)	2.578(3)[ss]	C	57
$Rh_2(O_2CCF_3)_4(\mu_2\text{-}\eta^2\text{:}\eta^2\text{-}C_{16}H_{10})$[tt]	2.423(1)	2.598(6) 2.672(6) 2.607(6) 2.735(6)	C	57
$Rh_2(O_2CCF_3)_4(\mu_2\text{-}\eta^2\text{:}\eta^1\text{-}C_{16}H_{10})$[tt]	2.426(1)	2.582(7)[uu] 2.571(8) 2.618(8)	C	57
$Rh_2(O_2CCF_3)_4(\eta^2\text{-}C_{10}H_{10})_2$[rr]	2.426(1)	2.554(5) 2.594(5)[oo]		57
$[Rh_2(O_2CCF_3)_4(\mu_2\text{-}\eta^2\text{:}\eta^2\text{-}C_{18}H_{12})]_\infty$[vv]	2.431(1)	2.528(9) 2.53(1) 2.60(1) 2.606(9)	C	57
$[Rh_2(O_2CCF_3)_4](\eta^2\text{-}C_{18}H_{12})_2$[ww]	2.425(1)	2.564(5) 2.707(5)[oo]	C	57
$[Rh_2(O_2CCF_3)_4]_3(\mu_3\text{-}\eta^2\text{:}\eta^2\text{:}\eta^2\text{-}C_{18}H_{12})_2$[ww]	2.422(2) 2.416(3)	2.56(2) 2.58(2) 2.59(2) 2.72(2) 2.73(2) 2.68(2)[oo]		57

Pictiva EX2004
Samsung v Pictiva
IPR2024-01094

Compound	r (Rh–Rh)[a] (Å)	r (Rh–L_{ax})[b] (Å)	Donor atom(s)	ref.
$\{[Rh_2(O_2CCF_3)_4](\mu_2\text{-}\eta^2\text{:}\eta^2\text{-}C_{18}H_{12})\}_\infty$ [xx]	2.427(1)	2.573(6) 2.601(6)[oo]	C	57
$\{[Rh_2(O_2CCF_3)_4]_3(\mu_4\text{-}\eta^2\text{:}\eta^2\text{:}\eta^2\text{:}\eta^2\text{-}C_{18}H_{12})\}_\infty$ [xx]	2.404(2) 2.421(2)	2.327(9)[f] 2.52(1) 2.62(1) 2.51(1) 2.61(1)[oo]	C O[g]	57
$\{[Rh_2(O_2CCF_3)_4](\mu_2\text{-}\eta^2\text{:}\eta^2\text{-}C_{20}H_{10})\}_\infty$ [yy]	2.431(1)	2.756(4) 2.531(4) 2.595(4) 2.564(4)	C	58
$[Rh_2(O_2CCF_3)_4]_3(\mu_3\text{-}\eta^2\text{:}\eta^2\text{:}\eta^2\text{-}C_{20}H_{10})_2$ [yy]	2.427(1) 2.425(1) 2.420(1)	2.636(3) 2.570(3) 2.548(3)	C	58
$\{[Rh_2(O_2CCF_3)_4]_3(\mu_4\text{-}\eta^2\text{:}\eta^2\text{:}\eta^2\text{:}\eta^1\text{-}C_{30}H_{12})\}$ [zz]	2.434(3) 2.418(3) 2.401(2)	2.46(2)[aaa] 2.50(2)[aaa] 2.54(2)[bbb]	C	59
$[Rh_2(O_2CCF_3)_4]_2(\mu_4\text{-TCNE})\cdot 2C_6H_6$	2.392(2) 2.399(2)	2.16(1) 2.19(1)	N	200
$[Rh_2(O_2CCF_3)_4(\text{DM-DCNQI})\cdot C_6H_6]_\infty$	2.412(1)	2.189(7)	N	203
$[Rh_2(O_2CCF_3)_4(\text{DCNNQI})\cdot C_7H_8]_\infty$	2.422(1)	2.212(2)	N	203
$\{[Rh_2(O_2CCF_3)_4]_2(\mu_4\text{-TCNQ})\cdot 3C_7H_8\}_\infty$	2.405(1)	2.174(4)	N	201
$[Rh_2(O_2CCF_3)_4(1,4\text{-bq})\cdot 3C_6H_6]_\infty$	2.407(1)	2.248(5)	O	242
$[Rh_2(O_2CCF_3)_4(2,3\text{-dmbq})\cdot 1.5C_6H_6]_\infty$	2.400(2)	2.247(9)	O	242
$[Rh_2(O_2CCF_3)_4(1,4\text{-nq})\cdot C_6H_6]_\infty$	2.405(1)	2.248(3)	O	242
$\{Rh_2(O_2CCF_3)_4[CH_3OC_6H_4C(CO_2CH_3)]_2\}_\infty$	2.398(1)	2.254(4)	O	308
$[Rh_2(O_2CCF_3)_4(\mu_2\text{-}\eta^1\text{:}\eta^1\text{-}3\beta\text{-acetoxylanostan-11}\beta\text{-olato})]_\infty$	2.417[c]	2.273[c,ccc] 2.284[c,lll]	O	241
$Rh_2(\mu\text{-}O_2CCF_3)_2\{C_6H_4[\mu\text{-}(CH_2)_2CO_2]_2\}(Me_2CO)_2$	2.397[c]	2.282[c]	O	109

Pictiva EX2004
Samsung v Pictiva
IPR2024-01094

Compound	r (Rh–Rh)[a] (Å)	r (Rh–L_{ax})[b] (Å)	Donor atom(s)	ref.
$Rh_2(O_2CC_2H_5)_4(DMSO)_2$	2.407(1)	2.453(1) 2.445(1)	S	227
$Rh_2(O_2CC_2H_5)_4(ACR)_2$	2.417(1)	2.413(3)	N	155
$Rh_2(O_2CC_2H_5)_4(AcrNH_2)_2$	2.405(1)	2.280(4)	N	65
$[Rh_2(O_2CC_2H_5)_4(\mu_2\text{-}\eta^1\text{:}\eta^1\text{-PHZ})]_\infty$	2.409(1)	2.362(4)	N	155
$[Rh_2(O_2CC_2H_5)_4(\mu_2\text{-}\eta^1\text{:}\eta^1\text{-DDA})]_\infty$	2.387(1)	2.324(6)	N	155
$Rh_2(O_2CC_2H_5)_4(metro)_2$	2.403(1)	2.259(5) 2.247(5)	N	177
$Rh_2(O_2CC_2H_5)_4(azin)_2$	2.403(1)	2.266(6)	N	155
$Rh_2(O_2CC_2H_5)_4(NO)_2$	2.512(2)	1.951(3)	N	218
$Rh_2(O_2CC_2H_5)_4(PPr^i_3)_2$	2.460(1)	2.498(1)	P	285
$Rh_2(O_2CC_2H_5)_4(PCy_3)_2$	2.462(1)	2.487(1)	P	285
$[Rh_2(O_2CC_3H_7)_4]_\infty$	2.366(1)	2.34[f]	O[g]	298
$Rh_2(O_2CC_3H_7)_4(CH_3OH)_2$	2.369(5)[ddd]	[eee]	O	186
$Rh_2(O_2CC_3H_7)_4(NO)_2$	2.519(1)	1.945(3)	N	218
$[Rh_2(O_2CC_3H_7)_4(Me_2SO)_2][Rh_2(O_2CC_6H_4\text{-}4\text{-}OH)_4(Me_2SO)_2]\cdot 2EtOH$	2.404(1)[fff] 2.410(1)[ggg]	2.427(1)[fff] 2.444(1)[ggg]	S	249
$Rh_4(O_2CC_3H_7)_4Cl_4(NCCH_3)_4$	2.555(1)	2.272(6)	N	197
$Rh_2(O_2CCMe_3)_4(H_2O)_2$	2.371(1)	2.295(2)	O	226
$[Rh_2(O_2CCMe_3)_4(NEt_3)_2]_\infty$	2.413(1)	2.391(8)	N	135
$[Rh_2(O_2CCMe_3)_4(4,4'\text{-bpy})]_\infty$	2.395(1)	2.225(5) 2.264(5)	N	135
$Rh_2(O_2CCMe_3)_4(\eta^1\text{-temyl})$	2.424[c]	2.057[c]	C	277
$[Rh_2(O_2CCMe_3)_4(1,4\text{-bq})]_\infty$	2.403(1) 2.375(1)	2.289(3)[ll] 2.439(4)[hhh] 2.488(5)[hhh]	O C	275
$[Rh_2(O_2CCMe_3)_4(1,4\text{-bq})]_\infty$	2.400(1) 2.377(1)	2.293(2)[ll] 2.435(4)[hhh] 2.486(5)[hhh]	O C	276

Pictiva EX2004
Samsung v Pictiva
IPR2024-01094

Compound	r (Rh–Rh)[a] (Å)	r (Rh–L_{ax})[b] (Å)	Donor atom(s)	ref.
$[Rh_2(O_2CCMe_3)_4(1,4\text{-nq})]_\infty$	2.402(1) 2.367(1)	2.338(7)[ll] 2.486(8)[hhh] 2.479(9)[hhh]	O C	276
$Rh_2(O_2CCMe_3)_4(Nic)_2$	2.386(5)	2.12(3) 2.36(1)	N	159
$\{Rh_2(O_2CCMe_3)_4[CH_3OC_6H_4C(CO_2CH_3)N]_2\}_\infty$	2.370(1)	2.420(2)	O	308
$[Rh_2(O_2CCH_2NMe_3)_4Cl_2]Cl_2{\cdot}4H_2O$	2.413(1)	2.557(1)	Cl	297
$(Bu^t{}_4N)_2[Rh_8(O_2CBu^t)_{16}(\mu_2\text{-}\eta^1{:}\eta^1\text{-}O_2CCH_3)_2]{\cdot}2C_6H_6$	2.38(1)	2.17(2)[h] 2.61(2)[f]	O[h] O[g]	239
cis-$[Rh_2(O_2CCPh_3)_2(O_2CCH_3)_2(NCCH_3)_2]{\cdot}C_6H_5Me$	2.388(2)	2.17(1) 2.21(2)	N	38
$Rh_2(O_2CCPh_3)_4(ErOH)_2$	2.365(1)	2.31(2)	O	68
$Rh_2[O_2C(CH_2)_3Ph]_4(metro)_2$	2.394(1)	2.232(3)	N	67
$Rh_2(O_2CC_6H_5)_4(DMSO)_2{\cdot}C_6H_5Me$	2.405(1)	2.454(2)	S	248
$Rh_2(O_2CC_6H_5)_4(py)_2$	2.402(1)	2.247(4)	N	124,151
$[Rh_2(O_2CC_6H_5)_4(pyz)_2]_\infty$	2.391(1)	2.185(6) 2.200(5)	N	207,208
$Rh_2(TTB)_4(py)_2$	2.374(3)	2.21(3)	N	39
$Rh_2(TTB)_3(\mu\text{-}O_2CCH_3)(py)_2{\cdot}0.37H_2O$	2.401(1)	2.18(2)	N	39
$Rh_2[\mu\text{-}O_2CCC_6H_2\text{-}3,4,5\text{-}(OEt)_2]_4(pyz)_2$	2.404(1)	2.252(2)	N	69
$Rh_2(\mu\text{-}O_2CC_6H_4\text{-}2\text{-}Ph)_4(NCCH_3)_2{\cdot}3C_6H_6$	2.396[c]	2.233(3)	N	38
$[Rh_2(O_2CC_6H_5)_4(\mu_2{:}\eta^1{:}\eta^1\text{-}btp)]_\infty$	2.404(1)	2.272(4)	N	149
$Rh_2(O_2CC_6H_4\text{-}2\text{-}OH)_4(EtOH)(H_2O)$	2.385(2)	2.30(1)[iii]	O	71
$(Rh_{0.88}Cu_{0.12})_2(O_2CCH_3)_4(H_2O)_2$[iii]	2.398(1)	2.276(5)	O	229
$[K(18\text{-crown-}6)(H_2O)]_2[K(18\text{-crown})(H_2O)_2]\{[Rh_2(O_2CC_6H_5)_4[Fe(CN)_6]\}{\cdot}8H_2O$	2.411(1)	2.207(3)	N	307
$(Et_4N)\{[Rh_2(O_2CCH_3)_4]_4[Cp^*Ir(CN)_3]\}$	2.402(2)	2.23(1)	N	306
$[Rh_2(O_2CCH_3)_4]_2[K_3Co(CN)_6]$	2.397(2)	2.20(1)	N	304
$\{[Rh_2(O_2CCH_3)_4][Mn(Mepyzca)_2(MeOH)_2{\cdot}2MeOH]\}_\infty$	2.398(1)	2.281(4)	N	309
$[Rh_2(\beta\text{-Ala})_4(H_2O)_2](ClO_4)_4{\cdot}2H_2O$	2.38[c]	2.34[c]	O	94

Pictiva EX2004
Samsung v Pictiva
IPR2024-01094

Compound	r (Rh–Rh)[a] (Å)	r (Rh–L_{ax})[b] (Å)	Donor atom(s)	ref.
$[Rh_2(\beta\text{-Ala})_4(H_2O)_2](ClO_4)_4{\cdot}4H_2O$	2.386(3)	2.33(1)	O	95
$Rh_2(N\text{-phthaloyl-}S\text{-phenylalaninate})_4(4\text{-Bu}^t\text{-py})_2$	kkk	kkk	N	151
$Rh_2[(R)\text{-mpa}]_4(THF)_2$	2.390[1]	2.289[9]	O	106
$Rh_2[(S)\text{-mand}]_4(EtOH)_2]{\cdot}0.43EtOH$	2.386[2]	2.295[7]	O	106
$\{Rh_2[(R)\text{-mtfpa}]_4(dmopehhypy)_2{\cdot}CHCl_3\}_\infty$	2.380(1) 2.377(1)	2.23(1) 2.30(1)	O	107
$Rh_2[Br_2calix[4]arene(CO_2)_2]_2(C_6H_5Me)_2$	2.399(2)	$2.968^{c,\infty}$ $3.027^{c,\infty}$	C	92
$[Rh_2(TBSP)_4(DMF)_2]{\cdot}0.5C_6H_5Me{\cdot}0.5n\text{-}C_5H_{12}$	2.391(1)	2.264(3) 2.262(3)	O	108
$Rh_2(TiPB)_4$	2.350(1)	iii	iii	16,75
$Rh_2(TiPB)_4(NCCH_3)$	2.354(1)	2.10(2)	N	75
$Rh_2(TiPB)_2(\mu\text{-}O_2CCH_3)_2(NCCH_3)_2$	2.400(1)	2.266(3)	N	75
$Rh_2(TiPB)_4(NCCH_3)_2{\cdot}CH_3CN$	2.388(1)	2.237[5]	N	75
$Rh_2(TiPB)_4(TiBPH)_2{\cdot}0.5C_6H_{14}$	2.367[1]	2.285[4]	O	75
$Rh_2(TiPB)_4(Me_2CO)_2{\cdot}0.90Me_2CO$	2.370[1]	2.31[1]	O	75
$Rh_2(TiPB)_4(H_2O)(\eta^2\text{-}C_6H_5CH_3)$	2.364(1)	$2.271(4)^{ymmm}$ $2.80^{c,nnn}$	O C^{nnn}	75
$Rh_2(TiPB)_3(\mu\text{-}O_2CCF_3)(TiPBH)_2$	2.367(1)	2.242[4]	O	75
$[Rh_2(TiPB)_3(\mu\text{-}O_2CCH_3)(TiPBH)]_2{\cdot}1.25C_6H_{14}$	2.358[1]	$2.279^{c,\infty\infty}$ $2.236^{c,\infty\infty}$ $2.395^{c,f}$ $2.361^{c,f}$	O O^g	75
$[Rh_2(TiPB)_2(\mu\text{-}O_2CCF_3)_2(TiPBH)]_2{\cdot}C_6H_{14}$	2.389(1)	$2.300[4]^{\infty\infty}$ $2.343^{c,f}$	O O^g	75
$[Rh_2(TiPB)_2(\mu\text{-}O_2CCF_3)_2(\eta^2\text{-}C_6H_5Me)]_2{\cdot}2C_6H_5Me$	2.396(1)	$2.652^{c,ppp}$ $2.752^{c,ppp}$ $2.300(3)^f$	O^g C^{ppp}	75

Pictiva EX2004
Samsung v Pictiva
IPR2024-01094

Compound	r (Rh–Rh)[a] (Å)	r (Rh–L_{ax})[b] (Å)	Donor atom(s)	ref.
$[Rh_2(TiPB)_2(\mu\text{-}O_2CCF_3)_2(Me_2CO)]_2$	2.392[1]	2.241[c,ll] 2.262[c,ll] 2.343[c,f] 2.345[c,f]	O O[g]	75
$Rh_2(TiPB)_2(\mu\text{-}O_2CCF_3)_2(Me_2CO)_2$	2.401(1)	2.268(4)	O	75
$Rh_2[O_2C(1\text{-adamantyl})]_4(MeOH)_2\cdot 5MeOH$	2.371(2)	2.296(9)	O	38
$Rh_2(camphanate)_4(MeOH)_2$	2.396[c]	2.24(1)	O	76
$Rh_2(O_2CC_3F_7)_4(DMF)_2\cdot 0.5C_6H_5Me$	2.416(1)	2.234[c] 2.232[c]	O	231
$Rh_2(O_2CC_3F_7)_4(dimenol)_2$	2.409(1)	2.387(4)	N	156
$Rh_2(O_2CC_3F_7)_4(Tempo)_2$	2.431(1)	2.235(5)	O	243,244
$Rh_2(O_2CC_9F_{19})_4(MeOH)_2\cdot 2MeOH$	2.404(3)	2.21(1)	O	231
(S, O) donor bridging groups				
$Rh_2(OSCCMe_3)_4(py)_2$	2.514(1)	2.253(5)	N	124
$Rh_2(OSCPh)_4(py)_2$	2.521(1)	2.236(7)	N	124
$Rh_2(OSCBu^t)_4(PPh_3)_2$	2.584(1)	2.475(2)	P	125
$Rh_2(\mu\text{-}OSCCH_3)_4(CH_3CSOH)_2$	2.550(3)	2.521(5)	S	117,118
Building blocks supported by carboxylate groups				
$\{[Rh_2(O_2CCF_3)_4]_3CH_3Si(C_5H_4N)_3(\eta^1\text{-}C_6H_6)_3\}\cdot C_6H_6$	2.420(1)	2.152(6)[qqq] 2.69(2)[rrr]	N C[rrr]	303
$\{Rh_2(O_2CCF_3)_4]_2(C_6H_5)_2Si(C_5H_4N)_2\}$	2.415(1)	2.150(5)[qqq] 2.776(8)[sss] 2.99(1)[sss]	N C[sss]	303

Pictiva EX2004
Samsung v Pictiva
IPR2024-01094

Compound	r (Rh–Rh)[a] (Å)	r (Rh–L_{ax})[b] (Å)	Donor atom(s)	ref.
{[$Rh_2(O_2CCF_3)_4$]$_3$[μ_5-(HO)C($C_5H_4N)_3$][η^1-C_6H_6)}·0.5C_6H_6	2.410(1) 2.413(1)	2.125(7)[qqq] 2.166(7)[qqq] 2.137(7)[qqq] 2.470(5)[rrr] 2.780[c,uuu] 2.66(3)[vvv]	N O C	303
Rh_2{[$O_2CC(CH_3)_2CH_2OCH_2$]$_2$C($CH_3)_2$}($py)_2$	2.402(1)	2.254(1)	N	110
Rh_2{$O_2CC(CH_3)_2OC_6H_4OC(CH_3)_2CO_2$}{$O_2C(CH_2)_{10}CO_2$}(4-Bu^t-$py)_2$	2.404[c]	2.251[c] 2.187[c]	N	112
Rh_2{$O_2CC(CH_3)_2OC_6H_4OC(CH_3)_2CO_2$}$_2$(4-Bu^t-$py)_2$	2.411[c]	2.237[c]	N	112
cis-Rh_2($O_2CCH_3)_2$){$O_2CC(CH_3)_2OC_6H_2Br_2OC(CH_3)_2CO_2$}($py)_2$	2.408[c]	2.228[c] 2.259[c]	N	112
Rh_2{$O_2CC(CH_3)_2OC_6H_2Br_2OC(CH_3)_2CO_2$}$_2$(4-Bu^t-$py)_2$	2.409[c]	2.209[c]	N	112
cis-Rh_2(μ-$O_2CCH_3)_2$){$O_2CC(CH_3)_2OC_6H_2$(Bu^t)$_2OC(CH_3)_2CO_2$}(4-Bu^t-$py)_2$	2.406[c]	2.239[c] 2.255[c]	N	112
{Rh_2($O_2CC(CH_3)_2OC_6H_2$(Bu^t)$_2OC(CH_3)_2CO_2$}$_2$($PhNMe_2$)}$_\infty$	2.405[c]	2.315[c] 2.709[c,www] 3.077[c,www]	N C[www]	112
cis-Rh_2(μ-$O_2CCH_3)_2$){$O_2CC(CH_3)_2OC_6H_4OC(CH_3)_2CO_2$}(4-Bu^t-$py)_2$	2.409(1)	2.24(1) 2.21(1)	N	111,112
{Rh_2($O_2CC_6H_4CO_2$)$_2$[$O_2CC(CH_3)_2OC_6H_4OC(CH_3)_2CO_2$][4-Bu^t-$py)_2$}$_4$·2$C_6H_{14}$[xxx]	2.411(3) 2.410(3)	2.239[c] 2.201[c] 2.259[c] 2.234[c]	N	111
[Rh_2(μ-$O_2CCH_3)_2$]$_2$[$O_2CC(CH_3)_2O$]$_2$PhPh[$OC(CH_3)_2CO_2$]$_2$}(4-Bu^t-$py)_4$	2.408[c]	2.247- 2.250[c,yyy]	N	115
trans-(HL)(O_2CCH_3)$Rh_2L_2Rh_2$($O_2CCH_3)_2$($THF)_2$[zzz,aaaa]	2.366[c] 2.371[c]	2.302[c] 2.315[c]	O[bbbb]	113
trans-(HL)(O_2CCH_3)$Rh_2L_2Rh_2$(O_2CCH_3)(HL)$(THF)_2$[zzz,aaaa]	2.367[c]	2.284[c]	O[bbbb]	113

Pictiva EX2004
Samsung v Pictiva
IPR2024-01094

Compound	r (Rh–Rh)[a] (Å)	r (Rh–L_{ax})[b] (Å)	Donor atom(s)	ref.
$\{Rh_2[O_2C(CH_3)_2OC_6H_4OC(CH_3)_2CO_2][O_2CC_6H_2(OH)_2CO_2]\}_4 \cdot 11EtOH \cdot 2CH_3CO_2C_2H_5 \cdot 2H_2O$[xxx]	2.383(1) 2.382(1)	2.238[c,ccc] 2.305[c,ll]	O	114
$\{Rh_2[O_2C(CH_3)_2OC_6H_4OC(CH_3)_2CO_2][O_2CC_{10}H_6CO_2]\}_4 \cdot 16CH_3OH \cdot H_2O$[xxx]	2.383(1) 2.379(1)	2.280[c,ccc] 2.294[c,ccc] 2.260[c,ccc] 2.264[c,ccc]	O	114
$\{Rh_2[O_2C(CH_3)_2OC_6H_4OC(CH_3)_2CO_2][O_2CC_6Cl_4CO_2]\}_4 \cdot 10EtOH \cdot 2CH_3CO_2C_2H_5$[xxx]	2.389(1) 2.388(1)	2.309[c,ccc] 2.299[c,ccc] 2.276[c,ccc]	O	114
$\{Rh_2[O_2C(CH_3)_2OC_6H_4OC(CH_3)_2CO_2][O_2CC_6(CH_3)_4CO_2]\}_4 \cdot 10CH_3OH \cdot 12H_2O$[xxx]	2.373(1) 2.380(1)	2.285[c,ccc] 2.261[c,ccc] 2.312[c,ccc]	O	114

[a] Distances are given with up to 3 decimal digits.
[b] In some cases the average Rh–L bond lengths are quoted. In these instances the estimated deviation, which is given in square brackets, is calculated as $[\ ] = [\Sigma_n \Delta_i^2/n(n-1)]^{1/2}$, in which Δ_i is the deviation of the ith of n values from the arithmetic mean of the set.
[c] Esds not reported.
[d] The longer of these two distances is Rh–O (H_2O), the shorter one is Rh–O (HCO_2^-).
[e] Crystal structure determined by X-ray powder diffraction.
[f] Rh–O distance to the carboxylate bridge of neighboring Rh_2^{4+} unit.
[g] Carboxylate bridge of neighboring Rh_2^{4+} unit.
[h] The compound contains *ax* acetate groups.
[i] The longer of these two distances is Rh–N (NO_2), the shorter one is Rh–N (NO).
[j] Low resolution structure (4 Å) due to poor quality of crystals.
[k] Different crystalline form from that in ref. 138.
[l] Distance to the pyridine coordination site.
[m] Distance to the amine coordination site.
[n] The crystal contains two kinds of dirhodium units: one with the *ax* sites occupied by pyridine nitrogen atoms and one with the *ax* sites occupied by amino nitrogen atoms.
[o] Nitrogen atom of the pyridine ring.
[p] The compound crystallizes in the space group $C2/c$.
[q] The compound crystallizes in the $P\bar{1}$ space group.
[r] Rh–N distance to pyrimidine ring nitrogen.
[s] Rh–N distance to the aminomethyl substituent nitrogen.
[t] Only the unit cell has been determined.
[u] Rh–P distance.
[v] Average distance.
[w] Binding takes place via a pendant NH_2 group of the acridine ligand.
[x] Centrosymmetric '*dimer of dimers*'.
[y] Distance to O of *ax* acetone molecule.
[z] Rh–S distance.
[aa] Rh–O distance.
[bb] There are three Rh_2^{4+} units with only O atoms at the ends, two with only S atoms and two with both O and S atoms.
[cc] Rh–O distance to the DMSO oxygen atom.

Pictiva EX2004
Samsung v Pictiva
IPR2024-01094

ddd Array of six rhodium atoms linked into infinite chains $[[Rh_2(\mu\text{-}O_2CCF_3)_2(CO)_4][Rh_2(\mu\text{-}O_2CCF_3)_4][Rh_2(\mu\text{-}O_2CCF_3)_2(CO)_4]]_\infty$.

eee Axial distance of $Rh_2(\mu\text{-}O_2CCF_3)_4$ Rh atom to Rh atom of neighboring $Rh_2(\mu\text{-}O_2CCF_3)_2(CO)_4$ unit.

fff Rh(I)···Rh(I) distance within the $Rh_2(\mu\text{-}O_2CCF_3)_2(CO)_4$ unit.

ggg Rh···Rh distance between two adjacent $Rh_2(\mu\text{-}O_2CCF_3)_2(CO)_4$ moieties.

hhh This Rh–Rh distance is encountered in the Rh_2^{4+} unit with two bidentate and two monodentate CF_3CO_2 ligands.

iii The Tempol ligand is bound through its hydroxyl group.

jjj Distance to alkyne carbon atom.

kkk Distance to arene carbon atom.

lll Distance to ax $O_{carbonyl}$.

mmm $C_{12}H_8$; acenaphthylene.

nnn $C_{12}H_{10}$; acenaphthene.

ooo The second set of Rh···C distances is the same.

ppp $C_{14}H_{10}$; anthracene.

qqq $C_{14}H_{10}$; phenanthrene.

rrr $C_{16}H_{10}$; pyrene.

sss All four Rh···C distances are the same.

ttt $C_{16}H_{10}$; fluoranthene.

uuu η^1-coordination.

vvv $C_{18}H_{12}$; 1,2-benzanthracene.

www $C_{18}H_{12}$; triphenylene.

xxx $C_{18}H_{12}$; chrysene.

yyy $C_{20}H_{10}$; corannulene.

zzz $C_{30}H_{12}$; hemibuckminsterfullerene.

aaaa Average value of two Rh–C distances for each *exo*-coordinated rhodium center; η^2-coordination mode.

bbbb Rh–C distance of *endo*-bound rhodium atom; η^1-coordination mode.

ccc Distance to ax $O_{alcohol}$.

ddd Distance determined by EXAFS.

eee No distance reported.

fff Distance in butyrate adduct.

ggg Distance in *p*-hydroxybenzoate adduct.

hhh Distance to carbon of double bond.

iii Same Rh–O distance to EtOH and H_2O molecules.

jjj Mixed Rh:Cu complex (88:12 ± 3%).

kkk No coordinates available.

lll Tetracarboxylate compound with no ax ligands.

mmm The value refers to the ax water molecule.

nnn There is a toluene molecule oriented in an η^2 fashion towards the other ax position at an average distance of 2.80 Å.

ooo Distance to the carbonyl group of an ax TiPBH molecule.

ppp A toluene molecule is oriented in a η^2 fashion towards the free ax position of each subunit at an average distance of 2.70 Å.

qqq Distance to N atom of pyridyl group.

rrr A benzene molecule is present at the open ax end of each dirhodium unit.

sss Metal-π interactions with the phenyl groups of the ligand.

ttt Distance to O of OH group.

uuu Distance to carbon atom of the pyridyl ring.

vvv Distance to carbon atom of the benzene molecule that occupies one ax site.

www Weak interactions with the aromatic carbons of the aniline ring axially bound to the flanking dirhodium unit.

xxx Molecular square.

yyy Range of distances.

zzz H_2L: 2,7-di-Bu^t-9,9-dimethyl-4,5-xanthenedicarboxylic acid.

aaaa Macrocyclic dimer.

bbbb THF oxygen atom.

Pictiva EX2004
Samsung v Pictiva
IPR2024-01094

The most commonly encountered $Rh_2(O_2CR)_4L_2$ compounds in the series adopt the discrete structure **12.11** and consist of the dirhodium core with essentially D_{4h} symmetry and almost invariably two *ax* ligands L that typically are identical. Exceptions include $Rh_2(O_2CC_6H_4$-2-$OH)_4(EtOH)(H_2O)$,[71] $Rh_2(O_2CCH_3)_4(NO)(NO_2)$,[134,216,217] $Rh_2(TiPB)_4(H_2O)(\eta^2$-$C_6H_5CH_3)$,[75] $Na[Rh_2(\mu$-$O_2CH)_4(\mu_3$-η^1:η^1:η^1-$O_2CH)(H_2O)]$,[235] the dimeric adduct $[Rh_2(O_2CCF_3)_4(Me_2CO)]_2$-$(\mu_2$-$\eta^2$:$\eta^2$-$C_4I_2)$[59] and the rare tetracarboxylate compound $Rh_2(TiPB)_4(NCCH_3)$, which has only one *ax* ligand.[75] The structural features of the monohydrate $Rh_2(O_2CH)_4(H_2O)$,[28,302] obtained from a formic acid solution containing small quantities of water, and the adducts $Rh_2(O_2CCH_3)_4L$ (L = DMSO, SEt_2), which were prepared as bulk materials by thermal decomposition of the corresponding bis-adducts,[43] have not been confirmed.

Another dirhodium tetracarboxylate group comprises 1:1 $Rh_2(O_2CR)_4L$ adducts arranged in polymeric infinite structures (Fig. 12.2a). In general, the *ax* ligands encountered in this group contain at least two binding sites, but there are a few exceptions such as those of the pyramidal complex $\{[Rh_2(O_2CCF_3)_4]_3CH_3Si(C_5H_4N)_3(\eta^1$-$C_6H_6)_3\}$ with three donor atoms of the pyridyl groups bridging three dirhodium units,[303] a few cases where the ligand exhibits tetradentate behavior (for $Rh_2(O_2CR)_4L$, with R = CF_3 and L = TCNE (Fig. 12.3),[200] R = CF_3 and L = TCNQ,[201] R = CH_3 and L = $Co(CN)_6^{3-}$,[304] and R = CF_3 and L = $(C_6H_5)_2Si(C_5H_4N)_2$ with the ligand binding via two N-donor atoms and two phenyl groups[303]), the adducts of the tetrakis(trifluoroacetate) with 1,4-diiodo-1,3-butadiyne,[59] and tri-, tetra- or multidentate aromatic hydrocarbons,[57,58] as well as the case of the unusual supramolecular assembly of $\{[Rh_2(O_2CCF_3)_4]_3[\mu_5$-$(HO)C(C_5H_4N)_3](\eta^1$-$C_6H_6)\}$.[303] There are a few examples, however, wherein a single donor atom of the ligand is engaged in bridging two Rh_2^{4+} units, leading to 1-D chain structures, e.g., $[Rh_2(O_2CCF_3)_4(\mu$-DMSO-*O*$)]_\infty$,[51] $[Rh_2(O_2CCF_3)_4(THF)]_\infty$ (Fig. 12.4),[49] $[Rh_2(O_2CCF_3)_4(Me_2SeO)]_\infty$[238] and $[Rh_2(O_2CCF_3)_4(Me_2Se)]_\infty$.[238]

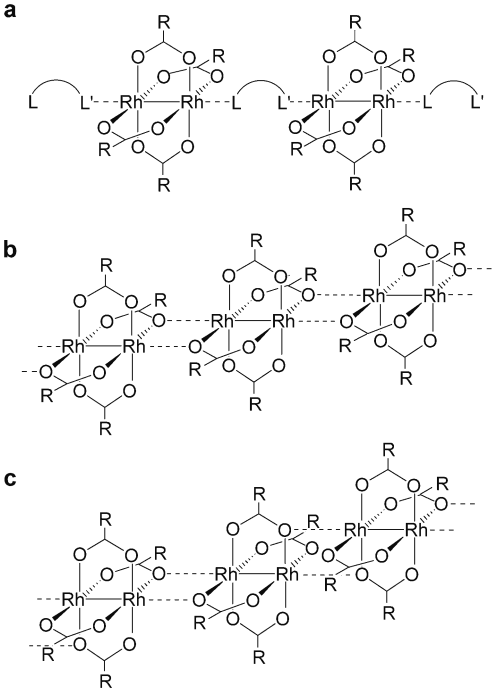


Fig. 12.2. Possible structural motifs of dirhodium tetracarboxylate compounds.

Pictiva EX2004
Samsung v Pictiva
IPR2024-01094

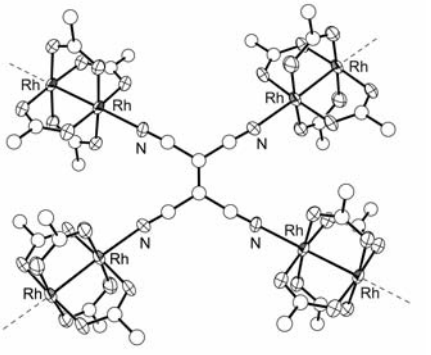


Fig. 12.3. Molecular structure of $[Rh_2(O_2CCF_3)_4]_2(\mu_4\text{-TCNE})$.

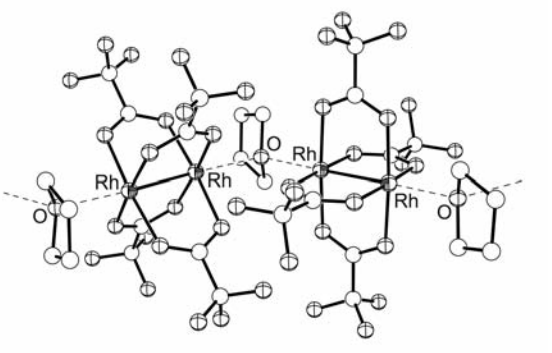


Fig. 12.4. A fragment showing the zig-zag chain structure $[Rh_2(O_2CCF_3)_4(THF)]_\infty$.

In the case of bidentate ligands L-L', the $Rh_2(O_2CR)_4$ units form infinite linear or zig-zag chains **a** (Fig 12.2), depending on the ligand and the hybridization of the donor atom. The ligand L-L' may employ the same donor atoms (L = L') such as in the cases of L-L' = PHZ (linear chain),[155] DDA,[155] NCPhCN,[198] I_2 (Fig. 12.5),[54] S_8,[56] TCNE,[202] DCNNQI and DM-DCNQI,[203] 4,4'-bpy,[135] 1,2-dimethoxy-4,5-bis[(2-pyridyl)ethynyl]benzene (dmpyethybz),[150] 1,3,5-tris[(2-pyridyl)ethenyl]benzene (tpyethebz; Fig. 12.6; zig-zag chain),[305] 2,6-bis-(*N*'-1,2,4-triazolyl)pyridine (btp),[149] *p*-quinones,[242] nickel biphenylbiguanide (linear chain),[148] $Cp^*Ir(CN)_3^-$,[306] $Fe(CN)_6^-$,[307] pyrazine (Fig. 12.7; linear chain),[207,208] dimeric azine molecules,[308] pyrazinecarboxylate compounds,[309] $[Rh_2(\mu\text{-}O_2CCF_3)_2(CO)_4]$ units (Fig. 12.8; linear chain),[50,310] substituted ferrocene[161,162] and ferrocenylphosphines.[311] In addition, there are examples where the *ax* ligands have the same type of donor atoms but these are part of different chemical functionalities as in L-L' = AAMP (*N*-coordination through pyrimidine and aminomethyl N atoms),[165] NITMe (*O*-coordination through nitrosyl and nitroxide oxygen atoms),[219] ammpy (pyridine and amine *N*-coordination),[147] and 3β-acetoxylanostan-11β-ol (hydroxy and acetoxy group *O*-coordination).[241] The same donor atom may also coordinate to the metal at opposite

Pictiva EX2004
Samsung v Pictiva
IPR2024-01094

sides of the molecule (*exo* and *endo* sides), as in the corannulene[58] (Fig. 12.9) and hemibuckminsterfullerene[59] adducts. Ligand donor atoms of different identity L-L' (L ≠ L') can be employed to link dimetal units, e.g., the *N,O* coordinated nitroxide radical IMMe,[219] *S,O*-bound DMSO,[51] *p*-quinones coordinated through the carbonyl group and the C=C double bond (Fig. 12.10)[275,276] and $PhNMe_2$ in the polymeric structure $\{Rh_2\{O_2CC(CH_3)_2OC_6H_2(Bu^t)_2OC(CH_3)_2CO_2\}_2(PhNMe_2)\}_\infty$;[112] *ax* interactions in the dirhodium units of the latter are mediated through the nitrogen and *p*-carbon atoms of *N,N'*-dimethylaniline.[112]

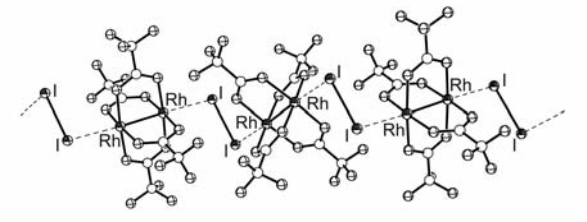


Fig. 12.5. A fragment showing the alternating arrangement of $Rh_2(O_2CCF_3)_4$ and weakly coordinated diiodine molecules in $\{[Rh_2(O_2CCF_3)_4I_2]\cdot I_2\}_\infty$.

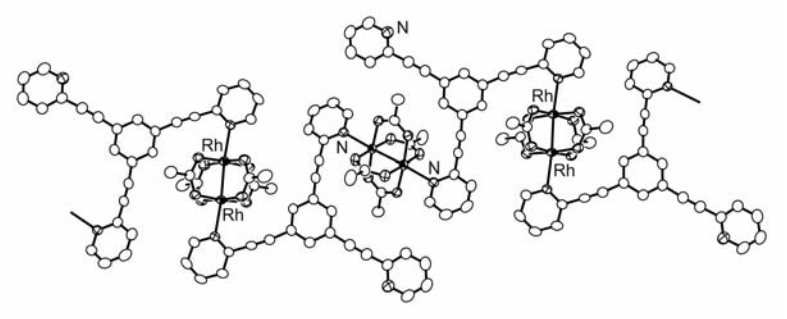


Fig. 12.6. A fragment of the 1-D zig-zag chain $[Rh_2(O_2CCH_3)_4(\mu_2\text{-}\eta^1{:}\eta^1\text{-tpyethebz})\cdot CH_2Cl_2]_\infty$.

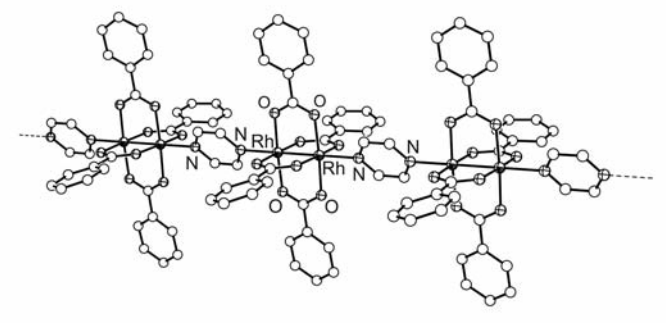


Fig. 12.7. A fragment of the linear chain structure $[Rh_2(O_2CC_6H_5)_4(pyz)_2]_\infty$.

Pictiva EX2004
Samsung v Pictiva
IPR2024-01094

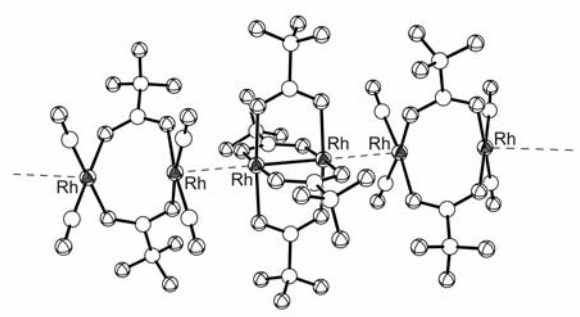


Fig. 12.8. A fragment of the arrangement of $Rh_2(O_2CCF_3)_4$ and $Rh_2(\mu\text{-}O_2CCF_3)_2(CO)_4$ units in the linear chain structure $\{Rh_2(O_2CCF_3)_4[Rh_2(\mu\text{-}O_2CCF_3)_2(CO)_4]_2\}_\infty$.

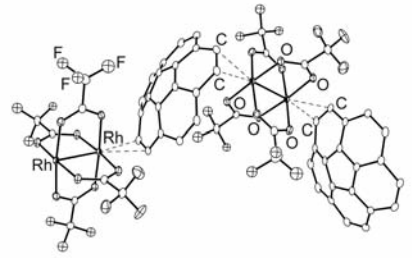


Fig. 12.9. A fragment of the 1-D infinite chain structure $\{[Rh_2(\mu\text{-}O_2CCF_3)_4]\text{-}(\mu_2\text{-}\eta^2\text{:}\eta^2\text{-}C_{20}H_{10})\}_\infty$.

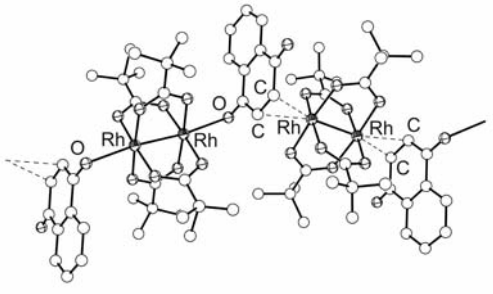


Fig. 12.10. A fragment of the infinite chain structure $[Rh_2(O_2CCMe_3)_4(1,4\text{-nq})]_\infty$.

In the absence of exogenous donor ligands, dirhodium units generally are arranged so that the *ax* sites of each dimer associate with the oxygen atoms of an adjacent carboxylate group to form structures with infinite chains, such as those in $[Rh_2(O_2CCH_3)_4]_\infty$ (Fig. 12.2b),[312] $[Rh_2(O_2CCF_3)_4]_\infty$ (Fig. 12.2b)[47] or $[Rh_2(O_2CC_3H_7)_4]_\infty$ (Fig. 12.2c).[298] These types of interactions are most likely present in other tetracarboxylate compounds, e.g., the linear chain alkanoates $Rh_2(O_2CC_nH_{2n+1})_4$ (n = 5, 7, or 11)[63,64] and the alkoxybenzoates $Rh_2(O_2CC_6H_4\text{-}4\text{-}OC_nH_{2n+1})_4$ (n = 8-14).[70] The latter compounds exhibit a conversion to a thermotropic discotic mesophase (i.e., a liquid crystalline phase) at 100-110 °C accompanied by structural changes from a crystalline compound to a

Pictiva EX2004
Samsung v Pictiva
IPR2024-01094

2-D rectangular or hexagonal columnar liquid-crystal phase.[63,64,70,313,314] Additionally, there are several adducts wherein the $Rh_2(O_2CR)_4$ core is associated with an adjacent Rh_2^{4+} unit through the O atoms of the carboxylate groups at one *ax* site only, whereas the opposite *ax* site is occupied by a different ligand L; such examples include the infinite chain $\{[Rh_2(O_2CCF_3)_4]_3(\mu_2\text{-DMSO-}S,O)_2\}_\infty$ (Fig. 12.11),[51] the adduct $(Bu^t{}_4N)_2[Rh_8(O_2CBu^t)_{16}(\mu_2\text{-}\eta^1\text{:}\eta^1\text{-}O_2CCH_3)_2]$[239] and the '*dimers of dimers*' $[Rh_2(O_2CCF_3)_4(THF)]_2$,[49] $[Rh_2(O_2CCF_3)_4(OCMe_2)]_2$,[315] $[Rh_2(O_2CCH_3)_4(CNPh)]_2$,[279] $[Rh_2(TiPB)_n(O_2CR)_{4-n}L]_2$ (R = CH_3, CF_3, L = TiPBH, Me_2CO, η^2-$C_6H_5CH_3$, n = 2, 3),[75] $[Rh_2(O_2CCH_3)_4(PPh_3)]_2$[279] and $\{Rh_2(O_2CCH_3)_4[Ph_2P(o\text{-}MeOC_6H_4)]\}_2$.[280] Despite the strong affinity of Rh_2^{4+} tetracarboxylate complexes for *ax* ligands (illustrated by the aforementioned structural motifs), the synthesis of the paddlewheel dirhodium compound $Rh_2(TiPB)_4$ (Fig. 12.12), with no *ax* ligands, has been accomplished.[16,75] The isolation of this complex as discrete, undimerized units is attributed to the presence of four sterically bulky 1,3,5-triisopropylphenyl groups which render impossible the association of each dirhodium unit with the carboxylate oxygen atoms of a neighboring Rh_2^{4+} core.[16,75]

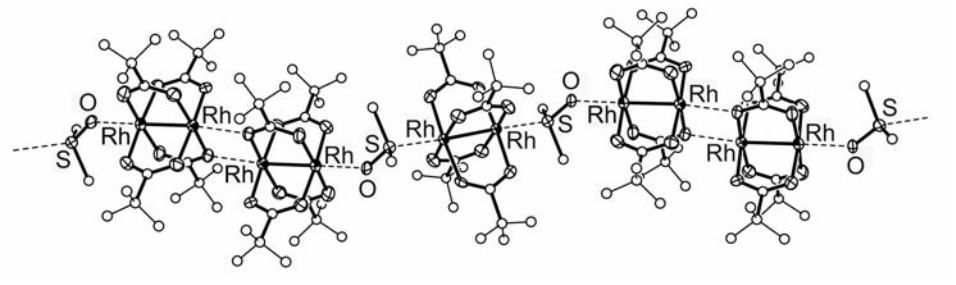


Fig. 12.11. A fragment showing the arrangement of $Rh_2(O_2CCH_3)_4$ and DMSO units in the extended structure $\{[Rh_2(O_2CCF_3)_4]_3(\mu_2\text{-DMSO-}S,O)_2\}_\infty$.

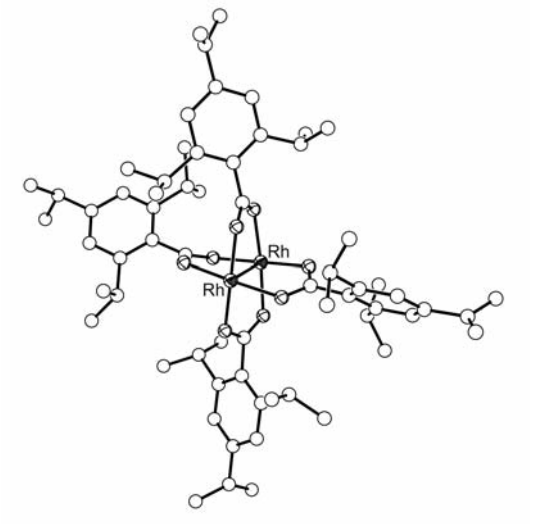


Fig. 12.12. Molecular structure of $Rh_2(TiPB)_4$.

Pictiva EX2004
Samsung v Pictiva
IPR2024-01094

The *ax* Lewis bases of $Rh_2(O_2CR)_4$ units may form 2-D sheets as in $[Rh_2(O_2CCF_3)_4]_2(\mu_4\text{-TCNE})$,[200] $\{[Rh_2(O_2CCF_3)_4]_2(\mu_4\text{-TCNQ})\}_\infty$,[201] $[Rh_2(O_2CCH_3)_4]_2[K_3Co(CN)_6]$,[304] $Na[Rh_2(\mu\text{-}O_2CH)_4(\mu_3\text{-}\eta^1\text{:}\eta^1\text{:}\eta^1\text{-}O_2CH)(H_2O)]\cdot H_2O$,[235] and $[Rh_2(O_2CCF_3)_4]_3(\mu_3\text{-}\eta^2\text{:}\eta^2\text{:}\eta^2\text{-}C_{20}H_{10})_2$,[58] 2-D extended organometallic networks as in $\{[Rh_2(O_2CCF_3)_4]_3(\mu_4\text{-}\eta^2\text{:}\eta^2\text{:}\eta^2\text{:}\eta^1\text{-}C_{30}H_{12})\}$,[59] pseudo 2-D architectures consisting of ribbon-type extended structures as those of $[Rh_2(O_2CCF_3)_4(S_8)]_\infty$ (Fig. 12.13)[56] and $\{[Rh_2(O_2CCF_3)_4]_3(\mu_3\text{-}\eta^2\text{:}\eta^2\text{:}\eta^2\text{-}C_{18}H_{12})_2\}$,[57] pyramids as in $\{[Rh_2(O_2CCF_3)_4]_3\text{-}CH_3Si(C_5H_4N)_3(\eta^1\text{-}C_6H_6)_3\}$,[303] as well as other unusual supramolecular assemblies.[149,303] Moreover, diacids have been employed as building blocks to prepare macrocyclic dimers with *transoid* arrangement of the bridging ligands,[113] covalently linked '*dimers of dimers*' that form square motifs,[115] and layered hexagonal networks of dirhodium units with chelating carboxylate groups.[112] The assembling of chelating[110] (Fig. 12.14) or linear diacids has produced a variety of molecular boxes with dirhodium units at the corners of the macrocycles;[111,114] the latter are discussed in Section 12.7.2. A notable reversible phase transition that generates 1-D channels takes place upon cooling samples of the host molecule $[Rh_2(O_2CC_6H_5)_4(pyz)_2]_\infty$ in a CO_2 atmosphere.[208]

The impact of a pure electronic change in the character of the metal atom on the preference of the ligand donor atoms is nicely demonstrated by the $Rh_2(O_2CR)_4$ adducts with the ambidentate ligand DMSO. For $Rh_2(O_2CR)_4$ adducts with DMSO, when R = CH_3, C_2H_5 and C_6H_5, the electron-donating substituents result in coordination to the sulfur atom,[226,227,248] whereas for R = CF_3, bonding changes to the oxygen atom.[227] The gas phase reaction between DMSO and $Rh_2(O_2CCF_3)_4$, however, affords $\{[Rh_2(O_2CCF_3)_4]_3(\mu_2\text{-DMSO-}S,O)_2\}_\infty$ (Fig. 12.11) and $[Rh_2(O_2CCF_3)_4]_7(DMSO)_8$ with *S*- and *O*-bound DMSO. Another example that supports the control of ligand coordination to $Rh_2(O_2CR)_4$, by changing the effective electronegativity of the carboxylate R group substituent, is that of 1,4-benzoquinone: for R = CF_3 ligation occurs only through the O atoms of the *p*-quinone carbonyl groups,[242] whereas for R = Bu^t, the increase in the '*softness*' of the Rh metal atoms enables coordination to the C=C double bond of *p*-quinone.[275] Other important interactions that determine the preferential ligand binding sites include intramolecular hydrogen-bonds between the substituents of the ligand and the O atoms of the bridging carboxylate; such interactions have been encountered in adducts with various pyridine, pyrimidine and triazine derivatives,[145,146,148] 1-methyladenosine,[184] and azathioprine.[188] This binding site preference is clearly demonstrated in $Rh_2(O_2CCH_3)_4(damt)_2$ (12.12); although damt has four nitrogen atoms that are potential binding sites, *ax* binding occurs through the site that favors formation of intramolecular hydrogen bonds between the exocyclic amino groups and the acetate *O* atoms.[146] The impact of these interactions is further demonstrated by biologically relevant compounds discussed in Section 12.7.3.

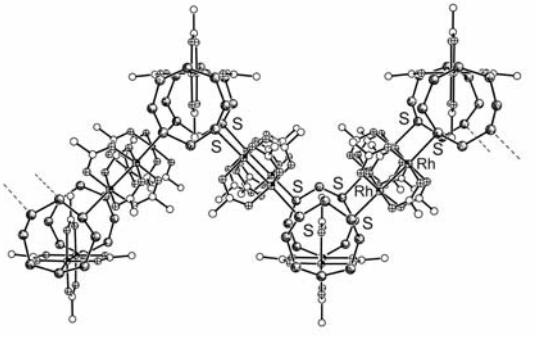


Fig. 12.13. The pseudo 2-D ribbon-type structure of $[Rh_2(O_2CCF_3)_4(S_8)]_\infty$.

Pictiva EX2004
Samsung v Pictiva
IPR2024-01094

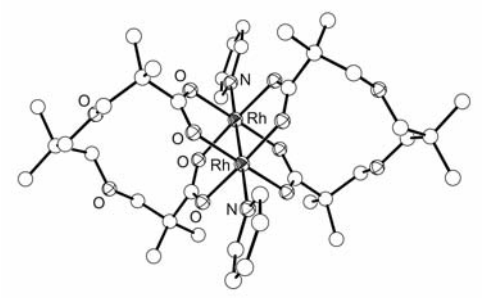
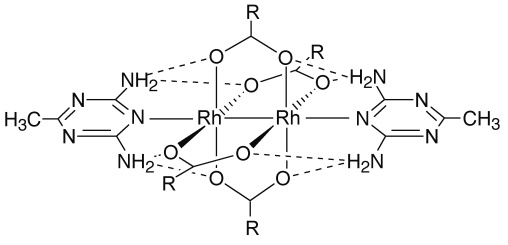


Fig. 12.14. Molecular structure of $Rh_2\{[O_2CC(CH_3)_2CH_2OCH_2]_2C(CH_3)_2\}(py)_2$.

In summary, characterization of dirhodium carboxylate compounds by X-ray crystallography has provided important information about the molecular structures of these compounds. These data are essential for interpretation of their spectroscopic properties and electronic structures[19,316-334] which are discussed in Chapter 16.



12.12

12.3 Other Dirhodium Compounds Containing Bridging Ligands

12.3.1 Complexes with fewer than four carboxylate bridging groups

Mixed carboxylate complexes of the type $Rh_2(O_2CCH_3)_{4-n}(O_2CR)_n$, n = 2 or 3, include those for which R = CPh_3,[38] C_6H_2-2,4,6-(p-tol)$_3$,[39] C_6H_4-2-OH,[72,335] and 1,3,5-triisopropylphenyl,[75] as well as $Rh_2(O_2CCF_3)_{4-n}(O_2CR)_n$, n = 2 or 3 for R = TiPB.[75] During exchange reactions of $Rh_2(O_2CR)_4$ carboxylate ligands, a stepwise replacement of RCO_2^- by $R'CO_2^-$ occurs with retention of the Rh_2^{4+} core. Monitoring the displacement of $CH_3CO_2^-$ with $CF_3CO_2^-$ by NMR spectroscopy has established that the rate constants for the first, second, third and fourth substitution reactions are in the approximate ratio 1:2:0.1:0.025,[36] an indication that there is a marked preference for the *cis*-$Rh_2(O_2CCH_3)_2(O_2CCF_3)_2$ isomer. This is in accordance with the prevalence and stability of compounds that contain the bis-carboxylate unit *cis*-$[Rh_2(O_2CR)_2]^{2+}$ (Table 12.2). The lability of carboxylate ligands is further demonstrated by the large number of neutral and cationic Rh_2^{4+} compounds with fewer than four carboxylate groups. Structural data for these compounds are provided in Table 12.2.

Pictiva EX2004
Samsung v Pictiva
IPR2024-01094

Table 12.2. Structural data for tris, bis and mono carboxylato Rh_2^{4+} compounds

Compound	r (Rh–Rh)[a] (Å)	r (Rh–L_{ax}) (Å)[b]	Donor atom(s)	ref.
Tris-carboxylato compounds				
$[Rh_2(\mu\text{-}O_2CCH_3)_3(py)_4]CF_3SO_3$	2.473(1)	2.25(1)	N	367
$[Rh_2(\mu\text{-}O_2CCH_3)_3(py)_4]CF_3SO_3$	2.474(1)	2.253(3) 2.235(4)	N	368
$Rh_2(\mu\text{-}O_2CCH_3)_3(\eta^2\text{-}O_2CCH_3)$(bpy)[c]	2.475(1)	2.12(1)[d] 2.466(8)[e]	N O	372,373
$[Rh_2(\mu\text{-}O_2CCH_3)_3(\eta^4\text{-bpnp})]PF_6$	2.405(2)	2.20(1) 2.19(1)	N	382,383
$\{[Rh_2(\mu\text{-}O_2CCH_3)_3]_2(\mu_2\text{-}\eta^4\text{:}\eta^4\text{-}L_1)\}(PF_6)_2$[f]	2.40[g]	2.16[g] 2.31[g,h]	N	384
$Rh_2(\mu\text{-}O_2CCH_3)_3$(*O*-TMPP)(MeOH)·EtOH	2.423(1)	2.351(2)[i] 2.251(2)[i]	O	565,566
$[Rh_2(\mu\text{-}O_2CCH_3)_3$(*O*-MPP)$](HO_2CCH_3)$	2.421(1)	2.300(5)[j] 2.342(4)[j]	O	516
$Rh_2(\mu\text{-}O_2CCH_3)_3$(*O*-MPP)$(NCCH_3)$	2.421(1)	2.373(3)[k] 2.203(4)	O N	568
$[Rh_2(\mu\text{-}O_2CCH_3)_3\{PhP(C_6H_4)(o\text{-}BrC_6H_4)\}P(C_6H_{11})_3]\cdot CHCl_3$	2.477(1)	2.400(1)	P	530
$Rh_2(\mu\text{-}O_2CCH_3)_3[PhP(C_6H_4)(o\text{-}ClC_6H_4)](HO_2CCH_3)_2$	2.410(1)	2.378(6) 2.26(1)	O	531
$Rh_2(\mu\text{-}O_2CCH_3)_3\{PhP(C_6H_4)(o\text{-}BrC_6H_4)\}(HOCCH_3)_2$	2.432(1)	2.273(4) 2.434(4)	O	532
$Rh_2(\mu\text{-}O_2CCH_3)_3\{(p\text{-}CH_3OC_6H_3)P(p\text{-}CH_3OC_6H_4)_2\}(HO_2CCH_3)_2$	2.421(1)	2.341(4) 2.257(4)	O	533
$\{Rh_2(\mu\text{-}O_2CCH_3)_3[Ph_2P(C_6H_4)]\}(HO_2CCH_3)_2$	2.430(2)	2.336(4) 2.301(4)	O	524,525

Pictiva EX2004
Samsung v Pictiva
IPR2024-01094

Compound	*r* (Rh–Rh)[a] (Å)	*r* (Rh–L_{ax}) (Å)[b]	Donor atom(s)	ref.
$[Rh_2(\mu\text{-}O_2CCF_3)_3(TMPP\text{-}O)]_2\cdot 1.25CH_2Cl_2$	2.452(2)	2.289(9) 1.995(9) 2.316(9) 2.287(9)	O	567
$[Rh_2(\mu\text{-}O_2CCF_3)_3\{Ph_2P(o\text{-}ClC_6H_3)\}(H_2O)_2]\cdot CHCl_3$	2.426(1)	2.325(2) 2.318(2)	O	534
$[Rh_2(\mu\text{-}O_2CCF_3)_3(\eta^1\text{-}O_2CCF_3)\{\eta^2\text{-}Ph_2P(o\text{-}ClC_6H_4)\}(H_2O)]$	2.469(1)	2.196(4)[l] 2.577(2)[m]	O Cl	379
$[Rh_2(\mu\text{-}O_2CCF_3)_3(\eta^1\text{-}O_2CCF_3)\{\eta^2\text{-}Ph_2P(o\text{-}ClC_6H_4)\}(H_2O)]$	2.449(1)	2.196(4)[l] 2.577(2)[m]	O Cl	378
Bis-carboxylato compounds				
cis-$[Rh_2(\mu\text{-}O_2CH)_2(bpy)_2Cl_2]\cdot 2H_2O$	2.584[g]	2.514(3)	Cl	344
cis-$[Rh_2(\mu\text{-}O_2CH)_2(bpy)_2Cl_2]\cdot 4H_2O$	2.578(1)	2.521(3)	Cl	345
cis-$Rh_2(\mu\text{-}O_2CH)_2Cl_2(phen)_2$	2.576(1)	2.504(1) 2.496(2)	Cl	343
cis-$[Rh_2(\mu\text{-}O_2CCH_3)_2(dmg)_2(PPh_3)_2]\cdot H_2O$	2.618(5)	2.476(9) 2.494(9)	P	336
cis-$Rh_2(\mu\text{-}O_2CCH_3)_2(CF_3COCHCOCH_3)_2(py)$	2.534(1)	2.13(1) 3.106[n]	N C[n]	341
cis-$Rh_2(\mu\text{-}O_2CCH_3)_2(CF_3COCHCOCF_3)_2(py)_2$	2.523(2)	2.27(1) 2.21(1)	N	340
cis-$[Rh_2(\mu\text{-}O_2CCH_3)_2(NCCH_3)_6](BF_4)_2\cdot 4CH_3CN$	2.534(1)	2.232(4)	N	361
cis-$[Rh_2(\mu\text{-}O_2CCH_3)_2(NCCH_3)_4(py)_2](BF_4)_2$	2.548(2)	2.231(9) 2.238(9)	N	361
cis-$[Rh_2(\mu\text{-}O_2CCH_3)_2(NCCH_3)_6(BF_4)_2][Re_2Cl_8]$	2.509(4)	2.23(3)	N	363
cis-$[Rh_2(\mu\text{-}O_2CCH_3)_2(NCCH_3)_3(PCy_3)_2](BF_4)_2$	°	°	P	742
cis-$[Rh_2(\mu\text{-}O_2CCH_3)_2(bpy)(NCCH_3)_4](BF_4)_2\cdot CH_3CN$	2.539(1)	2.188(6) 2.229(6)	N	373

Pictiva EX2004
Samsung v Pictiva
IPR2024-01094

Compound	r (Rh–Rh)[a] (Å)	r (Rh–L_{ax}) (Å)[b]	Donor atom(s)	ref.
cis-[Rh_2(μ-O_2CCH_3)$_2$(bpy)$_2$(H_2O)(CH_3)$_2$CHOH)][$B(C_6H_5)_4$]·H_2O	2.526(1)	2.231(2)[l] 2.264(2)[p]	O	358
cis-[Rh_2(μ-O_2CCH_3)$_2$(bpy)$_2Cl_2$]·$3H_2O$	2.574(1)	2.525(5)	Cl	350
cis-[Rh_2(μ-O_2CCH_3)$_2$(bpy)$_2Cl_2$]·$2H_2O$	2.601(1)	2.532(1)	Cl	358
cis-[Rh_2(μ-O_2CCH_3)$_2$(bpy)$_2Br_2$]·$3H_2O$	2.586(1)	2.672(1) 2.629(1)	Br	358
cis-[Rh_2(μ-O_2CCH_3)$_2$(bpy)$_2I_2$]	2.590(3)	2.769(4) 2.848(3)	I	358
cis-[Rh_2(μ-O_2CCH_3)$_2$(η^2-Hdpa)$_2Cl_2$]·$6H_2O$	2.593(1)	2.582(2) 2.562(2)	Cl	171
cis-[Rh_2(μ-O_2CCH_3)$_2$(bpy)$_2$($NCCH_3$)$_2$](PF_6)$_2$·$2CH_3CN$	2.548(1)	2.228(8) 2.185(8)	N	351
cis-[Rh_2(μ-O_2CCH_3)$_2$(phen)$_2Cl_2$]·H_2O	2.561(2)	2.509(5)	Cl	352
cis-[Rh_2(μ-O_2CCH_3)$_2$(phen)$_2Cl_2$]·$10.5H_2O$	2.554(1)	2.535(2)	Cl	352
cis-[Rh_2(μ-O_2CCH_3)$_2$(phen)$_2$(py)$_2$](PF_6)$_2$·$(CH_3)_2CO$	2.559(1)	2.242(4) 2.199(4)	N	356
cis-[Rh_2(μ-O_2CCH_3)$_2$(phen)$_2$(Me-Im)$_2$](ClO_4)$_2$	2.556(1)	2.188(3) 2.207(3)	N	349
cis-[Rh_2(μ-O_2CCH_3)$_2$(4,7-Me_2phen)$_2$(Me-Im)$_2$](ClO_4)$_2$	2.565(1)	2.223(4) 2.238(5)	N	349
cis-[Rh_2(μ-O_2CCH_3)$_2$(3,4,7,8-Me_4phen)$_2$(Me-Im)$_2$](ClO_4)$_2$	2.564(1)	2.18(1) 2.23(1)	N	349
cis-[Rh_2(μ-O_2CCH_3)$_2$(η^2-ampy)$_2$(py)$_2$](PF_6)$_2$	2.587(1)	2.281(9) 2.25(1)	N	357
cis-[Rh_2(μ-O_2CCH_3)$_2$(η^1-O_2CCH_3)(η^2-ampy)$_2$]ClO_4	2.525(1)	2.111(6)	N	357
cis-[Rh_2(μ-O_2CCH_3)$_2$(η^3-pynp)$_2$](BF_4)$_2$·C_7H_8	2.407(2) 2.408(2)	2.206(9) 2.20(1)	N	387,388
cis-[Rh_2(μ-O_2CCH_3)$_2$(η^3-pynp)(η^1-pynp)($NCCH_3$)$_2$](BF_4)(PF_6)·$2CH_3CN$	2.356(1)	2.158(5)[q] 1.997(5)[r]	N	388

Pictiva EX2004
Samsung v Pictiva
IPR2024-01094

Compound	r (Rh–Rh)[a] (Å)	r (Rh–L_{ax}) (Å)[b]	Donor atom(s)	ref.
$[Rh_4(\mu\text{-}O_2CCH_3)_2(\mu_2\text{-}\eta^3\text{:}\eta^3\text{-tppz})_2(MeOH)_4](PF_6)_4\cdot 2MeOH$[s]	2.606(1)	2.219(7) 2.252(7)	O	385
cis-$[Rh_2(\mu\text{-}O_2CCH_3)_2(\eta^2\text{-bpa})_2](PF_6)_2$[t]	2.568(1)	2.189[g]	N	206
cis-$[Rh_2(\mu\text{-}O_2CCH_3)_2(\eta^1\text{-bpa})_2](PF_6)_2$[u]	2.600(1)	2.180[g]	N	206
cis-$[Rh_2(\mu\text{-}O_2CCH_3)_2(\eta^1\text{-}O_2CCH_3)(\eta^2\text{-bpa})(\eta^2\text{-bpa})]PF_6\cdot 1.5H_2O$	2.565(1)	2.218[g]	N	206
cis-$[Rh_2(\mu\text{-}O_2CCH_3)_2(bpy)_2(py)_2](PF_6)_2$	2.584(2) 2.593(2)	2.24[g]	N	206
cis-$[Rh_2(\mu\text{-}O_2CCH_3)_2(dppz)_2(\eta^1\text{-}O_2CCH_3)(EtOH)]BF_4\cdot EtOH$	2.552(1)	2.187(3)[v] 2.334(3)[v]	O	822
cis-$[Rh_2(\mu\text{-}O_2CCH_3)_2(dppn)_2(\eta^1\text{-}O_2CCH_3)(MeOH)]BF_4\cdot 3MeOH$	2.552(1)	2.188(5)[y] 2.292(5)[y]	O	824
cis-$[Rh_2(\mu\text{-}O_2CCH_3)_2(bpy)(dppz)(MeOH)Cl]BF_4\cdot 3MeOH$	2.553(1)	2.273(3)[w] 2.498(1)[w]	O Cl	825
cis-$[Rh_2(\mu\text{-}O_2CCH_3)_2(py)_6](CF_3SO_3)_2$	2.639(2)	2.26(2) 2.23(1)	N	367
cis-$[Rh_2(\mu\text{-}O_2CCH_3)_2(py)_6](CF_3SO_3)_2$	2.653(1)	2.238(2) 2.229(2)	N	368
$(CN_3H_6)_5[(PO_4)W_{11}O_{35}(Rh_2(\mu\text{-}O_2CCH_3)_2(DMSO)_2)]\cdot 4H_2O$	2.525(2)	2.465(6) 2.535(6)	S	841
cis-$Rh_2(\mu\text{-}O_2CCH_3)_2(\mu\text{-}Ph_2Ppy)_2Cl_2$	2.518(1)	2.538(3) 2.537(3)	Cl	515
cis-$Rh_2(\mu\text{-}O_2CCH_3)_2Cl_2(dppm)_2\cdot 2CH_3CN$	2.622(1)	2.475(2) 2.492(2)	Cl	507
cis-$[Rh_2(\mu\text{-}O_2CCH_3)_2(bpy)(9\text{-EtGuaH})(H_2O)_2(CH_3SO_4)]CH_3SO_4\cdot H_2O$	2.511(1)	2.248(4)[l] 2.351(4)[x]	O	395
H-T *cis*-$[Rh_2(\mu\text{-}O_2CCH_3)_2(9\text{-EtGua})_2(MeOH)_2]\cdot 2MeOH$	2.483(2)	2.315(7) 2.317(7)	O	393
H-H *cis*-$[Rh_2(\mu\text{-}O_2CCH_3)_2(9\text{-EtGuaH})_2(Me_2CO)(H_2O)](BF_4)_2\cdot H_2O$	2.512(1)	2.27(1)[y] 2.32(1)[l]	O	394

Pictiva EX2004
Samsung v Pictiva
IPR2024-01094

Compound	r (Rh–Rh)[a] (Å)	r (Rh–L_{ax}) (Å)[b]	Donor atom(s)	ref.
H-T *cis*-[$Rh_2(\mu\text{-}O_2CCF_3)_2(9\text{-EtGuaH})_2(Me_2CO)_2$][$(CF_3CO_2)_2\cdot Me_2CO$	2.520(5)	2.18(1)	O	393
cis-[$Rh_2(\mu\text{-}O_2CCF_3)_2(\eta^1\text{-}O_2CCF_3)_2(bpy)_2$]$\cdot Me_2CO$	2.570(6)	2.19(3) 2.30(4)	O	351
$Rh_2(\mu\text{-}O_2CCF_3)_2(\eta^1\text{-}O_2CCF_3)_2(bpy)(THF)(H_2O)\cdot THF$	2.520(3)	2.25(1)[e] 2.27(1)[f]	O	373
$Rh_2(\mu\text{-}O_2CCF_3)_2(\eta^1\text{-}O_2CCF_3)_2(py)_4$	2.56(1) 2.54(1)	2.32(6) 2.26(3) 2.25(3) 2.22(3)	N	376
$Rh_2(\mu\text{-}O_2CCH_3)_2(\eta^1\text{-}O_2CCH_3)_2(CO)_2(MeOH)_2$	2.535(1)	2.202(3)	O	380
[$Rh_2(\mu\text{-}O_2CCH_3)_3(\eta^1\text{-}O_2CCH_3)(\eta^2\text{-}Ph_2P(o\text{-}CH_3OC_6H_4)(H_2O)$]	2.439(3)	2.25(1)[f] 2.35(1)[aa]	O	377
H-T *cis*-$Rh_2(\mu\text{-}O_2CCH_3)_2[Ph_2P(C_6H_4)]_2(HO_2CCH_3)_2$	2.508(1)	2.342(5)	O	522,523
H-T *cis*-$Rh_2(\mu\text{-}O_2CCH_3)_2[Ph_2P(P_6H_4)]_2(py)_2$	2.556(2)	2.281(9)	N	523
H-T *cis*-$Rh_2(\mu\text{-}O_2CCH_3)_2[Ph_2P(C_6H_4)]_2(PPh_3)_2\cdot 2C_7H_8$	2.630(1)	2.560(2)	P	547
H-T *cis*-{$Rh_2(\mu\text{-}O_2CCH_3)_2[Ph_2P(C_6H_4)][(p\text{-}ClC_6H_3)P(p\text{-}ClC_6H_4)_2](HO_2CCH_3)_2$}$\cdot 1/2C_6H_6$	2.513(1)	2.338(2) 2.346(3)	O	538
H-T *cis*-{$Rh_2(\mu\text{-}O_2CCH_3)_2[(p\text{-}FC_6H_3)P(p\text{-}FC_6H_4)_2]_2(HO_2CCH_3)_2$}	2.488(3)	2.29(1)	O	539
H-T *cis*-{$Rh_2(\mu\text{-}O_2CCH_3)_2[(m\text{-}CH_3C_6H_3)P(m\text{-}CH_3C_6H_4)_2]_2(HO_2CCH_3)_2$}$\cdot CH_3CO_2H$	2.502(3)	2.412(5) 2.317(4)	O	540
H-T *cis*-$Rh_2(\mu\text{-}O_2CCH_3)_2[\text{-}C_5H_9)_7Si_8O_{12}(CH_2)_2P(C_6H_4)Ph][Ph_2P(C_6H_4)](HO_2CCH_3)_2$	2.508(1)	2.346(3)	O	541
H-T *cis*-$Rh_2(\mu\text{-}O_2CCH_3)_2[PhP(C_6H_4)(o\text{-}BrC_6F_4)]_2$	2.475(1)	2.764(2)[m]	Br	555
H-T *cis*-$Rh_2(\mu\text{-}O_2CCH_3)_2[PhP(C_6H_4)(o\text{-}BrC_6F_4)]_2(H_2O)$	2.485(1)	2.983(1)[m] 2.292(6)[l]	Br O	555
cis-$Rh_2(\mu\text{-}O_2CCH_3)_2(\eta^2\text{-}O_2CCH_3)[PhP(C_6H_4)(o\text{-}BrC_6F_4)][Ph_2P(o\text{-}BrC_6F_4)]$[c]	2.519(3)	2.62(2)[m] 2.43(2)[e]	Br O	374
cis-$Rh_2(\mu\text{-}O_2CCH_3)_2(\eta^2\text{-}O_2CCH_3)[Ph_2P(C_6H_4)][Ph_2P(o\text{-}ClC_6H_4)]$[c]	2.529(1)	2.573(4)[m] 2.27(1)[e]	Cl O	375
H-T *cis*-$Rh_2(\mu\text{-}O_2CCH_3)_2[PhP(C_6H_4)(C_6F_5)]_2(H_2O)_2$	2.496(2)	2.367(1)	O	542

Pictiva EX2004
Samsung v Pictiva
IPR2024-01094

Compound	r (Rh–Rh)[a] (Å)	r (Rh–L_{ax}) (Å)[b]	Donor atom(s)	ref.
H-T *cis*-$Rh_2(\mu\text{-}O_2CCH_3)_2[(m\text{-}CH_3OC_6H_3)P(m\text{-}CH_3OC_6H_4)_2]_2(H_2O)(HO_2CCH_3)$	2.491(1)	2.313(9)[l] 2.363(1)	O	543
H-T *cis*-$Rh_2(\mu\text{-}O_2CCMe_3)_2[PhPMe(C_6H_4)]_2(py)_2{\cdot}2CHCl_3$	2.535(5)	2.27(1) 2.31(1)	N	544
H-T *cis*-$Rh_2(\mu\text{-}O_2CCMe_3)_2\{Me_2P(C_6H_4)\}_2(H_2O)_2$	2.492(1)	2.360(9) 2.351(9)	O	545
H-T *cis*-$Rh_2(\mu\text{-}O_2CCPh_3)_2[Ph_2P(C_6H_4)]_2(py)_2$	2.559(1)	2.302(4)	N	546
cis-$Rh_2(\mu\text{-}O_2CCF_3)_2$(TMPP-O)$_2{\cdot}2CH_2Cl_2$	2.562(2)	2.315(9) 2.323(9)	O	567
H-T *cis*-$Rh_2(\mu\text{-}O_2CCF_3)_2[Ph_2P(C_6H_4)]_2(py)_2$	2.582[g]	2.293[g] 2.263[g]	N	548
H-T *cis*-$Rh_2(\mu\text{-}O_2CCF_3)_2[Ph_2P(C_6H_4)]_2(HO_2CCF_3)_2$	2.515[g]	2.361[g] 2.335[g]	O	548
H-T *cis*-$Rh_2(\mu\text{-}O_2CC_2F_7)_2[PhP(C_6H_4)(C_6F_5)]_2(H_2O)_2$	2.530(2)	2.34(1)	O	542
H-T *cis*-$[Rh_2(\mu\text{-}O_2CCH_3)_2[PhP(C_6H_4)(C_5H_4)]Fe(C_5H_5)]_2(HO_2CCH_3)_2]$	2.504(1)	2.392(6) 2.295(6)	O	549
H-H *cis*-$Rh_2(\mu\text{-}O_2CCH_3)_2[Ph_2P(C_6H_4)]_2(HO_2CCH_3)_2$	2.493(1)	2.498(7) 2.198(5)	O	525
H-H *cis*-$Rh_2(\mu\text{-}O_2CCH_3)_2[(ClC_6H_3)P(p\text{-}ClC_6H_4)_2]_2(HO_2CCH_3)_2$	2.511(2)	2.39(1) 2.22(1)	O	525
H-H *cis*-$\{Rh_2(\mu\text{-}O_2CCH_3)_2[PhP(C_6H_4)(o\text{-}ClC_6H_4)][Ph_2P(C_6H_4)](PPh_3)\}{\cdot}2C_6H_6$	2.558(1)	2.370(2)	P	550
H-H *cis*-$[Rh_2(\mu\text{-}O_2CCH_3)_2\{\mu_2\text{-}(CH_2)PPh_2\}\{\mu_2\text{-}(C_6H_4)PPh_2\}(PPh_3)]{\cdot}2CH_2Cl_2$	2.532(2)	2.297(4)	P	551,552
H-H *cis*-$\{Rh_2(\mu\text{-}O_2CCH_3)_2[PhP(C_6H_4)(C_5H_4)]_2Fe\}(HO_2CCH_3)]{\cdot}CH_2Cl_2$	2.508(4)	2.26(2)	O	549
H-H *cis*-$Rh_2(\mu\text{-}O_2CCH_3)_2[(C_4H_3S)_2(C_4H_2S)P]_2(py)_2$	2.576(1)	2.145[g] 2.378[g]	N	553
cis-$Rh_2(\mu\text{-}O_2CCH_3)_2(\eta^2\text{-}Ph_2P(o\text{-}CH_3OC_6H_4)\}_2Cl_2$	2.560(1)	2.298(7) 2.342(7)	O	377
cis-$Rh_2(\mu\text{-}O_2CCH_3)_2(\eta^2\text{-}Ph_2P(o\text{-}ClC_6H_4)\}_2Cl_2$	2.569(1)	2.587(1) 2.592(1)	Cl	377

Pictiva EX2004
Samsung v Pictiva
IPR2024-01094

Compound	r (Rh–Rh)[a] (Å)	r (Rh–L_{ax}) (Å)[b]	Donor atom(s)	ref.
H-T *cis*-$Rh_2(\mu\text{-}O_2CCH_3)_2$(2*S*,5*S*-2,5-dimethyl-1-phenylphospholane)$_2(HO_2CCH_3)_2$	2.504(1)	2.370(3)	O	558
cis-$Rh_2(\mu\text{-}O_2CCF_3)_2(\eta^1\text{-}O_2CCF_3)_2$(*1S,2S,5R*-hprmph)$_2$	2.580(1)	2.262(1)	O	560
cis-$[Rh_2(\mu\text{-}O_2CCF_3)_2(\eta^1\text{-}O_2CCF_3)_2$(*1S,2S,5R*-hprmph)$_2]\cdot 1/2CHCl_3$	2.587(1)	2.250(5)	O	557,559
cis-$[Rh_2(\mu\text{-}O_2CCF_3)_2(\eta^1\text{-}O_2CCF_3)_2$(*1R,2R,5S*-hprmph)$_2]\cdot 2H_2O$	2.601(1)	2.25(1)	O	557
Mono-carboxylato compounds				
$[Rh_2(\mu\text{-}O_2CCH_3)(\eta^3\text{-tpy})_2Cl_2](H_3O)Cl_2\cdot 9H_2O$	2.634(1)	2.517(2)	Cl	205
$[Rh_2(\mu\text{-}O_2CPh)(\eta^3\text{-tpy})_2(NCCH_3)_2](BF_4)_3\cdot CH_3CN$	2.629(1)	2.154(5) 2.181(5)	N	351
$[Rh(\mu\text{-}O_2CCF_3)(\mu\text{-CO})(THF)]_4$	2.551(1) 2.624(1)	2.220(5)	O	310

[a] Distances are given with up to 3 decimal digits.
[b] Square brackets refer to average values; parentheses refer to unique values.
[c] Compound contains chelating acetate group.
[d] Axial bond to N of chelating bpy.
[e] Pseudoaxial bond to O of chelating acetate group.
[f] L_1: 2-aryl-4,6-bis(2-(7-pyridyl)-1,8-naphthyridyl)-pyrimidine.
[g] Esds not reported.
[h] Rh–N pyrimidine distance.
[i] The shorter of these two distances corresponds to Rh–O(methanol), the longer one to Rh–O(methoxy).
[j] The shorter of these two distances corresponds to Rh–O(carbonyl), the longer one to Rh–O(methoxy).
[k] Distance to the methoxy O atom of one phenyl ring.
[l] Distance to H_2O molecule.
[m] Distance to halogen atom of the phosphine.
[n] The vacant *ax* site of the dirhodium unit interacts with the γ-carbon atom of a β-diketonato ligand of an adjacent dimetal unit.
[o] Distance not reported due to crystallographic disorder.
[p] Distance to *ax* $(CH_3)_2CHOH$ molecule.
[q] Rh-N distance to a monodentate *ax* naphthyridine unit.
[r] Rh-N distance to the pynp ligand that is coordinated in a tridentate fashion.
[s] Tetranuclear Rh_4^{6+} compound.
[t] C_2 symmetry.
[u] C_s symmetry.
[v] The shorter of the two Rh–O distances corresponds to Rh–O(carboxylate), the longer one to Rh-O(alcohol).
[w] The longer distance corresponds to the Rh–Cl bond, the shorter one to Rh–O(MeOH).
[x] Distance to O of $CH_3SO_4^-$ group.
[y] Distance to O of carbonyl group.
[z] Distance to O of THF.
[aa] Axial bond to O atom of the phosphine.

Pictiva EX2004
Samsung v Pictiva
IPR2024-01094

The first such bis-carboxylate complex to be structurally characterized is the mixed acetate/dimethylglyoxime derivative *cis*-$Rh_2(\mu\text{-}O_2CCH_3)_2(\eta^2\text{-dmg})_2(PPh_3)_2$ with two acetate ligands in a *cisoid* arrangement, the dmg ligands chelating at *eq* positions, and the PPh_3 molecules occupying *ax* sites.[336] The Rh–Rh distance of 2.618(5) Å is longer than that in $Rh_2(O_2CCH_3)_4(PPh_3)_2$ (2.451(1) Å)[278] and far shorter than that in the related complex $Rh_2(dmg)_4(PPh_3)_2$ (2.936(2) Å);[337,338] the lengthening of the Rh–Rh bond compared to $Rh_2(O_2CCH_3)_4(PPh_3)_2$ has been attributed to the repulsion between the dmg ligands, which are close to achieving the maximum torsion angle, and the constraints imposed by the small '*bite*' of the bridging acetate groups.[299,336] The structure of *cis*-$Rh_2(\mu\text{-}O_2CCH_3)_2(\eta^2\text{-dmg})_2(PPh_3)_2$ serves as the prototype for a variety of neutral Rh_2^{4+} species that are supported by a pair of bridging carboxylate ligands in a *cisoid* arrangement. One such group comprises $Rh_2(\mu\text{-}O_2CCH_3)_2(\beta\text{-diketone})_2L_2$ compounds (the β-diketone ligand represents the anions of 2,4-pentanedione or its trifluoro or hexafluoro derivatives and L is pyridine).[339] Their close structural relationship to the dmg complex has been confirmed by the X-ray crystal structure determination of *cis*-$Rh_2(\mu\text{-}O_2CCH_3)_2(\eta^2\text{-}CF_3COCHCOCF_3)_2(py)_2$ (Fig. 12.15).[340] In both cases, the chelating ligands are not eclipsed, but have a significant twist of *c.* 10-20° with respect to each other. The mono-pyridine adduct *cis*-$Rh_2(\mu\text{-}O_2CCH_3)_2(\eta^2\text{-}CF_3COCHCOCH_3)_2(py)$ exhibits an unusual interaction (3.106 Å) between the vacant *ax* site of each dimetal unit and the γ-carbon atom of a β-diketonato ligand of an adjacent dirhodium unit.[341]

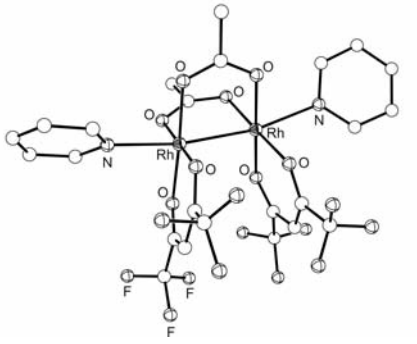


Fig. 12.15. Molecular structure of *cis*-$Rh_2(\mu\text{-}O_2CCH_3)_2(\eta^2\text{-}CF_3COCHCOCF_3)_2(py)_2$.

Compounds that possess similar structures to those previously described are those of general formulae $[Rh_2(\mu\text{-}O_2CR)_2(\eta^2\text{-N-N})_2]^{2+}$ (R = H, CH_3, or PhCH(OH); N-N = 2,2'-bipyridine-(bpy), 1,10-phenanthroline (phen) and substituted phen, ampy or HN=CHCH=NH) with the N-N donors chelating at *eq* sites of the dirhodium unit;[105,206,342-358] the reduced Rh_2^{3+} species for a number of these compounds have been studied by EPR spectroscopy.[359] Pertinent compounds of the aforementioned class, that have been crystallographically determined, are listed in Table 12.2.

Compounds in which the open *eq* sites of the bis-acetate dirhodium core are occupied by monodentate ligands (e.g., CH_3CN) were first obtained by treatment of $Rh_2(O_2CC_3H_7)_4$ with the weakly complexing acid CF_3SO_3H in CH_3CN; the $[Rh_2(O_2CC_3H_7)_2]^{2+}$ unit was detected by NMR spectroscopy, but the product was not fully characterized.[360] Subsequently, the compounds *cis*-$[Rh_2(O_2CCH_3)_2(NCCH_3)_6]X_2$, X = BF_4^- or $CF_3SO_3^-$, were prepared by treating $Rh_2(O_2CCH_3)_4$ with Me_3OBF_4 or CF_3SO_3H in CH_3CN.[361] The enhanced lability of *ax* CH_3CN molecules compared to those occupying *eq* sites is supported by the fact that the py ligands replace *ax* CH_3CN in the reactions of $[Rh_2(O_2CCH_3)_2(NCCH_3)_6]^{2+}$

Pictiva EX2004
Samsung v Pictiva
IPR2024-01094

with pyridine to afford *cis*-$[Rh_2(O_2CCH_3)_2(NCCH_3)_4(py)_2](BF_4)_2$,[361] or compounds of the type $[Rh_2(O_2CCH_3)_2(NCCH_3)_4L_2]^{2+}$ (L = H_2O, DMSO, thiourea and NSC^-) depending on the identity of the donor molecule.[362] The argument is further supported by the considerably shorter Rh–N_{eq} to Rh–N_{ax} distances in *cis*-$[Rh_2(O_2CCH_3)_2(NCCH_3)_6](BF_4)_2$ (e.g., Rh–N_{eq} = 1.985(4) Å and Rh–N_{ax} = 2.232(4) Å)[361] and the octachlorodirhenate salt *cis*-$[Rh_2(O_2CCH_3)_2(NCCH_3)_6(BF_4)_2][Re_2Cl_8]$ (e.g., Rh–N_{eq} = 1.97(3) Å and Rh–N_{ax} = 2.26(4) Å).[363] The substitutional inertness of the *eq* M-$NCCH_3$ bonds towards CD_3CN exchange in *cis*-$[Rh_2(\mu\text{-}O_2CCH_3)_2(NCCH_3)_4]^{2+}$, compared to the isostructural Mo species, has been attributed to the different M–M (M = Rh, Mo) MO configurations ($\sigma^2\pi^4\delta^2\delta^{*2}\pi^{*4}$ and $\sigma^2\pi^4\delta^{*2}$ for Rh_2^{4+} and Mo_2^{4+}, respectively).[364] On the other hand, the reactions of the dirhodium cation with acetate, bpy and phen proceed at reasonable rates at room temperature.[364]

Apart from the mixed acetate/acetonitrile ligand sets, cationic Rh_2^{4+} species with mixed acetate/water or acetate/pyridine ligands have been isolated. There is evidence that, in acidic aqueous solutions, the species $[Rh_2(O_2CCH_3)_3]^+$ and $[Rh_2(O_2CCH_3)_2]^{2+}$ are present.[365] It is also claimed that the cations $[Rh_2(O_2CCH_3)_3(H_2O)_4]^+$ and $[Rh_2(O_2CCH_3)_2(H_2O)_6]^{2+}$ have been isolated as their perchlorate salts and characterized by infrared and electronic spectroscopies.[366,367] Treatment of the two mixed acetate/water complexes with pyridine affords $[Rh_2(O_2CCH_3)_3(py)_4]^+$ and $[Rh_2(O_2CCH_3)_2(py)_6]^{2+}$;[366] the corresponding trifluoromethanesulfonate salts $[Rh_2(O_2CCH_3)_3(py)_4]CF_3SO_3$ and *cis*-$[Rh_2(O_2CCH_3)_2(py)_6](CF_3SO_3)_2$ have been structurally characterized.[367,368] Reports of mixed ligand Rh_2^{4+} species include several acetate/phosphate,[369] formate/carbonate,[370] acetate/sulfate complexes[371] as well as others that have been characterized by infrared and electronic spectroscopies but not structurally determined.[369,371]

Among adducts with three bridging acetate groups, an unusual structure is encountered in $Rh_2(\mu\text{-}O_2CCH_3)_3(\eta^2\text{-}O_2CCH_3)$(bpy) which has chelating acetate and bpy ligands (Fig. 12.16).[372,373] Not unexpectedly, the *ax* Rh–O bond of 2.466(8) Å is longer than the corresponding *eq* interaction of 2.051(8) Å. The appearance of a chelating acetate group is rather unusual but has been encountered in the orthometalated compounds *cis*-$Rh_2(\mu\text{-}O_2CCH_3)_2(\eta^2\text{-}O_2CCH_3)[PhP(C_6H_4)(o\text{-}BrC_6F_4)][Ph_2P(o\text{-}BrC_6F_4)]$[374] and *cis*-$Rh_2(\mu\text{-}O_2CCH_3)_2(\eta^2\text{-}O_2CCH_3)[Ph_2P(C_6H_4)][Ph_2P(o\text{-}ClC_6H_4)]$[375] (Table 12.2). Conversely, *eq* monodentate carboxylate groups are encountered more frequently as in $[Rh_2(\mu\text{-}O_2CCH_3)_2(\eta^1\text{-}O_2CCH_3)(\eta^3\text{-bpa})(\eta^2\text{-bpa})]PF_6$,[206] $[Rh_2(\mu\text{-}O_2CCH_3)_2(\eta^1\text{-}O_2CCH_3)(\eta^2\text{-ampy})_2]ClO_4$,[357] $Rh_2(\mu\text{-}O_2CCF_3)_2(\eta^1\text{-}O_2CCF_3)_2$(bpy)(THF)($H_2O$)·THF,[373] $Rh_2(\mu\text{-}O_2CCF_3)_2(\eta^1\text{-}O_2CCF_3)_2(py)_4$,[376] $[Rh_2(\mu\text{-}O_2CCH_3)_3(\eta^1\text{-}O_2CCH_3)\{Ph_2P(o\text{-}CH_3OC_6H_4)\}(H_2O)]$,[377] $[Rh_2(\mu\text{-}O_2CCF_3)_3(\eta^1\text{-}O_2CCF_3)\text{-}\{Ph_2P(o\text{-}ClC_6H_4)\}]$,[378] $[Rh_2(\mu\text{-}O_2CCF_3)_3(\eta^1\text{-}O_2CCF_3)\{\eta^2\text{-}Ph_2P(o\text{-}ClC_6H_4)\}(H_2O)]$[379] and $Rh_2(\mu\text{-}O_2CCH_3)_2(\eta^1\text{-}O_2CCH_3)_2(CO)_2(MeOH)_2$.[380]

Pictiva EX2004
Samsung v Pictiva
IPR2024-01094

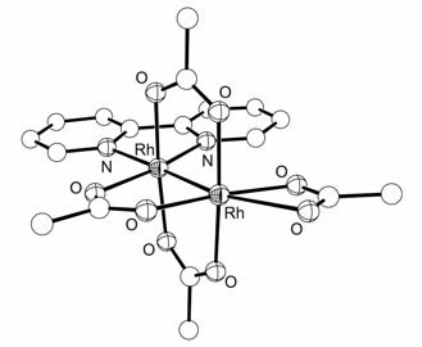


Fig. 12.16. Molecular structure of $Rh_2(\mu\text{-}O_2CCH_3)_3(\eta^2\text{-}O_2CCH_3)(bpy)$.

The *ax* ligands L in $Rh_2(O_2CR)_4L_2$ compounds generally are quite labile. Adduct formation starting with $Rh_2(O_2CR)_4$ is a stepwise process and studies of the formation constants have consistently shown that the first ligand is added much easier than the second.[19,175,181] Additionally, there is rapid ligand exchange of the groups in *ax* positions of tetracarboxylate compounds; the rate depends on the nature of the *ax* groups as well as the inductive effect and the lypophilicity of the carboxylate chain.[381] The X-ray crystal structural determinations of $Rh_2(\mu\text{-}O_2CCH_3)_3(\eta^2\text{-}O_2CCH_3)(bpy)$ and $[Rh_2(\mu\text{-}O_2CCH_3)_2(bpy)(NCCH_3)_4](BF_4)_2$ with *ax-eq* and *eq-eq* bpy moieties, respectively,[372,373] as well as those of a set of complexes with the bidentate ampy[357,206] and tridentate bpa ligands,[206] are important in a broader context as they provide insight into the mechanism of attack of N-donor chelates on the dinuclear unit. As illustrated in Fig. 12.17, a possible sequence of events for this reaction system involves a nucleophilic attack of the base at an *ax* site of $Rh_2(O_2CCH_3)_4$ to afford an axially bound monodentate adduct **a** followed by formation of a chelate ring by attack of a second donor atom at an *eq* site (**b**; *ax-eq* adducts) and conversion to the final *eq-eq* adducts **c**.[206,373]

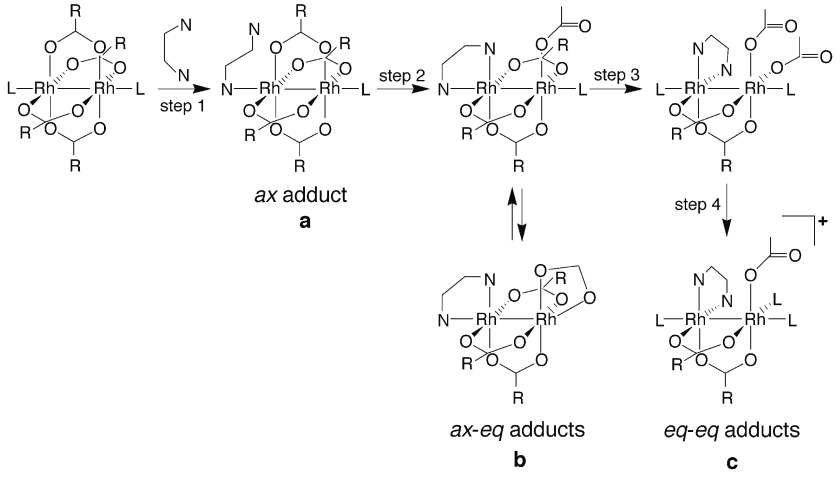
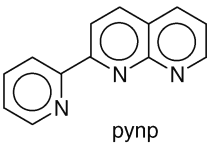
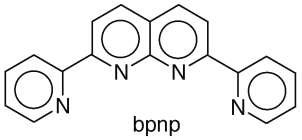
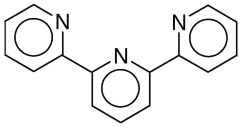


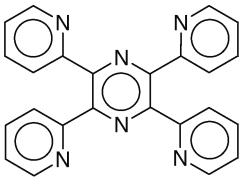
Fig. 12.17. Proposed mechanism of attack of a N-N donor chelate on the dirhodium core.

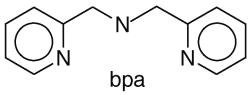
Pictiva EX2004
Samsung v Pictiva
IPR2024-01094

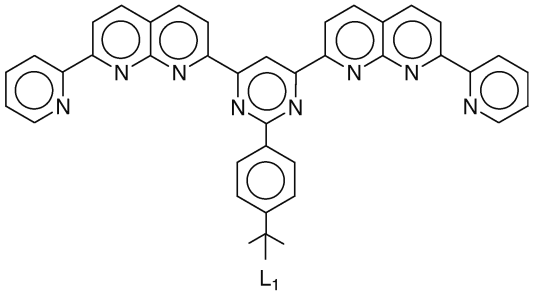

pynp
12.13


bpnp
12.14


tpy
12.15


tppz
12.17


bpa
12.16


L_1
12.18

A series of polyaza cavity-shaped (or crescent-shaped) ligands (**12.13**-**12.18**), that typically possess a central 1,8-naphthyridine fragment, have been found to form stable bis- and tris-acetate dirhodium complexes. In $[Rh_2(\mu\text{-}O_2CCH_3)_3(\eta^4\text{-bpnp})]PF_6$, the bpnp ligand (**12.14**) is binding to two *eq* and two *ax* sites of the dimetal unit (Fig. 12.18).[382,383] The ligand L_1 (L_1: 2-aryl-4,6-bis(2-(7-pyridyl)-1,8-naphthyridyl)-pyrimidine; **12.18**), which is composed of two bpnp type subunits, forms the tetranuclear complex $\{[Rh_2(\mu\text{-}O_2CCH_3)_3]_2(\mu_2\text{-}\eta^4\text{:}\eta^4\text{-}L_1)\}(PF_6)_2$ consisting of two separate dirhodium units bridged by a pyrimidine group.[384] Two unusual monocarboxylate cations $[Rh_2(\mu\text{-}O_2CCH_3)(\eta^3\text{-tpy})_2Cl_2]^+$ [205] and $[Rh_2(\mu\text{-}O_2CPh)(\eta^3\text{-tpy})_2(NCCH_3)_2]^{3+}$ [351] have been crystallized with tpy (**12.15**) binding in a tridentate fashion to the dirhodium core and both tpy molecules occupying *eq* planes. An extrapolation of this chemistry has involved 2,3,5,6-tetra-2-pyridylpyrazine (tppz; **12.17**) to afford the novel type metal-metal bonded molecular rectangle $[Rh_4(\mu\text{-}O_2CCH_3)_2(\mu_2\text{-}\eta^3\text{:}\eta^3\text{-tppz})_2(MeOH)_4]^{4+}$ (Fig. 12.19) with two linked reduced Rh_2^{3+} units.[385] The X-ray crystal structure of the disubstituted pynp cation $[Rh_2(\mu\text{-}O_2CCH_3)_2(\eta^3\text{-pynp})_2]^{2+}$, which was initially studied by NMR and electronic spectroscopies,[382,386] reveals both pynp ligands (**12.13**) behaving in a combined bridging/chelating fashion with each pynp moiety occupying one *ax* and two *eq* sites of the dimetal unit.[387,388] As expected, the Rh–N_{eq} distances are considerably shorter than Rh–N_{ax} (2.04(1) Å and 2.20(1) Å, respectively).[388] In another disubstituted pynp product that has been isolated, one pynp ligand is coordinated in the usual tridentate fashion and the second one acts as a monodentate *ax* ligand.[388] These complexes with polyaza, cavity-shaped molecules

Pictiva EX2004
Samsung v Pictiva
IPR2024-01094

exhibit rich electrochemistry: in addition to electrochemical processes corresponding to oxidation to the Rh_2^{5+} core, they exhibit two reduction processes,[382,386] which have been studied by EPR spectroscopy[389] and single-point energy theoretical calculations.[388] The carboxylate groups of the tetradentate 1,8-naphthyridine-2,7-dicarboxylate ligand (dcnp) presumably occupy *ax* positions in $Na[Rh_2(\mu\text{-}O_2CCH_3)_3(dcnp)]$.[390] The bpa ligands (**12.16**), in the two isomers of $[Rh_2(\mu\text{-}O_2CCH_3)_2(\eta^3\text{-bpa})_2]^{2+}$ (C_2 and C_s symmetry point groups), are coordinated in a tridentate fashion to each Rh atom.[206] It is notable that, among the disubstituted complexes, the carboxylate groups are usually found in the *cisoid* arrangement, except for *trans*-(2,2)$Rh_2(\mu\text{-}O_2CCH_3)_2(mhp)_2(Im)$[391] (mhp: anion of 6-methyl-2-hydroxypyridine); the latter is discussed with the monocarboxylate adduct *trans*-$[Rh_2(\mu\text{-}O_2CCH_3)(chp)_2(NCCH_3)_3]BF_4$[392] (chp: anion of 6-chloro-2-hydroxypyridine) in section 12.3.2. Likewise, mixed carboxylate/formamidinate and carboxylate/9-ethylguanine complexes[393-395] are discussed in Sections 12.3.3 and 12.7.3, respectively.

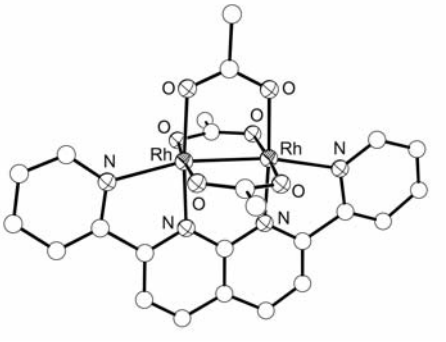


Fig. 12.18. The cation in $[Rh_2(\mu\text{-}O_2CCH_3)_3(\eta^4\text{-bpnp})]PF_6$.

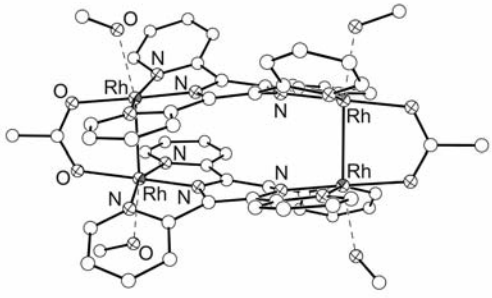


Fig. 12.19. The structure of the cationic rectangle $[Rh_4(\mu\text{-}O_2CCH_3)_2(\mu_2\text{-}\eta^3\text{:}\eta^3\text{-tppz})_2(MeOH)_4]^{4+}$.

12.3.2 Complexes supported by hydroxypyridinato, carboxamidato and other (N, O) donor monoanionic bridging groups

The quest for bridging ligands that preclude *ax* interactions led to the introduction of 6-X-oxopyridinate bridging groups (X = Me, F, and Cl; **12.4**).[391] In general, the Rh–Rh bond lengths for tetrahydroxypyridinato compounds vary between 2.36 Å and 2.41 Å, which is within the range of Rh–Rh distances for most tetracarboxylate complexes. The Rh–Rh bond distance in $Rh_2(mhp)_4$ (2.359(1) Å)[396,397] is comparable to that of the tetracarboxylate complex $Rh_2(TiPB)_4$ (Rh–Rh = 2.350(1) Å)[16] and to that of the pyrazolate bridged compound

Pictiva EX2004
Samsung v Pictiva
IPR2024-01094

$Rh_2(3,5\text{-}Me_2pz)_4(NCCH_3)_2$ (Rh–Rh = 2.353(3) Å),[398] which are among the shortest recorded Rh–Rh bond distances. The longest Rh–Rh bond distance among the compounds of this class is exhibited by $Rh_2(fhp)_4(DMSO)$ (X = F; Rh–Rh = 2.410(1) Å).[399] The significant increase in the Rh–Rh bond distance, as compared to $Rh_2(chp)_4$ (X = Cl; 2.379(1) Å),[391] is attributed mainly to the presence of the *S*-bound molecule of DMSO in the *ax* position, as well as to the electron withdrawing effect of the fluorine atoms.

The 6-X-oxopyridinate derivatives are prepared by one of the following procedures: reaction of the sodium salt, e.g., Na(mhp)[396] or Na(fhp),[399] with $RhCl_3{\cdot}xH_2O$; reaction of Na(mhp) with $Rh_2(O_2CCH_3)_4(MeOH)_2$,[396] or reaction of the molten ligands Hhp, Hmhp or Hchp with $Rh_2(O_2CCH_3)_4$.[391,400]

Homoleptic Rh_2^{4+} paddlewheel compounds supported by (N, O) 6-X-oxopyridinate bridging groups (X = Me, F, and Cl) (**12.4**) as well as other (N, O) donor groups (**12.5-12.6**) exhibit structural diversity. The crystal structures of a number of these compounds (Table 12.3) indicate that they exhibit four possible geometric isomers designated as *cis*-(2,2), *trans*-(2,2), (3,1) and (4,0) (Fig. 12.20).

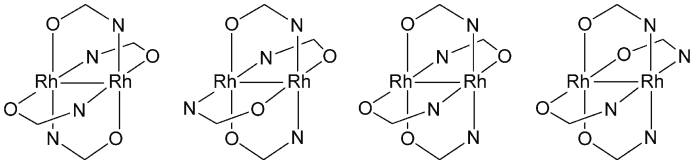


Fig. 12.20. Possible orientations of asymmetric bridging groups around the Rh_2 core and symmetry of the immediate coordination sphere.

Table 12.3. Structural data for Rh_2^{4+} compounds supported by carboxamidato and other (N, O) donor bridging groups

Compound	*r* (Rh–Rh)[a] (Å)	*r* (Rh–L_{ax})[b] (Å)	Donor atom(s)	ref.
trans-(2,2)-$Rh_2(mhp)_4$	2.359(1)	[c]	[c]	396,397
trans-(2,2)-$Rh_2(mhp)_4{\cdot}H_2O$	2.370(1)	[c]	[c]	391
trans-(2,2)-$[Rh_2(mhp)_4]{\cdot}CH_2Cl_2$	2.367(1)	[c]	[c]	285,401
(3,1)-$Rh_2(mhp)_4(NCCH_3)$	2.372(1)	2.152(7)	N	391
(3,1)-$[Rh_2(mhp)_4(Im)]{\cdot}0.5CH_3CN$	2.384(1)	2.144(4)	N	391
(3,1)-$[Rh_2(mhp)_4]_2{\cdot}2CH_2Cl_2$[d]	2.369(1)	2.236(3)[e]	O	402
(3,1)-$[Rh_2(mhp)_4(Hmhp)]{\cdot}0.5C_6H_5CH_3$	2.383(1)	2.195(4)	O	402
$[Rh_2(mhp)_3(\mu\text{-}OTs)]_2{\cdot}Et_2O$[d]	2.377(3) 2.376(3)	2.24(1)[e] 2.30(2)[e]	O	405
trans-(2,2)-$Rh_2(chp)_4$	2.379(1)	[c]	[c]	391
(3,1)-$[Rh_2(chp)_4(Im)]{\cdot}3H_2O$	2.385(1)	2.129(9)	N	391
trans-$[Rh_2(\mu\text{-}O_2CCH_3)(chp)_2(NCCH_3)_3]BF_4$	2.444(1)	2.149(6)	N	392
(4,0)-$Rh_2(fhp)_4(DMSO)$	2.410(1)	2.332(3)	S	399
$Rh_2(fhp)_4(THF)$[f]	2.34[g]	[f]	O	399
(3,1)-$[Rh_2(hq)_4(py)]{\cdot}1.5C_2H_4Cl_2$	2.396(1)	2.140(3)	N	404
trans-$Rh_2(\mu\text{-}O_2CCH_3)_2(mhp)_2(Im)$	2.388(2)	2.17(1)	N	391
trans-$[Rh_2(\mu\text{-}O_2CCH_3)_2(mhp)_2(Im)]{\cdot}2CH_2Cl_2$	2.388(1)	2.133(7)	N	391

Pictiva EX2004
Samsung v Pictiva
IPR2024-01094

Compound	*r* (Rh–Rh)[a] (Å)	*r* (Rh–L_{ax})[b] (Å)	Donor atom(s)	ref.
cis-[$Rh_4(mhp)_4(\mu_2\text{-}Cl)_4(PhCN)_2$]	2.537(3)	2.13(2)	N	197
cis-(2,2)-[$Rh_2(pyro)_4(Hpyro)_2$]·$2CH_2Cl_2$	2.445(1)	2.325(1)	O	430
cis-(2,2)-[$Rh_2(vall)_4(Hvall)_2$]·2Hvall	2.392(1)	2.357(3)	O	430
[$Rh_2(mphonp)_4$]·$C_6H_5OCH_3$·½Et_2O	2.566(3)	2.46(2) 2.42(2)	N[h]	406
cis-(2,2)-[$Rh_2(HNCOCH_3)_4(H_2O)_2$]·$3H_2O$	2.415(1)	2.352(2)	O	414
cis-(2,2)-[$Rh_2(HNCOCH_3)_4(DMSO)_2$]·H_2O	2.452(1)	2.414(1)	S	422
{[$Rh_2(HNCOCH_3)_4$]$_3(\mu_3\text{-}Cl)_2$·$4H_2O$}$_\infty$[i]	2.422(1) 2.424(1) 2.431(1)	2.552(1) 2.554(1) 2.610(1)	Cl	412
{[$Rh_2(HNCOCH_3)_4$]$(\mu_4\text{-}I)$·$6H_2O$}$_\infty$[j]	2.438(1)	2.975(1)	I	429
[$Rh_2(\mu\text{-}HNOCCH_3)_3(\mu\text{-}O_2CCH_3)(DMSO)_2$]·$2H_2O$	2.446(1)	2.413(1)	S	421
$Rh_2(\mu\text{-}HNCOCH_3)_3(\mu\text{-}O_2CCH_3)(AsPh_3)_2$	2.467(3)	2.553(4)	As	423
$Rh_2(\mu\text{-}HNCOCH_3)_3(\mu\text{-}O_2CCH_3)(SbPh_3)_2$	2.461(2)	2.699(3)	Sb	423
trans-(2,2)-$Rh_2(PhNCOCH_3)_4(NCPh)_2$	2.422[k]	2.205[k] 2.248[k]	N	420
(3,0)-$Rh_2(PhNCOCH_3)_4(DMSO)$	2.397(1)	2.395(1)	S	409
cis-(2,2)-$Rh_2(PhNCOCH_3)_4(DMSO)_2$	2.448(1)	2.606(2) 2.566(2)	S	409
cis-(2,2)-$Rh_2(HNCOCH_3)_4(AsPh_3)_2$	2.471(2)	2.540(2)	As	423
cis-(2,2)-$Rh_2(HNCOPh)_4(py)_2$	2.437(1)	2.227(7)	N	425
cis-(2,2)-[$Rh_2(HNCOPh)_4(SbPh_3)_2$]·CH_2Cl_2	2.463(1)	2.681(1)	Sb	425
cis-(2,2)-$Rh_2(HNCOCF_3)_4(py)_2$	2.472(3)	2.26(1) 2.31(1)	N	417
{$Rh_2(HNCOCF_3)_4(4,4'\text{-}bpy)$}$_\infty$	2.456(1)	2.222(4)	N	426
trans-[$Rh_2(\mu\text{-}O_2CCH_3)_2(\mu\text{-}HNCOCF_3)_2$-(9-MeAdeH$_2$)$_2$]$(NO_3)_2$[l]	2.430[k]	2.274(8)	N	411
trans-[$Rh_2(\mu\text{-}O_2CCH_3)_2(\mu\text{-}HNCOCF_3)_2$-(9-EtGuaH)$_2$]·2MeOH·$2H_2O$	2.427[k]	2.283(3)	N	411
$Rh_2(HNCOCF_3)_4(Guo)_2$·$3H_2O$	2.459[k]	2.27(1) 2.30(1)	N	411
trans-[$Rh_2(\mu\text{-}HNCOCH_3)_2(\mu\text{-}HNCOCF_3)_2$-(Guo)$_2$]·$3H_2O$	2.432[k]	2.296(7) 2.280(7)	N	411
[$Rh_2(HNCOCF_3)_4(dGuo)_2$]·$3H_2O$	2.475[k]	2.326[k] 2.250[k]	N	411
[$Rh_2(HNCOCF_3)_4(Ino)_2$]·$3H_2O$	2.455[k]	2.35(1) 2.27(1)	N	411
[$Rh_2(HNCOCF_3)_4(cyd)$]$_\infty$[m]	2.463(1)	2.326(5)[n] 2.247(5)[o]	N O	410
[$Rh_2(HNCOCF_3)_4(1\text{-}Mecyd)_2$]·$2H_2O$	2.469(1)	2.354(2)	N	410
cis-[$Rh_2(\mu\text{-}HNCOCF_3)_2(phen)_2(py)_2$]$(PF_6)_2$·$Et_2O$	2.612(1)	2.238(5) 2.241(5)	N	356
cis-$Rh_2(\mu\text{-}HNCOCF_3)_2(phen)_2Cl_2$	2.614(1)	2.540(2)	Cl	427
Homochiral Carboxamidate Compounds				
cis-(2,2)-Rh_2(5*R*-MEPY)$_4$(NCCH$_3$)$_2$(Pr^{i}OH)	2.457(1)	2.215(4) 2.236(4)	N	431

Pictiva EX2004
Samsung v Pictiva
IPR2024-01094

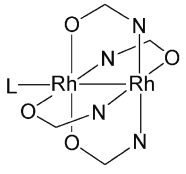
Compound	*r* (Rh–Rh)[a] (Å)	*r* (Rh–L_{ax})[b] (Å)	Donor atom(s)	ref.
Rh_2(5*S*-dFMEPY)$_4$($CH_3CO_2CH_2CH_3$)$_2$, Rh_2(5*S*-dFMEPY)$_4$($CH_3CO_2CH_2CH_3$)(H_2O)·1.5H_2O[p]	2.467(1)	2.362[k,q] 2.324[k,q] 2.286[k,q] 2.325[k,r]	O	432
cis-(2,2)-Rh_2(5*S*-DMAP)$_4$($NCCH_3$)$_2$·CH_3CN·6H_2O	2.454(1)	2.231(4) 2.224(4)	N	433
cis-(2,2)-Rh_2(4*S*-BNAZ)$_4$($NCCH_3$)$_2$	2.533(1)	2.210[k]	N	434
cis-(2,2)-Rh_2(5*S*-BNOX)$_4$($NCCH_3$)$_2$·CH_3CN	2.472(2)	2.205(8) 2.252(8)	N	431
cis-(2,2)-Rh_2(4*S*-PHOX)$_4$($NCCH_3$)$_2$·2CH_3CN	2.471(1)	2.19(1)	N	435
cis-(2,2)-[Rh_2(4*S*-MEOX)$_4$(NCPh)$_2$](C_6H_5CN)$_2$	2.477(1)	2.191(2)	N	436
cis-(2,2)-Rh_2(4*S*-THREOX)$_4$(NCPh)$_2$	2.474(1)	2.203(2)	N	436
cis-(2,2)-Rh_2(4*S*-MACIM)$_4$($NCCH_3$)$_2$·2CH_3CN	2.459(1)	2.220(3)	N	437
(3,1)-Rh_2(4*S*-MACIM)$_4$($NCCH_3$)$_2$·2CH_3CN	2.460(1)	2.223(4)	N	437
(4,0)-Rh_2(4*S*-MACIM)$_4$($NCCH_3$)$_2$	2.445(1)	2.179(4) 2.268(4)	N	438
cis-(2,2)-Rh_2(4*S*-MBOIM)$_4$($NCCH_3$)$_2$·2CH_3CN	2.461(1)	2.210(3)	N	437
cis-(2,2)-Rh_2(4*S*-MPPIM)$_4$($NCCH_3$)$_2$·2CH_3CN	2.464(1)	2.219(4)	N	437
cis-(2,2)-Rh_2(4*S*-MCHIM)$_4$($NCCH_3$)$_2$·2CH_3CN	2.451(1)	2.216(3)	N	437
cis-(2,2)-Rh_2(*S*,*S*-MANIM)$_4$($NCCH_3$)$_2$	2.467[k]	2.206[k]	N	439
cis-(2,2)-Rh_2(*S*,*R*-NaphthAZ)$_4$($NCCH_3$)$_2$	2.529(3)	2.22[2]	N	440

[a] Distances are given with up to 3 decimal digits.
[b] In some cases the average Rh–L bond lengths are quoted. In these instances the estimated deviation, which is given in square brackets, is calculated as [ ] = $[\Sigma_n\Delta_i^2/n(n-1)]^{1/2}$, in which Δ_i is the deviation of the *i*th of *n* values from the arithmetic mean of the set.
[c] No *ax* ligands.
[d] '*Dimer of dimers*'.
[e] Rh–O distance to mhp O atom of neighboring dirhodium unit.
[f] Unsatisfactory solution of crystal structure; only unit cell determined.
[g] Average approximate distance.
[h] Nitrogen atoms of mphonp ligand.
[i] Honeycomb arrangement of Rh_2^{4+} and Rh_2^{5+} units bridged by μ_3-Cl^- ions.
[j] Diamondoid arrangement of Rh_2^{4+} and Rh_2^{5+} units bridged by μ_4-I^- ions.
[k] Esds not reported.
[l] Each 9-methyladenine molecule is protonated at position *N1* of the purine ring.
[m] One dimensional zig-zag chain.
[n] Distance to the ring nitrogen N(3) of cytosine.
[o] Distance to the keto O(2) site of cytosine.
[p] The two molecules co-crystallize in the same crystal with 1.5 interstitial H_2O molecules.
[q] Rh–O distance to *ax* molecule of $CH_3CO_2CH_2CH_3$.
[r] Rh–O distance to *ax* molecule of H_2O.

The compounds $Rh_2(mhp)_4$,[396,397] $Rh_2(mhp)_4$·H_2O,[391] [$Rh_2(mhp)_4$]·CH_2Cl_2[285,401] and $Rh_2(chp)_4$[391] with D_{2d} molecular symmetry (i.e., symmetrical *trans*-(2,2) arrangement; Fig. 12.20b) lack *ax* ligands due to the presence of two 6-X hp bridging substituents located near each *ax* site; in the case of the hydrate, the H_2O molecules engage in hydrogen bonding with the mhp molecules. The (3,l) arrangement (Fig 12.20c) is encountered in the adducts $Rh_2(mhp)_4L$, (L = CH_3CN[391] or imidazole (Im),[391] Hmhp[402]), $Rh_2(chp)_4(Im)$,[391] as well as in the '*dimer of dimers*' [$Rh_2(mhp)_4$]$_2$.[402] The (3,1) arrangement permits binding of an *ax* ligand to the rhodium atom with the fewest N atoms coordinated to it (12.19), but in this case, the

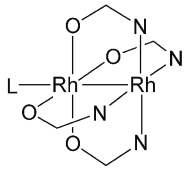
Pictiva EX2004
Samsung v Pictiva
IPR2024-01094

other *ax* site is even more blocked as compared to the (2,2) arrangement, which precludes *ax* ligands from occupying this position. The $[Rh_2(mhp)_4]_2$ structure[402] provides an example of the (3,1) arrangement wherein the molecules, which are denied access to other coordinating ligands, associate with the O atom from an mhp bridging group of an adjacent dirhodium unit. This association is evidenced by the ^{103}Rh NMR spectra of *trans*-(2,2)-$Rh_2(mhp)_4$ and (3,1)-$[Rh_2(mhp)_4]_2$; the former exhibits a singlet at δ = +5745 ppm, whereas the dimer exhibits a pair of doublets centered at $\delta \sim +7644$ ppm and $\sim +4322$, due to the two nonequivalent ^{103}Rh nuclei with $^1J(^{103}Rh, ^{103}Rh)$ coupling of ~35 Hz.[403] Another example of the (3,1) arrangement is that of the 2-quinolinol (Hhq) adduct $Rh_2(hq)_4(py)$, which has an *ax* py ligand coordinated to the Rh atom with the least steric hindrance.[404] The option of a single *ax* ligand is apparent in *trans*-$Rh_2(\mu\text{-}O_2CCH_3)_2(mhp)_2(Im)$ (Fig. 12.21), wherein not only are the acetate groups found in the unusual *transoid* arrangement, but the two mhp ligands point in the same direction, thus preventing *ax* coordination to one rhodium atom while leaving the other *ax* site accessible to the imidazole ligand.[391] In the '*dimer of dimers*' $[Rh_2(mhp)_3(\mu\text{-}OTs)]_2$, which is obtained from the reaction of $Rh_2(mhp)_4$ with toluene-*p*-sulfonic acid (TsOH), the 'open' *ax* sites are involved in intermolecular Rh···O(mhp) interactions (2.24(1) Å and 2.30(2) Å)[405] similar to those encountered in the '*dimer of dimers*' (3,1)-$[Rh_2(mhp)_4]_2$.[402]



(3,1)

12.19



(4,0)

12.20

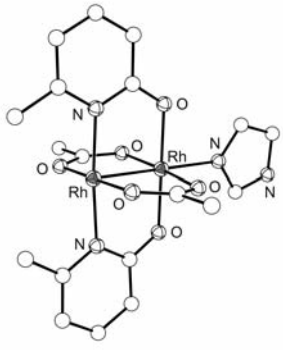


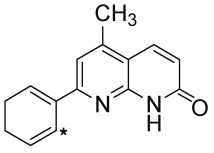
Fig. 12.21. Molecular structure of *trans*-$Rh_2(O_2CCH_3)_2(mhp)_2(Im)$.

The polar (4,0) ligand arrangement **12.20** is found in the fhp complexes $Rh_2(fhp)_4L$, L = EtOH, THF or DMSO,[399] which structurally resemble the Cr, Mo, and W analogs. In a similar vein to the (3,l) arrangement **12.19**, the *ax* ligands L bind to the rhodium atom with the fewest N atoms coordinated to it (in this case none), and the additional *ax* bond stabilizes the structure. It appears that steric effects are important in determining the type of isomer preferred. For example, it is less difficult to place four small fluorine atoms in the (4,0) arrange-

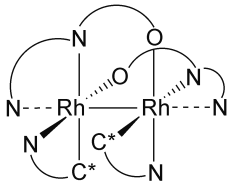
Pictiva EX2004
Samsung v Pictiva
IPR2024-01094

ment without creating significant repulsion, whereas four large chlorine or methyl groups would result in unfavorable repulsive interactions.[399] There is no general method, however, for predicting which isomer will be preferred, and the outcome depends on the interplay of various weak non-bonding attractions and repulsions. This argument is further supported by the polar arrangement of the chp ligands in *trans*-$[Rh_2(\mu\text{-}O_2CCH_3)(chp)_2(NCCH_3)_3]BF_4$, despite the fact that the two chlorine atoms of the chp pairs make contacts close to the sum of the van der Waals radii.[392]

In the cage-like structure *cis*-$[Rh_4(mhp)_4(\mu_2\text{-}Cl)_4(PhCN)_2]$, the two dirhodium units are linked by bridging chloride ions, the mhp ligands are in the usual *cis*-(2,2) arrangement, and the *ax* ligands are bound to the less hindered sites.[197] Unexpected binding modes are observed in the complex $Rh_2(mphonp)_4$ (Hmphonp = 5-methyl-7-phenyl-1,8-naphthyridin-2-one; **12.21**), which contains two bridging and two chelating mphonp anions in the unusual (N, C) mode (involving cyclometalation of the naphthyridine rings) as depicted in **12.22**.[406]



12.21



12.22

Interest in the compounds $Rh_2(O_2CR)_n(R'NCOR)_{4-n}$ (R = CH_3 or CF_3; R' = H or Ph; n = 0-3) supported by another class of mixed (N, O) donor anionic ligands, namely the carboxamidates (**12.5**), stems from the rich electrochemistry exhibited by these complexes due to the higher electron density of the Rh(II) centers as n increases.[407-409] The structural versatility of these compounds is notable, owing to the concomitant presence of hydrogen-bonding donor and acceptor sites on the bridging groups[410-412] (carboxylate groups function only as acceptors). Dirhodium compounds with carboxamidate bridging groups that have been studied by X-ray crystallography are listed in Table 12.3.

Reactions of $Rh_2(O_2CCH_3)_4$ with molten acetamide, trifluoroacetamide and *N*-phenylacetamide have been employed to prepare the fully substituted complexes $Rh_2(HNCOCH_3)_4$,[407,413-415] $Rh_2(HNCOCF_3)_4$,[416,417] and $Rh_2(PhNCOCH_3)_4$,[409,418] respectively. Partially substituted complexes are simultaneously formed and must be separated by liquid chromatography. Refluxing $Rh_2(O_2CCH_3)_4$ with acetamide in anhydrous chlorobenzene in a Soxhlet extraction apparatus (in the presence of sodium carbonate) affords only the tetra-substituted *cis*-(2,2)-$Rh_2(HNCOCH_3)_4$.[419] The compound $Rh_2(HNCOCF_3)_4$ is prepared by a molten reaction; the *cis*-(2,2) isomer was identified by X-ray diffraction studies of its bis(pyridine) analog as the most abundant product (>94%), whereas the next most abundant fraction (4%) is the (3,1) isomer, based on ^{19}F NMR spectroscopy.[417] These results indicate that the *cis*-(2,2) isomer (Fig 12.20a) is the most stable, although differences in free energy among the other isomers are small. Both the *cis*-(2,2) and (3,1) isomers of $Rh_2(PhNCOCH_3)_4$ have been synthesized (by molten reactions), separated by HPLC and subsequently crystallized as their DMSO adducts *cis*-(2,2)-$Rh_2(PhNCOCH_3)_4(DMSO)_2$ (Fig. 12.22) and (3,0)-$Rh_2(PhNCOCH_3)_4(DMSO)$; both adducts contain *S*-bound DMSO.[409] It is notable that the first *N*-substituted *trans*-(2,2)-$Rh_2(PhNCOCH_3)_4(NCPh)_2$ isomer has been synthesized (by using the Soxhlet extraction method) and structurally characterized.[420] The presence of two *ax* ligands in this adduct is reasonable due to the orientation of the phenyl rings attached to the N atoms of the bridging groups: the

Pictiva EX2004
Samsung v Pictiva
IPR2024-01094

rings are nearly perpendicular to the plane of the amidate bridging groups to avoid steric repulsion of their *ortho* protons with the CH_3 groups of the acetamide moieties.

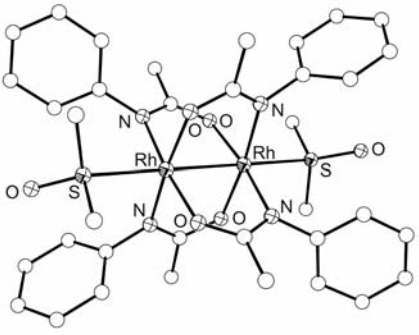


Fig. 12.22. Molecular structure of *cis*-(2,2)-$Rh_2(PhNCOCH_3)_4(DMSO)_2$.

Both acetamidate and trifluoroacetamidate complexes as well as the mixed carboxamidate/acetate complexes readily form adducts with H_2O,[414] DMSO,[421] pyridine,[413,417] acetonitrile,[408,422] PPh_3,[423] $AsPh_3$,[423] and $SbPh_3$.[423] The stability constants of the CO adducts with $Rh_2(O_2CCH_3)_n(R'NCOCH_3)_{4-n}$ (n = 0, 2, 3, 4) increase, whereas the frequency of the ν(CO) stretching mode decreases with increasing n, due to an increase in the degree of π-backbonding; these observations corroborate the enhanced electron-donating ability of acetamidate compared to carboxylate groups.[424] This is also supported by the formation constants of the ligand exchange reactions involving displacement of CH_3CN by DMSO, which indicate that different modes of DMSO binding (S vs O) exist for $[Rh_2(O_2CCH_3)_{4-n}(R'NCOCH_3)_n]^{0/+}$ as a function of the value n and the oxidation state.[422] Structural studies of the series of compounds $Rh_2(O_2CCH_3)(HNCOCH_3)_3L_2$, where L = DMSO,[421] $AsPh_3$[423] or $SbPh_3$[423] show them to be isostructural with each rhodium atom formally bound to a *cis* pair of carboxamide nitrogen atoms.

The benzamidate (**12.5**; R = Ph, R' = H) derivative $Rh_2(HNCOPh)_4$ readily forms adducts with benzamide, PPh_3, pyridine and $SbPh_3$; the crystal structure determinations of the compounds with the latter two ligands reveal that they possess the common *cis*-(2,2) geometry (Fig. 12.20a).[425] Polymeric adducts of $Rh_2(HNCOCF_3)_4$ with pyrazine, 1,4-diazabicyclo[2.2.2]octane and 4,4'-bipyridine have been prepared, and the compound $\{Rh_2(HNCOCF_3)_4(4,4'\text{-bpy})\}_\infty$ has been structurally characterized.[426] The bis-trifluoroacetamidate compounds *cis*-$[Rh_2(\mu\text{-}HNCOCF_3)_2(phen)_2(py)_2](PF_6)_2$[356] and *cis*-$Rh_2(\mu\text{-}HNCOCF_3)_2(phen)_2Cl_2$[427] with two chelating N-N groups occupying *eq* positions, and $Rh_2(HNCOCF_3)_4$ adducts with 2,4-diaminopyrimidine ligands[428] have been prepared. The unusual compound $\{[Rh_2(HNCOCH_3)_4]_3(\mu_3\text{-}Cl)_2\}_\infty$, which consists of Rh_2^{4+} and Rh_2^{5+} units bridged by chloride ions in a honeycomb arrangement, has low conductivity.[412] Alternatively, the diamondoid network of $\{[Rh_2(HNCOCH_3)_4]_2(\mu_4\text{-}I)\cdot 6H_2O\}_\infty$ units undergoes reversible dehydration-rehydration cycles of the interstitial water molecules with a 10^5 enhancement of its electrical conductivity in the hydrated form, most likely due to deformation of the hydrogen-bond network and localization of the odd electrons on some of the Rh_2 sites in the dehydrated form.[429] The carboxamidate adducts with DNA nucleobases and their nucleosides[410,411] are discussed in Section 12.7.3, and their electrochemical properties as well as their Rh_2^{5+} counterparts are presented in Section 12.6.

Several dirhodium complexes with (N, O) donor sets in which the nitrogen atom is incorporated into five membered rings are those with 2-pyrrolidinone (Hpyro) and δ-valerolactam

Pictiva EX2004
Samsung v Pictiva
IPR2024-01094

(2-piperidinone, Hvall) (12.6); their adducts $Rh_2(pyro)_4(Hpyro)_2$ and $Rh_2(vall)_4(Hvall)_2$ have been prepared from $Rh_2(O_2CCH_3)_4$ by ligand exchange of the acetate groups, and exhibit the usual *cis*-(2,2) arrangement (Fig 12.20a).[430] In weakly coordinating solvents, CO binding to $Rh_2(pyro)_4$ and $Rh_2(vall)_4$ is fast and CO dissociation is very slow, but in solvents such as CH_3CN, CO binding is reversible.[430] Homochiral dirhodium carboxamidate compounds[431-441] find extensive application in catalysis and are discussed in detail in Chapter 13.

12.3.3 Complexes supported by amidinato and other (N, N) donor bridging groups

Among the common monoanionic bridging ligands are *N*-donor bidentate amidinate groups (12.7), which have emerged as one of the more important classes. Amidinate bridging groups introduce chemical and structural diversity to dinuclear complexes, resulting in rich electrochemistry,[442] improvement of their biological activity,[443] and fine control in the design of supramolecular assemblies.[13,15] The robust nature and the strong *trans* influence of the amidinate bridging groups render the behavior of this class of compounds different, in many aspects, from that of the carboxylate series.

The parent compound of the formamidinate series, $Rh_2(DPhF)_4$ (12.7; R = H, Ar = Ph), is prepared by reaction of $Rh_2(O_2CCH_3)_4$ with molten HDPhF at 130 ºC,[444] a reaction that generally is applicable to the preparation of various formamidinate analogs.[442] An alternative method of preparation involves refluxing $RhCl_3$ with the neutral formamidine in $EtOH/Et_3N$, but the yields are better with the former method, especially for ligands with lower melting points; compounds with $ArNCHNAr^-$ bridging groups, Ar = XC_6H_4 (X = *p*-OMe, *p*-Me, H, *m*-OMe, *p*-Cl, *m*-Cl, *m*-CF_3, *p*-CF_3) or Ar = 3,4-$Cl_2C_6H_3$, 3,5-$Cl_2C_6H_3$, have been synthesized by the previous methods.[442] The reaction of $Rh_2(DTolF)_2(O_2CCF_3)_2(H_2O)_2$[445] with molten *N,N'*-di-*p*-tolylformamidine (HDTolF) at 135 °C affords $Rh_2(DTolF)_4$.[446] The analogous compound $Rh_2(DPhBz)_4$ (Fig. 12.23) is obtained from the reaction of $Rh_2(O_2CCH_3)_4$ with benzamidine (12.7; R = Ph, Ar = Ph).[447,448] Unlike $Rh_2(O_2CCH_3)_4(CO)_2$, which is stable only at low temperatures,[261] the monocarbonyl adducts of $Rh_2(DPhBz)_4$[448] and $Rh_2(DPhF)_4$[444,446] are very stable, most likely due to the presence of the amidinate groups which render the dirhodium core more electron-rich than carboxylate groups.

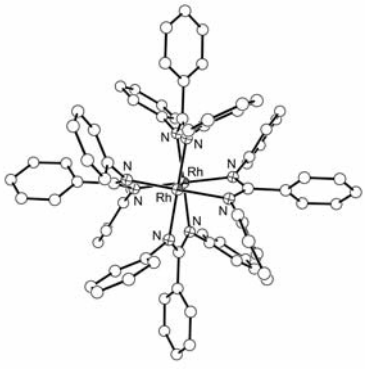


Fig. 12.23. Molecular structure of $Rh_2(DPhBz)_4$.

Molecular orbital calculations on the model species $Rh_2(HNCHNH)_4$ by the DV-Xα and Xα-SW methods revealed that the ground state electronic configuration is $\sigma^2\pi^4\delta^2\pi^{*4}\delta^{*2}$,[449,450] which accounts for the strong metal-ligand interactions in the cases of the bridging ligands $HNCHNH^-$ and $HNNNH^-$.[450] The adduct $Rh_2(DPhTA)_4$ with four

Pictiva EX2004
Samsung v Pictiva
IPR2024-01094

1,3-diphenyltriazenide moieties (**12.8**; Ar = Ph),[451] and several compounds with *eq* molecules of CO and 1,3-di-tolyltriazenide (**12.8**; Ar = *p*-tol),[452-457] or 1,3-diphenylacetamidinate (**12.7**; R = CH_3, Ar = Ph)[458] bridging groups, have been prepared and structurally characterized. In the '*dimer of dimers*' $\{[Rh_2(DTolTA)_2(CO)(bpy)(\mu\text{-}I)]_2\}(PF_6)_2$, the two dirhodium units are bridged by two iodide ions. Although the two Rh-I bond distances are not equivalent, they are in the range typical for Rh-halogen bonds encountered in carboxylate compounds.[453]

The asymmetric tris-formamidinate complexes $Rh_2(DTolF)_3(\eta^2\text{-}NO_3)L$ (L = PPh_3, pyridine, Me_2NH)[459] are formed by reaction of the paramagnetic Rh_2^{5+} complex $Rh_2(DTolF)_3(\eta^2\text{-}NO_3)_2$[460] with an excess of the neutral ligand L, via reductive elimination of one nitrate group. The adducts with L = PPh_3, pyridine (Fig. 12.24) have L occupying an *eq* site on one Rh atom and a chelating nitrate group bound to the other rhodium atom.[459] The nonequivalence of the two Rh atoms is consistent with the ^{103}Rh NMR spectra of these complexes, each of which shows two well-separated resonances.[459]

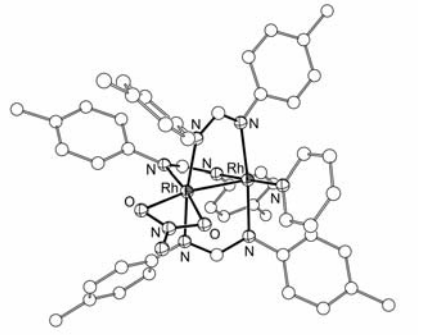


Fig. 12.24. Molecular structure of $Rh_2(DTolF)_3(\eta^2\text{-}NO_3)(py)$.

The mixed bis-trifluoroacetate complex *cis*-$Rh_2(DTolF)_2(O_2CCF_3)_2(H_2O)_2$[445] and the partially solvated *cis*-$[Rh_2(DTolF)_2(NCCH_3)_6](BF_4)_2$[461,462] are obtained by oxidation of $[Rh(COD)(DTolF)]_2$[463] (COD: cycloocta-1,5-diene) with AgO_2CCF_3 and $AgBF_4$, respectively, according to the reactions:

$$ArNHCHNAr \xrightarrow[CH_3CN,\ 0\ °C]{LiBu^t} ArNCHNAr^- \xrightarrow{[Rh(COD)Cl]_2} [Rh(COD)(DArF)]_2$$

$$[Rh(COD)(DArF)]_2 \xrightarrow[\text{or } AgO_2CCF_3]{AgBF_4} \begin{matrix} cis\text{-}[Rh_2(DArF)_2(CH_3CN)_6](BF_4)_2 \\ \text{or } cis\text{-}Rh_2(DArF)_2(O_2CCF_3)_2 \end{matrix}$$
$$\text{no light}$$

The *ax* water molecules of *cis*-$Rh_2(DTolF)_2(O_2CCF_3)_2(H_2O)_2$ are easily displaced by pyridine, DMSO, piperidine and methylimidazole, without altering the basic structure. The 1:1 adducts with various phosphorus donors PR_3, however, give rise to structures with a chelating $CF_3CO_2^-$ group and an *eq* phosphine on each Rh atom.[464] Contrary to the tetraformamidinate compounds which are inert to *eq* substitution,[465] both *cis*-$Rh_2(DTolF)_2(O_2CCF_3)_2(H_2O)_2$ and *cis*-$[Rh_2(DTolF)_2(NCCH_3)_6](BF_4)_2$ exhibit rich chemistry and are useful starting materials due to the increased lability of the ligands *trans* to the formamidinate groups (the latter exert a strong *trans* influence).[466,467] The polycyano acceptor molecules TCNE, TCNQ, DMDCNQI, DCNNQI,[468] and a variety of *meso*pyridyl-[469] and dicarboxylate-[470] porphyrins have been reacted with *cis*-$Rh_2(DTolF)_2(O_2CCF_3)_2(H_2O)_2$ to afford species with notable electro-

Pictiva EX2004
Samsung v Pictiva
IPR2024-01094

chemical properties. The same starting material has been used to prepare *cis*-$Rh_2(DTolF)_2$-$(\mu\text{-}O_2CC_6H_4CN)_2(py)_2$,[471] *cis*-$Rh_2(DTolF)_2(\mu\text{-}PPh_2Py)_2(O_2CCF_3)_2$[472] with (N, P) donor bridging 2-(diphenylphosphino)pyridine ligands, as well as two orthometalated compounds with only one formamidinate bridging group.[465,473] The complex *cis*-$[Rh_2(DTolF)_2(NCCH_3)_6](BF_4)_2$ has been employed to prepare the biologically relevant compounds *cis*-$[Rh_2(DTolF)_2(9\text{-}EtAdeH)_2$-$(NCCH_3)](BF_4)_2$,[462] *cis*-$[Rh_2(DTolF)_2(9\text{-}EtGuaH)_2(NCCH_3)](BF_4)_2$[462] (see Section 12.7.3) and *cis*-$[Rh_2(DTolF)_2(N\text{-}N)_n(NCCH_3)_m]^{2+}$, N-N = bpy or phen, n = 1 or 2, m = 1-4.[474] A notable aspect of *cis*-$[Rh_2(DTolF)_2(N\text{-}N)_n(NCCH_3)_m]^{2+}$ compounds is that the N-N ligands occupy *eq-eq* sites only[474] (e.g., *cis*-$[Rh_2(DTolF)_2(bpy)_2(NCCH_3)]^{2+}$; Fig. 12.25), unlike dirhodium carboxylate derivatives wherein the N-N ligands may occupy *ax-eq*[351,372] or *eq-eq*[351,373] positions (Figs. 12.16 and 12.17). This behavior is most likely due to the strong *trans* influence of the formamidinate groups, which render the groups *trans* to them more labile and thus *eq* positions readily available to N-N ligands.[474]

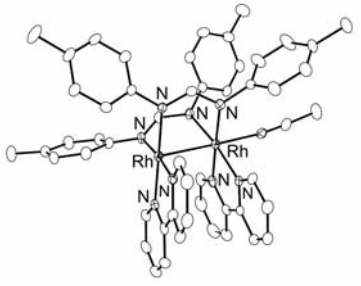


Fig. 12.25. Molecular structure of the cation in *cis*-$[Rh_2(DTolF)_2(bpy)_2(NCCH_3)](BF_4)_2$.

The amidinate compounds that have been structurally characterized are listed in Table 12.4. The Rh–Rh distances of the tetraamidinate compounds (2.389-2.570 Å) are longer than those of the carboxylate analogs; this can be partially ascribed to the '*bite*' of the amidinate groups.[299,445] Amidinate, e.g., $Rh_2(DPhF)_4$,[444] $Rh_2(DTolF)_4$,[446] $Rh_2(DPhF\text{-}m\text{-}OMe)_4$,[442] $Rh_2(DPhF\text{-}3,5\text{-}Cl_2)_4$,[442] $Rh_2(DPhBz)_4$,[448] and triazenide ($Rh_2(DPhTA)_4$[451] complexes lacking *ax* ligands, as well as others with only a small or linear *ax* ligand, e.g., $Rh_2(DPhF)_4(NCCH_3)$,[444] $Rh_2(DPhF)_4(CNPh)$,[475] $Rh_2(DPhBz)_4(CO)$,[448] $[Rh_2(DTolF)_2(bpy)(NCCH_3)_3](BF_4)_2$,[474] $[Rh_2$-$(DTolF)_2(phen)(NCCH_3)_3](BF_4)_2$[474] and *cis*-$[Rh_2(DTolF)_2(9\text{-}EtAdeH)_2(NCCH_3)](BF_4)_2$,[461,462] are not uncommon among complexes with (N, N) donor ligands. The absence of *ax* ligands in the foregoing compounds has been attributed primarily to steric crowding of (N, N) bridging groups as well as to electronic factors.[444,446,474,476] The aforementioned reasons are presumably responsible for the scarcity of tetraamidinate Rh_2^{4+} units associated in chains by *ax* ligands, in sharp contrast to tetracarboxylate complexes. Among the rare exceptions are the '*dimer of dimers*' $(DPhF)_4Rh_2(CNPhNC)Rh_2(DPhF)_4$,[475] the '*trimer of dimers*' $\{[Rh_2(DTolF)_4]_3(1,4\text{-}CNPhNC)_2\}$[477] and the polymer $[Rh_2(DTolF)_4(1,4\text{-}CNPhNC)]_\infty$[477] linked by the bidentate di-isocyano ligand 1,4-CNPhNC and the benzene ring acting as an appropriate spacer of the neighboring formamidinate ligands. Conversely, $[Rh_2(cis\text{-}DAniF)_2]^{2+}$ moieties, with two *cisoid* formamidinate anions as subunit precursors linked by polyfunctional ligands, e.g., dicarboxylate groups, have been assembled in 1- and 2-D molecular tubes, loops, squares, triangles, double helices and other supramolecular arrays,[13,15,469,470,478,483] as well as 'host' arrangements capable of encapsulating 'guest' molecules of appropriate size[484] (Section 12.7.2).

Pictiva EX2004
Samsung v Pictiva
IPR2024-01094

Table 12.4. Structural data for Rh_2^{4+} compounds supported by amidinato and other (N, N) donor bridging groups

Compound	*r* (Rh–Rh)[a] (Å)	*r* (Rh–L_{ax})[b] (Å)	Donor atom(s)	ref.
$Rh_2(DPhF)_4$	2.457(1)	[c]	[c]	444
$Rh_2(DPhF)_4(NCCH_3)$	2.459(1)	2.106(4)	N	444
$Rh_2(DPhF)_4(CNPh)$	2.480(1)	1.991(4)	C	475
$(DPhF)_4Rh_2(CNPhNC)Rh_2(DPhF)_4{\cdot}6CH_2Cl_2$	2.496(1)	1.988(9)	C	475
$Rh_2(DPhBz)_4$	2.389(1)	[c]	[c]	447,448
$Rh_2(DPhBz)_4(CO)$	2.435(1)	1.97(2)	C	448
$Rh_2(DTolF)_4$	2.434(1)	[c]	[c]	446
$[Rh_2(DTolF)_4(1,4\text{-}CNPhNC).2C_6H_6]_\infty$	2.570(1)	2.053(4)	C	477
$\{[Rh_2(DTolF)_4]_3(1,4\text{-}CNPhNC)_2\}.6H_2O$	2.520(2)	2.15(1)	C	477
$Rh_2(DTolF)_3(\eta^2\text{-}NO_3)(PPh_3){\cdot}0.5CH_2Cl_2$	2.498(2)	2.20(1)	O[d]	459
$Rh_2(DTolF)_3(\eta^2\text{-}NO_3)(py)$	2.476(1)	2.286(6)	O[d]	459
cis-$Rh_2(DTolF)_2(\mu\text{-}O_2CCF_3)_2(H_2O)_2{\cdot}0.5C_6H_6$	2.425(1)	2.311(3) 2.319(3)	O	445
cis-$Rh_2(DTolF)_2(\mu\text{-}O_2CCF_3)_2(NCCH_3)_2$	2.474(5)	2.265(5) 2.267(5)	N	462
cis-$[Rh_2(DTolF)_2(NCCH_3)_6](BF_4)_2$	2.559(1)	2.208(7) 2.235(7)	N	461,462
cis-$[Rh_2(DTolF)_2(bpy)(NCCH_3)_3](BF_4)_2.Me_2CO$	2.578(1)	2.107(3)	N	474
cis-$[Rh_2(DTolF)_2(bpy)(NCCH_3)_4](BF_4)_2$	2.638(3)	2.208(7) 2.316(5)	N	474
cis-$[Rh_2(DTolF)_2(bpy)_2(NCCH_3)](BF_4)_2$	2.5821(5)	2.116(4)	N	474
cis-$[Rh_2(DTolF)_2(phen)(NCCH_3)_3](BF_4)_2.2C_2H_5OC_2H_5$	2.581(1)	2.128(2)	N	474
cis-$[Rh_2(DPh^FF)_2(dppz)(NCCH_3)_4](BF_4)_2{\cdot}3.5C_6H_5Me$	2.581(1)	2.195(5) 2.173(5)	N	827
cis-$Rh_2(DTolF)_2(O_2CC_6H_4CN)_2(py)_2$	2.469(1)	2.296(5)	N	471
H-H *cis*-$[Rh_2(DTolF)_2(9\text{-}EtGuaH)_2(NCCH_3)](BF_4)_2$	2.514[e]	2.142[e]	N	462
H-T *cis*-$[Rh_2(DTolF)_2(9\text{-}EtAdeH)_2(NCCH_3)](BF_4)_2$	2.510(3)	2.06(2)	N	461,462

Pictiva EX2004
Samsung v Pictiva
IPR2024-01094

Compound	*r* (Rh–Rh)[a] (Å)	*r* (Rh–L_{ax})[b] (Å)	Donor atom(s)	ref.
cis-Rh_2(DTolF)$_2$(μ-PPh$_2$Py)$_2$(η^1-O_2CCF_3)$_2$	2.541(1)	2.327(4) 2.407(4)	O	472
cis-[Rh_2(DTolF)$_2$(μ-O_2CCF_3)(oxodmnp)(H$_2$O)]·½Et$_2$O	2.449(1)	2.186(4)	O	467
cis-[Rh_2(DTolF)$_2$(pypz)$_2$(DMSO)$_2$][O_2CCF_3]$_2$·DMSO	[f]	2.263(9)	O	467
Rh_2(DTolF)(μ-O_2CCF_3)(dppe)(η^1-O_2CCF_3)(*p*-toluidine)	2.606(1)	2.148(3)	N	473
[Rh_2(DTolF)(μ-O_2CCF_3)(Ph(C$_6$H$_4$)P(CH$_2$)$_2$PPh$_2$)(dppe)]O_2CCF_3·0.5H$_2$O[g]	2.733(1)	2.367(2)	P[g]	465
Rh_2(DAniF)$_4$	2.452(1) 2.415(1)	[c]	[c]	442
cis-Rh_2(DAniF)$_2$[Br_2calix[4]arene(CO$_2$)$_2$](CH$_3$OH$_{ax}$)$_2$[h]	2.438(1)	2.301(2)	O	484
Rh_2(DPhF-3,5-Cl$_2$)$_4$	2.458(1)	[c]	[c]	442
Rh_2(DPhTA)$_4$	2.377(3)	[c]	[c]	451
Rh_2(DTolTA)$_3$(CO)$_2$[i]	2.542(1)[j]	[c]	[c]	455
Rh_2(DTolTA)$_3$(NO)(CO)[k]	2.518(1)	[c]	[c]	455
[Rh_2(DTolTA)$_2$(CO)$_2$(PPh$_3$)$_2$][PF_6·CH_2Cl_2][i]	2.698(1)[j]	[c]	[c]	456
[Rh_2(DTolTA)$_2$(bpy)(CO)$_2$]BF_4·CH_2Cl_2[i]	2.646(1)[j]	[c]	[c]	453
[Rh_2(DTolTA)$_2$(bpy)(NCCH$_3$)$_2$](PF_6)$_2$	2.534(2)	2.080(9)	N	454
[Rh_2(DTolTA)$_2$(CO)(η^1-O_2PF_2)(μ$_2$-O_2PF_2)(bpy)]$_2$·2.3C_6H_{14}	2.505(4)	2.23(2) 2.38(1)	O	454
{[Rh_2(DTolTA)$_2$(CO)(bpy)(μ-I)]$_2$}(PF_6)$_2$·2.5CH_2Cl_2	2.544(1)	2.760(1) 2.670(1)	I[l]	453
[Rh_2(DPhAc)$_2$(PPh$_3$)$_2$(CO)$_2$]PF_6·2C_6H_{14}[i]	2.771(1)[j]	[c]	[c]	458
{Rh_2(DPhAc)$_2$[P(OPh)$_3$]$_2$(CO)$_2$}PF_6[i]	2.685(1)[j]	[c]	[c]	458
{Rh_2(DPhAc)$_2$(PPh$_3$)[P(OPh)$_3$](CO)$_2$}PF_6[i]	2.728(1)[j]	[c]	[c]	458
Rh_2(tpg)$_4$·CH_2Cl_2	2.408(1)	[c]	[c]	500
Supramolecular building blocks supported by (N, N) donor groups				
[Rh_2(*cis*-DAniF)$_2$(μ$_2$-C_2O_4)$_2$][m]	2.440(1) 2.454(1)	[n]	[n]	478
[Rh_2(*cis*-DAniF)$_2$(μ$_2$-C_2O_4)$_2$]$_3$[o]	2.457[2]	[n]	[n]	478

Pictiva EX2004
Samsung v Pictiva
IPR2024-01094

Compound	*r* (Rh–Rh)[a] (Å)	*r* (Rh–L_{ax})[b] (Å)	Donor atom(s)	ref.
$\{[Rh_2(cis\text{-}DAniF)_2]_2(\mu_2\text{-}O_2CCH_2CO_2)_2(NC_5H_4CHCHC_5H_4N)_2\cdot 3CH_2Cl_2\cdot 0.5Et_2O\}_\infty$[p]	2.434(1) 2.464(1)	2.317[e] 2.254[e] 2.263[e]	N	479
$\{[Rh_2(cis\text{-}DAniF)_2]_2(\mu_2\text{-}O_2CCH_2CO_2)_2(NCC_6H_4CN)_2\cdot 4CH_2Cl_2\}_\infty$[q]	2.442(1)	2.221[e] 2.216[e]	N	479
$\{[Rh_2(cis\text{-}DAniF)_2]_4(\mu_2\text{-}C_2O_4)_4(NCC_6F_4C_6F_4CN)_4\cdot 12.36CH_2Cl_2\}_\infty$[r]	2.418(2) 2.442(2)	2.333[e] 2.293[e] 2.248[e] 2.163[e]	N	479
$\{[Rh_2(cis\text{-}DAniF)_2]_2(\mu_2\text{-}O_2CCH_2CO_2)_2(NCC_6F_4C_6F_4CN)_2\cdot 6.8CH_2Cl_2\}_\infty$[p]	2.435(1)	2.204(9) 2.24(1)	N	480
$\{[Rh_2(cis\text{-}DAniF)_2]_2(\mu_2\text{-}O_2CCH_2CO_2)_2[C_3N_3(C_5H_4N)_3]_2\cdot 3CHCl_3\cdot CH_2Cl_2\}_\infty$[s]	2.465[2]	2.35[5]	N	481
$\{[Rh_2(cis\text{-}DAniF)_2]_2(\mu_2\text{-}O_2CCH_2CO_2)_2\}_3[C_3N_3(C_5H_4N)_3]_4\cdot 4.1CH_2Cl_2\cdot Et_2O\cdot H_2O\}_\infty$[t]	2.460[5]	2.31[1]	N	481
$\{[Rh_2(cis\text{-}DAniF)_2]_6[\mu_3\text{-}1,3,5\text{-}C_6H_3(CO_2)_3]_4(CH_3CN_{ax})_{7.5}\}\cdot 13.9CH_3CN$[o]	2.428- 2.438[e,u]	2.20[10]	N	482
$\{[Rh_2(cis\text{-}DAniF)_2(CH_3CN_{ax})_2]$(bicyclo[1.1.1]pentane-1,3-dicarboxylate)$\}_4\cdot 8CH_3CN$[m]	2.449(2)	2.228[e] 2.233[e] 2.245[e] 2.272[e]	N	483
$\{[Rh_2(cis\text{-}DAniF)_2(CH_3CN_{ax})_2](\mu_2\text{-}O_2CC_6F_4CO_2)\}_4\cdot 3CH_2Cl_2$[m]	2.446(1) 2.459(1)	2.196[e] 2.246[e] 2.251[e] 2.256[e]	N	483

Pictiva EX2004
Samsung v Pictiva
IPR2024-01094

Compound	*r* (Rh–Rh)[a] (Å)	*r* (Rh–L_{ax})[b] (Å)	Donor atom(s)	ref.
{[Rh_2(*cis*-DAniF)$_2$(CH_3CN_{ax})$_2$](1,4-cubanedicarboxylate)}$_4$·2.8CH_3CN[m]	2.432(2) 2.448(2)	2.162[e] 2.179[e] 2.236[e] 2.241[e] 2.246[e] 2.254[e] 2.255[e] 2.261[e]	N	483
{[Rh_2(*cis*-DAniF)$_2$(CH_3CN_{ax})$_2$](μ_2-$O_2CC_6H_4CO_2$)}$_4$·3CH_3CN·2CH_2Cl_2[m]	2.445(1) 2.453(2)	2.240[e] 2.254[e] 2.269[e] 2.263[e]	N	483
{Et_2O⊂[*cis*-Rh_2(DAniF)$_2$(CH_3CN_{ax})]$_4$[calix[4]arene(CO_2)$_4$]$_2$}·10CH_3CN[v]	2.429(1) 2.422(2)	2.16(1)	N	484
[{NEt_4⊂[*cis*-Rh_2(DAniF)$_2$L]$_4$[calix[4]arene(CO_2)$_4$]$_2$}]BF_4·3.5CH_3CN[v,w]	2.410(2) 2.413(4) 2.417(2) 2.428(2)	2.16(1)[x] 2.20(1)[x] 2.34(2)[y] 2.316(8)[y]	N[w] O[w]	484
Other (N, N) donor ligands				
Rh_2(3,5-Me_2pz)$_4$($NCCH_3$)$_2$·2CH_3CN	2.353(3)	2.202(5)	N	398
Rh_2(μ-pz)$_2$(I)$_2$(CO)$_2$[P(OMe)$_3$]$_2$	2.660(1)	2.741(1) 2.746(1)	I	486
cis-Rh_2I_2(CO)$_2$(μ-pz)$_2$(μ-dppm)	2.612(3)	2.710(3) 2.736(3)	I	520
trans-[Rh_2I_2(CO)$_2$(3,5-Me_2pz)(μ-dppm)$_2$]ClO_4	2.725(2)	2.757(2)	I	521
trans-(2,2)-Rh_2(ap)$_4$(NCPh)	2.412(1)	2.19(1)	N	493,494
[Rh_2(μ:η^3-pynp)$_2$(η^2-pynp)Cl_2](PF_6)$_2$·CH_3CN[z]	2.567(1)	2.190(5) 2.160(5)	N	498

Pictiva EX2004
Samsung v Pictiva
IPR2024-01094

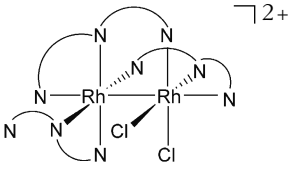
Compound	r (Rh–Rh)[a] (Å)	r (Rh–L_{ax})[b] (Å)	Donor atom(s)	ref.
$[Rh_2(\mu\text{-pdz})_2(pdz)_4(NCCH_3)_2](ClO_4)_4\cdot H_2O$[z]	2.557(2)	2.24(2) 2.19(2)	N	499
$Rh_2(\mu{:}\eta^3\text{-dpa})_2(\mu{:}\eta^2\text{-dpa})_2$	2.400(1)	2.386(3) 2.349(3)	N[aa]	171
$[Rh_2\{\mu\text{-}(C_5H_3N)NH(C_5H_4N)\}_2(\eta^2\text{-Hdpa})_2Cl_2]\cdot CH_3OH$	2.567(2)	2.205(9)	N	497
$Rh_2(pz)_2[Ph_2P(C_6F_4)]Br(CO)[Ph_2P(o\text{-}BrC_6F_4)]\cdot CHCl_2\cdot H_2O$	2.581(1)	2.561(2) 2.660(1)	Br	487
$Rh_2(3,5\text{-}Me_2pz)_2[\mu\text{-}P(o\text{-}C_6F_4)Ph_2]Br(CO)\{\eta^2\text{-}P(o\text{-}BrC_6F_4)Ph_2\}\cdot H_2O$	2.583(1)	2.597(1) 2.644(1)	Br	488
$Rh_2(mbzapH)_2(CO)_2Cl$	2.639(2)	2.466(4)	Cl	496

[a] Distances are given with up to 3 decimal digits.
[b] In some cases the average Rh–L bond lengths are quoted. In these instances the estimated deviation, which is given in square brackets, is calculated as $[\ ] = [\Sigma_n\Delta_i^2/n(n-1)]^{1/2}$, in which Δ_i is the deviation of the ith of n values from the arithmetic mean of the set.
[c] No *ax* ligand.
[d] Pseudoaxial bond to chelating nitrate group.
[e] Esds not reported.
[f] Distance not reported; quality of diffraction data insufficient for detailed structural analysis.
[g] The molecule contains an orthometalated bridging dppe and a chelating dppe.
[h] Br_2calix[4]arene$(CO_2H)_2$: 25,26,27,28-tetrapropoxy-5,17-dibromo-calix[4]arene-11,23-dicarboxylic acid.
[i] Mixed valence Rh_2^{3+} compound.
[j] Formal bond order 0.5.
[k] The compound contains a '*bent*' NO^- group.
[l] Iodide ions are bridging two Rh_2^{4+} units.
[m] Molecular square.
[n] Not reported.
[o] Molecular triangle.
[p] Tubular structure.
[q] Sheet-like structure.
[r] Infinite tubes of square cross sections.
[s] Zig-zag 1-D tunnel.
[t] Helices.
[u] Range of distances.
[v] calix[4]arene$(CO_2H)_4$: 25,26,27,28-tetra-*n*-propoxycalix[4]arene-5,11,17,23-tetracarboxylic acid.
[w] L = 50% CH_3CN and 50% H_2O; four of the eight *ax* sites are occupied by two CH_3CN and two H_2O molecules.
[x] Rh–N distance to *ax* CH_3CN molecule.
[y] Rh–O distance to *ax* H_2O molecule.
[z] Contains neutral nitrogen bridging ligands.
[aa] The two tridentate dpa ligands are involved in quasi-axial bonds which are unusual for Rh_2^{4+} compounds supported by (N, N) bridging groups.

Pictiva EX2004
Samsung v Pictiva
IPR2024-01094

An example of a symmetrically bridging (N, N) donor ligand is the anion of 3,5-dimethylpyrazole (3,5-Me_2pz; **12.9**), which upon reaction of its Na^+ salt with $Rh_2(O_2CCH_3)_4$ in CH_3CN, affords the yellow compound $Rh_2(3,5\text{-}Me_2pz)_4(NCCH_3)_2$;[398] its Rh–Rh bond length of 2.353(3) Å is the shortest among complexes supported by monoanionic nitrogen donor ligands.[398] The reaction of the bis-acetonitrile complex with pyridine affords $Rh_2(3,5\text{-}Me_2pz)_4(py)_2$ which converts, at 150 °C under vacuum, to the intense purple colored unsolvated compound $Rh_2(3,5\text{-}Me_2pz)_4$.[398] The corresponding unsubstituted pyrazolato complexes have been prepared,[398] as well as $\{[Rh_2(\mu\text{-}pz)_2(I)(CNBu^t)_4]_2(\mu\text{-}I)\}CF_3SO_3$, which consists of two $Rh_2(\mu\text{-}pz)_2(I)(CNBu^t)_4$ units linked by an iodide ion.[485] A few other Rh_2^{4+} compounds with pyrazolato bridging groups are $Rh_2(\mu\text{-}pz)_2(I)_2(CO)_2[P(OMe)_3]_2$[486] and the orthometalated compounds $Rh_2(pz)_2[Ph_2P(C_6F_4)]Br(CO)[Ph_2P(o\text{-}BrC_6F_4)]$[487] and $Rh_2(3,5\text{-}Me_2pz)_2[Ph_2P(C_6F_4)]Br(CO)[Ph_2P(o\text{-}BrC_6F_4)]$.[488] Various substituted pyrazolate Rh_2^{3+} compounds have been studied by fast atom bombardment and collision-induced dissociation mass spectrometry.[489]

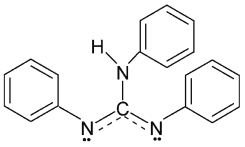
The sodium salt of 2-anilinopyridinate (ap; **12.10**) reacts with $RhCl_3{\cdot}xH_2O$ in refluxing ethanol to afford the dark-green, air-stable $Rh_2(ap)_4$.[490,491] This compound, which exhibits two accessible single-electron oxidations,[490-493] exists in four geometric isomers[490] (Fig. 12.20). The benzonitrile adduct $Rh_2(ap)_4(NCPh)$ is found as the *trans*-(2,2) isomer.[493,494] The brown microcrystalline adduct $Rh_2(ap)_4(CO)$, which presumably retains the same ap arrangement of the parent chloride, has been obtained by electrochemical reduction of $Rh_2(ap)_4Cl$ under a CO atmosphere;[493,495] the Rh_2^{5+} complex (4,0)-$Rh_2(ap)_4Cl$[492-494] is discussed in Section 12.6. The orthometalated compound $Rh_2(mbzapH)_2(CO)_2Cl_2$ contains two substituted ap groups (mbzap: 2-((α-methylbenzylidene)amino)pyridine) in a tridentate chelating mode.[496] The unusual complex $Rh_2[\mu\text{-}(C_5H_3N)NH(C_5H_4N)]_2(\eta^2\text{-Hdpa})_2Cl_2$ possesses two chelating 2,2'-dipyridylamine (Hdpa) ligands occupying *eq* sites and two bridged orthometalated dpa anions in the rare (N, C) coordination mode.[497] The adduct $Rh_2(\mu{:}\eta^3\text{-dpa})_2(\mu{:}\eta^2\text{-dpa})_2$ has the unusual feature of two tridentate dpa ligands forming quasi-axial bonds,[171] in contrast to the usual Rh_2^{4+} paddlewheel complexes supported by (N, N) donor ligands, which normally contain no *ax* ligands[442,444,446,448,451] or at most only one.[448,474,475,461,462] The dication in $[Rh_2(\mu{:}\eta^3\text{-pynp})_2(\eta^2\text{-pynp})Cl_2](PF_6)_2$ (pynp: 2-(2-pyridyl)-1,8-naphthyridine; **12.13**), depicted in **12.23**, contains one chelating and two bridging pynp ligands.[498] The 1,8-naphthyridine (np) complex is proposed to have the composition $[Rh_2(np)_4]Cl_4{\cdot}6H_2O$, although this has not been confirmed by X-ray crystallography.[382] The compound $[Rh_2(\mu\text{-pdz})_2(pdz)_4(NCCH_3)_2](ClO_4)_4$ (pdz: pyridazine), which is prepared by reacting $Na_4[Rh_2(\mu\text{-}SO_4)_4(H_2O)_2]$ with pdz, contains two bridging and four monodentate pdz groups,[499] whereas $[Rh_2(DTolF)_2(pypz)_2(DMSO)_2](O_2CCF_3)_2$ contains two short '*bite*' nitrogen pyridopyrazine (pypz) ligands in a *cisoid* arrangement.[467]



12.23

Among compounds supported by (N, N) donor groups with one of the shortest known Rh–Rh bond distances is the complex $Rh_2(tpg)_4$ (Fig. 12.26; Rh–Rh = 2.408(1) Å) with the strong organic base tpg (tpg: *N*,*N*',*N*''-triphenylguanidinate; **12.24**);[500] the photochemical and biological properties of this compound are succinctly discussed in Section 12.7.3.

Pictiva EX2004
Samsung v Pictiva
IPR2024-01094



12.24

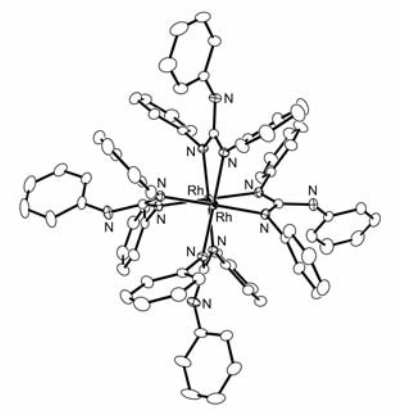


Fig. 12.26. Molecular structure of $Rh_2(tpg)_4$.

12.3.4 Complexes supported by sulfur donor bridging ligands

The structurally characterized compounds of this category are listed in Table 12.5. Apart from the thiocarboxylato group **12.3**, ω-thiocaprolactamate (tcl; **12.25**) is another example of an (S, O) donor bridging ligand. The compound $Rh_2(tcl)_4$ is prepared from $Rh_2(O_2CCH_3)_4$ by ligand exchange of the acetate groups with tcl.[501] In contrast to the analogous lactam adducts $[Rh_2(pyro)_4(Hpyro)_2]$ and $[Rh_2(vall)_4(Hvall)_2]$, which exhibit the usual *cis*-(2,2) arrangement[430] (Fig. 12.20a), $Rh_2(tcl)_4(tclH)$ and $Rh_2(tcl)_4(CO)$ exhibit the (4,0) polar geometry **12.20**; the tclH and CO molecules are coordinated to the S_4 end of the dirhodium unit.[501] In order to address the polarity of the Rh–Rh bond, *ab initio* calculations have been performed on the ground and lowest ionized states of the previous compounds.[502]

Table 12.5. Dirhodium compounds supported by (S, N), (S, O), (S, S), (P, N) donor and phosphine bridging ligands

Compound	*r* (Rh–Rh)[a] (Å)	*r* (Rh–L_{ax}) (Å)	Donor atom(s)	ref.
(4,0)-$Rh_2(tcl)_4(tclH)$	2.497(1)	2.388(1)	S	501
(4,0)-$Rh_2(tcl)_4(CO)$	2.495(1)	1.913(7)	C	501
$[Rh_2(\mu\text{-pyS})_2Cl_2(CO)_2(\eta^1\text{-pySH})_2]\cdot 2CHCl_3$	2.652(4)	2.547(4)	Cl	503
$Rh_2(Bu^t\text{-}S_4)_2\cdot 4.5Me_2CO$[b]	2.329(2)	2.341(2)	S	642
(4,0)-$Rh_2(mmtz)_4(PPh_3)$	2.603(1)	2.350(2)	P	504
H-T *cis*-$[Rh_2I_2(CO)_2(\mu\text{-mtz})_2(\mu\text{-dppe})]\cdot 0.5THF$	2.748(1)	2.794(1) 2.788(1)	I	505
H-T *cis*-$Rh_2(CO)_2Cl_4(\mu\text{-btmp})_2$	2.733(3)	2.418(1) 2.470(1)	Cl	506
$Rh_2(\eta^1\text{-}C_6H_5S)_2(\mu\text{-}C_6H_5S)_2(bpy)_2$	2.549(2)	2.243(4)	S	805

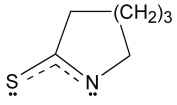
Pictiva EX2004
Samsung v Pictiva
IPR2024-01094

Compound	*r* (Rh–Rh)[a] (Å)	*r* (Rh–L_{ax}) (Å)	Donor atom(s)	ref.
Phosphine and (P, N) donor bridging groups				
cis-$Rh_2(\mu\text{-}Cl)_2(dppm)_2Cl_2\cdot 3CH_3CN\cdot H_2O$	2.523(2)	2.466(6) 2.457(6)	Cl	507
H-T *cis*-$Rh_2[Ph_2P(C_6H_4)]_2(dmpm)_2Cl_2\cdot CH_2Cl_2$	2.770(3)	2.561(6) 2.527(6)	Cl	507,563
$Rh_2[Ph_2P(C_6H_4)]_2(\mu\text{-}Cl)_2(PMe_3)_2\cdot C_7H_8\cdot C_4H_8O$	2.506(1)	2.363(4) 2.348(4)	P	562
$Rh_2[Ph_2P(C_6H_4)]_2(\mu\text{-}Cl)_2(PPh_3)_2$	2.499(1)	2.403(2)	P	562
$Rh_2(CO)(\mu\text{-}Cl)Cl_3(dppm)_2\cdot CH_2Cl_2\cdot C_6H_6\cdot H_2O$	2.691(3)	2.448(7) 2.384(7)	Cl	508
trans-$Rh_2(CO)_2Cl_4(dmpm)_2\cdot CH_2Cl_2$	2.759(5)	2.480(1) 2.478(1)	Cl	510
trans-$Rh_2(\mu\text{-}SO_2)(\mu\text{-}dppm)_2Cl_2$	2.784(1)	2.342(2) 2.341(2)	Cl	513
$Rh_2[\mu\text{-}PhP(py)_2]_2Cl_4$	2.687(1)	2.345(3)	Cl	516
$Rh_2(\mu\text{-}CO)Cl_2(\mu\text{-}Ph_2Ppy)_2$	2.612(1)	2.355(1)	Cl	519
trans-$Rh_2(\mu\text{-}Ph_2Ppy)_2(\mu\text{-}NO_3)(CO)Cl_3\cdot CH_2Cl_2$	2.589[c]	[d]	Cl	517
H-T Rh_2(succinimidate)$_2[Ph_2P(C_6H_4)]_2(H_2O)_2\cdot 2CH_2Cl_2$[e]	2.539(1)	2.358[c] 2.374[c]	O	561
H-T Rh_2(succinimidate)$_2[Ph_2P(C_6H_4)]_2$(succinimide)$(H_2O)\cdot CH_2Cl_2$[e]	2.555(1)	2.483[c,f] 2.284[c,f]	O	561
$Rh_2[CH_3N(PF_2)_2]_3Cl_4$	2.707(1)	2.416(2)	Cl	571
$Rh_2[CH_3N(PF_2)_2]_3Br_4$	2.750(8)	2.555(6)	Br	572
$Rh_2\{CH_3N[P(OCH_2CH_3{}^{F3})_2]_2\}_3Cl_4\cdot CH_2Cl_2$	2.669[c,g]	2.362[c,g]	Cl	569
cis-$\{Rh_2[Ph_2P(C_6H_4)]_2(NCCH_3)_6\}(BF_4)_2\cdot 0.5H_2O$[h,i]	2.656(1) 2.655(1)	2.202(6) 2.196(6)	N	564
$\{Rh_2[Ph_2P(C_6H_4)]_2(\mu_2\text{-}C_2O_4)(py)_2\}_3\cdot 6CH_3OH\cdot H_2O$[j,k]	2.565(1)	2.288(3)	N	564
$\{Rh_2[Ph_2P(C_6H_4)]_2(O_2CC_6H_4CO_2)(DMF)_2\}_3\cdot 6.5DMF\cdot 0.5H_2O$[j,l]	2.514(1) 2.507(1) 2.511(1)	2.285(7) 2.296(9) 2.304(8) 2.314(8) 2.322(9) 2.335(9)	O	564
$\{Rh_2[Ph_2P(C_6H_4)]_2(O_2CC_6H_4C_6H_4CO_2)(py)_2\}_3\cdot 4.5CH_3OH\cdot 0.75H_2O$[j,k]	2.541(3)	[m]	N	564
RRR-$\{Rh_6[Ph_2P(C_6H_4)]_6(\mu_2\text{-}C_2O_4)_3(py)_5(CH_2Cl_2)\}\cdot 3CH_2Cl_2$[j]	2.526(1) 2.555(1) 2.563(1)	2.304(5)[n] 2.284(4)[n] 2.269(5)[n] 2.265(4)[n] 2.231(4)[n] 2.650(1)[o]	N Cl	747
SSS-$\{Rh_6[Ph_2P(C_6H_4)]_6(\mu_2\text{-}C_2O_4)_3(py)_5(CH_2Cl_2)\}\cdot 3CH_2Cl_2$[j]	2.525(1) 2.557(1) 2.563(1)	2.229(4)[n] 2.253(5)[n] 2.265(5)[n] 2.272(5)[n] 2.303(5)[n] 2.636(2)[o]	N Cl	747

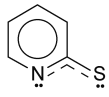
Pictiva EX2004
Samsung v Pictiva
IPR2024-01094

Compound	*r* (Rh–Rh)[a] (Å)	*r* (Rh–L_{ax}) (Å)	Donor atom(s)	ref.
SSS-{$Rh_2[Ph_2P(C_6H_4)]_2(O_2CC_6H_4CO_2)(py)_2\}_3$·6.5 CH_2Cl_2·1.5CH_3OH·4H_2O[j]	2.561(2) 2.556(2) 2.548(2) 2.533(2) 2.530(2)	2.22(1)- 2.35(1)[p]	N	747

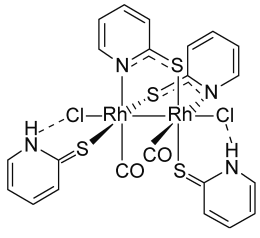
[a] Distances are given with up to 3 decimal digits.
[b] 'Bu^t-H_2S_4': 1,2-bis(2-mercapto-3,5-di-Bu^t-phenylthio)ethane.
[c] Esds not reported.
[d] Distance not reported.
[e] The compound has bridging succinimidate (N, O donor) and H-T phosphine groups.
[f] The longer distance corresponds to Rh–O(succinimidate), the shorter one to Rh–O(H_2O).
[g] Coordinates not available. The distances have been estimated from information provided in ref. 569.
[h] Molecule with two *cisoid* non-labile orthometalated phosphine bridging anions.
[i] First molecule with an inherently chiral metal-metal bonded unit. Racemic mixture; the asymmetric unit contains a pair of *S* and *R* molecules.
[j] Molecular triangle consisting of three singly bonded orthometalated *cis*-$\{Rh_2[Ph_2P(C_6H_4)]_2\}^{2+}$ units linked by two dicarboxylate anions.
[k] The compound exists as a mixture of *RRR* and *SSS* stereoisomers.
[l] The compound exists as a mixture of *RRS* and *SSR* stereoisomers.
[m] Distance not reported; quality of diffraction data insufficient for detailed structural analysis.
[n] Rh–N distance to N atom of pyridine ring.
[o] Distance of Rh to Cl of CH_2Cl_2.
[p] Range of distances.



12.25



12.26



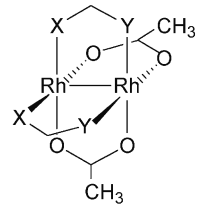
12.27

The bridging ligand 2-mercaptopyridine with (S, N) donor atoms reacts in chloroform with $Rh_2Cl_2(CO)_4$ to afford the blue-black complex $Rh_2(\mu\text{-pyS})_2Cl_2(CO)_2(\eta^1\text{-pySH})_2$[503] (**12.27**). The two 2-mercaptopyridinate (pyS; **12.26**) groups span the dirhodium unit in a *cis* disposition and a H-T orientation (for dirhodium compounds with two bridging ligands possessing different types of donor atoms X and Y, the compound is designated as H-H (**12.28**) or H-T (**12.29**) depending on whether the identical atoms of the two ligands are bound to the same or to opposite metal atoms, respectively), whereas the two pySH ligands are in their zwitterionic form. The *ax* chloride atoms are engaged in N–H···Cl hydrogen bonds that result in pseudo-chelate rings.[503] The long Rh–Rh bond distance of 2.652(4) Å may be a consequence of the π-accepting capability of the two *eq* CO ligands, a situation that leads to pronounced weakening of the Rh–Rh bond.[503]

Complexes of the (S, N) donor ligands 3-mercapto-5-methylthio-1,2-thiadiazoline (Hmmtz; **12.30**) and 2-mercaptothiazoline (Hmtz; **12.31**) have been structurally characterized. In particular, $Rh_2(mmtz)_4(PPh_3)$ is found in the polar (4,0) arrangement **12.20** and the *ax* phosphine ligand is coordinated to the Rh–S_4 metal center.[504] On the other hand, *cis*-$[Rh_2I_2(CO)_2(\mu\text{-mtz})_2(\mu\text{-dppe})]$ exhibits two mtz bridging ligands in a H-T arrangement and

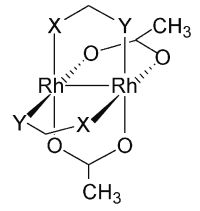
Pictiva EX2004
Samsung v Pictiva
IPR2024-01094

a bridging dppe moiety, rendering it the first example of a bridged dppe complex with a bifunctional ligand binding through different donor atoms.[505] A H-T arrangement of the bridging groups is also found in the (benzylthiomethyl)diphenylphosphine (btmp) complex *cis*-$Rh_2(CO)_2Cl_4(\mu\text{-btmp})_2$.[506]



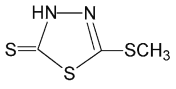
Head-to-Head (H-H)

12.28

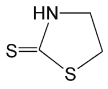


Head-to-Tail (H-T)

12.29



12.30



12.31

12.3.5 Complexes supported by phosphine and (P, N) donor bridging ligands

The most widely studied phosphine bridging ligands (Tables 12.2 and 12.5) are dmpm (dmpm: $Me_2PCH_2PMe_2$) and dppm (dppm: $Ph_2PCH_2PPh_2$). The reaction of $Rh_2(O_2CCH_3)_4$ with Me_3SiCl and dppm affords *cis*-$Rh_2(O_2CCH_3)_2Cl_2(dppm)_2$.[507] Further reaction with additional Me_3SiCl or the use of 4 equiv of Me_3SiCl affords $Rh_2(\mu\text{-}Cl)_2(\mu\text{-dppm})_2Cl_2$.[507] In contrast to the analogous $Re_2Cl_4(dppm)_2$ compound, which has a *transoid* arrangement of the phosphine groups, $Rh_2(\mu\text{-}Cl)_2(\mu\text{-dppm})_2Cl_2$ has a *cisoid* disposition of the dppm ligands and a 'cradle-like' structure (Fig. 12.27). The reaction of $Rh_2Cl_4(dppm)_2$ with CO under pressure affords the A-frame compound $Rh_2(CO)(\mu\text{-}Cl)Cl_3(dppm)_2$ (**12.32**).[508] The latter can also be prepared by electrochemical oxidation of *trans*-$Rh_2(CO)_2Cl_2(dppm)_2$ in the presence of chloride ions.[509] The dicarbonyl complex is directly obtained by reacting *trans*-$Rh_2(CO)_2Cl_2(dppm)_2$ with $PhICl_2$ in dilute CH_2Cl_2 solutions. As indicated by NMR spectroscopy, it most likely has the symmetrical structure **12.33**; this structure is analogous to the one established by X-ray crystallography for $Rh_2(CO)_2Cl_4(dmpm)_2$[510] and proposed for $Rh_2(CO)_2Cl_2I_2(dppm)_2$,[511] and the analogous compounds $Rh_2(CO)_2Br_2X_2(dpam)_2$ (X = Br or I; dpam: $Ph_2AsCH_2AsPh_2$).[512] Reactions of $Rh_2(CO)Cl_4(dppm)_2$ include its conversion to $Rh_2Cl_6(dppm)_2$ upon oxidation with $PhICl_2$ and the formation of the unsymmetrical complex $[Rh_2(CO)Cl_3(dppm)_2]PF_6$, when $Rh_2(CO)Cl_4(dppm)_2$ is reacted with $AgPF_6$. The latter has been structurally characterized as the methanol complex $[Rh_2(CO)Cl_3(dppm)_2(MeOH)]PF_6$ (**12.34**); the weak interaction between the metal atoms is indicated by their distance of 3.010(2) Å.[508] The compound *trans*-$Rh_2(\mu\text{-}SO_2)(\mu\text{-dppm})_2Cl_2$ displays a distorted A-frame geometry with a bridging sulfur dioxide group.[513] A-frame dirhodium compounds with bridging dppm groups have been studied by multinuclear NMR spectroscopy.[514]

The ligand Ph_2Ppy (Ph_2Ppy: 2-diphenylphosphinopyridine) reacts with $Rh_2(O_2CCH_3)_4(MeOH)_2$ and LiCl mixtures in refluxing toluene to afford the pink complex H-T *cis*-$Rh_2(\mu\text{-}O_2CCH_3)_2(\mu\text{-}Ph_2Ppy)_2Cl_2$ (**12.35**),[515] wherein the Ph_2Ppy ligands assume an (N, P) bridging mode, akin to the (C, P) mode encountered in orthometalated phosphine

Pictiva EX2004
Samsung v Pictiva
IPR2024-01094

compounds. Such (N, P) bridging groups spanning the dirhodium unit are encountered in $Rh_2[\mu\text{-}PhP(py_2)]_2Cl_4$.[516] Electrochemical oxidation of $Rh_2(\mu\text{-}CO)Cl_2(\mu\text{-}Ph_2Ppy)_2$ affords the unusual compound *trans*-$Rh_2(\mu\text{-}Ph_2Ppy)_2(\mu\text{-}NO_3)(CO)Cl_3$ with two Ph_2Ppy groups in H-T arrangement and a bridging nitrate ion.[517] Electrochemical oxidation of *trans*-$Rh_2(\mu\text{-}CO)Cl_2(\mu\text{-}Ph_2Ppy)_2$, in the presence of chloride ions affords *trans*-$Rh_2(CO)Cl_4(\mu\text{-}Ph_2Ppy)_2$, which is the starting material for *trans*-$Rh_2(CO)_2Cl_4(\mu\text{-}Ph_2Ppy)_2$.[518] The Rh–Rh distance in *trans*-$Rh_2(\mu\text{-}CO)Cl_2(\mu\text{-}Ph_2Ppy)_2$ (2.612(1) Å)[519] is essentially identical to that in the unusual heterobridged complex $Rh_2I_2(CO)_2(\mu\text{-}pz)_2(\mu\text{-}dppm)$ (2.612(3) Å), which contains a Rh–Rh bond supported by one dppm group and two bidentate (N, N) donor groups.[520] The Rh–Rh bond distance (2.725(2) Å) in *trans*-$[Rh_2I_2(CO)_2(3,5\text{-}Me_2pz)(\mu\text{-}dppm)_2]ClO_4$ (**12.36**), which is prepared by oxidation of *trans*-$[Rh_2(CO)_2(3,5\text{-}Me_2pz)(\mu\text{-}dppm)_2]ClO_4$ with I_2, is in the range of other similar A-frame compounds.[521]

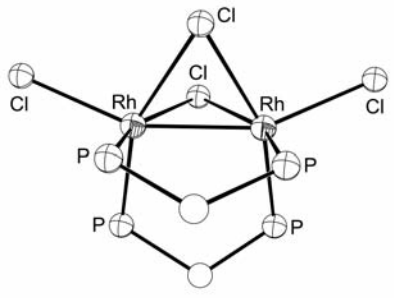
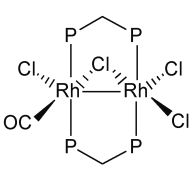
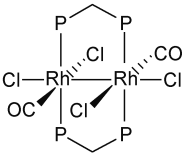


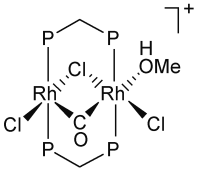
Fig. 12.27. The core of $Rh_2(\mu\text{-}Cl)_2(\mu\text{-}dppm)_2Cl_2$.



12.32



12.33

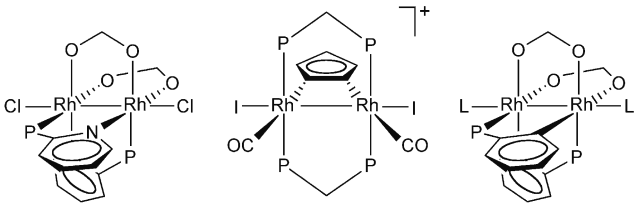


12.34

Reaction of $Rh_2(O_2CCH_3)_4$ with PPh_3 in refluxing acetic acid leads to isolation of the orthometalated product $Rh_2(\mu\text{-}O_2CCH_3)_2[Ph_2P(C_6H_4)]_2(HO_2CCH_3)_2$ with two bridging acetate ligands in a *cisoid* arrangement and two bridging $[Ph_2P(C_6H_4)]^-$ anions spanning the Rh–Rh bond in H-T orientation (**12.37**).[522,523] The reaction proceeds through formation of $Rh_2(\mu\text{-}O_2CCH_3)_3[Ph_2P(C_6H_4)](HO_2CCH_3)_2$ which reacts with an additional equiv of PPh_3, to afford the doubly orthometalated product.[524,525] Detailed studies that shed light into the role of the acid and the mechanism of the orthometalation reactions have been reported.[526-529] A number of dirhodium complexes of general formulae $Rh_2(\mu\text{-}O_2CR)_3(PC)$,[374,525,530-537] and *cis*-$Rh_2(\mu\text{-}O_2CR)_2(PC)_2$[522,523,536-553] (PC stands for orthometalated arylphosphines) with both H-H and H-T arrangements have been reported[554] to be highly active catalysts for certain intramolecular carbene insertion reactions (see Chapter 13). A structural characteristic of bis-orthometalated complexes is the elongation of the Rh–Rh bond compared to $Rh_2(O_2CR)_4$, the bond lengths ranging from 2.48 to 2.63 Å (Table 12.2). The longest Rh–Rh bonds are encountered in complexes with strong *ax* ligands such as PPh_3 (2.630(1) Å)[547] and the shortest in H-T *cis*-$Rh_2(\mu\text{-}O_2CCH_3)_2[PhP(C_6H_4)(o\text{-}BrC_6F_4)]_2$ (2.475(1) Å) wherein the bromine atom of

Pictiva EX2004
Samsung v Pictiva
IPR2024-01094

the C_6F_4Br ring occupies one of the dirhodium core *ax* sites.[555] Related compounds with chiral phosphines[556] and phosphanes[557-560] have been reported, as well as two dirhodium catalysts with two H-T metalated phosphine and two succinimidate (N, O donor) bridging groups.[561]



12.35 **12.36** **12.37**

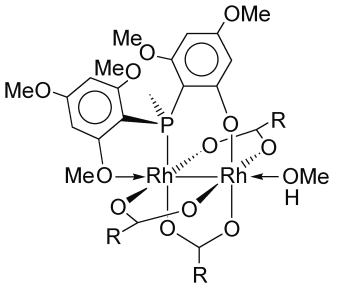
Reaction of $Rh_2(\mu\text{-}O_2CCH_3)_2[Ph_2P(C_6H_4)]_2$ with Me_3SiCl in warm THF and the monophosphine ligands PMe_3 or PPh_3 affords $Rh_2[Ph_2P(C_6H_4)]_2(\mu\text{-}Cl)_2(PMe_3)_2$ or $Rh_2[Ph_2P(C_6H_4)]_2(\mu\text{-}Cl)_2(PPh_3)_2$, respectively, which retain the H-T *cisoid* arrangement of the starting material.[562] A similar reaction of $Rh_2(\mu\text{-}O_2CCH_3)_2[Ph_2P(C_6H_4)]_2$ in warm THF, in the presence of Me_3SiCl and the bridging phosphine dmpm, affords $Rh_2(dmpm)_2[Ph_2P(C_6H_4)]_2Cl_2$ which has two *ax* Cl^- anions, two *cis* orthometalated bridging $[Ph_2P(C_6H_4)]^-$ anions in H-T arrangement and two *cis* bridging dmpm groups that also span the Rh–Rh bond.[507,563] The different outcome of the two previous reactions is attributed to the structure of dmpm, which precludes the chloride ligands from occupying bridging positions.[563] The long Rh–Rh bond distance (2.770(3) Å) in $Rh_2(dmpm)_2[Ph_2P(C_6H_4)]_2Cl_2$[507,563] (Table 12.5), compared to tetracarboxylate (Table 12.1) and mixed carboxylate/orthometalated phosphine (Table 12.2) compounds, is attributed to loss of the small '*bite*' carboxylate groups which act to hold the dirhodium unit together along with the addition of the *ax* chloride ligands.[507]

Reaction of *cis*-$Rh_2(\mu\text{-}O_2CCH_3)_2[Ph_2P(C_6H_4)]_2(HO_2CCH_3)_2$ with excess Me_3OBF_4 in CH_3CN results in formation of racemic *cis*-$\{Rh_2[Ph_2P(C_6H_4)]_2(NCCH_3)_6\}(BF_4)_2$ with two *cisoid* non-labile orthometalated phosphine bridging anions and six labile CH_3CN ligands occupying *eq* and *ax* positions.[564] This is the first structurally characterized orthometalated dirhodium compound in which the four additional *eq* positions (apart from those occupied by the bridging phosphine groups) are occupied by non-bridging ligands and, the first molecule with an inherently chiral metal-metal bonded unit.[564] Reaction of *cis*-$\{Rh_2[Ph_2P(C_6H_4)]_2(NCCH_3)_6\}(BF_4)_2$ with salts of linear dicarboxylate anions (e.g., oxalate, terephthalate) affords molecular triangles that employ orthometalated phosphine units as building blocks;[564] these are discussed in Section 12.7.2.

The highly basic and bulky phosphine ligand 2,4,6-trimethoxyphenylphosphine (TMPP) reacts with dirhodium carboxylate compounds to afford unusual products due to the 'noninnocence' of the ether functionalities. Reaction of TMPP with $Rh_2(O_2CCH_3)_4(MeOH)_2$ in the presence of ethanol, yields $Rh_2(\mu\text{-}O_2CCH_3)_3(O\text{-TMPP})(MeOH)$ (**12.38**), wherein the dirhodium unit is spanned by a tridentate oxygen-metalated *O*-TMPP ligand (demethylation of a methoxy substituent on one of the phenyl rings of TMPP takes place).[565,566] In the case of the TMPP reaction with the strong Lewis acid $Rh_2(O_2CCF_3)_4$, the ligand arrangement is similar to that in $[Rh_2(\mu\text{-}O_2CCH_3)_3(O\text{-TMPP})]$, with one important difference; namely, the phenoxide oxygen involved in the six-membered ring Rh–Rh–P–C–C–O is also bonded to another unit of $[Rh_2(\mu\text{-}O_2CCF_3)_3(O\text{-TMPP})]$ to afford the '*dimer of dimers*' $[Rh_2(\mu\text{-}O_2CCF_3)_3(TMPP\text{-}O)]_2$.[567] A tridentate oxygen-metalated binding mode, similar to that of TMPP in **12.38**, is observed with 2-methoxyphenylphosphine (MPP) in $Rh_2(\mu\text{-}O_2CCH_3)_3(O\text{-MPP})(HO_2CCH_3)$[516] and $Rh_2(\mu\text{-}O_2CCH_3)_3(O\text{-MPP})(NCCH_3)$.[568] Under refluxing conditions, $Rh_2(\mu\text{-}O_2CCF_3)_2(TMPP\text{-}O)_2$ is

Pictiva EX2004
Samsung v Pictiva
IPR2024-01094

obtained with each *O*-TMPP bound to a Rh center in a face-capping mode through the phosphorus and ether oxygen atoms as well as a phenoxide group.[567]



12.38

The homologous series of Rh_2^0, Rh_2^{2+}, Rh_2^{4+} complexes with bridging bis(difluorophosphin o)methylamine and its trifluoroethoxy[569] derivatives have been prepared and structurally characterized using the compounds $[RhCl(PF_3)_2]_2$,[570-572] $[RhBr(PF_3)_2]_2$,[571,572] or $[RhBr(C_8H_8)]_2$[11] as starting materials. Their electronic absorption spectra are dominated by intense bands that are characteristic of $d\sigma \rightarrow d\sigma^*$ transitions and each compound exhibits an emissive $d\sigma^*$ excited state.[570,571] The increase of the Rh–Rh and Rh–X distances in the $Rh_2[CH_3N(PF_2)_2]_3X_4$ family of compounds, upon replacement of Cl with Br, is consistent with the increasing size of the bridging atom.[572,573]

12.3.6 Complexes supported by carbonate, sulfate and phosphate bridging groups

Dirhodium compounds with bridging HCO_3^-, CO_3^{2-}, $H_2PO_4^-$, HPO_4^{2-}, HSO_4^-, and SO_4^{2-} anions have all been reported. Among them, carbonate compounds are similar to carboxylate-bridged compounds and will be discussed first. The structurally characterized dirhodium compounds with the aforementioned bridging groups are compiled in Table 12.6.

Table 12.6. Dirhodium compounds with bridging carbonate, sulfate and phosphate groups

Compound	*r* (Rh–Rh)[a] (Å)	*r* (Rh–L_{ax}) (Å)	Donor atom(s)	ref.
$Cs_4[Rh_2(CO_3)_4(H_2O)_2]\cdot 6H_2O$	2.378(1)	2.344(5)	O	575
$Cs_4Na_2[Rh_2(CO_3)_4Cl_2]\cdot 8H_2O$	2.380(2)	2.601(3)	Cl	575
$Na_4[Rh_2(SO_4)_4(H_2O)_2]\cdot 4H_2O$	2.449(3)	2.298(9)	O	580
trans-$[Rh_2(SO_4)_2(py)_6]\cdot 6H_2O$	2.604(2)	2.25(1)	N	580,581
trans-$[Rh_2(SO_4)_2(py)_6]\cdot 3H_2O$	2.592(3)	2.29(2)	N	580
$Rh_2(H_2PO_4)_4(H_2O)_2$	2.487(1)	2.292(7)	O	584,585
trans-$[Rh_2(HPO_4)_2(py)_6]\cdot(pyH)_2HPO_4$	2.598(2)	2.226(7)	N	581,587
	2.621(2)	2.246(8)		

[a] Distances are given with up to 3 decimal digits.

Early reports of carbonato-bridged dirhodium compounds formulated as $[C(NH_2)_3]_2$-$Rh(CO_3)_2$[574] and $[Rh_2(CO_3)_4]^{4-}$[40,370]noted that their properties resemble those of $Rh_2(O_2CR)_4L_2$ compounds but no specific structures were proposed. In particular, the $[Rh_2(CO_3)_4]^{4-}$ species was prepared by two different methods: treatment of a Rh_2^{4+}*(aq)* solution with an excess of CO_3^{2-} ions followed by addition of alkali metal ions (Na^+, K^+, Cs^+) to produce purple or dark-blue crystalline solids or, more directly by a ligand exchange procedure in which

Pictiva EX2004
Samsung v Pictiva
IPR2024-01094

$Rh_2(O_2CCH_3)_4$ is heated in the presence of a concentrated aqueous solution of the alkali metal carbonate.[40,41] The formulation of these compounds as salts of the $[Rh_2(CO_3)_4]^{4-}$ ion was based on elemental analyses, infrared and electronic absorption spectra, magnetic susceptibility measurements and electrochemical data.[40] The $[Rh_2(CO_3)_4]^{4-}$ formulation was confirmed in 1980 when the X-ray crystal structure determinations of $Cs_4[Rh_2(CO_3)_4(H_2O)_2]\cdot 6H_2O$ and $Cs_4Na_2[Rh_2(CO_3)_4Cl_2]\cdot 8H_2O$ were reported.[575] The Rh–Rh bond lengths in these two compounds, 2.378(1) Å and 2.380(2) Å, respectively, are not significantly shorter than the corresponding distance in $Rh_2(O_2CCH_3)_4(H_2O)_2$ (2.386(1) Å),[223] in contrast to the situation with dichromium compounds. The *ax* Cl^- ligands in $Cs_4Na_2[Rh_2(CO_3)_4Cl_2]\cdot 8H_2O$ are associated with the Rh atoms at 2.60 Å, a distance that implies weak interactions; this is most likely due to the high negative charge of the $[Rh_2(CO_3)_4]^{4-}$ unit.[575] There is also evidence that, in aqueous solution, species such as $[Rh_2(HCO_3)_2]^{2+}$ may exist.[40] Moreover, several bis-carbonate complexes that contain chelating 2,2'-bipyridine have been prepared from the formato complexes *cis*-$Rh_2(O_2CH)_2X_2(bpy)_2$ X = Cl, Br, and characterized by infrared and electronic absorption spectroscopies.[346]

Prior to recognition of carbonate-bridged dirhodium compounds, there was evidence of sulfate[40,576-579] and acetate/sufate[371] bridged species. Wilson and Taube reported that elution of the $Rh_2^{4+}(aq)$ ion from a cation exchange column with sulfate solutions allowed the isolation of a compound formulated as $(NH_4)_4[Rh_2(SO_4)_4]$.[40] The structure of $Na_4[Rh_2(SO_4)_4(H_2O)_2]\cdot 4H_2O$[580] revealed great similarity to that of the tetrakis-carbonate complex, i.e., the two metal centers are bridged by four sulfate groups.[580] Reaction of aqueous solutions of the sulfate compound with pyridine affords the crystalline hydrated adducts $[Rh_2(SO_4)_2(py)_6]\cdot nH_2O$, n = 3 or 6, with the bridging sulfate groups in a *transoid* arrangement,[580,581] in contrast to the *cisoid* arrangement of the acetate groups in $[Rh_2(O_2CCH_3)_2(py)_6](CF_3SO_3)_2$.[367,368] The relative ease of displacing the sulfate groups of $[Rh_2(SO_4)_4(H_2O)_2]^{4-}$ is demonstrated by reaction of its Na^+ salt with the nitriles RCN (R = CH_3, C_2H_5 or C_6H_5) in the presence of CF_3SO_3H.[582] In the case of CH_3CN, this reaction affords the cation $[Rh_2(NCCH_3)_{10}]^{4+}$ (Section 12.4.2).

Treatment of $Rh_2(O_2CCH_3)_4$ with aqueous H_3PO_4 affords mixed acetate/phosphate species[369] as well as $Rh_2(H_2PO_4)_4(H_2O)_2$,[583] which exhibits the expected paddlewheel structure with *ax* water molecules.[584,585] This compound gives acidic solutions when dissolved in H_2O and reacts with pyridine to afford $[Rh_2(HPO_4)_2(py)_6]\cdot 6H_2O$, $(pyH)_4[Rh_2(HPO_4)_4(py)_2]$ or $[Rh_2(HPO_4)_2(py)_6]\cdot(pyH)_2HPO_4$, depending on the reaction conditions.[581,584,586,587] The structure of $[Rh_2(HPO_4)_2(py)_6]\cdot(pyH)_2HPO_4$[581,587] reveals that the two HPO_4^{2-} ligands are in a *transoid* arrangement similar to *trans*-$[Rh_2(SO_4)_2(py)_6]$.[580,581] Addition of a 40% $HClO_4$ solution to $[Rh_2(HPO_4)_2(py)_6]\cdot(pyH)_2HPO_4$ yields $[Rh_2(H_2PO_4)_2(py)_4(H_2O)_2](ClO_4)_2\cdot 2H_2O$.[581] The electronic and CD spectra [588-590] of the tetraphosphate and tetrasulfate compounds have been reported.

12.4 Dirhodium Compounds with Unsupported Rh–Rh Bonds

12.4.1 The dirhodium(II) aquo ion

The dirhodium aquo species $[Rh_2(H_2O)_{10}]^{4+}$ was first generated[591] according to the reaction:

$$2[Rh(H_2O)_5Cl]^{2+} + 2Cr^{2+}(aq) \rightarrow [Rh_2(H_2O)_{10}]^{4+} + 2CrCl^{2+}(aq)$$

It is often written as $[Rh_2(H_2O)_{10}]^{4+}$ but the degree of hydration is speculative. The dimeric formulation of $Rh_2^{4+}(aq)$ is based on its cation exchange behavior, the similarity of its electronic absorption spectrum to that of $Rh_2(O_2CCH_3)_4(H_2O)_2$ and its diamagnetism, but attempts to

Pictiva EX2004
Samsung v Pictiva
IPR2024-01094

precipitate or crystallize it have failed to produce a solid form of $[Rh_2(H_2O)_{10}]^{4+}$.[40,591,592] It has been shown, however, that a number of Rh(III) species can be employed as starting materials and that electron transfer reactions between Cr(II) and Rh(III) proceed through bridged transition states (inner-sphere mechanism).[592]

The reaction of $Rh_2^{4+}(aq)$ with O_2 in a 2-3 M $HClO_4$ solution is postulated to produce the purple paramagnetic superoxo complex $[Rh_2(O_2^-)(OH)_2(H_2O)_n]^{3+}$.[593,594] Treatment of $[Rh_2(H_2O)_{10}]^{4+}$ in an aqueous solution of $HClO_4$ with NH_4OH/NH_3, py and/or en results in water exchange and formation of the corresponding $[Rh_2(H_2O)_{10-m}(base)_n(OH)_m]^{(4-m)+}$ derivatives.[595] Reaction of the latter with dioxygen affords superoxo and peroxo complexes, depending on the reaction conditions.[595]

An ^{17}O NMR investigation of aqueous solutions of $[Rh_2(H_2O)_{10}]^{4+}$ revealed the presence of $[Rh_2(eq\text{-}H_2O)_8(ax\text{-}H_2O)_2]^{4+}$ and it was noted that the exchange of the two *ax* H_2O ligands is at least a factor of 10^3 faster than the exchange of the *eq*-H_2O groups at 298 K.[596] The $[Rh_2(H_2O)_{10}]^{4+}$ ion decomposes within 1 h at 339 K forming metallic Rh and $[Rh(H_2O)_6]^{3+}$.[596]

12.4.2 The $[Rh_2(NCR)_{10}]^{4+}$ cations

In contrast to $[Rh_2(H_2O)_{10}]^{4+}$, the soluble organic analogs $[Rh_2(NCR)_{10}]^{4+}$, R = CH_3, CH_3CH_2, have been isolated by several independent routes and structurally characterized.[582,597,598] One method employs addition of excess Et_3OBF_4 to an acetonitrile solution of $Rh_2(O_2CCH_3)_4(MeOH)_2$, which initially produces the purple complex *cis*-$[Rh_2(O_2CCH_3)_2(NCCH_3)_6](BF_4)_2$.[361] Upon heating the reaction for several days, however, the purple colored solution turns orange and the dark orange-red homoleptic complex $[Rh_2(NCCH_3)_{10}](BF_4)_4$ (Fig. 12.28) is isolated.[597] Alternatively, $Me_3Si(CF_3SO_3)$ can be employed to remove the carboxylate ligands from the dinuclear unit as silylesters, or the acid $HBF_4{\cdot}Et_2O$ can be used to protonate them and liberate acetic acid, but the latter strategy leads to severe oiling problems which renders it less useful.[598] The use of the more labile $Rh_2(O_2CCF_3)_4$ reduces considerably the reaction time. In addition, $Rh_2(O_2CCH_3)_4$, $Na_4[Rh_2(CO_3)_4]{\cdot}nH_2O$, or preferably $Na_4[Rh_2(SO_4)_4(H_2O)_2]{\cdot}4H_2O$ can be heated in CH_3CN/CF_3SO_3H mixtures to afford $[Rh_2(NCCH_3)_8(H_2O)_2](PF_6)_4$ which has been structurally characterized;[599] when this compound is dissolved in CH_3CN, it forms $[Rh_2(NCCH_3)_{10}](PF_6)_4$,[582] and many compounds of the type $[Rh_2(NCCH_3)_8L_2](PF_6)_4$ (L = DMF, DMSO, NH_3, py, PPh_3) depending on the identity of the solvent.[582,600] Similar strategies have been employed to prepare $[Rh_2(NCEt)_{10}](CF_3SO_3)_4$, $[Rh_2(NCC_6H_5)_8L_2](ClO_4)_4$ (L = H_2O or py),[582] and $[Rh_2(NCEt)_{10}](BF_4)_4$, which has been the subject of single crystal X-ray studies.[598] The structurally characterized cations $[Rh_2(NCR)_{10}]^{4+}$ are listed in Table 12.7.

The Rh–Rh distances of the nitrile salts $[Rh_2(NCR)_{10}]^{4+}$ are in the narrow range 2.604-2.625 Å, a fact which suggests that the Rh–Rh bond is not highly influenced by the ligand identity or the different counterions.[598] Importantly, these nitrile Rh–Rh bonds are much shorter than in $Rh_2(dmg)_4(PPh_3)_2$ (2.936(2) Å)[337,338] and the unsupported isocyanide compound $[Rh_2(CN\text{-}p\text{-}tol)_8I_2]^{2+}$ (2.785(2) Å),[601] but longer than the average distance in tetracarboxylate systems (2.35-2.45 Å; Table 12.1). There is no significant repulsion between the essentially linear CH_3CN molecules in $[Rh_2(NCCH_3)_{10}](BF_4)_4$, contrary to $Rh_2(dmg)_4(PPh_3)_2$ (see Section 12.4.3), wherein the unfavorable interaction between the dmg groups induces considerable lengthening of the Rh–Rh bond.[337,338] Therefore the cation $[Rh_2(NCCH_3)_{10}]^{4+}$ with a fully staggered (χ_{av} = 44.8°) set of small *eq* ligands, which are neutral σ-donors, provides a reliable measure of the Rh–Rh bond distance in the absence of constraints or repulsions.

Pictiva EX2004
Samsung v Pictiva
IPR2024-01094

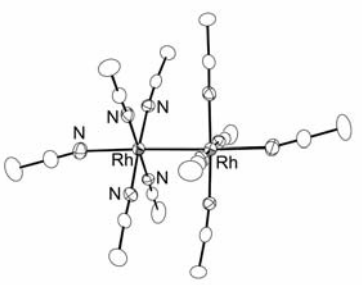


Fig. 12.28. The cation in $[Rh_2(NCCH_3)_{10}](BF_4)_4$.

Table 12.7. Dirhodium compounds with unsupported Rh–Rh bonds

Compound	r (Rh–Rh)[a] (Å)	r (Rh–L_{ax}) (Å)	Donor atom(s)	ref.
$[Rh_2(NCCH_3)_8(H_2O)_2](PF_6)_4{\cdot}2H_2O$	2.625(1)	2.23(2)	O	599
$[Rh_2(NCCH_3)_{10}](BF_4)_4$	2.624(1)	2.191(5)	N	597,598
$[Rh_2(NCCH_3)_{10}](O_3SCF_3)_4$	2.616(2)	2.15(1)	N	598
		2.14(1)		
$[Rh_2(NCEt)_{10}](BF_4)_4$	2.604(1)	2.180(6)	N	598
$[Rh_2(CN\text{-}p\text{-}tol)_8I_2](PF_6)_2$	2.785(2)	2.735(1)	I	601
$Rh_2(dmg)_4(PPh_3)_2{\cdot}H_2O{\cdot}C_3H_7OH$	2.936(2)	2.430(5)	P	337,338
		2.447(5)		
$Rh_2(dmg)_4(py)_2$	2.726(1)	2.219(8)	N	609
$Rh_2(hfacac)_4(py)_2$	2.590(1)	2.271(8)	N	582,610
		2.245(8)		
$Rh_2(tmtaa)_2$	2.619(6)	[b]	[b]	614
$Rh_2(tmtaa)_2{\cdot}3C_7H_8$	2.619(1)	[b]	[b]	144
$[Rh_2(pc)_2(py)_2]{\cdot}2C_6H_6$	2.741(2)	2.309(8)	N	617
$[Rh(CO)_2Cl_2]_2[Rh_2(quinCO)_2(CO)_2]$	2.671(1)	2.522(2)	Cl	612

[a] Distances are given with up to 3 decimal digits.
[b] No *ax* ligands.

A high-pressure ^1H NMR study[596] of CH_3CN exchange kinetics for $[Rh_2(NCCH_3)_{10}]^{4+}$ supports the presence of $[Rh_2(eq\text{-}NCCH_3)_8(ax\text{-}NCCH_3)_2]^{2+}$ in solution. Consistently with the findings for $[Rh_2(H_2O)_{10}]^{4+}$[596] and *cis*-$[Rh_2(O_2CCH_3)_2(NCCH_3)_6]^{2+}$,[364] the *ax* CH_3CN ligands are more labile than those in *eq* positions. Lastly, the cation $[Rh_2(NCCH_3)_{10}]^{4+}$ has been reported to exhibit unusual spectroscopic properties, including reversible photochemical heterolytic cleavage of the Rh–Rh bond at $\lambda < 600$ nm to yield the metastable photofragments $[Rh(NCCH_3)_6]^{3+}$ and $[Rh(NCCH_3)_4]^{+}$, which recombine to regenerate the original dimer in essentially quantitative yields.[602,603] Exposure of $[Rh_2(NCCH_3)_{10}](BF_4)_4$ to light after immobilization in ordered mesoporous silica promotes irreversible photodissociation to monomeric species.[604]

The mixed valence molecular wire $[Rh(NCCH_3)_4(BF_4)_{1.5}]_\infty$[598,605] is discussed with the rhodium blues in Section 12.5.2.

12.4.3 Complexes with chelating and macrocyclic nitrogen ligands

Compounds of this type that have been crystallographically determined are compiled in Table 12.7. The first example of a Rh_2^{4+} compound lacking bridging groups is $Rh_2(dmg)_4(PPh_3)_2$, which is prepared by reduction of $Rh_2(dmg)_2Cl(PPh_3)$ with an excess of $NaBH_4$.[606] Several

Pictiva EX2004
Samsung v Pictiva
IPR2024-01094

germane compounds with other *ax* donors (e.g., H_2O, DMSO, py), prepared by a synthetic procedure starting from $Rh_2(O_2CCH_3)_4$, have been reported.[607] The compound $Rh_2(dmg)_4(PPh_3)_2$ has a very long Rh–Rh distance of 2.936(2) Å.[337,338] Despite the staggered conformation of the dmg moieties, they are prevented from bending back by the PPh_3 ligands, thus repulsion between the dmg groups is primarily responsible for the long Rh–Rh distance.[608] An appreciable shortening of the Rh–Rh bond by 0.21 Å takes place upon replacing the *ax* phosphine groups with pyridine to form $Rh_2(dmg)_4(py)_2$.[609] The estimated dissociation energy for homolytic cleavage of the Rh–Rh bond in $Rh_2(dmg)_4(PPh_3)_2$ is *c.* 20 kcal.mol^{-1}.[608]

Heating aqueous solutions of $Na_4[Rh_2(SO_4)_4(H_2O)_2]\cdot 4H_2O$ with acetylacetone (acac) or hexafluoroacetylacetone (hfacac) to 80-90 °C under argon affords $Rh_2(acac)_4$ and $Rh_2(hfacac)_4(H_2O)_2\cdot 2H_2O$ with bidentate chelating diketonate groups.[582] In the pyridine adduct $Rh_2(hfacac)_4(py)_2$, the Rh–Rh bond of 2.590(1) Å[582,610] is shorter by *c.* 0.10 Å than that in $Rh_2(dmg)_4(py)_2$, a fact which clearly shows the effect of the bulky dmg groups on the Rh–Rh bond length. The chelate rings are not eclipsed, instead they are twisted by *c.* 42° with respect to each other. Reaction of $Rh_2(hfacac)_4L_2$, L = H_2O, py with PPh_3 in toluene, in the absence of O_2, is believed to form the paramagnetic species $Rh(hfacac)_2(PPh_3)$,[600] whereas in the presence of O_2, it produces the peroxo complex $(Ph_3P)(hfacac)_2Rh(\mu\text{-}O_2)Rh(hfacac)_2(PPh_3)$.[611]

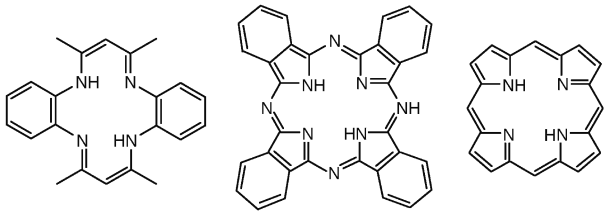
A related compound is the tetranuclear acylrhodium complex $[Rh(CO)_2Cl_2]_2[Rh_2(quinCO)_2(CO)_2]$ (quinCO: 8-quinoline acyl), which is formed by reacting $[(CO)_2RhCl]_2$ with 8-quinoline carboxaldehyde. The rather short unsupported Rh–Rh bond of 2.671(1) Å is mostly attributed to stacking interactions between the acylquinoline ligands.[612]

The macrocycle tetraaza[14]annulene, abbreviated H_2tmtaa (**12.39**), has a saddle-shaped conformation resulting from internal steric constraints which cause displacement of the coordinated metal from the N_4 plane.[613,614] This makes it possible for this 14-membered ring, which is an anti-aromatic system (4*n*), to coordinate in a tetradentate fashion to metal atoms that participate in metal-metal bonds. The reaction of H_2tmtaa with $Rh_2(O_2CCH_3)_4$ in EtOH[615] affords $Rh_2(tmtaa)_2$ with a Rh–Rh distance of 2.619(1) Å[144,614] (there is an earlier report quoting a similar Rh–Rh distance of 2.625 Å,[616] but full crystallographic details were not given). The shorter Rh–Rh bond distance compared to $Rh_2(dmg)_4(py)_2$ (2.726(1) Å)[609] and $[Rh_2(CN\text{-}p\text{-}tol)_8I_2](PF_6)_2$ (2.785(2) Å)[601] is attributed to the absence of *ax* ligands, whereas the longer Rh–Rh distance compared to $Rh_2(hfacac)_4(py)_2$ (2.590(1) Å), is likely a result of the 0.219 Å displacement from the N_4 plane.[144] The red diamagnetic di(pyridine)phthalocyaninatorhodium(II) complex, $[Rh(py)(pc)]_2$ (Fig. 12.29a) is another example of a dirhodium unit with a macrocycle, namely phthalocyanine (H_2pc; **12.40**), which has been structurally characterized.[617] The cofacial rhodium phthalocyaninate units have a Rh–Rh distance of 2.741(2) Å, which is comparable to that in $Rh_2(dmg)_4(py)_2$ (2.726(1) Å)[609] and suggests a strong unsupported Rh–Rh single bond. The pc-pc repulsions are minimized by their staggered conformation with a twist angle of 42° (Fig. 12.29b).[617]

Porphyrins (**12.41**) are 16-membered aromatic rings (4*n* + 2) that coordinate to metals in a tetradentate fashion. Dirhodium compounds with the tetraphenylporphyrin (TPP) and octaethylporphyrin (OEP) dianions have been extensively studied due to their rich radical chemistry and potential importance in biologically relevant processes. In the case of OEP, the Rh(III) hydrido complex Rh(OEP)H is converted, upon heating, to the dimeric complex $[Rh(OEP)]_2$, which has a Rh–Rh bond.[618,619] The reaction of $[Rh(OEP)]_2$ with O_2 at -80 °C affords the paramagnetic $Rh(OEP)(O_2)$ which, upon warming to room temperature, produces a peroxo species formulated as $[Rh(OEP)]_2(O_2)$.[620,621] A paramagnetic mononuclear compound formulated as $[Rh(TPP)]$ has been prepared by reaction of $[Rh(CO)_2Cl]_2$ with a solution of H_2TPP in refluxing acetic acid.[622] The similar behavior of 'Rh(TPP)' to $Rh(OEP)(O_2)$ suggested that it may actually

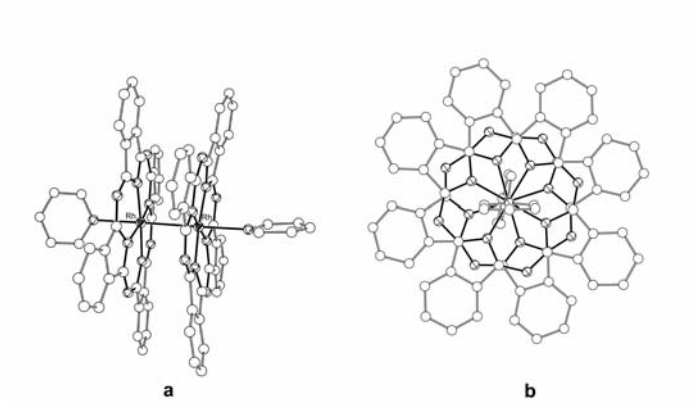
Pictiva EX2004
Samsung v Pictiva
IPR2024-01094

be Rh(TPP)(O_2); this is further supported by the fact that its sublimation in vacuum affords a diamagnetic compound consistent with the formula $[Rh(TPP)]_2$, which reacts with O_2 and NO similarly to $[Rh(OEP)]_2$.[620] The Rh–Rh bond dissociation energy of $[Rh(OEP)]_2$ has been estimated *c.* 16.5 kcal mol^{-1} by ^1H NMR line broadening measurements, but $[Rh(OEP)]_2$ and $[Rh(TPP)]_2$ have not been crystallographically characterized.[623,624] The radical-like reactivity of $[Rh(OEP)]_2$, initiated by dissociation of $[Rh(OEP)]_2$ to [Rh(OEP)], has been extensively studied.[625-633] The reactions of the dirhodium diporphyrin complexes Rh_2(DPB)[634] (DPB: diporphyrinatobiphenylene) and $[Rh(OMP)]_2$[635] (OMP: 2,3,7,8,12,13,17,18-octamethoxyporphyrin dianion), which have a Rh–Rh single bond, with various molecules have been studied.



H_2tmtaa — phthalocyanine (H_2pc) — porphyrin

12.39 **12.40** **12.41**



a **b**

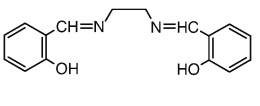
Fig. 12.29. The structure of the phthalocyanine (H_2pc) dirhodium complex $[Rh(pc)(py)]_2$; (a) side view, (b) view along the Rh–Rh axis.

For tetramesitylporphyrin (H_2TMP), the mononuclear radical $[Rh(TMP)]^{\bullet}$ is the stable form since ligand steric requirements preclude Rh–Rh bonding.[636,637] The focal point of subsequent studies has been the design of a series of tethered diporphyrin ligands, by linking two sterically demanding TMP derivatives with a series of diether spacers, in order to improve the kinetics and retain the selectivity of the stable bimetalloradical $^{\bullet}$Rh(porphyrin)-X-(porphyrin)Rh$^{\bullet}$ (X = spacer) reactions with substrates such as H_2 and CH_4.[638,639]

Although the Schiff base H_2salen (**12.42**) and the sulfur-based ligand 'Bu^t-H_2S_4' (**12.43**; 'Bu^t-H_2S_4': 1,2-bis(2-mercapto-3,5-di-Bu^t-phenylthio)ethane) are not macrocycles, they are mentioned here for practical purposes. Compounds formulated as $Rh_2(salen)_2(py)_2$,[640] $[Rh(salen)]_2$ and a few related derivatives with other Schiff bases have been reported but not structurally

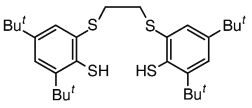
Pictiva EX2004
Samsung v Pictiva
IPR2024-01094

characterized.[641] The chelating ligand 'Bu^t-H_2S_4' (**12.43**) is coordinated in a tetradentate fashion in $Rh_2(Bu^t\text{-}S_4)_2$;[642] each thiolate group of the ligand bridges two rhodium centers.



H_2salen

12.42



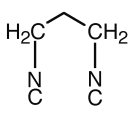
'Bu^t-H_2S_4'

12.43

12.5 Other Dirhodium Compounds

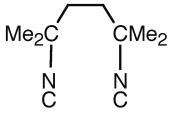
12.5.1 Complexes with isocyanide ligands

Although Rh(I) isocyanide complexes were known, it was not until much later that Rh_2^{4+} isocyanide species were obtained by reaction of $[Rh(CNR)]^+$ and $[Rh(CNR)_4X_2]^+$ (X = halide) in solvents of high dielectric constants, or by reaction of I_2 with $[Rh(NCR)_4]^+$ in a 1:2 mole ratio.[643,644] A species with a Rh–Rh bond, *ax* Rh-X bonds and no bridging groups is favored for the products $[Rh_2(CNR)_8X_2]^{2+}$ and confirmed by the crystal structure determination of $[Rh_2(CN\text{-}p\text{-}tol)_8I_2](PF_6)_2$.[601] A class of germane complexes with di-isocyanide ligands are formulated as $[Rh_2(LL)_4X_2]^{2+}$, LL: 1,3-di-isocyanopropane (abbreviated bridge, **12.44**),[645-648] 2,5-di-isocyano-2,5-dimethylhexane (abbreviated TMB, **12.45**),[648,649] and 1,8-di-isocyanomenthane (abbreviated dimen, **12.46**).[650] Salts of the $[Rh_2(LL)_4X_2]^{2+}$ cations (X = Cl, Br or I) are prepared by oxidation of $[Rh_2(LL)_4]^{2+}$ with molecular halogens.[648,650]



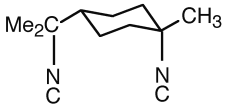
bridge

12.44



TMB

12.45



dimen

12.46

The structures of the isocyanide complexes $[Rh_2(bridge)_4Cl_2]Cl_2$[647] and $[Rh_2(TMB)_4Cl_2](PF_6)_2$[649] have been crystallographically determined (Table 12.8). Although the Rh–Rh bond lengths in these compounds (2.837(1) and 2.770(3) Å, respectively) are similar to that in $[Rh_2(CN\text{-}p\text{-}tol)_8I_2](PF_6)_2$ (2.785(2) Å),[601] the C–Rh–Rh–C torsion angles vary considerably. The isonitrile groups in $[Rh_2(bridge)_4Cl_2]Cl_2$ are eclipsed, whereas in $[Rh_2(TMB)_4Cl_2](PF_6)_2$ and $[Rh_2(CN\text{-}p\text{-}tol)_8I_2](PF_6)_2$, they are twisted by 33° and 28-35°, respectively, from the fully eclipsed geometry.[649]

Table 12.8. Other dirhodium compounds

Compound	*r* (Rh–Rh)[a] (Å)	*r* (Rh–L_{ax}) (Å)	Donor atom(s)	ref.
Rhodium blues				
$H_3[Rh_4\{CN(CH_2)_3NC\}_8Cl][CoCl_4]_4\cdot 6H_2O$[b]	2.932(4)[c] 2.923(3)[c] 2.775(4)[d]	2.613(8) 2.643(9)	Cl	653

Pictiva EX2004
Samsung v Pictiva
IPR2024-01094

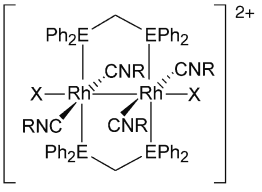
Compound	*r* (Rh–Rh)[a] (Å)	*r* (Rh–L_{ax}) (Å)	Donor atom(s)	ref.
$\{Rh(NCCH_3)_4](BF_4)_{1.5}\}_\infty$[e]	2.928(1) 2.844(1)			598,605
$\{[Rh(\mu\text{-pz})(CNBu^t)_2]_4\}(PF_6)_2$	2.721(4)[f] 2.723(4)[f] 2.713(4)[g]			673
$[Rh_4(\mu\text{-}O_2CH)_4(bpy)_4](PF_6)_2$	2.668(1)[h] 2.780(1)[i]			235
$\{[Rh_4(O_2CH)_4(bpy)_4]BF_4\cdot 0.5C_4H_8O_2\}_\infty$[j]	2.678(3)[h] 2.733(4)[i] 2.921(3)[k]			358
$\{[Rh_2(\mu\text{-}O_2CCH_3)_2(bpy)_2]BF_4\cdot H_2O\}_\infty$[e]	2.666(2)[l] 2.833(2)[m]			678
$\{[Rh_2(\mu\text{-}O_2CCH_3)_2(phen)_2]PF_6\cdot 0.5Me_2CHOH\}_\infty$[e]	2.652(1)[n] 2.739(1)[o] 2.832(1)[o]			677
$[Rh_3(CNCH_2Ph)_{12}I_2]Br_3$[p]	2.785(2)	2.735(1)	I	675
$[Rh_3(s\text{-pqdi})_4(pqdi)_2]Cl\cdot 3DMF$	2.754(2)[q]			676
Isocyanide compounds				
$[Rh_2\{CN(CH_2)_3NC\}_4Cl_2]Cl_2\cdot 8H_2O$	2.837(1)	2.447(1)	Cl	647
$[Rh_2(TMB)_4Cl_2](PF_6)_2$	2.770(3)	2.425[r]	Cl	649
$[Rh_2(CN\text{-}p\text{-tol})_8I_2](PF_6)_2$	2.785(2)	2.735(1)	I	601
trans-$[Rh_2(\mu\text{-pz})(CNBu^t)_2(dppm)_2Cl_2]PF_6$	2.768(1)	2.489(1) 2.471(1)	Cl	662
trans-$[Rh_2(\mu\text{-pz})(CNBu^t)_2(dppm)_2I_2]BF_4$	2.829(3)	2.738(3) 2.766(6)	I	663
$\{[Rh_2(\mu\text{-pz})_2(I)(CNBu^t)_4]_2(\mu\text{-I})\}CF_3SO_3$	2.632(1)	2.728(1) 2.754(1) 2.790(1) 2.812(1)	I	485

[a] Distances are given with up to 3 decimal digits.
[b] Rh(I)Rh(II)Rh(II)Rh(I) chain with an average oxidation state of +1.5 for each of the four Rh atoms in the tetranuclear unit.
[c] Rh(I)···Rh(II) distance within the binuclear unit.
[d] Rh(II)···Rh(II) distance between the two binuclear units Rh_2^{3+}.
[e] Mixed valence Rh(I)–Rh(II) infinite wire.
[f] Rh···Rh distance within $[Rh_2(pz)_2(CNBu^t)_4]^+$ unit.
[g] Rh···Rh separation between $[Rh_2(pz)_2(CNBu^t)_4]^{1+}$ units.
[h] Rh–Rh distance for entity supported by the formato group within the tetranuclear linear $[Rh_4(\mu\text{-}O_2CH)_4(bpy)_4]^+$ unit.
[i] Rh···Rh interaction within the tetranuclear linear $[Rh_4(\mu\text{-}O_2CH)_4(bpy)_4]^+$ unit.
[j] Infinite rhodium wire with each Rh atom in the +1.25 oxidation state.
[k] Rh···Rh interaction between the tetranuclear linear $[Rh_4(\mu\text{-}O_2CH)_4(bpy)_4]^+$ units.
[l] Rh–Rh distance within $[Rh_2(\mu\text{-}O_2CCH_3)_2(bpy)_2]^+$ units.
[m] Rh···Rh distance between $[Rh_2(\mu\text{-}O_2CCH_3)_2(bpy)_2]^+$ units.
[n] Rh–Rh distance within $[Rh_2(\mu\text{-}O_2CCH_3)_2(phen)_2]^+$ units.
[o] Rh···Rh separations between $[Rh_2(\mu\text{-}O_2CCH_3)_2(phen)_2]^+$ units.
[p] The molecule contains nearly linear I–Rh–Rh–Rh–I units.
[q] Average distance.
[r] Esd not reported.

Pictiva EX2004
Samsung v Pictiva
IPR2024-01094

Irradiation of the cation $[Rh_2(bridge)_4]^{2+}$, dissolved in acidic aqueous solutions (12 M HCl) at 550 nm, produces H_2 and $[Rh_2(bridge)_4Cl_2]^{2+}$.[646] The photochemical release of H_2 from water has been the subject of detailed mechanistic studies due to the interest stemming from the point of view of energy storage.[12,651-655] It has been proposed that the system initially involves reaction of $[Rh_2(bridge)_4]^{2+}$ with H^+ to form H_2 and the tetranuclear cluster $[Rh_2(bridge)_4Cl]_2^{4+}$ followed by a photochemical reaction that converts the latter to $[Rh_2(bridge)_4Cl_2]^{2+}$.[12] The structure of the tetranuclear cluster $H_3[Rh_4(bridge)_8Cl][CoCl_4]_4 \cdot 6H_2O$, which is a derivative of the chloride deficient $[Rh_4(bridge)_8Cl]^{5+}$ cation, has been crystallographically determined;[653] this complex is discussed with the rhodium blues in Section 12.5.2.

A number of dirhodium complexes of the type **12.47**, that are bridged by two *trans* $Ph_2PCH_2PPh_2$ (dppm) or $Ph_2AsCH_2AsPh_2$ (dpam) ligands and contain monodentate isocyanide groups, have been reported.[511,512,656] Electrochemical studies have established that oxidation of $[Rh_2(CNR)_4(dppm)_2]^{2+}$ is facilitated in the presence of various nitrogenous bases B, due to the increased stability of the $[Rh_2(CNR)_4(dppm)_2B_2]^{4+}$ cation.[657,658] Dirhodium compounds formulated as $[Rh_2(TMB)_2(dppm)_2X_2]^{2+}$ (X = Cl, Br or I) and $[Rh_2(dimen)_2(dppm)_2Cl_2]^{2+}$, which are supported by two *trans* dppm groups and the isocyanide ligands **12.44** and **12.45**, respectively, have also been reported.[659,660]



E = P, As; R = Me, Bu^n, Bu^t, C_6H_{11}; X = halogen or SCF_3^-

12.47

A series of paramagnetic complexes of the type $[Rh_2(\mu\text{-}Z)(CNBu^t)_2(\mu\text{-}LL')_2](PF_6)_2$ (Z = pyrazolate (**12.9**) or substituted pyrazolate ligand; LL' = $Ph_2PCH_2PPh_2$ (dppm), $Ph_2PCH_2AsPh_2$ (dpapm) or $Ph_2AsCH_2AsPh_2$ (dpam)) with a Rh_2^{3+} core and a mixed set of ligands have been prepared by controlled-potential electrolysis of the Rh_2^{2+} compounds $[Rh_2(\mu\text{-}Z)(CNBu^t)_2(\mu\text{-}LL')_2]PF_6$.[661] The two-electron oxidation of Rh_2^{2+} compounds to the Rh_2^{4+} analogs $[Rh_2(\mu\text{-}Z)(CNBu^t)_2(\mu\text{-}dppm)_2X_2]PF_6$ (X = Cl^-, Br^- I^-, SCN^-, NO_3^- or $CH_3CO_2^-$) has been electrochemically performed by treatment with halogens, HNO_3, CH_3CO_2H or disproportionation of the parent Rh_2^{3+} compound in the presence of anionic ligands.[662] An important structural feature of *trans*-$[Rh_2(\mu\text{-}pz)(CNBu^t)_2(\mu\text{-}dppm)_2Cl_2]PF_6$[662] (Fig. 12.30) is the orientation of the methylene moieties of the *transoid* bridging dppm ligands, which are folded away from the pyrazolate ligand, contrary to other *trans* dppm-bridged A-frame compounds. The analogous diiodide complex *trans*-$[Rh_2(\mu\text{-}pz)(CNBu^t)_2(dppm)_2I_2]BF_4$ has been reported as well.[663]

It is notable that the existence of stable dinuclear M–M bonded complexes with isocyanide groups in *eq* positions, even in the absence of bridging ligands, is unique to Rh_2^{4+} compounds.[265] Reaction of Cr_2^{4+}, Mo_2^{4+}, W_2^{4+} or Re_2^{6+} compounds, not supported by bridging groups, with isocyanide ligands results in disruption of the M–M bond and formation of mononuclear products.[664-666]

Pictiva EX2004
Samsung v Pictiva
IPR2024-01094

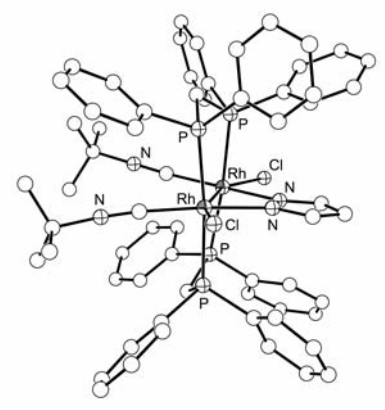


Fig. 12.30. The cation in *trans*-$[Rh_2(\mu\text{-pz})(CNBu^t)_2(\mu\text{-dppm})_2Cl_2]PF_6$.

12.5.2 Rhodium blues

Unlike platinum blues, which have been extensively studied (Section 14.4.7), the chemistry of the related rhodium blues is still at its nascence. Essential features of this class of compounds called 'blues', regardless of their color, are that they are tetranuclear (or oligonuclear) chains with at least one unsupported Rh–Rh bond, wherein the metal atoms possess non-integral oxidation numbers.[667] Special requirements apply to the ligands involved in the assembly of the chain. The rhodium blues that have been the subject of single crystal X-ray studies are listed in Table 12.8.

Mixed valence molecular wire $[Rh(NCCH_3)_4(BF_4)_{1.5}]_\infty$.

A remarkable example of a rhodium blue compound is that of the unprecedented mixed valence molecular wire $[Rh(NCCH_3)_4(BF_4)_{1.5}]_\infty$ (Fig. 12.31).[598,605] Electrochemical reduction of $[Rh_2(NCCH_3)_{10}](BF_4)_4$ at low currents produces single crystals of the 1-D chain polymeric product $[Rh(NCCH_3)_4(BF_4)_{1.5}]_\infty$ at the Pt electrode over a period of three weeks. This is the first example of an infinite metal-containing chain synthesized from a dimetal precursor.[668] Relevant features of $[Rh(NCCH_3)_4(BF_4)_{1.5}]_\infty$ are the two different Rh–Rh interactions of 2.844(1) and 2.928(1) Å present in the chain.[598,605] Both distances are significantly longer than the Rh–Rh single bond in $[Rh_2(NCCH_3)_{10}](BF_4)_4$ (2.624(1) Å), but considerably shorter than the typical Rh(I)-Rh(I) contacts of *c.* 3.16 Å found in $[Rh(CO)_2(NCCH_3)_2]^+$ which forms 1-D stacks in the solid state.[598] These results offer credible evidence for description of the material as being composed of Rh atoms in an average oxidation state +1.5. A view of the crystal packing is shown in Fig. 12.32. There are two different sets of torsional angles for the *eq* CH_3CN ligands coordinated to the square planar rhodium ions, namely 44.8° between the Rh atoms with the shorter contacts and 15.3° between the Rh atoms at longer separations. A slight bending of the CH_3CN ligands away from each other in the 'dimer' with the smaller torsion angle suggests that a minor steric effect is operative at $\chi = 15.5°$, which is alleviated when $\chi = 44.8°$.[598,605]

Pictiva EX2004
Samsung v Pictiva
IPR2024-01094

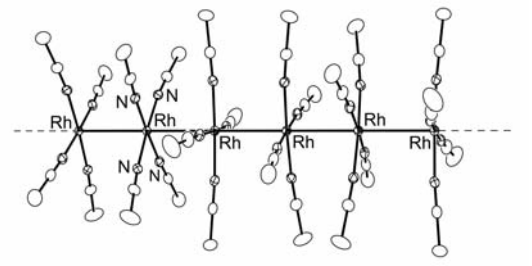


Fig. 12.31. Structure of the segment $[Rh_6(NCCH_3)_{24}]^{9+}$ in the molecular wire $[Rh(NCCH_3)_4(BF_4)_{1.5}]_\infty$.

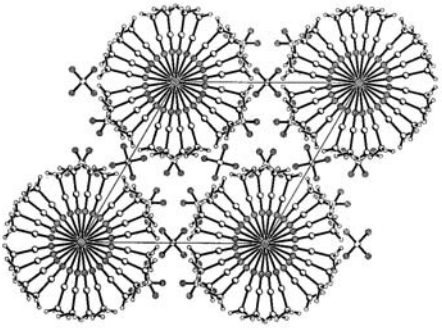


Fig. 12.32. Packing of $[Rh(NCCH_3)_4(BF_4)_{1.5}]_\infty$ along the *c* axis.

$H_3[Rh_4(bridge)_8Cl][CoCl_4]_4{\cdot}6H_2O$

This rhodium blue compound contains the oxygen- and light-sensitive mixed-valence cation $[Rh_4(bridge)_8Cl]^{5+}$ [12] (bridge: 1,3-di-isocyanopropane, **12.44**), which was crystallized as the tetranuclear green complex $H_3[Rh_4(bridge)_8Cl][CoCl_4]_4{\cdot}6H_2O$.[653] This salt is obtained by addition of $CoCl_2{\cdot}6H_2O$ to a solution of the photoactive complex $Rh_2(bridge)_4(BF_4)_2$ in 12 M HCl. The cation $[Rh_4(bridge)_8Cl]^{5+}$ is implicated in the visible light production of H_2 from aqueous acid solutions (see Section 12.5.1). It consists of two $[Rh_2(bridge)_4]^{3+}$ units linked by a Rh–Rh bond. The Rh(II)···Rh(II) separation of 2.775(4) Å between the dinuclear units is shorter than the Rh(I)···Rh(II) separations of 2.932(4) and 2.923(3) Å within the Rh_2^{3+} units, giving rise to a Rh(I)Rh(II)Rh(II)Rh(I) chain with an average oxidation state of +1.5 for each of the four Rh atoms in the tetranuclear unit.

Reduction of the tetranuclear Rh_4^{6+} unit produces higher nuclearity oligomers including Rh_6^{8+}, Rh_8^{10+} and Rh_{12}^{16+} cores with nonintegral average oxidation states of the metal atoms.[12,669] Despite the isolation of only few oligomers in the solid state,[669] the tetranuclear clusters and their higher homologs have been characterized by various spectroscopic[669,670] and electrochemical techniques.[671]

{[Rh(μ-pz)(CNBut)$_2$]$_4$}(PF$_6$)$_2$

Mixing equimolar amounts of the recently reported[485,672] yellow compounds $[Rh(I)(\mu\text{-pz})(CNBu^t)_2]_2$ and $[Rh(II)(\mu\text{-pz})(CNBu^t)_2]_2(PF_6)_2$ affords blue, EPR-silent solutions from which crystals of the tetranuclear rhodium blue complex $\{[Rh(\mu\text{-pz})(CNBu^t)_2]_4\}(PF_6)_2$ (Fig. 12.33) are isolated.[673] The success of this synthetic approach, which involves condensation

Pictiva EX2004
Samsung v Pictiva
IPR2024-01094

of dinuclear complexes with Rh atoms in different oxidation states, arises from the nucleophilic character of the Rh_2^{2+} entity induced by the very basic $CNBu^t$ ligands, [674] as well as by the presence of a vacant coordination site or a labile ligand *trans* to the Rh–Rh bond in the Rh_2^{4+} unit.[667] The unsupported Rh–Rh bond of 2.713(4) Å between the $\{[Rh(\mu\text{-}pz)(CNBu^t)_2]_4\}$ moieties is slightly shorter by 0.01 Å than those of 2.721(4) and 2.723(4) Å encountered within the dimers and, the average oxidation state of the Rh centers is +1.5. The two dinuclear moieties are in a staggered conformation, a situation which allows the two metals to form the Rh(2)–Rh(3) bond; the three metal bonds in the crystal structure are nearly linear.

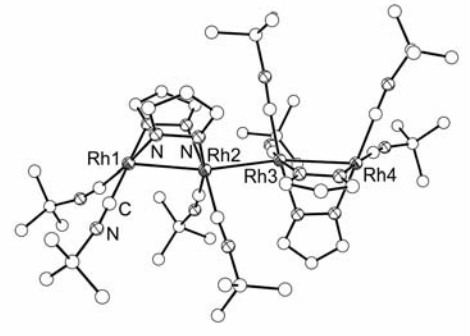


Fig. 12.33. The cation in $\{[Rh(pz)(CNBu^t)_2]_4\}(PF_6)_2$.

$[Rh_3(CNCH_2Ph)_{12}I_2]Br_3$

Another compound with mixed valence Rh atoms and ligands of the isocyanide family is $[Rh_3(CNCH_2Ph)_{12}I_2]Br_3$.[675] Each Rh atom is in a pseudooctahedral environment with four isocyanide ligands located at the corners of the square. The I–Rh–Rh–Rh–I unit is nearly linear with a Rh–Rh distance of 2.785(2) Å, which is the same as that in the related compound $[Rh_2(CN\text{-}p\text{-}tol)_8I_2](PF_6)_2$ (2.785(2) Å).[601]

$[Rh_4(O_2CH)_4(bpy)_4](PF_6)_2$

The tetranuclear Rh(I)–Rh(II) complex $[Rh_4(O_2CH)_4(bpy)_4](PF_6)_2$ (Fig. 12.34) is prepared under an Ar atmosphere by heating $Na_4[Rh_2(CO)_3]_4$ with bpy in a 10% aqueous solution of HCOOH. The molecule consists of two $[Rh_2(O_2CH)_2(bpy)_2]^+$ entities with a Rh–Rh separation between the dinuclear units of 2.780(1) Å.[235] The two rhodium atoms are bridged by two formato ligands with a Rh–Rh distance of 2.668(1) Å, which is among the shortest distances known for a Rh–Rh bond order of 0.5. The dinuclear units are linked in a *transoid* arrangement and the *eq* planes of the two rhodium atoms are partially staggered.[235]

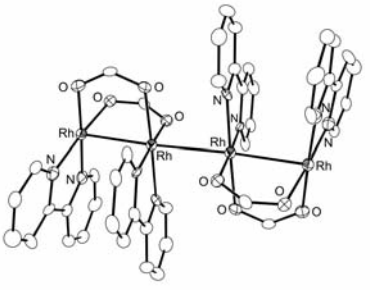


Fig. 12.34. The cation in $[Rh_4(O_2CH)_4(bpy)_4](PF_6)_2$.

Pictiva EX2004
Samsung v Pictiva
IPR2024-01094

$[Rh_3(s\text{-}pqdi)_4(pqdi)_2]Cl$

The red-purple linear trinuclear metal chain has an average Rh–Rh distance of 2.754(2) Å and all the ligands are in an eclipsed conformation (pqdi: 9,10-phenanthroquinonediimine and s-pqdi: 9,10-phenanthrosemiquinonediimine).[676]

Rhodium wires with dinuclear carboxylate-bridged complexes as building blocks

Two 1-D mixed valence Rh_2^{3+} infinite chains $\{[Rh_2(O_2CCH_3)_2(phen)_2]PF_6\}_\infty$ and $\{[Rh_2(O_2CCH_3)_2(bpy)_2]BF_4\}_\infty$, as well as the $Rh_2^{+2.5}$ infinite chain $\{[Rh_4(O_2CH)_4(bpy)_4]BF_4\}_\infty$, have been reported.

$\{[Rh_2(O_2CCH_3)_2(phen)_2]PF_6\}_\infty$. The molecular wire $\{[Rh_2(O_2CCH_3)_2(phen)_2]PF_6\}_\infty$[677] (Fig. 12.35) consists of dinuclear units linked in an infinite chain with unbridged Rh···Rh separations of 2.739(1) and 2.832(1) Å. The Rh–Rh distance of 2.652(1) Å within the $[Rh_2(O_2CCH_3)_2(phen)_2]^+$ units is the shortest known for a bond order of 0.5 and similar to the Rh(II)–Rh(II) distance of 2.624(1) Å for $[Rh_2(NCCH_3)_{10}]^{4+}$.[597,598] The chelating phen ligands occupy *transoid* coordination sites of adjacent dirhodium units.

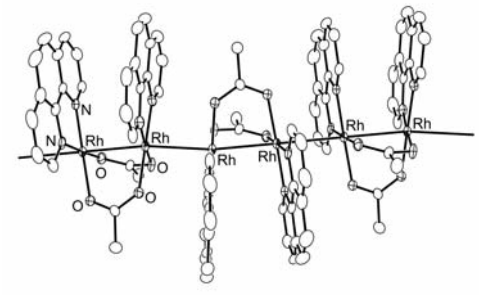


Fig. 12.35. A segment of the cationic chain in $\{[Rh_2(O_2CCH_3)_2(phen)_2]PF_6\}_\infty$.

$\{[Rh_2(O_2CCH_3)_2(bpy)_2]BF_4\}_\infty$. This infinite chain is formed by association of dinuclear $\{[Rh_2(O_2CCH_3)_2(bpy)_2]^+$ ions,[678] in which the rhodium atoms are bridged by two nearly eclipsed acetate ligands with a Rh–Rh distance of 2.666(2) Å. Unsupported Rh–Rh interactions between dinuclear entities display a distance of 2.833(2) Å. Similarly to $\{[Rh_2(O_2CCH_3)_2(phen)_2]PF_6\}_\infty$, the chelating bpy ligands on adjacent dirhodium units are in a *transoid* arrangement along the chain.

$\{[Rh_4(O_2CH)_4(bpy)_4]BF_4\}_\infty$. This infinite chain is formed by polymerization of tetranuclear linear $[Rh_4(O_2CH)_4(bpy)_2]^+$ units. It is the first metallic wire with the rhodium atoms in the +1.25 oxidation state.[358] The Rh–Rh distances of 2.678(3) and 2.733(4) Å are encountered in the tetranuclear fragment $[Rh_4(O_2CH)_4(bpy)_2]^+$, the shorter distance corresponding to the entity supported by the formato bridge. The molecular structure of $\{[Rh_4(O_2CH)_4(bpy)_4]BF_4\}_\infty$ is similar to those of $\{[Rh_2(O_2CCH_3)_2(bpy)_2]BF_4\}_\infty$ and $\{[Rh_2(O_2CCH_3)_2(phen)_2]PF_6\}_\infty$.

$\{Rh_2(O_2CCF_3)_4[Rh_2(\mu\text{-}O_2CCF_3)_2(CO)_4]_2\}_\infty$[50,310]

Although this remarkable compound is not a rhodium blue, it is included in this section because it consists of arrays of six rhodium atoms linked into infinite chains (Fig. 12.8); there is some degree of electron delocalization along the chain.[50] The Rh–Rh bond distance in $Rh_2(O_2CCF_3)_4$ is 2.412(1) Å, which is within the range of typical distances (2.35–2.45 Å) for tetracarboxylate

Pictiva EX2004
Samsung v Pictiva
IPR2024-01094

compounds (Table 12.2). The Rh–Rh distance of 2.960(1) Å for the $Rh_2(\mu\text{-}O_2CCF_3)_2(CO)_4$ unit is longer than that of 2.984(1) Å found for the dirhodium moieties in the infinite chain $\{[Rh_2(\mu\text{-}O_2CCF_3)_2(CO)_4]_2\}_\infty$,[310] a fact which suggests the absence of bonding interactions. The distance of 2.790(1) Å between a Rh atom of $Rh_2(O_2CCF_3)_4$ and a Rh atom of the neighboring $Rh_2(\mu\text{-}O_2CCF_3)_2(CO)_4$ unit is among the longest *ax* interactions known. Since each Rh atom of the $Rh_2(\mu\text{-}O_2CCF_3)_2(CO)_4$ moiety is essentially a square planar d^8 unit, it has the potential to act as a donor to an adjacent acceptor, which in this case is the Rh atom of a $Rh_2(O_2CCF_3)_4$ dimer. The entire repeat unit $\{[Rh_2(\mu\text{-}O_2CCF_3)_2(CO)_4][Rh_2(O_2CCF_3)_4][Rh_2(\mu\text{-}O_2CCF_3)_2(CO)_4]\}_\infty$ can be considered as being held together in the following manner: there is a Rh–Rh contact of 3.062(1) Å between two adjacent $Rh_2(\mu\text{-}O_2CCF_3)_2(CO)_4$ units,[50] which is shorter than that found between $Rh_2(\mu\text{-}O_2CCF_3)_2(CO)_4$ moieties in the chain $\{[Rh_2(\mu\text{-}O_2CCF_3)_2(CO)_4]_2\}_\infty$ (3.092(1) Å).[310] These findings give $\{Rh_2(O_2CCF_3)_4[Rh_2(\mu\text{-}O_2CCF_3)_2(CO)_4]_2\}_\infty$ unique features such as the electron delocalization along the chain.[50]

12.6. Reactions of Rh_2^{4+} Compounds

12.6.1 Oxidation to Rh_2^{5+} and Rh_2^{6+} species

Although the number of Rh_2^{5+} species that have been studied are far fewer than those with Rh_2^{4+} cores, the redox chemistry of Rh_2^{4+} compounds and their Rh_2^{5+} analogs has been the subject of considerable interest. The oxidation of complexes that contain the singly bonded Rh_2^{4+} core by one or two electrons gives rise to Rh_2^{5+} and Rh_2^{6+} species with ground state configurations $\sigma^2\pi^4\delta^2\delta^{*2}\pi^{*3}$ and $\sigma^2\pi^4\delta^2\delta^{*2}\pi^{*2}$ and bond orders of 1.5 and 2, respectively. The Rh_2^{5+} compounds that have been structurally characterized are listed in Table 12.9.

Table 12.9. Structural data for mixed valence Rh_2^{5+} compounds

Compound	*r* (Rh–Rh)[a] (Å)	*r* (Rh–L_{ax}) (Å)	Donor atom(s)	ref.
$[Rh_2(O_2CCH_3)_4(H_2O)_2]ClO_4\cdot H_2O$	2.315(2) 2.318(2)	2.22(1) 2.23(1)	O	693
$[Rh_2(O_2CC_2H_5)_4(PPr^i_3)_2]SbF_6$	2.510(1)	2.360(1)	P	285
$[Rh_2(O_2CC_2H_5)_4(PCy_3)_2]SbF_6\cdot 2CH_2Cl_2$	2.509(1)	2.375(1)	P	285
cis-(2,2)-$[Rh_2(HNCOCH_3)_4(H_2O)_2]ClO_4$	2.399(1)	2.281(2)	O	713
$[Rh_2(ClNCOCH_3)_4(H_2O)_2]ClO_4\cdot 2H_2O$	2.403(1)	2.250(9)	O	714
$[Rh_2(HNCOCH_3)_4(theophylline)_2]NO_3\cdot H_2O$	2.426(1) 2.428(1)	2.281(7) 2.294(7)	N	715
$\{[Rh_2(HNCOCH_3)_4](\mu_2\text{-}Cl)\}_\infty$	2.428(1)	2.581(1)	Cl	717
$\{[Rh_2(HNCOCH_3)_4](\mu_2\text{-}Cl)\cdot 7H_2O\}_\infty$	2.417(1)	2.564(1) 2.553(1)	Cl	716,717
cis-(2,2)-$[Rh_2(HNCOCH_3)_4(\mu_2\text{-}Br)]_\infty$	2.430(1)	2.684(1)	Br	716,717
cis-(2,2)-$\{[Rh_2(HNCOCH_3)_4](\mu_2\text{-}Br)\cdot 3H_2O\}_\infty$	2.427(1)	2.686(1) 2.674(1)	Br	717
cis-(2,2)-$\{[Rh_2(HNCOCH_3)_4](\mu_2\text{-}I)]\}_\infty$	2.442(1)	2.859(1)	I	717
cis-(2,2)-$[Rh_2(HNCOCH_3)_4(py)_2]BF_4$	2.434(1)	2.215(6)	N	719
trans-(2,2)-$[Rh_2(mhp)_4]SbCl_6\cdot 2C_2H_4Cl_2$	2.359(1)	[b]	[b]	720
(3,1)-$[Rh_2(mhq)_4(py)]PF_6\cdot 2C_2H_4Cl_2$	2.402(1)	2.111(7)	N	404
(3,1)-$[Rh_2(hq)_4(py)]SbCl_6\cdot CH_2Cl_2$	2.383[c]	2.103[c]	N	404
(3,1)-$[Rh_2(hq)_4(py)]PF_6$	2.403[c]	2.120[c]	N	404
(3,1)-$[Rh_2(hq)_4(py)]PF_6\cdot C_6H_4Cl_2$	2.396[c]	2.116[c]	N	404

Pictiva EX2004
Samsung v Pictiva
IPR2024-01094

Compound	r (Rh–Rh)[a] (Å)	r (Rh–L_{ax}) (Å)	Donor atom(s)	ref.
(3,1)-$[Rh_2(hq)_4(py)]CF_3SO_3\cdot 2C_2H_4Cl_2$	2.396(1)	2.097(4)	N	404
$[Rh_2(DPhF)_4(NCCH_3)]ClO_4$	2.466(1)	2.074(6)	N	444
$[Rh_2(DTolF)_4]ClO_4$	2.447(1)	[b]	[b]	285
$[Rh_2(DTolF)_4(H_2O)]O_2CCF_3$	2.452(2)	2.165(2)	O	722
$[Rh_2(DTolF)_4][C(CN)_3]$	2.463(4)	2.07(3)	N	468
$Rh_2(DTolF)_3(\eta^2\text{-}NO_3)_2$	2.485(1)	2.09(1) 2.38(1)	O	460
cis-$[Rh_2(DTolF)_2(\mu\text{-}O_2CCF_3)_2(O_2CCF_3)(AgO_2CCF_3)_2]_2$[d]	2.448(2)	2.20(1) 2.24(2)	O	723
$[Rh_2(DAniF)_4Cl]\cdot CHCl_3$	2.467(1)	2.400(2)	Cl	500
(4,0)-$Rh_2(ap)_4Cl$	2.406(1)	2.421(3)	Cl	493,494
(4,0)-$[Rh_2(ap)_4(C{\equiv}CH)]\cdot CH_2Cl_2$	2.439(1)	2.02(1)	C	730
(4,0)-$[(ap)_4Rh_2(C{\equiv}C)_2Si(CH_3)_3]\cdot \frac{1}{2}C_6H_{14}$	2.443(1)	2.028(7)	C	475
$(ap)_4Rh_2(C{\equiv}C)_2Rh_2(ap)_4$	[e]	[e]	C	475
(4,0)-$[Rh_2(2\text{-}Fap)_4Cl]\cdot 2CH_2Cl_2$	2.413(1)	2.431(3)	Cl	732
(4,0)-$[Rh_2(2,6\text{-}F_2ap)_4Cl]\cdot 2CH_2Cl_2$	2.416(1)	2.465(2)	Cl	732
(4,0)-$Rh_2(2,4,6\text{-}F_3ap)_4(C{\equiv}C)_2Si(CH_3)_3$	2.460(1)	2.00(1)	C	732
(3,1)-$[Rh_2(2,6\text{-}F_2ap)_4Cl]\cdot 2CH_2Cl_2$	2.420(1)	2.445(1)	Cl	732
(3,1)-$[Rh_2(F_5ap)_4Cl]\cdot 2CH_2Cl_2$	2.415(1)	2.438(1)	Cl	732
(3,1)-$[Rh_2(2,6\text{-}F_2ap)_4CN]\cdot 2CH_2Cl_2$	2.447(1)	2.031(5)	C	732

[a] Distances are given with up to 3 decimal digits.
[b] No *ax* ligand.
[c] Esds not reported.
[d] '*Dimer of dimers*' axially linked by CF_3CO_2 anions.
[e] No bond lengths determined due to disorder.

An early study describes the electrochemical oxidation of $Rh_2(O_2CCH_3)_4$ to the stable cation $[Rh_2(O_2CCH_3)_4]^+$;[679] the electron self-exchange rate constant of $[Rh_2(O_2CCH_3)_4(D_2O)_2]^{0/+}$ in aqueous media has been determined.[680] Chemical oxidation of $Rh_2(O_2CCH_3)_4$ with Br_2 and conc. HNO_3 affords $Rh_2(O_2CCH_3)_4Br$ and $Rh_2(O_2CCH_3)_4NO_3$, respectively.[681,682] Various electron-transfer reactions involving the $[Rh_2(O_2CCH_3)_4]^{+/0}$ couple have been performed in aqueous[683-686] and acetonitrile[687] solutions. Electrolytically generated solutions of the paramagnetic Rh_2^{5+} carboxylate species with various R groups have been the subject of detailed analyses by EPR, electronic absorption and Raman spectroscopies.[688-690]

Chemical oxidation of $Rh_2(O_2CCH_3)_4$ with Ce(IV) followed by elution of the crude product from cation exchange resins with 2 M $HClO_4$ leads to isolation[691,692] of $[Rh_2(O_2CCH_3)_4(H_2O)_2]$-$ClO_4\cdot H_2O$, which has been the subject of single crystal X-ray studies.[693] The structure of the cation is very similar to that of $Rh_2(O_2CCH_3)_4(H_2O)_2$[223] (Fig. 12.1), with the exception of the Rh–Rh bond distance which is shorter by *c.* 0.07 Å compared to the neutral molecule. This is attributable to the loss of an electron from a π^* orbital upon oxidation; SCF-Xα-SW calculations have been performed to account for the observed difference.[694] The Rh–Rh distance of 2.315(2) Å in $[Rh_2(O_2CCH_3)_4(H_2O)_2]ClO_4$ is the shortest known distance between two rhodium atoms (Tables 12.1-12.9). The compound $[Rh_2(O_2CCH_3)_4(DMSO)_2]ClO_4$ with *O*-bound DMSO has been prepared and spectroscopically studied.[695]

Electrochemical studies on $Rh_2(O_2CR)_4L_2$ compounds indicate that the ease of the Rh_2^{4+} core oxidation depends on the nature of both the R group[696-698] and the *ax* ligands.[136,408,697,699-701] It has been nicely shown that a linear free energy relationship exists between the $E_{1/2}(ox)_1$ and

Pictiva EX2004
Samsung v Pictiva
IPR2024-01094

the Hammett constant σ of the R group.[696] The effect of the R group on the values of $E_{1/2}$(ox) can be assessed from the oxidation potentials +0.56 V, +0.65 V and +0.99 V vs Ag/AgCl of the monothiocarboxylate compounds $Rh_2(OSCR)_4(PPh_3)_2$, for R = CMe_3, CH_3 and Ph, respectively.[125] Likewise, oxidation of $Rh_2(O_2CR)_4$ becomes more difficult upon substitution of R = CH_3 with CF_3 (Table 12.10) due to the electron-withdrawing effect of the latter group.[696] In $Rh_2(O_2CCF_3)_4$, the strong electron-withdrawing $CF_3CO_2^-$ ligands lower the energy of the highest occupied molecular orbital (HOMO), which is directly related to the $E_{1/2}$(ox) of the solvated dirhodium species. In the same vein, an increased donating ability of the *ax* ligand or solvent renders the oxidation process more favorable; a range of *c.* 0.60 V is spanned by the potentials measured for $Rh_2(O_2CC_3H_7)_4$ with various oxygen, nitrogen, sulfur and phosphorus ligands.[696] In addition to exhibiting a single-electron oxidation, $Rh_2(O_2CR)_4$ complexes undergo an irreversible reduction to $[Rh_2(O_2CR)_4]^-$, a species which is not stable but is immediately reduced by one or more electrons to afford a stable mononuclear Rh(I) complex or a reduced dinuclear species.[696] EPR spectra have been obtained for both cation and anion radical species of tetracarboxylate compounds.[702,703] The Rh_2^{6+} compound formulated as $Rh_2(\mu\text{-}O_2CCH_3)_2(OH)_2(\eta^1\text{-}O_2CCH_3)_2(NH_3)_2$ has been spectroscopically characterized.[704] The half-wave oxidation and reduction potentials of the compounds formulated as $Rh_2(O_2CR)_2(bpy)_2(H_2O)_2$ bear a linear relationship to the dissociation constant of the parent RCO_2H acid.[705] The species $[Rh_2(PhCHOHCO_2)_2(phen)_2(H_2O)_2]^{2+}$ catalyzes the electrochemical reduction of CO_2.[706]

Table 12.10. Half wave potentials (V vs SCE) of various dirhodium compounds in CH_3CN

Compound	$E_{1/2}(ox)_1$	$E_{1/2}(ox)_2$	$E_{1/2}$(red)	ref.
$Rh_2(O_2CCH_3)_4$	+1.17			407
$Rh_2(O_2CCH_3)_4$	+1.3[a]			409
$Rh_2(O_2CCF_3)_4$	+1.8[a]			696
$Rh_2(\mu\text{-}O_2CCH_3)_3(\mu\text{-}HNCOCH_3)$	+0.91			407
$Rh_2(\mu\text{-}O_2CCH_3)_2(\mu\text{-}HNCOCH_3)_2$	+0.62			407
$Rh_2(\mu\text{-}O_2CCH_3)(\mu\text{-}HNCOCH_3)_3$	+0.37	+1.65		407
$Rh_2(HNCOCH_3)_4$	+0.15	+1.41		407
$Rh_2(HNCOCF_3)_4$	+1.09			709
$Rh_2(\mu\text{-}O_2CCH_3)_3(\mu\text{-}PhNCOCH_3)$	+1.13[a]			678
$Rh_2(\mu\text{-}O_2CCH_3)_2(\mu\text{-}PhNCOCH_3)_2$	+0.97[a]			678
$Rh_2(\mu\text{-}O_2CCH_3)(\mu\text{-}PhNCOCH_3)_3$	+0.76[a]	+1.75		678
$Rh_2(PhNCOCH_3)_4$	+0.55[a]	+1.65[a]		710
$Rh_2(PhNCOCH_3)_4$	+0.34	+1.54		710
$Rh_2(pyro)_4$	+0.15	+1.33		430
$Rh_2(vall)_4$	+0.04	+1.30		430
$Rh_2(cap)_4$	+0.011[b]		−0.84	1,712
$Rh_2(DPhF)_4$	+0.34[a]	+1.15[a]	−1.21[a]	444
$Rh_2(DPhBz)_4$	+0.23[a]	+1.24[a]	−1.58[a]	447
$Rh_2(DTolF)_4$	+0.25[a]	+1.06[a]	−1.33[a]	446
$Rh_2(DTolF)_4$	−0.23[c]	+0.58[c]	−1.81[c]	446
$Rh_2(DTolF)_2(O_2CCF_3)_2(H_2O)_2$	+0.52	+1.36		445
$Rh_2(DTolF)_2(O_2CCF_3)_2(H_2O)_2$	+0.76[a]	+1.44[a]		445

[a] In CH_2Cl_2.

[b] The potential was measured vs Ag/AgCl in CH_3CN and is reported on the SCE scale by subtracting 0.044 V.

[c] Half wave potentials (V vs ferrocenium/ferrocene couple) measured in CH_3CN.

Pictiva EX2004
Samsung v Pictiva
IPR2024-01094

Oxidation of $Rh_2(O_2CC_2H_5)_4(PR_3)_2$ (R = Cy, Pr^i) with ferrocenium hexafluoroantimonate affords $[Rh_2(O_2CC_2H_5)_4(PCy_3)_2]SbF_6$ and $[Rh_2(O_2CC_2H_5)_4(PPr^i_3)_2]SbF_6$, which have been structurally characterized.[285] Interestingly, the Rh–Rh bond distances are by 0.05 Å longer and the Rh–P distances are by 0.12 Å shorter than the respective ones in the corresponding neutral precursors (Tables 12.1 and 12.9). These changes were anticipated by Xα-SW calculations performed on $Rh_2(O_2CCH)_4(PH_3)_2$[301] and EPR studies on $Rh_2(O_2CR)_4(PY_3)_2$ (R = Et, CF_3; PY_3 = PPh_3, $P(OPh)_3$, and the cyclic phosphite $P(OCH_2)_3CEt$),[707] and were later confirmed by DFT calculations for $Rh_2(O_2CEt)_4(PR_3)_2$.[285] The results are attributed to removal upon oxidation of an electron from the Rh–Rh σ orbital, which is primarily responsible for the lengthening of the Rh–Rh bond and, which becomes the HOMO in dirhodium adducts with *ax* phosphine molecules due to the strong antibonding interaction with the phosphine σ-donor orbitals.[301] Raman spectra have been performed on oxidized dirhodium compounds with variable R groups and the ν_{RhRh} frequency for each case has been identified.[708]

The class of carboxamidate (12.5) compounds $Rh_2(O_2CR)_n(R'NCOR)_{4-n}$ (R = CH_3 or CF_3; R' = H or Ph; *n* = 0-3) exhibits rich electrochemical properties due to the increased electron density on the Rh(II) centers as *n* increases. In the case of $Rh_2(O_2CCH_3)_n(HNCOCH_3)_{4-n}$, the progressive replacement of acetate ligands results in a more accessible one-electron oxidation, and for *n* = 3 and 4, the appearance of a second one-electron oxidation (Table 12.10).[407,408] Both oxidations of $Rh_2(HNCOCH_3)_4$ are reversible in CH_3CN and occur at $E_{1/2}$ = +0.15 V and +1.41 V.[407] Similar reversible diffusion-controlled oxidations are observed in DMSO ($E_{1/2}$ = +0.31 V) and pyridine ($E_{1/2}$ = +0.080 V), but, in both solvents, the second oxidation is obscured by the oxidation limit of the solvent.[408] Similarly to $Rh_2(O_2CCH_3)_4$, the values of $E_{1/2}$(ox) for $Rh_2(O_2CCH_3)_n(HNCOCH_3)_{4-n}$ are markedly dependent on the presence of *ax* ligands.[408,423,424] As expected, the substitution of CH_3 for CF_3 in the acetamidate complexes results in the single-electron oxidation of $Rh_2(HNCOCF_3)_4$ being less accessible than that of $Rh_2(HNCOCH_3)_4$. In a variety of nonaqueous solvents, a one-electron oxidation of $Rh_2(HNCOCF_3)_4$ is observed at potentials between +0.91 V and +1.09 V vs SCE.[709] The mixed acetate/*N*-phenylacetamidate complexes $Rh_2(O_2CCH_3)_n(PhNCOCH_3)_{4-n}$, *n* = 0-3, have been studied by cyclic voltammetry and, similarly to their acetate/acetamidate analogs, they show a steady decrease in the $E_{1/2}$(ox) values as the number of *N*-phenylacetamidate ligands increases;[409] for *n* = 0, 1, the compounds exhibit two reversible one-electron oxidation steps (Table 12.10).[710] The oxidation potential of the caprolactamate (cap; anion of 1-aza-2-cycloheptanone) complex $Rh_2(cap)_4$[711] is the least positive among all the carboxamidates (Table 12.10), thus $Rh_2(cap)_4$ is the most electron-rich member of the dirhodium carboxamidate series.[1,712]

Due to the low oxidation potential of $Rh_2(HNCOCH_3)_4$, it can be easily oxidized with 30-35% H_2O_2, in the presence of small amounts of $HClO_4$ or HNO_3, to afford $[Rh_2(HNCOCH_3)_4(H_2O)_2]ClO_4$.[713] The structural determination of $[Rh_2(HNCOCH_3)_4(H_2O)_2]$-$ClO_4$ revealed the preferred *cis*-(2,2) arrangement (Fig. 12.20a) and a Rh–Rh bond distance of 2.399(1) Å.[713] This distance is longer by 0.08 Å than the Rh–Rh distance of the Rh_2^{5+} tetraacetate adduct $[Rh_2(O_2CCH_3)_4(H_2O)_2]ClO_4$[693] and shorter by 0.016 Å than the Rh–Rh distance of the Rh_2^{4+} precursor *cis*-(2,2)-$[Rh_2(HNCOCH_3)_4(H_2O)_2]$.[414] The longer Rh–Rh bond distance compared to the tetraacetate adduct is attributed to steric factors,[713] whereas the shorter Rh–Rh distance compared to its neutral Rh_2^{4+} precursor is expected due to the higher bond order of $[Rh_2(HNCOCH_3)_4(H_2O)_2]ClO_4$. The crystal structure determination of the chlorinated analog $[Rh_2(ClNCOCH_3)_4(H_2O)_2]ClO_4$ reveals a similar *cis*-(2,2) arrangement to $[Rh_2(HNCOCH_3)_4$-$(H_2O)_2]ClO_4$ and essentially identical Rh–Rh bond distances (2.40 Å).[714] Oxidation of the reaction product between $Rh_2(HNCOCH_3)_4$ and theophylline with HNO_3 affords the reddish-

Pictiva EX2004
Samsung v Pictiva
IPR2024-01094

violet mixed-valence paramagnetic compound $[Rh_2(HNCOCH_3)_4(theophylline)_2]NO_3$ which has been structurally characterized (Section 12.7.3).[715]

The $[Rh_2(HNCOCH_3)_4]^+$ units have been successfully linked by bridging halide ions to form a series of infinite zig-zag chains of general formulae $\{[Rh_2(HNCOCH_3)_4](\mu_2\text{-}X)\}_\infty$ (X = Cl, Br, I), which have been structurally characterized (Fig. 12.36).[716,717] These infinite chains are mutually parallel in the crystal and represent the first such example of paddlewheel-type Rh_2^{5+} compounds. The chains are supported by hydrogen bonds between the NH and O groups of adjacent acetamidate bridging groups and occasionally by interstitial water molecules. The increase in the Rh–Rh bond length from the chloride to the iodide bridged complex (Table 12.9) is in accordance with the increasing σ-donating ability of the *ax* halide ions, Cl < Br < I.[717] The Rh–Rh bond distances (2.427(1)-2.442(1) Å) in $\{[Rh_2(HNCOCH_3)_4](\mu_2\text{-}X)\}_\infty$ (X = Cl, Br, I) are longer than that in $[Rh_2(HNCOCH_3)_4(H_2O)_2]^+$ (2.399 Å). The magnetic interactions along the chains of these compounds have been studied.[716-718] Polymeric complexes of acetamidate dimers linked by bidentate ligands have been prepared and magnetic measurements of their Rh_2^{5+} analogs have been reported.[719]

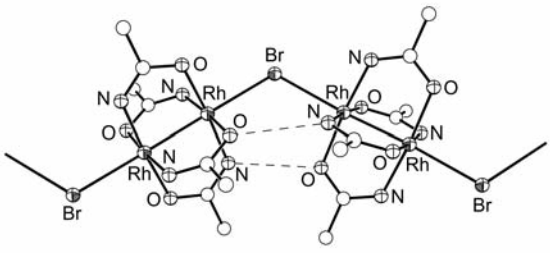


Fig. 12.36. The structure of the infinite zig-zag chain $\{[Rh_2(\mu\text{-}HNCOCH_3)_4](\mu_2\text{-}Br)\}_\infty$.

The crystal structure determination of the paramagnetic compound *trans*-(2,2)-$[Rh_2(mhp)_4]$-$SbCl_6{\cdot}2C_2H_4Cl_2$ revealed overlap of the neighboring aromatic rings and a Rh–Rh bond distance of 2.359(1) Å, [720] which is essentially the same as that of the neutral precursor[396,397] (Table 12.3). The lack of change in the Rh–Rh bond distance in the oxidized species is attributed to the fact that the antibonding character of the δ*(Rh–Rh*) orbital, from which the electron is removed, is not always sufficient to overcome the increased repulsion caused by the increase of the positive charge of the metal atoms.[720] The non-systematic changes of the Rh–Rh bond lengths among the different salts of the (3,1)-$[Rh_2(hq)_4(py)]^+$ ion (Table 12.9), which also has a δ*(Rh–Rh*) HOMO orbital compared to the neutral precursor, are accounted for by the foregoing argument.[404]

In contrast to dirhodium compounds supported by carboxylate ligands, which undergo only a single oxidation, complexes supported by tetraamidinate bridging groups (**12.7**) primarily undergo two metal centered one-electron oxidations. The latter correspond to stepwise removal of electrons from the δ*(Rh–Rh*) orbital (HOMO),[442,721] owing to the presence of the more basic amidinate groups which make the compounds more electron-rich. The electrochemical properties of $Rh_2(DArF)_4$ (DArF = DPhF, DTolF), $Rh_2(DPhBz)_4$ and the EPR spectra of the corresponding paramagnetic cations have been studied.[444,446,447] The previous compounds display reduction processes to Rh_2^{3+} species by addition of an electron to the σ*(Rh–Rh) orbital (LUMO)[444,446,447] but, in the case of $Rh_2(DTolF)_4$, the reduction process is irreversible.[446] A systematic study of the series $Rh_2(ArNCHNAr)_4$, (Ar = XC_6H_4, X = *p*-OMe, *p*-Me, H, *m*-OMe, *p*-Cl, *m*-Cl, *m*-CF_3, *p*-CF_3, or Ar = 3,4-$Cl_2C_6H_3$) revealed that the electrode potentials of the

Pictiva EX2004
Samsung v Pictiva
IPR2024-01094

compounds are linearly related to the Hammett constant σ of X and that both the $E_{1/2}$(ox) and $E_{1/2}$(red) potentials become more positive as the electron-withdrawing ability of the aryl substituent increases.[442] Therefore, electron-withdrawing and electron-donating substituents facilitate the corresponding reduction and oxidation processes occurring at the dirhodium core.[442] In contrast to $Rh_2(DPhF)_4$, which exhibits a single reduction at $E_{1/2}$ = -1.21 V (vs SCE) in CH_3CN, $Rh_2(DPhF)_4(CNPh)$ and $(DPhF)_4Rh_2(CNPhNC)Rh_2(DPhF)_4$ do not exhibit a reduction within the negative potential limit of the solvent (–1.8 V). This result suggests that the LUMOs of the latter compounds are higher in energy than the LUMO of $Rh_2(DPhF)_4$; this is accounted for by the σ-donation of electron density from the *ax* ligands CNC_6H_5 and CNPhNC to the antibonding orbitals of the dimetal core.[475]

Bulk electrolysis of $Rh_2(DPhF)_4$ at +0.65 V in the presence of $Bu^t_4NClO_4$ affords $[Rh_2(DPhF)_4(NCCH_3)]ClO_4$ which has been structurally characterized.[444] The Rh–Rh bond length of 2.466(1) Å is slightly longer than the Rh–Rh bond in the neutral precursor $Rh_2(DPhF)_4(NCCH_3)$ (2.459(1) Å) and the complex $Rh_2(DPhF)_4$ with no *ax* ligands (2.457(1) Å). The Rh–Rh bond distances in $[Rh_2(DTolF)_4]ClO_4$[285] and $Rh_2(DAniF)_4Cl$[500] are longer by *c.* 0.015(1) Å compared to the Rh_2^{4+} precursors (Tables 12.4 and 12.9). Likewise, the Rh–Rh bond in $[Rh_2(DTolF)_4(H_2O)]O_2CCF_3$ (2.452(2) Å)[722] is longer than that in $Rh_2(DTolF)_4$ (2.434(1) Å) and $[Rh_2(DTolF)_4]ClO_4$ (2.447(1) Å) with no *ax* ligands. It may thus be inferred that, for compounds with formamidinate bridging groups, the Rh–Rh bonds of the oxidized species are lengthened compared to the neutral counterparts, although changes of the Rh–Rh bond lengths are minimal with no apparent trend, when the electron is removed from a δ*(Rh–Rh*) orbital (HOMO).[285]

Correlations of the Rh–Rh bond distances of the Rh_2^{4+} precursors with that of the paramagnetic '*dimer of dimers*' *cis*-$[Rh_2(DTolF)_2(\mu\text{-}O_2CCF_3)_2(O_2CCF_3)(AgO_2CCF_3)_2]_2$ (2.448(2) Å),[723] can not be made due to the different *ax* ligands involved. The Rh–Rh distance in *cis*-$[Rh_2(DTolF)_2(\mu\text{-}O_2CCF_3)_2(O_2CCF_3)(AgO_2CCF_3)_2]_2$ is longer than that in *cis*-$Rh_2(DTolF)_2(O_2CCF_3)_2(H_2O)_2$ (2.425(1) Å), but shorter than that in *cis*-$Rh_2(DTolF)_2(O_2CCF_3)_2(NCCH_3)_2$ (2.474(5) Å). The single-electron oxidation of *cis*-$Rh_2(DTolF)_2(O_2CCF_3)_2(H_2O)_2$ affords the blue colored species $[Rh_2(DTolF)_2(O_2CCF_3)_2]^+$,[445] which has been isolated in the solid state as the paramagnetic complexes $[Rh_2(DTolF)_2(O_2CCF_3)_2(H_2O)_2]ClO_4$ and $Rh_2(DTolF)_2(O_2CCF_3)(NO_3)_2$.[723] Analytical data show that the oxidation of the Rh_2^{4+} precursor proceeds with elimination of a trifluoroacetate group, therefore $Rh_2(DTolF)_2(O_2CCF_3)(NO_3)_2$ most likely contains a bidentate nitrate group coordinated to each Rh center. Such a binding mode has been observed for the paramagnetic compound $Rh_2(DTolF)_3(\eta^2\text{-}NO_3)_2$ which has been structurally characterized.[460] The rather long Rh–Rh bond in $Rh_2(DTolF)_3(\eta^2\text{-}NO_3)_2$ (2.485(1) Å) is attributed to the reduced number of bridging ligands.[460] The second oxidation of *cis*-$Rh_2(DTolF)_2(O_2CCF_3)_2(H_2O)_2$ generates the Rh_2^{6+} species which is not stable, but undergoes changes that lead to further oxidizable products.[445] It is notable that the Rh_2^{4+}-porphyrin-based molecular boxes,[469,470] as well as the molecular triangle and square assembled from Rh_2^{4+} formamidinate units with oxalate linkers (Section 12.7.2), are multiredox systems with distinctly different electrochemical behavior depending on the structure of the compound, e.g., the second oxidation waves for the Rh_2 oxalate square and triangle are at 845 and 1125 mV, respectively.[13]

Reaction of $Rh_2(DTolF)_4$ with X = TCNE, TCNQ and DM-DCNQI proceeds via a single electron transfer from the dimetal unit to the cyano ligand to afford $Rh_2(DTolF)_4X$ which contains the $[Rh_2(DTolF)_4]^+$ cation radical and the cyano ligand as a radical anion.[468] Electrochemical and EPR measurements suggest a different extent of coordination between the polycyano fragment and the dirhodium unit, depending on the polarity of the solvents. Unexpectedly, for the TCNE complex, the tetracyanoethylenide ion is transformed to the tricyanomethanide

Pictiva EX2004
Samsung v Pictiva
IPR2024-01094

anion $[C(CN)_3]^-$, thus affording crystals of $[Rh_2(DTolF)_4][C(CN)_3]$, as shown by X-ray crystallography.[468]

The paramagnetic compound $Rh_2(DTolF)_4(C{\equiv}CC_5H_4N)$ has been synthesized and used as a starting material to prepare heterotrimetallic Rh/Re complexes with 4-ethynylpyridine as a bridging moiety;[724] the interactions between the Rh_2^{5+} and Re units, however, are weak as indicated by CV and EPR experiments.

The crystal structures and the redox properties of a number of Rh_2^{5+} complexes with the anilinopyridinate ligand **12.10** (ap) have been reported. The compound $Rh_2(ap)_4$ undergoes two accessible single-electron oxidations to the corresponding Rh_2^{5+} and Rh_2^{6+} species which have been spectroscopically characterized;[490-493] the latter dication is postulated to possess a Rh–Rh double bond.[491] The symmetric isomer *trans*-(2,2)-$Rh_2(ap)_4$ undergoes two single-electron oxidation processes at $E_{1/2}$ = +0.01 and +0.64 V vs Ag/AgCl.[490] The Rh_2^{5+} compound (4,0)-$Rh_2(ap)_4Cl$, which has been crystallographically characterized,[493,494] is prepared by reaction of $Rh_2(O_2CCH_3)_4$ with molten 2-anilinopyridine followed by dissolution in a CH_2Cl_2/CCl_4 mixture and separation on a silica gel column. The chloride ion source appears to be the solvent.[493] It has been reported that $Rh_2(ap)_4Cl$ can be prepared by refluxing $RhCl_3{\cdot}3H_2O$ and ap in anhydrous EtOH.[725] The compound $Rh_2(ap)_4Cl$ is reversibly reduced by one electron at -0.38 V and reversibly oxidized at +0.52 V vs SCE in CH_2Cl_2. The singly oxidized form of $Rh_2(ap)_4$ and the cation of $Rh_2(ap)_4Cl$ exhibit different UV and EPR spectra and therefore different distributions of the odd-electron density; the EPR spectra of $Rh_2(ap)_4$ and $Rh_2(ap)_4Cl$ are consistent with a singly occupied molecular orbital (SOMO) being equally distributed on both Rh atoms in the former complex and localized on one rhodium atom in the latter, respectively.[493] The (4,0)[726,727] and *trans*-(2,2)[727,728] isomers of $Rh_2(ap)_4$ react rapidly with dioxygen to form the stable superoxide complex $Rh_2(ap)_4(O_2)$ wherein molecular oxygen is axially bound to the dirhodium unit. Moreover, the compound $Rh_2(ap)_4Cl$ reduces dioxygen on a pure carbon paste electrode generating H_2O_2, which can be accurately measured.[729] The reaction of NaR or LiR (R = $C{\equiv}CH^-$, $C{\equiv}CPh^-$, $C{\equiv}CC_5H_{11}^-$ or $C{\equiv}C(CH_2)_4C{\equiv}CH^-$) with the chloride complex $Rh_2(ap)_4Cl$ in THF affords the paramagnetic compounds $Rh_2(ap)_4R$ with Rh–C σ-bonds.[730] These complexes have been characterized by EPR, infrared, electronic absorption and mass spectroscopies and, in the case of $Rh_2(ap)_4(C{\equiv}CH)$, by X-ray crystallography.[730] The increase in the Rh–Rh bond distance from 2.406(1) Å in $Rh_2(ap)_4Cl$ to 2.439(1) Å in $Rh_2(ap)_4(C{\equiv}CH)$ reflects the strong electron-donating properties of $C{\equiv}CH^-$. Electrochemical studies have shown that both the $E_{1/2}$(ox) and $E_{1/2}$(red) values for $Rh_2(ap)_4R$ are shifted cathodically from the potentials of the parent compound $Rh_2(ap)_4Cl$; the second oxidations are observed at *c.* +1.0 V. These changes reflect an increase in the electron density of the $Rh(N_{aniline})_4$ atom upon *ax* binding of the group R.[730] Disproportionation of $Rh_2(ap)_4X$ (X = Cl, Br), in the presence of acids, affords protonated Rh_2^{2+} dimers.[731]

A series of Rh_2^{5+} compounds of the type Rh_2L_4Cl (L: (2-fluoroanilino)pyridinate: 2-Fap; (2,6-difluoroanilino)pyridinate: 2,6-F_2ap; (2,4,6-trifluoroanilino)pyridinate: 2,4,6-F_3ap; (2,3,4,5,6-pentafluoroanilino)pyridinate: F_5ap) have been reported.[732] The compound Rh_2(2-Fap)$_4Cl$ exists only as the (4,0) isomer, whereas Rh_2(2,6-F_2ap)$_4Cl$, Rh_2(2,4,6-F_3ap)Cl and $Rh_2(F_5ap)_4Cl$ exist as both (4,0) and (3,1) isomers with a preference for the (3,1) structure. The EPR and magnetic data indicate that the SOMO is a δ*(Rh–Rh*) orbital and that the electronic configuration of these compounds is $\sigma^2\pi^4\delta^2\pi^{*4}\delta^{*1}$.[732] The compounds with 2,6-F_2ap and 2,4,6-F_3ap ligands undergo one reversible single-electron reduction and two reversible single-electron oxidations. The electronic effect of the substituents for these compounds can be quantified by a linear relationship between the $E_{1/2}$ values and the Hammett parameter σ of the bridging ligand substituents.[732] The preparation, electrochemistry and spectroscopic

Pictiva EX2004
Samsung v Pictiva
IPR2024-01094

properties of $(ap)_4Rh_2(C{\equiv}C)_2Si(CH_3)_3$ and $(ap)_4Rh_2(C{\equiv}C)_2Rh_2(ap)_4$ have been reported, and the structure of $(ap)_4Rh_2(C{\equiv}C)_2Si(CH_3)_3$ has been determined.[475] Both compounds exhibit redox processes associated with reduction to the species with Rh_2^{4+} units and oxidation to the species with Rh_2^{6+} units. For $(ap)_4Rh_2(C{\equiv}C)_2Rh_2(ap)_4$, the two reduction processes are separated by 130 mV, which is an indication of electronic interaction between the dirhodium units.[475]

Oxidation of $Na_4[Rh_2(SO_4)_4(H_2O)_2]{\cdot}5H_2O$ with Ce(IV) in sulfuric acid followed by cation exchange leads to the paramagnetic compounds $M_3[Rh_2(SO_4)_4(H_2O)]{\cdot}nH_2O$ (M = K, n = 3; M = Cs, n = 1), which have been studied by EPR and electronic spectroscopies.[733] Likewise, oxidation of $Na_4[Rh_2(CO_3)_4(H_2O)_2]{\cdot}4H_2O$ in acetonitrile with $(NH_4)_2[Ce(NO_3)_6]$ has been purported to afford $Na_3[Rh_2(CO_3)_4(H_2O)_2]{\cdot}2H_2O$.[366]

12.6.2 Cleavage of the Rh–Rh bond

A wide range of reagents and reaction conditions can lead to cleavage of the Rh–Rh bond. Reaction of $Rh_2(O_2CCH_3)_4$ with $ArSO_2H$ affords Rh_2^{6+} compounds,[734] whereas the hydrohalic acids HCl and HBr, as gases or in acetone or ethanol solutions, induce decomposition of $Rh_2(O_2CCH_3)_4$ to RhX_3 (X = Cl, Br) and rhodium metal.[735,736] Dirhodium tetraacetate is stable towards O_2, but is converted by O_3 to the $[Rh_3(\mu_3\text{-}O)(\mu\text{-}O_2CCH_3)_6(H_2O)_3]^+$ ion.[737,738] As stated in Section 12.4.1, reaction of $Rh_2^{4+}(aq)$ with O_2 in a 2-3 M $HClO_4$ solution is postulated to produce the purple paramagnetic superoxo complex $[Rh_2(O_2^-)(OH)_2(H_2O)_n]^{3+}$.[593,594] Reactions of $[Rh_2(H_2O)_{10}]^{4+}$ in the presence of Cl^-, Br^- or I^- ions lead to formation of Rh metal.[739] Carbon monoxide forms a labile adduct with $Rh_2(O_2CCH_3)_4$, which is isolated only at low temperatures,[261] whereas $Rh_6(CO)_{16}$ is formed at very high pressures of CO (300 atm) in C_4H_9OH above 120 °C.[262] Phosphines and phosphites readily react with dirhodium compounds to form products other than merely *ax* adducts. Thus, PPh_3 reacts with a solution of $Rh_2(O_2CCH_3)_4$ in MeOH/HBF_4 to afford $Rh(PPh_3)_3BF_4$[31,291] and reaction with excess of the bicyclic phosphite 4-ethyl-2,6,7-trioxa-1-phosphabicyclo[2.2.2]octane results in production of a mononuclear Rh(I) species.[281] Accordingly, reactions of $Rh_2(O_2CCF_3)_4$ with PMe_2Ph, PPh_3 and $P(OMe)_3$ lead to cleavage of the Rh–Rh bond and production of mononuclear Rh(I) and Rh(III) compounds.[142,290] In the presence of PMe_3, interaction between dialkyl- or diarylmagnesium and $Rh_2(O_2CCH_3)_4$ affords mononuclear Rh(I) compounds.[740,741] Reaction of *cis*-$[Rh_2(O_2CCH_3)_2(NCCH_3)_6](BF_4)_2$ with PCy_3 leads to cleavage of the Rh–Rh bond and formation of $[Rh(CH_3CN)_2(PCy_3)_2]BF_4$,[742] whereas reaction of $[Rh_2(NCCH_3)_{10}](BF_4)_4$ with (diphenylphosphino)tetrathiafulvalene affords mononuclear Rh(I) compounds.[743] Reaction of $Rh_2(O_2CCH_3)_4$ with dppm in the presence of Me_3SiCl affords $RhCl_3(dppm)(NCCH_3)$ in low yield[744] (the main product is $Rh_2(\mu\text{-}dppm)_2Cl_4$; Section 12.3.5).[507] Electrolysis of $Rh_2(HNCOCH_3)_4(SbPh_3)_2$ in CH_2Cl_2, in the presence of excess $SbPh_3$, produces the monomeric Rh(III) compound $Rh(Ph)(SbPh_3)_2Cl_2(NCCH_3)$.[745]

12.7 Applications of Dirhodium Compounds

12.7.1 Catalysis

Dirhodium tetracarboxylate compounds catalyze many reactions including asymmetric cyclopropanation and cyclopropenation, carbon–hydrogen insertion and carbenoid initiated C–C bond formation.[1-5] The catalytically active dirhodium compounds bearing orthometalated phosphine and homochiral carboxamidate groups that have been structurally characterized are listed in Tables 12.2 and 12.3, respectively. Further coverage of this topic is presented in Chapter 13.

Pictiva EX2004
Samsung v Pictiva
IPR2024-01094

12.7.2 Supramolecular arrays based on dirhodium building blocks

A pioneering contribution in promoting the assembly and dictating the main structural features of supramolecular arrays is the introduction of subunit precursors with Rh–Rh bonds linked by various *eq* and *ax* polyfunctional bridging groups such as polycarboxylate anions (**12.48-12.56**), polypyridyls (**12.57-12.58**), and polynitriles (**12.59-12.60**).[13,15] The precursors of choice have been Rh_2(*cis*-formamidinate)$_2^{2+}$ moieties (typically DAniF; **12.7**) with two *cisoid*, non-labile formamidinate anions. The dirhodium core with dicarboxylic acids has also been successfully employed as a substitutionally inert corner piece.[111,114] The remaining *eq* positions are typically occupied by labile ligands such as carboxylate or acetonitrile groups which are easily replaced by polyfunctional linkers (e.g., dicarboxylates). The strong *ax* interactions that the Rh_2^{4+} units usually engage in, renders them suitable candidates for linking by means of *eq* and *ax* connectors. This combination of both types of linking modes (Fig. 12.37) allows the formation of 1- and 2D molecular tubes, loops, squares, triangles, helices and other supramolecular arrays.[13,15] The judicious choice of both *eq* and *ax* elements provides fine control over the nature and degree of interaction between adjacent dimetal units and an enormous diversity in the emerging structures. The resulting oligomers and networks are neutral rather than highly charged species that retain their structural integrity upon oxidation in a controlled fashion. A wide variety of organic ligands may be used to vary the electrochemical behavior, solubility as well as the magnetic and spectroscopic properties. The supramolecular arrays function as hosts for medium size guest molecules, and the sizes of the pores, interstices and channels can be tuned to serve as sequestration and separation reagents. The dirhodium building blocks and the emerging supramolecular arrays that have been crystallographically determined are listed in Tables 12.1, 12.4 and 12.5.

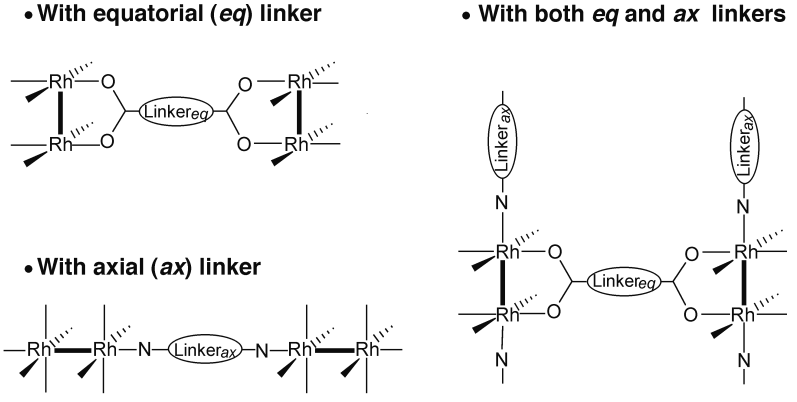


Fig. 12.37. Three basic modes of assembly of dirhodium units.

An example of a neutral Rh_2^{4+} molecular triangle is that of $[Rh_2(cis\text{-DAniF})_2(\mu_2\text{-}C_2O_4)]_3$ (Fig. 12.38).[478] The molecular triangle is formed exclusively by using 1 equiv of the oxalate anion **12.48** per equiv of $[Rh_2(cis\text{-DAniF})_2(NCCH_3)_4](BF_4)_2$, whereas the use of an excess of oxalate anions leads exclusively to the molecular square $[Rh_2(cis\text{-DAniF})_2(\mu_2\text{-}C_2O_4)]_4$[13,478] (Fig. 12.39). The distinct electrochemical signatures of the square and the triangle (the second and third oxidation processes take place at much higher potentials for the triangle) have allowed the study of the equilibrium between these species in solution (see Section 12.6.1).[13] Among systems built from dimetal units, the present one is unique in that the same linker

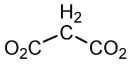
Pictiva EX2004
Samsung v Pictiva
IPR2024-01094

forms both a triangle and a square; the isolation of a particular structural motif is subject to kinetic as well as thermodynamic control. The square and the triangle have significantly different gel-permeation chromatography retention times and artificial mixtures of them have been successfully separated by this technique.[746] An interesting application of the redox properties of the square and the triangle is their use as potential switches to turn on and off their affinity for anions; in the oxidized (cationic) state, they could readily entrap suitably sized anions and in their reduced or neutral state, disgorge them.

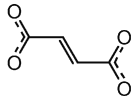
Equatorial Linkers



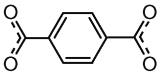
12.48



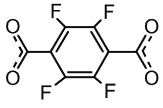
12.49



12.50



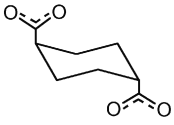
12.51



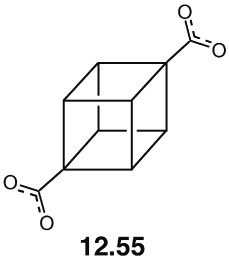
12.52



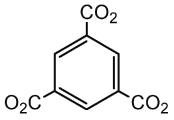
12.53



12.54

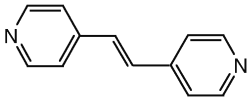


12.55

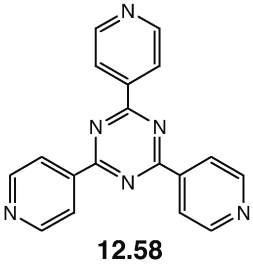


12.56

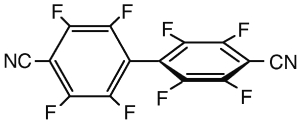
Axial Linkers



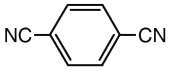
12.57



12.58



12.59



12.60

In contrast to the previous case where the formation of triangles or squares from the combination of $[Rh_2(cis\text{-}DAniF)_2]^{2+}$ units with oxalate anions depends on the reaction conditions,

Pictiva EX2004
Samsung v Pictiva
IPR2024-01094

only molecular triangles are formed when the orthometalated units $\{Rh_2[Ph_2P(C_6H_4)]_2\}^{2+}$ react with rigid linear dicarboxylate groups (e.g., *eq* linkers **12.48** and **12.51**).[564] This is partially due to the fact that the corner piece $\{Rh_2[Ph_2P(C_6H_4)]_2\}^{2+}$ has a preferred twist of *c.* 23° about the Rh–Rh bond (there is no inherent resistance to moderate twisting about the Rh–Rh axis, since there is only a net σ-bond), resulting in a very small strain in the triangular relative to the square structure; this allows the thermodynamic factor favoring the smaller ring (entropy) control the outcome of the reaction.[564] A number of these molecular triangles such as $\{Rh_2[Ph_2P(C_6H_4)]_2(\mu_2\text{-}C_2O_4)(py)_2\}_3$ (Fig. 12.40) have been structurally characterized (Table 12.5).[564,747]

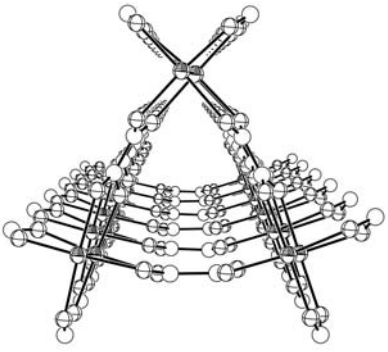


Fig. 12.38. Stacking arrangement for the Rh_2 molecular triangles $[Rh_2(cis\text{-}DAniF)_2(\mu_2\text{-}C_2O_4)]_3$.

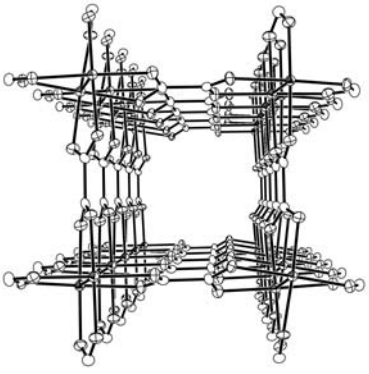


Fig. 12.39. Stacking arrangement for the Rh_2 molecular squares $[Rh_2(cis\text{-}DAniF)_2(\mu_2\text{-}C_2O_4)]_4$. The anisyl groups have been omitted for the sake of clarity.

Pictiva EX2004
Samsung v Pictiva
IPR2024-01094

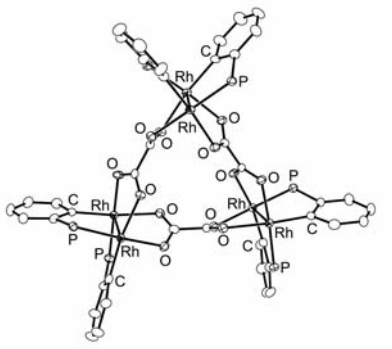


Fig. 12.40. The molecular triangle $\{Rh_2[Ph_2P(C_6H_4)]_2(\mu_2\text{-}C_2O_4)(py)_2\}_3$. The phenyl groups and the *ax* py ligands have been omitted for the sake of clarity.

A series of molecular squares of composition $[Rh_2(DAniF)_2(CH_3CN_{ax})_2(O_2CXCO_2)]_4$ (X = spacer group), have been prepared by reacting $[Rh_2(cis\text{-}DAniF)_2(NCCH_3)_4](BF_4)_2$ with each of the dicarboxylate linkers **12.49-12.55** in 1:1 ratio.[479,483] The molecular structure of the Rh_2 cubanedicarboxylate square is illustrated in Fig. 12.41. In all cases, the packing in the crystals creates infinite channels **12.61** that are capable of accommodating solvent molecules. Similar channels that can entrap small molecules are formed by molecular boxes with chelating dicarboxylate molecules capping the dirhodium units at the corners and substituted benzene-1,4-dicarboxylate side walls (Fig. 12.42).[111,114] A survey of the effect of the aromatic substituents on the basic box skeleton showed that substituents larger than the OH group cause distortion of the walls and an overall saddle-like distortion of the framework.[114]

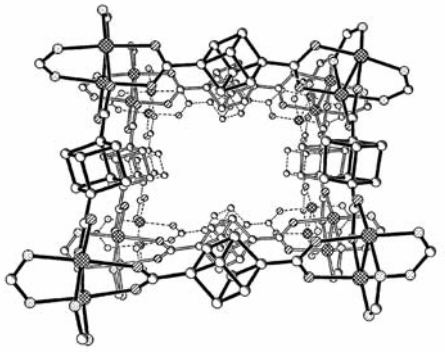
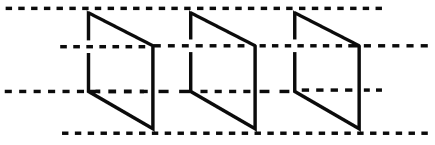


Fig. 12.41. Core of the Rh_2 cubanedicarboxylate square $\{[Rh_2(cis\text{-}DAniF)_2(CH_3CN_{ax})_2]$-(1,4-cubanedicarboxylate)$\}_4$. The anisyl groups and the *ax* ligands have been omitted for the sake of clarity.



12.61

Pictiva EX2004
Samsung v Pictiva
IPR2024-01094

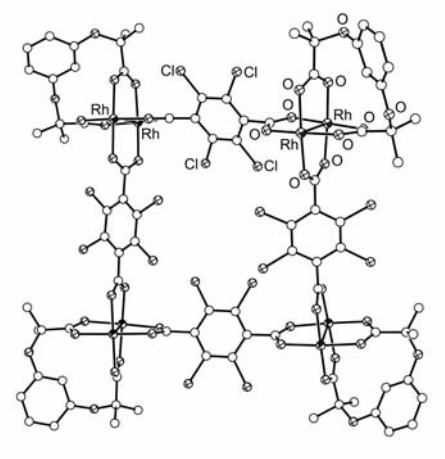


Fig. 12.42. The molecular square $\{Rh_2[O_2C(CH_3)_2OC_6H_4OC(CH_3)_2CO_2](\mu_2\text{-}O_2CC_6Cl_4CO_2)\}_4$.

A discrete molecular cage formulated as $\{[Rh_2(cis\text{-DAniF})_2]_6[\mu_3\text{-}C_6H_3(CO_2)_3]_4(CH_3CN_{ax})_{7.5}\}$ (Fig.12.43) has been assembled by reaction of 6 equiv of $Rh_2(cis\text{-DAniF})_2(NCCH_3)_4](BF_4)_2$ with 4 equiv of the anion of 1,3,5-tricarboxylatobenzene **12.56** (trimesic acid).[482] The ^1H NMR spectrum of the cage exhibits one resonance for all 12 aromatic protons on the four $C_6H_3(CO_2)_3^{3-}$ linkers and equivalent resonances for the 12 DAniF anions. The centers of the four six-membered rings define a tetrahedron, and the midpoints of the six Rh_2^{4+} units define an octahedron. The overall idealized symmetry is T_d and a well-ordered CH_2Cl_2 molecule is encapsulated in the center of the Rh_2 cage. Despite the propensity of dirhodium centers to bind *ax* ligands, only 2/3 of the *ax* sites are occupied by CH_3CN molecules due to steric crowding.[13,482]

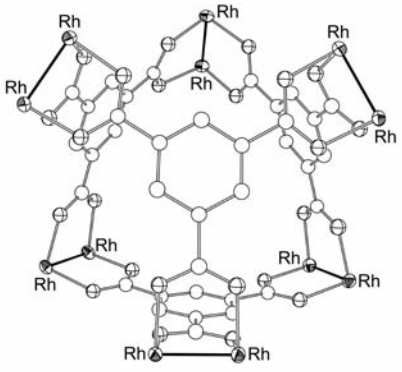
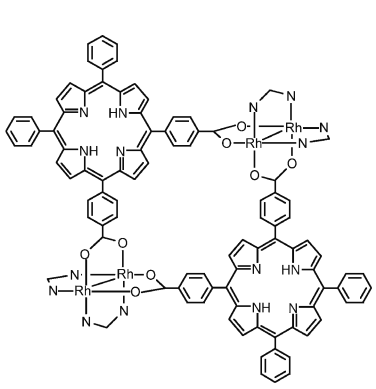


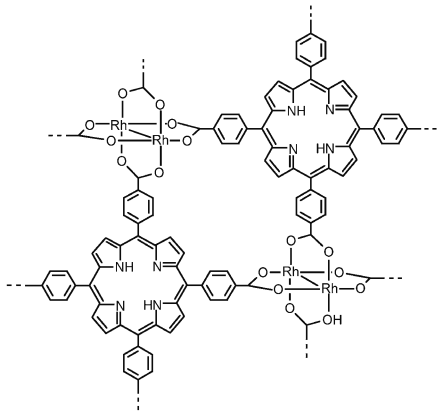
Fig. 12.43. The core of $\{[Rh_2(cis\text{-DAniF})_2]_6[\mu_3\text{-}C_6H_3(CO_2)_3]_4(CH_3CN_{ax})_{7.5}\}$.

Dirhodium-porphyrin-based molecular boxes exhibiting rich photochemical and redox properties have been prepared by reaction of $Rh_2(DTolF)_2(O_2CCF_3)_2$ with a variety of functionalized porphyrins.[469,470] Depending on the number and position of the peripheral pyridyl[469] or carboxylate[470] substituents, porphyrins can be employed as linear or angular connectors to form molecular boxes[470] **12.62** or 2-D layers **12.63** with high porosity,[748] but the compounds formed have not been structurally characterized.

Pictiva EX2004
Samsung v Pictiva
IPR2024-01094



12.62



12.63

In view of the affinity of Rh_2^{4+} units for *ax* ligands, the combination of *ax* and *eq* linkers has been employed to prepare extended 1-, 2- and 3-D arrays based on dirhodium building blocks. By using the Rh_2 molecular square $[Rh_2(cis\text{-}DAniF)_2(\mu_2\text{-}C_2O_4)]_4$ (Fig. 12.44a) with the *ax* linker **12.59**, the compound $\{[Rh_2(cis\text{-}DAniF)_2]_4(\mu_2\text{-}C_2O_4)_4(NCC_6F_4C_6F_4CN)_4\}_\infty$ is formed, exhibiting infinite tubes of square cross section and entrapped molecules of CH_2Cl_2 within the tube.[479] A portion of the extended structure is illustrated in Fig. 12.44b. When the *eq* linkers of the assembly units $Rh_2(cis\text{-}DAniF)_2^{2+}$ are changed from **12.48** (oxalate anion) to **12.49** (malonate anion), the molecular loop **12.64** is formed.[479] Reaction of loop **12.64** with the *ax* linker *trans*-1,2-bis(4-pyridyl)ethylene **12.57**, results in the formation of the 1-D tubular molecule $\{[Rh_2(cis\text{-}DAniF)_2]_2(\mu_2\text{-}O_2CCH_2CO_2)_2(NC_5H_4CHCHC_5H_4N)_2\}_\infty$ (**12.65**).[479] As can be observed from the schematic representation, the loops are related alternately by centers of inversion and two-fold axes in an overall linear structure and, interestingly, there are no guest molecules inside the tubes. Reaction of the loop **12.64** with the *ax* linker **12.59** affords another 1-D molecular tube $\{[Rh_2(cis\text{-}DAniF)_2]_2(\mu_2\text{-}O_2CCH_2CO_2)_2(NCC_6F_4C_6F_4CN)_2\}_\infty$ (**12.66**) with interstitial CH_2Cl_2 molecules located inside the tubes. Since the $[Rh_2(cis\text{-}DAniF)_2]_4(\mu_2\text{-}O_2CCH_2CO_2)]_2$ loop units impose significant steric demands, in the direction parallel to the metal-metal bond, only longer *ax* linkers that prevent the close approach of the bulky *p*-anisyl groups lead to formation of infinite columns. Shorter linkers such as 1,4-dicyanobenzene **12.60**, favor 2-D sheet-like structures **12.67**, which permit the C_6H_4OMe groups of the Rh_2^{4+} units to avoid steric interactions. As shown schematically, each rectangular sheet belongs to the 2-D group *Cmm*, which is the highest symmetry possible for such a case. Reaction of the loop **12.64** with the *ax* linker tri(4-pyridyl)triazine **12.58** in a stepwise fashion, by varying the stoichiometric ratio of the reactants, leads to construction of impressive self-assembled 3-D structures. When the reaction is performed in a 1:2 molar ratio of the Rh_2^{4+} loop unit to the linker **12.58**, a 1-D zig-zag molecular tunnel of composition $\{[Rh_2(cis\text{-}DAniF)_2]_2(\mu_2\text{-}O_2CCH_2CO_2)_2[C_3N_3(C_5H_4N)_3]_2\}_\infty$ (**12.68**) is formed, with no solvent molecules enclosed in the tunnel.[481] Reaction of the loop **12.64** with the *ax* linker tri(4-pyridyl)triazine **12.58** in a 3:4 molar ratio reveals that the additional loop is linking two zig-zag tunnels through the open nitrogen coordination sites of the triazine ligands to afford interpenetrating networks; the structure may be described as a collection of double helices formulated as $\{[Rh_2(cis\text{-}DAniF)_2]_2(\mu_2\text{-}O_2CCH_2CO_2)_2\}_3[C_3N_3(C_5H_4N)_3]_4\}_\infty$ (**12.69**), each with a pitch of *c.* 45° and surrounded by six other double helices.[13,15,481]

Pictiva EX2004
Samsung v Pictiva
IPR2024-01094

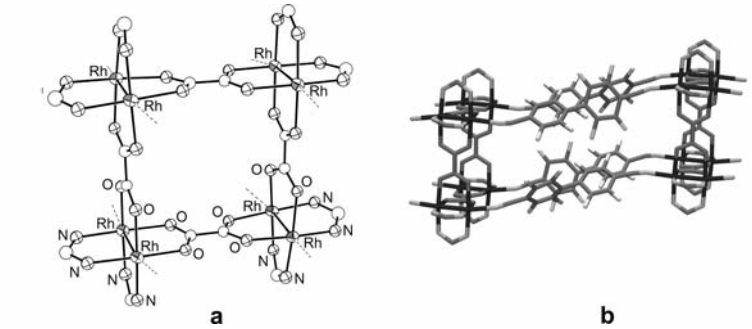
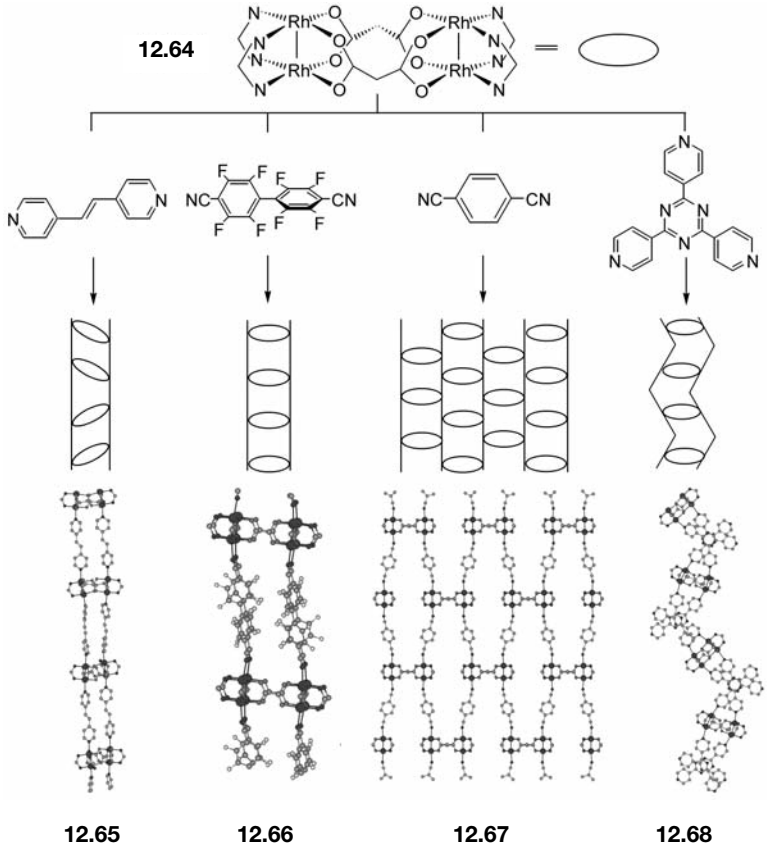


Fig. 12.44. (a) Molecular square $[Rh_2(cis\text{-}DAniF)_2(\mu_2\text{-}C_2O_4)]_4$ and (b) portion of the extended structure of the infinite tubes $\{[Rh_2(cis\text{-}DAniF)_2]_4(\mu_2\text{-}C_2O_4)_4(NCC_6F_4C_6F_4CN)_4\}_\infty$. The anisyl groups and the entrapped molecules of CH_2Cl_2 within the tube have been omitted.



Pictiva EX2004
Samsung v Pictiva
IPR2024-01094



12.69

A cage complex $[\{NEt_4 \subset [cis\text{-}Rh_2(DAniF)_2L]_4[calix[4]arene(CO_2)_4]_2\}]BF_4$ (Fig. 12.45), that is capable of permanently encapsulating imprisoned guest molecules, is formed by capping four $[Rh_2(cis\text{-}DAniF)_2]_2^{2+}$ corner piece precursors with two anions of the toroidal or chalice-like calix[4]arenetetracarboxylate ligands through the eight carboxylate groups of the two ligands.[484] The dirhodium units serve as 'fasteners' that hold together the two bowls of the calixarenes. The resulting carceplex encapsulates tetraethylammonium ions rather selectively to afford a stable species that remains intact in solution, even under the conditions necessary for mass spectroscopy.

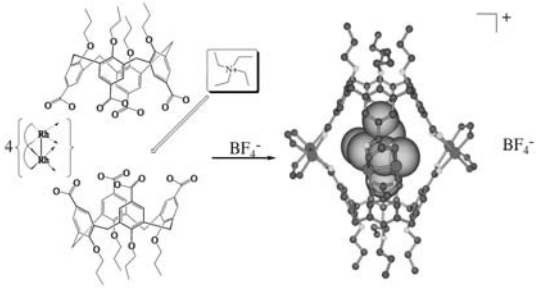


Fig. 12.45. Schematic drawing showing the formation of the carceplex $[\{NEt_4 \subset [cis\text{-}Rh_2(DAniF)_2L]_4[calix[4]arene(CO_2)_4]_2\}]BF_4$ (left) and the molecular structure (right). The NEt_4 ion is encapsulated in the cavity.

12.7.3 Biological applications of dirhodium compounds

The extraordinary success of *cis*-$Pt(NH_3)_2Cl_2$ (cisplatin) as a leading metal-based antitumor drug,[749-751] ushered to a new era in the development of other chemotherapeutic anticancer agents[752] with improved specificity, reduced toxicity and cell resistance. Among the promising non-platinum antitumor complexes are dirhodium compounds, a fact that has spawned a number of investigations of their biological effects upon encountering plausible cellular targets such as DNA, polymerases or other proteins.[753,754] Although their precise antitumor mechanism of action has not been elucidated, it has been demonstrated that dirhodium compounds, in a manner akin to that of cisplatin, bind to DNA[755-759] and inhibit DNA and protein synthesis.[177,760-764]

Pioneering studies that emanated in the 1970's showed that dirhodium carboxylate compounds $Rh_2(O_2CR)_4$ (R = Me, Et, Pr) exhibit significant *in vivo* antitumor activity against L1210 tumors,[765,766] Ehrlich ascites,[755,756,767-769] sarcoma 180 and P388 tumor lines.[770] It is notable that the antitumor activity increases in the series $Rh_2(O_2CR)_4$ (R = Me, Et, Pr) with the lipophilicity of the R group, but further lengthening of the carboxylate moiety beyond the pentanoate reduces the drugs' therapeutic efficacy;[756,766,767,771] this increase is independent of their

Pictiva EX2004
Samsung v Pictiva
IPR2024-01094

redox properties.[772] A small increase in effectiveness is achieved by modifications such as using the polyadenylic acid adduct of $Rh_2(O_2CC_2H_5)_4$ or $[Rh_2(O_2CC_2H_5)_4]^+$ instead of $Rh_2(O_2CC_2H_5)_4$ itself.[772,773] Moreover, dirhodium carboxylate compounds and their nitroimidazole adducts have been reported to increase the radiation sensitivity of hypoxic mammalian[774,775] and bacterial[776-778] cells *in vitro*.

A systematic variation of the *ax* and *eq* ligands on the dirhodium unit has provided valuable insight into the structure-activity relationships for this family of compounds. Substitution of the carboxylate ($pK_b = 9.25$) bridging groups of $Rh_2(O_2CCH_3)_4$ with trifluoroacetate ($pK_b > 13$) renders the dirhodium compound more reactive due to the greater lability and the strong electron withdrawing effect of the $CF_3CO_2^-$ groups. It has been reported that $Rh_2(O_2CCF_3)_4$and its adduct with sulfadiazine significantly increase the survival rate of mice bearing Ehrlich ascites cells and induce a higher mortality for these tumor cells *in vitro*.[779] When the basic trifluoroacetamidate bridging group CF_3CONH (**12.5**) is introduced into the dirhodium core, a 90% survival rate of the Ehrlich tumor-bearing population and an LD_{50} value of the same order as that of cisplatin to promote the same inhibitory effects on cell growth, are observed.[780,781] Cationic compounds of general formulae $[Rh_2(\mu\text{-}O_2CCH_3)_2(N\text{–}N)_2(H_2O)_2]^{2+}$ (N–N = 2,2' bipyridine (bpy) or 1,10 phenanthroline (phen)) exhibit anticancer activity against human oral carcinoma KB cell lines comparable to $Rh_2(O_2CCH_3)_4$[782] and, appreciable antibacterial activity.[783-786] Dirhodium compounds with tridentate oxygen-metalated methoxyphenylphosphine groups exhibit improved antitumor activity compared to dirhodium tetraacetate; the most active member of the series, $Rh_2(\mu\text{-}O_2CCH_3)_3[\mu\text{-}(o\text{-}OC_6H_4)P(o\text{-}OMeC_6H_4)_2](HOCCH_3)$,[568] exhibits higher antitumor activity than cisplatin against several cell lines.[543] The compound *cis*-$Rh_2(DTolF)_2(O_2CCF_3)_2(H_2O)_2$ with two robust formamidinate (**12.7**) and two labile trifluoroacetate bridging groups represents a favorable compromise between antitumor activity and toxic side-effects; it exhibits comparable antitumor activity to that of cisplatin against Yoshida ascites and T8 sarcomas with considerably reduced toxicity.[443] The homoleptic paddlewheel compound $Rh_2(DTolF)_4$, however, exhibits no appreciable biological activity,[787] presumably due to steric factors which preclude access of biological targets to *ax* and *eq* sites of the dirhodium core. Alternative strategies for improving dirhodium drug activity have paved the way to designing complexes with water soluble ligands such as carbohydrate and cyclophosphamide derivatives,[788,789] compounds with the dirhodium core attached to carrier ligands such as isonicotinic acid,[790,791] the substituted triazene Berenil,[169] metronidazole,[177] organic antimalarial drugs,[792] and cyclodextrin encapsulated compounds;[793,794] the latter offer a useful method for localized and controlled release of the drug with minimized side-effects.[795]

Human serum albumin (HSA) has been proposed as a pertinent transport protein for dirhodium carboxylate compounds[796,797] since it has been found to readily form adducts with the latter, most likely via the imidazole rings of the histidine residues.[798,799] The compound *cis*-$[Rh_2(\mu\text{-}O_2CCH_3)_2(bpy)_2(H_2O)_2](O_2CCH_3)_2$ also interacts with HSA and causes alterations to the secondary structure of the protein,[800] similarly to tetracarboxylate compounds.[796,798] The interactions of dirhodium compounds *vis-à-vis* several enzymes and sulfur-containing biomolecules have been explored owing to their biological relevance, but the conclusions have not been unequivocally established.[252,253,760,801-805]

Interactions with nucleobases, nucleos(t)ides and DNA

Nucleobases and nucleosides.[6] The reactions of dirhodium compounds with purine nucleobases (**12.70** and **12.71**) and nucleos(t)ides have received considerable attention because DNA is the primary target of most metal-based anticancer agents.[806] A perusal of the literature reveals that dirhodium compounds exhibit a strong preference for binding to adenine (**12.70**) compared

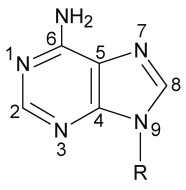
Pictiva EX2004
Samsung v Pictiva
IPR2024-01094

to guanine (**12.71**).[181,182,184,186,187,190-192,755,756,807-810] The immediate color change from green (or blue) to violet (or pink) upon replacing *ax* O donors with N donors attests to the interaction of dirhodium compounds with adenine and its derivatives. Binding of adenine bases predominantly takes place via *N7* and *N1* (**12.70**), which typically results in formation of polymeric bridged compounds of type **a** (Fig. 12.2);[182,184,190,807] in the cases of steric hindrance[182] or substitution of *N1*,[184] binding takes place via *N7* leading to adducts of type **12.11**.

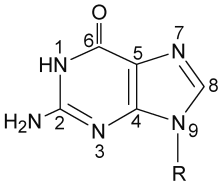
The crystal structure determinations of $Rh_2(O_2CCH_3)_4$(1-MeAdo)$_2$[184] and *trans*-[Rh_2(μ-$O_2CCH_3)_2$(μ-$HNCOCF_3)_2$(9-$MeAdeH_2)_2$]$(NO_3)_2$[411] indicate that preferential binding of adenine via *N7* may be attributed to intramolecular hydrogen bonds established between the exocyclic NH_2(6) amino group of the purine and the carboxylate oxygen atoms (**12.73**).[190,807] The argument is further supported by the fact that the guanine analog theophylline (**12.72**) binds axially to $Rh_2(O_2CCH_3)_4$ via *N9* to avoid electrostatic repulsion between the *06* exocyclic carbonyl group and the carboxylate oxygen atoms.[185] Conversely, in the case of [Rh_2($HNCOCH_3)_4$(theophylline)$_2$]NO_3,[715] theophylline binds via *N7* due to the favorable hydrogen bonding interactions between the theophylline site *06* and the NH hydrogen-donor group of the bridging acetamidate ligand. Similar favorable interactions have been established for dirhodium-acetamidate *ax* adducts of cytosine,[410] guanine (**12.71**) and its nucleosides,[411] as well as for the dirhodium adduct with the biologically relevant drug azathioprine.[188]

Electrostatic repulsion between the carboxylate oxygen atoms and the *06* exocyclic carbonyl group of guanine is responsible for its reduced reactivity towards $Rh_2(O_2CCH_3)_4$, a conclusion that is supported by the lack of perceptible color change upon $Rh_2(O_2CCH_3)_4$ reaction with guanine and its derivatives. This behavior led to early claims in the literature that dirhodium carboxylate compounds do not react with guanine and polyguanylic acids.[755,807] The issue was settled, however, with the crystal structural determinations of H-T *cis*-[Rh_2(μ-$O_2CCH_3)_2$(9-EtGua)$_2$(MeOH)$_2$],[393] (Fig. 12.46a), H-H *cis*-[Rh_2(μ-$O_2CCH_3)_2$(9-EtGuaH)$_2$(Me_2CO)(H_2O)]-$(BF_4)_2$[394] (Fig. 12.46b) and H-T *cis*-[Rh_2(μ-$O_2CCF_3)_2$(9-EtGuaH)$_2$(Me_2CO)$_2$]$(CF_3CO_2)_2$,[393] which revealed unprecedented bridging guanine groups that span the dirhodium unit via the *N7*/*06* sites in a *cis* disposition and H-H (**12.28**) or H-T (**12.29**) orientations. These crystal structures provided the first hard evidence for guanine *06* participation in binding to dimetal units. Notable features of H-T *cis*-[Rh_2(μ-$O_2CCH_3)_2$(9-EtGua)$_2$($MeOH)_2$] are the deprotonation of the purine site *N1*, i.e., the enolate form of guanine (9-$EtGua^-$) is stabilized[393] (**12.74**-**12.75**) and the substantial increase in the acidity of *N1–H* due to bidentate *N7*/*06* coordination (pH dependent ^1H and ^{13}C NMR titrations afford a pK_a value of *c.* 5.7 compared to 8.5 for *N7*-bound only and 9.5 for the unbound purine).[811] The importance of the *06*/*N1* guanine sites is obvious, given that they are involved in Watson-Crick hydrogen bonding in duplex DNA; alteration of these sites would lead to DNA base mispairing which bears directly on metal mutagenicity and cell death.[812] Bridging 9-EtGuaH and 9-EtAdeH groups, spanning the dirhodium unit in a similar fashion via *N7*/*06* (**12.71**) and *N7*/*N6* (**12.70**), respectively, have been observed in H-H *cis*-[Rh_2(DTolF)$_2$(9-EtGuaH)$_2$($NCCH_3$)]$(BF_4)_2$[462] and H-T *cis*-[Rh_2(DTolF)$_2$(9-EtAdeH)$_2$($NCCH_3$)]$(BF_4)_2$[461,462] (Fig. 12.47) wherein the dirhodium unit is supported by DTolF groups. In the case of H-T *cis*-[Rh_2(DTolF)$_2$(9-EtAdeH)$_2$($NCCH_3$)]$(BF_4)_2$, 9-EtAdeH (**12.76**) is present in the rare imino form **12.77**, as suggested by variable temperature ^1H NMR spectra.[461] The presence of the adenine imino form in DNA may lead to alteration of the base hydrogen bonding behavior and an increase in the acidity of *N1-H*, ultimately causing nucleobase mispairing and cell mutations.[812,813]

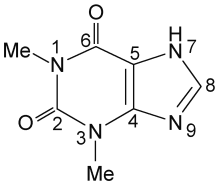
Pictiva EX2004
Samsung v Pictiva
IPR2024-01094



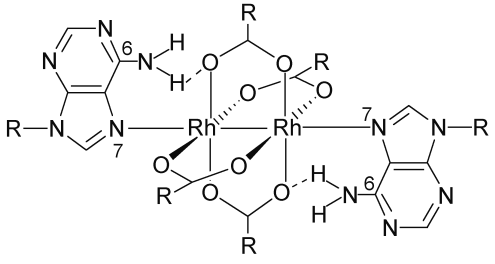
12.70



12.71



12.72



12.73

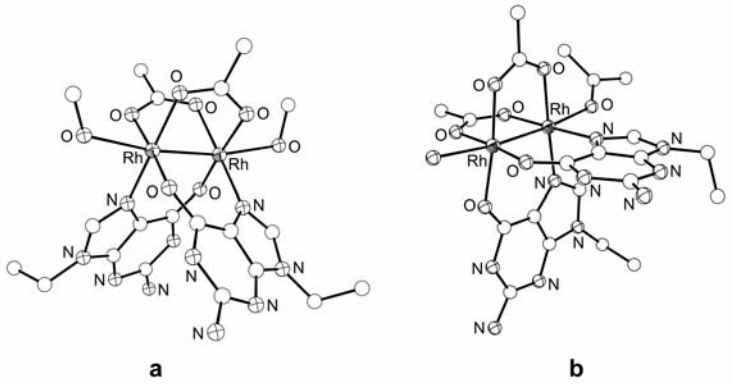
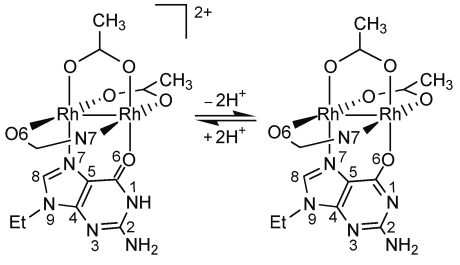
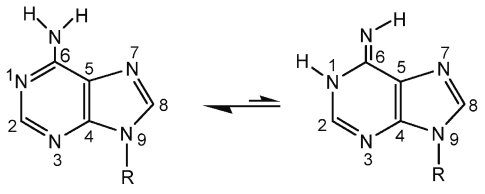


Fig. 12.46. The structures of (a) H-T *cis*-$[Rh_2(\mu\text{-}O_2CCH_3)_2(9\text{-EtGua})_2(MeOH)_2]$ and (b) the cation in H-H *cis*-$[Rh_2(\mu\text{-}O_2CCH_3)_2(9\text{-EtGuaH})_2(Me_2CO)(H_2O)](BF_4)_2$.



12.74 **12.75**

Pictiva EX2004
Samsung v Pictiva
IPR2024-01094



Amine form Imino form

12.76 **12.77**

The aforementioned crystal structures argue strongly for the prevalence of this *eq* bridging binding mode of guanine and adenine bases with dinuclear compounds. The crystal structure determination of *cis*-$[Rh_2(\mu\text{-}O_2CCH_3)_2(bpy)(9\text{-EtGuaH})(H_2O)_2(CH_3SO_4)]CH_3SO_4$ [395] revealed, however, that 9-EtGuaH may also bind in a monodentate fashion via *N*7 to a single rhodium center at an *eq* position, in the presence of a chelating agent (bpy) which occupies *eq* sites of the other rhodium center.[393,394] These findings provide insight into the possible mechanism of interaction between dirhodium compounds and biologically relevant nucleobases or nucleos(t)ides. This chemistry most likely involves initial attack of the nucleophilic base at the *ax* position of the dimetal core to afford an axially bound monodentate adduct followed by rearrangement to *eq* sites, as has been observed in the case of chelating N-N donor ligands (e.g., bpy; Fig. 12.17).[373] The rearrangement of ligands from *ax* to *eq* positions is a key feature in dictating the outcome of purine reactions with dirhodium units.

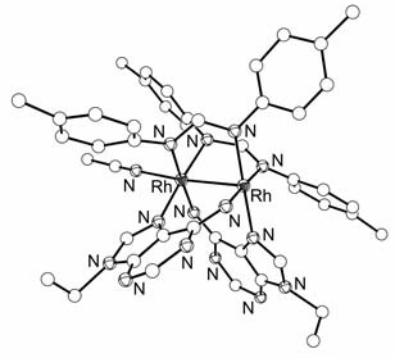


Fig. 12.47. Structure of the cation in H-H *cis*-$[Rh_2(DTolF)_2(9\text{-EtAdeH})_2(NCCH_3)](BF_4)_2$.

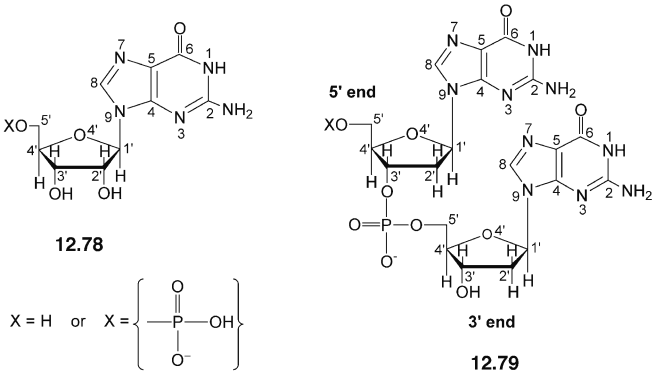
Nucleotides.[6] A natural extension of dirhodium reactions with model nucleobases is that with small DNA fragments. Early studies report the stepwise formation constants of 1:1 and 1:2 adducts of $Rh_2(O_2CCH_3)_4$ with adenine nucleotides, but the compounds were not isolated.[181] Subsequent studies based on ^1H NMR and infrared spectroscopies are consistent with *ax* binding of adenine nucleotides via *N*7 and *N1* to the dirhodium core.[182,814] Studies on the reaction of $Rh_2(O_2CCH_3)_4$ with guanosine-5'-monophosphate (GMP; **12.78** for X = PO_3H^-), performed by ^1H and ^{13}C NMR spectroscopies, suggest the formation of two isomers with the guanine rings spanning the Rh–Rh bond in a bridging fashion via *N7/06* and H-T or H-H arrangement of the bases, as in the case of 9-EtGuaH (Fig. 12.46a and 12.46b, respectively).[815]

Extension of the knowledge obtained from the dirhodium unit interactions with the basic building blocks of DNA, led to the reasonable hypothesis that the 90° '*bite*' angle displayed by the d(GpG)-cisplatin 'chelate' is well suited to accommodate two *cis eq* positions of one metal

Pictiva EX2004
Samsung v Pictiva
IPR2024-01094

atom in a dirhodium unit, despite the different geometries of the two metal complexes. Indeed, reactions of $Rh_2(O_2CCH_3)_4$ with the dinucleotides d(GpG) (**12.79**; X = H) and d(pGpG) (**12.79**; X = PO_3H^-) afford $Rh_2(O_2CCH_3)_2${d(GpG)} (**12.80**; X = H) and $Rh_2(O_2CCH_3)_2${d(pGpG)} (**12.80**; X = PO_3H^-), respectively, with bidentate *N7/06* bridging bases spanning the Rh–Rh bond.[811,815] For both dinucleotide complexes, intense H8/H8 ROE (Rotating frame nuclear Overhauser Effect) cross-peaks in the 2D ROESY NMR spectrum (Fig. 12.48) indicate H-H arrangement of the guanine bases (**12.80**).[811,815] The $Rh_2(O_2CCH_3)_2${d(GpG)} complex exhibits two major *right* handed conformers HH1R (~ 75%) and HH2R (~ 25%), which differ in the relative canting of the two bases.[811] In the case of $Rh_2(O_2CCH_3)_2${d(pGpG)}, the presence of the terminal 5'-phosphate group results in stabilization of *only* one left-handed $Rh_2(O_2CCH_3)_2${d(pGpG)} HH1L conformer due to the steric effect of the 5'-group favoring left canting, as in cisplatin-DNA adducts.[815] Detailed characterization of $Rh_2(O_2CCH_3)_2${d(GpG)}[811] and $Rh_2(O_2CCH_3)_2${d(pGpG)}[815] by 2D NMR spectroscopy, revealed notable structural features that resemble those of *cis*-[$Pt(NH_3)_2${d(pGpG)}]; the latter involve repuckering of the 5'-G sugar rings to the C3'-endo (N-type) conformation, retention of the C2'-endo (S-type) conformation for the 3'-G sugar rings and *anti* orientation of the bases with respect to the glycosyl bonds. The superposition of the low energy $Rh_2(O_2CCH_3)_2${d(pGpG)} conformer (Fig. 12.49a), generated by simulated annealing calculations, and the crystal structure of *cis*-[$Pt(NH_3)_2${d(pGpG)}][816] reveals remarkable similarities between the adducts (Fig. 12.49b); not only are the bases almost completely destacked (interbase dihedral angle 3'-G/5'-G ≈ 80°) upon coordination to the metal in both cases, but they are favorably poised to accommodate the *bidentate N7/06* binding to the dirhodium unit.[815] Contrary to conventional wisdom, two metal-metal bonded rhodium atoms are capable of engaging in *cis* binding to *GG* intrastrand sites by establishing *N7/06* bridges that span the Rh–Rh bond. The rigid steric demands of the tethered guanine bases bound to the square planar platinum atom in *cis*-[$Pt(NH_3)_2${d(pGpG)}] are also satisfied in metal-metal bonded dirhodium units. Our unprecedented findings that d(GpG) fragments establish bridging *eq* bonds via *N7/06* with the dirhodium core reveal new possibilities for metal-DNA interactions and lay a solid foundation for exploring similar structural motifs in related systems. Indeed, 1D and 2D NMR spectroscopic data of the dirhodium formamidinate dinucleotide complexes $Rh_2(DTolF)_2${d(GpG)}, $Rh_2(DTolF)_2${d(ApA)}, $Rh_2(DTolF)_2${d(GpA)} and $Rh_2(DTolF)_2${d(ApG)} (d(XpX) involves two purine bases X linked with a phosphodiester bond, X = adenine, **12.70**; guanine, **12.71**), corroborate *N7/06* and *N7/N6* binding of the guanine and adenine rings, respectively, with H-H arrangement of the tethered nucleobases.[817] Contrary to *cis*-[$Pt(NH_3)_2${d(pGpG)}] and $Rh_2(O_2CCH_3)_2${d((p)GpG)}, in the case of $Rh_2(DTolF)_2${d(GpG)} both sugar rings are of type N, a fact that implies possible conformational restriction for the compound. Variable temperature ^{1}H NMR studies of $Rh_2(DTolF)_2${d(ApA)} indicate that the adenine bases are present in the *rare* imino form **12.77**, as in the case of H-T *cis*-[$Rh_2(DTolF)_2(9\text{-EtAdeH})_2(NCCH_3)](BF_4)_2$.

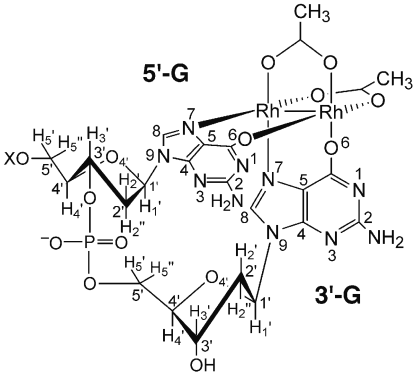
Pictiva EX2004
Samsung v Pictiva
IPR2024-01094



12.78

X = H or X = —P(=O)(O⁻)—OH

12.79



12.80

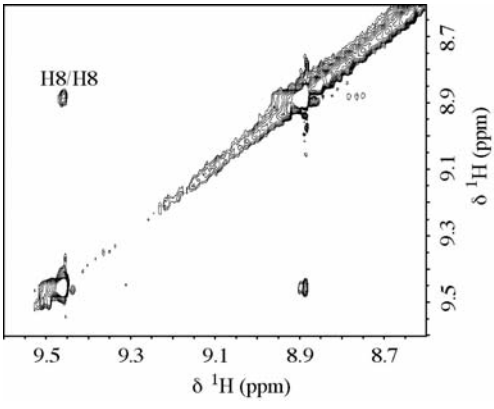


Fig. 12.48. Aromatic region of the 2D ROESY NMR spectrum of $Rh_2(O_2CCH_3)_2\{d(pGpG)\}$, in D_2O at 5 °C, pH 7.8, displaying the H8/H8 ROE cross-peaks of the two guanine bases in a H-H arrangement.

Pictiva EX2004
Samsung v Pictiva
IPR2024-01094

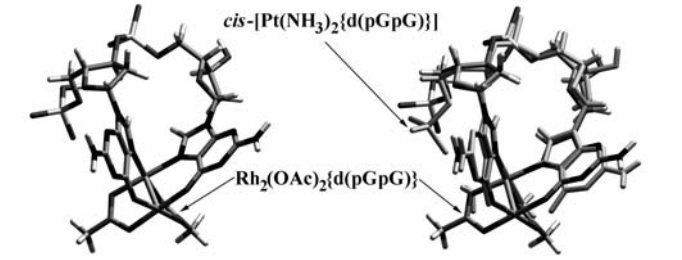


Fig. 12.49. (a) Low energy $Rh_2(O_2CCH_3)_2$\{d(pGpG)\} conformer resulting from simulated annealing calculations; (b) Superposition of the crystallographically determined *cis*-[$Pt(NH_3)_2$\{d(pGpG)\}] and the lowest energy $Rh_2(O_2CCH_3)_2$\{d(pGpG)\} conformer.

Oligonucleotides. Reactions of $Rh_2(O_2CCH_3)_4$, $[Rh_2(O_2CCH_3)_2(NCCH_3)_6]^{2+}$, and $Rh_2(O_2CCF_3)_4$ with single-stranded oligonucleotide tetramers, octamers and dodecamers containing *AA*, *GG*, *GA* and *GA* dipurine sites, e.g., d(T*GG*T), d(TTC*AA*CTC), d(CCTCT*GG*TCTCC), point to the following relative order of reactivity associated with the lability of the leaving groups: *cis*-$[Pt(NH_3)_2(H_2O)_2]^{2+}$ (activated cisplatin) ~ $Rh_2(O_2CCF_3)_4$ > *cis*-$[Pt(NH_3)_2Cl_2]$(cisplatin) >> *cis*-$[Rh_2(O_2CCH_3)_2(NCCH_3)_6](BF_4)_2$ > $Rh_2(O_2CCH_3)_4$.[758] Bis-acetate oligonucleotide adducts are the dominant species for the tetramers, whereas for longer oligonucleotides, the monoacetate and dirhodium species with no acetate bridging groups are detected. Although the metabolism of dirhodium carboxylate compounds in mammals involves displacement of *one* or *more* acetate bridges which are eventually oxidized to CO_2,[818] the dirhodium species detected in the aforementioned mass spectrometry study along with the kinetic stabilities of *cis*-$[Rh_2(NCCH_3)_{10}]^{4+}$ and $[Rh_2(H_2O)_{10}]^{4+}$ [596] suggest that the dirhodium core remains intact in the absence of carboxylate bridging groups. Electrospray ionization mass spectrometry permitted the observation of initial *ax* dirhodium-DNA adducts, followed by rearrangement to stronger *eq*-DNA species.[758] The detection of these adducts provides insight into the mechanism of interaction of dirhodium units with short oligonuleotides; the latter is most likely similar to that observed in the case of chelating N-N donor ligands, e.g., bpy; Fig. 12.17.[373] Enzymatic digestion studies with 3'→5' DNA and 5'→3' DNA exonucleases (Phosphodiesterase I and II, respectively) followed by MALDI and ESI MS, indicate that dipurine rather than pyrimidine sites of DNA oligonucleotides preferentially bind to the dirhodium core.[757,758]

Double-stranded (ds) DNA. Polyacrylamide Gel Electrophoresis (PAGE) studies address the long-standing issue of *if* and *how* dirhodium compounds bind to *ds*DNA. These studies refute earlier claims that no reaction between dirhodium compounds and *ds*DNA occurs, and indicate that interaction of *ds*DNA with dirhodium carboxylate compounds leads to covalent cross-linking of the two DNA strands.[819] The extent of DNA interstrand cross-link formation correlates with the lability of the leaving groups and is in the order $Rh_2(O_2CCF_3)_4$ > $[Rh_2(O_2CCH_3)_2(NCCH_3)_6](BF_4)_2$ >> $Rh_2(O_2CCH_3)_4$. The reversal behavior of the *ds*DNA interstrand cross-links in 5 M urea at 95 °C implies the presence of a mixture of monofunctional and/or bifunctional *ax*/*ax*, *ax*/*eq* or *eq*/*eq* dirhodium-DNA adducts. The less stable adducts in the isolated band are most likely *ax*-DNA adducts which are expected to exhibit enhanced exchange rates with heating compared to *eq*-DNA species.[596] The reversal of additional *ds*DNA-dirhodium adducts in the isolated band, by further heating in 40 mM thiourea, indicates the presence of another subset of products that are stable to more harsh conditions (most likely *eq*-DNA adducts).[819] These studies provide valuable insight into the possible underlying mechanism(s) of dirho-

Pictiva EX2004
Samsung v Pictiva
IPR2024-01094

dium antitumor behavior. In conclusion, it is important that DNA be considered a potential biological target of dirhodium compounds; the data obtained thus far constitute an excellent backdrop for further biochemical studies of metal-metal bonded systems.

Photochemistry and DNA photocleavage

Various dirhodium complexes have been investigated as potential antitumor agents in photochemotherapy, which involves triggering the toxicity of a compound by irradiation of the affected area with low energy visible or near-ir light to permit better tissue penetration.

It has been reported that $Rh_2(O_2CCH_3)_4$ exhibits a long-lived excited state (T = 3.5 μs) that can be accessed with visible light (λ_{exc} ~ 350–600 nm) and is able to undergo energy and electron transfer with a variety of acceptors.[7,8] Irradiation of $Rh_2(O_2CCH_3)_4$ with visible light (λ_{irr} = 400–610 nm), in the presence of electron acceptors, results in DNA photocleavage by the mixed-valent cation $[Rh_2(O_2CCH_3)_4]^+$ (Fig. 12.50).[9,820] The absorption of the related formamidinate (12.7) compounds $Rh_2(ArNCHNAr)_4$, Ar = XC_6H_4 (X = *p*-OMe, *p*-CF_3, *p*-Cl), as well as that of $Rh_2(tpg)_4$ (Fig. 12.26) extends to *c.* 880 nm, and irradiation of these complexes in the presence of various alkyl halide substrates results in formation of the corresponding mixed-valent Rh_2^{5+} compounds $Rh_2(ArNCHNAr)_4X$ (X = Cl, Br);[500,821] the compound $Rh_2(DAniF)_4Cl$ has been structurally characterized (Table 12.9).[500] The aforementioned complexes also effect DNA photocleavage in the presence of electron acceptors.[500]

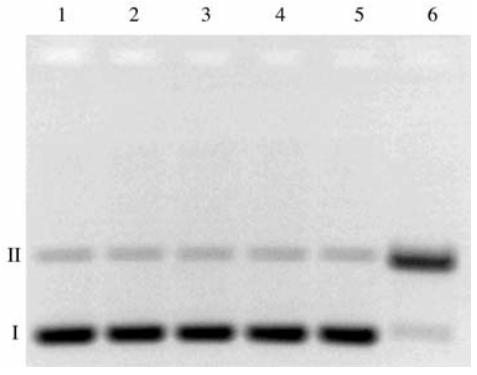
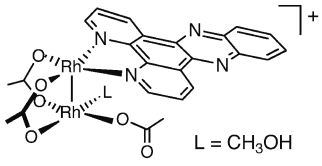


Fig. 12.50. Imaged agarose gel showing the photocleavage of 100 μM pUC18 plasmid (5 mM Tris buffer, pH 7.5) by 40 μM $Rh_2(O_2CCH_3)_4(H_2O)_2$ (Rh_2) in the presence of 2 mM py^+,10 min irradiation, $\lambda_{irr} \geq 395$ nm. **Lane 1:** plasmid only, dark. **Lane 2:** plasmid only, irradiated; **Lane 3:** plasmid + Rh_2, irradiated; **Lane 4:** plasmid +py^+, irradiated; **Lane 5:** plasmid + Rh_2 + py^+, dark; **Lane 6:** plasmid + Rh_2 + py^+, irradiated; 3-cyano-1-methylpyridinium tetrafluoroborate: py^+ (electron acceptor).

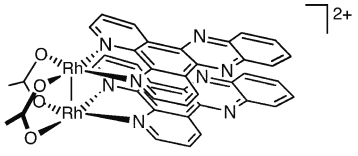
Unlike $Rh_2(O_2CCH_3)_4$, which requires an electron acceptor in solution, Rh_2^{4+} complexes with dppz (dppz: dipyrido[3,2-*a*:2',3'-*c*]phenazine), *cis*-$[Rh_2(\mu\text{-}O_2CCH_3)_2(dppz)(\eta^1\text{-}O_2CCH_3)(CH_3OH)]^+$ (**12.81**) and the structurally characterized[822] cis-$[Rh_2(\mu\text{-}O_2CCH_3)_2(dppz)_2]^{2+}$ (**12.82**), photocleave pUC18 plasmid *in vitro* upon near-uv ($\lambda_{irr} \geq 320$ nm) and visible ($\lambda_{irr} \geq 395$ nm) irradiation, resulting in the nicked, circular DNA (Fig. 12.51; lanes 4 and 6, respectively). An enhanced degree of photocleavage is observed for the former compared to the latter, which may be due to the ability of *cis*-$[Rh_2(\mu\text{-}O_2CCH_3)_2(dppz)(\eta^1\text{-}O_2CCH_3)(CH_3OH)]^+$ to intercalate DNA bases.[823] The compounds *cis*-$[Rh_2(\mu\text{-}O_2CCH_3)_2(dppn)_2]^{2+}$ [824] (dppn: benzo[*i*]dipyrido[3,2-*a*:2',3'-*c*]phenazine) and *cis*-$[Rh_2(\mu\text{-}O_2CCH_3)_2(dppz)_2]^{2+}$ [822] (Table 12.2) exhibit relatively low cytotoxicities in the dark, but their toxicities increase significantly (by 24- and 3.4-fold, re-

Pictiva EX2004
Samsung v Pictiva
IPR2024-01094

spectively) when the cell cultures are irradiated with visible light (400-700 nm, 30 min); the cation *cis*-$[Rh_2(\mu\text{-}O_2CCH_3)_2(dppn)_2]^{2+}$ has the added advantage of 18-fold lower toxicity than hematoporphyrin (key component in Photofrin©) in the dark. Likewise, the cytotoxicity of the heteroleptic species *cis*-$[Rh_2(\mu\text{-}O_2CCH_3)_2(bpy)(dppz)]^{2+}$ (Fig. 12.52) increases 5-fold upon irradiation, with the advantage of 10- and 7.5-fold lower toxicity than hematoporphyrin and *cis*-$[Rh_2(\mu\text{-}O_2CCH_3)_2(dppz)(\eta^1\text{-}O_2CCH_3)(CH_3OH)]^+$, respectively, in the dark.[825] The substitution of two *eq* labile groups in *cis*-$[Rh_2(\mu\text{-}O_2CCH_3)_2(dppz)(\eta^1\text{-}O_2CCH_3)(CH_3OH)]^+$ with a chelating bpy moiety apparently leads to reduction of its toxicity. The latter results render these compounds promising candidates for photochemotherapy. In the dirhodium series *cis*-$[Rh_2(\mu\text{-}O_2CCH_3)_2(dppz\text{-}X_2)_2]^{2+}$ (X = OCH_3, CH_3, Cl, NO_2) with substituted dppz (at positions 7 and 8 of the dppz ring), the percent of effected DNA photocleavage increases as the electron-donating ability of the group X increases.[826] The formamidinate derivatives *cis*-$[Rh_2(DPh^FF)_2(dppz)(NCCH_3)_4]^{2+}$ (Fig. 12.53) and *cis*-$[Rh_2(DPh^FF)_2(dppz)_2(NCCH_3)_2]^{2+}$ have also been prepared and will be the subject of future studies.[827] The ultimate goal of these investigations is to effectively control the photoreactivity and cytotoxicity of the previous compounds by tailoring both the *eq* bridging groups as well as the other ligands on the dimetal unit. Preliminary studies indicate that the cytotoxicity of dirhodium carboxylate compounds towards healthy human skin cells increases by substitution of acetate with the more labile trifluoroacetate bridging groups.[828]



12.81



12.82

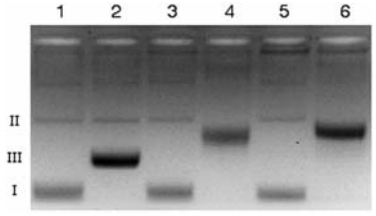


Fig. 12.51. Imaged agarose gel (2%) exhibiting the photocleavage ($\lambda_{irr} \geq 395$ nm, 20 min) of 100 μM pUC18 plasmid. **Lane 1:** plasmid only, dark; **Lane 2:** plasmid treated with SmaI to produce linear DNA; **Lane 3:** plasmid treated with: 10 μM *cis*-$[Rh_2(\mu\text{-}O_2CCH_3)_2(dppz)(\eta^1\text{-}O_2CCH_3)(CH_3OH)]^+$, dark ; **Lane 4:** plasmid treated with 10 μM *cis*-$[Rh_2(\mu\text{-}O_2CCH_3)_2(dppz)(\eta^1\text{-}O_2CCH_3)(CH_3OH)]^+$, irradiated; **Lane 5:** plasmid treated with 10 μM *cis*-$[Rh_2(\mu\text{-}O_2CCH_3)_2(dppz)_2]^{2+}$, dark; **Lane 6:** plasmid treated with10 μM *cis*-$[Rh_2(\mu\text{-}O_2CCH_3)_2(dppz)_2]^{2+}$, irradiated.

Pictiva EX2004
Samsung v Pictiva
IPR2024-01094

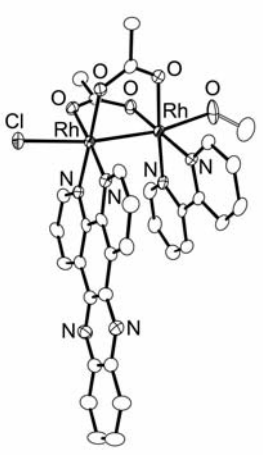


Fig. 12.52. The cation in *cis*-$[Rh_2(\mu\text{-}O_2CCH_3)_2(bpy)(dppz)(MeOH)Cl]BF_4$.

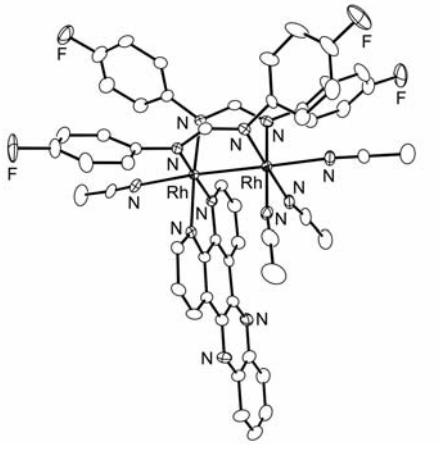


Fig. 12.53. The cation in *cis*-$[Rh_2(DPh^FF)_2(dppz)(NCCH_3)_4](BF_4)_2$.

Transcription inhibition in vitro

Transcription is the cellular process whereby mRNA is produced from a DNA template by the action of RNA polymerase.[829] Inhibition of this process leads to cell death. Contrary to cisplatin, which inhibits transcription by binding to the DNA template,[830] experiments designed to elucidate the mechanism of inhibition of dirhodium compounds indicate that, *in vitro* transcription inhibition is predominantly effected by interaction of the compounds studied with T7-RNA polymerase.[763,764] The imaged agarose gel illustrated in Fig. 12.54 exhibits the progressive decrease of the amount of mRNA produced during transcription relative to the control lane 1, as the concentration of $Rh_2(HNCOCF_3)_4$ increases (lanes 2-6).[764] The differences in reactivity and transcription inhibition mechanisms among the complexes $Rh_2(HNCOCH_3)_4$, $Rh_2(HNCOCF_3)_4$ and $Rh_2(O_2CCF_3)_4$ have been correlated to differences in the Lewis acidity of the *ax* sites as well as the lability of the bridging groups.[764] Studies aimed at gaining further understanding of dirhodium binding interactions with biomolecules are underway.

Pictiva EX2004
Samsung v Pictiva
IPR2024-01094

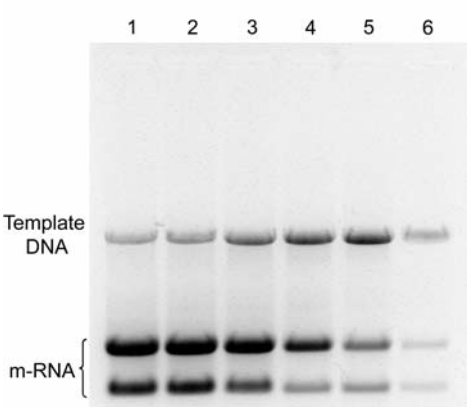


Fig. 12.54. Ethidium bromide stained agarose gel (1%) of transcribed mRNA in the presence of various concentrations of $Rh_2(HNCOCF_3)_4$. **Lane 1**: no metal compound; **Lane 2**: 2.4 μM; **Lane 3**: 3.6 μM; **Lane 4**: 4.8 μM; **Lane 5**: 0.60 μM; **Lane 6**: 7.2 μM. Both the DNA template and mRNA are imaged on the gel.

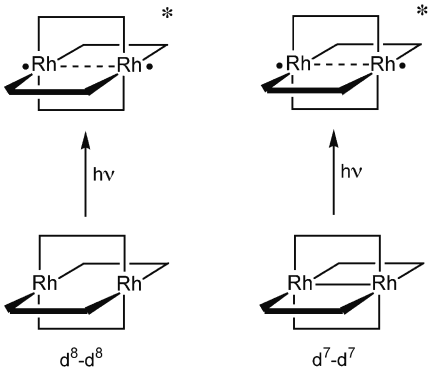
Nitric oxide sensors

The development of dirhodium tetracarboxylate scaffolds containing bound fluorophore conjugates for the reversible fluorescence-based detection of NO in biological fluids is underway[218] with very promising results: an immediate increase in fluorescence emission greater than 15-fold occurs when NO is admitted to solutions containing $Rh_2(O_2CCH_3)_4$ and the fluorophores Ds-im (dansyl-imidazole) or Ds-pip (dansyl-piperazine). The fluorescence response arises from the NO induced displacement of the axially coordinated fluorophore.[218]

12.7.4 Photocatalytic reactions

Dirhodium complexes have been investigated as potential systems for the conversion of solar energy by means of harnessing a photon to drive a multielectron redox event. Despite reversible photochemical homolytic cleavage of the Rh–Rh bond for the unsupported d^7-d^7 dirhodium complex $[Rh_2(NCCH_3)_{10}]^{4+}$ at $\lambda < 600$ nm, yielding mononuclear metal-centered radicals,[602-604] the bimetallic core remains intact in the radical photochemistry of bridged d^8-d^8 (**12.83**) and d^7-d^7 (**12.84**) dirhodium complexes. Several studies that focus on the photochemical release of H_2 from hydrohalic solutions HX in the presence of Rh_2^{2+} (d^8-d^8 system; **12.83**)[831] isocyanide compounds (section 12.5.1)[12,651-654] have been reported, but termination of the cycle that regenerates the initial photoreagent, due to formation of the highly stable Rh(II)-X bond, precludes catalytic turnover. Conversely, light excitation of the d^7-d^7 (**12.84**)[831] bimetallic complexes, bridged by bis(difluorophosphino)methylamine ($CH_3N(PF_2)_2$), results in formation of excited states that possess significant radical character centered on the metals ($d\sigma^*$ excited states) and provide a means of overcoming the energetic barrier to halogen atom elimination.[11,569] In seminal studies,[10,11] compounds such as $Rh_2[CH_3N(PF_2)_2]_3X_4$ (X = Cl, Br)[571,572] have been shown to enable the photocatalytic production of H_2 from homogeneous solutions of HX. An increased understanding of these systems is imperative to the development of efficient energy conversion photocatalysts with bimetallic cores.

Pictiva EX2004
Samsung v Pictiva
IPR2024-01094



12.7.5 Other applications

The absolute configuration of chiral alcohols, olefins, epoxides, ethers, amines and phosphines is determined from the NMR or CD spectra of their dirhodium carboxylate[270,274,832-835] and methoxytrifluoromethylphenylacetate (anion of Mosher's acid)[80-89] complexes, respectively. Chiral dirhodium carboxamidate catalysts are employed in highly enantioselective syntheses of therapeutic agents.[836-838] The electrochemical properties of a Doyle catalyst immobilized on a carbon paste electrode in the presence or absence of DNA,[839] as well as those of an acetamidate complex on a carbon paste electrode serving as a hydrazine sensor[840] have been explored. Likewise, the potential of dirhodium-substituted polyoxometalates, employed as catalysts, for the electrochemical oxidation of biomolecules has been addressed.[841-844] The entrapment of redox-active dimetal units into a siloxane framework produces promising materials for electrochemistry.[845] The design of several dirhodium compounds (with carboxylate ligands derived from fatty acids of varying length), that exhibit thermotropic columnar mesophase, is of considerable interest in view of their potential use as materials for molecular wires and electronics.[63,64,70,313,314]

References

1. M. P. Doyle and T. Ren, *Prog. Inorg. Chem.* **2001**, *49*, 113.
2. M. P. Doyle, *Catalysis by Di- and Polynuclear Metal Cluster Complexes*, R. D. Adams and F. A. Cotton, Eds., Wiley-VCH: New York, 1998, p 249.
3. M. P. Doyle and D. C. Forbes, *Chem. Rev.* **1998**, *98*, 911.
4. M. P. Doyle, *Acc. Chem. Res*. **1986**, *19*, 348.
5. M. P. Doyle, M. A. McKervey and T. Ye, *Modern Catalytic Methods for Organic Synthesis with Diazo Compounds – From Cyclopropanes to Ylides*, John Wiley & Sons: New York, 1998.
6. H. T. Chifotides and K. R. Dunbar, *Acc. Chem. Res.* **2005**, in press.
7. P. M. Bradley, B. E. Bursten and C. Turro, *Inorg. Chem.* **2001**, *40*, 1376.
8. P. M. Bradley, P. K.-L. Fu and C. Turro, *Comments Inorg. Chem.* **2001**, *22*, 393.
9. P. K.-L. Fu, P. M. Bradley and C. Turro, *Inorg. Chem.* **2001**, *40*, 2476.
10. A. F. Heyduk and D. G. Nocera, *Science* **2001**, *293*, 1639.
11. A. F. Heyduk, A. M. Macintosh and D. G. Nocera, *J. Am. Chem. Soc.* **1999**, *121*, 5023.
12. I. S. Sigal, K. R. Mann and H. B. Gray, *J. Am. Chem. Soc.* **1980**, *102*, 7252.
13. F. A. Cotton, C. Lin and C. A. Murillo, *Acc. Chem. Res.* **2001**, *34*, 759.
14. B. J. Holliday and C. A. Mirkin, *Angew. Chem., Int. Ed.* **2001**, *40*, 2022.

Pictiva EX2004
Samsung v Pictiva
IPR2024-01094

15. F. A. Cotton, C. Lin and C. A. Murillo, *Proc. Nat. Acad. Sci. U.S.A.* **2002**, *99*, 4810.
16. F. A. Cotton, E. A. Hillard and C. A. Murillo, *J. Am. Chem. Soc.* **2002**, *124*, 5658.
17. F. A. Cotton, G. Wilkinson, C. A. Murillo and M. Bochmann, *Advanced Inorganic Chemistry*, 6th ed., John Wiley & Sons: New York, 1999, p 1054.
18. T. R. Felthouse, *Prog. Inorg. Chem.* **1982**, *29*, 73.
19. E. B. Boyar and S. D. Robinson, *Coord. Chem. Rev.* **1983**, *50*, 109.
20. E. B. Boyar and S. D. Robinson, *Platinum Met. Rev.* **1982**, *26,* 65.
21. I. B. Baranovskii, *Russ. J. Inorg. Chem.* **1982**, *27*, 759.
22. T. Ren, *Coord. Chem. Rev.* **1998**, *175*, 43.
23. C. E. Housecroft, *Coord. Chem. Rev*. **1992**, *115*, 191.
24. C. E. Housecroft, *Coord. Chem. Rev*. **1995**, *146*, 235.
25. C. E. Housecroft, *Coord. Chem. Rev*. **1996**, *152*, 107.
26. I. I. Chernyaev, E. V. Shenderetskaya, A. G. Maiorova and A. A. Koryagina, *Russ. J. Inorg. Chem.* **1965**, *10,* 290.
27. I. I. Chernyaev, E. V. Shenderetskaya, A. G. Maiorova and A. A. Koryagina, *Russ. J. Inorg. Chem.* **1966**, *11,* 1383.
28. E. M. Shustorovich, M. A. Porai-Koshits and Yu. A. Buslaev, *Coord. Chem. Rev.* **1975**, *17,* 1.
29. S. A. Johnson, H. R. Hunt and H. M. Neumann, *Inorg. Chem.* **1963**, *2*, 960.
30. T. A. Stephenson, S. M. Morehouse, A. R. Powell, J. P. Heffer and G. Wilkinson, *J. Chem. Soc. (Abstracts)* **1965**, 3632.
31. P. Legzdins, R. W. Mitchell, G. L. Rempel, J. D. Ruddick and G. Wilkinson, *J. Chem. Soc. A* **1970**, 3322.
32. G. A. Rempel, P. Legzdins, H. Smith and G. Wilkinson, *Inorg. Synth.* **1972**, *13*, 90.
33. H. Brunner, H. Kluschanzoff and K. Wutz, *Bull. Soc. Chim. Belg.* **1989**, *98,* 63.
34. N. A. Ezerskaya, E. S. Toropchenova, I. V. Kubrakova, S. V. Krasheninnikova, T. F. Kudinova, T. A. Fomina and I. N. Kiseleva, *J. Anal. Chem*. **2000**, *55*, 1132.
35. G. Winkhaus and P. Ziegler, *Z. anorg. allg. Chem.* **1967**, *350,* 51.
36. J. L. Bear, J. Kitchens and M. R. Wilcotte, III, *J. Inorg. Nucl. Chem.* **1971**, *33*, 3479.
37. F. A. Cotton and J. G. Norman, Jr., *J. Am. Chem. Soc.* **1972**, *94,* 5697.
38. F. A. Cotton and J. L. Thompson, *Inorg. Chim. Acta* **1984**, *81,* 193.
39. H. J. Callot, A.-M. Albrecht-Gary, M. A. Joubbeh, B. Metz and F. Metz, *Inorg. Chem.* **1989***, 28,* 3633.
40. C. R. Wilson and H. Taube, *Inorg. Chem.* **1975**, *14*, 405.
41. G. H. P. Roos and M. A. McKervey, *Synth. Commun*. **1992**, *22*, 1751.
42. Yu. S. Varshavskii, T. G. Cherkasova, A. B. Nikol'skii and I. I. Vorontsov, *Russ. J. Inorg. Chem.* **2001**, *46*, 685.
43. J. Kitchens and J. L. Bear, *J. Inorg. Nucl. Chem.* **1970**, *32*, 49.
44. J. Kitchens and J. L. Bear, *Thermochim. Acta* **1970**, *1,* 537.
45. R. A. Howard, A. M. Wynne, J. L. Bear and W. W. Wendlandt, *J. Inorg. Nucl. Chem.* **1976**, *38,* 1015.
46. A. R. de Souza, R. Najjar and J. R. Matos, *Thermochim. Acta* **2000**, *343*, 119.
47. F. A. Cotton, E. V. Dikarev and X. Feng, *Inorg. Chim. Acta* **1995**, *237*, 19.
48. F. A. Cotton, E. V. Dikarev and S.-E. Stiriba, *Organometallics* **1999**, *18*, 2724.
49. F. A. Cotton, E. V. Dikarev and S.-E. Stiriba, *Inorg. Chem.* **1999**, *38*, 4877.
50. F. A. Cotton, E. V. Dikarev and M. A. Petrukhina, *J. Organomet. Chem.* **2000**, *596*, 130.
51. F. A. Cotton, E. V. Dikarev, M. A. Petrukhina and S.-E. Stiriba, *Inorg. Chem.* **2000**, *39*, 1748.
52. F. A. Cotton, E. V. Dikarev, M. A. Petrukhina and S.-E. Stiriba, *Organometallics* **2000**, *19*, 1402.
53. F. A. Cotton, E. V. Dikarev, M. A. Petrukhina and S.-E. Stiriba, *Polyhedron* **2000**, *19*, 1829.
54. F. A. Cotton, E. V. Dikarev and M. A. Petrukhina, *Angew. Chem., Int. Ed.* **2000**, *39*, 2362.
55. F. A. Cotton, E. V. Dikarev, M. A. Petrukhina and R. E. Taylor*, J. Am. Chem. Soc.* **2001**, *123*, 5831.
56. F. A. Cotton, E. V. Dikarev and M. A. Petrukhina, *Angew. Chem., Int. Ed.* **2001**, *40*, 1521.

Pictiva EX2004
Samsung v Pictiva
IPR2024-01094

57. F. A. Cotton, E. V. Dikarev and M. A. Petrukhina, *J. Am. Chem. Soc.* **2001**, *123,* 11655.
58. M. A. Petrukhina, K. W. Andreini, J. Mack and L. T. Scott, *Angew. Chem.*, *Int. Ed.* **2003**, *42*, 3375.
59. M. A. Petrukhina, K. W. Andreini, L. Peng and L. T. Scott, *Angew. Chem.*, *Int. Ed.* **2004**, *43*, 5477.
60. E. V. Dikarev, N. S. Goroff and M. A. Petrukhina, *J. Organomet. Chem.* **2003**, *683*, 337.
61. M. G. Bartlett, G. M. Haas, D. A. Bruce, S. M. Thomas, M. G. White, J. A. Bertrand and K. L. Busch, *Anal. Chim. Acta* **1997**, *346*, 223.
62. J. W. Trexler, Jr., A. F. Scheiner and F. A. Cotton, *Inorg. Chem*. **1988**, *27*, 3265.
63. A.-M. Giroud-Godquin, J.-C. Marchon, D. Guillon and A. Skoulios, *J. Phys. Chem.* **1986**, *90*, 5502.
64. O. Poizat, D. P. Strommen, P. Maldivi, A.-M. Giroud-Godquin and J.-C. Marchon, *Inorg. Chem.* **1990**, *29*, 4851.
65. D. M. L. Goodgame, C. J. Page and D. J. Williams, *Inorg. Chim. Acta* **1988**, *153*, 219.
66. R. Najjar, W. de Oliveira, J. B. Carducci and M. Watanabe, *Polyhedron* **1989**, *8*, 1157.
67. T. M. Dyson, E. C. Morrison, D. A. Tocher, L. D. Dale and D. I. Edwards, *Inorg. Chim. Acta* **1990**, *169*, 127.
68. F. A. Cotton, L. M. Daniels, P. A. Kibala, M. Matusz, W. J. Roth, W. Schwotzer, W. Wang and B. Zhong, *Inorg. Chim. Acta* **1994**, *215, 9*.
69. M. A. Castro, Z. D. Chaia, O. E. Piro, F. D. Cukiernik, E. E. Castellano and M. Rusjan, *Acta Crystallogr*. **2002**, *C58*, 393.
70. J. Barberá, M. A. Esteruelas, A. M. Levelut, L. A. Oro and J. L. Serrano, *Inorg. Chem.* **1992**, *31*, 732.
71. D. P. Bancroft, F. A. Cotton and S. Han, *Inorg. Chem.* **1984**, *23*, 2408.
72. R. N. Shchelokov, A. G. Maiorova, G. N. Kuznetsova, I. F. Golovaneva and O. N. Evstaf'eva, *Russ. J. Inorg. Chem.* **1980**, *25*, 1049.
73. A. Y. Ali-Mohamed and M. Fujita, *Transition Met. Chem*. **2003**, *28*, 361.
74. M. S. Nothenberg, A. R. de Souza and J. do R. Matos, *Polyhedron* **2000**, *19*, 1305.
75. F. A. Cotton, E. A. Hillard, C. Y. Liu, C. A. Murillo, W. Wang and X. Wang, *Inorg. Chim. Acta* **2002**, *337*, 233.
76. B. Kojic-Prodic, R. Marcec, B. Nigovic, Z. Raza and V. Sunjic, *Tetrahedron: Asymmetry* **1992**, *3*, 1.
77. Z. Rozwadowski, S. Malik, G. Tóth, T. Gáti and H. Duddeck, *Dalton Trans*. **2003**, 375.
78. H. Duddeck, S. Malik, T. Gáti, G. Tóth and M. I. Choudhary, *Magn. Reson. Chem*. **2002**, *40*, 153.
79. S. Malik, S. Moeller, G. Tóth, T. Gáti, M. I. Choudhary and H. Duddeck, *Magn. Reson. Chem*. **2003**, *41*, 455.
80. J. Jazwinski, Z. Rozwadowski, D. Magiera and H. Duddeck, *Magn. Reson. Chem*. **2003**, *41*, 315.
81. D. Magiera, J. Omelanczuk, K. Dziuba, K. M. Pietrusiewicz and H. Duddeck, *Organometallics* **2003**, *22*, 2464.
82. K. Wypchlo and H. Duddeck, *Tetrahedron: Asymmetry* **1994**, *5*, 27.
83. D. Magiera, W. Baumann, I. S. Podkorytov, J. Omelanczuk and H. Duddeck, *Eur. J. Inorg. Chem*. **2002**, 3253.
84. K. Wypchlo and H. Duddeck, *Chirality* **1997**, *9*, 601.
85. S. Rockitt, H. Duddeck and J. Omelanczuk, *Chirality* **2001**, *13*, 214.
86. D. Magiera, A. Szmigielska, K. M. Pietrusiewicz and H. Duddeck, *Chirality* **2004**, *16*, 57.
87. D. Magiera, S. Moeller, Z. Drzazga, Z. Pakulski, K. M. Pietrusiewicz and H. Duddeck, *Chirality* **2003**, *15*, 391.
88. C. Meyer and H. Duddeck, *Magn. Reson. Chem*. **2000**, *38*, 29.
89. T. Gáti, A. Simon, G. Tóth, A. Szmigielska, A. M. Maj, K. M. Pietrusiewicz, S. Moeller, D. Magiera and H. Duddeck, *Eur. J. Inorg. Chem*. **2004**, 2160.
90. T. Gáti, A. Simon, G. Tóth, D. Magiera, S. Moeller and H. Duddeck, *Magn. Reson. Chem*. **2004**, *42*, 600.
91. R. Najjar, F. S. dos Santos and W. Seidel, *An. Acad. Brasil. Cienc.* **1987**, *59*, 13.

Pictiva EX2004
Samsung v Pictiva
IPR2024-01094

92. J. Seitz and G. Maas, *Chem. Commun.* **2002**, 338.
93. M. A. Golubnichaya, I. B. Baranovskii, G. Ya. Mazo and R. N. Shchelokov, *Russ. J. Inorg. Chem.* **1981**, *26*, 1534.
94. A. M. Dennis, R. A. Howard, J. L. Bear, J. D. Korp and I. Bernal, *Inorg. Chim. Acta* **1979**, *37*, L561.
95. J. D. Korp, I. Bernal and J. L. Bear, *Inorg. Chim. Acta* **1981**, *51*, 1.
96. A. E. Bukanova, T. P. Sidorova, L. K. Shubochkin, Ya. V. Salyn' and N. A. Ezerskaya, *Russ. J. Inorg. Chem.* **1985**, *30*, 849.
97. P. R. Bontcev, M. Miteva, E. Zhecheva, D. Mechandjiev, G. Pneumatikakis and C. Angelopoulos, *Inorg. Chim. Acta* **1988**, *152*, 107.
98. M. Koralewicz, F. P. Pruchnik, A. Szymaszek, K. Wadja-Hermanowicz and K. Wrona-Grzegorek, *Transition Met. Chem*. **1998**, *23*, 523.
99. H. M. L. Davies, P. R. Bruzinski, D. H. Lake, N. Kong and M. J. Fall, *J. Am. Chem. Soc.* **1996**, *118*, 6897.
100. H. M. L. Davies and N. Kong, *Tetrahedron Lett.* **1997**, *38*, 4203.
101. H. M. L. Davies and S. A. Panaro, *Tetrahedron Lett.* **1999**, *40*, 5287.
102. R. N. Shchelokov, A. G. Maiorova, S. S. Abdullaev, O. N. Evstafeva, I. F. Golovaneva and G. N. Emel'yanova, *Russ. J. Inorg. Chem.* **1981**, *26*, 1774.
103. I. F. Golovaneva, S. S. Abdullaev and R. N. Shchelokov, *Russ. J. Inorg. Chem.* **1982**, *27*, 1468.
104. A. P. Klyagina, I. F. Golovaneva and A. A. Levin, *Russ. J. Inorg. Chem*. **1990**, *35*, 1138.
105. F. Pruchnik, B. R. James and P. Kvintovics, *Can. J. Chem.* **1986**, *64*, 936.
106. P. A. Agaskar, F. A. Cotton, L. R. Falvello and S. Han, *J. Am. Chem. Soc.* **1986**, *108*, 1214.
107. S. Rockitt, R. Wartchow, H. Duddeck, A. Drabczynska and K. Kiec-Kononowicz, *Z. Naturforsch.* **2001**, *56B*, 319.
108. D. C. Wynne, M. M. Olmstead and P. G. Jessop, *J. Am. Chem. Soc.* **2000**, *122*, 7638.
109. D. F. Taber, R. P. Meagley, J. P. Louey and A. L. Rheingold, *Inorg. Chim. Acta* **1995**, *239*, 25.
110. J. F. Gallagher, G. Ferguson and A. J. McAlees, *Acta Crystallogr.* **1997**, *C53*, 576.
111. R. P. Bonar-Law, T. D. McGrath, N. Singh, J. F. Bickley and A. Steiner, *Chem. Commun.* **1999**, 2457.
112. R. P. Bonar-Law, T. D. McGrath, N. Singh, J. F. Bickley, C. Femoni and A. Steiner, *J. Chem. Soc., Dalton Trans.* **2000**, 4343.
113. R. P. Bonar-Law, J. F. Bickley, C. Femoni and A. Steiner, *J. Chem. Soc., Dalton Trans.* **2000**, 4244.
114. J. F. Bickley, R. P. Bonar-Law, C. Femoni, E. J. MacLean, A. Steiner and S. J. Teat, *J. Chem. Soc., Dalton Trans.* **2000**, 4025.
115. R. P. Bonar-Law, T. D. McGrath, J. F. Bickley, C. Femoni and A. Steiner, *Inorg. Chem. Commun.* **2001**, 16.
116. J. F. Bickley, R. P. Bonar-Law, T. D. McGrath, N. Singh and A. Steiner, *New J. Chem*. **2004**, *28*, 425.
117. L. M. Dikareva, G. G. Sadikov, M. A. Porai-Koshits, M. A. Golubnichaya, I. B. Baranovskii and R. N. Shchelokov, *Russ. J. Inorg. Chem*. **1977**, *22*, 1093.
118. L. M. Dikareva, M. A. Porai-Koshits, G. G. Sadikov, I. B. Baranovskii, M. A. Golubnichaya and R. N. Shchelokov, *Russ. J. Inorg. Chem.* **1978**, *23*, 578.
119. I. B. Baronovskii, M. A. Golubnichaya, G. Ya. Mazo, V. I. Nefedov, Ya. V. Salyn' and R. N. Shchelokov, *Russ. J. Inorg. Chem*. **1976**, *21*, 591.
120. I. B. Baronovskii, M. A. Golubnichaya, G. Ya. Mazo and R. N. Shchelokov, *Russ. J. Inorg. Chem*. **1975**, *20*, 475.
121. R. H. Clark, D. J. West and R. Withnall, *Inorg. Chem*. **1992**, *31*, 456.
122. I. B. Baronovskii, M. A. Golubnichaya, G. Ya. Mazo and R. N. Shchelokov, *Sov. J. Coord. Chem.* **1975**, *1*, 1299.
123. I. B. Baranovskii, M. A. Golubnichaya, G. Ya. Mazo, V. I. Nefedov, Ya. N. Salyn' and R. N. Shchelokov, *Sov. J. Coord. Chem.* **1977**, *3*, 576.
124. N. Mehmet and D. A. Tocher, *Inorg. Chim. Acta* **1991**, *188*, 71.

Pictiva EX2004
Samsung v Pictiva
IPR2024-01094

125. E. C. Morrison and D. A. Tocher, *Inorg. Chim. Acta* **1989**, *156*, 99.
126. V. I. Nefedov, Ya. V. Salyn', A. G. Maiorova, L. A. Nazarova and I. B. Baranovskii, *Russ. J. Inorg. Chem.* **1974**, *19*, 736.
127. A. G. Maiorova, L. A. Nazarova and G. N. Emel'yanova, *Russ. J. Inorg. Chem*. **1973**, *18*, 986.
128. A. G. Maiorova, L. A. Nazarova and G. N. Emel'yanova, *Russ. J. Inorg. Chem*. **1973**, *18*, 989.
129. L. S. Volkova, V. M. Volkov and S. S. Chernikov, *Russ. J. Inorg. Chem*. **1971**, *16*, 1383.
130. J. Kitchens and J.L. Bear, *J. Inorg. Nucl. Chem.* **1969**, *31*, 2415.
131. L. Dubicki and R. L. Martin, *Inorg. Chem.* **1970**, *9*, 673.
132. L. A. Nazarova, I. I. Chernyaev and A. S. Morozova, *Russ. J. Inorg. Chem.* **1965**, *10*, 291.
133. L. A. Nazarova, I. I. Chernyaev and A. S. Morozova, *Russ. J. Inorg. Chem.* **1966**, *11*, 1387.
134. Y. B. Koh and G. G. Christoph, *Inorg. Chem.* **1979**, *18*, 1122.
135. M. Handa, M. Watanabe, D. Yoshioka, S. Kawabata, R. Nukada, M. Mikuriya, H. Azuma and K. Kasuga, *Bull. Chem. Soc. Jpn.* **1999**, *72*, 2681.
136. R. S. Drago, S. P. Tanner, R. M. Richman and J. R. Long, *J. Am. Chem. Soc.* **1979**, *101*, 2897.
137. R. S. Drago, J. R. Long and R. Cosmano, *Inorg. Chem.* **1981**, *20*, 2920.
138. Y.-B. Koh and G. G. Christoph, *Inorg. Chem.* **1978**, *17*, 2590.
139. T.A. Mal'kova and V. N. Shafranskii, *J. Gen. Chem. USSR* **1975**, *45*, 618.
140. K. Das, E. L. Simmons and J. L. Bear, *Inorg. Chem.* **1977**, *16*, 1268.
141. A. M. Dennis, R. A. Howard and J. L. Bear, *Inorg. Chim. Acta* **1982**, *66*, L31.
142. J. Telser and R. S. Drago, *Inorg. Chem.* **1984**, *23*, 2599.
143. F. A. Cotton and T. R. Felthouse, *Acta Crystallogr.* **1984**, *C40*, 42.
144. F. A. Cotton and J. Czuchajowska-Wiesinger, *Gazz. Chim. Ital.* **1992**, *122*, 321.
145. H. Kitamura, T. Ozawa, K. Jitsukawa, H. Masuda, Y. Aoyama and H. Einaga, *Inorg. Chem.* **2000**, *39*, 3294.
146. K. Aoki, M. Inaba, S. Teratani, H. Yamazaki and Y. Miyashita, *Inorg. Chem.* **1994**, *33*, 3018.
147. C. A. Crawford, E. F. Day, W. E. Streib, J. C. Huffman and G. Christou, *Polyhedron* **1994**, *13*, 2933.
148. H. Kitamura, T. Ozawa, K. Jitsukawa, H. Masuda and H. Einaga, *Chem. Lett*. **1999**, 1225.
149. Y. Kim, S.-J. Kim and A. J. Lough, *Polyhedron* **2001**, *20*, 3073.
150. J. E. Fiscus, S. Shotwell, R. C. Layland, M. D. Smith, H.-C. zur Loye and U. H. F. Bunz, *Chem. Commun*. **2001**, 2674.
151. S. Hashimoto, N. Watanabe, T. Sato, M. Shiro and S. Ikegami, *Tetrahedron Lett.* **1993**, *34*, 5109.
152. G.-P. Li and Y.-Z. Sun, *Acta Chim. Sinica* **1981**, *39*, 945.
153. J. Jazwinski and H. Duddeck, *Magn. Reson. Chem*. **2003**, *41*, 921.
154. D. M. L. Goodgame, C. A. O' Mahoney, C. J. Page and D. J. Williams, *Inorg. Chim. Acta* **1990**, *175*, 141.
155. F. A. Cotton and T. R. Felthouse, *Inorg. Chem.* **1981**, *20*, 600.
156. N. B. Behrens, G. M. Carrera, D. M. L. Goodgame, A. S. Lawrence and D. J. Williams, *Inorg. Chim. Acta* **1985**, *102*, 173.
157. N. Farrell and M. P. Hacker, *Inorg. Chim. Acta* **1989**, *166*, 35.
158. T. A. Mal'kova and V. N. Shafranskii, *Russ. J. Inorg. Chem.* **1975**, 20, 735.
159. I. L. Eremenko, M. A. Golubnichaya, S. E. Nefedov, I. B. Baranovskii, I. A. Ol'shnitskaya, O. G. Ellert, V. M. Novotortsev, L. T. Eremenko and D. A. Nesterenko, *Russ. J. Inorg. Chem.* **1996**, *41*, 1924.
160. W. Zhou, X. Wang, X. Liu, G. Le and A. Cui, *Beijing Daxue Xuebao, Ziran Kexueban* **1992**, *28*, 646.
161. W.-M. Xue, F. E. Kühn, E. Herdtweck and Q. Li, *Eur. J. Inorg. Chem*. **2001**, 213.
162. W.-M. Xue and F. E. Kühn, *Eur. J. Inorg. Chem*. **2001**, 2041.
163. K. Aoki and H. Yamazaki, *Acta Crystallogr.* **1989**, *C45*, 730.
164. M. A. Zoroddu, L. Naldini, F. Demartin and N. Masciocchi, *Inorg. Chim. Acta* **1987**, *128*, 179.
165. K. Aoki and H. Yamazaki, *J. Am. Chem. Soc.* **1984**, *106*, 3691.
166. L. A. Nazarova and A. G. Maiorova, *Russ. J. Inorg. Chem.* **1976**, *21*, 583.

Pictiva EX2004
Samsung v Pictiva
IPR2024-01094

167. T. A. Veteva and V. N. Shafranskii, *J. Gen. Chem. USSR* **1979**, *49*, 428.
168. R. D. Sinisterra and R. Najjar, *Spectrosc. Lett*. **1993**, *26*, 245.
169. N. Farrell, M. D. Vargas and Y. A. Mascarenhas and M. T. do P. Gambardella, *Inorg. Chem.* **1987**, *26*, 1426.
170. F. Nicolò, G. Bruno, S. Lo Schiavo, M. S. Sinicropi and P. Piraino, *Inorg. Chim. Acta* **1994**, *223*, 145.
171. J. F. Berry, F. A. Cotton, C. Lin and C. A. Murillo, *J. Cluster Sci*. **2004**, *15*, 531.
172. A. J. Holder, M. Schröder and T. A. Stephenson, *Polyhedron* **1987**, *6*, 461.
173. D. M. L.Goodgame, A. S. Lawrence, A. M. Z. Slawin, D. J. Williams and I. J. Stratford, *Inorg. Chim. Acta* **1986**, *125*, 143.
174. J. Chen and N. M. Kostic, *Inorg. Chem.* **1988**, *27*, 2682.
175. K. Das and J. L. Bear, *Inorg. Chem.* **1976**, *15*, 2093.
176. M. S. Nothenberg, G. K. F. Takeda and R. Najjar, *J. Inorg. Biochem.* **1991**, *42*, 217.
177. M. S. Nothenberg, S. B. Zyngier, A. M. Giesbrecht, M. T. P. Gambardella, R. H. A. Santos, E. Kimura and R. Najjar, *J. Braz. Chem. Soc.* **1994**, *5*, 23.
178. J. K. Bera, J. Bacsa, B. W. Smucker and K. R. Dunbar, *Eur. J. Inorg. Chem*. **2004**, 368.
179. J. K. Bera, T. T. Vo, R. A. Walton and K. R. Dunbar, *Polyhedron* **2003**, *22*, 3009.
180. T. A. Mal'kova and V. N. Shafranskii, *Russ. J. Inorg. Chem*. **1974**, *19*, 1366.
181. L. Rainen, R. A. Howard, A. P. Kimball and J. L. Bear, *Inorg. Chem.* **1975**, *14*, 2752.
182. G. Pneumatikakis and N. Hadjiliadis, *J. Chem. Soc., Dalton Trans.* **1979**, 596.
183. M. A. Zoroddu, G. Manca and S. Mosca, *Transition Met. Chem.* **1991**, *16*, 301.
184. J. R. Rubin, T. P. Haromy and M. Sundaralingam, *Acta Crystallogr.* **1991**, *C47*, 1712.
185. K. Aoki and H. Yamazaki, *J. Chem. Soc., Chem. Commun.* **1980**, 186.
186. N. Alberding, N. Farrell and E. D. Crozier, *J. Am. Chem. Soc.* **1985**, *107*, 384.
187. N. Alberding, N. Farrell and E. D. Crozier, *EXAFS and Near Edge Structure III; Proceedings of an International Conference*, K. O. Hodgson, B. Hedman and J. E. Penner, Eds., Berlin, New York: Springer-Verlag, 1984, vol. 2, 151.
188. H. T. Chifotides, K. R. Dunbar, J. H. Matonic and N. Katsaros, *Inorg. Chem.* **1992**, *31*, 4628.
189. H. T. Chifotides, N. Katsaros and G. Pneumatikakis, *Can. J. Appl. Spectrosc.* **1994**, *39*, 81.
190. N. Farrell, *J. Inorg. Biochem.* **1981**, *14*, 261.
191. D. Waysbort, E. Tarien and G. L. Eichhorn, *Inorg. Chem.* **1993**, *32*, 4774.
192. J. R. Rubin and M. Sundaralingam, *J. Biom. Struct. Dyn.* **1984**, *2*, 525.
193. K. Aoki and H. Yamazaki, *J. Am. Chem. Soc.* **1985**, *107*, 6242.
194. N. Kostic, *Comments Inorg. Chem*. **1988**, *8*, 137.
195. F. A. Cotton and J. L. Thompson, *Acta Crystallogr*. **1981**, *B37*, 2235.
196. F. A. Cotton and Y. Kim, *Eur. J. Solid State Inorg. Chem.* **1994**, *31*, 525.
197. Z. Yang, H. Oki, M. Ebihara and T. Kawamura, *J. Chem. Soc., Dalton Trans.* **1998**, 2277.
198. T. Niu, J. Lu, G. Crisci and A. J. Jacobson, *Polyhedron* **1998**, *17*, 4079.
199. T. Janecki, S. Shi, P. Kaszynski and J. Michl, *Collect. Czech. Chem. Commun.* **1993**, *58*, 89.
200. F. A. Cotton and Y. Kim, *J. Am. Chem. Soc.* **1993**, *115*, 8511.
201. H. Miyasaka, C. S. Campos-Fernández, R. Clérac and K. R. Dunbar, *Angew. Chem., Int. Ed.* **2000**, *39*, 3831.
202. F. A. Cotton, Y. Kim and J. Lu, *Inorg. Chim. Acta* **1994**, *221*, 1.
203. H. Miyasaka, C. S. Campos-Fernández, J. R. Galán-Mascarós and K. R. Dunbar, *Inorg. Chem.* **2000**, *39*, 5870.
204. C. J. Siemer, M. J. VanStipdonk, P. K. Kahol and D. M. Eichhorn, *Polyhedron* **2004**, *23*, 235.
205. F. P. Pruchnik, F. Robert, Y. Jeannin and S. Jeannin, *Inorg. Chem.* **1996**, *35*, 4261.
206. T. Yoshimura, K. Umakoshi and Y. Sasaki, I*norg. Chem.* **2003**, *42*, 7106.
207. S. Takamizawa, T. Hiroki, E. Nakata, K. Mochizuki and W. Mori, *Chem. Lett.* **2002**, 1208.
208. S. Takamizawa, E. Nakata, H. Yokoyama, K. Mochizuki and W. Mori, *Angew. Chem., Int. Ed.* **2003**, *42*, 4331.
209. B. Viossat, N. -H. Dung, J. C. Daran and J. C. Lancelot, *Acta Crystallogr.* **1993**, *C49*, 2084.

Pictiva EX2004
Samsung v Pictiva
IPR2024-01094

210. L. S. Hegedus, M. J. Sundermann and P. K. Dorhout, *Inorg. Chem.* **2003**, *42*, 4346.
211. P. Lemoine, A. Tomas, B. Viossat, Y. Mettey and J. M. Vierfond, *Acta Crystallogr.* **1995**, *C51*, 377.
212. P. B. Viossat, N.-H. Dung, F. Robert, J. C. Lancelot and M. Robba, *Acta Crystallogr.* **1991**, *C47*, 2550.
213. M. Selkti, A. Thomas, B. Viossat, G. Baziard-Mouysset and T. Prangé, *Z. Kristallogr.-New Cryst. Struct.* **1997**, *212*, 337.
214. Yu. N. Kukushkin, S. A. Simanova, V. K. Krylov, S. I. Bakhireva and I. A. Belen'kaya, *Russ. J. Gen. Chem*. **1976**, *46*, 885.
215. T. K. Martynova, V. A. Neverov, V. N. Byushkin, V. N. Shafranskii and T. A. Malkova, *Koord. Khim.* **1985**, *11*, 132.
216. E. M. Trishkina, M. A. Golubnichaya and I. B. Baranovskii, *Russ. J. Inorg. Chem*. **1990**, *36*, 687.
217. Y.-Koh, Ph.D. Thesis, The Ohio State University, 1979.
218. S. A. Hilderbrand, M. H. Lim and S. J. Lippard, *J. Am. Chem. Soc.* **2004**, *126*, 4972.
219. A. Cogne, A. Grand, P. Rey and R. Subra, *J. Am. Chem. Soc.* **1989**, *111*, 3230.
220. V. N. Shafranskii, T. A. Mal'kova and Yu. Ya. Kharitonov, *J. Struct. Chem.* **1975**, *16*, 195.
221. V. N. Shafranskii, T. A. Mal'kova and Yu. Ya. Kharitonov, *Sov. J. Coord. Chem.* **1975**, *1*, 297.
222. M. A. Porai-Koshits and A. S. Antsyshkina, *Dokl. Chem. Proc. Acad. Sciences USSR, Chem. Sect.* **1962**, *146*, 902.
223. F. A. Cotton, B. G. DeBoer, M. D. LaPrade, J. R. Pipal and D. A. Ucko, *Acta Crystallogr*. **1971**, *B27*, 1664.
224. F. A. Cotton, B. G. DeBoer, M. D. LaPrade, J. R. Pipal and D. A. Ucko, *J. Am. Chem. Soc.* **1970**, *92*, 2926.
225. T. A. Mal'kova and V. N. Shafranskii, *J. Gen. Chem. USSR* **1977**, *47*, 2365.
226. F. A. Cotton and T. R. Felthouse, *Inorg. Chem.* **1980**, *19*, 323.
227. F. A. Cotton and T. R. Felthouse, *Inorg. Chem.* **1980**, *19*, 2347.
228. F. A. Cotton and T. R. Felthouse, *Inorg. Chem.* **1982**, *21*, 431.
229. A. S. Antsyshkina, M. A. Mitryakina, E. N. Yurchenko and L. S. Gracheva, *Russ. J. Inorg. Chem.* **1991**, *36*, 975.
230. V. Noinville, B. Viossat and N.-H. Dung, *Acta Crystallogr.* **1993**, *C49*, 1297.
231. P. G. Jessop, M. M. Olmstead, C. D. Ablan, M. Grabenauer, D. Sheppard, C. A. Eckert and C. L. Liotta, *Inorg. Chem.* **2002**, *41*, 3463.
232. M. A. Porai-Koshits, L.M. Dikareva, G. G. Sadikov and I. B. Baranovskii, *Russ. J. Inorg. Chem.* **1979**, *24*, 716.
233. Q.-H. Zhao, W.-M. Bu, D.-Z. Liao, Z.-H. Jiang and S.-P. Yan, *Polish J. Chem.* **2000**, *74*, 285.
234. M. Moszner, T. Glowiak and J. J. Ziólkowski, *Polyhedron* **1985**, *4*, 1413.
235. F. P. Pruchnik, A. Jutarska, Z. Ciunik and M. Pruchnik, *Inorg. Chim. Acta* **2003**, *350*, 609.
236. V. N. Shafranskii and T. A. Mal'kova, *J. Gen. Chem. USSR* **1975**, *45*, 1051.
237. F. A. Cotton and T. R. Felthouse, *Inorg. Chem.* **1981**, *20*, 2703.
238. E. V. Dikarev, M. A. Petrukhina, X. Li and E. Block, *Inorg. Chem.* **2003**, *42*, 1966.
239. M. H. Chisholm, K. Folting, K. G. Moodley, J. E. Wesemann, *Polyhedron* **1996**, *15*, 1903.
240. X. Wei, M. H. Dickman and M. T. Pope, *Acta Crystallogr.* **1998**, *C54*, 351.
241. J. Frelek, J. Jagodzinski, H. Meyer-Figge, W. S. Sheldrick, E. Wieteska and W. J. Szczepek, *Chirality* **2001**, *13*, 313.
242. M. Handa, M. Mikuriya, Y. Sato, T. Kotera, R. Nukada, D. Yoshioka and K. Kasuga, *Bull. Chem. Soc. Jpn.* **1996**, *69*, 3483.
243. T.-Y. Dong, D. N. Hendrickson, T. R. Felthouse and H.-S. Shieh, *J. Am. Chem. Soc.* **1984**, *106*, 5373.
244. T. R. Felthouse, T.-Y. Dong, D. N. Hendrickson, H.-S. Shieh and M. R. Thompson, *J. Am. Chem. Soc.* **1986**, *108*, 8201.
245. A. Cogne, A. Grand, P. Rey and R. Subra, *J. Am. Chem. Soc.* **1987**, *109*, 7927.
246. C. Bilgrien, R. S. Drago, J. R. Stahlbush and T. C. Kuechler, *Inorg. Chem.* **1985**, *24*, 4268.
247. F. A. Cotton and T. R. Felthouse, *Inorg. Chem*. **1982**, *21*, 2667.

Pictiva EX2004
Samsung v Pictiva
IPR2024-01094

248. C. J. Simmons, A. Clearfield and Y. Sun, *Inorg. Chim. Acta* **1986**, *121*, L3.
249. N. N. Sveshnikov, M. H. Dickman and M. T. Pope, *Acta Crystallogr.* **2000**, *C56*, 1193.
250. R. J. H. Clark, A. J. Hempleman, H. M. Dawes, M. B. Hursthouse and C. D. Flint, *J. Chem. Soc., Dalton Tran.* **1985**, 1775.
251. R. J. H. Clark and A. J. Hempleman, *J. Mol. Struct*. **1989**, *197*, 105.
252. G. G. Christoph and M. Tolbert, *ACA, Ser. 2* **1980**, *7*, 39.
253. G. Pneumatikakis and P. Psaroulis, *Inorg. Chim. Acta* **1980**, *46*, 97.
254. G. Matsubayashi, K. Yokoyama and T. Tanaka, *J. Chem. Soc., Dalton Trans.* **1988**, 3059.
255. G. Faraglia, R. Graziani, L. Volponi and U. Casellato, *Inorg. Chim. Acta* **1988**, *148*, 159.
256. T. A. Mal'kova and V. N. Shafranskii, *Zhur. Fiz. Khim*. **1975**, *49*, 2805.
257. S. Ahmad, A. A. Isab and S. Ahmad, *J. Coord. Chem*. **2003**, *56*, 1587.
258. G. Faraglia, L. Volponi and S. Sitran, *Thermochim. Acta* **1988**, *132*, 217.
259. V. Kh. Kravtsov, Yu. A. Simonov, J. Lipkowski, O. A. Bologa, N. V. Gérbéléu and V. I. Lozan, *Cryst. Rep.* **2002**, *47*, 80.
260. T. A. Mal'kova, V. N. Shafranskii and Yu. Ya. Kharitonov, *Sov. J. Coord. Chem.* **1977**, *3*, 1371.
261. G. G. Christoph and Y.-B. Koh, *J. Am. Chem. Soc.* **1979**, *101*, 1422.
262. R. B. King, A. D. King, Jr. and M. Z. Iqbal, *J. Am. Chem. Soc.* **1979**, *101*, 4893.
263. C. Bilgrien, R. S. Drago, G. C. Vogel and J. Stahlbush, *Inorg. Chem.* **1986**, *25*, 2864.
264. V. N. Shafranskii and T. A. Mal'kova, *J. Gen. Chem. USSR* **1976**, *46*, 1181.
265. G. S. Girolami and R. A. Andersen, *Inorg. Chem.* **1981**, *20*, 2040.
266. C. T. Eagle, D. G. Farrar, C. U. Pfaff, J. A. Davies, C. Kluwe and L. Miller, *Organometallics* **1998**, *17*, 4523.
267. F. Mikes, V. Schurig and E. Gil-Av, *J. Chromatogr.* **1973**, *83*, 91.
268. V. Schurig, *Chem. -Ztg*. **1977**, *101*, 173.
269. V. Schurig, *Inorg. Chem.* **1986**, *25*, 945.
270. M. Gerards and G. Snatzke, *Tetrahedron: Asymmetry* **1990**, *1*, 221.
271. M. P. Doyle, M. R. Colsman and M. S. Chinn, *Inorg. Chem*. **1984**, *23*, 3684.
272. M. P. Doyle, S. N. Mahapatro, A. C. Caughey, M. S. Chinn, M. R. Colsman, N. K. Harn and A. E. Redwine, *Inorg. Chem*. **1987**, *26*, 3070.
273. V. Schurig, J. L. Bear and A. Zlatkis, *Chromatographia* **1972**, *5*, 301.
274. F. A. Cotton, L. R. Falvello, M. Gerards and G. Snatzke, *J. Am. Chem. Soc.* **1990**, *112*, 8979.
275. M. Handa, A. Takata, T. Nakao, K. Kasuga, M. Mikuriya and T. Kotera, *Chem. Lett.* **1992**, 2085.
276. M. Handa, T. Nakao, M. Mikuriya, T. Kotera, R. Nukada and K. Kasuga, *Inorg. Chem.* **1998**, *37*, 149.
277. J. P. Snyder, A. Padwa, T. Stengel, A. J. Arduengo III, A. Jockisch and H.-J. Kim, *J. Am. Chem. Soc.* **2001**, *123*, 11318.
278. G. G. Christoph, J. Halpern, G. P. Khare, Y. B. Koh and C. Romanowski, *Inorg. Chem.* **1981**, *20*, 3029.
279. G. G. Cristoph and D. J. Kountz, *ACA, Ser. 2* **1982**, *10*, 23.
280. C. J. Alarcón, P. Lahuerta, E. Peris, M. A. Ubeda, A. Aguirre, S. García-Granda and F. Gómez-Beltrán, *Inorg. Chim. Acta* **1997**, *254*, 177.
281. E. E. Nifantyev, A. T. Teleshev, L. F. Popova and V. A. Polyakov, *Phosphorus, Sulfur and Silicon* **1995**, *103*, 253.
282. A. B. Kudryavtsev, A. T. Teleshev, V. A. Polyakov, A. V. Shishin and W. Linert, *Inorg. Chim. Acta* **1998**, *267*, 293.
283. G. Zhang, J. Zhao, G. Raudaschl-Sieber, E. Herdtweck and F. E. Kühn, *Polyhedron* **2002**, *21*, 1737.
284. F. A. Cotton, T. R. Felthouse and S. Klein, *Inorg. Chem*. **1981**, *20*, 3037.
285. T. Kawamura, M. Maeda, M. Miyamoto, H. Usami, K. Imaeda and M. Ebihara, *J. Am. Chem. Soc.* **1998**, *120*, 8136.
286. E. B. Boyar and S. D. Robinson, *Inorg. Chim. Acta* **1982**, *64*, L193.
287. E. B. Boyar and S. D. Robinson, *J. Chem. Soc., Dalton Trans.* **1985**, 629.

Pictiva EX2004
Samsung v Pictiva
IPR2024-01094

288. M. A. S. Aquino and D. H. Macartney, *Inorg. Chem.* **1987**, *26*, 2696.
289. M. A. S. Aquino and D. H. Macartney, *Inorg. Chem.* **1988**, *27*, 2868.
290. J. Telser and R. S. Drago, *Inorg. Chem.* **1986**, *25*, 2989.
291. R. W. Mitchell, J. D. Ruddick and G. Wilkinson, *J. Chem. Soc. A* **1971**, 3224.
292. L. V. Slavina, L. S. Gracheva and V. K. Polovnyak, *Izv. Vyssh. Ucheb. Zaved., Khim. Khim. Tekhnol*. **2001**, *44*, 75.
293. L. M. Dikareva, G. G. Sadikov, I. B. Baranovskii and M. A. Porai-Koshits, *Russ. J. Inorg. Chem.* **1980**, *25*, 1725.
294. V. M. Miskowski, W. P. Schaefer, B. Sadeghi, B. D. Santarsiero and H. B. Gray, *Inorg. Chem.* **1984**, *23*, 1154.
295. V. M. Miskowski, R. F. Dallinger, G. G. Christoph, D. E. Morris, G. H. Spies and W. H. Woodruff, *Inorg. Chem.* **1987**, *26*, 2127.
296. E. Galdecka, Z. Galdecki, F. P. Pruchnik and R. Starosta, *Transition Met. Chem.* **1999**, *24*, 100.
297. Z.-H. Zhou, R.-J. Wang, T. C. W. Mak and C.-M. Che, *Inorg. Chim. Acta* **1991**, *180*, 1.
298. F. A. Cotton and K.-B. Shiu, *Rev. Chim. Minér.* **1986**, *23*, 14.
299. J. C. A. Boeyens, F. A. Cotton and S. Han, *Inorg. Chem.* **1985**, *24*, 1750.
300. J. G. Norman, Jr. and H. J. Kolari, *J. Am. Chem. Soc.* **1978**, *100*, 791.
301. B. E. Bursten and F. A. Cotton, *Inorg. Chem*. **1981**, *20*, 3042.
302. A. S. Ancyskina, *Acta Crystallogr.* **1966**, *S21*, A135 *& Part 7S*.
303. F. A. Cotton, E. V. Dikarev, M. A. Petrukhina, M. Schmitz and P. J. Stang, *Inorg. Chem.* **2002**, *41*, 2903.
304. J. Lu, W. T. A. Harrison and A. J. Jacobson, *Chem. Commun.* **1996**, 399.
305. C. T. Chapman, A. M. Goforth, N. G. Pschirer, M. D. Smith, U. H. F. Bunz and H.-C. zur Loye, *J. Chem. Crystallogr*. **2003**, *33*, 885.
306. S. M. Contakes, K. K. Klausmeyer and T. B. Rauchfuss, *Inorg. Chem.* **2000**, *39,* 2069.
307. Y. Kim, S.-J. Kim and W. Nam, *Acta Crystallogr.* **2001**, *C57*, 266.
308. M. A. Petrukhina, K. W. Andreini, A. M. Walji and H. M. L. Davies, *Dalton Trans*. **2003**, 4221.
309. C. T. Chapman, D. M. Ciurtin, M. D. Smith and H.-C. zur Loye, *Solid State Sciences* **2002**, *4*, 1187.
310. F. A. Cotton, E. V. Dikarev and M. A. Petrukhina, *J. Chem. Soc., Dalton Trans.* **2000**, 4241.
311. E.-J. Kim and T.-J. Kim, *Bull. Korean Chem. Soc.* **1994**, *15*, 990.
312. E. V. Dikarev, R. V. Shpanchenko, K. W. Andreini, E. Block, J. Jin and M. A. Petrukhina, *Inorg. Chem*. **2004**, *43*, 5558.
313. M. Bardet, P. Maldivi, A.-M. Giroud-Godquin and J.-C. Marchon, *Langmuir* **1995**, *11*, 2306.
314. M. Rusjan, B. Donnio, D. Guillon and F. D. Cukiernik, *Chem. Mater*. **2002**, *14*, 1564.
315. E. V. Dikarev, K. W. Andreini and M. A. Petrukhina, *Inorg. Chem*. **2004**, *43*, 3219.
316. D. L. Lichtenberger, J. R. Pollard, M. A. Lynn, F. A. Cotton and X. Feng, *J. Am. Chem. Soc.* **2000**, *122,* 3182.
317. F. A. Cotton and X. Feng, *J. Am. Chem. Soc.* **1998**, *120,* 3387.
318. D. V. Deubel, *Organometallics* **2002**, *21*, 4303.
319. R. J. H. Clark and J. Hempleman, *Inorg. Chem*. **1989**, *28*, 746.
320. R. J. H. Clark and J. Hempleman, *Inorg. Chem*. **1988**, *27*, 2225.
321. R. J. H. Clark, J. Hempleman and C. D. Flint, *J. Am. Chem. Soc.* **1986**, *108*, 518.
322. H. Nakatsuji, Y. Onishi, J. Uhio and T. Yonezawa, *Inorg. Chem*. **1983**, *22*, 1623.
323. C. Lacaze-Dufour, T. Mineva and N. Russo, *Int. J. Quantum Chem*. **2001**, *85*, 162.
324. S. Yanagisawa, T. Tsuneda and K. Hirao, *J. Comp. Chem*. **2001**, *22*, 1995.
325. H. Nakatsuji, J. Ushio, K. Kanda, Y. Onishi, T. Kawamura and T. Yonezawa, *Chem. Phys. Lett*. **1981**, *79*, 299.
326. P. Mougenot, J. Demuynck and M. Bénard, *Chem. Phys. Lett.* **1987**, *136*, 279.
327. R. D. Sinisterra, R. Najjar and L. F. C. de Oliveira, *Spectrosc. Lett*. **1993**, *26*, 305.
328. A. P. Ketteringham and C. Oldham, *J. Chem. Soc., Dalton Trans*. **1973**, 1067.
329. R. J. H. Clark and A. J. Hempleman, *Croat. Chem. Acta* **1988**, *61*, 313.

Pictiva EX2004
Samsung v Pictiva
IPR2024-01094

330. Yu. Ya. Kharitonov, G. Ya. Mazo and N. A. Knyazeva, *Russ. J. Inorg. Chem*. **1970**, *15*, 739.
331. A. V. Rotov, E. A. Ugolkova and Yu. V. Rakitin, *Russ. J. Inorg. Chem*. **1991**, *36*, 1024.
332. A. V. Rotov, E. A. Ugolkova and Yu. V. Rakitin, *Russ. J. Inorg. Chem*. **1991**, *36*, 1026.
333. A. M. Dennis, R. A. Howard, K. M. Kadish, J. L. Bear, J. Brace and N. Winograd, *Inorg. Chim. Acta* **1980**, *44*, L139.
334. F. M. O' Neill and J. C. A. Boeyens, *Inorg. Chem*. **1990**, *29*, 1301.
335. L. A. Nazarova and A. G. Maiorova, *Russ. J. Inorg. Chem.* **1973**, *18*, 904.
336. J. Halpern, E. Kimura, J. Molin-Case and C. S. Wong, *J. Chem. Soc., Chem. Commun.* **1971**, 1207.
337. K. G. Caulton and F. A. Cotton, *J. Am. Chem. Soc.* **1969**, *91*, 6517.
338. K. G. Caulton and F. A. Cotton, *J. Am. Chem. Soc.* **1971**, *93*, 1914.
339. S. Cenini, R.Ugo and F. Bonati, *Inorg. Chim. Acta* **1967**, *1*, 443.
340. H. J. McCarthy and D. A. Tocher, *Inorg. Chim. Acta* **1988**, *145*, 171.
341. H. J. McCarthy and D. A. Tocher, *Polyhedron* **1989**, *8*, 1117.
342. H. Pasternak and F. Pruchnik, *Inorg. Nucl. Chem. Lett.* **1976**, *12*, 591.
343. T. Glowiak, H. Pasternak and F. Pruchnik, *Acta Crystallogr.* **1987**, *C43,* 1036.
344. A. P. Kochetkova, L. B. Sveshnikova, V. M. Stepanovich and V. I. Sokol, *Sov. J. Coord. Chem.* **1982**, *8*, 281.
345. V. I. Sokol, M. A. Porai-Koshits, A. P. Kochetkova and L. B. Sveshnikova, *Sov. J. Coord. Chem.* **1984**, *10*, 461.
346. L. B. Sveshnikova, *Russ. J. Inorg. Chem.* **1987**, *32*, 1732.
347. F. Pruchnik, J. Hanuza, K. Hermanowicz, K. Wajda-Hermanowicz, H. Pasternak and M. Zuber, *Spectrochim. Acta* **1989**, *A45*, 835.
348. F. P. Pruchnik, *Pure Appl. Chem.* **1989**, *61*, 795.
349. M. Calligaris, L. Campana, G. Mestroni, M. Tornatore and E. Alessio, *Inorg. Chim. Acta* **1987**, *127*, 103.
350. E. Galdecka, Z. Galdecki, F. P. Pruchnik and P. Jakimowicz, *Trans. Met. Chem.* **2000**, *25*, 315.
351. C. A. Crawford, J. H. Matonic, J. C. Huffman, K. Folting, K. R. Dunbar and G. Christou, *Inorg. Chem.* **1997**, *36*, 2361.
352. T. Glowiak, F. P. Pruchnik and M. Zuber, *Polish J. Chem.* **1991**, *65*, 1749.
353. L. Natkaniec and F. P. Pruchnik, *J. Chem. Soc., Dalton Trans.* **1994**, 3261.
354. F. P. Pruchnik, M. Zuber, H. Pasternak and K. Walda, *Spectrochim. Acta* **1978**, *34A*, 1111.
355. F. P. Pruchnik and M. Zuber, *Rocz. Chem*. **1977**, *51*, 1813.
356. M. A. M. Daniels, N. Mehmet and D. A. Tocher, *J. Chem. Soc., Dalton Trans.* **1991**, 2601.
357. T. Yoshimura, K. Umakoshi and Y. Sasaki, *Chem. Lett.* **1999**, 267.
358. F. P. Pruchnik, A. Jutarska, Z. Ciunik and M. Pruchnik, *Inorg. Chim. Acta* **2004**, *357*, 3019.
359. F. Pruchnik, A. Jezierski and E. Kalecinska, *Polyhedron* **1991**, *10*, 2551.
360. J. Telser and R. S. Drago, *Inorg. Chem.* **1984**, *23*, 1798.
361. G. Pimblett, C. D. Garner and W. Clegg, *J. Chem. Soc., Dalton Trans*. **1986**, 1257.
362. I. B. Baranovskii, M. A. Golubnichaya, A. N. Zhilyaev and R. N. Shchelokov, *Sov. J. Coord. Chem.* **1987**, *13*, 369.
363. K. R. Dunbar, L. E. Pence and J. L. C. Thomas, *Inorg. Chim. Acta* **1994**, *217*, 79.
364. J. M. Casas, R. H. Cayton and M. H. Chisholm, *Inorg. Chem.* **1991**, *30*, 358.
365. C. R. Wilson and H. Taube, *Inorg. Chem.* **1975**, *14*, 2276.
366. A. N. Zhilyaev, A. T. Fal'kengof, M. A. Golubnichaya, I. B. Baranovskii and R. N. Shchelokov, *Sov. J. Coord. Chem.* **1986**, *12*, 977.
367. I. B. Baranovskii, M. A. Golubnichaya, L. M. Dikareva and R. N. Shchelokov, *Russ. J. Inorg. Chem.* **1984**, *29*, 872.
368. L. M. Dikareva, M. A. Golubnichaya and I. B. Baranovskii, *Russ. J. Inorg. Chem.* **1988**, *33*, 1179.
369. I. B. Baranovskii, S. S. Abdullaev, G. Ya. Mazo and R. N. Shchelokov, *Russ. J. Inorg. Chem.* **1982**, *27*, 1158.
370. R. N. Shchelokov, A. G. Maiorova, O. M. Evstafeva and G. N. Emel'yanova, *Russ. J. Inorg. Chem.* **1977**, *22*, 770.

Pictiva EX2004
Samsung v Pictiva
IPR2024-01094

371. I. B. Baranovskii and A. N. Zhilyaev, *Russ. J. Inorg. Chem.* **1984**, *29*, 607.
372. S. P. Perlepes, J. C. Huffman, J. H. Matonic, K. R. Dunbar and G. Christou, *J. Am. Chem. Soc.* **1991**, *113*, 2770.
373. C. A. Crawford, J. H. Matonic, W. E. Streib, J. C. Huffman, K. R. Dunbar and G. Christou, *Inorg. Chem.* **1993**, *32*, 3125.
374. F. Barceló, F. A. Cotton, P. Lahuerta, R. Llusar, M. Sanaú, W. Schwotzer and M. A. Ubeda, *Organometallics,* **1986**, *5*, 808.
375. A. García-Bernabé, P. Lahuerta, M. A. Ubeda, S. García-Granda and P. Pertierra, *Inorg. Chim. Acta* **1995**, *229*, 203.
376. P. Lahuerta, M. A. Ubeda, J. Payá, S. García-Granda, F. Gómez-Beltrán and A. Anillo, *Inorg. Chim. Acta* **1993**, *205*, 91.
377. F. Estevan, A. García-Bernabé, S. García-Granda, P. Lahuerta, E. Moreno, J. Pérez-Prieto, M. Sanaú and M. A. Ubeda, *J. Chem. Soc., Dalton Trans.* **1999**, 3493.
378. G. González, M. Martinez, F. Estevan, A. García-Bernabé, P. Lahuerta, E. Peris, M. A. Ubeda, M. R. Díaz, S. García-Granda and B. Tejerina, *New J. Chem.* **1996**, *20*, 83.
379. P. Lahuerta, E. Peris, M. A. Ubeda, S. García-Granda, F. Gómez-Beltrán and M. R. Díaz, *J. Organomet. Chem*. **1993**, *455*, C10.
380. Yu. S. Varshavskii, T. G. Cherkasova, I. S. Podkorytov and S. E. Nefedov, *Russ. J. Coord. Chem.* **1999**, *25*, 260.
381. J. L. Bear, R. A. Howard and J. E. Horn, *Inorg. Chim. Acta* **1979**, *32*, 123.
382. W. R. Tikkanen, E. Binamira-Soriaga, W. C. Kaska and P. C. Ford, *Inorg. Chem*. **1984**, *23*, 141.
383. W. R. Tikkanen, E. Binamira-Soriaga, W. C. Kaska and P. C. Ford, *Inorg. Chem*. **1983**, *22*, 1147.
384. A. Petitjean, J.-M. Lehn, R. G. Khoury, A. De Cian and N. Kyritsakas, *Chimie* **2002**, *5*, 337.
385. J. K. Bera, C. S. Campos-Fernández, R. Clérac and K. R. Dunbar, *Chem. Commun.* **2002**, 2536.
386. R. P. Thummel, F. Lefoulon, D. Williamson and M. Chavan, *Inorg. Chem.* **1986**, *25*, 1675.
387. C. S. Campos-Fernández, X. Ouyang and K. R. Dunbar, *Inorg. Chem.* **2000**, *39*, 2432.
388. C. S. Campos-Fernández, L. M. Thomson, J. R. Galán-Mascarós, X. Ouyang and K. R. Dunbar, *Inorg. Chem.* **2002**, *41*, 1523.
389. J. L. Bear, L. K. Chau, M. Y. Chavan, F. Lefoulon, R. P. Thummel and K. M. Kadish, *Inorg. Chem.* **1986**, *25*, 1514.
390. J.-P. Collin, A. Jouaiti, J.-P. Sauvage, W. C. Kaska, M. A. McLoughlin, N. L. Keder, W. T. A. Harrison and G. D. Stucky, *Inorg. Chem.* **1990**, *29*, 2238.
391. F. A. Cotton and T. R. Felthouse, *Inorg. Chem.* **1981**, *20*, 584.
392. F. A. Cotton and S.-J. Kang, *Inorg. Chim. Acta* **1993**, *209*, 23.
393. K. R. Dunbar, J. H. Matonic, V. P. Saharan, C. A. Crawford and G. Christou, *J. Am. Chem. Soc.* **1994**, *116*, 2201.
394. C. A. Crawford, E. F. Day, V. P. Saharan, K. Folting, J. C. Huffman, K. R. Dunbar and G. Christou, *Chem. Commun.* **1996**, 1113.
395. H. T. Chifotides, J. S. Hess, A. M. Angeles-Boza, J. R. Galán-Mascarós, K. Sorasaenee and K. R. Dunbar, *Dalton Trans*. **2003**, 4426.
396. M. Berry, C. D. Garner, I. H. Hillier, A. A. MacDowell and W. Clegg, *J. Chem. Soc., Chem. Commun.* **1980**, 494.
397. W. Clegg, *Acta Crystallogr.* **1980**, *B36*, 2437.
398. A. R. Barron, G. Wilkinson, M. Motevalli and M. B. Hursthouse, *Polyhedron* **1985**, *4*, 1131.
399. F. A. Cotton, S. Han and W. Wang, *Inorg. Chem.* **1984**, *23*, 4762.
400. D. A. Tocher and J. H. Tocher, *Inorg. Chim. Acta* **1987**, *131*, 69.
401. W. Clegg, C. D. Garner, L. Akhter and M. H. Al-Samman, *Inorg. Chem.* **1983**, *22*, 2466.
402. M. Berry, C. D. Garner, I. H. Hillier and W. Clegg, *Inorg. Chim. Acta* **1980**, *45*, L209.
403. C. D. Garner, M. Berry and B. E. Mann, *Inorg. Chem.* **1984**, *23*, 1500.
404. T. Kawamura, H. Kachi, H. Fujii, C. Kachi-Terajima, Y. Kawamura, N. Kanematsu, M. Ebihara, K. Sugimoto, T. Kuroda-Sowa and M. Munakata, *Bull. Chem. Soc. Jpn.* **2000**, *73*, 657.
405. W. Clegg, L. Akhter and C. D. Garner, *J. Chem. Soc., Chem. Commun.* **1984**, 101.

Pictiva EX2004
Samsung v Pictiva
IPR2024-01094

406. M. Mintert and W. S. Sheldrick, *Inorg. Chim. Acta* **1997**, *254*, 93.
407. T. P. Zhu, M. Q. Ahsan, T. Malinski, K. M. Kadish and J. L. Bear, *Inorg. Chem.* **1984**, *23*, 2.
408. M. Y. Chavan, T. P. Zhu, X. Q. Lin, M. Q. Ahsan, J. L. Bear and K. M. Kadish, *Inorg. Chem.* **1984**, *23*, 4538.
409. R. S. Lifsey, X. Q. Lin, M. Y. Chavan, M. Q. Ahsan, K. M. Kadish and J. L. Bear, *Inorg. Chem.* **1987**, *26*, 830.
410. K. Aoki and Md. A. Salam, *Inorg. Chim. Acta* **2001**, *316*, 50.
411. K. Aoki and Md. A. Salam, *Inorg. Chim. Acta* **2002**, *339*, 427.
412. Y. Takazaki, Z. Yang, M. Ebihara, K. Inoue and T. Kawamura, *Chem. Lett.* **2003**, *32*, 120.
413. I. B. Baranovskii and R. E. Sevast'yanova, *Russ. J. Inorg. Chem.* **1984**, *29*, 1025.
414. M. Q. Ahsan, I. Bernal and J. L. Bear, *Inorg. Chem.* **1986**, *25*, 260.
415. I. Bernal and J. L. Bear, *J. Chem. Crystallogr.* **2002**, *32*, 485.
416. A. M. Dennis, R. A. Howard, D. Lancon, K. M. Kadish and J. L. Bear, *J. Chem. Soc., Chem. Commun.* **1982**, 399.
417. A. M. Dennis, J. D. Korp, I. Bernal, R. A. Howard and J. L. Bear, *Inorg. Chem.* **1983**, *22*, 1522.
418. J. Duncan, T. Malinski, T. P. Zhu, Z. S. Hu, K. M. Kadish and J. L. Bear, *J. Am. Chem. Soc.* **1982**, *104*, 5507.
419. M. P. Doyle, V. Bagheri, T. J. Wandless, N. K. Harn, D. A. Brinker, C. T. Eagle and K.-L. Loh, *J. Am. Chem. Soc.* **1990**, *112*, 1906.
420. C. T. Eagle, D. G. Farrar, G. N. Holder, W. T. Pennington and R. D. Bailey, *J. Organomet. Chem.* **2000**, *596*, 90.
421. M. Q. Ahsan, I. Bernal and J. L. Bear, *Inorg. Chim. Acta* **1986**, *115*, 135.
422. M. Y. Chavan, X. Q. Lin, M. Q. Ahsan, I. Bernal, J. L. Bear and K. M. Kadish, *Inorg. Chem.* **1986**, *25*, 1281.
423. S. P. Best, P. Chandley, R. J. H. Clark, S. McCarthy, M. B. Hursthouse and P. A. Bates, *J. Chem. Soc., Dalton Trans.* **1989**, 581.
424. M. Y. Chavan, M. Q. Ahsan, R. S. Lifsey, J. L. Bear and K. M. Kadish, *Inorg. Chem.* **1986**, *25*, 3218.
425. A. R. Chakravarty, F. A. Cotton, D. A. Tocher and J. H. Tocher, *Inorg. Chim. Acta* **1985**, *101*, 185.
426. M. Handa, Y. Muraki, M. Mikuriya, H. Azuma and K. Kasuga, *Bull. Chem. Soc. Jpn.* **2002**, *75*, 1755.
427. A. M. Angeles-Boza, K. R. Dunbar, J. Bacsa and C. Turro, unpublished results.
428. M. A. Zoroddu and R. Dallocchio, *Transition Met. Chem.* **1989**, *14*, 267.
429. Y. Fuma, M. Ebihara, S. Kutsumizu and T. Kawamura, *J. Am. Chem. Soc.* **2004**, *126*, 12238.
430. J. L. Bear, R. S. Lifsey, L. K. Chau, M. Q. Ahsan, J. D. Korp, M. Chavan and K. M. Kadish, *J. Chem. Soc., Dalton Trans.* **1989**, 93.
431. M. P. Doyle, W. R. Winchester, J. A. A. Hoorn, V. Lynch, S. H. Simonsen and R. Ghosh, *J. Am. Chem. Soc.* **1993**, *115*, 9968.
432. M. P. Doyle, W. Hu, I. M. Phillips, C. J. Moody, A. G. Pepper and A. M. Z. Slawin, *Adv. Synth. Catal.* **2001**, *343*, 112.
433. M. P. Doyle, W. R. Winchester, S. H. Simonsen and R. Ghosh, *Inorg. Chim. Acta* **1994**, *220*, 193.
434. M. P. Doyle, Q.-L. Zhou, S. H. Simonsen and V. Lynch, *Synlett* **1996**, 697.
435. M. P. Doyle, W. R. Winchester, M. N. Protopopova, P. Müller, G. Bernardinelli, D. Ene and S. Motallebi, *Helv. Chim. Acta* **1993**, *76*, 2227.
436. M. P. Doyle, A. B. Dyatkin, M. N. Protopopova, C. I. Yang, C. S. Miertschin, W. R. Winchester, S. H. Simonsen, V. Lynch and R. Ghosh, *Recl. Trav. Chim. Pays-Bas* **1995**, *114*, 163.
437. M. P. Doyle, Q.-L. Zhou, C. E. Raab, G. H. P. Roos, S. H. Simonsen and V. Lynch, *Inorg. Chem.* **1996**, *35*, 6064.
438. M. P. Doyle, C. E. Raab, G. H. P. Roos, V. Lynch and S. H. Simonsen, *Inorg. Chim. Acta* **1997**, *266*, 13.
439. G. H. P.Roos, C. E. Raab, N. D. Emslie, M. P. Doyle and V. Lynch, *Aust. J. Chem.* **1998**, *51*, 1.
440. M. P. Doyle and D. J. Timmons, unpublished results.

Pictiva EX2004
Samsung v Pictiva
IPR2024-01094

441. M. P. Doyle and J. T. Colyer, *Tetrahedron: Asymmetry* **2003**, *14*, 3601.
442. T. Ren, C. Lin, E. J. Valente and J. D. Zubkowski, *Inorg. Chim. Acta* **2000**, *297*, 283.
443. V. Fimiani, T. Ainis, A. Cavallaro and P. Piraino, *J. Chemother.* **1990**, *2*, 319.
444. J. L. Bear, C.-L. Yao, R. S. Lifsey, J. D. Korp and K. M. Kadish, *Inorg. Chem.* **1991**, *30*, 336.
445. P. Piraino, G. Bruno, G. Tresoldi, S. Lo Schiavo and P. Zanello, *Inorg. Chem.* **1987**, *26*, 91.
446. P. Piraino, G. Bruno, S. Lo Schiavo, F. Laschi and P. Zanello, *Inorg. Chem.* **1987**, *26*, 2205.
447. J. C. Le, M. Y. Chavan, L. K. Chau, J. L. Bear and K. M. Kadish, *J. Am. Chem. Soc.* **1985**, *107*, 7195.
448. L.-P. He, C.-L. Yao, M. Naris, J. C. Lee, J. D. Korp and J. L. Bear, *Inorg. Chem.* **1992**, *31*, 620.
449. G. A. Rizzi, M. Casarin, E. Tondello, P. Piraino and G. Granozzi, *Inorg. Chem.* **1987**, *26*, 3406.
450. F. A. Cotton and X. Feng, *Inorg. Chem.* **1989**, *28*, 1180.
451. M. B. Hursthouse, M. A. Mazid, T. Clark and S. D. Robinson, *Polyhedron* **1993**, *12*, 563.
452. N. G. Connelly and G. Garcia, *J. Chem. Soc., Chem. Commun.* **1987**, 246.
453. T. Brauns, C. Carriedo, J. S. Cockayne, N. G. Connelly, G. G. Herbosa and A. G. Orpen, *J. Chem. Soc., Dalton Trans.* **1989**, 2049.
454. N. G. Connelly, T. Einig, G. G. Herbosa, P. M. Hopkins, C. Mealli, A. G. Orpen, G. M. Rosair and F. Viguri, *J. Chem. Soc., Dalton Trans.* **1994**, 2025.
455. N. G. Connelly, O. D. Hayward, P. Klangsinsirikul and A. G. Orpen, *J. Chem. Soc., Dalton Trans.* **2002**, 305.
456. N. G. Connelly, C. J. Finn, M. J. Freeman, A. G. Orpen and J. Stirling, *J. Chem. Soc., Chem. Commun.* **1984**, 1025.
457. N. G. Connelly and A. C. Loyns, *J. Organomet. Chem.* **1991**, *411*, 285.
458. D. C. Boyd, N. G. Connelly, G. G. Herbosa, M. G. Hill, K. R. Mann, C. Mealli, A. G. Orpen, K. E. Richardson and P. H. Rieger, *Inorg. Chem.* **1994**, *33*, 960.
459. P. Piraino, G. Bruno, G. Tresoldi, S. Lo Schiavo and F. Nicolò, *Inorg. Chem.* **1989**, *28*, 139.
460. P. Piraino, G. Bruno, F. Nicolò, F. Faraone and S. L. Schiavo, *Inorg. Chem.* **1985**, *24*, 4760.
461. K. V. Catalan, D. J. Mindiola, D. L. Ward and K. R. Dunbar, *Inorg. Chem.* **1997**, *36*, 2458.
462. K. V. Catalan, J. S. Hess, M. M. Maloney, D. J. Mindiola, D. L. Ward and K. R. Dunbar, *Inorg. Chem.* **1999**, *38*, 3904.
463. P. Piraino, G. Tresoldi and F. Faraoni, *J. Organomet. Chem.* **1982**, *224*, 305.
464. E. Rotondo, B. E. Mann, P. Piraino and G. Tresoldi, *Inorg. Chem.* **1989**, *28*, 3070.
465. G. Bruno, G. De Munno, G. Tresoldi, S. Lo Schiavo and P. Piraino, *Inorg. Chem.* **1992**, *31*, 1538.
466. S. Lo Schiavo, M. S. Sinicropi, G. Tresoldi, C. G. Arena and P. Piraino, *J. Chem. Soc., Dalton Trans.* **1994**, 1517.
467. G. Tresoldi, S. Lo Schiavo, F. Nicolò, P. Cardiano and P. Piraino, *Inorg. Chim. Acta* **2003**, *344*, 190.
468. S. Lo Schiavo, G. Bruno, P. Zanello, F. Laschi and P. Piraino, *Inorg. Chem.* **1997**, *36*, 1004.
469. S. Lo Schiavo, S. Serroni, F. Puntoriero, G. Tresoldi and P. Piraino, *Eur. J. Inorg. Chem.* **2002**, 79.
470. S. Lo Schiavo, G. Pocsfalvi, S. Serroni, P. Cardiano and P. Piraino, *Eur. J. Inorg. Chem.* **2000**, 1371.
471. S. Lo Schiavo, F. Nicolò, G. Tresoldi and P. Piraino, *Inorg. Chim. Acta* **2003**, *343*, 351.
472. E. Rotondo, G. Bruno, F. Nicolò, S. Lo Schiavo and P. Piraino, *Inorg. Chem.* **1991**, *30*, 1195.
473. G. Tresoldi, G. De Munno, F. Nicolò, S. Lo Schiavo and P. Piraino, *Inorg. Chem.* **1996**, *35*, 1377.
474. H. T. Chifotides, K. V. Catalan and K. R. Dunbar, *Inorg. Chem.* **2003**, *42*, 8739.
475. J. L. Bear, B. Han, Z. Wu, E. van Caemelbecke and K. M. Kadish, *Inorg. Chem.* **2001**, *40*, 2275.
476. F. A. Cotton and R. Poli, *Inorg. Chem.* **1987**, *26*, 3652.
477. M. Handa, M. Yasuda, Y. Muraki, D. Yoshioka, M. Mikuriya and K. Kasuga, *Chem. Lett.* **2003**, *32*, 946.
478. F. A. Cotton, L. M. Daniels, C. Lin and C. A. Murillo, *J. Am. Chem. Soc.* **1999**, *121*, 4538.
479. F. A. Cotton, C. Lin and C. A. Murillo, *Chem. Commun.* **2001**, 11.
480. F. A. Cotton, C. Lin and C. A. Murillo, *Inorg. Chem.* **2001**, *40*, 5886.
481. F. A. Cotton, C. Lin and C. A. Murillo *J. Chem. Soc., Dalton Trans.* **2001**, 499.
482. F. A. Cotton, C. Lin and C. A. Murillo, *Inorg. Chem.* **2001**, *40*, 6413.

Pictiva EX2004
Samsung v Pictiva
IPR2024-01094

483. F. A. Cotton, C. Lin, C. A. Murillo and S.-Y. Yu, *J. Chem. Soc., Dalton Trans.* **2001**, 502.
484. F. A. Cotton, C. Lin, C. A. Murillo, X. Wang, S.-Y. Yu and Z.-X. Zhang, *J. Am. Chem. Soc.* **2004**, *126*, 1518.
485. C. Tejel, M. A. Ciriano, J. A. López, F. J. Lahoz and L. A. Oro, *Organometallics* **1997**, *16*, 4718.
486. C. Tejel, M. Bordonaba, M. A. Ciriano, A. J. Edwards, W. Clegg, F. J. Lahoz and L. A. Oro, *Inorg. Chem.* **1999**, *38*, 1108.
487. F. Barceló, P. Lahuerta, M. A. Ubeda, C. Foces-Foces, F. H. Cano and M. Martínez-Ripoll, *J. Chem. Soc., Chem. Commun.* **1985**, 43.
488. F. Barceló, P. Lahuerta, M. A. Ubeda, C. Foces-Foces, F. H. Cano and M. Martínez-Ripoll, *Organometallics* **1988**, 7, 584.
489. J. D. Reynolds, J. L. E. Burn, B. Boggess, K. D. Cook and C. Woods, *Inorg. Chem.* **1993**, *32*, 5517.
490. D. A. Tocher and J. H. Tocher, *Inorg. Chim. Acta* **1985**, *104*, L15.
491. D. A. Tocher and J. H. Tocher, *Polyhedron* **1986**, *5*, 1615.
492. J. L. Bear, L.-M. Liu and K. M. Kadish, *Inorg. Chem.* **1987**, *26*, 2927.
493. J. L. Bear, C.-L. Yao, L.-M. Liu, F. J. Capdevielle, J. D. Korp, T. A. Albright, S.-K. Kang and K. M. Kadish, *Inorg. Chem.* **1989**, *28*, 1254.
494. L.-M. Liu and J. L. Bear, *Sci. China, Ser. B* **1990**, *33*, 513.
495. C.-L. Yao, F. J. Capdevielle, K. M. Kadish and J. L. Bear, *Anal. Chem.* **1989**, *61*, 2805.
496. D. Dowerah, L. J. Radonovich, N. F. Woolsey and M. J. Heeg, *Organometallics* **1990**, *9*, 614.
497. F. A. Cotton, C. A. Murillo and S.-E. Stiriba, *Inorg. Chem. Commun.* **1999**, *2*, 463.
498. A. T. Baker, W. R. Tikkanen, W. C. Kaska and P. C. Ford, *Inorg. Chem.* **1984**, *23*, 3254.
499. A. N. Zhilyaev, I. V. Kuz'menko, T. A. Fomina, G. N. Kuznetsova and I. B. Baranovskii, *Russ. J. Inorg. Chem.* **1991**, *36*, 1568.
500. D. A. Lutterman, N. N. Degtyareva, D. H. Johnston, J. L. Eglin and C. Turro, unpublished results.
501. R. S. Lifsey, M. Y. Chavan, L. K. Chau, M. Q. Ahsan, K. M. Kadish and J. L. Bear, *Inorg. Chem.* **1987**, *26*, 822.
502. J. M. Poblet and M. Benard, *Inorg. Chem*. **1988**, *27*, 2935.
503. A. J. Deeming, M. N. N. Meah, H. M. Dawes and M. B. Hursthouse, *J. Organomet. Chem.* **1986**, *299*, C25.
504. S. Gopinathan, C. Gopinathan, S. A. Pardhy, S. S. Tavale and V. G. Puranik, *Inorg. Chim. Acta* **1992**, *195*, 211.
505. J. Xiao and M. Cowie, *Can. J. Chem.* **1993**, *71*, 726.
506. Y. Fuchita, Y. Ohta, K. Hiraki, M. Kawatani and N. Nishiyama, *J. Chem. Soc., Dalton Trans.* **1990**, 3767.
507. F. A. Cotton, K. R. Dunbar and M. G. Verbruggen, *J. Am. Chem. Soc.* **1987**, *109*, 5498.
508. F. A. Cotton, C. T. Eagle and A. C. Price, *Inorg. Chem*. **1988**, *27*, 4362.
509. L. J. Tortorelli, P. W. Tinsley, C. Woods and C. J. Janke, *Polyhedron* **1988**, 7, 315.
510. J. A. Jenkins, J. P. Ennett and M. Cowie, *Organometallics* **1988**, 7, 1845.
511. A. L. Balch and B. Tulyathan, *Inorg. Chem*. **1977**, *16*, 2840.
512. A. L. Balch, *J. Am. Chem. Soc.* **1976**, *98*, 8049.
513. M. Cowie and S. K. Dwight, *Inorg. Chem.* **1980**, *19*, 209.
514. A. L. Davis and R. J. Goodfellow, *J. Chem. Soc., Dalton Trans*. **1993**, 2273.
515. F. A. Cotton and M. Matusz, *Inorg. Chim. Acta* **1988**, *143*, 45.
516. Z. Galdecki, E. Galdecka, A. Kowalski, F. P. Pruchnik, K. Wajda-Hermanowicz and R. Starosta, *Pol. J. Chem.* **1999**, *73*, 859.
517. L. J. Tortorelli, C. A. Tucker, C. Woods and J. Bordner, *Inorg. Chem.* **1986**, *25*, 3534.
518. C. Woods and L. J. Tortorelli, *Polyhedron* **1988**, 7, 1751.
519. J. P. Farr, M. M. Olmstead, C. H. Hunt and A. L. Balch, *Inorg. Chem*. **1981**, *20*, 1182.
520. L. A. Oro, M. T. Pinillos, A. Tiripicchio and M. Tiripicchio-Camellini, *Inorg. Chim. Acta* **1985**, *99*, L13.

Pictiva EX2004
Samsung v Pictiva
IPR2024-01094

521. L. A. Oro, D. Carmona, P. L. L. Pérez, M. Esteban, A. Tiripicchio and M. Tiripicchio-Camellini, *J. Chem. Soc., Dalton Trans.* **1985**, 973.
522. A. R. Chakravarty, F. A. Cotton and D. A. Tocher, *J. Chem. Soc., Chem. Commun.* **1984**, 501.
523. A. R. Chakravarty, F. A. Cotton, D. A. Tocher and J. H. Tocher, *Organometallics* **1985**, *4*, 8.
524. P. Lahuerta, J. Payá, E. Peris, M. A. Pellinghelli and A. Tiripicchio, *J. Organomet. Chem.* **1989**, *373*, C5.
525. P. Lahuerta, J. Payá, M. A. Pellinghelli and A. Tiripicchio, *Inorg. Chem.* **1992**, *31*, 1224.
526. P. Lahuerta and E. Peris, *Inorg. Chem*. **1992**, *31*, 4547.
527. P. Lahuerta, J. Payá and A. Bianchi, *Inorg. Chem*. **1992**, *31*, 5336.
528. F. Estevan, G. González, P. Lahuerta, M. Martinez, E. Peris and R. van Eldik, *J. Chem. Soc., Dalton Trans*. **1996**, 1045.
529. C. J. Alarcón, F. Estevan, P. Lahuerta, M. A. Ubeda, G. González, M. Martinez and S. E. Stiriba, *Inorg. Chim. Acta* **1998**, *278*, 61.
530. S. García-Granda, M. R. Díaz, F. Gómez-Beltrán, E. Peris and P. Lahuerta, *Acta Crystallogr.* **1994**, *C50*, 691.
531. P. Lahuerta, J. Payá, X. Solans and M. A. Ubeda, *Inorg. Chem.* **1992**, *31*, 385.
532. P. Lahuerta, J. Latorre, E. Peris, M. Sanaú and S. García-Granda, *J. Organomet. Chem.* **1993**, *456*, 279.
533. F. P. Pruchnik, R. Starosta, T. Lis and P. Lahuerta, *J. Organomet. Chem.* **1998**, *568*, 177.
534. P. Lahuerta, J. Payá, S. García-Granda, F. Gómez-Beltrán and A. Anillo, *J. Organomet. Chem.* **1993**, *443*, C14.
535. F. P. Pruchnik, R. Starosta, P. Smolenski, E. Shestakova and P. Lahuerta, *Organometallics* **1998**, *17*, 3684.
536. F. Estevan, J. Latorre and E. Peris, *Polyhedron* **1993**, *12*, 2153.
537. M. V. Borrachero, F. Estevan, P. Lahuerta, J. Payá and E. Perris, *Polyhedron* **1993**, *12*, 1715.
538. P. Lahuerta, J. Payá, E. Peris, A. Aguirre, S. García-Granda and F. Gómez-Beltrán, *Inorg. Chim. Acta* **1992**, *192*, 43.
539. F. Estevan, P. Lahuerta, J. Pérez-Prieto, M. Sanaú, S.-E. Stiriba and M. A. Ubeda, *Organometallics* **1997**, *16*, 880.
540. P. Lahuerta, R. Martinez-Mañez, J. Payá, E. Peris and W. Díaz, *Inorg. Chim. Acta* **1990**, *173*, 99.
541. M. Nowotny, T. Maschmeyer, B. F. G. Johnson, P. Lahuerta, J. M. Thomas and J. E. Davies, *Angew. Chem., Int. Ed.* **2001**, *40*, 955.
542. P. Lahuerta, I. Pereira, J. Pérez-Prieto, M. Sanaú, S.-E. Stiriba and D. F. Taber, *J. Organomet. Chem.* **2000**, *612*, 36.
543. F. P. Pruchnik, R. Starosta, Z. Ciunik, A. Opolski, J. Wietrzyk, E. Wojdat and D. Dus, *Can. J. Chem.* **2001**, *79*, 868.
544. E. C. Morrison and D. A. Tocher, *Inorg. Chim. Acta* **1989**, *157*, 139.
545. E. C. Morrison and D. A. Tocher, *J. Organomet. Chem.* **1991**, *408*, 105.
546. M. Barberis, P. Lahuerta, J. Pérez-Prieto and M. Sanaú, *Chem. Commun.* **2001**, 439.
547. F. Estevan, P. Lahuerta, E. Peris, M. A. Ubeda, S. García-Granda, F. Gómez-Beltrán, E. Pérez-Carreno, G. González and M. Martínez, *Inorg. Chim. Acta* **1994**, *218*, 189.
548. D. F. Taber, S. C. Malcolm, K. Bieger, P. Lahuerta, M. Sanaú, S.-E. Stiriba, J. Pérez-Prieto and M. A. Monge, *J. Am. Chem. Soc.* **1999**, *121*, 860.
549. F. Estevan, P. Lahuerta, J. Latorre, E. Peris, S. García-Granda, F. Gómez-Beltran, A. Aguirre and M. A. Salvadó, *J. Chem. Soc., Dalton Trans.* **1993**, 1681.
550. F. A. Cotton, F. Barceló, P. Lahuerta, R. Llusar, J. Payá and M. A. Ubeda, *Inorg. Chem.* **1988**, *27*, 1010.
551. M. V. Borrachero, F. Estevan, S. García-Granda, P. Lahuerta, J. Latorre, E. Peris and M. Sanaú, *J. Chem. Soc., Chem. Commun.* **1993**, 1864.
552. F. Estevan, S. García-Granda, P. Lahuerta, J. Latorre, E. Peris and M. Sanaú, *Inorg. Chim. Acta* **1995**, *229*, 365.

Pictiva EX2004
Samsung v Pictiva
IPR2024-01094

553. K. Bieger, F. Estevan, P. Lahuerta, J. Lloret, J. Pérez-Prieto, M. Sanaú, N. Siguero and S.-E. Stiriba, *Organometallics* **2003**, *22*, 1799.
554. P. Lahuerta and F. Estevan, *Metal Clusters in Chemistry*, P. Braunstein, L. A. Oro and P. R. Raithby, Eds., Wiley-VCH Verlag: Weinheim, Germany, 1999, *2*, 678.
555. F. Barcelo, F. A. Cotton, P. Lahuerta, M. Sanaú, W. Schwotzer and M. A. Ubeda, *Organometallics* **1987**, *6*, 1105.
556. F. Estevan, P. Lahuerta, J. Lloret, J. Pérez-Prieto and H. Werner, *Organometallics* **2004**, *23*, 1369.
557. P. Lahuerta, E. Moreno, A. Monge, G. Muller, J. Pérez-Prieto, M. Sanaú and S.-E. Stiriba, *Eur. J. Inorg. Chem.* **2000**, 2481.
558. F. Estevan, P. Krueger, P. Lahuerta, E. Moreno, J. Pérez-Prieto, M. Sanaú and H. Werner, *Eur. J. Inorg. Chem*. **2001**, 105.
559. R. E. Marsh, *Acta Crystallogr.* **2002**, *B58*, 893.
560. P. Lahuerta, J. Pérez-Prieto, M. Sanaú, N. Siguero and S.-E. Stiriba, *Inorg. Chim. Acta* **2001***, 323*, 152.
561. M. Barberis, F. Estevan, P. Lahuerta, J. Pérez-Prieto and M. Sanaú, *Inorg. Chem*. **2001**, *40*, 4226.
562. F. A. Cotton, K. R. Dunbar and C. T. Eagle, *Inorg. Chem.* **1987**, *26*, 4127.
563. F. A. Cotton and K. R. Dunbar, *J. Am. Chem. Soc.* **1987**, *109*, 3142.
564. F. A. Cotton, C. A. Murillo, X. Wang and R. Yu, *Inorg. Chem*. **2004**, *43*, 8394.
565. S. J. Chen and K. R. Dunbar, *Inorg. Chem.* **1990**, *29*, 588.
566. S. J. Chen and K. R. Dunbar, *Inorg. Chem.* **1991**, *30*, 2018.
567. K. R. Dunbar, J. H. Matonic and V. P. Saharan, *Inorg. Chem.* **1994**, *33*, 25.
568. F. P. Pruchnik, R. Starosta, M. W. Kowalska, E. Galdecka, Z. Galdecki and A. Kowalski, *J. Organomet. Chem.* **2000**, *597*, 20.
569. A. L. Odom, A. F. Heyduk and D. G. Nocera, *Inorg. Chim. Acta* **2000**, *297*, 330.
570. J. I. Dulebohn, D. L. Ward and D. G. Nocera, *J. Am. Chem. Soc.* **1988**, *110*, 4054.
571. J. I. Dulebohn, D. L. Ward and D. G. Nocera, *J. Am. Chem. Soc.* **1990**, *112*, 2969.
572. J. Kadis, Y. K. Shin, J. I. Dulebohn, D. L. Ward and D. G. Nocera, *Inorg. Chem*. **1996**, *35*, 811.
573. F. A. Cotton, K. R. Dunbar, C. T. Eagle, L. R. Falvello and A. C. Price, *Inorg. Chem*. **1989**, *28*, 1754.
574. L. A. Nazarova, I. I. Chernyaev, A. G. Maiorova, N. N. Borozdina and A. A. Koryagina, *Abstr. Proc. 10th Intl. Conf. Coord. Chem.* K. Yamasaki, Ed., Chemical Society of Japan: Tokyo and Nikko, Japan, 1967, 392.
575. F. A. Cotton and T. R. Felthouse, *Inorg. Chem.* **1980**, *19*, 320.
576. S. I. Ginzburg and N. N. Chalisova, *Russ. J. Inorg. Chem*. **1965**, *10*, 440.
577. S. I. Ginzburg and N. N. Chalisova, *Russ. J. Inorg. Chem*. **1965**, *10*, 1312.
578. S. I. Ginzburg, N. N. Chalisova and O. N. Evstafeva, *Russ. J. Inorg. Chem*. **1966**, *11*, 404.
579. I. B. Baranovskii, N. N. Chalisova and G. Ya. Mazo, *Russ. J. Inorg. Chem*. **1979**, *24*, 1893.
580. L. M. Dikareva, Yu. V. Zefirov, A. N. Zhilyaev, I. B. Baranovskii and M. A. Porai-Koshits, *Russ. J. Inorg. Chem.* **1987***, 32*, 64.
581. I. B. Baranovskii, A. N. Zhilyaev and L. M. Dikareva, *Russ. J. Inorg. Chem.* **1985***, 30*, 1015.
582. I. B. Baranovskii, A. N. Zhilyaev and L. M. Dikareva, *Russ. J. Inorg. Chem.* **1988**, *33*, 1802.
583. I. B. Baranovskii, S. S. Abdullaev and R. N. Shchelokov, *Russ. J. Inorg. Chem*. **1979**, *24*, 1753.
584. L. M. Dikareva, G. G. Sadikov, M. A. Porai-Koshits, I. B. Baranovskii and S. S. Abdullaev, *Russ. J. Inorg. Chem*. **1980**, *25*, 488.
585. L. M. Dikareva, G. G. Sadikov, M. A. Porai-Koshits, I. B. Baranovskii, S. S. Abdullaev and R. N. Shchelokov, *Russ. J. Inorg. Chem.* **1982**, *27*, 236.
586. I. B. Baranovskii, S. S. Abdullaev, G. Ya. Mazo, I. F. Golovaneva, Ya. V. Salyn' and R. N. Shchelokov, *Russ. J. Inorg. Chem.* **1981**, *26*, 925.
587. L. M. Dikareva, A. N. Zhilyaev and I. B. Baranovskii, *Russ. J. Inorg. Chem.* **1988**, *33*, 1176.
588. I. F. Golovaneva, S. A. Polonskii and A. P. Klyagina, *Russ. J. Inorg. Chem*. **1994**, *39*, 79.
589. A. P. Klyagina, S. A. Polonskii and I. F. Golovaneva, *Rhodium Express* **1993**, *2*, 8.
590. A. P. Klyagina, S. A. Polonskii and I. F. Golovaneva, *Rhodium Express* **1994**, *3*, 8.

Pictiva EX2004
Samsung v Pictiva
IPR2024-01094

591. F. Maspero and H. Taube, *J. Am. Chem. Soc.* **1968**, *90*, 7361.
592. J. J. Ziolkowski and H. Taube, *Bull. Acad. Pol. Sci. Ser. Sci. Chim.* **1973**, *21*, 113.
593. M. Moszner and J. J. Ziolkowski, *Inorg. Chim. Acta* **1988**, *145*, 299.
594. M. Moszner, M. Wilgocki and J. J. Ziolkowski, *J. Coord. Chem*. **1989**, *20*, 219.
595. M. Moszner, *Inorg. Chim. Acta* **2004**, *357*, 3613.
596. P.-A. Pittet, L. Dadci, P. Zbinden, A. Abou-Hamdan and A. E. Merbach, *Inorg. Chim. Acta* **1993**, *206*, 135.
597. K. R. Dunbar, *J. Am. Chem. Soc.* **1988**, *110*, 8247.
598. M. E. Prater, L. E. Pence, R. Clérac, G. M. Finniss, C. Campana, P. Auban-Senzier, D. Jerome, E. Canadell and K. R. Dunbar, *J. Am. Chem. Soc.* **1999**, *121*, 8005.
599. L. M. Dikareva, V. I. Andrianov, A. N. Zhilyaev and I. B. Baranovskii, *Russ. J. Inorg. Chem.* **1989**, *34*, 240.
600. A. N. Zhilyaev, A. V. Rotov, I. V. Kuz'menko and I. B. Baranovskii, *Dokl. Chem.* **1988**, *302*, 275.
601. M. M. Olmstead and A. L. Balch, *J. Organomet. Chem.* **1978**, *148*, C15.
602. C. A. James, D. E. Morris, S. K. Doon, C. A. Arrington, K. R. Dunbar, G. M. Finniss, L. E. Pence and W. H. Woodruff, *Inorg. Chim. Acta* **1996**, *242*, 91.
603. G. Knör, *Z. Naturforsch*. **2003**, *58b*, 741.
604. M. Pillinger, C. D. Nunes, P. D. Vaz, A. A. Valente, I. S. Gonçalves, P. J. A. Ribeiro-Claro, J. Rocha, L. D. Carlos and F. E. Kühn, *Phys. Chem. Chem. Phys*. **2002**, *4*, 3098.
605. G. M. Finniss, E. Canadell, C. Campana and K. R. Dunbar, *Angew. Chem., Int. Ed. Engl.* **1996**, *35*, 2772.
606. S. A. Shchepinov, E. N. Salnikova and M. L. Khidekel, *Izv. Akad. Nauk SSSR, Ser. Khim.* **1967**, 2128.
607. H. J. Keller and K. Seibold, *Z. Naturforsch.* **1970**, *25b*, 551.
608. U. Tinner and J. H. Espenson, *J. Am. Chem. Soc.* **1981**, *103*, 2120.
609. I. V. Kuz'menko, M. A. Golubnichaya and I. B. Baranovskii, *Russ. J. Inorg. Chem.* **1991**, *36*, 89.
610. L. M. Dikareva, V. I. Andrianov, A. N. Zhilyaev and I. B. Baranovskii, *Russ. J. Inorg. Chem.* **1989**, *34*, 219.
611. I. V. Kuz'menko, A. N. Zhilyaev, M. A. Porai-Koshits and I. B. Baranovskii, *Russ. J. Inorg. Chem*. **1990**, *35*, 648.
612. J. W. Suggs, M. J. Wovkulich, P. G. Williard and K. S. Lee, *J. Organomet. Chem*. **1986**, *307*, 71.
613. M. C. Weiss, B. Bursten, S.-M. Peng and V. L. Goedken, *J. Am. Chem. Soc.* **1976**, *98*, 8021.
614. F. A. Cotton and J. Czuchajowska, *Polyhedron* **1990**, *9*, 2553.
615. S. L. Van Voorhees and B. B. Wayland, *Organometallics* **1987**, *6*, 204.
616. L. F. Warren and V. L. Goedken, *J. Chem. Soc., Chem. Commun*. **1978**, 909.
617. H. Hückstädt, C. Bruhn and H. Homborg, *J. Porphyrins Phthalocyanines* **1997**, *1*, 367.
618. H. Ogoshi, J. Setsune and Z. Yoshida, *J. Am. Chem. Soc.* **1977**, *99*, 3869.
619. J. Setsune, Z. Yoshida and H. Ogoshi, *J. Chem. Soc., Perkin Trans. I* **1982**, 983.
620. B. B. Wayland and A. R. Newman, *J. Am. Chem. Soc.* **1979**, *101*, 6472.
621. B. B. Wayland and A. R. Newman, *Inorg. Chem.* **1981**, *20*, 3093.
622. B. R. James and D. V. Stynes, *J. Am. Chem. Soc.* **1972**, *94*, 6225.
623. B. B. Wayland, V. L. Coffin and M. D. Farnos, *Inorg. Chem.* **1988**, *27*, 2745.
624. B. B. Wayland, *Polyhedron* **1988**, *7*, 1545.
625. R. S. Paonessa, N. C. Thomas and J. Halpern, *J. Am. Chem. Soc.* **1985**, *107*, 4333.
626. B. B. Wayland and B. A. Woods, *J. Chem. Soc., Chem. Commun*. **1981**, 475.
627. B. B. Wayland and K. J. Del. Rossi, *J. Organomet. Chem*. **1984**, *276*, C27.
628. K. J. Del Rossi and B. B. Wayland, *J. Am. Chem. Soc.* **1985**, *107*, 7941.
629. B. B. Wayland, B. A. Woods and R. Pierce, *J. Am. Chem. Soc.* **1982**, *104*, 302.
630. B. B. Wayland, B. A. Woods and V. L. Coffin, *Organometallics* **1986**, *5*, 1059.
631. V. L. Coffin, W. Brennen and B. B. Wayland, *J. Am. Chem. Soc.* **1988**, *110*, 6063.
632. B. B. Wayland, K. J. Balkus, Jr. and M. D. Farnos, *Organometallics* **1989**, *8*, 950.
633. B. B. Wayland, Y. Feng and S. Ba, *Organometallics* **1989**, *8*, 1438.

Pictiva EX2004
Samsung v Pictiva
IPR2024-01094

634. J. P. Collman, Y. Ha, R. Guilard and M.-A. Lopez, *Inorg. Chem*. **1993**, *32*, 1788.
635. M. Feng and K. S. Chan, *J. Organomet. Chem*. **1999**, *584*, 235.
636. A. E. Sherry and B. B. Wayland, *J. Am. Chem. Soc.* **1989**, *111*, 5010.
637. A. E. Sherry and B. B. Wayland, *J. Am. Chem. Soc.* **1990**, *112*, 1259.
638. X.-X. Zhang and B. B. Wayland, *J. Am. Chem. Soc.* **1994**, *116*, 7897.
639. X.-X. Zhang and B. B. Wayland, *Inorg. Chem*. **2000**, *39*, 5318.
640. R. J. Cozens, K. S. Murray and B. O. West, *J. Organomet. Chem*. **1972**, *38*, 391.
641. S. Calmotti and A. Pasini, *Inorg. Chim. Acta* **1984**, *85*, L55.
642. D. Sellmann, G. H. Rackelmann, F. W. Heinemann, F. Knoch and M. Moll, *Inorg. Chim. Acta* **1998**, *272*, 211.
643. A. L. Balch and M. M. Olmstead, *J. Am. Chem. Soc.* **1976**, *98*, 2354.
644. A. L. Balch, *Ann. N. Y. Acad. Sci*. **1978**, *313*, 651.
645. N. S. Lewis, K. R. Mann, J. G. Gordon II and H. B. Gray, *J. Am. Chem. Soc.* **1976**, *98*, 7461.
646. K. R. Mann, N. S. Lewis, V. M. Miskowski, D. K. Erwin, G. S. Hammond and H. B. Gray, *J. Am. Chem. Soc.* **1977**, *99*, 5525.
647. K. R. Mann, R. A. Bell and H. B. Gray, *Inorg. Chem.* **1979**, *18*, 2671.
648. V. M. Miskowski, T. P. Smith, T. M. Loehr and H. B. Gray, *J. Am. Chem. Soc.* **1985**, *107*, 7925.
649. A.W. Maverick, T. P. Smith, E. F. Maverick and H. B. Gray, *Inorg. Chem*. **1987**, *26*, 4336.
650. M. R. Rhodes and K. R. Mann, *Inorg. Chem*. **1984**, *23*, 2053.
651. V. M. Miskowski, I. S. Sigal, K. R. Mann, H. B. Gray, S. J. Milder, G. S. Hammond and P. R. Ryason, *J. Am. Chem. Soc.* **1979**, *101*, 4383.
652. K. R. Mann and H. B. Gray, *Adv. Chem. Ser.* **1979**, *173*, 225.
653. K. R. Mann, M. J. DiPierro and T. P. Gill, *J. Am. Chem. Soc.* **1980**, *102*, 3965.
654. H. B. Gray, K. R. Mann, N. S. Lewis, J. A. Thich and R. M. Richman, *Adv. Chem. Series*, M. S. Wrighton, Ed., American Chemical Society: Washington, 1978, *168*, 44.
655. V. M. Miskowski, S. F. Rice, H. B. Gray and S. J. Milder, *J. Phys. Chem*. **1993**, *97*, 4277.
656. A. L. Balch, J. W. Labadie and G. Delker, *Inorg. Chem*. **1979**, *18*, 1224.
657. D. R. Womack, P. D. Enlow and C. Woods, *Inorg. Chem*. **1983**, *22*, 2653.
658. P. D. Enlow and C. Woods, *Inorg. Chem*. **1985**, *24*, 1273.
659. C.-M. Che and W.-M. Lee, *J. Chem. Soc., Chem. Commun*. **1986**, 616.
660. D. C. Boyd, P. A. Matsch, M. M. Mixa and K. R. Mann, *Inorg. Chem*. **1986**, *25*, 3331.
661. C. Woods, L. J. Tortorelli, D. P. Rillema, J. L. E. Burn and J. C. DePriest, *Inorg. Chem*. **1989**, *28*, 1673.
662. L. J. Tortorelli, C. Woods and A. T. McPhail, *Inorg. Chem.* **1990**, *29*, 2726.
663. D. Carmona, L. A. Oro, P. L. Pérez, A. Tiripicchio and M. Tiripicchio-Camellini, *J. Chem. Soc., Dalton Trans.* **1989**, 1427.
664. R. A. Walton, *ACS Symp. Ser.* **1981**, *No 155*, 207.
665. D. D. Klendworth, W. W. Welters, III and R. A. Walton, *Organometallics* **1982**, *1*, 336.
666. C. J. Cameron, S. M. Tetrick and R. A. Walton, *Organometallics* **1984**, *3*, 240.
667. C. Tejel, M. A. Ciriano and L. A. Oro, *Chem. Eur. J.* **1999**, *5*, 1131.
668. J. K. Bera and K. R. Dunbar, *Angew. Chem., Int. Ed*. **2002**, *41*, 4453.
669. I. S. Sigal and H. B. Gray, *J. Am. Chem. Soc.* **1981**, *103*, 2220.
670. V. M. Miskowski and H. B. Gray, *Inorg. Chem.* **1987**, *26*, 1108.
671. K. R. Mann and B. A. Parkinson, *Inorg. Chem*. **1981**, *20*, 1921.
672. C. Tejel, J. M. Villoro, M. A. Ciriano, J. A. López, E. Eguizábal, F. J. Lahoz, V. I. Bakhmutov and L. A. Oro, *Organometallics* **1996**, *15,* 2967.
673. C. Tejel, M. A. Ciriano, J. A. López, F. J. Lahoz and L. A. Oro, *Angew. Chem., Int. Ed.* **1998**, *37*, 1542.
674. L. A. Oro, M. A. Ciriano and C. Tejel, *Pure & Appl. Chem*. **1998**, *70*, 779.
675. A. L. Balch and M. M. Olmstead, *J. Am. Chem. Soc.* **1979**, *101*, 3128.
676. S.-S. Chern, G.-H. Lee and S.-M. Peng, *J. Chem. Soc., Chem. Commun.* **1994**, 1645.
677. F. P. Pruchnik, P. Jakimowicz and Z. Ciunik, *Inorg. Chem. Commun.* **2001**, *4*, 726.

Pictiva EX2004
Samsung v Pictiva
IPR2024-01094

678. F. P. Pruchnik, P. Jakimowicz, Z. Ciunik, K. Stanislawek, L. A. Oro, C. Tejel and M. A. Ciriano, *Inorg. Chem. Commun.* **2001**, *4*, 19.
679. R. D. Cannon, D. B. Powell, K. Sarawek and J. S. Stillman, *J. Chem. Soc., Chem. Commun*. **1976**, 31.
680. D. A. Foucher and D. H. Macartney, *J. Chem. Res., Synop.* **1992**, 346.
681. M. A. Golubnichaya, E. M. Trishkina, G. N. Kuznetsova, A. V. Rotov and I. B. Baranovskii, *Russ. J. Inorg. Chem*. **1989**, *34*, 1493.
682. I. B. Baranovskii and M. A. Golubnichaya, *Russ. J. Inorg. Chem*. **1984**, *29*, 1558.
683. R. D. Cannon, D. B. Powell and K. Sarawek, *Inorg. Chem*. **1981**, *20*, 1470.
684. R. B. Ali, K. Sarawek, A. Wright and R. D. Cannon, *Inorg. Chem*. **1983**, *22*, 351.
685. J. W. Herbert and D. H. Macartney, *Inorg. Chem*. **1985**, *24*, 4398.
686. J. W. Herbert and D. H. Macartney, *J. Chem. Soc., Dalton Trans*. **1986**, 1931.
687. M. A. S. Aquino, D. A. Foucher and D. H. Macartney, *Inorg. Chem*. **1989**, *28*, 3357.
688. T. Sowa, T. Kawamura, T. Shida and T. Yonezawa, *Inorg. Chem*. **1983**, *22*, 56.
689. R. S. Drago, R. Cosmano and J. Telser, *Inorg. Chem*. **1984**, *23*, 3120.
690. T. Kawamura, H. Katayama and T. Yamabe, *Chem. Phys. Lett*. **1986**, *130*, 20.
691. M. Moszner and J. J. Ziólkowski, *Bull. Acad. Pol. Sci., Ser. Sci. Chim*. **1976**, *24*, 433.
692. M. Moszner and J. J. Ziólkowski, *Transition Met. Chem*. **1982**, *7*, 351.
693. J. J. Ziólkowski, M. Moszner and T. Glowiak, *J. Chem. Soc., Chem. Commun.* **1977**, 760.
694. J. G. Norman, Jr., G. E. Renzoni and D. A. Case, *J. Am. Chem. Soc.* **1979**, *101*, 5256.
695. M. Moszner and J. J. Ziolkowski, *Rhodium Express* **1993**, *2*, 4.
696. K. Das, K. M. Kadish and J. B. Bear, *Inorg. Chem*. **1978**, *17*, 930.
697. L. A. Bottomley and T. A. Hallberg, *Inorg. Chem*. **1984**, *23*, 1584.
698. A. Szymaszek and F. P. Pruchnik, *Inorg. Chim. Acta* **1987**, *131*, 143.
699. Z.-S. Hu and T.-P. Zhu, *Acta Chim. Sinica* **1987**, *45*, 23.
700. A. Szymaszek and F. P. Pruchnik, *Polyhedron* **1990**, *9*, 1135.
701. S. Ö. Yaman, A. M. Önal and H. Isci, *Z. Naturforsch*. **2003**, *58b*, 563.
702. G. W. Eastland and M. C. R. Symons, *J. Chem. Soc., Dalton Trans*. **1984**, 2193.
703. T. Kawamura, K. Fukamachi and S. Hayashida, *J. Chem. Soc., Chem. Commun*. **1979**, 945.
704. G. Pannetier and J. Segall, *J. Less-Common Metals* **1970**, *22*, 293.
705. A. Szymaszek and F. P. Pruchnik, *Pol. J. Chem.* **1992**, *66*, 1859.
706. A. Szymaszek and F. P. Pruchnik, *Rhodium Express* **1994**, *5*, 18.
707. T. Kawamura, K. Fukamachi, T. Sowa, S. Hayashida and T. Yonezawa, *J. Am. Chem. Soc.* **1981**, *103*, 364.
708. S. P. Best, R. J. H. Clark and A. J. Nightingale, *Inorg. Chem*. **1990**, *29*, 1383.
709. K. M. Kadish, D. Lancon, A. M. Dennis and J. L. Bear, *Inorg. Chem*. **1982**, *21*, 2987.
710. J. L. Bear, T. P. Zhu, T. Malinski, A. M. Dennis and K. M. Kadish, *Inorg. Chem.* **1984**, *23*, 674.
711. M. P. Doyle, L. J. Westrum, W. N. E. Wolthuis, M. M. See, W. P. Boone, V. Bagheri and M. M. Pearson, *J. Am. Chem. Soc.* **1993**, *115*, 958.
712. A. J. Catino, R. E. Forslund and M. P. Doyle, *J. Am. Chem. Soc.* **2004**, *126*, 13622.
713. I. B. Baranovskii, M. A. Golubnichaya, L. M. Dikareva, A. V. Rotov, R. N. Shchelokov and M. A. Porai-Koshits, *Russ. J. Inorg. Chem*. **1986**, *31*, 1652.
714. M. A. Golubnichaya, L. M. Dikareva, A. V. Rotov and I. B. Baranovskii, *Russ. J. Inorg. Chem*. **1989**, *34*, 238.
715. K. Aoki, M. Hoshino, T. Okada, H. Yamazaki and H. Sekizawa, *J. Chem. Soc., Chem. Commun.* **1986**, 314.
716. Z. Yang, T. Fujinami, M. Ebihara, K. Nakajima, H. Kitagawa and T. Kawamura, *Chem. Lett.* **2000**, 1006.
717. Z. Yang, M. Ebihara, T. Kawamura, T. Okubo and T. Mitani, *Inorg. Chim. Acta* **2001**, *321*, 97.
718. M. Yamauchi, A. B. Koudriavtsev, R. Ikeda, Z. Yang and T. Kawamura, *Mol. Cryst. Liq. Cryst*. **2002**, *379*, 321.

Pictiva EX2004
Samsung v Pictiva
IPR2024-01094

719. M. Handa, Y. Muraki, S. Kawabata, T. Sugimori, I. Hiromitsu, M. Mikuriya and K. Kasuga, *Mol. Cryst. Liq. Cryst*. **2002**, *379*, 327.
720. T. Kawamura, M. Ebihara and M. Miyamoto, *Chem. Lett.* **1993**, 1509.
721. T. Kawamura, H. Katayama, H. Nishikawa and T. Yamabe, *J. Am. Chem. Soc.* **1989**, *111*, 8156.
722. G. Bruno, S. Lo Schiavo, G. Tresoldi, P. Piraino and L. Valli, *Inorg. Chim. Acta* **1992**, *196*, 131.
723. G. Bruno, G. Tresoldi, S. Lo Schiavo, S. Sergi and P. Piraino, *Inorg. Chim. Acta* **1992**, *197*, 9.
724. J.-L. Zuo, F. Fabrizi de Biani, A. M. Santos, K. Köhler and F. E. Kühn, *Eur. J. Inorg. Chem*. **2003**, 449.
725. M. Zuber, *Transition Met. Chem.* **1986**, *11*, 5.
726. J. L. Bear, C.-L. Yao, F. J. Capdevielle and K. M. Kadish, *Inorg. Chem*. **1988**, *27*, 3782.
727. L.-M. Liu, Y. Hu and S.-L. Gong, *Sci. China, Ser. B* **1990**, *33*, 897.
728. J.-D. Lee, C.-L. Yao, F. J. Capdevielle, B. Han, J. L. Bear and K. M. Kadish, *Bull. Korean Chem. Soc.* **1993**, *14*, 195.
729. C.-L. Yao, K. H. Park and J. L. Bear, *Anal. Chem*. **1989**, *61*, 279.
730. C.-L. Yao, K. H. Park, A. R. Khokhar, M.-J. Jun and J. L. Bear, *Inorg. Chem.* **1990**, *29*, 4033.
731. M. Zuber, *Pol. J. Chem*. **1992**, *66*, 433.
732. K. M. Kadish, T. D. Phan, L. Giribabu, E. Van Caemelbecke and J. L. Bear, *Inorg. Chem*. **2003**, *42*, 8663.
733. I. B. Baranovskii, A. N. Zhilyaev and A. V. Rotov, *Russ. J. Inorg. Chem*. **1985**, *30*, 1822.
734. J. G. Norman and E. D. Fey, *J. Chem. Soc., Dalton Trans.* **1976**, 765.
735. H. D. Glicksman, A. D. Hamer, T. J. Smith and R. A. Walton, *Inorg. Chem*. **1976**, *15*, 2205.
736. H. D. Glicksman and R. A. Walton, *Inorg. Chim. Acta* **1979**, *33*, 255.
737. I. B. Baranovskii, G. Ya. Mazo and L. M. Dikareva, *Russ. J. Inorg. Chem*. **1971**, *16*, 1388.
738. S. Uemura, A. Spencer and G. Wilkinson, *J. Chem. Soc., Dalton Trans*. **1973**, 2565.
739. E. F. Hills, M. Moszner and A. G. Sykes, *Inorg. Chem*. **1986**, *25*, 339.
740. R. A. Andersen, R. A. Jones and G. Wilkinson, *J. Chem. Soc., Dalton Trans*. **1978**, 446.
741. R. A. Jones and G. Wilkinson, *J. Chem. Soc., Dalton Trans*. **1979**, 472.
742. M. H. Chisholm, J. C. Huffman and S. S. Iyer, *J. Chem. Soc., Dalton Trans*. **2000**, 1483.
743. M. Fourmigué, C. E. Uzelmeier, K. Boubekeur, S. L. Bartley and K. R. Dunbar, *J. Organomet. Chem*. **1997**, *529*, 343.
744. F. A. Cotton, K. R. Dunbar, C. T. Eagle, L. R. Falvello, S.-J. Kang, A. C. Price and M. G. Verbruggen, *Inorg. Chim. Acta* **1991**, *184*, 35.
745. S. P. Best, A. J. Nightingale and D. A. Tocher, *Inorg. Chim. Acta* **1991**, *181*, 7.
746. C. R. Graves, M. L. Merlau, G. A. Morris, S.-S. Sun, S. T. Nguyen and J. T. Hupp, *Inorg. Chem*. **2004**, *43*, 2013.
747. F. A. Cotton, C. A. Murillo, X. Wang and R. Yu, unpublished results.
748. T. Sato, W. Mori, C. N. Kato, T. Ohmura, T. Sato, K. Yokoyama, S. Takamizawa and S. Naito, *Chem. Lett*. **2003**, *32*, 854.
749. E. R. Jamieson and S. J. Lippard, *Chem. Rev.* **1999**, *99*, 2467.
750. S. M. Cohen and S. J. Lippard, *Prog. Nucl. Acid Res. Mol. Biol.* **2001**, 67, 93.
751. J. Reedijk, *Proc. Nat. Acad. Sci. U.S.A.* **2003**, *100*, 3611.
752. C. X. Zhang and S. J. Lippard, *Curr. Op. Chem. Biol*. **2003**, 7, 481.
753. M. J. Clarke, F. Zhu and D. R. Frasca, *Chem. Rev*. **1999**, *99*, 2511.
754. N. Katsaros and A. Anagnostopoulou, *Crit. Rev. Oncol. Hematol*. **2002**, *42*, 297.
755. A. Erck, L. Rainen, J. Whileyman, I.-M. Chang, A. P. Kimball and J. L. Bear, *Proc. Soc. Exp. Biol. Med.* **1974**, *145*, 1278.
756. J. L. Bear, H. B. Gray, Jr., L. Rainen, I. M. Chang, R. Howard, G. Serio and A. P. Kimball, *Cancer Chemother. Rep*. **1975**, *59*, 611.
757. J. M. Asara, J. S. Hess, E. Lozada, K. R. Dunbar and J. Allison, *J. Am. Chem. Soc.* **2000**, *122*, 8.
758. H. T. Chifotides, J. M. Koomen, M. Kang, K. R. Dunbar, S. Tichy and D. Russell, *Inorg. Chem.* **2004**, *43*, 6177.
759. E. Tselepi-Kalouli and N. Katsaros, *J. Inorg. Biochem*. **1990**, *40*, 95.

Pictiva EX2004
Samsung v Pictiva
IPR2024-01094

760. P. N. Rao, M. L. Smith, S. Pathak, R. A. Howard and J. L. Bear, *J. Nat. Cancer Inst*. **1980**, *64*, 905.
761. P. N. Rao, M. L. Smith, S. Pathak, R. A. Howard and J. L. Bear, *Curr. Chemother., Proc. 11th Int. Cong. Chemother. Infect. Dis.* J. D. Nelson and C. Grassi, Eds., Am. Soc. Microbiol.: Washington, D.C. 1980, p 1627.
762. L. D. Dale, T. M. Dyson, D. A. Tocher, J. H. Tocher and D. I Edwards, *Anti-Cancer Drug Design* **1989**, *4*, 295.
763. K. Sorasaenee, P. K.-L. Fu, A. M. Angeles-Boza, K. R. Dunbar and C. Turro, *Inorg. Chem.* **2003**, *42*, 1267.
764. H. T. Chifotides, P. K.-L. Fu, K. R. Dunbar and C. Turro, *Inorg. Chem.* **2004**, *43*, 1175.
765. R. G. Hughes, J. L. Bear and A. P. Kimball, *Proc. Am. Assoc. Cancer Res*. **1972**, *13*, 120.
766. R. A. Howard, A. P. Kimball and J. L. Bear, *Cancer Res.* **1979**, *39*, 2568.
767. R. A. Howard, E. Sherwood, A. Erck, A. P. Kimball and J. L. Bear, *J. Med. Chem.* **1977**, *20*, 943.
768. I. Chang and W. S. Woo, *Korean Biochem. J*. **1976**, *9*, 175.
769. S. Zyngier, E. Kimura and R. Najjar, *Braz. J. Med. Biol. Res*. **1989**, *22*, 397.
770. J. L. Bear, *Precious Metals 1985: Proceedings of the Ninth International Precious Metals Conference*; E. D. Zysk and J. A. Bonucci, Eds.; Int. Precious Metals: Allentown, PA, 1986, p 337.
771. L. M. Hall, R. J. Speer and H. J. Ridgway, *J. Clin. Hematol. Oncol*. **1980**, *10*, 25.
772. K. M. Kadish, K. Das, R. Howard, A. Dennis and J. L. Bear, *Bioelectrochem. Bioenerg.* **1978**, *5*, 741.
773. J. L. Bear, R. A. Howard and A. M. Dennis, *Curr. Chemother., Proc. 10th Int. Cong. Chemother.* W. Siegenthaler and R. Lüthy, Eds., Am. Soc. Microbiol.: Washington, D.C. 1978, p 1321.
774. R. Chibber, I. J. Stratford, P. O' Neill, P. W. Sheldon, I. Ahmed and B. Lee, *Int. J. Radiat. Biol*. **1985**, *48*, 513.
775. R. Chibber, I. J. Stratford, I. Ahmed, A. B. Robbins, D. Goodgame and B. Lee, *Int. J. Radiat. Oncol. Biol. Phys.* **1984**, *10*, 1213.
776. R. C. Richmond, N. P. Farrell, T. J. Curphey and H. K. Mahtani, *Radiat. Res*. **1989**, *120*, 416.
777. R. C. Richmond, N. P. Farrell and H. K. Mahtani, *Radiat. Res*. **1989**, *120*, 403.
778. R. C. Richmond and H. K. Mahtani, *Radiat. Res*. **1991**, *127*, 36.
779. E. M. Reibscheid, S. B. Zyngier, D. A. Maria, R. J. Mistrone, R. D. Sinisterra, L. G. Couto and R. Najjar, *Braz. J. Med. Biol. Res*. **1994**, *27*, 91.
780. B. P. Esposito, S. B. Zyngier, A. R. Souza and R. Najjar, *Met. Based Drugs* **1997**, *4*, 333.
781. B. P. Esposito, S. B. Zyngier, R. Najjar, R. P. Paes, S. M. Ykko Ueda and J. C. A. Barros, *Met. Based Drugs* **1999**, *6*, 17.
782. F. P. Pruchnik and D. Dus, *J. Inorg. Biochem*. **1996**, *61*, 55.
783. F. P. Pruchnik, G. Kluczewska, A. Wilczok, U. Mazurek and T. Wilczok, *J. Inorg. Biochem*. **1997**, *65*, 25.
784. F. P. Pruchnik, M. Bien and T. Lachowicz, *Met. Based Drugs* **1996**, *3*, 185.
785. M. Bien, F. P. Pruchnik, A. Seniuk, T. M. Lachowicz and P. Jakimowicz, *J. Inorg. Biochem*. **1999**, *73*, 49.
786. M. Bien, T. M. Lachowicz, A. Rybka, F. P. Pruchnik, L. Trynda, *Met. Based Drugs* **1997**, *4*, 81.
787. P. Piraino, G. Tresoldi and S. Lo Schiavo, *Inorg. Chim. Acta* **1993**, *203*, 101.
788. E. de Souza Gil, M. I. de Almeida Gonçalves, E. I. Ferreira, S. B. Zyngier and R. Najjar, *Met. Based Drugs* **1999**, *6*, 19.
789. E. de Souza Gil, E. I. Ferreira, A. C. Valderrama, S. B. Zyngier and R. Najjar, *Anal. Real. Acad. Farm*. **2000**, *66*, 229.
790. A. R. Souza, R. Najjar, S. Glikmanas and S. B. Zyngier, *J. Inorg. Biochem*. **1996**, *64*, 1.
791. A. R. Souza, R. Najjar, E. de Oliveira and S. B. Zyngier, *Met. Based Drugs* **1997**, *4*, 39.
792. D. G. Craciunescu, C. Molina, E. Parrondo-Iglesias, M. P. Alonso, C. Lorenzo Molina, J. C. Doadrio-Villarejo, M. T. Gutierrez-Rios, M. I. de Frutos, E. Gaston de Iriarte, G. Certad Fombona and N. Ercoli, *Ann. Real. Acad. Farm*. **1991**, *57*, 15.
793. R. D. Sinisterra, V. P. Shastri, R. Najjar and R. Langer, *J. Pharm. Sci*. **1999**, *88*, 574.

Pictiva EX2004
Samsung v Pictiva
IPR2024-01094

794. R. D. Sinisterra, R. Najjar, O. L. Alves, P. S. Santos, C. A. Alves de Carvalho and A. L. Conde da Silva, *J. Inclusion Phenom. Mol. Recognit. Chem*. **1995**, *22*, 91.
795. A. E. Burgos, J. C. Belchior and R. D. Sinisterra, *Biomaterials* **2002**, *23*, 2519.
796. B. P. Espósito, A. Faljoni-Alário, J. F. Silva de Menezes, H. F. de Brito and R. Najjar, *J. Inorg. Biochem*. **1999**, *75*, 55.
797. B. P. Espósito, E. de Oliveira, S. B. Zyngier and R. Najjar, *J. Braz. Chem. Soc.* **2000**, *11*, 447.
798. L. Trynda and F. Pruchnik, *J. Inorg. Biochem*. **1995**, *58*, 69.
799. B. P. Espósito and R. Najjar, *Coord. Chem. Rev*. **2002**, *232*, 137.
800. L. Trynda-Lemiesz and F. P. Pruchnik, *J. Inorg. Biochem*. **1997**, *66*, 187.
801. R. A. Howard, T. G. Spring and J. L. Bear, *Cancer Res*. **1976**, *36*, 4402.
802. R. A. Howard, T. G. Spring and J. L. Bear, *J. Clin. Hematol. Oncol.* **1977**, *7*, 391.
803. P. Jakimowicz, L. Ostropolska and F. P. Pruchnik, *Met. Based Drugs* **2000**, 7, 201.
804. K. Sorasaenee, J. R. Galán-Mascarós and K. R. Dunbar, *Inorg. Chem*. **2002**, *41*, 433.
805. K. Sorasaenee, J. R. Galán-Mascarós and K. R. Dunbar, *Inorg. Chem*. **2003**, *42*, 661.
806. M. R. Moller, M. A. Bruck, T. O'Connor, F. J. Armatis, Jr., E. A. Knolinksi, N. Kottmair and R. S. Tobias, *J. Am. Chem. Soc.* **1980**, *102*, 4589.
807. N. Farrell, *J. Chem. Soc., Chem. Comm*. **1980**, 1014.
808. E. de Souza Gil, S. H. P. Serrano, E. I Ferreira and L. T. Kubota, *J. Pharm. Biomed. Anal*. **2002**, *29*, 579.
809. R. P. Singhal and Y. Sarwar, *J. Radioanal. Nucl. Chem*. **1988**, *128*, 377.
810. B. S. Yu, S. Y. Choo and I. M. Chang, *J. Pharm. Soc. Korea* **1975**, *19*, 215.
811. H. T. Chifotides, K. M. Koshlap, L. M. Pérez and K. R. Dunbar, *J. Am. Chem. Soc.* **2003**, *125*, 10703.
812. B. Lippert, *Prog. Inorg. Chem*. **2005**, Vol 54, Chapter 6, in press.
813. A. C. G. Hotze, M. E. T. Broekhuisen, A. H. Velders, K. van der Schilden, J. G. Haasnoot and J. Reedijk, *Eur. J. Inorg. Chem*. **2002**, 369.
814. A. Koutsodimou and N. Katsaros, *J. Coord. Chem*. **1996**, *39*, 169.
815. H. T. Chifotides, K. M. Koshlap, L. M. Pérez and K. R. Dunbar, *J. Am. Chem. Soc.* **2003**, *125*, 10714.
816. S. E. Sherman, D. Gibson, A. H.-J. Wang and S. J. Lippard, *J. Am. Chem. Soc.* **1988**, *110*, 7368.
817. H. T. Chifotides and K. R. Dunbar, unpublished results.
818. A. Erck, E. Sherwood, J. L. Bear and A. P. Kimball, *Cancer Res.* **1976**, *36*, 2204.
819. S. U. Dunham, H. T. Chifotides, S. Mikulski, A. E. Burr and K. R. Dunbar, *Biochemistry* **2005**, *44*, 996.
820. P. M. Bradley, P. K.-L. Fu and C. Turro, *Spectrum* **2001**, *14*, 12.
821. L. Liu and J. L. Bear, *Acta Phys. Chim. Sinica* **1989**, *5*, 644.
822. A. M. Angeles-Boza, P. M. Bradley, P. K.-L. Fu, S. E. Wicke, J. Bacsa, K. R. Dunbar and C. Turro, *Inorg. Chem*. **2004**, *43*, 8510.
823. P. M. Bradley, A. M. Angeles-Boza, K. R. Dunbar and C. Turro, *Inorg. Chem.* **2004**, *43*, 2450.
824. A. Chouai, M. Shatruk, A. M. Angeles-Boza, N. N. Degtyareva, P. K.-L. Fu, K. R. Dunbar and C. Turro, unpublished results.
825. A. M. Angeles-Boza, P. M. Bradley, P. K.-L. Fu, M. G. Hilfiger, M. Shatruk, K. R. Dunbar and C. Turro, unpublished results.
826. A. Chouai, A. M. Angeles-Boza, N. N. Degtyareva, P. K.-L. Fu, Y. Liu, K. R. Dunbar and C. Turro, unpublished results.
827. A. M. Angeles-Boza, P. M. Bradley, P. K.-L. Fu, J. Bacsa, K. R. Dunbar and C. Turro, unpublished results.
828. A. M. Angeles-Boza, H. T. Chifotides, P. K.-L. Fu, K. R. Dunbar and C. Turro, unpublished results.
829. D. Voet and J. G. Voet, *Biochemistry*, John Wiley & Sons: New York, 1995, p 919.
830. Y. Jung and S. J. Lippard, *J. Biol. Chem*. **2003**, *278*, 52084.

Pictiva EX2004
Samsung v Pictiva
IPR2024-01094

831. C. M. Partigianoni, C. Turro, C. Hsu, I.-J. Chang and D. G. Nocera, *Photosensitive Metal-Organic Systems: Mechanistic Principles and Recent Applications, Advances in Chemistry Series*, No 238, C. Kutal and N. Serpone, Eds., American Chemical Society: Washington D.C. 1993, p 147.
832. J. Frelek and W. J. Szczepek, *Tetrahedron: Asymmetry* **1999**, *10*, 1507.
833. M. Gerards and G. Snatzke, *Tetrahedron: Asymmetry* **1990**, *1*, 221.
834. J. Frelek, *Polish J. Chem*. **1999**, *73*, 229.
835. W. Diener, J. Frelek and G. Snatzke, *Collect. Czech. Chem. Commun.* **1991**, *56*, 954.
836. M. P. Doyle and W. Hu, *Chim. Oggi* **2003**, *21*, 54.
837. W. Kurosawa, T. Kan and T. Fukuyama, *J. Am. Chem. Soc.* **2003**, *125*, 8112.
838. S. M. Berberich, R. J. Cherney, J. Colucci, C. Courillon, L. S. Geraci, T. A. Kirkland, M. A. Marx, M. F. Schneider and S. F. Martin, *Tetrahedron* **2003**, *59*, 6819.
839. E. S. Gil and L. T. Kubota, *Bioelectrochem*. **2000**, *51*, 145.
840. E. de S. Gil and L. T. Kubota, *J. Braz. Chem. Soc.* **2000**, *11*, 304.
841. X. Wei, M. H. Dickman and M. T. Pope, *Inorg. Chem*. **1997**, *36*, 130.
842. M. E. Tess and J. A. Cox, *Electroanalysis* **1998**, *10*, 1237.
843. J. A. Cox, S. D. Holmstrom and M. E. Tess, *Talanta* **2000**, *52*, 1081.
844. A. M. Kijak, R. K. Perdue and J. A. Cox, *J. Solid State Electrochem*. **2004**, *8*, 376.
845. S. Lo Schiavo, C. Forte, B. Pignataro, G. Tresoldi and P. Piraino, *Macromol. Rapid Commun*. **2004**, *25*, 1033.

Pictiva EX2004
Samsung v Pictiva
IPR2024-01094

13

Chiral Dirhodium(II) Catalysts and Their Applications

Daren J. Timmons, *Virginia Military Institute*
Michael P. Doyle, *University of Maryland*

13.1 Introduction

Dirhodium(II) acetate has been known to catalyze organic transformations by the decomposition of diazo compounds since the early 1970s.[1] Development and understanding of both the mechanism and the synthetic uses have placed $Rh_2(OAc)_4$ in a unique position among transition metal catalysts. Although demonstrably effective for reactions involving metal carbene intermediates,[2] this catalyst is also recognized for its ability to catalyze oxidation[3] and reduction[4-10] reactions, and to serve as a Lewis acid capable of catalyzing those transformations.[11] In reactions with diazo compounds, the effectiveness of rhodium acetate for addition, insertion, and ylide reactions are well established. Only recently have homochiral dirhodium(II) complexes containing carboxylate[12-14] (described in the previous chapter) and carboxamidate ligands, and dirhodium(II) complexes bearing orthometalated phosphine ligands, been shown to provide high selectivity in the formation of chiral organic molecules.[2] However, their structural uniqueness and stereoselection in catalytic chemical reactions place them among the most important asymmetric catalysts employed for chemical transformations.[15] This chapter describes the structures of these important chiral dirhodium(II) complexes and their synthetic utility.

13.2 Synthetic and Structural Aspects of Chiral Dirhodium(II) Carboxamidates

The best characterized of the dirhodium(II) carboxamidate complexes are those bearing chiral carboxamidate ligands. Primarily through the work of Doyle and co-workers, a large number of chiral dirhodium(II) carboxamidate complexes have been synthesized and utilized in catalytic asymmetric metal carbene transformations.[2,15-17] Each catalyst has a paddlewheel structural motif defined by four bridging carboxamidate ligands about a Rh_2^{4+} core with, preferentially,[18-20] two nitrogens and two oxygens bound to each rhodium, and the two nitrogen atoms (or oxygen atoms) cis to each other (Fig. 13.1). The rhodium-to-rhodium bond is formally a single bond[21] with the electronic configuration $\sigma^2\pi^4\delta^2\delta^{*2}\pi^{*4}$. With acetonitrile or benzonitrile coordinated in the axial positions, these air stable complexes typically crystallize as red solids. The axial ligands, which are derived from the solvent in which the complex is crystallized, can be easily removed by placing the solid under vacuum or in a poorly coordinating solvent (e.g,. dichloromethane) yielding a blue species. The standard preparation of these catalysts involves the reaction of $Rh_2(OAc)_4$ with an excess of the neutral carboxamidine ligand

Pictiva EX2004
Samsung v Pictiva
IPR2024-01094

in boiling chlorobenzene. The reaction is driven to completion by use of a Söxhlet continuous extractor in which the inner thimble is filled with a mixture of sodium carbonate and sand to trap the evolved acetic acid.[2] Product formation is typically followed by HPLC using a chiral reverse-phase support and purified by column chromatography.

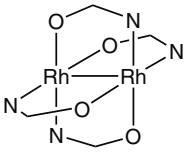
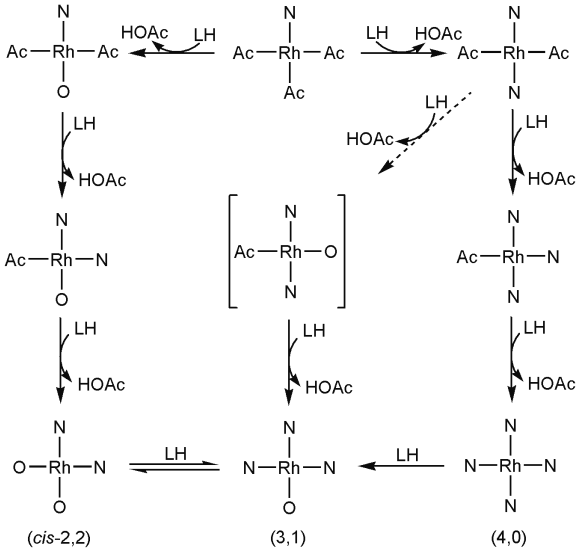


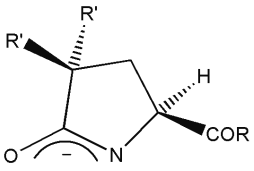
Fig. 13.1. Typical paddlewheel arrangement for dirhodium(II) carboxamidates.

Carboxamidate catalysts can be divided by ligand type into four primary classes: 2-oxopyrrolidinates, **13.1**,[22-25] 2-oxooxazolidinates, **13.2**,[22,26] 1-acyl-2-oxoimidiazolidinates, **13.3**,[25,27-31] and 2-oxoazetidinates, **13.4**.[32-35] The use of over 30 different ligands has provided the successful preparation of many dirhodium(II) complexes. Like the achiral carboxamidates (Chapter 12), the chiral carboxamidate ligands are unsymmetrical bridges and, therefore, four different geometries are possible about the Rh_2^{4+} core: *cis*-(2,2), *trans*-(2,2), (3,1) and (4,0) (see Fig. 1.10). The *cis*-(2,2) isomer is dominant or exclusive in these preparations, and the *trans*-(2,2) isomer has never been observed for this class of chiral compounds.[16] A detailed study has been performed to explain the formation of all three isomers in reactions with oxoimidazolidinate ligands, and the proposed mechanism is shown in Scheme 13.1 (Ac = acetate).[28] Ligand substitution is initiated through coordination at the axial site. Replacement of acetate by the first carboxamidate ligand activates the acetate that is *trans* to the carboxamidate for the second substitution. For ligand types **13.1**, **13.2** and **13.4**, steric considerations lead directly to the formation of the *cis*-(2,2) isomer, and there is no evidence for the formation of other isomers. However, when using ligand type **13.3**, an increased level of steric repulsion exists between the *N*-acyl moieties and the ester groups of neighboring ligands. This can lead to initial formation of the (4,0) isomer, followed by isomerization to the (3,1) and *cis*-(2,2) geometries.



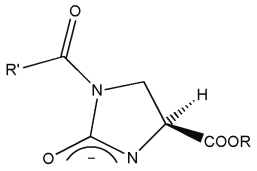
Scheme 13.1. Mechanism for the formation of dirhodium(II) carboxamidate isomers.

Pictiva EX2004
Samsung v Pictiva
IPR2024-01094



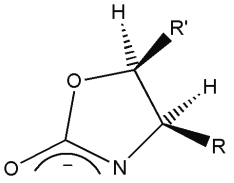
13.1

(5*S*)-MEPY (R = OMe, R' = H)
(5*S*)-dFMEPY (R = OMe, R' =F)
(5*S*)-DMAP (R = NMe_2, R' =H)
(5*S*)-NEPY (R = OCH_2CMe_3, R' = H)
(5*S*)-ODPY (R = $O(CH_2)_{17}CH_3$, R' = H)

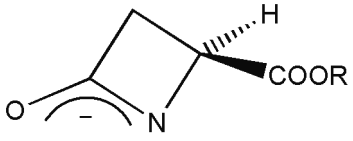


13.3

(4*S*)-MACIM (R = R' = Me)
(4*S*)-BACIM (R = Bu^i, R' = Me)
(4*S*)-MBOIM (R = Me, R' = Ph)
(4*S*)-MPAIM (R = Me, R' = $PhCH_2$)
(4*S*)-MPPIM (R = Me, R' = $PhCH_2CH_2$)
(4*S*)-MCHIM (R = Me, R' = *c*-$C_6H_{11}CH_2$)
(4*S*)-MANIM (R = Me, R' = *R*,*S*,-Ph(MeO)CH)
(4*S*)-EPPIM (R = Et, R' = $PhCH_2CH_2$)
(4*S*)-BPPIM (R = Bu^i, R' = $PhCH_2CH_2$)



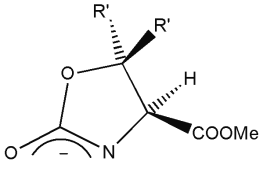
13.2a



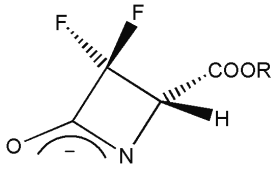
13.4a

(4*S*)-IPOX (R = Pr^i, R' = H)
(4*S*)-PHOX (R = Ph, R' = H)
(4*S*)-BNOX (R = $PhCH_2$, R' = H)
(4*S*)-MPOX (R = CH_3, R' = Ph)

(4*S*)-IBAZ (R = Pr^i)
(4*S*)-BNAZ (R = $PhCH_2$)
(4*S*)-MEAZ (R = Me)
(4*S*)-CHAZ (R = *c*-C_6H_{11})
(*S*,*S*/*R*)-MENTHAZ (R = *S*/*R*-menthyl)
(*S*,*S*/*R*)-NAPHTHAZ (R = *S*/*R*-naphthylethyl)



13.2b



13.4b

(4*S*)-MEOX (R = R' = H)
(4*S*)-THREOX (R = H, R' = Me)

(4*R*)-dFIBAZ (R = Pr^i)
(4*R*)-dFCHAZ (R = *c*-C_6H_{11})

The structures of 16 different dirhodium(II) carboxamidates, including all three isomers of $Rh_2(MACIM)_4$,[27,28] have been determined by X-ray diffraction, and selected distances are given in Table 13.1. Each of the first three classes of ligands (**13.1**-**13.3**) is based on a 5-membered azacycle, and all the Rh–Rh bond distances fall within a narrow range (2.445-2.477 Å). Ligands of either *S*- or *R*- configuration can be used, and Fig. 13.2 shows the structure of

Pictiva EX2004
Samsung v Pictiva
IPR2024-01094

$Rh_2(5R\text{-MEPY})_4$ with acetonitrile molecules occupying axial coordination sites.[22] This dirhodium carboxamidate incorporated an interstitial isopropyl alcohol molecule (not shown in Fig. 13.2). The mirror image ligand configuration of these complexes is displayed in the structure of $Rh_2(4S\text{-MEOX})_4$[26] in which axial benzonitrile molecules have been removed (Fig. 13.3). Only two crystal structures exist for ligand type **13.4** with rhodium-to-rhodium bond distances up to 0.09 Å longer than the others (2.533 Å[32] and 2.530 Å[34]). The four-membered azacycle-ligated $Rh_2(4S\text{-BNAZ})_4$ is presented in Fig. 13.4. The average Rh–N bond distance in types **13.1-13.3** (2.01 Å) is longer than that in type **13.4** (1.96 Å), and the average Rh–O bond distance in types **13.1-13.3** (2.08 Å) is somewhat shorter than that in type **13.4** (2.10 Å). It is clear in structures containing ligand type **13.4** that maximization of the Rh–N overlap has occurred at the expense of the Rh–O overlap.[16] These structural differences in catalysts of group **13.4** have been attributed primarily to the larger bite angle of the NCO bridge imposed by the 4-membered azacycle. This strain causes increased reactivity toward diazo substrates.[33]

Table 13.1. Structural data for chiral Rh_2^{4+} carboxamidinato compounds[a]

Compound[b]	Rh–Rh	Rh–N	Rh–O	Rh–N_{ax}	Axial Ligand	Isomer	ref.
$Rh_2(5R\text{-MEPY})_4$[c]	2.457(1)	2.015[5]	2.079[5]	2.226[6]	CH_3CN	*cis*-(2,2)	22
$Rh_2(5S\text{-dFMEPY})_4$[c,d]	2.467(1)	2.01[1]	2.08[9]	2.30[1]	EtOAc	*cis*-(2,2)	24
	2.467(1)	2.01[1]	2.09[1]	2.362(8)	EtOAc	*cis*-(2,2)	24
				2.324(8)	H_2O		
$Rh_2(5S\text{-DMAP})_4$[c]	2.454(1)	2.004[4]	2.082[4]	2.228[6]	CH_3CN	*cis*-(2,2)	23
$Rh_2(4S\text{-PHOX})_4$[c]	2.471(1)	2.01[1]	2.08[1]	2.19(1)	CH_3CN	*cis*-(2,2)	26
$Rh_2(5S\text{-BNOX})_4$[c]	2.472(2)	2.019[8]	2.088[7]	2.23[1]	CH_3CN	*cis*-(2,2)	22
$Rh_2(4S\text{-MEOX})_4$[c]	2.477(1)	2.009[3]	2.083[3]	2.191(2)	C_6H_5CN	*cis*-(2,2)	26
$Rh_2(4S\text{-THREOX})_4$[c]	2.474(1)	2.018[4]	2.081[4]	2.203(2)	C_6H_5CN	*cis*-(2,2)	26
$Rh_2(4S\text{-MACIM})_4$[e]	2.459(1)	2.009[2]	2.081[1]	2.220[3]	CH_3CN	*cis*-(2,2)	27
$Rh_2(4S\text{-MACIM})_4$[e]	2.460(1)	2.023[3]	2.054[2]	2.223[4]	CH_3CN	(3,1)	27
$Rh_2(4S\text{-MACIM})_4$[d]	2.445(1)	2.039[4]	2.047[4]	2.224[6]	CH_3CN	(4,0)	28
$Rh_2(4S\text{-MBOIM})_4$[e]	2.461(1)	2.008[2]	2.072[2]	2.210[3]	CH_3CN	*cis*-(2,2)	27
$Rh_2(4S\text{-MPPIM})_4$[e]	2.464(1)	2.012[2]	2.063[2]	2.219[4]	CH_3CN	*cis*-(2,2)	27
$Rh_2(4S\text{-MCHIM})_4$[e]	2.451(1)	2.007[1]	2.073[1]	2.216[3]	CH_3CN	*cis*-(2,2)	27
$Rh_2(S,S\text{-MANIM})_4$[c]	2.467()	2.005[6]	2.071[4]	2.206(2)	CH_3CN	*cis*-(2,2)	29
$Rh_2(4S\text{-BNAZ})_4$[c]	2.533(1)	1.977[3]	2.112[3]	2.210[6]	CH_3CN	*cis*-(2,2)	32
$Rh_2(S,R\text{-NaphthAZ})_4$[c]	2.529(3)	1.95[1]	2.09[1]	2.22[2]	CH_3CN	*cis*-(2,2)	34

[a] All bond distances reported in Angstroms (Å).

[b] See list of abbreviations for MEPY, dFMEPY, DMAP, PHOX, BNOX, MEOX, THREOX, MACIM, MBOIM, MPPIM, MCHIM, MANIM, BNAZ, NaphthAZ.

[c] For average bond lengths, the estimated standard deviation given in square brackets is calculated as $[\ ] = [\Sigma_n\Delta_i^2/(n\text{-}1)]^{1/2}$ where Δ_i is the esd of each bond length contributing to the average.

[d] Compound crystallized in two forms in the same crystal.

[e] For average bond lengths (reported in the original literature), the estimated standard deviation given in square brackets is calculated as $[\ ] = [1/\Sigma_i(1/\sigma_i)]^{1/2}$ where σ_i is the esd of each bond length contributing to the average.

Pictiva EX2004
Samsung v Pictiva
IPR2024-01094

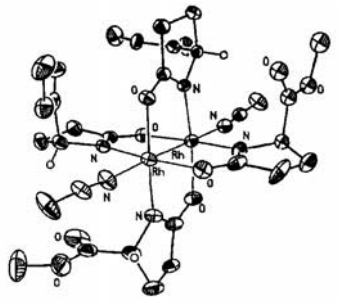


Fig. 13.2. The structure of $Rh_2(5R\text{-MEPY})_4(CH_3CN)_2$.

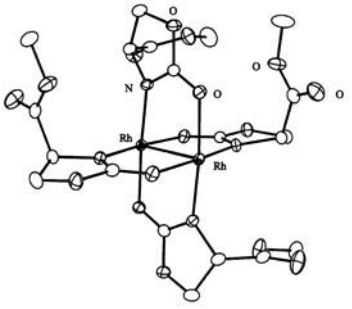


Fig. 13.3. The structure of $Rh_2(4S\text{-MEOX})_4$ with axial PhCN molecules removed.

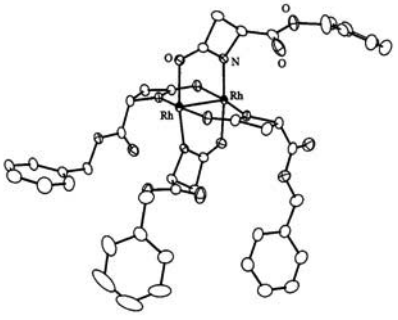


Fig. 13.4. The structure of $Rh_2(4S\text{-BNAZ})_4$ with axial CH_3CN molecules removed.

The structures of the dirhodium(II) carboxamidates (and, more specifically, the structures of the ligands) have a dramatic influence on their selectivity and reactivity in carbene transformations.[16] The complex $Rh_2(BNOX)_4$ (**13.2a**, Fig. 13.5) without a pendant carboxylate group but containing a benzyl group in its place exhibited much lower enantioselectivity in its catalytic reactions.[22] The dimethylamide derivative of $Rh_2(5S\text{-MEPY})_4$ also exhibited lower selectivity in reactions with diazo compounds.[23] In fact, only ligands containing an ester functionality on the chiral carbon atom alpha to nitrogen have resulted in significant control over product formation.[22] In the imidazolidinone series of carboxamidate catalysts[27,28] the *cis*-(2,2) isomers are the most selective, as the protruding ester groups form a balanced and well defined chiral

Pictiva EX2004
Samsung v Pictiva
IPR2024-01094

pocket around the axial coordination site of each rhodium atom. The general ligand framework is rigid, while a variety of ester alkyl groups allow for moderate differentiation at the active site–primarily due to steric effects. The chiral ester functionality on the ligand can be either *S* (13.5) or *R* (13.6) and gives an identical chiral pocket at each rhodium site.

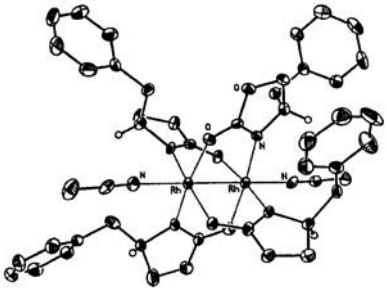
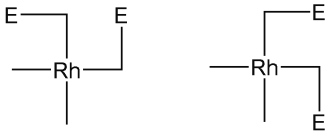


Fig. 13.5. The structure of $Rh_2(4S\text{-BNOX})_4(CH_3CN)_2$.



(*S*) (*R*)

13.5 **13.6**

N-Acyl and ester substituents of imidazolidinone-ligated compounds have provided even greater definition to the space around each rhodium atom.[17] *N*-Acyl groups of various size have been employed to produce deeper or more restricted pockets to enhance catalytic selectivity (e.g., $Rh_2(MPPIM)_4$, Fig. 13.6).[27] Additional variations of *N*-acyl attachments with ethyl (EPPIM) and isobutyl (BPPIM, BACIM) ester moieties have been reported and display some of the subtleties involved in optimizing the chiral pocket.[31] Attempts to synthesize *N*-alkylimidazolidinone-ligated dirhodium(II) compounds have failed.

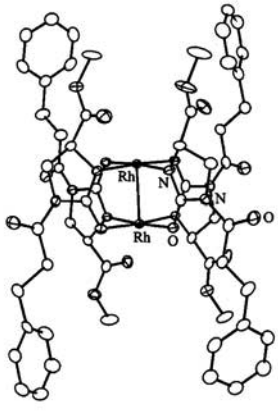
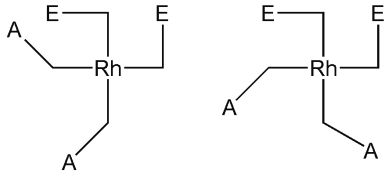


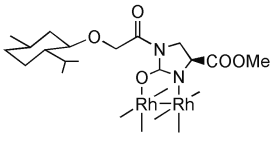
Fig. 13.6. The structure of $Rh_2(4S\text{-MPPIM})_4$ with axial CH_3CN molecules removed.

Pictiva EX2004
Samsung v Pictiva
IPR2024-01094

Chiral *N*-acyl groups on imidazolidinone ligands have also been used to explore match/mismatch concepts, as shown with **13.7** and **13.8**, where E is an ester group and A is the *N*-acyl attachment. Here, the chiral *N*-acyl attachments of the imidazolidinone-carboxylate catalysts are designed to potentially reinforce the inherent stereocontrol provided by the core ligand system. Use of ligand diastereomers to form $Rh_2(MLMIM)_4$ (**13.9**) and $Rh_2(MDMIM)_4$ (**13.10**) revealed remarkable differences in diastereo- and enantiomeric product selectivity.[30] The *S,R*-MENTHAZ catalyst (**13.11**) was significantly more selective than its diasteriomer *S,S*-MENTHAZ, which itself was less selective than the structures reported as $Rh_2(IBAZ)_4$.[35] Several other systems are under development, but structural data have not yet been reported.

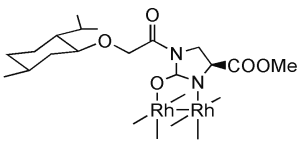


13.7 **13.8**



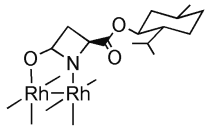
$Rh_2(MLMIM)_4$

13.9



$Rh_2(MDMIM)_4$

13.10



$Rh_2(S,R\text{-MENTHAZ})_4$

13.11

To increase catalyst activity, fluorinated ligand derivatives of MEPY (**13.1**), IBAZ (**13.4a**) and CHAZ (**13.4a**) were substituted onto the dirhodium(II) core.[24] A structural determination of $Rh_2(dFMEPY)_4$ (Fig. 13.7) showed very little change in the distances and geometry about the core relative to $Rh_2(MEPY)_4$, but two ligated structures of this compound crystallized, one with two axial ethyl acetate ligands and the other having one ethyl acetate ligand and one water ligand occupying the axial sites. The dirhodium(II) complexes bearing the fluorinated ligands are much more reactive towards diazo decomposition because of the electron withdrawing influence of the fluorine substitution.[24]

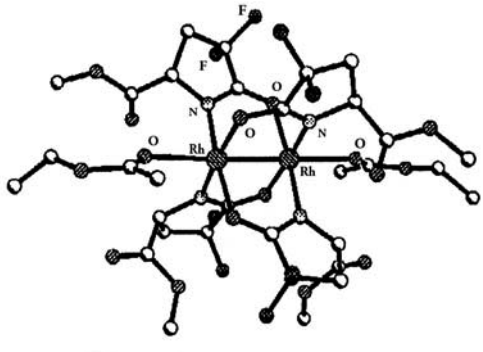
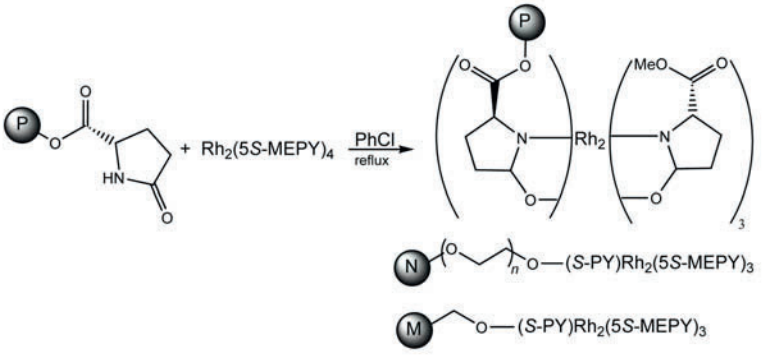


Fig. 13.7. The structure of $Rh_2(5S\text{-}dFMEPY)_4(EtOAc)_2$.

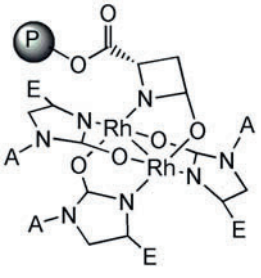
Pictiva EX2004
Samsung v Pictiva
IPR2024-01094

Recently, some of these carboxamidate catalysts have been covalently linked to polymer (P) supports with great initial success.[36-38] A pyrrolidinone[37] (PY) or azetidinone[38] (AZ) ligand was bound to either a NovaSynTG (N) or a Merrifield (M) resin through ester formation to give **13.12**. Different catalysts (e.g., $Rh_2(MEPY)_4$, $Rh_2(MPPIM)_4$) were then heated in chlorobenzene with the substituted resin causing ligand exchange and attachment of $Rh_2(carboxamidato)_3$ to the polymer (e.g., **13.13**).[37] Elemental analysis determined the loading ratio. The solid-supported catalysts N-PY-$Rh_2(MEPY)_3$ and M-PY-$Rh_2(MEPY)_3$ were equally selective in cyclopropanation reactions as their solution phase counterparts.[37] Reuse of the immobilized catalyst up to eight times with no loss in selectivity demonstrated the stability of the system.



13.12 **13.13**

Heteroleptic chiral dirhodium(II) carboxamidates were made by immobilizing one ligand type on the resin and using a different homogeneous catalyst during the ligand exchange step. Mixed ligands on the Rh_2^{4+} core can be controlled in this way, and they provide information not otherwise possible about catalytic reactivity. For example, the attachment of the four-membered-ring azetidinone ligand to the resin and subsequent coordination of the five-membered-ring ligand catatyst $Rh_2(MPPIM)_4$ resulted in the mixed ligand system *N*-AZ-$Rh_2(MPPIM)_3$ (**13.14** where E = COOMe and A = $PhCH_2CH_2C(O)$).[38] An elongated Rh–Rh bond is implicated by increased reactivity with diazo substituents over the homogeneous $Rh_2(MPPIM)_4$; this is consistent with other catalysts bearing ligands of type **13.4**.[38] Other ligand combinations have also been prepared, and they show advantageous effects.

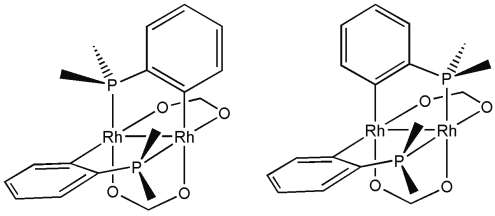


13.14

Pictiva EX2004
Samsung v Pictiva
IPR2024-01094

13.3 Synthetic and Structural Aspects of Dirhodium(II) Complexes Bearing Orthometalated Phosphines

Dirhodium(II) complexes, with two cisoid bridging acetate groups (OAc) and two orthometalated aryl phosphines (PC) with inherent backbone chirality, have also received attention as catalysts. They have been reported to be active in the decomposition of diazo compounds,[39-46] as well as in hydroformylation[47] and reductive coupling[48] reactions. The first complex was reported in 1984 by Cotton and co-workers who boiled $Rh_2(OAc)_4$ and PPh_3 in acetic acid to form the purple complex *cis*-$Rh_2(OAc)_2[(C_6H_4)PPh_2]_2 \cdot 2HOAc$ with a molecule of acetic acid at each axial site (Fig 13.8).[49,50] The Rh–Rh bond distance (2.508 Å) is longer than those for tetracarboxylate complexes (see previous chapter), and becomes even longer (2.556 Å) when the axial ligand is pyridine.[50] In both of these complexes, the *cis*-orthometalated phosphines are oriented in a head-to-tail arrangement (*cis-H,T*; **13.15**, Fig. 13.8) around the Rh_2^{4+} core, while the *cis*-head-to-head arrangement (*cis-H,H*; **13.16**) is also known (Fig. 13.9).[51]



13.15 **13.16**

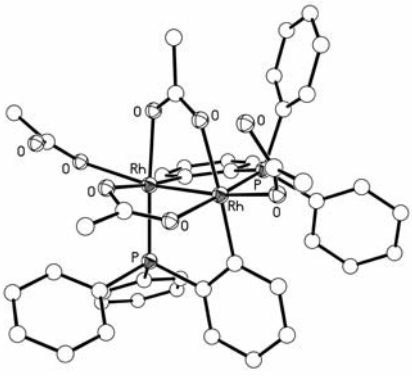


Fig. 13.8. The structure of cis-H,T-$Rh_2(OAc)_2[(C_6H_4)PPh_2]_2 \cdot 2HOAc$.

Reaction pathways to these two structural types have been detailed.[51,52] The *cis-H,H*-$Rh_2(OAc)_2(PC)_2$ complexes generally show poor reactivity with diazo compounds, but the *cis*-H,T isomers can be modified to give high reactivity and selectivity in competitive C–H insertion reactions of selected diazo-esters and diazo-ketones.[41] Variation of acetate ligands and of the substituents on the metalated phenyl ring provided dramatic differences in chemoselectivity during C–H insertion and aromatic substitution competition reactions, and there was a high level of selectivity for cyclopropanation.[39] A variety of *bis*-orthometalated complexes with different aryl phosphines, carboxylates, and axial ligands have been characterized.[39,42-45,50,51,53-62] Important bond distances are recorded in Table 13.2. The Rh–Rh bond distances range from 2.485 Å to 2.630 Å with an average of 2.516 Å. The Rh–O bond lengths vary according to the

Pictiva EX2004
Samsung v Pictiva
IPR2024-01094

trans effect with those *trans* to carbon (average = 2.18 Å) longer than those *trans* to phosphorus (average = 2.13 Å).

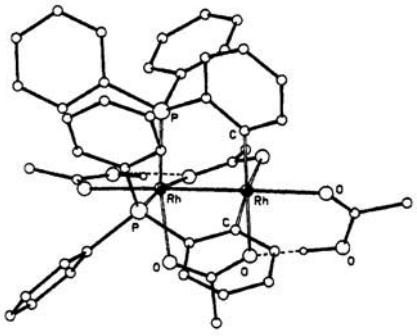


Fig. 13.9. The structure of cis-H,H-$Rh_2(OAc)_2[(C_6H_4)PPh_2]_2 \cdot 2HOAc$.

Carboxylate exchange for orthometallated phosphines happens in a straightforward manner, and modification of catalyst electronic and steric characteristics has been achieved.[46] Complexes bearing trifluoroacetate ligands, *cis-H,T*-$Rh_2(O_2CCF_3)_2(PC)_2$, were expectedly more reactive towards diazo decomposition than those with acetate ligands.[39,45]

The first separation of catalyst enantiomers was accomplished by column chromatography on silica gel after the acetate ligands of $Rh_2(OAc)_2[(C_6H_4)PPh_2]_2$ were substituted with chiral Protos (*N*-(4-methylphenylsulfonyl)-(*L*)-prolinate) ligands.[42] A subsequent substitution of the prolinate ligands using trifluoroacetic acid provided the (*P*)- and (*M*)- enantiomers of *cis-H,T*-$Rh_2(O_2CCF_3)_2[(C_6H_4)PPh_2]_2$ in 98% optical purity. These structures are shown in Fig. 13.10 and Fig. 13.11, respectively.[42] When used for a C–H insertion reaction of a diazoketone, the two enantiomers gave identical but opposite enantiocontrol (36% ee). [42] A subsequent study showed low diastereoselectivity, but high enantioselectivity in a typical reaction between styrene and ethyl diazoacetate.[44] Use of (*M*)-$Rh_2(O_2CCF_3)_2[(C_6H_4)PPh_2]_2$ resulted in a substantial reduction in enantioselectivity for the same reaction.[44]

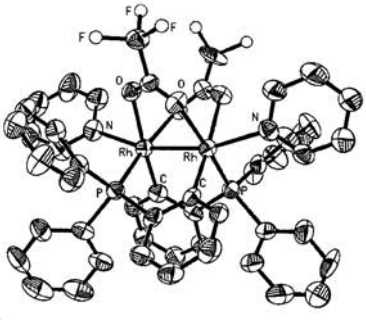


Fig. 13.10. The structure of (*P*)-cis-H,T-$Rh_2(O_2CCF_3)_2[(C_6H_4)PPh_2]_2 \cdot 2C_5H_5N$.

Pictiva EX2004
Samsung v Pictiva
IPR2024-01094

Table 13.2. Structural data for cis-$Rh_2(OAc)_2(PC)_2L_n$[a]

Compound[b]	Rh—Rh	Rh—O[c]	Rh—O[d]	Rh—P	Rh—C	Rh—L	ref.
H,T-$Rh_2(OAc)_2[(C_6H_4)PPh_2]_2\cdot(HOAc)_2$[e]	2.508(1)	2.136[4]	2.190[4]	2.210(2)	1.996(6)	2.342(5)	50
H,T-$Rh_2(OAc)_2[(C_6H_4)PPh_2]_2\cdot(C_5H_5N)_2$[e]	2.556(2)	2.118[8]	2.182[7]	2.216(3)	2.01(1)	2.281(9)	50
H,T-$Rh_2(OAc)_2[(C_6H_4)PPh_2][(p\text{-}ClC_6H_3)P(p\text{-}ClC_6H_4)]\cdot(HOAc)_2$[e]	2.513(1)	1.982[6]	2.140[4]	2.211[1]	1.982[6]	2.342[4]	57
H,T-$Rh_2(OAc)_2\{[(C_6H_4)PhP(C_5H_4)]Fe(C_5H_5)\}_2\cdot(HOAc)_2$[e]	2.504(1)	2.164[9]	2.192[9]	2.201[3]	2.00[1]	2.344[9]	58
H,T-$Rh_2(OAc)_2[(m\text{-}MeC_6H_3)P(m\text{-}C_6H_4)_2]_2\cdot(HOAc)_2$[e]	2.502(3)	2.158[4]	2.185[4]	2.213[4]	1.984[6]	2.365[6]	55
H,T-$Rh_2(O_2CCMe_3)_2[(C_6H_4)PMe_2]_2\cdot(H_2O)_2$[e]	2.492(1)	2.18[1]	2.16[1]	2.191[6]	1.99[2]	2.36[1]	56
H,T-$Rh_2(O_2CCF_3)_2[(C_6H_4)PPh_2]_2\cdot(PPh_3)_2$[e]	2.630(1)	2.187[5]	2.184[5]	2.237(2)	2.011(7)	2.560(2)	59
H,T-$Rh_2(OAc)_2[(p\text{-}FC_6H_3)P(p\text{-}FC_6H_4)_2]_2\cdot(HOAc)_2$[e]	2.488(3)	2.12[1]	2.19[1]	2.213(4)	1.99(2)	2.29(1)	39
H,T-$Rh_2(OAc)_2[(C_6H_4)PPh(C_6H_4Br)]_2$[e]	2.475(1)	2.129[8]	2.175[8]	2.203(3)	2.03(1)	2.764(2)	53
(*M*)-*H,T*-$Rh_2(OAc)_2(PC^*)_2$[f]	2.504(1)	2.139(2)	2.196(2)	2.219(1)	1.992(4)	2.370(3)	45
(P)-*H,T*-$Rh_2(O_2CCF_3)_2[(C_6H_4)PPh_2]_2\cdot(C_5H_5N)_2$[e]	2.583(1)	2.176[9]	2.200[9]	2.218[4]	2.00[1]	2.28[1]	42
(*M*)-*H,T*-$Rh_2(O_2CCF_3)_2[(C_6H_4)PPh_2]_2\cdot(HOAc)_2$[e]	2.513(2)	2.21[3]	2.22[3]	2.21[1]	2.01[3]	2.35[2]	42
(*M*)-*H,T*-$Rh_2(O_2CCPh_3)_2[(C_6H_4)PPh_2]_2\cdot(C_5H_5N)_2$	2.559(1)	2.151(3)	2.164(3)	2.28(1)	2.005(5)	2.302(4)	44
H,T-$Rh_2(O_2CC_3F_7)_2[(C_6H_4)PPh(C_6F_5)]_2\cdot(H_2O)_2$[e]	2.530(2)	2.18[2]	2.18[2]	2.212[9]	2.00[3]	2.34[2]	43
H,T-$Rh_2(OAc)_2[(C_6H_4)PPh(C_6F_5)]_2\cdot(H_2O)_2$[e]	2.496(2)	2.12[2]	2.15[2]	2.207[7]	2.01[3]	2.34[2]	43
H,T-$Rh_2(OAc)_2[(C_6H_4)PPh_2]\{(C_6H_4)PPh[c\text{-}(C_5H_9)_7Si_8O_{12}(CH_2)_2]\}$[e]	2.508(2)	2.152[4]	2.187[4]	2.212	1.998[6]	2.349[4]	60
H,T-$Rh_2(OAc_2)[(C_6H_4)PPh(C_6H_4Br)]_2\cdot H_2O$[e]	2.485(1)	2.128[8]	2.170[9]	2.220[3]	1.99[1]	2.983(1)[g] 2.292(6)[h]	53
H,H-$Rh_2(OAc)_2[(C_6H_4)PPh_2]_2\cdot(HOAc)_2$[e]	2.493(1)	2.133[6]	2.185[6]	2.229[3]	1.990[9]	2.348[9]	51
H,H-$Rh_2(OAc)_2[(ClC_6H_3)P(p\text{-}ClC_6H_4)_2]_2\cdot(HOAc)_2$[e]	2.511(2)	2.13[1]	2.178[9]	2.237[4]	2.01[1]	2.31[1]	51
H,H-$Rh_2(OAc)_2[(CH_2)PPh_2][(C_6H_4)PPh_2]\cdot PPh_3$[e]	2.532(2)	2.11[1]	2.20[1]	2.226[6]	2.06[1]	2.297(4)	61,62
H,H-$Rh_2(OAc)_2\{[(C_6H_4)PhP(C_5H_4)]_2Fe\}\cdot(HOAc)$[e]	2.508(4)	2.13[3]	2.22[3]	2.22[1]	1.98[4]	2.26(2)	58
H,H-$Rh_2(OAc)_2[(C_6H_4)P(o\text{-}ClC_6H_4)Ph][(C_6H_4)PPh_2]\cdot PPh_3$[e]	2.558(1)	2.099[8]	2.182[8]	2.219[3]	2.04[1]	2.370(2)	54

[a] Where OAc = acetate; PC = orthometalated phosphine; L = axial ligand
[b] *H,T* = head-to-tail arrangement, 13.15; *H,H* = head-to-head arrangement, 13.16
[c] *trans* to P
[d] *trans* to C
[e] For average bond lengths, the estimated standard deviation given in square brackets is calculated as $[\ ] = [\Sigma_n\Delta_i^2/(n\text{-}1)]^{1/2}$ where Δ_i is the esd of each bond length contributing to the average
[f] PC* = orthometalated (2*S*,5*S*)-2,5-dimethyl-1-phenylphospholane
[g] Rh—Br
[h] Rh—O

Pictiva EX2004
Samsung v Pictiva
IPR2024-01094

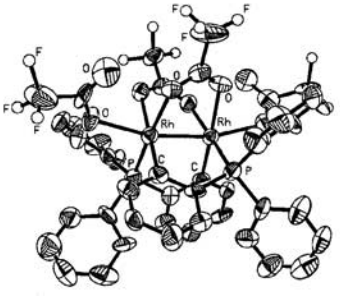


Fig. 13.11. The structure of (M)-cis-H,T-$Rh_2(O_2CCF_3)_2[(C_6H_4)PPh_2]_2 \cdot 2CF_3CO_2H$.

When a chiral phosphane was boiled with $Rh_2(OAc)_4$, two chromatographically separable *cis-H,T*-$Rh_2(OAc)_2(PC^*)_2$ diastereomers were isolated.[45] One of the structures, shown in Fig. 13.12, gave moderate enantioselectivity during selected intramolecular C–H insertion and cyclopropanation reactions using diazoketones.[45] The acetate ligands of *cis-H,T*-$Rh_2(OAc)_2(PC)_2$ have also been replaced with bridging succinimidate ligands to yield two complexes, neither of which exhibited high selectivity in intramolecular diazoketone cyclopropanation reactions.[40] In one of the diastereoisomers, the succinimidate ligands are oriented head-to-head about the Rh_2^{4+} core, and one succinimidine moiety and one water molecule serve as axial ligands.[40] In the other, the succinimidate ligands are bridging in a head-to-tail orientation with a water molecule in each axial position (Fig. 13.13).[40] The Rh–Rh bond distances (2.555 Å and 2.539 Å, respectively) fall within the range of *cis*-$Rh_2(OAc)_2(PC)_2$ complexes.[40]

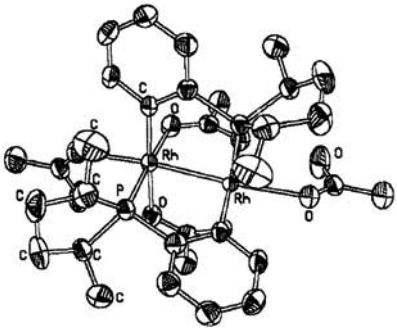


Fig. 13.12. The structure of (M)-cis-H,T-$Rh_2(OAc)_2(PC^*)_2(acetone)_2$ where PC* is orthometalated (2S, 5S)-2,5-dimethyl-1-phenylphospholane.

Modified arylphosphines [e.g., $PPh_2(C_6F_4X)$, X = Cl, Br] are orthometalated at one phenyl ring while the halogenated aryl ring becomes a chelating, bidentate ligand (P, X) at a rhodium atom.[53] The shortest Rh–Rh bond distance (2.475 Å) in the $Rh_2(OAc)_2(PC)_2$ series has been recorded in $Rh_2(OAc)_2[(C_6H_4)PPh(C_6F_4Br)]_2$ which has each axial site occupied by a bromine atom from a modified aryl ring (Fig. 13.14).[53] Several other structures have been reported

Pictiva EX2004
Samsung v Pictiva
IPR2024-01094

with functionalized aryl phosphine ligands acting as chelating, bidentate ligands,[53,54] but some contain only one orthometalated arylphosphine,[63-66] while others have none.[67-69] Little catalytic activity has been reported for these complexes.[69,70]

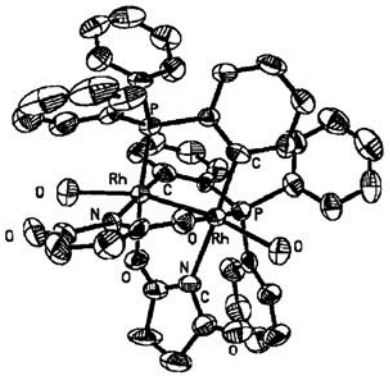


Fig. 13.13. The structure of cis-$Rh_2(C_4H_4NO_2)_2[(C_6H_4)PPh_2]_2 \cdot 2H_2O$.

A reaction between $Rh_2(OAc)_4$ and 1,1'-bis(diphenylphosphino)ferrocene resulted in the formation of $Rh_2(OAc)_2\{[(C_6H_4)PhP(C_5H_4)]_2Fe\} \cdot HOAc$ containing a *cis-H,H* orientation of the bidentate phosphine (Fig. 13.15).[58] One axial site is blocked by the steric bulk of the ferrocene, while an acetic acid molecule occupies the other. Use of diphenylphosphinoferrocene in a similar reaction resulted in the isolation of a typical *cis-H,T*-$Rh_2(OAc)_2(PC)_2$ complex with two pendant ferrocene groups.[58] While neither dirhodium(II) complex has any reported catalytic activity, each shows two well-defined oxidation processes (one from ferrocene; one from the Rh_2^{4+} core).[58]

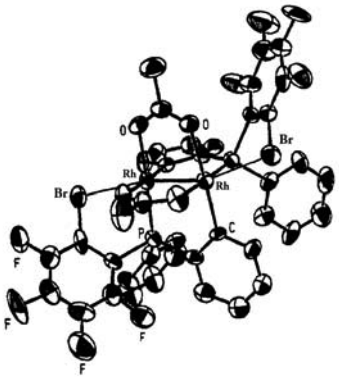


Fig. 13.14. The structure of $Rh_2(OAc)_2[(C_6H_4)P(C_6H_5)(C_6F_4Br)]_2$.

Pictiva EX2004
Samsung v Pictiva
IPR2024-01094

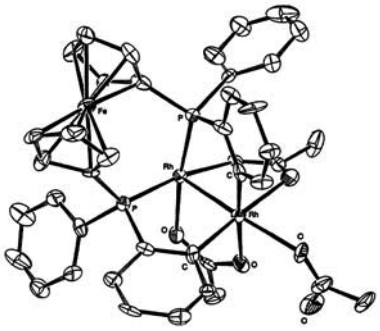


Fig. 13.15. The structure of H,H-$Rh_2(OAc)_2\{[(C_6H_4)PhP(C_5H_4)]_2Fe\}\cdot HOAc$.

The monoorthometalated complex, $Rh_2(OAc)_3[(C_6H_4)PPh_2]$ (Fig. 13.16)[51] and others of this type[52,71-76] have been synthesized, and there are reports of their catalytic activities and selectivities, none of which are remarkable.[41,43] These monoorthometalated complexes have been used primarily for the formation of complexes bearing two different metalated arylphosphines.[60-62] A complex similar to that in Fig. 13.16 containing an orthometalated diphenylphosphinomethane was reacted with PPh_3 causing orthometalation of the PPh_3 and rearrangement of the metalated $PMePh_2$ ligand to give metalation at the methyl group. This complex, *cis-H,H*-$Rh_2(OAc)_2[(CH_2)PPh_2][(C_6H_4)PPh_2]$ (Fig. 13.17) contains a four-membered Rh-P-C-Rh ring and only one axial PPh_3 with a short Rh–P bond distance (2.297 Å).[61,62]

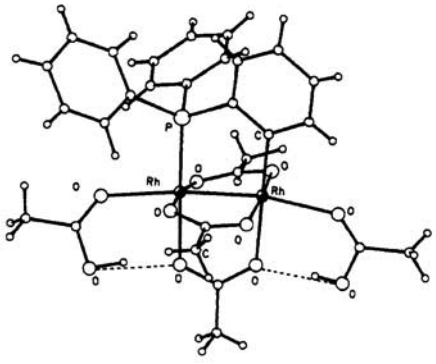


Fig. 13.16. The structure of $Rh_2(OAc)_3[(C_6H_4)PPh_2]\cdot 2HOAc$.

Immobilized $Rh_2(OAc)_2(PC)_2$ on silica and MCM-41 have been used in hydroformylation reactions of styrene with >99% aldehyde formation.[60] A model for the surface chemistry of these immobilized catalysts was prepared by a reaction between a phosphane-modified silsequioxane, $(c\text{-}C_5H_9)_7Si_8O_{12}(CH_2)_2PPh_2$, with $Rh_2(OAc)_3[(C_6H_4)PPh_2]$. Successful orthometalation of the pendant diphenylphosphine produced the complex shown in Fig. 13.18. Typical distances and geometries were observed for the Rh_2^{4+} moiety.[60]

Pictiva EX2004
Samsung v Pictiva
IPR2024-01094

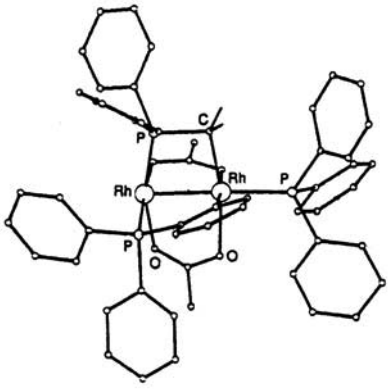


Fig. 13.17. The structure of cis-H,H-$Rh_2(OAc)_2[(CH_2)PPh_2][(C_6H_4)PPh_2]\cdot PPh_3$.

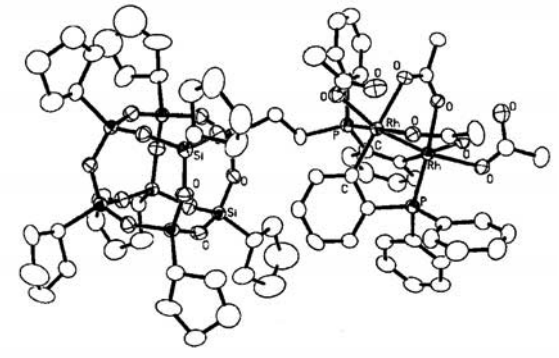
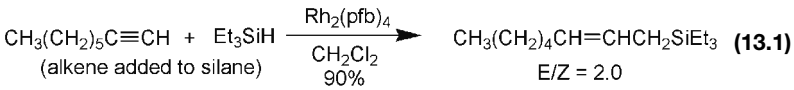


Fig. 13.18. The structure of H,T-$Rh_2(OAc)_2[(C_6H_4)PPh_2]\{(C_6H_4)PPh[c\text{-}(C_5H_9)_7Si_8O_{12}(CH_2)_2]\}$.

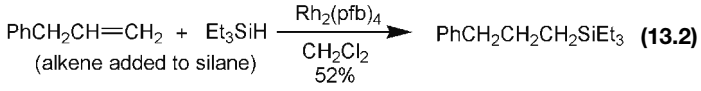
13.4 Dirhodium(II) Compounds as Catalysts

Few classes of transition metal compounds have received as much attention in recent years as have those of dirhodium(II) in their role as catalysts. The subject of numerous reviews,[2,15,16,77-86] the catalytic applications of these compounds continues to grow. The initial and most diverse set of applications has been in catalytic reactions of diazo compounds (Scheme 13.2, $ML_n = Rh_2L_4$), but advantages have also been realized in hydrosilylation (13.1, 13.2, pfb = perfluorobutyrate),[87,88] highly selective organosilane alcoholysis (13.3),[89] silylformylation (13.4),[90] and as Lewis acids in the hetero-Diels-Alder reaction (13.5).[11] Descriptions of the processes exemplified by (13.1-13.4) were reported in the earlier edition of this book and will not be further described here. Details of the catalytic applications of dirhodium(II) compounds as applied to reactions of diazo compounds, particularly those that relate to asymmetric catalysis, and as Lewis acids will be emphasized here. In their applications dirhodium(II) compounds are employed with low catalyst loadings under mild conditions and generally without degassing, and it is believed that the dimetallic structure imparts additional stability for catalytic uses.

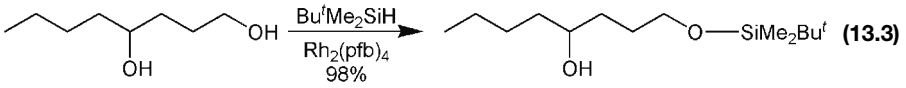
Pictiva EX2004
Samsung v Pictiva
IPR2024-01094



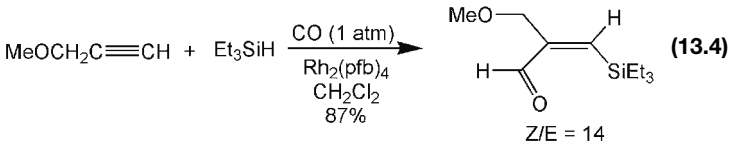
(13.1)



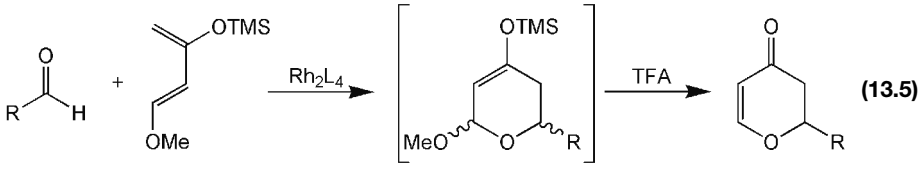
(13.2)



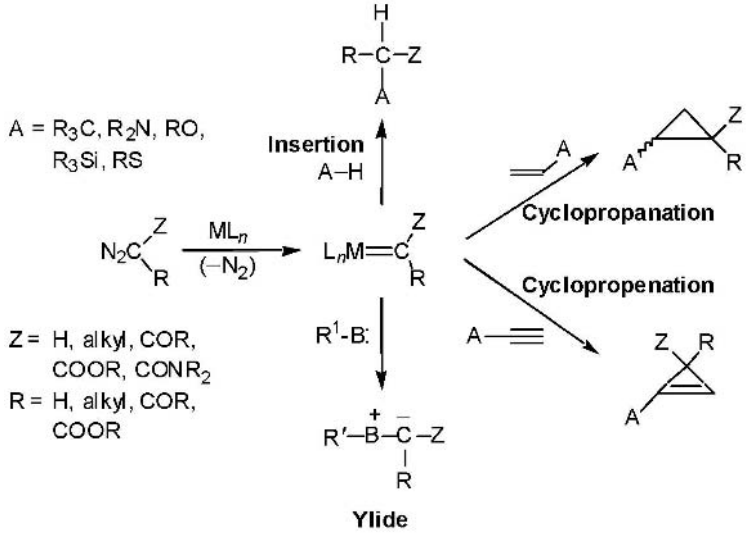
(13.3)



(13.4)



(13.5)

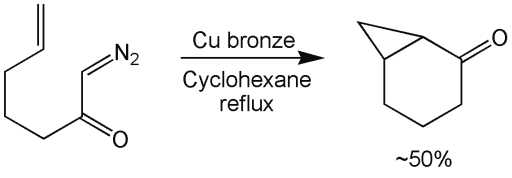


Scheme 13.2. Applications for catalytic reactions of diazo compounds.

Pictiva EX2004
Samsung v Pictiva
IPR2024-01094

13.5 Catalysis of Diazo Decomposition

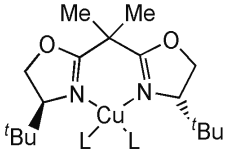
Dirhodium(II) tetraacetate came relatively late to the list of catalysts that were effective for the extrusion of dinitrogen from a diazo compound and, thereby, promote reactions that involved carbene-like intermediates. Copper and copper salts that included copper(II) sulfate were known since the beginning of the twentieth century to be effective, although they were characteristically unselective (both diastereoselection and regioselection) in their reactions. By 1960 there was uniform recognition that copper salts could cause the loss of dinitrogen from diazocarbonyl compounds with addition of the resulting carbene intermediate to a carbon-carbon double bond to form a cyclopropane product. That this reaction could occur in an intramolecular fashion, first reported by G. Stork in 1961 (13.6),[91] and thus avoid the formation of geometrical isomers, as was the case in intermolecular transformations, ushered in the first significant synthetic applications beyond insecticide pyrethroid syntheses from the reactions between 2,5-dimethyl-2,4-hexadiene or its dichloro analog and ethyl diazoacetate. Extensions of this intramolecular cyclopropanation methodology led to the preparation of a large number of natural products,[92] but neither the mechanism of this transformation, nor methods to control reaction selectivity, were well understood. It was during this decade that new catalysts were developed, eventually resulting in those now recognized to be the most reactive and selective for cyclopropanation (13.17-13.22).[2,15,93-100] Copper catalysts preceded those of dirhodium(II), and those of ruthenium and cobalt were more recent.



(13.6)

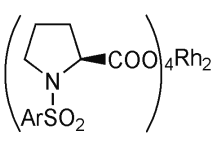
Achiral Catalysts For Diazo Decomposition	$Cu(acac)_2$ *low reactivity stable*	CuOTf *high reactivity easily oxidized*	$Rh_2(OAc)_4$ *moderate reactivity stable*	$PdCl_2$ *high reactivity stable*

Chiral Catalysts For Diazo Decomposition



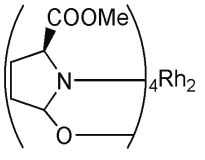
moderate reactivity easily oxidized

13.17



moderate reactivity stable

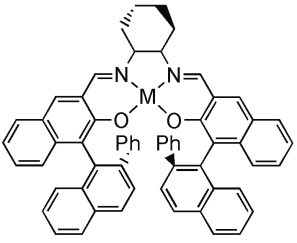
13.18



low reactivity stable

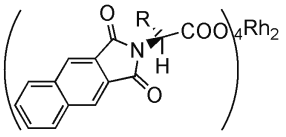
13.19

Pictiva EX2004
Samsung v Pictiva
IPR2024-01094



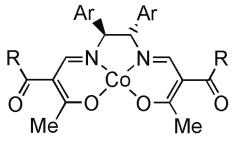
M = Ru(NO)Cl
low reactivity
stable

13.20



moderate reactivity
stable

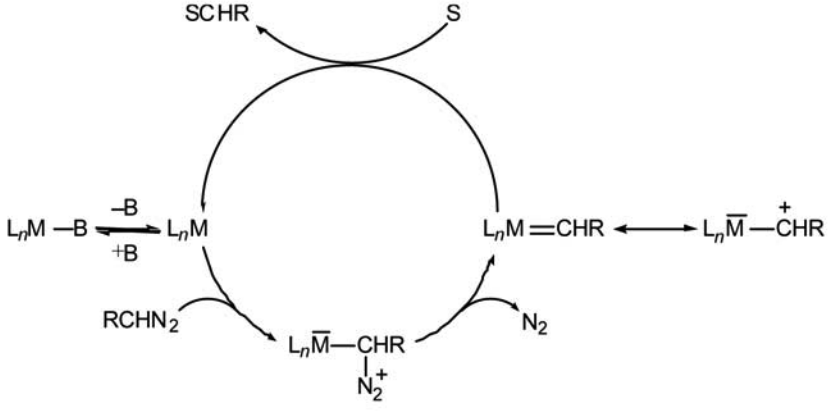
13.21



moderate reactivity
activated with N-methyl-
imidazole

13.22

The mechanism for diazo decomposition is now widely understood.[87,88] The metal unit, having an open coordination site and acting as a Lewis acid, undergoes electrophilic addition to the diazo compound at carbon. Loss of dinitrogen from the diazonium ion intermediate then forms the metal carbene that is able to transfer the carbene from the metal to a substrate and thereby regenerate the catalytically active ligated metal (Scheme 13.3). It is in the carbene transfer step that selectivity is achieved. The rate-limiting step is either electrophilic addition or loss of dinitrogen, and mechanistic determinants are both Lewis acidity from the 16*e* ligated metal and backbonding from the metal-stabilized carbocation. Confirmation of this pathway was originally established by correlation of reactivity and selectivity between reactions of pentacarbonyltungsten(phenylcarbene) with alkenes and reactions of phenyldiazomethane and alkenes catalyzed by rhodium(II) acetate.[101]

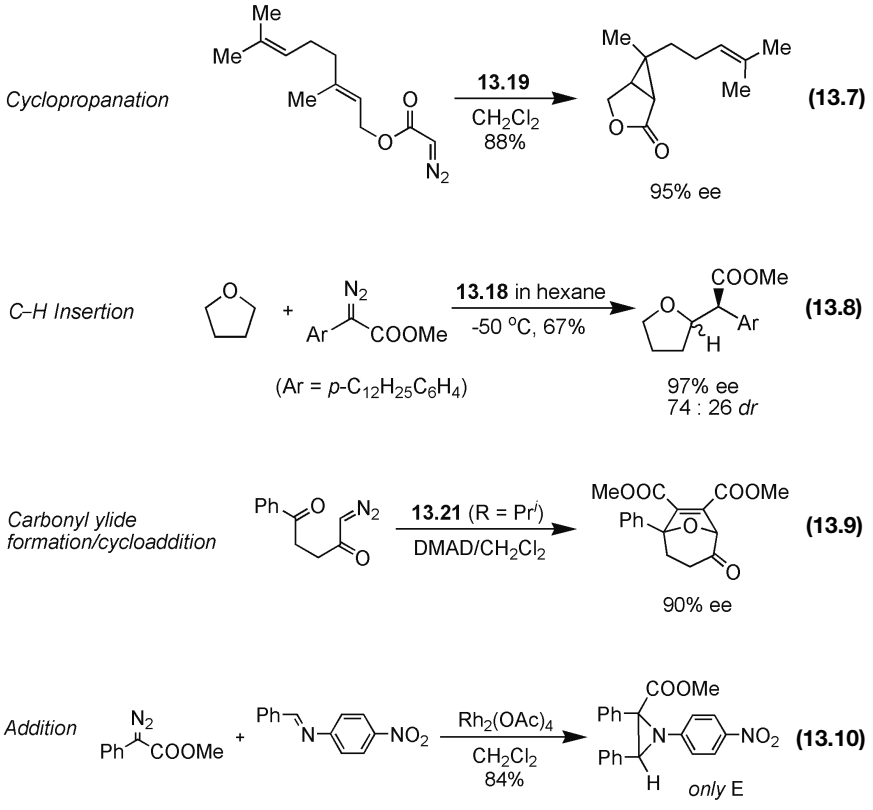


Scheme 13.3. Mechanism for catalytic decomposition of diazo compounds.

The transfer of the carbene may occur to any of a variety of substrates and be in an intermolecular or intramolecular fashion. Cyclopropanation is perhaps the best known catalytic transformation (13.7),[25] but carbon-hydrogen insertion (13.8),[102] ylide formation and rearrangement or cycloaddition (13.9),[99] and addition to multiple bonds other than C=C (13.10)[103] are also well established.[2,15,78-81] In all cases the reaction rate for carbene formation is increased with substrates having electron-rich substituents. Catalytic cyclopropanation of α,β-unsaturated carbonyl compounds with diazo compounds does not occur.[2,15]

Pictiva EX2004
Samsung v Pictiva
IPR2024-01094

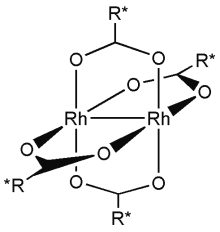
Diazocarbonyl compounds are best for these transformations, and they may be readily prepared by a variety of methods, and dirhodium(II) compounds are generally the catalysts of choice. The use of iodonium ylides has also been developed,[104] and their reactions are also catalyzed by dirhodium(II) compounds, but they exhibit no obvious advantage for selectivity in carbene transfer reactions. Enantioselection is much higher with diazoacetates than with diazoacetoacetates or diazomalonates.



13.6 Chiral Dirhodium(II) Carboxylates

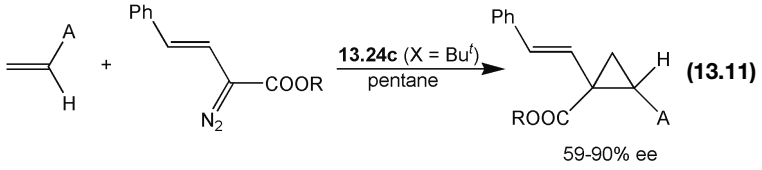
Dirhodium(II) carboxylates, especially $Rh_2(OAc)_4$, have emerged as the most generally effective catalysts for metal carbene transformations and, because of this, there is continuing interest in the design and development of dirhodium(II) complexes that possess chiral ligands. They are structurally well defined, having idealized D_{4h} symmetry, with axial coordination sites at which carbene formation occurs in reactions with diazo compounds.[105] With chiral dirhodium(II) carboxylates the asymmetric center is relatively far removed from the carbene center in the metal carbene intermediate. The first of these to be reported with applications to cyclopropanation reactions was developed by Brunner[106] who prepared thirteen chiral dirhodium(II) tetrakis(carboxylate) derivatives (**13.23**) from enantiomerically pure carboxylic acids $R^1R^2R^3CCOOH$ with substituents that were varied from H, Me, and Ph to OH, NHAc, and CF_3. However, reactions performed using ethyl diazoacetate and styrene yielded cyclopropane products whose optical purities were less than 12%.

Pictiva EX2004
Samsung v Pictiva
IPR2024-01094

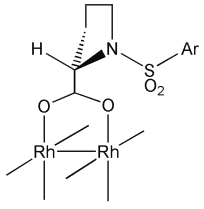


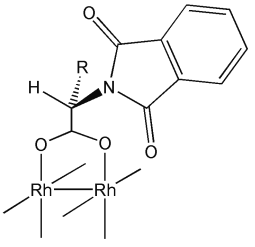
13.23

Reports appeared of the use of chiral *N*-sulfonamidoprolinate catalysts (**13.24**)[107] and of dirhodium(II) catalysts with ligands that were phthalimide derivatives of phenylalanine (**13.25a**), *tert*-leucine (**13.25b**), and alanine (**13.25c**),[108,109] but they were similarly unselective in intermolecular cyclopropanation reactions of ethyl diazoacetate. Only when Davies applied chiral prolinate **13.24a** and **13.24c** (X = Bu^t, $C_{12}H_{25}$) to cyclopropanation reactions of vinyldiazocarboxylates (13.11) did the significance of these catalysts for cyclopropanation reactions become evident.[94,110] An advantage of **13.24c** (X = $C_{12}H_{25}$) is its solubility in pentane, even at -78 °C.



(13.11)



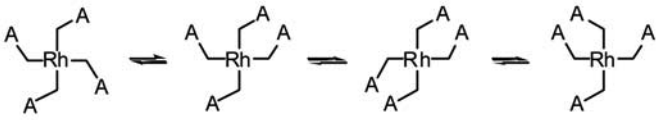


13.24a Ar = Ph
13.24b Ar = Nap
13.24c Ar = C_6H_4X

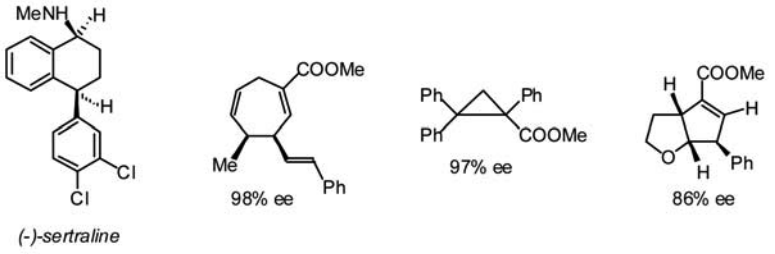
13.25a R = Ph CH_2
13.25b R = Bu^t
13.25c R = Me

Reactions of methyl phenyldiazoacetate with alkenes exhibit similar selectivities.[111,112] The use of pentane as the solvent, rather than dichloromethane, has a significant influence on enantioselectivities, increasing ee values to ≥90%. The cause for this solvent influence is the change in the relative conformations of prolinate ligands,[111] depicted in Scheme 13.4, with solvation by pentane favoring the structural alignment shown at the far left. (-)-Sertraline,[113] chiral 1,4-cycloheptadienes,[114] and select cyclopentenes[115] (Scheme 13.5) have been prepared using these catalysts and vinyldiazocarboxylates, and this approach has also been applied to the enantioselective synthesis of functionalized tropanes[116] and of the four stereoisomers of 2-phenylcyclopropane-1-amino acid.[94]

Pictiva EX2004
Samsung v Pictiva
IPR2024-01094



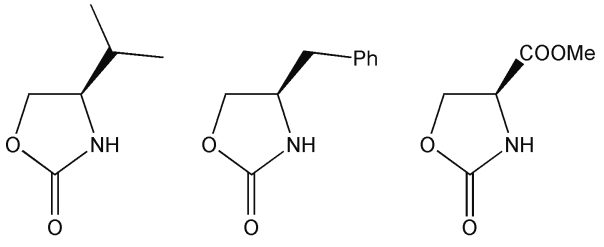
Scheme 13.4. Conformational orientations of prolinate ligands: A = $ArSO_2$.



Scheme 13.5. Products from the decomposition of vinyldiazo compounds.

13.7 Chiral Dirhodium(II) Carboxamidates

Based on reports of Bear and coworkers[18,19,117] and the discovery that carboxamidate ligands could be introduced onto dirhodium(II) by semi-automated methods,[118] Doyle and coworkers began development of carboxamidate ligands for dirhodium with oxazolidinones (e.g., **13.26** and **13.27**), but with limited success in achieving high enantiocontrol.[119,120] Only when a carboxylate attachment, as in pyrrolidinone **13.28**, rather than an isopropyl or benzyl group, as in **13.26** or **13.27**, was placed in proximity to the reaction center could high enantiocontrol be achieved.[22] The key developments here were the methodology for the semi-automated synthesis of dirhodium(II) carboxamidates by trapping acetic acid with sodium carbonate in a Söxhlet extraction apparatus (13.12),[96,97,118] the operation of the trans effect in the ligand exchange process,[28] and the discovery of the high selectivity enhancement afforded by the carboxylate attachment.[121]



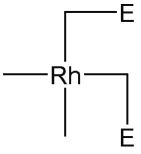
13.26 **13.27** **13.28**

$$Rh_2(OAc)_4 + 4\,LH \xrightarrow[\text{reflux}]{PhCl} Rh_2L_4 + 4\,HOAc \quad \textbf{(13.12)}$$

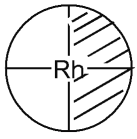
(trapped by Na_2CO_3)

Pictiva EX2004
Samsung v Pictiva
IPR2024-01094

In dirhodium(II) carboxamidates the ligands are tightly bound and undergo slow exchange only at temperatures at or above 80 °C. If the COOMe "chiral attachment" is viewed as a chemical entity that occupies the space around rhodium, two adjacent quadrants of a circle are occupied, leaving two quadrants for open access to the reaction center (e.g., **13.29** and **13.30**). The accessibility of the electrophilic carbene center in these catalysts to approach by nucleophiles makes them especially advantageous for highly selective intramolecular metal carbene reactions of diazo compounds.[2,15] Because of the rigidity of the carboxamidate ligands, selectivities in metal carbene reactions are independent of solvent.

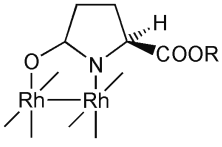


13.29
E = COOMe



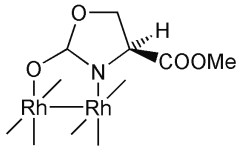
13.30

A broad selection of chiral ligands is now available, and each has specific advantages.[2,15,16,77-81] Dirhodium(II) carboxamidates have been synthesized with chiral pyrrolidinones (**13.31**),[22] oxazolidinones (**13.32**),[26] imidazolidinones (**13.33**),[27,122] and azetidinones (**13.34**)[24,32] ligands. They differ in reactivities and selectivities for metal carbene reactions based on their steric and/or electronic influences. Because of the wider bite angle of the azetidinone OCN attachment, the rhodium-rhodium bond length is longer (2.53 Å versus 2.46 Å) than in those constructed from five-membered ring lactams. The longer Rh–Rh distance imparts a greater electrophilic reactivity in these catalysts.[33]



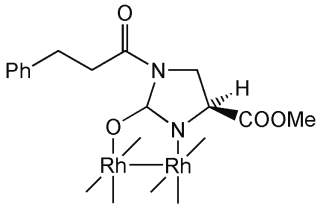
13.31

R = Me : Rh_2(5S-MEPY)$_4$
R = $(CH_2)_{17}CH_3$: Rh_2(5*S*-ODPY)$_4$



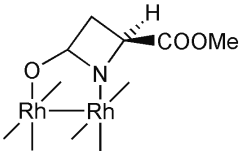
13.32

Rh_2(4*S*-MEOX)$_4$



13.33

Rh_2(4S-MPPIM)$_4$



13.34

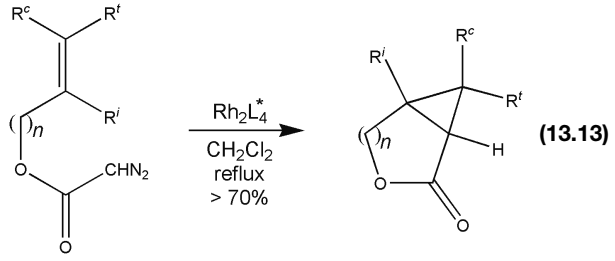
Rh_2(4S-MEAZ)$_4$

Pictiva EX2004
Samsung v Pictiva
IPR2024-01094

13.8 Catalytic Asymmetric Cyclopropanation and Cyclopropenation

13.8.1 Intramolecular reactions

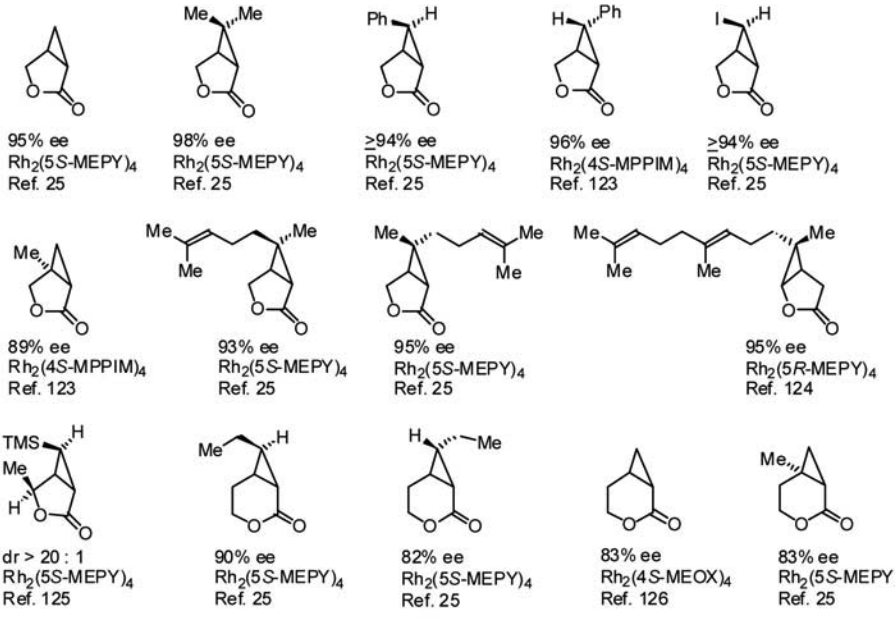
Chiral dirhodium(II) carboxamidates are preferred for intramolecular cyclopropanation of allylic and homoallylic diazoacetates (13.13).



(13.13)

(n = 1,2) (n = 1,2)

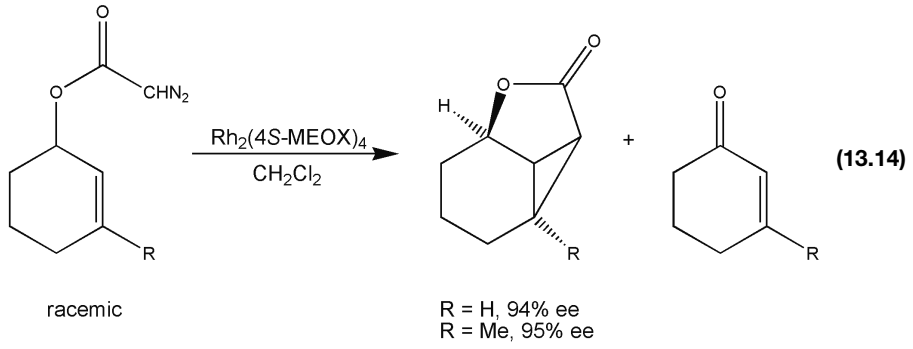
The catalyst of choice is $Rh_2(MEPY)_4$ when R^c and R^i are H, but $Rh_2(MPPIM)_4$ gives the highest selectivities when these are alkyl or aryl groups. Representative examples of the applications of these catalysts are listed in Scheme 13.6.[25,123-126] Use of the mirror image catalyst produces the enantiomeric cyclopropane with the same selectivity.[78-81,127] However, enantioselectivities fall off to a level of 40-70% ee when n in 13.12 is increased beyond 2 up to 8,[126] and in these cases use of the chiral bis-oxazoline copper complexes is advantageous.[128]



Scheme 13.6. Examples of enantioselection for intramolecular cyclopropanation of diazoacetates.

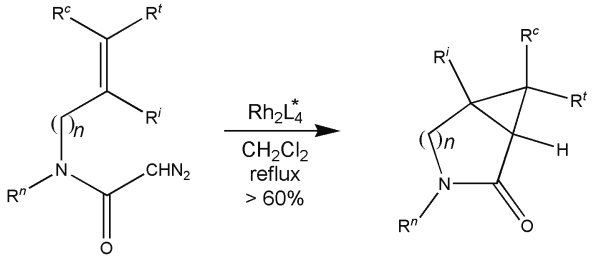
Pictiva EX2004
Samsung v Pictiva
IPR2024-01094

"Kinetic resolution" (enantiomer differentiation) of cycloalkenyl diazoacetates has been achieved in a novel fashion (e.g., 13.14).[129] In these cases one enantiomer of the racemic reactant matches with the catalyst configuration to produce the intramolecular cyclopropanation product in high enantiomeric excess, whereas the mismatched enantiomer preferentially undergoes hydride abstraction from the allylic position to yield the corresponding cycloalkenone.[130] With acyclic secondary allylic diazoacetates the hydride abstraction pathway is relatively unimportant, and diastereoselection becomes the outcome of enantiomer differentiation.[125]



(13.14)

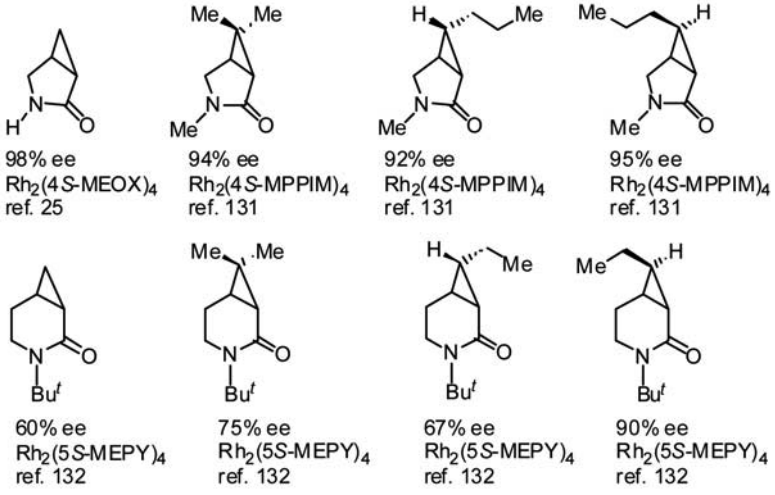
Diazoacetamides undergo intramolecular cyclopropanation with similarly high enantioselectivities (13.15).[78-81,131,132] In these cases, however, competition from intramolecular dipolar cycloaddition can complicate the reaction process. Therefore, use of R^n = Me or Bu^t has been required to achieve good yields of reaction products. Representative examples of uses of chiral dirhodium(II) carboxamidates for enantioselective intramolecular cyclopropanation of diazoacetamides are listed in Scheme 13.7.



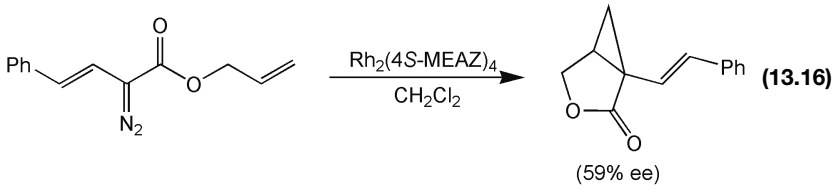
(13.15)

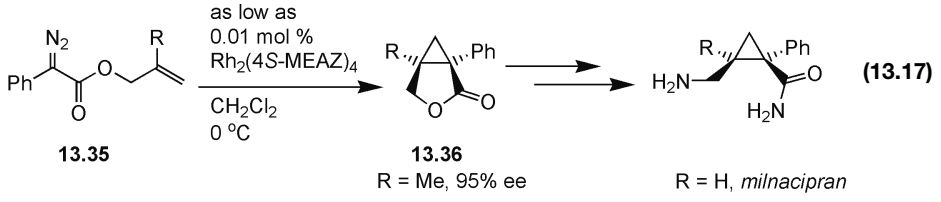
Dirhodium(II) carboxamidates are less reactive towards diazo decomposition than are dirhodium(II) carboxylates.[16] This has usually meant that they could not be used for reactions with aryl- and vinyldiazoacetates or with diazomalonates. However, azetidinone-ligated catalysts such as Rh_2(4*S*-MEAZ)$_4$ (**13.34**) offer distinct advantages for rapid diazo decomposition and for achieving the highest levels of enantioselectivity reported (e.g., 13.16).[33] This catalytic system has been used to prepare *milnacipran* and its analogs.[133] When Rh_2(4*S*-MEAZ)$_4$ catalyzed the reaction of **13.35** to form **13.36**, a turnover number of 10,000 and a selectivity of 95% ee were achieved (13.17).

Pictiva EX2004
Samsung v Pictiva
IPR2024-01094



Scheme 13.7. Examples of enantioselection for intramolecular cyclopropanation of diazoacetamides.





These chiral catalysts have also been linked to polymeric resins (**13.13**) for multiple use/reuse without significant loss in enantiocontrol (Fig. 13.19).[37,38] Both Novasyn and Merrifield resins proved effective, and mixed ligand systems (**13.14**) with enhanced electronic and steric characteristics could be produced by this methodology.[38] Davies has used an alternate approach in which dirhodium(II) tetraprolinates are bound non-covalently in highly cross-linked macroporous polystyrene resins, and high turnover numbers and selectivities have been achieved.[134]

Pictiva EX2004
Samsung v Pictiva
IPR2024-01094

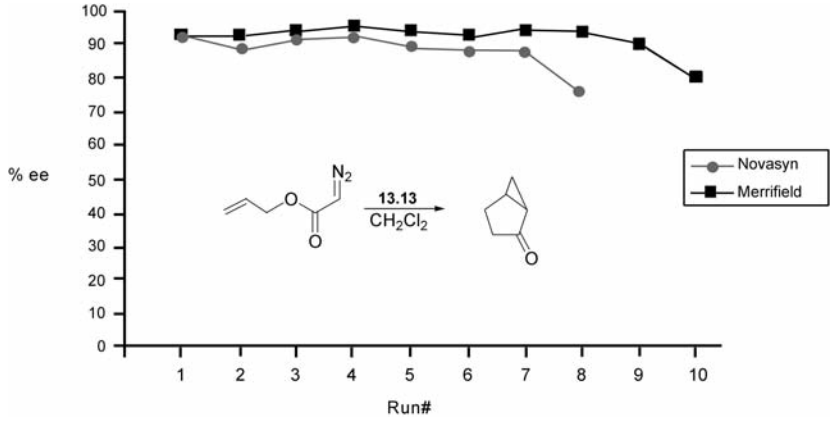
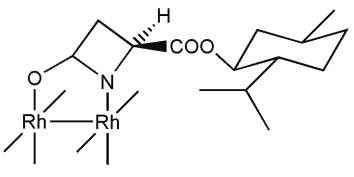


Fig. 13.19. Immobilized chiral dirhodium(II) pyrrolidinone-carboxylates and their application to intramolecular cyclopropanation of allyl diazoacetate.

Intramolecular cyclopropanation of diazo ketones have long been a challenge for enantioselection.[2,15,135,136] Copper catalysts were reported to effect up to 94% ee with the ketone analog of homoallyl diazoacetate, but lower selectivities were more common.[137] Lahuerta's chiral metalated aryl phosphine derivatives of rhodium(II) carboxylates, $Rh_2(O_2CCF_3)_2(PC)_2$,[42] show promise in giving enantiomeric excesses above 80% for intramolecular diazo ketone cyclopropanation when these reactions are performed in pentane.[138] In contrast, chiral dirhodium(II) carboxamidates exhibit low enantiocontrol.[139]

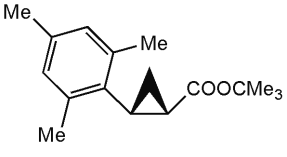
13.8.2 Intermolecular reactions

Dirhodium(II) catalysts with carboxamidate ligands show a propensity to form the *cis*-isomer in preference to the thermodynamically favored *trans*-isomer in intermolecular cyclopropanation reactions (e.g., 13.18).[139] Using an azetidinone with a menthyl-carboxylate attachment (**13.37**), diastereoselectivities as high as 92:8 (*cis*:*trans*) were achieved in the synthesis of **13.38**.[35] This methodology has been employed for the synthesis of a cyclopropane-configured urea-PETT analog (**13.39**) that is an HIV-1 reverse transcriptase inhibitor (13.19).[35] Although the Katsaki salen-binol-ligated cobalt and ruthenium catalysts[98,140] exhibit virtually complete *cis*-selectivity for cyclopropanation of styrene, their reactivities are problematic and they have not been examined with substrates other than styrene.



Rh_2(4*S*,*R*-MenthAZ)$_4$

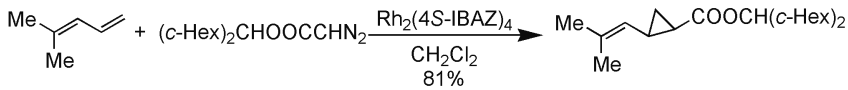
13.37



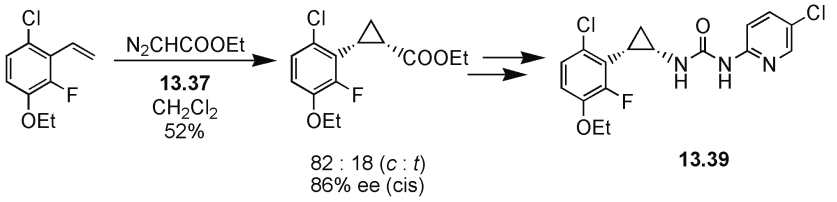
92 : 8 (*c* : *t*)
97% ee (*cis*)
76% ee (*trans*)

13.38

Pictiva EX2004
Samsung v Pictiva
IPR2024-01094



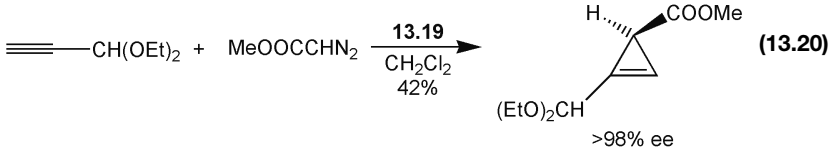
(13.18)



(13.19)

13.8.3 Cyclopropenation

The addition of a carbene to a carbon-carbon triple bond results in the formation of a cyclopropene product,[141] and with diazoacetates the catalyst of choice for asymmetric intermolecular addition is the dirhodium(II) carboxamidate **13.19** (e.g., 13.20).[142,143] The reactions are general, except for phenylacetylene and 1,3-enynes whose cyclopropene products undergo [2+2]-cycloaddition, and selectivities are high. Catalytic hydrogenation of the cyclopropene yields the *trans*-disubstituted cyclopropane.



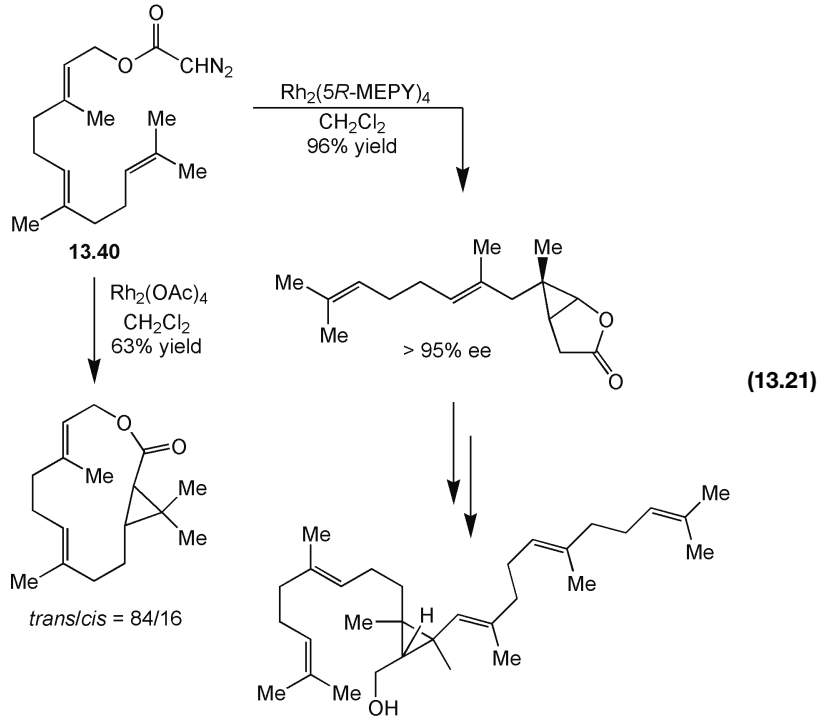
(13.20)

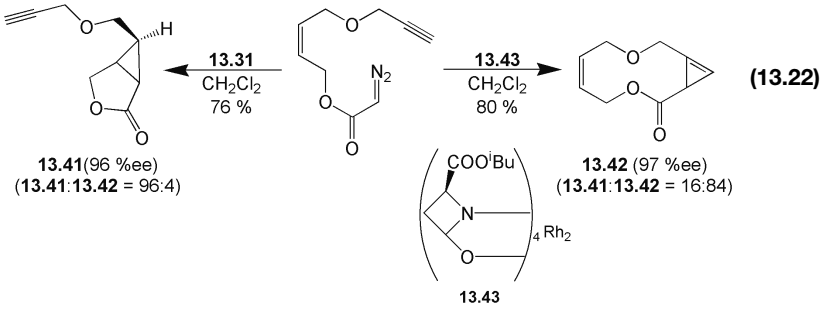
13.8.4 Macrocyclization

Intramolecular addition reactions are not limited to the formation of 5- to 7-membered rings, as once believed. They occur with high stereocontrol and product yield for reactions that produce large rings.[128,142,143] First observed with rhodium acetate in the attempted cyclopropanation of the allylic position of *trans,trans*-farnesyl diazoacetate (**13.40**),[144] the preference for addition to the terminal double bond was found to be highly ligand-dependent with carboxamidates preferring allylic cyclopropanation while rhodium(II) carboxylates preferred macrocyclization (e.g., 13.21).[145] Ring sizes of 15-20, have been formed in high yield and without dilution common to macrocyclization procedures. However, in reactions where intramolecular carbon-hydrogen insertion is possible, rhodium(II) carboxamidates prefer that pathway rather than macrocyclic cyclopropanation.[126,146-148] Intramolecular cyclopropenation is also a facile process with ring sizes of ten or higher.[149,150] High levels of enantiocontrol can be achieved in these reactions with catalysts appropriate to the transformation (e.g., 13.22).[151] Note that the choice of catalyst can influence chemoselectivity (**13.41**, **13.42**) as well as stereoselectivity, and the cause of prefential cyclopropenation with the Rh_2(4*S*-IBAZ)$_4$ catalyst (**13.43**) is its higher reactivity resulting from the stretching of the Rh–Rh bond. As the length of the chain increases, selectivity approaches outcomes that can be predicted from intermolecular reactions.[146-148]

Pictiva EX2004
Samsung v Pictiva
IPR2024-01094

Macrocyclic addition reactions, including novel processes with aromatic compounds,[152,153] are now well represented in the literature with dirhodium(II) catalysts, but there are numerous opportunities for expansion in this area.



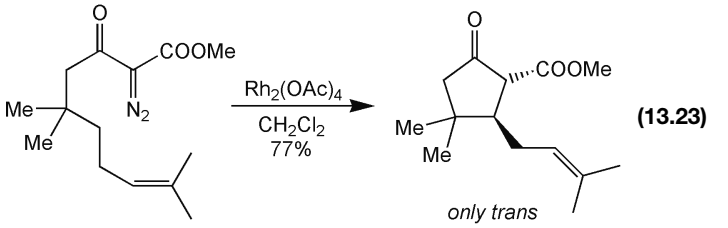


Pictiva EX2004
Samsung v Pictiva
IPR2024-01094

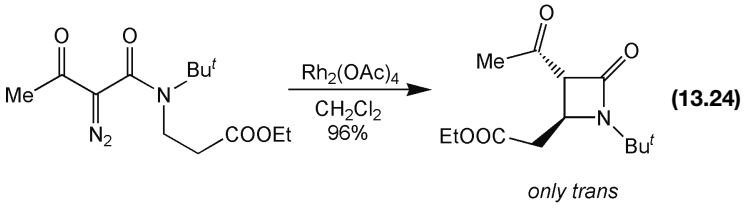
13.9 Metal Carbene Carbon-Hydrogen Insertion

13.9.1 Intramolecular reactions

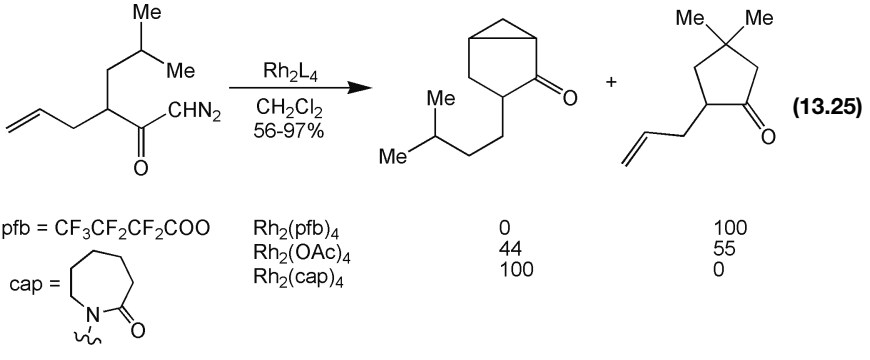
One of the unique advantages of dirhodium(II) catalysts in synthesis is their ability to effect carbon-hydrogen insertion reactions. [2,15,16,77-81,154] Here dirhodium(II) catalysts are far superior to those of copper or other transition metal catalysts. Insertion into the gamma position is virtually exclusive in intramolecular reactions, and only when this position is blocked or deactivated does insertion occur into the beta or delta C–H position (e.g., 13.23-13.25).[155-157] The electrophilic character of these insertion reactions is suggested by C–H bond reactivity in competitive experiments (3° > 2° >> 1°)[158,159] and by the enhancement due to heteroatoms such as oxygen[160] or nitrogen. A recent theoretical treatment[161] confirmed the mechanistic proposal (Scheme 13.8) that C–C and C–H bond formation with the carbene carbon occurs synchronously as the ligated metal dissociates.[157] As indicated by the influence of ligands on selectivity in (13.25), one transformation may be turned on and the other turned off with the proper selection of ligand for dirhodium.[84,86,127]



(13.23)

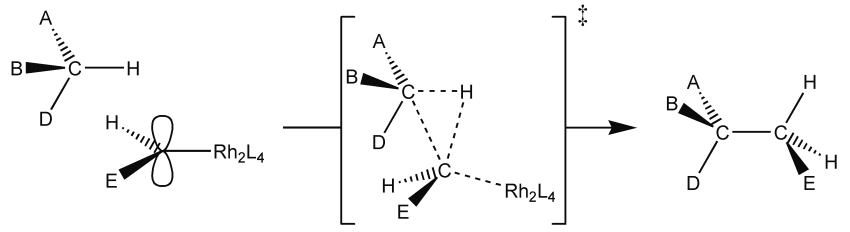


(13.24)



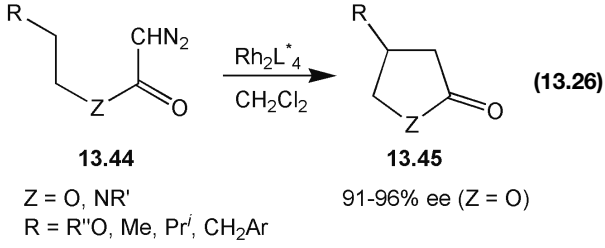
(13.25)

Pictiva EX2004
Samsung v Pictiva
IPR2024-01094



Scheme 13.8. Synchronous mechanism.

Dirhodium(II) carboxamidates, and especially the $Rh_2(MPPIM)_4$ (13.33) catalysts, are exceptionally effective for highly enantioselective intramolecular insertion reactions of diazoacetates and diazoacetamides.[2,15,16,77-81] These reactions take place with high regioselectivity for γ-lactone (lactam) formation (13.26),[162] and enantioselectivities greater than 90% ee are commonly achieved. In reactions of **13.44**, use of the *S*-configured catalyst yields **13.45** having the *S*-configuration, and with the *R*-configured catalyst the *R*-configured product is formed preferentially. Examples of biologically-active compounds that have been prepared in greater than 90% ee by this methodology include the lignan lactones (e.g., enterolactone **13.46**),[162] the sugar-based 2-deoxyxylolactone **13.47**,[163,164] and the GABA receptor agonist (*R*)-baclofen **13.48**.[165]

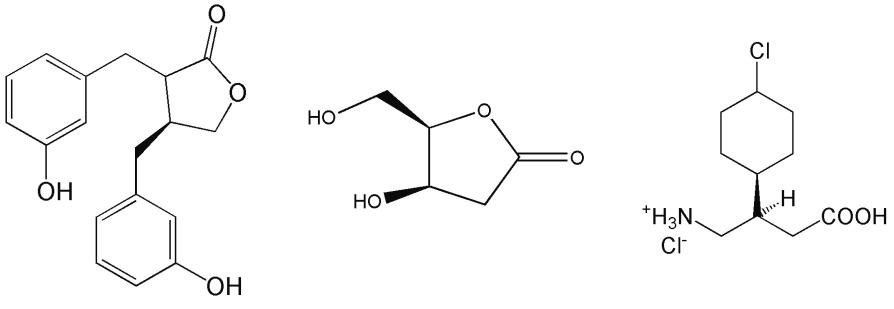


13.44

Z = O, NR'
R = R''O, Me, Pr^i, CH_2Ar

13.45

91-96% ee (Z = O)



13.46
(-)-enterolactone

13.47
2-deoxyxylolactone

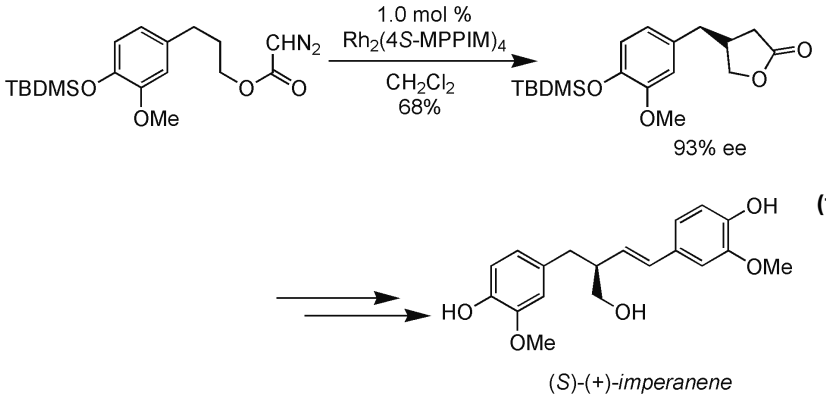
13.48
(*R*)-(-)-baclofen

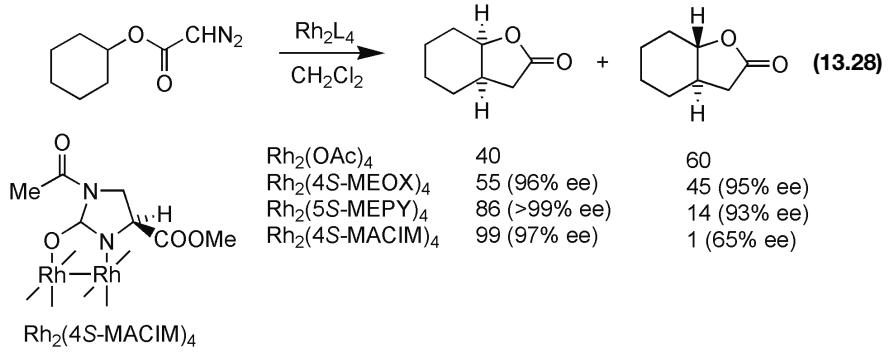
Recently, this methodology has been used for the synthesis of naturally occurring (*S*)-(+)-imperanene (e.g., 13.27),[166] whose absolute configuration was established in the insertion process. In all cases selectivities were high with less than 5% insertion into other C–H positions.

Because of the synthetic interest in their lactone products, and the potential for control of both diastereoselectivity and enantioselectivity in their C–H insertions, catalytic reactions

Pictiva EX2004
Samsung v Pictiva
IPR2024-01094

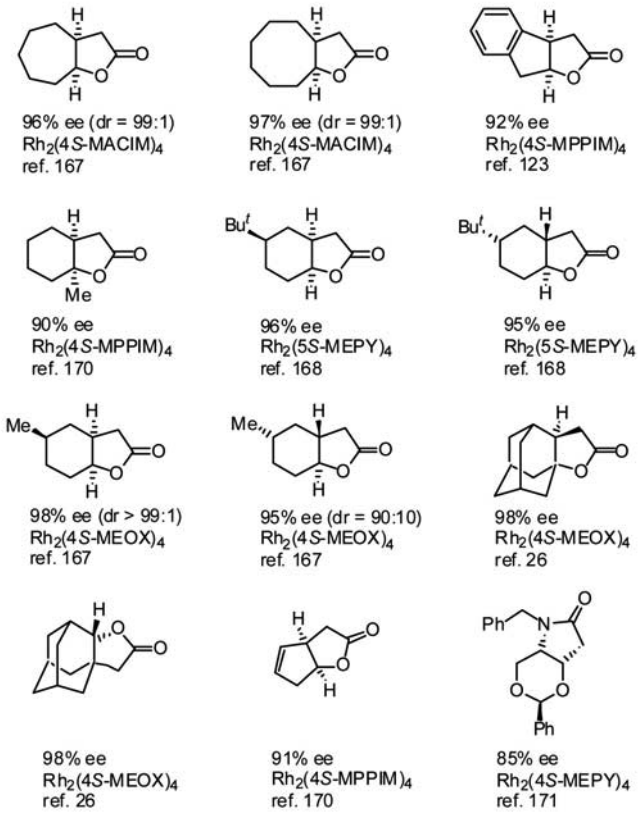
of cycloalkyl diazoacetates have received a great deal of attention.[167-169] With cyclohexyl diazoacetate, for example, both *cis*- and *trans*-bicyclic products are formed (13.28),[167] and control of this diastereoselectivity, as well as enantiocontrol, was the goal. Use of $Rh_2(OAc)_4$ suggested that there was no inherent selectivity attributable to the coordinated carbene or to dirhodium(II). However, ligand modification for dirhodium(II) to imidazolidinones, specifically $Rh_2(MACIM)_4$, provided exceptional diastereocontrol, obtained by influencing the conformational energies of the intermediate metal carbene, [2,15,78-81] as well as high enantiocontrol. Representative examples of products from these highly selective intramolecular C–H insertion reactions with cyclic systems is found in Scheme 13.9.[26,123,167,168,170,171] Additional examples of effective insertion reactions in systems which form diastereomeric products can be found in processes for the synthesis of 2-deoxyxylolactone (13.47).[163,164] Others in acyclic systems without heteroatom activation, as in the synthesis of 13.47, confirm this preference.[123]





Configurational match/mismatch governs these reactions so that different products may be produced in high yield and selectivity when enantiomeric catalysts are applied to the same substrate.[169,170] This is illustrated by the reaction processes with chiral nonracemic 2-methylcyclohexyl diazoacetates in Scheme 13.10,[169] and additional examples in the steroidal field have also been reported.[172] In the steroidal cases the formation of four-membered ring β-lactones is a common outcome of configurational mismatch.

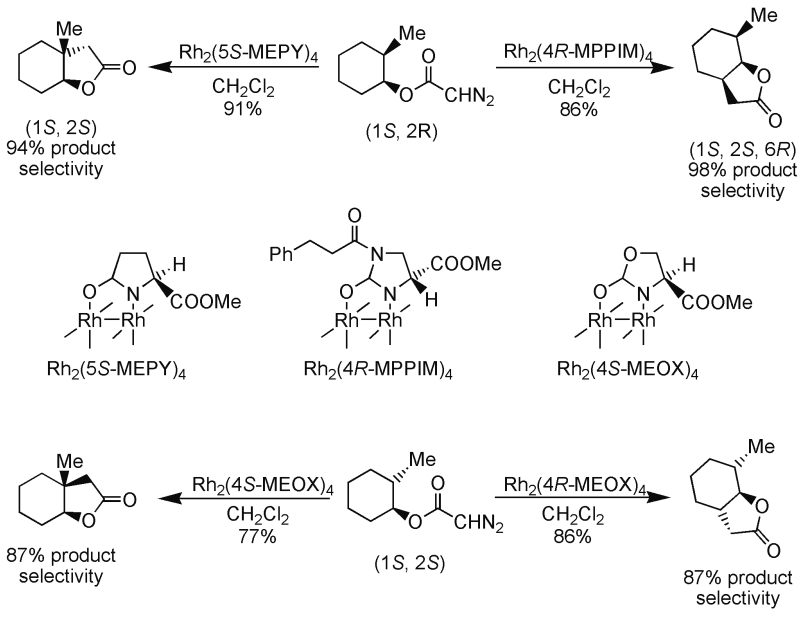
Pictiva EX2004
Samsung v Pictiva
IPR2024-01094



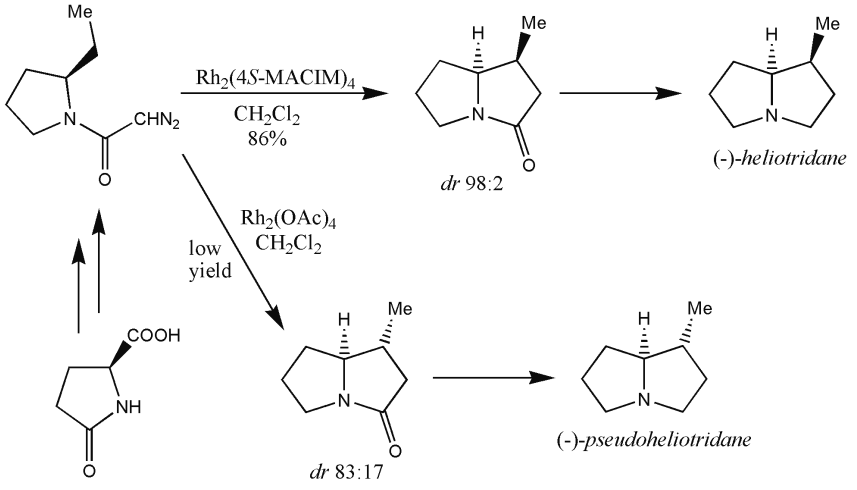
Scheme 13.9. Enantioselectivity for intramolecular carbon-hydrogen insertion reactions of diazoacetates and diazoacetamides.

Lactam systems have also been synthesized by reliance on configurational matching as, for example, in the synthesis of the pyrrolizidine alkaloid (-)-heliotridane (Scheme 13.11).[173] Here use of the achiral $Rh_2(OAc)_4$ catalyst gave a low yield of the C–H insertion product, and the dominant isomer was the one opposite to the natural product produced with the use of the chiral $Rh_2(4S\text{-MACIM})_4$ catalyst. β–Lactams have also been prepared by C–H insertion, and some of them with high enantiocontrol,[174] but the generality of this process has not yet been established.

Pictiva EX2004
Samsung v Pictiva
IPR2024-01094



Scheme 13.10. Diastereocontrol in carbon-hydrogen insertion reactions with chiral dirhodium(II) carboxamidate catalysts.

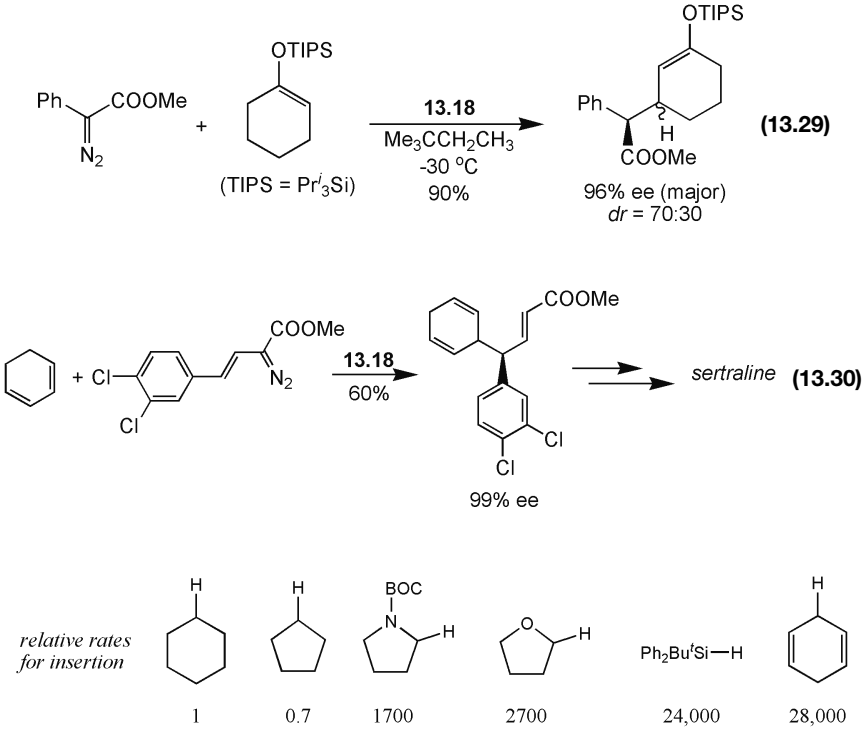


Scheme 13.11. Synthesis of (-)-heliotridane.

Pictiva EX2004
Samsung v Pictiva
IPR2024-01094

13.9.2 Intermolecular reactions

Until recently, intermolecular C–H insertion reactions were more a curiosity than a synthetically productive undertaking. Davies discovered in the late 1990's that aryl- and vinyldiazoacetates undergo intermolecular insertion with a wide variety of hydrocarbons in high yield.[175] With Rh_2(*S*-DOSP)$_4$ (**13.18**, Ar = $C_{12}H_{25}C_6H_4$), moderate to high enantioselectivities have been achieved (e.g., 13.29, 13.30).[176,177] These reactions are generally performed under mild conditions in hexane, and with few exceptions[102,178] diastereoselectivity is moderate. The relative rates of insertion using methyl phenyl-diazoacetate with catalysis by **13.18** (Scheme 13.12) suggest significant charge separation in the transition state;[176] for comparison, the carbene addition to styrene had a relative rate of 24,000.



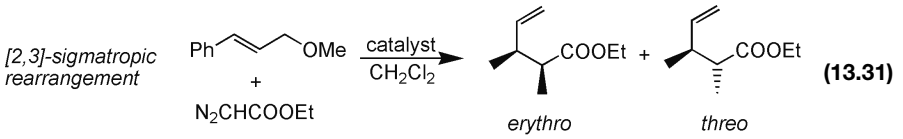
Scheme 13.12. Relative rates of insertion.

13.10 Catalytic Ylide Formation and Reactions

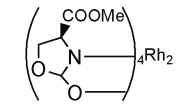
As electrophiles in one of the major achievements with dirhodium(II) compounds, metal carbene intermediates in catalytic reactions capture Lewis bases to form ylide intermediates that, in turn, undergo a vast array of chemical transformations.[2,15,179-181] Alternative base-promoted methodologies do not have the generality afforded by these catalytic methods. Recent efforts have been primarily directed to establishing asymmetric induction, which arises when the chiral catalyst remains bound to the intermediate ylide during bond formation—a possibility that was originally considered to be unlikely. In the [2,3]-sigmatropic rearrangement depicted in (13.31)[182] the transition metal catalyst is associated with the ylide **13.49** in the

Pictiva EX2004
Samsung v Pictiva
IPR2024-01094

product forming step. The *threo* product is dominant with the use of the chiral $Rh_2(MEOX)_4$ catalysts but is the minor product with $Rh_2(OAc)_4$. That this process occurs through the metal-stabilized ylide rather than a chiral "free ylide" was demonstrated from asymmetric induction using allyl iodide and ethyl diazoacetate. Somewhat lower enantioselectivites have been observed in other systems.[99,183-185]

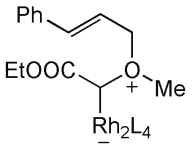


(13.31)

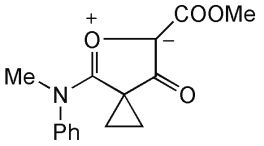


$Rh_2(4S\text{-MEOX})_4$ (**13.32**)

$Rh_2(OAc)_4$	83	17
$Rh_2(4S\text{-MEOX})_4$	15 (94% ee)	85 (98% ee)
$Rh_2(4R\text{-MEOX})_4$	15 (94	85 (98% ee)

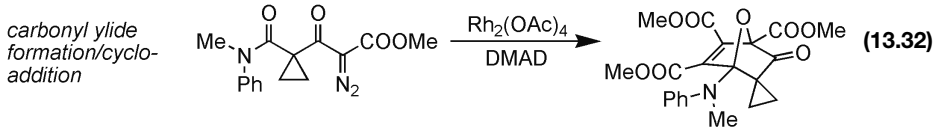


13.49



13.50

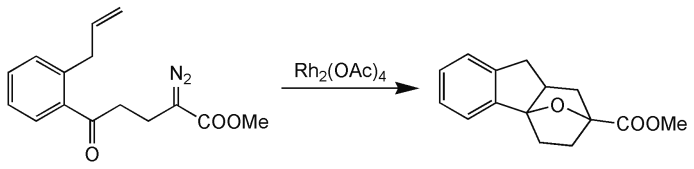
However, this is not the case with all oxygen-centered ylides, and rarely, if at all, with nitrogen or sulfur ylides. The trapping of carbonyl ylides (e.g., **13.50**) by dipolarophiles such as DMAD (dimethyl acetylenedicarboxylate) provides versatility to the overall transformation (13.32),[183] and high enantioselectivity has been achieved in one case (13.9).[99] Although catalytic entry into ylides has been widely investigated and is known to be highly versatile for synthesis,[82,83] stereoselectivity in ylide transformations remains a significant challenge.[186-188]



(13.32)

Using achiral dirhodium(II) catalysts Padwa and coworkers have developed a broad selection of tandem reactions of which that in (13.33) is illustrative;[189] these intramolecular reactions indicate the multiplicity of processes catalyzed by dirhodium(II) compounds that can be used for the synthesis of complex organic compounds. More recently carbonyl ylides and corresponding imino ylides generated from aryl- and vinyldiazoacetates have been shown to undergo a variety of processes not previously encountered (13.10).[103,190,191] The difference in these results from those obtained with the use of diazoacetates[192] is due to differences in the internal stabilities of the intermediate onium ylides, and one can anticipate a spectrum of outcomes that may result from reactions with variously constituted diazo compounds.

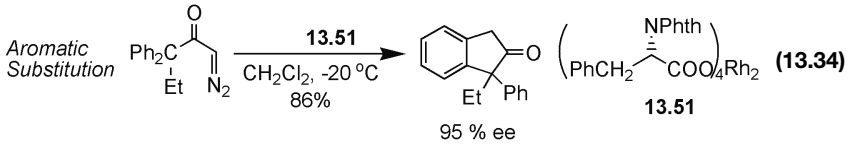
Pictiva EX2004
Samsung v Pictiva
IPR2024-01094



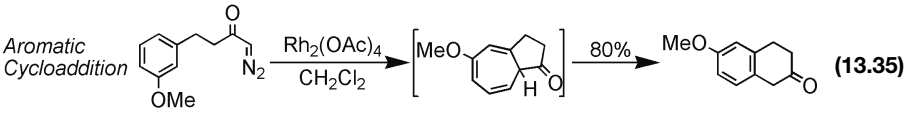
(13.33)

13.11 Additional Transformations of Diazo Compounds Catalyzed by Dirhodium(II)

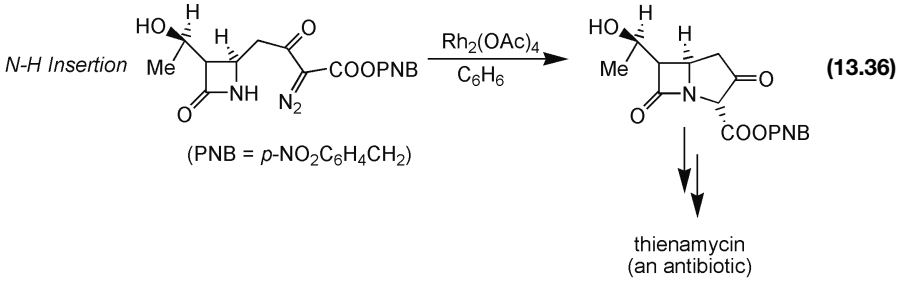
Transition metal catalysts also promote reactions of diazocarbonyl compounds that are significantly different from standard addition, insertion, and ylide transformations (e.g., 13.34-13.37).[2,15,193-196] These demonstrate the enormous versatility of diazo compounds as metal carbene precursors in organic synthesis. In most cases the substrate to catalyst ratio is 100, but ratios up to 10,000 have been reported, so catalyst cost is not a major factor in potential pharmaceutical uses.



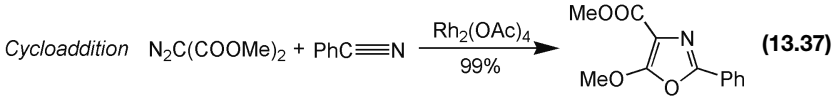
(13.34)



(13.35)



(13.36)



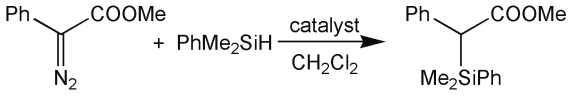
(13.37)

13.12 Silicon-Hydrogen Insertion

Early work by Landais and coworkers established the viability of aryl- and vinyldiazoacetates for silicon-hydrogen insertion which, like C–H insertion, occurs in rhodium(II) catalyzed reactions in a concerted fashion.[197,198] Subsequently, Doyle, Moody, and Davies showed that chiral dirhodium(II) catalysts could be used to effect asymmetric induction.[199,200] Not surprisingly, the highest enantiomeric excess achieved at room temperatures or in refluxing CH_2Cl_2 was

Pictiva EX2004
Samsung v Pictiva
IPR2024-01094

with the $Rh_2(MEPY)_4$ catalysts (13.38);[199] however, these reactions were sluggish and generally impractical. Work by Davies showed that $Rh_2(S\text{-DOSP})_4$, operating at -78 °C in pentane for 48 h, gave **13.52** in 50% yield with 85% ee;[200] and even higher selectivity could be obtained with vinyldiazoacetates.



(13.38)

13.52

References

1. R. Paulissenen, H. Reimlinger, E. Hayez, A. J. Hubert and P. Teyssie, *Tetrahedron Lett.* **1973**, 2233.
2. M. P. Doyle, M. A. McKervey and T. Ye. *Modern Catalytic Methods for Organic Synthesis with Diazo Compounds*, John Wiley & Sons, Inc.: New York, 1998.
3. M. P. Doyle, J. W. Terpstra, C. H. Winter and J. H. Griffin, *J. Mol. Catal.* **1984**, *26*, 259.
4. G. A. Devora and M. P. Doyle, *Main Group Chemistry* **1994**, 7, 395.
5. M. P. Doyle, L. J. Westrum, M. N. Protopopova, M. Y. Eismont and M. B. Jarstfer, *Mendeleev Commun.* **1993**, 81.
6. M. P. Doyle and M. S. Shanklin, *Organometallics* **1993**, *12*, 11.
7. M. P. Doyle, K. G. High and C. L. Nesloney, In *Catalysis of Organic Reactions*, W. E. Pascoe, Ed., Marcel Dekker, Inc.: New York, 1992, p. 293.
8. E. B. Boyar and S. D. Robinson, *Coord. Chem. Rev.* **1983**, *50*, 109.
9. T.R. Felthouse, *Prog. Inorg. Chem*. **1982**, *50*, 73.
10. B. C. Y. Hui, W. K. Teo and G. L. Rempel, *Inorg. Chem.* **1973**, *12*, 757.
11. M. P. Doyle, I. M. Phillips and W. Hu, *J. Am. Chem. Soc.* **2001**, *123*, 5366.
12. D. C. Wynne, M. M. Olmstead and P. G. Jessop, *J. Am. Chem. Soc.* **2000**, *122*, 7638.
13. S. Hashimoto, N. Watanabe, T. Sato, M. Shiro and S. Ikegami, *Tetrahedron Lett.* **1993**, *34*, 5109.
14. P. A. Agaskar, F. A. Cotton, L. R. Falvello and S. Han, *J. Am. Chem. Soc.* **1986**, *108*, 1214.
15. M. P. Doyle. In *Catalytic Asymmetric Synthesis*, I. Ojima, Ed., John Wiley & Sons, Inc.: New York, 2000, Chapter 5.
16. M. P. Doyle and T. Ren, *Prog. Inorg. Chem.* **2001**, *49*, 113.
17. D. J. Timmons and M. P. Doyle, *J. Organometal. Chem.* **2001**, *617-618*, 98.
18. A. M. Dennis, J. D. Korp, I. Bernal, R. A. Howard and J. L. Bear, *Inorg. Chem.* **1983**, *22*, 1522.
19. M. Q. Ahsan, I. Bernal and J. L. Bear, *Inorg. Chem.* **1986**, *25*, 260.
20. R. S. Lifsey, X. Q. Xin, M. Y. Chavan, M. Q. Ahsan, K. M. Kadish and J. L. Bear, *Inorg. Chem.* **1987**, *26*, 830.
21. F. A. Cotton and R. A. Walton. *Multiple Bonds between Metal Atoms*, 2nd ed., Oxford University Press: Oxford, 1993.
22. M. P. Doyle, W. R. Winchester, J. A. A. Hoorn, V. Lynch, S. H. Simonsen and R. Ghosh, *J. Am. Chem. Soc.* **1993**, *115*, 9968.
23. M. P. Doyle, W. R. Winchester, S. H. Simonsen and R. Ghosh, *Inorg. Chim. Acta* **1994**, *220*, 193.
24. M. P. Doyle, W. Hu, I. M. Phillips, C. J. Moody, A. G. Pepper and A. M. Z. Slavin, *Adv. Syn. Catal.* **2001**, *343*, 112.
25. M. P. Doyle, R. E. Austin, A. S. Bailey, M. Dwyer, A. B. Dyatkin, A. V. Kalinin, M. M. Y. Kwan, S. Liras, C. J. Oalmann, R. J. Pieters, M. N. Protopopova, C. E. Raab, G. H. P. Roos, Q. L. Zhou and S. F. Martin, *J. Am. Chem. Soc.* **1995**, *117*, 5763.
26. M. P. Doyle, A. B. Dyatkin, M. N. Protopopova, C. I. Yang, C. S. Miertschin, W. R. Winchester, S. H. Simonsen, V. Lynch and R. Ghosh, *Recl. Trav. Chim. Pays-Bas* **1995**, *114*, 163.

Pictiva EX2004
Samsung v Pictiva
IPR2024-01094

27. M. P. Doyle, Q.-L. Zhou, C. E. Raab, G. H. P. Roos, S. H. Simonsen and V. Lynch, *Inorg. Chem.* **1996**, *35*, 6064.
28. M. P. Doyle, C. E. Raab, G. H. P. Roos and V. Lynch, *Inorg. Chim. Acta* **1997**, *266*, 13.
29. G. H. P. Roos, C. E. Raab, N. D. Emslie, M. P. Doyle and V. Lynch, *Aust. J. Chem.* **1998**, *51*, 1.
30. M. P. Doyle, D. J. Timmons, M. M. R. Arndt, A. Duursma, J. T. Colyer and H. Brunner, *Russ. Chem. Bull.* **2001**, *50*, 2156.
31. M. P. Doyle and J. T. Colyer, *J. Mol. Catal. A: Chem.* **2003**, *196*, 93.
32. M. P. Doyle, Q. L. Zhou, S. H. Simonsen and V. Lynch, *Synlett* **1996**, 697.
33. M. P. Doyle, S. B. Davies and W. Hu, *Org. Lett.* **2000**, *2*, 1145.
34. M. P. Doyle and D. J. Timmons, unpublished results.
35. W. Hu, D. J. Timmons and M. P. Doyle, *Org. Lett.* **2002**, *4*, 901.
36. M. P. Doyle, M. Y. Eismont, D. E. Bergbreiter and H. N. Gray, *J. Org. Chem.* **1992**, *57*, 6103.
37. M. P. Doyle, D. J. Timmons, J. S. Tumonis, H. -M. Gau and E. C. Blossey, *Organometallics* **2002**, *21*, 1747.
38. M. P. Doyle, M. Yan, H.-M. Gau and E. C. Blossey, *Org. Lett.* **2003**, *5*, 561.
39. F. Estevan, P. Lahuerta, J. Pérez-Prieto, M. Sanaú, S.-E. Stiriba and M. A. Ubeda, *Organometallics* **1997**, *16*, 880.
40. M. Barberis, F. Estevan, P. Lahuerta, J. Pérez-Prieto and M. Sanaú, *Inorg. Chem.* **2001**, *40*, 4226.
41. F. Estevan, P. Lahuerta, J. Pérez-Prieto, I. Pereira and S.-E. Stiriba, *Organometallics* **1998**, *17*, 3442.
42. D. F. Taber, S. C. Malcolm, K. Bieger, P. Lahuerta, M. Sanaú, S.-E. Stiriba, J. Pérez-Prieto and M. A. Monge, *J. Am. Chem. Soc.* **1999**, *121*, 860.
43. P. Lahuerta, I. Pereira, J. Pérez-Prieto, M. Sanaú, S.-E. Stiriba, and D. F. Taber, *J. Organometal. Chem.* **2000**, *612*, 36.
44. M. Barberis, P. Lahuerta, J. Pérez-Prieto, and M. Sanaú, *Chem. Commun.* **2001**, 439.
45. F. Estevan, P. Krueger, P. Lahuerta, E. Moreno, J. Pérez-Prieto, M. Sanaú and H. Werner, *Eur. J. Inorg. Chem.* **2001**, 105.
46. J. Pérez-Prieto, S.-E. Stiriba, E. Moreno and P. Lahuerta, *Tetrahedron: Asymmetry* **2003**, *14*, 787.
47. C. Claver, N. Ruiz, P. Lahuerta and E. Peris, *Inorg. Chim. Acta* **1995**, *233*, 161.
48. M. Fontaine, A. Demonceau, R. Messere, A. F. Noels, E. Peris and P. Lahuerta, *J. Mol. Catal. A: Chem.* **1995**, *96*, 107.
49. A. R. Chakravarty, F. A. Cotton and D. A. Tocher, *J. Chem. Soc., Chem. Commun.* **1984**, 501.
50. A. R. Chakravarty, F. A. Cotton, D. A. Tocher and J. H. Tocher, *Organometallics* **1985**, *4*, 8.
51. P. Lahuerta, J. Payá, M. A. Pellinghelli and A. Tiripicchio, *Inorg. Chem.* **1992**, *31*, 1224.
52. P. Lahuerta, J. Payá, X. Solans and M. A. Ubeda, *Inorg. Chem.* **1992**, *31*, 385.
53. F. Barceló, F. A. Cotton, P. Lahuerta, M. Sanaú, W. Schwotzer and M. A. Ubeda, *Organometallics* **1987**, *6*, 1105.
54. F. A. Cotton, F. Barceló, P. Lahuerta, R. Llusar, J. Payá and M. A. Ubeda, *Inorg. Chem.* **1988**, *27*, 1010.
55. P. Lahuerta, R. Martínez-Mañez, J. Payá, E. Peris and W. Diaz, *Inorg. Chim. Acta* **1990**, *173*, 99.
56. E. C. Morrison and D. A. Tocher, *J. Organometal. Chem.* **1991**, *408*, 105.
57. P. Lahuerta, J. Payá, E. Peris, A. Aguirre, S. García-Granda and F. Gómez-Beltrán, *Inorg. Chim. Acta* **1992**, *192*, 43.
58. F. Estevan, P. Lahuerta, J. Latorre, E. Peris, S. García-Granda, F. Gómez-Beltrán, A. Aguirre and M. A. Salvadó, *J. Chem. Soc., Dalton Trans.* **1993**, 1681.
59. F. Estevan, P. Lahuerta, E. Peris, M. A. Ubeda, S. García-Granda, F. Gómez-Beltrán, E. Pérez-Carreño, G. González and M. Martínez, *Inorg. Chim. Acta* **1994**, *218*, 189.
60. M. Nowotny, T. Maschmeyer, B. F. G. Johnson, P. Lahuerta, J. M. Thomas and J. E. Davies, *Angew. Chem., Int. Ed.* **2001**, *40*, 955.
61. M. V. Borrachero, F. Estevan, S. García-Granda, P. Lahuerta, J. Latorre, E. Peris and M. Sanaú, *J. C. S., Chem. Commun.* **1993**, 1864.

Pictiva EX2004
Samsung v Pictiva
IPR2024-01094

62. F. Estevan, S. García-Granda, P. Lahuerta, J. Latorre, E. Peris and M. Sanaú, *Inorg. Chim. Acta* **1995**, *229*, 365.
63. F. Barceló, P. Lahuerta, M. A. Ubeda, C. Foces-Foces, F. H. Cano and M. Martinez-Ripoll, *J. Chem. Soc., Chem. Commun.* **1985**, 43.
64. F. Barceló, F. A. Cotton, P. Lahuerta, R. Llusar, M. Sanaú, W. Schwotzer and M. A. Ubeda, *Organometallics* **1986**, *5*, 808.
65. F. Barceló, P. Lahuerta, M. A. Ubeda, C. Foces-Foces, F. H. Cano and M. Martínez-Ripoll, *Organometallics* **1988**, 7, 584.
66. A. García-Bernabé, P. Lahuerta, M. A. Ubeda, S. García-Granda and P. Pertierra, *Inorg. Chim. Acta* **1995**, *229*, 203.
67. P. Lahuerta, E. Peris, M. A. Ubeda, S. García-Granda, F. Gómez-Beltrán and M. R. Diaz, *J. Organometal. Chem.* **1993**, *455*, C10.
68. G. González, M. Nartinez, F. Estevan, A. García-Bernabé, P. Lahuerta, E. Peris, M. A. Ubeda, M. R. Diaz, S. García-Granda and B. Tejerina, *New J. Chem.* **1996**, *20*, 83.
69. F. Estevan, A. García-Bernabé, S. García-Granda, P. Lahuerta, E. Moreno, J. Pérez-Prieto, M. Sanaú and M. A. Ubeda, *J. Chem. Soc., Dalton Trans.* **1999**, 3493.
70. P. Lahuerta, J. Pérez-Prieto, S.-E. Stiriba and M. A. Ubeda, *Tetrahedron Lett.* **1999**, *40*, 1751.
71. P. Lahuerta, J. Payá, E. Peris, M. A. Pellinghelli and A. Tiripicchio, *J. Organometal. Chem.* **1989**, *373*, C5.
72. P. Lahuerta, J. Latorre, E. Peris, M. Sanaú and S. García-Granda, *J. Organometal. Chem.* **1993**, *456*, 279.
73. P. Lahuerta, J. Payá, S. García-Granda, F. Gómez-Beltrán and A. Anillo, *J. Organometal. Chem.* **1993**, *443*, C14.
74. S. García-Granda, M. R. Diaz, F. Gómez-Beltrán, E. Peris and P. Lahuerta, *Acta Crystallogr.* **1994**, *C50*, 691.
75. S. García-Granda, P. Lahuerta, J. Latorre, M. Martínez, E. Peris, M. Sanaú and M. A. Ubeda, *J. Chem. Soc., Dalton Trans.* **1994**, 539.
76. F. P. Pruchnik, R. Starosta, T. Lis and P. Lahuerta, *J. Organometal. Chem.* **1998**, *568*, 177.
77. M. P. Doyle. In *Catalysis by Di- and Polynuclear Metal Complexes*, R. D. Adams and F. A. Cotton, Eds., VCH Publishers: New York, 1998, Chapter 7.
78. M. P. Doyle and D. C. Forbes, *Chem. Rev.* **1998**, *98*, 911.
79. H. M. L. Davies and E. G. Antoulinakis. In *Organic Reactions (N. Y.)*, Vol. 57, L. Overman et al, Eds., John Wiley & Sons, Inc.: New York, 2001, pp. 1-326.
80. M. P. Doyle and M. N. Protopopova, *Tetrahedron* **1998**, *54*, 7919.
81. M. P. Doyle and M. A. McKervey, *J. Chem. Soc., Chem. Commun.* **1997**, 983.
82. D. M. Hodgson, F. Y. T. M. Pierand and P. A. Stupple, *Chem. Soc. Rev.* **2001**, *30*, 50.
83. A. Padwa and S. F. Hornbuckle, *Chem. Rev.* **1991**, *91*, 263.
84. A. Padwa and D. J. Austin, *Angew. Chem., Int. Ed.* **1994**, *33*, 1797.
85. M. P. Doyle, *Enantiomer* **1999**, *4*, 621.
86. H. M. L. Davies, *Eur. J. Org. Chem.* **1999**, 2459.
87. M. P. Doyle, G. A. Devora, A. O. Nefedov and K. G. High, *Organometallics* **1992**, *11*, 549.
88. M. P. Doyle, K. G. High, C. L. Nesloney and T. W. Clayton, Jr. and J. Lin, *Organometallics* **1991**, *10*, 1225.
89. M. P. Doyle, K. G. High, V. Bagheri, R. J. Pieters, P. J. Lewis and M. M. Pearson, *J. Org. Chem.* **1990**, *55*, 6082.
90. M. P. Doyle and M. S. Shanklin, *Organometallics* **1994**, *13*, 1081.
91. G. Stork and J. Ficini, *J. Am. Chem. Soc.* **1961**, *83*, 467.
92. S. D. Burke and P. A. Grieco. In *Organic Reaction (N. Y.)*, W. G. Dauben, Ed. Chapter 2, Vol. 26, John Wiley & Sons, Inc.: New York, 1979, pp. 361-475.
93. D. A. Evans, K. A. Woerpel, M. M. Hinman and M. M. Faul, *J. Am. Chem. Soc.* **1991**, *113*, 726.
94. H. M. L. Davies, P. R. Bruzinski, D. H. Lake, N. Kong, and M. J. Fall, *J. Am. Chem. Soc.* **1996**, *118*, 6897.

Pictiva EX2004
Samsung v Pictiva
IPR2024-01094

95. M. A. McKervey and T. Ye, *J. C. S., Chem. Commun.* **1992**, 823.
96. M. P. Doyle, R. J. Pieters, S. F. Martin, R. E. Austin, C. J. Oalmann and P. J. Müller *J. Am. Chem. Soc.* **1991**, *113*, 1423.
97. M. P. Doyle, W. R. Winchester, M. N. Protopopova, A. P. Kazula and L. J. Westrum, *Org. Synth.* **1996**, *73*, 13.
98. T. Uchida, R. Irie and T. Katsuki, *Tetrahedron* **2000**, *56*, 3501.
99. S. Kitagaki, M. Anada, O. Kataoka, K. Matsuno, C. Umeda, N. Watanabe and S. Hasimoto, *J. Am. Chem. Soc.* **1999**, *121*, 1417.
100. T. Ikeno, M. Sato, H. Sekino, A. Nishizaka and T. Yamada, *Bull. Chem. Soc. Jpn.* **2001**, *74*, 2139.
101. M. P. Doyle, J. H. Griffin, V. Bagheri and R. L. Dorow, *Organometallics* **1984**, *3*, 53.
102. H. M. L. Davies, T. Hansen and M. R. Churchill, *J. Am. Chem. Soc.* **2000**, *122*, 3063.
103. M. P. Doyle, W. Hu and D. J. Timmons, *Org. Lett.* **2001**, *3*, 933.
104. P. Müller and C. Boléa, *Helv. Chim. Acta* **2001**, *84*, 1093.
105. M. P. Doyle, *Acc. Chem. Res.* **1986**, *19*, 348.
106. H. Brunner, H. Kluschanzoff and K. Wutz, *Bull. Soc. Chem. Belg.* **1989**, *98*, 63.
107. M. Kennedy, M. A. McKervey, A. R. Maguire and G. H. P. Roos, *J. Chem. Soc., Chem. Commun.* **1990**, 361.
108. S. Hashimoto, N. Watanabe and S. Ikegami, *Tetrahedron Lett.* **1990**, *31*, 5173.
109. N. Watanabe, T. Ogawa, Y. Ohtake, S. Ikegami and S. Hashimoto, *Synlett* **1996**, 85.
110. H. M. L. Davies and D. K. Hutcheson, *Tetrahedron Lett.* **1993**, *34*, 7243.
111. M. P. Doyle, Q.-L. Zhou, C. Charnsangavej, M. A. Longoria, M. A. McKervey and C. F. Garcia, *Tetrahedron Lett.* **1996**, *37*, 4129.
112. H. M. L. Davies, P. R. Bruzinski and M. J. Fall, *Tetrahedron Lett.* **1996**, *37*, 4133.
113. E. J. Corey and T. G. Grant, *Tetrahedron Lett.* **1994**, *35*, 5373.
114. H. M. L. Davies, D. G. Stafford, B. D. Doan and J. H. Houser, *J. Am. Chem. Soc.* **1998**, *120*, 3326.
115. H. M. L. Davies, N. Kong and M. R. Churchill, *J. Org. Chem.* **1998**, *63*, 6586.
116. H. M. L. Davies, J. J. Matasi, L. M. Hodges, N. J. Huby, C. Thornley, N. Kong and J. H. Houser, *J. Org. Chem*. **1997**, *62*, 1095.
117. J. L. Bear, T. P. Zhu, T. Malinski, A. M. Dennis and K. M. Kadish, *Inorg. Chem.* **1984**, *23*, 674.
118. M. P. Doyle, V. Bagheri, T. J. Wandless, N. K. Harn, D. A. Brinker, C. T. Eagle and K.–L. Loh, *J. Am. Chem. Soc.* **1990**, *112*, 1906.
119. M. P. Doyle, B. D. Brandes, A. P. Kazala, R. J. Pieters, M. B. Jarstfer, L. M. Watkins and C. T. Eagle, *Tetrahedron Lett.* **1990**, *31*, 6613.
120. P. Müller, C. Baud, D. Ene, S. Motallebi, M. P. Doyle, B. D. Brandes, A. B. Dyatkin and M. M. See, *Helv. Chim. Acta* **1995**, *78*, 459.
121. M. P. Doyle, *Rec. Trav. Chim. Pays-Bas* **1991**, *110*, 305.
122. M. P. Doyle and J. T. Colyer, *Tetrahedron: Asymmetry* **2003**, *14*, 3601.
123. M. P. Doyle, Q.-L. Zhou, A. B. Dyatkin and D. A. Ruppar, *Tetrahedron Lett.* **1995**, *36*, 7579.
124. D. H. Rogers, E. C. Yi and C. D. Poulter, *J. Org. Chem.* **1995**, *60*, 941.
125. S. F. Martin, M. R. Spaller, S. Liras and B. Hartmann, *J. Am. Chem. Soc.* **1994**, *116*, 4493.
126. M. P. Doyle and I. M. Phillips, *Tetrahedron Lett.* **2001**, *42*, 3155.
127. C. A. Merlic and A. L. Zechman, *Synthesis* **2003**, 1137.
128. M. P. Doyle and W. Hu, *Synlett* **2001**, 1364.
129. M. P. Doyle, A. B. Dyatkin, A. V. Kalinin, D. A. Ruppar, S. F. Martin, M. R. Spallar and S. Liras, *J. Am. Chem. Soc.* **1995**, *117*, 11021.
130. M. P. Doyle, A. B. Dyatkin and C. L. Autry, *J. Chem. Soc., Perkin Trans. 1* **1995**, 619.
131. M. P. Doyle and A. V. Kalinin, *J. Org. Chem.* **1996**, *61*, 2179.
132. M. P. Doyle, M. Y. Eismont, M. N. Protopopova and M. M. Y. Kwan, *Tetrahedron* **1994**, *50*, 1665.
133. M. P. Doyle and W. Hu, *Adv. Synth. & Catal.* **2001**, *343*, 299.
134. T. Nagashima and H. M. L. Davies, *Org. Lett.* **2002**, *4*, 1989.
135. H. Hirai and M. Matsui, *Agr. Biol. Chem.* **1976**, *40*, 169.
136. W. G. Dauben, R. T. Hendricks, M. J. Luzzio and H. P. Ng, *Tetrahedron Lett.* **1990**, *31*, 6969.

Pictiva EX2004
Samsung v Pictiva
IPR2024-01094

137. C. Piqúe, B. Fähndrich and A. Pfaltz, *Synlett* **1995**, 491.
138. M. Barberis, J. Pérez-Prieto, S.-E. Stiriba and P. Lahuerta, *Org. Lett.* **2001**, *3*, 4325.
139. M. P. Doyle, S. B. Davies and W. Hu, *J. C. S., Chem. Commun.* **2000**, 867.
140. T. Niimi, T. Uchida, R. Irie and T. Katsuki, *Tetrahedron Lett.* **2000**, *41*, 3647.
141. P. Müller and C. Gränicher, *Helv. Chim. Acta* **1995**, *78*, 129.
142. M. P. Doyle, C. S. Peterson and D. L. Parker, Jr., *Angew. Chem., Int. Ed.* **1996**, *35*, 1334.
143. M. P. Doyle and W. Hu, *Chinese J. Chem.* **2001**, *19*, 22.
144. M. P. Doyle, M. N. Protopopova, C. D. Poulter and D. H. Rogers, *J. Am. Chem. Soc.* **1995**, *117*, 7281.
145. M. P. Doyle, C. S. Peterson, M. N. Protopopova, A. B. Marnett, D. L. Parker, Jr., D. G. Ene and V. Lynch, *J. Am. Chem. Soc.* **1997**, *119*, 8826.
146. M. P. Doyle and W. Hu, *J. Org. Chem.* **2000**, *65*, 8839.
147. M. P. Doyle, W. Hu, B. J. Chapman, A. B. Marnett, C. S. Peterson, J. P. Vitale and S. A. Stanley, *J. Am. Chem. Soc.* **2000**, *122*, 5719.
148. M. P. Doyle and W. Hu, *Tetrahedron Lett.* **2000**, *41*, 6265.
149. M. P. Doyle, M. N. Protopopova, P. Müller, D. G. Ene and E. A. Shapiro, *J. Am. Chem. Soc.* **1994**, *116*, 8492.
150. P. Müller and H. Imogaï, *Tetrahedron: Asymmetry* **1998**, *9*, 4419.
151. M. P. Doyle, D. G. Ene, C. S. Peterson and V. Lynch, *Angew. Chem., Int. Ed.* **1999**, *38*, 700.
152. M. P. Doyle, M. N. Protopopova, C. S. Peterson, J. P. Vitale, M. A. McKervey and C. F. Garcia, *J. Am. Chem. Soc.* **1996**, *118*, 7865.
153. M. P. Doyle, B. J. Chapman, W. Hu, C. S. Peterson, M. A. McKervey and C. F. Garcia, *Org. Lett.* **1999**, *1*, 1327.
154. D. F. Taber. In *Houben-Wehl: Methods of Organic Chemistry*, G. Helmchen, Georg Thiem Verlag, Stuttard, Germany, **1995**, Chapter 1.2.
155. D. F. Taber and E. H. Petty, *J. Org. Chem.* **1982**, *47*, 4808.
156. M. P. Doyle, M. S. Shanklin, S. M. Oon, H. Q. Pho, F. R. Van der Heide and W. R. Veal, *J. Org. Chem.* **1988**, *53*, 3384.
157. A. Padwa, D. J. Austin, A. T. Price, M. A. Semones, M. P. Doyle, M. N. Protopopova, W. R. Winchester and A. Tran, *J. Am. Chem. Soc.* **1993**, *115*, 8669.
158. D. F. Taber and R. E. Ruckle, Jr., *J. Am. Chem. Soc.* **1986**, *108*, 7686.
159. M. P. Doyle, L. J. Westrum, W. N. E. Wolthuis, M. M. See, W. P. Boone, V. Bagheri and M. M. Pearson, *J. Am. Chem. Soc.* **1993**, *115*, 958.
160. P. Wong and J. Adams, *J. Am. Chem. Soc.* **1994**, *116*, 3296.
161. E. Nakamura, N. Yoshikai and M. Yamanaka, *J. Am. Chem. Soc.* **2002**, *124*, 7181.
162. J. W. Bode, M. P. Doyle, M. N. Protopopova and Q.-L. Zhou, *J. Org. Chem.* **1996**, *61*, 9146.
163. M. P. Doyle, J. S. Tedrow, A. B. Dyatkin, C. J. Spaans and D. G. Ene, *J. Org. Chem.* **1999**, *64*, 8907.
164. M. P. Doyle, A. B. Dyatkin and J. S. Tedrow, *Tetrahedron Lett.* **1994**, *35*, 3853.
165. M. P. Doyle and W. Hu, *Chirality* **2002**, *14*, 169.
166. M. P. Doyle, W. Hu and M. V. Valenzuela, *J. Org. Chem.* **2002**, *67*, 2954.
167. M. P. Doyle, A. B. Dyatkin, G. H. P. Roos, F. Cañas, D. A. Pierson, A. Van Basten, P. Müller and P. Polleux, *J. Am. Chem. Soc.* **1994**, *116*, 4507.
168. P. Müller and P. Polleux, *Helv. Chim. Acta* **1994**, *77*, 645.
169. M. P. Doyle, A. V. Kalinin and D. G. Ene, *J. Am. Chem. Soc.* **1996**, *118*, 8837.
170. M. P. Doyle and A. J. Catino, *Tetrahedron: Asymmetry* **2003**, *14*, 925.
171. M. P. Doyle, M. Yan, I. M. Phillips and D. J. Timmons, *Adv. Syn. Catal.* **2002**, *344*, 91.
172. M. P. Doyle, S. B. Davies and E. J. May, *J. Org. Chem.* **2001**, *66*, 8112.
173. M. P. Doyle and A. V. Kalinin, *Tetrahedron Lett.* **1996**, *37*, 1371.
174. M. P. Doyle and A. V. Kalinin, *Synlett* **1995**, 1075.
175. H. M. L. Davies and E. G. Antoulinakis, *J. Organometal. Chem.* **2001**, *617-618*, 47.
176. H. M. L. Davies and P. Ren, *J. Am. Chem. Soc.* **2001**, *123*, 2070.

Pictiva EX2004
Samsung v Pictiva
IPR2024-01094

177. H. M. L. Davies, D. G. Stafford and T. Hansen, *Org. Lett.* **1999**, *1*, 233.
178. H. M. L. Davies, T. Hansen, D. W. Hopper and S. A. Panaro, *Tetrahedron Lett.* **1991**, *32*, 6509.
179. A. H. Li, L. X. Dai and V. K. Aggarwal, *Chem. Rev.* **1997**, *97*, 2341.
180. V. K. Aggarwal, E. Alonso, G. Hynd, K. M. Lydon, M. J. Palmer, M. Porcelloni and J. R. Studley, *Angew. Chem., Int. Ed.* **2001**, *40*, 1430.
181. V. K. Aggarwal, E. Alonso, G. Fang, M. Ferrara, G. Hynd and M. Porcelloni, *Angew. Chem., Int. Ed.* **2001**, *40*, 1433.
182. M. P. Doyle, D. C. Forbes, M. M. Vasbinder and C. S. Peterson, *J. Am. Chem. Soc.* **1998**, *120*, 7653.
183. A. Padwa, J. P. Snyder, E. A. Curtis, S. M. Sheehan, K. J. Worsencroft and C. O. Kappe, *J. Am. Chem. Soc.* **2000**, *122*, 8155.
184. S. Kitagaki, Y. Yanamoto, H. Tsutsui, M. Anada, M. Nakajima and S. Hashimoto, *Tetrahedron Lett.* **2001**, *42*, 6361.
185. N. McCarthy, M. A. McKervey, T. Ye, M. McCann, E. Murphy and M. P. Doyle, *Tetrahedron Lett.* **1992**, *40*, 5963.
186. D. M. Hodgson, R. Glen, G. H. Grant and A. J. Redgrave, *J. Org. Chem.* **2003**, *68*, 581.
187. H. Ishitani and K. Achiwa, *Heterocycles* **1997**, *46*, 153.
188. M. C. Pirrung and J. Zhang, *Tetrahedron Lett.* **1992**, *40*, 5987.
189. A. Padwa, Z. J. Zhang and L. Zhi, *J. Org. Chem.* **2000**, *65*, 5223.
190. M. P. Doyle, W. Hu and D. J. Timmons, *Org. Lett.* **2001**, *3*, 3741.
191. M. P. Doyle, M. Yan, W. Hu and L. S. Gronenberg, *J. Am. Chem. Soc.* **2003**, *125*, 4692.
192. M. P. Doyle, D. C. Forbes, M. N. Protopopova, S. A. Stanley, M. M. Vasbinder and K. R. Xavier, *J. Org. Chem.* **1997**, *62*, 7210.
193. N. Watanabe, Y. Ohtake, S.-I. Hashimoto, M. Shiro and S. Ikegami, *Tetrahedron Lett.* **1995**, *36*, 1491.
194. M. Kennedy, M. A. McKervey, A. R. Maguire, S. M. Tuladhar and M. F. Twohig, *J. Chem. Soc., Perkin Trans. 1* **1990**, 1047.
195. T. N. Salzmann, R. W. Ratcliffe, B. G. Christensen and F. A. Bouffard, *J. Am. Chem. Soc.* **1980**, *102*, 6161.
196. R. Connell, F. Scavo, P. Helquist and B. Akermark, *Tetrahedron Lett.* **1986**, *27*, 5559.
197. Y. Landais and D. Planchenault, *Tetrahedron Lett.* **1994**, *35*, 4565.
198. P. Bulugahapitiya, Y. Landais, L. Parra-Rapado, D. Planchenault and V. Weber, *J. Org. Chem.* **1997**, *62*, 1630.
199. R. T. Buck, M. P. Doyle, M. J. Drysdale, L. Ferris, D. C. Forbes, D. Haigh, C. J. Moody, N. D. Pearson and Q. L. Zhou, *Tetrahedron Lett.* **1996**, *37*, 7631.
200. H. M. L. Davies, T. Hansen, J. Rutberg and P. R. Bruzinski, *Tetrahedron Lett.* **1997**, *38*, 1741.

Pictiva EX2004
Samsung v Pictiva
IPR2024-01094

14

Nickel, Palladium and Platinum Compounds

Carlos A. Murillo,
Texas A&M University

14.1 General Remarks

The most common oxidation state for the group 10 elements is two which gives rise to the very stable d^8 electronic configuration. For Pd and Pt (and to a lesser extent Ni), the stereochemistry of such d^8 species is dominated by square planar compounds. The tetravalent state is often found in Pd and Pt compounds but all of them are mononuclear or without metal-metal bonds when they associate. Whenever bridging ligands couple divalent square planar species, compounds of the paddlewheel type form, but these again are devoid of metal-to-metal bonds as all bonding and antibonding MOs are occupied giving a $\sigma^2\pi^4\delta^2\delta^{*2}\pi^{*4}\sigma^{*2}$ configuration with a net bond order of zero. Thus, only when the d^8 electronic configuration is altered, i.e., by oxidation of the metal centers, can metal-metal bond formation occur. Therefore, a one-electron oxidation of a non-bonded paddlewheel complex would be expected to yield a paramagnetic species with an M_2^{5+} core and an electronic configuration $\sigma^2\pi^4\delta^2\delta^{*2}\pi^{*4}\sigma^*$ (or a variation thereof) with a bond order of 0.5. A 2-electron oxidation would be expected to give a diamagnetic M_2^{6+} core with an electronic configuration of $\sigma^2\pi^4\delta^2\delta^{*2}\pi^{*4}$ and a single M–M bond. Since higher oxidation states are typically favored for the heavier elements of a given group of the periodic table, Pt would be expected to be most readily oxidized. Indeed, almost all of the M_2^{6+} complexes in this group contain singly-bonded Pt_2^{6+} units. In this chapter we will focus our attention primarily to those dimetal compounds in which each metal atom unit possesses a square planar configuration and two square planes (with or without additional axial ligands) parallel to each other.

A useful review of quadruply bridged dinuclear complexes of platinum, palladium and nickel has appeared.[1] There are also several reviews covering various aspects of paddlewheel Pt chemistry. These will be referenced, as appropriate, later on.

14.2 Dinickel Compounds

To date, no authentic singly bonded dinickel(III) complex has been isolated in the solid state and characterized, although several closely related dinickel(II) species without metal-metal bonds have been prepared and various attempts made to oxidize them. The dithioacetato complex $Ni_2(S_2CCH_3)_4$, in which the Ni···Ni separation is 2.564(1) Å, has been oxidized[2] to $[Ni_2(S_2CCH_3)_4I]_\infty$ which consists of linear chains of ···I···$[Ni_2S_8]$···I···$[Ni_2S_8]$··· with Ni–Ni and

Pictiva EX2004
Samsung v Pictiva
IPR2024-01094

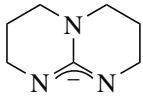
Ni–I distances of 2.514(3) Å and *c.* 2.93 Å, respectively. Within the individual Ni_2S_8 units the torsional angle is 28°. This compound is said to be EPR-silent. This is in contrast to the EPR-active $[Ni_2(DTolF)_4]^+$ cation, where DTolF = [(*p*-tol)NCHN(*p*-tol)]$^-$, which can be generated by the electrochemical oxidation of $Ni_2(DTolF)_4$ ($E_{1/2}$(ox) = +0.73 V in $Bu^n_4NPF_6/CH_2Cl_2$ versus Ag/AgCl).[3,4] This spectrum is consistent with axial symmetry, with $g_\perp$ = 2.210 and $g_\parallel$ = 2.038. Thus the oxidation can be considered as metal centered. The dark-green complex $[Ni_2(DTolF)_4]BF_4$ has been prepared[4] by oxidizing $Ni_2(DTolF)_4$ with $[Ag(NCCH_3)_2]BF_4$ in dichloromethane. The Ni–Ni distance in the Ni_2^{5+} complex (2.418(4) Å) is appreciably shorter than that in $Ni_2(DTolF)_4(H_2O)_2$ (2.485(2) Å) while the torsional angle is larger (27.4° versus 16.85°). A SCF-Xα-SW calculation on the model species $Ni_2(HNCHNH)_4$ and $[Ni_2(HNCHNH)_4]^+$, along with the EPR spectral results indicates that the electron is lost from an orbital with partial metal-based δ* character, thereby explaining the Ni–Ni bond shortening upon oxidation. Interestingly, the electrochemical oxidation of $[Ni_2(DTolF)_4]^+$ to $[Ni_2(DTolF)_4]^{2+}$ occurs at $E_{p,a}$ = +1.25 V versus Ag/AgCl,[3,4] but the dication is not stable and this process is irreversible.

14.3 Dipalladium Compounds

The number of compounds of Pd^{III} that have been isolated and characterized is very limited. There is no aqua ion nor any classical anionic complexes, PdX_6^{3-}; the latter have been made only in the solid state under harsh conditions.[5] There are no binary compounds ("PdF_3" is a mixed Pd^{II}, Pd^{IV} compound).[6] In 1987 the compound $(H_3O)[PdL_2](ClO_4)_4 \cdot 3H_2O$, L = 1,4,7-trithiacyclononane, was reported with a structure determination.[7]

14.3.1 A singly bonded Pd_2^{6+} species

The only authentic paddlewheel compound having a Pd_2^{6+} core is $Pd_2(hpp)_4Cl_2$. Here, hpp is the anion of the guanidinate derivative 1,3,4,6,7,8-hexahydro-2*H*-pyrimido[1,2-*a*]pyrimidine depicted in **14.1**. This was prepared in low yield by oxidation of the non-metal–metal-bonded Pd^{II} complex $Pd_2(hpp)_4$ with $PhICl_2$, $NOPF_6$ or $NOBF_4$ but always as a mixture of compounds.[8] Hand-picked crystals are quite stable, even in air. The paddlewheel structure shown in Fig. 14.1 is centrosymmetric with the chloride ions occupying axial positions of the paddlewheel. Except for the absence of chlorine atoms in the precursor, the structures are similar. However, the Pd–Pd distance in the Pd_2^{6+} compound of 2.391(1) Å is considerably shorter by 0.164 Å than that of the precursor and 0.36 Å shorter than that in Pd metal itself. The Pd–Cl distance is 2.474(4) Å and the crystallographically unique Pd–N distance is 2.034(6) Å. A cyclic voltammogram of the precursor $Pd_2(hpp)_4$ in CH_2Cl_2 showed a wave at -0.12 V vs. Ag/AgCl and another less reversible wave at +0.82 V.



14.1

Geometry optimization by the Hartree-Fock self-consistent field method has shown excellent agreement between the calculated and experimental results with a Pd–Pd distance of 2.402 vs the observed 2.391 Å and a torsion angle of 22.6° vs the experimental value of 24°. The HOMO/LUMO gap is calculated to be 167 kcal mol^{-1}. The calculations indicate that the Pd–Pd bond is a σ-bond formed mainly by d_{z^2}–d_{z^2} overlap. The electronic configuration to be assigned to the dipalladium core appears to be $\pi^4\delta^2\delta^{*2}\pi^{*4}\sigma^2$. This is shown in Fig. 14.2.

Pictiva EX2004
Samsung v Pictiva
IPR2024-01094

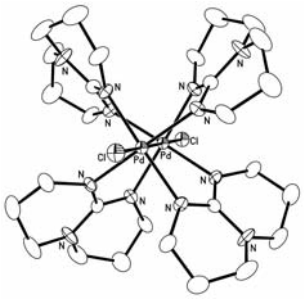


Fig. 14.1. The structure of the singly-bonded guanidinate compound $Pd_2(hpp)_4Cl_2$.

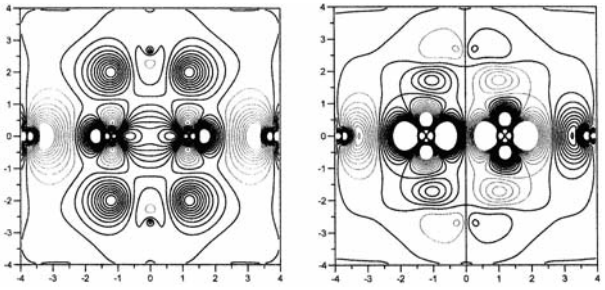


Fig. 14.2. Contours of the HOMO (left) and LUMO (right) of the molecule $Pd_2(hpp)_4Cl_2$ showing the Pd–Pd single bond on the plane formed by the Cl–Pd–Pd–Cl unit and four nitrogen atoms from two of the guanidinate ligands hpp. Positive and negative contours are in heavy and light lines, respectively. Both are antibonding with respect to the Pd–Cl interaction.

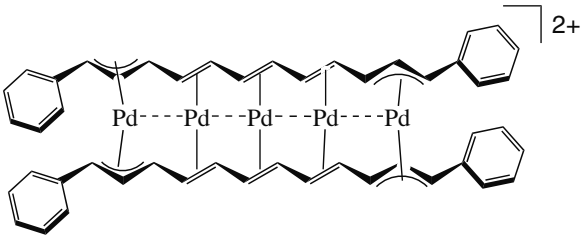
14.3.2 Chemistry of Pd_2^{5+} and similar species

The redox chemistry of the dipalladium(II) complex $Pd_2(DTolF)_4$, which is analogous to the nickel complex described in Section 14.2, has also been investigated.[3,4] The cyclic voltammogram of solutions of this compound in $Bu^n_4NPF_6/CH_2Cl_2$ shows reversible one-electron oxidations at $E_{1/2}$ = +0.81 V and +1.19 V versus Ag/AgCl, but only the one-electron oxidized product $[Pd_2(DTolF)_4]PF_6$ has been prepared and structurally characterized.[4] For this paramagnetic species the EPR spectrum suggests that the odd electron occupies a ligand-based molecular orbital,[4] but SCF-Xα-SW calculations show that the odd electron is located on an orbital with very significant metal character.[4] Furthermore, it has been reported[9] that the complex $Pd_2(DPhBz)_4$, where DPhBz = $[PhNC(Ph)NPh]^-$, undergoes a reversible one-electron oxidation at +0.65 V to form the radical cation $[Pd_2(DPhBz)_4]^+$. This shows an axially symmetric EPR signal at $g_\perp$ = 2.17 and $g_\parallel$ = 1.98 that has been interpreted,[9] in terms of the oxidation being metal-centered. The dipalladium(II) complex with 2-mercaptopyridine, $Pd_2(pyS)_4$, undergoes[10] an irreversible one-electron oxidation at $E_{p,a}$ = +0.61 V versus Ag/Ag^+ in $Bu^n_4NClO_4/CH_2Cl_2$, but in the presence of halide ion (Cl^- or Br^-) a new quasi-reversible two-electron couple appears at a much more negative potential ($E_{1/2}$ = +0.13 V for Cl^- and +0.15 V for Br^-). This has been attributed[10] to the generation of the dipalladium(III) species $[Pd_2(pyS)_4X]^+$, but such a entity has not been isolated or characterized further.

Pictiva EX2004
Samsung v Pictiva
IPR2024-01094

14.3.3 Other compounds with Pd–Pd interactions

There are compounds with Pd–Pd interactions e.g., those in which two square planar Pd^{II} units are held together by bridging ligands such as the precursor to $Pd_2(hpp)_4Cl_2$ in Section 14.3.1. However, these compounds do not have a formal metal-metal bond. Compounds with chains of three and four Pd atoms have also been made.[11] The chains are cationic having BF_4 or $B(3,5\text{-}(CF_3)_2C_6H_3)_4$ counteranions. The Pd_n chains are sandwiched between two *all-trans*-1,8-diphenyl-1,3,4,7-octatetraene molecules (DPOT). In **14.2**, the Pd–Pd–Pd–Pd skeleton is essentially linear with the outer Pd···Pd separations of 2.7322(8) and the inner one of 2.654(1) Å. The overall formal oxidation number for the Pd_4 unit is +2, $Pd^{+0.5}$. Since molecules of this type do not fall in the category of metal–metal bonded species with a paddlewheel structure, no further comments will be made.



14.2

14.4 Diplatinum Compounds

Singly bonded diplatinum complexes having Pt_2^{6+} cores are second only to dirhodium(II) species in the number of compounds that possess the $\sigma^2\pi^4\delta^2\delta^{*2}\pi^{*4}$ configuration. With the exception of a few mononuclear species such as $Bu^n_4N[Pt(C_6Cl_5)_4]$[12,13] and $[Pt(1,4,7\text{-trithiacyclononane})_2]^{3+}$,[14] the vast majority of Pt^{III} complexes are those that possess a Pt_2^{6+} core. Those with bridging oxyanions (sulfate, acetate, phosphate and pyrophosphite) and mixed N–O donor sets (such as hydroxypyridinato) predominate. For historical reasons we shall discuss the oxyanion-containing systems first. Several reviews have appeared covering diverse aspects of the chemistry of species containing Pt^{III} units such as the chemistry of quadruply bridged dinuclear complexes of platinum, palladium and nickel,[1] the preparation and properties of paddlewheel complexes,[15] sulfate complexes,[16] pyrophosphite complexes,[17-19] complexes of 2-pyridone and its derivatives.[20] There are also a series of reviews on chains such as those in the so-called platinum blue compounds and related species which also discuss chemistry relevant to complexes with a Pt_2^{6+} core.[21-24] Assignment of electronic spectra of Pt_2^{6+} complexes will be discussed in Chapter 16. Some relevant papers should be consulted.[25-28] Structural data for the Pt–Pt bonded complexes are given in Table 14.1.

Pictiva EX2004
Samsung v Pictiva
IPR2024-01094

Table 14.1. Structural data for diplatinum(III) compounds

Compound[a]	r(Pt–Pt) (Å)	r(Pt–L) (Å)[b]	Donor atom(s) L	ref.
$K_2[Pt_2(SO_4)_4(H_2O)_2]$	2.461(1)	2.111(7)	O	32
$K_2[Pt_2(SO_4)_4(DMSO)_2]$	2.471(1)	2.126(6)	O	33
$[Pt(pydz)_4][Pt_2(SO_4)_4(pydz)_2]\cdot 2H_2O$	2.482(1)	2.140(6)	N	35
$(pyH)_2[Pt_2(SO_4)_4(py)_2]$	2.489(1)	2.15(1)	N	34
$Na_2[Pt_2(HPO_4)_4(H_2O)_2]$	2.486[2][c]	2.15[1][c]	O	32,41
$(3,4\text{-}Me_2C_5H_3NH)_2[Pt_2(HPO_4)_4(3,4\text{-}Me_2C_5H_3N)_2]$	2.494(1)	2.16(1)	N	42
$(Ph_4As)_2[Pt_2(HPO_4)_4(THT)_2]\cdot 2H_3PO_4$	2.525(1)	2.462(1)	S	43
$(pyH)[Pt_2(H_2PO_4)(HPO_4)_3(py)_2]\cdot H_2O$	2.494(1)	2.14[4]	N	40
$(Et_4N)_2[Pt_2(H_2PO_4)_2(HPO_4)_2Cl_2]\cdot H_2O$	2.529(1)	2.448(4)	Cl	32
$Na_{10}[Pt_2(PO_4)_4(gu)_2]\cdot 22H_2O$	2.534(1)	2.141(2)	N	46
$K_4[Pt_2(pop)_4Cl_2]\cdot 2H_2O$	2.695(1)	2.407(2)	Cl	54,61
$K_4[Pt_2(pop)_4(CH_3)I]\cdot 2H_2O$	2.782(1)	2.18(2)	C	58
		2.816(3)	I	
$(Bu^n{}_4N)_4[Pt_2(pop)_4Br_2]$	2.716(1)	2.572(1)	Br	59
$K_4[Pt_2(pop)_4Br_2]\cdot 2H_2O$	2.723(4)	2.555(5)	Br	60
$K_4[Pt_2(pop)_4I_2]$	2.754(1)	2.746(1)	I	59
$K_2(Bu^n{}_4N)_2[Pt_2(pop)_4I_2]$	2.742(1)	2.721(1)	I	59
$(Bu^n{}_4N)_2[Pt_2(pop)_4(SEt_2)_2]$	2.766(1)	2.479(5)	S	62
$K_4[Pt_2(pcp)_4Cl_2]\cdot 8H_2O$	2.750(1)	2.442(1)	Cl	51
$K_4[Pt_2(pop)_4(SCN)_2]\cdot 2H_2O$	2.760(1)	2.466(4)	S	66
$K_4[Pt_2(pop)_4(NO_2)_2]\cdot 2KNO_2\cdot 2H_2O$	2.754(1)	2.147(6)	N	66
$K_4[Pt_2(pop)_4(IM)_2]\cdot 7H_2O$	2.745(1)	2.13(2)	N	66
$(Bu^n{}_4N)_2[Pt_2(pop)_4(NCCH_3)_2]$	2.676(1)	2.09(1)	N	67
$Na_8[Pt_2(pop\text{-}H)_4(NO_2)_2]\cdot 18H_2O$	2.733(1)	2.153(6)	N	65
$[Pt_2(O_2CCH_3)_4(H_2O)_2](ClO_4)_2$	2.391(1)	2.17(1)	O	83
$[Pt_2(O_2CCH_3)_4(H_2O)_2](CF_3SO_3)_2\cdot 4H_2O$	2.393(1)	2.115(4)	O	83
$Cs_3[Pt_2(O_2CCH_3)_2(CH_2CO_2)_2Cl_2]Cl\cdot 3H_2O$ (H,T)	2.451(1)	2.44[2]	Cl	92

Pictiva EX2004
Samsung v Pictiva
IPR2024-01094

Compound[a]	r(Pt–Pt) (Å)	r(Pt–L) (Å)[b]	Donor atom(s) L	ref.
$Pt_2[S_2CCH(CH_3)_2]_4I_2{\cdot}I_2$	2.578(1)	2.764[2]	I	94
$Pt_2[S_2CCH_2Ph]_4I_2$	2.598(2)	2.753(3)	I	94
$Pt_2[S_2CC_2H_5]_4I_2$	2.582(2)	2.764[1]	I	95
cis-$Pt_2(O_2CCF_3)_2(CH_3)_4(4\text{-Mepy})_2$	2.557(1)	2.13[4]	N	99
cis-$Pt_2(O_2CCH_3)_2(CH_3)_4(py)_2$	2.529(1)	2.20(1)	N	100
$Pt_2(DPhF)_4Cl_2{\cdot}THF$	2.517(1)	2.435(2)	Cl	86
$Pt_2(hpp)_4Cl_2$	2.438(1)	2.483(4)	Cl	101
$Pt_2(Bu^tCONH)_4Cl_2{\cdot}1.5H_2O$	2.448(2)	2.427(5)	Cl	110
$Pt_2(CH_3CONH)_4I_2{\cdot}8H_2O$	2.473(2)	2.733(3)	I	109
$[Pt_2(PPh_3)_2(Bu^tCONH)_4](NO_3)_2{\cdot}2CHCl_3$	2.504(1)	2.460(4)	P	112
$[Pt_2(H_2O)(PPh_3)(Bu^tCONH)_4](NO_3)_2$	2.468(1)	2.404(3) 2.279(6)	P O	112
cis-$[Pt_2(\mu\text{-}CH_3CONH)_2(CH_3CONH)_2(en)_2]I_2$ (H,T)	2.567(1)	2.16(2)	N	113
cis-$[Pt_2(Bu^tCONH)_2(NH_3)_4(NO_2)(NO_3)]{\cdot}H_2O$ (H,H)	2.609(1)	2.29(1)	$O(NO_3^-)$	114
		2.10(1)	$N(NO_2^-)$	
cis-$[Pt_2(Bu^tCONH)_2(NH_3)_4(CH_2COCH_3)](NO_3)_3{\cdot}H_2O$ (H,H)	2.689(1)	2.095(9)	C	114
		2.667(7)	O	
cis-$[Pt_2(Bu^tCONH)_2(NH_3)_4(CH_2CH(CH_3)_2O](NO_3)_3{\cdot}7H_2O$ (H,H)	2.711(1)	2.11	C	119
cis-$[Pt_2(Bu^tCONH)_2(NH_3)_4(CH_2CHO)](NO_3)_3{\cdot}H_2O$ (H,H)	2.749(1)	2.121(9)	C	119
cis-$[Pt_2(Bu^tCONH)_2(NH_3)_4(CH_2COPh)](NO_3)_3{\cdot}PhCOCH_3$ (H,H)	2.676(1)	2.15(2)	C	120
cis-$[Pt_2(Bu^tCONH)_2(NH_3)_4(CH_2COCH_2COCH_3)](NO_3)_3$ (H,H)	2.721(1)	2.114(8	C	120
cis-$[Pt_2(Bu^tCONH)_2(NH_3)_4(CH_2CHCH(OH)Me)](NO_3)_3$ (H,H)	2.734(1)	2.12(1)	C	122
cis-$[Pt_2(Bu^tCONH)_2(NH_3)_4(CH_2CHCH(OH)Et)](NO_3)_3$ (H,H)	2.735(1)	2.06(1)	C	122
cis-$[Pt_2(Bu^tCONH)_2(NH_3)_4(CH_2CMeCH(OH)Me)](NO_3)_3$ (H,H)	2. 740(1)	2.14(1)	C	122
cis-$[Pt_2(Bu^tCONH)_2(NH_3)_4(CH_2CHCMe(OH)Me)](NO_3)_3$ (H,H)	2.732(1)	2.11(1)	C	122
cis-$[Pt_2(Bu^tCONH)_2(NH_3)_4(CHC(OH)CH_2CH_2)](NO_3)_3$ (H,H)	2.734(2)	2.11(3)	C	121
cis-$[Pt_2(Bu^tCONH)_2(NH_3)_4(CH_2C(O)CH_2CH_2CH_3)](NO_3)_3{\cdot}H_2O$ (H,H)	2.688(1)	2.10(2)	C	123
cis-$[Pt_2(Bu^tCONH)_2(NH_3)_4(CH_2C(O)CH_2OH](NO_3)_3{\cdot}0.5C_3H_5O$ (H,H)	2.700(1)	2.10(1)	C	123

Pictiva EX2004
Samsung v Pictiva
IPR2024-01094

Compound[a]	r(Pt–Pt) (Å)	r(Pt–L) (Å)[b]	Donor atom(s) L	ref.
cis-[Pt_2(Bu^tCONH)$_2$(NH_3)$_4$($CH_2C(O)CH_2$)$_3$OH](NO$_3$)$_3$ (H,H)	2.688(1)	2.10(2)	C	123
cis-[Pt_2(Bu^tCONH)$_2$(NH_3)$_4$($CH_2C(O)CH_2OCH_3$](NO$_3$)$_3$ (H,H)	2.693(1)	2.09(1)	C	123
cis-[Pt_2(Bu^tCONH)$_2$(NH_3)$_4$($CH_2(CH_3)C(O)CH_3$](NO$_3$)$_3$ (H,H)	2.722	2.15(1)	C	123
cis-[Pt_2(hp)$_2$(NH_3)$_4$(NO_3)(H$_2$O)](NO$_3$)$_3$·2H$_2$O (H,H)	2.540(1)	2.193(7)	O(NO_3^-)	132
		2.122(6)	O	
cis-[Pt_2(hp)$_2$(NH_3)$_4$(NO_3)$_2$](NO$_3$)$_2$·0.5H$_2$O (H,T)	2.547(1)	2.17(1)	O(NO_3^-)	132
cis-[Pt_2(hp)$_2$(NH_3)$_4$(NO_2)$_2$](NO$_3$)$_2$·0.5H$_2$O (H,T)	2.576(1)	2.170[2]	N(NO_2^-)	133
cis-[Pt_2(hp)$_2$(NH_3)$_4$Cl$_2$](NO$_3$)$_2$ (H,T)	2.568(1)	2.436[8]	Cl	133
cis-[Pt_2(hp)$_2$(NH_3)$_4$Br$_2$](NO$_3$)$_2$·0.5H$_2$O (H,T)	2.582(1)	2.568[6]	Br	133
cis-[Pt_2(hp)$_2$(en)$_2$(NO_2)(NO_3)](NO$_3$)$_2$·0.5H$_2$O (H,H)	2.638(1)	2.307(9)	O(NO_3^-)	134
		2.11(1)	N	
cis-[Pt_2(1-MeC)$_2$(NH_3)$_4$(NO_2)$_2$](NO$_3$)$_2$·2H$_2$O (H,T)	2.584(1)	2.12[2]	N	135,136
cis-[Pt_2(1-MeC)$_2$(NH_3)$_2$(gly-*N,O*)$_2$](NO$_3$)$_2$·3H$_2$O (H,T)	2.527(1)	2.17[1]	N	137
cis-[Pt_2(1-MeC)$_2$(NH_3)$_4$(NO_3)$_2$](NO$_3$)$_2$·HNO$_3$·3H$_2$O (H,T)	2.552(1)	2.138(8)	O	138
cis-[Pt_2(1-MeC)$_2$(NH_3)$_4$(NO_2)(H$_2$O)](ClO$_4$)$_3$·3.5H$_2$O (H,T)	2.604(1)	2.091(8)	N	138
		2.311(6)	O	
cis-[Pt_2(1-MeC)$_2$(NH_3)$_4$(H$_2$O)$_2$](ClO$_4$)$_4$·H$_2$O (H,T)	2.565(1)	2.16[4]	O	138
cis-[Pt_2(1-MeC)$_2$(NH_3)$_4$(EtguaH)$_2$](NO$_3$)$_4$·9H$_2$O (H,T)	2.586(1)	2.184[7]	N	138,139
cis-Pt_2(hp)$_2$(CH_3)$_4$(py)$_2$·2CHCl$_3$ (H,T)	2.550(1)	2.18[2]	N	100
cis-Pt_2(hp)$_2$(CH_3)$_4$(py) (H,H)	2.556(1)	2.034(8)	N	127
cis-Pt_2(fhp)$_2$(CH_3)$_4$(py)$_2$·0.17C_6H_6 (H,T)	2.551(1)	2.20[1]	N	100
cis-Pt_2(fhp)$_2$(CH_3)$_4$(py) (H,H)	2.554(1)	2.04(1)	N	127
cis-Pt_2(chp)$_2$(CH_3)$_4$(py) (H,H)	2.543(1)	2.06(1)	N	100
cis-Pt_2(mhp)$_2$(CH_3)$_4$(py) (H,H)	2.545(1)	2.030(8)	N	100
cis-Pt_2(bhp)$_2$(CH_3)$_4$(py) (H,H)	2.551(1)	2.06(2)	N	127
cis-Pt_2(hp)$_2$(CH_3)$_4$(SEt_2)·0.5C_7H_8 (H,H)	2.568(1)	2.292(4)	S	128
cis-Pt_2(fhp)$_2$(CH_3)$_4$(SEt_2)·0.5C_7H_8 (H,H)	2.571(1)	2.285(4)	S	128
cis-Pt_2(mhp)$_2$(CH_3)$_4$(SEt_2) (H,H)	2.561(1)	2.303(4)	S	128

Pictiva EX2004
Samsung v Pictiva
IPR2024-01094

Compound[a]	r(Pt–Pt) (Å)	r(Pt–L) (Å)[b]	Donor atom(s) L	ref.
cis-[Pt_2(1-MeU)$_2$(NH_3)$_4$(NO_2)$_2$(H_2O)][NO_3]$_3$·5H_2O (H,T)	2.574(1)	2.08(1)	N	142
		2.253(9)	O	
cis-[Pt_2(1-MeU)$_2$(NH_3)$_4$(NO_3)(H_2O)][NO_3]$_3$·3H_2O (H,T)	2.556(1)	2.14(1)	O(NO_3^-)	143
		2.18(1)	O	
cis-[Pt_2(1-MeU)$_2$(NH_3)$_4$(NO_3)(H_2O)][NO_3]$_3$·2H_2O (H,T)	2.560(1)	2.12(1)	O(NO_3^-)	143
		2.17(1)	O	
cis-[Pt_2(1-MeU)$_2$(NH_3)$_4$(NO_2)][NO_3]$_3$·H_2O (H,H)	2.607(1)	2.06(2)	N	144
cis-[Pt_2(1-MeU)$_2$(NH_3)$_4$Cl$_2$]Cl$_2$·3.5H_2O (H,H)	2.573(1)	2.44[2]	Cl	145
cis-Pt_2(1-MeU)$_2$(NH_3)$_2$Cl$_4$·2H_2O (H,H)	2.543(1)	2.44[2]	Cl	145
cis-[Pt_2(1-MeU)$_2$(NH_3)$_4$(1-MeU)][SiF_6](NO_3)·7H_2O (H,H)	2.685(1)	2.037(9)	C	146
cis-[Pt_2(pyrr)$_2$(NH_3)$_4$(NO_2)(NO_3)][NO_3]$_2$·H_2O (H,H)	2.644(1)	2.01[1]	N(NO_2^-)	148
		2.00[1]	O(NO_3^-)	
cis-[Pt_2(pyrr)$_2$(NH_3)$_4$Cl$_2$][NO_3]$_2$ (H,H)	2.637(1)	2.395(3)	Cl	150
		2.455(3)	Cl	
cis-[Pt_2(pyrr)$_2$(NH_3)$_4$Cl(NO_3)][NO_3]$_2$·H_2O (H,H)	2.624(1)	2.361(4)	Cl	150
		2.30(3)	O	
cis-[Pt_2(pyrr)$_2$(NH_3)$_3$(H_2O)(μ-OH)]$_2$(NO_3)$_6$·4H_2O (H,T)	2.553(1)	2.188(6)	O(H_2O)	150
		NA	O(OH)	
cis-[Pt_2(pyrr)$_2$(NH_3)$_4$($C_{10}H_{13}N_5O_4$)(SO_4)]·4H_2O (H,H)	2.584(1)	2.13(1)	N	152
		2.199(8)	O	
cis-[Pt_2(pyrr)$_2$(NH_3)$_3$(μ-NH_2)(NO_3)]$_2$(NO_3)$_4$·4H_2O (H,H)	2.608(1)	1.98(1)	N	151
		2.29(1)	O	
cis-[Pt_2(1-MeT)$_2$(NH_3)$_4$(NO_2)][NO_3]$_3$ (H,H)	2.651(1)	2.079(7)	N	155
cis-[Pt_2(1-MeT)$_2$(NH_2CH_3)$_2$$Cl_3$]$ClO_4$ (H,H)	2.612(2)	2.31(1)	Cl	155
cis-[Pt_2(1-MeT)$_2$(NH_3)$_2$$Cl_3$($H_2O$)][$PrCl_6$]$_{0.5}$·$H_2O$·0.4HCl	2.556(1)	d		140
cis-2,2-[Pt_2(1-MeC)$_4$(NH_3)$_2$](ClO_4)$_2$·2H_2O	2.465(1)	2.178[7]	N	156
cis-2,2-[Pt_2(1-MeC)$_4$(NH_3)(H_2O)](ClO_4)$_2$·1.6H_2O	2.451(1)	2.112(7)	N	156
		2.259(6)	O	

Pictiva EX2004
Samsung v Pictiva
IPR2024-01094

Compound[a]	*r*(Pt–Pt) (Å)	*r*(Pt–L) (Å)[b]	Donor atom(s) L	ref.
cis-2,2-$[Pt_2(1\text{-}MeC)_4(NO_2)]ClO_4\cdot 6H_2O$	2.498(1)	2.044(1)	N	156
$Pt_2(pymS)_4Cl_2$	2.518(1)	2.45[1]	Cl	158
$Pt_2(pymS)_4I_2$	2.554(1)	2.774[6]	I	157
$Pt_2(2\text{-}TU)_4I_2$	2.546(2)	2.771[5]	I	158
$Pt_2(pyS)_4Cl_2\cdot 2CHCl_3$	2.532(1)	2.458(2)	Cl	159
$[Pt_2(5\text{-}MepyS)_4Cl]S_4[Pt_2(5\text{-}MepyS)_4Cl]\cdot 0.5S_8\cdot 2CHCl_3$	2.556(2) 2.558(2)	2.603(7) 2.567(8) 2.435(8) 2.424(9)	Cl Cl S S	161
$[Pt_2(5\text{-}MepyS)_4Br]S_4[Pt_2(5\text{-}MepyS)_4Br]\cdot 0.5S_8\cdot 2CHCl_3$	2.560(2) 2.552(2)	2.705(5) 2.660(6) 2.42(1) 2.41(1)	Br Br S S	161
cis-$Pt_2Cl_6[HN{=}C(OH)CMe_3]_4$[e]	2.694(1)	2.458(3)	Cl	163
cis-$Pt_2Cl_6[(E)HN{=}C(OMe)Me]_4\cdot C_6H_6$[e]	2.765(2)	2.474(7) 2.465(7)	Cl Cl	164
trans-$Pt_2Cl_6[(E)HN{=}C(OH)CMe_3]_4\cdot C_6H_6$[e]	2.758(3)	2.450(6)	Cl	164
$Pt_2(C_8H_{12}(=NO)H)_4Cl_2$[e]	2.696(1)	2.40[1]	Cl	166
$Pt_2(phpy)_4Cl_2$[e]	2.727(1)	2.16[1]	N	165
$Pt_2(OBQDI\text{-}H)_4(CF_3SO_3)_2$[e]	3.031(1)			167

[a] In those cases where a head-to-tail or head-to-head arrangement of *cis* bridging ligands is possible, the actual isomer characterized is denoted by (H,T) or (H,H).

[b] In some cases the average Pt–L lengths are quoted. In these instances the estimated deviation, which is given in square brackets, is calculated as $[\ ] = [\sum_n \Delta_i^2/n(n\text{-}1)]^{1/2}$, in which Δ_i is the deviation of the *i*th of *n* values from the arithmetic mean of the set.

[c] Average value for two crystallographically independent molecules in the unit cell.

[d] Not reported.

[e] This complex contains an unsupported Pt–Pt bond.

Pictiva EX2004
Samsung v Pictiva
IPR2024-01094

14.4.1 Complexes with sulfate and phosphate bridges

The first entirely unequivocal identification of a diplatinum(III) complex was the tetrakis-μ-sulfato derivative $K_2[Pt_2(SO_4)_4(H_2O)_2]$, whose crystal structure was determined but only incompletely reported in 1976.[29] The anion has the same type of sulfato-bridged structure, with two axial water molecules, as that of the $[Re_2(SO_4)_4(H_2O)_2]^{2-}$ ion and several other similar ones. The Pt–Pt distance of 2.466 Å (quoted without an esd) is consistent with the assumption that a single bond, based on a $\sigma^2\pi^4\delta^2\delta^{*2}\pi^{*4}$ configuration, exists between the Pt^{III} atoms. The dinuclear anion is formed in a complex reaction,[29,30] which is said to have the following overall stoichiometry:

$$2Pt(NO_2)_2(NH_3)_2 \xrightarrow{H_2SO_4} (NH_4)_2[Pt_2(SO_4)_4(H_2O)_2] + 2NO + 2NH_4HSO_4$$

This compound has also been prepared by using $K_2[Pt(NO_2)_4]$ in place of $Pt(NO_2)_2(NH_3)_2$.[31] A subsequent redetermination of this structure gave[32] a Pt–Pt bond distance of 2.461(1) Å, essentially identical to the previously reported[29] value. The lability of the axial water molecules is shown[33] by their ease of displacement by dimethylsulfoxide to form $K_2[Pt_2(SO_4)_4(DMSO)_2]$. In this complex the DMSO ligands are O-bound, and the Pt–Pt distance is a little longer (by *c.* 0.01 Å) than in the aquo adduct.[33] From boiling pyridine, yellow crystals of $(pyH)_2[Pt_2(SO_4)_4(py)_2]$ can be isolated.[34] This complex, shown in Fig. 14.3, reacts with a 50% solution of boiling acetic acid for 20 h displacing only two of the four bridging sulfate groups by acetate anions. The axial water molecules in $K_2[Pt_2(SO_4)_4(H_2O)_2]$ can be easily replaced also by heating with pyridazine in aqueous solution but partial reduction also occurs. This gives $[Pt(pydz)_4][Pt_2(SO_4)_4(pydz)_2]$.[35] Further heating cleaves the Pt–Pt bond giving compounds with the $[Pt(pydz)_4]^{2+}$ ion exclusively. Other derivatives with various neutral and monoanionic axial ligands (e.g., NH_3, NH_2CH_3, ROH, Cl^-, Br^-, CN^-, NO_2^-, SCN^- or OH^-) have also been described.[30,31,36,38] Measurements have been made of the ^{195}Pt NMR spectra of several of these complexes.[31,37] Of special interest is the chiral complex $K_2[Pt_2(SO_4)_4(Amb)_2]$, where Amb is the optically active R(-)-2-amino-1-butanol. This adduct has been studied by circular dichroism, IR, XPS and NMR spectroscopies.[38]

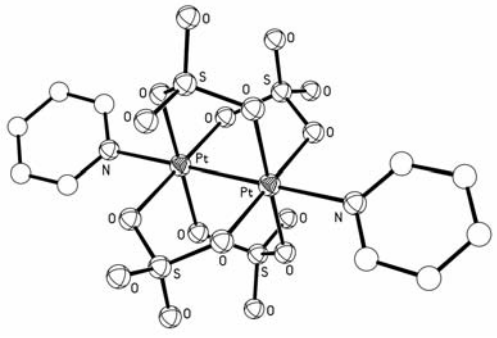


Fig. 14.3. The structure of the $[Pt_2(SO_4)_4(py)_2]^{2-}$ anion.

Several phosphato-bridged diplatinum(III) complexes have also been prepared and structurally characterized. Most of these have been shown to contain the dianionic monohydrogenphosphate ligand $[HPO_4]^{2-}$. The synthesis of a complex purported to be $(NH_4)_2\{(H)_4[Pt_2(PO_4)_4(H_2O)_2]\}$, as well as several of its derivatives in which the H_2O molecules are

Pictiva EX2004
Samsung v Pictiva
IPR2024-01094

replaced by NH_3, py, OH^- or NO_2^-, was first reported in 1980.[39] Compounds with the chiral alcohol R(-)-2-amino-1-butanol (Amb), similar to that of the sulfate reported above,[38] are also known to have formulas $K_2[Pt_2(HPO_4)_4(Amb)_2](Amb)$, $NH_4(Amb)[Pt_2(HPO_4)_4(Amb)_2]$-(Amb) and $(AmbH)_2[Pt_2(HPO_4)_4(Amb)_2](Amb)$. The synthetic strategy for the preparation of $[Pt_2(HPO_4)_4L_2]^{2-}$, which is similar to that used to prepare $[Pt_2(SO_4)_4]^{2-}$, involves the reaction of *cis*- or *trans*-$Pt(NO_2)_2(NH_3)_2$ with concentrated H_3PO_4, usually with heating.[32,39,40] The use of $K_2[Pt(NO_2)_4]$ in place of $Pt(NO_2)_2(NH_3)_2$ has also been advocated.[31] The structural identity of these compounds has been established from crystal structure determinations[32,41-43] on several salts of the type $M_2^{II}[Pt_2(HPO_4)_4(L)_2]$, the results of which are summarized in Table 14.1. Detailed studies have been made of the stepwise displacement of the H_2O molecules in $[Pt_2(HPO_4)_4(H_2O)_2]^{2-}$ by halide (Cl^- and Br^-),[44] and various amine, thioether and thiolato ligands[43] and rate constant data and equilibrium constants determined for several of these systems. In these studies,[43,44] use was made of the sensitivity of the metal-based $\sigma\rightarrow\sigma^*$ transition to the nature of the axial ligand. For example, in the cases where L is H_2O, py, Cl^-, Br^- and I^-, this band is at 224, 294, 296, 342 and 410 nm, respectively.[43,44] Luminescence from the $d\sigma^*$excited state of $[Pt_2(HPO_4)_4(H_2O)_2]^{2-}$ and $[Pt_2(HPO_4)_4X_2]^{4-}$ (X = Cl or Br) has been studied[45] for solids and low-temperature solution glasses. ^{195}Pt NMR spectral measurements on adducts of $[Pt_2(HPO_4)_4]^{2-}$, including those where the two axial ligands are different, show[31,37] that ^1J(Pt–Pt) is always larger in magnitude than for the corresponding sulfato-bridged complexes, although ν(Pt–Pt) from the Raman spectra and X-ray structural data do not indicate a stronger Pt–Pt bond.

In a few instances, diplatinum(III) complexes have been isolated that contain monoanionic dihydrogenphosphato $[H_2PO_4]^-$ bridges. Complexes of the type $(BH)[Pt_2(H_2PO_4)$-$(HPO_4)_3(B)_2]\cdot H_2O$, where B = pyridine, 4-methylpyridine or 3,4-dimethylpyridine, are apparently present as minor contaminants in the complexes of stoichiometry $(BH)_2[Pt_2(HPO_4)_4(B)_2]$ that are formed by reacting these heterocyclic tertiary amines with phosphoric acid solutions of $[Pt_2(HPO_4)_4]^{2-}$.[40] However, when 4-phenylpyridine is used as the base (4-PhpyH)-$[Pt_2(H_2PO_4)(HPO_4)_3(4\text{-Phpy})_2]\cdot H_2O$ is the major product.[40] During attempts to grow single crystals of $(pyH)[Pt_2(HPO_4)_4(py)_2]$, a crystalline sample of $(pyH)[Pt_2(H_2PO_4)$-$(HPO_4)_3(py)_2]\cdot H_2O$ was obtained and structurally characterized.[40] Subsequently, crystals of the bis-dihydrogenphosphato complex $(Et_4N)_2[Pt_2$-$(H_2PO_4)_2(HPO_4)_2Cl_2]\cdot H_2O$ were obtained upon treating $(NH_4)_2[Pt_2(HPO_4)_4(H_2O)_2]$ with Et_4NCl in water.[32] The measured Pt–Pt distance (Table 14.1) is one of the longest of all the structurally characterized phosphato (and sulfato) bridged diplatinum(III) anions.

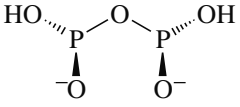
The reaction of $Na_2[Pt_2(HPO_4)_4(H_2O)_2]$ with the ligand guanine (guH_2) gives the complex $Na_2[Pt_2(HPO_4)_4(guH_2)_2]$,[43] which upon dissolution in aqueous NaOH has been found[46] to afford crystals of composition $Na_{10}[Pt_2(PO_4)_4(C_5H_3N_5O)_2]\cdot 22H_2O$, where $C_5H_3N_5O$ is the dianion of guanine. This complex is the first example[46] of a structurally characterized diplatinum(III) complex with a fully deprotonated phosphate bridge.

Other than studies of the substitutional lability of the axial ligands of the aforementioned diplatinum(III) phosphate complexes, investigations of their reactivity have been limited. The salt $(NH_4)_2[Pt_2(HPO_4)_4(H_2O)_2]$ reacts with concentrated H_2SO_4 to afford the corresponding sulfate derivative $(NH_4)_2[Pt_2(SO_4)_4(H_2O)_2]$.[40] Other reactions have demonstrated that the Pt–Pt bond is subject to reductive cleavage. Thus, the reaction of $(pyH)_2[Pt_2(HPO_4)_4(py)_2]$ with PPh_3 in water gives a product that has been formulated as $Pt_2(HPO_4)_3(PPh_3)_3(H_2O)_2$, whereas in refluxing glacial acetic acid this reaction proceeds further to give mononuclear $Pt(O_2CCH_3)_2(PPh_3)_2$.[40] The complex $Pt(CN)_2(CNBu^t)_2$ is formed[40] when $(pyH)_2[Pt_2(HPO_4)_4(py)_2]$ is treated with Bu^tNC in refluxing methanol.

Pictiva EX2004
Samsung v Pictiva
IPR2024-01094

14.4.2 Complexes with pyrophosphite and related ligands

Another very important class of diplatinum(III) complexes are those that contain the dianionic pyrophosphite ligand $[P_2O_5H_2]^{2-}$ shown as **14.3**. This chemistry has its origins in the important discovery of the non-metal-metal-bonded diplatinum(II) complex $K_4[Pt_2(P_2O_5H_2)_4]\cdot 2H_2O$ by Roundhill and co-workers[47] in 1977. This compound, which is usually referred to as "platinum pop", is prepared by the reaction of K_2PtCl_4 with phosphorous acid.[47,48] Some minor modifications in the original procedure have been recommended,[49] and this procedure has also been adapted for the synthesis of other salts of the type $M^I_4[Pt_2(pop)_4]$ (M^I = Na^+, $Bu^n_4N^+$, Ph_4As^+ or $\frac{1}{2}Ba^{2+}$)[49] as well as the corresponding derivative with the dianion of methylenebis(phosphinic acid), $CH_2[PH(O)(OH)]_2$, (pcpH), which is of composition $K_4[Pt_2(pcp)_4]\cdot 6H_2O$.[50,51] Several properties of these complexes have proven to be of great interest, including the excited-state chemistry of $[Pt_2(pop)_4]^{4-}$ which appears to be[18,52,53] the richest of that exhibited by any d^8-d^8 complex. However, of most significance to the subject of our monograph is the ease of the oxidation of $[Pt_2(pop)_4]^{4-}$ and $[Pt_2(pcp)_4]^{4-}$ to diplatinum(III) species.



14.3

The thermal and photochemical oxidative-additions of halogens (Cl_2, Br_2, I_2)[49,54-56] and alkyl[54,57] and aryl halides[57] to $[Pt_2(pop)_4]^{4-}$ provide a ready route to diplatinum(III) complex anions of the types $[Pt_2(pop)_4X_2]^{4-}$ and $[Pt_2(pop)_4(R)X]^{4-}$, several of which have been structurally characterized (Table 14.1).[54,58-62] The electrochemical oxidation of $[Pt_2(pop)_4]^{4-}$ in the presence of X^- also provides a means of generating $[Pt_2(pop)_4X_2]^{4-}$,[63] while the photolysis of $[Pt_2(pop)_4]^{4-}$ in methanolic solutions of $CHCl_3$ and CCl_4 produces $[Pt_2(pop)_4Cl_2]^{4-}$,[64] as does the thermal reaction of $[Pt_2(pop)_4]^{4-}$ with NOCl.[65] The analogous halogen-containing pcp species $[Pt_2(pcp)_4X_2]^{4-}$ are prepared from the reactions of $[Pt_2(pcp)_4]^{4-}$ with X_2 (X = Cl, Br or I), and the complex $K_4[Pt_2(pcp)_4Cl_2]\cdot 8H_2O$ has been structurally characterized by X-ray crystallography.[51] The lability of the axial halide ligand sites in $[Pt_2(pop)_4X_2]^{4-}$ has been used[49,55,56] as a means to generate mixed-halide species of the type $[Pt_2(pop)_4XY]^{4-}$.

Other diplatinum(III)-pop complexes have been prepared from the reactions between $[Pt_2(pop)_4]^{4-}$ and various nucleophiles under oxidizing conditions (e.g., the presence of O_2 or H_2O_2). By this means, salts of the types $[Pt_2(pop)_4X_2]^{4-}$ (X = NO_2^- or SCN^-) and $[Pt_2(pop)_4L_2]^{2-}$ (L = H_2O, nicotinamide, py or CH_3CN) have been prepared,[49,66,67] and several have been crystallographically characterized (Table 14.1).[66,67] As an alternative means of synthesizing the bis-nitrito complex, the reaction between $[Pt_2(pop)_4]^{4-}$ and NO_2 can be used.[65] Interestingly, when attempts were made to grow single crystals of a salt of this complex anion by the reaction of an acidic solution of $K_4[Pt_2(pop)_4]\cdot 2H_2O$ with $NaNO_2$ in a sealed tube over a period of 30 days, the product turned out to be of composition $Na_8[Pt_2(pop\text{-}H)_4(NO_2)_2]\cdot 18H_2O$, and contained the monodeprotonated pop ligand.[65] However, the anion is structurally very similar to that of $[Pt_2(pop)_4(NO_2)_2]^{4-}$ as characterized in the salt $K_4[Pt_2(pop)_4(NO_2)_2]\cdot 2KNO_2\cdot 2H_2O$.[66] The reactions of $[Pt_2(pop)_4(NO_2)_2]^{4-}$ with Cl^- or Br^- give $[Pt_2(pop)_4(NO_2)X]^{4-}$, while the reaction of 1 equiv of *N*-iodosuccinimide produces $[Pt_2(pop)_4(NO_2)I]^{4-}$.[65] When $[Pt_2(pop)_4(NO_2)_2]^{4-}$ is treated with CO the following redox reaction is believed[65] to occur:

$$[Pt_2(pop)_4(NO_2)_2]^{4-} + 2CO \rightarrow [Pt_2(pop)_4]^{4-} + 2NO + 2CO_2$$

Pictiva EX2004
Samsung v Pictiva
IPR2024-01094

There is no evidence for the stabilization of diplatinum(III) by the nitrosyl ligand.[65] Indeed, the reaction of $[Pt_2(pop)_4]^{4-}$ with NOCl produces only $[Pt_2(pop)_4Cl_2]^{4-}$.

Crystal structure data for the pyrophosphito-bridged and methylenebis(phosphito)-bridged diplatinum(III) complexes (Table 14.1) reveal closely related structures in all cases (see, for example, Fig. 14.4). These differ only to the extent of having either P–O–P (for pop) or P–CH_2–P (for pcp) bridgehead units. The Pt–Pt distances, which vary over a range of about 0.1 Å (i.e. 2.676(1) Å to 2.782(1) Å), are shorter than the distances of 2.925(1) Å and 2.9801(2) Å in the diplatinum(II) analogs $K_4[Pt_2(pop)_4]\cdot 2H_2O$[68,69] and $K_4[Pt_2(pcp)_4]\cdot 6H_2O$,[51] respectively. The variations in Pt–Pt distances reflect a *trans* influence of the axial ligands. The P–O bond distances fall into three classes: P–OH, P=O and P–O(bridging). The terminal P–O groups are linked through O–H···O hydrogen bonds around the periphery of each planar PtP_4 unit (see Fig. 14.4). In the case of $Na_8[Pt_2(pop\text{-}H)_4(NO_2)_2]\cdot 18H_2O$, which contains singly deprotonated pop ligands,[65] the hydrogen-bonding network is more complicated and the Na^+ ions are variously O–bonded to terminal P–O and H_2O groups.

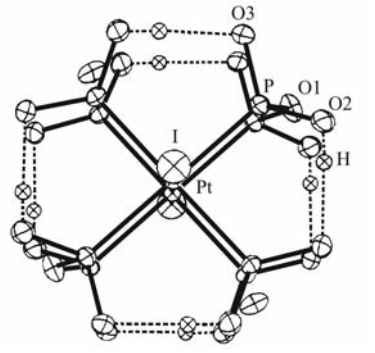


Fig. 14.4. The structure of the $[Pt_2(pop)_4I_2]^{4-}$ anion as viewed down the Pt–Pt bond showing the O–H···O bonding around the periphery of each PtP_4 unit.

The spectroscopic properties of these diplatinum(III) complexes have proven to be of considerable interest. Several studies have focused on the electronic absorption[49,51,54,57,66,67] (including the MCD)[70] and vibrational spectra,[59,71,72] with a particular focus upon the $d\sigma \rightarrow d\sigma^*$ electronic transition and the influence of the axial ligands upon it and the vibrations of the X–Pt–Pt–X unit. Both ν(Pt–Pt) and ν(Pt–X) (X = halide) vibrations have been assigned. NMR spectral characterizations (especially the ^{195}Pt and ^{31}P spectra) have also attracted attention.[51,57,65] Although electronic emission from singly-bonded d^7-d^7 complexes does not normally occur, salts of $[Pt_2(pop)_4X_2]^{4-}$ (X = Cl, Br, SCN) and $[Pt_2(pop)_4(py)_2]^{2-}$ have been found[73] to exhibit strong red luminescence at 77 K.

The $d\sigma^*p\sigma$ ($^3A_{2u}$) excited state of $[Pt_2(pop)_4]^{4-}$ is a powerful one-electron reductant.[18] Among its many interesting reactions are those with various hydrogen donors[74-77] to give $[Pt_2(pop)_4H_2]^{4-}$. Detailed NMR and IR spectroscopic studies[77] show that like other diplatinum(III)-pop complexes with X–Pt–Pt–X units, this compound possesses a linear H–Pt–Pt–H unit. Among the reactions of the electronically excited state of $[Pt_2(pop)_4]^{2-}$ is that with HNO_3 in which NO_2^- is formed.[78] The species $[Pt_2(pop)_4]^{3-}$ and $[HNO_3]^-$ have been identified as intermediates. This same mixed-valence Pt_2^{5+} species $[Pt_2(pop)_4]^{3-}$ has also been formed by the photoionization of $[Pt_2(pop)_4]^{4-}$ in aqueous solution and by its thermal reaction with $OH^\bullet$ radicals generated by pulse radiolysis.[79] This unstable species has been spectroscopically characterized but it rapidly disproportionates to $[Pt_2(pop)_4]^{4-}$ and $[Pt_2(pop)_4]^{2-}$.[79] Interestingly, pulse radiolysis

Pictiva EX2004
Samsung v Pictiva
IPR2024-01094

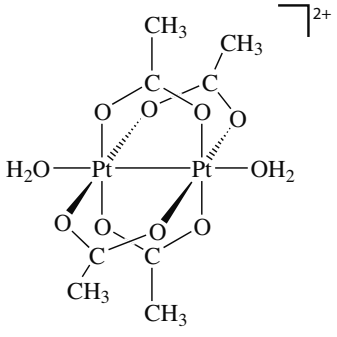
has also been used[80] to reduce aqueous solutions of several diplatinum(III) complexes to their Pt_2^{5+} congeners.[81] The species $[Pt_2(pop)_4X_2]^{4-}$ (X = Cl, Br, SCN, imidazolyl) and $[Pt_2(pop)_4(1\text{-MeIm})_2]^{2-}$ (1-MeIm = 1-methylimidazole) have been reduced by this means; they exhibit a very characteristic, intense $\sigma \rightarrow \sigma^*$ transition in the near-UV region (X = 1-MeIm or Im, 310; Cl, 330; Br, 370; SCN, 390 nm).[80] The UV-visible irradiation of these $[Pt_2(pop)_4X_2]^{4-}$ species in methanol leads to reduction to $[Pt_2(pop)_4]^{4-}$ in essentially quantitative yield.[82] In a similar context, irradiation at 313 nm into the $\sigma \rightarrow d\sigma^*$ absorption band of $[Pt_2(pop)_4H_2]^{4-}$ quantitatively produces $[Pt_2(pop)_4]^{4-}$ and H_2.[77] The thermal chemistry of $[Pt_2(pop)_4H_2]^{4-}$ includes its reactions with HCl and DCl to produce H_2 and HD.[77]

A class of mixed-valence Pt_2^{5+} complexes that have attracted attention are the potassium salts of composition $K_4[Pt_2(pop)_4X]\cdot 3H_2O$ (X = C1, Br, I). These are described in Section 14.4.6.

14.4.3 Complexes with carboxylate, formamidinate and related ligands

In contrast to the proclivity of the singly-bonded Rh_2^{4+} species to be stabilized by a wide range of carboxylate bridging ligands, the isoelectronic Pt_2^{6+} species are rare. The only authentic, simple diplatinum(III) carboxylates that have been structurally characterized are of the type $[Pt_2(O_2CCH_3)_4(H_2O)_2]X_2$, X = ClO_4[83,84] and CF_3SO_3.[83] The cation is represented as 14.4. The corresponding Pt–Pt distances of 2.391(1) and 2.393(1) Å are the shortest distances known for any Pt_2^{6+} species (Table 14.1). The perchlorate compound has been prepared by reaction of $K_2[Pt_2(NO_2)_4]$ and a 1:1 mixture (by volume) of acetic acid and 1 M perchloric acid while carefully controlling the temperature at 100 °C for 4 h:

$$K_2[Pt(NO_2)_4] \xrightarrow[100\ ^\circ C]{CH_3COOH/HClO_4} [Pt_2(CH_3COO)_4(H_2O)_2](ClO_4)_2$$



14.4

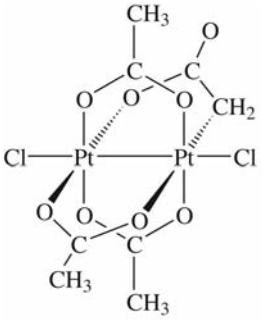
It is noteworthy that use of a mixture of acetic acid and perchloric acid is very important for the success of the reaction. Otherwise mixtures of compounds having Pt in oxidation states of 2, 3 and 4 are observed.[85] Nitric acid is also useful but the yield of the corresponding nitrate is lower and the product is sometimes contaminated with $K_2[Pt(NO_2)_6]$. As in the sulfate and phosphate analogs, the axial water molecules can be substituted by a series of donor molecules such as DMF, SMe_2 and pyridine or anions such as Cl^- and Br^-. The substitution reactions have been followed by ^{195}Pt and ^{13}C NMR spectroscopy.[83] Preparation of $Pt_2(CH_3COO)_4Cl_2$ has been accomplished in nearly 100% yield by reaction of $[Pt_2(CH_3COO)_4(H_2O)_2](CF_3SO_3)_2$ and $SOCl_2$.[86]

The compound $Pt_2(O_2CCH_3)_6$ has also been claimed[87] as a product of the reaction of $K_2Pt(OH)_6$ with formic acid in glacial acetic acid. The analogous trifluoroacetate, $Pt_2(O_2CCF_3)_6\cdot 4H_2O$, as

Pictiva EX2004
Samsung v Pictiva
IPR2024-01094

well as the mixed acetate-trifluoroacetate of composition $Pt_2(O_2CCH_3)_3(O_2CCF_3)_3$ have also been reported.[88] The reaction conditions that are used for the preparation of $Pt_2(O_2CCH_3)_6$ can apparently be modified to produce materials that have been formulated as $Pt_4(O_2CCH_3)_4(OH)_8(H_2O)_4$,[89] $Pt_4(O_2CCH_3)_{10}(OH)_2$[90] and $Pt_4(O_2CCH_3)_4(OH)_8(H_2O)_2$.[90] The last two of these have been characterized by the EXAFS technique.[89] These tetranuclear formulations, if correct, may accord with a similar nuclearity for the 'parent' platinum(III) acetate, viz $Pt_4(O_2CCH_3)_{12}$, a possibility that is supported[87] by molecular weight measurements. It is noteworthy that platinum(II) acetate is tetranuclear $Pt_4(\mu\text{-}O_2CCH_3)_8$, with short Pt–Pt distances (2.49-2.50 Å).[91] The correctness of these earlier structural conclusions remains clouded.

Another structurally characterized diplatinum(III) acetate complex is encountered in the salt $Cs_3[Pt_2(\mu\text{-}O_2CCH_3)_2(\mu\text{-}CH_2COO\text{-}C,O)_2Cl_2]Cl\cdot 3H_2O$,[92] (**14.5**) in which there are two *cis* bridging O,O-bound acetate ligands as well as two singly deprotonated ones that have an unusual C,O-bridging mode. This complex, which was isolated in very low yield from a $K_2PtCl_4/CH_3CO_2Ag/CH_3CO_2H–H_2O$ (10:1) reaction mixture,[92] has ^1H and ^{13}C NMR spectra that are fully consistent with this structural result. The Pt–Pt distance of 2.451(1) Å is slightly longer than those mentioned above where all carboxylate groups are bound through the oxygen atoms.



14.5

Many dithiocarboxylates $Pt_2(S_2CR)_4X_2$ (X = Cl, Br, I) have been prepared and structurally characterized.[93-95] Treatment of the diplatinum(II) complexes $Pt_2(S_2CR)_4$[95,96] with the halogens gives diamagnetic $Pt_2(S_2CR)_4X_2$ compounds (R = CH_3, for X = Cl and Br, and R = CH_3, $(CH_3)_2CH$, CH_2Ph or C_2H_5 for X = I).[93-95] The iodo complexes where R = $(CH_3)_2CH$,[94] CH_2Ph,[94] and C_2H_5[95] have been structurally characterized and found to have Pt–Pt distances of 2.598(2), 2.578(1) and 2.582(2) Å, respectively. By adjusting the stoichiometry of the $Pt_2(S_2CCH_3)_4/I_2$ reaction, the mixed-valence compound $Pt_2(S_2CCH_3)_4I$ can be isolated.[93,95] This work is described in Section 14.4.6.

Several diplatinum(III) complexes of stoichiometry $Pt_2(O_2CR)_2R'_4(SR"_2)_2$ that contain a pair of *cis* bridging carboxylate ligands (R = CH_3, CF_3 or $(CH_3)_2CH$), four equatorial alkyl or aryl groups (R' = CH_3, Ph or *p*-tolyl) and two axial thioether ligands (R" = Et, Pr^n or Pr^i) have been prepared[97,98] by the oxidation of $Pt_2(\mu\text{-}SR"_2)_2(CH_3)_4$ with AgO_2CR, $Hg(O_2CR)_2$ or $Tl(O_2CCH_3)_3$. The axial thioether ligands can be replaced by pyridine, 4-methylpyridine, $PhNH_2$ or Cl^-, giving $Pt_2(O_2CR)_2R'_4L_2$ complexes. The structural identity of these compounds has been substantiated by crystal structure determinations of *cis*-$Pt_2(O_2CCF_3)_2(CH_3)_4(4\text{-Mepy})_2$[99] and *cis*-$Pt_2(O_2CCH_3)_2(CH_3)_4(py)_2$.[100] When PEt_3 or $P(OMe)_3$ are reacted with $Pt_2(O_2CCH_3)_2R'_4(SR"_2)_2$, the 1:1 adducts $Pt_2(O_2CCH_3)_2R'_4(PR_3)$ are formed.[98] These probably have asymmetric structures with one Pt center six coordinate and the other five coordinate.

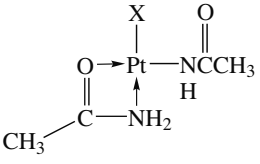
Pictiva EX2004
Samsung v Pictiva
IPR2024-01094

There are only two paddlewheel compounds having a Pt_2^{6+} core surrounded by four bridging ligands having *all-N* donor atoms. These are the formamidinate complex $Pt_2(DPhF)_4Cl_2$ which has a rather long Pt–Pt distance of 2.517(1) Å[86] and the guanidinate compound $Pt_2(hpp)_4Cl_2$ that has a significantly shorter Pt–Pt distance of 2.438(1) Å.[101,102] The latter is just slighly longer than those in the carboxylate analogs mentioned above (Table 14.1). The formamidinate compound has been prepared using a reaction of $Pt_2(CH_3COO)_4Cl_2$ and molten HDPhF according to:

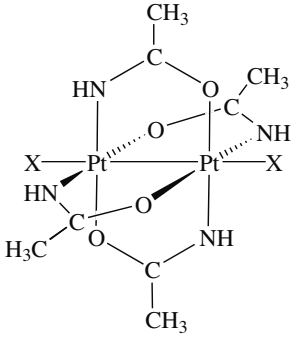
$$Pt_2(CH_3COO)_4Cl_2 + 4HDPhF \xrightarrow{\Delta} Pt_2(DPhF)_4Cl_2 + 4CH_3COOH$$

14.4.4 Complexes containing monoanionic bridging ligands with N,O and N,S donor sets

There are some *amidate* analogs of the $Pt_2(CH_3COO)_4X_2$ compounds described above. This is a group of compounds for which the existence of a Pt–Pt bond had been proposed but direct proof had been lacking until recently. This story goes back to the early 1950s when a series of what were then assumed to be acetamido-Pt(II) complexes was reported.[103] Formulae such as **14.6** were suggested. However, in 1967, it was proposed,[104] without evidence, that the compounds are in fact diplatinum(III) compounds with structures such as **14.7.** Subsequently, XPS studies[105] provided evidence that the platinum atoms are equivalent and in oxidation state +3. Thus, in six compounds the binding energies (Pt $4f_{7/2}$, eV) were 75.0 ± 0.2, while the typical values for Pt^{II} and Pt^{IV} are 73.6 ± 0.8 and 76.3 ± 1.5, respectively. A value of 75.2 eV has been found for the sulfato compound $K_2[Pt_2(SO_4)_4(H_2O)_2]$.[106] An analysis of the radial distribution functions, obtained from the X-ray powder diffraction patterns, has been used[107] to determine the structure of the nitrito derivative $Pt_2(CH_3CONH)_4(NO_2)_2$. The structure was concluded to be as represented in **14.7**, except that the disposition of equatorial ligands about each Pt atom gives a *trans*-PtN_2O_2 geometry. The Pt–Pt distance was reported to be 2.455 Å.[107]



14.6



14.7

Another synthetic procedure for the preparation of $Pt_2(CH_3CONH)_4Cl_2{\cdot}2H_2O$ involves the reaction at 90 °C for 16 h of an amide and a 1:1 mixture of K_2PtCl_6 and K_2PtCl_4 in aqueous solution.[108] In these complexes axial ligands are labile and they can be replaced by other donor groups, e.g., pyridine.

The first compound of this class to be fully characterized crystallographically was $Pt_2(CH_3CONH)_4I_2$. It has a Pt–Pt distance of 2.473(2) Å.[109] The chloro derivative having pivaloamide bridges is also known and has a metal-metal distance of 2.448(2) Å.[110] These distances are short but slightly longer than those in the acetate analogs (Table 14.1). In the

Pictiva EX2004
Samsung v Pictiva
IPR2024-01094

two compounds interstitial water molecules help stabilize the crystal by forming a complex network of hydrogen bonds. In the solid state the compounds are symmetrical with two *cis* amidate ligands having the nitrogen atoms pointing in one direction and the other two cis ligands having the oxygen atoms pointing in the same direction as the nitrogen atoms of the other ligands. However, isomers are observed in the NMR spectra. In the presence of halogens, the acetamidate ligands retain the binuclear Pt_2^{6+} cores at low temperature but halogenation occurs at the methyl and NH group of the acetamidate ligand.[111] At higher temperature further oxidation to Pt^{IV} species occurs.

The axially coordinated halide ions are substituted by the neutral ligands triphenylphosphine or water after reaction with $AgNO_3$.[112] In this way, compounds with formulae $[Pt_2(PPh_3)_2(RCONH)_4](NO_3)_2$, R = CH_3, Bu^t and $[Pt_2(H_2O)(PPh_3)(Bu^tCONH)_4](NO_3)_2$ have been prepared. The corresponding Pt–Pt distances for the Bu^t derivatives are 2.504(1) and 2.468(1) Å.[112] In solution, these compounds form isomers differing in the arrangement of the sets of equatorial ligands around each platinum atom, N^3O/NO^3 or N^2O^2, and for the latter there are *cis* and *trans* arrangements.

Reactions of $Pt_2(CH_3CONH)_4X_2$, X = Cl and I, with aqueous ethylenediamine solutions give the mixed acetamido-ethylenediamine complexes *cis*-$[Pt_2(CH_3CONH)_4(en)_2]X_2$. The crystal structure of the iodide has been determined (Fig. 14.5).[113] There are two acetamidato bridges in a *cis* disposition to one another, two monodentate, monodeprotonated acetamide ligands and two chelating en ligands that show equatorial and axial binding. The Pt–Pt distance of 2.566(1) Å is significantly longer than those of the precursors, a common occurrence in dimetal complexes that have less than four bridging ligands. An even longer Pt–Pt distance of 2.609(1) Å is found in *cis*-$[Pt_2(Bu^tCONH)_2(NH_3)_4(NO_2)(NO_3)]$.[114] The interaction of *cis*-$[Pt_2(CH_3CONH)_4(en)_2]Cl_2$ with chlorine has been studied at room temperature and on heating. In both cases the Pt_2^{6+} core is retained but chlorination occurs at the methyl group at room temperature but on heating replacement of the H atom of the NH group occurs also.[115] Several platinum acetamide complexes, including some where the ethylenediamine ligands have been replaced by bipyridine, have been studied by XAFS photoelectron spectroscopy and other techniques such as XANES and EXAFS.[116]

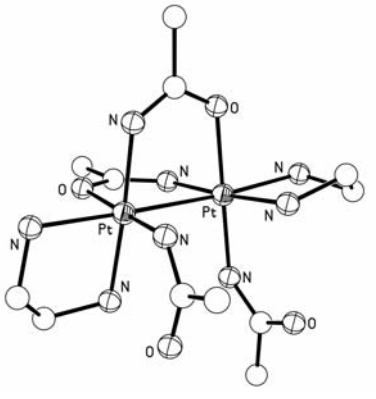
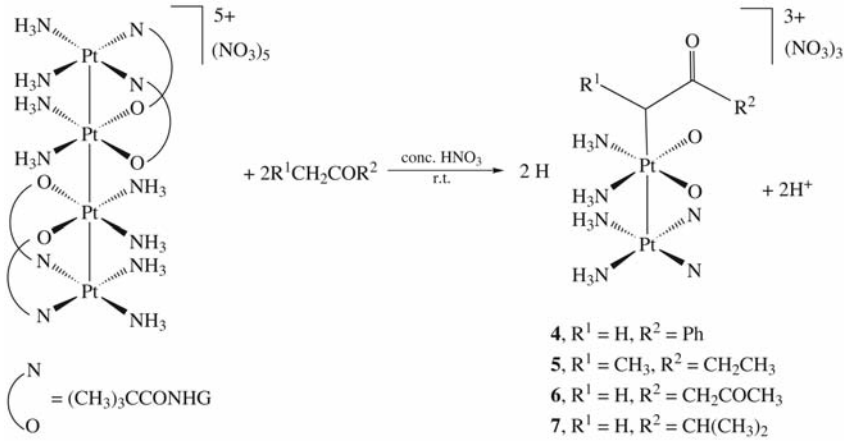


Fig. 14.5. The structure of the $[Pt_2(CH_3CONH)_4(en)_2]^{2+}$ cation, where en = ethylendiamine.

There is also an extensive *organometallic chemistry* of amidate-bridged, singly-bonded Pt_2^{6+} species, particularly where the bridges are pivalamidate (Bu^tCONH). These compounds commonly contain cations of the type *cis*-$[Pt_2(Bu^tCONH)_2(NH_3)_4(alkyl)]^{3+}$. In one axial position

Pictiva EX2004
Samsung v Pictiva
IPR2024-01094

there is an alkyl group with a strong Pt–C bond; the other axial position is generally empty or occupied by a very weakly bound anion such as nitrate. These studies have been done primarily in K. Matsumoto's laboratory and have been reviewed recently.[117,118] Most of these compounds are made by reaction of the platinum blue species $[Pt_4(Bu^tCONH)_4(NH_3)_4]^{5+}$ (see Section 14.4.7). For example, reaction with ketones in the presence of either HNO_3 or $Na_2S_2O_8$ gives the corresponding ketonylplatinum^{III} complexes according to:



When the ketone has two α-C–H bonds, a mixture of isomers is possible. Several of these compounds have been structurally characterized (Table 14.1).[114,119,120] One example is shown in Fig. 14.6. In general, there is a strong trans effect of the Pt–Pt bond that makes the $Pt–O_{(nitrate)}$ separation very long (more than 2.6 Å.) This is significantly longer than typical $Pt–O_{(nitrate)}$ distances of 2.16-2.36 Å found in other complexes with Pt_2^{6+} cores.

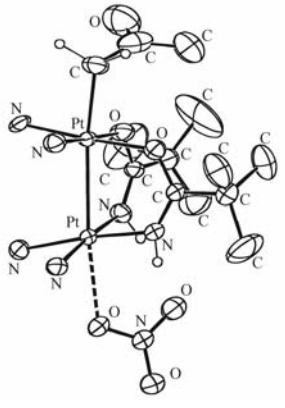
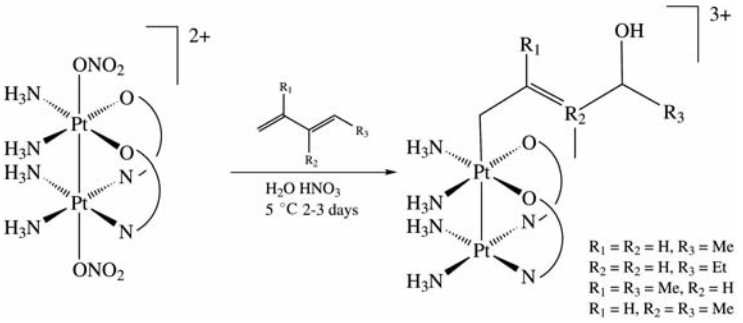


Fig. 14.6. The structure of the cation in the organometallic compound *cis*-$[Pt_2(Bu^tCONH)_2(NH_3)_4(CH_2COCH_3)(NO_3)](NO_3)_2$.

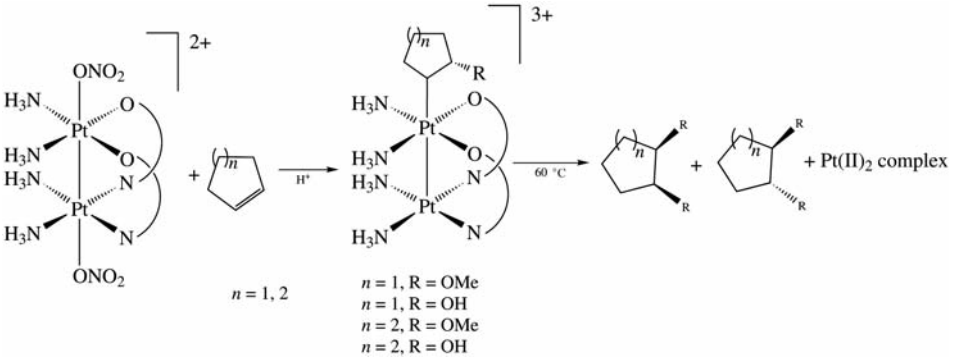
Structurally characterized Pt–C bonds can be made also by reaction of *cis*-$Pt_2(Bu^tCONH)_2(NH_3)_4(NO_3)_2$ with olefins,[121] 1,3 conjugated dienes[122] and alkynes[123] in aqueous solution. With dienes, the 4-hydroxy-(*E*)-2-alkenyl-Pt^{III} dinuclear complexes are formed. In these compounds, the α-carbon atom of the axially coordinated alkenyl ligand bound to the

Pictiva EX2004
Samsung v Pictiva
IPR2024-01094

Pt^{III} atom is electrophilic and is easily attacked by water to release (*E*)-2-alkene-1,4,diol. Some reactions are summarized in the equation below:



With monoolefins such as cyclopentane or cyclohexane, double nucleophilic attacks by methanol and water occurs according to:

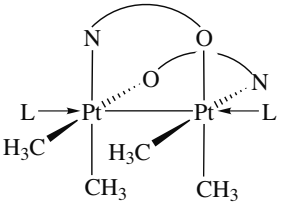


Mechanistic studies of ketone and alcohol formation from alkenes and alkynes,[124] and of axial ligand substitution reactions of the olefin derivatives with *p*-styrenesufonate or 4-pentanediol,[125] and of replacement of various axial ligands with halide ions[126] have been published.

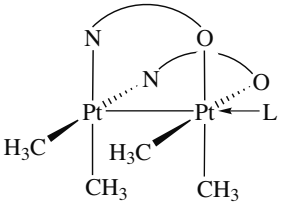
The type of structure shown in Fig. 14.5 in which there are only two bridging ligands in a *cis* arrangement is actually quite common for diplatinum(III). Thus it is not surprising that the bis-μ-carboxylato complexes of the general type $Pt_2(O_2CR)_2R'_4L_2$ that were mentioned in the preceding section have analogs in which various *2-hydroxypyridinato* (also known as α-pyridonato) ligands replace the acetates.[100,127-129] The reactions of $Pt_2(\mu\text{-}SEt_2)_2(CH_3)_4$ and Ag(Xhp), where Xhp represents the monoanion of 2-hydroxypyridine (hp), 2-hydroxy-6-fluoropyridine (fhp), 2-hydroxy-6-chloropyridine (chp), 2-hydroxy-6-bromopyridine (bhp) or 2-hydroxy-6-methylpyridine (mhp), in benzene followed by filtration and the addition of pyridine affords[100,127] the pyridine adducts $Pt_2(Xhp)_2(CH_3)_4(py)_n$, with $n = 2$ for X = H or F and $n = 1$ for X = Cl, Br or CH_3. For all five complexes there is a *cis* arrangement of bridging Xhp ligands, with the details of the geometry and stoichiometry being dependent upon the size of X.[100,127] When X is relatively small (H or F) the complex contains a non-polar arrangement (head-to-tail) of bridging ligands and has both axial positions occupied (**14.8**). An increase in the size of X (to Cl, Br or CH_3) leads to a polar (head-to-head) arrangement of *cis* bridging Xhp ligands with only one axial site occupied by pyridine, namely, that which is less sterically congested and involves the Pt center which is coordinated by two O atoms from the Xhp ligands (**14.9**).

Pictiva EX2004
Samsung v Pictiva
IPR2024-01094

When the bis-pyridine adducts $Pt_2(hp)_2(CH_3)_4(py)_2$ and $Pt_2(fhp)_2(CH_3)_4(py)_2$ are subjected to chromatography on a silica gel column they convert to the polar head-to-head monopyridine adducts,[127] a conversion that can be reversed upon treatment of the latter with pyridine. The analogous 1:1 adducts with diethylsulfide have also been isolated for the bis-hp, fhp and mhp complexes, and all have been structurally characterized (Table 14.1). These have the expected head-to-head arrangement of Xhp ligands. NMR spectral properties have been used[129] to determine the formation constants of the 1:2 pyridine adducts from the reactions of the 1:1 head-to-head isomers with pyridine. It has been suggested[129] that the head-to-head → head-to-tail rearrangement may involve a pre-equilibrium with pyridine, and the opening of a Xhp bridge followed by its rearrangement. A mechanism involving rupture of the Pt–Pt bond is not favored.



14.8



14.9

It should be noted that the beginnings of this chemistry had its origins in efforts during the early 1980s to unravel the structural secrets of the oligomeric platinum blues (see Section 14.4.7). In a series of reports that were published in the period 1981-83, Stephen J. Lippard and co-workers described[130-133] the synthesis of several diplatinum(III) species of the type $[Pt_2(hp)_2(NH_3)_4XY]^{n+}$,where $n = 3$ when X = H_2O and Y = NO_3, and $n = 2$ when X = Y = NO_3, NO_2, Cl or Br, by the chemical oxidation of *cis*-diammineplatinum α-pyridone blue with nitric acid,[130,132] or the oxidation of the diplatinum(II) complex $[Pt_2(hp)_2(NH_3)_4](NO_3)_2{\cdot}2H_2O$ with nitric acid, either alone[130-132] or in the presence of NO_2^-, Cl^- or Br^-.[133] The structural characterization of these compounds (Table 14.1) shows that all of them have very similar structures, with *cis* bridging hp ligands that are in a head-to-tail arrangement except when the axial ligands are different (i.e. X = H_2O when Y = NO_3). The structure of the latter complex cation is shown in Fig. 14.7. The Pt–Pt bond lengths are dependent upon the nature of the axial ligands and follow the order $Br^- \approx NO_2^- > Cl^- > NO_3^-$,[133] a trend that parallels the known *trans*-influence for these ligands. An electrochemical study on the head-to-tail nitrate isomer shows[132] that it undergoes a concerted two-electron reversible reduction, the Pt_2^{6+} and Pt_2^{4+} species being cleanly interconverted upon controlled potential electrolysis. For the head-to-head isomer the reduction takes place in two one-electron steps which differ by 50 mV; exhaustive electrolytic reduction of this complex forms the corresponding α-pyridone blue.[132]

The mixed nitrito-nitrato complex *cis*-$[Pt_2(hp)_2(en)_2(NO_2)(NO_3)](NO_3)_2{\cdot}0.5H_2O$, which possesses a head-to-head arrangement of *cis* bridging hp ligands, is formed[134] upon oxidation of $[Pt_2(hp)_2(en)_2](NO_3)_2$ with nitric acid or $NaNO_2$ in nitric acid; the second method gives the higher yield. The complex retains its structure in freshly prepared aqueous or DMF solutions as shown by ^{195}Pt NMR spectroscopy.[134] However, decomposition to the diplatinum(II) species slowly occurs by a mechanism that is believed[134] to involve the reductive elimination of the capping nitrito ligand as the nitronium ion, NO_2^+.

Pictiva EX2004
Samsung v Pictiva
IPR2024-01094

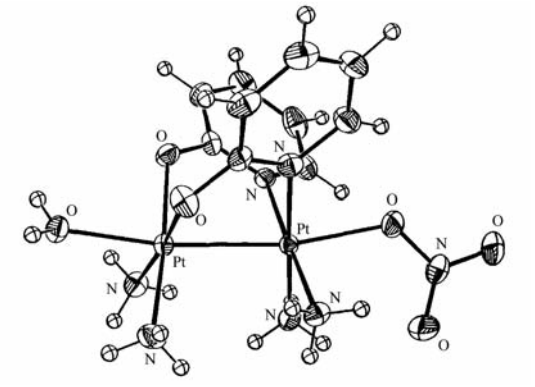


Fig. 14.7. The structure of the *cis*-$[Pt_2(hp)_2(NH_3)_4(NO_3)(H_2O)]^{3+}$ with a head-to-head arrangement of the α-pyridonate ligands.

While the structure determination of the compound $[Pt_2(hp)_2(NH_3)_4(H_2O)(NO_3)](NO_3)_3 \cdot 2H_2O$ was the first to be published[130] for a diplatinum(III) derivative of the so-called platinum blues, an earlier report[135] on a complex whose composition was purported to be $(H_5O_2)[Pt_2(1\text{-MeC})_2(NH_3)_4(NO_2)_2](NO_3)_2$, where 1-MeC represents the monoanion of *N*,*N*-bound *1-methylcytosine*, i.e. a Pt_2^{5+} complex, is in reality probably that of a Pt_2^{6+} complex. It was pointed out by Lippard[130,133] that the Pt–Pt distance of 2.584(1) Å accords with it being a single bond. Subsequently, it has been confirmed[136] that the correct formulation is *cis*-$[Pt_2(l\text{-MeC})_2(NH_3)_4(NO_2)_2](NO_3)_2 \cdot 2H_2O$ (see Table 14.1). More recently, several compounds containing 1-methylcytosinate ligands and Pt_2^{6+} cores have been characterized with various axial ligands including nucleobases.[137,138] For example, the structure of the head-tail *cis*-$[Pt_2(1\text{-MeC})_2(NH_3)_2(\text{gly-}N,O)_2](NO_3)_2$ has been reported[137] but an *L*-alanine analog of the latter compound has not been crystallographically characterized. In solution, two diastereomeric forms are observed in the NMR spectrum.[137] Other compounds have the nucleobase 9-ethylguanine (EtguaH),[138,139] NO_3^- or water or a mixture of NO_2^- and water occupying the two axial positions.[138] The Pt–Pt distances are in the range 2.55–2.60 Å as shown in Table 14.1. Some compounds of this family can interact with DNA and exhibit antitumor activity.[140,141]

Another series of diplatinum(III) complexes that are closely related to those that contain a pair of bridging hp ligands have been prepared in which the monoanion of 1-methyluracil (1-MeU) replaces hp.[142-147] Bernhard Lippert and co-workers[142-144,146] have generally obtained these compounds by the oxidation of diplatinum(II) precursor complexes. The compounds that have been structurally characterized are listed in Table 14.1. The unsymmetrical mixed aquo-nitrito and aquo-nitrato species *cis*-$[Pt_2(1\text{-MeU})_2(NH_3)_4X(H_2O)]^{3+}$, where X = NO_2 or NO_3,[142,143] have a head-to-tail disposition of the 1-MeU ligands and therefore differ structurally from *cis*-$[Pt_2(hp)_2(NH_3)_4(NO_3)(H_2O)]^{3+}$ and *cis*-$[Pt_2(hp)_2(NH_3)_4(NO_2)(NO_3)]^{2+}$ which are in their head-to-head isomeric forms.[132,134] All other diplatinum(III) 1-MeU complexes that have been structurally characterized contain head-to-head arrangements, including the 1:1 adducts with nitrite[144] and carbon-bound 1-methyluracilato (bound through its deprotonated C(5) position).[146] In both structures the single axial ligand is bound to the Pt atom that has the PtN_2O_2 ligand set. The cis-$[Pt_2(l\text{-MeU})_2(NH_3)_4(1\text{-MeU})]^{3+}$ cation[146] has a short strong Pt–C(axial) bond and a long Pt–Pt distance (2.685(1) Å) (see Table 14.1) which reflects a high structural trans-influence of this C-bound 1-MeU ligand.

Pictiva EX2004
Samsung v Pictiva
IPR2024-01094

In aqueous solution, axial ligands such as Cl^-, ONO_2^- and NO_2^- readily undergo solvolysis with the resulting formation of $[Pt_2(1\text{-}MeU)_2(NH_3)_4(H_2O)_2]^{4+}$. The lability of the axial ligands has been taken advantage of in the conversion of the 1:1 head-to-head nitrito complex *cis*-$[Pt_2(l\text{-}MeU)_2(NH_3)_4(NO_2)](NO_3)_3\cdot H_2O$ to *cis*-$[Pt_2(l\text{-}MeU)_2(NH_3)_4Cl_2]Cl_2\cdot 3.5H_2O$ upon its reaction with aqueous HCl.[145,147] This dichloride has also been prepared by chlorination of $[Pt_2(l\text{-}MeU)_2(NH_3)_4]Cl_2\cdot H_2O$,[143] but this reaction is complicated and other products, including mononuclear ones, are formed. Also, chlorination of the 1-MeU ligand can occur at the 5-position.[143] Ligand lability is not restricted to the axial ligands, as illustrated by the reaction of *cis*-$[Pt_2(1\text{-}MeU)_2(NH_3)_4Cl_2]Cl_2\cdot 3.5H_2O$ with HCl over a period of several days[145,147] to give the neutral complex *cis*-$Pt_2(l\text{-}MeU)_2(NH_3)_4Cl_2$, in which a pair of *cis*-NH_3 ligands have been replaced by Cl^-.

Another example of a series of diplatinum(III) complexes with monoanionic N,O bridging ligands is that of the α-*pyrrolidonato-containing compounds* with the core *cis*-$[Pt_2(pyrr)_2(NH_3)_n]^{4+}$, where pyrr = the anion of $C_4H_6(O)NH$. The earliest compound structurally characterized is *cis*-$[Pt_2(pyrr)_2(NH_3)_4(NO_2)(NO_3)](NO_3)_2\cdot H_2O$. This is formed[148,149] by the nitric acid oxidation of the tetranuclear complex $[Pt_4(pyrr)_4(NH_3)_8](NO_3)_6\cdot 2H_2O$ and resembles structurally other compounds of this type. Crystallographic data[149-151] for a total of six compounds of this family, including one with one axial position occupied by the deoxyribonucleoside 2N-deoxyguonosine,[152] are given in Table 14.1. The Pt–Pt distances are generally over 2.6 Å except for the latter and for the dimer of dimers *cis*-$[Pt_2(pyrr)_2(NH_3)_3(H_2O)(\mu\text{-}OH)]_2(NO_3)_6\cdot 4H_2O$ (H,T)[150] in which it is only 2.553(1) Å. The exceptionally short distance has been attributed to hydrogen bonding between an amine group and the oxygen atom of the bridging OH unit between the dimer. Kinetic and equilibrium studies on the axial-ligand substitution reactions of the head-to-head and head-to-tail α-pyridonate-bridged dinuclear compounds have been done.[153,154]

A final example of a series of diplatinum(III) complexes with monoanionic N,O bridging ligands is that containing *1-methylthyminato* (1-MeT) and *1-ethylthyminato* (1-EtT) nucleobase ligands.[155] These have been studied in solution and they are of general composition *cis*-$[Pt_2L_2(amine)_4XY]^{n+}$ where L = thymine nucleobase, amine = NH_3 or NH_3CH_3 and the axial groups X and Y are ligands such NO_2^-, Cl^-, water or no ligand at all. These are made by oxidation of Pt_2^{4+} precursors. The reaction proceeds via purple and blue-green intermediates, which are likely mixed-valence species. Unfortunately, synthetic procedures are sometimes poorly reproducible as a consequence of facile substitution reactions of the axial ligands and X-ray crystallography is usually the only reliable method of establishing the nature of the X and Y ligands. The compounds *cis*-$[Pt_2(1\text{-}MeT)_2(NH_3)_4(NO_2)](NO_3)_3$ and *cis*-$[Pt_2(1\text{-}MeT)_2(NH_2CH_3)_2Cl_3]ClO_4$ have been crystallographically characterized and have Pt–Pt distances of 2.6507(6) and 2.612(2) Å, respectively.[155] The most relevant structural feature is the *head–head* arrangement. This is similar to that of the 1-methyluracil described above. Thus one platinum atom is six-coordinate while the other is five-coordinate. The two units are held together by hydrogen bonding as shown in Fig. 14.8 for the 1-Met complex.

A few compounds having *four bridging nucleobases* have been made in low yield by heating the heteronuclear complex *trans*-$[(NH_3)_2Pt(N4\text{-}1\text{-}MeC\text{-}N3)_2Cu(H_2O)_2](ClO_4)_2$ in water.[156] By small modification of the reaction conditions, *cis*-2,2-$[Pt_2(1\text{-}MeC)_4L_n](ClO_4)_2$ complexes have been isolated and structurally characterized for L_n = $(NH_3)_2$, NH_3/H_2O. Another complex has only one axial NO_2^- group. The Pt–Pt distances are in the range of 2.452(1) to 2.498(1) Å (Table 14.1). These are about 0.1 Å shorter than those in species with only two bridging nucleobases such as [*cis*-$Pt_2(1\text{-}MeC)_2(NH_3)_4(NO_3)_2]^{2+}$ but similar to those in $Pt_2(Bu^tCONH)_4Cl_2$ (2.448(2) Å).

Pictiva EX2004
Samsung v Pictiva
IPR2024-01094

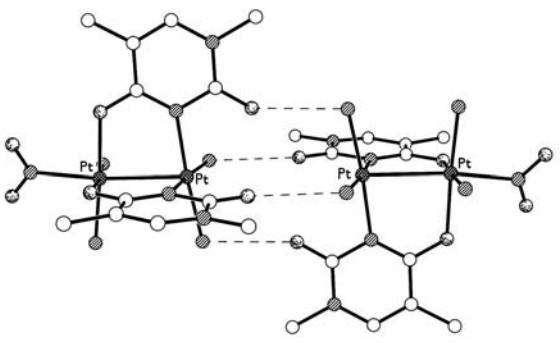


Fig. 14.8. The structure of the centrosymmetric pair of cations joined by hydrogen bonding in the 1-methylthiminato derivative *cis*-$[Pt_2(1\text{-MeT})_2(NH_3)_4(NO_2)](NO_3)_3$ (HH). Note that the platinum atom binds to the NO_2 group through the N atom.

Several compounds that contain monoanionic bridging ligands with *N,S donor sets* are known and a few of these have been structurally characterized (Table 14.1).[157-159] The reactions of aqueous solutions of K_2PtX_4 (X = Cl, Br or I) with methanol or ethanol solutions of pyrimidine-2-thione (pymSH) lead to oxidation of the platinum to produce diplatinum(III) compounds of the type $Pt_2(pymS)_4X_2$ (X = Cl, Br or I).[157,158] A compound of composition $Pt_2(pymS)_5Cl$ has also been prepared,[158] and similar synthetic methods to these have been used[158] to prepare $Pt_2(4\text{-MepymS})_4X_2$ (4-MepymS is the anion of 4-methylpyrimidine-2-thione; X = Cl or I) and $Pt_2(2\text{-TU})_4I_2$ (2-TU is the anion of 2-thiouracil). Crystal structure determinations of the iodo complexes $Pt_2(pymS)_4I_2$[157] and $Pt_2(2\text{-TU})_4I_2$[158] show similar structures with *cis*-PtN_2S_2 geometries present about each Pt center. This *cis*-2,2 arrangement contrasts with the less symmetric structure of $Pt_2(pymS)_4Cl_2$, in which there is a 3,l ligand arrangement, i.e. PtN_3S and $PtNS_3$ ligand atom sets about the two Pt atoms in the dimer.[158] All three complexes have rotational geometries that are twisted considerably from the fully eclipsed arrangement (χ in the range 25° to 29°).[157,158] A partial structure determination has been carried out[158] on a crystal of composition $Pt_2(pymS)_4Br_{1.2}(pymS)_{0.8}$, in which the axial sites of $Pt_2(pymS)_4Br_2$ are partially occupied by pymS. The Pt–Pt distance of 2.554(1) Å is the same as that of the di-iodide.

The diplatinum(II) complexes $Pt_2(pyS)_4$ and $Pt_2(4\text{-MepyS})_4$, where pyS and 4-MepyS represent the monanions of 2-mercaptopyridine and 4-methyl-2-mercaptopyridine, are oxidized by chloroform to give $Pt_2(pyS)_4Cl_2$ and $Pt_2(4\text{-MepyS})_4Cl_2$, respectively.[159] When this $CHCl_3$ oxidation of $Pt_2(pyS)_4$ is carried out in the presence of NaBr, NaI or NaSCN, then exchange of the axial ligands occurs to give $Pt_2(pyS)_4X_2$, where X = Br, I or SCN.[159] The reaction of $Pt_2(pyS)_4$ with $CHBr_3$ also gives $Pt_2(pyS)_4Br_2$.[159] The structure of $Pt_2(pyS)_4Cl_2$ is that of the *cis*-2,2 isomer; the Pt–Pt distance of 2.532(1) Å[159] is a little longer than that in $Pt_2(pymS)_4Cl_2$.[158] The electrochemical behavior of $Pt_2(pyS)_4$ and $Pt_2(4\text{-MepyS})_4$ in DMF are characterized[159] by quasi-reversible two-electron processes that result in oxidation to $[Pt_2(pyS)_4(DMF)_2]^{2+}$ and $[Pt_2(4\text{-MepyS})_4(DMF)_2]^{2+}$. The $E_{1/2}$ values are +0.28 and +0.26 V versus Ag/Ag[Cryp(2,2)]$^+$. A detailed study[159] of the cyclic voltammetry of $Pt_2(pyS)_4Cl_2$ shows that it conforms to a four-component scheme which involves an ECEC mechanism. More recently, these compounds have been isolated from reactions of $K_2[PtCl_4]$ with mercaptopyridine in hot alcohol.[160] Reaction of $Pt_2(5\text{-MepyS})_4X_2$, X = Cl or Br, and WS_4^{2-} or S_2^{2-} in $CHCl_3$ forms compounds of the type $[Pt_2(5\text{-MepyS})_4X]S_4[Pt_2(5\text{-MepyS})_4X]$ where the two Pt_2^{6+} units are held together by a chain of sulfur atoms from an S_4^{2-} anion.[161] In refluxing acetonitrile, these compounds decompose into $Pt_2(5\text{-MepyS})_4X_2$, $Pt_2(5\text{-MepyS})_4$ and S_8. The Pt–Pt distances for the corresponding

Pictiva EX2004
Samsung v Pictiva
IPR2024-01094

chloride and bromide compounds are 2.556(2) and 2.560(2) Å, respectively.[161] Treatment of $Pt_2(5\text{-MepyS})_4Cl]S_4[Pt_2(5\text{-MepyS})_4Cl$ with H_2 in DMF at 150 °C produces 3-picoline which was generated by C–S bond cleavage of the bridging 5-MepyS ligands.[162]

14.4.5 Unsupported Pt–Pt bonds

A growing number of unbridged diplatinum(III) complexes has emerged. These are often unstable towards disproportionation to Pt^{II} and Pt^{IV} species. The first such complex was *cis*-$Pt_2Cl_6[HN{=}C(OR)CR'_3]_4$ where R = H and R' = CH_3 (Pt–Pt distance of 2.694(1) Å).[163] Here, each Pt atom has two mutually *cis* iminoether groups in equatorial positions. The other equatorial and the axial positions are occupied by Cl atoms. Later, two analogous compounds were made by reacting the Pt^{II}-iminoether precursors *cis*- and *trans*-$PtCl_2[HN{=}C(OR)CR'_3]_4$ (R = CH_3 and R' = H) with Cl_2 at low temperature in the dark producing the corresponding *cis*- and *trans*-$Pt_2Cl_6[HN{=}C(OR)CR'_3]_4$ complexes.[164] At room temperature these compounds readily disproportionate. In this case the iminoether ligands can have either *E* or *Z* configuration depending upon the relative position of the methoxy and platinum residues with respect to the C=N double bond. The crystals are stabilized by N–H···Cl bonds and there are long Pt–Pt distances (2.765(2) and 2.758(3) Å for the *cis* and *trans* isomers, respectively).

Reaction of $Pt(phpy)_2$ (phpy is the anion of phenylpyridine) with an equimolar amount of $AuCl(SMe_2)$ in dichloromethane yields metallic gold and unsupported $Pt_2(phpy)_4Cl_2$.[165] The dimer has an approximate 2-fold axis bisecting the metal-metal bond and each phpy adopts a chelating mode. However, one is *ax-eq* while the other is *eq-eq*. The Pt–Pt distance of 2.7269(3) Å is similar to those mentioned above. In solution it is stable in the dark for several days.

Controlled oxidation with $PhICl_2$ of a Pt^{II} compounds having two C_8 carbocyclic α-dioximato ligands produces $Pt_2(C_8H_{12}(=NO)H)_4Cl_2$.[166] The unsupported metal-metal bond length is 2.6964(5) Å. The two square units are capped by axially coordinated chloride ions. A Raman absorption at 139 cm^{-1} has been assigned to the Pt–Pt stretch.

There is also an unusual Pt_2^{6+} compound devoid of bridging and axial ligands. This is obtained by oxidation of Pt(OBQDI-H)$_2$ (OBQDI = *o*-benzoquinodiimine) with AgO_3SCF_3.[167] In spite of the long Pt–Pt distance of 3.031(1) Å in $Pt_2(OBQDI\text{-}H)_4(CF_3SO_3)_2$, the Pt–Pt unit appears to be stable in solution, as shown by NMR spectroscopy. In the solid state, the diamagnetic molecule has an important number of hydrogen bonds between the triflate anions and each of the N–H groups in the cation.

Oxidation by controlled addition of chlorine to chilled solutions of various Pt^{II}-substituted acetylacetonates having formulae Pt(acacRR')$_2$ with R/R' = Me/Me, Ph/Ph and Me/CF_3 produces coupling of the planar Pt(acacRR')$_2$ moieties.[168] These compounds have not been crystallographically characterized but the ^{195}Pt NMR resonance at around 1300 ppm (which is between those of -216 to -771 ppm for the Pt^{II} precursors and those of about 1900 ppm for the corresponding Pt^{IV} compounds) supports the presence of Pt_2^{6+} species. The Raman stretch at 144 cm^{-1} is very similar to that of $Pt_2(C_8H_{12}(=NO)H)_4Cl_2$.[166] There is also a very strong absorption band at 24,000 cm^{-1}. This band is very weak in Pt(acacRR')$_2$ compounds and disappears upon further oxidation to Pt^{IV} species.

Another important species having unsupported the Pt–Pt units is that of the dimeric anion $[Pt_2(CN)_{10}]^{4-}$ which has been made in solution but not isolated in the solid state by addition of an aqueous solution of $Tl(ClO_4)_3$, NaCN at a pH of 2 to a solution of $Na_2Pt(CN)_4$.[169] The dimeric nature has been determined by EXAFS that shows a Pt–Pt distance of 2.729(3) Å and Pt–C distances of 2.008(2) Å.[170] Each platinum atom has one axial and four equatorial CN groups. Thus the structure is similar to that of the $[Co_2(CN)_{10}]^{6-}$ anion[171] which is discussed in Section 11.3.2. The Pt–Pt Raman stretching frequency of 144 cm^{-1} is similar to those of other

Pictiva EX2004
Samsung v Pictiva
IPR2024-01094

unsupported Pt_2^{6+} units as well as those in $[Pt_2(pop)_4X_2]^{4-}$ species[15] but significantly lower than those in the anion $[Pt_2(SO_4)_4(H_2O)_2]^{2-}$ and $Pt_2(SO_4)_4X_2$, X= Cl and Br, where such a vibration is at 333 cm^{-1}.[28]

14.4.6 Dinuclear Pt_2^{5+} species

The understanding of the chemistry and electronic structure of dinuclear Pt_2^{5+} units is not as well-developed as that for other M_2^{5+} paddlewheel species. When a compound with an M_2 core has four bridging mononegative ligands, the additional anion occupies an axial position, and an unsymmetrical species would be expected to form. However, that is not commonly found as the fifth mononegative ligand, e.g., a halide, is often shared and an infinite chain of the type ···M–M···X···M–M···X forms. Generally, these are paramagnetic compounds and EPR spectra clearly show that the unpaired electron is localized in the corresponding M_2 unit, as has been shown for example for Cr_2^{5+},[172] Mo_2^{5+},[172] W_2^{5+} [173] and other dimetal units (see Chapters 8 and 9). The metal-metal bond distance is generally between those of the corresponding M_2^{4+} and M_2^{6+} species.

Undoubtedly, this model can be applied to the formamidinate derivative $[Pt_2(DTolF)_4]PF_6$.[174] The bond distance of 2.5304(6) Å is between 2.649(2) Å in $Pt_2(DPhF)_4$ [174] and 2.5169(7) Å in $Pt_2(DPhF)_4Cl_2$.[86] This is in agreement with a bond order of 0.5 and an electronic configuration of $\sigma^2\pi^4\delta^2\delta^{*2}\pi^{*4}\sigma^*$. In the crystal, the molecules pack in such a way that there is a PF_6 anion between each $[Pt_2(DTolF)_4]^+$ unit as shown in Fig. 14.9. The Pt to F separation of 4.34 Å is too long to imply the presence of bonds and thus the cations are essentially isolated from each other.

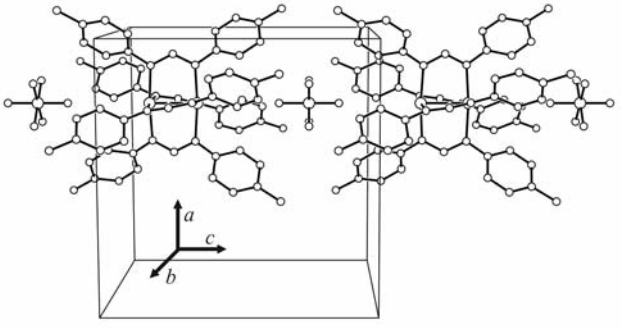


Fig. 14.9. Packing of the mixed-valence $[Pt_2(DTolF)_4]PF_6$ species along the *c* axis. The Pt···F separations of over 4 Å are too long to imply Pt to F bonding.

The bonding situation appears more complex in a class of mixed-valence Pt_2^{5+} complexes that have attracted a lot of attention.[15,18,23,175] These are salts of composition $A_4[Pt_2(pop)_4X]\cdot nH_2O$ (X = C1, Br, I), A = Li, K, Cs or NH_4 and n = 2 or 3. These are prepared by the partial oxidation of $A_2[Pt_2(pop)_4]$ (see Section 14.4.2) in aqueous solution using chlorine water, bromine water and KI_3, respectively,[61] or by the comproportionation reaction between $K_2[Pt_2(pop)_4]$ and $K_2[Pt_2(pop)_4X_2]$ in water.[61,72] These materials, which are linear-chain semiconductors, have a golden metallic appearance and while the finer points of their structures have prompted considerable debate,[60,61,72,176] the situation now seems to have been clarified. Based upon the results of resonance Raman spectral studies,[72,176] their electronic absorption spectra,[72] and magnetic susceptibility properties,[176] as well as a series of X-ray crystal structure determinations at room temperature (X = Cl[60,176] and Br[61]) and at *c*. 20 K (X = Cl and Br),[176] some differences are seen

Pictiva EX2004
Samsung v Pictiva
IPR2024-01094

in the structures of the chloride and bromide. For the chloride, the translational symmetry is such that there appears to be a combination of equal amounts of Pt_2^{4+} and $Pt_2Cl_2^{4+}$ units alternating along the chains (as in **14.10**) both at 300 K and 22 K. This gives rise[176] to inequivalent Pt–Pt distances (2.685(2) and 2.969(2) Å at 22 K) and sets of Pt–Cl (short) and Pt–Cl (long) distances. The bromide, on the other hand, is best modeled as containing equivalent Pt–Pt bonds (2.793(1) Å at 300 K and 2.781(1) Å at 22 K).[61,176] These measured distances are actually the average given by superimposing Pt^{II}–Pt^{II} and Pt^{III}–Pt^{III} distances. While the Pt–Br distances appear the same at 300 K, i.e. the Br atoms are equidistant between adjacent pairs of Pt_2 units,[61] at 19 K they resolve into a short–long disposition (2.579(4) Å and 2.778(4) Å).[176]

$$\cdots Pt^{2+}–Pt^{2+}\cdots Cl–Pt^{3+}–Pt^{3+}–Cl\cdots$$

14.10

A structure determination on $(NH_4)_4[Pt_2(pop)_4Cl]$ at room temperature likewise reveals an arrangement as in **14.10**.[177] The 'averaged' Pt–Pt distance is 2.830(1) Å, and the bridging Cl atom displays positional disorder over two sites so that the short Pt–Cl distance is 2.363(4) Å and the long one is 3.022(4) Å in the chain. The dihydrates of $K_4[Pt_2(pop)_4X]$ (X = C1, Br) have also been structurally characterized.[178] Structure determinations at room temperature (X = Cl) and 125 K (X = Br) accord with the results of the previous studies; the only significant differences are that the chains deviate slightly from linearity and the short and long Pt–X distances differ by an amount greater than in the corresponding trihydrates.

In Section 14.4.3 the preparation of the singly bonded $Pt_2(S_2CCH_3)_4I_2$ complex was mentioned. By adjusting the stoichiometry of the reaction, the mixed-valence compound $Pt_2(S_2CCH_3)_4I$ can be isolated.[93] It has also been prepared from the reaction of $Pt_2(S_2CCH_3)_4$ and $Pt_2(S_2CCH_3)_4I_2$ in toluene at reflux.[93] It is a semiconductor material and has a linear chain structure of the type $\cdots Pt_2S_8\cdots I\cdots Pt_2S_8\cdots I\cdots$ in which the Pt–Pt distance is 2.677(2) Å and the Pt–I distances are essentially identical.[93] The latter feature is different from the disparity in Pt–X distances encountered in compounds that contain the $\{[Pt_2(pop)_4X]^{4-}\}_\infty$ chains. The $[PtS_4]$ units are twisted ≈21° away from the full eclipsed conformation.[93] Although the crystallographic data accord with an essentially symmetrical structure, an intervalence band is observed[93] in the electronic absorption spectrum at 7800 cm^{-1}. The compound exhibits metallic conduction above room temperature.[179] Theoretical investigations indicate a noticeable reduction of electron–phonon coupling through the bridging halogen atoms.[180] Crystallographic studies on $Pt_2(S_2CC_2H_5)_4I$ at temperatures ranging from 115 to 377 K show only small variations in the Pt–Pt distances with bond distances changing from 2.680(1) Å at 115 K to 2.686(1) Å at 377 K.[95] The Pt–I distances change from 2.954(1) Å to 2.989(1) Å but they are essentially the same for each of the two axial iodide ligands. This compound shows a relatively high electrical conductivity at room temperature (5–30 C cm^{-1}) and undergoes a metal–semiconductor transition at $T_{M\text{-}S}$ = 205 K.[95]

There is also a class of tetranuclear compounds with a formal oxidation state of $Pt^{2.5+}$ but these are best described with the platinum blues in the following section.

14.4.7 The platinum blues

While the oligomeric compounds that encompass this very important class of molecules all formally contain at least one Pt^{III} atom, the average oxidation state is usually far less than 3.0 and the average Pt–Pt bond order is therefore less than one. Accordingly, while a discussion of these materials is appropriate in order to point out their relationship to the diplatinum(III) compounds that have been described in previous sections (especially Section 14.4.4), a compre-

Pictiva EX2004
Samsung v Pictiva
IPR2024-01094

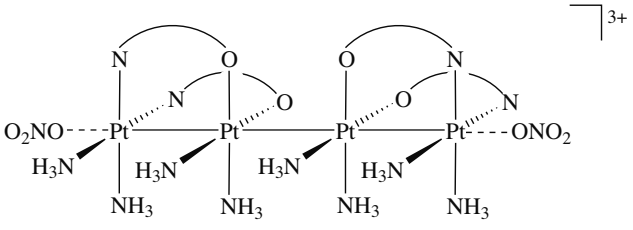
hensive and detailed coverage of the literature falls outside the scope of this text. Many review articles that touch upon the platinum blues can be consulted for additional details.[21,22,181-183]

The oxidation state nuclearity relationships that commonly exist between diplatinum(II) and diplatinum(III) species and the platinum blues can be summarized as follows:

$$2[Pt(2+)]_2 \underset{+e^-}{\overset{-e^-}{\rightleftharpoons}} [Pt(2.25+)]_4 \underset{+e^-}{\overset{-e^-}{\rightleftharpoons}} [Pt(2.5+)]_4 \underset{+e^-}{\overset{-e^-}{\rightleftharpoons}} [Pt(2.75+)]_4 \underset{+e^-}{\overset{-e^-}{\rightleftharpoons}} 2[Pt(3+)]_2$$

However, a full understanding of these relationships has taken most of the twentieth century to evolve. The first platinum blues, the platinum-acetamide blues, were reported in 1908 and formulated as $Pt(CH_3CONH)_2(H_2O)$.[184] This same formula was proposed again in 1964[185] augmented by some speculation as to the presence of Pt–Pt bonds. On the other hand two more studies[186,187] then appeared in which it was proposed that the platinum blues are Pt^{IV} compounds, e.g., $Pt(CH_3CONH)_2(OH)_2$. In connection with the anticancer action of platinum compounds,[181] a second set of blue platinum compounds were made and studied in the 1970s. The reaction between a solution of *cis*-$PtCl_2(NH_3)_2$ which has wholly or partially undergone aquation and various pyrimidines such as thymine, uridine, uracil, 1-methyluracil and polyuracil gives deep-blue products[188,189] which also have anticancer activity.[190,191] These developments led to a resurgence of efforts to obtain a better characterization of platinum blues, or at least some of the compounds that have been included under this name.

By using 2-hydroxypyridine (α-pyridone or Hhp), Lippard and co-workers[191] were able to isolate and structurally define what is now recognized as being an analog of the previously described platinum blues. A combination of X-ray crystallography,[191,192] XPS data,[106] magnetic susceptibility,[192] EPR spectroscopy,[192] optical spectroscopy and scattered-wave Xα calculations[193] have been applied to the characterization of the paramagnetic complex *cis*-$[Pt_4(hp)_4(NH_3)_8(NO_3)_2](NO_3)_3{\cdot}H_2O$ in which the mean oxidation state is +2.25 and $S = ½$. The structure is as shown in 14.11. The Pt–Pt distances are 2.774(1) Å for the pair of outer bonds and 2.877(1) Å for the inner Pt–Pt bond.[192] While the net σ-bonding interaction between the end pairs of Pt atoms in the chain is stronger than between the middle pair,[193] it is not possible for either type of bond to be a full single bond. Note that this α-pyridone blue and other closely related tetranuclear analogs (see below) bear a structural relationship to the mixed-valence tetranuclear compounds $Ir_4(\mu\text{-}C_7H_4NS_2)_4I_2(CO)_8$ (Section 11.4.4) and $[Rh_4(1,3\text{-di-isocyanopropane})_8Cl]^{5+}$ (Section 12.5.2), both of which also contain linear M_4 units.



14.11

The reactions that ultimately give rise to the formation of *cis*-diammine-platinum α-pyridone blue from the reaction of *cis*-$[Pt(NH_3)_2(H_2O)_2]^{2+}$ and 2-hydroxypyridine (α-pyridone) have been shown to involve a variety of mononuclear Pt^{II} and Pt^{IV} complexes[194-196] as well as the head-to-tail and head-to-head isomers of $[Pt_2(hp)_2(NH_3)_4]^{2+}$.[194,196]

Pictiva EX2004
Samsung v Pictiva
IPR2024-01094

The chemistry of the *cis*-diammineplatinum α-pyridone blue is representative of that of other closely related platinum blues. The analogous ethylenediamineplatinum α-pyridone blue $[Pt_4(hp)_4(en)_4(NO_3)_3](NO_3)_3{\cdot}H_2O$ has been prepared and characterized,[197,198] and several *cis*-diammineplatinum α-pyrrolidone ($[cis\text{-}Pt_2(C_4H_6NO)_2]_m^{n+}$) species have been obtained.[150,199-202] The latter include phases that have been described as 'α-pyrrolidone green'[199] and 'α-pyrrolidone violet'[200] and which have the compositions $[Pt_4(pyrr)_4(NH_3)_8](NO_3)_{5.48}{\cdot}3H_2O$ and $[Pt_4(pyrr)_4(NH_3)_8](PF_6)_2(NO_3)_{2.56}{\cdot}5H_2O$, respectively. These 'non-stoichiometric' crystalline materials have been purported to be mixtures of the $[Pt(2.25+)]_4/[Pt(2.5+)]_4$ and $[Pt(2+)]_4/[Pt(2.25+)]_4$ species, respectively. The so-called 'α-pyrrolidone tan', which is of composition $[Pt_4(pyrr)_4(NH_3)_8](NO_3)_6{\cdot}3H_2O$,[201,202] has a structure similar to **14.11** but without axial coordination by nitrate. In the solid state hydrogen bonding between the two Pt_2 units appear to stabilize the structure. The Pt–Pt distances are very similar to one another (2.702(6) Å, 2.710(5) Å and 2.706(6) Å in sequence down the chain), but are shorter than those in the α-pyridone blue. This is consistent with the α-pyrrolidone tan being in the higher average oxidation state of Pt(2.5+). Kinetic studies indicate that in solution this compound disproportionates into $[Pt^{III}_2(NH_3)_4(pyrr)_2]^{4+}$ and $[Pt^{II}_2(NH_3)_4(pyrr)_2]^{2+}$, both of which are diamagnetic.[203] This "tan" complex can be oxidized further[204] by $[S_2O_8]^{2-}$ in a strongly acidic medium to give the yellow tetranuclear cation $[Pt_4(pyrr)_4(NH_3)_8]^{8+}$ in which each platinum is formally Pt^{III}. This diamagnetic species has been isolated in various salts in which there are mixtures of anions present (e.g., $[Pt_4(pyrr)_4(NH_3)_8](SO_4)_2(ClO_4)_4{\cdot}6H_2O$), and it has the interesting property of oxidizing water to molecular oxygen.[204] The reaction of $[Pt_4(pyrr)_4(NH_3)_8](NO_3)_6{\cdot}2H_2O$ with excess pyrazine in water has given the $[Pt^{III}]_4$ complex $[(NO_3)(NH_3)_2Pt(pyrr)_2Pt(NH_3)(\mu\text{-}NH_2)]_2(NO_3)_4$ in very low yield.[205] The Pt–Pt distances are 2.608(1) Å for the outer Pt–Pt bonds and 3.160(2) Å for the interdimer separation.

An early study[206] of the spectroscopic, redox and chemical properties of *cis*-diammineplatinum α-pyridone blue established its close relationship to various other platinum blues, including the platinum acetamide blue and *cis*-diammineplatinum uracil blue. Such materials were shown to share the properties of mixed valence and oligomeric structure. More recent studies have confirmed these conclusions. Of special note is the isolation and structural characterization of a linear octanuclear platinum acetamide complex $[Pt_8(NHCOCH_3)_8(NH_3)_{16}](NO_3)_{10}{\cdot}4H_2O$, in which the average oxidation state is Pt(2.25+).[207] The Pt–Pt bonds are alternately supported (short) and unsupported (long) by bridging acetamido ligands and have lengths of 2.880(2) Å, 2.900(1) Å, 2.778(1) Å and 2.934(1) Å in this centrosymmetric structure. The complex is diamagnetic and shows no EPR signal.[207] Another important result has been the confirmation that the tetranuclear uracil blue $[Pt_4(1\text{-}MeU)_4(NH_3)_8](NO_3)_5{\cdot}H_2O$, where 1-MeU is the monoanion of 1-methyluracil, has the expected structure, and a chemistry that closely mirrors that of the α-pyridone blues.[197,208-210] Platinum uridine blue and uridine green compounds have also been prepared and characterized by a variety of spectroscopic methods.[140] The uridine green species exhibits antitumor activity. Cationic platinum blues based on isonicotinamide, malonamide and biuret have been described.[211]

With the base 1-methylthymine, a complex of composition $\{[Pt_2(MeT)_2(NH_3)_2Cl_2]_2Cl\}(PtCl_6){\cdot}6H_2O$ has been obtained in which the average oxidation state is Pt(2.75+).[212] However, this contains two *cis*-$[(NH_3)_2Pt(\mu\text{-}MeT)_2PtCl_2]$ units that are linked by a single chloride bridge and so is not a tetranuclear Pt_4 linear cluster of the type usually encountered. The Pt–Pt distance within the individual Pt_2 units is 2.699(1) Å.[212] Platinum blue compounds containing acetamide and bypyridine groups have been described[213] and the structure of a tetranuclear compound shows long outer distances of 2.908(2) Å and even longer inner distances of 3.209(4) Å.

Pictiva EX2004
Samsung v Pictiva
IPR2024-01094

Recently, a series of partially oxidized 1-D platinum chain complexes consisting of carboxylate-bridged *cis*-diammineplatinum dimer units have been crystallographically characterized. These compounds have the formulae $[Pt(2.2+)_2(acetato)_2(NH_3)_4](NO_3)_{2.4}\cdot 2H_2O$ and $[Pt(2.2+)_2(propionato)_2(NH_3)_4](NO_3)_2(ClO_4)_{0.4}\cdot 2H_2O$. In both compounds the intra Pt–Pt distances range from 2.81 to 2.85 Å while the interdimer distances are *c.* 3.0 Å.[214] The dimer-dimer associations are stabilized by four hydrogen bonds formed between the ammine groups and the carboxylate anions.

A strategy has been developed[215,216] for the synthesis of trinuclear mixed Pt_2Pd complexes of composition *cis*-$[A_2PtL_2PdL_2PtA_2]X_2$ and *cis*-$[A_2PtL_2PdL_2PtA_2]X_3$, where L = 1-methyluracilato (1-MeU) or 1-methylthyminato (1-MeT), $A_2 = 2NH_3$ or en, and X = NO_3^- or ClO_4^-. In the paramagnetic tri-cations the average metal oxidation state is M(2.33+), so that one of the three metals is M^{III}; this is believed to be Pd^{III}. These intensely purple-blue colored compounds are considered models of a trinuclear platinum pyrimidine blue.

While it should be emphasized that the platinum blues which are the most thoroughly characterized, and whose chemistry is the most fully developed, are those that contain monoanionic bridging ligands with N,O donor atoms, other blues have been described. Examples include diammine platinum blues that are said to contain bridging monohydrogenphosphato and nitrito ligands,[217] although full structural details of these compounds remain to be elucidated.

14.4.6 Other compounds

Some unusual molecules contain *C*-bound quinone or quinone-like bridges between the singly-bonded Pt_2^{6+} units such $(Bu^n_4N)_2[Pt_2(\mu\text{-}C_6F_4O)_2(C_6F_5)_4]$ and $(Bu^n_4N)_2[Pt_2(\mu\text{-}C_6F_4O(CH_3)_2)_2(C_6F_5)_4]$. The Pt–Pt distances are 2.570(1) and 2.584(1) Å, respectively.[218] Reaction of mesotetraphenylporphyrin dimethyl ether, H_2MP, and $K_2[PtCl_6]$ in boiling pyridine produces a compound of composition $ClPt^{III}MP$,[219] which has not been structurally characterized. It is possible that it might resemble compounds such as those of Ru and Ir which are known to contain unsupported metal–metal bonds. Several hydroxide and peroxide containing platinum compounds have been claimed to be diplatinum(III) species, but confirmation is lacking.[220] As yet, there is no proof of their identity from X-ray crystallographic studies, their structures having been inferred from microanalytical data, infrared spectroscopy and potentiometric titrations. Finally, electrochemical and chemical oxidation using NO^+ of the antitumor, organometallic compound $[Pt\{((p\text{-}HC_6F_4)NCH_2)_2\}(py)_2]$ have produced some moderately stable diamagnetic species that have been attributed to the formation of bridged complexes containing Pt–Pt bonds but no structural characterization has been offered.[221]

References

1. K. Umakoshi and Y. Sasaki, *Adv. Inorg. Chem.* **1993**, *40*, 187.
2. C. Bellitto, G. Dessy and V. Fares, *Inorg. Chem.* **1985**, *24*, 2815.
3. F. A. Cotton, M. Matusz and R. Poli, *Inorg. Chem.* **1987**, *26*, 1472.
4. F. A. Cotton, M. Matusz, R. Poli and X. Feng, *J. Am. Chem. Soc.* **1988**, *110*, 1144.
5. A. Tressaud, S. Khairoun, J. M. Dance and P. Hagenmuller, *Z. anorg. allg. Chem.* **1984**, *517*, 43.
6. A. Tressaud, M. Winterberger, N. Bartlett and P. Hagenmuller, *C. R. Acad. Sci.* **1976**, *282*, 1069.
7. A. Blake, A. J. Holder, T. I. Hyde and M. Schröder, *J. Chem. Soc., Chem. Commun.* **1987**, 987.
8. F. A. Cotton, J. Gu, C. A. Murillo and D. J. Timmons, *J. Am. Chem. Soc.* **1998**, *120*, 13280.
9. C.-L. Yao, L.-P. He, J. D. Korp and J. L. Bear, *Inorg. Chem.* **1988**, *27*, 4389.
10. K. Umakoshi, A. Ichimura, I. Kinoshita and S. Ooi, *Inorg. Chem.* **1990**, *29*, 4005.
11. T. Murahashi, E. Mochizuki, Y. Kai and H. Kurosawa, *J. Am. Chem. Soc.* **1999**, *121*, 10660.
12. R. Usón, J. Forniés, M. Tomás, B. Menjón, K. Sunkel and R. Bau, *J. Chem. Soc., Chem. Commun.* **1984**, 751.

Pictiva EX2004
Samsung v Pictiva
IPR2024-01094

13. R. Usón, J. Forniés, M. Tomás, B. Menjón, R. Bau, K. Sunkel and E. Kuwabara, *Organometallics* **1986**, *5*, 1576.
14. A. J. Blake, R. O. Gould, A. J. Holder, T. I. Hyde, A. J. Lavery, M. O. Odulate and M. Schröder, *J. Chem. Soc., Chem. Commun*. **1987**, 118.
15. J. D. Woollins and P. F. Kelly, *Coord. Chem. Rev*. **1985**, *65*, 115.
16. A. N. Zhilyaev and T. A. Fomina, *Russ. J. Coord. Chem.* **1997**, *23*, 525.
17. A. P. Zipp, *Coord. Chem. Rev.* **1988**, *84*, 47.
18. D. M. Roundhill, H. B. Gray and C.-M. Che, *Acc. Chem. Res.* **1989**, *22*, 55.
19. R. J. Sweeney, E. L. Harvey and H. B. Gray, *Coord. Chem. Rev.* **1990**, *105*, 23.
20. J. M. Rawson and R. E. P. Winpenny, *Coord. Chem. Rev.* **1995**, *139*, 313.
21. K. Matsumoto and K. Sakai, *Adv. Inorg. Chem.* **2000**, *49*, 375.
22. B. Lippert, *Coord. Chem. Rev.* **1999**, *182*, 263.
23. R. J. H. Clark, *Chem. Soc. Rev.* **1990**, *19*, 107.
24. T. V. O'Halloran and S. J. Lippard, *Isr. J. Chem*. **1985**, *25*, 130.
25. R. Stranger, S. C. Nissen, M. T. Mathieson and T. G. Appleton, *Inorg. Chem.* **1997**, *36*, 937.
26. R. Stranger, G. A. Medley, J. E. McGrady, J. M. Garrett and T. G. Appleton, *Inorg. Chem.* **1996**, *35*, 2268.
27. G. Gökagac, H. Isci and W. R. Mason, *Inorg. Chem.* **1992**, *31*, 2184.
28. R. A. Newman, D. S. Martin, R. F. Dallinger, W. H. Woodruff, A. E. Stiegman, C.-M. Che, W. P. Schaefer, V. M. Miskowski and H. B. Gray, *Inorg. Chem.* **1991**, *30*, 4647.
29. G. S. Muraveiskaya, G. A. Kukina, V. S. Orlova, O. N. Evstaf'eva and M. A. Porai-Koshits, *Dokl. Akad. Nauk SSSR* **1976**, *226*, 596; *Dokl. Chem*. **1976**, *226*, 76.
30. G. S. Muraveiskaya, V. S. Orlova and O. N. Evstaf'eva, *Russ. J. Inorg. Chem.* **1974**, *19*, 561.
31. T. G. Appleton, J. R. Hall and D. W. Neale, *Inorg. Chim. Acta* **1985**, *104*, 19.
32. D. P. Bancroft, F. A. Cotton, L. R. Falvello, S. Han and W. Schwotzer, *Inorg. Chim. Acta* **1984**, *87*, 147.
33. F. A. Cotton, L. R. Falvello and S. Han, *Inorg. Chem.* **1982**, *21*, 2889.
34. A. N. Zhilyaev, E. V. Shikhaleeva, S. B. Katser and I. B. Baranovskii, *Russ. J. Inorg. Chem.* **1994**, *39*, 568.
35. P. A. Koz'min, T. B. Larina, M. D. Surazhskaya, A. N. Zhilyaev and G. N. Kuznetsova, *Russ. J. Inorg. Chem.* **1993**, *38*, 797.
36. V. S. Orlova, G. S. Muraveiskaya and O. N. Evstaf'eva, *Russ. J. Inorg. Chem.* **1975**, *20*, 753.
37. T. G. Appleton, J. R. Hall, D. W. Neale and S. F. Ralph, *Inorg. Chim. Acta* **1983**, *77*, L149.
38. I. F. Golovaneva, S. A. Polonskii, A. P. Klyagina and G. S. Muraveiskaya, *Russ. J. Inorg. Chem*. **1993**, *38*, 1679.
39. G. S. Muraveiskaya, V. E. Abashkin, O. N. Evstaf'eva, I. F. Golovaneva and R. N. Shchelokov, *Sov. J. Coord. Chem*. **1980**, *6*, 218.
40. H. L. Conder, F. A. Cotton, L. R. Falvello, S. Han and R. A. Walton, *Inorg. Chem.* **1983**, *22*, 1887.
41. F. A. Cotton, L. R. Falvello and S. Han, *Inorg. Chem.* **1982**, *21*, 1709.
42. F. A. Cotton, S. Han, H. L. Conder and R. A. Walton, *Inorg. Chim. Acta* **1983**, *72*, 191.
43. R. El-Mehdawi, F. R. Fronczek and D. M. Roundhill, *Inorg. Chem.* **1986**, *25*, 1155.
44. R. El-Mehdawi, S. A. Bryan and D. M. Roundhill, *J. Am. Chem. Soc*. **1985**, *107*, 6282.
45. Y. K. Shin, V. M. Miskowski and D. G. Nocera, *Inorg. Chem.* **1990**, *29*, 2308.
46. R. El-Mehdawi, F. R. Fronczek and D. M. Roundhill, *Inorg. Chem.* **1986**, *25*, 3714.
47. R. P. Sperline, M. K. Dickson and D. M. Roundhill, *J. Chem. Soc., Chem.Commun*. **1977**, 62.
48. K. A. Alexander, S. A. Bryan, M. K. Dickson, D. Hedden and D. M. Roundhill, *Inorg. Synth*. **1986**, *24*, 211.
49. C.-M. Che, L. G. Butler, P. J. Grunthaner and H. B. Gray, *Inorg. Chem.* **1985**, *24*, 4662.
50. C. King, R. A. Auerbach, F. R. Fronczek and D. M. Roundhill, *J. Am. Chem. Soc*. **1986**, *108*, 5626.
51. C. King, D. M. Roundhill, M. K. Dickson and F. R. Fronczek, *J. Chem. Soc., Dalton Trans*. **1987**, 2769.

Pictiva EX2004
Samsung v Pictiva
IPR2024-01094

52. D. J. Thiel, P. Livins, E. A. Stern, A. Lewis, *Nature* **1993**, *362*, 40.
53. I. V. Novozhilova, A. V. Volkov and P. Coppens, *J. Am. Chem. Soc*. **2003**, *125*, 1079.
54. C.-M. Che, W. P. Schaefer, H. B. Gray, M. K. Dickson, P. B. Stein and D. M. Roundhill, *J. Am. Chem. Soc.* **1982**, *104*, 4253.
55. S. A. Bryan, M. K. Dickson and D. M. Roundhill, *J. Am. Chem. Soc*. **1984**, *106*, 1882.
56. S. A. Bryan, M. K. Dickson and D. M. Roundhill, *Inorg. Chem.* **1987**, *26*, 3878.
57. D. M. Roundhill, M. K. Dickson and S. J. Atherton, *J. Organomet. Chem*. **1987**, *335*, 413.
58. C.-M. Che, T. C. W. Mak and H. B. Gray, *Inorg. Chem.* **1984**, *23*, 4386.
59. K. A. Alexander, S. A. Bryan, F. R. Fronczek, W. C. Fultz, A. L. Rheingold, D. M. Roundhill, P. Stein and S. F. Watkins, *Inorg. Chem.* **1985**, *24*, 2803.
60. R. J. H. Clark, M. Kurmoo, H. M. Dawes and M. B. Hursthouse, *Inorg. Chem.* **1986**, *25*, 409.
61. C.-M. Che, F. H. Herbstein, W. P. Schaefer, R.E. Marsh and H.B. Gray, *J. Am. Chem. Soc*. **1983**, *105*, 4604.
62. C.-M. Che, M.-C. Cheng, Y. Wang and H. B. Gray, *Inorg. Chim. Acta* **1992**, *191*, 7.
63. S. A. Bryan, R. H. Schmehl and D. M. Roundhill, *J. Am. Chem. Soc*. **1986**, *108*, 5408.
64. C.-M. Che and W.-M. Lee, *J. Chem. Soc., Chem. Commun*. **1986**, 512.
65. D. Hedden, D. M. Roundhill and M. D. Walkinshaw, *Inorg. Chem.* **1985**, *24*, 3146.
66. C.-M. Che, W.-M. Lee, T. C. W. Mak and H. B. Gray, *J. Am. Chem. Soc*. **1986**, *108*, 4446.
67. C.-M. Che, T. C. W. Mak, V. M. Miskowski and H. B. Gray, *J. Am. Chem. Soc*. **1986**, *108*, 7840.
68. M. A. F. Dos Remedios Pinto, P. J. Sadler, S. Neidle, M. R. Sanderson, A. Subbiah and R. J. Kuroda, *J. Chem. Soc., Chem. Commun*. **1980**, 13.
69. R. E. Marsh and F. H. Herbstein, Acta Crystallogr. **1983**, *B39*, 280.
70. H. Isci and W. R. Mason, *Inorg. Chem.* **1985**, *24*, 1761.
71. P. Stein, M. K. Dickson and D. M. Roundhill, *J. Am. Chem. Soc*. **1983**, *105*, 3489.
72. M. Kurmoo and R. J. H. Clark, *Inorg. Chem.* **1985**, *24*, 4420.
73. A. E. Stiegman, V. M. Miskowski and H. B. Gray, *J. Am. Chem. Soc*. **1986**, *108*, 2781.
74. D. M. Roundhill, *J. Am. Chem. Soc*. **1985**, *107*, 4354.
75. A. Vlćek, Jr and H. B. Gray, *J. Am. Chem. Soc*. **1987**, *109*, 286.
76. A. Vlćek, Jr and H. B. Gray, *Inorg. Chem.* **1987**, *26*, 1997.
77. E. L. Harvey, A. E. Stiegman, A. Vlćek, Jr and H. B. Gray, *J. Am. Chem. Soc*. **1987**, *109*, 5233.
78. C.-M. Che and K.-C. Cho, *J. Chem. Soc., Chem. Commun*. **1987**, 133.
79. D. M. Roundhill and S. J. Atherton, *J. Am. Chem. Soc*. **1986**, *108*, 6829.
80. C.-M. Che, H. B. Gray, S. J. Atherton and W.-M. Lee, *J. Phys. Chem*. **1986**, *90*, 6747.
81. Note that the reductions of $[Pt_2(pop)_4]^{4-}$ to $[Pt_2(pop)_4]^{5-}$ and $[Pt_2(pop)_4]^{6-}$ have also been reported: C.-M. Che, S. J. Atherton, L. G. Butler and H. B. Gray, *J. Am. Chem. Soc*. **1984**, *106*, 5143; K. A. Alexander, P. Stein, D. B. Hedden and D. M. Roundhill, *Polyhedron* **1983**, *2*, 1389.
82. C.-M. Che, W.-M. Lee and K.-C. Cho, *J. Am. Chem. Soc*. **1988**, *110*, 5407.
83. T. G. Appleton, K. A. Byriel, J. M. Garrett, J. R. Hall, C. H. L. Kennard, M. T. Mathieson and R. Stranger, *Inorg. Chem.* **1995**, *34*, 5646.
84. T. G. Appleton, K. A. Byriel, J. M. Garrett, J. R. Hall, C. H. L. Kennard and M. T. Mathieson, *J. Am. Chem. Soc.* **1992**, *114*, 7305.
85. T. G. Appleton, K. J. Barnham, K. A. Byriel, J. R. Hall, C. H. L. Kennard, M. T. Mathieson and K. G. Penman, *Inorg. Chem.* **1995**, *34*, 6040.
86. F. A. Cotton, J. H. Matonic and C. A. Murillo, *Inorg. Chim. Acta* **1997**, *264*, 61.
87. R. I. Rudyi, N. V. Cherkashina, G. Ya. Mazo, Ya. V. Salyn' and I. I. Moiseev, *Izv. Akad. Nauk SSSR, Ser. Khim*. **1980**, 29,754; *Bull. Acad. Sci. USSR* **1980**, *29*, 510.
88. I. I. Moiseev, R. I. Rudyi, N. V. Cherkashina, G. Ya. Mazo and J. Salins, *Dokl. Akad. Nauk SSSR* **1980**, *253*, 624; *Dokl. Chem*. **1980**, *253*, 364.
89. R. I. Rudyi, N. V. Cherkashina, Ya. V. Salyn' and I. I. Moiseev, *Izv. Akad. Nauk SSSR. Ser. Khim*. **1983**, *32*, 1866; **1983**, *32*, 1691.
90. D. I. Kochubei, M. A. Kozlov, N. V. Cherkashina, R. I. Rudyi, K. I. Zamaraev and I. I. Moiseev, *Koord. Khim*. **1985**, *11*, 846; *Sov. J. Coord. Chem*. **1985**, *11*, 479.

Pictiva EX2004
Samsung v Pictiva
IPR2024-01094

91. M. A. A. F. de C. T. Carrondo and A. C. Skapski, *Acta Crystallogr*. **1978**, *B34*, 1857 and 3576.
92. T. Yamaguchi, Y. Sasaki and T. Ito, *J. Am. Chem. Soc*. **1990**, *112*, 4038.
93. C. Bellitto, A. Flamini, L. Gastaldi and L. Scaramuzza, *Inorg. Chem.* **1983**, *22*, 444.
94. C. Bellitto, M. Bonamico, G. Dessy, V. Fares and A. Flamini, *J. Chem. Soc., Dalton Trans*. **1986**, 595.
95. M. Mitsumi, T. Murase, H. Kishida, T. Yoshinari, Y. Ozawa, K. Toriumi, T. Sonoyama, H. Kitagawa and T. Mitani, *J. Am. Chem. Soc*. **2001**, *123*, 11179.
96. C. Bellitto, *Comments Inorg. Chem.* **1988**, *8*, 101.
97. J. Kuyper and K. Vrieze, *Transition Met. Chem*. **1976**, *1*, 208.
98. B. R. Steele and K. Vrieze, *Transition Met. Chem*. **1977**, 2, 169.
99. J. D. Schagen, A. R. Overbeek and H. Schenk, *Inorg. Chem.* **1978**, 17, 1938.
100. D. P. Bancroft, F. A. Cotton, L. R. Falvello and W. Schwotzer, *Inorg. Chem.* **1986**, 25, 763.
101. F. A. Cotton, C. A. Murillo, X. Wang and C. C. Wilkinson, *Inorg. Chim. Acta* **2003**, *351*, 183.
102. R. Clérac, F. A. Cotton, L. M. Daniels, J. P. Donahue, C. A. Murillo and D. J. Timmons, *Inorg. Chem.* **2000**, *39*, 2581.
103. I. I. Chernyaev and L. A. Nazarova, *Izv. Sektora Platiny Akad. Nauk SSSR* **1951**, *26*, 101; **1952**, *27*, 175; **1955**, *30*, 21.
104. L. A. Nazarova, I. I. Chernyaev, A. G. Maiorova, A. A. Koryagina and N. N. Borozdina, *Proc. 10th Int. Conf. Coord. Chem., Tokyo* **1967**, 391.
105. V. I. Nefedov, Ya. V. Salyn, I. B. Baranovskii and A. G. Maiorova, *Zh. Neorg. Khim*. **1980**, *25*, 216; *Russ. J. Inorg. Chem.* **1980**, *25*, 116.
106. J. K. Barton, S. A. Best, S. J. Lippard and R. A. Walton, *J. Am. Chem. Soc*. **1978**, *100*, 3785.
107. V. I. Korsunskii and G. N. Kuznetsova, *Zh. Neorg. Khim*. **1988**, *33*, 1624; *Russ. J. Inorg. Chem.* **1988**, *33*, 923.
108. T. N. Fedotova, G. N. Kuznetsova, L. Kh. Minacheva and I. B. Baranovskii, *Russ. J. Inorg. Chem.* **1990**, *35*, 840.
109. T. N. Fedotova, L. Kh. Minacheva, G. N. Kuznetsova, V. G. Sakharova, M. I. Gel'fman and I. B. Baranovskii, *Russ. J. Inorg. Chem.* **1997**, *42*, 1838.
110. A. Dolmella, F. P. Intini, C. Pacifico, G. Padovano and G. Natile, *Polyhedron* **2002**, *21*, 275.
111. T. N. Fedotova, G. N. Kuznetsova, L. Kh. Minacheva and I. B. Baranovskii, *Russ. J. Inorg. Chem.* **1993**, *38*, 84.
112. G. Bandoli, A. Dolmella, F. P. Intini, C. Pacifico and G. Natile, *Inorg. Chim. Acta* **2003**, *346*, 143.
113. L. Kh. Minacheva, I. B. Baranovskii, V. G. Sakharova and M. A. Porai-Koshits, *Russ. J. Inorg. Chem*. **1991**, *36*, 348.
114. K. Matsumoto, J. Matsunami, K. Mizuno and H. Uemura, *J. Am. Chem. Soc.* **1996**, *118*, 8959.
115. T. N. Fedotova, G. N. Kuznetsova, V. I. Korsunskii and I. B. Baranovskii, *Russ. J. Inorg. Chem*. **1994**, *39*, 1287.3
116. Ya. V. Zubavichus, Yu. L. Slovokhotov, T. N. Fedotova, G. N. Kuznetsova and I. L. Emerenko, *Russ. J. Inorg. Chem.* **2001**, *46*, 5.
117. K. Matsumoto and M. Ochiai, *Coord. Chem. Rev.* **2002**, *231*, 229.
118. K. Matsumoto, in: B. Lippert, Ed. *Cisplatin: Chemistry and Biochemistry of a Leading Anticancer Drug*, Wiley-VCH: Weinheim, Germany, 1999, p. 455.
119. K. Matsumoto, Y. Nagai, J. Matsunami, K. Mizuno, T. Abe, R. Somazawa, J. Kinoshita and H. Shimura, *J. Am. Chem. Soc.* **1998**, *120*, 2900.
120. Y.-S. Lin, H. Misawa, J. Yamada and K. Matsumoto, *J. Am. Chem. Soc.* **2001**, *123*, 569.
121. Y.-S. Lin, S. Takeda and K. Matsumoto, *Organometallics* **1999**, *18*, 4897.
122. M. Ochiai and K. Matsumoto, *Chem. Lett. 2002*, 270.
123. M. Ochiai, Y.-S. Lin, J. Yamada, H. Misawa, S. Arai and K. Matsumoto, *J. Am. Chem. Soc*. **2004**, *126*, 2536.
124. N. Saeki, N. Nakamura, T. Ishibashi, M. Arime, H. Sekiya, K. Ishihara and K. Matsumoto, *J. Am. Chem. Soc.* **2003**, *125*, 3605.
125. M. Arime, K. Ishihara and K. Matsumoto, *Inorg. Chem*. **2004**, *43*, 309.

Pictiva EX2004
Samsung v Pictiva
IPR2024-01094

126. K. Shimazaki, H. Sekiva, H. Inoue, N. Saeki, K. Ishihara and K. Matsumoto, *Eur. J. Inorg. Chem*. **2003**, 1785.
127. D. P. Bancroft and F. A. Cotton, *Inorg. Chem.* **1988**, *27*, 1633.
128. D. P. Bancroft and F. A. Cotton, *Inorg. Chem.* **1988**, *27*, 4022.
129. E. S. Peterson, D. P. Bancroft, D. Min, F. A. Cotton and E. H. Abbott, *Inorg. Chem.* **1990**, *29*, 229.
130. L. S. Hollis and S. J. Lippard, *J. Am. Chem. Soc*. **1981**, *103*, 6761.
131. L. S. Hollis and S. J. Lippard, *Inorg. Chem.* **1982**, *21*, 2116.
132. L. S. Hollis and S. J. Lippard, *Inorg. Chem.* **1983**, *22*, 2605.
133. L. S. Hollis, M. M. Roberts and S. J. Lippard, *Inorg. Chem.* **1983**, *22*, 3637.
134. T. V. O'Halloran, M. M. Roberts and S. J. Lippard, *Inorg. Chem.* **1986**, *25*, 957.
135. R. Faggiani, B. Lippert, C. J. L. Lock and R. A. Speranzini, *J. Am. Chem. Soc*. **1981**, *103*, 1111.
136. See footnote 12 in Ref. 135.
137. T. Wienkötter, M. Sabat, G. Fusch and B. Lippert, *Inorg. Chem.* **1995**, *34*, 1022.
138. G. Kampf, M. Willermann, E. Freisinger and B. Lippert, *Inorg. Chim. Acta* **2002**, *330*, 179.
139. G. Kampf, M. Willermann, E. Zangrando, L. Randaccio and B. Lippert, *Chem. Commun.* **2001**, 747.
140. See, for example, T. Uemura, T. Shimura, H. Nakanishi, T. Tomohiro, Y. Nagawa and H. Okuno, *Inorg. Chim. Acta* **1991**, *181*, 11 and references cited therein.
141. G. Cervantes, M. J. Prieto and V. Moreno, *Metal–Based Drugs* **1997**, *4*, 9.
142. B. Lippert, H. Schöllhorn and U. Thewalt, *Z. Naturforsch* **1983**, *38b*, 1441.
143. H. Schöllhorn, P. Eisenmann, U. Thewalt and B. Lippert, *Inorg. Chem.* **1986**, *25*, 3384.
144. B. Lippert, H. Schöllhorn and U. Thewalt, *J. Am. Chem. Soc*. **1986**, *108*, 525.
145. B. Lippert, H. Schöllhorn and U. Thewalt, *Inorg. Chem.* **1986**, *25*, 407.
146. H. Schöllhorn, U. Thewalt and B. Lippert, *J. Chem. Soc., Chem. Commun*. **1986**, 258.
147. B. Lippert, *New J. Chem*. **1988**, *12*, 715.
148. T. Abe, H. Moriyama and K. Matsumoto, *Chem. Lett*. **1989**, 1857.
149. T. Abe, H. Moriyama and K. Matsumoto, *Inorg. Chem.* **1991**, *30*, 4198.
150. K. Sakai, Y. Tanaka, Y. Tsuchiya, K. Hirata, T. Tsubomura, S. Iijima and A. Bhattacharjee, *J. Am. Chem. Soc.* **1998**, *120*, 8366.
151. K. Matsumoto and K. Harashima, *Inorg. Chem.* **1991**, *30*, 3032.
152. K. Ito, R. Somazawa, J. Matsunami and K. Matsumoto, *Inorg. Chim. Acta* **2002**, *339*, 292.
153. N. Saeki, Y. Hirano, Y. Sasamoto, I. Sato, T. Toshida, S. Ito, N. Nakamura, K. Ishihara and K. Matsumoto, *Eur. J. Inorg. Chem.* **2001**, 2081.
154. N. Saeki, Y. Hirano, Y. Sasamoto, I. Sato, T. Toshida, S. Ito, N. Nakamura, K. Ishihara and K. Matsumoto, *Bull. Chem. Soc. Jpn.* **2001**, *74*, 861.
155. M. Peilert, S. Weißbach, E. Freisinger, V. I. Korsunsky and B. Lippert, *Inorg. Chim. Acta* **1997**, *265*, 187.
156. J. Müller, E. Freisinger, P. J. Sanz Miguel and B. Lippert, *Inorg. Chem*. **2003**, *42*, 5117.
157. D. M. L. Goodgame, R. W. Rollins and A. C. Skapski, *Inorg. Chim. Acta* **1984**, *83*, L11.
158. D. M. L. Goodgame, R. W. Rollins, A. M. Z. Slawin, D. J. Williams and P. W. Zard, *Inorg. Chim. Acta* **1986**, *120*, 91.
159. K. Umakoshi, I. Kinoshita, A. Ichimura and S. Ooi, *Inorg. Chem.* **1987**, *26*, 3551.
160. J. Jolly, W. I. Cross, R. G. Pritchard, C. A. McAuliffe and K. B. Nolan, *Inorg. Chim. Acta* **2001**, *315*, 36.
161. K. Umakoshi and Y. Sasaki, *Inorg. Chem*. **1997**, *36*, 4296.
162. K. Umakoshi, T. Yamasaki, A. Fukuoka, H. Kawano, M. Ichikawa and M. Onisji, *Inorg. Chem*. **2002**, *41*, 4093.
163. R. Cini, F. P. Fanizzi, F. P. Intini and G. Natile, *J. Am. Chem. Soc*. **1991**, *113*, 7805.
164. G. Bandoli, P. A. Caputo, F. P. Intini, M. F. Sivo and G. Natile, *J. Am. Chem. Soc.* **1997**, *119*, 10370.
165. T. Yamaguchi, O. Kubota and T. Ito, *Chem. Lett.* **2003**, *33*, 190.

Pictiva EX2004
Samsung v Pictiva
IPR2024-01094

166. L. A. M. Baxter, G. A. Heath, R. G. Raptis and A. C. Willis, *J. Am. Chem. Soc.* **1992**, *114*, 6944.
167. A. A. Sidorov, M. O. Ponina, S. E. Nefedov, I. L. Eremenko, Yu. A. Ustynyuk and Yu. M. Luzikov, *Russ. J. Inorg. Chem.* **1997**, 42, 853.
168. P. D. Prenzler, G. A. Heath, S. B. Lee and R. G. Raptis, *Chem. Commun.* **1996**, 2271.
169. M. Maliarik, J. Glaser and I. Tóth, *Inorg. Chem.* **1998**, *37*, 5452.
170. F. Jalilehvand, M. Maliarik, J. Mink, M. Sandström, A. Ilyukhin and J. Glaser, *J. Phys. Chem. A* **2002**, *106*, 3501.
171. G. L. Simon, A. W. Adamson and L. F. Dahl, *J. Am. Chem. Soc.* **1972**, *94*, 7654.
172. F. A. Cotton, N. S. Dalal, E. A. Hillard, P. Huang, C. A. Murillo and C. M. Ramsey, *Inorg. Chem.* **2003**, *42*, 1388.
173. D. J. Santure, J. C. Huffman and A. P. Sattelberger, *Inorg. Chem.* **1985**, *24*, 371.
174. F. A. Cotton, J. H. Matonic and C. A. Murillo, *Inorg. Chem.* **1996**, *35*, 498.
175. M. Yamashita, S. Miya, T. Kawashima, T. Manabe, T. Sonoyama, H. Kitagawa, T. Mitani, H. Okamoto and R. Ikeda, *J. Am. Chem. Soc*. **1999**, *121*, 2321.
176. L. G. Butler, M. H. Zietlow, C.-M. Che, W. P. Schaefer, S. Sridhar, P. J. Grunthaner, B. I. Swanson, R. J. H. Clark and H. B. Gray, *J. Am. Chem. Soc*. **1988**, *110*, 1155.
177. S. Jin, T. Ito, K. Toriumi and M. Yamashita, *Acta Crystallogr*. **1989**, *C45*, 1415.
178. M. Yamashita and K. Toriumi, *Inorg. Chim. Acta* **1990**, *178*, 143.
179. H. Kitagawa, N. Onodera, T. Sonoyama, M. Yamamoto, T. Fukawa, T. Mitani, M. Seto and Y. Maeda, *J. Am. Chem. Soc.* **1999**, *121*, 10068.
180. V. Robert, S. Petit and S. A. Borshch, *Inorg. Chem*. **1999**, *38*, 1573.
181. S. J. Lippard, *Science* **1982**, *218*, 1075.
182. A. I. Stetsenko and L. S. Tikhonova, *Koord. Khim*. **1989**, *15*, 867; *Sov. J. Coord. Chem*. **1989**, *15*, 515.
183. B. Lippert, *Prog. Inorg. Chem.* **1989**, *37*, 1.
184. K. A. Hofmann and G. Bugge, *Ber*. **1908**, *41*, 312.
185. R. D. Gillard and G. Wilkinson, *J. Chem. Soc*. **1964**, 2835.
186. D. B. Brown, R. D. Burbank and M. B. Robin, *J. Am. Chem. Soc*. **1969**, *91*, 2895.
187. A. K. Johnson and J. D. Miller, *Inorg. Chim. Acta* **1977**, *22*, 219.
188. C. M. Flynn, Jr, T. S. Viswanathan and R. B. Martin, *J. Inorg. Nucl. Chem*. **1977**, *39*, 437.
189. J. P. Davidson, P. J. Faber, R. G. Fischer, Jr, S. Mansy, H. J. Peresie, B. Rosenberg and L. Van Camp, *Cancer Chemother. Rep*. **1975**, *59*, 287.
190. B. Rosenberg, *Cancer Chemother. Rep*. **1975**, *59*, 589.
191. J. K. Barton, H. N. Rabinowitz, D. J. Szalda and S. J. Lippard, *J. Am. Chem. Soc*. **1977**, *99*, 2827.
192. J. K. Barton, D. J. Szalda, H. N. Rabinowitz, J. V. Waszczak and S. J. Lippard, *J. Am. Chem. Soc*. **1979**, *101*, 1434.
193. A. P. Ginsberg, T. V. O'Halloran, P. E. Fanwick, L. S. Hollis and S. J. Lippard, *J. Am. Chem. Soc*. **1984**, *106*, 5430.
194. L. S. Hollis and S. J. Lippard, *J. Am. Chem. Soc*. **1983**, *105*, 3494.
195. L. S. Hollis and S. J. Lippard, *Inorg. Chem.* **1983**, *22*, 2708.
196. L. S. Hollis and S. J. Lippard, *J. Am. Chem. Soc*. **1981**, *103*, 1230.
197. T. V. O'Halloran, M. M. Roberts and S. J. Lippard, *J. Am. Chem. Soc*. **1984**, *106*, 6427.
198. T. V. O'Halloran, P. K. Mascharak, I. D. Williams, M. M. Roberts and S. J. Lippard, *Inorg. Chem.* **1987**, *26*, 1261.
199. K. Matsumoto, H. Takahashi and K. Fuwa, *J. Am. Chem. Soc*. **1984**, *106*, 2049.
200. K. Matsumoto, *Bull. Chem. Soc. Jpn.* **1985**, *58*, 651.
201. K. Matsumoto and K. Fuwa, *J. Am. Chem. Soc*. **1982**, *104*, 897.
202. K. Matsumoto, H. Takahashi and K. Fuwa, *Inorg. Chem.* **1983**, *22*, 4086.
203. K. Sakai, T. Tsubomura and K. Matsumoto, *Inorg. Chim. Acta* **1993**, *213*, 11.
204. K. Matsumoto and T. Watanabe, *J. Am. Chem. Soc*. **1986**, *108*, 1308.
205. K. Matsumoto and K. Harashima, *Inorg. Chem.* **1991**, *30*, 3032.
206. J. K. Barton, C. Caravana and S. J. Lippard, *J. Am. Chem. Soc*. **1979**, *101*, 7269.

Pictiva EX2004
Samsung v Pictiva
IPR2024-01094

207. K. Sakai and K. Matsumoto, *J. Am. Chem. Soc*. **1989**, *111*, 3074.
208. B. Lippert and D. Neugebauer, *Inorg. Chem.* **1982**, *21*, 451.
209. P. K. Mascharak, I. D. Williams and S. J. Lippard, *J. Am. Chem. Soc*. **1984**, *106*, 6428.
210. B. Lippert, H. Schöllhorn and U. Thewalt, *Inorg. Chem.* **1987**, *26*, 1736.
211. A. I. Stetsenko, L. S. Tikhonova, L. I. Iozep, A.M. Demkin and Yu. P. Kostikov, *Koord. Khim.* **1990**, *16*, 1570; *Sov. J. Coord. Chem*. **1990**, *16*, 837.
212. O. Renn, A. Albinati and B. Lippert, *Angew. Chem., Int. Ed. Engl.* **1990**, *29*, 84.
213. T. N. Fedotova, P. A. Koz'min, G. N. Kuznetsova, M. D. Surazhskaya and I. B. Baranovskii, *Russ. J. Inorg. Chem*. **1999**, *44*, 659.
214. K. Sakai, E. Ishigami, Y. Konno, T. Kajiwara and T. Ito, *J. Am. Chem. Soc.* **2002**, *124*, 12088.
215. W. Micklitz, G. Muller, J. Riede and B. Lippert, *J. Chem. Soc., Chem. Commun*. **1987**, 76.
216. W. Micklitz, G. Muller, B. Huber, J. Riede, F. Rashwan, J. Heinze and B. Lippert, *J. Am. Chem. Soc.* **1988**, *110*, 7084.
217. G. S. Muraveiskaya, V. E. Abashkin, O. N. Evstaf'eva and I. F. Golovaneva, *Zh. Neorg. Khim*. **1989**, *34*, 921; *Russ. J. Inorg. Chem.* **1989**, *34*, 516.
218. R. Usón, J. Forniés, L. R. Falvello, M. Tomás, J. M. Casas, A. Martín and F. A. Cotton, *J. Am. Chem. Soc.* **1994**, *116*, 7160.
219. E. Yu. Tyulyaeva, T. N. Lomova and L. G. Andrianova, *Russ. J. Inorg. Chem*. **2001**, *46*, 371.
220. See ref. 15 for a summary of the literature and a critical appraisal of these results.
221. D. N. Mason, G. B. Deacon, L. J. Yellowlees and A. M. Bond, *Dalton Trans*. **2003**, 890.

Pictiva EX2004
Samsung v Pictiva
IPR2024-01094

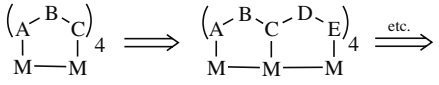
15

Extended Metal Atom Chains

John F. Berry,
Texas A&M University

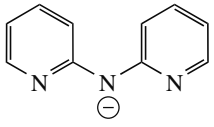
15.1 Overview

The previous chapters of this book have shown that the chemistry of dinuclear compounds with metal–metal bonds is extensive. But why should this chemistry be limited to bonds between only two metal atoms? As will be seen in this chapter, it is not. By using expanded bridging ligands as in **15.1**, it is possible to synthesize extended metal atom chain (EMAC) compounds. Such EMACs with polypyridylamido or related ligands will be the main subject of this chapter. Brief reviews on this subject have appeared.[1]



15.1

The first EMAC was synthesized serendipitously in 1968 by Hurley and Robinson and formulated as $Ni_3(dpa)_4Cl_2$ (dpa is the anion of di-2-pyridylamine; see **15.2**).[2]



di-2,2'-pyridylamide (dpa)

15.2

Though Hurley and Robinson were able to ascertain the trinickel formula $Ni_3(dpa)_4Cl_2$ from careful elemental analysis, they postulated a structure which was shown in 1991 by X-ray crystallography[3] to be incorrect. The correct structure, as determined by Aduldecha and Hathaway,[3] is shown in Fig. 15.1a, and an end-on view along the Ni_3 axis is shown in Fig. 15.1b. This compound contains only d^8 Ni^{2+} ions and therefore Ni–Ni bonds are not expected, though subsequently, tricobalt,[4] triruthenium,[5] trirhodium,[5] and trichromium[6] complexes of dpa have been synthesized, all of which have metal–metal bonds.

Pictiva EX2004
Samsung v Pictiva
IPR2024-01094

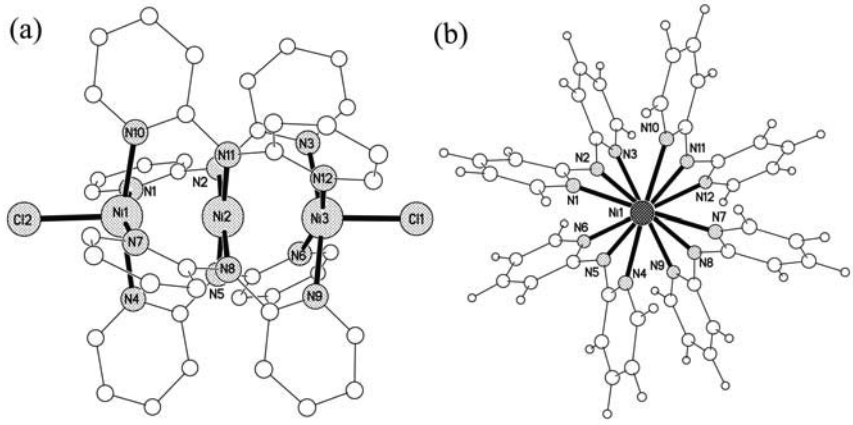
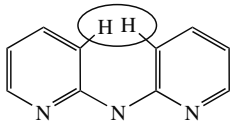


Fig. 15.1. The structure of $Ni_3(dpa)_4Cl_2$ shown (a) perpendicular to the Ni_3 axis, and (b) along the Ni_3 axis.

The type of structure in Fig. 15.1 is typical of the compounds discussed in this chapter. Four dpa anions wrap helically around the trimetal chain with a considerable torsion angle, typically ~50° from end to end. This torsion angle can be attributed to steric repulsions between opposite pyridyl hydrogen atoms as in **15.3**.



15.3

The metal ions are most often in the +2 oxidation state, though other oxidation states are known, and anionic ligands, usually in axial positions, are present in order to balance the charge. These range from simple halides (Cl, Br) to pseudohalides (CN, NCS) to more complex anions (C≡CPh, $Ag(CN)_2$). Neutral molecules such as water or acetonitrile are also known to occupy axial positions.

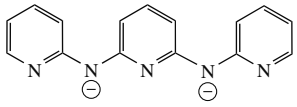
The dpa ligand is the shortest in a series of polypyridylamide ligands (see **15.4**), which have been shown to stabilize linear arrays of five,[7] seven,[8] and even nine[9] metal atoms in compounds with the general formula $M_n(L)_4X_2$ (for n = 5, L = tpda; n = 7, L = teptra; n = 9, L = peptea).[†] The synthetic methodology exists to produce ligands which can hold greater numbers of metal atoms.

The study of EMACs focuses primarily on their interesting physical properties. The magnetic properties of polypyridylamido complexes are of importance, since the large majority of these compounds contain unpaired electrons. For example, $Co_3(dpa)_4Cl_2$ has been shown to undergo a thermally induced spin transition from a low-spin (S = ½) to a high-spin (S = $^3/_2$ or $^5/_2$) state.[10] Also, the structural results are often complicated. Both $Cr_3(dpa)_4Cl_2$[11] and $Co_3(dpa)_4Cl_2$[10] have

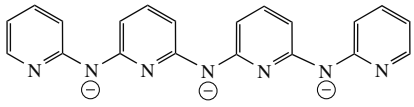
[†] The nomenclature for these ligands follows from the number of pyridyl groups and amido groups of the ligand. The ligand shown in **15.4** which holds five metal atoms has three pyridyl groups and two amido groups and is thus called "tripyridyldiamide," with the abbreviation tpda. The ligand teptra is thus "tetrapyridyltriamide," and peptea is "pentapyridyltetraamide."

Pictiva EX2004
Samsung v Pictiva
IPR2024-01094

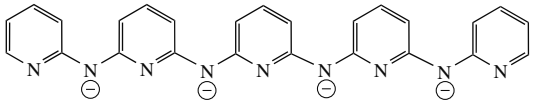
been shown to exist in crystalline polymorphs with drastically different metal-metal distances. In some forms, the two M–M distances of the compound are equivalent yielding a symmetrical D_4 core structure. In other cases, the compounds are distinctly unsymmetrical (C_4 symmetry) with a short M–M distance and a long M···M separation with Δd(M–M) (i.e. the difference between the two independent M–M distances) as much as 0.18 Å (see **15.5**). This phenomenon is relevant to Cr_5 chains also.[12]



tripyridyldiamide = tpda

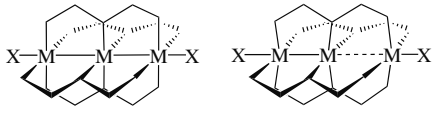


tetrapyridyltriamide = teptra



pentapyridyltetraamide = peptea

15.4



s-$M_3(dpa)_4X_2$ *u*-$M_3(dpa)_4X_2$

15.5

Theoretical work on EMACs is important to the understanding of their properties. The molecular orbital (MO) theory of metal-metal bonds as presented in Chapter 1 is useful in describing the electronic structures of oligomeric chains. Calculations have been performed using DFT for $Co_3(dpa)_4Cl_2$[13] and $Cr_3(dpa)_4Cl_2$[14] in order to explain some of the experimental results. Also, qualitative MO diagrams for $M_3(dpa)_4Cl_2$[15] and $M_3(tpda)_4Cl_2$[16] have been proposed. At some point, as the EMACs become longer, the discrete molecular orbitals must be viewed as comprising continuous bands, and simple MO theory must give way to the band theory for a proper description of the electronic structure. Detailed descriptions of this are beyond the scope of this book, though it should be noted that band calculations on a hypothetical infinite chain of equally spaced Cr^{2+} atoms with a polypyridylamido backbone have been performed.[17]

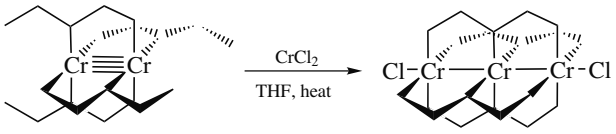
The remainder of the chapter will discuss the synthetic, structural, physical, and theoretical work done for polypyridylamido complexes of chromium, cobalt, nickel, and second row metals. Other recent developments in the chemistry of EMACs will be discussed lastly.

15.2 EMACs of Chromium

The parent trichromium dipyridylamido compound, $Cr_3(dpa)_4Cl_2$, is prepared in high yield in a straightforward reaction between excess $CrCl_2$ and lithium dipyridylamide in THF.[6,11] In

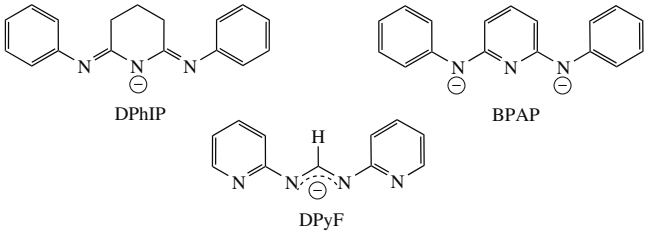
Pictiva EX2004
Samsung v Pictiva
IPR2024-01094

the early stages of the reaction, red quadruply-bonded $Cr_2(dpa)_4$ is formed, which is then converted to the green $Cr_3(dpa)_4Cl_2$ upon heating to reflux as shown in **15.6**. A ligand shuffling process is proposed in this transformation of the ligands from a *trans*-2:2 geometry in $Cr_2(dpa)_4$ to the μ_3 bridging mode in the trinuclear species.[18] Such a ligand shuffling process has recently been studied by variable temperature NMR spectroscopy for a dichromium complex with multidentate ligands.[19]



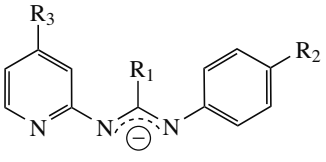
15.6

This synthetic method is also employed in the preparation of trichromium complexes of the ligands DPhIP[20] (di(phenylimino)piperidinate), BPAP[21] (2,6-bisphenylaminopyridinate), and DPyF[22] (dipyridylformamidinate), shown schematically in **15.7**.



15.7

Unsymmetrical amidinate ligands have also been used, with various substituents on the aryl rings, as in **15.8**.[23]



PhPyF: $R_1 = R_2 = R_3 = H$
PhPyBz: $R_1 = Ph$, $R_2 = R_3 = H$
AniPyF: $R_1 = R_3 = H$, $R_2 = OMe$
TolPyF: $R_1 = R_3 = H$, $R_2 = Me$
^{F}PhPyF: $R_1 = R_3 = H$, $R_2 = F$
PhPcF: $R_1 = R_2 = H$, $R_3 = Me$

15.8

Replacement of one of the axial Cl ions by a BF_4[6] or PF_6[11] anion is achieved by metathesis with one equivalent of the corresponding silver reagent, but reaction with more than one equivalent of silver causes oxidation of the Cr_3^{6+} unit to Cr_3^{7+}.[24] For example, reaction of $Cr_3(dpa)_4Cl_2$ with two equivalents of $AgBF_4$ yields the oxidized complex $[Cr_3(dpa)_4F(BF_4)]BF_4$ shown in Fig. 15.2. The axial Cl ions can also be replaced by phenylacetylide by reaction of $Cr_3(dpa)_4Cl_2$ with LiC≡CPh.[11,18] This reaction was difficult to control, and pure products were not obtained. Recently, $Cr_3(dpa)_4(CCPh)_2$ has been prepared in good yields and excellent purity by using $[Cr_3(dpa)_4(NCCH_3)_2](PF_6)_2$ as starting material.[25]

Pictiva EX2004
Samsung v Pictiva
IPR2024-01094

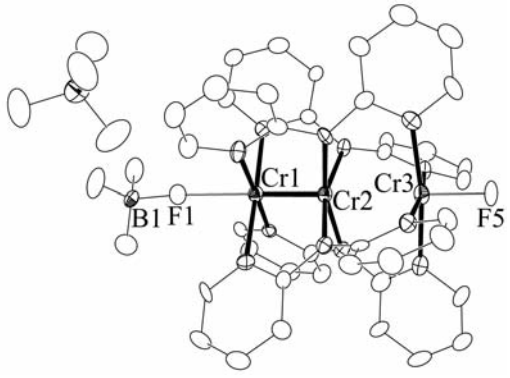


Fig. 15.2. Structure of $[Cr_3(dpa)_4F(BF_4)]BF_4$.

By far the most facile reactions are oxidations. The parent compound $Cr_3(dpa)_4Cl_2$ has a reversible one-electron oxidation wave at $E_{½}$ = 74 mV vs Ag/AgCl[11] and thus mild oxidants such as ferrocenium salts react to convert $Cr_3(dpa)_4Cl_2$ to the corresponding cation $[Cr_3(dpa)_4Cl_2]^+$.[24]

$$Cr_3(dpa)_4Cl_2 + [Cp_2Fe]X \rightarrow [Cr_3(dpa)_4Cl_2]X + Cp_2Fe$$

Structurally characterized Cr_3^{6+} and Cr_3^{7+} compounds are listed in Table 15.1. The variability of the Cr–Cr bond lengths in these structures is compounded by the fact that the Cr_3 chains can exist in symmetric (D_4) or unsymmetric (C_4) forms. The question of whether a Cr_3^{6+} chain is symmetrical or unsymmetrical appears to have its answer in the properties of the bridging and axial ligands. For $Cr_3(dpa)_4Cl_2$, all of the known structures contain unsymmetrical molecules, though replacement of the chloride ligands by cyanide ligands results in a symmetrical complex of D_4 symmetry.[26] Complexes of the unsymmetrical amidinates also form symmetrical chains.[23,27] Trichromium complexes of the ligands DPyF,[22] DPhIP,[20] and BPAP[21] are all unsymmetrical, however, each with a very short Cr–Cr quadruple bond (< 2.0 Å) and a long distance to the isolated Cr(II) species (2.59 to 2.74 Å). Complexes with an unsymmetrical set of axial ligands, or no axial ligands at all, are in all cases unsymmetrical. Furthermore, all known Cr_3^{7+} compounds have unsymmetrical chains with short Cr_2^{4+} quadruple bonds and long distances to the isolated Cr^{3+} ions.[24]

All of the known trichromium compounds are paramagnetic. Variable temperature magnetic susceptibility data for both symmetrical and unsymmetrical Cr_3^{6+} compounds follow the Curie law with μ_{eff} = 4.6 - 5.1 μ_B corresponding to four unpaired electrons.[11] Thus, it is not possible to distinguish between symmetrical and unsymmetrical compounds by magnetic susceptibility data alone. For the unsymmetrical Cr_3^{6+} compounds, the four unpaired electrons are thought to be localized on the isolated high spin Cr^{2+} ion (since the quadruply bonded Cr_2^{4+} unit is diamagnetic). In the case of the symmetrical Cr_3^{6+} species, the four unpaired electrons are thought to be delocalized over the Cr_3 chain. A qualitative MO scheme for the symmetrical Cr_3 compounds has been presented to account for this[15] and it is shown in 15.9a. Since the Cr–Cr distances are fairly long, the δ interactions of the d_{xy} orbitals are neglected. Thus, the δ orbitals and the π nonbonding orbitals are essentially degenerate, and using Hund's rule to fill in the 12 electrons for a Cr_3^{6+} unit, the ground state therefore has S = 2.

Pictiva EX2004
Samsung v Pictiva
IPR2024-01094

Table 15.1. Structural data for trimetal EMACs

Cr_3^{6+} Compounds

Compound	Space Group	Cr1–Cr2, Å	Cr2–Cr3, Å	μ_{eff}, μ_B	Remark[a]	ref.
$Cr_3(dpa)_4Cl_2 \cdot CH_2Cl_2$	*P*nn2	2.254(4)	2.477(4)	5.1	U	26[c]
$Cr_3(dpa)_4Cl_2 \cdot C_6H_6$	*P*na2$_1$	2.227[9], 2.236[9][b]	2.483[9], 2.481[9][b]	NR	U	26[c]
$Cr_3(dpa)_4Cl_2 \cdot C_7H_8$	*P*ca2$_1$	2.24[1][e]	2.48[1][e]	NR	U	26[c]
$Cr_3(dpa)_4Cl_2 \cdot THF$	*P*$\bar{4}$n2	2.365(2)[d]	2.365(2)[d]	NR	S	11[d]
$Cr_3(dpa)_4Cl(BF_4) \cdot CH_2Cl_2$	*C*2/c	1.9952(8)	2.6427(8)	3.29	U	6
$Cr_3(dpa)_4Cl(PF_6) \cdot 2CH_2Cl_2$	*C*2/c	2.008(1)	2.614(1)	4.62	U	11
$Cr_3(dpa)_4(NCS)_2 \cdot 2C_2H_4Cl_2$	*P*2$_1$/c	2.277(2)	2.391(2)	NR	U	67
$Cr_3(dpa)_4(C{\equiv}CPh)_2$[f]	*P*2$_1$/c	2.415(2)	2.422(2)	NR	S	11
$[Cr_3(DPhIP)_4Cl]Cl \cdot 1.5CH_2Cl_2 \cdot 0.5H_2O$	*P*2$_1$/c	1.932(2)	2.659(2)	NR	U	20
$[Cr_3(DPhIP)_4(NCMe)](PF_6)_2 \cdot H_2O \cdot 4CH_3CN$	*P*4/n	1.907(2)	2.633(2)	4.3	U	20
$(NBu_4)_2[Cr_3(BPAP)_4] \cdot THF$	*C*2/c	1.904(3)	2.589(2)	NR	U	21
$Cr_3(PhPyBz)_4Cl_2 \cdot 1.64CH_2Cl_2 \cdot 0.52hexane \cdot 0.42THF$	*P*$\bar{1}$	2.269(1)	2.513(1)	5.3	U	23
$Cr_3(PhPyF)_4Cl_2 \cdot CH_2Cl_2$	*P*4$_3$2$_1$2	2.4380(8)	2.4602(8)	4.78(2)	S	27
$Cr_3(AniPyF)_4Cl_2$	*P*2$_1$/c	2.4789(7)	2.4759(7)	4.69(1)	S	27
$Cr_3(TolPyF)_4Cl_2 \cdot 2H_2O$	*P*ccn	2.4298(9)	2.4298(9)	NR	S	27
$Cr_3(^FPhPyF)_4Cl_2$	*P*$\bar{1}$	2.460(1)	2.500(1)	NR	S	27
$Cr_3(PhPcF)_4Cl_2 \cdot THF \cdot 0.5hexane$	*C*2/c	2.4743(8)	2.4743(8)	4.65(2)	S	27
$Cr_3(PhPcF)_4Cl_2 \cdot 0.61Et_2O$	*P*2/n	2.216(1)	2.646(1)	4.70(1)	U	27

Pictiva EX2004
Samsung v Pictiva
IPR2024-01094

Cr_3^{7+} Compounds, All Are Unsymmetrical

Compound	Space Group	Cr–Cr, Å	Cr···Cr, Å	μ_{eff}, μ_B	ref.
$[Cr_3(dpa)_4Cl_2]Cl\cdot 2CH_2Cl_2\cdot THF$	*I*bca	2.12(1)[e]	2.47(1)[e]	3.85(5)	24
$[Cr_3(dpa)_4Cl_2]AlCl_4\cdot CH_2Cl_2$	$P2_1/n$	2.010(1)	2.555(1)	3.85(5)	24
$[Cr_3(dpa)_4Cl_2]FeCl_4\cdot CH_2Cl_2$	$P2_1/n$	2.009(1)	2.562(1)	NR	24
$[Cr_3(dpa)_4Cl_2]I_3\cdot THF\cdot 2H_2O$	$P2_1/c$	2.08(1), 2.09(2)[e]	2.49(1), 2.48(2)[e]	NR	24
$[Cr_3(dpa)_4Cl_2]PF_6\cdot 2CH_2Cl_2$	$P2_1/n$	2.09(2), 2.09(2)[e]	2.48(2), 2.48(2)[e]	NR	24
$[Cr_3(dpa)_4F(BF_4)]BF_4\cdot 2CH_2Cl_2\cdot C_6H_{14}$	$Pna2_1$	1.900(2), 1.906(2)[b]	2.596(3), 2.579(3)[b]	4.4	6
$[Cr_3(dpa)_4ClF]BF_4\cdot CH_2Cl_2\cdot C_6H_{14}$	$P2_1/n$	2.039(5), 2.066(9)[e]	2.507(4), 2.491(9)[e]	NR	24
$[Cr_3(DPhIP)_4F(NCMe)](BF_4)_2\cdot 5MeCN$	$P4/n$	1.968(2)	2.594(2)	NR	20

Crystal Structures of $Co_3(dpa)_4Cl_2$

Interstitial Molecules	T, K	Space Group	Co1–Co2	Co2–Co3	μ_{eff}, μ_B	Remark[a]	ref.
$2CH_2Cl_2\cdot H_2O$		$I4$[g]	2.290(3)	2.472(3)	2.6	U	4
$Co(dpa)_2$		$P4/n$	2.285(1)	2.459(1)	NR	U	31
CH_2Cl_2	296	*P*nn2	2.3369(4)	2.3369(4)	2.9	S	10
	168	*P*nn2	2.3178(9)	2.3178(9)	NR	S	31,32
	109	*P*n	2.3224(8)	2.3214(8)	NR	S	10
	20	*P*n	2.34(1)	2.34(1)	NR	S	10
$2CH_2Cl_2$	298	$I\bar{4}$	2.299(1)	2.471(1)	4.4	U	10
	213	$I\bar{4}$	2.294(1)	2.466(1)	NR	U	39
	173	$I\bar{4}$	2.2958(9)	2.457(1)	NR	U	10
	133	$I\bar{4}$	2.295(1)	2.440(1)	NR	U	10
	20	$I\bar{4}$	2.3035(7)	2.3847(8)	NR	U	10

Pictiva EX2004
Samsung v Pictiva
IPR2024-01094

Interstitial Molecules	T, K	Space Group	Co1–Co2	Co2–Co3	μ_{eff}, μ_B	Remark[a]	ref.
$0.85Et_2O{\cdot}0.15CH_2Cl_2$	296	$P2_1/c$	2.3230(3)	2.3667(4)	3.5	S	40
	213	$P2_1/c$	2.3193(3)	2.3352(3)	NR	S	40
	120	$P2_1/c$	2.3191(3)	2.3304(3)	NR	S	40
THF	295	$Pccn$	2.3484(4)	2.4234(8)	4	sl. U	40
	120	$Pccn$	2.3111(4)	2.4402(7)	NR	U	40
cyclohexane	295	$Pccn$	2.3620(5)	2.3620(5)	4	S	40
	213	$Pccn$	2.3311(5)	2.3311(5)	NR	S	40
	120	$P2_1/c$	2.3127(5)	2.3253(5)	NR	S	40
benzene	316	$Pca2_1$	2.3417(9)	2.3665(9)	4.2	S	40
	260	$Pna2_1$	2.324(1), 2.323(1)[b]	2.350(1), 2.346(1)[b]	NR	S	40
	213	$Pna2_1$	2.323(1), 2.326(2)[b]	2.344(2), 2.338(2)[b]	NR	S	40
	170	$Pna2_1$	2.3135(8), 2.3189(8)[b]	2.3280(8), 2.3283(8)[b]	NR	S	40
1.75toluene·0.5hexane	298	$P\bar{1}$	2.310(2), 2.312(2)[b]	2.471(2), 2.442(2)[b]	4.25	U U	40
	170	$P\bar{1}$	2.3046(6), 2.3084(6)[b]	2.4216(6), 2.3622(6)[b]	NR	U sl. U	40
	110	$P\bar{1}$	2.3135(6), 2.3174(6)[b]	2.3728(6), 2.3245(6)[b]	NR	sl. U S	40
	90	$P\bar{1}$	2.3098(6), 2.3139(6)[b]	2.3660(6), 2.3196(6)[b]	NR	sl. U S	40

Other Co_3^{6+} Compounds

Compound	T, K	Space Group	Co1–Co2	Co2–Co3	μ_{eff}, μ_B	Remark[a]	ref.
$Co_3(dpa)_4Cl(BF_4){\cdot}2CH_2Cl_2$		$C2/c$	2.277(2)	2.504(2)	NR	U	32
$Co_3(dpa)_4(BF_4)_2{\cdot}2CH_2Cl_2$		$P2_1/c$	2.254(2)	2.252(2)	NR	S	32

Pictiva EX2004
Samsung v Pictiva
IPR2024-01094

Compound	T, K	Space Group	Co1–Co2	Co2–Co3	μ_{eff}, μ_B	Remark[a]	ref.
$Co_3(dpa)_4(CN)_2 \cdot CH_2Cl_2$		*P*nn2	2.3392(2)	2.3392(2)	2.1	S	35
$Co_3(dpa)_4(NCS)_2 \cdot 1.5CH_2Cl_2$		$P2_1/c$	2.3223(6)	2.3087(6)	2.5	S	35
$Co_3(dpa)_4(NCS)_2 \cdot 2CH_2Cl_2$		$P\bar{1}$	2.300(2)[b]	2.344(2)[b]	NR	sl. U	67
			2.311(2)[b]	2.324(2)[b]		S	
$Co_3(dpa)_4(NCS)_2 \cdot 5THF$		$P\bar{1}$	2.313(2)	2.309(2)	NR	S	35
$Co_3(dpa)_4(NCS)_2 \cdot 2toluene$		*F*dd2	2.3140(8)	2.3140(8)	NR	S	35
$Co_3(dpa)_4(NCNCN)_2 \cdot 2CH_2Cl_2$		$P2_1/c$	2.3194(8)	2.3184(8)	2.2	S	35
$[Co_3(dpa)_4(NCMe)_2](PF_6)_2 \cdot 3MeCN$		$P\bar{1}$	2.301(1)	2.304(1)	2.25	S	33
$[Co_3(dpa)_4(NCMe)_2](PF_6)_2 \cdot MeCN \cdot 2Et_2O$	213	$P2_1$	2.300(1)	2.298(1)	NR	S	33
	163	$P2_1$	2.301(1)	2.299(1)	NR	S	33
$Co_3(dpa)_4Br_2 \cdot CH_2Cl_2$	240	*P*nn2	2.3234(6)	2.3234(6)	2.7	S	34
	147	*P*nn2	2.3182(8)	2.3182(8)	NR	S	34
	111	*P*nn2	2.3164(8)	2.3164(8)	NR	S	34
$Co_3(dpa)_4Br_2 \cdot cyclohexane$	298	*P*2/n	2.3830(3)	2.3830(3)	NR	S	34
	213	*P*2/n	2.3566(3)	2.3566(3)	NR	S	34
	150	*P*2/n	2.3262(3)	2.3262(3)	NR	S	34
	110	*P*2/n	2.3188(2)	2.3188(2)	NR	S	34
$Co_3(dpa)_4Br_2 \cdot 1.75toluene \cdot 0.5hexane$	295	$P\bar{1}$	2.312(1),	2.469(1),	NR	U	34
			2.323(1)[b]	2.433(1)[b]		U	
	213	$P\bar{1}$	2.305(1),	2.451(1),	NR	U	34
			2.3099(9)[b]	2.392(1)[b]		sl. U	
	170	$P\bar{1}$	2.3062(9),	2.4313(9),	NR	U	34
			2.3118(8)[b]	2.3536(9)[b]		sl. U	
	110	$P\bar{1}$	2.3097(9),	2.3892(9),	NR	sl. U	34
			2.3173(8)[b]	2.3162(8)[b]		S	

Pictiva EX2004
Samsung v Pictiva
IPR2024-01094

Compound	T, K	Space Group	Co1–Co2	Co2–Co3	μ_{eff}, μ_B	Remark[a]	ref.
$Co_3(depa)_4Cl_2$	213	$P\bar{4}n2$	2.3611(7)	2.3611(7)	NR	S	36
$Co_3(depa)_4Cl_2 \cdot 0.5$hexane	213	$P\bar{4}n2$	2.3609(5)	2.3609(5)	NR	S	36
	297	$P\bar{4}n2$	2.3787(7)	2.3787(7)	4.9	S	36
$Co_3(depa)_4Cl_2 \cdot$acetone	213	$P\bar{4}n2$	2.352(1)	2.352(1)	NR	S	36
$Co_3(depa)_4Cl_2 \cdot 4CH_2Cl_2 \cdot 2H_2O$	213	$I\bar{4}c2$	2.3309(8)	2.3309(8)	NR	S	36
$Co_3(depa)_4(CN)_2 \cdot 0.5$hexane	213	$P\bar{4}n2$	2.3371(4)	2.3371(4)	2.7	S	36
$Co_3(depa)_4(CN)_2 \cdot 4CH_2Cl_2 \cdot 2H_2O$	213	$I\bar{4}c2$	2.3357(7)	2.3357(7)	NR	S	36
Co_3^{7+} Compounds							
$[Co_3(dpa)_4Cl_2]BF_4 \cdot xCH_2Cl_2$	300	$P2_1/n$	2.325(1)	2.341(1)	2.5	S	37
	213	$P2_1/n$	2.321(1)	2.327(1)	NR	S	37
	100	$P2_1/n$	2.3168(8)	2.3289(8)	NR	S	37

Ni_3^{6+} Compounds				
Compound	**Space Group**	**Ni···Ni, Å**	**μ_{eff}, μ_B**	**ref.**
$Ni_3(dpa)_4Cl_2 \cdot 0.23H_2O \cdot 0.5(CH_3)_2CO$	$C2/c$	2.443(1), 2.443(1); 2.431(1)[h]	3.5	3
$Ni_3(dpa)_4Cl_2 \cdot 2CH_2Cl_2$	$I\bar{4}$	2.4386(9), 2.422(1)	2.8	47
$Ni_3(dpa)_4Cl_2 \cdot$THF	$Pccn$	2.4172(8)	NR	47
$Ni_3(dpa)_4Cl_2 \cdot Et_2O$	$P2_1/c$	2.438(1), 2.433(1)	NR	15
$Ni_3(dpa)_4Cl_2 \cdot 2$toluene$\cdot 0.5$hexane	$P\bar{1}$	2.4249(9), 2.4253(9); 2.4265(9), 2.4386(9)[b]	NR	15
$Ni_3(dpa)_4(NO_3)_2$	$P2_12_12_1$	2.3982(5), 2.4074(5)	NR	52
$Ni_3(dpa)_4(N_3)_2$	$P2_1/c$	2.4325(7), 2.4356(7)	2.7	53

Pictiva EX2004
Samsung v Pictiva
IPR2024-01094

Compound	Space Group	Ni···Ni, Å	μ_{eff}, μ_B	ref.
$[Ni_3(dpa)_4(N_3)]PF_6 \cdot 3CH_2Cl_2$	$P2_1/n$	2.389(2), 2.385(2)	3.2	53
$Ni_3(dpa)_4[Ag(CN)_2]_2 \cdot Me_2CO$	$C2/c$	2.4030(7)	NR	55
$[Ni_3(dpa)_4F_2][Ni_3(dpa)_4(H_2O)_2](BF_4)_2 \cdot 2MeOH$	$P\bar{1}$	2.3888(7), 2.3917(7), 2.3924(7), 2.3896(7)	NR	56
$[Ni_3(dpa)_4(C_4O_4Me)]BF_4 \cdot Et_2O$	$C2/c$	2.400(1), 2.403(1)	NR	53
$Ni_3(dpa)_4(4\text{-}PyCO_2)_2$	$P2_1/n$	2.4176(4), 2.4297(5)	NR	48
$Ni_3(dpa)_4(3\text{-}PyCO_2)_2$	$P2_1/n$	2.4214(5), 2.4136(5)	NR	48
$[Ni_3(dpa)_4(4\text{-}PyCO_2)_2][ZnTPP]_2$	$P\bar{1}$	2.4212(6), 2.4067(6)	NR	48
$\{[Ni_3(dpa)_4(4\text{-}PyCO_2)_2][MnTPP]\}_n(ClO_4)_n$	$C2/c$	2.4088(4)	4.97	48
$\{[Ni_3(dpa)_4(3\text{-}PyCO_2)_2][MnTPP]\}_n(ClO_4)_n$	$P2_1/c$	2.4156(5), 2.4206(5)	5.28	48
$[Ni_3(dpa)_4(NCMe)_2](PF_6)_2 \cdot 3.14CH_3CN$	$P\bar{1}$	2.376(2), 2.371(2)	2.37	48
$Ni_3(dpa)_4(CN)_2 \cdot CH_2Cl_2$	$Pnn2$	2.4523(3)	2.68	54
$Ni_3(dpa)_4(NCS)_2 \cdot CH_2Cl_2$	$Fddd$	2.4285(9)	NR	67
$Ni_3(dpa)_4(NCNCN)_2 \cdot 2.5CH_2Cl_2$	$P\bar{1}$	2.4044(8), 2.4082(8)	2.53	54
$Ni_3(dpa)_4(CCPh)_2 \cdot 0.3CH_3OH$	$C2$	2.477(1), 2.474(1), 2.4861(7), 2.4467(8)[b]	2.83	54
$Ni_3(depa)_4Cl_2 \cdot 0.5hexane$	$P\bar{4}n2$	2.4325(3)	2.68	50
$[Ni_3(depa)_4(NCMe)_2](PF_6)_2 \cdot 0.33H_2O$	$Pn\bar{3}n$	2.415(1)	2.53	50
$[Ni_3(PhPyF)_4(NCMe)_2](BF_4)_2$	$I4_1/a$	2.469(5)	NR	51
$[Ni_3(PhPyF)_4Cl]Cl$	$P4/ncc$	2.443(3), 2.454(3)	3.08	51
$Ni_3(PhPyF)_4Cl_2$	$P4_32_12$	2.508(1), 2.503(1)	NR	51
$(NBu_4)_2[Ni_3(BPAP)_4] \cdot 2THF$	$C2/c$	2.368(1)	diamagnetic	21

Pictiva EX2004
Samsung v Pictiva
IPR2024-01094

Ni_3^{7+} Compounds

Compound	Space Group	Ni–Ni, Å	μ_{eff}, μ_B	ref.
$[Ni_3(dpa)_4(PF_6)_2]PF_6 \cdot 5CH_2Cl_2$	$P2/n$	2.2851(6), 2.2885(7)	2.0	15,44
$[Ni_3(depa)_4(PF_6)_2]PF_6 \cdot 3CH_2Cl_2$	$P2_1/n$	2.296(1), 2.289(1)	1.79	50

Cu_3^{6+} Compounds

Compound	T,K	Space Group	Cu···Cu, Å	μ_{eff}, μ_B	ref.
$Cu_3(dpa)_4Cl_2$		$Pnn2$	2.4712(4)	NR	46
$Cu_3(dpa)_4Cl_2 \cdot H_2O$		$Pnn2$	2.471(1)	2.4	45
$Cu_3(dpa)_4Cl_2 \cdot CH_2Cl_2$	298	$Pnn2$	2.492(2)	2.02	49
	160	$Pnn2$	2.4688(9)	NR	49
$Cu_3(dpa)_4Cl_2 \cdot$toluene		$Pca2_1$	2.4710(9), 2.4688(9)	NR	49
$Cu_3(dpa)_4Cl_2 \cdot Et_2O$		$P2_1/c$	2.4672(8), 2.4735(8)	NR	49
$Cu_3(dpa)_4(BF_4)_2$		$P2_1/c$	2.4035(8), 2.4029(8)	2.1	49

Cu_3^{7+} Compounds

Compound	Space Group	Cu···Cu, Å	μ_{eff}, μ_B	ref.
$[Cu_3(dpa)_4Cl_2]SbCl_6 \cdot 2.86C_2H_4Cl_2 \cdot 0.792C_6H_{12}$	$I4/m$	2.510(1), 2.516(1)	2.83	15
$[Cu_3(dpa)_4Cl_2]SbCl_6 \cdot 2.44Me_2CO$	$P2_1/c$	2.506(1), 2.505(1)	NR	15

Pictiva EX2004
Samsung v Pictiva
IPR2024-01094

Ru_3^{6+} Compounds

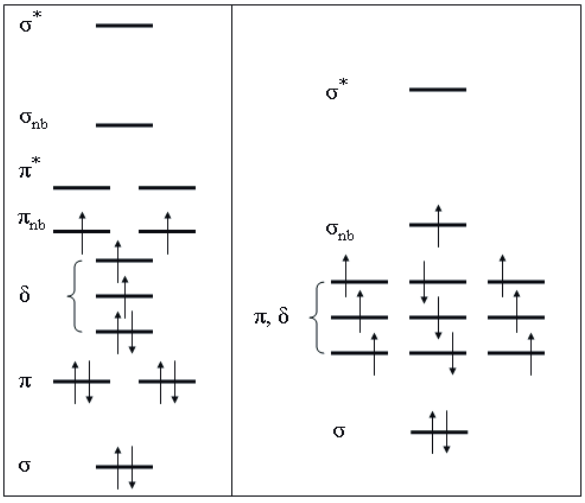
Compound	Space Group	Ru–Ru, Å	μ_{eff}, μ_B	ref.
$Ru_3(dpa)_4Cl_2 \cdot CH_2Cl_2$	*P*nn2	2.596(2)	diamagnetic	5

Rh_3^{6+} Compounds

Compound	Space Group	Rh–Rh, Å	μ_{eff}, μ_B	ref.
$Rh_3(dpa)_4Cl_2 \cdot CH_2Cl_2$	*P*nn2	2.586(1)	1.9	5

[a] S = symmetrical, U = unsymmetrical, sl. U = slightly unsymmetrical.
[b] Asymmetric unit contains two molecules.
[c] These structures were reported (ref.11) to contain symmetrical molecules, but have been reinvestigated (ref. 26) and found to contain *un*symmetrical molecules.
[d] The symmetrical arrangement in this structure is believed to be an artifact due to pseudomerohedral twinning of the crystals (see ref. 26).
[e] Disorder in the positions of the Cr atoms leads to high esd's.
[f] Recently this has been shown to have the formula $Cr_3(dpa)_4(CCPh)_{1.8}Cl_{0.2}$; see ref. 25.
[g] This structure has been reinterpreted in space group $I\bar{4}$, see ref. 31.
[h] Asymmetric unit contains one and a half molecules.

Pictiva EX2004
Samsung v Pictiva
IPR2024-01094



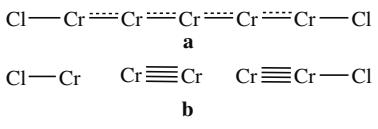
15.9

A different model is based on results of DFT calculations.[14] In this, the δ and π orbital interactions are both considered to be negligible, leading to nine degenerate orbitals, three localized on each Cr atom (see **15.9**b). By filling these orbitals and maximizing the spin multiplicity, the result is ten unpaired electrons. Since nine of these are localized on the individual Cr atoms in sets of three, they couple antiferromagnetically with each other. They also couple ferromagnetically (because of orthogonality) with the remaining electron in the σ nonbonding orbital to yield an $S = 2$ ground state and a net $3c3e$ sigma bond. The $S = 5$ excited state is calculated to lie 30.8 kcal mol^{-1} (> 10,000 cm^{-1}) above the ground state, precluding any evidence of its population in the variable temperature magnetic susceptibility data.

Although no potential energy minimum for an unsymmetrical Cr_3 chain is found, further calculations on $Cr_3(dpa)_4Cl_2$ showed that a very unsymmetrical geometry exists in a quintet excited state at +10 kcal mol^{-1} vs that of the ground state.[28] Though this observation does not justify an extremely unsymmetrical $Cr_3(dpa)_4Cl_2$, it is proposed that exchanging the axial Cl ligands with an unsymmetrical set of ligands (e.g., Cl and PF_6) could stabilize the unsymmetrical excited state and cause it to be favored.[28]

The Cr compounds of higher nuclearity, Cr_n^{2n+} and $Cr_n^{(2n+1)+}$ with $n \geq 4$, are listed in Table 15.2. These are synthesized similarly to the trinuclear complexes,[12] but $Cr_5(tpda)_4Cl_2$ and $Cr_7(teptra)_4Cl_2$ have also been synthesized from $CrCl_2$, H_2tpda or $H_3teptra$, and KO^{t}Bu in molten naphthalene.[17] In the tetranuclear ion $[Cr_4(DPyF)_4Cl_2]^{2+}$, the Cr atoms pair up to form two isolated Cr_2^{4+} quadruply bonded units (av. Cr–Cr = 2.01 Å) with a distance of 2.73 Å separating them (see Fig. 15.3).[22] The pentachromium complexes of the $tpda^{2-}$ ligand are the most studied, but the results are still controversial.[12,29,30] Both localized and delocalized models for the structure of $Cr_5(tpda)_4Cl_2$ have been proposed as shown schematically in **15.10**. Crystallographic disorder in the positions of the metal atoms is an important issue in deciding whether the model of **15.10**a (delocalized) or **15.10**b (with alternating Cr–Cr quadruple bonds) is more applicable.[30] The compounds $Cr_5(tpda)_4(NCS)_2$[29] and heptanuclear $Cr_7(teptra)_4Cl_2$[17] (shown in Fig. 15.4) have been reported as being consistent with model **15.10a**, though the elongated thermal ellipsoids for the Cr atoms in the crystal structures suggest that **15.10b** is probably a better description.[30]

Pictiva EX2004
Samsung v Pictiva
IPR2024-01094



15.10

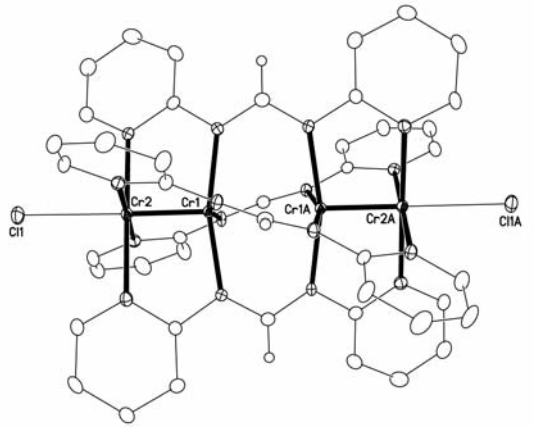


Fig. 15.3. Structure of the dication $[Cr_4(DPyF)_4Cl_2]^{2+}$.

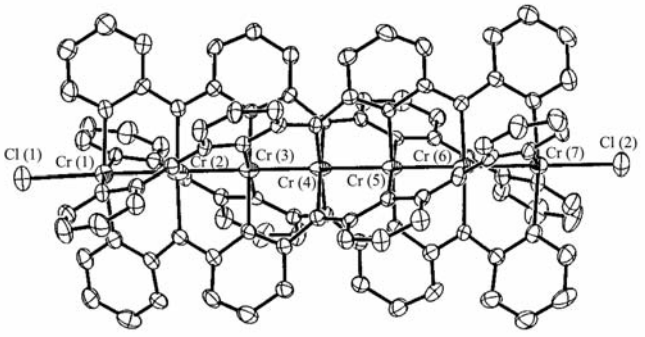


Fig. 15.4. Structure of $Cr_7(teptra)_4Cl_2$.

In the pentachromium complexes, interpretation of the magnetic data has also been debated. For $Cr_5(tpda)_4Cl_2$, the observed μ_{eff} of 4.0-4.2 μ_B has been interpreted as indicative of either two[29] or four[12,30] unpaired electrons, though it is not very close to either of the spin-only values (2.83 and 4.90 μ_B, respectively) expected for these situations. A thorough and conclusive magnetic study of these pentachromium complexes has not been reported.

For the oxidized $Cr_5(tpda)_4^{3+}$ compounds $[Cr_5(tpda)_4F_2]BF_4$ and $[Cr_5(tpda)_4F(OTf)]OTf$,[29] the structural results clearly indicate that model **15.10**b is applicable, with the isolated Cr atom being the one oxidized to Cr(III) and responsible for the magnetic moment of 4.0 μ_B corresponding to three unpaired electrons.

Pictiva EX2004
Samsung v Pictiva
IPR2024-01094

Table 15.2. Structural data for EMACs having more than three metal atoms

Cr_n^{2n+} Compounds

Compound	Cr≡Cr, Å	Cr···Cr, Å	μ_{eff}, μ_B[b]	ref.
$[Cr_4(DPyF)_4Cl_2]Cl_2 \cdot 5Me_2CO$	1.9832(8)	2.709(1)	diamagnetic	22
$[Cr_4(DPyF)_4Cl_2]Cl_2 \cdot 4MeOH$	2.013(2), 2.001(2)	2.726(2)	diamagnetic	22
$Cr_5(tpda)_4Cl_2 \cdot CH_2Cl_2$	1.901(6), 2.031(6)	2.578(7), 2.587(6)	4.2	12
$Cr_5(tpda)_4Cl_2 \cdot 2Et_2O \cdot 4CHCl_3$[a]	1.872(2), 1.963(3)	2.598(3), 2.609(2)	NR	30
$Cr_5(tpda)_4Cl_2 \cdot Et_2O$	1.862(3), 1.931(3)	2.661(3), 2.644(3)	NR	30
	Outer Cr–Cr	**Inner Cr–Cr**		
$Cr_5(tpda)_4Cl_2 \cdot 2Et_2O \cdot 4CHCl_3$[a]	2.284(1), 2.284(1)	2.2405(8), 2.2405(8)	4.0	29
$Cr_5(tpda)_4(NCS)_2$	2.285(2), 2.285(2)	2.246(1), 2.246(1)	NR	29
$Cr_7(teptra)_4Cl_2 \cdot 6THF$	2.291(2), 2.280(2)	2.243(2), 2.211(2), 2.215(2), 2.243(2)	NR	17

$Cr_n^{(2n+1)+}$ Compounds

Compound	Cr≡Cr	Cr···Cr	μ_{eff}, μ_B[b]	ref.
$[Cr_5(tpda)_4F_2]BF_4 \cdot 1.5CH_3CN \cdot 2H_2O \cdot THF$	1.969(2), 2.138(2)	2.487(2), 2.419(2)	4.0	29
$[Cr_5(tpda)_4F(OTf)]OTf \cdot 2CHCl_3$	1.846(1), 1.922(1)	2.610(1), 2.596(1)	NR	29

Co_5^{10+} Compounds

Compound	Outer Co–Co	Inner Co–Co	μ_{eff}, μ_B[b]	ref.
$Co_5(tpda)_4(NCS)_2 \cdot CH_2Cl_2 \cdot 0.5Et_2O \cdot 0.5H_2O$	2.276(2), 2.271(2)	2.232(2), 2.232(2)	1.90	7,43
$Co_5(tpda)_4Cl_2 \cdot 2CHCl_3 \cdot Et_2O$	2.282(1)	2.235(1)	NR	43
$Co_5(tpda)_4(N_3)_2 \cdot 2CH_2Cl_2 \cdot 1/3H_2O$	2.258(1), 2.264(1)	2.223(1), 2.221(1)	NR	43
$Co_5(tpda)_4(CN)_2 \cdot 3CH_2Cl_2 \cdot Et_2O$	2.279(1), 2.286(1)	2.227(1), 2.231(1)	NR	43
$Co_5(tpda)_4(OTf)_2 \cdot 2CH_2Cl_2$	2.253(1)	2.225(1)	NR	43

Pictiva EX2004
Samsung v Pictiva
IPR2024-01094

Co_5^{11+} Compounds

Compound	Outer Co–Co	Inner Co–Co	μ_{eff}, μ_B[b]	ref.
$[Co_5(tpda)_4(NCS)_2]ClO_4$	2.292(1), 2.276(1)	2.238(1), 2.243(1)	2.93	43
$[Co_5(tpda)_4Cl_2]ClO_4 \cdot 3CH_2Cl_2$	2.300(2), 2.285(2)	2.246(2), 2.244(2)	3.18	43
$[Co_5(tpda)_4(OTf)_2]OTf$	2.282(1), 2.290(1)	2.253(1), 2.241(1)	2.86	43

Ni_n^{2n+} Compounds

Compound	Outer Ni···Ni	Inner Ni···Ni	μ_{eff}, μ_B[b]	ref.
$Ni_4(phdpda)_4 \cdot C_5H_{12}$	2.3269(6), 2.3280(6)	2.3010(6)	diamagnetic	8
$Ni_5(tpda)_4Cl_2 \cdot 4CH_2Cl_2$	2.385(2)	2.305(1)	4.0	7,68
$Ni_5(tpda)_4(CN)_2 \cdot CH_2Cl_2$	2.400(3)	2.296(2)	3.7	68
$Ni_5(tpda)_4(N_3)_2$	2.379(2)	2.298(2)	3.85	68
$Ni_5(tpda)_4(NCS)_2 \cdot 4CH_2Cl_2$	2.367(2), 2.371(2)	2.298(2), 2.294(2)	3.94	68
$[Ni_5(tpda)_4(NCMe)_2](PF_6)_2 \cdot 4MeCN$	2.346(3)	2.291(2)	3.81	68
$Ni_5(tpda)_4(NCFe(dppe)Cp)_2$	2.384(1)	2.306(1)	NR	38
$Ni_5(etpda)_4Cl_2 \cdot 6CHCl_3$	2.389(2), 2.383(2)	2.304(2), 2.304(2)	4.3	65
$Ni_7(teptra)_4Cl_2 \cdot 3CHCl_3$	2.383(1), 2.374(2)	2.310(1), 2.225(2), 2.215(2), 2.304(1)	4.0	8,69
$Ni_7(teptra)_4(NCS)_2 \cdot 4CHCl_3$	2.375(2), 2.354(2)	2.300(2), 2.194(2), 2.206(2), 2.303(2)	NR	69
$Ni_9(peptea)_4Cl_2 \cdot 10C_2H_4Cl_2$	2.391, 2.380, 2.375[c]	2.297, 2.253, 2.237, 2.243, 2.255, 2.286, 2.296, 2.263, 2.247[c]	4.0	9

$Ni_n^{(2n+1)+}$ Compounds

Compound	Outer Ni–Ni	Inner Ni–Ni	μ_{eff}, μ_B[b]	ref.
$[Ni_5(tpda)_4(H_2O)(BF_4)](BF_4)_2 \cdot 4CH_2Cl_2$	2.337(1), 2.300(1)	2.261(1), 2.245(1)	2.25	66
$[Ni_5(tpda)_4(OTf)_2]OTf \cdot CH_2Cl_2 \cdot 3.5H_2O$	2.358(2), 2.304(1)	2.276(2), 2.245(2)	2.75	66
$[Ni_5(etpda)_4](PF_6)_3 \cdot 4Me_2CO$	2.289(2), 2.292(2)	2.233(2), 2.235(2)	2.0	65

[a] This structure was determined twice and refined using two different models.
[b] NR = Not reported.
[c] No values are listed in ref. 9. Ni···Ni distances are reported from the Cambridge database without esd's.

Pictiva EX2004
Samsung v Pictiva
IPR2024-01094

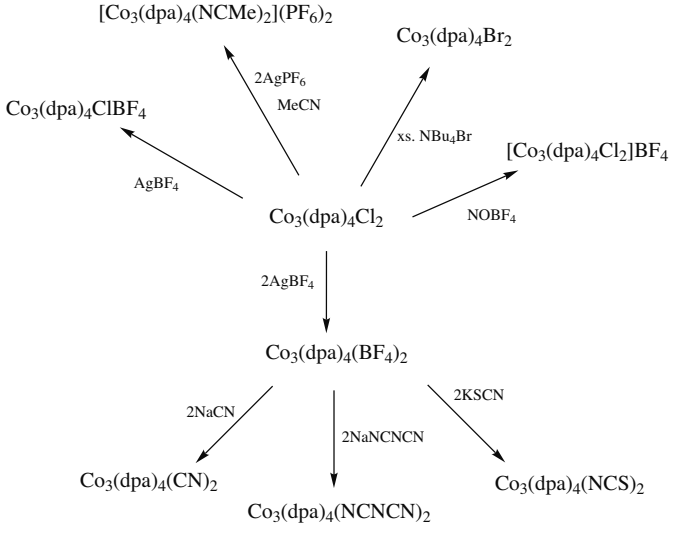
The model **15.10a** has been used to calculate the band structure of a hypothetical Cr_∞ chain.[17] The results indicate that Cr_n^{2n+} wires of the type **15.10a** should be one-dimensional metallic conductors.

15.3 EMACs of Cobalt

Because the first synthesis of the parent tricobalt complex $Co_3(dpa)_4Cl_2$ reported very low yields,[4] its chemistry was not studied in detail until a straightforward, high yield synthesis was devised. Reaction of anhydrous $CoCl_2$ with Lidpa in refluxing THF gives black microcrystalline $Co_3(dpa)_4Cl_2$ in > 40% yield.[31]

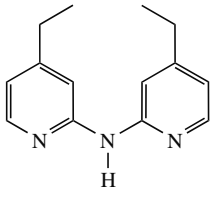
$$3CoCl_2 + 4Lidpa \rightarrow Co_3(dpa)_4Cl_2 + 4LiCl$$

The chemistry of this complex is summarized in **15.11**, and involves substitutions and oxidations. The chloride ions are easily exchanged for tetrafluoroborate or hexafluorophosphate anions by metathesis with the corresponding silver reagents.[32,33] Replacement of Cl by Br, however, is slow, and complete reaction takes ~5 days using a 50 fold excess of NBu_4Br.[34] $Co_3(dpa)_4(BF_4)_2$ was found to react more quickly than the chloride precursor with pseudohalogens to form $Co_3(dpa)_4X_2$ compounds with X = CN, NCS, and NCNCN.[35]



15.11

Tricobalt complexes with axial Cl and CN ligands have also been reported for the ethyl substituted depa ligand (**15.12**).[36]



Hdepa

15.12

Pictiva EX2004
Samsung v Pictiva
IPR2024-01094

The cyclic voltammogram of $Co_3(dpa)_4Cl_2$ shows two reversible one-electron oxidation waves at $E_{1/2}$ of 0.32 V and 1.24 V vs ferrocene. The oxidant $NOBF_4$ was used to convert $Co_3(dpa)_4Cl_2$ to the corresponding one-electron oxidized cation.[37] Oxidation of $Co_3(depa)_4Cl_2$ and $Co_3(depa)_4(CN)_2$ are more easily achieved, due to the increased basicity of the depa ligand.[36] Tricobalt chains with Fe, Ru or Cr complexes attached through axial cyanide linkages have been reported and electrochemical studies have shown that the axially coordinated metal ions are oxidized at essentially the same potential.[38]

Like the trichromium compounds, tricobalt compounds can exist with either equivalent or very different Co–Co distances.[4,31,32,39] The solvates of $Co_3(dpa)_4Cl_2$ with symmetrical and unsymmetrical structures have been viewed as examples of bond-stretch isomerism,[31,40] although this claim has been debated.[13,41] Because of this unusual situation, a wealth of crystallographic information has been obtained for this compound alone. As shown in Table 15.1, the structure has been determined with various interstitial solvent molecules, and at various temperatures.[10,40]

The dichloromethane solvates are unique in that the orthorhombic form ($Co_3(dpa)_4Cl_2{\cdot}CH_2Cl_2$, *P*nn2) and the tetragonal form ($Co_3(dpa)_4Cl_2{\cdot}2CH_2Cl_2$, $I\bar{4}$) have symmetrical (D_4) and unsymmetrical (C_4) molecular structures, respectively, though they crystallize simultaneously from the same solution.[10,39] The crystal habits of these solvates are sufficiently differentiable that they can be separated by hand under a microscope (see Fig. 15.5).

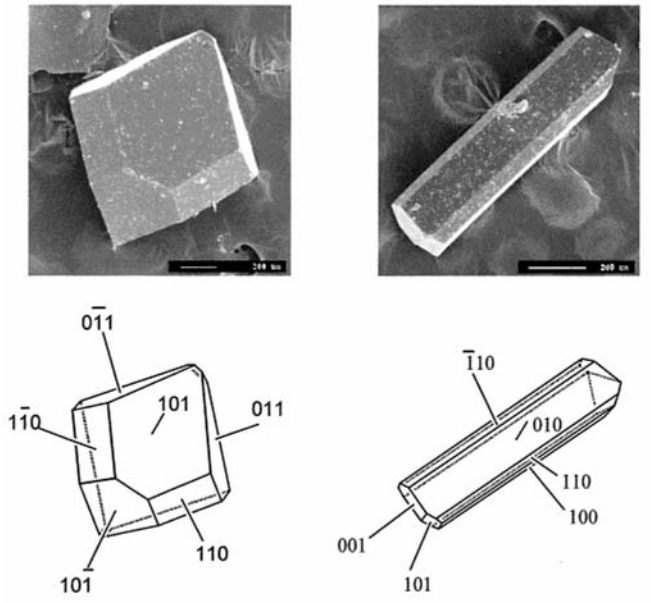


Fig. 15.5. STM images (above) and face-indexed drawings (below) of $Co_3(dpa)_4Cl_2{\cdot}CH_2Cl_2$ (left) and $Co_3(dpa)_4Cl_2{\cdot}2CH_2Cl_2$ (right).

The molecular structure of $Co_3(dpa)_4Cl_2$ in these crystals is temperature dependent, as shown in Table 15.1. Between 168 K and 109 K, the symmetric structure undergoes a phase transition from the orthorhombic *P*nn2 form to a monoclinic *P*n form. This breaks the crystallographically imposed equivalence of the Co–Co distances, though the compound remains symmetrical within experimental error (Co–Co distances of 2.3224(8) and 2.3214(8) Å at 109 K). For the unsymmetri-

Pictiva EX2004
Samsung v Pictiva
IPR2024-01094

cal tetragonal $I\bar{4}$ form, the Co–Co distances become more symmetrical as the temperature is lowered, reaching 2.3035(7) and 2.3847(8) Å at 20 K (as compared to 2.299(1) and 2.47(1) Å at room temperature).[10]

The other solvates of $Co_3(dpa)_4Cl_2$ also have temperature dependent structures.[40] Though most of these contain symmetrical molecules for which *d*(Co–Co) increases with temperature, there are a few that do not. For example, $Co_3(dpa)_4Cl_2$·cyclohexane, like $Co_3(dpa)_4Cl_2$·CH_2Cl_2, undergoes a phase transition between 213 K and 120 K, causing loss of the crystallographic equivalence of the Co–Co distances. The molecule, however, remains symmetrical at 120 K with Co–Co distances of 2.3127(5) and 2.3253(5) Å. $Co_3(dpa)_4Cl_2$·THF crystallizes in the orthorhombic *P*ccn space group, and contains a slightly unsymmetrical molecule at 295 K, which becomes *less* symmetrical at lower temperature, contrary to the behaviour of tetragonal $Co_3(dpa)_4Cl_2$·$2CH_2Cl_2$.

The most complex crystal form is $Co_3(dpa)_4Cl_2$·1.75toluene·0.5hexane. Though this compound crystallizes in the triclinic space group $P\bar{1}$, the asymmetric unit contains two independent molecules which are both unsymmetrical at room temperature. The crystal structures determined at lower temperatures show increasing similarity of the Co–Co distances. At 90 K, one molecule is completely symmetrical (Co–Co = 2.3139(6) and 2.3196(6) Å) while the other is still slightly unsymmetrical (Co–Co = 2.3098(6) and 2.3660(6) Å).

Similar results were found for $Co_3(dpa)_4Br_2$,[34] but only one dichloromethane solvate was observed with equal Co–Co distances of 2.3234(6) Å at 240 K. The crystals of $Co_3(dpa)_4Br_2$·1.75toluene·0.5hexane show complex behavior similar to that of the chloride analog.

The molecular structure of $Co_3(dpa)_4Cl_2$ was also characterized in solution by ^1H and ^{13}C NMR spectroscopy, despite the paramagnetism of the compound.[42] In the ^1H NMR spectrum, only four signals are detected and assigned to the pyridyl hydrogen atoms. The five signals of the ^{13}C NMR spectrum are due to the pyridyl carbon atoms. The assignments are consistent with D_4 molecular symmetry in solution. This could either be because the molecule actually *is* symmetrical in solution, or it could be that the molecule is unsymmetrical and that the central Co atom shifts positions more quickly than the timescale of the NMR experiment. Nevertheless, it should be noted that solutions made by dissolving crystals of either symmetrical or unsymmetrical $Co_3(dpa)_4Cl_2$ result in the same NMR spectrum.

The only other unsymmetrical tricobalt compound known is $Co_3(dpa)_4Cl(BF_4)$, which has two different axial ligands.[32] The tricobalt complexes with axial cyanide,[35] dicyanamide,[35] thiocyanate,[35] and acetonitrile[33] are all symmetrical with Co–Co distances ranging from 2.30 to 2.34 Å. $Co_3(dpa)_4(BF_4)_2$ (shown in Fig. 15.6) has the shortest Co–Co distances of the known symmetrical molecules (2.25 Å).[32]

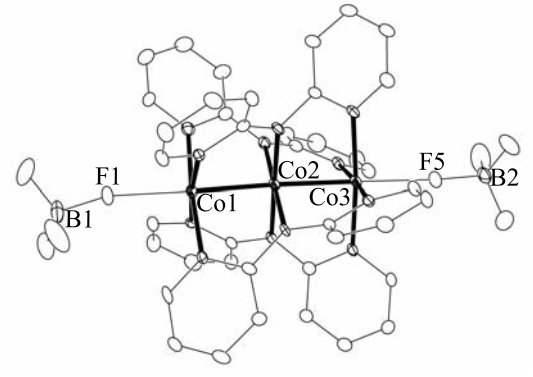


Fig. 15.6. Structure of $Co_3(dpa)_4(BF_4)_2$.

Pictiva EX2004
Samsung v Pictiva
IPR2024-01094

The temperature dependence of the Co–Co distances in these compounds is mirrored to a degree by the temperature dependence of their magnetic moments. $Co_3(dpa)_4Cl_2$ has been shown to exist in an equilibrium between low spin (S = ½) and high spin (S = $^3/_2$ or S = $^5/_2$) states.[4,10,40,42] At low temperatures, only the S = ½ state is populated, but as the temperature is increased, population of the high spin state occurs which leads to a temperature dependence of μ_{eff} as shown in Fig. 15.7. This spin crossover phenomenon has been studied in other tricobalt complexes also.[33,34,35] For $Co_3(dpa)_4Cl_2$, the magnetic data at high temperatures show incomplete population of the high spin state and therefore it is not possible to determine whether this state is S = $^3/_2$ or S = $^5/_2$. For the ethyl-substituted $Co_3(depa)_4Cl_2$, however, population of the high spin state is complete at 400 K and this state clearly has S = $^3/_2$.[36]

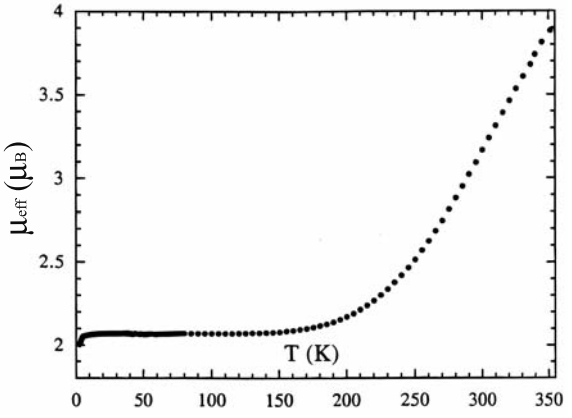


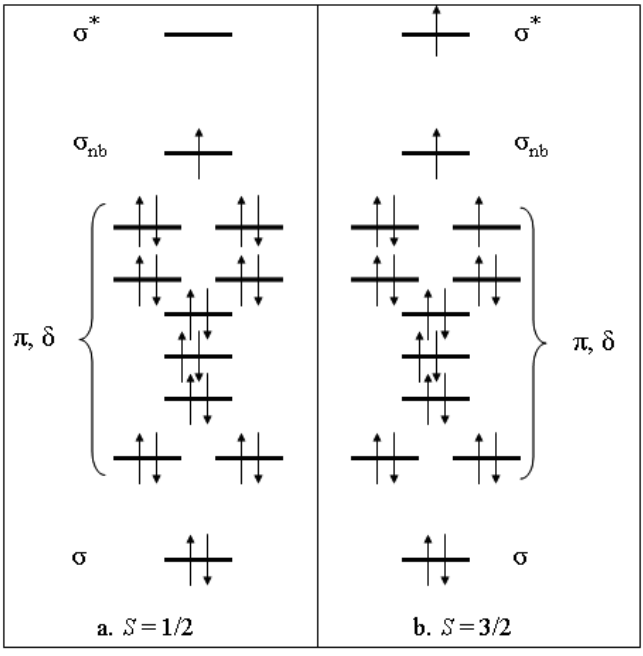
Fig. 15.7. Plot of μ_{eff} vs T for *s*-$Co_3(dpa)_4Cl_2$.

A qualitative model of the symmetrical $Co_3(dpa)_4Cl_2$ molecular orbitals accounts for the spin equilibrium.[36] By filling the 21 cobalt based electrons in the MO scheme described earlier for chromium, the result is that all the π and δ orbitals are filled, and a $3c3e$ σ bond exists in the compound as shown in **15.13**a. The spin crossover process to achieve an S = $^3/_2$ state therefore involves removing an electron from the π* orbitals and placing it in the σ* orbital as in **15.13**b (resulting in longer Co–Co distances in the high spin state). This accounts for the lengthening of the Co–Co bonds with increasing temperature because population of the high spin state implies population of the σ* orbital, and the reason that the Co–Co bond distances in $Co_3(depa)_4Cl_2$ (2.3787(7) Å) are longer than those of $Co_3(dpa)_4Cl_2$ (2.3369(4) Å) is because in the former, the high spin state is nearly 90% occupied at room temperature, whereas in the latter it is only ~50 % occupied.

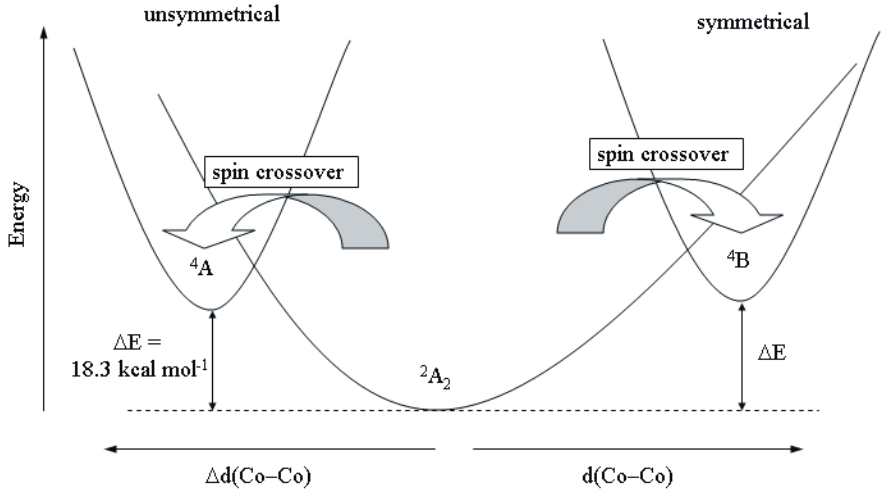
Density functional calculations on $Co_3(dpa)_4Cl_2$ are consistent with this scheme and support the view of a three-center three-electron bond in the symmetrical complex, very similar to the DFT results for $Cr_3(dpa)_4Cl_2$.[13,14] The calculations have shown that the potential energy surface of symmetrical $Co_3(dpa)_4Cl_2$ (which is the only observed potential energy minimum) is very broad and that distortions to C_4 symmetry cause changes in energy of only 1 to 4 kcal mol^{-1} vs the symmetrical ground state.[13b] No potential energy minimum could be found, however, for an unsymmetrical complex.[13] Scheme **15.14** summarizes the DFT results in which the ground $^2A_2$ state undergoes two different types of distortions. If the Co–Co distances lengthen in a symmetrical manner (from the middle towards the right in **15.14**), spin crossover to the symmetrical ^4B state occurs while as Δd(Co–Co) becomes larger (i.e. the compound becomes more unsymmetrical), spin crossover to the ^4A state can be achieved. The molecular geometry

Pictiva EX2004
Samsung v Pictiva
IPR2024-01094

of $Co_3(dpa)_4Cl_2$ in the ^4A excited state was calculated and found to be very similar to that observed in the unsymmetrical compound. It is postulated that population of this state at low temperatures gives rise to the unsymmetrical "isomer" of $Co_3(dpa)_4Cl_2$, despite the large energy difference of 18 kcal mol^{-1} vs the ground state. It should be mentioned that no transitions to spin sextet states were postulated in this study.



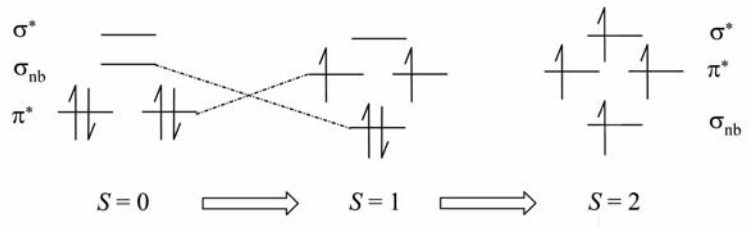
15.13



15.14

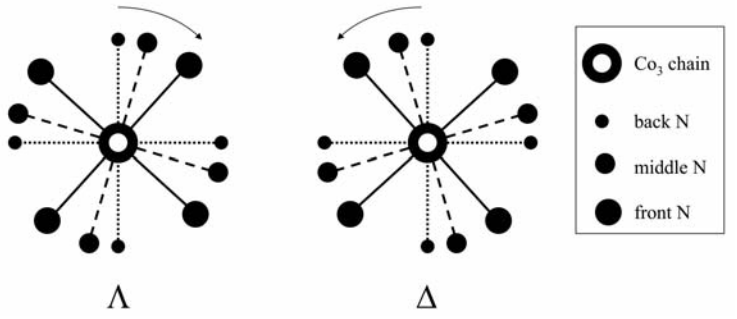
Pictiva EX2004
Samsung v Pictiva
IPR2024-01094

The DFT calculations also explain the behavior of the one-electron oxidized $[Co_3(dpa)_4Cl_2]BF_4$. As shown in Table 15.1, the Co–Co distances (2.32 Å) in this cation are not only equivalent, but similar to those of the neutral species.[37] The major structural difference between $Co_3(dpa)_4Cl_2$ and $[Co_3(dpa)_4Cl_2]^+$ is that the Co–Cl bond lengths are 0.15 Å shorter in the latter.[37] The lack of change in the Co–Co distances and the major change in the Co–Cl distances is consistent with the DFT calculation indicating that the SOMO of $Co_3(dpa)_4Cl_2$ (containing the electron which is removed upon oxidation) has Co–Co nonbonding character and Co–Cl antibonding character.[13] Moreover, the oxidized $[Co_3(dpa)_4Cl_2]^+$ cation undergoes *two* stepwise, thermal, spin crossover transitions (evidenced by magnetic susceptibility measurements in the solid state and in solution) from the $S = 0$ ground state to an intermediate $S = 1$ state, and then an $S = 2$ state.[37] The partial MO diagram in **15.15** accounts for this.[37]



15.15

In addition, the polypyridylamido EMACs are helical and therefore chiral. They exist as Λ and Δ enantiomers as shown in **15.16**.



15.16

As seen in Table 15.1, often these compounds crystallize in noncentrosymmetric space groups. The compound $[Co_3(dpa)_4(NCMe)_2](PF_6)_2$ has been found in the centrosymmetric group $P\bar{1}$ and also in the noncentrosymmetric and chiral group $P2_1$.[33] The monoclinic $P2_1$ crystals were examined and the absolute configuration of several of these were determined crystallographically. Crystals containing only the Λ or Δ isomers were separated this way, and circular dichroism spectra were obtained for solutions of the Λ and Δ enantiomers.[33] These spectra, shown in Fig. 15.8, are related by mirror symmetry, as expected for an enantiomeric pair. This experiment also shows that the pure enantiomers do not racemize in solution, because conversion from the Λ to the Δ isomer would involve the difficult process of interchanging the constrained pyridyl hydrogen atoms shown in **15.3**.

Pictiva EX2004
Samsung v Pictiva
IPR2024-01094

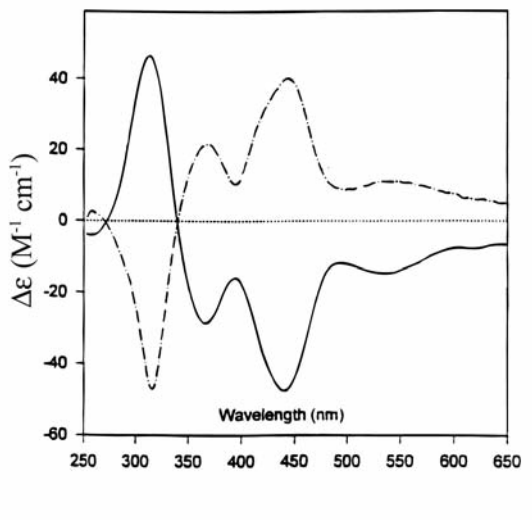
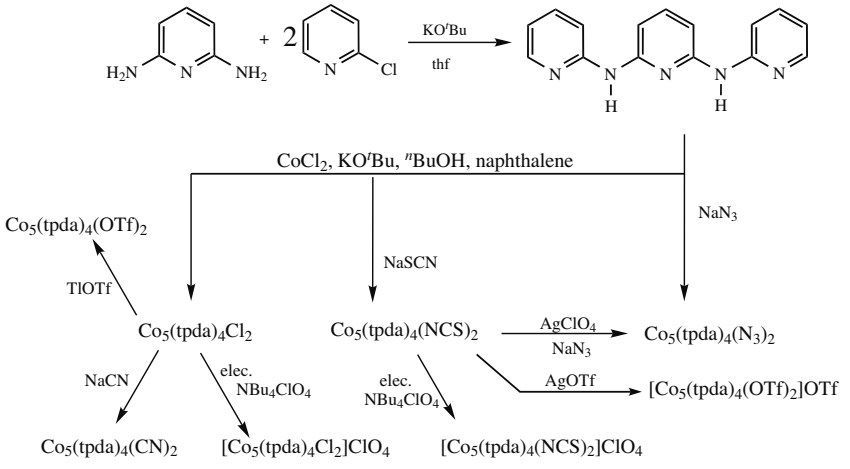


Fig. 15.8. CD spectra of Δ- (solid line) and Λ- (dashed line) $[Co_3(dpa)_4(NCCH_3)_2](PF_6)_2$.

The complex structural behavior of the tricobalt complexes is not seen to any degree in the pentacobalt complexes with the tpda ligand. These are prepared in useful yield from $CoCl_2$, H_2tpda and KOBu^t in molten naphthalene in an Erlenmeyer flask.[7,43] This chemistry is summarized in 15.17.



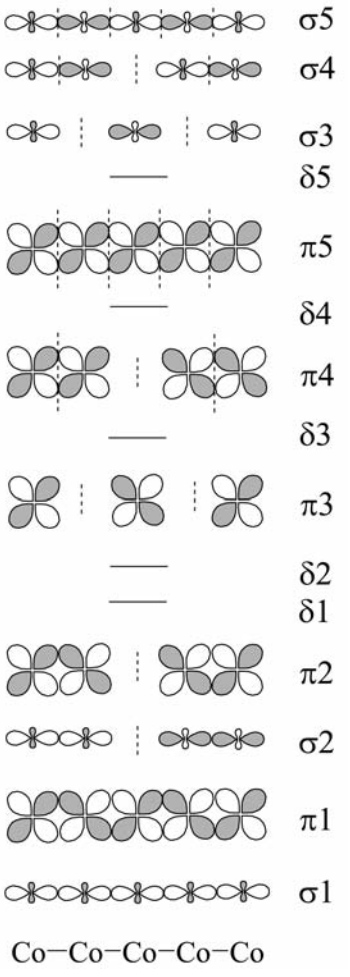
15.17

Upon treatment of $Co_5(tpda)_4Cl_2$ or $Co_5(tpda)_4(NCS)_2$ with AgOTf, oxidation occurs yielding $[Co_5(tpda)_4(OTf)_2]OTf$, while use of the non-oxidizing TlOTf yields $Co_5(tpda)_4(OTf)_2$. The one-electron oxidized $[Co_5(tpda)_4Cl_2]^+$ and $[Co_5(tpda)_4(NCS)_2]^+$ cations are readily obtained by bulk electrolysis of a solution containing the neutral Co_5^{10+} compound and NBu_4ClO_4 at $E_{appl.}$ = +0.55 V vs Ag/AgCl.[43] The reaction is monitered by UV-Vis spectroscopy, and the products are obtained by recrystallization when the reaction is complete.

Pictiva EX2004
Samsung v Pictiva
IPR2024-01094

In contrast to the tricobalt complexes, all $Co_5(tpda)_4^{2+/3+}$ compounds have symmetrical chains (i.e. the inner two Co–Co distances are indestinguishable within experimental error, as are the outer two distances). The outer Co–Co distances are typically ~ 0.05 Å longer than the inner ones due to interactions of the outer Co atoms with the axial ligands. All of the Co–Co distances are short (2.22 to 2.30 Å); therefore five-center Co–Co bonds are proposed.

The $Co_5(tpda)_4^{2+}$ complexes are paramagnetic with one unpaired electron (μ_{eff} of 1.90 μ_B) and the $Co_5(tpda)_4^{3+}$ complexes contain two unpaired electrons (μ_{eff} = 2.86 - 3.18 μ_B). These observations were rationalized by the MO scheme presented by Peng[43] shown in **15.18** filled with the 35 *d* electrons from the five cobalt atoms. Therefore, the unpaired electron of the $Co_5(tpda)_4^{2+}$ complexes is believed to occupy the σ3 nonbonding orbital. Since the oxidized species have triplet ground states, upon oxidation the electron therefore is said to be removed from the δ^*5 orbital.



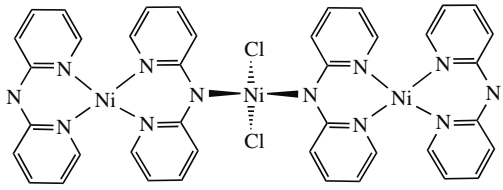
15.18

Pictiva EX2004
Samsung v Pictiva
IPR2024-01094

15.4 EMACs of Nickel and Copper

Polynickel(II) complexes have no nickel-nickel bonds, but are included in this book for two reasons: EMACs of nickel provide examples of the longest discrete metal chains,[9] and more importantly, oxidation of Ni_n^{2n+} EMACs to $Ni_n^{(2n+1)+}$ involves the formation of delocalized Ni–Ni bonds.[44] Tricopper complexes also have no Cu–Cu bonds, but are included for the following reasons: (1) Dipyridylamido tricopper complexes were the first EMACs to be recognized as such and structurally characterized.[45,46] (2) Oxidation of $Cu_3(dpa)_4Cl_2$ provides a remarkable contrast to the oxidation of $Ni_3(dpa)_4Cl_2$.[15] (3) Tricopper complexes are known for ligands other than those already described in this chapter which may be useful in the future for synthesizing metal-metal bonded EMACs of other metals.

The earliest known polypyridylamido EMAC, $Ni_3(dpa)_4Cl_2$, was synthesized in 1968 by high temperature reaction of $NiCl_2(Hdpa)_2$ (an octahedral, mononuclear Ni(II) complex with two *cis* chelating Hdpa ligands) with $KOBu^n$ in molten naphthalene.[2] The product was characterized by elemental analysis, room temperature magnetic susceptibility measurements, a molecular weight determination, IR and UV-Vis spectroscopy. Based on these measurements, a structure (**15.19**) with two square planar Ni atoms and one tetrahedral Ni atom was proposed.[2]



15.19

While at the time, this structure was reasonable, an X-ray crystallographic study showed over 20 years later that the compound possesses the linear structure shown in Fig. 15.1.[3] Synthetic routes to this compound are various, and are summarized in the following equations:

$$3NiCl_2(Hdpa)_2 + 4KOBu^n \xrightarrow[\text{naphthalene}]{Bu^nOH} Ni_3(dpa)_4Cl_2 + 4KCl + 2Hdpa$$

$$3NiCl_2 + 4Lidpa \xrightarrow{thf} Ni_3(dpa)_4Cl_2 + 4LiCl$$

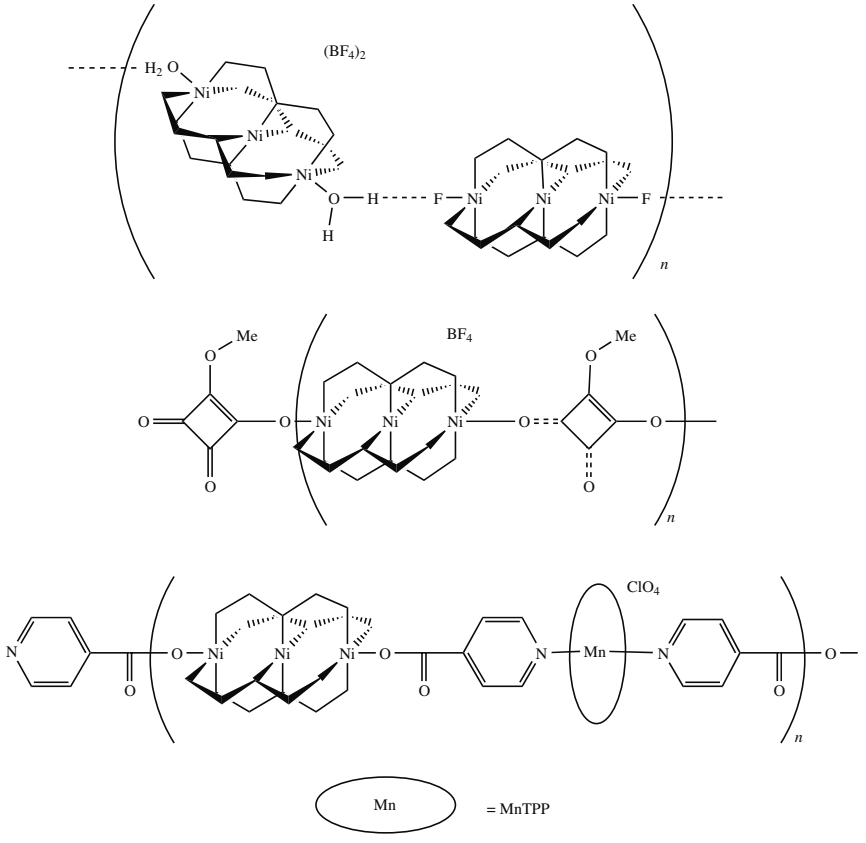
$$3NiCl_2(Hdpa)_2 + 4MeLi \xrightarrow{thf} Ni_3(dpa)_4Cl_2 + 4LiCl + 4CH_4 + 2Hdpa$$

$$3NiCl_2 + 4Hdpa + 4KOBu^t \xrightarrow[\text{naphthalene}]{Bu^tOH} Ni_3(dpa)_4Cl_2 + 4KCl + 2Bu^tOH$$

All four of these reactions give $Ni_3(dpa)_4Cl_2$ in high yields,[2,3,15,47,48] and the product is easily purified by recrystallization from dichloromethane and hexanes. Method 2 has been used to synthesize a Ni_3^{6+} chain with the ligand BPAP,[21] and an analogous method starting with $CuCl_2$ was used to obtain $Cu_3(dpa)_4Cl_2$ in high yields.[49] Method 4 claims the highest yield[48] (95 %) and has been used to synthesize an ethyl-substituted analog, $Ni_3(depa)_4Cl_2$.[50] Trinickel complexes of the unsymmetrical formamidinate ligand PhPyF have also been synthesized, but only in low yields as minor reaction products.[51] From $Ni_3(dpa)_4Cl_2$, many new derivatives have been made by substitution of different axial ligands. These $Ni_3(dpa)_4X_2$ compounds are known for X = NO_3,[52] N_3,[53] MeCN,[50] C≡N,[54] NCNCN,[54] C≡CPh,[54] $Ag(CN)_2$,[55] mixed F and H_2O ligands,[56] C_4O_4Me,[53] and also carboxylates.[48] The latter three sets of ligands have been used to

Pictiva EX2004
Samsung v Pictiva
IPR2024-01094

connect together trinickel units either by hydrogen bonding, direct connection, or through another metal-containing linker as shown in **15.20**.



15.20

$Ni_3(dpa)_4Cl_2$ has been shown to react incompletely with X anions to give products with mixed Cl and X ligands, so two methods have been developed to improve this type of reaction. In one, $Ni_3(dpa)_4Cl_2$ is first allowed to react with $AgBF_4$ to remove the Cl anions and then the desired axial ligand is added.

$$Ni_3(dpa)_4Cl_2 \xrightarrow[2.\ X^-]{1.\ 2AgBF_4} Ni_3(dpa)_4X_2$$

In the other, $[Ni_3(dpa)_4(NCMe)_2](PF_6)_2$ is first prepared from $Ni_3(dpa)_4Cl_2$ by reaction with $AgPF_6$ in MeCN.[50] This complex with labile acetonitrile ligands then reacts quickly with X anions to give $Ni_3(dpa)_4X_2$.[54]

$$Ni_3(dpa)_4Cl_2 + 2AgPF_6 \xrightarrow{MeCN} [Ni_3(dpa)_4(NCMe)_2](PF_6)_2$$

$$[Ni_3(dpa)_4(NCMe)_2](PF_6)_2 + 2NaX \xrightarrow{methanol} Ni_3(dpa)_4X_2 + 2NaPF_6$$

Pictiva EX2004
Samsung v Pictiva
IPR2024-01094

The bis-phenylacetylide complex is prepared in high yield from $[Ni_3(dpa)_4(MeCN)_2](PF_6)_2$ by reaction with sodium hydroxide and phenylacetylene in methanol.[54]

$$[Ni_3(dpa)_4(NCMe)_2](PF_6)_2 + 2NaOH + 2HCCPh \xrightarrow{\text{methanol}} Ni_3(dpa)_4(CCPh)_2 + 2NaPF_6 + 2H_2O$$

Oxidation of Ni_3^{6+} to Ni_3^{7+} is quite difficult because the potential for this process is high ($E_{1/2}$ = 0.908 V vs Ag/AgCl for $Ni_3(dpa)_4Cl_2$). Reaction of $Ni_3(dpa)_4Cl_2$ with excess $AgPF_6$ leads to the formation of the oxidized $Ni_3(dpa)_4^{3+}$ cation.[15,44] The blue crystalline compound $[Ni_3(dpa)_4](PF_6)_3$ is unstable at room temperature. Solutions revert to Ni_3^{6+} within a day, and the solid decomposes in air in about a week. For the ethyl-substituted analog $Ni_3(depa)_4Cl_2$, the potential for this process is 0.130 V lower (due to the increased bacisity of the depa ligand), and the blue compound resulting from oxidation (i.e. $[Ni_3(depa)_4](PF_6)_3$) is stable for several weeks, even in solution:[50]

$$Ni_3(dpa)_4Cl_2 + 3AgPF_6 \rightarrow [Ni_3(dpa)_4](PF_6)_3 + 2AgCl + Ag$$

The Ni···Ni distances in Ni_3^{6+} compounds range from 2.37 Å in $Ni_3(BPAP)_4^{2-}$ to 2.51 Å in $Ni_3(PhPyF)_4Cl_2$ (see Table 15.1). In all of these compounds, the Ni···Ni distances are similar enough to consider the Ni_3^{6+} core as having idealized D_4 symmetry. No unsymmetrical Ni_3^{6+} compounds are known. All $Ni_3(dpa)_4^{2+}$ compounds have strongly bound axial ligands, which cause the terminal Ni^{2+} ions to be high spin. This is manifested in the magnetic properties (vide infra), and also structurally in the fact that the Ni–N distances for the terminal, 5-coordinate Ni atoms are typically ~0.2 Å longer than the Ni–N distances for the central Ni(II) species (which is square planar and thus diamagnetic). A compound with the PhPyF ligand is known with only one axial ligand, namely $[Ni_3(PhPyF)_4Cl]Cl$, which contains two diamagnetic square planar Ni atoms and only one high spin, five coordinate Ni(II) ion which is responsible for the observed μ_{eff} of 3.08 μ_B.[51] The only Ni_3 compound known without axial ligands is $Ni_3(BPAP)_4^{2-}$ (shown in Fig. 15.9) which has three square planar Ni(II) units with equivalent Ni–N bond lengths, and is diamagnetic.[21]

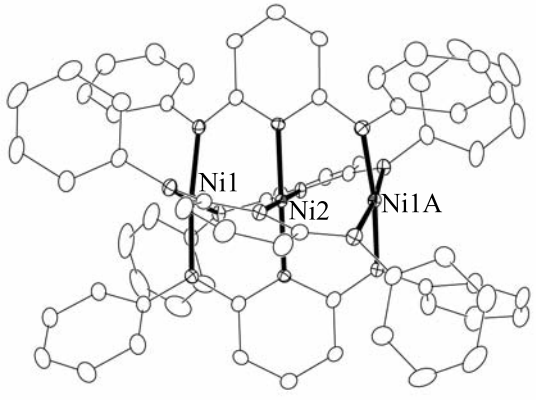


Fig. 15. 9. Structure of the dianion $[Ni_3(BPAP)_4]^{2-}$.

Oxidation of $Ni_3(dpa)_4Cl_2$ to $[Ni_3(dpa)_4](PF_6)_3$ causes major structrural changes to the trinickel unit.[15,44] Most notably, the Ni–Ni distances in the Ni_3^{7+} compounds are 0.07 Å shorter than the

Pictiva EX2004
Samsung v Pictiva
IPR2024-01094

shortest distances in any Ni_3^{6+} compound and 0.14 Å shorter than the Ni···Ni distances in the precursor $Ni_3(dpa)_4Cl_2$ (2.43 Å). The axial PF_6 anions are not strongly coordinated to the terminal nickel atoms (Ni···F distances are over 2.4 Å), and the Ni–N distances for all three nickel atoms are shorter than in the precursor. These structural results are explained by the formation of 3*c* Ni–Ni bonds in the Ni_3^{7+} species. A similar result is observed in the ethyl-substituted analog.

In contrast to this, the Cu···Cu distances in $Cu_3(dpa)_4Cl_2$ are in the range of 2.47 to 2.49 Å,[45,46,49] while the oxidized $[Cu_3(dpa)_4Cl_2]SbCl_6$ has Cu···Cu separations of 2.51 to 2.52 Å.[15] The modest increase of ~0.05 Å in the Cu···Cu distances upon oxidation is the result of increased electrostatic repulsion between the more highly charged Cu atoms. These results show *inter alia* that neither the Cu_3^{6+} nor the Cu_3^{7+} compounds have Cu–Cu bonds. In the oxidized species, the central Cu atom with shorter Cu–N distances (1.89 Å, as compared to the outer Cu–N distances of 2.06 Å) is believed to be the Cu atom oxidized to Cu^{III}.

If a delocalized MO scheme such as the one shown in **15.9** is considered for Ni_3^{6+} compounds, the 24 *d* electrons would fill all the bonding, nonbonding, and antibonding MOs leaving no net bond. Moreover, the compound is expected to be diamagnetic, since all the MOs are occupied by an electron pair. This cannot be the case, however, because $Ni_3(dpa)_4Cl_2$ is paramagnetic at room temperature.[3,47] The reason for this apparent discrepancy is that since there are no Ni–Ni bonds, each Ni atom behaves independently. The central Ni atom is square planar and diamagnetic while the outer ones are five coordinate and high spin with $S = 1$. The spins of the two outer Ni atoms couple antiferromagnetically so that μ_{eff} is a complex function of temperature as shown in Fig. 15.10. All known Ni_3^{6+} compounds show this type of magnetic behavior except for $[Ni_3(BPAP)_4]^{2-}$ which, as mentioned above, is diamagnetic since it has no axial ligands.[21]

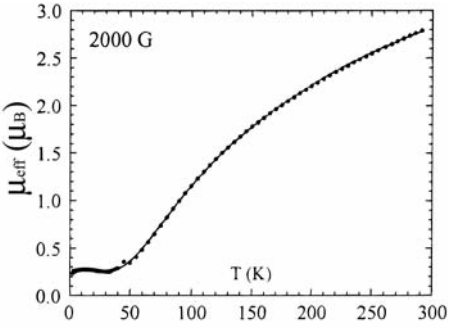


Fig. 15.10. Plot of μ_{eff} vs T for $Ni_3(dpa)_4Cl_2$.

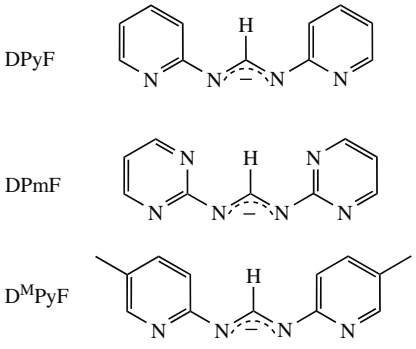
Oxiation to Ni_3^{7+} changes the magnetic behavior of the trinickel chain. The magnetic moment of 2.0 μ_B for $[Ni_3(dpa)_4](PF_6)_3$ is constant over the entire temperature range signifying that there is only one unpaired electron delocalized over the Ni_3 chain.[44] More evidence for delocalization of this electron comes from EPR measurements. The X-band EPR spectra of $Ni_3(dpa)_4^{3+}$ and $Ni_3(depa)_4^{3+}$ are axial, and the $g_\parallel$ components are split into three lines, consistent with coupling of the unpaired electron with the two axially coordinated fluorine atoms of the molecule.[15] Thus, the unpaired electron is believed to reside in the three-center σ^* orbital, which has small but significant contributions from the axial ligands.

Exchange coupled multinuclear Cu(II) complexes are perhaps the most well studied systems in the field of magnetochemistry.[57] As may be expected from the vast work done on dinuclear Cu_2^{4+} paddlewheel-type complexes,[58] the tricopper complexes $Cu_3(dpa)_4Cl_2$ and $Cu_3(dpa)_4(BF_4)_2$

Pictiva EX2004
Samsung v Pictiva
IPR2024-01094

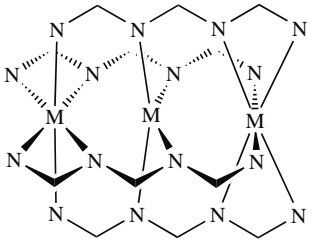
show antiferromagnetic coupling between the three nonbonded d^9 Cu(II) ions.[49] In the oxidized Cu_3^{7+} complex, only two unpaired electrons remain, and these couple antiferromagnetically.[15] This is consistent with the view that the central, square planar Cu atom is the one oxidized to a d^8 Cu(III) species. Further evidence is seen in the crystal structure (vide supra) and in the electronic spectrum. The band at 487 nm is assigned to the d^8 square planar Cu^{III} species, and a band at 1310 nm is believed to be an intervalence charge transfer band.

Several complexes with non-metal-metal bonded tricopper chains are known which employ bridging ligands other than dpa. For example, Cu(II) complexes of tetradentate bis-pyridyl or bis-pyrimidyl formamidinates are known for those ligands shown in **15.21**.[59,60]



15.21

Table 15.3 summarizes the structural information and magnetic data for these compounds and also for the known Cr_3^{6+}, Fe_3^{6+}, and Co_3^{6+} complexes which employ DPyF and related ligands. An unsymmetrical Cr_3^{6+} chain with the DPyF ligands has been characterized which, as mentioned in Section 15.2,[22] can be described as having a short Cr–Cr quadruple bond and a longer Cr···Cr separation leaving an isolated high spin Cr^{2+} ion. The corresponding Co_3^{6+}, Cu_3^{6+}, and Fe_3^{6+} compounds are isomorphous to $[Cr_3(DPyF)_4](PF_6)_2$, but do not show any sign of metal-metal bonding.[61] The M···M distances in this group of complexes (except for the Cr_3^{6+} compound) are all long, ranging from 2.64 Å in $[Cu_3(DPmF)_4](OTf)_2$[60] to 2.78 Å in $[Fe_3(DPyF)_4](PF_6)_2$ and 2.87 Å in $[Co_3(DPyF)_4](PF_6)_2$.[61] Rather than forming metal-metal bonds in these complexes, the outer two metal atoms are pulled away from the central, square-planar one by the extra dangling pyridyl groups resulting in a distorted octahedral geometry for the former as in **15.22**.



15.22

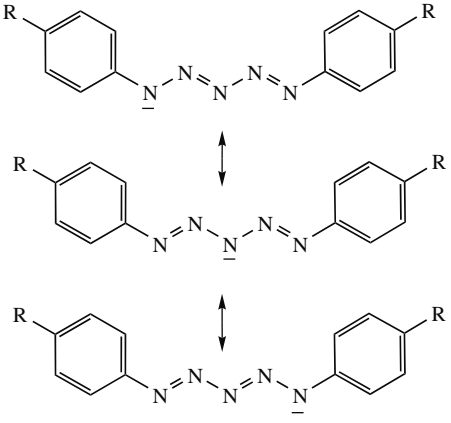
Pictiva EX2004
Samsung v Pictiva
IPR2024-01094

Table 15.3. Structural data for EMACs of DPyF and related ligands

Compound	Space Group	M···M	μ_{eff}, μ_B[a]	ref.
$[Cr_3(DPyF)_4](PF_6)_2 \cdot 4CH_3CN \cdot 2Et_2O$	$P2_1/c$	1.949(7) 2.738(7)	4.6	22
$[Cu_3(DPyF)_4](PF_6)_2 \cdot 4CH_3CN \cdot 2Et_2O$	$P2_1/c$	2.649(1) 2.649(1)	NR	61
$[Co_3(DPyF)_4](PF_6)_2 \cdot 4CH_3CN \cdot 2Et_2O$	$P2_1/c$	2.865(1) 2.849(1)	6.60	61
$[Fe_3(DPyF)_4](PF_6)_2 \cdot 4CH_3CN \cdot 2Et_2O$	$P2_1/c$	2.782(1) 2.783(1)	11.33	61
$[Cu_3(DPyF)_4](OTf)_2 \cdot 1.5EtOH$	$P2_1/c$	2.6618(8) 2.6676(8)	2.6	59
$[Cu_3(DPmF)_4](OTf)_2 \cdot 0.5H_2O$	$P\bar{1}$	2.637(3) 2.625(3)	2.6	60

[a] NR = not reported.

Also relevant are some chains of Cu^I ions with N-donor ligands. These include the remarkable trigonal complexes of pentaazadienide ligands[62] (shown in **15.23** and Fig. 15.11) among others.[63,64]



15.23

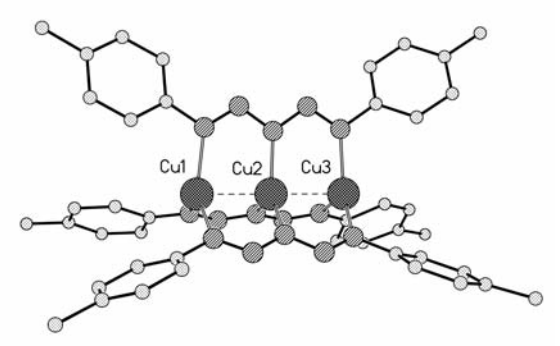


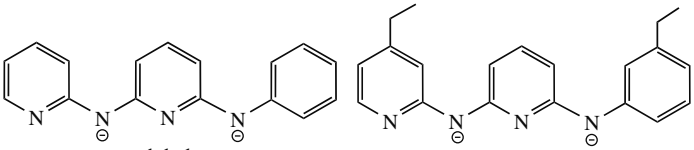
Fig. 15.11. Structure of $Cu_3(TolN_5Tol)_3$.

Pictiva EX2004
Samsung v Pictiva
IPR2024-01094

The trigonal chain complexes $Cu_3(TolN_5Tol)_3$ and $Cu_3(p\text{-}EtOPhN_5PhOEt)_3$ feature some of the shortest known Cu···Cu distances: 2.36 and 2.35 Å, respectively. The weak paramagnetism of these compounds is not well understood.[62]

It is for nickel that the longest discrete EMACs are known. The Ni_n^{2n+} compounds with n = 4,[8] 5,[7,65] 7,[8] and 9[9] have been synthesized and structurally characterized. Since these contain only d^8 Ni(II) ions, no Ni–Ni bonds are present. Oxidation to Ni–Ni bonded $Ni_n^{(2n+1)+}$ has only been achieved so far with pentanickel compounds (i.e. n = 5).[65,66] There is some evidence to suggest that EMACs with axial NCS ligands adhere to Au (111) surfaces.[67]

The longer Ni_n^{2n+} chains are synthesized by the reaction of $NiCl_2$ or $Ni(OAc)_2$ with the free ligand (those shown in **15.4** as well as H_2phdpda for the tetranickel chain and H_2etpda, which are shown in **15.24**) and $KOBu^t$ in molten naphthalene.[68,69] High temperatures appear to be necessary for the formation of the longer Ni_n chains. As seen already for the pentacobalt complexes, addition of excess NaX (X = CN, N_3, SCN) to the reaction mixtures yields complexes with axial X ligands.[68,69]



15.24

The pentanickel complexes are easier to oxidize than the corresponding trinickel complexes by ~0.4 V.[65] Reaction of $Ni_5(tpda)_4Cl_2$ or $Ni_5(etpda)_4Cl_2$ with excess Ag^+ gives the green oxidized complexes as follows:[65,66]

$$Ni_5(tpda)_4Cl_2 + 3AgOTf \xrightarrow{CH_2Cl_2} [Ni_5(tpda)_4(OTf)_2]OTf + 2AgCl + Ag$$

$$Ni_5(etpda)_4Cl_2 + 3AgPF_6 \xrightarrow{CH_2Cl_2} [Ni_5(etpda)_4](PF_6)_3 + 2AgCl + Ag$$

By using $AgBF_4$ in non-rigorously dry conditions the reaction occurs similarly, but the crystallographically characterized product has H_2O coordinated to the Ni_5 chain.[66]

The tetranuclear complex $Ni_4(phdpda)_4$ is unique among the longer EMACs of nickel because it has no axial ligands and is thus diamagnetic.[8] All four of the Ni atoms have similar Ni–N bond lengths, and the average Ni···Ni separations (2.32 Å) are nearly the same, with the outer Ni···Ni separations longer than the inner one by 0.02 Å. The unsymmetrical ligands wrap the tetranickel chain in a *cis* 2:2 geometry with each ligand pointing the opposite direction from the ligand *trans* to it.

The Ni_5^{10+} EMACs with the $tpda^{2-}$ ligand[7,68] and the $etpda^{2-}$ ligand[65] have fairly short inner Ni···Ni separations in the range 2.29-2.31 Å. The outer Ni···Ni separations are longer (2.35 - 2.40 Å) due to interactions with the axial ligands. Similar to the trinickel chains, the outer Ni atoms are high spin. Thus, the Ni–N bond distances of the outer Ni atoms are typically ~ 0.2 Å longer than the corresponding distances to the inner Ni atoms.

As seen previously for $Ni_3^{6+/7+}$ compounds, oxidation of Ni_5^{10+} to Ni_5^{11+} leads to major structural changes in the pentanickel chain. The inner Ni–Ni distances in the Ni_5^{11+} compounds shorten to between 2.23 and 2.28 Å and the outer Ni–Ni distances shrink to 2.29 - 2.36 Å consistent with five-center Ni–Ni bond formation. Attachment of Fe, Ru, Mo and W complexes to pentanickel chains

Pictiva EX2004
Samsung v Pictiva
IPR2024-01094

through axial cyanide linkages leads to very complex cyclic voltammograms in which it is difficult to assign the waves as being due to oxidation of the pentanickel core or of the axial metal ions.[38]

For hepta-[8,69] and nonanickel[9] compounds (an example is shown in Fig. 15.12), few are known and no metal-metal bonded oxidation products have been synthesized yet. The compounds which are known follow trends adumbrated by the tri- and pentanickel compounds. The inner Ni atoms are square planar and diamagnetic with shorter Ni–N bond lengths (*c.* 1.92 Å) and shorter Ni···Ni distances in the range of 2.19 to 2.31 Å. The two terminal Ni atoms are high spin with $S = 1$ and have Ni–N distances ~ 0.2 Å longer than the inner Ni atoms and Ni···Ni distances in the range 2.35 - 2.39 Å.

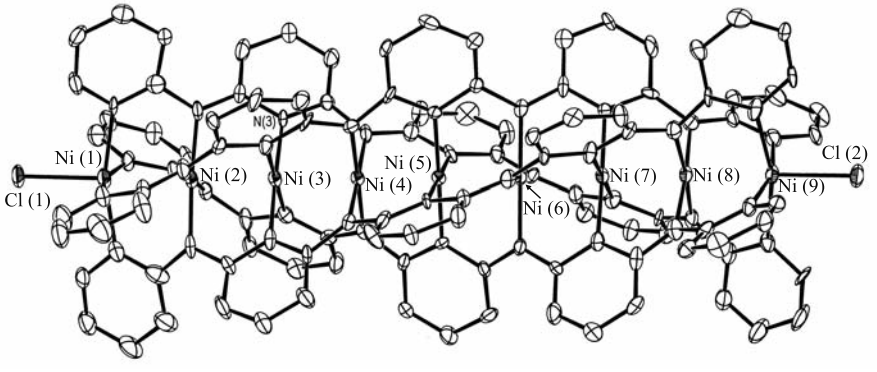


Fig. 15.12. Structure of $Ni_9(peptea)_4Cl_2$.

In Ni_n^{2n+} compounds with $n = 3$, 5, 7, and 9, the values of J for the antiferromagnetic coupling of the spins of the terminal Ni atoms of $Ni_3(dpa)_4Cl_2$, $Ni_5(tpda)_4Cl_2$, $Ni_7(teptra)_4Cl_2$, and $Ni_9(peptea)_4Cl_2$ are -198, -16.6, -7.6, and -3.4 cm^{-1}, respectively.[9,‡] These values are proportional to $1/d^3$, where d is the distance between terminal Ni atoms. The J value for $Ni_3(dpa)_4Cl_2$, however, was redetermined by another group with the result that $J = -218.2(7)$ cm^{-1}.[50] Also, the value of J for $Ni_5(tpda)_4Cl_2$ given above has been shown to be in error and has been redetermined to be -33.54(4) cm^{-1}.[65] Despite the controversy in the derived J values, it is clear from the magnetic data that the trinickel compounds have the most strongly coupled spins, and the coupling appears to decline rapidly as the Ni_n chain becomes longer.

The magnetic properties of the oxidized $Ni_5(tpda)_4^{3+}$ complexes have been described and modeled by the view that only one of the two terminal Ni atoms is oxidized to Ni^{3+} and antiferromagnetic coupling between the terminal high spin Ni^{2+} ($S = 1$) and Ni^{3+} ($S = ½$) with $J = -1110$ and -636 cm^{-1} for $[Ni_5(tpda)_4(H_2O)(BF_4)](BF_4)_2$ and $[Ni_5(tpda)_4(OTf)_2]OTf$ occurs.[66] This view has been contested and evidence for a delocalized Ni_5^{11+} unit with $S = ½$ has been shown for $Ni_5(etpda)_4(PF_6)_3$.[65]

15.5 EMACs of Ruthenium and Rhodium

The compounds $Ru_3(dpa)_4Cl_2$ and $Rh_3(dpa)_4Cl_2$ were described in a short communication lacking many basic experimental details.[5] $Ru_3(dpa)_4Cl_2$ was prepared in 2% yield from $Ru_2(OAc)_4Cl$, $KOBu^t$, and Hdpa in naphthalene. There is no indication of the preparation of $Rh_3(dpa)_4Cl_2$ except that it is prepared "similarly." Both complexes feature symmetrical chains

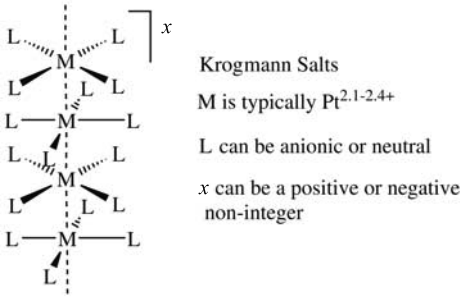
‡ These J values have all been normalized to accord with the Hamiltonian = $-JS_1 \cdot S_2$. Therefore, values which were determined in ref. 9 with the Hamiltonian = $-2JS_1 \cdot S_2$ have been multiplied by 2.

Pictiva EX2004
Samsung v Pictiva
IPR2024-01094

with M–M distances of 2.25 (Ru_3) and 2.39 Å (Rh_3) and long M···Cl contacts > 2.5 Å. The Ru_3^{6+} complex is reported to be diamagnetic, and its ^1H NMR spectrum is reported to consist, oddly, of seven unresolved multiplets which were not assigned. $Rh_3(dpa)_4Cl_2$ is paramagnetic with one unpaired electron.

15.6 Other Metal Atom Chains

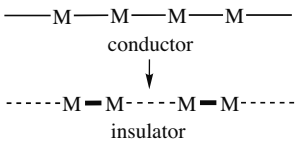
The compounds described above can be viewed as the newest addition to an old family of metal atom chains. The most notable of these are the platinum blues which have been known since 1908[70] and are briefly reviewed in Section 14.4.7, and Krogman salts (mixed-valence chains, shown schematically in **15.25**) which were shown in the 1960s to possess metallic properties in one dimension[71] and have been the subject of three monograph texts.[72] More recently, face-sharing $M_3X_{12}^{n-}$ compounds[73] and organometallic complexes with metal atom chains have been reported,[74] along with rhodium and iridium blues[75] and new rhodium chains.[76] Certain aspects of this chemistry are similar to issues discussed above for polypyridylamido complexes and will be discussed briefly here, along with selected examples of chain compounds with metal-metal bonds from the recent literature. Strong $d^{10}\cdots d^{10}$ interactions in compounds of heavy elements such as gold often give rise to extended chains as well, though these will not be discussed in detail here since formal Au–Au bonding is not involved. A major review by Pyykkö[77] summarizes this chemistry rather comprehensively.



15.25

A major impetus for the study of solids with one-dimensional metal atom chains is their ability to conduct electrical current, although the photophysical properties[78] and superconductivity[79] have also been of interest. The study of conductivity in systems such as Krogmann salts has been intimately related with the band theory of solids which is far too complicated to describe in this monograph, though interested readers may consult some introductory texts.[80] In a hypothetical infinite metal atom chain where the metal atoms are evenly spaced and allowed to form bonds to their neighbors, electron delocalization about the metal-based orbitals may be expected to give rise to conductivity in the same way that the π orbitals of polyacetylene[81] (i.e. $(CH)_x$) are conducting. But things are not always this straightforward. Peierls showed that in one dimensional systems, a conducting structure with equally spaced metal atoms is often unstable with respect to a phase with alternating long and short metal-metal distances.[82] In one dimensional systems, such insulator-conductor phase transitions (also called Peierls transitions) are common as shown in **15.26**.

Pictiva EX2004
Samsung v Pictiva
IPR2024-01094

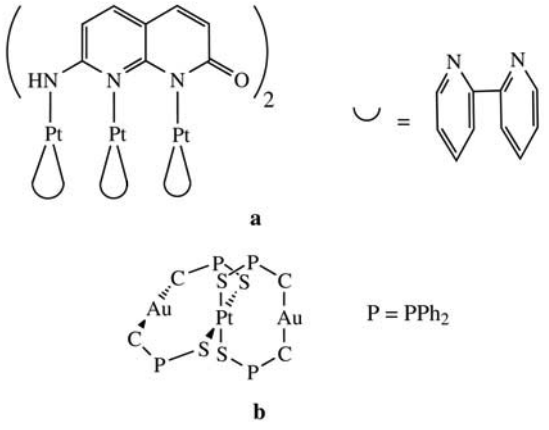


15.26

It is useful here to look back at the Cr_5^{10+} and Co_5^{10+} compounds described above in connection with the Peierls instability. The issue which must be addressed is the relative stability of the localized M_2^{4+} units vs the delocalized M_5^{10+} unit. For chromium, the pairing of 8 *d* electrons to form a Cr_2^{4+} quadruple bond appears to favor the Peierls (insulator) state, which tends to agree with the experimental evidence that several unsymmetrical crystal structures of $Cr_5(tpda)_4Cl_2$ are known with alternating long and short Cr–Cr distances. On the other hand, a Co_2^{4+} unit has only a single electron rich bond. In this case, the Co_5^{10+} unit appears to be favored, though the possibility of a Peierls phase transition at very low temperatures cannot be ruled out.

Square planar complexes of d^8 metals such as $Pt(CN)_4^{2-}$ often pack to form metal atom chains in the solid state. Partial oxidation of these complexes to form mixed valence chains or Krogmann salts typically results in a one dimensional conducting material.[71] Discrete oxidized oligomers of this type with Pt_4^{9+} chains are known as platinum blues for their deep blue color.[83] This chemistry is similar to the chemistry of $Ni_3^{6+/7+}$ and $Ni_5^{10+/11+}$ chains discussed earlier. The unoxidized species have only d^8 Ni^{2+} ions and no Ni–Ni bonds, but upon oxidation, Ni–Ni bonds form in the mixed-valence state and the compounds are expected to be conducting.

Similar chemistry is known in the oxidation to Pt_3^{8+} of a discrete Pt_3^{6+} compound with a linear $[Pt(bpy)]_3$ chain stabilized by the ligand 7-amino-1,8-naphthyridin-2-one (see **15.27**a).[84] Also, linear Au···Pt···Au compounds with the bridging ylide ligand shown in **15.27**b have been oxidized from Au_2Pt^{4+} to Au_2Pt^{6+} whereupon Au–Pt bonds (2.67 Å) form.[85] It is worth noting that the corresponding Au_2Pb^{4+} complex does not undergo similar oxidation.[86]



15.27

Pictiva EX2004
Samsung v Pictiva
IPR2024-01094

References

1. (a) L.-G. Zhu and S.-M. Peng, *Wuji Huaxue Xuebao*, **2002**, *18*, 117. (b) J. K. Bera and K. R. Dunbar, *Angew. Chem., Int. Ed.* **2002**, *41*, 4453.
2. T. J. Hurley and M. A. Robinson, *Inorg. Chem.* **1968**, *7*, 33.
3. S. Aduldecha and B. Hathaway, *J. Chem. Soc., Dalton Trans.* **1991**, 993.
4. E.-C. Yang, M.-C. Cheng, M.-S. Tsai and S.-M. Peng, *J. Chem. Soc., Chem. Commun.* **1994**, *20*, 2377.
5. J.-T. Sheu, C.-C. Lin, I. Chao, C.-C. Wang and S.-M. Peng, *Chem. Commun.* **1996**, *3*, 315.
6. F.-A. Cotton, L. M. Daniels, C. A. Murillo and I. Pascual, *J. Am. Chem. Soc.* **1997**, *119*, 10223.
7. S.-J. Shieh, C.-C. Chao, G.-H. Lee, C.-C. Wang and S.-M. Peng, *Angew. Chem., Int. Ed. Engl.* **1997**, *36*, 56.
8. S.-Y. Lai, T.-W. Lin, Y.-H. Chen, C.-C. Wang, G.-H. Lee, M.-H. Yang, M.-K. Leung and S.-M. Peng, *J. Am. Chem. Soc.* **1999**, *121*, 250.
9. S.-M. Peng, C.-C. Wang, Y.-L. Jang, Y.-H. Chen, F.-Y. Li, C.-Y. Mou and M.-K. Leung, *J. Magn. Magn. Mater.* **2000**, *209*, 80.
10. R. Clérac, F. A. Cotton, L. M. Daniels, K. R. Dunbar, K. Kirschbaum, C. A. Murillo, A. A. Pinkerton, A. J. Schultz and X. Wang, *J. Am. Chem. Soc.* **2000**, *122*, 6226.
11. R. Clérac, F. A. Cotton, L. M. Daniels, K. R. Dunbar, C. A. Murillo and I. Pascual, *Inorg. Chem.* **2000**, *39*, 748.
12. F. A. Cotton, L. M. Daniels, T. Lu, C. A. Murillo and X. Wang, *J. Chem. Soc., Dalton Trans.* **1999**, 517.
13. (a) M.-M. Rohmer and M. Bénard, *J. Am. Chem. Soc.* **1998**, *120*, 9372. (b) M.-M. Rohmer, A. Strich, M. Bénard and J.-P. Malrieu, *J. Am. Chem. Soc.* **2001**, *123*, 9126.
14. N. Benbellat, M.-M. Rohmer and M. Bénard, *Chem. Commun.* **2001**, 2368.
15. J. F. Berry, F. A. Cotton, L. M. Daniels, C. A. Murillo and X. Wang, *Inorg. Chem.* **2003**, *42*, 2418.
16. C.-Y. Yeh, C.-H. Chou, K.-C. Pan, C.-C. Wang, G.-H. Lee, Y.-O. Su and S.-M. Peng, *J. Chem. Soc., Dalton Trans.* **2002**, 2670.
17. Y.-H. Chen, C.-C. Lee, C.-C. Wang, G.-H. Lee, S.-Y. Lai, F.-Y. Li, C.-Y. Mou and S.-M. Peng, *Chem. Commun.* **1999**, 1667.
18. F. A. Cotton, L. M. Daniels, C. A. Murillo and I. Pascual, *Inorg. Chem. Commun.* **1998**, *1*, 1.
19. R. Clérac, F. A. Cotton, S. P. Jeffery, C. A. Murillo and X. Wang, *Dalton Trans*. **2003**, 3022.
20. R. Clérac, F. A. Cotton, L. M. Daniels, K. R. Dunbar, C. A. Murillo and H.-C. Zhou, *Inorg. Chem.* **2000**, *39*, 3414.
21. F. A. Cotton, L. M. Daniels, P. Lei, C. A. Murillo and X. Wang, *Inorg. Chem.* **2001**, *40*, 2778.
22. F. A. Cotton, L. M. Daniels, C. A. Murillo and X. Wang, *Chem. Commun.* **1998**, 39.
23. F. A. Cotton, P. Lei, C. A. Murillo and L.-S. Wang, *Inorg. Chim. Acta* **2003**, *349*, 165.
24. R. Clérac, F. A. Cotton, L. M. Daniels, K. R. Dunbar, C. A. Murillo and I. Pascual, *Inorg. Chem.* **2000**, *39*, 752.
25. J. F. Berry, F. A. Cotton, C. A. Murillo and B. K. Roberts, *Inorg. Chem.* **2004**, *43*, 2277.
26. J. F. Berry, F. A. Cotton, T. Lu, C. A. Murillo, B. K. Roberts and X. Wang, *J. Am. Chem. Soc*. **2004**, *126*, 7082.
27. F. A. Cotton, P. Lei and C. A. Murillo, *Inorg. Chim. Acta* **2003**, *349*, 173.
28. M.-M. Rohmer and M. Bénard, *J. Cluster Sci.* **2002**, *13*, 333.
29. H.-C. Chang, J.-T. Li, C.-C. Wang, T.-W. Lin, H.-C. Lee, G.-H. Lee and S.-M. Peng, *Eur. J. Inorg. Chem.* **1999**, 1243.
30. F. A. Cotton, L. M. Daniels, C. A. Murillo and X. Wang, *Chem. Commun.* **1999**, 2461.
31. F. A. Cotton, L. M. Daniels and G. T. Jordan, IV, *Chem. Commun.* **1997**, 421.
32. F. A. Cotton, L. M. Daniels, G. T. Jordan, IV and C. A. Murillo, *J. Am. Chem. Soc.* **1997**, *119*, 10377.
33. R. Clérac, F. A. Cotton, K. R. Dunbar, T. Lu, C. A. Murillo and X. Wang, *Inorg. Chem.* **2000**, *39*, 3065.

Pictiva EX2004
Samsung v Pictiva
IPR2024-01094

34. R. Clérac, F. A. Cotton, L. M. Daniels, K. R. Dunbar, C. A. Murillo and X. Wang, *J. Chem. Soc., Dalton Trans.* **2001**, 386.
35. R. Clérac, F. A. Cotton, S. P. Jeffery, C. A. Murillo and X. Wang, *Inorg. Chem.* **2001**, *40*, 1265.
36. J. F. Berry, F. A. Cotton, T. Lu and C. A. Murillo, *Inorg. Chem.* **2003**, *42*, 4425.
37. R. Clérac, F. A. Cotton, K. R. Dunbar, T. Lu, C. A. Murillo and X. Wang, *J. Am. Chem. Soc.* **2000**, *122*, 2272.
38. T. Sheng, R. Appelt, V. Comte and H. Vahrenkamp, *Eur. J. Inorg. Chem*. **2003**, 3731.
39. F. A. Cotton, C. A. Murillo and X. Wang, *J. Chem. Soc., Dalton Trans.* **1999**, 3327.
40. R. Clérac, F. A. Cotton, L. M. Daniels, K. R. Dunbar, C. A. Murillo and X. Wang, *Inorg. Chem.* **2001**, *40*, 1256.
41. M.-M. Rohmer and M. Bénard, *Chem. Soc. Rev.* **2001**, *30*, 340.
42. F. A. Cotton, C. A. Murillo and X. Wang, *Inorg. Chem.* **1999**, *38*, 6294.
43. C.-Y. Yeh, C.-H. Chou, K.-C. Pan, C.-C. Wang, G.-H. Lee, Y.-O. Su and S.-M. Peng, *J. Chem. Soc., Dalton Trans.* **2002**, 2670.
44. J. F. Berry, F. A. Cotton, L. M. Daniels and C. A. Murillo, *J. Am. Chem. Soc.* **2002**, *124*, 3212.
45. L.-P. Wu, P. Field, T. Morrissey, C. Murphy, P. Nagle, B. Hathaway, C. Simmons and P. Thornton, *J. Chem. Soc., Dalton Trans.* **1990**, 3853.
46. G. J. Pyrka, M. El-Mekki and A. A. Pinkerton, *J. Chem. Soc., Chem. Commun.* **1991**, 84.
47. R. Clérac, F. A. Cotton, K. R. Dunbar, C. A. Murillo, I. Pascual and X. Wang, *Inorg. Chem.* **1999**, *38*, 2655.
48. T.-B. Tsao, G.-H. Lee, C.-Y. Yeh and S.-M. Peng, *Dalton Trans.* **2003**, 1465.
49. J. F. Berry, F. A. Cotton, P. Lei and C. A. Murillo, *Inorg. Chem.* **2003**, *42*, 377.
50. J. F. Berry, F. A. Cotton, T. Lu, C. A. Murillo and X. Wang, *Inorg. Chem.* **2003**, *42*, 3595.
51. F. A. Cotton, P. Lei and C. A. Murillo, *Inorg. Chim. Acta* **2003**, *351*, 183.
52. L.-G. Zhu, S.-M. Peng and G.-H. Lee, *Anal. Sci.* **2002**, *18*, 1067.
53. C.-H. Peng, C.-C. Wang, H.-C. Lee, W.-C. Lo, G.-H. Lee and S.-M. Peng, *J. Chin. Chem. Soc. (Taipei)* **2001**, *48*, 987.
54. J. F. Berry, F. A. Cotton and C. A. Murillo, *Dalton Trans.* **2003**, 3015.
55. L.-G. Zhu, S.-M. Peng and G.-H. Lee, *Chem. Lett.* **2002**, 1210.
56. H. Li, G.-H. Lee and S.-M. Peng, *Inorg. Chem. Commun.* **2003**, *6*, 1.
57. O. Kahn, *Molecular Magnetism*, Wiley-VCH, Inc.: New York, 1993.
58. (a) M. Gerloch and J. H. Harding, *Proc. R. Soc. London* **1978**, *A 360*, 211. (b) M. Kato and Y. Muto, *Coord. Chem. Rev.* **1988**, *92*, 45.
59. G. A. van Albada, I. Mutikainen, U. Turpeinen and J. Reedjik, *Eur. J. Inorg. Chem.* **1998**, 547.
60. G. A. van Albada, P. J. van Koningsbruggen, I. Mutikainen, U. Turpeinen and J. Reedjik, *Eur. J. Inorg. Chem.* **1999**, 2269.
61. F. A. Cotton, C. A. Murillo and X. Wang, *Inorg. Chem. Commun.* **1998**, *1*, 281.
62. (a) J. Beck and J. Strähle, *Angew. Chem., Int. Ed. Engl.* **1985**, *24*, 409. (b) R. Schmid and J. Strähle, *Z. Naturforsch.* **1989**, *446*, 105.
63. M.-S. Tsai and S.-M. Peng, *J. Chem. Soc., Chem. Commun.* **1991**, 514.
64. R. Clérac, F. A. Cotton, L. M. Daniels, J. Gu, C. A. Murillo and H.-C. Zhou, *Inorg. Chem.* **2000**, *39*, 4488.
65. J. F. Berry, F. A. Cotton, P. Lei, T. Lu and C. A. Murillo, *Inorg. Chem.* **2003**, *42*, 3534.
66. C.-Y. Yeh, Y.-L. Chiang, G.-H. Lee and S.-M. Peng, *Inorg. Chem.* **2002**, *41*, 4096.
67. S.-Y. Lin, I.-W. P. Chen, C.-h. Chen, M.-H. Hsieh, C.-Y. Yeh, T.-W. Lin, Y.-H. Chen and S.-M. Peng, *J. Phys. Chem. B* **2004**, *108*, 959.
68. C.-C. Wang, W.-C. Lo, C.-C. Chou, G.-H. Lee, J.-M. Chen and S.-M. Peng, *Inorg. Chem.* **1998**, *37*, 4059.
69. S.-Y. Lai, C.-C. Wang, Y.-H. Chen, C.-C. Lee, Y.-H. Liu and S.-M. Peng, *J. Chin. Chem. Soc. (Taipei)* **1999**, *46*, 477.
70. K. A. Hofmann and G. Bugge, *Ber. Dtch. Chem. Ges.* **1908**, *41*, 312.

Pictiva EX2004
Samsung v Pictiva
IPR2024-01094

71. (a) K. Krogmann and P. Dodel, *Chem. Ber.* **1966**, *99*, 3402. (b) K. Krogmann and P. Dodel, *Chem. Ber.* **1966**, *99*, 3408. (c) K. Krogmann, *Z. anorg. allg. Chem.* **1968**, *358*, 97. (d) K. Krogmann, *Angew. Chem., Int. Ed. Engl.* **1969**, *8*, 35.
72. (a) *Extended Linear Chain Compounds* Miller, J. S., Ed. Vol. 1, Plenum Press: New York, 1982. (b) *Extended Linear Chain Compounds* Miller, J. S., Ed. Vol. 2, Plenum Press: New York, 1982. (c) *Extended Linear Chain Compounds* Miller, J. S., Ed. Vol. 3, Plenum Press: New York, 1983.
73. (a) J. C. Fettinger, S. P. Mattamana, C. J. O'Connor, R. Poli and G. Salem, *J. Chem. Soc., Chem. Commun.* **1995**, 1265. (b) F. A. Cotton, M. Matusz and R. C. Torralba, *Inorg. Chem.* **1989**, *28*, 1516. (c) F. A. Cotton and R. C. Torralba, *Inorg. Chem.* **1991**, *30*, 2196. (d) F. A. Cotton and R. C. Torralba, *Inorg. Chem.* **1991**, *30*, 4386. (e) F. A. Cotton and R. C. Torralba, *Inorg. Chem.* **1991**, *30*, 4386.
74. (a) T. Murahashi, E. Mochizuki, Y. Kai and H. Kurosawa, *J. Am. Chem. Soc.* **1999**, *121*, 10660. (b) T. Murahashi, Y. Higuchi, T. Katoh and H. Kurosawa, *J. Am. Chem. Soc.* **2002**, *124*, 14288. (c) T. Murahashi and H. Kurosawa, *Coord. Chem. Rev.* **2002**, *231*, 207. (d) T. Murahashi, T. Uemura and H. Kurosawa, *J. Am. Chem. Soc.* **2003**, *125*, 8536. (e) M.-D. Su, H.-Y. Liao, S.-Y. Chu, Y. Chi, C.-S. Liu, F.-J. Lee, S.-M. Peng and G.-H. Lee, *Organometallics* **2000**, *19*, 5400. (f) F. A. Cotton, E. V. Dikarev and M. A. Petrukhina, *J. Organomet. Chem.* **2000**, *596*, 130. (g) F. A. Cotton, E. V. Dikarev and M. A. Petrukhina, *J. Chem. Soc., Dalton Trans.* **2000**, 4241. (h) T. Murahashi, S. Ogashi and H. Kurosawa, *Chem. Record* **2003**, *3*, 101.
75. C. Tejel, M. A. Ciriano and L. A. Oro, *Chem. Eur. J.* **1999**, *5*, 1131.
76. (a) G. M. Finniss, E. Canadell, C. Campana and K. R. Dunbar, *Angew. Chem., Int. Ed. Engl.* **1996**, *35*, 2772. (b) F. P. Pruchnik, P. Jakimowicz, Z. Ciunik, K. Stanislawek, L. A. Oro, C. Tejel and M. A. Ciriano, *Inorg. Chem. Commun.* **2001**, *4*, 19. (c) K. R. Mann, M. J. DiPierro and T. P. Gill, *J. Am. Chem. Soc*. **1980**, *102,* 3965.
77. P. Pyykkö, *Chem. Rev.* **1997**, *97*, 597.
78. (a) V. M. Miskowski and V. H. Houlding, *Inorg. Chem.* **1991**, *30*, 4446. (b) J. W. Brill, M. Mégnamisi-Bélombé and M. Novotny, *J. Chem. Phys.* **1978**, *68*, 585. (c) A. Lechner and G. Gliemann, *J. Am. Chem. Soc.* **1989**, *111*, 7469.
79. S. T. Carr and A. M. Tsvelik, *Phys. Rev. B* **2002**, *65*, 195121/1.
80. (a) I. Božović and J. Delhalle, *Phys. Rev. B* **1984**, *29*, 4733. (b) J. S. Miller and A. J. Epstein, *Prog. Inorg. Chem*. **1976**, *20*, 1.
81. (a) A. J. Heeger, *Rev. Mod. Phys.* **2001**, *73*, 681. (b) A. G. MacDiarmid, *Rev. Mod. Phys.* **2001**, *73*, 701. (c) H. Shirakawa, *Rev. Mod. Phys.* **2001**, *73*, 713.
82. R. E. Peierls, *Quantum Theory of Solids*, Oxford University Press: Oxford, 1955, p. 108.
83. S. J. Lippard, *Science* **1982**, *218*, 1075.
84. B. Osuki and W. S. Sheldrick, *Eur. J. Inorg. Chem.* **1999**, 1325.
85. (a) H. H. Murray, D. A. Briggs, G. Garzón, R. G. Raptis, L. C. Porter and J. P. Fackler, Jr., *Organometallics* **1987**, 6, 1992. (b) J. P. Fackler, Jr. *Inorg. Chem.* **2002**, *41*, 6959.
86. S. Wang, G. Garzón, C. King, J.-C. Wang and J. P. Fackler, Jr., *Inorg. Chem.* **1989**, *28*, 4623.

Pictiva EX2004
Samsung v Pictiva
IPR2024-01094

16

Physical, Spectroscopic and Theoretical Results

F. Albert Cotton,
Texas A&M University

16.1 Structural Correlations

16.1.1 Bond orders and bond lengths

Throughout the preceding chapters of this book we have reported and in some cases discussed the lengths of the multiple bonds between metal atoms. We have reported in tabular form most of the M–M distances that have been determined crystallographically. It is now time to make some general comments on these distances in relation to our understanding of the M–M bonds.

It is a general qualitative rule in chemistry that bond lengths and bond orders are inversely related. In some limited areas, particularly with the first-row elements carbon, nitrogen, and oxygen, quantitative relationships expressing bond length as a single-valued function of bond order are well known. However, these quantitative relationships are based heavily on faith, as well as fact. Bond lengths are facts; bond orders are not. In the process of inferring a bond order from a bond length one is often getting out no more than what was put in to begin with.

We shall not further digress into a discussion of the philosophical ambiguities of these quantitative bond order-bond length correlations because they have proven to be useful, within their own sphere of application. However, there is no *a priori* reason to expect that similar procedures will (or will not!) work in the very different realm of metal-to-metal bonds. Experience is the only test, and experience thus far has shown that M–M bonds cannot usefully be treated in such a way.

In the realm of M–M bonds it is best to invoke only a qualitative inverse relationship between bond order and bond length and to define bond order only in a qualitative or ordinal way. In this book we have used the term M–M bond order only to indicate how many electron pairs are believed, on the basis of essentially qualitative considerations, to play a significant part in holding the pair of metal atoms together. We condemn as foolish and hopeless any effort to associate a unique, precise, quantitative bond order with each and every M–M internuclear distance.

In principle, M–M bond lengths, like others, should be amenable to treatment by the method of molecular mechanics, and some efforts[1-4] (hampered by a dearth of necessary experimental data) to do this have been reported. In general the results are encouraging and can account for

Pictiva EX2004
Samsung v Pictiva
IPR2024-01094

variations in the lengths and vibrational frequencies of a given type (i.e. order) of M–M bond by taking into consideration the way in which the entire set of intra-ligand bonds and ligand-ligand repulsions contribute to the net result. One major result of this work has been to support and clarify the concept that bridging ligands (RCO_2^- and stereoelectronically similar ones) favor shorter M–M distances (see Section 4.4.5 for Mo–Mo bonds) and high M–M stretching frequencies. Such molecular mechanics calculations have also provided some estimates of the barriers to internal rotation that arise from a combination of the δ-bonding and the end-to-end ligand–ligand repulsive forces (see Section 16.1.6).

Another point worth noting here is that even the statement just made concerning "how many electron pairs... play a significant part in holding the metal atoms together" has a simplicity that is very deceptive. The classic molecular orbital definition of bond order, as an ordinal number, is valid only when the bond is described by a single electron configuration. But, as we have already noted for Cr–Cr bonds in Chapter 3, and will discuss more generally later, multiple bonds between metal atoms can rarely if ever be described accurately without including configuration interaction (CI). This means that the best description of the ground state (or any other state, for that matter) entails the mixing in of configurations having fewer bonding electrons and more antibonding electrons. Thus the net value of $(n_b - n_a)/2$ (i.e. bonding pairs minus antibonding pairs) in general is a fractional number, with a value that keeps changing as the CI calculation is extended.

Thus, when we have referred to double bonds, triple bonds, and quadruple bonds, i.e. bond orders of 2, 3, and 4, we have been using somewhat fictional or formal numbers, often corresponding to what we would deduce if we carried out a simple (i.e. one-configuration) Hartree-Fock calculation, then used the results to calculate an integral or half-integral bond order, and ignored CI. Despite the reservations we must have about this procedure, the bond orders so obtained provided a much-needed framework for classifying and discussing the subject.

Even at the most empirical level both the shortcomings and the utility of the nominal bond orders are apparent. For example Mo–Mo quadruple bond distances range from about 2.07 Å to about 2.18 Å, as noted in Section 4.5.5. There is a range of values for Mo–Mo triple bonds as well, running from 2.167 Å in $Mo_2(CH_2SiMe_3)_6$ to 2.222(2) Å in $Mo_2(OCH_2CMe_3)_6$. If one were to insist that every different Mo–Mo distance must be associated with a different bond order, there would be, in addition to the irksome difficulty of devising a meaningful way of establishing the proper numerical values, the insuperable inconsistency of having to assign a higher bond order in the triply bonded $Mo_2(CH_2SiMe_3)_6$ than in the quadruply bonded $[Mo_2(NCS)_8]^{4-}$ ion.

Deeper insight into some of the reasons why bond order and bond length seldom have a truly simple relationship (even if there is sometimes an apparently simple one) is provided by the following story.[5] The following data for an essentially isostructural series of compounds appear to provide a straightforward example of bond length increasing simply as a function of decreasing bond order:

	Bond length (Å)	Elect. conf.	Bond order
$[Mo_2(SO_4)_4]^{4-}$	2.111(1)	$\sigma^2\pi^4\delta^2$	4.0
$[Mo_2(SO_4)_4]^{3-}$	2.167(1)	$\sigma^2\pi^4\delta$	3.5
$[Mo_2(HPO_4)_4]^{2-}$	2.223(2)	$\sigma^2\pi^4$	3.0

From this it would seem to follow straightforwardly that on oxidizing the $[Tc_2Cl_8]^{3-}$ ion, which has a $\sigma^2\pi^4\delta^2\delta^*$ configuration, to $[Tc_2Cl_8]^{2-}$, the loss of the δ* electron should strengthen and shorten the bond, by something of the order of 0.05-0.10 Å. The actual results, shown below are opposite to this expectation.

Pictiva EX2004
Samsung v Pictiva
IPR2024-01094

	Bond length (Å)	Elect. conf.	Bond order
$[Tc_2Cl_8]^{3-}$	2.105(1), 2.117(2)	$\sigma^2\pi^4\delta^2\delta^*$	3.5
$[Tc_2Cl_8]^{2-}$	2.151(1)	$\sigma^2\pi^4\delta^2$	4.0

The reason for this initially surprising result is as follows. First, we must recognize that the σ and π components of these bonds are far stronger than the δ (or δ*) component, the latter supplying only a few per cent of the total bond strength. Therefore even a small change (2-3%) in the σ and π contributions will be as important as a 50% change in the δ-bonding. Second, in all of the five compounds just discussed, the changes in bond order (by removing δ or δ* electrons) are also accompanied by increases in the oxidation states of the metal atoms. An increase in the effective positive charge on the metal atoms may be expected to cause some contraction of the *d*-orbitals and hence a diminution of the overlaps in all components of the M–M bonds, including the strong σ and π components.

In the case of the three molybdenum compounds, there is an increase in formal positive charge along with the reduction in bond order. Thus, both factors tend to increase the M–M distance, and increases are, therefore, necessarily observed. It is a mistake, however, to attribute them entirely to the reduction in bond order. In the case of the two technetium compounds, however, the two factors work in opposite directions, and evidently the bond-weakening effect of increased effective charge on the metal atoms outweighs the bond-strengthening effect of removing the δ* electron. A net increase in Tc–Tc distance thus results despite the increase in bond order.

While the line of argument just developed might be regarded as simply *ad hoc* on the basis of only two cases, convincing support has been provided by the data for the following series of compounds,[6] as well as others.

	Bond length (Å)	Elect. conf.	Bond order
$Re_2Cl_6(PEt_3)_2$	2.222(3)	$\sigma^2\pi^4\delta^2$	4.0
$Re_2Cl_4(PEt_3)_4$	2.232(6)	$\sigma^2\pi^4\delta^2\delta^{*2}$	3.0
$Re_2Cl_4(PMe_2Ph)_4$	2.241(1)	$\sigma^2\pi^4\delta^2\delta^{*2}$	3.0
$[Re_2Cl_4(PMe_2Ph)_4]^+$	2.218(1)	$\sigma^2\pi^4\delta^2\delta^*$	3.5
$[Re_2Cl_4(PMe_2Ph)_4]^{2+}$	2.215(2)	$\sigma^2\pi^4\delta^2$	4.0

The first two compounds show a possible slight lengthening with decreasing bond order, but evidently the charge factor, while not outweighing the bond order factor, is of approximately equal importance. An even better illustration of these effects is provided by the last three species, where there is no change in composition. The steady increase in bond order produces only a small and irregular decrease in bond length as a result of the countervailing effect of the steady increase in effective charge on the metal atoms.

Further support for the foregoing analysis is provided by the results of several kinds of experiments in which the bond order is changed without changing the formal oxidation states of the metal atoms. Two ways to do this, both of which will be discussed in detail later, are:

1. to reduce the δ-bond strength by twisting the rotational conformation away from eclipsed towards the staggered, and
2. to excite an electron from a bonding to an antibonding orbital, as for example, in a δ→δ* type transition.

The very disparate importance of π (or π*) and δ (or δ*) electrons is clearly illustrated by two ruthenium compounds.

	Bond length (Å)	Elect. conf.
$Ru_2(mhp)_4$	2.235(1)	$\sigma^2\pi^4\delta^2\pi^{*2}\delta^{*2}$
$Ru_2(PhN_3Ph)_4$	2.399(1)	$\sigma^2\pi^4\delta^2\pi^{*4}$

Pictiva EX2004
Samsung v Pictiva
IPR2024-01094

Here there is no change in bond order, but two δ* electrons are replaced by two π* electrons. Since the former are only weakly antibonding and the latter strongly so, a large increase in bond length would be expected, and is found.

Finally, we note that the very short Tc–Tc distance in $K_2Tc_2Cl_6$, 2.04 Å, is, in fact, consistent with other Tc–Tc distances, such as 2.15 Å in $[Tc_2Cl_8]^{2-}$ and 2.11 Å in $[Tc_2Cl_8]^{3-}$, because we now have $[Tc_2Cl_8]^{4-}$ ions fused together in chains. Within each such unit the low formal charge (Tc_2^{4+}) allows strong σ and π overlap even though there are two δ*-electrons.

16.1.2 Internal rotation

The strength of the σ and π components of multiple M–M bonds is essentially independent of the angle of internal rotation, since the σ overlap and the two π overlaps jointly are cylindrically symmetrical. Thus, in bonds of order 3 there is no inherently preferred angle of internal rotation, and the angle adopted is not prejudiced by the M–M bonding. In quadruple bonds (and to a lesser extent those of order 3.5) the presence of δ bonding introduces an additional factor. The δ overlap is angle-sensitive in a way that is easily determined[7] from the angular wave function of the d_{xy}-orbitals, with the M–M direction as the *z* axis. If we define the angle of internal rotation, χ, as zero for the eclipsed structure and 45° for the perfectly staggered structure (symmetries of D_{4h} and D_{4d} for an M_2X_8 species), the overlap (*S*) varies as cos2χ. A plot of S_δ versus χ is shown in Fig. 16.1. Naturally, a plot of S_δ versus cos2χ should be a straight line from $S_\delta = 1$ (at $\chi = 0$) to $S_\delta = 0$ (at $\chi = 45°$).

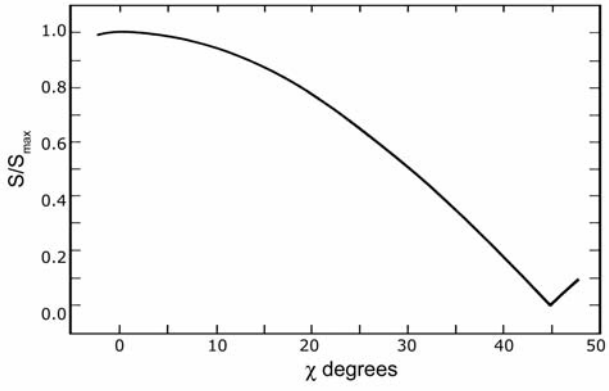


Fig. 16.1. A plot of the δ overlap vs torsion angle χ.

The fact that the strength of the δ-bond is greatest for $\chi = 0$ does not necessarily mean that this is the preferred angle when *all* factors are taken into account, however. The δ bond is a relatively weak one, and the minimization of nonbonded repulsions, operating between the sets of ligands at the two ends of an $L_4M{\equiv}ML_4$ unit, may favor a rotation away from the eclipsed ($\chi = 0$) conformation. The value of χ where these two forces are balanced may be expected, in general, to be other than zero. There are, of course, still other factors bearing on the result, including intermolecular (packing) forces. When some of the ligands are bidentate ones, such as $Ph_2PCH_2CH_2PPh_2$, that span the two metal atoms, the conformational preferences of the resulting M_2-containing rings often favor twist angles quite different from zero. It is precisely this phenomenon that has allowed us to obtain the data required to map quantitatively the δ manifold, as explained in Section 16.4.1.

Pictiva EX2004
Samsung v Pictiva
IPR2024-01094

From Fig. 16.1 it can be seen that small values of χ_{av} cause little diminution in the strength of the δ-bond. A rotation of 22.5° (halfway toward a staggered conformation) costs only 30% of the δ overlap, and even a 30° rotation leaves 50% of the δ overlap intact. Thus, it is to be expected that in most cases when a quadruply bonded species is unconstrained by its surroundings, the optimum angle may well be > 0.

In some experimentally determined structures a C_4 axis makes all four torsion angles equal, Fig. 16.2(a). In general, however, we require a practical rule for specifying the torsion angle. The rule that has been normally used is to define the four torsion angles as shown in Fig. 16.2(b) and use their average value (algebraic sum divided by 4). There are many examples where symmetry considerations result in the torsion angle (sometimes also called the twist angle) being rigorously zero when so defined. Thus, if there is a center of inversion at the midpoint of the M–M bond, the four torsion angles must form two pairs each of the same value but opposite in sign. This is a rather common occurrence but there are also other cases when the average of individually non-zero torsion angles is zero because of a plane or C_2 axis of symmetry.

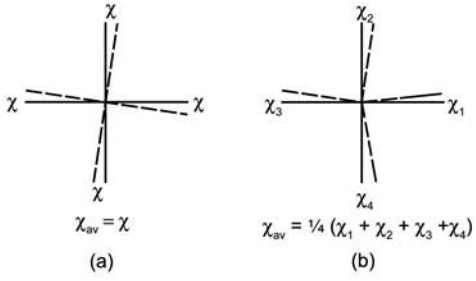


Fig. 16.2. Diagrams defining the angle of internal rotation for $L_4M–ML_4$ systems. (a) The case where four fold symmetry prevails and all four L–M–M–L torsion angles are equal; (b) a general case where there is no overall symmetry and all four torsion angles may have different magnitudes and directions. Directions are defined consistently, so that if χ1 and χ4 are + or –, χ2 and χ3 are – or +.

If bond length is linearly related (inversely) to the magnitude of S_δ, then for a series of compounds in which only the twist angle is changed, a plot of the M–M distance versus cos2χ should be linear. Compounds of the type β-$Mo_2X_4(PP)_2$, where X = Cl or Br and PP is a diphosphine, are a series that can be used to test this proposal.[8,9] The results are shown in Fig. 16.3. The best straight line, shown in the figure, has a correlation coefficient of 0.995, and from it a change in Mo–Mo distance of 0.097 Å for complete loss of the δ-bond (change in χ from 0 to 45°) is derived.

To make a quantitative estimate of the barrier to internal rotation, either experimentally or theoretically, experimental efforts have been devoted to ^{1}H NMR line-shape measurements on dimolybdenum and ditungsten porphyrin compounds.[10-13] In all cases the results have been in the range of 10-13 kcal mol^{-1}. The "barrier to rotation" measured in this way is the difference in free energy between the most stable rotational conformation (not necessarily of D_{4h} symmetry but probably close) and the least stable one (not necessarily of D_{4d} symmetry, but probably close). How much these barriers tell us about the strength of the δ bonding per se is more problematical than one might suppose. To say that the measured barrier and the δ bond strength are equal is not justified.

Conversely, from theoretical calculations of the difference between the electronic energies of the D_{4h} and D_{4d} ground states, it is problematic to infer the measurable barrier to rotation.

Pictiva EX2004
Samsung v Pictiva
IPR2024-01094

Efforts to estimate this electronic energy difference (see Section 16.3.2) have been made for $Re_2Cl_8^{2-}$ and for $Mo_2Cl_4(PH_3)_4$, with results in the neighborhood of 12 kcal mol^{-1}.

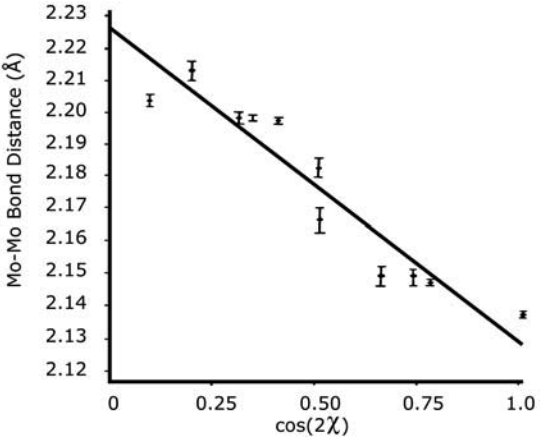


Fig. 16.3. A plot of Mo–Mo distances versus cos2χ for eleven β-Mo2X4(LL)2 compounds, where LL is a diphosphine.

More recently, DFT calculations have been reported on $Mo_2Cl_4(PH_3)_4$ type molecules, both the 1,3,6,8 and 1,2,7,8 isomers.[14-16] While such calculations are less rigorous electronically, they have the advantage of allowing for structural relaxation. They support previous calculations of an electronic barrier of 10-13 kcal mol^{-1}. An interesting new result is that for $Mo_2Cl_4(PH_3)_4$ the 1,2,7,8 (C_{2h}) structure is about 27 kcal more stable than the 1,2,5,6 (C_{2v}) rotamer.

16.1.3 Axial ligands

There are many cases where a multiply bonded M_2X_8 or paddlewheel species also has axial ligands (or, less commonly, one axial ligand). The question of how the formation of bonds to these axial ligands affects the length of the M–M bond is an important one. Some qualitative generalizations are possible, but the magnitude of the effect varies greatly from one metal and one class of compound to another. As a broad generalization, however, the presence of axial ligands causes elongation of the M–M bond. This is best demonstrated by cases where a given M_2X_8 species has been structurally characterized both with and without axial ligands.

We have seen in Chapter 3 that the lengths of Cr–Cr bonds are extremely sensitive to the presence of axial ligands, and to the number and basicity of such ligands. The dichromium compounds are exceptional, however, and most other M–M multiple bonds are less responsive to the attachment of axial ligands and bind them less strongly. Consider, for example, the marked contrast between dichromium and dimolybdenum species. For the molybdenum compounds,[17,18] even when axial ligands are attached, they are very weakly bound and the Mo–Mo distance is lengthened by only a few hundredths of an Angstrom.

With dirhenium compounds there is also only a small tendency to bind axial ligands and only small consequences. A good illustration of this is provided by the structure[19] of $Cs_2Re_2Cl_8{\cdot}H_2O$, which contains one $[Re_2Cl_8]^{2-}$ ion with no axial water molecules, and r(Re–Re) = 2.237(2) Å, and another with axially coordinated water molecules where r(Re–Re) = 2.252(2) Å. The water molecules in the latter are very loosely held, with r(Re–O) = 2.66(3) Å. Of course, the tendency of $[Re_2Cl_8]^{2-}$ to attract additional ligands is probably reduced by the fact that it is an anion. An $[Re_2(O_2CR)_4]^{2+}$ unit, being a cation, tends to form stronger bonds to axial ligands such as

Pictiva EX2004
Samsung v Pictiva
IPR2024-01094

Cl^-, with Re–Cl distances of 2.477(3) Å in $Re_2(O_2CCMe_3)_4Cl_2$,[20] which may be compared with Re–Cl distances[19] of about 2.32 Å in $[Re_2Cl_8]^{2-}$.

An interesting assessment of the effect of axial ligation in weakening M–M quadruple bonds was derived from the vibrational spectra of the cisoid $M_2(O_2CCH_3)_2Cl_4L_2$ compounds, where M = Tc, Re and L was varied through the series H_2O, DMF, dimethylacetamide, DMSO, Ph_3PO and pyridine.[21] As the donor strength of L increased (in the above order), the metal–metal stretching frequencies decreased from 311 cm^{-1} to 282 cm^{-1} for Tc and from 274 cm^{-1} to 258 cm^{-1} for Re.

It has been recognized[22] that the interrelationship of an M–M multiple bond with axial ligands (**16.1**) is quite comparable to that of multiple M–O and M–N bonds to *trans* ligands in octahedral complexes (**16.2**) and that the reasons, whatever they may be in detail, are presumably similar.

M≡M–L X=M–L

16.1 **16.2**

The $W_2(O_2CR)_4R'_2$ compounds[23,24] constitute a special case. Here we find that in going from $W_2(O_2CR)_4$ to $W_2(O_2CR)_4R'_2$ the W–W bond is not significantly lengthened, while the axial W–C bonds are fairly strong (*c.* 2.19 Å in length). Detailed calculations by the Xα-SW method, with relativistic corrections[25] have been carried out and provide a satisfactory explanation for this unusual behavior. They show that it arises because of properties peculiar to the tungsten atoms (with some possibility of molybdenum behaving similarly) and is not to be expected in general. The W–C axial bonds do not form in direct competition with the W–W σ-bond (as would normally be expected) because considerable *6s* (and even some *6p*) character is introduced. The molecular orbital mainly responsible for W–W σ bonding in $W_2(O_2CR)_4$ is scarcely affected by the axial ligation in this case.

16.1.4 Comparison of second and third transition series homologs

There are several aspects to the comparison of second and third transition series homologs:

1. the relative stabilities of stoichiometrically analogous compounds (e.g., Mo and W, Tc and Re, Ru and Os, to mention the most common pairs),
2. the structural differences between pairs of homologous species when both can be isolated and characterized,
3. electronic structure differences.

There are some very striking differences in homologous pairs of compounds, while in many cases the differences are negligible. In comparing triply-bonded dimolybdenum and ditungsten compounds, there are few major stability differences. All types of M_2X_6 compounds are known for both elements, although a few specific differences do exist. For example, the metathesis reactions of $W_2(OCMe_3)_6$ with acetylenes do not occur for any $Mo_2(OR)_6$ compound. There are more marked differences between the Mo-Mo and W–W quadruple bonds, however, consistently in the direction of the W_2^{4+} species being less stable, more easily oxidized, and more reactive generally. There are, however, many homologous pairs that exhibit considerable similarity, viz. the $M_2(mhp)_4$ and $M_2Cl_4(PR_3)_4$ compounds, and MoW^{4+} compounds are numerous and stable. Notably, no $MoWX_6$ species has been made.

Greater susceptibility of W_2^{4+} compounds to attack by acids or other oxidizing agents is probably due to their having weaker δ bonds, leaving the δ electrons more open to attack. The W–W quadruple bonds are typically 0.1 Å longer than corresponding Mo–Mo bonds, and for the inherently small δ overlap this might make a crucial difference. For the triple bonds, the W–W distances are also consistently greater, by 0.08-0.10 Å, but the σ and π electrons are so

Pictiva EX2004
Samsung v Pictiva
IPR2024-01094

much more strongly held in both the Mo_2 and W_2 species that this may have little influence on their stabilities.

A few observations concerning differences in other groups are the following:

1. The reduction of $[Tc_2Cl_8]^{2-}$ to $[Tc_2Cl_8]^{3-}$ is easy, while conversion of $[Re_2Cl_8]^{2-}$ to $[Re_2Cl_8]^{3-}$ can be accomplished only below room temperature.
2. While $Mo_2(O_2CCH_3)_4$ is easily obtained by direct reaction of $Mo(CO)_6$ with CH_3CO_2H, analogous chemistry does not occur for tungsten.
3. While over 1500 Rh_2^{4+} compounds are known and are generally easy to make, Ir_2^{4+} compounds of the M_2X_8 or paddlewheel of type are few. Whether thermodynamic instability or synthetic difficulties are responsible is an open question.
4. There are numerous singly-bonded Pt_2^{6+} compounds but only one Pd_2^{6+} complex, $Pd_2(hpp)_4Cl_2$. Similarly, species with formal Pt_2^{5+} cores have been more extensively studied than those of the Pd analogs.

One generalization that clearly emerges from all of the above facts is that for the dinuclear species as well as for the conventional mononuclear complexes, higher oxidation states are favored for the third transition series as compared to the second. Among the reasons for this is the much greater magnitude of relativistic effects on ionization energies and spin-orbit coupling in the third series atoms.[26]

With particular respect to the formation of short M–M multiple bonds, it is of major importance that the third row elements, which follow the lanthanides, have very dense and relatively incompressible cores inside their valence-shell regions. The main consequence of the difference in core densities, which is displayed in Fig. 16.4 for molybdenum and tungsten, is that M–M bond lengths are affected strongly, but metal-ligand bond lengths are not. The M–L internuclear distances are much the same for Mo–L and W–L bonds in the M_2 species, just as they are in mononuclear complexes, because the small ligand atom cores do not encounter the metal atom cores appreciably in either case. Thus, the valence-shell radii (Pauling's R_1 values) are practically the same. However, the core-core repulsions are significantly greater for W–W bonds than for Mo–Mo bonds, because for the former *both* of the bonded atoms have much denser cores than for the latter. This leads to the general result that for a given bond order (3 or 4) and the same or similar ligand sets, the W–W bond is 0.09-0.12 Å longer than the Mo–Mo bond.

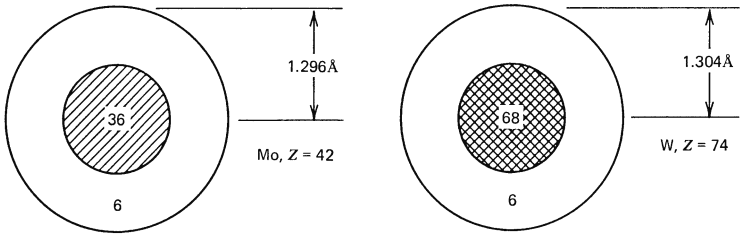


Fig. 16.4. A comparison of the single-bond radii (Pauling R_1 values) and core densities for molybdenum and tungsten atoms.

Pictiva EX2004
Samsung v Pictiva
IPR2024-01094

In quadruply bonded heteronuclear Mo–W molecules, changes in the metal-metal distances are in qualitative accord with these considerations. Some pertinent results[27,28] are:

$Mo_2(mhp)_4$		$MoW(mhp)_4$		$W_2(mhp)_4$
2.065(1) Å		2.091(1) Å		2.161(1) Å
	Δ = 0.026(2) Å		Δ = 0.070(2) Å	
$Mo_2(O_2CCH_3)_4$		$MoW(O_2CCH_3)_4$		$W_2(O_2CCF_3)_4$
2.091(1) Å		2.080(1) Å		2.209(2) Å
	Δ = -0.011(2) Å		Δ = 0.129(3) Å	

It is seen that the differences between Mo–Mo and Mo–W bond lengths are small and may be of either sign, whereas the change from Mo–W to W–W is consistently larger and positive.

16.1.5 Disorder in crystals

In addition to the kinds of crystallographic disorders that may occur in compounds of any kind, the tetragonal shapes of M_2^{n+} molecules favor a characteristic type of orientational disorder in which the M_2^{n+} unit within a cube-like set of ligands can display more than one orientation. This was first observed for the $[Mo_2Cl_8]^{4-}$ ion and is now known to occur very generally in $M_2X_8^{n-}$ ions and in some of their substitution products.

$[M_2X_8]^{n-}$ ions.

There is usually one primary orientation and one secondary one, but in a few cases there are two secondary ones. In two cases all three orientations are equally represented. Table 16.1 lists the pertinent compounds in which disorder has been reported.

Table 16.1. Orientational disorder in compounds of $M_2X_8^{n-}$ ions

Compound	Occupancy (%) of orientations			ref.
$(Bu^n_4N)_2Re_2Cl_8$	74	26		29
$(PHPr_3)_2Re_2Cl_8$	76	24		30
$(PMePh_3)_2Re_2Cl_8$	61	39		30
$(Et_4N)_2Re_2Cl_8$	67	17	16	31
$[ReCl_2(depe)_2]_2Re_2Cl_8$	74	26		32
$(Bu^n_4N)_2Re_2Br_8$	62	38		33
$(PMePh_3)_2Re_2Br_8$	82	18		30
$(PPh_4)_2Re_2Br_8$	95	5		34
$(DMAA_2H)_2Re_2Br_8$[a]	57	36	7	35
$(Bu^n_4N)_2Re_2I_8$	33	33	33	36
$(Bu^n_4N)_2Tc_2Cl_8$	69	31		37
$K_4Mo_2Cl_8{\cdot}2H_2O$	90	10		38
$(1,3\text{-}C_3H_6N_2H_6)_2Mo_2Cl_8{\cdot}4H_2O$	53	47		38
$(PMePh_3)_2Os_2Cl_8$	63	37		39
$[(C_3Me_5)_2OsH]_2Os_2Br_8$	33	33	33	40

[a] $DMAA_2H = [(CH_3CON(CH_3)_2)_2H]$

At the root of this type of disorder in $[M_2X_8]^{n-}$ compounds is the fact that these square parallelepipids are practically cubes, as shown in Fig. 16.5. They are only about 0.05 Å (*c.* 2%) higher than wide. Since vibrational amplitudes are greater than this, as sensed by its surround-

Pictiva EX2004
Samsung v Pictiva
IPR2024-01094

ings in a crystal, an $[M_2X_8]^{n-}$ ion fits nearly as well in one direction as in either of the others. Disorder in the $Re_2Br_8^{2-}$ ion,[30] as shown in Fig. 16.6, is a typical example.

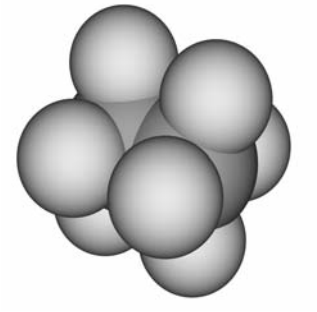


Fig. 16.5. A space-filling drawing of the $Mo_2Cl_8^{4-}$ ion showing its practically cubic proportions.

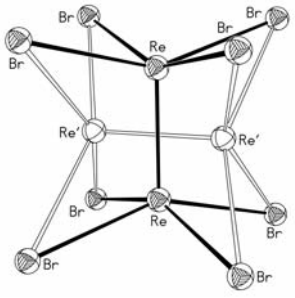


Fig. 16.6. The 82:18 disorder in the $Re_2Br_8^{2-}$ ion in $(PMePh_3)_2[Re_2Br_8]$

The positive charge on the M_2^{n+} unit within the cube of X^- ion is not uniformly distributed at all three opposite pairs of faces, and in general this leads to a preferred orientation of the $M_2X_8^{n-}$ ion. In about 70% of the reported structures there was no detectable secondary orientation.[38,41] However, no quantitative correlation between the nature or distribution of the surrounding positive charges and orientational disorder of the $M_2X_8^{n-}$ ion has been established.[38]

The question of whether the extent of disorder (when it is not governed by crystallographic symmetry) is reproducible has been examined in a study of $(Bu^n_4N)_2Re_2Cl_8$.[42] It was found that the percentages (74 and 26) are reproducible and are reliable to ± 0.5%.

Disordered crystal structures have also been found for some mixed-ligand species, $M_2X_nL_{8-n}$. The largest class of mixed-ligand compounds are the neutral $M_2X_4L_4$ molecules, where M = Mo, W or Re, X = a halide, pseudohalide or alkoxide ion, and L is usually a phosphine, although in a few cases L is an amine, alcohol, or nitrile. Only about 20% of the structures reported show disorder, and most (if not all) that do are listed in Table 16.2. All these molecules have the 1,3,6,8 distribution of ligands. Note that in three cases the disorder is complete (i.e., one third in each direction). Moreover, all of the disordered structures occur for molecules with L = PR_3. In these cases the three identical R groups permit a certain "sloppiness" in their own orientations although generally the X and PR_3 ligands each have their distinct locations. For the three $M_2Cl_4(PEt_3)_4$ molecules, the Cl and PEt_3 ligands are also randomly disordered over the eight ligand sites.

Pictiva EX2004
Samsung v Pictiva
IPR2024-01094

Table 16.2. Orientational disorder in $M_2X_nL_{8-n}$ compounds

Compound	Occupancy (%) of orientations			ref.
1,3,6,8-$M_2X_4L_4$ and $M_4X_4Y_2L_2$ compounds				
$Re_2Cl_4(PEt_3)_4$	33	33	33	43
$Mo_2F_4(PMe_3)_4$	33	33	33	44
$Mo_2Cl_4(PEt_3)_4$	33	33	33	43
$Re_2Cl_4(PPr^n_3)_4$	43	29	28	45
$Re_2Br_4(PPr^n_3)_4$	50	32	18	45
$W_2Cl_4(PBu^n_3)_4$	88	8.5	3.5	45
$Mo_2(OC_6F_4)_4(PMe_3)_4$	56	44	–	46
$Tc_2Cl_4(PEt_3)_4$	33	33	33	47
$Tc_2Cl_4(PMe_2Ph)_4$	94	6	–	47
$Mo_2Cl_4(NH_2Pr^n)_4$	79	19	12	48
$Mo_2Cl_4(NH_2Bu^t)_4$[a]	97	3	–	48
$Mo_2Cl_4(NH_2Bu^t)_4$[a]	92	8	–	48
$Mo_2Cl_4(NH_2Bu^t)_4$[a]	33	33	33	48
$W_2Cl_4(NEt_2)_2(NHEt_2)_2$	98	2	–	121
$W_2Cl_4(NHBu^n)_2(PMe_3)_2$	94	6	–	122
1,3,6-$M_2X_5L_3$ molecules				
$W_2Cl_5(PMe_3)_3$	98	2	–	49
$Re_2Cl_5(PEt_3)_3$	64	32	4	50
$Tc_2Cl_5(PMe_2Ph)_3$	96	2	2	51
$Re_2Cl_5(PMe_3)_3$	62	38	–	52
$Re_2Cl_5(PPr^n_3)_3$	90	5	5	53
$Re_2I_5(PMe_3)_3$	92	6	2	54
1,7-$M_2X_6L_2$ molecules or ions				
$Re_2Cl_6(PMe_3)_2$	33	33	33	55
$Re_2Cl_6(PEt_3)_2{\cdot}C_7H_8$	33	33	33	56
$(Bu^n_4N)[Re_2I_6(PEt_3)_2]{\cdot}{}^1/_3C_6H_6$[b]	86	10	4	54
$(Bu^n_4N)[Re_2I_6(PEt_3)_2]{\cdot}{}^1/_3C_6H_6$[b]	82	13	5	54
1,6-$M_2X_6L_2$ molecule				
$[Re_2Cl_6(PPr^n_3)_2]^-$	82	18	–	57

[a] In a monoclinic form there are two independent molecules with 3% and 8% secondary orientations. In a cubic polymorph there is a three-way disorder.
[b] Two molecules in the asymmetric unit.

Molecules of the type $M_2X_4(\mu\text{-LL})_2$ also display disorder, of a type that can be approximately described as two orientations of the M_2^{4+} unit relative to a given configuration of the ligands. This is illustrated for the case of $Mo_2Cl_4(dppe)_2$ in Fig. 16.7.[58] It is important to note that the two differently oriented molecules are *different molecules*. They are geometric isomers, and they also have opposite chiralities with regard to the helical twist about the Mo–Mo axis. This form of disorder has been found for numerous other $M_2X_4(\mu\text{-LL})_2$ compounds as well, as shown in Table 16.3.

Pictiva EX2004
Samsung v Pictiva
IPR2024-01094

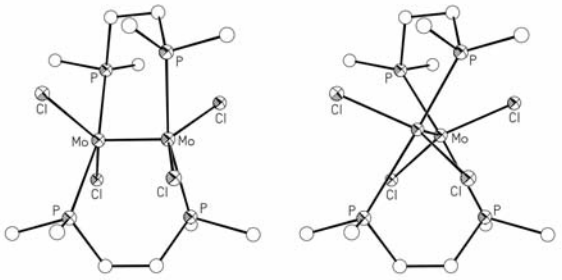


Fig. 16.7. Disorder in the structure of $Mo_2Cl_4(dppe)_2$; phenyl groups are omitted for clarity. Note that the ligand arrangement is the same in both molecules and only the orientation of the Mo_2 units is changed.

Table 16.3. Orientational disorder in $M_2X_4(\mu\text{-}LL)_2$ compounds

Compound	% of orientations		ref.
$Mo_2Cl_4(dppe)_2$	87	13	58
$Mo_2Cl_4(dmpe)_2$	90	10	59
$Mo_2Cl_4(dmpe)_2$	96	4	60
$Mo_2Cl_4(dppee)_2$	83	17	61
$Mo_2Cl_4(R\text{-}DIOP)_2$	89	11	62
$Mo_2Br_4(dppe)_2$	74	26	63
$Mo_2Br_4(arphos)_2$	77	23	64
$W_2Cl_4(dppe)_2$	93	7	65
$Re_2Cl_4(dppe)_2$	94	6	66
$Re_2Cl_4(dppee)_2$	80	20	67
$Re_2Cl_4(dpae)_2$	86	14	68

16.1.6 Rearrangements of M_2X_8 type molecules

As soon as two to six of the X ligands in an M_2X_8 type ion or molecule are replaced by other ligands, isomers of the mixed-ligand complex must be considered. This, in turn, raises the question of whether, and if so how, isomers may be interconverted. In general, as already noted in Section 16.1.2 barriers to rotation about the M–M bond axis are low (*c.* 40 kJ mol^{-1}) so that in any multistep rearrangement process where the rate-determining step has a significantly higher barrier, such a rotation (or rotations) may be a step in the overall process. The crucial question is what sort of processes with activation energies greater than about 60 kJ mol^{-1} are plausible.

An early suggestion[69] was an internal flip of the M_2 unit within the box of eight ligand atoms, as shown in Fig. 16.8. Such a net change could occur by either of two pathways, as also shown in Fig 16.8. The most intensively studied rearrangement processes have been those in which $\alpha\text{-}M_2X_4(diphos)_2$ isomers are converted to equilibrium α/β mixtures, or in some cases completely to the β isomers.[70-74] In solution these reactions are unimolecular, with rates independent of excess diphos and activation energies in the range of 80-120 kJ mol^{-1}. In each case the flip mechanism is consistent with but not necessarily required by the facts. The flip mechanism has also been invoked in other cases.[75-82]

Pictiva EX2004
Samsung v Pictiva
IPR2024-01094

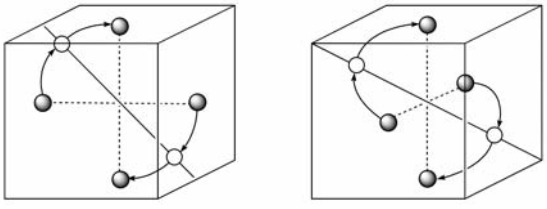


Fig. 16.8. The two distinct pathways for internal reorientation of a dimetal unit within a quasicubic cage of ligands.

The strongest positive evidence for the flip mechanism is provided by two special cases. One is the α→β transformation of $Mo_2Cl_4(dppe)_2$ in the solid state.[58,74] It proceeds quantitatively over two days at 80 °C with an activation energy of 335 ± 30 kJ mol^{-1} (80 ± 7 kcal mol^{-1}). It is hard to imagine any process (e.g., bond dissociation, etc) more complicated than the internal flip occurring cleanly in the solid state. Of course, the fact that the Ea is more than 3 times higher than those in solution might be used as an argument that it cannot be the internal flip that occurs in solution.

On the other hand, a demanding stereochemical test for the flip process in solution was carried out on a system in which a diphos ligand has differentiated ends, namely, $Ph_2PCH_2CH_2(4\text{-}Me_3CC_6H_4)_2$, and it gave results consistent with that process.[73] The logic of the experiment is shown in Fig. 16.9. Of all possible interconversions, only (1), (2), (3), and (4), shown by full arrows, are permitted by the internal flip mechanism. This means that if a mixture of α-isomers with a given *syn*/*anti* ratio is prepared and dissolved, the same *syn*/*anti* ratio must appear in the β-isomers formed, and must persist indefinitely in the α-isomers as well. This was found to be the case. While even this result does not demand the flip mechanism uniquely, there does not appear to be any other mechanism capable of accounting for all the observations. It has also been shown[83] that the flip process is probably not symmetry-forbidden (in the Woodward-Hoffmann sense).

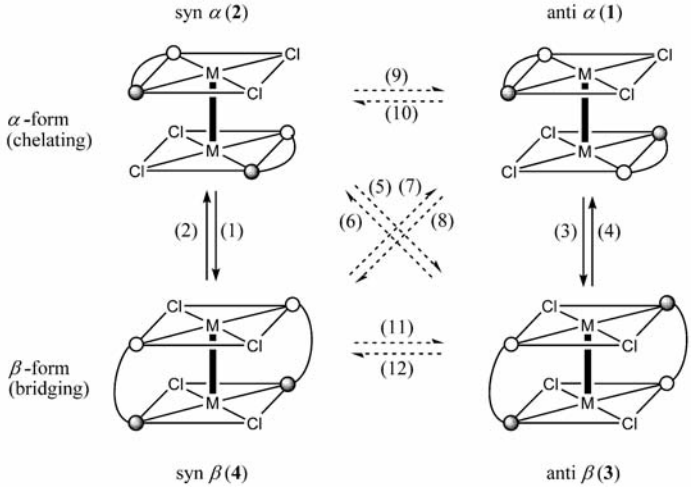


Fig. 16.9. Diagrams of the *syn* and *anti* forms of α- and β-$M_2Cl_4(LL')_2$ molecules. Interconversions allowed by the internal flip mechanism, (1), (2), (3), (4), are shown by full arrows, while all others, shown by broken arrows are excluded for this mechanism.

Pictiva EX2004
Samsung v Pictiva
IPR2024-01094

With the advent of efficient computer codes for the application of density functional theory (DFT) to relatively large molecules, a quantitative avenue for computationally testing rearrangement pathways became available. DFT studies[84,85] have found that calculated activation energies for the flip mechanism are much higher than those measured for α-$Mo_2Cl_4(diphos)_2 \rightarrow \beta$-$Mo_2Cl_4(diphos)_2$ processes in solution. An alternative process in which one end of the phosphine slips into a bridging position and then continues on to give a transition state in which one metal atom is three-coordinate ($MoCl_2P$) which the other is five-coordinate ($MoCl_2P_3$), was found preferable. By the way, the calculated activation energy (*c* 360 kJ mol^{-1}) for a flip process was *not* inconsistent with that measured 335 ± 30 kJ mol^{-1}) for the $\alpha \rightarrow \beta$ isomerization in the solid state.[58]

Another type of isomerization is shown in Fig. 16.10 for the three isomers of $W_2Cl_4(NHEt)_2(PMe_3)_2$.[78-80] In the reports of the experimental results, mechanisms featuring internal flips were proposed. It should be noted that an extra factor comes into play in this case, because in each isomer there are two N–H···Cl hydrogen bonds and for a reaction path in which these must be broken there will accordingly be a significant increment to the activation energy. The entire problem is too complex to be recapitulated in detail here, but DFT calculations[86,87] militate against the suggested internal flip pathways and favor others in which hopping of chloride ligands as well as hopping and/or dissociation of phosphine ligands are the rate-determining steps.

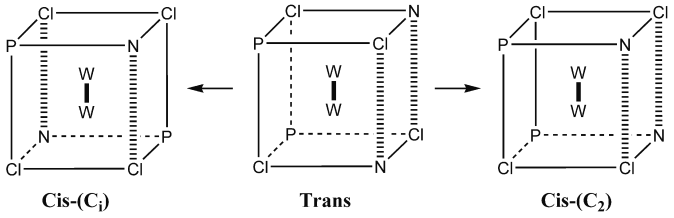


Fig. 16.10. Unimolecular *trans* to *cis* transformations. Note that vertical N–H···Cl hydrogen bonds are present in each isomer.

16.1.7 Diamagnetic anisotropy of M–M multiple bonds

It is well known that unsaturated organic molecules (olefins, alkynes, and aromatics) show relatively large diamagnetic anisotropies associated with the π-electrons. An understanding of these is useful in the assignment and interpretation of their NMR spectra. The same considerations apply, *a fortiori,* to M–M multiple bonds. It was J. San Filippo who first pointed this out for M–M multiple bonds in 1972.[88] The most important effect of diamagnetic anisotropy is seen in NMR chemical shifts. The basic theory will be found in a paper by McConnell.[89] If $\chi_\parallel$ represents the magnetic susceptibility parallel to the bond direction and $\chi_\perp$ the susceptibility perpendicular to it, $\chi_\parallel$-$\chi_\perp$ defines the magnetic anisotropy of the bond in the case where the bond has axial symmetry. When axial symmetry is lacking it is necessary to employ two $\chi_\perp$ values, $\chi_\perp$' and $\chi_\perp$", defined in directions orthogonal to each other. The difference between a measured chemical shift and that which would be expected if there were no anisotropy, is then given by the following equations[90] for the axial and non-axial cases, respectively, where subscript *i* refers to the *i*-th nucleus located at a distance *r* along a direction making an angle θ from the M–M bond direction, both measured from the center of the M–M bond:

$$\Delta\sigma_i = (1/3r^3)\,[\,(\chi_\parallel - \chi_\perp)\,(1-3\cos^2\theta)]/4\pi$$

$$\Delta\sigma_i = (1/3r^3)\,[(\chi_\parallel - \chi_\perp')\,(1-3\cos^2\theta'_\perp) + (\chi_\parallel - \chi_\perp'')(1-3\cos^2\theta''_\perp)]/4\pi$$

Pictiva EX2004
Samsung v Pictiva
IPR2024-01094

In early work the factor of 4π was sometimes omitted, leading, naturally, to $\chi_{\parallel}$-$\chi_{\perp}$ values that were too high by this factor. For the axial case the spacial zones of positive (upfield) and negative (down field) shifts are shown in Fig. 16.11. They are separated by a double cone of revolution determined by the value of θ which makes $\cos^2\theta = 1/3$, namely 55.44°. Thus, protons (or other resonant nuclei) lying in the equatorial region will be observed downfield from their "normal" position, and those in the axial region will be observed upfield in the NMR spectra.

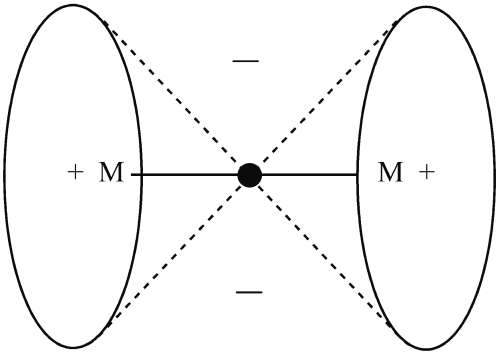


Fig. 16.11. Zones for positive and negative chemical shifts due to diamagnetic anisotropy about an axially symmetric metal–metal bond.

Examples of the former abound,[90-93] the methyl protons of μ-acetate ligands being representative. Only recently has a well-defined instance of protons shifted upfield been reported.[94] Table 16.4 provides some values for a range of multiple bonds.

Table 16.4. Diamagnetic anisotropies[a] for some M–M[b] and other[c] multiple bonds

Bond	Diamagnetic anisotropy	Bond	Diamagnetic anisotropy
C≡C	-340	Mo≡Mo[e]	-4700 – -5100
N=O	1300[d]	Ru=Ru[e]	-3800
C=O	420[d]	W≡W[e]	-5500
V≡V[e]	-7300	Re≡Re[e]	-4400
Cr≡Cr[e]	-5200		

[a] In units of 10^{-36} m^3 per molecule.
[b] See refs 91-93.
[c] R. K. Harris, *Nuclear Magnetic Resonance Spectroscopy*, Longman (UK), 1986.
[d] Perpendicular to the nodal plane of the π-bond.
[e] For formamidinate paddlewheel M_2^{4+} compounds.

16.2 Thermodynamics

16.2.1 Thermochemical data

Thermochemical data on compounds containing M–M multiple bonds have been gathered primarily because of interest in the M–M bond energies. Since these bonds have such high bond orders and are so short, the question of how strong they may be in a thermodynamic sense naturally arises. However, there are very serious difficulties involved in estimating the bond strengths from measurable thermodynamic quantities. It is even difficult to obtain accurate,

Pictiva EX2004
Samsung v Pictiva
IPR2024-01094

unambiguous data.[95] The most extensive sets of data have been obtained for the following reactions:[96-98]

$$W_2(NMe_2)_6\,(s) + 24O_2\,(g) \rightarrow 2WO_3\,(s) + 18H_2O\,(l) + 3N_2\,(g) + 12CO_2\,(g)$$

$$M_2(NMe_2)_6\,(s) + [14H^+ + Cr_2O_7^{2-} + H_2O]\,(aq) \rightarrow 2H_2MO_4\,(ppt/soln) + [2Cr^{3+} + 6NMe_2H_2^+]\,(aq)\ \ (M = Mo, W)$$

$$Mo_2(OPr^i)_6\,(s) + [6FeCl_3 + 4NaCl + 8H_2O]\,(aq) \rightarrow 2Na_2MoO_4\,(ptt/soln) + [6FeCl_2 + 6Pr^iOH + 10HCl]\,(aq)$$

$$MM'(O_2CMe)_4\,(s) + [8FeCl_3 + 4\,NaCl + 8H_2O]\,(aq) \rightarrow [Na_2MO_4 + Na_2M'O_4]\,(ppt/soln) + [8FeCl_2 + 4MeCO_2H + 12HCl]\,(aq)$$
(M, M' = Mo, Cr)

Similar reactions were used to obtain enthalpies of formation of several related mononuclear compounds containing comparable metal-ligand bonds, viz. $Ta(NMe_2)_5$, $W(NMe_2)_6$, and $Mo(NMe_2)_4$. Enthalpies of sublimation were measured in a few cases, but were mostly estimated. The available data are collected in Table 16.5.

Table 16.5. Thermochemical results for triply and quadruply bonded dimetal compounds.

Compound	ΔH_f° (kJ mol^{-1})		ΔH_{sub}^{298} (kJ mol^{-1})	ΔH_{disr} (kJ mol^{-1})	ref.
	Solid	Gas			
$Mo_2(NMe_2)_6$	+(17.2±10)	+(128.2±13)	111±8[a]	1929±28	96
$W_2(NMe_2)_6$	+(19.2±9)	+(132.5±11)	113±6	2328±29	96
$Mo_2(OPr^i)_6$	-(1662±9)	-(1549±14)	113±10	2508±62	98
$Mo_2(O_2CCH_3)_4$	-(1970.7±8.4)	-1826	145[a]	—[b]	97
$MoCr(O_2CCH_3)_4$	-(2113.9±6.4)	-1969	145[a]	—[b]	97
$Cr_2(O_2CCH_3)_4$	-(2297.5±6.6)	-2153	145[a]	—[b]	97
$Cr_2(O_2CCH_3)_4{\cdot}2H_2O$	-(2875.4±6.7)	-2725	150[a]	—[b]	97
$Mo_2(O_2CCH_3)_2(acac)_2$	-(1805.0±8.9)	-1660	145[a]	—[b]	97

[a] Estimated.
[b] Not reported.

From the enthalpies of formation plus collateral data it is possible, and in some cases useful, to derive what have been called enthalpies of disruption, ΔH_{disr}, which represent the energy needed to break a mole of the gaseous substance into individual metal atoms and ligands; in other words, ΔH_{disr} is the sum of the M–M and all metal-ligand bond energies. These values are also given in Table 16.5.

One other thermochemical measurement has been reported,[99] namely, for $Cs_2Re_2Br_8$, but there have been no new thermochemical data for many years.

16.2.2 Bond energies

The estimation of individual bond energies from thermochemical data is difficult. Assumptions of highly uncertain accuracy are required. The essential difficulties are clearly evident, in a representative way, for the $M_2(NMe_2)_6$ molecules.[96,100] The disruption energy for such a molecule corresponds to the process

$$M_2(NMe_2)_6\,(g) \rightarrow 2M\,(g) + 6NMe_2\,(g)$$

Pictiva EX2004
Samsung v Pictiva
IPR2024-01094

ΔH_{disr} and the equation relating this to bond energies is

$$\Delta H_{disr} = D(M–M) + 6\ D(M–NMe_2)$$

Clearly, to calculate D(M–M) it is necessary to know D (M–NMe_2), and to know it accurately, since the uncertainty therein is multiplied by six.

Unfortunately, there is no rigorous way to estimate D (M–NMe_2), and even the uncertainty in any given estimate is difficult to fix[100,101] Thus, for $M_2(NMe_2)_6$, D(Mo–Mo) values could be as low as 200 and as high as 790 kJ mol^{-1} although they are likely to be from 350-600 kJ mol^{-1}. Similarly, the likely range for D(W–W) is 550-775 kJ mol^{-1}. No doubt the most definite and useful result of these efforts is that, other things being equal, the W≡W bond is appreciably stronger than the Mo≡Mo bond. For $Mo_2(OCHMe_2)_6$, D(Mo≡Mo) has been estimated in the range 310-395 kJ mol^{-1}.

For quadruply-bonded species, the problem is even worse since there are eight M–L bonds. By using thermochemical data for $M(acac)_3$ compounds to estimate D(M–O) values, the following D(M–M) values (in kJ mol^{-1}) in $M_2(O_2CCH_3)_4$ compounds were proposed:[97] Cr–Cr, 205; Mo–Cr, 249; Mo–Mo, 334. From the measured enthalpy of formation[99] of $K_2Re_2Br_8$ and estimates of lattice energy and D(Re–Br), D(Re–Re) was calculated to be 408 ± 50 kJ mol^{-1}.

A few attempts have been made to estimate the dissociation energies of weaker M–M bonds. From thermodynamic data for solutions, it has been suggested that in the corresponding $M_2(O_2CCH_3)_4(H_2O)_2$ compounds of Cr and Cu, the Cr–Cr bond is about 45 kJ mol^{-1} stronger than the Cu–Cu bond.[102] The latter is so weak that this may well be tantamount to an estimate of the Cr–Cr bond energy. The dissociation energy of the Rh–Rh bond[103] in $Rh_2(OEP)_2$ has been shown to be 69 ± 3 kJ mol^{-1}.

Spectroscopic and theoretical methods have also been used to estimate the dissociation energies of some triple and quadruple bonds. There is a procedure in the spectroscopy of diatomic molecules, the Birge-Sponer extrapolation, in which a progression of overtones in the stretching frequency of the diatomic molecule is employed to evaluate ω and χ, the harmonic stretching frequency and the anharmonicity constant, respectively. With these constants, the bond energy can be estimated as $(\omega^2/4\chi)-\omega/2$. This is only an approximate relationship and tends to give results that are too high, but it is generally reliable to within 20%.

If the assumption is made that a stretching vibration localized in the M_2 unit in the center of a $[M_2X_8]^{n-}$ ion can be treated like the vibration of a diatomic molecule, the Birge-Sponer procedure can be employed for several $[Mo_2X_8]^{4-}$ and $[Re_2X_8]^{2-}$ species that have long progressions in that fundamental mode believed to be essentially a metal-metal stretching motion. Bond energies estimated in this way[104] are in the range 530-790 kJ mol^{-1} for $[Mo_2Cl_8]^{4-}$, 635 ± 80 kJ mol^{-1} for $[Re_2Cl_8]^{2-}$, and 580 ± 100 kJ mol^{-1} for $[Re_2Br_8]^{2-}$.

Attempts have been made to estimate bond energies directly from theory;[105] the reliability of the results is difficult to assess but unlikely to be high. The final conclusion[105] was that the best theoretical estimate for the dissociation energy of the Mo≡Mo triple bond in Mo_2X_6 compounds is about 284 kJ mol^{-1}. A generalized valence bond method[106] especially adapted to the particular difficulties presented by M–M multiple bonds, gave a bond energy of 367 kJ mol^{-1} for the $[Re_2Cl_8]^{2-}$ ion. This is appreciably lower than the Birge-Sponer estimates but in fair agreement with the thermochemical estimate 408 ± 50 kJ mol^{-1} for $[Re_2Br_8]^{2-}$. This same calculation indicated that the δ-bond contributes only 25 ± 12 kJ mol^{-1}, which is probably too low. SCF-Xα-SW calculations on Mo_2, $[Mo_2Cl_8]^{4-}$, and $Mo_2(O_2CH)_4$ gave 305 and 406 kJ mol^{-1} for $[Mo_2Cl_8]^{4-}$ and $Mo_2(O_2CH)_4$, respectively.[107]

Pictiva EX2004
Samsung v Pictiva
IPR2024-01094

Another theoretical attack[108,109] gave the following estimates of M–M bond energies (in kJ mol^{-1}):

$Mo_2(OH)_6$	258	$Mo_2Cl_4(PH_3)_4$	371	$Tc_2Cl_4(PH_3)_4$	337
$W_2(OH)_6$	360	$W_2Cl_4(PH_3)_4$	460	$Re_2Cl_4(PH_3)_4$	441

The preceding summary of the published efforts to estimate D(MM) values for triple and quadruple bonds suggests that the results obtained, at least individually, are very unreliable. However, when they are taken all together, the results show a moderate degree of consistency. It is very likely (in our opinion) that the highest estimates are, in fact, too high. Most likely, the D(Mo≡Mo) values are around 300 kJ mol^{-1}, and the D(W≡W) ones somewhat higher, say about 350 kJ mol^{-1}. For quadruple bonds, it is likely that D(Mo≡Mo) is about 350 kJ mol^{-1} while D(Re≡Re) is between 400 and 450 kJ mol^{-1}.

To put these values in context, they are somewhat above the range, 250-350 kJ mol^{-1} of single bonds between lighter elements. Suitable comparisons are provided by D(C–C) = 350, D(S–S) = 265, D(Cl–Cl) = 244 kJ mol^{-1}. However, they are well below the values for such multiple bonds as C=C (622), C≡C (715) and N≡N (950). Thus, in spite of the exceptional shortness of M–M multiple bonds (in relation to the atomic sizes) they are not exceptionally strong. They probably are adversely affected by the rather large cores and consequent core-core repulsions that come into play at these short distances.

16.3 Electronic Structure Calculations

16.3.1 Background

Multiple bonds between transition metal atoms pose exceptional challenges to the quantitative theory of molecular electronic structure. At the time these bonds were first recognized and qualitatively described, and for some years thereafter, these challenges were insuperable.

Early attempts were made to employ approximate semiempirical methods[110-113] to the quadruple bond, but the results were then of doubtful reliability and are today of little value or interest. We shall not discuss them here at all, nor shall we consider qualitative valence bond,[114] or other less rigorous treatments.[115-118]

The first encouraging developments began in the early 1970s with the modification of certain theoretical techniques, originally developed by Slater's school for dealing with the band theory of metals, to make them applicable to molecular problems. This work, pioneered by John C. Slater and Keith Johnson, resulted in what became known as the SCF-Xα-SW method; the abbreviation means self-consistent field Xα scattered wave.

The term Xα refers to an approximate way of evaluating the mean exchange energy. This way of setting up the problem led to equations that lent themselves to machine solution even when the atoms have many electrons and the molecule is large. More recent advances in both theory *per se* and computer codes for its implementation, make it possible to employ the Hartree-Fock equations, including the density functional modifications, to the whole field of multiple bonds between metal atoms. In general the SCF-Xα-SW method has been superceded, but many of the results previously obtained have not been and are still an excellent guide to electronic structures.

Underlying all Hartree-Fock calculations on M–M multiple bonds is the fact that a one-electron orbital picture, so familiar and so straightforwardly useful in many other types of chemistry, is often a poor approximation for these very electron-rich systems. The idea behind the usual Hartree-Fock MO treatment is that the energies of interaction between electrons are much smaller than orbital energy differences. As more electrons (upwards of 6 to as many as 14)

Pictiva EX2004
Samsung v Pictiva
IPR2024-01094

are crowded together in the space between two close (1.8-2.4 Å) metal atoms, this idea becomes less valid. The most difficult problems have been encountered with the simple diatomics (e.g., Cr_2, Mo_2) and among isolable compounds, with those of Cr_2^{4+} and others formed by metals in the first transition series. There are several papers that specifically deal with this so-called 'electron correlation' problem.[119,120]

16.3.2 $[M_2X_8]^{n-}$ and $M_2X_4(PR_3)_4$ species

The first quantitative calculations performed on metal-metal multiple bonds were carried out by the SCF-Xα-SW method on the $[Mo_2Cl_8]^{4-}$ ion[123] and the $[Re_2Cl_8]^{2-}$ ion.[124,125] These calculations are major landmarks because they provided reliable, detailed, and quantitative descriptions of the ground state electronic structures of these ions (along with descriptions of the lower unoccupied MOs) and verified the essential correctness of the qualitative description of the quadruple bond originally given.[126] Later, calculations for the $[Tc_2Cl_8]^{3-}$, $[W_2Cl_8]^{4-}$ ions,[127] and the $[Os_2Cl_8]^{2-}$ ion[128] were presented. In addition, a calculation[129] on $[Re_2Cl_8]^{2-}$ was done by the discrete variational Xα method, giving results in good general agreement with those by the SCF-Xα-SW method. A pictorial comparison of all SCF-Xα-SW results for $[M_2X_8]^{n-}$ species, taken from the paper[128] dealing with the osmium compound is shown in Fig. 16.12. It can be seen that all the electronic structures are qualitatively similar.

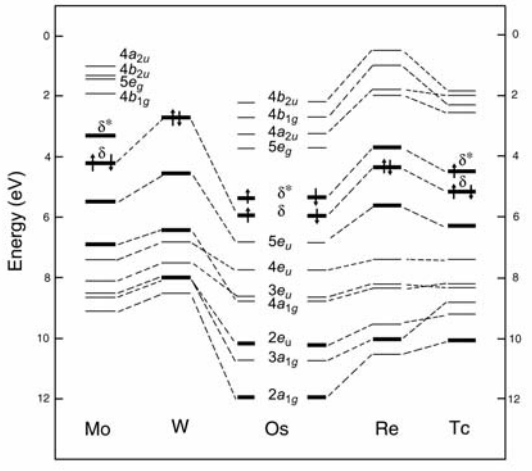


Fig. 16.12. Selected energy levels for the $[M_2X_8]^{n-}$ species that have been calculated by the SCF-Xα-SW method. Levels drawn with heavier lines have > 50% metal character.

In all these $[M_2Cl_8]^{n-}$ species the pattern of orbitals has $2b_{1u}$ (δ*) > $2b_{2g}$ (δ) > 5 e_u (π), with a rather large gap from the δ* orbital up to the next lowest antibonding orbital. Below the e_u (π) type orbital, there is a fairly dense array of closely spaced orbitals of mainly M–Cl and Cl lone pair character, but among them are three a_{1g}-orbitals which must, in varying degrees, enter into M–M and M–Cl σ-bonding. This can be better discussed by employing the energy level diagrams in Fig. 16.13 for $[Re_2Cl_8]^{2-}$.

In more recent years improvements in computer hardware and increasing sophistication in software have permitted more accurate and sophisticated calculations (at least in principle) to be made. One obvious improvement is to include relativistic effects, at least approximately, for compounds of third-transition series metals. This was done for $[Re_2Cl_8]^{2-}$ in 1983,[130] by a

Pictiva EX2004
Samsung v Pictiva
IPR2024-01094

method that was believed to be about 90% effective. As shown in Fig. 16.13 some levels are shifted significantly, although the qualitative picture is not changed. Subsequently full inclusion of relativistic effects became possible, including the calculation of spin-orbit coupling.[131] One of the first of such calculations was done on the $[W_2Cl_8]^{4-}$ ion, where a change from the nonrelativistic to the relativistic calculation had about the same results as those in Fig 16.13. Another interesting result in the relativistic $[W_2Cl_8]^{4-}$ calculation is that spin-orbit coupling is predicted to split the e_u (π) orbitals by 0.33 eV, which is very close to the splitting observed by PES for $W_2(mhp)_4$ (*c.* 0.4 eV).

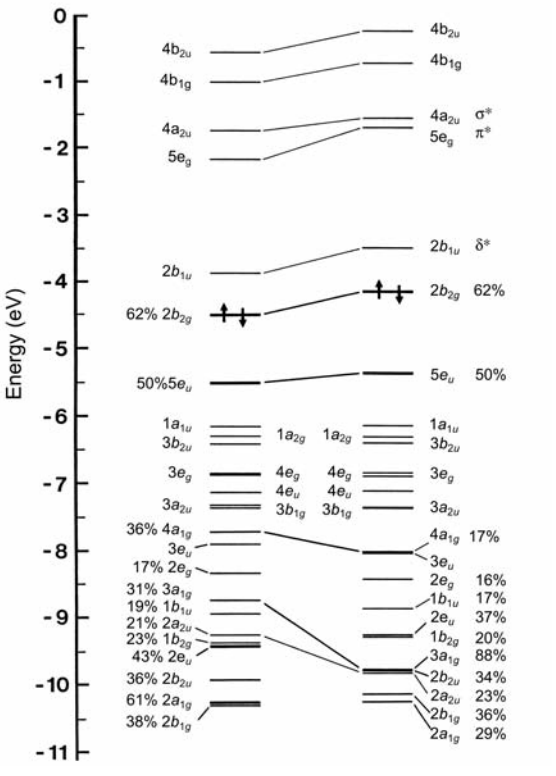


Fig. 16.13. Energy levels of $[Re_2Cl_8]^{2-}$ calculated by the SCF-Xα-SW method without (left) and with (right) relativistic corrections.

Various other calculations have more recently been done on $[Re_2Cl_8]^{2-}$, by a variety of methods.[132] While these have illuminated certain details, from the point of view of the chemist the essentials are unchanged.

The effect of replacing four Cl^- ligands in $[Re_2Cl_8]^{2-}$ by phosphine ligands was investigated by relativistic SCF-Xα-SW calculations.[133] As shown in Fig. 16.14 the pattern of the frontier orbitals is not much changed on going to the model phosphine compound $Re_2Cl_4(PH_3)_4$.

Beginning in the late 1990s efficient computer programs for a computational methodology called density functional theory (DFT)[134] have become available, and DFT is now a popular choice for ground states of molecules. The computational efficiency of DFT methods is very high and it has the ability to provide computed bond lengths, bond angles and vibrational frequencies that usually approximate very closely to experimental values, especially when large basis sets and well crafted functionals are used.

Pictiva EX2004
Samsung v Pictiva
IPR2024-01094

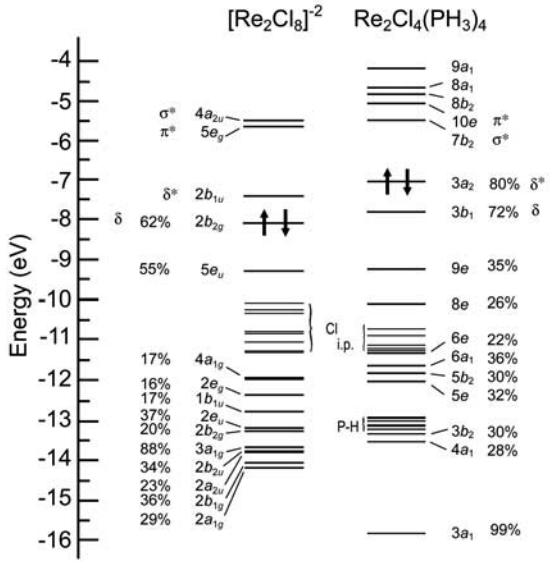


Fig. 16.14. A comparison of the energy levels in $[Re_2Cl_8]^{2-}$ and $Re_2Cl_4(PH_3)_4$, both calculated by the SCF-Xα-SW method with relativistic corrections. HOMOs are indicated by paired arrows and percentage metal character is given for some. The two diagrams have been vertically aligned to match the lowest Cl lone-pair orbital energies.

The first tests of DFT on compounds with multiple bonds between transition metal atoms were made by Cotton and Feng.[135] The molecules included in the first study were $M_2(O_2CH)_4$, (M = Nb, Mo, Tc), $M_2(HNCHNH)_4$ (M = Nb, Mo, Tc, Ru, Rh), $M_2(HNNNH)_4$ (M = Mo, Ru, Rh), and $M_2Cl_4(PH_3)_4$ (M = Nb, Mo, Tc). In all cases where real molecules of the same or similar types were known, the calculated structures were generally quite accurate provided the most appropriate functional (B3LYP) was used and all-electron calculations were done. For example, for $M_2(O_2CH)_4$ the following results were obtained:

	Mo–Mo (Å)	**Mo–O (Å)**	**<Mo–Mo–O (°)**	**<O–Mo–O (°)**
Calc.	2.11	2.11	92.1	89.9
Exp.	2.09	2.11	92.0	90.0

For $M_2(O_2CH)_4$, $M_2(O_2CH)_4(H_2O)_2$ and $Mo_2(O_2CCH_3)_4$ (M = Mo, Rh) vibrational spectra were also calculated, and again in very good agreement with experiment.

For the calculation of electronic spectra, it is advantageous to use an extension of DFT called time-dependent DFT.[136] This method provided helpful results in assigning the spectra of $[Mo_2(DAniF)_3](O_2C(CH{=}CH)_nCO_2)[Mo_2(DAniF)_3]$ (n = 0-4) molecules,[137] although quantitative agreement was not attained.

$Mo_2Cl_8^{4-}$ and $Mo_2Cl_4(PR_3)_4$.

These species have also been treated theoretically several times, beginning with SCF-Xα-SW calculations on $Mo_2Cl_8^{4-}$ as already noted.[123] From these calculations emerged the first orbital contour diagrams for multiple metal–metal bonds. They are shown in Fig. 16.15. Although there is some mixing of metal and ligand orbitals in the $Mo_2Cl_8^{4-}$ ion, the pictures clearly show that the mixing is not great and these M–M bonding MOs display their metal orbital parentage very clearly.

Pictiva EX2004
Samsung v Pictiva
IPR2024-01094

In connection with PES studies of $Mo_2Cl_4(PMe_3)_4$ and $W_2Cl_4(PMe_3)_4$, to be discussed in Section 16.5, relativistic SCF-Xα-SW calculations were done.[138] These gave results that fitted well with the experimental data including even the spin-orbit splitting of the π ionization peak. Hypothetical molecules containing PH_3 were used for these calculations.

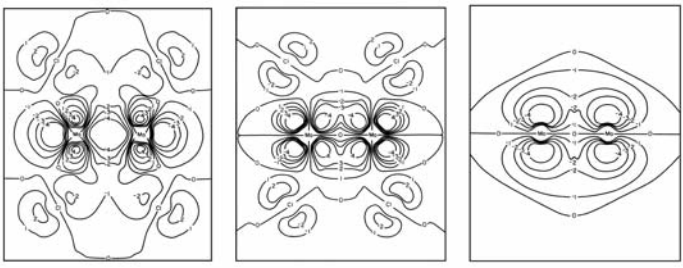


Fig. 16.15. Contour diagrams for the σ (left), π (center), and δ (right) bonding orbitals of $[Mo_2Cl_8]^{4-}$ from SCF-Xα-SW calculations.

Two particularly careful and important calculations have been done on the electronic structure of $Mo_2Cl_4L_4$ (L = PH_3[139] or ½$H_2PCH_2CH_2PH_2$[140]) type compounds as a function of rotation about the Mo-Mo bond. CASSCF calculations[139] on the model $Mo_2Cl_4(PH_3)_4$ showed that the $^1A_{1g}$ - $^3A_{2u}$ gap decreases to 1550 cm^{-1} at the exactly staggered conformation while DFT calculations[140] on the model $Mo_2Cl_4(H_2PCH_2CH_2PH_2)_2$ molecule gave values in the range 700-1600 cm^{-1}. The experimental data indicate a value of *c.* 1300 cm^{-1}. Thus, even though the δ–δ overlap goes to zero at 45°, the singlet ($^1A_{1g}$) ground state persists. This point is pursued further in Section 16.4.1.

16.3.3 The $M_2(O_2CR)_4$ (M = Cr, Mo, W) molecules

The first attempt to deal rigorously with such molecules was the SCF-Xα-SW calculation on $Mo_2(O_2CH)_4$ by Norman.[141,142] The greater complexity of the four HCO_2^- ligands as compared to eight Cl^- ligands introduces a few additional features, but the Mo–Mo bonding picture remains basically the same. Eight of the sixteen C–O π and O 2*p* lone-pair orbitals of the formate ions mix with metal atom orbitals, and thus eight MOs responsible for Mo–O bonding are engendered. These bonds, in which considerable charge transfer from the HCO_2^- ions to the Mo_2^{4+} unit occurs, greatly reduce the charge on the metal atoms, thereby expanding the metal orbitals and enhancing the Mo–Mo bonding interactions.

The highest filled orbital is again the b_{2g} δ bonding orbital, and this has 89% metal *d*-character. The next orbital down is the $6e_u$-orbital, which has 65% metal *d*π-character, but also 32% oxygen character; it contributes substantially to Mo–Mo π-bonding, but also to Mo–O π-bonding. The next e_u level down, $5e_u$, has 38% metal character and 48% oxygen character, and it too makes significant contributions to both Mo–Mo and Mo–O π bonding, but in this case, the Mo–O bonding is preponderant. The Mo–Mo π-bonding obtains substantial contributions from both the $6e_u$ and the $5e_u$ MOs. The Mo–Mo σ-bonding is also provided by two MOs. This is in contrast to the case of $[Mo_2Cl_8]^{4-}$, where the highest filled a_{1g} orbital, with 83% metal character, is mainly responsible. In this case it is actually the second-highest filled a_{1g} orbital, $4a_{1g}$, with 75% metal character, that makes the principal contribution, while the $5a_{1g}$ orbital (48% Mo) makes a smaller contribution and is more involved in Mo–O σ-bonding.

A few years after the SCF-Xα-SW calculations appeared, the first of a series of Hartree-Fock calculations were published.[143] It was found that the single configuration of lowest energy was the quadruple bond configuration ($\sigma^2\pi^4\delta^2$). After the introduction of a moderate amount of

Pictiva EX2004
Samsung v Pictiva
IPR2024-01094

configuration interaction (CI), the $\sigma^2\pi^4\delta^2$ contributed about 66% to the ground state of the molecule.

Numerous other HF-CI calculations have been reported for $Mo_2(O_2CH)_4$ and comparisons with the $Cr_2(O_2CH)_4$ molecule have also been stressed.[144-149] For example[148,147] calculations done in the same way for the two systems gave the results shown in Table 16.6. It is clear that while the $\sigma^2\pi^4\delta^2$ configuration makes only a small (16%) contribution to the ground state of $Cr_2(O_2CH)_4$ it makes up such a large fraction (67%) in the $Mo_2(O_2CH)_4$ case that by itself it can be considered a useful description of the electronic structure.

Table 16.6. Contributions of various configurations to ground state wave functions of $M_2(O_2CH)_4$ molecules

Configuration	Coefficient and percentage in wave functions	
	$Mo_2(O_2CH)_4$	$Cr_2(O_2CH)_4$
$\sigma^2\pi^4\delta^2$	0.817 (67%)	0.398 (16%)
$\sigma^{*2}\pi^4\delta^2$	-0.185 (3%)	-0.223 (5%)
$\sigma^2\pi^2\pi^{*2}\delta^2$	-0.235 (6%)	-0.318 (10%)
$\sigma^2\pi^4\delta^{*2}$	-0.382 (15%)	-0.354 (13%)
$\sigma^{*2}\pi^{*2}\pi^2\delta^2$	0.053	0.178 (3%)
$\sigma^{*2}\pi^4\delta^{*2}$	0.087 (1%)	0.199 (4%)
$\sigma^2\pi^{*4}\delta^2$	0.067	0.253 (6%)
$\sigma^2\pi^2\pi^{*2}\delta^{*2}$	0.110 (1%)	0.283 (8%)
$\sigma^{*2}\pi^{*2}\pi^2\delta^{*2}$	-0.025	-0.159 (3%)
$\sigma^2\pi^{*4}\delta^{*2}$	-0.032	-0.226 (5%)
$\sigma^{*2}\pi^{*4}\delta^2$	-0.015	-0.142 (2%)
$\sigma^{*2}\pi^{*4}\delta^{*2}$	0.007	0.127 (2%)

For the mixed species, $CrMo(O_2CH)_4$, two calculations have been reported. Both show that the bonding closely resembles that in $Mo_2(O_2CH)_4$. In one calculation[121] the method was conventional Hartree-Fock with extensive inclusion of configuration interaction, whereas the other calculation was done by the CASSCF method.[150] It appears that the polarizability of the molybdenum *4d* orbitals leads to a substantial overlap with the contracted *3d* orbitals of chromium.

The inadequacy of the HF-CI method for describing the electronic structure of $Cr_2(O_2CH)_4$ or any other Cr_2^{4+} complexes[151] has not yet been remedied, even by much more elaborate methods.[152]

16.3.4 $M_2(O_2CR)_4R'_2$ (M = Mo, W) compounds

These compounds, first reported and extensively investigated[153] by Chisholm and co-workers, are remarkable because in spite of the presence of strong axial M–C bonds (W–C ≈ 2.2 Å), the M–M bonds remain essentially the same length as they are in the corresponding $M_2(O_2CR)_4$ compounds. Normally, axial ligation causes a lengthening of the M–M multiple bond, but a theoretical analysis[154,155] has shown why the present examples are exceptions. We have already referred to this in Section 16.1.3.

The problem was treated by the SCF-Xα-SW method and the essential results are shown in Fig. 16.16. It is evident, and not surprising, that the formation by $W_2(O_2CH)_4$ of the two axial W–C bonds leaves the W–W π, π*, δ, and δ* orbitals essentially unaltered. The important

Pictiva EX2004
Samsung v Pictiva
IPR2024-01094

consequences of introducing the two CH_3 units result from the interaction of their frontier orbitals (which form a_g and b_u combinations) with the various σ orbitals of the W_2 unit.

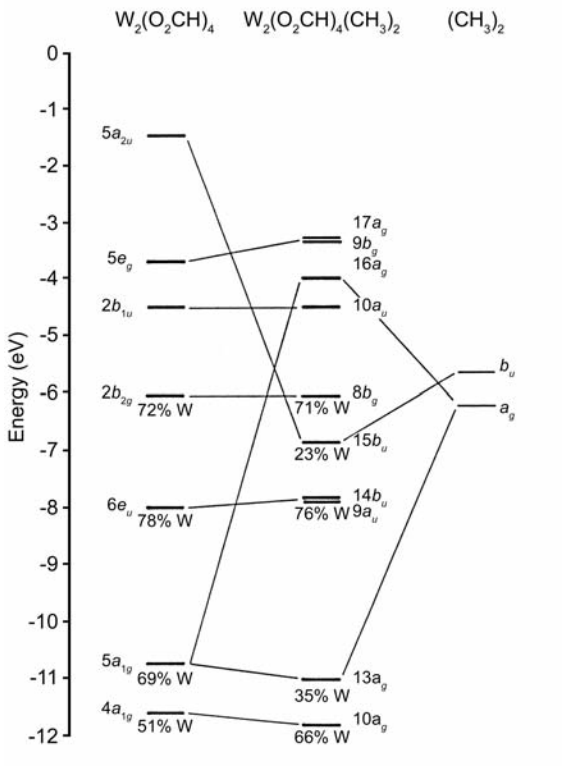


Fig. 16.16. MO energy level diagram from relativistically corrected SCF-Xα-SW calculations, showing the correlation of orbitals in $W_2(O_2CH)_4$ and $2CH_3$ with those in $W_2(O_2CH)_4(CH_3)_2$.

The symmetric combination (a_g) of the CH_3 frontier orbitals interacts strongly (for both spatial and energetic reasons) with the $5a_{1g}$ orbital of $W_2(O_2CH)_4$, resulting in the formation of the $13a_g$ (W–C bonding) and $16a_g$ (W–C antibonding) orbitals of $W_2(O_2CH)_4(CH_3)_2$. The former is occupied; the latter is empty. A critical (and perhaps surprising) result of this interaction is that the $4a_{1g}$ orbital of $W_2(O_2CH)_4$ is stabilized and increases its metal character in becoming the $10a_g$ MO of the $W_2(O_2CH)_4(CH_3)_2$ molecule. Thus W–W σ-bonding is actually enhanced, because in $W_2(O_2CH)_4$ the $4a_{1g}$ orbital makes the major contribution to W–W σ-bonding. The new $13a_g$ orbital of $W_2(O_2CH)_4(CH_3)_2$, while derived from the $5a_{1g}$ orbital, differs from it in having a much larger contribution from the tungsten 6*s*-orbitals. Thus, the new W–C bonds are to a significant extent made possible not by stealing from the W–W σ-bond but by bringing other orbitals, namely, the W 6*s*-orbitals, into play.

The b_u combination of CH_3 frontier orbitals interacts mainly with the $5a_{2u}$ orbital of $W_2(O_2CH)_4$. It thereby generates the filled $15b_u$ orbital, which is W–C bonding and consists of 6*s*, 6*p*, and 5*d* metal orbitals, but also generates an empty W–C antibonding orbital. This interaction slightly lessens the W–W σ-bond strength. However, together with the increase provided by the $10a_g$-orbital, the net result of binding the two CH_3 groups is to leave the W–W σ-bond strength essentially unaltered.

Pictiva EX2004
Samsung v Pictiva
IPR2024-01094

16.3.5 Dirhodium species

The earliest, qualitative attempt to describe the electronic structure of $Rh_2(O_2CR)_4L_2$ species, by Dubicki and Martin,[110] led to the conclusion that there is a bond order of 1, based on an electron configuration of $\sigma^2\pi^4\delta^2\delta^{*2}\pi^{*4}$. While the short Rh–Rh distance (2.39 Å) in $Rh_2(O_2CMe)_4(H_2O)_2$ seemed at first a little difficult to reconcile with such a low bond order, all subsequent theoretical work has fully supported this view, and there is abundant experimental evidence that either positively supports it or is fully consistent with it.

Taking the electron configuration of $Mo_2(O_2CR)_4$ as a point of departure, it would seem straightforward to conclude, as mentioned above, that for $Rh_2(O_2CR)_4$, where there are six more electrons, the configuration should be $\sigma^2\pi^4\delta^2\delta^{*2}\pi^{*4}$. However, this is not entirely correct and, besides, the tetracarboxylato dirhodium compounds always contain axial ligands, which are strongly enough attached to have important effects on the ordering of the one-electron orbitals.

The first attempt at a rigorous treatment[156] gave the results shown in Fig. 16.17. A notable and important feature of the orbital pattern for $Rh_2(O_2CH)_4$ is that the δ^*-orbital is higher than the π^*-orbital, contrary to the simple expectation mentioned above. This was the earliest indication that the ordering of δ^*- and π^*- orbitals, in species where they are occupied, may be variable, depending on the metal atoms, type of bridging and axial ligands, and charge. More important, however, was the indication this calculation gave as to the important influence of axial ligands. It should be noted that the introduction of two axial ligands (H_2O molecules or other) generally lowers the symmetry, thus splitting all degeneracies and requiring a relabeling of all orbitals.

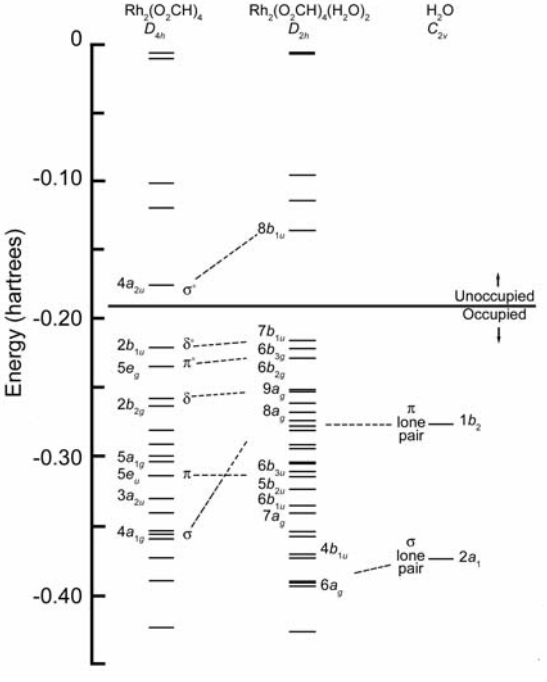


Fig. 16.17. Orbital energies calculated for $Rh_2(O_2CH_4)_4$ and $Rh_2(O_2CH_4)_4(H_2O)_2$ by the SCF-Xα-SW method.

Pictiva EX2004
Samsung v Pictiva
IPR2024-01094

Following this early work[156] and greatly stimulated by the observations made by EPR (see Section 16.7.1) on the $[Rh_2(O_2CR)_4L_2]^+$ ions, where it is possible to get direct experimental evidence as to the nature of the SOMO, which may or may not have been the HOMO in the parent Rh_2^{4+} compound, additional theoretical work was done.[157-160] An SCF-CI calculation[158] showed that for $[Rh_2(O_2CR)_4(H_2O)_2]^+$ species the odd electron ought to be in the π^*-orbital, as indicated by EPR spectra. On the other hand, the observation that for species with PPh_3 and $AsPh_3$ as axial ligands the $[Rh_2(O_2CR)_4L_2]^+$ ions have the odd electron in an orbital of σ type with strong coupling to the ^{31}P nuclei, occasioned a theoretical investigation of this type of compound.[157] Because in PPh_3 the lone-pair electrons are much closer in energy to the $4a_{2u}$ MO of $Rh_2(O_2CR)_4$, the outcome is quite different from that for H_2O as an axial ligand. The essentials of the situation are shown in Fig. 16.18. The much higher lone-pair energy for PH_3, as compared to H_2O, forces the $17a_g$ MO of $Rh_2(O_2CH)_4(PH_3)_2$ to become the highest occupied orbital of the complex. We thus obtain a picture in which the highest occupied orbital is axially symmetric and yet the Rh–Rh bond remains single in complete accord with the EPR results on the $Rh_2(O_2CR)_4(PY_3)_2$ cations.[161-163] Recent DFT calculations and structural studies have provided additional support for this picture.[164]

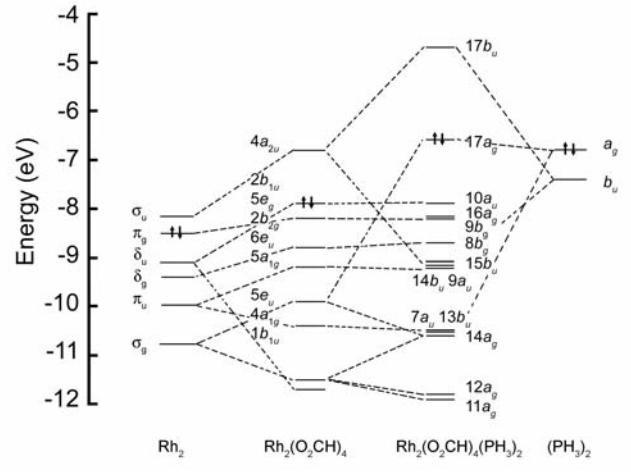


Fig. 16.18. Orbital energies calculated for $Rh_2(O_2CH)_4$ and $Rh_2(O_2CH)_4(PH_3)_2$ by the SCF-Xα-SW method.

There have been two calculations, one by the SCF-Xα-SW[165] and one by the DV-Xα[166] method on $Rh_2(HNCHNH)_4$ and both have shown that the RNCHNR-type ligand has a strong interaction between one of its π MOs and the δ^*-orbital such that the energy of the latter is driven up well above (*c.* 1.7 eV) the π^*-orbital.

16.3.6 Diruthenium compounds

Diruthenium compounds have a rather curious history. The $[Ru_2(O_2CR)_4]X$ compounds were the first ones discovered (1966) and the presence of three unpaired electrons as well as the stability of the fractional oxidation state were considered puzzling. These questions were not addressed until a dozen years later by an SCF-Xα-SW calculation,[167] with the results shown in Fig. 16.19. The presence of three unpaired electrons was accounted for by the near degeneracy of the π^* and δ^* orbitals. These calculations also provided a starting point for interpreting the electronic absorption spectra of the $[Ru_2(O_2CR)_4]X_n$ ions.

Pictiva EX2004
Samsung v Pictiva
IPR2024-01094

As indicated in Fig. 16.19, it was suggested that the accidental degeneracy of the π* and δ* orbitals should persist in the $Ru_2(O_2CR)_4$ molecules with a $\pi^{*3}\delta^*$ arrangement of the top four electrons being preferred. This, however, has turned out not to be true, according to a detailed magnetic study[168] of such compounds. The magnetic data are well accommodated by a ${}^3A_{2g}$ ground state derived from a $\delta^{*2}\pi^{*2}$ configuration. It is probable that the calculation is not seriously in error since interelectronic interactions may become the controlling factor in such a situation. With the $Ru_2(Xhp)_4$ (X = CH_3, Cl, Br) compounds the same ground state was again indicated by magnetic data.[169] As noted in Chapter 9, in certain cases, magnetic and structural data have been able to distinguish between alternatives such as π^{*4}, $\pi^{*3}\delta^*$ and $\pi^{*2}\delta^{*2}$, or π^{*3}, $\pi^{*2}\delta^*$ and $\delta^{*2}\pi^*$, or π^{*2}, $\pi^*\delta^*$ and δ^{*2}.

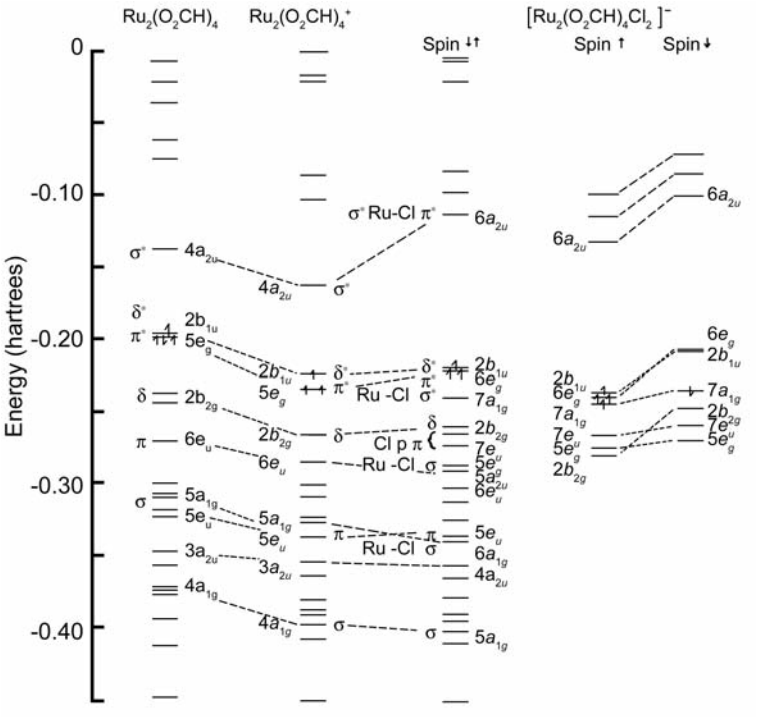


Fig. 16.19. Orbital energies calculated for $Ru_2(O_2CH)_4$, $[Ru_2(O_2CH)_4]^+$ and $[Ru_2(O_2CH)_4Cl_2]^-$.

An SCF-Xα-SW calculation[165] on $Ru_2(HNCHNH)_4$ showed that this type of ligand has the capacity (not found for RCO_2^- ligands) to drive the δ* orbital well above (*c.* 1 eV) the π* orbital, thus causing such a compound to have a diamagnetic ground state derived from the $\sigma^2\pi^4\delta^2\pi^{*4}$ configuration.

The most recent theoretical work[170] on $Ru_2(O_2CH)_4$, $Ru_2(O_2CH)_4L_2$ and $Ru_2(O_2CH)_4X$ molecules, employing a semiempirical INDO method as well as DFT reconfirms that the π* and δ* orbitals have very similar energies and that unambiguous, a priori assignment of the ground states of these molecules is generally likely to be difficult.

16.3.7 M_2X_6 molecules (M = Mo, W)

Calculations by the SCF-Xα-SW method on the Mo_2X_6 species (X = OH, NH_2, NMe_2, and CH_3) have given a very detailed and satisfactory (as judged by comparison with PES) account

Pictiva EX2004
Samsung v Pictiva
IPR2024-01094

of the bonding in these molecules.[171,172] Of the four species mentioned, only $Mo_2(NMe_2)_6$ is known, the others being only models for real molecules (i.e. $Mo_2(OH)_6$ for $Mo_2(OR)_6$ compounds, $Mo_2(NH_2)_6$ for $Mo_2(NR_2)_6$ compounds, and $Mo_2(CH_3)_6$ for Mo_2R_6 molecules in general). These models were chosen to lessen the expense of the calculations. Comparison of the results for $Mo_2(NMe_2)_6$, which can be checked against the PES, with those for its model, $Mo_2(NH_2)_6$, confirms that the chosen models are valid, provided due allowance is made for the greater inductive effects of R groups compared to H atoms.

The results for the three model compounds are shown as energy level diagrams in Fig. 16.20. In addition, the numerical wave functions for all three compounds have been resolved into contributions from atomic orbital basis sets. These results are given in Table 16.7 for $Mo_2(OH)_6$. We shall discuss here only this molecule in detail, but complete discussions of all three will be found in the literature.[172] It must be noted that in the D_{3d} symmetry of these molecules, both π and δ AOs and MOs belong to the same representations, e_g or e_u, and thus, in contrast to the X_4MMX_4 molecules with fourfold symmetry, π and δ character is not rigorously differentiated.

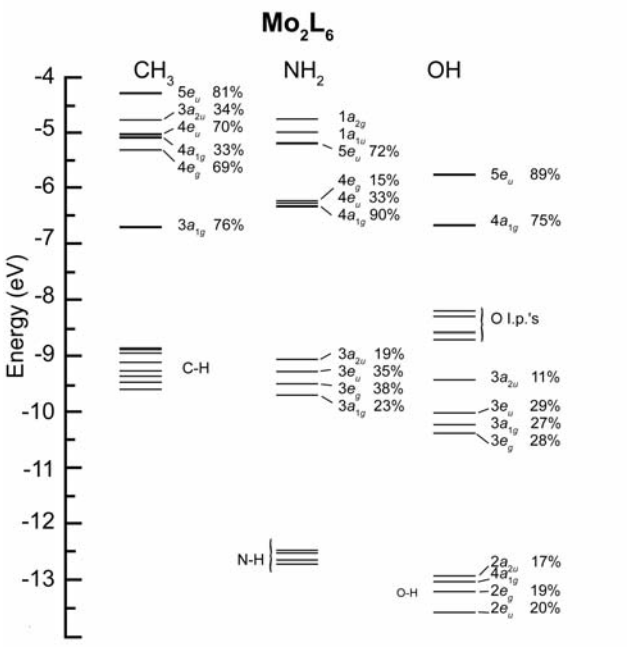


Fig. 16.20. SCF-Xα-SW energy levels for Mo_2L_6 model compounds. Only the higher filled orbitals are shown. The percentage metal character is shown for some levels.

On the basis of the information contained in Fig. 16.20 and Table 16.7, the following statements can be made concerning $Mo_2(OH)_6$. First, the valence orbitals of $Mo_2(OH)_6$ are grouped energetically into four sets:

1. the Mo–Mo bonding orbitals, $5e_u$ and $4a_{1g;}$
2. oxygen lone-pair levels;
3. Mo–O σ-bonding orbitals;
4. O–H σ-bonding and Mo–O π-bonding orbitals.

Second, the Mo–Mo bonding orbitals are largely made up of metal *d*-orbital contributions and conform closely to what is expected from the simple *d*-orbital overlap picture.

Pictiva EX2004
Samsung v Pictiva
IPR2024-01094

Table 16.7. Energies and percent characters of the highest occupied orbitals of $Mo_2(OH)_6$

Level	ε(ev)	Mulliken percent contributions						
		Mo[a,b]					O	
		σ	π	δ	5*s*	5*p*	2*s*	2*p*
$5e_u$	-5.75		80.8	3.4		4.6	2.5	6.6
$4a_{1g}$	-6.66	63.2			11.8			19.2
$1a_{2g}$	-8.19							99.1
$1a_{1u}$	-8.30							99.1
$4e_g$	-8.59		2.8					96.2
$4e_u$	-8.72		2.8					96.2
$3a_{2u}$	-9.42	11.2					0.9	86.5
$3e_u$	-10.02			28.6				71.0
$3a_{1g}$	-10.23	27.2						71.8
$3e_g$	-10.39			28.6			1.6	69.8
$2a_{2u}$	-12.95				17.4		5.4	55.8
$2a_{1g}$	-13.05				5.3		7.2	64.0
$2e_g$	-13.23		7.0	5.0		7.1	4.0	54.0
$2e_u$	-13.59		14.2	5.9			4.5	47.8

[a] $\sigma = 4d_{z^2}$; $\pi = 4d_{xz}$, $4d_{yz}$; $\delta = 4d_{xy}$, $4d_{x^2-y^2}$.

[b] Spaces indicate contributions less than 0.4%. Hydrogen 1*s* contributions are not listed but are the difference between the sum of the contributions shown and 100%.

The HOMO, i.e. the $5e_u$ orbital, has 89% metal character, most of which (81%) is metal $d\pi$ character. Fig. 16.21 shows a contour plot of one component of the MO, and it is clear that it is essentially the result of overlapping of two d_{xz} (or two d_{yz}) orbitals of the metal atoms, although slight Mo–O π*-antibonding character is also evident both from the plot and from the oxygen 2*p* percentage in Table 16.7.

The next lowest MO is the $4a_{1g}$ orbital, which is strongly Mo–Mo bonding, as can be seen from the contour diagram in Fig. 16.22. The total metal contribution here is 75%, although 12% is derived from the Mo 5*s*-orbital. It can also be seen in the contour plot that the $4a_{1g}$ orbital is Mo–O antibonding.

The clean separation of the Mo–Mo σ- and π-bonding orbitals from all the lower-lying MOs that we find for $Mo_2(OH)_6$ is lost when we go to the $Mo_2(NH_2)_6$ and $Mo_2(CH_3)_6$ cases, as can be seen in Fig. 16.20. The lower effective nuclear charge felt by the valence-shell electrons of nitrogen atoms causes the lone-pair electrons of these atoms to lie at energies equal to, and even slightly above, those of the metal *d*-orbitals. Thus, in $Mo_2(NH_2)_6$ the two highest filled orbitals, $1a_{2g}$ and $1a_{1u}$, are 100% nitrogen 2*p* in character. The $5e_u$ MO, which is responsible for Mo–Mo π-bonding, comes next, and it has now only 72% Mo character and 24% nitrogen 2*p* character. It is not until we reach the sixth highest filled orbital, $4a_{1g}$, that the principal Mo–Mo σ-bonding orbital is found.

In the case of $Mo_2(CH_3)_6$, the result of the carbon AOs being of comparable energy to that of the Mo *d*-orbitals is that Mo–C bonding orbitals are in the same energy range as the Mo-Mo π- and σ-orbitals. The mixing is now quite extensive in all respects, and no simple account of the bonding suffices. The Mo–Mo π-bonding is now effected by two MOs, $5e_u$ and $4e_u$; moreover, in both of these the $d\pi$ and the $d\delta$ type AOs make substantial contributions. It is again the sixth highest MO (now $3a_{1g}$ rather than $4a_{1g}$, since the totally symmetric Mo–C bonding orbital is $4a_{1g}$) that constitutes the principal instrument of Mo–Mo σ- bonding.

Pictiva EX2004
Samsung v Pictiva
IPR2024-01094

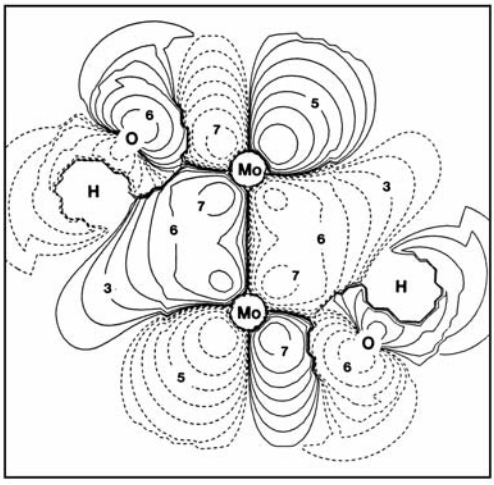


Fig. 16.21. A contour plot of the $5e_u$ orbital of $Mo_2(OH)_6$. Full and broken contours represent positive and negative regions.

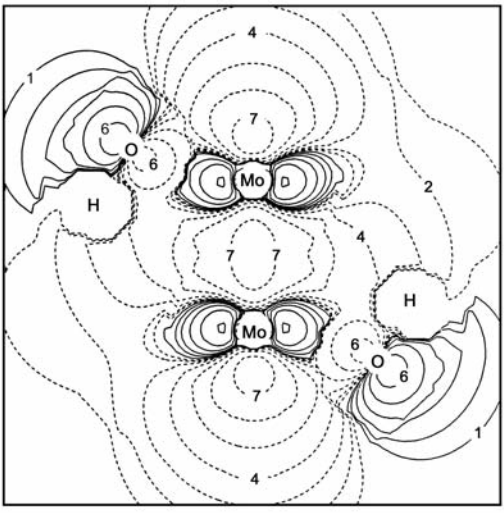


Fig. 16.22. A contour plot of the $4a_{1g}$ orbital of $Mo_2(OH)_6$.

The question of how well the model compounds, containing only hydrogen atoms appended to the ligating atoms, serve their purpose was addressed by comparing the results of the $Mo_2(NH_2)_6$ calculation with those for $Mo_2(NMe_2)_6$. As will be shown later, the photoelectron spectrum of the latter shows that the theoretical results for it are essentially correct. The computational results for the two compounds are juxtaposed in Fig. 16.23.

Since there are many more MOs in the case of $Mo_2(NMe_2)_6$ that in $Mo_2(NH_2)_6$, the numbers of orbitals with corresponding character in the two compounds do not correspond. Three of the six highest orbitals, including the two highest that are of a_{2g} and a_{1u} symmetry, are essentially pure nitrogen lone-pair orbitals in both cases. Two other orbitals in this group of six are, in each case, two e_u-orbitals that jointly provide the Mo–Mo π-bonding. However, the apportionment

Pictiva EX2004
Samsung v Pictiva
IPR2024-01094

of metal character is different. For $Mo_2(NH_2)_6$, the upper e_u-orbital ($5e_u$) plays a greater role than the lower one ($4e_u$). In $Mo_2(NMe_2)_6$, the situation is reversed, with the lower orbital $10e_u$, being the main instrument of Mo–Mo π-bonding.

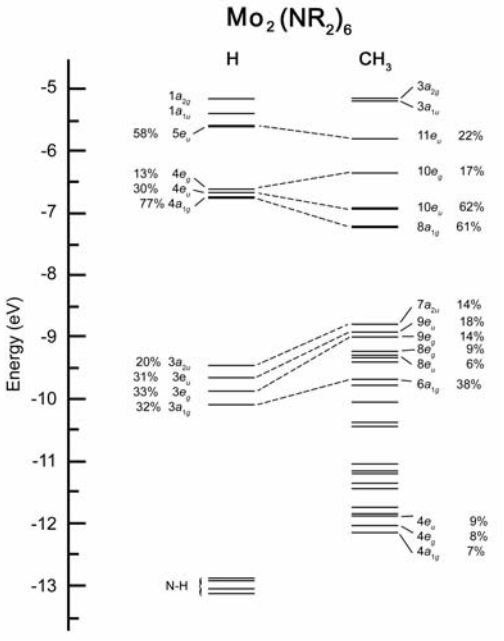


Fig. 16.23. SCF-Xα-SW energy levels for $Mo_2(NH_2)_6$ and $Mo_2(NMe_2)_6$. Percentages give atomic sphere molybdenum contributions.

The M_2X_6 type molecule has also been treated by other theoretical methods, with the question of the rotational potential energy function being particularly addressed. From the SCF-Xα-SW calculations just described, one would conclude that the M≡M bond *per se* does not imply any rotational preference and that the staggered conformation invariably found in all these molecules is dictated by the nonbonded repulsive forces between the ligands.

However, an examination of this question by an essentially qualitative frontier orbital analysis was said to show that the M≡M bond is inherently biased (by 45 kJ mol^{-1}) toward an eclipsed conformation.[173] It was also suggested that for an X_3MMX_3 molecule with small enough ligands, such a conformation would be observed,[173] but this "prediction" is incapable of being experimentally proven wrong. So long as no eclipsed X_3MMX_3 molecule is found, it can simply be said that small enough ligands have not been used. It seems unlikely that the overall analysis is correct, since it supposes that:

1. the metal atoms form octahedral hybrid orbitals of the d^2sp^3 type;
2. they use a mutually *cis* set of three to form M–X bonds; and
3. the two X_3M units then approach each other along a common threefold axis with a relative rotational relationship that maximizes the overlaps of the two sets of three hybrid orbitals.

The overlap is maximized when the X_3M–MX_3 relationship is eclipsed. The validity of this analysis requires significant involvement of the metal *p*-orbitals in the M–M bonding, but there is little likelihood that the degree of involvement is very great, certainly not to the extent of corresponding to full d^2sp^3 hybridization.

Pictiva EX2004
Samsung v Pictiva
IPR2024-01094

In quantitative calculations[174] on H_3MoMoH_3 by the Hartree-Fock method, it was found that at the SCF (i.e. single configuration) level the eclipsed conformation was favored by only 1.0 kcal mol^{-1} and that when CI was introduced this preference vanished and free rotation was predicted. This is equivalent to attributing the Mo≡Mo bonding to pure *4d*-*4d* overlaps with negligible 5*p* participation.

Other Hartree-Fock calculations[175,176] have also concluded that there is no inherent rotational barrier in the M≡M bond, but that the staggered conformations result essentially from repulsive interactions between vicinal metal-ligand bonding electrons.

16.3.8 Other calculations

An SCF-Xα-SW calculation[177] has been carried out on $Mo_2(HNCHNH)_4$ and $Mo_2(HNCHNH)_4^+$. The results were similar to those for $Mo_2(O_2CH)_4$, but the greater basicity of the formamidinate ligand led to understandable shifts in some orbitals.

SCF-Xα-SW calculations[178] on $Rh_2(O_2CH)_4(H_2O)_2$ and $[Pt_2(O_2CH)_4(H_2O)_2]^{2+}$ have shown that there is extensive and complex mixing of metal–metal and metal–ligand character in nearly all the molecular orbitals, but more so in the case of the platinum compound. In each case, however, the LUMO is mainly an M–M σ* orbital and an orbital of significant δ* character lies either immediately below it (Rh) or not far below (Pt). Thus, in each case the metal–metal bond may be roughly described as a single bond of σ character.

The $Re_2(allyl)_4$ molecule is an example of a $\sigma^2\pi^4\delta^2\delta^{*2}$ triply-bonded system, but of a special type both structurally and electronically. The structure, which has D_{2d} symmetry and the nature of the C_3H_5 ligands introduces bonding features not encountered in molecules of the usual X_4MMX_4 type. SCF-Xα-SW calculations[179] show that the functions of the d_{xy} and $d_{x^2-y^2}$ orbitals are not markedly differentiated and there are, in effect, two sets of δ-orbitals and two sets of δ* orbitals. Moreover, there are MOs arising mainly from combinations of the π-nonbonding and π* orbitals of the individual C_3H_5 groups, and one of the resulting MOs, 10*e*, turns out to be the HOMO of the $Re_2(C_3H_5)_4$ molecule.

There have been a few calculations of electron density maps (summed over all occupied orbitals) and comparisons have been made with experimental results. The latter are of uncertain accuracy, but agreement has been reported[180] for $Cr_2(O_2CCH_3)_4(H_2O)_2$, and $Mo_2(O_2CCH_3)_4$. Two dichromium compounds with very short bonds,[181] $Cr_2[(CH_2)_2PMe_2]_4$ and $Cr_2(mhp)_4$, were studied by theory and experiment, respectively, and each was found to have a buildup of electron density consistent with a $\sigma^2\pi^4\delta^2$ bonding pattern.

16.4 Electronic Spectra

The electronic absorption spectra of compounds with M–M multiple bonds have presented some unusual and fascinating problems. Dinuclear species in which the metal atoms are strongly bonded to each other have spectral properties entirely different from those of mononuclear complexes, where many techniques of interpretation (i.e. ligand field and crystal field models) that rely on the survival of the central-field, atomic character of the metal orbitals can be employed. The simplifications and approximations that arise from the fact that the mononuclear complex can be treated as a perturbed atom, with symmetry lowered from spherical to O_h or T_d, do not exist for dinuclear species with strong M–M bonds. More rigorous and complex theoretical arguments are needed. There is, however, one special advantage that the dinuclear species have, and that is the existence of a unique molecular axis of high symmetry. This can be utilized to classify orbitals, molecular states, electronic transitions, vibrations, and so on, and thus aids greatly in the interpretation of the spectroscopic data.

Pictiva EX2004
Samsung v Pictiva
IPR2024-01094

The material that follows will be mainly concerned with species having $\sigma^2\pi^4\delta^2$ configurations, with some attention also paid to the $\sigma^2\pi^4\delta^2\delta^{*m}\pi^{*n}$ species. There has been relatively little study, and thus little to be said here, of the electronic spectra of M_2X_6 type compounds.[182] For all of them the lowest metal-centered, allowed transition should be a $\pi\rightarrow\pi^*$ transition and bands in the 25 500-27 800 cm^{-1} region have been so assigned. Strong charge transfer bands in the $M_2(NMe_2)_6$ compounds ($N_{2p}\rightarrow\pi^*$) are also observed.

While many types of electronic transition contribute to the electronic absorption spectra observed from compounds containing M_2^{n+} cores,[183,184] the one that has dominated the experimental study and the discourse involves the photon-induced promotion of an electron from a δ orbital to a δ^* orbital. Before presenting a review of the data on such $\delta\rightarrow\delta^*$ transitions, it will be appropriate to look carefully at the δ-bond itself. In Sect. 16.4.1, a generally useful approximate way of looking at the bond in cases where there are two δ electrons present in the ground state will be explained in detail. It should be pointed out that an alternative so-called valence bond (VB) approach based on resonance interaction between covalent and ionic states also provides insight and can also be computationally feasible.[185,132b]

16.4.1 Details of the δ manifold of states

While the δ^2 bond is weak, because of the relatively small overlap (compared to σ and π overlaps) between the δ atomic orbitals on the two metal atoms, it displays all of the basic characteristics of any two-electron bond. What makes it unique is that it is possible to obtain experimental data on the entire manifold of four states that are associated with it as the strength of the bond is changed from maximal to minimal.[186,187]

The idea that wave functions for the interaction between a pair of bonded atoms could be constructed as linear combinations of overlapping atomic orbitals (LCAO-MOs) was fully implemented in 1949 by Coulson and Fischer [188,189] for the σ bond in the hydrogen molecule, H_2. The Coulson and Fischer treatment (a) described an entire manifold of four states, (b) showed in theory how their energies should change as the internuclear distance increased from the equilibrium value to the dissociation limit, and (c) drew attention to the critical role of configuration interaction. All of this can be done for the δ bond manifold, except that for part (b), the weakening of the bond is actually accomplished experimentally, not by stretching it (which is not experimentally realizable) but by twisting it (which is).

The theoretical argument proceeds in three steps. We begin by aligning the two ends of an M_2X_8 type ion or molecule so the δ-δ overlap is maximized, as shown in Fig 1.5 (a). Designating the two atomic orbitals as γ_1 and γ_2 we write bonding, ϕ and antibonding, χ, LCAO-MOs (neglecting overlap) as follows:

$$\phi = \tfrac{1}{\sqrt{2}}(\gamma_1 + \gamma_2)$$

$$\chi = \tfrac{1}{\sqrt{2}}(\gamma_1 - \gamma_2)$$

The energies of these MOs are

$$\begin{aligned} E_\phi &= \phi|H|\phi \\ &= \int\gamma_i H\gamma_i d\tau + \int\gamma_1 H\gamma_2 d\tau \quad \text{where } i = 1 \text{ or } 2 \\ &= E_\gamma + W \quad (W < 0) \\ E_\chi &= E_\gamma - W \end{aligned}$$

Pictiva EX2004
Samsung v Pictiva
IPR2024-01094

Since E_γ is the energy of one electron in the atomic orbital γ_1 or γ_2, we may take this as the zero of energy and write

$$E_\phi = W \quad \text{and} \quad E_\chi = -W$$

If there is only one electron to occupy these MOs, we have a very simple (and very familiar) picture, in which there are only two *states*, ϕ and χ, and only one electronic transition, namely, that from the ground state to the excited state, whose energy is exactly $2W$.

When there are two electrons, we must write determinantal wave functions for the four states that can arise. If both electrons occupy the ϕ MO, to give a full bond, we have

$$\psi_1 = \left|\overset{+}{\phi}\quad\overset{-}{\phi}\right| = \frac{1}{\sqrt{2}}\begin{vmatrix}\overset{+}{\phi}(1) & \overset{-}{\phi}(1)\\ \overset{+}{\phi}(2) & \overset{-}{\phi}(2)\end{vmatrix}$$

$$= \frac{1}{\sqrt{2}}\left[\overset{+}{\phi}(1)\,\overset{-}{\phi}(2) - \overset{-}{\phi}(1)\,\overset{+}{\phi}(2)\right]$$

After separating orbital and spin functions, using α ($S = \frac{1}{2}$) and β ($S = -\frac{1}{2}$) for the latter, we obtain

$$\psi_1 = \frac{1}{\sqrt{2}}\phi(1)\phi(2)[\alpha\beta - \beta\alpha]$$

where the antisymmetrization required by the Pauli principle is accomplished by the spin function. We could also place both electrons in the χ MO and get an analogous expression,

$$\psi_4 = \frac{1}{\sqrt{2}}\chi(1)\chi(2)[\alpha\beta - \beta\alpha]$$

Both of these represent spin singlet states.

When we develop the corresponding expressions for the states arising from placing one electron in ϕ and the other in χ, the Pauli principle no longer restricts us to antisymmetrizing the wave function by way of the spins. Antisymmetrization can also be done if both electrons have the same spin by way of an antisymmetric orbital (i.e., spatial) function, giving a triplet state. Altogether, we have the following four states in what is called the bond manifold:

$$\psi_1 = \frac{1}{\sqrt{2}}\phi(1)\phi(2)[\alpha\beta - \beta\alpha]$$

$$\psi_2 = \frac{1}{\sqrt{2}}[\phi(1)\chi(2) - \phi(2)\chi(1)]\begin{cases}[\alpha\alpha]\\ \frac{1}{\sqrt{2}}[\alpha\beta + \beta\alpha]\\ [\beta\beta]\end{cases}$$

$$\psi_3 = \frac{1}{\sqrt{2}}[\phi(1)\chi(2) + \phi(2)\chi(1)][\alpha\beta - \beta\alpha]$$

$$\psi_4 = \frac{1}{\sqrt{2}}\chi(1)\chi(2)[\alpha\beta - \beta\alpha]$$

The two-term orbital factors in ψ_2 and ψ_3 arise because of the indistinguishability of electrons; we cannot assert that electron 1 is in ϕ and electron 2 in χ rather than the reverse, so we must give both assignments equal weight.

Pictiva EX2004
Samsung v Pictiva
IPR2024-01094

For δ bonding in a unit such as $Mo_2Cl_8^{4-}$ or $Re_2Cl_8^{2-}$, where the symmetry is D_{4h}, the symmetries of these four wave functions, and the corresponding MO configurations are as follows:

ψ_1 ($^1\delta\delta$) $^1A_{1g}$

ψ_2 ($^3\delta\delta^*$) $^3A_{2u}$

ψ_3 ($^1\delta\delta^*$) $^1A_{2u}$

ψ_4 ($^1\delta^*\delta^*$) $^1A_{1g}$*

To obtain the energies of the four states in the manifold, the following equations, obtained by inserting the wave functions into the wave equation, $E = \int\psi_n H \psi_n^* d\tau$, must be solved:

$$\begin{vmatrix} 2W + J_{\phi\phi} - E & K \\ K & -2W + J_{\chi\chi} - E \end{vmatrix} = 0$$

where $E_- = E_1$ and $E_+ = E_4$

$E_2 = J_{\phi\chi} - K$

$E_3 = J_{\phi\chi} + K$

Note that ψ_1 and ψ_4 have the same symmetry, and the energies E_1 and E_4 cannot be obtained independently because ψ_1 and ψ_4 interact to give the off-diagonal matrix elements, K.

In these equations, ± *W* has the same meaning as before, namely, it is the energy by which φ or χ, as a one-electron orbital, is lowered or raised, respectively, from their average value. $J_{\phi\phi}, J_{\chi\chi}, J_{\phi\chi}$ are Coulomb integrals, inherently positive, and represent the repulsive interaction between the charge clouds of two electrons that are either in the same orbital ($J_{\phi\phi}, J_{\chi\chi}$) or in different orbitals ($J_{\phi\chi}$). Finally we have *K,* the exchange integral, which is simply half the energy required, for two atoms, X, infinitely far apart, to convert from X + X to $X^+ + X^-$.

The approximation of neglecting the small δ-δ overlap was used to write the bonding and antibonding LCAO wave functions with which we began. It may, consistently, be invoked once more[190] to simplify the energy equations by assuming that $J_{\phi\phi}$ and $J_{\chi\chi}$ (which are, of course, equal) are about equal to $J_{\phi\chi}$ Since all the *J*'s are additive to the E_n values, they may all be omitted and the energies will come out as shown in Fig. 16.24. The large magnitude of *K* relative to *W* is a consequence of the small δ-δ overlap. In $Mo_2Cl_8^{4-}$ $2K/W$ is about 4.

Let us now return to the wave functions previously written for the four states and see what they tell us about the electron distribution in each state. If we take the state wave functions and substitute in the LCAO expressions for φ and χ, we obtain the following results:

	Ionic		Covalent
ψ_1 =	$[\gamma_1(1)\gamma_1(2) + \gamma_2(1)\gamma_2(2)]$	+	$[\gamma_1(1)\gamma_2(2) + \gamma_2(1)\gamma_1(2)]$
ψ_2 =			$[\gamma_1(1)\gamma_2(2) + \gamma_2(1)\gamma_1(2)]$
ψ_3 =	$[\gamma_1(1)\gamma_1(2) + \gamma_2(1)\gamma_2(2)]$		
ψ_4 =	$[\gamma_1(1)\gamma_1(2) + \gamma_2(1)\gamma_2(2)]$	–	$[\gamma_1(1)\gamma_2(2) + \gamma_2(1)\gamma_1(2)]$

Pictiva EX2004
Samsung v Pictiva
IPR2024-01094

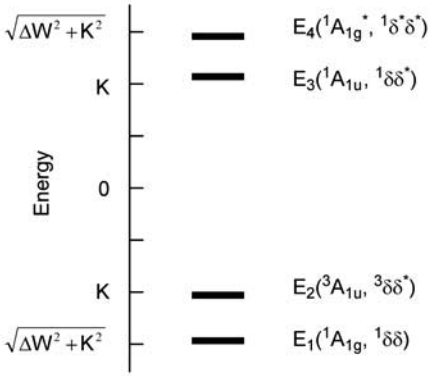


Fig. 16.24. Energy level diagram for the states of the δ manifold when two electrons are present. $\Delta W = E_\chi - E_\phi$.

ψ_1 to ψ_4 here correspond to those numbered E_1 to E_4 in Figure 16.24. We see that ψ_2 and ψ_3 which are the actual wave functions (so long as we treat the δ manifold alone), are, respectively, purely covalent and purely ionic. On the other hand, ψ_1 and ψ_4 both have half covalent and half ionic character. These are not credible wave functions as they stand. It is not, for example, believable that in the $^1A_{1g}$ state there are two electrons on one atom half the time. The ionic distribution must be of much higher energy than the covalent one and, accordingly should contribute mainly to the $^1A_{1g}$* state, while the $^1A_{1g}$ ground state should be mainly covalent. This is, in fact, exactly what occurs. The wave functions ψ_1 and ψ_4 are not really the orbital wave functions for the $^1A_{1g}$ and $^1A_{1g}$* states; through the off-diagonal element, these two orbital wave functions are mixed (configuration interaction) and the true orbital wave functions for these two states are given by

$$\psi\,(^1A_{1g}) = \psi_1 - \lambda\psi_4$$

$$\psi\,(^1A_{1g}^*) = \psi_4 + \lambda\psi_1$$

If we examine the expressions for ψ_1 and ψ_4 given above we see that as λ increases, $\psi\,(^1A_{1g})$ becomes more covalent and $\psi\,(^1A_{1g}^*)$ becomes more ionic. This mixing contributes to the stability of the $^1A_{1g}$ ground state and raises the energy of the $^1A_{1g}$* state.

With the LCAO picture of the fully developed δ bond (i.e. an eclipsed molecule with a δ^2 configuration and an empty δ* orbital) we may inquire how the δ manifold will evolve as we weaken the bond. As has been shown in Sect. 16.1.2, with an increase in the torsion angle χ from 0° to 45°, the δ-δ overlap decreases, linearly with cos 2χ. In a series of actual molecules of the type $Mo_2X_4(PR_3)_4$ and Mo_2X_4 (diphos)$_2$ (see Sect 4.3.4) the angle χ has been found to vary from 0° to ~ 40°, and for each of these molecules the energy of the $^1A_{1g} \rightarrow {}^1A_{2u}$ transition (which is commonly called "the δ→δ* transition", but more precisely, the $\delta^2 \rightarrow \delta\delta^*$ transition), has been measured.[191] These energy differences which have already been shown in Fig 16.4. may be replotted as shown in Fig. 16.25 (a). Since we are interested only in energy differences within the manifold, it is convenient to keep the energy of the $A_{2u}{}^1$ state horizontal.

Pictiva EX2004
Samsung v Pictiva
IPR2024-01094

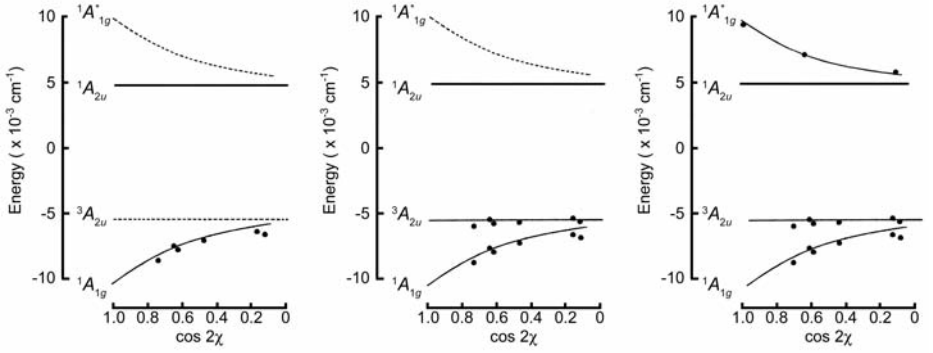


Fig. 16.25. The experimental evolution of the manifold of states for the δ bond in $Mo_2Cl_4(diphos)_2$ molecules. (a) The $^1A_{1g}$ and $^1A_{2u}$ states. (b) Adding the $^3A_{2u}$ state. (c) Adding the $^1A_{1g}$* state.

Theory leads us to expect that in addition to the $^1A_{1g}$ and $^1A_{2u}$ states which are shown in full lines in Fig 16.25 (a) there should be $^3A_{2u}$ and $^1A_{1g}$* states as shown by the broken lines. Experimental data to support the theory has been obtained. In principle, spectroscopic observations of the $^1A_{1g} \rightarrow {}^3A_{2u}$ transitions could provide verification of the position of the line for the $^3A_{2u}$ state in Fig 16.24, but such transitions are too weak to be observed. The problem of measuring the $^1A_{1g} \rightarrow {}^3A_{2u}$ gap was solved by a non-spectroscopic method. When the torsion angle is in the range of 20-40°, the gap is of the order kT at and below room temperature. Therefore, there is enough thermal population of the $^3A_{2u}$ state, following a Boltzmann distribution, to cause a measurable change in the chemical shift of the ^{31}P resonance, without making the line too broad for accurate measurement. This NMR method was used[192] for several of the $Mo_2Cl_4(P\text{-}P)_2$ compounds to afford $^1A_{1g} \rightarrow {}^3A_{2u}$ energy gaps for six compounds of the $Mo_2Cl_4(P\text{-}P)_2$ type, with χ values of 20.6, 24.7, 25.5, 30.5, 40.0 and 41.4°. These data define a line that is parallel to the one for the $^1A_{2u}$ state and separated from it by 10,400 ± 200 cm^{-1}, which is the value of 2 K. In this way we proceed from Fig 16.25 (a) to Fig. 16.25 (b).

To verify the remaining broken line (for the $^1A_{1g}$* state) by conventional spectroscopic measurement is also impossible because of the weakness of a one-photon, two-electron transition. However, the $^1A_{1g} \rightarrow {}^1A_{1g}$* transition is allowed in the two-photon absorption spectrum.[193,194] Here, two δ electrons are promoted to the δ* level by the simultaneous absorption of two photons whose energies sum to the energy required. Because we can estimate the $^1A_{1g} \rightarrow {}^1A_{1g}$* transition energy from that of $^1A_{1g} \rightarrow {}^1A_{2u,}$ it follows that the two exciting photons must be in the near-infrared frequency range. The simultaneous absorption of two photons is an unlikely event, but the probability increases with the square of the intensity of the absorbing light, so the flux of the exciting photons must be intense.

These demanding conditions of intense and tunable near-infrared photons can be satisfied with the output from optical parametric oscillators. But providing the necessary laser excitation source constitutes only one half of the experimental problem. There is also the question of how to show that the $^1A_{1g} \rightarrow {}^1A_{1g}$* transition is occurring. To measure the transmittance is impractical for a two-photon experiment and especially so when the spin-allowed transitions are weak, as is the case within the δ manifold. Instead one can monitor a fluorescence intensity that is dependent on the population of the $^1A_{1g}$* state. Although $^1A_{1g}$* is sure to be photon-silent, its neighboring $^1A_{2u}$ excited state may be emissive for selected quadruple bond metal complexes. Because the $^1A_{1g}* \rightarrow {}^1A_{2u}$ conversion is fully allowed, $^1A_{1g}$* may internally convert

Pictiva EX2004
Samsung v Pictiva
IPR2024-01094

to $^1A_{2u}$ on a much faster time scale than that associated with emissive decay from the $^1A_{2u}$ state. Therefore, as the two-photon laser excitation frequency is tuned into the $^1A_{1g}$* excited state, emission from $^1A_{2u}$ can be observed. Conversely, no $^1A_{2u}$-based luminescence will be generated when the two near-infrared photons are off resonance from the $^1A_{1g} \rightarrow {}^1A_{1g}$* transition. In this manner, the absorption profile of the $^1A_{1g}$* state was mapped out (at twice the excitation frequency) by monitoring the laser-induced fluorescence from the $^1A_{2u}$ excited state as the near-infrared spectral region is scanned.

Three points have been obtained to establish experimentally the energies of $^1A_{1g}$* states and when these are introduced we obtain Fig 16.25 (c). It is clear that the classic theoretical picture of a two-electron bond and its manifold of four states is quantitatively borne out by experiment for metal-metal δ-bonding.

It must be understood, however, that it is one thing to see that theoretical concepts can be combined with experimentally determined numbers to provide a complete quantitative picture of the δ manifold, as just shown. However, the problem of making quantitative a priori calculations of the numbers is quite another problem for which no entirely satisfactory solution has yet been found.

16.4.2 Observed δ→δ* transitions

While the electronic absorption spectra of M_2^{n+} complexes afford a plethora of observed transitions, the greatest attention has been directed to those which may be described generically as δ→δ* type transitions. There are three subclasses, depending on the number of electrons present in δ and δ* orbitals in the ground state:

1. $\delta^2 \rightarrow \delta\delta^*$
2. $\delta \rightarrow \delta^*$
3. $\delta^2\delta^* \rightarrow \delta\delta^{*2}$

The transition in subclass (1) is the $^1A_{1g} \rightarrow {}^1A_{2u}$ transition discussed in the previous section.

In all three subclasses the transition is orbitally allowed with *z* polarization (i.e. along the M–M axis). In class (1) the singlet - singlet transition is spin-allowed, while the singlet-triplet transition is spin-forbidden and not observed. As explained in Section 16. 4.1 the energies of the class (1) transitions are not simply related to orbital energy differences. On the other hand the class (2) and class (3) transitions both have energies that are equal to the difference in the energies of the δ and δ* orbitals. This is immediately obvious for class (2); for class (3) it results from the fact that interelectronic interaction energies are about the same in the ground and excited states and thus cancel out.

All three types of δ→δ* transitions are of low intensity, despite being dipole allowed. The reason for this is that the overlap of the two *d*-orbitals that form the δ bond is quite small.[195] Moreover, as Mulliken showed[196] many years ago, oscillator strength in a transition of this nature is approximately proportional to the square of the overlap integral. Thus, inherently low intensity is a straight-forward consequence of the weakness of the δ bond. However, the intensities actually observed are all somewhat greater than the inherent or intrinsic intensities because both the δ and δ* orbitals mix with ligand orbitals, but to different degrees. This has the effect of giving δ→δ* transitions some charge transfer (usually LMCT) character. It is because of the variability of such mixing from one compound to another that δ→δ* transitions, while always weak vary considerably in their intensities. For example, in the series of molecules $Mo_2X_4(PMe_3)_4$, the energy range is only from 15 700 cm^{-1} (X = I) to 17 000 cm^{-1} (X = Cl) but the intensity changes by nearly a factor of 2, as the X→M LMCT transitions approach the δ→δ* transitions in energy and therefore mix in more strongly.[197] With ligands such as RCO_2^-,

Pictiva EX2004
Samsung v Pictiva
IPR2024-01094

SO_4^{2-} or H_2O mixing of δ or δ* orbitals with ligand orbitals is very small and the intensities become extremely low, with ε_{max} values of *c.* 10^2 instead of 10^3.

A representative class (1) transition is found in $K_4[Mo_2(SO_4)_4]\cdot 2H_2O$.[198] As shown in Fig. 16.26, the $\delta^2 \rightarrow \delta\delta^*$ band at about 19 x 10^3 cm^{-1} narrows and the peak height increases on lowering the temperature from 300 K to 15 K, but the integrated intensity does not change, which is appropriate for an orbitally allowed (as opposed to a vibronically allowed) transition. Moreover, when the orientation of the Mo–Mo bonds relative to the crystal axes is taken into account (23.7° angle with the *c* axis), the relative intensities of the peak in the two spectra are in quantitative agreement with what would be expected for a *z*-polarized transition.

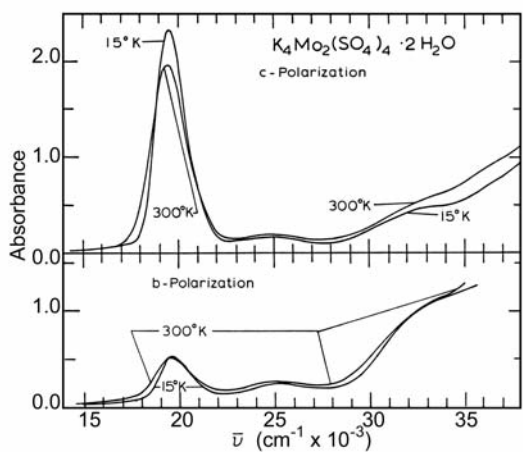


Fig. 16.26. Polarized crystal spectra of $K_4[Mo_2(SO_4)_4]\cdot 2H_2O$.

The case of $K_4[Mo_2(SO_4)_4]\cdot 2H_2O$ is exceptional in that the absorption band shows no vibrational structure, even at 15 K. In other cases such structure is seen at low temperatures and occasionally even at room temperature. An example of detectable structure even at 300 K is provided by $K_3[Tc_2Cl_8]$,[199] as shown in Fig. 16.27. It should also be noted that this is a class (3) transition and is at much lower energy than the class (1) transitions shown in Figs. 16.26 and 16.28. On the other hand, the situation in $K_4[Mo_2Cl_8]\cdot 2H_2O$, due to a $\delta^2 \rightarrow \delta\delta^*$,[200] shown in Fig. 16.28, is more typical in that the vibrational structure is observed only at the lower temperature. In each of these cases the resolved vibrational structure, consists of a single series of equally spaced components. In the $\delta^2 \rightarrow \delta\delta^*$ transition only one internal coordinate (the M–M distance) is expected to change very much on going to the excited state. The molecule therefore goes from the vibrational ground state to a series of states in which the totally symmetric vibration corresponding to this internal coordinate has various degrees of excitation, and a progression in ν' (M–M) (i.e. ν', 2ν', 3ν', etc.) in the excited electronic state is seen. Since the M–M bond is weaker in the electronically excited state, this frequency (ν') is lower (by *c.* 30 cm^{-1}) than that (ν) in the ground state. We shall discuss these questions in more detail in Sections 16.4.6 and 16.6.1.

Pictiva EX2004
Samsung v Pictiva
IPR2024-01094

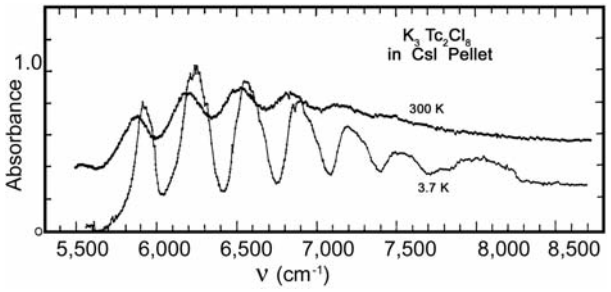


Fig. 16.27. The $\delta^2 \rightarrow \delta\delta^*$ transition in the $[Tc_2Cl_8]^{3-}$ ion at 300 K and 3.7 K.

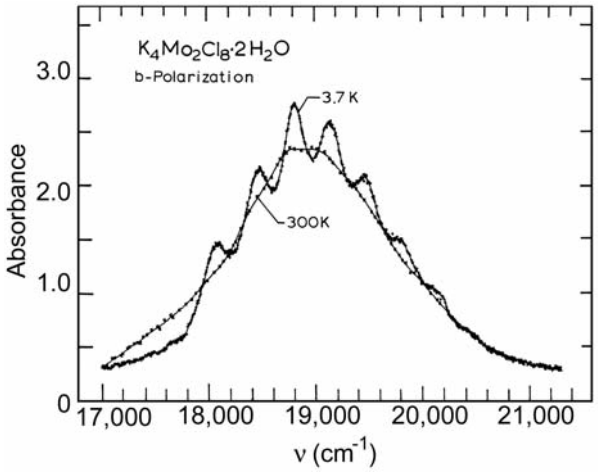


Fig. 16.28. The $\delta^2 \rightarrow \delta\delta^*$ transition in the $[Mo_2Cl_8]^{4-}$ ion at 300 K and 3.7 K.

In the case of the $[Re_2Cl_8]^{2-}$ ion [201-203] the $\delta^2 \rightarrow \delta\delta^*$ transition contains two progressions, one being in the ν' (Re–Re) vibration, as expected. The other involves the totally symmetric Re–Re–Cl bending mode δ', the progression being δ', $\delta' + \nu'$, $\delta' + 2\nu'$, etc. This type of participation by two totally symmetric vibrations is not unusual. The band intensity shows no temperature dependence and is *z*-polarized. Thus, its assignment to the $\delta^2 \rightarrow \delta\delta^*$ transition is completely secure. Similar results were reported for the $[Re_2Br_8]^{2-}$ analog.[203]

Further support for the assignment of the $\delta^2 \rightarrow \delta\delta^*$ transition to the weak ($\varepsilon \approx 10^3$) band at 14,500 cm^{-1} is provided by a Raman excitation profile study[204] which also supports this assignment for similar bands at 17,900, 13,700 and 13,000 cm^{-1} in $[Re_2F_8]^{2-}$, $[Re_2Br_8]^{2-}$ and $[Re_2I_8]^{2-}$, respectively.

In keeping with the expected relationship between class (1) and class (3) transitions, twenty $\delta^2\delta^* \rightarrow \delta\delta^{*2}$ transitions in a variety of Re_2^{5+} compounds including $Re_2Cl_8^{3-}$ [205] are found[206] in the range 6500 - 7600 cm^{-1}, as compared to the $\delta^2 \rightarrow \delta\delta^*$ transition in $Re_2Cl_8^{2-}$ at about 14,700 cm^{-1}. Similarly, comparisons of class (1) and class (2) transitions also show the expected relationship.[207] In $[Re_2Cl_8]^{1-}$ the class (2) transition occurs at 4700 cm^{-1}.

For complexes of the Mo_2^{4+} core numerous other observations of the $\delta^2 \rightarrow \delta\delta^*$ transition are scattered throughout the literature. There would be little point in attempting to collect

Pictiva EX2004
Samsung v Pictiva
IPR2024-01094

all of these, but a few are worth mentioning, such as the following ones (cm^{-1}) for homoleptic species:[208]

$[Mo_2(NH_3)_8]^{4+}$	20,000	$[Mo_2Cl_8]^{4-}$	19,000
$[Mo_2(en)_4]^{4+}$	20,900	$[Mo_2(CH_3)_8]^{4-}$	19,500
$[Mo_2(MeCN)_8]^{4+}$	18,000	$[Mo_2(NCS)_8]^{4-}$	14,500
$[Mo_2(DMF)_8]^{4+}$	19,400		
$[Mo_2(H_2O)_8]^{4+}$	18,800		

There are two classes of compounds in which $\delta^2 \rightarrow \delta\delta^*$ transitions which might naively have been expected are not seen. In $Mo_2(O_2CAr)_4$ compounds, strong LMCT transitions occur in the region where the relatively weak $\delta^2 \rightarrow \delta\delta^*$ transitions must be and completely cover them up.[209] In compounds of the type shown in Fig. 4.40 in Section 4.5.6, the δ bonds that were originally present on the two short, unbridged edges of the rectangles have opened and the δ orbitals and their electrons have become engaged in forming Mo-Mo single bonds along the two long, bridged edges. No simple $\delta^2 \rightarrow \delta\delta^*$ transitions remain.[210]

While the behavior of the $[M_2X_8]^{n-}$ ions is conventional and fairly easily interpreted, that of the carboxylato species $M_2(O_2CR)_4$ and some others is not. In fact, several of these species present examples of complicated vibronic interactions that were previously so rare that it was some time before the true situation was recognized and the spectra were correctly interpreted. We may begin the discussion as it began in the literature, namely, with the low-temperature, oriented single-crystal spectra of $[Mo_2(O_2CCH_2NH_3)_4](SO_4)_2{\cdot}4H_2O$,[211] shown in Fig. 16.29. This compound forms tetragonal crystals in which the Mo–Mo bonds are all aligned with the crystal *c* axis, thus making cleanly polarized spectra quite easy to record.

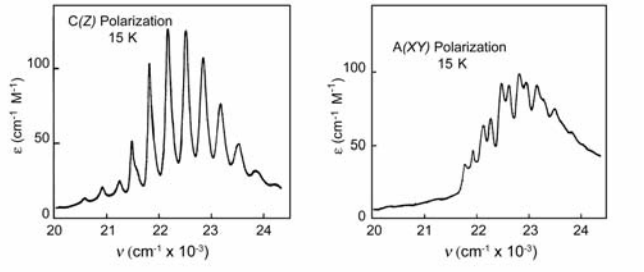


Fig. 16.29. Single crystal polarized spectra of $[Mo_2(O_2CCH_2NH_3)_4]^{4+}$ at 15 K.

In view of the fact that for $[Mo_2Cl_8]^{4-}$ the $\delta^2 \rightarrow \delta\delta^*$ transition is found at 18.0-20.0 x 10^3 cm^{-1}, it had seemed natural to suppose that the weak transitions exhibited by $Mo_2(O_2CR)_4$ compounds in the range 20.0-23.0 x 10^3 cm^{-1} should be similarly assigned. It will be recalled, however, that this transition was expected to appear exclusively in *z* polarization. As Fig. 16.29 shows, in the glycinate it is present with comparable intensities in both *z* and *xy* polarizations. This was taken as evidence that, contrary to expectation, the absorption in this region could not be assigned to the $\delta^2 \rightarrow \delta\delta^*$ transition, but must be assigned to some electronically forbidden transition, with several different vibrations being involved in conferring vibronic intensity upon it. Some specific suggestions were made as to the assignment.[211]

Pictiva EX2004
Samsung v Pictiva
IPR2024-01094

It was soon shown that $Mo_2(O_2CH)_4$ has very similar behavior,[198] with vibrational progressions of comparable intensities appearing in both *xy* and *z* polarizations, again implying that the transition should not be assigned to the $\delta \rightarrow \delta^*$ transition. A very detailed investigation[212] of the acetate, $Mo_2(O_2CCH_3)_4$, then showed that not only was there intensity in *xy* polarization, but that this was predominant. From a detailed analysis of the observed vibrational structure, the temperature dependence of hot bands, and the characteristics of the emission spectrum of $Mo_2(O_2CCF_3)_4$, it was concluded that the absorption band at *c.* 23.0 x 10^3 cm^{-1} in $Mo_2(O_2CCH_3)_4$ was best assigned to an orbitally forbidden, metal-localized $\delta \rightarrow \pi^*$ transition, which derived its intensity from vibronic coupling.

The trouble with having all of this evidence against assigning the bands at *c.* 23.0 x 10^3 cm^{-1} in $Mo_2(O_2CR)_4$ molecules to the $\delta^2 \rightarrow \delta\delta^*$ transition was that there are no bands at lower energy in the visible spectrum, and it hardly seemed likely that this transition could come at an energy below the visible (i.e. at < 12 000 cm^{-1}). On the other hand, the next higher bands are at 30.0 x 10^3 cm^{-1} and above, which seemed too high. For a short time, the problem appeared to have no reasonable solution, until, in 1979, Martin, Newman, and Fanwick provided the definitive explanation.[213] They showed that the characteristics of the band in $Mo_2(O_2CCH_3)_4$ at *c.* 23.0 x 10^3 cm^{-1} and similar bands in other $Mo_2(O_2CR)_4$ compounds are *not* inconsistent with their being assigned to the $\delta^2 \rightarrow \delta\delta^*$ transition. They pointed out that there were inconsistencies in the earlier study[212] of $Mo_2(O_2CCH_3)_4$ and that all observations could be explained in the following way.

Because of the small overlap of the d_{xy} orbitals, $\delta^2 \rightarrow \delta\delta^*$ transitions have rather low intensities, even though they meet the symmetry requirements to be orbitally allowed in z polarization. In other words, while there is a purely orbital dipolar intensity mechanism, it is an unusually week one. To understand how this affects the appearance of the absorption band (other than making it very weak), we must consider in detail the following expression for the transition moment:

$$\mathbf{M}_{fg}(Q) = \mathbf{M}_0 + \mathbf{m}_i Q_i \quad \text{where } \mathbf{m}_i = \left[\frac{\delta M}{\delta Q i}\right]_{Qi} = 0$$

This expression takes account of vibronic coupling to first order and must be squared to give the intensity values for each vibrational component. When this is done using the adiabatic Born-Oppenheimer approximation we obtain:

$$\mathbf{M}_{g0fv'_i} = [\mathbf{M}_0^2 \langle g0||fv'_i\rangle^2 + 2\mathbf{M}_0\mathbf{m}_i\langle g0||fv'_i\rangle\langle g0|Q_i|fv'_i\rangle + \mathbf{m}_i^2\langle g0|Q_i|fv'_i\rangle^2]\prod_{j\neq i}\langle g0||fv'_i\rangle^2$$

The functions $\langle g0|$ and $|fv'_i\rangle$ denote the zeroth vibrational level of the electronic ground state and the *i*th vibrational level of the upper electronic state, respectively. As a normal rule, when a transition is orbitally dipole-allowed, $\mathbf{M}_0$ is so large that $\mathbf{M}_0^2 >> \mathbf{M}_0\mathbf{m}_i >>> \mathbf{m}_i^2$ and we see only the vibrational progression in a totally symmetric frequency represented by the first term on the RHS of the equation. Moreover, this occurs only in parallel polarization. For dipole-forbidden transitions ($\mathbf{M}_0 = 0$) only the third term survives; we then see vibronic progressions in one or both polarizations, but not in the totally symmetric frequencies. The curious situation we have with the weaker $\delta \rightarrow \delta^*$ transitions is that $\mathbf{M}_0 \approx \mathbf{m}_i$ so that *all three* terms in the equation are of similar importance.

It is therefore possible to see in *z* polarization not only the "expected" progressions in one or more totally symmetric vibrations, but also one or more other progressions in which the

Pictiva EX2004
Samsung v Pictiva
IPR2024-01094

Franck-Condon factors (that is, the relative intensities of the lines in the progression) may be different from those in the totally symmetric progressions. In addition, vibronic components of similar intensities will also be seen in *xy* polarization.

Subsequent study of other amino acid complexes[214] has further confirmed the general applicability of Martin, Newman, and Fanwick's analysis to all $Mo_2(O_2CR)_4$ compounds. Moreover, this sort of situation has been shown to prevail in several other compounds, and it now appears to have been only a happy accident that in the $[M_2X_8]^{n-}$ systems first examined, no 'anomalous' features were present. This is because in the $[M_2X_8]^{n-}$ ions the $\delta\rightarrow\delta^*$ type transitions have molar intensities of 800 M^{-1} cm^{-1} or greater, and the conventional allowed-band characteristics (i.e. *z* polarization and all progressions having identical Franck-Condon factors) dominate. In the tetracarboxylates, however, the intensities are only about 100 M^{-1} cm^{-1}, and this leads to the complex behavior characteristic of these species.

While the assignment of the $\delta^2\rightarrow\delta\delta^*$ transition in $Mo_2(O_2CR)_4$ compounds to the absorption band at *c.* 23 x 10^3 cm^{-1} was placed almost entirely beyond doubt by the work of Martin, Newman, and Fanwick,[213] as just explained, there have been several more recent experimental studies that also contribute, in varying degrees, to supporting this conclusion.[200,215-218] The polarized crystal spectra of $Mo_2(O_2CCF_3)_4$ and $Mo_2(O_2CCF_3)_4py_2$ display well-developed vibrational progressions on this band that can be interpreted in a manner fully consistent with the $\delta^2\rightarrow\delta\delta^*$ assignment.[200] In two new crystal forms of $Mo_2(O_2CCMe_3)_4$, a wealth of vibronic structure is observed and can be fully explained by employing the $\delta^2\rightarrow\delta\delta^*$ assignment.[217] Similarly, in a study of $Mo_2(O_2CCPh_3)_4\cdot n CH_2Cl_2$, the vibronic structure is extremely rich and detailed, and all of it entirely consistent with the $\delta^2\rightarrow\delta\delta^*$ assignment.[218]

A study of $Re_2(O_2CCMe_3)_4Cl_2$ has provided corroboration of the analysis of the $Mo_2(O_2CR)_4$ $\delta^2\rightarrow\delta\delta^*$ bands.[219] This compound forms tetragonal crystals which, as in the case of $Mo_2(O_2CCPh_3)_4$ and several others, makes the interpretation of polarized crystal spectra as straightforward as possible. A band maximizing at 20,200 cm^{-1} is strongly but not totally *z*-polarized; there is a weak (15%) band at 20, 500 cm^{-1} in *xy* polarization. The intensity of the *z*-polarized band is also temperature independent (from 300 to 6 K). Thus, assignment to the $\delta^2\rightarrow\delta\delta^*$ transition is indicated. The weak *xy*-polarized absorption at slightly higher energy can be attributed to vibronic activation of the same transition. Because the allowed transition (*z*-polarized) is here about four times as strong as in the $Mo_2(O_2CR)_4$ molecules, the vibronic contribution is much less important.

It is interesting that the appearance of progressions with two different sets of Franck-Condon factors for a single vibration is observed in an even more startling and unequivocal fashion[220] in the compound $Mo_2[(CH_2)_2P(CH_3)_2]_4$, as shown in Fig. 16.30. It can be seen that there are five origins for vibrational progressions, all of which are built on the excited state ν'(M–M) of 345 cm^{-1} (the ground state value is 388 cm^{-1}). It is obvious, however, that the two series, labeled 0 and a, have very different Franck-Condon factors: the former has its strongest peak second (02), while the latter has it third (a3). From a detailed interpretation of these results it has been deduced that the Mo-Mo distance in the excited state $\delta^2\pi^4\delta\delta^*$ is about 0.09 Å longer than that in the $\delta^2\pi^4\delta^2$ ground state.

In $Tc_2(hp)_4Cl$ (hp = anion of 2-hydroxypyridine the $\delta\rightarrow\delta^*$ type transition has a more complex plethora of vibrational components than in any other case.[221] Fortunately, this compound forms tetragonal crystals, with the molecules all parallel to the *c*-axis, and the polarized spectra were therefore cleanly accessible. It would probably have been impossible to separate the many components had the molecules not been entirely parallel to one another. The results are shown in Fig. 16.31. In *z* polarization only, there is a peak at 12,194 cm^{-1} and this must be the 0-0 component of the orbitally allowed $\delta^2\delta^*\rightarrow\delta\delta^{*2}$ transition, but following it there are clearly

Pictiva EX2004
Samsung v Pictiva
IPR2024-01094

other progressions of equal or greater intensity. There are also numerous progressions in *xy* polarization that are as strong, or stronger. Again, we have a case where vibronic intensity is equal to or greater than the orbital dipole intensity.

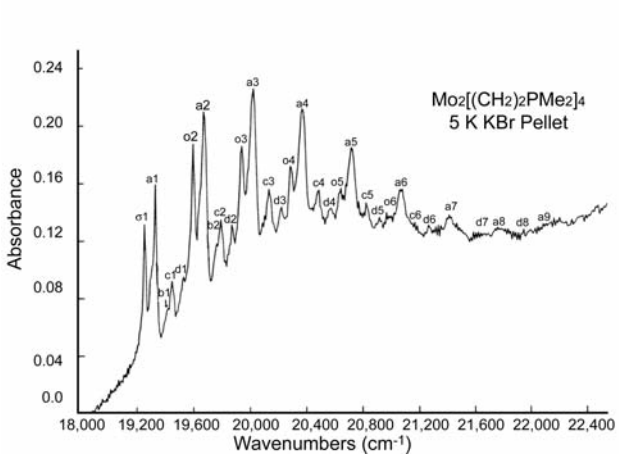


Fig. 16.30. The $\delta^2 \rightarrow \delta\delta^*$ transition in polycrystalline $Mo_2[(CH_2)_2PMe_2]_4$ at 5 K.

A complete analysis of the *z*-polarized spectrum and a partial analysis of the *xy*-polarized spectrum showed that not only the ν_1'(Tc–Tc) vibration (339 cm^{-1}), but also the Tc–O and Tc–N vibrations ν_2' and ν_3' (264 and 298 cm^{-1}) are involved. Thus, after the 0-0 band we have peaks corresponding to ν_1', ν_2', and ν_3'. Following this, however, we have not only the expected continuation of progressions in all possible overtones of ν_1' and ν_2' but also in their combinations. Thus, for example in the fifth collection of peaks we identify $5\nu_2'$, $4\nu_2' + \nu_1'$, $3\nu_2' + 2\nu_1'$, $2\nu_2'$, $3\nu_1'$, $\nu_2' + 4\nu_1'$, and $5\nu_1'$. This spectrum may well be the most complex example of vibronic coupling yet observed and analyzed.

It is interesting to note that while the $[Mo_2(SO_4)_4]^{4-}$ ion, with which we began this discussion, shows no vibrational structure for the $\delta^2 \rightarrow \delta\delta^*$ transition even at 15 K, the $[Mo_2(SO_4)_4]^{3-}$ ion (like $[Tc_2Cl_8]^{3-}$) shows such structure even at room temperature[222] and in solution.[223] At low temperature (5.3 K) the resolution is enormously enhanced and the details are found to be complex, which is, in part, a result of there being two crystallographically distinct $[Mo_2(SO_4)_4]^{3-}$ ions present in the compound $K_3[Mo_2(SO_4)_4]\cdot 3.5H_2O$. All data, including polarization, are consistent with the $\delta \rightarrow \delta^*$ assignment. The energy of the electronic transition is *c.* 6400 cm^{-1}, which is very similar to that for $[Tc_2Cl_8]^{3-}$. Thus we see again, now for the $\delta^2\pi^4\delta$ case, that when electron correlation effects are not involved, $\delta \rightarrow \delta^*$ transitions have energies of *c.* 6000 cm^{-1}, whereas, when correlation effects come into play, as they do for the quadruply bonded $\delta^2\pi^4\delta^2$ configuration, the energies are 14,000 ($[Re_2Cl_8]^{2-}$) to 23,000 cm^{-1} ($Mo_2(O_2CR)_4$).

The $M_2(mhp)_4$ (M = Cr, Mo) molecules also display $\delta^2 \rightarrow \delta\delta^*$ transitions, with origins at about 21,000 and 19,400 cm^{-1}, respectively.[224] For the Mo compound a vibrational progression of 344 cm^{-1} separation is assigned to ν'(Mo-Mo), while a progression of 305 cm^{-1} in the Cr compound was not considered to have this assignment, but the situation is ambiguous. The related $Mo_2(mhp)_2Cl_2(PEt_3)_2$ has its $\delta^2 \rightarrow \delta\delta^*$ transition[225] with an origin at *c.* 17,600 cm^{-1} (maximum at *c.* 18,500 cm^{-1}) and shows progressions in ν'(Mo-Mo) ≈ 370 cm^{-1}.

Pictiva EX2004
Samsung v Pictiva
IPR2024-01094

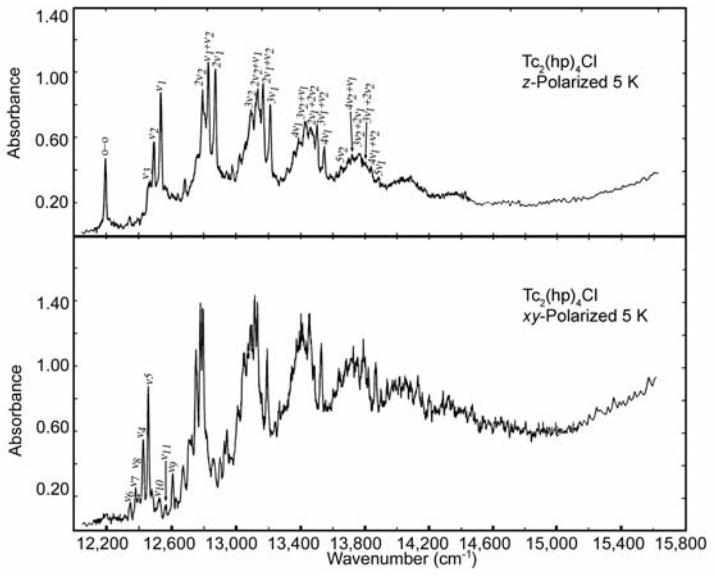


Fig. 16.31. Polarized crystal spectra of the $\delta^2\delta^* \rightarrow \delta\delta^{*2}$ transition of $Tc_2(hp)_4Cl$ at 5 K.

16.4.3 Other electronic absorption bands of Mo_2, W_2, Tc_2 and Re_2 species

The literature records a vast array of other electronic absorption spectra in addition to those due to $\delta \rightarrow \delta^*$ type transitions. Some of these results will be presented here, more or less briefly.

$[Re_2X_8]^{n-}$ ions.

In the $[Re_2Cl_8]^{2-}$ ion there are several absorption bands that occur below 50,000 cm^{-1} but above the $\delta^2 \rightarrow \delta\delta^*$ transition in these species and attempts to assign them began as early as 1975.[125] Two strong bands (ε = 5000-10000) at 30,900 and 39,200 cm^{-1} were reported to have *xy* polarization and to show MCD A-terms. Both of these characteristics imply that the excited states have E_u symmetry and the high intensities indicate that allowed transitions are responsible. It was therefore proposed that the first band is due to an $e_g \rightarrow b_{1u}$ transition and it was described as a charge-transfer transition where electron density from an orbital mainly occupied by Cl lone pair electrons is transferred to the metal-based δ^* orbital.

Support for this assignment has since come from RR excitation profile studies,[204] which also suggest that bands in $[Re_2Br_8]^{2-}$ (23,800 cm^{-1}) and $[Re_2I_8]^{2-}$ (14,800 cm^{-1}) can be given the same assignment. The other band was assigned [125] to the $\pi \rightarrow \pi^*$ transition but it has been suggested [130] that this is incorrect.

Between the $\delta \rightarrow \delta^*$ and the $\pi(Cl) \rightarrow \delta^*$ transitions in $[Re_2Cl_8]^{2-}$ there are several other transitions, all weak and presumably forbidden. This region of the spectrum is shown in Fig. 16.32. It has been suggested that bands I and II are not singlet→triplet transitions,[226] but only on the basis of negative evidence. The earliest set of assignments[104] are unreliable due to uncertainties in the (nonrelativistic) calculations, inadequacies in the data, and a simplistic approach.

Pictiva EX2004
Samsung v Pictiva
IPR2024-01094

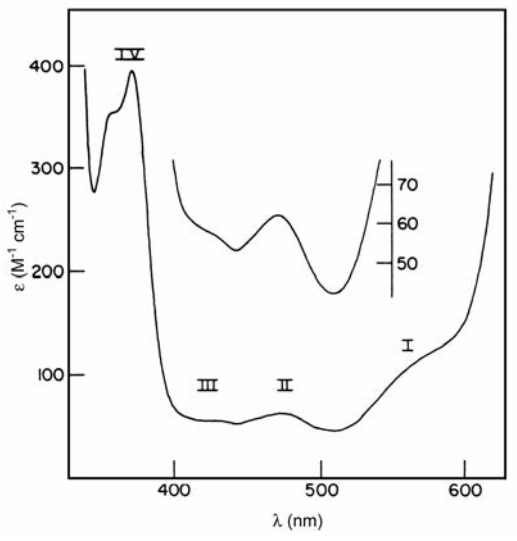


Fig. 16.32. The visible absorption spectrum of $(NBu^n_4)_2[Re_2Cl_8]$ in acetonitrile.

At the present time the best interpretation of the region shown in Fig. 16.32, is to be found in a later paper[130] in which a relativistically corrected SCF-Xα-SW calculation is employed as well as calculations of actual transition energies by the transition state method (as opposed to mere subtraction of orbital energies). To illustrate the importance of this, the energy of the $e_g \rightarrow b_{1u}$ ($\pi \rightarrow \delta^*$) LMCT band at 31.4 x 10^3 cm^{-1} in $[Tc_2Cl_8]^{3-}$ is calculated to be about 22.0 x 10^3 cm^{-1} by using only orbital energy differences, but when a relaxation correction using Slater's transition state method is introduced, a value of *c.* 29 x 10^3 cm^{-1} is predicted. In addition new measurements of crystal spectra were made whereby errors in the older data were corrected. These new measurements failed to confirm the existence of the questionable-looking band III in Fig. 16.32. Bands I and II were examined under better resolution and their polarizations correctly determined.

Band I was assigned to two overlapping transitions, $\pi \rightarrow \delta^*$ and $\delta \rightarrow \pi^*$, and band II to a spin forbidden $^3(\pi \rightarrow \pi^*)$ transition. The assignment of the pair of bands labeled IV remains uncertain. One suggestion[104] was that these might be singlet-triplet transitions related to the strong, spin-allowed LMCT band at 30,800 cm^{-1}, but other assignments are possible in the absence of further experimental data.

Some work on $[Re_2Br_8]^{2-}$ has also been published [125,227] but it is inconclusive. It was carried out before the existence of disorder in the $(NBu^n_4)_2[Re_2Br_8]$ crystals was recognized and thus the interpretation of polarization data requires reconsideration.

Other dirhenium species.

For $Re_2(O_2CCMe_3)_4Cl_2$, in addition to the firm assignment of the $^1(\delta^2 \rightarrow \delta\delta^*)$ transition at 20,200 cm^{-1}, a much weaker band at 16,500 cm^{-1} with *xy* polarization was tentatively assigned to the spin-forbidden $^1A_{1g}(\delta^2) \rightarrow {}^3A_{2u}(\delta\delta^*)$ transition.[219] Bands at 24,700 and 29,000 cm^{-1} have been assigned to the vibronically activated $\pi \rightarrow \delta^*$ and $\delta \rightarrow \pi^*$ transitions, respectively.

There have been some spectroscopic data reported for the $Re_2Cl_5(PR_3)_3$ and $Re_2Cl_4(PR_3)_4$ species.[228] The former are $\sigma^2\pi^4\delta^2\delta^*$ species and would be expected to have $\delta^2\delta^* \rightarrow \delta\delta^{*2}$ transitions at quite low energy, by analogy with $[Tc_2Cl_8]^{3-}$. In fact, all such species have absorption bands at *c.* 7000 cm^{-1} that can be so assigned. The $Re_2X_4(PR_3)_4$ compounds often appear

Pictiva EX2004
Samsung v Pictiva
IPR2024-01094

to have similar bands, but it has been shown that these come not from such molecules, but from their oxidation products, the $[Re_2X_4(PR_3)_4]^+$ ions, and they may again be assigned as $\delta^2\delta^* \rightarrow \delta\delta^{*2}$ bands. The spectrum of the compound $[Re_2Cl_4(PPr^n_3)_4]PF_6$ has been investigated in detail at 5 K and a complete assignment proposed.[133] The band at *c.* 6600 cm^{-1} is, indeed, the $\delta^2\delta^* \rightarrow \delta\delta^{*2}$ transition, and assignments in keeping with the general picture developed for $[Re_2Cl_8]^{2-}$ have been made for the entire spectrum on the basis of an SCF-Xα-SW calculation with relativistic corrections.[133]

The $[Tc_2Cl_8]^{3-}$ ion.

For the $[Tc_2Cl_8]^{3-}$ ion a complete assignment has been proposed,[199] in part on the basis of guidance provided by an SCF-Xα-SW calculation.[127] The observed spectrum is shown in Fig. 16.33 (except for the $\delta^2\delta^* \rightarrow \delta\delta^{*2}$ transition, which is off-scale at *c.* 1600 nm), and the proposed assignment is give in Table 16.8. Again there are no allowed transitions between $\delta^2\delta^* \rightarrow \delta\delta^{*2}$ and the first LMCT transitions in the near-UV, except that here, because of the presence of a δ^* electron, there is an allowed $\delta^* \rightarrow \pi^*$ transition that cannot occur for $[Re_2Cl_8]^{2-}$ and other such species. In general, the fit of calculated and observed energies is very good. It will be recalled that for $[Re_2Cl_8]^{2-}$ this was not the case. While part of the problem with $[Re_2Cl_8]^{2-}$ may have been the result of relativistic effects, it is likely, in view of the work on $[Tc_2Cl_8]^{3-}$, that the underestimation of the actual energy is largely attributable to the failure to include relaxation energy in the calculation.

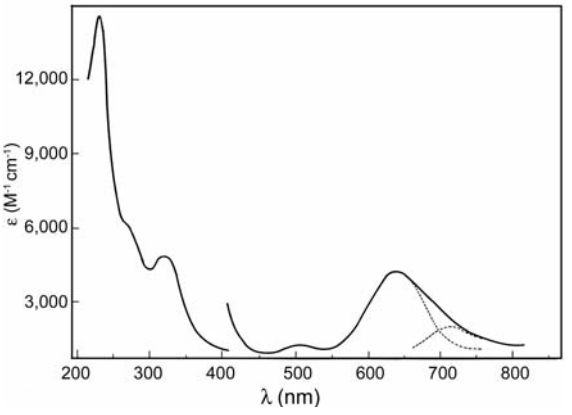


Fig. 16.33. The absorption spectrum of the $[Tc_2Cl_8]^{3-}$ ion in aqueous HCl solution.

The spectrum of the $[Mo_2Cl_8]^{4-}$ ion was first reported and assigned by Norman and Kolari,[123] and subsequent work[200,227] has only served to confirm their proposals, which are shown in Table 16.9. The polarization of the band at 31.4 x 10^3 cm^{-1} was shown to be in accord with the assignment,[200] and the absorption band at about 37.0 x 10^3 cm^{-1} has been shown to have an MCD *A* term as required for a $^1A_{1g} \rightarrow {}^1E_u$ transition. It should be noted that there is again good agreement between calculated and observed energies (except for $\delta^2 \rightarrow \delta\delta^*$), as in the case of $[Tc_2Cl_8]^{3-}$, because here too the transition state method of Slater was used. The assignments suggested for the weak absorption at around 24.0 x 10^3 cm^{-1} are like those proposed for similar bands in $[Re_2Cl_8]^{2-}$.

Pictiva EX2004
Samsung v Pictiva
IPR2024-01094

Table 16.8. Spectrum of $[Tc_2Cl_8]^{3-}$ and possible assignments

Observed band			Possible assignment		
ν^a_{max}	ε_{max}	f(x 10^3)	Calculated energy[a]	No.[b]	Type
5.9[c]	630	5.4	6.0	1	δ→δ*
13.6	35		16.3	3	π→δ*
15.7	172	2.0	15.8	2	δ*→π*
20.0	10		17.7	4	δ*→$d_{x^2-y^2}$
			20.2	7	δ*→σ*
			21.3	9	δ→π*
			23	11	δ→$d_{x^2-y^2}$
31.4	3 9000		28.3	14	LMCT
			29.1	**15**	LMCT
			31.2	**17**	π→π*
			32.5	**18**	π→$d_{x^2-y^2}$
37.2	5 600		~42[d]	**19**	LMCT
43.5	14 000		~41[d]	**21**	LMCT
			~44[d]	**24**	LMCT

[a] Energies in cm^{-1} x 10^3; ε in liters mol^{-1} cm^{-1}; f is the oscillator strength (dimensionless).
[b] Bold numbers indicate electric dipole-allowed transitions.
[c] Energy of first vibrational component.
[d] Estimated; see text.

Table 16.9. Calculated and experimental electronic spectrum of $[Mo_2Cl_8]^{4-}$ below 40 kcm^{-1}[a]

Transition	Excited state	Type[b]	Calculated	Experimental[c]
$2b_{2g}$→$2b_{1u}$	$^1A_{2u}$	δ→δ*	13.7	18.8
$5e_u$→$2b_{1u}$	^1E_g	π→δ*	23.7	~24
$2b_{2g}$→$4b_{1g}$	$^1A_{2g}$	δ→$d_{x^2-y^2}$	24.6	
$5e_u$→$4b_{1g}$	^1E_u	π→$d_{x^2-y^2}$	34.1	31.4
$4e_g$→$2b_{1u}$	^1E_u	Cl→δ*	37.5	
$3e_g$→$2b_{1u}$	^1E_u	Cl→δ*	38.6	>34
$5e_u$→$5e_g$	$^1A_{2u}$	π→π*	39.4	

[a] Band positions in kcm^{-1}, obtained using the relation 1 hartree = 219.4746 kcm^{-1}. All calculated spin- and dipole-forbibben transitions that should not be obscured by dipole-allowed bands are listed. All observed peaks in the range 4.8-40 kcm^{-1} are listed plus the strong unresolved absorption that begins above 34 kcm^{-1} and apparently maximizes above 40 kcm^{-1}.
[b] Largely metal orbitals are denoted σ, π, δ, δ*, π*, σ*, and $d_{x^2-y^2}$ according to their character. Largely ligand orbitals are represented by Cl.
[c] From the mineral oil mull spectrum of $K_4Mo_2Cl_8{\cdot}2H_2O$.

The bands in $[Tc_2Cl_8]^{3-}$ at 13,600 (ε 35) and 15,700 cm^{-1} (ε 172) were assigned as $^2B_{1u}$→^2E_u (π→δ*) and $^2B_{1u}$→^2E_g (δ*→π*), respectively. The weakness of the π→δ* transition can be attributed to its being Laporte-forbidden in D_{4h} symmetry. Although the δ*→π* transition is fully allowed, the extinction coefficient of 172 M^{-1} cm^{-1} indicates that it is quite

Pictiva EX2004
Samsung v Pictiva
IPR2024-01094

weak. The transitions at 17,000 and 18,000 cm^{-1} are broad and weak, and it was not possible to obtain definitive polarization data from the crystal spectrum.

$Mo_2(O_2CR)_4$ molecules.

The correct assignment of the $\delta \rightarrow \delta^*$ transition in $Mo_2(O_2CR)_4$ molecules, at *c.* 23.0×10^3 cm^{-1}, was achieved only after considerable effort, with much confusion along the way, as already recounted in Section 16.4.2. So much attention has been concentrated on this question that the rest of the spectrum has not yet been studied very thoroughly. The SCF-Xα-SW calculation[142] suggested several assignments of the solution spectrum, but agreement between calculated and observed peaks is not especially good. There is a band at 26.5×10^3 cm^{-1} in the spectrum of $Mo_2(O_2CCH_3)_4$, which may be the $\delta \rightarrow \pi^*$ transition,[213] that had previously been erroneously assigned to the 23.0×10^3 cm^{-1} band. The spectra of the $Mo_2(O_2CR)_4$ species need further experimental (and perhaps also theoretical) study.

The $[Mo_2(HPO_4)_4]^{2-}$ ion.

The $[Mo_2(HPO_4)_4]^{2-}$ ion is doubtless the best characterized example of a $\sigma^2\pi^4$ configuration within the M_2X_8 D_{4h} structural context. It has been carefully studied and the principal features of its electronic absorption assigned[229] as shown in Table 16.10. From these assignments one calculates a separation of ~ 5500 cm^{-1} between the one-electron δ and δ^* orbitals, in reasonable accord with expectation from theory. The separation between the π and π^* orbitals is then about 40,000 cm^{-1} (5 eV), also in agreement with the strength of the π-bonding indicated by MO calculations.

Table 16.10. Electron transitions in $[Mo_2(HPO_4)_4]^{2-}$

Orbital transition	Obs. freq. (cm^{-1})	Upper state
$\pi \rightarrow \delta$	15,000	^3E_u
$\pi \rightarrow \delta$	18,500	^1E_u
$\pi \rightarrow \delta^*$	24,000	^1E_g
$\pi \rightarrow \pi^*$	40,000	$^1A_{2u}$

$Mo_2X_4(PR_3)_4$ compounds.

We conclude this section by citing work on the $Mo_2X_4(PR_3)_4$ compounds, which have been rather extensively investigated[197,230-232] and provide some important insight into the relationship of the $\delta^2 \rightarrow \delta\delta^*$ transition (energy and intensity) to the other properties of the molecule, as well as data on other electronic transitions. For a series of $Mo_2Cl_4(PR_3)_4$ molecules, the position of the $\delta^2 \rightarrow \delta\delta^*$ transition is sensitive to the π-acidity of the phosphine.[230] It moves to lower energy as the π-acidity of the phosphine increases. However, it is not clear how to account for this. When the phosphine is kept constant (as PMe_3) and the halide is changed[197,231] from Cl to Br to I, the position of the $\delta^2 \rightarrow \delta\delta^*$ transition is little affected but the intensity increases markedly. This has been attributed to borrowing from an LMCT band at 30,860 (Cl), 29,990 (Br), and 25,320 (I) cm^{-1}. The nature of this LMCT transition was described as $\sigma(M–P) \rightarrow \delta^*$ (Mo_2) with substantial X→M character as well. In addition, there are several weak bands lying between the $\delta^2 \rightarrow \delta\delta^*$ and the LMCT bands, one of which lies in the 20,000-23,000 cm^{-1} range and has been assigned to the $\pi \rightarrow \delta^*$ transition.

Pictiva EX2004
Samsung v Pictiva
IPR2024-01094

16.4.4 Spectra of Rh_2, Pt_2, Ru_2 and Os_2 compounds

$Rh_2(O_2CR)_4L_2$ molecules.

All such molecules have two principal electronic absorption bands: band A around 17,000 cm^{-1} and band B around 23,000 cm^{-1}, whose assignments have been controversial. The polarized crystal spectra of $Rh_2(O_2CCH_3)_4(H_2O)_2$ are shown in Fig. 16.34 for band A.

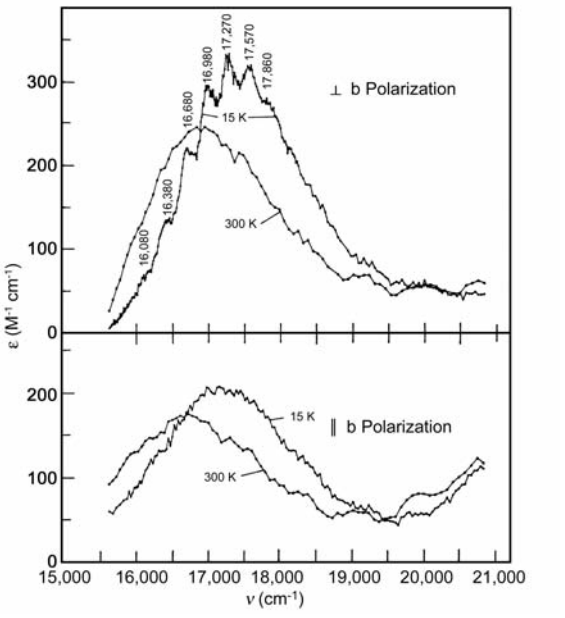


Fig. 16.34. Polarized crystal spectra of $Rh_2(OCCH_3)_4(H_2O)_2$ in the region of band A.

As early as 1970 it was proposed that band A, on the basis of its *xy* polarization, temperature-independent intensity, and sensitivity to changes in the axial ligand, should be assigned to a $\pi^*(Rh_2) \rightarrow \sigma^*(Rh_2)$, $5e_g \rightarrow 4a_{2u}$ transition.[110] The MO calculations of Norman and Kolari[156] as well as further measurements of crystal spectra[233,234] supported this assignment. One of the observations used to support this assignment was the appearance of a vibronic progression with a frequency of 297 cm^{-1}. This was assumed to be due to ν(Rh–Rh) in the excited state and such an assignment seemed consistent with the then accepted assignment of ν(Rh–Rh) in the ground state of 320 cm^{-1}. The moderate (23 cm^{-1}) lowering of the frequency was considered reasonable for a $\pi^* \rightarrow \sigma^*$ transition, where an electron goes from one antibonding orbital to another (presumably) more strongly antibonding one. Finally, a further theoretical treatment[167] also supported this assignment.

In 1984, however, the assignment of this electronic transition was challenged and a change proposed.[235] The main reason given was that a ν(Rh–Rh) frequency in the ground state of 320 cm^{-1} was considered to be too high. By attributing this ground state Raman frequency to the A_{1g} Rh–O stretching mode these authors[235] were led to reassign band A as a $\pi^*(Rh_2) \rightarrow \sigma^*$ (Rh–O), $5e_g \rightarrow 4b_{2u}$, transition. However, it is now known that the Rh–Rh stretching mode is in the neighborhood of 300 cm^{-1} (see Section 16.6.1).

Pictiva EX2004
Samsung v Pictiva
IPR2024-01094

In 1988 the results of an MCD measurement[236] showed that the sign of the MCD for band A agreed with expectation for an upper A_{2u} ($\sigma(Rh_2)$) orbital but was the reverse of that expected for an upper B_{2u} ($\sigma^*(Rh–O)$) orbital, thus supporting the original assignment, which is now accepted.

The assignment of band B, also *xy*-polarized and showing no resolved vibrational structure,[233,235] is at present still uncertain. It has been assigned as a $\pi(Rh–O)\rightarrow\sigma^*$ (Rh–O) transition.[235] There are also strong absorption bands in the near UV (40,000-45,000 cm^{-1}) for which a $\sigma(Rh_2)\rightarrow\sigma^*(Rh_2)$ assignment has been proposed.[163,235]

$Pt_2(O_2CR)_4L_2$, $Pt_2(O_2SO_2)_4L_2$ and $Pt_2(O_2P(O)OH)_4L_2$.

While these have the same type of ground state electron configuration, $\sigma^2\pi^4\delta^2\delta^{*2}\pi^{*4}$, as their Rh_2^{4+} analogs, there is a great deal more mixing of metal and ligand orbitals. Spectra are, accordingly, more complex and difficult to assign,[237-240] and the details are beyond the scope of this discussion. For any given set of bridging ligands, the axial ligands may be varied (e.g., H_2O, Cl^-, Br^-, NCS^-) and such variations result in large changes in the spectra. There is no doubt that essentially all observed bands have considerable LMCT character. It should be noted that the MCD results in ref 238 appear to refute some of the assignments proposed in ref 237. The assignments in ref 239 and ref 240 appear to be the most reliable.

$[Ru_2(O_2CR)_4]^{n+}$ and related compounds.

Many spectroscopic observations have been mentioned in Chapter 9. For Ru_2^{5+} species with a quartet ground state derived from a $\sigma^2\pi^4\delta^2$ $(\delta^*\pi^*)^3$ configuration, a $\delta\rightarrow\delta^*$ type transition should occur effectively as a one-electron transition and thus at about the calculated energy. This is the case. The calculations[167] place it at about 8800 cm^{-1} and polarized crystal spectra [241-243,] confirm this assignment for a band with an origin near 9000 cm^{-1} and displaying a progression in ν'(Ru–Ru). A very weak absorption at *c.* 7000 cm^{-1} has been assigned to a $\pi^*\rightarrow\delta^*$ transition.[243,244]

The most prominent feature in the spectra of all the molecules is an intense band around 21,000 cm^{-1} and all the evidence[243,245] as well as theory[167] favor assigning this to the $6e_u\rightarrow 6e_g$ transition, where $6e_u$ is essentially a π-orbital that shares both oxygen and metal π character and $6e_g$ is the $\pi^*(Ru_2)$ orbital.

$Os_2(O_2CR)_4Cl_2$ molecules.

These have been discussed in Chapter 10. Like their ruthenium homologs, they have $\sigma^2\pi^4\delta^2$ $(\delta^*\pi^*)^2$ ground states.[246] Their spectra are complex, but plausible assignments have been made. A *z*-polarized $\delta\rightarrow\delta^*$ transition occurs at *c.* 12,000 cm^{-1} and displays a progression in the excited state ν(Os–Os) vibration (220 cm^{-1}).

$[Os_2X_8]^{2-}$.

The $[Os_2X_8]^{2-}$ ions (to which there are no ruthenium homologs) have also been discussed in Chapter 10. They have D_{4d} symmetry and $\sigma^2\pi^4\delta^2\ \delta^{*2}$ ground state configurations. The absorption spectra for X = Cl, Br, and I have been reported.[247] All of them display a plethora of bands between 250 and 750 nm of which only the lowest in each case has been assigned, namely, to a $\delta\rightarrow\pi^*$ excitation. The lengths of the progressions and the considerable reductions in frequency from the ground state values (*c.* 90 cm^{-1}) are consistent with this assignment.

Pictiva EX2004
Samsung v Pictiva
IPR2024-01094

16.4.5 CD and ORD spectra

Compounds containing M–M quadruple bonds can be chiral and when they are they display CD and ORD effects (optical activity). In practice only the CD effects have been studied. As is true of optically active compounds in general, there are two major categories:

1. The inherently chiral chromophore.
2. The achiral chromophore in a chiral environment.

Examples of category A are provided by molecules in which one to four chiral ligands bridge the metal atoms and impose a twist about the M–M bond so that it is no longer in an eclipsed state. The commonest, but not the only, examples are the β-$Mo_2X_4(PP)_2$ species, in which PP represents a 1,2-diphosphinoethane ligand. Because the chromophore itself, that is, the M–M quadruple bond and its coordinated atoms, has a helical conformation, it is inherently chiral. Examples of category B are provided by carboxylato-bridged species, $M_2(O_2CR)_4L_2$ in which the eclipsed conformation exists but either R or L is chiral, or by the chelated (α) isomers of $M_2X_4(diamine)_2$, in which the diamine is chiral. These two cases require rather different theoretical analyses, case A being much more straightforward, and we shall now discuss them separately, beginning with type A.

The prototype compound to illustrate case A, the inherently chiral chromophore, is Λ-[Mo_2Cl_4(*S,S*-dppb)$_2$], where the diphosphine ligand is (*S,S*)-$Ph_2PCHMeCHMePPh_2$. Conformational analysis predicts and crystallography confirms[248,249] that with the (*S,S*)-ligand the Λ sense of rotation about the Mo–Mo bond should be induced. This molecule is shown in Fig. 16.35. As viewed straight down the Mo–Mo axis, the left or counterclockwise twist (by *c.* 23°) is clearly evident. Fig 16.35 also shows the CD spectrum of the same molecule and it can be seen that there are two very prominent features: a negative CD band corresponding to the $\delta^2 \rightarrow \delta\delta^*$ absorption (*c.* 13,500 cm^{-1}) and a positive CD band at *c.* 21,300 cm^{-1}. Similar CD spectra are observed for many other similar molecules. [250-252] All such results can be understood in terms of the following straightforward analysis.[248,249,251]

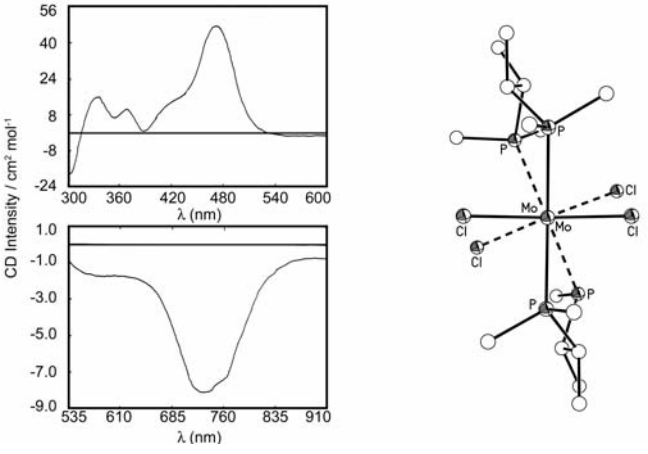


Fig. 16.35. The β-Mo_2Cl_4(*S,S*-dppb)$_2$ molecule viewed down the Mo–Mo axis (right) and its CD spectrum (left).

For the $\delta^2 \rightarrow \delta\delta^*$ transition, whose assignment is securely established, the transient charge distribution during the transition is shown diagrammatically in Fig. 16.36. It can be seen that based on this diagram we can state that the $\delta \rightarrow \delta^*$ transition has a movement of charge both

Pictiva EX2004
Samsung v Pictiva
IPR2024-01094

along and around the Mo–Mo bond. This means that it is both electric dipole allowed and (due to the rotation) magnetic dipole allowed. The combination of these two qualities makes it CD active. Moreover, it is possible, as also shown in Fig. 16.36, to infer the sign of the CD band because this is a consequence of the direction of charge rotation. We take the dipole direction to be given by the + → – direction. We then take the charge rotation in the same sense, and assign a vector to the rotation according to the right hand rule: if fingers point in the direction of rotation, the thumb points in the vector direction. We can thus see in Fig. 16.36 (a) that for the Λ molecule the electric and magnetic vectors point in opposite directions (down and up, respectively). This means that the CD band should be negative for the $\delta^2 \rightarrow \delta\delta^*$ transition of a Λ-$M_2X_4(PP)_2$ type molecule, as observed for Λ-Mo_2Cl_4(*S*, *S*-dppb)$_2$.

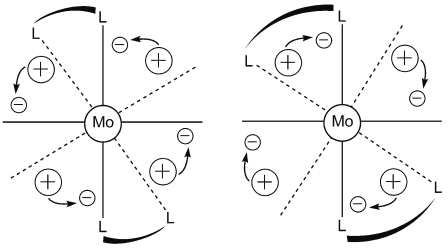


Fig. 16.36. Diagrams of the transient charge distributions for the δ→δ* transition in twisted $Mo_2X_4(LL)_2$ molecules with twist angle θ (a) in the range 0 to -45° and (b) in the range -45 to -90°. Note that the two ranges, though in the same direction geometrically, give transient charge distributions of opposite rotational sense.

This analysis can be generalized into a sign rule as shown in Fig. 16.37. This sign rule has the following important feature. For a rotation of > 45°, the CD sign again changes (see Fig. 16.36 (b)) and it therefore turns out that for rotations of ± θ the sign of the CD will be the same as for rotations ∓ θ. The first actual test of this complete relationship was provided[250] by the compound Mo_2Cl_4(*S*, *S*-chiraphos)$_2$, in which the mean P–Mo–Mo–P torsion angle is *c*. -80°, that is, into the region where the CD band for the δ→δ* transition should be positive, and it is.

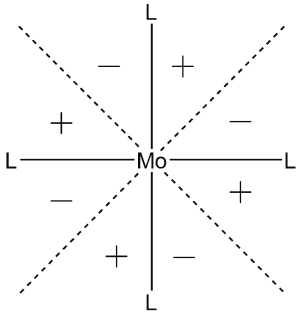


Fig. 16.37. The sign rule for the CD of the δ→δ* transition. The sign of the CD refers to the sector in which the rear set of ligand atoms is found.

Pictiva EX2004
Samsung v Pictiva
IPR2024-01094

As would be expected, the CD spectrum of the $[Re_2Cl_4(S,S\text{-dppb})_2]^{2+}$ ion (which has a $\sigma^2\pi^4\delta^2$ configuration) conforms to the same sign rule as the isostructural and isoelectronic molybdenum compounds.[253] The $Mo_2Cl_4(LL)_2$ (LL = (R)-$H_2NCH(CH_3)CH_2NH_2$) molecule also appears to be of type A, and it too, follows the octant sign rule.[254]

In the type A compounds we have just discussed, the CD band at around 22,000 cm^{-1} is opposite in sign to the CD band for the $\delta^2 \rightarrow \delta\delta^*$ transition. This is naturally, and without exception, explained by assigning the 22,000 cm^{-1} band to the transition $\delta_{xy} \rightarrow \delta_{x^2-y^2}$, for which it is easily shown[251] that an octant type sign rule also applies, but rotated 45° from the one we have derived for the $\delta \rightarrow \delta^*$ transition. Thus, by the correct use of CD spectra one can conclusively refute the suggestion[255] that the lowest-energy band in the spectra of quadruply-bonded species should be assigned to a $\delta_{xy} \rightarrow \delta_{x^2-y^2}$ transition rather than to a $\delta \rightarrow \delta^*$ transition.

We now turn to compounds of class B, in which there is no internal twist to make the M–M bond inherently chiral, but instead an essentially eclipsed M_2X_8 core within a set of ligands some or all of which are chiral. The earliest attempt[256] to deal with such a compound was concerned with rhodium compounds of the type $Rh_2(O_2CR)_4L_2$, where R = CPh(OH)H and CPh(OMe)H. As explained fully at the time[256] this situation is more difficult to analyze because *within the chromophore* no transition is both electrically and magnetically allowed. Hence, a perturbation method whereby some magnetic component is mixed into a nominally dipole-allowed transition, or vice versa must be employed. The details are too complex to be spelled out here and the original papers dealing with the dirhodium compounds[236,256] and others that belong to the same class[257,258] should be consulted.

A different type of class B compound was more recently examined, namely $[Mo_2(O_2CCF_3)_2(S,S\text{-dach})_2(CH_3CN)_2](BF_4)_2$ in which the *S,S*-dach (dach = 1,2-diaminocyclohexane) ligands are chelated, one to each Mo atom. The *R,R*-dach enantiomer was also characterized.[259] In an earlier report in which structure was not determined, it was assumed that the dach ligands were bridging and the CD spectrum was treated as a class A case.[260]

A final point of importance has to do with the employment of M_2^{n+} complexes as tools for studying the absolute chiralities of colorless organic compounds in solution. Organic chemists have long been interested in the idea of adding some metal-containing species with electronic absorption in the visible region to a solution containing the organic compound of interest so that when the former forms a complex with the latter, it will acquire a CD spectrum in the conveniently observed visible region. No really practical and general way to do this was found until recently. Snatzke and co-workers[261] made a number of attempts to employ $Mo_2(O_2CCH_3)_4$, whose $\delta^2 \rightarrow \delta\delta^*$ transition is conveniently placed (*c.* 450 nm) but without finding a fully satisfactory method. However, it has recently been found that $Rh_2(O_2CCF_3)_4$ can bind essentially every type of organic molecule at its axial positions,[262] including even olefins,[263] and then display CD effects whose signs can be related to the absolute configuration of the attached organic molecule. It appears that $Rh_2(O_2CCF_3)_4$ may turn out to be the long-sought general reagent for absolute chirality determinations.

16.4.6 Excited state distortions inferred from vibronic structure

It is well known that in principle it is possible to calculate, at least approximately, structural changes in a molecule upon electronic excitation or ionization from the vibrational patterns observed in the electronic absorption band or PES ionization band. This has been done for several $Mo_2(O_2CR)_4$ compounds, $Mo_2[(CH_2)_2PMe_2]_4$, and $Rh_2(O_2CMe)_4L_2$. Extensive work has been done on the Mo compounds, where progressions in the ν'(Mo–Mo) vibration are employed and the process is commonly referred to as Franck-Condon analysis. The first such result was for $Mo_2(O_2CCH_3)_4$ where the progression in ν'(Mo-Mo) on the $\delta^2 \rightarrow \delta\delta^*$ excitation

Pictiva EX2004
Samsung v Pictiva
IPR2024-01094

(then thought to be a $\delta \rightarrow \pi^*$ excitation) was used.[212] The Mo–Mo distance was estimated to be *c* 0.1 Å longer in the excited state. From the analogous vibronic data for $Mo_2(O_2CCF_3)_4$ and $Mo_2[(CH_2)_2PMe_2]_4$ estimates of 0.045[264] and 0.09 Å,[220] respectively, have been made, while for the $[Mo_2X_6(H_2O)_2]^{2-}$ ions (X = Cl, Br) the derived values are 0.12-0.13 Å.[265] A combined study of resonance Raman and electronic absorption spectra of $Mo_2X_4(PMe_3)_4$ molecules has also led to a value of 0.10 Å for the Mo–Mo bond length increase in the singlet state of the $\sigma^2\pi^4\delta\delta^*$ configuration.[266]

A related but more sophisticated approach which employs both a Franck-Condon analysis of the $\delta^2 \rightarrow \delta\delta^*$ absorption band and the intensities of resonance Raman overtones for the ν'M–M vibration is called the sum-over-states method. It has been applied to the $[Re_2Br_8]^{2-}$, $[Re_2I_8]^{2-}$ and $[Mo_2Cl_8]^{4-}$ ions.[267] The results are similar to those previously obtained, namely an increase of 0.08 Å in the Re–Re bond distances and 0.15 for Mo–Mo, on going from the $^1A_{1g}$ ground state to the $^1A_{2u}$ excited state.

From the vibration progression in the δ ionization of $Mo_2(O_2CCH_3)_4$ (see Fig. 16.44) it was estimated[268] that the Mo–Mo distance in the $[Mo_2(O_2CCH_3)_4]^+$ ion is 0.13-0.18 Å longer than that in the neutral molecule. This result must be considered surprising because the ionization process abolishes only half of the δ-bond whereas the $\delta^2 \rightarrow \delta\delta^*$ transition abolishes all of it. It was proposed[268] that the increase in oxidation state of the Mo atoms upon ionization also makes a substantial contribution to bond lengthening, but this would still leave some inconsistency between the two types of result. This inconsistency prompted a reanalysis[269] of the ionization results, from which it was concluded that the change in distance was probably 0.11 Å.

These spectroscopic results may be compared with some X-ray crystallographic results which were summarized in Section 16.1.1. In the series $[Mo_2(SO_4)_4]^{4-}$, $[Mo_2(SO_4)_4]^{3-}$, $[Mo_2(HPO_4)_4]^{2-}$ where at each step there is loss of one δ-electron and a one-unit increase in oxidation state, the Mo–Mo bond length increases are each about 0.06 Å. This is reasonably consistent with the recalculated increase on photoionization of $Mo_2(O_2CCH_3)_4$, 0.11 Å. On the other hand, the structures of $Mo_2(DTolF)_4$ and $Mo_2(DTolF)_4^+$ show only a 0.037 Å increase on ionization.[177]

For the $Rh_2(O_2CCH_3)_4L_2$, L = Ph_3P or Ph_3As, molecules, Franck-Condon analysis[270,271] of the progressions seen in a band believed to be due to a $\pi^* \rightarrow \sigma^*$ transition, have led to Δ(Rh–Rh) ≈ 0.045 Å and also Δ(Rh–O) ≈ 0.038 Å. The σ* state is believed to be one in which the excited electron is in an orbital that is primarily Rh–Rh antibonding, but some σ* Rh–O character can also not be excluded.

For the most commonly observed $\delta \rightarrow \delta^*$ type transition, namely from a $^1A_{1g}$ (δ^2) ground state to a $^1A_{2u}$ ($\delta\delta^*$) excited state the molecule passes on a very fast time scale (*c.* 10^{-16} sec) from an electronic structure in which there is a δ-bond strong enough to maintain an internal rotation angle of *c.* 0° to an electronic structure in which no δ-bond exists and the most stable structure would be one in which the preferred internal rotation angle is 45°. In other words, the spectroscopically observed $^1A_{2u}$ state, which is responsible for the observed vibrational structure of the absorption band, is an unrelaxed state for the molecule having a $\sigma^2\pi^4\delta\delta^*$ electron configuration. The relaxed configuration, as in molecules with $\sigma^2\pi^4$ or $\sigma^2\pi^4\delta^2\delta^{*2}$ configurations, should have a torsion angle of 45° (D_{4d} symmetry instead of D_{4h}).

The existence of such relaxed $\sigma^2\pi^4\delta\delta^*$ molecules has been demonstrated in two ways. One approach is to use time-resolved resonance Raman (TR^3) spectroscopy. In this way the excited state geometry can be probed.[272] For solids containing $[Re_2X_8]^{2-}$ (X = Cl, Br) ions it is seen that until the eclipsed $^1A_{2u}$ excited state decays back to the ground state, it retains its D_{4h} structure because it is constrained by crystal packing forces. In solution, however, the conformation changes within nanoseconds to D_{4d} as evidenced by the Raman spectrum. A second type of experiment entailing the study of emission spectra will be discussed in the next section.

Pictiva EX2004
Samsung v Pictiva
IPR2024-01094

16.4.7 Emission spectra and photochemistry

Emission spectra.

The emission spectra of the $[Mo_2Cl_8]^{4-}$, $[Re_2Cl_8]^{2-}$, and $[Re_2Br_8]^{2-}$ ions and especially the $Mo_2X_4(PR_3)_4$ compounds have been studied in detail. The earliest reported observations of the $[M_2X_8]^{n-}$ ions were as follows. Excitation of solid compounds containing $[Re_2Cl_8]^{2-}$ and $[Re_2Br_8]^{2-}$ ions at 650 nm or $[Mo_2Cl_8]^{4-}$ at 540 nm, at 1.3 K, generated broad emission bands at frequencies below those of the respective $\delta^2 \rightarrow \delta\delta^*$ absorption bands.[273] The two most important features of these results were that:

1. the absorption and emission spectra were not mirror images, and
2. the absorption and emission envelopes did not overlap at the frequency of the 0-0 transition in the absorption band.

It was therefore concluded that these emissions could not be attributed to simple radiative decay of the $^1A_{2u}$ ($\delta\delta^*$) state. Instead, it was suggested, the emission is from one of the spin-orbit components of the $^3A_{2u}$ state arising from the same configuration. This work was followed up by a study[274] of the emission behavior of $Mo_2Cl_4(PBu^n_3)_4$ which gave the results shown in Fig. 16.38. Here the absorption and emission envelopes are essentially mirror images and overlap at the 0-0 band; this is clearly a simple case of prompt emission from the singlet excited state. The obvious question was, then, why this case is so different from that of $[Mo_2Cl_8]^{4-}$ and the $[Re_2X_8]^{2-}$ ions. There are also further details concerning the emission behavior of the $[Re_2Cl_8]^{2-}$ ion that are not easily reconciled with the previously proposed $^3A_{2u} \rightarrow {}^1A_{1g}$ emission process.[274,275]

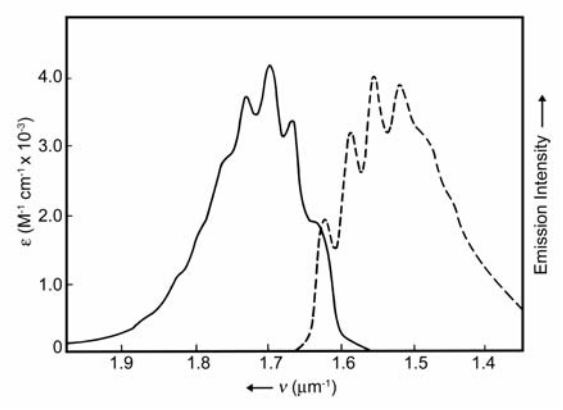


Fig. 16.38. Absorption (left) and emission (right) spectra of $Mo_2Cl_4(PBu^n_3)_4$ at 80 K in a 2-methylpentane glass.

It was then proposed[274,275] that the foregoing observations can be reconciled by recognizing that in the $\delta\delta^*$ excited state the eclipsed rotational conformation is no longer stable relative to the staggered one (the δ-bond has been abolished). From the $[M_2X_8]^{n-}$ ions, then, the emitting state is one in which a rotation to (or towards) the staggered conformation has occurred. That being the case, no mirror image relationship to the absorption spectrum is to be expected. In $Mo_2Cl_4(NBu^n_3)_4$ such a rotation is prevented by the tight interlocking of the large and small ligands and the ground state and excited state structures are so similar that the mirror image relationship is seen.

Pictiva EX2004
Samsung v Pictiva
IPR2024-01094

Further work[276-278] has been done on the three $Mo_2X_4(PMe_3)_4$ compounds with X = Cl, Br, and I, which also show emission spectra indicative of close geometrical similarity of the ground and excited states, but to different degrees, with the iodide providing the most and the chloride the least perfect mirror images. Only recently[279] has emission from the $^3A_{2u}$ state been shown to occur, namely in $Re_2(DAniF)_4Cl_2$.

It was noted in Section 16.4.6 that a TR^3 study of the $Re_2Cl_8^{2-}$ ion had shown that while it rapidly internally rotates to a D_{4d} structure in solution (as would be expected), it cannot and does not do so in a crystalline environment. This, along with other subsequent work,[280] in which it was shown that an earlier report on solid $(NBu^n_4)_2[Re_2Cl_8]$ was incorrect, puts an end to the need for strained rationalizations.[274,275] Solid $(NBu^n_4)_2[Re_2Cl_8]$ emits from the $^1A_{2u}$ state of the D_{4h} anion.

In an important study[281] employing picosecond excitation followed by transient absorption spectroscopy, it was found that in fluid solution at room temperature, both $[Re_2Cl_8]^{2-}$ and $[Mo_2Cl_8]^{4-}$ give, in less than 20 picoseconds, a transient that is reasonably attributable to the twisted, singlet excited state. This same study produced other interesting information about transient excited states in quadruply bonded species. This accords with the TR^3 study which showed[272] that after a few nanoseconds $[Re_2Cl_8]^{2-}$ in its $^1A_{2u}$ ($\delta\delta^*$) excited state has a staggered conformation when it is *in solution*.

It has also been shown that the emission of $Mo_2Cl_4(PMe_3)_4$ can be electrogenerated.[282] This is done by pulsing the applied potential from a value more positive than that required for oxidation to one more negative than that for reduction, thus generating both cation and anion radicals in close proximity. Because the energy released on recombination exceeds that required for an excitation to the $\delta\delta^*$ state (the $[Mo_2Cl_4(PMe_3)_4]^*$ species, which emits) we have the following reaction sequence:

$$[Mo_2Cl_4(PMe_3)_4]^- + [Mo_2Cl_4(PMe_3)_4]^+ \rightarrow Mo_2Cl_4(PMe_3)_4 + [Mo_2Cl_4(PMe_3)_4]^*$$

$$[Mo_2Cl_4(PMe_3)_4]^* \rightarrow Mo_2Cl_4(PMe_3)_4 + h\nu$$

Only a few other observations of emission from excited states have been reported. For $Mo_2(O_2CCF_3)_4$ structured emission has been observed at 1.3 K with an origin 1800 cm^{-1} below that of the absorption band, which was then assigned to a $\delta\rightarrow\pi^*$ transition,[212] and the emission to the reverse triplet$\rightarrow$singlet transition. Since we now know that the absorption band is the $\delta^2\rightarrow\delta\delta^*$ absorption, the emission should be reassigned also, to the $^3A_{2u}\rightarrow{}^1A_{1g}$ transition. The long life of the excited molecule (2 ms as compared to an estimated 2 μs for a $^1A_{2u}$ state) as well as the 1800 cm^{-1} separation of the origins are the basis for designating the emitting state as $^3A_{2u}$ rather than $^1A_{2u}$.

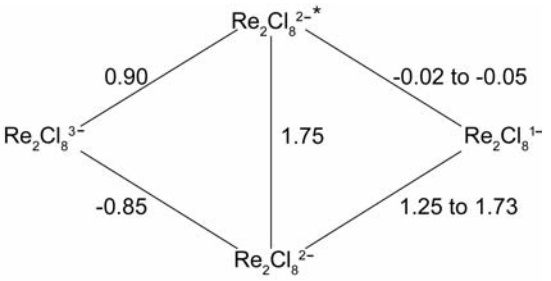
The compounds $Mo_2(mhp)_4$, $Mo_2(chp)_4$ and $W_2(mhp)_4$ have been observed to emit upon excitation into the $\delta^2\rightarrow\delta\delta^*$ absorption band.[283] All show vibrational structure (at 15 K) and in the case of $Mo_2(mhp)_4$ it is highly resolved. It was not possible, however, to make a firm assignment of the emitting state.

Photochemistry.

The photochemistry of $[Re_2Cl_8]^{2-}$, via its singlet $\delta\delta^*$ excited state has been developed in an interesting way by Nocera and Gray. They first showed[284] that the luminescence of this species, hereafter $[Re_2Cl_8]^{2-*}$, is quenched by both electron acceptors, which remove the δ^*-electron to give $[Re_2Cl_8]^-$, and electron donors (aromatic amines), which add a δ-electron to give $[Re_2Cl_8]^{3-}$ as a strongly associated ion pair, (amine$^+$) ($[Re_2Cl_8]^{3-}$). Back reactions in both cases are extremely fast. A diagram showing the energetic relationships of the four pertinent

Pictiva EX2004
Samsung v Pictiva
IPR2024-01094

Re_2Cl_8 species was deduced and is as shown below, where the units are eV or V versus SCE in CH_3CN solution:



These workers then showed[285] that the uninteresting thermal back reaction of $[Re_2Cl_8]^-$ and the quencher, Q, can be obviated by the presence of Cl^- ion. In this case, one of two things will happen, depending on whether Q is a relatively weak oxidizing agent, or a stronger one, as the following two reactions show:

$$[Re_2Cl_8]^{2-*} + Q + Cl^- \rightarrow Q^- + [Re_2Cl_9]^{2-}$$

$$[Re_2Cl_8]^{2-*} + 2Q + Cl^- \rightarrow 2Q^- + [Re_2Cl_9]^-$$

Irradiation of $[Mo_2(SO_4)_4]^{4-}$ in aqueous H_2SO_4 at 254 nm causes the following reaction[223,286] (quantum yield, 17%):

$$2[Mo_2(SO_4)_4]^{4-} + 2H_3O^+ \xrightarrow{h\nu} 2[Mo_2(SO_4)_4]^{3-} + 2H_2O + H_2$$

Generation of hydrogen can also be caused by irradiation of other Mo_2^{4+} species.[286] Thus Mo_2^{4+} (aq) in CF_3SO_3H undergoes the following reaction (in low quantum yield, 3.5 per cent):

$$Mo_2^{4+}(aq) + 2H_2O \rightarrow [Mo_2(\mu\text{-}OH)_2]^{4+}(aq) + H_2$$

More recently it has been shown[287] that $[Mo_2(HPO_4)_4]^{4-}$ displays similar, but even more elaborate photochemistry. Here there is a series of three species, the 4-, 3-, and 2- ions, and irradiating either of the first two leads to the 2- ion, with evolution of $\frac{1}{2}H_2$ at each step. From a study of the wavelength profile for photoactivity and the absorption spectra, it was concluded that the photoactive state is in each step one that is produced by a $\pi \rightarrow \pi^*$ excitation. The highly reducing $\pi \rightarrow \pi^*$ excited state then directly reduces H^+ to H, and the H atoms rapidly combine to form H_2.

When $[Mo_2X_8]^{4-}$, X = Cl, Br, are irradiated in aqueous HX solution,[286] $[Mo_2X_8H]^-$ is first formed and then undergoes decomposition to give H_2 and $[Mo_2(\mu\text{-}OH)_2]^{4+}$. The glycine complex, $[Mo_2(O_2CCH_2NH_3)_4]^{4+}$, does not react in this way.[286] Given the high energy of the photons used (254 nm) in these reactions, it is not the singlet $\delta\delta^*$ state that is generated, but some more highly excited one, perhaps again one resulting from a $\pi \rightarrow \pi^*$ excitation.

In contrast to the systems just discussed where a $\pi \rightarrow \pi^*$ or other high-energy excited state is responsible for the photochemistry, the $Mo_2[O_2P(OPh)_2]_4$ molecule has allowed for the study of photochemistry in nonaqueous media where the $\delta^2 \rightarrow \delta\delta^*$ excitation is responsible for photoactivation.[288] Using 510 nm light (the $\delta^2 \rightarrow \delta\delta^*$ transition causes absorption maximizing at 515 nm) the following reaction can be carried out with a quantum yield of 4%:

$$2Mo_2[O_2P(OPh)_2]_4 + ClCH_2CH_2Cl \rightarrow 2\,Mo_2[O_2P(OPh)_2]_4Cl + C_2H_4$$

Pictiva EX2004
Samsung v Pictiva
IPR2024-01094

This overall stoichiometry is consistent with either of two pathways, once the activated Mo_2 species, Mo_2^{4+}*, has reacted with $ClCH_2CH_2Cl$ to give $Mo^{II}Mo^{III}Cl + ClCH_2CH_2$. If these two are held in a tight solvent cage, further reaction to give C_2H_4 and $ClMo^{III}Mo^{III}Cl$ probably ensues. There is then a comproportionation of $ClMo^{III}Mo^{III}Cl$ with $Mo^{II}Mo^{II}$ to give $Mo^{II}Mo^{III}Cl$. On the other hand a free $ClCH_2CH_2$ radical may react with $Mo^{II}Mo^{II}$ to give $Mo^{II}Mo^{III}Cl$ and C_2H_4.

In all of the photochemistry of quadruply-bonded dimetal compounds so far discussed, only one-electron transfers occurred; overall two-electron redox reactions occurred stepwise. One of the goals in investigations of the photochemistry of these binuclear systems was to see if any genuine two-electron process could be discovered.[289] In the photochemical reaction of $W_2Cl_4(dppm)_2$ with CH_3I, this goal has been reached.[290] While thermal additions to quadruply-bonded molecules, which proceed by radical processes, give scrambling of ligands, the photoaddition of CH_3I to $W_2Cl_4(dppm)_2$ gives a single pure product. It is believed[289] that the photoactivation occurs through a $\delta\rightarrow\pi^*$ or a $\pi\rightarrow\delta^*$ excitation (or both, since the two excited states are accidently almost degenerate).

A few other results of a photochemical nature have been reported. Irradiation of a solution of $[Re_2Cl_8]^{2-}$ in acetonitrile[291] with a 1000-watt Hg-Xe lamp equipped with a pyrex filter causes cleavage of the dinuclear species and allows isolation of $ReCl_3(CH_3CN)_3$ as well as a small amount of $[ReCl_4(CH_3CN)_2]^-$. Further study[292] left the detailed mechanism still in doubt.

While it is not, strictly speaking, photo*chemistry*, since no net chemical change occurs, flash photolysis of $Mo_2(O_2CCF_3)_4$ in acetonitrile or benzene at 337 nm causes bleaching, followed by the reappearance of ground state absorption on a microsecond time scale; the recovery follows first-order kinetics, with a half-life of 33 μs in benzene.[293] The principal species present at the end of a 10 ns flash was postulated to be a triplet state derived from the $\sigma^2\pi^4\delta\delta^*$ configuration (incorrectly assigned in the paper because of the confusion generally prevailing at the time concerning the absorption bands at *c.* 23.0 x 10^3 cm^{-1} for $Mo_2(O_2CR)_4$ compounds as a class). Some speculative discussion was presented concerning possible intermediate adducts with CH_3CN solvent.

An odd observation[294] of uncertain significance is that four $Rh_2(O_2CCH_3)_4L_2$ (L = CH_3OH, THF, PPh_3, py) compounds are excited by "visible light" to a transient excited state of 3-5 μs lifetime which has an absorption band at *c.* 760 nm. No suggestion was made as to what this transient is.

Effects of high pressure.

It is well known that the compression of liquid solutions and molecular solids entails mainly decreasing the intermolecular distances where the softest (van der Waals) resistance is encountered. Nevertheless, at sufficiently high (50-150 kbar) pressures molecular shapes and dimensions are also affected and there are consequences seen spectroscopically.[377,421-425] Interpretation of the observations is somewhat speculative and there are differences of opinion. Increasing pressure causes increases in ν(M–M) and decreases in the energy of the $\delta\rightarrow\delta^*$ type transition in, for example $Re_2Cl_8^{2-}$. Both have been, reasonably, attributed to concomitant twisting, which lessens the δ bond strength, and shortening of the Re–Re distance. It is easier to compress the Re–Re bond when the conformation is twisted away from the eclipsed state. For $Mo_2Cl_4(PMe_3)_4$, it has been proposed that the smaller spectroscopic changes result from compression alone.

Pictiva EX2004
Samsung v Pictiva
IPR2024-01094

16.5 Photoelectron Spectra

Photoelectron spectra (PES) provide the most direct and least equivocal experimental information about valence electrons in molecules. In this context we are referring to the use of UV light to photodetach valence shell electrons. Inner shell electron spectroscopy, denoted XPS, will be mentioned in Section 16.7.2.

16.5.1 Paddlewheel molecules

Since the entire field to which thus book is devoted commenced with the $Re_2Cl_8^{2-}$ ion, we turn first to the PES of that species. The experimental methodology for PES measurements on gaseous ions, which is novel, was applied to $Re_2Cl_8^{2-}$ in 2000 and gave the results[295] shown in Fig. 16.39. It is self-evident that these data confirm unequivocally the original proposal of a quadruple bond in the $Re_2Cl_8^{2-}$ ion (see Section 1.2.2). Distinct δ, π and σ ionizations, preceding a plethora of peaks from other ionizations, exactly as expected from theory, are clearly to be seen.

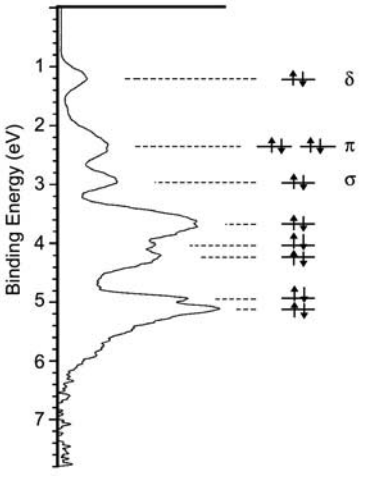


Fig. 16.39. The photoelectron spectrum of $[Re_2Cl_8]^{2-}$ showing the assignment of the features to the molecular orbitals.

We turn now to a historical account of PES studies. The easy volatility and relative simplicity of the group 6 $M_2(O_2CCH_3)_4$ molecules made them early subjects of study,[296-302] although some parts of the interpretations accepted today differ from those first proposed.[304] The He(I) PE spectra of these molecules[304] are shown in Fig. 16.40. There is a marked difference between the lower-energy region for the chromium compound and the other two. As shown in Fig. 16.41, the first broad band in $Cr_2(O_2CCH_3)_4$ can be deconvoluted into three overlapping bands in an approximately 1:2:1 intensity ratio. It is generally believed that these correspond to the δ, π and σ ionizations, in increasing order of energy.

The $Mo_2(O_2CCH_3)_4$ and $W_2(O_2CCH_3)_4$ spectra each begin with a distinct weak band that can be assigned to the δ ionization. The spectra of the Mo and W carboxylates differ in their next highest bands, the Mo compound showing only a single (although slightly unsymmetrical) band while the W compound has two bands, the one at the higher energy being very sharp. $W_2(O_2CCF_3)_4$ has been shown to display this same pattern.[305] According to an early assignment of the molybdenum spectrum, the single observed band, at *c.* 9 eV. corresponds to the π ionization only, with the σ ionization lying at least 1.5 eV higher and thus buried in the first

Pictiva EX2004
Samsung v Pictiva
IPR2024-01094

group of ligand ionizations. Another proposal was that the σ ionization also contributes to the *c*. 9 eV peak and is unresolved. Results on the $W_2(O_2CR)_4$ compounds provide support for this second proposal, the argument being that the accidental overlap occurring in the Mo case is now replaced by two non-overlapping bands. The sharp band for the tungsten compounds is then assigned to the σ ionization, but this raises a question (or at least an eyebrow) because such a narrow band implies that the σ-bond is relatively weak, which may seem counter-intuitive. However, because of the very close approach of the two metal atoms in M–M quadruple bonds, it is possible that the d_{z^2}-d_{z^2} overlap is not entirely favorable to M–M bonding.[304]

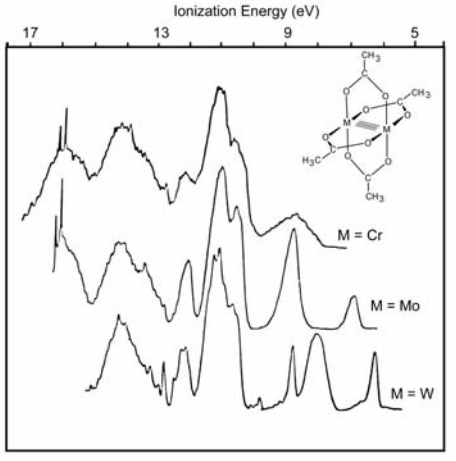


Fig. 16.40. The PES (He I) of the $M_2(O_2CMe)_4$ molecules in the gas phase.

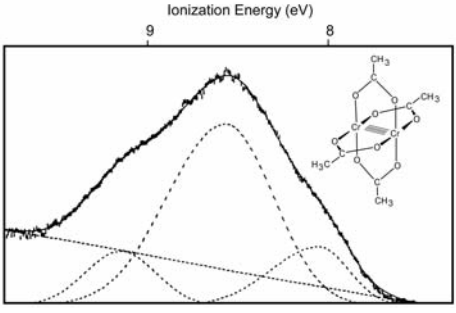


Fig. 16.41. The first band in the PES of $Cr_2(O_2CMe)_4$.

An important result[304] in this regard was obtained by comparing the PES spectrum of $MoW(O_2CCH_3)_4$ with those of the Mo_2 and W_2 compounds, as shown in Fig. 16.42. It seems clear that on going from the W_2 to the MoW compound the gap between σ- and π-bonds is closing and that by carrying this process one step further, the unresolved superposition found in the Mo_2 case would be a logical result. It should be noted that in spite of all efforts to effect some resolution of the two bands in an $Mo_2(O_2CR)_4$ compound by changing the R group, no such observation has been made.

Pictiva EX2004
Samsung v Pictiva
IPR2024-01094

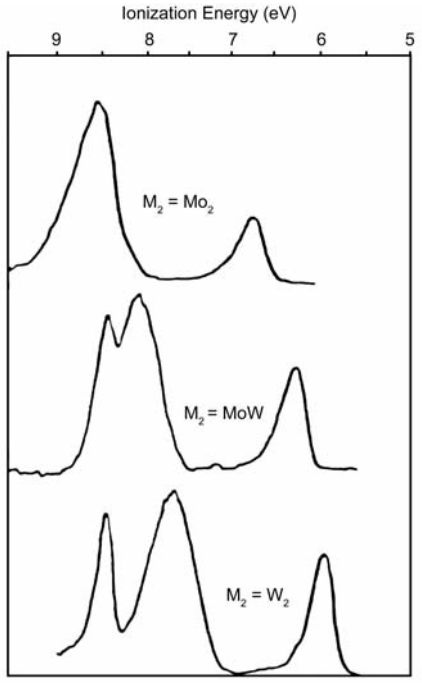


Fig. 16.42. The PES of MM'$(O_2CMe)_4$ molecules with MM' = MoMo, MoW and WW.

A study of the PES of solid $M_2(O_2CCH_3)_4$ compounds,[306] as thin films deposited from the vapor phase, and a comparison of these spectra with the vapor phase spectra previously studied has provided results that in no way contradict the interpretations just discussed. Fig. 16.43 presents the results. It should be recalled that for all three compounds there is intermolecular linking via oxygen atoms into infinite chains, but this is much stronger in the chromium case. In fact, for $Cr_2(O_2CCH_3)_4$ the Cr–Cr distance changes greatly from the gas phase (1.97 Å) to the solid phase (2.29 Å) whereas for $Mo_2(O_2CCH_3)_4$ the change is slight (2.079 Å to 2.093 Å). Presumably the change for $W_2(O_2CCH_3)_4$ is also very small.

It can be seen in Fig 16.43 that the first band for $Cr_2(O_2CCH_3)_4$ shifts quite a bit (*c.* 0.5 eV) toward lower binding energy from the gas to the solid phase, in keeping with the large increase in Cr–Cr distance. For $Mo_2(O_2CCH_3)_4$ there is no significant change in band energies, but a shoulder on the low energy side of the second band emerges in the solid state. It has been suggested[304] that this represents a partial breaking out of the σ ionization. For $W_2(O_2CCH_3)_4$ it is clear that the proposed σ band has moved down in energy and is no longer resolved from the π band. The π/δ intensity ratio correspondingly increases from *c.* 3:1 to *c.* 5:1.

The behavior of the thin film $Mo_2(O_2CCH_3)_4$ PES as the photon energy is varied[307] provides more insight into the makeup of the σ, π and δ orbitals. The π orbitals have the largest metal 4*d* character, while the σ and δ orbitals show more mixing with orbitals of the acetate ions.

A study of $Mo_2(O_2CCF_3)_4$ in the gas phase[308] gave results similar to those for $Mo_2(O_2CCH_3)_4$ but displaced to higher ionization energies. The displacement for the δ ionization is *c.* 1.8 eV.

Pictiva EX2004
Samsung v Pictiva
IPR2024-01094

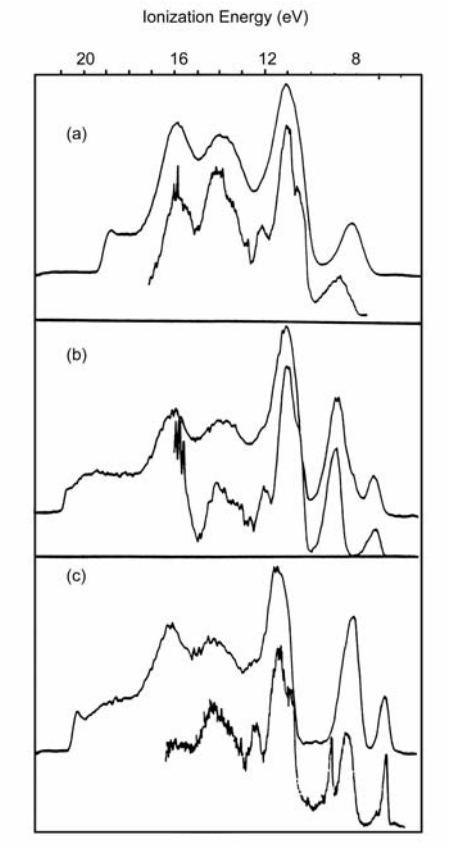


Fig. 16.43. Comparison of PES (He I) spectra in thin solid films (upper) and gases (lower) for $Cr_2(O_2CMe)_4$ (a), $Mo_2(O_2CMe)_4$ (b), and $W_2(O_2CMe)_4$ (c).

One of the most beautiful PES results obtained in the M–M multiple bond field, is the vibrationally resolved δ ionization band for $Mo_2(O_2CCH_3)_4$.[268] Fig. 16.44 shows the experimental band and a schematic indication of how a Franck-Condon analysis was carried out. The progression is in the ν(Mo-Mo) frequency for the $[Mo_2(O_2CCH_3)_4]^+$ ion in its $^2B_{2g}$ ground state (360 ± 10 cm^{-1}). This may be compared to 406 cm^{-1} for the neutral molecule in its $\sigma^2\pi^4\delta^2(^1A_{1g})$ ground state and 390 cm^{-1} in its $\sigma^2\pi^4\delta\delta^*(^1A_{2u})$ excited state. A quantitative Franck-Condon analysis from which an Mo–Mo distance in the ion of 2.26 ± 0.02 Å was deduced is not so simple as Fig. 16.44 makes it appear.

Fortunately, other group 6 paddlewheel molecules can also be vaporized in ultra high vacuum without decomposition, and thus the influence of more basic ligands has been determined. A major study dealt with the $M_2(DPhF)_4$ molecules (M = Cr, Mo, W) and the $Mo_2(DCyF)_4$ molecule.[309] It was found that in contrast to the acetate compounds, several formamidinate-based ionizations derived from the nitrogen $p\pi$ orbitals occur among the metal-metal σ, π, and δ ionization bands. Although these formamidinate-based levels are close in energy to the occupied metal–metal bonding orbitals, there is little direct mixing. All in all, there appears to be a greater degree of metal–ligand covalency than with the carboxylate compounds and the greater basicity of the formamidinates pushes the M–M orbitals to lower energies.

Pictiva EX2004
Samsung v Pictiva
IPR2024-01094

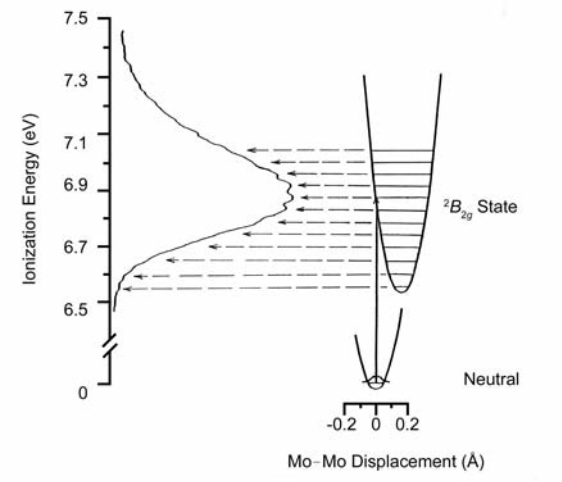


Fig. 16.44. The vibrational structure of the δ ionization band in the PES of gaseous $Mo_2(O_2CMe)_4$ (left) and a diagrammatic indication of how the Franck-Condon analysis is carried out (right).

The most recent and exciting development in the PES study of paddlewheel complexes concerns the $M_2(hpp)_4$ compounds with M = Cr, Mo and W, especially $W_2(hpp)_4$.[310] There is abundant evidence that the hpp ligand has the greatest general ability of any ligand to stabilize high charges on M_2^{n+} cores, for all metals. Conversely, this means that for $M_2(hpp)_4$ compounds the lowest ionization energies (and least positive electrode potentials) should be found. This has its most extreme manifestation in the fact that the $W_2(hpp)_4$ molecule is the most easily oxidized molecule known: its δ ionization has an onset value of 3.51 eV and a peak (vertical) value of 3.76 eV. Even the cesium atom is not this easily ionized (IP = 3.89 eV). There is a filled-filled interaction between the W_2^{4+} δ orbital and a symmetry-appropriate combination of hpp^- π orbitals that makes a key contribution to the high position of the HOMO of $W_2(hpp)_4$.

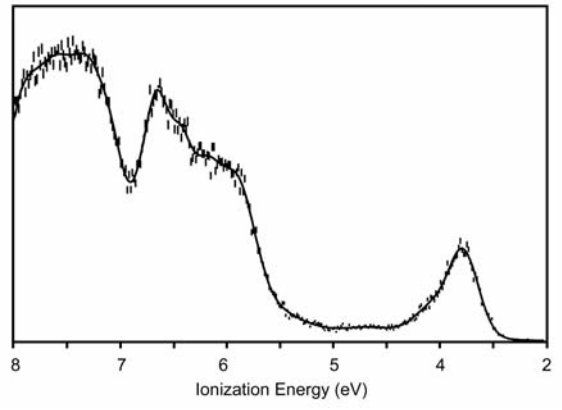


Fig. 16.45. The (He (I) PES of $W_2(hpp)_4$, supplied by Prof. D. L. Lichtenberger (University of Arizona).

Pictiva EX2004
Samsung v Pictiva
IPR2024-01094

Photoelectron spectroscopy has also been able to address the question of how strongly M–M σ bonding is sacrificed when $M_2(O_2CCH_3)_4$ compounds of Mo and W are converted to the $M_2(O_2CCH_3)_4(CH_2CMe_3)_2$ compounds.[304,311]

Finally, we note that the paddlewheel compounds of the 6-methyl-2-oxopyridine (mhp^-) ligand provide a unique set, ranging over CrCr, CrMo, MoMo, MoW and WW cores. There have been several studies of some[302,312] or all[313] of them. Some of the results of the study covering them all are shown in Fig. 16.46. In all compounds, (with the possible exception of the Cr_2 compound) it seems clear that the lowest peak is due solely to the δ ionization. As the MM' unit changes through the series from CrCr to WW, this peak moves to lower energy and increases in relative intensity, both of which are expected for ionization from an MO of essentially pure metal character.

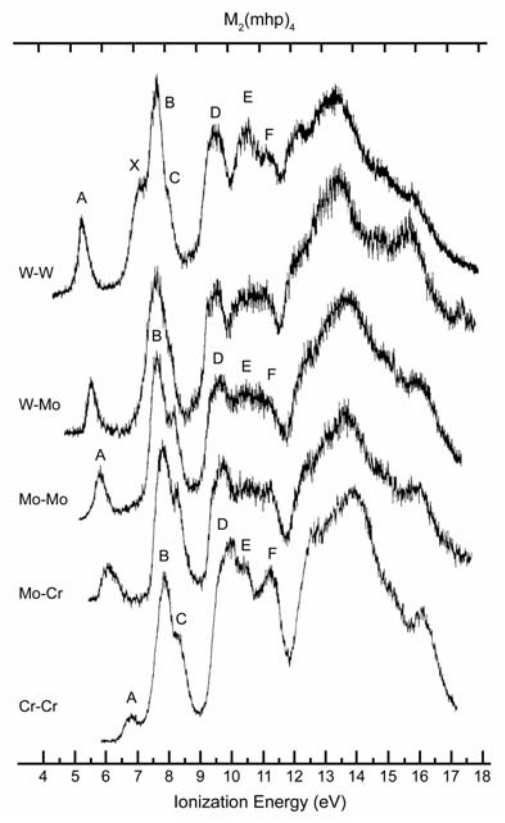


Fig. 16.46. The PES (He I) for five $MM'(mhp)_4$ compounds.

Unfortunately, the flexibility in the choice of MM' is countered, insofar as the overall value of these studies is concerned, by the fact that the ligand has a strong band that comes right where the π or π + σ band is expected. The first ionization of Hmhp occurs at 8.81 eV and the partial negative charge remaining on the coordinated hmp^- ion causes a shift to lower energy, viz. to *c*. 7.7 eV.

Pictiva EX2004
Samsung v Pictiva
IPR2024-01094

16.5.2 Other tetragonal molecules

Informative PES results have been obtained[314,315] for volatile $M_2X_4(PMe_3)_4$ molecules. The comparison between the spectra for molecules with M = Mo, W, and Re gives insight into the consequences of relativistic effects (both energy shifts and spin-orbit coupling) and of the filling of the δ* orbitals (for the Re compound). Some of the pertinent results are displayed in Figs. 16.47 and 16.48. In the spectra of all three compounds there is a band at 8.42 ± 0.07 eV that is assigned to phosphorus lone pairs.

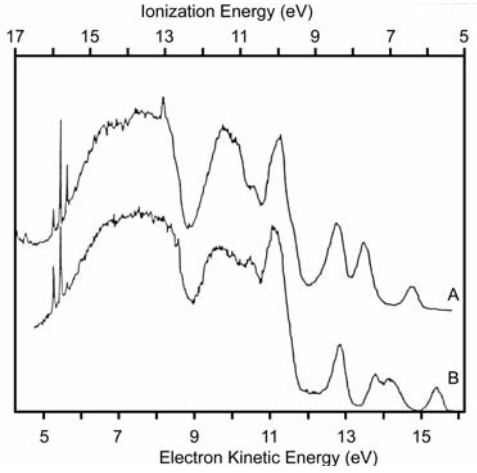


Fig. 16.47. The PES (He I) of (A) $Mo_2Cl_4(PMe_3)_4$, and (B) $W_2Cl_4(PMe_3)_4$.

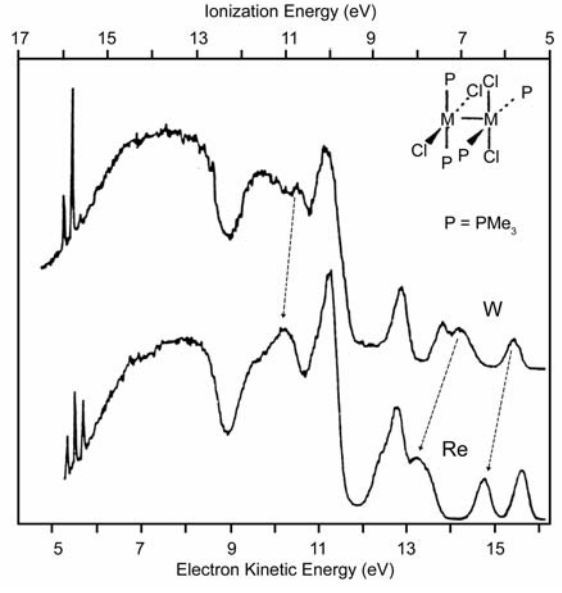


Fig 16.48. The PES (He I) of the $W_2Cl_4(PMe_3)_4$ (upper) and $Re_2Cl_4(PMe_3)_4$ (lower) molecules.

Pictiva EX2004
Samsung v Pictiva
IPR2024-01094

For the Mo and W compounds, one important result is that the δ ionization (the lowest one in each case) is significantly easier (by *c*. 0.6 eV) for the tungsten compound, in keeping with the well-known fact that W–W quadruple bonds are far more easily oxidized than Mo–Mo quadruple bonds. The π ionization is also easier for the W than for the Mo compound (7.05/7.45 eV versus 7.70 eV). The splitting of the π ionization band in the tungsten case, by *c*. 0.4 eV, has been attributed to spin-orbit coupling. However, when the results for the rhenium compound became available, they prompted a reconsideration of this assignment, and it was proposed instead that the broad band at 7.05 eV contains both components of the spin-orbit split π ionization and the band at 7.45 eV is due to the σ ionization. A similar assignment has been proposed for the PES of $MoWCl_4(PMe_3)_4$.[316] In the Re compound the σ and π ionizations are assigned at 8.83 eV and *c*. 7.93 eV. The latter band is broad and can be deconvoluted into two spin-orbit components at 7.78 and 8.09 eV. The Re compound also displays a δ* ionization, as expected.

16.5.3 M_2X_6 molecules

Only those of Mo and W have been studied although a few Ru_2R_6 species exist. The PES spectra of the Mo and W compounds[171,172,317] have provided very good evidence for the $\sigma^2\pi^4$ triple bonds and detailed information about them. The $Mo_2(OCH_2CMe_3)_6$ molecule, whose PES is shown in Fig 16.49 provides an excellent example. Theory predicts that the HOMO should be the Mo–Mo π bonding orbital with the σ orbital lying about 0.9 eV below it, and then a gap of about 1.5 eV to the next levels, which are essentially pure oxygen lone-pair orbitals. Clearly, the observed spectrum agrees very well with this.

There is, in fact, virtually quantitative agreement between the observed and calculated PES for the $Mo_2(OR)_6$ systems. The actual ionization energies, with due allowance for relaxation, as well as relative intensities, were calculated for $Mo_2(OH)_6$, and reasonable line-shape functions were applied to the resulting line diagram, with the results shown by the smooth lower curve in Fig. 16.49. The calculated spacing between the first two peaks is slightly (0.2 eV) too large and the relative intensity of the first one is apparently slightly overestimated, but the agreement with the measured spectrum is remarkably good. The apparent discrepancy for the large peak covering the oxygen lone-pair ionizations is actually not an error. Because the calculation is for OH groups while the measurement is for $OCH_2C(CH_3)_3$ groups, the disagreement of *c*. 0.90 eV is in the right direction and of about the magnitude to be expected empirically for the greater inductive effect of the neopentyl group compared to a hydrogen atom.

In a recent detailed study[317] of the σ and π region for the three $Mo_2(OR)_6$ compounds with R = $CHMe_2$, CH_2CMe_3, and CMe_3, these three spectra have been shown to be very similar, with peak separations in the range 0.62-1.01 eV. For $W_2(OCMe_3)_6$ the separation was significantly greater, namely 1.52 eV.

For $Mo_2(NMe_2)_6$ and $Mo_2(CH_2SiMe_3)_6$ the measured PE spectra also agree well with those computed for the simplified models, $Mo_2(NH_2)_6$ and $Mo_2(CH_3)_6$. The pattern of $\sigma^2\pi^4$ bonding in these molecules is unambiguously supported.

Pictiva EX2004
Samsung v Pictiva
IPR2024-01094

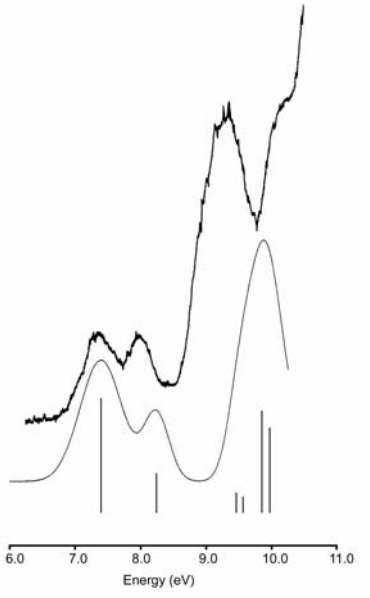


Fig. 16.49. Upper curve: Observed PES (He I) of $Mo_2(OCH_2CMe_3)_6$. Lower curve and bars: calculated PES (by SCF-Xα-SW method) for $Mo_2(OH)_6$. Energies are photoionization energies.

16.5.4 Miscellaneous other PES results

The only $Rh_2(O_2CR)_4$ compound that can be vaporized without decomposition is that with R = CF_3, and a combined PES and theoretical study has been reported for this molecule.[318] The fourteen metal-based electrons are predicted by DFT calculations to occupy the Rh–Rh bonding orbitals in the following order of increasing energy: $\sigma^2\pi^4\delta^2\delta^{*2}\pi^{*4}$. The PES (both He(I) and He(II)) supports this, with the π^* (9.55 eV) and δ^* (9.77 eV) ionizations being so close that their vibrational spreads overlap. The δ (10.61 eV) and then the overlapping σ and π (11.08 eV) ionizations follow. This same paper also gives more information on the PES of $Mo_2(O_2CCF_3)_4$.

Other dirhodium compounds, namely $Rh_2(mhp)_4$,[319] $Rh_2(DTolF)_4$,[166] and $Rh_2(DTolF)_2(O_2CCF_3)_2$[166] have also been studied. In these cases, the spectra have been assigned to a $\sigma^2\pi^4\delta^2\pi^{*4}\delta^{*2}$ configuration, with the δ^*-π^*-δ spacings being *c*. 0.85 and 0.75 eV, respectively. In the case of the $Rh_2(DTolF)_4$ compound, discrete variational-Xα calculations show how the change from a carboxyl to an amidinate ligand causes a large increase in the π^* to δ^* separation, namely from *c*. 0 eV to about 1 eV.

Ru_2 compounds.

The PE spectra of $Ru_2(O_2CCF_3)_4$ and $Ru_2(O_2CCF_3)_4(NO)_2$ have been recorded and the assignment discussed.[320,321] With regard to the former, the observed spectrum was assignable to either a $\sigma^2\pi^4\delta^2\delta^{*2}\pi^{*2}$ or a $\sigma^2\pi^4\delta^2\pi^{*3}\delta^*$ configuration. A preference for the former was expressed on the basis of some MO calculations. The result of strongly attaching NO groups at each end is that the σ-orbital is so much raised in energy that a σ ionization is responsible for the lowest energy band in the PE spectrum of $Ru_2(O_2CCF_3)_4(NO)_2$.

Pictiva EX2004
Samsung v Pictiva
IPR2024-01094

The PE spectrum of $Ru_2(mhp)_4$ was reported and assigned in accordance with a $\sigma^2\pi^4\delta^2\pi^{*3}\delta^*$ configuration.[322] However, there was no convincing basis for this and the spectrum can be at least as well explained by a $\sigma^2\pi^4\delta^2\delta^{*2}\pi^{*2}$ configuration, for which there is other evidence.

$M_2(C_3H_5)_4$ molecules.

$M_2(C_3H_5)_4$ molecules, with M = Cr or Mo, have been studied by two groups[301,323] only one of which has presented the results in detail. Because of the low symmetry of these molecules (only a mirror plane perpendicular to the M–M bond) and the lack of any MO calculations, interpretation is at best tentative. In each case, there is a weak low-energy peak (6.90 eV for Cr and 6.72 eV for Mo) that can be assigned to δ ionization with reasonable certainty. Beyond this there are many peaks at higher energies, most of which are due to ligand-based orbitals. The intensity changes from He(I) to He(II) spectra indicate that the M–M π ionizations are probably in the region of 7.89 eV.

The $Re_2(C_3H_5)_4$ molecule constitutes a quite separate case since its structure is very different from those of the group 6 $M_2(C_3H_5)_4$ molecules. $Re_2(C_3H_5)_4$ has D_{2d} symmetry and a combined MO study (by SCF-Xα-SW, including relativistic corrections but no spin-orbit coupling) and PES study has been reported.[179] The observed spectrum could be satisfactorily assigned with the δ* and δ ionizations being the lowest metal-based ones, as expected.

16.6 Vibrational Spectra

We shall discuss here only *tetragonal* systems (e.g., $M_2X_8^{n-}$, $M_2(O_2CR)_4$, $M_2X_4L_4$, etc.). There have been only a few efforts to do full vibrational analyses, whereby accurate force constants and realistic descriptions of the normal modes could be obtained. Some early attempts were a bit sketchy[324-326] but more thorough work has been done on the four $[Re_2X_8]^{2-}$ (X = F, Cl, Br, I) ions, the $[Tc_2X_8]^{n-}$ (X = Cl, Br and n = 2, 3) ions, and the $[Os_2X_8]^{2-}$ (X = Cl, Br, I) ions.[327] Significant amounts of mixing of other totally symmetric modes ($\nu_{M\text{-}X}$ and δ_{MMX}) into the normal mode generally labeled $\nu_{M\text{-}M}$ were found. In the cases of $Mo_2(O_2CCH_3)_4$[328] and the $[Mo_2(SO_4)_4]^{n-}$ species[329] it has been found that the frequency shifts resulting from ^{92}Mo for ^{95}Mo substitution support the assumption that the "Mo–Mo stretch" is reasonably pure. On the other hand, there are cases (vide infra) in which this normal mode entails significant mixing of other internal coordinates.

There are a great many data scattered through the literature; many were simply noted in passing as part of studies having others purposes. No claim is made here to have vacuumed the literature for all reported vibrational data. Major emphasis is placed on the normal mode that can be called, with varying degrees of rigor, the metal-metal stretching mode, $\nu_{(M\text{-}M)}$, in both the ground electronic state, $^1A_{1g}$ (δ^2), and the $^1A_{2u}$ ($\delta\delta^*$) excited state, but in most cases the extent of coupling is assumed (or known) to be small.

16.6.1 M–M stretching vibrations

The first vibrational studies[324,330] of L_4MML_4 compounds were published in 1971; the data were derived only from conventional Raman spectra and infrared spectra. In 1973 it was first observed that impressive resonance Raman (RR) effects could be obtained[331] and this has since been widely exploited and with very telling effect by R. J. H. Clark and co-workers.[332]

The most thoroughly studied feature of the vibrational spectra of the L_4MML_4 systems is the Raman band attributed to metal-metal stretching. This totally symmetric vibration, ν(M–M), is active only in the Raman spectrum for the homonuclear molecules and is especially susceptible to resonance enhancement when excitation occurs in the $\delta\rightarrow\delta^*$ band of the visible spectrum. Other electronic bands that produce excited states in which the M–M distance is

Pictiva EX2004
Samsung v Pictiva
IPR2024-01094

appreciably changed have also been used for resonance enhancement of ν(M–M) and in certain cases transitions that involve excitation into M–L antibonding orbitals have been observed to give resonance enhancement to the totally symmetric M–L stretching mode, ν(M–L), as discussed in Section 16.6.2.

Resonance Raman (RR) spectra have been employed in two ways. One is to obtain greater intensity for the relevant totally symmetric vibration as well as many of its overtones and combination bands. An early and excellent example[333] of this is shown in Fig. 16.50. From the frequencies of so many overtones the anharmonicity constant for ν(M–M) can be accurately determined and this, in turn, allows estimation of the M–M bond dissociation energy by means of a Birge-Sponer extrapolation, as already mentioned in Section 16.2.2.

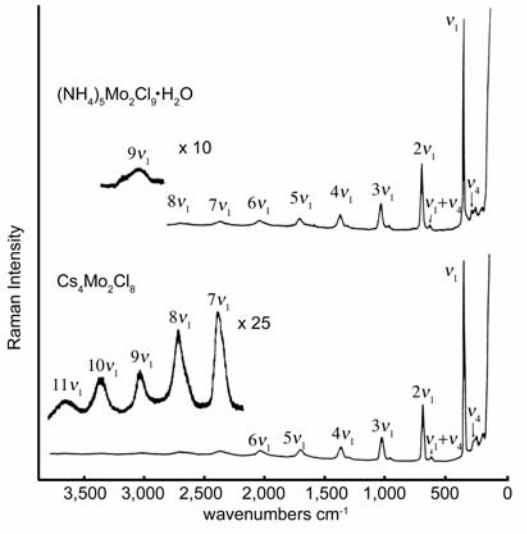


Fig. 16.50. Resonance Raman spectra of two compounds containing the $[Mo_2Cl_8]^{4-}$ ion, recorded with a 514.5 nm exciting line.

On the other hand, it is possible to use the dependence of the RR effect upon the frequency of the exciting line to provide evidence for assignments in the electronic spectrum. This entails the measurement of the *excitation profile* of a particular Raman line, as for example the ν(M–M) line. Such a profile is shown in Fig. 16.51 for $[Re_2F_8]^{2-}$. It can be seen that the excitation profile corresponds closely to the shape and position of an absorption band in the electronic spectrum, which shows that the electronic transition responsible for the absorption band must entail an excited state in which the M–M distance is changed. This provides a criterion of correctness that any proposed assignment of that band must satisfy. In the case shown, the RR evidence supports the $\delta^2 \rightarrow \delta\delta^*$ assignment.

In the unique case[334] of $MoWCl_4(PMe_3)_4$ the metal–metal stretch, ν(Mo–W), has been seen in the infrared as a band of medium intensity at a frequency of 326 cm^{-1} in as well as in the Raman at 322 cm^{-1}.

Especially thorough studies[335,336] have been made of the $M_2X_4L_4$ compounds in which M = Mo or W, X = Cl, Br, I, and L = and R_3P or R_3As ligands. For the series $Mo_2X_4(PMe_3)_4$ with X = Cl, Br and I, the ν(Mo–Mo) frequencies are nearly invariant, viz., 355, 352 and 342 cm^{-1}, respectively. A normal coordinate analysis of $Mo_2Cl_4(PMe_3)_4$ showed that the vibration at 355 cm^{-1} is 86% localized in the Mo–Mo bond.

Pictiva EX2004
Samsung v Pictiva
IPR2024-01094

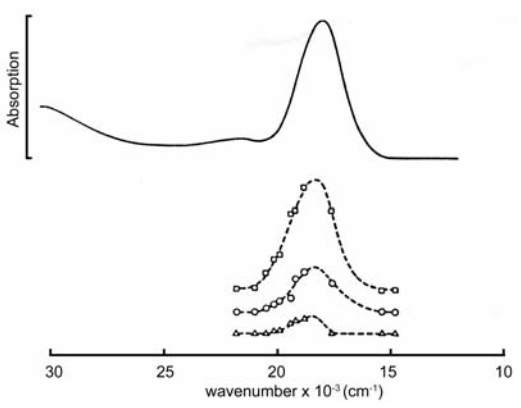


Fig. 16.51. An example of excitation profiles in RR spectra. Upper curve is the electronic absorption spectrum of the $[Re_2F_8]^{2-}$ ion, featuring the $\delta^2 \rightarrow \delta\delta^*$ transition. Below are plots of Raman line intensities versus frequency for the ν(Re–Re) line and its first two overtones.

An instructive example[337] of the danger of superficial interpretation is afforded by the $[Mo_2(CN)_8]^{4-}$ ion, where isotopomers containing (nearly) all ^{12}C and (nearly) all ^{13}C can be compared. The Raman band at 411 cm^{-1} in the ^{12}C ion which is resonance-enhanced by excitation in the $\delta \rightarrow \delta^*$ band (at *c.* 600 nm) would, loosely speaking, be called the ν(Mo–Mo) band. Yet, with data from both isotopomers, this band (which shifts only a little to 406 cm^{-1}, in the ^{13}C isotopomer) is found to be far from a pure Mo–Mo stretch. In fact, the normal coordinate for this vibration has only 50-60% ν(Mo–Mo) character, and 30-40% Mo–C–N wagging character.

Similarly, in $Mo_2(CCH)_4(PMe_3)_4$ a normal coordinate analysis based on data for isotopomers showed that the "ν(Mo–Mo)" Raman band has only about 54% ν(Mo–Mo) character combined with 18% ν(Mo–C), 12% δ(Mo–Mo–C) and 8% of Mo–C≡C wagging.[336]

When the purity of the ν(M–M) vibrations can be accepted as a valid approximation, force constants may be calculated for the M–M bonds by assigning the frequencies to a diatomic harmonic oscillator, M_2. The values so obtained, some of which are listed in Table 16.11, are useful for comparative purposes even though they do not have absolute validity.

Table 16.11. ν(M–M) frequencies for multiply bonded dimetal species

Compound	ν(M–M) (cm^{-1})	k (mdyne $Å^{-1}$)[a]	ref.
	A. Quadruple bonds		
$(NEt_4)_4[Mo_2(CN)_8]$	411		338
$K_4[Mo_2Cl_8]$	345		331,333
$K_4[Mo_2Cl_8]\cdot 2H_2O$	345		331
$Cs_4[Mo_2Cl_8]$	340		333
$Rb_4[Mo_2Cl_8]$	338		333
$(enH_2)_2[Mo_2Cl_8]\cdot 2H_2O$	348		331,333
$(NH_4)_5[Mo_2Cl_8]Cl\cdot H_2O$	350,338		331,333
$[Mo_2(CH_3)_8]^{4-}$ in benzene	336		339
$(C_4H_8ONH)_2[Mo_2Cl_6(H_2O)_2]$	357		340
$(C_4H_8ONH)_2[Mo_2Br_6(H_2O)_2]$	350		340
$(C_5H_5NH)_2[Mo_2I_6(H_2O)_2]$	340		340

Pictiva EX2004
Samsung v Pictiva
IPR2024-01094

Compound	ν(M–M) (cm^{-1})	k (mdyne $Å^{-1}$)[a]	ref.
$Mo_2(O_2CH)_4$	406		341
$Mo_2(O_2CH)_4H_2O$	410		341
$Mo_2(O_2CH)_4(DMSO)_2$	360		341
$Mo_2(O_2CCH_3)_4$	404		324,342, 343,344
$Mo_2(O_2CCD_3)_4$	403		344
$Mo_2(O_2CCH_3)_4{\cdot}2py$	363		345
$Mo_2(O_2CCF_3)_4$	397		342,345
$Mo_2(O_2CCF_3)_4{\cdot}2py$	367		342,345
$[Mo_2(O_2CCH_3)_4]^+$ (gas)	360		268
$CrMo(O_2CCH_3)_4$	393		346
$Mo_2[(CH_2)_2P(CH_3)_2]_4$	388		220
$Mo_2[O_2C(2,4,6\text{-}Me_3C_6H_2)]_4$	404		347
$Mo_2[O_2C(4\text{-}CN\text{-}C_6H_4)]_4$	397		347
$Mo_2[O_2C(4\text{-}MeO\text{-}C_6H_40]_4$	402		347
$K_2[Mo_2(SO_4)_4]{\cdot}2H_2O$	371		229,331, 348,349
$Mo_2[PhNC(Ph)NPh]_4$	410		350
$Mo_2[(tol)NC(Ph)N(tol)]_4$	416		350
$Mo_2Cl_4(PMe_3)_4$	355	3.54	197,276,334, 335,336
$Mo_2Br_4(PMe_3)_4$	352		197,276,335
$Mo_2I_4(PMe_3)_4$	343		197,276,335
$Mo_2Cl_4(AsMe_3)_4$	356		197,335
$Mo_2Cl_4(PBu^n_3)_4$	350	3.46	334,342
$Mo_2Cl_4[P(OMe)_3]_4$	347		342
$Mo_2Cl_2(O_2CPh)_2(PBu^n_3)_2$	392		347
$Mo_2Br_2(O_2CPh)_2(PBu^n_3)_2$	383		347
$Mo_2Br_2[O_2C(2,4,6\text{-}Me_3C_6H_2)]_2(PBu^n_3)_2$	383		347
$Mo_2(OEP)_2$	341	3.29	351
$Cr_2(mhp)_4$	556	4.73	18
$CrMo(mhp)_4$	504	5.03	313
$Mo_2(mhp)_4$	425	5.10	352
$MoW(mhp)_4$	384	5.45	352
$MoWCl_4(PMe_3)_4$	322(R), 326(ir)		334
$W_2(O_2CCH_3)_4$	204		353
$W_2(O_2CCMe_3)_4$	313		353
$W_2(O_2CCMe_3)_4(PPh_3)_2$	287		353
$W_2(O_2CCF_3)_4$	310		354
$W_2(O_2CCF_3)_4(PPh_3)_2$	280		354
$W_2(mhp)_4$	284	4.71	18
$W_2Cl_4(PBu^n_3)_4$	260	3.65	334,355
$Re_2(O_2CR)_4Cl_2$[b]	288-295		330,342
$Re_2(O_2CR)_4Br_2$[b]	277-284		330,342
$Re_2(O_2CCH_3)_2Cl_4{\cdot}2H_2O$	279		330,342
$Re_2(O_2CCH_3)_2Br_4{\cdot}2H_2O$	277		330,342
$(Bu^n_4N)_2[Re_2F_8]$	318	5.55	204,356,357

Pictiva EX2004
Samsung v Pictiva
IPR2024-01094

Compound	ν(M–M) (cm^{-1})	k (mdyne $Å^{-1}$)[a]	ref.
$(Bu^n_4N)_2[Re_2Cl_8]$	272,275	4.12	204,280,342, 357,358
$(Bu^n_4N)_2[Re_2Br_8]$	276	4.18	204,342,357, 358
$(Bu^n_4N)_2[Re_2I_8]$	257		204,357,359
$Re_2Cl_6(PPr^n_3)_2$	278		342
$Re_2Cl_6(PPh_3)_2$	278		360
$Re_2Br_6(PPh_3)_2$	285		360
$Re_2Cl_6[Me_2N)_2CS]_2$	276		342
$[Mo_2(HPO_4)_4]^{4-}$	345		287
$Tc_2(O_2CCH_3)_2Cl_4(CH_3C(O)NMe_2)_2$	290	3.38	237
$Re_2(O_2CCH_3)_2Cl_4(CH_3C(O)NMe_2)_2$	265		237
$Mo_2(O_2CH)_4L_2$ (L = various aromatic amines)	350-361		361
B. Lower bond orders			
$K_3Mo_2(SO_4)_4 \cdot 3.5H_2O$	373,385[c]		235,348
$K_4[Mo_2(SO_4)_4]Cl \cdot 4H_2O$	369		349
$K_4[Mo_2(SO_4)_4]Br \cdot 4H_2O$	370		349
$[Mo_2(HPO_4)_4]^{3-}$	352		287
$Cs_2[Mo_2(HPO_4)_4] \cdot 2H_2O$	358		229,287
$(C_5H_5NH)_3[Mo_2(HPO_4)_4]Cl$	361		229
$Re_2Cl_5(MeSCH_2CH_2SMe)_2$	267		342
$Re_2Cl_5(PEtPh_2)_3$	277		362
$[Re_2(OEP)_2]^+$ (in THF)	290	4.61	351
$Ru_2(O_2CH)_4Cl$	331,339		244,245
$K[Ru_2(O_2CH)_4Cl_2]$	335		244
$Ru_2(O_2CCH_3)_4Cl$	326		242,245
$[Ru_2(O_2CCH_3)_4(H_2O)_2]^+$	326		245
$Ru_2(O_2CEt)_4Cl$	338		242,245
$Ru_2(O_2CPr)_2Cl$	328,331		242,245
$Ru_2(O_2CCH_3)_4Br$	321		242
$(Bu^n_4N)[Ru_2(O_2CEt)_4Br_2]$	325		242
$Ru_2(O_2CPr)_4Br$	329		242
$Ru_2(OEP)_2$	285	2.42	351
$[Ru_2(OEP)_2]^+$ (in THF)	301	2.70	351
$[Ru_2(OEP)_2]^{2+}$ (in THF)	310	2.86	351
$(NBu_4)_2[Os_2Cl_8]$	285		247
$(NBu_4)_2[Os_2Br_8]$	287		247
$(NBu_4)_2[Os_2I_8]$	270		247
$Os_2(O_2CCH_2Cl)_4Cl_2$	236		363
$Os_2(O_2CC_2H_5)_4Cl_2$	233		363
$Os_2(O_2CC_3H_7)_4Cl_2$	228		362 363
$Os_2(O_2CCH_3)_4Cl_2$	229		364
$Os_2(O_2CCD_3)_4Cl_2$	230		364
$Os_2(OEP)_2$	233	2.94	351
$[Os_2(OEP)_2]^+$ (in THF)	254	3.46	351
$[Os_2(OEP)_2]^{2+}$ (in THF)	266	3.79	351
$[Rh_2(O_2CCH_3)_4Br_2]^-$	286		365

Pictiva EX2004
Samsung v Pictiva
IPR2024-01094

Compound	ν(M–M) (cm^{-1})	k (mdyne Å^{-1})[a]	ref.
$[Rh_2(O_2CCH_3)_4I_4]^-$	314		365
$Rh_2(O_2CCH_3)_4(PPh_3)_2$	289		366,367,368,369
$Rh_2(O_2CCH_3)_4(AsPh_3)_2$	297		370,371
$Rh_2(O_2CCH_3)_4(SbPh_3)_2$	307		367,371
$Rh_2(O_2CCH_3)_4(PPh_3)_4$	226		372
$Rh_2(O_2CH)_4(PPh_3)_2$	286		368
$Rh_2(O_2CC_2H_5)_4(PPh_3)_2$	287		368
$Rh_2(O_2CC_3H_7)_4(PPh_3)_2$	299		368
$Rh_2(CH_3CONH)_4(PPh_3)_2$	275		369,371
$Rh_2(CH_3CONH)_4(AsPh_3)_2$	283		369,371
$Rh_2(CH_3CONH)_4(SbPh_3)_2$	294		371
$Rh_2(CF_3CONH)_4(PPh_3)_2$	277		369
$[Rh_2(O_2CCH_3)_4(PPh_3)_2]^+$	302		369
$[Rh_2(CH_3CONH)_4(PPh_3)_2]^+$	264		369
$[Rh_2(CH_3CONH)_4(AsPh_3)_2]^+$	283		369
$[Rh_2(CF_3CONH)_4(PPh_3)_2]^+$	277		369
$Rh_2(O_2CCH_3)_4$	355[d]		373
$Rh_2(O_2CCH_3)_4(H_2O)_2$	~340[d]		371

[a] Force constants in md Å^{-1} are calculated from $k = (5.889 \text{ H } 10^{-7})\nu^2\mu$, where 10 pt is the frequency in cm^{-1} and $\mu = M_AM_B/(M_A + M_B)$ with M_A and M_B representing atomic masses in Daltons.

[b] R may be CH_3, C_2H_5, C_3H_7, C_6H_{11} or C_6H_5.

[c] There are two crystallographically distinct $[Mo_2(SO_4)_4]^{3-}$ units in the solid.

[d] These values are far higher than any other ν(Rh–Rh) reported, but they occur in compounds with the shortest Rh–Rh bonds, viz. 2.385 Å in $Rh_2(O_2CCH_3)_4(H_2O)_2$ compared to 2.450 Å in $Rh_2(O_2CCH_3)_4(PPh_3)_2$.

The data in Table 16.11 provide some useful comparisons. For example, within the series of five $MM'(mhp)_4$ compounds, with M and M' representing Cr, Mo or W, as well as $MM'Cl_4(PR_3)_4$ (M,M' = Mo, W), we see that the mixed metal species, especially the MoW ones, have bonds that are stronger than would be predicted by linear interpolation between the homonuclear species.

A number of data in Table 16.11 show that axial ligands appreciably lower the stretching frequencies of M–M quadruple bonds. For example, for $Mo_2(O_2CR)_4$ molecules, the axial ligands lower ν(Mo–Mo) by 30-40 cm^{-1} even though the Mo–Mo bond lengths change by only *c*. 0.02 Å.

When electronic transitions are examined at low temperatures with sufficient resolution, they often display vibrational fine structure, as we have already noted in Section 16.4. For an allowed transition, such as δ→δ*, the vibrational progressions should be in the totally symmetric skeletal modes, i.e. in ν(M–M), in the totally symmetric M–L stretching mode, ν(M–L), and in the totally symmetric M–M–L bending mode, δ(M–M–L). The extent to which each of these contributes depends on how much the electronic excitation alters the internal coordinate (that is, *d*(MM), *d*(ML) or <MML) involved in the vibrational mode. For a δ→δ* transition the main effect is on *d*(MM) and hence strong progressions in ν(M–M) (or its combination with another mode) are the predominant vibrational feature. Thus, since much of the work on electronic spectra has dealt with δ→δ* transitions, a body of data has accumulated on the frequencies of M–M stretching in the state $^1A_{2u}$, arising from the $\sigma^2\pi^4\delta\delta^*$ configuration. Some of these are listed in Table 16.12 where they are designated ν'(M–M) to distinguish them from the ground state ν(M–M) values. A δ→δ* promotion lowers the M–M stretching frequency by amounts ranging from 10 to 50 cm^{-1}.

Pictiva EX2004
Samsung v Pictiva
IPR2024-01094

Table 16.12. Metal–metal stretching frequencies in the ground state and δ→δ* excited state,[a] ν(M–M) and ν'(M–M), respectively, in cm^{-1}.

Compound	ν(M–M)	ν'(M–M)	ν–ν'	ref
$[Mo_2Cl_8]^{4-}$	346	336	10	200,333
$(NH_4)_4[Mo_2Br_8]$	336	320	16	374
$Mo_2[(CH_2)_2P(CH_3)_2]_4$	388	345	43	220
$K_3[Mo_2(SO_4)_4]\cdot 3.5H_2O$	373,385	350,357	25	222,223,348
$K_3[Mo_2(HPO_4)_4]$	352	334	18	287
$(C_4H_8ONH)_2[Mo_2Cl_6(H_2O)_2]$	357	320	27	340
$(C_4H_8ONH)_2[Mo_2Br_6(H_2O)_2]$	350	320	30	340
$(C_5H_5NH)_2[Mo_2I_6(H_2O)_2]$	340	320	20	340
$Mo_2(O_2CH)_4$	403	360	43	122,375
$Mo_2(O_2CCH_3)_4$	406	370	36	212,331,342
$Mo_2(O_2CCH_3)_4$ (in argon matrix)	–	390	–	215
$Mo_2(O_2CCF_3)_4$	397	356	41	212,342,345
$Mo_2(O_2CCF_3)_4py_2$	367	331	36	376
$Mo_2Cl_4(PMe_3)_4$	358	335	22	276
$Mo_2Br_4(PMe_3)_4$	353	340	13	276
$Mo_2I_4(PMe_3)_4$	345	320	25	276
cis-$[Mo_2(mhp)_2Cl_2(PEt_3)_2]$	–	370	–	225
$Ru_2(O_2CH)_4Cl$	331	280	51	244
$K[Ru_2(O_2CH)_4Cl_2]$	335	312	23	244
$(NBu^n_4)_2[Re_2Cl_8]$	272	247	25	104,358
$(NBu^n_4)_2[Re_2Br_8]$	275	255	20	201,280, 358,203
$(NBu^n_4)_2[Re_2I_8]$	257	240	17	377
$K_3[Tc_2Cl_8]\cdot 2H_2O$	370	320	50	199,221
$Tc_2(hp)_4Cl$	383	337	46	221
$(NBu^n_4)_2[Os_2Cl_8]$[b]	285	195	90	247
$(NBu^n_4)_2[Os_2Br_8]$[b]	287	211	76	247
$(NBu^n_4)_2[Os_2I_8]$[b]	270	183	87	247

[a] Unless otherwise stated.

[b] In these the excitation is believed to be δ→π*.

Most values of ν' have been obtained in low-temperature studies of crystalline compounds. Under these conditions it seems likely that the $^1A_{2u}$ excited state is constrained to remain in an eclipsed or nearly eclipsed conformation. In the case of $(NBu^n_4)_2[Re_2Cl_8]$ there is direct evidence for this.[280] For $[Re_2Cl_8]^{2-}$ in solution, a time-resolved RR study[272] has allowed measurement of the ν(Re–Re) vibration for the relaxed, staggered excited state, and this frequency, 262 cm^{-1} is intermediate between those for the eclipsed ground state (276 cm^{-1}) and the eclipsed $^1A_{2u}$ (δδ*) state (249 cm^{-1}). This seems reasonable and by an empirical rule relating bond lengths to force constants it has been estimated that the Re–Re distances are 2.239, 2.276, and 2.320 Å for the $^1A_{1g}(\delta^2)$, staggered excited, and $^1A_{2u}$ (δδ*) states, respectively.

16.6.2 M–L stretching vibrations

Of the many other modes of vibration for M_2X_8, $M_2(O_2CR)_4L_2$ and similar species, those of next most interest, after ν(M–M) and ν'(M–M) are the metal-ligand stretching modes for the equatorial ligands, especially the totally symmetric ones.

Pictiva EX2004
Samsung v Pictiva
IPR2024-01094

In the $[Re_2X_8]^{2-}$ ions and $Mo_2X_4L_4$ molecules the totally symmetric M–X frequencies have been observed by Raman spectroscopy. The results are given in Table 16.13. These values are approximately those one would expect from those known in classical MX_6^{n-} and MX_4^{n-} complexes.

Table 16.13. Some metal–ligand stretching frequencies[a]

Compound	M–L	ν (cm^{-1})	ref.
$[Mo_2Cl_6(H_2O)_2]^{2-}$	Mo–Cl	325	265
$[Mo_2Br_6(H_2O)_2]^{2-}$	Mo–Br(?)	168	265
$[Mo_2I_6(H_2O)_2]^{2-}$	Mo–I	149	265
$Mo_2Cl_4(PMe_3)_4$	Mo–Cl	274 (284)[b]	197,276[b]
	Mo–P	235	197
$Mo_2Cl_4(AsMe_3)_4$	Mo–Cl	278	197
	Mo–As	217	197
$Mo_2Br_4(PMe_3)_4$	Mo–Br	159 (165)[b]	197,276[b]
	Mo–P	235	197
$Mo_2I_4(PMe_3)_4$	Mo–I	105[c] (143)[b]	197[c],276[b]
	Mo–P	217	197
$[Re_2F_8]^{2-}$	Re–F	623.5[d]	204,357
$[Re_2Cl_8]^{2-}$	Re–Cl	361	204,245
$[Re_2Br_8]^{2-}$	Re–Br	211	204,245
$[Re_2I_8]^{2-}$	Re–I	152	204

[a] These are the totally symmetric modes in the ground state unless otherwise noted.
[b] From emission spectra.
[c] Doubtful value. Also band at 148 cm^{-1} that agrees better with emission value.
[d] IR-active modes at 568, 560, 552 cm^{-1}.

The assignment of M–O stretching frequencies, especially the totally symmetric one, in $M_2(O_2CR)_4$ molecules has been of importance in connection with assigning electronic absorption bands. In several cases, e.g., the $Rh_2(O_2CR)_4L_2$ molecules (see Section 16.4.3), transitions to π*(M–O) orbitals are prominent and the assignment of such transitions can be supported by the observation of progressions in the totally symmetric M–O stretching mode of the excited state.

It is not always obvious which frequency should be assigned to ν(M–M) and which to the totally symmetric ν(M–O) mode since the two often occur in the same frequency range. Some representative data are collected in Table 16.14.

Table 16.14. Some totally symmetric M–O stretching frequencies in $M_2(O_2CR)_4L_2$ molecules

Compound	Frequency (cm^{-1})	ref.
$Mo_2(O_2CH)_4L_2$[a]	350-400	341
$Mo_2(O_2CCH_3)_4$	323	344,328
$[Ru_2(O_2CCH_3)_4(H_2O)_2]^+$	371	245
$Ru_2(O_2CH)_4Cl$	432,440	243,245
$Ru_2(O_2CCH_3)_4Cl$	371	245
$Ru_2(O_2CC_2H_5)_4Cl$	395	245
$Ru_2(O_2CC_3H_7)_4Cl$	377,435	242,245

Pictiva EX2004
Samsung v Pictiva
IPR2024-01094

Compound	Frequency (cm^{-1})	ref.
$Os_2(O_2CCH_3)_4Cl_2$	393	364
$Os_2(O_2CCD_3)_4Cl_2$	375	364
$Os_2(O_2CCH_2Cl)_4Cl_2$	271	363
$Os_2(O_2CC_2H_5)_4Cl_2$	321	363
$Os_2(O_2CC_3H_7)_4Cl_2$	256	363
$Rh_2(O_2CCH_3)_4(CH_3CN)_2$	344	365
$Rh_2(O_2CCH_3)_4(H_2O)_2$	342	365
$[Rh_2(O_2CCH_3)_4Cl_2]^{2-}$	342	365
$[Rh_2(O_2CCH_3)_4Br_2]^{2-}$	338	365
$[Rh_2(O_2CCH_3)_4I_2]^{2-}$	338	365
$Rh_2(O_2CH)_4(PPh_3)_2$	402	368
$Rh_2(O_2CCH_3)_4(PPh_3)_2$	338	368
$Rh_2(O_2CC_2H_5)_4(PPh_3)_2$	310	368
$Rh_2(O_2CC_3H_7)_4(PPh_3)_2$	289	368
$Rh_2(^{18}O_2CCH_3)_4(PPh_3)_2$	332	367
$Rh_2(O_2CCD_3)_4(PPh_3)_2$	325	367

[a] See text.

It is evident that the frequency of the totally symmetric M–O stretching mode (and, presumably, the other ν(M–O) modes) is enormously sensitive to the mass of the group R in $M_2(O_2CR)_4L_2$ compounds. Thus in the Rh compounds, $Rh_2(O_2CR)_4(PPh_3)_2$ through the series R = H, CH_3, C_2H_5, C_3H_7, the frequency drops: 402, 338, 310, 289 cm^{-1}, respectively. Simply replacing CH_3 by CD_3 changes the frequency from 338 to 325 cm^{-1}. Similar changes occur with the other metals.

16.7 Other types of Spectra

16.7.1 Electron Paramagnetic Resonance

EPR spectra have not played a general role in the characterization of compounds with metal-metal bonds because relatively few of them are suitable for EPR study. However, in certain cases, EPR spectra afford valuable information. Unless otherwise noted, spectra mentioned were recorded at X-band frequency (*c.* 9.5 GHz)

Seven-electron Compounds.

The $Mo_2Cl_8^{3-}$ ion is short-lived and its EPR spectrum has not been detected.[378] However, numerous paddlewheel Mo_2^{5+} species have been observed. The first report[378] of an $Mo_2(O_2CR)_4^{+}$ ion was for the electrogenerated ion with R = *n*-C_3H_7. The spectrum indicated that the unpaired electron is delocalized over both Mo atoms and was fitted with $g_{\parallel} = g_{\perp} = 1.941$. An X-band spectrum[379] of the ion with R = 2, 4, 6-triisopropylphenyl, showed a resonance at $g_{\parallel} = g_{\perp} = 1.936$ with coupling to both Mo atoms, while a W-band (92.5 GHz) spectrum,[380] at 10 K showed $g_{xx} = 1.9310$, $g_{yy} = 1.9358$ and $g_{zz} = 1.9427$, although resolution of g_{xx} and g_{yy} was uncertain and would not be expected for axial symmetry.

A few other Mo_2^{5+} species have given EPR spectra. The $[Mo_2(SO_4)_4]^{3-}$ ion was one of the earliest,[381] for which $g_{\parallel} = 1.891$ and $g_{\perp} = 1.901$. These g values are consistent with the $\sigma^2\pi^4\delta$ configuration.[382] The $[Mo_2(HPO_4)_4]^{3-}$ ion has a very similar spectrum with $g_{\parallel} = 1.886$ and $g_{\perp} = 1.894$.[287]

Pictiva EX2004
Samsung v Pictiva
IPR2024-01094

Data for Cr_2^{5+} and V_2^{3+} have only recently become available. The paddlewheel complex $\{Cr_2[PhN)_2CN(CH_2)_4]_4\}PF_6$ has been examined at W-band frequency (95 GHz) at 295 K and found to have $g_{\parallel}$ = 1.9701 and $g_{\perp}$ = 1.9767.[380] The anion $[V_2(DPhF)_4]^+$ displays an X-band spectrum at 6 K which consists of 15 hyperfine components (coupling to two ^{51}V nuclei each with I = $^7/_2$) with g_{av} = 1.9999,[383] thus showing one unpaired electron delocalized over the V_2^{3+} core.

Nine-electron compounds.

The $[Tc_2Cl_8]^{3-}$ ion provided the first example of the $\sigma^2\pi^4\delta^2\delta^*$ configuration, and the most conclusive evidence for its authenticity is undoubtedly its EPR spectrum.[384] Liquid solutions gave no spectrum, but certain frozen solutions (*c.* 10^{-3} M in a mixture of aqueous HCl and ethanol) at 77 K gave good spectra. Both X- and Q-band spectra were obtained. These spectra showed unequivocally the presence of one unpaired electron with hyperfine coupling to two equivalent ^{99}Tc (I = 9/2) nuclei. Analysis afforded the following parameters: $g_{\parallel}$ = 1.912, $g_{\perp}$ = 2.096, $|A_{\parallel}|$ = 166 x 10^{-4} cm^{-1}, and $|A_{\perp}|$ = 67 x 10^{-4} cm^{-1}. The qualitative facts, $g_{\parallel} < 2.00$ and $g_{\perp} > 2.00$, have been shown[382] to be consistent with the assignment of the unpaired electron to the δ^*-orbital, although it cannot be said that they uniquely demand this assignment.

Numerous Re_2^{5+} compounds have been shown to have EPR spectra consistent with the $\sigma^2\pi^4\delta^2\delta^*$ configuration. These, which have all been discussed in Chapter 8, include $Re_2Cl_8^{3-}$, $[Re_2(O_2CR)_4X_2]^-$, $[Re_2X_4(PR_3)_4]^+$, $[\beta\text{-}Re_2Cl_4(diphos)_2]^+$, $\beta\text{-}Re_2Cl_5(dppm)_2$, *inter alia.* Because of the large number of hyperfine components, detailed interpretation of the signals in elusive, but they are always consistent with delocalization of one electron over the two rhenium atoms.

It is uncertain whether the configuration in $[Os_2(hpp)_4Cl_2]^+$ is $\sigma^2\pi^4\delta^2\delta^*$ or $\sigma^2\pi^4\delta^2\pi^*$, but the observed EPR signal[385] is very unusual. It appears at a g value of 0.8 which is consistent with the bulk magnetic susceptibility, but the line width is about 6000 G.

Eleven-electron compounds.

The EPR spectra of Ru_2^{5+} and Os_2^{5+} compounds [386-389] are all affected by very large zero-field splitting of their S = $^3/_2$ ground states, which has made complete development of the spin Hamiltonian impossible. The g values for the Ru_2^{5+} compounds are generally 2.1 to 2.2 for S = ½. Similar results were obtained for a few Os_2^{5+} compounds.[390,391]

Thirteen-electron compounds.

These are the compounds of cobalt, rhodium and iridium with M_2^{5+} cores. For M_2^{4+} cores, there is a metal–metal bond of order one, based, unambiguously, on a $\sigma^2\pi^4\delta^2\delta^{*2}\pi^{*4}$ configuration. In many cases, stable singly oxidized species, where the configuration is probably $\sigma^2\pi^4\delta^2\delta^{*2}\pi^{*3}$ (but might be $\sigma^2\pi^4\delta^2\pi^{*4}\delta^*$) have been studied by EPR spectroscopy. The EPR spectrum of the electrochemically generated (but not isolated) $[Co_2(PhNCPhNPh)_4]^+$ ion shows a signal at $g_{\parallel}$ = 1.98, split into 15 equally spaced lines by two cobalt atoms, each with I = $^7/_2$.[392] The compound $Ir_2(DAniF)_4(O_2CCF_3)$, which was isolated and structurally characterized,[393] has an EPR spectrum in frozen CH_2Cl_2 (-100 °C) with g_{iso} of 2.14.

Compounds containing the Rh_2^{5+} core are very numerous and have been extensively studied. These have been cited in Chapter 12 where literature references that need not be repeated here were given. Many of these compounds show axial spectra, which have $2.05 \leq g_{\perp} \leq 2.09$ and $1.91 \leq g_{\parallel} \leq 1.98$. The $g_{\parallel}$ component nearly always shows hyperfine coupling to one or both $Rh(I_s = 1/2)$ nuclei, depending on whether the Rh_2^{5+} core is in a symmetric environment that allows the unpaired electron to be delocalized or whether the electron is constrained to only one rhodium atom. For example the symmetric $[Rh_2(PhNCPhNPh)_4]^+$ ion displays a triplet

Pictiva EX2004
Samsung v Pictiva
IPR2024-01094

($A_{||}$ = 19.5x10^{-4} cm^{-1})[394] while in the unsymmetrical (3,1) $Rh_2(ap)_4Cl$ molecule there is a doublet ($A_{||}$ = 20.5 x 10^{-4} cm^{-1})[395]. Such spectra are believed to be due to a $\sigma^2\pi^4\delta^2\pi^{*4}\delta^*$ electron configuration.[162,396,397]

For many $[Rh_2(OCCH_3)_4L_2]^+$ with L = H_2O, CH_3OH, THF, CH_3CN and $(CH_3)_2CO$ the g values, which are $0.6 \leq g_\perp \leq 1.87$ and $3.38 \leq g_{||} \leq 4.00$ have been interpreted as evidence for a $\sigma^2\pi^4\delta^2\delta^{*2}\pi^{*3}$ configuration.[396,397]

Fifteen-electron compounds.

Some compounds of the elements Ni, Pd and Pt with M_2^{4+} cores are known and have M–M bond orders of zero. Some of the M_2^{5+} species have been obtainable by oxidation,[398] and their EPR spectra are consistent with a $\sigma^2\pi^4\delta^2\delta^{*2}\pi^{*4}\sigma^*$ configuration. In the case of $[Ni_2(DTolF)_4]^+$ in frozen CH_2Cl_2, the X-band spectrum clearly shows that it is a metal-centered radical with axial symmetry ($g_{||}$ = 2.038 and $g_\perp$ = 2.210). Under the same conditions the palladium analog displayed only a symmetric line with g = 2.014 and it was proposed on this basis, plus structural evidence, that the unpaired electron might be delocalized essentially on the ligands.[398] However, later work on a powder sample at 10 K, with a 92.5 GHz field revealed $g_{||}$ = 1.9945 and $g_\perp$ = 2.0202, thus supporting a metal-centered radical here too.[399] It has also been reported that the $Pd_2[(PhNCPhNPh)_4]^+$ ion has an axially symmetrical EPR signal with $g_{||}$ = 1.98 and $g_\perp$ = 2.17.[400]

Another fifteen-electron configuration is found in $Rh_2[(PhN)_2CPh]_4^-$, generated electrochemically.[394] It has $g_\perp$ = 2.181 and $g_{||}$ = 2.003 (triplet) and indicates that the odd electron is in a symmetrical σ_{RhRh} orbital.

Irradiation of $Rh_2(O_2CR)_4$ compounds with gamma rays gave unstable species with EPR spectra consistent with the presence of a lone σ^* electron.[401]

Miscellaneous.

The trigonal molecule $Fe_2(DPhF)_3$ has a ground state with seven unpaired electrons (μ_{eff} = 7.81 BM). Consistent with this, it has an EPR spectrum in frozen toluene glass that presents two signals corresponding to g values of 1.99 and 7.94.[402]

16.7.2 X-Ray spectra, EXAFS, and XPS

Core electron binding energies of a variety of dinuclear multiply-bonded complexes, which have been recorded using the X-ray photoelectron spectroscopic technique (XPS), are consistent with those expected for low-valent "electron-rich" metal centers. Extensive Re 4*f* and Mo 3*d* binding energy data are available for quadruply-bonded dirhenium[403-407] and dimolybdenum[408,409] complexes. It was suggested[410] on the basis of Mo 3*d* XPS studies that Mo-silica catalysts prepared from $Mo_2(O_2CR)_4$ may have different metal-support interactions from other Mo catalysts. In the case of chlorine-containing dinuclear complexes, measurements of the Cl 2*p* binding energies can be used to distinguish between terminal and bridging M–Cl bonds, since the core electron binding energies of these two environments fall in the order $Cl_b > Cl_t$.[411,412]

X-Ray emission spectra can, in principle, provide detailed information on the valence shell configuration, but such spectra suffer from poor resolution and only one such study has been reported. The Mo $L\beta_{2,15}$ X-ray emission spectrum of $K_4Mo_2Cl_8$ is consistent with the order σ, π, δ for the Mo–Mo bond.[413]

EXAFS measurements [414] on the Mo_2^{4+} ion in aqueous CF_3SO_3H gave an Mo–Mo distance of 2.12 Å and Mo–O distances of 2.14 Å, both in reasonable accord with expectation. An EXAFS study[415] of the $[Ru_2(OEP)_2]^n$ species with n = 0, +1, + 2 has given Ru–Ru distances of 2.40 Å (2.408 Å by crystallography), 2.29 Å and 2.24 Å, respectively. The L_2 and L_3 absorption edge

Pictiva EX2004
Samsung v Pictiva
IPR2024-01094

spectra were also measured for these species and interpreted to indicate a separation of *c*. 2 eV between the σ* and π* energies. The EXAFS and Re L_3 absorption edge have also been measured[357] for $[Re_2F_8]^{2-}$, the former giving Re–F and Re–Re distances in reasonable agreement with those subsequently determined by crystallography.

The XPS spectra of $Mo_2Cl_4(PMe_3)_4$, $MoWCl_4(PMe_3)_4$, and $W_2Cl_4(PMe_3)_4$ have been measured[334] and interpreted to indicate that in the heteronuclear compound there is a net shift of electron density from W to Mo. Several other XPS studies of Cr_2^{4+} and Mo_2^{4+} compounds have been reported.[375,416,417,418]

Nonlinear optical properties have been reported for $M_2Pd_2Cr_2(pyphos)_4$ molecules (M = Cr, Mo)[419] and for Mo_2 and W_2 compounds of the $M_2(O_2CBu^t)_4$, $M_2Cl_4(PMe_3)_4$, $M_2(OR)_6$ and $M_2(NMe_2)_6$ types.[420]

References

1. F. M. O'Neill and J. C. A. Boeyens, *Inorg. Chem.* **1990**, *29*, 1301.
2. J. C. A. Boeyens and D. J. Ledwidge, *Inorg. Chem.* **1983**, *22*, 3587.
3. J. C. A. Boeyens, *Inorg. Chem.* **1985**, *24*, 4149.
4. J. C. A. Boeyens, F. A. Cotton and S. Han, *Inorg. Chem.* **1985**, *24*, 1750.
5. F. A. Cotton, *Chem. Soc. Rev.* **1983**, *12*, 35.
6. F. A. Cotton, K. R. Dunbar, L. R. Falvello, M. Tomas and R. A. Walton, *J. Am. Chem. Soc.* **1983**, *105*, 4950.
7. For the derivation, see F. A. Cotton, P. E. Fanwick, J. W. Fitch, H. D. Glicksman and R. A. Walton, *J. Am. Chem. Soc.* **1979**, *101*, 1752.
8. F. L. Campbell, III, F. A. Cotton and G. L. Powell, *Inorg. Chem.* **1984**, *23*, 4222.
9. F. L. Campbell, III, F. A. Cotton and G. L. Powell, *Inorg. Chem.* **1985**, *24*, 4384.
10. J.P. Collman, J. M. Garner, R. T. Hembre and Y. Ha, *J. Am. Chem. Soc.* **1992**, *114*, 1292.
11. J.P. Collman and H. J. Arnold, *J. Cluster Sci*. **1994**, *5*, 37.
12. J. C. Kim, V. L. Goedkin and B. M. Lee, *Polyhedron* **1996**, *15*, 57.
13. J. P. Collman, S. T. Hartford, S. Franzen, T. A. Eberspacher, R. K. Shoemaker and W. H. Woodruff, *J. Am. Chem. Soc.* **1998**, *120*, 1456.
14. A. Lledos and Y. Jean, *Chem. Phys. Lett*. **1998**, *287*, 243.
15. I. Demachy, Y. Jean and A. Lledos, *Chem. Phys. Lett*. **1999**, *303*, 621.
16. S. Blasco, I. Demachy, Y. Jean and A. Lledos, *Inorg. Chem. Acta* **2000**, *300-302*, 837.
17. D. M. Collins, F. A. Cotton and C. A. Murillo, *Inorg. Chem.* **1976**, *15*, 1861.
18. F. A. Cotton, M. W. Extine and L. D. Gage, *Inorg. Chem.* **1978**, *17*, 172.
19. F. A. Cotton and W. T. Hall, *Inorg. Chem.* **1977**, *16*, 1867.
20. D. M. Collins, F. A. Cotton and L. D. Gage, *Inorg. Chem.* **1979**, *18*, 1712.
21. J. Skowronek, W. Preetz and S. M. Jesson, *Z. Naturforsch*. **1991**, *46b*, 1305.
22. E. M. Shustorovich, M. A. Porai-Koshits and Yu. A. Busalaev, *Coord. Chem. Rev.* **1975**, *17*, 1.
23. (a) M. H, Chisholm, H. T. Chiu and J. C. Huffman, *Polyhedron* **1984**, *3*, 759. (b) M. H. Chisholm, D. M. Hoffman, J. C. Huffman, W. G. Van Der Sluys and S. Russo, *J. Am. Chem. Soc.* **1984**, *106*, 5386.
24. M. H. Chisholm, D. L. Clark, J. C. Huffman, W. G. Van Der Sluys, E. M. Kober, D. L. Lichtenberger and B. E. Bursten, *J. Am. Chem. Soc.* **1987**, *109*, 6796.
25. M. D. Braydich, B. E. Bursten, M. H. Chisholm and D. L. Clark, *J. Am. Chem. Soc.* **1985**, *107*, 4459.
26. (a) K. S. Pitzer, *Acc. Chem. Res.* **1979**, *12*, 271. (b) P. Pykkö and J. P. Desclaux, *ibid.* **1979**, *12*, 279. (c) T. Ziegler, J. G. Snijders and E. J. Baerends, *Chem. Phys. Lett.* **1980**, *75*, 1. (d) J. G. Snijders and P. Pykkö, *ibid*. **1980**, *75*, 5.
27. F. A. Cotton, P. E. Fanwick, R. H. Niswander and J. C. Sekutowski, *J. Am. Chem. Soc.* **1978**, *100*, 4725.
28. V. Katovic and R. E. McCarley, *J. Am. Chem. Soc.* **1978**, *100*, 5586.

Pictiva EX2004
Samsung v Pictiva
IPR2024-01094

29. F. A. Cotton, B. A. Frenz, B. R. Shultz and T. R. Webb, *J. Am. Chem. Soc.* **1976**, *98*, 2768.
30. F. A Cotton, A. C. Price, R. C. Torralba and K. Vidyasagar, *Inorg. Chim. Acta* **1990**, *175*, 281.
31. K. Gelman, N. S. Grigoriev, F. A. Cotton, S. V. Kryutchkov and L. Falvello, *Koord. Khim.* **1991**, *17*, 1230.
32. F. A. Cotton and L. M. Daniels, *Inorg. Chim. Acta* **1988**, *142*, 255.
33. H. W. Huang and D. S. Martin, *Inorg. Chem.* **1985**, *24*, 96.
34. F. A. Cotton and K. Vidyasagar, unpublished results.
35. P. A. Koz'min, *Sov. J. Coord. Chem.* **1986**, *12*, 647.
36. F. A. Cotton, L. M. Daniels and K. Vidyasagar, *Polyhedron* **1988**, *7*, 1667.
37. F. A.Cotton, L. M. Daniels, A. Davison and C. Orvig, *Inorg. Chem.* **1981**, *20*, 3051.
38. F. A. Cotton, J. H. Matonic and D. de O. Silva, *Inorg. Chim. Acta* **1995**, *234*, 115.
39. F. A. Cotton and K. Vidyasagar, *Inorg. Chem*. **1990**, *29*, 3197.
40. C. L. Gross, S. R. Wilson and G. S. Girolami, *Inorg. Chem*. **1995**, *34*, 2582.
41. F. A. Cotton and J. L. Eglin, *Inorg. Chim. Acta* **1992**, *198-200*, 13.
42. F. A. Cotton and J.-D. Chen, unpublished results.
43. F. A. Cotton, L. M. Daniels, M. Shang and Z. Yao, *Inorg. Chim. Acta* **1994**, *215,* 103.
44. F. A. Cotton and K. J. Wiesinger, *Inorg. Chem.* **1992**, *31*, 920.
45. F. A. Cotton, J. G. Jennings, A. C. Price and K. Vidyasagar, *Inorg. Chem.* **1990**, *29*, 4138.
46. F. A. Cotton and K. J. Wiesinger, *Inorg. Chem.* **1991**, *30*, 750.
47. C. J. Burns, A. K. Burrell, F. A. Cotton, S. C. Haefner and A. P. Sattelberger, *Inorg. Chem*. **1994**, *33*, 2257.
48. F. A. Cotton, E. V. Dikarev and S. Herrero, *Inorg. Chem*. **1999**, *38*, 2649.
49. F. A. Cotton and E. V. Dikarev, *Inorg. Chem*. **1995**, *34*, 3809.
50. F. A. Cotton, A. C. Price and K. Vidyasagar, *Inorg. Chem*. **1990**, *29*, 5143.
51. F. A. Cotton, S. C. Haefner and A. P. Sattelberger, *Inorg. Chem*. **1996**, *35*, 1831.
52. F. A. Cotton and E. V. Dikarev, *Inorg. Chem*. **1996**, *35*, 4738.
53. F. A. Cotton, E. V. Dikarev and M. A. Petrukhina, *Inorg. Chem.* **1999**, *38*, 3384.
54. P. Angaridis, F. A. Cotton, E. V. Dikarev and M. A. Petrukhina, *Polyhedron* **2001**, *9-10*, 755.
55. F. A. Cotton, E. V. Dikarev and M. A. Petrukhina,. *J. Am. Chem Soc.* **1997**, *119*, 12541.
56. F. A. Cotton and K. Vidyasagar, *Inorg. Chim Acta* **1989**, *166*, 105.
57. F. A. Cotton, E. V. Dikarev and M. A. Petrukhina, *Inorg. Chem*. **1999**, *38*, 3889.
58. P. A. Agaskar and F. A. Cotton, *Inorg. Chem.* **1984**, *23*, 3383.
59. F. A. Cotton and G. L. Powell, *Inorg. Chem.* **1983**, *22*, 1507.
60. F. A. Cotton and G. L. Powell, *Inorg. Chem.* **1985**, *24*, 177.
61. M. Bakir, F. A. Cotton, L. R. Falvello, C. Q. Simpson and R. A. Walton, *Inorg. Chem.* **1988**, *27*, 4197.
62. J.-D. Chen, F. A. Cotton and L. R. Falvello, *J. Am. Chem. Soc.* **1990**, *112*, 1076.
63. P. A. Agaskar and F. A. Cotton, *Rev. Chim. Miner.* **1985**, *22*, 302.
64. F. A. Cotton, P. E. Fanwick, J. W. Fitch, H. D. Glicksman and R. A. Walton, *J. Am. Chem. Soc.* **1979**, *101*, 1752.
65. F. A. Cotton and T. R. Felthouse, *Inorg. Chem.* **1981**, *20*, 3880.
66. F. A. Cotton, G. G. Stanley and R. A. Walton, *Inorg. Chem.* **1978**, *17*, 2099.
67. M. Bakir, F. A. Cotton, L. R. Falvello, K. Vidyasagar and R. A. Walton, *Inorg. Chem.* **1988**, *27*, 2460.
68. J. Ferry, J. Gallagher, D. Cunningham and P. McArdle, *Polyhedron* **1989**, *8*, 1733.
69. P. A. Agaskar, F. A. Cotton, D. R. Derringer, G. L. Powell, D. R. Root and T. J. Smith, *Inorg. Chem.* **1985**, *24*, 2786.
70. I. F. Fraser, A. McVitie and R. D. Peacock, *J. Chem. Res. (S)* **1984**, 420.
71. P. A. Agaskar and F. A. Cotton, *Inorg. Chem.* **1986**, *25*, 15.
72. S. Christie, I. F. Fraser, A. McVitie and R. D. Peacock, *Polyhedron* **1986**, *5*, 35.
73. F. A. Cotton and S. Kitagawa, *Polyhedron* **1988**, *7*, 463.
74. A. McVitie and R. D. Peacock, *Polyhedron* **1992**, *11*, 2531.

Pictiva EX2004
Samsung v Pictiva
IPR2024-01094

75. F. A. Cotton and R. L. Luck, *Inorg. Chem*. **1989**, *28*, 4522.
76. R. G. Abbott, F. A. Cotton and L. R. Falvello, *Polyhedron* **1990**, *9*, 1821.
77. H. Chen, F. A. Cotton and Z. Yao, *Inorg. Chem*. **1994**, *33*, 4255.
78. F. A. Cotton, E. V. Dikarev and W.-Y. Wong, *Inorg. Chem.* **1997**, *36*, 2670.
79. F. A. Cotton, E. V. Dikarev and W.-Y. Wong, *Inorg. Chem.* **1997**, *36*, 80.
80. F. A. Cotton, E. V. Dikarev and W.-Y. Wong, *Inorg. Chem.* **1997**, *36*, 3268.
81. M. H. Chisholm, J.-H. Huang, J. C. Huffman and I. P. Parkin, *Inorg. Chem.* **1997**, *36*, 1642.
82. M. H. Chisholm, K. Folting, W. E. Streib and D.-D. Wu, *Inorg. Chem.* **1998**, *37*, 50.
83. R. H. Cayton and M. H Chisholm, *Inorg. Chem* **1991**, *30*, 1422.
84. Y. Jean and A. Lledos, *Chem. Commun*. **1998**, 1443.
85. I. Demachy, A. Lledos and Y. Jean, *Inorg. Chem*. **1999**, *38*, 5443.
86. A. Magistrato, J. VandeVondele and U. Rothlisberger, *Inorg. Chem*. **2000**, *39*, 5553.
87. J. VandeVondele, A. Magistrato and U. Rothlisberger, *Inorg. Chem*. **2001**, *40*, 5780
88. J. San Filippo, Jr, *Inorg. Chem.* **1972**, *11*, 3140
89. H. N. McConnell, *J. Chem. Phys*. **1957**, *27*, 226.
90. F. A. Cotton and S. Kitagawa, *Polyhedron* **1988**, *7*, 1673.
91. F. A. Cotton and T. Ren, *J. Am. Chem. Soc.* **1992**, *114*, 2237.
92. F. A. Cotton, L. M. Daniels and C. A. Murillo, *Angew. Chem., Int. Ed. Engl.* **1992**, *31*, 737.
93. C. Liu, J. D. Protasiewicz, E. T. Smith and T. Ren, *Inorg. Chem.* **1996**, *35*, 6422.
94. F. A. Cotton, L. M. Daniels, P. Lei, C. A. Murillo and X. Wang, *Inorg. Chem.* **2001**, *40*, 2778.
95. J. A. Connor and H. A. Skinner, *Reactivity of Metal-Metal Bonds,* M. H. Chisholm, Ed. ACS Symposium Series, No. 155, 1981.
96. F. A. Adedeji, J. J. Cavell, S. Cavell, J. A. Connor, G. Pilcher, H. A. Skinner and M. T. Zafarani-Moattar, *J. Chem. Soc., Dalton Trans.* **1979**, 1714.
97. K. J. Cavell, C. D. Garner, G. Pilcher and S. Parkes, *J. Chem. Soc., Dalton Trans.* **1979**, 1714.
98. K. J. Cavell, J. A. Connor, G. Pilcher, M. A. V. Riveiro, M. D. M. C. Riveiro da Silva, H. A. Skinner, Y. Virmani and M. T. Zafarani-Moattar, *J. Chem. Soc., Faraday Trans. 1* **1981**, *77*, 1585.
99. L. R. Morss, R. J. Porcja, J. W. Nicoletti, J. San Filippo, Jr and H. D. B. Jenkins, *J. Am. Chem. Soc.* **1980**, *102*, 1923.
100. J. A. Connor, G. Pilcher, H. A. Skinner, M. H. Chisholm and F. A. Cotton, *J. Am. Chem. Soc.* **1978**, *100*, 7738.
101. D. V. Drobot and E. A. Pisarev, *Russ. J. Inorg. Chem.* **1981**, *26*, 1.
102. R. D. Cannon, *Inorg. Chem.* **1981**, *20*, 2341.
103. (a) B. B. Wayland, V. L. Coffin and M. D. Farnos, *Inorg. Chem.* **1988**, *27*, 2745. (b) B. B. Wayland, *Polyhedron* **1988**, *7*, 1545.
104. W. C. Trogler, C. D. Cowman, H. B. Gray and F. A. Cotton, *J. Am. Chem. Soc.* **1977**, *99*, 2993.
105. R. A. Kok and M. B. Hall, *Inorg. Chem.* **1983**, *22*, 728.
106. D. C. Smith and W. A. Goddard, III, *J. Am. Chem. Soc.* **1987**, *109*, 5580.
107. J. G. Norman, Jr and P. B. Ryan, *J. Comput. Chem.* **1980**, *1*, 59.
108. T. Ziegler, V. Tschinke and A. Becke, *Polyhedron* **1987**, *6*, 685.
109. T. Ziegler, *J. Am. Chem. Soc.* **1983**, *105*, 7543.
110. L. Dubicki and R. L. Martin, *Inorg. Chem.* **1970**, *9*, 673.
111. F. A. Cotton and C. B. Harris, *Inorg. Chem.* **1967**, *6*, 924.
112. R. A. Evarestov, *Zh. Strukt. Khim.* **1973**, *14*, 955.
113. V. N. Pak and D. V. Korol'kov, *Zh. Strukt. Khim.* **1973**, *14*, 956.
114. L. Pauling, *Proc. Natl. Acad. Sci. USA* **1975**, *72*, 3799 and 4200.
115. R. G. Woolley, *Inorg. Chem.* **1979**, *18*, 2945.
116. T. F. Block, R. F. Fenske, D. L. Lichtenberger and F. A. Cotton, *J. Coord. Chem.* **1978**, *8*, 109.
117. F. A. Cotton and M. W. Extine, *J. Am. Chem. Soc.* **1978**, *100*, 3788.
118. M. Biagini-Cingi and E. Tondello, *Inorg. Chim Acta* **1974**, *11*, L3.
119. M. B. Hall, *Polyhedron* **1987**, *6*, 679.
120. P. M. Atha, I. H. Hillier, A. A. MacDowell and M. F. Guest, *J. Chem. Phys.* **1982**, *77*, 195.

Pictiva EX2004
Samsung v Pictiva
IPR2024-01094

121. F. A. Cotton, E. V. Dikarev and W.-Y. Wong, *Inorg. Chem.* **1997**, *36*, 559.
122. F. A. Cotton, E. V. Dikarev and W.-Y. Wong, *Inorg. Chem.* **1997**, *36*, 2670.
123. J. G. Norman, Jr and H. J. Kolari, *J. Am. Chem. Soc.* **1975**, *97*, 33.
124. A. P. Mortola, J. W. Moskowitz and N. Rösch, *Int. J. Quantun Chem., Symp. No. 8* **1974**, 161.
125. A. P. Mortola, J. W. Moskowitz, N. Rösch, C. D. Cowman and H. B. Gray, *Chem. Phys. Lett.* **1975**, *32*, 283.
126. F. A. Cotton, *Inorg. Chem.* **1965**, *4*, 334.
127. F. A. Cotton and B. J. Kalbacher, *Inorg. Chem.* **1977**, *16*, 2386.
128. P. A. Agaskar, F. A. Cotton, K. R. Dunbar, L. R. Falvello, S. M. Tetrick and R. A. Walton, *J. Am. Chem. Soc.* **1986**, *108*, 4850.
129. W. C. Trogler, D. E. Ellis and J. Berkowitz, *J. Am. Chem. Soc.* **1979**, *101*, 5895.
130. B. E. Bursten, F. A. Cotton, P. E. Fanwick and G. G. Stanley, *J. Am. Chem. Soc.* **1983**, *105*, 3082.
131. R. A. Perez and D. A. Case, *Inorg. Chem.* **1984**, *23*, 3271.
132. (a) L. Gagliardi and B. O. Roos, *Inorg. Chem*. **2003**, *42*, 1599. (b) J.-P. Blaudeau, R. B. Ross, R. M. Pitzer, P. Mouqeuot and M. Benard, *J. Phys. Chem*. **1994**, *98*, 7123.
133. B. E. Bursten, F. A. Cotton. P. E. Fanwick, G. G. Stanley and R. A. Walton, *J. Am. Chem. Soc.* **1983**, *105*, 2606.
134. R. G. Parr and W. Yang, *Density-Functional Theory of Atoms and Molecules*, Oxford University Press: Oxford, 1989.
135. (a) F. A. Cotton and X. Feng, *J. Am. Chem. Soc*. **1997**, *119*, 7514. (b) F. A. Cotton and X. Feng, *J. Am. Chem. Soc*. **1998**, *120*, 3387.
136. M. E. Casida, C. Jaorski, K. C. Casida and D. R. Salahub, *J. Chem. Phys.* **1998**, *108*, 4439.
137. F. A. Cotton, J. P. Donahue, C. A. Murillo and L. M. Perez, *J. Am. Chem. Soc*. **2003**, *125*, 5486.
138. F. A. Cotton, J. L. Hubbard, D. L. Lichtenberger and I. Shim, *J. Am. Chem. Soc.* **1982**, *104*, 679.
139. F. A. Cotton and X. Feng, *J. Am. Chem. Soc*. **1993**, *115*, 1074.
140. I. Demachy, A. Lledos and Y. Jean, *Inorg. Chem*. **1999**, *38*, 5443.
141. J. G. Norman, Jr and H. J. Kolari, *J. Chem. Soc., Chem. Commun.* **1975**, 649.
142. J. G. Norman, Jr, H. J. Kolari, H. B. Gray and W. C. Trogler, *Inorg. Chem.* **1977**, *16*, 987.
143. M. Bénard, *J. Am. Chem. Soc.* **1978**, *100*, 2354.
144. M. F. Guest, I. H. Hillier and C. D. Garner, *Chem. Phys. Lett.* **1977**, *48*, 587.
145. M. Bénard and A. Veillard, *Nouv. J. Chim.* **1977**, *1*, 97.
146. M. Bénard, *J. Chem. Phys.* **1979**, *71*, 2546.
147. M. F. Guest, C. D. Garner, I. H. Hillier and I. B. Walton, *J. Chem. Soc., Faraday Trans. 2* **1978**, *74*, 2092.
148. P. M. Atha, I. H. Hillier and M. F. Guest, *Mol. Phys.* **1982**, *46*, 437.
149. T. Ziegler, *J. Am. Chem. Soc.* **1985**, *107*, 4453.
150. (a) F. A. Cotton, J. G. Norman, Jr., B. R. Stults and T. R. Webb, *J. Coord. Chem.* **1976**, *5*, 217. (b) R. Wiest, A. Strich and M. Bénard, *New J. Chem*. **1991**, *15*, 801.
151. A. Mitschler, B. Rees, R. Wiest and M. Bénard, *J. Am. Chem. Soc.* **1982**, *104*, 7501.
152. K. Andersson, C. W. Bauschlicher, B. J. Persson and B. O. Roos, *Chem. Phys. Lett*. **1996**, *257*, 238.
153. M. H. Chisholm, D. L. Clark, J. C. Huffman, W. G. Van Der Sluys, E. M. Kober, D. L. Lichtenberger and B. E. Bursten, *J. Am. Chem. Soc.* **1987**, *109*, 6796.
154. M. D. Braydich, B. E. Bursten, M. H. Chisholm and D. L. Clark, *J. Am. Chem. Soc.* **1985**, *107*, 4459.
155. B. E. Bursten and D. L. Clark, *Polyhedron* **1987**, *6*, 695.
156. J. G. Norman, Jr and H. J. Kolari, *J. Am. Chem. Soc.* **1978**, *100*, 791.
157. B. E. Bursten and F. A. Cotton, *Inorg. Chem.* **1981**, *20*, 3042.
158. P. Mougenot, J. Demuynck and M. Bénard, *Chem. Phys. Lett.* **1987**, *136*, 279.
159. H. Nakatsuji, J. Ushio, K. Kanda, Y. Onishi, T. Kawamura and T. Yonezawa, *Chem. Phys. Lett.* **1981**, *79*, 299.
160. H. Nakatsuji, Y. Onishi, J. Ushio and T. Yonezawa, *Inorg. Chem.* **1983**, *22*, 1623.

Pictiva EX2004
Samsung v Pictiva
IPR2024-01094

161. T. Kawamura, K. Fukamachi and S. Hayashida, *J. Chem. Soc., Chem. Commun.* **1979**, 945.
162. T. Kawamura, K. Fukamuchi, T. Sowa, S. Hayashida and T. Yonezawa, *J. Am. Chem. Soc.* **1981**, *103*, 364.
163. T. Sowa, T. Kawamura, T. Shida and T. Yonezawa, *Inorg. Chem.* **1983**, *22*, 56.
164. T. Kawamura, M. Maeda, M. Miyamoto, H. Usami, K. Imaeda and M. Ebihara, *J. Am. Chem. Soc*. **1998**, *120*, 8136.
165. F. A. Cotton and X. Feng, *Inorg. Chem.* **1989**, *28*, 1180.
166. G. A. Rizzi, M. Casarin, E. Tondello, P. Piraino and G. Granozzi, *Inorg. Chem.* **1987**, *26*, 3406.
167. J. G. Norman, Jr, G. E. Renzoni and D. A. Case, *J. Am. Chem. Soc.* **1979**, *101*, 5256.
168. F. A. Cotton, V. M. Miskowski and B. Zhong, *J. Am. Chem. Soc.* **1989**, *111*, 6177.
169. F. A. Cotton, T. Ren and J. L. Eglin, *J. Am. Chem. Soc.* **1990**, *112*, 3439.
170. G. Estiu, F. D. Cukiernik, P. Maldivi and O. Poizat, *Inorg. Chem*. **1999**, *38*, 3030.
171. F. A. Cotton, G. G. Stanley, B. J. Kalbacher, J. C. Green, E. Seddon and M. H. Chisholm, *Proc. Natl. Acad. Sci. USA* **1977**, *74*, 3109.
172. B. E. Bursten, F. A. Cotton, J. C. Green, E. A. Seddon and G. G. Stanley, *J. Am Chem. Soc.* **1980**, *102*, 4579.
173. T. A. Albright and R. Hoffman, *J. Am. Chem. Soc.* **1978**, *100*, 7736.
174. M. B. Hall, *J. Am. Chem. Soc.* **1980**, *102*, 2104.
175. T. Ziegler, *J. Am. Chem. Soc.* **1983**, *105*, 7543.
176. K. D. Dobbs, M. M. Francl and W. J. Hehre, *Inorg. Chem.* **1984**, *23*, 24.
177. F. A. Cotton, X. Feng and M. Matusz, *Inorg. Chem.* **1989**, *28*, 594.
178. R. Stranger, G. A. Medley, J. E. McGrady, J. M. Garrett and T. G. Appleton, *Inorg. Chem*. **1996**, *35,* 2268.
179. F. A. Cotton, G. G. Stanley, A. H. Cowley and M. Lattman, *Organometallics* **1988**, 7, 835.
180. M. Bénard, P. Coppens, M. L. DeLucia and E. D. Stevens, *Inorg. Chem.* **1980**, *19*, 1924.
181. K. Hino, Y. Saito and M. Bénard, *J. Am. Chem. Soc.* **1982**, *104*, 7501.
182. M. H. Chisholm, D. L. Clark, E. M. Kober and W. G. Van Der Sluys, *Polyhedron* **1987**, *6*, 723.
183. V. M. Miskowski, M. D. Hopkins, J. R. Winkler and H. B. Gray, *Inorganic Electronic Structure and Spectroscopy, Vol II, Application and Case Studies,* E. I. Solomon and A. B. P. Lever, Eds., John Wiley & Sons: New York, 1999**,** p. 343.
184. W. C. Trogler and H. B. Gray, *Acc. Chem. Res.* **1978**, *11*, 232.
185. L. Noodleman and J. G. Norman, Jr, *J. Chem. Phys.* **1979**, *70*, 4903.
186. F. A. Cotton and D. G. Nocera, *Acc. Chem. Res.* **2000**, *33*, 483.
187. B. E. Bursten and T. W. Cayton, Jr, *J. Cluster Sci.* **1994**, *5*, 157.
188. C. A. Coulson and I. Fischer, *Philos. Mag.* **1949**, *40*, 386.
189. D. G. Nocera, *Acc. Chem. Res.* **1995**, *28*, 209.
190. M. D. Hopkins, H. B. Gray and V. M. Miskowski, *Polyhedron* **1987**, 6, 705.
191. F. L. Campell, III, F. A. Cotton and G. L. Powell, *Inorg. Chem.* **1985**, *24*, 177.
192. F. A. Cotton, J. L. Eglin, B. Hong and C. A. James, *Inorg. Chem.* **1993**, *32*, 2104.
193. D. S. Engebretson, J. M. Zaleshi, G. E. Leroi and D. G. Nocera, *Science* **1994**, *265*, 729.
194. D. S. Engebretson, E. M. Graj, G. E. Leroi and D. G. Nocera, *J. Am. Chem. Soc.* **1999**, *121*, 868.
195. W. C. Trogler and H. B. Gray, *Acc. Chem. Res.* **1978**, *11*, 232.
196. R. S. Mulliken, *J. Chem. Phys.* **1939**, 7, 20.
197. M. D. Hopkins, W. P. Schaefer, M. J. Bronikowski, W. H. Woodruff, V. M. Miskowski, R. F. Dallinger and H. B. Gray, *J. Am. Chem. Soc.* **1987**, *109*, 408.
198. F. A. Cotton, D. S. Martin, P. E. Fanwick, T. J. Peters and T. R. Webb, *J. Am. Chem. Soc.* **1976**, *98*, 4681.
199. F. A. Cotton, P. E. Fanwick, L. D. Gage, B. Kalbacher and D. S. Martin, *J. Am. Chem. Soc.* **1977**, *99*, 5642.
200. P. E. Fanwick, D. S. Martin, F. A. Cotton and T. R. Webb, *Inorg. Chem.* **1977**, *16*, 2103.
201. C. D. Cowman and H. B. Gray, *J. Am. Chem. Soc.* **1973**, *95*, 8177.
202. F. A. Cotton, N. F. Curtis, B. F. Johnson and W. R. Robinson, *Inorg. Chem.* **1965**, *4*, 326.

Pictiva EX2004
Samsung v Pictiva
IPR2024-01094

203. H. W. Huang and D. S. Martin, *Inorg. Chem.* **1985**, *24*, 96.
204. R. J. H. Clark and M. J. Stead, *Inorg. Chem.* **1983**, *22*, 1214.
205. G. A. Heath and R. Raptis, *Inorg. Chem.* **1991**, *30*, 4106.
206. S. K. D. Strubinger, C. L. Hussey and W. E. Cleland, Jr, *Inorg. Chem.* **1991**, *30*, 4276.
207. G. A. Heath and R. G. Raptis, *J. Am. Chem. Soc.* **1993**, *115*, 3768.
208. G. Comrie, A. McVitie and R. D. Peacock, *Polyhedron* **1994**, *13*, 193.
209. M. H. Chishlom, J. C. Huffman, S. S. Lyer and M. A. Lynn, *Inorg. Chem. Acta* **1996**, *243*, 283.
210. W. W. Beers, R. E. McCarley, D. S. Martin, V. M. Miskowski, H. B. Gray and M. D. Hopkins, *Coord. Chem. Rev.* **1999**, *187*, 103.
211. F. A. Cotton, D. S. Martin, T. R. Webb and T. J. Peters, *Inorg. Chem.* **1976**, *15*, 1199.
212. W. C. Trogler, E. I. Solomon, I. Trabjerg, C. J. Ballhausen and H. B. Gray, *Inorg. Chem.* **1977**, *16*, 828.
213. D. S. Martin, R. A. Newman and P. E. Fanwick, *Inorg. Chem.* **1979**, *18*, 2511.
214. A. Bino, F. A. Cotton and P. E. Fanwick, *Inorg. Chem.* **1980**, *19*, 1215.
215. M. C. Manning and W. C. Trogler, *Inorg. Chem.* **1982**, *21*, 2797.
216. M. C. Manning, G. F. Holland, D. E. Ellis and W. C. Trogler, *J. Phys. Chem.* **1983**, *87*, 3083.
217. D. S. Martin and H.-W. Huang, *Inorg. Chem.* **1990**, *29*, 3674.
218. F. A. Cotton and B. Zong, *J. Am. Chem. Soc.* **1990**, *112*, 2256.
219. D. S. Martin, H.-W. Huang and R. A. Newman, *Inorg. Chem.* **1984**, *23*, 699.
220. F. A. Cotton and P. E. Fanwick, *J. Am. Chem. Soc.* **1979**, *101*, 5252.
221. F. A. Cotton, P. E. Fanwick and L. D. Gage, *J. Am. Chem. Soc.* **1980**, *102*, 1570.
222. P. E. Fanwick, D. S. Martin, Jr, T. R. Webb, G. A. Robbins and R. A. Newman, *Inorg. Chem.* **1978**, *17*, 2723.
223. D. K. Erwin, G. L. Geoffroy, H. B. Gray, G. S. Hammond, E. I. Solomon, W. C. Trogler and A. A. Zaggers, *J. Am. Chem. Soc.* **1977**, *99*, 3620.
224. P. E. Fanwick, B. E. Bursten and G. B. Kaufmann, *Inorg. Chem.* **1985**, *24*, 1165.
225. P. E. Fanwick, *Inorg. Chem.* **1985**, *24*, 258.
226. A. W. Maverick, L. G. Butler, W. Lewis, C. H. Gallegos, J. D. Goettee, D. G. Rickel and C. M. Fowler, *Inorg. Chim. Acta* **1996**, *243*, 309.
227. C. D. Cowman, W. C. Trogler and H. B. Gray, *Isr. J. Chem.* **1977**, *15*, 308.
228. J. R. Ebner and R. A. Walton, *Inorg. Chim. Acta* **1975**, *14*, L45.
229. M. D. Hopkins, V. M. Miskowski and H. B. Gray, *J. Am. Chem. Soc.* **1986**, *108*, 959.
230. F. A. Cotton, L. M. Daniels, G. L. Powell, A. J. Kahaian, T. J. Smith and E. Fiore Vogel, *Inorg. Chim. Acta* **1988**, *144*, 109.
231. M. D. Hopkins, V. M. Miskowski and H. B. Gray, *J. Am. Chem. Soc.* **1988**, *110*, 1787.
232. V. M. Miskowski, H. B. Gray and M. D. Hopkins, *Inorg. Chem*. **1992**, *31*, 2085.
233. D. S. Martin, Jr, T. R. Webb, G. A. Robbins and P. E. Fanwick, *Inorg. Chem.* **1979**, *18*, 475.
234. G. Bienek, W. Tuszynski and G. Gliemann, *Z. Naturforsch.* **1978**, *33b*, 1095.
235. V. M. Miskowski, W. P. Schaefer, B. Sadeghi, B. D. Santarsiero and H. B. Gray, *Inorg. Chem.* **1984**, *23*, 1154.
236. J. W. Trexler, Jr, A. F. Schreiner and F. A. Cotton, *Inorg. Chem.* **1988**, *27*, 3265.
237. R. A. Newman, D. S. Martin, R. F. Dallinger, W. H. Woodruff, A. E. Stiegman, C.-M. Che, W. P. Schaefer, V. M. Miskowshi and H. B. Gray, *Inorg. Chem.* **1991**, *30*, 4647.
238. G. Gokagac, H. Isci and W. R. Mason, *Inorg. Chem.* **1992**, *31*, 2184.
239. R. Stranger, G. A. Medley, J. E. McGrady, J. M. Garrett and T. G. Appleton, *Inorg. Chem.* **1996**, *35*, 2268.
240. R Stranger, S. C. Nissen, M. T. Mathieson and T. G. Appleton, *Inorg. Chem.* **1997**, *36*, 937.
241. D. S. Martin, R. A. Newman and L. M. Vlasnik, *Inorg. Chem.* **1980**, *19*, 3404.
242. V. M. Miskowski, T. M. Loehr and H. B. Gray, *Inorg. Chem.* **1987**, *26*, 1098.
243. V. M. Miskowski and H. B. Gray, *Inorg. Chem.* **1988**, *27*, 2501.
244. V. M. Miskowski, T. M. Loehr and H. B. Gray, *Inorg. Chem.* **1988**, *27*, 4708.
245. R. J. H. Clark and L. T. H. Ferris, *Inorg. Chem.* **1981**, *20*, 2759.

Pictiva EX2004
Samsung v Pictiva
IPR2024-01094

246. V. M. Miskowski and H. B. Gray, *Topics in Current Chemistry* **1997**, *191*, 41.
247. W. Preetz, P. Hollmann, G. Thiele and H. Hillebrecht, *Z. Naturforsch.* **1990**, *45b*, 1416.
248. P. A. Agaskar, F. A. Cotton, I. F. Fraser and R. D. Peacock, *J. Am. Chem. Soc.* **1984**, *106*, 1851.
249. P. A. Agaskar, F. A. Cotton, I. F. Fraser, L. Manojlovic-Muir, K. W. Muir and R. D. Peacock, *Inorg. Chem.* **1986**, *25*, 2511.
250. J.-D. Chen, F. A. Cotton and L. R. Falvello, *J. Am. Chem. Soc.* **1990**, *112*, 1076.
251. R. D. Peacock, *Polyhedron* **1987**, *6*, 715.
252. I. F. Fraser, A. McVitie and R. D. Peacock, *Polyhedron* **1986**, *5*, 39.
253. I. F. Fraser and R. D. Peacock, *J. Chem. Soc., Chem. Commun.* **1985**, 1727.
254. R. D. Peacock and I. F. Fraser, *Inorg. Chem.* **1985**, *24*, 988.
255. (a) K. B. Mathisen, U. Wahlgren and L. G. M. Pettersson, *Chem. Phys. Lett.* **1984**, *104*, 336. (b) A. Stromberg, L.G. M. Pettersson and U. Wahlgren, *Chem. Phys. Lett.* **1985**, *118*, 389.
256. P. A. Agaskar, F. A. Cotton, L. R. Falvello and S. Han, *J. Am. Chem. Soc.* **1986**, *108*, 1214.
257. J.-D. Chen and F. A. Cotton, *Inorg. Chem.* **1990**, *29*, 1797.
258. J.-D. Chen and F. A. Cotton, *J. Am. Chem. Soc.* **1991**, *113*, 2509.
259. C.-Y. Pan, M.-C, Suen, Y.-Y. Wu, J.-D. Chen, T.-C. Keng and J.-C. Wang, *Inorg. Chim. Acta* **2001**, *312*, 111.
260. M. Gerards, *Inorg. Chim. Acta* **1995**, *229*, 101.
261. See, for example, A. Liptak, J. Frelek, G. Snatzke and I. Vlakov, *Carbohydr. Res.* **1987**, *164*, 149 and earlier references therein.
262. M.Gerards and G. Snatzke, *Tetrahedron: Asymmetry* **1990**, *1*, 221.
263. F. A. Cotton, L. R. Falvello, M. Gerards and G. Snatzke, *J. Am. Chem. Soc.* **1990**, *112*, 8979.
264. C. S. Yoo and J. I. Zink, *Inorg. Chem.* **1983**, *22*, 2472.
265. V. K. Ceylan, C. Sourisseau and J. V. Brencic, *J. Raman Spectrosc.* **1985**, *16*, 128.
266. C. Svendsen, M. J. Nilsen, O. S. Mortensen, S. J. R. Allers and R. J. H. Clark, *Chem. Phys.* **1997**, *215*, 477.
267. R. J. H. Clark, S. J. R. Owens, C. Svendsen, M. J. Nielsen and O. S. Mortensen, *Inorg. Chim. Acta* **1996**, *243*, 249.
268. D. L. Lichtenberger and C. H. Blevins, II, *J. Am. Chem. Soc.* **1984**, *106*, 1636.
269. V. M. Miskowski and D. E. Brinza, *J. Am. Chem. Soc.* **1986**, *108*, 8296.
270. K.-S. Shin, R. J. H. Clark and J. I. Zink, *J. Am. Chem. Soc.* **1989**, *111*, 4244.
271. K.-S. K. Shin and J. I. Zink, *Inorg. Chem.* **1989**, *28*, 4358.
272. J. R. Schoonover, D. F. Dallinger, P. M. Killough, A. P. Sattelberger and W. H. Woodruff, *Inorg. Chem.* **1991**, *30*, 1093.
273. W. C. Trogler, E. I. Solomon and H. B. Gray, *Inorg. Chem.* **1977**, *16*, 3031.
274. V. M. Miskowski, R. A. Goldbeck, D. S. Kliger and H. B. Gray, *Inorg. Chem.* **1979**, *18*, 86.
275. C. G. Morgante and W. S. Struve, *Chem. Phys. Lett.* **1979**, *63*, 344.
276. M. D. Hopkins and H. B. Gray, *J. Am. Chem. Soc.* **1984**, *106*, 2468.
277. I. F. Fraser and R. D. Peacock, *Chem. Phys. Lett.* **1983**, *98*, 620.
278. C. S. Yoo and J. I. Zink, *Inorg. Chem.* **1983**, *22*, 2474.
279. P. M. Bradley, L. T. smith, J. L. Eglin and C. Turro, *Inorg. Chem.* **2003**, *42*, 7360.
280. I. F. Fraser and R. D. Peacock, *Chem. Phys. Lett.* **1987**, *137*, 583.
281. J. R. Winkler, D. G. Nocera and T. L. Netzel, *J. Am. Chem. Soc.* **1986**, *108*, 4451.
282. J. Ouyang, T. C. Zietlow, M. D. Hopkins, F. F. Fan, H. B. Gray and A. J. Bard, *J. Phys. Chem.* **1986**, *90*, 3841.
283. M. C. Manning and W. C. Trogler, *J. Am. Chem. Soc.* **1983**, *105*, 5311.
284. D. G. Nocera and H. B. Gray, *J. Am. Chem. Soc.* **1981**, *103*, 7349.
285. D. G. Nocera and H. B. Gray, *Inorg. Chem.* **1984**, *23*, 3686.
286. W. C. Trogler, D. K. Erwin, G. L. Geoffroy and H. B. Gray, *J. Am. Chem. Soc.* **1978**, *100*, 1160.
287. I.-J. Chang and D. G. Nocera, *J. Am. Chem. Soc.* **1987**, *109*, 4901.
288. I.-J. Chang and D. G. Nocera, *Inorg. Chem.* **1989**, *28*, 4309.
289. C. M. Partigianoni, I.-J. Chang and D. G. Nocera, *Coord. Chem. Rev.* **1990**, *97*, 105.

Pictiva EX2004
Samsung v Pictiva
IPR2024-01094

290. C. M. Partigianoni and D. G. Nocera, *Inorg. Chem.* **1990**, *29*, 2033.
291. G. L. Geoffroy, H. B. Gray and G. S. Hammond, *J. Am. Chem. Soc.* **1974**, *96*, 5565.
292. R. H. Fleming, G. L. Geoffroy, H. B. Gray, A. Gupta, G. S. Hammond, D. S. Kliger and V. M. Miskowski, *J. Am. Chem. Soc.* **1976**, *98*, 48.
293. V. M. Miskowski, A. J. Twarowski, R. H. Fleming, G. S. Hammond and D. S. Kliger, *Inorg. Chem.* **1978**, *17*, 1056.
294. P. M. Bradley, B. E. Bursten and C. Turro, *Inorg. Chem.* **2001**, *40*, 1376.
295. X. B. Wang and L. S. Wang, *J. Am. Chem. Soc*. **2000**, *122*, 2096.
296. J. C. Green and A. J. Hayes, *Chem. Phys. Lett.* **1975**, *31*, 306.
297. F. A. Cotton, J. G. Norman, Jr, B. R. Stults and T. R. Webb, *J. Coord. Chem.* **1976**, *5*, 217.
298. I. H. Hillier, C. D. Garner, G. R. Mitcheson and M. F. Guest, *J. Chem. Soc., Chem. Commun.* **1978**, 204.
299. A. W. Coleman, J. C. Green, A. J. Hayes, E. A. Seddon, D. R. Lloyd and Y. Niwa, *J. Chem. Soc., Dalton Trans.* **1979**, 1057.
300. I. H. Hillier, *Pure Appl. Chem.* **1979**, *51*, 2183.
301. M. Berry, C. D. Garner, I. H. Hillier, A. A. MacDowell and I. B. Walton, *Chem. Phys. Lett.* **1980**, *70*, 350.
302. C. D. Garner, I. H. Hillier, A. A. MacDowell, I. B. Walton and M. F. Guest. *J. Chem. Soc., Faraday Trans. 2* **1979**, *75*, 485
303. Reference withdrawn.
304. D. L. Lichtenberger and R. L. Johnston, in *Metal-Metal Bonds and Clusters in Chemistry and Catalysis,* ed. J. P. Fackler, Jr, Plenum Press: New York, 1990, pp. 275-298.
305. G. M. Bancoft, E. Pellach, A. P. Sattelberger and K. W. McLaughlin, *J. Chem. Soc., Chem. Commun.* **1982**, 752.
306. D. L. Lichtenberger and J. G. Kristofzski, *J. Am. Chem. Soc.* **1987**, *109*, 3458.
307. D. L. Lichtenberger, C. D. Ray, F. Stepniak, Y. Chen and J. H. Weaver, *J. Am. Chem. Soc*. **1992**, *114*, 10492.
308. J. Brennan, G. Cooper, J. C. Green, M. P. Payne and C. M. Redfern, *J. Electron Spectr*. **1995**, *73*, 157.
309. D. L. Lichtenberger, M. A. Lynn and M. H. Chisholm, *J. Am. Chem. Soc.* **1999**, *121*, 12167.
310. F. A. Cotton, N. E. Gruhn, J. Gu, P. Huang, D. L. Lichtenberger, C. A. Murillo, L. O. Van Dorn and C. C. Wilkinson, *Science* **2002**, *298*, 1971.
311. M. H. Chisholm, D. L. Clark, J. C. Huffman, W. G. Van Der Sluys, E. M. Kober, D. L. Lichtenberger and B. E. Bursten, *J. Am. Chem. Soc.* **1987**, *109*, 6796.
312. C. D. Garner, I. H. Hillier, M. J. Knight, A. A. MacDowell, I. B. Walton and M. F. Guest, *J. Chem. Soc., Faraday Trans.* **1980**, *76*, 885.
313. B. E. Bursten, F. A. Cotton, A. H. Cowley, B. E. Hanson, M. Lattman and G. G. Stanley, *J. Am. Chem. Soc.* **1979**, *101*, 6244.
314. F. A. Cotton, J. L. Hubbard, D. L. Lichtenberger and I. Shim, *J. Am. Chem. Soc.* **1982**, *104*, 679.
315. D. R. Root, C. H. Blevins, D. L. Lichtenberger, A. P. Sattelberger and R. A. Walton, *J. Am. Chem. Soc.* **1986**, *108*, 953.
316. G. M. Bancroft, J.-A. Bice, R. H. Morris and R. L. Luck, *J. Chem. Soc., Chem. Commun.* **1986**, 898.
317. E. M. Kober and D. L. Lichtenberger, *J. Am. Chem. Soc.* **1985**, *107*, 7199.
318. D. L. Lichtenberger, J. R. Pollard, M. A. Lynn, F. A. Cotton and X. Feng, *J. Am. Chem. Soc*. **2000**, *122*, 3182.
319. M. Berry, C. D. Garner, I. H. Hillier, A. A. MacDowell and W. Clegg, *J. Chem. Soc., Chem. Commun.* **1980**, 494.
320. D. L. Clark, J. C. Green, C. M. Redfern, G. E. Quelch, I. H. Hillier and M. F. Guest, *Chem. Phys, Lett.* **1989**, *154*, 326.
321. D. L. Clark, J. C. Green and C. M. Redfern, *J. Chem. Soc.,Dalton Trans.* **1989**, 1037.
322. M. Berry, C. D. Garner, I. H. Hillier, A. A. MacDowell and W. Clegg, *Inorg. Chim Acta* **1981**, *53*, L61.

Pictiva EX2004
Samsung v Pictiva
IPR2024-01094

323. J. C. Green and E. A. Seddon, *J. Organomet. Chem.* **1980**, *198*, C61.
324. W. K. Bratton, F. A. Cotton, M. Debeau and R. A. Walton, *J. Coord. Chem.* **1971**, *1*, 121.
325. A. P. Ketteringham, C. Oldham and C. J. Peacock, *J. Chem. Soc., Dalton Trans.* **1976**, 1640.
326. E. M. Larson, T. M. Brown and R. B. Von Dreele, *Acta Crystallogr.* **1986**, *B42*, 533.
327. W. Preetz, G. Peters and D. Bublitz, *J. Cluster Sci.* **1994**, *5*, 83.
328. B. Hutchinson, J. Morgan, C. B. Cooper, Y. Mathey and D. F. Shiver, *Inorg. Chem.* **1979**, *18*, 2048
329. A. Bino, F. A. Cotton, D. O. Marler, S. Farquharson, B. Hutchinson, J. Kincaid and B. Spencer, *Inorg. Chim. Acta* **1987**, *133*, 295.
330. C. Oldham, J. E. D. Davies and A. P. Ketteringham, *J. Chem. Soc., Chem. Commun.* **1971**, 572.
331. C. L. Angell, F. A. Cotton, B. A. Frenz and T. R. Webb, *J. Am. Chem. Soc., Chem. Commun.* **1973**, 399.
332. R. J. H. Clark and T. J. Dines, *Angew. Chem., Int. Ed. Engl.* **1986**, *25*, 131.
333. R. J. H. Clark and M. L. Franks, *J. Am. Chem. Soc.* **1975**, *97*, 2691.
334. R. T. Carlin and R. E. McCarley, *Inorg. Chem.* **1989**, *28*, 280.
335. M. D. Hopkins, V. M. Miskowski, P. M. Killough, A. P. Sattelberger, W. H. Woodruff and H. B. Gray, *Inorg. Chem*. **1992**, *31*, 5368.
336. K. D. John, V. M. Miskowski, M. A. Vance, R. F. Dallinger, L. C. Wang, S. J. Geib and M. D. Hopkins, *Inorg. Chem*. **1998**, *37*, 6858.
337. I. M. Bell, R. J. H. Clark and D. G. Humphrey, *J. Chem. Soc., Dalton Trans*. **1997**, 1225.
338. R. J. H. Clark, S. Firth, A. Sella, V. M. Miskowski and M. D. Hopkins, *J. Chem. Soc., Dalton Trans.* **2000**, 2928.
339. A. P. Sattelberger and J. P. Fackler, *J. Am. Chem. Soc.* **1977**, *99*, 1258.
340. V. K. Ceylan, C. Sourisseau and J. V. Brencic, *J. Raman Spectrosc.* **1985**, *16*, 128.
341. E. L. Akhmedov, A. S. Kotel'nikova,O. N. Eustaf'eva, Y.Y. Kharitonov, A. N. Smirnov, A. Y. Tsivadze, I. Z. Babievskaya and A. M. Abbasov, *Sov. J. Coord. Chem.* **1987**, *13*, 273.
342. J. San Filippo, Jr and H. J. Sniadoch, *Inorg. Chem.* **1973**, *12*, 2326.
343. A. P. Ketteringham and C. Oldham, *J. Chem. Soc., Dalton Trans.* **1973**, 1067.
344. R. J. H. Clark, A. J. Hempleman and M. Kurmoo, *J. Chem. Soc., Dalton. Trans.* **1988**, 973.
345. F. A. Cotton and J. G. Norman, Jr, *J. Am. Chem. Soc.* **1972**, *94*, 5697.
346. C. D. Garner, R. G. Senior and T. J. King, *J. Am. Chem. Soc.* **1976**, *98*, 647.
347. J. San Filippo, Jr and H. J. Sniadoch, *Inorg. Chem,* **1976**, *15*, 2215.
348. A. Lowenshuss, J. Shamir and M. Ardon, *Inorg. Chem.* **1976**, *15*, 238.
349. A. Bino, F. A. Cotton, D. O. Marler, S. Farquharson, B. Hutchinson, J. Kincaid and B. Spencer, *Inorg. Chim. Acta* **1987**, *133*, 295.
350. F. A. Cotton, T. Inglis, M. Kilner and T. R. Webb, *Inorg. Chem.* **1975**, *14*, 2023.
351. C. D. Tait, J. M. Garner, J. P. Collman, A. P. Sattelberger and W. H. Woodruff, *J. Am. Chem. Soc.* **1989**, *111*, 9072.
352. F. A. Cotton and B. E. Hanson, *Inorg. Chem.* **1978**, *17*, 3237.
353. D. J. Santure, J. C. Huffman and A. P. Sattelbeger, *Inorg. Chem.* **1985**, *24*, 371.
354. D. J. Santure, K. W. McLaughlin, J. C. Huffman and A. P. Sattelberger, *Inorg. Chem.* **1983**, *22*, 1877.
355. P. R. Sharp and R. R. Schrock, *J. Am. Chem. Soc.* **1980**, *102*, 1430.
356. G. Henkel, G. Peters, W. Preetz and J. Skowronek, *Z. Naturforsch.* **1990**, *45b*, 469.
357. S. D. Conradson, A. P. Sattelberger and W. H. Woodruff, *J. Am. Chem. Soc.* **1988**, *110*, 1309.
358. R. J. H. Clark and M. L. Franks, *J. Am. Chem. Soc.* **1976**, *98*, 2763.
359. W. Preetz, G. Peters and L. Rudzik, *Z. Naturforsch.* **1979**, *34b*, 1240.
360. C. Oldham and A. P. Ketteringham, *J. Chem. Soc., Dalton Trans.* **1973**, 2304.
361. E. L. Akgmedov, G. G. Kassaev, L. T. Abullaeva, M. S. Khiyalov, A. Y. Tsivadze, T. K. Kirbanov, K. S. Khalilov, *Koord. Khim.* **1992**, *18*, 64. (b) E. L. Akhmedov, A. Y. Tsivadze, T. K. Kurbanov, G. G. Khassaev, *Koord. Khim*. **1992**, *18*, 594.
362. J. R. Ebner and R. A. Walton, *Inorg. Chem.* **1975**, *14*, 1987.
363. R. J. H. Clark and A. J. Hempleman, *J. Chem. Soc., Dalton Trans.* **1988**, 2601.

Pictiva EX2004
Samsung v Pictiva
IPR2024-01094

364. R. J. H. Clark, A. J. Hempleman and D. A. Tocher, *J. Am. Chem. Soc.* **1988**, *110*, 5968.
365. V. M. Miskowski, R. F. Dallinger, G.G. Christoph, D. E. Morris, G. H. Spies and W. H. Woodruff, *Inorg. Chem.* **1987**, *26*, 2127.
366. R. J. H. Clark, A. J. Hempleman and C. D. Flint, *J. Am. Chem. Soc.* **1986**, *108*, 518.
367. R. J. H. Clark and A. J. Hempleman, *Inorg. Chem.* **1988**, *27*, 2225.
368. R. J. H. Clark and A. J. Hempleman, *Inorg. Chem.* **1989**, *28*, 746.
369. S. P. Best, R. J. H. Clark and A. J. Nightingale, *Inorg. Chem.* **1990**, *29*, 1383.
370. R. J. H. Clark and A. J. Hempleman, *Inorg. Chem.* **1989**, *28*, 92.
371. S. P. Best, P. Chandley, R. J. H. Clark, S. McCarthy, M. B. Hursthouse and P. A. Bates, *J. Chem. Soc., Dalton Trans.* **1989**, 581.
372. R. J. H. Clark, D. J. West and R. Withnall, *Inorg. Chem.* **1992**, *31*, 456.
373. R. J. H. Clark and A. J. Hempleman, *Croat. Chem. Acta* **1988**, *61*, 313.
374. R. J. H. Clark and N. R. D'Urso, *J. Am. Chem. Soc.* **1978**, *100*, 3088.
375. P. Brant, *J. Electron Spectroscopy and Related Phenomena*, **1982**, *27*, 63.
376. D. S. Martin, R. A. Newman and P. E. Fanwick, *Inorg. Chem.* **1982**, *21*, 3400.
377. J. R. Shapley and H. G. Drickamer, *J. Cluster Sci.* **1994**, *5*, 145.
378. F. A. Cotton and E. Pedersen, *Inorg. Chem.* **1975**, *14*, 399.
379. F. A. Cotton, L. M. Daniels, E. A. Hillard and, C. A. Murillo, *Inorg. Chem.* **2002**, *41*, 1639.
380. F. A. Cotton, N. S. Dalal, E. A. Hillard, P. Huang, C. A. Murillo and C. M. Ramsey, *Inorg. Chem.* **2003**, *42*, 1388.
381. F. A. Cotton, B. A. Frenz, E. Pedersen and T. R. Webb, *Inorg. Chem.* **1975**, *14*, 391.
382. F. A. Cotton and E. Pedersen, *J. Am. Chem. Soc.* **1975**, *97*, 303.
383. F. A. Cotton, E. A. Hillard, C. A. Murillo and X. Wang, *Inorg. Chem.* **2003**, *42*, 6063.
384. F. A. Cotton and E. Pedersen, *Inorg. Chem.* **1975**, *14*, 383.
385. F. A. Cotton, N. S. Dalal, P. Huang, C. A. Murillo, A. C. Stowe and X. Wang, *Inorg. Chem.* **2003**, *42*, 670.
386. F. A. Cotton and E. Pedersen, *Inorg. Chem.* **1975**, *14*, 388.
387. B. K. Das and A. R. Chakravarty, *Inorg. Chem.* **1992**, *31*, 1395.
388. A. J. Lindsay, G. Wilkinson, M. Motevalli and M. B. Hursthouse, *J. Chem. Soc., Dalton Trans*. **1987**, 2723.
389. J. Telser and R. S. Drago, *Inorg. Chem.* **1984**, *34*, 3114; **1985**, *24*, 4765.
390. S. M. Tetrick, V. T. Coombe, G. A. Heath, T. A. Stephenson and R. A. Walton, *Inorg. Chem.* **1984**, *23*, 4567.
391. F. A. Cotton, K. R. Dunbar and M. Matusz, *Inorg. Chem.* **1986**, *25*, 1585.
392. L.-P. He, C.-L. Yao, M. Naris, J. C. Lee, J. D. Korp and J. L Bear, *Inorg. Chem.* **1992**, *31*, 620.
393. F. A. Cotton, C. Lin and C. A. Murillo, *Inorg. Chem.* **2000**, *39*, 4574.
394. J. C. Le, M. Y. Chavan, L. K. Chau, J. L. Bear, K. M. Kadish, *J. Am. Chem. Soc.* **1985**, *107*, 7195.
395. K. M. Kadish, T. D. Phan, L. Giribabu, E. V. Caemelbecke and J. L. Bear, *Inorg. Chem.* **2003**, *42*, 8663.
396. T. Kawamura, H. Katayama and T. Yamabe, *Chem. Phys. Lett.* **1986**, *130*, 20.
397. T. Kawamura, H. Katayama, H. Nishikawa and T. Yamabe, *J. Am. Chem. Soc.* **1989**, *111*, 8156.
398. F. A. Cotton, M. Matusz, R. Poli and X. Feng, *J. Am. Chem. Soc.* **1988**, *110*, 1144.
399. F. A. Cotton, N. S. Dalal, S. Ibragimov, C. A. Murillo and J. M. North, unpublished work.
400. C.-L. Yao, L.-P. He, J. D. Korp and J. L. Bear, *Inorg. Chem.* **1988**, *27*, 4389.
401. G. W. Eastland and M. C. R. Symons, *J. Chem. Soc., Dalton Trans.* **1984**, 2193.
402. F. A. Cotton, L. M. Daniels, L. R. Falvello, J. H. Matonic and C. A. Murillo, *Inorg. Chim. Acta* **1997**, *256*, 269.
403. D. G. Tisley and R. A. Walton, *J. Chem. Soc., Dalton Trans.* **1973**, 1039.
404. D. G. Tisley and R. A. Walton, *J. Mol. Struct.* **1973**, *17*, 401.
405. J. R. Ebner and R. A. Walton, *Inorg. Chem.* **1975**, *14*, 2289.
406. J. R. Ebner, D. R. Tyler and R. A. Walton, *Inorg. Chem.* **1976**, *15*, 833.

Pictiva EX2004
Samsung v Pictiva
IPR2024-01094

407. V. I. Nefedov, Ya. V. Salyn, A. V. Shtemenko and A. S. Kotelnikova, *Inorg. Chim. Acta* **1980**, *45*, L49.
408. R. A. Walton, in *Proceedings of the Climax Second International Conference on the Chemistry and Uses of Molybdenum,* ed. P. C. H. Mitchell, Climax Molybdenum Co. Ltd. **1976**, p. 35.
409. S. A. Best, T. J. Smith and R. A. Walton, *Inorg. Chem.* **1978**, *17*, 99.
410. S. A. Best, R. G. Squires and R. A. Walton, *J. Catal.* **1979**, *60*, 171.
411. J. R. Ebner, D. L. McFadden, D. R. Tyler and R. A. Walton, *Inorg. Chem.* **1976**, *15*, 3014.
412. R. A. Walton, *Coord. Chem. Rev.* **1976**, *21*, 63 and references therein.
413. (a) D. E. Haycock, D. S. Urch, C. D. Garner, I. H. Hillier and G. R. Mitcheson, *J. Chem. Soc., Chem. Commun.* **1978**, 262. (b) D. Haycock, D. S. Urch, C. D. Garner and I. H. Hillier, *J. Electron Spectrosc.* **1979**, *17*, 345.
414. S. P. Cramer, P. K. Eidem, M. T. Paffett, J. R. Winkler, Z. Dori and H. B. Gray, *J. Am. Chem. Soc.* **1983**, *105*, 799.
415. H. Asahina, M. B. Zisk, B. Hedman, J. T. MeDevitt, J. P. Collman and K. O. Hodgson, *J. Chem. Soc., Chem. Commun.* **1989**, 1360.
416. P. M. Atha, M. Berry, C.D. Garner, I. H. Hillier and A. A. MacDowell, *J. Chem. Soc., Chem. Commun.* **1981**, 1027.
417. P. M. Atha, J. C. Campbell, C. D. Garner, I. H. Hillier and A. A. MacDowell, *J. Chem. Soc., Dalton Trans.* **1983**, 1085.
418. P. M. Atha, P. C. Ford, C. D. Garner, A. A. MacDowell, I. H. Hillier, M. F. Guest and V. R. Saunders, *Chem. Phys. Lett.* **1981**, *84*, 172.
419. K. Mashima et al, *Chem. Letters,* **1997**, 411.
420. B. D. Pate, J. R.G. Thorne, D. R. Click, M. H. Chisholm and R. G. Denning, *Inorg. Chem.* **2002**, *41*, 1975.
421. D. E. Morris, C. D. Tait, R. B. Dyer, J. R. Schoonover, M. D. Hopkins, A. P. Sattelberger and W. H. Woodruff, *Inorg. Chem.* **1990**, *29*, 3447.
422. T. L. Carroll, J. R. Shapley and H. G. Drickamer, *J. Chem. Phys.* **1986**, *85*, 6787.
423. D. E. Morris, A. P. Sattelberger and W. H. Woodruff, *J. Am. Chem. Soc.* **1986**, *108*, 8270.
424. R. T. Roginski, T. L. Carroll, A. Moroz, B. R. Whittlesey, J. R. Shapley and H. G. Drickamer, *Inorg. Chem.* **1988**, *27*, 3701.
425. T. L. Carroll, J. R. Shapley and H. G. Drickamer, *J. Am. Chem. Soc.* **1985**, *107*, 5802.

Pictiva EX2004
Samsung v Pictiva
IPR2024-01094

Abbreviations

The following list provides a selection of the less common abbreviations used in this book. Those of common usage such as py, acac, THF, NMR, DFT have been left out. The abbreviations are listed in alphabetical order. When a number, a Greek letter or another special character precedes the abbreviation, this is listed ignoring such character.

A	
AAMP	4-amino-5-(aminomethyl)-2-methylpyrimidine
aampy	2-acetylamino-6-methylpyridine
acbt	anion of 2-amino-4-chlorobenzothiazole
ACR	acridine
Acr-4-carboxamide	N-[2-(dimethylamino)hexyl]acridine-4-carboxamide
$AcrNH_2$	9-(2-aminoethyl)amino-6-chloro-2-methoxyacridine
$AcrNMe_2$	6-chloro-9-(2-dimethylaminoethyl)amino-2-methoxyacridine
adbtz	11-aminodibenzo[b,f](1,4)thiazepine
admp	2-amino-4,6-dimethylpyridinate
admpym	2-amino-4,6-dimethylpyrimidinate
β-Ala	alanine zwitterion ($^+NH_3CH_2CO_2^-$)
Amb	*R*(-)2-amino-1-butanol
ambt	anion of 2-amino-4-methylbenzothiazole
ammpy	2-(aminomethyl)pyridine
amp	2-aminopyridine
ampy	2-amino-6-methylpyridine
AniPyF	*N*,*N*'-*p*-anisylpyridylformamidinate

Pictiva EX2004
Samsung v Pictiva
IPR2024-01094

ap	anion of 2-anilinopyridine
8-aq	8-aminoquinoline
asp	2-acetoxybenzoate
AZ	azathioprine
azin	anion of 7-azaindole

B

4*S*-BACIM	2-methyl-1-propyl 1-acetyl-2-oxoimidazolidine-4(*S*)-carboxylate
BAII	bis(pyridylimino-isoindolinate)
bcnp	1,8-naphthyridine-2,7-dicarboxylate
bdppp	2,6-di[$(C_6H_5)_2P$]pyridine
bhp	anion of 6-bromo-2-hydroxypyridine
BINO	binaphthoxide
BNAZ or 4*S*-BNAZ	benzyl-2-oxoazetidine-4(*S*)-carboxylate
BNOX or 4*S*-BNOX	4(S)-benzyl-2-oxooxazolidine
bpa	bis(2-pyridylmethyl)amine
BPAP	2,6-bisphenylaminopyridinate
bpbg	biphenylbiguanide
bpnp	2,7-bis(2-pyridyl)-1,8-naphthyridine
4*S*-BPPIM	2-methyl-l-propyl 1-(3-phenylpropanoyl)-2-oxoimidazolidine-4(*S*)-carboxylate
bpynap	2,7-bis(2-pyridyl)-1,8-naphthyridine
1,4-bq	1,4-benzoquinone
Br_2calix[4]arene$(CO_2H)_2$	25,26,27,28-tetrapropoxy-5,17-dibromo-calix[4]arene-11,23-dicarboxylic acid
5-Brsalpy	(2-pyridyl)-2-oxy-5-bromobenzylaminato
btmp	(benzylthiomethyl)diphenylphosphine
btp	2,6-bis-(*N*'-1,2,4-triazolyl)pyridine
Bu^t_2bipy	4,4'-bis(*tert*-butyl)-2,2'-bipyridine
Bu^t-H_2S_4	1,2-bis(2-mercapto-3,5-di-Bu^tphenylthio)ethane
4-Bu^t-py	4-*tert*-butylpyridine
Bu^t-salophen	*N*,*N*'-*o*-phenylenebis(salicylidenamine)

Pictiva EX2004
Samsung v Pictiva
IPR2024-01094

C

$CH_3N[P(OCH_2CH_3^{F3})_2]_2$	bis(bis(trifluoroethoxy)phosphine)methylamine
$C_4H_4NCO_2$	pyrrole-2-carboxylate
$C_4H_3SCO_2$	thiophene-2-carboxylate
C_4H_3SCONH	thiophene-2-amidate
$C_{10}H_{15}CO_2$	1-adamantylcarboxylate
calix[4]arene$(CO_2H)_4$	25,26,27,28-tetra-*n*-propoxycalix[4]arene-5,11,17,23-tetracarboxylic acid
cap	caprolactamate (anion of 1-aza-2-cycloheptanone)
carb	anion of carboline
CEP	$P(NCCH_2CH_2)_3$
4*S*-CHAZ	cyclohexyl 2-oxoazetidine-4(*S*)-carboxylate
chea	1-cyclohexylethylamine
CHIP	anion of 1'-3'-dihydrospiro[cyclohexane-1,2'-[2*H*]imidazo-[4,5*b*]pyridine
chp	anion of 6-chloro-2-hydroxypyridine
5-Clsalpy	(2-pyridyl)-2-oxy-5-chlorobenzylaminate
Cl-tpy	4'-chloro-2,2':6,2"-terpyridine
CNPh	phenylisocyanide
$CNPhCF_3$	trifluoromethylphenylisocyanide
$CNPhNMe_2$	*p*-dimethylaminophenylisonitrile
4-CN-py	4-pyridinecarbonitrile
COD	cycloocta-1,5-diene
COT	1,3,5,7-cyclooctatetraene
(*S*,*R*)-CPFA-P	(*S,R*)-(1-*N*,*N*'-dimethylaminoethyl)-2-(dicyclohexylphosphi-no)-ferrocene
18-crown-6	the crown ether 1,4,7,10,13,16-hexaoxacyclooctadecane
Cy	cyclohexyl or *c*-C_6H_{11}
cyt	cytosine

D

daapy	2,6-diacetylaminopyridine
dabco	1,4-diazabicyclooctane

Pictiva EX2004
Samsung v Pictiva
IPR2024-01094

dach	1,2-diaminocyclohexane
damt	2,4-diamino-6-methyl-s-triazine
DAniF	*N*,*N*'-di-*p*-anisylformamidinate
DAni^{m}F	*N*,*N*'-di-*m*-anisylformamidinate
DAni^{o}F	*N*,*N*'-di-*o*-anisylformamidinate
dapy	2,6-diaminopyridine
DArF	*N*,*N*'-diarylformamidinate
D^{Cl}PhF	*N*,*N*'-di-*p*-chlorophenylformamidinate
D^{Cl2}PhF	$[(3,5\text{-}Cl_2C_6H_3)_2N)_2CH]^-$
DCNNQI	*N*,*N*'-dicyanonaphthaquinone diimine
DCyF	*N*,*N*'-dicyclohexylformamidinate
DDA	2,3,5,6-tetramethyl-*p*-phenylenediamine (durenediamine)
dedp	$Et_2PCH_2CH_2PPh_2$
DEtBz	*N*,*N*'-di(ethyl)benzamidinate
depa	4,4'-diethyl-2,2'-dipyridylamide
depe	$CH_3CH_2PCH_2CH_2PCH_2CH_3$
dFMEPY or 5*S*-dFMEPY	methyl-(5*S*)-3,3-difluoro-2-oxopyrrolidine-carboxylate
dGuo	deoxyguanosine
diglyme	$CH_3O(CH_2)_2O(CH_2)_2OCH_3$
DMAD	dimethyl acetylene dicarboxylate
dimen	1,8-di-isocyanomenthane
dimenol	5,7-dimethyl-1,8-naphthyridine-2-ol
dippp	$Pr^i_2P(CH_2)_3PPr^i_2$
DMAA or dma	*N*,*N*'-dimethylacetamide
DMAP or 5*S*-DMAP	*N*,*N*'-dimethyl-2-pyrrolidone-5(*S*)-carboxamide
dmapd	2,6-dimethyl-4-aminopyrimidine
dmat	4,5-dimethyl-2-methylaminothiazolato
2,3-dmbq	2,3-dimethyl-1,4-benzoquinone
DM-DCNQI	2,5-dimethyl-*N*,*N*'-dicyanoquinonediimine
dmdppm	$Ph_2PCH_2PMe_2$
dme	dimethoxyethane, $CH_3O(CH_2)_2OCH_3$
DMeBz	*N*,*N*'-di-methylbenzamidinate

Pictiva EX2004
Samsung v Pictiva
IPR2024-01094

DMeODMBz	*N*,*N*'-dimethyl-3,5-dimethoxybenzamidinate
dmf	dimethylformamide
dmg	anion of dimethylglyoxime
dmhp	anion of 2, 4-dimethyl-6-hydroxypyrimidine
dmmp	anion of 4,6-dimethyl-2-mercaptopyrimidine
dmopehhypy	1,3-dimethyl-2,4-dioxo-9-(1-phenylethyl)-1,3,6,7,8,9-hexahydropyrimido[2,1-*f*]purine
dmp	anion of 2,6-dimethylpyridine
dmpe	bis(dimethylphosphino)ethane, $Me_2P(CH_2)_2PMe_2$
dmph	anion of 2,4-dimethyl-6-oxopyrimidine
dmpm	bis(dimethylphosphino)methane, $Me_2PCH_2PMe_2$
dmptsczda	dimethyl-4-phenylthiosemicarbazidediacetate
dmpyethybz	1,2-dimethoxy-4,5-bis[(2-pyridyl)ethynyl]benzene
$D^{M}PyF$	*N*,*N*'-5,5'-dimethyl-2,2'-dipyridylformamidinate
$D^{m\text{-}Me}PhF$	$[(m\text{-}MeOC_6H_4N)_2CH]^-$
DMSO or dmso	dimethylsulfoxide
DMTF	*N*,*N*'-dimethylthioformamide
DOSP	*N*-dodecylbenzenesulfonylprolinate
dpa	anion of 2,2'-dipyridylamine
dpae	$Ph_2AsCH_2CH_2AsPh_2$
dpam	bis(diphenylarsino)methane, $Ph_2AsCH_2AsPh_2$
dpapm	diphenylarsinodiphenylphosphinomethane, $Ph_2PCH_2AsPh_2$
DPB	diporphyrinatobiphenylene
dpcp	$Ph_2P\overline{CH(CH_2)_3CH}PPh_2$
dpdbp	$Ph_2PCH_2CH_2P(p\text{-}Bu^tC_6H_4)_2$
dpdt	$Ph_2PCH_2CH_2P(p\text{-tol})_2$
DPhAc	$[PhNC(CH_3)NPh]^-$
DPhBz	*N*,*N*'-diphenylbenzamidinate
DPhF	*N*,*N*'-diphenylformamidinate
$D^{p\text{-}Br}PhF$	$(p\text{-}BrC_6H_4N)_2CH^-$
$D^{p\text{-}Cl}PhF$	$(p\text{-}ClC_6H_4N)_2CH^-$
$D^{p\text{-}F}PhF$	$(p\text{-}FC_6H_4N)_2CH^-$

Pictiva EX2004
Samsung v Pictiva
IPR2024-01094

DPh$^{3,5\text{-diCl}}$F	*N*,*N*'-di-3,5-dichlorophenylformamidinate
DPh^{F}F	*N*,*N*'-di-*p*-fluorophenylformamidinate
DPh$^{m\text{-Cl}}$F	*N*,*N*'-di-*m*-chlorophenyl-formamidinate
DPhIP	anion of 2,6-di(phenylimino)piperidine
DPhTA	*N*,*N*'-di-phenyltriazenate
DPmF	dipyrimidinylformamidinate
dpmp	$(Ph_2PCH_2)_2PPh$
dpnapy	2,7-bis(diphenylphosphino)-1,8-naphthyridine
dppa	$(Ph_2P)_2NH$
dppb	$Ph_2PCH(Me)CH(Me)PPh_2$
dppbe	1,2-bis(diphenylphosphino)benzene
dppe	1,2-bis(diphenylphosphino)ethane, $Ph_2P(CH_2)_2PPh_2$
dppee	*cis*-$Ph_2PCH{=}CHPPh_2$
dppm	bis(diphenylphosphino)methane, $Ph_2PCH_2PPh_2$
dppma	$(Ph_2P)_2NMe$
dppn	benzo[*i*]dipyrido[3,2-*a*:2',3'-*c*]phenazine
1,3-dppp	$Ph_2P(CH_2)_3PPh_2$
dppz	dipyrido[3,2-*a*:2',3'-*c*]phenazine
DPyF	*N*,*N*'-di-2,2'-pyridylformamidinate
ds-im	dansyl-imidazole
ds-pip	dansyl-piperazine
DTBN	di-Bu^t-nitroxide
dtd	4,7-dithiadecane
dtdd	5,8-dithiadodecane
DTolF	*N*,*N*'-di-*p*-tolylformamidinate
DTolTA	*N*,*N*'-di-*p*-tolyltriazenato
DV-Xα	discrete variational calculations
DXyl^{2,6}F	*N*,*N*'-di-2,6-xylylformamidinate

E

EMAC	extended metal atom chain
en"	*N*,*N*-dimethylethylenediamine, $CH_3(H)N(CH_2)_2N(H)CH_3$

Pictiva EX2004
Samsung v Pictiva
IPR2024-01094

EPPIM	ethyl 1-(3-phenylpropanoyl)-2-oxoimidazolidine-4(*S*)-carboxylate
ESBO	edge-sharing bioctahedra
9-EtAdeH	9-ethyladenine
9-EtGH or 9-EtGuaH	9-ethylguanine
etpda	diethyltripyridyldiamide
1-EtT	anion of 1-ethylthymine

F

2-Fap	anion of (2-fluoroanilino)pyridine
2,5-F_2ap	anion of 2-(2,5-difluoroanilino)pyridine
2,6-F_2ap	anion of (2,6-difluoroanilino)pyridine
2,4,6-F_3ap	anion of (2,4,6-trifluoroanilino)pyridine
F_5ap	anion of (2,3,4,5,6-pentafluoroanilino)pyridine
$FcCO_2$	ferrocenecarboxylate
Fcpe	3-ferrocenyl-2-propenate
FHMO	Fenske-Hall Molecular Orbital
fhp	anion of 6-fluoro-2-hydroxypyridine
form	any formamidinate ligand
^{F}PhPyF	*N*,*N*'-*p*-fluorophenylenepyridylformamidinate
FSBO	face-sharing bioctahedron

G

gly	glycine
GudH	guanidinium cation
guH_2	guanine
Guo	guanosine

H

Hadmp	2-amino-4,6-dimethylpyridine
HBPAP	2-(PhN)-6-(PhN)py
Hdpa	bis-2-(pyridyl)amine
HDPhTA	*N*,*N*'-diphenyltriazine
HDXyl^{2,6}F	*N*,*N*'-di-2,6-xylylformamidine

Pictiva EX2004
Samsung v Pictiva
IPR2024-01094

hedp	1-hydroxyethylidenediphosphonato
hfacac	hexafluoroacetylacetonato
H-H	head-to-head
Hhq	2-quinolinol
Hmhq	4-methyl-2-quinolinol
Hmphonp	5-methyl-7-phenyl-1,8-naphthyridin-2-one
hp	anion of 2-hydroxypyridine
H_2pc	phthalocyanine
hpp	anion of 1,3,4,6,7,8-hexahydro-2*H*-pyrimido[1,2-*a*]pyrimidine
1R,2R,5S-hprmph	*1R,2R,5S*-2-hydroxy-5-isopropenyl-2-methylcyclohexyl-diphenylphosphane
1S,2S,5R-hprmph	*1S,2S,5R*-2-hydroxy-5-isopropenyl-2-methylcyclohexyl-diphenylphosphane
Hpyro	2-pyrrolidinone
H-T	head-to-tail
H_2TMP	tetramesitylporphyrin
Hvall	2-piperidinone (δ-valerolactam)

I

4*S*-IBAZ	isopropyl 2-oxoazetidine-4(*S*)-carboxylate
Im	imidazole
IMMe	2,4,4,5,5-pentamethyl-4,5-dihydro-1*H*-imidazolyl-1-oxy
indenyl	$C_9H_7^-$
Ino	inosine
4*S*-IPOX	isopropyl 2-oxooxazolidine-4(S)-carboxylate

L

lut	lutidine

M

MACIM or 4*S*-MACIM	methyl 1-acetyl-2-oxoimidazolidine-4(*S*)-carboxylate
mand	mandelate (α-hydroxy-α-phenylacetate, $PhCH(OH)CO_2^-$)
MANIM or *S*,*S*-MANIM	mandaloylimidazolidinone-4-carboxylate or methyl 4(*S*)-1-[(2'S)-methoxy-2'-phenylacetyl]-2-oxoimidazolidine-4-carboxylate

Pictiva EX2004
Samsung v Pictiva
IPR2024-01094

map	anion of 2-amino-6-methylpyridine
MBOIM or 4*S*-MBOIM	methyl 1-benzoyl-2-oxoimidazolidine-4(*S*)-carboxylate
mbzap	2-((α-methylbenzylidene)amino)pyridine
MCHIM or 4*S*-MCHIM	methyl 1-(cyclohexylacetyl)-2-oxoimidazolidine-4(*S*)-carboxylate
MDMIM	methyl 1-(*d*-menthoxyacetyl)-2-oxoimidazolidine-4(*S*)-carboxylate
9-MeAdeH	9-methyladenine
1-MeAdo	1-methyladenosine
2-Meap	2-(2-methylanilino)pyridinate
4*S*-MEAZ	methyl 2-oxoazetidine-4(*S*)-carboxylate
1-MeC	anion of 1-methylcytosine
1-Mecyd	1-methylcytosine
Me-DuPHOS	(+)-1,2-bis(2*S*,5*S*)-2,5-dimethylphospholano)benzene or its corresponding *R* enantiomer
Me-Im or 1-MeIm	*N*-methylimidazole
menapo	7-methyl-1,8-naphthyridin-2-onato-N,N'
MENTHAZ	menthyl 2-oxoazetidine-4(*S*)-carboxylate
mentholate	anion of menthol
meonp	7-methyl-1,8-naphthyridin-2-one
MEOX or 4*S*-MEOX	methyl 2-oxooxazolidine-4(*S*)-carboxylate
4,7-Me_2phen	4,7-dimethyl-1,10-phenanthroline
3,4,7,8-Me_4phen	3,4,7,8-tetramethyl-1,10-phenanthroline
mephnapo$^{N,N'}$	5-methy-7-phenyl-1,8-naphthridin-2-onato-N,N'
mephnapo^{N,O}	5-methy-7-phenyl-1,8-naphthridin-2-onato-N,O
mephonp	5-methyl-7-phenyl-1,8-naphthyridin-2-one
4*S*-MPAIM	methyl 1-phenylacetyl-2-oxoimidazolidine-4(*S*)-carboxylate
4*S*-MPOX	4(*S*)-methyl-5(*S*)-phenyl-2-oxooxazolidine
4*S*-MPPIM	methyl 1-(3-phenylpropanoyl)-2-oxoimidazolidine-4(*S*)-carboxylate
MEPY or 5*R*-MEPY	methyl 2-oxopyrrolidine-5(*R*)-carboxylate
4-Mepy	4-methylpyridine
4-Mepyms	anion of 4-methylpyrimidine-2-thione

Pictiva EX2004
Samsung v Pictiva
IPR2024-01094

4-MepyS	anion of 4-methyl-2-mercaptopyridine
5-MepyS	anion 5-methylpyridine-2-thiolate
3,5-Me_2pz	anion of 3,5-dimethylpyrazole
Mepyzca	anion of 2-methylpyrazine-5-carboxylic acid
Mes	mesityl, 2,4,6-$C_6H_2(CH_3)_3$
5-Mesalpy	(2-pyridyl)-2-oxy-5-methylbenzylaminato
1-MeT	anion of 1-methylthymine
metro	metronidazole
1-MeU	anion of 1-methyluracil
mhp	anion of 6-methyl-2-hydroxypyridine
m-MeODMB	dimethyl-3-methoxybenzamidinate
MLMIM	methyl 1-(*l*-menthoxyacetyl)-2-oxoimidazolidine-4(*S*)-carboxylate
mmtz	5-methylthio-2-mercaptothiadiazolinate
m-nitpy	2-(3-pyridyl)-4,4,5,5-tetramethyl-4,5-dihydro-1*H*-imidazol-1-oxyl-3-N-oxide
mpa	α-methoxy-α-phenylacetate
mphamnp	2-acetamido-5-methyl-7-phenyl-1,8-naphthyridine
MPP	2-methoxyphenylphosphine
MPPIM or 4*S*-MPPIM	methyl 1-(3-phenylpropanoyl)-2-oxoimidazolidine-4(*S*)-carboxylate
2-mq	anion of 2-mercaptoquinoline
mtfpa	(*R*)-α-methoxy-α-(trifluoromethyl)phenylacetate
mtz	2-mercaptothiazolinate

N

Nap	naphthyl
NaphthAZ	(*R*)-1-naphthalen-1-yl-ethyl 2-oxoazetidine-4(*S*)-carboxylate
NCPhCN	1,4-dicyanobenzene
5*S*-NEPY	neopentyl 2-oxopyrrolidine-5(*S*)-carboxylate
Nic	*N*-nitroxyethyl-nicotinamide
nitet	2-ethyl-4,4,5,5-tetramethyl-4,5-dihydro-1*H*-imidazol-1-oxyl-3-*N*-oxide

Pictiva EX2004
Samsung v Pictiva
IPR2024-01094

nitme	2,4,4,5,5-pentamethyl-4,5-dihydro-1*H*-imidazol-1-oxyl-3-*N*-oxide
nitph (NITPh)	2-phenyl-4,4,5,5-tetramethyl-4,5-dihydro-1*H*-imidazol-1-oxyl-3-*N*-oxide
5-NO_2salpy	(2-pyridyl)-2-oxy-5-nitrobenzylaminato
np	1,8-naphthyridine
1,4-nq	1,4-naphthoquinone

O

OBQDI	*o*-benzoquinodiimine
O_2CAr^{tol}	2,6-di(*p*-tolyl)benzoate
5*S*-ODPY	octadecyl 2-oxopyrrolidine-5(*S*)-carboxylate
OEP	dianion of 2,3,7,8,12,13,17,18-octaethylporphyrin
OMP	dianion of 2,3,7,8,12,13,17,18-octamethoxyporphyrin
OTf	triflate
OTs	anion of toluene-*p*-sulfonic acid
oxodmnp	2-oxo-5,7-dimethyl-1,8-naphthyridine

P

PC	orthometalated phosphine
pcp	methylenbis(phosphinate), $CH_2[P(O)OH]_2^{2-}$
PCy_3	tris(cyclohexyl)phosphine
pdc	pyroledithiocarbamate
pdz	pyridazine
c-Pen	*cyclo*-$C_5H_{10}O$
peptea	pentapyridyltetraamide
Ph_2Ppy	2-diphenylphosphinopyridine
phdpda	phenyldipyridyldiamide
phen	1,10-phenanthroline
PhIP	anion of 2-phenyliminopiperidine
PhNPy	anion of 2-anilinopyridine
PHOX or 4*S*-PHOX	4(*S*)-phenyl-oxooxazolidine
PhPcF	phenylpicolylformamidinate
$PhPpy_2$	phenylbis(2-pyridyl)phosphane

Pictiva EX2004
Samsung v Pictiva
IPR2024-01094

phpy	anion of phenylpyridine
PhPyBz	phenylpyridylbenzamidinate
PhPyF	phenylpyridylformamidinate
Phth	phthlamide
phz	phenazine
plpyz	2-pyrrolyl-1-pyrazine
p nitpy	2-(4-pyridyl)-4,4,5,5-tetramethyl-4,5-dihydro-1*H*-imidazol-1-oxyl-3-*N*-oxide
PNP	2,6-di[$(C_6H_{11})_2P$]pyridine
pop	pyrophosphate, $O[P(O)OH]_2^{2-}$
pqdi	9,10-phenanthroquinonediimine
pydz	pyridazine, $N_2C_4H_4$
pymSH	pyrimidine-2-thione
pynp	2-(2-pyridyl)-1,8-naphthyridine
pyphos	6-(diphenylphosphino)-2-pyridonate
pypz	pyrido[2,3-*b*]pyrazine
pyrimethamine	2,4-diamino-5-*p*-chlorophenyl-6-ethylpyrimidine
pyrr	α-pyrrolidonate, $C_4H_6NO^-$
pyS	anion of 2-mercaptopyridine
pySH	2-mercaptopyridine
pyz	pyrazine
pz	anion of pyrazole

Q

quin	quinuclidine
quinCO	8-quinoline acyl

R

$RcCO_2$	ruthenocenecarboxylate
Roll-3696	1-(2-hydroxy-3-methoxypropyl)-2-methyl-5-nitroimidazole

S

salpy	(2-pyridyl)-2-oxy-benzylaminate
SCF-Xα-SW	self consistent field-Xα-scattered wave

Pictiva EX2004
Samsung v Pictiva
IPR2024-01094

silox	$OSi(Bu^t)_3$
s-pqdi	9,10-phenanthrosemiquinonediimine
stf-CN	[2]staffane-3-carbonitrile

T

TBDMS	*tert*-butyldimethylsilyl
TBSP	1-[(4-Bu^t-phenyl)sulfonyl]-(2*S*)-pyrrolidinecarboxylate
Tcbiim	dianion of tetracyanobisimidazole
tclH	ω-thiocaprolactam
TCNE	tetracyanoethene
TCNQ	7,7,8,8-tetracyanoquinodimethane
tdpm	$(Ph_2P)_3CH$
tempo	2,2,6,6-tetramethylpiperidine-1-oxyl
tempol	2,2,6,6-tetramethyl-4-hydroxypiperidinyl-1-oxy
temyl	1,3,4,5-tetramethylimidazol-2-ylidene
teptra	tetrapyridyltriamide
tetraphos-1	$Ph_2P(CH_2)_2P(Ph)(CH_2)_2P(Ph)(CH_2)_2PPh_2$
tetraphos-2	$P(CH_2CH_2PPh_2)_3$
TFA	trifluoroacetate
tfepma	bis(bis(trifluoroethoxy)phosphino)methylamine, $MeN[P(OCH_2CF_3)_2]_2$
2-$THCO_2$	2-thienylcarbonylate
3-$THCO_2$	3-thienylcarbonylate
2,5-$TH(CO_2)_2$	2,5-thienyldicarboxylate
THREOX or 4*S*-THREOX	threonine-based-oxooxazolidinone-4(*S*)-carboxylate (5(*R*)-methyl-2-oxooxazolidine-4(*S*)-carboxylate)
tht	tetrahydrothiophene
TiPB	2,4,6-tri-isopropylbenzoic acid
TMB	2,5-di-isocyano-2,5-dimethylhexane
tmed or tmeda	$Me_2N(CH_2)_2NMe_2$, tetramethylethylenediamine
tmph	thiamin monophosphate (phosphate ester of vitamin B1)
TMP	2,4,6-trimethoxyphenyl anion
TMPP	2,4,6-trimethoxyphenylphosphine

Pictiva EX2004
Samsung v Pictiva
IPR2024-01094

tpyethebz	1,3,5-tris[(2-pyridyl)ethenyl]benzene
tmtaa	dianion of 5,7,12,14-tetramethyldibenzo[*b*,*i*]-[1,4,8,11]-tetraazacyclotetradecine (benzotetramethyltetraaza[14]annulene)
tmtu or tmu	1,1,3,3-tetramethyl-2-thiourea
TOEP	meso-(4'-tolyl)octaethylporphyrin dianion
$TolN_5Tol$	di-*p*-tolylpentaazadienate
TolPyF	*p*-tolylpyridylformamidinate
tpda	tripyridyldiamide
TPG or tpg	*N*,*N'*,*N"*-triphenylguanidinate anion
TPP or tpp	tetraphenylporphyrin dianion
tppz	2,3,5,6-tetra-2-pyridylpyrazine
tpy	2,2':6,2"-terpyridine
trimethoprim	2,4-diamino-5-(3',4',5'-trimethoxybenzyl)pyrimidine
triphos	$Ph_2P(CH_2)_2P(Ph)(CH_2)_2PPh_2$
$tRNA^{phe}$	transfer RNA of the amino acid phenylalanine
TTB	2,4,6-tri-*p*-tolylbenzoate
ttf	tetrathiafulvalene
2-TU	thiouracil anion

X

Xhp	substituted 6-hydroxypyridinate anion

Pictiva EX2004
Samsung v Pictiva
IPR2024-01094

Index

A

assemblies containing
- Mo_2^{4+} complexes 148-168, 222-223
- Re_2^{n+} complexes (n = 6, 5 or 4) 287, 291, 332, 338-340, 357
- Rh_2^{4+} complexes 483-485, 487-492, 516-518, 548-555
- Ru_2^{5+} complexes 400-401
- W_2^{4+} complexes 188

B

bond energies of M–M bonds 721-724

bond lengths
- atomic number, dependence on 713-715
- bond order, dependence on 707-710
- effect of axial ligands on 712-713

bond orders
- bond length correction with 707-710
- definition of 13

bridging ligands stabilizing metal–metal multiple bonds, classification of 18

C

CD spectra of compounds with M–M quadruple bonds 758-760

cobalt compounds, metal–metal bonding in 451-455

Cr_2^{5+} compound 56-57

Cr_2^{4+} compounds
- affect of axial ligation in 40-43
- A-frame-like structures in 64
- amidate ligands in 50-52
- amidinate ligands in 52-55, 58-59
- bridging amido ligands in 49, 57-58, 64
- carbonate ligands in 38
- carboxylate ligands in 35-43, 46, 55, 61
- Cr–C bonds in 43-46, 52-53, 60-61
- Cr–Cr bond distances in 36-37, 50-51, 54
- electronic structures of 65
- guanidinate ligands in 56
- intramolecular axial interactions in 57-59
- macrocyclic anionic chelating ligands in 61-62
- 2-methoxyphenyl ligands in 43-45
- N–C–N type divergent-bite ligands in ... 62-64
- 2-oxophenyl ligands in 45-46
- 2-oxopyridinate and related ligands in 47-50, 59
- 'super-short' Cr–Cr bonds in 43-50

D

δ–δ* transitions
- Cr_2^{4+} compounds 750
- Mo_2^{5+} compounds 750
- Mo_2^{4+} compounds 744-750, 758-759
- Os_2^{6+} compounds 757
- Re_2^{6+} compounds 746, 749, 760
- Re_2^{5+} compounds 746, 752-753
- Ru_2^{5+} compounds 757
- Tc_2^{5+} compounds 745-746, 749-751
- theory of 739-744

double metal–metal bonds
- Ir_2^{6+} compounds containing 457
- Nb_2^{6+} compounds containing 31-32
- Os_2^{4+} compounds containing 438, 442-444
- Re_3^{9+} compounds containing 3
- Re_2^{6+} compounds containing 300-301, 331-332
- Ru_2^{4+} compounds containing 405-414, 422

Pictiva EX2004
Samsung v Pictiva
IPR2024-01094

E

electron density maps, calculation of.....738

electronic absorption spectra
Cr_2^{4+} compounds.....750
effect of pressure on.....765
Mo_2^{5+} compounds.....750
Mo_2^{4+} compounds.....745-750, 753-755
Os_2^{6+} compounds.....442-443, 757
Pt_2^{6+} compounds.....757
Re_2^{6+} compounds.....746, 749, 751-752
Re_2^{5+} compounds.....746, 752-753
Rh_2^{4+} compounds.....756-757
Ru_2^{5+} compounds.....757
Tc_2^{5+} compounds.....745-746, 749-755

electronic structure calculations
Cr_2^{4+} compounds.....728-729
Mo_2^{6+} compounds.....729-730, 733-738
Mo_2^{5+} compounds.....738
Mo_2^{4+} compounds.....725, 727-729
Nb_2^{4+} compounds.....727
Os_2^{6+} compounds.....725
Pt_2^{6+} compounds.....738
Re_2^{6+} compounds.....725-727
Re_2^{4+} compounds.....738
Rh_2^{4+} compounds.....727, 731-732, 738
Ru_2^{5+} compounds.....732-733
Ru_2^{4+} compounds.....727, 733
Tc_2^{5+} compounds.....725
Tc_2^{4+} compounds.....727
W_2^{6+} compounds.....729-730, 737
W_2^{4+} compounds.....725-726, 728

electron paramagnetic resonance spectra.....441-442, 783-785

emission spectra of compounds with M–M quadruple bonds.....762-763

EXAFS measurements.....785-786

excited state distortions of M–M bonded compounds.....760-761

extended metal atom chains (EMACs)
chromium compounds with.....671-673, 682-683, 686, 698, 703
cobalt compounds with.....686-693, 703
copper compounds with.....694, 697-700
iridium compounds with.....461-462, 702
iron compounds with.....698
ligand bridges present in.....669-671, 698-700
metal–metal distances present in.....674-681, 684-685, 699
nickel compounds with.....694-697, 700-701, 703
platinum compounds with.....658-661, 702-703
rhodium compounds with.....536-540, 701-702
ruthenium compounds with.....701-702

F

formal shortness ratios for multiple bonds.....47

H

heteronuclear diatomic compounds
$[CrMo]^{4+}$ core in.....43, 145-146
$[MoOs]^{n+}$ core (n = 4 or 5) in.....146, 148, 438-439
$[MoRe]^{5+}$ core in.....146, 148, 291
$[MoRu]^{n+}$ core (n = 4 or 5) in.....146, 148, 422
$[MoW]^{5+}$ core in.....196
$[MoW]^{4+}$ core in.....145-148, 196-197
$[OsW]^{4+}$ core in.....438
$[RuOs]^{4+}$ core in.....422, 438
$[RuW]^{4+}$ core in.....422

I

internal flips of M_2 units.....718-720

internal rotation
effect on bond length of.....711-712
effect of δ bonding on.....710-712

Ir_2^{6+} compounds.....456-457

Ir_2^{5+} compounds.....455-457

Ir_2^{4+} compounds
anionic bridging ligands in.....455-461
intramolecular disproportionation in.....456-458
Ir–Ir bond distances in.....455-456
π-acceptor ligands in.....458-461
unsupported Ir–Ir bonds in.....458

iridium blues.....461-462

iron compounds, metal–metal bonding in.....447-450

isomers of $M_2X_{8-n}L_n$ species
types of.....17
mechanisms for the interconversion of.....718-720

Pictiva EX2004
Samsung v Pictiva
IPR2024-01094

M

Mo_4^{12+} tetranuclear clusters.....218-223

Mo_4^{8+} compounds of the type $Mo_4X_8(PR_3)_4$ (X = Cl or I).....165-166

Mo_2^{6+} compounds
alkoxide ligands in.... 205-207, 210, 213-228, 230-234, 236-237, 239
alkynes, reactions with.....234
amido ligands in..... 205-206, 210-217, 224-228
arsenate ligand bridges in.....94
bonding in triply bonded Mo_2L_6 molecules.....208-209
calixarene ligands in.....228
carboxylate ligands in.....229
cleavage of triple bond in.....231-234
CO, reactions with.....232-233
COT ligands in.....207-208, 210
cyclopentadienyl ligands in.....210-211
β-diketonate ligands in.....225
ethane-like structures of.....203-204
intramolecular disproportionation in.....226
isocyanides, reactions with.....234
Mo–C bonds in..... 204, 207-208, 210-217, 222-223, 228-229
Mo–Mo bond distances in..204-205, 213, 224
$Mo_2X_{6-n}Y_n$ molecules.....210-218
nitriles, reactions with.....236-237
phosphate ligand bridges in.....94
oxidation of Mo_2^{4+} compounds to give.....139
phosphido ligands in.....210, 213-216
phosphine ligands in.....223, 228
redox chemistry of.....230-232
thiolate/selenate ligands in.....208, 213, 215-216, 236
triazenate ligands in.....227

Mo_2^{5+} compounds
oxidation of Mo_2^{4+} compounds to give.....139
phosphate ligand bridges in.....94
sulfate ligand bridges in.....92, 139

Mo_2^{4+} compounds
affect of axial ligation in.....73
alkoxide ligands in..... 116, 134-135, 217-218
amidate ligands in..... 97, 152-153, 156-159
amidinate ligands in.....98, 101-103, 141-142, 155-167
anionic N,N bridging ligands in..98-103, 217
anionic O,S and S,S ligands in.....103-105
carbonate ligands in..... 161-163, 167-168
carboxylate ligands in.... 69-92, 106, 138-139, 151-152, 154-158, 160-164, 166-167
cationic complexes of.....130-132
cleavage of quadruple bond in.....136-137
guanidinate ligands in.....141
halide anions of the type $[Mo_2X_6(H_2O)_2]^{2+}$ (X = Cl, Br or I) in.....106-108
halide ligands in, see $[Mo_2X_8]^{4-}$ ions
homoleptic acetonitrile cations of.....130-131
hydride ligands in.....142
intramolecular disproportionation in.135, 218
macrocyclic anionic chelating ligands in.....132-133
mixtures of carboxylate with other anionic ligands in.....79-92, 99-100, 106
Mo–C bonds in..... 115-116, 137, 142-145
Mo–Mo bond distances in..... 71-73, 80-84, 92, 96, 106, 115-118, 131-132, 148, 156-157, 161, 163-164
$[Mo_2X_8H]^{3-}$ salts (X = Cl, Br or I) formed by oxidation of.....108-110
2-oxopyridinate ligands in.....95-97, 127
phosphine ligands in..... 77-78, 87-90, 112-130, 137, 142-144
polyoxoanion bridges in.....92-95
porphyrin ligands in.....132-133
redox chemistry of..... 92-94, 108-110, 127-130, 134, 137-142, 153-154

Mo_2^{2+} compound containing $F_2PN(CH_3)PF_2$ ligands.....138

$[Mo_2X_8]^{4-}$ ions (X = Cl, Br, CN or NCS), salts containing
molecular structure of.....69-70, 106
synthesis of.....69, 97, 106-107

$Mo_2X_4(PP)_2$ compounds (X = halide; PP = bidentate phosphine),
α- and β- isomers of..... 113-114, 117-118, 120, 123-129

multiple bonding, distribution within the transition elements.....16-17

N

Nb_2^{6+} compounds, double bonds in.....31-32

Nb_2^{4+} compounds
7-azaindole ligands in.....30-31
calix[4]arene ligands in.....31-32

Pictiva EX2004
Samsung v Pictiva
IPR2024-01094

guanidinate ligands in.....29-30
Nb–Nb bond distances in 29

nickel compounds, metal–metal
bonding in.....633-634

Noddack, Walter and Ida, discovery of
rhenium by.....271-272

O

ORD spectra, see CD spectra

orientation disorder of M–M units
in crystals 715-718

Os_2^{7+} compounds
guanidinate ligands in.....435
magnetic properties of.....439
Os–Os bond distances in 435

Os_2^{6+} compounds
amidate ligands in.....432, 441
amidinate ligands in.....432, 440
anionic N,N bridging
ligands in.....432-433, 442
carboxylate ligands in..... 432-436, 438-443
cleavage of triple bond in 434-437
electronic structures of 439-443
halide ligands in, see $[Os_2X_8]^{2-}$ ions
magnetic properties of..... 435-436, 439-442
orthometalated ligands in.....433-434, 441
Os–C bonds in 432-436
Os–Os bond distances in 434-435, 437
2-oxopyridinate ligands in.....432-433, 441
phosphine ligands in 433-434, 441
porphyrin ligands in.....434-444
redox chemistry of.....437, 439
spectroscopic properties of.....442-443

Os_2^{5+} compounds
carboxylate ligands in.....437-438, 441
electronic structures of 441-442
magnetic properties of.....435, 441-442
Os–Os bond distances in 435
2-oxopyridinate ligands in.....437, 441-442
phosphine ligands in 438
porphyrin ligands in.....434-444
spectroscopic properties of.....441-442

Os_2^{4+} compounds, porphyrin
ligands in 438, 442-444

$[Os_2X_8]^{2-}$ ions (X = Cl, Br or I), salts containing
cleavage of triple bond in 436-437
electronic structure of.....441
molecular structures of 436
redox chemistry of.....442-443
synthesis of.....436

P

paddlewheel molecules with
unsymmetrical ligands, regioisomers of 18

palladium compounds, metal–metal
bonding in.....634-636

Peligot, Eugéne-Melchoir, discovery of
dichromium (II) carboxylates by 10-11

photochemical reactions of compounds
with M–M quadruple bonds 763-765

photoelectron spectra (UV)
allyl compounds 775
Cr_2^{4+} compounds 766-771, 775
M_2X_6 (M = Mo or W) molecules 773-774
$M_2Cl_4(PMe_3)_4$ compounds
(M = Mo, W or Re) 772
Mo_2^{6+} compounds.....773-774
Mo_2^{4+} compounds.....766-775
paddlewheel molecules..... 766-771, 774-775
Re_2^{6+} compounds.....766
Re_2^{4+} compounds.....772-773, 775
Rh_2^{4+} compounds 774
Ru_2^{4+} compounds 773-774
W_2^{6+} compounds.....773
W_2^{4+} compounds.....766-773

platinum blues 658-661

Pt_2^{6+} compounds
amidate ligands in.....648-651
amidinate ligands in.....648
anionic N,O bridging ligands in 648-654
anionic N,S bridging ligands in 655-656
carboxylate ligands in.....646-647
electronic structures of 636
guanidinate ligands in.....648
2-oxopyridinate ligands in.....651-652
polyoxoanion bridges in 642-643
Pt–C bonds in 647, 649-653, 661
Pt–Pt bond distances in 637-641
pyrophosphite ligand bridges in 644-646
unsupported Pt–Pt bonds in.....656-657

Pt_2^{5+} compounds.....657-658

Pictiva EX2004
Samsung v Pictiva
IPR2024-01094

Q

quadruple metal–metal bonds
Cr_2^{4+} compounds containing..... 10-12, 35-65
discovery and initial characterization of $Mo_2(O_2CCH_3)_4$.....9-10
Mo_2^{4+} compounds containing..... 8-10, 69-168
qualitative bonding treatment of.....13-15
Re_2^{6+} compounds containing 7-8, 273-301, 364-365
recognition of existence in $Cr_2(O_2CCH_3)_4 \cdot 2H_2O$ 10-12
Tc_2^{6+} compounds containing.....252-260
W_2^{4+} compounds containing 183-196

R

Re_3^{9+} clusters, recognition of Re=Re bonding in.....3

Re_2^{8+} compounds, electron-poor triple bond in 360-361

Re_2^{7+} compounds, paddlewheel structure of.....307

Re_2^{6+} compounds
alkyl ligands in 289, 300
amidate ligands in.....296-297, 365
amidinate ligands in.....295-296
carboxylate ligands in.....282-292
cleavage of quadruple bond in 362-363, 365
β-diketonate ligands in 292-293
halide ligands in, see $[Re_2X_8]^{2-}$ ions (X = F, Cl, Br or I)
intramolecular disproportionation reactions of 290-292, 302
2-mercaptopyridinate ligands in.....294-295
2-oxopyridinate ligands in.....294-295
phosphine ligands in 298-300
polyoxoanion bridges in 293
Re–Re bond distances in 275-278, 364-365
redox chemistry of.....303-308
thiocyanate ligands in 280-281
thioether ligands in 301

Re_2^{5+} compounds
amidate ligands in.....307
amidinate ligands in.....307, 333, 360
bidentate phosphine ligands in.....322-327, 333, 335-338, 340-341
bidentate thioether ligands in.....302-303
carboxylate ligands in.....306-307, 333, 335-338, 340-341
2-mercaptopyridinate ligands in.....306-307
monodentate phosphine ligands in 309, 314-322, 335, 337
2-oxopyridinate ligands in.....306-307
Re–Re bond distances in 312-313
redox chemistry of.....315-322, 335

Re_2^{4+} compounds
alkyl ligands in 309, 327
allyl ligands in 359-360
amidinate ligands in.....365
bidentate and tridentate phosphine ligands in.....322-341
carboxylate ligands in.....333-341
cleavage of triple bond in 362-363, 365
β-diketone ligands in 340-342
electron-rich triple bond in 302, 313-314
homoleptic acetonitile cation of.....360
monodentate phosphine ligands in.....309-322, 329, 359
phthalocyanine ligand in 360
porphyrin ligands in.....360
Re–Re bond distances in 310-312
redox chemistry of..... 315-322, 326-327, 331-332, 334-335, 359

$[Re_2X_8]^{2-}$ ions (X = F, Cl, Br or I), salts containing
molecular structure of 6, 274-275, 278-280, 364-365
recognition of existence of multiple bonding in 7-8
redox chemistry of..... 303-304, 307-308
synthesis of..... 273-274, 278-279

$Re_2Cl_6(\mu\text{-dppm})_2$, the Re=Re bond in..... 300-301, 331-332

$Re_2X_4(PP)_2$ compounds (X = halide; PP = bidentate phosphine), α- and β- isomers of.....321-325

$Re_2X_4(\mu\text{-dppm})_2$ (X = halide) complexes, see also Re_2^{4+} compounds, reactions with CO, isocyanides, nitriles and alkynes with retention of Re–Re bonding in 342-359

$[Re_2X_3(\mu\text{-dppm})_2(CO)(CNR)]^+$ cations (X = Cl or Br; R = alkyl or aryl), structural isomers of 343-344, 353-355

$[Re_2Cl_2(\mu\text{-dppm})_2(CO)(CNXyl)_3]^{n+}$ species (n = 2, 1 or 0), structural isomers of.....356

rhenium, discovery of the element 271

Rh_2^{6+} compounds.....540, 542, 546-547

Pictiva EX2004
Samsung v Pictiva
IPR2024-01094

Rh_2^{5+} compounds
amidate ligands in.....543-544
amidinate ligands in.....544-546
anionic N,N bridging ligands in 544-547
carboxylate ligands in.....541-543, 545
electronic structures of 540, 543-544, 546
Ru–C bonds in.....546-547
Rh–Rh bond distances in 540-541

Rh_2^{4+} compounds
amidate ligands in..... 510-511, 543-544, 557, 565-566, 591-598, 611-612
amidinate ligands in..... 512-514, 544-545, 548-555, 557, 559-560, 563-656
anionic N,N bridging ligands in 512-521, 544-546
anionic N,O bridging ligands in 505-512
biological significance of 555-566
carboxylate ligands in..... 466-506, 509-514, 525-531, 541-543, 548-567, 599-605, 609-611
catalytic activity and applications of...591-627
chiral ligands in 591-598, 609-612
cleavage of the Rh–Rh bond in 547
β-diketone ligands in 501, 531
electronic structure of.....465, 512
homoleptic aquo cation 528-529
homoleptic nitrile cations.....529-530, 566
isocyanide ligands in 533-535
macrocyclic ligands in 531-533
multidentate heterocyclic amine ligands in..... 501-505, 511, 513-514, 520, 553-554, 556, 563-565
nitrile ligands in 487-488, 492, 501-506, 510, 513-514, 520, 526, 545, 548, 551-554, 562, 564, 566
organic transformations catalyzed by ..591-627
orthometalated ligands in.....502, 520, 525-526, 551-552, 599-605
2-oxopyridinate ligands in.....505-510
phosphine containing bridging ligands in..... 524-527, 535, 551-552, 556, 566, 599-605
photochemistry of 563-564, 566-567
polyoxoanion bridges in 527-528, 547
porphyrin ligands in..... 531-532, 552-553
redox chemistry of.....535, 540-547
Rh–Rh bond distances in .. 471-485, 494-500, 506-508, 515-519, 521-523, 527, 530, 594, 601
(S,N), (S,O) and (S,S) anionic bridging ligands in 468, 521-524
triazenate ligands in 512-513
unsupported Rh–Rh bonds in 528-533

Rh_2^{3+} compounds.....535-536, 542, 544

rhodium blues 536-539

rhodium, mixed-valence molecular wires containing 536-537, 539

Ru_2^{6+} compounds
amidinate ligands in.....418-421
anionic N,N bridging ligands in 416-422
electronic structures of 415-422
guanidinate ligands in.....421-422
macrocyclic ligands in 422
magnetic properties of..... 415-416, 421-422
polyoxoanion bridges in 415-416
redox chemistry of.....418-422
Ru–C bonds in.....417-421
Ru–Ru bond distances in 414-415

Ru_2^{5+} compounds
amidate ligands in.....391-393
amidinate ligands in.....399-401
anionic N,N bridging ligands in 396-404
biological significance of 423-424
carbonate ligands in 390-391
carboxylate ligands in.....382-389, 394, 398-404, 423-424
catalytic activity of.....422-423
cleavage of Ru–Ru bond in 385
electronic structures of 386-389, 404
macrocyclic ligands in 422
magnetic properties of.....388-389, 393, 395-396, 399, 401, 403-404
naphthyridine ligands in 401-402
2-oxopyridinate ligands in.....393-396
polyoxoanion bridges in 390
redox chemistry of.....386, 392-393, 395, 398, 400, 403
Ru–C bonds in.....397-401
Ru–Ru bond distances in 378-382

Ru_2^{4+} compounds
amidinate ligands in.....411-412
carboxylate ligands in..... 405-409, 422-423
catalytic activity of.....422-423
cleavage of Ru–Ru bond in 406-407
electronic structures of 406-408, 410-414
macrocyclic ligands in 422
magnetic properties of..... 407-411, 413-414
naphthyridine ligands in 413-414
2-oxopyridinate ligands in.....409-410
redox chemistry of.....407, 411-414
Ru–Ru bond distances in 404-405

Pictiva EX2004
Samsung v Pictiva
IPR2024-01094

triazenate ligands in 412-413

S

supramolecular assemblies and arrays,
see assemblies containing

T

tantalum compounds, metal–metal
bonding in.....32

Tc_8^{n+} octanuclear clusters
(n = 13 or 12).....266-267

Tc_6^{n+} hexanuclear clusters
(n = 12, 11 or 10).....265-267

Tc_2^{6+} compounds
carboxylate ligands in.....257-259
halide ligands in, see $[Tc_2X_8]^{2-}$ ions
(X = Cl or Br)
sulfate ligand bridges in.....260
Tc–Tc bond distances in 253

Tc_2^{5+} compounds
amidinate ligands in.....259-260
carboxylate ligands in.....258-259
halide ligands in, see $[Tc_2X_8]^{3-}$ ions
(X= Cl or Br)
2-oxopyridinate ligands in.....259
phosphine ligands in 260-261
redox chemistry of.....259-260
Tc–Tc bond distances in 253

Tc_2^{4+} compounds
cleavage of triple bond in 264-265
homoleptic acetonitrile cation of 263-265
phosphine ligands in 262-263
polymeric $\{[Tc_2X_6]^{2-}\}_n$ anions in.....261-262
redox chemistry of.....259, 262-263
Tc–Tc bond distances in 253

$[Tc_2X_8]^{2-}$ ions (X = Cl or Br), salts containing
molecular structure of 255
redox chemistry of.....255
synthesis of.....254-256

$[Tc_2X_8]^{3-}$ ions, (X = Cl or Br), salts containing
molecular structure of 254
recognition of existence of multiple
bonding in.....9
redox chemistry of.....254
synthesis of.....252, 254-257
Tc–Tc bond of order 3.5 in 252

$Tc_2Cl_4(PP)_2$ compounds (PP = bidentate
phosphine), α- and β- isomers of 263

technetium, synthesis and properties of 251

triple metal–metal bonds
discovery of the first compound
containing 8, 302-303
Mo_2^{6+} compounds containing 94, 139-141,
165-166, 203-242
Mo_2^{2+} compound containing.....138
Nb_2^{4+} compounds containing 29-32
Os_2^{6+} compounds containing 431-437,
439-444
Re_2^{4+} compounds containing 302-361, 365
Ru_2^{6+} compounds containing.....416-417,
420-422
Tc_2^{4+} compounds containing 261-265
V_2^{4+} compounds containing.....23-27
W_2^{6+} compounds containing 198-199,
203-242

V

V_2^{4+} compounds
amidinate ligands in.....24-26
2-aminopyridinate ligands in 26
guanidinate ligands in.....26
stabilization by bridging anionic
ligands of.....24-26
V–V bond distances in 26

V_2^{3+} compounds, bonds of order 3.5 in 26-28

vibrational spectra
M–L stretches.....781-783
M–M stretches 775-778
M–M stretches in the excited state 780-781

W

W_4^{12+} tetranuclear clusters.....218-223

W_2^{6+} compounds
aldehydes, reactions with.....239
alkoxide ligands in 205-207, 210-214,
217-221, 224-228, 230-241
alkynes, reactions with 234-236, 239
amido ligands in 205-206, 210-215,
217-218, 221, 224-228, 236
Bloomington Shuffle process 219-220
bonding in ethane-like molecules.....208-209
calixarene ligands in.....198-199, 228
C=C bonds, reactions with 237-240

Pictiva EX2004
Samsung v Pictiva
IPR2024-01094

carboxylate ligands in.....207-208, 217, 229
cleavage of triple bond in 231-237
CO, reactions with 232-234
COT ligands in 207-208, 210-212, 214-215, 218
cyclopentadienyl ligands in 210-211, 213, 217-218, 241-242
β-diketonate ligands in 225
ethane-like structures of.....203-204
H_2, reactions with 240, 242
isocyanides, reactions with 234
ketones, reactions with 239
nitrile containing ligands, reactions with.....236-237
organometallic molecules, reactions with...241
oxidation of W_2^{4+} compounds to give 190, 194-195, 197-198
phosphido ligands in 210-215, 218
phosphine ligands in 224-226
redox chemistry of.....230-232,
thiolate/selenate ligands in 208, 213, 218
triazenate ligands in 227
W–C bonds in..... 204, 207-208, 210-215, 217-218, 221, 229, 236, 240
W–W bond distances in.....205, 213-214, 224-225
$W_2X_{6-n}Y_n$ molecules 210-218

W_2^{5+} compounds 186, 190, 194, 197-198

W_2^{4+} compounds
amidinate ligands in.....189-190
anionic N,N bridging ligands in 189-190
carboxylate ligands in.....183-188, 197, 217
guanidinate ligands in.....189, 197-198
halide ligands in, see $[W_2Cl_8]^{4-}$ ion
2-oxopyridinate ligands in.....189-190, 192
phosphine ligands in 184-185, 187-188, 192-195
porphyrin ligands in.....192
redox chemistry of.....186, 190, 194-195, 197-198
W–C bonds in.....189, 191
W–W bond distances in.....184-185

$[W_2Cl_8]^{4-}$ ion, salts containing 191-192

$W_2X_4(PP)_2$ compounds (X = halide; PP = bidentate phosphine),
α- and β- isomers of.....192-194

X

X-ray photoelectron spectra (XPS).....785-786

Pictiva EX2004
Samsung v Pictiva
IPR2024-01094